ECR 2017 – BOOK OF ABSTRACTS

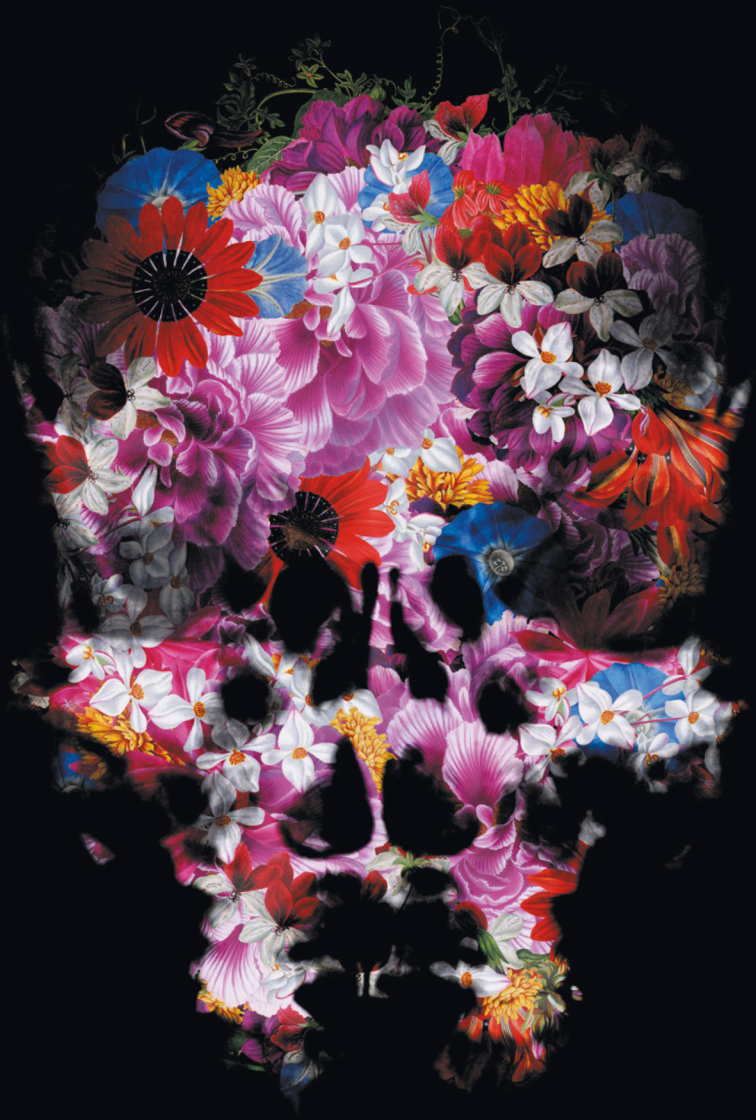

CONTENTS:

Insights Imaging (2017) 8 (Suppl 1):S1–S583
DOI 10.1007/s13244-017-0546-5

A

Postgraduate Educational Programme

EFOMP Workshop (EF)
ESR/EFRS meets Sessions (EM)
European Excellence in Education (E³)
Headline Sessions
Joint Sessions
Mini Courses (MC)
Multidisciplinary Sessions (MS)
New Horizons Sessions (NH)
Professional Challenges Sessions (PC)
Pros & Cons Session (PS)
Refresher Courses (RC)
Special Focus Sessions (SF)
State of the Art Symposia (SA)

Wednesday, March 1

08:30 - 10:00 **Room A**

E³ - ECR Academies: Interactive Teaching Sessions for Young (and not so Young) Radiologists

E³ 121
Emergency radiology I

A-001 08:30
A. Brain trauma
M. Smits; *Rotterdam/NL (marion.smits@erasmusmc.nl)*

Neurotrauma is a major cause of death and disability and accounts for up to 10% of all emergency department visits. Most patients with head trauma are classified as having minor head injury, defined as no or brief loss of consciousness, amnesia and a Glasgow Coma Score (GCS) of 13-15. Brain injury is, however, fatal in 10% of all head injury patients, while 5-10% suffer permanent serious neurological deficits. A further 20-40% of patients are left moderately disabled. CT is the modality of choice for assessment of brain injury in the acute setting, while MRI is more commonly used as a secondary modality in the subacute or chronic stage. Direct consequences of brain injury include fracture, contusion, haematoma and vascular injury, which are generally well known and easily appreciated. Findings of indirect consequences, however, such as herniation, brain swelling and vascular complications, are sometimes subtle and easy to overlook. In this case-based presentation, I will outline the common findings of direct brain injury consequences and specifically focus on the less common findings of indirect consequences.

Learning Objectives:
1. To understand the different types of brain trauma.
2. To become familiar with the differential diagnosis.

A-002 09:15
B. Peripheral vascular injury
J. Ferda; *Plzen/CZ (ferda@fnplzen.cz)*

Penetrating vascular trauma is caused by direct vessel damage, which exhibits visible bleeding with an extensive blood loss. Blunt trauma injures vessels by crushing, distraction or shearing which leads to dissection, thrombosis and consequent ischaemia and/or invisible bleeding. Unrecognised and uncontrolled haemorrhage can rapidly lead to the demise of the trauma patient. Unrecognised and untreated ischaemia can lead to limb loss, stroke and multiple organ failure. Proper imaging has to be done to recognise the vascular injury and to decide if surgical or endovascular repair should be used. In injuries caused by high energy and/or high velocity, CT angiography is the method of choice to determine the site of active extravasation or the vessel occlusion even if the patient is in the condition of centralised circulation. Some bleedings are delayed after restoration of systemic blood pressure, especially in pelvic region. In low-energy low-velocity trauma, the development of the signs of vascular trauma could be hidden - ultrasound aims to detect the pseudoaneurysms as well as the intramural haematoma or thrombosis. The imaging of the bleeding artery or occluded vessel is crucial to consequent therapy. The injuries with tissue loss and destruction of the skeleton are preferably indicated to surgical treatment. Where it is possible to penetrate the injured segments by the wire, the endovascular approach is preferable, with the exception of the simple embolization to stop bleeding. During the presentation, the illustrative cases of penetrating injury, the blunt injury including the crossroads of imaging and treatment will be shown.

Learning Objectives:
1. To understand the different types of peripheral vascular injury.
2. To become familiar with the different imaging techniques.
3. To become familiar with interventional treatment options.

08:30 - 10:00 **Room B**

GI Tract

RC 101
Assessing inflammation and fibrosis in Crohn's disease

A-003 08:30
Chairman's introduction
A. Laghi; *Latina/IT (andrea.laghi@uniroma1.it)*

Diagnostic imaging plays a major role in the decision-making process of patients affected by Crohn's disease (CD), both at the time of diagnosis and throughout the course of the disease. One of the most relevant clinical problems in current management of patients affected by CD is represented by the assessment of inflammation and fibrosis. The two entities should not be considered separately, since they coexist in most of the patients. A correct quantification of the prevalent entity is extremely important, since the patient should be referred for medical therapy if inflammation predominates, whereas either endoscopic dilatation of the stricture or surgery becomes necessary if fibrosis is prevalent. Cross-sectional imaging (CSI) modalities, including ultrasound (US), multidetector-CT (MDCT) and MR imaging (MRI), can provide useful information, particularly for inflammation, less for fibrosis. Contrast-enhanced US (CEUS) has been shown to correlate with disease activity and severity, in comparison with endoscopic score of severity. Data about CEUS and fibrosis are controversial, although a quantitative data analysis seems the most valuable approach. Very promising results have been recently obtained with US elastography. Current data with MDCT highly correlate with disease activity and severity, but not with fibrosis. Dual-energy analysis might improve MDCT performances. MRI correlates not only with inflammation, but also with fibrosis, particularly if multiparametric analysis is performed. This analysis includes the evaluation of pattern of enhancement, late enhancement and the analysis of T2 signal. In the next future, other MR techniques are under evaluation, such as T1 mapping and magnetization transfer contrast.

A-004 08:35
A. Is sonography (CEUS and elastography) the right tool?
E. Quaia; *Edinburgh/UK (equaia@ex sede.ed.ac.un)*

Crohn's disease (CD) is a chronic transmural inflammatory disease of the gastrointestinal tract which can be assessed by ultrasound. Unenhanced ultrasound may evaluate the localization and the length of the affected intestinal segments and may suggest the presence of mural fibrosis based on the layered appearance of the bowel wall. Contrast-enhanced ultrasound of the bowel is performed by wide-band transducers including the microbubble resonance frequency. Contrast-enhanced ultrasound has become an important imaging modality in patients with CD for the grading of disease activity, the differentiation between small bowel stricture due to inflammation or mural fibrosis, and for the assessment of the response to specific pharmacologic therapy. New dedicated software packages allow the accurate quantification of the enhancement within the small bowel wall after microbubble contrast agent injection to obtain different kinetic parameters - percentage of the maximal enhancement, the time-to-the peak enhancement, and the area under the time-intensity curve - which may differentiate mural inflammation from fibrosis and responders from non-responders to the specific pharmacologic therapy. The main advantage of contrast-enhanced ultrasound in the real-time assessment of the perfusion of the bowel wall but the scan is necessarily limited to one single loop each time. US real-time elastography can be considered an additional tool to complete US assessment of the bowel wall in patients with CD. US real-time elastography allows to assess the bowel wall stiffness to distinguish acute inflammation from fibrosis in patients with CD and increases the diagnostic confidence if compared to contrast-enhanced US alone.

Learning Objectives:
1. To learn about CEUS technique, including imaging acquisition and data post-processing.
2. To become familiar with US elastography, particularly with those techniques useful in the assessment of the small bowel.
3. To understand potential advantages and possible limitations of CEUS and elastography in the assessment of inflammation and fibrosis in Crohn's disease.

Author Disclosure:
E. Quaia: Speaker; Bracco Imaging and GE Healthcare Board Speaker.

A-005 08:58

B. Is there space for MDCT (spectral imaging, iodine map)?

J. Podgorska; *Warsaw/PL (jpodgo@gmail.com)*

Many aspects of managing patients suffering from Crohn's disease (CD) remain unclear. It is still unknown which factors trigger disease chronicity, and which promote the development of intestinal fibrosis. On the other hand, anti-inflammatory treatment such as steroids, immunosuppressants and anti-TNF-alpha have serious side effects; moreover, the decision for surgical treatment is also difficult. Because of many factors that influence the disease management, there is a strong need for a reliable tool of inflammatory activity and fibrosis assessment. Recently, apart from MR enterography (MRE), CT enterography (CTE) is being used to detect and monitor intestinal inflammation. Bowel wall and mesenteric changes such as mural thickening and hyperenhancement, increased attenuation of perienteric fat, and mesenteric hyperaemia have been reported to indicate CD activity. Recently introduced dual-energy CT modality allows creating monochromatic spectral images at energy levels ranging from 40 to 140 keV and water and iodine-based material decomposition with quantitative analysis. This method has already been applied in abdominal imaging, e.g. urinary stones, renal cell carcinoma and hepatocellular carcinoma. There are also preliminary reports about implementation of spectral imaging in CTE technique for an objective assessment of Crohn's disease activity and coexistent fibrosis. The aim of this lecture is to give an overview of the CTE bowel inflammatory changes, and the possible advantages of spectral imaging for assessing activity and fibrosis in CD.

Learning Objectives:

1. To understand basic principles of spectral imaging, including data post-processing.
2. To appreciate the strengths and limitations of spectral imaging in the abdomen.
3. To learn about advantages and possible limitations of spectral imaging in the assessment of inflammation and fibrosis in Crohn's disease.

A-006 09:21

C. Will MRI (DWI and perfusion) solve the problem?

S.A. Taylor; *London/UK (csytaylor@yahoo.co.uk)*

Crohn's disease (CD) is a relapsing and remitting inflammatory condition of the GI tract. Clinical management essentially resolves around use of immunosuppressive medication and surgery. Crucial to clinical decision making is assessment of the underlying inflammatory activity, those with active inflammatory disease tend to undergo immunosuppressive therapy whereas those with fibrosis may benefit from surgical resection. In reality, however, inflammation and fibrosis tend to coexist. Both DWI and perfusion are abnormal in CD. However, the relationship between both DWI and contrast enhancement and the histopathological phenotype is complex. Whist data suggest active Crohn's disease tends to result in restricted DWI, the balance between increased inflammatory infiltrate and tissue oedema influences ADC values and recent data using surgical resection specimens suggest fibrosis also leads to restricted diffusion. Similarly, whilst perfusion tends to increase in active CD, tissue angiogenesis which increases in chronic disease also affects contrast uptake. Enhancement patterns may help radiologist grade activity. For example, a layered enhancement pattern is reported in active disease, but again overlap with fibrosis is seen. Recent data suggest delayed contrast-enhanced sequences at around 7 minutes can help quantify fibrosis. This presentation will describe clinical protocols used to acquire DWI and perfusion imaging in CD and present the data as to their utility in clinical practice.

Learning Objectives:

1. To understand basic principles of DWI applied to Crohn's disease.
2. To learn about MR-perfusion protocols and data analysis.
3. To learn about advantages and possible limitations of MRI in the assessment of inflammation and fibrosis in Crohn's disease.

Author Disclosure:

S.A. Taylor: Investigator; Robarts.

09:44

Panel discussion: How do I approach a case in my routine clinical practice?

08:30 - 10:00 **Room C**

Chest

RC 104
Pneumonia

A-007 08:30

Chairman's introduction

I.E. Tyurin; *Moscow/RU (igortyurin@gmail.com)*

Pneumonia is a major health care and economic problem because of high morbidity and mortality rate, and due to direct and indirect costs of its management. The most common cause is community-acquired pneumonia, caused by common bacteria like S. Pneumonia as well as different viral agents. Tuberculosis is one of the most important respiratory infections in developing countries and in immune-compromised patients with AIDS everywhere. Tuberculosis pneumonia can easily mimic bacterial CAP and other pulmonary infections. Viral and mycotic infections represent a common course of febrile neutropenia in immune-compromised patients under aggressive therapy. In most of all these patients, a diagnosis is made on the basis of a combination of clinical, radiographic, and laboratory findings. High-resolution CT is usually performed in patients with nonspecific clinical and radiologic findings and in patients with progression of disease despite therapy. A large number of acute and chronic infectious and noninfectious diseases may also result in parenchymal lung disease in both immune-competent and immune-compromised patients. Thin section CT is also performed in patients with noninfectious causes of acute parenchymal lung disease such as organizing pneumonia, acute interstitial pneumonia, hypersensitivity pneumonitis, acute eosinophilic pneumonia, pulmonary oedema and haemorrhage. These diseases often have clinical and functional features similar to one another but obviously requiring different treatment. Therefore, the differential diagnosis of these entities is important in daily clinical practice.

Session Objectives:

1. To review the role of imaging in infectious lung diseases.
2. To become confident in recognising typical patterns.

A-008 08:35

A. Community-acquired pneumonia

I. Hartmann; *Rotterdam/NL (i.j.c.hartmann@gmail.com)*

Community-acquired pneumonia (CAP) refers to pneumonia acquired outside of hospitals or extended-care facilities and is one of the most common infectious diseases. CAP is an important cause of mortality and morbidity worldwide. According to the IDSA/ATS/AAFP guidelines, a chest radiograph is required for the routine evaluation of patients with suspected CAP to exclude conditions that mimic CAP (e.g., acute bronchitis) and to confirm the presence of an infiltrate compatible with the presentation of CAP. Although chest radiography findings usually do not allow identifying the causative organism, they may be helpful in narrowing down the differential diagnosis, prognosis, and detection of associated conditions. Serial chest radiography can be performed to observe the progression of CAP. CT scanning is increasingly used in clinical practice. Performing CT should be considered if any of the abnormalities at presentation or at follow-up are not consistent with the diagnosis of pneumonia, if concomitant disease is suspected such as an underlying bronchogenic carcinoma, for the confirmation of pleural effusion, and for the detection of pulmonary complications. The aim of the presentation is to provide an overview of the imaging findings of the most common aetiologic organisms in patients with CAP. In addition, imaging findings that may help in the differentiation between pneumonia and other common non-infectious causes of abnormal chest radiographs in patients with suspected CAP will be discussed.

Learning Objectives:

1. To appreciate the role of imaging in the management of community-acquired pneumonia.
2. To consolidate knowledge of how to discriminate from noninfectious diseases.

A-009 08:58

B. Tuberculosis

E. Castañer; *Sabadell/ES (ecastaner@tauli.cat)*

Pulmonary tuberculosis (TB) remains a common worldwide infection that produces high mortality and morbidity, especially in developing countries. In 2013, an estimated 9.0 million (360 000 of whom were HIV-positive) people developed TB and 1.5 million died from the disease. Chest radiographs play a major role in the screening, diagnosis and response to treatment of patients with TB. However, the radiographs may be normal or show only mild or nonspecific findings in patients with active disease. We will review the chest

radiograph findings of TB, which vary widely in function of several host factors, age, prior exposure to TB, and underlying immune status. CT is useful, in detecting TB incidentally, in resolving cases with inconclusive findings on chest radiographs and in assessing disease activity. Cavities, centrilobular nodules and tree-in-bud appearance are the most common CT findings of active pulmonary tuberculosis. We will discuss the classic, and some not-so-classic, signs that should suggest the diagnosis of TB.

Learning Objectives:

1. To appreciate typical and atypical tuberculosis manifestations on imaging.
2. To differentiate between acute and chronic tuberculosis infection.

A-010 09:21

C. Fungal pneumonia in immunocompromised hosts

C.P. Heussel; *Heidelberg/DE (heussel@uni-heidelberg.de)*

The radiological characterisation of infiltrates gives a first and rapid hint to differentiate between different types of infectious (e.g. typical bacterial, atypical bacterial, fungal) and non-infectious aetiologies. Follow-up investigations need careful interpretation according to disease, recovery, concomitant treatment and eventually vessel erosion requiring contrast-enhanced angio-CT. Due to a high incidence of fungal infiltrates in immunocompromised hosts, interpretation of the follow-up of an infiltrate must use further parameters besides the lesion size.

Learning Objectives:

1. To learn the patterns of fungal lung infection depending on the type of immune depression.
2. To become familiar with CT signs suggesting angioinvasive fungal infection.

Author Disclosure:

C.P. Heussel: Consultant; Schering-Plough, Pfizer, Basilea, Boehringer Ingelheim, Novartis, Roche, Astellas, Gilead, MSD, Lilly, Intermune, Fresenius, Olympus. Grant Recipient; Siemens, Pfizer, MeVis, Boehringer Ingelheim. Patent Holder; Method and Device For Representing the Microstructure of the Lungs. IPC8 Class: AA61B5055FI, PAN: 20080208038, Inventors: W Schreiber, U Wolf, AW Scholz, CP Heussel. Shareholder; Stada, GSK. Speaker; Gilead, Essex, Schering-Plough, AstraZeneca, Lilly, Roche, MSD, Pfizer, Bracco, MEDA Pharma, Intermune, Chiesi, Siemens, Covidien, Pierre Fabre, Boehringer Ingelheim, Grifols, Novartis, Basilea, Bayer.

09:44

Panel discussion: What is the role of radiologists in the diagnosis and management of lung infections?

08:30 - 10:00 **Room Z**

ESR Working Group on Ultrasound

WG 1

Ultrasound of the lung parenchyma: a diagnostic tool for the paediatric radiologist or for the clinician?

Moderator:
C. Owens; London/UK

A-011 08:30

How I perform and interpret lung parenchymal ultrasound

M. Riccabona; *Graz/AT (michael.riccabona@medunigraz.at)*

The objective of this presentation is to present and discuss the role, the potential and the limitations of ultrasonography (US) in paediatric lung and chest conditions. The technical equipment, transducer selection and device setting will be listed. Furthermore, the course of the examination is demonstrated. Requirements for standardisation will be discussed, such as sitting position for quantifying potentially associated effusions. Typical queries that can be addressed by US will be listed and normal as well as abnormal findings will be demonstrated. Besides the great potential of US in pleural and lung conditions, limitations have to be respected and artefacts have to be known to avoid pitfalls and mismanagement. Particularly, one needs to accept that US cannot replace plain film or chest CT, despite its huge potential for many queries. Lung (and chest) US have become a valuable tool for addressing chest conditions in childhood both for diagnosis as well as for follow-up. US helps to reduce other irradiating imaging, but restrictions and artefacts have to be acknowledged and other imaging such as plain film and CT need to be considered as additional methods helping to solve sonographically equivocal findings.

Learning Objectives:

1. To define technical requirements and main protocols for use in lung ultrasound.
2. To describe normal and abnormal findings in childhood.
3. To understand artefacts and limitations in lung ultrasound.

A-012 08:55

How does lung parenchymal ultrasound change the clinical management of the sick child: the paediatric radiologists' perspective

P. Tomà; *Rome/IT (paolo.toma@opbg.net)*

The imaging of the chest in paediatrics needs a specific cultural approach planned to integrate and optimise the techniques available. The prevalence of air represents a particular challenge for the radiologist. It limits the intrathoracic ultrasound (interfaces between soft tissue and lung generate very strong echoes due to a large acoustic impedance gradient), is a problem for the MRI (low proton density and the susceptibility differences between tissue and air), determines an excellent contrast resolution for the conventional radiology and CT that remains the gold standard. Technically, CT is conditioned by a cost/benefit ratio that means dose/diagnosis relationship. Risk of chest PA and lateral is negligible. Classical indications for chest US (in the presence of an acoustic window) are opaque hemi-thorax, assessment of vascular abnormalities, evaluation of diaphragmatic motion and juxta-diaphragmatic processes, detection characterisation of a suspected mediastinal disease, evaluation of chest wall lesions, to confirm and characterise pleural effusions guiding for pleural drainage procedures. New extensive use of sonography as clinical portable tool takes information also from physical acoustic phenomena that are not directly convertible into images of the human body. These artefacts are non-anatomical images, which are at best a sensitive but, unfortunately, a very nonspecific sign of lung injury common to many conditions. Young paediatric radiologists can easily learn the traditional chest ultrasound and they should know strengths and weaknesses of “new” imaging.

Learning Objectives:

1. To discuss the appropriate use of US, x-ray, CT and MRI in the management of children presenting with thoracic diseases.
2. To define if and how paediatric radiologists should be trained in chest US.

A-013 09:20

How does lung parenchymal ultrasound change the clinical management of the sick child: the clinicians' perspective

L. Cattarossi; *Udine/IT (luigi.cattarossi@asuiud.sanita.fvg.it)*

In the last two decades, lung ultrasound (LUS) has become popular both in adult and children for the clinical evaluation of pulmonary diseases. In neonatal and paediatric age, LUS has been utilized by the clinician as point of care tool to address the decision making process. LUS features of the most common neonatal respiratory diseases (respiratory distress syndrome, transient tachypnoea of the newborn, meconium aspiration, pneumothorax, pleural effusion, pulmonary haemorrhage) as well as its functional application on the respiratory therapy will be presented.

Learning Objectives:

1. To illustrate the role of bedside lung parenchymal US in comparison with x-ray and CT in management of sick children.
2. To define and discuss the paediatricians perspective.

09:45

Panel discussion

08:30 - 10:00 **Room O**

Special Focus Session

SF 1

Assessing age, based on bone maturation: scientific and ethical aspects

A-014 08:30

Chairman's introduction

K. Rosendahl; *Bergen/NO (karen.rosendahl@helse-bergen.no)*

Age assessment is an important, yet complex and challenging issue that authorities may need to perform to determine whether an individual is an adult or a child in circumstances where their age is unknown. There is currently no method which can identify the exact age of an individual and there are concerns about the invasiveness and accuracy of the methods in use, namely analysis of documentary evidence, interviews, physical or other form of medical examination such as imaging. The main imaging methods include carpal, collar bone and dental examinations. Whilst many countries make use of these methods they do not apply them in the same way and often use different combinations and/or order. One of the main reasons for this is the fact that age assessment procedures remain to a large extent determined by national legislation, with procedures evolving through national jurisprudence (Ref.: European Asylum Support Office (EASO Age Assessment Practice in Europe)). During this session, different methods of bone age assessment, their precision and accuracy will be addressed by experts within the field, followed by a presentation/discussion on ethical and legal aspects of using bone age to determine age.

Session Objectives:

1. To become familiar with current indications for bone age assessment.
2. To learn about the methods' precision and accuracy.
3. To appreciate the caveats in using bone maturation to determine chronological age.

A-015 08:35

Bone age assessment: indications and methods

F. Dedouit, P. Baumann, T. Uldin, S. Grabherr; *Lausanne/CH (fabded2@hotmail.com)*

The use of appropriate methods for determining the age is necessary for medical, medico-legal, and sporting contexts. Paediatric endocrinologists have an important interest for bone maturation to evaluate children for advanced or delayed growth and physical development. The developmental status of a child can be assessed by analysing various parameters such as height, weight, secondary sexual characteristics, bone age (BA) and dental age. The factors determining a normal skeletal maturational pattern are not clearly defined; however, genetic, nutritional, metabolic, social and emotional as well as environmental factors and hormones have an impact on bone development. BA assessment is a common procedure used in the management of children with various endocrinopathies and growth disorders. A significant discrepancy between BA and chronological age (CA) indicates abnormalities in skeletal development. When integrated with other clinical findings, clinicians can separate the normal from the relatively advanced or retarded physical development. The literature concerning age assessment, especially hand and wrist radiographies is oversized. Besides chronological methods, some morphological methods can be performed with a citation method (Tanner-Whitehouse, Fels, Sempé, Fishman) or with an atlas (Greulich and Pyle [GP], Gilzang-Ratib, Thiemann-Nitz-Schmeling). Different automated software have been developed for this purpose. The future seems to be represented by non-ionizing techniques like MRI. Nevertheless, the GP atlas, published in the 1950s, is still the most world-wide used method, although the reference sample compared to contemporary European population presents a different socio-economic status and a different ethnics.

Learning Objectives:

1. To learn about current medical indications for bone-age assessment.
2. To become familiar with the different methods.
3. To understand the differences between the different methods.

A-016 08:50

Precision and accuracy of an automated radiographic method

H.H. Thodberg; *Holte/DK (thodberg@visiana.com)*

The automated method for assessing bone age from radiographs has recently been extended up to 19 years of bone age for boys. The precision of the automated method is defined as its ability to give the same results on repeated x-rays of the hand, and it is reported as the SD = 0.18 years of such repeated determinations. Manual reading by different rater has a precision error of SD = 0.58 years. The accuracy of the automated method is defined as the SD error when compared to manual rating and it has been determined to be 0.75 years, when comparing to a single rater and to 0.52 years when compared to the average of many raters. When the automated method is used to predict the age, the accuracy is larger, with SD approx. 1 years. This holds for Caucasians in Western Europe; for other populations, the age assessment is biased to the extent that maturation proceeds differently in these populations. This has been studied by the automated method by presenting bone age reference curves, where the average bone age advancement (i.e. average BA-CA, BA = bone age, CA = chronological age) is shown versus CA. Such curves have been established for eight populations. The magnitude of BA-CA can be up to 1 year, in particular at the end of puberty. Such differences should be taken into account when using bone age to estimate age, so new studies need to be performed in countries wherefrom asylum seekers originate.

Learning Objectives:

1. To learn about an automated radiographic method.
2. To understand the difference between the method's precision and its accuracy.
3. To acknowledge the need for different reference standards by ethnicity.

Author Disclosure:

H.H. Thodberg: Owner; Owner of Visiana, which develops and markets the BoneXpert method.

A-017 09:10

Precision and accuracy of MRI

S. Diaz; *Stockholm/SE (sandra.diaz@med.lu.se)*

Magnetic resonance imaging (MRI) emerged as a potential technique in the assessment of bone age maturity in the context of international football competitions supported by the Fédération Internationale de Football Association - FIFA - due to the need to estimate the 'real' age of healthy adolescent football players. Meanwhile, the clinical use of MRI in the assessment of bone age is limited to the field of endocrine disorders related to alterations in developmental age. Lately, and due to war situation in different countries, MRI has been proposed as a forensic tool to establish the age of migrant unaccompanied children without official documents evidencing their 'real' age. MRI technique not only avoids the radiation that conventional radiography leads to but also provides detailed image of the growth plate. With this purpose, several groups in the world have been working with different magnetic fields (0.2, 0.3, 1.5, 3T), sequences and gradients (T1 tse, ge, vibe/flash, T2, PD, FFE), body areas (wrist, hand, clavicle, knee, ankle), grade scales and consequently with different results. The majority of the studies have been conducted with males and Caucasians. No consideration regarding other potential factors of influence such as ethnicity, gender, height and weight, nutritional level and socioeconomic factors was taken into account. Whatever the purpose to use MRI for assessment of bone age, there is a pressing need to coordinate our efforts to get consensus not only elaborating standard MRI protocols and grade scales to use, but also in other influencing factors.

Learning Objectives:

1. To learn about MRI in the assessment of bone age.
2. To become familiar with the method's precision and accuracy.
3. To appreciate potential pitfalls.

A-018 09:30

Ethical and legal aspects of using bone age to determine age

K. Chaumoitre; *Marseille/FR (kathia.chaumoitre@ap-hm.fr)*

Numerous bone age (BA) methods have been used by clinical practitioners in assessing growth or developmental disorders. BA does not reflect the child's chronological age, which is an objective element that does not take account of individual variability. Many studies carried out in diverse populations have not always yielded concordant results, but one constant finding emerges: large individual variability exists whatever the method. A princeps study, revealed a link between socioeconomic, health level and BA. The existence in the Greulich and Pyle (GP) atlas of age categories of up to 19 years in boys may perpetuate the illusion that the GP atlas enables classification of individuals aged under or over 18 years. It appears indispensable to apply the recommendations of the Study Group for Forensic Age Estimation. To assess the age of persons who are assumed to be at least 18 years, an additional CT examination of the clavicles is possible. The use of methods of BA estimation in a judicial context raises a number of ethical problems, especially for a delinquent minor. The width of the prediction intervals and the limits of agreement make it possible to emphasize some restrictions when a BA method is used to estimate the age of an individual in a judicial context. In individuals with a bone age of more than 10 years, the prediction interval is nearly 4 years. This raises the question of whether it is relevant to use bone age in judicial context.

Learning Objectives:

1. To understand the difference between bone age as "a marker of disease", and "a substitute for age".
2. To become familiar with ethical aspects.
3. To appreciate legal aspects.

09:50

Panel discussion: Should bone age be used to estimate chronological age - alone or in combination with additional methods?

08:30 - 10:00 **Room N**

Head and Neck

RC 108

Head and neck imaging: don't sell your ultrasound yet!

Moderator:
D.W. Tshering Vogel; Berne/CH

A-019 08:30

A. Salivary gland imaging with ultrasound

P. Gołofit; Koszalin/*PL (piotrgolofit@gmail.com)*

Ultrasound examination is often the first-line modality for imaging patients suspected of having salivary gland disease. Indications for this procedure include swelling with suspected sialadenitis or obstructing calculus, autoimmune diseases, palpable solitary or multiple masses suggestive of a benign or malignant neoplasm or floor of the mouth lesion. A thorough knowledge of the anatomy is crucial for reliable diagnosis of the pathology in this area. Although having considerable limitations (e.g. limited visualization of the deep lobe of the parotid gland) ultrasound can be very useful in selecting patients who require CT or MR imaging, provide biopsy guidance and, in some cases, gives the final diagnosis.

Learning Objectives:

1. To understand the limitations of clinical examination.
2. To learn about the diagnostic approach to salivary glands.
3. To appreciate how to differentiate salivary gland pathology.

A-020 09:00

B. Masses of the soft parts of the neck

P.K. Srivastava; *Lucknow/IN (yashdeep.pks@gmail.com)*

The neck constitutes a broad anatomic region, which has many aero-digestive, salivary glands, lymphatic, endocrine, neural and vascular structures. A good number of pathological conditions affecting these organs system are very well evaluated on high-resolution ultrasound. It is also very useful for ultrasound-guided needle aspiration for cytology, culture and hormone assay, ultrasound-guided core biopsy and molecular markers. The excellent tissue details and anatomical landmarks in the neck such as thyroid cartilage, trachea, strep muscles and neck vessels have made assessment of the neck masses a practical proposition. The neck masses are divided into two major groups: 1. thyroid neck masses; 2. non-thyroid neck masses. The non-thyroid neck masses include congenital masses, cervical masses, lymph node mass, salivary gland masses, nerve tumours, vascular masses, inflammatory masses, parasitic infestations, foreign body, benign and malignant neck tumours. High-resolution ultrasound is a multi-planner, non-invasive, cost-effective imaging modality which is having advantage of CT scan and MRI as the spatial resolution of ultrasound is much better than CT and MRI. The biggest advantage is that it is a dynamic modality which does not require any sedation or special preparation for evaluation of neck masses. The excellent tissue characterization of various structures in the neck on ultrasound clearly differentiate different pathology. The 3D ultrasound with multi-planner, panoramic and colour flow imaging increases the diagnostic accuracy.

Learning Objectives:

1. To become familiar with cervical ultrasound anatomy.
2. To learn about benign neck masses.

A-021 09:30

C. Lymph nodes: differential diagnosis and fine-needle aspiration

R. Maroldi; *Brescia/IT (roberto.maroldi@unibs.it)*

There are several clinical scenarios where imaging is required to investigate the neck lymph nodes. 1. Imaging is indicated to integrate the clinical examination in the evaluation of unknown neck masses. In this clinical setting, the first task of imaging is to differentiate between non-nodal lesions and adenopathies. If the clinical examination cannot detect a primary neoplasm in the head and neck area, fine-needle aspiration (FNAC) is indicated. Ultrasound (US) is the technique of choice for the initial evaluation and for FNAC. 2. In case of acute/subacute neck infection with enlarged adenopathies, imaging is required to assess nodal changes (abscess), spread outside the lymph node capsule, potential extent into deep neck spaces, with great risk of mediastinal involvement. While US can be accurate in assessing superficial cervical node changes, CT with contrast agent is indicated to survey the deep spread of infections. 3. If a malignant neoplasm arising from the mucosa of the upper aerodigestive tract (UADT) is identified at clinical examination, imaging techniques are required to detect nodal metastases in the ipsilateral (if the primary tumour arises far from midline) and the contralateral neck. Besides detecting the abnormal node, extra-nodal spread and key vessels invasion (carotid, jugular vein) are key information to be acquired by imaging. US, MDCT and MR can be used: their greatest limitation is the low sensitivity for non-enlarged metastatic nodes. A different setting is the assessment of thyroid papillary carcinoma where microcalcifications inside even very small metastatic nodes can be detected by US.

Learning Objectives:

1. To get acquainted with normal and abnormal findings.
2. To understand the patterns of nodal involvement.
3. To learn about technique of fine-needle aspiration.

08:30 - 10:00 **Room E1**

Professional Challenges Session

PC 1

Will emerging technology replace the radiologist?

A-022 08:30

Chairman's introduction

L. Donoso; *Barcelona/ES (ldonoso@clinic.ub.es)*

Call it artificial intelligence, deep learning, cognitive computing; whatever its name, it is the same thing, machines recognizing clinical problems in digital images ahead of the radiologists charged with making the diagnosis. Regardless of whether machine- or human-based aids are leveraged, radiology needs such aids. Never has improving performance been so important to its future. The liquid biopsy as a test is done on a sample of blood to look for cancer cells from a tumour that are circulating in the blood or for pieces of DNA from tumour cells that are in the blood. A liquid biopsy may be used to help find cancer at an early stage. It may also be used to help plan treatment or to find out how well treatment is working or if cancer has come back. The clinical impact of these developments together with the ones in molecular imaging, quantification and biomarkers will be discussed in this session.

Session Objectives:

1. To become familiar with the emerging technologies in the imaging field.
2. To learn about the new concepts behind the computerised image analysis and diagnosis.
3. To understand the potential benefits and threats related to its implementation.

A-023 08:35

Computer-aided and computer-determined diagnosis

K.J. Dreyer; *Boston, MA/US*

As computers outperform humans at complex cognitive tasks, disruptive innovation will increasingly remap the familiarity with waves of creative destruction. In healthcare, nowhere is this more apparent or imminent than at the crossroads of radiology and the emerging field of clinical data science. As leaders in our field, we must shepherd the innovations of cognitive computing by defining its role within diagnostic imaging, while first and foremost ensuring the continued safety of our patients. If we are dismissive, defensive or self-motivated, industry, payers and provider entities will innovate around us achieving different forms of disruption, optimized to serve their own needs. To maintain our leadership position, as we enter the era of machine learning, it is essential that we serve our patients by directly managing the use of clinical data science towards the improvement of care. In this session, we will explore the state of clinical data science in medical imaging and its potential to improve the quality and relevance of radiology as well as the lives of our patients. Attendees will learn the basics of clinical data science, understand the potential impact of data science on the field of radiology, understand the transition of radiology from visualization to quantification in preparation for precision healthcare, and understand the value of deep learning in the era of MACRA and MIPS payment reform policies.

Learning Objectives:

1. To lean about the different tools related with "computer assisted" diagnosis.
2. To understand the challenges in management and radiologist practice of introducing these technologies.
3. To become familiar with "real-life" implementations.

A-024 08:50

Liquid biopsy: a new kid on the block

M. Ignatiadis; *Brussels/BE (michail.ignatiadis@bordet.be)*

Circulating tumour cells and circulating tumour DNA often referred as a 'liquid biopsy' are promising tools that have the potential to improve cancer diagnosis, prognosis assessment and real-time monitoring of treatment efficacy. In June 2016, the Food and Drug Administration (FDA) approved a test to screen for EGFR mutations in plasma samples to identify patients with metastatic non-small cell lung cancer that are eligible for treatment with erlotinib. In the future, more liquid biopsy tests are expected to complement other approaches used today for the prediction of treatment efficacy towards precision medicine.

Learning Objectives:

1. To understand the concept of liquid biopsy.
2. To learn about the advantages of liquid biopsy in the diagnostic process.
3. To understand the impact that these techniques will have on clinical practice.

Author Disclosure:

M. Ignatiadis: Consultant; Novartis, Roche. Research/Grant Support; Roche, Janssen Diagnostics.

A-025 09:05

Novelties in molecular imaging

K. Riklund; *Umea/SE (katrine.riklund@umu.se)*

Molecular imaging with hybrid imaging such as PET/CT is integrated in many clinical pathways. The selected tracer for the PET part will determine which biochemical or molecular information the examination with the PET part will return. On the other hand, the section of study protocol for the CT or MR on the case of PET/MR imaging will decide which information that part of the examination will return. The major role for PET/CT or PET/MR is staging of oncologist diseases but applications in cardiac and neuro-imaging are emerging. There are also non-oncologic applications for these modalities. In the field of oncology, we are aware of several hallmarks in cancer that are involved in disease development as well as in treatment strategies and treatment response. A major challenge is to develop imaging so we can visualize the behaviour of these hallmarks and during the talk the possibility of using hybrid imaging to do this will be discussed. The interest and attempts to quantifying biomarkers is higher than ever; however, there are many challenges in this field. Quantification and how it can be used will be briefly discussed.

Learning Objectives:

1. To understand the role of hybrid imaging in the current clinical practice.
2. To become familiar with the new hybrid imaging applications in relationship to disease presentations.
3. To learn about quantification in hybrid imaging: its benefits and limitations.

A-026 09:20

Deep learning and biomarkers: the engineer's view

A. Alberich-Bayarri; *Valencia/ES (alberich_ang@gva.es)*

Quantitative imaging biomarkers are driving the paradigm shift in radiology towards precision medicine. Although the lack of standardization can hinder their appropriate use in clinical practice and drug development trials, alliances like QIBA and EIBALL allow for arriving to a consensus in image acquisition and image processing algorithms, which are the main current sources of uncertainty. The adoption of quantitative imaging solutions in the clinical setting requires, however, from the synthesis of the most relevant information, moving from redundancy to relevancy in the data evaluated by the radiologist and the clinical specialist, avoiding information overload. Therefore, data clustering and data reduction techniques, consisting of machine learning approaches have to be implemented. One of the most promising artificial intelligence techniques in the field of medical imaging is deep learning, which allows for the supervised (based on given features like imaging biomarkers) or non-supervised (learning features from data) by means of convolutional neural networks (CNN). Such networks have been applied for the automated classification of medical images as computer-aided detection (CAD) systems; however, the high number of data (millions of cases) required to train the CNNs and obtain efficacy is influencing the research evolution to new network configurations such as generative adversarial nets (GAN), which are expected to have a highly significant impact in the field of artificial intelligence and medical imaging.

Learning Objectives:

1. To learn about the specific engineering challenges of developing new quantification methods.
2. To become familiar with the process of adapting the use of biomarkers in the clinical setting.
3. To understand the impact of deep learning on these diagnostic tools.

Author Disclosure:

A. Alberich-Bayarri: CEO; QUIBIM. Patent Holder; Lung Emphysema quantification. Shareholder; QUIBIM.

09:38

Panel discussion: Should we start to worry?

08:30 - 10:00 **Room E2**

Neuro

RC 111

Management of acute stroke

Moderator:
P. Vilela; Almada/PT

A-027 08:30

A. A critical appraisal of the current literature

W. van Zwam; *Maastricht/NL (w.van.zwam@mumc.nl)*

In 2015 and 2016, eight randomised controlled trials were published, reporting a clear benefit of endovascular treatment over standard care for patients with an acute ischaemic stroke caused by a large vessel occlusion of the anterior intracranial circulation. Individual patient data from five of these trials were pooled in the HERMES collaboration project and first results were published in 2016. After publication of the first positive trial, MRCLEAN, stroke treatment underwent a revolutionary change since the introduction of intravenous therapy with thrombolytics more than twenty years before. The different trials used different inclusion criteria and showed differences in outcome. In this lecture, a short history of acute stroke treatment trials, an overview of the differences between the 2015 and 2016 trials, new studies with subgroup analyses, and the pooled data from the HERMES collaboration will be presented and discussed.

Learning Objectives:

1. To understand the strengths and shortcomings of the relevant multicentre trials assessing the role of endovascular treatment in patients with acute ischaemic stroke.
2. To understand the outcomes of these trials, the context in which they were achieved and how they can be ensured in a different environment.
3. To appreciate potential differences in management of patients with anterior vs posterior circulation strokes.

Author Disclosure:

W. van Zwam: Grant Recipient; Dutch Brain Council, Dutch Heart Foundation. Speaker; Codman, Stryker.

A-028 09:00

B. Which techniques can we use to reopen an occluded cerebral blood vessel?

T. van der Zijden; *Edegem/BE (thijsvanderzijden@hotmail.com)*

Since the 90s, the mainstay of primary stroke treatment is the use of clot-dissolving medication. Nowadays, mechanical thrombectomy has established itself as a very powerful tool in the management of acute ischaemic stroke in the (hyper)acute setting. The number of mechanical thrombectomy procedures has increased considerably in the last few years. An occluded cerebral blood vessel can be reopened in a swift and efficient way with quite acceptable complication risk rates using stent retrievers and/or thrombosuction catheters. In this presentation, not only an illustration of different mechanical thrombectomy techniques will be provided, but, next to an introduction to intra-arterial primary stroke treatment, also an overview of several accessory matters, such as tandem lesions, stenting and complications, will be discussed.

Learning Objectives:

1. To understand the principles underlying endovascular clot aspiration.
2. To become familiar with the different materials available for mechanical clot retrieval.
3. To understand the circumstances in which stenting of an intracranial blood vessel is needed.

A-029 09:30

C. Endovascular stroke treatment: ethical and economical concerns

K.-O. Løvblad; *Geneva/CH (karl-olof.lovblad@hcuge.ch)*

While stroke has known advances both in imaging and treatment since the 1990s, it has been the breakthrough with the use of stentrievers that has caused the most response. We have seen that with these methods, it is now possible to on the one hand extract safely and quickly the thrombus without the adverse effects of secondary haemorrhage. While this is extremely encouraging, a few things need to be considered: on the one hand, there will be an enormous demand in a very strictly organized stroke treatment system based on stroke units and stroke centres. Some that will carry out the initial examination and maybe treatment while the patients that need endovascular treatment may be referred to centres that dispose of 24/7 state-of-the-art imaging and post-treatment setups. The costs incurred will be caused on the one hand by and increase in treated patients, then an increase in the management and treatment costs themselves due to the stents. However, this should be counterbalanced by a decrease in morbidity and mortality with decreased readaptation costs. One major concern is the case of the increased need for improved informed consent ways for these patients that may not be initially be able to agree or disagree to the treatment, which is critical due to the short time-window available. Also while the industry is necessary to continue to support the needed R&D in this field, it should allow physicians freedom to provide the best choice of materials adapted to the patient.

Learning Objectives:

1. To appreciate the structure that is necessary to organise interventional stroke treatment for a large population.
2. To understand the cost implications and their mitigation.
3. To become familiar with the associated ethical concerns (such as informed consent) and the different ways of addressing them.

08:30 - 10:00 **Room F1**

E³ - Rising Stars Programme: Basic Session

BS 1

Neuroradiology

Moderator:
E. Tali; Ankara/TR

A-030 08:30

White matter disorders

A. Rovira-Cañellas; *Barcelona/ES (alex.rovira@idi.gencat.cat)*

MR imaging is highly sensitive for the detection of white matter signal abnormalities, which can be identified in 5-10% of the adult population. Evaluation of this focal white matter hyperintensities (WMHs) on MR imaging, particularly in young adults, is always challenging since clinical and imaging features are commonly non-specific. Although most of these signal abnormalities are incidental and age related, or secondary to different types of vascular disorders, they also may be caused by a wide variety of infectious, inflammatory, neoplastic, and demyelinating disorders. In this regard, the most common difficulty, by far, is to distinguish multiple sclerosis from acquired hypoxic/ischaemic small-vessel disease, due to the high prevalence of this last group of disorders even in young adults. While it is recognized that a combination of findings from clinical history, physical examination, and laboratory tests is commonly required to correctly establish a firm and clear aetiological diagnosis, a detailed analysis of different MR imaging features should also be considered essential, e.g. lesions shape, size, and distribution; contrast-uptake; associated structural lesions (microbleeds, infarctions, etc.). Knowledge of these features, will assist the diagnostic workup of patients presenting with WMHs, and should be considered a first step to take full advantage of the potential of MRI, and in doing so should result in a reduced chance of misdiagnoses and facilitate the correct diagnosis of sometimes treatable disorders.

Learning Objectives:

1. To have a basic understanding of classification of white matter disorders.
2. To describe the typical imaging features of noninfectious, noninflammatory disorders.
3. To identify and describe the imaging features of brain infectious-inflammatory disorders.

A-031 09:00

Brain tumours

J. Walecki; *Warsaw/PL (jerzywalecki@o2.pl)*

Neuroimaging techniques are essential tools for the diagnostic process and management of brain tumours. Early and accurate diagnosis is usually possible using various brain imaging techniques. Brain tumours are classified by cell origin and how the cells behave, from the least aggressive (benign) to the most aggressive (malignant). Malignant tumours can be divided into two categories: primary and metastatic. A malignant tumour usually grows rapidly and often invades or crowds healthy areas of the brain, where most benign brain tumours are characterised by slow growth. Based on analysis of all imaging features/imaging biomarkers/tumours are rated or graded by their level of malignancy. Many factors which determine tumour grade include how fast the tumour is growing, how much blood is supplying the tumour's tissue, the presence of the tumour necrosis and peritumoural oedema leading to high intracranial pressure/mass effect. Brain tumours are one of the most challenging disorders encountered; however, experiences of numerous authors as well as my own affirm the highest efficacy in the diagnostic process using multiparametric MR imaging: DWI, PWI or MRS. Lecture will present most common brain tumours and selected imaging modalities to their detection as well as postoperative follow-up and/or tumour's recurrence.

Learning Objectives:

1. To identify and describe the imaging appearance of malignant tumours.
2. To identify and describe the imaging features of benign tumours.
3. To have a basic knowledge of postsurgical evaluation of brain.

A-032 09:30

Stroke

E.T. Tali; *Ankara/TR (turgut.tali@gmail.com)*

Ischaemic stroke results from a sudden cessation of adequate amounts of blood reaching the brain. Imaging workup should be fast, readily available and reliable to detect early and subtle abnormal findings to suggest parenchymal hypoperfusion and, therefore, facilitate early diagnosis and intervention. Initial ischaemic stroke imaging using non-contrast CT has been effectively applied to exclude haemorrhage, estimate parenchymal abnormality and other intracranial pathologies that may mimic stroke. Even though non-contrast CT remains the mainstay of imaging, it has limited sensitivity in the acute setting of the ischaemic changes. Detection depends on the territory, time of the examination from onset of symptoms and experience of the interpreting radiologist. CT perfusion and angiography as a second step is a critical tool in increasing the accurate diagnosis. CT perfusion shows both the core of the infarct and the surrounding penumbra, the region which can be salvaged. CT angiography may be helpful to identify the thrombus within an intracranial vessel, establishing the stroke aetiology and also may guide treatment planning. MRI has significantly higher sensitivity and specificity in the diagnosis of hyperacute stage of ischaemic stroke. However, MRI is more time-consuming and less available than CT particularly in the emergency departments. Diffusion-weighted MR imaging shows infarct core within minutes following the onset of ischaemia. MR perfusion imaging also provides information almost similar to the CT perfusion. Treatment planning can be done under the guidance of the imaging findings and can be performed as various reperfusion techniques (intravenous or intra-arterial thrombolysis, mechanical thrombectomy, etc.).

Learning Objectives:

1. To learn about typical imaging features of haemorrhagic stroke.
2. To discuss current imaging techniques for evaluation of ischaemic stroke.
3. To have a basic knowledge of neuroradiological interventions - revascularisation in stroke.

08:30 - 10:00 **Room F2**

E³ - ECR Master Class (Oncologic Imaging)

E³ 126a

Oncologic imaging in the age of precision medicine

Moderator:
H. Hricak; New York, NY/US

A-033 08:30

A. Precision medicine
G. Frija; *Paris/FR (guy.frija@egp.aphp.fr)*

According to the National Institutes of Health (NIH), precision medicine (PM) is "an emerging approach for disease treatment and prevention that takes into account individual variability in genes, environment, and lifestyle for each person". Its development is stimulated by the progresses in data intensive basic science, and is characterized by a high level of complexity. The key pillars of PM are: to develop a new taxonomy of diseases based on biological mechanisms, to develop correlations of phenotyping with genotyping, to increase the statistical power of research in developing networking and integrated databases. The main national plans or programmes, which are currently being developed, will be briefly presented in order to highlight the cost and the complexity of this concept. Imaging has certainly an important role in this framework: the development of reliable quantitative biomarkers and the delivery of structured data are crucial. Correlations between phenotype and genotype through radiogenomic approaches appear promising. Concrete examples will be presented to illustrate the potential of imaging in this context mostly in oncology (tumour heterogeneity mapping). The importance of companion diagnostics will be discussed as well as liquid biopsy, which potentially is a strong competitor as well.
Learning Objectives:
1. To understand the meaning of precision medicine.
2. To document the role of radiologists in precision medicine.
3. To understand how precision imaging will have an influence on the practice of radiology.

A-034 08:55

B. Radiomics: the role of imaging in precision medicine
R. Kikinis; *Boston, MA/US (kikinis@bwh.harvard.edu)*

Radiogenomics is the correlation between image-derived features and gene expression. Recent scientific progress has enabled the treatment of cancer based on targeting of specific mutations. Imaging, in contrast to biopsies, allows the assessment of the entire tumour volume. The presentation will explain the state of the art in the field and discuss the contributions that radiology can make.
Learning Objectives:
1. To review how radiologists can contribute to radiomics investigation.
2. To explain state-of-the-art of radiomics, from science to practise.
3. To learn about the idea of radiomics.

A-035 09:20

C. Precision medicine and imaging-guided interventions
S.B. Solomon; *New York, NY/US (SolomonS@mskcc.org)*

Modern oncologic care is centred on the molecular characteristics of an individual's cancer in what is termed precision medicine. The image-guided needle biopsy has been the key tool used to access the cancer for molecular analysis. Radiologists as central players in needle biopsy, thus, play a critical role in precision medicine. Recent data show that many specimens are insufficient to provide enough material for molecular analysis. This lecture will focus on optimising biopsies through improved techniques, tools and work flow. In addition, we will see how radiologists can use molecular status to help distinguish between responders and non-responders of locoregional therapies.
Learning Objectives:
1. To explain what is the present and the future of imaging-guided interventions.
2. To learn about current concepts for precise imaging guidance during IR procedures.
3. To understand the practical implementation of such tools.
Author Disclosure:
S.B. Solomon: Consultant; AstraZeneca, Medtronic, Aperture, Innoblative. Research/Grant Support; GE Healthcare.

09:45
Panel discussion: Precision medicine in oncology: what can imaging provide?

08:30 - 10:00 **Room D**

Musculoskeletal

RC 110

The elbow: a comprehensive approach

A-036 08:30

Chairman's introduction
A. Alcalá-Galiano; *Madrid/ES (aalcalagaliano@gmail.com)*

The elbow is a complex hinge joint commonly injured in trauma and subject to chronic overuse syndromes in both athletic and non-athletic individuals. Understanding of the anatomy, systematic image evaluation as well as structured reporting are crucial for accurate diagnosis and to assist in surgical decision making. Recognised pitfalls and normal variants should not be confounded with pathology. Chronic overuse injuries or instability may have subtle imaging manifestations and some injuries may clinically emulate or exacerbate other entities; therefore, imaging prior to intervention is essential. Relevant parameters of tendon injury for treatment planning and the imaging appearance of the different instability patterns of the elbow joint due to lesion of the valgus/varus stabilizers need to be identified. Ulnar neuropathy at the elbow is the most common and best recognised, but there are other nerve entrapment syndromes that should not be missed. The choice of imaging modality for soft tissue derangement at the elbow includes MR and US, whereas CT is usually reserved for osteoarticular evaluation. US allows dynamic evaluation and may demonstrate findings which would otherwise be missed at static examinations. This session will provide a profound review of the imaging appearance of tendon anatomy and pathology, ligament injury and instability and nerve entrapment syndromes at the elbow with different imaging modalities. Interventional techniques for treating elbow tendon disease will also be discussed
Session Objectives:
1. To understand that assessing this joint requires a multimodality approach with careful attention to technique, imaging protocol, choice of coils and sequences.
2. To learn about the pivotal role of the radiologist in evaluating elbow imaging to provide relevant information to the arthroscopist.

A-037 08:35

A. The tendons: anatomy, pathology and intervention
P. Peetrons; *Brussels/BE*

"no abstract submitted"
Learning Objectives:
1. To become familiar with the normal imaging anatomy and pathological appearances of the elbow tendons.
2. To learn about interventional radiological techniques for treating elbow tendon disease.

A-038 08:58

B. Ligament injury and instability: what to look for and what to say
M.C. De Jonge; *Amsterdam/NL (mdjonge@zuwehofpoort.nl)*

The elbow joint is an intrinsic very unstable joint. It derives its stability from the capsula, joint crossing muscles, tendons and ligaments. Ligament injuries are not frequent although it depends upon the patient population. In sports people, e.g. throwing sports like baseball, it is quite common. The most common stabilising ligaments are on the ulnar and radial side. On the ulnar side, the ulnar collateral ligament (UCL) is the most important one often injured in situations where acute (severe) valgus stress is applied to the elbow. The most common chronic instability due to a ligament injury of the elbow, however, is the posterolateral instability. The most important structure on the radial side involved in this type of instability is the lateral ulnar collateral ligament (LUCL). At the same time this is also one of the most challenging ligaments to visualise for the radiologist. After a brief introduction of the anatomy, the mechanisms of injury to the medial and lateral ligaments will be discussed. Optimisation of the imaging protocol will be reviewed with the respective values of ultrasound and MRI.
Learning Objectives:
1. To become familiar with patterns of abnormality seen in elbow instability.
2. To learn about the imaging findings of elbow instability.

A-039 09:21

C. Nerve entrapment at the elbow

L.M. Sconfienza; *San Donato Milanese/IT (io@lucasconfienza.it)*

The most common condition around the elbow is the cubital tunnel syndrome. It is a compression neuropathy that can occur either at the condylar groove or at the edge of the arcuate ligament. Causes of compression include direct extrinsic compression on the condylar groove, bone abnormalities, and soft tissue lesions. Clinical findings include elbow pain and sensory symptoms in the innervated area. Diagnosis is mainly based on electrophysiological studies but US may demonstrate the presence of nerve thinning/thickening and associated abnormalities. Ulnar nerve instability at the cubital tunnel is also common but is asymptomatic in up to 47% of patients. When symptoms are present, US may demonstrate nerve thickening with hypervascularisation. The median nerve is infrequently impinged around the elbow. Anterior interosseous neuropathy occurs where nerve branches off the median nerve, in proximity to the pronator teres and the tendinous bridge connecting the heads of the flexor digitorum superficialis. When this syndrome is clinically suspected, US evaluation is usually inconclusive. However, abnormal reflectivity of innervated muscles can be seen. The median nerve may also be impinged as passing the pronator teres muscle. Posterior interosseous neuropathy is an uncommon condition of impingement at three different locations around the elbow, but more typically near or behind the supinator muscle at the proximal third of the forearm, where the nerve enters a strong fibrous arcade (i.e. arcade of Frohse). Clinical presentation is typical and US is able to identify the thickened nerve impinging in the arcade of Frohse.

Learning Objectives:

1. To understand the radiological anatomy of the peripheral nerves at the elbow.
2. To learn about the imaging findings of nerve entrapments at the elbow.

Author Disclosure:

L.M. Sconfienza: Author; Springer Verlag. Other; Travel grants from Bracco Imaging Srl and Esaote.

09:44

Panel discussion: US, CT, conventional MR, high field MR: making the right choice

08:30 - 10:00 **Room G**

Physics in Medical Imaging

RC 113

Single-dual-multi-energy CT

A-040 08:30

Chairman's introduction

J. Damilakis; *Iraklion/GR*

Dual-energy CT acquisition is possible using either single-source CT or dual-source CT. In single-source CT units, a generator switches x-ray tube potential from 80 kVp to 140 kVp corresponding to photon energies from about 40 keV to 140 keV. For each exposure, the exposure time is only 0.5 msec, allowing simultaneous acquisition of low-kVp and high-kVp images. Dual-source CT scanners are composed of 2 tubes and 2 detector arrays. The 2 tubes are positioned at 90 degrees from each other. For dual-energy CT the potential applied across the 2 tubes is 80 kVp to 140 kVp. The tube load (mAs) is adjusted accordingly to 50 mAs for the high-kVp tube and 200 mAs for the low-kVp tube. Other approaches have been introduced through energy-sensitive detectors and photon counting detectors. All CT examinations should be optimised to achieve diagnostic image quality with the lowest radiation dose possible. Dose optimisation of dual-energy examinations is an area of great interest for both medical physicists and radiologists. The replacement of pre-contrast imaging by virtual non-contrast-enhanced imaging provides a great opportunity of radiation dose reduction. Moreover, several techniques and tools have been developed for CT dose optimisation and these methods are also applicable for dual-energy CT studies. For example, application of new iterative reconstruction algorithms, use of automatic exposure control and other dose saving tools may help to reduce patient doses considerably.

Session Objectives:

1. To learn about the basics of dual-energy CT (DECT).
2. To understand today's photon counting detector technology.
3. To learn how DECT is applied in clinical practice.

A-041 08:35

A. Basics of diagnostic dual-energy CT

T. Klinder; *Hamburg/DE (tobias.klinder@philips.com)*

Although the first applications of dual-energy CT (DECT) were already introduced in the 1980s, they were not adopted in clinical practice. However, with advancements in the CT systems, DECT experienced its comeback and is now clinically emerging. In this talk, we will explain the technological basics of diagnostic DECT and show its clinical potential. First, the general idea of CT acquisition is reviewed to acknowledge the spectral information that DECT provides. The fundamental underlying physics of DECT is explained. In particular, it is derived how spectral acquisition allows to parameterise the energy-dependent attenuation coefficient inaccessible to single-energy CT. The different techniques for acquisition of DECT will be shortly compared. Dual-energy data can be post-processed and presented in various ways (e.g. monochromatic images, iodine maps or virtual non-contrast images). The individual possibilities are thereby described on the basis of the introduced physical principles. Finally, an overview of main clinical applications of DECT is given including the detailed review of different clinical example cases. Where appropriate, a comparison to single-energy CT is given to fully appreciate the additional value of DECT.

Learning Objectives:

1. To learn about the underlying physics and today's technology.
2. To see potential advantages compared to single-energy CT.
3. To appreciate the rationale behind clinical applications.

A-042 08:58

B. Photon counting detector technology for diagnostic CT

I. Blevis; *Haifa/IL (ira.blevis@philips.com)*

Medical CT imaging has recently advanced due to the introduction of dual-energy techniques. Material composition and density in the body are disentangled using the energy information in the x-rays traversing the body. The added information can be combined with the conventional image using colours or other techniques. Realizing the full potential of the newly tapped energy information will require a major technological change from the scintillating crystals and light sensing electronics in current use to semiconductor detectors and electronics sensitive to each photon and its energy, individually. The current technology is called indirect and integrating detection, and the new and emergent technology is called direct conversion photon counting. Photons are absorbed in high Z, high band gap, high crystallinity, thick semiconductors, notably Cd(Zn)Te, producing a very compact ball of electric charge that is transferred to external electronics by a fine grid of contact electrodes on the semiconductor surface. The small size of the charge ball also permits a high resolution and contrast improvement in CT, potentially without an increase of patient dose. The new technology has been introduced commercially in the past decade in less demanding SPECT imaging at 10^{-1}photons/s/mm^2 and now in our CT research prototypes the detector development has permitted close to the 10^{9}photons/s/mm^2 needed for CT. Verification images from phantoms and preclinical trials, including resolution tests, and high Z contrast agents will be shown.

Learning Objectives:

1. To learn about the underlying physics and technological solutions.
2. To understand the potential advantages compared to dual-energy CT.
3. To appreciate how mature today's photon counting technology is.

Author Disclosure:

I. Blevis: Employee; Philips Healthcare. Investigator; H2020 Grant Agreement No 668142.

A-043 09:21

C. Do we really need multi-energy CT?

S.T. Schindera; *Aarau/CH (sschindera@aol.com)*

Dual-energy CT has been introduced more than ten years ago and since then various clinical applications from head to toe have been described in the scientific literature. A clear added value of each clinical application needs to be proven to transfer them into clinical routine. Besides optimization of the clinical workflow of dual-energy CT, including post-processing of the additional datasets, the radiation exposure to the patient is an important aspect which decides if dual energy maintains a success story. To promote the wide-spread use of dual-energy CT, there is a definite need for future investigations on the outcome of dual-energy CT, such as patient care, costs and workflow.

Learning Objectives:
1. To learn about medical applications and potential benefits.
2. To see which single energy applications should be replaced by dual-energy applications, and why.
3. To find out what additional multi-energy CT applications would be nice to have.

Author Disclosure:
S.T. Schindera: Advisory Board; Bayer Healthcare.

09:44
Panel discussion: How many 'energies' do we need in CT?

08:30 - 10:00 **Room K**

Radiographers

RC 114
MRI technology and techniques

Moderators:
V. Syrgiamiotis; Athens/GR
A. Mizzi; Msida/MT

A-044 08:30
A. Recent developments in structural and quantitative spinal cord imaging at 3T
M.C. Yiannakas; *London/UK*

In this presentation I would be discussing new developments in acquisition and analysis protocols for spinal cord imaging using a clinical 3T MR system, which are suitable for use in a number of neurological diseases, such as multiple sclerosis (MS), spinal cord injury (SCI), amyotrophic lateral sclerosis (ALS), neuromyelitis optica (NMO) and multiple system atrophy (MSA). In terms of acquisition, protocols which allow depiction of grey matter (GM) and white matter (WM) within the cord will be presented along with examples on how these may facilitate further tissue-specific (i.e. GM/WM) quantitative investigations such as the estimation of tissue volume, diffusion tensor imaging (DTI) metrics and magnetisation transfer ratio (MTR). In terms of analysis methods, recent advances in semi- and fully-automated image segmentation will be presented and discussed.

Learning Objectives:
1. To understand the technical challenges associated with spinal cord imaging.
2. To learn about new structural and quantitative spinal cord acquisition and analysis protocols.
3. To discuss some of the clinical applications in neurological disease.

A-045 08:55
B. RF-related heating in clinical MRI
T. Owman; *Lund/SE (Titti.Owman@gmail.com)*

Magnetic resonance is a frequently used diagnostic tool and considered a fairly safe modality. It is well known that MR is not only exclusively used for diagnostic purposes but also used in interventional care, research and functional studies of various kinds. Clinical demands for faster examinations and higher resolution, and in combination with advanced research has resulted in a development toward stronger magnetic fields and a more powerful and complex technology. This with the consequence that clinical MR of today uses higher frequencies and increased energy deposition in patients and volunteers. There are several known risks in MR and the radiofrequency (rf)-induced heating problem in patients has increased significantly parallel to the fast technological development. Several efforts are made to improve the situation since MR-related rf-burns occur more and more frequent in clinical practice. The rf-heating problem is relatively difficult to predict and may even cause various degrees of burns during regular clinical MR scanning. Improved knowledge and better understanding of this hazard is necessary to minimize risks and avoid unnecessary damage. Heat-related accidents (rf) can be reduced and the situation considerably improved by careful patient preparations and good safety routines prior to MR examinations.

Learning Objectives:
1. To learn about b1-related problems in clinical MRI.
2. To understand RF-related heating and current efforts to improve the situation.
3. To discuss how to avoid RF-burns in clinical practice.

A-046 09:20
C. The benefits of diffusion imaging
J. Castillo; *Msida/MT (josecast@melita.com)*

Diffusion-weighted magnetic resonance imaging (DWI) derives its image contrast from differences in the motion of water molecules between tissues. Such imaging can be performed very quickly without the need for exogenous contrast medium administration. A series of technological advances have made it feasible to translate DWI measurements to extra-cranial sites, such as the abdomen and pelvis. The application of DWI in oncology has been widely explored. DWI for tumour detection has been shown for a variety of tumour types in adult and paediatric oncology. Used together with other MR imaging techniques, DWI can aid tumour characterization and in distinguishing tumour from non-tumour tissues. DWI is usually performed using an echo-planar imaging technique, in breath-hold, free-breathing or with the use of respiratory and/or cardiac gating. Meticulous attention to technique is important to ensure high-quality images can be consistently obtained. This is one of the key competence of MR radiographers. There is now considerable interest in using DWI for the monitoring of treatment response. Several studies have already shown that the apparent diffusion coefficient (ADC) of tumour in response to successful chemotherapy, radiotherapy and other minimally invasive interventional procedures. Diffusion-weighted MRI is being increasingly used in paediatric body imaging. Its role is still emerging. It holds great promise in the assessment of therapy response in body tumours, with ADC value as a potential biomarker. Body DWI is a technique that can be quickly performed on clinical MR systems, and can be incorporated into existing clinical protocols.

Learning Objectives:
1. To appreciate the role of diffusion imaging in oncology imaging.
2. To discuss the responsibility of radiographers in the application of DWI.
3. To discuss the clinical application of diffusion imaging in MR enterography and paediatric imaging.

09:45
Discussion and questions: How is patient care affected by MRI technology and techniques?

08:30 - 10:00 **Room M 1**

Vascular

RC 115
Peripheral vascular malformations: light after darkness

A-047 08:30
Chairman's introduction
J.A. Reekers; *Amsterdam/NL (j.a.reekers@amc.uva.nl)*

Treatment of peripheral vascular malformations is a combination of diagnostics, skills and experience. This treatment is done by specialised interventional radiologists in dedicated centres. Treatment is always a team effort. There is a wide variety of diagnostic pathways used to establish the final diagnosis and to plan treatment. These pathways will be discussed. Based on the clinical diagnosis specific imaging algorithms can be used. In the workshop this will be discussed. Treatment of peripheral vascular malformations is often not a medical necessity but mainly closely related to the wishes and expectations of the patients. Every procedure is tailored by this “shared dissection making” and, therefore, planning of a treatment procedure should also be patient tailored. How to define success is, therefore, sometimes difficult. This planning of treatment will also be discussed. Children are a specific entity within the spectrum of vascular malformations and special knowledge is needed not only to treat but also to support these patients and their family. Also in children interventional techniques are tailored and this will be discussed in the session.

Session Objectives:
1. To review classification and description.
2. To identify the role of imaging modalities.
3. To understand the role of interventional radiologist in management and treatment.

A-048 08:35
A. The diagnostic assessment
M. Köcher; *Olomouc/CZ (martin.kocher@seznam.cz)*

Vascular malformations are categorized into the low-flow malformations and high-flow malformations. From imaging methods it is expected to distinguish between the low-flow lesions and high-flow lesions, localisation, volume and range of lesion and relationship to the surrounding tissues and organs. Colour

Doppler ultrasonography (DUS) can offer good differentiation between high-flow and low-flow lesions. Magnetic resonance (MR) offers good differentiation between high-flow and low-flow lesions also and, moreover, good evaluation of volume and extent of lesion, good interpretation of anatomical relationship to the surrounding tissues and organs. On DUS the low-flow malformations are demonstrated as hypoechogenic or heterogenous lesions with minimal flow inside, flow during augmentation and normal arterial flow volumes and normal high arterial resistance flow. The high-flow malformations are heterogeneous lesions with tortuous feeding arteries, high-velocity and low-resistance flow in feeding arteries, multiple arteriovenous shunts and pulsatile flow in draining veins. On MR, the low-flow malformations typically have low signal intensity in T1-weighted images in abnormal vascular structures and high signal intensity in T2-weighted images whereas the high-flow lesions usually demonstrate signal voids in abnormal vascular structures on most sequences. At follow-up, DUS demonstrates thrombosis and fibrosis of the low-flow lesion. In the high-flow lesion, the waveform will normalised and the resistive indexes and the flow volumes will become normalized as well. MR demonstrates thrombosis and fibrosis of low-flow malformation by the loss of high signal in T2-weighted images and loss of signal voids in high-flow lesions.

Learning Objectives:

1. To learn about classification and terminology.
2. To understand the role of US, CT and MRA in diagnostic assessment.
3. To learn the optimal imaging algorithm for diagnosis and follow-up.

A-049 08:58

B. Percutaneous or endovascular treatment: when and how?

B. Peynircioglu; *Ankara/TR (borapeynir@gmail.com)*

Vascular anomalies are divided into two different categories which carry different prognosis and management: "vascular tumours" and "vascular malformations" (VM). Their precise identification is crucial and involves a good knowledge of the biological classification published by Mulliken and Glowacki and that has recently been updated by the International Society for the Study of Vascular Anomalies (ISSVA). Vascular malformations are always congenital and growth with the child. They can involve type of vessels solely or combined with others. A rheologic differentiation between low and high flow malformations is essential to characterize the seriousness of the lesion. Interventional radiology (IR) plays major role in both curative and palliative treatments of these VM. Transcatheter/endovascular (transarterial or transvenous) or direct percutaneous puncture under imaging guidance are the 2 main techniques for treating these lesions. Depending on the type, nature, location and surroundings of the VM, one should decide the best strategy for treatment. Another key point is to decide whether to use embolization or sclerotherapy. Again, the type, location of the VM is vital and the patient-based decision is to be made carefully by a multidisciplinary team. Operator's experience is of most importance in determining all of the above variables, together with the local circumstances. There are many different types of embolic and sclerotherapy agents available around the world.

Learning Objectives:

1. To recognise the indications and the real need for treatment.
2. To learn about technical approach - how to plan the intervention?
3. To understand possible limitations and the final result prediction.

A-050 09:21

C. Paediatric vascular malformations: diagnosis and treatment

S. Stuart, D. Roebuck; *London/UK (derek.roebuck@gosh.nhs.uk)*

The current accepted method for classification of vascular malformations is straightforward and clinically relevant. Vascular malformations can be divided into high flow lesions such as arteriovenous malformation (AVM) or low flow lesions such as venous or lymphatic malformations. In children, 90% of vascular anomalies can be diagnosed by clinical history and examination alone. Imaging predominantly with US or MRI can confirm the diagnosis, evaluate extent of a lesion or flow within it. In children ultrasound is particularly useful for aiding the diagnosis. Many vascular malformations require no treatment, if they are not causing symptoms. A multidisciplinary team approach to the management of these conditions is vital. Non-interventional treatments such as physiotherapy and occupational therapy are vital. The use of compression garments can help symptomatically in venous malformations. Interventional radiology plays a role in treatment principally with injection sclerotherapy of low flow lesions and embolization of the much rarer AVM. Many sclerotherapy agents are available with sodium tetradecyl sulphate the most commonly used for venous malformations and doxycycline commonly used for lymphatic malformations. Different sclerotherapy agents have different characteristics and uses which will be covered. Symptomatic relief is often achieved with treatment but multiple treatment episode may be needed to achieve the wanted outcome. Ensuring the child and family understand this is vital to ensure they are satisfied with the management of the condition.

Learning Objectives:

1. To understand the specifics of vascular malformations in children.
2. To recognise when to observe and when to intervene?
3. To learn about interventional techniques used and results of treatment.

09:44

Panel discussion: How could we improve diagnosis and optimise the results of our interventions?

08:30 - 10:00 **Room M 3**

Interventional Radiology

RC 109

Musculoskeletal interventions: what's new?

Moderator:
A. Gangi; Strasbourg/FR

A-051 08:30

A. Musculoskeletal ablation and embolisation

A. Basile; *Catania/IT (basile.antonello73@gmail.com)*

In a modern era of interventional strategies, ablation and embolization use is not anymore limited to usual target organs but these techniques are finding new rooms, remarkably in MSK tumours. In the literature, the most encountered benign tumours treated via ablation and/or embolization are osteoid osteoma, osteoblastoma, chondroblastoma and osteochondroma, giant cell tumour, aneurysmal bone cyst, eosinophilic granuloma, vertebral haemangioma and fibrous dysplasia. In turn, malignancies of the soft tissue and bones (primary sarcomas) are rare, likely spinal metastases are the most common (derived by carcinomas of the breast, lung, prostate, kidney and uterus). Shall be underlined that in most cases palliative measures are related to malignant cancer and patient's quality of life and motility are the priority. Among first weapon such as thermal ablation (both MW, RF and Laser) cryotherapy is raising the interest of the IR's community due to the powerful pain management feature and the possibility of an instant check of the ice ball, preserving nervous tissues, specially for vertebral metastases use. Nevertheless, ablation may be applied both for curative and palliative strategies when combined with cement injection, allowing a precise patient's selection to be made. Embolization has a strong importance applied to hypervascular lesions, may also reduce recurrence rate and potentially extend survival one. New heroes of oncologic interventions and probably future fashion are MR-guided HIFU and irreversible electroporation (IRE), even though bringing higher cost. Improved research of the field is strongly needed to assess a proper cost-benefit analysis and limits of these approaches.

Learning Objectives:

1. To appreciate the indications for ablations and embolisation.
2. To learn about different techniques and combination of them.
3. To discuss the results and literature data of interventional radiology procedures.

A-052 09:00

B. Vertebral augmentation and discectomy techniques: can we challenge surgery?

D. Filippiadis; *Athens/GR (dfilippiadis@yahoo.gr)*

Vertebral augmentation techniques include standard vertebroplasty, balloon kyphoplasty and percutaneous implant insertion combined to PMMA injection. Indications include osteoporotic, traumatic, pathologic and cancer-related fractures as well as benign (e.g. symptomatic atypical aggressive haemangiomas) or malignant (e.g. metastatic) lesions. Under proper patient selection, these techniques provide pain relief and functional improvement along with spine alignment height restoration and endplate reduction. Additionally, kyphotic angle restoration or maintenance seems to prevent future vertebral fracture in the adjacent levels and improved sagittal balance. Studies in the literature report that load distribution in patients with vertebral fractures post-vertebroplasty returns to values of normal population. Variety in the morphology, location, and aetiology of vertebral fractures demands a tailored patient-centred approach. Percutaneous technique for intervertebral disc herniation and discogenic pain can be either decompression or biomaterial implantation techniques. The former can be classified into mechanical (discectomy), thermal (RF, laser, coblation, IDET) or chemical (Discogel, ozone) methods whilst the latter includes hydrogel, PRP and stem cell therapies. Decompression techniques are indicated for small- to medium-sized symptomatic contained hernias. Percutaneous techniques are performed as outpatient, low-cost procedures and are governed by good patient compliance, high success (75-85%) and low complication rates (<1-2%). In case of treatment failure, percutaneous techniques can be repeated without interfering

with surgery at a later stage. Percutaneous vertebral augmentation and discectomy techniques compared to surgical approaches are favoured in terms of reduced blood loss and operating time, shorter hospital stay, fewer complications and less postoperative pain.

Learning Objectives:

1. To appreciate the rationale for the using of interventional radiology procedures.
2. To learn about different techniques and treatment strategy.
3. To discuss results and literature data in comparison with other treatments.

A-053 09:30

C. Bone biopsy and pain treatment using cone-beam CT (CBCT)

L. Tselikas; *Villejuif/FR (lambros.tselikas@gustaveroussy.fr)*

Cone beam-CT imaging (CB-CT) is actually widely available and allows, because of high-quality multiplanar reconstructions and using dedicated guiding software, to perform various bone interventions. Bone biopsies are feasible using CB-CT guidance with the same accuracy as CT-scan guidance and requiring less radiation exposure for patients and operators. Furthermore, pain palliation procedures such as cementoplasty and percutaneous osteosynthesis are actually possible with very high accuracy and technical success rates. New techniques and software are under development to decrease radiation dose, improve guidance for in case where CB-CT acquisition can be complicated and be easily integrated in an everyday workflow.

Learning Objectives:

1. To appreciate the high imaging quality and guidance accuracy using CBCT for biopsy and pain treatment.
2. To learn about the advantages of CBCT guided interventions, reconstruction algorithms, image enhancement and dose reduction.
3. To discuss about techniques, limitations of CBCT and future applications.

Author Disclosure:

L. Tselikas: Consultant; General Electric.

08:30 - 10:00 **Room M 4**

E³ - ECR Academies: Tips and Tricks in Liver, Bile Ducts and Pancreas Imaging

E³ 118

Liver, bile ducts and pancreas: improving your technique with advanced tools

A-054 08:30

Chairman's introduction

Y. Menu; *Paris/FR (yves.menu@sat.aphp.fr)*

Optimal imaging technique is absolutely critical in abdominal studies, as many parameters may interfere in the production of final images. Despite technical advances, or may be as a consequence, settings and fine-tuning of machines is the only way to reach clinical relevance of images. The radiologist has to be familiar with the most important parameters that may influence image quality and relevance. In this session, the purpose is to learn the best and the most simple way to obtain optimized results with recent and advanced imaging technique, with a special interest on how to integrate it while driving these machines for clinical practice.

A-055 08:35

A. Liver specific contrast: how, why, when?

E. Neri; *Pisa/IT*

The so-called liver-specific (or hepatobiliary) contrast agents (gadobenate dimeglumine, Gd-BOPTA, and gadoxetic acid, Gd-EOB-DTPA), are characterised by a dual behaviour by exhibiting elimination through both renal and hepatic excretion pathways and thereby possessing both early perfusion information (renal elimination pathway) and, later, hepatocyte-selective information (hepatic excretion pathway) mediated through protein transporters, located in the canalicular or sinusoidal pole of the hepatocytes. As a basic rule of MR technique all non-blood pool gadolinium chelate-based contrast agents are suitable for dynamic liver MRI, but the use of liver-specific contrast agents is mandatory to obtain the hepatobiliary phase in addition to the dynamic phase. The workup of solid focal liver lesions should include: axial breath-hold heavily T2-weighted half-Fourier single-shot turbo spin-echo sequences; navigator triggered intermediate T2-weighted turbo spin-echo sequences, breath-hold T1-weighted two-dimensional dual gradient-echo in-phase and opposed-phase sequences, and dynamic contrast enhanced fat-suppressed three-dimensional spoiled gradient-echo breath-hold sequence, acquired before and during the late arterial, portal venous and late dynamic phase. Hepatocyte phase can be considered adequate when Gd-EOB is detected in the intrahepatic bile ducts and the vessels are definitely hypointense in comparison to the background parenchyma. Liver specific contrast agents improves the characterisation of benign liver lesions, malignant liver lesions in non-cirrhotic, focal lesions in cirrhotic patients; they are also helpful to to depict the degree of fibrotic changes in liver fibrosis.

Learning Objectives:

1. To learn about physiology of liver specific contrast media physiology, and to be able to optimise liver MRI protocols.
2. To understand why they are useful for the detection and characterisation of liver masses.
3. To learn and understand the limitations.

A-056 09:03

B. Diffusion-weighted imaging (DWI): how, why, when?

D.-M. Koh; *Sutton/UK*

Diffusion-weighted MRI (DWI) is now routinely applied for the evaluation of abdominal diseases. The principles of optimising DWI are similar on both 1.5T and 3.0T, which includes maximising image signal to noise and minimising artefacts. In this regard, free-breathing DWI acquisition is most widely used to achieve the best image quality. DWI can be used to improve disease detection in the liver, hepatobiliary tract and the pancreas. It can be applied to support disease characterisation, but potential pitfalls should be appreciated. There is an increasing role for its deployment for the early evaluation of tumour response to treatment. Monoexponential DWI model to derive the apparent diffusion coefficient (ADC) of tissue is still the most widely used approach in the clinical setting. However, there is interest in applying non-monoexponential approaches including IVIM (intravoxel incoherent motion) and DKI (diffusion kurtosis imaging). These approaches should be utilised with full knowledge of their measurement repeatability so that it allows for meaningful data interpretation.

Learning Objectives:

1. To become familiar with the different acquisition techniques and to be able to adapt to a specific machine, including field strength.
2. To understand the role of DWI in the detection and characterisation of hepatobiliary and pancreatic diseases.
3. To learn about the potential technical future developments.

A-057 09:31

C. Advances in hybrid imaging: new tracers and MR/PET

E.J. Rummeny; *Munich/DE (rummeny@roe.med.tu-muenchen.de)*

In both PET/CT and MR/PET, radioactive tracers are used to detect primary tumours and metastases. During the lecture, we will discuss those tracers which are used for PET imaging of the abdomen and pelvis. By far the most commonly applied tracer is 18F-FDG which is used to study glucose metabolism in tumours and metastases. Increasingly, other more specific tracers, primarily marked with 68 Ga, are used for abdominal tumours such as DOTA-TATE and DOTA TOC. These tracers exhibit high affinity to somatostatin receptors and can be used to detect endocrine tumours (NET) with low or moderate proliferation rate (G1 and G2). To quantify tumour response to therapy, standard uptake values (SUV) can be calculated. Newer tracers like 68 Ga-PSMA-ligand are primarily used to diagnose prostate cancer (PCa) and its metastases to lymph nodes and bones. Furthermore, this tracer may be also useful to diagnose other tumours of the urinary tract. Bound to 90 Yttrium or 177 Lutetium, these carriers, i.e. DOTA-NOC and PSMA-ligand, can be used as so-called theranostics which are employed successfully to treat tumour metastases of certain cancers. All those markers can be used for PET/CT and MR/PET. While PET/CT is in clinical use already, MR/PET systems are still under evaluation. MR has better soft tissue contrast and radiation dose from MR/PET is substantially less than PET/CT. However, MR/PET takes longer than PET/CT and is only feasible in certain patients. Therefore, MR/PET is currently available for patients with selected indications and primarily used for clinical research studies.

Learning Objectives:

1. To understand why alternative tracers to FDG may be useful in exploring liver and pancreatic diseases.
2. To learn about the role of PET in the follow-up of tumours and quantification of tumour response.
3. To become familiar with the specific advantages of MR/PET over PET/CT in abdominal diseases.

08:30 - 10:00 **Room M 5**

E³ - ECR Master Class (Genitourinary)

E³ 126b

Functional MRI of the kidneys: ready for prime time?

Moderator:
H.C. Thoeny; Berne/CH

A-058 08:30

A. Diffusion-weighted MRI
N. Grenier; *Bordeaux/FR (nicolas.grenier@chu-bordeaux.fr)*

Diffusion-weighted MRI of the kidney has multiple applications in morphological renal imaging. Its applications in the functional field of parenchymal renal diseases are still to be defined. For morphological applications such as renal tumours or infections, 3 b-values are enough with calculation of an ADC-map based on a mono-exponential fit. For functional applications, the tendency goes toward more sophisticated approaches such as the IVIM technique with more b-values and a bi-exponential fit or characterisation of the diffusion tensor, based on acquisition of at least 6 directions, of diffusion encoding. All functional and tissue changes decreasing water movements or increasing the cell density in renal parenchyma can decrease diffusion coefficients. Renal ADC decrease is correlated with the degree of renal dysfunction in parenchymal diseases. Urinary obstruction and parenchymal processes such as inflammation or fibrosis also decrease the diffusion coefficients. In chronic diseases, tissue changes and fibrosis induce changes of the microarchitecture responsible for a decrease of renal anisotropy shown by diffusion tensor imaging.

Learning Objectives:
1. To learn about the technical issues of DWI.
2. To understand the physiological determinants of diffusion measurements.
3. To assess the role of DWI in clinical practice.

Author Disclosure:
N. Grenier: Advisory Board; Supersonic Imagine.

A-059 09:00

B. Perfusion MRI
M. Claudon; *Vandoeuvre-les-Nancy/FR (m.claudon@chu-nancy.fr)*

Because of its high spatial resolution, magnetic resonance urography has demonstrated high accuracy in the morphologic assessment of urinary tract. More recently, functional MRU (fMRU) has shown feasibility in adults and children, using dynamic pulse sequences performed after injection of an intravenous bolus of gadolinium chelates (DCE-MRU), which allow calculating the split renal function (SRF) from time-intensity curves, where the Patlak method should be preferred to the area under the curve method. Using MRU to obtain both anatomical and functional information in a single examination without radiation would be beneficial, especially for follow-up in young patients. Complementary medico-economic analysis confirms the interest of a potential substitution of nuclear renal scintigraphy by fMRU as an adjunct to morphological MRU.

Learning Objectives:
1. To learn about the clinical indications for kidney perfusion imaging.
2. To become familiar with perfusion protocols for kidney perfusion imaging.
3. To learn about difficulties in kidney perfusion imaging.

A-060 09:30

C. BOLD and ASL
A. Boss; *Zurich/CH (andreas.boss@usz.ch)*

In functional renal magnetic resonance imaging (MRI) advanced techniques are used to obtain functional and molecular information from the state of the kidney. In blood oxygenation level-dependent (BOLD) MRI, the susceptibility difference between oxyhaemoglobin (diamagnetic) and deoxyhaemoglobin (paramagnetic) is used to extract information on tissue oxygenation, which is interesting because of the physiological hypoxia in the renal medulla. BOLD MRI, therefore, may be applied to non-invasively assess renal oxygenation and the oxygen metabolism of the kidneys. Arterial spin labelling (ASL) is a non-invasive technique, which uses radiofrequency-labelled blood water as endogenous tracer to visualize and quantify renal perfusion. Using the extended Bloch equations, quantitative perfusion values in ml/100 g/min can be calculated.

Learning Objectives:
1. To understand the physiological and technical basis of blood oxygen level-dependent (BOLD) imaging of the kidneys.
2. To learn typical findings of BOLD-MRI in patients with kidney disease.
3. To review the physics and technique of arterial spin labelling (ASL) perfusion measurements of the kidneys.
4. To see typical findings of ASL measurements in patients with kidney diseases.

10:30 - 12:00 **Room A**

E³ - ECR Academies: Interactive Teaching Sessions for Young (and not so Young) Radiologists

E³ 221

MR imaging in sports medicine I

A-061 10:30

A. Muscle injury in sports
M.G. Mack; *Munich/DE (m.mack@radiologie-muenchen.de)*

According to the UEFA injury study 2014, almost 50% of all injuries in professional soccer players are related to muscles, tendon and the musculotendinous junction. During this lecture, you will learn how normal and injured muscle will look like. The standard imaging protocol is including axial T1- and fsPD sequences, angulated coronal and sagittal fsPD sequences with a slice thickness between 1 and 6 mm. You will learn to differentiate between functional muscle disorders without structural injuries (like fatigue-induced muscle disorder (Type 1a), delayed-onset muscle soreness (Type 1b) and spine (Type 2a) or muscle-related neuromuscular disorder (Type 2b)) and structural injuries (minor partial tear (Type 3a), moderate partial tear (Type 3b) and total/subtotal tear (Type 4) of the muscle, the musculotendinous junction and tendinous avulsion). Most structural injuries are stretch-induced injuries and have to be differentiated from contusion injury and distraction injury. In soccer, 92% of all muscle injuries affect the four major muscle groups of the lower limbs (hamstrings, adductors, quadriceps and calf muscles) and occur mainly in non-contact situations.

Learning Objectives:
1. To understand the anatomy of the most common injured muscles.
2. To learn the evaluation of muscle injuries and the impact regarding recover.

A-062 11:15

B. Knee trauma
M. Shahabpour; *Brussels/BE*

"no abstract submitted"

Learning Objectives:
1. To learn the anatomy of the most common injured structures.
2. To recognise typical combinations of injuries.

10:30 - 12:00 **Room F1**

E³ - Rising Stars Programme: Basic Session

BS 2

Lungs

Moderator:
T. Franquet; Barcelona/ES

A-063 10:30

Congenital anomalies
J. Ley-Zaporozhan; *Munich/DE*

Imaging in lung anomalies is usually started off by plain film radiography. This projection technique gives a first overview of the anatomical situs and allows for a first assessment of expected anomaly. Depending on the individual setting an ultrasound of the chest can be added for further assessment of the vascular structures or cystic components. A more sophisticated imaging technique like computed tomography or magnetic resonance imaging will allow for definite classification of the anomaly. The different imaging techniques and especially CT and MRI protocols used will be covered. Anatomical variants are most often detected within the tracheobronchial tree, namely with anomalous branching pattern of the upper lobe bronchi. Congenital lung anomalies are a heterogeneous group of developmental disorders with a wide distribution in imaging appearance and clinical manifestations. The most frequent ones are: congenital pulmonary airway malformation (CPAM), congenital lobar hyperinflation, bronchial atresia, bronchiogenic cyst and pulmonary

sequestration. For these anomalies, the embryologic background, clinical presentation and imaging findings will be demonstrated.
Learning Objectives:
1. To discuss current imaging techniques for evaluation of normal lung anatomy.
2. To learn and understand possible anatomical variants.
3. To describe the typical imaging features of the most common anatomical anomalies.

A-064 11:00

Infection

T. Franquet; *Barcelona/ES (tfranquet@santpau.cat)*

Inflammation is a response of vascularised tissues to infections to eliminate the offending agents. Pneumonia occurs when the host mounts an inflammatory response, centred on the lung parenchyma, usually against a microorganism which has reached this normally sterile site. Bacteria are the most common causative microorganisms. Pneumococci usually spare alveolar walls and cause lobar pneumonia that resolves completely, whereas Staphylococci and Klebsiella species destroy alveolar walls and form abscesses that heal with scar formation. Combination of pattern recognition with knowledge of the clinical setting is the best approach to pulmonary infectious processes. When pulmonary infection is suspected, knowledge of the varied radiographic manifestations will narrow the differential diagnosis, helping to direct additional diagnostic measures, and serving as an ideal tool for follow-up examinations. Management of immunocompromised patients is challenging and difficult because of the diversity of causative organisms. Although diagnostic information may also be obtained by means of bronchoalveolar lavage and transbronchial needle aspiration, the radiologist plays an important role in the diagnosis and management of patients with suspected pneumonia.
Learning Objectives:
1. To recognise the most common imaging patterns of lung infections.
2. To understand the temporal relationship between the immune status and diverse lung infections.
3. To have a basic knowledge of CT-path correlation of some pulmonary infectious diseases.

A-065 11:30

Tumours

I. Hartmann; *Rotterdam/NL (i.j.c.hartmann@gmail.com)*

Non-small cell lung carcinoma (NSCLC) comprises the largest group of which the imaging appearance can be variable. It can present as centrally or peripherally located nodule or mass that may invade mediastinal structures or the chest wall. Tumour margins may be smooth, lobulated, ill defined, irregular or spiculated. Other findings include cavitation, consolidation and ground glass opacity (GGO). Accompanying post-obstructive pneumonia and/or lung collapse can be seen in central tumours. Small cell lung carcinoma (SCLC) is the most common primary pulmonary neuroendocrine tumour. Most SCLCs are a centrally located large mass invading or metastasising to regional lymph nodes. 5-10% of SCLCs present as a peripherally located spiculated nodule without associated lymphadenopathy. Pulmonary metastasis: the lung is frequently involved in metastatic disease. Typical radiological features include multiple round nodules with variable size, peripherally located (haematogenous metastasis) and diffuse thickening of the interstitium (lymphangitic carcinomatosis). Atypical features such as cavitation, calcification, air bronchogram and GGO are often encountered. Pulmonary lymphoma imaging findings of parenchymal disease in both primary (rare entity) and more frequently occurring secondary pulmonary lymphoma are variable and non-specific. They include single or multiple nodules, masses or consolidations, cavitation and air bronchogram. Ancillary findings include lymphadenopathy, bronchial wall thickening, interlobular septal thickening and pleural effusion. CT is the workhorse of imaging in bronchogenic carcinoma, metastasis and lymphoma, and plays together with PET/CT a crucial role in staging bronchogenic carcinoma and lymphoma. Due to the variety in CT imaging appearances, tissue confirmation is usually warranted to confirm the diagnosis.
Learning Objectives:
1. To describe the typical imaging appearance of bronchogenic carcinoma.
2. To describe the typical imaging features of pulmonary metastases.
3. To describe the manifestations and the role of imaging in pulmonary lymphoma.

10:30 - 12:00 **Room M 4**

E³ - ECR Academies: Tips and Tricks in Liver, Bile Ducts and Pancreas Imaging

E³ 218

Benign liver tumours: daily questions

A-066 10:30

Chairman's introduction

S.M. Ertürk; *Istanbul/TR (smerturk@gmail.com)*

The session will focus on the imaging features of the cystic and solid liver lesions. The new classification system of the hepatic adenomas will be discussed in detail. Sample cases of haemangiomas and FNHs will be another focus of the session since these lesions are very frequently encountered in imaging studies of the liver. Imaging strategies to increase accuracy regarding the detection and characterisation of focal hepatic lesions will be summarised.
Author Disclosure:
S.M. Ertürk: Speaker; General Electric, Siemens, Bayer, Guerbet.

A-067 10:35

A. Cystic lesions: always biliary cysts?

O. Benjaminov; *Petach Tikva/IL (obenjaminov@gmail.com)*

Liver cysts are increasingly found on abdominal imaging studies. They cause a diagnostic challenge. There are no current management guidelines that help in their management. In most cases they are asymptomatic and follow a benign course. However, it is essential to differentiate between benign and malignant liver cysts. The majority are of a biliary origin. Others are non-biliary and include hydatid and other infectious cystic lesions, cystic neuroendocrine lesions and cystic metastases. Other lesions which contain a fluid attenuation component may mimic liver cysts such as necrotic changes within lesions following chemotherapeutic treatment. Clinical history, laboratory findings and previous imaging may help in reaching an accurate diagnosis. An important step in narrowing the differential diagnosis is in determining the presence of complex structures within the lesions.
Learning Objectives:
1. To be able to list the different conditions that may present as cystic liver masses.
2. To understand the diagnostic multimodality strategy.
3. To become familiar with assessment challenges.

A-068 11:03

B. Solid benign lesions: how to solve the conundrum?

F. Caseiro-Alves; *Coimbra/PT (caseiroalves@gmail.com)*

Benign hepatocellular neoplasms are being recognized with increased frequency using cross-sectional imaging. One of the main goals is to be able to make a clear-cut differential diagnosis between focal nodular hyperplasia (FNH) and hepatocellular adenoma (HCA) since patient management is substantially different. Despite the sound knowledge acquired in the last few years about the morphological features of FNH using various cross-sectional imaging techniques, new players in the field have arisen such as diffusion-weighted MR imaging (DWI) and use of hepatobiliary contrast agents. These new biomarkers offer a different view over FNH and allow a more accurate characterization even in more atypical cases. Concerning HCA, current knowledge implies that the sub-types of this neoplasm should be known since, again, patient management differs and these patients are no longer seen as compulsory surgical candidates. These sub-types will be further discussed and the role of imaging for risk stratification (haemorrhage and malignant transformation) will be addressed. Further, illustrative cases of combined FNH/HCA cases will be demonstrated along with the main imaging clues for a successful differential diagnosis.
Learning Objectives:
1. To become familiar with the recent classification of liver cell adenoma and its justification.
2. To learn about the typical and atypical appearance of focal nodular hyperplasia.
3. To understand the treatment strategy and the modalities of follow-up when appropriate.

A-069 11:31

C. From images to strategy: tough cases of benign liver tumours

M. Nadrljanski; *Belgrade/RS (dr.m.nadrljanski@gmail.com)*

Benign liver tumours are often diagnosed incidentally. The most common lesions include haemangioma, focal nodular hyperplasia (FNH) and hepatocellular adenoma (HCA). Liver nodule(s), often detected on the initial abdominal ultrasound (US), are characterized by contrast-enhanced imaging studies: contrast-enhanced US (CEUS), computed tomography (CT) and magnetic resonance imaging (MRI). Clinical context determines the association with the development of liver disease. Lesions with atypical features ("tough cases") require additional attention. The most common atypical findings in haemangioma - rapidly filling and giant haemangiomas - may be diagnosed on MRI. In case of the slow-filling and calcified lesions - sclerosing haemangiomas - the diagnostic imaging is less reliable. In case of the growing lesions, the lesion management is made according to multidisciplinary team (MDT). The diagnosis of FNH is based on the combined radiological features, not considered as lesion specific. Atypical forms (FNH without a central scar, FNH with significant steatosis) require particular attention, as the sensitivity of MRI is lower, especially in the absence of the central scar. The use of the specific hepatobiliary contrast agents may contribute to the increase of MRI sensitivity. HCA, not considered the unique entity, reflects the subtype radiological features. The presence of fat and telangiectatic features requires the appropriate imaging technique(s) - MRI for fat and dilated vascular spaces visualization. MRI lesion subtyping is important, as MRI is considered superior to other modalities. In case of atypical benign lesions, MDT will decide on the patient management, including the indication for biopsy/resection.

Learning Objectives:

1. To be able to define a diagnostic strategy when facing an unknown case of solid liver lesion, likely to be benign.
2. To become familiar with the unusual appearance of common lesions like focal nodular hyperplasia or haemangioma.

12:15 - 12:45 **Room B**

Headline Session

Guest Lecture

Breaking News from Latin America

Presiding:
P.M. Parizel; Antwerp/BE

A-070 12:15

Imaging findings in Zika virus infection

M. Vasco Aragao; *Recife/BR (fatima.vascoaragao@gmail.com)*

Zika virus (ZIKV) was discovered in 1947 in monkeys (Zika forest) and human infection was identified in 1952. The first epidemic happened in 2007, at Micronesia and Yap Islands and the second in 2013, at French Polynesia. In Brazil (March 2015) begun the third epidemic and, surprisingly, in the second half of 2015, a microcephaly epidemic was identified. The relationship between the two epidemics is established. The diagnosis is based on clinical and radiological findings, associated with laboratory exclusion of other congenital infections or hereditary conditions. The imaging abnormalities are subcortical calcifications and malformations of cortical development (frontal predominance), ventriculomegaly, decreased brain volume, enlarged cisterna magna, corpus callosum abnormalities and delayed myelination. In patients with arthrogryposis, the abnormalities are reduced spinal cord thickness and anterior nerve roots. Immunologic tests specific for the ZIKV are in development and not available for clinical routine. Thus, the role of radiologists is extremely important in recognizing the radiological pattern of presumed cases of the congenital Zika syndrome, mainly in mild cases, when the disease is not suspected by the paediatrician. There is a possibility that we have been seeing just the most severe extreme of the disease spectrum. Guillain-Barre syndrome, myelitis and encephalitis have been found in adults. Prevention remains the only way to control the disease. The disease has already spread across the world. Up to October 19th, 2016, 73 countries had reported ZIKV transmission, while 23 countries had reported ZIKV-related microcephaly (WHO). In Brazil, there are 2,033 confirmed cases of microcephaly.

Learning Objective:

1. To describe the neuroimaging findings of the Zika virus (ZIKV) syndrome, the new emerging epidemic that is writing a new chapter in the history of medicine.

12:30 - 13:30 **Room C**

E³ - The Beauty of Basic Knowledge: Chest Imaging

E³ 25A

Useful signs in chest radiology

Moderator:
N. Howarth; Chêne-Bougeries/CH

A-071 12:30

A. Lung parenchyma

G.R. Ferretti; *Grenoble/FR (GFerretti@chu-grenoble.fr)*

CXR remains the keystone for the diagnosis of pulmonary diseases, as it is performed in the vast majority of patients complaining of chest symptoms, because is it largely available, simple to realize, low cost and delivers low radiation dose. However, indications of CXR for imaging the lung parenchyma are challenged by ultra-low-dose HRCT. In this presentation, we will focus on useful signs to detect lung parenchymal abnormalities such as airspace opacities, air bronchogram, silhouette sign, atelectasis and interstitial pattern. Pulmonary distribution of abnormalities such as butterfly-wing distribution, anti-butterfly-wing distribution and migratory consolidations may increase the value of CXR. Difficulties in the interpretation and limitations of CXR will be discussed along with correlations with HRCT results.

Learning Objectives:

1. To review the most useful signs on the chest x-ray.
2. To learn how to interpret the chest x-ray more accurately.
3. To know the appropriate indications of the chest x-ray.

A-072 13:00

B. Mediastinum and chest wall

N. Howarth; *Chêne-Bougeries/CH (nigel.howarth@grangettes.ch)*

The presentation will explain useful signs in chest radiology using side-by-side plain film and CT imaging to help understand the imaging features of common pathologies of the mediastinum and chest wall. Although the clinical value of the chest x-ray remains undiminished, errors of interpretation of the chest x-ray remain one of the most frequent causes of malpractice issues. The skills required for accurate interpretation of imaging of the mediastinum and chest wall will be explored. The objective is to help you improve your performance in plain film interpretation and CT imaging of the chest.

Learning Objectives:

1. To review the most useful signs on the chest x-ray.
2. To learn how to interpret the chest x-ray more accurately.
3. To know the appropriate indications of the chest x-ray.

12:30 - 13:30 **Room D**

E³ - The Beauty of Basic Knowledge: A Survival Guide to Musculoskeletal Imaging

E³ 24A

Degenerative disorders

Moderator:
V.N. Cassar-Pullicino; Oswestry/UK

A-073 12:30

Degenerative disorders

A. Cotten; *Lille/FR (anne.cotten@chru-lille.fr)*

Osteoarthritis is the most common joint disease worldwide. It is a major source of pain, disability, and socioeconomic cost. The epidemiology of the disorder is complex and multifactorial, with genetic, biological and biomechanical components. Conventional x-ray is the standard diagnostic method to confirm the clinical diagnosis, to evaluate the degree of severity of osteoarthritis and to look for predisposing conditions. CT can be performed for the assessment of bone stock, anatomic conditions and bone deformation. MRI can be used to confirm early forms and to clarify possible damage and/or wear and tear, which cannot be seen on x-rays. Finally, intraarticular administration of contrast will be performed in selected cases, when a precise assessment of the cartilage or fibrocartilage is required. This lecture will focus on: the role of imaging in clinical practice, the typical and atypical imaging features of OA, the radiological features which should not be read as OA, the main predisposing factors that have to be known and searched.

Learning Objectives:
1. To appreciate the musculoskeletal imaging manifestations of degenerative disorders.
2. To understand the underlying pathomechanisms involved in these imaging abnormalities.
3. To appreciate the strengths and weaknesses of imaging modalities in assessing these disorders.

14:00 - 15:30 **Room F1**

E³ - Rising Stars Programme: Basic Session

BS 3
Gastrointestinal diseases

Moderator:
N. Papanikolaou; Lisbon/PT

A-074 14:00
Oesophagus
F.-T. Fork; *Malmö/SE (thomas.fork@med.lu.se)*

Double-contrast barium fluoroscopy is today almost substituted for endoscopy, because the oesophageal mucosa is better evaluated and locally treated by therapeutic endoscopy. Single-contrast studies are used for diagnosing swallowing disorders, sometimes in combination with oesophageal manometry, for food impaction, stent function and achalasia. Computed tomography of thorax and abdomen is done for staging malignant diseases. Combined with FDG-PET the number of metastases increases. Magnetic resonance imaging of thorax with diffusion techniques may improve detectability of metastatic deposits. Local tumour spread, TNM-stage 1 to 4, is imaged by endoscopic ultrasound. The majority of benign oesophageal lesions emanate from the mucosal lining, i.e. adenoma, all kinds of inflammatory conditions, be it gastric reflux, overgrowth in immunosuppressive patients, or noxious contact lesions. As with varices these superficial lesions are diagnosed and biopsied and, when appropriate treated endoscopically. However, diverticular disease is best evaluated radiographically. Small neoplastic lesions are vague in symptoms and incidentally found on routine examination for other reasons and seldom diagnosed by radiological means. Local wall thickening and dislocation are suspicious signs, whereas local lymph nodes grown in size and number are ominous. Oesophageal cancer is endemic in Asia and with us seen in individuals with an overconsumption of tobacco and alcohol. Due to anatomy of the lymphatic system with lymph vessels reaching into the mucous membrane, early tumour spread is mostly encountered. Radiology plays an important role in detecting peripheral disease prior to a MDT-meeting but also after surgical resection to document any post-operative complication or recurrent tumour.
Learning Objectives:
1. To discuss current imaging techniques for evaluation of normal anatomy.
2. To describe the imaging features in most common benign pathologies.
3. To review and illustrate the imaging features of malignant pathologies.

A-075 14:22
Stomach
M. Laniado; *Dresden/DE (michael.laniado@uniklinikum-dresden.de)*

Today, the stomach is well accessible for endoscopic evaluation. Therefore, double-contrast barium studies of the stomach have almost completely disappeared from the armamentarium of imaging studies in radiology. However, abdominal computed tomography (CT) - not so much magnetic resonance imaging (MRI) - has become the number one procedure in many scenarios if ultrasonography fails to provide a conclusive diagnosis. As the stomach is always imaged when abdominal CT is performed knowledge of normal anatomy, incidental findings, and the most often benign and malignant gastric pathologies is mandatory. Depending on the clinical request, imaging techniques are slightly different. If the main focus is on a lesion of the stomach, maximum wall distention should be achieved by oral administration of up to 2 L of water shortly before the study and i.v. administration of a hypotonic agent. In addition, i.v. administration of iodinated contrast material is mandatory. The presentation will cover normal anatomy of the stomach including vascular supply/drainage and loco-regional lymph nodes. Examples of common and uncommon gastric lesions (e.g. carcinoma, lymphoma, GIST, NET, metastases, ulcer, portal gastropathy, pneumatosis, ischaemia) will be shown and discussed. Also examples of postoperative anatomy and potential complications will be part of the presentation.
Learning Objectives:
1. To discuss current imaging techniques for evaluation of normal anatomy.
2. To describe the imaging features in most common benign pathologies.
3. To review and illustrate the imaging features of malignant pathologies.

A-076 14:45
Small bowel
N. Papanikolaou; *Lisbon/PT (npapan@npapan.com)*

Magnetic resonance imaging (MRI) provides excellent soft tissue contrast without radiation exposure and three-dimensional imaging capabilities, which are important when studying the small intestine. Various sequences and contrast agents have been proposed for MRI examination of the small bowel. The development of high-performance gradient systems improved the performance of ultra-fast sequences and allowed comfortable breath-hold acquisition times. For a more detailed evaluation of small bowel diseases, MRI examination should be performed in conjunction with duodenal intubation and administration of a suitable contrast agent, i.e. iso-osmotic water solution (PEG) for homogeneous lumen opacification and adequate distention. A comprehensive MR enteroclysis imaging protocol should comprise single shot turbo spin echo (SSTSE), diffusion weighted imaging, true FISP, HASTE and fat suppressed T1 FLASH sequences. SSTSE is utilized for monitoring the infusion process and performing MR fluoroscopy while true FISP and HASTE, classified as sequential ultrafast techniques insensitive to motion, are mainly used for anatomic demonstration and detection of the pathology. T1 FLASH sequences after intravenous gadolinium injection may aid tissue characterization. For the assessment of Crohn's disease activity other alternative techniques may be used including perfusion and calculation of the magnetization transfer ratio of the bowel wall. These techniques may be useful for differentiating oedematous or inflammatory bowel thickening from fibrotic thickening but a more extensive evaluation is required to determine the clinical utility of these methods.
Learning Objectives:
1. To discuss current imaging techniques for evaluation of normal anatomy.
2. To describe the imaging features in most common benign pathologies.
3. To review and illustrate the imaging features of malignant pathologies.

A-077 15:07
Colon
R.G.H. Beets-Tan; *Amsterdam/NL*

CT, US and colonoscopy are the main diagnostic tools for detection of benign and malignant diseases involving the colon. Bowel ischaemia, infectious enterocolitis, diverticulitis and appendicitis are causes of the acute abdomen that often needs prompt diagnosis. This lecture will deal with the typical features on imaging that will lead to the correct diagnosis. CT is part of the staging work up of patients with colonic cancer. It does not only provide information on distant disease but also on the local status. The latter information will help surgeons in choosing the right surgical approach. In this lecture attendees will learn about the current role for CT and potential new role for MRI in the management of colon cancer.
Learning Objectives:
1. To discuss current imaging techniques for evaluation of normal anatomy.
2. To describe the imaging features in most common benign pathologies.
3. To review and illustrate the imaging features of malignant pathologies.

14:00 - 15:30 **Room M 1**

Professional Challenges Session

PC 3
Excellence and innovation in undergraduate teaching of radiology

A-078 14:00
Chairman's introduction: Innovative approaches to undergraduate teaching, impact on student learning
V. Válek; *Brno/CZ (vlvalek@med.muni.cz)*

Over the past several decades, the practice of radiology has undergone substantial change primarily related to advances in imaging technology, changes in the infrastructure of healthcare delivery, and evolution of reimbursement systems. Rapid technological innovation in radiology has led to continual advances in importance of radiology in clinical praxis. This trend is, however, unfortunately without significant implications for radiology teaching and the educational system has not substantially changed. Radiology training programs around the world face a challenging task in both teaching a common knowledge base across all the imaging modalities and in imparting deep knowledge within each imaging domain. Today medical school teaching of radiology includes anatomy, imaging, interventions and new technology. Cross-sectional and virtual anatomy is extremely important. Clinical procedures performed without such a relevant anatomical knowledge could result in serious harm to patients. Important part of the training programs are

radiological e-learning activities. E-learning has been used recently in dental and general medicine curricula to support traditional learning methods. Effectiveness of e-learning in radiology education when compared with traditional classroom learning methods is very good and the students had positive attitude when using e-learning. Second example is incorporation of ultrasound education into medical school curricula. Even if the ultrasound imaging is incorporated into the curricula of most of medical schools, actual hands-on training is less widespread. It is time for the changes. 80 hours, which is a common duration of medical school teaching of radiology, is insufficient. Radiology must be incorporated into clinical teaching programmes.

Session Objectives:

1. To learn about innovation of didactic and learning strategies in radiology.
2. To evaluate the impact of technology for developing and transforming undergraduates teaching.
3. To analyse student organisation experiences.

A-079 14:05

How to keep students engaged

C. Nyhsen; *Sunderland/UK (nyhsenc@doctors.org.uk)*

When teaching medical students, PowerPoint presentations are often chosen as the preferred lecture format as they can be reliably shown year after year. Although presented material may be of excellent quality, published surveys have shown that students prefer interactive sessions, in particular when real-case scenarios are discussed with close relation to daily medical practice. The objective of this talk is to inspire attendees to try implementing different teaching methods, thus breaking down teaching sessions into smaller elements, engaging students to a higher degree (thereby hopefully improving learning outcomes and retention of information) as well as making it more enjoyable for teachers. The focus will be on "low tech" teaching methods which do not require sophisticated software or hardware facilities. Possibilities of how to integrate quizzes and assessments in a positive way will also be included.

Learning Objectives:

1. To learn about tips and tricks to connect with students.
2. To analyse the learning outcomes of students and specify what they expect as a result of a learning activity.
3. To define the methods to achieve excellence in undergraduate training and usefulness of teaching evidence-based radiology.

A-080 14:23

Excellence in undergraduate teaching

B. Ertl-Wagner; *Munich/DE (Birgit.Ertl-Wagner@med.uni-muenchen.de)*

To attract the best and the brightest medical students into a carrier in radiology, it is important that they become acquainted with the principles of radiology early on in their medical studies, preferentially already during preclinical studies. Cross-sectional and radiographic anatomy, radiation biology, radiation protection and imaging physics can already form an integral part of preclinical training and can be integrated into other teaching modules, e.g. in anatomy. During the clinical part of undergraduate medical education, radiology is a crucial part in almost all clinical aspects - the diagnostic workup and/or image-guided therapeutic principles are highly pertinent for almost all disease entities. In addition, radiology is an integral and important part of many oral and/or written examinations throughout undergraduate medical education. To ascertain that radiology is well represented during undergraduate medical education, it is very important that radiologists become and remain involved in curricular planning. The U-level curriculum of the ESR provides a basis for undergraduate curricular planning. In addition, mentoring programmes can be an important part in undergraduate medical education.

Learning Objectives:

1. To learn about the usefulness of curricula.
2. To discuss how to introduce to the students during the undergraduates teaching programmes radiology as an attractive specialisation.
3. To analyse the importance of mentoring undergraduates.

A-081 14:41

Teaching with technology: a challenging experience

P. Pokieser; *Vienna/AT (peter.pokieser@meduniwien.ac.at)*

Direct communication with the students remains the basis of medical education. The big difference to the past before information technology is the great advantage that the students' self-directed learning process is supported by online information and their new ability to navigate within the free available resources and the journals and other contents, by university access. For radiology training, for example, they can even use eurorad, epos or radiopaedia and other valuable data bases. This paradigmatic change does not mean more or less, that the modern student has most interest to hear, what is not accessible online. First, direct contact and interaction with experienced doctors (teachers, tutors), best near the daily work is and will stay as the most appreciated contribution we can give to our students. Second, doctors' experience, ideally combined with own original case studies; nowadays more and more interdisciplinary (e.g. board cases) represents a good starting point of training. Other new challenges in education are the international new undergraduate curricula, with focus on problem orientation, interdisciplinary perspectives of clinical decisions and dedication to organ systems more than clinical disciplines. Sessions in undergraduate's education are enriched by new tools to allow the students to interact with teachers, communication platforms and webinar applications open the space to include online live and remote blended learning.

Learning Objectives:

1. To emphasise on how to communicate with the students.
2. To evaluate new challenges in education, informatics tools available to encourage education.
3. To analyse the advantages of interactive sessions in undergraduate's education.

A-082 14:59

Evidence-based radiology for diagnostic imaging: do we need to teach the undergraduates?

R. Iezzi; *Rome/IT (roberto.iezzi.md@gmail.com)*

Evidence-based practice (EBP) has been defined as the 'interpretation of the best research evidence with clinical expertise and the patient's unique values and circumstances'. EBP teaching to future healthcare professionals has mainly been documented in medical students. Many different educational interventions of varying duration, frequency, and forma to teach EBP in a variety of settings exist. It showed that educational strategies adopted were found to improve students' overall EBP competence and their EBP knowledge and skills. Students felt more confident to accurately interpret the literature, could better assess the reliability/validity of information on the web and felt more comfortable with the concepts of EBP. It indicated that EBP is a learnable skill and the question is not whether EBP can or should be taught, but how to best teach. The use of technology to promote EBP through mobile devices, simulation, and the web is on the rise and web-based educational platforms have been demonstrated as an effective and desirable mechanism to deliver educational content to health professionals.

Learning Objectives:

1. To analyse the key concepts of teaching evidence-based radiology.
2. To learn about new approaches in teaching and learning radiology.
3. To discuss the importance of teaching evidence-based radiology among students.

15:17

Panel discussion: How do new approaches contribute to excellence in undergraduate teaching?

14:00 - 15:30 **Room M 4**

E³ - ECR Academies: Tips and Tricks in Liver, Bile Ducts and Pancreas Imaging

E³ 318

Chronic liver disease: guidelines for the radiologist

A-083 14:00

Chairman's introduction

B.J. Op de Beeck; *Antwerp/BE (bart.op.de.beeck@uza.be)*

Chronic liver disease is a substantial worldwide problem. Its major consequence is increasing deposition of fat, iron and fibrous tissue within the liver, leading to the development of cirrhosis with its consequences, portal hypertension, hepatic insufficiency and HCC. During this session, the question "how accurate are we in measuring fat and iron with MRI" will be answered. The goal is to become familiar with the different acquisition techniques, to understand the correspondence between MRI evaluation and histological scores and to learn about the limitations of the method. A second problem will be discussed concerning the question "can we reliably identify and quantify liver fibrosis and cirrhosis". It is important to understand the basic principles of fibrosis evaluation with US and MRI, how these methods could be implemented in daily practice, and how to make a radiological report. Fibrosis is independently associated with the viscoelastic parameters and is less associated with the diffusion parameters than is steatosis. There is a need for non-invasive detection and follow-up of these chronic liver diseases. Elastographic techniques are rapidly becoming the method of choice for the assessment of liver fibrosis, replacing liver biopsy for diagnosis, evaluation of disease progression and treatment monitoring. Finally, the problem of a small liver nodule in a patient with chronic liver disease will be discussed with the focus on characterisation and the international guidelines presenting diagnostic

and follow-up strategy. Not only HCC presents as a hypervascular nodule, but also FNH, FNH-like lesions, adenoma, capillary haemangioma and nodular regenerative hyperplasia.

A-084 14:05

A. Measuring fat and iron with MRI: how accurate?

M.M. França; *Porto/PT (mariamanuela.franca@gmail.com)*

Liver steatosis is the hallmark of non-alcoholic fatty liver disease (NAFLD) but is also commonly found in different diffuse liver diseases. Iron overload is found not only in genetic haemochromatosis, transfusional haemosiderosis and iron loading anaemias, but also in chronic liver diseases. Because liver biopsy has several limitations, magnetic resonance (MR) imaging biomarkers have been developed for fat and iron quantification. Liver fat quantification can be accurately performed by MR spectroscopy or using multi-echo chemical shift encoded (MECSE) MR sequences. For precise quantification of proton density fat fraction (PDFF), MECSE MR sequences must be corrected for T1 bias, T2* decay effect, noise and fat spectral complexity. Nowadays, PDFF is being considered as the best imaging biomarker of liver steatosis. Quantification of liver iron using MR imaging can be performed with signal intensity ratio (SIR) methods as well as R2 and R2* relaxometry techniques. As MR imaging does not depict iron itself, but the effect of iron in nearby protons, all these different MR methods require calibration against liver biopsies, to generate empirical calibration curves. Both R2 and R2* values are increasingly being used for quantification of liver iron concentration, either for diagnosis or treatment monitoring, but they must be performed with validated acquisition and analysis protocols. MECSE-MR sequences have the advantage of simultaneously quantifying steatosis and siderosis and are promising as fast non-invasive biomarkers of liver fat and iron, also providing spatial coverage of all liver parenchyma.

Learning Objectives:

1. To become familiar with the different acquisition techniques allowing measurement of fat and iron with MRI.
2. To understand the correspondence between MRI evaluation and histological scores.
3. To learn about the limitations of the method.

A-085 14:33

B. Can we reliably identify/quantify liver fibrosis and cirrhosis

V. Vilgrain; *Clichy/FR (valerie.vilgrain@aphp.fr)*

Diagnosis of cirrhosis on imaging is not difficult as there are striking features, the most common being surface nodularity and morphologic changes of the liver (atrophy of segment 4 and hypertrophy of the caudate lobe). Diagnosis and staging of fibrosis was done on pathologic examination of the liver for years but quantitative imaging has changed the paradigm. First, diffusion-weighted MR has enabled to assess liver fibrosis as the ADC decreases with increasing fibrosis stage. More recently, imaging-based elastography (using ultrasound or MR imaging) has shown high diagnostic performance to stage fibrosis. The principle of these two methods is to measure the speed of shear waves propagating in the organ. The shear-wave speed is related to tissue stiffness and, therefore, to the fibrosis. The first technique that has been extensively validated is the fibroscan (transient elastography). More recently ultrasound-based techniques such as ARFI and shear-wave elastography have shown comparable or even better performance over fibroscan. They are nowadays performed in clinical practice. Some limitations are patient overweight and increased intercostal thickness. There are confounding factors that should be known. MR-based elastography is a very accurate technique that has been recently validated in multicentric studies. Its advantages is the 3D assessment of the liver and the ability to go deeper in tissue characteristics (elasticity and viscosity). MR elastography is performed in many centres nowadays but still more in research than for daily use. Both approaches compare favourably with liver biopsy and are particularly helpful for monitoring patients.

Learning Objectives:

1. To understand the basic principles of fibrosis evaluation (US and MRI), how these methods could be implemented in daily practice, and how to make a radiological report.
2. To learn about the correlation between imaging tools and other methods and to understand the clinical strategy.
3. To become familiar with the necessity for non-invasive detection and follow-up of chronic liver disease.

A-086 15:01

C. The small liver nodule and chronic liver disease

G. Brancatelli; *Palermo/IT (gbranca@yahoo.com)*

The enrolment of patients with chronic liver disease into surveillance programs has determined a steady increase in the number of small hepatic masses being detected. In addition, technological advances have improved the spatial, contrast and temporal resolution of imaging modalities allowing for higher rates of detection. However, detection and characterization of a lesion in a cirrhotic liver is oftentimes a challenging task, due to the intrinsic features of a fibrotic/cirrhotic organ and to a different epidemiology in comparison to the noncirrhotic population. While most lesions in a cirrhotic liver are hepatocellular, a wide array of other observations can be encountered, such as haemangioma, nodule-like arterial phase hyperenhancement, focal fibrosis, cholangiocarcinoma and metastases. Moreover, small HCC frequently present with atypical findings, such as lack of enhancement, lack of washout or no capsule. Furthermore, HCC <1cm grows very slowly; therefore, stability (i.e. lack of growth) over a few months does not entirely rule out malignancy, and a negative biopsy is not helpful due to the high false-negative sampling rate. In these instances, two possible options are 1) further imaging with a different technique or 2) imaging follow-up.

Learning Objectives:

1. To become familiar with the problem of characterisation of liver nodule on cirrhosis/fibrosis.
2. To understand the imaging strategy.
3. To learn about the international guidelines presenting diagnostic and follow-up strategy.

Author Disclosure:

G. Brancatelli: Speaker; Bayer Healthcare. Other; Funding for travel to educational meetings, Bayer Healthcare and Bracco.

16:00 - 17:30 **Room B**

Abdominal Viscera

RC 401

The spleen: the forgotten organ

A-087 16:00

Chairman's introduction

L.H. Ros Mendoza; *Zaragoza/ES (lhrosmendoza@gmail.com)*

The spleen has been considered as the forgotten organ of the abdominal cavity; nevertheless, a wide range of diseases can affect the spleen. The finding of an incidental splenic mass is frequently encountered at imaging studies that are performed on patients for other reasons. Pathologic conditions of the spleen can be classified into the following categories: congenital: accessory spleen, polysplenia and asplenia, true cyst; inflammatory: pyogenic abscess, fungal abscess, hydatid cyst, sarcoidosis; vascular: infarction, peliosis: haematologic: sickle cell disease, extramedullary haematopoiesis; posttraumatic: haematoma, false cyst; neoplastic: benign tumours: haemangioma, hamartoma, lymphangioma; malignant tumours: lymphoma, metastases, angiosarcoma. Other disease processes affect the spleen diffusely: Gaucher disease, portal hypertension and sickle cell disease. The findings in the different imaging techniques (ultrasound, computed tomography and magnetic resonance imaging) of these splenic lesions are reviewed, considering three different scenarios: the incidental lesion, acute and chronic diseases, and malignant tumours, emphasizing the key differences that in many cases can help narrow the differential diagnosis. An imaging algorithm is proposed to ease the diagnostic workup in cases of incidental splenic lesions. In some cases, these radiologic findings could have substantial overlap, which precludes the rendering of a specific diagnosis on the basis of imaging findings alone; in these instances, correlation of radiologic features with clinical and histological findings is needed to confirm the diagnosis.

A-088 16:05

A. Acute and chronic splenic disease

G. Zamboni; *Verona/IT (gzamboni@hotmail.com)*

The spleen can harbour different types of acute and chronic non-malignant disease. The radiologist should be aware of these entities, to recognize them on imaging performed with the specific purpose of evaluating the spleen, or to characterize them when incidentally discovered. Congenital abnormalities range from very common entities, like accessory spleens, to rare conditions like polysplenia and asplenia syndromes. Focal non-malignant diseases include cystic lesions, the different types of haemangioma, sclerosing angiomatous nodular transformation (SANT), hamartoma and abscess, among others. Diffuse non-malignant diseases include granulomatous diseases, such as sarcoidosis, and parenchymal infiltrative diseases such as siderosis. In addition, the spleen can undergo vascular diseases, with resulting infarction, and rupture, both traumatic and spontaneous. Aim of this talk will be to describe the imaging features of the most common diseases, with emphasis on the imaging findings that, coupled with clinical information, can allow a diagnosis.

Learning Objectives:
1. To describe the most common causes of acute and chronic splenic disease, excluding malignant lesions.
2. To define imaging protocols, including functional and metabolic techniques, to apply for the detection and characterisation.

A-089 16:28

B. The incidental splenic lesion

M. Laniado; *Dresden/DE (michael.laniado@uniklinikum-dresden.de)*

Incidental findings are defined as lesions detected by CT, MRI, or another imaging modality performed for an unrelated reason. The overall reported incidence is around 30% for CT, and 25% if the initial diagnosis involved the genitourinary and gastrointestinal tract. About 20% of incidental findings are located in the abdomen. The frequency of either clinical follow-up or clinical confirmation accounts for approximately 65% and 45%, respectively. Compared to other abdominal viscera, incidental findings in the spleen have not been evaluated in great detail. Few available data in the literature report a low incidence of less than 2% for splenic granulomas, haemangiomas, cysts, abscesses, etc. Unfortunately, both incidentally detected and other splenic lesions often show overlapping imaging features. Therefore, differentiation of benign lesions from indeterminate or malignant lesion may be a challenge. On the other hand, most isolated splenic lesions are benign and without clinical relevance. To further characterise incidentalomas of the spleen, clinical correlation (e.g. pain, fever, immunocompromised state, neoplasm, trauma) and other imaging findings (e.g. liver lesions, lymphadenopathy) are often the key to diagnosis. It is essential for the radiologist to know how to deal with splenic incidentalomas, namely what should be written in the report and when additional studies have to be recommended. This issue will also be addressed in the presentation.

Learning Objectives:
1. To describe the most common causes of splenic incidentaloma and their imaging appearance.
2. To define imaging protocols, including functional and metabolic techniques, for the differential diagnosis.
3. To propose an algorithm for the management of incidental splenic lesions.

A-090 16:51

C. Malignant lesions

S. Gourtsoyianni; *London/UK (sgty76@gmail.com)*

Malignant splenic lesions are quite rare; however, incidentally picked up splenic lesions on cross-sectional imaging performed in patients with suspected or known malignancy certainly pose a diagnostic challenge. Most common malignant lesion of the spleen is lymphoma, primary or secondary. In Hodgkin disease, splenic involvement results in up-staging while in non-Hodgkin lymphoma if spleen is the predominant site of involvement therapeutic approach might change, thus degree of splenic involvement influences treatment and prognosis. Imaging appearances of malignant splenic lesions, including besides lymphoma, angiosarcoma, leiomyosarcoma and metastases can overlap and imaging alone is not adequate for accurate characterization in all cases. Percutaneous image-guided biopsy of the spleen using 18-gauge needles or smaller has reported a high diagnostic accuracy and a complication rate similar to that reported for liver and kidney rendering it a better alternative to splenectomy.

Learning Objectives:
1. To describe the clinical presentation and imaging findings for focal and diffuse neoplastic malignant lesions.
2. To discuss the indication of splenic lesion biopsy and its diagnostic contribution.

17:14

Panel discussion: How to manage incidental findings in clinical routine practice

16:00 - 17:30 **Room C**

Chest

RC 404

Pulmonary embolism: persistent controversies

A-091 16:00

Chairman's introduction

M. Rémy-Jardin; *Lille/FR (martine.remy@chru-lille.fr)*

The utility of CT angiography is not questioned as a first-line diagnostic test for pulmonary embolism. However, technological advances and incidental findings on chest CT examinations have raised practical questions regarding the most efficient use of CT in this clinical context. The purpose of this session is to cover some of these issues, emphasizing the diagnostic and prognostic role of CT.

Session Objectives:
1. To review the current controversies regarding PE diagnosis.
2. To appreciate the need for defining a standardised management.

Author Disclosure:
M. Rémy-Jardin: Research/Grant Support; Siemens Healthcare.

A-092 16:05

A. Subsegmental PE, incidental PE: diagnosis and management

C.M. Schaefer-Prokop; *Amersfoort/NL*

Attention to subsegmental PE (SSPE) has increased with the ability of CT pulmonary angiography (CTPA) to show such small emboli. The advent of multi-detector computed tomographic pulmonary angiography (CTPA) allows increased visualization of the peripheral pulmonary arteries. More cases of peripheral PEs, such as isolated subsegmental PE (SSPE) and incidental PE, have thereby been identified. The prevalence of SSPE in patients with suspected PE varies between 0.4% and 18% according to the literature. It is likely that this variability is caused by patient characteristics, reading methodology but last not least by scanner technology used. A systematic review mentions a prevalence of SSPE of 4.7% in a group examined with a single slice scanner, and of 9.4% in a patient group examined with a multi-slice CT scanner. In the PIOPED II trial the positive predictive value (PPV) of CTPA when compared to a composite reference was 98% for central but only 25% for SSPE pointing towards the lower diagnostic accuracy and reader confidence in diagnosing SSPE. Clinical relevance and management of patients with symptomatic SSPE is still controversial. A Cochrane meta-analyses of 2014 and 2015 summarized that there is no randomized controlled trial evidence for the effectiveness and safety of anticoagulation therapy versus no intervention in patients with isolated subsegmental pulmonary embolism (SSPE) or incidental SSPE. More and more publications occur describing outcome of untreated patients with SSPE that have no associated DVT. Recent recommendations from the European Society of Cardiology suggest an individualized approach for the management of patients with newly diagnosed SSPE based on the risk/benefit ratio of anticoagulation and the presence of lower limb DVT. Results of a still ongoing prospective trial (NCT 01455818) are expected to provide more evidence in that respect.

Learning Objectives:
1. To learn about the characteristics of subsegmental and incidental PE.
2. To appreciate an appropriate management in both situations.

A-093 16:28

B. CT not available, contraindicated or inconclusive: what to do?

E.J.R. van Beek; *Edinburgh/UK (edwin-vanbeek@ed.ac.uk)*

The utility of CT pulmonary angiography (CTPA) as a first-line diagnostic test for imaging of pulmonary embolism (PE) is one of the great developments for this commonly encountered disease. It has enabled a fast triage service, allowing safe exclusion and early discharge for patients with symptoms, thus avoiding unnecessary treatment and complications. In approximately 5% of cases, CTPA is inconclusive. In most of these patients, repeat CTPA is an accepted method to detect or rule out PE. In some hospitals, CTPA may not be available around the clock, and in these situations the aim would be to positively diagnose the presence of venous thromboembolic disease using ultrasound or rule out the disease using perfusion scintigraphy. Finally, there are situations where radiation dose is of concern, e.g. in young female patients or during pregnancy. Although the risk-benefit for diagnosis of PE is beyond doubt, alternative approaches such as ultrasound for the detection of DVT or MR angiography for detection or exclusion of PE may be considered. This lecture will describe some potential approaches using a combination of

ultrasonography, perfusion scintigraphy and MR angiography as an alternative to CTPA.

Learning Objectives:

1. To review the role of US and V/Q scan.
2. To learn about the current performance of MR.

Author Disclosure:

E.J.R. van Beek: CEO; QCTIS Ltd. Founder; QCTIS Ltd. Research/Grant Support; Siemens Healthineers.

A-094 16:51

C. Can we predict outcome from imaging?

B. Ghaye; *Brussels/BE (benoit.ghaye@uclouvain.be)*

The mortality risk of unselected patients with proven pulmonary embolism (PE) is around 10%, although it may be superior to 50% in some selected patient categories. Recent international guidelines have refined the stratification of early mortality risk in patient with PE as this may influence the therapeutic strategies and the duration of hospitalization. Clinical findings as cardiogenic shock or persistent arterial hypotension remain the most powerful predictors and identify patients at high risk of mortality. Absence of such findings requires further risk stratification. Clinical prognostic scores, such as the PESI, cardiac biomarkers dosage and signs of right ventricle (RV) dysfunction on an imaging test (echocardiography or CT pulmonary angiography) are used to discriminate patients with intermediate or low risk. Therefore, it is recommended to indicate the ratio between the diameters of RV and left ventricle (RV/LV) on each report of CT pulmonary angiography. Meta-analyses have confirmed RV/LV diameter ratio as measured on CT to be significantly associated with increased risk of mortality. However, taken individually, RV/LV diameter ratio is limited by a 95% NPV and a 5-30% PPV for predicting mortality. RV/LV diameter ratio should be, therefore, combined with other factors, including biomarkers and clinical findings to increase the prognostic value. This lecture will also discuss more recent and potentially more powerful predictor CT findings, including among others RV/LV surface and volume ratios, atrial measurements, severity of "perfusion" defect and cardiac function parameters as calculated from ECG-gated acquisition.

Learning Objectives:

1. To learn how clinical findings influence the selection of the imaging strategy.
2. To learn how imaging may predict the outcome of the patient.
3. To learn about the follow-up.

17:14

Panel discussion: How to optimise patient management?

16:00 - 17:30 **Room Z**

ESR Working Group on Ultrasound

WG 2
Image fusion

A-095 16:00

Chairmen's introduction: Basic principles of image fusion (part 1)

M. Bachmann Nielsen; *Copenhagen/DK (mbn@dadlnet.dk)*

This technique is optional and only available in high-end US machines. It requires a positioning device connected to the US apparatus and corresponding images in DICOM format (CT, MRI, PET/CT). Theoretically also US-US fusion can be performed. Several techniques can be used to align the image data, and not all will be available from all manufacturers. There is probably no distinct advantage of any of these except time consumption. Co-registration should be repeated when scanning at a distance from the primary co-registration area. Using the technique requires good patient cooperation. Training of the doctor is also required to become familiar with the technique and pitfalls. Image fusion will extend the examination time 10-15 minutes and, therefore, used in selected patient cases. When US is used as the modality for patient follow-up the fusion will facilitate comparison with the measurements on the primary imaging modality. Image fusion may also be of help in patients with poor image quality on US, e.g. obese patients and where the target area is partially covered of air in bowels or abscesses. It is also used as assistance for US-guided biopsy of lesions seen by CT, MRI or PET/CT, and to identify lesions which stand out in PET-imaging. However, since the US examination is the only live procedure, care must be taken not to rely fully on the projected needle path on previous recorded datasets. The session will give examples on how the image fusion can be used in the kidney, liver and prostate.

Session Objectives:

1. To become familiar with the technical requirements for performing image fusion.
2. To learn about the technologies used to fuse CT-US, MR-US and PET-MR/CT -US-images.
3. To understand the different option of image registration (point to point, plane, auto registration).
4. To understand how to use them in clinical practice and difficult cases.

A-096 16:07

Chairmen's introduction: Basic principles of image fusion (part 2)

L.E. Derchi; *Genoa/IT (derchi@unige.it)*

Image fusion techniques have gained an important role in clinical practice. Their value is mainly during interventional procedures, to guide more accurately therapeutic manoeuvres; there are, however, also diagnostic situations in which added value is provided by simultaneous co-registered display of US images with those from other techniques. Different technologies can be used to fuse CT-US, MR-US and PET-MR/CT-US images and it is important to understand the main advantages of each of them, the problems that may be encountered and the need for a learning curve to provide good results. This session will demonstrate situations in which image fusion can provide clinical advantage in the use of US in renal, hepatic and prostatic applications.

Session Objectives:

1. To become familiar with the technical requirements for performing image fusion.
2. To learn about the technologies used to fuse CT-US, MR-US and PET-MR/CT -US-images.
3. To understand the different option of image registration (point to point, plane, auto registration).
4. To understand how to use them in clinical practice and difficult cases.

A-097 16:15

Image fusion of the kidney (part 1)

M. Claudon; *Vandoeuvre-les-Nancy/FR (m.claudon@chu-nancy.fr)*

Image fusion of kidney is now more currently used to facilitate the realization of second-row ultrasound (US) examination in complex cases, when contrast-enhanced ultrasound (CEUS), guided biopsy or interventional procedure is required. Fusion is usually obtained using CT series of images, generally after contrast injection, but T2-weighted sequences or post-Gd T1-weighted series are more commonly considered. Fusion can be made using various fusion protocols, which require some training phase. Examples of various pathological cases of complex cystic lesions, tumours, vascular pathologies will be presented to illustrate the interest of the technique.

Learning Objectives:

1. To understand the imaging features of kidney lesions.
2. To become familiar with unclear cystic lesions by using the Bosniak classification.
3. To learn about the differential diagnoses of complex cystic renal masses and compare the modalities by using the image fusion tool.
4. To understand the potential pitfalls in image fusion.

Author Disclosure:

M. Claudon: Speaker; Philips Ultrasound.

A-098 16:25

Image fusion of the kidney (part 2)

D.A. Clevert; *Munich/DE (Dirk.Clevert@med.uni-muenchen.de)*

Ultrasound is a widely accepted imaging technique for the diagnosis and monitoring of cystic renal lesions. The widely used Bosniak classification (I-IV) categorises renal cystic lesions in five distinctive groups by the help of ultrasound and CT image criteria. In unclear cases, contrast-enhanced ultrasound (CEUS) and MRI/CT ultrasound image fusion are able to detect and characterise difficult pathologies. In contrast to multi-slice CT (MS-CT), ultrasound image fusion is a real-time imaging technique that can be used in combination with other cross-sectional imaging techniques. This talk explains the latest possibilities of image fusion with CEUS and MS-CT to detect and characterise unclear renal pathologies.

Learning Objectives:

1. To understand the imaging features of kidney lesions.
2. To become familiar with unclear cystic lesions by using the Bosniak classification.
3. To learn about the differential diagnoses of complex cystic renal masses and compare the modalities by using the image fusion tool.
4. To understand the potential pitfalls in image fusion.

Author Disclosure:

D.A. Clevert: Advisory Board; Samsung, Siemens, Philips, Bracco. Speaker; Samsung, Siemens, Philips, Bracco.

A-099 16:35

Image fusion of the liver

G.H. Mostbeck; *Vienna/AT (gerhard.mostbeck@wienkav.at)*

US image fusion may be defined as overlaying US (real-time US, colour Doppler and CEUS) images with CT, MRT or PET-CT data. Spatial co-registration is needed to make sure that US volume data and CT/MRT/PET-CT data represent the same volume, which is of major importance in the liver. This is obtained by defining standard registration points, either by external fiducials or by defining specific anatomic structures in the specific patient. All US image fusion systems available work based on an electromagnetic tracking system, where sensors and transmitters on the US scan head inform the system about the orientation and position of the current imaging plane. In liver imaging, fusion might be useful in various clinical situations. First, in diagnostic imaging, overlying US with CT/MRT/PET data may be useful to get information on focal lesions not seen by real-time US and/or CEUS. Specifically, small or superficial or lesions deep in the liver might be able to be detected and classified regarding their aetiologies. Second, in patients with contraindications to CT or MR contrast media (especially in renal insufficiency) fusion between CEUS and CT/MRT might gain vascular information and allow lesions classification. Third, in US-guided diagnostic and therapeutic interventions (biopsy and ablation) various studies have demonstrated advantages for fusion-guided procedures regarding lesion conspicuity, needle path safety and ablation evaluation with US and CT/MRT/PET and US/US (pre- and post-intervention) fusion. Needle tracking is another option to improve outcome in diagnostic and therapeutic procedures.

Learning Objectives:

1. To learn about the advanced liver imaging fusion technique.
2. To learn how to optimise scanning protocols by using the image fusion tool.
3. To learn about common benign and malignant lesions and differential diagnosis by using image fusion.
4. To understand how to use fusion imaging of US, CT and MRI for treatment of liver tumour.

A-100 16:55

Image fusion of the prostate

D.A. Clevert; *Munich/DE (Dirk.Clevert@med.uni-muenchen.de)*

Transrectal prostate biopsy is currently performed one million times annually in the USA to diagnose or exclude prostate cancer under ultrasound-guided technique. However, many of the currently performed prostate biopsies yield misleading information. Multiparametric MRI of the prostate is capable of detecting clinically relevant prostate cancer. Image fusion is the process of combining relevant information from MRI and real-time ultrasound into a single image, which provides more information than the separate image. Targeted biopsy through MRI-ultrasound fusion offers a way to localise and sample suspected cancers with precision.

Learning Objectives:

1. To explain the PIRADS system in prostate imaging.
2. To become familiar with the technical requirements for performing image fusion of the prostate.
3. To understand how to detect and biopsy guided suspicious MR-lesions using the ultrasound image fusion technique.
4. To understand the potential pitfalls and discuss the evidence for the use of these technologies in routine clinical practice.

Author Disclosure:

D.A. Clevert: Advisory Board; Siemens, Philips, Samsung. Speaker; Siemens, Philips, Samsung.

17:15

Panel discussion

16:00 - 17:30 **Room O**

Paediatric

RC 412

Chest imaging in paediatrics

Moderator:
B. Ahuja; Agra/IN

A-101 16:00

A. Congenital anomalies of the chest

M. Haliloglu; *Ankara/TR (mithath@hacettepe.edu.tr)*

Advances in both foetal ultrasonography (US) and magnetic resonance (MR) imaging resulted in increased recognition of congenital anomalies of the chest prenatally. Despite the role of US and/or MR imaging in the prenatal diagnosis of congenital lung malformations, chest radiography and computed tomography still have an important role for postnatal diagnosis. Congenital lung anomalies have a broad spectrum ranging from small and asymptomatic to large and symptomatic lesions. They may involve lung parenchyma, bronchi, arterial supply and venous drainage. Currently there is no organizational structure or system of nomenclature to define all lung abnormalities. Congenital lung anomalies can be divided into three categories including isolated bronchopulmonary anomalies, combined lung and vascular abnormalities and vascular anomalies. Congenital thoracic wall anomalies involve sternum, clavicle, rib and scapula anomalies. Malformations of the chest wall can be a manifestation of a syndrome or skeletal dysplasia. The management of congenital lung and thoracic wall anomalies depends on the type of malformation and symptoms. Radiologists should perform individualized proper imaging techniques and should be familiar with characteristic imaging findings in paediatric patients for appropriate patient management.

Learning Objectives:

1. To discuss best imaging techniques when evaluating congenital chest anomalies.
2. To have an overview of antenatal and postnatal appearances of common congenital chest anomalies.
3. To understand the clinical significance and management of congenital lung and thoracic wall anomalies.

A-102 16:30

B. Lung infection and its complications

M.L. Lobo; *Lisbon/PT (mluisalobo@gmail.com)*

Lung infection is one of the most common causes of illness in children, and a leading cause of mortality in developing as well as in developed countries. Chest radiography is the imaging cornerstone in the diagnosis of pneumonia. While most previously healthy children with community acquired pneumonia treated as an outpatient will not clearly benefit from chest radiography, imaging plays an important role in the approach of paediatric patients with more severe lung infection, atypical presentation, complicated clinical course as well as in those with recurrent infections or infection in the immunocompromised children. Radiological findings are usually nonspecific, but in the appropriate clinical setting (including patient's age, immune status, seasonal epidemiology and clinical presentation) some radiological patterns may allow to narrow the differential diagnosis, thus helping to guide treatment. Furthermore, imaging is crucial in the assessment of complicated pneumonia and development of potential late complications. Ultrasound is an invaluable imaging modality in the evaluation of pleural effusion/empyema and peripheral lung consolidations, with chest computed tomography reserved for centrally located complicated pneumonia, bronchopleural fistula and bronchiectasis, as well as unusual infections, infection in the immunocompromised children and suspicion of underlying pulmonary or systemic conditions (e.g. foreign body, congenital malformation, immunodeficiency). Although not routinely used in many places, lung MRI should be considered as a potential alternative to CT for diagnosing at least some complications of infection, particularly in patients with chronic lung diseases (e.g. cystic fibrosis), thus contributing for reduction of radiation exposure from CT.

Learning Objectives:

1. To understand the justification for imaging children with lower respiratory tract infection.
2. To provide tips for accurate diagnosis and to understand differential diagnosis.
3. To become familiar with complications and potential underlying conditions.

A-103 17:00

C. Imaging interstitial lung disease in children: update 2017

E. Alexopoulou[1], A. Pastroma[1], G. Papaioannou[1], M. Raissaki[2]; *[1]Athens/GR, [2]Iraklion/GR (ealex64@hotmail.com)*

Paediatric interstitial lung diseases (ILDs) include a range of diseases, which involve the pulmonary interstitium, causing defective gas exchange. The current classification of paediatric ILDs is based on aetiology, clinical characteristics, genetics, child's lung growth and histology. Some of the diseases are common, or even unique in infants or younger children. The clinical presentation varies from mild, subclinical respiratory symptoms, which may disorientate the initial diagnosis, to severe respiratory failure. Correct diagnosis of ILDs is crucial for early treatment and better prognosis, when possible. Imaging and especially CT scan plays a significant role in this, as for some types of ILDs CT findings are quite specific, while in others laboratory tests or lung biopsy may be needed for definitive diagnosis. CT scan can also suggest a short list of the most likely diagnosis, and guide further investigation including lung biopsy. Child's age is an essential tool to approach the diagnosis as some ILDs have a predisposition in infancy-early childhood (developmental, growth, or genetic disorders). Disorders related to systemic diseases, infections, or environmental exposures are commoner in older children. Additionally, CT scan is helpful for monitoring disease activity and assessing response to therapy. The use of low-dose techniques is mandatory in paediatric population, to minimize patient's radiation exposure. High-resolution computed tomography (HRCT) is a valuable technique to gain information on the pattern and anatomical distribution of lung diseases.

Learning Objectives:

1. To understand optimised protocols.
2. To learn about updated nomenclature of interstitial lung diseases in children.
3. To discuss a systematic approach for the diagnosis of common entities diffusely affecting the paediatric lung.

16:00 - 17:30 **Room N**

Head and Neck

RC 408

Pathways for tumour spread

Moderator:
J. Huyskens; Antwerp/BE

A-104 16:00

A. Pathways for oral cavity and oropharynx tumour spread

A. Borges; *Lisbon/PT*

90% of oral cavity and oropharyngeal malignancies originate from the epithelial lining and spread superficially along the mucosa, deeply into the submucosa, adjacent muscles and bone and along neighbouring cranial nerves used as elevator shafts for tumour spread. There are 8 tumour subsites in the oral cavity each with different patterns of spread and implications on patient's management. Those with direct impact on tumour staging or surgical management are the midline raphe, extrinsic tongue muscles, bone and oropharyngeal spread. Tumours of the retromolar trigone have a complex pattern of spread as they sit on the crossroad between the oral cavity, masticator space and oropharynx. Whereas gingival tumours of the superior alveolar ridge can invade the maxilla and spread along the superior alveolar nerves and V2, tumours of the inferior alveolar ridge can invade the mandible, the inferior alveolar nerve and spread along V3. Invasion of the neurovascular tongue bundle prone tumours to spread along the lingual or hypoglossal nerves. There are 4 different oropharyngeal subsites. The palatine tonsil has the highest association with lymph node metastases. Local spread is through the palatoglossus muscle and transgression of the constrictor muscles and pterygomandibular raphe leads to tumour extent into the retromolar trigone and pterygoid plates. Tongue base tumours can spread anteriorly to the tongue root and floor of the mouth and posteriorly into the supraglottic larynx. Palatal tumours spread inferiorly into the palatine fossa, laterally into the parapharyngeal space and are prone to perineural spread along the greater and lesser palatine nerves.

Learning Objectives:

1. To become familiar with the anatomy of the oral cavity and oropharynx.
2. To learn which imaging technique to use.
3. To understand the typical local and remote spread of oral cavity and oropharynx tumours.

A-105 16:30

B. Pathways for nasopharyngeal tumour spread including perineural spread

V. Chong; *Singapore/SG (vincent_chong@nuhs.edu.sg)*

Most nasopharyngeal carcinomas (NPC) originate in the fossa of Rosenmuller and spread along well-defined routes. Tumours often spread into the nasal and pterygopalatine fossa. From the nasal cavity tumours can infiltrate the pterygopalatine fossa which may lead to perineural infiltration of the maxillary nerve and further extend into the intracranial cavity. Tumours may infiltrate further into the orbital apex and enter the intracranial cavity through the superior orbital fissure. Lateral spread involves the parapharyngeal and masticator spaces. When tumour enters these spaces, there is a risk of perineural infiltration along the mandibular nerve. Perineural spread along the mandibular nerve is a frequent route of intracranial extension. When NPC spreads superiorly, it erodes the skull base with subsequent direct extension into the intracranial cavity. Lesions may also be seen to spread through the foramen lacerum. Cervical nodal metastasis is very common and up to 80% of patients have enlarged nodes at presentation. Nodal metastasis show an orderly inferior spread and the affected nodes are larger in the upper neck. Spread to the supraclavicular nodes has grave prognostic significance. Up to 50% of patients with supraclavicular lymphadenopathy will eventually have distant metastases. NPC shows a high frequency of distant metastasis compared with other tumours of the head and neck. The frequency of distant spread varies between 5% and 41%. Common sites of distant metastases include bone (20%), lung (13%) and liver (9%).

Learning Objectives:

1. To become familiar with the anatomy of the nasopharynx.
2. To learn which imaging technique to use.
3. To understand the typical local and remote spread of nasopharyngeal tumours, including perineural spread.

A-106 17:00

C. Pathway for laryngeal and hypopharyngeal tumour spread

N. Chidambaranathan; *Chennai/IN (drchidam55@gmail.com)*

Supraglottic tumours constitute 30% of laryngeal tumours. Epiglottic tumours primarily invade the pre-epiglottic space (PES), base of tongue and the paraglottic space (PGS) laterally. Tumours from petiole of epiglottis invade the low PES and extend to the glottis/subglottis through the anterior commissure. Tumours originating from the false vocal cord, laryngeal ventricle or aryepiglottic fold primarily infiltrate the PGS. Tumours arising from arytenoids and inter-arytenoid regions tend to infiltrate post-cricoid region of hypopharynx. Lymphatic spread (levels II,III&IV nodes) is common. Glottic tumours (~65%) arise from the anterior half of the true vocal cords and spread anteriorly to the anterior commissure, contralateral cord and thyroid cartilage via Broyle's ligament, or posteriorly into the posterior commissure, arytenoids, cricoarytenoid joint and cricoid cartilage. The tumour can extend superiorly to the PES and PGS or inferiorly to the subglottis. Lymphatic spread is uncommon. Subglottic tumours (~5%) are usually inferior extensions of glottic or supraglottic tumours. Primary subglottic tumours spread to the trachea, thyroid gland and cervical oesophagus. Lymphnode metastases involve pre/para-tracheal nodes. Hypopharynx consists of pyriform sinus, posterior hypopharyngeal wall and post-cricoid region. Pyriform sinus tumours spread to thyroid cartilage laterally, endolarynx medially, post-cricoid region infero-medially, posterior pharyngeal wall posteriorly and base of tongue superiorly. Growths in the posterior pharyngeal wall invade the pre-vertebral fascia, whereas post-cricoid growths spread inferiorly to the cervical oesophagus and antero-laterally to thyroid. CT is the preferred imaging modality for evaluating laryngeal carcinoma, while MRI is useful as a problem-solving adjunct, especially early cartilage involvement.

Learning Objectives:

1. To become familiar with the anatomy of the larynx and hypopharynx.
2. To learn which imaging technique to use.
3. To understand the typical local and remote spread of laryngeal and hypopharyngeal tumours.

16:00 - 17:30 **Room L 8**

Joint Session of the ESR and UEMS

ESR and UEMS: a strong professional partnership

A-107/A-108 16:00

Chairmen's introduction

L. Bonomo; *Rome/IT (lorenzo.bonomo@unicatt.it)*
P. Ricci; *Rome/IT (paolo.ricci@uniroma1.it)*

The UEMS - European Union of Medical Specialists is the oldest European medical organisation representing the interests of more than 50 different medical specialities and involving more than 1.6 million of healthcare professionals. The ESR - European Society of Radiology is the world's biggest radiological society, encompassing 67.500 members from 155 different countries. It was founded in 2005 by merging the European Congress of Radiology and the European Association of Radiology, aiming at establishing a single, powerful and unified voice for European radiologists. Through the section of radiology, UEMS and ESR share the same ambitious objective of promoting the highest quality of care and medical practice in radiology, by serving the needs of patients and general public, harmonizing radiological training and defending free movement and professional interests of European radiologists. This Joint Session will focus in particular on the function of the UEMS section of radiology within EU institutions and legislation, with specific regard to the harmonisation of radiological training, to the definition of clear boundaries towards other specialities and to the competence-based format of European Training Curricula. It will further investigate the value of European Diploma in Radiology, the impact of professional qualifications directive on radiologists and the importance of joint effort for EU lobbying and interest representation. Finally, particular attention will be dedicated to the working methodologies of EACCME (European Accreditation Council for Continuing Medical Education) and ACI (Accreditation Council in Imaging) in the framework of CME - Continuing Medical Education and CPD - Continuing Professional Development programmes.

Session Objectives:

1. To describe the role of the UEMS within the EU.
2. To understand the difference between ESR and UEMS.
3. To understand the importance of cooperation between ESR and UEMS.

Author Disclosure:

P. Ricci: Board Member; UEMS SECTION of RADIOLOGY - PRESIDENT.

A-109 16:05

Structure of the UEMS and position of the UEMS within the EU

B. Maillet; *Brussels/BE (bernie.mail@skynet.be)*

The harmonisation of post graduate training in Europe: a challenge for the medical profession. The diploma in medicine is automatically recognised in the European Union but for the specialities things are different, the European directive on recognition of Professional qualification has an Annex V where the specialities are listed that can be enjoying automatic recognition if the speciality is mentioned as recognised in the home as well as the host country. This is only the case for 19 specialities that are recognised in all the EU Member States while for other specialities it varies from country to country. Until now, the only criterion that is taken into account is the length of training while it would be also good to include competences, and that is the reason why the UEMS is working on the European Training Requirements (ETR) for all the specialities that are mentioned in Annex V. The UEMS is also working for more than ten years now to increase the harmonisation of training by developing European exams in those specialities and this through the Council for European Specialist Medical Assessment (CESMA). Of course being licensed to practice is not the endpoint of the learning process and afterwards, the physician should demonstrate that he or she is working on keeping up to date his or her knowledge, skills and attitudes and here the UEMS has created the European Accreditation Council for Continuous Medical Education (EACCME) to harmonise the process of CME-CPD accreditation also at European level.

Learning Objectives:

1. To understand the structure of the UEMS and the position of the UEMS radiology section within the UEMS.
2. To understand the UEMS political involvement in EU affairs.
3. To understand the influence of EU directives on national legislation and daily practice.

A-110 16:25

Harmonising radiology training in Europe (part I)

P. Ricci; *Rome/IT (paolo.ricci@uniroma1.it)*

Free exchange of persons and services within the European medical sector has been achieved by mutual recognition of basic and specialist medical qualifications brought into effect by the Commission of the European Communities in 1975. The directives have been consolidated in the Directive 93/16/EEC of 5 April 1993, establishing a European training charter for medical specialists. The charter describes the requirements for adequate training, which prepares specialists for practice of their speciality at an appropriate level in any EU member state. The same charter divides the requirements regarding content of training into a general part, defined by the European Union of Medical Specialists (UEMS), and a specific part for each recognized speciality, defined by the UEMS Specialized Sections (Chapter 6). For the speciality of radiology, the charter states radiology involves all aspects of medical imaging which provide information about the anatomy, pathology and function of normal and disease states and interventional techniques for diagnosis and minimally invasive therapy involving image-guided systems. The Council for European Specialist Medical Assessment (CESMA) is an advisory body of the UEMS created in 2007 with an aim to provide recommendation and advice on the organisation of European examinations and improve the quality of European postgraduate training examinations. Its main tasks include: to promote harmonisation of European board assessments, to provide guidelines to the boards on the conduct of assessments, to encourage take up of board assessments as a quality mark, and to offer an alternative to national assessments, where appropriate.

Learning Objectives:

1. To become familiar with Chapter 6 and the current competence-based European Training Curricula.
2. To learn about the Council for European Specialist Medical Assessment (CESMA).

Author Disclosure:

P. Ricci: Board Member; UEMS SECTION of RADIOLOGY - PRESIDENT.

A-111 16:35

Harmonising radiology training in Europe (part II)

L. Oleaga Zufiría; *Barcelona/ES (lauraoleaga@gmail.com)*

The European Training Curriculum (ETC) represents a guide to standardize education and harmonize skills and competencies among radiologists in Europe. The ETC outlines a five-year training period to acquire the knowledge to practice radiology, consisting of Level I training over the first three years, followed by Level II training, with potential special interest rotations during the last two years. Level III corresponds to full subspeciality training with consecutive subspecialization after this five-year training period. It is important to satisfy the needs and integrity of the radiology profession, to avoid fragmentation and take over by other specialities. Endorsement of the curriculum by the UEMS Council is critical to provide support to the defense of the profession and as a guaranty of training, to assure quality and safety in radiology practice. The European Diploma in Radiology (EDIR) is available to radiologists and radiology residents in their fifth year of training. To certify knowledge and competency in line with the ESR ETC for radiology, it represents a valuable additional qualification and a recognised certificate to standardize and facilitate the accreditation of radiologists across the EU borders.

Learning Objectives:

1. To learn about the different levels of curricula within radiology on a European level.
2. To understand the importance of endorsement of the curriculum by the UEMS Council (i.e. the importance to secure and defend the practice of radiology against hostile take-over by other specialties).
3. To know about the value of the European Diploma in Radiology (EDiR).

A-112 16:45

Recognition of qualifications (part I)

Z. Fras; *Ljubljana/SI*

"No abstract submitted."

Learning Objective:

1. To know about the EU Directive on Professional Qualifications Recognition.

A-113 16:55

Recognition of qualifications (part II)

E.J. Adam; *London/UK (drjaneadam@gmail.com)*

The ESR is actively engaged in EU affairs related to radiology, with an office in Brussels. Only by direct engagement can the profession's voice be heard. The EU Directive on Professional Qualifications aims to facilitate the free movement of some professionals, including doctors within the EU. The ESR has been active in consultations on this subject and, alongside the UEMS, broadly supports the aims of the directive. However, it has emphasised that quality should not be compromised, and that language issues and differences in radiological training across the EU should be acknowledged. Fortunately the European training curriculum developed by the ESR is a potential means of addressing the latter together with the EDiR examination. Both are supported by the UEMS, as tools to promote uniform standards. Collaboration between the ESR and UEMS has been very successful in the past, and this is another area where a unified approach and shared goals may prove fruitful.

Learning Objectives:

1. To know how ESR is involved in the political lobby at the EU using the EU Directive on Professional Qualifications Recognition as an example.
2. To understand the importance of cooperation between ESR and UEMS using the EU Directive on Electromagnetic fields as an example.

A-114 17:05

Continuing professional development (CPD) (part I)

M. Adriaensen; *Heerlen/NL (miraude@gmail.com)*

Continuing Professional Development (CPD) has been defined as the educative means of updating, developing and enhancing how doctors apply the knowledge, skills and attitudes required in their daily practice. In January 2000, the European Accreditation Council for Continuing Medical Education (EACCME®) was established by the European Union of Medical Specialists (UEMS) with the aim of encouraging high standards in the development, delivery and harmonisation of Continuing Medical Education (CME) by the establishment of an independent, dual, peer-reviewed system for the accreditation of international CME events and international recognition of CME credit points, i.e. European CME credits (ECMEC®s). The EACCME® also provides for accreditation of e-learning materials. The EACCME® is solely financed by the application fees paid by CPD-providers. Independent accreditation, based on cooperation of all medical specialities, is important to foster professional autonomy and self-regulation, and deliver high-quality CME with the ultimate goal to assure high-quality patient care.

Learning Objectives:

1. To learn about the European Accreditation Council for Continuing Medical Education (EACCME®).
2. To understand why an international independent, dual reviewing process is important.
3. To know about the existence of European CME Credit (ECMEC®).

A-115 17:15

Continuing professional development (CPD) (part II)

D. Negru; *Iasi/RO (draneg@gmail.com)*

In January 2016, the ACI was officially launched. It was established under the umbrella of the European Board of Radiology (EBR) to cooperate and collaborate with the accreditation council of the UEMS, the European Accreditation Council for Continuing Medical Education (EACCME). The structure of the ACI, whose committees are composed of active experts in radiology, members of the EBR and the UEMS Radiology Section, allows to maximise the synergies between both organisations. Continuing Professional Development (CPD) is considered a cornerstone of quality assurance in medical care and recognition by the EACCME® is a contributing factor as well as a necessary step towards European harmonisation of educational standards in radiology.

Learning Objectives:

1. To learn about the set-up and structure of the Accreditation Council in Imaging (ACI).
2. To understand the importance of cooperation with and recognition by the EACCME®.

17:25
Questions

16:00 - 17:30 **Room E1**

Breast

RC 402
Screening for breast cancer

A-116 16:00

Chairman's introduction

E.A. Morris; *New York, NY/US*

Breast cancer screening as currently practised is not a perfect test, nor is it ever likely to be. Improvements on current digital techniques are available; however, the question whether these techniques move the needle far enough in the direction of detection of biologically relevant invasive cancers with the minimization of call backs and biopsies. Furthermore, there is the question of size of cancer at detection - the average size of cancer detected is still over 1 cm which has not dramatically improved over decades. If we are to make a difference in breast cancer mortality we need a technique that can detect breast cancer when it is very small - likely well under a cm - before it has a chance to become heterogeneous and undergo clonal expansion. Resistance to treatment and development of subclones which may be different from the original tumour contribute to the mortality. There is a need to be able to differentiate those cancers requiring aggressive detection and treatment from those that do not.

Author Disclosure:

E.A. Morris: Advisory Board; Delphinus, Devicor. Board Member; Avon. Consultant; Grail. Research/Grant Support; Hologic.

A-117 16:05

A. Screening with mammography only

R.M. Pijnappel; *Utrecht/NL (r.m.pijnappel@umcutrecht.nl)*

Screening with mammography has proven to save lives. The reduction in mortality is substantial. In the Netherlands, woman who attend all biannual offered screening rounds from 50-75 years reduce their chance of dying from breast cancer before the age of 80 to 50%. The basis for this positive effect from screening with mammography is only training and auditing. The shift from analogue form to digital between 2005 and 2010 has improved these results and showed that more high-risk tumours were detected by mammography. The cost-effectiveness of screening with mammography only is acceptable. The drawbacks of screening with mammography, false positive and overdiagnosis will be discussed. So far no other modality has proven to save lives and no information is available regarding the aggressiveness of other modalities that detected breast cancers. The positive predictive value of ultrasound is substantially lower and quality control (operator dependent) is difficult. For these reasons, screening with mammography only still is the gold standard for population-based screening with an average risk.

Learning Objectives:

1. To learn about benefits and limitations of mammography screening.
2. To become familiar with common findings, recall rates and assessment outcomes.
3. To appreciate errors.

A-118 16:30

B. Screening with mammography and ultrasound

T.H. Helbich; *Vienna/AT (Thomas.Helbich@meduniwien.ac.at)*

The sensitivity and specificity of mammography are limited in highly fibroglandular breasts. Digital mammography provides increased sensitivity in young women and those with moderately dense breasts, and digital three-dimensional mammography (tomosynthesis) promises further improvement. For women with the densest breasts, however, radiography is unlikely to be the optimum solution. MRI, although not affected by breast density, is expensive and access is often limited. Ultrasonography is attractive for breast cancer screening because, likewise, it is not impaired by breast density, and it avoids the use of ionising radiation and the need for breast compression. Nevertheless, enthusiasm for the use of ultrasonography has been limited because its specificity has been much lower than that of mammography, but technical developments have given rise to sharper, more informative images. These improvements foster the use of ultrasound particular in those women with higher breast density. Different trials have been preformed and promising results have been reported. This talk will focus on benefits, harms, and cost-effectiveness of supplemental ultrasonography screening for women with dense breasts.

Learning Objectives:
1. To learn about the added value of US in screening and its indication.
2. To become familiar with the common level of evidence.
3. To appreciate its role in clinical practice.
Author Disclosure:
T.H. Helbich: Grant Recipient; EU Horizon 2020. Research/Grant Support; Siemens, Guerbet, Angiomed, Medicor.

A-119 16:55

C. Screening with tomosynthesis
U. Bick; *Berlin/DE (Ulrich.Bick@charite.de)*

By eliminating ambiguity from superposition of normal breast parenchymal structures, digital breast tomosynthesis (DBT) holds the potential to improve cancer detection rates while at the same time reducing call-backs related to false-positive findings. The magnitude of these two effects will depend on the clinical setting. In European population-based screening programs, where recall rates are kept low, DBT will primarily increase detection rates. On the other hand, in screening practices with high recall rates such as in North America, the main effect of DBT will be to lower recall rates by improving specificity. In screening, the advantages of DBT must be weighed against the potential disadvantages of DBT such as higher costs (higher equipment and image storage costs, longer reading times) and possible increases in radiation exposure, especially if DBT is used as an adjunct to 2D mammography. Synthetic 2D views reconstructed from the DBT dataset can be used to replace 2D mammography in screening; however, the impact of this especially on the detection of microcalcifications is still unclear. Despite the very promising data from the available first DBT screening trials, which all showed a significant increase in detection rates with DBT; further studies are needed before DBT can replace 2D mammography in population-based screening programs. The key question still unanswered up to now is whether the additional cancers found by DBT are in the majority clinically relevant and contribute to a reduction in advanced-stage interval cancers.
Learning Objectives:
1. To learn about the role of tomosynthesis in the screening setting.
2. To become familiar with the different protocols.
3. To appreciate potential advantages of tomosynthesis in screening.
Author Disclosure:
U. Bick: Patent Holder; Patent Royalties, Hologic, Inc. Research/Grant Support; Institutional Research Collaboration until August 2014, Siemens AG, Institutional research collaboration, GE Healthcare.

17:20
Panel discussion: What is the best modality approach to screen for breast cancer?

16:00 - 17:30 **Room E2**

Multidisciplinary Session

MS 4
Neuroimaging and mental health disorders

A-120 16:00

Chairman's introduction
T.A. Yousry; *London/UK (t.yousry@ucl.ac.uk)*

Over the last decade, neuroimaging has been central to research in mental illness elucidating disorders of the underlying rather complex network. However, neuroimaging has not only been relevant to research but also to clinical management of patient. This can be illustrated in two diseases: Obsessive compulsive disorder (OCD) and Tourette syndrome (TS). Neuroimaging was central to the process of identifying anatomic targets for surgical intervention. In this intervention - functional stereotactic neurosurgery - electrodes are placed in these targets, an intervention known as "deep brain stimulation". This intervention in turn is also reliant on imaging. This session will, therefore, clarify the important role of imaging in the understanding and treatment of mental health disorders.
Session Objectives:
1. To understand the concept of mental illness as illustrated by obsessive compulsive disorder (OCD) and Tourette-Syndrome (TS).
2. To show how neuroimaging is furthering our understanding of OCD and TS.
3. To understand the central role of neuroimaging in functional neurosurgery of OCD and TS.
Author Disclosure:
T.A. Yousry: Advisory Board; Biogen Idec; Genzyme, Ixico. Board Member; Neuroradiology. Grant Recipient; Medical Research Council, MS Society of Great Britain and Northern Ireland, Stroke Association, British Heart Foundation. Research/Grant Support; BRC. Speaker; Novartis.

A-121 16:05

Unpicking obsessive compulsive disorder (OCD) networks with neuroimaging
E. Joyce; *London/UK*

Obsessive compulsive disorder (OCD) has a life time prevalence world wide of 1-2% and is the 11th leading cause of non-fatal burden (WHO). OCD is characterised by anxiety provoking thoughts, images and impulses which trigger mental or motor rituals designed to neutralise the anxiety. This leads to temporary relief only and patients become trapped in a vicious circle of disabling thoughts and actions. Effective treatments are available but 10-20% remain resistant. Deep brain stimulation (DBS) has been shown to be effective in 50-60% of such cases who have extremely severe OCD. Understanding the neural basis of OCD is important in order to develop new treatments and better targets for DBS. This talk will review how our understanding of OCD has developed over the past 20 years following advances in neuroimaging. Early PET findings showed that patients with OCD have increased metabolism in fronto-striatal circuitry which is decreased following successful pharmacological treatment. This concept of OCD as a network disorder has been elaborated since then but has also been found to be more complex. For example, tractography studies have shown altered topography and connectivity between the orbitofrontal cortex and striatum; structural MRI has shown reduced volumes of not only prefrontal and cingulate cortex but also hippocampus and increased volumes of pallidum and thalamus. MRI spectroscopy has contributed to our understanding of the neurochemical basis of OCD with abnormalities of GABA and glutamate being implicated. In the light of these neuroimaging findings the psychological understanding of the behavioural characteristics of OCD has been modified which might pave the way for better interventions.
Learning Objectives:
1. To understand the concept of severe mental illness exemplified by OCD.
2. To demonstrate the impact of neuroimaging - structural and functional MRI and PET - to our understanding of OCD as a neural network disorder.
3. To show the central role of neuroimaging in enabling us to pinpoint the critical neural target for successful treatment with deep brain stimulation.
Author Disclosure:
E. Joyce: Speaker; Boston Scientific

A-122 16:25

Bridging movement and mind: neuroimaging in Tourette-Syndrome
T. Foltynie; *London/UK (t.foltynie@ucl.ac.uk)*

In this lecture I will describe the potential of deep brain stimulation as a treatment for severe, medication refractory Tourette syndrome. I will introduce the concept of patient-specific simulations of the DBS electrical field using neuroimaging. I will show how the clinical efficacy of DBS for Tourette syndrome can be related to simulated electrical field on a voxel by voxel basis.
Learning Objectives:
1. To understand the importance on neuroimaging in understanding Tourette-Syndrome as a neural network disorder.
2. To introduce the concept of DBS as a treatment for severe medication refractory Tourette-Syndrome and the role of neuroimaging of the DBS electrical field.
3. To show how the clinical efficacy of DBS for Tourette-Syndrome can be related to simulated electrical field on a voxel by voxel basis.
Author Disclosure:
T. Foltynie: Advisory Board; BIAL. Research/Grant Support; MJ Fox Foundation, European Union, Brain Research Trust, John Black Charitable Foundation.

A-123 16:45

Precision neurosurgical targeting in Tourette's and obsessive compulsive disorder (OCD): critical role of neuroimaging
L. Zrinzo; *London/UK (l.zrinzo@ucl.ac.uk)*

Functional neurosurgery involves precise surgical targeting of anatomic structures to modulate neurologic function. Preoperative stereotactic localization places several demands on image acquisition that go beyond those required for diagnostic imaging. MRI coils must accommodate the relevant stereotactic frame. Target structures are often small placing demands on image resolution. Specific MR sequences that provide high tissue contrast between the target structure and the surrounding tissues must be used while ensuring clinically practical acquisition times. Geometric distortion represents a significant obstacle to accurate spatial representation and can render MR images useless for the purpose of accurate anatomic targeting. Numerous anatomical targets have been proposed in the management of Tourette syndrome (e.g. globus pallidus, centromedian/parafascicular nucleus) and obsessive compulsive disorder (ventral capsule / ventral striatum, anterior cingulate gyrus, anteromedial subthalamic nucleus). A vital step to assessing the efficacy of each anatomical target is confirming the anatomical location of

the intervention, whether after placement of a stereotactic lesion or a deep brain stimulation lead. Many commercially available DBS leads are MR conditional and the gold standard in verification is obtaining a stereotactic MRI as part of the surgical procedure. It is imperative that appropriate safety precautions be followed when obtaining such images. Likewise, it is inappropriate that a radiology department places a blanket ban on MR imaging of DBS patients. MR physicists and neuroradiologists are an essential part of the multidisciplinary team that offers neurosurgical interventions in patients with mental health disorders, including Tourette syndrome and obsessive compulsive disorder.

Learning Objectives:

1. To understand the essential differences between diagnostic and stereotactic MR imaging.
2. To introduce the concept of image-guided and image-verified DBS surgery.
3. To provide an overview of the different anatomical targets used for DBS in Tourette syndrome and OCD surgery and describe their radiological correlates.

Author Disclosure:

L. Zrinzo: Advisory Board; Medtronic, Boston Scientific.

17:05

Multidisciplinary case presentation and discussion

16:00 - 17:30 **Room F1**

E³ - Rising Stars Programme: Basic Session

BS 4

Gynaecology and obstetrics

Moderator:
M. Bekiesinska-Figatowska; Warsaw/PL

A-124 16:00

Benign gynaecological pathologies

R.N. Lucas; *Lisbon/PT (ritalucas1@gmail.com)*

The internal reproductive organs in the female include the vagina, uterus, uterine tubes and ovaries. Ultrasound and MRI are the most useful imaging modalities for female reproductive organs evaluation. Leiomyomas, are the most common benign tumours of the uterus made up of smooth muscle cells fascicles. Histologically, different subtypes are distinguished, of which cellular, myxoid leiomyoma and lipoleiomyoma can have particular MRI features. Benign ovarian masses include functional cysts and benign ovarian tumours. Cystic mature teratomas and cystadenomas comprise the majority being followed by benign stromal tumours fibromas/fibrothecomas and Brenner tumours. Ultrasound is usually the first imaging modality to identify the ovarian lesion and MRI is used for further characterisation.

Learning Objectives:

1. To describe the normal anatomy of the female reproductive organs.
2. To describe the imaging features of uterine leiomyomas.
3. To learn the key features of benign ovarian tumours.

A-125 16:30

Gynaecological malignancies

A.G. Rockall; *London/UK (a.rockall@imperial.ac.uk)*

Gynaecologic malignancies are initially detected either clinically or on ultrasound examination. Cervix cancer, which is increasingly rare in Europe due to screening, is detected clinically and histologically. Staging of disease is usually undertaken with MRI; PET/CT may also be used in cases of advanced disease. Features suitable for fertility-preserving surgery will be illustrated. Endometrial cancer is often first suspected on ultrasound and the diagnosis is confirmed histologically by endometrial sampling. Staging may be performed with CT and/or MRI. The stages of disease will be illustrated. Ovarian cancer is usually first detected on ultrasound. Further staging of disease for treatment planning may include CT and MRI. The typical appearances of ovarian cancer will be demonstrated on the different modalities.

Learning Objectives:

1. To describe the imaging appearance of malignant tumours of myometrium.
2. To review and illustrate the imaging features of cervical cancer.
3. To describe the imaging features of malignant ovarian tumours.

A-126 17:00

Foetal imaging

M. Bekiesinska-Figatowska; *Warsaw/PL (m.figatowska@gmail.com)*

Ultrasonography (US) is a method of choice in foetal imaging. It is obligatory in many European countries at certain points of pregnancy and is also used whenever it is necessary to follow-up suspected pathology. It is usually performed by gynaecologists-obstetricians and not by radiologists. Magnetic resonance imaging (MRI) is the second line method, performed always after US, to confirm, correct or complete the sonographic findings. It is not dependent on foetal or placental position, maternal obesity, oligohydramnios and other factors that limit US. It offers an "all in one" evaluation of complex malformations, is more illustrative for surgeons and parents and is more and more widely used for decision making in the pre- and postnatal period as it provides additional useful information that helps in the management of the foetus and the newborn. MRI can be safely performed after 18-19 weeks of gestation and does not require sedation or other preparation. Single-shot T2-weighted sequence, balanced steady-state gradient echo sequence, T1-weighted images, echo-planar gradient-echo T2*-weighted sequence, susceptibility- and diffusion-weighted sequences are nowadays available in foetal MRI, allowing for detailed analysis and diagnosis of various abnormalities of the foetal brain and body. Each sequence performed serves as a pilot study for the next one, taking into consideration foetal motility. The knowledge of the normal appearance of the foetal organs and its changes with gestational age is obligatory to be able to differentiate normal and abnormal anatomy and to point out and name the pathology.

Learning Objectives:

1. To discuss current imaging techniques for evaluation of normal anatomy.
2. To have a basic knowledge about the role of ultrasonography in foetal imaging.
3. To have a basic knowledge about foetal magnetic resonance imaging.

16:00 - 17:30 **Room F2**

Special Focus Session

SF 4a

Image-guided interventions in oncology: the pieces of the jigsaw

A-127 16:00

Chairman's introduction

J.I. Bilbao; *Pamplona/ES (jibilbao@unav.es)*

Establishing a program that includes continuous assessment of clinical outcomes ensures patient safety and increases the quality of the services. It is thus important to organise an accurate auditing system that will allow the identification and minimisation of risks and the maintenance of a low incidence of complications. Several safety practices can substantially reduce errors and medical complications and provide an optimal standard of care to patients. Imaging in oncology has dramatically evolved with the inclusion of functional information of the underlying process. A better understanding of which tumoural areas still remain active after therapy ensures the obtaining of accurate information that may improve the targeting of percutaneous biopsies or the direct guidance of selective therapies. If interventional radiologists are willing to be a robust pillar in the management of cancer patients they must be part of multidisciplinary teams, acquire skill in clinical responsibilities and obtain solid support, based in evidence, for the procedures they perform. For obtaining such conditions, interventional radiologists must have dedicated programs of training, must improve their social visibility and must conduct research and clinical trials.

Session Objectives:

1. To explain the importance of quality assurance in image-guided interventions in oncology and their effect on treatment outcomes.
2. To describe how developments in functional imaging are affecting clinical practice in oncology.
3. To summarise the current evidence regarding the treatment of cancer patients by interventional radiologists and explain the methods being employed to obtain the relevant data.

Author Disclosure:

J.I. Bilbao: Advisory Board; Boston Scientific, Cook Medical, Bayer. Speaker; Sirtex Medical Europe.

A-128 16:04

How molecular imaging and image fusion are shaping oncology

E. de Kerviler; *Paris/FR (eric.de-kerviler@sls.aphp.fr)*

Molecular and functional imaging has become an integral step in the evaluation of cancer patients. Most primary tumours are now biopsied under image-guidance to determine the best therapeutic strategy. However, the standard image-guided biopsy entails sampling a small portion of a tumour. Tumours are notoriously heterogeneous so that a small amount of tissue may not adequately represent the most aggressive component. Serial biopsies to account for variable expression of molecular targets throughout the tumour (tumour heterogeneity) are typically not practical. To optimize tissue sampling, molecular imaging can provide a more complete insight into living tumours. The ability of PET/CT to demonstrate malignancies, which are not visible on

anatomic images, increases the number of biopsy requests based on foci of tracer uptake. In addition, some neoplasms may demonstrate non-uniform tracer uptake and can be mostly necrotic or contain metabolically active tumour cells in only a small portion of the total mass. Whenever no PET tracers are available, SPECT/CT may be used as well for image guidance. Image fusion with MR can also be used to target biopsies toward areas with restricted diffusion. Lastly, dynamic contrast enhancement studies using MRI, CT or ultrasound nicely demonstrate foci of microvascular anomalies suitable for biopsy.

Learning Objectives:

1. To summarise the main developments in molecular imaging.
2. To highlight the importance of image fusion in the diagnosis and treatment of cancer.
3. To explain how functional imaging is changing oncological practice.

Author Disclosure:

E. de Kerviler: Consultant; Galil Medical.

A-129 16:23

Registries, trials and the evidence base

P.L. Pereira; *Heilbronn/DE (philippe.pereira@slk-kliniken.de)*

Medicine, in some instances more than other fields, undergoes a constant development process, making guidelines and standard operative procedures an important tool for the medical community. This is especially true in oncology, a discipline for which multidisciplinarity and combined therapies are essential for treatment success or better outcomes. Principles of clinical guidelines are based on current scientific knowledge with participants coming from different medical societies and on the consensus of medical experts, sometimes called good clinical practice. Furthermore, high-quality guidelines are necessary not only for a structured knowledge transfer, but they also find their place in the structures of the health system, being more and more a reference for discussions with reimbursement institutes and insurances. At least, evidence-based guidelines serve as a basis for creating and updating of disease management programs and to define quality indicators that will be used for the certification process of comprehensive cancer centres. If one refers to the number of papers, lectures and conferences focused on interventional radiology, we are forced to admit that the interventional oncology is taking a large place in interventional radiology. Over the last 30 years, interventional oncology has not only developed palliative monotherapies but could also obtain curative treatment for selected patients with renal, hepatic or pulmonal cancers.

Learning Objectives:

1. To explain the methods of gathering evidence in practical disciplines.
2. To outline the evidence base for image-guided interventions in oncology.
3. To outline the main current trials and registries in image-guided interventions in oncology.

A-130 16:42

Clinical practice: why it matters and how to do it

A. Adam; *London/UK (andy.adam@kcl.ac.uk)*

Interventional radiologists working in the field of cancer care have an excellent understanding of imaging and a diversity of interventional skills. However, they lack formal training in oncology and have a relatively poor understanding of chemotherapy and radiotherapy. Furthermore, their relative lack of sub-specialisation in interventional oncology is a disadvantage when communicating with other disciplines. It is very important to consider the patient and not the image. Talking to the patient, establishing his/her general state of physical and psychological health and their family and domestic circumstances is very important. In addition, the interventional oncologist should understand the disease and should be familiar with treatment alternatives other than those offered by interventional radiology. Sub-specialisation in interventional oncology is likely to increase and has substantial advantages because it provides a clear path for referrals and makes it easier for interventional oncologists to participate fully at multidisciplinary meetings. Participation at multidisciplinary meetings is very important because interaction with other disciplines improves decision-making and reduces the risk of error. Interventional oncologists should practise as clinicians at every stage in the patient pathway. Delegation of care to other disciplines can lead to inadequate consideration of the indications for and limitations of interventional radiological treatment, is wasteful of resources and is frustrating and unkind to patients. Practising as a clinician makes it easier for the interventional radiologist to prepare the patient appropriately, obtain true informed consent and ensure adequate follow-up.

Learning Objectives:

1. To explain the importance of clinical practice in image-guided interventions in oncology.
2. To describe how interventional radiologists can practice as clinicians rather than technicians.
3. To outline the curriculum being developed for image-guided interventions in oncology.

A-131 17:01

Quality assurance: an essential development

L.M. Kenny; *Brisbane/AU (lizkenny@bigpond.net.au)*

In acknowledgement of the overwhelming importance of standards of practice and their ultimate incorporation into a quality assurance programme, CIRSE has developed a set of practice standards for interventional oncology. The framework is based on the Australian and New Zealand Radiation Oncology Practice Standards and they follow the entire care pathway for patients undergoing interventional cancer procedures. They will support safe quality care for patients and will also act as a basis on which interventional oncologists can work with facilities to improve the infrastructure and processes required for their teams to practise effectively. There are 14 standards, broadly divided into three areas, and each follows a standard format: facility management (7 standards), treatment planning and delivery (3 standards), safety and quality management (4 standards). There is a consistent format for each standard, as follows: i. each standard refers to a corresponding goal or outcome, ii. criteria describe the key processes required to attain that goal, iii. a commentary provides information which outlines how a criterion applies in everyday practice and iv. the required evidence that documents the records that the facility should be able to provide to demonstrate compliance with the standards. These draft standards have been piloted in a number of interventional oncology units during the second half of 2016. Upon completion, CIRSE will incorporate the standards into a quality assurance and credentialing programme.

Learning Objectives:

1. To highlight the importance of quality assurance in image-guided interventions in oncology.
2. To explain how quality assurance affects clinical outcomes in cancer care.
3. To summarise the content and practical implications of the framework developed for quality assurance in image-guided interventions in oncology.

17:20

Panel discussion: What will be the future of image-guided interventions in oncology?

16:00 - 17:30 **Room D**

Musculoskeletal

RC 410

Bone trauma in the axial skeleton: patterns of injury and how I describe them

Moderator:

A. Barile; L'Aquila/IT

A-132 16:00

A. Thoracic and lumbar spine

V.N. Cassar-Pullicino; *Oswestry/UK (Victor.Pullicino@rjah.nhs.uk)*

Thoracolumbar spinal injuries occur in up to 4% of blunt trauma cases with an incidence of associated neurological deficit in up to 50%. The radiologist is pivotal in the evaluation of these patients. Plain film radiology, CT and MRI all play a role in the evaluation of the injury. They are often complementary as all imaging modalities have inherent strengths and weaknesses. The aim is to expedite prompt and accurate characterisation of the injured segment with the added task of excluding concomitant non-contiguous injury in the rest of the spine. The patterns of injury differ, reflecting underlying unique differences in the anatomy and biomechanics of each region, and this also varies with age and pre-morbid states such as the fused spine. The primary objective is for the radiologist to become familiar with the types of injury to ensure accurate description based on sound image interpretation. Although many classification systems have evolved with time they are primarily descriptors and not predictors of outcome. More recent classification systems include a prognostic theme. Although they are a clinical tool aiding in therapeutic decision making, the radiologist needs to have a basic understanding of the ones that are commonly used. With this in mind, the report should present the imaging data to the clinician.

Learning Objectives:

1. To become familiar with the types of injury seen in the thoracic and lumbar spine.
2. To learn how to describe the injuries in a manner useful to the clinician.

A-133 16:30

B. Pelvis

K. Verstraete; *Ghent/BE*

Bone injury to the pelvis may be caused by high-energy trauma, stress fractures, and avulsion fractures. Pelvic ring fractures are a common consequence of motor vehicle accidents or falls from heights. Major patterns of injury include lateral compression, anteroposterior compression, vertical shear injury, or complex injury due to a combination of these fracture forces. Anteroposterior radiographs are still included in the initial evaluation, but pelvic inlet and outlet views and lateral projection are replaced by CT, which allows multiplanar reformatted imaging for diagnosis, classification and surgical planning. CT angiography is essential to detect active bleeding from cancellous bone, injured vessels or soft tissues. The typical sites of pelvic stress fractures are the sacrum and pubic rami. Fatigue or overuse stress fractures occur in athletes due to repetitive microtrauma. Insufficiency fractures are caused by normal, physiologic stress on weakened bone, usually in elderly women with osteoporosis, corticotherapy or after pelvic irradiation. These stress fractures can be undetectable on radiography in initial stages, and have an aggressive lytic appearance in late stages when patient keeps on moving. CT demonstrates fracture lines or sclerosis, and on MR bone marrow oedema is an early sign of bone stress injury. Apophyseal avulsion fractures occur in young recreational or competitive athletes (sprinters, gymnasts, football, baseball players, etc.), usually teenagers. Radiography is the technique of first choice in acute avulsion injuries. Comparison with the contralateral side is important, and in selected cases, ultrasound, CT, MRI and bone scintigraphy may be needed.

Learning Objectives:

1. To become familiar with the types of injury seen in the pelvis.
2. To learn how to describe the injuries in a manner useful to the clinician.

A-134 17:00

C. Acetabulum

A. Kassarjian; *Majadahonda/ES (akassarjian@gmail.com)*

Acetabular trauma can present a challenge to radiologists given the complex nature of the anatomy of the acetabulum and the various configurations of fractures. The objectives of this lecture on acetabular trauma are: to become familiar with the types of injury seen in the acetabulum and to learn how to describe the injuries in a manner useful to the clinician.

Learning Objectives:

1. To become familiar with the types of injury seen in the acetabulum.
2. To learn how to describe the injuries in a manner useful to the clinician.

Author Disclosure:

A. Kassarjian: Consultant; Arthrosurface.

16:00 - 17:30 **Room G**

Professional Challenges Session

PC 4

Design and implementation of structured reporting

A-135 16:00

Chairman's introduction

W.H. Sommer; *Munich/DE (Wieland.sommer@med.uni-muenchen.de)*

The role of the radiologist will evolve during the next years and decades from the interpretation of imaging data by free-text to providing sets of quantitative and mineable data based on these images. In this context, structured reporting has become one of the most discussed topics. When talking about this topic, one should consider the different forms of structured reporting, ranging from the simple introduction of fixed subsection headers in a free-text report on the one hand to complex decision support algorithm and synoptic reporting on the other hand. The form of structured reporting determines the challenges of integration into the workflow as well as the possible goals which can be obtained by the implementation. The aim of this session is to give an overview on different forms of structured reporting and describe possible achievements of each of these forms, such as quality improvement, educational aspects, improvement of referring physicians' satisfaction and the possibility of data mining. The session presents several ongoing initiatives, such as the ESR/RSNA structured reporting initiative. There will be a special focus on the combination of structured reporting and natural language processing and how this can be implemented into clinical routine for quality management.

Session Objectives:

1. To get an overview on different initiatives for structured reporting.
2. To understand pros and cons of different forms of structured reporting, including template-based reporting, decision support and modular structured reporting.
3. To appreciate the wide range of possibilities for quality management which become possible with structured reporting.
4. To become familiar how different institutions integrate structured reporting in the clinical workflow.

Author Disclosure:

W.H. Sommer: Founder; Smart Reporting GmbH.

A-136 16:10

Beyond templates: modular multilingual structured reporting

M. Fatehi; *Tehran/IR (fatehi@irsr.org)*

Structured reporting is still following the traditional concept of putting the report together through the template library. So, the efforts and applications are based mostly on the template-driven concepts. But in practice, even using the templates the radiologists address a particular part of the text that may be called sub-templates or modules. These modules can be presented in detailed or brief format or even deleted from the final report. The ideal solution is an expandable flexible dynamic template builder where the modules are selected according to the need letting the user to tailor the length and order of the report to the problem of the patient. Currently available template libraries mostly provide templates for normal findings. But the missing component is the structure for description of abnormal findings. But a library of modules is required to let radiologists report their abnormal cases in a similar manner to achieve the best from the data storage and mining in radiological reports. Using structured reporting to store a report technically means to follow a tabular data structure which bears the potential to be codified rather than being stored as a character set. So, the codes may be presented in any pre-defined languages and one of the major advantages of structured reporting is the potential to be language independent. In this presentation, multiple models of structured reporting applications will be shown as examples of modular, language-independent, problem-specific approach.

Learning Objectives:

1. To get familiar with advantages of modular structured reporting to template-based approach.
2. To know challenges in language independent reporting in radiology.
3. To understand importance of availability of modules for structured description of abnormal findings.
4. To learn about already developed modular structured reporting tools and apps.
5. To understand features of a problem specific flexible structured reporting application to tailor the template to clinical condition of the patient.

A-137 16:30

Introducing quality management for radiology reports

C. Wald; *Boston, MA/US (christophwald@me.com)*

Modern radiology reporting quality assurance must ascertain that radiologists understand the hallmarks of a high-quality report and implement proper reporting. A value-added report is the most important and visible work product of our profession, increasingly expected by our patients and referring clinicians. Required specifications may include use of a standard document model, inclusion of required data elements, qualitative and quantitative image descriptors and the use of building blocks of standardized language. Considering the large number of reports routinely issued in a radiology department, systematic, scalable quality control tools are needed to efficiently assess and improve compliance of radiologists. Modern, natural language processing-based methods can check for errors (laterality, gender), check compliance with reporting requirements (Bi-Rads, LungRads, etc.), completeness of reporting, but also help evaluate more elusive concepts such as frequency of self-referral and use of ambiguous language. The lecture presents a novel reporting quality toolbox that can facilitate those assessments while also analysing report generation metrics. Result can be used for change management in the department. In the future, many of these quality assessments can be performed on the fly to allow the radiologist to make immediate adjustments prior to report issuance. Other approaches to increasing the value of reports, such as multimedia reporting and dashboard presentation of report content, are also presented.

Learning Objectives:
1. To learn about available options for basic quality control of radiology reporting.
2. To understand challenges of current prevailing practice for consumers of radiology reports and risk management.
3. To appreciate the importance of performing systematic report quality control and reporting compliance control.
4. To become familiar with tools for Q/C as well as structured data generation and presentation, including multimedia reports and dashboard presentation of report content.

Author Disclosure:
C. Wald: Advisory Board; Philips Medical.

A-138 16:50

Structured reporting: two decades of surveys and subcommittees, but what do we wish to achieve?

J.M.L. Bosmans; *Ghent/BE (janbosmans@telenet.be)*

Since the beginning of this century, a considerable number of surveys have shown that radiologists as well as referring physicians prefer structured reporting (SR) to reporting in free text, at least for complex imaging studies. Comparison of these studies, however, shows a wide variety in the definition of SR. Although the quantitative results of the surveys are very similar, it is possible that they reflect preferences on vastly different forms of reporting, the common factor being that findings should be presented in a predefined, orderly way, in the interest of clarity, coherence and comparability. Several authors have challenged this minimal interpretation. A limited number of studies have also revealed a preference for SR based on an underlying lexicon. Initiatives have been undertaken to create a coherent system of SR templates and a radiology-oriented coded lexicon, the most conspicuous being the ESR/RSNA structured reporting initiative. A new concept in the development of SR is the creation of common data elements (CDE), units of information used in a shared, predefined fashion, that can improve the ability to exchange information among information systems. While in surveys the preference for SR was mainly based on well-chosen, theoretical examples, a few real-life applications of SR have been greeted with enthusiasm by referring clinicians. Many obstacles, however, hinder its acceptance, e.g. the absence of SR-based radiology information systems, the slow introduction of the electronic health record in many countries and, particularly in Europe, the rich variety in languages other than English.

Learning Objectives:
1. To learn about the preferences of radiologists and referring physicians concerning text-oriented vs structured reporting.
2. To understand the definition of structured reporting, and the evolution in thinking about the objectives to attain.
3. To become familiar with initiatives to create a framework for structured reporting, including a SWOP analysis.

17:10
Panel discussion: Structured reporting in 10 years: large-scale or fairy-tale?

16:00 - 17:30 **Room K**

Radiographers

RC 414

Modern imaging of major trauma

Moderators:
P.H. Hogg; Salford/UK
L. van den Hauwe; Antwerp/BE

A-139 16:00

A. Use of MSCT in disaster victim identification

J. Kroll; *Maastricht/NL (j.kroll@mumc.nl)*

Radiology, mainly as a tool for forensic odontology, has long been an essential discipline in the post-mortem identification of human remains. Because forensic radiology is a rapidly developing field due to the fast technical developments of CT scanners, the possible applications are increasing. A whole body CT scan contains a wealth of identification information that can be used in an identification process. This presentation will highlight the contribution of forensic radiology, and more specific a whole body CT scan, for a DVI-process, discussing its applications, equipment, advantages and positioning within a DVI-process. It will also discuss future developments, opportunities and challenges which future DVI-processes will face.

Learning Objectives:
1. To appreciate the role of forensic radiology in a disaster victim identification process.
2. To learn about the methods using forensic radiology in a disaster victim identification process.
3. To discuss added value of forensic radiology in a disaster victim identification process.

A-140 16:25

B. Conventional radiography in major trauma: role, technique modification and impact on interpretation

M. Hardy; *Bradford/UK (M.L.Hardy1@bradford.ac.uk)*

The role of imaging in major trauma is to inform life-saving medical intervention and assist in the prioritization of patient care pathways. The modality of choice to undertake this is CT. However, what happens when cross-sectional imaging is not available due to equipment malfunction, planned service or lack of availability locally? In these situations, image referrals may revert back to conventional radiographic imaging. But with so little opportunity to undertake these examinations in the modern trauma setting, the radiographic skills and decision-making necessary to produce diagnostic images may be limited. This talk revisits the acquisition of chest and pelvis radiographs following major trauma and, through a series of case studies, provides an overview of important diagnostic features and explores the impact that radiographic technique may have on these.

Learning Objectives:
1. To appreciate the limited role of conventional radiography in major trauma.
2. To learn key radiographic indicators and signs of major trauma.
3. To discuss the impact of technique modification on anatomical appearances and the accurate identification of trauma on conventional radiographs.

Author Disclosure:
M. Hardy: Author; Multiple Journals & textbooks. Grant Recipient; ISRRT Award, HEE Award, CCIP HEIF Award. Other; President UKRC, Associate Editor JMIRS Journal, Editorial Board Member Radiography Journal.

A-141 16:50

C. Applications of ultrasound in the evaluation of major trauma

T. Herlihy; *Dublin/IE (therese.herlihy@ucd.ie)*

Ultrasound is the most widely used and readily available imaging modality in the world. In recent years, ultrasound has moved from its classic use in the radiology department to playing a useful and sometimes vital role in the assessment and management of the trauma patient. Focused assessment with sonography for trauma (FAST), chest abdominal-focused assessment sonography for trauma (CA-FAST) and extended-FAST (E-FAST) are now widely performed in cases of both penetrating and non-penetrating trauma. Despite this, more research needs to be done to elicit the affect ultrasound has on patient prognosis and survival. As ultrasound is portable it can be used both in the hospital and ambulance setting. FAST is now an integral part of the training of emergency physicians; however, there is a lack of standardisation around education and clinical competencies and there are also variations in the use of FAST between centres. While ultrasound on trauma patients is primarily performed by physicians, some countries are now training and using paramedics to perform ultrasound in the field and in ambulances before the patient is moved/arrives at the hospital. Ultrasound is extremely operator dependent and so anyone using ultrasound to assess patients must be properly trained and understand the advantages and limitations of ultrasound scanning. As ultrasound machines become cheaper and more accessible ultrasound is being used more and more in the emergency setting.

Learning Objectives:
1. To appreciate the role ultrasound can play in assessing the trauma patient, both in the hospital and ambulance setting.
2. To learn about focused assessment with sonography for trauma (FAST) and what training is required to perform FAST scanning.
3. To discuss the expanding role of ultrasound in the accident and emergency room. Who does what and when and how does it impact on patient care?

17:15
Discussion and questions: Imaging of major trauma - what are the challenges?

16:00 - 17:30 **Room M 1**

EuroSafe Imaging Session

EU 1

Clinical diagnostic reference levels

Moderators:
G. Simeonov; Luxembourg/LU
G. Frija; Paris/FR

A-142 16:00

Introduction
G. Frija; *Paris/FR (guy.frija@egp.aphp.fr)*

Diagnostic reference levels (DRLs) are an important tool for optimisation. With the new Basic Safety Standards Directive (Council Directive 2013/59/Euratom) DRLs have been included in European legislation. The BSS Directive defines DRLs as "dose levels in medical radiodiagnostic or interventional radiology practices, or, in the case of radio-pharmaceuticals, levels of activity, for typical examinations for groups of standard-sized patients or standard phantoms for broadly defined types of equipment". A working group on clinical DRLs has been established under the umbrella of EuroSafe imaging, the European Society of Radiology's campaign to promote quality and safety in medical imaging. Clinical DRLs take into account the different clinical tasks of the same area, which do not require the same image quality. The working group aims at developing a first set of DRLs for clinical indications to transform the requirements of the BSS Directive into concrete action for users. This presentation will give an overview of the concept of DRLs and the standard-sized patient generally used to define DRLs, although most patients do not comply with the definition. In addition, the preliminary results of the "Is your Imaging EuroSafe?" surveys, which have collected data on CT DRLs for different indications, will be briefly presented.
Session Objectives:
1. To become familiar with the concept of local and clinical diagnostic reference levels.
2. To discuss the need for DRLs specific to body size, disease distribution and clinical indication.
3. To present the results of the first EuroSafe Imaging Stars survey.

A-143 16:15

Clinical diagnostic reference levels: from concept to impact in clinical practice
R.W.R. Loose; *Nürnberg/DE (Loose@klinikum-nuernberg.de)*

Today most diagnostic reference levels (DRL) are based on modalities and anatomical body regions to be examined (e.g. CTDIvol and DLP in CT, or DAP in radiography). In film-based radiography, the detector dose is given by the film-screen sensitivity and can be modified only within narrow limits. Introduction of digital radiography enabled substantial dose reduction with increased image noise for specific clinical questions (e.g. control of metal removal after surgery or measurement of scoliosis angles in children). CT as a digital modality with the highest collective medical dose contribution enabled dose modifications from the first beginning. Because of digital viewing conditions (window width) high-contrast objects in general require lower CT doses than low-contrast objects. A CT of the brain (window width ~80 HU) requires a typical CTDIvol of ~50 mGy which is significantly higher than a CT of the lung parenchyma (window width 1500-2000 HU) with a CTDIvol < 10 mGy. Typical clinical DRLs with reduced dose in CT are screening for lung nodules, sinusitis or ureteral stones. In addition, clinical DRLs have to include the number of required CT scan series. In fluoroscopy, setting up clinical DRLs is more complex, as in addition to image quality the complexity and duration of a procedure have a major impact. Setting up more clinical DRLs requires a classification of patient conditions where different dose levels for one anatomical region are reasonable. Such a process will increase the number of DRLs but probably reduce the overall dose to patients.
Learning Objectives:
1. To understand the different quality requirements to answer specific clinical imaging questions in CT exams of the same body region.
2. To learn about the steps needed for a transition to clinical DRLs.
3. To appreciate the practical impact of clinical reference levels.

A-144 16:30

ICRP perspective: from methodological region-related DRLs to DRLs based on clinical indications
E. Vaño; *Madrid/ES (eliseov@med.ucm.es)*

The International Commission on Radiological Protection (ICRP) has recently completed a report updating the recommendations on "Diagnostic Reference Levels - DRLs - in Medical Imaging". DRLs have been proven to be an effective tool that aids in optimisation of protection in the medical exposure of patients for diagnostic and interventional procedures. There are issues related to definitions of the terms used in previous guidance, determination of the values for DRLs, the appropriate interval for re-evaluating and updating these values, appropriate use of DRLs in clinical practice, methods for practical application of this tool, and application of the DRL concept to newer imaging technologies. The report has already been submitted to public consultation and it is expected to be published in 2017. According to ICRP recommendations, DRL quantities should be appropriate to the imaging modality being evaluated, should assess the amount of ionising radiation applied to perform a medical imaging task, and should be easily measured or determined. Data for determining DRL values are obtained from surveys or registries of the DRL quantities for procedures performed on appropriate samples of patients. The 75th percentile value of the distribution of median values of a DRL quantity at healthcare facilities throughout a country is used as the 'national DRL'. DRLs are not intended to be used for individual patients or as a trigger (alert or alarm) level for individual patients or individual examinations. The appropriate image quality or diagnostic information needed for the clinical task should be a priority when setting DRL values.
Learning Objectives:
1. To become familiar with ICRP's term of 'DRLs for a defined clinical task'.
2. To learn about methodological requirements for establishing DRLs.
3. To understand the potential uses and limitations of DRLs.

A-145 16:45

EuroSafe Imaging clinical DRLs: detailed results of the pilot survey and lessons learnt for the survey among the EuroSafe Imaging Stars
P. Vock; *Spiegel/CH*

While the reasons for using clinical DRLs have been demonstrated by the previous speakers of the session, there is still a lack of concrete indication-based DRLs. The ESR has performed a pilot survey to overcome this deficit, concentrating on CT examinations of a few frequent indications. The results of this survey will be analysed: no matter what indication, there was a wide spread of exposure levels for one clinical task. The most important sources of variation - the equipment and protocol used, patient body size, and locally different specifications of a general indication - will be discussed. Different image quality needs for frequent indications are illustrated. Based on the experience of the ESR pilot study and of other European DRL projects, the methodological approach to reducing variation has been defined and will be used for a survey among EuroSafe Imaging Stars. This project will not compete with the establishment of national DRLs: based on dose management software tools it will be a faster way to see the trends in DRL evolution over time in European centres dedicated to radiation protection whereas national DRLs, by the fact that they have to be representative for all providers and all equipment in use, will take longer time and more efforts to be established.
Learning Objectives:
1. To present results of the pilot survey.
2. To learn about the different exposure levels needed in important indications.
3. To appreciate complimentary uses of EuroSafe Imaging and national DRLs.

A-146 17:00

North American DRLs: a view from across the pond
R.L. Morin; *Jacksonville, FL/US (morin.richard@mayo.edu)*

The purpose of this work was to use the American College of Radiology Computed Tomography (CT) Dose Index Registry (DIR) to develop diagnostic reference levels (DRLs) and achievable doses (ADs) for the 10 most common adult CT examinations in the US as a function of patient size. These examinations are: head brain without contrast, cervical spine without contrast, neck with contrast, chest without contrast, chest with contrast, chest with pulmonary embolism protocol, chest abdomen pelvis with contrast, abdomen pelvis with contrast, abdomen pelvis without contrast, and abdomen pelvis nephrolithiasis protocol without contrast. For the head exams, lateral thickness dimension was used as an indicator of patient head size. For neck, c-spine, chest, abdomen and pelvis exams, effective diameter was used. Data from over 1.3 million examinations were used to determine median values (AD) as well as mean, 25th and 75th (DRL) percentiles of $CTDI_{vol}$, DLP and SSDE. The median CTDIvol did not vary significantly but DLP increased with lateral thickness for head exams. For neck and c-spine, the median CTDIvol and the 75th percentile did not vary significantly but the median DLP did with effective diameter. Similar trends were seen for the median CTDIvol and SSDE for

chest, abdomen and chest-abdomen-pelvis exams. Our data agree well with the data from other resources. This talk will enable facilities to compare their patient doses to size-specific national benchmarks and optimize their CT protocols resulting in lower dose at the appropriate image quality.
Learning Objectives:
1. To present the US approach to quantitative benchmarking in optimisation and the role of DRLs.
2. To understand how the ACR finds consensus about minimal image quality requirements in different clinical indications.
3. To share the ACR experience with DRLs.
Author Disclosure:
R.L. Morin: Board Member; RSNA Research and Education Board of Trustees. Employee; Mayo Clinic. Speaker; Over 100 meetings and confernces.

17:15
Panel and public discussion
1. To discuss advantages and limitations of clinical DRLs. 2. To appreciate the initial cooperation among EuroSafe Imaging Stars. 3. To discuss the future role of EuroSafe Imaging DRLs and national/European DRLs.

16:00 - 17:30 **Room M 2**

Special Focus Session

SF 4b
The female pelvis

A-147 16:00
Chairman's introduction
R.A. Kubik-Huch; *Baden/CH (rahel.kubik@ksb.ch)*

Gynaecologic emergencies are disorders typically characterised by acute pelvic pain related to the female genital organs, related or unrelated to pregnancy. In an acute clinical setting, gynaecologic conditions must be separated from gastrointestinal diseases. Diagnoses implicate potentially profound consequences for the patient. Imaging plays an increasing role in the emergency setting by 1) assisting clinicians to diagnose acute gynaecological pathology and 2) helping to guide surgical or medical treatment. Therefore, it is important to accurately interpret the imaging findings in the context of the clinical signs. Chronic pelvic pain is a common problem. It presents a major challenge because of its unclear aetiology and often poor response to therapy. The condition is best managed using a multidisciplinary approach. Common gynaecologic and non-gynaecological causes as well as the role of imaging will be discussed. The aim of this session is to illustrate frequently encountered gynaecologic pathologies responsible for acute and chronic pelvic pain to raise awareness among radiologists and to ensure adequate patient care.
Session Objectives:
1. To discuss the differential diagnosis of acute and chronic pelvic pain with a special emphasis on the female genital organs.
2. To learn how to optimise the imaging work-up for pelvic pain in the pregnant and non-pregnant patient.

A-148 16:05
Acute pelvic pain
R. Manfredi; *Verona/IT (riccardo.manfredi@univr.it)*

Acute pelvic pain is a common symptom necessitating emergent medical evaluation, to make a prompt diagnosis and perform ovary-sparing or life-saving surgery. Clinical evaluation and laboratory testing are essential when a gynaecologic condition is suspected to be the cause of acute pelvic pain. For the initial diagnostic imaging evaluation, ultrasonography (US) is the modality of choice; however, the role of computed tomography (CT) in the evaluation of abdominal and pelvic pain continues to expand. In recent years, magnetic resonance (MR) imaging has been increasingly employed to assess those patients, because of the lack of ionizing radiation beneficial in possibly pregnant patients. Given the many possible causes of pelvic pain, a structured approach to image interpretation is necessary to narrow the differential diagnosis. First, the distinction between pregnant and non-pregnant patients, as determined by beta human chorionic gonadotropin (β-hCG) levels in correlation with menstrual history, is crucial. This clinical information portends the physiologic changes that may be expected and allows accurate image interpretation. Among ovarian causes of acute pelvic pain are follicular cysts, cystic corpus luteum, haemorrhagic ovarian cysts, endometriomas, teratomas and cystadenomas. Any mass ovarian lesion predisposes the ovary to torsion on its vascular pedicle, although torsion also occurs in the absence of an ovarian mass in pre-puberal girls. Among non-ovarian causes of acute pelvic pain are para-ovarian cysts, hydrosalpinx, peritoneal inclusion cysts, ectopic pregnancy and pelvic inflammatory disease. Among uterine causes, fibroids are the most common tumours of the uterus causing pelvic pain in as many as 30% of cases.
Learning Objectives:
1. To learn about the underlying aetiologies of acute pelvic pain.
2. To recognise various emergencies of the female pelvis and to take appropriate action.
3. To learn how to optimise MRI of the female pelvis in patients with acute pelvic pain.

A-149 16:30
Chronic pelvic pain
R. Forstner; *Salzburg/AT (r.forstner@salk.at)*

Chronic pelvic pain refers to pain of at least 6 months duration. It is a major issue in health care due to its often debilitating nature and its estimated prevalence of up to 18%. It is also a common cause of both diagnostic and curative surgeries. The spectrum of aetiologies is broad and comprises gynaecologic and non-gynaecologic conditions. The latter include gastrointestinal, urological, musculoskeletal, neurological and psychological disorders. MRI is most useful to differentiate between the gynaecological causes of chronic pelvic pain including endometriosis, adenomyosis and uterine leiomyomas. Clinical history and meticulous analysis of the character of pain may help to identify deep endometriosis, which is the most common cause of chronic pain in the reproductive age. A structured analysis of the MRI findings will assist in assessing also subtle findings of endometriosis, e.g. of the bowel or along the uterosacral ligaments. Unlike sonography, MRI allows also differentiation of adenomyosis and uterine leiomyomas. Although a controversial topic, pelvic congestion syndrome may be treated by interventional radiology. Due to its multifactorial character, patients with chronic pain often will require interdisciplinary management, with radiology rendering crucial information.
Learning Objectives:
1. To learn about prevalence and aetiologies of chronic pelvic pain.
2. To become familiar with gynaecologic causes of chronic pelvic pain.
3. To become familiar with common non-gynaecological causes of chronic pelvic pain.
4. To understand the role of imaging in the interdisciplinary management.

A-150 16:55
Pain in pregnant women
M. Weston; *Leeds/UK (michael.weston2@nhs.net)*

The pregnant woman may suffer pain related to her pregnancy or the pain may be co-incidental, related to other systems outside of the gravid uterus. Ultrasound is the starting point for imaging in the pregnant woman and has a recognised role in ectopic pregnancy, fibroid degeneration, adnexal torsion and appendicitis. There are sometimes when ultrasound is not enough and MR is required. This may be so in renal colic, uterine dehiscence and placental abruption. A radiologist should use the test that is most likely to answer the question in their hands. So, to use appendicitis as an example, it maybe that the best chance of an accurate diagnosis will be with CT, if the radiologist has not used MR in this scenario before. CT is often the imaging test of choice in significant trauma or suspected pulmonary embolus. The merits of each imaging modality and typical appearances will be discussed.
Learning Objectives:
1. To learn about causes of pain specific to pregnancy, such as ectopic pregnancy, placental abruption, fibroid degeneration and uterine dehiscence.
2. To learn about causes of pain in other organs that may present during pregnancy, such as appendicitis, renal colic and ovarian torsion.
3. To understand how pregnancy alters the way imaging is undertaken.
4. To appreciate the relative risk to the mother and foetus of imaging irradiation and misdiagnosis.
5. To become familiar with the increasing role that MR can play.

17:20
Panel discussion: The management of pelvic pain: is imaging always needed?

16:00 - 17:30 **Room M 3**

Molecular Imaging

RC 406

Molecular imaging: what can we quantify?

Moderator:
O. Clément; Paris/FR

A-151 16:00

A. Advanced MRI techniques
M. Smits; *Rotterdam/NL (marion.smits@erasmusmc.nl)*

Functional MR imaging (fMRI) and diffusion tensor imaging (DTI) are used extensively in the research arena to study an infinite number of questions regarding the brain's function and structure under normal conditions, as well as with neurological and psychiatric disease. The clinical use of these techniques, however, is by comparison fairly limited. The current main indication is the presurgical assessment of the relationship between the brain tissue to be resected and functionally eloquent brain tissue. In the context of brain tumour surgery, the aim is maximum tumour resection, while at the same time avoiding functional deficit. With tumour localisation in or near presumed eloquent brain areas, such as the motor or language areas, additional fMRI and DTI may be advantageous to guide the neurosurgical approach, shorten surgery duration and obtain prognostic information prior to surgery. fMRI is used to localise eloquent cortex, which is particularly useful when normal anatomy is obscured by tumour mass effect or in cases of cortical plasticity. With DTI the anatomy and involvement of white matter tracts may be evaluated. Inadvertent transection of white matter tracts during surgery leads to severe neurological deficit. DTI-tractography offers attractive visualisation of the major white matter tracts such as the corticospinal tract and the arcuate fasciculus, and offers valuable preoperative information on their relationships with the brain tumour to be resected. As well as providing such anatomical information, colour-coded eigenvector maps obtained with DTI can be used to categorise involvement of the white matter tracts by brain tumour.

Learning Objectives:
1. To learn about functional MRI (fMRI, DCE-MRI), diffusion tensor imaging (DTI) and diffusion-weighted imaging (DWI).
2. To understand the application of these techniques in the study of the healthy and diseased.
3. To learn about quantification using MR.

A-152 16:30

B. Advanced PET imaging techniques
T. Beyer; *Vienna/AT (thomas.beyer@meduniwien.ac.at)*

PET is a non-invasive imaging technique that provides reproducible and fully quantitative information on preselected metabolic/signalling pathways. PET is highly sensitive, thus, requiring only small amounts of biomarkers to be used for visualization and quantification purposes. Today, clinical PET imaging systems are offered almost exclusively in combination with CT and MR systems. Advantages of these imaging combinations are manifold and include, mainly for PET/CT, a marked reduction in total acquisition time, and improved spatio-temporal alignment of the complementary image information. Advancing PET-imaging technology into combined PET-based imaging technology included methodological input and technical innovation. We will highlight the most important advances of PET instrumentation that help increase volume sensitivity, improve spatial resolution and overall image quality. PET imaging in the context of combined PET/MRI was made possible only through the introduction of completely revised PET detectors that can operate in high-strength magnetic fields. Overall, increased volume sensitivity helps reduce the amount of radiotracer injected into patients or shorten the emission scan time, in combination with increased signal-to-noise in the emission images it helps increase sensitivity and reader accuracy of PET images. Lastly, advances in image reconstruction have brought the level of PET, and the appearance of the PET images, closer to the common understanding of radiologically useful images. Following this presentation, the audience will 1. learn about the benefits and challenges of quantification in PET, 2. understand the fundamentals of PET physics relevant to PET/MR imaging and 3. appreciate the advantages of PET/MR and its complementary role in diagnostic oncology.

Learning Objectives:
1. To understand the fundamentals of PET physics relevant to MR/PET imaging.
2. To appreciate the advantages of MR/PET and its complementary role in diagnostic oncology.
3. To learn about the benefits and challenges of quantification in PET.

Author Disclosure:
T. Beyer: Research/Grant Support; Siemens Healthcare. Other; Manging Director cmi-experts GmbH.

A-153 17:00

C. Clinical applications of quantitative hybrid imaging in oncology
L. Umutlu; *Essen/DE (Lale.Umutlu@uk-essen.de)*

Over the past 15 years, hybrid imaging, in terms of PET/CT, has become an essential part of clinical oncologic imaging. It has been well demonstrated to provide fast, high-quality, quantifiable imaging for numerous application fields, including whole-body staging and restaging in cancer patients, therapy monitoring and for radiation therapy planning. The combined assessment of morphological and metabolic features of tumours has not only been shown to add valuable non-invasive information concerning tumours, but also improve the diagnostic competence to higher levels than sole morphological cross-sectional imaging. The successful introduction of simultaneous PET/MRI into clinical imaging, in terms of the interchange of the CT component for anatomical correlation to MRI, has leveraged hybrid imaging onto utterly new and emerging platforms of tumour assessment. The application of multi-parametric PET/MRI imaging, comprising high-resolution morphological imaging as well as functional parameters such as diffusion-weighted imaging, perfusion parametrics and tumour metabolism, facilitates an improved understanding of tumour biology as well as prognostic factors. Furthermore, it enables improved therapy monitoring to better differentiate between potential responders and non-responders to chemo- and/or radiation therapy.

Learning Objectives:
1. To become familiar with the role of hybrid imaging in clinical oncology.
2. To learn about quantification in oncology: its benefits and limitations.
3. To understand hybrid imaging applications in relationship to disease presentations.

16:00 - 17:30 **Room M 4**

E³ - ECR Academies: Tips and Tricks in Liver, Bile Ducts and Pancreas Imaging

E³ 418

Bile ducts imaging: not so simple

A-154 16:00

Chairman's introduction
S.A. Jackson; *Plymouth/UK (simon.jackson1@nhs.net)*

Despite rapid technological advances, which have resulted in significant improvements when imaging the biliary tree, the accurate assessment and diagnosis of bile duct pathology still offers challenges for the clinical radiologist. Multi-modality imaging techniques remain central to optimal multi-disciplinary patient management with this interactive ECR academy covering the presentation and imaging appearances of both benign and malignant biliary diseases. In particular, lectures will focus on the imaging features of cholangiocarcinoma and the underlying differential diagnosis of patients presenting with chronic cholangitis. Tips and tricks for accurate diagnosis and the importance of clear diagnostic algorithms will also be emphasised using a range of challenging illustrative clinical cases.

A-155 16:05

A. Cholangiocarcinoma
S. Kim; *Seoul/KP (sykim.radiology@gmail.com)*

Cholangiocarcinoma (CCA) is a malignant epithelial neoplasm with biliary differentiation, which arises from any portion of the biliary system including epithelium and peribiliary gland. Although it shows the highest incidence in Asia, the incidence appears to be increasing recently in western countries. Of late, the concepts of CCA has been progressed regarding precancerous lesions of CCA, biliary disease with a pancreatic counterpart, and the relationship of CCA with cancer stem cells. Based on its anatomic location, CCA is classified as intrahepatic (iCCA), perihilar (pCCA), and distal (dCCA) CCA. CCA exhibits three growth patterns: mass-forming (MF), periductal infiltrating (IF), and intraductal growing (IG). The list of radiologic differential diagnosis is varied according to its gross morphology. For MF CCA, tumours with abundant fibrosis such as metastasis, sclerosing HCC, combined HCC-CC are important mimickers. PI CCA looks similar to sclerosing cholangitis. IG CCA has various morphology depending on tumour location and mucin production. Patients with CCA are usually treated with surgery. Because of its various morphology, infiltrative nature and underlying diseases, it can be a challenge to diagnose and stage CCA accurately. Although contrast-enhanced CT and MRI play an important role to assess resectability, a multidisciplinary approach is needed to accomplish best results.

Learning Objectives:
1. To become familiar with the different presentations of cholangiocarcinoma (including hilar and peripheral) tumours.
2. To learn about the role of imaging in staging the lesion and its limitations.
3. To understand the principle of surgical and non-surgical treatment.

A-156 16:33

B. Chronic cholangitis

M. Ronot; *Clichy/FR (maxime.ronot@bjn.aphp.fr)*

Chronic cholangitis are a group of diseases resulting in a chronic inflammation of the bile ducts, with variable causes and consequences. They can be roughly divided into two main groups: sclerosing cholangitis (SC) and secondary cholangitis. The first group includes primary and IgG4-related SC. They correspond to the biliary lesion of chronic extrahepatic/systemic diseases, respectively, inflammatory bowel diseases and IgG4-related disease. Secondary cholangitis is associated with specific identified causes: biliary ischaemia, trauma, chronic infections, iatrogeny, etc. The diagnosis of chronic cholangitis is difficult and relies on four pillars: laboratory tests, associated diseases and medical history, pathology, and of course imaging. The latter plays a central role. Magnetic resonance imaging including MR cholangiography is now considered as the best imaging technique. On imaging, the affected segments demonstrate irregular stenosis, focal, or diffuse circumferential thickening of the wall with contrast enhancement. Ultrasound can be useful to detect small biliary lesions and stones. It remains difficult to distinguish IgG4-SC from primary SC or bile duct malignancy based on imaging features alone. Careful analysis of cholangiograms can be helpful. Nevertheless, biopsy should be used in all patients with a suspicion of malignancy.

Learning Objectives:
1. To understand the appropriate technique for the non-invasive evaluation of bile ducts.
2. To become familiar with the main causes for chronic cholangitis, including primary sclerosing, autoimmune and ischaemic cholangitis.

A-157 17:01

C. Tough clinical cases

E.M. Merkle; *Basle/CH (emerkle@uhbs.ch)*

In this interactive session, various clinical cases that focused on the biliary system will be presented. Case presentations will include a wide range of pathologic entities, both benign and malignant. Images will be shown from various modalities including but not limited to percutaneous ultrasound, computed tomography, magnetic resonance imaging including magnetic resonance cholangiography and positron emission tomography. Case presentations are intended to represent typical clinical scenarios; as such information regarding the patient's history and physical exam will be shown first, followed by laboratory data. Subsequently, the audience will be asked to recommend the most appropriate imaging modality and to participate in solving these cases!

Learning Objectives:
1. To be able to define the most likely diagnosis facing an unknown case.
2. To understand the diagnostic strategy.

Author Disclosure:
E.M. Merkle: Advisory Board; Siemens Healthineers. Equipment Support Recipient; Siemens Healthineers. Research/Grant Support; Bayer, Bracco, Guerbet. Speaker; Siemens Healthineers.

16:00 - 17:30 **Room M 5**

E³ - ECR Master Class (Cardiac)

E³ 426

Assessment and lifelong follow-up of congenital heart disease

A-158 16:00

Chairman's introduction

L. Saba; *Cagliari/IT (lucasaba@tiscali.it)*

Congenital heart disease (CHD) identifies several cardiac and vasculature prenatal defects and CHD is the most common birth defect: in 2013, they were present in 34.3 million people globally. Many congenital heart defects can be diagnosed prenatally by foetal echocardiography when the woman is 18-24 weeks pregnant and thanks to the evolution of interventional and surgical treatment, the survival of newborns with CHD has improved dramatically over the past half century. A number of classification systems exist for CHD and to correctly identify these pathologies, it is mandatory a knowledge of the anatomy and pathophysiology because the broad spectrum of diseases ranges from small septal defects and minor valvar obstructions to complex single ventricle malformations. Sometimes CHD improves without treatment whereas other defects are so small that they do not require any treatment. However, most of the time CHD is serious and requires surgery and/or medications. A vital component to the multidisciplinary management of newborn with the CHD is adequate imaging of the heart and circulation. The development of those complementary non-invasive techniques has made decrease the need for invasive catheterization. CT, MRI and TTE have potentialities and pitfalls but allow obtaining a tailored imaging, fundamental to offer the best chances to CHD subjects. Although MRI is generally more flexible and appropriate for congenital imaging, it is not entirely free of limitations whereas CT is likely to become an increasingly important imaging technique for the CHD population, in part because of greater access to CT than MRI.

Session Objectives:
1. To enhance knowledge of anatomy and physiology of common congenital cardiac conditions as well as the surgical/interventional procedures used to treat them.
2. To discuss the appropriate use and performance/interpretation of non-invasive tests examining patients with CHD.

A-159 16:10

A. A primer: what do the most important anomalies look like?

O. Rompel; *Erlangen/DE (oliver.rompel@uk-erlangen.de)*

Congenital heart disease (CHD) has an incidence of 6-8 per 1,000 live births. CHD is a term for a variety of cardiac and vasculature prenatal defects. The broad spectrum of diseases ranges from small septal defects and minor valvar obstructions to complex single ventricle malformations. The concept of developmental “errors” helps us to explain, define and classify these inborn diseases. A common pathophysiological classification of CHD is based on the clinical consequence of structural defects on the physiology of blood circulation: CHD with increased pulmonary blood flow can be differentiated from CHD with decreased pulmonary flow, CHD with obstruction to blood progression and no septal defects and CHD so severe as to be incompatible with postnatal blood circulation. For diagnostic management of patients with CHD, knowledge of the underlying pathophysiology is essential. This is also true for the effects of catheter-based intervention or surgical repair on anatomical and haemodynamic changes. Physicians must be familiar with the complex terminology used in CHD to effectively communicate findings. Due to further development of interventional and surgical treatment concepts, the life expectancy of newborns with CHD has improved dramatically over the past decades. For instance, more and more patients with ventricular hypoplasia can nowadays be treated successfully, either by biventricular repair or refined functionally single ventricle palliation. Thus, an increasing number of adults with CHD can now be followed up in tertiary cardiac care centres.

Learning Objectives:
1. To get an overview on the spectrum of congenital heart disease (CHD), from the foetus and newborn through adults with congenital heart disease.
2. To explain the pathophysiology, manifestations, diagnosis and management of cyanotic, acyanotic and obstructive congenital cardiac anomalies.
3. To discuss the implications of cardiac anomalies on complexity and urgency of treatment indications.

A-160 16:30

B. CT for assessment and follow-up

J.-N. Dacher; *Rouen/FR (Jean-Nicolas.Dacher@chu-rouen.fr)*

The number of grown-ups requiring lifelong follow-up for congenital heart disease is increasing continuously due to the improvement of surgical and medical treatments. In this context, trans-thoracic echocardiography (TTE), MRI and CT appear complementary and help decrease the use of invasive angiography. Today, using the most recent CT equipment, it is possible to obtain high-resolution images of the heart and great vessels with minimal radiation and contrast medium doses. Prospective gating, low x-ray power and current intensity protocols, iterative reconstruction, limited field of views and number of scans all contribute to limit the radiation dose to a strict minimum. The advantages of CT match the MRI (and TTE) limitations, so that we believe that radiologists involved in one of both techniques should also practice the other one. The target organs of CT are small moving vessels such as coronary arteries (origin and course). The 2D and 3D CT depiction of pulmonary arteries, pulmonary veins and thoracic aorta is excellent. CT is very efficient in showing stented vessels or conduits. Finally, its capability to evaluate the lung (infection, pleural fluid, arterial venous malformation) and thoracic cage is unique. CT remains limited in cardiac functional information (ejection fraction, regurgitations and stenosis) that would require multiphase acquisition, e.g. retrospective gating involving significant dose. A series of illustrative examples will be shown.

Learning Objectives:

1. To learn how to decide which imaging modality is the most appropriate for which indication in CHD patients, and to recognise their advantages and limitations.
2. To integrate the most up-to-date CT imaging techniques for CHD patient management, including dose reduction strategies.
3. To be able to perform a complex CT protocol in CHD, and how to systematically read and evaluate CT imaging in CHD patients.

Author Disclosure:

J. Dacher: Equipment Support Recipient; GE HealthCare. Investigator; Shire. Speaker; GE, Siemens, Guerbet, Bayer.

A-161 16:50

C. MR imaging for assessment and follow-up

N. Schicchi; *Ancona/IT (schicchi.n@alice.it)*

The number of patients with congenital heart disease (CHD) is rapidly increasing in the adult population, mainly due to the improved long-term survival. Serial follow-up with cardiac magnetic resonance imaging (CMR) is very appealing due to its non-invasive nature. CMR exam is able to provide specific information about cardiac function, haemodynamics, anatomy and tissue characterization unlikely achievable by other diagnostic techniques. CMR in CHD plays a role both in early diagnosis and in post-operative follow-up. Black-blood T1-weighted sequences are used to acquire morphological information. Cine steady-state free precession sequences are mainly used to provide data about cardiac function and kinesis. Haemodynamic assessment is routinely performed using phase contrast sequences, which provide reliable information concerning vessel flow pattern, cardiac output and intracardiac shunts. Magnetic resonance angiography (MRA) and 3D coronary MRA of the whole thorax can provide detailed morphological information regarding great vessels and proximal coronary arteries. Presence of late gadolinium enhancement suggesting myocardial macroscopic fibrosis seems to play a prognostic and diagnostic role even in this field.

Learning Objectives:

1. To learn how to decide which imaging modality is the most appropriate for which indication in CHD patients, and to recognise their advantages and limitations.
2. To learn about the role of MRI in the diagnosis and planning of therapy of CHD in both paediatric patients and adults, in comparison and correlation to echocardiography.
3. To be able to perform a complex MRI protocol in CHD, and how to systematically read and evaluate MR imaging in CHD patients.

17:10

Panel discussion: How to best assess congenital anomalies?

Thursday, March 2

08:30 - 10:00 **Room A**

E³ - ECR Academies: Interactive Teaching Sessions for Young (and not so Young) Radiologists

E³ 521

Integrating diagnostic tools in breast imaging

A-162 08:30

A. Multimodality breast imaging

K. Kinkel; *Chêne-Bougeries/CH (karen.kinkel@grangettes.ch)*

The different tasks of breast imaging concern screening, characterization and staging breast cancer as well as diagnosing patients with symptomatic breasts. This lecture gives an overview of the respective place and complementarity of imaging modalities for a variety of clinical situations taking into account evidence-based medical recommendation and recent advances in breast imaging. Case-based teaching covers choice of imaging modalities for breast pain, breast mass, nipple discharge, positive screening mammography, multiple breast imaging abnormalities, complex lesion characterization and known breast cancer staging. The information provided by imaging requires adequate ranking and organization into a final report with a final risk of malignity translated into a BIRADs category. Multi-modality imaging of the breast takes advantage of the strength of each imaging modality to allow an optimal diagnostic procedure. Examples of a variety of breast problems are documented using state-of-the-art imaging techniques and reporting.

Learning Objectives:

1. To choose the adequate imaging modality according to the clinical question taking into account the performance and the cost of ultrasound, mammography and MRI.
2. To combine information provided by different imaging modalities into a final report with special focus on mammography/tomosynthesis and ultrasound.
3. To update your BI-RADS knowledge.

A-163 09:15

B. Multiparametric breast MRI

J. Camps Herrero; *Valencia/ES (juliacamps@gmail.com)*

Breast MRI's main sequence is dynamic contrast-enhanced T1-weighted 3D (DCE-MRI), but there are other MRI techniques that can add very useful information due to the fact that they convey different functional information based on varying approaches to the biological hallmarks governing breast cancer. Angiogenesis is the basis for DCE-MRI, as the newly formed blood vessels show endothelial gaps that allow for the passage of gadolinium-based contrast media thus making it possible for tumours to enhance earlier than normal tissue. Diffusion-weighted imaging reflects the thermally induced movement of water molecules in the tissues and through the ADC or apparent diffusion coefficient is able to improve specificity of DCE-MRI in the characterisation of breast lesions, as well as response evaluation to neoadjuvant chemotherapy treatment. DWI and its 3D counterpart, diffusion tensor imaging or DTI, are breakthrough techniques in breast MRI characterisation, response evaluation and also in breast cancer screening. Spectroscopy MRI assesses elevated membrane metabolism through analysis of altered phospholipid metabolites; this technique remains, however, subject to cutting-edge research.

Learning Objectives:

1. To learn about the different technical and clinical aspects of the MRI sequences that are used currently in breast imaging.
2. To know how to unify the information thereof provided in everyday clinical practice.

Author Disclosure:

J. Camps Herrero: Advisory Board; Bayer.

08:30 - 10:00 **Room B**

E³ - ECR Master Class (Abdominal Viscera)

E³ 526a

The obesity epidemic: what is radiology's role?

A-164 08:30

Chairman's introduction

E.M. Merkle; *Basle/CH (emerkle@uhbs.ch)*

In the chairman's introduction, the history of the obesity epidemic in the western world will be briefly described followed by outlining the evolution of the various invasive treatment options. These main surgical procedures may cause specific complications with radiology playing a key role in the detection and management of these.

Session Objectives:

1. To learn about the obesity epidemic and the relevance of fat disorders for the Western world.
2. To understand the methodical and diagnostic challenges when imaging obese patients including postoperative conditions after bariatric surgery.
3. To appreciate the role of radiology in abdominal fat quantification.

Author Disclosure:

E.M. Merkle: Advisory Board; Siemens Healthineers. Equipment Support Recipient; Siemens Healthineers. Research/Grant Support; Bayer, Bracco, Guerbet.

A-165 08:36

A. The metabolic syndrome: what the radiologist needs to understand

H.J. Lamb; *Leiden/NL (h.j.lamb@lumc.nl)*

Recently, the concept of the 'metabolic syndrome' was introduced, which is a constellation of risk factors of metabolic origin that are accompanied by increased risk for cardiovascular disease and type 2 diabetes. The two major underlying risk factors for the metabolic syndrome are obesity and insulin resistance. Metabolic imaging and total body fat distribution may be used to determine if obese subjects are an increased risk for developing type 2 diabetes. In this situation, more intensive lifestyle intervention can be advised and monitored. MR techniques offer unique possibilities for monitoring effects of new dietary strategies. Whole body imaging may also allow one to study interaction between different organs. For example, initial results show that high liver triglyceride content in type 2 diabetes is associated with decreased myocardial perfusion, glucose uptake and high-energy phosphate metabolism, in conjunction with impaired whole body insulin sensitivity. Multi-organ imaging in a single patient opens interesting possibilities to study interaction between key organs involved in the metabolic syndrome, such as liver, pancreas, kidney and heart, in relation to vascular morphology and function. In summary, metabolic MR imaging and total body fat distribution may be used in the future for risk assessment and personalised medicine in patients with the metabolic syndrome. Furthermore, multi-organ MR imaging is promising for evaluation of interaction between different organs in the metabolic syndrome.

Learning Objectives:

1. To learn about the causes and consequences of the metabolic syndrome.
2. To become familiar with the abdominal manifestations of the metabolic syndrome.
3. To understand the role of radiology in surveillance of the population at risk.

A-166 08:57

B. Imaging the obese patient presenting as an emergency: challenges and solutions

M. Rengo; *Latina/IT (marco.rengo@gmail.com)*

Laparoscopic sleeve gastrectomy, Roux-en-Y gastric bypass and laparoscopic gastric banding are the dominant bariatric procedures. All these techniques may be associated with short- or long-term complications which can become an emergency. We will discuss the appearance of common and uncommon complications associated with the bariatric procedures on MDCT and fluoroscopy. We will discuss the technical features of imaging modalities and the indications according to the clinical setting.

Learning Objectives:

1. To understand the most common abdominal causes leading to an emergency presentation.
2. To become familiar with the specific technical difficulties and challenges that obese patients present for the imaging department in an emergency situation.
3. To learn about tips and tricks in order to optimally image the obese patient in this situation.

A-167 09:18

C. Evidence and recommendations for quantification of hepatic and visceral fat

C.B. Sirlin; *San Diego, CA/US (csirlin@ucsd.edu)*

Obesity is associated with the accumulation of excess fat in solid organs such as liver and in adipose tissues such as visceral adipose tissue. Quantification of hepatic and visceral fat accumulation are increasingly important for research and it is anticipated that they will become important for clinical care in the years to come. This lecture reviews confounder-corrected chemical shift-encoded MRI methods to quantify the proton density fat fraction (PDFF) as a marker of hepatic fat accumulation as well as semi-automated MRI-based segmentation methods to quantify the volume of visceral abdominal tissue.

Learning Objectives:

1. To understand the current evidence for the role of imaging in the quantification of hepatic and visceral fat.
2. To become familiar with the various techniques and recommendations used for fat quantification.
3. To learn about future directions for accurate fat quantification.

Author Disclosure:

C.B. Sirlin: Advisory Board; Bracco, Virtual Scopics, Pfizer, Tobira, Guerbet. Investigator; Alexion, AstraZeneca, Bioclinica, BMS, Fibrogen, Galmed, Genentech, Genzyme, Gilead, Icon, Intercept, Isis, Janssen, NuSirt, Perspectum, Pfizer, Profil, Sanofi, Shire, Synageva, Tobira, Takeda. Research/Grant Support; GE, Siemens, Guerbet.

A-168 09:39

D. Bariatric surgery: normal postoperative imaging appearances and spectrum of complications

A. Blachar; *Tel Aviv/IL (ablachar@gmail.com)*

Recently, there has been a tremendous increase in the utilization of laparoscopic surgery to control morbid obesity that is very common and increasing in incidence in Western nations. Bariatric restrictive procedures include reduction of the gastric capacity causing an early sensation of fullness after ingestion of small quantities of food. In bariatric combination procedures, a part of the digestive tract is bypassed, thus causing decreased absorption of nutrients and calories. In this lecture, we discuss the most common laparoscopic bariatric procedures: Roux-en-Y gastric bypass, gastric sleeve surgery, both combination procedures and adjustable silastic ring gastric banding, a restrictive procedure. Imaging plays an important role in the evaluation and management of patients before and after bariatric surgery. Imaging findings relating to these bariatric procedures will be discussed, focusing on the role of fluoroscopy and CT in evaluation of the normal post-operative anatomy and gastrointestinal complications.

Learning Objectives:

1. To become familiar with the common bariatric surgical procedures.
2. To learn about the normal postoperative anatomy and imaging appearances.
3. To understand the role of imaging for the assessment of both, early and late postoperative complications.

08:30 - 10:00 **Room C**

State of the Art Symposium

SA 5

Lung cancer screening: past, present, future

A-169 08:30

Chairman's introduction

L. Bonomo; *Rome/IT (lorenzo.bonomo@unicatt.it)*

This state-of-the-art symposium (SA) aims to inform the audience about the real state of the art of the lung cancer screening. The session includes three lecturers each of whom will focus in some specific aspects of the lung cancer screening. The design, conduct, results and limitations of the largest randomised trial, the NLST, will be discussed by the first lecturer. The results and the latest insights from European trials will be presented by the second lecturer. The opportunities for future screening research will be discussed by the third lecturer. The panel discussion will focus on how to implement lung cancer screening in Europe.

Session Objective:

1. To learn about the results of European and international lung cancer screening and to appreciate opportunities for future screening research.

A-170 08:35

What did we know: NLST and previous trials

S. Diederich; *Düsseldorf/DE (stefan.diederich@vkkd-kliniken.de)*

Radiologic examinations have been used since the 1960s to identify asymptomatic lung cancers in at-risk populations. Chest radiography alone or in combination with sputum cytology was used in several randomized trials and was able to detect more cases of lung and more early cancer stages in the study groups compared to the control groups with no chest radiography. However, no study was able to demonstrate mortality reduction from chest radiography screening. In the 1990s, unenhanced low radiation dose computed tomography was used in feasibility studies to screen for asymptomatic lung cancer in risk populations, mainly active or ex-smokers. Several non-randomized trials were able to demonstrate that low-dose CT had a much improved sensitivity for asymptomatic lung cancers compared to chest radiography with an acceptable rate of invasive procedures for false-positive findings, although the rate of false-positive findings was high.The first randomized controlled trial of low-dose CT versus chest radiography screening in active or (maximum 15 years) ex-smoker aged 55 -74 years with a minimum of 30 pack years of cigarette smoking in the US (National Lung Screening Trial: NLST) to publish results on mortality reduction showed a 20% reduction of mortality from lung cancer.

Learning Objectives:

1. To understand the design, conduct, results and limitations of the randomised NLST trial.
2. To learn about the results of previous trials in terms of mortality reduction.
3. To understand the results of feasibility studies in terms of prevalence and incidence of screening detected lung cancer.

A-171 09:00

What do we know: latest insights from European trials, modelling studies and current screening programmes

M. Prokop; *Nijmegen/NL*

"no abstract submitted"

Learning Objectives:

1. To learn how to select participants for maximum yield of screening.
2. To understand how to optimise reading and nodule management.
3. To learn how to improve patient outcome by quality control of screening and treatment.

A-172 09:25

What don't we know: opportunities for future research

A. Devaraj; *London/UK*

Opportunities for future research for lung cancer screening with CT will be guided by the need to answer specific questions related to implementation. Many of these questions are relevant to radiology. How frequently should participants be screened? How can nodule follow-up or biopsy be minimised without impacting on cancer diagnosis and patient outcomes? How can the reading process be optimized? Since many lung cancer screening trials are already completed or nearing completion, the methods by which these areas could be addressed and their challenges will be discussed.

Learning Objectives:

1. To understand the limitations of existing screening protocols.
2. To learn about opportunities for optimisation of future screening protocols.
3. To appreciate questions, not answered by current trials, for future screening research.

Author Disclosure:

A. Devaraj: Advisory Board; GrailBio.

09:50

Panel discussion: How to implement lung cancer screening in Europe

08:30 - 10:00 **Room X**

EIBIR Session

EIBIR 1

VPH-DARE@IT: Novel biomarkers and platforms for earlier dementia diagnosis

A-173 08:30

Introduction

Z.A. Taylor; *Sheffield/UK (z.a.taylor@sheffield.ac.uk)*

Dementia, in all its forms, is recognised as one of the key healthcare problems facing Western societies, especially as populations age, and concomitant economic and societal costs of the condition expand. Enabling more objective, earlier, predictive and individualised diagnosis and prognosis of dementias will support health systems worldwide to cope with this burden. The VPH-DARE@IT integrated project aims at precisely this. To this end, it pursues, first, a unique programme of biomarker discovery founded on a combination of patient-specific mechanistic and phenomenological models of disease. Second, it supports development of two new IT infrastructures aimed at clinical research and clinical decision support, respectively, which facilitate the complete pipeline from biomarker discovery and validation, to clinical deployment and evaluation. In this session, we will present latest developments in these areas.

Session Objective:

1. To learn about the VPH-DARE@IT project and the use of its results.

A-174 08:40

Patient care platform

M. van Gils; *Tampere/FI (Mark.vanGils@vtt.fi)*

Diagnosing complex diseases, such as dementia, is a challenging task. Clinicians need to combine in their minds a multitude of data from different sources, to consider a high number of different possible reasons behind clinical symptoms, to take into account the background information based on the precision medicine concepts, and finally to apply existing economic constraints. This complexity easily leads to suboptimal decision making, even with profound clinical expertise available. Clinical decision support systems (CDSS) based on the principles of data-driven medicine hold potential for making the process more quantitative and objective. In VPH-DARE@IT, the Patient Care Platform (PCP) implements a CDSS integrating heterogeneous biomarkers from medical images, neuropsychological tests and other measurements, and helping to form a holistic view of the patient's status based on the principles of data-driven medicine. The PCP uses a data-driven approach where large databases of previously diagnosed patients are used for building models of several dementing diseases, including Alzheimer's disease (AD), frontotemporal dementia (FTD), vascular dementia (VaD) and dementia with Lewy bodies (LBD). When a new patient arrives at a clinic, studies and tests are done, after which all available patient data are contrasted to the disease models, revealing the most likely reasons for dementia. The software architecture enables the CDSS to access heterogeneous patient data from several data sources. Furthermore, it communicates with the VPH-DARE@IT Clinical Research Platform to allow incorporation of novel biomarkers into the decision making.

Learning Objectives:

1. To learn about dementia patient's needs.
2. To understand the VPH-DARE@IT patient care platform.

A-175 09:00

Clinical research platform

S. Varma; *Sheffield/UK (susheel.varma@sheffield.ac.uk)*

This presentation will inform the audience about the VPH-DARE@IT project that will deliver the first patient-specific predictive models for early differential diagnosis of dementias and their evolution using an integrative and validated multi-scale modelling platform for biomedical research and clinical decision support, underpinned by a set of unique databases and modelling paradigms. This platform will tackle the early and differential diagnosis of dementias using a combination of mechanistic and phenomenological models of the ageing brain, taking into account the environmental context.The objectives of the project are: deliver a systematic, multi-factorial and multi-scale modelling approach to understanding dementia, explore the lifestyle and environmental factors that predispose individuals to the development of dementia, deliver more objective and accurate differential diagnoses than those currently available in Europe, shorten the current average time-lapse between the onset of cognitive and memory deficits and its specific clinical diagnosis. We will present the VPH-DARE@IT clinical research platform that has integrated existing datasets, tools and workflows focused on dementia research, providing a single framework where new generation workflows will be created focusing on multi-scale patient-specific treatment for dementia. By means of this platform, novel modelling strategies will be developed and disseminated to unravel the brain ageing processes and progression of dementia through high-throughput analysis of clinical, biological and environmental data.

Learning Objectives:

1. To learn about the setup of a research platform.
2. To understand the data in the VPH-DARE@IT clinical research platform.

A-176 09:20

Mechanistic model-based biomarkers

Y. Ventikos; *London/UK (y.ventikos@ucl.ac.uk)*

Chronic cerebral hypoperfusion has been identified as a possible initiator of neurodegenerative processes leading to dementia. Lifestyle and environmental factors (LEFs), such as smoking, have an effect on the vascular system physiology. Pathophysiological changes in this system are, therefore, going to have an effect on the functioning of the brain. We propose to relate LEFs that act via the cardiovascular system and that have been shown to associate with AD. These LEFs are garnered from the preliminary data of a cross-sectional case-control study (Lido study). This multi-modal dataset is used to drive a patient-specific circulation model that provides predictions of CBF. The additional mechanistic components include a poroelasticity model used to acquire 4D maps of perfusion, clearance and ICP, in addition to a high-throughput imaging pipeline capable of providing anisotropic tissue permeability to capture the patterns of interstitial flow in addition to the parenchymal tissue and cerebroventricular representations required by the poroelasticity model. Preliminary simulation results indicate that predisposition to cognitive loss may be linked to modifiable risk factors, such as those witnessed relating to ICP, perfusion and clearance. Based on the preliminary data obtained from the Lido study, the CBF parameters that were found to be associated with MCI status were: reduced total CBF, reduced total perfusion (in women), increased APP (in very old subjects) and increased PI. The multiscale model of brain fluid transport developed in VPH-DARE@IT will be used to account for the long-term response to hypothetical LEF patterns and timings.

Learning Objectives:

1. To learn about mechanistic model-based biomarkers for dementia.
2. To understand the biomarkers used in the VPH-DARE@IT project.

A-177 09:40

Phenomenological model-based biomarkers

S. Klein; *Rotterdam/NL (s.klein@erasmusmc.nl)*

Both normal ageing and neurodegenerative disorders such as Alzheimer's disease cause morphological changes (i.e. atrophy) in the brain, which can be visualised using magnetic resonance imaging (MRI). However, it is often difficult to distinguish normal ageing from neurodegenerative disorders by visual inspection of these images. In the VPH-DARE@IT project, we have developed a novel method for distinguishing between normal and abnormal brain morphology, based on a quantitative phenomenological modelling approach. A comprehensive spatiotemporal model of normal brain morphology is derived, in a data-driven and hypothesis-free fashion, from MRI brain data collected in a large-scale population study (the Rotterdam scan study). Based on this model, percentile curves are constructed that characterise the distribution of brain morphology in the general population as a function of age. These percentile curves serve as reference charts to which patient data can be compared. Experiments using data of the Alzheimer's disease neuroimaging initiative (ADNI) show that the model generalises across study populations, and that it could be used to quantify a patient's brain health.

Learning Objectives:

1. To learn about phenomenological model-based biomarkers for dementia.
2. To understand the biomarkers used in the VPH-DARE@IT project.

08:30 - 9:30 **Room Z**

ESR Working Group on Ultrasound

WG 3

Minimising the risk of cross infection: how to keep patients safe in ultrasound

A-178 08:30

Chairman's introduction

M. Claudon; *Vandoeuvre-les-Nancy/FR (m.claudon@chu-nancy.fr)*

Ultrasound (US) is considered one of the safest imaging modalities. However, a survey undertaken by the US working group of the European Society of Radiology (ESR) to know about potential risk of cross-infection showed large diversity in protocols and practice throughout European countries. This leads to present detailed results and discuss how to establish currently applied infection control measures in US and highlight the importance of good medical practice in this area.

Session Objectives:

1. To understand how the issue of infection transmission risks in ultrasound was raised and what the US WG has done to investigate and address concerns.
2. To gain an overview of current infection control practice in Europe.
3. To become familiar with best practice recommendations to prevent cross transmission of infection in ultrasound.
4. To understand different viewpoints of practitioners, patients as well as the industry.

Author Disclosure:

M. Claudon: Speaker; Philips Ultrasound.

A-179 08:35

Risk of cross transmission of infection in ultrasound: current European practice (ESR survey results) and best practice recommendations prepared by the ESR US WG

C. Nyhsen; *Sunderland/UK (nyhsenc@doctors.org.uk)*

Ultrasound is generally considered one of the safest diagnostic modalities available. Causing significant harm to imaged patients by performing ultrasound is not anticipated by professionals or patients. However, risks of infection transmission through ultrasound have been highlighted increasingly in the last years and patient groups are becoming more concerned. Current European infection prevention standards in ultrasound were evaluated by a survey of the ESR ultrasound working group which has just been published, showing a very wide range of practice. Survey results highlight the need to raise awareness of the risk of infection transmission through ultrasound probes/gel and the need for stricter guidance to safeguard patients. The ultrasound working group, in close collaboration with expert microbiologists, have, therefore, worked on a consensus statement on best practice, which will also be presented in this talk.

Learning Objectives:

1. To gain an overview of the current infection control practice in Europe by presenting the main results of the ESR US WG survey undertaken.
2. To become familiar with the issued US WG recommendations for best practice, which are aimed to minimise the risk of cross infection.

A-180 08:50

Comments from the ESR Patient Advisory Group regarding infection control practice in Europe

J. Birch; *Poole/UK (judy_b@dsl.pipex.com)*

This presentation will assess patient knowledge and concerns relating to hygiene in ultrasound procedures. Current practice in several countries regarding the level of disinfection and various methods of ultrasound probe decontamination in particular will be discussed. I will also refer to anecdotal information regarding personal experience of ultrasound examinations and hygiene procedures.

Learning Objective:

1. To understand the patient's perspective regarding cross contamination risks in ultrasound.

A-181 09:00

Comments from industry representation

N. Denjoy; *Brussels/BE*

"No abstract submitted."

Learning Objective:

1. To understand the industry's perspective.

09:10

Panel discussion: How can safer practice be achieved?

08:30 - 10:00 **Room O**

Paediatric

RC 512

Paediatric musculoskeletal imaging

Moderator:
A.C. Offiah; Sheffield/UK

A-182 08:30

A. The occurrence of bone marrow oedema, joint fluid, ganglion cysts and erosion like features in the normal paediatric wrist

D. Avenarius; *Tromsø/NO (Derk.Avenarius@unn.no)*

Normal variations in the amount of joint fluid, ganglion cysts, bone marrow oedema, and bony depressions that resemble erosions are frequent in the wrists of children. The results of a follow-up of a healthy cohort aged 6-17 will be presented. The cohort was examined twice with MR of the wrist, and the second time also with a cartilage sequence for better visualization of the bony depressions. Knowledge of these normal variations is important because they can resemble disease.

Learning Objectives:

1. To discuss MRI protocols for the paediatric wrist.
2. To give an overview of normal development and variations in MR anatomy and signal patterns.
3. To provide an understanding of features indicative of pathology.

A-183 09:00

B. MRI of the temporomandibular joints: findings that can mimic arthritis

T. von Kalle; *Stuttgart/DE (t.vonkalle@klinikum-stuttgart.de)*

Arthritis of the temporomandibular joint (TMJ) is common in children and adolescents with juvenile idiopathic arthritis (JIA). Early treatment is warranted to prevent severe growth disturbances and joint deformities. As TMJ arthritis is often clinically silent, MRI with contrast-enhancement has been considered to be the most reliable method to assess signs of inflammation. To reliably guide therapeutic decisions and monitor outcomes it would be of utmost importance to clearly define the MR characteristics of a normal TMJ as a basis for the assessment of minor pathologies. However, similar to other small joints in children, we are just beginning to understand its developmental, physiological and anatomical characteristics as well as its reaction to inflammatory diseases and their treatment. Recent studies on normal TMJ in children have revealed age-dependent changes in shape and angulation of the mandibular condyle as well as typical time-intensity curves of contrast-enhancement in the soft joint tissue and the condyle. To date, the differentiation between normal synovial findings and mild signs of synovitis remains challenging. This lecture presents typical MR images of normal and inflamed TMJs in children and adolescents, including age-dependent anatomical variations. It discusses the available data on possible cutoffs between normality and pathology, the impact of the temporal dynamics of contrast enhancement, and presents findings that can mimic arthritis. It summarizes the minimum requirements of image quality and spatial resolution, the best image orientation, as well as the advantages of fat suppression and subtraction analysis in contrast-enhanced imaging.

Learning Objectives:

1. To discuss MRI protocols for imaging of the temporomandibular joints (TMJ).
2. To give an overview of MR imaging finding in arthritis of the TMJ.
3. To highlight the major differential diagnoses of TMJ arthritis and its MR imaging characteristics.

A-184 09:30

C. Skeletal trauma in children

I. Barber; *Esplugues de Llobregat/ES (ibarber@hsjdbcn.org)*

Paediatric fracture patterns, mechanisms of Injury and complications are different to those in adults. Differences are related to the dynamic state of a growing skeleton and its decreased mechanical strength. Imaging skeletal trauma is based on orthogonal radiographs but we will also discuss the role of other imaging techniques such as US, CT and MR imaging. Differential diagnosis with normal developmental variant and tumours, and recognition of an underlying metabolic syndrome are also important in children. Finally, complications of paediatric fractures will also be reviewed including growth arrest, malunion, nonunion, synostosis and avascular necrosis. We will try to give a rationale for diagnostic imaging based on the clinical and surgical demand.

Learning Objectives:

1. To become familiar with the types of injuries seen in children.
2. To understand the basic mechanisms.
3. To learn about the diagnostic imaging approach.

08:30 - 10:00 **Room N**

Cardiac

RC 503

Imaging of cardiac valves: new trends

Moderator:
H. Alkadhi; Zurich/CH

A-185 08:30

A. Echocardiography remains the reference technique

F. Knebel; *Berlin/DE (fabian.knebel@charite.de)*

Echocardiography is the most widely used technology to assess the valves. The talk will focus on the current guidelines and standards on the assessment of valvular heart disease by echocardiography. The transthoracic and transoesophageal techniques will be presented. Furthermore, there will be critical discussion of the role of other imaging technologies (MRI and CT) in this field.

Learning Objectives:

1. To learn about state-of-the-art echo techniques to evaluate cardiac valves.
2. To provide a practical approach to assessing valve pathology based on echocardiography.
3. To become familiar with the role of echo in the diagnosis, clinical management and prognosis.

A-186 09:00

B. MRI is the best comprehensive approach

M. Francone; *Rome/IT (marco.francone@uniroma1.it)*

Valvular heart disease has a direct impact on cardiac morphology and haemodynamics requiring comprehensive morphological and functional imaging for its assessment, which includes the evaluation of anatomy (leaflets, chordae tendineae and papillary muscles) and quantification of trans-valvular flow (i.e. degree of stenosis and regurgitation). Cardiac magnetic resonance (CMR) represents an ideal, non-invasive diagnostic tool on this regard, which has emerged as an alternative or complementary modality to echocardiography providing insight into the pathophysiology of the disease including the consequences of a valvular lesion, from the effects of ventricular volume or pressure overload to alterations in systolic function. A further unique strength of the exam is its ability to characterise myocardial tissue changes, which has further expanded with the recent implementation of T1/T2 mapping techniques providing potentially relevant information regarding the amount and distribution of replacement fibrosis in valvular pathology. CMR is also indicated to follow-up post-operative patients and as a reference tool for planning before TAVI procedures with some relevant advantages towards MDCT. Present lecture will overview principles of CMR technique and recommended acquisition protocol with particular emphasis on phase-contrast pulse sequences analysing its respective strength and weaknesses. Pathophysiology with common and less common imaging findings in left- and right-sided valve disease will also be presented and discussed.

Learning Objectives:

1. To learn about the role of MRI in diagnosis and evaluation of valvular disease.
2. To become familiar with state-of-the-art MRI techniques to evaluate valvular disease.
3. To learn about typical imaging findings in MRI with impact on clinical management.

Author Disclosure:
M. Francone: Speaker; Bracco Medical Imaging Invited Speaker.

A-187 09:30

C. Does CT have a role in diagnosing valvular disease?

G. Feuchtner; *Innsbruck/AT (Gudrun.Feuchtner@i-med.ac.at)*

Imaging of cardiac valves by computed tomography is an emerging topic. Technical development has created new horizons in the clinical triage of patients and changed old-fashioned paradigms. Therefore, the aim of of this course is to learn "how-to" evaluate cardiac valves and prosthesis by cardiac computed tomography, including the entire spectrum of valvular disease and prosthesis malfunction. Clinical implementations based on current scientific evidence and AHA /ESC guidelines will be discussed. Multimodality imaging will be highlighted.

Learning Objectives:

1. To learn about state-of-the-art CT techniques to evaluate cardiac valves at low dose.
2. To review CT appearance of the most common conditions causing valvular disease.
3. To become familiar with the role of CT in the diagnosis and clinical management.

08:30 - 10:00 **Studio 2017**

New Horizons Session

NH 5

Hyperpolarised MRI: imaging tissue metabolism in real time

A-188 08:30

Chairman's introduction

J.M. Gomori; *Jerusalem/IL (moshe.gomori@mail.huji.ac.il)*

Conventional MRI can access only 10-4-10-5 of the potential nuclear magnetic polarisation. Hyperpolarisation can achieve greater than 10% polarisation, i.e. more than 10,000 increase in polarisation and MRI signal of atoms such as 13C, 15N, 3He and 129Xe. This hyperpolarisation is achieved by transfer of polarisation from: polarised laser light, polarised supercooled electrons or polarised parahydrogen. Its short in-vivo T1 is usually much less than a minute. Since the hyperpolarisation is achieved outside the body, it must be quickly injected or inhaled and rapidly imaged with sequences adapted to optimal utilisation of the non-renewable nuclear magnetisation. Despite the hyperpolarisation, the signal is still relatively low, and large, usually non-physiologic, doses are required for imaging. In SNR it cannot compete with PET which has picomolar sensitivity. However, PET is not spectroscopic, i.e. it is not sensitive to the chemical bonds of the reporter atom. PET also has a much lower temporal resolution and does not have available the rich family of MRI sequences that can probe diffusion, motion, etc. Therefore, the promise and uniqueness of hyperpolarised MRI is in metabolic and physiologic quantitation and imaging. In our New Horizon session, some of the leading experts in the field will present the current status and research on applications of hyperpolarised MRI. We will finish off with a panel discussion and speculation on the future of hyperpolarised MRI.

Session Objectives:

1. To understand the basic principles of hyperpolarisation (how is it achieved, how long does it last, and how does it compare to PET).
2. To present clinical and preclinical applications of hyperpolarisation.
3. To explore potential future applications of hyperpolarisation.

A-189 08:35

Hyperpolarised MRI in oncology

F.A. Gallagher; *Cambridge/UK (fag1000@cam.ac.uk)*

There is increasing evidence to support a role for metabolism in tumour development, for example, deregulation of cellular energetics is now considered to be one of the key hallmarks of cancer. Changes in tumour metabolism over time are now known to be early biomarkers of successful response to chemotherapy and radiotherapy. There are a number of imaging methods that have been used to probe cancer metabolism: the most widely

available is 18F-fluorodeoxyglucose (FDG), an analogue of glucose, used in PET. Hyperpolarised carbon-13 MRI (13C-MRI) is an emerging molecular imaging technique for studying cellular metabolism, particularly in the field of oncology. This method allows non-invasive measurements of tissue metabolism in real time. To date, the most promising probe used in conjunction with hyperpolarised MRI has been 13C-labelled pyruvate: pyruvate is metabolised into lactate in normal tissue in the absence of oxygen, but in tumours this occurs very rapidly even in the presence of oxygen. Results from many animal models have shown that there is a reduction in the metabolism of pyruvate following successful treatment with chemotherapy. Tumour lactate labelling has also been shown to correlate with the grade of some tumour types. There are now a small number of sites performing human hyperpolarised carbon-13 MRI imaging. This talk will discuss the progress that has been made in this field within the area of oncology and potential clinical applications.

Learning Objectives:

1. To explore the role of metabolism in cancer development.
2. To understand how these changes in metabolism can be exploited using hyperpolarised 13C-pyruvate.
3. To review the current evidence for hyperpolarised carbon-13 imaging in oncology.
4. To understand potential clinical applications for hyperpolarised carbon-13 imaging.
5. To consider the role of new hyperpolarised molecules in oncology.

Author Disclosure:

F.A. Gallagher: Grant Recipient; GSK, GE Healthcare.

A-190 08:52

Hyperpolarised MRI in cardiology

A. Comment; *Lausanne/CH (arnaud.comment@epfl.ch)*

The tremendous polarization enhancement afforded by dissolution dynamic nuclear polarization (DNP) can be taken advantage of to perform molecular and metabolic imaging. Following the injection of molecules that are hyperpolarized via dissolution DNP, real-time measurements of their biodistribution and metabolic conversion can be recorded. This technology, therefore, provides a unique and invaluable tool for probing cellular metabolism *in vivo* in a noninvasive manner. It gives the opportunity to follow and evaluate disease progression and treatment response without requiring *ex vivo* destructive tissue assays. Five sites across the globe are currently performing human studies using hyperpolarized ^{13}C-pyruvate and several other institutions are on the brink of being ready to inject their first patients. One of the most promising fields of application of this technology is cardiology. Cardiac dysfunction is often associated with a shift in substrate preference for ATP production and hyperpolarized ^{13}C magnetic resonance has the unique ability to detect real-time metabolic changes *in vivo* due to its high sensitivity and specificity. Several proposed methods for assessing metabolic flux through different enzymatic pathways will be presented. It will be shown how hyperpolarized ^{13}C magnetic resonance enables mechanistic studies of the changing myocardial energetics often associated with disease.

Learning Objectives:

1. To become familiar with the principles of hyperpolarised MRI.
2. To understand the key parameters required to integrate a hyperpolariser into a MRI facility.
3. To learn about the cardiac metabolic pathways that can be probed by hyperpolarised MR.

Author Disclosure:

A. Comment: Employee; General Electric Healthcare. Research/Grant Support; ERC Consolidator grant ASSIMILES.

A-191 09:09

Hyperpolarised MRI in respirology

J. Vogel-Claussen; *Hannover/DE (vogel-claussen.jens@mh-hannover.de)*

In the last decade, functional imaging of the lungs using hyperpolarized noble gases has entered the clinical stage. Both helium (3He) and xenon (129Xe) gas have been thoroughly investigated for their ability to assess both the global and regional patterns of lung ventilation. With advances in polarizer technology and the current transition towards the widely available 129Xe gas, this method is ready for translation to the clinic. Also advantages and disadvantages of hyperpolarized gas functional lung imaging are highlighted and compared to MRI techniques for regional ventilation quantification without the need for hyperpolarization such as 19F MRI and Fourier decomposition ventilation MRI.

Learning Objectives:

1. To learn about the promises and challenges to build a hyperpolarised gas enhanced lung imaging programme.
2. To compare hyperpolarised gas enhanced lung MRI with emerging multinuclear functional lung MRI techniques without the need for hyperpolarised gas.

Author Disclosure:

J. Vogel-Claussen: Advisory Board; Boehringer Ingelheim, Novartis,. Research/Grant Support; Siemens. Speaker; Bayer, Siemens.

A-192 09:26

Available and potential hyperpolarised molecular targets

R. Katz-Brull; *Jerusalem/IL (rkb@hadassah.org.il)*

The dissolution-dynamic nuclear polarization technology had revolutionized the way small molecules can be imaged and their chemical evolution monitored, in physiologically relevant doses, by magnetic resonance imaging and spectroscopy. In this presentation, we will review several molecules that have proven useful as such molecular imaging probes. The specific stable isotopes with which these molecules were labelled will be reviewed (13C, 15N, 2H). The basis for these labelling strategies will be explained, predominantly the effects on MR visibility and T1. Naturally abundant nuclei such as protons and yttrium that are useful for hyperpolarized MRI will also be introduced. The main biochemical pathways that can be followed with hyperpolarized MRI and spectroscopy of these molecular imaging probes will be reviewed in the context of the potential emerging applications for hyperpolarized MRI and spectroscopy.

Learning Objectives:

1. To get an overview of the many targets available for hyperpolarised molecular targets.
2. To understand the basic chemical properties of hyperpolarised MRI molecular imaging probes.
3. To understand the role of stable-isotopes in hyperpolarised MRI.
4. To understand the biochemical processes that can be imaged with hyperpolarised MRI.

09:43

Panel discussion: Is hyperpolarisation worth all the hype?

08:30 - 10:00 **Room L 8**

ESR Research Committee Session

A few examples of European structures for imaging research

A-193 08:30

Chairman's introduction

O. Clément; *Paris/FR*

Session Objectives:

1. To explain the different research activities of ESR.
2. To learn how to set up a research project with EIBIR.
3. To learn how to organise research in an imaging department.
4. To learn how to use imaging biomarkers in clinical studies.

A-194 08:40

How EIBIR can help to prepare and manage a H2020 project

G.P. Krestin; *Rotterdam/NL*

With decreasing national R&D budgets and a substantial increase of the European budget for research, the new framework program Horizon 2020 became an attractive source for funding for many researchers in Europe. However, the competition is fierce and success rates around 3% are discouraging many scientists to engage into a complicated, time-consuming application process with unsecure outcomes. The European Institute for Biomedical Imaging Research (EIBIR) has developed a track record of successful services for imaging scientists engaging into the adventure of submitting a grant application within the Horizon 2020 funding scheme. The European Institute for Biomedical Imaging Research is a non-profit limited liability company that was founded in 2006 by the European Society of Radiology (ESR), dedicated to the coordination of research. EIBIR aims to deliver services to scientists involved in biomedical imaging research by fostering multidisciplinary collaboration. The platform supports research networking activities and plays a key role in spreading good practice, promoting common initiatives and interoperability in the field of biomedical imaging research. The mission of EIBIR is to coordinate research in, and innovation of, biomedical imaging technologies within Europe and support the dissemination of knowledge with the ultimate goal of improving prevention, detection, diagnosis and treatment of disease. EIBIR offers expert advice,

project management and coordination, and dissemination and exploitation services for research projects and clinical studies. This allows researchers to save time and focus on the scientific aspects and ensure the best possible outcome. EIBIR can support both the preparation and the execution of projects.

Learning Objectives:

1. To explain the mission of EIBIR and its organisational structure.
2. To learn about the activities of EIBIR and its Joint Initiatives.
3. To learn about the services offered by EIBIR related to project application and management.

A-195 08:55

Imaging biobanks and big data

E. Neri; *Pisa/IT (emanuele.neri@med.unipi.it)*

Biobanks are collections, repositories and distribution centres of all types of human biological samples. In 2014 the European Society of Radiology established an Imaging Biobanks Working Group of the Research Committee, aimed at defining the concept and scope, exploring the existence, and providing guidelines for the implementation of imaging biobanks. The WG defined imaging biobanks as "organised databases of medical images, and associated imaging biomarkers (radiology and beyond), shared among multiple researchers, linked to other biorepositories" and suggested that biobanks (which focus only on the collection of genotype data) should simultaneously come with a system to collect related clinical or phenotype data. Imaging biobanks may be developed to collect data from the general population. The aim of population-based biobanks is to identify risk factors in the development of disease, to develop prediction models for the stratification of individual risk or to identify markers for early detection of disease. Imaging biobanks may be developed to collect data from a specific disease cohort, such as neurodegenerative disorders, or oncologic diseases in order to understand the genetic nature of cancer or assess the efficacy of drugs and to identify features that may predict treatment response as early on in disease as possible.

Learning Objectives:

1. To understand the concept of imaging biobanks.
2. To learn about the different types of biobanks and imaging biobanks.
3. To have an overview of the existing network of biobanks in Europe and the collaboration between BBMRI and ESR.

A-196 09:10

Role of EIBALL and EORTC to promote imaging biomarkers in clinical studies

N.M. deSouza; *Sutton/UK (nandita.desouza@icr.ac.uk)*

The European Imaging Biomarkers Allowance (a subcommittee of the ESR) works to identify and validate new imaging biomarkers prior to their introduction into clinical trials. In partnership with the EORTC Imaging Group, it is possible to standardise acquisitions for implementation in a multicentre setting and arrange a QA and QC process together with central reading. Both EIBALL and EORTC interact with North America's QIBA in the development of standardised test objects, procedures and protocols for their use in trial set-up and monitoring. The EIBALL-EORTC partnership ensures that imaging biomarkers can be embedded into clinical trials of multiple cancer types through the EORTC's disease oriented groups.

Learning Objectives:

1. To learn the requirements for biomarker standardisation.
2. To understand the requirements for qualitative and quantitative biomarker assessments.
3. To learn how to address biomarker variability.

A-197 09:25

How to organise an imaging research unit within a clinical department: the Force Imaging French project

L.S. Fournier; *Paris/FR*

Radiology and nuclear medicine imaging provide independent and complementary information from clinical examination and biological explorations, such as drug development and validation. In these cases, imaging is not the object of the research but a tool to measure outcomes, therefore its quality must be assured to guarantee the quality of the overall research data. This clinical research occurs on imaging platforms in public or private structures, most of which are part of clinical departments organised to deal with clinical care. There are several challenges to integrate a research among a clinical workflow. First, the volume of imaging dedicated to clinical research is steadily increasing, as imaging is recognised as giving useful biomarkers of disease and drug efficacy. Second, the quality assurance and quality control required are also becoming more stringent. However, there has not been a proportional investment in departments in terms of material and personnel resources. Faced with this, we formed a working group named FORCE Imaging dedicated to make recommendations for the organisation of imaging research units in clinical departments, including image standardisation, quality control, archiving and processing. The issue of financing was also addressed, proposing a unified national grid for overcosts intended for supporting dedicated imaging CRAs.

Learning Objectives:

1. To learn about the French national initiative to organise imaging research units in clinical departments.
2. To understand the challenges of managing research patients among a clinical routine workflow.
3. To learn about solutions to allow an economically viable organisation for clinical research in imaging departments.

09:40

Panel discussion: Imaging biomarkers as a roadmap for promoting imaging research in Europe

08:30 - 10:00 **Room E1**

Breast

RC 502

The high-risk lesions enigma

Moderator:
F. Kilburn-Toppin; Cambridge/UK

A-198 08:30

A. Lesions with an elevated risk for breast cancer

G. Forrai; *Budapest/HU (forrai.gabor@t-online.hu)*

The histological, clinical presentation, together with the mammography and US appearance of the high-risk lesions would be demonstrated. They have very different probability figures of developing cancer, this would be detailed for each type of lesion. The concept and the global problem of the management of these lesions will be explained, together with the conflict of over/under-diagnosis/treatment.

Learning Objectives:

1. To learn about different types of high-risk lesions.
2. To become familiar with the risk of developing a cancer.
3. To appreciate the different imaging modalities for diagnosis.

A-199 09:00

B. Value of breast MRI: rate of underestimation and impact on treatment decision

R.M. Mann; *Nijmegen/NL (r.mann@rad.umcn.nl)*

The evaluation of high-risk lesions on biopsy with MRI is commonly performed. One of the major ideas is to ascertain that there is not more disease present than seen with other techniques. As many high-risk lesions are in fact accidental findings on needle biopsy the absence of enhancement within the breast reduces the likelihood of more extensive disease. Nevertheless, the underestimation rate with MRI is dependent on the type of high-risk lesion initially found and is still substantial for lesions like atypical ductal hyperplasia and lobular neoplasia. Moreover, several high-risk lesions may in fact enhance strongly in breast MRI, but are not upgraded at subsequent pathological assessment. In this lecture, MRI features of common and less common high-risk lesions will be discussed. In general, MRI cannot preclude the need for extensive tissue sampling, but it may be used for guiding of the biopsy and may obviate complete surgical excision.

Learning Objectives:

1. To learn about the evidence based on MRI in evaluating high-risk lesions.
2. To become familiar with different imaging appearances of high-risk lesions.
3. To appreciate the added value for diagnosis and treatment decision.

Author Disclosure:

R.M. Mann: Advisory Board; Screenpoint. Grant Recipient; Siemen Healthcare. Investigator; Siemens Healthcare, Bayer Healthcare, Seno medical, IDS.

A-200 09:30

C. Could surgery be avoided?

S.J. Vinnicombe; *Dundee/UK (s.vinnicombe@dundee.ac.uk)*

Within the UK National Health Service Breast Screening Programme (NHSBSP), a median of 7% of screen detected lesions subjected to needle core biopsy are categorised as B3, of uncertain malignant potential. These lesions are either heterogeneous (such that, though the area sampled by needle core is benign, this may not be representative) or they may be associated with malignancy (in-situ or invasive) - or both. They comprise a group of pathological entities with or without epithelial atypia, which have a variable rate of upgrade to malignancy on surgical excision biopsy, which until recently has been the diagnostic procedure of choice. With increasing

concerns about overdiagnosis (and subsequent overtreatment) in breast screening programmes and widespread availability of large bore vacuum-assisted biopsy (VAB) or excision (VAE), it is timely to consider alternative minimally invasive modes of treatment for these lesions. Various techniques are available, from large bore vacuum-assisted devices where the lesion is removed in a piecemeal fashion, through to devices which remove the lesion in its entirety with a single pass. These approaches to management of B3 lesions are cost-effective and well tolerated, but oncological safety must be the key consideration. In this respect, the literature is challenging to synthesise, since there is wide variability in the rates of surgical excision in differing series and it seems likely that B3 lesions that are surgically excised differ from those treated non-operatively, introducing a source of bias. Nonetheless, many countries are adopting minimally invasive approaches and some consensus has been achieved.

Learning Objectives:

1. To learn about the different non-invasive modalities to excise high-risk lesions.
2. To become familiar with the risk of avoiding surgery.
3. To appreciate the standard protocols in different countries.

08:30 - 10:00 **Room E2**

Special Focus Session

SF 5a

Stroke, beyond the usual suspects

A-201 08:30

Chairman's introduction

O. Jansen; *Kiel/DE (olav.jansen@uksh.de)*

Stroke is the third leading cause for death and the most often reason for invalidation in modern societies. With the introduction of endovascular thrombectomy, medicine has found a sufficient answer for the most vesting cause of severe strokes; however, acute occlusion of larger brain supplying vessels is responsible for only 10-15% of all acute strokes. Besides microvascular disease and acute haemorrhage, there are more rare causes for acute stroke symptoms which have to be kept in mind in the imaging workup of acute stroke patients. This special focus session will take care for three of these more rare but nevertheless important diseases which can result in acute stroke symptoms.

Session Objectives:

1. To learn that stroke can be a more complex disease than only acute arterial vessel occlusion.
2. To understand the possibilities of advance imaging.
3. To appreciate different diagnostic approaches.

A-202 08:35

Understanding watershed infarcts

P. Mordasini; *Berne/CH*

"no abstract submitted"

Learning Objectives:

1. To understand the pathophysiology of cerebral circulation.
2. To review the difference between “internal” and “external” watershed infarcts.
3. To demonstrate how to diagnose watershed infarcts.

A-203 09:00

Reversible cerebral vasoconstriction syndrome

J. Linn; *Munich/DE*

"no abstract submitted"

Learning Objectives:

1. To understand the pathophysiology and clinical presentation of RVCS.
2. To review imaging findings on CT and MR.
3. To show how the diagnosis can be confirmed on angiography.

A-204 09:25

Thrombosis of cerebral veins and dural sinuses

V. Costalat; *Montpellier/FR*

"no abstract submitted"

Learning Objectives:

1. To review the radiologic anatomy of the intracranial venous system (vascular territories, imaging techniques).
2. To diagnose deep vein and dural sinus thrombosis.
3. To understand cortical vein occlusions.

09:50

Panel discussion: Rational imaging in patients with acute stroke symptoms

08:30 - 10:00 **Room F1**

E³ - Rising Stars Programme: Basic Session

BS 5

Head and Neck

Moderator:

S.S. Özbek; Izmir/TR

A-205 08:30

Sinuses

R. Maroldi; *Brescia/IT (roberto.maroldi@unibs.it)*

Paranasal sinuses are air-filled cavities developed within the bones of the face and skull from invaginations of the nasal cavity. They are composed of four paired sinuses: maxillary and ethmoid (present at birth), frontal and sphenoid (develop during infancy). A mucous blanket covers their ciliated epithelium. The mucus is moved by cilia towards the ostium, from which it eventually drains into the nasal cavity along narrow passages, which may be longer (frontal recess, ethmoid infundibulum) or shorter (superior meatus, spheno-ethmoidal recess). Conditions impairing the drainage may lead to the accumulation of mucus inside the sinuses. The most frequent condition is acute sinusitis (AS), usually due to viral infection, which causes inflammation (and thickening) of the nasal mucosa, consequently blocking the drainage passages. The diagnosis is clinical. Imaging is required only when symptoms suggest bacterial superinfection with possible involvement of the orbit or intracranial structures (veins, meninges). Chronic rhinosinusitis (CRS) is an inflammatory process involving the nose and paranasal sinuses, persisting for 12 weeks or longer. Though frequently a continuation of an unresolved AS, CRS may be noninfectious, related to allergy or other conditions. CRS may manifest as one of three major clinical syndromes: CRS without nasal polyps, CRS with nasal polyps, or allergic fungal rhinosinusitis. CT is indicated to identify the causes of impaired mucus drainage, to map the changes of the mucosa and bone, to precisely delineate the unique individual anatomy of sinuses, which may increase the risk in case of endonasal surgery or hamper the mucus drainage.

Learning Objectives:

1. To discuss current imaging techniques for evaluation of normal anatomy.
2. To describe common imaging manifestations of inflammatory diseases.
3. To review tumour and tumour-like lesions.

A-206 08:52

Thyroid and parathyroid

A. Levai; *Budapest/HU (andrealevai@freemail.hu)*

The main objectives of this lecture are to review the normal imaging findings and to emphasize the main radiological features in different modalities in benign and malignant thyroid and parathyroid conditions. Normal anatomy and main radiological features of the thyroid and parathyroid gland are covered briefly including description of developmental abnormalities, followed by demonstration of inflammatory diseases and main benign and malignant lesions of the thyroid. Imaging characteristics of Grave’s thyrotoxicosis and common subtypes of thyroiditis will be detailed. Thyroid malignancy - predominantly papillary carcinoma as the most frequent type of thyroid cancer - will be characterized comprehensively. High-resolution ultrasonography is commonly used in the detection of thyroid and parathyroid abnormalities; however, it is frequently unhelpful in distinguishing between benign and malignant lesions. In case of undetermined nodules, diagnosis can be obtained by ultrasound-guided biopsy. Ultrasound can be sufficient in early staging of thyroid cancer; however, CT and MRI is required in more advanced cancer stages to determine extra-thyroid extension and metastatic spread. Imaging of the parathyroid glands revolves around the detection of parathyroid adenomas and hyperplastic parathyroid glands in the setting of hyperparathyroidism. Imaging is also key to determine pre-operative localization of ectopic

parathyroid glands. Scintigraphy and ultrasound are usually the first-line imaging modalities; CT and MRI can be helpful to reveal supernumerary glands, unusual localizations of ectopic parathyroid, as well as persistent/recurrent disease after surgery.

Learning Objectives:

1. To discuss current imaging techniques for evaluation of normal anatomy.
2. To describe common imaging manifestations of inflammatory diseases.
3. To identify and describe the imaging appearance of malignant pathologies.

A-207 09:15

Salivary glands

S.J. Golding; *Oxford/UK (stephen.golding@nds.ox.ac.uk)*

This presentation offers a clinically orientated approach to imaging salivary gland disease in which the alignment between findings and further management is defined. Salivary imaging has been changed dramatically by the development of cross-sectional imaging. Ultrasound, CT and MRI have consigned radiographs and sialograms to a subsidiary role. Scintigraphy offers the best measure of global salivary gland function but currently is not widely used in practice. Today investigation is closely related to the underlying pathology of salivary disorders and to providing reliable guide to surgical or medical treatment. Masses are well detected by cross-sectional imaging, which provides accurate guidance on appropriate approaches for surgical management. Differential diagnosis cannot always be achieved but this is rarely a clinical problem because biopsy or resection is usually indicated. Sialography remains a reliable method of showing calculi and ductal changes in sialadenitis but cross-sectional techniques, especially ultrasound and MRI, have advantages in inflammatory disease and complete sensitivity in detecting ductal disease may not be necessary in practice because patients may be treated symptomatically. A strong case can be made for using MRI as sole investigation as this has been shown to be sensitive to both surgical and medical conditions. On this basis, the radiologist may be well placed to offer a primary referral service with triage, directing clinical management of patients or further referral on the basis of findings on MRI. Salivary interventional techniques have more recently extended the role of the radiologist.

Learning Objectives:

1. To discuss current imaging techniques for evaluation of normal anatomy.
2. To describe common imaging manifestations of inflammatory diseases.
3. To identify and describe the imaging appearance of malignant pathologies.

A-208 09:37

Lymph nodes

S.S. Özbek; *Izmir/TR (sureyya.ozbek@ege.edu.tr)*

In case of a visible or palpated neck mass, lymph node enlargement is routinely included in the differential diagnosis list. Medical imaging can be effectively used to distinguish other causes of cervical swelling, as well as normal lymph nodes from abnormal ones. Characteristically, normal lymph nodes have well-defined borders, reniform shape and central fatty hilum contiguous with adjacent cervical fat tissue. Although commonly used as a criterion, nodal size is not reliable in characterizing abnormal lymph nodes. Apart from enlargement, imaging parameters including internal structure, vascularity pattern, degree of enhancement and perinodal tissue changes shed light on the aetiology of any lymphadenopathy, which may be reactive hyperplasia, infection, inflammation or neoplastic infiltration. In children, and in most of the adult cases with a low risk of malignancy, ultrasound is the first choice of imaging modality owing to its radiation-free nature, and due to practical reasons. However, when further characterization of nodal abnormality or evaluation of sonographically inaccessible anatomic locations is required, use of other cross-sectional techniques such as CT and MRI is mandatory. These modalities provide not only more detailed information including anatomic localization, size, number, internal structure and enhancement characteristics of lymph nodes, but also important data about perinodal soft tissue and other associated pathologic processes in the region. Although the choice of imaging modalities to be used in the evaluation of cervical lymph nodes changes according to the means, experience and preferences of institutions, the role of medical imaging remains pivotal and decisive in this common indication.

Learning Objectives:

1. To discuss current imaging techniques for evaluation of normal anatomy.
2. To describe the imaging features of infectious and inflammatory disorders.
3. To describe the imaging appearance of neoplastic disorders.

08:30 - 10:00 **Room F2**

Oncologic Imaging

RC 516

A multidisciplinary approach to prostate cancer: can we make a difference?

A-209 08:30

Chairman's introduction

B. Hamm; *Berlin/DE (bernd.hamm@charite.de)*

The session deals with the multidisciplinary approach to prostate cancer. First, we will learn about the diagnostic challenges in prostate cancer from the urologist's point of view. This includes an outline of current treatment options and the role of imaging in therapeutic decision-making. Next, the radiologist's point of view will be presented, providing an outline of how to perform and interpret multiparametric MRI and how to use the PIRADS classification system. A radiation oncologist will then outline the rationale for focal treatment of prostate cancer including strategies as to how these treatments can be guided by multiparametric MRI. The session will conclude with a discussion among the speakers and the audience.

Session Objectives:

1. To understand the pathophysiological properties of prostate cancer and its impact on diffusion-weighted imaging and dynamic contrast-enhanced MRI.
2. To understand the necessity of functional MRI (compared with mere morphological MRI) in the assessment of prostate cancer.
3. To learn about PiRADS classification system.
4. To learn about the role of MRI in selecting patient-tailored therapy.
5. To learn about the option of active surveillance vs immediate treatment.

Author Disclosure:

B. Hamm: Board Member; Deutsche Röntgengesellschaft, ECR, ESR, ESRMRMB, ESOR, Deutsche Forschungsgemeinschaft. Consultant; Toshiba. Grant Recipient; Abbott, Kendle/MorphoSys AG.

A-210 08:35

A. The urologist: evidence-based clinical decision making

N. Mottet; *St. Etienne/FR (nicolas.mottet@chu-st-etienne.fr)*

Prostate cancer is the third cause of cancer death in men. While systematic screening is not promoted, an individual early diagnosis is standard of care. Based on risk factors (such as family history), PSA and DRE, pathology obtained after sonography-guided biopsies is the only diagnostic possibility. If indicated a normal mpMRI should not rule out the biopsy decision. Although a systematic mpMRI before a first biopsy is not yet recommended, it is standard of care before rebiopsying. This increases the biopsy reliability using a combination of 12 systematic plus targeted scores. The treatment policy is based on individual life expectancy, patient's wishes and staging. The classical risk categories (known as d'Amico's classification) are more and more challenged by information from image results. Apart from biopsy results (number of positive scores, Gleason score) and DRE, the local staging (T stage) is based on MRI. Its sensitivity is mild (intraprostatic localisation, microscopic extracapsular extension). But its specificity is acceptable and the MRI is a must in intermediate-/high-risk situations. It is also mandatory before considering active surveillance. N staging is poorly done, even with the PET. As for M staging, PSMA might represent the future, but remain experimental in 2017. For M staging, bone scan should be replaced by a whole body MRI. However, for mCRPC progression characterisation, bone and CT scan remain standard, as no consensus definition of progression with MRI exists yet.

Learning Objectives:

1. To understand how a diagnosis is established by PSA evaluation and biopsy.
2. To learn about different treatment options: surgery, radiotherapy, local ablative and hormonal treatment; as well as active surveillance.
3. To learn how imaging impacts treatment selection.
4. To understand what the urologist needs to know from the radiologist.

A-211 08:58

B. The radiologist: evidence-based use of multiparametric MRI

H.-P. Schlemmer; *Heidelberg/DE (h.schlemmer@dkfz.de)*

Prostate cancer diagnosis is challenged by significant variability in cancer multifocality and biologic heterogeneity. Risk stratification is urgently required for individualized patient management, particularly as active surveillance and various focal therapy options are nowadays emerging. Several clinical studies have demonstrated that multiparametric MR imaging (mpMR) is advantageous for detection and localisation of significant cancer, for biopsy guidance as well as for local staging. Transrectal or transperineal TRUS/MR image fusion biopsy

methods with targeted +/- random biopsies have been proven beneficial for improved diagnosis and risk assessment, particularly also in case of negative (cancer free) results. In active surveillance the combination of morphologic and functional MR data represent important objective and reproducible biomarkers for monitoring individual temporal changes of cancer size and aggressiveness. Standardization and quality assurance of mpMR is challenging, however, particularly concerning DWI, which has been proven most important for detection and characterisation of peripheral zone cancers. Standardised high-quality mpMR including standardized reporting according to PI-RADS has been proven to be important for individualised decision making. Standardisation is of clinical relevance concerning improved image acquisition, interpretation, documentation and communication. This lecture will provide detailed knowledge about evidence-based "state-of-the-art" mpMRI according to PI-RADS. It will specify how mpMRI can improve the complex management of prostate cancer patients.

Learning Objectives:

1. To learn how to perform and interpret multiparametric MRI.
2. To become familiar with the PiRADS classification system.
3. To become familiar with the role of imaging for patient stratification and treatment planning.

Author Disclosure:

H.-P. Schlemmer: Advisory Board; Siemens Healthineers. Author; Thieme Verlag. Consultant; Curagita AG. Employee; German Cancer Research Center, Mediacal University of Heidelberg. Speaker; Siemens Healthineers, Bayer Healthcare, Curagita AG.

A-212 09:21

C. The radiation oncologist

D. Georg; *Vienna/AT (dietmar.georg@meduniwien.ac.at)*

Various treatment techniques are successfully used for treating prostate cancer (PCa) with irradiation. In conventional radiation therapy, the tumour volume is irradiated with a homogeneous dose and clinical practice is to carry out treatment planning based on a computed tomography (CT). A morphological MRI is often used in addition. However, technology developments and achievements made in radiation oncology during the last decade enable to focus the high-dose irradiation very precisely on the tumour, while sparing of the surrounding normal tissue. Improved precision of treatment planning and delivery warrant equally precise tumour definition; moreover, new treatment concepts are stimulated by the advancements in medical imaging to visualize and quantify biological, physiological and pathological processes. During the last years, positron emission tomography (PET), perfusion computed tomography (CT) and especially multiparametric magnetic resonance imaging (mp-MRI) have been continuously explored for lesion characterization, improved target definition and response assessment for radiotherapy of PCa. Elucidating tumour biology and identifying subvolumes of more aggressive behaviour, which are often radiotherapy resistant, are feasible with mp-MRI. The concept of inhomogeneous tumour irradiation according to its biological behaviour, called dose painting, is motivated by selective dose escalation based on biological tumour characteristics. This approach may lead not only to higher local control but also to better sparing of normal surrounding tissue. With the clinical implementation of dose painting, improvements in the therapeutic outcome can be expected. Due to the existing technical challenges, extensive collaboration between radiation oncologists, radiologists, medical physicists and radiation biologists is needed.

Learning Objectives:

1. To learn the rationale and scientific basis for focal therapies for prostate cancer.
2. To learn how focal therapies are performed in prostate cancer.
3. To learn through personal experience and from literature how multiparametric MRI can guide focal therapies of the prostate.

09:44

Panel discussion: Prostate cancer: evidence-based multidisciplinary approach to imaging and treatment

08:30 - 10:00 **Room D**

Musculoskeletal

RC 510

Musculoskeletal ultrasound in the management of sports injuries

Moderator:
C. Cyteval; Montpellier/FR

A-213 08:30

A. Ultrasound of foot and ankle injuries: technique and diagnosis

C. Martinoli; *Genoa/IT (carlo.martinoli@libero.it)*

In sports injuries, the role of ultrasound (US) has become increasingly important in the assessment of tendons, joints, ligaments and other soft tissue injuries about the foot and ankle. With many structures to be examined, the US examination should be focused on clinical findings in an attempt to save time and increase the efficacy of the study. In eversion trauma, the status of the anterior tibiotalar, anterior tibiofibular and calcaneofibular ligaments can be assessed with effective results by means of static and dynamic scans. Some midtarsal ligaments (e.g. dorsal calcaneocuboid, superior talonavicular, bifurcate) can be also evaluated. In inversion injuries, US can detect abnormalities affecting the individual bundles of the medial ligamentous complex (i.e. tibiotalar, tibiocalcanear, tibiospring and tibionavicular). US can diagnose peroneal tendon instability based on tendon displacement relative to the malleolar groove and recognize retinacular/periosteal tears. Dynamic scanning can help to detect cases of intermittent subluxation. Longitudinal splits of the peroneus brevis is well recognized with this technique. Occult fractures (i.e. lateral talar process) and ankle neuropathies (i.e. superficial, deep peroneal) may be detected occasionally in sports injuries. At hindfoot level, US can provide diagnosis and percutaneous treatment of Achilles tendinopathy and plantar fascia injuries.

Learning Objectives:

1. To become familiar with ultrasound findings seen in ankle instability.
2. To learn about the ultrasound patterns of tendon abnormalities.

A-214 09:00

B. Ultrasound of the hip and knee: what is it good for and what are its limitations?

E. Rowbotham; *Leeds/UK (emmarowbotham@doctors.org.uk)*

The high-resolution nature of ultrasound coupled with its dynamic capabilities make this an ideal modality for assessing the soft tissues about the hip and knee joints. Assessment of the tendons for tendinopathy, tears or rupture is a common indication alongside evaluation of the collateral ligaments at the knee and snapping hip syndromes at the hip. In the athletic population, muscle tears are extremely common; ultrasound may be used to demonstrate both the site and extent of a muscle tear in the majority of situations. However, ultrasound is less sensitive than MRI to low-grade tears where there is little in the way of muscle fibre disruption or where the injury is imaged very early following the event. Ultrasound is particularly useful when image-guided intervention around either the hip joint or knee joint is performed to ensure accurate placement or injectate or aspiration of haematoma. However, it is also important to recognise the limitations of this technique and where either plain film, MRI or CT may be needed either in addition or instead of ultrasound. These indications include assessment of cartilage, bone marrow oedema, intra articular bodies, low grade muscle injuries and assessment of the meniscus at the knee and the labrum at the hip.

Learning Objectives:

1. To become familiar with examination technique and typical findings of ultrasound of the hip and knee.
2. To understand the limitations of ultrasound of the hip and knee.

A-215 09:30

C. Ultrasound-guided intervention in the athlete: indications and techniques

H. Guerini; *Paris/FR (henri.guerini@gmail.com)*

Diagnostic and interventional ultrasound is a rapidly evolving field in sports medicine. The use of ultrasound has increased exponentially during the past decade. Ultrasound-guided procedure is performed for joint and tendon sheath injections with PRP or steroïd drugs. We will discuss of the the indications, technical considerations about interventional ultrasound in sports medicine.

Learning Objectives:

1. To become familiar with the indications for ultrasound-guided interventions in the athlete.
2. To learn about the different injection techniques.

08:30 - 10:00 **Room G**

Special Focus Session

SF 5b

Diffusion-weighted imaging (DWI): from physics to practice

A-216 08:30

Chairman's introduction

N. Papanikolaou; *Lisbon/PT (npapan@npapan.com)*

Diffusion-weighted MR imaging (DWI), based on the thermally driven random motion of water molecules (otherwise called Brownian motion) has been increasingly applied in the evaluation of a wide variety of oncological diseases not only in the brain but in the body during recent years. Promising results for improved detection and treatment evaluation, in terms of prediction and early response assessment, have been reported. DWI is probing water mobility propelled by thermal energy, and since water molecules are interacting with cellular membranes or other structures, DWI has the potential to provide us with information regarding the cellular architecture in a non-invasive manner. The apparent diffusion coefficient (ADC) is a property of tissue that reflects local water mobility. In the presence of pathology, ADC, has been correlated with important histologic properties, including the tumour proliferation index, tumour grade, the presence of necrosis, and tumour cell apoptosis. The model that is used to calculate the ADC value is based on a mono-exponential function that generally works well. However, in the presence of increased vascularity, there is a second component that is called microperfusion and needs to be taken into consideration. In that case, the use of a bi-exponential function where ADC is decomposed into D and D*, the true diffusion coefficient and the microperfusion coefficient is providing more accurate modelling of diffusion signals. In the presence of increased tissue heterogeneity, a non-Gaussian diffusion model should be considered to take into account the interactions between water molecules and local tissue architecture components.

Session Objectives:

1. To review the basic theoretical and technical aspects behind DWI.
2. To discuss the clinical yield of DWI in the brain and body.
3. To compare DWI with other modalities like PET/CT for whole-body applications.

A-217 08:35

The physics behind the images: diffusion in oncology

T. Scheenen; *Nijmegen/NL (tom.scheenen@radboudumc.nl)*

Next to T1- and T2-weighted MR imaging, diffusion-weighted imaging plays an increasing role in the detection and characterization of cancer in a variety of soft tissues. DWI probes the random displacement of water molecules by applying a pair of pulsed magnetic field gradients with a certain amplitude, duration and spacing (the labelling time), summarized in the so-called b-value. From DWI of at least two b-values, the apparent diffusion coefficient image (ADC) can be calculated. Within DWI labelling times, in the order of tens of milliseconds, the random displacements are usually restricted by the presence of cells, cell organelles and extracellular structure elements. Differences herein will cause differences in the mean displacements of water in the DWI labelling time, which results in contrast in the ADC image. Cancer tissue often exhibits high cellular densities, restricting water motion, lowering the ADC values compared to nearby healthy or non-cancer tissue. In this talk, the concepts of DWI, the origin of its contrast and examples of clinical applications will be shown.

Learning Objectives:

1. To understand the basics of measuring diffusion with MRI.
2. To understand the concept of b-value, and its shortcomings.
3. To explain contrast mechanism of DWI.
4. To review established and potential clinical applications of DWI in oncology.

A-218 08:58

Diffusion in the brain

A. Radbruch; *Heidelberg/DE*

"no abstract submitted"

Learning Objectives:

1. To differentiate pseudoprogression from pseudoresponse in glioma patients with DWI.
2. To analyse the contribution of DWI in glioma radiomics.
3. To define the role of DWI in ischaemic stroke.

A-219 09:21

Whole-body diffusion

A.R. Padhani; *London/UK (anwar.padhani@talk21.com)*

The disease detection and response assessment performance of WB-MRI is enhanced by adding DWI sequences, which also help to overcome some of the limitations of morphologic sequences. When evaluating test performance, it should be noted that there are intrinsic verification biases particularly prevalent on lesion-level analyses because it is simply not possible to obtain histopathology for every lesion detected. The potential exists that WB-MRI are suitable for wide deployment in disease detection settings, given their test performance, potential wide availability, and multiorgan evaluation capabilities. Sufficient data now indicate that WB-MRI has better accuracy for detecting bone metastases than bone scans to confidently recommend use for bone metastasis detection. Preclinical and small-scale clinical studies indicate that ADC changes can be useful for assessing therapy response but there are few systematic studies. To date, however, there are few data on the benefits of treatment modifications based on the earlier detection of treatment failure or primary resistance or on the negative quality of life effects of continued treatments with ineffective drugs. Nevertheless, a recent EORTC position paper concluded that MRI offers a good “one size fits all” solution for patients who do not have substantial non-bone disease to assess therapy effectiveness. The MET-RADS-P imaging recommendations have recently been developed to address that need for standardisation of acquisition, interpretation and reporting of WB-MRI.

Learning Objectives:

1. To provide a rationale for the use of DWI to supplement morphologic assessments in whole-body MRI examination.
2. To show how measurements are acquired in the body and to distinguish between tumour detection and response assessment protocols.
3. To provide interpretation guidelines for disease detection and response assessments including how to recognise false positive and negative cases.
4. To provide the scientific evidence comparing WB-MRI with PET/CT, bone and CT scans for disease detection including areas of potential synergy.

Author Disclosure:

A.R. Padhani: Speaker; Siemens heathcare.

09:44

Panel discussion: What's new in diffusion-weighted imaging?

08:30 - 10:00 **Room K**

Radiographers

RC 514

CT imaging: the role of the radiographer and technological developments

Moderator:

C. Beardmore; London/UK

R. Siemund; Lund/SE

A-220 08:30

A. The role of the radiographer in interventional CT procedures

J. Santos; *Coimbra/PT (joanasantos@estescoimbra.pt)*

Computed tomography (CT) is a valuable medical tool to plan and guide interventional or therapeutic procedures. The interventional procedures can be performed based in 2 dimensions images (2D), image reconstructions (3D) or using CT fluoroscopy. These procedures allow continuous monitoring of needle course to the lesion. CT interventional typical diagnostic procedures are biopsies, which can be done as aspiration or fine-needle biopsies, punch biopsies, or drill biopsies. The goal is to acquire material for a microbiological analysis, to classify tumours before treatment or search for remaining living tumour cells after treatment. Various therapeutic procedures were drainages, tumour/ablation therapy, neurolysis, anesthesia injection and skeletal interventions can also be performed by CT. Several authors described CT fluoroscopy as successful method for percutaneous interventional procedures in the chest, spine, abdomen, and pelvis, however it is particularly more useful for deep structures, liver and lungs. Despise this applications CT fluoroscopy is the high radiation exposure procedure and radiation protection safety measures must apply. However the use of fluoroscopy CT is controversial and interventional procedures are regularly performed based on 2D images. Sterile conditions are required in all the interventions, the scanner room and the CT scanner needs to be carefully cleaned and disinfected, especially the CT table and the gantry. Planning the procedure is recommended in order to protect the staff and decrease the risk of patient’s over exposure and procedures complications. CT interventional procedures require teamwork and

radiographers must be aware and involved in all the phases promoting the safety.

Learning Objectives:

1. To appreciate the clinical role of the most common CT interventional procedures.
2. To understand the role of the radiographer in CT interventional procedures.
3. To be aware of procedure optimisation in order to promote patient and staff safety.

A-221 08:55

B. Optimising CT doses

F. Zarb; *Msida/MT (francis.zarb@um.edu.mt)*

Computed tomography (CT) is well documented as a main contributor to the radiation dose in medical imaging and constitutes the largest provider of radiation exposure to the population from medical imaging examinations. Once justified, CT examinations should be optimised to provide images from which a diagnosis can be obtained using the lowest radiation dose. The purpose of this presentation is to 1) outline the importance of the role of the radiographer throughout the optimisation process which should include all the links of the imaging chain, i.e. x-ray production, x-ray detection, image processing, image display and image interpretation; 2) learn about available methods in evaluating image quality during CT optimisation (the resultant image being the final link in the imaging chain) and 3) discuss the impact of CT optimisation on patient dose and image quality, i.e. limiting radiation exposure to the patient without compromising diagnostic efficacy.

Learning Objectives:

1. To appreciate the role of the radiographer in CT optimisation.
2. To learn about different ways of evaluating image quality resulting from CT dose optimisation strategies.
3. To discuss the impact of CT dose optimisation on patient radiation dose and image quality.

A-222 09:20

C. State-of-the-art CT technology

S.D. Mørup; *Odense/DK (sdmo@ucl.dk)*

In recent years, the manufacturers of computed tomography (CT) have developed several new applications that continue to make it possible to improve the image quality and reduce the radiation dose to the patient in CT. Radiographers must understand and appreciate these new applications and be able to use them wisely to achieve a dose reduction without compromising the image quality. There is no single method that works perfectly for all diagnostic challenges in CT and, therefore, the radiographer should be aware of the advantages and disadvantages when applying different new methods for dose reduction or for improving the image quality. This presentation discusses present challenges related to the new developments in CT, some of the developments are the organ effective modulation, which is a technique that delivers safer exams for patients by limiting the dose to radiosensitive organs like the breast or lens. Other applications are the automatic kV selection and improved software that can reduce metal artefacts without the use of dual energy or increasing the radiation dose.

Learning Objectives:

1. To appreciate new development in hardware and software with regards to image quality and radiation dose in CT.
2. To learn about the disadvantages of the new technologies in regards to the image quality and radiation dose.
3. To discuss how the radiographer can combine these new technologies with regard to image quality and radiation dose.

09:45

Discussion and questions: Optimisation of care in CT: what else may be done?

08:30 - 10:00 **Room M 1**

E³ - ECR Master Class (Vascular)

E³ 526b

What's new in arterial embolisation? Current and future trends

Moderator:

D.K. Tsetis; Iraklion/GR

A-223 08:30

A. New beads and new drugs: new indications

S.N. Goldberg; *Jerusalem/IL (sgoldber@bidmc.harvard.edu)*

Primary liver cancer is the second most common cause of cancer-related deaths worldwide. As most patients present with intermediate to advanced stage disease, non-amendable to curative therapies (i.e. ablation, resection or liver transplant), catheter-based intra-arterial therapies have meanwhile become officially incorporated into treatment guidelines. The most commonly used modality, transarterial chemoembolization or TACE, uses the preferentially arterial blood supply of liver tumours (both primary and metastatic) to deliver a highly concentrated cocktail of embolic material and chemotherapeutic agents directly to the target lesion while preserving healthy liver tissue with is preferentially supplied by the portal vein. This talk will discuss the rationale for TACE in a variety of clinical scenarios and provide an overview of the most recently available data on different drug-eluting particles and drug delivery platforms. Furthermore, most recent evidence and clinical trial data for the combination of TACE with systemically applicable anti-angiogenic agents will be discussed. Finally, novel intra-procedural imaging technologies for improved targeting as well as assessment of treatment response will be summarized.

Learning Objectives:

1. To explain new technological improvement with regards beads.
2. To discuss about new drugs potentially used for chemoembolisation.
3. To review experimental literature as well as preliminary experience on the use of new devices and drugs for liver chemoembolisation.

Author Disclosure:

S.N. Goldberg: Consultant; Angiodynamics, Cosman Instruments. Research/Grant Support; Angiodynamics.

A-224 09:00

B. Prostate arterial embolisation

H. Rio Tinto; *Lisbon/PT (hugo.tinto@gmail.com)*

Benign prostatic hyperplasia (BPH) has a prevalence of more than 50% in men over 60 years. It is associated with lower urinary tract symptoms (LUTS). The indication treatment depends on disease staging. Medical therapy is usually the first-line treatment. TURP is the gold standard surgical treatment for BPH. There are several minimally invasive treatments that offer safety and efficacy and are valid options without the burden and risk of operative morbidity. Prostatic arterial embolisation (PAE) for BPH has been shown as a safe and effective procedure after failure of medical therapy. Unilateral femoral approach is routinely used; a catheter is advanced to the anterior division of the internal iliac artery. First angiograms with specific angulations are performed to identify the prostatic arteries. Deep knowledge of the pelvic arterial anatomy is essential since there are several variations. Selective access is performed with a micro-catheter. The embolisation material of choice is spherical particles. Controlled embolisation is crucial to avoid non-target embolisation until near stasis is achieved. It is a minimally invasive treatment that can be performed as an outpatient procedure. Short and mid-term studies in BPH have shown that PAE also improves LUTS related to BPH. Potential major complications are associated with non-target embolisation but in experienced hands the rate is extremely low. The most frequent minor complications are perineal pain, haematuria, haematospermia, transient urinary retention and others associated with femoral access.

Learning Objectives:

1. To learn about anatomic variations of prostatic vasculature and technical difficulties of embolisation.
2. To understand clinical indications - who is a good candidate for embolisation?
3. To review the results and possible advantage for minimally invasive treatment.

A-225 09:30

C. Haemorrhoid embolisation

T. Jargiello; *Lublin/PL (tojarg@interia.pl)*

Haemorrhoidal disease is the most common proctologic pathology with the prevalence of up to 35%. Anorectal discomfort, pain and of course bleeding are typical symptoms. Evaluating pathophysiology of this disease it was stated that haemorrhoids are not varicose veins but they are the normal tissue - a sort of physiological network of small arterioles and venous spaces. This part of rectum is called the corpus cavernosum recti and its role is not to bring oxygen but to create the cushion with functional role as the anal closure. This pathophysiologic mechanism together with theory of high arterial flow causing haemorrhoids gave basic thinking of possible arterial embolization of superior rectal arteries in the endovascular treatment of the disease. Minimally invasive embolization seems to be less harmful for the patient and similarly effective when compared with alternative surgical therapies like: open haemorrhoidectomy, Longo technique or Doppler-guided haemorrhoid artery ligation. The technique of haemorrhoid embolization is not very sophisticated - it is routine microcoil placement into both superior rectal arteries, usually at the level of superior edge of pubic arch. Some operators use also embolic particles. The potential benefit of endovascular treatment is the absence of direct anorectal trauma but we still do not know which arteries should be embolised (possible anastomoses) and how to choose the ideal patient?

Learning Objectives:

1. To understand vascular anatomy of the rectum and arterial physiology of haemorrhoids.
2. To review other treatment options.
3. To learn about haemorrhoid embolisation technique.

08:30 - 10:00 **Room M 2**

ESR Audit and Standards Session

How (Euro)safe is your department?

Moderator:
B.E. Kelly; Belfast/IE

A-226 08:30

Audit and raising the standard: the role of audit in 2017

M.F.J. Ryan; *Cork/IE*

Clinical Audit is considered to be a tool designed to improve the quality of patient care experiences and outcomes though the formal review of systems, pathways and outcomes of care against defined standards and the implementation of change on the basis of the results. There is wide variation in the understanding and implementation of clinical audits in Europe.

Learning Objectives:

1. To understand the definition and function of audit.
2. To learn about the distinction between audit and research.
3. To appreciate the importance of reaudit.

A-227 08:50

Auditing the auditors: safe health care professionals in safe departments

P. Soffia; *Santiago/CL (psoffia@alemana.cl)*

For radiologists to change the way they are perceived they will have to establish their value, not just as report generators, but as guardians of patient safety through efficient management with justification of every study and optimization of radiation exposure. Appraisal and revalidation of radiologists is mandatory for today standards. In most developed countries, there are official mechanisms for certification and re-certification of radiologists, but every department should have its own appraisal system for evaluating staff on a regular basis. This evaluation should consider not only both knowledge and technical skills but also soft skills, such as communication, ethics and professionalism. Professionalism is a key issue for most doctor and radiologists are not an exception. Disruptive behaviour of radiologists is not an uncommon problem in large imaging departments having a significant medical, economic and emotional consequences. Thus, every medical organization has to establish essential aspects to deal with disruptive behaviour. An organized and standarized approach is recommended and must be documented. Most authors recommend including a zero tolerance policy. Considering that reporting errors is a key indicator of quality, discrepancy meetings are an excellent way to improve practice learning from errors. These meeting should take place periodically and should not be punitive. Finally, communications within the radiology department are crucial, specially in organ-based practices with little interaction between staff radiologists from different subspecialities. An effective way to improve communication is a schedule of weekly meetings of quality and safety with participation of radiologists from different sections within the department.

Learning Objectives:

1. To learn about appraisal and revalidation.
2. To learn about managing the failing doctor.
3. To understand discrepancy meetings, root cause analysis and no blame culture.
4. To hear examples of effective communication within and between radiology departments.

A-228 09:10

Audit: what a regulator needs to know

S. Ebdon-Jackson; *Didcot/UK (steve.ebdon-jackson@phe.gov.uk)*

Within the European Union, legislation and regulations relating to the hazards of ionising radiation in medical exposures are addressed in Euratom Directives 97/43 and 2013/59. These directives both require that clinical audits are carried out in accordance with national procedures and national regulations should reflect this. The directives deliberately avoid detail, recognising that clinical audit has wide application across medicine and not just in radiation specialities. Member states may wish to transpose this requirement in different ways, but all European regulators will wish to see that implementation of the directives is meaningful. There is widespread acceptance that the processes of inspection by regulators and professionally led clinical audit should and will differ. Nevertheless, regulators will wish to see how clinical audit can help to demonstrate appropriate implementation of the key principles of justification and optimisation as well as other legal requirements.

Learning Objectives:

1. To learn about National Standards and local guidelines.
2. To understand systems to ensure patient safety.
3. To learn about minimising ionizing radiation exposure to staff and patients.

A-229 09:30

Audit and the patient journey

E. Briers; *Brussels/BE (erikbriers@telenet.be)*

The radiology department is part of medical professionals involved in the care of patients. The patient is referred to the department by his clinician who may have explained the purpose of the visit but maybe not what to expect once in the department. We can state that once the patient crosses the threshold of the department, the department is in charge of the patient, as well for optimal results (outcome) as for a smooth journey through the department. The quality of the journey is influenced by the quality of communication. Modern patients want to know what will happen, meaning before it happens. This requires that this information is available in different forms (print, internet kiosk, etc.) and addressing different levels of literacy. It is clear that the retired university professor of philosophy will need another brochure (if any) compared to the cleaner, and both are entitled to be well informed. Understanding what will happen gives the patient a safe feeling, his first issue may not be the radiation that will be applied but perhaps where the next toilet is, or if the contrast will cause discomfort. Most of communication is “patient” listening to patients to learn what their concerns are so that this smooth journey can be assured. Discussing examination results is no easy task, in serious pathologies the multi-professional approach (example a tumour board) is the preferred route to bring together the information from the many experts, and to only have one line of communication to the patient.

Learning Objectives:

1. To learn about communicating with the patient before, during and after their examination.
2. To appreciate the patient-centred department.
3. To appreciate well thought-through, timely and accurate discussion of examination results.

09:50

Panel discussion: Can an auditless department prove that it's a safe department?

08:30 - 10:00 **Room M 3**

Interventional Radiology

RC 509

Introduction to percutaneous interventional procedures: a practical guide

A-230 08:30

Chairman's introduction

R. Iezzi; *Rome/IT (roberto.iezzi.md@gmail.com)*

Percutaneous imaging-guided interventions are making an increasing contribution to the treatment of patients with many non-vascular conditions. Minimally invasive techniques enable effective treatment that is followed by rapid recovery, with a low complication rate. However, the effectiveness of such methods of treatment is enhanced by an accurate preprocedural planning, an adequate selection of image guidance technique, as well as an optimal intra/periprocedural sedation. In detail, analgesia and sedation before, during, and after interventional procedures allow a safe, comfortable, and technically successful procedure to be performed. This session will explore different imaging-guided methods to define advantages, disadvantages, as well as tips and tricks for successful percutaneous intervention.

Session Objectives:

1. To appreciate the importance of pre-procedure planning and selection of image guidance technique.
2. To learn about intra-procedure patient analgesia and adjunctive techniques for access to sites for intervention.
3. To discuss tips and tricks for successful percutaneous intervention.

A-231 08:35

A. How to safely perform US-guided procedures

D. Akinci; *Ankara/TR (akincid@hotmail.com)*

Ultrasound (US) guidance is a frequent modality of choice in percutaneous biopsy, drainage and ablation procedures, because it enables continuous real-time visualization, is radiation free, has a lower cost and is better for angled access. In most of the abdominal organ biopsies (e.g. liver, kidney, pancreas and spleen) and drainage of fluid collections, local ablation of liver tumours, drainage of pleural collections, biopsy of peripheral pleural-based thoracic lesions, US guidance is utilized. Endocavitary approaches can be used safely in pelvic biopsy and drainage procedures with transvaginal or transrectal US guidance. Fusion techniques combine US images with CT or MRI images, enabling targeted US-guided biopsy for lesions that are difficult to see on US.

Learning Objectives:

1. To learn about patient positioning for US-guided percutaneous and endocavitary approaches to sites in the body.
2. To learn about real time guidance advantages of US-guided intervention.
3. To explain image fusion techniques for US-guided intervention.

A-232 08:58

B. How to safely perform CT-guided procedures

R. García Marcos; *Valencia/ES (raulgamar@hotmail.com)*

Percutaneous computed tomography (CT) guided is a minimally invasive approach for interventional procedures. Although is a procedure with few complications precise planning and knowledge of the indications, technique and material. CT-guided interventions may be divided into diagnostic (biopsies) and therapeutic interventions (drainages, thermal ablation, vertebroplasty, etc.). The main problems of access to lesions depend on the situation due to poor imagery, mobility and distance. Therefore, we are obliged to know and identify the structures along the established route. Different techniques of CT exist. Multidetector CT is commonly used for guiding percutaneous biopsy and catheter drainage of fluid collections. CT fluoroscopy has the potential to improve the efficacy of CT-guided interventions and to reduce the procedure time. C-arm cone-beam CT (CBCT) is a real-time needle guidance technique that can be used to visualise the needle trajectory from skin to target lesions. The aim of this study is to present the types and advantages of the CT-guided interventions, the patient positioning and adjunctive techniques for access to sites for intervention.

Learning Objectives:

1. To learn about patient positioning for CT-guided percutaneous approaches to sites in the body.
2. To learn the types of CT guidance and advantages of CT-guided intervention.
3. To learn about adjunctive techniques for access to sites for intervention.

A-233 09:21

C. Post-procedure follow-up and complication management

M. Seidensticker; *Magdeburg/DE (max.seidensticker@med.ovgu.de)*

Biopsy procedures bare - although commonly at a low rate - potentially life-threatening risks. To know about potential complications and proper patient monitoring is the key to identify the complications and to react accordingly. The lecture will give information about common and uncommon complications after biopsy procedures and help will be given to identify the patient at risk and how to avoid/reduce specific complications. Further on, management of complications will be addressed. Of note, not all complications are avoidable, but proper patient management helps to reduce associated morbidity and mortality.

Learning Objectives:

1. To appreciate the potential for complications in common biopsy procedures.
2. To learn about management of post-procedure complications.
3. To discuss the role of quality improvement.

Author Disclosure:

M. Seidensticker: Advisory Board; Bayer. Grant Recipient; Bayer, Sirtex medical. Speaker; Sirtex medical, Cook, BTG, Bayer, LIAM, DAFMT.

09:44

Panel discussion: Tips and tricks for choosing your first cases. Controversial case-based review of approaches to difficult lesions

08:30 - 10:00 **Room M 4**

E³ - ECR Academies: Tips and Tricks in Liver, Bile Ducts and Pancreas Imaging

E³ 518

New challenges of pancreatitis

A-234 08:30

Chairman's introduction

M.A. Bali; *Sutton/UK (mantoniettabali@icr.ac.uk)*

The 1992 Atlanta Classification aimed to promote uniformity in terminology to facilitate communication among clinicians. The 2012 revision provides a more comprehensive classification of AP and peripancreatic collections and gives new information about the aetiology, pathophysiology, severity and radiologic findings. The role of imaging is: 1. to confirm the diagnosis (non-conclusive clinical/laboratory findings); 2. to detect the cause; 3. to stage the severity; 4. to detect the complications; 5. to guide the treatment. Autoimmune pancreatitis is a distinct form of pancreatitis presenting with obstructive jaundice, periductal lymphoplasmacytic infiltrate (IgG4-positive cells) and fibrosis at histology and response to corticosteroids. Type I (IgG4-related lymphoplasmacytic sclerosing pancreatitis, pancreatic manifestation of IgG4-related diseases demonstrates diffuse pancreatic enlargement ("sausage-shaped" in 30-50%), delayed enhancement at the venous phase, highly specific low-attenuating rim (30-40% of cases), long main pancreatic duct stricture without marked upstream dilatation. Other organs can be involved (bile ducts, kidneys, retroperitoneum). It responds to corticosteroids but 20-60% of the cases will relapse. Type II (idiopathic duct-centric pancreatitis) is less common with pancreatic-limited disease and no extra-pancreatic involvement . The imaging findings are similar to type I. Disease relapse after corticosteroids is rare. Pancreatic cystic lesions (PCL) represent a significant clinical entity. According to WHO, PCL include epithelial and non-epithelial neoplasm classified as benign, potentially malignant and malignant. The diagnosis includes patient clinical data, imaging findings and cystic-fluid analysis. Several imaging findings allow differential diagnosis and may be suggestive of malignancy. However, cystic lesions smaller than 3 cm may lack specific morphologic features.

A-235 08:35

A. Understanding the Atlanta 2012 classification of acute pancreatitis

W. Schima; *Vienna/AT (wolfgang.schima@khgh.at)*

According to the Revised Atlanta Classification of 2012, acute pancreatitis is categorized as interstitial oedematous or necrotizing pancreatitis. In interstitial oedematous pancreatitis, acute peripancreatic fluid collections may occur early (< 4 weeks from). In the late phase, these either resolve or evolve into pseudocysts, which are hypodense at CT and hyperintense on T2w MRI. Treatment of pseudocysts is indicated in symptomatic patients or if complications (gastric outlet obstruction, cholestasis or haemorrhage) develop. Necrotizing pancreatitis may present with combined pancreatic and peripancreatic or pancreatic necrosis or peripancreatic necrosis alone. Acute necrotic collections may evolve into walled-off necrosis (WON) in the late stage (≥ 4 weeks). A WON containing digested fat and parenchyma must not be confused with a pseudocyst. They are similar on CT, but US/MRI reveal the

predominantly solid nature of WON. Secondary infection of necrotizing pancreatitis results in high mortality. Diagnosis of infection is difficult based on imaging. Gas within a collection is not sensitive, but specific. If feasible, CT-guided abscess drainage is recommended. Necrotic collections with debris require a more aggressive approach. In general, MDCT for diagnosis of pancreatitis should be performed no less than 2-3 days from clinical onset, because development of necrosis may take some time. In case of suspected biliary pancreatitis, early MRCP guides further treatment (ERCP and stone removal). The Revised Atlanta Classification system introduces a uniform terminology for imaging features of pancreatitis. Contrast-enhanced CT is the primary tool of diagnostic imaging and image-guided therapy. MRCP characterizes fluid collections and delineates the duct system.

Learning Objectives:

1. To be aware of the new terminology for the evaluation of acute pancreatitis.
2. To learn about how to report imaging findings.
3. To understand the relationship between imaging findings and prognosis.

A-236 09:03

B. Autoimmune pancreatitis and its relatives

G. Morana; *Treviso/IT (gmorana@ulss.tv.it)*

Autoimmune pancreatitis (AIP) is a immune disorder affecting the pancreas, with or without a pancreatic mass, characterized by a dramatic clinical response to steroids. Symptoms are similar to that of pancreatic cancer: fluctuating obstructive jaundice, vague abdominal pain, weight loss, steatorrhoea and diabetes due to decline in exocrine function. AIP is subdivided into: Type 1: is the pancreatic manifestation of an IgG4-related systemic disease and is characterized by elevated IgG4 serum levels, infiltration of IgG4-positive plasma cells and extrapancreatic lesions. Type 2: usually has none or very few IgG4-positive plasma cells, no serum IgG4 elevation and appears to be a pancreas-specific disorder without extrapancreatic involvement. There are three patterns of autoimmune pancreatitis: diffuse disease is the most common type, with a “sausage-like” diffuse pancreatic enlargement with sharp margins and loss of the lobular contours; focal disease is less common and manifests as a focal mass, mimicking a pancreatic malignancy. Focal disease tends to be relatively well demarcated and, when present, upstream dilation of the main pancreatic duct is typically milder than what is observed in patients with pancreatic carcinoma. Multifocal involvement can also be evident. Established imaging criteria allow a confident diagnosis. Differential diagnosis with pancreatic carcinoma is of utmost importance to establish the optimal therapeutic strategy and to avoid unnecessary laparotomy or pancreatic resection in AIP patients. Non-invasive imaging plays also an important role in OOI in case of Type I AIP, therapy monitoring, in follow-up and in early identification of disease recurrence.

Learning Objectives:

1. To understand the various forms of autoimmune pancreatitis, especially cases that are associated with extra pancreatic disease.
2. To learn about the usual and unusual appearance of autoimmune pancreatitis.
3. To understand the principles of the follow-up.

Author Disclosure:

G. Morana: Speaker; BRACCO IMAGING SpA.

A-237 09:31

C. Tough clinical cases of cystic pancreatic lesions

M. Karcaaltincaba; *Ankara/TR (musturayk@yahoo.com)*

Cystic lesions are the most common lesion in pancreas, particularly in the elderly. Crucial points in reporting of a cystic lesion will be reviewed, which are size, location, septal enhancement, mural nodule and pancreatic duct dilatation. In the absence of worrisome features, cysts can be safely followed up. Weaknesses and strengths of radiologic modalities will be emphasized. The most common cystic lesions of pancreas are serous cystadenoma, intraductal papillary mucinous tumour, mucinous cystadenoma and pancreatitis-related cysts. Typical and atypical forms of these entities and distinction from malignant lesions will be discussed during the lecture. Finally, difficult cystic pancreatic lesions will be reviewed and imaging findings for correct diagnosis and management will be presented.

Learning Objectives:

1. To understand how to report a cystic pancreatic lesion, including recommendation for imaging strategy.
2. To become familiar with the most common cystic neoplasms of the pancreas.
3. To learn how to differentiate neoplasms and inflammatory cystic lesions of the pancreas.

Author Disclosure:

M. Karcaaltincaba: Speaker; GE Healthcare, Koninklijke Philips Healthcare, Pfizer.

08:30 - 10:00 **Room M 5**

Joint Course of ESR and RSNA (Radiological Society of North America): Hybrid Imaging

MC 528

The ABCs of hybrid imaging

Moderators:
A. Drzezga; Cologne/DE
K. Riklund; Umea/SE

A-238 08:30

A. What you need to know about PET-physics

J. Axelsson; *Umea/SE (jan.e.axelsson@vll.se)*

This lecture covers PET physics without equations, to give a basic understanding of how radioactive decay of anti-matter, positrons, lead to acquisition of positional information of radioactively labelled molecules. In a further step, quantitative tomographic image reconstruction is described. In this step, attenuation correction and the benefits and problems arising from CT-based attenuation correction is described.

Learning Objectives:

1. To understand the basics of physics in PET imaging.
2. To learn about the different approaches of PET attenuation correction.
3. To learn about potential artefacts in hybrid imaging.

A-239 09:00

B. How MR physics influence image quality in hybrid imaging

C. Catana; *Boston, MA/US (ccatana@nmr.mgh.harvard.edu)*

The introduction of combined PET/MR scanners allows the PET emission data to be corrected for photon attenuation effects using the anatomical MR images. This approach has both advantages and limitations. On the one hand, MR eliminates the radiation exposure associated with CT scans. On the other hand, assumptions regarding the composition of the body based on the available morphological information have to be made since the MR signal does not reflect electron densities. MR physics influences PET in several ways, potentially leading to artefacts and bias that could affect qualitative and quantitative PET studies. The purpose of this presentation is to present such artefacts, describe their origin and impact on PET attenuation correction and discuss strategies to overcome them. Artefacts related to bone and lung tissue misclassification, B0 field inhomogeneity, aliasing/wrap-around, positron-range effects, metallic implants, MR contrast agents, MR hardware, image quality phantoms and subject motion will be discussed.

Learning Objectives:

1. To learn about MR for attenuation and motion correction.
2. To learn about MR artefacts influencing PET-quality.
3. To understand the complexity of physics in MR/PET.

Author Disclosure:

C. Catana: Consultant; Cubresa, Inc..

A-240/A-241 09:30

C. Interactive case discussion

J. Axelsson; *Umea/SE*
C. Catana; *Boston, MA/US*

Learning Objectives:

1. To learn how to identify common MR artefacts.
2. To learn how to identify common PET artefacts.
3. To learn how to identify common CT artefacts.

10:30 - 12:00 **Room A**

E³ - ECR Academies: Interactive Teaching Sessions for Young (and not so Young) Radiologists

E³ 621
Emergency radiology II

A-242 10:30
A. Abdominal vascular emergencies
A. Palkó; *Szeged/HU (palkoand@gmail.com)*

The goal of this problem-oriented, case-based presentation is to involve the audience in an interactive communication aimed at clarifying and clearly understanding the role and clinical significance of imaging and image-guided intervention in the diagnosis and treatment of abdominal vascular emergencies. We will discuss and solve typical but also unusual cases to introduce the proper diagnostic algorithm providing the fastest possible treatment to the patient in these most frequently very severe, potentially lethal conditions; in which time elapsing between onset of symptoms and correct diagnosis is critical from the point of view of successful therapy and chance of survival.

Learning Objectives:
1. To understand the different types of abdominal vascular emergencies.
2. To learn about imaging findings and treatment options.

Author Disclosure:
A. Palkó: Advisory Board; Affidea.

A-243 11:15
B. Chest trauma
J. Biederer; *Heidelberg/DE (juergen.biederer@med.uni-heidelberg.de)*

Chest trauma involves the respiratory system and the main cardiovascular structures of the body. The respiratory system is the functional unit of lung parenchyma, pleura, airways, vasculature, mediastinum, chest wall and diaphragm. Any trauma to single or multiple of these structures directly or indirectly impairs the genuine task of this complex system, which is to guarantee gas exchange by ventilation and perfusion. The spectrum of traumatic mechanisms to the respiratory system covers blunt and perforating trauma, barotrauma and aspiration of foreign bodies or gases and fluids, or any combination of these. The typical scenarios for blunt trauma of the chest are motor vehicle accidents or deep falls with deceleration leading to lung contusion/laceration and aortic or cardiac injury. Perforating trauma is typically related to stabbing or gunshot. Depending on the intensity of trauma and the structures involved, chest trauma is an immediately life-threatening condition. For ER imaging (whole body CT or “classical” x-ray/ultrasound), this requires fast imaging and an efficient concept for data management, reading and reporting. In severely injured patients, the first look of the radiologist should be for ABC: airway/breathing/circulation. The key diagnostic signs are abnormal lung opacity (aspiration, bleeding, atelectasis, pleural fluid accumulation, chest wall haematoma), pneumothorax/pneumomediastinum (alveolar rupture, tracheobronchial rupture or esophageal injury) or widened mediastinum (aortic/arterial injury, venous injury or fracture of sternum/spine). Fractures of the spine, sternum, clavicle, or scapula are indicative of extreme forces and a high probability of life-threatening injury, such as aortic rupture or cardiac contusion.

Learning Objectives:
1. To understand the imaging technique.
2. To become familiar with the differential diagnosis.

10:30 - 12:00 **Room X**

EuroSafe Imaging Session

EU 2
Focus on appropriate image quality: what we have to know

Moderators:
W. Stiller; Heidelberg/DE
J. Damilakis; Iraklion/GR

A-244 10:30
EuroSafe Imaging on "appropriate image quality": Introduction
S.T. Schindera; *Aarau/CH (sschindera@aol.com)*

To define the appropriate image quality in diagnostic imaging (e.g. CT) is a very challenging task, as many factors, such as the diagnostic task, patient size and technical parameters, can impact the image quality. The goal of the radiologist is to achieve the best diagnosis without harming the patient, which means that the image quality has to be set at a level, where the clinical question can be answered at the lowest achievable dose. Various subjective and objective measurements for image quality have been introduced in the past, which unfortunately have all limitations. To date, a robust, meaningful and easy-to-use measurement for image quality in CT is still missing.

Learning Objectives:
1. To become familiar with the goals and methods of the work on appropriate image quality.
2. To learn about preliminary results and future work for ensuring appropriate image quality in daily imaging routine.

A-245 10:40
Metrics and methods for quantitative image quality determination: a physicist's perspective
C. Hoeschen; *Magdeburg/DE (christoph.hoeschen@ovgu.de)*

The physicist would like to measure image quality as objective as possible to be able to a) compare systems, b) assure constant quality, c) have direct access to procedure optimisation outcomes. The measured image quality should in addition be directly related to the diagnostic quality. The latter is sometimes not a trivial condition. First of all, the talk will present the mathematical basics for Fourier-based (modulation transfer function - MTF, noise power spectrum - NPS, detective quantum efficiency - DQE) as well as task-based image quality metrics (as signal-to-noise ratio - SNR or contrast-to-noise ration - CNR and others) on an easy to understand basis. Possible interlinks will be presented. Afterwards, various options to measure these image quality parameters will be discussed e.g. grating or edge method for projectional image MTF determination, wire or ball characterisation for 3D MTF and noise analysis with Fourier methods or eigenvector and-eigenvalue determination for task based measures. All these will be shown on easy to understand examples from own measurements. Afterwards, a discussion about advantages and potential limitations will follow. Here, the focus will be on aspects of measurement time, generality appropriateness in terms of fulfilment of mathematical conditions, predictivity of diagnostic outcomes. This will be separately investigated for Fourier-based and task based image quality descriptors using examples. The final comments will show the importance of accurate determination of radiation exposure for tasks of quantitative image quality investigations. Again, this will be shown for example on measurements of CNR for mammography image quality evaluation.

Learning Objectives:
1. To learn about mathematical metrics used for the quantitative description of image quality.
2. To become familiar with the methods employed for measuring image quality quantitatively.
3. To understand advantages and limitations of quantitative image quality assessment.

A-246 11:00
Balancing diagnostic image quality and radiation exposure in clinical routine: a radiologist's perspective
H. Geijer; *Örebro/SE (hakan.geijer@regionorebrolan.se)*

The balance between image quality and radiation exposure is not easy to optimise. The goal should be to choose an image quality that is good enough for the diagnostic task at hand, at a radiation exposure that is as low as reasonably achievable according to the ALARA concept. One way to do this is to adjust equipment settings such as tube current (mA) or tube potential (kV). Iterative reconstruction might give the opportunity to reduce the dose settings in CT. Sometimes a change of modality can reduce the radiation exposure.

This was often seen when moving from storage phosphor radiography to flat-panel detectors. Another approach is to improve the diagnostic potential of a method without necessarily reducing the dose. This can sometimes be achieved by moving from radiography to low-dose CT. In the lecture, the efficacy of diagnostic imaging will also be mentioned. Many studies of diagnostic methods stop at measuring the physical characteristics of the image or the sensitivity and specificity of the method, while the really important test of a method is if it benefits the patients, for example, by reducing the mortality or morbidity for those who undergo the test.

Learning Objectives:

1. To learn about the image features mainly determining diagnostic image quality in clinical routine.
2. To become familiar with the factors influencing image quality in clinical practice.
3. To raise awareness of the interrelation between image quality and radiation exposure.

A-247 11:20

Image quality assessment via model observers: connecting objective and subjective perspectives

F.R. Verdun; *Lausanne/CH (Francis.Verdun@chuv.ch)*

The course will focus on the description and implementation of mathematical model observers for objective image quality assessment in CT. The limitations of the standard methods when dealing with iterative reconstruction will be first presented. Then the concept of model observers will be introduced with some background theory in psychophysics. The concept of ideal and anthropomorphic model observers will be discussed together with their strengths and weaknesses. Then practical examples will be given to show how model observers could be used in the framework of the patient dose optimisation. Finally some work in progress will be presented.

Learning Objectives:

1. To become familiar with the concept of model observers for objectively assessing image quality for clinically relevant tasks.
2. To learn about how objective measurements of physical parameters characterising image quality in CT connect to clinically task-based assessment of image quality.
3. To understand the potential and limitations of automated image quality assessment by means of model observers.

A-248 11:40

Implementing a review process on image quality: experiences from a EuroSafe Imaging Star

F. Deferme; *Edegem/BE (filip.deferme@uza.be)*

Implementing a review process on image quality is the logical next step in documenting justified use of ionising radiation. At Antwerp University Hospital, we are implementing a review process on image quality in 3 different areas. The first step is to implement daily quality control (QC) of all x-ray equipment, using a phantom or copper filter. Depending on the outcome, ”thumbs up” or “thumbs down” dashboard view is provided for management (modality-related QC). The second step involves registration of patient age, weight and gender. For every patient group and for every procedure, the radiographer performing the study is profiled for fluoroscopy time, number of retakes and dose per study. This generates an anonymized dashboard overview of all the radiographers within the department. Individual performances are compared to the “Dose Reference Levels” (DRL), with Belgian and European outcomes in a management dashboard (dose-related QC). The third step entails assessment of image quality by identifying: correct use of lead letters for laterality, positioning, radiation exposure, image noise, and absence of artefacts (removal of jewellery, clothing, etc.). This step is done by the radiologist during reporting (image-related QC). The outcomes of all 3 steps are converted into “Key Performance Indicators” (KPI) for modality, workflow and patient safety. KPI can be used for process improvement and education. In conclusion, it is essential to implement this review process in a fully automated software environment, in conjunction with a dose management and registration system.

Learning Objectives:

1. To learn about the criteria employed for assessing image quality of radiologic examinations.
2. To become familiar with the structure and course of the review process and its routine implementation.
3. To learn about the results of the image quality review process, the intervention levels identified, and the actions taken.

10:30 - 12:00 **Room F1**

E³ - Rising Stars Programme: Basic Session

BS 6

Oncologic therapies

Moderator:
O. Akhan; Ankara/TR

A-249 10:30

Kidney

O. Akhan; *Ankara/TR (oakhan@hacettepe.edu.tr)*

RCC is the most common malignant renal tumour accounting for an estimated 2% to 3% of all malignancies in the United States. Although the incidence of renal tumours has reached to a plateau in the developed countries in recent years it is still increasing in developing countries. As the incidence of the incidentally detected renal masses is increased in the last decade, the management of RCC has greatly changed from radical nephrectomy to nephron-sparing treatment options such as partial nephrectomy or local ablative therapies with RFA, microwave or cryoablation. Although guideline of American Urological Association suggests partial nephrectomy as a standard treatment option for the T1 renal masses, local ablative approach with RFA, microwave or cryoablation are getting to be more applied for the treatment. Relative contraindications for the ablative procedures include proximity to the central collecting system, bowel and adrenal glands. These limitations are overcome by the fluid injection along the margin of the targeted lesion by displacing these anatomical structures. The main indications for renal artery embolization (RAE) include preoperative embolization before nephrectomy, treatment of angiomyolipoma, an adjunctive treatment for RCC ablation and for palliation of advanced-stage RCC. RAE is also indicated to reduce blood loss before resection of metastatic RCC.

Learning Objectives:

1. To have a basic knowledge about indications and limitations of interventional radiology procedures in renal malignancies.
2. To have a basic knowledge about embolisation of renal tumours.
3. To become familiar with ablation of renal tumours.

A-250 10:52

Lungs

M. Bezzi; *Rome/IT (mario.bezzi@uniroma1.it)*

Percutaneous needle biopsy has been a mainstay of oncologic diagnosis for more than three decades, since the advent of CT and ultrasound, and has become the standard of care in the diagnosis of most lung tumours and often in lung inflammation. The technique is also beneficial in the staging of patients with cancer, particularly when another treatment method may be more appropriate than surgical resection. Advantages of percutaneous biopsy over surgical excisional biopsy include time and cost savings and reduction in morbidity. Aim of this presentation is to discuss the practical aspects of lung biopsy, needle selection and guidance techniques and to show how to approach difficult lesions and avoid complications. About 70% of patients with lung cancer are not surgical candidates, either due to advanced disease or comorbidities. Thermal ablation is a minimally invasive treatment that is commonly used in this group of patients, with promising results. Currently, the most widely used ablation techniques in the treatment of lung malignancies are radiofrequency ablation (RFA), microwave ablation, and cryoablation. This presentation reviews the application of thermal ablation in the thorax, including patient selection, basics of procedure technique, imaging follow-up, and treatment results.

Learning Objectives:

1. To have a basic knowledge about indications and limitations of interventional radiology procedures in lung malignancies.
2. To have a basic knowledge about image-guided biopsy.
3. To become familiar with ablation of lung cancer.

A-251 11:15

Bones

A. Gangi; *Strasbourg/FR*

"No abstract submitted."

Learning Objectives:

1. To have a basic knowledge about indications and limitations of interventional radiology procedures in bone malignancies.
2. To understand the basic concepts of embolisation of bone tumours.
3. To have a basic knowledge about bone tumours ablation.

A-252 11:37

Liver

J.I. Bilbao; *Pamplona/ES (jibilbao@unav.es)*

The liver has a dual vascular supply with seventy-five percent of the blood coming from the portal vein and the rest from the hepatic artery. Small (<1mm) tumours are initially nourished by portal branches; however, when they start growing they deliver pro-angiogenic agents which may create an arterial network that ensures its vascularisation. Thus, liver tumours are almost exclusively vascularised by the hepatic artery and can be safely treated by an endovascular approach. The angiographic appearance of a liver tumour depends on the amount of the arterio-capillary network and hypervascular tumours are easily detected and more adequate for receiving endovascular treatments. One therapeutic possibility is to occlude the vascular network and close the afferent vessels ("embolisation") provoking ischaemia that will lead to necrosis. However, since the tumour sends continuously pro-angiogenic signals, if there is a decrease in the blood supply the ischaemic effect will trigger an increase in angiogenesis. For abolishing such effect it is possible to add chemotherapeutic agents ("chemoembolisation"), together with the occluding particles, with the aim of obtaining a more complete antineoplastic effect. A different approach consists in the use of small particles just as carriers, with no occluding effect, that will place an anticancer agent intratumourly. When the agent is a radioisotope the procedure is called "radioembolisation", a form of brachytherapy. Using a percutaneous access, some tumours (<3cm) can be punctured with probes through which energy (heat-radiofrequency/microwaves or cold-cryotherapy) is delivered which will lead to tumoural necrosis ("ablation").

Learning Objectives:

1. To understand the basic concepts of chemoembolisation in liver malignancies.
2. To understand the basic concepts of radioembolisation in liver malignancies.
3. To have a basic knowledge about liver tumours ablation.

Author Disclosure:

J.I. Bilbao: Advisory Board; Boston Scientific, Cook Medical, Bayer. Speaker; Sirtex Medical Europe.

10:30 - 12:00 **Room M 4**

E³ - ECR Academies: Tips and Tricks in Liver, Bile Ducts and Pancreas Imaging

E³ 618

Pancreatic tumours

A-253 10:30

Chairman's introduction

J. Votrubová; *Prague/CZ (votrubovajana@seznam.cz)*

Pancreatic tumours represent a major challenge to radiologists in their recognition and characterisation. Appropriate radiological examination has become increasingly important for appropriate treatment and survival. A variety of imaging studies, including CT, endoscopic ultrasound (EUS), MR and positron emission tomography with 18F-fluorodeoxyglucose (FDG PET) have important roles to play in the diagnosis, initial staging and follow-up of pancreatic tumours. Primary epithelial neoplasms of the pancreas arise either from the endocrine islet cells or from the exocrine parenchymal tissue. The most often pancreatic malignancy represents pancreatic ductal adenocarcinoma, accounting for 75 to 92% of all pancreatic neoplasms. The extent of surgery may depend on tumour size, location, extrapancreatic extension, vascular involvement , lymph nodes involvement and metastases. The primary goals of imaging include accurate diagnosis and staging and, in patients with locally advanced and/or metastatic disease avoidance of inappropriate radical surgery. Among endocrine pancreatic tumours, insulinoma and gastrinoma often cause symptoms of hormone excess despite their inconspicuous size, but they can be successfully removed with improved pre- and intraoperative localization. Other tumours -glucagonoma, VIPoma and non-functioning endocrine pancreatic tumours - are often large or metastasizing, but generally require surgical debulking to alleviate hormonal symptoms and have favourable survival. In some patients, neuroendocrine pancreatic tumours occur as a part of multiple neuroendocrine neoplasia (MEN 1) syndrome. We herein discuss the currently available imaging modalities and their applications in tumour detection and staging as well as in choice of therapy, imaging follow-up and prediction of response, with emphasis on the recent knowledge.

A-254 10:35

A. Staging adenocarcinoma

N. Kartalis; *Stockholm/SE (nikolaos.kartalis@me.com)*

Pancreatic cancer is a disease with very dismal prognosis. The 5-year survival is around 5% and has been stable over the last decades. The only potential curative treatment is surgical resection combined with adjuvant and/or neoadjuvant medical therapy. However, at diagnosis less than 20% of patients have a resectable tumour, while the rest have tumours that are locally advanced and/or have distant metastases. To improve survival, there is a need to increase the number of patients that undergo surgery. However, for the surgical removal to be meaningful, the goal is to achieve complete macroscopic and microscopic removal of tumour (R0-resection). For the identification of patients who will benefit from surgery, the so-called "resectability status" was developed. It is based on the presence and extent of tumour contact with the major peripancreatic vessels such as portomesenteric axis (PV/SMV), hepatic artery, celiac artery and superior mesenteric artery. Depending on the degree of the circumferential tumour-vessel contact, the tumours are classified into one of the three categories: resectable, borderline resectable and unresectable. The criteria of the various existing classification systems will be discussed and their differences outlined. Furthermore, the role of CT, MRI and PET-CT in the evaluation of these patients will be analysed and, finally, important aspects of the post-operative imaging follow-up will be presented.

Learning Objectives:

1. To understand the rationale behind local staging of pancreatic adenocarcinoma.
2. To learn about the respective role of CT, MRI and PET-CT.
3. To become familiar with the principle of postoperative follow-up.

A-255 11:03

B. Neuroendocrine tumours

R. Manfredi; *Verona/IT (riccardo.manfredi@univr.it)*

Neuroendocrine tumours account for 1.2%-1.5% of all gastrointestinal neoplasms, with an incidence of 1.6-2.0 new cases per 100,000 persons per year. The majority of neuroendocrine tumours occur sporadically, that is, they are non-familial. However, they sometimes occur as part of complex familial endocrine cancer syndromes such as type 1 multiple endocrine neoplasia (MEN 1) and neurofibromatosis type 1. Immunohistochemical staining has played an important role in the diagnosis of neuroendocrine tumours. The neuroendocrine cells of the diffuse neuroendocrine system are characterized by the expression of certain marker protein, such as chromogranin, synaptophysin and neuron-specific enolase (NSE). Clinically, neuroendocrine tumours of the pancreas are classified into functioning and non-functioning tumours, according to the symptoms. Non-functioning, hormonally silent, neuroendocrine tumours (NF-NET) represent 68-80% of all NETs, and are diagnosed because of the mass effect exerted by the tumour. Abdominal pain is the most frequent presenting symptom (35-78%), followed by weight loss (20-35%), anorexia and nausea (45%), palpable mass (7-40%) and jaundice (17-50%). According to the 2010 WHO classification, neuroendocrine neoplasms are classified according to the percentage of Ki67, a protein index of cell replication, on the pathologic specimen. There are three categories: G1, Ki-67 index ≤2%; G2, Ki-67 index between 3% and 20%; G3, with Ki-67 index >20%. At diagnostic imaging, neuroendocrine neoplasms are hypervascular compared to adjacent pancreas in 74% of the cases. Hyper- or isovascularity represents the most suggestive features of neuroendocrine neoplasms that are helpful in the differential diagnosis with adenocarcinoma.

Learning Objectives:

1. To understand the basics of histological classification of neuroendocrine tumours.
2. To learn about the natural history of these tumours.
3. To become familiar with the usual appearance and imaging specificities of neuroendocrine tumours.

A-256 11:31

C. Tough clinical cases

T.C. Lauenstein; *Essen/DE (thomas.lauenstein@evk-duesseldorf.de)*

The ability to non-invasively diagnose and characterise pancreatic tumours has vast therapeutic implications. However, there are several aspects that may impede a reliable characterisation of a pancreatic lesion. While some pancreatic tumours exhibit typical imaging findings, there is often an overlap of imaging findings between different lesions, e.g. pseudotumours due to chronic pancreatitis and adenocarcinoma of the pancreas. We often face the same dilemma as far as cystic pancreatic lesions are concerned since some cystic tumours have a potential for malignant transformation including IPMN or mucinous cystadenomas. Furthermore, there is a large variety of diagnostic tools available for the assessment of pancreatic disease, including ultrasonography, endosonography, CT, MRI and PET. It is important to

understand strengths and weaknesses of these diagnostic modalities particularly in equivocal cases of pancreatic lesions. Eventually, biopsy samples are often needed either to establish a diagnosis or to allow for a more profound histopathological analysis of tumour tissue. Several challenging cases of pancreatic tumours will be presented in this lecture. Differential diagnoses will be discussed and a diagnostic algorithm for each case will be proposed.

Learning Objectives:
1. To be able to define diagnostic probabilities when facing an unknown case of solid mass in the pancreas.
2. To understand the role of multimodality approach, including endosonography and biopsy.

10:30 - 12:00 **Room M 5**

Joint Course of ESR and RSNA (Radiological Society of North America): Hybrid Imaging

MC 628
Hybrid imaging in the female

Moderators:
A. Drzezga; Cologne/DE
K. Riklund; Umea/SE

A-257 10:30
A. Pelvic tumours
F. Dehdashti; *St. Louis, MO/US (dehdashtif@mir.wustl.edu)*

This presentation summarizes the literature in PET/CT and PET/MRI in the evaluation of the three most common gynaecologic malignancies: cervical, endometrial and ovarian cancers. The advantages and challenges of each hybrid modality will be briefly discussed. In addition to clinically used 2-[^{18}F]fluoro-2-deoxy-D-glucose (FDG), novel tracers such as ^{18}F-fluorooestradiol (FES), an oestrogen-receptor imaging tracer, 3´-deoxy-3´-[^{18}F]fluorothymidine (FLT), a proliferative tracer and ^{18}F-fluoroazomycinarabinoside (FAZA), a hypoxic tracer that are currently used for research purposes in these malignancies will be briefly discussed.

Learning Objectives:
1. To learn about different tracers.
2. To understand how to interpret hybrid imaging examinations of the pelvis.
3. To learn about the role of hybrid imaging in staging, treatment evaluation and follow-up.

A-258 11:00
B. Breast cancer
O. Ratib; *Geneva/CH*

Hybrid imaging has gained important role in staging and treatment monitoring as well as in detection of recurrence of breast cancers. From SPECT-CT applications of bone metastases, to whole-body staging with PET-CT to the newer applications of hybrid PET-MR that allow to benefit from that added value of functional imaging and tissue characterization of MRI combined with metabolic and imaging biomarkers of PET. In this refresher course, we will review the current state of recommended applications of hybrid imaging in breast cancers. The basic applications of FDG - PET in staging of regional lymph nodes and distance metastases as well as its added value in monitoring the responses to neoadjuvent chemotherapy. Beyond these well-established applications a review of upcoming new tracers and their potential advantages will also be addressed. Finally a detailed evaluation of hybrid PET-MRI applications in management of breast cancers will be presented highlighting the added value of complementary information gathered from these two modalities.

Learning Objectives:
1. To learn about pathophysiology and relation to different tracers.
2. To understand how to interpret hybrid imaging examinations of the breast.
3. To learn about the role of hybrid imaging in staging, treatment evaluation and follow-up.

A-259 11:30
C. Interactive case discussion (part 1)
F. Dehdashti; *St. Louis, MO/US (dehdashtif@mir.wustl.edu)*

Imaging is critical for staging, determining prognosis and treatment strategy, and in predicting prognosis in gynaecological malignancies. In this case presentation session, common clinical applications of PET/CT and PET/MRI in the evaluation of the most common gynaecologic malignancies will be presented. In addition, the advantages and disadvantages of each hybrid modality will be illustrated and discussed.

Learning Objectives:
1. To understand how to interpret hybrid imaging in female pelvic tumours.
2. To understand how to interpret hybrid imaging in breast cancer.
3. To learn how to avoid common pitfalls.

A-260 11:45
C. Interactive case discussion (part 2)
O. Ratib; *Geneva/CH*

Learning Objectives:
1. To understand how to interpret hybrid imaging in female pelvic tumours.
2. To understand how to interpret hybrid imaging in breast cancer.
3. To learn how to avoid common pitfalls.

12:15 - 12:45 **Room A**

Headline Session

HL 1
Wilhelm Conrad Röntgen Honorary Lecture

Presiding:
P.M. Parizel; Antwerp/BE

A-261 12:15
Dissatisfaction, burnout and inequality: three major challenges in radiology
M. Castillo; *Chapel Hill, NC/US (Mauricio_castillo@med.unc.edu)*

Are you working more? Is your salary higher? Are you hiring more, or less women in your practice? Recent statistics show that radiologist's salaries are decreasing and that only one half of us feel fairly compensated and would become radiologists again given the opportunity. This has led to radiologists leaving our profession to work for the industry at record numbers. With less radiologists, we work more. Studies show that radiology residents have a high burnout rate and that nearly 20% of them feel clinically depressed. These rates are even higher for radiologists in practice in whom depression rates reach 40% and suicidal ideation reaches 7%. Perfectionism, self-critical, inflexible and idealism are personality traits that contribute to burnout. At my school, the University of North Carolina, the School of Medicine has now adopted "improving the life of the provider" as one of its main aims in an attempt to prevent burnout. Dissatisfaction and burnout have resulted in an all-time low number of applications to radiology residencies and fellowships, especially from women who find the speciality incompatible with their lifestyle and family responsibilities. Only 16% of all radiologists are female, in academia Radiology departments have one of the lowest percentages of women, and overall women make 25% less salary than males. Thus, we must work to improve our life-work balance, our purpose-values balance, our professional-personal health, and end salary and academic inequalities for women.

12:30 - 13:30 **Room C**

E³ - The Beauty of Basic Knowledge: Chest Imaging

E³ 25B
How to avoid misdiagnosis on the chest x-ray

Moderator:
N. Howarth; Chêne-Bougeries/CH

A-262 12:30
A. Neoplastic lesions
J. Vlahos; *London/UK*

"no abstract submitted"

Learning Objectives:
1. To review the reasons for misdiagnosis on the chest x-ray.
2. To learn how to focus on blind areas.
3. To know the consequences of a misdiagnosis.

A-263 13:00

B. Non-neoplastic lesions

A.R. Larici; *Rome/IT (annarita.larici@unicatt.it)*

Although the clinical value of chest x-ray remains undiminished, errors in interpreting chest x-ray is still one of the most frequent issue in clinical practice, also in the context of benign lesions. This presentation will cover the predefined learning objectives using side-by-side plain film and CT imaging to help understand how to systematically review chest x-ray and improve radiologist's performance and accuracy in interpreting images. Observer error is one of the most important cause of misdiagnosis when looking at the chest x-ray, and includes scanning error, recognition error, decision-making error and satisfaction of search. Technical considerations, such as image quality and patient positioning and movement, are also factors that can contribute to the likelihood of missing lung lesions. Lesion characteristics also play a critical role and include lesion size, conspicuity and location. Imaging features of the common chest diseases, including those of the diaphragm, pleura and chest wall, as well as diseases of the mediastinum, pulmonary hilum and vascular system, will be reviewed on a case-based approach. The possible consequences of misdiagnosing a benign lesion at chest x-ray will be shown by discussing some explicative clinical cases. The skills required for an accurate interpretation of imaging of the mediastinum, pleura and chest wall will be explored and provided.

Learning Objectives:

1. To review the reasons for misdiagnosis on the chest x-ray.
2. To learn how to interpret the chest x-ray more accurately.
3. To know the consequences of a misdiagnosis.

12:30 - 13:30 **Room D**

E³ - The Beauty of Basic Knowledge: A Survival Guide to Musculoskeletal Imaging

E³ 24B

Chronic trauma: spectrum of bone response

Moderator:
V.N. Cassar-Pullicino; Oswestry/UK

A-264 12:30

Chronic trauma: spectrum of bone response

A.H. Karantanas; *Iraklion/GR (akarantanas@gmail.com)*

The bones are able to develop adaptive mechanisms which are sensitive to their mechanical environment. Thus, bone is constantly remodelled, throughout life, by the coordinated action of bone-resorbing osteoclasts and bone-forming osteoblasts. This remodelling process serves to prevent and heal fatigue-related micro-injuries due to overloading. The balance between the amount of bone resorption and formation determines whether the process of bone remodelling leads to a net loss or gain of bone mass. Chronic trauma may be applied on normal or weakened bone and on mature or immature skeleton. The imaging findings of the resulting painful syndromes cover a wide spectrum. Chronic overload ranges from stress reaction to stress fracture. The former is occult and the latter rarely obvious on radiographs. Fatigue injuries result from stress on normal bone and insufficiency injuries from stress on abnormal bone. Both pathomechanisms may coexist in certain groups of adults. In the immature skeleton, repetitive injury may cause in addition osteochondritis dissecans, osteochondral lesions, physiolysis and chronic apophysitis. Abnormal loading matched with various parameters may result in periprosthetic fractures. Bisphosphonates may induce suppression on the bone turnover, particularly in jaw and proximal femur, resulting in osteonecrosis and insufficiency fractures. Plain films remain the first imaging modality for exploring a pain response in chronic trauma. However, very often, plain films are normal. MRI is able not only to show even subtle findings, responsible for the clinical syndrome, but also to grade the lesions and match with known risk factors to guide the treatment.

Learning Objectives:

1. To become familiar with the pathomechanisms that can affect the axial and peripheral skeleton in chronic trauma.
2. To understand the radiological manifestation of these pathological mechanisms.
3. To appreciate how to best use imaging modalities in diagnosing occult and overt injury and monitoring the response to Treatment.

14:00 - 15:30 **Room A**

E³ - ECR Academies: Interactive Teaching Sessions for Young (and not so Young) Radiologists

E³ 721

MR imaging in sports medicine II

A-265 14:00

A. Sports injuries of the ankle

P. Robinson; *Leeds/UK (philip.robinson10@nhs.net)*

Acute ankle injuries are among the commonest problems encountered at all levels of sporting activity and thus even rare chronic sequelae are still a significant problem. Radiologists play an important role in imaging and treatment of athletes with acute and chronic injuries as clinical assessment is often difficult and non-specific. This presentation will illustrate ankle anatomy and the most significant sports-related acute and chronic injury processes and demonstrate the use of MR imaging and ultrasound in the diagnosis and management of these conditions, where appropriate image-guided therapy will also be discussed. Acute sports injury processes will include osseous, osteochondral and ligament injury. Chronic overuse injuries to the tendons, osteochondral unit and soft tissue impingement syndromes will be illustrated.

Learning Objectives:

1. To learn the anatomy of the ankle.
2. To learn the evaluation of common ankle injuries.

A-266 14:45

B. Shoulder injury

M. Zanetti; *Zurich/CH (marco.zanetti@hirslanden.ch)*

Standard radiographs, MR imaging, CT and ultrasound provides clinically useful information in detecting and characterizing injuries of the rotator cuff, cartilage, labrum and bone. The appropriate use of these modalities in common and uncommon shoulder injuries will be demonstrated in an interactive session. Tips and tricks will be given with the special focus on the normal anatomy, variants and potential pitfalls.

Learning Objectives:

1. To review the anatomy of the shoulder in three dimensions.
2. To learn the evaluation of common shoulder injuries.

14:00 - 15:30 **Studio 2017**

Joint Session of the ESR and ERS

ESR/ERS

Novel strategies in idiopathic interstitial pneumonia

Moderators:
K.M. Antoniou; Iraklion/GR
C.M. Schaefer-Prokop; Amersfoort/NL

A-267 14:00

Updated clinical practice guidelines for classification

A.U. Wells; *London/UK (RBHILD@rbht.nhs.uk)*

Updated clinical practice guidelines for classification. The 2011 ATS/ERS/JRS/ALAT guidelines for the diagnosis of idiopathic pulmonary fibrosis (IPF) serve to identify a large sub-group of IPF patients in whom a confident diagnosis can be made with, based upon a) typical HRCT findings of usual interstitial pneumonia (UIP) or b) UIP at surgical biopsy when HRCT appearances are atypical. However, guideline criteria fail to diagnose at least 50% of IPF patients, due to concerns about mortality associated with diagnostic surgical biopsy. Developments related to classification and the diagnostic tools by which disease is classified include: 1) in the 2013 ATS/ERS updated classification of the idiopathic interstitial pneumonia, a category of "unclassifiable disease" is formalised and a disease behaviour classification is proposed as a guide to treatment goals and their achievement. This category includes a large sub-group of IPF patients not diagnosed using current criteria. 2) The development of cryobiopsy should allow increased use of histologic data in the formulation of an IPF diagnosis with particular reference to older patients with greater pulmonary function impairment. 3) A current ERS task force has proposed an algorithm allowing the formulation of a working diagnosis of IPF in multidisciplinary discussion in cases not meeting guideline criteria.

Learning Objectives:
1. To appreciate the rationale for the roles of pathology, radiology, and pneumology.
2. To understand strengths and weaknesses of pathology.
3. To become familiar with novel developments in histopathology.
Author Disclosure:
A.U. Wells: Advisory Board; Roche/Intermune, Boehringer Ingeleim, Bayer. Consultant; Roche/Intermune, Gilead, Boehringer Ingelheim, Bayer. Speaker; Roche/Intermune, Chiesi, Boehringer Ingelheim, Bayer.

A-268 14:22

CT patterns for classification
N. Sverzellati; *Parma/IT*

In 2013, the consensus statement on idiopathic interstitial pneumonias (IIPs) was updated, with the aim of adding further precision to the diagnosis/management of the IIPs. Radiologists are central to the evaluation of patients with IIPs. Radiologists should first distinguish fibrosing from non-fibrosing entities. The main computed tomography (CT) differential of fibrosing lung disease is between the usual interstitial pneumonia (UIP) pattern and other fibrotic patterns such as non-specific interstitial pneumonia (NSIP). When definite UIP pattern is not fulfilled, the differential between UIP and NSIP should rely on CT characteristics of reticular opacities and clinical features, notably age. An important addition is a disease behaviour classification, which provides a framework for management of cases that are unclassifiable or where a histologic diagnosis cannot be obtained.
Learning Objectives:
1. To consolidate knowledge about the anatomical and pathological correlates.
2. To learn about the criteria for usual interstitial pneumonia (UIP).
3. To learn about the criteria for non-specific interstitial pneumonia (NSIP).
Author Disclosure:
N. Sverzellati: Speaker; Dr. Sverzellati reports personal fees from Roche and Boehringer Ingelheim.

A-269 14:45

Updated clinical practice guidelines for treatment
V. Poletti; *Forli/IT (venerino.poletti@gmail.com)*

IPF is a disorder with a sort of unpredictable behaviour with, broadly speaking, rapid progressions and slow progressions. Biomarkers such as specific autoantibodies, morphologic features might be valid indicators of the incoming lung function decline. The use of less invasive procedures such as transbronchial cryobiopsy may strengthen the clinical-radiologic correlation and allow identification of new imaging markers of the disorder that could have diagnostic and prognostic impact (presence of upper lobe subpleural thickening-elastotic fibrosis, nodular calcifications, peripheral bronchiolar proliferation, etc.). Also genomic studies on lung samples or even culture of cells obtained by this method could increment the "personalized diagnostic and therapeutic" approach. So far, however, specific antifibrotic drugs are identified as efficacious in reducing the functional decline in IPF subject and in reducing the mortality risk. Clinicians' task is to clearly define patients with a high probability diagnosis of IPF (not only according to rigid guidelines but also taking into account the clinical profile/clinical behaviour, data provided by biomarkers, CT scan and morphology) to adjust the therapy for the single patient. Learning points: clinical diagnosis of IPF, treatment of patients with a high probability diagnosis of IPF, identification of new effective endpoints to design clinical trials and identification of new efficacious drugs.
Learning Objectives:
1. To learn about the clinical course and prognosis.
2. To consolidate knowledge about the standard therapy.
3. To become familiar with novel therapies.
Author Disclosure:
V. Poletti: Advisory Board; oche, Boehringer Ing. Speaker; oche, Boerhinger Ing, Chiesi.

A-270 15:07

CT and MRI for monitoring therapy response and inflammatory activity
J.A. Verschakelen; *Leuven/BE (johny.verschakelen@uz.kuleuven.ac.be)*

Being an integral tool in the multidisciplinary team approach of idiopathic interstitial pneumonias (IIPs), CT helps to make the diagnosis and may predict prognosis and survival. However, since it is clear now that less typical CT patterns may also be predictive of pulmonary fibrosis and especially since the recent successful introduction of antifibrotic therapy, there is a growing need for a more accurate prognostic evaluation and for an accurate assessment of longitudinal behaviour and response to treatment. While monitoring prognosis and therapy response is predominantly based on clinical data (pulmonary function tests), many methods to quantify disease with CT (and few with MRI) ranging from visual estimates to the use of sophisticated software were developed and used although mostly in study circumstances. In this presentation, the need for prognostic and therapy response imaging and the potentials and pitfalls of (semi)quantitative imaging biomarkers will be discussed. Using imaging biomarkers is challenging since both qualitative and (semi)quantitative measurement results reflect the effect of different processes like inflammation, fibrosis and lung destruction that interact with each other, vary in time and may be different in different parts of the lung. In addition, some of these processes are not well understood. Especially, estimating the amount of inflammation may be difficult, although novel techniques to image inflammation have been proposed. A short review of these techniques will be given.
Learning Objectives:
1. To consolidate knowledge about the rationale for therapy response imaging.
2. To learn about quantitative imaging biomarkers.
3. To become familiar with novel options of imaging inflammation.

14:00 - 15:30 **Room M 3**

ESOR Session

How to gain and maintain quality education in radiology

Moderators:
N. Gourtsoyiannis; Athens/GR
P.M. Parizel; Antwerp/BE

A-271 14:00

Introduction
P.M. Parizel; *Antwerp/BE*

A-272 14:05

ESOR in action 2017
N. Gourtsoyiannis; *Athens/GR (gournick@gmail.com)*

A-273 14:15

How to improve education in radiology
S.J. Golding; *Oxford/UK (stephen.golding@nds.ox.ac.uk)*

Most radiologists require teaching skills: there is always someone to teach, whatever the professional setting. Academic radiologists have undergraduate and postgraduate students but all radiologists may teach clinicians, technicians and nurses. These skills begin with understanding both the needs and the viewpoint of the particular student and ensuring that teaching exchange is bilateral and interactive. An ability to understand and set an appropriate learning environment is essential, as is a broad knowledge of the methods of teaching delivery which may be employed. In addition to traditional methods, these include computer-based methods, e-learning approaches and use of social media: radiology lends itself well to such methods. An understanding of the mental process which takes place in learning and the role of student assessment in driving this should be acquired by all teachers. The effective teacher of radiology will possess the widest armamentarium of approaches to teaching and will be able to adapt these to the needs and circumstances of the individual student. They will also proactively practice self-improvement by obtaining regular feedback from their students and colleagues and by attending courses and studying the educational literature. Ideally, radiologists will always be represented on the bodies which set students' curricula and define their learning outcomes.

A-274 14:30

Feeling confident? Evaluating competencies
O. Kolokythas; *Seattle, WA/US (orpheus@uw.edu)*

Development of competency and professionalism of medical trainees is fostered by regular self-reflection and assessment. While promoted and recommended by national and local educational authorities, the implementation of a robust evaluation process in clinical routine might be challenged by many factors including lack of formal assessment tools, time constraints, absence of incentives, subjective decision making and non-separation of performance related and professional issues. Two basic forms of assessments are being distinguished: A) verbal feedback, which is based on informal communication, is instant, spontaneous, personal and specific, is given by one peer and is related to one situation; B) written evaluation, which is based on a standardized structured approach, is scheduled to occur regularly, done by more than one peer, assessing competency and professionalism over a period of time. Requirements to a robust assessment process include standardization, consistency, objectivity, specificity, relevance, validity, impact, practicability, timeliness, efficiency, availability, comparability, confidentiality, transparency and stability of systems. Since a purely number-based approach on competency and professionalism is of poor prognostic value, individual comments are a precious asset to the assessment process and allow for documentation of more specific nuances without jeopardizing overall efficiency

of the process for all. Demands on trainees and peers to successfully participate in a standardized evaluation process include the willingness to promote the quality of education, the commitment to regularly participate in the process, readiness for realistic self-reflection of trainees and commitment of peers to openly address deficiencies of trainees using a fair and non-subjective approach.
Author Disclosure:
O. Kolokythas: Other; Editor of SOCRATES digital evaluation system.

A-275 14:45

Lifelong learning: stay sharp in the field of radiology
B. Ertl-Wagner; *Munich/DE (Birgit.Ertl-Wagner@med.uni-muenchen.de)*

The performance and reporting of radiological procedures and of image-guided interventions is a complex clinical act, which only appropriately trained physicians should embark on. The European Training Curriculum for Radiology recommends a five-year training period in radiology, consisting of Level I training for the first three years followed by two years of a more flexible Level II training scheme with potential special interest rotations during the last two years. Its content is based on knowledge, skills, competences and attitudes. The European Diploma in Radiology (EDiR) can be undertaken after a five-year training period in radiology. In addition to the Level I and II curricula of the ETC, the level III curriculum provides the content basis for subspecialisation. To stay sharp in the field of radiology, it is of utmost importance to remain on a path of lifelong learning. Important tools include not only lectures and workshops at conferences but also online resources.

A-276 15:00

Find your mentor and stick together
C.A. Minoiu; *Bucharest/RO (costin.minoiu@gmail.com)*

Mentorship is widely accepted as an important component of development in most medical specialities; however, radiology residents, in many training centres in Europe, lack mentoring. The present talk highlights the importance of a reciprocal collaboration between junior and senior professionals with the primary goal being the nurturing of the junior professional's future pathway, mentoring relationships being critical for the professional development and career advancement. The role of the mentor should be focused both on professional and personal development of the mentees based on their needs and according to a well-defined specific teaching agenda. For a successful mentoring relationship, potential barriers should be understood, and specific pathways for improved implementation of mentor programmes should be defined to allow a good matching system between compatible mentors and mentees. Although the importance of mentorship in facilitating both professional and academic research careers has been largely described, little is understood about early career research mentorship for residents. Successful mentoring programs have been associated with increased involvement in research, enhanced career satisfaction, and pursuit for academic careers. Such programs can help at an individual level as well as at an institutional one, widening networking and cross-disciplinary research and clinical collaborations.

15:15
Awards

14:00 - 15:30 **Room M 4**

E³ - ECR Academies: Spinal Imaging

E³ 719
Spine: osseous lesions

A-277 14:00

Chairman's introduction
F. Kainberger; *Vienna/AT*

Osseous lesions of the vertebra, mainly manifesting as signal alterations of the bone marrow, are challenging because of the sometimes only subtle differences among these entities. Indications drive the proper work-up especially in these situations: Spondylarthropathies may be suspected clinically with a sensitivity of more than 70 percent. Skeletal metastasis, plasmocytoma and primary bone tumours are in many cases part of a step-wise oncologic workup. Bone marrow hyperplasia can be better differentiated from hematopoetic diseases better when knowing the life-style parameters. The red-flags concept has only in part been proven helpful and may be replaced by more sophisticated questionnaires. The investigation with projection radiography and MRI should include in many of these cases the whole-spine. In rheumatic and infectious inflammatory diseases the sacrum and the sacroiliac joints must be included. The interpretation of focal spinal lesions relies on the differentiation of osteolytic or sclerotic bone lesions. Pitfalls may be avoided by exactly differentiating the localisation within the vertebra and the patterns of bone marrow edema. Tricky lesions are atypical hemangioma, metastasis with a mixed pattern, lytic-expansile fibrous dysplasia and SAPHO. Diffuse spinal abnormalities mainly manifest as osteoporotic on projection radiographs or bone marrow changes with MRI. Diffuse haematopoetic marrow hyperplasia may be due to chronic anaemia, infection, chemotherapy, adiposity in females, heavy smoking and long-distance running. In conclusion, the diagnostic workup of osseous spinal lesions, mainly the indications for imaging, has changed and is continuously changing.
Session Objectives:
1. To establish a structured indication basing on clearly pre-defined questions.
2. To understand the distinct patterns of osseous spine lesions on projection radiographs and MRI.

A-278 14:05

A. Primary bone tumours
J.L. Bloem; *Leiden/NL (j.l.bloem@lumc.nl)*

Metastases and myeloma are much more frequent than primary tumours of the spine. Only mature haemangiomas and enostosis are frequent asymptomatic incidental findings in the spine. In patients younger than 30 years, primary osseous tumours do occur with an incidence of <5% of primary osseous tumours, and may present with pain, associated scoliosis, or neurological symptoms. Most of these, with the exception of Ewing sarcoma (and its metastases) and osteosarcoma are benign and include osteoid osteoma, osteoblastoma, ABC, Langerhans cell histiocytosis, giant cell tumour, and vascular haemangiomas. These aforementioned tumours constitute 80% of all primary osseous tumours in the spine. In patients >30 years, some of these benign conditions are also seen (giant cell tumour), but malignant tumours (chordoma, lymphoma) are becoming more frequent. Benign lesions that are increasingly diagnosed and have specific features are hibernoma and benign notochord tumour. Normally primary osseous tumours of the spine can be differentiated using radiologic criteria from metastases and infection. Radiological features used in diagnosis that will be discussed include location in the spine (sacrum: chordoma, GCT. Location in posterior elements: osteid osteoma, osteoblastoma, osteochondroma), MR signal intensity (low SI in GCT), presence of marked reactive changes (osteoid osteoma, osteoblastoma, Langerhans cell histiocytosis, chondroblastoma), CT density, morphology, way of extending into nearby anatomical structures.
Learning Objectives:
1. To learn how to use MR parameters to suggest a specific diagnosis.
2. To learn how to use radiographic and clinical parameters to suggest a specific diagnosis.
3. To identify the new types of spinal tumours and their radiological features.

A-279 14:33

B. Early diagnosis of spondyloarthropathies
J.A. Narvaez; *Barcelona/ES (jose_a_narvaez@hotmail.com)*

The use of magnetic resonance imaging (MRI) has changed the understanding of SpA. The ability of MRI to directly detect typical inflammatory changes makes possible to establish the diagnosis early in the disease, when radiographs are normal (non-radiographic axial SpA). Detection of inflammatory changes (bone oedema) on MRI of the sacroiliac joints has been included as a major criterion in the Assesment of Spondyloarthritis International Society (ASAS) classification criteria for axial SpA. Although not included in these ASAS criteria, MRI of the spine is an useful tool in the diagnosis, because spinal involvement may occur prior to or even without sacroiliitis. The lesion type most characteristic for SpA on spinal MRI is bone oedema at one or more of the four corners of vertebral bodies (called anterior/posterior spondylitis). Bone oedema in the lateral body and posterior arch of the spine (costovertebral arthritis, spinal ligaments enthesitis) is highly specific, but their use for diagnostic purposes was limited by low sensitivity. Fatty deposition at the vertebral corners is typical for axial SpA, but lacks specificity, because may also be seen as a consequence of degenerative disc disease. MRI of the spine may also be used to: a) assess and monitor disease activity, b) predict outcome/severity, since MRI vertebral corner inflammatory or fatty lesions are associated to the development of new radiographic syndesmophytes, and c) predict treatment effect, because extensive bone oedema on MRI, particularly in the spine in patients with AS, is a good predictor to clinical response to anti-TNF-alpha treatment in axial SpA.
Learning Objectives:
1. To identify the MR features in the axial skeleton of early spondyloarthropathies.
2. To differentiate systemic inflammatory changes from other entities.
3. To learn the importance of imaging in patients managing and outcome.

A-280 15:01

C. Diffuse bone marrow disorders: myeloma and metastases

A. Baur-Melnyk; *Munich/DE (Andrea.Baur@med.uni-muenchen.de)*

Multiple myeloma represents a malignant bone marrow neoplasia in which a monoclonal strain of atypical plasma cells proliferate. Due to various therapeutical options and due to the large variance in survival, the sensitive detection of myeloma involvement of the skeleton is mandatory to enable for an accurate staging. In MRI, 5 different infiltration patterns can be found. The most sensitive imaging method for multiple myeloma is MRI. Whole body MRI is superior to conventional skeletal survey and whole body MDCT. On the other hand, MDCT is the method of choice for displaying osteolysis and determining the fracture risk. Durie and Salmon staging system created in 1975 is the most widely used clinical staging system. It combines laboratory and imaging data (x-rays). In 2003, the Durie and Salmon PLUS staging system has been released, which includes whole body MRI and or PET-CT data. Bone metastases are the most common secondary bone tumours of the spine. CT can clearly demonstrate tumour matrix and the extent of osseous destructions. The radiologist should give a fracture risk assessment. MRI is the most sensitive method for metastasis detection by showing directly bone marrow involvement. Different pseudotumours and bone marrow lesions and variations can mimic metastases. Sometimes malignant collapse of a vertebra is the first sign of a malignancy. It is of clinical importance to differentiate it from an acute benign osteoporotic vertebral collapse. Morphologic as well as special sequences, such as DWI, can help in finding the correct diagnosis.

Learning Objectives:

1. To discuss the advantages and disadvantages of MR, CT, and PET/CT in diagnosis.
2. To identify MR features in multiple myeloma and metastasis.
3. To know the imaging role in treatment planning and monitoring therapy of metastases and myeloma.

14:00 - 15:30 **Room M 5**

Joint Course of ESR and RSNA (Radiological Society of North America): Hybrid Imaging

MC 728

Hybrid imaging of the brain

Moderators:
A. Drzezga; Cologne/DE
K. Riklund; Umea/SE

A-281 14:00

A. Neurodegenerative disorders

H. Barthel; *Leipzig/DE (Henryk.Barthel@medizin.uni-leipzig.de)*

Integrated PET/MRI systematically offers a complementary combination of two modalities which has often proven itself superior to the single modality approach in the diagnostic workup of neurodegenerative diseases. Emerging brain PET tracers, like amyloid or tau tracers, technical advances in multi-parametric brain MRI and obvious workflow advantages may enable brain PET/MRI to significantly improve diagnostics of dementia disorders and Parkinsonian syndromes. Moreover, simultaneous PET/MRI is well suited to study complex brain function in which fast fluctuations of brain signals (e.g. related to task processing or in response to pharmacological interventions) need to be monitored on multiple levels. Further, brain PET/MRI is considered the ideal tool for anti-neurodegenerative drug testing.

Learning Objectives:

1. To learn about pathophysiology in neurodegenerative disorders.
2. To learn about different tracers and how to interpret the findings.
3. To understand the role of hybrid imaging in neurodegenerative disorders.

Author Disclosure:
H. Barthel: Consultant; Piramal Imaging. Speaker; Siemens Healthcare, Piramal Imaging.

A-282 14:30

B. Brain tumours

J. McConathy; *St. Louis, MO/US (jmcconathy@uabmc.edu)*

Neuroimaging with positron emission tomography (PET) and magnetic resonance imaging (MRI) plays a critical role in the diagnosis, treatment planning, and post-treatment evaluation of patients with primary and metastatic brain tumours. This presentation will discuss the use of molecular neuroimaging in conjunction with MRI for neuro-oncology. The use of [F-18]FDG and radiolabeled amino acids will be reviewed, and the potential applications of PET/MRI for brain tumour imaging will be presented.

Learning Objectives:

1. To get an overview of brain tumours and tracers used.
2. To learn how to interpret the examinations.
3. To understand the role of hybrid imaging of brain tumours.

Author Disclosure:
J. McConathy: Advisory Board; Blue Earth Diagnostics. Consultant; Siemens Healthcare, GE Healthcare.

A-283 15:00

C. Interactive case discussion (part 1)

H. Barthel; *Leipzig/DE (Henryk.Barthel@medizin.uni-leipzig.de)*

Integrated PET/MRI systematically offers a complementary combination of two modalities which has often proven itself superior to the single modality approach in the diagnostic workup of neurodegenerative diseases. In this presentation, interesting case examples of neurodegenerative disorders will be discussed. It will be demonstrated how combined PET/MRI simplifies and improves early and differential diagnosis.

Learning Objectives:

1. To learn about evaluation of hybrid imaging in neurodegenerative disorders.
2. To learn about evaluation of hybrid imaging of brain tumours.

Author Disclosure:
H. Barthel: Consultant; Piramal Imaging. Speaker; Siemens Healthcare, Piramal Imaging.

A-284 15:15

C. Interactive case discussion (part 2)

J. McConathy; *St. Louis, MO/US (jmcconathy@uabmc.edu)*

Learning Objectives:

1. To learn about evaluation of hybrid imaging in neurodegenerative disorders.
2. To learn about evaluation of hybrid imaging of brain tumours.

Author Disclosure:
J. McConathy: Advisory Board; Blue Earth Diagnostics. Consultant; Siemens Healthcare, GE Healthcare.

16:00 - 17:30 **Room A**

E³ - ECR Academies: Interactive Teaching Sessions for Young (and not so Young) Radiologists

E³ 821

Paediatric radiology for the general radiologist

A-285 16:00

A. Fractures in children

K.J. Johnson; *Birmingham/UK (karl.johnson@bch.nhs.uk)*

Traumatic injury and fracturing is one of the commonest reasons why children present to hospital and undergo radiological investigation. The anatomy and physiology of the growing skeleton is different to that of adults and as a consequence, some of the fractures and injuries are unique to children. This presentation will demonstrate the various types of incomplete fracture which occur within the more plastic skeleton of the child. It will detail the different types of Salter-Harris fractures which can occur across the unfused growth plate. The differences in relative strength of bone and ligamental attachments which are seen in children and the consequences of the different types of injuries which can occur will be illustrated. The importance of recognising normal variants of growth from pathological change will also be highlighted. The importance of understanding the child's development and mobility and how this correlates with the injury patterns seen in normal childhood will be discussed along with an understanding of the injury patterns and fracture types which occur from inflicted physical injury.

Learning Objectives:

1. To become familiar with different traumatic fracture types.
2. To identify possible criteria for child abuse.

A-286 16:45

B. MRI-typical paediatric applications in musculoskeletal imaging

A.M.J.B. Smets; *Amsterdam/NL (a.m.smets@amc.uva.nl)*

Musculoskeletal MRI plays an important role in the diagnosis of developmental, metabolic, infectious, inflammatory, traumatic and oncologic diseases in children and adolescents. Before skeletal maturity, imaging characteristics are influenced by the transformation of cartilage to bone and the conversion of red to yellow bone marrow. These features are to be taken into account both for the choice of sequences and parameters as for image interpretation. The

processes of growth also affect the mechanisms of trauma and infection and the types of conditions that can be encountered in childhood and adolescence. Indications for paediatric musculoskeletal MRI and MRI findings in paediatric musculoskeletal disorders will be discussed.

Learning Objectives:

1. To learn indications of paediatric MRI.
2. To become familiar with MR imaging findings in children.

16:00 - 17:30 **Room B**

Special Focus Session

SF 8

The postoperative abdomen: lost in translation?

A-287 16:00

Chairman's introduction: Presentation of a challenging case

Y. Menu; *Paris/FR (yves.menu@sat.aphp.fr)*

Previous surgery is always a major difficulty when reporting on abdominal imaging. Some surgery is quite obvious, like hepatectomy or colectomy, some may be less apparent like by-pass, complex bowel surgery or even atypical liver resection. Knowledge of the exact surgical procedure is critical for the radiologist. This is even more true when looking for complications as some are quite specific. Differentiating fistulae, abscesses and bowel loops can be really challenging. Defining criteria for bowel obstruction is tricky. This session intends to clarify the most common clinical situations, allowing the radiologist to fully understand the specific situations and to enhance the dialogue with the surgeon.

Session Objectives:

1. To learn about the most common complications following abdominal surgery, either immediate or delayed.
2. To become familiar with the most common surgical procedures and to understand the mechanism of complications.
3. To be able to detect these complications with imaging methods, and to understand the principle of management, including conservative, interventional and/or surgical treatments.

A-288 16:05

Inflammatory complications (peritonitis, abscess)

Z. Tarján; *Budapest/HU (ztarjan@gmail.com)*

Postoperative complications can be general or specific to particular operations. Infections may occur in the operative site or organ, like wound infection, biliary infection or UTI and the peritoneum may be contaminated during or after surgery. Anastomotic leaks, traumatic organ injuries like lacerations and haematomas may develop to form abscesses. Abscesses can be categorised as intraperitoneal retro/subperitoneal or visceral. Pathways of infection are related to well-defined anatomical structures but may extend to contiguous structures and erode boundaries. In the early postoperative period, fever may be caused by tissue necrosis at the operation site. In a few days later sepsis, wound infection and abscess formation may start. Around 5 days after surgery anastomosis breakdown, fistula formation, wound infection and distant site infections may occur. Pelvic collections usually form in the first week, while subphrenic collections tend to form later. Inflammatory damage of vessels in the operation field often results in late postoperative bleeding. CT is the most widely used modality to detect postoperative conditions. Exams should be tailored to be able to demonstrate the altered anatomy, signs of peritonitis, possible source of leakage and collections. Imaging features of inflammatory complications and checklist of critical findings related to different abdominal and pelvic operations will be shown. The team of clinicians, surgeons and radiologists should always discuss treatment options and minimal invasive techniques are preferred; therefore, radiological intervention plays a major role. CT, US, EUS and image fusion (technical or cognitive) may help to guide the intervention.

Learning Objectives:

1. To learn about the incidence of immediate postoperative inflammatory complications and their outcome.
2. To understand the surgical procedures that are most commonly exposed to inflammatory complications.
3. To be able to detect inflammation and abscesses and to identify direct and indirect signs of leakage.
4. To understand the discussion about treatment, conservative, surgical or interventional.

A-289 16:23

Vascular complications (bleeding, thrombosis, ischaemia)

R. Nolz; *Vienna/AT (richard.nolz@meduniwien.ac.at)*

Immediate vascular complications after abdominal surgery require early detection and treatment. Their incidence depends on different factors, including patient characteristics, complexity of surgery and surgeon's learning curve. Transplantations are the surgical procedure most frequently affected by vascular complications in up to 20%. Imaging has a fundamental role in the postoperative period to screen for complications and to monitor the recovery process. Multidetector contrast material-enhanced computed tomography (MDCT) is the gold standard to detect immediate vascular complications. Delayed application of MDCT is leading to a higher patients mortality and morbidity. Accurate interpretation of postoperative findings requires that radiologists have sound knowledge and understanding of surgical procedures and related surgical anatomy. Most postoperative vascular complications provide a fertile ground for interventional radiology (IR), which can circumvent a major surgery on most occasions. The minimally invasive nature and lower morbidity associated with IR procedures make them preferable to similar surgical procedures.

Learning Objectives:

1. To learn about the incidence of immediate postoperative vascular complications and their outcome.
2. To understand the surgical procedures that are most commonly exposed to vascular complications.
3. To be able to manage the diagnostic strategy using appropriate imaging modalities.
4. To understand the role of intervention.

A-290 16:41

Postoperative obstruction

A. Palkó; *Szeged/HU (palkoand@gmail.com)*

Post-operative complications, including gastrointestinal obstruction may be responsible for increasing morbidity and mortality. Recognition of early signs and identification of cause, location and type of immediate and late postoperative obstruction is a difficult task that may not be accurately accomplished by clinical examination. Imaging plays a paramount role in properly detecting and characterising such conditions, allowing for a timely and adequate treatment. Detection, diagnosis and differential diagnosis may be challenging because of the atypical postoperative anatomy and the effect of the underlying disease. Understanding their influence on imaging appearance is critical for correct diagnosis. Plain abdominal x-ray examination may be of little use in the immediate postoperative cases because of the commonly present paralytic ileus obscuring any characteristic signs and also not sufficiently accurate in most late postoperative cases. Barium examinations are usually not performed in acute abdominal conditions. Ultrasound does not play a significant role in the exploration of gastrointestinal pathology. Computed tomography with or without endoluminal contrast is the proper diagnostic modality to establish the definitive diagnosis; however, being familiar with typical signs of postoperative conditions (inflammation, infection, adhesion, dysfunction, volvulus, herniation, etc.) resulting in mechanical obstruction is mandatory to make an accurate and timely diagnosis.

Learning Objectives:

1. To learn about the incidence of immediate and long-term intestinal obstruction after surgery and/or radiotherapy.
2. To understand the mechanism of obstruction related to previous surgery, including adhesion, volvulus, internal hernia and recurrence/complication of initial disease.
3. To be able to detect obstruction, characterise the mechanism and evaluate the severity.
4. To feed the discussion of conservative vs surgical treatment.

Author Disclosure:

A. Palkó: Advisory Board; Affidea.

A-291 16:59

Complications of weight-loss surgery

M. Rengo; *Latina/IT (marco.rengo@gmail.com)*

Obesity is a disease that has reached epidemic proportions around the world. During the past 20 years bariatric surgery has become an increasingly popular form of treatment for morbid obesity. The most common bariatric procedures performed include laparoscopic Roux-en-Y gastric bypass, laparoscopic adjustable gastric banding and laparoscopic sleeve gastrectomy. Fluoroscopic upper gastrointestinal examinations and abdominal computed tomography (CT) are the major imaging tests used to evaluate patients after these various forms of bariatric surgery. We will illustarate the common bariatric surgical procedures, the imaging procedures accordingly to become familiar with the normal post-operative anatomy and to appreciate the role of imaging in the

assessment of suspected immediate and long-term postoperative complications.
Learning Objectives:
1. To learn about the main surgical techniques of bariatric surgery and to understand the mechanism of the most common immediate and delayed complications.
2. To be able to identify the normal post-surgical appearance on imaging methods.
3. To detect the main complications associated with bariatric surgery on imaging methods.

17:14
Panel discussion: Where might we go wrong and how can we avoid it?

16:00 - 17:30 **Room C**

Chest

RC 804
CT - patterns in chest radiology: back to basics and beyond

A-292 16:00
Chairman's introduction
H. Prosch; *Vienna/AT (helmut.prosch@meduniwien.ac.at)*

The diagnosis of diffuse parenchymal lung diseases (DPLD) is one of the most challenging tasks in radiology. As DPLD include more than 200 diseases, the diagnosis frequently requires an extensive workup in which HRCT plays a central role. HRCT is not only essential in the detection of DPLD, but even more important in providing a brief differential diagnosis. Some DPLD, like Langerhans cell histiocytosis or lymphangioleiomyomatosis, can even be diagnosed confidently with HRCT alone. Given the large number of DPLD, the HRCT diagnosis of DPLD requires a systematic approach, and should be based on an analysis of the CT patterns, which can be classified into four categories: increased lung densities, decreased lung densities, a linear pattern and a nodular pattern. A prerequisite for the analysis of the CT pattern is a knowledge of the anatomy of the lung, with a fundamental understanding of the architecture of the secondary pulmonary lobule in particular. The secondary pulmonary lobule is the smallest anatomical unit of the lung, bordered by connective tissue septa. An analysis of HRCT images should aim to narrow the differential diagnosis by attributing CT patterns to the components of the secondary pulmonary lobule: the interlobular septa, the centrilobular structures, or the lobular parenchyma. Such a structured approach can provide a narrow list of differential diagnoses and thereby guide additional steps to diagnose the underlying disease.
Session Objectives:
1. To emphasise the importance of anatomy in reading CT.
2. To appreciate the necessity of defining patterns to improve CT diagnoses.
Author Disclosure:
H. Prosch: Advisory Board; Boehringer Ingelheim, Roche. Speaker; Boehringer Ingelheim, Roche.

A-293 16:05
A. Secondary pulmonary lobule anatomy: essential to tackle with the nodular pattern
T. Frauenfelder; *Zurich/CH (thomas.frauenfelder@usz.ch)*

The goal of this lecture is to provide information about the anatomy of the lung and to provide a structured approach to nodular pattern. High-resolution CT gives detailed morphologic information about lung structures. This allows distinguishing findings by their typical predominance in certain anatomical compartments. The anatomy of secondary lobule, therefore, plays a key role. Based on the distribution of nodular lesions in relation to the bronchial, vascular and lymphatic structure of the secondary lobule the number of possible pathologies can be narrowed down. For example, centrilobular predominance of nodules is a frequent sign of bronchiolitis. Perilymphatic predominance in the periphery of the lobules is associated with sarcoidosis or lymphangitic spread of cancer. Random distribution of nodules is interpreted as a sign of haematogenic spread of disease. Therefore, a subtle interpretation can contribute substantially to clinical decision making. Nevertheless, these signs may not always replace biopsy and histologic workup. During this lecture, a stepwise algorithm for differentiating nodular pattern will be provided that allows a pragmatic approach for a successful reading of HRCT.
Learning Objectives:
1. To become confident in recognising the anatomical compartments of the lung.
2. To describe typical nodular imaging patterns of lung disease using appropriate terminology.

A-294 16:28
B. Linear and reticular pattern
F. Molinari; *Lille/FR (francescomolinari.dr@gmail.com)*

The reticular pattern is one of the imaging findings that may suggest the presence of a diffuse parenchymal lung disease at HRCT. Reticulations are typically formed by a collection of innumerable small linear opacities that by summation produce an appearance resembling a "net". Lines may vary from smooth to nodular and irregular. The resulting "net" may alter the normal HRCT appearance of the lung and become suspected for an underling lung disease. Chest radiologists typically use a structured approach to interpret this finding and eventually to propose a diagnosis. The radiologic approach consists in identifying the dominant types of lines, in establishing what portion of the lung interstitium is predominantly involved, and in correctly classifying the type of reticulation (namely inter-lobular, peri-lobular, intra-lobular). When all the radiologic features are correctly interpreted, the radiologist can differentiate reticulations that represent an acute disease from those that indicate a chronic inflammatory or fibrotic change in the lung. In addition, by integrating clinical and laboratory data, it is possible to significantly narrow the final differential diagnosis.
Learning Objectives:
1. To recognise and interpret typical reticular imaging patterns.
2. To differentiate acute and chronic diseases which cause septal patterns.

A-295 16:51
C. Ground glass opacities (GGO) and consolidation
J. Vogel-Claussen; *Hannover/DE*

Ground glass opacity (GGO) is a nonspecific finding on computed tomography (CT) scans of the chest that indicates a partial filling of air spaces in the lungs by exudate or transudate, as well as interstitial thickening or partial collapse of lung alveoli. The term derives from the similarity in appearance of the small objects to small chips of glass that are a by-product of glass grinding. The differential diagnosis of the many causes of GGO includes pulmonary oedema, infections (including cytomegalovirus and Pneumocystis jirovecii pneumonia), various noninfectious interstitial lung diseases (such as hypersensitivity pneumonitis, Hamman-Rich syndrome), diffuse alveolar haemorrhage, and cryptogenic organising pneumonia. Thus, clinical correlation and disease dynamics are important to narrow down the differential diagnosis. The aim of this refresher course is to distinguish ground glass opacities from consolidations on chest CT and give practical instructions for daily clinical routine.
Learning Objectives:
1. To appreciate the different conditions which cause GGO pattern and consolidation.
2. To learn how to interpret GGO and consolidation in different clinical settings.
Author Disclosure:
J. Vogel-Claussen: Advisory Board; Boehringer Ingelheim, Novartis, Bayer. Research/Grant Support; Siemens.

17:14
Panel discussion: Is it always easy to detect a pattern? Tips for success

16:00 - 17:30 **Room X**

Joint Session of the ESR and EORTC

Imaging biomarker and education for multicentre clinical oncological trials

Moderators
N.M. deSouza; Sutton/UK
Y. Liu; Brussels/BE

A-296 16:00

Imaging as primary endpoint in clinical trials: perspective of the EORTC
Y. Liu; *Brussels/BE (yan.liu@eortc.be)*

Imaging biomarkers have evolved in clinical trials, thanks to improvements in conventional imaging and innovation in advanced imaging techniques. Imaging biomarkers play key roles as outcome measures in trials, and are also used for patient selection, stratification, and safety monitoring tools (measure harm or lack of harm related to treatment). Despite the obvious values of imaging, the integration of imaging biomarkers into trials faces various challenges, such as the complexity of imaging techniques, lack of standardization across multivendor platforms, and paucity of optimized trial design and operational support. Those pitfalls become more apparent, especially in centers with little experience in clinical trials that involve imaging. A risk management approach will be introduced in the presentation, to manage trials with imaging endpoints. It could be a useful tool for prioritization, and avoid undue cost and eventually decreases trial attrition rate. An initial risk assessment plan should be performed before study initiation, which might be achieved with a multidisciplinary team, including imaging experts, clinicians, and study project managers. The risk plan should also be reviewed and updated throughout the trial, to ensure that actions have been or will be taken. This session will set the scene for discussion with imaging experts, to improve the implementation and utilization of imaging biomarkers within clinical trials.
Learning Objectives:
1. To become familiar with the importance of imaging biomarker in oncologic trials.
2. To learn about the role of the Imaging group of the EORTC.
3. To appreciate how standardisation and quality assessment enhances the role of imaging in oncologic trials.

A-297 16:22

Imaging biomarker for clinical trials in brain tumours
M. Smits; *Rotterdam/NL (marion.smits@erasmusmc.nl)*

Gliomas are the most common primary brain tumours and constitute a group of tumours with heterogeneous clinical behaviour, with many therapeutic agents under investigation for their effectiveness. The assessment of treatment effect is, however, not without difficulty. It is on the one hand hampered by therapy-related changes which can be indistinguishable from tumour progression, such as pseudoprogression or radiation necrosis, and on the other hand by a phenomenon called pseudoresponse, occurring in the context of anti-angiogenic treatment, in which contrast enhancement diminishes unrelated to an actual anti-tumoural effect. New, preferably quantitative, markers of response are desperately needed to assess treatment response as accurately and early as possible within the context of a clinical trial. Furthermore, recent insights indicate that the clinical heterogeneity of glioma behaviour can - at least in part - be attributed to the tumour genotype. In the context of clinical trials, it is adamant that patients are correctly stratified according to their tumour genotype, which at this point in time can only be determined from tumour tissue acquired through biopsy/surgery. To avoid such invasive procedures, as well as to obtain a full overview of the tumour and its heterogeneity, and to be able to follow changes over time, imaging can play an important role using a radiogenomic approach. In this presentation, I will discuss the current and potential imaging markers of glioma biological behaviour and response to treatment, and the challenges for implementation in clinical, multicentre trials.
Learning Objectives:
1. To consolidate knowledge about state-of-the-art quantitative MRI.
2. To learn about standardisation and validation.
3. To appreciate the value of quantitative MRI in tumour grading and therapy response.
Author Disclosure:
M. Smits: Consultant; Independent reviewer for Parexel Intl. Corp. for the trial EORTC-1410.

A-298 16:45

The importance of collaboration between the European Initiative on Biomarkers Alliance (EIBALL) and EORTC
S. Trattnig; *Vienna/AT (siegfried.trattnig@meduniwien.ac.at)*

EORTC performs many clinical multicentre trials per year, has 150,000 patients in its database, with 50,000 in the follow-up stage, and comprises 2000 collaborators. Organizationally, EORTC is subdivided into 18 disease-oriented groups with their own respective steering committees in which multicentre trials are planned and performed. The imaging group (comprising radiologists, nuclear medical physicians, physicists and imaging scientists) is part of the "Translational Research and Imaging Department" within EORTC, and is responsible for imaging protocols in multicentre trials, in collaboration with the disease-specific groups and their steering committees in EORTC. The role of EIBALL is to strengthen the collaboration with the imaging group of EORTC with the integration of more radiologists into the imaging group. There is also a need to integrate more imaging people, particularly radiologists, into the disease-oriented groups and their respective steering committees of EORTC where multicentre studies are developed and to which imaging protocols can be implemented. This will allow clinical validation of different imaging biomarkers in multicentre trials. Imaging protocols, including quantitative imaging biomarkers, should be proposed and distributed to the members of EIBALL, and an expert consensus should be achieved, which then should be integrated within the EORTC multicentre studies. Imaging protocols that are acceptable for a number of sites should be established and a program of quality assurance/quality control should be implemented prior to imaging in multicentre trials. In planned multicentre projects, potential sites should be recruited based on a site qualification process for clinical validation of imaging biomarkers.
Learning Objectives:
1. To become familiar with recent developments of collaboration between EIBALL and EORTC.
2. To learn about the increasing role of radiologists in oncologic trials.
3. To appreciate the importance of imaging biomarker in multicentre trials.

A-299 17:07

Training possibilities for radiologists involved in clinical multicentre trials
L.S. Fournier; *Paris/FR*

Learning Objectives:
1. To become familiar with education of radiologists for oncologic trials.
2. To learn about the advantages of education for implementation and evaluation of clinical trials.
3. To appreciate the value of educational courses on clinical multicentre trials for radiologists.

16:00 - 17:30 **Room Z**

ESR Working Group on Ultrasound

WG 4

Simulation training in ultrasound

Moderators:
M. Bachmann Nielsen; Copenhagen/DK
V. Cantisani; Rome/IT

A-300 16:00

How to evaluate simulation training
L. Konge; *Copenhagen/DK (lars.konge@regionh.dk)*

Naturally, we treat our patients according to the best available evidence and the same principle should be applied to the way we train our future colleagues. High-quality research in medical education using assessment tools with solid evidence of validity is needed to create the most efficient training programs. Learner satisfaction or self-assessed competence is not a valid measure of learning outcome. Evidence shows that simulation-based training is cheaper and more effective than traditional apprenticeship training in the early part of the learning curve. Specific examples of this will be presented at the lecture.
Learning Objectives:
1. To learn the theories behind training assessment in medical education.
2. To understand why some study designs are valid and others are not.
3. To learn about simulation studies in radiology and other medical specialties (e.g., OB/GYN).

A-301 16:15

Different ultrasound simulators for different purposes

A. Kabaalioglu; *Antalya/TR (adnank@akdeniz.edu.tr)*

Simulation training is increasingly becoming an essential part of many educational activities. Simulation methods have long been used for training the military personnel, pilots, astronauts and engineers. Medical use of simulation training is not only limited to basic teaching of "blood draw" or other interventions that are helpful for the patient safety. Complex interactive simulator mannequins have been developed for helping medical students to learn how to act in several clinical scenarios. Moreover, this environment is regarded as a better standardised evaluation or assessment system. Ultrasound simulators have been introduced for training the medical personnel before having "troubled times" during real life scanning. The patients may complain of the time spent on their body, especially when they have a serious illness and/or severe pain and anxiety. Besides these factors, safety concerns regarding tissue heating with long exposures to sound waves, especially prolonged Doppler use in pregnancy, inhibit the trainer and the trainee to spend sufficient time on a patient. Ultrasound simulators have been successfully developed for use in abdominal, obstetrics/gynaecological and cardiac exams. Interventional models for abdominal and breast biopsies and vascular access are also available for training the residents or fellows. In this part of the session, several ultrasound simulators used for medical training will be presented with advantages and disadvantages. Their potential for future applications will be discussed.

Learning Objectives:

1. To learn about different types of simulators on the market.
2. To learn about which are suitable for beginners or advanced levels, for OB/GYN or abdominal, and which can be used for training interventional ultrasound.
3. To learn about advantages and disadvantages of different types of ultrasound simulators.

A-302 16:30

US simulation training in student education

R. Badea; *Cluj-Napoca/RO (rbadea2012@gmail.com)*

Ultrasound is a operator-dependent procedure. Source of errors that should be avoided are: multimodal picture, real-time data, artefacts, large number of transducers, diversity and lack of standardisation of machines. Because of these, ultrasonography is apparently unfriendly and medical students are reluctant in practising it. Main purpose of implementation of ultrasonography in education of students should be "sonovisualisation" of some areas to improve and accelerate the clinical diagnosis. Simulators are educational instruments that replace the human body. A combination between a model and a ultrasound machine like computer can replace the ultrasound examination. Some devices explain images by comparing ultrasound and anatomical/imaging slices, other devices explain images focusing on small anatomical area to facilitate "point of care" diagnosis. Advantages are: good real-time picture; friendly utilisation. Disadvantages are: insufficient connection to the student curriculum; insufficient versatility; low possibility of simulation of clinical syndromes or signs (e.g. compressibility, pain, etc). Outcomes depend on the year of study and educational objectives. In a linear curriculum, ultrasonography should make the student to understand anatomy and physiology including pathological phenomenon (blood flow; vascular stenosis/obstruction; shape/function of heart; anatomical relation between organs; pathological processes like inflammation, angiogenesis, tumoural detection/characterisation; evaluation of fluids). Next step should be integration of ultrasonography into the clinical judgement as geste part of the physical examination of the patient. Final step should be integration of ultrasound evaluation in a emergency situation and ultrasound guidance of some simple invasive procedures.

Learning Objectives:

1. To learn about the basis for training in medical students in US.
2. To learn about reported outcomes from ultrasound simulation training of medical students.
3. To learn about possible ways of its implementation.

A-303 16:45

Experience with ultrasound simulators in training radiologists

M.L. Østergaard; *Copenhagen/DK (mia.louise.ostergaard@gmail.com)*

The traditional apprenticeship training is being challenged by multiple factors such as time restraints, supervisor shortage, patient's safety and sub-specialised clinical setups. Simulation-based training may be the answer to a lot of these challenges and could secure adequate training time and skill level. In combination with the prevailing approach of competency-based education it could provide a setup for evidence-based education. In this session, I will give a recap of what we know about simulation-based training in ultrasound, present a simulation-based test with solid validity evidence and offer a perspective on what simulation-based assessment might bring to ultrasound education.

Learning Objectives:

1. To learn about the present literature on simulation training in abdominal ultrasound.
2. To understand the level of evidence for the effect of ultrasound simulation training.
3. To learn about the experience from starting simulation training as part of the curriculum in Denmark.

17:00

Panel discussion

16:00 - 17:30 **Room O**

Professional Challenges Session

PC 8

How to make best use of cardiac imaging in a radiology department

A-304 16:00

Chairman's introduction

G.I. Kirova-Nedialkova; *Sofia/BG (gal.kirova@gmail.com)*

Over the past two decades, almost all aspects of imaging diagnostic have undergone fundamental change. In the light of the advances in technology, the health care environment and the transit to the patient-oriented medicine, the need of a reform of the organization and practice is unambiguous. As the equipment becomes increasingly sophisticated, the ability of the general radiologist to keep up with the advancing technology will be even further outperformed. The main goal of the session will be to stress the audience's attention to the new tendencies in the development of noninvasive cardiac radiology and how to narrow the gap between the needs of the society and the ability of the profession to respond. The relationship between the science and practice, the applicability and cost effectiveness of new guidelines and the challenges in implementation working training programmes in a real situation will be discussed. The panel discussion will focus on the integration of cardiac imaging in the routine radiology workload and the role of the radiologist into the multidisciplinary team, addressing the medical decision-making.

Session Objectives:

1. To focus on the needs for and challenges in organising a non-invasive cardiac imaging programme.
2. To learn about the main factors driving cost-effectiveness in the setting of cardiac imaging.
3. To understand the process of credentialing and accreditation in the practice of cardiac imaging.
4. To understand the radiologists' role as a team player.

A-305 16:06

Starting a cardiac imaging programme

G.A. Krombach; *Giessen/DE (gabriele.krombach@uniklinikum-giessen.de)*

To successfully initiate an imaging programme serving the needs of an interdisciplinary team consisting of cardiologists, paediatric cardiologists, vascular surgeons and cardiac surgeons requires dedicated knowledge regarding the typical spectrum of questions raised by these referring colleges as well as of the current guidelines. The radiologist needs to choose the appropriate modality and to apply the best suited imaging protocol. Reading the images implies the description of all cardiac pathologies, quantifying cardiac function, describing extra cardiac pathologies, summarizing all findings to a final diagnosis and writing a comprehensive report. A specific training program certified by the respective National radiological society or by the European society of radiology itself that consists of courses and practical training provides the necessary knowledge and ensures high quality of cardiac imaging. A team of technicians must be trained as well to accurately carry out

imaging protocols. To finally gain the best value from imaging, consistent ways of communication with the referring physicians have to be established. In addition to the written report, regular multidisciplinary conferences might be best suited for radiological departments in larger hospitals, while a timely structured written report combined with regular personal communication with the referring physicians might be best suited for radiological practices. With a structured approach, starting a cardiac imaging programme will be successful. It gains quality for patients and referring physicians by providing the exact diagnosis, allowing to choose the best suited therapy and monitoring the response to the treatment.

Learning Objectives:

1. To understand the challenges for starting a cardiac imaging programme.
2. To learn about requirements for starting a cardiac imaging programme.
3. To learn about the steps necessary for starting a successful cardiac imaging programme.

A-306 16:28

Cost-effectiveness of cardiac imaging

M.G.M. Hunink; *Rotterdam/NL (m.hunink@erasmusmc.nl)*

Coronary artery disease (CAD) is one of the leading causes of mortality and morbidity. This presentation reviews the evidence on comparative cost-effectiveness of imaging strategies for patients presenting with stable chest pain symptoms suggestive for CAD. The literature was systematically reviewed for formal economic evaluations or decision analyses written in English. The identified studies compared very different testing strategies using very different methods and provided mostly short-term results. Strategies of no-testing and stress ECG were underrepresented. Nonetheless, the findings suggest that for patients with a low to intermediate prior probability of having obstructive CAD, CT coronary angiography (CTCA) is cost-effective as an initial diagnostic imaging test in comparison with catheter angiography or other non-invasive diagnostic tests. If functional testing is required, stress echocardiography or SPECT are suggested to be cost-effective initial strategies in patients with intermediate prior probability of CAD. Other functional testing strategies such as stress ECG and PET scanning have not been studied as extensively. Catheterisation angiography is cost-effective in patients at a high prior probability of having obstructive CAD whom may benefit from revascularisation.

Learning Objectives:

1. To understand the issues related to cost-effectiveness calculations.
2. To learn how cost-effectiveness in cardiac imaging can be influenced by different parameters.
3. To learn about the thresholds for cost-effectiveness in cardiac imaging.

Author Disclosure:

M.G.M. Hunink: Advisory Board; EIBIR. Grant Recipient; ESR iGuide. Other; CUP: Royalties for textbook.

A-307 16:50

Training cardiac imaging in the radiology department

F. Pugliese; *London/UK (f.pugliese@qmul.ac.uk)*

Due to advances in imaging technology and improved infrastructure availability, advanced cardiac and cardiovascular imaging applications (cardiac magnetic resonance, cardiac computed tomography) have become appealing diagnostic tools in increasing numbers of patients with a range of cardiac conditions. While a growing body of literature and recently issued clinical guidelines stress the role of cardiac imaging in contemporary clinical cardiology, to date the availability of trained staff performing and reading cardiac imaging appears patchy, geographically variable and insufficient.

Learning Objectives:

1. To understand the challenges of training cardiac imaging.
2. To learn about the ideal training conditions for cardiac imaging.
3. To learn about how to implement cardiac imaging training programmes.

17:12

Panel discussion: Are we ready to integrate cardiac imaging in routine radiology workload?

16:00 - 17:30 **Room N**

Head and Neck

RC 808

Pitfalls in interpretation of head and neck disease

Moderator:
S. Robinson; Vienna/AT

A-308 16:00

A. Anatomical variants without clinical consequence

F.A. Pameijer; *Utrecht/NL (f.a.pameijer@umcutrecht.nl)*

Variant: "Something that is slightly different". Imaging methods can provide an extraordinary amount of useful data to specialists treating head and neck (cancer) patients. It is crucial that these data are used to full advantage of individual patients. The most important factor in this process is mutual cooperation between the physicians in charge of patient care and the diagnostic imaging specialist. Anatomical variants in the head and neck are frequently encountered and may result in interpretation problems for the radiologist. Usually, anatomical variants are without clinical consequence. However, normal variants may simulate diseases not recognized, normal variants may lead to unnecessary interventions. The presentation aims to familiarize general radiologists, who have an interest in head and neck imaging, with common anatomical variants encountered on head and neck CT and MR studies. Many examples from daily practice will be discussed.

Learning Objectives:

1. To gain insight into the great variability of head and neck anatomy.
2. To be able to recognise pseudo lesions.

A-309 16:30

B. Anatomical variants posing surgical risks

D. Farina; *Brescia/IT (nappaje@yahoo.it)*

Several anatomic variants may pose a threat during surgery. A large part is found in the sinonasal region basically due to the widespread use of endoscopy which, inherently, provides the operator with narrow accesses and limited exposition of submucosal anatomic structures. Onodi cell is probably the most feared anatomic threat, because if not correctly indicated by the radiologist and identified by the surgeon, it generates a high risk of disastrous intracranial penetration. Similarly, bone dehiscence of the lamina papyracea of the ethmoid increases the risk of iatrogenic damage, mainly of intrinsic ocular muscles. The inferior alveolar nerve is at high risk of surgical damage during molar teeth extraction, particularly when the curved apex of roots embrace the inferior wall of the nerve canal. In the neck, the main threats are related to anomalous course of major vessels: not infrequently the common or internal carotid artery display a medialized course reaching the lateral aspect of the pharyngeal wall or even protruding in the retropharyngeal space towards the midline. Simultaneous medial deviation of the arteries on both sides is referred to as kissing (common or internal) carotids. The risk in these eveniences are mainly related to the possible effects of a deep biopsy performed by an unaware surgeon. At the cervicomediastinal junction, vascular rings may embrace the trachea or the esophagus and, consequently, pose a threat during intubation or tracheostomy.

Learning Objectives:

1. To learn about structures at risk during functional endoscopic sinus surgery (FESS).
2. To become familiar with vascular variants in the head and neck.
3. To appreciate surgical anatomical landmarks in the head and neck.

A-310 17:00

C. Distinct head and neck disease or systemic disease?

M.G. Mack; *Munich/DE (m.mack@radiologie-muenchen.de)*

Head and neck manifestations of systemic disease is characterized by a multitude of maladies that have manifestations in the head and neck. This lecture relates commonly encountered head and neck symptoms and signs to an array of diseases and disorders that should be considered in the differential diagnosis. During this lecture, systemic disorders with head and neck manifestation (e.g. Sjögren's syndrome, Adamantiades-Behcets disease, granulomatous disease like Wegener's granulomatosis), infectious disease (e.g. tuberculosis fungal rhinosinusitis and HIV-related disease), malignant disease (e.g. lymphoma, myeloproliferative disorders and leukaemia, malignant melanoma, histiocytosis, sickle cell anaemia and rhabdomyosarcoma) or other systemic disorders (e.g. Paget's disease of bone and fibrous dysplasia) will be presented.

Learning Objectives:

1. To recognise head and neck manifestations of systemic disease.
2. To categorise lesions into different pathologic entities.

16:00 - 17:30 **Studio 2017**

Genitourinary

RC 807

Imaging of the prostate

Moderator:
P. Puech; Lille/FR

A-311 16:00

A. MRI staging of prostate cancer

G.M. Villeirs; *Ghent/BE*

Staging involves the correct assessment of the local tumour situation (T), involvement of lymph nodes (N) and of distant metastases (M). According to the European Association of Urology (EAU) Guidelines, assessment of lymph nodes is only useful in patients with a PSA >10, Gleason score >7, >cT2b. Imaging can be performed using the well-known size criteria (round node >8mm, short axis of oval node >10mm) on CT or MRI, but this approach clearly lacks both sensitivity and specificity. Diffusion-weighted MRI incorporating morphologic features, MR-lymphangiography using ultra-small particles of iron oxide (USPIO), and nuclear medicine techniques such as choline- and PSMA-PET/CT offer higher sensitivity and specificity, but cannot (yet) replace the current gold standard (pelvic lymphadenectomy). The search for distant metastases (T) primarily involves skeletal assessment in patients at increased risk (PSA >20, Gleason >8, cT3-cT4). The current gold standard is the bone scan, but whole body MRI and new PET tracers seem to be on track to replace the bone scan as gold standard. In the absence of N+ or M+ disease, MRI can be used to assess the local status (T). High-resolution T2-weighted images are used to assess potential extracapsular extension or seminal vesicle invasion. Although this is a recommended approach according to the EAU guidelines, the accuracy of such T-staging is currently still quite variable. However, standardization of scanning techniques for staging and standardization of diagnostic criteria may solve this problem.

Learning Objectives:

1. To understand the current role of prostate MRI.
2. To learn how to optimise imaging and reporting.
3. To illustrate the staging approach.

A-312 16:30

B. Pitfalls in MRI of the prostate

V. Panebianco; *Rome/IT (valeria.panebianco@uniroma1.it)*

Currently, high-quality multi-parametric magnetic resonance imaging (mpMRI) represents a promising modality for the diagnosis, characterisation and treatment planning of prostate cancer. However, some physiological changes in the peripheral and central zone may simulate prostate cancer. Consequently, mp-MRI often leads to interpreting doubts and misdiagnosis due to the many interpretative pitfalls that a tissue, whether healthy or treated, may cause. The detection of prostate cancer on mpMRI can be confounded by false-positive or false-negative findings. These “false-positive/negative” findings may occur in each stage of the disease history, from the primary diagnosis and staging, to post-treatment stage and their recognition is critical for proper treatment and management. Knowledge of these known pitfalls and their interpretation can help radiologist to avoid misdiagnosis and consequently a wrong treatment. PI-RADS score often is decisive for definitive diagnosis and in particular PIRADS vers. 2 even more based on “dominant sequence” for each portion of the gland. In the lecture, a wide spectrum of prostate mp-MRI pitfalls that may occur in clinical practice will be presented, with radiological and pathological correlation. In addition, some difficult cases focusing on the presence of cancer in pitfalls will be discussed. In summary, the purpose of this course is to provide a practical guide to the radiologist for imaging interpretation in prostate cancer, with a focus on how to discriminate pathological tissue from the most common pitfalls that may be encountered during daily clinical practice with the aid of PI-RADS v. 2.

Learning Objectives:

1. To illustrate the classification of the most common pitfalls on mpMRI of the prostate.
2. To discuss the role of PI-RADS version 2 in interpreting pitfalls in prostate MRI.
3. To learn how to avoid pitfalls.

A-313 17:00

C. Imaging of PSA recurrence

H.-P. Schlemmer; *Heidelberg/DE (h.schlemmer@dkfz.de)*

Although radical prostatectomy and radiotherapy are first-line treatment options for patients with organ-confined prostate cancer, subsequent biochemical recurrence develop in ca. 40% of the cases. Early detection and precise localisation of local recurrence and/or systemic cancer spreading is essential for optimised treatment. Early detection of local cancer recurrent after radical prostatectomy is particularly challenging, as salvage radiotherapy with curative intention is achievable only in case of low tumour load and accordingly low PSA serum levels. Conventional TRUS has limited sensitivity and specificity for detection of local recurrence. Multiparametric MRI (mpMRI) has been shown to be superior for detection of local recurrence, although early detection of small cancer foci is also significantly limited. mpMRI is, furthermore, significantly limited concerning early detection of lymph node and/or bone marrow metastases, which is on the other hand essential for prognostic stratification and individualised therapy. In case of PSA recurrence after therapy highest sensitivity for cancer detection is achieved by PET, although the accuracy strongly depends on the radiotracer. In clinical routine, C-11 or F-18 choline and Ga-68 or F-18 PSMA PET/CT is used most notably. PET/MR imaging provides additional advantaged by combining the highest sensitivity of PET with best anatomical referencing and functional tissue characterisation by mpMR. This lecture will provide an overview about the currently available imaging methods for detection of recurrence in case of PSA recurrence. Their clinical relevance will be discussed against the background of the potential therapy options.

Learning Objectives:

1. To understand the clinical need and indications for advanced imaging in patients with PSA recurrence.
2. To learn about the potentials of multiparametric MR for the detection of locoregional recurrence.
3. To become familiar with the clinical impact of PET/CT and PET/MRI using different radiotracers.

Author Disclosure:

H.-P. Schlemmer: Advisory Board; Siemens Healthineers. Author; Thieme Verlag. Consultant; Curagita AG. Employee; German Cancer Research Center, Medical University of Heidelberg. Speaker; Siemens Healthineers, Bayer Healthcare, Curagita AG.

16:00 - 17:30 **Room L 8**

EuroSafe Imaging Session

EU 3

European Alliance for Medical Radiation Protection Research (EURAMED)

Moderator:
G. Frija; Paris/FR

A-314 16:00

Introduction of EURAMED

C. Hoeschen; *Magdeburg/DE (christoph.hoeschen@ovgu.de)*

EURAMED is currently a Joint Initiative of EIBIR. It has been launched in September as a platform at the Radiation Protection Week 2016. EURAMED is a platform which is intended to be a counterpart and partner of the existing platforms MELODI, ALLIANCE, NERIS and EURADOS representing radiation protection research in Europe. The last four mentioned platforms kind of determined the research topics in radiation protection research funding in Europe in the last few years due to their existing Strategic Research Agendas (SRAs). MELODI and EURADOS did sign memoranda of understanding with the five associations representing use of ionizing radiation in medical application (EANM - European Association of Nuclear Medicine; EFOMP - European Federation of Organisations for Medical Physics; EFRS - European Federation of Radiographer Societies; ESR and ESTRO - European SocieTy

for Radiotherapy and Oncology) reviewing the impact of use of ionising radiation in medicine. The associations initiated with the help of the EU Project OPERRA the development of a "medical strategic research agenda". This SRA is available for the public using the EIBIR webside. The importance of medical radiation protection research got more prominent and the associations therefore decided to set up a platform. This platform was already able to foster the preparation of a proposal for a EURATOM call and to determine a subtopic for the second CONCERT call. The platform plans to do biannual actualisations of the SRA and to foster medical radiation protection research by helping with European calls and develop a corresponding researcher database. Further developments are planned.

Learning Objectives:

1. To be introduced to EURAMED.
2. To become familiar with how EURAMED has been developed.
3. To learn what its objectives are.
4. To understand how EURAMED could benefit the ESR.

A-315 16:18

Cardiovascular effects of radiotherapy in breast cancer patients: potential mechanisms

W. Dörr; *Vienna/AT (wolfgang.doerr@meduniwien.ac.at)*

Most of the clinical endpoints of radiation effects in the heart are clearly promoted by factors like pre-existing vascular disease, such as atherosclerosis, and hence must be considered multifactorial. Radiation effects are observed in the peri- and myocardium, cardiac valves, coronary arteries and the microvasculature, as well as in the conduction system. In the pericardium, early inflammatory reactions are uncommon even at high doses of ionizing radiation. Late pericardial changes are usually asymptomatic, but can develop into chronic and/or constrictive pericarditis. The dominant late change is pericardial fibrosis. Myocardial changes follow three phases: acute (within 6 h after exposure) inflammation, a clinically silent latent phase where myocardial capillary endothelial cell damage results in capillary obstruction and thrombi formation, and then local ischaemia and consequent myocardial cell death and fibrosis. The cardiac valves are also subject to fibrotic transformation, with unclear radiopathological mechanisms - independent of microvascular changes, as the valves are avascular - potentially related to direct radiation-induced differentiation of fibroblasts into collagen-producing fibrocytes. Both types of cardiovascular morbidity, i.e. coronary artery disease (mainly left anterior descending and right coronary arteries) through the acceleration of age-related atherosclerosis and a decrease in capillary density causing chronic ischaemia and focal myocardial degeneration, are relevant for radiation effects in the heart. The radiation exposure of the surrounding tissues (particularly the lung, but also the liver) seems to impact on the clinical manifestation.

Learning Objectives:

1. To become familiar with which CV effects we see in breast cancer treated patients.
2. To learn how these effects could be optimised in terms of endpoint specificity.

A-316 16:36

Circulating biomarkers reflecting dose exposure

R. Tamarat; *Fontenay-aux-Roses/FR (radia.tamarat@irsn.fr)*

Microparticles (MPs) are extracellular membrane vesicles with potent biological activities. Circulating levels of MPs have been associated with outcome of several cardiovascular and inflammatory diseases. We conducted a large prospective study to determine whether the number and/or the type of circulating MPs could be used as potential biomarkers of rectorragic grade and severe complications in patients with prostate adenocarcinoma overexposed to radiation. We also assessed their biological activity with regard to their pro-coagulant and pro-inflammatory potential. Blood samples were obtained from a cohort of 217 patients overexposed to irradiation during their radiotherapy. Flow cytometry analysis of platelet-free plasmas indicated that circulating levels of Annexin V+ MPs were increased by 3-fold in grade 3/4 patients compared to grade 0, 1 and 2 patients according to the rectorragic grade. Platelet-derived MPs constituted the major MPs sub-population while the endothelial cell and monocyte-derived MPs were increased in grade 3/4 patients compared to the other grades. Clotting assays revealed a trend towards decreased pro-coagulant activity of MPs in grade 3/4 patients compared to other groups. MPs from grade 3/4 patients affected the endothelium activation in a P-selectin manner. High levels of circulating MPs derived from platelets, endothelial cells and monocytes correlate with grade 3/4 chronic radiation enteritis patients. MPs could be considered as a biomarker and may be valuable for the prognostic of radiation therapy complications.

Learning Objectives:

1. To learn about the extracellular vesicles (EV) as circulating biomarkers.
2. To understand how to evaluate the different EV and their origins.
3. To learn how to use EV as biomarkers in a prostate adenocarcinoma cohort.

A-317 16:54

General physical principles used for optimisation

G. Paulo; *Coimbra/PT (graciano@estescoimbra.pt)*

For an optimisation strategy to be effective, all health professionals involved in the use of x-ray equipment need to have knowledge and access to the results of performance tests and patient dose surveys. In addition, there should be a continuing programme of assessment to track any changes in equipment performance. Links between the radiographer, the medical physicist and the radiologist to provide a greater opportunity for optimisation are essential. The main objective of optimisation of radiological procedures is to adjust imaging parameters and implement measures in such a way that the required image is obtained with the lowest possible radiation dose and maximised benefit, considering patient characteristics and clinical indication. To achieve this goal, good practice in radiographic technique is needed and, therefore, special attention must be given, simultaneously, to several aspects of the procedure, such as (a) patient positioning and immobilisation, (b) accurate field size and correct x-ray beam limitation, (c) the use of protective shielding, when appropriate and (d) optimisation of radiographic exposure factors. Using a correct beam limitation is crucial to avoid unnecessary radiation dose outside the area of interest, and prejudice the image contrast and resolution by increasing the scattered radiation. Applied research in radiology is the necessary tool to analyse the problems and find the solutions on how to best optimize the medical imaging procedure. Translating the research results into clinical practice will contribute to improve the quality of care delivered to our patients.

Learning Objectives:

1. To learn how optimisation should take place.
2. To understand that image quality and dose depends on the class of patients.
3. To learn how to transfer this optimisation into clinical practice.

A-318 17:12

Dose distribution in interventional radiology

H. Schlattl; *Munich/DE (helmut.schlattl@helmholtz-muenchen.de)*

The small field sizes applied during radiological interventions lead to significant dose gradients in organs close to the region of interest. Thus, mean organ doses might be misleading when estimating the actual radiation risk of the patient. With the largest skin entrance doses observed for coronary angiographic interventions, these are examined in more detail. Local dose conversion coefficients are computed using Monte Carlo simulations by employing human models which represent the average Caucasian adult man and woman as defined by the International Commission on Radiological Protection. In the 21 investigated projections, the mean organ dose conversion coefficients vary from a few 0.01 to 2 mGy/(Gy cm²), depending on the projections. Especially in portions of the lungs and the active bone marrow, the conversion coefficients can locally amount up to 10 mGy/(Gy cm²), i.e., half the average conversion coefficient of the skin at the field entrance. The dependence of the patient dose on the projection has been estimated too. Highest patient doses are observed for left anterior oblique views with strong caudal or cranial orientation, while for the remaining image-intensifier positions no significant dose differences could be identified.

Learning Objectives:

1. To learn how to determine dose distributions by simulations.
2. To understand reasons for dose differences in organs for interventions.
3. To understand optimisation of dose distributions in interventional radiology, e.g. to avoid deterministic effects.

16:00 - 17:30 **Room E1**

Breast

RC 802
Radio-pathological correlation: more important than you thought

A-319 16:00
Chairmen's introduction
F.J. Gilbert; *Cambridge/UK (fjg28@cam.ac.uk)*
M.R. Parizel; *Antwerp/BE (maxim.parizel@gmail.com)*

In breast imaging, correlation of the pathology results with imaging findings is essential to properly carry out triple assessment of clinical examination, imaging and core biopsy. This approach has a very high sensitivity and if correctly implemented will result in very few cancers being missed. Multidisciplinary team meetings ensure that women's biopsy findings are reviewed to ensure that the correct area has been targeted and that the pathological findings are appropriate for the clinical and imaging diagnosis.
Author Disclosure:
F.J. Gilbert: Research/Grant Support; Hologic, GE Healthcare.

A-320 16:05
A. Pretreatment planning
C.K. Kuhl; *Aachen/DE*

"no abstract submitted"
Learning Objectives:
1. To know the role of the imaging methods for preoperative staging.
2. To understand the need for imaging-guided needle sampling and localisation for a tailored surgery.
3. To appreciate the need for changing surgical guidelines for treating breast cancer.

A-321 16:28
B. Intraoperative specimen evaluation
J. Camps Herrero; *Valencia/ES (juliacamps@gmail.com)*

After a thorough integrated radiological diagnosis in breast cancer staging, the following phase is as important as the rest to achieve a thorough and exact map of the cancer's extent and minimize the risk of positive margins. Preoperative planning together with the surgeon is essential, especially in those instances which are complex and have higher possibilities of yielding positive margins if the surgical decision is to preserve the breast: extensive DCIS, extensive multifocal disease, cancers with extensive intraductal component (EIC) and rare instances of multicentric cancers in which the surgeon chooses to preserve the breast. After the patient is marked with one of the many available options (hook-wire, radioactive seeds, SNOLL, ROLL), the next step is to evaluate the specimen obtained during surgery. The most common technique is the radiography of the specimen, although ultrasound has also been used in nodular lesions and lately, tomosynthesis is also being used. The most important issues in peroperative evaluation of specimens are: to know well the orientation protocol used by the surgeon, to know with detail the patients' staging results and to be fast conveying the information on margins to the surgeon.
Learning Objectives:
1. To learn about different imaging techniques for preoperative marking and intraoperative specimen evaluation.
2. To become familiar with methods for specimen orientation and handling.
3. To understand the need for immediate reporting/reaction from radiological department to surgical room.
Author Disclosure:
J. Camps Herrero: Advisory Board; Bayer.

A-322 16:51
C. The breast radiologist sitting down with the pathologist
T. Tot; *Falun/SE (tibor.tot@ltdalarna.se)*

Most breast carcinomas exhibit complex subgross morphology already in the in situ phase. If the cancer is located in the terminal ductal-lobular units, it may manifest as unifocal or multifocal disease and may be associated with clustered calcifications. Cancer in situ that develops predominantly in larger ducts is most often diffuse, extensive, high grade, and may be associated with linear branching (casting type) calcifications or may cause architectural distortion. The invasive component of the tumour usually manifests as circular/oval or stellate density, and rarely as architectural distortion only. One third of invasive cases are unifocal, with a single invasive focus and in situ component within and/or in the vicinity of this focus. Another third of the cases are characterized by the presence of a single invasive focus, but associated with a diffuse or multifocal in situ component. The final third of the cases exhibit a multifocal invasive component. Almost half of these cases are extensive in which the individual foci occupy a tissue volume of greater than 4 cm in the largest dimension. Multimodality breast radiology is able to asses this complexity of subgross morphology with high and ever increasing accuracy. Small samples of the specimen with invasive cancer used in conventional pathology may be fully sufficient for typing and grading the tumour and for molecular and genetic analysis, but a special technique using non-fragmented contiguous tissue slices including the cut surface of the entire specimen (large-format histology) is required for detailed and systematic radiological-pathological correlation.
Learning Objectives:
1. To understand the importance of using imaging to guide the pathologist in complex lesions.
2. To know the different ways of correlating radiology and pathology.
3. To learn how to enhance this cooperation in order to achieve the best results in terms of tumour extension and tumour margins.

17:14
Panel discussion: How to enhance the interaction between radiologists and pathologists?

16:00 - 17:30 **Room E2**

Neuro

RC 811
Toxic brain disorders
Moderator:
P. Due-Tønnessen; Oslo/NO

A-323 16:00
A. Alcohol-related changes in the brain
M. Knauth; *Göttingen/DE*

Alcoholism is a major problem (not only, but also) in the western industrial societies, including Europe, of course. Therefore, every radiologist has to be familiar with the MRI detectable changes that can occur in the brain in acute, chronic or acute on chronic alcohol intoxication. This does not only include alterations of the brain structure that are directly caused by ethanol, but also those that are more correctly attributable to the circumstances of chronic alcohol addiction, i.e. malnutrition. Also, the lecture will deal with the reversibility potential of some of these brain changes when alcohol abstinence can finally be achieved. The main focus will be the ethanol-induced brain changes, but we will glance at "neighbouring" alcohols as well.
Learning Objectives:
1. To document how imaging can help to make the diagnosis of acute alcohol poisoning and chronic alcoholic encephalopathy.
2. To discuss Wernicke encephalopathy.
3. To present the imaging findings in methanol and ethylene glycol poisoning.

A-325 17:00
B. Recreational drugs and occupational hazards
L. van den Hauwe; *Antwerp/BE (lucvdhauwe@mac.com)*

Drug abuse is a substantial problem in society and is associated with significant morbidity and mortality. It is an epidemic that crosses racial, socioeconomic, and age barriers. According to the 2016 Global Drug Survey, besides alcohol, tobacco and caffeine products the top 10 drugs used across the world are: cannabis, MDMA, cocaine, amphetamines, LSD, magic mushrooms, prescribed & non-prescribed opioid medication, nitrous oxide, ketamine and poppers. Various drugs may cause central nervous system (CNS) complications and include neurovascular complications, toxic leukoencephalopathy, atrophy, infection, changes in the corpus callosum, etc. The lecture will focus on acute neurovascular complications: the most frequent drug-related emergencies. They include ischaemic stroke, subarachnoid and intracerebral haemorrhage. Multiple drugs are associated with neurovascular complications, but cocaine is the hallmark drug. Mechanisms of action contributing to these ischaemic strokes include direct vasospasm, enhanced platelet aggregation, cardioembolic sources, accelerated atherosclerosis, and cerebral vasculitis. Subarachnoid haemorrhage may be found as a result of aneurysm rupture; up to 50% of patients have aneurysms and arteriovenous malformations. Also toxic leukoencephalopathies have been described. A specific pattern has been ascribed to the inhalation of heroin vapour when the drug is heated on tinfoil, a practice known as "chasing the dragon". A more nonspecific leukoencephalopathy is seen in chronic inhalant abuse of industrial solvents, e.g. toluene. Such lesions can be explained by the high affinity of

these lipophilic volatile agents for myelin. Imaging changes as a result of occupational exposure to other chemical substances such as lead, mercury, and cyanide will be discussed.

Learning Objectives:

1. To present an overview of recreational drugs and how they influence the brain.
2. To illustrate the effect of drugs on imaging studies (amphetamines, ecstasy, cocaine, heroin, methadone, …).
3. To understand how occupationally used toxic substances can influence the brain (including toluene, cyanide, organophosphates, lead and mercury poisoning, …).

Author Disclosure:

L. van den Hauwe: Consultant; icometrix, Leuven/BE.

A-324 16:30

C. Treatment-induced effects on the brain parenchyma

T. Lim; *Singapore/SG (tchoyoson_lim@nni.com.sg)*

Radiation and chemotherapy are the most common causes of iatrogenic CNS damage. The consequences of brain irradiation can be early (within weeks) early delayed (1-4 months) or late delayed (years after therapy). MRI features of contrast-enhancing mass surrounded by oedema and mass effect are not specific, and surgical brain biopsy is often needed for definitive diagnosis. Magnetic resonance spectroscopy and perfusion-weighted imaging showing increased choline/creatine ratio and increased relative cerebral blood volume in recurrent high-grade neoplasia, and increased tumour metabolism detected using fluorodeoxyglucose positron emission tomography and thallium 201 single photon emitted computed tomography may be helpful to distinguish recurrent neoplasm from radiation necrosis. Intrathecal chemotherapy drugs (especially methotrexate) can cause bilaterally symmetrical leucoencephalopathy, especially in patients receiving concurrent radiotherapy. Other examples of iatrogenic effects include posterior reversible encephalopathy syndrome (PRES, vasogenic oedema in the posterior part of the brain particularly the subcortical white matter). Causes include cyclosporin and cancer chemotherapy. Patients with systemic lupus erythematosus may develop post progressive multifocal leucoencephalopathy associated with intensive immunosuppressive therapy. Finally, transient diffusion-weighted imaging hyperintensity of the splenium of the corpus callosum has been reported, associated with antiepileptics and capecitabine. Radiologists should be familiar with the patterns of neuroimaging abnormality associated with treatment-induced effects, especially radiotherapy and chemotherapy in cancer treatment.

Learning Objectives:

1. To show the imaging findings after radiation therapy in the acute, early and late delayed stages.
2. To present an overview of long-term sequelae after radiation therapy.
3. To discuss treatment induced leukoencephalopathy after chemotherapy (especially methotrexate).

16:00 - 17:30 **Room F1**

Joint Session of the ESR and ESOR

ESR/ESOR 1

Radiologic anatomy: abdomen

Moderator:
S. Gourtsoyianni; London/UK

A-326 16:00

Liver

G. Brancatelli; *Palermo/IT (gbranca@yahoo.com)*

The liver is the largest organ in the human body. The penetration and branching of the hepatic artery, portal vein and hepatic veins allow to divide the organ into the eight traditional segments of the Couinaud scheme. Knowledge of vascular and segmental anatomy is important to correctly locate the site of disease and to perform increasingly demanding and challenging liver resection and transplantation. Anatomy of the liver can be altered by congenital variants, diseases causing hepatic dysmorphy and after surgery.

Learning Objectives:

1. To locate and identify, using cross sectional medical imaging, superficial and internal structures of common liver anatomy.
2. To learn and understand how the vasculature define the eight Couinaud segments.
3. To explain how common pathological conditions affect the structure of the liver.

Author Disclosure:

G. Brancatelli: Author; Springer; Elsevier. Speaker; Bayer. Other; funding for travel to educational meetings from Bayer Healthcare and Bracco..

A-327 16:30

Biliary tree

O. Benjaminov; *Petach Tikva/IL (obenjaminov@gmail.com)*

"no abstract submitted"

Learning Objectives:

1. To discuss current imaging techniques for evaluation of normal biliary anatomy.
2. To learn and understand possible anatomical variants that may occur.
3. To explain how common pathological conditions affect the bile ducts.

A-328 17:00

Pancreas

M. Dioguardi Burgio; *Clichy/FR (marco_dioguardi@hotmail.it)*

The pancreas is a retroperitoneal gland, which is anatomically divided into 4 portions: head, neck, body and tail. Main anatomical relationships of the head are duodenal loop, the porta hepatis, and the superior mesenteric vessels. Body and tail anatomical relationship includes left kidney and adrenal gland, posterior gastric wall and lesser sac, splenic hilum, celiac region and duodenojejunal junction. Main pancreatic duct (Wirsung) drains into the major papilla most of the pancreatic secretions. A common biliopancreatic tract may be present. An accessory duct (Santorini) is usually present draining the anterior part of the pancreatic head in the minor papilla. Pancreatic gland is the result of the fusion of two buds. During the seventh gestational week the ventral bud rotates around the duodenum and it locates inferiorly and posteriorly to the dorsal bud. The fusion of the two buds leads to anastomosis of the ductal systems. Anomalies of this fusion process are at the base of the wide spectrum of anatomical variants which pancreatic parenchyma and ductal system may present. Those variants include pancreas divisum, ansa pancreatica, annular pancreas, ectopic pancreas, pancreatic hypoplasia or agenesis. Pathological involvement of the pancreas may be focal or diffuse. Radiological appearance of the gland is modified depending on aetiology and chronology of pancreatic involvement. Moreover, ductal system and peripancreatic tissue/organ changes are often associated. Knowledge of basic CT and MR modifications induced by common pancreatic pathologies is necessary to reach a proper diagnosis and to orientate patient's follow-up and therapeutic strategy.

Learning Objectives:

1. To review and illustrate the imaging features of normal pancreatic anatomy.
2. To review the possible congenital variants and anomalies of the pancreas and pancreatic duct.
3. To explain how common pathological conditions affect the pancreas.

16:00 - 17:30 **Room F2**

Oncologic Imaging

RC 816

Evaluating lymph node involvement: an impossible task?

A-329 16:00

Chairman's introduction

P. Lalitha; *Hyderabad/IN*

Session Objectives:

1. To understand diagnostic imaging difficulties in the evaluation of nodal involvement.
2. To understand the complementary information obtained with CT, MRI and PET.
3. To learn about advanced imaging techniques (CT - dual-energy; MRI - DWI, and PET) for evaluating nodal involvement.
4. To recognise pitfalls in evaluating nodal involvement using CT, MRI and PET.

A-330 16:05

A. The current criteria for nodal involvement MRI/CT

D. Tse; *Hong Kong/HK (donald.tse@gmail.com)*

Lymph nodes are often the first site of metastasis in many of the common cancers. Presence or absence of regional lymph node metastasis is a critical component of the UICC/AJCC TNM classification, now in its 8th edition. Nodal(N) staging has therapeutic significance in a number of cancers in determining operable vs inoperable disease, and use of neo-adjuvant or adjuvant therapy. For most malignancies, CT and MRI (and ultrasound) remain the main imaging modalities for nodal staging. Differentiation of metastatic lymph nodes from normal or benign reactive nodes relies on various

parameters afforded by CT/MRI; size is most widely used, and the only parameter used for nodal classification in the RECIST v1.1 criteria. In RECIST, 10mm is used as cutoff for non-pathological nodes, though in the chest and abdomen location-specific threshold sizes have been described. However, using size criteria alone has limited diagnostic accuracy when compared with the reference standard of histology; in rectal cancer, there is significant overlap in the sizes of benign and malignant nodes. Thus, various other imaging parameters, including attenuation, signal, homogeneity, border regularity, location, number, clustering and contrast enhancement, are also used for nodal classification in routine clinical practice. While each feature individually offers relatively poor diagnostic accuracy, with possible pitfalls such as necrotic nodes in infection, combinations of multiple imaging parameters can lead to improved sensitivity and specificity for diagnosing malignant nodes. Techniques including computer-aided algorithms have been explored to provide more quantitative nodal assessment. Nevertheless, nodal staging on CT and MRI remains a challenge.

Learning Objectives:

1. To understand the role of local nodal staging and its importance for management and prognosis.
2. To become familiar with the current imaging criteria for assessment of nodal metastases.
3. To understand the diagnostic performance of cross-sectional imaging.

A-331 16:28

B. Advanced MRI techniques: what do they contribute?

H.C. Thoeny; *Berne/CH (harriet.thoeny@insel.ch)*

Up-to-date lymph node staging is based on size and shape criteria only; however, micrometastases can also be present in normal-sized lymph nodes and nodes can be enlarged due to inflammatory changes. New contrast agents in MRI such as ultrasmall particles of iron oxide (USPIO) have substantially improved the diagnostic accuracy of lymph node staging. Unfortunately, USPIO are not commercially available on the market. DW-MRI is a noninvasive method that provides tissue microstructural information, and several studies mainly in the pelvis have shown promising results for lymph node detection and differentiation between benign and malignant nodes. These studies reported sensitivities of 79-100% and specificities of 74-93% using the underlying ADC-value; lower ADCs were reported in malignant nodes as compared to benign ones. On the other hand, it has been shown that there is a considerable overlap between ADC values of benign and malignant nodes. A recent prospective study in 120 patients with bladder and prostate cancer and normal-sized pelvic LNs on conventional cross-sectional imaging compared DW-MRI to histopathology based on extended pelvic lymph node dissection. It has been shown that the combination of DW-MRI findings and meticulous analysis of morphological findings allowed to detect malignant lymph nodes even in normal-sized nodes. The combination of USPIO with DW-MRI might further facilitate and improve lymph node staging in the future, provided that USPIOs will become available for clinical use. Initial promising results on the use of ferumoxytol in this context have already been publishes recently.

Learning Objectives:

1. To understand the principle of DWI of nodes.
2. To learn about the appearances of malignant nodes on diffusion-weighted MRI.
3. To become familiar with node-specific enhanced MRI.

Author Disclosure:

H.C. Thoeny: Advisory Board; Guerbet.

A-332 16:51

C. PET and other nuclear medicine techniques

T. Barwick; *London/UK (tara.barwick@imperial.nhs.uk)*

PET/CT imaging using 18-fluoro-deoxyglucose (FDG), a glucose analogue, has an established role in oncology for the staging and response assessment of a variety of tumours. For the assessment of nodal involvement visual analysis and semi-quantitative SUV analysis are utilised. However, there are no reliable absolute SUV cutoffs to differentiate between benign and malignant lymph nodes. It is very important to be familiar with the typical patterns of spread of the specific cancer being assessed as this also influences the likelihood of disease involvement. Glucose metabolism is not specific for malignancy and false positives can occur with inflammation, infection and other processes such as a sarcoid-like reaction to malignancy. Further pitfalls are that some well-differentiated malignancies have only low-level glucose metabolism and the limited spatial resolution of PET means involvement of small nodes may be missed or the level of metabolic activity may be underestimated in small nodes. New radiotracers which target more specific pathways such as C-11/ F-18 fluorocholine which target cell membrane metabolism and Ga-68 prostate-specific membrane antigen (PMSA) which targets a cell surface protein are gaining increasing use in prostate cancer imaging and the Ga-68 Dota-peptide tracers for somatostatin receptor imaging of neuroendocrine tumours.

Learning Objectives:

1. To learn the typical appearance on nodal metastatic disease on FDG.
2. To recognise the pitfalls for interpretation.
3. To become familiar with new radiotracers, including choline and PSMA PET, for the demonstration of nodal disease.

17:14

Panel discussion: Will imaging ever make diagnostic biopsy unnecessary?

16:00 - 17:30 **Room D**

Musculoskeletal

RC 810

Inflammatory arthritis: beyond the radiograph

A-333 16:00

Chairman's introduction

M. Reijnierse; *Leiden/NL (m.reijnierse@lumc.nl)*

Radiographs have been the cornerstone of rheumatology for a long time. Hand and foot radiographs are scored in rheumatoid arthritis patients to assess baseline bone destruction and are used in follow-up. In spondyloarthritis, pelvic radiographs are used to detect sacroiliitis. Radiographs and scoring methods are based on the identification of structural changes secondary to disease. Since new effective medication has become available, the focus in rheumatology has shifted towards early disease detection to treat early and prevent damage. Ultrasound and MRI might play a role in this since they detect active inflammation. With the use of colour Doppler in ultrasound, hypervascularisation can be appreciated and (teno)synovitis diagnosed. MRI has the additional value of the detection of bone marrow oedema and shows subclinical inflammation. The exact position of these imaging techniques in rheumatology is still under debate; however, they are increasingly used in research and daily practice. This refresher course aims to give an update on the diagnosis of inflammatory arthritis beyond the radiograph.

Session Objectives:

1. To gain insight into the merits of various imaging modalities in the daily practice of radiology of rheumatology.
2. To appreciate the crucial radiological contribution we need to provide in order to support optimal clinical decision making.

Author Disclosure:

M. Reijnierse: Grant Recipient; Dutch Arthritis Foundation.

A-334 16:05

A. Rheumatoid arthritis: what does MRI show and how do I do it?

I. Sudoł-Szopińska; *Warsaw/PL (sudolszopinska@gmail.com)*

Magnetic resonance imaging is being increasingly used both in RA research and in clinical practice due to its capacity to provide insight into pathogenesis of RA, the ability to identify the key pathologic features of this entity at presentation, to follow up patients' treatment results, and to establish remission. This presentation will cover two issues: 1. MRI techniques used in the assessment of rheumatoid arthritis, including sequences and protocols most frequently applied in imaging of various peripheral joints and the spine; 2. MRI findings in rheumatoid arthritis within synovial joints, tendons' sheaths, subchondral bone marrow, articular and extraarticular fat tissue. This part will make us aware that next to the synovium, which is a well-known source of inflammatory cells and a site for aggressive pannus formation, the same process may occur within the subchondral bone marrow or adipose tissue. In addition, the following issues will be addressed: 1. the importance of MRI in subclinical and early diagnosis of RA. 2. Monitoring the disease activity and progression, including the clinical relevance of synovitis and BME in terms of their role as an erosion precursor. 3. Assessing remission/residual synovitis, tenosynovitis, osteitis. 4. Identification of disease complications, especially within the spine.

Learning Objectives:

1. To become familiar with MRI techniques used in the assessment of rheumatoid arthritis.
2. To learn about the MRI findings in rheumatoid arthritis and their significance.

A-335 16:28

B. The axial skeleton in spondyloarthritis: conventional radiograph to MRI

R. Campbell; *Liverpool/UK (Rob.Campbell@rlbuht.nhs.uk)*

Inflammatory spondyloarthropathy (SpA) includes ankylosing spondylitis, psoriatic and reactive arthritis, enteropathic SpA, juvenile SpA and undifferentiated SpA. The assessment of spondyloarthritis (ASAS) International Society criteria for diagnosis of SpA includes MRI for disease staging. Imaging should include the sacro-iliac (SI) joints, and the dorsal and lumbar spine, utilising a combination of T1W and STIR or T2W fat-saturated sequences. In the SI joints, bone marrow oedema and sclerosis are present in areas of sub-chondral inflammation. Identification of bone erosion helps differentiate inflammatory disease from stress related or degenerative change. In the spine, inflammatory corner lesions of the vertebral bodies are one of the earliest signs of SpA, with bone marrow oedema on MRI. They may become sclerotic (previously termed Romanus lesions on radiographs), or fatty replacement may occur in inactive lesions. Inflammatory lesions also involve the facet joints, spinous processes, and costovertebral joints. Other features include disco-vertebral erosion, and syndesmophyte formation. Syndesmophytes may progress to profuse spinal ossification, with ankylosis across the intervertebral disc. Ankylosis of the facet joints, intervertebral ligaments and costovertebral joints also occurs in advanced disease. The proliferative bone formation in psoriasis and reactive arthritis tends to show more asymmetry than ankylosing spondylitis and enteropathic SpA, with more pronounced bony excrescences and paravertebral ossification. The radiologic patterns of inflammatory SpA must be differentiated from the bone formation associated with spondylosis deformans and DISH. Disco-vertebral erosion may mimic Modic changes associated with disc degeneration, cartilaginous Schmorl nodes an even infective discitis.

Learning Objectives:

1. To become familiar with imaging findings seen in the axial skeleton in spondyloarthritis.
2. To understand features on imaging which distinguish spondyloarthritis from other spinal diseases.

A-336 16:51

C. Ultrasound in inflammatory arthritis: what does it show and what does it mean?

A. Klauser; *Innsbruck/AT*

Ultrasound (US) is an established imaging modality for early detection, characterisation and follow-up of various forms of inflammatory arthritis, performed by radiologists and rheumatologists as well. It allows for the detection and characterisation of changes like synovial thickening, synovial proliferation, destructive pannus, effusion, erosions and enthesitis. Using PDUS a further assessment of synovitis and erosions can be obtained by classifying them in active versus nonactive, what has implication for the therapeutic management. Beside intraarticular inflammatory changes also periarticular and extraarticular inflammation in terms of tenosynovitis and enthesitis can be sensitively detected, not always easy to differentiate from articular inflammation by clinical investigation. However, as every imaging modality when assessing arthritis, the initial analysis has to start from the "joint-organ" concept, by dividing the imaging findings in synovial disease, cartilage disease or enthesis disease. This allows not only for basic differential diagnosis but is fundamental especially in more challenging cases, which will be also discussed in this lecture.

Learning Objectives:

1. To become familiar with US techniques used in the assessment of inflammatory arthritis.
2. To learn about the US findings in inflammatory arthritis and their significance.

17:14

Panel discussion: How practical is it for radiologists to support ultrasound and MRI for clinical rheumatology? Is it something the rheumatologists should undertake themselves?

16:00 - 17:30 **Room G**

State of the Art Symposium

SA 8

Forensic and post-mortem imaging

A-337 16:00

Chairman's introduction

P.A.M. Hofman; *Maastricht/NL (paul.hofman@mumc.nl)*

Radiology has always played a role in forensic and death investigations but only after the introduction of high-resolution cross-sectional imaging techniques both forensic and clinical postmortem radiology are evolving into a new subspeciality. There are two application fields: court procedures or law enforcement and the clinical use as a quality assurance or teaching tool. In all these cases, imaging can be an independent examination and the combination with an external examination, an autopsy and toxicological examination will provide more comprehensive information on the cause and manner of death and disease processes. The questions in a forensic setting will differ from a clinical setting but in both applications the level of expertise of the interpreter will determine the quality of the examination. It is, therefore, essential that radiologists are involved in these procedures. As in all new applications of imaging techniques it is important to establish a scientific basis, which positions forensic and postmortem radiology as a reliable method. The last decade many studies have been publishes but there are still many issues that need to be addressed. This includes pathologies that are difficult visualize. Another important question that needs to be answered during a forensic examination deals with injury patterns, and injury mechanisms and most research has been focused on individual injury rather than on injury patterns. Also the timing of injury and the time of death are important forensic issues that are still challenging for imaging. Therefore, more and larger studies are needed to establish a scientific basis.

Session Objectives:

1. To update delegates on the role of radiologists in post-mortem and forensic radiology.
2. To update delegates on the radiology in death investigations.
3. To discuss the role of various imaging modalities.
4. To highlight areas where further research is required.

A-338 16:07

Introduction to post-mortem radiology

T. Ruder; *Zurich/CH (Thomas.Ruder@irm.uzh.ch)*

Over the last 20 years, forensic radiology underwent tremendous growth and today, pre-autopsy post-mortem CT or MR are standard practice in many countries worldwide. Imaging is used for personal identification, documentation of injury, as evidence in court and for research and teaching in forensic sciences. The aim of this lecture is to provide an introduction to the field of forensic radiology and entice radiologists to get involved in this growing sub-speciality area. The lecture includes a discussion about the role and the potential of radiologic imaging in forensic medicine; a description of imaging modalities used in post-mortem imaging such as CT, CTA and MR; an outline of minimum standards for image acquisition in post-mortem forensic radiology; a review of current applications of cross-sectional imaging in forensic death investigations, including forensic identification, documentation of injury, disease and death; a note on legal aspects and peculiarities of reading, reporting and presenting findings in forensic radiology.

Learning Objectives:

1. To understand the potential role of post-mortem imaging and forensic imaging.
2. To discuss the different imaging techniques and protocols for post-mortem imaging.
3. To learn about the typical imaging findings and pitfalls.
4. To discuss relevant legal issues related to forensic radiology.

A-339 16:24

Post-mortem imaging: a pathologist's perspective

D. Ranson; *Melbourne/AU (david.ranson@vifm.org)*

PMCT is completely integrated with Coroners' death investigation procedures in Melbourne and this has been associated with a halving of the autopsy rate over the past 15 years. In Australia, the reliance on PMCT as a death investigation tool is becoming firmly established. The historical background to this change in death investigations and the medical, social and legal advantages that have accrued will be explored. We believe that considering autopsies to be the main medical tool (or the 'gold standard') of medico-legal death investigation is an outdated approach today. Unfortunately, legislation is often focused on these traditional approaches and this has influenced some of

the case law that has emerged following family objections to autopsy. These views have also driven the academic and community debate that seeks to address the question as to whether PMCT can replace autopsy. We believe this approach is fundamentally flawed and it should be replaced by a consideration of how PMCT can provide part of the evidence base that helps identify what are procedures are appropriate in a particular death investigation. This paper outlines the benefits that arise when you analyse the medico-legal death investigation process and re-engineer it so that PMCT, autopsy, 24-hour toxicology, 24-hour DNA, fast electronic access to medical records, scene photography/video and early external examinations are seen as equally valuable tools in the death investigation. The way in which these various modalities are chosen by the legal investigator (coroner) in partnership with forensic pathologists in Melbourne will be explored.

Learning Objectives:

1. To understand the potential role of post-mortem imaging in relation to pathology.
2. To become familiar with relevant questions in a death investigation.
3. To discuss the contribution of imaging to a death investigation.

A-340 16:41

Paediatric forensic post-mortem radiology

R.R. van Rijn; *Amsterdam/NL (r.r.vanrijn@amc.uva.nl)*

Postmortem radiology is mostly focussed on imaging of foetuses and neonates. However, in recent years it has found its way into the field of forensic medicine. The advantage of post-mortem imaging is the fact that imaging can be reviewed indefinitely and images can easily be shared between experts. Using post-processing techniques imaging findings can be used as illustrations for laymen in forensic reports. This lecture will present legal cases and the advantage and limitations of post-mortem imaging.

Learning Objectives:

1. To learn about the role of imaging in child abuse.
2. To discuss the different imaging techniques and protocols in paediatric forensic radiology.
3. To discuss relevant legal issues related to paediatric forensic radiology.

Author Disclosure:

R.R. van Rijn: Author; Several books, bookchapters and publications.

A-341 16:58

Post-mortem CT and MRI: imaging techniques

A. Persson; *Linköping/SE (anders.persson@cmiv.liu.se)*

Postmortem imaging has been used for more than a century as a complement to medico-legal autopsies. The technique has also emerged as a possible alternative to compensate for the continuous decline in the number of clinical autopsies. The diagnostic accuracy of postmortem imaging for various types of findings are depending of the imaging acquisition technique that has been used. Only recently quantitative post-mortem magnetic resonance imaging (PMMRI) technique has been introduced. A particular quantitative MRI sequence feasible for simultaneous quantification of T1 and T2 relaxation times as well as proton density (PD) can be used to quantify and characterize post-mortem tissue. This technique has the potential to reduce the temperature dependents in PMMRI examinations. Another promising imaging technique is postmortem dual-energy computed tomography (PMDECT). This technique enables to some extent quantification and determination of soft tissues and other foreign materials in the body. These new quantification techniques lay the foundation for new advanced visualization techniques and the use of big data, machine learning tools and radiomics in future forensic radiology.

Learning Objectives:

1. To learn about quantitative MRI and temperature independent imaging.
2. To learn about DECT in post-mortem imaging.
3. To learn about advanced visualisation techniques in post-mortem and forensic radiology.
4. To understand areas where further research is needed.

17:15

Panel discussion: What should be the focus of future research?

17:27

Chairman's closing remarks

P.A.M. Hofman; *Maastricht/NL (paul.hofman@mumc.nl)*

16:00 - 17:30 **Room K**

Radiographers

RC 814

The education and training of radiographers

Moderators:
H.H. Hjemly; Oslo/NO
E. Papadaki; Iraklion/GR

A-342 16:00

A. E-learning and blended learning approaches to continuing professional development (CPD): is this the way forward?

E. Metsälä; *Helsinki/FI (eija.metsala@metropolia.fi)*

There are various ways of understanding blended learning. Most common definitions refer to the so-called media blend, activity blend, space blend or time blend. In 2015, it was performed an integrative review dealing with blended learning outcomes in health care staff education. Search engines EBSCO Host, Science Direct and Pro Quest comprising several databases were used to search studies being published during the years 2005-2015. Measures used comparing blended learning and traditional learning are competency, skills and knowledge; student satisfaction; effectiveness of learning; the capacity of BL in relating theory and practice; the 'blended' nature of the blended learning modules; cost-effectiveness. The selected studies reported that blended learning was either superior or equal to conventional class room teaching. Blended learning outcomes are little or not at all dependent on the learning content or the topic being taught. It seems to be a suitable teaching method for various types of content in health care education. Blended learning should be implemented into health care education in a controlled way, with the support of organizational leadership, by offering the educational staff strong support in curriculum construction, pedagogics, and user-friendly technology.

Learning Objectives:

1. To discuss about the concepts used related to e-learning and blended learning.
2. To learn about the measures used and outcomes received comparing blended learning and traditional learning.
3. To appreciate the possibilities of e-learning and blended learning in health care staff CPD.

A-343 16:25

B. The assessment of clinical knowledge, skills and competences for pre- and post- registration radiographers

L. Robinson; *Salford/UK (l.robinson@salford.ac.uk)*

Participants will be provided with an overview of the principles and good practices for the assessment of clinical competence, exploring the difference between skills and knowledge for practice. Examples from the UK context will be provided, looking at both pre- and post-registration. Post-registration will also be broadened out to consider extended skill roles versus advanced practice. In small groups, participants will then be facilitated to consider the barriers and potential solutions to measuring clinical competence, which exist within their own context. Each participant will leave with their own action plan for further work which may also include a list of potential collaborative partners and sources of reference.

Learning Objectives:

1. To appreciate the complexities involved in designing pre- and post-graduate assessments.
2. To learn about the differences between assessing and extended role skills and post-graduate cognition.
3. To discuss the differences between advanced practice and extended roles for radiographers.

A-344 16:50

C. Clinical placements: the challenges ahead

L.A. Rainford; *Dublin/IE (louise.rainford@ucd.ie)*

In medical imaging, the application and frequency of specific imaging modalities are ever-changing. The scope of imaging across all sub-specialities is expanding, however, clinical practice is partly determined by the availability of advancing technologies, reliant on social economic factors; therefore, training needs will not change in a standardised manner across European jurisdictions. Radiography education needs to keep abreast of these changes and modify curricula and training schemes to meet the needs of the clinical environment. Radiography role development is also progressing at different rates across Europe and requires consideration with respect to guideline

documents focused on professional education. With a growing list of subjects considered as graduate radiography requirements, the depth to which subjects are taught is challenging. In many jurisdictions, the presence/evolution of national regulatory agencies for allied healthcare professions drive the clinical training needs for radiographers; however, the mobility of the radiography workforce across Europe requires consideration. Clinical training enhancement requires equality of training opportunity and high standards of teaching across radiography programmes, which is evidenced. To ensure safe practice the supervisory staff should be adequately trained and all patient safety issues need to be fully addressed and form an integral part of competency verification. A further challenge to clinical training is the commencement of graduate entry pathways; training programmes must fulfil the needs of two socially different student cohorts. Additionally, the methods of recording clinical placement experience and assessment is moving from traditional written logs to ePortfolios which presents notable challenges. The presentation will address these issues.

Learning Objectives:

1. To appreciate the challenges of clinical practice placement enhancement for radiography students.
2. To review methods of addressing the challenges ahead.
3. To discuss how to best address safe clinical practice for radiography students.

17:15

Discussion and questions: Education and training: what is the way forward?

16:00 - 17:30 **Room M 1**

Vascular

RC 815

Carotid artery disease: so what's new?

Moderator:
T. Jargiello; Lublin/PL

A-345 16:00

A. The diagnostic assessment of carotid arteries: do we still need US?
R. Iezzi; *Rome/IT (roberto.iezzi.md@gmail.com)*

Stroke is the third leading cause of death in industrialized nations, behind heart disease and cancer, and a leading cause of long-term disability. The current indication for intervention in patients with carotid artery stenosis is based primarily on the degree of stenosis and symptoms. Carotid ultrasonography, CTA and MRA can provide the information needed to guide the choice of medical, endovascular, or surgical treatment. As each imaging modality has strengths and weaknesses, choosing among the available vascular imaging modalities, deciding when to combine multiple modalities, and judicious application of angiography are challenging aspects of evaluation in patients with carotid artery disease. These features will be discussed and highlighted in the presentation to obtain a suggested diagnostic algorithm for diagnosis and follow-up of patients with carotid artery disease. The final section of the presentation will be dedicated on the discussion about plaque instability that in recent studies seems to be crucial in the aetiology of acute cerebral ischaemic events in patients with carotid disease. Some authors advocate the possibility that patients may soon be selected for intervention based more on plaque vulnerability than on the degree of stenosis or symptoms. The challenge could be to identify patients at high risk who have lesions that are vulnerable to thrombosis, so-called "vulnerable-plaques", before the event occurs. Moreover, to tailor and improve treatment strategies, appropriate diagnostic methods must be chosen that are able to determine the patient-specific risk of experiencing a cardiovascular event, the so-called "vulnerable-patient".

Learning Objectives:

1. To understand the role of US, CT, MR and DSA in diagnostic assessment.
2. To learn the optimal imaging algorithm for diagnosis and follow-up.
3. To appreciate the role of plaque characterisation in routine practice.

A-346 16:30

B. Carotid stenting vs endarterectomy: is the jury back yet?
K.D. Mathias; *Hamburg/DE*

In symptomatic patients with carotid artery stenosis invasive treatment with removal of the stenosis is international standard based on the data of numerous trials. Less clear is the choice of the treatment modality. Carotid endarterectomy (CEA) and carotid stenting (CAS) have recently shown similar early and late outcomes. The anatomy of the aortic arch and supra-aortic arteries as well as the characteristcs of the lesion are important information for the choice of the method. Carotid stenting is preferred in patients with the so called "hostile neck". Carotid endarterectomy is the better option in dense circular calcifications of the carotid stenosis and in elongated carotid arteries with kinks and loops. The preference for one or the other treatment modality concerns about 10 to 15% of the patients. In more than 80% of the patients both methods can be applied with similar results. Actual technical progress of endovascular devices makes carotid stenting safer than in the past. But sufficient volume of interventions (>100 CAS/year) is necessary to reach good results. In asymptomatic patients best medical treatment has shown that the annual stroke risk can be reduced to 1% or even less. Therefore, the selection criteria for invasive treatment are different. Invasive treatment requires a rate of morbidity and mortality of less than 3% and a life expectancy of the patient of at least 5 years to gain a benefit for the patient. The degree of stenosis should exceed 70%. Additional other vascular pathologies like multiple vessel disease, incomplete circle of Willis, isolated middle cerebral artery etc. increase the stroke risk and should be treated invasively. The international and european guidelines support this process. CAS should be performed when the complication rate of the intervention is in the range of 1 to 2% and clearly below 3%. In acute carotid occlusion endovascular treatment is the method of choice as long as a good penumbra is shwon by perfusion CT or MRI. In carotid T-occlusions thrombectomy should be performed as fast as possible. In bifurcational carotid occlusion thrombectomy is combined with CAS. After stenting of the underlying stenosis the thrombus is retrieved. Carotid stenting has some additional advantages in comparison to carotid endarterectomy. In patients with contra-lateral carotid artery occlusion the stroke risk of CEA is increased (NASCET 14.7%, SPACE 13%), but not of CAS. Endovascular treatment can also manage additional lesions in the same session such as ostial stenosis of the common carotid artery or stenosis of the distal internal carotid artery close to the skull base or intracranially.

Learning Objectives:

1. To understand the evidence supporting surgery and endovascular therapy.
2. To understand why the trials have been slow to bring clarity to optimal therapy.
3. To learn how best to triage patients for surgery or endovascular therapy.

A-347 17:00

C. Carotid interventions in the setting of acute stroke
S. Sencer; *Istanbul/TR (serrasencer@gmail.com)*

Leaning objectives in this lecture are to understand the indications and contraindications to carotid stenting, appreciate how MR/CT can aid patient selection for carotid stenting and learn about carotid stenting in the setting of acute thrombosis/dissection. Carotid stenting is a well-established method of revascularization in patients with carotid stenosis. Indications for carotid stenting are based upon the symptomatic status of the patient, degree of stenosis and possibly other factors (patient features such as co-morbidities, life expectancy, age, sex). In pre-treatment evaluation, Doppler ultrasound, CTA and MRA can be used to investigate the degree of stenosis and plaque character. Catheter angiography is usually reserved for cases where there is a discrepancy between noninvasive vascular imaging techniques. Cerebral MRI with diffusion-weighted imaging is used for assessing ischemic lesions (symptomatic and silent) in the territory of intended treatment as well as other findings. In patients with acute CVA, non-contrast head CT and advanced imaging techniques such as CT perfusion and perfusion MR studies can also be utilized for selecting the suitable treatment strategy. In the setting of acute stroke treatment, carotid angioplasty and/or stenting can be performed as an adjunct to thrombectomy/thrombolysis or as the primary choice of therapy depending on the angiographical findings. Dissection of the carotid artery may also present as an acute clinical picture and can also be treated with carotid stenting.

Learning Objectives:

1. To understand the indications and contraindications to carotid stenting.
2. To appreciate how MR/CT can aid patient selection for carotid stenting.
3. To learn about carotid stenting in the setting of acute thrombosis/dissection.

16:00 - 17:30 **Room M 2**

Computer Applications

RC 805
Daily use of mobile devices in radiology

A-348 16:00
Chairman's introduction
O. Ratib; *Geneva/CH*

Session Objectives:
1. To give an overview of tools available on mobile devices for education and exam reporting.
2. To underline the impact of mobile devices in routine clinical activity.
3. To learn about the legislative backbone and potential drawbacks of mobile technology.

A-349 16:05
A. What did mobile devices change in radiology education?
E. Kotter; *Freiburg/DE*

Mobile devices and fast networks are ubiquitous today. E-learning has been used in radiology for more than 30 years. The lecture will give an introduction to and an overview of e-learning systems for radiology with emphasis on e-learning on mobile devices. Advantages and limitations of mobile e-learning will be discussed. An outlook to future development of e-learning will be given.
Learning Objectives:
1. To give an overview of tools available for e-learning.
2. To explore the potential impact of e-learning in the daily radiological practice.
3. To explore future developments and limits of e-learning.
Author Disclosure:
E. Kotter: Consultant; Thieme Verlag - eRef.

A-350 16:28
B. Is it appropriate to read a study on a smartphone or a tablet?
E. Neri; *Pisa/IT*

The presentation will address the technological limitations and security concerns that arise for radiologists looking to go mobile. With regard to the technological aspect, while it is acceptable to occasionally read images on a smartphone or tablet for a second expert opinion or learning purposes, they should not be used in daily practice for primary diagnosis. Even then, only devices with a screen size of 9 inches or more, with a high-resolution display, are appropriate for medical imaging. Moreover, new high resolution retina displays with increased size (as the IPAD Pro) are bringing mobile devices closer to a standard medical monitor. Security concerns are now better clarified by the recent general data protection directive of the EU. It clearly addresses the need to protect patient's data with respect to privacy, and also highlights the importance of an informed consent to the use of data for any purpose, even in regard to the portability of such confidential information. Even if mobile devices make the reading, the portability and the exchange of patient's data easier, their use must be strongly regulated at a national level and across countries.
Learning Objectives:
1. To give an overview of available DICOM viewers and software for reporting imaging studies.
2. To discuss technical requirements of mobile devices for use in imaging interpretation.
3. To provide insight on future developments of imaging viewing technology.

A-351 16:51
C. Security and ethical issues of mobile device technology
E.R. Ranschaert; *Mol/BE (ranschaert@telenet.be)*

In clinical practice medical specialists use mobile devices to quickly exchange medical images and patient information with other health care professionals. Frequently they want to ask a colleague for advice regarding a diagnosis or treatment, sometimes even in an acute setting. Often popular messaging services such as WhatsApp are being used for this purpose. Transmission of patient data by public social media and messaging services, however, does have several limitations from an ethical point of view, which are mostly related to the security and privacy of patients. Some critical questions need to be answered: is this unsafe and/or illegal, and if yes, why? Are there any regulations and/or guidelines available? Are there any secure and legal alternatives? In this refresher course these issues will be discussed in more detail.
Learning Objectives:
1. To provide an overview of technical solutions for patients' image and data mobility.
2. To provide a risk assessment analysis (data loss, privacy, etc.) of mobile technology.
3. To give an overview of European legislation in relation to patient image and data mobility.
Author Disclosure:
E.R. Ranschaert: Board Member; EUSOMII. Shareholder; Diagnose.me.

17:14
Panel discussion: Will mobile technology overcome stationary technology in radiology?

16:00 - 17:30 **Room M 3**

Interventional Radiology

RC 809
Imaging and endovascular treatment of pulmonary embolism

A-352 16:00
Chairman's introduction
G. O'Sullivan; *Galway/IE (gerard.osullivan2@hse.ie)*

Venous thrombo-embolism (VTE) is an enormous healthcare issue. This session focuses on state of the art, cutting edge, and yet absolutely practical imaging of pulmonary embolus (PE), which is a bigger killer in Western Europe than AIDS, breast cancer, road traffic accidents, and prostate cancer all COMBINED. All radiologists need to know how to diagnose and interpret this important condition. Following diagnosis, interventional radiologists have the ability to treat PE by aggressive catheter-based therapy and the latter 2/3 of this session will focus on the evidence to support this and the "how to" application of same.
Session Objectives:
1. To appreciate the value of imaging in therapy planning and follow-up.
2. To learn about patient selection and evidence in catheter directed therapies for PE.
3. To learn about recent and ongoing trials in the endovascular treatment of PE.
Author Disclosure:
G. O'Sullivan: Advisory Board; iemens Healthcare. Author; New Horizons in Venous Disease. Speaker; Cook Medical, Straub, Bard, BSCI, Marvao Medical.

A-353 16:05
A. Imaging algorithm for pulmonary embolism
B. Ghaye; *Brussels/BE (benoit.ghaye@uclouvain.be)*

The diagnosis of pulmonary embolism (PE) is difficult since the clinical signs and symptoms are non-specific. Unstable patients usually undergo thrombolysis following demonstration of right ventricle (RV) dysfunction at echocardiography. Diagnostic algorithm strategies in stable patients have been developed to limit the number of patients requiring an imaging test. The first step includes the assessment of clinical probability of PE and D-dimers testing. Patients with either a high clinical probability or a positive D-dimers test should undergo further imaging test. Incompliance to such diagnostic algorithms has been demonstrated to increase the rate of PE recurrence and the rate of false-positive CT pulmonary angiographies. In patients not at high-risk of mortality (i.e. without clinical findings as cardiogenic shock or persistent arterial hypotension), signs of RV dysfunction (at echocardiography or CT pulmonary angiography) are used together with clinical prognostic scores, such as the PESI, and cardiac biomarkers dosage to discriminate patients with *intermediate* or *low* risk. This is usually performed by measuring the ratio between the diameters of RV and the left ventricle (RV/LV). More recent and potentially more powerful predictor CT findings have been reported, including among others RV/LV surface and volume ratios, severity of "perfusion" defect and cardiac function parameters as calculated from ECG-gated acquisition. Evidence concerning the follow-up of unselected patients after treatment is limited in the literature. Short-term follow-up after systemic thrombolysis or endovascular treatment has been performed using various techniques, including RV/LV dimensions, pulmonary arterial obstruction scores or pulmonary perfusion comparison.
Learning Objectives:
1. To learn how clinical findings influence the selection of the imaging strategy in PE.
2. To learn about the follow-up after treatment.
3. To learn how imaging may predict the outcome of the patient.

A-354 16:28

B. What is new in the recently published guidelines for pulmonary embolism treatment?

R. Uberoi; *Oxford/UK (Raman.Uberoi@ouh.nhs.uk)*

PE is a major cause of mortality, morbidity, and hospitalization in Europe. 317 000 deaths related to VTE were reported in six countries of the European Union (with a total population of 454.4 million) in 2004. 34% present with sudden fatal PE and 59% postmortem. Only 7% who died early were correctly diagnosed with PE before death. Following diagnosis, patients should undergo risk stratification using a scoring system such as the pulmonary embolism severity index and patients stratified into high-, intermediate- and low-risk groups based on the clinical status of the patient, i.e. shock , hypotension, signs of RV dysfunction and cardiac biomarkers. Patients with scores of PESI of III-IV will have a 30-day mortality of 24.5%. High-risk and intermediate-high-risk patients should undergo consideration for rapid primary pharmacologic treatment, or surgery and where available interventional treatment to rapidly clear thrombus. Acute right ventricular dysfunction critical determinant of outcome and persistent arterial hypotension and cardiogenic shock carries a high risk of early death. Primary reperfusion treatment, particularly systemic thrombolysis is currently the treatment of choice. This can result in early reduction of pulmonary resistance and improvement in RV function. The maximum benefit is in the first few days, ideally within 48 hours with 90% of patients showing improvement, with no benefit at one week. Low-risk patients, i.e. PESI scores I-II or sPESI 0 should be considered for early discharge and outpatient treatment with anticoagulation.

Learning Objectives:

1. To learn about the recently published guidelines for PE treatment in stable patients.
2. To learn about the recently published guidelines for PE treatment in unstable patients.
3. To learn about recent therapeutic algorithms in PE treatment.

Author Disclosure:

R. Uberoi: Grant Recipient; Bolton medical.

A-355 16:51

C. Updates on the endovascular treatment of massive and submassive pulmonary embolism

S.C. Spiliopoulos; *Athens/GR (12461)*

Minimal invasive percutaneous endovascular treatment of massive and submassive pulmonary embolism (PE) offer the benefit of low-risk, more aggressive management than systemic anticoagulation and have been correlated with reduced morbidity and mortality rates. Traditional endovascular methods include thrombus dissolution using standard pigtail catheters or balloons, presenting reasonable technical success rates of approximately 86%. Local low-dose catheter-directed thrombolysis combined with thrombectomy (e.g. pharmacomechanical thrombolysis) seems to improve outcomes, without increasing the risk of bleeding. The rationale of recent and ongoing trials is based on the fact that systemic thrombolysis, although more effective than anticoagulation alone, increases 5-fold the risk of major bleeding and 10-fold that of haemorrhagic stroke, while is contraindicated in many patients mainly due to recent surgery or intracranial haemorrhage. On the other hand, the majority of evidence for catheter-based interventions is based on few single-centre case series and prospective trials. Over the past few years, a number of prospective, multi-centre, randomized trials and large registries investigated novel pharmacological and pharmacomechanical thrombectomy techniques, such as ultrasound accelerated thrombolysis, providing high level of evidence regarding the safety and efficacy of endovascular treatment options in acute PE. However, studies comparing various endovascular modalities versus systemic fibrinolysis are missing, while additional large-scale, well-designed randomized trials are required to improve the level of evidence of currently available interventional radiology techniques. In this lecture, outcomes of available and ongoing clinical data will be presented and future perspectives will be discussed.

Learning Objectives:

1. To learn about the rationale of recent and ongoing trials.
2. To learn about the level of evidence for interventional radiology techniques in PE treatment.
3. To learn about clinical results and possible further developments.

17:14

Panel discussion: Appropriate diagnosis and risk stratification in the management of acute massive and acute submassive pulmonary embolism

16:00 - 17:30 **Room M 4**

E³ - ECR Academies: Spinal Imaging

E³ 819

Spinal trauma

A-356 16:00

Chairman's introduction

L. Manfrè; *Catania/IT (lmanfre@me.com)*

A-357 16:05

A. Looking for fractures

E.J. Ulbrich; *Zurich/CH (erika.ulbrich@usz.ch)*

In trauma patients, the spine is often involved with the thoracolumbar spine as the most common portion, especially T11-L2. The necessity of a radiography after trauma may be weighed with the help of the national emergency x-radiography use study (NEXUS) criteria and the Canadian C-spine rule (CCR). According to the clinical NEXUS criteria, the probability of absence of a fracture is 99.6% in patients with no posterior midline cervical-spine tenderness, no evidence of intoxication, a normal level of alertness, no focal neurologic deficit and no painful distracting injuries. The CCR defines clinical criteria for a low-risk patient for C-spine fractures after blunt trauma with a 100% sensitivity. Comparing the CCR with the NEXUS criteria, CCR performed somehow better. If imaging is indicated by clinical criteria (NEXUS, CCR) the American College of Radiology (ACR) Appropriateness Criteria list the precise indications of imaging modalities (x-ray, CT, MRI, myelography, angiography). Concerning thoracolumbar spinal fractures, the Magerl classification (exclusively applicable for assessment of CT findings) is used which is based on the three-column concept by Denis and the McAfee classification. The Magerl AO concept differentiates between compression (type A), distraction (type B) and rotation (type C). The thoracolumbar injury classification and severity (TLICS) scale is a guideline for management of treatment regarding thoracolumbar injuries. Based on the three major categories (injury morphology, posterior ligamentous complex integrity and patient neurology) patient scores determine a management plan for surgeons depending on the presence of injuries and co-morbidities.

Learning Objectives:

1. To understand the different standard clinical criteria for spine imaging (Canadian C-spine rule, Nexus criteria).
2. To understand the essential traumatic spinal mechanisms.
3. To become familiar with the different classification systems, from Denis to TLICS.

A-358 16:33

B. Looking for spinal cord and soft tissue injuries

F. Bonneville; *Toulouse/FR (bonneville.f@chu-toulouse.fr)*

In spinal trauma, MRI is the modality of choice for evaluation of ligamentous and other soft tissue structures, disc, spinal cord and vessels. Complete spinal ligamentous tears appear as interruption of those structures normally appearing as low signal intensity bands. It is best depicted on T2-weighted and STIR images. Spinal instability is defined by the involvement of two of the three vertical parallel columns biomechanically forming the vertebral column. Acute disk herniation can also occur and may worsen the symptoms. Neurological deficits may be due to cord compression by epidural or subdural haematoma, or intrinsic spinal cord injury. Axial gradient echo T2-WI is mandatory to identify such haemorrhagic lesions, especially within the cord, because haemorrhagic contusions and haematomyelia are correlated to worse outcome. They appear hypointense while cord oedema returns T2 hyperintensity. Spinal cord trauma usually demonstrates a mixture of both oedema and haemorrhage. In cervical spinal trauma, vascular injuries should be sought as asymptomatic injuries can subsequently lead to cerebral and cerebellar infarctions. Vertebral arteries are more commonly involved than carotid arteries. Main cervical traumas at risk for vascular injuries include C1-C3 fractures, fracture extending into a foramen transversarium, cervical spine luxation and expanding neck haematoma. Most of the vascular injuries can be seen as irregularity or loss of normal flow void on T2WI, and should be confirmed by adequate and dedicated vascular imaging.

Learning Objectives:

1. To understand which soft tissue structures are relevant for spinal stability.
2. To learn how to detect subtle soft tissue injuries.
3. To become familiar with the different traumatic cord injuries.

A-359 17:01

C. Looking for spinal injuries in children
P.C. Maly Sundgren; *Lund/SE (Pia.Sundgren@med.lu.se)*

Spinal injuries are generally less common in the paediatric population compared to adults with cervical spine injuries being most frequent spine injury of all spine injuries occurring in up to 40-60% of all injuries in children. The specific biomechanics of the paediatric cervical spine leads to a different distribution of injuries and distinct radiological features and represent a distinct clinical entity compared to those seen in adults. Young children have a propensity for injuries to the CCJ, upper cervical injuries (i.e. cranial base to C2) whereas older children are prone to lower cervical injuries similar to those seen in adults. In this lecture, typical injuries in the paediatric population will be presented including normal variants that can be misleading in the diagnosis of fractures.

Learning Objectives:
1. To understand that children are prone to different types and locations of injuries when compared to adults.
2. To become familiar with normal anatomy and anatomic variants that may mimic fractures in children.
3. To learn how to select the appropriate imaging modality in the individual patient.

16:00 - 17:30 **Room M 5**

Joint Course of ESR and RSNA (Radiological Society of North America): Hybrid Imaging

MC 828

Hybrid imaging in the male

Moderators:
A. Drzezga; Cologne/DE
K. Riklund; Umea/SE

A-361 16:00

A. Prostate cancer: novel tracers
S.P. Rowe; *Baltimore, MD/US*

"No abstract submitted."

Learning Objectives:
1. To learn about novel tracer and their biochemical properties.
2. To understand the differences of information given by the use of different tracers.
3. To understand how to interpret examinations with different tracers.

A-360 16:30

B. Prostate cancer: PET, MR or both?
M. Eiber; *Los Angeles, CA/US*

Currently national and international guidelines for imaging procedures for high-risk and advanced prostate cancer (PCa) include abdomino-pelvic cross sectional imaging, multiparametric prostate MRI, bone scintigraphy and in the case of therapy monitoring of mCRPC whole-body cross-sectional imaging mainly by means of computed tomography. Positron emission tomography (PET) has became increasingly important in the work-up of prostate cancer. In the past, the use was mainly limited to radiolabeled choline-derivatives which showed considerable limitations and did not always meet the diagnostic needs. Recently, a 68 Gallium-labelled ligand of the prostate-specific membrane antigen (68Ga-PSMA) has been introduced in PET-imaging of PCa with first promising results. Due to relatively exclusive expression of PSMA in prostatic tissue as well as increased expression in PCa 68Ga-PSMA was reported to exhibit a favourable lesion to background ratio compared to presently used choline- or fluorodeoxyglucose-based PET examinations. Together with the novel development of combined PET/MR, the combination of excellent morphological detail, multiparametric functional information and molecular PET data might lead to a significant improvement in detection and staging of PCa and thus may help to optimise oncological treatment. The talk encompasses: 1. The molecular basis of prostate cancer imaging targeting the prostate-specific membrane antigen (PSMA), review of the various PSMA-tracers. 2. The diagnostic performance and potential role of PSMA PET/CT and PET/MR for high-risk primary and advanced prostate cancer. 3. Comparison of the use of PSMA PET-imaging with conventional imaging as included in the guidelines.

Learning Objectives:
1. To learn about pathophysiology in prostate cancer.
2. To understand how to interpret hybrid imaging of prostate cancer.
3. To learn about the role of hybrid imaging in staging, treatment evaluation and follow-up.

A-362/A-363 17:00

C. Interactive case discussion (part 1)
M. Eiber; *Los Angeles, CA/US*
S.P. Rowe; *Baltimore, MD/US*

The third part of this session will contain interactive cases based on the previous teaching points.

Learning Objectives:
1. To learn how to interpret hybrid imaging of prostate cancer.
2. To understand the pathophysiology in relation to imaging.

Friday, March 3

08:30 - 10:00 **Room A**

E³ - ECR Academies: Interactive Teaching Sessions for Young (and not so Young) Radiologists

E³ 921
Use of staging and classification systems

A-364 08:30
A. RECIST 1.1 training
A. Graser; *Munich/DE (a.graser@radiologie-muenchen.de)*

RECIST 1.1 has been developed as an improvement of RECIST 1.0 to allow for reproducible and exact measurement of overall tumour load in patients with metastatic disease that are being treated as part of clinical trials. Furthermore, it can be used to guide decision-making in everyday clinical practice. This lecture will explain basic RECIST rules, teach about types of lesions (target versus non-target), and measurement strategies. Furthermore, clinical cases will be used to train correct use of the system. Recent additions to RECIST, e.g. Choi criteria, will also be covered. Finally, limitations of RECIST in clinical practice will be discussed.

Learning Objectives:
1. To understand the principle of the RECIST system.
2. To become familiar with the daily oncological work-up.

Author Disclosure:
A. Graser: Consultant; Pfizer Pharma AG. Speaker; Pfizer Pharma, Novartis Pharma, Siemens AG.

A-365 09:15
B. Gastrointestinal-abdominal masses
A. Ba-Ssalamah; *Vienna/AT (ahmed.ba-ssalamah@meduniwien.ac.at)*

The spectrum of abdominal masses is broad, as is the differential diagnosis. Cross-sectional imaging modalities, in particular computed tomography (CT) and magnetic resonance imaging (MRI), are routinely used to evaluate the size, morphology, location and relationship of the lesion to adjacent organs. It is essential to understand how to tailor the exam to the clinical indication, i.e. which modality is best, and which contrast agent to use for MRI. The role of PET-CT and PET-MRI, with various radiotracers, that can give us further insight into the metabolic properties of these masses, will be discussed. Furthermore, we will explain the enhancement pattern and tracer behaviour of the mass which may help us to narrow the differential diagnosis. Demonstrating the content of the lesion, such as fat, fluid, solid components or calcifications, is an important imaging clue, too. Malignant entities, including peritoneal carcinomatosis and pseudomyxoma peritonei, as well as lymphoma and GIST, will be demonstrated. We will include some uncommon entities that may present with and without symptoms, such as epiploic appendagitis, omental infarction and mesenteric panniculitis. Finally, we will illustrate exophytic masses originating from abdominal organs, such as the liver, pancreas and bile ducts, causing diagnostic challenges.

Learning Objectives:
1. To learn the characteristic features of some common and atypical abdominal masses.
2. To identify the key imaging findings that assist surgeons or oncologists treating specific abdominal masses.

08:30 - 10:00 **Room B**

GI Tract

RC 901
CT colonography today

A-366 08:30
Chairman's introduction
M. Hellström; *Gothenburg/SE*

A-367 08:35
A. How I perform it
P. Lefere; *Roeselare/BE (radiologie@skynet.be)*

According to the ESGE/ESGAR guidelines and the second ESGAR CTC consensus on CT colonography (CTC), correct technique of performing CT colonography is essential to obtain good results of polyp/tumour detection. CTC technique is related to an adequate preparation of the colon, optimal distension of the colon and the correct use of scanning protocols adapted to the specific requirements of CTC. 1. Bowel preparation and faecal tagging: a) principles of state-of-the-art preparation: diet, laxatives, faecal tagging, b) application according to the clinical presentation of the patient, c) full cathartic preparation vs reduced cathartic preparation: when, advantages/disadvantages, the future? and d) pitfalls related to preparation. 2. Colon distension: a) principles of state-of-the-art colonic distension, b) practical application of optimal colonic distension, c) possible issues/complications and how to prevent and d) pitfalls related to colonic distension. 3. Scanning protocols: a) acquisition of CTC in clinical practice, adapted to the different clinical presentations/indications, b) dose considerations: how to reduce dose in CTC and c) pitfalls related to acquisition.

Learning Objectives:
1. To learn about modern approaches to bowel preparation and faecal/fluid tagging.
2. To become familiar with colon distention, including prevention of possible complications.
3. To learn about different scanning protocols and their use according to patient status and clinical needs.

A-368 08:58
B. How I interpret it
T. Mang; *Vienna/AT (thomas.mang@meduniwien.ac.at)*

The evaluation of CT colonography (CTC) studies is based on detection, interpretation, and documentation of colonic findings. It is performed on a computer workstation equipped with dedicated CTC software by a primary 2D or a primary 3D approach. In either case, the alternative viewing technique must be available for rapid correlation and characterization of any suspicious findings. Primary 2D evaluation is based on “lumen tracking” by interactively scrolling through the axial slices and multiplanar reformatted images, focusing only on the air-distended colonic lumen from one end to the other one. Primary 2D evaluation provides information about the attenuation of findings during the search process. It is time-efficient. Primary 3D evaluation is based on 3D virtual endoscopy in an antegrade and retrograde fashion. It increases both, the conspicuity, especially of small and medium-sized polyps, and the duration of visualization. The use of advanced 3D displays like virtual dissection or unfolding techniques may reduce the interpretation time for primary 3D evaluation at the expense of increased image distortion. Colonic findings can be systematically characterized by their morphology, attenuation characteristics and mobility. Knowledge of the CTC imaging features of common colonic lesions and artefacts is necessary for characterization of findings and differentiation of genuine colonic lesions from pseudo-lesions. Computer-assisted detection (CAD) algorithms, used in CTC, can automatically detect polypoid findings. Specifically, if used as a second reader, CAD was found to reduce the number of perceptual errors by pointing out possible abnormalities that might otherwise be missed.

Learning Objectives:
1. To become familiar with different image presentations: 2D, 3D, enhanced views.
2. To appreciate the strengths and limitations of primary 2D and primary 3D reading.
3. To learn about the use of Computed Assisted Diagnosis (CAD) software.

A-369 09:21

C. Screening with CTC

D. Regge; *Turin/IT (daniele.regge@ircc.it)*

Colorectal cancer screening reduces cancer-specific mortality significantly and is cost-effective, or even cost-saving, with respect to not performing a screening test. In some European countries, tests with different lesion yield and costs (i.e. faecal occult blood test, sigmoidoscopy and colonoscopy) have been chosen for population screening programs. CT colonography has been approved by the American Cancer Society in 2008 as a test to detect polyps and colorectal cancer and has since then been adopted on an individual basis. Recently CT colonography has also been endorsed by US preventive services task force as a screening test paving the way to reimbursement by medicare and private insurers. In Europe, CT colonography has been explored in a screening context mainly in randomized controlled trials where CT colonography lesion yield and subject participation into running screening programs have been compared to that of other tests. These data are now available as those related to costs of the CT colonography arm. The lecture will focus on the evidence cumulated in the last decade on the use of CT colonography as a screening test, to review current guidelines and present possible scenarios for its future adoption in colorectal cancer screening.

Learning Objectives:

1. To understand basic principles of population and opportunistic screening.
2. To become familiar with data on accuracy of CTC in screening populations.
3. To learn about current guidelines on the use of CTC in screening.

Author Disclosure:

D. Regge: Author; Springer. Speaker; GE Medical Systems.

09:44

Panel discussion: Challenging cases from clinical practice

08:30 - 10:00 **Room C**

Chest

RC 904

Low-dose and no-dose chest imaging: opportunities and limitations

Moderator:
D. Tack; Baudour/BE

A-370 08:30

A. CT

C. de Margerie-Mellon; *Paris/FR (constancedemm@gmail.com)*

Radiation dose in CT scan must be as low as reasonably achievable. High natural contrast of lung parenchyma makes it particularly suitable for radiation dose reduction. Various technical parameters have to be optimized, especially tube current, tube potential, and reconstruction algorithm, to obtain the better trade-off between radiation dose level and image quality. Iterative reconstruction algorithms take currently a dominant role in radiation reduction by lowering image noise induced by reduced-dose examinations. On the other hand, reduced-dose CT protocols should be adapted to the clinical situation. Their relevancy have been largely investigated for solid nodules detection on non-enhanced CT and for pulmonary emboli diagnosis on CT pulmonary angiography. Other potential applications include infectious pneumonia and pleural abnormalities detection (especially in asbestos-exposed workers) and neoplasia follow-up. However, radiation dose reduction is still limited for obese patients and in case of interstitial pneumonia.

Learning Objectives:

1. To learn about techniques for decreasing the radiation dose.
2. To know in which clinical situations low-dose CT should be performed.

A-371 09:00

B. MRI

J. Dinkel; *Munich/DE*

Although many studies have advocated a valuable role for thoracic MRI, it has currently limited clinical utilization with the exception of cardiovascular imaging. However, new technical developments and MRI sequences have continuously improved the quality and broadened the clinical indications for thoracic MRI. Furthermore, due to its high soft tissue contrast and the lack of radiation exposure, MRI allows for repeated measurements of the lung structures and, therefore, appears to be appropriate for functional investigation of lung. The purpose of this presentation is to review the currently available MR techniques useful in thoracic imaging and to provide an overview of present and emerging clinical applications of thoracic MRI.

Learning Objectives:

1. To learn about the current lung MR protocols.
2. To know in which clinical situations lung MRI is a helpful adjunct to diagnosis.

A-372 09:30

C. US

F. Gleeson; *Oxford/UK (fgleeson@mac.com)*

Ultrasound has historically been used to determine the presence of pleural fluid prior to a decision on chest drain insertion. More recently it has been used to characterise pleural effusions, and is now being investigated as a potential tool to identify cardiac failure and pulmonary oedema. It is now also used to identify pneumothorax in patients in place of or more often as an adjunct to the CXR. Recent publications have also highlighted the ability to identify the intercostal vessels using colour Doppler to avoid potential laceration during biopsy or drain insertion.

Learning Objectives:

1. To learn when, how and why to perform a US study of the chest.
2. To become familiar with the strengths and limitations of the technique.

Author Disclosure:

F. Gleeson: Advisory Board; lue Earth Diagnostics, olarean. Board Member; ptellum. Consultant; lliance Medical Ltd. Equipment Support Recipient; eneral Electric. Grant Recipient; IHR.

08:30 - 10:00 **Room X**

Joint Session of the ESR and ESTRO

Radiomics and imaging databases for precision radiation oncology

A-373 08:30

Chairmen's introduction (part 1)

K. Riklund; *Umea/SE (katrine.riklund@umu.se)*

In this session, biomarkers in imaging will be discussed as used in treatment planning, prognosis and prediction. Furthermore, we will learn about the potential of using big data analysis in imaging in radiation treatment. When using quantitative imaging biomarkers, it is also important to be aware of potential shortnesses of the methods and you will also hear about this in the joint session between ESR and ESTRO.

Session Objectives:

1. To discuss how radiomics will change the clinical practice both in radiology and oncology.
2. To understand the impact of quantitative imaging data uncertainties in the prognosis and predictive models.
3. To discuss the potential and challenges of large multicentre imaging datasets.

A-374 08:31

Chairmen's introduction (part 2)

V. Valentini; *Rome/IT (vvalentini.it@gmail.com)*

Radiomics is gaining an always greater attention in our scientific communities. Images are always less pictures and more mines of information that can be used by clinicians as decision-making tools, from prognosis assessment to therapy choice and outcome prediction. New paradigms, new uncertainty measurements, new statistical and mathematical tools are required to take advantage of radiomics potentialities and to become familiar with these approaches is unavoidable. Facing the entity of the challenge, an interdisciplinary approach is mandatory with all the imaging-based medical specialities hinged on imaging knowledge and images sharing in big data biobanks and DICOM repositories.

Session Objectives:

1. To discuss how radiomics will change the clinical practice both in radiology and oncology.
2. To understand the impact of quantitative imaging data uncertainties in the prognosis and predictive models.
3. To discuss the potential and challenges of large multicentre imaging datasets.

A-375 08:33

Radiomics in radiology, what are the parameters of interest for different imaging modalities?

H. Ahlström; *Uppsala/SE (HAKAN.AHLSTROM@AKADEMISKA.SE)*

CT, MRI, PET, PET-CT and PET-MRI datasets contain huge amounts of spatially detailed morphological, functional and metabolic information. Today, when analysed, these detailed datasets are typically heavily reduced to a few

measurements of a priori specified measurements of interest (e.g. volumes, areas, diameters, average/maximum tracer concentrations, etc.) and/or visually - and, therefore, inevitably subjectively - assessed by a human operator. As a result, normality/non-normality can only be assessed on these measurements and not on the entire data collected, and statistical interaction with non-imaging parameters can also be assessed only on these a priori specified measurements. To utilise the full potential of these image datasets, new analysis tools included in the concept radiomics, which allow objective or quantitative assessment of all imaging data (including, e.g. previously discarded information about texture), are needed. Radiomics can be divided into distinct processes: (a) image acquisition and reconstruction, (b) image segmentation and rendering, (c) feature extraction and feature qualification and (d) databases and data sharing with non-imaging data (e.g. different "omics" and clinical data) for (e) informatics analyses. Statistical knowledge of the normal range of radiomics features are needed for the analyses. These analyses are anticipated to bring out new associations and understandings that traditional approaches could not achieve. Radiomics features can, together with non-imaging data, be included in models that have shown to provide valuable diagnostic, prognostic or predictive information for oncological diseases. This information aims at improving individual patients' outcomes by a better treatment selection.

Learning Objectives:

1. To learn how radiomics can be measured with imaging methods.
2. To discuss how radiomics can be integrated in "omics" analysis.
3. To explore the potential of radiomics analysis in cancer care.

Author Disclosure:

H. Ahlström: Founder; one of four owner of Antaros Medical AB. Owner; 20% owner of Antaros Medical AB. Shareholder; 20% of the shares of Antaros Medical AB.

A-376 08:53

Radiomics in radiotherapy: how is it used to personalise treatment and to predict toxicity and/or tumour control

C. Gani; *Tübingen/DE (cihan.gani@gmail.com)*

Radiomics is defined as the automated or semi-automated extraction of a large number of features from imaging datasets resulting an individual "imaging phenotype". These features and the imaging phenotype can then be correlated with a variety of other parameters: from genetic phenotypes to oncological outcome data. Radiomics as a non-invasive procedure is of particular interest for the radiation oncologist in times of precision radiation oncology: The radiomics phenotype might help to identify patients at high risk for treatment failure and, therefore, candidates for more aggressive treatment. Furthermore, radiomics can also be a helpful tool to predict the risk for radiation-induced toxicities and guide the dose distribution within normal tissues. This lecture will give an overview about the existing data on radiomics in the field of radiation oncology.

Learning Objectives:

1. To understand how radiomics can be used to identify patients at high risk for failure after radiotherapy.
2. To discuss how radiomics can be integrated into radiotherapy treatment planning.
3. To explore the potential of radiomics to predict acute and long-term toxicity after radiotherapy.

A-377 09:13

Uncertainties in imaging: how they should be reported and propagated in prediction models using radiomics

L.P. Muren; *Aarhus/DK*

"no abstract submitted"

Learning Objectives:

1. To understand how to incorporate radiomics into RT response models.
2. To discuss how uncertainties should be estimated and reported.
3. To explore the effect of image uncertainties in RT response models.

A-378 09:33

Imaging banks: challenges and opportunities

A. Van der Lugt; *Rotterdam/NL (a.vanderlugt@erasmusmc.nl)*

An imaging biobank can be defined as an organised database of medical images and associated imaging biomarkers (radiology and beyond) shared among multiple researchers, and linked to other biorepositories. An imaging biobank is designed for scientific use. Image data are systematically analysed visually, manual, or (semi)-automated with the main aim to extract imaging biomarkers than can be related to patient characteristics such as medical history, genomic data, and outcome or disease characteristics such as genomic data, biomaterials or response to treatment. The data storage is structured in a way that the database can be queried and retrieved based on available metadata. To exploit the available information interactions with other databases are a perquisite. General requirements with respect to the data collection are, therefore, a database facilitating storage of image data and metadata, storage of derived image-based measurements, and storage of associated non-imaging data, taking into account the need to deal with longitudinal data, and to cope with multiple file formats. Finally, automated retrieval is needed for image analysis pipelines that extract image features for radiomics signatures or for hypothesis-free deep learning algorithms.

Learning Objectives:

1. To understand what is an imaging biobank.
2. To discuss how an imaging biobank can be integrated in cancer care.
3. To explore the intraoperability of clinical imaging biobank and other data repositories.

09:53
Discussion

08:30 - 10:00 **Room Z**

Joint Session of the ESR Working Group on Ultrasound with EFSUMB

Handheld devices: a game changer?

A-379/A-380 08:30

Chairmen's introduction

P.S. Sidhu; *London/UK (paulsidhu@btinternet.com)*
M. Claudon; *Vandoeuvre-les-Nancy/FR (m.claudon@chu-nancy.fr)*

Middle and high-quality portable ultrasound machines are now widely available in the market. There is a large range in commercial offer, with various levels of performances but most of these units allow for grayscale and Doppler mode. The basic concept is to meet patients at the point-of-care, in the hospital and in the outpatient clinic and take benefit form a fast, early imaging examination. Alternative interest has been proposed for education of medical and non-medical students.

Session Objectives:

1. To learn about which handheld devices are available and the price range in rent or buy setups.
2. To learn about the requirements for image quality and image storage.
3. To learn about the training requirements for medical personnel and how to potentially bring US into the medical school.

Author Disclosure:

P.S. Sidhu: Speaker; Bracco, Siemens, Philips, Samsung, GE Healthcare, Hitachi.**M. Claudon:** Speaker; Philips Ultrasound.

A-381 08:45

Reviewing the market

M. Bachmann Nielsen; *Copenhagen/DK (mbn@dadlnet.dk)*

Most ultrasound (US) manufacturers offer handheld or portable devices in addition to their more traditional larger mid- and high-end machines. The price of handheld devices is generally lower, but they may lack features like elastography, contrast agent imaging and biopsy guidance. An advantage of handheld US devices is that due to their small size they fit into the pockets of a physician's lab coat. The smallest handheld devices are composed of a transducer with a USB connection to a tablet or a smartphone. Many of the large companies we know from radiology now also offer handheld devices, e.g., GE Healthcare, Philips. Some comes with a screen; some connects to the user's own smartphone. Philips sell their Lumify system only as a rental product for a low monthly fee and only in the USA. In addition, a large market exists on the internet for cheap wireless or USB transducers and for portable devices on web-based marketplaces like Alibaba. Another addition to the market is a cloud-based telehealth service by some seen as another business case to distribute ultrasound to users with little experience in diagnostic ultrasound.

Learning Objectives:

1. To learn about which handheld US devices are available on the market.
2. To learn about different pricing levels of the US equipment based on rent or buy models.

A-382 09:00

Who can use the equipment and reimbursement

R.F. Havre; *Bergen/NO (roald.flesland.havre@helse-bergen.no)*

Ultrasound scanners have become portable and cheaper, while the image quality has improved. Several clinicians have discovered the usefulness of the portable ultrasound (US) scanners and they are increasingly used in general practice, by hospital departments and even in ambulances. The users of ultrasound should be health care professionals including medical doctors, sonographers and in some countries US midwifes. It is important that users of US equipment have adequate training to perform US examinations in their clinical practice. The responsibility for this should be the departments in which

the examinations take place and be defined by training curriculums for the medical specialities. US training can also be included in medical school. Basic or more advanced US courses arranged by national and international US societies. Not all portable devices have interfaces for easy and safe storage of images. This is an important issue as images serve as documentation. It is important that safe storage is provided preferably to the PACS systems of the department in charge of medical treatment. The solutions for image storing may be an important for selection of models. The reimbursement for ultrasound scanning is depending on the group of health care personnel who perform the examination and not by the type of equipment used. Medical doctors in general practice in Norway have reimbursement for specific US examinations. When point of care US is performed in hospitals as a part of a clinical examination of in-patients, it is generally not reimbursed specifically.

Learning Objectives:

1. To learn about the possible requirements for image quality and storage for handheld devices.
2. To learn about the requirements for training and profession for using the equipment.
3. To learn about different reimbursement requirements and practices in selected European countries.

A-383 09:15

Appropriate training

H. Prosch; *Vienna/AT (helmut.prosch@meduniwien.ac.at)*

Ultrasound (US) is an indispensable diagnostic tool, not only in radiology, but also in almost all clinical specialities. In addition to its use for thorough, systematic examinations, US is used more and more in point-of-care examinations where single, specific clinical questions are addressed (i.e. the search for pleural effusions or ascites, pneumothorax, hydronephrosis). With the use of ultrasound contrast media, the diagnostic value of US increases even further. As with all imaging modalities, specific training is required to gain the required skills. Consequently, the radiologic training curricula of most European countries, as well as the European training curriculum for radiology of the European Society of Radiology, demand that residents must learn US skills. In addition to a profound theoretical knowledge about the technical aspects of ultrasound, anatomy, and pathology, US requires substantial hands-on training to reach sufficient expertise. A comprehensive hands-on training necessitates a case-by-case teaching protocol in which the attending physician supervises the examination. Simulation-based training has proven to be an effective means to further improve US training, particularly to achieve mastery in ultrasound-guided biopsies. Only a structured training curriculum that combines all these different aspects of US training can make it possible for US to fulfil its role as the stand-alone diagnostic tool and the problem solving tool it can and should be.

Learning Objectives:

1. To get an overview on the current status of ultrasound training in radiology.
2. To appreciate the pivotal role of ultrasound in the understanding of basic anatomy and pathology.
3. To become familiar with the importance of one to one teaching in ultrasound.

A-384 09:30

Ultrasound to train students

V. Cantisani; *Rome/IT (vito.cantisani@uniroma1.it)*

Ultrasound is an effective method used throughout the world for clinical workup of patients with a wide range of diseases, particularly as first-line imaging modality. Technological advancements have made the equipment accessible and affordable up to hand-held ultrasound devices. Therefore, education and subsequently preparation and updating of US knowledge is crucial. EFSUMB (European Federation of Societies for Ultrasound in Medicine and Biology) and others have published an atlas on anatomy and examination technique of handheld devices. Medical student education is traditionally based on “classical” training methods such as presentations, courses and workshops. However, new technologies and web-based sources of information have opened novel educational applications in medical practice. The European Federation of Societies for Ultrasound in Medicine and Biology (EFSUMB) recommends that ultrasound should be used systematically as an easily accessible and instructive educational tool in the curriculum of modern medical schools. Medical students should acquire theoretical knowledge of the modality and hands-on training should be implemented and adhere to evidence-based principles. EFSUMB policy statements on medical student education in ultrasound, update of the actual status on US Medical Education worldwide and the activities already decided will be discussed.

Learning Objectives:

1. To provide current status of education in ultrasound of medical student.
2. To provide EFSUMB proposal and strategy in student education.

Author Disclosure:

V. Cantisani: Speaker; Samsung, Toshiba, Bracco.

09:45

Panel discussion: Handheld devices - should we be happy or concerned?

08:30 - 10:00 **Room O**

Paediatric

RC 912

Understanding paediatric neuroradiology

Moderator:
A. Rossi; Genoa/IT

A-385 08:30

A. Imaging of the premature brain

N. Khandelwal; *Chandigarh/IN (khandelwaln@hotmail.com)*

Dramatic reduction in mortality rates of premature infants in recent times due to better perinatal care has not really translated to exceptional neurodevelopmental outcomes in these patients. Neuroimaging has taken a front stage in evaluation, diagnosis and prognostication of premature neonates. Ultrasound (US) forms the backbone of current neuroimaging practice in small babies. Magnetic resonance imaging (MRI) has matured recently as an excellent modality to better identify and classify intracranial structures. The premature brain is significantly different in terms of volume, structure, maturity (myelination pattern) and disease appearance as compared to childhood brain. Myelination progresses in the following order in human brain - caudal to cranial, centre to periphery and posterior to anterior. Identification of brain maturity by means of myelination pattern helps us in identifying and classifying white matter disorders. The distinctly variable patterns of involvement of susceptible structures, namely the deep grey nuclei and white matter in hypoxic-ischaemic brain injury in premature and mature brains is worth understanding as helps in evaluating and prognosticating such patients. MRI helps in comprehensive brain evaluation while US is a good, handy, radiation-free tool for follow-up.

Learning Objectives:

1. To discuss the roles of US, (CT) and MRI in preterm imaging.
2. To give an overview of the different imaging findings in the preterm brain related to age.
3. To discuss the prognostic role preterm brain imaging.

A-386 09:00

B. Abusive head trauma: the role of CT and MRI

C. Adamsbaum; *Le Kremlin-Bicêtre/FR (c.adamsbaum@bct.aphp.fr)*

Abusive head trauma (AHT) is a leading cause of morbidity and mortality in infants. The presence of a diffuse subdural haematoma (SDH) with no evidence of accident is a key diagnostic clue. The haematoma is due to rupture of the cerebral bridging veins due to violent shaking. Neuroimaging is crucial for the diagnosis of AHT. The presence of SDHs, especially in multiple locations, such as the interhemispheric region, over the convexity and in the posterior fossa, is significantly associated with AHT. CT is the first-line imaging modality for suspected AHT, particularly in case of acute or subacute symptoms. CT exquisitely demonstrates intracranial haemorrhages, skull fractures and soft tissue swelling of the scalp. In addition of CT, early MRI within the first week provides a better estimation of parenchymal injuries (hypoxic-ischaemic insult, contusions). MRI can also disclose subtle key signs for the diagnosis of AHT such as rupture/thrombosis of bridging veins at the convexity and/or ligamentous cervical injuries. Both CT and MRI offer wide ranges for dating the causal event. In particular, mixed density/intensity pattern of SDHs is frequent and provides no reliable clues for assessing repeated violence. Only the finding of different density in two distant SDHs argues in favour of "age-different" injuries. As a reminder, in all cases of suspicion of AHT, the full skeletal survey is also mandatory.

Learning Objectives:

1. To discuss the role of CT and MRI in imaging of abusive head trauma (AHT).
2. To give an overview of common CT and MRI findings in AHT.
3. To understand the strengths and limitations of CT and MRI in imaging AHT.

A-387 09:30

C. Imaging in hypoxic-ischaemic injury and hypothermia: an update

F.M. Triulzi; *Milan/IT (Fabio.triulzi@policlinico.mi.it)*

The incidence of hypoxic ischaemic encephalopathy (HIE) ranges from 1 to 8 per 1000 live births in developed countries, it accounts for approximately 15%-20% of neonatal mortality in full-term neonates. Differently from adults, in whom acute anoxic-ischaemic injury causes diffuse brain injury predominantly involving gray matter, neonatal HIE is generally more selective. The most frequent type of injury on MRI in term newborns consists of selective involvement of areas with higher energy requirements, i.e. the lateral thalami, posterior lentiform nuclei, hippocampi and perirolandic cortex. Moreover, the absence of a normal PLIC on T1-weighted images in asphyxiated infants has a high positive predictive value (100% of abnormal neurodevelopmental

outcome). In order of frequency, other locations of brain involvement in full-term newborns with HIE include the perirolandic and primary auditory cortex and optic radiation, the hippocampal formation and limbic cortex and the dorsal mesencephalic structures. Conventional MR sequences, diffusion, spectroscopy and more recently perfusion have been widely used in the last twenty years to find out the more reliable prognostic biomarker. There are now several evidences of benefits in neuroprotection by cooling treatment. No major complications are associated with therapeutic hypothermia and the predictive value of MRI for subsequent neurological impairment seems to be not affected by this kind of therapy. Being cooling therapy effective in the acute phase of HIE the role of MRI is now predominantly related to a better assessment of the brain damage in the subacute phase of asphyxia, when lesion load is well established.

Learning Objectives:

1. To discuss the role of US, (CT) and MRI in hypoxic-ischaemic injury (including advanced MR techniques).
2. To give an overview of common imaging findings in hypoxic-ischaemic injury (HIE).
3. To understand the importance of timing and prognostic value of imaging in HIE.

08:30 - 10:00 **Room N**

Cardiac

RC 903

Novel ways to assess myocardial tissue

Moderator:
O. Duvernoy; Uppsala/SE

A-388 08:30

A. T1 mapping: technical considerations
M.R. Makowski; *Berlin/DE (marcus.makowski@charite.de)*

In this refresher course, the current role of cardiac MRI for the characterisation of myocardial diseases with a focus on novel mapping techniques will be discussed. The limitations of current imaging techniques will be highlighted. The potential of novel T1 mapping technical approaches will be introduced. This refresher course will finish with clinical case examples.

Learning Objectives:

1. To learn about the principles of T1 mapping.
2. To learn about specific issues of T1 mapping.
3. To learn how to do and assess T1 mapping.

A-389 09:00

B. T2 mapping: technical considerations
C. Tessa; *Lido di Camaiore/IT (ctessa@sirm.org)*

Cardiac T2 mapping represents an alternative approach to traditional T2-weighted imaging that allows to quantify myocardial T2 relaxation times. Parametric T2 maps are obtained by collecting multiple images with different T2-weighting, providing multiple points along the T2 decay curve for fitting of an exponential signal decay model. To this purpose, T2-prepared steady-state free precession (SSFP) sequences as well as multi-echo-spin-echo (MESE) or gradient-spin-echo (GRASE) sequences can be employed. They can be acquired both in breath-hold and during free breathing, utilizing respiratory navigators. Optional motion correction algorithms may be applied to compensate for mis-registrations between the images used to generate the parametric maps. The maps are usually acquired in diastole, but they can also be obtained in systole to reduce partial-volume effect. T2 maps can be analysed both visually and quantitatively, by means of ROIs or automatic thresholds. T2 mapping sequences are less prone to artefacts than traditional T2-weighted sequences, and their reproducibility is very good. However, T2 relaxation time is very sensitive to co-factors and it is, therefore, necessary to generate reference values specific for each site, technique and imaging setting. Furthermore, studies in healthy controls have found a relatively large inter-subject variability in T2 measures that may potentially cause problems when trying to define cutoff values at single subject level. To date, there have been only a few single-centre studies. Further multi-centres trials in larger sample are needed to fully explore the potential of T2 mapping techniques.

Learning Objectives:

1. To learn about the principles of T2 mapping.
2. To learn about specific issues of T2 mapping.
3. To learn how to do and assess T2 mapping.

A-390 09:30

C. Clinical use of T1 and T2 mapping
H.J. Lamb; *Leiden/NL (h.j.lamb@lumc.nl)*

This lecture will provide an overview of the current and future application of MR multi-parametric imaging using T1- and T2-mapping techniques. The main field of application in cardiology is to determine tissue properties in a broad range of cardiomyopathies and metabolic disease such as metabolic syndrome and diabetes type 2. Based on an MR physics of multi-parametric MR imaging, first clinical applications will be discussed, followed by more advanced future application of T1-/T2-mapping. The overview aims in general to show the potential of quantitative MR imaging, which is also applicable in other organs than the heart, such as liver and kidney.

Learning Objectives:

1. To learn about the main fields of application for T1-T2 mapping.
2. To learn the specific parameters useful for the clinical implementation of T1-T2 mapping.
3. To understand the incremental value of T1-T2 mapping over current methodologies.

08:30 - 10:00 **Studio 2017**

Professional Challenges Session

PC 9

Implementing and evaluating clinical decision support (CDS) for imaging referral guidelines

A-391 08:30

Chairman's introduction
L. Oleaga Zufiría; *Barcelona/ES (lauraoleaga@gmail.com)*

Clinical decision support systems (CDS) represent computer application systems to enhance decision-making in the clinical workflow. These tools include clinical recommended guidelines, condition-specific order sets, computerized alerts and relevant reference information. Among the benefits of the use of CDS, we can include increase of quality and safety of care, avoidance of errors and improved efficiency. Implementation strategies and outcomes in the hospitals depend on their culture and resources. The introduction of a CDS includes a number of steps, such as identifying the needs and functional requirements, designing or configuring the system for use in the local environment, planning the implementation process and determining how to assess the needs identified. Most research has evaluated the effects of CDS, it has been focused primarily on clinician decision-making, but little has been published on how those decisions affect patient's outcomes. It is important to involve clinicians to avoid misconceptions about the use of CDS. Finally, an application of the CDS includes its application in medical schools to train students on the appropriateness of the imaging techniques in the clinical setting.

Session Objectives:

1. To understand the challenges to implementing CDS.
2. To learn from practical experiences of CDS implementation.
3. To understand how a CDS implementation can be evaluated and impact measured.
4. To understand the perspective of CDS users: referring physicians.

A-392 08:35

The role of basic and advanced CDS in value-centred radiology
H.-U. Kauczor; *Heidelberg/DE (Hans-Ulrich.Kauczor@med.uni-heidelberg.de)*

Radiologists are participating in the transition from the volume-centred pay-for-service to the value-centred pay-for-performance. Thus, clinical and economic outcomes are driving the reimbursement. However, the definition of metrics to measure performance, quality and outcome within the complex web of the healthcare system is challenging. Overall, the goal-directed behaviour of patients, ordering physicians, radiologists and specialists has to be aligned. As workflow is critical, incentives for improvements in collaborative care are pivotal. CDS will play an important role in improving quality and efficacy of the workflow and the radiology service in value-centred medicine. Basic CDS will check the appropriateness of CT or MRI for a given clinical scenario, mainly based on evidence and guidelines. Major challenges of CDS are 1) the deep integration into an existing multi-vendor environment of HIS and RIS as well as image acquisition devices and PACS; 2) data security and patient privacy issues between different health care providers and the integration of a cloud-based service into the system; 3) the adaptation of the basic "guidelines" of the CDS provider to the specific requirements of the institution and its imaging

department(s). This in particular relates to the level of healthcare (in- or outside, prevalence of disease), complexity of cases, comorbidities, local, regional and national standard of care and operating procedures. Advanced CDS should also check for already available imaging studies and reports as well as whether intravenous contrast should be given. If yes, contraindications (allergies, renal insufficiency, etc.) should automatically be checked from the electric patient record.

Learning Objectives:

1. To learn about challenges in the implementation of CDS.
2. To understand the opportunities of advanced functions of CDS.
3. To appreciate the contribution of CDS to value-centred radiology.

A-393 08:50

Evaluating CDS implementation and measuring outcomes

M.G.M. Hunink; *Rotterdam/NL (m.hunink@erasmusmc.nl)*

Background: guidelines and appropriateness criteria have been published to help physicians choose the right test for the right patient at the right time. These are typically implemented through computerized decision support systems (CDSSs) so that the advice is presented at the point-of-care. ACR select and ESR iGuide are such systems. The results of implementation of CDSSs for guiding imaging referrals is, however, not (yet) convincing: are CDSSs really cost-effective in guiding the justified use of imaging procedures? Study designs to evaluate CDSSs: to evaluate interventions, ideally a parallel group double-blinded RCT is performed but this is not feasible in this context given the nature of the intervention. A pragmatic parallel group RCT may be feasible but contamination effects between care-givers could easily occur invalidating such a study and this study design would be logistically difficult to perform. More realistic is a stepped-wedge cluster RCT or a matched pair cluster RCT. So far single-centre before-after studies have been published with their limitations. Outcome measures to evaluate CDSSs: ideally mortality, morbidity, quality of life and costs are evaluated to determine the cost-effectiveness of implementing CDSSs, requiring large studies with long follow-up. More realistic is to measure short-term quality of life, complications of testing and costs of the diagnostic workup. So far studies have focused on diagnostic yield and the number of exams ordered which provides only a very limited picture.

Learning Objectives:

1. To understand the difficulties in evaluating the impact of CDS and guideline use.
2. To learn about what can be measured and how.
3. To understand how comparisons between different hospitals can be drawn and lessons learned.

Author Disclosure:

M.G.M. Hunink: Advisory Board; ElBIR. Grant Recipient; ESR iGuide. Other; CUP: Royalties for textbook.

A-394 09:05

Using CDS: referring physicians' perspective: GPs

J.F.M. Metsemakers; *Maastricht/NL*

"no abstract submitted"

Learning Objectives:

1. To understand how referrers view and what they expect from imaging referral guidelines.
2. To learn how CDS can best be integrated into referral workflows and what to avoid.
3. To learn how general practitioners can best be involved in the process of introducing CDS.

A-395 09:20

CDS implementation in the classroom: ESR eGuide

L. Donoso; *Barcelona/ES (ldonoso@clinic.ub.es)*

Imaging referral guidelines are not only a legally recognised concept to ensure imaging is used appropriately or an evidence-based tool to improve clinical practice, but also a vital educational tool. Over the past years, the ESR has worked to create CDS-compatible guidelines based on the American College of Radiology Appropriateness Criteria which are now available at the point of care through ESR iGuide. Building on this effort, the ESR eGuide project aims to reap the educational benefits of referral guidelines and clinical decision support. An ESR Education Committee Taskforce is creating case studies on appropriate imaging to be solved with decision support using the ESR's referral guidelines. Taking a long-term approach to improving appropriateness in medical imaging, the overall purpose of this project is to educate doctors-in-training about appropriate imaging using evidence-based referral guidelines, while introducing the concept of clinical decision support and familiarising them with a technology they will encounter in their professional careers. The ESR eGuide project is part of the implementation of the EuroSafe Imaging Call for Action with regard to Action 1 on Clinical Decision Support and Action 6 focusing on educational activities including the development of e-learning tools. The objectives of ESR eGuide are: improving the quality of medical education with regard to diagnostic imaging, educating medical students about the appropriateness of different imaging modalities for given clinical indications, familiarising medical students with CDS technology, demonstrating the efficacy and utility of CDS, reinforcing the concept of evidence-based medicine.

Learning Objectives:

1. To understand how guidelines and CDS can be used for education.
2. To understand how test cases are developed and hear about user experiences.
3. To learn about the ESR eGuide project and how to participate.

09:35

Panel discussion: Introducing CDS for medical imaging referrals: what to do and how to measure

08:30 - 10:00 **Room E1**

Breast

RC 902

Minimally-invasive local treatment of breast cancer: the time is now

A-396 08:30

Chairman's introduction

M. Sklair-Levy; *Tel Aviv/IL (mirisklair@gmail.com)*

Breast cancer is the most common cancer among women in the western world. The aim of early diagnosis is to detect smaller cancers.Since we can detect smaller tumours, there is a shift towards less invasive treatment. With a transition from Radical mastectomy to breast conserving therapy is a well established practice. The question is are we ready for the next step to minimally/non-invasive therapy of small breast cancer. Are we ready to the NEXT REVOLUTION of Non-Surgical Ablation of breast cancer. Using minimally invasive image-guided tumour ablation techniques. There are many techniques available, such as radiofrequency ablation (RFA); laser ablation (ILT); microwave ablation; focused US ablation - high-intensity focused (MR-guided focused ultrasound - MRgFUS); cryoablation - ablates tumour tissue by cooling; MRg-FUS - is a noninvasive thermal ablation method using high-intensity focused ultrasound - US thermal ablation beam that heats and destroys targeted tissue, non-invasively using an accurate MRI guidance. It can achieve precise thermal ablation following target definition, treatment planing and control of energy deposition during treatment. Integrating FUS and MRI as a therapy delivery system enables to localise, target, treat, monitor in real time without damaging surrounding tissue. The different techniques will be described in detail.

A-397 08:35

A. High intensity focused ultrasound (HIFU) therapy

B. Cavallo Marincola; *Rome/IT (beatrice.cavallomarincola@gmail.com)*

Surgical treatment of breast cancer has changed overtime, evolving from radical mastectomy to more conservative approaches. This has been possible thanks to technical advantages in the field of diagnostic imaging that allowed early diagnosis of breast cancers with very small dimensions. Mini-invasive technologies (radiofrequency ablation, cryoablation, etc.) can preserve the original breast volume avoiding glandular resections and surgical scars and ensuring at the same time complete tumour ablation. Ablation with high-intensity focused ultrasound (HIFU) is based on the use of an extra-corporeal ultrasound transducer that selectively destroys target tissue avoiding thermal damages to surrounding structures. The technique can be performed under ultrasound or magnetic resonance (MR) guidance. MR guidance offers several advantages that improve safety and efficacy of the procedure: a visualization of the planned US beam during each phase of the procedure, a real-time monitoring of the progressive temperature increase within the target tissue and surrounding tissues, an accurate treatment planning, an evaluation of the treatment efficacy thanks to the use of intravenous gadolinium-based contrast agent. HIFU ablation of breast cancer is a new and promising technique that deserves large interest in the field of clinical research in order of its potential application in the clinical practice.

Learning Objectives:

1. To learn about the basics of HIFU therapy.
2. To become familiar with the different types of imaging guidance.
3. To appreciate its role in treating benign and malignant lesions.

A-398 09:00

B. Radiofrequency ablation therapy

B. Brkljačić; *Zagreb/HR (boris@brkljacic.com)*

Radiofrequency ablation (RFA) is a promising but quite rarely used minimally invasive modality to treat small breast cancer in patients in whom general anaesthesia is contraindicated or who refuse surgery. In most studies, cancers were surgically excised shortly after RFA. In very few studies, RFA was used as the only treatment modality, instead of surgery. The procedure is most conveniently performed under ultrasound guidance, in local analgesia, which allows constant contact with the patient during the procedure. Precise preprocedural imaging is crucial, and should include contrast-enhanced MRI in addition to mammography and ultrasound. Preprocedural core biopsy is mandatory, with the precise assessment of the tumour type, grade, and immunohistochemical features. Typical US findings of hyprechogenicity of ablated mass are noted during the procedure. Postprocedural mammographic and MRI findings are characteristic and will be presented. The complete ablation can be achieved in small T1-2 N0 M0 breast cancers that present as masses of maximum 2-3 cm in diameter, with the sufficient distance from the skin and pectoral muscle to avoid the thermal lesion of these tissues. In larger lesions only partial ablation may be achieved. Only solitary, unicentric, invasive ductal cancers, preferably ER/PR positive should be treated. Invasive lobular cancers should not be treated with RFA. Our results will be presented in a small group of patients who were treated with RFA, and who refused surgery, had contraindication to general anaesthesia and opted for RFA. The technique, preprocedural, intraprocedural and postprocedural imaging findings, as well as long-term result will be presented.

Learning Objectives:

1. To learn about how radiofrequency works.
2. To become familiar with its use in clinical practice.
3. To appreciate the advantages and disadvantages.

Author Disclosure:

B. Brkljačić: Speaker; Guerbet, Bayer.

A-399 09:25

C. Cryotherapy

M.H. Fuchsjäger; *Graz/AT (michael.fuchsjaeger@medunigraz.at)*

Cryotherapy is a new, minimal-invasive image-guided treatment option for breast tumours. A specific 12-17G probe is applied into the tumour. Argon gas making use of the Joule-Thomson effect cools down the needle tip to minus 187 degrees centigrade. An ice ball covering lesion and an adequate safety margin is formed. Coagulative necrosis of the tumour cells after two freezing cycles is the result. Cryoablation for breast tumours can be performed under US, CT or MRI guidance. Several studies showed an overall success rate of more than 90%. Indications for cryotherapy are small tumours, contraindications to general anaesthesia or increased risk of complications, support of standard therapies and palliative approach. Cryotherapy can be performed under local anaesthesia on out-patient basis with a potential better cosmetic outcome than standard surgical therapies. Minimal-invasive therapies ask for a paradigm-shift as the eradicated tumour is left in situ and resection with clear margins will not be proven histopathologically but functionally by MR imaging. It is important to emphasize that radiology is not aiming to take over therapy of breast cancer patients but to help with innovative, less invasive treatment options as a member of a multidisciplinary team. Close cooperation with our clinical partners (surgery, gynaecology, oncology, radiation therapy, etc.) is the key to success and avoidance of turf battles. The goal for the future should be minimal-invasive ablation therapy for breast cancer as a valid therapeutic option.

Learning Objectives:

1. To learn about cryotherapy technique.
2. To become familiar with its use in clinical practice.
3. To appreciate its role in treating benign and malignant lesions.

09:50

Panel discussion: How can we overcome resistance of clinical partner specialties to refer eligible women to radiology?

08:30 - 10:00 **Room E2**

Neuro

RC 911

Cerebrovascular disease

Moderator:
A. Krainik; Grenoble/FR

A-400 08:30

A. Vascular distribution territories: arterial and venous

A. Dörfler; *Erlangen/DE (arnd.doerfler@uk-erlangen.de)*

After a short overview on the vascular anatomy of the brain with a focus on vascular distribution territories, the main aim of this presentation is to present different neurovascular pathologies closely associated with arterial and venous vascular distribution territories. A focus is here put on acute stroke and particularly imaging-based patient selection for interventional stroke therapy and venous pathologies. Another aim is to provide a better understanding of pathophysiology of different neurovascular disease in an interactive matter. In addition, advantages and limitations of CTA and MRI compared to conventional angiography are presented.

Learning Objectives:

1. To become familiar with a comprehensive vascular anatomy of the brain.
2. To understand the advantages and limitations of CTA and MRA.
3. To recognise the different imaging patterns in stroke and their prognostic value.

A-401 09:00

B. Arterial dissection and vasculitis

P.C. Maly Sundgren; *Lund/SE (Pia.Sundgren@med.lu.se)*

This lecture will focus on imaging findings with arterial dissection and the best method of choice for diagnosis. Also underlying causes will be briefly reviewed. Vasculitis is a rare condition. It is not always easy to diagnoses and multiple imaging modalities might be needed to come to final diagnosis. In this lecture, typical imaging patterns of the more common disease with vasculitis changes will be discussed, as well as discussion over which imaging method to use and the clinical implications for patients with vasculitis.

Learning Objectives:

1. To learn how to image dissections of the neck vessels and intracranial arteries.
2. To learn about the imaging features of cerebral vasculitis and how to differentiate it from reversible cerebral vasoconstriction syndrome.
3. To become familiar with the most important causes of secondary vasculitis, including infectious causes such as TB and HIV.

Author Disclosure:

P.C. Maly Sundgren: Research/Grant Support; SUS donation founds Lund, Sweden, Gustav V 80 years foundation, Swedish rheumatology Foundation, Kocks foundation, Sweden.

A-402 09:30

C. Cerebral perfusion studies in cerebrovascular disease: techniques, indications and applications

H.R. Jäger; *London/UK*

"no abstract submitted"

Learning Objectives:

1. To understand how imaging can help select patients for treatment of acute ischaemic stroke.
2. To show the importance of collateral flow in ischaemic patients.
3. To discuss the current evidence-based medicine (EBM) for treatment of patients with acute ischaemic stroke.

08:30 - 10:00 **Room F1**

Joint Session of the ESR and ESOR

ESR/ESOR 2

Radiologic anatomy: lower extremities

Moderator:
U. Aydingoz; Ankara/TR

A-403 08:30

Hip

A.H. Karantanas; *Iraklion/GR (akarantanas@gmail.com)*

The painful hip is a common clinical problem in all age groups. Magnetic resonance imaging (MRI) is an invaluable tool to assess the hip joint because of its ability to directly visualize bone marrow, cartilage and soft tissues in multiple planes. MR arthrography (MRa) using intra-articular contrast material is the standard method for imaging labral lesions and cartilage degeneration. Understanding normal hip anatomy and common variants is important, to accurately detect and localize areas of pathology and to prevent misinterpreting normal structures as abnormal ones. Plain radiographs should always be available when reporting MRI because basic measurements allow assessment of underlying deformities which might explain the clinical and MRI findings. The most important to know are: joint space width (JSW), CE angle, VCA angle, alpha angle, acetabular retroversion and ischiofemoral space. Among the disorders causing hip pain, osteoarthritis (OA) is the most common one. Age is a risk factor strongly correlated with OA. Early OA is related to CAM type femoroacetabular impingement, developmental dysplasia and previous trauma. The diagnosis of OA is based on a combination of radiographic findings and characteristic subjective symptoms. The progression of OA traditionally has been measured using radiographic JSW. Weight-bearing radiographs centred on the hip are the most reproducible and reliable ones. The sequence of degeneration includes the following radiographic findings: joint space narrowing, osteophyte formation, subchondral sclerosis and cyst formation. In cases that radiographs show minor changes and high clinical suspicion of early disease, OA can be confirmed with MRI and/or MRa.

Learning Objectives:
1. To identify intra- and extra-articular anatomy on MRI.
2. To learn what we see and what we miss on plain film.
3. To understand osteoarthritis and learn its key features on imaging.

A-404 09:00

Knee

M. Klontzas; *London/UK (miklontzas@gmail.com)*

The prevalence of knee pain is constantly increasing worldwide, together with life expectancy and the prevalence of obesity. Advances in imaging technology over the last decades have rendered MRI the modality of choice for the evaluation of knee disorders. The use of MRI offers a comprehensive evaluation of the cartilage, the bone marrow and the soft tissues of the knee, providing high sensitivity and specificity for the diagnosis of common pathology such as cruciate ligament and meniscal tears, which cannot be visualized with plain radiographs. Knowledge of the normal cross-sectional anatomy of the knee is, therefore, of utmost importance for the evaluation of knee disorders and the discrimination between anatomical variations and clinically significant knee lesions. Menisci are among the most commonly injured knee structures, with a low signal intensity on MRI. Understanding of the variants of normal meniscal anatomy and awareness of meniscal injury patterns on MRI, combined with clinical history and examination data, can prove indispensable for the diagnosis of meniscal injuries and the avoidance of unnecessary diagnostic arthroscopic procedures.

Learning Objectives:
1. To identify intra- and extra-articular anatomy on MRI.
2. To learn what we see and what we miss on plain film.
3. To understand and learn the key features of meniscal injury.

A-405 09:30

Ankle

M. Maas; *Amsterdam/NL (m.maas@amc.nl)*

Injury of the ankle joint is a common entity, of which inversion is the most frequently seen trauma mechanism. This means that after applying Ottawa ankle rules conventional radiology of the ankle still occurs often in every day practice. And then things become difficult. Identifying a fracture on conventional AP, AP-Mortise (20 degrees of endorotation) and lateral views, being mainstay, is not that difficult, yet ruling out a fracture anywhere along the inversion line of the lateral ankle and foot is a challenge. In this presentation, anatomical landmarks will be provided to ease assessment and to aid structured reporting. So why is this difficult? Many bony landmarks that get injured are easily obscured on standard conventional radiology. Understanding biomechanics of this inversion trauma helps to analyse the images. Assessing according to the Lauge Hansen Classification of ankle trauma and subsequently ankle fracture makes things a bit better to understand. But the most important problem is the limitation of plain radiology in identifying soft tissue injury. Since both the lateral ligamentous complex, the syndesmotic network as well as the medial deltoid ligamentous network are prone to injury in inversion trauma, we need to be able to assess these soft tissue structures. For this purpose, cross-sectional imaging, preferably with MRI, yet also possible to a lesser extent with the use of CT scanning, is extremely helpful. Finally, cartilage injury of the talar dome might be caused by ankle inversion injury and needs assessment, preferably with MRI.

Learning Objectives:
1. To identify intra- and extra-articular anatomy on MRI.
2. To learn what we see and what we miss on plain film.
3. To understand and learn key features of ankle sprain.

08:30 - 10:00 **Room F2**

Special Focus Session

SF 9

The revival of lymphangiography

A-406 08:30

Chairman's introduction

B.A. Radeleff; *Heidelberg/DE (Boris.radeleff@med.uni-heidelberg.de)*

For decades, conventional bi-pedal lymphangiography has been considered the preferred technique for the evaluation of the lymphatic system and its disorders. Lymphangiography provides excellent architectural detail of the lymph nodes and lymphatic ducts. Intranodal lymphangiography (INL) was first reported in 1967 but the technique has been refined in the last 5 years. The lymph nodes are entered with ultrasound with a 25-23 G needle which provides an easy access to inject lipiodol and opacify the lymphatic system. This approach has simplified the technique, has shortened the time required for the procedure and, finally, has made it reproducible. Non-contrast MR lymphography is a new imaging technique and may be used for the diagnosis and classification of primary and secondary upper and lower limb lymphoedema. Therefore, it can be used for positive diagnosis, differential diagnosis and specific evaluation of lymphoedema pattern. Non-contrast MR lymphography may also be used as the modality of reference for the diagnosis of the so-called cystic lymphangioma but also for various lymphatic disorders such as lymphatic injuries resulting in chylous collections, chylous ascites and chylothorax. A postoperative (most common after oesophagectomy) or posttraumatic thoracic chyle leak is highly morbid and can carry significant mortality, if treatment is delayed. The gold standard for treatment of a chyle leak or postoperative chylothorax (e.g. after oesophagectomy) is a re-operation, either open or thoracoscopic, to ligate the thoracic duct. In this talk, I will discuss the technique of thoracic duct embolisation in cases of chyle leak and chylothorax.

Session Objectives:
1. To learn and to become familiar about the radiological diagnostic tools and therapy options (indication, technique and success) of lymphatic disease.
2. To understand the most important sequences and tricks for MR-lymphography for diagnosis and treatment steps leading to occlusion of chyle leaks.
3. To appreciate that diagnostics by non-contrast magnetic resonance lymphography in a near future could become the imaging modality of reference for investigation of lymphatic disorders.

A-407 08:35

"Theranostic" lymphangiography

E. Santos Martín; *New York, NY/US (ernessantos@gmail.com)*

Lymphangiography is a radiological image technique in which a radiopaque contrast medium (ethiodized oil) is injected into the lymphatic system. Lymphangiography provides excellent architectural detail of the lymph nodes and lymphatic ducts. For decades, conventional bipedal lymphangiography has been considered the preferred technique for the evaluation of the lymphatic system and its disorders, particularly in patients with lymphomas. The number of lymphographic studies performed in oncology centres has declined since the advent of simpler, less difficult and less morbid diagnostic tests (CT, MRI and PET), which have rendered the technique obsolete. Lymphangiography still has a role in the diagnosis, management and treatment of the lymphatic disorders, particularly in patients with lymphatic leaks and obstruction of the lymphatic vessels. Intranodal lymphangiography (INL) was first reported in 1967 but the technique has been refined in the last 5 years. The technique appears to be safer and faster than the old method. The lymph nodes are

entered with ultrasound with a 25-23 G needle which provides an easy access to inject lipiodol and opacify the lymphatic system. This approach has simplified the technique has shortened the time required for the procedure and, finally, has made it reproducible. INL has allowed to streamline the management of the patients with chylous leaks. Due to embolic properties of the lipiodol, lymphangiography can have therapeutic properties in patients with chylous effusions, ranging from 51% to 97%. This success is linked to the volume of the lymphatic drainage per day.

Learning Objectives:

1. To learn and to become familiar about the indication, technique and success of intranodal lymphangiography (INL).
2. To understand that intranodal lymphangiography is an effective option for further treatment method e.g. for chyle leaks.
3. To appreciate that if conventional lymphography is impossible, percutaneous intranodal lymphangiography is a valuable alternative.

A-408 09:00

MR lymphangiography

L. Arrivé; *Paris/FR (lionel.arrive@sat.aphp.fr)*

Non-contrast MR lymphography uses very heavily T2-weighted fast spin echo sequences with 3D acquisition and very thin section source images which obtain a specific display of lymphatic vessels. The raw data can be processed with different algorithms such as maximum intensity projection (MIP) algorithm. Lymphatic vessels are demonstrated with MR lymphography as alternating areas of constriction and dilatation representative of valves and contractile units. Non-contrast MR lymphography may be used in different fields. It is a unique non-invasive imaging modality for the diagnosis and classification of upper and lower limb lymphoedema. It can be used for positive diagnosis, differential diagnosis and specific evaluation of lymphoedema pattern (aplasic, hypoplasic and hyperplasic). Non-contrast MR lymphography is the modality of reference for the diagnosis of the so-called cystic lymphangioma which is a developmental abnormality characterised by lack of communications of regional lymphatic vessels resulting in marked dilatation. Non-contrast MR lymphography demonstrates that there is a continuous spectrum of change from normal variants to cystic lymphangioma. Non-contrast MR lymphography may also be used in various lymphatic disorders such as lymphatic injuries resulting in chylous collections, chylous ascites and chylothorax but also in lymphatic pathology of liver, spleen, kidney and chest. Non-contrast MR lymphography is a relative new imaging technique. The main limitation today is still the suboptimal spatial resolution. However, because of ongoing advances in software and hardware, in a near future it could become the imaging modality of reference for investigation of lymphatic pathology.

Learning Objectives:

1. To learn and to become familiar about the indication, technique and success of non-contrast magnetic resonance lymphography.
2. To understand the most important sequences and tricks for the non-contrast magnetic resonance lymphography.
3. To appreciate that non-contrast magnetic resonance lymphography in a near future could become the imaging modality of reference for investigation of lymphatic disorders.

A-409 09:25

Thoracic duct embolisation

H.H. Schild; *Bonn/DE (Schild@uni-bonn.de)*

Interventional thoracic duct occlusion has become an established alternative to surgical thoracic duct ligation in patients with a chylothorax that does not respond to conservative treatment. The first step of the procedure involves lymphographic delineation of abdominal and thoracic lymphatics. A lymph vessel that by course and size is a suitable access route to the thoracic duct is punctured transabdominally under fluoroscopy (or CT) with a 22 G needle. After insertion of a microwire, the puncture needle is removed, and a microcatheter advanced over the guide wire into the thoracic duct. After delineation of the anatomy to exclude anatomic variants, the duct is then occluded using first coils and then tissue adhesive. If for anatomical reasons the thoracic duct cannot be entered, percutaneous destruction of lymph vessels (by “scratching”) may be performed, or it may be tried to enter the duct transvenously in a retrograde fashion. Reported clinical success rates vary between 55 and 90%, depending on anatomy and cause of the chylothorax. The complication rate of the procedure is around 7%, with major complications being rare.

Learning Objectives:

1. To learn and to become familiar about the indication, technique and success of minimal-invasive therapies for thoracic chyle leaks.
2. To understand that thoracic duct embolisation is an effective treatment method for chylothorax.
3. To appreciate that if thoracic duct embolisation is impossible, percutaneous lymphatic destruction or injection of sclerosants/tissue adhesive next to the thoracicare valuabe therapeutic alternatives.

09:45

Panel discussion: Lymphangiography, are you convinced?

08:30 - 10:00 **Room D**

Multidisciplinary Session

MS 9

Primary bone tumours

A-410 08:30

Chairman's introduction

A.M. Davies; *Birmingham/UK*

Session Objectives:

1. To recognise the importance of a multidisciplinary approach to the diagnosis of bone tumours.
2. To appreciate the challenges faced by pathologists in making a diagnosis.
3. To appreciate the role of imaging from diagnosis to surgical planning.

A-411 08:35

Fundamental imaging

S.L.J. James; *Birmingham/UK (stevenjames@nhs.net)*

In this session, the fundamental requirements for bone tumour imaging will be discussed. The importance of radiographs will be stressed along with the important radiographic features to describe within a report. Local, regional and distant staging will also be described including a review of the current literature regarding the optimal modalities to perform this.

Learning Objectives:

1. To appreciate the diverse radiographic appearances of bone tumours.
2. To understand the importance of reviewing all imaging when making a diagnosis.
3. To become familiar with local and distant imaging strategies for staging.

A-412 08:55

Why I need the radiologist: the pathologist's perspective

L.-G. Kindblom; *Billdal/SE*

"no abstract submitted"

Learning Objectives:

1. To provide a reasoned differential diagnosis based on imaging findings.
2. To communicate the precise anatomical location and origin of the tumour.
3. To correlate imaging features of malignancy with histological findings.

A-413 09:15

The surgeon's perspective

L. Jeys; *Birmingham/UK (lee.jeys@nhs.net)*

"no abstract submitted"

Learning Objectives:

1. To orchestrate the multidisciplinary discussion of management based on combined imaging and histological findings.
2. To appreciate the significance of local and distant extent on management.
3. To learn about the imaging requirements for robotic surgery.

09:35

Multidisciplinary case presentation and discussion

08:30 - 10:00 **Room G**

EFOMP Workshop: Radiation incidents and accidents in medical imaging: can we prevent them?

EF 1

Radiation incidents and accidents in medical imaging and their management (part I)

Moderators:
J. Damilakis; Iraklion/GR
A. Torresin; Milan/IT

A-414 08:30

Chairman's introduction
J. Damilakis; *Iraklion/GR*

There are radiation incidents involving the exposure of a patient to a dose much greater than intended. Main reasons for these very high doses are a) lack of knowledge in medical radiation protection, b) poor equipment knowledge and c) use of inappropriate protocols. Accidental irradiation of pregnant patients during the first post-conception weeks leads to unnecessary termination of pregnancies. To avoid these radiation accidents, proper pregnancy screening is needed. In fluoroscopically guided interventional procedures with very long screening time, there is a possibility of cell killing sufficient to result in radiation-induced injuries in certain tissues of patients. There are also other causes of accidental exposure, for example, failure of staff to properly check the identity of patients. This may lead to radiation exposure of a patient who undergoes an x-ray procedure intended for another patient. Accidental medical exposures are a source of continuing concern. All measures should be taken to minimise the probability of accidental or unintended exposures of individuals subject to medical exposure.

Session Objectives:
1. To learn about the common reasons for radiation incidents and accidents in CT and interventional suites.
2. To learn about the common reasons for accidental exposure during pregnancy.
3. To be informed about the EU BSS requirements on radiation incidents and accidents in medical imaging and their management.

A-415 08:35

Radiation incidents and accidents in CT
M. Mahesh; *Baltimore, MD/US (mmahesh@jhmi.edu)*

Radiation incidents in diagnostic radiology are rare and may not be as life threatening as in radiation oncology, yet it is equally important to devise plans of action to address radiation incidents in diagnostic radiology. This talk will discuss various measures medical physicists can do to address such situations with focus on CT studies. Radiation incidents/accidents can lead to deterministic effects such as hair loss or skin erythema, which are rare but possible in CT scans (CT perfusion studies) due to incorrect settings or improper scanning. When radiation incidents occur, a physicist can do the following. First, physicist should record details of scan settings that have led to the radiation incident. Next, assess and make necessary changes to avoid future incidents. This should be followed by detail assessment of radiation exposure to patients (skin dose and organ dose) and work with the radiologists and other physicians to address the radiation events. Further, medical physicists can take precautions to avoid such incidents in future. Recently introduced 'CT dose alert' can be customized for each CT protocol such that incorrect settings that could lead to unintended high radiation exposure can be flagged prior to CT scan. In addition, features such as CT dose notification can further assist in periodic CT dose audits. This presentation will discuss in detail about the CT dose alert and CT dose notifications, which are key to avoid unintended radiation exposure to patients undergoing CT studies.

Learning Objectives:
1. To give an overview of radiation incidents and accidents in CT.
2. To discuss the lessons learnt from these incidents and accidents.
3. To learn how to manage incidents and accidents in CT.

Author Disclosure:
M. Mahesh: Author; Book Royalty for 'MDCT Physics - The Basics, Technology, Image Quality and Radiation Dose.

A-416 09:05

Radiation incidents and accidents in interventional suites
R.W.R. Loose; *Nürnberg/DE (Loose@klinikum-nuernberg.de)*

The majority of radiation incidents and accidents in interventional suites are related to patients. Radiation accidents of staff members are very rare but may occur under specific circumstances. For example, staff members are at risk if parts of their body are for too long in the primary beam or if safety measures for new practices like SIRT with 90-Y are inadequate. A radiation accident to a patient means normally a deterministic injury - in most cases of the skin. Depending on the individual patient condition the threshold dose for accidents with skin injuries is above 2-5 Gy. Incidents may be unintended overexposures in the dose range of stochastic effects without injuries or "near miss" events without patient exposure. Incidents and accidents during interventional procedures can be avoided by precise and comprehensive standard operating procedures (SOP) and extensive training of all staff members involved. Every incident or accident should trigger a workup of the team to minimize the risk of a second occurrence. After a patient injury the patient and/or his relatives and the referring physician should be informed about recommendations for follow-up of possible lesions. The time delay in the occurrence of lesions may be in the range between 2 weeks and one year. Until February 6th 2018, the Council Directive 2013/59/Euratom has to be transposed into national regulations of member states requiring a recording and reporting of accidental and unintended exposures. Up to now, the approach of this transposition is unclear for many member states.

Learning Objectives:
1. To give an overview of radiation incidents and accidents in interventional radiology.
2. To discuss the lessons learnt from these incidents and accidents.
3. To learn how to manage incidents and accidents in interventional radiology.

A-417 09:35

Accidental exposure during pregnancy
J. Damilakis; *Iraklion/GR*

Accidental irradiation of pregnant patients occurs during the first weeks of gestation. During the first 2 weeks postconception, radiation will terminate pregnancy or the embryo will either recover completely (all or nothing effect). From the 3rd to 8th week postconception, the most possible form of damage is organ malformations. However, these effects are not likely to be observed after diagnostic imaging. After accidental exposure of pregnant patients, conceptus dose estimation is needed. CODE (COnceptus Dose Estimation) is a free web-based software tool for the estimation of embryo dose from radiography, diagnostic fluoroscopy, CT and fluoroscopically guided procedures. For more information about CODE, please visit embryodose.med.uoc.gr. Careful screening is needed to avoid accidental irradiation during pregnancy. X-ray departments must have posters in the waiting area asking female patients to inform the radiographer or radiologist about a possible pregnancy. According to ICRP publication 84, 'investigation of the reproductive status of a female of childbearing age prior to x-ray imaging' is needed. Article 62 of the new EU BSS states that 'Member States shall ensure that the referrer or the practitioner, as appropriate, inquire, as specified by Member States, whether the individual subject to medical exposure is pregnant or breastfeeding, unless it can be ruled out for obvious reasons or is not relevant to the radiological procedure'.

Learning Objectives:
1. To provide information about the frequency of accidental exposure of pregnant patients in imaging departments.
2. To learn how cases of accidental exposure of pregnant patients in imaging departments can be reduced.
3. To learn how to manage pregnant patients in case of accidental exposure to x-rays.

08:30 - 10:00 **Room K**

Radiographers

RC 914

Patient safety: professional and clinical responsibility of the radiographer

Moderators:
T. Roding; Haarlem/NL
P. Due-Tønnessen; Oslo/NO

A-418 08:30

A. Patient and staff safety in medical imaging: what can be done?
S. Mc Fadden; *Newtownabbey/UK (S.McFadden@ulster.ac.uk)*

A wide variety of legislation and guidelines exist internationally to ensure that patient and staff safety in medical imaging is maintained. The systems for radiation protection for the 28 member states of the EU were initially based on the requirements of Council Directive 96/29/Euratom, i.e. European basic safety standards (EU BSS). The more recent Council Directive 2013/59/Euratom revises these standards and contains important changes to the legislation. In addition, a deadline of February 6, 2018 has been set whereby each member state must bring into force the laws and regulations necessary to comply with the new requirements. Free movement of health professionals within the European Union was established by Directive 2005/36 of the European Commission. This directive states that EU countries should recognise professional qualifications from other member states. However, the profession of radiography does not have specific requirements regarding training and education, or identification of required competencies defined at European level. Current research highlights great variation in the different education frameworks and competencies acquired during training by radiographic staff across the EU. Further work is required to standardise these qualifications and ensure safe movement of radiographic staff across member states. As technology continues to advance, the practice of radiography is continually evolving and new staff roles are emerging across all departments to accommodate these changes. A clear standardised framework recognising the different roles/competencies of radiographic staff, i.e. referrers, practitioners and operators across the EU is required to ensure safe autonomous practice is maintained.

Learning Objectives:
1. To appreciate the current guidelines and legislation across the EU.
2. To learn about current research and different roles of the radiographer.
3. To discuss different ways to ensure patient safety is maintained.

A-419 08:55

B. Aspects of safety: what should be considered?
K. Azevedo[1], C.A. Silva[2], A.F.C.L. Abrantes[1], L.P.V. Ribeiro[1], A.M. Ribeiro[1]; [1]*Faro/PT*, [2]*Évora/PT (kbazevedo@ualg.pt)*

The radiographer is a key element in the radiology department. To perform the examinations, from their programming, to their execution and evaluation, there are several factors that may influence patient safety, not only at the department level, but also at the healthcare facility level. It is clear that the main goal is to diagnose and treat the patient, but at the same time do no unnecessary harm. Incidents or accidents, more commonly seen as errors are one of the most assessed measurements when the topic is patient safety; however, as James Reason alerted, to err is human and healthcare is always a potentially hazardous sector. To maximize patient safety, the first step is to make it a cultural issue in the department and in the institution. Only if every healthcare worker understands the importance of this subject and feels like a link in the chain of safety, it becomes possible to achieve higher levels of safety. The professional responsibility in safety starts even before the first contact with the patient and ends after the last contact with the patient. During this period, several steps can be taken to increase safety and it is always important to check the progress in patient safety, by looking at indicators and to the healthcare worker perceptions.

Learning Objectives:
1. To appreciate the core competencies and the radiographer's role as a key element to ensure patient safety at the imaging department.
2. To learn about the main concepts of patient safety related to the radiographer's professional responsibility and ethics outlines at the imaging department level from a public or private hospital or even at the private practice level.
3. To discuss ways to promote patient safety and quality in imaging.

A-420 09:20

C. Patient safety: opportunities and challenges ahead in medical imaging
J. McNulty; *Dublin/IE (jonathan.mcnulty@ucd.ie)*

Patient safety is a major priority for all healthcare professions and undergraduate health professions education has the potential to improve patient safety. While patient safety curricula have been developed by many organisations to help support the introduction and promotion of patient safety within educational curricula, patient safety in medical imaging requires particular attention. There is a paucity of reports regarding the inclusion of patient safety topics within undergraduate radiography curricula and within radiology training programmes. We have reached a point where a comprehensive approach to patient safety from education and training through to service delivery cannot be viewed as optional. While some patient safety topics within medical imaging are stated to be comprehensively addressed across Europe, such as radiation protection, other topics may be being neglected. The starting point for addressing patient safety and any associated challenges is through an initial mapping exercise of how and where all topics are addressed in education and training programmes and how risk is minimised in clinical departments. While resourcing of new initiatives is often problematic, it would be negligent of educational and clinical service providers to overlook initiatives targeting patient safety on this basis. Education and training providers should actively engage with clinical departments and professional bodies to ensure the medical imaging department so that risks are minimised. European professional societies such as the European Federation of Radiographer Societies (EFRS) and European Society of Radiology (ESR) have significant roles to play in driving this activity.

Learning Objectives:
1. To appreciate the current status and challenges ahead with ensuring patient safety in medical imaging.
2. To learn about new ways of addressing the challenges ahead.
3. To discuss the implementation of patient safety focused curricula and the benefits for clinical departments.

09:45
Discussion and questions: Ensuring patient safety in medical imaging: what else can be done?

08:30 - 10:00 **Room M 1**

Vascular

RC 915

Post-treatment evaluation: what every radiologist should know

A-421 08:30

Chairman's introduction
P. Haage; *Wuppertal/DE (patrick.haage@helios-kliniken.de)*

Suitable post-treatment evaluation after any intervention is crucial for a good outcome and high long-term success rates. Consequently, it is necessary to supervise the outcomes, define follow-up strategies and to identify potential complications and possibly prepare for re-intervention. Herein most common complications after thoracic aortic interventions, abdominal aorta surgical and endovascular repair and endovascular peripheral arterial disease treatment will be presented including imaging specifics, i.e. normal and pathological appearances and indications for reintervention. Information on the selection of modality (ultrasonography, CT, MRI), the typical phase interval between follow-up examinations and some specific suggestions including items to cover in a structured report will be delivered.

Session Objectives:
1. To briefly introduce the distinctive role of proper post-treatment evaluation after intervention.
2. To control the results and to know possible complications - to prepare re-intervention.

A-422 08:35

A. Thoracic aorta
T. Leiner; *Utrecht/NL (t.leiner@umcutrecht.nl)*

Cross-sectional imaging techniques play an important role when following up patients after endovascular or surgical repair of aortic disease. Depending on the disease in question, imaging is indicated at regular intervals after intervention and in many cases for the rest of a patients' life. Structured evaluation and reporting is very important to standardize the follow-up and to minimize interobserver variation. In my presentation, I will discuss the various endovascular and surgical techniques used to repair aortic disease and their

normal post-operative appearance. I will also discuss the most common complications and potential imaging pitfalls in the postoperative period including mimickers of pathologic processes such as felt pledgets, graft folds, and nonabsorbable haemostatic agents. Postoperative complications that may be encountered include pseudoaneurysms, infection, prosthetic valve dysfunction, dehiscence as well as graft kinking, stent fracture and endoleak. Specific attention will be paid to follow up intervals and which findings necessitate reintervention.

Learning Objectives:

1. To learn about the most common complications after thoracic aortic interventions.
2. To understand imaging specifics after thoracic aortic interventions.
3. To know indications for re-intervention.

Author Disclosure:

T. Leiner: Board Member; Society of Cardiovascular Magnetic Resonance (SCMR); European Society for Magnetic Resonance in Medicine and Biology (ESMRMB). Grant Recipient; Netherlands Heart Foundation, Technology Foundation STW, Netherlands Organisation for Scientific Research,. Research/Grant Support; Bayer, Bracco, Philips. Speaker; Philips.

A-423 08:58

B. Abdominal aorta

C. Loewe; *Vienna/AT (christian.loewe@meduniwien.ac.at)*

The endovascular treatment of infrarenal aortic aneurysms (EVAR) has become a well-established treatment option. On the contrary to patients after surgical repair, patients after EVAR require lifetime follow-up imaging since the chronic and progressive character of atherosclerosis can cause progression of aortic dilatation leading to prosthesis movement or insufficient aneurysm exclusion with time. Additionally, persistent perfusion of the aneurysm sac (endoleaks) can occur even years after stentgraft placement. Finally, the life expectancy of the materials used for endovascular treatment might be limited. CT angiography was established as the first method of choice for follow-up after abdominal aortic repair. The advantages of CT angiography are manifold and include optimal comparability with the pre-treatment examination (usually done by means of CT angiography), high resolution, direct visualization of the device itself and the possibility of multiphasic acquisition to detect even slow flow endoleaks. As its true for all treatment follow-up examinations, knowledge about primary procedure and typical post-therapeutic findings as well as about most common complications is a prerequisite in patient care after abdominal aortic repair. Device migration, device fracture and/or persistent sac perfusion - in most of the cases related to each other and - are the most common procedure-related complications. In this presentation, different therapeutic means for abdominal aortic disease will be presented as well as the typical, normal findings after treatment. Furthermore, most common complications will be introduced and discussed based on clinical examples. Finally, possible follow-up strategy depending on disease and procedure should be proposed.

Learning Objectives:

1. To learn about the most common complications after abdominal aortic interventions.
2. To understand imaging specifics after thoracic aortic interventions.
3. To know indications for re-intervention.

Author Disclosure:

C. Loewe: Speaker; GE Healthcare, BRACCO, Medtronic.

A-424 09:21

C. Peripheral arterial disease

M. Anzidei; *Rome/IT (michele.anzidei@gmail.com)*

CT and MR angiography (CTA and MRA) substantially changed the diagnostic approach in planning and follow-up of treatment for peripheral arterial disease (PAD), enabling early identification of treatment failure or treatment-related complications after endovascular and surgical procedures. Doppler Ultrasound is the first-line imaging modality during follow-up after treatment, but CTA and MRA enable more detailed and panoramic imaging that is extremely valuable in the assessment of treatment outcome. The aim of this presentation is to review the imaging findings in the most common complications after endovascular treatment for PAD, to discuss the best imaging modality in the various clinical scenarios and to explain when and how to re-intervene on the basis of imaging findings.

Learning Objectives:

1. To learn about the most common complications after PAD endovascular repair.
2. To understand what imaging technique is preferred (any diagnostic).
3. To explain when to re-intervene and how to prepare it?

09:44

Panel discussion: How to optimise post-treatment imaging: getting proper diagnosis without performing too many examinations

08:30 - 10:00 **Room M 2**

EIBIR Session

EIBIR 2

EU Research on cancer imaging

A-425 08:30

Introduction

Y. Liu; *Brussels/BE (yan.liu@eortc.be)*

Imaging biomarkers are involved throughout cancer research, and serve many purposes other than providing surrogate endpoints. Nevertheless, novel imaging biomarkers must be qualified before they can be used to reliably guide clinical decisions. Imaging biomarker qualification requires strong collaboration between imagers in industry and academia, as well as insight from regulators and payers, utilizing the different strengths of each stakeholder. The European Union has launched Horizon 2020, the biggest EU Research and Innovation programme with nearly €80 billion of funding available over 7 years (2014 to 2020), in calls for proposals or actions. Of the total Horizon 2020 budget, around € 6.8 billion has been committed to fund "Health, demographic change and well-being" research, which is one of the seven challenges of the Societal Challenges pillar of Horizon 2020. The Innovative Medicines Initiative (IMI) is a partnership between the European Union and the European pharmaceutical industry, and it is also the world's biggest public-private partnership in the life sciences. Through the IMI 2 programme, it has a €3.3 billion budget for the period 2014-2024. The European Institute for Biomedical Imaging Research (EIBIR) has a significant amount of experience in the field of biomedical imaging research funding, and has achieved high successful rates in the past Horizon 2020 calls. It is in a stronger position to provide knowledgeable support for imaging proposal preparation and project management. Three granted imaging projects will be introduced in this session.

Session Objectives:

1. To understand cancer imaging research in Europe.
2. To learn about current funding opportunities for cancer imaging research in Europe.

A-426 08:45

Multimodal imaging with diffuse optics for cancer theranostics

T. Durduran; *Barcelona/ES (turgut.durduran@icfo.es)*

Near-infrared diffuse optical methods provide unique contrasts based on haemodynamics (microvascular blood flow, blood oxygen saturation and blood volume) and tissue structure (cell density, size) as well as the water and other chromophore concentrations. These can be measured in a non-invasive, relatively safe manner. I will describe the current state-of-the-art in the context of theranostics for oncology and relate them to ongoing European projects. In particular, the focus of my research is on the development of hybrid technologies that combine diffuse correlation spectroscopy (DCS) and diffuse optical spectroscopy (DOS) to be utilized in biomedicine. Our international efforts involve the validation, research as well as clinical translation of these technologies from "mice to men". The translational aspect of this effort is strengthened by the utilization of same/similar instrumentation on both small animals and on clinical feasibility testing. I will describe the background physics, the basics of the technology, different approaches to probes and illustrate the state of the art using examples from different studies. Finally, I will describe the LUCA project (http://www.luca-project.eu) where a European consortium is working towards building and validating a prototype that combines optics with ultrasound.

Learning Objectives:

1. To understand a new multimodal imaging technology.
2. To learn about the Horizon 2020 research project LUCA.

Author Disclosure:

T. Durduran: Patent Holder; TD is an inventor on two relevant patents.. Research/Grant Support; TD receives grant support from the European Commission H2020 programme, Spanish health ministry , Spanish science ministry and two private foundations.. Other; ICFO has equity ownership in the spin-off company HemoPhotonics. Potential financial conflicts of interest and objectivity of research have been monitored by ICFO's Knowledge & Technology Transfer Dep.

A-427 09:10

Hybrid PET/MRI for breast cancer detection

C.K. Kuhl; *Aachen/DE*

"no abstract submitted"

Learning Objectives:

1. To discover the importance of hybrid imaging for cancer detection.
2. To learn about the Horizon 2020 research project HYPMED.

A-428 09:35

Using GlucoCEST MRI to visualise cancer

X. Golay; *London/UK (x.golay@ucl.ac.uk)*

Cancer accounts for 13% of all deaths worldwide and despite recent medical improvements remains one of the most deleterious diseases in the world. Early detection is very important as it increases the chances of survival. In addition, the high level of sophistication towards treating cancer has generated a new problem: the differentiation between treatment effect, regrowth or pseudo-progression of the tumour, which are all poorly differentiated on most imaging methods. Tumour cells preferentially uptake glucose over normal cells, as they rely on enhanced aerobic glycolysis for their energy supply, which distinguishes them from normal tissue (the Warburg effect. We have exploited this finding to both develop and demonstrate the sensitivity of a new radiation-free magnetic resonance imaging (MRI) technique, named glucose-based chemical exchange saturation transfer (GlucoCEST), which will provide additional information over and above current medical in vivo imaging techniques in oncology (1). GlucoCEST has been shown to detect both native glucose and glucose (Glc) analogues such as 3-O-methyl-D-glucose (3OMG) uptake in tumour models. We, therefore, established a consortium (GlucoCEST imaging of neoplastic tumours - GLINT) to bring the combination of Glc and 3OMG as a combined exam to the clinics, thereby providing a wide-ranging new diagnostic tool for one of the most devastating diseases in the world. Thus, GLINT aims, therefore, to provide a cheap, available, comprehensive, non-invasive, radiation-free complementary method to nuclear medicine techniques currently used for cancer assessment. Ref: 1) Walker-Samuel et al, Nature Medicine, 19(8):1067-73 (2013).

Learning Objectives:

1. To discover an innovative MRI method to visualise cancer.
2. To learn about the Horizon 2020 research project GLINT.

Author Disclosure:

X. Golay: CEO; Gold Standard Phantoms Ltd. Consultant; Olea Medical. Founder; Imgenious Ltd. Research/Grant Support; Olea Medical.

08:30 - 10:00 **Room M 3**

Molecular Imaging

RC 906

Translational research in molecular imaging: how to do the translation

A-429 08:30

Chairman's introduction

J. Hodler; *Zurich/CH (juerg.hodler@usz.ch)*

Radiologists are good organisers with excellent knowledge of technology and with an important role in patient care. They are not necessarily at the forefront of basic research. Although radiologists do not all need to perform animal studies, we need to understand methodology, to recognize new findings with clinical potential and to reduce the well-known time lag between “bench and bedside”. This session contributes knowledge about preclinical imaging and its translation into clinical radiology by experts in their fields.

Session Objectives:

1. To learn the translational potential of preclinical research.
2. To understand the needs of preclinical research.
3. To know the physiological differences between small animals and humans.

Author Disclosure:

J. Hodler: Research/Grant Support; Bayer, Guerbet, Siemens.

A-430 08:36

A. Preclinical MR/PET imaging of cancer

C. Kuntner-Hannes; *Seibersdorf/AT (claudia.kuntner@ait.ac.at)*

Small animal molecular imaging has become an important technique for the development of new drugs, radiotracers and therapies. Positron emission tomography (PET) together with magnetic resonance imaging (MRI) provides unique in vivo information about specific molecular pathways in different diseases. How to decide what settings or conditions to use is not straightforward, as the experimental design is dependent on the particular science being investigated. In small animal imaging there are different multi-modal techniques available starting from using two stand-alone scanners to fully integrated PET/MRI scanners. From physics to physiology, there are many factors to consider when setting up an experiment, each of which can have a significant impact upon quantitative PET/MRI data. Standardization from animal models, animal handling, data acquisition protocols, and image data analysis should help to generate data that can be reproduced by the same or other laboratories to enhance scientific importance. This talk examines the most common factors related to all types of quantitative PET imaging.

Learning Objectives:

1. To learn the use of preclinical PET/MR imaging.
2. To understand the needs of standardisation in preclinical imaging.
3. To understand the challenges in quantitative preclinical PET imaging.

A-431 08:59

B. What about nanotechnology?

F.M.A. Kiessling; *Aachen/DE (fkiessling@ukaachen.de)*

The design of a molecular imaging agent should follow its clinical demands. This sounds trivial but often basic questions are not asked, which leads to failure in translation. Therefore, the following questions should be answered positively before starting research and development: is there a clinical need for the envisioned diagnostic procedure? Does its application impact the therapeutic conduct? Are all alternative drug designs less promising? Will the agent fulfil the required pharmacokinetic demands? Are toxic side effects not expected? Is the imaging method sufficiently robust and sensitive to draw a clear conclusion from the application of the nanodiagnostic agent also when analysing individual patients instead of comparing groups? Is there sufficient market potential for commercialisation and can the production be controlled and upscaled? Asking these questions will substantially help researchers to find ideal indication for nanomedicines and nanodiagnostics. For example, if fast compartmental exchange and renal clearance are required, the nanoparticles must be below 5 nm. If EPR-dependent accumulation is desired, the particles should be larger but neutrally charged. In turn, charged particles are preferred for labelling the MPS (mononuclear phagocyte system) and cells in vitro. Active targeting, may be used to enhance local retention and cellular uptake but it will not improve (even rather decrease) accumulation due shortening blood half-life. Using examples of our and others research on nanodiagnostics, nanotherapeutics and theranostics, the above questions will be addressed and according concepts and their strengths and limitations will be explained and discussed in detail.

Learning Objectives:

1. To understand advantages and limitations of nanomedicines.
2. To gain knowledge on elimination routes of nanoprobes.
3. To understand the potential benefit of active targeting.

Author Disclosure:

F.M.A. Kiessling: Consultant; Bracco, Molecular Targeting Inc., invivoContrast GmbH. Research/Grant Support; DFG, EU, BMBF, Bayer, Bracco. Shareholder; invivoContrast GmbH.

A-432 09:22

C. The transition from preclinical to clinical

A. Kjaer; *Copenhagen/DK*

"no abstract submitted"

Learning Objectives:

1. To learn the benefits of preclinical imaging for clinical activities.
2. To learn how to translate the knowledge from preclinical to clinical applications.
3. To understand the limitations of translation.

09:45

Panel discussion: How to perform translational research in molecular imaging

08:30 - 10:00 **Room M 4**

E³ - ECR Academies: Spinal Imaging

E³ 919

Degenerative cervical spine

A-433 08:30

Chairman's introduction

V.N. Cassar-Pullicino; *Oswestry/UK (Victor.Pullicino@rjah.nhs.uk)*

The degenerative process targeting the intervertebral discs and synovial joints can affect single or multiple levels in the cervical spine with variable severity. The changes are usually progressive and proliferative promoting instability and encroachment on the cord and exiting nerve roots. However, imaging evidence of these changes even when severe is not always related to symptoms. The objective of this session is to specifically focus on the relevant imaging features that a) are likely to be clinically relevant, b) require treatment and c) aid in treatment planning.

A-434 08:35

A. Normal ageing process

C.W.A. Pfirrmann; *Zurich/CH*

Ageing of the spine is a normal process, occurring in any subject. The prevalence of neck problems accounts for 1% of all health issues. Normal ageing; however, is not necessarily linked to symptoms. Ageing of the cervical intervertebral disc involves several processes, such as decrease of proteoglycan content and decrease of water content. Ageing of the disc starts with adolescence. The prevalence is around 16% in adolescence and close to 90% in subjects over 60 years. Already at 40 years of age, at least one finding representing a degenerative phenomenon is seen on two thirds of MR images of the spine. Cross-sectional studies have shown that all factors but age, such as physical activity, gender, smoking, body mass index are not significantly linked to the progression of degeneration. About one third of previously asymptomatic subject develops symptoms over a 10-year period. The most common MR imaging findings in the 10-year follow-up of an asymptomatic cohort are drop in signal of the nucleus pulposus, narrowing of the interspace, compression of the dural sac or the spinal cord and formational stenosis.

Learning Objectives:

1. To understand normal ageing process.
2. To describe biomechanical spinal changes with ageing.
3. To learn MR age-related findings.

A-435 09:03

B. MR findings: what's relevant?

M.-A. Weber; *Heidelberg/DE (MarcAndre.Weber@med.uni-heidelberg.de)*

This lecture will summarise typical MRI patterns of degenerative cervical spine disease, will explain which imaging findings may explain pain and are useful in planning treatment and will also include a discussion of the role of the different modalities, especially MRI vs. CT. Modern CT and MRI techniques provide excellent anatomical images of the cervical spine. MRI is best suitable for evaluation of the soft tissues, including the intervertebral discs, ligaments, bone marrow and spinal cord, whereas CT offers delineation of osseous components with high spatial resolution. MR imaging has a key role for exploration of spine degenerative disease. Intervertebral disc fissures are optimally depicted on T2-weighted imaging. Disc herniation and neural foraminal stenosis are common changes seen associated with neck pain with or without radiculopathy. Questions concerning pathologies of the neuroforamina, multiplanar reconstructions and/or additional angulated imaging sequences of the spine should particularly be included in routine examinations for improved delineation and depiction of neuroforaminal pathologies, especially if there is a need to evaluate surgical therapy. Whenever possible, a 3D sequence is preferred and thus post-imaging reconstructions can be compiled that not merely reduce examination time but also offers advantages for multiple planar reconstructions as well as simplifying the MR exam. Kinematic MRI might be beneficial for revealing disc bulges, which are not shown by traditional neutral views and should be considered in dedicated cases for the evaluation of the cervical spine. Cervical spine MRI should systematically be performed for cases of neck pain associated with neurologic deficit.

Learning Objectives:

1. To summarise typical MRI patterns of degenerative cervical spine disease.
2. To identify which imaging findings explain pain and are useful in planning treatment.
3. To discuss the role of the different modalities, MR vs CT.

A-436 09:31

C. Spinal stenosis: what is it?

M. Muto; *Naples/IT (mutomar2@gmail.com)*

Spinal canal stenosis represents a frequent cause of pain with relevant impact on the quality of life and daily activities. Spondylosis, trauma and malignancies are the most frequent causes and their incidence depends on patient age. Radiology has a crucial role in the diagnosis of spinal stenosis as well as in the recognition of the aetiologies using different imaging modalities: x-ray, CT, MR and dynamic studies. Furthermore, mini-invasive image-guided treatments are nowadays commonly included in the clinical practice dedicated to this category of patients. This presentation aims to describe the most frequent causes of spinal stenosis, to propose a correct diagnostic approach and planning the treatment strategies.

Learning Objectives:

1. To learn the most frequent causes of spinal stenosis.
2. To learn how to make a correct diagnosis of spinal stenosis using different imaging modalities.
3. To identify imaging features of spinal stenosis that determine outcome and treatment strategies.

08:30 - 10:00 **Room M 5**

E³ - ECR Master Class (Emergency Imaging)

E³ 926

Multimodality imaging of the acute female pelvis

Moderator:
R. Basilico; Chieti/IT

A-437 08:30

A. Ultrasound: making a more specific diagnosis

M. Weston; *Leeds/UK (michael.weston2@nhs.net)*

Acute conditions in the female pelvis may be related to the gynaecological tract, namely ectopic pregnancy, ovarian cyst accidents, adnexal torsion, fibroid degeneration and pelvic inflammatory disease. Or, they may be related to other systems within the pelvis such as appendicitis, diverticulitis, urinary tract infections and stones, aneurysms and musculoskeletal conditions. The patient history and clinical findings are an important part of the differential diagnosis. However, having taken these into account it is important to be familiar with the typical ultrasound appearances of the common presentations and to keep an open mind regarding atypical alternatives. Ultrasound may be enough to make the diagnosis and guide treatment and follow-up, typically in self-limiting conditions such as a cyst accident. It is important to be aware of limitations and to know when other imaging modalities are needed.

Learning Objectives:

1. To be familiar with common and uncommon clinical scenarios in acute female pelvis.
2. To know the typical and atypical imaging findings.
3. To review the influence of findings on patient management.

A-438 09:00

B. When can CT give a definite answer?

I. Millet; *Montpellier/FR (milletingrid@wanadoo.fr)*

In the acute female pelvis setting, transvaginal and transabdominal pelvic sonography is the preferred imaging modality especially when gynaecologic causes are suspected. However, enhanced computed tomography (CT) can be helpful if the sonography is not conclusive or in a first line if the clinical symptoms are non-specific. Many gynaecologic causes of pain can be detected with some specific CT findings at enhanced CT and conversely, no additional imaging is recommended if pelvic CT examination is normal. Pelvic inflammatory disease should be considered if there is a symmetric low epiploic fat haziness especially when the fallopian tubes are thickened and enhanced. Adnexal torsion should be considered when an enlarged asymmetric ovary is adjacent to a thickened fallopian tube. CT can assert the gynaecologic origin of a haemoperitoneum by identifying the sentinel clot and/or an active bleeding in the pelvis. In pregnant women, CT remains the primary diagnostic tool in case of hypovolemic blunt or penetrating trauma or severe sepsis. CT may also be needed during pregnancy to assess common causes of acute abdominal pain such as suspected appendicitis, bowel obstruction, obstructing urinary tract calculi and pancreatitis especially if other imaging techniques such as ultrasound and magnetic resonance imaging are inconclusive. Protocols should then minimize the use of multi-phase studies and should use optimized settings to reduce the dose as much as possible without losing image quality. The estimated foetal dose using a single CT phase remains always below the 50-mGy limit above which there is a statistically higher risk of teratogenesis.

Learning Objectives:

1. To understand the role of CT in different female pelvic pathologies.
2. To become familiar with CT findings useful for differential diagnoses.
3. To know the strict indications for the use of CT in pregnant women.

A-439 09:30

C. Is MRI a game-changer?

G. Masselli; *Rome/IT (gabrielemasselli@libero.it)*

Rapid and accurate diagnosis is essential for the appropriate management of acute female pelvic conditions in the emergency department. Magnetic resonance (MR) imaging provides an additional imaging alternative to CT that does not involve the use of ionizing radiation or iodinated contrast material. MR imaging has several advantages over CT in terms of safety profile, diagnostic efficacy and ease of use. An issue that is causing increasing concern, both in the general population and in the medical community, is the potential adverse effects of overuse of ionizing medical radiation, of which CT remains the primary source. MR imaging does not make use of ionizing radiation, which is of particular concern in young women and pregnant patients. Recent advances in MR imaging hardware and software have allowed the development of rapid

imaging techniques that are particularly suited for emergency department indications. MR imaging enables assessment of the entire pelvis within several minutes without ionizing radiation and due MR to its high contrast resolution the administration of contrast agents is not mandatory. The value of MR imaging has been assessed in many acute conditions of the lower abdomen and pelvis, in particular MRI is accurate in differentiating gynaecological from no gynaecological disorders. Due to its advantages, depending on the local availability, MR imaging may be considered as the modality of first choice in the patients with acute pelvic pain.

Learning Objectives:

1. To be familiar with clinical conditions which are the clear indications for MRI examination.
2. To learn MRI protocols which are used in imaging of acute pelvic diseases.
3. To comprehend the advantage of MRI over US and CT in particular clinical settings.

10:30 - 12:00 **Room B**

ESR meets Belgium

EM 1

Emergency radiology

Presiding:
G.M. Villeirs; Gent/BE
P.M. Parizel; Antwerp/BE

A-440 10:30

Introduction

G. Villeirs; *Gent/BE*

Introduction to the "European Society of Radiology (ESR) Meets Belgium" session, by the President of the Belgian Society or Radiology. During this session, various topics in emergency medicine will be presented and illustrated by eminent Belgian radiologists. The session will also be animated by an interlude about radiology of Belgian food and a video about the Belgian Museum of Radiology.

Session Objectives:

1. To learn more about various topics presented by eminent Belgian radiologists.
2. To illustrate imaging applications in the Belgian context.
3. To show the diversity of emergency radiology.

A-441 10:35

Additional value of dual-energy CT in abdominal emergencies

E. Danse; *Brussels/BE (etienne.danse@uclouvain.be)*

CT plays a major role in the management of emergency situations. Its role is increased because the diagnostic performance of imaging methods takes benefit of the continuous technological CT improvements. Our goal is to present our recent experience of using spectral CT for the diagnostic workup of adult patients admitted for acute abdominal disorders. This presentation will be focused on the main applications of the spectral modalities for the diagnostic management of patients having severe trauma with abdominal consequence, suspicion of acute intestinal ischaemia, bowel obstruction, acute renal disorders (renal colic, acute pyelonephritis, renal infarct), acute pancreatitis and biliary tract disorders and some uncommon situations. Some basic key points about the spectral technique and the imaging flow management will also be presented.

Learning Objectives:

1. To explain the basics of dual-energy CT.
2. To illustrate the application of dual-energy CT in the abdominal emergency setting.
3. To demonstrate the incremental value of dual-energy CT in abdominal emergencies.

A-442 10:55

High-end CT imaging in forensic medicine: experience after recent Brussels terror attacks

W. Develter; *Leuven/BE*

"No abstract submitted."

Learning Objectives:

1. To learn more about the challenges in forensic medicine after major calamities.
2. To explain the need for high-end CT imaging in forensic medicine.
3. To illustrate the value of high-end CT in the aftermath of the Brussels terror attacks.

A-443 11:15

Interlude: Imaging Belgian food

K. Verstraete; *Ghent/BE (koenraad.verstraete@ugent.be)*

The purpose of this lecture is to present the imaging characteristics of a classical Belgian meal, including delicious Belgian desserts and beers. The methods used are plain radiography, CT and MR imaging. Results show the different absorption and resonance characteristics of Belgian food and drinks. Attendants should try to guess what we eat and drink by analysing the images.

Author Disclosure:

K. Verstraete: Other; Part of Belgian Food presented was prepared by Sodexo.

A-444 11:25

Imaging genetics and beyond: facial reconstruction and identification

P. Claes; *Leuven/BE (peter.claes@kuleuven.be)*

The phenotypic complement to genomics is phenomics which aims to obtain high-throughput and high-dimensional phenotyping. The paradigm shift is simple and similar to the one made in the human genome project, instead of 'phenotyping as usual' or measuring a limited set of simplified features that seem relevant, why not measure it all? With the advent of ever more consumer-worn sensors, the technological hardware exists for extensively (wide variety of measurements from different sensors) and intensively (in great detail and high resolution) collecting quantitative phenotypic data. In my research, e.g. 3D surface imaging and medical scanning devices, provide the optimal means to capture information of human morphology and appearance to the level of phenomics. In this seminar, I guide you through the science and the complexities of imaging genetics and elaborate on the genetic architecture of the human brain and face captured using MRI and 3D surface scanning, respectively. I will illustrate a computational framework that is able to match given faces to probe DNA. This facilitates the ability to perform facial identification and/or verification from DNA. Towards the future, this will generate innovative applications in forensics and biometrics, arming investigators with new and powerful tools to establish human identity from DNA.

Learning Objectives:

1. To demonstrate the application of imaging in genetic assessment.
2. To illustrate the use of imaging for identification.
3. To illustrate the use of imaging after facial reconstruction.

A-445 11:45

Interlude: The Belgian Museum of Radiology

R. Van Tiggelen; *Brussels/BE (info@radiology-museum.be)*

Some years ago, the Science Museum of London performed a survey among the visitors on the most important discoveries in medicine. Out of over 40,000 answers, radiology was number one. Radiology came ahead of, e.g. the discovery of penicillin of the description of DNA. This was a supplementary reason why we created, in 1990, the Belgian Museum of Radiology. Remember also that radiology is used in many fields in medicine and in many fields different from medicine . It is a fact that due to radiology, more than 30 Nobel Laureates have gained their prizes with the practical implementation of this technology. In the world, museums of radiology are rather scarce. What we do and what you can see in our institution is developed with the projection of our short video. We hope to see you in the near future.

11:50

Panel discussion: Acute pathology: emergency radiologists or organ subspecialists?

10:30 - 12:00 **Room G**

EFOMP Workshop: Radiation incidents and accidents in medical imaging: can we prevent them?

EF 2

Radiation incidents and accidents in medical imaging and their management (part II)

Moderators:
M. Brambilla; Novara/IT
D.J. Lurie; Aberdeen/UK

A-446 10:30

Chairman's introduction
M. Brambilla; *Novara/IT (marco.brambilla@maggioreosp.novara.it)*

This session will review the current safety issues related to MRI and nuclear medicine environment for both the patients as well as the staff members. Hazards intrinsic to the MRI and nuclear medicine environment must be understood, acknowledged and respected. Incidents occurring in imaging departments shall be properly documented and reported. An overview of incidents and accidents in MRI and nuclear medicine will be provided together with a critical discussion of the lessons learnt from these incidents and accidents. Information and guidelines will be provided on how to properly manage and report incidents and accidents. Finally, the role of the medical physicist in managing incidents and accidents in imaging departments will be outlined by identifying duties and responsibilities of medical physicists associated with the management of radiation incidents and accidents.

Session Objectives:
1. To learn about the common reasons for radiation incidents and accidents in MRI and nuclear medicine departments.
2. To appreciate why we need to manage radiation incidents and accidents properly.

A-447 10:35

Incidents and accidents in MRI
D.J. Lurie; *Aberdeen/UK (d.lurie@abdn.ac.uk)*

MRI is considered “safe”, due to the lack of ionising radiation and the absence of cumulative “dose” from the scanner’s static, switched and radiofrequency magnetic fields. Nevertheless, hazards associated with MR scanning exist and accidents and incidents of varying severity do occur. The most obvious hazard arises from the “missile effect”, whereby large ferromagnetic objects (chairs, compressed gas tanks) are accelerated into the magnet bore. More common, and harder to control, are the effects of the static magnetic field on small, treatment-related objects (e.g. endotracheal tube components) and on non-MR-safe implanted devices including pacemakers, stents, aneurysm clips or capsule-endoscopy devices. The most significant hazard from MRI is associated with radiofrequency pulses transmitted by the scanner. Non-resonant absorption of energy can potentially cause overheating of tissues, but these effects are well controlled by scanner software. Burns may arise from the unintended concentration of radiofrequency fields. This may be caused by conductive (non-ferromagnetic) objects within or near to the patient, including implanted pacemaker leads (remaining after pacemaker removal), non-MR-compatible or wrongly placed ECG leads, and drug-delivery patches. Burns may also arise from malfunction or incorrect setup of radiofrequency coils. The primary means of minimising adverse incidents are the design and control of MR facilities, education of all staff (from radiologists to cleaners) with regular updates, patient screening techniques and the flagging of patient notes and request forms. It is vital that all incidents are recorded and discussed locally and that lessons learned are disseminated to the wider MRI community.

Learning Objectives:
1. To give an overview of radiation incidents and accidents in MRI.
2. To discuss the lessons learnt from these incidents and accidents.
3. To learn how to manage incidents and accidents in MRI.

A-448 11:05

Radiation incidents and accidents in nuclear medicine
M. Brambilla; *Novara/IT (marco.brambilla@maggioreosp.novara.it)*

In addition to hazards associated with every imaging modality, such as patient’s over or underexposure due to non-optimized acquisition protocols, defective equipment, wrong manoeuvres, there are specific hazards in nuclear medicine procedures associated with the storage, manipulation and administration of unsealed radioactive sources, targeted with radiopharmaceuticals. As a consequence, accidents of varying severity do occur which involves not only patients but also staff workers. All the steps involved in the nuclear medicine workflow are subjected to potential accidents: from patient reception, to patient preparation, radiopharmaceutical preparation, administration and uptake phase of the examination, examination and quality controls of the equipment. The potential accidents must be understood, acknowledged and respected. The most diffuse accidents in nuclear medicine are contamination events, followed by overexposure of patients and failure in the managements of radioactive materials. The primary means of minimising adverse accidents are education of all staff (from nuclear medicine doctors, to radiographers and nurses) with regular updates, blank or dry tests during radiopharmaceutical preparation, clear identification of duties and responsibilities of the staff involved, traceability of procedural steps from patient reception to patient leaving the department, and the flagging of patient notes and request forms. Incident reporting is crucial. Accidents should be discussed locally and lessons learned should be disseminated to the wider NM community. Nuclear medicine departments may also be involved in the health managements of nuclear incidents and accidents in emergency scenarios occurring in nuclear power plants and during radioactive transportation.

Learning Objectives:
1. To give an overview of radiation incidents and accidents in nuclear medicine.
2. To discuss the lessons learnt from these incidents and accidents.
3. To learn how to manage incidents and accidents in nuclear medicine.

A-449 11:35

Management of incidents and accidents in imaging departments: the role and responsibilities of medical physicists
V. Tsapaki; *Athens/GR (virginia@otenet.gr)*

Modern imaging systems such as CT, MR, nuclear medicine machines and other interventional x-ray equipment are widely used by clinicians to pledge a more successful clinical outcome. There are occasionally cases, though, that incidents and accidents can occur during the use of these highly sophisticated systems. Medical physicists are working with technologists, radiologists, regulators, as well as various imaging systems manufacturers to ensure that such incidents and/or accidents do not occur in imaging departments. They are also cooperating closely with x-ray technologists and radiologists, cardiologists and other related physicians to reduce the radiation dose to the patient as well as to the staff. The role of medical physicists in ensuring high-quality and low-risk management system is vital in the attempt to build up a robust safety structure and culture and reduce or prevent radiation incidents/accidents or reduce hazards in MR departments both for the patients and also for the staff. All these issues will be discussed in more detail in the particular lecture. A number of recommendations will be given to guide all related imaging department personnel on the responsibilities of medical physicists regarding the management of incidents and accidents in imaging departments.

Learning Objectives:
1. To provide information about the role of medical physicists in managing incidents and accidents in imaging departments.
2. To identify the duties and responsibilities of medical physicists associated with the management of radiation incidents and accidents.

10:30 - 12:00 **Room M 2**

Professional Issues and Economics in Radiology (PIER)

PIER 1

Improving efficiency in radiology departments

Moderators:
J.A. Brink; Boston, MA/US
S. Morozov; Moscow/RU

A-450 10:30

A. How to identify radiology productivity bottlenecks?
S. Morozov; *Moscow/RU (npcmr@zdrav.mos.ru)*

The shared radiology workflow consists of physician’s referral, study approval, scheduling, patient arrival, imaging, reporting, validating, and results distribution. The performance of this process can be measured on different levels: resources utilization, current operations and outcomes. The end-result of the process is defined by the goal, which can also vary. The major goals are effectiveness (e.g. high-quality, high-safety, high-volume, high-accessibility services, patients’ and physicians’ satisfaction), efficiency (cost-effectiveness, cost-control, revenue generation) and health improvement (better treatment because of accurate diagnostics, less morbidity and mortality because of early diagnostics). The problem with the radiology services is that we often incorrectly measure incorrect metrics. Wherever we see systematic measurement of results in health care—no matter what the country—we see

those results improve (R.S. Kaplan, M.E. Porter). Hence, we should move from current radiology operational metrics (report turn-around-time, back-log time, discrepancies, equipment utilization rate, revenue) to clinical operational metrics (diagnosis-related delays of treatment, time to begin treatment) and outcome measurements (patients' and clinicians' satisfaction, gross margin of services, involvement in disease-specific clinical teams). The best method for tackling 'bottlenecks' is time-driven activity-based costing (TDABC) through better resource utilization, standardized processes, proper staffing, and logistics optimization. Building an enabling IT platform is the key for embedding the changes in the system. Ideal physician measurements are aligned to electronic data collection, attributable to individuals, cascade from organizational goals, supported by evidence and physicians, comparative, and transparent.

Learning Objectives:

1. To review the metrics of shared radiology workflow in the domains of efficiency, quality and safety (what).
2. To demonstrate various methods and techniques for total productivity improvement (how).
3. To delineate the roles of individuals and teams in productivity improvement cycle (who).

Author Disclosure:

S. Morozov: Advisory Board; Philips. CEO; Radiology research and practice center, Moscow.

A-451 10:48

B. How to optimise radiology with big data: Medical Analytics Group (MAG) project

O.S. Pianykh; *Newton Highlands, MA/US (opiany@gmail.com)*

With medical technology becoming increasingly complex, and expected outcomes - more demanding, the cost of medical errors, delays and guesswork grows prohibitively high. To deal with these challenges, contemporary radiology has to rely on objective metrics and knowledge, applied to optimize its operations and decision-making. These metrics and their performance patterns can be most efficiently learned from the (big)data that our hospitals have been accumulating since the beginning of the digital era. Currently, most of these data are recorded and used only when the patients are examined; then it gets warehoused in the RIS, PACS and similar databases, remaining completely idle and forgotten. Transforming these data into the most effective and objective problem solver was the main idea behind the Medical Analytics Group (MAG) project, recently launched by the Department of Radiology at Massachusetts General Hospital. The principal purpose of MAG is to apply data science to routine radiology problems, looking for the best possible solutions. In this presentation, we will share our most interesting results, important successes, and thought-provoking challenges.

Learning Objectives:

1. To highlight the need for big data analysis in radiology management.
2. To provide examples of already implemented data-driven radiology optimisation.
3. To illustrate the challenges of big-data analysis and project implementation.

A-452 11:06

C. How to implement system changes?

G. Paulo; *Coimbra/PT (graciano@estescoimbra.pt)*

Health care organizations are complex sociotechnical environments where highly differentiated health professionals come together to provide, what is expected to be, the best quality of care to the patients. However, it is important to be aware that an asymmetric scientific and professional knowledge between health professionals and even inside each profession is a reality and consequently a barrier to implement a harmonized practice. To improve efficiency in radiology departments it is crucial to deliver patient care based on a well-established teamwork model, by providing team members with clear guidance, as a tool to allow them to be capable to undertake their role with professionalism and be able to identify when errors occur and how to recover and correct those errors. The department leaders have the responsibility to create and maintain a good working atmosphere by developing well-established communication channels and by empowering all staff members. Implementing system changes demands for understanding the paradigm shift of the social behaviour, influenced by the digital era and make adequate adaptations. Health care organizations are opened systems, influencing and being influenced by the internal and external environments. It is crucial for radiology departments to adapt to the new era. The challenges are manifold: to improve efficiency; to increase visibility in patient clinical workflow; to avoid commoditization, amongst other important aspects that will be presented during this session.

Learning Objectives:

1. To learn about the importance of teamwork towards the establishment of a good work environment.
2. To understand the impact of good communication strategies in increasing staff satisfaction.
3. To discuss about the influence of the organisational culture in professional empowerment.

A-453 11:24

D. Making the business case for patient-centred imaging care

M.H. Maurer; *Berne/CH (martin.maurer@insel.ch)*

Patient-centred health care aims to organize health care facilities around the needs of patients and their families. Also in radiology, the traditional business model of radiologists being "doctors to other doctors" is changing towards a patient-centred imaging care where the patient is placed at the centre of the health care environment and the imaging service is organized around the patient's needs and preferences. In this talk, the different dimensions of patient-centred imaging care (e.g. effective communication, education of the patient, emotional support) will be discussed to empower patients to participate in their medical care and decision-making. Several key indicators to build a patient-centred environment such as appropriateness of imaging procedures, scheduling and registration, physical comfort during imaging procedures, management of radiation exposure, and development of reporting programs will be presented as well as methods to redesign radiology processes towards a patient-centred imaging care.

Learning Objectives:

1. To identify health system priorities around patient-centred care.
2. To develop reporting and improvement programmes that align with health system priorities.
3. To build influence through leadership and performance in patient-centred care.

11:42
Panel discussion

10:30 - 12:00 **Room M 4**

E³ - ECR Academies: Spinal Imaging

E³ 1019
Spinal cord abnormalities

A-454 10:30

Chairman's introduction

S. Gaudino; *Rome/IT (simona.gaudino@gmail.com)*

Spinal imaging is a very wide and challenging topic and requires an integrated approach of clinical data, traditional and so-called advanced protocols. The objective of this academies course is to provide a deep and comprehensive discussion of the different fields of the spine/spinal cord pathology that are more frequently observed in clinical practice. The aim of the organizers was to provide a complete discussion on how to integrate the technical aspects of MRI examination of the spinal cord, the MRI semeiotics of both intradural extramedullary and intramedullary lesions, and the "pattern" approach to intramedullary lesions, to ultimately offer a helpful overview of the spinal pathologies that a radiologist may encounter during his professional career. Prof. Van Goethem will address the technical aspects of the MRI study of the spinal cord, discussing how to exploit MRI ranging from the basics to the most updated state-of-the-art techniques. He will specifically discuss the importance to include the "advanced" techniques in the evaluation of the spinal cord diseases. In the second lecture, Dr. Lycklama will discuss the fundamental topic of differential diagnosis between intra- and extra-medullary tumours, discussing semiotic, pathology and MR features. Finally, during the closing lecture, Prof. Turner will address one of the most difficult scenario that a neuroradiologist may deal with, non-tumoural spinal cord lesions, with the objective to make the audience familiar with the "pattern" approach, with whom, at least, reduce the number of differential diagnosis.

A-455 10:35

A. MR imaging of the spinal cord: how to do it?

J. Van Goethem; *Antwerp/BE (johan.vangoethem@uantwerpen.be)*

Magnetic resonance imaging (MRI) of the spinal cord is challenging in many ways. The spinal cord is a small structure and is located in an environment prone to artefacts. I will cover many types of artefacts, including truncation artefacts, motion artefacts caused by breathing and swallowing, CSF pulsation artefacts, aliasing artefacts, susceptibility artefacts and radiofrequency artefacts. The origin of these artefacts and the countermeasures that can be

taken will be discussed. I will also provide an overview of the different sequences that should be used in basic and advanced spinal cord imaging, briefly touching upon diffusion and perfusion imaging, spectroscopy and fMRI of the spinal cord.
Learning Objectives:
1. To understand the challenges for acquiring high-quality MR images of the spinal cord.
2. To learn current state-of-the-art sequences for spinal cord imaging.
3. To be aware of the importance of advanced neuroimaging techniques for the evaluation of spinal cord diseases.

A-456 11:03

B. Differentiating intradural mass lesions
G. Lycklama à Nijeholt; *The Hague/NL (g.lycklama@mchaaglanden.nl)*

Intradural lesions are primarily characterized by their location: intra- vs extramedullary. Intramedullary tumours will expand the spinal cord, while extramedullary lesions will deform it. MRI workup should include high-resolution axial T2 (for example, CISS) to better differentiate intra- from extramedullary. Susceptibility sensitive images show blood products as found, for example, in ependymoma and cavernoma. In addition, MRA may be useful, for example, to demonstrate vessels in a haemangioblastoma. Repeat MRIs are often needed to make a diagnosis and to rule out 'tumour mimickers'. The most common intramedullary tumour in adults is ependymoma. Usually they present with an enhancing component, some haemorrhage and cysts, and for the surgeon it is important to define the cystic components into tumour cyst, peritumoural cyst and secondary syringomyelia. Usually, the whole neuraxis is imaged to detect 'drop' metastases. In children, spinal cord tumours are very rare, and when occurring, astrocytoma is the most common - presenting with less strong enhancement and more vaguely defined than ependymoma. Other primary spinal cord tumours are rare - and 'tumour mimickers' should always be considered. Extramedullary tumours are most often benign: meningioma and Schwannoma. These can usually be distinguished by their growth pattern and signal characteristics, Schwannoma usually following the nerve root into the neuroforamen and expanding it. Other extramedullary lesions include metastasis, haemangioblastoma and cavernoma. It is, however, important to realize that some tumours which usually occur extramedullary, may also occur within the cord, for example, Schwannoma and haemangioblastoma.
Learning Objectives:
1. To understand how to differentiate intradural-extramedullary mass lesions from intrinsic spinal cord tumours.
2. To become familiar with the most common types of tumours arising within the spinal canal, both in children and in adults.
3. To learn the typical MR imaging features of these lesions.

A-457 11:31

C. Pattern recognition of non-tumoural spinal cord lesions
M.M. Thurnher; *Vienna/AT (majda.thurnher@meduniwien.ac.at)*

The choice of strategy for diagnostic problem solving depends on the perceived difficulty of the case and on knowledge of content. The list of non-tumoural pathology affecting the spinal cord includes demyelinating, vascular, metabolic and degenerative conditions. However, MR imaging findings are overlapping and sometimes confusing. Knowledge of coexisting brain lesions is crucial for narrowing the differential diagnosis. Clinical information (onset of symptoms, history of travels, immune status, etc.) will be helpful to confirm or exclude specific diagnoses. In this lecture, a simplified approach including tips and tricks to non-tumoural spinal cord lesions will be presented.
Learning Objectives:
1. To become familiar with the epidemiology and clinical manifestations of the most common diseases affecting the spinal cord.
2. To recognise the most common intramedullary lesions.
3. To learn how to identify these lesions based on the pattern of involvement.

12:30 - 13:30 **Room C**

E³ - The Beauty of Basic Knowledge: Chest Imaging

E³ 25C

Reporting interstitial lung disease made easy

Moderator:
N. Howarth; Chêne-Bougeries/CH

A-462 12:30

A. Five golden rules
S.R. Desai; *London/UK*

"no abstract submitted"
Learning Objectives:
1. To review diagnostic signs of common interstitial lung disease.
2. To learn how to avoid overdiagnosis.
3. To know the limitations of radiological diagnoses.

A-463 13:00

B. Multidisciplinary approach to diagnosis in interstitial lung disease: the role of HRCT
N. Sverzellati; *Parma/IT*

Surgical lung biopsy is no longer the reference standard for histological diagnosis in interstitial lung disease (ILD). Indeed, its traditional role has been supplanted by multidisciplinary diagnosis, over the last 15 years. It was shown that multidisciplinary discussion between clinicians, radiologists, and pathologists may often change initial individual subspeciality diagnosis. Interpretation of high-resolution computed tomography (HRCT) plays pivotal role in the multidisciplinary diagnosis. A number of scenarios can be outlined in the ILD, in which, clinical, HRCT, and histologic information can be combined in a complementary fashion: 1. HRCT appearance is pathognomonic in the correct clinical context. 2. The combination of HRCT and clinical features, including bronchoalveolar lavage, is sufficient for diagnosing ILD. 3. Clinical features and HRCT appearance can be combined to any biopsy to secure the diagnosis.
Learning Objectives:
1. To understand the role of radiologists in diagnosing interstitial lung disease.
2. To know the limitations of radiological diagnoses.
3. To understand what to say when the diagnosis is not obvious.

12:30 - 13:30 **Room D**

E³ - The Beauty of Basic Knowledge: A Survival Guide to Musculoskeletal Imaging

E³ 24C

Bone tumours

Moderator:
V.N. Cassar-Pullicino; Oswestry/UK

A-464 12:30

Bone tumours
K. Wörtler; *Munich/DE (klaus.woertler@tum.de)*

The diagnosis of a bone tumour is based on clinical findings, the age of the patient, the location of the lesion, its radiologic appearance, and, if imaging does not allow for a specific diagnosis, its histopathologic features. Radiography remains the initial imaging modality for evaluation of the localisation of the lesion with respect to the longitudinal and axial planes of the involved bone, for the depiction of matrix mineralisations, and for estimation of biologic activity by analysing the patterns of bone destruction and periosteal response. CT is typically used to obtain “radiographic” information in regions of complex skeletal anatomy such as the skull, spine, pelvis and shoulder girdle. MR imaging is best suited to determine the local extent of a bone tumour (local staging), but can also be helpful to narrow the differential diagnosis in specific lesions such as cysts and cartilage-forming tumours. With a clear emphasis on conventional radiography, this course will review the basic imaging features of benign and malignant bone tumours. Important radiographic findings, such as bone destruction patterns, types of periosteal reactions and matrix mineralisation, will be explained in correlation with histopathology as well as advanced imaging techniques.

Learning Objectives:
1. To become familiar with the imaging features of benign and malignant bone tumours.
2. To appreciate their imaging characteristic hallmarks on plain film radiography.
3. To learn how best to use imaging modalities in differential diagnosis.

13:00 - 13:30 **Room A**

Headline Session

HL 2
Josef Lissner Honorary Lecture

Presiding:
P.M. Parizel; Antwerp/BE

A-465 13:00

The future of CT: from hardware to software
M. Prokop; *Nijmegen/NL (mathias.prokop@radboudumc.nl)*

The introduction of computed tomography in the 1970s has changed the field of radiology for good: we radiologists became cross-sectional imagers and moved to the center of the diagnostic process for millions of patients worldwide. CT became one of the exponential technologies in medicine: from the 1980s to the 2000s, speed and longitudinal spatial resolution doubled every two years. Since roughly 2010, this development has slowed down considerably, and the focus shifted from slice wars towards radiation dose reduction and dual energy imaging. While CT is nowadays a mature technology, further improvements in spatial resolution, photon counting detectors and overall optimization of the imaging chain will push its performance forward. Phase contrast imaging, x-ray lasers and inverse geometry scanners are far on the horizon. In the coming decades, however, technological progress in CT will shift from hardware solutions to software and novel applications. Already now, iterative reconstruction has reduced dose requirements more profoundly than most hardware solutions. Novel software techniques for motion correction offer temporal resolutions that outperform the most advanced hardware technology. Subtraction imaging becomes a competitor for contrast-enhanced dual energy CT. The main break-through for our patients, however, will come from a shift from morphological analysis to functional analysis for risk prediction and selection of appropriate treatments. Software solutions that keep radiation dose at bay, use radiomics and deep learning will transform the way we do radiology in the future. The same economic pressure that makes us report ever faster and cheaper will push automated image analysis forward for most of our routine work. By embracing the novel functional and predictive diagnostic opportunities of CT and MR, we will be able to remain at the center of the diagnostic process.

14:00 - 15:30 **Room K**

EFRS meets Belgium

EM 4
EFRS meets Belgium

Presiding:
S. Bogaert; Ghent/BE
H.H. Hjemly; Oslo/NO
A. Tempels; Lodelinsart/BE

Moderators:
G. Alleman; Beernem/BE
J.-L. Greffe; Lodelinsart/BE

A-466/A-467/A-468 14:00

Introduction
H.H. Hjemly; *Oslo/NO (Hakon@radiograf.no)*
S. Bogaert; *Ghent/BE*
A. Tempels; *Lodelinsart/BE (atempels@hotmail.be)*

The European Federation of Radiographer Societies has since 2013 had the pleasure and honour of being invited by the European Society of Radiology to host this dedicated 'EFRS meets' session at ECR. During the EFRS meets sessions, radiographers have the opportunity to get information about the role and education of radiographers in the different European countries. In line with the tradition, we choose as our guests the home country of the ECR Congress President. Previous EFRS meets session was in 2013 dedicated Spain, 2014 it was Russia, 2015 we met Germany and last year we met Sweden, and for 2017 EFRS welcomes you all to EFRS meets Belgium. The EFRS meets session will give a picture of the history and challenges of the radiographers profession and education in Belgium and the aims to achieve in the near future. Important items as patient safety, quality improvement and radiation protection will be presented. There will also be focus on Belgium itself, cultural highlights and how Belgium sees the world.
Session Objective:
1. To give an overview of Belgian radiographers and the radiographers' profession in Belgium.

A-469 14:05

A picture of the radiographers' profession and education
P. Van Laer; *Lovendegem/BE (Philippe.vanlaer@odisee.be)*

The Belgian radiographers educational system as well as the radiographers profession are relatively young in comparison with the rest of Europe. Belgium, with its multilingual organisation, is very complex. To get an overview on both themes, education and profession, it is necessary to look at Belgium as a country, to look at the different parliaments/legislation throughout Belgium and to look at how the profession has developed over the last 20 years. Furthermore, we have to look at the changes that have been realised in legislation during the last four years and at the opportunities that are in front of us.
Learning Objectives:
1. To learn about the education system for radiographers in Belgium.
2. To understand the history of the profession and the complexity of the legislation system in Belgium.
3. To become familiar with what has changed in Belgium in the last five years and what aims are to be achieved in the near future.

A-470 14:23

Belgium: the beautiful 'city'
K. Van Belle; *Sint-Andries/BE (kurt.vanbelle@odisee.be)*

What to say about Belgium? Is it as abstract as we think? Not that long ago Belgium was formed, so you would think not a great story. But before that, the Belgians had a great and rich history in Europe as it was the centre for trading luxury goods and great architecture. Today, Belgium is still known as a country with high standards and has many desirable goods such as chocolate and diamonds. On a cultural level, Belgium has many great artists from our medieval Van Eyck, modern Magritte and even Tintin from Hergé could conquer the world. Belgium is seen by the world as very Burgundian. Which is true: the highest density in high-end culinary and gastronomical cuisine can be found in our little country. Conclusion: Belgium stands for a cultural, gastronomical, rich history and a place to discover with many fantastic treats.
Learning Objectives:
1. To arouse curiosity about Belgian cultural highlights.
2. To explain how Belgium sees Belgium.
3. To discuss how the world sees Belgium.
4. To understand how Belgium sees the world.

A-471 14:41

Patient safety and quality improvement in Belgian radiology departments
S. Germonpré; *Brussels/BE (sofie.germonpre@odisee.be)*

In this study, we focus on the use of fluoroscopy-guided positioning (FGP) techniques in radiography. In Belgium, FGP is common practice. We investigate the importance of knowledge, skills and attitudes of imaging staff and organizational factors with respect to applying non-FGP. In addition, we study the usefulness of the UTAUT-model to investigate the acceptance of non-FGP by Belgian radiographers. A mixed method approach was used. To develop an in-depth understanding of imaging practices, radiographers and radiologists were interviewed (n=40), complemented with non-participative observations (200 hours) and image and document analyses. To study the usefulness of the UTAUT-model, we applied a cross-sectional survey research at 17 Belgian radiology departments. Clinical leadership of radiologist and chief radiographers as well as suitable x-ray devices and positioning aids were identified as important determinants. Furthermore, a lack of skills and knowledge of (advanced) positioning techniques and negative attitudes towards non-FGP was present. More precisely, staff expressed concerns with respect to the impact on the workload and workflow. Adequate supervision, regularly feedback and coaching were identified as important enabling factors for increasing the quality of the applied imaging techniques. The UTAUT model proved to be an adequate model for predicting the acceptance to use non-FGP. The intention to use non-FGP depends on the usefulness, the ease of use of and the positive attitudes towards non-FGP. A holistic approach considering knowledge, attitudes and contextual-organizational factors is needed to improve imaging practices. Clinical leadership of physicians, supervisor and peers are important enablers.

Learning Objectives:
1. To promote the implementation of best professional practices in patient positioning; knowledge, attitudes, organisational factors.
2. To highlight the usefulness of the UTAUT model to study professional behaviour outside the context of new technology.

A-472 14:59

Radiation protection in Belgium
O. Bran; *Louette-Saint-Pierre/BE*

"no abstract submitted"
Learning Objectives:
1. To learn about dose limits and radiation protection regulations in Belgium.
2. To explain the daily practice of radiographers in Belgium under the present laws.
3. To promote implementation of radiation protection best practice for radiographers.

15:17
Panel discussion

14:00 - 15:30 **Room M 1**

EuroSafe Imaging Session

EU 4

European CT dose repository

Moderators:
J.A. Brink; Boston, MA/US
J. Damilakis; Iraklion/GR

A-473 14:00

The technical implementation of dose tracking tools
A. Torresin; *Milan/IT (alberto.torresin@unimi.it)*

In the medical area, technological and scientific developments have led to a remarkable increase in radiation exposure. The need to implement radiation-dose-index monitoring (RDIM) systems for the most important ionizing radiation procedures in connection with stochastic and deterministic risks has become important. RDIM systems are software which passively or actively collect all the radiation-dose-index (RDI) from ionizing radiation modalities. RDIM systems store RDI data in a database along with patient demographic and exam information allowing the final user to visualize the RDI according to study type and patient. These data can be used both for quality assurance procedures in the diagnostic department and as a benchmark in the regional and national registries. To successfully implement an RDIM system, careful commissioning, testing and data analysis are needed in advance in full collaboration with the manufacturer. An interdisciplinary team of lead radiologist, lead medical-physics-expert, lead technologist, PACS IT leader and clinical engineers need to work together to choose, implement and ensure the proper use of the RDIM software based on the specific needs of the institution. RDIM systems are not intended solely as databases for patient exposure: collected RDIs do not represent the absorbed dose in an individual patient because they are related to the x-ray beam output and absorption at the image receptor.
Learning Objectives:
1. To discuss the strategy of implementation in the PACS.
2. To understand the open issues of the integration (standards, reporting, etc.).

A-474 14:15

How do dose tracking tools change the practice of radiographers?
S.J. Foley; *Dublin/IE (shane.foley@ucd.ie)*

This presentation aims to discuss the features of dose tracking systems that can be practically useful to radiographers in their role within CT. In particular, the radiographers' responsibility regarding dose optimisation will be examined, considering how dose tracking tools can influence behaviour and encourage protocol optimisation and support quality improvement initiatives.
Learning Objective:
1. To understand the impact of dose tracking tools on the radiographer's responsibility and behaviour towards CT protocols.

A-475 14:30

How do dose tracking tools change the practice of radiologists?
F. Zanca; *Leuven/BE (federica.zanca@ge.com)*

Dose tracking systems and their utilisation are an emerging topic of interest, with focus being on whether to track or not dose, what to track and how. However, another important aspect is how a dose tracking system can impact the practice of radiologists. This talk will identify and report examples of outcomes related to the implementation of a dose tracking system in a radiology department. We will talk about the role of such a tool for procedures standardization and optimisation, legislation compliance, individual patient risk assessment and research purposes. The primary rationale is indeed to avoid exposing patients to unnecessary radiation by engaging radiologists in a new practice of exams justification, protocols standardisation and optimisation. Such a system is also helpful for being compliant with the coming EU directive 2013/59/Euratom. A dose tracking system can also help in: identifying unusual high radiation dose and implementing patient follow-up process (patient safety); identifying studies with parameters outside pre-defined reference levels and optimize protocols (optimisation); identifying patient populations that receive a relatively large number of imaging studies and propose patient-specific protocol development; standardizing the workflow and operator-dependent protocol parameters; optimising dose level versus image quality. Similarly, it can act as a conduit of data to national benchmarking databases or as a tool to support the tracking of radiological procedures of individual patients and radiation dose. This presentation will end with some examples of dose tracking systems implementations in clinical practice.
Learning Objective:
1. To understand the impact of dose tracking tools on the radiologist's daily practice and behaviour towards CT protocols.
Author Disclosure:
F. Zanca: Employee; GE Healthcare.

A-476 14:45

European CT Dose repository working group: summary of activities
E. Neri; *Pisa/IT*

The CT Dose repository is the 3rd EuroSafe imaging subgroup, whose members are D. Caramella (IT), G. Paulo (PT), J. Damilakis (Gr) and A. Torresin (IT), with S. Ebdon-Jackson, a co-opted member from HERCA (European Radiological protection Competent Authorities). The subgroup was created and aimed at exploring the clinical impact of tools for automatic dose monitoring and provide recommendations, best practice in CT, to reassure radiologists about the reliability of statistics obtained from such systems. To reach that goal, the subgroup drafted a questionnaire that will be distributed to ESR members. The results of the questionnaire could be helpful to prepare recommendations on how to improve the CT dosimetric behaviour in radiological departments (with the help of such tools). The dose monitoring tools allows a precise internal audit of the dose behaviour in the radiological department, tracking the general dosimetric trend that mainly depends on the adopted imaging protocols. Such imaging protocols are frequently designed by an anatomical orientation with few concern about the specific clinical context in which the exam is performed. In parallel the attention of dose reference levels (DRL) is oriented to the anatomical segments, and not the clinical context. One example: lung CT for screening has the same scan length of a lung CT for nodule characterisation, as well as for pulmonary embolism, but the 3 exams are strongly different by indication and as a consequence by imaging protocols that influence the dose levels. Therefore it is clear that the actual dose reference levels, based on the anatomical focus, do not reflect the standard of dose anymore. Even more, in a same clinical context, there is a potential variability of patients anatomy, physiology, and target disease, which influences the CT imaging protocols. Dose monitoring systems could be therefore a helpful tool for building new dose reference levels based on the clinical indications and on the patient's specific factors, driving the actual DRL based on anatomy toward clinical indication reference levels.
Learning Objective:
1. To become familiar with the summary of activities of the working group.

A-477 15:00

The ACR Dose Index Registry
R.L. Morin; *Jacksonville, FL/US (morin.richard@mayo.edu)*

The ACR Dose Index Registry (DIR) is designed to assist practices, and institutions in comparison of dose indices with national values. The DIR was conceived in 2004 to address the uncertainty of dose in various imaging examinations. The key features of the DIR is the automatic extraction of dose indices, patient features (e.g. gender, age, exam type, etc.) and technical parameters. Facilities can then compare their values with national or local values to make decisions on altering their protocols to optimise the use of radiation for each examination. The DIR was launched in May 2011 and now has over 1600 institutions participating, both domestic and international. Over 33 million exams are currently in the DIR. The biggest challenge that was discovered was the large variation in examination names. This was narrowed by providing registry users with a mapping tool to map each examination name to the standardised RSNA RadLex® terminology. The other challenge was the automatic modulation of the x-ray beam as the tube circulates about the patient; hence, indices are larger for big patients than small patients. This is being addressed by the automatic measurement of the patient thickness and calculation of the size-specific dose estimate (developed by the AAPM). These solutions have improved the accuracy and utility of the DIR. In the future, the

DIR will address CR/DR, then fluoroscopy and it is hoped that the widespread use will contribute significantly to the management of radiation dose in medical imaging.
Learning Objective:
1. To learn the impact of the ACR Dose Index Registry in the clinical practice.
Author Disclosure:
R.L. Morin: Board Member; RSNA sub Board. Employee; Mayo Clinic Jacksonville. Speaker; Over 100 meetings and conferences.

15:15
Questions and answers

14:00 - 15:30 **Room M 2**

Professional Issues and Economics in Radiology (PIER)

PIER 2

Perspectives on radiology equipment management

Moderators:
B. Brkljačić; Zagreb/HR
P. Leander; Malmö/SE

A-478 14:00

A. Renewal of equipment and procurement: central vs local procedures
B. Brkljačić; *Zagreb/HR (boris@brkljacic.com)*

Advances in radiology equipment provide accurate and fast diagnosis, and offer new options for treatment guidance, thus improving the health outcomes and quality of life for the patients. The fast development of technology also resulted in accelerated technical and functional obsolescence of imaging equipment, consequently creating a need for renewal. Radiological equipment has a definite life cycle span and older equipment has a high risk of failures and breakdowns. The unavoidable decrease or loss of image quality renders equipment useless after the certain period. This may cause delays in diagnosis and treatment of the patient and safety problems both for the patient and the medical staff. European society of radiology is promoting the use of up-to-date equipment, especially in the context of the EuroSafe imaging campaign, as the use of up-to-date equipment will improve quality and safety in medical imaging. Reduction in radiation dose when utilising state-of-art equipment is of utmost clinical importance. Every healthcare institution or authority should have a plan for medical imaging equipment upgrade or renewal, since the equipment older than ten years is no longer state-of-the art equipment and the replacement is essential. Operating costs of older equipment will be high when compared with new one and sometimes maintenance will be impossible if no spare parts are available. Public procurement is another important issue in the renewal of equipment. Situation in Europe is very heterogeneous and often long and complicated procurement procedures hinder timely equipment renewal. The issues of different procurement strategies will be discussed.
Learning Objectives:
1. To discuss the need for the regular renewal of radiology equipment.
2. To present controversies in public procurement of radiology equipment.
3. To discuss advantages and disadvantages of different types of procurement.
Author Disclosure:
B. Brkljačić: Speaker; Guerbet, Bayer.

A-479 14:18

B. Utilisation of equipment: what is appropriate? The public healthcare system's perspective
P. Leander; *Malmö/SE (peter.leander@med.lu.se)*

Medical imaging equipment utilisation needs to be optimised for managing capital equipment budgets. Health economics talk about scarcity and that economics are needed for the only reason of scarcity of resources. Cost analysis for imaging equipment is a straightforward analytic task. Fixed costs are mainly the initial investment and service contracts. Running costs are mainly personnel and contrast media (CM). Personnel costs are not fully proportional to worked hours, as early and late hours are more costly. For MRI and CT, CM costs are relatively small but for PET/CT this a substantial part of the exam cost. On the other hand, if cyclotron is in-house this may come into another situation. All together the different costs can be put down in spread sheets showing cost per exam in relation to operating hours. Other factors to consider are the willingness of personnel to work and the possibility to have the imaging facility open at non-office hours. Traditionally personnel in imaging departments work daytime beside their duty on call. There may be an educational challenge to explain why the funder/hospital have such an urge to open up scanners early in the morning and run them into the evening. In addition, aside ER imaging the departments are often not built to be open at non-office hours. All stated above need to be worked through to come to best practice and a reasonable compromise between the radiological department and the public funder.
Learning Objectives:
1. To describe how a cost analysis of system utilisation can be performed.
2. To discuss how other factors than economical influence the utilisation.
3. To come to a reasonable common goal of utilisation between the radiological department and the public funder.

A-480 14:36

C. Utilisation of equipment: what is appropriate? The private healthcare system's perspective
A. Palkó; *Szeged/HU (palkoand@gmail.com)*

Private companies tend to be more sensitive to cost and efficacy than community/government-financed service providers. It explains why several of the key focus points from management point of view, in their case, are cost management, optimisation in scheduling and patient involvement, and best practice maintenance concepts. The purpose of this lecture is to explain the paradigm shift in cost management from traditional cost management to total cost of ownership and optimization of company-owned inventory; from breakdown or corrective to preventive maintenance; from traditional to lean-based scheduling, workflow-optimisation and patient satisfaction-based management.
Learning Objectives:
1. To understand the basics of cost management.
2. To learn about optimisation in scheduling and patient involvement.
3. To present best-practice maintenance concepts.
Author Disclosure:
A. Palkó: Advisory Board; Affidea.

A-481 14:54

D. Radiology: a cost factor? The hospital manager's perspective
P. Garel; *Brussels/BE (sg@hope.be)*

In-house and outsourced radiology are often opposed on different grounds, for example, on: quality and patient safety, availability of human resources, financial incentives, organisational reasons, etc. Those different elements should be perceived through the huge diversity of the healthcare systems in place in Europe. Success or failures of both options will depend much more on context factors than on theoretical approaches. Not only this cannot be anymore limited to the local or even national context as cross-border care is developing but this has to be perceived in the context of the development of integrated concept diversely defined and put in place. Integrated care is bringing new issues of collaboration, coordination between the different levels of care as well as new ways of financing.
Learning Objectives:
1. To discuss reasons for in-house vs outsourced radiology.
2. To explain cost-models (e.g. internal budgeting).
3. To discuss new concepts for integrated care and the consequences for radiology.

15:12
Panel discussion

14:00 - 15:30 **Room M 4**

Joint Session of the ESR and ESMRMB

MR imaging biomarkers: what we have and what we need

Moderators:
D. Sappey-Marinier; Lyon/FR
M. Smits; Rotterdam/NL

A-482 14:00

Preclinical MRI: multimodal markers for neuroscience drug discovery?
M. von Kienlin; *Basle/CH (markus.von_kienlin@roche.com)*

One of the biggest bottlenecks in drug development for brain disorders is the lack of reliable and predictive biomarkers during early clinical testing; this makes very difficult the development of novel therapies which respond to the huge unmet medical need in many neurological or psychiatric diseases. Pharmacological magnetic resonance imaging and spectroscopy (phMRI/MRS) have the potential to serve as early indicators for target engagement or proof of mechanism studies in clinical phase I/II trials. This contribution will address the topic from a preclinical perspective, i.e. how MR approaches in rodents can elucidate pharmacologically induced changes in structure or function, and how confidence can be increased that preclinical results are relevant to the patient situation. Preclinical imaging in drug discovery serves three main purposes. First, it is used to qualify animal models, ensuring that the molecular

mechanisms in the model appropriately reflect human disease processes; whenever possible, this “back-translation” is based on genetic and proteomic evidence, and is also linked to further phenotypic characteristics of the model. Second, phMRI supports milestone transition decisions for advanced compounds in the discovery portfolio, by characterising the mechanistic and functional properties of potential new medical entities. Last but not least, preclinical results identify imaging biomarkers to be deployed in early clinical development. These three domains will be illustrated with examples from neurodegenerative and neurodevelopmental disorders.

Learning Objectives:

1. To become familiar with potential MR biomarkers for diagnosis and therapeutic monitoring of specific brain diseases.
2. To learn about advanced MR techniques and methods providing quantitative biomarkers.
3. To learn how MR imaging biomarkers can help to evaluate specific effects of novel pharmaceuticals upon brain function in preclinical animal models.
4. To understand how brain imaging markers could be included in clinical trials.

Author Disclosure:

M. von Kienlin: Employee; F. Hoffmann-La Roche AG. Shareholder; F. Hoffmann-La Roche AG.

A-483 14:30

Clinical MRI: whole-body markers for cancer detection/response

F. De Keyzer; *Leuven/BE (frederik.dekeyzer@uzleuven.be)*

While T1- and T2-weighted magnetic resonance imaging has been feasible in the body for several decades, anatomical information does not always reflect underlying biological information, which limits its diagnostic and prognostic value. In the last decade, hardware and software improvements have led to applicability of functional MR techniques that fill in that gap. At the same time, there has been a huge expansion of possible treatments and combinations, whereby optimal treatment success very much depends on patient-specific information, of which imaging is an important part. In this session, we will focus mainly on applications of diffusion-weighted (DW-) and dynamic contrast-enhanced (DCE-) MR imaging and the biomarker information these can provide, both as a diagnostic tool, and as a tool for predicting and evaluating response to therapy. While the strengths of these techniques make them worthwhile in a whole range of oncologic applications, they also have drawbacks regarding standardization of acquisition, handling of motion effects, use of post-processing strategies and image interpretation. These drawbacks need to be discussed and overcome to set up multicentre studies aiming to bring these imaging biomarkers into widespread clinical domain.

Learning Objectives:

1. To become familiar with the biomarker content of WB-MRI protocols.
2. To review the literature showing that WB-MRI biomarkers can aid in the detection and characterisation of cancers and by extension to response assessment to therapies.
3. To highlight that WB-MRI BM qualification requires frameworks for development and that we are now at efficacy testing stage.

A-484 15:00

Molecular MRI: where are the limits for MRI biomarkers?

L. Schröder; *Berlin/DE (lschroeder@fmp-berlin.de)*

MRI suffers from intrinsic low sensitivity and relies on abundant tissue water as the signal source in most conventional imaging applications. However, there are two emerging concepts that can improve this situation and thus contribute to the field of molecular and metabolic imaging for advancing the understanding of many diseases on a molecular level. The first one is CEST (chemical exchange saturation transfer) that amplifies the signal from dilute metabolites or contrast agents through labile protons or exchangeable water molecules by encoding it as signal loss in the abundant tissue water signal. CEST works both with certain endogenous substances and synthetic contrast agents that can also sense the presence of distinct analytes. The second technique is based on increasing the detectable magnetization through special preparation of the spin system prior to the encoding and detection. The achieved condition outside the thermal equilibrium is called hyperpolarization. Though being of transient nature, it is a powerful approach that has enabled various applications for metabolic, molecular and cellular imaging. Both approaches can be combined in the so-called hyper-CEST approach that is currently under investigation for ultra-sensitive MRI that visualizes the distribution of targeted sensors in the picomolar concentration range. Altogether, clinical and preclinical imaging applications will benefit significantly from specific contrast agents or metabolites with enhanced sensitivity since a biochemical or cell biological response to a certain treatment usually occurs much earlier than mesoscopic changes in morphology.

Learning Objectives:

1. To become familiar with the wide range of new potential markers provided by new contrast mechanisms for MR imaging, in particular chemical exchange saturation transfer (CEST) and hyperpolarisation.
2. To understand the role, benefits and limitations of molecular imaging.
3. To learn about the potential future use of targeted contrast agents that combine the benefits from both CEST and the sensitivity gain of hyperpolarised agents.

Author Disclosure:

L. Schröder: Grant Recipient; DFG Koselleck Program; HFSP Program Grant; MJ Fox Foundation for Parkinson's Research.

16:00 - 17:30 **Room A**

E³ - ECR Academies: Interactive Teaching Sessions for Young (and not so Young) Radiologists

E³ 1221

Basic breast imaging

A-485 16:00

A. Calcifications in mammography

C.S. Balleyguier , S. Moalla, J. Arfi-Rouche, A.-M. Tardivel, M. Attard, M.-C. Mathieu; *Villejuif/FR (Corinne.BALLEYGUIER@gustaveroussy.fr)*

Breast calcifications are common findings detectable on mammography. Breast calcifications are most likely benign; nevertheless irregular microcalcifications cluster may be the only imaging findings suggesting a ductal carcinoma in situ (DCIS). Analysis of microcalcifications on mammography remains on magnification views; size, density, number, pleomorphism and distribution within the breast have to be carefully analysed to differentiate benign and suspicious microcalcifications clusters. Benign calcifications are categorised as BI-RADS 2 and are more likely round, regular, with a calcified rim, tea-cup or egg-shell shape. Suspicious microcalcifications may be amorphous, irregular, with a linear or segmental distribution. When a microcalcifications cluster is categorised as BI-RADS 4, a stereotactic biopsy should be performed. Ultrasound may be performed first to detect non-calcified mass. Vacuum assisted stereotactic biopsy with at least 6 11 Gauge samples must be performed. New technologies such as BLES biopsy, associating biopsy and radiofrequency can be performed to entirely remove the cluster. In this topic, biopsy techniques and diagnostic strategies to diagnose microcalcifications will be presented on a basis of clinical cases.

Learning Objectives:

1. To become familiar with different types of calcifications.
2. To learn the differential diagnosis of different calcifications.
3. To learn the different tools to biopsy calcification clusters.

A-486 16:45

B. Asymmetry and architectural distortion

L.J. Pina Insausti; *Pamplona/ES (ljpina@unav.es)*

Asymmetries are unilateral deposits of fibroglandular tissue not conforming to the definition of a mass. Four types of asymmetries can be considered: asymmetry as an area of fibroglandular tissue visible on only one mammographic projection, mostly caused by superimposition of normal breast tissue. Focal asymmetry visible on two projections, hence a real finding rather than superposition. Global asymmetry consisting of an asymmetry over at least one quarter of the breast and is usually a normal variant. Developing asymmetry new, larger and more conspicuous than on a previous examination. After the detection of one of the previous asymmetries, it is mandatory to compare with previous mammograms, if available. Palpation and additional techniques can be used to study the lesion, such as spot compressions, tomosynthesis, US and in some cases MRI. A biopsy is needed if malignancy cannot be excluded. The term architectural distortion is used when the normal architecture is distorted with no definite mass visible. This includes thin straight lines or spiculations radiating from a point and focal retraction, distortion or straightening at the edges of the parenchyma. Architectural distortion can also be seen as an associated feature. Tomosynthesis is a very sensitive technique to detect architectural distortions. Surgery, radial scar and carcinoma are the most common causes of distortions. A biopsy is mandatory if a surgical scar is excluded. The management of radial scars needs further workup after a core needle biopsy: both surgery or vacuum-assisted biopsy can be used.

Learning Objectives:

1. To understand the concept of asymmetry and architectural distortion.
2. To become familiar with the respective imaging features.
3. To learn about the diagnostic approach using all breast imaging modalities.

Author Disclosure:

L.J. Pina Insausti: Speaker; Speaker invited by SIEMENS for other lectures.

16:00 - 17:30 **Room B**

New Horizons Session

NH 12
The increasing clinical impact of MR/PET

A-487 16:00
Chairman's introduction
L. Umutlu; *Essen/DE (Lale.Umutlu@uk-essen.de)*

Within the past 5 years, simultaneous PET/MRI has been successful introduced into clinical oncologic imaging. It has demonstrated its strength and superiority, particularly in application fields that require high soft tissue contrast imaging such as head and neck cancers or cardiac imaging, questioning the need and or benefit for PET/CT imaging in particular clinical investigations. Apart from its high soft tissue contrast, the interchange from CT to MRI for morphological correlation facilitates another favourable topic, by means of the reduction of the applied ionizing radiation. The applied amount of ionizing radiation can be reduced to 1/3 of the amount in full-dose diagnostic PET/CTs. This is of particular interest for paediatric imaging as well as in the setting for therapy monitoring, when repetitive scans are required.

Session Objectives:
1. To understand the increasing clinical impact of MR/PET in diverse application fields.
2. To understand the benefits of MR/PET over PET/CT in paediatric and head and neck imaging.
3. To become familiar with indications for MR/PET in cardiac and musculoskeletal imaging.

A-488 16:05
MR/PET in paediatric oncology?
P.D. Humphries; *London/UK (humphriespaul@gmail.com)*

Advances in paediatric oncology over the past decades have led to a much improved success rate in the treatment of children with cancer, with some tumours having a 5-year survival over 90%. This success increases the relevance of diagnostic radiation exposure, given the greater radiosensitivity of children and, therefore, increased chance of inducing a second malignancy following treatment. Imaging modalities that can reduce ionising exposure are, therefore, very attractive for paediatric imaging. MRI has been a preferred method of imaging childhood tumours for some time, owing to excellent soft tissue depiction, lack of ionising radiation and the ability to derive “functional” data from DWI and spectroscopy, for example. PET imaging is well established for some paediatric tumours, notably FDG-PET in lymphoma, but is also gaining traction in other cancers, such as sarcomas and choline-PET for CNS neoplasms. Given the above considerations a hybrid platform of PET-MRI is particularly relevant for paediatric oncology, with the potential for future multi-parametric tumour modelling allowing evaluation at both at staging and therapy response assessment.

Learning Objectives:
1. To understand the gain of using MRI instead of CT together with PET.
2. To become familiar with current application fields in paediatric imaging.
3. To give an insight into future application fields.

Author Disclosure:
P.D. Humphries: Grant Recipient; Great Ormond Street Hospital Charity Grant.

A-489 16:25
MR/PET in cardiac imaging?
M. Dewey; *Berlin/DE (marc.dewey@charite.de)*

MR/PET is the new kid on the block, enabling hybrid imaging of anatomy and function. I will summarise the new horizons of MR/PET for providing clinical impact in patients with known or suspected cardiac diseases. For this purpose, we will discuss myocardial area-at-risk definition, differentiation of cardiac tumours (from thrombus) and assessment of myocarditis by MR/PET. Finally, technical challenges and potential solutions will be discussed together with patients’ experience of the examination.

Learning Objectives:
1. To understand the gain of using hybrid MR/PET in cardiac imaging.
2. To become familiar with current application fields in cardiac imaging.
3. To give an insight into the clinical impact and potential future applications of MR/PET in cardiac imaging.

Author Disclosure:
M. Dewey: Author; “Coronary CT Angiography”, Springer, 2009, “Cardiac CT”, Springer 2011 and 2014. Consultant; Guerbet. Patent Holder; Joint patent with Florian Michallek on dynamic perfusion analysis using fractal analysis. Research/Grant Support; Heisenberg Program of the German Research Foundation (DFG) for a Professorship (DE 1361/14-1), FP7 Program of the European Commission for the randomized multicenter DISCHARGE trial (603266-2, HEALTH-2012.2.4.-2), European Regional Development Fund (20072013 2/05, 20072013 2/48), German Heart Foundation/German Foundation of Heart Research (F/23/08, F/27/10), Joint program of the DFG and the German Federal Ministry of Education and Research (BMBF) for meta-analyses (01KG1013, 01KG1110, 01KG1210), GE Healthcare, Bracco, Guerbet, Toshiba Medical System. Speaker; Toshiba Medical Systems, Guerbet, Cardiac MR Academy Berlin, Bayer-Schering. Other; Cardiac CT Courses in Berlin: www.ct-kurs.de, Institutional master research agreements with Siemens Medical Solutions, Philips Medical Systems, Toshiba Medical Systems. Terms of arrangements are managed by the legal Dept. of Charité Berlin.

A-490 16:45
MR/PET in head and neck imaging?
M. Becker; *Geneva/CH*

PET/CT and MRI with diffusion-weighted imaging (DWI) are complementary techniques for the assessment and staging of head and neck tumours. This lecture focuses on clinical applications of MR/PET in head and neck tumours with special emphasis on multiparametric imaging using high-resolution morphological MRI, DWI and perfusion imaging. First, advantages of using MRI instead of CT in head and neck oncology are summarized and current evidence regarding clinical feasibility, image quality, optimized imaging protocols and quantification with MRI-based attenuation algorithms and with DWI in the head and neck is reviewed. Then the current state of knowledge regarding the diagnostic performance of MR/PET in head and neck cancer is discussed and typical tumour manifestations are presented. The appearance of primary and recurrent squamous cell cancers, lymph node metastases and distant metastases on MR/PET, as well as the value of multiparametric imaging are summarized. The variable appearance of functional phenomena mimicking disease, as well as potential pitfalls of image interpretation due to morphological or functional post-treatment changes are addressed. Illustrative cases of concordant and discrepant multiparametric evaluations are discussed, as well as the dilemma how to deal with discrepant multiparametric data in clinical routine.

Learning Objectives:
1. To understand the gain of using MRI instead of CT together with PET.
2. To become familiar with current application fields in head and neck imaging.
3. To give an insight into the clinical impact of MR/PET in head and neck imaging.

Author Disclosure:
M. Becker: Research/Grant Support; Swiss National Science Foundation.

A-491 17:00
MR/PET in musculoskeletal imaging?
G. Andreisek; *Münsterlingen/CH (gustav@andreisek.de)*

Hybrid MR/pet is an increasing and fast-growing topic in musculoskeletal research. This talk will highlight current applications in the field of musculoskeletal imaging and gives an insight into potential future applications of MR/PET in musculoskeletal imaging. Therefore, a short introduction is provided about the necessity for MR/PET in certain musculoskeletal pathologies. After that, the current gold standard imaging modalities and their limitations are reviewed, and then potential advantages of MR/PET are discussed. Examples for clinical applications are provided as well as a review of the corresponding literature. The audience should get an impression what is clinically available, what is “evidence-based” and what applications are currently purely reserved for research.

Learning Objectives:
1. To understand the gain of using hybrid MR/PET in MSK imaging.
2. To become familiar with current application fields in MSK imaging.
3. To give an insight into the clinical impact and potential future applications of MR/PET in musculoskeletal imaging.

Author Disclosure:
G. Andreisek: Advisory Board; Otsuka. Author; Springer Book. Patent Holder; US patent (USPTO Number 12/947,256).

17:15
Panel discussion: Are we ready to fully integrate MR/PET into clinical diagnostic work-up?

16:00 - 17:30 **Room C**

Chest

RC 1204

Thoracic manifestations of systemic disease

Moderator:
A. Chodorowska; Wroclaw/PL

A-492 16:00

A. Systemic sclerosis
M. Silva; *Parma/IT (mariosilvamed@gmail.com)*

Systemic sclerosis (SSc) is variably associated with pulmonary involvement, which is a paramount prognostic factor. Interstitial fibrosis and small vessel abnormalities are the two elementary lung wounds in SSc, they can occur independently of each other. Chest radiograph has low sensitivity in the assessment of early interstitial lung disease (ILD) associated with SSc. Whereas, basal symmetric reticulonodular opacities and bronchiectasis, even honeycombing can be seen in advanced SSc-ILD. Oesophageal dilation can be the only apparent finding. High-resolution computed tomography (HRCT) is pivotal in baseline staging and follow-up of lung involvement. HRCT findings of SSc-ILD include confluent ground-glass opacities, traction bronchiectasis/bronchiolectasis, fine reticulation and honeycombing. The HRCT pattern of non-specific interstitial pneumonia (NSIP) is common, actually reflecting 75% frequency of histologic NSIP. The combination of HRCT and pulmonary function tests (PFTs) has been proposed for prognostication of SSc. ILD extent <10% has lower risk compared to >30%, with minor influence from PFTs. On the other hand, PFTs can further stratify prognosis among subjects with ILD extent 10-30%. Quantitative CT methods are being developed to measure ILD extent. SSc patients are at increased risk of lung cancer, its surgical treatment is mostly prevented by extensive ILD. Pulmonary hypertension (PH) can occur independently of ILD, reflected by isolated reduction of DLCO at PFTs. In particular, PH is more common in the limited cutaneous systemic sclerosis, also known under the acronym CREST syndrome. Echocardiography is used for indirect non-invasive assessment of PH, whereas right heart catheterization is more accurate albeit invasive.
Learning Objectives:
1. To learn about the typical radiological appearances.
2. To be aware of the clinical relevance of scoring.
3. To know how vascular complications affect patient prognosis.

A-493 16:30

B. Granulomatosis and polyangiitis
S. Bayraktaroglu; *Izmir/TR (selenb2000@gmail.com)*

Granulomatosis with polyangiitis (GPA) is characterized by chronic granulomatous necrotizing vasculitis that involves mainly small and medium-sized vessels. It is the most common of the ANCA-associated vasculitis. The classic clinical triad includes upper airway diseases (such as sinusitis, nasalmucosal ulcerations, subglottic stenosis), lower respiratory tract involvement and glomerulonephritis. The upper respiratory tract is affected in almost all patients, and the lungs and kidneys are involved in 90% and 80% of patients, respectively. The most common findings with GPA are nodules and masses of varying sizes, seen in up to 70% of the patients. Cavitation within these lesions may be seen due to the necrotic nature of the disease. Diffuse ground-glass opacity and consolidation occur in 25-50% of patients representing DAH secondary to capillaritis. Tracheobronchial involvement is also common typically occurring at the subglottic area in the form of circumferential thickening. Patients are treated with immunosuppressive therapy. Ground-glass attenuation, cavitated nodules and masses appear to represent active inflammatory lesions. In patients treated with immunosuppressive therapy, the ground glass areas, nodules and mass lesions generally decrease or resolve.
Learning Objectives:
1. To learn about the radiological appearances of small-vessels vasculitis.
2. To learn how clinical and radiological features help in differential diagnosis.
3. To appreciate the actual role of imaging in assessing disease activity.

A-494 17:00

C. Histiocytosis and lymphangioleiomyomatosis
A. Oikonomou; *Toronto, ON/CA (anastasia.oikonomou@sunnybrook.ca)*

PLCH is a rare type of histiocytosis occurring in smokers, characterized by infiltration of tissues with dendritic Langerhans cells. PLCH may exclusively involve lungs or rarely be part of multisystem disease. HRCT findings include nodules, combination of nodules and cysts or only cysts with upper lobe distribution and sparing of lung bases. Coexistence of cysts with GGO is common. Cysts are bizarre-shaped, thin or thick-walled and variable in number and size. Nodules with or without cavitation have a centrilobular location. Pneumothorax may be the initial manifestation. Lymphangioleiomyomatosis (LAM) is a rare cystic lung disease caused by infiltration of the lungs with smooth muscle cells. It occurs in patients with tuberous sclerosis (TSC-LAM) and in a “sporadic” form (S-LAM), exclusively seen in women of reproductive age. Parenchymal lesions in LAM mainly include cysts, which are thin-walled, well-defined, rounded, may reach large numbers and have no zonal predominance. Nodules are extremely rare in S-LAM and may be seen in TSC-LAM. They represent multifocal micronodular pneumocyte hyperplasia. Chylothorax and pneumothorax are common. When both cysts and nodules coexist then PLCH has to be differentiated from LIP, amyloidosis or light-chain disease. When only nodules or only cysts are present then differential diagnosis includes nodular diseases (only for PLCH) such as sarcoidosis, silicosis, tuberculosis, amyloidosis and metastases or cystic lung diseases (both for PLCH and LAM) such as LAM and PLCH, respectively, Birt-Hogg-Dube, LIP and amyloidosis. If cysts coexist with GGO then PLCH is differentiated from PJP, DIP and LIP.
Learning Objectives:
1. To learn about the typical radiological features and complications.
2. To discuss the possible overlap with other cystic and non-cystic lung diseases.
3. To appreciate the clinical relevance of differentiating these two entities.

16:00 - 17:30 **Room Z**

Headline Session

European Radiology 25th Anniversary Session

Moderators:
M.F. Reiser; Munich/DE
A.L. Baert; Kessel-Lo/BE
A.K. Dixon; Cambridge/UK

A-500 16:00

Introduction: 25 years of European Radiology
M.F. Reiser; *Munich/DE (Maximilian.Reiser@med.uni-muenchen.de)*

At this ECR, we celebrate the 25th anniversary of European Radiology. For this occasion, 25 articles published during the past 25 years were picked to reflect the immense progress radiology and imaging sciences have made over this period. The selection was based on number of citations and whether the work was influential for the development and changing practise of imaging and image guided interventions. Furthermore, we attempted to achieve a balance and to represent the diversity within the different subspecialties. 10 of these 25 articles are presented in this session. We invite you to join this journey through time with a perspective towards the future.

A-501 16:05

How to present research data consistently in a scientific paper
M. Laniado; *Dresden/DE (Michael.Laniado@uniklinikum-dresden.de)*

Scientific writing is an integral part of academic radiology, and it is professionally rewarding. One of the duties of academic mentors is to motivate and help young radiologists to successfully pass the primary hurdle of knowing how to begin. As with the research project as such, thoughtful planning of the manuscript is an important step. There are many ways to begin but the writer typically drafts the methods section first, followed by the results, the discussion, and the introduction. Information given in both the introduction and the discussion may function as a clip between which data provided in materials and methods and results are embedded. The conclusions should exactly reflect what was reported in the results section. The abstract has to be written as a comprehensive but very short summary of purpose, materials and methods, results, and conclusions. It is of utmost importance that the author edits the manuscript carefully and follows the target journal's instructions to contributors. Once the manuscript has gone through peer review and revisions are requested (provisional acceptance) it is recommended to respond to the comments point by point. This will facilitate reevaluation of the manuscript by the same reviewer(s) and enhances the likelihood that the revised version will be accepted for publication. In conclusion, writing scientific articles is a form of mental exercise that has to be practised to be successful.

A-502 16:13

Cost considerations regarding an integrated CT-PET system

G.K. von Schulthess; *Zurich/CH (gustav.vonschulthess@usz.ch)*

Integrating two modalities into one system, like PET and CT into PET/CT has advantages and drawbacks. The advantages are: the patient gets "two examinations in one", which is time efficient (patient preparation in the scanner is half), a hybrid exam is more agreeable to the patient, and there are synergies in siting and technology. The disadvantages are mainly due to added inflexibility. Separate modalities can be used in parallel for two patients, scheduling is much more flexible and, therefore, amortization of equipment and revenue generation may become easier with separate systems. It turns out that PET/CT seems quite efficient. First, all oncologic PET (the majority) examinations require PET and CT. Second, the time gained in pre-and post-scan patient handling using PET/CT is a critical bonus. CT being so fast makes PET/CT cost-effective. Cost-effectiveness with SPECT/CT (e.g. in cardiac imaging) or in PET/MR are much more difficult to attain. In summary, when purchasing a hybrid system, one has to carefully weigh advantages and disadvantages, so as to stay on the cost-effective side.

Author Disclosure:

G.K. von Schulthess: Advisory Board; INtl. Diagnostic Course Davos (IDKD). Board Member; Intl. Diagnostic Course Davos (IDKD). Consultant; GE Healthcare. Research/Grant Support; Bayer, GE, Guerbet, Lilly,.

A-503 16:21

Role of contrast-enhanced helical CT in the evaluation of acute thoracic aortic injuries after blunt chest trauma

M. Scaglione; *Naples/IT (scaglionefun@gmail.com)*

The purpose of this retrospective study was to determine the value of contrast-enhanced helical CT for detecting/managing acute thoracic aortic injury (ATAI). Between June 1995 and February 2000, 1419 consecutive chest CT examinations were performed in the setting of major blunt trauma. The following CT findings were considered indicative of ATAI: intimal flap; pseudoaneurysm; contour irregularity; lumen abnormality; extravasation of contrast material. On the basis of these direct findings no further diagnostic investigations were performed. Isolated mediastinal haematoma on CT scans was considered an indirect sign of ATAI. In these cases, thoracic aortography was performed even if CT indicated normal aorta. Seventy-seven patients had abnormal CT scans: among the 23 patients with direct CT signs, acute thoracic aortic injuries was confirmed at thoracotomy in 21. Two false-positive cases were observed. The 54 remaining patients had isolated mediastinal haematoma without aortic injuries at CT and corresponding negative angiograms. The 1342 patients with negative CT scans were included in the 8-month follow-up program and did not show any adverse sequela. Contrast-enhanced helical CT has a critical role in the exclusion of thoracic aortic injuries in patient with major blunt chest trauma and prevents unnecessary thoracic aortography. Direct CT signs of ATAI do not require further diagnostic investigations: isolated aortic bands or contour vessel abnormalities should be first considered as possible artefacts or related to non-traumatic aetiologies especially when mediastinal haematoma is absent. In cases of isolated mediastinal haematoma other possible sources of bleeding should be considered before directing patients to thoracic aortography.

A-504 16:29

CT angiography of pulmonary embolism in patients with underlying respiratory disease: impact of multislice CT on image quality and negative predictive value

M. Remy-Jardin; *Lille/FR (martine.remy@chru-lille.fr)*

Our objective was to evaluate the impact of multislice CT (MSCT) on image quality and diagnostic value of spiral CT angiograms. Over an 8-month period (January 2000 to August 2000), 134 consecutive patients, including 55 patients with underlying lung disease, underwent MSCT (group 1). Image quality and diagnostic results of CT angiograms were compared with those obtained in 125 consecutive patients, including 58 patients with underlying lung disease, evaluated with thin-collimation single-slice CT (SSCT; group 2) over a similar period of time (January 1999 to August 1999). A 3-month clinical follow-up was systematically obtained in all patients who were not anticoagulated in the two groups. For a significantly longer mean z-axis coverage, the mean duration of data acquisition was significantly shorter with MSCT. The frequency of examinations devoid of motion artefacts was significantly higher in group 1 than in group 2. In the absence of significant difference in the quality of vascular enhancement, mainly coded as good or excellent, the proportion of examinations interpretable down to the subsegmental arteries was higher in group 1 (57.5%) than in group 2 (13%) ($p<0.0001$). The benefits of MSCT were more marked for patients with underlying respiratory disease and did not lead to a higher detection rate of peripheral pulmonary embolism. The negative predictive values of single-slice and multislice CT were 100 and 99%, respectively. Improvement in image quality on MSCT scans accounts for the improved diagnostic accuracy of CT angiography, in particular for patients with impaired respiratory function.

Author Disclosure:

M. Remy-Jardin: Research/Grant Support; Siemens Healthcare.

A-505 16:37

CT colonography: effect of experience and training on reader performance

S. Halligan; *London/UK (s.halligan@ucl.ac.uk)*

The purpose of this paper was to investigate the effect of radiologist experience and increasing exposure to CT colonography on reader performance. Three radiologists of differing general experience (consultant, research fellow, trainee) independently analysed 100 CT colonographic datasets. Readers had no prior experience of CT colonography and received feedback and training after the first 50 cases from an independent experienced radiologist. Diagnostic performance and reporting times were compared for the first and second 50 datasets and compared with the results of a radiologist experienced in CT colonography. Before training only the consultant reader achieved statistical equivalence with the reference standard for detection of larger polyps. After training, detection rates ranged between 25 and 58% for larger polyps. Only the trainee significantly improved after training ($P=0.007$), with performance of other readers unchanged or even worse. Reporting times following training were reduced significantly for the consultant and fellow ($P<0.001$ and $P=0.03$, respectively), but increased for the trainee ($P<0.001$). In comparison to the consultant reader, the odds of detection of larger polyps was 0.36 (CI 0.16, 0.82) for the fellow and 0.36 (CI 0.14, 0.91) for the trainee. There is considerable variation in the ability to report CT colonography. Prior experience in gastrointestinal radiology is a distinct advantage. Competence cannot be assumed even after directed training via a database of 50 cases.

Author Disclosure:

S. Halligan: Grant Recipient; Multiple peer-reviewed competitive research grants from Research Councils/Charities. Research/Grant Support; Multiple peer-reviewed competitive research grants from Research Councils/Charities.

A-506 16:45

First performance evaluation of a dual-source CT (DSCT) system

T. Flohr; *Forchheim/DE (thomas.flohr@siemens.com)*

We present the first performance evaluation of a new dual source CT (DSCT) system equipped with two x-ray tubes and two corresponding detectors that are mounted onto the rotating gantry with an angular offset of 90°. We introduce the system concept and potential benefits for ECG-controlled cardiac CT and for general radiology applications. We evaluate both temporal and spatial resolution by means of phantom scans. We present first patient scans to illustrate the performance of DSCT for ECG-gated cardiac imaging, and we demonstrate first results using a dual-energy acquisition mode. The evaluated DSCT system provides 83 ms temporal resolution independent of the patient's heart rate for cardiac CT. In a centred z-resolution phantom, 0.4-mm cylinders can be resolved at all heart rates, owing to the z-flying focal spot technique. The scan time to cover the heart volume (12 cm) is 5-9 s, depending on the patient's heart rate. First clinical experience shows a considerably increased robustness of the method for the imaging of patients with high heart rates. As a potential application of the dual-energy acquisition mode the automatic separation of bones and iodine filled vessels, e.g. for CT angiographic examinations, is demonstrated. Retrospect after 10 years: DSCT has been a significant step in introducing cardiac CT into clinical routine. Dual-energy CT has been reinvigorated by DSCT, resulting in some applications on their way to mainstream clinical use.

Author Disclosure:

T. Flohr: Employee; Siemens Healthcare GmbH.

A-507 16:53

Gd-EOB-DTPA-enhanced magnetic resonance images of hepatocellular carcinoma: correlation with histological grading and portal blood flow

T. Murakami[1], Y. Imai[2]; [1]*Osaka/JP*, [2]*Ikeda City/JP*
(murakami@med.kindai.ac.jp)

The objective of this study is to retrospectively investigate enhancement patterns of hepatocellular carcinoma (HCC) and dysplastic nodule (DN) in the hepatobiliary phase of gadolinium-ethoxybenzyl-diethylenetriamine (Gd-EOB-DTPA)-enhanced MRI in relation to histological grading and portal blood flow. Sixty-nine consecutive patients with 83 histologically proven HCCs and DNs were studied. To assess Gd-EOB-DTPA uptake, we calculated the EOB enhancement ratio, which is the ratio of the relative intensity of tumorous lesion to surrounding non-tumorous area on hepatobiliary phase images (post-contrast EOB ratio) to that on unenhanced images (pre-contrast EOB ratio). Portal blood flow was evaluated by CT during arterial portography. Post-contrast EOB ratios significantly decreased as the degree of differentiation declined in DNs (1.00 ± 0.14) and well, moderately and poorly differentiated HCCs (0.79 ± 0.19, 0.60 ± 0.27, 0.49 ± 0.10, respectively). Gd-EOB-DTPA

uptake, assessed by EOB enhancement ratios, deceased slightly in DNs and still more in HCCs, while there was no statistical difference in the decrease between different histological grades of HCC. Reductions in portal blood flow were observed less frequently than decreases in Gd-EOB-DTPA uptake in DNs and well-differentiated HCCs. Reduced Gd-EOB-DTPA uptake might be an early event of hepatocarcinogenesis, preceding portal blood flow reduction. The hepatobiliary phase of Gd-EOB-DTPA-enhanced MRI may help estimate histological grading, although difficulties exist in differentiating HCCs from DNs.

A-508 17:01

ESUR prostate MR guidelines 2012

J.O. Barentsz; *Nijmegen/NL (j.barentsz@rad.umcn.nl)*

The aim was to develop clinical guidelines for multi-parametric MRI of the prostate by a group of prostate MRI experts from the European Society of Urogenital Radiology (ESUR), based on the literature evidence and consensus expert opinion. True evidence-based guidelines could not be formulated, but a compromise, reflected by “minimal” and “optimal” requirements has been made. The scope of these ESUR guidelines is to promulgate high-quality MRI in acquisition and evaluation with the correct indications for prostate cancer across the whole of Europe and eventually outside Europe. The guidelines for the optimal technique and three protocols for “detection”, “staging” and “node and bone” are presented. The use of endorectal coil vs. pelvic phased array coil and 1.5 vs. 3T is discussed. Clinical indications and a PI-RADS classification for structured reporting are presented.

A-509 17:09

Nephrogenic systemic fibrosis and gadolinium-based contrast media: updated ESUR Contrast Medium Safety Committee guidelines

H. Thomsen; *Aalborg/DK*

The purpose of the session is to update the guidelines of the Contrast Media Safety Committee (CMSC) of the European Society of Urogenital Radiology (ESUR) on nephrogenic systemic fibrosis and gadolinium-based contrast media. Topics reviewed include the history, clinical features and prevalence of nephrogenic systemic fibrosis and the current understanding of its pathophysiology. The risk factors for NSF are discussed and prophylactic measures are recommended. The stability of the different gadolinium-based contrast media and the potential long-term effects of gadolinium in the body have also been reviewed.

A-510 17:17

Iterative reconstruction techniques for computed tomography Part 1: Technical principles

M.J. Willemink; *Utrecht/NL (m.willemink@umcutrecht.nl)*

The objectives are to explain the technical principles of and differences between commercially available iterative reconstruction (IR) algorithms for computed tomography (CT) in non-mathematical terms for radiologists and clinicians. Technical details of the different proprietary IR techniques were distilled from available scientific articles and manufacturers' white papers and were verified by the manufacturers. Clinical results were obtained from a literature search spanning January 2006 to January 2012, including only original research papers concerning IR for CT. IR for CT iteratively reduces noise and artefacts in either image space or raw data, or both. Reported dose reductions ranged from 23% to 76% compared to locally used default filtered back-projection (FBP) settings, with similar noise, artefacts, subjective, and objective image quality. IR has the potential to allow reducing the radiation dose while preserving image quality. Disadvantages of IR include blotchy image appearance and longer computational time. Future studies need to address differences between IR algorithms for clinical low-dose CT.

Author Disclosure:

M.J. Willemink: Speaker; Philips Healthcare speaker bureau.

17:25

Awards

16:00 - 17:30 **Room O**

Paediatric

RC 1212

Dose reduction: tips and tricks

Moderator:

C. Granata; Genoa/IT

A-511 16:00

A. Dose reduction in paediatric CT

D. Aadnevik; *Bergen/NO (daniel.aadnevik@helse-bergen.no)*

Computed tomography (CT) is an invaluable tool in diagnostics and the use of CT has rapidly increased since the 1970s. Ionising radiation can damage human tissues, and is associated with an increased risk of cancer. The effect is of particular concern in children as they have a higher radiosensitivity and longer life expectancy. Modern CT scanners have a high level of automatisation regarding acquisition parameters which may leave the imaging professionals insecure whether the radiation dose is appropriate for the diagnostic task at hand. Studies have shown that in some cases adult protocols are directly implemented in paediatric imaging, resulting in unnecessary high doses. As radiation professionals, it is our duty to keep the radiation dose as low as reasonably achievable (ALARA). It is important to have a basic understanding of how technical factors influence image quality and how to properly balance the output parameters of the scanner in accordance with the ALARA principle. The benefits of low tube voltage, automatic exposure control (AEC), helical pitch and iterative reconstruction techniques will be discussed with respect to radiation dose and examples from local optimisation studies will be presented. Vendor-specific solutions for dose reduction will be explained.

Learning Objectives:

1. To explain the factors that affect patient radiation exposure from CT exams.
2. To discuss the importance of dose reduction in paediatric CT.
3. To give an overview of CT dose reduction strategies and techniques.

A-512 16:30

B. Diagnostic reference levels in paediatric imaging: international recommendations

R. Seuri; *Helsinki/FI (raija.seuri@hus.fi)*

In many institutions the number of paediatric patients is fairly small, which makes optimization challenging. Diagnostic reference levels are an important method for optimization. The DRLs offer a way to compare institution's own patient dose levels, which are expected to comply with good practices. In this comparison dose should always be considered together with the indication of imaging and image quality. DRLs are used by collecting patient dose values and comparing their median values to DRLs. Paediatric DRLs have usually been established for different age-groups. Both ICRP and EC now recommend the use of weight for grouping of paediatric patients. Instead of different groups, also a continuous DRL-curve can be used. The guidelines also provide recommended dose metrics for each modality to be used in DRL comparison. Quite a few countries have set their national DRLs (NDRLs) for at least the most common paediatric examinations, mostly for radiography. By European recommendation the NDRLs should be based on collection of doses from representative institutions in the country, not phantom measurements. The NDRL is then determined by calculating the third quartile level of the collected doses, or the local median values. The PiDRL project was organized by EC to collect the existing national DRLs in Europe to establish European DRLs for optimization in those countries, which have not established their own NDRLs. The report with the European DRLs for the most common paediatric radiological procedures including all modalities was published in 2016.

Learning Objectives:

1. To discuss the need for establishing diagnostic reference levels (DRLs) in paediatric diagnostic imaging.
2. To give an overview of DRL values for typical paediatric examinations.
3. To understand the way of implementation and use of DRLs in dose reduction and protocol optimisation.

A-513 17:00

C. The impact of dose management systems

L.A. Rainford; *Dublin/IE (louise.rainford@ucd.ie)*

The importance of radiation dose monitoring, particularly for high-dose medical examinations, is clearly stated in international radiation protection guidelines, with specific reference to paediatrics. It is mandated by European Directive that the establishment and use of DRLs is fulfilled by all member states. Existing levels of dose information varies across imaging sub-specialities, as evidenced by the recent European PiDRL project. Specific challenges continue to

confound paediatric dose data collections, including reduced frequency of examinations compared to adults, patient age/weight/size variations, procedural variability and varied data survey methodologies. Increasing numbers of dose tracking software packages, including those providing web-based dose data collection, tracking and analytics are available. These systems although varied in scope of content offer services, including dose documentation, dose reference levels setting, performance benchmarking, imaging protocol management and outlier identification. A summary overview of products and their management of big data will be provided. Furthermore, the current clinical reality that substantial amounts of both unstructured and structured dose data are routinely being captured, with the employment of varied mechanisms of data recording, will be evidenced. Why this information is potentially not being used optimally will be discussed, as will communication matters relevant to dose management products. Practical issues relevant to clinical data required for dose and imaging protocol evaluation will be incorporated. Finally, the role of dose management systems in the review of population dose data and protocol optimisation will be discussed and the potential barriers to the successful completion of multi-centre surveys will be considered.

Learning Objectives:

1. To discuss the importance of dose monitoring in paediatric imaging.
2. To have an overview of the features and functions of dose monitoring systems.
3. To understand the role of dose monitoring systems in the evaluation of population dose and protocol optimisation.

16:00 - 17:30 **Room N**

Special Focus Session

SF 12a

My most scary head and neck mistakes

A-514 16:00

Chairman's introduction: Misses, misinterpretations and mistakes

A. Borges; *Lisbon/PT*

At the same time imaging became a major player in the diagnostic process it has also become a major source of diagnostic error. Although errors in radiology are multifold, most are attributable to image interpretation errors by radiologists which can grossly be subdivided into perceptual and cognitive. Radiologists are put under a great amount of pressure by the urgency of the diagnosis requiring rapid reporting, on top of increasing workload, increasing complexity of imaging techniques and increasing complexity of clinical cases. While the number of images and post-processing requirements have increased dramatically in the past decades the reporting time has decreased at the same pace, leaving more room for error. This session will cover misses, perceptual errors defined as important imaging findings that are not seen by the radiologist and mistakes, cognitive errors defined as visually detected findings which are misinterpreted by the radiologist, in head and neck imaging using illustrative clinical cases. We will also provide strategies both at the individual and departmental level to prevent these mistakes in a solution-oriented approach and to cope with mistakes once they eventually occur.

Session Objectives:

1. To become familiar with the most common mistakes in head and neck imaging and their causes.
2. To learn strategies to avoid mistakes.
3. To learn how to deal with different types of mistakes.

A-515 16:05

What I missed and why

M.G. Mack; *Munich/DE (m.mack@radiologie-muenchen.de)*

This lecture will give you an overview of diagnosis which can be missed easily. The reason for missed diagnosis can be variable and includes the following: the radiologists know only common disease; radiologists are only able to diagnose lesions, which they have seen before; radiologist did not get the full clinical Information; lack of time; radiologists can have the "hammer-and-nail" bias; radiologists want to save money by not doing an additional examination (e.g. with another modality); radiologists have different skill levels.

Learning Objectives:

1. To become familiar with different types of missed findings.
2. To appreciate common radiologist's bias.
3. To learn strategies to avoid different categories of misses.

A-516 16:28

What I misinterpreted and why

L. Ginsberg; *Houston, TX/US (lginsberg@mdanderson.org)*

Head and neck cancer imaging is fraught with opportunity for error. These errors include but are not limited to failure to observe, failure to synthesize and integrate findings into the correct interpretation and various types of knowledge gaps that can produce an incomplete, inaccurate or otherwise inadequate reading. This presentation will reflect on my own personal shortcomings in several cases, serving as a cautionary tale to others.

Learning Objectives:

1. To appreciate different causes of misinterpretation of imaging findings in the head and neck.
2. To review common misinterpreted findings in the head and neck.
3. To learn how to avoid misinterpretations.

A-517 16:51

How to deal with mistakes: the report, the radiologist and the department

S.J. Golding; *Oxford/UK (stephen.golding@nds.ox.ac.uk)*

Errors always occur in radiology, as a result of the nature of the subject, clinical circumstances and the complexity of human individuality. Individuals and departments must have a strategy for dealing with these incidents. The initial question to address is whether an error has actually occurred and whether it is clinically significant. Radiological reporting is open to discrepancies (a better description than "errors") in medical opinion and each discrepancy should be graded in a system which allows for justifiable variation in opinion and judges the potential clinical impact. Where a significant discrepancy is found the appropriate action potentially involves the radiologist, the referring clinician and the patient. It also depends on the grade of discrepancy. Any actions taken should be documented at the time: retrospective alteration of medical records should be avoided. Departments should have methods of recording discrepancies that change the impact of previously issued reports, whether or not these have impact extending to duty of disclosure to the patient. Where an individual radiologist is found to generate an excessive number of discrepancies the grading system can be used to evaluate their competence objectively, but must be statistically robust, i.e. it employs a sufficient number of blinded viewers who independently grade an adequate number of the same reports, randomly selected. Regular evaluation of all radiologists in this way could be used to demonstrate the overall clinical performance of individual departments. Where substandard performance is found departments must have arrangements for retraining or altering the content of that radiologist's practice.

Learning Objectives:

1. To learn how to deal with mistakes: your own and other's.
2. To understand the value of clinical audits.
3. To become familiar with different steps of clinical action.

17:14

Panel discussion: Mistakes - can they be avoided and how?

16:00 - 17:30 **Studio 2017**

Genitourinary

RC 1207

MRI for gynaecologic imaging: how I do it

A-518 16:00

Chairman's introduction

K.H. Härmä; *Berne/CH (kirsihannele.haermae@insel.ch)*

Optimising gynaecologic magnetic resonance imaging (MRI) incorporates the understanding of the concepts of multiparametric MRI, the combination of thin section high-resolution T2-weighted anatomical sequences and diffusion-weighted imaging (DWI). In DWI, the random Brownian motion of water molecules is measured within a voxel of tissue, being related to cellularity and the integrity of the cellular membranes of tissues providing qualitative and quantitative information compared to morphologic criteria only. DWI has potential to differentiate between malignant and benign tumours, to monitor therapy response or to detect recurrence. It also may have its value in predicting tumour aggressiveness or heterogeneity. Patient preparation includes intramuscular antispasmodic drug administration to last through the scanning. Indications of using MR-contrast media vary among different gynaecologic diseases. Contrast agents are not recommended in pregnancy, despite of lacking evidence of adverse foetal effects. Linear gadolinium chelates should be avoided when imaging breast feeding mothers. MRI has a growing role as a non-invasive diagnostic tool while decisions of treatment management move towards personalised medicine, for example, in ovarian

cancer patients. Developed methods in debulking surgery, such as peritonectomy, resection of diaphragm or suspicious cardiophrenic lymph nodes via thoracoscopy, aimed to optimal debulking without any residual tumour, require accurate pre-operative knowledge of the tumour extent. Increasingly used whole body DW-MRI may have potential in assessing disease extent, also in supradiaphragmatic tumour sites. Radiologists should be active in interdisciplinary workshops to communicate the new development and possibilities of multiparametric MRI in gynaecologic imaging.

Session Objectives:

1. To learn how to optimise MRI of the female pelvis.
2. To understand the diagnostic benefit of integration of advanced techniques.

A-519 16:05

A. Basics of patient preparation and T2W-imaging

N.M. deSouza; *Sutton/UK (nandita.desouza@icr.ac.uk)*

T2-W MR imaging provides exquisite soft tissue contrast for diagnosis and evaluation of benign and malignant pelvic pathology. It is essential to achieve images free of artefact with maximal spatial and optimal contrast resolution. Sequence acquisition parameters that deliver the best tissue contrast must be implemented and image degradation by patient-related factors must be avoided. Physiological motion in the pelvis arises largely from bowel peristalsis and bladder filling. Intramuscular administration of antiperistaltic agents (Buscopan [hyoscine butylbromide] 20mg or glucagon 1mg) is important; intravenous delivery results in a very short period of antiperistaltic action insufficient to last through the scanning period. Bladder filling during the scan also degrades image quality. An empty bladder at the outset is preferred. To minimise diuresis during scanning, diuretic-inducing caffeine containing drinks or excessive fluid intake should be discouraged for 4 hours prior. Images dedicated to a particular anatomical structure, e.g. uterus should be acquired in planes along the long and short axis of the organ, with as small a field-of-view as feasible without compromising signal-to-noise ratio. For large field-of-view images, T2-W scans in true orthogonal planes to the B0 field are preferred. The sagittal plane is best for visualising the uterus, while the transverse plane is ideal for assessing parametria, adnexae and pelvic side wall. For the ovaries, the coronal plane may be helpful. High-quality T2-W imaging in orthogonal planes are usually sufficient for detecting, characterising, staging pelvic malignancy, monitoring treatment response and assessing disease recurrence of a range of gynaecological pathologies.

Learning Objectives:

1. To understand the value of patient preparation.
2. To learn how to optimise and tailor protocols in female pelvic imaging.
3. To understand the role of T2WI, and how and when to use 3D techniques.

A-520 16:28

B. Contrast agents

R.A. Kubik-Huch; *Baden/CH (rahel.kubik@ksb.ch)*

Gadolinium-based contrast material is not usually necessary for evaluating benign uterine disease, but is recommended in fibroid evaluation. Gadolinium-enhanced sequences are performed for staging endometrial carcinoma, being useful in the assessment of the depth of myometrial tumour invasion. The optimal tumour/myometrial contrast timing was reported between 90 and 150 seconds. Thus, the utility of dynamic acquisition has been debated. Contrast-enhanced imaging will not be routinely performed in cervical carcinoma. It is recommended that the MR assessment of sonographically indeterminate adnexal masses are mandatory for staging ovarian carcinoma. Dynamic contrast-enhanced MRI may provide quantitative information about tumour perfusion, being useful for monitoring therapeutic effects and predicting therapeutic outcome. MR angiography should be performed in patients scheduled for fibroid embolization or in suspected pelvic congestion syndrome. Gadolinium-based contrast agents will cross the placenta and enter the foetal bloodstream. The agents are excreted into the amniotic fluid and will not be removed effectively from the foetal environment. Although there is currently no evidence of adverse foetal effects, contrast agents should be avoided in the pregnant patient. Only a small amount of gadolinium is excreted into the breast milk and absorbed by the infant, without any adverse effects being reported. Therefore, breast feeding can be continued, but it might be the preference of the mother to discard the breast milk in the 24 hours after contrast medium. If contrast agents need to be administered in these patients, linear gadolinium chelates should be avoided.

Learning Objectives:

1. To become familiar with the safety considerations and guidelines for the use of gadolinium with a special focus on imaging pregnant and lactating patients.
2. To learn why, how and when to use IV contrast-enhanced imaging in MRI of the female pelvis.
3. To understand different gadolinium T1W techniques and their clinical value in routine imaging, as well as to become familiar with quantification techniques.

A-521 16:51

C. Diffusion and ADC

E. Sala; *New York, NY/US (salae@mskcc.org)*

DW-MRI is a functional imaging technique that displays information about water mobility, tissue cellularity and the integrity of the cellular membranes. It also permits the quantitative evaluation of the apparent diffusion coefficient (ADC) from images with different b-values. The ADC value is measured in mm^2/s and is calculated by the slope of the line of the natural algorithm of signal intensity versus b-values. DW-MRI should be performed at two or more b-values, which include one or more low b-values (50-100 s/mm^2) since perfusion contribution to diffusion is then eliminated and a very high b-value (750-1000 s/mm^2). Both breath hold and non-breath hold DW sequences can be used. However, the type of DW sequence differs among manufacturers and the radiologist should be familiar with the strengths and limitations of their own scanners. Combination of DWI with conventional MRI sequences improves lesion detection and radiologist confidence in imaging interpretation. DW-MRI can be useful for accurately determining the depth of myometrial invasion in endometrial cancer. This can be particularly helpful in cases of tumours that are either iso- or hyper-intense relative to the myometrium or when the use of intravenous contrast medium is contraindicated. In addition, ADC values are inversely related to the cellularity of tumours which may be useful for distinguishing between benign and malignant tissues and for monitoring tumour response to treatment in cervical and ovarian cancer.

Learning Objectives:

1. To understand the technical principles of DWI.
2. To learn how to optimise and integrate DWI in pelvic imaging.
3. To illustrate the added diagnostic value of DWI in female pelvic imaging.

17:14

Panel discussion: Multiparametric MRI of the female pelvis - should it replace tailored protocols?

16:00 - 17:30 **Room E1**

Special Focus Session

SF 12b

Challenges in the diagnosis of acute appendicitis

A-522 16:00

Chairman's introduction

J. Stoker; *Amsterdam/NL (j.stoker@amc.uva.nl)*

Acute appendicitis is the most common urgent cause of acute abdominal pain at the emergency department. Ultrasound and computed tomography play an important role in diagnosing acute appendicitis, while magnetic resonance imaging can be considered in certain situations. Knowledge on the accuracy, pros and cons and cost-effectiveness of either technique and the possible imaging strategies (e.g. in specific groups or clinical settings) are crucial for proper management, including discriminating between complicated and uncomplicated appendicitis.

Session Objectives:

1. To become familiar with the topics on imaging in acute appendicitis discussed in this session.
2. To learn the optimal diagnostic strategy in diagnosing acute appendicitis in specific populations (paediatric, pregnant, obese, elderly).
3. To understand the role of imaging in the management of acute appendicitis in specific populations (paediatric, pregnant, obese, elderly).

Author Disclosure:

J. Stoker: Research/Grant Support; Robarts Clinical Trials.

A-523 16:05

Acute appendicitis during pregnancy: high-end ultrasonography, ultra-low dose CT or unenhanced MRI?

P.-A. Poletti; *Geneva/CH (pierre-alexandre.poletti@hcuge.ch)*

Imaging is important in the diagnostic management of pregnant patients with suspicion of appendicitis, since the risk of foetal loss dramatically increases (20-25%) in case of perforation, when compared to unperforated appendicitis (3-5%). Ultrasonography is unanimously advocated as first-line imaging; however, this operator-dependent technique is limited by an uncertain sensitivity (20-100%) and by a high rate of indeterminate results (88-96%), especially in the last trimester of pregnancy. MRI is often recommended to be used as second-line imaging method, because it has a good sensitivity (80-100%) and specificity (93-98%) for appendicitis and delivers no ionizing radiations. However, there are many drawbacks to its use: MRI is not available

24/24 in every centre, being absolute innocuous for the foetus is not demonstrated, it is time consuming, requires patients collaboration and its value for identifying alternative diagnoses is debated. Because of reluctance to ionizing radiation exposure, especially during the first trimester, i.v. contrast-enhanced CT is usually only recommended when ultrasonography and MRI are inconclusive or unavailable. The accuracy of CT is equivalent to that of MRI for the diagnosis of appendicitis, but has been reported better for alternative diagnoses. Preliminary, not yet published series suggest that ultra-low-dose unenhanced CT (<2mSv), with iterative reconstruction, might be a practical alternative to MRI and to standard dose i.v. enhanced CT, as second-line imaging tool, after an indeterminate ultrasound, for an acceptable dose of radiation. This will be discussed in the presentation.

Learning Objectives:

1. To learn about the pros and cons of high-end ultrasonography, ultra-low dose CT and unenhanced MRI in diagnosing appendicitis in pregnancy.
2. To appreciate the role of high-end ultrasonography, ultra-low dose CT and unenhanced MRI in diagnosing appendicitis in pregnancy.
3. To understand of the role of high-end ultrasonography, ultra-low dose CT and unenhanced MRI in relation to clinical findings to differentiate between diagnosing appendicitis uncomplicated vs complicated appendicitis in pregnancy.

A-524 16:23

Imaging algorithms for acute appendicitis in difficult patients (obese, elderly, other)

J.B.C.M. Puylaert; *The Hague/NL (dr.jbcmpuylaert@wxs.nl)*

The clinical diagnosis of appendicitis is classically unreliable: 25% of appendectomies are unnecessary, while significant surgical delay occurs in 20% of patients with appendicitis. US, CT and MR have brought down these numbers to 3% and 5%, respectively, by accurately diagnosing both acute appendicitis as well as many of its clinical masqueraders. The inflamed appendix presents as a blind-ending, concentrically layered, firm sausage-like structure, often surrounded by inflamed fat. This is in contrast to the normal appendix, which is compressible, mobile and usually, but not always, smaller than 7mm. Appendicitis can be excluded by demonstrating a normal appendix over its full length or by reliably demonstrating an alternative diagnosis. This may involve principally conservatively manageable conditions such as Crohn's disease, infectious ileocolitis, haemorrhagic follicle, pneumonia, necrotic myoma, non-perforated peptic ulcer, pyelonephritis, ureterolithiasis, right colonic and sigmoid diverticulitis, rectus sheath haematoma, familial Mediterranean fever, adnexitis, ovarian cyst, segmental omental infarction and primary epiploic appendagitis, or principal surgical conditions such as perforated peptic ulcer, ectopic pregnancy, ovarian torsion, cholecystitis, small bowel obstruction, colonic carcinoma, intussusception, ruptured aneurysm and Meckel diverticulitis. Various imaging appearances of appendicitis and its differential diagnosis will be shown as well as many possible pitfalls. Specific pitfalls and management in difficult patients (obese, the elderly and the pregnant patient) will be highlighted.

Learning Objectives:

1. To learn about the pros and cons of high-end ultrasonography, ultra-low dose CT and MRI in diagnosing appendicitis in 'difficult' patients.
2. To appreciate the role of high-end ultrasonography, ultra-low dose CT and unenhanced MRI in diagnosing appendicitis in 'difficult' patients.
3. To understand the role of high-end ultrasonography, ultra-low dose CT and unenhanced MRI in relation to clinical findings to differentiate between uncomplicated vs complicated appendicitis in 'difficult' patients.
4. To understand the pros and cons of different imaging strategies in diagnosing appendicitis in 'difficult' patients.

A-525 16:41

What is the cost-effectiveness of different imaging modalities in acute appendicitis?

M. Zins; *Paris/FR (mzins@hpsj.fr)*

Use of imaging in the diagnostic workup of patients with clinically suspected appendicitis reduced the rate of negative appendectomies, surgical complications and the costs. There is a high level of evidence that the most cost-effective method of imaging appendicitis is to start with a US study and follow each negative US study with a CT examination (conditional CT strategy). During pregnancy, following indeterminate US, magnetic resonance imaging is the most cost-effective strategy. For pregnant women with suspected appendicitis, an extremely high level of clinical diagnostic certainty must be reached prior to proceeding to operation without pre-operative imaging. In the general population, the accuracy of conditional or immediate MR imaging is similar to that of conditional CT in patients suspected of having appendicitis. Paradigm shifts to MRI owing to concerns over radiation should be considered only if high MRI test performance is reliably achievable.

Learning Objectives:

1. To learn about the level of evidence concerning cost effectiveness of imaging in acute appendicitis.
2. To learn about the cost effectiveness of high-end ultrasonography, ultra-low dose CT and MRI in diagnosing appendicitis (including uncomplicated vs complicated).
3. To understand the cost-effectiveness of different imaging strategies in diagnosing appendicitis in the general population, in pregnancy and in 'difficult' patients.

A-526 16:59

Evidence-based treatment of acute appendicitis: conservative vs surgical management?

M.A. Boermeester; *Amsterdam/NL (m.a.boermeester@amc.uva.nl)*

In the past only clinical evaluation was used to evaluate patients with suspected appendicitis, but this is imperfect. Unnecessary surgical exploration is not without downsides. It carries an increased risk of mortality, of prolonged hospital stay, and of wound infections. Based only on clinical evaluation, 10-20 per cent of patients with appendicitis would be missed. Such a missed diagnosis results in a treatment delay. Perforated appendicitis is associated with higher mortality and morbidity rates. Because of negative appendectomy rates, missed appendicitis cases and differentiation between uncomplicated and complicated appendicitis, imaging has become widely used in first world countries to aid the clinical evaluation of acute abdominal pain. Appendiceal perforation has long been considered an advanced state of acute appendicitis. However, the relation between time and progression of disease (from simple uncomplicated to gangrenous or perforated appendicitis) is being questioned. Perforated and non-perforated appendicitis are suggested to have different pathophysiologies. Conservative management has been proposed as an alternative for selected patients with uncomplicated or simple appendicitis. Several randomized trials have indicated that treatment with antibiotics is as safe and effective as appendectomy for patients with uncomplicated appendicitis, with low failure rates which then can be treated with appendectomy without a higher complication rate. However, preoperative identification of patients with uncomplicated appendicitis has proven to be a challenge.

Learning Objectives:

1. To learn about the evidence concerning conservative vs surgical management in acute appendicitis.
2. To learn about the role of clinical history, physical examination and laboratory findings in the management of acute appendicitis.
3. To appreciate the role of imaging in management of acute appendicitis (including uncomplicated vs complicated).

Author Disclosure:

M.A. Boermeester: Advisory Board; J&J, Acelity. Consultant; Acelity, Bard. Research/Grant Support; J&J, Baxter, Mylan, Ipsen, Bard, Acelity. Speaker; J&J, Bard, Acelity.

17:12

Panel discussion: Optimised imaging algorithms in the diagnosis of acute appendicitis

16:00 - 17:30 **Room E2**

Neuro

RC 1211

Reporting the degenerative lumbar spine

Moderator:
E.T. Tali; Ankara/TR

A-527 16:00

A. Disc nomenclature: how I make my report

E. Arana; *Valencia/ES (aranae@uv.es)*

For the clinical management of degenerative spine lesions, the radiologist is of major importance for the discrimination of normal ageing and probable relevant imaging findings. A systematic review will include key anatomic and radiologic features in disc pathology. Standardized disc nomenclature (version 2.0) is mandatory and its key imaging characteristics are showed. Emphasis is placed on pain generators and clear-cut imaging findings such as neural compression. Elusive relationship among other imaging findings and symptoms are also explained. Overall, challenges and pitfalls will be reviewed for the management of potentially relevant lesions using MRI on the background of symptoms relevance. Hints are provided to increase reproducibility and consistency of radiological reports and what clinicians need in our report.

Learning Objectives:
1. To become familiar with the different nomenclatures in degenerative disc disease and their anatomic substrates.
2. To learn how to differentiate between the different types of disc disease.
3. To appreciate how the different types of degenerative disc diseases determine the therapeutic approach.

A-528 16:30

B. Don't forget the facet joints and posterior elements
L. van den Hauwe; *Antwerp/BE (lucvdhauwe@mac.com)*

Many radiologists reading imaging studies of the spine performed in patients with low back pain (LBP), neck pain, and radicular symptoms tend to focus on the anterior part of the spine, and more specifically on the intervertebral disc. They are often unaware that the posterior elements (facet joints, pedicles, spinal ligaments, spinous processes, etc.). may also be a source of pain. Moreover, radiologists are faced with the low specificity of the morphological abnormalities found on plain film radiography, computed tomography (CT) and magnetic resonance (MR) imaging which are also a frequent finding in the general - often asymptomatic - population. Conversely, the source of LBP (and neck pain) may remain unrecognized unless more dedicated MR imaging sequences such as fat-suppressed (FS) T2-weighted images (e.g. short-tau inversion recovery (STIR)) and FS contrast-enhanced (CE) T1-weighted images are added to the standard spinal MR imaging protocol. These FS-sequences are more sensitive in demonstrating bone marrow oedema, soft tissue inflammation, and hypervascularity that are often associated with degenerative changes of the posterior elements, e.g. facet joint osteoarthritis, synovitis, neural arch intervertebral or spinous process neoarthrosis, etc. Also nuclear medicine techniques such as single-photon emission computed tomography (SPECT), SPECT/CT, etc. are additional imaging techniques that may correctly identify the source of the pain.
Learning Objectives:
1. To become familiar with the anatomy of the facet joints and the posterior elements.
2. To understand the pathophysiological principle underlying the degenerative changes of these structures.
3. To appreciate the effect of these changes on the therapeutic approach.
Author Disclosure:
L. van den Hauwe: Consultant; icometrix, Leuven/BE.

A-529 17:00

C. What to say and not to say in your report
M.M. Thurnher; *Vienna/AT (majda.thurnher@meduniwien.ac.at)*

Following a degenerative spine diagnosis, many issues can be successfully treated with various conservative treatments. These options do not work for every patient, some will need surgical pain relief. Variability in radiologists' reporting styles and recommendations for spinal studies can lead to confusion among clinicians and may contribute to inconsistent patient care. Reporting spine studies requires a systematic approach. The report on MRI of the spine should have following elements: perispinal tissue, bones, disks, spinal canal, facet joints, spinal cord and cauda equina. Adequate techniques and sequences are mandatory for optimal evaluation of spinal structures. In this lecture, the recommendations to improve documentation and reporting of spine MRI will be discussed.
Learning Objectives:
1. To understand the legal value of a report.
2. To demonstrate how detailed a report should be.
3. To understand the importance of a clinical information and the relevance of assessing previous examinations.
Author Disclosure:
M.M. Thurnher: Consultant; Guerbet.

16:00 - 17:30 **Room F1**

Joint Session of the ESR and ESOR

ESR/ESOR 3

Radiologic anatomy: neuro

Moderator:
M.A. Lucic; Sremska Kamenica/RS

A-530 16:00

Cortical anatomy and primary functional areas
T.A. Yousry; *London/UK (t.yousry@ucl.ac.uk)*

The anatomy of the brain is often perceived as being complicated. Especially the cortex is seen as an irregular arrangement of variable structures, which are difficult to differentiate and to identify. We will review the overall subdivision of the brain into lobes and describe their boundaries and their major gyri and sulci. We will then describe the location of specific functions. 1. Primary sensorimotor cortex: motor is located in the precentral gyrus, sensory in the postcentral gyrus around the central sulcus (CS), hence the importance of always correctly identifying the CS. We will present 4 interlocked methods to identify the CS in the axial plane: a) knob, b) lateral axial, c) medial axial and d) gyral/cortical thickness and 3 to identify it in the sagittal plane: a) lateral sagittal, b) hook and c) medial sagittal. 2. Primary auditory cortex (A1): centred at the postero-medial part of Heschl's gyrus (HG), we will present simple landmarks in each of the 3 planes: a) axial: adhaesio interthalamica, b) sagittal: omega/heart shape of HG, c) coronal: omega shape of HG. 3. Primary visual cortex (V1): centred on the calcarine sulcus, we will discuss the characteristic shape that allows the identification of this structure in all 3 planes. At the end of this lecture, you will know the subdivision of the cortex; the methods and landmarks necessary to identify the primary sensorimotor, speech, auditory and visual areas.
Learning Objectives:
1. To understand the basic concepts of cortical subdivision.
2. To be able to identify critical cortical structures.
3. To learn to localise primary functional areas.
Author Disclosure:
T.A. Yousry: Advisory Board; Biogen Idec; Genzyme. Board Member; Neuroradiology. Grant Recipient; Medical Research Council, MS Society of Great Britain and Northern Ireland, Stroke Association, British Heart Foundation, Wellcome Trust. Research/Grant Support; BRC. Speaker; ESOR, Novartis.

A-531 16:30

Vascular distribution territories: arterial and venous
A. Dörfler; *Erlangen/DE (arnd.doerfler@uk-erlangen.de)*

After a short overview on the vascular anatomy of the brain with a focus on vascular distribution territories, the main aim of this presentation is to present different neurovascular pathologies closely associated with arterial and venous vascular distribution territories. A focus is here put on acute stroke and particularly imaging-based patient selection for interventional stroke therapy. Another aim is to provide a better understanding of pathophysiology of different neurovascular disease in an interactive matter. In addition, advantages and limitations of CTA and MRI compared to conventional angiography are presented.
Learning Objectives:
1. To become familiar with a comprehensive vascular anatomy of the brain.
2. To recognise patterns of various pathologies attributed to vascular distribution territories.
3. To recognise the different imaging patterns in stroke and their prognostic value.

A-532 17:00

The basal ganglia of the brain revisited
D. Zlatareva; *Sofia/BG (dorazlat@yahoo.com)*

The deep grey matter nuclei include the basal ganglia and thalamus. These paired symmetric structures are located in the telencephalon, diencephalon, and mesencephalon. The lenticular nucleus includes putamen and globus pallidus. Together with caudate nucleus these structures are named corpus striatum. The term "basal ganglia" refers to caudate nucleus, putamen, globus pallidus, substantia nigra and subthalamic nucleus. All these structures are part of extrapyramidal system and have wide connections not only with each other but also with the midbrain, thalamus and cerebral cortex. The striatum is the main recipient of afferents from the entire cerebral cortex and from thalamus to the basal ganglia. In the motor regions of the basal ganglia, there is a motor homunculus similar to that seen in the primary motor cortex. The major output structures of the basal ganglia are the globus pallidus internal

segment and the substantia nigra pars reticulate. Both of these structures make GABAergic, inhibitory connections on their targets. The basal ganglia and thalami have five functional divisions which are sensorimotor, supplementary motor, premotor, association and limbic territories. These divisions take part in functional cortical-basal-ganglial-thalamocortical circuits which enable the execution of automatic and semi-automatic motor programs, modulation of muscle tone and the harmonisation of movement. If one or more of these regulatory circuits are interrupted the result will be either a net removal of inhibition, leading to excessive movement like tremor or dystonia, or a net decrease in motor activation causing impaired movement (e.g. rigidity, akinesia).

Learning Objectives:

1. To recall the basal ganglia nuclei and their topography.
2. To identify the classic functional organisation of the basal ganglia and its current concepts.
3. To elucidate the pathophysiology of various movement disorders.

16:00 - 17:30 **Room F2**

Oncologic Imaging

RC 1216

Monitoring response: the essential guide for all radiologists

A-533 16:00

Chairman's introduction

P. Brader; *Graz/AT (peter@brader.md)*

Imaging-based therapy monitoring is essential to visualise and quantify the effect of cancer therapy. Therefore, criteria-based reporting methods were established to ensure standardised and reproducible results for response evaluation of oncologic patients. Response evaluation criteria in solid tumours (RECIST) as the most widely accepted morphologic, size-based evaluation system is based on imaging assessment of change in tumour burden, to determine if the tumour has shrunk or grown. However, they only evaluate the size of the lesion, not its viability, proliferative rate or physiologic state. In recent years, a broad range of novel molecular cancer therapeutics were introduced into clinical use. These new therapy regimes demonstrated significant effects on tumour angiogenesis and tumour metabolism, but often only subtle effects on tumour morphology. Established methods of monitoring cytotoxic tumour therapies such as RECIST have been shown to be not sufficiently sensitive for monitoring the therapeutic effects of molecular anti-cancer agents to allow for a timely differentiation of responders from non-responders because such treatments are less likely to result in tumour shrinkage. The complementary acquisition of morphological, functional and molecular information using advanced imaging methods such as diffusion-weighted imaging or perfusion imaging as well as hybrid imaging techniques (PET/CT, PET/MRI) allows for a higher sensitivity and specificity in the timely differentiation of responders from non-responders. The tremendous development in oncology and technical innovations in imaging present a particular challenge for radiology.

Session Objectives:

1. To understand the correlation of functional imaging evaluation with the pathophysiological effect of treatment on oncological pathology.
2. To understand the necessity of functional imaging for an accurate (early) evaluation of the therapy regimen on the response (or non-response) of oncological disease.
3. To learn about the added value of functional imaging for evaluating treatment (e.g. anti-angiogenic treatment).
4. To learn about the technical principles of functional imaging in correlation with the impact of therapy on tumour cells and neo-vasculature.

A-534 16:05

A. RECIST made easy

A.G. Rockall; *London/UK (a.rockall@imperial.ac.uk)*

A significant part of modern-day cancer imaging involves the assessment of change in the extent of tumour in the context of a clinical trial or research study. The reporting requirements for these imaging studies are documented in the research protocol. A standardized response assessment is important to be able to collate data between different centres, as well as to evaluate published data from different studies. Response evaluation criteria in solid tumours (RECIST) were developed and published in 2000. RECIST criteria have been widely adopted for the evaluation of treatment response in the clinical trial setting. A revised version, RECIST 1.1 was subsequently published in 2009, to address several problems that had been encountered with RECIST 1.0. New studies frequently use RECIST 1.1 but in some cases, new studies will still use RECIST 1.0 to allow direct comparison with a previous similar study. In this lecture, the key features of RECIST will be presented with worked examples. Selection of appropriate target lesions will be illustrated. Frequently asked questions will be addressed and the criteria for response will be illustrated.

Learning Objectives:

1. To learn about the basic idea of RECIST.
2. To understand how to use RECIST in daily clinical practice.
3. To become familiar with the detailed rules of RECIST.

A-535 16:28

B. PERCIST: PET response criteria

C.C. Cyran; *Munich/DE (clemens.cyran@med.uni-muenchen.de)*

With the implementation of novel oncologic strategies and prolonged survival of cancer patients, early and longitudinal monitoring of therapy response to treatment in individual patients has become a key request to imaging. Known limitations of morphological size-based criteria (e.g. RECIST) for the monitoring of tumour response led to the investigation of additional functional and molecular imaging techniques to allow for a reliable and timely distinction of responders and non-responders, particularly under novel molecular cancer therapies. Particularly hybrid imaging techniques, such as PET/CT or PET/MRI, demonstrated significantly improved diagnostic accuracy for the evaluation of treatment response in different tumour entities under a variety of treatments with a reported change-in-intended management of up to 35% in oncologic indications compared to conventional imaging alone. To allow for a standardised evaluation of therapy response, criteria-based reporting of target and non-target lesions has been established to classify therapy response into different categories ranging from complete response to progressive disease and has found broad application particularly within clinical studies. Similar to the size-based RECIST (response criteria in solid tumours) criteria, PERCIST (PET response criteria in solid tumour) criteria were developed to provide a systematic, standardised approach for the criteria-based evaluation of metabolic tumour response to therapy using 18F-FDG PET. Studies evaluating PERCIST criteria suggest that the inclusion of standardised metabolic criteria may allow for an increased sensitivity, specificity and diagnostic accuracy in the evaluation of therapy response compared to morphological imaging criteria alone.

Learning Objectives:

1. To learn about the basic principles of PERCIST.
2. To understand how to use PERCIST for structured quantitative research and clinical reporting.
3. To appreciate the advantages of PERCIST over mere morphological methods.

Author Disclosure:

C.C. Cyran: Research/Grant Support; Novartis.

A-536 16:51

C. Assessment of response using functional MR and CT imaging: the essentials

C.A. Cuénod; *Paris/FR (ca@cuenod.net)*

The assessment of the morphological changes detected by imaging is the most common way to evaluate response to treatment. The most frequently used criteria being the RECIST criteria. However, changes in cell metabolism and tissue physiology, which precede morphological changes, cannot be detected by the conventional imaging techniques. The development of functional imaging techniques such as dynamic contrast-enhanced CT (DCE-CT) or MRI (DCE-MRI) and diffusion MRI has enabled the assessment of information such as tumour vascularity, permeability and cellularity non-invasively. Therefore, there is a growing interest in using these new techniques to early assess the response of treatment as well as to follow patients during treatment. These methods may be of great help, not only to test the effect of new drugs and determine the groups of patients and tumours that could benefit from a new drug, but also to monitor the treatment of an individual patient. After reviewing the basic principles and the theory involved in DCE-CT, DCE-MRI and diffusion

MRI, we will address the technical aspects and requirements of these functional imaging methods. The spread of these techniques, however, is slowed down by many limitations that will be discussed. Not only they tend to be more complex to implement than routine morphological protocols, but they are very sensitive to the acquisition parameters and the mathematical models and software models used to extract the parameters. Consensus and normalization are still required.

Learning Objectives:

1. To learn about the portfolio of functional imaging response methods in CT and MRI.
2. To understand the current clinical value of each technique.
3. To appreciate potential advantages compared to PERCIST.

Author Disclosure:

C.A. Cuénod: Grant Recipient; travelling expenses Schering and Guerbet, Research grant GE.

17:14

Panel discussion: When and how will functional imaging overcome morphological assessment?

16:00 - 17:30 **Room D**

Musculoskeletal

RC 1210

Imaging the hip and thigh

Moderator:

V. Njagulj; Sremska Kamenica/RS

A-537 16:00

A. Femoroacetabular impingement: what is it, how do I image it and does it matter?

R. Sutter; *Zurich/CH*

The last decade has seen a constant rise in the number of patients diagnosed and treated for femoroacetabular impingement (FAI). However, there are ongoing controversies about the accuracy of measurements for assessing FAI and an associated overdiagnosis of FAI. This refresher course covers the pathophysiology of FAI, the classic osseous hallmarks, and the characteristic damage to the articular cartilage and labrum. It gives an overview of state-of-the-art FAI imaging with different radiological modalities, including the use of traction at MR arthrography, and addresses possible pitfalls when evaluating the hip joint. Additional anatomical factors are described that contribute to the development of FAI, such as abnormal femoral antetorsion and acetabular version, and finally the relevance of the different parts of the diagnostic algorithm for evaluating FAI are discussed.

Learning Objectives:

1. To understand the mechanism of femoroacetabular impingement.
2. To learn about the imaging findings in patients with femoroacetabular impingement.

A-538 16:30

B. Groin pain in the athlete: what causes it and what does imaging contribute?

M. Maas; *Amsterdam/NL (m.maas@amc.nl)*

The diagnosis and classification of groin pain in athletes is a topic of ongoing debate and extensive research, since groin pain comprises 2 to 5 percent of all sports injuries that is potentially career-ending. How come the trouble arriving at an easy to treat diagnosis? First of all there is a very complex anatomy. Besides the complex anatomy that will be discussed in the presentation, differential diagnosis is quite broad, including intra-abdominal pathology, genitourinary abnormalities, referred lumbosacral pain and hip joint disorders. Secondly, in the field of sports medicine only recently there is an improvement of diagnostic dedicated tests allowing better narrowing of the differential. Adductor strains and osteitis pubis are the most common musculoskeletal causes of groin pain in athletes. And then there still is the debatable sportman's hernia. In the field of imaging, the mainstay is to start with pelvic radiography, also in young athletes. The not completely matured symphysis pubis will not be easy to distinguish normal from abnormal. Features will be discussed. In the field of MRI recently The Copenhagen standardized MRI protocol is launched that can assess the pubic symphysis and adductor regions in athletes. We will provide details on this strategy. We also will enlighten on the role of US imaging and US-guided intervention in this specific population. Most important topic is to stress the team effort in this complex type of injury in these athletes. We will illustrate this with our initiatives in the IOC centre of scientific excellence ACES in Amsterdam.

Learning Objectives:

1. To understand the anatomy of the groin region.
2. To learn about the imaging findings in athletes with groin pain.

A-539 17:00

C. Muscle injury of the hip and thigh

M.-A. Weber; *Heidelberg/DE (MarcAndre.Weber@med.uni-heidelberg.de)*

This lecture will focus on MRI for the assessment of muscle injuries at the hip and thigh using fluid-sensitive sequences. Muscle injuries include a large variety of imaging patterns from occasionally subtle changes in muscle strain to complete muscle tears. Exercise-related chronic changes such as delayed onset muscle soreness, compartment syndrome and muscle hernias, as well as complications of muscle injuries such as myositis ossificans may be encountered. The MRI appearance of a muscle contusion may be similar to a muscle strain/tear. Mild post-exercise oedema can persist for some time and can mimic a low-grade muscle strain injury. 35% of all soccer injuries are muscle injuries and they are the most frequent cause for missing a game. The myotendinous junction is the weakest link in the muscle-tendon-bone chain. The widely used grading system for muscle injuries divides muscle injuries into four grades (grade 0: normal MRI, i.e. functional injury of the muscle, grade 1: oedema, grade 2: partial rupture, grade 3: complete tear). However, this grading system is only a rough estimate, because grade 2 injuries comprise a wide range from tiny fibre discontinuities to subtotal muscle ruptures. Measures of the longitudinal length as well as the percentage and volume of the muscle injury in MRI have some predictive value with respect to time to return to sports activities. Moreover, injury to the intramuscular component of the tendon has prognostic significance. A complete tear (grade 3) may require surgery.

Learning Objectives:

1. To understand the imaging patterns of muscle injury at the hip and thigh.
2. To learn about grading and prognostic values of muscle injuries.

16:00 - 17:30 **Room G**

Multidisciplinary Session

MS 12

Transcatheter aortic valve implantation (TAVI)

A-540 16:00

Chairman's introduction: A brief history of TAVI

A. Cribier; *Rouen/FR (alain.cribier@chu-rouen.fr)*

Aimed at redressing the limitations of balloon aortic valvuloplasty developed by our group in 1985 for the treatment of inoperable patients with aortic stenosis (AS), TAVI (transcatheter aortic valve implantation) emerged in 2002 to profoundly alter the landscape of cardiovascular medicine. This new disruptive technology is among the important "medical breakthroughs" till date. It evoked scepticism and criticism in the beginning. But, thanks to innumerable clinical trials and evidence-based investigations, it is widely accepted by the medical community now and this acceptance is continuing to grow. In the last decade, TAVI has been performed in about 300 000 patients around the world and its use keeps growing 40% annually. The field of TAVI is rapidly evolving, with major refinements in technology and procedural techniques, patient selection and biomedical engineering.With the development of better devices, new approaches and new implantation strategies, TAVI has become much simpler and safer. The indications were initially limited to elderly AS patients with multiple co-morbidities. The same are now cautiously and appropriately growing to include a broader population of patients with lower surgical risk and degenerated surgical bioprosthesis. There are few examples of clinical fields in medicine that match the rapid and careful evolution of TAVI.

Session Objectives:

1. To understand the clinical needs of non-surgical techniques for aortic valve replacement.
2. To understand the difficult process of developing a breakthrough innovative technology in interventional cardiology.
3. To understand the importance of "translational research" for the success and expansion of TAVI.

Author Disclosure:

A. Cribier: Consultant; Edwards Lifesciences.

A-541 16:15

The TAVI procedure

H. Eltchaninoff; *Rouen/FR (helene.eltchaninoff@chu-rouen.fr)*

In 2016, TAVR is clearly turning into a routine procedure. This is driven by a number of factors: increased operator's experience, better patient selection and improved 3D adjunctive imaging. But, mainly, striking technology enhancements have changed the world of TAVR with improved systems, and the development of "minimalist strategies" making the procedure faster, simpler safer and more cost-effective. In 2016 was demonstrated the efficiency of new devices provided by the two leading companies, Edwards Lifesciences with its balloon-expandable Sapien 3 valve, and Medtronic with its self-expanding Evolut-R valve. With these new devices, the main complications of TAVR, mortality, paravalvular regurgitation (PV), vascular complications and stroke have been considerably improved. In the US, PARTNER Sapien 3 trial reported this year (583 patients), all cause mortality has decreased at 1 month to 1.1% (13% at 1 year), disabling stroke to 1.0%, PV leak to 3%, major bleeding and vascular complications to 5%. Similar improved results with the Evolut-R in a smaller series of patients were reported. In 2016, with the decreased size of the new devices, TAVR can now be performed using the transfemoral approach (the default access site) in almost 90% of cases, under local anaesthesia, allowing early discharge home within 3 days in a majority of cases (60% in Rouen). In patients non-suitable for transfemoral approach, alternative approaches include trans-aortic, trans-apical, trans-carotid and subclavian routes. TAVR is confirmed to be a breakthrough technology addressing an unmet clinical need validated by rigorous evidence-based studies.

Learning Objectives:

1. To learn the current indications of TAVI and the process of patient selection.
2. To learn the different phases of the procedure using the transfemoral approach.
3. To learn the prevention and treatment of complications.

Author Disclosure:

H. Eltchaninoff: Speaker; edwards lifesciences.

A-542 16:30

The cardiac surgeon's perspective

P.-Y. Litzler; *Rouen/FR (pierre-yves.litzler@chu-rouen.fr)*

During many years, the only treatment of calcific aortic stenosis was surgical aortic valve replacement. Despite excellent results, numerous patients were not eligible to surgery due to comorbidities or frailty. In April 2002, the first human transcatheter aortic valve implantation(TAVI) was performed in Rouen leading to a new era in the treatment of aortic stenosis. The first cases of TAVI were performed with a surgical cut down of the groin under local anaesthesia. But, due to the large diameter of the first catheters (24Fr) and the presence in numerous patients of small calibre vessels, the idea of a transapical approach emerged and, the first patients were implanted in 2005. Few years later, new surgical approaches were developed with transaortic, trans-sub-clavian or transcarotid artery procedure. Transapical approach could be a secure procedure if a perfect analysis of the aortic valve is managed prior to surgery to avoid drastic complication. The measurement of the distances between annulus and coronary ostia, the aortic valve area and the annulus plan are the key points of procedural success. At the beginning of the procedure, a transthoracic echocardiography to determine the position of the apex of the heart is strongly recommended. Multiple studies have reported excellent results whatever the approach (transfemoral, transapical, etc.) and the initial goal, i.e. "to provide an alternative to non-surgical patients" has been reached. However, the long-term durability of the transcatheter valves still unknown and today, the use of TAVI in low risk or younger patients remains controversial.

Learning Objectives:

1. To learn the different mini-surgical approaches for TAVI and the current indications.
2. To learn the different phases of TAVI using the mini-surgical approaches.
3. To learn from a cardiac surgeon the perspectives of surgical valve replacement in the TAVI era.

Author Disclosure:

P. Litzler: Other; Edwards Proctor.

A-543 16:45

Pre-interventional assessment by CT

J.-N. Dacher; *Rouen/FR (Jean-Nicolas.Dacher@chu-rouen.fr)*

In recent years, transcatheter aortic valve intervention (TAVI) gained wide acceptance in patients with severe aortic stenosis contraindicated to surgical valve replacement. Pre-operatively, CT of the heart, aorta and iliac vessels is recommended. Various CT techniques can be performed depending on CT generation. Basically, ECG-gated examination of the heart and aortic root should be performed, completed by non-gated coverage of the abdominal aorta and ilio femoral vessels. Systolic reconstruction of the heart should be obtained to evaluate the aortic valve area and measure the annulus (diameters and planimetry). Diastolic reconstruction can be used for evaluating distances between annulus and coronary ostia, the sub-aortic septum, the calcification and cuspidity of the valve, the extent of the calcification (i) to the annulus (increasing the risk of per procedural rupture) (ii) to the septum (risk of conduction abnormality) and (iii) mitral valve. Vascular route should be evaluated from the access up to the aortic valve. All images should be transmitted to the Cath. Lab. with a structured report, including any other thoraco-abdominal abnormality/disease, a frequent situation is those elderly patients.

Learning Objectives:

1. To learn about the technical principles of MDCT acquisition in pre-TAVI assessment.
2. To learn about the advantages of a structured MDCT report (including key images) validated by the cardiology team.
3. To know the medical impact of the radiology team in the management of TAVI patients.

A-544 16:58

Why use dual-energy CT in TAVI patients?

B. Dubourg; *Rouen/FR (benjamin.dubourg@chu-rouen.fr)*

Since the first introduction of transcatheter aortic valve implantation (TAVI), the number of procedures has increased worldwide. A comprehensive cardiac and aorto-iliac arteries CT angiography before the procedure has become a common and recommended clinical practice. Dual-energy CT (DECT) allows to quantify iodine within a voxel and to display two different data sets : (1) virtual monoenergetic images and (2) Iodine maps. The virtual monoenergetic images allow to increase iodine attenuation at post-processing hence to reduce the injected iodine load. This property is of importance in TAVI population with frequent impaired renal function. Up to 50% reduction of iodine volume can be attained at the expense of an increased image noise which remains acceptable for diagnosis. The iodine maps allow to measure iodine concentration within a voxel. Myocardial extracellular volume fraction (ECV) is a validated myocardial fibrosis marker; it is directly measurable from iodine maps. The ECV calculated from DECT is comparable and/or highly correlated to ECV calculated from MRI. A single delayed post-contrast DECT acquisition could add a prognosis value to the actual standard anatomic comprehensive CT evaluation.

Learning Objectives:

1. To know how to decrease the dose of iodine with new CT technology including dual-energy.
2. To know how to control the radiation dose with new CT technology.
3. To know how to characterise the myocardium with new CT technology.

A-545 17:11

Common and uncommon complications seen by CT

J. Caudron; *Rouen/FR (drjeromecaudron@gmail.com)*

Computed tomography angiography (CTA) is a suitable technique for assessing potential vascular and cardiac complications occurring after TAVI thanks to its good spatial and contrast resolution. Vascular complications are easily evaluated by CTA. Some cardiac complications can be assessed by CT. The cardiac CTA (CCTA) protocol will depend on the clinical context and the degree of emergency. A retrospectively ECG-gated CCTA is adapted in these patients with frequent tachycardia and difficulties to use beta-blockers. Prior acquisition without injection can be useful in case of suspicion of annulus rupture to distinguish the calcifications from extravasation of contrast agent. A normally implanted valve is properly deployed (i.e. with diameter and surface in adequation with the valve size implanted), with good circularity. Its basal portion is located at the level of the native annulus, often some millimetres below. The coronary ostia are free, distant from native valvular calcification. The main complications leading the realization of CTA are 1) vascular complication, often at the point of puncture; 2) malpositioning and/or misdeployment in the aortic root which can lead to paravalvular leak or disturb the opening/closing of the valvular leaflets; 3) valve migration or embolization; 4) annulus rupture, the most severe complication with poor prognosis.

Learning Objectives:

1. To learn the basic cardiac CTA protocol in implanted patients.
2. To know the normal CT findings in implanted patients.
3. To know the complications of TAVI and potential yield of CT.

17:24

Multidisciplinary case presentation and discussion

16:00 - 17:30 **Room K**

Pros & Cons Session

PS 1227

Providing an effective ultrasound service: how and by whom?

Moderators:
L.E. Derchi; Genoa/IT
V. Gibbs; Bristol/UK

A-546 16:00

A. Who provides US services? The situation in Europe
H. Edwards; *Stevenage/UK (hazel.edwards@nhs.net)*

For many years, the majority of ultrasound examinations in the United Kingdom (UK), both obstetric and non-obstetric, have been performed by radiographers who have undergone post-graduate training in ultrasound. These 'sonographers' scan, interpret and report their own examinations. Today, sonographer-led ultrasound services are essential and well established. The second largest professional group performing ultrasound in the UK is radiologists. Other groups including midwives, obstetricians, emergency physicians and aortic screening technicians also contribute to services. This model is successful yet it appears to be unique. No other country relies so heavily on sonographers. Throughout mainland Europe physicians and general practitioners perform the majority of ultrasound examinations. In countries like Australia, Canada and the United States, ultrasound may be performed by sonographers but reporting remains the domain of the overseeing physician. However, as demand for ultrasound services continues to escalate, changes are afoot with small numbers of sonographers now practising in Sweden, Denmark and The Netherlands, some as part of pilot studies. Furthermore, physicians in Germany are beginning to view UK ultrasound services with interest. Evidence supporting the success of UK ultrasound practice will be offered in this presentation. Possible reasons behind the historical development and emerging trends will be discussed. Recommendations for supporting future practice of sonographers outside the UK will be made.
Learning Objectives:
1. To discuss the three models of ultrasound scanning undertaken across Europe.
2. To outline the differences in ultrasound services provided across European countries.

A-547 16:15

B. Should US services be provided by radiologists? (performed and reported on)
M. Claudon; *Vandoeuvre-les-Nancy/FR (m.claudon@chu-nancy.fr)*

Ultrasound (US) is an imaging technique which is now widely expanded among countries and specialties. The increase in daily activity as well as off-hours requests are a challenge for most teams. The possibility of educating technicians for doing the first part of examination has been raised in several European countries on a model partly inspired from the position of sonographers in UK and the USA. However, there are still some challenges which should moderate such an evolution: the level and control of competences and practice of such new activities for technicians, the way technicians should be covered by radiologists in case of complex cases, the difficulty in checking the content of the examination performed by the technician and compared to previous examinations. Therefore, caution should be emphasized before going in this direction, and a careful control of US should be maintained by radiologists
Learning Objectives:
1. To discuss why US examinations should be performed directly by the radiologist.
2. To underline why US examinations should be reported only by the radiologist.
Author Disclosure:
M. Claudon: Speaker; Philips Ultrasound.

A-548 16:30

C. Can or should US services be provided by radiographers/sonographers? Educational needs
G. Harrison; *London/UK (G.Harrison@city.ac.uk)*

In 1977 the College of Radiographers set the standard for ultrasound training in the UK by launching the highly respected Diploma of Medical Ultrasound (DMU). Then, in the early 1990s, radiography education changed to degree level and universities were able to develop their own post-graduate ultrasound programmes, set standards and assessments, independent of the professional body. This allowed entry into ultrasound training to MSc level for radiographers and other health care professionals, such as nurses and midwives. In 1993 the Consortium for the Accreditation of Sonographic Education (CASE) was formed by a number of professional bodies and ultrasound interest groups, to ensure that the standards of these postgraduate programmes met the needs of the health care service. The current remit of CASE includes ensuring high standards of training for ultrasound practitioners and stipulates that reporting should be an integral part of the examination. Ultrasound education is changing to meet the growing demands on the ultrasound service in the UK. There are new programmes being delivered as direct entry programmes at undergraduate and postgraduate levels, for non-health care professionals, and some training is being provided outside the university setting. These will be discussed in relation to other international training models.
Learning Objectives:
1. To outline ultrasound training programmes and curricula in countries where US is undertaken and reported by sonographers.
2. To compare this with other international training models available.

A-549 16:45

D. Is it possible to standardise a 'real-time' examination? Sometimes it is possible, but not always
C. Nyhsen; *Sunderland/UK (nyhsenc@doctors.org.uk)*

Ultrasound is a real-time investigation and has a great variety of indications and uses. The advantage is that practitioners can directly communicate with patients, which allows tailoring of scans for each individual case. This can be very helpful allowing areas to be scanned that may not even have been requested, but on the other hand a thorough investigation is still needed as important pathology may otherwise be missed. This presentation will focus on the ability and limitations of standardising exams and highlight the importance of good team working between sonographers and radiologists.
Learning Objectives:
1. To discuss when and how this is possible.
2. To be able to recognise when an additional examination by the radiologist is needed.

A-550/A-551 17:00

Discussion on the pros and cons
L.E. Derchi; *Genoa/IT*
V. Gibbs; *Bristol/UK (vivien.gibbs@uwe.ac.uk)*

This session will include invited speakers presenting their views on which are the most appropriate groups of healthcare professionals to provide an effective ultrasound service. An overview of the current models in places across Europe will be explored. This will be followed by a facilitated discussion on the advantages and disadvantages of each model.

16:00 - 17:30 **Room M 1**

EuroSafe Imaging Session

EU 5

EuroSafe Imaging Stars

Moderators:
L. Bonomo; Rome/IT
S. Ebdon-Jackson; Didcot/UK

A-552 16:00

Value and limitations of the 'Is your Imaging EuroSafe' surveys
L. Bonomo; *Rome/IT (lorenzo.bonomo@unicatt.it)*

Eurosafe imaging stars is an initiative designed to identify and recognize imaging facilities worldwide that embody best practice in radiation protection. One important contribution Eurosafe imaging stars is making is to participate in the data collection efforts through the "Is your imaging Eurosafe" surveys on CT doses making the resulting benchmarks more reliable. "Is your imaging Eurosafe" comprises a series of surveys on CT DRLs for different indications.The core aim of "Is your imaging Eurosafe" is to build a European repository based on dose exposures for specific clinical indications that would be most useful for self-benchmarking and for future establishment of DRLs. In addition, this repository would provide insights into the influence of the age of the equipment on dose exposures which may be helpful at the local level to stimulate a policy of upgrading or replacing equipment. Finally, repeating the survey in the same centre over a period of three years will provide important information on the evolution of DRLs.

Learning Objectives:
1. To learn about the value of EuroSafe Imaging surveys.
2. To understand how useful the EuroSafe Imaging surveys' findings in our daily clinical activity can be.
3. To understand how data can be collected and what actions are needed to enhance radiation protection of patients.

A-553 16:15

Integration of the 'EuroSafe Imaging Clinical Audit Pack' in imaging departments

B.E. Kelly; *Belfast/UK (barryekelly@mac.com)*

Audit simply means comparing an element of clinical practice against an agreed standard. In radiological practice, this might mean what we do; how we do it; what equipment we use; how we interact with our patients; our colleagues and our environment. To put it another way, audit asks one question: 'are we safe?' Audit should be achievable, local, practical, inexpensive, non-threatening and easy (ALPINE). In February 2018, the Euratom 2013/59 Directive will come into effect. This directive will set comprehensive standards for radiological best practice across the European Union. These standards will become the benchmarks against which our practice is measurable. The audit subcommittee, under the auspices of the ESR, has designed an audit pack to help you get started and to demonstrate how easy audit can be. The purpose of this lecture is not only to do that, but also suggest why you should do it, how it protects you, your patients, optimizes your equipment and your working environment.

Learning Objectives:
1. To gain an appreciation of the place for audit in radiological practice in the 21st century.
2. To understand the difference between audit and research.
3. To appreciate the importance of re-audit in the audit spiral (helix).

A-554 16:30

Benchmarking: why, how and when?

J. Hakumäki; *Kuopio/FI (juhana.hakumaki@kuh.fi)*

Benchmarking is the comparison of processes and performance with peer organizations. The objectives are usually threefold: to determine what type of functions need to be improved, how top performers achieve their performance, and to use this information for performance improvement. In the context of radiation protection, the main goal is not only the reduction of radiation in particular imaging studies but also the employment of alternative imaging techniques with significantly lower (CBCT) or negligible dose (MRI/US), and how this is best done. The employees and the organization using radiation are ultimately responsible for radiation protection and employment of the ALARA (as-low-as-reasonably-achievable) principles. Guidelines, regulations or vendor efforts always require implementation and may not always be sufficient. Benchmarking serves this goal well by providing performance data from peers to peers. Collection of dosage data is usually simple and standardized, and modern imaging information systems store these data already. Data inspection and analysis, however, usually requires dedicated professionals, such as a medical/hospital physicists to partake in the process. The Eurosafe imaging initiative provides guidelines for compatibility, which is introduced in more detail. Scheduling is governed usually by combination of benchmarking requests initiated by authorities, self-initiated assessment work, as well as those implemented or recommended by the Eurosafe imaging initiative for compatible institutions. The extent of this will naturally be limited by personnel and time devoted to such activity. Benchmarking is normally not especially cost-intensive and integrates well into workflow.

Learning Objectives:
1. To understand why to benchmark radiation doses among institutions.
2. To learn how to collect and compare data and how to be compatible with the EuroSafe Imaging initiative.
3. To understand the scheduling and motives for benchmarking.

A-555 16:45

The value of achieving star status

D. Akata; *Ankara/TR (dakata@hacettepe.edu.tr)*

Stars are often used as symbols for classification and ranking purposes. It is a way to announce publicly the level of quality of the service provider. For the first time in radiology, it is used by ESR to promote and endorse institutions for safer and better radiological practice as part of the Eurosafe imaging campaign. The number of examinations using ionizing radiation is tremendously increasing each year. In this regard, justification of the exams and maintaining doses within diagnostic reference levels, to develop a patient safety culture in medical imaging is highly important. When an institution applies to become a EuroSafe imaging star, it revisits the most updated principles for radiation protection to perform safe imaging. Although one of the goals is to harmonize the patient safety standards, it should be regarded differently from an accreditation process. It is not a pass or fail system. It is a system aiming to achieve for the better. With this voluntary action, an institution can do self-auditing and learn their weaknesses, but also in a way declares to be bound and determined to improve. With the star project, awareness of the basic concepts for safe imaging is created not only by the providers, but also for the patients. Moreover, it will be a motivation for institutions to be in the network of imaging departments committed to best practice in radiation protection for future cooperation in projects.

Learning Objectives:
1. To cause awareness of the basic concepts for safe imaging in order to harmonize patient safety standards.
2. To understand criteria and goals to perform the best clinical practice in radiation protection.
3. To learn to do self-auditing and to identify strengths and weaknesses.
4. To gain an insight in the network of imaging departments committed to best practice in radiation protection for future cooperation in projects.

A-556 17:00

How to improve the EuroSafe Imaging Stars concept?

L. Donoso; *Barcelona/ES (ldonoso@clinic.ub.es)*

Launched in February 2016, the EuroSafe imaging stars initiative has been designed to identify and recognise imaging facilities that embody best practice in radiation protection and that are committed to putting the principles advocated and concepts developed by the European society of radiology into practice. By recruiting a network of imaging departments committed to best practice in radiation protection, the stars initiative will give radiation protection efforts greater visibility, have a direct impact on clinical practice, and enable the ESR to collect data for analysis and benchmarking. To become a EuroSafe imaging star, the applicant facility has to perform a self-assessment according to a list of criteria defined by the ESR. The list of criteria is divided into five sections and imaging facilities will be awarded up to five Stars depending on how many criteria of a certain level they fulfil, i.e. from 'EuroSafe imaging star *' to 'EuroSafe imaging star *****'. After the first year of implementation, it is now time to consider the first experiences and lessons learnt, as well as to review the current criteria; e.g. the EuroSafe imaging stars initiative is currently not targeted towards specialised hospitals, like orthopaedic or paediatric hospitals. These facilities cannot complete the current 'Is your imaging EuroSafe?' surveys, although participation is a prerequisite for becoming a star. Thus, measures have to be considered to improve the EuroSafe imaging stars initiative, e.g. the establishment of additional surveys to collect paediatric patient data.

Learning Objectives:
1. To review the current criteria for the different levels of accreditation.
2. To present the experience and the lessons learned after the first year of implementation.
3. To discuss the possible ways for the improvement of the EuroSafe Imaging Stars initiative.

A-557 17:15

Improving the integration of radiation protection in the clinical setting

G. Frija; *Paris/FR (guy.frija@egp.aphp.fr)*

The basic principles of radiation protection are justification, optimisation and dose limitation. The optimisation process is essential to ensure the necessary image quality with minimal exposure of the patient to radiation dose and to maintain diagnostic efficacy at the same time. The ALARA principle ("as low as reasonable achievable") is followed in the optimisation process, which also has to consider different factors, e.g. equipment, type of examination and body region. Image quality in relation to clinical need would be much more relevant than only dose reduction as part of the optimisation process. When a CT is performed, it is clear that the technical protocol is driven by the clinical indication. The resultant image quality needed for a reliable interpretation is consequently also directly linked to the clinical indication. Therefore, it is very important to record the dose exposure on the basis of the clinical indication rather than on technical and/or anatomical protocols. The development of automatic dose recording systems would also facilitate the establishment of local diagnostic reference levels (LDRLs), which have the advantage of better reflecting the distribution of the patient's body characteristics as well as the disease's prevalence and the performance of the used modalities. In addition, it has already been shown that LDRLs would be an effective tool for improving the clinical practice, as one can only improve what one can measure.

Learning Objectives:
1. To clarify the concept of optimisation in relation to the clinical indication.
2. To show why local diagnostic reference levels are appropriate.

16:00 - 17:30 **Room M 2**

Professional Issues and Economics in Radiology (PIER)

PIER 3

Tailoring radiology departments towards patients' needs

Moderators:
C.D. Becker; Geneva/CH
H. Hricak; New York, NY/US

A-558 16:00

A. Visibility of radiology

N.H. Strickland; *London/UK (nicola.strickland@imperial.nhs.uk)*

Radiologists must raise their visibility with their patients, clinical peers and managers if they are to survive as doctors in the hospital environment, and not be relegated to distant report-producing commodities, or be replaced by non-radiologist doctors and/or non-medical personnel. Their reports must add value by being diagnostic and actionable, and not merely observational descriptions devoid of medical interpretation. Their interventions must be based upon their own informed, collaborative clinical assessment of their patients, not carried out in response to directed instruction from their clinical peers. Diagnostic and interventional radiology underpins the whole of modern medicine and surgery. Radiologists must raise their profile by actively involving themselves in a wide gamut of clinical activity including: medical student and postgraduate teaching, advising upon the patient pathway, multidisciplinary team meetings, patient interactions, multidisciplinary research and managerial decisions. Visibility, accessibility and excellent communication skills are key to raising radiologists' profile and making them an indispensable and valued part of the clinical team.

Learning Objectives:

1. To discuss ways of raising the visibility of radiology with our clinical colleagues.
2. To explore the pros and cons of raising the visibility of radiology with patients.
3. To consider how to make radiology the centre of managers' vision.

A-559 16:18

B. Outsourcing in radiology: costs and quality matters

A. Giovagnoni; *Ancona/IT (a.giovagnoni@univpm.it)*

Outsourcing is defined as buying labour, parts or services from a source outside the company rather than using the company's own staff or resources. Over the last five years, outsourcing has become a global trend in business because, when performed properly, it can produce efficiencies not attainable when these functions are performed internally by an organization. Outsourcing in hospitals is becoming more and more popular. The most common services that are outsourced are non-medical tertiary services; in recent years, however, hospitals have started to outsource medical services, so-called "secondary services", which include laboratory, pathology as well as radiology services. Structured and operated effectively, outsourcing can produce significant benefits while enabling hospitals to focus limited resources and management efforts on other areas. Radiology is increasingly being considered for outsourcing due to its unique operating and funding challenges and because of interest expressed by radiologists and outside vendors. The challenge of responding to constant technological advancement, labour shortages and increasing customer service expectations in the face of declining reimbursement, managed care, capital constraints and outpatient competition are compelling hospitals to consider outsourcing. Moreover, the daunting financial and operational challenge of transitioning radiology from an analogue world to a digital one makes management and funding of radiology even more of a challenge for hospitals. Radiology outsourcing arrangements can be tremendous win-win opportunities for radiologists and hospitals; they are very significant undertakings and should be entered into only with realistic goals, commitment, due diligence and confidence by both parties.

Learning Objectives:

1. To define the various types of outsourcing and discussing advantages and disadvantages.
2. To know and analyse the different stages of the outsourcing process.
3. To analyse the legal issues and professional responsibility.

A-560 16:36

C. Demonstrating the added value of the radiologist: the European approach

P.M.A. van Ooijen; *Groningen/NL (p.m.a.van.ooijen@umcg.nl)*

We live in a world that is constantly changing at a high pace. Many of these changes are related to the advances in computer science and can be quite disruptive and turn things around. These changes also have their effects on healthcare in general and radiology in particular. Many technologies have a disruptive effect on the way radiology is practised now and in the near future. The tasks in the patient treatment process will be re-distributed among healthcare professionals and radiologists should understand this and claim their part of this workload based on their knowledge and experience in medical imaging. This will pose threats to the radiological speciality but it also holds tremendous opportunities that will allow radiology to keep adding value to patient care in the future.

Learning Objectives:

1. To know and acknowledge which disruptive technologies will influence future radiology.
2. To know about different workload distribution models between professionals.
3. To determine new possibilities for radiology to add value to patient care.

A-561 16:54

D. Demonstrating the added value of the radiologist: the US/Canadian approach

G. McGinty; *New York, NY/US (geraldinemcginty@gmail.com)*

Advances in technology such as PACS and voice recognition have made radiologists more efficient and productive but have rendered them largely invisible to their referring physician colleagues and patients. Whereas in the past consultation in the radiology department was common, now many physicians do not know where the radiology department is located and worse, if they find it, the door might be locked because the radiologist is too busy to talk to them! As the US healthcare system has sought to embrace value rather than volume in the "Obamacare" era, radiologists risked being considered a commodity and indeed reductions in reimbursement reflected this misperception. The ACR's imaging 3.0 initiative ignited a culture change among radiologists and has led to greater visibility for radiologists. The radiology community has used its advocacy efforts to shape payment policy to incentivise even more engagement with patients and colleagues as well as provide meaningful metrics and reporting methodologies by which radiologists can demonstrate their value. This presentation will discuss the journey that has taken radiologists "out of the shadows" and provide a vision of the future where the value of radiologists is not only recognised but rewarded.

Learning Objectives:

1. To see the change of radiology as a discipline over the last decades and threats out of this.
2. To learn about opportunities of radiology today.
3. To understand about the continuity of care and the role of radiology in this context.

17:12
Panel discussion

16:00 - 17:30 **Room M 3**

Interventional Radiology

RC 1209
Portal hypertension and interventional radiology (IR)

A-562 16:00
Chairman's introduction
V. Vilgrain; *Clichy/FR (valerie.vilgrain@aphp.fr)*

Portal hypertension (PHT) is a common complication of chronic liver cirrhosis. It is defined by an increase in portal pressure. Complications occur (mostly gastro-oesophageal bleeding and ascites) when the portal pressure exceeds 10 mmHg. The role of imaging is twofold: diagnosis of PHT using morphologic imaging and tissue elasticity and performing interventional procedures (TIPS) when indicated. Such procedures are decided in multidisciplinary team sessions.
Session Objectives:
1. To appreciate the role of multidisciplinary treatment of portal hypertension.
2. To learn about imaging and intervention in portal hypertension.
3. To discuss outcomes of interventions in portal hypertension.

A-563 16:05
A. Imaging of portal hypertension
I. Bargellini; *Pisa/IT (irenebargellini@hotmail.com)*

Portal hypertension (PH) represents a fearful complication of several diseases (most frequently liver cirrhosis), being associated with a significant increase in morbidity and mortality. Ultrasound and cross-sectional imaging (CT and MR) are required to evaluate presence and extent of PH complications (such as varices, splenomegaly, ascites), providing essential information for patient's management and treatment planning. Moreover, several surrogate signs have been described in the attempt to reach a confident non-invasive diagnosis of PH. Nonetheless, as of today, definitive diagnosis of PH is based on the measurement of hepatic venous pressure gradient (HVPG). PH is diagnosed by an HVPG higher than 6mmHg, it is considered clinically significant when HVPG is higher than 10mmHg and severe when HVPG is higher than 12mmHg. A direct relation has been demonstrated between HVPG and risk of variceal bleeding, hepatic decompensation and liver-related mortality, and HVPG has become a surrogate endpoint in the assessment of treatment response and reduction of risk of liver-related mortality. However, HVPG measurement is invasive and is routinely available and reliably standardized only in expert centres. Thus, non-invasive methods, such as elastography, are under investigation, able to identify PH, grade its severity and predict presence, extent and risk of variceal bleeding.
Learning Objectives:
1. To appreciate imaging features of portal hypertension.
2. To discuss the appropriate choice and timing of imaging technique in investigation of portal hypertension and its complications.
3. To learn about relevant findings that influence therapy choice in portal hypertension.
Author Disclosure:
I. Bargellini: Advisory Board; Bayer. Speaker; Bayer, Ge Healthcare, Biocompatibles UK Ltd, Sirtex,.

A-564 16:28
B. Embolisation of varices and splenic artery in portal hypertension
I.E. Keussen; *Lund/SE (inger.keussen@med.lu.se)*

Portal hypertension is the most common secondary to liver cirrhosis; however, it can also be caused by portal/splenic vein thrombosis or occlusion. A bleeding secondary to portal hypertension usually originates from esophageal or gastric varices, other sites may be duodenal, stomal or rectal varices. A bleeding from oesophageal varices is primarily most often treated endoscopically with sclerotherapy or rubber banding. Gastric varices are less prevalent but more difficult to treat endoscopically. If medical and endoscopic treatment methods fail, interventional treatment is the next option, which includes embolisation of varices, TIPS, BRTO and partial splenic arterial embolisation. Embolisation of varices may be performed by percutaneous or transjugular-transhepatic approach, but trans-splenic route or direct puncture of the stomal varices are also reported. A BRTO may be applied in patients with a spleno-renal shunt and secondary gastric varices. Partial splenic embolisation may decrease inflow of blood to the portal vein and secondary decrease the portal hypertension. In most cases, a combination of different techniques is necessary to achieve good results.
Learning Objectives:
1. To discuss the rationale for embolisation.
2. To learn about the selection of technique and choice of material.
3. To understand outcomes from embolisation techniques.

A-565 16:51
C. Transjugular intrahepatic portosystemic shunt (TIPS): critical appraisal of techniques and guidelines for treatment
A. Krajina; *Hradec Králové/CZ (antonin.krajina@fnhk.cz)*

TIPS is a percutaneous, minimally invasive method of creating a portosystemic shunt for decompression of portal hypertension (PH). Using transjugular approach, long needle, balloon angioplasty, and stent-graft, a side-to-side shunt of determined diameter is created to shunt blood flow from the portal vein (PV) to hepatic vein or inferior vena cava above the liver. The most often indication for TIPS is cirrhotic ascites, which is sometimes combined with severe hydrothorax. However, TIPS should be used only in those patients who are intolerant of repeated large-volume paracentesis. TIPS has been used as a rescue treatment in rare cases of endoscopically uncontrollable variceal bleeding, especially from gastric fundal varices. Emergent TIPS (in 72 hours) performed in patients with severe PH and high risk of early rebleeding has been proved to have better bleeding control and survival in 1 year. Partial or complete PV thrombosis does not change usual technique of TIPS. TIPS is technically difficult in chronic extrahepatic PV obstruction, in children, and in patients with massive hepatic veins thrombosis (Budd Chiari Syndrome - BCS). The absence of hepatic veins and distorted anatomy due to the caudate lobe hypertrophy requires sometimes direct transcaval approach to the PV in patients with BCS. Moreover, these patients must be anticoagulated life long due to underlying hypercoagulopathy. TIPS demonstrated good control of ascites and reversal of liver failure in large series of patients with BCS. All patients with TIPS must be followed regularly in specialized multidisciplinary centre, and the surveillance of TIPS function is mandatory.
Learning Objectives:
1. To discuss the selection of patients for TIPS.
2. To learn about the techniques for TIPS formation.
3. To discuss outcomes of TIPS and role of imaging surveillance.

17:14
Panel discussion: Appropriate selection of patients for IR including the role of balloon-occluded retrograde transvenous obliteration (BRTO) for gastric varices

16:00 - 17:30 **Room M 4**

Special Focus Session

SF 12c
Gadolinium contrast agents: a Yin and Yang story

A-566 16:00
Chairman's introduction
B. Hamm; *Berlin/DE (bernd.hamm@charite.de)*

Reports that gadolinium is deposited in the body (e.g. brain, bone and skin), though in very small amounts, have shaken the radiological community. This session will first present the latest preclinical data on gadolinium deposition and possible mechanisms of gadolinium tissue accumulation. Next, we will proceed from preclinical insights to the latest clinical findings regarding gadolinium deposition and possible strategies to deal with the challenges faced by radiologists using gadolinium-based contrast agents in MR imaging. Finally, for our daily clinical work, we are also interested in possible future guidelines of the regulatory authorities. The session will conclude with a discussion among the speakers and the audience.
Session Objectives:
1. To become familiar with our current understanding of gadolinium deposition in the body.
2. To learn about the latest clinical and preclinical findings regarding gadolinium deposition.
3. To understand possible mechanisms underlying gadolinium deposition in the body.
4. To learn about the current opinion and strategy of the regulatory authorities.
5. To learn about possible strategies to deal with the challenge of gadolinium deposits.
Author Disclosure:
B. Hamm: Board Member; Deutsche Röntgengesellschaft, ECR, ESR, ESMRMB, ESOR, Deutsche Forschungsgemeinschaft. Grant Recipient; Abbott, Kendle/MorphoSys AG.

A-567 16:05

Latest preclinical data on gadolinium deposition

H.A. Rowley; *Madison, WI/US (hrowley@uwhealth.org)*

This section will provide an update and synthesis of basic science aspects and preclinical studies relevant to gadolinium deposition, with an emphasis on brain findings. To understand gadolinium deposition we must first understand the physiology of transportation, uptake, elimination, localization, and potential retention for metals in general, not just gadolinium. Animal investigations, clinical MRI, and pathologic studies show evidence for iron, calcium, and manganese preferentially localizing to the same deep grey nuclei in the brain as those areas 'stained' with gadolinium, suggesting shared mechanisms of deposition. Tissue levels of gadolinium deposition seen after clinically relevant doses are far below known toxic thresholds, and to date, no signs of tissue damage (e.g. gliosis or neuronal dropout) or corresponding neurologic deficits have been observed. It is important to recognize that all marketed gadolinium agents have been linked to varying levels of gadolinium retention in the body, regardless of specific agent or structural class (e.g. linear vs macrocyclic). Due to underlying physics and chemistry, we must recognize that MRI metrics (T1 signal hyperintensity or relaxometry changes) and tissue data may or may not be well correlated. MRI detection of T1 shortening relies on gadolinium species that are bound to either a chelate or macromolecules; gadolinium phosphates and other salts do not contribute to MRI signal changes but can still be detected using tissue assays. Levels of deposition depend on the organ, cumulative dose, time after injection, the specific pharmaceutical agent, and host factors including prior radiation or chemotherapy.

Learning Objectives:

1. To become familiar with the latest preclinical data on gadolinium deposition.
2. To learn about possible mechanisms of gadolinium deposition in tissues.
3. To be informed about ongoing preclinical studies to avoid gadolinium deposition.

Author Disclosure:

H.A. Rowley: Consultant; GE, Bracco, Bayer, Guerbet, Gore, Genentech.

A-568 16:28

Current clinical situation based on published data

V. Runge; *Berne/CH*

Omniscan, Magnevist, and MultiHance (all being linear gadolinium chelates) are now known to be associated with dentate nucleus hyperintensity, specifically high signal intensity within the dentate nucleus on T1-weighted scans seen pre-contrast after 5 or more prior injections. Dotarem, Gadovist and ProHance, the macrocyclic chelates, are not so associated. Dentate nucleus hyperintensity is likely to reflect more general gadolinium deposition throughout the body in these patients with normal renal function. In patients receiving a very high number of injections, hyperintensity is observed in many other nuclei and structures within the brain. Initial reports suggest associated clinical symptomatology, but are not definitive. The following recommendation has been made by the National Institutes of Health - "When GBCAs are required, consider the use of a macrocyclic GBCA (e.g. gadobutrol, gadoteridol, gadoterate meglumine) rather than a linear agent". The EMA is likely soon to act, with a possible outcome of this and other actions being the withdrawal of multiple agents.

Learning Objectives:

1. To learn about the latest clinical findings regarding gadolinium deposition.
2. To be informed about the latest trends concerning gadolinium deposition in academia.
3. To learn about possible strategies to deal with the challenge of gadolinium deposits.

Author Disclosure:

V. Runge: Advisory Board; Bayer. Research/Grant Support; Bayer, Guerbet. Speaker; Bayer.

A-569 16:51

What is the position of the regulatory authorities?

O. Clément; *Paris/FR*

There are a considerable amount of studies published in the last 3 years showing hyperintensities in the dentate nucleus in patients having received multiple injections of gadolinium chelates, especially with linear chelates. This new safety concern about gadolinium chelates is happening 6 years after the nephrogenic systemic fibrosis crisis where the European Medicines Agency (EMA) released decisions concerning the classification and use of gadolinium chelates in renal insufficiency. Here, new clinical aspects have to be taken into account: who are the populations at risks? Which chelates are involved? Should the marketing authorisations be changed? On March 2016, the European Commission triggered a procedure under article 31 of Directive 2001/83/EC and asked the Pharmacovigilance Risk Assessment Committee (PRAC) to assess the impact of the new findings on the benefice/risk balance of gadolinium chelates and to issue recommendation concerning the marketing authorisations. The procedure included questions to the pharmaceutical companies, and the organisation of an ad hoc expert group at the EMA. The final conclusions are still awaited at the time of writing this abstract, but might be public during ECR 2017.

Learning Objectives:

1. To learn about the current opinion and strategy of the regulatory authorities.
2. To learn about possible strategies to deal with the challenge of gadolinium deposits.
3. To learn whether alternative contrast agents will become available in the near future.

17:14

Panel discussion: After all that, what are you doing?

16:00 - 17:30 **Room M 5**

Joint Session of the ESR and the EANM

Common diagnostic guidelines on diabetic foot, osteomyelitis and prosthetic joint infection

Moderators:
V.N. Cassar-Pullicino; Oswestry/UK
A. Signore; Rome/IT

A-570 16:00

Guidelines on osteomyelitis (part 1)

L.M. Sconfienza; *San Donato Milanese/IT (io@lucasconfienza.it)*

Although the bone was one of the first organs to be evaluated in radiology, the diagnosis of osteomyelitis still remains a challenge. Over time, plain radiography, computed tomography and magnetic resonance imaging have been variously used to detect acute and chronic osteomyelitis in different locations of the body. On the other hand, nuclear medicine has been also used with good diagnostic performance. From 2013 onwards, a collaboration between ESR, EANM and the relevant clinical societies has taken place to develop common guidelines on the topic. In this session, we present the process which led to the development of these guidelines and the results of such a work.

Learning Objectives:

1. To learn about the current literature evidence on the diagnosis of osteomyelitis using radiological and nuclear medicine modalities.
2. To understand the consensus process that led to build common diagnostic flowcharts on osteomyelitis.
3. To become familiar with diagnostic flowcharts on osteomyelitis involving radiological and nuclear medicine modalities.

Author Disclosure:

L.M. Sconfienza: Equipment Support Recipient; Travel grants by Bracco Imaging Srl / Esaote.

A-571 16:15

Guidelines on osteomyelitis (part 2)

A. Glaudemans; *Groningen/NL (a.w.j.m.glaudemans@umcg.nl)*

In this session the latest version of the joint guidelines on the imaging of peripheral bone infection are presented. These guidelines have been prepared with the collaboration of delegates from ESR, EANM, ESCMID and EBJIS. The focus in this nuclear medicine part will be on the statements presented in the guidelines that focus on nuclear medicine techniques.

Learning Objectives:

1. To learn about the current literature evidence on the diagnosis of osteomyelitis using radiological and nuclear medicine modalities.
2. To understand the consensus process that led to build common diagnostic flowcharts on osteomyelitis.
3. To become familiar with diagnostic flowcharts on osteomyelitis involving radiological and nuclear medicine modalities.

A-572 16:30

Guidelines on prosthetic joint infection (part 1)

L.M. Sconfienza; *San Donato Milanese/IT (io@lucasconfienza.it)*

With ageing of general population, prosthetic substitution of joints has become extremely diffuse. Prosthetic joint infection (PJI) is a complication occurring in about 3% of patients undergoing prosthetic substitution of joints. The diagnosis of PJI still remains a challenge. Over time, plain radiography, computed tomography and magnetic resonance imaging have been variously used to detect the presence of infection around metallic implants. On the other hand, nuclear medicine has been also used with good diagnostic performance. From 2013 onwards, a collaboration between ESR, EANM and the relevant clinical

societies has taken place to develop common guidelines on the topic. In this session, we present the process which led to the development of these guidelines and the results of such a work.

Learning Objectives:

1. To learn about the current literature evidence on the diagnosis of prosthetic joint infection using radiological and nuclear medicine modalities.
2. To understand the consensus process that led to build common diagnostic flowcharts on prosthetic joint infection.
3. To become familiar with diagnostic flowcharts on prosthetic joint infections involving radiological and nuclear medicine modalities.

Author Disclosure:

L.M. Sconfienza: Equipment Support Recipient; Travel grants Bracco Imaging / Esaote.

A-573 16:45

Guidelines on prosthetic joint infection (part 2)

O. Gheysens; *Leuven/BE (olivier.gheysens@uzleuven.be)*

The number of joint prosthesis replacements is still increasing due to an increased life expectancy. Even though in the majority of patients, better joint function and pain relief is obtained, prosthetic joint infection (PJI) is a complication with an incidence between 2 and 4%, which leads to a high socio-economic burden. Early diagnosis of PJI is of utmost importance to save the prosthesis and joint function. In this session, we will present the latest joint guidelines for the diagnosis of PJI. These guidelines have been prepared in collaboration between EANM and ESR as well as the clinical societies (EBJIS and ESCMID).

Learning Objectives:

1. To learn about the current literature evidence on the diagnosis of prosthetic joint infection using radiological and nuclear medicine modalities.
2. To understand the consensus process that led to build common diagnostic flowcharts on prosthetic joint infection.
3. To become familiar with diagnostic flowcharts on prosthetic joint infections involving radiological and nuclear medicine modalities.

A-574 17:00

Guidelines on diabetic foot complications (part 1)

A. Leone; *Rome/IT (a.leonemd@tiscali.it)*

Soft tissue and bone superimposed infection involving the foot is one of the most common long-term complications of diabetes mellitus. Diagnosing these complications is crucial to make proper decisions regarding therapeutic strategies, and should be clinically based on the presence of local or systemic signs or symptoms of inflammation. However, a probable diagnosing is reasonable if there are positive results on a combination of diagnostic tests such as probe-to-bone, serum inflammatory markers, and imaging modalities. Each imaging modality, however, does not provide enough information alone and a multimodal approach should be used for an accurate diagnosis. In an effort to provide guidance for diagnosing diabetes-related foot complications, this presentation is divided into 3 parts: part 1 will review diabetic foot complications and illustrate their major radiological imaging features. Part 2 will present the consensus process that led to build common diagnostic flowcharts on diabetic foot complications. Part 3 will illustrate some cases to become familiar with these diagnostic flowcharts.

Learning Objectives:

1. To learn about the current literature evidence on the diagnosis of diabetic foot complications using radiological and nuclear medicine modalities.
2. To understand the consensus process that led to build common diagnostic flowcharts on diabetic foot complications.
3. To become familiar with diagnostic flowcharts on diabetic foot complications radiological and nuclear medicine modalities.

A-575 17:15

Guidelines on diabetic foot complications (part 2)

A. Signore; *Rome/IT (alberto.signore@uniroma1.it)*

In this session, we will present the latest version of the joint guidelines prepared in collaboration between EANM and ESR on the imaging of infections in several musculoskeletal diseases, such as the diabetic foot, spondylodiscitis, prosthetic joint infections and peripheral bone osteomyelitis. These guidelines have been prepared also with the collaboration of other clinical European societies such as the EASD, the ESCMID, the ESNR and the EBJIS.

Learning Objectives:

1. To learn about the current literature evidence on the diagnosis of diabetic foot complications using radiological and nuclear medicine modalities.
2. To understand the consensus process that led to build common diagnostic flowcharts on diabetic foot complications.
3. To become familiar with diagnostic flowcharts on diabetic foot complications radiological and nuclear medicine modalities.

Saturday, March 4

08:30 - 10:00 **Room A**

E³ - ECR Academies: Interactive Teaching Sessions for Young (and not so Young) Radiologists

E³ 1321
Imaging of abdominal tumours

A-576 08:30
A. Liver tumours
A. Luciani; *Créteil/FR (alain.luciani@aphp.fr)*

Imaging of liver tumours relies on optimal imaging instrumentation, thorough understanding of the key underlying liver diseases, and on key diagnostic elements. This session should provide attendees with the main elements allowing an accurate management of patients suspected of baring liver tumours. Current guidelines recommend that MRI and ultrasound, especially contrast-enhanced ultrasound (CEUS) should be preferred to CT for the diagnosis of benign liver tumours. The lecture will provide the opportunity to review key diagnostic features of liver cysts, haemangiomas and focal nodular hyperplasia (FNH). The differential diagnosis with liver hepatocellular adenomas and the specific role of hepatobiliary contrast agents in that context will also be discussed. Current guideline for the detection and characterisation of patients with underlying chronic liver disease will be reviewed, including the most up-to-date criteria for non-invasive HCC characterisation. Last, the imaging management strategies of liver metastases will be presented.
Learning Objectives:
1. To become familiar with the differential diagnosis.
2. To identify the key imaging findings.
Author Disclosure:
A. Luciani: Grant Recipient; Bracco. Investigator; GEMS. Research/Grant Support; GEMS, Siemens Helathcare. Speaker; GEMS.

A-577 09:15
B. Pancreatic tumours
C. Matos; *Lisbon/PT (celso.matos@fundacaochampalimaud.pt)*

Despite the advent of more and more sophisticated imaging techniques (US, CEUS, EUS, MDCT, MRI, PET-CT) the diagnosis and staging of pancreatic solid lesions remains a challenge. As for other organs and disease entities no single imaging modality is perfect. Differential diagnosis and management decisions are based on a mixture of clinical information and imaging findings involving multiple modalities. This lecture will familiarise the attendees with old truths, main challenges and new trends in the diagnosis of pancreas tumours, differential diagnosis with pancreas inflammation, and in identifying features that may help to select surgical candidates.
Learning Objectives:
1. To become familiar with the differential diagnosis.
2. To identify the key imaging findings.

08:30 - 10:00 **Room B**

GI Tract

RC 1301
Difficult challenges in imaging the acute abdomen
Moderator:
S.K. Puri; New Delhi/IN

A-578 08:30
A. Perforation of the GI tract
V. Maniatis; *Aabenraa/DK (vmaniatis67@gmail.com)*

Perforation of the gastrointestinal tract represents an emergency and life-threatening condition. Causes of perforation may be traumatic (endoscopy, blunt trauma, ingested foreign body), inflammatory (peptic ulcer disease, diverticulitis, appendicitis, Crohn's disease or other enteritis), bowel ischaemia and neoplasms. Clinical diagnosis may be difficult and patients may be first radiologically evaluated with plain radiographs or ultrasound but with limited information in cases of perforation. CT scanning is by far the imaging method of choice in cases of perforation. CT findings of gastrointestinal tract perforation can be direct or indirect. Direct findings include free air or/and oral contrast either intra- or retroperitoneal. Indirect findings comprise inflammatory mass surrounding an appendicolith or a radiopaque foreign body. Non-specific findings include bowel wall thickening, mesenteric infiltration, interloop free fluid and abnormal bowel wall enhancement. With the use of both direct and indirect findings, the sensitivity of CT in diagnosing gastrointestinal tract perforation is up to 92%. False-positive results usually occur in post-operative patients, where free air as a result of previous operation can be misdiagnosed as a sign of anastomotic leak or iatrogenic bowel trauma. CT is also able to depict the site of perforation with an overall accuracy between 82 and 90% and the cause of perforation in up to 67% of cases. It is well documented that CT plays a crucial role in the assessment of patients with gastrointestinal tract perforations, by offering fast and accurate essential information to the clinicians and enabling the most correct therapeutic choice.
Learning Objectives:
1. To learn about the main causes and clinical symptoms of GI tract perforation.
2. To become familiar with the imaging methods used to detect GI tract perforation and with relevant diagnostic algorithms.
3. To appreciate the important imaging appearances indicative of GI tract perforation. What should radiologists not miss?

A-579 09:00
B. Bowel obstruction
A.J.B.S. Madureira; *Porto/PT (ajbmadureira@gmail.com)*

Bowel obstruction is an important cause of surgical admissions for acute abdominal pain, with high morbidity and mortality if left untreated. The diagnosis can be suggested by plain abdominal films but CT plays a crucial role in the diagnosis and management of these patients. It can confirm the diagnosis, grade the severity of the obstruction, locate it, and provide the aetiology. A dedicated technique is necessary and multiplanar reconstructions are mandatory. The causes of small bowel obstruction can be divided into intrinsic (inflammatory diseases, neoplasia), extrinsic (adhesions, hernias), and intraluminal (gallstones, bezoars). The three most frequent causes of large bowel obstruction are neoplasm, volvulus, and diverticulitis. The imaging findings vary according to the cause, and some are very specific. CT can provide a quick diagnosis and allow an early and optimal management of these patients, contributing to an improved survival.
Learning Objectives:
1. To learn about the different types and causes of bowel obstruction.
2. To become familiar with relevant imaging signs in both small and large bowel obstruction including complications.
3. To appreciate the most widely used imaging approach for detection and evaluation of bowel obstruction.

A-580 09:30
C. Acute biliary conditions
C.D. Becker; *Geneva/CH*

Acute cholangitis is a serious condition which occurs most commonly in the context of bile duct obstruction du to stone disease or strictures. Unless diagnosed and treated correctly, acute cholangitis may lead to liver abscess formation, septicemia and multiorgan failure. The role of noninvasive imaging is to determine the presence of obstruction of the biliary tree, as well as its level and its cause. Although ultrasonography or computed tomography are most commonly used in the emergency situation, magnetic resonance imaging offers the most detailed diagnostic results, especially with regard to the cause obstruction. Depending on the level and the cause of bile duct obstruction, decompression of the biliary tree may be done by means of minimally invasive interventional techniques either via the endoscopic-retrograde or the percutaneous-transhepatic approach. Acute gallbladder disease is most often associated with calculous disease and obstruction of the cystic duct, although it may also occur without the presence of calculi (acalculous cholecystitis). Ultrasonography should always be used as the first line method in suspected gallbladder disease.
Learning Objectives:
1. To learn about the most common pathologies leading to acute biliary conditions.
2. To become familiar with the relevant multimodality imaging appearances in this group of patients.
3. To appreciate the role of interventional radiology in the management of these conditions.

08:30 - 10:00 **Room C**

Special Focus Session

SF 13a
Cases I'll never forget in chest imaging

A-581 08:30
Chairman's introduction
A.P. Parkar; *Bergen/NO (apparkar@gmail.com)*

Errors in radiology reporting occur regularly, and the underlying causes are well studied and documented. Most errors are recognized early and do not cause permanent harm, but sometimes the delays caused by errors lead to serious harm to patients. The errors can be divided into perceptual (observational) and cognitive (interpretative) errors, the prior being the most common, up to 80% of errors. The pathology is not seen or observed, often as it is hidden behind another structure or in an uncommon location. Sometimes the reason why it was missed initially cannot be found when reviewed retrospectively. In addition, an additional finding may be missed due to so-called “satisfaction of search”. Cognitive errors are when the pathology is seen but interpreted incorrectly. This may be because the reader is misled by irrelevant clinical information, or simply lacks the knowledge to understand the clinical relevance of the finding. In chest radiology, there are pitfalls in the plain radiographs related to certain anatomical areas, to the way the image has been performed (supine or with insufficient inspiration) or inherent limitations of the modality. Lung cancers are frequently missed, and up to 50% of nodules below 10mm are missed initially on radiography. A systematic approach to reading chest radiographs and CT images is necessary to avoid common reporting errors.
Session Objectives:
1. To become familiar with the common mistakes in chest imaging.
2. To understand the value and limitation of pattern recognition.
3. To appreciate the value of combing pattern recognition and clinical information.

A-582 08:34
Nodules (0.4-2 cm)
A.R. Larici; *Rome/IT (annarita.larici@unicatt.it)*

Errors in imaging interpretation are the principal causes that bring a radiologist to remember a certain case for the whole life, and this eventuality may occur both in chest radiographs and CT scans. Observer error is one of the most important mechanisms leading to a misdiagnosis of a pulmonary nodule and includes scanning error, recognition error, decision-making error and satisfaction of search. Technical considerations, such as image quality and patient positioning and movement, are also factors that can contribute to the likelihood of missing lung nodules, mainly on chest radiographs. Nodule characteristics also play a critical role and include size, conspicuity and location. Up to 96% of nodules are less than 10 mm, with a reported malignancy rate of 1-12%. These nodules may be easily missed on chest radiographs, particularly if they show ill-defined margins or ground-glass density, or if they are masked by superimposed chest structures or have endobronchial location. To learn about chest anatomical details and to become familiar with the possible appearance and differential diagnosis of pulmonary nodules is helpful in avoiding misinterpretation. This presentation will cover the learning objectives using side-by-side plain films and CT scans in most of the selected cases, to help understand how to systematically review chest x-ray and improve radiologist’s accuracy in interpreting this challenging topic.
Learning Objectives:
1. To understand the anatomical and pathological basis.
2. To learn about typical diagnoses and differentials.
3. To appreciate typical caveats and pitfalls.

A-583 08:43
Masses and consolidation (> 2 cm)
C.P. Heussel; *Heidelberg/DE (heussel@uni-heidelberg.de)*

A mass is any pulmonary, pleural, or mediastinal lesion seen on chest radiographs as an solid or partly solid opacity greater than 3 cm in diameter (Fleischner Society: Glossary of Terms for Thoracic Imaging, Radiology 246). Radiologists are expected to identify masses sensitive and easy on chest x-ray; however, detectability might be difficult due to, e.g. superimposition. Consolidations, however, suffer mainly from correct differential diagnosis taking clinical information into account. Knowledge of anatomy, sensibility to the weaknesses of conventional radiology, and differential diagnoses are helpful for correct image reading and interpretation. Similar to masses, a consolidation appears as a homogeneous increase in pulmonary parenchymal attenuation that obscures the margins of vessels and airway walls usually giving an positive pneumobronchogram. Therefore, a series of abnormal chest x-ray is demonstrated with giving the audience the possibility for own image analysis like a quiz. Furthermore, characterization will be discussed in other lesions.
Learning Objectives:
1. To understand the anatomical and pathological basis.
2. To learn about typical diagnoses and differentials.
3. To appreciate typical caveats and pitfalls.

A-584 08:52
Ground glass opacity
M.-P. Revel; *Paris/FR (marie-pierre.revel@aphp.fr)*

Ground glass opacity (GGO) is defined by a hazy increased opacity which does not obscure the underlying vascular markings of the lung parenchyma. It may result from a partial filling of the alveolar spaces, a thickening of the alveolar walls or septal interstitium, or from a combination of these changes. On CT, it is important to evaluate whether the GGO is focal or diffuse, and in diffuse forms to look for homogeneity, distribution and ancillary findings such as traction bronchiectasis, intralobular lines resulting in a crazy-paving pattern, the presence of cysts, of lobule sparing. The main differential diagnosis is mosaic perfusion, characterized by an asymmetry of vessels between the low and high attenuating areas. Diffuse GGO may also be overlooked, but can be suspected if the “dark bronchus sign” is present. To find out the cause, it is important to take into account the chronicity of symptoms, the patient's immune status, smoking history and preexisting medical condition.
Learning Objectives:
1. To understand the anatomical and pathological basis.
2. To learn about typical diagnoses and differentials.
3. To appreciate typical caveats and pitfalls.

A-585 09:01
Reticular pattern
J. Coolen; *Leuven/BE (johan.coolen@uzleuven.be)*

When a collection of innumerable small linear opacities on CXR or HRCT merges into an network we speak about reticulation. On HRCT it is one of the imaging findings that may suggest the presence of a diffuse interstitial lung disease (ILD). The Fleischner Society propose this ‘reticular pattern’ in the glossary of terms, because this pattern approach is not purely descriptive but already contains some interpretation of what is seen and hence narrows the differential diagnosis. The key points are to identify the dominant types of linear opacities (interlobular/perilobular/intralobular), to establish what portion of the lung is predominantly involved (central/peripheral and upper/mid/lower zone) and to describe the appearance of reticulation (smooth/nodular/irregular). When all the radiological patterns (ground glass/nodular/honeycombing/mosaic attenuation) or other radiological signs are correctly interpreted, the radiologist must be aware whether these findings fit with acute disease or are more likely to be associated with chronic inflammatory or even fibrotic change of lung tissue. This format provides mostly a pattern-based specific diagnosis or a shortened list of differential diagnoses. However, in ILD establishing the correct diagnosis, mostly an integrated pathologic-radiologic-clinical correlation is mandatory.
Learning Objectives:
1. To understand the anatomical and pathological basis.
2. To learn about typical diagnoses and differentials.
3. To appreciate typical caveats and pitfalls.

A-586 09:10
Cystic pattern
S.R. Desai; *London/UK*

"no abstract submitted"
Learning Objectives:
1. To understand the anatomical and pathological basis.
2. To learn about typical diagnoses and differentials.
3. To appreciate typical caveats and pitfalls.

A-587 09:19
Airway abnormalities
E. Castañer; *Sabadell/ES (ecastaner@tauli.cat)*

Radiologists are crucial in the diagnosis of airway abnormalities. Conventional radiography is the first step but often lesions are identified only when large. MDCT plays an important role in the characterization of lesions and improved planning for interventional procedures. The radiologist is often the first to suggest the diagnosis of a diffuse tracheal disease. A systematic approach to a large-airway lesion considers the focality or diffuseness of the lesion, the airway that is involved, and whether the posterior airway membrane is

involved. By noting the wall portion affected and its abnormal characteristics sometimes a diagnosis can be suggested. Some entities cause circumferential wall thickening (Wegener´s granulomatosis, amyloidosis, intestinal inflammatory disease), whereas others affect mainly the tracheal cartilage (relapsing polychondritis, tracheobronchopathia osteochondroplastica). We will review the anatomy and histology of the airways, and present some demonstrative cases. Most errors in diagnosing central airway disease are caused by our failure to look at these structures. If we remember to look at the airways, we usually have no difficulties in recognizing disease.

Learning Objectives:

1. To understand the anatomical and pathological basis.
2. To learn about typical diagnoses and differentials.
3. To appreciate typical caveats and pitfalls.

A-588 09:28

Vascular abnormalities

M. Das; *Maastricht/NL*

"no abstract submitted"

Learning Objectives:

1. To understand the anatomical and pathological basis.
2. To learn about typical diagnoses and differentials.
3. To appreciate typical caveats and pitfalls.

A-589 09:37

Pleural disease

C. Beigelman; *Lausanne/CH*

Common reporting errors regarding pleural disorders may be related to the difficult recognition of findings with chest x-ray such as those related to a pneumothorax in supine position or intrafissural in location. The projection of a device or the presence of an underlying lung disease such as bullae of emphysema may also be responsible of an underestimation (satisfaction of search) of a pneumothorax. All these mistakes are usually solved using CT. Errors in interpretation may also delay the accurate diagnosis. This is especially the case for focal pleural thickening (PT) that may be related to typical pleural plaques, but may also correspond to normal structures, previous tuberculosis, pleural metastasis, silicosis, or other rarer conditions. Furthermore, postero-basal PT in supine examination may be reversible on prone position. In all cases, a careful analysis of other CT findings, of previous imaging studies and the clinical history (previous malignancy, talc pleurodesis) are determinant for the final diagnosis. Features suggestive of malignancy include circumferential pleural thickening, nodular pleural thickening, parietal pleural thickening greater than 1 cm and mediastinal pleural involvement. However, atypical aspects such as pleural effusion even without plaque and pleural irregularity may be observed in mesothelioma and slight changes in the mediastinal or interlobar pleura should be considered suspicious of this diagnosis. The correct recognition of such potential pitfalls will ensure the best diagnostic quality for the patients.

Learning Objectives:

1. To understand the anatomical and pathological basis.
2. To learn about typical diagnoses and differentials.
3. To appreciate typical caveats and pitfalls.

09:46

Panel discussion: How to avoid common mistakes in the interpretation of chest imaging?

08:30 - 10:00 **Room O**

Special Focus Session

SF 13b

Cardiac imaging in prevention and screening: who, when and how?

A-590 08:30

Chairman's introduction

T. Leiner; *Utrecht/NL (t.leiner@umcutrecht.nl)*

The widespread availability of ultrasonography, multidetector row CT and fast-gradient MR systems has enabled high-quality cardiac imaging in many centres. This has converged with the recognition that early and subtle alterations in cardiac structure and function can be detected before becoming clinically relevant. In this session, we explore the role of cardiac imaging in prevention and screening. In the first part, the role of cardiac imaging in athletes is discussed, including the ability of imaging techniques to differentiate effects of physical training from cardiac disease. The second lecture will focus on the complementary role of imaging in individuals with elevated cardiac risk factors over clinical risk scoring systems. The third lecture will cover the role of imaging in screening for cardiac disease of suspected or known genetic origin.

Session Objectives:

1. To recognise and interpret cardiac alterations in athletes, individuals with elevated cardiac risk factors and patients with suspected genetic cardiac disease.
2. To understand when and in whom cardiac imaging is indicated according the best available evidence today.
3. To perscribe practical MR and CT approaches in populations that qualify for prevention and screening using imaging.

Author Disclosure:

T. Leiner: Board Member; Society for Cardiovascular Magnetic Resonance (SCMR), European Society for Magnetic Resonance in Medicine and Biology (ESMRMB). Grant Recipient; Netherlands Heart Foundation, Technology Foundation STW, Netherlands Organisation for Scientific Research,. Research/Grant Support; Bayer, Bracco, Philips. Speaker; Philips.

A-591 08:35

Cardiac imaging in athletes: what is normal, what is abnormal?

B.K. Velthuis; *Utrecht/NL (b.k.velthuis@umcutrecht.nl)*

High levels of sports training generate physiological cardiac adaptation with balanced increase in biventricular size and ventricular hypertrophy. The degree of ventricular dilatation and myocardial wall thickness depends on several factors, including sex, ethnicity, sport discipline, training level and doping. Understanding these changes is essential to distinguish normal variance and sport-adaptation from mild forms of cardiomyopathy. The largest dimensions are usually seen in male endurance athletes. African/Afro-Caribbean athletes can show higher wall thickness and more hypertrabeculation which should not be confused with hypertrophic or non-compaction cardiomyopathy. Long-term high-level endurance sports can induce atrial fibrillation, myocardial fibrosis, more coronary artery calcification and ARVC-like right ventricular dilatation and arrhythmias. Cardiac events in young athletes (<35 years of age) are rare and mostly caused by cardiomyopathy, channelopathies, malignant coronary artery anomalies and myocarditis. Echocardiography is the first imaging investigation if screening reveals abnormalities or athletes are symptomatic, but cardiac MRI is the most all-round imaging modality. Cardiac MRI is better for assessing possible cardiomyopathies, myocardial fibrosis and ischaemia detection. Most cardiac events occur in older male recreational sportsmen and the majority are related to atherosclerotic coronary artery disease (CAD). Low-dose coronary CT, with non-contrast CT to evaluate coronary artery calcium and CT angiography to assess the full extent of the atherosclerotic burden and degree of stenosis, has additional value to a sports-medical examination for screening older athletes or in athletes with atypical complaints. Cardiac events can be triggered by demand ischaemia, even without a significant coronary stenosis.

Learning Objectives:

1. To recognise the spectrum of cardiac alterations due to physical activity and how to differentiate these from disease.
2. To understand the differences in cardiac alterations due to different types of physical activity and training duration.
3. To understand the benefits and limitations of coronary CT in athletes.

A-592 08:58

Screening of individuals with cardiac risk factors: what to look for?

M. Dewey; *Berlin/DE (marc.dewey@charite.de)*

Addressing patients with an increased cardiac risk clinically is difficult. Magnetic resonance (MR) imaging and/or computed tomography (CT) might improve the discrimination of patients with an increased cardiac event risk from those without. The strengths and weaknesses of MR imaging and CT will be discussed. Randomised controlled trials such as PACC, FACTOR-64 and EISNER as well as large-scale population studies such as MESA, SHIP, SCAPIS, UK Biobank, German NaKo, and ROBINSCA will be introduced. Finally, I will outline when and in whom cardiac imaging might be beneficial as a screening approach to better target preventive therapies.

Learning Objectives:

1. To understand the role of imaging techniques in patients with elevated risk for cardiovascular events.
2. To understand the strengths and weaknesses of different imaging modalities.
3. To understand when and in whom cardiac imaging is indicated.

Author Disclosure:

M. Dewey: Author; “Coronary CT Angiography”, Springer, 2009, “Cardiac CT”, Springer 2011 and 2014. Consultant; Guerbet. Patent Holder; Joint patent with Florian Michallek on dynamic perfusion analysis using fractal analysis. Research/Grant Support; Heisenberg Program of the German Research Foundation (DFG) for a Professorship (DE 1361/14-1), FP7 Program of the European Commission for the randomized multicenter DISCHARGE trial (603266-2, HEALTH-2012.2.4.-2),

European Regional Development Fund (20072013 2/05, 20072013 2/48), German Heart Foundation/German Foundation of Heart Research (F/23/08, F/27/10), Joint program of the DFG and the German Federal Ministry of Education and Research (BMBF) for meta-analyses (01KG1013, 01KG1110, 01KG1210), GE Healthcare, Bracco, Guerbet, Toshiba Medical System. Speaker; Toshiba Medical Systems, Guerbet, Cardiac MR Academy Berlin, Bayer-Schering. Other; Cardiac CT Courses in Berlin: www.ct-kurs.de, Institutional master research agreements with Siemens Medical Solutions, Philips Medical Systems, Toshiba Medical Systems. Terms of arrangements are managed by the legal Dept. of Charité Berlin.

A-593 09:21

Evidence base and guidelines for screening genetic cardiac diseases

J. Moon; *London/UK*

"no abstract submitted"

Learning Objectives:

1. To review cardiac imaging findings that can provide clinically important information in patients with suspected genetic cardiac disease.
2. To understand when and in whom cardiac imaging is indicated for screening for manifestations of genetic diseases involving the heart.

09:44

Panel discussion: Who, when and how to screen?

08:30 - 10:00 **Room N**

Head and Neck

RC 1308

Post-treatment imaging of the head and neck

A-594 08:30

Chairman's introduction

H.B. Eggesbø; *Oslo/NO (h.b.eggesbo@medisin.uio.no)*

Head and neck cancer in the Western countries accounts for 3-4% of all cancers. Worldwide incidence is estimated to be 500,000, in Europe 250,000. Three times as many men as women are affected. Squamous cell carcinoma constitutes more than 80% of the head and neck cancers. Though, the histopathology depends on the anatomical region. At the time of the diagnosis 1/3 is in stage I or II and 2/3 in stage III or IV. The recurrence rates for stage I and II is relatively low, with 5-year survival of 70-90%. However, the risk of a secondary primary cancer after radiation therapy (RT) may be higher than the risk of recurrence. For stage III and IV, the local recurrence rates vary from 25 to 80%, and metastases from 10 to 30%. 5-year survival is 10-55%. For stage I and II, the treatment options are surgery and/or RT, while for stage III and IV chemo- and RT are the main options. Common for all treatments are major alterations to the treated tissue that challenge the post-treatment imaging interpretation, independent of modality. This session will focus on expected changes after RT and surgery, including the most frequent surgical procedures. Then finally, when and how to perform post treatment imaging, to depict early cancer recurrence.

Session Objectives:

1. To become familiar with different ways of treatment.
2. To understand post-surgical and post-RT complications.
3. To know how to follow-up patients in order to depict early recurrence.

A-595 08:35

A. Normal findings after radiotherapy

R. Hermans; *Leuven/BE (Robert.Hermans@uzleuven.be)*

After radiotherapy, imaging may be used to monitor tumour response, and to detect recurrent or persistent disease before it becomes clinically evident. Early tumour recurrence may be difficult to distinguish from treatment-induced tissue changes. Therefore, the expected imaging changes after radiotherapy of a head and neck cancer should be well known. These tissue changes depend on the radiation dose, the irradiated volume, and the time elapsed since treatment. Reticulation of fat layers, retropharyngeal space oedema, postirradiation sialadenitis, lymphatic tissue atrophy, and thickening of the pharyngeal and laryngeal structures may be seen. These expected tissue changes often appear symmetrical, unless asymmetric radiation portals were used. However, at the site of a bulky tumour, scar tissue may cause an asymmetric appearance also after successful treatment. Therefore, obtaining a baseline CT or MR study after therapy for a neoplasm with a high risk for recurrence is recommended, best 3-6 months post-treatment. By comparing subsequent studies with this baseline study, tumour recurrences or treatment complications can be detected with more confidence. Some recommend PET-CT as initial baseline study, as this technique has a high negative predictive value; the positive predictive value is lower, as therapy-induced inflammatory changes may cause false-positive results. Tissue necrosis is a rare complication of radiotherapy in the head and neck region, usually appearing late after treatment. Both soft tissue, cartilage and bone necrosis may be encountered; differentiation from tumour recurrence at an early stage may be difficult. Other long-term complications may occur, such as development of a secondary tumour.

Learning Objectives:

1. To get acquainted with changes in tissues during and after radiotherapy.
2. To understand expected changes after radiotherapy in CT and MR imaging.
3. To recognise treatment complications from expected tissue changes after radiotherapy.

A-596 08:58

B. Normal findings after surgery

A. Trojanowska; *Lublin/PL (agnieszka30@yahoo.com)*

Nowadays, the management of head and neck cancer involves multidisciplinary evaluation and treatment, which usually includes surgery, radiation therapy and chemotherapy. The various approaches to surgical resection and tissue reconstruction, the types of neck dissection, different radiation therapy techniques and the addition of concurrent and neoadjuvant chemotherapy regimens may complicate imaging findings. Differentiating post-treatment changes from tumour recurrence with the use of different imaging modalities is challenging because of the presence of altered anatomy secondary to resection, flap reconstructions, oedema, inflammation and the presence of scar tissue. Therefore, it is essential to be familiar with normal findings after surgery and radiotherapy, to distinguish these characteristics from tumour recurrence and treatment-related complications.

Learning Objectives:

1. To get acquainted with most frequent surgical procedures in head and neck.
2. To understand how to evaluate post-surgical patients.
3. To learn how to assess microvascular flaps.

A-597 09:21

C. Treatment monitoring for early detection of recurrence

A.D. King; *Hong Kong/HK (king2015@cuhk.edu.hk)*

Head and neck tumour recurrence occurs in ~25-50% of patients with squamous cell carcinoma treated by CRT, the majority occur “in field” and are detected on the post-treatment assessment or within 3 years of follow-up. Imaging aims to identify early recurrence amenable to curative salvage surgery and avoid unnecessary biopsy or surgery. Reported size criteria for recurrence include ≥1cm primary focal mass and ≥1cm nodal short axis/<75%-90% size reduction. However, size criteria have limitations, notably in HPV+ disease which is associated with large sterile post-treatment nodes. Extracapsular tumour spread and persistent necrosis are also inaccurate signs of persistent nodal disease. The main advantages of MRI over CT are T2 and diffusion-weighted images. Tumour recurrence has similar signal intensity to the pre-treatment tumour, T2 intermediate signal and restricted diffusion (b-1000 high + ADC map low signal), compared to inflammation (high signal) or mature scar tissue (low signal) on the T2 images and ADC maps. Contrast enhancement tends to be moderate in recurrence and between that of mature scar tissue (mild/absent) and granulation tissue/inflammation (marked), but there is overlap on the conventional T1W post-contrast images. False-negative findings arise from microscopic disease such as that found at tumour margins or in pre-treatment occult nodal metastases, and also from small/infiltrating tumours mixed with benign post-treatment change. False-positive findings arise from post-treatment changes, especially granulation tissue/inflammation, sterile component of necrotic node (ADC map low signal) and complications such as radionecrosis, radiation-induced tumours and granulomatous polyps.

Learning Objectives:

1. To get acquainted with problem of recurrence in imaging studies.
2. To understand how to estimate signs of recurrence on CT and MRI.
3. To learn about false positive and false negative findings.

09:44

Panel discussion: What are the challenges in differentiating post-treatment changes from tumour recurrence?

08:30 - 10:00 **Studio 2017**

Genitourinary

RC 1307

Management of incidental findings in the genitourinary tract

Moderator:
R.H. Oyen; Leuven/BE

A-598 08:30

A. Adrenals
L.E. Derchi; *Genoa/IT (derchi@unige.it)*

Adrenal gland abnormalities are unexpectedly identified in 5% to 8% of abdominal imaging studies. Most of them are benign and a source of little or no concern; others are potentially fatal. Clinical and imaging criteria make differentiation between benign and malignant lesions possible in most cases. When there is no history of malignancy, adrenal lesions are almost always non-malignant (usually an adenoma), while in subjects with known malignancy up to 50% of them are malignant, and most metastatic. Imaging criteria based on macroscopic appearance of these lesions can easily identify those containing mature fat (myelolipomas), the hyperdense haematomas and fluid-filled cysts. However, when lesions have non-specific appearance it is necessary to analyse their structure with lipid-sensitive techniques (density measurement at unenhanced CT; chemical shift evaluation at MR), using perfusion/wash-out imaging after contrast medium injection (absolute or relative percentage wash-out calculation) or with metabolic imaging during PET and CT/PET studies. This presentation will discuss how to behave when an unexpected adrenal lesion is detected and how to proceed in its diagnostic workup.

Learning Objectives:
1. To understand the definition of incidental findings in adrenal pathology.
2. To learn about the imaging characteristics of common adrenal incidental masses.
3. To become familiar with the algorithm approach and evidence-based recommendations for management of adrenal incidentalomas.

A-599 09:00

B. Kidneys
H.C. Thoeny; *Berne/CH (harriet.thoeny@insel.ch)*

Cystic and small solid renal masses are frequently detected incidental renal lesions with increasing incidence in the elderly population. Therefore, renal cell carcinomas are also increasingly detected as incidental findings on imaging. Nephron-sparing surgery has been the method of choice for the treatment of small solid renal masses. However, a large percentage of these solid renal lesions is benign and most of the incidentally detected malignant renal tumours such as renal cell carcinomas (RCCs) are smaller, with lower stage and are less aggressive than symptomatic RCCs. In addition, a correlation with size of the solid lesion and growth rate has been described ranging from 0.13 to 0.31 cm per year. Therefore, active surveillance is now a more frequently applied approach to deal with these incidentally detected small solid renal lesions (<3-4cm). Whereas in solid enhancing lesions <1cm in diameter active surveillance is the treatment of choice at any age, in larger lesions management is mainly depending on clinical factors including the age and the performance state of the patient. The role of the radiologist is to exclude benign lesions such as Bosniak I and II cysts and angiomyolipomas as well as non-neoplastic conditions mimicking a tumour (infection, infarct, vascular anomalies and aneurysms). In patients with small solid renal lesions stratified for active surveillance close follow-up with note of the growth rate has to be performed not to miss the time point of delayed treatment in case of a fast growth rate or clinical progression.

Learning Objectives:
1. To understand the definition of incidental findings in renal pathology.
2. To learn about the imaging characteristics of common renal incidental masses, namely cystic.
3. To become familiar with the algorithm approach and evidence-based recommendations for management of renal incidentalomas.

A-600 09:30

C. Adnexa
C.S. Balleyguier [1], T.M. Cunha[2], N. Perrot[3], F.M. Danza[4], I. Thomassin-Naggara[3]; *[1]Villejuif/FR, [2]Lisbon/PT, [3]Paris/FR, [4]Rome/IT (Corinne.BALLEYGUIER@gustaveroussy.fr)*

Incidental adnexal lesions are non-symptomatic lesions diagnosed on ultrasound, CT or MRI performed for an unrelated reason. They have increased in frequency with increased use of cross-sectional imaging. The majority is benign, even in patients with known malignancy or postmenopausal women. However it is important to reliably differentiate malignant from benign lesions to avoid delays in treating ovarian cancer and prevent unnecessary interventions in benign lesions. To try to characterise these findings, age, menopausal status, previous medical and family history and tumour marker such as CA 125 have to be known. Further management will depend on whether the lesion is clearly benign or malignant, or indeterminate. Specific diagnoses have to be suggested in case of fatty content (teratoma, lipoid cell tumour, ...), calcified content (ovarian leiomyoma, teratoma, brenner struma, ...), and in extra-gynaecological origin (lipoleiomyoma, pelvic teratoma, liposarcoma, ...). Diagnostic algorithms in cystic and solid incidentaloma will be presented in this session, including differential diagnoses. A specific focus will be made on diagnostic strategy in post-menopausal cystic ovarian lesions. Treatment strategy will also been described.

Learning Objectives:
1. To understand the definition of incidental findings in adnexal pathology.
2. To learn about the imaging characteristics of common adnexal incidental masses.
3. To become familiar with the algorithm approach and evidence-based recommendations for management of adnexal incidentalomas.

08:30 - 10:00 **Room L 8**

E³ - Rising Stars Programme: EFRS Radiographers' Basic Session

The professional roles of the radiographer

A-601/A-602 08:30

Introduction
H.H. Hjemly; *Oslo/NO (hakon@radiograf.no)*
D. Katsifarakis; *Athens/GR (d_katsifarakis@yahoo.gr)*

The session will highlight the variety of professional pathways radiographers have the opportunity to persuade, emphasising how to conduct service need analysis as a driver for development and the education required to underpin radiographer advanced and consultant practice. It will present and discuss the pathway from clinical practice to management, requirements to ensure a successful transition from clinical practice to management and challenges encountered during the transition and at management level. It will also present how radiographers can have an academic career and/or become a researcher, the main areas of work for radiographer academics in research, teaching and administration. Radiographers are attractive for vendors of medical imaging industry and an experience-based presentation on this possibility will discuss why radiographers should make the move, the breadth of available opportunities, demands of industry and role progression opportunities.

A-603 08:35

Becoming a clinical radiographer: role, role development and specialisation
N.H. Woznitza; *London/UK (nicholas.woznitza@nhs.net)*

Worldwide there has been sustained and significant increases in the number of imaging investigations, driven by an ageing population, new and emerging technologies and dissemination of practice. Radiographers are fundamental to the diagnostic pathway, are integrated into clinical teams and have a unique position from which to improve patient care and outcomes. Clinical radiographers have a varied career pathway, from graduate radiographer to consultant practitioner. Key opportunities for career development will be discussed, as well as an introduction to the evidence base that underpins radiographer reporting. To facilitate role development for radiographers, an outline of service need analysis will be included. The education required to underpin radiographer advanced and consultant practice will be identified. Key points covered: challenges facing a newly qualified radiographer in settings with limited radiologist cover. Becoming a reporting radiographer, with education and audit requirements. Progression from advanced to consultant practice, including research evidence to support role development.

Learning Objectives:
1. To understand the opportunities for different career pathways across the radiography profession.
2. To be aware of the educational requirements underpinning each of the different careers which will be presented within the session.
3. To support radiographers in making choices about their own career development and career pathway.

Author Disclosure:
N.H. Woznitza: Research/Grant Support; College of Radiographers.

A-604 08:53

Becoming a clinical manager

E. Kelly; *Galway/IE (eileenma.kelly@hse.ie)*

Making the transition from clinical practice into clinical management requires extensive consideration. For some the transition results from 'stepping up' into the role of clinical manager while others actively pursue promotion to management and undertake formal managerial studies in preparation for the challenges encountered in a management role. Pre-requisites for a managerial role include excellent communication and people skills, excellent organisational, administrative and project management skills and the ability to adapt in a rapidly changing environment. While it is not essential in Ireland to possess a managerial postgraduate qualification a manager does require six years of post-graduate experience. The role of a clinical manager can be extremely fulfilling with the ability to improve the service provided to patients and support and develop staff in their own professional roles. Managers also encounter many challenges including budget restrictions which impact on technology advances and education and development and ultimately on the quality of service delivery. However, a successful clinical manager overcomes those daily challenges through continued commitment in effective leadership and by empowering and motivating staff.

Learning Objectives:
1. To understand the opportunities that may be available for clinical managers.
2. To be aware of the requirements and qualifications needed for this role.
3. To support prospective radiographers when choosing a managerial role.

A-605 09:11

Becoming an academic and/or researcher

S.J. MacKay; *Liverpool/UK (S.Mackay@liverpool.ac.uk)*

This talk will begin with a description of the role of the radiographer as an academic/researcher drawing on the recognised role from the UK experience. It will explain the main areas of work for radiographer academics in research, teaching and learning and administration. It will then describe the educational requirements to obtain an academic/research post in the UK. Finally, it will discuss the opportunities available for a career in research and academia.

Learning Objectives:
1. To understand the role of the radiographer as an academic person and researcher.
2. To be aware of the educational requirements underpinning this career pathway.
3. To support radiographers by providing the required information on the opportunities in these fields.

A-606 09:29

Working in industry

P. Doherty; *Forchheim/DE (doherty.patrick@siemens.com)*

The healthcare environment is one which is rapidly changing. Consolidation and industrialisation of services are changes which are evident worldwide. Industry partners are evolving to meet these changes. This evolution places unique demands on these companies and one integral cohort of employees for such companies are those who have clinical training. For imaging companies, radiographers are uniquely positioned to leverage their extensive training in a wide variety of areas. The potential for radiographers is vast, but it is imperative that radiographers entering into industry are not only aware of the unique challenges associated with the transition but also of the unlimited rewards that can be attained.

Learning Objectives:
1. To understand the opportunities of working in industry.
2. To be aware of the fast developments that take place in industry and be knowledgeable of the requirements to occupy such a post.
3. To provide the necessary support for radiographers in making the choices to pursue a career in industry.

09:47
Discussion, questions and conclusion

08:30 - 10:00 **Room E1**

Breast

RC 1302

Rethinking ductal carcinoma in situ (DCIS)

Moderator:
F. Pediconi; Rome/IT

A-607 08:30

A. New radiologic-pathologic knowledge on DCIS

A. Frigerio; *Turin/IT (alfonso.frigerio@gmail.com)*

A modern rethinking of ductal carcinoma in situ must take off from the awareness of the utter inadequacy of the terminology currently in use. Already in 1976, Jensen, Rice and Wellings remarked that "ductal carcinoma in situ of the human breast is of lobular (acinar) origin". While the latest (2012) WHO Classification decided to omit the name 'ductal' from the definition of the most common type of invasive breast carcinoma, it still failed to recognize the inconsistency of this descriptor for its intra-epithelial counterpart. It is time to move to a new inter-disciplinary approach where a mutually respectful interaction between radiologists and pathologists should take full advantage of new imaging techniques and new pathologic methods to achieve better characterization of the different types of breast lesions and their clinico-biological potential. A new classification and terminology based on the site of tumour origin (acinar vs ductal), as best displayed by diagnostic imaging paired with modern pathologic techniques as large-format histologic sections, should open the way to a better understanding of the lesion biology, eventually improving treatment planning decisions. This lecture will include a discussion of different subtypes of in situ lesions neoductgenesis as an important feature that should be recognized and reported, the potential of mammographic tumour features as synergistic prognostic factors alongside classical pathological and modern molecular patterns. Overcoming long-lasting barriers to effective communication would be the prerequisite to a new professional setting where all specialists involved mutually enhance the benefits of their clinical knowledge.

Learning Objectives:
1. To learn about different types of DCIS.
2. To become familiar with risk of developing a cancer.
3. To appreciate the radiologic-pathologic correlations.

A-608 09:00

B. Diagnosing DCIS

S. Schrading; *Aachen/DE (sschrading@ukaachen.de)*

The presentation gives an overview over the current role and recent data of dynamic contrast-enhanced (DCE) breast MRI for diagnosis ductal carcinoma in situ (DCIS). Special attention is paid on the description and illustration of typical imaging features as well as pitfalls and difficult differential diagnosis of DCIS at MRI. In addition, the impact of DCE MRI on DCIS treatment and recent discussion on overdiagnosis and overtreatment of DCIS are discussed.

Learning Objectives:
1. To learn about the evidence based on MRI in evaluating DCIS.
2. To become familiar with different imaging appearance of DCIS.
3. To appreciate added value of MRI for diagnosis.

A-609 09:30

C. Reducing overtreatment of DCIS

M.G. Wallis; *Cambridge/UK (matthew.wallis@addenbrookes.nhs.uk)*

Breast screening has led to an inexorable rise in the number of women living with a diagnosis of DCIS predominantly but not exclusively as a result of the detection of micro-calcification. It is clear from long-term follow-up that conventional treatment fails the 15 to 20% who develop invasive disease a few of whom then die from breast cancer. There is larger group that never progresses with in their lifetime which means we have either cured them or just overtreated them. Traditional pathology and genetics suggest that there is a low-risk group that either never progresses or if they do, they develop 'low-risk' invasive disease. I will describe the 3 international trials LORIS (The LOw RISk DCIS trial), LORD (LOw Risk DCIS) & COMET (Comparison of Operative versus Medical Endocrine Therapy for Low-Risk DCIS); in particular, commenting on their differences. Using LORIS as my main example I will discuss how we have attempted to resolve the hurdles of setting up a 'no treatment trial' and talk about some of the lessons learnt from successfully steering LORIS from feasibility to full trial. Anecdotally patient views have been more entrenched than those of surgeons and to my surprise the radiology second opinion service set up to reduce the risks of 'active monitoring' up by annual VAB has not been overwhelmed.

Learning Objectives:
1. To learn about the risk of overdiagnosis and overtreatment.
2. To become familiar with the risk of avoiding surgery.
3. To appreciate the prospective for the future.

08:30 - 10:00 **Room E2**

Neuro

RC 1311
White spots in the brain

Moderator:
E. Maj; Warsaw/PL

A-610 08:30
A. White spots and blots in the brain: what are they?
T.A. Yousry; *London/UK (t.yousry@ucl.ac.uk)*

White matter lesions (WMLs) often present a diagnostic challenge. They can be incidental, associated with ageing, or reflect an underlying disease. The differential diagnosis is, therefore, wide reaching from vascular, such as small vessel disease (SVD) to inflammatory causes, such as multiple sclerosis (MS). Although the clinical presentation often leads to the right diagnosis, overlap in the clinical presentation as well as in the MR findings is frequent. The correct interpretation of the corresponding imaging is, therefore, essential. To be able to put WMLs in the right context, they need to be categorised and related to their pathological substrate, which is the basis for the nomenclature that should be used. MRI criteria have been developed to support the differential diagnosis. They are based among other features on shape (oval in MS), distribution (subcortical in MS, basal ganglia in SVD), enhancement (MS), involvement of spinal cord (MS) and occurrence of other changes (lacunes and microhaemorrhages in SVD). New findings from 7T high-field MRI have contributed to the development of new criteria, such as the central vein in MS lesions, which can be also identified at 3T. These findings determine the imaging strategy that needs to be adopted. This strategy also needs to take into account the MRI criteria to diagnose MS - the 2010 “McDonald criteria” - which are based on the demonstration of dissemination in space (DIS) and time (DIT) and after exclusion of alternative causes.
Learning Objectives:
1. To understand what white spots are.
2. To make differential diagnoses in brain white spots.
3. To demonstrate how to study patients with brain white spots.
Author Disclosure:
T.A. Yousry: Advisory Board; Biogen Idec; Genzyme, Ixico. Board Member; Neuroradiology. Grant Recipient; Medical Research Council, MS Society of Great Britain and Northern Ireland, Stroke Association, British Heart Foundation, Wellcome Trust. Speaker; Novartis.

A-611 09:00
B. How can I improve my reporting of T2-hyperintense lesions?
A. Rovira-Cañellas; *Barcelona/ES (alex.rovira@idi.gencat.cat)*

Focal white matter bright spots on T2-weighted images (BS) are commonly observed on brain MRI, not only in the elderly, but also in middle-aged subjects, particularly those with migraine or chronic headache. In addition, a large list of different disorders should be considered in these patients as hypoxic-ischaemic vasculopathies, multiple sclerosis, primary and systemic vasculitis and acquired metabolic and toxic conditions, among others. While it is recognized that a combination of findings from clinical history, physical examination and laboratory tests is commonly required to correctly establish a firm and clear etiological diagnosis, a detailed analysis of different MRI features should also be considered essential, e.g. lesions shape, size and distribution; contrast-uptake; associated structural lesions (microbleeds, infarctions, etc.). Knowledge of these features, will assist the diagnostic workup of patients presenting with BS and should be considered a first step to take full advantage of the potential of MRI, and in doing so should result in a reduced chance of misdiagnoses and facilitate the correct diagnosis of sometimes treatable disorders. Detailed description of these features and their interpretation must be translated into a written and structured radiological report, which should be accurate with inclusion of relevant positive and negative findings and clinically focused, to properly assist with the further management of these patients. These standardized reports are more time-efficient than simply dictation, support analysis for research and decision support and improve communication of radiology results, which has important clinical implications in the management of patients presenting with brain BS.

Learning Objectives:
1. To understand if it is possible to use a structured report with white brain abnormality.
2. To learn how to define a comprehensive imaging protocol for those patients.
3. To appreciate the role of modern imaging techniques for defining white brain hyperintense T2 lesions.

A-612 09:30
C. Is there a need for quantitative reporting of white matter lesions?
W. van Hecke; *Antwerp/BE (wim.vanhecke@icometrix.com)*

Brain white matter lesions occur in different brain disorders, such as vascular disease, dementia, multiple sclerosis, etc. As the number, location, shape and size of these lesions are relevant for diagnosis, follow-up or clinical decision making, they should be assessed in the radiological report. However, studies have demonstrated that a visual evaluation of white matter lesions is labour intensive and observer dependent, leading to a low reproducibility of the reported values. In recent years, image processing techniques were developed to obtain quantitative white matter lesion information in a semi-automatic or automatic way. Some of these techniques are now also approved for and available in a clinical routine setting, allowing to integrate quantitative information on brain white matter lesions in the radiological report.
Learning Objectives:
1. To understand the importance of quantitative analysis in white matter lesions.
2. To show how to perform the quantitative analysis.
3. To understand the importance of follow-up in patients with white matter lesions.
Author Disclosure:
W. van Hecke: Board Member; icometrix. Founder; icometrix.

08:30 - 10:00 **Room F1**

E³ - European Diploma Prep Sessions

E³ 1323
Chest

A-613 08:30
Chairman's introduction
J. Vilar; *Valencia/ES*

Session Objectives:
1. To understand the most important signs in chest imaging.
2. To learn the imaging features of benign and malignant lesions of the lung.
3. To become familiar with the imaging appearance of common lesions of the mediastinum, pleura and chest wall.
4. To understand the role of different imaging modalities including hybrid imaging in diagnosing and staging neoplasms of the chest.

A-614 08:36
A. Fundamentals of chest imaging
D. Tack; *Baudour/BE (denis.tack@skynet.be)*

This lecture intends to review the basic technical requirements for performing chest radiographs and chest CT, the radiation dose descriptors suited for CXR and CT, the basic anatomical landmarks for image interpretation and numerous signs in chest imaging used for radiographic or CT examinations. In addition, rules for checking for lines and tubes will be illustrated with quiz cases.
Learning Objectives:
1. To learn the anatomy and normal variants of the respiratory system, heart and vessels, mediastinum and chest wall and to confidently identify these on radiographs, CT and MRI.
2. To understand the technical aspects, exposure doses and post-processing of radiographs and CT of the chest.
3. To gather an in-depth understanding of the most common chest radiography signs (including silhouette sign, air bronchogram, air crescent sign, cervicothoracic sign, tapered margins, gloved finger sign, golden sign, deep sulcus sign).
4. To learn the appearance and correct position of monitoring and support devices (tubes and lines).

A-615 09:04

B. Inflammation and tumours of the lung

H. Prosch; *Vienna/AT (helmut.prosch@meduniwien.ac.at)*

Inflammatory and neoplastic diseases of the lung are frequently encountered on chest CTs. As both inflammatory and neoplastic diseases, as well as some congenital disorders, present with an increase in lung density, the differential diagnosis is challenging. Increased lung densities may present as ground glass opacities or consolidations. Ground glass opacities are defined as an increase in lung density, with preservation of bronchial and vascular margins. Ground glass opacities may be caused by a thickening of the pulmonary interstitium or a partial filling of the air spaces with fluids or cells. Pulmonary opacities, in which the bronchial or vascular margins are obscured, are defined as consolidations. Consolidations are the result of a complete filling of the alveolar spaces with fluids or cells, or a thickening of the pulmonary interstitium with complete displacement of the air from the parenchyma. The diagnosis of diseases that present with an increase in lung density requires a systematic analysis of the predominant CT pattern and ancillary CT findings. Furthermore, clinical data, such as information on the immunological status of the patient as well as laboratory findings, have to be taken into account to narrow the differential diagnosis. If CT findings and clinical data are inconclusive, percutaneous or transbronchial biopsies are often required to confirm or rule out a presumptive diagnosis. Biopsies are particularly important in cases in which a presumed benign process does not respond to treatment or a malignant process is suspected.

Learning Objectives:

1. To understand the imaging features and differential diagnoses of diffuse infiltrative and alveolar lung disease and atelectasis.
2. To become familiar with thoracic diseases in immunocompetent, immunocompromised and post-transplant patients.
3. To become familiar with the differentiation of solitary and multiple pulmonary nodules, benign and malignant neoplasms, hyperlucencies and their potential aetiology and evaluation.
4. To understand the role of different imaging modalities including hybrid imaging in diagnosing and staging neoplasms of the chest.

Author Disclosure:

H. Prosch: Advisory Board; Boehringer Ingelheim, Roche. Speaker; Boehringer Ingelheim, Roche, Roche.

A-616 09:32

C. Mediastinum, pleura and chest wall

N. Howarth; *Chêne-Bougeries/CH (nigel.howarth@grangettes.ch)*

The presentation will cover the predefined learning objectives using side-by-side plain film and CT imaging to help understand the imaging features of common pathologies of the diaphragm, pleura and chest wall, concentrating on causes of mediastinal and hilar diseases, disorders of the pulmonary vascular system and great vessels and the postoperative chest. Although the clinical value of the chest x-ray remains undiminished, errors of interpretation of the chest x-ray remains one of the most frequent causes of malpractice issues. The skills required for accurate interpretation of imaging of the mediastinum, pleura and chest wall will be explored. The topics will be disease orientated. The objective is to help you improve your performance in plain film and CT imaging of the chest.

Learning Objectives:

1. To become familiar with the imaging features of common pathologies of the diaphragm, pleura and chest wall on radiography, CT and MRI of the chest.
2. To learn the imaging features and causes of mediastinal and hilar diseases.
3. To understand the imaging features of disorders of the pulmonary vascular system and great vessels.
4. To learn the typical imaging features of the postoperative chest.

08:30 - 10:00 **Room F2**

Emergency Imaging

RC 1317

Acute pain: hallmark in emergency radiology

A-617 08:30

Chairman's introduction: Management and therapeutic pathways in patients with acute pain

D.R. Kool; *Nijmegen/NL*

Acute pain in head, chest or abdomen is a common reason for patients to visit an emergency department. The differential diagnosis in these patients is often diverse and diagnostic imaging will help the clinician to make the correct diagnosis and start appropriate treatment. Depending on the available clinical information, the radiologist decides together with the treating physician what image modality or imaging pathway is the most suitable and efficient for that patient, with those symptoms, in that hospital, at that time. In this refresher course, the clinical conditions presenting with acute pain in head, chest and abdomen will be addressed. The ratio behind the choice of imaging modality will be discussed and the imaging findings will be demonstrated. In the panel discussion, the role of radiology and the radiologist in the diagnostic journey of these patients will be addressed.

A-618 08:35

A. Head

S. Wirth; *Munich/DE (stefan.wirth@med.uni-muenchen.de)*

Severe headache is a common reason for presentation to emergency services. While many headaches resolve spontaneously, some patients require further examination including neuroimaging. The international classification of headache disorders differentiates 1) primary headaches, 2) secondary types with a known structural or biochemical cause and 3) cranial neuralgias. Consequently, imaging has a relatively low diagnostic yield in primary headache whereas it plays an important role in the differential diagnosis of secondary forms. Worldwide, the most common form of headaches is caused by primary tension-type headaches and migraines (90%). Danger signs or other potential indicators of secondary headache are: history of recent head trauma, new onset or change in headache in patients over 50 years of age, time to peak intensity of less than 5 minutes, any new or worsened abnormal neurological examination. In such circumstances, patients should undergo neuroimaging. Typical imaging findings for the most common clinical scenarios will be presented. Particular attention will be paid to sudden onset (thunderclap) headache, which requires urgent evaluation as such headaches may be signs of intracranial and in particular of subarachnoid haemorrhage - mainly caused by trauma or aneurysm rupture. Besides traumatic and non-traumatic bleeding, typical other aetiologies of headache will be discussed: cerebral venous thrombosis, cervical artery dissection, spontaneous intracranial hypotension, pituitary apoplexy, retroclival haematoma, ischaemic stroke, acute hypertensive crisis, headache associated with sexual activity, third ventricular colloid cysts, meningitis, complicated sinusitis and reversible cerebral vasoconstriction syndromes.

Learning Objectives:

1. To become familiar with common clinical conditions resulting in acute headache.
2. To understand the choice of the best-suited imaging modality.
3. To learn about typical imaging findings in the most common clinical scenarios.

A-619 09:00

B. Chest

E. Dick; *London/UK (elizabeth.dick@imperial.nhs.uk)*

General radiologists need to be able to confidently review CT in patients with acute chest pain since this is a common emergency presenting complaint which is increasingly investigated with CT. This case-based talk will consider the cardiac, aortic, pulmonary, oesophageal and chest wall causes of pain. It will review the best imaging protocols for different patient groups according to their risk factors. Take-home tools will include a reporting pro forma and checklist of 'Don't miss' sites.

Learning Objectives:

1. To become familiar with clinical conditions resulting in acute pain.
2. To understand which additional data will influence the choice of the correct imaging modality.
3. To learn about typical imaging findings in patients with acute chest pain.

Author Disclosure:
E. Dick: Board Member; British Society of Emergency Radiology, European Society of Emergency Radiology.

A-620 09:25

C. Abdomen
R. Basilico; *Chieti/IT (rbasilic@unich.it)*

Acute abdominal pain is a common main complaint in patients examined in the emergency department and can be related to a wide range of diseases. On the basis of the results of the initial diagnostic steps for these patients, represented by clinical evaluation and laboratory investigations, the clinicians will consider imaging examinations to help establish the correct diagnosis. The diagnostic approach for acute abdominal pain is not only one of the most difficult for the clinician but it is also a great challenge for the radiologist because differential diagnoses include a myriad of disorders, ranging from life-threatening to benign self-limiting conditions. The diagnostic workup of patients admitted with acute abdominal pain is based on various imaging modalities such as abdominal plain film, ultrasound, CT and MRI: the topographic classification of acute abdominal pain (pain in one of the four abdominal quadrants, diffuse abdominal pain, flank or epigastric pain) with reference to the age and gender of patients, facilitates the choice of the imaging technique and allows to narrow the range of possible diagnoses. The most practical approach to acute abdominal pain is to confirm or to exclude the most common disease and to look for general signs of pathology such as inflamed fat, bowel wall thickening, ileus, free fluid and free air. Moreover, knowledge of atypical imaging findings is of great importance to improve the diagnostic orientation. In any case, results have to be confronted with clinical findings to obtain the correct diagnosis.
Learning Objectives:
1. To become familiar with common clinical conditions resulting in acute abdominal pain.
2. To understand what clinical information influences the choice of the best-suited imaging modality.
3. To learn typical and less typical imaging findings in patients with acute abdominal pain.

09:50
Panel discussion: Where does radiology fit in the pathway?

08:30 - 10:00 **Room D**

Musculoskeletal

RC 1310
Shoulder MRI: mastering technique and making my report relevant

A-621 08:30

Chairman's introduction
J. Kramer; *Linz/AT (kramer@ctmri.at)*

General considerations regarding the following lectures are made focused on the question: what the patient/surgeon want to know together with clues how to make a reasonable report. Beginning with demonstration of normal anatomy including subtle details and variants, new insights into rotator cuff disorders (from degenerative changes to full thickness tear) pathologic alterations in patients with shoulder instability are demonstrated and discussed.
Session Objectives:
1. To understand the level of expertise that patients expect for adequate performance and reading of shoulder MRI.
2. To gain insight into differentiating normal age-related changes from clinical relevant MR features.

A-622 08:35

A. The normal MRI: techniques and anatomy
E. Llopis; *Valencia/ES (evallopis@gmail.com)*

The shoulder has a large range of motion making it susceptible for instability. To maintain shoulder stability there are a combination of static and dynamic structures. Bone structures, humeral head and glenoid, are essential to keep shoulder normal function, and its role is being redefined as key for success of arthroscopy treatments. Intraarticular the glenoid ligaments, bicipitolabral complex and labrum help act in combination with the strong rotator cuff muscles (supraspinatus, infraspinatus, subscapularis and teres minor) to allow all the normal range of motion of the shoulder. We will review the normal anatomy and different techniques to study the shoulder, with especial emphasis on MR and MR arthrography. Including how to perform MR and CT arthrography in one single procedure. We will provide some tricks such as forced external rotation or ABER position that allow to diagnose small subtle lesions.
Learning Objectives:
1. To become familiar with MRI techniques for imaging the shoulder.
2. To understand normal MRI shoulder anatomy, and normal variants seen.

A-623 08:58

B. Rotator cuff tears: what are they and what do they look like?
K.-F. Kreitner; *Mainz/DE (Karl-Friedrich.Kreitner@unimedizin-mainz.de)*

Rotator cuff (RC) disease is common and may be a significant cause of shoulder pain. Thorough assessment of the RC by MR imaging may enable accurate diagnosis and facilitate appropriate management by the orthopaedic surgeon. The tendons of the rotator muscles are highly organized structures where five distinct histologic layers have been described. Over the last decade, the rotator cable has received increasing attention as it acts as a supporting limb of the cuff. The cable is adjacent to the crescent zone of the RC and can be seen on most MR imaging studies. Pathologically, tendinosis/tendinopathy can be differentiated from partial- and full-thickness tears of the cuff. Whereas tears at the rotator crescent are often due to ischaemia and degeneration, tears of the footprint have obtained increased attention as they affect younger patients and have implications on the appropriate operative procedure. Partial-thickness tears can be described as articular, bursal or intrasubstance partial tears and should be further characterized with regard to the degree of tendon involvement. Full-thickness tears allow communication between the glenohumeral joint and the subacromial-subdeltoid bursa and can be pinhole in size or involve an entire tendon. It is further of utmost importance to assess atrophy or fatty infiltration in case of an RC tear as these findings influence therapy and outcome of the affected patients. Tears of the subscapularis tendon typically begin in the cranial part of the tendon are often associated with lesions of the long biceps tendon and the rotator interval.
Learning Objectives:
1. To become familiar with the anatomical basis of rotator cuff tears.
2. To learn about the MRI findings of rotator cuff pathology.

A-624 09:21

C. Patterns of instability: what does the MRI show?
A.J. Grainger; *Leeds/UK (andrewgrainger@nhs.net)*

Two patterns of injury are seen in patients dislocating their shoulder. Younger patients will tend to disrupt the labroligamentous complex, whereas the older population tends to disrupt the integrity of the rotator cuff. In this latter group, tears of supraspinatus are seen along with tears of subscapularis and avulsion fractures of the greater tuberosity. Rotator cuff disruption forms the subject of other talks so will not be discussed further here. Anterior dislocation leading to avulsion of the anteroinferior labral-ligamentous complex from the glenoid is termed the Bankart lesion, or bony Bankart if accompanied by a fracture. Avulsion occurs due to the pull of the anterior band of the inferior glenohumeral ligament (AIGHL) at its attachment to the anteroinferior labrum. The AIGHL is the primary restraint to movement when the arm is abducted and externally rotated. Avulsion of the labrum is well shown at MR arthrography and a number of variants exist which will be discussed. Posterior dislocation will produce a reverse pattern of shoulder injury which will also be discussed.
Learning Objectives:
1. To become familiar with patterns of abnormality seen in shoulder instability.
2. To learn about the MRI findings of shoulder instability.
Author Disclosure:
A.J. Grainger: Consultant; medivir AB. Equipment Support Recipient; Siemens Healthcare. Speaker; GE Healthcare.

09:44
Panel discussion: How are the indications for MR arthrography in the shoulder changing?

08:30 - 10:00 **Room G**

Physics in Medical Imaging

RC 1313
Motion management in medical imaging

A-625 08:30
Chairman's introduction
A. Torresin; *Milan/IT (alberto.torresin@unimi.it)*

Motion management in medical imaging is very important for diagnostic and therapeutic application. Its quantification and control can increase image quality in diagnostic imaging and optimize the final results in radiotherapy for delivering ablative doses to tumours with limited normal tissue toxicity. The methods for quantification and control are modality and clinical application dependent. Respiratory induces motion artefacts, particularly those occurring in the abdomen and lung. It poses a hefty problem in diagnostic imaging and cardiac motion leads to blurred images with reduction of spatial and contrast resolution. In diagnostic application many methods can be applied in MRI, US, CT, CBCT, SPECT, PET where different image modalities should be registered in the same reference coordinates and a lot of methods have to be applied for different clinical applications. A modern radiotherapy tenet is to accurately identify the treatment target to follow and secure high-dose treatment target volume. Respiratory motion can induce errors in target volume delineation and dose delivery in radiation therapy for thoracic and abdominal cancers. 4D computed tomography and 4D magnetic resonance imaging are the most common contemporary imaging technique for identifying tumour motion. Radiotherapy application is not directly discussed during the section but imaging corrected for motion will support also this application.
Session Objectives:
1. To learn about the origins of motion management in medical imaging.
2. To understand image motion in medical imaging.
3. To learn about solutions and work-arounds.

A-626 08:35
A. Managing respiratory motion with CT and CBCT: conventional approaches and motion compensating techniques
J. Sijbers; *Antwerp/BE (jan.sijbers@ua.ac.be)*

Motion in x-ray imaging is a common problem. It generally leads to blurred images and loss of spatial resolution. In this talk, various strategies for motion compensation will be discussed, on acquisition as well as tomographic image reconstruction level. In addition, it will be shown that motion blur in the acquired x-ray projections can be beneficial instead of disadvantageous with respect to CT image quality.
Learning Objectives:
1. To learn about conventional techniques for respiratory motion compensation.
2. To learn about new methods for respiratory motion compensation.
3. To contrast the available and up-and-coming respiratory motion compensation methods.

A-627 08:58
B. Managing cardiac motion with CT and CBCT: conventional approaches and motion compensating techniques
M. Kachelrieß; *Heidelberg/DE (marc.kachelriess@dkfz.de)*

Diagnostic CT is the workhorse of the radiologist: highly quantitative images with very high spatial resolutions (0.3 mm isotropic) for complete anatomical areas are acquired in scan times as short as about 1 s. CT further routinely achieves an unprecedented temporal resolution of 63 ms, which is one quarter of the rotation time, for complete anatomical regions. For moving objects, however, even 63 ms may introduce motion blurring. Given the spatial resolution of 0.3 mm, objects moving at a speed of about 4 mm/s or faster will introduce blurring. Such velocities occur in the thorax due to breathing and, even more dominantly, in the heart, where velocities of 70 mm/s are typical. In CBCT, a slowly scanning non-diagnostic modality, the situation becomes even worse because not only the temporal duration of the scan is long but also because respiratory motion cannot be ignored anymore and will be superimposed with the cardiac motion. The simplest methods to manage cardiac motion are cardiac-correlated (prospectively or retrospectively gated) scans performed during a single breath-hold. Gating may include scanning during a single heart beat (either in circle, in spiral, or in high-pitch spiral mode) or during multiple heart beats. Recently, new algorithms that have the ability to compensate for the motion during image reconstruction are being developed: they have the potential to significantly increase the temporal resolution or to improve the dose usage to 100%. The lecture discusses the methods in use, and those that are being developed.
Learning Objectives:
1. To learn about conventional techniques for cardiac motion compensation.
2. To learn about new methods for cardiac motion compensation.
3. To contrast the available and up-and-coming cardiac motion compensation methods.

A-628 09:21
C. Motion compensation in MR and PET imaging
C. Kolbitsch; *Berlin/DE (christoph.kolbitsch@ptb.de)*

MR image quality and diagnostic accuracy can be considerably impaired by physiological organ motion (e.g. breathing, heartbeat or swallowing). Advances in MR hardware, plus novel image acquisition and reconstruction approaches, now allow for faster MR imaging; nevertheless, up to 20% of MR scans experience severe motion artefacts and require repeated data acquisition. A wide range of techniques to minimise motion artefacts has been developed for different MR applications. In clinical practice, this is commonly motion prevention (e.g. asking a patient to hold their breath) and motion gating (i.e. restricting data acquisition to a certain motion state). More advanced approaches measure displacement of organs due to physiological motion and utilise this information to correct motion artefacts. PET images are affected by motion twofold. Movement of organs can lead to blurring of the imaged structures and impair detectability, particularly of small features. In addition, quantitative PET requires correction for different tissue densities using so-called attenuation correction maps. Motion can lead to a mismatch between these and PET image data, resulting in severe errors in PET quantification. The recent introduction of simultaneous PET-MR now offers us the possibility to improve PET image quality and accuracy by utilising MR-based motion information.
Learning Objectives:
1. To learn about motion measurement and compensation in MR.
2. To understand how patient motion affects PET images.
3. To learn about how MR data can be used to motion-compensate PET images, in PET/MR.

09:44
Panel discussion: How to optimise motion management in different imaging modalities?

08:30 - 10:00 **Room K**

Professional Challenges Session

PC 13a
Radiography and radiology: more than the sum of their parts

A-629 08:30
Chairmen's introduction: Working together (part 1)
P. Bezzina; *Msida/MT (Paul.bezzina@um.edu.mt)*

To sustain a good medical imaging department and to ensure a positive atmosphere at work, a place where most of us spend the majority of our daily time, it is important to work together and support each other. It is only in a positive working environment that radiologists and radiographers can understand and respect each other, acknowledge the competences of all the individuals, and have joint goals to develop and strengthen radiology and radiography so as to improve practice in a department. Among many of the topics in which working together is practically important is patient safely where we all need to be on the same path and committed to this. The same goes for improvement of protocols, new ideas and testing of new sequences and method. In other words, it has to be done jointly if it is to work and has to be implemented with the support of all staff regardless of background. This session will focus on these topics as well as to give an insight into how you as radiologist and radiographers working together, with different but important skills and knowledge, can achieve a lot to improve your daily practice. For sure two work better than one.
Session Objectives:
1. To appreciate the challenges facing radiography and radiology.
2. To emphasise the importance of a patient safety culture.
3. To understand the need for care and compassion in medical imaging.

A-630 08:33

Chairmen's introduction: Working together (part 2)

P.C. Maly Sundgren; *Lund/SE (Pia.Sundgren@med.lu.se)*

This is a joint chairman session to introduce the following lectures that are focused on the need and benefits of working together as radiologists and radiographers in the clinical and research setting to improve quality, to learn from each other and to move the field forward with the best interest in patient care and quality.

Session Objectives:

1. To appreciate the challenges facing radiography and radiology.
2. To emphasise the importance of a patient safety culture.
3. To understand the need for care and compassion in medical imaging.

A-631 08:37

Opportunities and challenges facing radiography and radiology

G. Paulo; *Coimbra/PT (graciano@estescoimbra.pt)*

Medical imaging is the main pillar of modern health care systems. The equipment technological development combined with the new medical devices have increased medical importance in healthcare delivery. However, evidence shows an exponential growth of the number of medical imaging procedures and a decrease of radiographers and radiologists. One of the main reasons related to this evidence is related to the fact that medical imaging is slowly being fragmented and taken by others, which represents a real threat to our professions. This new reality calls for a development of a common strategy to make us more visible in the patient clinical pathway, enhancing our importance in patient care delivery avoiding medical imaging to be transformed into a commodity. Radiologists must increase their “clinical” role in the management of patient disease and radiographers must increase knowledge, skills and competences towards a consistent and structured role development into advance practice. The future of medical imaging professions depends on our capability of building a team-work model based on roles and responsibilities, as a tool to develop professional satisfaction and increase our visibility in healthcare systems.

Learning Objectives:

1. To highlight the current challenges facing radiographers and radiologists.
2. To discuss the opportunities for radiographers and radiologists.
3. To suggest approaches to meeting current and future needs for the delivery of effective patient care in clinical departments.

A-632 09:00

Patient safety culture: a combined responsibility

S.J. Foley; *Dublin/IE (shane.foley@ucd.ie)*

This presentation aims to familiarise attendees with the recent European Basic Safety Standards Directive (2013/59) which is due to be transposed by all member states into national law by February 2018. The directive consolidates five previous directives into one single document and aims to modernise radiation protection in Europe. It strengthens a number of key radiation protection principles such as justification, the need for and use of DRLs and the requirements for appropriate education of all individuals involved in the delivery of radiation. New requirements are also stipulated for the education of patients as to potential risks while undergoing radiological procedures, the need for dose monitoring devices on all CT and interventional equipment as well as the requirement to transfer patient dose data to the radiological report. In particular, new legislative requirements will be discussed with a particular focus on the increased responsibilities regarding patient safety that will be required of both radiographers and radiologists under the directive. Finally, the potential for the directive to improve the culture of radiation safety within clinical environments will be discussed by consideration of the cumulative effect of both the new and strengthened articles contained within, to change professional behaviours.

Learning Objectives:

1. To familiarise attendees with the European BSS Directive (2013/59).
2. To discuss the responsibilities for radiographers and radiologists within the Directive.
3. To consider how the Directive can improve the culture of radiation safety within the clinical environment.

A-633 09:23

Skills and competences in care and compassion

A. England; *Salford/UK (A.England@salford.ac.uk)*

Ever since Robert Francis QC published his report into the mid-Staffordshire NHS trust inquiry care and compassion have been the forefront of many public and professional debates. The subject of care and compassion is in itself huge and one which has implications for both undergraduate radiography education and post-qualification clinical practice. Questions have arisen as to how these two topics can be adequately embedded into high-quality radiographic practice. What skills are necessary to practice with appropriate care and compassion and how can these be assessed at both pre- and post-qualification levels. Care and compassion is highly topical but often difficult to quantify, will these two topics remain at the forefront of radiographic practice and what can we do as professionals to encourage this. This lecture serves to identify and discuss the key issues of skills and competencies in the delivery of care and compassion within radiographic practice.

Learning Objectives:

1. To focus on the specific aspects of care and compassion within radiography and radiology.
2. To discuss the issue of continuous professional development in care and compassion.
3. To emphasise the importance of care and compassion within training curricula.

09:46

Panel discussion: A winning team: radiographers and radiologists?

08:30 - 10:00 **Room M 1**

Professional Challenges Session

PC 13b

Burnout of radiologists

A-634 08:30

Chairman's introduction

M.G.M. Hunink; *Rotterdam/NL (m.hunink@erasmusmc.nl)*

Do you feel more-and-more overwhelmed? Are you often physically and emotionally exhausted? Have you lost your passion and commitment? Are you not accomplishing what you could and should? Are you disillusioned with your job or career (or life in general)? Are you becoming cynical and emotionally detached? Insomnia, headaches, neck pain, GI upsets? You probably have burnout. If you recognise these signs in yourself, your colleagues or your employees, it is time to act. The cost of burnout is high: personally, to the department and to the hospital! Burnout among physicians is becoming an epidemic. Radiologists are particularly vulnerable to burnout due to a host of factors related to their work: declining income, limited interaction with patients and peers, severe time constraints, work overload, too many bureaucratic tasks, and too much computer work. About 50% of radiologists in the USA have at least one symptom of burnout. The percentage in Europe is unknown. Burnout has negative consequences for the individual and also for his/her practice and patients: it can have adverse effects on performance, professionalism, patient safety, relationships, personnel retention and patient satisfaction. Prevention is better than cure when it comes to burnout. Important preventive measures can and should be taken both at the personal and organisational level. Personal measures include mindfulness training, attention for work-life balance, and focusing on meaningful activities. Organisational measures include tracking and supporting physician well-being, monitoring physician burnout, implementing programs teaching personal preventive measures, leadership skills training and flexibility in work hours.

Session Objectives:

1. To learn about the silent epidemic of physician burnout.
2. To learn to recognise the symptoms of burnout.
3. To understand what factors contribute to burnout in radiologists.
4. To learn what preventive measures can be taken to prevent burnout in radiologists.
5. To understand what interventions work in treating burnout.

Author Disclosure:

M.G.M. Hunink: Advisory Board; EIBIR. Grant Recipient; ESR iGuide. Other; CUP: Royalties for textbook.

A-635 08:40

A personal story

M.F. Berger; *Nottwil/CH (mberger@access.ch)*

In this talk I shall present my own experience with burnout from a first person point of view: early warning signs, failed attempts at self-help, sudden break-out of symptoms, medical workup, interventions and, finally, resolution and consequences. I shall also briefly touch on how I witnessed burnout in two colleagues of mine. Mindfulness played a major role in the recovery of all three of us. I shall describe my personal approach to mindfulness and explain how the practice can not only improve your resilience to stressful life events, both private and professional, but also how it may actually help you become a better radiologist.

Learning Objectives:
1. To learn to recognise the early symptoms of burnout in oneself.
2. To understand how life events and work stress in radiology contribute to burnout.
3. To appreciate the challenges in dealing with burnout.
4. To learn how mindfulness can help in prevention and treatment.
5. To appreciate the value of mindfulness in being a better radiologist.

A-636 09:00

Mindfulness-based interventions for burnout of physicians

A. Speckens; *Nijmegen/NL (Anne.Speckens@radboudumc.nl)*

Mindfulness-based interventions (MBIs) are increasingly applied in health care settings to reduce psychological distress in both patients with psychiatric disorders and those with somatic illnesses. Originally, mindfulness-based cognitive therapy (MBCT) was offered to patients with recurrent depressive disorder to reduce relapse/recurrence. The current evidence suggests that MBCT might be at least as effective as antidepressant medication in preventing relapse/recurrence. Increasingly, MBIs are also offered to patients with other psychiatric disorders, such as somatoform disorders and ADHD. In addition, MBIs have demonstrated to be effective in reducing symptoms of anxiety and depression in patients with chronic somatic conditions, such as cancer and multiple sclerosis. MBIs have not only been applied in clinical populations, but also in health care professionals. Mindfulness-based stress reduction (MBSR) has been shown to reduce burnout and improve psychological well-being and empathy in medical students, residents, general practitioners and consultants. In this presentation, recent findings of two randomised controlled trials in 167 medical students and in 148 residents from different medical specialities will be presented. In addition, the results from two pilot studies in 50 general practitioners and 52 medical consultants will be discussed.

Learning Objectives:
1. To appreciate the impact of the practice environment and the risk factors that lead to physician burnout.
2. To understand the impact of physician burnout on patient care.
3. To learn what we can do to prevent and treat physician burnout.
4. To learn what the research says about the effectiveness of mindfulness for burnout.
5. To appreciate what leaders can do to enhance the lives of staff and residents.

Author Disclosure:
A. Speckens: Employee; Radboudumc Nijmegen, the Netherlands. Founder; Radboudumc Centre for Mindfulness. Grant Recipient; Dutch Organisation for Scientific Research, Dutch Cancer Society, Dutch Assocation for Mental Health. Research/Grant Support; See above.

A-637 09:25

Interventions to prevent and treat burnout

B. Trück; *Brussels/BE (beate.trueck@brusselsmindfulness.be)*

Mindful awareness is about learning to pay attention. It is like training a muscle - training attention to be where you want it to be. This reduces our tendency to work on autopilot, allowing us to us choose how we respond and react in stressful situations. Mindfulness is cultivated in a variety of ways. This includes sitting down (on a chair) and observing your thoughts, emotions or your breath. But mindfulness can also be developed by simply focusing on the task at hand whether you are at work in a meeting or at home cooking a meal. In this talk we will be discussing what it means to be most of the time on autopilot and how this can lead to symptoms of stress and burnout. I will give a practical insight into how mindfulness helps to step out of the autopilot. We will be practising some short mindfulness meditations and share our experiences. We will also be talking about how one can be more mindful in daily life and how short moments of stopping and becoming aware can bring about a great change. I will present some concrete tips of how to integrate mindfulness in your daily life without much additional time.

Learning Objectives:
1. To learn what interventions are available to prevent and treat burnout.
2. To experience what mindfulness/meditation can do for you.
3. To appreciate that attention to the present moment enhances feelings of happiness.
4. To appreciate that mindfulness enhances focus in all activities.

09:50

Panel discussion and discussion with the audience

08:30 - 10:00 **Room M 2**

ESHI (European Society for Hybrid Medical Imaging) Session

Hybrid imaging: case-based diagnosis in PET/CT

Moderator:
K. Nikolaou; Tübingen/DE

A-638 08:30

FDG indications in oncology: case-based

K. Riklund; *Umea/SE (katrine.riklund@umu.se)*

Hybrid imaging with PET/CT and sometimes PET/MR is used on daily basis in the clinical workup, staging procedure, treatment planning and evaluation of several oncologic diagnoses. The most commonly used tracer is oncology is 18F-fluorodeoxyglucose (FDG) and the presented cases are examined with FDG. We will also discuss the evidence base for FDG PET/CT and the impact on clinical handling.

Learning Objectives:
1. To learn about the evidence for common indications.
2. To become familiar with PET and CT findings.
3. To learn about the impact on clinical decision.

A-639 09:00

Non-FDG indications in oncology: case-based

O. Ratib; *Geneva/CH*

Learning Objectives:
1. To learn about the evidence for common indications.
2. To get familiar with PET and CT findings.
3. To learn about the impact on clinical decision.

A-640 09:30

Pitfalls in PET/CT: case-based

G. Antoch; *Düsseldorf/DE (antoch@med.uni-duesseldorf.de)*

Coupling CT with PET adds additional information to morphologic and functional imaging alone. However, bringing both modalities together gives way to new types of image artefacts and pitfalls caused by interaction of morphology and function. In addition, pitfalls known from CT and PET alone still exist in hybrid imaging. The reader has to be aware of these pitfalls to avoid misinterpretation of the imaging data. This course gives an overview regarding different pitfalls in PET/CT imaging that have to be known and dealt with when reading an reporting hybrid imaging studies.

Learning Objectives:
1. To learn about the cause of pitfalls in PET/CT.
2. To get familiar with the appearance of pitfalls in PET/CT.
3. To learn about how to avoid pitfalls in PET/CT.

08:30 - 10:00 **Room M 3**

E³ - ECR Master Class (Interventional Radiology)

E³ 1326

Image-guided liver interventions: update and level of evidence

Moderator:
P.L. Pereira; Heilbronn/DE

A-641 08:30

A. Hepatocellular carcinoma (HCC)

L. Crocetti; *Pisa/IT (laura.crocetti@med.unipi.it)*

Hepatocellular carcinoma (HCC) represents one of the few cancers for which locoregional treatments are recognized as being able to cure and/or prolong survival and included in international guidelines. This is due to the unique nature of HCC, in most cases occurring in patients with underlying virus- or alcohol-related cirrhosis. Treatment choice in patients with HCC is, therefore, driven not only by tumour staging, but also by careful evaluation of liver function and physical status. These characteristics configure a complex scenario and prompt the need for close cooperation among interventional oncologists, surgeons and hepatologists. The Barcelona Clinic Liver Cancer (BCLC) classification has emerged during recent years as the standard classification that is used for clinical management of patients with HCC. This classification links stage stratification with a recommended treatment strategy and defines standard of care for each tumour stage. According to the BCLC

staging system, image-guided tumour ablation is recommended in patients with very early and early-stage HCC. Despite the widespread implementation of surveillance programs, more than half of the patients with HCC are diagnosed late, when curative treatments cannot be applied. For patients presenting with multinodular HCC and relatively preserved liver function, absence of cancer-related symptoms, and no evidence of vascular invasion or extrahepatic spread, i.e. those classified as intermediate-stage - transcatheter arterial chemoembolization (TACE) is the current standard of care. Transarterial radioembolization (TARE), despite non yet included in current guidelines, is a valuable treatment tool entering the clinical practice especially for the early advanced HCCs.

Learning Objectives:

1. To evaluate the clinical indication for interventional radiological approaches for HCC.
2. To evaluate pro and contra of endovascular vs percutaneous treatment options.
3. To highlight recent research and emerging developments in the treatment of HCC.

A-642 09:00

B. Liver metastases of colorectal cancer (mCRC)

T.K. Helmberger; *Munich/DE (Thomas.Helmberger@klinikum-muenchen.de)*

Among the approximately 450,000 colorectal cancer patients per year about 30% will present with synchronous, and 50% with metachronous metastases, whereas about 35% will have “liver only” metastases. Primarily, only up to 20% of the metastases will be resectable. According to current guidelines, various local and locoregional cytoreductive therapies might apply after primary systemic therapy for induction of response. Interventional oncology (IO) provides mainly three image-guided local and locoregional cytoreductive therapeutic approaches: (1) percutaneous thermal-ablation (mainly radiofrequency and microwave ablation) got established over the last 20 years. With current techniques 3 cm metastases can safely be coagulated achieving 5-year survival rates of around 50% - comparable to surgical results. (2) Transarterial chemo-ablation for larger, multifocal, or diffuse metastases is currently adopted parallel to the experiences made in the treatment of HCC. While the results of hepatic arterial infusion (HAI) are still not convincing, transarterial chemo-embolisation with drug-eluting beads (DEB-TACE) is gaining promising results with comparable response rates to systemic chemotherapy (sCTx) but less side effects. Nevertheless, long-term survival data are still lacking. (3) Transarterial radio-embolisation (TARE, SIRT) could prove its efficacy in chemo-refractory patients but also with sCTx in first-line therapy regimens achieving response rates over 90% and a significantly improved hepatic progression-free survival. Current research in IO focus on refinement of techniques and identifying (and probably utilising) secondary effects as immune-stimulation triggered, e.g. by thermal- or radio-ablation.

Learning Objectives:

1. To outline the current status of image-guided therapeutic approaches for mCRC.
2. To discuss the application of endovascular vs percutaneous treatment options in different clinical scenarios.
3. To highlight recent research and emerging developments in this field.

Author Disclosure:

T.K. Helmberger: Consultant; BTG, TERUMO, SIRTEX. Speaker; TG, TERUMO, SIRTEX.

A-643 09:30

C. Liver metastases of neuro-endocrine tumours (NET)

J. Kettenbach; *St. Pölten/AT (joachim.kettenbach@stpoelten.lknoe.at)*

Neuroendocrine tumours (NET) usually arise from the gastrointestinal tract or the pancreas and often metastasise in the liver. NETs are not easily detected and their clinical symptoms are often non-specific; thus, they pose a particular clinical challenge and most patients present with tumours at an already advanced stage. Incidence and prevalence of NETs have been increasing significantly over last decades and survival rates remain low. Somatostatin analogues have proven effective for several NET types. Recently, molecular targeted drugs against pancreatic NETs are also effective. Systemic chemotherapy may be beneficial, but often lacks clear supporting evidence. Attaching isotopes (such as ^{68}Ga, ^{90}Y or ^{177}Lu) to somatostatin-receptors makes them usable for both diagnosis and therapy, showing reduction in disease progression and no relevant toxicity. Since NETS metastasise in the liver, these metastases can be targeted by intra-arterial therapies such as chemo-, radio-, and bland embolisation as well. Radioembolisation has the advantage of not being affected by portal thrombosis, a contraindication to TACE/TAE. Currently grade 1-2, liver-only or liver-dominant disease, tumour progression and symptoms are defined as indications for embolotherapy. In addition, 18F-FDOPA PET/CT-guided RFA ablation has shown very promising results recently. There is no clear consensus which therapy technique for NETs to favour. However, these technique require careful consideration and dedicated patient care and there are still many diagnostic and therapy challenges. All local and systemic therapies do have specific characteristics and should not be seen as competing, as survival is linked to the number of treatment lines.

Learning Objectives:

1. To outline the current status of image-guided therapeutic approaches for NETs.
2. To discuss indications and advantages of endovascular vs percutaneous treatment options.
3. To evaluate literature data on interventional treatments of NETs.

08:30 - 10:00 **Room M 4**

E³ - ECR Academies: Multiparametric Ultrasound (MPUS)

E³ 1320

Multiparametric US in paediatric radiology

A-644 08:30

Chairman's introduction

K. Rosendahl; *Bergen/NO (karen.rosendahl@helse-bergen.no)*

Multi-parametric ultrasound (US) integrates B-mode anatomical information with information on an organ’s vascularity and stiffness. During this session, the role of contrast-enhanced US in paediatric imaging, focusing on trauma, liver and kidneys will be addressed, followed by a presentation on Doppler and CEUS in chest imaging. Moreover, issues on off-label use of CEUS in children will be discussed.

A-645 08:35

A. Contrast-enhanced US (CEUS) in paediatric trauma

M. Riccabona; *Graz/AT (michael.riccabona@medunigraz.at)*

The objective of this lecture is to present basic knowledge about the use, the findings and the limitations of contrast-enhanced ultrasound (CEUS) in paediatric trauma. First basics of CEUS will be revisited including a short discussion of visualization tools, implications of the off-label use of ultrasound contrast agents (UCA) in children and safety precautions. Then tips and tricks about “how to perform the exam” will be presented. Finally, indications when intravenous or intracavitary applications of UCA are useful will be listed - with examples of the typical imaging findings and discussion of restrictions of CEUS. The pros and cons of CEUS in children with trauma are discussed with respect to other imaging, particularly CT which remains the gold standard imaging technique particularly in severe and multiple trauma in childhood. CEUS is a promising option for imaging children with blunt abdominal trauma or for follow-up after trauma. When restrictions are respected, the non-ionizing nature of the investigation with a good safety profile suggest the use of CEUS in paediatric (mild to moderate) trauma as an alternative to standard CT imaging - in spite of the off-label application of UCA in Europe.

Learning Objectives:

1. To understand the role of off-label use of US contrast agents in paediatric patients.
2. To become familiar with CEUS in the assessment of paediatric trauma patients.
3. To learn about limitations of CEUS in trauma compared to CT.

A-646 09:03

B. CEUS in paediatrics: liver, kidney and beyond

E.-M. Jung; *Regensburg/DE (Ernst-Michael.Jung@klinik.uni-regensburg.de)*

The objective of this lecture is the comparison of the diagnostic liver findings of MRI, CT and CEUS in children. Methods include analysis of the diagnostic findings of CEUS, MRI and CT scans in 56 children (age 0-17 years) with a total of 60 benign and malignant liver lesions and anomalies of the portal vein/perfusion. All patients underwent CEUS using sulphur hexafluoride microbubbles and a multi-frequency probe (1-5 MHz, 6-9 MHz). MRI was performed in 38 lesions. CT was performed in 8 lesions. Out of the 56 patients, 49 liver lesions (48 benign, 1 malignant), 9 anomalies of the portal vein/perfusion and 2 of the biliary system were detected. 16/49 lesions were analysed histopathologically. Using CEUS, the characterisation of the lesions was possible in 45 out of 49 cases. In 32 cases, CEUS provided the exact diagnosis. Findings of MRI and CEUS were concordant in 84% of cases (n=32/38). CEUS considered 1 benign lesion to be malignant. 2 lesions were not detectable and in 3 lesions no definite diagnosis was established using MRI. Findings of CT and CEUS were concordant in 5 of 8 cases. In 21 lesions, CEUS as the only imaging modality was found to be sufficient. Despite the restricted indications for using CEUS in children, it offers a high diagnostic detection rate (93%) of liver lesions.

Learning Objectives:
1. To understand established indications for off-label use of CEUS.
2. To learn how to perform CEUS in different age groups.
3. To become familiar with US contrast enhancement in parenchymal organs.

A-647 09:31

C. Multiparametric US of the paediatric chest: more than effusion
P. Tomà; *Rome/IT (paolo.toma@opbg.net)*

Indications for use of thoracic ultrasound are (in descending order): to confirm and characterize pleural effusions, evaluation of a radiological opacities, follow-up of lung diseases in neonates, thoracic wall lesions (i.e. fractures, etc.), congenital malformations such as CPAM, and in several cases the pneumothorax. Colour and pulsed Doppler, wherever possible, due to motion artefacts (i.e. flash artefacts) are helpful to identify the vascular supply in congenital malformations, detection vascularity of consolidations and atelectasis. About CEUS, use in paediatrics is off label. In adults, pattern of enhancement detected by chest CEUS does not distinguish between CAP and lung cancer and overly optimistic beliefs on this matter should be debated. The limits about CAP are operator dependency, limited access of deeper areas hidden by aerated lung, no evaluation of air trapping, limited assessment of mediastinal and hilar lymphadenopathy, perihilar opacities, restrictions in appraising pulmonary vascularity, potentially non-recognition of other underlying pulmonary conditions. About the management of complicated paediatric pneumonia improving by CEUS the detection of ischaemia and necrotic tissue is useless as does not change the approach (CT experience).
Learning Objectives:
1. To understand established indications for chest US in children.
2. To learn the different roles of real-time US, Doppler and CEUS to diagnose pulmonary and mediastinal lesions, especially pneumonia.
3. To understand the limitations of percutaneous US of the chest.

08:30 - 10:00 **Room M 5**

E³ - ECR Academies: Neuroradiology: from Morphology to Function

E³ 1322
Cerebral blood flow quantification

A-648 08:30

Chairman's introduction
T. van der Zijden; *Edegem/BE (thijsvanderzijden@hotmail.com)*

Obviously, physiological and pathophysiological processes in the brain have repercussions on the cerebral perfusion. The cerebral perfusion is influenced by many regulatory mechanisms. Both systemic and local processes play a role in entities such as vasoreactivity, autoregulation and neurovascular coupling in the brain. Imaging of brain perfusion can play an important role in not only detecting pathological processes, such as stroke, neurodegenerative disease and tumour, but also in directing treatment of these diseases and in the follow-up after treatment. Nowadays, a shift from invasive to non-invasive CBF imaging has occurred. Several methodologies with different techniques have been developed to detect and measure variations in blood flow components. In this session, an overview of functional and physiological properties of cerebral vasculature in health and disease will be given. A demonstration of how to conduct functional imaging of perfusion will be given as well. In particular, the use of arterial spin-labelling techniques will be discussed. Last but not least an overview will be demonstrated of how these MRI-based cerebrovascular reactivity measurements can be implemented in a clinical setting.

A-649 08:36

A. Functional imaging of cerebral perfusion
A. Krainik; *Grenoble/FR (akrainik@chu-grenoble.fr)*

The lecture presents the functional properties of the cerebral vasculature, including neurovascular coupling, autoregulation and cerebral vascular reactivity (CVR) to circulating gases (CO2 and O2). We describe how to conduct functional imaging of perfusion, especially CVR mapping using MRI under hypercapnic challenge. We show that CVR fMRI allows to estimate the impact of functional changes of perfusion on activation BOLD fMRI in ageing and brain lesioned patients referred for stroke and tumour. CVR fMRI also provides interesting information on adaptative physiology in healthy subjects under hypoxia, and on pathophysiology in various diseases such as cerebral steno-occlusive disease, neurodegenerative diseases, brain tumour and seizure.

Learning Objectives:
1. To understand that functional imaging of perfusion enables the study of properties such as vasoreactivity to circulating gases, autoregulation and neurovascular coupling.
2. To show that functional imaging of perfusion can influence therapeutic strategy through estimation of the vascular reserve and the risk of ischaemia.
3. To learn that functional MRI of vasoreactivity is of value in understanding functional MRI activation.

A-650 09:04

B. Cerebral blood flow measurements with arterial spin-labelling
X. Golay; *London/UK (x.golay@ucl.ac.uk)*

Arterial spin labelling (ASL) is a magnetic resonance (MR) imaging technique used to assess cerebral blood flow non-invasively by magnetically labelling of the inflowing blood. One of the most attractive reasons to use ASL is that it can provide a quantitative assessment of cerebral blood flow (CBF). There are currently two main approaches used to implement ASL, pulsed ASL (PASL) and pseudo-continuous ASL (pCASL). A recent position paper has been published, indicating that the second one is preferred, as it provides a more robust SNR than PASL (1). Here, the basic model describing the biophysics of perfusion will be demonstrated and the assumptions behind its use will also be discussed. In particular, examples showing where such assumptions fail will be highlighted, so that they can be recognised and interpreted appropriately. Finally, examples of applications will be shown, in particular in stroke and as an early biomarker of disease onset in dementia. Ref: 1) Alsop et al, Magnetic Resonance in Medicine 73:102-116 (2015).
Learning Objectives:
1. To reveal how arterial spin labelling (ASL) can accurately measure cerebral blood flow (CBF).
2. To present an overview of the advantages and limitations of using ASL in adult and paediatric subjects.
3. To show that the use of subject-specific model parameters (for example particularly blood and tissue T1) can improve the accuracy of CBF estimates.
Author Disclosure:
X. Golay: CEO; Gold Standard Phantoms Ltd. Consultant; Olea Medical. Founder; Imgenious Ltd. Grant Recipient; Olea Medical.

A-651 09:32

C. Cerebrovascular reserve imaging and the consequences of neurovascular uncoupling
J. Hendrikse; *Utrecht/NL (j.hendrikse@umcutrecht.nl)*

The presence of cerebrovascular reserve (CVR) can be assessed when a challenge is applied that causes a change in the cerebral vasculature (such as a vasodilation). For a patient with already a change (vasodilation) in the resting condition only a small change upon this challenge will be detected relative to a healthy subject with a normal baseline condition of the cerebral vasculature. To measure the cerebrovascular reserve two important parts can be distinguished. First, the type of challenge that is used. Second, the methods that are used to measure the cerebrovascular reserve. In the current presentation we focus on the MRI methods that used to measure the cerebrovascular reserve. Challenges that are most often used are either a carbon dioxide challenge, a breath-holding challenge, a simple functional MRI challenge (visual), or medication such as acetazolamide. For MRI measurement methods, a change in BOLD signal during the challenge is most often used. Other quantitative MRI methods that can be used are arterial spin labelling (ASL) perfusion MRI, or other quantitative methods such as phase-contrast MRA. Challenge of the CVR measurements is the setup of these measurements with, for the carbon dioxide, the delivery of the gas mixture to the patient in the MRI scanner during the MRI scan. The patient needs a gas mask and the images need to be processed after the MRI exam. In patients with cerebrovascular disease, the CVR may indicate the patients with the most severe haemodynamic impairment (reduced CVR) that might benefit most from revascularisation procedures.
Learning Objectives:
1. To understand the consequences of severely reduced CVR in terms of future risk of stroke as well as cortical thinning that can occur in the absence of acute ischaemic events.
2. To review the challenges facing clinical implementation.
3. To understand the potential of CVR for informing patient selection for revascularisation.

10:30 - 12:00 **Room A**

E³ - ECR Academies: Interactive Teaching Sessions for Young (and not so Young) Radiologists

E³ 1421

Genitourinary and gastrointestinal radiology

A-652 10:30

A. Prostate MRI using PI-RADS

H.C. Thoeny; *Berne/CH (harriet.thoeny@insel.ch)*

Prostate imaging is based on the so-called PI-RADS (prostate imaging and reporting data system) system that provides clinical guidelines for performing and interpreting multiparametric MRI (mpMRI) of the prostate. To perform correct mpMRI all sequences should be acquired with the same angle, slice thickness and location. PI-RADS is an objective tool based on a 5-point scoring system to define the probability of the presence of a significant prostate cancer and to exclude significant prostate cancer with a high likelihood. Furthermore, interreader variability should be decreased. PIRADS allows to improve and standardise communication between radiologists and urologists. In PIRADS vs 2 an overall score based on all mpMR techniques (high-resolution T2, DW-MRI and DCE-MRI) is provided for each detected lesion. PIRADS 1 and 2 mean that clinical significant cancer is unlikely to be present, PIRADS 3 means an indeterminate lesion and PIRADS 4 and 5 suggest that clinically significant cancer is highly likely to be present, in PIRADS 4 the size of the lesion is smaller than 1.5 cm, whereas PIRADS 5 means that the tumour is larger than 1.5 cm. Most of the prostate cancers are located in the peripheral zone and DW-MRI is the dominant sequence to detect a significant cancer in this location, whereas T2 is the dominant sequence to detect significant prostate cancer in the transition zone. If a sequence is technically inadequate, this should be assigned assessment category "X".

Learning Objectives:

1. To learn the clinical indications for prostate MRI.
2. To assess technical considerations for performance of multiparametric prostate MRI.

A-653 11:15

B. New aspects of renal tumours

N. Grenier; *Bordeaux/FR (nicolas.grenier@chu-bordeaux.fr)*

Renal tumours can be solid or cystic or mixed. Clear cell, papillary and chromophobe are the three most frequent types of carcinomas but many other types are possible. Angiomyolipomas, oncocytomas and leiomyomas remain the three most frequent types of benign tumours. New aspects of renal tumours include integrated MR and contrast-enhanced US criteria within Bosniak's classification for cystic masses and multiparametric MR patterns for solid tumours. These new imaging criteria should provide reliable criteria for patient management and decrease the number of inadequate follow-up and tumour biopsies. Separating atypical cystic masses and low- or non-enhancing solid tumours often requires contrast-enhanced US or MRI. One of these two techniques is now mandatory in CT-based type IIF cystic lesions for reclassification. In solid tumours, multiparametric MR imaging must include chemical shift gradient echo (GRE) sequences, signal intensity on T2-weighted images, dynamic contrast-enhanced sequences, diffusion-weighted sequences and late contrast-enhanced images. Using different combinations of two or several parameters, now makes it possible to clearly distinguish certain renal tumours. A larger validation of all these combinations is still necessary to define those having a clinical significance for routine practice.

Learning Objectives:

1. To become familiar with the different types and classifications of renal tumours.
2. To understand the key imaging findings of the different tumours.

Author Disclosure:

N. Grenier: Advisory Board; Supersonic Imagine.

10:30 - 12:00 **Room B**

ESR meets the United States of America

EM 2

Precision imaging and patient experience

Presiding:
J.A. Brink; Boston, MA/US
R.L. Ehman; Rochester, MN/US
P.M. Parizel; Antwerp/BE

A-654/A-655/A-656 10:30

Introduction

P.M. Parizel; *Antwerp/BE,*
J.A. Brink; *Boston, MA/US,*
R.L. Ehman; *Rochester, MN/US*

Session Objectives:

1. To document the growing significance of clinical decision support software for radiologists.
2. To demonstrate how radiologists can use quantitative imaging biomarkers to enhance their role in scientific research and clinical practice.
3. To illustrate how ACR and RSNA are helping radiologists to provide better patient-centred care and improve patient experience with medical imaging.

A-657 10:45

Clinical decision support

K.J. Dreyer; *Boston, MA/US*

As computers outperform humans at complex cognitive tasks, disruptive innovation will increasingly remap the familiar with waves of creative destruction. In healthcare, nowhere is this more apparent or imminent than at the crossroads of radiology and the emerging field of clinical data science. As leaders in our field, we must shepherd the innovations of cognitive computing by defining its role within diagnostic imaging, while first and foremost ensuring the continued safety of our patients. If we are dismissive, defensive or self-motivated - industry, payers and provider entities will innovate around us achieving different forms of disruption, optimised to serve their own needs. To maintain our leadership position, as we enter the era of machine learning, it is essential that we serve our patients by directly managing the use of clinical data science towards the improvement of care - a position which will only strengthen our relevance in the care process as well as in future federal, commercial and accountable care discussions. In this session, we will explore the state of clinical data science in medical imaging and its potential to improve the quality and relevance of radiology as well as the lives of our patients.

Learning Objectives:

1. To understand how decision support systems may improve appropriate utilisation of medical imaging.
2. To understand the role of decision support systems in reducing variation in radiologists' reporting.
3. To consider future opportunities for decision support for medical imaging.

11:05

Interlude/Commentary: Future directions in decision support (ESR/ACR/RSNA Leaders)

A-658 11:10

Quantitative Imaging Biomarkers Alliance

E.F. Jackson; *Madison, WI/US (efjackson@wisc.edu)*

The RSNA quantitative imaging biomarkers alliance (QIBA, www.rsna.org/qiba) unites imaging scientists, healthcare professionals and industry and regulatory stakeholders to advance quantitative imaging and the use of quantitative imaging biomarkers (QIBs) in clinical trials and clinical practice. The QIBA mission is to improve the value and practicality of QIBs by reducing variability across devices, patients and time. This mission is accomplished by 1) collaborating to develop, test, and promulgate methods for obtaining consistent and valid QIB results across imaging platforms, clinical sites, and time and 2) accelerating the development and adoption of hardware and software standards needed to achieve accurate and reproducible QIB results. The work of QIBA is accomplished primarily by stakeholder volunteers who contribute to the efforts of four modality-specific coordinating committees (CT, MR, nuclear medicine, ultrasound) and twelve biomarker committees. In addition, a metrology work group has developed standard terminology and a rigorous statistical framework for research and clinical applications of QIBs. Selected QIBs that are considered to be transformational, translational, feasible, practical and collaborative are addressed by profiles, which are technical standards that include one or more performance claims and inform users what quantitative results can be achieved by following the profile. Sources of bias

and variance, and methods to minimize each, are considered in profile development. This presentation will summarize the goals and objectives of QIBA, including international efforts. The QIBA perspective on opportunities for QIB applications in the practice of precision medicine, challenges to be overcome, and approaches to addressing such challenges will be presented.

Learning Objectives:

1. To understand the need for quantitative imaging biomarkers in clinical trials and clinical practice.
2. To understand key challenges to the implementation of standardised quantitative imaging techniques.
3. To describe some of the current approaches to resolving such key challenges.

11:30

Interlude/Commentary: Future directions in quantitative imaging (ESR/ACR/RSNA Leaders)

A-659/A-660 11:35

Imaging 3.0/Radiology Cares

G. McGinty; *New York, NY/US (geraldinemcginty@gmail.com),*
R.L. Ehman; *Rochester, MN/US*

This session will describe campaigns that have been created by professional radiology organisations in the US to promote patient-centred practice and a thoughtful understanding of the radiologist's role in shaping care delivery and improving the health of the patients they serve. The session will describe resources and tools that have been created for these campaigns which may be useful to the radiology community worldwide. The radiology cares campaign, developed by the Radiological Society of North America (RSNA) focuses on optimising the experience of patients during their radiologic care. Through online resources and educational materials the initiative helps radiologists take patient-centred radiology from concept to practice. The imaging 3.0 campaign of the American College of Radiology (ACR) was designed as a blueprint for the future of radiology as the US healthcare delivery system transitions from a volume-based payment methodology to a value-based one. Its specific aim is to position the radiologist as the steward of appropriate imaging and an integral member of the care delivery team. Together these efforts aim to refocus radiologists' practice around the patient's needs rather than those of the physician and staff. An important component of both campaigns has been the development of tools such as the RadiologyInfo site that teaches patients about their imaging care as well as data registries such as the dose index registry that allows radiologists to benchmark against peers and measure quality improvement efforts. These campaigns have also helped promote advocacy efforts to include meaningful value-based incentives and metrics for radiologists.

Learning Objectives:

1. To understand the principles of the Imaging 3.0 initiative.
2. To understand the principles of the Radiology Cares initiative.
3. To consider potential opportunities for improved patient experience with medical imaging.

Author Disclosure:

R.L. Ehman: Board Member; Radiological Society of North America.

11:55

Interlude/Commentary: Future directions in patient experience (ESR/ACR/RSNA Leaders)

10:30 - 12:00 **Room O**

RTF - Radiology Trainees Forum

TF 1

Highlighted Lectures

Moderators:
L. Andrade; Coimbra/PT
A. Svare; Riga/LV

A-661 10:30

Ovarian cancer staging: where and what to look for?

M.M. Otero-García; *Santiago de Compostela/ES (milagros.otero.garcia@sergas.es)*

Ovarian cancer (OC) is the 5th most common cancer among women worldwide and the second most common gynaecological malignancy. More than 70% of women are diagnosed at an advanced stage (Stages III, IV) and, therefore, with a low 5-year survival rate. Imaging findings of OC depend on the route of dissemination. The first route is the direct extension to the pelvis and surrounding structures, followed by peritoneal extension with ascites and implants in abdominal gravity-dependent areas. Other routes include lymphatic spread throughout para-aortic and pelvic pathways, and haematogenous dissemination. OC treatment requires radical cytoreductive surgery followed by chemotherapy or neoadjuvant chemotherapy followed by interval debulking. An accurate mapping of tumour burden and distribution of disease by imaging plays a central role in treatment stratification. Contrast-enhanced CT is the first imaging technique to use in OC staging because it identifies eligible patients for complete cytoreductive surgery, establishes a precise mapping of peritoneal lesions, detects possibly non-resectable disease and possible complications (e.g. intestinal obstruction). MRI detects implants smaller than 1 cm, especially those adjacent to tissues with similar signal intensity and bladder or rectal involvement. MRI provides helpful functional information regarding response monitorization. An increase in the ADC value in the diffusion sequence indicates a good response to chemotherapy. MRI is the first imaging tool in pregnant women or those with allergy to iodinated contrast. PET/CT has the greatest utility in those patients with rising CA 125 levels and negative CT/MR imaging results during OC follow-up.

Learning Objectives:

1. To become familiar with the different radiological findings in ovarian cancer.
3. To learn where to look for metastatic ovarian cancer.
3. To investigate the role of different imaging modalities in ovarian cancer staging.
4. To understand the potential clinical impact of imaging in treatment planning.

A-662 11:00

Update in breast ultrasound

B. Brkljačić; *Zagreb/HR (boris@brkljacic.com)*

Modern US scanners use compound and harmonic imaging, and as colour Doppler for evaluation of vascularisation of lesions. High-frequency transducers may demonstrate most of lesions containing malignant microcalcifications. 3D ultrasound is available for hand-held and automated high-resolution linear 3D transducers. US-guided biopsies should be performed for all lesions visible by ultrasound. US-guided wire localisation and clip placement can be performed, as well as US-guided minimally invasive therapy, like RFA. Automated whole-breast ultrasound might have important role in screening. Fusion of ultrasound and MRI images, as second look US in MRI-examined patients decreases proportion of false-positive findings, increases specificity and decreases number of MR-guided biopsies. Hand-held ultrasound is highly operator dependent and requires proper examination technique, experience and education to visualise all breast parts and axilla. The best US scanner should be used, with high-frequency linear transducers for breast examination. Ultrasonographic findings should be compared with mammographic and MRI findings. Features of the breast lesions that need to be analysed are: shape, relation of anteroposterior to laterolateral diameter, margins, internal structure, sound absorption (distal acoustic phenomena), and stiffness. Sonoelastography is a dynamic technique that uses US to estimate the stiffness of tissues by measuring the degree of distortion under application of external force. Elastogram is superimposed over B-mode image in different colours depending on the type of elastography. Strain elastography requires compression with the transducer and is mostly qualitative, while shear wave elastography does not require compression and enables quantification of the stiffness of the lesion.

Learning Objectives:

1. To learn about technique and clinical applications of breast ultrasound.
2. To understand the role of ultrasound for guidance of breast biopsies and minimally invasive treatment.
3. To understand the role of ultrasound in screening for breast cancer.
4. To become familiar with clinical use of sonoelastography and automated whole-breast ultrasound systems.

Author Disclosure:

B. Brkljačić: Speaker; Guerbet, Bayer.

A-663 11:30

Multiparametric MRI evaluation in brain tumours

A. Santa; *Sibiu/RO (adriansanta@ymail.com)*

MRI is definitely the method of choice in evaluating brain tumours, it is multiparametric approach permitting a very good characterisation and identification of many different types of brain masses. For the best diagnosis, one should have a good knowledge not only of what sequences are to be applied in the examination, but most importantly, what any of these sequences is really dealing with, what kind of information are they revealing and how to exploit such information for the better characterisation of tumour. The presentation explains via clinical examples the position and role of each sequence, from the morphological T1, T2 and FLAIR images to more sophisticated acquisitions, such as diffusion and ADC mapping, susceptibility weighted images, tractography, perfusion and rCBV, emphasising what properties of the mass these sequences are exploring. The multimodal approach to brain tumours is a speculative science, in which each sequence brings a different sort of data, the final result being "constructed" from the rapport that every sequence brings to the radiologist.

Learning Objectives:
1. To learn about how we assess MRI images regarding brain tumours.
2. To understand the role of each type of sequence in evaluating the pathology.
3. To appreciate how the decision of diagnostic progresses along with the various sequences acquired, the data that each sequence bring to the reader.
4. To become familiar with more sophisticated modalities of assessment of brain tumours, e.g. diffusion, ADC, spectroscopy, perfusion and with the way they add to positive and differential diagnosis.

10:30 - 12:00 **Room L 8**

ESR Patient Advisory Group (ESR-PAG)

ESR-PAG 1

Improving patient safety and quality of care in clinical radiology

A-664 10:30

Chairmen's introduction (part 1)

N. Bedlington; *Vienna/AT (nicola.bedlington@eu-patient.eu)*

This session will focus on improving patient safety and quality of care in clinical radiology. Different presentations will be included. The first one will present the work of the ESR Audit & Standards Subcommittee in collaboration with the ESR Patient Advisory Group. It will highlight methods and examples of good practice and how to improve the patient-doctor relationship. Thereafter, the patients' perspective will be provided with a focus on the driver diagram as well as on information over-/underload. The final presentation is dedicated to the implementation of a patient satisfaction questionnaire in the radiology department. It will point out the benefits of patient satisfaction assessment and how to understand the gathered feedback. The session will conclude with a panel discussion.

Session Objectives:
1. To understand how ESR is improving patient safety and quality of care through audit and standards.
2. To explore concrete examples of best practice on implementing these standards in the radiology department and how these might be replicated.

A-665 10:35

Chairmen's introduction (part 2)

B.E. Kelly; *Belfast/UK (barryekelly@mac.com)*

Audit measures something against an agreed standard. As radiological health care professionals, we tend to think of this as equipment and process driven. Whilst this is an important component, audit can, and should, also be used to measure our interaction with each other and with our patients. By doing this, we ensure that a patient-centred approach leads to a safe, professional and harmonious institution.

Session Objectives:
1. To understand how ESR is improving patient safety and quality of care through audit and standards.
2. To explore concrete examples of best practice on implementing these standards in the radiology department and how these might be replicated.

A-666 10:40

The work of the ESR Audit & Standards Subcommittee in collaboration with ESR-PAG

B.E. Kelly; *Belfast/UK (barryekelly@mac.com)*

A driver diagram (DD) is used to conceptualise an issue and to determine its system components, thus creating a pathway to achieve the goal of patient-centred care. The DD that shall be discussed provides guidance on how to embed this patient-centred care within radiology departments for the benefit of all. One way to measure patient contentment is with a patient satisfaction questionnaire. Such a document has been produced by Dr Dominque Carrie. This has been reviewed and refined by both the Patient Advisory Group and the Audit committees and will be disseminated to radiology departments throughout Europe. Overwhelming evidence shows that doctors are patients too. Ten percent of medical students and doctors have significant psychological and dependency issues. Two percent are bipolar and one percent suicidal. In addition it is known that these traits are longstanding, continuing from school, college, university through long medical careers. It is vital, for professional, pastoral and ethical reasons that these issues are recognised and treated.

Learning Objectives:
1. To become familiar with methods and examples of good practice and on how to improve the patient-doctor relationship.
2. To understand the need for balance between professional responsibility and patient autonomy.

A-667 10:55

Patients' perspective (part I)

D. Walsh; *Dublin/IE (executivedirector@efna.net)*

This presentation will explore what neurology patients view as 'quality care', using examples of good and bad radiology practice from relevant disease areas. It will then question if such good practice can be further enabled - and bad practice minimized - through patient involvement in monitoring the implementation of the driver diagram. To facilitate this process, good communication between doctor, patient and the wider multidisciplinary team is essential, and this will be considered from the patient perspective. The presentation will aim to analyse the potential phases of patient involvement, for example, including ways to identify the most relevant patient-reported outcome measures, and ways to collect and analyse patient-generated evidence. The evidence - in this case, a patient relevant audit of driver diagram implementation - must then be disseminated to allow prospective patients to engage in more informed decision-making in their approach to choosing treatment and management options, e.g. services, treatment centres and health care professionals.

Learning Objectives:
1. To learn that implementing the driver diagram in their department will be a step-by-step process that can be monitored by patients.
2. To learn that a fair knowledge of the upcoming procedure is part of feeling safe for the patient.
3. To learn that an overload of information is equally detrimental to a safe feeling as no information, putting the patient central means an adjusted offering of information.

Author Disclosure:
D. Walsh: Grant Recipient; EFNA, as an organisation, is funded - in part - by a consortia of pharmaceutical sponsors. The list can be found here: http://efna.net/about-us/finance-and-funding/. Speaker; As Executive Director of EFNA, I am occasionally invited to speak at events held by the pharmaceutical industry. However, no payment is received..

A-668 11:10

Patients' perspective (part II)

E. Briers; *Hasselt/BE (erikbriers@telenet.be)*

The perfect radiology department does not exist there is always room for improvement. The driver diagram can be seen as an inventory of good practice objectives. A comparison between this standard and the actual situation in the department should show weak point and elements to be improved. Ideally this is realised through a good set of procedures (ISO meaning) that guide the work in the department. These procedures need verification in the execution. In this, patients play a vital role as they go where radiologists do not go and they undergo the procedures. To ensure patients a safe and comfortable journey through the department they need to know and understand what they are up to. Patients present themselves to the department they are sent by a clinician with a diagnostic issue. The diagnostic issues are very diverse from a simple broken wrist to a cancer diagnosis. The patients on the other hand have different levels of literacy and on top of that different level of coping. This boils down to the fact that there is not one answer that will fit all patient and diagnostics needs. What is not enough information for one patient is an overload for another and overload is as bad as no information at all as it makes the patient deaf to new and potentially important info. Good information is provided at the level of the individual patient with adequate complexity, respect and compassion for the intellectually underprivileged.

Learning Objectives:
1. To learn that implementing the driver diagram in their department will be a step-by-step process that can be monitored by patients.
2. To learn that a fair knowledge of the upcoming procedure is part of feeling safe for the patient.
3. To learn that an overload of information is equally detrimental to a safe feeling as no information, putting the patient central means an adjusted offering of information.

A-669 11:25

Example of good practice: implementing a patient satisfaction questionnaire in your radiology department

D.-G. Carrié; *Toulouse/FR (dominiquecarrie@wanadoo.fr)*

Patients of modern medical imaging require from us doctors radiologists, very high-quality technical performances, carried out on the most modern equipment, in complete efficiency and safety. They also demand that they are carried out as quickly as possible, in pleasant places, by well-trained staff

attentive to all their requests. For 9 years, in our department of medical imaging in Toulouse (France), it has, therefore, appeared necessary to assess their satisfaction by a questionnaire after they benefited from a diagnostic or interventional (CT or MRI) imaging. This experience showed us that it is easy to implement such a questionnaire in any structure of medical imaging. The proposed items may be discussed between radiologists, with the service personnel, with patient-users organisations you know, in relation to the supposed expectations of your patients and potential problems or limits to each structure (for example, appointment delays, times of waiting, results retrieval, direct access to the radiologist). The questions must be simple and understandable by each patient. For the responses obtained to be sufficiently numerous and representative, incentives to respond to the questionnaires must be implemented (proposed systematically after any delivery of the result for instance). The results obtained must be regularly collated, their evolution over time analysed, modifications in your daily practice implemented, their presentation to the entire team regularly made. This allows us to better understand the expectations of our patients, to improve our practices to satisfy them better, and thus offer a radiology service closer to them.

Learning Objectives:

1. To understand the benefits of patient satisfaction assessment.
2. To learn how to implement a questionnaire (means to be used, items to estimate).
3. To understand the feedback you will obtain.

11:40

Panel discussion: Does your department perform well in patient-centred care?

10:30 - 12:00 **Room F1**

E³ - European Diploma Prep Sessions

E³ 1423
Gastrointestinal and abdominal

A-670 10:30

Chairman's introduction

C. Stoupis; *Männedorf/CH (c.stoupis@spitalmaennedorf.ch)*

The role of radiologist in the diagnosis of abdominal diseases is crucial. Knowledge of the key imaging features of the different abdominal disorders including the benign and malignant lesions of the parenchymal organs and the GI tract, based on the underlying anatomy, physiology and pathology is essential to approach the correct diagnosis. Awareness of strengths and limitations of the different imaging techniques will increase the diagnostic confidence of radiologist, providing important information about lesion detection and characterization and will guide to the specific diagnosis and the decision making in patient management.

Session Objectives:

1. To understand the typical imaging features of benign and malignant lesions of the hepatobiliary system.
2. To learn the typical imaging features of benign and malignant lesions of the pancreas and spleen.
3. To become familiar with the methodological basis and to differentiate typical features in imaging examinations of the gastrointestinal tract.
4. To understand the role of different imaging modalities including hybrid imaging in diagnosing and staging neoplasms, gastrointestinal and abdominal organ systems.

A-671 10:36

A. Hepatobiliary system

Y. Menu; *Paris/FR (yves.menu@sat.aphp.fr)*

Detailed understanding of liver and biliary anatomy and segmentation and vessel anatomy (hepatic artery, portal vein, hepatic veins, inferior vena cava) including variants in vascular anatomy that may affect surgical planning is critical. Focal liver lesions include benign and malignant tumours, as well as infections. Distinction can be done with imaging in most cases using an algorithmic approach, helped with clinical and biological data. Multimodality may be necessary, sometimes leading to the necessity of imaging-guided biopsy. Imaging is more and more prominent in the evaluation of diffuse liver diseases, based on morphological changes as well as quantification of fat, iron and fibrosis. Bile duct imaging requires relevant technique and good understanding of the appearance of main diseases like tumours and inflammation. Overall, imaging is a prominent step for the evaluation of hepatobiliary diseases, while the radiologist's role is also to choose the relevant method, or association of methods, for the clinical question.

Learning Objectives:

1. To learn the anatomy, normal variants and congenital disorders of the hepatobiliary system.
2. To become familiar with the primary and secondary imaging features of acute and chronic diffuse liver diseases.
3. To understand the causes and imaging features of benign and malignant focal liver lesions, including cysts, haemangiomas, adenomas, focal nodular hyperplasia, hepatocellular carcinomas and metastases.
4. To learn the various causes and imaging features of benign and malignant diseases of the biliary tract and gallbladder.

A-672 11:04

B. Pancreas and spleen

W. Schima; *Vienna/AT (wolfgang.schima@khgh.at)*

In general, contrast-enhanced MDCT is the primary tool of pancreatic imaging, and MRCP is very valuable for assessment of the ductal system. There is a variety of anatomic variants and anomalies of the pancreas and the ductal system. Pancreas divisum and annular pancreas are the result of either failure of fusion or of rotation of the pancreas anlagen during the foetal period. Both anomalies may result in significant morbidity. Ductal adenocarcinoma is by far the most common malignant tumour of the pancreas, with approximately 80% of patients having non-resectable (advanced) disease at the time of diagnosis. In patients with equivocal CT findings, contrast-enhanced MRI is the technique of choice for visualization of small tumours. A wide differential diagnosis exists for cystic masses: from benign pseudocysts to benign, borderline and invasive malignant neoplasms. Contrast-enhanced MRI is the best modality for characterization of these lesions and to guide follow-up in these patients. Acute pancreatitis is classified as interstitial oedematous or necrotizing pancreatitis according to the revised Atlanta classification, which has brought a consistent terminology for fluid collections and complications of pancreatitis. Imaging of splenic masses is one of the less esteemed tasks in abdominal imaging. The reason for this is that the imaging appearances of many splenic lesions may overlap, which makes noninvasive characterization quite challenging. However, imaging findings of the most important benign lesions such as haemangiomas, hamartomas and abscesses should be familiar. If noninvasive characterization of focal splenic lesions is not possible, US-guided core needle biopsy may be of help.

Learning Objectives:

1. To understand the anatomy, normal variants and congenital disorders of the pancreas.
2. To become familiar with the causes and imaging features of benign and malignant pancreatic tumours.
3. To understand the imaging features of acute and chronic pancreatitis and its potential complications.
4. To learn the causes and imaging features of focal and diffuse splenic abnormalities.

A-673 11:32

C. Imaging of the gastrointestinal tract

R.G.H. Beets-Tan; *Amsterdam/NL*

Fluoroscopy, US, CT and MRI are the cornerstones in GI tract imaging. Fluoroscopy has a role in congenital anomalies and functional disorders of GI tract. Transabdominal US is accurate to detect appendicitis and abdominal free fluid and fluid/abscess collections. Contrast-enhanced CT identifies post-traumatic complications such as lacerations, the causes of bowel obstruction and dilatation. CT shows postoperative complications such as leakage of surgical anastomosis, abscesses, internal herniation, bowel strangulations and bowel ischaemia. Inflammation of the bowel, diverticulitis, epiploic appendagitis are well detected on CT. In recent years, MR enterography has gained field for the assessment of Crohn's disease activity and extent. Endoscopic US is the mainstay in staging oesophageal and gastric tumours, CT is the method of choice for local and distant staging of duodenal, small and large bowel tumours, while endorectal US and MRI have been widely adopted for staging of rectal tumours. This lecture will deal with the various GI diseases and its imaging features.

Learning Objectives:

1. To become familiar with the anatomy, normal variants and congenital disorders of the oesophagus, stomach, duodenum, small bowel, colon, rectum and anal canal.
2. To understand the imaging features of colonic diverticulosis, diverticulitis, tumour stenosis, ileocolic intussusception, colonic fistula, paracolic abscess, epiploic appendagitis, intraperitoneal fluid collection, colonic pneumatosis and pneumoperitoneum.
3. To learn typical radiological manifestations of inflammatory bowel diseases, malabsorption syndromes, infection and bowel ischaemia.
4. To become familiar with the staging of tumours of the gastrointestinal tract, including features that indicate nonresectability, and to understand the role of different imaging modalities including hybrid imaging in diagnosing and staging.

10:30 - 12:00 **Room M 4**

E³ - ECR Academies: Multiparametric Ultrasound (MPUS)

E³ 1420
Multiparametric US of small parts

A-674 10:30
Chairman's introduction
D.-A. Clevert; *Munich/DE (Dirk.Clevert@med.uni-muenchen.de)*

Ultrasound is a sensitive and accurate technique for the evaluation of small part abnormalities, and is widely accepted as the first-line imaging technique and the gold standard for many common and uncommon small part diseases but does not provide a histological diagnosis. Due to the continuous development of modern ultrasonography, such as high frequency transducers, colour Doppler and real-time elastography, ultrasonography is considered the imaging modality of choice in small parts disorders. Real-time elastography has been introduced over 20 years ago for making non-invasive measurements of the mechanical properties of tissue and for imaging the elasticity of biological tissue. Real-time elastography in detection and differentiation of nodules in the breast, prostate, thyroid gland lymph nodes and scrotal mass has already demonstrated its promising value.
Author Disclosure:
D. Clevert: Advisory Board; Samsung, Siemens, Philips, Bracco. Speaker; Samsung, Siemens, Philips, Bracco.

A-675 10:35
A. Thyroid
S.S. Özbek; *Izmir/TR (sureyya.ozbek@ege.edu.tr)*

Thyroid nodules are detected in more than half of the general population. Given the fact that only about 5-15% of them are malignant, characterization of them during clinical management becomes highly important. Contrary to its high performance in detecting nodules, real-time grey-scale ultrasonography (US) is not perfect in differentiating malignancy. Nodular features including marked hypoechogenicity, solid structure, irregular margins, taller-than-wider shape, internal microcalcifications and evidence of extrathyroidal disease have been used for characterization. However, no single parameter has been shown to be completely reliable in this regard. Thus, some sonographic patterns and guidelines with combined use of these features have been suggested in recent years, resulting better rates of characterization. Up to now, research focusing on Doppler US and sonoelastographic techniques has yielded only complementary value to enhance the conclusion deduced from grey-scale examinations, rather than being a substitute. A sonoelastographic result in favour of a “soft” lesion is suggested to be used to impose benignancy, when grey-scale US results are inconclusive. Thanks to the gland’s superficial location, new generations of colour Doppler US systems provide highly detailed vascular depiction of nodular vascularity, which results in scarcity of contrast-enhanced US (CEUS) research in thyroid gland. Currently, the use of CEUS agents is largely limited to depiction of residual tissue following therapeutic ablation. In conclusion, the characterization of thyroid nodules are mainly based on combined use of grey-scale US criteria indicating highly suspicious for malignancy. In cases of equivocal results, sonoelastographic findings may be of value in enhancing diagnostic accuracy.
Learning Objectives:
1. To understand the current roles of real-time US, Doppler techniques, US elastography and CEUS to differentiate between benign and malignant thyroid nodules.
2. To learn about current guidelines for thyroid nodule assessment.
3. To become familiar with the advantages and limitations of the various US techniques.

A-676 11:03
B. Lymph nodes
P.-Y. Marcy; *Ollioules/FR (brozpy@gmail.com)*

Multiparametric ultrasound (MPUS) assessment of superficial lymph nodes (LN) is well established. This includes diagnosis, prognosis, selecting and monitoring treatment, beyond the diagnosis itself (cancer, lymphoma, or inflammatory nodes). Diagnosis of a unilateral metastatic N+ reduces by 50%/25% the epidermoid head and neck cancer patient's 5-year survival rate when ipsilateral/in the lower/contralateral neck. Metastasis is site specific with respect to H&N primary location. Differences between benign and malignant nodes are based upon size, shape, echotexture, echogenic hilum and vasculature. Malignant nodes are typically hypoechoic, without echogenic hilum, round shaped, with L/T ratio <2, and with vessels predominant in periphery. Typical US features of LN include reactive adenitis (germinative centres); cystic (tuberculosis, H&N & thyroid carcinomas) and reticulated patterns (malignant lymphoma), and microN+. Combining Fine Needle Aspiration Cytology (FNAC) increases US specificity up to 93%. US guided-FNAC makes the diagnosis of microN+ (subcortical foci), thus should improve oncology prognosis. FNA biopsy makes the subtype diagnosis of malignant lymphoma. Thyroglobulin/Calcitonin wash-out improves the diagnostic accuracy of N+ of follicular/medullary thyroid origin. CEUS can assess nodal architecture and depicts abnormal vascular patterns, where results are uncertain. Elastography may detect a subset of malignant LN. US landmarks knowledge of axillary and inguinal regions, and of the Robbins classification in the neck is mandatory to define the correct anatomical location of LN to the surgeon/oncologist. Assessment of sentinel lymph nodes is useful in breast/penile, vulva/head and neck, and thyroid cancers.
Learning Objectives:
1. To understand the current roles of real-time US, Doppler techniques, US elastography and CEUS to differentiate between benign and malignant superficial lymph nodes.
2. To understand MPUS criteria and their limitations.
3. To learn about MPUS in the assessment of sentinel lymph nodes.

A-677 11:31
C. Scrotum
M. Bertolotto; *Trieste/IT (bertolot@units.it)*

Ultrasonography (US) is the imaging modality of choice for examination of the scrotum. It can provide information valuable for the differential diagnosis of a variety of disease processes involving the scrotum with similar clinical manifestations. Beside grey-scale US, several modes have been adopted to improve characterization of scrotal lesions, including Doppler US modes, sonoelastography and CEUS. A multiparametric approach to scrotal pathologies has potential to improve the diagnostic performance of grey-scale US. Doppler modes are used in association with grey-scale investigation in virtually all patients. Their ability to demonstrate testicular perfusion aids in reaching a specific diagnosis in patients with acute scrotal pain, and in characterization of solid tumours. A number of hypovascular lesions, however, still appear avascular. Differentiation between truly avascular and hypovascular lesions is clinically important, since there is increasing evidence that the former are usually benign, while the latter are more often malignant. CEUS can be used to clearly demonstrate presence or absence of lesion vascularization when colour Doppler findings are equivocal. Reason for the use of elastographic modes stems from the existence of large differences in stiffness between surrounding normal and pathologic tissues that may otherwise possess similar image contrast with conventional modes. Generally speaking, when a hard lesion is identified malignancy is suspected, while soft masses are more often benign. However, exceptions exist to this rule. A variety of benign testicular lesions may appear hard at elastography and, on the contrary, malignant tumours may be softer than expected. Moreover, some lesions change consistency over time.
Learning Objectives:
1. To become familiar with the US morphology of the normal scrotal content as assessed by real-time US, Doppler techniques, US elastography and CEUS.
2. To learn the advantages and limitations of these US modalities in the assessment of the acute scrotum.
3. To understand the current roles of real-time US, Doppler techniques, US elastography and CEUS to differentiate between benign and malignant testicular and extratesticular scrotal mass lesions.
Author Disclosure:
M. Bertolotto: Board Member; ESUR Board Member.

10:30 - 12:00 **Room M 5**

E³ - ECR Academies: Neuroradiology: from Morphology to Function

E³ 1422
Advanced imaging techniques in brain tumours

A-678 10:30
Chairman's introduction
P.C. Maly Sundgren; *Lund/SE (Pia.Sundgren@med.lu.se)*

As session chairman, I will give a brief introduction to the topics related to advanced techniques in brain tumour imaging that will be discussed in this session and give some highlight as well as some future ideas regarding advanced brain tumour imaging with respect to new magnetic resonance imaging sequences.

A-679 10:36

A. Clinical utility of perfusion imaging for differentiating brain tumours
I.N. Pronin; *Moscow/RU*

"no abstract submitted"
Learning Objectives:
1. To provide practical tips and tricks for performing CT and MR perfusion in patients with brain tumours.
2. To illustrate how certain perfusion derived parameters (rCBV) can be correlated with tumour histology (e.g. angiogenesis, capillary leakage, malignancy grade).
3. To show that intense contrast enhancement is not identical to perfusion.

A-680 11:04

B. Clinical applications of amino acid PET in brain tumour patients
N. Galldiks; *Cologne/DE (norbert.galldiks@uk-koeln.de)*

In the last years, PET using radiolabelled amino acids has gained increasing interest in the diagnostics of brain tumour patients and has been established in many neurooncological centres as a complementary diagnostic tool to conventional MRI. Amino acid PET offers important additional information in the diagnosis of unclear space-occupying brain lesions and an improved delineation of glioma extent, which is helpful for biopsy guidance, planning of resection and radiation therapy. Furthermore, amino acid PET imaging may provide prognostic information in untreated, newly diagnosed glioma patients, helps to differentiate tumour progression or recurrence from treatment-related changes in low- and high-grade gliomas as well as in brain metastasis (e.g. pseudoprogression, radiation necrosis) and allows to evaluate the metabolic response following brain tumour therapy, particularly chemoradiation, alkylating chemotherapy and antiangiogenic therapy, earlier than with conventional MRI.
Learning Objectives:
1. To show that amino acid PET is gaining increasing importance in assessment of tumour activity and malignancy.
2. To demonstrate how amino acid PET can be useful in glioma delineation for treatment planning (e.g., resection, biopsy, radiation), detection of post-therapeutic effects, assessment of treatment response, and prognostication.
3. To provide information on new PET tracers (targeting tumour hypoxia, enzymes in neoplastic metabolic pathways, etc.) and the combination of tracers with therapeutic agents.

A-681 11:32

C. Assessment of brain tumour perfusion and abnormal vascular structure using arterial spin-labelling
X. Golay; *London/UK (x.golay@ucl.ac.uk)*

Haemodynamic alterations are present in many brain tumours, and in general, CBF and cerebral blood volume (CBV) increase with grade. Much of our MR imaging-based knowledge about these changes has been gained from Gd-based techniques, in particular dynamic susceptibility contrast (DSC) and dynamic contrast-enhanced (DCE) imaging. Thus, so far, most literature has focused on relative CBV changes, because it is easier to assess using such techniques than CBF, and most of the data available are of relatively poor spatial resolution and prone to artefacts, due to the rapid passage of the intravascularly confined tracer necessitates. ASL cannot measure relative CBV, but provides a straightforward assessment of CBF. In particular, since water has high permeability in the normal and neoplastic tissue, there is no need with ASL to use complicated leakage-correction algorithms to obtain quantitative results. Initial reports demonstrated that ASL and DSC show largely concordant results in glioblastoma multiformae (GBM) (for reference, see 1). Higher CBF in GBM correlates with genetic markers and is associated with shorter progression-free survival time. Lower grade tumours typically demonstrate lower CBF. In fact, some have suggested that CBF quantification provides a better estimate of event-free survival for a wide range of gliomas than does a histologic grading scale. Finally, CBF has also been used to assess metastatic disease and treatment response, in particular in the assessment of radiation necrosis vs. recurrence. Ref: 1) Haller et al., Radiology, 281(2):337-356 (2016).
Learning Objectives:
1. To offer a short update on the physical principles and technique of arterial spin-labelling in assessing brain tumour perfusion.
2. To review the advantages and disadvantages of ASL as compared to contrast-enhanced perfusion imaging.
3. To provide clinical examples where ASL has contributed significantly to management and clinical decision making in brain tumour patients.
Author Disclosure:
X. Golay: CEO; Gold Standard Phantoms Ltd. Consultant; Olea Medical. Founder; Imgenious Ltd. Research/Grant Support; Olea Medical.

12:15 - 12:45 **Room A**

Headline Session

HL 3

Arthur de Schepper Honorary Lecture

Presiding:
P.M. Parizel; Antwerp/BE

A-682 12:15

From features to function: breakthroughs in breast imaging
F.J. Gilbert; *Cambridge/UK (fjg28@cam.ac.uk)*

The imaging phenotype of breast cancer is used to decide the likelihood of a lesion being invasive or in situ disease which affects the diagnostic approach. The morphological appearance can give a clue as to the grade or aggressiveness of a cancer. Functional imaging gives information about the vascularity, metabolism or cellular activity of a lesion or organ. Functional magnetic resonance imaging (MRI) techniques include dynamic contrast-enhanced (DCE) MR, diffusion-weighted imaging (DWI), blood oxygen level-dependent (BOLD) MR and these give insight into pathology and pathological processes that cannot be gained from traditional anatomical imaging. Molecular imaging with radioisotopes gives information on metabolism and proliferation and this has been exploited in PET using different radiotracers. Breast cancer has a marked degree of tumoural heterogeneity reflecting clonal diversity which exhibits various metabolic and functional phenotypic characteristics. This variation can result in different prognosis and also a differential response to treatment creating a challenge in the identification of the best therapeutic regimen for each patient. Vascular and proliferation measures can be used to predict response to treatment. This lecture will focus on the move from morphological imaging in breast cancer to a more functional approach and examine whether or not there is sufficient evidence for us to change our practice.
Author Disclosure:
F.J. Gilbert: Research/Grant Support; Hologic, GE Healthcare.

12:30 - 13:30 **Room C**

E³ - The Beauty of Basic Knowledge: Chest Imaging

E³ 25D

The most important measurements you need to know in chest radiology

Moderator:
N. Howarth; Chêne-Bougeries/CH

A-683 12:30

A. Heart and great vessels: how, why, when?
G. Fassa-Ashrafpoor; *Chêne-Bougeries/CH (golmehr.fassa@grangettes.ch)*

Cross-sectional imaging techniques such as computed tomography (CT) and magnetic resonance imaging (MRI) are increasingly being performed, allowing unrestricted assessment of the heart and great vessels. ECG-gated acquisition protocols are crucial in reducing motion artefacts. Measurement of the thoracic aorta is performed at different anatomic levels using a multi-plane double-oblique reconstruction perpendicular to the lumen, allowing for identification of patients requiring surgical management. Assessment of the heart includes measurement of right and left atrial areas, end-systolic and end-diastolic right and left ventricular volumes (allowing determination of ejection fraction) and left ventricular end-diastolic wall thickness, which are relevant for the diagnosis of cardiomyopathies. Moreover, structural analysis of the heart should also be performed. The anatomy, connections and dimensions of the pulmonary veins can be easily analysed. The presence of thrombosis in cardiac cavities, mainly in the left atrial appendage and the left ventricular apex should also be sought, most importantly in patients with a history of systemic embolism. Other structures, such as the coronary arteries and cardiac valves can also be accurately assessed by CT and MRI. Finally, cross-sectional techniques are indicated for follow-up of patients after surgical intervention of the heart and great vessels.
Learning Objectives:
1. To review the most useful measurements on cross-sectional imaging of the heart and great vessels.
2. To learn how to accurately perform these measurements.
3. To know when the measurements are of clinical importance.

A-684 13:00

B. Lung nodules: is volume better than size?

M. Prokop; *Nijmegen/NL*

"no abstract submitted"

Learning Objectives:

1. To review the management of pulmonary nodules seen on CT.
2. To learn how to accurately perform the measurement of nodule volume and size.
3. To know the limitations of the lung nodule measurement.

12:30 - 13:30 **Room D**

E³ - The Beauty of Basic Knowledge: A Survival Guide to Musculoskeletal Imaging

E³ 24D

Acute trauma: patterns in the peripheral skeleton

Moderator:
V.N. Cassar-Pullicino; Oswestry/UK

A-685 12:30

Acute trauma: patterns in the peripheral skeleton

J. Teh; *Oxford/UK (jamesteh1@googlemail.com)*

A systematic approach to analyse trauma imaging of the peripheral skeleton is presented. Typically, imaging begins with x-rays. A step-wise approach may reveal subtle abnormalities that should prompt further action. For example, the presence of a Segond fracture on x-ray suggests an ACL injury and thus should lead to an MRI scan. It should be recognized that in trauma, certain injuries cannot occur in isolation; therefore, a dislocated radial head on elbow x-ray should prompt imaging of the whole forearm, as Monteggia fracture-dislocation may be present. Understanding mechanisms of injury allows the radiologist to predict patterns of injury. So if bone bruising is present on MRI in the lateral femoral condyle and medial patella, a lateral patellar dislocation should be suspected and a specific search for an injury of the medial retinaculum should be made. Conversely, recognizing classic patterns of injury can allow the mechanism of injury to be deduced. This lecture will focus on classical patterns of acute trauma in the peripheral skeleton.

Learning Objectives:

1. To become familiar with the imaging manifestations of common important injuries in the upper and lower limb.
2. To understand the underlying mechanism that result in combination of injuries.
3. To learn how to best employ imaging modalities in their diagnosis.

14:00 - 15:30 **Room A**

E³ - ECR Academies: Interactive Teaching Sessions for Young (and not so Young) Radiologists

E³ 1521

Imaging of the skull base

A-686 14:00

A. Non-tumoural pathology of the temporal bone

B. Ozgen Mocan; *Ankara/TR (burce@hacettepe.edu.tr)*

The temporal bone has a complex anatomy but the pathologies involving the temporal bone structures are somewhat limited with specific and diagnostic imaging findings. During this lecture, the most common non-tumoural causes of conductive and sensorineural hearing loss will be reviewed in an interactive manner with an emphasis on the most commonly seen pathologies such as chronic inflammation, cholesteatoma, otosclerosis and labyrinthitis ossificans.

Learning Objectives:

1. To learn the most common inflammatory lesions of the temporal bone.
2. To become familiar with malformations and common pathologies.

A-687 14:45

B. Tumours of the skull base

T. Beale; *London/UK (timothy.beale@uclh.nhs.uk)*

The lecture will describe a classification system for tumours of the skull base that will aid in the differential diagnosis. Using clinical cases the imaging features of the common skull base tumours will be highlighted. The important review areas for the individual tumours will be discussed including those features that may alter the clinical management and help in the differential diagnosis. The common pitfalls and non-neoplastic differential diagnosis will be highlighted and an imaging technique for assessing the skull base will be discussed.

Learning Objectives:

1. To become familiar with the imaging technique of the skull base.
2. To identify imaging criteria for improved differential diagnosis.

14:00 - 15:30 **Room B**

Special Focus Session

SF 15a

My three top tips for abdominal imaging

A-688 14:00

Chairman's introduction

M. Zins; *Paris/FR (mzins@hpsj.fr)*

In this session including focused short lectures we will learn how to avoid common mistakes in abdominal radiology and we will understand how to get over an area of difficulty through the clinical expertise of selected abdominal radiologists. Common liver, pancreatic and biliary diseases will be discussed as well as Inflammatory bowel diseases and acute abdominal conditions.

Session Objectives:

1. To learn how to avoid common mistakes in abdominal radiology.
2. To understand how to get over an area of difficulty through the clinical expertise of selected abdominal radiologists.

A-689 14:05

Postoperative abdomen

D.J.M. Tolan; *Leeds/UK*

"no abstract submitted"

Learning Objectives:

1. To learn how to optimise detection of anastomotic leaks on CT using radiological signs and positive luminal contrast.
2. To recognise material in the abdomen surgeons may leave deliberately.
3. To recognise material in the abdomen surgeons may leave by accident.

A-690 14:13

Appendicitis

J.B.C.M. Puylaert; *The Hague/NL (dr.jbcmpuylaert@wxs.nl)*

Abdominal ultrasound plays a pivotal role in the imaging workup of patients with suspected appendicitis. It should be the primary modality, and only in case of a negative or inconclusive examination, should be followed by CT or MR. The specific advantages of US over CT are: US has an image definition in the close range which is much higher than that of CT. US is more interactive than CT. Patient's history as well as the painful area or palpable mass can directly be correlated with the US findings. US is real-time and shows peristalsis, pulsations and blood flow. US also shows the effects of respiration, Valsalva manoeuvre, gravity and compression with the probe, allowing to assess whether the appendix or other organs as bowel and gallbladder are soft or rigid. US allows immediate US-guided puncture of intraperitoneal fluid and drainage of pus. US in appendicitis should be performed with graded compression. Compression is necessary to displace or compress bowel to eliminate the disturbing influence of bowel gas and to approach the pathological structure closely. This allows the use of a high-frequency transducer with a better image quality. The final US report should be integrated with the clinical findings, laboratory data, CT scan and possible other radiological examinations. It is clear that the US examination, as described here, should not be performed by a technician nor by a clinician, but by an experienced (abdominal) radiologist.

Learning Objectives:

1. To learn that US has a pivotal and unique role in appendicitis and should be done prior to CT.
2. To learn that US in acute abdomen allows the radiologist to get closer to the patient than CT and MRI.
3. To learn that US should be performed by abdominal radiologists, and not by clinicians or technicians.

A-691 14:21

Bile duct stones

J.A. Guthrie; *Leeds/UK (Ashley.Guthrie@leedsth.nhs.uk)*

1. Whilst the investigation of choice for the diagnosis of gallstones within the gall bladder is US, it is less reliable for stones in the bile ducts. Risk factors in patients with known stones (either pre- or post-cholecystectomy) include right upper quadrant pain, deranged liver function tests and a dilated common bile duct. MRCP is a reliable quick non-invasive examination. 2. 2D HASTE/SS-FSE/FSE-ADA/FASE without fat saturation in 2 planes (oblique coronal and axial) will establish a diagnosis in most cases and are the “work horse” sequences in most patients, and can usually be acquired over a limited number of breathholds. The ducts are outlined by fluid in the lumen and fat outside the duct. Stones are identified as dependent filling defects on 2 planes. The lack of fat saturation allows for a better appreciation of the bile duct wall and adjacent anatomical structures. 3D sequences often take a long time to acquire and may yield poor images. 3. FISP/GRASS/FFE/SARGE (which can be gated) are a useful adjunct especially in those patients that have difficulty holding their breath, if they are struggling turn to this class of sequence before the patient is exhausted.

Learning Objectives:

1. To learn that in patients with a high index of clinical suspicion of bile duct stone, MRCP should be employed early.
2. To know that 2D HASTE/SS-FSE/FSE-ADA/FASE without fat saturation in 2 planes (oblique coronal and axial) - will establish a diagnosis in most cases and are the "work horse" sequences in most patients.
3. To understand that FISP/GRASS/FFE/SARGE (which can be gated) are a useful adjunct especially in those patients that have difficulty holding their breath.

Author Disclosure:

J.A. Guthrie: Speaker; Bayer Healthcare, Siemens AG.

A-692 14:29

Dilated pancreatic duct

R. Manfredi; *Verona/IT (riccardo.manfredi@univr.it)*

The prognosis of pancreatic adenocarcinoma is very poor, and little improvement has been reported in the past several decades. Only a low percentage of patients in whom pancreatic cancer is detected at an early stage without local infiltration have the potential for long-term survival after surgical resection. The earliest possible diagnosis may be the most effective way to improve the prognosis. Dilatation of the main pancreatic duct may represent a secondary sign of pancreatic adenocarcinoma. Therefore, the diagnosis of dilated main pancreatic duct may be a predictive sign of pancreatic adenocarcinoma; therefore, careful follow-up in people with such signs have been recommended and eventually prompt treatment. Pancreatic endocrine neoplasms are relatively rare, with an incidence rate of approximating five cases per one million person-years. Some pancreatic endocrine neoplasms release hormones into the blood stream that cause clinical syndromes, whereas others are non-syndromic and present as a mass lesion. At diagnostic imaging, pancreatic endocrine neoplasms typically produce hyperenhanced well-demarcated lesions that are best seen on arterial phase images. Pancreatic endocrine neoplasms may be responsible for pancreatic duct stenosis, even when they are small in size (<2 cm) and be responsible for marked dilatation of the main pancreatic duct and/or marked atrophy of upstream pancreas. Intraductal papillary mucinous neoplasm (IPMNs) originates from the ductal epithelium and overproduce mucin which is responsible for dilatation of the main pancreatic duct and/or the side branches. Diagnostic imaging is helpful in the diagnosis and follow-up of these patients.

Learning Objectives:

1. To learn how to diagnose and manage adenocarcinoma of the pancreas mimickers: autoimmune pancreatitis and paraduodenal pancreatitis.
2. To appraise how to manage incidental cystic lesions of the pancreas.
3. To learn how to diagnose and manage neuroendocrine neoplasms of the pancreas.

A-693 14:37

Liver biopsy

V. Vilgrain; *Clichy/FR (valerie.vilgrain@aphp.fr)*

Liver biopsy is the most common invasive procedure of the liver. Indications of biopsy in diffuse liver diseases have declined due to improvements in non-invasive assessment of fibrosis and steatosis. On the contrary, biopsy of liver tumours is still indicated mostly for diagnostic purpose and to a lesser extent for assessing the prognosis or the prediction of tumour response. Three keys are important: first, check the indication. There are very few contraindications (mostly related to coagulation disorders) and the most important is to ensure that there is a good indication for liver biopsy; second, use ultrasound guidance, which is faster, easier and more accurate than CT. It allows real-time control; third, if a primary tumour liver is considered, always perform a biopsy in the adjacent liver. This will help the pathologist for the diagnosis.

Learning Objectives:

1. To understand the risk/benefit of liver biopsy.
2. To know the absolute contraindications.
3. To be aware of the most important technical tricks.

A-694 14:45

Bowel ischaemia

A. Filippone; *Chieti/IT (a.filippone@rad.unich.it)*

Mesenteric ischaemia is associated with a high mortality rate, especially in the acute setting. A high index of suspicion is necessary to achieve early diagnosis. The main challenge is to differentiate acute mesenteric ischaemia from other more common causes of acute abdominal pain. Nonvascular CT findings including bowel wall appearance, mesenteric involvement, intestinal pneumatosis, and portal venous gas play a crucial role to reach a prompt diagnosis. Therefore, the radiologist has to be aware either of the meaning of all these signs in terms of diagnosis and prognosis or of their mimics to avoid an incorrect treatment. We will review the typical CT pattern of mesenteric pneumatosis which allows to distinguish it from the so-called “pseudopneumatosis”. Furthermore, we will discuss those conditions of mesenteric pneumatosis not associated with acute ischaemia. Since the bowel wall appearance plays a crucial role to understand the pathogenesis of mesenteric ischaemia and, therefore, its treatment planning, we will describe the different patterns to understand their meaning and the possible differential diagnosis. Then, we will review the value of peritoneal involvement to figure out its role in terms of diagnosis and prognosis.

Learning Objectives:

1. To understand the reliability of mesenteric pneumatosis.
2. To learn about the different faces of ischaemic bowel wall.
3. To understand the meaning of peritoneal fluid.

A-695 14:53

Colon polyp

F. Iafrate; *Rome/IT (francoiafrate@gmail.com)*

Colorectal cancer (CRC) is a major cause of morbidity and mortality in western societies. According to the adenoma-carcinoma sequence, the vast majority of CRC arise from benign polyps over a very long period of time so that screening based on polyp detection has been universally accepted. Among the available options, CT colonography (CTC) has shown an excellent accuracy for large polyps and carcinomas and it has been included among the recommended options for CRC screening in average-risk people. CT colonography (CTC) interpretation using a combined three-dimensional/two-dimensional (3D/2D) approach requires a specific set of diagnostic tools to facilitate this strategy. The software viewing platform should provide these tools to maximize the advantages of this interpretation algorithm. Recent advances in CTC software have given rise to a number of new features aimed to facilitate analysis and improve diagnostic accuracy. In this respect, endoluminal data can be analysed by virtual colon dissection, which virtually dissects and unfolds the colon to obtain a quick view of the entire colonic surface without requiring antegrade or retrograde fly-through. One of the key components of effective polyp detection at CT colonography (CTC) involves the bowel preparation for the study and up to now faecal tagging technique represents a crucial step and strong weapon in the hand of radiologists to obtain greatest accuracy in detecting large and small polyps. In addition, advanced post-processing tools such as electronic fluid cleansing or computer-aided detection (CAD) may help readers.

Learning Objectives:

1. To quickly review different morphological aspects and "weapons" in the hand of radiologist to detect colonic polyps with CT colonography with small focus on correct preparation and the use of CAD.
2. To define large, small and intermediate polyp size and to review polyp pathology including the risk of cancer and high grade dysplasia moreover in small and intermediate polyps.
3. To summarise the current debate with regard to intermediate polyps (conservative management vs polypectomy) and the rational for non-reporting of diminutive polyps.

A-696 15:01

Acute pancreatitis

W. Schima; *Vienna/AT (wolfgang.schima@khgh.at)*

For the diagnosis of acute pancreatitis, at least 2 of the 3 following criteria, (1) abdominal pain consistent with pancreatitis, (2) increase (≥threefold) in serum amylase or lipase levels and (3) imaging findings of acute pancreatitis, have to be fulfilled. According to the Revised Atlanta Classification, the disease is categorized as interstitial oedematous or necrotizing pancreatitis. Development of necrosis may take some time, so that CT imaging should not be performed earlier than 2-3 days after clinical onset. Imaging too early may lead to

underestimation of disease severity. Necrotizing pancreatitis may present with either combined pancreatic and peripancreatic necrosis (most common) or with pancreatic necrosis or with peripancreatic necrosis alone. These acute necrotic collections (ANC) in the early phase may evolve into walled-off necrosis (WON) in the late stage (≥ 4 weeks). A WON containing chunks of digested fat and parenchyma must not be confused with a pseudocyst containing enzymatic fluid. They may appear similarly hypoattenuating in CT imaging, but US or MRI will show the predominantly solid nature of a WON. Secondary infection of necrotizing pancreatitis usually occurs in the 3rd week after onset (or later). Diagnosis of infection is difficult based on imaging alone. Infection is more likely if collections have broad contact with bowel. Gas within a collection is not a sensitive sign, but quite specific. In case of infection percutaneous aspiration is sought, followed by drainage in positive cases. However, necrotic collections with large proportions of debris require a more aggressive approach for clearance.

Learning Objectives:

1. To learn about the proper timing of imaging studies in acute pancreatitis.
2. To learn about the imaging manifestations of necrotising pancreatitis.
3. To understand the different nature of fluid collections with regard to further therapy.

A-697 15:09

Crohn's disease

J. Rimola; *Barcelona/ES (jrimola@clinic.ub.es)*

Bowel imaging had experienced relevant clinical advances in the last decade and represents the first diagnostic tool for assessing bowel inflammation in patients with Crohn's disease (CD). There is growing evidence that cross-sectional imaging is able to accomplish main endpoints in the diagnosis of CD, including the detection of active disease, especially severe lesions, and the achievement of healing of inflammatory lesions. The identification of structuring and penetrating complications is also a key aspect that has implications in the therapeutic management as well as in the determination of bowel damage. The lecture will provide the key points to confidently diagnose activity and complications related to CD.

Learning Objectives:

1. To learn about useful signs indicating active Crohn's disease.
2. To understand the changes which occur after treatment of intestinal inflammation.
3. To become familiar with complications related to Crohn's disease.

Author Disclosure:

J. Rimola: Consultant; Robarts Clinical Trials.

A-698 15:17

Liver metastases follow-up

Y. Menu; *Paris/FR (yves.menu@sat.aphp.fr)*

Liver metastasis follow-up is dramatically important in patients with systemic chemotherapy. The first tip is to identify if the treatment is adjuvant, neo-adjuvant or palliative. The goals and evaluation methods will be completely different. For adjuvant therapy, the question is detection of new lesions. For neo-adjuvant therapy, the question is to select the optimal schedule for curative treatment if relevant, mostly surgery. For palliative treatment, the role of imaging is to evaluate treatment efficacy. The second tip is to understand if the treatment is cytotoxic, targeted or immune. Evaluation criteria and complications are different for each category. Knowledge of the treatment details is critical. The third tip is to apply the relevant evaluation standard for the tumour and for the treatment. RECIST, CHOIs, irRC, irRECIST may apply for liver metastases. The report should be structured according to these criteria.

Learning Objectives:

1. To learn how to quickly identify three most common systemic treatments of liver metastases (cytotoxic, targeted and immune), and to understand why knowledge of the regimen is essential for the radiological report.
2. To understand the rationale of international standards for the evaluation of response to treatment, and how to build accordingly a useful report.
3. To appraise the respective objectives of neoadjuvant and palliative chemotherapy, and to be able to explain the specific endpoints for each clinical situation.

14:00 - 15:30 **Room C**

E³ - ECR Master Class (Chest)

E³ 1526a

Large airway disease

Moderator:
M. Occhipinti; Florence/IT

A-699 14:00

A. Diseases of the trachea

P.A. Grenier; *Paris/FR (philippe.grenier@aphp.fr)*

Multidetector CT (MDCT) using thin collimation during a single breath hold has become the preferred imaging technique for assessing tracheal diseases. MDCT acquisition is performed from the larynx to the termination of the left main bronchus or beyond, at full suspended inspiration. Axial images are reconstructed with thin slice thickness and overlap (50% overlap is optimal). Additional acquisition at full continuous (dynamic) forced expiration using reduced dose technique is useful for assessing tracheobronchial collapsibility. Multiplanar reformations along the long axis of the trachea are helpful to display tracheal abnormalities. Minimum intensity projections can highlight diverticulas and fistulas. Volume rendering techniques can segment the airway lumen wall interface and can be useful to detect subtle changes in airway calibre and to facilitate understanding of complex tracheobronchial abnormalities. Virtual bronchoscopy provides an internal rendering of the tracheobronchial inner surface and can better depict subtle mucosal abnormalities such as neoplasia and granulomatous disease. The different CT patterns of tracheal disease include luminal filling defect, multinodular appearance of the inner surface of the airway, focal tracheal narrowing, diffuse tracheobronchial wall thickening, tracheal bronchial diverticula, fistulas and cysts, and tracheobronchial collapsibility. Dynamic expiratory MDCT can offer a feasible alternative to bronchoscopy in patients with suspected tracheobronchomalacia. It shows complete collapse or collapse of greater than 80% of the airway lumen.

Learning Objectives:

1. To appreciate standard and dynamic techniques in assessing large airways.
2. To learn what is normal and what is disease in adults.
3. To know how imaging can help clinicians in assessing tracheal disease.

A-700 14:30

B. Tracheobronchial instability

M.O. Wielpütz; *Heidelberg/DE (mark.wielpuetz@med.uni-heidelberg.de)*

Advanced-stage chronic obstructive pulmonary disease (COPD) is associated with severely altered respiratory dynamics. Progressive inflammation may lead to malacia of cartilaginous airways, resulting in a collapse during tidal breathing and exercise, which often remains undiagnosed when employing pulmonary function testing (PFT) only. The diagnosis of tracheobronchomalacia (TBM) is traditionally made by invasive flexible bronchoscopy, and TBM has been reported in up to 44% of patients with chronic bronchitis. TBM is differentiated from excessive dynamic airway collapse (EDAC), characterized mainly by a bowing of the posterior membranous part of the trachea. Bronchoscopic examination and severity estimation is not standardized and user dependent, and may also influence the visibility of a collapse due to stabilization of the airways. Thus, airway instability has subsequently been assessed by imaging techniques. 1) Paired inspiratory-expiratory computed tomography (CT) scans may detect airway instability, but is an inherently static technique and limited by patient cooperation. 2) Dynamic cine-CT (2D+t CT) is used to continuously monitor a pre-defined airway segment (single-slice acquisitions to stack of few slices) during shallow or forced breathing. These acquisitions are effective in detecting and quantifying airway instability, but are limited in z-axis direction. 3) Dynamic 4D-CT (3D+t), either using a large detector or as respiratory-gated CT of the whole chest, finally allows for the evaluation of airway instability by volumetric time-resolved datasets. These different techniques will be addressed and compared with respect to individual advantages and drawbacks for the safe and precise diagnosis of airway instability of the trachea and large conducting airways.

Learning Objectives:

1. To appreciate the possible causes of tracheobronchial instability and its differential diagnosis.
2. To learn how to assess airway instability with 4D-CT.
3. To understand how 4D-CT could help in treatment planning.

Author Disclosure:

M.O. Wielpütz: Advisory Board; Boehringer Ingelheim.

A-701 15:00

C. Quantitative analysis and imaging biomarkers of chronic obstructive pulmonary disease (COPD)

H.A. Gietema; *Enschede/NL (hester.gietema@gmail.com)*

Airflow limitation in COPD is a result of combination of small airway remodelling, emphysema and large airway disease. The presence and extent of emphysema can easily be assessed with CT by calculating the number of voxels with density below a certain threshold, usually -950HU, as percentage of the total number of voxels. This method has been shown to correlate well to the extent of emphysema in pathology specimens. The thresholding method can also be used to quantify airtrapping, an indirect marker of small airways disease. Furthermore, CT can be used to establish bronchial wall thickening as marker of chronic bronchitis. Presence of CT emphysema has been shown to correlate to COPD-related symptoms as cough, phlegm production and dyspnoea, independent of smoking history or lung function. COPD patients with emphysema show more exercise-induced oxygen desaturation than those with a chronic bronchitis (CB) phenotype. While spirometry is still the main tool to diagnose COPD, imaging has become more and more important to assess the relative contributions of emphysema and airway disease in COPD patients to predict patient response to therapeutic interventions. While patients with airway predominant disease may show better response to drugs, patients with emphysema predominant disease and a heterogeneous distribution may be eligible for endoscopic lung volume reduction (ELVR) therapy. CT markers as extent of emphysema, distribution and completeness of fissures are crucial in patient selection for ELVR.

Learning Objectives:

1. To consolidate knowledge of post-processing image tools and imaging biomarkers.
2. To understand how imaging biomarkers are related to clinical events and patient prognosis.
3. To discuss about the clinical relevance of phenotyping COPD and identifying COPD patients in a lung cancer screening setting.

14:00 - 15:30 **Room O**

E³ - ECR Master Class (Paediatric)

E³ 1526b

Imaging in child abuse: an update

Moderator:
G.M. Magnano; Genoa/IT

A-702 14:00

A. Skeletal fractures

R.R. van Rijn; *Amsterdam/NL (r.r.vanrijn@amc.uva.nl)*

In childhood, fractures are a common cause for presentation in an emergency department. Estimates in the USA report that approximately 15% of all emergency department presentations in this population are related to fractures. Although the vast majority of all fractures are accidental they also represent the second most common finding in cases of physical child abuse. Radiologists may, therefore, be amongst the first caregivers to discover an indication of child abuse. To detect indicators of child abuse it is of importance to interpret all childhood fractures in relation to the provided clinical history and trauma mechanism. In this lecture, attention will be given to imaging techniques and the applicable protocols as well as fractures, frequently seen in child abuse, and their differential diagnosis. Finally, the need for collaboration with clinicians in the diagnosis of child abuse will be discussed, this as the diagnosis can never be solely based on radiological imaging but always on a combination of clinical, investigative and social findings.

Learning Objectives:

1. To understand the basic mechanisms.
2. To learn about fracture patterns suggestive of abuse and the evidence behind.
3. To become familiar with the most important differentials.

Author Disclosure:
R.R. van Rijn: Author; Royalties from Springer and Thieme.

A-703 14:30

B. Abusive head trauma

C. Adamsbaum; *Le Kremlin-Bicêtre/FR (c.adamsbaum@bct.aphp.fr)*

Radiologists play a key role in the early diagnosis of child abuse. Imaging must be performed and interpreted with rigour. The recommended guidelines for imaging in children younger than 2 years suspected of abuse include a highly detailed complete skeletal survey with centred views, and brain CT (or MRI if the child is free of neurological symptom). The use of abdominal imaging is debatable if the child has no symptoms. All siblings younger than 2 years should be assessed in the same way. To determine if the pattern may be of "age-different" lesions is a major point and must be assessed on robust criteria. This provides a strong argument for the diagnosis of abuse and also indicates repetitive violence which occurs in more than half of the cases. The differential diagnoses must be exhaustively discussed. However, they are usually easy to rule out. A changing or absent history of trauma in a non-ambulatory child is a key diagnostic sign for abuse. Radiologists must communicate clearly the suspicion of abuse and its degree of certainty to clinicians. The medical challenge is only to protect the child.

Learning Objectives:

1. To understand the basic mechanisms.
2. To learn about imaging findings suggestive of abuse.
3. To become familiar with the differentials and the controversies.

A-704 15:00

C. The medico-legal issues

A.C. Offiah; *Sheffield/UK (amaka.offiah@nhs.net)*

The presentation will be given in the context of suspected child physical abuse and will cover both the written report and court attendance. The various types of written report (clinical report, police statement, witness statement and expert report) will be covered, including what is expected from the individual who is providing the report or statement. The importance of the 3 Rs (retain, record, reveal) and 3 Is (independence, impartiality, integrity) will be emphasised and the manner in which witnesses should conduct themselves while giving oral evidence will be addressed. Common pitfalls in both written and oral evidence that should be avoided will be highlighted where relevant throughout the talk.

Learning Objectives:

1. To learn about the information required by any court, and how to structure the radiological report.
2. To recognise imaging markers suggestive for abuse and how to raise the suspicion.
3. To become familiar with the terms that should be used when highly specific imaging markers for abuse are identified in an otherwise normal infant.

Author Disclosure:
A.C. Offiah: Consultant; Expert witness for Her Majesty's Courts, UK.

14:00 - 15:30 **Room N**

Cardiac

RC 1503

Imaging of cardiac function, perfusion and viability by MR

A-705 14:00

Chairman's introduction

M. Francone; *Rome/IT (marco.francone@uniroma1.it)*

Ischaemic cascade is usually triggered by the presence of a flow-limiting stenosis inducing a perfusion defect which is initially reversible and progressively evolves to tissue necrosis with a subendocardial to transmural expansion of necrotic frontwave. Cardiac MR is able to comprehensively assess the entire spectrum of events characterizing this complex process from the regional and global functional impairment occurring in the early phase of ischaemia usually combined with rest-stress perfusion, to the direct visualization of necrotic areas/scars in post-infarct imaging. This has been achieved already almost twenty years ago and was recently integrated with novel imaging techniques providing further insight into the pathophysiology of ischaemic heart disease. Present session will focus on this crucial indication of cardiac MR offering precious information regarding image quality optimization in this setting and imaging features for differentiation between ischaemic vs non-ischaemic heart disease. An overview about CMR application of tissue perfusion in congenital heart disease will also be presented and session will close with a discussion focusing on the real and clinical reliability of CMR "comprehensiveness" in this clinical scenario.

Author Disclosure:
M. Francone: Speaker; Bracco Medical Imaging Invited Speaker.

A-706 14:05

A. Getting the best image quality

B. Jankharia; *Mumbai/IN (bhavin@jankharia.com)*

Reading cardiac MRIs require high-quality scans to be available to the radiologist interpreting the scan. There are many issues to be considered to ensure optimal quality, signal-to-noise and artefact-free scans. Current advances are 1. 3T scanning: it has become easier to scan on 3.0T as compared to 1.5T scanners and the situation a few years ago. The differences

will be discussed along with current state-of-the art cine and perfusion sequences. 2. Parametric imaging and tissue characterization: T1 and T2 mapping, STIR images and late gadolinium enhancement help us assess myocardial oedema, inflammation, infiltration and fibrosis. These will be discussed. Pitfalls are 1. shim artefacts: these can create bad-looking scans. 2. Rhythm abnormalities: these affect the quality of the scans but can be taken care off, with a little understanding of cardiac physiology. 3. Artefactual enhancement: this occurs in some segments of the myocardium and can simulate disease. 4. Wall motion pitfalls: left bundle branch block can simulate septal hypokinesia. These and other such issues need to be understood. Integrated approach: different clinical questions need different protocols. A viability scan has a different protocol from a scan for suspected amyloidosis or arrhythmogenic right ventricular cardiomyopathy (ARVC). While some aspects of scanning (basic cine imaging) remain the same for all types of indications, there are many other differences that allow us to highlight the specific issue at hand.

Learning Objectives:

1. To become familiar with the latest technical and methodological advances in cardiac MRI.
2. To learn about important and typical pitfalls in cardiac MRI and how to avoid or overcome these.
3. To consolidate the knowledge about an optimised, integrated approach using cardiac MRI depending on the clinical question.

A-707 14:28

B. Differentiation of ischaemic and non-ischaemic cardiomyopathy

P. Croisille; *Saint-Etienne/FR*

"no abstract submitted"

Learning Objectives:

1. To correctly define various causes of cardiomyopathies and compare functional and structural changes occurring with ischaemic and non-ischaemic cardiomyopathies.
2. To recognise common and less common signal intensity abnormalities and late enhancement patterns to provide etiological differentiation of the various forms of cardiomyopathies.
3. To review the prognostic significance of various functional and tissue abnormalities observed by cardiac magnetic resonance in cardiomyopathies.

A-708 14:51

C. Best applications in congenital heart disease

J. Schäfer; *Tübingen/DE (juergen.schaefer@med.uni-tuebingen.de)*

Congenital heart disease (CHD) comprises a wide-ranging of specific anomalies of the heart and the pulmonary vessels. Detailed knowledge of embryology, anatomy, and pathophysiology is crucial for diagnosis by imaging. Additionally, patient's age ranges from newborn to adults with an increasing life expectancy due to advancing in treatment. Apart from cardiac ultrasound and catheterization, traditionally in the hand of the cardiologist, cardiac MRI and MDCT are integral parts of the diagnostic workup. In this context, radiologists should be familiarized with indications, imaging protocols and standardized reporting. Advances in imaging technology are resulting in higher temporal resolution with better assessment of disorders and patient's comfort. Furthermore, radiation exposure essentially decreases in the past decade. In the case of MRI, 4D-imaging of blood flow opens a new horizon for treatment planning. The applications are related to patient management and treatment options. The domain of MDCT is the detailed visualization of morphology whereas MRI is the reference standard for functional analysis. However, there is overlap for both modalities. Thus, very complex anatomy or emergency cases are suitable indications for MDCT, while MRI determines the time point of (re)intervention by assessment of cardiac function.

Learning Objectives:

1. To decide which modality (MDCT/MRI) is the most appropriate for which indication in CHD.
2. To learn about the role of various MR applications in the diagnosis and planning of therapy of CHD.
3. To be able to perform a morphological and functional assessment of the right and left ventricle in CHD.

15:14

Panel discussion: Has MRI matured to a one-stop shop in cardiac imaging?

14:00 - 15:30 **Studio 2017**

New Horizons Session

NH 15

Large cohorts: imaging biobanks

A-709 14:00

Chairmen's introduction

M.H. Fuchsjäger, M. Pasterk; *Graz/AT (michael.fuchsjaeger@medunigraz.at)*

This session will offer insights not only into why biobanks should include imaging data, but also into the technological basis required to integrate imaging data and on how to deal with potential incidental findings in these large cohorts. Furthermore, the potential future benefits - specifically for radiology and radiologists - of including imaging data in large biobanks will be discussed.

Session Objectives:

1. To understand why biobanks should include imaging data.
2. To learn about the relevance of incidental findings in large cohorts.
3. To consolidate knowledge on integration and analysis of imaging data in biobanks.

A-711 14:05

Why biobanks should include imaging data

R.L. Vanninen; *Kuopio/FI (ritva.vanninen@kuh.fi)*

Imaging e-infrastructure is based on radiomics, a new omic science which provides a comprehensive quantification of tissue phenotypes by extracting large number of quantitative image features to higher dimensional data and the subsequent mining of these data for improved decision support. Correlating imaging phenotype with genomic information (referred to as radiogenomics), to better understand genetic variability and the ability to predict prognosis or response to therapy, is a new field of research. It has been initiated mainly in oncology and neuroradiology studies, but it is applicable to other diseases and can be performed with several diagnostic imaging modalities.The overlap between image-based tumour phenotype features and genomic characteristics is not currently well established. Image features are extracted from regions or volumes of interest, which can be either entire tumours or defined sub-volumes within tumours, known as habitats. Recently, the interest is increased in clinical research. Radiomics is potentially useful in the diagnosis of many diseases and can be used in decision support of personalised medicine. Development of "omics" analyses in parallel with growing interests towards translational research has also created a need for quality-assured sample sets with available clinical, imaging, epidemiological and treatment data. Imaging biobanks can be defined as organised databases of medical images and associated imaging biomarkers (radiology and beyond) shared among multiple researchers, and linked to other biorepositories. European Society of Radiology contributes to develop imaging e-infrastructures combined with work on digital pathology.

Learning Objectives:

1. To understand why inclusion of imaging data is the logical next step of phenotypical characterisation in cohorts.
2. To learn about the importance of enriching clinical datasets in biobanks with imaging data.
3. To learn about biobanks in which imaging data have already been included.

A-712 14:30

Incidental findings in large cohorts (German national cohort)

S. Weckbach; *Heidelberg/DE (sabine.weckbach@med.uni-heidelberg.de)*

The German National Cohort (GNC) is a long-term, multi-centre population-based cohort study in Germany with the goal of investigating the development of common chronic diseases. 30.000 out of 200.000 participants are being examined by whole body MR imaging at 3 Tesla. Incidental findings (IF) are findings deemed beyond the aims of a study and an expected consequence of imaging studies with potential high impact. By the use of national and international ethical guidelines and the current literature, a system was developed within the GNC to classify and report incidental findings that might be detected on whole body MR imaging and possibly are of risk to the participant's health. This system focuses on guiding radiologists in the decision of reporting or not-reporting a finding in an attempt to balance the risk of over- and underreporting and to minimize false-positive and false-negative findings. In the centre of that process is a (constantly updated and online available) list of defined incidental findings separating them into reportable and not reportable - taking into account study-specific limitations and confounders. In the talk, the necessary steps to develop such a reporting system are explained, particular challenges and ethical dilemmas are summarized. Quality assurance

tools to guarantee high quality and consistency for incidental finding reporting in large multicentre studies are presented.
Learning Objectives:
1. To consolidate knowledge on the significance of incidental findings in large cohorts.
2. To learn about how incidental findings may be detected in large cohorts.
3. To understand the management of incidental findings in large cohorts.

A-713 14:55

Analysis of big imaging data (UK Biobank)
A. Jackson; *Manchester/UK (Alan.Jackson@manchester.ac.uk)*

Collection of large datasets, often with many thousands of subjects poses specific problems for data analysis. Although specific analyses might be used by individual investigators on selected subsets this does not make optimal use of the availability of datasets, characterised by extensive imaging and other data derived from soluble and tissue biomarkers and genomic analysis. The analysis of by biobank imaging data must be considered from the inception of the imaging protocols. Automated image analysis techniques must be applicable so that quality control of individual imaging datasets across the database is essential. Selection of acquisition protocols for MRI and other imaging techniques should be designed to facilitate automated analysis with generation of quantitative imaging biomarkers. To facilitate information extraction series of preselected quantitative imaging biomarkers should be identified. These might include relatively standard biomarkers such as regional grey matter volume and CSF volume cardiac ejection fraction. The important features of these analytical techniques is that they should produce a reliable and reproducible qualitative imaging biomarker that can be included in combined biomarker databases for analysis using data extraction and informatics methodologies.
Learning Objectives:
1. To consolidate knowledge on the technological basis necessary to enable analysis and interpretation of big data.
2. To learn about how imaging data can be integrated in large research databases.
3. To understand the importance of imaging on new biomarker development.

15:20
Panel discussion: What are the benefits of linking imaging and biobanks?

14:00 - 15:30 **Room L 8**

EIBIR Session

EIBIR 3

Innovative solutions for diagnosis and treatment concepts for GIST patients from the MITIGATE project

Moderator:
S.O. Schönberg; Mannheim/DE

A-714 14:00

Introduction to the state-of-the-art therapy in GIST
P. Hohenberger; *Mannheim/DE*
(peter.hohenberger@medma.uni-heidelberg.de)

GIST primarily affects the GI tract with the stomach being most frequently involved, followed by the small intestine, the rectum and the duodenum and oesophagus. This disease entity represents "the" role model for the efficacy of molecular-based targeted therapy, molecular imaging and minimally invasive treatment. The detection of the *KIT*-protooncogene in 1988 and the *KIT*-receptor antagonist TKI imatinib provided an effective treatment in the advanced stage of the disease. Unlike other tumours, no valid blood tumour markers exist for monitoring the course of the disease, rendering functional and molecular imaging-based approaches of high importance. Patients with completely resected primary tumour, but imatinib-resistant progressive oligometastatic disease are quite frequent. Tumour types as those with a platelet-derived growth factor receptor-alpha (PDGFRA)-D842V mutation or SDH mutant GIST, or so-called quadruple-negative GIST represents 10-15% of all GIST patients. They are insensitive to imatinib or other TKI drugs as are the huge group of patients who no longer respond to imatinib due to secondary mutations in the *KIT* protooncogene. Therefore, for a major group of patients with metastatic GIST no treatment alternatives currently exist as tumours are neither sensitive to large-field external irradiation nor cytotoxic chemotherapy. Thus, interventional techniques such as SIRT, RFA or radionuclide therapy such as ion is the clinical focus when treating patients who live for 10 to 15 years at very good QoL with a disease that has metastasized but is still to be controlled by various measures and interventions.
Learning Objectives:
1. To learn about current therapy options for GIST patients.
2. To understand specificity of GIST treatment.
Author Disclosure:
P. Hohenberger: Advisory Board; Novartis; Pfizer; Bayer;. Grant Recipient; Novartis;. Investigator; Novartis; Bayer; Infinity; AROG, Pfizer. Research/Grant Support; Novartis. Speaker; Novartis; Bayer; AROG; Pfizer.

A-715 14:10

Improving the diagnostic imaging approach in GIST patients
C. Decristoforo; *Innsbruck/AT (Clemens.Decristoforo@tirol-kliniken.at)*

Gastrointestinal stromal tumour (GIST) is a rare disease and can be treated with tyrosine kinase inhibitors (TK). Resistance to TK is a common problem limiting therapeutic options and life expectancy. The MITIGATE project aims to develop new approaches to diagnose and treat patients with metastatic GIST resistant to the standard TK treatment. PET/CT is a widely used molecular imaging tool in oncology, usually investigating glucose metabolism with FDG. More specifically targeted radiopharmaceuticals are sought to better identify and characterise tumour lesions. Within the MITIGATE project, a novel ^{68}Ga-labelled peptide, NeoBOMB1 was selected to be investigated in GIST patients within the MITIGATE clinical study. ^{68}Ga-NeoBOMB1 binds specifically to gastrin-releasing peptide (GRP) receptors highly overexpressed on GIST tumour cells. The combination of ^{68}Ga, an ultra-short-lived, generator-derived positron emitter, with a small bombesin peptide analogue with antagonistic receptor properties provides a unique basis for highly sensitive and specific imaging of GIST tumours. The MITIGATE study aims not only to assess safety and pharmacokinetics of this novel imaging approach, but also to provide a basis for better characterisation of GIST tumours by molecular imaging opening new therapeutic options in this rare disease. Preclinical development of ^{68}Ga-NeoBOMB1, clinical trial design and first clinical results of PET/CT imaging in GIST patients will be presented.
Learning Objectives:
1. To learn about the current imaging approach in GIST patients.
2. To discover the novel imaging approach applied in the MITIGATE clinical study.

A-716 14:35

Minimally invasive treatment of GIST patients in a compassionate use programme
S. Diehl; *Mannheim/DE (Steffen.Diehl@umm.de)*

Several minimal invasive treatments are currently available for GIST patients. In case of multiple liver metastases, radioembolization (RE) offers a safe and effective treatment for patients with GIST liver metastases who do not show a response to TKIs. In case of oligometastatic disease, percutaneous ablations such as microwave ablation (MWA) or irreversible electroporation (IRE) can be used in lung, liver and soft tissue metastases. Besides a brief description of the methods, the use within the MITIGATE compassionate use programme will be presented. The focus will be on the combination of several minimal invasive therapeutic options.
Learning Objectives:
1. To understand minimally invasive treatment options.
2. To learn about the MITIGATE compassionate use programme and its minimally invasive treatment options.

A-717 15:00

Impact of the MITIGATE project on European GIST patients
A. Bruno-Lindner; *Vienna/AT*

Learning Objectives:
1. To learn about the need of European GIST patients.
2. To discover how patients might benefit from the developments of the MITIGATE project.

15:25
Discussion

14:00 - 15:30 **Room E1**

Special Focus Session

SF 15b

Breast cancer screening with tomosynthesis: the time is now

A-718 14:00

Chairman's introduction

P. Skaane; *Oslo/NO (PERSKA@ous-hf.no)*

A main limitation of conventional mammography (FFDM) is the poor sensitivity in women with dense breast parenchyma. During the last decade there has been much discussion how to improve the quality of breast cancer screening, especially for women at increased risk. Focusing on personalized (individualized) screening, ultrasound and MRI has been considered the most important adjuncts to mammography. It is important to distinguish between low-volume ("individualized") and high-volume ("population-based") screening regarding implementation of new techniques. An emerging mammographic technique that might significantly improve screening is digital breast tomosynthesis (DBT). Cancer visibility and conspicuity is increased using tomosynthesis, and DBT has significantly higher sensitivity (cancer detection rate) than FFDM. DBT has also a higher specificity (lower recall rates). Furthermore, DBT can replace conventional cone-mag views for evaluation of non-calcified indeterminate lesions, which also is an important contribution for reducing recalls in screening programs. Implementation of DBT with synthetic 2D reconstructed from the 3D data has several advantages compared with other modalities: Ultrasound is time-consuming and has a low specificity; MRI is expensive and availability is limited. Other modalities are still at a research level. DBT might easily be incorporated into existing programs, and transition from FFDM to DBT would be less challenging than the transition from screen-film to FFDM a decade ago. DBT might be the next improvement of population-based breast cancer screening. Cost-effectiveness studies and studies on outcomes including number and stage of interval cancers and subsequent round cancers are still to be desired.

Session Objectives:

1. To learn about the need for improving breast cancer screening.
2. To learn about alternative screening techniques.
3. To learn about the potential benefits of DBT as compared with other modalities.

Author Disclosure:

P. Skaane: Grant Recipient; Has previously received travel costs and fee for lectures from Hologic. Research/Grant Support; Financial and technical support for the Oslo Tomosynthesis Screening Trial was provided by Hologic.

A-719 14:05

Screening with digital breast tomosynthesis in the USA: performance indicators and breast density

E.A. Morris; *New York, NY/US*

Mammography is the best screening test for the early detection of breast cancer. Mammography had not changed for many years until the advent of digital imaging technology. Digital technology allowed the development of digital breast tomosynthesis (DBT), an advanced application, informally called 3D mammography (in contrast to conventional 2D DM). DBT has arrived on the world stage in time to address many of the limitations of mammography. Dense tissue has always been the challenge of mammography due to the masking effect. Trials have shown that cancer detection rate with DBT is improved as the cancers are "unmasked" as the issue of overlapping tissue or summation artefacts are eliminated. Additionally, recent criticism of mammography has centred false-positive examinations and overdiagnosis. In numerous trials, the call back rates are lower when DBT is used compared to standard DM. Fewer women are asked to return for summation shadows as DBT easily resolves these at interpretation. A recent multicentre study published in the Journal of the American Medical Association (JAMA) found that when tomosynthesis is used in addition to digital screening mammography, there is a 41% increase in invasive cancer detected, 15% decrease in unnecessary callbacks for false alarms and a 29% increase in the detection of all breast cancers. The conclusion is that DBT finds more of the invasive, harmful cancers and saves women the anxiety and cost of having additional screenings for what turns out to be a false alarm.

Learning Objectives:

1. To learn about recalls and cancer detection in the USA DBT screening studies.
2. To understand the false positive and the false negative interpretations in screening with tomosynthesis.
3. To understand the influence of breast density and age on the performance of DBT screening.

Author Disclosure:

E.A. Morris: Advisory Board; Delphinus, Devicor. Board Member; Avon. Consultant; Grail. Research/Grant Support; Hologic.

A-720 14:30

Screening with digital breast tomosynthesis in Europe: tumour characteristics and potential harms including overdiagnosis

F.J. Gilbert; *Cambridge/UK (fjg28@cam.ac.uk)*

The introduction of a new more expensive technique to breast screening requires careful analysis of the cost-benefit. DBT has been shown to increase the sensitivity and specificity of the detection of breast cancer especially in younger women, those with increased breast density (BIRADS C & D) and for those readers who are less experienced. However, it should not be assumed there will be a mortality benefit. One method is to use surrogate end points - tumour size and stage. However, information on tumour aggressiveness determines whether the additional cancers might have caused harm. There is increased sensitivity in cancers presenting as spiculate masses and also asymmetric density or distortion both of which tend to be associated with less aggressive cancers. In the prospective studies, there were relatively few additional DCIS cases being found and slightly more grade 1 cancers compared to grade 2 & 3 cancers. The three large prospective trials cannot report interval cancer rates as each case was read by all combinations but one small American series has reported a non-significant decrease in the number of interval cancers. Tumour size should decrease in incident rounds following the introduction of DBT. The potential harms of DBT are increased number of biopsies for benign lesions or even further excision. The radiation dose is small but can be avoided using synthetic 2D with DBT. The unknown harm is the increase in "overdiagnosis" (diagnosis of cancers that would not otherwise have been found in the woman's lifetime).

Learning Objectives:

1. To learn about the tumour characteristics of cancers detected with tomosynthesis.
2. To understand the potential influence of DBT screening on interval cancer rate and next round cancers.
3. To learn about the potential harms of tomosynthesis screening with special focus on so-called "overdiagnosis".

Author Disclosure:

F.J. Gilbert: Research/Grant Support; Hologic, GE Healthcare.

A-721 14:55

Which challenges should we consider prior to tomosynthesis screening implementation?

G. Gennaro; *Padua/IT (gisella.gennaro@ioveneto.it)*

Clinical benefits of digital breast tomosynthesis (DBT) in screening application have been demonstrated. However, there is concern about some technical aspects which should be analysed before implementing tomosynthesis in screening. The first concern regards radiation dose, which is supposed to be minimized when x-ray techniques are used to image healthy population. Dose differences depending on the tomosynthesis and the number of projections will be discussed, along with dose dependence from the clinical protocol (number of views, tomosynthesis alone or in combination with standard mammography), and the role of synthetic mammograms in this respect. The second negative aspect associated to the introduction of tomosynthesis is the increase of the interpretation time; learning curve is crucial, but also software developments like navigation tools or computer-aided detection (CAD) systems might help the reduction of the reading time. Appropriate hanging protocols should be defined to allow comparison with prior DBT examinations in subsequent screening rounds. Finally, the large amount of data produced by DBT versus standard mammography have a significant IT impact. IT infrastructure should be adapted to handle datasets that can be from 10 to 20 times the size of standard digital mammography images. The storage space needs to be increased, but also pre-fetching mechanism could be necessary to cope with the time necessary to retrieve DBT datasets from the PACS. Advantages of the implementation of the DICOM standard format for DBT images will be shortly discussed.

Learning Objectives:

1. To discuss radiation dose, number of DBT projections, and the need for conventional or synthetic 2D images in combination with DBT.
2. To learn about hanging protocols, reading time, and potential solutions for reducing the interpretation time.
3. To understand the "IT issues" in DBT screening implementation.

15:20

Panel discussion: Is tomosynthesis ready for replacing 2D mammography in organised breast cancer screening?

14:00 - 15:30 **Room E2**

Professional Challenges Session

PC 15a
Radiology at the core of interdisciplinary communication

A-722 14:00
Chairman's introduction
E.J. Adam; *London/UK (drjaneadam@gmail.com)*

The role of a radiologist is the same as any other doctor - to help patients. In diagnostic radiology, this is often done through written communication (report) to the referrer. The radiologist should understand the needs of the referrer and ensure that the radiological findings are clearly described and interpreted in the light of the clinical information. It should also be communicated in a timely manner to prevent patient harm. The means of communication should be secure and ensure that patient data are processed in line with data protection legislation.The challenges to effective communication can be significant, even when the radiologist and referrer are in the same institution, but are potentially magnified with offsite teleradiology. Direct verbal discussion in clinico-radiological meetings can add considerable value, and discussion directly with patients is recognised to be important for the future of radiology, but is increasingly 'squeezed out' by the volume of work.
Session Objectives:
1. To appreciate the importance of communicating in a timely and clear way.
2. To understand the particular issues related to communicating verbally or using written or electronic information.
3. To appreciate how the communication style and needs will be different for different groups of people.

A-723 14:05
Sharing information within the hospital
D. Regge; *Turin/IT (daniele.regge@ircc.it)*

Communication within hospital walls is a difficult process due to the multiple interconnections between individuals having different professional profiles. Furthermore, sharing information implies knowledge of management of sensitive information, including patient medical records. In this lecture, both the behavioural and technological aspects of knowledge sharing within the hospital will be explored, and tips will be provided to avoid miscommunication or misunderstanding. Effective communication through information sharing of electronic health records and the role of multidisciplinary team meetings on patient assessment, management and outcome will be reviewed.
Learning Objectives:
1. To identify who you will be communicating with within the hospital and who will be communicating with you.
2. To learn how to avoid miscommunication or misunderstanding.
3. To learn how to promote effective communication.
Author Disclosure:
D. Regge: Board Member; Springer. Speaker; GE Medical Systems.

A-724 14:30
Sharing information beyond the hospital
W.R. Jaschke; *Innsbruck/AT (werner.jaschke@i-med.ac.at)*

Communication between radiologists and referring physicians depends mainly on 4 columns: referral forms, radiology reports, individual consultations and clinical conferences. If radiologists and referring physicians are familiar with each other, communication is usually easy and efficient. Years of collaboration and "problem solving" generate a positive working environment supporting a trustworthy communication between equal partners. This positive attitude between radiologists and clinical partners supports a concise and team-oriented communication. Thus, the most important clinical information (previous/chronic illnesses, current complaints; risk factors for adverse events related to the planned procedure) is usually included in the referral forms. If this is not the case, direct consultation of the referring physician or of the electronic patient record is possible in an in-house setting. The same applies to questions regarding the indication for an radiological exam/procedure and the choice of exam/procedure. Communication beyond the hospital is sometimes hampered because of technical reasons and misunderstanding due to lack of appropriate information and a lack of knowledge regarding the requested radiological exam/procedure. Typical technical obstacles to efficient communication are lacking clinical information, ill-defined indications for exam/procedure and non-availability of the person you want to talk to in case of missing information. Triage of patients in case of workforce overload is another problem which cannot be easily dealt in case of an outside referral. Typical examples will be given which illustrate the above-mentioned scenarios. In addition, solutions how to avoid bad communication will be given.
Learning Objectives:
1. To identify the key routes of communication outside the hospital, including teleradiology.
2. To understand barriers to good communication.
3. To learn how to promote good communication.

A-725 14:55
Sharing information with the patient
E. Briers; *Hasselt/BE (erikbriers@telenet.be)*

The average patient is a statistical invention and does not attend the radiology department. Even the equipment used has a set of possibilities to adjust to the individual size of a patient. The same is true with the communication capabilities of the patients. This is caused by the differences is coping capacity and literacy. The information that a patient needs or wishes when he enters the radiology department is at different levels. The internal level of the department is really linked to what is done in the department, how it is done, etcetera. This should be known by the patient and can be provided on paper or any other means that are effective. But, as patients are so diverse this information should also be offered in a multi-layered system, and the radiologist should be available to answer questions or have someone available who can. The other level is the pathology, the reason why the patient is coming to the department. This can be quite simple a broken rib or wrist, questions on this can be answered in the department as the clinical data are rather clear. But complex pathologies require knowledge of the patient file, his past, family situation and more, only known by the clinician who did the referral. In these cases, the best option is the interdisciplinary consult with the clinician where the radiologist can transmit his feelings about the patient and findings. In these cases, the clinician would be the ideal person to speak with the patient.
Learning Objectives:
1. To understand what information patients require before they attend a radiology department.
2. To appreciate the communication needs of patients when they are undergoing investigations, and when they receive results.
3. To learn how to communicate effectively with patients.

15:20
Panel discussion: Conveying information clearly. Do we still need to 'speak' to each other?

14:00 - 15:30 **Room F1**

E³ - European Diploma Prep Sessions

E³ 1523
Musculoskeletal

A-726 14:00
Chairman's introduction
F.M.H.M. Vanhoenacker; *Antwerp/BE (filip.vanhoenacker@telenet.be)*

Diagnosis of acute-onset musculoskeletal trauma is usually straightforward on plain radiographs. Despite its higher radiation dose than CR and the longer interpretation time, CBCT is a very valuable technique for evaluation of trauma of small bones and joints in patients with negative radiographs or doubtful fractures and a high clinical suspicion for fractures or when complex fractures are suspected. MRI is the imaging technique of choice for evaluation of chronic-onset trauma and stress fractures, particularly in sports-related injuries. If atypical fractures of the femoral shaft are encountered, one should think of underlying bisphosphonates treatment. Analysis of clinical features (age, location, concomitant diseases) is a prerequisite for characterization of bone tumours. For imaging characterization, plain films are the mainstay, as they accurately depict matrix, cortical permeation or disruption, and periosteal reaction. MRI has an additional role as most tumours have a low SI on T1-WI and a high SI on T2-WI. The major role of MRI consists of local tumour staging and monitoring of treatment. Whole body MRI and PET-(CT) may evaluate distant tumour spread. Meticulous analysis of distribution and morphology of imaging findings are the clues to distinguish inflammatory arthritides and degenerative joint disorders. Whereas ultrasound has an emerging role for grading of synovitis and early detection of erosions of peripheral joints in RA, MRI is the preferred technique for early diagnosis and detection of active inflammatory lesions by demonstrating bone marrow oedema in axial spondyloarthropathy. MRI is a powerful imaging modality for monitoring treatment response of inflammatory arthritis treatment.

Session Objectives:
1. To understand typical and atypical imaging features of traumatic disorders of the musculoskeletal system.
2. To learn typical imaging features of benign and malignant bone tumours.
3. To become familiar with the imaging appearance of degenerative and inflammatory disorders of the musculoskeletal system.

A-727 14:06

A. Traumatic disorders of the musculoskeletal system
M. Maas; *Amsterdam/NL (m.maas@amc.nl)*

Assessing post-traumatic situations is common practice in MSK radiology. It is often thought easy, already learned in first year of residency and most often topic of radiological education in medical school. Very often films are read by on call clinicians first, often without very much proper training, and radiology reading is done later. This brings important responsibilities to us as radiology community when dealing with trauma. We need to provide an everyday meeting with emergency room physicians and supervising trauma surgeon focused on quality and on teaching. We need to be experts in the field of trauma radiology, adding information to the discussion and providing advise concerning consequential imaging steps. We need to understand and talk the language of traumatology, we need to be aware of the consequences there are for the surgeon; when is conservative treatment first option, when will be decided for surgery. If we can provide all the answers to the questions that influence surgical planning, we are performing most optimally. This session will take two complex small joints as focus, ankle-foot and wrist-hand. We will discuss normal radiological anatomy, we will describe standards in positioning, and we will enhance present guidelines in a given clinical situation. We will stress the value of adding cross-sectional imaging early, and will emphasise which answers need to be provided. A special focus lies on sports-related injury of bone and soft tissue. This goes for high-performing athletes as well as the so-called weekend warriors.
Learning Objectives:
1. To understand the anatomy and normal variants of the musculoskeletal system.
2. To become familiar with common imaging presentations of acute and chronic trauma involving the skeleton and soft tissue.
3. To learn common pitfalls in trauma imaging of the musculoskeletal system.

A-728 14:34

B. Bone tumours
S.L.J. James; *Birmingham/UK (stevenjames@nhs.net)*

Diagnosis and characterisation of bone tumours still relies heavily on the radiographic features to reach a differential diagnosis. An approach to radiograph interpretation will be presented. The radiographic features that give an indication of rate of growth will be discussed along with illustrations of the common patterns of matrix mineralisation. This will allow a description of a potential bone tumour to be provided so that the so-called "don't touch" lesions can be assessed. In the latter part of the presentation, some common patterns of haematological malignancy will be discussed.
Learning Objectives:
1. To learn the typical imaging features of common bone tumours.
2. To understand the typical imaging features of "don't touch" ("leave-me-alone") lesions.
3. To become familiar with the imaging manifestations of haematological disorders.

A-729 15:02

C. Degenerative and inflammatory disorders of the musculoskeletal system
D. Spira; *Heidelberg/DE (daniel.spira@med.uni-heidelberg.de)*

In most cases, inflammatory arthritides can be contrasted from primarily degenerative disorders according to their distribution and morphology. A subset of patients, however, presents with overlap syndromes, e.g. erosive degenerative disorders such as erosive osteoarthritis, or florid stages of activated osteoarthritides. Radiography and magnetic resonance imaging both help the clinician in characterising inflammatory arthritides. Commonly, rheumatoid arthritis and seronegative spondyloarthropathies are differentiated by their characteristic distribution, imaging appearance and concomitant soft tissue and bone involvement. Metabolic diseases such as gout and connective tissue diseases such as lupus and scleroderma also involve joints and can present in a typical manner. Several anti-inflammatory drugs are used in the treatment of inflammatory and degenerative arthropathies. In this context, magnetic resonance imaging may complement the clinical course and further assist in therapy response monitoring.
Learning Objectives:
1. To understand the imaging presentation of degenerative disorders of the joints and to appreciate their clinical relevance.
2. To learn the imaging features and clinical features of degenerative disease of the spine, disc and facet joints.
3. To become familiar with the typical imaging manifestations of infection, inflammation and metabolic diseases of the musculoskeletal system.

14:00 - 15:30 **Room F2**

Emergency Imaging

RC 1517
The latest update in imaging of polytrauma patients

A-730 14:00

Chairman's introduction: the role of proper imaging and management in patients after severe trauma
M. Stajgis; *Poznan/PL (stajgis@gmail.com)*

The rationale of emergency procedures in severe trauma patients is based on time factor and adequate selection of imaging modalities. The “Golden Hour” concept describes the need for as-fast-as-possible management of these patients very well. The present-day diagnostic workup of polytrauma patients is mostly based on whole body CT (WBCT); however, this method is thought to be overused in some clinical scenarios. Therefore, we should very carefully look again at advantages and limitations of still evolving all modern diagnostic modalities such as ultrasound, CT and MR. All 3 lectures in this session are dedicated to effective imaging of polytrauma patients, management priorities in different clinical situations and suggested practical approach.
Session Objectives:
1. To understand the role of early and fast diagnostic imaging in patients after severe trauma.
2. To recognise the basic statistics in management of polytrauma patients, which have the impact on practical approach regarding selection of proper diagnostic modalities.
3. To be aware of the position and responsibilities of radiologist in "decision-making team".

A-731 14:05

A. Ultrasound: when, why and by whom?
P.-A. Poletti; *Geneva/CH (pierre-alexandre.poletti@hcuge.ch)*

"FAST" (Focused assessment with sonography for trauma), which is now part of the ATLS^{R} guidelines, refers to real-time sonographic scanning of four regions for depiction of intra-peritoneal, pericardial and pleural blood, without visualization of parenchymal injuries, during the primary survey of a polytrauma patient. Depiction of a large haemoperitoneum mandates urgent exploratory laparotomy, while a negative FAST directs a search toward extra-abdominal sources of haemorrhage. The adequate training schedule of non-radiologist FAST operators is subject to controversy; there is no consensus with regard to the number of proctored examinations necessary before an operator can be considered capable to perform a FAST examination. This number varies from 10 to 200 according to the different societies. Some recent reports advocate to extend FAST (E-FAST) to the screening of large pneumothoraces during the primary survey, while others also recommend to evaluate the efficiency of fluid resuscitation by assessing the inferior vena cava diameter. This raises further concerns about the training of the operators. In haemodynamically stable patients, ultrasound may be useful for the triage of mild trauma patients towards CT or clinical observation, when time constraint is no major issue and/or CT not immediately available. However, the absence of free intra-peritoneal fluid is not sufficient per se to rule out potentially life-threatening injuries and ultrasound achieves low sensitivity (40 to 55%) for the direct depiction of parenchymal injuries. Contrast-enhanced sonography can be useful to improve the detection of solid-organ lesions and for the detection of vascular injuries, such as delayed splenic pseudoaneurysms.
Learning Objectives:
1. To become familiar with the role of modern ultrasound in polytrauma patients.
2. To comprehend the rationale of using FAST protocol in selected patients.
3. To know the advantages and limitations of ultrasound imaging in emergency setting.

A-732 14:31

B. CT: is it always whole-body?

F.H. Berger; *Toronto, ON/CA (fhberger@gmail.com)*

In the western world, polytrauma is the major cause of mortality in people under 45 years of age. Furthermore, it is a major contributor to loss of quality of life and ability to work. The setting of polytrauma is almost always chaotic, not a favourable environment to come to timely diagnosis and treatment. To decrease morbidity and mortality, time is everything. It is our job as radiologist to contribute to the trauma team and help facilitate timely diagnosis - and in many cases, also timely treatment by interventional radiology. To reach the best treatment strategy for the patient as quick and accurate as safely possible, is the goal. In this update on imaging of polytrauma patients, I will focus on the role of CT to achieve this goal. With the progress in CT scanner development, different protocol options arise. Which CT protocols are being used and what factors do they depend upon? In addition, there is a widespread increase in use of whole body CT internationally, is this a good thing or should we be more selective? What is the current evidence to select patients for targeted CT examinations in polytrauma? A lot of these questions have not been definitively resolved. This lecture aims to provide an update of the current insights into the use of CT for trauma care, with the goal to choose wisely how to investigate the polytrauma patient in a timely and meaningful fashion.

Learning Objectives:

1. To be familiar with currently worldwide accepted protocols in polytrauma CT imaging.
2. To know clinical conditions requiring whole-body CT.
3. To comprehend the selection of trauma patients for targeted CT examinations.

A-733 14:57

C. Where is the proper place for MRI?

K. Katulska; *Poznan/PL (katarzyna_katulska@op.pl)*

A multimodality of imaging should be involved in the diagnosis and management of severely injured multi-trauma patients. The current role of magnetic resonance imaging (MRI) is confident in the spinal cord and brain injuries. MRI examination is the imaging method of choice in assessment of lesion morphology, extent and severity of trauma. In case of neurological symptom not completely explained in CT findings, an MRI must be performer. Among all post-traumatic intracranial pathologies, the diagnosis of diffuse axial injury remains more complex. In fact, about 30% of negative CTs are already positive on MRI. MRI is a powerful diagnostic tool that can detect signs of injury such as minute bleeding (microhaemorrhage), small areas of bruising (contusion) or scarring (gliosis), which are invisible to the CT scan. Newer, specialized types of MRI can assess brain structure at an even finer level or measure brain function to detect alterations in brain structure and function due to traumatic spinal cord and brain injury (TBI, SCI). Protocol for routine MRI of patients with TBI and SCI, which consists of SE and GRE sequences, is proposed. MRI techniques such as SWI, DWI and DTI are discussed, as a new standard protocol. In the acute setting, MRI can determine the presence and extent of injury and guide surgical planning and minimally invasive interventions. Neuroimaging also can be important in the chronic therapy of injury, identifying chronic sequel, determining prognosis and guiding rehabilitation.

Learning Objectives:

1. To learn which patients are the best candidates for post-traumatic MRI.
2. To be familiar with standard and short MRI examination protocols.
3. To understand the impact of MR findings on further management of polytrauma patients.

15:23

Panel discussion: Comprehensive guidelines how to qualify post-traumatic patients for the proper imaging modality - summary

14:00 - 15:30 **Room D**

E³ - ECR Master Class (Musculoskeletal)

E³ 1526c

MRI developments and techniques in musculoskeletal (MSK) radiology

Moderator:
C.W.A. Pfirrmann; Zurich/CH

A-734 14:00

A. Whole-body MRI (WBMRI) and diffusion-weighted imaging (DWI) in MSK: where is it (not) useful and how do I do it?

F.E. Lecouvet; *Brussels/BE (frederic.lecouvet@uclouvain.be)*

WB-MRI has growing indications in many oncologic and rheumatologic disorders, as a tool for early diagnosis, quantification of disease extent and assessment of treatment response. The technique is refining and efforts are made to decrease examination durations and to tailor sequences to the targeted disease. WB-MRI studies should at least include anatomical (morphological) sequences, most commonly T1, STIR, sometimes acquired in a 3D approach. These may be sufficient to assess multifocal inflammatory conditions affecting bones, joints, muscles. In oncology, diffusion-weighted imaging (DWI) sequences are very sensitive and have become mandatory, but should not be acquired without anatomic sequences, as some findings may be confusing. This lecture illustrates the protocols, imaging findings, strengths and pitfalls of WB-MRI in oncologic indications, including metastatic disease, lymphoma and myeloma, and in rheumatologic disorders. It also highlights how the technique extends the exploration of the body beyond the musculo-skeletal system.

Learning Objectives:

1. To know the indications for WBMRI in MSK imaging.
2. To understand the advantages and limitations of diffusion-weighted imaging of the MSK system.

A-735 14:30

B. MR neurography: how to optimise and interpret your images

G. Andreisek; *Münsterlingen/CH (gustav@andreisek.de)*

Evaluation of peripheral nerve disorders is an emerging field and may make up to 20% of the daily musculoskeletal magnetic resonance imaging studies in some centres, where MR neurography techniques are well established. Whereas nerve ultrasound is today mainly performed by neurologists in their clinics along with the clinical examination and the traditional electrodiagnostic studies such as electromyography and nerve conduction studies, dedicated clinical programs in MR neurography are currently available at relatively few centres around the world; however, interest in the techniques and clinical indications is spreading rapidly. The focus of this lecture will, therefore, be on the common clinical MR neurography techniques, which are particularly methods that use fairly basic MR pulse sequences for high-resolution cross-sectional imaging of nerves. Often mentioned advanced imaging techniques such as diffusion-weighted, diffusion tensor imaging and tractography will only be described briefly because to date, those techniques only play a limited role in the clinical routine. Even in specialized MR centres where nerve imaging is an established part of the daily clinical business, DWIT/DTI/tractography is only used as complementary to standard imaging techniques.

Learning Objectives:

1. To know the pathophysiology and grades of peripheral nerve lesions.
2. To understand the need for a MR neurography protocol.
3. To learn how to interpret MR neurography examinations.

Author Disclosure:

G. Andreisek: Advisory Board; Otsuka Pharmaceuticals.

A-736 15:00

C. 3D-spin echo (3D-SE) and radial imaging: uses and limitations

J. Fritz; *Tübingen/DE (jfritz9@jhmi.edu)*

Three-dimensional spin echo MRI has evolved into a powerful technique for the non-invasive assessment of joint, cartilage, ligament, tendon, muscle, and nerve abnormalities. In addition to interactive multi-planar imaging evaluation for the evaluation of fine detail, standard transverse, sagittal and coronal images can be created from a single isotropic 3D volume. The high spatial resolution of such isotropic data sets further allow for the creation of radial MR images as well as individualized curved and oblique planar image reconstructions, which improve the visualization of oblique ligaments and curved tendons. Recent advances in acceleration techniques have dramatically increased the speed of 3D spin echo data acquisition. With the use of optimized parallel imaging techniques and compressed sensing data sampling,

high-quality isotropic 3D spin echo sequences can now be acquired in under 5 minutes and further enable rapid high-resolution 3D MR imaging protocols of joints within an acquisition time of 10-15 min.
Learning Objectives:
1. To understand the MR imaging techniques used for 3D MR imaging of joints.
2. To know the strength and limitations for 3D MR imaging of joints.
3. To learn about new imaging acceleration techniques used for 3D MR imaging of joints.
Author Disclosure:
J. Fritz: Advisory Board; Siemens AG, Alexion Pharmaceuticals, Inc.. Research/Grant Support; Siemens AG. Other; Speaker's Honorarium Siemens AG.

14:00 - 15:30 **Room G**

Physics in Medical Imaging

RC 1513
Dose reduction using iterative image reconstruction in CT

A-737 14:00
Chairman's introduction
V. Gershan; *Skopje/MK (vesna.gershan@pmf.ukim.mk)*

Filtered backprojection (FBP) was the primary method for reconstructing CT images for many years. Advancements in algorithm design and computer hardware have led to development of iterative reconstruction (IR) algorithms for CT images. Iterative algorithms can model many of the physical parameters that FBP cannot, such as the x-ray spectrum, the blurring of the focal, etc. The first type of IR algorithms goes through a series of iterations applied on first-pass FBP raw datasets. This technique results in longer reconstruction time, but also in substantially less image noise. Degree of the noise reduction can be taken as either improved image quality or as a reduction of patient dose, typically up to 40%. Recently, more complex IR algorithm called fully model based has become available. It uses both backward and forward projections datasets. By combining many more iterations, image noise can be reduced to a higher degree, enabling 80-90% patient dose reduction compared to FBP. The last developed IR algorithm is called partial model-based IR. It takes much less reconstruction time than fully model based, but results also in substantially greater noise reduction. The patient dose reduction is 50-60% compared to FBP. Images reconstructed by IR techniques have different appearance compared to FBP, mainly due to decrease in overall noise and different pattern of tissue depiction. Therefore, radiologists need a period of adaptation on the new image appearance. Over time, as they became accustomed to the look of images, the iterative strength level may be decreased and reduce the patient dose even further.
Session Objectives:
1. To learn about the origins of dose reduction using iterative image reconstruction in CT.
2. To understand dose reduction using iterative image reconstruction in CT.
3. To learn about solutions and workarounds.

A-738 14:05
A. Basics of iterative image reconstruction in CT
M. Kortesniemi; *Helsinki/FI (mika.kortesniemi@hus.fi)*

Computed tomography image reconstruction is a mathematical process where the raw data projections (sinogram data) acquired during rotational CT scan exposure are transformed into volumetric (3D) image data. As such, reconstruction is an inverse problem, with no direct analytical solution. Traditional algorithms (filtered back projection, FBP) approximate the true acquisition method and are prone to artefacts and noise. Iterative reconstruction methods approach the final solution gradually in steps and may take quantum statistics, physical properties and limitations of image acquisition more faithfully into account. Thus, a more accurate and correct outcome may be achieved. However, more detailed modelling of the actual CT acquisition system, physics, optics and object also increases the calculation time and related CPU requirements. Especially, the forward projection phase (calculation of simulated raw-data) on each iteration step is computationally intensive. More optimised reconstruction techniques with clinically acceptable reconstruction times are under active research. As the main diagnostic benefit, higher image quality in terms of lower noise and artefacts can be achieved using iterative methods, and/or a lower radiation dose. However, users should be aware that current iterative reconstructions potentially alter the image texture in different clinically relevant contrast and detail levels. Therefore, sufficient clinical image quality should be verified when applying iterative techniques on new exam indications and protocol optimization.
Learning Objectives:
1. To learn about the basic aspects of iterative reconstruction.
2. To learn about potential dose reduction via iterative reconstruction.
3. To compare iterative reconstruction with other techniques.

A-739 14:28
B. Iterative image reconstruction in clinical practice (dos and don'ts)
H. Alkadhi; *Zurich/CH (hatem.alkadhi@usz.ch)*

The increasing use of computed tomography (CT) for clinical imaging in patients has raised concerns about its potential risks, leading to the development of various strategies for optimizing and reducing the radiation dose associated with CT. Of those techniques, iterative reconstruction algorithms have gained wide acceptance as powerful tools for improving image quality on dose-optimized CT studies through image noise reduction. This presentation reviews the clinical challenge of applying iterative reconstruction techniques to computed tomography (CT) examinations, and especially to low radiation dose CT examinations. The various currently available techniques are discussed, and their potential for improving image quality and increasing the diagnostic accuracy are discussed. Practical aspects of the different iterative reconstruction techniques are emphasized, along with their benefits, pitfalls and potential clinical implementations.
Learning Objectives:
1. To understand the radiologist's requirements for image reconstruction.
2. To learn about current best practice in image reconstruction for clinical CT.
3. To learn about the potential benefits and pitfalls of using iterative reconstruction in clinical CT.

A-740 14:51
C. Image quality assessment of iterative reconstruction: pitfalls and future directions
C. Ghetti; *Parma/IT (CGhetti@ao.pr.it)*

The use of iterative reconstruction algorithms in computed tomography (CT) has become a crucial issue for dose reduction in CT examinations. The main advantage of iterative algorithms as opposed to filtered back projection (FBP) is the incorporation of physical models, which allow for CT studies at reduced doses with preserved image quality and low levels of image noise. The most common iterative reconstruction methods and the solutions introduced by CT manufacturers will be briefly presented. A simple phantom-based approach will be described to explore the features of iterative algorithms. Quantitative parameters that can be evaluated are image noise, impact of different reconstruction kernels on noise reduction, noise power spectrum (NPS), contrast-to-noise ratio (CNR), spatial resolution, and linearity and accuracy of CT numbers. The evaluation of noise properties of a CT image using standard deviation metric is not exhaustive because the image appearance depends also on the noise distribution in frequencies, described by noise power spectrum NPS. Usually the shape of NPS curves are different from FBP; peaks are shifted towards low frequencies and this effect is more marked if the iteration is applied with a greater strength. In iterative reconstruction, a blotchy image quality impression is commonly reported by radiologists, for this reason it is important to measure NPS to give at the radiologists a feedback on how to reach a good compromise between dose reduction and a familiar image appearance.
Learning Objectives:
1. To learn about basic image quality metrics employed in CT.
2. To understand why image quality assessment is difficult with iterative reconstruction.
3. To learn about up-and-coming methods for image quality assessment.

15:14
Panel discussion: How low can we go?

14:00 - 15:30 **Room K**

Professional Challenges Session

PC 15b

A team approach towards ensuring patient safety and care

A-741 14:00

Chairmen's introduction: A team approach - why is this necessary?

T. Owman[1], J. McNulty[2]; [1]*Lund/SE*, [2]*Dublin/IE (Titti.Owman@gmail.com)*

In this session, we will discuss and present different ways in which teamwork and cooperation can change and improve our daily work in medical imaging departments. Team-based solutions is a concept that is growing in a wide variety of professions and medical imaging is no exception. Due to an increasing awareness of value-based healthcare and rapidly rising healthcare costs it is of utmost importance that we take care of, and use, available competences and resources as well and efficiently as we possibly can. A well-functioning team constellation may be the future for an increasing number of medical imaging procedures as we continue to move from what used to be imaging-only modalities toward a more complex diagnostic reality where physiology, functional measurements and therapies are included in our daily work. We need persons on our medical imaging teams with unique skills, overlapping knowledge and different levels of expertise to optimise the results from our departments and clinics. The specialised team approach is also dependent on a good leadership, trust and a well-functioning information system. When this is done in a successful way we end up with better procedures, enhanced quality and improved safety for both patients and staff members. Well-functioning teamwork would also mean increased motivation and involvement among all personnel.

Session Objectives:

1. To explore the added value of a team approach to radiological procedures.
2. To understand the impact of radiographer reporting on clinical practice.
3. To explore the benefits provided by a team approach in interventional procedures.

A-742 14:06

A team-based approach to delivering safe practice

J. Damilakis; *Iraklion/GR (damilaki@med.uoc.gr)*

A considerable number of medical accidents, incidents and omissions can be attributed to lack of communication. Medical physicists, radiographers and radiologists should work collaboratively with colleagues and clinicians to develop effective radiation dose reduction strategies, increase patient safety and optimize the outcomes of patient care. Medical physics experts (MPEs) are involved in medical imaging departments to measure the radiation output to estimate the radiation dose, monitor doses using dose tracking methods, maintain patient doses within diagnostic reference levels, reduce doses while maintaining the image quality needed for diagnosis, establish appropriate acquisition techniques and train staff in radiation protection. These activities are of great importance for all modalities and especially for CT and interventional radiology, where radiation doses are high. A team approach is needed in medical radiation protection to ensure patient safety and care.

Learning Objectives:

1. To understand a team-based approach to ensuring patient safety during radiological procedures.
2. To consider how a joint approach may improve the culture of radiation safety within the clinical environment.
3. To highlight how a collaborative approach to practice leads to improved effectiveness and patient safety.

A-743 14:29

The radiographer and radiologist: joint responsibility for reporting

S. Rowe; *London/UK (Susan.Rowe@homerton.nhs.uk)*

Effective efficient utilisation of all staff within radiology departments has the potential to maintain and improve patient experience, minimising the impact of increasing demand for imaging services on a background of financial continued austerity and shortage of radiology consultants. Allied health professionals (AHPs) have provided both acquisition and reporting of radiology diagnostic examinations for many years in the UK, initially largely in ultrasound. Over the last 2 decades, reporting radiographers have been providing x-ray reports in many UK departments and more recently in specific areas of MR reporting. Due often to complex local factors utilisation of their skills has been highly variable between different hospitals leaving many UK hospitals paying potentially expensive independent sector providers to report examinations, often as part of backlog recovery programmes rather than real-time service. Apart from reporting, AHPs have successfully undertaken intervention work, including biopsies and therapeutic joint injections, supporting service provision traditionally undertaken by radiologists. Embracing a diverse workforce increases resilience during periods of acute workforce shortages or spikes in demand and potentially enables more extensive provision of 7-day services. In addition, it facilitates deployment of consultant radiologist skills to areas that require their different levels of expertise and more varied clinical experience and training. Ensuring appropriate development of the whole clinical team while working in a supportive integrated service enables decreased length of imaging pathway from request to report and the increased availability of consultants for more complex work/discussions centred around improving patient care.

Learning Objectives:

1. To discuss the concept of joint reporting and responsibility and how this system may be developed within clinical practice.
2. To highlight the benefit of reporting abnormality detection by radiographers.
3. To discuss future opportunities for radiographers and radiologists in this area.

A-744 14:52

A team approach in interventional procedures

C. McLaren; *London/UK (clare.mclaren@gosh.nhs.uk)*

A team approach in interventional procedures advanced practice is well established in the UK, in nursing and other allied health professions. At Great Ormond Street Hospital, we responded to poor staff retention and low morale by implementing advanced practice in interventional radiology. There was strong support for this from the medical director of the hospital and lead consultant interventional radiologist. The establishment of the role of consultant radiographer in the interventional radiology team has created a strong link between the radiologists and radiographers. The consultant radiographer provides a similar service to the radiologist by being an expert in specific areas of paediatric interventional radiology. This role incorporates clinical work, research and maintaining an expert knowledge of complex radiographic techniques, for example cone beam CT-guided procedures. The consultant radiographer is also heavily involved with multi-disciplinary team meetings, presenting imaging findings to referring teams. Incorporation of the WHO safety checklist into everyday practice has led to interaction with the whole team involved in the planning of procedures for the day. All team members are encouraged to voice their opinions and concerns at the team brief. National safety standards for invasive procedures were implemented in the UK in September 2016. These standards have been set to reduce never events, such as wrong site surgery, serious incidents and near misses. The standards promote multi-disciplinary team working in the operating department and interventional radiology.

Learning Objectives:

1. To familiarise attendees with the active role of the radiographer when performing interventional procedure.
2. To discuss the professional issues and responsibilities within such a team.
3. To emphasise the benefits for patient care and patient safety.

15:15

Panel discussion: Can a team-based approach ensure patient safety?

14:00 - 15:30 **Room M 4**

E³ - ECR Academies: Multiparametric Ultrasound (MPUS)

E³ 1520

Vascular multiparametric US

A-745 14:00

Chairman's introduction

P.S. Sidhu; *London/UK (paulsidhu@btinternet.com)*

A-746 14:05

A. Deep venous thrombosis and chronic venous insufficiency of the lower extremity

G. O'Sullivan; *Galway/IE (gerard.osullivan2@hse.ie)*

Ultrasound is the first modality for diagnosis of deep vein thrombosis (DVT). The purpose of this session is to familiarise attendees with the various ultrasound modalities, including compression, colour, Doppler, the use of respiratory and augmentation manoeuvres and their use. In addition, the limitations of US particularly above the groin will be stressed. Diagnosis of reflux is an important component of venous ultrasound and it is quite a specific technical skill. Ultrasound guidance for catheterisation of superficial and deep venous structures will be elaborated. Lastly, the place of intra-vascular

ultrasound (IVUS) will be discussed and its use will be illustrated with examples.
Learning Objectives:
1. To learn about the current role of MPUS to diagnose DVT.
2. To become familiar with the US examination technique: compression US and Doppler.
3. To learn how US is used to diagnose varicose veins and valve insufficiency.
Author Disclosure:
G. O'Sullivan: Advisory Board; Siemens Healthcare. Author; New Horizons in Venous Disease. Speaker; Cook Medical, Straub, Bard, BSCI, Marvao Medical.

A-747 14:33

B. Abdominal vascular emergencies: ruptures and occlusions
D.A. Clevert; *Munich/DE (Dirk.Clevert@med.uni-muenchen.de)*

Conventional ultrasound is the most widely used imaging modality in routine clinical practice worldwide. The limitations of conventional ultrasound in the detection of aortic lesions vs multi-slice computed tomography angiography (MS-CTA) are well known. Conventional unenhanced ultrasound is in direct comparison with contrast-enhanced CTA probably inappropriate given the fact that without contrast enhancement the performance of CT may well be equal or even inferior to that of ultrasound. Due to the introduction of microbubbles (MB), ultrasound contrast might be a way of bridging the gap between these modalities. In the last three years, recent articles have focused on the use of contrast-enhanced ultrasound (CEUS) for diagnosis of ruptured abdominal aortic aneurysm and other vascular disorders.
Learning Objectives:
1. To understand MPUS findings in arterial rupture (aneurysm, other).
2. To learn about Doppler techniques and CEUS to improve diagnosis of vascular occlusions and infarcts.
3. To understand the advantages and limitations of US techniques compared to CT.
Author Disclosure:
D.A. Clevert: Advisory Board; Samsung, Siemens, Philips, Bracco. Speaker; Samsung, Siemens, Philips, Bracco.

A-748 15:01

C. Upper and lower extremity arterial emergencies
B. Brkljačić; *Zagreb/HR (boris@brkljacic.com)*

B-mode ultrasound enables evaluation of arterial anatomy and of the vessel wall, it detects early atherosclerotic changes, allows detection of stenosis and occlusions, but tends to overestimate the degree of stenosis and should not be used for the stenosis grading. Colour duplex Doppler ultrasound (CDUS) enables fast visualization of vessel to be examined. It demonstrates haemodynamic changes, including velocity increase. Underestimation of disease is likely if only colour is used and the precise assessment of haemodynamic disturbances is impossible without the spectral analysis. In general, CDUS has high diagnostic accuracy, it is cheap, widely available, there is no exposure to ionizing radiation, and no contrast media injection. However, the examination is time consuming and requires high operator dependence. The thorough understanding of haemodynamics and physics is needed for adequate interpretation of Doppler findings. The factors influencing spectral morphology will be discussed in the lecture and different types of spectra presented. Waveform changes will be presented in stenosis and occlusion. The typical findings of pseudoaneurysms and arteriovenous fistulas will be presented. Findings in acute occlusion and collateral flow will be discussed, both for native arteries and for bypass grafts. The role of ultrasound in endovascular recanalizations will be discussed, both in planning and performing of the procedure and in the follow-up. The role of CEUS will be discussed. Several clinical examples will be presented.
Learning Objectives:
1. To understand the MPUS imaging techniques to diagnose arterial occlusion.
2. To learn how to improve diagnosis by Doppler techniques and CEUS.
3. To learn US limitations, challenges and pitfalls.
Author Disclosure:
B. Brkljačić: Speaker; Guerbet, Bayer.

14:00 - 15:30 **Room M 5**

E³ - ECR Academies: Neuroradiology: from Morphology to Function

E³ 1522

Functional MRI of the brain opens new horizons

A-749 14:00

Chairman's introduction
T.A. Yousry; *London/UK (t.yousry@ucl.ac.uk)*

Since their development about 25 years ago, functional MRI and diffusion-weighted imaging have been central in research and also in clinical patient management. This session will explore the latest developments in terms of techniques and postprocessing as well as their clinical applications. Consideration will be given to pitfalls, limitations and practical guidelines for quality control and analysis.
Author Disclosure:
T.A. Yousry: Advisory Board; Biogen Idec; Genzyme, Ixico. Board Member; Neuroradiology. Grant Recipient; Medical Research Council, MS Society of Great Britain and Northern Ireland, Stroke Association, British Heart Foundation, Wellcome Trust. Research/Grant Support; BRC. Speaker; Novartis.

A-750 14:06

A. No function without structure: challenges in diffusion MRI and fibre tractography for clinical research
C. Tax; *Cardiff/UK (taxc@cardiff.ac.uk)*

Diffusion MRI (dMRI) has the unique ability to characterise tissue microstructure in vivo, and has been widely used in clinical and biomedical research applications to infer valuable information about the brain's structural connectivity. dMRI is based on the fundamental principle that water molecules randomly move due to thermal energy, and that this motion is modulated by tissue structures. With diffusion tensor imaging (DTI) the anisotropic behaviour of diffusion can be characterised in a three-dimensional fashion. This allows for the virtual reconstruction of pathways - a process called fibre tractography. In the first part of this presentation, the basic principles of diffusion, dMRI, and tractography will be explained. Due to the growing interest in dMRI, the society has been continuously triggered to develop novel dMRI image processing approaches. Such approaches are necessary to 'prepare' the data for subsequent analysis. In the second part of this talk several preprocessing steps are highlighted, including data quality assessment and correction for artefacts. Subsequently, some analysis strategies will be summarised. With the overwhelming amount of processing and analysis strategies available and still being developed, it is unfortunately not always evident how dMRI can be optimally used in applications and which conclusions can and cannot reliably be drawn from dMRI data. In the final part, methodological challenges related to dMRI will be discussed.
Learning Objectives:
1. To present an introduction to the use of diffusion MRI and fiber tractography of the brain.
2. To illustrate how these techniques have provided new insights into functional neuroanatomy.
3. To raise awareness about methodological challenges and limitations for clinical applications.

A-751 14:34

B. Clinical utility of fMRI for preoperative brain mapping
H. Urbach; *Freiburg/DE (horst.urbach@uniklinik-freiburg.de)*

Subtle epileptogenic lesions (mainly focal cortical dysplasias) are often missed on standard MRI. To find them, a 3 Tesla 3D T1-weighted MPRAGE (for morphometric analysis), a FLAIR SPACE, and a coronal highly resolved T2-weighted TSE sequence in-plane resolution 0.45x0.45 mm (for visual inspection) are key sequences within a epilepsy-dedicated protocol. In further presurgical workup language, laterality (which is related to the verbal memory capacity of the ipsilateral anterior temporal lobe and hippocampus) and spatial relationship of lesions to eloquent cortex and white matter tracts must be evaluated. With clear left laterality language fMRI is sufficient, in atypical laterality electrical stimulation mapping rather than a Wada test is added. Primary motor cortex and corticospinal tract on one and visual cortex and optic radiation on the other side are displayed with fMRI and diffusion tensor tractography. For the corticospinal tract, a "global" tracking algorithm and for the optic radiation including Meyer's loop, which may be damaged in anterior temporal lobe resections, a probabilistic algorithm are best suited. However,

most neuronavigation systems only process white matter tracts calculated with the FACT algorithm.
Learning Objectives:
1. To reveal how morphometric analysis of 3D data sets can help to reveal the true extent of a cerebral lesion in the presurgical work-up.
2. To demonstrate how fMRI is useful for documenting the spatial relationship of brain lesions to the adjacent eloquent cerebral cortex.
3. To illustrate how diffusion tensor tractography can reveal important white matter tracts such as the corticospinal tract and optic radiation.
Author Disclosure:
H. Urbach: Board Member; Clinical Neuroradiology, Neuroradiology. Investigator; Stryker. Research/Grant Support; BMBF. Speaker; Bayer, Stryker, UCB.

A-752 15:02

C. Introduction to resting state fMRI and functional connectomics
M. Oldehinkel; *Nijmegen/NL (m.oldehinkel@donders.ru.nl)*

Our brain consists of networks formed by structurally as well as functionally connected brain areas. Functional communication between brain regions is assumed to play a key role in the various functions of the brain. This makes the investigation of 'functional connectivity' in the human brain of high importance as it provides insights into the basic organisation of the brain. Regions are said to be functionally connected if their activation patterns (as measured with a functional MRI (fMRI) scan) are highly correlated. An fMRI scan can be acquired while participants or patients are performing a specific cognitive task, but also at 'resting state' during which participants are instructed to relax and to not think of anything in particular. Various studies have reported that the functional architecture of brain networks is altered in neurological and psychiatric diseases. However, before resting-state fMRI (rfMRI) can be used for diagnosis and predicting disease outcome, the field needs to overcome several challenges. In this talk I will cover the basic concepts of rfMRI and functional connectivity, give some examples of innovative rfMRI applications for studying brain function in neurological and psychiatric disorders and discuss the current challenges in the field.
Learning Objectives:
1. To understand how spontaneous fluctuations in activity in different parts of the brain can be used to study functional brain networks.
2. To review how resting-state functional MRI (rfMRI) can be used to map the macroscopic functional connectome.
3. To highlight some upcoming challenges in functional connectomics, using high-quality rfMRI data being generated by the Human Connectome Project.

16:00 - 17:30 **Room A**

E³ - ECR Academies: Interactive Teaching Sessions for Young (and not so Young) Radiologists

E³ 1621
Imaging of the chest

A-753 16:00

A. Fibrosing lung diseases
F. Molinari; *Lille/FR (francescomolinari.dr@gmail.com)*

The diagnostic approach to patients with fibrosing interstitial lung disease (FILD) is often complicated even when clinical history and physical findings are correctly assessed at presentation. In fact, many disorders of known and unknown aetiology may result in lung fibrosis and have overlapping clinical and radiographic features. Surgical lung biopsy is a viable tool for establishing the diagnosis. However, the procedure is associated to morbidity and mortality risks. HRCT remains the most important noninvasive modality for the diagnosis and management of patients with FILD. HRCT findings such as parenchymal reticulation, ground-grass attenuation, traction bronchiectasis and bronchiolectasis, architectural distortion and honeycombing indicate the presence of FILD. Honeycombing also indicates that lung fibrosis is irreversible and potentially progressive. To differentiate the most commonly encountered FILDs, current guidelines recommend to consider the presence of subpleural and basilar reticulation associated with honeycombing, altogether as the "UIP pattern". In the absence of known causes of lung fibrosis, a "definite" UIP is consistent with a diagnosis of idiopathic pulmonary fibrosis and does not require lung biopsy. The forms of FILD that manifest at HRCT as "possible" UIP and for which an alternative diagnosis of NSIP exists require lung biopsy. Finally, if the FILD manifests with HRCT findings that are inconsistent with UIP, the potential diagnosis of chronic HP is considered and lung biopsy is usually not indicated. This clinical-HRCT interpretative algorithm facilitates the assessment of HRCT scans that show the presence of lung fibrosis and provides guidance in the management of patients with FILD.
Learning Objectives:
1. To become familiar with the differential diagnosis.
2. To identify the key imaging findings.

A-754 16:45

B. Pleural disease
C. Beigelman; *Lausanne/CH*

Diffuse or focal pleural disorders are commonly encountered in routine practice, including pleural effusions, pleural thickenings, calcified or not, pneumothoraces or masses. Differential diagnosis must be known. In particular, focal pleural thickening (PT) may be related not only to typical pleural plaques, but also to normal structures, previous tuberculosis, pleural metastasis, silicosis, or other rarer conditions. Furthermore, postero-basal PT in supine examination may be reversible on prone position. Any atypical shape, location or change of a PT should suggest a pleural metastasis in a context of malignancy. In all cases, a careful analysis of other CT findings, previous imaging studies and clinical history are determinant for the final diagnosis. Parenchymal bands or rounded atelectasis are helpful for the diagnosis of benign diffuse pleural thickening. Features suggestive of malignancy include circumferential pleural thickening, nodular pleural thickening, parietal pleural thickening greater than 1 cm, and mediastinal pleural involvement. Atypical aspects such as pleural effusion even without plaque and pleural irregularity may be observed in mesothelioma, and slight changes in the mediastinal or interlobar pleura should be considered as suspicious of this diagnosis. Mistakes may be related to the difficult recognition of features such as in case of pneumothorax in supine position or to atypical features such as loculated effusions or atypical presentations of malignant pleural involvement that may lead to a delayed diagnosis.
Learning Objectives:
1. To become familiar with the differential diagnosis.
2. To identify the key imaging findings.

16:00 - 17:30 **Room B**

Abdominal Viscera

RC 1601
Abdominal MRI: from standard to advanced protocols

A-755 16:00

Chairman's introduction
F. Caseiro-Alves; *Coimbra/PT (caseiroalves@gmail.com)*

Abdominal MR imaging is a continuously evolving technique where researchers, vendors and clinical users get together to push it to the next level of medical practice. Recent advances in the MR field include the development of dedicated DWI sequences, increased spatial resolution and functional imaging capabilities to name a few. Therefore, there is a clear-cut need to use and take advantage of the most recent and best suited protocols. In this session, we will deal with three important common clinical situations: a) the suspected pancreatic cancer where MR appears not only as a problem-solving tool but also as a competitive diagnostic modality compared with MDCT ranging from DWI to high-resolution MRCP and time-resolved dynamic imaging; b) inflammatory bowel disease that, as a chronic relapsing disease, is one of the cases where MR may contribute to drive patient management exquisitely monitoring the inflammatory activity of the disease; c) MRI of pelvic floor disorders that consists in the use of high-resolution morphological data together with functional information under straining conditions. Its diagnostic power and contribution to patient management is well acknowledged today but protocol optimisation and proper quantification assumes a vital importance. To enhance the educational value of this session an illustrative clinical case for each clinical problem will be presented exploring the benefits and/or MR limits.

A-756 16:05

A. Suspected pancreatic tumour
R. Manfredi; *Verona/IT (riccardo.manfredi@univr.it)*

Pancreatic cancer is the fourth leading cause of cancer-related death. Surgical resection is the sole curative treatment option; however, only 15%-20% of them are resectable at the time of diagnosis. Furthermore, the prognoses for patients with pancreatic cancer remains poor. Although the 5-year survival rate is up to 20% after complete resection, it is further improved to more than 75%, in patients with a diagnosis of stage 1 disease. Computed tomography (CT) remains the initial imaging modality of choice for pancreatic solid neoplasms, even because recent improvements in multidetector CT technology, including improved temporal and spatial resolution, have facilitated more precise timing

of multiphasic imaging and increased the accuracy of CT for the detection and staging of pancreatic adenocarcinoma. Recently magnetic resonance (MR) imaging has developed a role in the early diagnosis of adenocarcinoma, because of diffusion-weighted (DW) MR imaging. By means of DW imaging MRI is able to depict changes in water mobility caused by interactions with cell membranes, macromolecules and alterations to the tissue environment, and thus provides a tissue contrast that is different from that on conventional T1- and T2-weighted images. DW imaging plays a role in oncology for tumour detection in general. DW imaging allows detection of pancreatic adenocarcinomas with high sensitivity and specificity, because it appears hyperintense compared with the rest of the gland. DW-MR imaging is also useful in finding small functioning neuroendocrine neoplasm, responsible for a clinical syndrome, but difficult to diagnose because of their small size.

Learning Objectives:

1. To learn about the role of MRI in the assessment of a patient with suspected pancreatic tumour.
2. To become familiar with the optimal MRI protocols including the role of DWI and secretin in this group of patients.
3. To appreciate the advantages and limitations of MRI in comparison with other imaging techniques.

A-757 16:28

B. Inflammatory bowel disease

J. Rimola; *Barcelona/ES (jrimola@clinic.ub.es)*

Magnetic resonance enterography (MRE) examinations are increasingly used in bowel imaging in particular for Crohn's disease assessment. In this setting, MRE has an evolving role not only for detecting and grading inflammation and their complications, but also for monitoring the course of the disease. MRE has unique technical characteristics including the distension of the bowel and the scanning of large areas of the body. Knowledge about patient preparation (bowel distension, anti-peristaltic drugs, etc.), scan technique and sequence parameters optimization as well as being familiar with commonly encountered problems that can arise during scan acquisition is of paramount importance. In this session, we will outline the most common sequences employed in routine MRE and its application in clinical practice. The potentialities and limitations of new functional sequences such as diffusion-weighted imaging and motility will be also discussed.

Learning Objectives:

1. To learn about the role of MRI in patients with IBD.
2. To become familiar with the optimal MRI protocols including bowel distension in this group of patients.
3. To appreciate the role of functional imaging techniques for assessment of IBD.

Author Disclosure:

J. Rimola: Consultant; Robarts Clinical Trials.

A-758 16:51

C. Pelvic floor disorder

D. Weishaupt; *Zurich/CH (dominik.weishaupt@triemli.zuerich.ch)*

Imaging of the female pelvic floor is of rising interest due to an ageing population, harbouring an increasing incidence of pelvic floor disorders (PFD) and the rising need for comprehensive diagnosis and treatment. Magnetic resonance imaging (MRI) of the female pelvic floor combines high-resolution imaging with an excellent soft tissue contrast and provides the possibility to assess noninvasively and objectively a spectrum of possible disorders affecting the pelvic floor in one examination. There is general agreement that MRI of the pelvic floor should encompass static and dynamic MR images, whereas dynamic means imaging under maximum stress to the pelvic floor and MR defecography. Static MR images visualize pelvic floor anatomy and defects of the supporting structures, while dynamic MR images visualize pelvic organ mobility, pelvic floor weakness, pelvic organ prolapse (POP) and associated compartment defects. In this lecture, a standardized approach regarding indications, patient preparation, sequences acquisition, interpretation and reporting of MRI for diagnosis and grading of PFD is presented. Due to the different views of the clinical specialists involved in the treatment of PFD, adapting the MRI reporting scheme according to the speciality of the referring physician is discussed. Finally, the limitations of the technique are addressed.

Learning Objectives:

1. To learn about the clinical relevance of MRI in the management of patients with pelvic floor disorders.
2. To become familiar with the optimal patient preparation and MRI protocols in this group of patients.
3. To appreciate the advantages of MRI relative to other imaging modalities including conventional defecography.

17:14

Panel discussion: How to create an efficient MR protocol in abdominal diseases

16:00 - 17:30 **Room C**

State of the Art Symposium

SA 16

Detection and management of small renal masses

A-759 16:00

Chairman's introduction

H.C. Thoeny; *Berne/CH (harriet.thoeny@insel.ch)*

Small renal masses are often incidentally detected on cross-sectional imaging. Management of these focal renal lesions depends on the underlying histology, age and comorbidities of the patient. However, characterisation of these small renal masses is often a big challenge. Cystic real lesions are classified according to Bosniak. In recent years, differentiation of solid renal lesions has improved substantially mainly thanks to a multiparametric approach using MRI. In the past years, solid renal lesions were surgically resected in most centres; however, in recent years, active surveillance and imaging-guided minimally invasive treatment are increasingly used alternatives to partial nephrectomy depending on histology of the tumour and various patient factors. As a consequence treatment monitoring is not only based on change in size or macroscopic tumour recurrence, but needs more detailed knowledge of the performed treatment including normal and pathological findings and knowledge of functional imaging techniques to early evaluate treatment success or recurrence.

Session Objectives:

1. To understand the imaging features of small benign and malignant renal masses.
2. To learn about the treatment options using imaging-guided minimally invasive treatment.
3. To appreciate typical normal and abnormal imaging findings during treatment monitoring.

Author Disclosure:

H.C. Thoeny: Advisory Board; Guerbet SA.

A-760 16:05

Detection and characterisation of small renal masses

N. Grenier; *Bordeaux/FR (nicolas.grenier@chu-bordeaux.fr)*

Imaging is the main source of detection of small renal masses. Primary detection is based on US and CT. MRI may help in indeterminate cases, DWI playing a major role. Characterisation of solid component of a small renal mass is based on CT-contrast enhancement, but, when doubtful, DCE-MRI and CEUS are more sensitive. Considering cystic masses, Bosniak classification is required. Considering solid masses, characterisation of fat-rich angiomyolipomas is based on plain CT, but fat-poor AMLs can be distinguished from carcinomas by multiparametric MRI only. Multiparametric MRI includes chemical shift gradient echo (GRE) sequences, signal intensity on T2-weighted images, DCE sequences, diffusion-weighted sequences and late contrast-enhanced images. Using different combinations of two or several parameters, now makes it possible to clearly distinguish some renal tumours such as fat-poor AMLs, papillary carcinomas and clear cell carcinomas, the latter being difficult to separate from oncocytoma when a central scar is absent. A larger validation of all these combinations is still necessary to define those having a clinical significance for routine practice. Percutaneous biopsy remains mandatory before such a validation, as soon as pathological result is supposed to have an impact on tumour management.

Learning Objectives:

1. To understand the definition of small renal masses.
2. To understand the typical imaging findings of small renal masses on CT.
3. To become familiar with multiparametric MRI to characterise small renal masses.

Author Disclosure:

N. Grenier: Advisory Board; Supersonic Imagine.

A-761 16:30

Image-guided minimally invasive treatment

M. Krokidis; *Cambridge/UK (mkrokidis@hotmail.com)*

The clinical management of small renal masses generates significant controversy. The gold standard still remains surgical excision; nevertheless, nephron sparing minimal invasive percutaneous ablation appears to offer similar oncologic outcomes and less complication than surgery. Active surveillance is only reserved for patients that are not suitable for any kind of treatment. Percutaneous ablation (radiofrequency, cryo or microwave) may be performed under local or general anaesthesia with minimal hospital stay;

guidance may be performed under CT, MRI or US guidance and with the use of fusion and navigation systems. Long-term results and comparative data are now available. Psutka et al. [Eur Urol. 2013] report the results of 185 patients with Stage I renal tumour (median size 3 cm) treated with RFA and followed up for a median of 6.43 years (range: 5.3-7.7). Local recurrence occurred in 6.5% of the patients after a median time of 2.5 years; however, the 5-year recurrence-free survival was 96.1%. Olweny et al. [Eur Urol. 2012] identified no significant difference between RFA and open partial nephrectomy for the treatment of T1a RCC in terms of 5-year disease-free survival, metastasis-free survival and local recurrence-free survival. Furthermore, Thompson et al. [Eur Urol. 2015] recently published a retrospective single-centre comparison of ablation with partial nephrectomy for Stage I RCC of 1424 patients with no difference on recurrence-free survival and comparative oncologic results. Ablation is offering excellent long-term results for the management of small renal tumours and should be considered as a first-line therapy for T1a tumours.

Learning Objectives:

1. To become familiar with the clinical management of small renal lesions.
2. To understand the minimally invasive treatment options of small renal lesions.
3. To learn about the current evidence on the minimal invasive treatment of small renal tumours.

A-762 16:55

Treatment monitoring with imaging

G. Cardone; *Milan/IT (cardoneg@tin.it)*

Most frequent treatments for small renal masses (SRM) are partial nephrectomy, radiofrequency ablation, cryoablation and active surveillance. CT and MR are commonly used in the imaging follow-up of patients treated for SRM. Parenchymal changes after partial nephrectomy are the presence of postoperative granulomas, fat, scars or parenchymal defects at the excision site. Imaging patterns of recurrence are the presence of a mass with enhancement, increasing in size during the follow-up, at the excision site or perinephric space. Radiofrequency ablation and cryoablation are minimally invasive approach for the treatment of SRM. Both ablative treatments, performed with percutaneous approach under US or CT guidance, provide tissue necrosis. Since it is not possible to document histopathologically the complete tissue necrosis after renal ablation, an adequate radiological follow-up is mandatory. Recurrence patterns after ablative treatments are the presence of an enhancing nodule in the treated area, increasing in size during the follow-up. Active surveillance has emerged as an alternative to extirpative or ablative treatments for SRM, in elderly and comorbid patients. Serial abdominal imaging (CT/MR) is performed to monitorize tumour size, with delayed intervention reserved for those tumours that show clinical progression during follow-up. In treated kidneys imaging follow-up, the most effective imaging techniques were multiphasic acquisition (CT) and morphologic TSE T2w and dynamic ce-FS-GRE T1w sequences before and after digital subtraction technique (MR). MR diffusion-weighted imaging may also be helpful to identify foci of residual tumour when contrast enhancement is difficult to evaluate, or when contrast cannot be administered due to renal insufficiency.

Learning Objectives:

1. To become familiar with imaging techniques for patients under active surveillance.
2. To understand typical imaging findings after minimally invasive treatment.
3. To appreciate functional imaging techniques to assess early treatment response.

17:20

Panel discussion: What to do with small renal masses?

16:00 - 17:30 **Room O**

Paediatric

RC 1612

Imaging children with cancer

Moderator:
C. Balassy; Vienna/AT

A-763 16:00

A. Imaging of abdominal masses at diagnosis: clues for benignity vs malignancy

Ø.E. Olsen; *London/UK (oystein.e.olsen@googlemail.com)*

Radiology is a probabilistic discipline since there is no test-diagnosis pair with perfect sensitivity and specificity. This also means that the definition of what distinguishes a likely benign vs. a likely malignant lesion must change depending on pre-test likelihoods. In most instances, the accuracy of imaging to make this distinction is low, hence the pretest likelihood is more important than the imaging findings themselves. So, for example, if you work in a general hospital you will very rarely see malignant tumours in children, so you are rarely wrong calling all lesions benign. The opposite is true in a specialised paediatric cancer centre. Similarly, it is possible to make decision rules based on clinical presentation, age, etc. There are, however, a few clues that often help shift these pre-test likelihoods, albeit none is absolute. Almost always benign: 1) origin splenic, hepatic in children <3 months of age, gastrointestinal, dermal. 2) Perfusion pattern similar to organ of origin. 3) Uptake of tissue-specific contrast agent. 4) Typical appearance of hamartoma. 5) Sharply demarcated lytic bone lesions. Almost always malignant: solid tissue with any pattern of growth. Most other characteristics must be interpreted with caution. Specifically, the following are NOT good predictors: 1) Doppler features (a vascular tumour is not always a haemangioma). 2) Heterogeneity (teratomas may contain malignant elements). 3) Containment (renal tumour are typically very large yet rarely breach the renal capsule). 4) Lack of enhancement (embryonal tumours often do not enhance much). 5) Apparent diffusion coefficient.

Learning Objectives:

1. To become familiar with clinical characteristics and imaging features of a mass suggesting benignity.
2. To emphasise clinical and imaging manifestations of abdominal malignancies.
3. To learn how to report according to international standards.

A-764 16:30

B. From whole-body MRI to MR/PET

W. Hirsch; *Leipzig/DE (wolfgang.hirsch@medizin.uni-leipzig.de)*

Whole body MR (WB-MR) and PET-MR are suitable methods to determine precisely the spread pattern of diseases. Whole body MRI is routinely used in paediatric oncology. It is very effective in the initial staging in multifocal oncological diseases. In restaging, the PET MRI has been shown to be more specific and sensitive in many diseases than the WB-MR. The new hybrid technique of whole body PET-MR leads, particularly in children, to significantly less radiation compared to whole body PET-CT. The radiation dose derives only from the PET part. The radiation exposure in PET-MR equals 3-4 mSv in 3D-mode. In contrast to this, a typical effective dose for a child on PET-CT is about 25 mSv. Therefore, it is likely that by establishing PET-MR 80% of radiation exposure can be prevented compared to PET-CT. A lot of radiotracers are used for PET imaging. For paediatric PET-MR mainly ^{18}F-fluorodeoxyglucose (^{18}F-FDG) and ^{11}C-methionine (^{11}C-MET) are used. However, other tracers are available, e.g. ^{68}Ga-DOTATOC for neuroendocrine tumours or meningioma. Using case studies, typical clinical indications and findings of hybrid imaging in children will be demonstrated, such as PET-MR for oncologic issues, or to locate biopsy areas for brain tumours (hotspot-biopsy). However, the diagnostic usefulness and impact on patient management (“diagnostic imaging efficacy”) must be weighed against the exposure of radiation and also the costs.

Learning Objectives:

1. To understand differences and pitfalls of whole-body MRI and MR/PET in children compared to adults.
2. To compare PET/MRI to PET/CT.
3. To discuss the impact of whole-body MRI and PET/MRI in paediatric oncology.

16:00 - 17:30 **Room N**

Cardiac

RC 1603

Coronary CT angiography: how to get it done?

Moderator:
K. Pagonidis; Iraklion/GR

A-766 16:00

A. Beautiful cases from clinical practice I

S. Feger; *Berlin/DE (sarah.feger@charite.de)*

Coronary computed tomography angiography (CTA) is a non-invasive diagnostic test with high diagnostic accuracy in detecting coronary artery disease (CAD). Due to its very high negative predictive value, it is especially suitable for ruling out CAD in patients with low to intermediate pretest probability. For stable chest pain patients in this pretest probability range, the current European guidelines already recommend the use of CTA. Additionally, in patients with unstable chest pain and a low CAD probability, CTA can be considered to detect relevant differential diagnoses. Different acquisition techniques are applied in clinical practice. Initially, retrospective ECG-gated

CTA was routinely used. While this approach is very robust, especially for high or irregular heart rates, radiation exposure is relatively high. Prospective axial scanning reduces radiation exposure, since data acquisition is only performed in predefined ranges within the RR interval with the tube current entirely being turned off outside the acquisition window. Further approaches to reduce radiation exposure are the adjustment of scanning parameters, ECG-gated tube current modulation, automatic tube potential selection and, recently, the introduction of iterative reconstructions.

Learning Objectives:

1. To learn about cardiac CT acquisition techniques, pitfalls, and dose reduction strategies.
2. To summarise current indications and clinical applications of CT coronary angiography.
3. To review the diagnostic performance of CT for the diagnosis of coronary artery disease.

A-767 16:35

B. Staff training and technical requirements

M. Francone; *Rome/IT (marco.francone@uniroma1.it)*

The complexity of cardio-thoracic motion combined with the need of scanning small and tortuous vessels like the coronary arteries pushes technical requirements for cardiac CT to the maximum level. Image quality is directly influenced by the spatial and temporal resolution of the scanners adopted, which are pivotal parameters to consider when selecting a machine to be used for setting up a cardiac CT programme. High temporal resolution is needed, in particular, to minimize cardiac-motion artefacts, and can be raised by increasing gantry rotation speed, or using multisegment reconstructions or by means of a dual-tube solutions. Different technical solutions have been adopted in last years to improve diagnostic performances. After an initial phase of “slice-wars” in which different vendors adopted the strategy of increasing number of slices, there has been a more articulated differentiation in technological proposals ranging from the diffusion of dual tube and dual energy scanners to the availability of “single heart-beat” machines characterized by full-volumetric z-coverage increase; scanner’s tubes have also been implemented to minimize noise and reduce patient’s dose. An additional focus regards the training of personnel, which highly varies geographically all over Europe and, mostly, between different specialities (radiology vs. cardiology) reflecting the still-existing deep differences in training and formation between various backgrounds. On completion of this lecture, participants will be provided an overview of updated technological proposals to implement a cardiac CT programme. Training requirements for radiologists will also be reviewed and compared between different scientific societies and specialities.

Learning Objectives:

1. To become familiar with technical prerequisites and post-processing tools for coronary CT angiography.
2. To discuss a necessary team setup and training modules for radiologists and technical staff.
3. To evaluate the role of coronary CT angiography and requirements for the radiological team in routine imaging and in emergencies.

Author Disclosure:

M. Francone: Speaker; Bracco Medical Imaging Invited Speaker.

A-768 16:55

C. Beautiful cases from clinical practice II

F. Plank; *Innsbruck/AT*

Content of this refresher course will be to illustrate a coronary CTA exam of patients with coronary stents and coronary artery bypass grafts, including step by step accomplishment of a CT exam and differences to usual coronary CTAs, technical and post-processing tools, anatomical configurations of different types of stents, advantages and limitations of CT to visualise stents, appearance of different types of CABG, case discussions, possible pit falls, strategies to improve visualisation and decrease false results.

Learning Objectives:

1. To outline the technical and contrast administration parameters and post-processing tools for the assessment of coronary stents and coronary artery bypass grafts (CABG).
2. To review anatomical configurations and CT appearance of different types of CABG.
3. To discuss current limitations and spectrum of artefacts produced by different types of stents and strategies to improve visualisation of stents.

16:00 - 17:30 **Studio 2017**

Special Focus Session

SF 16a
The male pelvis

A-769 16:00

Chairman's introduction

J.J. Fütterer; *Nijmegen/NL (jurgen.futterer@radboudumc.nl)*

Urogenital organs include the testes, epididymis, vas deferens, ejaculatory ducts, urethra, penis, prostate and seminal vesicles. The male reproductive system consists of those organs whose function is to accomplish reproduction. This consists of testes, which produce spermatozoa and hormones, a series of ducts that store and transport the sperm, seminal vesicles, the prostate and the penis. Imaging has given radiology a significant role in the characterization, diagnosis and staging of tumours in these organs.

Session Objective:

1. To provide an overview of indications, biopsy techniques and multiparametric MR imaging of the prostate.

A-770 16:05

Update on prostate MR

O. Rouvière; *Lyon/FR (olivier.rouviere@chu-lyon.fr)*

Typically, prostate multiparametric MRI (mpMRI) combines T2-weighted imaging (T2WI) with at least diffusion-weighted imaging (DWI) and dynamic contrast-enhanced imaging (DCEI). The use of spectroscopic imaging is optional, as is the use of an endorectal coil. Recent works suggest that the added value of DCE imaging is limited, especially in some settings (history of radiation therapy), but whether DCE can be systematically omitted in all patients remains controversial. Correlations to prostatectomy specimens showed that mpMRI could detect 88-92% of cancers with a volume ≥0.5cc and a Gleason score of 7, and more than 95% of cancers with a Gleason score ≥8. Although many benign conditions can mimic cancer, existing scoring systems can stratify the risk of malignancy and the aggressiveness of the tumours. The recent PIRADS V2 score introduced the concept of a dominant pulse sequence (DWI in the peripheral zone, T2WI in the transition zone), and should help standardizing mpMRI interpretation, even if further refinements of the PIRADS score are to be expected. Quantitative approaches have also shown promising results and will probably be increasingly used in the future.

Learning Objectives:

1. To become familiar with indications and technique.
2. To demonstrate new developments in prostate imaging.
3. To raise awareness about prostate imaging.

Author Disclosure:

O. Rouvière: Consultant; EDAP-TMS, Bracco.

A-771 16:23

Template biopsy vs TRUS/MR-fusion guided biopsy

T. Fischer; *Berlin/DE (thom.fischer@charite.de)*

Prostate cancer is the most common malignancy in men and its incidence is continuously increasing. As with other malignant tumours, early and adequate diagnosis improves the chances of cure. Patients who underwent organ-sparing treatment should be risk-stratified based on localisation, extent, and actual Gleason score of the cancer. Real-time magnetic resonance imaging/ultrasound (MRI/US)-fusion-guided biopsy detects more clinically significant prostate cancers than conventional transrectal ultrasound (TRUS) biopsy. The aim of this session is to discuss state-of-the-art ultrasound techniques for MRI/US-fusion-guided biopsy in daily practice in comparison with transperineal template biopsy, which has high sensitivity (>90%) in detecting aggressive prostate cancer but is also much more invasive. Both techniques are useful in planning organ-sparing approaches (active surveillance, focal therapy). In addition, we use ultrasound contrast agents to characterise focal prostate lesions and to monitor irreversible electroporation (IRE) as well as for molecular imaging.

Learning Objectives:

1. To become familiar with the different fusion techniques.
2. To review the pros and cons of each approach.
3. To show complications and outcome.

Author Disclosure:

T. Fischer: Advisory Board; Bracco, Toshiba. Consultant; Toshiba. Speaker; Toshiba, Siemens, Hitachi, Bracco.

A-772 16:41

Imaging after focal prostate therapy

C. Allen; *London/UK*

"no abstract submitted"

Learning Objectives:

1. To understand image findings of the post-treated gland.
2. To show imaging characteristics of local recurrent disease.
3. To highlight some challenges in the follow-up after focal therapy.

A-773 16:59

Biopsy strategy

A. Briganti; *Milan/IT*

"no abstract submitted"

Learning Objectives:

1. To become familiar with indications and technique.
2. To demonstrate different biopsy strategies.
3. To show complications and outcome.

17:17

Panel discussion: Is there a role for MR imaging to steer the biopsy?

16:00 - 17:30 **Room L 8**

ESR Patient Advisory Group (ESR-PAG)

ESR-PAG 2

Big data - data management, standardisation, access and protection: the way forward in developing personalised/precision medicine

A-774 16:00

Chairmen's introduction

B. Brkljačić[1], N. Bedlington[2]; [1]*Zagreb/HR*, [2]*Vienna/AT (boris@brkljacic.com)*

The session about the management of big data, standardisation, access and protection will include presentations of several perspectives. The perspective of European Society of Radiology will be provided, with presentation of current European situation and future developments. Then patient's perspective will be provided, demonstrating that patients are entitled to personal care and understand that sharing and access to images is needed for their proper precision care. Finally, the US perspective will be provided, where the lessons learnt so far in the top US institution will be highlighted, and US perspective as a whole will be presented.

Session Objectives:

1. To understand the importance of wider recognition for medical imaging and its role in personalised/precision medicine.
2. To understand the key issues of medical imaging in the development of personalised medicine.
3. To learn how patient involvement and education can facilitate the development of personalised medicine.

Author Disclosure:

B. Brkljačić: Speaker; Guerbet, Bayer.

A-775 16:10

European developments within data management, standardisation, access and protection

P. Mildenberger; *Mainz/DE (mildenbe@uni-mainz.de)*

Development in imaging strategies is clearly providing new and exciting opportunities in, e.g. functional or molecular imaging, image processing and many others. These techniques generate a lot of different data, which require more sophisticated workup than conventional x-ray or CT imaging. Therefore, for research or analysis, very often multi-site collaboration will be necessary. For individual treatment, patients will try to find the 2nd opinion outside their primary care-centre seeking for experts throughout their country or even on international level. The EU directive on cross-border healthcare supports this. Several countries have already regional or national eHealth strategies, which help to communicate information between different care providers or patients themselves. One internationally accepted way of standardised communication in healthcare is the application of IHE-profiles. Many of such profiles are already recommended for procurement by the EC. Building such networks could enable access for patients to experts, or pseudonomized/anonymized imaging data could be used to feed national or international registers for benchmarking quality parameters, e.g. for radiation exposure optimisation. Some more work has to be organised to build such registers and to have consensus on coding systems to be used in such environments.

Learning Objectives:

1. To define the current status of play from ESR leadership.
2. To advise on future developments.
3. To highlight advantages of improvements from patient perspective.

A-776 16:25

Patients' point of view (part I)

N. Bedlington; *Vienna/AT (nicola.bedlington@eu-patient.eu)*

The presentation will outline European patients' forum's work to date on big data and data management in the policy context, and describe key principles from the perspective of patients. The changing role of patients will be explored, as will concepts such as informed consent, patients' ownership of data, and transparency. Finally, the presentation will highlight EPF's work on precision medicine and our contribution to the policy debate, with particular emphasis on data management.

Learning Objectives:

1. To understand that patients are entitled to personal care (medicine) as this is to be seen as a minimal requirement.
2. To understand that patient wants precision medicine that their treatment is to be adjusted to the specific properties of their disease - genetic or otherwise.
3. To understand that, from a patients view, data sharing is a necessary instrument to improve the patient journey through her or his disease and that images are also data that need to be shared.

A-777 16:40

Patients' point of view (part II)

E. Briers; *Hasselt/BE (erikbriers@telenet.be)*

Patients are entitled to personal care, care that is tailored to the personal needs of the individual patient, taking into consideration not only the pathology to be taken care of but also the patients' needs and wishes, medical or otherwise, in as far as humanely possible. Precision medicine is tailored to the genetic characteristics of the disease, which will guide the treatment options. Precision medicine can prevent the application of new medicines that would not work or precisely identify a medicine that could be effective eventually from another cancer. To gather knowledge on personalized and precision medicine it is not enough to perform some clinical trials as the level of information is potentially too large. This kind of information can best be distilled from large data sets in which not only many patients are present but of these patients a lot of data. At the start you do not know which data will be relevant. Patients with life-threatening diseases that depend for their treatment on innovative new medicines know that these are the fruit of tenacious research over many years. Those who participate in the trial do so for their own benefit but also from an altruistic point of view for others. In the same reasoning patients know that the analysis of "good" data could allow better treatment options for other patients in the future. Therefore, patients are willing to share their data for their own benefit and the benefit of research but they want to be asked in advance.

Learning Objectives:

1. To understand that patients are entitled to personal care (medicine) as this is to be seen as a minimal requirement.
2. To understand that patient wants precision medicine that their treatment is to be adjusted to the specific properties of their disease - genetic or otherwise.
3. To understand that, from a patients view, data sharing is a necessary instrument to improve the patient journey through her or his disease and that images are also data that need to be shared.

A-778 16:55

Current US status pros and cons and issues

J.A. Brink; *Boston, MA/US (JABRINK@partners.org)*

To enable research in clinical data science, the radiology community must embrace a number of initiatives intended to establish several important standards. International image sharing networks with robust, clean image data sets are needed to serve as reference data sets of proven cases against which new artificial intelligence programs can be tested. Moreover, standardized imaging protocols are critical for subsequent analysis by new machine learning tools. Watermarking methods are needed to ensure the integrity of images in image sharing networks. Image data may be altered intentionally or inadvertently corrupted in transmission or storage, making it difficult to reproduce studies and conclusions in more than a single institution. Watermarks that have been altered will allow recognition of disruptions of data integrity.

Learning Objectives:

1. To discuss the US perspective.
2. To understand the issues from an US perspective.
3. To highlight the lessons learnt.

Author Disclosure:

J.A. Brink: Research/Grant Support; NVIDIA Corporation.

17:10

Panel discussion: Importance of data management in modern medicine - what are the main issues to be addressed?

16:00 - 17:30 **Room E1**

Multidisciplinary Session

MS 16

Virtual autopsy imaging in children: the role of pathologist vs radiologist, one big happy family?

A-779 16:00

Chairman's introduction

C. Owens; *London/UK (owensc@gosh.nhs.uk)*

In this session, we intend to present a multidisciplinary approach to state-of-the art virtopsy imaging in children. We have contributions from radiologists and pathologists, working in harmony to achieve the best possible outcome for bereaved parents, with a conjoint, highly accurate but sympathetic approach. Advances in postmortem imaging and tissue sampling techniques will be outlined to provide a comprehensive autopsy service in the most clinically appropriate setting, whilst respecting the bereaved parents' wishes.

Session Objectives:

1. To learn about the multidisciplinary nature of perinatal autopsy, with reference to the scientific contribution of radiology and pathology.
2. To learn about the limitations of both conventional autopsy, and conventional imaging techniques.
3. To appreciate the role that novel imaging and pathology techniques have to play in future service provision.

A-780 16:05

Minimally invasive autopsy: setting the scene - why, how and by whom?

N.J. Sebire; *London/UK (neil.sebire@gosh.nhs.uk)*

The approach to standard paediatric autopsy has changed little over many years, remaining predominantly based on external examination, dissection and subsequent organ examination and then histological evaluation. Minimally invasive autopsy is a new approach encompassing external examination, non-invasive comprehensive cross-sectional postmortem imaging, and limited tissue sampling to permit the most appropriate tissue sampling techniques necessary to reach a final diagnosis or cause of death which is more acceptable to parents and families.

Learning Objectives:

1. To learn about novel minimally invasive autopsy techniques.
2. To understand how imaging fits into a modern clinical autopsy service.

A-781 16:25

State-of-the-art post-mortem imaging: the way it works and how we do it

O.J. Arthurs; *London/UK (owen.arthurs@gosh.nhs.uk)*

Postmortem (PM) magnetic resonance imaging (MRI) has high diagnostic accuracy for the majority of perinatal and paediatric diagnoses, when accompanied by other non-invasive investigations, and compared to traditional autopsy. Comprehensive whole body imaging using PM MRI performs particularly well for cardiac, neurological and abdominal diagnoses, but less well for thoracic and skeletal abnormalities. PM MRI performs better than PM CT in the same individual, although ventilated PMCT and CT angiography have been proposed to increase PMCT diagnostic detection rates. However, both modalities become increasingly non-diagnostic with reducing foetal size, typically below 500g body weight or at early foetal gestations. Postmortem ultrasound is yet to be assessed in a comprehensive trial.

Learning Objectives:

1. To learn about the recent advances in cross-sectional imaging in a post-mortem setting.
2. To learn about the advantages and disadvantages of conventional PMCT and PMMR techniques.

A-782 16:45

Latest advances: the new kid on the block micro-CT - when and how?

J.C. Hutchinson; *London/UK (ciaran.Hutchinson@gosh.nhs.uk)*

Microfocus computed tomography has been proposed as an alternative to MR or CT in small specimen foetal imaging. Diagnostic accuracy is high for excised foetal hearts and kidneys, with appropriate tissue and image optimisation parameters. Whole body foetal autopsy may be possible with micro-CT in future. However, several issues remain to be addressed for widespread implementation of micro-CT scanning, including tissue colouration, distortion due to fixation, data storage of large files, and comprehensive reconstruction and post-processing.

Learning Objectives:

1. To learn how novel techniques like micro-CT can be used in the perinatal autopsy setting.
2. To appreciate how micro-CT works.
3. To learn what high resolution imaging can offer within a clinical setting.

17:05

Multidisciplinary case presentation and discussion

16:00 - 17:30 **Room E2**

Special Focus Session

SF 16b

Black and white spots in the brain

A-783 16:00

Chairman's introduction

H.R. Jäger; *London/UK*

Session Objectives:

1. To learn about the differential diagnosis of white matter lesions and cerebral microhaemorrhages (including small vessel disease, demyelination and trauma).
2. To understand clinical correlates including the prognostic and therapeutic impact of black spots and white spots.
3. To appreciate the best MR sequences used for detection of white and black spots and tools for quantitative analysis of disease burden.

A-784 16:05

White spots in the brain on T2 and FLAIR: what are they?

A. Rovira-Cañellas; *Barcelona/ES (alex.rovira@idi.gencat.cat)*

White matter hyperintensities (WMHs) are common findings on brain MRI, especially in middle-aged and elderly individuals, and are usually regarded as surrogates of small vessel disease. However, evaluation of WMHs in any age group is challenging because their cause may vary from infectious, inflammatory, or demyelinating findings to nonspecific findings related to ageing and other systemic conditions. Even in the absence of any clue in the clinical data, many WMHs are classified as 'vascular', particularly in elderly individuals, implying a presumed hypoxic-ischaemic pathogenesis and the expression of arteriolosclerotic disease. However, mechanisms other than arteriolosclerosis should also be considered, such as amyloid angiopathy, Wallerian degeneration due to cortical atrophy, or Alzheimer disease-related pathological changes. A more specific diagnosis within the group of hypoxic/ischaemic disorders may be suggested when certain MRI features are

present, such as haemorrhage (amyloid angiopathy), significant asymmetry of the WMHs (ipsilateral carotid disease), and involvement of the external capsule and temporal poles (CADASIL) or the central part of the corpus callosum (SUSAC). In young adults, presence of WMHs commonly suggests the diagnosis of multiple sclerosis, leading to an overdiagnosis of this disease. Therefore, in the absence of typical clinical and MRI features of multiple sclerosis, alternative conditions must always be considered such as migraine, systemic inflammatory diseases, or genetic-related vascular disorders, which are commonly associated with WMHs. In this presentation, we will review different disorders that may present with WMHs and the value of MRI in the diagnosis and management of them.

Learning Objectives:

1. To learn about the differential diagnosis of white spots.
2. To understand semi-quantitative and quantitative approaches for measuring the burden of white spots.
3. To appreciate the role of white spots as biomarkers for natural history and treatment of disease.

A-785 16:30

Black spots in the brain on SWI: differential diagnosis

M. Vernooij; *Rotterdam/NL (m.vernooij@erasmusmc.nl)*

Compounds which distort the local magnetic field may result in 'black spots' in the brain on MRI sequences that are susceptible to such paramagnetic effects, such as susceptible-weighted imaging (SWI). These black spots may result from various tissue changes, such as iron deposition, calcifications or microbleeds. In turn, these changes can reflect different underlying conditions, ranging from traumatic- or radiation-induced pathology, to amyloid angiopathy or hypertensive small vessel disease. Detection of these 'black spots' strongly depends on the MR pulse sequence and field strength used. Cerebral microbleeds in particular have been an important topic of research in (clinical) populations in the past decade, in view of their emergence of a marker of small vessel disease with links to both stroke (ischaemic as well as haemorrhagic) and dementia.

Learning Objectives:

1. To learn about the differential diagnosis of black spots.
2. To understand semi-quantitative and quantitative approaches for measuring the burden of black spots.
3. To appreciate the role of black spots as biomarkers for natural history and treatment of disease.

A-786 16:55

Advanced MR imaging and quantification techniques: do they help?

S. Haller; *Carouge/CH (Sven.Haller@affidea.ch)*

The third and final presentation of this special focus session discusses example applications of advanced imaging methods in the context of the diseases discussed before, notably traumatic brain injury and cerebral microbleeds. The first part will discuss diffusion tensor imaging (DTI) as an example of an advanced MR technique in the context of mild traumatic brain injury (MTBI). DTI may detect subtle trauma-related changes in the brain, which are not visible using standard MR imaging sequences. Given the recent public interest in sports-related MTBI and concussion, such as the movie "Concussion" featuring Will Smith, recent DTI brain imaging in American football and soccer players are critically discussed. The second part will critically discuss an example of quantitative MRI, notably automatic counting of cerebral microbleeds in cerebral amyloid angiopathy (CAA) as well as traumatic microbleeds/haemorrhagic diffuse axonal injuries (DAI).

Learning Objectives:

1. To understand how diffusion tensor imaging (DTI) might be helpful to detect subtle structural brain changes related to minor traumatic brain injury, which are not visible using standard structural MR sequences.
2. To understand the limitations of DTI for clinical applications and notably the need for strict standardisation of both data acquisition and data analysis.
3. To understand the principle potential of quantitative imaging analysis tools of brain MR imaging, based on the example of cerebral micro bleeds.

17:20

Panel discussion: How to image, quantify and report black and white spots in the brain?

16:00 - 17:30 **Room F1**

E³ - European Diploma Prep Sessions

E³ 1623

Breast

A-787 16:00

Chairman's introduction

F. Pediconi; *Rome/IT (federica.pediconi@uniroma1.it)*

Radiology is a medical speciality that involves all aspects of medical imaging. It provides information about the anatomy, physiology, and function of organs and systems of the human body in normal and abnormal status, allowing for imaging-based diagnosis, tissue sampling, and therapy. This is even more applicable to the breast radiology subspeciality where only appropriately trained physicians should carry out this duty. The fundamentals of undertaking and interpreting a wide range of imaging techniques and disease manifestations remain essential for breast radiologists. Mammography is the main investigation for breast cancer. It is used primarily to detect and diagnose breast cancer and to evaluate palpable masses and non-palpable breast lesions. So starting from the anatomical and pathological knowledge of the breast disease, the first step is to understand the principles of the mammography and how to apply them. This will be followed by all the other imaging modalities currently available to gain an appropriate diagnosis (US, MR, biopsy, etc.). What it is desirable for all the radiologist embracing the breast subspeciality is to interpret and report mammograms, breast ultrasound and breast MRI examinations using a standardized diagnostic categorization system such as the ACR Breast Imaging Reporting and Data System (BI-RADS®) and put the patient into a correct diagnostic pathway. It is important to have the appropriate breast imaging knowledge to choose the best suited method for evaluating the breast disorder in each patient. Finding breast cancers early greatly improves women's chance for successful treatment and it really affects their prognosis.

Session Objectives:

1. To understand the methodological principles of mammography.
2. To learn the mammographic appearance of benign and malignant lesions of the breast.
3. To become familiar with the imaging appearance of benign and malignant breast lesions.

A-788 16:06

A. Fundamentals of mammography

S. Barter; *Cambridge/UK (suebarter@btinternet.com)*

In this lecture anatomy, normal variants and common abnormalities of the female breast will be discussed, with particular emphasis on breast cancer detection. The importance of technical aspects of diagnostic mammography especially with regard to positioning, dose and image quality will be discussed. Quality can be lost at different points in the mammography process, positioning of the patient, the x-ray beam and dose, the detector and display. Viewing conditions must be optimised to ensure accurate detection of abnormalities. There is good evidence from two population-based screening programmes that poor image quality can reduce cancer detection on screening mammograms by 15% to 24%. Finally, the principles of current practice and risk/benefit analysis in breast cancer screening will be explained. Screening is the practice of mammograms performed regularly in asymptomatic women. The goal of screening is to ensure detection of breast cancer in the examined population at the earliest possible stage to reduce breast cancer mortality, and minimise potential side effects and unnecessary interventions in the screened population. Fundamental to a successful program is strict quality assurance.

Learning Objectives:

1. To understand the anatomy, normal variants and abnormalities of the female breast.
2. To become familiar with the technical aspects of diagnostic mammography, especially in regard to dose and image quality.
3. To become familiar with the principles of current practice and risk/benefit analysis in breast cancer screening.

Author Disclosure:

S. Barter: Board Member; Co -editor ESR E-Learning board. Speaker; ECR 2017.

Saturday

A-789 16:34

B. Breast cancer diagnosis and interventions

M. Müller-Schimpfle; *Frankfurt a. Main/DE (MMS@KlinikumFrankfurt.de)*

Mammography, ultrasound and MRI are the imaging modalities of choice for diagnosing breast diseases. The ability to detect lesions depends on density, glandular heterogeneity or background enhancement. The most important typical types of findings that can be differentiated are masses, non-mass lesions, architectural distortions, asymmetries and additional findings. Masses can be characterised by shape and margin, non-mass lesions by morphology and distribution, suggesting a category of suspicion for malignancy. Further elements such as density, echogenicity, contrast kinetics, pre-test probability or individual risk can modify a category of suspicion. Whenever a lesion shows a probability of malignancy >2% a needle biopsy should be considered. The modality of choice as well as the needle used depends on the detection method and lesion type. The same is true for pre-surgical localisations. Most masses will show a correlating finding in ultrasound which subsequently can guide a fine needle, a 14G needle biopsy or a wire, clip/coil marker online. Non-mass lesions such as microcalcifications or lesions in breast MRI will typically be biopsied by vacuum-assisted techniques to diminish sampling error.

Learning Objectives:

1. To learn the different presentation of normal breast patterns and the appearance of common benign diseases and of breast cancer at mammography, ultrasound, and MRI.
2. To understand principles and basic application of a standardised diagnostic categorisation systems such as the ACR breast imaging reporting and data system (BI-RADS®).
3. To become familiar with indications, contraindications and technical aspects of image-guided interventional breast procedures (fine needle aspiration, core needle biopsy, vacuum-assisted biopsy, presurgical localisation).

Author Disclosure:

M. Müller-Schimpfle: Equipment Support Recipient; Fujifilm, Tomosynthesis cooperation. Patent Holder; Cook Company: tumor marker coil.

A-790 17:02

C. Advanced imaging of the female breast

R.M. Mann; *Nijmegen/NL (r.mann@rad.umcn.nl)*

While mammography, ultrasound and MRI are the basis for current breast imaging, the field is rapidly evolving. Tomosynthesis is rapidly replacing mammography in the clinic and is in some countries already implemented in mass screening. Supplemental screening techniques for women with dense breasts are constantly under development. Automated breast ultrasound is already clinically available and in use for whole breast ultrasound evaluation, other modalities are tested in several trials. For lesion classification other techniques become important. Contrast-enhanced mammography may play an important role in the evaluation of women recalled from screening. Similarly, several add-ons for ultrasound have found their way to the clinic. Doppler is widely employed and also elastography is still gaining momentum, while opto-acoustic imaging as the next step is around the corner. Also in MRI many techniques help to classify lesions beyond what can be achieved with BIRADS evaluation alone, while simultaneously ultrafast techniques are under development to improve its value as a screening tool. In the evaluation of known cancers it becomes increasingly important to understand the biologic profile of a cancer. This is more and more determining the therapy given. Also translation of image findings to therapy is a major challenge. Multimodal evaluation and integration of imaging findings with clinical and histopathological parameters hence becomes a must. Advanced imaging techniques such as breast PET and spectroscopy might have an important role in this field in the near future.

Learning Objectives:

1. To understand the role of advanced imaging techniques in evaluation of the breast.
2. To use the added value of new techniques for lesion classification in mammography, ultrasound and MRI.
3. To recognise the major imaging issues for common indications of breast imaging.

Author Disclosure:

R.M. Mann: Advisory Board; Screenpoint. Equipment Support Recipient; Elswood. Grant Recipient; Siemens Healthcare, Seno Medical. Investigator; Siemens Healthcare, Bayer Healthcare, Seno Medical, IDS.

16:00 - 17:30 **Room F2**

Emergency Imaging

RC 1617

Abdominal trauma: things not to forget

Moderator:
G. Schueller; Opfikon/CH

A-791 16:00

A. Liver and spleen

M. Scaglione; *Castel Volturno/IT (scaglionefun@gmail.com)*

Abdominal injuries are a significant cause of death in the polytraumatised patients. Early recognition and communication of life-threatening hepatic and splenic injuries is crucial for an early and tailored management approach. The vast majority of the hepatic and splenic injuries are now treated non-operatively, independently from their volume, depth and location, thanks to the extensive use of MDCT technology in the emergency rooms. From a management viewpoint, size, depth or location of a contusion/laceration are relatively important if the patient is haemodynamically stable. However, using MDCT, the radiologists have to carefully scrutinise the images in the liver and spleen to look for vascular lesions, such as pseudoaneurysms, A-V fistula and active bleeding. Actually, the evidence of pseudoaneurysms, A-V fistula and/or active bleeding change injury grade and patients' management and outcome! This is our task, to look for such injuries within lacerations or haematomas in a pre-clinic stage, i.e. before the patents may develop haemodynamic instability. Thus, in this lecture, high-grade hepatic and splenic injuries will be illustrated, with special emphasis on vascular injuries as well as the value of post-processing techniques, protocols, pitfalls, tips and tricks. Furthermore, the importance of a rational and integrated imaging approach will be pointed out and, finally, the role of the radiologist in emergency room will be emphasised.

Learning Objectives:

1. To become familiar with traumatic injuries of the liver and spleen that can result in haemodynamic instability and other clinical complications.
2. To learn how to optimise scanning protocols to diagnose these injuries.
3. To understand the impact of these imaging findings on further management of patients and report accordingly.

A-792 16:30

B. Pancreas, bowel and mesentery

M.A. Patak; *Zurich/CH (Michael.Patak@hirslanden.ch)*

Imaging in abdominal trauma is crucial to get a fast overview of the situation and to plan treatment according to the different injuries. Injuries of the pancreas, the bowel and the mesenteries are a rather rare conditions and happens mostly to severely injured patients. It is important to actively rule out any possible injury to one of these organs. The presentation will show the typical aspects of traumatic injuries to pancreas, bowel and mesenteries. CT is the most often performed modality in acute trauma and will be discussed extensively. Treatment consequences according to imaging will be discussed.

Learning Objectives:

1. To become familiar with traumatic injuries of the pancreas, bowel and mesentery that can result in haemodynamic instability and other clinical complications.
2. To learn how to optimise scanning protocols to diagnose these injuries.
3. To understand the impact of these imaging findings on further management of patients and report accordingly.

A-793 17:00

C. Urogenital tract

R.H. Oyen; *Leuven/BE (Raymond.Oyen@uzleuven.be)*

Whatever cause (blunt, penetrating, iatrogenic), traumatic injury to the urogenital tract in the majority of cases requires dedicated multiphase scanning protocols (1) to assess the location and extent of lesions and (2) to tailor appropriate therapeutic strategies. With haemorrhagic complications optimised scan timing is essential to recognise active bleeding, and to evaluate whether interventional procedures are indicated to avoid invasive surgery. When urinary leakage is suspected, delayed scanning is essential to clearly demonstrate the site of the leakage. Retrograde opacification of the bladder can be useful to demonstrate subtle leakages and to gain time. Percutaneous procedures including nephrostomy, and antegrade or retrograde ureteral stenting may be therapeutic or supportive. Ultrasound with colour Doppler is the imaging modality of choice to assess penile and scrotal trauma. Detailed evaluation of penile and testicular integrity and vascularity are crucial to differentiate surgical from non-surgical cases. Urethral trauma deserves specific attention, with (conventional) imaging during retrograde and antegrade contrast opacification to assess the site and length of the urethral injury. For the evaluation of

iatrogenic injury it is essential to understand the surgical technique performed (organ sparing surgery, pouch constructions, bowel derivations, etc.). Some surgery is prone to more procedure-related complications as partial nephrectomy compared to total nephrectomy (9% versus 3%), including (active) bleeding and urinary leakage, and the reintervention rate is higher (2.5% versus 0.6%).

Learning Objectives:

1. To become familiar with traumatic injuries of the urogenital tract that can result in haemodynamic instability and other clinical complications.
2. To learn how to optimise scanning protocols to diagnose these injuries.
3. To understand the impact of these imaging findings on further management of patients and report accordingly.

16:00 - 17:30 **Room D**

Professional Challenges Session

PC 16
Ensuring the future role of radiologists

A-794 16:00

Chairman's introduction

J. Van Goethem; *Antwerp/BE (johan.vangoethem@uantwerpen.be)*

The role of radiologists has changed enormously in the past decades. With the advent of PACS most clinicians have gained direct and immediate access to radiology images. Many clinicians have at least the basic knowledge and capacities to interpret radiology studies and some clinicians are even highly skilled in interpreting studies in their specific field of expertise. Many radiologists on the other hand work disconnected from the 'patient flow' and report studies on their own pace. Together with the development of intelligent computer systems the traditional role of radiologists becomes less and less meaningful. We as radiologists will need to reinvent ourselves in we want our profession to stay relevant and meaningful in the future.

Session Objectives:

1. To understand what challenges lie ahead.
2. To learn how to deal with these challenges.
3. To learn what you can do as a radiologist.

A-795 16:05

SWOT analysis of the radiologic profession

J.-Y. Meuwly; *Lausanne/CH (jean-yves.meuwly@chuv.ch)*

Since decades, radiology has to face up to multiple challenges to survive as an independent medical speciality. Existential questions surge from everywhere, inside and outside the medical profession. At the same time, technology improvements in radiology open every day new horizons and expand the frontiers of radiological venture. How to find one's way in the extreme complexity of this perpetually evolving world? How to keep one's identity and propose the adequate answers to these multiple challenges? The SWOT analysis brings tools to identify the internal and external factors that are favourable or unfavourable to achieve the specific objectives of the radiological profession. In the SWOT analysis, the internal factors of the organization, as the strengths (S) and weaknesses (W), and the external factors, like opportunities (O) and threats (T) are analysed on the light of the defined objectives. Identification of SWOTs clarifies the challenges and helps in planning how to achieve the objectives.

Learning Objectives:

1. To understand our strengths and weaknesses within the medical world.
2. To recognise opportunities.
3. To identify threats lying ahead.

A-796 16:28

Turf battles: how to respond to the challenges

C. Loewe; *Vienna/AT (christian.loewe@meduniwien.ac.at)*

Different turf battles within or around radiology are challenging, and the way how radiologists deal with these challenges will decide about the future of radiology and radiologists. The "invasions" into our radiological world include not only activities by other medical specialities, but even from the technical evolution within radiology. With further improvement of post-processing, big-data handling and image-guided diagnostic tools, radiology will look completely different in 10 years. If radiologists are not able to adapt to this evolution, they might be replaced. The change from detection to communication, integration and interpretation, describing an evolution from classic "technical" speciality into an integrative clinical speciality is required. Radiology already represents the processor of the modern hospitals, and radiologists are the trigger for clinical decision-making. Beside these challenges from inside there are continuous invasions from outside. However, with view from a distance, it becomes obvious that radiology invades other specialities as well. With every newly implemented minimally invasive treatment offered by radiology, we are competing with other medical specialities and open a new border for turf battles. As more successful such new methods are higher the interest to overtake them will be. This moving target of invasion and being invaded produces many turf battles in many different fields. In this presentation, different "burning" turf battles such as cardiac imaging, stroke treatment as well as vascular IR will be addressed. Although there is no general clue to survive, some possible strategies to further strengthen radiology and to compete with the challenges around will be discussed.

Learning Objectives:

1. To identify possible future invasions in our radiological world.
2. To learn how to deal with turf battles.
3. To learn how to change battles in opportunities.

Author Disclosure:

C. Loewe: Speaker; GE Healthcare, BRACCO, Medtronic.

A-797 16:51

Always on the forefront: ensuring the future of radiology

G.P. Krestin; *Rotterdam/NL*

Imaging is the key diagnostic tool in many diseases and has an important role in monitoring treatment and predicting outcome. As the practice of medicine moves away from an intuitive, experience-based model to empirical, evidence-based and to personalized medicine, diagnostic precision becomes paramount to select the particular treatment that will best help each individual patient. "Precision imaging" requires objective quantitative and standardized assessment of all features available in digital images. This "deep image phenotyping" is at the basis of radiomics and radio-genomics and allows to use the big image data for prediction, diagnosis and monitoring of disease. Deep machine learning using neural networks on large image data repositories will allow computers to take over much of the repetitive interpretation work carried out by radiologists in today's practice. Is the profession in danger? The threat to radiology as a distinct speciality can be overcome only by adapting and embracing this change. Focusing on technological innovation and on high-level super-specialized consulting services and less on image interpretation activities will guarantee the future of the profession. Research into new applications of imaging and value-based imaging are some of the solutions for proving the added value of radiologists in daily practice.

Learning Objectives:

1. To become familiar with new emerging radiological techniques.
2. To learn how to be ahead.
3. To safeguard the future of our profession.

Author Disclosure:

G.P. Krestin: Advisory Board; Zebra Medical Vision, Technion Israel Institute of Technology. Consultant; Bracco Imaging. Research/Grant Support; Siemens AG, GEHC, Bayer AG. Other; Supervisory Board of Quantib BV..

17:14

Panel discussion: The real challenge for radiologists is "how to change ourselves"

16:00 - 17:30 **Room G**

Physics in Medical Imaging

RC 1613
MR: artefacts and devices

A-798 16:00

Chairman's introduction

M. Tosetti; *Pisa/IT (michela.tosetti@fsm.unipi.it)*

The course intends to describe causes and cures of a variety of artefacts encountered in MRI: the purpose is to promote understanding them, so they can be prevented or properly interpreted to optimise diagnostic effectiveness. First, we learn about the artefacts raised from the MRI chain (static magnetic field uniformity; eddy currents resulting from imperfect gradient pulses; nonuniformity of the transmit RF system; defects in the receive portion of the RF system) and from sampling strategies of the MR signals (unwanted signals and noise spikes as zipper or banding artefacts; aliasing effects). We follow up analysing what happens in the presence of metallic implants, which gives rise to important artefacts in the images of patients. Such artefacts impair the information contained in the image, namely near the metallic device. The extent of the artefact is dependent on the object's magnetic susceptibility, size, shape, position in the patient's body, the technique used for imaging and the processing method. Last, the advance MR techniques are particularly sensitive either to artefacts related to the MR system but also to those produced by different sources of physiological noise. Furthermore, it is also necessary to

look closely to the pitfalls in the analysis pipelines, which ultimately lead to the robustness of the advance MR studies. Recognise and understand artefacts encountered in MRI, together with the knowledge of the imaging and post-processing strategies to mitigate or treat them, will allow audience to obtain robust data to make sound interpretations and to do not lead to diagnostic errors.

Session Objectives:

1. To learn about MR image distortions.
2. To appreciate the appearance of metal-induced image distortions in MRI.
3. To appreciate image distortions in perfusion- and diffusion-weighted imaging.

A-799 16:05

A. Image artefacts in MRI and their mitigation

D.J. Lurie; *Aberdeen/UK (d.lurie@abdn.ac.uk)*

No imaging modality can reproduce the original object under study in a completely faithful manner because all imaging technology is susceptible to artefacts. It is very important that the sources of artefacts are understood so that the fidelity of images can be maximised. Artefacts in MRI can be discussed according to their primary source, under the following four categories. (a) Physics: artefacts include those arising from magnetic susceptibility differences, often around tissue/air interfaces, and chemical-shift artefacts, at fat/water boundaries. These effects can be mitigated by manipulation of gradient strengths and directions, and sampling bandwidths. (b) Hardware: examples include RF or gradient miscalibration or instability, leading to image shading and ghosting; RF interference, causing zipper artefacts; gradient nonlinearity, causing geometric distortion. These issues can be addressed by careful calibration and quality control procedures, and sometimes by post-processing. (c) Pulse sequence: this includes artefacts due to aliasing and slice-overlap shading (slice cross-talk); these can usually be reduced by careful setting of gradient directions and acquisition parameters. Other artefacts arising from pulse sequences are related to signal sampling and Fourier transformation, including Gibbs ringing artefacts at boundaries. (d) Physiological: artefacts can arise due to regular motion of the heart, or of abdominal organs during the breathing cycle. Mitigation is by gating, breath-holding and the use of rapid pulse sequences. Irregular, involuntary motion such as peristalsis in the gut can also lead to ghosting artefacts, which can be reduced by the administration of pre-scan medication and by ultra-rapid MR pulse sequences.

Learning Objectives:

1. To identify common types of artefacts in MR images.
2. To learn about the physical origins of artefacts in MRI.
3. To learn methods of minimising artefacts on MR images.

A-800 16:28

B. Imaging around metal implants: artefact reduction in MRI

C. McGrath[1], A. Fagan[2]; [1]*Belfast/IE,* [2]*Dublin/IE*

The presence of metallic implants within a patient distorts the main static magnetic field of an MRI scanner and can lead to very severe image artefacts that may render the resultant images non-diagnostic. The physics behind these artefacts is described. Acquisition parameter changes, such as matrix size, receive bandwidth and pulse sequence choice, are described that can reduce the impact of these artefacts and improve the diagnostic quality of these scans. Advanced metal artefact reduction techniques are also discussed.

Learning Objectives:

1. To review the origin of signal in MRI.
2. To understand the MRI physics of artefact reduction around metal implants.
3. To understand the parameters used in an optimised imaging protocol.

Author Disclosure:

C. McGrath: Speaker; GE: Invited speaker at 2 GE MRI symposia (honoraria recieved). Other; Bayer: Regional MRI education day sponsored (venue, catering and printing) by Bayer, twice and one upcoming, Bayer: assistance to attend ECR 2016.

A-801 16:51

C. Artefacts in perfusion and diffusion MRI

I. Tsougos; *Larissa/GR (tsougos@uth.gr)*

Accurate brain damage diagnosis plays an essential role in the selection of the optimum treatment strategy, as the nature of the damage and the definition of nature and grade defines the therapeutic approach. Advanced magnetic resonance imaging (MRI) techniques have added incremental diagnostic information regarding brain damage characterisation over conventional MRI alone. Particularly, diffusion-weighted imaging, diffusion tensor imaging and perfusion imaging provide, non-invasively, significant structural and functional information in a microscopic level, revealing aspects of the underlying pathophysiology. Although over the last 10 to 20 years, diffusion and perfusion MRI have become established techniques with a great impact on differential diagnosis, like any other MRI technique they remain subject to artefacts and pitfalls. Hence, it is evident that obtaining reliable data and drawing meaningful and robust inferences is of utmost importance. The current exhibit aims to: review the artefacts and pitfalls of diffusion MRI on a qualitative basis, especially in terms of eddy currents and sensitivity to motion; review and evaluate the possible issues that can affect the accuracy of measurements regarding dynamic susceptibility contrast (DSC)-MRI (measurements of cerebral blood flow (CBF), cerebral blood volume (CBV), and mean transit time (MTT)). Introduce possible strategies that have been developed to mitigate or overcome these artefacts and pitfalls.

Learning Objectives:

1. To review the artefacts and pitfalls of diffusion MRI on a qualitative basis, especially in terms of eddy currents and sensitivity to motion.
2. To review and evaluate the possible issues that can affect the accuracy of measurements regarding dynamic susceptibility contrast (DSC)-MRI (measurements of cerebral blood flow (CBF), cerebral blood volume (CBV), and mean transit time (MTT)).
3. To introduce possible strategies that have been developed to mitigate or overcome these artefacts and pitfalls.

17:14

Panel discussion: Clinically applicable tools/strategies for minimising/avoiding MR imaging artefacts

16:00 - 17:30 **Room K**

EFRS Workshop

EFRS authorship and reviewer workshop

A-802 16:00

Chairman's introduction: Establishing the evidence base in radiology and radiography

G. Paulo; *Coimbra/PT (graciano@estescoimbra.pt)*

A profession is defined by the Australian Council of Professions as a disciplined group of individuals who adhere to high ethical standards and uphold themselves to, and are accepted by, the public as possessing special knowledge and skills in a widely recognised, organised body of learning derived from education and training at a high level, and who are prepared to exercise this knowledge and these skills in the interest of others. Radiography profession adheres to all the principals expressed in the definition. However, it is important to understand that the development of the radiographer specific field of knowledge is only possible through research and that research is only accepted and adopted by the peers, if published: “It doesn’t exist if it isn’t written down”. The invited speakers for this session will give an overview about the reasons why we should publish; on how to select the most adequate journal; the ethical principles of publication; an explanation about the reviewer process and finally some tips on how to increase the success of acceptance. At the end of this session, an interaction is expected with the audience to discuss the solutions to increase the research and publications in the field of medical imaging and radiotherapy.

Session Objectives:

1. To consider why publishing is important for the development of radiology and radiography.
2. To highlight the value of collaboration in medical imaging research.

A-803 16:05

Why publish your work?

F. Zarb; *Msida/MT (francis.zarb@um.edu.mt)*

Research is the contribution to the body of knowledge in a particular area/expertise. Any research finding, if contributing to this body of knowledge, should be shared and made available to fellow professionals. One of the ways of sharing this body of knowledge is through publication. Publication is the process of producing written material and making it available to others. The aim of this presentation is to highlight the importance of publishing for both the individual researcher/practitioner and to the clinical/academic departments they represent. The publication process may not always seem easy and straightforward, requiring a commitment and perseverance in the work it entails. However, the benefits and satisfaction associated with getting work accepted for publication outweigh the hard work involved.

Learning Objectives:

1. To explore the importance of publishing for individual researchers and practitioners.
2. To explore the importance of publishing for clinical and academic departments.

A-804 16:20

Journal selection: aims and scope, audience and metrics

J.M. Nightingale; *Salford/UK (j.nightingale@salford.ac.uk)*

A wide selection of professional peer-reviewed journals are available to radiography and radiology authors and researchers. Selecting the most appropriate journal for a particular article will depend upon many factors, the most important being the aims of the journal and the size and scope of the readership. A high-quality article will be of little value if it is never read by people who can potentially use it to develop knowledge or effect change. Journal selection may also be influenced by a number of metrics which can be used to indicate the impact or influence of a journal on the professional field. This presentation will explore the strengths and limitations of a range of traditional and contemporary citation-based metrics that are often used for journal comparisons.

Learning Objectives:

1. To highlight the classifications of journals available to radiography and radiology authors (generalist, specialist and methodological).
2. To consider the benefits and limitations of publishing in different journal formats.
3. To explore the role of traditional (Impact Factor) and contemporary journal metrics in demonstrating impact, speed and reach of a journal.

A-805 16:35

Ethics of publishing

J. McNulty; *Dublin/IE (jonathan.mcnulty@ucd.ie)*

The publication of our research in peer-reviewed journals is a fundamental step in contributing to the body of professional knowledge which may then contribute to evidence-based professional practice. When submitting an article to a journal for consideration for publication the authors have a number of responsibilities in terms of publishing ethics. These considerations go beyond the ethical considerations within the research itself and associated ethical approvals or exemptions. For the purpose of this presentation the topics of authorship, originality and plagiarism, data access and retention, multiple or concurrent publication, disclosures and conflicts of interest, and acknowledgements (of sources, limitations and errors) will be briefly explored. Plagiarism, often due to inappropriate citation, can vary significantly in severity and is readily detected by journals. What constitutes a potential conflict of interest must also be considered by authors in the name of transparency and objectivity. It is important that all authors are aware of these ethical issues and novice authors should make sure that they are fully informed by following guidelines and through good mentorship by senior colleagues and co-authors. It is also important to note that the editor and reviewers handling a particular submission must also adhere to guidelines on publication ethics.

Learning Objectives:

1. To understand the ethical implications of article authorship.
2. To consider the nature of plagiarism in publishing and how it can be avoided.
3. To highlight potential conflicts of interest and how these should be managed and declared.

Author Disclosure:

J. McNulty: Board Member; Associate Editor, Radiography journal (Elsevier).

A-806 16:50

Things to consider: the reviewer's perspective

A. England; *Salford/UK (A.England@salford.ac.uk)*

Undertaking a review of a journal article is a serious but rewarding task. There are many personal benefits but a high-quality review is also a valuable contribution to the profession and of importance to the authors. From a personal perspective, undertaking a review can help generate understanding of what the requirements of a journal article are. It allows the reviewer to develop an understanding of the art of journal manuscript writing. For the author, the reviewer provides an important role in giving feedback on both the good and bad elements of the manuscript but ultimately how it can be improved. If this is via a recommendation to accept the paper, then the role of the reviewer is to provide feedback and and a list of tasks which allow the manuscript to reach its full potential. If the decision is to reject, then it is down to the reviewer to provide some justification and direct the authors appropriately for any future submissions. This may include details of any changes needed in the research design and manuscript structure. Ultimately, it is a balance of aiming for high-quality manuscripts whilst providing the readership with new information which is likely to positively influence the profession and clinical practice. Reviewing a journal article is a skill and with experience this can develop into a significant contribution for developing authors and support the publication of high-quality research papers.

Learning Objectives:

1. To identify the purpose of peer review.
2. To explain the steps within the peer review process.
3. To understand the qualities of a good reviewer.

A-807 17:05

Editor's ten top tips for publishing success

J.M. Nightingale; *Salford/UK (j.nightingale@salford.ac.uk)*

The peer review process is a well-established method of improving the quality of articles published within a journal. Very few articles will be accepted at first submission; the majority will require either minor or major revision to bring them to the standard required of the journal. This will often require more work for the authors and will delay the publication of the article, but the published article will be of better quality than the original submission. However, for some papers the editor makes a decision to reject the manuscript before sending it for peer review, or they reject it following peer review because the revisions required are significant. This presentation explores the most common reasons why a paper may be rejected before and after peer review, and offers some simple guidelines to help authors to avoid the common errors and pitfalls. The presentation concludes with a reminder of the author's responsibilities in ensuring that their published article is promoted widely.

Learning Objectives:

1. To discuss reasons why a manuscript may be rejected.
2. To emphasise how common manuscript errors can be avoided.
3. To highlight the author's responsibilities in promoting their article.

17:15

Panel discussion: What are the barriers to publishing your research or becoming a reviewer and how can they be overcome?

16:00 - 17:30 **Room M 2**

Computer Applications

RC 1605

Will the good old PACS disappear?

A-808 16:00

Chairman's introduction

D. Regge; *Turin/IT (daniele.regge@ircc.it)*

Picture Archiving Communication Systems (PACS) have originally been conceived as local archives of medical images originating from different modalities interconnecting using DICOM, a universal format for image storage and transfer. This course will approach the changing world of PACS pragmatically, by providing helpful information and tips on when and how to implement a new PACS system and how to perform data migration safely even in complex environmental conditions. The course will include an overview of different cloud healthcare solutions and on how to improve interconnectivity by the implementation of vendor-neutral archiving systems. PACS has paved the way to the filmless department, but a paperless department is still a long way off. Advantages and challenges of a truly paperless infrastructure will be discussed in this course.

Session Objectives:

1. To explain when and how to replace PACS.
2. To provide insight on how to improve interconnectivity and information sharing in medicine.
3. To envisage the role of off-site archiving solutions in radiology.

Author Disclosure:

D. Regge: Author; Springer. Speaker; GE Medical Systems, GE Medical Systems.

A-809 16:05

A. It's time for PACS replacement: how-to guide, recommendations and pitfalls

S. Morozov; *Moscow/RU (npcmr@zdrav.mos.ru)*

PACS has made a great progress from a pure storage and a radiologist's tool to a platform for interdisciplinary collaboration and big data analysis. It has allowed transition from analogue to digital workflow and further in the direction of decentralized enterprise clinical imaging. Major drivers for PACS development are expansion of imaging into clinical areas, EHR integration, and radiological practices consolidation on regional and international levels. The major trends of PACS development are the following: cross-functionality, cross-integration, patient-centric solutions and analytic tools development. Any PACS with a lack of standardization, workflow optimization and comprehensive viewing tools limits interoperability and efficiency of a radiology practice. PACS should enable communications, feedback, collaboration, second opinion, report

interpretation, clinical integration, tumour board applications, reports dispersal to patients, and tracking of outcomes. It should be affordable, faster, integrated with voice recognition, EMR and prior studies. The typical lifetime of a PACS is 7-10 years. New PACS selection process considers in-house or cloud-based solutions, VNA, modular approach, division of storage/diagnostics functionality. Capital costs for a new PACS purchase should be justified in terms of productivity increase and return of investment. New PACS adoption includes resource, workflow and cut-over planning, risk assessment, test version installation, integration, implementation, data migration and changeover. Major pre-requisites for a successful PACS installation are planning, standardization, team involvement, iterative testing, over-communication, feedback analysis and correction.

Learning Objectives:

1. To explain why and when PACS should be replaced.
2. To provide recommendations for PACS replacement and risk assessment analysis including image migration issues.
3. To give a practical example of how PACS is replaced in a large health facility or region.

Author Disclosure:

S. Morozov: Advisory Board; Philips. CEO; Radiology research and practice center, Moscow.

A-810 16:28

B. The paperless radiology department

C. Heilmaier; *Zurich/CH (christina.heilmaier@triemli.zuerich.ch)*

Within the last 30 years, radiology underwent tremendous changes. The implementation of radiology information systems (RIS), picture archiving and communication systems (PACS), and electronic health records (EHR) has considerably altered the workflow and cleared the way for an (almost) paperless radiology department. The next step within the electronic environment is to further improve the interoperability of one system with another to achieve a seamless communication, data exchange and interactivity (e.g. dose information from dose management software is automatically added to image report, which is automatically sent to EHR). At the same time, the electronic environment enables the formation of imaging portals, so that patients can access their health data. This might motivate them to fully participate in their healthcare and might increase their satisfaction, medical knowledge and self-care. However, as shown by recent experience, not only transition from hard-copy practice to a paperless department but also improving the interoperability of different systems comes along with many challenges. To name just a few, it needs to be assured that all modalities are digital-ready, that the department has the required infrastructure and that the management of the electronic environment is clearly structured to address issues such as data correction and user support. The major problem in establishing data exchange between different systems (and also between different radiology departments) is that standards are often not uniform. While, for example, for PACS the DICOM 3 standard is nowadays broadly accepted, sometimes multiple standards are available to accomplish a given task, which considerably impairs interoperability.

Learning Objectives:

1. To provide reasons to give patient direct access to their medical imaging data.
2. To describe the challenges and infrastructure needed to implement an imaging portal.
3. To discuss first experiences and lessons learned.

A-811 16:51

C. Does PACS into the cloud means PACS evaporates?

J. Schillebeeckx; *Knokke/BE (jan@schillebeeckx.com)*

Cloud computing is a model for enabling ubiquitous on-demand network access to a shared pool of computing resources that can be rapidly provisioned with minimal management effort or service provider interaction. This cloud model is composed of five essential characteristics, three service models, and four deployment models. Service models are provision models of applications, hardware, software, data, operation systems, telecom, etc. managed by external parties in the cloud. The three types of service models are Software as a Service (SaaS), Platform as a Service (PaaS) and Infrastructure as a Service (IaaS). Deployment models mean different environments (clouds) where different service models are located. The characteristics of those four types of environment are the private cloud, the community cloud, the public cloud and as a combination, the hybrid cloud. PACS in the cloud has several advantages and weaknesses. Clear advantages are less upfront costs, access to on-demand capacity, reliable back-up and recovery, easier management of IT staff and better financial planning. Weaknesses are performance, data migration and portability of data. Most likely PACS will not evaporate but become a game player in the enterprise imaging model.

Learning Objectives:

1. To explain the concept of cloud archiving and its advantages.
2. To address limitations and risks of cloud PACS solutions.
3. To give insight on future developments of cloud technology.

Author Disclosure:

J. Schillebeeckx: Advisory Board; NDSC Europe. Consultant; Agfa Healthcare. Shareholder; Qaelum NV.

17:14

Panel discussion: How will increased interconnection affect radiologists' day-to-day life?

16:00 - 17:30 **Room M 3**

E³ - ECR Master Class (Molecular Imaging)

E³ 1626

Molecular imaging in oncology

A-812 16:00

Chairman's introduction

K. Nikolaou; *Tübingen/DE (Konstantin.Nikolaou@med.uni-tuebingen.de)*

Today, radiology is playing a central role in the set-up of multidisciplinary cancer centres and in the comprehensive work-up of oncologic patients, integrating an ever increasing amount of qualitative and quantitative diagnostic information. Still, radiology is facing significant challenges, as “precision medicine” develops and matures. Integrating functional and molecular information in a quantitative fashion and adding complementary multimodality information is crucial. In detail, molecular imaging is regarded as the direct or indirect non-invasive monitoring and recording of the spatial and temporal distribution of in vivo molecular, genetic, and/or cellular processes for biochemical, biological, diagnostic, or therapeutic applications. Molecular images that indicate the presence of malignancy can be acquired using an abundance of modalities, including optical, ultrasonic, radiologic, radionuclide, and magnetic resonance techniques. In this session, molecular and functional imaging of oncologic processes are reviewed with respect to their physical basics and imaging characteristics, including attributes of hypoxia, proliferation, and metabolism. Also, the role, development and standardisation of prognostic, predictive and therapy response oncologic imaging biomarkers will be discussed, and current and future clinical applications in oncologic diagnosis will be reviewed.

Session Objectives:

1. To understand the basics of molecular imaging.
2. To appreciate the unmet needs of oncological imaging.
3. To learn the role of molecular imaging in oncology.

A-813 16:05

A. Imaging of hypoxia

V.J. Goh; *London/UK (vicky.goh@kcl.ac.uk)*

Tumour hypoxia is present in up to 60% of locally advanced solid tumours. Tumour hypoxia is a significant challenge to successful therapy, contributing to treatment resistance and a poor prognosis. Intra-tumoural hypoxia may be assessed by molecular markers including hypoxia inducible factor 1 (HIF-1) and carbonic anhydrase isoenzyme IX (CA-IX). However, hypoxia is a dynamic process and alters depending on perfusion and oxygenation status. Non-invasive imaging of intra-tumoral hypoxia provides an opportunity to better stratify patients to improve local control. Tumour hypoxia may be assessed in vivo by direct and indirect imaging techniques. Positron emission tomography (PET) imaging targets hypoxic cells with tracers including18F-fluoromisonidazole (18F-MISO), 18F-fluoroazomycin arabinofuranoside (18F-FAZA) and 64Cu-diacetyl-bis(N4-methylthiosemicarbazone (64Cu-ATSM). Hypoxia imaging may also be undertaken by magnetic resonance imaging (MRI) with techniques such as blood oxygenation level-dependent (BOLD) MRI and oxygen enhanced MRI measuring R2* and R1 changes, respectively. This lecture will review the biological basis and fundamentals of hypoxia imaging and potential clinical applications including radiotherapy.

Learning Objectives:

1. To review the fundamentals of hypoxia imaging.
2. To review the advantages and disadvantages of hypoxia imaging and its relation to perfusion.
3. To learn about hypoxia imaging in radiation treatment.

Author Disclosure:

V.J. Goh: Research/Grant Support; Siemens Healthcare, GE Healthcare. Speaker; Lilly, Bayer Healthcare.

A-814 16:23

B. Imaging of proliferation

A. Kjaer; *Copenhagen/DK*

"No abstract submitted."

Learning Objectives:

1. To understand basic principles of proliferation imaging.
2. To become familiar with imaging of proliferation.
3. To learn about difficulties in liver proliferation imaging.

A-815 16:41

C. Imaging of metabolism

C. Nanni; *Bologna/IT (cristina.nanni@aosp.bo.it)*

18F-FDG PET/CT is an imaging technique that is aimed to evaluate glucose metabolism of tissues and organs. PET/CT scanners consist of a combination of a PET scanner and a CT scanner providing both morphological and functional images. The procedure is standard and includes several steps. Patients are not allowed to consume any food or sugar for at least 6 h prior to the start of the PET study. Injection should be fully intravenous. Optimal uptake time is 60 minutes. In general, for a 3D system and 3 MBq/Kg of FDG, 2 min/bed position is enough, leading to an average overall acquisition time of 14 minutes. Low-dose CT (120 kV, 80 mA) is necessary both for attenuation correction and for image interpretation. Once reconstructed, images must be interpreted on a dedicated workstation. SUV max based on body weight is the standard semi-quantitative index. FDG PET/CT was proved to be accurate for several malignancies for the definition of TNM at staging and in the suspect of relapse. Furthermore, changing in SUV max are related to the response to systemic therapies, both during and after treatment. This parameter is considered a non-invasive surrogate for therapy assessment. Some particular kinds of malignant tumours are not detectable by FDG PET. In particular, mucinous cancers, transitional cell cancers, clear cell cancers, indolent HCC and some adenocarcinomas fail to significantly concentrate FDG. Low accuracy can also be found in some particular areas of the body where FDG is physiologically concentrated such the brain and the urinary tract.

Learning Objectives:

1. To learn the clinical indications for FDG imaging.
2. To become familiar with imaging protocol.
3. To learn about difficulties in FDG imaging.

A-816 16:59

D. Biomarker imaging with MR

M.E. Mayerhöfer; *Vienna/AT (marius.mayerhoefer@meduniwien.ac.at)*

Originally regarded as a morphological imaging technique with excellent soft-tissue contrast, MRI today is recognised as a technique that can also provide functional biomarkers through different approaches. For treatment response assessment, diffusion-weighted imaging (DWI), which indirectly provides information on cell density in tumours, is quite well-established. In lymphoma, for instance, it is even considered as an alternative to [18F]FDG-PET after treatment with chemo- or immunochemotherapy. Nevertheless, limitations for DWI include artefacts and standardisation of apparent diffusion coefficients between different DWI pulse sequences, and between MR scanners of different vendors. Perfusion-weighted imaging (PWI) is another technique that is increasingly being used in the response evaluation of hypervascular tumours, such as hepatocellular carcinoma. In the body, PWI is most commonly performed on the basis of dynamic contrast-enhanced sequences (relying on T1 shortening), with k-trans, a measure of capillary permeability, as one of several quantitative parameters. Alternatively, PWI may be performed using arterial spin labelling, without contrast media. MR spectroscopy (MRS), which today is most frequently based on protons, is another technique that can be used to assess biomarkers in the form of metabolites, such as lactate and choline. While several studies reported encouraging data, for instance in breast cancer and prostate cancer, limitations such as long acquisition times and difficulties in terms of standardisation and quantification have prevented MRS from being introduced into routine clinical imaging. Cutting-edge techniques, such as chemical exchange saturation transfer (CEST) imaging, may overcome the limitations of MRS.

Learning Objectives:

1. To learn the clinical indications for biomarker imaging.
2. To become familiar with quantification.
3. To learn about difficulties in quantification.

17:17

Panel discussion: The pros and cons of molecular imaging in oncology

16:00 - 17:30 **Room M 4**

E³ - ECR Academies: Multiparametric Ultrasound (MPUS)

E³ 1620

Multiparametric US in musculoskeletal applications

A-817 16:00

Chairman's introduction

P. Peetrons; *Brussels/BE*

A-818 16:05

A. Sports-related lower extremity injuries

P.J. O'Connor; *Leeds/UK*

"No abstract submitted."

Learning Objectives:

1. To learn about muscle and tendon injuries in athletes.
2. To know how to perform MPUS in this setting and how to interpret findings.
3. To understand the advantages and limitations of US compared to MRI.

A-819 16:33

B. Entrapment neuropathies of extremity nerves

H. Gruber; *Innsbruck/AT (hannes.gruber@i-med.ac.at)*

Entrapment neuropathies are rather frequent issues: the “standard” neuropathies in this field are clinically fast forward and “standard” measures are to be taken to solve the typical clinical problem. So why do we need imaging and why should one modality be superior in comparison to another (e.g. sonography vs. MRI)? What are features of interest or features relevant for further therapy and prognosis? In this rather wide field, however, tricky features and constellations can be depicted sometimes using, e.g. a functional access to a pretended “banal” problem (“Do the right thing at the right time”): I will try to present the banal and the special imaging to provide a more profound knowledge and understanding of radiologic options and relevance of imaging entrapment neuropathies.

Learning Objectives:

1. To learn imaging anatomy of entrapment neuropathies.
2. To become familiar with the specific US techniques and US findings in this setting.
3. To know the advantages and limitations of US compared to MRI.

A-820 17:01

C. Inflammatory joint disease

A. Klauser; *Innsbruck/AT*

The standard for diagnosing and differentiating arthritis is based on clinical examination, laboratory exams, and imaging findings. B-mode ultrasound (US) and PDUS are established imaging modalities for early detection, characterisation and follow-up of various forms of inflammatory arthritis. They allow for detection and characterisation of synovial thickening, synovial proliferation, destructive pannus, effusion, erosions and enthesitis. PDUS allows a further assessment of synovitis and erosions by classifying them into active versus nonactive, what has implication for therapy. CEUS (contrast-enhanced US) with and without the use of quantification, such as parametric mapping of contrast uptake is an emerging sensitive tool for assessing vascularization and disease activity at the angiogenetic level with the possibility of quantitative assessment performed at the region of interest level. Beside intraarticular inflammatory changes also periarticular and extraarticular inflammation in terms of tenosynovitis and enthesitis assessment are of importance. SEL (sonoelastography) has a proven role in tendon assessment and might give new insights into enthesitis. A summary and analysis of the current evidence on the role of multiparametric ultrasound in the assessment of inflammatory joint disease will be presented.

Learning Objectives:

1. To learn how to apply various US techniques in inflammatory joint disease.
2. To understand the indications, contraindications, challenges and limitations US in the specific clinical setting.
3. To know the advantages and disadvantages of US compared to XR, CT and MRI.

16:00 - 17:30 **Room M 5**

E³ - ECR Academies: Neuroradiology: from Morphology to Function

E³ 1622
Functional imaging of the spine

A-821 16:00
Chairman's introduction
D. Balériaux; *Brussels/BE (dbaleri@me.com)*

When considering "spine" for functional imaging very different areas may be studied: the spinal cord proper, well protected in a bony canal, surrounded by CSF and the spinal column. Imaging the spinal cord has been very challenging and the functional aspects remain even more challenging. Still, recently, diffusion-based imaging provides a new in vivo inside information of the spinal cord. MRI and its sensitivity to flow allows better information about CSF flow. Finally, the spinal bony structures are continuously solicitated to enable movement of the human whilst assuring protection of the nervous structures. Dynamic MRI helps in analysing spinal movements in an unmatched noninvasive manner. In this session those different aspects will be discussed. A tricky though simple case of a conus medullaris lesion associated with a lumbar fracture will be discussed emphasizing the necessity to know the clinical history of the patient as always to achieve the right diagnosis.

A-822 16:06
A. Measuring CSF flow: technique and clinical usefulness
B. Ertl-Wagner; *Munich/DE (Birgit.Ertl-Wagner@med.uni-muenchen.de)*

The cardiac cycle is the motor of cerebrospinal fluid (CSF) flow. During systole, there is an inflow of volume into the cranial vault. As the skull is nearly rigid, a compensatory downward flow of CSF ensues. During diastole, there is an upward flow of CSF from the spinal canal into the cranial vault with a nearly simultaneous venous outflow. Using MR phase contrast sequences, it is possible to quantify and assess the direction of CSF flow and the arterial inflow and venous outflow. When measuring flow, it is important to acquire the imaging planes perpendicular to the main axis of flow. Branching vessels or vascular loops should be avoided. Moreover, the velocity encoding (VENC) needs to be carefully chosen to ascertain a reliable quantification of flow and to avoid aliasing. To measure aqueductal flow, the measurement plane should be positioned perpendicular to the aqueduct. This also enables the quantification of the aqueductal net flow and an estimation of the CSF production rate. To quantify the cerebrospinal CSF volume shift, the imaging plane should be positioned at the level of C2 above the most cranial pair of exiting nerve roots. When combining the measurements of arterial inflow and venous outflow to and from the cranial vault as well as the craniospinal volume shift, the intracranial pressure can be estimated. Chiari malformations can lead to an impaired craniospinal CSF flow. The assessment of CSF flow parameters can be combined with the evaluation of morphological parameters to enhance diagnostic decision making.
Learning Objectives:
1. To review the physiology of CSF flow during the cardiac cycle.
2. To evaluate the reliability of the quantification of CSF flow rates by use of phase contrast MRI.
3. To show examples where alterations of CSF flow in the craniocervical junction can influence clinical management (e.g. in patients with Chiari Malformation Type I).

A-823 16:34
B. Diffusion tensor imaging of the spinal cord in the assessment of intramedullary changes
M. Sasiadek; *Wroclaw/PL (marek.sasiadek@umed.wroc.pl)*

Conventional MRI sequences provide limited information of the spinal cord pathology. Diffusion tensor imaging (DTI), including tractography (DTT), might improve qualitative and quantitative assessment of the spinal cord lesions. DTI is based on anisotropic, one-direction diffusion, which theoretically is ideally suited to imaging of the spinal cord. However, due to the small size of the spinal cord and many artefacts, obtaining a good quality spinal cord DTI is a challenge. Fortunately, technical improvements (e.g. parallel imaging, decrease of slice thickness, increased number of diffusion directions, use of 3T MR) have improved the quality of DTI images. The main clinical applications of the spinal cord DTI include degenerative myelopathy, intraspinal tumours, spine trauma, demyelinating and inflammatory diseases of the spinal cord. In degenerative disease of the spine DTI can detect, on the base of fractional anisotropy (FA), mean diffusivity (MD) or average diffusion coefficient (ADC) metrics, myelopathic changes, not visible on plain MRI and correlated with the degree of spinal canal stenosis and spinal cord compression. In traumatic spinal cord injury DTI can evidence changes in the spinal cord at and away the site of trauma. In intraspinal tumours DTI and DTT are helpful in differentiation compression from infiltration of the spinal cord adjacent to tumour. In multiple sclerosis and other demyelinating diseases DTI metrics might detect changes in normal appearing spinal cord. The advantages of spinal cord DTI described above should increase the role of this technique in diagnosis, prognosis and follow-up of the spinal cord diseases.
Learning Objectives:
1.To review the technique of diffusion tensor imaging (DTI) in the assessment of the spinal cord.
2.To document the usefulness of DTI in the detection of cervical spinal cord integrity alterations in different stages of degenerative spine disease.
3.To discuss the value of DTI in other diseases of the spinal cord.

A-824 17:02
C. Dynamic MR lumbar evaluation in degenerative spine disease
M. Muto; *Naples/IT (mutomar2@gmail.com)*

Thanks to its peculiarity in recognizing soft tissues pathologies entailing articular structures and nerve roots, great interest emerged in the last two decades on new MR scanners able to perform dynamic acquisitions in upright. Dynamic MR allows a correct evaluation of structures involved in lumbar back pain due to radicular conflict and spondylolisthesis; in supine position relevant factors can be underestimated or hidden and become evident only patient standing upright. Lumbar lordotic angle, flavum ligament thickness, herniated discs, spinal canal area, spinal canal and dural sac antero-posterior diameters and spinal alignment can be measured and compared in both supine and upright positions. The standard protocols include supine standing: sagittal T1- and T2-weighted turbo spin echo, sagittal short tau inversion recovery and axial T2-weighted turbo spin echo; upright standing: sagittal turbo spin echo T2-weighted and axial turbo spin echo T2-weighted turbo spin echo. This technique entails some limitations: low-field magnet, long scanning time, difficulty in evaluating the most lateral areas of the spine. This presentation aims to discuss technical aspects, advantages and disadvantages of dynamic MRI, supported by illustrative case studies.
Learning Objectives:
1. To provide technical information on how to perform dynamic MRI of the lumbar spine.
2. To discuss the advantages and disadvantages of dynamic MRI, as compared with static MRI.
3. To document the added value of dynamic MRI of the lumbar spine in selected, illustrative case studies.

Sunday, March 5

08:30 - 10:00 **Room A**

E³ - ECR Academies: Interactive Teaching Sessions for Young (and not so Young) Radiologists

E³ 1721
Brain tumours

A-825 08:30
A. Paediatric brain tumours
M.I. Argyropoulou; *Ioannina/GR (margyrop@cc.uoi.gr)*

Primary brain tumours in childhood are the second most common malignancy after leukaemia. The presenting symptoms depend on age with macrocephaly and failure to thrive in infants and headache, morning vomiting, diplopia, ataxia motor and sensory deficits, seizures endocrinological symptoms in older children. Brain tumours may be of glial origin (astrocytomas, ependymomas), neuronal or neuroglial (gangliogliomas, gangliocytomas, DNET), embryonal (PNET, ATRT) and from germ cells (germinomas, teratomas). Tumours arising in the sellar and parasellar region (craniopharyngiomas, hypothalamic hamartomas and pituitary adenomas) may also occur. Neurinomas and meningiomas are rare in children arising mainly in the context of neurofibromatosis type II. Secondary brain tumours arise mainly from CSF seeding while haematogenous metastases are rare. MRI is the modality of choice to for the diagnostic workup of brain tumours. Imaging protocols may include T2W, T1W plain and contrast-enhanced images, diffusion tensor imaging, dynamic susceptibility-weighted contrast-enhanced perfusion imaging (DSC), functional MRI (fMRI) and MR spectroscopy (MRS). Brain tumours may be heterogeneous with cystic and solid components. The latter appears with low signal on T1W and high signal on T2W images. A low signal intensity on T2W images associated with restricted diffusion and increased perfusion indexes on DSC may be suggestive of a more aggressive tumour. Increased choline and lactate and decreased N-acetyl aspartate in MRS is also suggestive of malignant tumours. Tractography and f-MRI are useful for preoperative evaluation to assess major white matter tracts and eloquent areas of the brain related with the tumour.

Learning Objectives:
1. To become familiar with different paediatric brain tumours.
2. To learn the imaging criteria for differentiation.

A-826 09:15
B. Adult brain tumours
P.C. Maly Sundgren; *Lund/SE (Pia.Sundgren@med.lu.se)*

Glioblastomas are the most common malignant neoplasms and together with metastatic tumours comprise half of all malignant tumours in the adult population. The latest WHO classification is from 2016 and several changes has occurred with respect to classification of brain tumours. The grading of tumours presumes biological behaviour or phenotype of a lesion and is of high importance clinically by guiding therapy selection: adjuvant radiation, chemotherapy, surgical or palliative treatment of brain tumours. MRI is considered the standard modality for diagnosis and prognosis of brain tumours, based primarily on gadolinium (Gd) enhancement. However, this concept has become more and more challenging due to the fact that not all high-grade gliomas demonstrate Gd enhancement while low-grade tumours might enhance in up to 30% of the cases. This lecture will review the more common primary and secondary brain tumours in adults, their imaging characteristics on CT and MRI. The use of advanced imaging for diagnosis and treatment follow-up will be discussed.

Learning Objectives:
1. To become familiar with the different types of brain tumours.
2. To learn the imaging criteria for differentiation.

08:30 - 10:00 **Room B**

Abdominal Viscera

RC 1701
IgG4-related disease: what is it and what do I need to know?

A-827 08:30
Chairman's introduction
S.A. Jackson; *Plymouth/UK (simon.jackson1@nhs.net)*

IgG4-related disease represents a systemic fibro-inflammatory condition, which includes autoimmune pancreatitis. The condition was first reported in 2003 by Kamisawa and colleagues and during the same year autoimmune pancreatitis was also sub-classified into two histologically separate sub-types, with the “classical” type 1 form comprising part of the IgG4-related disease spectrum. Multiple modality imaging plays a central role in the diagnosis of both pancreatic and extra-pancreatic disease involvement which can affect multiple organs. This session will review the systemic manifestations of IgG4-related disease, including both pancreatic and hepatobiliary findings. In particular, various tips and tricks will be presented, to aid a confident imaging diagnosis in patients with IgG4-related disease.

A-828 08:35
A. Pancreatic manifestations
R. Pozzi-Mucelli; *Verona/IT (roberto.pozzimucelli@univr.it)*

The pancreatic manifestation of IgG4-related disease is autoimmune pancreatitis (AIP) which represents a distinct form of chronic pancreatitis. Histologically, AIP is characterised by a dense lymphoplasmacytic infiltrate of mainly CD4+ T lymphocytes and immunoglobulin G4 plasma cells, located around the pancreatic ducts with mass-forming regions of fibrosis. AIP has been classified into focal or diffuse forms. The differential diagnosis between focal AIP and pancreatic adenocarcinoma represents a medical need, since AIP responds to steroid therapy and surgery should be avoided. CT and MRI findings of AIP are characterised by an enlargement of the gland, either focal or diffuse. In CT, the affected areas are isodense before contrast enhancement, hypodense (due to hypovascularity) in the arterial phase with progressive increase in density in the venous and late phases following contrast administration. The involved areas appear hypointense on T1-weighted MR images, mild hyperintense on T2-weighted images with reduced diffusion at DWI. The lesion appears hypovascular during the arterial phase, with progressive enhancement and delayed retention of contrast in the venous and late phases. MRCP is able to assess the involvement of the pancreatic duct system and these features are important in the differential diagnosis with the pancreatic adenocarcinoma in which the main pancreatic duct is characterised by single short stenosis, with marked dilation of the upstream ductal system. In cases in which AIP involves the head of the pancreas, dilatation of the common bile ducts and the intrahepatic ducts can be seen.

Learning Objectives:
1. To describe clinical and biological presentation of IgG4-related pancreatitis.
2. To describe morphological and functional (DWI, PET/CT, etc.) imaging features of IgG4-related pancreatitis.
3. To identify imaging findings for the differential diagnosis with other solid pancreatic lesions, i.e. pancreatic cancer, and to avoid unnecessary invasive therapeutic procedures.

A-829 08:58
B. Hepatobiliary manifestations
M. Ronot; *Clichy/FR (maxime.ronot@bjn.aphp.fr)*

IgG4-related cholangitis is frequent in patient with IgG4-related disease. IgG4-RC should be carefully diagnosed based on a combination of clinical, serological, morphological, and histopathological features. Asian Diagnostic Criteria (Japan-Korea Consensus) and Mayo Clinic Diagnostic Criteria (The HISORt Criteria) have been commonly accepted. On imaging, the affected segments demonstrate irregular stenosis, focal, or diffuse circumferential thickening of the wall with contrast enhancement. The most commonly involved segment are the intrapancreatic segment of the common bile duct showing tapering with upstream biliary dilatation and the biliary convergence. It remains difficult to distinguish IgG4-RC from primary sclerosing cholangitis (PSC) or bile duct malignancy based on imaging features alone. The presence of other organs' involvement, especially pancreatic abnormalities, and elevated serum IgG4 level favour a diagnosis of IgG4-RC. The presence of an inflammatory bowel disease is more frequent in PSC. Biopsy should be used in all patients with a suspicion of malignancy. Although some patients may respond to biliary drainage or surgical resection, IgG4-RC displays a good response to steroid

therapy, as is the case for pancreatic lesions. Thus, early introduction of steroid therapy is recommended, especially for patients with obstructive jaundice.

Learning Objectives:

1. To describe clinical, biological presentation and morphological and functional imaging findings for the diagnosis of IgG4-related cholangitis.
2. To discuss the role of imaging to avoid unnecessary invasive diagnostic and/or therapeutic procedures.
3. To discuss the diagnostic criteria to differentiate IgG4-related cholangitis from other causes of cholangitis and biliary cancer.

A-830 09:21

C. Systemic manifestations

G. Morana; *Treviso/IT (gmorana@ulss.tv.it)*

IgG4 related diseases include swelling of involved organs, a lymphoplasmacytic infiltrate with IgG4-positive plasma cells and a variable degree of fibrosis. Elevated serum concentrations of IgG4 are found in 60-70 percent of patients. IgG4-RD often affects more than one organ. Immunoglobulin G4-related disease (IgG4-RD) generally occurs most commonly in middle-aged and older men, although disease extent and severity appear to be similar in men and women. IgG4-RD-associated disorders - other than Type 1 AIP and IgG4-related sclerosing cholangitis - include: aalivary and lachrymal gland involvement: dacryoadenitis/sialadenitis and sclerosing sialadenitis: about 40 percent of patients with AIP also have salivary or lachrymal gland involvement (despite marked lachrymal and salivary gland enlargement, these patients experience relatively mild dryness of the eyes and of the mouth than patients with Sjogren's syndrome); inflammatory orbital pseudotumour: account for 25 to 50 percent of all orbital pseudotumours; idiopathic retroperitoneal fibrosis and mesenteritis, chronic sclerosing aortitis and periaortitis: it involves the infrarenal aorta and simultaneously affect the iliac arteries (chronic inflammatory and fibrotic change can involve regional tissues, such as the ureters, leading to obstructive uropathy); Riedel's thyroiditis; interstitial pneumonitis and pulmonary inflammatory pseudotumours, which may mimic sarcoidosis; tubulointerstitial nephritis and membranous glomerulonephritis, in most cases with involvement of other organs. The likelihood of IgG4-RD is significantly increased if high serum levels of IgG4, allergic symptoms, and/or other fibrotic processes are also present. Because of the systemic nature of the disease, imaging workup of IgG4-RD should always include whole body examinations to detect multiorgan involvement.

Learning Objectives:

1. To describe extra-pancreatic and extra-biliary manifestation of IgG4-related disease.
2. To describe the imaging findings of the most common extra-pancreatic and extra-biliary organ involvement.
3. To discuss the role of "whole-body" imaging modality for the diagnosis and the follow-up of IgG4-related systemic disease.

Author Disclosure:

G. Morana: Speaker; Bracco Spa.

09:44

Panel discussion: Tips and tricks in clinical practice

08:30 - 10:00 **Room C**

Chest

RC 1704

Novelties in lung cancer imaging

Moderator:
B. Feragalli; Chieti/IT

A-831 08:30

A. New approaches to the management of pulmonary nodules

A. Nair; *London/UK (arjun7764@gmail.com)*

Small pulmonary nodules are an increasingly common incidental finding, as the indications for thoracic CT widen while the threshold for performing the investigation is lowered. Although the majority are benign, the difficulty in histologically verifying such nodules inevitably means that CT follow-up using pragmatic algorithms is mandated. Such algorithms aim to minimise over-investigation while detecting potentially malignant nodules early. Most recommendations have been extrapolated from lessons learnt from lung cancer screening trials, and have relied on measuring diameter to prove stability. In 2015, the British Thoracic Society (BTS) published novel guidelines combining the use of semi-automated volumetric measurement (where possible) and malignancy risk calculation using the Brock model to guide nodule management. Volumetric measurements are more repeatable and reproducible than diameter measurements, but the radiologist should be aware of patient, technical and vendor factors that influence this reliability. With the sanctioning of low-dose CT screening in the USA, the American College of Radiology released Lung-RADS version 1.0 in 2014, a standardised reporting system for nodules found at baseline and incidence rounds of lung cancer screening stratified by diameter. As with the BTS guidelines, Lung-RADS recommends using the Brock model to estimate malignancy for more suspicious nodules, but also allows the radiologist to use their judgement to move a nodule into a more suspicious category. In this lecture, we review the categories, similarities and differences between BTS and the most recent version of Lung-RADS, and discuss how both BTS and Lung-RADS can affect the management of incidental- and screening-detected nodules, respectively.

Learning Objectives:

1. To learn about strengths and limitations of the recent British Thoracic Society guidelines in managing pulmonary nodules.
2. To become familiar with LungRads classification and reporting system in pulmonary nodule assessment.
3. To understand how LungRads may affect results in a lung cancer screening programme.

A-832 09:00

B. CT phenotypes of lung adenocarcinoma

M. Lederlin; *Rennes/FR (Mathieu.LEDERLIN@chu-rennes.fr)*

Adenocarcinoma, the most prevalent type of lung cancer, represents a heterogeneous group of tumour with a large spectrum of genetics, histologic subtype, CT appearance, clinical behaviour and prognosis. The IASLC/ATS/ERS histopathological classification of lung adenocarcinoma defines a wide range of subtypes showing interesting correlations with CT findings. These correlations are particularly strong for pre-invasive lesions (i.e. atypical adenomatous hyperplasia, adenocarcinoma in situ and minimally invasive adenocarcinoma), appearing as sub-solid nodules at CT. AAH and AIS typically exhibit no ground-glass opacity, while MIA has a tiny solid component within ground glass opacity. The growth rate of the solid component may be critically informative for the prognosis and the management of these lesions. Invasive adenocarcinomas usually display suggestive CT features such as peripheral location, lobulated margins, or pleural tags. Intra-tumoural mixed attenuation with ground-glass opacity and internal bronchogram suggest the presence of lepidic pattern, a subtype defined by preserved alveolar architecture, which conveys a less aggressive behaviour. Furthermore, some CT findings might be associated with genomic alterations such as EGFR and KRAS mutations, as well as ALK rearrangements. Invasive mucinous adenocarcinoma is a rare separate entity characterised by areas of ground-glass opacity or consolidation with a tendency to spread along the airways and lung parenchyma. Beyond visual analysis, radiomics is a new trend which aims to capture information of the tumour phenotype by extracting a large number of quantitative descriptors from medical images. In lung adenocarcinomas, some radiomics features have been shown to be significantly associated with prognosis and survival.

Learning Objectives:

1. To become familiar with CT assessment of lung adenocarcinoma phenotypes.
2. To learn how CT-based radiomic features can capture information on phenotypes.
3. To understand if non-invasive evaluation of phenotypes can predict patient prognosis.

A-833 09:30

C. Imaging of immune-related response criteria (irRC)

O.L. Sedlaczek; *Heidelberg/DE (sedlaczek@web.de)*

Imaging of immune-related response criteria (irRC) cancer immunotherapy is a broad field of approach employing the immune system to treat cancer. They can be divided into active priming of the endogenous immune system and the passive delivery of compounds that may use immune system as an effector (monoclonal antibodies/adoptive cell transfer). In contrast to cytotoxic agent anti-tumour response, immunotherapy may take longer and in the initial phase the response to immune therapies can manifest in a morphologic "progressive disease", therefore, called "pseudoprogression". In this situation a early discontinuation of the treatment would not be appropriate, unless PD is confirmed. On the contrary to standard RECIST criteria, initially "clinically insignificant" PD including even the detection of new lesions can be called "stable disease" and may in the long run result in an long-term tumour control reflecting the ongoing antitumour activity. Checkpoint inhibitors will play a major role in the first-line treatment of lung-cancer and, therefore, the broad use of adjusted response criteria a major need. Morphologic patterns of cancer-specific immunologic mechanisms and those of cytotoxic agents will be shown and examples of the evaluation of immune therapies using irRC compared to the conventional ones will be given.

Learning Objectives:
1. To become familiar with mechanisms of inducing lung cancer-specific immune response.
2. To learn about the response imaging patterns beyond those of cytotoxic agents.
3. To understand the clinical benefits from immune therapies using irRC compared to the conventional ones.

08:30 - 10:00 **Room O**

Special Focus Session

SF 17a

Paediatric parenchymal lung disease: what imaging technique to choose?

A-834 08:30

Chairman's introduction

H. Ducou le Pointe; *Paris/FR (hubert.ducou-le-pointe@aphp.fr)*

Chest x-ray should be performed prior to considering advanced imaging. It is an useful procedure for evaluating the airways, lungs and others chest components. Ultrasound is a well-known technique to explore to investigate the pleura and the mediastinum. It could be also a tool to explore the lung. To perform this exam, one must know the physical basis of the ultrasonographic method because images of the lung are based on artefacts. Chest CT is the method of choice to explore lung disease. Multidetector CT is now widely available and is characterized by high, almost isotropic resolution. Despite this fact, the main disadvantage of CT is the radiation exposure. Low HRCT protocols are mandatory to explore lung disease in children. MRI combines structural and functional information. MRI could be an effective tool to explore lung diseases because most lung diseases are accompanied by an increase in the quantity of tissue, cells, or blood within the lungs. Recent technical advances have helped MRI to become an effective tool to explore lung diseases.

Session Objectives:
1. To be familiar with paediatric parenchymal lung disease.
2. To learn the advantages and drawbacks of each imaging modalities.
3. To understand the optimal use of the different imaging modalities.

A-835 08:35

Chest x-ray

P. Tomà; *Rome/IT (paolo.toma@opbg.net)*

Parenchyma refers to the gas-exchanging part of the lung, consisting of the alveoli and their capillaries. The parameters for a normal lung size are: less than one third of the heart is below the hemi-diaphragm, the diaphragm is not flattened and the sixth anterior rib crosses the diaphragm. Complete increase of transparency of the thorax in association with low flattened diaphragms is commonly associated to air trapping as in asthma, bronchiolitis, cystic fibrosis, etc. In a child with asymmetric lung transparency, usually the lung with less vascularity is the abnormal one. Air bronchogram is the radiological sign of alveolar space involvement. It stands for air in patent airways surrounded by high-density alveolar spaces. This sign is frequent in consolidations and in atelectasis. Consolidation relates to a product of disease that substitutes alveolar air, solidifying the lung (as in infective pneumonia). In atelectasis reduced volume is seen, accompanied by increased opacity. About the aetiologies of pneumonia in infants and young children (<5 years), the majority of infections are viral: respiratory syncytial virus, metapneumovirus and adenovirus. In older children (5-18 years), main causes are viruses and atypical bacteria. Imaging studies have limited value in the differentiation between viral and bacterial respiratory tract infections. Probably, type of pattern is related to age and not to aetiologic agent.

Learning Objectives:
1. To learn about the aetiologies of paediatric parenchymal lung diseases.
2. To understand the differential diagnosis based on clinical and imaging findings.
3. To discuss the radiographic appearances of paediatric parenchymal lung diseases.

A-836 08:55

US

S.P. Deftereos; *Alexandroupolis/GR (sdefter@med.duth.gr)*

According to the basics of lung ultrasound (LUS), from the physics point of view (physical acoustic phenomena that produces special signs: sliding sign, A-lines, B-lines, etc.) the resulting images from LUS do not represent a clear image. Actually images are artefacts that are (or may) combined with disease-specific profiles with the assumption that the disease patterns correlate with the amount of fluid in the lung. Based on the presence or absence of those artefacts and with the estimation of the amount of B-lines, “imaging models” or lung ultrasound (LUS) findings have described both for the lung diseases of new-born (respiratory distress syndrome, transient tachypnoea of the new-born, bronchopulmonary dysplasia, etc.) and for lung diseases of infant and child, e.g. bronchiolitis, community acquired pneumonia etc. Of course, specific LUS findings are present in conditions such as pneumothorax, pleural effusion, opacification, etc. The use of LUS is advantageous in terms of radiation protection but there are a lot of limitations with the inability to have an overview of the entire thorax being the first (but not the only) weakness of the LUS. Furthermore, the acoustic phenomena are not always satisfactory corresponding to the pathology and thus the idea of routinely replacing chest radiography with LUS is unenforceable. The LUS has no ground to replace conventional chest radiology, but when appropriately applied, can save time to achieve a critical diagnosis especially in neonatal intensive care unit and also is a very useful follow-up tool (easy/safe/cheap/without radiation but of course operator dependent).

Learning Objectives:
1. To learn about the role of ultrasonography (US) in paediatric parenchymal lung diseases.
2. To discuss the ultrasonographic appearances of parenchymal lung pathology in children.
3. To understand pitfalls and limitations of US of the chest/lung.

A-837 09:15

CT

P. Ciet; *Rotterdam/NL (p.ciet@erasmusmc.nl)*

Despite chest radiograph (CR) being the most used technique for paediatric thoracic imaging, chest computed tomography (Chest-CT) remains the gold standard imaging modality to characterize parenchymal lung diseases. Chest-CT enables high-quality images both in non-collaborative and collaborative children. In non-collaborative children, fast acquisition CT protocols can be used to avoid sedation or anaesthesia without compromising image quality. Conversely, collaborative children can be trained prior to the CT scan to perform specific inspiratory and expiratory manoeuvres using a spirometer. The use of the spirometer improves protocol standardization and image quality. Nonetheless, the main limitation of chest-CT remains radiation exposure, which always conveys a risk of developing cancer related to its stochastic nature. However, dose reduction measures have been introduced to minimize this risk and nowadays chest-CT can be performed at the same radiation dose of a CR. Further radiation dose reduction might be achieved through chest-CT protocol standardization across vendors, which is still lacking. Finally, chest-CT has enabled to shift from qualitative to quantitative radiology. Newly developed imaging analysis techniques allows today to extract numbers from CT images that can be used to assess treatment’s efficacy or to determine patient’s prognosis. In this presentation will be shown a series of clinical examples where the combination of clinical, laboratory and CT imaging data allowed to obtain an integrated report jointly written by radiologist and clinician.

Learning Objectives:
1. To learn about the role of CT in paediatric parenchymal lung diseases.
2. To discuss the technique and protocols of CT of the lung parenchyma in children.
3. To learn about the differential diagnosis based on clinical and imaging findings.

Author Disclosure:
P. Ciet: Speaker; Vertex Pharmaceuticals.

A-838 09:35

MRI

M.O. Wielpütz; *Heidelberg/DE (mark.wielpuetz@med.uni-heidelberg.de)*

Using magnetic resonance imaging (MRI) for the management of paediatric patients with lung disease has obvious advantages: comprehensive structural and functional imaging without ionizing radiation. Functional imaging with MRI comprises measurements of perfusion, blood flow, ventilation, gas exchange as well as respiratory motion and mechanics. However, MRI of the lung is challenging for three reasons: 1) low tissue density containing few protons to generate signal; 2) multiple air-tissue interfaces causing susceptibility artefacts and fast signal decay; 3) respiratory, vascular, and cardiac motions requiring fast imaging or triggering and gating techniques. Most lung diseases are associated with an increase in tissue per volume (“plus pathology”), due to the interstitial, alveolar, bronchial or pleural accumulation of cells, extracellular matrix or fluid, displacing air content inside a voxel. Subsequently, proton MRI signal is enhanced. On the other hand, lung diseases may present with tissue loss or loss of blood volume attributable to hypoxic vasoconstriction (“minus pathology”), posing additional challenges to MRI. Still, lung MRI has benefited much from recent research in obstructive lung diseases such as cystic fibrosis, propelling its introduction in clinical routine and broadening experience with lung MRI in paediatric population. Nowadays, lung MRI provides robust

protocols for paediatric oncology, inflammatory lung diseases (especially pneumonia) and airways disease, which will be discussed in the talk.
Learning Objectives:
1. To learn about the (potential) role of MRI in paediatric parenchymal lung diseases.
2. To discuss the technique and protocols of MRI of the lung parenchyma in children.
3. To learn about the differential diagnosis based on clinical and imaging findings.
Author Disclosure:
M.O. Wielpütz: Advisory Board; Boehringer Ingelheim.

09:55
Panel discussion: What imaging modality to choose and when?

08:30 - 10:00 **Room N**

E³ - ECR Master Class (Head and Neck)

E³ 1726a
Functional imaging in head and neck radiology: beyond morphology

Moderator:
M.M. Lemmerling; Ghent/BE

A-839 08:30
A. Diffusion-weighted MRI: apparent diffusion coefficient (ADC) and beyond
A.D. King; *Hong Kong/HK (king2015@cuhk.edu.hk)*

The apparent diffusion coefficient (ADC), obtained from DWI images, measures diffusion of water molecules in head and neck tumours. Many factors influence the ADC but in general malignant tumours show greater impairment of diffusion and lower ADC values compared to benign lesions. When used in the correct clinical context ADC aids MRI lesion characterisation. Lower ADCs are reported in metastatic compared to benign /reactive nodes; malignant salivary gland tumours compared to pleomorphic adenomas; malignancy compared to infection/ inflammation; lymphoma compared to squamous cell carcinoma (SCC); poorly compared to well differentiated SCC. However, ADC thresholds overlap and low ADC values occur in benign processes. The ADC of SCC shows associations with chemoradiotherapy response, an unfavourable outcome reported for tumours with high ADC pre-treatment, smaller %ADC rise early intra-treatment and low ADC post-treatment. ADC is obtained usually from a monoexponential model using b-values from 0 to 800/1000 sec/mm^2, but the choice of b-values influences ADC values and provides diffusion parameters beyond ADC. Intravoxel incoherent motion (IVIM) uses lower b-values (~0-200 sec/mm^2) to measure pseudodiffusion related to the microcirculation (D* and f) and higher b-values (~400-1000 sec/mm^2) to measure pure diffusion (D). Diffusion kurtosis imaging extends the range to even higher b-values (>1000 sec/mm^2) and takes into account non-Gaussian diffusion to obtain a diffusion parameter (Dapp) and also a kurtosis parameter (Kapp) which is believed to better reflect tumour heterogeneity and cell complexity. Methods of analysing the diffusion maps also are evolving to take into account tumour heterogeneity.
Learning Objectives:
1. To understand the concept of diffusion in oncology.
2. To learn how to evaluate diffusion images and numeric values.
3. To understand new trends and restrictions of the method.

A-840 09:00
B. Perfusion imaging in head and neck: what is new?
R. Maroldi; *Brescia/IT (roberto.maroldi@unibs.it)*

As chemo-radiation therapy is increasingly applied to head and neck cancer, there is a growing need to develop non-invasive surrogate-biomarkers to predict and assess the response to a non-surgical treatment. Therefore, imaging techniques exploring tumour properties other than CT density, T2-T1 weighting or the single-phase "static" enhancement pattern have been devised. These "functional techniques" aim at targeting tumour micro-architecture, perfusion and heterogeneity (texture analysis). In particular, CT and MR perfusion techniques have been developed to investigate the changes induced by neo-angiogenesis in the microcirculation of tumour. This has been accomplished by analysis of the kinetics of the passage through the tissues of a bolus of contrast agent (DCE-CT, DCE-MR) or of an endogenous bolus (blood, ASL-MR perfusion). These kinetics can be explored with different strategies to obtain visual information, semi-quantitative or quantitative parameters. Though quantitative parameters should reproduce tissue microvascular physiology more precisely than semi-quantitative parameters, they are less simple to calculate. Presently, most of the medical literature on perfusion analysis encompasses pilot studies only. In addition, these studies share several limitations, not only linked to the complexity of the physiological model used to extract quantitative parameters but also correlated to the variety of the acquisition techniques, outcome measures as well calculation procedures. These limitations deter the reproducibility of results. Nevertheless, one emerging finding is that neoplasms showing great heterogeneity of a parameter like Ktrans are associated with a poorer prognosis; probably related to the presence of areas capable of surviving in conditions of hypoxia.
Learning Objectives:
1. To review the clinical usefulness of perfusion imaging in head and neck.
2. To understand advantages and disadvantages of perfusion.
3. To become familiar with the value of perfusion imaging in monitoring the early effects of non-surgical treatment.

A-841 09:30
C. MR/PET: the way to go
M. Becker; *Geneva/CH*

This lecture focuses on clinical applications of MR/PET in head and neck tumours with special emphasis on squamous cell carcinoma. First, principles of MR/PET are discussed and the current evidence regarding clinical feasibility, image quality, optimized imaging protocols and quantification with MRI-based attenuation algorithms in the head and neck are reviewed. Typical tumour manifestations are presented and the recent literature on the diagnostic performance of MR/PET in head and neck cancer is reviewed. The appearance of primary and recurrent squamous cell cancers, lymph node metastases and distant metastases on MR/PET is summarized and the appearance of benign lesions mimicking malignant tumours, such as scar tissue, granulation tissue, soft tissue necrosis and osteonecrosis is addressed. We present illustrative cases of multiparametric evaluations of malignant and benign lesions with MRI, diffusion-weighted imaging, perfusion and PET and we discuss the dilemma how to deal with discrepant multiparametric data.
Learning Objectives:
1. To become familiar with the technique of MR/PET.
2. To discuss the value of MR/PET in head and neck oncology.
3. To be aware of the possible pitfalls.
Author Disclosure:
M. Becker: Research/Grant Support; Swiss National Science Foundation.

08:30 - 10:00 **Studio 2017**

Genitourinary

RC 1707
Pitfalls in gynaecologic oncologic imaging: how to avoid them and minimise risks

A-842 08:30
Chairman's introduction
A. Sahdev; *London/UK (anju.sahdev@bartshealth.nhs.uk)*

The increasing use of pelvic MRI for staging and assessing treatment response in gynaecological cancers opens a new world of pathology and pitfalls in pelvic imaging. These pitfalls are commonly encountered and may be due to poor acquisition, incorrect technical parameters, mimicking pathology or pitfalls in interpretation of the MR image. Functional imaging with diffusion-weighted imaging and dynamic contrast enhancement in particular, confer unique challenges at acquisition and image interpretation. This session will highlight pitfalls in common gynaecological MRI practice and relate these pitfalls to their consequences on patient management. The panel will also provide handy tips and solutions, where possible, to avoid and minimise the pitfalls.
Session Objectives:
1. To provide an overview of pitfalls and errors in interpretation of gynaecologic cancers.
2. To become familiar with strategies for avoiding pitfalls.

A-843 08:35
A. Mistakes in assessment of cervical cancer
M.M. Otero-García; *Santiago de Compostela/ES (milagros.otero.garcia@sergas.es)*

Cervical cancer (CC) continues to be staged at clinical examination but the International Federation of Gynaecology and Obstetrics (FIGO) staging system and different guidelines acknowledge the benefits of MRI staging. MRI is the best single imaging method for determining prognostic factors such as lymphatic involvement, tumour size, and depth of stromal invasion. High-resolution T2 images are a mainstay for tumour detection. Oblique axial T2W

images perpendicular to the cervical long axis provide more accurate assessment of stromal involvement and parametrial invasion. Diffusion-weighted imaging (DWI) and dynamic multiphase contrast (Gd)-enhanced T1 sequence are useful complementary sequences. Possible pitfalls in assessing CC staging and follow-up are as follows: overstaging when a wrong oblique axial acquisition is performed, or cervical oedema secondary to post-biopsy changes or large tumours is present; difficult tumour delimitation (e.g. early CC, isointense tumours in young women, cervical versus endometrial in adenocarcinoma); nearby structures invasion misinterpretation (e.g. bladder bullous oedema as direct invasion); misdiagnosis in unusual appearance of CC; benign conditions are mistaken as tumour (e.g. "burned out'' endometriosis, polypoid adenomyoma, vaginal vault nodularity after hysterectomy, etc.); post-chemoradiation changes produce soft tissue stranding in the cervix and parametria simulating recurrent tumour. To avoid pitfalls it is very important to plan MRI exploration correctly and to review all the sequences together including DWI and dynamic multiphase contrast (Gd)-enhanced T1 sequences. PET/CT can help in evaluating equivocal findings in post-treatment setting.

Learning Objectives:

1. To become familiar with pitfalls in staging of cervical cancer and in monitoring treatment response.
2. To learn how to differentiate mimics of cervical cancer.
3. To understand the central role of MRI in treatment planning.

A-844 08:58

B. Mistakes in assessment of endometrial cancer

T.M. Cunha, M. Horta; *Lisbon/PT (tmargarida@gmail.com)*

Endometrial carcinoma represents 4.8% of all cancers in women worldwide with approximately 75% of cancers diagnosed at an early stage. Although magnetic resonance imaging is not considered in the International Federation of Obstetrics (FIGO) 2009 staging classification, it plays an important role in the diagnosis and pre-operative staging of endometrial carcinoma; thus being a crucial tool for defining the surgical and therapeutic approach of these tumours. To help preventing diagnostic errors and to guide appropriate therapeutic management, radiologists should be aware of common magnetic resonance imaging mistakes in assessment of endometrial carcinoma. Pitfalls that may mask or simulate endometrial carcinoma include: a cervical adenocarcinoma misinterpreted as an endometrial adenocarcinoma; benign endometrial pathology misinterpreted as malignant pathology; specific tumoural locations and uncommon cancer enhancing patterns. Several common mistakes in staging endometrial carcinoma will also be outlined. Knowledge of the existence of these diagnostic pitfalls should help prevent misinterpretation of a pelvic magnetic resonance for assessment of endometrial carcinoma.

Learning Objectives:

1. To become familiar with pitfalls in local tumour spread in endometrial cancer.
2. To learn how to differentiate benign and malignant mimics.
3. To appreciate the complementary value of functional MRI techniques.
4. To understand the potential clinical impact of these mistakes in treatment planning.

A-845 09:21

C. Mistakes in assessment of ovarian masses

I. Thomassin-Naggara; *Paris/FR*

Pelvic MR imaging allows to avoid most of the mistakes in the assessment of ovarian masses made using transvaginal ultrasonography or CT scan. However, even using pelvic MR imaging, there are some pathologies that may mimic primitive ovarian cancer including pelvic inflammatory disease, uterine myoma, digestive tumour or ovarian metastases. Preoperative diagnosis of these pathologies is crucial because the therapeutic strategy is completely different and the absence of a diagnosis may impact the prognosis. Thus, this lecture will present three clinical situations where the radiologist needs to accurately analyse MR images to not misdiagnose a wide variety of pelvic pathologies as ovarian cancer.

Learning Objectives:

1. To become familiar with benign masses mimicking ovarian cancer.
2. To demonstrate benign and malignant diseases mimicking peritoneal carcinomatosis.
3. To learn about imaging strategies for avoiding these pitfalls.

09:44

Panel discussion: How can we improve interdisciplinary communication and avoid misunderstanding in our reports?

08:30 - 10:00 **Room E1**

E³ - ECR Master Class (Breast)

E³ 1726b

Taking clinical breast MRI to the next level

A-846 08:30

Chairman's introduction

J. Camps Herrero; *Valencia/ES (juliacamps@gmail.com)*

This masterclass will tackle three issues that are currently at the forefront of the breast MRI debate: imaging biomarkers, preoperative staging and so-called "overdiagnosis". Breast MRI should have already passed the phase of diagnostic validation and must now head towards the definition of imaging biomarkers that are capable of sampling the whole cancer in its entire heterogeneity as well as allowing serial measures in response evaluation. Imaging biomarkers must be solid, reproducible and standardised. This lecture will define common imaging biomarkers in the clinical setting as well as set the path for their further development in the future. Preoperative breast MRI is still being questioned as a valid indication and the MIPA study has been designed to answer the questions raised by published evidence on the contrary (excess mastectomies, no significant difference in mastectomy rates, etc) tainted by methodological biases which will be highlighted during this session. The number of high-risk (B3) lesions has increased after the use of breast MRI, being considered traditionally false-positive diagnoses, when in fact they have underlying prognostic implications. This lecture outlines these implications and lets us see breast MRI under a different light, when pathology correlates are considered.

Session Objectives:

1. To understand the concept of breast MR imaging biomarker and its role in the standardisation of the MRI technique.
2. To know how the results of the MIPA trial might influence the general approach to staging with breast MRI.
3. To understand the close relationship between pathology and MRI in the characterisation of high-risk lesions.

Author Disclosure:

J. Camps Herrero: Advisory Board; Bayer.

A-847 08:35

A. Breast MRI biomarkers for the clinical setting

E.A. Morris; *New York, NY/US*

Enhancement of the existing underlying fibroglandular tissue has been termed background parenchymal enhancement (BPE). As BPE is related to vascular flow, it has been proposed that this may represent an imaging biomarker of the underlying proliferation of fibroglandular tissue. Investigations have shown that there is an extremely strong association between BPE and risk of breast cancer, at least a strong as the association between mammographic density and breast cancer. BPE is also affected by treatment changes and hormonal manipulation. Tamoxifen and aromatase inhibitors decrease BPE, demonstrating an imaging treatment response. Radiation therapy to the breast causes a permanent reduction in BPE. Rim enhancement: MRI phenotypic features can predict aggressiveness of breast cancer. For example, we know that spiculation on MRI is associated with a lower histologic grade and lower ki67 expression and is more commonly seen in ER+ cancer. Rim enhancement has been shown to be associated with cancers that are higher in grade and ER-. Rim enhancement is associate with a worse distant metastatic survival. It has been shown that triple-negative tumours without rim enhancement are associated with tumour infiltrating lymphocytes. High TIL levels are associated with pCR following NAC and improved survival in TNBC. Peritumoural oedema: peritumoural oedema is caused by increased vascular permeability and release of cytokines. It is seen in <10% of breast cancer and is associated with early distant metastases (<2.5 y). In TNBC, peritumoural oedema was a significant independent predictor of worse recurrence-free survival.

Learning Objectives:

1. To explain which are the most common MRI biomarkers for breast cancer.
2. To understand the value of biomarkers in clinical practice.
3. To know the new possibilities for the future.

Author Disclosure:

E.A. Morris: Advisory Board; Delphinus, Devicor. Board Member; Avon. Consultant; Grail. Research/Grant Support; Hologic.

A-848 09:00

B. Preoperative MRI: which changes to expect after the MIPA trial?

F. Sardanelli; *San Donato Milanese/IT (f.sardanelli@grupposandonato.it)*

Preoperative MRI (pMRI) is highly debated. Context: established breast conserving surgery (BCS), with 10-40% positive margins rate; low ipsilateral recurrence rate after BCS plus radiation therapy (9% at 20 years); 0.5-1% annual risk of contralateral breast cancer (BC). Of 4 published RCTs, 2 against, 2 in favor; meta-analyses found 11-12% of wider ipsilateral surgery (8% mastectomies), 3-4% of contralateral surgery for true-positive pMRI; all observational studies have an intrinsic selection bias. An overdiagnosis/overtreatment risk by pMRI exists: some ipsilateral/contralateral cancers are cured by radiation therapy and/or adjuvant therapy. Guidelines by EUSOBI and ACR included pMRI indication for contralateral screening; the former also suggested ipsilateral MRI for dense breasts and invasive lobular cancer (ILC), the latter for tumour extent, additional cancers, invasion deep to fascia; both societies noted the lack of evidence for a pMRI effect on patient outcome. A multidisciplinary EUSOMA working group agreed on four indications: 1) ILC; 2) high risk; 3) mammography/US size discrepancy >1 cm; 4) selection for partial breast irradiation. Other indications: Paget; multifocal/multicentric/bilateral BC at conventional imaging; skin-/nipple-sparing mastectomy; positive margins after BCS. The ongoing multicentre MIPA study is enrolling two concurrent series of first-BC patients, not candidate to neoadjuvant therapy, receiving or not receiving pMRI. First results on 2,500 patients (50%/50% MRI/no-MRI): 40% of pMRIs are requested by surgeons; 20% of MRI-group had mastectomy already planned before pMRI; only 1% of mastectomies prompted by pMRI; after pMRI, more extensive BCS (14.2%) compensated by less extensive BCS (12.7%); re-operation rate 8.3% (MRI-group), 13.4% (no-MRI group).

Learning Objectives:

1. To understand which methodological issues of evidence-based medicine are implied in preoperative breast MRI (PB-MRI).
2. To become aware of the intrinsic bias of observational studies reporting only series of breast cancer patients who had PB-MRI.
3. To become aware of the first results of the MIPA study showing from the real clinical world that: a) surgeons are largely involved in requesting PB-MRI; b) PB-MRI is often requested as a confirmation tool for an already planned mastectomy; c) the additional rate of mastectomies really induced by PB-MRI is very low; d) PB-MRI allows for tailoring the breast conservative treatment balancing more and less extensive surgery.

Author Disclosure:

F. Sardanelli: Advisory Board; Bracco, General Electric. Research/Grant Support; Bracco, Bayer. Speaker; Bracco, Bayer.

A-849 09:25

C. Is breast MRI increasing the number of high-risk lesions?

C.K. Kuhl; *Aachen/DE*

"No abstract submitted."

Learning Objectives:

1. To describe MR imaging findings of DCIS, ADH/ALH, FEA.
2. To list common pathophysiological correlates of false positive diagnoses made by MRI vs conventional imaging.
3. To describe the different prognostic implications of false positive diagnoses made by MRI vs conventional imaging.

09:50

Panel discussion: Breast MRI: what more evidence do we need?

08:30 - 10:00 **Room E2**

E³ - ECR Master Class (Neuro)

E³ 1726c

Imaging of traumatic brain injury

Moderator:

M. Karlovic-Vidakovic; Mostar/BA

A-850 08:30

A. New MRI techniques in the diagnosis of patients with traumatic brain injury

D. Galanaud; *Paris/FR (galanaud@gmail.com)*

Traumatic brain injury (TBI) is a major cause of disability among younger patients. MRI is emerging as the leading method to evaluate the extent of brain damage in this setting, especially using advanced sequences such as diffusion tensor imaging (DTI), MR spectroscopy and functional imaging. Each of these sequences has its own promises and challenges. DTI allows a precise and direct evaluation of the extent of white matter damage, which is the leading lesional mechanism in TBI. It is currently the most widely used and promising sequence for TBI evaluation. Its main limitation is significant inter-machine variability, still difficult to correct with controls or phantoms. MR spectroscopy, performed on the brain stem and the thalamus has shown promising results but suffers from a limited acceptance and availability. Functional MRI may show brain reorganisation following TBI and has shown promising results in evaluating the level of consciousness in vegetative/minimally conscious subjects. However, it is much less reliable in the acute setting due to the confounding effects of sedations. Large-scale studies are currently under way to standardise the acquisition procedures and determine the best approach to perform a reliable assessment of TBI severity based on MRI data.

Learning Objectives:

1. To learn about different types of traumatic brain injuries.
2. To understand how to use advanced MR techniques in brain injury.
3. To enhance the value of DTI in traumatic brain injury.

A-851 09:00

B. Computer-aided diagnosis in trauma imaging: status and developments and the role of deep learning

R. Manniesing; *Nijmegen/NL (rashindra.manniesing@radboudumc.nl)*

Computed tomography (CT) is the first-line imaging technique in the acute situation of traumatic brain injuries (TBI) and has high sensitivity for visualising haemorrhages and bone fractures. MR has superior soft tissue contrast and is capable of visualising diffuse axonal injuries including cerebral microbleeds, which may have long-term prognostic value and which are frequently present in all severities of TBI. However, detecting, quantifying, and characterising these lesions are time-consuming tasks and subject to observer variability. Furthermore, imaging data from trauma patients have additional complexity because of the typical heterogeneity of the patient group and the variability inherent to the image acquisition protocols. Computer-aided diagnosis (CAD), therefore, has an important role. For example, CAD systems can be developed to detect and measure the volume of intracerebral haemorrhages in CT, or to count and determine the laterality of cerebral microbleeds in MR. In this talk I give an overview of the current status of computer-aided diagnosis in trauma imaging. I identify the areas of interest which has a high potential and need for automation. As an example, a recently developed CAD system for cerebral microbleed detection is described. Finally, future developments and the potential role of deep learning in trauma imaging are discussed.

Learning Objectives:

1. To learn how automated image analysis can aid diagnosis and prognosis in traumatic brain injury.
2. To demonstrate the potential of computer-aided detection of cerebral microbleeds.
3. To discuss future developments of computer-aided diagnosis in trauma imaging.

Author Disclosure:

R. Manniesing: Research/Grant Support; Toshiba Medical Systems Corporation, Japan.

A-852 09:30

C. Structured reporting of traumatic brain injury lesions: introducing common data elements

T. Vande Vyvere; *Antwerp/BE (thijs.vandevyvere@icometrix.com)*

Conventional interpretation of radiologic findings in brain-injured patients is prone to error and highly variable between observers. It is believed that the visual, qualitative and subjective nature of interpretation, combined with a narrative form of reporting, are the root causes of these differences in evaluation. Agreement is especially low in cases with multiple coexistent lesion types. Reporting skills are commonly transmitted through the master-apprentice model, but unfortunately, agreement is low, even between experts. Novel up-and-coming structured scoring systems show a lot of promise to standardize the way traumatic brain injuries are interpreted and reported. The National Institute of Neurological Disorders and Stroke (NINDS) Common Data Elements (CDEs) were specifically designed to minimize inter- and intra-reader variability. Using specific operational definitions to describe each type of lesion, and by providing a framework of structured templates, the narrative report can be replaced by a more reliable and mineable structured report. Drop-down menus can be completed for each lesion using tiers of progressive complexity. Studies have shown high inter-reader reliability for reporting primary and secondary lesions when using this structured scoring system. However, significant variability is still found in some tiers with higher complexity where subclassification is required. Reported features which still show high variability when using structured reporting could be tackled by including more quantitative techniques. A combination of human-computer interpretation could, therefore, not only significantly increase the reliability of imaging-outcome research, it can also pave the way towards new hybrid reporting initiatives in radiology training and practice.

Learning Objectives:
1. To demonstrate the different patterns of primary and secondary extra-axial and intra-axial traumatic brain lesions.
2. To understand assessment of intracranial hypertension and cerebral herniation.
3. To discuss the issue of paediatric brain trauma and stress the importance of MRI in non-accidental injury.

Author Disclosure:
T. Vande Vyvere: Employee; icometrix NV, Leuven, Belgium.

08:30 - 10:00 **Room F1**

Special Focus Session

SF 17b
Errors in emergency radiology

A-853 08:30
Chairman's introduction: Why do radiological errors occur?
A. Brady; *Cork/IE (abrady@muh.ie)*

Errors and discrepancies in radiology practice are uncomfortably common, with an estimated day-to-day rate of 3-5% of studies reported, and much higher rates reported in many targeted studies. Nonetheless, the meaning of the terms “error” and “discrepancy”, and the relationship to medical negligence are frequently misunderstood. This session will outline the incidence of these events, the ways they can be categorised to aid understanding and potential contributing causes, personal and system based. Possible strategies to minimise error and means of dealing with perceived underperformance when it is identified will be considered. The inevitability of imperfection will be explained, while the importance of striving to minimise such imperfection will be emphasised.

Session Objectives:
1. To learn about the frequency of errors in radiology practice.
2. To understand some of the contributing factors.
3. To prepare for a discussion later in the session of possible strategies to minimise errors.
4. To understand the frequency of and reasons for errors in radiological interpretation.
5. To learn about common errors in trauma radiology and non-traumatic abdominal emergency imaging.
6. To learn about the physical and human factors that can influence radiology error rates, and strategies that can influence the frequency of such errors.
7. To appreciate the personal and environmental influences that can contribute to a radiologist’s error rate, and how to optimise conditions to keep error to a minimum.

A-854 08:40
Imaging in multiple trauma
U. Linsenmaier; *Munich/DE (Ulrich.Linsenmaier@helios-kliniken.de)*

Multiple injury due to penetrating or blunt trauma is common and associated with significant morbidity and mortality and many of these injuries are or can become critical. They have to be characterized fully by diagnostic imaging in an early clinical phase. With the introduction of fast MDCT an established emergent diagnostic modality is now available for imaging multiple trauma that allows the detection and characterization of a large variety of parenchymal, vascular and skeletal injuries. Beside ultrasound (US) and conventional radiography (CR) it allows now in the emergency setting a thorough morphologic characterization of injuries and its potential bleeding dynamics. This presentation reviews the role of MDCT and spectrum of blunt and penetrating injuries as well as the imaging algorithm commonly used in the acute trauma setting. The diagnostic process is complex and difficult; possible sources of error are: A. technical errors: availability and proper use of the CT scanner and monitoring and life support equipment; B. logistic errors: availability and proper use of transportation equipment and organization and staffing of the trauma team; C. management errors: availability and proper use of a shock room algorithm based on ATLS, organization of diagnostic and therapeutic procedures; D. diagnostic errors: availability and proper use of a whole body CT protocol, individual errors, impact of delayed lesions in CT; E. current controversies.

Learning Objectives:
1. To learn about possible sources of error in imaging of multiple trauma.
2. To appreciate guidelines and algorithms in use in the imaging of multiple trauma.
3. To become familiar with current controversies in imaging of multiple trauma.
4. To understand state-of-the-art of imaging in multiple trauma.

A-855 09:00
Non-traumatic abdominal emergencies
A. Pinto; *Naples/IT (antopin1968@libero.it)*

Non-traumatic abdominal emergencies include a large spectrum of medical and surgical conditions. The clinical outcome depends on different factors based on the diagnosis, severity of the disease, and management. Imaging plays a major role in diagnosing these conditions, as well as in identifying associated complications. The imaging workup of patients with abdominal pain often starts with radiographs including supine and upright abdominal radiographs, and upright chest radiograph. The main cause of diagnostic error in the emergency department is the failure to correctly interpret chest and abdominal radiographs. Leading factors contributing to missed diagnosis on radiographs are lack of relevant clinical information, inappropriate or insufficient radiographs performed, failure of perception, lack of knowledge and error in interpretation. Ultrasonography (US) is an inexpensive and widely available imaging modality for evaluation of abdominal pain in the emergency department. Causes of error in emergency US are multifactorial, frequently exist in combination as in other diagnostic imaging techniques and include lack of attention to the clinical history, lack of communication with the patient, lack of knowledge of the technical equipment, failure of perception, lack of knowledge of the possible differential diagnoses, failure to suggest further ultrasound examinations or other imaging techniques. The utility of multidetector row computed tomography in the diagnosis and management of non-traumatic abdominal emergencies is well established. Technical factors, lack of knowledge, error in interpretation, satisfaction of search, error due to multitasking and increased workload may all play an important role in missed diagnosis on MDCT performed in patient with abdominal pain.

Learning Objectives:
1. To review the spectrum of diagnostic errors related to radiographs and CT performed in patient with non-traumatic abdominal pain.
2. To understand the leading factors contributing to missed diagnosis on radiographs and CT.
3. To learn how to reduce errors in radiographic and CT evaluation of patient with non-traumatic abdominal pain.

A-856 09:20
How not to fail in emergency radiology
P. McCoubrie; *Bristol/UK (paul.mccoubrie@nbt.nhs.uk)*

Most concepts of error in radiology concentrate on the technical expertise of the individual. In emergency radiology, a radiologist needs to work quickly and their decisions are increasing central in the management of the critically ill patients. However, many mistakes that happen in radiology are often little to do with the individual and their radiological prowess. The error is precipitated as the individual radiologist has been ‘set up to fail’. Even the best technically skilled radiologists will make the worst mistakes when working in a challenging environment and when they lack certain non-technical skills. First, the radiologist may be attempting in an unsuitable physical environment. Any number of factors may interfere with productive and effective reporting, including room temperature, lighting, background noise. Second, the workflow of the whole radiology department is crucial. Without the department being well organised (e.g. efficient teamwork, adequate staffing, adequate rest, a manageable workload and minimal interruptions) radiologists will make more mistakes. Third, technical skill is not all a radiologist needs. A radiologist needs a number of non-technical skills to prevent errors inadvertently entering their work. Primarily, they need to be a consummate communicator, both written and verbal. They also need excellent consultation skills to effectively help clinicians. A radiologist also needs the ability to make decisions safely and effectively, often under considerable pressure and stress. Only by concentrating on these topics will radiologists be truly ‘set up to succeed’.

Learning Objectives:
1. To list the key factors in improving a physical layout of a radiologist’s working environment that optimise performance.
2. To explain the non-technical, non-interpretative skills necessary for a radiologist to reduce error.
3. To enumerate the key concepts behind successful working with other healthcare professions to reduce the risk of errors.

09:40
Panel discussion: Errors in radiology, inevitable or preventable?

08:30 - 10:00 **Room F2**

Oncologic Imaging

RC 1716

Diffusion-weighted imaging (DWI) in oncology: how I do it

A-857 08:30

Chairman's introduction

D.-M. Koh; *Sutton/UK*

Diffusion-weighted MRI (DWI) is now widely used for the routine management of patients in clinical practice both at 1.5T and 3.0T. There is significant interest in going beyond simple ADC calculations for disease assessment. Such non-monoexponential models (e.g. intravoxel incoherent motion, diffusion kurtosis and stretched exponential) can provide additional information about underlying tissue characteristics. However, knowledge of the strengths and limitations of such approaches are important for their wider application. There is also increasing interest in using whole body DWI for disease assessment, particularly for the evaluation of bone marrow disease.

Session Objectives:

1. To understand the technical principles on DWI and to understand DWI-tailored protocols in function of the clinical questions to be answered.
2. To learn about calculation of true diffusion and perfusion fraction using DWI.
3. To learn about whole-body MRI vs DWI dedicated to one organ: strengths and weaknesses of both approaches.

A-858 08:35

A. DWI: how to optimise protocols

N. Papanikolaou; *Lisbon/PT (npapan@npapan.com)*

Diffusion-weighted imaging (DWI) is a modality that can be used to study microscopic motion of water molecules. Therefore, the presence of macroscopic physiological motion, like respiration or peristalsis affecting abdominal organs, poses certain challenges. Several methods have been proposed including breath holding, respiratory triggering or free breathing to overcome respiratory-related image degradation. Additionally, ultrafast pulse sequences, like single-shot echo planar imaging, are preferable for diffusion applications due to their capability to freeze macroscopic motion; however, they are sensitive to susceptibility artefacts. Efficient fat suppression is a prerequisite for adequate image quality. Different approaches including spectral fat sat pulses or inversion recovery methods (DWIBS) have been proposed. Geometrical distortions represent another potential problem, since it may hamper diagnostic efficacy of DWI images. To minimise the latter effects, strong gradients need to be recruited to achieve short echo times and furthermore, make the right selection of the phase encoding direction. In the context of a reliable and accurate analysis of the DWI data, the choice of a sufficient number of b-values and an optimal distribution is mandatory and still under discussion. Literally, signal attenuation due to capillary blood flow (perfusion) is most apparent at low b-values with their range varying depending on the tissue of interest. On the other hand, diffusivity is highlighted in higher b-values. Therefore, choosing the optimum number and group of b-values can substantially minimise the overall measurement error of the diffusion metrics that lead to better quantitative and qualitative results.

Learning Objectives:

1. To learn about examination protocols and techniques.
2. To understand the different models describing diffusion in various organs and diseases.
3. To become familiar with basic and advanced post-processing aspects.

A-859 08:58

B. DWI in abdominal oncology: ready for clinical practice?

D.M. Lambregts; *Amsterdam/NL (doenja.lambregts@gmail.com)*

Diffusion-weighted MRI plays a central role nowadays in oncologic MR imaging. In the abdomen, important applications of DWI include lesion detection (for example, in the prostate and liver), lesion characterisation, response monitoring (for example, in rectal cancer), response prediction and prognostication. The strengths and weaknesses for these different applications of DWI within the abdomen will be discussed. Moreover, important pitfalls of using DWI in the abdomen will be addressed with specific emphasis on how to avoid them.

Learning Objectives:

1. To learn about the different ways diffusion imaging protocols can be used for qualitative and quantitative evaluation of malignant tumours in the abdomen.
2. To understand the pitfalls of using DWI in abdominal oncology.
3. To become familiar with the current clinical applications for DWI in abdominal oncology.

A-860 09:21

C. DWI: whole-body imaging

V. Vandecaveye; *Leuven/BE (vincent.vandecaveye@uzleuven.be)*

Diffusion-weighted imaging (DWI) uses differential tissue microstructural properties for tumour detection, staging and response assessment. Technical developments have enabled clinically efficient whole body DWI (WB-DWI) and is warranted in oncology due to the increasing need for assessment of multifocal disease. WB-DWI brings a number of challenges in terms of correct selection of indications, optimisation of sequences and qualitative and quantitative interpretation protocol. WB-DWI is best applied in indications where metabolic imaging has lower diagnostic yield due to inflammatory background such as in the post-treatment setting, in case of expected small volume disease such as in peritoneal carcinomatosis in ovarian or colorectal cancer or in case of cancer with low metabolic profile such as lobular breast cancer or gastric cancer. The DWI sequence is the core of the imaging protocol but requires anatomical sequences for correlation and exact interpretation. The types of applied anatomical sequences vary depending on the indication but with contrast-enhanced sequences being indispensable in abdominal cancer and non-enhanced T1 sequences being mandatory for assessing skeletal metastases. WB-DWI benefits most from the application of the short tau inversion recovery (STIR) prepulse as it is robust to inhomogeneity-induced fat suppression and susceptibility artefacts and facilitates the detection of small tumoural lesions. Image interpretation should be qualitative as much as possible for clinical efficiency and to enhance communication with referring clinicians. Quantitative image evaluation in case of response assessment of nodal staging requires development of computer-aided imaging interpretation tools. This presentation outlines indications, optimised imaging and interpretation protocols for WB-DWI.

Learning Objectives:

1. To learn about the most common indications of whole-body diffusion imaging in cancer staging and treatment planning.
2. To become familiar with normal anatomy and physiological signal at whole-body diffusion imaging.
3. To understand how to integrate qualitative and quantitative interpretation criteria into a structured report to optimise communication with the referring clinician.

09:44

Panel discussion: How to optimise DWI for clinical practice?

08:30 - 10:00 **Room D**

Musculoskeletal

RC 1710

MRI of articular cartilage and bone: areas of imaging confusion and practical solutions

Moderator:

O. Papakonstantinou; Athens/GR

A-861 08:30

A. Bone oedema syndromes and avascular necrosis

B. Vande Berg; *Brussels/BE (bruno.vandeberg@uclouvain.be)*

The bone marrow oedema (BME) pattern is defined as an ill-delimited marrow area of homogeneous decrease in signal intensity on T1-weighted SE images and of intermediate to high signal intensity on fluid-sensitive sequences.The BME pattern is non-specific and can be observed in epiphyseal marrow in association with numerous bone or joint disorders. We will emphasize the significance of BME in association with systemic osteonecrosis. We will also review specific imaging features that enable distinction between the three most common causes of non-traumatic epiphyseal fractures, i.e. systemic osteonecrosis, insufficiency stress fractures and osteoarthritis.

Learning Objectives:

1. To understand the aetiologies of bone marrow oedema syndromes.
2. To learn about the imaging characteristics of avascular necrosis of bone.

A-862 09:00

B. Osteochondral injury, subchondral fractures and traumatic bone oedema: what is important and how do I describe it

F.W. Roemer; *Erlangen/DE (frank.roemer@uk-erlangen.de)*

Bone marrow contusions are frequently identified on MRI after an injury to the musculoskeletal system. These osseous injuries may result from a direct blow to the bone, from compressive forces of adjacent bones impacting one another, or from traction that occurs during an avulsion injury. Commonly these injuries resolve without long-term sequelae. However, they may also involve the cartilaginous surface with or without an associated fracture line defining these as osteochondral injuries, which may have a different prognostic relevance. Subchondral fractures have been implicated in the genesis of some destructive articular conditions whose cause was previously undetermined, such as rapidly progressive osteoarthritis or spontaneous osteonecrosis of the knee. Subchondral fractures may ultimately lead to bone collapse, secondary osteonecrosis and severe articular damage. It should be suspected in the appropriate clinical setting, as in early stages it is usually indistinct on initial plain radiographs and MRI is required for a definitive diagnosis. The fracture line usually appears as a band of low signal intensity in the subchondral bone plate, adjacent to the articular surface, most often surrounded by bone marrow oedema. As these injuries may be occult on radiographs, the differentiation of bone contusions from osteochondral injuries or subchondral fractures is possible only with MRI including fat-suppressed and non-fat suppressed sequences. While purely subchondral lesions may have a good prognosis if diagnosed early, disruption of the articular surface may lead to early degenerative alterations including focal cartilage loss and other features of osteoarthritis.

Learning Objectives:

1. To understand the pathomechanisms of osteochondral injury and subchondral fractures.
2. To learn about the imaging techniques and prognostic values.

Author Disclosure:

F.W. Roemer: Shareholder; Boston Imaging Core Lab (BICL), LLC.

A-863 09:30

C. Is this osteomyelitis? If not what else could it be?

A.B. Rosskopf; *Zurich/CH (andrea.rosskopf@balgrist.ch)*

This talk will cover the most important key points for radiologists to diagnose osteomyelitis and to successfully distinguish other mimicking diseases, such as bone and soft tissue tumours, Charcot arthropathy and Langerhans cell histiocytosis. Diagnosis of osteomyelitis may require the combination of different imaging techniques depending on disease stage (acute, subacute, or chronic). Plain radiographs have low sensitivity and specificity for bone infection, but should be the primary imaging modality to start with. Magnetic resonance imaging (MRI) is the most sensitive and specific modality for detection of osteomyelitis: pattern and location of a signal drop on unenhanced T1-weighted sequences can distinguish between osteomyelitis and reactive bone marrow oedema. The so-called “penumbra sign” helps to differentiate subacute osteomyelitis from bone tumour lesions, and a positive “ghost-sign” can be helpful in patients with a diabetic foot. Ultrasound plays a key role for surrounding soft tissue abnormalities and periosteal involvement in children. In chronic osteomyelitis, computed tomography provides valuable information regarding the presence of involucrum, sequestrum, or cloaca formation.

Learning Objectives:

1. To understand the imaging characteristics of osteomyelitis.
2. To learn the value of different imaging modalities for the diagnosis of osteomyelitis.

08:30 - 10:00 **Room G**

Physics in Medical Imaging

RC 1713

Artefacts and pitfalls in tomography

A-864 08:30

Chairman's introduction

V. Tsapaki; *Athens/GR (virginia@otenet.gr)*

A number of imaging techniques are currently present to facilitate clinical diagnosis. More specifically, CT, PET/CT and MR/PET are excellent imaging modalities for evaluation of a wide variety of pathologies, due to either their spatial resolution and/or tissue contrast. Furthermore, hybrid imaging can provide clinicians with tools for making an accurate diagnosis prior to making treatment recommendations. Their use, however, is occasionally restricted by a variety of associated artefacts. Artefacts degrade image quality leading in some cases in diagnostically useless images. In some cases, they also appear due to the inevitable consequence of natural properties of the human body. There are many different types of artefacts such as noise, beam hardening, scatter, pseudoenhancement, motion, cone beam, helical, ring or metal artefacts. Understanding the technical basics of hybrid imaging is vital to avoid misinterpreting artefacts as pathological findings. In addition, a deeper understanding of the origins and imaging characteristics of artefacts will reduce the likelihood of misdiagnosis and optimise the image. As accurate CT, PET/CT and MR/PET imaging is a question of knowledge, the particular refresher course intends to refresh the participants’ knowledge of the physical origins of artefacts. The course will present different methods for minimising artefacts, how to image regions of the body close to metal implants, as well as solutions to frequent image distortion.

Session Objectives:

1. To learn about the origins of image artefacts in tomographic imaging.
2. To understand image distortions in hybrid imaging.
3. To learn about solutions and workarounds.

A-865 08:35

A. CT

J. Kuntz; *Heidelberg/DE (j.kuntz@dkfz.de)*

Although CT is the most quantitative diagnostic tomographic imaging modality, its images still suffer from several kinds of artefacts. Among the CT artefacts the most prominent, severe, and well known one in diagnostic CT is the metal artefact, mainly because larger metal implants are almost opaque to the x-ray radiation and thus x-rays that are scattered from the surrounding tissue into the metal shadow cause a very high scatter-to-primary ratio. In addition, there are many less dominating sources of artefacts. Among those are beam hardening and scatter causing dark streaks between dense objects such as bones, motion causing motion blurring and partial cycloid artefacts, very large patients causing truncation artefacts, sampling issues causing aliasing artefacts, as well as the finite detector size which causes linear and non-linear partial volume artefacts. Last but not least, there are artefacts that are known mainly to experts in CT physics because the manufacturers typically correct for them: defect detector pixel artefacts, detector afterglow artefacts, and geometric misalignment artefacts. The lecture discusses the source of artefacts and gives, wherever applicable, examples and points towards approaches of how to reduce such artefacts.

Learning Objectives:

1. To understand the source of artefacts in clinical CT.
2. To understand the most important correction methods.
3. To find out what artefact correction techniques are actually provided by the CT vendors in their systems.

A-866 08:58

B. PET/CT

T. Beyer, I. Rausch; *Vienna/AT (ivo.rausch@meduniwien.ac.at)*

A proposal to combine PET with CT was made in the early 1990s by Townsend, Nutt et al. In addition to the intrinsic alignment of complementary images, the anticipated benefit of PET/CT was to use the CT images to derive the mandatory attenuation maps for the PET data. In short, CT-based attenuation correction (CT-AC) is based on the assumption that CT image can be segmented into bone and non-bone tissues; voxels in each tissue class are then scaled with corresponding scale factors. CT-AC is prone to several errors arising from the methodological shortcomings of the segmentation-scaling method in light of CT-transmission measurements in clinical conditions. These include: truncation artefacts, artefacts from high-density implants and positive contrast agents and others. More frequently, errors from patient motion during the examination propagate through CT-AC into the final emission images and lead to distortions/bias of the reconstructed data. In addition, artefacts and biases may occur from involuntary mistakes made during the set-up/conduct of the imaging procedure. During this presentation, we will rehearse the principles of CT-AC in PET/CT and point to source of artefacts arising from the methodology of CT-AC and from specific imaging workflow scenarios not optimized for routine PET/CT.

Learning Objectives:

1. To understand image distortions, artefacts and bias from methodological pitfalls.
2. To appreciate and understand solutions to frequent image distortions.
3. To understand the methodological limitations of PET/CT.

Author Disclosure:

T. Beyer: Research/Grant Support; Siemens Healthcare. Other; Manging Director cmi-experts GmbH. **I. Rausch:** None.

A-867 09:21

C. MR/PET

H.H. Quick; *Essen/DE (Harald.Quick@uni-due.de)*

Each new imaging modality and technical system introduces new types of artefacts and in MR/PET hybrid imaging the potential for new artefacts is even higher than just considering two independent systems. Artefacts in MR/PET might affect the visual impression of either MR or PET data and, furthermore, may also have an effect on quantification in MR and even stronger on PET being a quantitative method. Artefacts in integrated MR/PET may result from technical crosstalk between the MR and the PET components. Both imaging centres might not be co-aligned correctly. Differences in the data acquisition speed between MR and PET might lead to local misalignments due to patient motion. MR-based attenuation correction (AC) is still a new concept to support PET data quantification in the best possible way. All deviations from the real physical gamma quanta attenuation will ultimately lead to false values in PET quantification following AC. Administration of contrast agents before application of MR-based AC due to changes in tissue contrast potentially may lead to errors in tissue segmentation. The MR field-of-view is limited which may lead to truncation of patient tissues exceeding the constraints of the field-of-view. Consequently, the arms are not fully considered in AC leading to false PET quantification. Metal implants might introduce signal voids or local distortions in MR-AC that exceed the physical implant volume. Such signal voids might then be assigned with the low linear attenuation coefficients of air in image segmentation. Typical artefacts, pitfalls, and their avoidance will be presented.

Learning Objectives:

1. To identify common artefacts.
2. To understand the physical origin of and methods to resolve artefacts.
3. To understand the interrelation of MR artefacts and bias in PET quantification.

09:44

Panel discussion: Imagine imaging without artefacts: dos and don'ts in your clinical practice

08:30 - 10:00 **Room K**

Special Focus Session

SF 17c

How do radiographers enhance paediatric imaging?

A-868/A-869 08:30

Chairmen's introduction: The role of the radiographer when imaging a paediatric patient

L.J.O.C. Lança; *Lisbon/PT (luis.lanca@estesl.ipl.pt)*
E. Sorantin; *Graz/AT (erich.sorantin@medunigraz.at)*

The radiographer knowledge, skills and competences regarding the paediatric patient-centred care needs to be highlighted to pursue the enhancement of paediatric imaging. In the paediatric radiology department, radiographers and radiologists, among other healthcare professionals, develop their work that may be involved in child care. The associated risks information and the justified procedures to be undertaken for any radiological examination need to be appropriately and confidently communicated to child carers. Informed consent procedures would encourage radiographers and radiologists to be more attentive to consistently provide patients with adequate benefit-risk information relating to imaging examinations. Therefore, it is important that radiographers are aware on how to confidently communicate to paediatric patients and their families, as well as to other health professionals that may be involved in their care. Promoting a paediatric patient radiation safety culture for radiographers assumes a major relevance in paediatric imaging as the biological effects and lifetime risks of ionising radiation are higher in children than in adults. Identifying the types of traits that radiographers working with children have identified as being important to their practice emphasises how emotional intelligence impacts on their ability to gain the cooperation of paediatric patient and parents or carers, producing a high-quality clinically justified diagnostic examination. This special focus session will provide an opportunity for radiographers, radiologists and other healthcare professionals to share their experiences and their views about how to enhance paediatric imaging in a paediatric patient-centred care environment.

Session Objectives:

1. To learn about informed consent in paediatric imaging.
2. To emphasise the need of dose reduction practices in paediatric imaging.
3. To discuss emotional intelligence in paediatric imaging as a requirement for practice.

A-870 08:35

Informed consent: is this possible in paediatric imaging?

J. Portelli; *Msida/MT (jonathan.portelli@um.edu.mt)*

Concerns about the possible development of cancer as a result of the use of ionising radiation during medical imaging examinations are increasing. Consequently in a era driven towards patient-centred care, it has been argued that it is time for imaging departments to adopt informed consent procedures for imaging examinations that are considered to pose higher risks to patients, such as those performed in paediatric patients and those involving higher radiation doses. Such recommendations have been made on the presumption that an informed consent procedure would encourage referring physicians, radiographers and radiologists to be more attentive to consistently provide patients with adequate benefit-risk information relating to imaging examinations, unlike current practice whereby it appears that such information is not always disclosed. Subsequently, adequately informed patients and parents would be empowered to take a more active role in shared decisions concerning what would be best for them or their child. It is in this context that this lecture will seek to analyse and discuss the issue of informed consent in paediatric imaging, as well as highlight potential challenges radiographers face when imaging paediatric patients. Subsequently this lecture will seek to emphasise the importance of radiographers being knowledgeable and skilled on how to confidently communicate benefit-risk information to paediatric patients and their families, as well as to other health professionals that may be involved in their care.

Learning Objectives:

1. To discuss informed consent in paediatric imaging.
2. To highlight the challenges for radiographers in paediatric imaging.
3. To focus on risk communication as part of informed consent during paediatric imaging.

A-871 08:58

Dose reduction in paediatric imaging

G. Paulo; *Coimbra/PT (graciano@estescoimbra.pt)*

It is interesting to observe that over 120 years after the revolution triggered by Roentgen's discovery, there are still persisting problems, similar to those described in 1910 by Eddy German, one of the pioneers of the radiographer profession in the United States: "It was difficult to find two operators who were anywhere near in accord regarding technical procedure. Some would advise certain procedures and others entirely different programs". Despite the scientific knowledge and the technological development in the last decades, the reality described by Eddy German in 1910 still applies to today's practice of medical imaging. The reasons are manifold: (a) the lack of harmonisation of professional practice at all levels; (b) a communication gap between science and professional practice; (c) a delay in integrating the new technology concepts of medical imaging into curricular programmes of health professions; (d) a barrier between manufactures/equipment developers and clinical practice. Current research evidence shows that by developing applied research in radiography, involving clinical and academic radiographers, a significant dose reduction without compromising diagnostic image quality is achieved. The link between radiographers, radiologists and hospital management in the process of developing and translating research evidence into clinical practice, is the key for success in promoting a radiation safety culture, contributing to the development of best practice. The implementation of a radiation safety culture assumes particular relevance in the field of paediatric imaging due to the fact that the biological effects and lifetime risks of ionising radiation are higher in children than in adults.

Learning Objectives:

1. To discuss the current research findings and their implications for paediatric imaging.
2. To illustrate essential practical approaches to minimising doses.
3. To highlight the importance of radiation safety culture in paediatric imaging.

A-872 09:21

Personality traits: a way of maximising cooperation during paediatric imaging

S.J. MacKay; *Liverpool/UK (S.Mackay@liverpool.ac.uk)*

This paper will begin by defining and explaining trait, ability and tripartite models of emotional intelligence. It will then focus on the trait model and identify the types of traits that paediatric radiographers have identified as being important to their practice. It will then give examples from current clinical practice at a specialist paediatric hospital in the UK of how emotional intelligence impacts on their ability to gain the cooperation of patients and parents and produce a high-quality diagnostic image. Finally, it will give some examples of how radiographers can improve their emotional intelligence in paediatric radiography.

Learning Objectives:
1. To define and explain the different models of emotional intelligence (EI).
2. To discuss aspects of paediatric practice that require EI in order to deliver a quality paediatric radiography service for the patient and parent/guardian.
3. To discuss methods of improving emotional intelligence in radiographers.

09:44
Panel discussion: Challenges and opportunities when imaging paediatric patients

10:30 - 12:00 **Room A**

E³ - ECR Academies: Interactive Teaching Sessions for Young (and not so Young) Radiologists

E³ 1821
Dementia and movement disorders

A-873 10:30
A. MR contribution to diagnosis and differential diagnosis in dementia
M. Sasiadek; *Wroclaw/PL (marek.sasiadek@umed.wroc.pl)*

Imaging methods play an increasing role in diagnosing, differentiating, prognosis and follow-up of dementia. The most important imaging methods are: CT, MR, SPECT and PET. Among them MR, including MR spectroscopy (MRS), perfusion MR (PWI), diffusion tensor imaging (DTI) or functional MRI (fMRI), appears to be the most valuable modality. Plain MR might provide valuable contribution to the diagnostics of dementia. The distribution of the brain atrophy indicates the specific dementia disease, e.g. hippocampal atrophy is highly suggestive for Alzheimer disease and frontotemporal atrophy for frontotemporal dementia. There are also specific MR patterns of progressive supranuclear palsy (mesencephalic atrophy) or multiple system atrophy (cerebellar/brainstem or putaminal atrophies). Vascular dementia changes (e.g. small vessel disease, CADASIL, amyloid angiopathy) could be reliably diagnosed with MR, including MR angiography and susceptibility weighted sequences. There are also typical MR patterns of many other diseases, which may be accompanied by dementia, e.g. normal pressure hydrocephalus, multiple sclerosis, Wilson disease, Fahr disease, Creutzfeldt-Jakob disease, etc. Advanced MR techniques provide further contribution to diagnosing dementia by adding quantitative data. MRS could reveal increase of myoinositol level in degenerative diseases or of choline in multiple sclerosis. PWI shows decrease of perfusion in vascular dementia, but also in Alzheimer disease. DTI detects decrease of fractional anisotropy in white matter tracts affected by degenerative or inflammatory process. fMRI provides assessment of the impairment of cognitive functions in dementia disorders. MR, due to the advantages described above, should be a part of routine diagnostic protocol in patients with dementia.
Learning Objectives:
1. To become familiar with imaging in different types of dementia.
2. To learn the imaging criteria for differentiation.

A-874 11:15
B. Imaging in Parkinsonism and other extrapyramidal disorders
T. Stosic-Opincal; *Belgrade/RS (stosic.tanja@yahoo.com)*

Extrapyramidal disorders can be classified as pathologies that affect basal ganglia (*caudate*, *putamen*, and *globus pallidus*), subthalamic nucleus and structures that are functionally connected with them (substantia nigra). On histological level, affected tissues exhibit high level of deposits of paramagnetic ions (presumably iron and copper) and loss of neural tissue. This is manifested in loss of volume of brain structures and dysfunction of specific neural tracts. Parkinsonism refers to any condition that causes a combination of the movement abnormalities such as tremors, slow movement, impaired speech or muscle stiffness. Besides idiopathic Parkinson's disease, a several conditions fulfil definition, such as progressive supranuclear palsy, multisystem atrophy and corticobasal degeneration. Role of imaging techniques is assessment of structural and physiological changes caused by EPD. Magnetic resonance imaging is the primary choice since it provides morphological, structural and physiological insight into changes caused by extrapyramidal disorders. Positron emission tomography gives additional information about physiological changes by using neurotransmitters labelled with positron emitters. Computerized tomography has limited possibilities which are restricted to assessment of morphological changes.
Learning Objectives:
1. To become familiar with the different imaging modalities.
2. To learn the imaging criteria.

10:30 - 12:00 **Room B**

ESR meets Peru

EM 3
Peru in the radiological world

Presiding
J.L. Guerrero Gil; Lima/PE
P.M. Parizel; Antwerp/BE

A-875 10:30
Introduction: Peruvian radiology: how is it going?
J.L. Guerrero Gil; *Lima/PE (jguerrero@auna.pe)*

Peru is a South American country. We are about 30 million people. Our geography is very difficult and our cities have different conditions of life. That is why we have few modern cities specially at seaside with good level of health and education facilities and many other cities in the mountains and jungle regions with not so good level. The best hospitals, clinics and universities are in the main cities. There are 25 universities in Peru, 15 of them have medical schools. There is only one national program of residency and a 3-year training of radiology is included. Approximately 10 universities in different hospitals and clinics are able to train 30 or 40 radiologists a year and most of those are in Lima. There are about 500 radiologists in Peru and almost a half of them live and work in Lima, and are not yet members of the radiology society. We do not have official programs of fellows yet, but this is not bad at all because a Peruvian radiologist usually has to resolve a lot of problems in US, CT, MRI, x-ray in thorax, abdomen, etc. in different patients such as children, adults or old patients every day and that makes them very good general radiologists. We have a few modern hospitals and clinics with modern equipment such as PET CT, MRI, CT scans and digital mammography. They are distributed in the seaside cities specially in Lima; digital mammography, ultrasounds, digital radiography are spread out in almost all the cities of the country.
Session Objectives:
1. To become familiar with the Peruvian situation in the radiological world.
2. To show some radiological tools and their distribution over the country.
3. To give some information about radiological training in Peru.

A-876 10:35
MRI findings in CNS tuberculosis
R. Marquina Diaz; *Lima/PE (rmarquina@cinternacional.com.pe)*

In Peru, tuberculosis is a major cause of morbidity in the group of young adults, 82% of TB cases reported in 2013 and 2014 primarily affected the lungs. 77% of cases were diagnosed with pulmonary TB smear positive and nearly 40% with smear with a high bacillary load (2-3 crosses). Almost 18% of cases of extra pulmonary tuberculosis and pleural location had the highest percentage (54%), lymph nodes (11.1%) and meningeal/nervous system (9%) was reported. Magnetic resonance (MR) imaging has been shown to be superior to CT in evaluating patients with suspected meningitis and its associated complications. Complications of meningitis include hydrocephalus, vasculitis, cranial nerve involvement, and associated multiple tuberculomas. Tuberculomas are among the most common intracranial mass lesions and the most common manifestation of parenchymal TB and less than 2 to 3 cm in size. Tuberculous abscess are generally larger. In tuberculous spondylodiscitis, MR imaging is currently the imaging modality of choice, given its superior ability in the detection of soft tissue and bone marrow changes. Finally, numerous conditions can mimic tuberculomas on conventional imaging. Other imaging techniques such as diffusion imaging, perfusion and MR spectroscopy may help in differentiating these conditions.
Learning Objectives:
1. To give information about the characteristics of the MRI signs of the CNS tuberculosis in Peruvian patients.
2. To understand the accuracy of the MRI signs in CNS tuberculosis.
3. To show MRI images of CNS tuberculosis simulating other pathologies.

A-877 10:55
Interlude: From Peruvian mummies to bones: use of x-rays in Peruvian archaeology (part 1)
J.L. Guerrero Gil; *Lima/PE (jguerrero@auna.pe)*

X-rays are not only useful in medicine but are also particularly useful in other studies like archaeology. We are going to show you some of those applications in the study of mummies in Paracas a Pre Inca civilization types of mummifications, some results about the uses of conventional x-ray and CT scans and differences between dry and freezing mummifications.

A-878 11:00

MRI findings in non-tuberculosis infectious diseases in the CNS

P. Tapia Puente Arnao; *Lima/PE (tapiapedro@hotmail.com)*

CNS infectious diseases in Peru are still one of the leading causes of morbidity and mortality. We still have socioeconomic barriers that have limited the physicians from offering the best diagnostic method for the patient. MRI and CT reveal structural abnormalities and play a critical role in the initial diagnosis of new onset of neurologic symptoms in general. Nowadays due to techniques like diffusion, perfusion and spectroscopy associated with clinical and laboratory tests a more detailed analysis can be made that may significantly improve the sensitivity and specificity of MRI. The role of radiology in the diagnosis of infectious diseases is enormous. We need to identify the extension of the disease, the geographic region, and evaluate response of the diseases to different treatments. There are many infectious pathogens known to cause CNS infection, including broad categories of bacteria, viruses, fungi, mycobacteria, and parasites. In most cases, it is impossible for the radiologist with certainty to identify a specific organism as the cause of an observed radiographic abnormality in the CNS. In Peru, we can see cases of infection such as *Balamuthia mandrillaris* amoeba and co-infection of rhinocerebral mucormicosis and sinonasal aspergillosis. Geographical information, exposures, and clinical information supplied in the medical record can significantly aid in developing a more specific differential diagnosis. Different areas of Peru are well known for specific infectious pathology; for example, the leading cause of late-onset seizures and epilepsy in the north of Peru is neurocysticercosis.

Learning Objectives:

1. To learn about some infectious illness of the CNS in Peru and their MRI signs.
2. To give information about the accuracy of MRI signs in infection diseases.
3. To show MRI images of CNS infections simulating other pathologies.

A-879 11:20

Interlude: From Peruvian mummies to bones: use of x-rays in Peruvian archaeology (part 2)

J.L. Guerrero Gil; *Lima/PE (jguerrero@auna.pe)*

X-rays are not only useful in medicine but are also particularly useful in other studies such as archaeology. We are going to show you some of those applications in the study of mummies in Paracas a Pre Inca civilization types of mummifications, some results about the uses of conventional x-ray and CT scans and differences between dry and freezing mummifications.

A-880 11:25

Non-diagnosed spondyloarthritis in MRI of the spine for lower back pain

J. Carpio; *Lima/PE (jeremy.carpio@resocentro.com)*

Spondyloarthropathies (SpA) include a group of long-term (chronic) diseases of joints as well as the spine and sacroiliac joints. It is divided into axial spondyloarthritis axSpA (ankylosing spondylitis AS) and peripheral spondyloarthritis. They share clinical and radiologic manifestations as well as familial aggregation and a strong association with HLA B27 antigen. Inflammatory back pain is the leading symptom of the SpA. ASAS criteria to diagnose axial SpA include MRI of sacroiliac joints to find bone marrow oedema (BME). However, MRI-identified structural lesions are not included (contradictory due to the fact that it is criteria in simple x-ray) as neither are spinal lesions. 23% to 50% of patients with ankylosing spondylitis (with disease clinically active) or “non-radiographic’’ axial SpA can have acute spinal inflammatory lesions without evidence of acute sacroiliitis by MRI. Chronic back pain is often investigated by nonrheumatologists and SI joint scanning may be excluded. On the other hand, ASAS criteria only evaluate sacroiliac joints leaving spine without evaluation. Are current criteria sufficiently capable of including all those patients with potential diagnosis of spondyloarthropathies? In any case, what can modify to achieve a greater range of sensitivity in our studies?

Learning Objectives:

1. To demonstrate that routine spine MRI for lower back pain is not sufficient for finding osteitis in spondyloarthritis.
2. To understand the MRI signs in lumbosacral spondyloarthritis.

11:45

Panel discussion: Is MRI the gold standard in CNS infection disease?

10:30 - 12:00 **Room F1**

E³ - European Diploma Prep Sessions

E³ 1823

Principles of imaging and radiation protection

A-881 10:30

Chairman's introduction

P. Vock; *Spiegel/CH (peter.vock@med.unibe.ch)*

This short introduction to the session will point out the importance of the three basic subjects covered in every radiologist's professional life. While it will not be possible to cover the full body of knowledge in each area, the speakers will discuss important principles and their application in the daily clinical work.

Session Objectives:

1. To understand the technical and methodological principles of computed tomography.
2. To understand the technical and methodological principles of magnetic resonance tomography.
3. To learn the principles of radiation biology and radiation protection.

A-882 10:36

A. Principles of computed tomography

W.A. Kalender; *Erlangen/DE (willi.kalender@imp.uni-erlangen.de)*

The introduction of x-ray computed tomography (CT) in 1972 meant the transition from conventional 2D projection imaging to superposition-free slice imaging. To understand the basic principles of CT to a certain degree, the data acquisition and the image reconstruction process will be explained in a general form. The resulting CT images do not only provide morphology but also give quantitative CT values according to the Hounsfield scale which will be explained in detail. There is an impressively broad spectrum of technical solutions and CT scanner types. It all started with single-slice imaging, was developed further into true 3D imaging by the introduction of spiral scanning approaches, and was augmented significantly by the introduction of multi-row detectors. Multi-slice imaging is today’s standard. In addition to the typical clinical scanner design, a variety of scanner types such as dual source CT and C-arm CT have to be mentioned; small dedicated peripheral CT scanners also gain increasing acceptance in clinical practice. Aspects of image quality and dose efficiency are of great importance. High spatial resolution and low image noise are contradictory goals and both may imply elevated radiation dose levels. Many innovative technical means for dose reduction are available today and are used to reduce dose at unimpaired image quality. Some important options, such as the use of optimized spectra, will be explained. Modern CT allows imaging at very high quality with effective dose values in the low mSv or even sub-mSv range.

Learning Objectives:

1. To understand the physical basis of image formation of computed tomography and of the physics of helical, multidetector and dual-source CT.
2. To learn the scale of Hounsfield units and the principle of window centre and width.
3. To become familiar with modern CT technology.
4. To understand the principles of optimising CT protocols with a focus on patient dose reduction.

Author Disclosure:

W.A. Kalender: CEO; AB-CT GmbH, Erlangen, Germany. Consultant; Bayer Healthcare Berlin, Germany. Founder; AB-CT GmbH, Erlangen, Germany.

A-883 11:04

B. Principles of magnetic resonance imaging

T. Metens; *Brussels/BE (tmetens@ulb.ac.be)*

Magnetic resonance imaging (MRI) is based on proton nuclear magnetic resonance (liquid NMR) inside a strong magnetic field (1.5T/3T). The tissue NMR signal is a Faraday induction in coils consecutive to radiofrequency pulse sequences. Magnetic field gradients are furthermore used in MRI to provide signal spatial encoding. The MRI signal provides an excellent soft tissue contrast. Indeed the signal intensity depends on NMR relaxation times T1 and T2 (spin-echo sequences) or T2* (magnetic susceptibility-dependent gradient-echo sequences) and soft tissue contrast occurs because relaxation times are tissue dependent. The sequence structure controls the image contrast: T1-weighted or T2-weighted (or T2*-weighted) images are commonly used for diagnostic purpose. When an inversion radiofrequency pulse precedes the main sequence by a time delay TI, a T1-based selective tissue suppression can be achieved (fat suppression in STIR, fluid suppression in FLAIR sequences). The presence of a paramagnetic agent inside a tissue shortens

the tissue T1 relaxation time and contributes to lesion detection or characterisation. The agent can be intrinsic (like methemoglobin after haemorrhage) or exogenous (intravenous injection of a gadolinium chelate). The MRI signal can be made sensitive to blood flow: flow-void in spin-echo or inflow hyper-intensity in gradient-echo sequences. Angiography is also obtained with Gd-enhanced gradient-echo sequences. Sequence structure, operator choices and tissue characteristics influence image quality, including signal-to-noise ratio and artefacts. MRI contraindications and staff or patient safety issues are mostly related to the strong magnetic field, to RF and gradient pulses or to contrast agent use.

Learning Objectives:

1. To become familiar with the physical basis of image formation in MRI including the principles of pulse sequences and relaxation times.
2. To understand the principles and main diagnostic applications for the most commonly used sequences in MRI, including T2-weighted sequences, T1-weighted sequences, STIR sequences, FLAIR sequences, other inversion recovery sequences, T2*- / susceptibility-weighted sequences and MR angiography sequences.
3. To learn typical artefacts on MR imaging and to discuss their respective causes.
4. To understand absolute or relative contraindications against MR imaging and safety issues in the MR environment with regard to patients and staff.

A-884 11:32

C. Radiation protection

M. Mahesh; *Baltimore, MD/US (mmahesh@jhmi.edu)*

The number of medical imaging procedures is growing exponentially across the globe. The overall benefit from medical imaging procedures far outweighs any associated risks. However, increasingly patients and families undergoing medical imaging are enquiring about radiation dose and risks. Hence, it is upon us as providers (radiologists, cardiologists, and any other physicians) of medical imaging studies to ensure the studies are justified and optimally performed with the focus of keeping any associated risks to a minimum. This lecture will focus on the biological effects of radiation and fundamental concepts of radiation protection applicable to both patients and staff alike. Three pillars of radiation protection, namely time, distance and shielding will be discussed with illustrations. Since there is an increasing demand from patients to know more about their radiation doses and risks, this lecture will also describe various radiation dose descriptors in CT, fluoroscopy and radiography. Finally, the lecture will summarize key radiation protection strategies for all those working in a radiation environment.

Learning Objectives:

1. To understand the phenomena of x-ray interaction with matter and the consequences for image generation, image quality and radiation exposure.
2. To become familiar with the types and magnitudes of radiation exposure from natural and artificial sources and the concepts of dose determination and dose measurement for patients, occupationally exposed personnel and the public.
3. To learn the types and magnitudes of radiation risk from radiation exposure in medicine.
4. To understand the basic principles of radiation protection, as outlined by the ICRP (International Commission on Radiological Protection).
5. To become familiar with the concepts and tools for dose management in radiology with regard to adult and paediatric patients.

Author Disclosure:

M. Mahesh: Author; Book Royalty for 'MDCT Physics - The Basics, Technology, Image Quality and Radiation Dose.

12:30 - 13:30 **Room C**

E³ - The Beauty of Basic Knowledge: Chest Imaging

E³ 25E

Still tricky after all these years

Moderator:
N. Howarth; Chêne-Bougeries/CH

A-885 12:30

A. The hila

B. Ghaye; *Brussels/BE (benoit.ghaye@uclouvain.be)*

Anatomy of the hila on plain films is generally considered as a difficult matter. Some simple anatomical landmarks are important to know to make easier interpretation of chest plain films, including the hilar angle, the infrahilar window and the normal anisomerism of both hila. Right upper lobe bronchus is eparterial and the left one is hyparterial. The left hilum is higher than the right in 97% while opacity and dimension of both hila are equivalent in about 90%. On lateral view, the right hilum and the left upper pulmonary vein are located in front of and the left hilum behind the tracheobronchial lumen. Knowing those simple findings makes easier the recognition of pathologies such as discrete lobar volume loss, small hilar lymphadenopathies or substantial congenital abnormalities that would be otherwise overlooked, including isomerism or persistent ductus arteriosus. On the other hand, knowledge of hilar and pulmonary vessels anatomy will avoid wrong diagnosis of pulmonary nodule or tumour due the 2D-projection of normal vascular structures. During this presentation, the side-by-side analysis of chest plain films and CT will present a comprehensive review of the most important anatomical and pathological findings in the hila and the proximal pulmonary vessels.

Learning Objectives:

1. To review the anatomy of the hila.
2. To learn how to identify hilar lesions.
3. To know the limitations of plain radiographic signs.

A-886 13:00

B. The mediastinum

M. Occhipinti; *Florence/IT (mariaelena.occhipinti@gmail.com)*

Hilar mass or pulmonary mass? Middle mediastinum or posterior mediastinum? Vessel or not? Normal or abnormal? CT or MRI? Many questions can arise during daily clinical practice on evaluating the complex anatomical region called mediastinum. Whether clinicians or radiologists bring up the question, the patient awaits an accurate answer. This answer is essential to address patient diagnostic workup and management. Chest radiography, CT and MRI are invaluable tools to study the mediastinum with a non-invasive approach. However, knowledge of the most appropriate technique to use in each context as well as knowledge of specific imaging signs and features are needed to narrow the differential diagnosis and to address the majority of the questions that have arisen when a mediastinal mass is either seen or suspected.

Learning Objectives:

1. To review the mediastinal anatomy according to old and new classifications.
2. To learn how characteristic features can be helpful in the differential diagnosis.
3. To know how to choose the most appropriate imaging modality according to the diagnostic question.

12:30 - 13:30 **Room D**

E³ - The Beauty of Basic Knowledge: A Survival Guide to Musculoskeletal Imaging

E³ 24E

Infective/inflammatory disorders

Moderator:
V.N. Cassar-Pullicino; Oswestry/UK

A-887 13:00

Infective/inflammatory disorders

F.M.H.M. Vanhoenacker; *Antwerp/BE (filip.vanhoenacker@telenet.be)*

Osteomyelitis is divided into acute, subacute and chronic osteomyelitis. Pathophysiological factors that determine imaging are patient's age, route of contamination, virulence of the causative micro-organism and the immune status of the patient. In haematogenous spread, the site and extent of the infection depends primarily on the vascularisation. The metaphysis is the common site for haematogenous osteomyelitis in children over 18 months, due to stasis of slow-flowing blood. In infants and adults, the presence of transphyseal vessels may cause spread of the infection to the epiphysis. Imaging plays a pivotal role in confirming the diagnosis of musculoskeletal infection, determining the disease extent and guiding early treatment. Plain radiography is not very sensitive for early diagnosis. Ultrasound is a reliable tool to detect subperiosteal spread in children, but its use in adults is restricted to evaluation of soft tissue infection and for aspiration of infected joints. In adults, MRI is the preferred modality, although CT may detect sequestrum formation in chronic osteomyelitis. SpA consists of a spectrum of chronic inflammatory disorders that are distinct from RA. Ultrasound is useful for grading of synovitis and early detection of erosions of peripheral joints in RA. SpA has a predilection for the axial skeleton. MRI is the preferred technique for early diagnosis and detection of active inflammatory lesions by demonstrating bone marrow oedema at the sacro-iliac joints. Two or more areas of BME or one focus of BME on at least two consecutive 3 mm slices is needed to reliably diagnose axial SpA.

Learning Objectives:
1. To learn about the pathomechanisms involved in inflammatory and infections disorders.
2. To understand the imaging appearances and their differential diagnosis in the acute, sub-acute and chronic phases of infection.
3. To become familiar with the spectrum of imaging features of inflammatory disorders in the axial and peripheral skeleton.

14:00 - 15:30 **Room F1**

E³ - European Diploma Prep Sessions

E³ 1923
Neuro

A-894 14:00
Chairman's introduction
C. Manelfe; *Toulouse/FR*

Session Objectives:
1. To learn relevant imaging and interventional algorithms and important imaging features of neurovascular disorders of the brain and spine.
2. To understand imaging features and prognostic implications of tumours of the brain and spine.
3. To become familiar with the role of different imaging modalities including hybrid imaging in diagnosing disorders of the central nervous system.

A-895 14:06
A. Congenital and white matter disorders of the brain
A. Rossi; *Genoa/IT (andrearossi@gaslini.org)*

Understanding of normal maturational steps and myelination is crucial for interpreting MR imaging scans of the brain in infants and children correctly. Planning of sequence parameters tailored to the water-rich brain environment of small children is also crucial for image quality. Among the several pitfalls, pineal gland cysts are extremely common in children and their significance will be highlighted. The principal features of the commonest brain malformations (corpus callosum, cortical, and cerebellar) and neurocutaneous syndromes (NF1, NF2, tuberous sclerosis, and Von Hippel-Lindau) will be discussed. Finally, a road map for differentiating congenital from acquired white matter disorders will be presented.
Learning Objectives:
1. To understand the development, normal anatomy and normal variants of the brain.
2. To become familiar with common congenital disorders of the brain and neurocutaneous syndromes.
3. To learn imaging features and differential diagnoses of white matter disease, inflammation and neurodegeneration.
Author Disclosure:
A. Rossi: Consultant; Bracco Imaging Italia SrL.

A-896 14:34
B. Neurovascular disorders and trauma of the brain
M. Forsting; *Essen/DE*

"No abstract submitted."
Learning Objectives:
1. To become familiar with the normal anatomy and normal variants of the craniocervical arterial and venous system and its relevance to interventional neuroradiology.
2. To learn the causes and imaging features of stroke, haemorrhage and other common vascular lesions of the brain.
3. To understand the imaging features of traumatic injury to the brain and spine.

A-897 15:02
C. Tumours of the brain and spine
M.M. Thurnher; *Vienna/AT (majda.thurnher@meduniwien.ac.at)*

Standardised MR brain tumour protocol is crucial for the preoperative evaluation and interpretation of postoperative changes. Brain tumour imaging objectives include: the diagnosis of brain tumour and the ability to distinguish it from non-tumoural lesions, assessment of histological grade of the tumour, delineation of the tumour borders and extension, differentiation between tumour and peritumoural oedema, and finally the evaluation of possible recurrence and therapy induced phenomena. In this lecture, the following issues will be discussed: how to distinguish between benign and malignant brain tumours; the value of different conventional and advanced MRI techniques in evaluation of CNS tumours; most common spine tumours not to miss.
Learning Objectives:
1. To understand the normal anatomy and normal variants of the spine, spinal cord and nerve roots.
2. To learn imaging features of benign and malignant tumours of the neurocranium.
3. To become familiar with the imaging features of benign and malignant tumours of the spine.

B

Scientific Sessions and Clinical Trials in Radiology (B)

Scientific session numbers are prefixed by SS.
Presentation numbers are prefixed by the letter B.
Sessions and abstracts are listed by days.

The Clinical Trials in Radiology sessions are listed at the end of section B. (page 484)

Wednesday, March 1

10:30 - 12:00 **Room B**

Abdominal Viscera

SS 201a

Hepatocellular carcinoma (HCC): detection, characterisation and therapeutic response

Moderators:
D. Ippolito; Monza/IT
N.N.

B-0001 10:30

Feasibility of 10-min delayed hepatocyte phase imaging using a 30° flip angle in Gd-EOB-DTPA-enhanced liver MRI for the detection of hepatocellular carcinoma in patients with cirrhosis

J. Choi, E.-S. Cho, J. Kim, Y. Choi; *Seoul/KR (justice-cjm@yuhs.ac)*

Purpose: To compare 10-min delayed hepatocyte phase imaging (HPI) using a 30° flip angle (FA) (10m-FA30) and 20-min delayed HPI using a 10° FA (20m-FA10) or 30° FA (20m-FA30) in Gd-EOB-DTPA-enhanced MRI in patients with chronic hepatitis or cirrhosis, in terms of contrast-to-noise ratio (CNR) for hepatocellular carcinoma (HCC) and detection sensitivity for focal hepatic lesions (FHLs).
Methods and Materials: 104 patients with 168 HCCs and 55 benign FHLs who underwent Gd-EOB-DTPA-enhanced MRI with 10m-FA30, 20m-FA10, and 20m-FA30 were enrolled. Patients were divided into two groups according to the Child-Pugh classification: group A with Child-Pugh A cirrhosis and group B with Child-Pugh B or C cirrhosis. CNR for HCCs and the detection sensitivity for FHLs were compared between 10m-FA30 and 20m-FA10 or 20m-FA30.
Results: In group A, the CNR for HCCs on 10m-FA30 (165.8±99.7) was significantly higher than that on 20m-FA10 (113.4±71.4) and lower than that of 20m-FA30 (210.2±129.3). However, there was no significant difference in the detection sensitivity between 10m-FA30 (95.0%) and 20m-FA10 (94.7%) or 20m-FA30 (94.7%). In group B, the CNR (54.0±36.4) for HCCs and the detection sensitivity (94.2%) for 10m-FA30 were significantly higher than those for 20m-FA10 (41.8±36.4 and 80.8%, respectively) and were not different from those for 20m-FA30 (62.7±44.4 and 93.3%, respectively).
Conclusion: The diagnostic performance of 10m-FA30 was similar to or higher than 20m-FA10 or 20m-FA30 in both groups A and B. This finding indicates that 10m-FA30 could replace 20-min delayed HPIs regardless of patient's liver function and reduce the delay time by 10 minutes.

B-0002 10:38

Assessment of gadoxetic acid-enhanced MRI phases for LI-RADS categorisation and non-invasive grading of hepatocellular carcinoma

M. Wutschke, U. Teichgräber, T. Lehmann, K. Katenkamp, T. Franiel; *Jena/DE (martin.wutschke@web.de)*

Purpose: This retrospective study evaluated the impact of transitional and hepatobiliary phase on LI-RADS classification and non-invasive grading in patients with hepatocellular carcinoma (HCC).
Methods and Materials: 61 patients with 61 histologically confirmed HCCs underwent MRI with gadoxetic acid. In all phases (arterial [AP], portal venous [PVP], transitional [TP], hepatobiliary [HP]) signal intensities (SI) of HCC and adjacent liver parenchyma were measured. For quantitative assessment ratio between SI of HCC and SI of normal liver were calculated. LI-RADS classification (LR-1 to LR-5) were done in A) LI-RADS major criterions with assessment of washout criterion only in PVP, B) same as A + ancillary feature "transitional phase hypointensity" and C) same as B + ancillary feature "hepatobiliary phase hypointensity". Histopathological HCC grading results were correlated with the SI HCC ratio (= SI mass HP / SI mass AP).
Results: None HCC was graded as LR-1 or LR-2. The inclusion of the feature "transitional phase hypointensity" led to a non-significant upgrading of 5/9 HCC from LR-3 to LR-4 (p = 0.062). The addition of the feature "hepatobiliary phase hypointensity" led to a statistical significant upgrading of 8/9 HCC from LR-3 to LR-4 (p = 0.008). None HCC with initial LR-4 was upgraded. None lesions were downgraded. The HCC SI ratios between G1 vs. G2/G3 tumours were statistically significant different (p = 0.008).
Conclusion: The addition of transitional and hepatobiliary gadoxetic acid-enhanced MRI phases improves LI-RADS categorisation. Quantitative assessment of HCC SI ratio enables non-invasive grading.

B-0003 10:46

Comparison between acoustic radiation force impulse quantification data and perfusion-CT parameters in hepatocellular carcinoma

M. Esser, S. Schneeweiß, M. Kolb, M. Kurucay, C. Ruff, K. Nikolaou, M. Horger; *Tübingen/DE (michael.esser@med.uni-tuebingen.de)*

Purpose: To find out, if ultrasound elastography of hepatocellular carcinoma (HCC) can predict patterns of tumour perfusion in volume perfusion computed tomography (VPCT).
Methods and Materials: 25 consecutive patients (mean age, 68.9; range, 51 - 85 years) with liver cirrhosis suspected of HCC underwent VPCT and acoustic radiation force impulse (ARFI) elastography the same day. Quantitative elasticity values were registered, while blood flow (BF), blood volume (BV) and hepatic perfusion index (HPI) of the HCC lesions were calculate. Additionally, we identified histologic WHO grading, lesion size and localisation. The Siemens Acuson S 3000 HELX-System with Virtual Touch™-Software and Siemens Somatom Definition Flash with Syngo® software were used.
Results: A total of 43 HCC lesions were assessed. Mean shear wave velocity was 2.6 m/s (range, 1.1 - 4.3 m/s). There was no significant linear correlation between the elasticity values and BF (p=0.751), BV (p=0.426) and HPI (p=0.437). However, elasticity values were higher, the larger the tumour was (p=0.008). Shear wave velocity declined with increasing distance of the HCC to the skin surface (p=0.028) and depending on liver segment. In addition, elasticity values were higher in less differentiated HCCs. This trend was not statistically significant (p=0.842).
Conclusion: Tissue elasticity in HCC does not correlate with the degree of tumour vascularisation, but calculated values are influenced both by the tumour size and localization inside the liver.

B-0004 10:54

Evolution of indeterminate hepatocellular nodules at initial Gd-EOB-DPTA-enhanced MRI in cirrhotic patients

F. Agnello, M. Galia, G. Sparacia, M. Miroddi, F. Midiri, G. Brancatelli; *Palermo/IT (fra.agnello@libero.it)*

Purpose: To retrospectively evaluate the evolution of indeterminate hepatic nodules at initial Gd-EOB-DPTA-enhanced MRI in cirrhotic patients.
Methods and Materials: 33 cirrhotic patients (24 males; mean age 64.9 years) with 69 indeterminate nodules (mean diameter 1.1 cm; range 0.5-2) at initial Gd-EOB-DPTA-enhanced MRI and a Gd-EOB-DPTA-enhanced MRI follow-up of at least 2 years (mean 805 days; range 745-2440) were evaluated. Indeterminate hepatocellular nodules were defined as nodules that cannot be diagnosed as HCC according to ASSLD 2010 criteria. Based on signal intensity at initial MRI, each nodule was classified into 6 groups: A) hyperintense on precontrast T1 phase (12/69); B) hyperintense on precontrast T1 and hepatobiliary phase (4/69); C) hyperintense on hepatobiliary phase (23/69); D) hypointense on hepatobiliary phase (9/69); E) hypointense on transitional and hepatobiliary phase (20/69); F) hypointense on portal-venous, transitional and hepatobiliary phase (1/69). Changes in size (disappearance, regression, no change, growth) and rate of progression to HCC were compared among groups using Chi-square test. Diagnosis of HCC was done by pathology and ASSLD 2010 criteria.
Results: 5/69 (7%) nodules (3 Group E; 2 group D) become HCC. There was no statistically significant difference in progression to HCC among groups. There was no statistically significant difference in rate of nodule disappearance (6%; 8/69); regression (4%; 7/69), no change (55%; 38/69) and growth (23%; 16/69) among groups.
Conclusion: Indeterminate hepatic nodules at Gd-EOB-DPTA-enhanced MRI in cirrhotic patients rarely progress to HCC.

B-0005 11:02

Fate of subcentimeter arterially enhancing and hepatobiliary hypointense lesions seen on gadoxetate-enhanced MRI in patients at risk of HCC

C. Park, C. An, J.-Y. Choi, M.-J. Kim; *Seoul/KR (CHANSIKAN@yuhs.ac)*

Purpose: To investigate the significance of subcentimeter (≤1 cm) arterially enhancing and hepatobiliary hypointense lesions (SAELs) found on gadoxetate-enhanced MRI in patients at risk of hepatocellular carcinoma (HCC).
Methods and Materials: Two radiologists jointly reviewed gadoxetate-enhanced MRI obtained from September 2008 to March 2013 in 2,311 patients at high risk of HCC, and found 52 SAELs that were confirmed histologically or followed by imaging over 12 months: 17 isolated SAELS in patients without accompanying HCC and 35 in patients with early-stage HCC (solitary or up to 3 nodules ≤ 5cm in size without vascular invasion). SAELs found in patients at beyond early stages were excluded. The imaging findings were compared between the malignant and benign SAELs.
Results: Of total 52 SAELs (in 46 patients), 30 (57.7%) were finally diagnosed as HCCs: 10 (58.8%) among 17 isolated SAELs and 20 (57.1%) among 35 SAELs accompanying early-stage HCCs. All HCCs were resectable with

curative intention at the time of diagnosis. Diagnostic accuracy of HCC based on imaging findings of arterial enhancement and venous-phase washout yielded the sensitivity, specificity, and positive predictive values of 83.3%, 50%, and 69.4%, respectively. Venous-phase washout was more frequently observed in the malignant SAELs than in the benign SAELs (57.7% vs. 30.6%; $P = 0.01$).
Conclusion: SAELs found on gadoxetate-enhanced MRI in patients at risk of HCC have a high malignant potential. Close observation can be an appropriate strategy for isolated SAELs. Venous-phase washout may be helpful to predict malignant SAELs.

B-0006 11:10

Hypovascular hypointense nodules on hepatobiliary phase without T2 hyperintensity on gadoxetic acid-enhanced MRI: long-term outcomes and risk factors of hypervascularisation

H. Yang, J. Song, E. Choi, E. Park; *Jeonju-si/KR (yphot@naver.com)*

Purpose: To evaluate the long-term outcome and risk factors associated with hypervascularisation in hypovascular hypointense nodules on hepatobiliary phase (HBP) without T2 hyperintensity on gadoxetic acid-enhanced magnetic resonance (MR) images in patients with chronic liver disease.
Methods and Materials: The institutional review board-approved retrospective analysis included 97 chronic liver disease patients with 222 hypovascular hypointense nodules on HBP without T2 hyperintensity on gadoxetic acid-enhanced MRI. The following MR features were analysed: nodule size, presence of fat, degree of hypointensity on HBP, degree of signal intensity on diffusion-weighted images (DWI) and T1-weighted images (T1WI). Baseline clinical characteristics were also obtained. Univariate and multivariate analysis with a Cox proportional hazard regression model was used for statistical analysis.
Results: The mean follow-up interval was 997 days (range, 137-1804 days). Of them, 41 nodules (18.5 %) became hypervascular hepatocellular carcinoma (HCC). Both univariate and multivariate Cox analysis identified that previous history of HCC, follow-up nodule size, degree of hyperintensity on T1WI and DWI were significant risk factors for hypervascularisation ($P<0.05$). The mean growth rate of hypervascularised nodule was 2.89×10^{-3}/days and 0.68×10^{-3}/days for non-hypervascularised nodule. The cumulative incidence of hypervascularisation was 3.7 % at 1 year, 12.9 % at 2 years, 21.3 % at 3 years.
Conclusion: The previous history of HCC, follow-up nodule size, degree of hyperintensity at T1WI and DWI were associated with progression to hypervascular HCC.

B-0007 11:18

Is CT perfusion a useful tool to predict response early after transarterial chemoembolisation?

D. Tamandl, F. Waneck, S. Unterhumer, A. Ba-Ssalamah, C. Loewe; *Vienna/AT (dietmar.tamandl@meduniwien.ac.at)*

Purpose: To determine the value of CT perfusion (CTP) to predict complete response early after transarterial chemoembolisation (TACE).
Methods and Materials: This prospective study was approved by the institutional review board, written informed consent was obtained from all patients. CTP was performed before and one day (interquartile range[IQR]: 1-2 days) after TACE in 18 patients. 46 lesions (41 hepatocellular carcinoma [HCC] and 5 hypervascular cholangiocarcinoma [CCC]) were amenable for analysis. Blood flow (BF), Blood volume (BV), time to start (TTS), arterial liver perfusion (ALP), portal liver perfusion (PVP) and hepatic perfusion index (HPI) were measured in all lesions, and values before and after TACE, as well as relative change was compared to clinical response on biphasic CT using mRECIST criteria 6 weeks after the procedure. Optimal cut-off values for detecting response were calculated using area under the ROC curves (AUROC). Long-term outcome was assessed using Kaplan-Meier estimates.
Results: CTP parameters were all significantly reduced after TACE in responding patients (PR, CR) while no difference was observed in non-responders. ALP_{post} was superior in prediction of CR compared to BF_{post} and BV_{post} ($AUROC_{ALP}$ 0.953 vs. $AUROC_{BF}$ 0.859 and $AUROC_{BV}$ 0.831, $p<0.001$) with a sensitivity, specificity, PPV, NPV and accuracy of 91%, 92%, 91%, 92% and 91%. Only 4/22 lesions with CR recurred with a median progression local-recurrence free survival of 22.7 months.
Conclusion: CT Perfusion is a feasible tool for early response assessment after transarterial chemoembolisation and can reliably detect lesions with complete response.

B-0008 11:26

HCC showing complete response according to mRECIST on CT after a first session of TACE: is lipiodol deposition a good predictor of local recurrence?

M. Dioguardi Burgio, M. Ronot, M. Lagadec, C. Garcia-Alba, M. Zappa, A. Sibert, V. Vilgrain; *Clichy/FR (marco_dioguardi@hotmail.it)*

Purpose: To evaluate if the lipiodol deposition pattern can predict local recurrence in hepatocellular carcinoma (HCC) nodules with complete response (CR) according to mRECIST on CT after a first session of conventional chemoembolisation (cTACE).
Methods and Materials: From January 2012 to May 2014 all consecutive patients undergoing a first cTACE for HCC were identified. Inclusion criteria were presence of ≤3 HCCs and available pre- and post-cTACE CECT. Each treated tumour response was classified according to mRECIST. The analysis focused on tumours showing CR. For them, the lipiodol deposition pattern was classified as complete (C-Lip, covering the entire tumour volume), or incomplete (I-Lip). Local recurrence was defined as the reappearance of enhancing areas on arterial phase showing washout on portal/delayed phase within 2 cm from treated tumours on follow-up CT.
Results: Final population included 50 patients (mean age 62+/-12 y; 45 male (90%)) with 82 HCCs (mean 26.8+/-14.2 mm). A total of 46 (52%) HCCs were classified as CR, including 16 (35% - mean 22.9+/-8 mm) with incomplete, and 30 (65% - mean 22.8+/-10 mm) with complete lipiodol deposition. After a median follow-up of 14 months (range 3.2-35.9 months), 15/16 (94%) and 10/30 (30%) of I-Lip and C-Lip HCCs showed local recurrence on CT ($p<0.001$). No statistical difference regarding delay of recurrence was noted between I-Lip and C-Lip HCCs (mean 334 vs 401 days $p=0.519$).
Conclusion: Despite showing CR according to mRECIST, HCCs with incomplete lipiodol deposition have a high risk of recurrence and should be considered as incompletely treated.

B-0009 11:34

Role of IVIM in the verification of response to locoregional therapy in HCC

W.R.A. Abdel Hamid, R. Salah Eldein, Y. Abbas; *Cairo/EG (w.gforever@yahoo.com)*

Purpose: Liver cirrhosis and HCC constitute an important cause of morbidity and mortality in Egypt. Our work aimed at evaluating the role of intravoxel incoherent motion (IVIM) as a non-contrast imaging biomarker in follow-up of HCC after locoregional therapy to reduce study cost.
Methods and Materials: Our study included 20 patients with liver cirrhosis accommodating 100 HFLs. They were assessed using 3T MR scanner with addition of IVIM both initially and in the follow-up after loco-regional therapy. Post-processing analysis was performed to measure IVIM parameters including D, D*, fp & ADC. fp was compared to the % of arterial enhancement of hepatic focal lesions in both initial and follow-up studies using Pearson correlation test. Moreover, we assessed the correlation between D and ADC initially and on follow-up using t test.
Results: Moderate correlation between fp and % of arterial enhancement of hepatic focal lesions ($r= 0.686$). Significant difference between fp initially and in follow-up with $P<0.01$. Better performance of D compared to ADC in follow-up studies regarding differentiating viable malignant tissue from non-malignant entities with $P=0.03$ and 0.04, respectively.
Conclusion: fp shows moderate correlation with % of arterial enhancement in differentiating well-treated lesions from residual malignancy. D value is better in assessing residual component compared to ADC. Thus, fp and D values can be considered reliable non-contrast MR tools in the verification of response to therapy.

B-0010 11:42

Role of DW-MRI in the evaluation of HCC response to DEB TACE: correlation with DCE MRI

M.M.H. Faheem[1], M.I. Youssef[1], M.M. Reffat[1], I.M. Hamed[2]; [1]*Banha/EG*, [2]*Cairo/EG (dr.mohamed.yousef@fmed.bu.edu.eg)*

Purpose: Aim of study is to evaluate accuracy of DW-MRI in evaluating HCC response post-DEB TACE and compare results with DCE MRI.
Methods and Materials: 42 patients with 59 lesions underwent conventional precontrast abdominal MR, DWI, ADC map with ADC value measurement and DCE MR. According to DCE MR, the lesions have been classified into 4 groups (complete response, heterogeneous enhancement, partial nodular enhancement, diffuse enhancement groups). Qualitative DWIs and ADC values were correlated to the DCE MR findings.
Results: Upon comparing qualitative DWI findings to DCE MRI in the evaluation of HCC response to DEB TACE, it showed sensitivity of 83.9%, a specificity of 64.3%, a positive predictive value of 72.2%, and a negative predictive value of 78.3% and overall accuracy of 74.5%. The measured ADC values showed significant difference (P value <0.05) between ADC values

measured in active tumoural areas and those measured in necrotic areas with no significant difference between areas of active tumoural enhancement in the different groups. ROC analysis was performed for ADC values showing area under curve 0.7 and maximum combined sensitivity and specificity of 79% and 69.6%, respectively, at cutoff ADC value of 1.395mm²/sec.
Conclusion: DW-MRI is a useful highly sensitive technique in the evaluation of HCC response to DEB TACE, yet it has low specificity related to high number of false-positive results preventing using it solely. In addition, DWI is a reliable method in differentiation between active tumour residue/recurrence and benign perilesional enhancement.

B-0011 11:50

Liver stiffness measured by 2D shear-wave elastography: prognostic values after radiofrequency ablation for hepatocellular carcinoma
D. Lee; *Seoul/KR (dhlee.rad@gmail.com)*

Purpose: Liver stiffness (LS) measured by supersonic shear-wave elastography (SWE) can estimate the degree of liver fibrosis. We prospectively evaluated the prognostic value of LS measured using SWE in patients with hepatocellular carcinoma (HCC) treated by radiofrequency ablation (RFA).
Methods and Materials: We prospectively enrolled a total of 145 patients with up to three HCCs≤5cm treated by RFA and who underwent pre-procedural 2D-SWE from January 2012 to December 2013. LS values were measured using real-time SWE (Aixplorer; Supersonic Imagine, France). After a mean follow-up of 32.2±11.5 months, we analysed overall survival (OS) after RFA using the Kaplan-Meier method and Cox proportional hazard regression model. The optimal cut-off LS value to predict OS was determined by the minimal P-value approach.
Results: During the follow-up period, 22 patients died and 11 patients underwent liver transplantation. The estimated 1- and 3-year OS was 96.4% and 85.8%, respectively. The LS value measured by 2D-SWE was a significant predictive factor for OS after RFA for HCC, as was the presence of extrahepatic metastases. The optimal cut-off LS value to predict OS was set at 13.3 kilopascal (kPa). Seventy-nine patients had an LS value ≥13.3kPa, and the estimated 3-year OS was 77.5%, compared to 96.4% in 66 patients with an LS value <13.3kPa. This difference was statistically significant (hazard ratio=5.27 [1.35-20.5]; P=0.017).
Conclusion: The LS value ≥3.3kPa measured by 2D-SWE is a significant predictive factor for OS after RFA for HCC.

10:30 - 12:00 **Room C**

GI Tract

SS 201b

Rectal cancer: response assessment and diagnostic biomarkers

Moderators:
L. Cevasco; Genoa/IT
S. Schmidt; Lausanne/CH

B-0012 10:30

Performance of high-resolution MRI in predicting tumoural response to neoadjuvant chemoradiotherapy in patients with rectal cancer
D.S. Feier, A. Cote, A. Lebovici, C. Caraiani, D. Florian, F. Epure, C. Iancu, S.M. Dudea; *Cluj-Napoca/RO (diana.feier@gmail.com)*

Purpose: To determine the performance of high-resolution MRI parameters in predicting complete tumoural response in patients with locally advanced rectal cancer treated with neoadjuvant chemoradiotherapy (CRT).
Methods and Materials: Population consisted of 52 patients with rectal cancer, who underwent pre-treatment 1.5-T MRI. Tumour ADC (DWI) measurements (10^{-3} mm^2/s), lesion site, tumour longitudinal extent, distance between lesion and puborectalis muscle, levator ani muscles infiltration, depth of extramural spread and lymph nodes involvement were appreciated. After CRT, all patients underwent complete surgical resection and the surgical specimen served as gold standard. Area under receiver operating characteristic curve (AUROC) analysis was performed to assess the discriminatory power of MRI parameters to predict complete response.
Results: Pathological complete response, partial response and no response were found in 6, 22 and 23 patients, respectively. Among analysed parameters mean ADC values, depth of extramural spread and lymph nodes involvement were independent predictors of pathological complete response (p<0.0001). Independently, pathological complete response can be predicted by mean ADC values (AUROC=0.90, Se=93.8%, Sp=73.3%), depth of extramural spread (AUROC=0.72, Se=36.73%, Sp=97.78%) and absence of lymph nodes involvement (AUROC=0.87, Se=80.82%, Sp=93.33%), respectively. Together, the three parameters can accurately assess pathological complete response with an AUROC of 0.92 (Se=79.59%, Sp=93.33%).
Conclusion: Baseline high-resolution MRI parameters have the potential to act as imaging biomarkers of tumoural response to neoadjuvant chemoradiotherapy.

B-0013 10:38

DWI predictive value of response to CRT in local advanced rectal cancer
A. Palmisano, A. Di Chiara, A. Esposito, P. Passoni, L. Albarello, A. Del Maschio, F. De Cobelli; *Milan/IT (palmisano.anna@hsr.it)*

Purpose: A complete response to CRT may candidate patients with local advanced rectal cancer (LARC) to a conservative management. Hence, the non invasive prediction of response to CRT is of pivotal importance. Aim was to assess the value of DWI in the prediction of pathological response to CRT in LARC.
Methods and Materials: 29 pts with LARC underwent 1.5T MRI before the beginning of CRT (preMRI), after 6 week of CRT (midMRI), and at the end of CRT (postMRI). High-resolution axial-T2w sequences on the three planes and DWI sequences (b:0-200-600-1000) were acquired. Cancer volume was segmented on T2w (V_{T2}) and b:1000 (V_{b1000}) images, and the percentages of modification over time (ΔV) were evaluated. V_{T2} was coregistered on ADC map, and a volumetric histogram-analysis of ADC performed. After surgery patients were classified according to Tumour Regression Grade (TRG) in Non-Responder (NR) when TRG=0-2, Partial Responder (PR) when TRG=3, and Complete Responder (CR) when TRG=4.
Results: At histopathology 8 patients were CR, 13 PR, 8 NR. A good correlation between V_{T2} and V_{b1000} was observed at each time point (p<0.01), with lower V_{b1000} values than V_{T2} (p<0.01). At multivariate analysis ΔV_{T2} >81.5% at midMRI, V_{b1000}<3 cc at postMRI and mean ADC>1,4 at preMRI resulted able to predict CR with an accuracy of 86%, 89% and 76%, respectively. At preMRI ADC was higher in CR as well as ADC skewness (p<0.01).
Conclusion: DWI may improve the MRI capability to predict the LARC response to CRT; in particular, V_{b1000} at postMRI increases its accuracy.

B-0014 10:46

The value of ADC measurements for assesing treatment response of neoadjuvant chemoradiotherapy in patients with localy advanced rectal cancer
A. Lebovici, A. Cote, D.S. Feier, C. Caraiani, D. Florian, F. Graur, C. Iancu, S. Dudea; *Cluj-Napoca/RO (andrei1079@yahoo.com)*

Purpose: To evaluate the diagnosis performance of ADC measurements in assessing treatment response to neoadjuvant chemoradiation therapy (CRT) in patients with locally advanced rectal cancer.
Methods and Materials: Forty-eight consecutive patients with pathologically confirmed rectal adenocarcinoma, who had undergone pretreatment MRI (1.5T; T2TSE/DWI) were retrospectively collected. ADC measurements based on variable b-value (50,400,800 x 10^{-3} mm^2/s) were performed using a variable ROI size and six diagnostic measurement tools were computed: min ADC, max ADC, mean ADC and their corresponding ratio with ADC values of normal rectal wall. Patients were classified as responders and non-responders according to rectal cancer regression grade. Univariate and multivariate logistic regression models were performed to predict complete response to treatment and the diagnostic performance was assessed using the area under the receiver operating characteristic curve analysis (AUROC).
Results: Mean ADC values presented significantly lower values in patients with complete response compared to those with partial or no response (692.16±43.7 vs 835.17±88.38, p<0.001) and had the best diagnostic performance (AUROC=0.91, Se=100%, Sp=82.50%, cut-off 0.758 × 10(-3) mm(2)/s) in predicting complete response after CRT.
Conclusion: Mean ADC values perform best in predicting complete response after CRT in patients with locally advanced rectal cancer.

B-0015 10:54

Locally advanced rectal cancer: predicting response to neoadjuvant chemoradiotherapy using apparent diffusion coefficient textures
L. Liu, Z. Wang, Z. Yang, E. Jin; *Beijing/CN (llh9821@163.com)*

Purpose: To evaluate whether ADC textures could predict patient with locally advanced rectal cancer (LARC) who would not response to neoadjuvant chemoradiotherapy (NCRT).
Methods and Materials: Thirty-two patients who underwent MRI including diffusion-weighted imaging at a 3.0 T system before NCRT were enrolled. Texture analysis of pre-therapy ADC mapping was performed, and a total of 135 ADC textures as well as routine mean ADC value of the primary tumour were extracted for each patient. Texture parameters and mean ADC value were compared between responsive group and non-responsive group. Receiver operating characteristic (ROC) curves were performed to evaluate the predictive performance of each significant parameter.

Results: Among the texture parameters, skewness, energy, Gabor-43, high-intensity emphasis, and low-intensity small area emphasis significantly differed between responsive and non-responsive groups (0.72 vs 0.30, p = 0.020; 0.11 vs 0.08, p = 0.045; 3.34 vs 2.19, p = 0.028; 65.67 vs 98.06, p = 0.045; 21.49 vs 8.06, p = 0.038). Further, skewness, high-intensity emphasis and low-intensity small area emphasis were identified as independent predictors for non-responders to NCRT, with areas under the ROC curves (AUC) of 0.754, 0.729, and 0.739, respectively.
Conclusion: Several texture features derived from pre-therapy ADC image could potentially be helpful to predict patients with LARC who would not response to NCRT.
Author Disclosures:
L. Liu: Research/Grant Support; Supported by the Health Industry Special Scientific Research Project (201402019), China. **Z. Wang:** Research/Grant Support; Supported by the Health Industry Special Scientific Research Project (201402019), China.

B-0016 11:02

DCE-MRI shows slower flow and more homogeneous vascularity in responding tumours after CRT for rectal cancer
R.A.P. Dijkhoff[1], M. Maas[1], G. Shakirin[2], D.M.J. Lambregts[1], J. van Griethuysen[1], M. Weibrecht[2], M. Perkuhn[2], M. de Boer[1], R.G.H. Beets-Tan[1]; [1]*Amsterdam/NL*, [2]*Aachen/DE* *(rebeccadijkhoff@hotmail.com)*

Purpose: To evaluate whether pre-chemoradiation(CRT) DCE-MRI can predict response to CRT in rectal cancer.
Methods and Materials: 20 patients with locally advanced rectal cancer underwent DCE-MRI with the contrast agent gadofosveset-trisodium before CRT. DCE-MRI was processed with the Intellispace Discovery research platform(Philips Healthcare). One reader delineated whole-tumour volumes on DWI. Semiquantitative DCE-parameters based on the enhancement curve(AUC(60), (AUC of)time to peak(TTP), maximum enhancement, bolus arrival time(BAT), initial signal excess (ISE), mean transit time(MTT), wash-in- and wash-out-parameters) were compared between patients with complete(CR;ypT0) or good response(GR;ypT0-2) and non-responders. Additionally, heterogeneity of DCE parameters (measured by coefficient of variance(CoV:sd/mean)) was compared.
Results: 8/20(40%) had CR. Almost all DCE-parameters were lower in CR and GR (p>0.05). MTT and BAT were higher in CR, with BAT significantly higher(p=0.015). In good responders the BAT was also significantly higher(p=0.028). Heterogeneity was higher in CR for almost all DCE-parameters, except for BAT and wash-out, that had somewhat lower heterogeneity (p>0.05). The higher heterogeneity of AUCTTP, wash-in and AUC60 in CR showed a trend towards statistical significance (p=0.062-0.099). In good responders AUC60 and TTP were significantly more heterogeneous than in poor responders(p=0.024-0.041). Washout slope(>0.05) and BAT (p=0.012) were less heterogeneous in good responders.
Conclusion: Bolus arrival time is longer and less heterogeneous in CR and GR after CRT, potentially reflecting slower but more homogeneous inflow of the contrast bolus. This could represent prolonged and more homogeneous exposure to chemotherapy and reduced hypoxia, leading to more response. Most other DCE parameters were lower and more heterogeneous in responders.
Author Disclosures:
G. Shakirin: Employee; Philips Research. **M. Weibrecht:** Employee; Philips Research. **M. Perkuhn:** Employee; Philips Research.

B-0017 11:10

A modified 3-point MRI-predicted tumour regression grade incorporating diffusion-weighted image: locally advanced rectal cancer
B. Park, S. Cho, M. Lee; *Taegu/KR (redzon7543@gmail.com)*

Purpose: To evaluate the prognostic relevance of a modified 3-point MRI-predicted tumour regression grade (mrTRG) incorporating diffusion-weighted image (DWI) in patients with locally advanced rectal cancer (LARC) after preoperative chemoradiotherapy (PCRT).
Methods and Materials: Between March 2012 and September 2013, 118 consecutive patients with mid/lower LARC, who underwent PCRT followed by surgery, were enrolled in this retrospective study. Two radiologists in consensus assessed the mrTRG based on T2-weighted images and high b-value DWIs (0, 1000 s/mm2) using the following grade: Grade 0, good regression (no obvious tumour); Grade 1, intermediate regression (dominant fibrosis; regression > 50%); Grade 2, poor regression (dominant tumour; regression ≤ 50%). A multivariate Cox proportional-hazard regression was performed to evaluate the association of the modified mrTRG with the 3-year disease-free survival (DFS). A Kaplan-Meier analysis with a log-rank test was used to compare the DFS rate between responder (Grade 0 and 1) and non-responder (Grade 2) groups.
Results: The modified mrTRG (adjusted HR, 2.505; 95% CI 1.231 - 5.100) was independently associated with the 3-year DFS (P = 0.011). Additionally, there was a significant difference in the 3-year DFS rate between responder (73.8%; 95% CI 64.2 - 81.3%) and non-responder (41.7%; 95% CI 10.9 - 70.8%) groups (P = 0.028).
Conclusion: In patients with mid/lower LARC, the modified 3-point mrTRG incorporating DWI was independently associated with the 3-year DFS after PCRT followed by surgery. The grading scale may be used as a surrogate for expected prognosis to PCRT prior to surgery. Further prospective trials are warranted.

B-0018 11:18

Validity of MRI tumour volumetry as a biomarker in rectal cancer
E. Qasem; *Swansea/UK (eyasqasem@doctors.org.uk)*

Purpose: MRI tumour volumetry (TV) is a recently described imaging concept that may have advantages over radiological TNM staging of rectal cancer in assessing tumour response to chemoradiotherapy. This study aims to investigate the performance of TV against traditional radiological and pathological staging modalities, and introduces the novel concept of tumour volumetry to mesorectal volume ratio (TMVR).
Methods and Materials: Patients with histologically proven rectal cancer treated at a single cancer institute by surgery alone were selected from a prospective database. Axial MRI images for T2 to T4 disease were selected and transferred to an offline workstation (Prosoma ®). A single investigator delineated each axial slice for the rectal tumour and mesorectum defining the tumour (TV) and mesorectal volumes. The ratio of tumour volume to mesorectal volume (TMVR) was calculated. Correlations between the tumour volume, TMRV and tumour length were compared with MRI and pathological T staging
Results: 35 patients with rectal cancer treated without neoadjuvant therapy were analysed. A distinct correlation was observed between increasing TV and advancing ordinal T stage (p=0.027 , Logistic regression). TV correlated better with pathological T stage than radiological T stage. In particular there was improved prediction of pathological T3 subset (a-d) with volumetric over MR-T stage. Correction of TV with mesorectal volume did not improve accuracy.
Conclusion: Tumour volumetry is a promising predictor of final pathological T stage. This reflects that volumetry is a scale which potentially smooths out differences between discrete T staging categories.
Author Disclosures:
E. Qasem: Author; R J Egan, R Hugtenburg, R Taylor, P Chowdhury, T Wells, D A Harris.

B-0019 11:26

Accuracy of MRI for predicting anterior peritoneal reflection involvement for locally advanced rectal cancer: prospective comparison with operation findings
K. Sim, B. Park, M. Kim, D. Sung, N. Han, S. Cho; *Seoul/KR (ha2sky@hanmail.net)*

Purpose: To assess the diagnostic accuracy of preoperative rectal MRI for rectal cancer involvement through anterior peritoneal reflection (PR) in comparison with operation findings.
Methods and Materials: This prospective study was approved by Institutional review board; informed consent was waived. Eighty-three consecutive patients (Group 1: direct surgery, n=56; Group 2: neoadjuvant CCRT and surgery, n=27) with locally advanced rectal cancer were enrolled in this prospective study. All patients underwent rectal MR imaging using 3T systems. The identification of anterior PR was assessed using a 5-point scale. The possibility of anterior PR involvement was designated as positive or negative and all radiologic assessment were obtained in independent review by two radiologists. Diagnostic accuracy of MRI was obtained by operation findings and surgical record.
Results: More than 90% patients showed relatively good anterior PR identification regardless of neoadjuvant CCRT (Chi square test, P = .580) and there was no statistical difference in two reviewers (McNemar test, P = .443). The fifteen patients (15 of 83 patients, 18.1%) were clinically suspected anterior PR involvement during surgery. The sensitivity, specificity, positive predictive value, and negative predictive value of anterior PR involvement in the preoperative MRI were 69.2%, 78.3%, 47.4%, and 90%, respectively. The diagnostic accuracy of MRI for predicting for anterior peritoneal reflection involvement was 76.3%.
Conclusion: MR assessment of tumour involvement through anterior peritoneal reflection has relatively low sensitivity and positive predictive value, although preoperative rectal MR provides accurate anatomical information regarding anterior PR with high conspicuity.

B-0020 11:34

MRI can accurately predict sphincter preservation after chemoradiation

J. Krdzalic[1], M. Maas[2], S. Engelen[3], J.J.M. Van Griethuysen[2], D.M.J. Lambregts[2], M.J. Lahaye[2], G.L. Beets[2], R.G.H. Beets-Tan[2]; [1]*Heerlen/NL*, [2]*Amsterdam/NL*, [3]*Maastricht/NL (jasenkokrdzalic@hotmail.com)*

Purpose: It is believed that chemoradiation for low rectal cancer increases sphincter preservation. Aim was to evaluate with MRI whether sphincter preservation is increased by chemoradiation and whether MRI can predict sphincter preservation after chemoradiation.
Methods and Materials: A radiologist independently evaluated the T2-weighted MRIs (in 3 directions) in 47 patients before and after CRT with tumours <5 cm from the anorectal junction (ARJ) and measured distance of the lower tumour pole to the ARJ. Also, a confidence level score for feasibility of sphincter preservation was scored (CL=0 definitely no sphincter preservation, CL4=sphincter preservation definitely possible). Likelihood for sphincter preservation before and after CRT was compared and receiver operator characteristics(ROC) curves with area under the curve (AUC) were calculated.
Results: Mean distance from ARJ increased significantly during CRT from 21±16mm pre-CRT to and 31±18mm post-CRT (P<0.001). In 42% sphincter preservation was deemed not feasible pre-CRT, which decreased to 23% after CRT. AUC for sphincter preservation based on confidence level score was 0.84(0.72-0.96), with sensitivity of 100% and specificity of 44%. Based on post-CRT height measurement AUC was 0.87(0.76-0.98), with optimal size cut-off at 26 mm (sens: 86%, spec: 71%).
Conclusion: This is the first study to show that CRT increases the distance to the ARJ and thus leads to a higher rate of sphincter preservation. MRI can accurately predict sphincter preservation after CRT.

B-0021 11:42

Organ preservation for clinical complete responders after chemoradiation for rectal cancer, does timing of selection matter?

M. Maas[1], B. Hupkens[2], M. Martens[3], M. van der Sande[1], J. Melenhorst[2], D. Lambregts[1], G. Beets[1], R.G.H. Beets-Tan[1]; [1]*Amsterdam/NL*, [2]*Maastricht/NL*, [3]*Sittard/NL (d.lambregts@nki.nl)*

Purpose: Wait-and-see policy could be offered to clinical complete responders(cCR) after neoadjuvant chemoradiation(CRT). In patients with near cCR a second restaging can be considered to evaluate whether response becomes complete. Aim was to evaluate whether timing of inclusion influences outcome, by comparing patients included for wait-and-see at initial assessment with patients who were included after a second assessment 3 months later.
Methods and Materials: (Near) CRs underwent endoscopy+MRI+DWI ±8 weeks post-CRT. 103 had typical cCR and were selected for wait-and-see (W&S-1). The other 67 patients had near cCR, 19 underwent TEM and the 48 had a second assessment after 3 months, after which 43 were included for wait-and-see (W&S-2); 5 had TME. 3-6 monthly follow-up (MRI+DWI+endoscopy) was performed. 2-year local regrowth (LR), disease-free survival (DFS) and overall survival (OS) were compared between W&S-1 and W&S2. Multivariable Cox regression analyses were performed to assess whether inclusion timing was predictive for higher LR.
Results: 2-year LR in W&S-1 was 18% and 23% in W&S-2. 2-year DFS was 82% in W&S-1 and 78% in W&S-2. 2-year OS was 99% in W&S-1 and 98% in W&S-2 (all: p>0.05). The timing of inclusion was not predictive of more local regrowth or lower DFS. All LRs were detected early, so that they could be easily salvaged with standard TME.
Conclusion: A second response assessment 3 months after the first post-CRT staging can offer wait-and-see to more patients, who would otherwise be referred for TME. However, the 2-year LR is slightly higher in the late inclusion group, but this does not affect OS.

B-0022 11:50

Air artefacts on diffusion-weighted MRI of the rectum: effect of applying a rectal micro-enema

J.J.M. van Griethuysen, E.M. Bus, M. Hauptmann, L. Molenaar, A. Kint, M.J. Lahaye, M. Maas, G.L. Beets, R.G.H. Beets-Tan, D.M.J. Lambregts; *Amsterdam/NL (j.v.griethuysen@nki.nl)*

Purpose: Diffusion-weighted imaging (DWI) is increasingly included in standard rectal MRI-protocols. Single-shot echo planar imaging (EPI) is the most commonly used DWI-method. DWI-EPI is prone to susceptibility artefacts, mainly caused by air in the rectal lumen. Aim was to assess whether application of a micro-enema can reduce these artefacts.
Methods and Materials: 50 patients were included who underwent sequential DWI-MRIs (1.5T; highest b-value b1000) during follow-up as part of a wait-and-see approach after chemoradiotherapy. Until March 2014 DWI-MRIs were acquired without bowel preparation, thereafter a micro-enema (Microlax®;5 ml) was routinely given ±15 minutes prior to the DWI-MRI. The presence/severity of air artefacts was scored by 2 readers in consensus on each b1000 DWI-scan with a confidence level, ranging from 0 (no artefact) to 5 (severe artefact). A score >= 3 (moderate-severe) was considered significant. The presence/severity of artefacts was compared between DWI-scans with/without a micro-enema. Potential confounding factors (age, gender, DWI acquisition parameters, MRI-scanner, endoscopy prior to MRI) were taken into account.
Results: In total 335 DWI-MRIs were assessed. Significant air artefacts were seen in 24.3% (no micro-enema) vs 3.7% (with micro-enema). Using binary logistic regression with samples clustered by patient, the odds ratio between the use of a micro-enema and presence of significant artifacts was 0.12 (95% CI 0.04-0.40), p=0.0005. None of the parameters assessed for possible confounding significantly altered this effect.
Conclusion: The use of a micro-enema prior to rectal EPI-DWI examinations significantly reduces the amount and severity of air artefacts, compared to examinations without bowel preparation.

10:30 - 12:00 **Room X**

Vascular

SS 215

Blood flow assesment / experimental

Moderators:
J.I. Bilbao; Pamplona/ES
F. Takis; Keratea/GR

B-0023 10:30

Experimental ex-vivo flow studies in pig kidneys by multimodal angiography using DSA, MRA, and magnetic particle imaging

M.G. Kaul, I. Molwitz, J. Salamon, C. Jung, T. Knopp, G. Adam, H. Ittrich; *Hamburg/DE*

Purpose: Magnetic particle imaging (MPI) is a new imaging modality providing a high temporal resolution scanning magnetic particle distributions in 3D. To evaluate MPI for vessel imaging and perfusion studies a flow phantom is mandatory. To mimic in-vivo applications we established an experimental set-up and a work flow for multimodal evaluation of flow and perfusion in ex-vivo pig kidneys.
Methods and Materials: Kidneys of sacrificed pigs were perfused with heparin and saline. The main blood vessels and the ureter were connected to tubes allowing in and out flow of fluids. Flow was generated by a perfusion pump.
To minimize dislocations, kidneys were placed on a couch compatible with digital subtraction angiography (DSA), magnetic resonance imaging (MRI), and MPI. Measurements were performed in a clinical DSA (Allura, Philips), a preclinical high field MRI scanner (7T ClinScan, Bruker) and preclinical MPI scanner (Bruker/Philips). With each modality a dynamic sequence was performed and a dedicated DSA/MRI contrast agent (Imeron 300, Bracco) / (Ominscan, Ge Healthcare) and MPI tracer (Resovist, Bayer-Schering) was standardized injected by the pump.
Results: It was feasible to detect in and out flowing contrast agents/tracer and to produce angiograms with all three systems. Because flow can be steered temporal resolution can be traded for spatial resolution in MRI. Perfusion experiments for diffusion weighted intra voxel incoherent motion analysis are feasible as well.
Conclusion: Flow phantoms are essential when evaluating imaging and image analysis techniques. An experimental flow phantom was successfully established and will serve in future for detailed analysis procedures.

B-0024 10:38

The application of fat-water single-echo Dixon acquisition to time-resolved contrast-enhanced MRA

S. Riederer, E. Stinson, J. Glockner, J. Trzasko, P. Young; *Rochester, MN/US (riederer@mayo.edu)*

Purpose: Describe how fat-water decomposition using single-echo Dixon acquisition can be applied to time-resolved contrast-enhanced MR angiography (CE-MRA) for fat suppression.
Methods and Materials: The Dixon technique of fat-water decomposition has recently been applied to CE-MRA to eliminate background signal from fat and reduce the motion-induced misregistration artifacts. The first of these matches the performance of standard subtraction of pre- from post-contrast time frames ("time subtraction") while the second is an advantage over time subtraction methods. Such Dixon imaging has previously been performed using two echoes. Compared to time subtraction this requires double the amount of data and can also prolong the repetition time, TR. In this work we describe how the Dixon technique using a single echo can be applied to CE-MRA. The echo time is intentionally chosen so that water and fat are out of phase by 90 degrees. Corrections for other effects such as B_0 inhomogeneity are made using a pre-contrast calibration which also includes determination of coil sensitivities. The method was studied analytically and implemented experimentally.

Results: Results in phantoms demonstrate the feasibility of the technique. Results acquired in vivo in the lower extremity with 10 sec frame times show the ability of the method to reliably provide fat suppression over a large field of view. The increased intrinsic signal-to-noise ratio (SNR) of single-echo Dixon vs. that of time subtraction is shown in improved portrayal of small, enhancing vessels.
Conclusion: Fat suppression can be performed in time-resolved CE-MRA using the Dixon technique with a single echo.

B-0025 10:46

Getting rid of the grind: automated analysis of large quantity data and intraindividual stability on MRI aortic blood flow measurements for vascular age assessment

A. Knorr[1], T. Re[1], B. Stieltjes[1], D. Yates[2], R. Schmieder[3], J. Bremerich[1], T. Heye[1]; [1]*Basle/CH*, [2]*Cambridge, MA/US*, [3]*Erlangen/DE (alexander.knorr@usb.ch)*

Purpose: Aortic blood flow (ABF) characteristics are useful indicators for structural and functional vascular changes. We assessed the capabilities of an in-house developed algorithm to automatically analyze ABF curves obtained from MRI and to evaluate intraindividual curve stability over time.
Methods and Materials: 101 patients (70 male, age 60±11yrs.) were included from a multicenter trial on antihypertensive treatment. All patients underwent 3 standardized cardiovascular 3T MRI scans (0, 12, 52wks.). ABF in ascending and descending aorta was measured using semi-automatic analysis software on axial phase-contrast scans. Flow measurements were evaluated for all 303 examinations for 40 curve-defining characteristics using a sophisticated algorithm. Intraindividual ABF variability over time was characterized by full width half maximum (FWHM), peak acceleration and systolic area under the curve (AUC) coefficient of variation (COV). Observer-results-dependence was assessed by five observers for 45 patients.
Results: The automated analysis tool was able to process ABF curves for 303 examinations with speed and accuracy. Calculation of the entire data took 2.6s for 40 curve parameters in each data set including various time periods, functional ratios and AUCs. Median FWHM, peak acceleration and systolic AUC COV in the ascending aorta were 8.44%, 7.13% and 7.57% (range 0-31.96%, 0-24.80% and 0.63-28.06%). Median intra- and inter-observer COV was 0.67% (range 0.48-1.20%) and 1.54%.
Conclusion: Fully automated curve analysis facilitates evaluation of ABF data, enabling scalable and fast analysis thus shifting radiologist's time and focus from time-intensive manual evaluation to data interpretation. ABF characteristics show clear stability over time independent of the observer.

B-0026 10:54

Is there more to aortic flow curves than meets the eye? - MRI blood flow analysis of large quantity data as a substitute marker for vascular age assessment

A. Knorr[1], T. Re[1], B. Stieltjes[1], D. Yates[2], R. Schmieder[3], J. Bremerich[1], T. Heye[1]; [1]*Basle/CH*, [2]*Cambridge, MA/US*, [3]*Erlangen/DE (alexander.knorr@usb.ch)*

Purpose: Aortic blood flow (ABF) characteristics are useful indicators for structural and functional vascular changes. In this study we assessed ABF curve parameters of a large number of magnetic resonance imaging (MRI) measurements to assess their potential as substitute markers for aortic stiffness.
Methods and Materials: A subset of 101 adult patients (70 male, age 60±11 yrs) with essential arterial hypertension were included from a multicenter trial (3 sites, 140 patients total) on antihypertensive treatment. All patients underwent cardiovascular 3T MRI with a standardised imaging protocol at 3 different time points (0, 12, 52 wks). ABF in the ascending and descending aorta was measured by one reader using semi-automatic analysis software on axial phase-contrast scans (100 frames/RR-interval). Aortic stiffness was estimated via aortic strain calculations on maximum/minimum area measurements on cine gradient-echo scans. The flow measurements were then evaluated for all 303 examinations simultaneously for several curve-defining characteristics using a sophisticated Python algorithm. Pearson's product moment correlations and clustering between variables was done in RStudio.
Results: Peak acceleration, systolic, acceleration and deceleration time, as well as areas under the curve before and after peak flow of the ascending aorta emerged as significantly correlated to strain in the proximal descending aorta (r=0.44, -0.40, -0.37, -0.19, -0.27 and -0.23; p<0.001).
Conclusion: ABF measurements are a simple, reproducible and fast technique compared with other approaches to obtain aortic strain or stiffness and shows promise as a substitute marker for vascular age/aortic stiffness thus facilitating long-term prediction of vascular health.

B-0027 11:02

Dual-energy CT angiography in peripheral arterial stents: an investigation of optimal scanning protocols with regard to image quality and radiation dose

A.M. Almutairi[1], Z. Sun[2], Z. Al Safran[1], S.A. Al Zaabi[1]; [1]*Dammam/SA*, [2]*Perth/AU (aa1ss@hotmail.com)*

Purpose: To determine optimal scanning protocols of dual-energy computed tomography angiography (DECTA) in terms of radiation dose and image quality at different keV levels compared with conventional computed tomography angiography (CTA) in patients treated with peripheral artery stents.
Methods and Materials: Twenty-nine patients with prior stent placement in peripheral arteries were evaluated with DECTA. Images were reconstructed with virtual monochromatic spectral imaging (VMS) at 65, 68, 70 and 72 keV and adaptive statistical iterative reconstruction (ASIR) at 50% compared with CTA. Image quality comprising image noise, SNR and CNR were assessed and radiation dose were compared.
Results: A total of 56 identified stents, which were located in the main formal peripheral arteries were evaluated. At subject's level, the results show that DECTA (VMS) had less noise than the CTA for CIA, EIA and SFA stents, with lowest noise at 72 keV. In addition, the VMS set had greater SNR than the CTA for the EIA stents (P< 0.05); and that the VMS set had greater CNR than the CTA for CIA, EIA and SFA stents (P< 0.001). Also, with respect to CT attenuation, VMS continued to outperform CTA, but to a lesser extent. At between subjects level, average VMS noise varied significantly with the type of stent (P=0.025) for CIA stents. Radiation dose was highly significant between DECTA and CTA scans (P< 0.0001).
Conclusion: An optimal scanning protocol consisting of 72keV and 50% ASIR leads to better image quality for DECTA in peripheral arterial stenting when compared to CTA.

B-0028 11:10

High pitch sub-second chest CT angiography using third-generation dual-source CT scanner: intra-patient comparison with standard acquisition

F. Sodagari, H. Savas, R. Agrawal, A. Arslanoglu, V. Yaghmai; *Chicago, IL/US (Rishi.Agrawal@nm.org)*

Purpose: To evaluate image quality and contrast attenuation in chest CT angiography (CTA) on a third-generation dual-source CT scanner using high-pitch mode.
Methods and Materials: Fifty-four patients underwent chest CTA for pulmonary emboli evaluation. Previous chest CTA studies of the same patients on standard-pitch were used for comparison. Main pulmonary artery attenuation, overall image quality, vascular opacification, noise, CNR, and DLP were compared.
Results: Of 54 scans with standard-pitch, 42 scans (77.8%) had been performed with 100kV and 12 scans (22.2%) with 120kV. On high-pitch protocol, patients had been scanned with lower kV (30/54, 56%), same kV (12/54, 22%), or higher kV (12/54, 22%), compared to the standard-pitch protocol. Acquisition time was less than a second for all high-pitch CTAs (mean, 0.48±0.06s). The overall mean percentage radiation reduction on high-pitch for lower, same, and higher kVs was 64.7±10.8%, 57.5±13.7%, and 19.5±20.2%, respectively. In 12 patients with similar kVs at both scans, high- and standard-pitch scans had comparable attenuation (327.5±146.6 vs 298.5±95.8HU; P=0.35) and noise (22.3±6.4 vs 22.7 ±7.2; P=0.86). Vascular opacification score on high-pitch (4.1) was significantly higher than standard-pitch (3.5) (P=0.002). Overall image quality was acceptable for both high- and standard-pitch scans (3.8 vs 3.9; P=0.67). Mean CNR on high-pitch (12.0±6.4) and standard-pitch (13.4±5.9) was comparable (P=0.41). Mean DLP on high-pitch (219.0±116.2 mGy-cm) was significantly lower than the standard-pitch (555.5±282.4) (P=0.001).
Conclusion: High-pitch chest CTA with third-generation dual-source CT scanner provides excellent pulmonary artery visualisation at lower radiation dose with short acquisition times and without compromising the image quality.
Author Disclosures:
F. Sodagari: Grant Recipient; Educational Grant, Siemens. **A. Arslanoglu:** Grant Recipient; Educational Grant, Siemens.

B-0029 11:18

4D flow can visualise and quantitatively analyse the characteristic reflection flow in infrarenal aorta and suction flow in renal arteries during diastole

M. Sugiyama[1], Y. Takehara[2], M. Alley[3], T. Wakayama[4], H. Nasu[1], S. Yamashita[1], A. Nozaki[4], H. Kabasawa[4], H. Sakahara[1]; [1]*Hamamatsu/JP*, [2]*Nagoya/JP*, [3]*Stanford, CA/US*, [4]*Hino/JP (m-sugi@hama-med.ac.jp)*

Purpose: Fusiform aneurysm is more commonly seen in infrarenal abdominal aorta (AAA), but hardly seen in descending thoracic aorta. We hypothesize that this is due to the characteristic flow dynamics in this specific portion affected by

the reflection flow from the common iliac arteries (CIAs) and suction by renal arteries (RAs) at diastole. Since inconsistent flow dynamics create fluctuated wall shear stress, the endothelium eventually stimulates atherosclerotic drive (J Biomech28(12):1515,1995). The purpose of our study is to quantitatively and visually analyse this characteristic blood flow dynamics that makes this area prone to atherogenic AAA using 3D cine PC MR imaging (4D-Flow).
Methods and Materials: 15 patients (40-84 y.o.) underwent 3.0T MRI including 4D flow and Gd-3DMRA. The maximum and minimal blood flow volume was measured at sections in supra and infrarenal abdominal aorta, celiac artery, superior mesenteric artery, RAs and CIAs. Streamlines within the supra and infrarenal aorta was visually assessed.
Results: The average minimal diastolic blood flow within suprarenal aorta was antegrade (11.93 +/- 6.74ml/sec), whereas that of infrarenal aorta was retrograde (-6.33 +/- 7.17ml/sec). The average minimal diastolic blood flow within RAs and other mesenteric arteries were antegrade. The average minimal diastolic blood flow of CIAs was negative, reflecting the reflection wave. Streamlines of infrarenal aorta depicted more turbulent flow than that of suprarenal aorta during diastole.
Conclusion: The retrograde flow due to RA suction and the reflection wave from the CIAs may be responsible for inconsistent flow within the infrarenal aorta, which may develop atherogenic AAA.
Author Disclosures:
T. Wakayama: Employee; GE Healthcare Japan. **A. Nozaki:** Employee; GE Healthcare Japan. **H. Kabasawa:** Employee; GE Healthcare Japan.

B-0030 11:26

Differences in MRI and tonometry measured pulse wave velocity: effect of arterial composition, arterial length or technique bias?
J. Weir-McCall, A. Thakur, D. Cassidy, F. Khan, S. Matthew, H. Colhoun, J. Belch, G. Houston; *Dundee/UK (jweirmccall@doctors.net.uk)*

Purpose: Carotid-femoral pulse wave velocity (cf-PWV) and MRI-PWV show good correlation, but with a significant bias of 2m/s difference between the techniques across studies. The aim of the current study was to evaluate whether the differences between cf-PWV and MRI-PWV can be accounted for by inaccuracies of currently used distance measurements.
Methods and Materials: 109 study participants underwent cf-PWV and whole body MR angiography (WBMRA). 80 participants also underwent MRI-PWV. cf-PWV_{EXT} was performed using tonometric measures at the carotid and femoral arteries. WBMRA was performed on a 3T scanner using a dual bolus contrast injection of gadoteric acid and a 4-station acquisition protocol. From this, a true intra-arterial pathlength from the bifurcation of the common carotid to the aortic arch was measured. This MRA derived distance was then used to recalculate the cf-PWV_{EXT} to give a cf-PWV_{MRA}.
Results: MRI-PWV was significantly lower than cf-PWV_{EXT} (MRI-PWV= 8.8±3.4 vs. cf-PWV_{EXT} =10.77±2.67ms^{-1}, p<0.001). When cf-PWV was recalculated using the inter-arterial distance from WBMRA, this difference was lost (MRI-PWV=8.41±3.43ms^{-1} vs. cf-PWV_{MRA} 8.96±2.15 ms^{-1}, p=0.14). Recalculation of the cf-PWV using this MRA arterial distance also improved the correlation of PWV with age (cf-$PWV_{EXT:}$ r=0.49, p=<0.001; cf-PWV_{MRA}: r=0.59, p=<0.001) and global atheroma burden as measured on WBMRA (cf-$PWV_{EXT:}$ r=0.39, p=<0.001; cf-PWV_{MRA}: r=0.42, p=<0.001).
Conclusion: Differences in cf-PWV and MRI-PWV can be predominantly explained by inaccuracies introduced by the use of simple surface measurements to represent the convoluted arterial path between the carotid and femoral arteries. Correction of this also improves the association between cf-PWV and age and arterial atheroma burden.

B-0031 11:34

Optimising contrast media injection protocols in CT angiography at different tube voltages: evaluation in a circulation phantom using third generation dual-source CT
D. De Santis[1], U.J. Schoepf[1], D. Caruso[2], M. Eid[1], M.H. Albrecht[1], A. Varga Szemes[1], V.W. Lesslie[1], C.N. De Cecco[1]; [1]*Charleston, SC/US*, [2]*Latina/IT (domenico.desantis@hotmail.it)*

Purpose: To investigate the minimum iodine delivery rate and contrast media volume required for diagnostic contrast enhancement of 350 HU in the ascending aorta at different kV settings.
Methods and Materials: Dynamic CT acquisitions from 70 to 150 kV were performed in a circulation phantom. First, injections with iodine delivery rate ranging from 0.1 grams of Iodine/second (gI/s) to 2.0 gI/s were tested for each kV. In the second part, the iodine delivery rate was held constant with the contrast media volume reduced from 50 to 10 mL. Diagnostic aortic peak enhancement for each kV was compared using the Kruskal-Wallis test. A $p<0.05$ was considered statistically significant.
Results: The mean aortic peak enhancement for all diagnostic iodine delivery rates was 368.7±11.1 HU. Diagnostic iodine delivery rates returned similar aortic peak enhancement values for all protocols (all $p \geq 0.18$). For the second part of the study, a diagnostic enhancement was yielded by using a minimum of 30 mL of contrast media for 110 kV, 25 mL for 100 kV and 90 kV, 15 mL for 80 and 70 kV.
Conclusion: Our study suggests that a differentiated approach reducing the contrast media volume for tube voltages <120 kV and increasing the iodine delivery rate for higher kV settings seems the most effective approach.
Author Disclosures:
U.J. Schoepf: Consultant; Guerbet. Research/Grant Support; Astellas, Bayer, Bracco, GE, Medrad, Siemens. **A. Varga Szemes:** Consultant; Guerbet. **C.N. De Cecco:** Consultant; Guerbet. Research/Grant Support; Siemens.

B-0032 11:42

Radiologic and biochemical correlates of arterial stiffness in patients with peripheral artery disease and in clinically healthy subjects
M. Zagura, J. Kals, M. Serg, P. Kampus, M. Zilmer, M. Jakobson, E. Unt, J. Eha; *Tartu/EE (Maksim.Zagura@kliinikum.ee)*

Purpose: Arterial stiffness is an independent predictor of cardiovascular outcome in patients with atherosclerosis. Angiographic score (ASc) reflects severity of atherosclerosis in patients with peripheral artery disease (PAD). Osteopontin (OPN) and oxidized LDL (oxLDL) are involved in the pathogenesis of atherosclerosis. The aim of the present study was to evaluate the association between arterial stiffness, ASc, serum OPN, and oxLDL in patients with symptomatic PAD and in clinically healthy subjects.
Methods and Materials: We studied 79 men with symptomatic PAD (mean age 64±7 years) and 84 healthy men (mean age 63±8 years). Calculation of the ASc was based on severity and location of atherosclerotic lesions in the arteries of the lower extremities. Aortic pulse wave velocity (aPWV) was evaluated by applanation tonometry using the Sphygmocor device. Serum OPN and oxLDL levels were determined by ELISA.
Results: The aPWV (10±2.4 vs. 8.4±1.7 (m/s); p<0.001), OPN (75 (62.3-85.8) vs. 54.8 (47.7-67.9) (ng/ml); p<0.001), and oxLDL (67 (52.5-93.5) vs. 47.5 (37-65.5); p<0.001) were different for the patients and for the controls. In multiple regression models, aPWV was independently determined by ASc, log-OPN, log-oxLDL, and eGFR in the patients (R^2=0.44; p<0.001) and with log-OPN, log-oxLDL, age, and heart rate in the controls (R^2=0.38; p<0.001).
Conclusion: The independent relationship of aPWV with ASc and serum levels of OPN and oxLDL in the patients with PAD indicates that radiologic severity of atherosclerosis as well as OPN and oxLDL might influence arterial stiffening in patients with atherosclerosis.

B-0033 11:50

Investigation basis for the resistive factors in blood circulation by MRI and CT
G. Beraia, M. Beraia; *Tbilisi/GE (beraiaguram@gmail.com)*

Purpose: Purpose of the study is, to identify the reason for the formation of the restrictive factors in blood flow: inertial flow in aorta and vena cava, high turbulence and resistivity associated with the pulsatile blood flow at the branching, extraction of the lymph from the blood, with the increasing erythrocyte aggregation in the venous blood flow.
Methods and Materials: Blood flow velocity measurements were made in the ascending, thoracic aorta and inferior vena cava of 35 adult normal subjects (15 men, 20 women, age 21-49 years) with the use of Magnetic Resonance Angiography. Blood mean density (HU) was measured by the CT scanner at the same levels. Blood flow pulsatility index and density were carried out.
Results: Pulsatility index for the ascending aorta - 6.0±0.3, thoracic aorta - 4.3±0.2, inferior vena cava - 1.2±0.1. (P<0.01). Blood density (HU) ascending aorta - 57.3±3.5, thoracic aorta - 35.7±3.1, inferior vena cava -59.3±3.3 (P<0.05).
Conclusion: Heart energy is stored in the elastic deformation of the blood cells and large vessel walls, in kinetic energy of the blood flow. Elasticity of the structure is associated with the inertiality. Inertial blood flow due to oscillation in the large arteries, transforms to the flow with high fluidity in capillaries - entropy of the system increases and changes Gibbs free energy, enabling chemical reaction to proceed spontaneously. In the venous blood flow, low oscillation with the reduced amount of the plasma and increased erythrocyte aggregation, decreases entropy of the system.

10:30 - 12:00 **Room Z**

Interventional Radiology

SS 209
Oncological embolisation

Moderators:
Z. Bánsághi; Budapest/HU
N.N.

K-01 10:30
Keynote lecture
N.N.

B-0034 10:39
Transarterial bland embolisation for HCC using cyano-acrylate glue and 40-100µm microspheres
E. Lanza, V. Pedicini, D. Poretti, M. Tramarin, R. Ceriani, F. Procopio, D. Del Fabbro, M. Donadon, G. Torzilli; *Rozzano/IT (vittorio.pedicini@humanitas.it)*

Purpose: To present a modified technique of TAE for HCC, using both microspheres and cyano-acrylate glue. To report on its feasibility and effects on disease progression and tumour devascularisation.
Methods and Materials: Inclusion criteria were: a) HCC according to the AASLD criteria, b) unsuitable for surgery and c) multidisciplinary consensus on performing TAE. Exclusion criteria were: 1) Child-Pugh C, 2) GI bleeding, 3) encephalopathy and 4) portal thrombosis. All patient underwent preoperative MDCT or CE-MRI. TAE was performed entering the artery feeding the tumour, sparing the most healthy liver. Cone-beam CT was used for confirmation. After full embolisation with 40 or 100µm microspheres, a mixture of averagely 0.3mL cyano-acrylate/Lipiodol in a 1:10 ratio was injected. Follow-up was at 30days, 3months and every 6months. Response rates were assessed with mRECIST criteria.
Results: Between 2013 and 2016, 64 patients and 78 HCCs were treated. Overall survival was 93%; 54 patients at one year follow-up resulted in 24 complete responses (44%), 20 partial responses (37%), 4 stable disease (7%) and 16 progressive disease (30%). Forty-six tumours were completely devascularised at 1 year control (71%), 17 had a residual supply (26%), two did not show any devascularisation (3%). One case was complicated by a late-onset abscess of the treated lesion; another patient had postoperative pancreatitis. Both complications were treated conservatively.
Conclusion: TAE with microspheres and cyano-acrylate glue for HCC is safe and feasible, offering desirable rates of one-year disease control and tumour devascularisation. These appear in line and in some cases better to those reported in the current literature for standard TAE.

B-0035 10:47
Tumour response and survival outcomes of very small drug eluting beads used in trans-arterial chemoembolisation for unresectable hepatocellular carcinoma
A.M.K. Abdel Aal, S. Moawad, M. Hanaoka, S. Tatum, B. Jackson, C. Baalmann, N. Ertel, A. Abouarab, S. Saddekni; *Birmingham, AL/US (akamel@uabmc.edu)*

Purpose: The purpose of the study is to evaluate the tumour response rate and survival outcomes of a transarterial chemoembolisation (TACE) of unresectable hepatocellular carcinoma (HCC) using 75 microns Oncozene (Boston Scientific, MA, USA) drug-eluting beads (DEB).
Methods and Materials: We retrospectively reviewed the medical records and radiologic studies of 109 patients who had their first TACE for HCC between November 2013 and August 2016 using 75 microns Oncozene DEB. The primary endpoint of the study was tumour response rate which was categorised according to mRECIST and the toxicity profile using Common Terminology Criteria for Adverse Events (CTCAE) version 4.0. The secondary endpoint was patient survival.
Results: The study included 89 (81.7%) males with a mean age of 64.1 years. Overall tumour response was 23% complete response (CR), 66% objective response (OR) and 90% disease control (DC). CR, OR and DC were 27%, 64%, and 89% respectively in Child-Pugh A patients, and 27%, 72% and 92% respectively in BCLC stages A and B patients. CR, OR and DC were 15%, 71% and 91% respectively in Child-Pugh B and C patients, and 16%, 55% and 87% respectively in BCLC stages C and D patients. Grades 3 toxicity was seen in 10% of the patients and only 1 with grade 4. The 6, 12 and 18-month survival were 97%, 84%, and 72% respectively.
Conclusion: The present study shows very good tumour response rate and survival outcomes for TACE using 75 microns Oncozene DEB, with very low toxicity profile.
Author Disclosures:
A.M.K. Abdel Aal: Consultant; St Jude Medical, Boston Scientific, WL Gore, Baxter Healthcare, Brad Peripheral Vascular Inc.. Grant Recipient; BTG, Covidien, Brad, Boston Scientific, Sirtex. Research/Grant Support; Celonova, Boston Scientific. **S. Saddekni:** Consultant; St Jude Medical.

B-0036 10:55
Evaluation of a newly developed biodegradable embolic agent for transcatheter arterial embolisation in a rabbit renal model
H. Wittgenstein, M. Stechele, J. Breinl, J. Schnorr, B. Rudolph, C. Schmidt, B. Hamm, R. Günther, F. Streitparth; *Berlin/DE (h.wittgenstein@gmx.de)*

Purpose: Evaluation of embolic effect, biocompatibility and biodegradability of a novel temporary embolic agent
Methods and Materials: Superselective embolization of the lower kidney pole was performed with bland (n=15) and SPIO-loaded (n=9) polydioxanone microspheres (90-500 µm) in 24 New Zealand White rabbits (female; 2,5-3,5 kg; 12-16 weeks) under fluoroscopy. Embolization effect was evaluated on DSA and MRI (T1-TSE pre/post-contrast, T2-TSE, T2*-GRE). 4 animals were sacrificed immediately after embolization. 20 animals underwent control angiograms and MRI 1 (n=3), 4 (n=3), 8 (n=3), 12 (n=8) and 16 weeks (n=3) post embolization. Final angiograms were compared with post-embolization angiograms for evaluation of embolization success and arterial reperfusion. Kidneys were harvested for histopathological analysis of embolic effect, biocompatibility and biodegradability.
Results: Evaluation of imaging modalities showed successful target embolization in 18/20 animals. In 2/20 animals the whole kidney was affected due to reflux. T2*-GRE images demonstrated the distributon of SPIO-loaded microspheres. Comparison of angiograms showed evidence of partial and complete reperfusion in 93 %. Macro- and microscopic pathological analysis revealed cell necrosis/infarct in the embolized areas. A mild acute inflammatory reaction was detected throughout and a foreign body reaction at advanced time intervals. The microspheres were increasingly degraded at sixteen weeks (Ø degradation score: 2,92/3).
Conclusion: Novel bioresorbable microspheres led to an effective occlusion of target vessels while simultaneously demonstrating good biocompatibility. The agent appeared extensively reabsorbed at sixteen weeks, thus offering advantages as a temporary embolic agent. SPIO-loaded microspheres allowed a non-invasive visualization of the microsphere distribution in MRI.

B-0037 11:03
Evaluation of the effectiveness of transpulmonary chemoembolisation (TPCE) and intraarterial chemoperfusion (TACP) in treatment of colorectal lung metastases
A.I. Mekkawy[1], A. Hassan[1], M. El-Sharkaway[1], H.M. Kamel[1], D.B. Thabet[1], N.E. Nour-Eldin[2], N.N.N. Naguib[2], T.J. Vogl[2]; [1]*Assiut/EG*, [2]*Frankfurt a. Main/DE (time_dr@yahoo.com)*

Purpose: To assess the response, mean time to progression and mean survival time for patients with colorectal lung metastasis after palliative TPCE and TACP.
Methods and Materials: This study included 45 patients (mean age 57.3 ±13 years; 21 females, 24 males) with unresectable colorectal lung metastases, who failed or refused systemic chemotherapy, and underwent either repetitive TPCE (Group1; n= 16), TACP (Group2; n= 9) or both techniques (Group3; n= 20), between 2006 and 2015. Bilateral lung involvement was seen in 95.6% of patients and the median number of lung nodules was 14. Patients who underwent subsequent ablation were excluded. Chemotherapeutic agents were applied either through the pulmonary artery followed by embolisation (TPCE) or by means of intra-aortic chemoperfusion (TACP). The response according to Response Evaluation Criteria in Solid Tumours (RECIST 1.1) was evaluated and survival parameters were statistically analysed.
Results: After evaluation of the tumour response; partial response (PR) was 4.5% (n=2), stable disease (SD) 62.2% (n=28) and progressive disease (PD) 33.3% (n=15). The estimated mean survival time and mean time to progression were 21 months (±2.7 SE) and 5.5 ± 0.5 months, respectively. The mean survival time was significantly ($P < 0.05$) higher in Group3 with mixed treatment (27.8 ± 7 months) than the other two groups; Group1 and Group2 (18.9 ± 4.2 months and 14.2 ± 4.7 months, respectively).
Conclusion: TPCE and TACP could be a promising palliative treatment with acceptable survival for patients with colorectal lung metastases who failed or are not eligible for other treatment options.

B-0038 11:11

Effectiveness of intra-arterial steroid administration (IASA) for the treatment of steroid-refractory acute gastrointestinal GvHD

V. Bérczi, A. Tóth, J. Fábián, P. Reményi, T. Masszi; *Budapest/HU (Berczi@hotmail.com)*

Purpose: The aim of this study was to retrospectively assess clinical effectiveness of intra-arterial steroid-administration (IASA) treatment in adult patients, non-responsive to systemic corticosteroids, with grade III or IV GI-aGvHD.
Methods and Materials: Clinical data of 10 adult patients (age range, 19-61 years; mean age, 42 years) with GI-aGvHD (≥grade III) non-responsive to intravenous methylprednisolone (at least 2 mg/kg/day) and received IASA into the superior and/or inferior mesenteric artery between March 2015 and January 2016 were collected. The severity of acute GvHD was determined according to the Glucksberg grading system before, 12±3 [SD], 27±4 and 54±6 days after IASA. Long-term outcomes were also recorded in 4 cases (range, 87-370 days; median, 246 days).
Results: Seven patients had grade IV and 3 patients had grade III aGvHD prior to IASA treatment, with 4 patients having stage II, 2 patients having stage III, and 4 patients having stage IV gastrointestinal involvement. After IASA treatment 6 patients at 12 days, 7 patients at 27 days, 5 patients at 54 days had gastrointestinal response. Among them, 1 patient at 12 days, 4 patients at 27 days and the same 4 patients at 54 days showed complete remission of GI-aGVHD. Seven patients were alive 54 days after treatment. At follow-up evaluation time, 5 patients were alive. Among the 4 patients who were discharged from the hospital, 3 had no gastrointestinal symptoms, 1 patient had complains about occasional symptoms.
Conclusion: IASA treatment seems to be an effective second-line treatment in adult patients suffering from steroid-refractory GI-aGvHD.

B-0039 11:19

Adjuvant stereotactic body radiotherapy following transarterial chemoembolisation using small diameter drug eluting beads in patients with unresectable hepatocellular carcinoma

A.M.K. Abdel Aal, S. Moawad, M. Hanaoka, A. Abouarab, S. Tatum, K. Mahmoud, R. Jacob, B. Jackson, S. Saddekni; *Birmingham, AL/US (akamel@uabmc.edu)*

Purpose: The purpose of this study is to assess tumour response and locoregional control in patients with unresectable intermediate-stage hepatocellular carcinoma (HCC) treated with transarterial chemoembolisation using small diameter drug-eluting beads (DEB-TACE) compared to DEB-TACE followed by adjuvant stereotactic body radiotherapy (DEB-TACE-SBRT).
Methods and Materials: We retrospectively reviewed the medical records of patients with HCC and tumour size ≥3cm between November 2013 and June 2016 who underwent DEB-TACE using 75µm Oncozene beads (Boston Scientific) (n=56) or DEB-TACE-SBRT using 45Gy over 3 fractions (n=12). Tumours response was assessed using m-RECIST criteria.
Results: There were no significant baseline differences between the two groups. The number of lesions was not statistically significant between the 2 group (p=0.771). However, the diameter of the largest lesion as well as the total tumour diameter was larger in the DEB-TACE group (p=0.025 and 0.006 respectively). The tumour response according to mRECIST criteria did not show any significant difference between the 2 groups (p=0.251). After censoring for liver transplantation, the DEB-TACE-SBRT group showed better progression free survival (PFS) of 18 months compared to 9 months in the DEB-TACE group (p=0.006).
Conclusion: The study suggests that in patients with HCC of ≥3cm, treatment with DEB-TACE-SBRT provides better locoregional control with longer PFS, compared to DEB-TACE. Further prospective randomised controlled trial with larger number of patients is required to validate these results and to determine if there is an overall survival advantage.
Author Disclosures:
A.M.K. Abdel Aal: Consultant; St Jude Medical, Boston Scientific, WL Gore, Baxter Healthcare, Bard Peripheral Vascular Inc.. Grant Recipient; BTG, Covidien, Bard, Boston Scientific, Sirtex. Research/Grant Support; Celonova, Boston Scientific. **S. Saddekni:** Consultant; St Jude Medical.

B-0040 11:27

Extended liver venous deprivation: the most powerful interventional radiology technique for liver preparation before major hepatectomy?

B. Guiu, L. Escal, L. Piron, M.-A. Pierredon, E. Deshayes; *Montpellier/FR (b-guiu@chu-montpellier.fr)*

Purpose: Relatively high rates of post-hepatectomy liver failure (PHLF) have been reported after portal vein embolization (PVE) or ALPPS despite adequate future remnant liver (FRL) volume. FRL function is probably a better endpoint than FRL volume to decide for resection and can be calculated by ^{99m}Tc-mebrofenin hepatobiliary scintigraphy (HBS). The aim of this study was to assess safety and efficacy of extended liver venous deprivation (eLVD), i.e. combination of right PVE and right and middle hepatic vein embolization before major hepatectomy for FRL functional increase.
Methods and Materials: eLVD was performed in non-cirrhotic patients referred for major hepatectomy in a context of small FRL (baseline FRL<25% of the total liver volume or FRL function <2.69%/min/m^2). All patients underwent ^{99m}Tc-mebrofenin HBS and computed tomographic evaluations.
Results: Ten consecutive patients underwent eLVD before surgery for liver metastases (n=8), Klatskin tumour (n=1) and gallbladder carcinoma (n=1). FRL function increased by 64.3% (range=28.1-107.5%) at day 21. In patients with serial measurements, FRL function was maximum at day 7 (+65.7±16%). The FRL volume increased by +53.4% at 7 days (+25±8 cc/day). Thirty-one days (range=22-45 days) after eLVD, 9/10 patients were resected. No PHLF ("50-50" criteria or peak bilirubin >7 mg/dL) was reported. Two grade II and one grade III complications (Dindo-Clavien classification) occurred. No patient died within 90 days following surgery.
Conclusion: eLVD is safe and provides marked and very rapid increase in liver function, unprecedented for an interventional radiology procedure. If these results are confirmed prospectively, this technique could replace PVE and challenge ALPPS.

B-0041 11:35

Prototype metal artifact reduction algorithm in flat panel CT: performance in patients with intraarterial angiography during hepatic selective internal radiotherapy

Q.M. Hamie[1], A. Kobe[1], L. Mietzsch[1], M. Manhart[2], T. Pfammatter[1], R. Guggenberger[1]; [1]*Zurich/CH*, [2]*Forchheim/DE (mustafa.hamie@usz.ch)*

Purpose: To retrospectively compare the effect of a prototype metal artifact reduction (MAR) algorithm in flat panel (FP)-CT on quantitative and qualitative image parameters in patients undergoing intraarterial (ia)-angiography during selective internal radiotherapy (SIRT) of hepatic masses.
Methods and Materials: After ia-catheter placement in celiac trunk application of 36ml contrast-agent (Ultravist®300 18ml + 18ml NaCl 0.9%) a FP-CT was acquired (Artis zeego, Siemens Healthineers) using a 8s rotation protocol (200 degrees rotation, 397 projections) in 29 patients (11 female), including 16 patients with arterial metallic coils. Image reconstructions with and without MAR were evaluated quantitatively by region-of-interest (ROI) measurements of attenuation in most pronounced streak-artifacts and qualitatively assessing visibility of hepatic parenchyma and vessels in near (2cm) and far field (5cm) of artifact sources (catheter curvature and coils). Paired Wilcoxon sign rank and Student t-test were used to compare quantitative measurements and qualitative scores of corrected and uncorrected images.
Results: Quantitative evaluation showed significant reduction of near field streak-artifacts with MAR (p<0.001), while remaining stable in far field and unaffected organs (all p>0.05). Qualitative image scores in near field were significantly improved after MAR (all p<0.005). Standard deviation of attenuation values in the near field decreased significantly after MAR (p<0.05). There was no significant difference in the amount of artifact reduction between catheter curvature and metallic coils (p<0.01).
Conclusion: MAR quantitatively and qualitatively improves image quality for visibility of hepatic parenchyma and vessels in near field of artifact sources in patients undergoing FP-CT ia-angiography for SIRT.
Author Disclosures:
M. Manhart: Employee; Siemens Healhineers GmbH, Germany. Other; industrial cooperation..

B-0042 11:43

Locoregional treatments for HCC in patients with high risk for intraprocedural bleeding: is single-step combined therapy safe and feasible?

A. Posa, R. Iezzi, F. Carchesio, A. Gasbarrini, C. Colosimo, L. Bonomo; *Rome/IT (alessandro.posa@gmail.com)*

Purpose: To assess feasibility, safety, and efficacy of single-step combined therapy with radiofrequency ablation and drug-eluting beads transarterial chemoembolisation (RFA+TACE) in patients with HCC and low platelet count. Primary endpoints were major and minor complications, and death rates during and after the procedure.
Methods and Materials: Our single-centre retrospective study involved 115 cirrhotic patients (Child-Pugh A5-B7) with HCC, who underwent combined treatment between 2010 and 2015. Patients were divided into 3 groups by platelet count (>150.000/mm^3, low risk; >50.000/mm^3-<150.000/mm^3, average risk; <50.000/mm^3, high risk). Single-step combined treatment was performed with RFA during balloon occlusion of the tumour-feeding artery followed by selective TACE. Feasibility, safety, and efficacy were evaluated in terms of technical success, peri-procedural mortality and morbidity rates, laboratory values variations, blood transfusion needing, and 1-month TC follow-up.
Results: Technical success was obtained in all patients. There were no major complications. There was a significant increase of minor complications rate in group C after RFA only, all successfully treated with the subsequent TACE. No

patient required blood transfusion, nor post-procedural surgical treatment. The 3 groups did not significantly differ in terms of platelet count, INR and haemoglobin before and after the procedure, nor in terms of complete response rates at 1-month CT-follow-up.
Conclusion: Single-step combined treatment with RFA+TACE seems to be a safe, feasible, and effective treatment in patients with HCC at high risk for intraprocedural bleeding due to low platelet count, broadening the range of curative treatment. Chemoembolisation after radiofrequency ablation helps preventing iatrogenic hepatic bleeding.

B-0043 11:51

Prospective randomised FAST II trial: evaluation of the response after regional chemoembolisation (TACE) of hepatocellular carcinoma (HCC) with two different protocols

T.J. Vogl, M. Langenbach, R. Hammerstingl, T. Gruber-Rouh;
Frankfurt a. Main/DE (t.vogl@em.uni-frankfurt.de)

Purpose: To compare two different embolisation protocols for transarterial chemoembolisation (TACE) regarding tumour volume, RECIST/mRECIST criteria and apparent diffusion coefficient (ADC) in a double-blinded randomised study.
Methods and Materials: In total 49 patients (32 men; 17 women; mean 70 years; range 43-84) with hepatocellular carcinoma (HCC) were included. The treatment protocol included three TACE sessions in 4-week intervals with MRI prior to TACE and four weeks after the last TACE. Two treatment groups were determined using a randomisation sheet: in group 1 TACE was performed using Lipiodol only, in group 2 using Lipiodol combined with EmboCept®S. Tumour volume, RECIST and mRECIST were evaluated for every scan, ADC only for first and last MRI.
Results: An average tumour volume reduction of 2.15% was documented in group 1 vs 1.39% in group 2 (p=0.3849), diameter reduction was 11.8% (group 1) vs 18.32% (group 2; p=0.72). Regarding the RECIST/mRECIST criteria group 1 showed stable disease (SD) in 18 cases, progressive disease (PD) in 4 cases and partial response (PR) in 1 case. Group 2 showed PR in 4 cases, SD in 20 cases and PD in 2 cases. During treatment the ADC coefficient raised on average 878.46mm^2/s in group 1 vs 578.91mm^2/s in group 2 (p=0.4336).
Conclusion: No significant benefit in local tumour-control was documented in group 1 vs group 2. A correlation of the decrease of tumour volume after TACE and an increase in the ADC was observed. This indicates that the ADC might be an individual predictor for success of TACE.

10:30 - 12:00 **Room O**

Chest

SS 204

Lung cancer: from diagnosis to prognosis

Moderators:
C.M. Schaefer-Prokop; Amersfoort/NL
A. Snoeckx; Antwerp/BE

B-0044 10:30

Comparison of the capability for differentiating malignant from benign nodules among quantitatively assessed dynamic perfusion ADCT and MR indexes and FDG-PET/CT

W. Tani[1], Y. Ohno[1], Y. Kishida[1], S. Seki[1], T. Yoshikawa[1], Y. Fujisawa[2], M. Yui[2], S. Ohyu[2], N. Sugihara[2]; [1]*Kobe/JP*, [2]*Otawara/JP (yosirad@kobe-u.ac.jp)*

Purpose: To compare the capability for differentiating malignant from benign nodules among quantitatively assessed dynamic first-pass contrast-enhanced (CE-) perfusion area-detector CT (ADCT) and magnetic resonance imaging (MRI) indexes and FDG-PET/CT.
Methods and Materials: 57 consecutive patients (38 male, 29 female; mean age 73 years) with 71 nodules underwent dynamic CE-perfusion ADCT and MRI at 3T, PET/CT, and microbacterial and/or pathological examinations. 71 nodules were classified into malignant (n=45) and benign nodules (n=26). In each patient, total nodule perfusion (TNP) and nodule perfusions from pulmonary (NP_P) and systemic (NP_S) circulations calculated by dual-input maximum slope method from on dynamic ADCT and MRI data and SUV_{max} on PET/CT were assessed by ROI measurements. On each index, ROC analysis was performed, and feasible threshold value was determined. Finally, sensitivity, specificity and accuracy were compared each other by using McNemar's test.
Results: Area under the curves (Azs) of TNPs of dynamic ADCT (Az=0.89) and MRI (Az=0.88) were significantly larger than that of NP_Ss on both methods (ADCT: Az=0.75, p<0.05; MRI: Az=0.81, p<0.05). When feasible threshold values adopted, accuracy of TNP on dynamic ADCT (87.3 [62/71] %) and MRI (87.3 [62/71] %) was significantly higher than that of NP_Ss (ADCT: 77.5 [55/71] %, p=0.008; MRI: 77.5 [55/71] %, p=0.008) and SUV_{max} (78.9 [56/71] %, p=0.02).
Conclusion: Quantitatively assessed dynamic first-pass CE-perfusion ADCT and MRI indexes have better potential than PET/CT for differentiating malignant from benign nodules. In addition, both quantitative perfusion methods were considered as having same potential in this setting.
Author Disclosures:
Y. Ohno: Research/Grant Support; Toshiba Medical Systems Corporation.
S. Seki: Research/Grant Support; Toshiba Medical Systems Corporation.
T. Yoshikawa: Research/Grant Support; Toshiba Medical Systems Corporation. **Y. Fujisawa:** Employee; Toshiba Medical Systems Corporation.
M. Yui: Employee; Toshiba Medical Systems Corporation. **S. Ohyu:** Employee; Toshiba Medical Systems Corporation. **N. Sugihara:** Employee; Toshiba Medical Systems Corporation.

B-0045 10:38

Comparison of capability for differentiation of malignant from benign pulmonary lesions among CEST imaging, DWI and FDG-PET/CT

Y. Ohno[1], M. Yui[2], Y. Kishida[1], S. Seki[1], T. Yoshikawa[1], M. Miyazaki[3], K. Kyotani[1], K. Sugimura[1]; [1]*Kobe/JP*, [2]*Otawara/JP*, [3]*Vernon Hills, IL/US (yosirad@kobe-u.ac.jp)*

Purpose: To directly and prospectively compare the capability for differentiation of malignant from benign pulmonary nodules and/or masses among chemical exchange saturation transfer (CEST) imaging targeted to amide (-NH)groups, diffusion-weighted MR imaging (DWI) and FDG-PET/CT.
Methods and Materials: 88 consecutive patients with pulmonary nodules and/or masses underwent CEST imaging and DWI at a 3T MR system, FDG-PET/CT and pathological and/or follow-up examinations. According to final diagnoses, all lesions were divided into malignant (n=49) and benign (n=39) groups. On CEST imaging, magnetisation transfer ratio asymmetry (MTR_{asym}) was calculated from z-spectra at 3.5ppm in each pixel, and MTR_{asym} map was computationally generated. To evaluate the capability for differentiation between two groups at each lesion, MTR_{asym}, apparent diffusion coefficient (ADC) and SUV_{max} were assessed by ROI measurements. To compare each index between two groups, Student's t-test was performed. Then, ROC analysis was performed to determine each feasible threshold value for differentiation of two groups. Finally, sensitivity, specificity and accuracy were compared each other by McNemar's test.
Results: Mean MTR_{asym}, ADC and $SUV_{max}$of malignant group had significant difference with those of benign group (p<0.05). Results of ROC analysis showed that there were no significant differences of area under the curve (Az) among all indexes (p>0.05). When applied each feasible threshold value, there were no significant differences of diagnostic performance among all indexes (p>0.05).
Conclusion: CEST imaging is considered at least as valuable as DWI and FDG-PET/CT for differentiation of malignant from benign pulmonary lesions.
Author Disclosures:
Y. Ohno: Research/Grant Support; Toshiba Medical Systems Corporation.
M. Yui: Employee; Toshiba Medical Systems Corporation.
S. Seki: Research/Grant Support; Toshiba Medical Systems Corporation.
T. Yoshikawa: Research/Grant Support; Toshiba Medical Systems Corporation. **M. Miyazaki:** Employee; Toshiba Medical Research Institute USA, Inc. **K. Sugimura:** Research/Grant Support; Guerbet.

B-0046 10:46

The role of diffusion weighted MR imaging for the characterisation of mediastinal lymphnodes

M.K. Garg, E. Ramamoorthy, P. Singh, A.N. Aggarwal, N. Gupta;
Chandigarh/IN (gargmandeep@hotmail.com)

Purpose: To assess the diagnostic performance and additional value of diffusion-weighted (DW) magnetic resonance imaging (MRI) in the characterisation of mediastinal lymphadenopathy.
Methods and Materials: This prospective study was approved by the institutional review board, and written informed consent was obtained from all patients. A total of 43 patients [23 males and 20 females with mean age of 49 years] with mediastinal lymphadenopathy underwent DW and T2 weighted MRI and pathological examination in the period of January 2015 to June 2016. Diffusion restriction pattern, apparent diffusion coefficient (ADC) mean value, size and T2 heterogeneous signal intensity of the nodes were evaluated. Receiver operating characteristic curve analysis was used to determine ADC mean threshold values. The best predicting combinations of these four parameters were selected by means of stepwise logistic regression analysis.
Results: ADC mean value of malignant lymphadenopathy (0.873±0.109×10−3 mm2/s) was significantly different from that of benign lymphadenopathy (1.663±0.311×10−3 mm2/s) (P<0.001). When an ADC mean value of 1.0955×10^{-3} mm^2/s was used as a threshold value for differentiating malignant from benign nodes, the best results were obtained with a sensitivity of 94%, a specificity of 96% and area under the curve of 0.996. The three other predictor

variables didn't add anything statistically significant to the regression equation with ADC mean.
Conclusion: ADC mean value of malignant mediastinal lymphadenopathy was significantly different from the benign lymphadenopathy. The ADC mean value was the strongest independent predictor of malignancy.

B-0047 10:54

Whole body MRI with diffusion-weighted imaging (DWI) for preoperative assessment of lymph node involvement in NSCLC patients: ADC value of primary tumour as prognostic factor

L. Calandriello, M. Ciliberto, G. Sica, D. Coviello, A. Larici, L. Bonomo;
Rome/IT

Purpose: To determine whether ADC (apparent diffusion coefficient) values of the primary tumour are a predictor of lymph node involvement in NSCLC patients and to compare its diagnostic capability with qualitative assessment of DWI images.
Methods and Materials: Twenty-eight patients with NSCLC underwent preoperative whole body MRI with DWI (b value: 0-1000mm^2/sec). A qualitative analysis of lymph node involvement was performed analysing DWI images and defining patients as N+ or N- (presence or absence of lymph node metastasis). Afterwards ADCmean and ADCmin of primary tumours were calculated for a quantitative analysis. Pathology reports served as the reference standard. Diagnostic accuracy of qualitative and quantitative analysis was calculated with receiver operating characteristic (ROC) curve analysis. Student's t test was used to compare ADC values of N+ and N- patients.
Results: Pathology reports showed 12 N+ patients and 16 N- patients. Qualitative analysis showed fair diagnostic accuracy with an AUC (area under the curve) of 0.75. ADCmin of the primary tumour showed a good diagnostic accuracy with an AUC value of 0.81. The cutoff ADCmin value to discriminate between N+ and N- patients was set as 0.77x10^{-3}mm^2/s with sensitivity, specificity, PPV and NPV of 83%, 75%, 71% and 85%. ADCmin differed significantly (p=0.007) between N+ and N- patients (ADCmin 0.63x10^{-3}mm^2/s vs ADCmin 0.86x10^{-3}mm^2/s). No statistically significant result was obtained with regards to ADCmean.
Conclusion: ADCmin of primary tumour can be used as a predictor of lymph node involvement in NSCLC with a better diagnostic accuracy compared to qualitative analysis of DWI images.

B-0048 11:02

Lung cancer: short-term reproducibility of diffusion-weighted magnetic resonance imaging and intravoxel incoherent motion parameters at 3.0T

J. Jiang[1], L. Cui[1], J. Yin[1], X. Gu[2], S. Gong[1]; [1]*Nantong/CN*, [2]*Suzhou/CN (1021809719@qq.com)*

Purpose: To prospectively evaluate the short-term test-retest reproducibility of Diffusion-weighted imaging (DWI) and Intravoxel Incoherent Motion (IVIM) parameters in lung cancer, and to investigate the influence of lung cancer type, size and location.
Methods and Materials: 38 lung cancer patients underwent free breathing DWI (b=0, 800s/mm^2) and IVIM (10 b-values, 0-1000s/mm^2) scans twice (0.5-1 h interval). Regions of interests were drawn on apparent diffusion coefficient (ADC) maps, DWI (b=800s/mm^2) and IVIM images to derive ADCs, LSR_{800}(lesion-to-spinal cord ratio) and IVIM parameters D, D*, f . All parameters were compared between repeated measurements , readers, and scans. Intra- and inter-observer, test-retest reproducibility and variability was assessed with interclass correlation coefficient (ICC), within coefficient of variation (WCV), and Bland-Altman analysis. Effects of lung cancer type, size and location on the short-term reproducibility were compared by WCVs.
Results: There were no significant differences between repeated measurements , readers, and scans (P> 0.05). All parameters showed good intra- and inter-observer agreement (ICC 0.845-0.986). The test-retest reproducibility of D was best (WCV 8.91%), ADC and LSR_{800} were good to moderate (WCV 12.12%, 21.84%), while D* and f was poor (WCV 54.83% ,33.87%). The test-retest WCVs of D and ADC were greater for central lung cancer or lesions smaller than 2cm or in the lower field. While f and LSR800 was less reproducible in larger lesions,and LSR800 was less reproducible in the upper field. D* was greatly influenced by lung cancer type, size, and location.
Conclusion: If the change of D, D*, f , ADC, LSR_{800} is less than 8.91%, 54.83%, 33.87% 12.12%, 21.84% respectively, it may be caused by measurement error. The type, size and location of lung cancer are the potential influencing factors.

B-0049 11:10

A comparative analysis of dual-phase dual-energy CT and FDG-PET/CT for the prediction of histopathological invasiveness of non-small-cell lung cancer

R. Ito, S. Iwano, H. Shimamoto, H. Umakoshi, S. Ito, K. Kato, S. Naganawa;
Aichi/JP (rintaro-ito@med.nagoya-u.ac.jp)

Purpose: To compare dual-phase dual-energy CT (DE-CT) with FDG-PET/CT for predicting histopathological locoregional invasiveness of non-small-cell lung cancers (NSCLCs).
Methods and Materials: We selected 57 consecutive patients with NSCLC lesions (34 males, 23 females; age range, 44-85 years; mean age, 69 years) who were evaluated preoperatively by both DE-CT and PET/CT. Postoperative microscopic invasiveness (lymphatic permeation, vascular invasion, or pleural involvement) was reviewed, and we defined locoregional invasive tumours as tumours that had at least one positive finding of microscopic invasiveness. DE-CT scanning in the arterial and delayed phases was performed after injection of iodinated contrast media using 140kVp and 80kVp tube voltages. Three-dimensional iodine-related attenuation of primary tumours in the arterial and delayed phases was quantified automatically using application software, and the ratio of arterial phase to delayed phase enhancement (A/D ratio) was calculated. The A/D ratio and SUVmax on PET/CT were evaluated with respect to postoperative invasiveness by univariate logistic regression analysis.
Results: The A/D ratio was significantly correlated with lymphatic permeation, vascular invasion and pleural involvement (p=0.017, p=0.024, and p=0.035, respectively). On the other hand, the SUVmax was significantly correlated with pleural involvement (p=0.012) but not with lymphatic permeation or vascular invasion (p=0.179 and p=0.303, respectively). In the subgroup of patients with lesion diameters ≤2cm, the A/D ratio was significantly correlated with locoregional invasiveness (p=0.048), while the SUVmax was not (p=0.160).
Conclusion: For the prediction of microscopic invasiveness of NSCLCs, the diagnostic performaof dual-phase DE-CT may be comparable to that of FDG-PET/CT.

B-0051 11:18

Comparison of capability for therapeutic outcome prediction among dynamic perfusion MRI, dynamic ADCT and FDG-PET/CT: in NSCLC patients with chemoradiotherapy

W. Tani[1], Y. Ohno[1], Y. Kishida[1], S. Seki[1], T. Yoshikawa[1], Y. Fujisawa[2], M. Yui[2], S. Ohyu[2], N. Sugihara[2]; [1]*Kobe/JP*, [2]*Otawara/JP (yosirad@kobe-u.ac.jp)*

Purpose: To directly compare the capability for therapeutic outcome prediction between dynamic first-pass CE-perfusion area-detector CT (ADCT) and MRI assessed by same mathematical method and FDG-PET/CT in non-small cell lung cancer (NSCLC) patients treated with chemoradiotherapy.
Methods and Materials: 43 consecutive Stage IIIB NSCLC patients underwent PET/CT, dynamic CE-perfusion ADCT and MRI, chemoradiotherapy, and follow-up examination. Then, all patients were divided into two groups according to the RECIST guidelines as follows: 1) CR+PR (n=23) and 2) SD+PD (n=20) groups. In each patient, total perfusion (TP) and tumour perfusions from pulmonary (TP_P) and systemic (TP_S) circulations calculated by dual-input maximum slope method from ADCT and MRI data and SUV_{max} on PET/CT were assessed. To compare the capability for distinguishing two groups, ROC analyses were performed. Then, disease free and overall survivals between responders and non-responders assessed by each index were compared by Kaplan-Meier method followed by log-rank test.
Results: Area under the curves (Azs) of TP (MRI: Az=0.90, ADCT: Az=0.87) and TP_S (MRI: Az=0.84, ADCT: Az=0.84) were significantly larger than that of TP_P (MRI: Az=0.72, p<0.05; ADCT: Az=0.72, p<0.05). Disease free survivals of responder were significantly longer than that of non-responder by TP (p<0.05) and TP_S (p<0.05). Overall survivals of responder were also significantly longer than that of non-responder by TP (p<0.05), TP_P (ADCT: p=0.008), TP_S (p<0.05) and SUV_{max} (p=0.04).
Conclusion: Dynamic first-pass CE-perfusion ADCT and MRI has equal to or better potential to predict therapeutic outcome than PET/CT in NSCLC patients treated with chemoradiotherapy.
Author Disclosures:
Y. Ohno: Research/Grant Support; Toshiba Medical Systems Corporation. **S. Seki:** Research/Grant Support; Toshiba Medical Systems Corporation. **T. Yoshikawa:** Research/Grant Support; Toshiba Medical Systems Corporation. **Y. Fujisawa:** Employee; Toshiba Medical Systems Corporation. **M. Yui:** Employee; Toshiba Medical Systems Corporation. **S. Ohyu:** Employee; Toshiba Medical Systems Corporation. **N. Sugihara:** Employee; Toshiba Medical Systems Corporation.

B-0052 11:26

Radiomics features provide reliable measurements from manual contouring of tumours in lung cancer

A. Eilaghi, M.A. Haider, Y. Zhang, A. Oikonomou, L. Jimenez-Juan, F. Khalvati; *Toronto, ON/CA (armin.eilaghi@utoronto.ca)*

Purpose: The purpose of this study was to quantify the inter-rater reliability of a set of grey level co-occurrence matrix features in a cohort of non-small-cell lung cancer patients who underwent stereotactic body radiotherapy.
Methods and Materials: 159 patients with overall 183 tumours, mean age (range) =71(52-92), were included in the study. Manual contouring of the tumours was performed on PET and CT images of staging PET/CT studies by two radiologists independently using ProCanVAS. Radiomics features were extracted using an in-house developed prototype for each slice and averaged across slices. Cohen's Kappa test was used to assess inter-rater agreement in 3 dimensions between two contouring sets. Intra-class correlation (ICC) was used to measure the reliability between the two contoured datasets. ICC>0.8 is equivalent to high reliability. Statistical analysis was performed using R Statistical Software.
Results: For CT images, 1608 slices were assessed. Tumours appeared in 1304 and 1399 slices according to radiologist 1 and 2, respectively. For CT images, the inter-rater agreement in tumour appearance, Cohen's kappa was 0.56 and the average ICC for image features was 0.899. For PET images, 899 slices were assessed. Tumours appeared in 558 and 582 slices according to radiologist 1 and 2, respectively. The agreement in tumour co-appearance was 0.893 and average ICC for PET image features was 0.835. No significant difference was found between ICC from PET and CT images (p=0.09).
Conclusion: Studied radiomics features showed high reliability in CT and PET images and moderate agreement in tumour appearance between radiological contours.

B-0053 11:34

CT texture analysis in metastatic lung adenocarcinoma treated with tyrosine kinase inhibitors: prediction of survival

J. Cardinale, V. Bettoni, G. Agazzi, M. Ravanelli, E. Roca, D. Farina, A. Berruti, R. Maroldi; *Brescia/IT (marcoravanelli@hotmail.it)*

Purpose: To assess the predictive and prognostic value of pre-treatment CT texture features in lung adenocarcinoma treated with tyrosine kinase inhibitors (TKI).
Methods and Materials: Texture analysis was performed with a commercially available software (TexRAD Ltd, UK) on pre-treatment contrast-enhanced CT studies of 27 patients with metastatic lung adenocarcinoma treated by TKI. Texture features were quantified on a 5-mm thick central slice of the primary tumour and were correlated with progression-free and overall survival (PFS and OS) using uni- and multi-variable analysis.
Results: Mean PFS and OS were 77.4±71 and 110±87 weeks, respectively. At multivariable analysis, kurtosis of 3-mm texture was independently correlated with PFS, tumours with high kurtosis (>0.98) had a 11.4 relative risk of progression compared with tumours with low kurtosis (p<0.0001); kurtosis on unfiltered images was correlated with OS, tumours with high kurtosis (>1.74) had a 10.3 relative risk of death compared with tumours with low kurtosis (p 0.0006). Among clinical variables, only age<60 years correlated with shorter PFS (relative risk 4.1, p0.02).
Conclusion: Texture features, in particular kurtosis, are strongly associated with PFS and OS in lung adenocarcinoma treated with TKI.

B-0054 11:42

Early lung adenocarcinomas appearing as subsolid nodules: is systematic nodal dissection always essential?

S. Jeon, C. Park, J. Goo; *Seoul/KR (sunkyung417@gmail.com)*

Purpose: To assess whether nodule size or solid portion size of early lung adenocarcinomas appearing as subsolid nodules can predict lymph node (LN) metastasis at preoperative CT.
Methods and Materials: For training set for model build up, 473 patients (pure ground-glass nodules (GGNs)=116; part-solid GGNs=357) who underwent surgery for clinical stage I adenocarcinomas were included. In addition to training set, another independent patients group (N=242) with same inclusion criteria except period when the patients underwent surgery were included for the test set. Presence of LN metastasis was confirmed through LN dissections (n=413) or 1-year follow-up (n=60). Maximal diameters of whole lesions including ground-glass opacities (D_{whole}) and solid components only (D_{solid}) were measured. Solid proportion [D_{solid}/D_{whole} x100(%)] was also calculated.
Results: Among 473 patients, 11 (2.33%) patients had LN metastasis (pN+). All patients with pure GGNs did not demonstrate LN metastasis (pN0)(n=116). All patients with D_{whole}≤15mm (n=214) or D_{solid}≤5mm (n=229) were pN0. Nodal metastases only occurred in 11 among 194 patients with D_{whole}>15mm and D_{solid}>5mm (*P*<0.001 versus the other 279cases). When we made diagnostic algorithm using pure GGN, D_{solid}≤5mm, and D_{whole}≤15mm, sensitivity of 59.1% and specificity of 100% were achieved. In addition, when we apply this diagnostic algorithm in the test set, sensitivity of 41.5% and specificity of 100% in prediction of LN metastasis were achieved.
Conclusion: Pure GGN, nodule size≤15mm or solid portion size≤5mm may be reliable predictors of the absence of lymph node involvement in early-stage clinically N0 lung cancers, making it possible to avoid unnecessary nodal dissections.

10:30 - 12:00 **Room N**

Genitourinary

SS 207

Kidney and urinary tract I

Moderators:
G.P. Krestin; Rotterdam/NL
R. Salvador; Barcelona/ES

B-0055 10:30

Do clinicians follow imaging recommendations on renal artery duplex ultrasound reports?

A.H. Rajaram; *Bangalore/IN (akashrajaram@gmail.com)*

Purpose: To characterise the use of renal artery duplex ultrasound (RADUS) in assessing renal artery stenosis (RAS) as well as the rate of provider compliance with follow-up with CT or MR angiogram.
Methods and Materials: RADUS examinations conducted from 2009 to 2016 were retrospectively reviewed by one radiologist. Patients with sonographic features of RAS were identified. Recommendations for additional imaging were recorded. Subsequent CTA or MRA examinations were identified, and the reports were reviewed for concordance with RADUS findings as well as incidental findings that required further workup. We used an unpaired t-test to assess the differences in basic demographics between patients who underwent CTA or MRA versus those who were not imaged.
Results: 103 patients (mean age ± SD, 67.9 ± 15.7 years; range, 12-92 years; 53 men, 50 women) with sonographic findings of RAS were included. All patients had been recommended for CTA or MRA. Only 24 patients underwent further imaging with CTA (n=10) or MRA (n=14). Of the 24 patients undergoing additional CTA or MRA, 11 were had unilateral or bilateral RAS. However, 13 patients who were suspected to have RAS were found to have widely patent bilateral renal arteries on CTA or MRA. Incidental findings on CTA or MRA triggering additional work-up was found in only two patients, one with hydronephrosis and another with a pulmonary nodule.
Conclusion: Our study suggests that referring clinicians do not always follow recommendations on RADUS reports, even in the presence of sonographically suspected renal artery stenosis.

B-0056 10:38

Evaluation of image quality and radiation dose for low kilovoltage peak (kVp) with an adaptive statistical iterative reconstruction algorithm in computed tomography urography

L. Zheng, Z. Zhou; *Shanghai/CN (zhenglinfeng04@aliyun.com)*

Purpose: To evaluate the image quality and radiation dose in CTU images acquired with a low kVp in combination with an ASiR algorithm.
Methods and Materials: A total of 45 subjects who underwent CTU with kV assist software for automatic selection of the optimal kVp were included and divided into groups A and B based on kVp and the image reconstruction algorithm: group A consisted of a 80-100 kVp and image reconstruction with 50% ASiR algorithm (n=32); group B consisted of a 120 kVp and image reconstruction with the FBP algorithm(n=13). The images were reconstructed with VR and MIP, respectively. Image quality was evaluated using image score, CT attenuation, image noise, CNR and SNR. Radiation dose was assessed using volume CT dose index (CTDIvol), dose length product (DLP) and effective dose(ED).
Results: No significant difference was found (p>.05) between the two group's image scores for either the volume rendering (VR) or maximum intensity projection (MIP) reconstruction images. The mean attenuation of the bilateral renal pelvis in group A was significantly higher than that in group B (p<.05), whereas the image noise in group A was significantly lower than that in group B (p<.05). The CNR and SNR in group A were both significantly higher than in group B (p<.05). The CTDIvol, DLP and ED in group A were significantly lower than in group B (p<.05).
Conclusion: The low kVp CTU images with 50% ASiR reconstruction exhibit sufficient image quality and facilitate up to a 44% radiation dose reduction.

B-0057 10:46

Split-bolus vs single-bolus MDCT urography: comparison of urinary tract opacification and radiation dose exposure

C. Valle[1], P.A. Bonaffini[1], F. Invernizzi[1], A. Barletta[1], S. Faenza[1], A.S. Casiraghi[2], A. Pappini[1], S. Sironi[3]; [1]*Desio/IT*, [2]*Monza/IT*, [3]*Bergamo/IT (clarissa.valle1987@icloud.com)*

Purpose: To evaluate the urinary tract opacification and the radiation dose exposure of split-bolus MDCT urography (CTU) as compared to standard single-bolus protocol.
Methods and Materials: Forty-eight patients (18-83 years), undergone a CTU study on a 64-row scanner (Aquilion, Toshiba) after i.v. administration of 90-110mL of iodinated contrast medium (350mg/mL), were retrospectively analysed: 24 were studied using a split-bolus protocol, including mainly a combined nephrographic-pyelographic phase (study group), 24 a single-bolus CTU (control group). Quantitative analysis of opacification in pyelographic phase (HU) was achieved by placing ROIs within the lumen of renal pelvis, ureters and bladder. Two radiologists (1-consultant, 2-resident) also qualitatively evaluated the opacification by using a 4-point scale. The radiation dose exposure was calculated as dose-length product (DLP, mGy*cm) and CTDIvol (mGy). All data were statistically analysed.
Results: The split-bolus protocol demonstrated a mean urinary attenuation significantly lower than the standard CTU (left pelvis 909 vs 1326HU, right pelvis 877 vs 1253HU, left ureter 810 vs 1114HU, right ureter 655 vs 1127HU, respectively) but no differences between the two groups were observed concerning the qualitative evaluation of urinary opacification. Mean split-bolus DLP was significantly lower (1869 mGy*cm; p=0.045) as compared to the single-bolus protocol (3002 mGy*cm), with a dose exposure reduction of 37%; no significant differences were achieved for CTDIvol.
Conclusion: The urinary tract opacification, even if quantitatively lower, was qualitatively comparable between the two protocols; moreover, the split-bolus DLP was significantly lower, with an overall dose reduction of 37%.

B-0058 10:54

Rescanning in prone position in CT urography: is it really necessary for the evaluation of an incompletely opacified bladder?

P. Martingano, M. Muca, M.F. Cavallaro, M. Iannelli, M.A. Cova; *Trieste/IT (pmartingano@sirm.org)*

Purpose: To assess diagnostic confidence in bladder malignancy detection of CT urography (CTU) performed with split bolus technique in case of incomplete bladder opacification due to urine retention.
Methods and Materials: From January 2014 to February 2015, 100 consecutive patients who underwent both CTU and cystoscopy were retrospectively identified. One investigator with 10 year genitourinary imaging experience evaluated bladder wall in the supine position and then, when available, in the prone position to detect bladder malignancy. Cystoscopy was considered as reference standard to calculate receiver operating characteristic (ROC) curves of diagnostic confidence.
Results: 62 out of 100 CTU exams met inclusion criteria (38 were rule out for absence of unopacified urine or presence of artifacts due to hip prosthesis), and 35/62 were performed in both supine and prone position. In these 35 exams there were not statistically significant difference between the evaluation of the supine scan alone and both scans. In the 62 exams the overall accuracy of the supine scans was 94.6%, with a 94.7% sensitivity and a 94.4% specificity (ROC Area: 0.985).
Conclusion: The split-bolus technique, with a single scan in a nephro-excretory phase, allows a good evaluation of bladder wall also in patients with distended but not entirely opacified bladder. Its high diagnostic confidence spare in most cases rescanning in prone position, with consequent radiation exposure reduction and time saving.

B-0059 11:02

Role of diffusion-weighted magnetic resonance imaging in predicting renal dysfunction in chronic kidney disease patients

M.S. Shaaban, M. Sakr, A. Fathy, G. Kortam; *Alexandria/EG (mohamed.shaban@gmail.com)*

Purpose: To assess the relationship between ADC of renal parenchyma and serum markers of renal function and stage of chronic kidney disease (CKD), and to establish cut-off ADC values to identify CKD.
Methods and Materials: This is a prospective study conducted from December 2013 to April 2016. Subjects divided into 2 groups: Group I included 15 CKD patients at different stages and aetiologies, Group II included 15 individuals control group who have normal renal function indicated for MRI for other aetiologies. Both groups underwent DWI. ADC values were determined for renal parenchyma and compared. ROC curves were drawn to establish cut-off ADC values. Pearson's correlation coefficient (R) was calculated between ADC and renal function parameters.
Results: ADC values in patients with renal dysfunction were significantly lower than in patients with normal renal function. There was significant inverse correlation between ADC and serum creatinine, and significant linear correlation with eGFR. ADC values showed a statistically significant decreasing trend with increasing stage of CKD. ROC curve for average ADC of both kidneys revealed ADC cut-off value ≤1.866 with 86.67% sensitivity and 78.57% specificity.
Conclusion: ADC values may serve as an additional marker for the presence and degree of renal dysfunction.

B-0060 11:10

Observational study on the incidence of nephrogenic systemic fibrosis in patients with renal impairment following gadoteric acid administration

A.I.B. De Backer; *Ghent/BE (adelard.debacker@azstlucas.be)*

Purpose: To determine the incidence of Nephrogenic Systemic Fibrosis (NSF) in patients with renal impairment after gadoteric acid (DOTAREM, Guerbet, France) administration.
Methods and Materials: Worldwide post-marketing study including 540 patients with at least moderate renal impairment scheduled to undergo a routine contrast-enhanced Magnetic Resonance Imaging (MRI) using gadoteric acid. Medical history, MRI indication(s) and Adverse Events (AEs) were recorded for each patient. Patients were followed up over 2 years with 3 visits separated by at least 3 months in order to detect any signs of NSF.
Results: Among the 540 patients (mean age: 69.6 years [min-max: 21-95]; men: 58.5%), renal impairment was evaluated as moderate for 69.3% of patients, severe for 16.1% and end-stage for 12.0%; 2.6% of patients had undergone a previous kidney transplant. Mean eGFR was 37.6 ± 15.7 ml/min/1.73 m2 [4.0-74.2]. Main MRI indication was to assess suspected abnormalities of the central nervous system (34.6%). As of 1st September 2016, 97.3% of patients attended the first follow-up visit, 76.9% attended the second and 55.4% attended the third. Neither AE considered to be related to the administration of gadoteric acid, nor NSF suspicion were reported.
Conclusion: Intermediate data of the NSsaFe study show no cases of NSF after gadoteric acid administration, confirming its good safety profile in patients with renal impairment.
Author Disclosures:
A.I.B. De Backer: Investigator; Dr De Backer is a study investigator with no other financial relationship with Guerbet. The NSsaFe Study is a Guerbet-sponsored study. The investigators who participated in the study, including Dr, received funding from Guerbet for participating in the study. Dr De Backer is not a party to a consulting agreement with Guerbet..

B-0061 11:18

Perfusion MRI in early detection of renal fibrosis in patient with ADPKD: a preliminary study

A. Di Gaeta, E.L. Indino, S. Lai, D. Mastroluca, C. Catalano, V. Panebianco; *Rome/IT (alessandro.digaeta@hotmail.it)*

Purpose: The aim of our study is the evaluation through perfusional MRI (PMR) of Total Kidney Volume (TKV), Total perfusional volume (TPV) and the Total Fibrotic Volume (TFV) correlating to clinical data in patient with Autosomal Dominant Polycystic Kidney Disease (ADPKD).
Methods and Materials: Twenty-five ADPKD patient (mean age 39 years), thirteen of them ADPKD-hypertensive, with eGFR > 50 ml/min and blood aldosterone levels measurement. All patient enrolled underwent perfusional MRI (MRP) with Magnet 3T (Discovery MR 750, 3T, GE Healthcare) and 32-channels surface coil. PMR protocol included morphological sequences T2-W single shot (SSFS), and T1-W Gradient Echo (GRE). During MRP were used ultrafast T1-W 3D-GRE sequences high time resolution repeated for 8 minutes. Perfusion was evaluated with qualitative and quantitative approaches. The former based on two colour maps (showing functional parenchyma and the late parenchymal enhancement); the latter obtained by using a post-processing 3D-Volume Rendering software to quantify TPV and TFV. Mean follow-up period of 15±2 months, in which MRP was repeated.
Results: All correlations were obtained with Spearman's rho coefficient and was considered significant $p<0.05$. Time 1 eGFR negatively correlates with TKV ($r = -0.059$, $p<0.02$), with TFV ($r= -0.61$, $p<0.04$) and TPV/TKV(%) ($r= -0.59$, $p<0.02$). TFV positively correlates with aldosterone blood levels ($r= 0.50$, $p<0.05$).
Conclusion: PMR is a useful tool in monitoring progression of the disease and to evaluate early ADPKD, highlighting early changes in terms of fibrotic evolution in renal parenchyma even when renal function is preserved.

B-0062 11:26

DW-MRI as an alternative to biopsy in renal allograft patients with deteriorating renal function: a preliminary study

S. Barbieri, P. Steiger, A. Kruse, M. Ith, H.C. Thoeny; *Berne/CH (sebastiano.barbieri@insel.ch)*

Purpose: To assess the accuracy of diffusion-weighted MRI (DW-MRI) used to classify renal allograft patients with deteriorating renal function into two groups: the "biopsy-mild" group consisting of patients with normal or mild grade I interstitial fibrosis and tubular atrophy and the "biopsy-severe" group with grade II-III interstitial fibrosis and tubular atrophy, rejection, or other pathologies not due to rejection. At our institution, "biopsy-severe" patients are associated with a change in clinical management.
Methods and Materials: Forty kidney transplant patients underwent DW-MRI (1.5T, 10 b-values) and biopsy (the reference standard) within 10 days. Patients were classified in two subsequent steps: at first patients with allografts appearing heterogeneous on b=900 sec/mm^2 images were assigned to the "biopsy-severe" group; the remaining patients were classified by applying a threshold to the average or minimal ADC or intravoxel incoherent motion parameters (pseudodiffusion D*, diffusion D, perfusion fraction f) measured within the upper, middle, and lower pole of the allograft.
Results: According to histopathology 15 patients were in the "biopsy-mild" group and 25 in the "biopsy-severe" group. Classification based on minimal ADC or minimal f led to the highest accuracy of 80% (sensitivity 84.0% and 92.0%; specificity 73.3% and 60.0%, respectively). Patients were considered "biopsy-severe" if the allografts appeared heterogeneous or the minimal ADC was less than $179.5 \cdot 10^{-5}$ mm^2/sec or the minimal f was less than 14%.
Conclusion: DW-MRI is a promising technique to predict the severity of histopathologic findings in renal allograft patients and might, in the future, reduce the number of biopsies.

B-0063 11:34

Usefulness of transplanted kidney evaluation by multiparametric ultrasonography: including two different types of ultrasound elastography

M. Yoo, D. Jung, Y. Oh, S. Park, K. Han; *Seoul/KR (placeborain@yuhs.ac)*

Purpose: The purpose of this study was to investigate the association between microscopic abnormalities of transplanted kidney and ultrasonography based imaging biomarkers including elasticity, venous impedance index, arterial resistive index and renal size.
Methods and Materials: Between 2011 and 2015, ultrasonography was performed in 159 recipients who would be planned to undergo transplanted kidney biopsy. Maximal longitudinal length on greyscale images, arterial resistive index, and venous impedance index on Doppler images, and shear wave velocity on Acoustic Radiation Force Impulse imaging or Young's modulus on Supersonic Shear Imaging were measured before biopsy. Ultrasonography parameters and clinical variables were analysed with individual and sum of Banff scores derived from the tissue samples.
Results: On Spearman's rank correlation coefficient and ordinal logistic regression, no ultrasonography parameters were associated with sum of Banff scores. Only the duration between kidney transplantation and biopsy was significantly associated with sum of Banff scores (r=0.588, B=0.018, p<0.05). On univariate logistic regression analysis with individual Banff scores, mm were associated with arterial resistive index; t, cg, mm with venous impedance index; and t, cg, ct, ci, mm, ah with duration between transplantation and biopsy (p<0.05). Shear wave velocity or Young's modulus were not associated with any individual Banff scores.
Conclusion: Both types of elastography were not significantly associated with any histopathologic change of the transplanted kidney. Although arterial resistive index and venous impedance index were related to a few individual Banff scores, time after transplantation showed stronger correlation with renal allograft deterioration than imaging biomarkers.

B-0064 11:42

Diffusion-weighted imaging and diffusion tensor imaging in the evaluation of transplanted kidneys before and after furosemide

D.C. Caltabiano, L. Mammino, V. Costanzo, P. Foti, P. Milone, L. Mauro, N. Sinagra, M. Veroux, S. Palmucci; *Catania/IT (daniele.788@gmail.com)*

Purpose: To evaluate renal function in a population of kidney transplant recipients using diffusion-weighed imaging (DWI) and diffusion tensor imaging (DTI) before and after furosemide administration.
Methods and Materials: 29 patients with transplanted kidneys were studied using 1.5 Tesla MRI; DWI and DTI sequences were performed before and after intravenous administration of furosemide. Patients were divided into 2 groups according to their creatinine clearance values: group A, including patients with normal clearance value (≥60 ml/min), and group B, including patients with low clearance value (<60 ml/min). Apparent diffusion coefficient (ADC) and fractional anisotropy (FA) were calculated placing region of interests both in renal cortex and medulla; their values - before and after furosemide administration - were compared among groups using Mann-Whitney U test.
Results: Cortical ADC values were statistically different between groups before furosemide, with p=0.01; after furosemide administration, a higher statistical difference was observed between groups A and B, with p=0.007. No statistical differences were found for cortical FA before and after furosemide stimulation, with p values, respectively, of 0.329 and 0.723. Medullar ADC and FA values were statistically different between groups, showing respectively p values of 0.001 and 0.041 before functional furosemide administration; after diuretic stimulation bolus, p values of 0.017 and 0.023 were observed comparing, respectively, ADC and FA among groups.
Conclusion: In functional MRI with DTI, furosemide improves differentiation between normal and abnormal transplanted kidneys; however, a certain degree of overlap remains between groups. Medullar FA is a reliable parameter for renal function evaluation.

B-0065 11:50

CT diagnosis and follow-up of urolithiasis using ultra-low dose hybrid and pure iterative reconstruction algorithms based on size

V. Vardhanabhuti[1], S. Tenant[2], C.-L. Pang[2], P. Dissanayake[2], C. Gutteridge[2], C.J. Hyde[3], C.A. Roobottom[2]; [1]*Hong Kong/HK*, [2]*Plymouth/UK*, [3]*Exeter/UK*

Purpose: The aim of this study was to evaluate the accuracy of scans for the primary investigation and follow up of urolithiasis, comparing MBIR with as low a dose as possible with a standard ASIR reconstruction algorithm.
Methods and Materials: A single-centre IRB-approved prospective study recruited 125 patients with written consent. Standard-dose (SD) and low-dose (LD) were performed. Scans were reconstructed with adaptive statistical iterative reconstruction (ASIR) and model-based iterative reconstruction algorithms (MBIR). Accuracy of detection of urolithiasis were analysed. Dose was recorded.
Results: Mead doses were as follows: SD: $CTDI_{vol}$ 4.7 mGy, DLP 223.6 mGy.cm, SSDE 5.3 mGy; LD: $CTDI_{vol}$ 2.2 mGy, DLP 102.6 mGy.cm, SSDE 2.3 mGy. Primary end-point (the presence of obstructive uropathy), for each reader, review of the reduced-dose MBIR scan was found to concur perfectly with that reader's review of the standard-dose scan. In all cases the obstructing calculus was correctly observed. By contrast, the reduced-dose scans reconstructed using ASIR were of reduced accuracy, with a sensitivity of only 0.81 and 0.86 for readers 1 and 2 respectively. MBIR had excellent sensitivity for stones of 3mm (95.7% identified) and performed perfectly for stones above this size. Accuracy dropped off between 2mm and 1mm, where sensitivity fell from 90% to 67.5%.
Conclusion: Significantly reduced-dose CT KUB scans can be performed with the use of model-based iterative reconstruction without any loss in diagnostic accuracy for obstructing calculi and whilst maintaining very high accuracy for renal calculi of 3mm and above.

10:30 - 12:00 **Room L 8**

Head and Neck

SS 208

New technical developments in head and neck imaging

Moderators:
N.J.M. Freling; Amsterdam/NL
N.N.

B-0066 *10:30*

US localisation of abnormal findings in neck PETCT or scintiscan: a preliminary experience with 3D and 2D virtual navigation (VN) and bodymap technology (BMT) vs cognitive approach

G. Bizzarri, A. Bianchini, D. Valle, L. Velari, S. De Nuntis, A. Dell'Era, L. Di Vito, L. Forzoni, E. Papini; *Albano Laziale/IT (bizzarrigiancarlo@libero.it)*

Purpose: US is the modality of choice for neck examination and for image guided neck biopsies. However scintiscan and PETCT can provides specific functional information which are useful for detecting pathologies. Cognitive correlation between US findings and functional findings can be challenging. We report a preliminary experience using 3D VN and 2D navigation with BMT.
Methods and Materials: MyLabTwice ultrasound scanner equipped with 2D navigation with BodyMark and 3D VN was used (Esaote S.p.A., Italy). 20 patients with different findings (abnormal uptake in thyroid nodules, residual uptake after thyroidectomy, lymph nodes pathologic uptake, parathyroid pathologic uptake) at Scintiscan and PETCT were enrolled. Functional images were loaded on the equipment before performing US examination. After a standard US scan, US was co-registered with scintiscan or PETCT using anatomical landmarks (linear probe LA533, 5-13 MHz with magnetic sensor

support CIVCO, USA). Each patients was examined by 3 operators that were asked about the confidence in localization with cognitive versus VN or BMT technology. The time necessary for cognitive and VN or BMT were recorded.
Results: Operators reported that VN and BMT increased the confidence in localization of pathologic uptake in 76% of cases. The mean time necessary for cognitive, VN and BMT was 4, 2 and 5 minutes respectively.
Conclusion: 3D VN and 2D Navigation with BMT increase the confidence in US localization of abnormal or pathologic functional findings on scintiscan and PETCT compared to cognitive approach. Furthermore the navigation techniques are not time consuming.

B-0067 10:38

TSE or SPACE for high-resolution dental-MRI?
T. Hilgenfeld, M. Prager, S. Schwindling, A. Heil, S. Kuchenbecker, P. Rammelsberg, M. Bendszus, S. Heiland; *Heidelberg/DE (tim.hilgenfeld@med.uni-heidelberg.de)*

Purpose: Dental MRI is a new, radiation free diagnostic tool. Unfortunately, the application is often limited due to poor resolution and artefacts due to metallic dental-materials. Here, we for the first time systematically evaluated whether the turbo spin echo (TSE) or sampling perfection with application optimized contrasts using different flip angle evolution (SPACE) sequence is advantageous for the demanding requirements of Dental MRI.
Methods and Materials: Sequences were optimized on a 3T MRI for maximal resolution and artefact suppression. Normalised signal-to-noise ratio (nSNR), artefact volume and image quality were assessed in vitro in T1- and T2-weighted images. Image quality was assessed by two blinded reader's on a five-point scale. Four titanium and one zirconia dental implants provided with different single crowns were studied: porcelain-fused-to-metal precious-alloy (GP-T), porcelain-fused-to-metal non-precious-alloy (CCT-T), porcelain-fused-to-zirconia (ZC-T) and monolithic-zirconia (Z-T, Z-Z).
Results: Amount of artifact volume depended on used sequence and material composition. Smaller artefacts were always observed for the optimised TSE sequence beside the Z-Z sample (mean reduction over all samples 73.9±12.9%; maximum reduction for GP-T sample 87.8±3.9%). nSNR was significantly higher for the SPACE sequence (241% of the TSE) but no significant difference in image quality was noted. Fewest MRI artefacts were observed for the Z-Z sample and largest for the CCT-T sample. Smaller and comparable artefact volumes were noted for the GP-T, ZC-T, and Z-T samples.
Conclusion: The optimised TSE performs better in terms of artefacts reduction. However, for materials with small differences in magnetic susceptibility the optimised SPACE sequence performs as good as the TSE sequence while offering a higher resolution and higher normalised SNR.

B-0068 10:46

Multiparametric MRI of velopharyngeal inadequacy in patients who underwent primary palatoplasty
R. Magnani, N. Flor, F. Galli, M. Zaffaroni, S. Sbaraini, G. Carrafiello; *Milan/IT (roberta.magnani@hotmail.it)*

Purpose: To evaluate the prospectively role of MR in diagnosis and treatment of cleft palate patients who developed velopharyngeal inadequacy (VPI) and speech deficit, after primary palatoplasty.
Methods and Materials: After our institution review board approval, from January to May 2016 we recruited 17 patients (11 M; 6 F) older than 4 years-of-age (mean age 18; age range 4-42), who previously underwent primary palatoplasty, 10 with velopharyngeal inadequacy and 7 with normal speech function. We performed 1,5 T MR of the soft palate to all patients, without any sedation, at rest and during phonation of vowel "I". Statistical analysis was carried out by means of t-test and Pearson correlation coefficient.
Results: Among cleft palate patients with impaired speech the length and thickness of levator veli palatini muscle (LVP) and velar eminence angle are respectively shorter, thinner and wider in comparison with cleft palate patients with normal speech function (p-value $p<0.0015$, $p<0.02$ and $p=0.014$). All normal speakers have no lateral sphincterial gap during phonation, while most of the patients with speech deficit have.
Conclusion: MR is a consistent and well-tolerated test to investigate patients with velopharyngeal inadequacy, complementary to videofluoroscopy with the significative advantage of the absence of radiation exposure.

B-0069 10:54

Facial vascular anomalies: MRI and TRICKS-MR angiography diagnostic approach
O. Hassanien, U. Ghieda, R.L. Younes, E.A.I.N. Shaban; *Mehalla/EG (ekhlas_radiology@med.tanta.edu.eg)*

Purpose: To evaluate the role of MRI and TRICKS-MR angiography in diagnosis of facial vascular anomalies.
Methods and Materials: This prospective study was performed upon 30 patients presented with suspected facial vascular anomalies. Eight patients were excluded (5 patients because of lack proved diagnosis & 3 patients because of poor image quality secondary to inadequate sedation). The remaining 22 patients with proved facial vascular anomalies on basis of interventional/surgical procedures (n=19) or clinical follow up (n=3) were included .The age range, 2months-23 years; mean age 9 years) .They underwent routine MRI examination with TRICKS-MRA. Images were evaluated for lesion location, extent , signal characteristics, nidus size , presence of feeding arteries and draining veins
Results: AVM was diagnosed in 15patients, haemangiomas were in 5 patients and 2 patients were diagnosed as low flow venous malformation. TRICKS-MRA was more accurate in assessment of the size of AVM nidus and in detection of feeding arteries and draining veins. AVM patients were treated with sclerotherapy (4/15), embolization (6/15) and combined embolization and surgery (5/15). Surgery was done in 2patients with haemangioma while the other three patients underwent clinical follow up for 2 years with stationary course. The 2 patients with venous malformation underwent successful sclerotherapy.
Conclusion: MRI & TRICKS-MR angiography provide excellent diagnostic data for accurate assessment of facial vascular anomalies regarding their size and nature which greatly helps in planning of their therapeutic approach. We recommend addition of TRICKS- MR angiography in MR examination of cases with suspected facial vascular anomalies.

B-0070 11:02

Intravoxel incoherent motion imaging of the head and neck: comparison of quantitative parameters between turbo spin-echo and echo-planar imaging
R. Mikayama, H. Yabuuchi, K. Kobayashi, S. Sonoda, M. Kimura, H. Honda; *Fukuoka/JP (mt_mika_jan_5@yahoo.co.jp)*

Purpose: Echo-planar imaging (EPI), diffusion-weighted imaging (DWI) in the head and neck area is frequently deteriorated by susceptibility artifacts. On the other hands, turbo spin-echo (TSE)-DWI is less sensitive to susceptibility artifacts for using the repeated radio frequency refocusing pulse. The purpose of our study was to compare apparent diffusion coefficient (ADC) and intravoxel incoherent motion (IVIM) parameters between TSE-DWI and EPI-DWI of the head and neck.
Methods and Materials: Fourteen healthy volunteers underwent head and neck DWI of two sequences (TSE-DWI and EPI-DWI). All the examinations were performed using a 3T magnetic resonance unit with a 16-channel-SENSE neurovascular coil. We manually set the regions of interest (ROIs) in the bilateral submandibular glands, sublingual glands, and palatine tonsils, as large as possible avoiding vessels or grand ducts. ADC and IVIM parameters (true diffusion coefficient, D; perfusion fraction, f, respectively) in each ROI were calculated for the two DWI sequences. Bland-Altman analysis was performed to detect systematic errors and calculate limits of agreement (LoA) between TSE-DWI and EPI-DWI.
Results: There are no systematic errors; however, Bland-Altman analysis showed unacceptable LoA (minimum-maximum LoA for each parameter; ±22.8-33.6 % for ADC, ±32.5-56.6 % for D, and ±110.2-153.6 % for f) between TSE-DWI and EPI-DWI.
Conclusion: There are large variance in ADC and IVIM parameters between two sequences. ADC and IVIM parameters of TSE-DWI could not be used as equivalent parameters of EPI-DWI in the head and neck.

B-0071 11:10

Computed tomography of the head and neck region: comparison of dual energy vs single energy
M. May, R. Heiss, M. Wiesmueller, M. Uder, W. Wuest; *Erlangen/DE (wolfgang.wuest@uk-erlangen.de)*

Purpose: Aim of this study was to intra-individually compare the image quality obtained by dual-energy examinations and different virtual monoenergetic images to low kV single-energy scanning.
Methods and Materials: Third-generation dual-source dual-energy CT was performed in 49 patients with histologically proven malignant disease of the head and neck region. A second scan aligned to the jaw covering the oral cavity was obtained to reduce artefacts caused by dental hardware. Single energy with a 70kV setting was used for the second scan. Tube current settings in single- and dual-energy scans were adapted to obtain comparable radiation dose levels. Objective image quality was assessed as contrast to noise ratio (CNR) and subjective image quality on a 5-point Likert scale.
Results: For vessel attenuation, 40keV CNR (28±12) was significantly higher compared to all other keV and kV settings (all $p<0.05$). For tumour attenuation, 40keV and 60keV yielded the highest CNR (9.6±5.6 vs. 6.5±3.4) with no significant difference to each other ($p=0.09$ and 0.08). 60keV CNR was comparable to 70kV ($p=1.0$). Overall subjective image quality was comparable for 40keV, 60keV, 70kV and the weighted average image (all $p>0.05$). CTDIvol was not significantly different (70kV: 19.4 mGy vs. DE neck: 18.6 mGy, $p=0.10$).

Conclusion: 40keV yielded the highest objective image quality in comparison to the other keV reconstructions and to the 70kV scan. Scanning at 70kV might be an option in CT scanners not capable of the dual-energy technique.
Author Disclosures:
M. May: Speaker; Siemens. **M. Uder:** Speaker; Siemens, Bayer, Bracco. **W. Wuest:** Speaker; Siemens.

B-0072 11:18

Dental implant artefact reduction using novel dual-layer spectral CT
M.J. Willemink, S. Wiersma, R.W. van Hamersvelt, B. Peltenburg, R. de Bree, P.A. de Jong, T. Leiner, J.W. Dankbaar; *Utrecht/NL (m.willemink@umcutrecht.nl)*

Purpose: Dental implant artefacts can be reduced with dual-energy CT (DECT) using virtual-monochromatic images at high photon energies (High-MonoE). However, image quality of virtual-monochromatic images is inferior to conventional images for current DECT systems. Dual-layer spectral CT (DLCT) is a novel DECT technique that uses an anti-correlated noise reduction algorithm. We evaluated artefact reduction and image quality of High-MonoE images of head and neck DLCT with anti-correlated noise reduction.
Methods and Materials: Sixty-one patients with dental implants who underwent a head and neck CT on a DLCT system were retrospectively included. Conventional images and High-MonoE (200keV) images were reconstructed from standard 120kVp-acquisitions. Dental artefact reduction was evaluated using a 5-point Likert scale on three levels adjacent and distal to the implants (resulting in 61*3*2=366 evaluations). Regions-of-interest (ROIs) were drawn at the mandible level in the sternocleidomastoid and spinal muscles and carotid arteries. CT-densities (HU), noise (standard deviations) and signal-to-noise ratios (SNRs) were calculated.
Results: Artefacts influenced adjacent structures in 254/366 evaluations (69.4%) on conventional images, which decreased to 203/366 (55.5%) for High-MonoE. Averaged muscle noise levels were 22.4±4.5HU at conventional images, whereas High-MonoE noise levels reduced to 17.4±3.6HU. Average CT densities of the carotid arteries decreased from 211.8±71.1HU on conventional images to 63.4±20.9HU on High-MonoE, respectively. As CT densities decrease at High-MonoE, averaged muscle SNRs were similar (3.0±0.7 vs 3.1±0.7, respectively).
Conclusion: Noise and dental artefacts reduced with anti-noise-correlated High-MonoE images acquired on novel DLCT compared to conventional CT. Therefore, this study indicates that DLCT may allow for head and neck evaluation on High-MonoE images with improved image quality.
Author Disclosures:
M.J. Willemink: Speaker; Philips Speaker Bureau.

B-0073 11:26

Lateral position with gantry tilt further improves CT image quality reconstructed by single energy metal artifact reduction algorithm in the oral cavity
M. Onodera, K. Aratani, T. Shonai, K. Ogura, M. Hatakenaka; *Sapporo/JP (monodera8@gmail.com)*

Purpose: Single Energy Metal Artefact Reduction (SEMAR) algorithm reduces metal artefacts on CT. However, image quality is not sufficiently improved in cases with multiple dental metals. The objective of this study is to investigate whether lateral position (LP) with gantry tilt (GT) resolves this limitation in the oral cavity (OC).
Methods and Materials: Our institutional review board approved this prospective study and written informed consent was obtained from all patients. We recruited 74 patients (45 men and 29 women) who had dental metals in multiple locations, and underwent head and neck CT between September 2014 and March 2015 in two positions: First, standard supine position (SP) without GT, and second, LP with 15 degrees of GT. Both images were reconstructed with SEMAR. Two radiologists assessed image quality in two areas, outside (OUT) and inside the dental arch (IN), using a 4-point scale: 1= severe artefact, 2= moderate artefact, 3= slight artefact, 4= no artefact. Image-quality score was compared between two positions using Wilcoxon signed-rank test. A *P* value < 0.05 was regarded as statistically significant.
Results: The image-quality score was significantly higher in LP with GT than SP in both areas (OUT: 3.1±0.4 vs. 2.3±0.4; IN: 2.6±0.7 vs. 1.9±0.5; $P < 0.0001$).
Conclusion: LP with GT resolved the limitation of SEMAR in the OC, probably through separating right and left dental metals into different planes.

B-0074 11:34

Evaluation of laryngopharyngeal structures by CT scan using dynamic "eee" phonation maneuver
K.K. Obeng, P. Ignaciuk, J. Kim, F. Appiah, N. Darboe, E.J. Escott; *Lexington, KY/US (kob223@uky.edu)*

Purpose: To determine if we could prospectively produce clearer delineation of pertinent structures of the pharynx and larynx by imaging patients with head and neck ailments with dynamic "eee" phonation.
Methods and Materials: One hundred and sixty patients were randomly divided into 2 groups; group A (n=80) underwent CT imaging in 'quiet respiration and group B (n=80) underwent CT imaging with an "eee" phonation maneuver. A control group C (n=82) imaged prior to beginning the study were selected randomly from our PACS. Images were evaluated independently by; (1) a neuroradiologist evaluating by consensus with a senior radiology trainee and (2) a neuroradiologist alone. Each evaluated subject was assigned numerical values for the valleculae, piriform sinuses and laryngeal ventricles distention (0 - no distention to 2- excellent distension). True vocal cord position was also assigned a numerical value (0,1,2). Chi-square test was used to examine the relationship between the experiments outcome and the control. .
Results: There was a mild to moderately high agreement between the two reviewing personnel with respect to the experimental and control measures. There was a statistically significant delineation with respect to laryngeal ventricles (p-value=0.009), piriform sinuses (p-value<0.001), and true vocal cords (p-value<0.001), of the experimental groups compared to the control group.
Conclusion: There is improved delineation of pertinent laryngopharengeal structures when CT scan of the neck is performed by employing the 'eee' phonation maneuver.

B-0075 11:42

The role of CB-CT on the planning, surgical technique and follow-up of pterygoid implants: a controlled prospective study
G. Ferrero[1], F. Fiz[2], C. De Angelis[2], E. Fabbro[1], A. Corazza[2], D. Orlandi[2], I. Fiz[2]; [1]*Pietra Ligure/IT*, [2]*Genoa/IT (giulio.ferrero@gmail.com)*

Purpose: Pterygoid implant (PI) is an emerging treatment option for posterior maxillary edentulism. Pre-operatory planning is the key: CB-CT examination performed with the use of a radiologic template allows to obtain an accurate intraoperatory 3D-printed model as surgical referral, thus improving the surgical outcome. In this study, the PI made with the guidance of a preoperative CB-CT obtained with a radiologic template was compared with the traditional implanting technique without radiologic template.
Methods and Materials: Forty patients (group A:27 females, mean age 58, range 38-85) underwent 52 PI procedures with the guidance of a 3D intraoperatory model obtained from CB-CT performed with radiological template. Patients' comorbidities at the time of implant, PI positioning (I or II quadrant) and presence of post-operative pain were recorded. These parameters were compared with the ones derived from 40 patients (group B,controls: 14 females, mean age 59, range 35-93, 52 procedures), treated with CB-CT-based solutions without radiological template.
Results: Dental elements loss was less pronounced in group A with respect to group B, occurring in 2 patients (3/52 PI) in the first 12 months and in 17 patients (17/52 PI) in group B (p<0.001). Follow-up at 24 months up confirmed this trend (3/52 vs 29/52, p<0.001). Advanced age and diabetes mellitus resulted as risk factors for this occurrence (p<0.01). Persistent post-operative pain was less prevalent in group A patients compared with group B (5/40 vs 31/40, p<0.001) and was a hallmark of possible procedure failure (in 3/3 failed and 2/47 successful procedures of group A; in 17/17 failed and in 2/35 successful procedures in group B; p<0.001).
Conclusion: PI guided by CB-CT examination performed with the use of a radiologic template is a viable therapeutic option for posterior edentulism.

B-0076 11:50

Quantitative and analytic assesment of incidental findings in patients exposed to CBCT
M. Iodice; *Milan/IT (maiodice@gmail.com)*

Purpose: The aim of this study was to evaluate topology and incidence of incidental findings in patients who had undergone to cone-beam computed tomography (CBCT) and the consequences on diagnostic and therapeutic path.
Methods and Materials: A group of expert radiologist examined retrospectively 5000 CBCT reports of two diagnostic radiology centres (using respectively NewTom VGi Evo and Planmeca ProMax 3D Mid) executed between January 2013 and November 2015. We divided findings according to the anatomic belongings: odontogenic, airways, soft tissues, bone, and temporo-mandibular joint (TMJ). Moreover they were divided into three groups: a group 1 of patients who needed intervention or postponement, a group 2 of

patients with monitoring pathologies and a group 3 of patients who did not need intervention.
Results: On 5000 patients, we found 3021 incidental findings (60%). The most significative findings were referred to airways (68%), bone (15%), odontogenic (10,5%), soft tissues (5%), TMJ (1%) and blood vessels (0.5%). 21% of our findings belonged to group 1, 11% to group 2 and 68% to group 3. We did not find malignant neoplastic lesions.
Conclusion: This study underlines the necessity of accurate examination of all the anatomic parts included in the volume of acquisition of CBCT, to avoid the oversight of important clinical findings.

10:30 - 12:00 **Room E1**

Breast

SS 202

Breast ultrasound and computer-aided diagnosis (CAD) systems

Moderators:
A. Domingo; Tarragona/ES
G. Esen; Istanbul/TR

B-0077 10:30

Targeted ultrasound for breast lesions detected at MRI: a systematic review and meta-analysis
N. Berger[1], J. Wiederer[2], N. Voyvoda[3], L.A. Carbonaro[4], R.M. Trimboli[4], G. Di Leo[4], F. Sardanelli[4]; [1]*Zurich/CH*, [2]*Würzburg/DE*, [3]*Derince/Kocaeli/TR*, [4]*San Donato Milanese/IT (Nicole.Berger@usz.ch)*

Purpose: To perform a systematic review and meta-analysis on the detection rate of second look ultrasound(SLUS) in breast lesions detected by Magnet Resonance Imaging(MRI).
Methods and Materials: No ethics committee approval was needed. A systematic literature search was performed (MEDLINE,EMBASE,WEB OF SCIENCE) for articles evaluating SLUS after MRI with follow up or histologic proof as reference standard. Three independent readers selected eligible articles published until April 2016. The quality of studies was assessed using the Quality Assessment of Diagnostic Accuracy Studies 2(QUADAS-2). Effect size with a 95% confidence interval(CI) and heterogeneity of the studies were calculated. The Egger test was performed for assessing the publications bias and a meta-regression was performed to analyze the publication date and the size of the lesions. Subgroup analyses were performed for cancers, mass lesions, non-mass enhancement and foci.
Results: Thirty-three articles were included. The study quality was mostly high. The detection rate of all lesions was very heterogeneous (I^2=93.7%; P=0.0001) with a point estimate of 64.2% (95%CI=57.5%-70.4%). The risk of publication bias was significant (P=0.033). Year of publication and mean lesion diameter were not significant (P=0.935 and 0.184, respectively). The detection rate at SLUS of cancers, mass lesions, non-mass enhancement and foci showed a point estimate of 77.5%, 66.5%, 37.5% and 48.1%, respectively.
Conclusion: SLUS is a reasonable examination-tool after finding a previously unknown lesion in breast-MRI, especially in cancerous or mass lesions. Nevertheless negative SLUS does not exclude malignancy and MRI-guided biopsies or follow-up examinations have to be considered for further work-up.

B-0078 10:38

How does switching from mammography to tomosynthesis impact the use of breast ultrasound
A. Stolz[1], A. Poncet[2], H. Stolz[2], N. Howarth[3], K. Kinkel[3]; [1]*Neuchâtel/CH*, [2]*Geneva/CH*, [3]*Chêne-Bougeries/CH (alexandre.stolz@h-ne.ch)*

Purpose: The aim of this study was to evaluate changes in the daily use of secondary breast ultrasound after mammography when switching from digital mammography (DM) to systematic digital breast tomosynthesis (DBT).
Methods and Materials: A total of 2000 women (mean age, 57,9yrs ; range, 46-69yrs) with diagnostic mammographies were evaluated between December 2014 and November 2015 in a breast clinic. Three experienced radiologists filled a questionnaire before performing or not any additional breast ultrasound (US). Questionnaires include age, menopausal status, hormonal treatment, indication for additional ultrasound decided by the radiologist (clinical either/or imaging findings, dense breasts, familial high risk or personal history of breast cancer) and the time required for completion of the US.
Results: Secondary ultrasound was performed in 447/476 (93.9%) patients after DM and in 1415/1524 (92,8%) patients after DBT and showed no difference in proportion. There were no significant differences in clinical findings, familiar risk and treated cancer patient between the DM and DBT groups. The proportion of examinations followed by US for positive imaging findings or dense breasts did not differ between the two groups. The mean time required for performing US after a DBT was 5.06min compared to 5.07min after a DM, the difference of -0.01 minutes, 95% CI [-0.26 ; 0.25], p = 0.9565) was not significant and did not differ when compared by radiologist.
Conclusion: The introduction of DBT does not change the proportion of secondary ultrasound of the breast after mammography nor the time required to perform it.

B-0079 10:46

Breast ultrasound: can 3D multiplanar reconstructions aid in the differentiation of benign from malignant lesions?
P. Kapetas, P. Clauser, R. Woitek, M. Bernathova, K. Pinker, T.H. Helbich, P.A.T. Baltzer; *Vienna/AT (panagiotis.kapetas@meduniwien.ac.at)*

Purpose: To evaluate the added value of three-dimensional (3D) multiplanar reconstructions (MPRs) to the two-dimensional (2D) B-mode ultrasound (US) for differentiating benign from malignant breast lesions.
Methods and Materials: 99 patients with 101 breast lesions planned to undergo US-guided biopsy were examined with 2D B-mode US. A 3D volume of each lesion was subsequently recorded. 2 readers (R) independently evaluated the 2D image of each lesion according to the breast imaging reporting and data system (BI-RADS) lexicon and assigned a BI-RADS classification. Then, they evaluated the MPRs of each lesion and assigned a new BI-RADS classification, while also recording the presence or absence of retraction in the coronal plane. They were also asked to score their degree of confidence for the BI-RADS classification in a 10-point scale. Receiver-operating characteristics analysis was used to evaluate reader performance and confidence. Logistic regression was used to evaluate the different BI-RADS descriptors in 2D and 3D US.
Results: 53 lesions were malignant and 48 benign. Area under the curve did not differ significantly between 2D and 3D BI-RADS classification for neither of the readers (R1:0.829 vs 0.866, p>0.05, R2:0.847 vs 0.810, p>0.05). Retraction phenomenon showed high specificity (R1:96.55%, R2:89.58%) but low sensitivity (R1:31.82%, R2:42.31%). In multivariate logistic regression significant association with malignancy was shown for margin (p<0.05) in 2D and margin (p<0.001) and shape (p<0.01) in 3D US. A (non-significant) tendency towards higher confidence was shown for 3D US.
Conclusion: 3D MPRs have a similar diagnostic performance as 2D breast US. A positive retraction phenomenon is highly suggestive of malignancy.

B-0080 10:54

Usefulness of computer-aided diagnosis conjunction to breast ultrasound depending on experience of breast imaging
J.-h. Choi[1], B. Kang[2], E. Kim[2], S. Kim[2]; [1]*Gyeonggi-do/KR*, [2]*Seoul/KR (mchjjh2@naver.com)*

Purpose: To evaluate the usefulness of computer-aided diagnosis (CAD) conjunction to breast ultrasound depending on the experience of breast imaging.
Methods and Materials: Between October 2015 and January 2016, the expert group of two breast radiologists consecutively performed general breast ultrasound for women with screening and diagnostic purposes. When there was suspicious or probable benign lesion, they added the newly developed CAD system (S-detect™) on them. And, they choose the proper BI-RADS lexicons and categories on general ultrasound, CAD, and general ultrasound with CAD. For the same cases, two first-grade residents without breast imaging experience choose the BI-RADS lexicons and categories on them (general ultrasound, CAD, and general ultrasound with CAD). And then an uninvolved expert radiologist concluded enrolment and assessed the final result correlated with mammography, old ultrasound, and histopathology. Finally we compared the diagnostic performance depending on the experience of breast imaging.
Results: A total of 200 cases were enrolled in this study. These were sensitivities of expert (91.7%), resident (75%), and CAD (75% & 66.7%). These were specificities of CAD (78.2% & 76.1%), expert (76.6%), and resident (71.8%). After combination with CAD, the specificity was improved (76.6% to 80.3%) without change of sensitivity (91.7%) in expert group. After combination with CAD, the sensitivity and specificity were improved in resident group (75% & 71.8% to 83.3% & 77.1%).
Conclusion: CAD is more useful for less experienced radiologists. When combined the CAD to ultrasound, the specificity is improved in any radiologists.

B-0081 11:02

Evaluation of a computer-aided-diagnosis system in breast ultrasound (S-Detect): intrinsic value and effect on junior radiologist's performance
M. Attard, S. Ammary, E. Pottier, F. Mihoubi, A. Dunant, C. Balleyguier; *Villejuif/FR (marie_attard@hotmail.fr)*

Purpose: To evaluate diagnosis performance and effect of S-Detect™ on junior radiologist's interpretation in breast ultrasound. This Computer-Aided Diagnosis (CAD) is based on Breast Imaging Reporting and Data System (BI-RADS).
Methods and Materials: 189 biopsied lesions were included, 111 were malignant and 78 were benign. CAD sensitivity and specificity was calculated.

Four junior radiologists read ultrasound images without and with CAD, and their sensitivity (Se), specificity (Sp), and Receiving Operating Characteristic (ROC) analysis were compared. Readers had classified lesions using American College of Radiology (ACR) BI-RADS score, and a binary classification benign/malignant (BM).
Results: CAD sensitivity and specificity were calculated respectively at 82% and 81%. Its use has resulted in an increasing trend with all reader's sensitivity for either classification used: reader 1: 92% vs. 90% (classification BM and BI-RADS score); reader 2: 78% vs. 77% (classification BM); 91% vs. 88% (BI-RADS score); reader 3: 85% vs. 80% and 98% vs. 97%; and reader 4: 90% vs. 88% (BI-RADS score); and also with the ROC for 3 readers: reader 1: 0.87 vs. 0.86; reader 3: 0.89 vs. 0.87; and reader 4: 0.81 vs. 0.78. These results were not statistically significant ($p > 0.01$). No significant decrease in specificity was identified after using CAD.
Conclusion: S-Detect™ has good intrinsic performances, but its use did not allow significant modifications for the 4 junior radiologists' performance; nevertheless, an improving trend could be noted.

B-0082 11:10

Breast ultrasound computer-aided diagnosis: diagnostic performance, merits and pitfalls

M. Jeong[1], B. Kang[2], E. Kim[2], S. Kim[2]; [1]*Gyeonggi-do/KR*, [2]*Seoul/KR*
(mkjpretty@gmail.com)

Purpose: The aim of this study was to evaluate diagnostic performance of a computer-aided diagnosis (CAD) system for breast ultrasound to distinguish between benign and malignant lesions and to analyse features of lesions interpreted with errors retrospectively.
Methods and Materials: Between October 2015 and August 2016, 338 women (mean age, 48.7± 11.5 years) with 397 lesions were enrolled and underwent breast ultrasound with ultrasound CAD system (S-detect™). We assessed accuracy, sensitivity, specificity, positive predictive value (PPV) and negative predictive value (NPV). In addition, we evaluated causes and patterns of misinterpretation in false positive and negative groups.
Results: Accuracy, sensitivity, specificity, PPV and NPV of breast ultrasound CAD were 77.1 %, 81.6 %, 76.5 %, 32.7 and 96.7 %, respectively. Eight false negative lesions were all oval in shape and parallel in orientation. Among 82 false positive lesions, 31 lesions were benign lesions with suspicious features such as fat necrosis or post-operative change. Second leading cause of misinterpretation in 23 lesions was inappropriate demarcation of lesions due to heterogeneous echogenicity, large size, adjacent parenchyma or posterior acoustic shadowing. 21 lesions with suspicious features with good demarcation and proper description were confirmed as benign histologically. And 7 lesions with good demarcation and descriptions implying benignity showed possible malignancy as a final conclusion.
Conclusion: Breast ultrasound CAD is expected to be helpful in avoiding unnecessary biopsy due to its high NPV. And operators need to know characteristics of lesions prone to misinterpretation and to consider clinical history and findings of other imaging modality.

B-0083 11:18

Quantitative multiparametric ultrasound of the breast

P. Kapetas, R. Woitek, P. Clauser, K. Pinker-Domenig, M. Bernathova, T.H. Helbich, P.A.T. Baltzer; *Vienna/AT*
(panagiotis.kapetas@meduniwien.ac.at)

Purpose: To evaluate quantitative multiparametric ultrasound of the breast for the differentiation of benign and malignant lesions.
Methods and Materials: 118 patients, each with one biopsy-proven, sonographically evident lesion were included in this prospective, IRB-approved study. Each lesion was examined with B-mode ultrasound (US), elastography (Acoustic Radiation Force Impulse-ARFI), Doppler US and Contrast Enhanced US (CEUS). Quantitative indices were recorded for each modality as follows: Shear Wave Velocity (SWV) for ARFI, Pulsatility (PI) and Resistive Index (RI) for Doppler US, and Peak Enhancement (PE), Wash-in Area Under the Curve (WiAUC), Rise Time (RT), mean Transit Time (local) (mTTI), Time To Peak (TTP), Wash-in Rate (WiR), Wash-in Perfusion Index (WiPI), Wash-out AUC (WoAUC), Fall Time (FT) and Wash-out Rate (WoR) for CEUS. Paired and unpaired nonparametric statistics were applied for comparisons as appropriate. Diagnostic accuracy of measurements was compared using Receiver Operating Characteristics (ROC) analysis. Multivariate logistic regression was used to determine independent predictors of malignancy.
Results: 64 lesions were malignant and 54 benign. SWV and RI showed the highest diagnostic performance as measured by the area under the ROC curve (0,871 and 0,805 respectively). At a cut-off value of 3.1 m/s, SWV showed sensitivity of 85.94% and specificity of 85.19%. An RI cut-off of 0.68 revealed sensitivity of 77.78% and specificity of 80.56%. Multivariate logistic regression showed that SWV, RI and mTTI were independent predictors of malignancy.
Conclusion: Multiparametric ultrasound of the breast offers quantitative indices that can aid in the differentiation of benign and malignant breast lesions.

B-0084 11:26

Diagnostic performance of assist strain ratio (ASR) in computing fat-to-lesion ratio (FLR) in ultrasound breast elastography

R.G. Barr[1], R.A. Managuli[2]; [1]*Campbell, OH/US*, [2]*Seattle, WA/US*
(rgbarr@zoominternet.net)

Purpose: ASR is a new application tool developed to differentiate benign from malignant lesions in breast US elastography. This ASR would potentially eliminate current user dependency in outlining tumour and fat area while computing FLR manually. The objective here is to compare the clinical performance of ASR against manual strain ratio (MSR) in the computation of FLR.
Methods and Materials: 42 breast lesions (24 malignant and 18 benign) scheduled for biopsy were included in this IRB approved and HIIPA complaint study. Skilled physician (RGB) performed the elastography exam and selected a frame for computing FLR. MSR was computed manually while ASR was computed with minimal user input. Hitachi's HIVISION Ascendus with L75P was used for this study. An average of three measurements was used as a cut-off for differentiating lesions.
Results: Cut-off point were determined to be 2.2 for both MSR and ASR using Youden index. Diagnostic performance of MSR were: sensitivity-96%, specificity-67%, accuracy-83 %, PPV-79%, and NPV-92%. Corresponding performance of ASR were: sensitivity-96%, specificity-83%, accuracy-91%, PPV-89%, and NPV-94%. The AUC for MSR and ASR were 0.86 and 0.95, respectively and average coefficient of variation (COV) were 30% and 43% respectively.
Conclusion: ASR demonstrated excellent diagnostic performance compared to MSR. In addition, COV of ASR is lower than MSR implying reduced intra- and inter-operator dependency. Next, we will use auto-frame-select with ASR to minimise manual dependency in selecting the frame as well.
Author Disclosures:
R.G. Barr: Advisory Board; Bracco Diagnostics, Lantheus Medical. Equipment Support Recipient; Siemens Ultrasound, Philips Ultrasound, SuperSonic Imagine, B and K Ultrasound, Hitahi Ultrasound. Speaker; philips Ultrasound, Bracco Diagnostics, Lantheus Medical. **R.A. Managuli:** Employee; Hitachi Healthcare.

B-0085 11:34

Strain elastography with quality control: auto strain ratio system

K. Nakashima, S. Sakurai, A. Mizutou; *Okayama/JP*
(urbandoc@med.kawasaki-m.ac.jp)

Purpose: Strain elastography (SE) and shear wave speed imaging provide us with tissue stiffness information, important for breast diagnosis. SE allows us to visualise tissue stiffness that reflects the pathological information. However, it can be associated with operator bias in image formation, scanning technique, the selection of the appropriate frame, and ROI setting for strain ratio measurement. To overcome these problems, we have developed an "Auto Strain Ratio System (ASRS)", which requires no manual compression whilst scanning, full auto frame selection on freeze and fully automatic ROI target selection. A preliminary prospective clinical study was performed in 2015.
Methods and Materials: 232 breast masses assessed as BI-RADS Category 3 or above by B-mode, were scanned using SE. The new ASRS was compared to conventional manual strain ratio measurement (MSR) by experienced doctors and the diagnostic performance and quality evaluated.
Results: There was a significant correlation between the MSR and ASRS with $R=0.79$ ($p<0.001$). The MSR (cut-off=3.8) had a sensitivity of 89%, a specificity of 75%, an accuracy of 78%, a positive predictive value (PPV) of 52%, and a negative predictive value (NPV) of 96%. The ASRS (cut-off=3.9) had a sensitivity of 82%, specificity of 89 %, an accuracy of 87%, a PPV of 69%, and a NPV of 94%. The AUCs were 0.88 on MSR and 0.89 on ASRS.
Conclusion: We have demonstrated that it is possible to quantify SE and control its accuracy. The ASRS is expected to contribute to the standardisation of breast elastography.

B-0086 11:42

Mass-like focal breast fibrosis a bening entity mimicking malignancy on ultrasound

E. Horvath, A. Altamirano S., M. Pinochet, E. Soto, M. Uchida, F. Pizzolon; *Santiago de Chile/CL (aleenaltamirano@gmail.com)*

Purpose: To determine the sonographic characteristics of core biopsy-proven mass-like focal breast fibrosis (MFBF).
Methods and Materials: IRB approved, retrospective study. Between April 2007 and January 2015, 3051 US-guided breast biopsies with 14G core needle, were performed, 251 of them with a diagnosis of stromal breast fibrosis. We excluded 128 cases where fibrosis was not the primary histologic diagnosis, only MFBF cases were included. Imaging features were tabulated and analysed. Follow-up imaging was reviewed to document lesion stability.

Results: In 121 women (median age: 50 years, range: 25-83) we found 123 cases of MFBF. Lesion size ranged from 4 to 35mm (median: 10mm), non-palpable in 94% of the cases. Eighty-seven (71%) of them developed in dense breast (ACR 4 and 3). Only 7 (6%) were evident on mammography. We identified two distinct sonographic patterns of MFBF. Pattern A (28%): well-circumscribed, hypoechoic, avascular mass. Pattern B (72%): ill defined, irregular, avascular, markedly hypoechogenic, spiculated with shadowing, located intraparenchymatous or under Cooper ligament. Sixty-seven (54%) lesions were reported as BI-RADS 5, 4C or 4B. MRI was performed in 7 patients with negative outcome. One lesion was surgically removed and 4 new biopsies were performed due to discordance, obtaining the same results. Patients remain in follow-up (30 months), without malignancy.
Conclusion: The MFBF is a benign entity with the potential to mimic malignancy. Is important that radiologists know the specific US patterns and if proven on core needle biopsy, it may be taken as a concordant diagnosis.

B-0087 11:50

Clinical usefulness of repeated short-term follow-up imaging in young patients with initial diagnosis of BI-RADS 3 lesions

M. Marcon, T. Frauenfelder, A. Becker, K. Dedes, A. Boss; *Zurich/CH (Magda.Marcon@usz.ch)*

Purpose: To evaluate the clinical usefulness of repeated short-term follow-up with ultrasound in patients younger than 35 years with a BI-RADS 3 lesion at first ultrasound examination and proven lesion stability at the 6-month follow-up.
Methods and Materials: In this IRB-approved study, 492 women, aged 18-34 years (mean±standard deviation, 28±4.5 years) with first breast ultrasound examination in 2012-2014 were retrospectively evaluated. Inclusion criteria were: at least one BI-RADS3 lesion and (a) biopsy/surgical excision or (b) follow-up of at least 18 months (including a 6-month follow-up). BI-RADS category assigned during follow-up and pathologic findings in cases undergoing biopsy/surgical excision were collected. Recommended biopsy rates (RBR) after 6 and 18 months and positive predictive value (PPV) for biopsy after recommendation due to interval changes (PPV_{bio}) were calculated.
Results: In 97 patients, 151 BI-RADS3 lesions were identified. Biopsy/surgical excision was performed after initial assessment in 25/151 (16.5%) lesions. At 6-month follow-up, assessment category was changed to BI-RADS 1 or 2 in 23/126 (15.3%) and to BI-RADS 4 in 9/126 lesions (7.1%) due to interval growth. Pathological diagnosis of these lesions was fibroadenoma in 5 cases and benign phyllodes tumour in 4 cases (RBR 7%, PPV_{bio} 44.4%). At 18-month follow-up one lesion was classified BI-RADS 4 due to interval growth and pathological diagnosis was fibroadenoma (RBR 1.1%, PPV_{bio} 0%).
Conclusion: Follow-up imaging performed after 18 months from a first BI-RADS3 diagnosis does not affect clinical treatment and 6-month follow-up may be sufficient to assess the stability of probably benign lesions and to discern those which entail further investigation.

10:30 - 12:00 **Room E2**

Neuro

SS 211a

Stroke: aetiology, diagnosis and prognosis

Moderators:
A.Y. Oner; Ankara/TR
M. Taina; Kuopio/FI

B-0088 10:30

Inter-rater variability when scoring CT scans in acute ischaemic stroke using the ASPECTS score

C. Goncalves[1], O. Joly[2], A.L. Kühn[3], S. Shah[1], S. Kelavkar[1], C. Law[4], P. Harman[1], I.Q. Grunwald[5]; [1]*Southend-on-Sea/UK*, [2]*Oxford/UK*, [3]*Worcester, MA/US*, [4]*Palo Alto, CA/US*, [5]*Chelmsford/UK*

Purpose: Plain computed tomography (CT) remains the most common imaging modality for acute ischaemic stroke. For mechanical thrombectomy, recommended selection criteria include an ASPECTS score of ≥ 6. However, detection of early ischaemic signs can be challenging, even for senior neuroradiologists. The purpose of our study was to assess the inter-rater agreement for the detection of early ischaemic signs in the ASPECTS regions between senior neuroradiologists.
Methods and Materials: Plain CT images from 132 patients with acute ischaemic stroke were included in this study. Three neuroradiologists, experienced with stroke imaging and evaluation of ASPECTS, independently scored all the cases. They were blinded to any clinical information. Cohen's Kappa and Fleiss' Kappa were computed both for 20 region-based agreement and for dichotomised ASPECTS (ASPECTS ≥6) as a measurement of agreement between the raters.
Results: At the regional level, paired Cohen's Kappa were 0.35, 0.51, 0.34. The regional agreement was summarised as a Fleiss' Kappa of 0.37. When considering dichotomised ASPECTS (≥6), paired Cohen's Kappa were 0.36, 0.51, 0.25. Overall dichotomised ASPECTS was summarised as a Fleiss' Kappa of 0.31.
Conclusion: We have found only a fair level of inter-rater agreement between neuroradiologists for the evaluation of early ischaemic changes. Our results are within the range of slight to moderate interrater agreement reported recently (Farzin et al., Neurology 2016). Clinicians should be encouraged to evaluate the inter-rater variability for evaluation of ASPECTS in their own center in order to design an optimal clinical pathway for acute stroke management.
Author Disclosures:
O. Joly: Employee; Brainomix Limited. **I.Q. Grunwald:** Founder; Brainomix Limited. Shareholder; Brainomix Limited.

B-0089 10:38

Diagnostic accuracy for detection of intracranial haemorrhage in low-dose unenhanced head single-energy and dual-energy third generation dual-source computed tomography

J.-E. Scholtz, J.L. Wichmann, D.W. Bennett, D. Leithner, M.H. Albrecht, S. Martin, R.W. Bauer, T.J. Vogl, B. Bodelle; *Frankfurt a. Main/DE (janerikscholtz@gmail.com)*

Purpose: To determine diagnostic accuracy for detection of intracranial haemorrhage (ICH), image quality, and radiation dose of low-dose single-energy (SE) and dual-energy (DE) unenhanced head computed tomography (CT) on third-generation dual-source CT.
Methods and Materials: 123 patients with suspected ICH were examined on a 192-slice dual-source CT. Standard-dose SE (120-kV, Group A,n=36) and DE (80-/Sn150-kVp, Group B,n=30) images were compared with low-dose SE (Group C,n=32) and DE (Group D,n=25) using automated-tube-current-modulation (ATCM). Advanced-modeled-iterative-reconstruction (ADMIRE) was used for all protocols. Detection of ICH was performed by three blinded readers. Image quality was assessed quantitative and qualitative. Interobserver agreement was calculated using Fleiss' Kappa. Radiation dose was assessed as dose-length product (DLP).
Results: Detection of ICH was excellent (sensitivity,94.9-100%; specificity,94.7-100%) in all protocols (p=1.00) with perfect interobserver agreement (0.83-0.96). Qualitative ratings showed significantly better ratings for both standard-dose protocols regarding gray-matter-to-white-matter (GM-WM) contrast (p≤0.014), whereas highest GM-WM CNR was observed in low-dose DE-CT (all,p≥0.057). Lowest posterior-fossa-artifact-index was measured for standard-dose DE-CT with significantly lower values compared to low-dose protocols (both p≤0.034). Delineation of ventricular margins and subarachnoidal spaces sharpness were rated excellent in all protocols (p≥0.096). Low-dose SE lowered radiation dose by 26% (DLP, 575.0±72.3mGy*cm vs. 771.4±146.8mGy*cm, p<0.001) and by 24% in DE (DLP, 587.0±103.2mGy*cm vs. 770.6±90.2mGy*cm, p<0.001). No significant differences were observed between low-dose protocols (p=1.00).
Conclusion: Low-dose unenhanced head SE and DE-CT using ATCM and ADMIRE provide excellent diagnostic accuracy for detection of ICH with good quantitative and qualitative image quality in third-generation dual-source CT while allowing for significant radiation dose reduction.
Author Disclosures:
R.W. Bauer: Speaker; Siemens Healthcare.

B-0090 10:46

Leptomeningeal score (LMs) on computed tomography angiography (CTA) and effect of endovascular reperfusion (ER) on clinical outcome in patients with acute ischaemic stroke (AIS)

E. Puglielli, R. Lattanzi, G. Esposito, V. Di Egidio; *Teramo/IT (edopug@hotmail.com)*

Purpose: Aim of this study was to review the importance of LMs on the outcome after ER and to evaluate a reliable score system for grading the collateral state.
Methods and Materials: In our database, we identified 125 consecutive AIS patients (mean age 59,8 y, April 2009 - September2016), with classic on-set, that undergoing to ET after basal CT/CTA. We assessed the baseline ASPECT on non-enhanced (NCCT), CTA images, collaterals, clot burden score (CBS) on CTA and degree of reperfusion after ET (TICI 0-III) with clinical data. Two readers, blinded to clinical informations, evaluated the images in parallel and LMs was based on scoring pial and lenticulostriate collaterals (0, no; 1, less; 2, equal or more prominent compared with matching region in opposite hemisphere) in 6 ASPECTS regions (M1-6) plus anterior region and basal ganglia. Good clinical outcome (GCO) was defined as mRS≤2 at 90 days.
Results: TICI III-IIb (OR 27.50; 95%-CI 9.34-81.63) and good collaterals (OR 9.76; 95%-CI 3.28-56.72) were independent predictors of favourable outcome,

such as female sex (OR 0.27; 95%-CI 3.45-8.63), younger age (OR 75.30; 95%-CI 7.44-87.31) and higher NCCT ASPECT (OR 2.56; 95%-CI 1.34-6.33). On multivariate analysis GCO well matched with good LMs and TICI III-IIb, but there was no statistical association between LMs and reperfusion (p=0.5).
Conclusion: LMs alone appear to be as a strong imaging parameter for GCO after ET in AIS patients and it might be suitable for imaging based selection.The effect of reperfusion on outcome seems to be strong as the LMs.

B-0091 10:54

Causes of acute intracranial large vessel occlusion in patients with acute ischemic stroke

K. Compagne[1], Y. Roos[2], D. Dippel[1], R. van Oostenbrugge[3], W. van Zwam[3], C. Majoie[2], H. Marquering[2], A. van der Lugt[1], B. Emmer[1]; [1]*Rotterdam/NL*, [2]*Amsterdam/NL*, [3]*Maastricht/NL (c.compagne@erasmusmc.nl)*

Purpose: Intracranial large vessel occlusion (LVO) in patients with acute ischemic stroke (AIS) has multiple pathogenic causes. Identification of the underlying cause of LVO may have major implications for clinical decisions, treatment, and outcome. The aim of this study is to identify the most likely cause of intracranial LVO.
Methods and Materials: Data (n=500) from the MR CLEAN trial which investigated the effectiveness of intra-arterial treatment were reanalysed. Patients with AIS are classified in one of the four pre-defined categories of presumed causes of AIS: carotid dissection, carotid atherosclerosis, cardiac embolism, or undefined. Categorization was based on clinical data (atrial fibrillation (AF) and myocardial infarction (MI)), electrocardiogram (ECG), and CT angiography (CTA). Atherosclerotic carotid disease was defined by the presence of an occlusion, stenosis (>50%), plaque ulcerations or severe calcifications (upper quartile of volume of calcifications at bifurcation) on the symptomatic side.
Results: Data of 426 patients could be analysed. Carotid dissection was identified in 21 patients (4,9%) and cardiac embolism in 126 (29,6%) patients (AF (n=92) and MI (n=47)). Carotid atherosclerosis was present in 154 (36,2%) patients subdivided in occlusion (n=61), significant stenosis (n=49), ulcerations (n=25), and severe calcifications (n=19). The cause of LVO could not be classified in 125 patients (29,3%) according to our criteria.
Conclusion: Based on clinical information, ECG and CTA the most likely cause of AIS due to LVO can be classified in more than 70% of the patients. Carotid vessel atherosclerosis and cardiac embolism are major causes of LVO in patients with AIS.
Author Disclosures:
D. Dippel: Grant Recipient; Stryker. **A. van der Lugt:** Grant Recipient; Stryker, GE healthcare.

B-0092 11:02

Acute ischaemic stroke CT imaging and clinical score in patients with isolated intracranial distal artery occlusion

A. Velasco González, N. Münnich, B. Buerke, W. Schwindt, J. Spieker, J. Minnerup, C. Sauerland, W. Heindel; *Münster/DE (Aglae.VelascoGonzalez@ukmuenster.de)*

Purpose: Evaluation of CT characteristics in patients with acute ischemic stroke by isolated intracranial distal artery occlusion in correlation with acute and subacute neurological symptoms due to the final infarction area.
Methods and Materials: 55 consecutive stroke patients with an acute distal cerebral artery occlusion were retrospectively analysed. The following criteria were evaluated: presence of infarct demarcation at stroke onset in the non-contrast CT (NECT), localisation of the thrombus and collaterals in CT-angiography [M2- and M3-segment of the middle cerebral artery (n =46), A2-segment of the anterior cerebral artery (n=5), P2-segment of the posterior cerebral artery (n=1) and superior cerebellar artery (n=1)], presence of mismatch in the CT-perfusion and final infarction in the follow up NECT after 24 hours. NIHSS scores of the first and the 4th day and type of therapy were evaluated.
Results: Initial versus follow up NECT showed no significant differences regarding rates of no infarct (49% vs 41.3%), partial (20% and 20%) and complete demarcation (30.9% vs 37.7%). Nevertheless, an overall significant improvement of the neurological symptoms was observed [mean initial NIHSS:11.2±5.6 versus NIHSS on day 4: 3.5±0.86(P=.017)]. Patients with an initial perfusion mismatch had no significant better outcome than those with an initial match. No significant better outcomes were found in the group treated with iv thrombolysis versus without iv thrombolysis or mechanical thrombectomy (P>0.05).
Conclusion: Our data suggest that distal intracranial occlusions without concomitant proximal stenosis or occlusion have a relative benign course poorly improved by the use of iv thrombolysis or mechanical thrombectomy.

B-0093 11:10

Intra-arterial thrombus detection by multi-echo SWI in acute ischaemic stroke patients

B. Kong, H. Choi, Y. Nam, J. Jang, S.-L. Jung, K.-J. Ahn, B.-S. Kim; *Seoul/KR (blacksky1218@hotmail.com)*

Purpose: Detection of intra-arterial thrombus is important to decide treatment plan and to monitor treatment response. Previously, precontrast CT, T2*-weighted gradient echo, FLAIR, and SWI were studied for detection of intra-arterial thrombus. However, to the best of our knowledge, there was no study using multi-echo SWI in detection of intra-arterial thrombus. The purpose of this study is to compare multi-echo SWI (mSWI) with single-echo SWI (sSWI), FLAIR and T2-weighted image (T2WI) in detection of intra-arterial thrombus in acute stroke patients.
Methods and Materials: Between March 2015 and April 2016, 89 consecutive patients with acute infarct (positive on DWI) were reviewed from stroke registry. Among them, 74 patients who were examined by MRI including multi-echo SWI, FLAIR, and T2WI were included in this study. Four MR sequences (mSWI, sSWI, FLAIR, and T2WI) were evaluated by two radiologists with consensus, where separate reading sessions for each sequences were made with the interval of 3 days. McNemar test was performed to compare detection rates of intra-arterial thrombus.
Results: The age of study population was 67.16±13.63 years (mean ± standard deviation). Detection rates of intra-arterial thrombus were 0.19 on mSWI; 0.09 on sSWI; 0.07 on FLAIR; and 0.04 on T2WI. The detection rate of mSWI was superior to sSWI (p=0.016), FLAIR (p=0.004), and T2WI (p<0.001).
Conclusion: Multi-echo SWI showed superior detection rate of intra-arterial thrombus compared with single-echo SWI, FLAIR, and T2-weighted image.

B-0094 11:18

Prediction of malignant cerebellar oedema development after acute ischaemic stroke using multiparametric CT

M.P. Fabritius, K.M. Thierfelder, F. Schuler, M.F. Reiser, W.H. Sommer, W.G. Kunz; *Munich/DE (matthias.fabritius@med.lmu.de)*

Purpose: Malignant cerebellar oedema (MCE) is a life-threatening complication after acute cerebellar stroke. Aim of this study was to identify imaging predictors using multiparametric CT including whole-brain CT perfusion (WB-CTP).
Methods and Materials: We consecutively selected all subjects with cerebellar WB-CTP alterations and follow-up-confirmed infarction from a cohort of 3254 patients who underwent multiparametric CT. Follow-up imaging was assessed for the presence of MCE, measured using an established 10-point scale, of which scores ≥4 are considered malignant. posterior-circulation-Acute-Stroke-Prognosis-Early-CT-Score (pc-ASPECTS) was determined to assess ischemic changes on non-contrast CT (NCCT), CT angiography (CTA), and on parametric WB-CTP maps (cerebral blood flow, CBF; cerebral blood volume, CBV; mean transit time, MTT; time to drain, TTD). Chi-square, Mann-Whitney-U tests and receiver operating characteristics (ROC) analyses were performed for statistical analyses.
Results: Forty-seven patients were included. 38 patients (80.9%) were categorized as MCE- and 9 (19.1%) as MCE+. MCE+ patients had larger CBF, CBV, MTT and TTD deficit volumes (each with p<0.001) and showed significantly lower median pc-ASPECTS assessed using WB-CTP (CBF: 5 vs. 8; CBV: 8 vs. 9; MTT: 5 vs. 8; TTD: 5 vs. 8; each with p<0.001) compared to MCE- patients, while median pc-ASPECTS on NCCT was not significantly different (9 vs. 10, p=0.097). ROC analyses yielded the largest area-under-the-curve values for CBF (0.977) and CBV deficit volumes (0.952) and pc-ASPECTS on CBF (0.934), whereas pc-ASPECTS on NCCT (0.681) and CTA (0.712) provided significantly less diagnostic value.
Conclusion: WB-CTP provides added diagnostic value regarding the prognosis of MCE development after stroke.

B-0095 11:26

Increased PS of basal ganglion on CTP predicting HT in acute ischaemic stroke patients with cerebral proximal large vessel occlusion

Q. Li, H. He; *Shanghai/CN (liqiao1227@gmail.com)*

Purpose: PS measured with CTP reflects the permeability of the blood-brain barrier, and is related to pathophysiology of haemorrhagic transformation (HT). Basal ganglia haemorrhage (BGH) can be found after treatment of cerebral proximal large vessel occlusion and is related with poor clinical outcome. We aimed to determine the relationship between BGH and the site of occlusion, PS of basal ganglia region, and collateral status.
Methods and Materials: 121 consecutive patients with acute ischaemic stroke (AIS) within 6 hours of symptom onset and with cerebral proximal artery occlusion were evaluated. CTP data were postprocessed into PS of ipsilateral and contralateral basal ganglion. A blinded reader assigned collateral score using a previous 5-point scale and proximal MCA -M1 status (with or without

absolute occlusion). We assessed the relationship between HT occurrence and PS value of BG.
Results: Increased basal ganglia PS were associated with earlier HT outcome after AIS. In logistic regression analysis after adjustment for age, sex, onset time, baseline NIHSS, poor collateral status (p=0.009; OR 7.8) and proximal MCA-M1 occlusion (p=0.045; OR 4.12, 95%CI 1.03-16.52;) were independently associated with increase of basal ganglia PS. The rPS value (AUC=0.94) was the most accurate parameter to predict HT, with an optimal threshold at 2.89.
Conclusion: Increasing basal ganglia PS predicts the HT after distal inter-carotid artery or M1 middle cerebral artery occlusion. In this situation, the absolute occlusion of proximal MCA-M1 was a prerequisite for PS aggravation, but poor collateral status appeared a critical determinant of ultimate outcome.

B-0096 11:34

Diffusion-MRI detects protection effects of DAPT treatment following stroke

X. Hao, Y. Yang, L. Yin, X. Zhang, J. Tian; *Shanghai/CN (haoxiaozhu123@sohu.com)*

Purpose: To evaluate the effects of γ-secretase inhibitor treatment after transient cerebral ischaemia using diffusion magnetic resonance imaging (d-MRI).
Methods and Materials: 20 middle cerebral artery occlusion (MCAO) rats were divided into two groups: control group (n = 10) and treated group (n = 10), receiving γ-secretase inhibitor (N-[N- (3,5-difluorophenacetyl)-1-alanyl]-S-phenylglycine t-butylester, DAPT) at 3 days after ischemia. All rats were performed with behavioral test, MRI and immunofluorescence staining (IF) at 24h and 7d after MCAO. Percent changes of all values of striatum (STR) were measured and compared between the two groups, that including MR T2 signal intensity (T2 SI), fractional anisotropy (FA), mean diffusivity (MD), mean kurtosis (MK), as well as intensity fluorescence of microglia/NICD.
Results: At 7 days after stroke, percent changes of all values in the treated group were more closer to the baseline compared to the control group (treated vs control: T2 SI, 19.67±7.23% vs 33.33±2.52%, P=0.037; FA, -24.67±6.02% vs -44.67± 5.51%, P=0.039; MD, -6.7±4.04% vs 16.67±8.51%, P=0.033; MK, 49±12.53% vs 123.67±40.15%, P=0.037). Corroborated by IF, microglia and Notch activation were markedly reduced in treated group (treated vs control: micrglia, 57±3.61% vs 125.67±6.43%, P=0.001; NICD, 33±7.51% vs 166.33±12.22%, P=0.000). Significant therapeutic DAPT effects on functional recovery were detected at 7 days after stroke (treated vs control: 4.25±0.5 vs 7.0±0.816, P=0.001).
Conclusion: Our data demonstrate that d-MRI can dynamically identify and quantitatively characterize white matter recovery after DAPT treatment. And DKI parameters in treated group, be closer to the baseline, were in agreement with reduced activation of microglia/NICD.

B-0097 11:42

Diagnostic importance of brain CT perfusion 4D in the detection of acute suptratentorial infarctions

K. Davidovic, A. Stankovic, J. Kostic, F. Crnovrsanin, D. Masulovic, R. Maksimovic; *Belgrade/RS (k_cina@yahoo.com)*

Purpose: CT brain perfusion 4D aids with assessing the certain part of the brain and evaluating perfusion deficits by displaying 4D-DSA views of blood flow in vessels and 3D perfusion maps. It can be performed rapidly and aids in the detection of salvageable tissue (penumbra) from the unsalvageable core infarct.
Methods and Materials: We included 258 patients with symptoms of acute ischemic stroke admitted to Emergency Room for the last 10 months CT perfusion was performed on 160-slice scanner (Toshiba Aquilion Prime) using 50 mL of nonionic iodinated contrast media. Total coverage was 80mm. This acquisition also allows generation of intracranial angiographic data as well as perfusion maps. Whole brain non-contrast CT (NCCT) was performed before CTP.
Results: The study was designed as a retrospective study and included 258 patients. We compared brain tissue involvement on NCCT with CTP (T max, cerebral blood volume [CBV], and cerebral blood flow [CBF]). The sensitivity of CTP (92,1%) was significantly higher compared with that of NCCT (15%). CTP detected significantly more ischemic lesions.
Conclusion: Perfusion CT has proven to be a valuable tool in the diagnosis of acute ischemic stroke. The use of CTP and the advances of this technology will hopefully lead to an extended time window for the use of drugs like tPA for the revascularization of the stroke-affected tissue.

B-0098 11:50

Differentiation of thrombus composition using dual-layer computed tomography

J. Borggrefe[1], J. Kottlors[1], M. Mirza[2], V. Maus[1], C. Kabbasch[1], N. Abdullayev[1], V.-F. Neuhaus[1], D. Maintz[1], A. Mpotsaris[1]; [1]*Cologne/DE*, [2]*Galway/IE (Jan.Borggrefe@uk-koeln.de)*

Purpose: For differentiation of blood-clot-types in stroke-workups, we tested if dual-layer computed tomography (DLCT) can characterise predefined clots of varying red-blood-count (RBC) in native and contrast-enhanced scans.
Methods and Materials: Five clots of three ovine blood-clot-types (n=15) containing histologically confirmed RBC composition of 0% (fibrin-rich), 36% (intermediate) and 99% (RBC-rich) were provided by Neuravi-Ltd. (Galway, Ireland). The clots were scanned in a DLCT (Philips, Amsterdam, Netherlands) with 250 mAs, 120 kVp and 0.6 mm slice-thickness and three different settings; a) in a tube containing saline, b) 5 minutes and c) 3 days after exposure to a 1:50 dilution of Accupaque-350 (GE-Healthcare, Boston, USA). The ROI-density of the clots was measured in Hounsfield-units in regular CT datasets as well as Virtual-Non-Contrast (VNC) reconstructions of DLCT.
Results: In native saline-environment the clots differed in density (mean HU±SD) (fibrin-rich 23.6±1.1, intermediate 34.9±1.6, RBC-rich 46.7±1.6). Blood-clots did not show any overlap of density in the native scans and VNC-reconstructions at different time-points (p<0.0001 for each setting and clot-type).However, they could not be differentiated in the regular early contrast-enhanced scan (b) (fibrin-rich 108.5±7.8, intermediate 105.3±3.5, RBC-rich 104.8±3.8). In the late scan, the fibrin-rich clots showed a further increase of density due to uptake of contrast-medium (fibrin-rich 163.6±3.6, intermediate 138.3±4.1, RBC-rich 109.6±5.4).
Conclusion: DLCT allows differentiating the blood-clot-types both in native as well as contrast enhanced scans.The fibrin content of the clots is associated with uptake of contrast medium after prolonged exposure to contrast agents which can be used as an independent predictor of clot type.
Author Disclosures:
J. Borggrefe: Other; The blood-clots were provided by Neuravi LTD (Galway, Ireland). **M. Mirza:** Employee; Employee of Neuravi LTD.

10:30 - 12:00 **Room F2**

Emergency Imaging

SS 217

Traumatic emergencies

Moderators:
M. Maas; Amsterdam/NL
S. Vaidya; London/UK

B-0099 10:30

A new low-dose multi-phase trauma CT-protocol and its impact on diagnostic assessment and radiation dose in multitrauma patients

Z. Alagic, A. Eriksson, S. Rezaei Motamed, M.C. Wick; *Stockholm/SE (zlatan.alagic@karolinska.se)*

Purpose: During spring 2015, the Karolinska University Hospital installed the latest generation of a 16cm-detector 258-slices Multi-Detector-Computed-Tomography (MDCT) scanner. Concomitantly, a modification of the multitrauma CT-protocol has been performed. This study investigates if a novel multitrauma CT-protocol, combining latest dose-reduction techniques with multi-phase whole-body-CT-(WBCT)-scans, is superior for trauma patients.
Methods and Materials: 109 patients (Group A) underwent acute trauma CT with the novel MDCT and multi-phase CT-protocol whereas 120 patients (Group B) underwent single-phase trauma CT at 64-slices MDCT. The diagnostic accuracy to trauma-related injuries, radiation dose, quantitative and qualitative image quality parameters, subjective image quality scorings, and workflow time parameters were compared.
Results: In group A, statistically significantly more arterial injuries (p=0.04) and arterial dissections (p=0.002) were detected. In group A, the mean (±SD) DLP value was 1681±183mGy*cm and markedly lower when compared to group B (p<0.001). SD of the mean HU-values of brain, liver and abdominal aorta were lower in group A (p<0.001). Mean SNRs for the brain, liver and abdominal aorta were significantly higher in group A (p<0.001). Group A had significantly higher image quality scores for all analysed anatomical locations (p<0.02). The mean time from patient registration until completion of examination was significantly longer for group A (p<0.001).
Conclusion: The novel multi-phase CT-protocol improves diagnostic accuracy for trauma-related arterial injuries and image quality at markedly reduced radiation. However, the amount of electronic information leads to an increase in examination time, which reduces work-flow for acute emergency situations when time is one of the most relevant factors.

B-0100 10:38

Are follow-up ultrasound (US) studies of severely injured patients after negative multi-detector computed tomography (MDCT) a waste of time?

M. Schürer, T. Kahn, C. Josten, J.K.M. Fakler, P. Stumpp; *Leipzig/DE (Matti.Schuerer@medizin.uni-leipzig.de)*

Purpose: To evaluate the diagnostic significance and clinical relevance of routinely performed follow-up ultrasound studies on severely injured patients with initial whole-body MDCT.
Methods and Materials: Over a period of 48 months, we identified 611 severely injured patients, who received an initial whole-body MDCT and a follow-up US six hours afterwards. Patients were divided into two cohorts: patients with (A) and without (B) a trauma-related abdominal pathology in the initial MDCT. Both cohorts were then evaluated regarding the presence of findings in US, changes compared to initial MDCT and change of the therapeutic management.
Results: 150 patients have been categorised in cohort A and 461 in cohort B. Only 2 patients (1.3%) in cohort A showed new findings in the US and one of them needed clinical intervention. In cohort B, 6 patients (1.3%) showed minimal new findings in the form of small amounts of free fluid, and none of them needed any form of clinical intervention. This means that due to follow-up US, only in 1 of 611 patients (0.16%) the treatment plan had to be changed.
Conclusion: Since there were no new findings with need for clinical intervention in patients without trauma related pathology in the initial whole-body MDCT, this group of patients does not benefit from a routinely performed follow-up US.

B-0101 10:46

Blunt cervical spine injury in adult polytrauma: incidence, injury patterns and predictors of significant ligament injury on CT

G. Chilvers, U. Janjua, S. Choudhary; *Birmingham/UK (geoffreyschilvers@gmail.com)*

Purpose: Recent guidelines suggest the cervical spine can be safely cleared solely on multi-detector computed tomography (MDCT) scans. However, available literature defining CT findings of significant ligament injury in the absence of cervical spine fractures is limited. We aim to identify CT parameters which predict significant ligament injury in the cervical spine when fractures are absent or subtle.
Methods and Materials: In this retrospective study all polytrauma patients imaged with MDCT over a 5-year period were identified. Patients with cervical spine fracture and/or suspected ligament injury were collated based on CT report and their imaging was reviewed. Predefined predictors of ligament injury were recorded for each study with comparison to subsequent MRI as reference standard.
Results: CT predictors of significant ligament injury at the craniocervical junction include basion-dens interval >10mm, widened C0/C1 facet joint space >3mm or loss of congruity, widened C1/2 facet joint space >6mm, increased AADI >3mm and atlas offset >/=2mm. In the subaxial cervical spine, facet subluxation >50% was the only reliable predictor of ligament injury. Asymmetry of lateral atlanto-dens interval, subluxation at C1/C2 facet, subaxial facet joint widening or minor incongruence and asymmetry of disc space were seen in many studies with normal MRIs.
Conclusion: When fractures are absent, signs of significant ligament injury on CT at the craniocervical junction are increased basion-dens interval, lateral offset of atlas, widened or incongruent anterior atlanto-dens interval and widened C0/C1 and C1/C2 facet joints. In the subaxial cervical spine, >50% subluxation of a facet joint is an indicator of significant injury.

B-0102 10:54

Traumatic arterial injuries of the extremities: MDCT angiography evaluation in emergency setting

C. Liguori, G. Russo, T. Cinque, S. Daniele, N. Gagliardi, C. Acampora, L. Romano; *Naples/IT (carlo.liguori@gmail.com)*

Purpose: To retrospectively assess the accuracy of MDCT angiography as the initial diagnostic technique to depict arterial injury in patients with extremity trauma.
Methods and Materials: Over 36 months, 90 patients (16-87 y) with clinically suspected arterial injury after extremity trauma underwent 64-MDCT angiography and 80 ultimately underwent surgery or interventional radiology treatment. 67 pts had blunt injuries, and 23 had penetrating injuries. Each detected arterial lesion was then characterised as a spasm, stenosis, occlusion, pseudoanurism or rupture. 2 CT experienced radiologists performed separately images evaluation. The standard of reference was surgery (54 pts) or angiography (26 pts); clinical and radiologic follow-up was used in 10 pts. Image quality, lesion depiction, and artefacts were assessed.
Results: 72 traumatic arterial lesions were confirmed. MDCT showed sensitivity and specificity 95% and 87%, respectively, in vascular lesion depiction. Image quality and lesion depiction on MDCT angiograms were considered good and artefacts were considered mild with substantial interobserver agreement.
Conclusion: MDCT angiography provides significant and reproducible technique for detection and characterisation of arterial injuries to the extremities with high image quality and vascular delineation.

B-0103 11:02

Structured reporting of facial skeletal trauma CT scan as a tool to reduce report turnaround time (TAT)

B.M. Jain, K.A. Bhagwat, R.B. Shashikiran, P.T. Reddy, K. P, N. Rathod, M. Karanji, V. Dev; *Davanagere/IN (bharat454@gmail.com)*

Purpose: Treating patients with facial skeletal trauma is a multi-departmental task. In an emergency setting, the report turnaround time (TAT) is very crucial. Descriptive reporting of facial skeletal trauma was increasingly cumbersome. Hence we devised a structured reporting format in a tabular form in order to reduce the TAT and ease of inter departmental communication.
Methods and Materials: Structured report was designed keeping anatomical structures, laterality, accuracy and ease of reporting as main purpose. Prospectively we started reporting facial skeletal trauma using structured format as well as conventional method of reporting and recorded time taken to finalise the report by each of the methods by to separate double blinded radiologists. Total of 500 cases were included in the study.
Results: The average time taken for structured reporting was significantly less than traditional method. (10 to 11 minutes for traditional reporting Vs 6-7 minutes for structured reporting). This validated our assumption of structured reporting reducing the report turnaround time. We also noted that some findings were missed by traditional descriptive reporting as compared to structured reporting.
Conclusion: Structured reporting of facial trauma CT reduces report turnaround time, increases accuracy, ease of reporting findings, objectively conveys information to all treating team flawlessly. Total reduction in report turnaround time was by about 30- 40%. Structured reporting also opens the gate for Big Data analysis of facial skeletal trauma and also will be back bone for computer aided neural network based pattern matching and reporting of facial skeletal trauma in near future.

B-0104 11:10

CT injury score of blunt pancreatic trauma is useful in decision-making for treatment

Y.-C. Wong, L.-J. Wang, C.-H. Wu; *Taiwan/TW (ycwong@cgmh.org.tw)*

Purpose: To evaluate if CT injury score of blunt pancreatic trauma is useful for deciding the choice of treatment.
Methods and Materials: Between 2010 January to 2016 August, 44 patients of blunt pancreatic trauma were treated at our institution. Their clinical data and CT examinations were retrospectively analysed. Six patients were excluded because of poor CT quality (n=3) and unavailability of pre-treatment CT (n=3). A total of 38 patients (22 men, 16 women) with a median age of 28.5 years (IQR 19.0, 41.3 years) were finally included. All CT examinations were reviewed and each pancreas trauma was graded by a CT injury score based on a modified Wong's pancreas injury severity scheme. The CT injury scores were compared with the choice of management (observation or intervention). A p-value <0.05 was considered statistically significant.
Results: Of 38 pancreas trauma, 24 receive observational management, 14 underwent intervention (partial pancreatectomy=9, pancreas repair=1, pancreatic duct stenting=3, percutaneous catheter drainage=1). Their injuries included grade A (n=9), grade BI (n=6), grade BII (n=5), grade BIII (n=10), CI (n=5), CII (n=2), CIII (n=1). Among them, twenty had score 1, seven had score 2, eleven had score 3. Of twenty score 1, 20 (100.0%) received observational management. Four (4/7, 57.1%) patients of score 2 and ten (10/11, 90.9%) patients of score 3 underwent intervention. The comparison of CT injury scores with choice of management was statistically significant (p<0.001).
Conclusion: Injury score of pancreas trauma derived from CT severity is crucial in decision-making for choices of treatment.

B-0105 11:18

Correlation of traumatic skin and subcutaneous injuries with the severity of trauma - analysis of whole-body emergency CT scans in 250 patients

A. Klempka, C. Fischer, D. Spira, H.-U. Kauczor, M.-A. Weber; *Heidelberg/DE (Anna.Klempka@med.uni-heidelberg.de)*

Purpose: To assess correlations between skin and subcutaneous lesions such as bruises and haematomas, deep abrasions, soft tissue emphysema and internal post-traumatic injuries, as support by clinical triage of injured patients, to avoid unnecessary radiation by whole-body computed tomography (WBCT).
Methods and Materials: WBCT emergency scans for suspected polytrauma were retrospectively analysed in 250 patients from June until November 2015. The scan included the entire head, neck, thorax, and abdomen and was indicated after fulfilling criteria of standard operating procedures for WBCT emergency scans in our institution.

Results: A skin lesion of thorax wall was detected in 19 cases, whereas in 17 of those cases an internal injury of the thorax was present. Only two patients with haematoma of chest wall had no internal injury. Skin and subcutaneous lesions of the thorax had the strongest association with internal injury (Fisher's exact test, p<0.001). Skin lesions of abdominal wall were observed in 30 cases. In only 11 cases, these lesions were correlated with internal damages, such as fractures or active bleeding. Fifty-two skin and subgaleal lesions of the scalp were observed. In 20 of these patients an intracranial or internal injury was detected. In 3 patients skin abrasions of the neck were present, and in only one was connected with internal injury.
Conclusion: Clinical triage of injured patients is crucial to decide whether WBCT is appropriate. When cutaneous lesions are observed and the trauma mechanism is appropriate, an internal lesion must be taken into consideration.

B-0106 11:26

Assessment of CT scan need for patients with delayed presentation of head trauma

M.S. Khan, Y.B. Hadi, B. Ibrahim, M. Irfani, M. Aslam, U.F. Bhatti, W. Memon; *Karachi/PK (salmankhan3935@gmail.com)*

Purpose: The National Institute for Health and Care Excellence (NICE) guidelines are commonly used to triage patients presenting with head trauma for need of CT scan. This tool was validated and developed with data for patients presenting within 24 hours of trauma. Thus it is not clear whether these guidelines hold true for patients presenting after 24 hours of injury. Our purpose was to estimate the proportion of CT scans done for late presenters, compare their rate of abnormalities on CT with early presenters, and compare the sensitivity of NICE guidelines in both groups.
Methods and Materials: We conducted a retrospective cohort study of all CT head examinations performed in the Radiology department at Aga Khan University Hospital Karachi on adult patients presenting to the ER with head injury from July 2014 to 2016.
Results: Out of the 2009 eligible patients in the study period, 2002 patients with complete records were included. 52% showed some traumatic abnormality, and mortality rate was 2.3% in the cohort. 32.2% of scans were conducted on patients presenting after 24 hours of trauma. The proportion of CT scans with any traumatic finding was 46.7% for those presenting within and 63% for those presenting after 24 hours of injury. The sensitivity of NICE guidelines for intracranial injury was 93% for early and 83% for late presenters.
Conclusion: Patients presenting after 24 hours of head injury form a significant proportion. NICE guidelines are not as sensitive in this population, and may miss significant injuries.

B-0107 11:34

Maxillo-facial trauma: a surgical approach to CT reporting

G. Pasinati, A. Sorbo, F. Romano, M. Altiero, G. Avitabile, E. Laccetti, M. Scaglione; *Castel Volturno/IT*

Purpose: The role of radiology emergency in CT for the evaluation of maxillo-facial trauma identification and classifying fractures avoiding complications clearly apprising the surgeon to encourage a perfect management of patient.
Methods and Materials: 432 patients were evaluated who presented suspicious injuries or clinically evident maxillo-facial injuries. The research has been led to focus on sustaining structures and on soft tissue lesions.
Results: Our study showed that a ready fast and schematic reporting CT would be diriment for the treatment of these patients obviously giving clear information to the surgical team.
Conclusion: The quick and correct maxillo-facial fractures classification and their related complications allow to decisive patient surgical treatment.

B-0108 11:42

Structured reporting of calcaneal CT in trauma: a checklist for daily practice

I. Altmann-Schneider, K. Bartlema, I. Dekkers, A. van der Molen; *Leiden/NL (i.altmann-schneider@hotmail.com)*

Purpose: Neither on a national nor on an international level there is consensus on how to report CT examinations in calcanea trauma in a structured manner. We aimed to systematically review the literature on CT in calcaneal trauma and to develop an evidence-based checklist for structured reporting in daily practice.
Methods and Materials: A systematic review was performed using Pubmed. A search strategy was developed in consensus. All original studies written in English about CT in human calcaneal trauma from 1/1/2000 - 1/10/2016 were included. Reviews, letters and case reports were excluded. Included articles were used to determine the frequency of possible relevant reporting items and in case available reported prognostic value was scored.
Results: The search strategy yielded 156 articles of which 26 met the inclusion criteria. Sanders CT classification system of (intra-articular) calcaneal fractures was used most frequently (18 of 26 articles; 69%) and the only classification system which is of prognostic value for patient outcome. The following items are considered crucial in radiological reports of calcaneal CT in trauma: Congruence of the posterior talocalcaneal and calcaneocuboid joints and the middle facet and involvement of the anterior process of the talus (8 of 26 articles; 31%), Böhler angle and critical angle of Gissane (9 of 26 articles; 35%), joint relationship between talus and sustentaculum tali, hind foot widening, and calcaneal height (3 of 26 articles; 12%).
Conclusion: Based on a systematic literature review a checklist for structured reporting of CT in calcaneal trauma is proposed.

B-0109 11:50

Post-traumatic active bleeding in dual-phase CT: identification, characterisation and management implications

F. Guida, F. Romano, M. Altiero, E. Laccetti, I. Iadevito, M. Tanga, G. Pasinati, M. Scaglione; *Castel Volturno/IT (fraguida@hotmail.com)*

Purpose: To characterise active bleeding according to its entity using MDCT and, on this base, to establish a tailored management.
Methods and Materials: A retrospective study was performed by selecting in our department data (June 2015-March 2016) all high-energy blunt trauma patients with CT diagnosis of active abdominal bleeding. Bleeding was classified into three main categories, according to morphology (spot, jet and pooling) and origin (arterial or venous). All patients underwent a bi/triphasic contrast-enhanced dual-source CT, with iterative reconstruction algorithm. Spot was defined as punctiform self-limiting bleeding, jet as linear bleeding with no significant changes in morphology during different study phases while pooling was defined as active extravasation of intravenous contrast media with significant changes in its entity and morphology. Patients were randomised and two radiologists were asked to evaluate such bleedings. Interobserver agreement was assessed by the weighted Cohen kappa.
Results: 56 patients were selected in our study, classified as follows: 29 patients as spots, 16 patients as jets and 11 patients as poolings. 3/16 jet had worsened as pooling and were managed with surgery, while 13/16 jets and all spots were managed non-operatively. In particular, 18/29 spots and 11/13 jet underwent endovascular treatment. All the cases of pooling were managed with surgery. Overall interobserver agreement was k=0.98.
Conclusion: Although haemodynamic state represents the major factor influencing patient management in abdominal blunt trauma, it is mandatory to characterise the entity of active bleeding in MDCT for addressing therapeutic decisions, with almost perfect interobserver agreement.

10:30 - 12:00 **Room D**

Musculoskeletal

SS 210

Nerve and muscle

Moderators:
M.A. Fischer; Zurich/CH
S. Peer; Innsbruck/AT

B-0110 10:30

Peripheral nerve ultrasound examinations without peripheral nerve abnormalities: prevalence and further assessment of extraneural findings

B. Bignotti, F. Zaottini, S. Airaldi, F. Rossi, G. Succio, C. Martinoli, A. Tagliafico; *Genoa/IT (bignottibianca@gmail.com)*

Purpose: To evaluate the prevalence and further assessment of extraneural findings detected during peripheral nerve US examinations.
Methods and Materials: A retrospective query of Institutional database identified 278 peripheral nerves US examinations of 229 patients performed between December 2014 and December 2015. Reports were reviewed to assess the number of US without peripheral nerve abnormalities and among these examinations, the prevalence and further assessment of extraneural findings. An extraneural finding was defined as a finding of non-neural origin (eg. muscle, tendon, bone). Standard statistic was used to describe extraneural finding and the 95% confidence interval (CI) was calculated.
Results: In a total of 107 peripheral nerve US examinations of 90 patients (49 male; 41 female; mean age: 55 ± 16 years) no peripheral nerve abnormalities were detected. Among these, extraneural findings were detected in 24 examinations (22.4%). A total of 15 of the 278 (5.4% [95% CI: 2.7%, 8.1%]) peripheral nerve US examinations performed in a year led to a recommendation for additional imaging or clinical evaluation of an extraneural finding.
Conclusion: At least 5.4% (15 of 278) of peripheral nerve US led to additional clinical or imaging assessment.

B-0111 10:38

Sciatic nerve diffusion tensor imaging in muscular disease

S. Keller[1], A. Golsari[1], Z.J. Wang[2], G. Adam[1], J. Yamamura[1]; [1]*Hamburg/DE*, [2]*Dallas, TX/US (j.yamamura@uke.de)*

Purpose: To assess the feasibility of sciatic nerve magnetic resonance neurography (MRN) using diffusion tensor imaging (DTI) adapted for skeletal muscle in patients with muscular dystrophy and healthy controls.
Methods and Materials: DTI of the thigh was conducted using b-values of 0 and 500 s/mm^2 on a 3T system in 12 consecutive patients (m:f 7:5, 52±17y) with various muscular disorders, and in 10 controls. For detection of the sciatic nerve, anatomical T1w images were co-registered geometrically to fractional anisotropy colour encoded images (FA CEI). The apparent diffusion coefficient (ADC), FA and fibre track length (FTL) were analysed by two operators using a *freehand-ROI* and a single-point ROI covering the sciatic nerve. Both ROI methods and the inter-operator agreement were statistically assessed using Bland-Altman analysis and parametric tests.
Results: The inter-operator agreement of DTI-metrics using the freehand-ROI and single-point-ROI technique showed no significant difference between both methods (mean bias 0.02 ± 0.07, 95% confidence interval -0.16 - 0.12). Three-dimensional visualization of sciatic fiber composition and maximum FTL was achievable using both techniques. DTI-metrics of the freehand-ROI and single-point ROI technique in controls corresponded to the literature (ADC 1.45 ± 0.14 mm^2/sx10^{-3}; FA 0.46 ± 0.07).
Conclusion: The skeletal muscle adapted DTI protocol shows a high reproducibility and inter-operator agreement for analysis of the sciatic nerve.

B-0112 10:46

Ultrasound anatomy of the infrapatellar branch of the saphenous nerve

G. Riegler, J. Mayer, C. Pivec, H. Platzgummer, P. Brugger, S. Jengojan, G. Bodner; *Vienna/AT (georg.riegler@meduniwien.ac.at)*

Purpose: Neuropathy of the infrapatellar-branch-of-the-saphenous-nerve (IPSBN) is a common iatrogenic complication of knee surgery and its diagnosis is limited. This study aimed to visualize the IPSBN with high-resolution-ultrasound (HRUS) and to provide a detailed description of its variable course.
Methods and Materials: HRUS with high-frequency probes (15-22MhZ) was used to locate the IPSBN in 14 fresh anatomical specimens. The correct identification of the IPSBN was verified by ink-marking and consecutive dissection. Moreover, the IPSBN was located in both knees of 20 healthy volunteers (n=40). The visibility of the branches was rated on a five-point scale (1= not visible, 5 excellent) and their course was marked on the volunteers' skin in the flexed-knee position. Distances were measured from the IPSBN branch closest to the median of the patella-base (D1), center (D2), and apex (D3), and in a 45°(D4) and 0°(D5) relation to the median patella-apex. Standardized photographs of all knees were mapped on one typically shaped knee. Descriptive statistics, coefficient of variation (CV), and paired t-tests were performed.
Results: Dissection confirmed the correct identification of the IPBSN in 12/14 knees (86%). In volunteers, the visibility-median was four. Significant intra-individual differences for distance measurements were observed for D1(p<.001) and D2(p=.002). The CV was highest for D5(0.86) and lowest for D1(0.14). Mapping of the nerve branches on a typical knee demonstrated a highly variable course for the IPBSN.
Conclusion: This study confirms the ability to reliably visualize the IPSBN and its variations with HRUS, which may allow for selective diagnosis of its neuropathy.

B-0113 10:54

Ultrasound of the median nerve in patients with diabetes

F. Steinkohl, A. Loizides, L. Gruber, M. Krapf, G. Mörsdorf, I. Gruber, B. Glodney, H. Gruber; *Innsbruck/AT (fabian.steinkohl@tirol-kliniken.at)*

Purpose: Carpal tunnel syndrome (CTS) is the most frequent nerve entrapment syndrome. Diabetes mellitus (DM) is a common metabolic disease and its steadily incidence is rising. Therefore there is a high probability of encountering patients with both CTS and DM. Ultrasound has a very important role in diagnosing CTS. Often the cross sectional area (CSA) of the median nerve is measured to calculate the Wrist-to-Forearm-Ratio (WFR). A ratio of >1.4 is considered pathologic. DM causes neuropathies, but it is unclear if this has an effect on the CSA. If this is the case, WFR should not be used in diabetic patients. We want to find out if WFR is a suitable method in diabetic patients.
Methods and Materials: 233 wrists of 153 patients were examined. Three groups were formed: Patients with DM and CTS, patients without DM and with CTS, and patients with DM and without CTS. CSA of the median nerve was obtained by using a linear array probe. WFR was calculated.
Results: Both diabetic patients without CTS and with CTS had significantly lower WFR values (p = 0.002 and 0.029, respectively) than non-diabetic patients with CTS. There was no difference between WFR of diabetics with and without CTS (p = 0.06). Diagnostic accuracy to discriminate diabetics with and without CTS was low for measurements of WFR and median nerve CSA and the carpal tunnel.
Conclusion: Our findings suggest that WFR in diabetic patients with CTS has a low diagnostic accuracy and should not be used in those patients.

B-0114 11:02

Role of real time and shear wave sonoelastography in the follow up of muscle thigh injuries in athletes: a three-years longitudinal study

A. Corazza[1], D. Orlandi[1], G. Ferrero[2], C. Messina[3], R. Sartoris[1], E. Silvestri[1], L.M. Sconfienza[3]; [1]*Genoa/IT*, [2]*Pietra Ligure/IT*, [3]*Milan/IT*

Purpose: The aim of the current study is to assess the reliability and effectiveness of real-time sonoelastography (RTE) and shear-wave sonoelastography (SWE) in the evaluation and follow-up of traumatic lower limb muscle tears in a cohort of professional athletes using MRI as a reference standard.
Methods and Materials: 143 male athletes (aged 27 ± 4) with MRI confirmed indirect thigh muscle injury was included in our study and evaluated with US over a period of 36 months. Muscle tears were evaluated with B-mode US, RTE and SWE using two different US machines (LOGIQ E9, GE Healthcare; RS80 Prestige, Samsung Medical) at baseline, 2, 4 and 6 weeks in order to evaluate the healing process of the injury also comparing the obtained results with the healthy contralateral side. Statistical analysis of the obtained data was performed, also assessing intra- and inter-observer reproducibility with the Bland-Altmann test.
Results: The results derived from the current study highlight a direct relationship between the clinical recovery of the injured muscle and the elastic features of the regenerative scar tissue. In particular SWE quantitative elasticity assessment was able to provide meaningful data about the quality of the regenerated tissue furnishing thresholds, with high measurement reliability index (RMI): 0.7 ± 0.2.
Conclusion: The dynamic features of US, combined with RTE and SWE techniques are able to provide qualitative and quantitative elasticity assessment of the healing process of an injured muscle. This can be crucial in the management and early recovery of athletes.

B-0115 11:10

Shear wave elastography of median nerve at carpal tunnel in upper extremity spasticity

H. Aslan, P.D. Analan; *Adana/TR (hul_yaaslan@hotmail.com)*

Purpose: To compare the median nerve elasticity of the paretic side with that of the nonparetic side of patients with wrist spasticity using shear wave elastography (SWE) at the carpal tunnel and to assess the correlations between shear wave velocities (V_s) and clinical outcomes.
Methods and Materials: This prospective study included 25 patients with one-sided wrist spasticity following stroke. The Modified Ashworth Scale (MAS) of wrist and the Brunnstrom's motor staging (BMS) of hand were performed. The patients underwent median nerve ultrasound (US) and SWE of their paretic and nonparetic sides at the carpal tunnel. V_{mean} and V_{max} of both sides were compared for each patient. The correlations between SWE results, duration of stroke and clinical outcomes were assessed.
Results: The mean age of the study population was 56.4±13.64 years. V_{mean} and V_{max} on the paretic side were 2.94 ± 0.51 and 3.11 ± 0.54 m/s, respectively, and on the nonparetic side were 3.01 ± 0.71 and 3.16 ± 0.78 m/s, respectively. No significant difference was found in the V_s of both sides (P > 0.05). Moreover, no significant correlation existed between the V_s of the median nerve with MAS and BMS scores and time since stroke (r < 0.3, P > 0.05).
Conclusion: These results suggested that SWE could not be a helpful imaging tool in detecting the possible changes in the median nerve following wrist spasticity, or less likely the median nerve could have increased the capacity to adapt to the long-standing effects of muscle spasticity.

B-0116 11:18

Quantification of muscle degeneration in patients with late-onset Pompe disease by MRI

A. Lollert, C. Stihl, A.M. Hötker, E. Mengel, J. König, K. Laudemann, C. Düber, G. Staatz; *Mainz/DE (andre.lollert@unimedizin-mainz.de)*

Purpose: To evaluate the value of two quantitative methods based on T1- and T2-weighted magnetic resonance imaging, to assess fatty muscular degeneration in patients with late-onset Pompe disease (LOPD) in comparison with the standard semi-quantitative visual evaluation.
Methods and Materials: MRI of the lumbar spine was performed using T1- and T2-weighted turbo spin echo (TSE) sequences in 41 patients with LOPD. Images were semi-quantitatively evaluated with respect to fatty degeneration of the psoas and paraspinal muscles by two independent observers, using a well-established 4-point scoring system (the Mercuri score), as well as quantitatively by manual signal intensity measurements, and semi-automated muscle and fat

tissue separation using the ImageJ programme. Correlations with clinical parameters were assessed.
Results: Inter-observer agreement was higher for the semi-automated compared to manual quantitative method. Mercuri scores correlated well with clinical parameters, especially for the six-minute walk test and forced vital capacity in the supine position. Measurements derived from the semi-automated method correlated well with MRC scores of muscle strength (P<0.001). Moderate correlations were found for the six-minute walk test (ρ=-0.52, P=0.001), the four-step stair climb test (ρ=0.52, P=0.001), and spirometry in the supine position (ρ=-0.587, P<0.001).
Conclusion: Quantification of fatty muscle degeneration using the semi-automated method resulted in a superior inter-observer agreement compared with manual signal intensity measurements, and greater accuracy than Mercuri-scoring. MRI-derived muscle-specific data correlate with clinical strength tests.
Author Disclosures:
A. Lollert: Research/Grant Support; Genzyme-Sanofi. **G. Staatz:** Research/Grant Support; Genzyme-Sanofi.

B-0117 11:26

Automated artifact correction of diffusion tensor data allows unbiased muscle fiber tracking in the thigh

C. Giraudo[1], S. Motyka[1], M. Weber[1], C. Resinger[1], T. Feiweier[2], H. Traxler[1], U. Koller[1], S. Trattnig[1], W. Bogner[1]; [1]*Vienna/AT*, [2]*Erlangen/DE*
(chiara.giraudo@meduniwien.ac.at)

Purpose: To optimise a robust protocol for fiber tracking of thigh muscles and evaluate an automated post-processing method for correction of artifacts (i.e., signal loss areas) affecting STEAM-based DTI images.
Methods and Materials: Ten healthy volunteers (5 males; mean age 30.8 yrs) were scanned at rest on a 3T-MR using a STEAM-DTI sequence. Thighs' native images were automatically corrected using the formula $\mu_{weighted}=\sum_i^N w_i x_i / \sum_i^N w_i$, computing a weighted mean of all six averages (avg) for each DTI-direction and b-value.Fiber tracking of the entire datasets and of ROIs, placed where artifacts occurred, were done using the native images, with one and six averages (1avg, 6avg), and the corrected datasets (c6avg). Differences in tracts' mean number (tr_n), length (tr_l), volume (tr_v), fractional anisotropy (FA), mean- (MD), axial- (AD) and radial-diffusivity (RD) were investigated with one-way-ANOVA test post-hoc Bonferroni corrected Greenhouse-Geisser.
Results: In the entire datasets, tr_n, tr_l, tr_v increased comparing 1avg with 6avg and c6avg (+41.6%,+59.7%,+75.8% and +43.9%,+65.6%,+81.1%;all p<0.001).No significant changes occurred for FA (p>0.05);AD decreased whereas RD increased using 6avg and c6avg rather than 1avg (-1.8%,-1.9% and +3.2,+2.1%;all p<0.05).MD and RD decreased using c6avg rather 6avg (-0.6%,-1.1%;p<0.05).In the ROIs, tr_n, tr_l, tr_v increased comparing 1avg with 6avg and c6avg likewise 6avg with c6avg (+83.4%,+67.6%,+122.9% and +131.0%,+97.3%,+180.8% and +25.9%,+17.7%,+26%;all p<0.05);RD decreased comparing 6avg with c6avg (-2.1%;p=0.001).No significant changes occurred for MD, FA, AD (all p>0.05)
Conclusion: The STEAM-based DTI protocol including six averages and the artifact correction improved fiber tracking of thigh's muscle and it's expected to enable robust clinical DTI musculoskeletal applications.
Author Disclosures:
C. Giraudo: Research/Grant Support; Austrian Science Fund (FWF; Project KLIF 382). **S. Motyka:** Research/Grant Support; OeNB Jubilaeumsfond (Grant #16133). **T. Feiweier:** Employee; Senior Researcher Healthcare Siemens.

B-0118 11:34

Proton density fat-fraction of rotator cuff muscles is associated with isometric strength 10 years after rotator cuff repair: a quantitative MR imaging study of the shoulder

P.M. Jungmann, D.C. Karampinos, C. Holwein, S. Buchmann, S. Ruschke, A.B. Imhoff, E.J. Rummeny, T. Baum; *Munich/DE*

Purpose: To investigate the relationship of proton density fat fraction (PDFF) of the rotator cuff muscles with semi-quantitative MR-scores, cartilage T2 relaxation times and isometric strength measurements in patients 10 years after rotator cuff repair.
Methods and Materials: Bilateral shoulder MR imaging was performed in n=13 patients (11 male, 2 female; age 72±8 years) 10.9±0.4 years after unilateral autologous periosteal flap augmented rotator cuff repair (total shoulders assessed, N=26). Goutallier classification, muscle atrophy, rotator cuff tendon integrity and cartilage defects were determined based on morphological MR sequences. A paracoronal 2D multi-slice multi-echo sequence was used for quantitative cartilage T2 mapping. A chemical shift encoding-based water-fat separation technique (based on a six-echo 3D spoiled gradient echo sequence) was used for quantification of the PDFF of rotator cuff muscles. Isometric shoulder abduction strength was measured clinically. Mean and standard deviation, Pearson correlation and partial Spearman correlation were calculated.
Results: The mean PDFF of rotator cuff muscles was 11.7±10.4%. High supraspinatus PDFF correlated significantly with higher Goutallier scores (R=0.75, P<0.001) and with lower isometric muscle strength (R=-0.49, P=0.011), also after adjustment for muscle area measurements and tendon rupture (R=-0.41, P=0.048). More severe cartilage defects at the humerus were associated significantly with higher supraspinatus PDFF (R=0.44; P=0.023). Cartilage T2 values did not correlate with muscle PDFF (P>0.05).
Conclusion: Since MR imaging-derived rotator cuff muscle PDFF is associated with isometric strength independently of muscle atrophy and tendon rupture it may provide complementary, clinically important information in tracking rotator cuff muscle composition on a quantitative level.
Author Disclosures:
D.C. Karampinos: Grant Recipient; Dimitrios C. Karampinos receives grant support from Philips Healthcare. **S. Buchmann:** Consultant; consultant of Arthrex Inc. (Naples, FL, USA). **A.B. Imhoff:** Consultant; consultant of Arthrex Inc. (Naples, FL, USA).

B-0119 11:42

Ultrasound elastography in detection of supraspinatus muscle atrophy and fatty degeneration in the reference to MRI

V. Gazhonova, M. Emelianenko, M. Onishchenko; *Moscow/RU*
(vx969@yandex.ru)

Purpose: To investigate the possibilities of US-sonoelastography (SE) in detection of supraspinatus muscle (SSM) atrophy and fatty degeneration (FD) with reference to MRI.
Methods and Materials: 29 patients with shoulder pain and disability underwent US with and without SE before MRI study. Occupational ratio of SSM with and without SE was calculated for evaluation of muscle atrophy in oblique sagittal plane. Modified Goutallier classification was used for assessment of FD on B-mode US and with SE. Soft areas on SE reflects fatty infiltration of SSM. All data was compared to MRI for atrophy and FD. Correlation finding of US alone and US SE in detection of SSM atrophy and FD was achieved in the reference to MRI. Interobserver variability was estimated for US SE data.
Results: US SE improved the diagnosis of fatty degeneration and atrophy compared to US alone. Inter-observer reliability of SE showed ''almost perfect agreement'', kappa 0.83. For SSM atrophy US SE had a positive correlation (r = 0.829, p=<0.001), without SE (r=0.679, p=<0.05) with reference to MRI. For FD grades US SE also had a positive correlation (r =0.873, p=<0.001), US alone (r= 0.713, p=<0.05) with reference to MRI. SE provided more accurate measurements of occupational ratio of SSM atrophy by highlighting area of FD.
Conclusion: US with SE had excellent interobserver reliability and better correlation with MRI findings than conventional ultrasonography for SSM atrophy and FD.

B-0120 11:50

Evaluation of lower back muscle activity with functional magnetic resonance imaging

B. He; *Kunming/CN (henri5437@sina.com)*

Purpose: To evaluate the exercise-induced changes of transverse proton relaxation time (T2) and blood oxygenation level-dependent (BOLD) effect in the lumbar extensor muscles of healthy volunteers by applying muscle functional MRI (mfMRI).
Methods and Materials: In 20 healthy participants, mean age 27 years, the cross-sectional area (CSA), T2 and R2* values were calculated for the multifidus, longissimus and iliocostalis at the level of superior margin of L4 at rest and after following trunk extension exercise by using 3.0T MR.
Results: The CSA of all muscles at L4 level were significantly bigger after exercise than at rest (P<0.05). In resting state, the average T2 value of multifidus, longissimus and iliocostalis were 50.89±6.87ms, 49.35±5.00ms and 44.88±4.26ms, after loading which separately were 59.30±10.11ms, 56.81±7.99ms and 51.12±6.33ms. After exercise, the T2 value was significantly increased (P<0.05). In resting state, the average R2* value of multifidus, longissimus and iliocostalis were 42.90±5.06Hz, 43.88±5.28Hz and 41.89±5.32Hz, after loading which separately were 36.70±4.79Hz,36.72±4.60Hz and 37.63±4.48Hz. After exercise, the R2* value was significantly decreased (P<0.05).
Conclusion: Muscle functional MRI can be used to evaluate lower back muscle activity by measuring T2 and R2*.
Author Disclosures:
B. He: Author; Jialong Zhou, Jianqiang Huang, Wei Zhao.

10:30 - 12:00 **Room G**

Physics in Medical Imaging

SS 213
CT technology and reconstruction algorithms

Moderators:
A. Alberich-Bayarri; Valencia/ES
A. Stadler; Vienna/AT

B-0121 10:30

Identification and quantification of multiple high-Z materials by spectral CT

M. Moghiseh, R. Aamir, J. Healy, A.P.H. Butler, N.G. Anderson;
Christchurch/NZ (mahdieh_moghiseh@yahoo.com)

Purpose: Spectral (multi-energy) CT using photon-counting x-ray detector technology has the potential to image multiple high-Z contrast agents whether targeted or non-targeted. The aim was to identify and quantify iodine, gadolinium, and gold contrast agents in a spectral CT scan of a mouse.
Methods and Materials: We used a multi-spectral micro-CT and Medipix3RX detector bonded to Cadmium-Zinc-Telluride, and four energy thresholds from 27-118 keV selected to include the K-edges of iodine (I), gadolinium (Gd) and gold (Au) containing contrast agents. We imaged a 38-mm PMMA (Polymethyl methacrylate) phantom containing Iodixanol (4.5, 9, 18 mg I/mL), gold nanoparticles (AuNPs) (2, 4, 8 mg Au/mL), gadopentetate dimeglumine (2.1, 8.4 mg Gd/mL) and calcium hydroxyapatite (HA) (200, 800 mg HA/mL) to determine calibration curves of attenuation versus concentration. Three mice injected intravenously with 16 mg iodine and 16 mg AuNPs, then 8 mg gadolinium introduced into the stomach and rectum were scanned with the same imaging protocol along with the calibration phantom.
Results: We identified, discriminated, and quantified all concentrations of iodine, gadolinium, and AuNPs. In the phantom, the material was correctly identified in 90%, 100% and 82% of voxels for 18 mg/mL iodine, 8 mg/mL gadolinium and 8 mg/mL AuNPs respectively. In the mice, iodine, gadolinium, gold, and hydroxyapatite could all be distinguished from each other.
Conclusion: Iodine, gadolinium, gold and hydroxyapatite were distinguished and discriminated simultaneously by spectral CT using an imaging protocol which could be translated to human imaging. If these agents can be targeted to different biomarkers, then simultaneous use of these agents may help imaging biological or disease processes on one scan.
Author Disclosures:
A.P.H. Butler: Board Member; MarsBioImaging Ltd. **N.G. Anderson:** Shareholder; Mars BioImaging Ltd.

B-0122 10:38

Modified dual-energy-based three material decomposition for calcium plaque removal on spectral CT data

B. Schmidt[1], B. Krauss[1], A. Pourmorteza[2], D.A. Bluemke[2], K. Grant[3], T. Flohr[1];
[1]*Forchheim/DE*, [2]*Bethesda, MD/US*, [3]*Malvern, PA/US*
(bernhard.schmidt@siemens.com)

Purpose: Removal of calcified plaques from small vessels is one of the remaining challenges in CT. Threshold-based plaque removal typically fails due to calcium blooming. Traditional dual-energy (DE)-based 2-material decomposition into water and iodine leads to an incomplete subtraction of calcium. Here we assess the ability of a modified 3-material decomposition algorithm for the removal of calcium-related enhancement from iodinated vessels.
Methods and Materials: Instead of iodine and soft tissue alone, a 3-material decomposition into calcium as a first base material and a mixture of different contributions of soft tissue/iodine as the remaining materials, is performed. To evaluate our method, first tubes with different mixtures of calcium plaque equivalent solution and soft tissue/iodine were measured on a SOMATOM Force (Siemens) and on a prototype CT-system equipped with a detector using photon counting technology in an anthropomorphic environment and then decomposed. Second, specimen vessels with iodinate contrast and calcified plaques at different stenosis levels were evaluated with both CT technologies.
Results: For both CT technologies, decomposed images showed a good separation of calcium from soft tissue/iodine. The processed data from the specimen showed excellent calcium removal for medium and large calcifications. Data from photon counting technology showed a superior performance for small calcifications.
Conclusion: The presented modified 3-material decomposition allows for an improved visualisation of vessel lumen, and a more reliable removal of plaque. For smaller structures counting technology leads to slightly better results. The proposed technique may allow for substantially improved confidence in stenosis quantification.
Author Disclosures:
B. Schmidt: Employee; Siemens Healthcare GmbH. **B. Krauss:** Employee; Siemens Healthcare GmbH. **K. Grant:** Employee; Siemens Healthcare. **T. Flohr:** Employee; Siemens Healthcare GmbH.

B-0123 10:46

Comparison of metal artefact reduction in dual- and single-source CT: a vertebra phantom study

P. Jagoda, D. Schmitz, S. Wagenpfeil, A. Buecker, P. Minko; *Homburg/DE (peterminko@yahoo.com)*

Purpose: To compare the capability of OMAR and iMAR, two algorithms for metal artefact reduction and FAST DE, a metal artefact reduction application for dual-source CT.
Methods and Materials: A bovine vertebra phantom with 16 artificial osteolyses and two osteosynthesis screws was scanned on two different single source CT scanners (Brilliance 64, Phillips and Somatom 64, Siemens) at 80, 100, 120 and 140kV with 150mAs and on a dual-source CT scanner with a selective photon shield (Force, Siemens) at tube voltages 100/150kV at doses identical to single source acquisition. Data sets were reconstructed with OMAR, iMAR and FAST DE. Blinded to the methods 3 independent observers evaluated metal artefacts, bone and muscular tissue using a 4-point scale. Depicted osteolyses were counted and screws diameters measured for each reconstruction.
Results: FAST DE showed the best metal artefact reduction capability among evaluated methods; overall artefacts were rated 1.0±0 for FAST DE, 3.1±0.7 for iMAR and 3.7±0.5 for O-MAR ($p<0.001$). FAST DE could provide better reconstructions of bone structure in vicinity to metallic hardware than OMAR or iMAR algorithm (1.4±0.5 FAST DE, 3.7±0.5 iMAR, 4.0±0 OMAR; $p<0.001$) and was superior regarding muscular tissue reconstruction (1.3±0.5 FAST DE, 3.2±0.6 iMAR, 2.9±0.5 OMAR; $p<0.001$). Meanwhile with 14.6±1.7 the detection rate for osteolyses was best on OMAR reconstructions (iMAR 13.1±1.3, FAST DE 12.1±0.7; $p<0.001$).
Conclusion: FAST DE application for dual-energy CT is superior to OMAR and iMAR algorithm regarding metal artefact reduction, tissues and metallic hardware reconstruction but is lacking in a total depiction of all osteolysis.
Author Disclosures:
A. Buecker: Founder; Aachen Resonance GmbH. Research/Grant Support; Siemens AG Consultant, Bracco Group Speaker, Bracco Group Consultant, Medtronic plc Speaker, Medtronic plc Research Grant, Novartis AG Research Grant, GlaxoSmithKline plc Research Grant, Biotest AG, OncoGenex Pharmaceuticals, Inc Research Grant, Bristol-Myers Squibb Company Research Grant, Eli Lilly & Company Research Grant, Pfizer Inc Research Grant, F. Hoffmann-La Roche Ltd Research Grant, sanofi-aventis Group Research Grant, Merrimack Pharmaceuticals, Inc Research Grant, Sirtex Medical Ltd Research Grant, Concordia Healthcare Corp Research Grant, AbbVie Inc Research Grant, Takeda Pharmaceutical Company Limited Research Grant, Merck & Co, Inc Research Grant, Affimed NV Research Grant, Bayer AG Research Grant, Johnson & Johnson Research Grant, Seattle Genetics, Inc Research Grant, Onyx Pharmaceuticals, Inc Research Grant, Synta Pharmaceuticals Corp Research Grant, Siemens AG Research Grant, iSYMED GmbH Research Grant, St. Jude Medical. **P. Minko:** Speaker; Straub Medical AG.

B-0124 10:54

Metal artefact reduction in CT: objective evaluation of three commercial algorithms

K.N. Bolstad, S. Flatabo, D. Aadnevik, I. Dalehaug, N. Vetti; *Bergen/NO (kirsten.bolstad@helse-bergen.no)*

Purpose: Metal implants may introduce artefacts in CT images. The aim of this study was to evaluate metal artefact reduction algorithms (MAR) when imaging different metal implants using single energy acquisition.
Methods and Materials: Three clinical metal implants were taped on the leg of an anthropomorphic phantom; surgical steel, chromium cobalt (CrCo) and titanium. A tissue equivalent material was placed on top to simulate skin surface. Three commercial MAR were investigated; SEMAR (Toshiba), O-MAR (Philips) and iMAR (Siemens). The images were reconstructed without and with MAR. The images were analysed objectively by calculating the rate of HU pixels above 500HU in a region of interest around the metal.
Results: For steel, the rate of HU pixels above 500HU decreased from 39% to 24% when using O-MAR, 29% to 14% using iMAR and 33% to 10% using SEMAR. For CrCo, the rate of HU pixels above 500HU decreased from 35% to 25% when using O-MAR, 31% to 17% using iMAR and 32% to 12% using SEMAR. For titanium the rate of HU pixels above 500HU increased from 8% to 12% when using O-MAR, the rate decreased from 7% to 5% using iMAR and 13% to 6% using SEMAR.

Conclusion: MAR reduces metal artefacts and improves the image quality for CT images containing metal implants of steel and CrCo. SEMAR decreased the rate of HU pixels better than O-MAR and iMAR for CrCo and steel when using single energy acquisition. When using MAR on titanium, all algorithms introduced new visible artefacts.

B-0125 11:02

Accurate reconstruction of x-ray spectra in CT from simple transmission measurements

C. Leinweber, J. Maier, M. Kachelrieß; *Heidelberg/DE (carsten.leinweber@dkfz.de)*

Purpose: To determine the x-ray spectra of CT systems from transmission measurements without additional hardware.
Methods and Materials: The proper knowledge of x-ray spectra is important for several CT applications. Often, assessing the x-ray spectrum requires the use of additional hardware. On the other hand, available methods to reconstruct the x-ray spectrum from nothing but transmission measurements are not very accurate. This is because the reconstruction of x-ray spectra from transmission measurements is a highly ill-conditioned inverse problem. We face this ill-conditioning in three steps. Prior to the calculation of a singular value decomposition (SVD) we weight the input data according to their signal noise. In the second step we regularize the SVD solution with help of the L-curve criterion. The resulting spectra accurately reproduce the incident transmission measurements. However they also tend to exhibit an unphysical shape that leads to deviations in reproducing transmission data that have not been included into the reconstruction process. We solve this by incorporating prior knowledge about the x-ray target material. Our method is applied to simulated and measured data.
Results: For noiseless simulated data our reconstructed spectra perfectly reproduce the input spectra. For noisy data we outperform the standard transmission-based spectrum estimation methods, in particular when testing absorbers that have not been included in the estimation process. These finding are confirmed by results of measured data.
Conclusion: Our hybrid spectrum reconstruction method is simple to use and accurate in reproducing both transmission data as well as the physical shape of the spectral distribution.

B-0126 11:10

Advanced electron density reconstruction for single-energy computed tomography

A. Ritter, R. Raupach, B. Schmidt; *Forchheim/DE (andre.ritter@siemens.com)*

Purpose: A new reconstruction allows estimating electron density images from single-energy computed tomography. We discuss the technical foundation of this method and show first results of a phantom evaluation.
Methods and Materials: The reconstruction is based on a water-bone material decomposition, computed partly in image and projection domain. The bone content is approximated via thresholding in the image domain. Water-bone decomposition is completed in the projection domain, using a scanner- and spectrum-specific relationship between attenuation and effective water and bone thicknesses. Both effective thicknesses are used to synthesize line integrals of electron density, from which images of electron density are reconstructed. The reconstruction is tested with the Gammex 467 Tissue Characterisation Phantom using different tube voltages.
Results: We observe that image values reconstructed with this method are nearly proportional to electron density. The accuracy of the electron density reconstruction increases with higher tube voltage. Additionally an intrinsic correction of beam hardening artifacts is included with this method.
Conclusion: The presentation provides a basic understanding of this new method and helps to assess its capabilities for potential applications, in the diagnostic and the radiation therapy field.
Author Disclosures:
A. Ritter: Employee; Siemens Healthcare GmbH. **R. Raupach:** Employee; Siemens Healthcare GmbH. **B. Schmidt:** Employee; Siemens Healthcare GmbH.

B-0127 11:18

Iterative reconstruction algorithm in CT protocol optimisation

C.R. Gigliotti, A. Loria, F. De Cobelli, R. Nicoletti, G. Bianco, R. Calandrino, A. del Vecchio; *Milan/IT (gigliotti.carmen@hsr.it)*

Purpose: The use of the iterative algorithm for CT image reconstruction led to the possibility to drastically reduce patients' doses, maintaining, or even improving, the image quality. The aim of this study is to optimize the CT clinical protocols of the Philips Somatom Definition Flash 64 for different anatomical districts and clinical questions.
Methods and Materials: Different protocols, concerning four districts (head, thorax, abdomen, orthopedic) were investigated exposing Catphan 600 CT image quality phantom. The routinely used protocols were considered as references. Starting from reference protocol parameters, the medium current was gradually reduced while the level of the iterative algorithm (Philips iDose) was progressively raised. Non-uniformity, low contrast, noise power spectrum (NPS) and spatial resolution (MTF) were evaluated for each image reconstruction. Furthermore, the Rose and Impact quality indexes were evaluated.
Results: In order to preserve the radiologist image perception resulted necessary to select parameters that produce images with NPS shape and frequency peak comparable to the reference image ones. Furthermore, non-uniformity, low contrast details detectability and MTF resulted comparable to, or better than, the reference image ones. The protocols optimized in such a way were proposed to radiologists as alternatives to the reference ones permitting dose reduction between 15% and 35%.
Conclusion: The optimization of the iterative reconstruction algorithm use in clinical protocols permits to sensibly reduce patients' dose. It is mandatory to tailor this optimization on specific anatomical district and clinical question keeping constant the radiologists' image perception.

B-0128 11:26

Effects of five iterative reconstruction algorithms on low-contrast detectability in patients with varying abdominal diameters: a CT phantom study

A. Viry[1], D. Racine[1], C. Aberle[2], S. Schmidt[1], S. Schindera[3], F.R. Verdun[1], F. Becce[1]; [1]*Lausanne/CH*, [2]*Basle/CH*, [3]*Aarau/CH (anais.viry@chuv.ch)*

Purpose: To objectively compare the effects of FBP and various iterative reconstruction (IR) algorithms on low-contrast detectability (LCD) in patients with varying abdominal diameters.
Methods and Materials: An anthropomorphic abdominal phantom with an optional ring (equivalent diameters, 24cm and 35cm) and containing 5mm targets of 20HU contrast was scanned on four CTs using routine abdominal protocols (CTDIvol, 5.9-16mGy): Revolution, Discovery CT750 HD (GE), Somatom Definition Flash, Somatom Definition Edge (Siemens). Images were reconstructed using both FBP and various IR algorithms: statistical IR (ASIR50% on Discovery), statistical model-based IR (MBIR, ASIR-V50% on Revolution, SAFIRE3 on Flash, ADMIRE3 on Edge), or the full MBIR (VEO on Discovery). Slice thickness/interval were 2/1mm (Siemens) or 2.5/1.25mm (GE), except 0.625/0.625mm for VEO. A channelized Hotelling observer with 10 dense differences of Gaussian channels was used to assess LCD, with the area under the curve as a figure of merit.
Results: With the smaller phantom, we found no significant difference between FBP and various IR algorithms for all CTs ($p \geq 0.07$). For the larger phantom, a slight but statistically significant improvement in LCD was observed with statistical IR (2.3%, $p=0.0003$) and statistical MBIR algorithms (1.7%-2.3%, $p<0.0004$), as compared with FBP. VEO enabled a greater significant improvement in LCD (8.5%, $p<0.0001$) together with a four times higher longitudinal spatial resolution.
Conclusion: For smaller-sized patients, the various IR algorithms have no effect on LCD. For larger-sized patients, the full MBIR algorithm substantially improves LCD at higher longitudinal spatial resolution, whereas other IR algorithms have a smaller effect on LCD.

B-0129 11:34

The impact of new generation scanner CT and ASIR-V on dose reduction and image quality

M. Gatti, M. Fronda, D. Castellano, P. Isoardi, F. Marchisio, O. Rampado, R. Ropolo, P. Fonio, G. Gandini; *Turin/IT (marcogatti17@gmail.com)*

Purpose: To evaluate the impact on dose reduction and image quality of a new generation scanner CT equipped with adaptive statistical iterative reconstruction (ASIR-V) in oncologic patients.
Methods and Materials: 38 oncologic patients (66.3±10.0 years, 13 females, BMIndex 24.4±5.0kg/m^{-2}) acted as case-control undergoing during their follow-up a CT scan both with GE Healthcare Optima 660 + 50% ASIR (Optima+ASIR) and with a GE Healthcare Revolution CT + 40% ASIR-V (Revolution+ASIR-V). The image noise (IN) was measured by placing a circular region of interest (ROI) in three standard locations: liver parenchyma, gluteal subcutaneous fat and aorta. Absolute visual grading (AVG) analysis evaluating the subjective noise, sharpness, and diagnostic quality and relative visual grading (RVG) analysis evaluating the overall image quality on a 5-point scale were performed independently by 2 radiologists.
Results: Revolution+ASIR-V dose-length product [DLP=448.5(Interquartiles 362.8-489.1) mGy-cm] and CT dose index [CTDI=7.1(6.60-7.98) mGy] were significantly lower ($p<0.0001$) than those of Optima+ASIR [DLP=696.36(566.9-807.2) mGy-cm and CTDI= 12.20(10.57-14.22) mGy]. Revolution+ASIR-V significantly reduced IN: $IN_{Revolution+ASIR-V}$=10.46(9.61-11.58) vs $IN_{Optima+ASIR}$=12.37(11.65-14.21) for liver parenchyma ($p<0.0001$); $IN_{Revolution+ASIR-V}$=9.54(8.61-10.35) vs $IN_{Optima+ASIR}$=10.38(9.97-12.47), for gluteal subcutaneous fat ($p=0.003$) and $IN_{Revolution+ASIR-V}$=12.07(10.31-13.86) vs $IN_{Optima+ASIR}$=18.03(16.40-20.8), for aorta ($p<0.0001$). Revolution+ASIR had a higher AVG than Optima+ASIR for the subjective noise only ($p=0.01$), but the other parameters were similar.

Conclusion: New generation scanner CT equipped with ASIR-V facilitates a radiation dose reduction of 38% with a significant reduction of IN, a reduction of subjective noise and an equal subjective image quality when compared with the last generation scanner CT equipped with ASIR.

B-0130 11:42

Utilizing model-based iterative reconstruction to minimise radiation dose in chest CT examinations for diagnosing lung metastases of sarcoma patients: a phantom study

T. Kaasalainen, T. Mäkelä, A. Kelaranta, M. Kortesniemi; *Helsinki/FI (touko.kaasalainen@hus.fi)*

Purpose: To develop and evaluate ultra-low-dose chest CT protocols using model-based iterative reconstruction (MBIR) for diagnosing lung metastases in sarcoma patients.
Methods and Materials: An adult female anthropomorphic phantom was scanned using a 64-slice CT scanner with different ultra-low-dose and standard dose protocols. Mean absorbed organ doses in the chest area (lungs, liver, heart, thyroid gland and breasts) were measured with ten metal-oxide-semiconductor field-effect transistor (MOSFET) dosimeters. Additionally, Monte Carlo simulations were performed to validate the MOSFET measurements, and effective doses were calculated. Image quality in terms of image noise, contrast, and modulation transfer function (from cylinder contrast targets) was determined from the CT images reconstructed with conventional filtered back projection (FBP), adaptive statistical iterative reconstruction (ASIR), and MBIR algorithms. All the results were compared with those obtained using the standard dose protocol.
Results: Mean absorbed organ and effective doses were reduced by up to almost 95% when using the lowest ultra-low-dose protocol compared to the standard dose chest CT protocol, while still resulting in an acceptable image quality for diagnosing round-shaped lung metastases. The image noise level of the ultra-low-dose MBIR images was comparable to the standard dose FBP images.
Conclusion: According to our phantom study, patient organ and effective doses can be reduced remarkably when using the ultra-low-dose chest CT protocols and the MBIR technique to reconstruct images, while at the same time, image quality is maintained at a diagnostically acceptable level for detecting round-shaped lung metastases in the lungs.

B-0131 11:50

Monte-Carlo simulation of iodine enhancement in an anthropomorphic abdomen phantom: effects of different primary MDCT x-ray spectra on energy deposition

A. Steuwe, H.-U. Kauczor, W. Stiller; *Heidelberg/DE (andrea.steuwe@med.uni-heidelberg.de)*

Purpose: To compare the effect of different primary MDCT x-ray spectra on energy deposition in organs in absence and in presence of iodinated contrast agents.
Methods and Materials: The influence of different primary x-ray spectra (Toshiba CXB-750D MegaCool measured in-house at 120kV$_p$, spectra of the "Siemens Healthcare Online tool for the simulation of x-ray Spectra" at 80/100/120/140kV$_p$ with/without aluminium filtration) on energy deposition in an anthropomorphic abdomen phantom was determined using Monte Carlo simulations with Geant4. Furthermore, energy deposition and relative energy absorption increase ($\Delta E_{rel}=[E_{iodine}-E_{native}]/E_{iodine}$) in presence of iodinated contrast agent (iodine weight fraction ψ=0.005; ~5mg/ml) in the organs pancreas, spleen, kidney, and liver were studied.
Results: Total energy deposition increases with increasing tube potential and mean spectral energy, independent of the presence of iodinated contrast agent. In its presence, energy absorption increases for the specified organs, but decreases (~-3%) in surrounding tissues. For the measured spectrum, Δ_{rel} was 44.0% (pancreas), 36.1% (spleen), 44.0% (kidney) and 29.5% (liver). For simulated spectra with 3.3mm aluminium filtration, Δ_{rel} ranges are: 43.4%-46.7% (pancreas), 32.9%-37.1% (spleen), 40.7%-44.5% (kidney), and 24.8%-30.3% (liver). At each respective tube potential, Δ_{rel} was lower in absence and higher in presence of thicker aluminium filtration.
Conclusion: Differences in ΔE_{rel} between different tube potentials are small. However, aluminium filtration enlarges the fraction $F_{55\text{-}74keV}$ of photon energies between 55keV and 74keV by suppressing the low-energy photon fraction of the spectrum, thereby increasing ΔE_{rel}. Maximizing ΔE_{rel} will cause a large difference between enhanced and non-enhanced tissues, thereby optimising image contrast.
Author Disclosures:
H.-U. Kauczor: Research/Grant Support; Siemens, Bayer. Speaker; Böhringer Ingelheim, Bracco, GSK, Novartis, Siemens, Almirall.

10:30 - 12:00 **Room K**

Radiographers

SS 214
CT imaging

Moderators:
K. Muscat; Birkirkara/MT
A. Palkó; Szeged/HU

K-03 10:30

Keynote lecture

F. Zarb; *Msida/MT*

B-0132 10:39

Using of eye Bismuth shields in CT scan: its influence on ESD and image quality

P.A.T. Gamboa[1], A.P.N. Batista[2], M.M.C.P. Ribeiro[2], A.L.C.F. Vieira[2], H.N. Sousa[3]; [1]*Vila Franca de Xira/PT*, [2]*Lisbon/PT*, [3]*Torres Vedras/PT (patricia24.gamboa@hotmail.com)*

Purpose: Evaluate the impact of using the eye Bismuth shields in ESD (Entrance Skin Dose) and the effect on image quality in brain CT scans.
Methods and Materials: Two CT routine acquisitions of the brain were performed using a CT Activation 16 scanner and an anthropomorphic phantom RSD: with and without Bismuth shields placed over the orbital region. The ESD was evaluated by four TLD-100(LiF:Mg) dosimeters, two for each acquisition (one placed on the nasion -frontal bone - and the other on the inion - occipital bone). The acquisition parameters were fixed. The image quality was quantitatively analysed by five ROI's (two placed in the anterior, one in the middle and two in the posterior region of the brain), and qualitatively by three experienced neuroradiologists through a survey based on a comparative visual analysis test, under the criterias: image contrast; noise; anatomical evaluation; pathological evaluation, dose reduction and global image quality.
Results: The ESD values show a reduction of 61% in the crystalline, with the use of these shields (34,13mGy vs 58,03mGy in average). The observers considered their beneficial use in selected cases. The quantitative results show that the Bismuth shields cause artefacts and increase image noise in the frontal brain parenchyma.
Conclusion: The Bismuth shields are advantageous in certain areas/pathologies, and disadvantageous for studies of the anterior brain parenchyma. Radiographers and doctors should consider the advantages and disadvantages of these shields application in each specific case.

B-0134 10:47

A multi-site head CT topogram acquisition protocol analysis based on DICOM metadata

M. Santos, L. Bastião, N. Rocha, A. Silva; *Aveiro/PT (mrs@ua.pt)*

Purpose: Several international initiatives and scientific studies emphasise the need to promote a greater focus on patient safety when choosing Computed Tomography (CT) scan parameters. This work aimed to analyse the CT Topogram dimension and scan parameters used in Head CT studies conducted in three distinct CT equipment and based on DICOM metadata stored at PACS facilities from two health institutions.
Methods and Materials: The metadata produced by three different Computed Tomography (CT) equipment and stored in two health care PACS facilities were systematically analysed using a DICOM Metadata mining approach. For studies characterisation several DICOM tags were analysed (e.g. mAs, KvP, Exposure Time, Modality, Patient Age) within different queries. The CT Topogram dimension was obtained from the Exposure Time value and the table feed during the topograma acquisition.
Results: The DICOM metadata from 1.274.927 images, bellowing to 19.180 studies performed on 16.169 patients (including 768 paediatric patients) were analysed. The number of CT Topogram images performed per patient ranged from 1 to 2,33 and its dimension between 20,76 cm and 25,16 cm depending on the equipment (CT1=20,8cm±0,04; CT2=24,01cm±0,4; CT3=25,01cm±0,5), namely in paediatrics studies (CT1=20,78cm±0,01; CT2=23,61cm±0,71; CT3=24,98cm±0,01). With regard to CT Topogram scan parameters, no significant changes were identified when the x-ray Tube Current (CT1=10mA±0,02; CT2=49,98 mA±0,03; CT3=39,47 mA±2,29) and KvP values were analysed (CT1= 119,54KvP±1,65; CT2=120,02KvP±0,04; CT3=90KvP).
Conclusion: The age groups (including the paediatric patients) are not factors determining significant changes in the values of the exposure factors and size of the area exposed to radiation upon topogram acquisition.

B-0135 10:55

Investigating optimal abdominal CT protocol for obese patients

A.A. Qurashi[1], L.A. Rainford[1], A. Ajlan[2], K. Khashoggi[2], L. Ashkar[2], M. Alraddadi[3], M. Alghamdi[2], M. Althobaiti[2], S. Foley[1]; [1]*Dublin/IE*, [2]*Jeddah/SA*, [3]*Medina/SA (qetharah@hotmail.com)*

Purpose: To investigate optimal CT parameters when scanning obese patients.
Methods and Materials: With ethical permission, abdominal CT scans for 47 obese patients (AP diameter>26cm, BMI>30kgm-2) were retrospectively collected from 3 different CT models from a single manufacturer over three-month period. Patients were scanned using 5 different protocols, due to various settings used locally (kV: 100/120, mAs: ATCM reference mA: 150, 190, 218, 250, 300). When available, images were retrospectively reconstructed using various SAFIRE strengths (2,3,4 and 5) and FBP. Subjective image quality was determined by three experienced radiologists using visual grading analysis in accordance to EUR 16262. Comparison between radiation dose and image quality was performed using one-way-anova test.
Results: Patients ranged in weight from 65-190 kg with DLP ranging from 345-1525mGy.cm. Mean dose was lowest (up to 60%) for the protocol using 100 kVp technique with statistical differences noted between this protocol and all other scanning techniques ($p<0.05$). All mean image quality scores for all the protocols being examined were deemed suitable for diagnostic interpretation. Images reconstructed with FBP for the protocol with 100 kVp were given the lowest score ($p<0.05$) compared to 120 kVp protocols, especially those with higher reference mAs. However, when the images for the low dose protocol were reconstructed using SAFIRE no significant difference was seen.
Conclusion: Numerous CT protocols are being used clinically for obese patients, with wide variations in dose and image quality. 100kVp protocols produced acceptable image quality for obese patients with up to 60% dose reduction than 120 kVp protocols when IR is used.

B-0136 11:03

Optimisation of CT via analysis of computational fluid dynamics in cerebral aneurysm

M. Ogasawara[1], T. Hirano[1], T. Yagi[2], M. Nakamoto[2], H. Nagahama[1]; [1]*Sapporo/JP*, [2]*Tokyo/JP (mogasawa@sapmed.ac.jp)*

Purpose: Computational fluid dynamics (CFD) in a cerebral aneurysm (CA) is a recently reported method for analyses of CA haemodynamics. However, the reliability of analytical data and optimal CT scan conditions remain unclear. The objective of this study was to investigate optimal scan conditions and contrast medium concentrations for CFD.
Methods and Materials: We performed scans using a 320-slice CT scanner (Aquilion ONE; Toshiba Medical Corporation) and CFD analysis software (hemoscope; EBM Co., Ltd). The hand-made CA phantom contained enclosed concentrations of contrast medium (CT values: 200-500 HU) and silicon (straight line and clinical model). We obtained images using varying noise index values and reconstruction FOVs and used these images to investigate wall shear stress (WSS).
Results: The CFD analytical results indicated a stable maximum WSS (WSSmax) at CT values of 300-500 HU and scan doses of SD20, SD15, and SD10 [straight line model: 2.63 ± 0.42 (16.1%) Pa, clinical model: 16.82 ± 3.80 (22.6%) Pa]. Our results indicated a tendency of the reconstruction FOV (image resolution) and WSSmax-WSSmin (exponential) to converge. Therefore, this technique seems to improve analytical accuracy by setting a smaller reconstruction FOV.
Conclusion: We determined that for CT-based CFD analysis of CA, the optimal scan conditions include a CT value >300 HU, scan dose >SD20, and smaller reconstruction FOV. Under these conditions, all users will be able to obtain a stable, accurate WSS analysis.
Author Disclosures:
T. Yagi: Employee; EBM Corporation. **M. Nakamoto:** Employee; EBM Corporation.

B-0137 11:11

Evaluate the effect of contrast media on patient dose in CT examination of abdomen-pelvic performed with AEC

O. Seraydarmansour; *Tehran/IR (mansour.omid@yahoo.com)*

Purpose: The aim of our study was to investigate the relative dose increase when an abdomen-pelvic CT examination is carried out after administration of oral and IV contrast medium with respect to the same CT scan without contrast medium.
Methods and Materials: Forty patients who underwent both unenhanced and contrast-enhanced abdomen-pelvic CT scan. All examinations were performed using an automatic tube potential selection tool on a 16MDCT scanner (Ingenuity, Philips) with the following protocol: Collimation 16X1.5mm, 120Kvp, pitch 1.37, rotation time 0.5sec. All CT images were reconstructed at 5-millimeter section thickness with a standard reconstruction algorithm. The oral contrast agent was made up of 40ml of meglumine compound (370mgI/ml) mixes in 1 litre of water 3 hours before scanning. Iodinated contrast medium (Ultravist 350) containing 350mgI/ml was administered IV at a dose of 1.2ml/kg of patient weight. Contrast-enhanced CT examination was performed 60 seconds after the start of injection. Two abdominal radiologists evaluated the images for diagnostic confidence.
Results: CTDI vol values obtained for each patient on dose report at the end of CT examinations. An increase in patient dose was noted in all CT examinations with IV and oral contrast compared to unenhanced CT examinations. Average dose increase was 11%.
Conclusion: Our evaluation showed an increase in patient dose when iodinated contrast medium is used in CT examination of abdomen-pelvic basing on the increment in Hounsfield units on the organs.
Author Disclosures:
O. Seraydarmansour: Author; Ghazal Jafarinosar.

B-0138 11:19

Impact of acquisition protocol variations on effective dose for CT head examinations

M.R. Benhalim, A. England; *Salford/UK (A.England@salford.ac.uk)*

Purpose: For range of acquisition protocols, determine the most dominant acquisition factors which impact on effective dose for paediatric CT brain examinations.
Methods and Materials: An ATOM phantom (1-year old child) was implanted with metal oxide semiconductor field effect transducer (MOSFET) dosimeters; these were inserted into 24 organs (167 predrilled holes). Helical CT brain scanning was undertaken using 54 protocols; protocol variations included changes in rotation times, gantry angulation, tube current/potential and fixed slice thickness (0.5x16). ED was calculated for each acquisition protocol.
Results: ED ranged from 1.01 mSv and 4.81 mSv. Organs located within the scan volume consistently received the highest absorbed doses; organs at the periphery and outside of the scan volume still received a radiation dose. ED trends were as follows: ED increased consistently by around 33% when increasing kVp from 100 to 120 (mean ED 2.35 SD 0.75 mSv versus 3.52 SD 1.21 mSv, respectively; $P<0.05$). Changes in gantry angle had minimal effect on ED, when moving from a zero gantry angle to +27 degrees the mean ED decreased by 0.04 mSv ($P>0.05$). Changing the tube current from 120 to 200 mAs lead to increase in ED by 27.7% (mean ED 1.50 SD 0.40 mSv vice versa 2.23 SD 0.65 mSv, respectively; $P<0.05$). Increasing the rotation time from 0.5 seconds to 1 seconds showed increase in ED by 33.4% (mean 1.52 SD 0.46 mSv versus 2.25 SD 0.80 mSv; $P<0.05$).
Conclusion: The most dominant factors affecting ED are tube current, tube potential and scan rotation time.

B-0139 11:27

Effective dose comparison between fixed tube current FTC and automatic tube current ATC methods for abdominal CT examinations

M. Alrowily, A. England, P. Hogg; *Manchester/UK (P.Hogg@Salford.ac.uk)*

Purpose: Fixed tube current (FTC) and automatic tube current modulation ATCM are options used during abdominal CT exams. The aim of this study was to evaluate the effective radiation dose E when comparing FTC and ATCM techniques, using different detector configurations and pitch factors, for abdominal CT scans.
Methods and Materials: Using a Toshiba Aquilion 16 CT scanner 120 kVp, 0.5 seconds tube rotation an adult ATOM dosimetry phantom was exposed to a series of FTC and ATCM CT protocols with variation in detector configuration 0.5mmx16; 1.0mmx16 and 2.0mmx16 and pitch factors 0.688, 0.938 and 1.438. Effective dose E estimations were undertaken using two methods, one using mathematical modelling with k-factors and DLP and the other using Metal Oxide Semiconductor Field Effect Transistor MOSFET dosimeters and tissue weighting factors.
Results: The mean E for ATCM and FTC methods using MOSFET were 5.9mSv and 4.7mSv, respectively. The mean E using DLP and k-factors were 6.3mSv and 5.1mSv, respectively. Using both E estimation methods the radiation doses from ATCM techniques were around 20% higher $P<0.006$. Good correlation existed between ATCM and FTC doses $R^2>0.82$.
Conclusion: In this study, ATCM effective doses were higher than FTC using both dosimetry techniques. E estimated by DLP and k-factors were higher than when directly measured by MOSFET. Differences between the two methods could be due to the limitations of Monte Carlo modelling used in the DLP/k factors approach.

B-0140 11:35

Establishment of diagnostic reference levels in computed tomography

D. Castro, P. Sousa, S. Rodrigues, A.F. Abrantes, R.P.P. Almeida, K.B. Azevedo, L.P.V. Ribeiro; *Faro/PT (kbazevedo@ualg.pt)*

Purpose: To measure radiation dose levels in computed tomography of two regional public hospitals (A and B) and to compare them with international guidelines.
Methods and Materials: A survey of technical parameters (type of exam, patient age, *kV*, *mAs*, $CTDI_{vol}$ and DLP) from 446 CT exams was used to establish the Diagnostic Reference Levels (DRLs). For viability measurements, the dose rate and quality control using the RF detector Unfors Xi and PMMA (polymethylmethacrylate) phantom were carried out.
Results: The Diagnostic Reference Levels established for the Hospital A were 883.22 mGy.cm (Head), 302.18 mGy.cm (Neck), 371.46 mGy.cm (Cervical spine), 406.97 mGy.cm (Lumbar spine), 225.08 mGy.cm (Chest), 274.82 mGy.cm (Abdomen), 463.62 mGy.cm (Abdomen/Pelvis) and 582.78 mGy.cm (Ches/Abdomen/Pelvis). For the Hospital B and considering the same CT exams, DRLs values were, respectively, 959.37 mGy.cm, 339.45 mGy.cm, 306.73 mGy.cm, 480.73 mGy.cm, 243.59 mGy.cm, 278.24 mGy.cm, 606.22 mGy.cm and 674.33 mGy.cm. Despite the DRLs of the Hospital B being generally higher than the Hospital A, they are both lower than all international guidelines considered.
Conclusion: DRLs of both regional hospitals are in general greatly lower than the international guidelines. However, it is important to optimise the protocols used and similar studies in other hospitals are necessary in order to establish a National Dose Reference Level.

B-0141 11:43

Single- and dual-energy quantitative CT adjacent to acetabular prosthetic components: a reliability study

B.R. Mussmann, P.E. Andersen, T. Torfing, S. Overgaard; *Odense/DK (bo.mussmann@rsyd.dk)*

Purpose: Density measurements adjacent to acetabular prosthetic components are challenged by artifacts and the complex anatomy. Three-dimensional ROIs are needed to assess the bone stock. The purpose was to test the intraobserver agreement and reliability of custom segmentation software and to compare BMD measurements in single and dual energy CT (SECT and DECT).
Methods and Materials: 10 male patients with uncemented hip prosthetics were scanned and rescanned using 120 kVp SECT and DECT with virtual monochromatic images reconstructed at 130 keV. Hemispherical ROIs were defined slice-by-slice and bone mineral density was calculated using a calibration phantom. Median time between ROI drawings was 6 days.
Results: The mean BMD for repeated SECT scans was 430 mg/ccm with a between scan difference of 18 mg/ccm, p=0.001. ICC was 0.98 (95%CI: 0.73 to 1). For DECT the mean BMD was 162 mg/ccm with a difference of 11 mg/ccm, p<0.0001. ICC was 0.94 (95%CI: 0.36 to 0.99). Bland-Altman Limits of Agreement were -51 to 15 in SECT and -30 to 7 in DECT. Repeatability coefficients were 33 and 18 mg/ccm for SECT and DECT respectively. The difference was not statistically significant.
Conclusion: The intraobserver reliability was high for both scan modes with statistically significant differences between the repeated measurements in SECT and DECT. The limits of agreement were slightly narrower in DECT, but with no statistically significant difference between repeatability coefficients. The results suggest that the intraobserver agreement of the scan modes is equal. BMD cannot be measured interchangeably with SECT and DECT.
Author Disclosures:
B.R. Mussmann: Equipment Support Recipient; Stryker Corp., Kalamazoo, Michigan, US.

10:30 - 12:00 **Room M 1**

Cardiac

SS 203

Cardiac CT: contrast agent and radiation dose

Moderators:
A. Esposito; Milan/IT
G. Feuchtner; Innsbruck/AT

B-0142 10:30

Reducing iodinated contrast agent concentrations with dual energy CT: a multivendor dynamic phantom study

R.W. van Hamersvelt[1], N.G. Eijsvoogel[2], C. Mihl[2], P.A. de Jong[1], N. Buls[3], M. Das[2], J.E. Wildberger[2], T. Leiner[1], M.J. Willemink[1]; [1]*Utrecht/NL*, [2]*Maastricht/NL*, [3]*Brussels/BE (R.w.vanhamersvelt-3@umcutrecht.nl)*

Purpose: To evaluate the feasibility of reduction of iodinated contrast agent (ICA) concentration with dual energy computed tomography (DECT) systems from 3 major vendors.
Methods and Materials: A circulation phantom simulating physiological conditions (heart rate 60bmp, blood pressure 120/80mmHg) was scanned with dual source CT (DSCT), rapid kVp switching CT (GSI) and dual-layer CT (DLCT). Reference scans were acquired using standard CT (SECT) mode at 120kVp. Subsequently, scans were made in SECT mode at lowest tube potential possible (70, 70, 80kVp) and DECT mode (80-150Sn, 80-140,140kVp respectively). ICA was injected in different concentrations (300, 240, 180, 120, 60, 30mgI/mL) using a fixed protocol (flow rate 6.0mL/s, volume 40mL). Virtual monochromatic images (VMI) between 40-120keV were reconstructed for each DECT acquisition. CT attenuation values (HU) were obtained in the coronary artery and aorta.
Results: Mean attenuation at reference (120kVp,300mgI/mL) was 361±7, 320±15 and 312±5HU for DSCT, GSI and DLCT. With SECT at lowest possible kVp, attenuation values at 180mgI/mL (DSCT and GSI) and 240mgI/mL (DLCT) were 429±13, 339±2.7 and 420±15HU and were significantly higher compared to the reference values (P<0.01). For all vendors in DECT mode, VMI at 40keV resulted in significantly higher HU (528±7, 442±5 and 430±8, respectively) at 120mgI/mL compared to reference (P<0.01). For both SECT and DECT, lower iodine concentrations yielded significantly lower attenuation compared to reference (P<0.01).
Conclusion: Standard CT at lowest possible kVp allows for iodine reductions of 20-40% without loss of intravascular attenuation. In DECT mode, VMI at 40keV allows for a further reduction down to 120mgI/mL (60% reduced), for all 3 vendors.
Author Disclosures:
M. Das: Research/Grant Support; Institutional research grants.
J.E. Wildberger: Research/Grant Support; institutional grants from Siemens, Philips, GE, Bracco, Bayer, and AGFA. Speaker; Siemens, GE, Bayer.
T. Leiner: Research/Grant Support; Bayer A, Bracco Group.G Research Grant. Speaker; Speakers Bureau, Koninklijke Philips NV. **M.J. Willemink:** Speaker; Speakers Bureau, Koninklijke Philips NV..

B-0143 10:38

Individualisation of injection protocols to the individual patients blood volume and automated tube voltage selection in coronary CTA

N.G. Eijsvoogel, B.M.F. Hendriks, B. Horehledova, J.L. Willigers, B.L.J.H. Kietselaer, H.J.G.M. Crijns, J.E. Wildberger, M. Das; *Maastricht/NL (nienke.eijsvoogel@mumc.nl)*

Purpose: Assessing the performance of individualised contrast media (CM) protocols based on patients' blood volume (BV) and automated tube voltage selection (ATVS) in coronary computed tomography angiography (CCTA).
Methods and Materials: 110 consecutive patients referred for CCTA were included. Scans were prospectively ('High pitch'/'dual-step prospective triggering') or retrospectively helical ECG-triggered on a 3rd-generation dual-source CT (Somatom Definition Force, Siemens) with: 70-120 kV (ATVS) and 330 mAs_{ref}. CM volume and flow rate were adapted to BV (Nadlers' formula), scan time and kVp setting. Objective/subjective image quality (OIQ/SIQ) were assessed in a 17-segment model (AHA) with help of attenuation values (HU), contrast-to-noise (CNR), signal-to-noise (SNR) ratio and a 4-point Likert scale (1=poor/2=sufficient/3=good/4=excellent).
Results: Selected kVp settings: 55(70 kVp), 29(80 kVp), 15(90 kVp), 2(100 kVp) and 9(120 kVp). Mean BV (men/women): 5.0±0.9L/4.7±0.9L. Mean CM volume and flow rate were 30.6±6 mL and 3.3±0.5 mL/s (70 kVp); 41.7±6.7 mL and 4.6±0.6 mL/s(80 kVp); 54.5±8.1 mL and 5.8±0.6 mL/s(90 kVp); 55.9±1.3 mL and 5.9±1.0 mL/s(100 kVp); 66.5±16.8 mL and 6.3±1.4 mL/s(120 kVp). Mean attenuation was >300 HU for most proximal segments, 18 proximal

segments <300 HU due to late scanning/stenosis/artefacts. Distal segments were <300 HU due to stenosis/frail artery. Of 1.605 segments 93.5% was assessable (6.5% not assessable due to artefacts or frail arteries). Mean CNR/SNR was 9.4±3.4/9.9±2.4(70 kVp); 9.0±3.5/10.0±2.2(80 kVp); 7.9±2.9/9.0±2.0(90 kVp); 8.0±1.4/10.0±1.4(100 kVp); 11.8±4.3/10.2±2.4(120 kVp). No significant difference was found in CNR/SNR between groups. Overall SIQ was diagnostic in all scans (excellent in 50%) and excellent-sufficient in 89.9% of segments (poor due to artefacts/<HU).
Conclusion: Adaptation of CM protocols to BV and ATVS in CCTA is a promising technique for tailoring CM administration to the individual patient, while maintaining diagnostic image quality.
Author Disclosures:
N.G. Eijsvoogel: Research/Grant Support; Bayer. **B.M.F. Hendriks:** Research/Grant Support; Bayer. **B. Horehledova:** Research/Grant Support; Siemens. **J.E. Wildberger:** Research/Grant Support; Bayer, Siemens, Philips, AGFA. Speaker; Siemens, Bayer. **M. Das:** Research/Grant Support; Bayer, Siemens, Philips, Cook.

B-0144 10:46

Image quality and radiation dose of dynamic stress myocardial perfusion imaging at 70kV using third generation dual-source CT: comparison with second-generation scanner

M. Takafuji, K. Kitagawa, S. Nakamura, A. Yamada, Y. Goto, N. Nagasawa, H. Sakuma; *Tsu Mie/JP (amaranth.0521mt@gmail.com)*

Purpose: With the 2nd generation dual-source CT (2nd-DSCT), dynamic myocardial perfusion imaging (CTP) with 7cm z-axis coverage can be performed at 80kV with mean effective dose of 5mSv. The 3rd-DSCT has 50% wider coverage which is sufficient to cover the entire LV myocardium in most patients. However, increase of radiation as a result of the increased coverage should be avoided. New x-ray tube installed in 3rd-DSCT allows dynamic CTP at 70kV. The purpose of this study was to evaluate image quality and radiation dose of CTP using 3rd-DSCT in comparison with 2nd-DSCT.
Methods and Materials: Thirteen patients with known or suspected coronary artery disease who underwent stress CTP of 30 seconds using 2nd-DSCT at 80kV and 3rd-DSCT at 70kV with 24±7months interval were retrospectively enrolled. Tube current was determined by using automatic exposure control system with the quality reference of 350-mAs/rot at 120kV for both scans. Contrast-to-noise ratio (CNR) and dose length product (DLP) were compared.
Results: Dynamic CTP with 3rd-DSCT showed 7% higher maximal enhancement (708 ± 99 vs 661± 90HU; P=0.19) and 14% greater noise (20.4± 2.8 vs 17.8 ± 2.8; P=0.03) compared to 2nd-DSCT without significant difference in CNR (33.1 ± 7.1 vs 35.1 ± 6.6; P=0.42). Radiation dose was 28.6% lower with 3rd-DSCT (mean DLP, 229±53 vs 320±86mGy·cm; P=0.005).
Conclusion: Dynamic CTP can be performed with mean effective dose of 3.2mSv with 3rd-DSCT. In spite of the increased 10.5cm coverage in z-axis, 70kV imaging with 3rd-DSCT allows dose reduction without compromising image quality compared to 2nd-DSCT, which may expand the clinical utility of dynamic CTP.
Author Disclosures:
K. Kitagawa: Research/Grant Support; Siemens. **H. Sakuma:** Research/Grant Support; Siemens.

B-0145 10:54

Low injection speed study on prospectively high-pitch coronary CT angiography: iodinated contrast media injection protocol with a flow rate at 3.5 ml/s scanned at 70 kVp

L. Zhang, X. Liu, B. Feng; *Shenyang/CN (270973226@163.com)*

Purpose: To evaluate the feasibility and image quality of prospectively ECG-triggered high-pitch coronary CTA with low-contrast medium injection rate at 70 kVp.
Methods and Materials: 104 patients with suspected coronary artery disease (BMI<26 kg/m^2, sinus rhythm and HR<70 bpm) were prospectively enrolled in this study. All patients were randomly divided into two groups. Group A was set as experiment group in which 28 mL of 370 mg/mL iodinated contrast media was administrated at a flow rate of 3.5 mL/s. Group B was set as control group in which 40 ml of 370 mg/mL iodinated contrast media was administrated at a flow rate of 5 mL/s. All patients underwent prospectively ECG-triggered high-pitch coronary CTA on a dual-source CT system at 70 kVp. Main coronary artery CT value, noise, signal-to-noise ratio and contrast-to-noise ratio with regard to adjacent fat tissue were evaluated. Subjective evaluation was also performed based on AHA 15 segment model using 4-point grading scale.
Results: All patients successfully conducted CT examinations. Objective evaluation: CT values for main coronary arteries in both groups were all above 350 HU, SNRs and CNRs were of diagnostic quality. Subjective evaluation: no statistical difference in image quality was observed between the two groups (image quality scores: 3.04 ± 0.75 [group A] vs. 3.0 ± 0.79 [group B]; detectability ratio: 96.1% (50/52) vs. 94.2% (49/52).
Conclusion: Prospectively ECG-triggered high-pitch coronary CTA at 70 kVp with 28 mL of contrast media and injection rate of 3.5 mL/s could provide promising image quality for normal-weight patients with heart rate <70bpm.

B-0146 11:02

Systemic hypotension following intravenous administration of non-ionic contrast medium: a randomised controlled double-blinded phase IV clinical trial

G. Widmann, R. Bale, H. Ulmer, D. Putzer, P. Schullian, F.-J. Wiedermann, W. Lederer; *Innsbruck/AT (gerlig.widmann@i-med.ac.at)*

Purpose: Intravenous administration of non-ionic contrast medium may lead to self-limited systemic hypotension. Objective was to quantify this effect during CT scans in patients under general anesthesia with invasive blood pressure monitoring and to compare iso-osmolar iodixanol and low-osmolar iopromide.
Methods and Materials: In this study (EudraCT No.: 2013-002051-15) forty consecutive patients were randomly assigned to receive either iopromide or iodixanol. For each patient normo-saline solution (NSS) was administered as a placebo control. Systemic blood pressure and heart rate were recorded one minute before, during and three minutes after each administration of contrast medium and NSS. Per-hour urine output was recorded. Analysis of variance for repeated measurements together with t-testing and/or non-parametric testing was applied for significance testing of the study endpoints (α=0.05).
Results: Iopromide showed self-limited mean systolic/diastolic drops of 31/26mmHg (P<0.001). In contrast, iodixanol only produced mean changes for the lowest values of 2/0mmHg, similar to 3/2mmHg after NSS (P>.640). Compared with iodixanol, iopromide showed a statistically significant higher increase in heart rate (P=0.042) and 2-fold higher per-hour urine output (P=0.006).
Conclusion: Iso-osmolar iodixanol did not show the effect of systemic hypotension of low-osmolar iopromide. Radiologists and anesthetists should be aware of this effect during observation of anesthetized patients undergoing contrast-enhanced CT scans.

B-0147 11:10

The effect of iterative beam hardening correction on Agatston score: adaptive tube voltage modulation comes to calcium scoring

H. Haubenreisser[1], M. Meyer[1], N. Vogler[1], T. Allmendinger[2], S.O. Schönberg[1], T. Henzler[1]; [1]*Mannheim/DE*, [2]*Forchheim/DE (Holger.Haubenreisser@medma.uni-heidelberg.de)*

Purpose: To investigate the effect of lower tube voltages on Agatston scores processed with an adjusted iterative beam hardening correction (IBHC) filter.
Methods and Materials: 30 patients referred for cardiac CT examinations were included in the study. The patients were examined on a 3rd generation dual-source CT system, using 2 scans for calcium scoring. The first scan (gold standard) was done using accepted clinical parameters (120 kV tube voltage), while the second scan performed immediately after the first utilised adaptive tube voltage modulation (CareDose 4D, Siemens Healthcare, Forchheim, Germany), with an additional IBHC filter applied using an offline reconstruction workstation. The data was then re-imported to a clinical workstation and both scans (with and without IBHC) were each evaluated for vessel calcification.
Results: Compared to the gold standard, Agatston scored performed with lower tube voltages without an additional IBHC filter were found to vary by as much as ±27%. After the IBHC filter was applied, the overall variation was reduced to ±4%.
Conclusion: Utilising an adjusted IBHC filter for calcium scoring examinations opens up the possibility of performing these scans with adaptive tube voltage modulation activated, thus potentially reducing the applied radiation dose by a significant amount.
Author Disclosures:
H. Haubenreisser: Speaker; Siemens Healthcare, Bayer Healthcare. **M. Meyer:** Speaker; Siemens Healthcare. **T. Allmendinger:** Employee; Siemens Healthcare. **T. Henzler:** Speaker; Siemens Healthcare.

B-0148 11:18

CT imaging of the tricuspid valve in patients with tricuspid regurgitation: tailored contrast media protocol and dynamic analysis of the annulus

R.M.M. Hinzpeter[1], M. Eberhard[1], P. Burghard[2], F.C. Tanner[1], M. Taramasso[1], R. Manka[1], F. Maisano[1], G. Feuchtner[2], H. Alkadhi[1]; [1]*Zurich/CH*, [2]*Innsbruck/AT (Ricarda.Hinzpeter@usz.ch)*

Purpose: To introduce a tailored contrast media (CM) protocol for visualization of the tricuspid valve (TV) with cardiac CT and to analyse the dynamic dimensions of the tricuspid annulus (TA) in healthy subjects and patients with functional tricuspid regurgitation(FTR).
Methods and Materials: Fifteen patients with no cardiac abnormalities (=controls), 15 patients with FTR<3+ and 13 with FTR≥3+ (determined by echocardiography) underwent a three-phasic CM protocol for optimised visualization of the right heart. Using a segmentation and image analysis software, the annular area, the entire annular circumference, its anterior,

posterior and septal annular parts, and the antero-posterior and septo-lateral diameters were measured by two independent, blinded readers in end-systole and mid-diastole in 3D and 2D. Attenuation and standard deviation of attenuation (indicating homogeneity) were determined.
Results: The homogeneity of attenuation in the right heart showed a negative correlation with the degree of FTR (r=-0.61, P<.001). The interreader agreement was excellent for all measurements (ICC=0.995-0.999). Annular area, annulus and diameters were larger in patients with FTR as compared to controls (P<.05). There were significant differences between systole and diastole in controls, patients with FTR<3+ and those with FTR≥3+ for the area and annulus (all, P<.05). Anterior, posterior, septal and entire annulus were significantly smaller (all,P<.05) in 2D compared to 3D measurements (systematic underestimation 1.0-1.3mm), the difference decreasing with increasing FTR grades.
Conclusion: Using a tailored CM protocol allows for the dynamic analysis of the TA with cardiac CT, showing differences within and between patients with FTR and demonstrates systematic errors for 2D assessments.

B-0149 11:26

False-positive calcifications and radiation dose in coronary artery calcium scoring using iterative reconstruction with a noise threshold
M. Garmer, C. Lehrenfeld, F. Metz, O. Klein-Wiele, B. Brandts, D. Grönemeyer; *Bochum/DE (garmer@groenemeyer.com)*

Purpose: To determine the effect of iterative reconstruction in coronary artery calcium (CAC) scoring on false-positive lesions and radiation dose using a noise threshold in a large patient population. Semiautomatic software-based quantification of calcifications may be impaired by reduced signal-to-noise ratio. Noise-based thresholds have been previously suggested to reduce false-positive lesions in lower dose protocols.
Methods and Materials: The institutional review board approved this retrospective study of 388 matched pairs of patients with identical sex, age±5 years and BMI±2 points. We performed CAC scoring using a 320-row CT scanner with standard dose filtered backprojection (FBP) and lower dose adaptive iterative dose reduction in 3D (AIDR 3D). Patient-dependent dose modulation was based on a noise threshold. Radiation dose, image quality, CAC scores and extent of false-positive calcifications were obtained.
Results: AIDR 3D versus FBP showed reduced effective radiation dose (median mSv 0.85 versus 1.04; p<0.001), less noise (median SD 14.71 versus 18.07; p<0.001) and higher signal-to-noise ratio (median 4.01 versus 3.14; p<0.001). Using AIDR 3D in 388 patients, a low quantity of false-positive calcifications was found in 302 patients, a moderate quantity in 76 patients and a high quantity in 10 patients, while using FBP, the corresponding distribution of patients was 79, 175 and 134 (p<0.001).
Conclusion: CAC scoring using iterative reconstruction and a noise threshold is an appropriate technique for the reduction of radiation dose and improvement of image quality with the avoidance of false-positive calcifications.

B-0150 11:34

57% dose reduction in coronary artery calcium scanning by using lower kVp and advanced modeled iterative reconstruction
M. Vonder[1], G. Pelgrim[1], T. Henzler[2], R. Vliegenthart[1], M. Oudkerk[1]; [1]*Groningen/NL*, [2]*Mannheim/DE (marleenvonder@gmail.com)*

Purpose: To develop a dose-reduced coronary calcium scan protocol by using advanced dose reduction techniques, yielding similar outcomes as a conventional protocol.
Methods and Materials: A calcium insert with 100 small calcifications (size: 0.5-2.0mm, density: 90-540mgHA) was placed inside a thorax phantom and was scanned with 3rd generation dual-source CT. Scans were acquired at 90 ref mAs with 70,80,90,100,110 kVp and reconstructed with filtered back projection (FBP) and ADMIRE levels 1-5, resulting in 30 different scan protocols. For protocols that showed similar results as the conventional protocol of 120kVp-FBP, extra scans were acquired at 18-72 ref mAs. Differences and trends in image quality and calcium scores between the dose-reduced and reference protocol were analysed using Mann-Whitney U test, Independent samples median test and Kendall's τ_b.
Results: Overall, the number of detected calcifications (detection) and calcium scores (Agatston, volume, mass) decreased at increasing tube voltage (τ_b<-0.679, p<0.001) and levels of ADMIRE. (τ_b<-0.825, p<0.001). Detection and calcium scores were similar for 90kVp-IR 3 (p>0.206) and 100kVp-IR1 (p=0.206) compared to the conventional protocol. Detection and calcium scores (p>0.206) remained similar at 36-72 ref mAs with 90kVp-IR3 and 72 ref mAs with 100kVp-IR1 and image quality were similar or higher than the conventional protocol (0.008<p<0.206). Dose reduction from the conventional dose of 0.46mGy could be reduced to 0.20mGy and 0.36mGy for respectively 90kVp-IR3 and 100kVp-IR1.
Conclusion: A dose reduction of 22-57% can be achieved at 90kVp-IR3 and 100kVp-IR1, yielding similar calcium scores and image quality as the conventional protocol.

B-0151 11:42

High-pitch coronary CT angiography using the 3rd generation dual-source CT: initial experience in patients with high heart rate
L. Zhang, X. Liu, B. Feng; *Shenyang/CN (270973226@163.com)*

Purpose: To evaluate the feasibility, image quality and radiation dose of prospectively high-pitch coronary CT angiography in patients with high heart rate using the 3rd generation dual-source CT.
Methods and Materials: 100 consecutive high heart rate (HR) patients (male=56, female=44, 70<HR<100bpm) with suspected coronary artery disease and sinus rhythm were enrolled into this study. All patients were divided into two groups. Patients in group A (n=46) were performed CCTA with prospectively Electrocardiogram (ECG)-triggered high-pitch scan mode, image acquisition was triggered at the end-systolic phase about 30% in the R-R interval. Patients in group B (n=56) were underwent prospectively Electrocardiogram (ECG)-triggered sequential acquisition mode with acquisition window at 30%-50% of the R-R interval. The ascending aorta CT value, noise, signal-to-noise ratio (SNR) and contrast-to-noise ratio (CNR) with regard to adjacent fat tissue were evaluated. Subjective evaluation was also performed by using 4-point grading scale.
Results: In total, 100 patients, 400 coronary arteries and 1270 vessel segments were included in the statistical analysis. No statistical differences were found in image noise, SNR, CNR and subjective assessment of image quality between two groups. Diagnostic ratios were 89.1% vs 94.4% (patient-based), 95.1% vs 97.7% (vessel-based) and 97.8% vs 98.8% (segment-based), respectively (all p>0.05). However, radiation dose was significantly lower in group A (0.53±0.14mSv vs 1.33±0.17mSv, p<0.01).
Conclusion: In patients with HR > 70 bpm without cardiac arrhythmia, the prospectively high-pitch spiral acquisition at end-systolic phase can provide images with high diagnostic rate and significant low radiation dose as comparing with prospectively sequential acquisition mode.

B-0152 11:50

Non-inferior image quality in low-dose CCTA with knowledge-based iterative model reconstruction for overweight patient: unnecessary tube current modulation according to the body size
I.K. Park, C.H. Park, T.H. Kim; *Seoul/KR (serene@yuhs.ac)*

Purpose: The purpose of this study was to evaluate the feasibility of low-dose coronary CT angiography (CCTA), using knowledge-based iterative model reconstruction (IMR) and a fixed tube current in overweight subjects.
Methods and Materials: 40 non-overweight subjects (group A; body-mass index [BMI] < 25 kg/m2) and 40 overweight subjects (group B; BMI = 25-30 kg/m2), who underwent CCTA for coronary artery disease screening were retrospectively enrolled. All CT scans were performed on a 64-slice CT scanner at 100-kVp tube voltage and 150-mA tube current. CT images were reconstructed using IMR techniques. The CCTA images were qualitatively evaluated using a four-point scale (1=poor, 4=excellent) and further analyzed using a non-inferiority test with a pre-defined non-inferiority margin of -0.2.
Results: The mean noise of group A and group B was 26.0 ± 4.8 HU and 28.9 ± 4.3 HU, each (p = 0.005). The noise reduction ratio of IMR was 65.0% in Group A and 68.1% in Group B, compared to filtered back projection. The mean scale of image quality between two groups was insignificantly different (3.75 ± 0.04 vs. 3.71 ± 0.04, p = 0.478). The non-inferiority of the CCTA image quality in Group B was demonstrated using a pre-defined non-inferiority margin of -0.2 (mean difference = -0.043, 95% CI = -0.162-0.077).
Conclusion: Low-dose CCTA with IMR can be applied to overweight subjects, without tube current modulation based on the patient's body size.

10:30 - 12:00 **Room M 2**

Paediatric

SS 212

Paediatric cardiothoracic imaging

Moderators:
A. Secinaro; Rome/IT
E. Sorantin; Graz/AT

B-0153 10:30

Evaluation of paediatric radiology services in hospitals in the UK

K. Halliday[1], K. Drinkwater[2], D.C. Howlett[3]; [1]*Nottingham/UK*, [2]*London/UK*, [3]*Eastbourne/UK (kath.halliday@nuh.nhs.uk)*

Purpose: To compare paediatric radiology provision across the UK with national standards published by the Department of Health and the Royal College of Radiologists (RCR).
Methods and Materials: Audit standards and indicators for paediatric imaging were derived from "Delivering quality imaging services for children", "Standards for imaging in cases of suspected non-accidental injury" and "Improving paediatric interventional radiologyservices"and agreed jointly by the Clinical Radiology Audit Committee and the British Society of Paediatric Radiology. A questionnaire was sent to all hospitals and NHS trusts imaging children aged 16 or younger in the UK in October 2013. The target for all indicators was 100%. Eighty-seven of 196 (44%) eligible institutions submitted data.
Results: Only 65% of paediatric images were obtained by staff who had had specific training and only 60% were reported by radiographers or radiologists with appropriate training. Sixty-two percent of centres did not have access to a paediatric opinion 24 hours a day, 7 days a week all year; only 34% of radiographers who regularly imaged children had had any access to continuing professional development (CPD) in the 12 months of the audit. Although all hospitals had facilities for image transfer, only 57% had any formal funding arrangements in place for external reporting of images.
Conclusion: The standards set for a network approach to paediatric radiology provision in "Delivering quality imaging services for children" are largely unmet. This failure to make the most of the workforce and resources puts vulnerable children at risk.

B-0154 10:38

CT lung perfusion in the long-term follow-up of congenital left-sided diaphragmatic hernia: results in a cohort of 28 children

M. Remy-Jardin, T. Duchaussoy, A. Deschildre, V. Deken, A. Duhamel, J. Remy; *Lille/FR (martine.remy@chru-lille.fr)*

Purpose: To evaluate lung perfusion on dual-energy (DE) lung-perfused blood volume (PBV) images in the long-term follow-up of left-sided congenital diaphragmatic hernia.
Methods and Materials: CT angiographic examinations were obtained in 28 children (mean age: 10.9±-3.6 yr) with evaluation of the following parameters: (a) on CT angiograms, ipsilateral and controlateral lung appearance (volume; attenuation); (b) on iodine maps, the pattern of lung perfusion and level of attenuation on both sides.
Results: For 11 children (Group 1; 39%): (a) lung perfusion was homogeneous and symmetrical (left: 38.20±10.64HU; right: 42.01±14.24HU; p=0.08); (b) the left lung showed mild hypoplasia (6/11) or normal volume (5/11); (c) the right lung had normal volume and attenuation in all cases. For 17 children (Group 2; 61%): (a) lung perfusion on the left side was abnormal with a mean attenuation on iodine maps significantly lower than that measured on the right lung (39.0±17.9HU vs 52.53 ±20.97HU; p<0.0001); (b) the left lung showed various degrees of hypoplasia (15/17) or a normal volume (2/17); (c) the right lung showed morphological and/or perfusion alterations in 6 children (6/17). Perfusion alterations observed on the right lung were depicted in 21% of the study group (6/28), always seen in Group 2 patients.
Conclusion: Lung perfusion alterations were identified in the lungs of children who underwent congenital diaphragmatic hernia ipsilateral to the hernia side in 61% of cases and in the controlateral lung in 21% of cases.
Author Disclosures:
M. Remy-Jardin: Research/Grant Support; Siemens Healthcare. **J. Remy:** Consultant; Siemens Healthcare.

B-0155 10:46

High-temporal resolution chest CT examinations in infants and young children without sedation or general anesthesia: frequency and severity of motion artifacts

S. Khung, M. Remy-Jardin, N. Lassalle, T. Santangelo, A. Deschildre, J. Remy; *Lille/FR (martine.remy@chru-lille.fr)*

Purpose: To evaluate the frequency and severity of motion artifacts on chest CT examinations acquired without sedation nor general anesthesia in infants and children younger than 5 years.
Methods and Materials: The study population included all consecutively registered infants and young children (age <5 years) who had been referred for a standard chest CT examination on a third-generation, dual-source CT system (pitch: 3.0; rotation time: 250 ms). For each examination, we recorded (a) the number of acquisitions necessary to reach a diagnostic image quality, (b) the frequency and severity of motion artifacts using a 4-point scale (0: no artifact ; 1: mild; 2: moderate ; 3: severe) and (c) the diagnostic value of each acquisition.
Results: The study population comprised 343 patients (mean age: 14.92 months); the mean duration of data acquisition was 0.23±0.05s. For 330 patients (96.2%), the investigation comprised a single acquisition, rated as follows: (a) no motion artifact over the entire thorax (n=193); (b) presence of motion artifacts that did not affect the overall diagnostic value of the examination (n=137) with a mean score of artifact of 0.72. In 13 patients (3.8%): (a) the acquisition was rated as nondiagnostic due to the presence of severe artifacts (mean score: 1.62); (b) a second acquisition was then performed, rated as diagnostic in 13 cases (mean score of artifact: 0.47) and non-diagnostic in 1 patient.
Conclusion: Diagnostic image quality is obtained with a single examination in 96.2% of children scanned while freely breathing.
Author Disclosures:
M. Remy-Jardin: Research/Grant Support; Siemens Healthcare. **J. Remy:** Consultant; Siemens Healthcare.

B-0156 10:54

Functional magnetic resonance imaging compared to lung function in primary ciliary dyskinesia

S. Nyilas[1], G. Bauman[2], G. Sommer[2], O. Pusterla[2], F. Singer[1], O. Bieri[2], C. Heyer[3], C. Koerner-Rettberg[3], P. Latzin[1]; [1]*Berne/CH*, [2]*Basle/CH*, [3]*Bochum/DE (sylvia.nyilas@insel.ch)*

Purpose: Primary ciliary dyskinesia (PCD) is characterised by functional abnormalities of the cilia, leading to chronic airway infection and remodeling. Lung function tests like inert gas washout measurements detect ventilation inhomogeneity, but cannot determine its origin. Novel magnetic resonance imaging (MRI) methods such as Matrix Pencil (MP) decomposition MRI can visualise functional changes in the lung without the administration of contrast agents and the need for breathing maneuvers. This study investigates the correlation between functional and morphological MRI and lung function indices in patients with PCD.
Methods and Materials: Thirty-one patients with PCD (mean age 13.5 years, range 5-28) underwent MRI and lung function tests on the same day. Functional MP-MRI provided semi-quantitative measures of the perfusion (RQ) and ventilation (RFV) impairment as percentages of the affected lung volume. Morphological MRI was evaluated using a score derived from cystic fibrosis. Lung function tests provided information about global (lung clearance index, LCI) ventilation inhomogeneity.
Results: Both MP-MRI and inert gas washout measurements detected functional impairment in PCD: R_{FV} ranged from 12% to 27% and R_Q ranged from 11% to 28%. R_{FV} and R_Q were moderately correlated with LCI (r=0.5, p=0.03; r=0.4, p=0.05, respectively). Total morphology scores as well as sub-scores strongly correlated with LCI.
Conclusion: Functional MP-MRI is a novel, sensitive and non-invasive method to detect and visualise perfusion and ventilation abnormalities. For the first time we could show a correlation between a lung function test and a functional and structural MRI in patients with PCD.

B-0157 11:02

3T MR T1 mapping after arterial switch operation in patients with transposition of the great arteries

K. Rydén Suther, E. Hopp, O. Geier, H. Brun, B. Nguyen, A. Tomterstad, H. Lindberg, A.E. Fiane, C. de Lange; *Oslo/NO (kathrine79@me.com)*

Purpose: Coronary artery patency is of major concern in young patients corrected for transposition of the great arteries (TGA), but is there development of diffuse myocardial fibrosis? We explored coronary ostia and presence of myocardial fibrosis in this patient group corrected with arterial switch operation (ASO).
Methods and Materials: Thirty-three corrected TGA individuals(10-15 years) were examined with 3T MR and compared to 15 healthy controls(18-25 years).

Gd-enhanced 3D fast low-angle shot coronary MRA was performed (n=45), in addition to modified look-locker inversion recovery before (n=48) and after intravenous contrast (n=45) followed by late gadolinium enhancement (LGE) (n=45). Native T1 was measured and extracellular volume fraction (ECV) was calculated in the coronary artery distribution territories of the left ventricular wall. Statistical analyses were performed using independent t-test and Mann-Whitney test.
Results: No LGE was observed and all coronary artery ostia were visualised. Mean(SD) native T1 measurements were in right coronary artery (RCA) 1228(62) ms, left anterior descending artery (LAD) 1260(134) ms, circumflex artery (CX) 1226(86) ms in the TGA group, and in the controls 1226(57) ms, 1197(51) ms and 1168(59) ms respectively (p=.02). ECV was increased in all the coronary distribution territories in the TGA group; RCA 0,30(0,05), LAD 0,29(0,05) and CX 0,29(0,06) in comparison to the controls 0,27(0,04), 0,26(0,03) and 0,25(0,04), respectively (p<.02).
Conclusion: All ASO corrected TGA patients had patent coronary artery ostia but compared to controls they had increased pre-contrast T1 values and ECV. This indicates diffuse myocardial fibrosis in all distribution areas of the coronary arteries.

B-0158 11:10

Image quality comparison of applied and exploratory weight-dependent exposure charts of lower doses in paediatric chest radiography: a multi-centre study of a mobile DR systems
K. Shahgeldi, T. Svahn, R. Lesanu; *Gävle/SE*
(kaveh.shahgeldi@regiongavleborg.se)

Purpose: To compare the image quality of different applied exposure charts in paediatric chest radiography and settings associated with lower doses.
Methods and Materials: Two clinics employed imaging charts of different x-ray energy spectrum (tube load and tube voltage) for paediatric chest imaging (patient weight: 10-20 / 20-30kg) for the same model of mobile x-ray unit. Using these clinical charts, and settings of lower doses, images were acquired in the anterior-posterior projection view of a paediatric anthropomorphic phantom (~20 kg). Fourteen radiologists evaluated the quality of images in a blinded side-by-side study. The different settings were compared in a multiple-reader multiple-case analysis using one of the clinical charts as a reference. Effective dose for the different exposure settings was computed using a Monte-Carlo-based software, PCXMC (Finnish Radiation and Nuclear Safety Authority, Helsinki, Finland).
Results: The different clinical imaging charts, high vs. intermediate x-ray spectrum, had comparable image quality and resulted in approximately the same effective dose. When lowering the tube voltage from that of the applied exposure charts, the lower kV-settings (75/85kV) had comparable quality at a reduced effective dose with 35%. For settings resulting in 50% lower doses, differences were detected ($p < 0.05$) but were mainly recognised as being of slightly worse quality (relative the reference settings).
Conclusion: Effective dose could be decreased with up to 35% of that of the applied settings, while maintaining image quality. Lower energies in paediatric chest radiography offer dose savings by yielding a higher image quality/effective dose.

B-0159 11:18

Quality of paediatric AP/PA chest radiographs based on EC-guidelines - realisable in daily routine at an academic paediatric radiology division?
P.-C. Krüger, F. Schmidt, S. Otto, S. Langner; *Greifswald/DE*
(paul-ch.krueger@uni-greifswald.de)

Purpose: In a paediatric population, as the most radiation-sensitive patients, accurate collimination to reduce unnecessary irradiation and improve image quality are of utmost importance. For AP/PA chest radiographs the European Commission (EC) guideline 16261 provides minimal field size with an age-dependent tolerance. Quality criteria of this guideline were evaluated qualitatively and quantitatively in an academic paediatric radiological division.
Methods and Materials: During a one year period 1238 chest radiographs (58% male, 42% female, age: 0-17years) were evaluated using a semi-automatic tool. Quality criteria, minimal field size and overexposure were assessed based on EC guideline criteria.
Results: Overall only 4,4% of all images completely fulfilled the EC-guidelines. Most correct radiographs (14,1%) were made of infants (1-12 months). Generally, 46,3% were rated as under-, 43,9% as overexposed. Mean overexposure (52,2%±29,2%; range: 4,7% to 325,6%) and tissue overexposure (41,5%±27,5%; range: 0,0% to 272,7%) were differentiated. Diagnostic requirements were virtually confirmed, except deep inspiration and rotation/tilting. Age-dependently both criteria increased (successful deep inspiration: newborn: 21,2%; early adolescents: 81,6%). Furthermore, images were analysed to the commissioned radiological section. Overexposure was significantliy increased when images were acquired on newborn ICU (69,6%) compared to paediatric ICU (56,7%; $p<0.05$) and the radiological department (44,6%; $p<0.05$).
Conclusion: The EC-guidelines are indispensable to protect children from unnecessary radiation exposure. In daily routine the feasibility was constricted, especially on ICU. Semi-automated quality assessment is a fast and reliable tool to improve patient care.

B-0160 11:26

Role of lung ultrasound in the evaluation of pneumonia in children
I. Sefic-Pasic, A. Dzananovic, A. Pasic, S. Vegar Zubovic; *Sarajevo/BA*
(irmina.sefic@gmail.com)

Purpose: To introduce basic principles of lung ultrasound (analysis of appearance of specific ultrasound artifacts) technique and ultrasound findings in community acquired pneumonia found in paediatric population, and to compare it with x-ray.
Methods and Materials: Lung ultrasound were performed prospectively (Feb 2015 - Sep 2016) in 40 children (23 boys and 17 girls) with positive clinical and laboratory signs of impaired pulmonary function, suspected to pneumonia and ultrasound findings were compared with chest x-ray. All ultrasound examinations were performed with linear-array probes 7,5 and 10 MHz. Right and left lung were examined with anterior, posterior and lateral approach. Interpretations of findings have been done by two radiologists, one blinded to x-ray study and vice versa and results were compared with statistical analysis.
Results: In the cohort of 40 patients, bacterial pneumonia was confirmed in 37. On ultrasound we found pathological findings presented with B lines, consolidation of parenchyma, pleural effusion, empyema and abnormalities of pleural line. Sensitivity of ultrasound was 97%, specificity 75%, positive predictive value 94.8% and negative predictive value of x-ray 60%. Low specificity of lung ultrasound can be explained with the fact that consolidations of lung parenchyma found in two patients have been differentiated as tuberculous infections,and were considered statistically as false positive.
Conclusion: Lung ultrasonography is suitable for routine use, diagnosing and follow-up, and it can sufficiently replace chest x-ray in mild and uncomplicated cases of pneumonia in children. It should be incorporated in diagnostic algorithm of lungs evaluation in paediatric population.

B-0161 11:34

Role of lung ultrasound in paediatric intensive care units: comparison with bedside chest radiography
M. Mughetti, G. Napoli, A.M. Chiesa, F. Ciccarese, P. Bertaccini, M. Zompatori; *Bologna/IT (martinamughetti@gmail.com)*

Purpose: To compare the diagnostic performance of lung ultrasonography and chest radiography for the detection of common pathologic abnormalities.
Methods and Materials: Thirty-three children admitted in intensive care-unit were prospectively studied, for a total amount of 64 LUS and 64 CXR performed. Consolidation, alveolar-interstitial syndrome, pneumothorax, and pleural effusion were evaluated.
Results: Pleural effusion was demonstrated in 6 CXR examinations, while 20 LUS exams resulted positive. Pneumothorax was detected in 1 CXR exam as well as in LUS. Alveolar-interstitial syndrome was detected in 44 CXR while in 39 LUS. Consolidation was diagnosed in 33 CXR while in 43 LUS. Agreement analysis showed perfect overall agreement between LUS and CXR for pneumothorax diagnosis (100% agreement, Cohen Kappa coefficient 1), substantial agreement for pulmonary consolidation (84%, K 0,68), moderate agreement for alveolar-interstitial syndrome (76%, K 0,49) and fair agreement for pleural effusion (75%, K 0,28). The Z score was statistically significant for the 4 abnormalities detected with CXR and LUS. 3 LUS examinations were negative versus 7 negative CXR (94% agreement, K 0,000).
Conclusion: LUS is both feasible and convenient in the critical care paediatric units and may eventually replace CXR and HRCT at least if it results negative and eventually for the follow up of these common pathologic entities.

B-0162 11:42

The effect of iodinated contrast administered during a CT pulmonary angiogram during pregnancy on neonatal thyroid function
S. Culleton, A. Egan, B. Buckley, T. Tarmey, D. O'Donovan, P. Mayne, D. Sheppard; *Galway/IE (cullets@tcd.ie)*

Purpose: CT pulmonary angiogram (CTPA) is a frequently performed test to evaluate for pulmonary emboli in pregnancy. Current guidelines recommend checking neonatal thyroid function in the first week of life as there is a risk of hypothyroidism. This retrospective study assessed the effect of in utero exposure to iodinated contrast on neonatal thyroid stimulating hormone (TSH) screening results.
Methods and Materials: All CTPAs performed on pregnant females at Galway University Hospital during 2011-2015 were reviewed. The neonatal TSH screening records were reviewed. A control group of 106 unexposed infants was from same time period were chosen.
Results: TSH neonatal screening records for 81 babies were identified. In the exposed group two infants had abnormal screening results and were normal when repeated. There were no confirmed cases of neonatal hypothyroidism

due to exposure to contrast in utero. The control group of 106 neonates had no abnormal results. There was no statistically significant difference between the control and exposed values for TSH (p =0.4). This study also looked at the number of weeks pre-delivery that the babies had been exposed to iodine from weeks 1-5, 5-10 and greater than 10 weeks and there was no significant difference between the groups (p =0.6).
Conclusion: This study showed no adverse effect on neonatal thyroid function following a single exposure to iodinated contrast in utero.

B-0163 11:50

Effect of high concentration iodinated contrast medium in euthyroid children

A. Clemente, F. Avogliero, A. Di Giambattista, D. Della Latta, D. Chiappino; *Massa/IT (andreadigia@gmail.com)*

Purpose: To assess the effect of administration of high concentration iodinated contrast medium (HCICM) on the thyroid function in a population of children <4 years of age undergoing CT-angiography for cardiac surgery planning.
Methods and Materials: We evaluated 46 patients (m = 26, f = 20, mean age:1 ± 0.86 years) from April 2013 to October 2015 admitted for congenital heart disease. Preoperative CTA was performed by administration of non-ionic triiodate contrast medium (iopromide 370 mg / ml, 1.14± 0.17 ml / kg). Exclusion criteria: thyroid hormone abnormalities at admission. TSH, fT3, fT4 were collected at admission, 48 hours after the CT scan and at discharge (20 ± 21 days) and indexed for haematocrit.
Results: TSH/Ht (admission): 0.11±0.10; TSH/Ht (48h): 0.02±0.03; TSH/Ht (discharge):0.08±0.06. fT3/Ht (admission): 0.08±0.02; fT3/Ht (48h): 0.07±0.03; fT4/Ht (discharge): 0.09±0.03. fT4/Ht (admission): 00:03±0.01; fT4/Ht (48 h): 0.03±0.01; fT4/Ht (discharge):0:03±0.01. Compared to admission values, a significant decrease was found in TSH at 48h ($p<0.05$). TSH to 48 hours was reduced respect to normal values indexed for haematocrit in 29 patients (63% of cases). A non-statistically significant trend was found in reduction of fT3 at 48 h (14 cases, 30%). No significant differences were found in comparison of the other values.
Conclusion: The use of HCICM in children is associated with a temporary but significant reduction in TSH values at 48h with normalised valued at discharge. Thyroid hormonal status in not significantly altered by HCICM in euthyroid children.

10:30 - 12:00 **Room M 3**

Oncologic Imaging

SS 216

Imaging and predicting treatment response and outcome in oncology

Moderators:
A. Fohlen; Caen/FR
J. Sosna; Jerusalem/IL

B-0164 10:30

Histogram analysis of ADC from whole-body DW-MRI (WB DW-MRI) to predict very early response to chemotherapy in patients with metastatic colorectal cancer (mCRC): preliminary results

I. Lavdas, E. Daulton, A.G. Rockall, L. Honeyfield, K. Kozlowski, E. Aboagye, R. Sharma; *London/UK (emilydaulton@doctors.org.uk)*

Purpose: We evaluated apparent diffusion coefficient (ADC) histogram analysis parameters from WB DW-MRI as very early predictors of response to chemotherapy in patients with mCRC.
Methods and Materials: 11 patients with histologically confirmed mCRC were scanned with WB DW-MRI (b=0, 50, 150, 500, 900 s/mm^2) at 1.5T, before and 10.8±2.7 days after commencing chemotherapy. Response was assessed by the final clinical RECIST 1.1. For analysis, patients were grouped as progressive or non-progressive disease. Mean ADC and histogram analysis parameters (skewness, kurtosis, 25th., 50th. and 75th. percentile) were calculated. Parameters were compared between baseline and follow-up scans using a Wilcoxon signed rank test.
Results: 8 patients did not progress and 3 patients progressed on treatment. Skewness and kurtosis were significantly lower at follow-up (2.57±2.65 vs. 0.93±1.09 and 26.6±36.1 vs. 5.9±6.5 with P=0.003 and P=0.001 respectively) for non-progressors, whilst for progressive disease skewness and kurtosis was higher at follow-up (1.16±0.63 vs. 1.35±1.30 and 6.08±3.44 vs. 11.10±14.04 with P=0.89 and P=0.57 respectively). There was no significant difference between baseline and follow-up in the mean ADC and percentiles for any of the groups.
Conclusion: Skewness and kurtosis are ADC histogram parameters that can potentially separate between progressive and non-progressive disease in patients with mCRC, scanned with WB DW-MRI. This promising 'one-stop-shop' response assessment methodology is ready for use in a larger trial.

B-0165 10:38

Comparison of imaging response criteria in metastatic melanoma patients treated with immune checkpoint inhibitors: a single institution analysis

M. Morone[1], L. Spain[1], J. Winfield[2], T. Schmid[2], D.-M. Koh[1], C. Messiou[1], D. Collins[1], A. Sohaib[1], J. Larkin[2], M. Bali[1]; [1]*Sutton/UK*, [2]*London/UK (mariomorone@libero.it)*

Purpose: Immune-related response criteria (irRC) is increasingly used for assessing tumour response in patients treated with immunotherapy. However, it is unclear how response categorisation by irRC is directly compared with other criteria. We applied Response Evaluation Criteria in Solid Tumours (RECIST 1.1), irRC, Choi and revised-Choi response criteria and compared their associated progression free survival (PFS) and overall survival (OS) in melanoma patients treated with immunotherapy.
Methods and Materials: After institutional review board approval, 144 patients (65% male, mean age 59) treated with Ipilimumab (Group 1, n=100) and Pembrolizumab or Nivolumab (Group 2, n=44) were identified. CT images acquired at baseline, 3- and 6-months after treatment were analysed. A radiologist categorised response according to the above four criteria. Patients demonstrating complete response (CR), partial response (PR) or stable disease (SD) were responders (R); patients with disease progression (PD) were non-responders (NR).
Results: For Group 1, all criteria showed significant differences between R and NR for PFS and OS at 3- and 6-months after therapy (log-rank test $p<0.05$; hazard ratio between 2.7 and 3.6 for PFS, and between 2.2 and 3.4 for OS, across four criteria). For Group 2, all criteria showed significant differences between R and NR for PFS at 3- and 6-months ($p<0.05$; hazard ratio between 4.2 and 14.4) but not for OS ($p>0.05$).
Conclusion: The four imaging response criteria were comparable for patient categorisation of R and NR and for stratification of PFS and OS. IrRC may not provide additional information for the majority of patients on immunotherapy.

B-0166 10:46

3D imaging biomarkers: prediction of survival in patients with non-small cell lung cancer brain metastases treated with stereotactic body radiation therapy

M. Della Seta[1], D. Kaul[1], J. Chapiro[2], B. Hamm[1], F. Collettini[1]; [1]*Berlin/DE*, [2]*New Haven, CT/US (marta.della-seta@charite.de)*

Purpose: To investigate the value of 3D-quantitative tissue enhancement as an early imaging biomarker for patient survival in patents with non-small cell lung cancer (NSCLC) brain metastases treated with stereotactic body radiation therapy (SBRT).
Methods and Materials: 27 patients with NSCLC brain metastasis were treated with SBRT. Baseline contrast-enhanced MRI (ceMRI) was used for image analysis using the qEASL tool (IntelliSpace Portal V.8, Philips Healthcare). A segmentation-based 3D-quantification was performed in each patient to measure the relative tumour enhancement in each lesion. A cut-off value of 65% lesion enhancement was used to stratify the patient cohort in two groups (<65% and >65% volumetric lesion enhancement). Survival was evaluated using Kaplan-Meier analysis and compared using the Mantel-Cox Log-rang test as well as proportional hazard ratios (HR).
Results: Median OS of the entire population was 6.0 months. The stratification of the cohort according to the 65% cut-off for the relative enhancing tumour volume achieved statistical significance p=0.0452 (HR, 2.2 [95% CI, 1.1-6.8]). Patients with >65% enhancing lesion volume survived significantly longer than patients with relatively less-enhancing tumour lesions (8.15 months vs. 2,09 months [HR 0.25; 95% CI, 0.11-0.58], respectively). The total tumour volume did not achieve a statistically significant separation of survival curves.
Conclusion: As opposed to the total tumour which currently is the most commonly used staging marker, volumetric assessment of metastatic NSCLC lesion enhancement on baseline ceMRI is strongly associated with patient survival after SBRT. Specifically, patients with hyper-enhancing lesions demonstrated improved survival as compared to those with hypo-enhancing lesions.
Author Disclosures:
J. Chapiro: Research/Grant Support; Philips Healthcare, GIF, Günther Foundation, NIH/NCI RO1. **B. Hamm:** Research/Grant Support; Toshiba Corporation Research Grant, Koninklijke Philips NV Research Grant, Siemens AG Research Grant, General Electric Company Research Grant, Elbit Imaging Ltd Research Grant, Bayer AG Research Grant, Guerbet SA Research Grant, Bracco Group Research Grant, B. Braun Melsungen AG Research Grant, KRAUTH medical KG Research Grant. **F. Collettini:** Research/Grant Support; Berlin Institute of Health, GIF.

B-0167 10:54

DWI and ADC in assessing early response to angiogenesis inhibitors in metastatic renal cell carcinoma

C. Marigliano, C. Sgrazzutti, A. Vanzulli; *Milan/IT (kiarmn@gmail.com)*

Purpose: Angiogenesis inhibitors have a potential role in treating metastatic renal-cell carcinoma, but it is still not clear why only some patients can benefit of this treatment protocol. Objective was to look for DWI parameters able to identify early response to angiogenesis inhibitors in patients with metastatic renal-cell carcinoma, considering RECIST1.1 as reference Standard.
Methods and Materials: We prospectively enrolled twenty-four patients candidate to start angiogenesis inhibitors with at least one target lesion and who underwent 1,5T MRI examination with multiple b-values DWI sequences (0,40,200,300,600) in specific timeline: one week before (T0), 2 weeks after (T2) and 8 weeks after (T8) treatment beginning. ADC value was calculated drawing ROIs on the lesions. Twenty-one patients with 30 lesions had adeguate data for comparative evaluation.
Results: At T2 six patients had early response. At T8 4 patients had partial response (PR), 15 disease control (DC), 2 progression disease (PD); average progression free survival was 273 days. PR group, as compared to DC or to PD showed higher T0 ADC values at b40 (respectively 5,5(1,4),3,6(1,2), 1,7(0,9) avg(SD)): we can assess that more vascularised lesions are more responsive to treatment. PD group have significantly lower ADC values then both other groups, at T0, T2 and T8, for all b-values.
Conclusion: Results show that ADC at T0 may help selecting patients with promising good response to angiogenesis inhibitors. Moreover at T0 and at T2 ADC has the potential to select patients who wouldn't benefit from treatment (early progression disease).

B-0168 11:02

CT texture analysis as a predictor of response to therapy and prognosis in patients with metastatic renal cell carcinoma treated with first-line tyrosine kinase inhibitors

G. Bonera, G. Agazzi, M. Ravanelli, D. Farina, V. Ferrari, A. Berruti, R. Maroldi; *Brescia/IT (gei.bonera@gmail.com)*

Purpose: To investigate if texture analysis (TA) on pretreatment contrast-enhanced CT (CECT) images can predict response to tyrosine kinase inhibitors (TKI) and prognosis in patients with metastatic renal cell carcinoma (mRCC).
Methods and Materials: 65 pretreatment CECT studies of mRCC patients treated with first-line TKI were retrospectively reviewed. Objective response was assessed every 3 months according to RECIST 1.1 and modified Choi (mChoi) criteria. TA was performed on a 5-mm-thick central slice for each target lesion using a commercially available software (TexRAD Ltd, UK). Primary texture features and a novel HeteroDensity Index (HDI), accounting for size-standardised heterogeneity and mean pixel density, were quantified using different spatial-scale filters (ssf). Per-patient texture features were correlated with objective response, progression-free and overall survival (PFS, OS) using logistic regression and survival analysis, statistical significance was corrected to control false discovery rate.
Results: Primary texture features were not able to discriminate responders and non-responders. HDI obtained with a 3-mm ssf (ssf3) was positively correlated with objective response (odds ratio 0.14 for RECIST and 0.2 for mChoi criteria, p 0.018 and 0.026, respectively). Low ssf3 HDI was associated with worse PFS (hazard ratio 4.14, p 0.0001) and OS (hazard ratio 3.36, p 0.0008).
Conclusion: TA on pretreatment CECT helps to predict objective response and prognosis in mRCC patients treated with first-line TKI.

B-0170 11:10

DCE-MRI to assess pathological response to neoadjuvant chemotherapy for high-grade soft tissue sarcomas

A. Crombe[1], X. Buy[1], N. Alberti[2], M. Toulmonde[1], E. Stoeckle[1], J.-M. Coindre[1], A. Italiano[1], M. Kind[1]; [1]*Bordeaux/FR*, [2]*Contamines-sur-Arve/FR (crombeamandine2@gmail.com)*

Purpose: Aim of this pilot study is to determine if DCE-MRI parameters or their changes show significant differences between good and poor responders to neoadjuvant chemotherapy in high-grade soft tissue sarcomas.
Methods and Materials: 23 patients underwent DCE-MRIs after 2 courses of chemotherapy (MRI-1) and at the end of neoadjuvant protocol, before curative surgery (MRI-2), in our tertiary referral center. 17/23 patients had an available initial MRI (MRI-0). MRIs were performed on two 1.5T-MR-systems with same acquisition parameters and post-processing. Surgical specimens pathological analysis was the gold standard: good response was defined as <10% of viable tumour (11/23) and poor response as ≥50% (12/23). Morphological features on conventional sequences and their changes were reported by two radiologists. For DCE-MRI analysis, ROIs were manually and consensually drawn on tumoural tissue component and on healthy muscle to obtain ratio for each parameter. The wash-in (WI), peak-enhancement (PE), area-under-curve 180s (AUC180) were calculated for semi-quantitative analysis using Olea software. The volume transfer constant (Ktrans) was calculated using extended-Tofts-Kety model. Permeability-curves and AUC180 density-histogram were obtained and scored according to an 8-points qualitative scale.
Results: WI-ratio, PE-ratio, AUC-ratio and Ktrans-ratio on MRI-2 were significantly decreased in good responders (respectively, p=0.04, 0.015, 0.017, 0.018) while differences did not reach significance on early MRI-1. Evaluation of permeability-curve and AUC180 histogram showed early and late significant modifications (p=0.025 and 0.0005).
Conclusion: Qualitative, semi-quantitative and quantitative DCE-MRI may be helpful as an additional technique in evaluating response to chemotherapy in high-grade soft tissue sarcoma.

B-0171 11:18

Response to neoadjuvant chemotherapy of skeletal-osteosarcoma/Ewing sarcoma on the basis of MRI 18-FDG-PET by correlating with pathological necrosis

D.P. Wali[1], S. Gupta[2]; [1]*Bangalore/IN*, [2]*Mumbai/IN (wali.praveen@gmail.com)*

Purpose: To establish pre/post-chemotherapy MRI and PET-CT scans are as effective as histopathological assessment in assessing response to neoadjuvant-chemotherapy.
Methods and Materials: 34 biopsy proven patients of osteosarcoma/Ewing sarcoma prospectively studied pre/post-chemotherapy for response evaluation by MRI and PET-CT in P. D. Hinduja Hospital-Mumbai. Comparison by assessing post-chemotherapy response in these patients using dynamic contrast MRI/DW-MRI. Post-chemotherapy scans analysed by radiologist and nuclear-medicine specialist without knowledge of neoadjuvant-chemotherapy status.
Results: Paired sample t-test used to analyse change in percentage volume of tumour in pre/post-chemotherapy patients. Mean ADC values in pre/post-chemotherapy were 0.8964 and 2.8043. ADC values in post-chemotherapy responders and non-responders were 3.5437 and 1.8536. Positive correlation between necrosis rate and increased ADC values in post-chemotherapy patients was observed. In post-chemotherapy patients positive correlation was observed between percentage change of volume and percentage change of SUV value. Change in DCE curve types in post-chemotherapy patients were evaluated using chi square test.
Conclusion: Advanced MRI techniques complement standard MRI but remain insufficiently used. DWI/DCE sequences are significantly effective in preoperative response evaluation to chemotherapy in patients with osteosarcoma/Ewing sarcoma patients. Conventional MRI not effective in response evaluation to chemotherapy as much as PET-CT. Preoperative response evaluation by non-invasive imaging modality like MRI helps deciding management and surgical procedure to be either limb salvage or amputation.

B-0172 11:26

Can diffusion-weighted MR imaging be used for prediction and monitoring of treatment response in gall bladder carcinoma?

L. Singh, R. Sharma, D. Kandasamy, M. KS, S. Gamanagatti, R. Sahoo, A. Sharma, P. Garg, P. Sahni; *New Delhi/IN (luv_ldh@yahoo.co.in)*

Purpose: Response evaluation in gall bladder carcinoma (Ca GB) is traditionally done after completion of 3-4 cycles of chemotherapy according to size criteria based on Response Evaluation Criteria in Solid Tumours (RECIST). We hypothesised that apparent diffusion coefficient (ADC) value can be used as an early marker of response to chemotherapy in Ca GB.
Methods and Materials: In this study 23 patients were evaluated. MRI was done at baseline, after 1st (early time point) and 3rd cycle of chemotherapy. Percentage change in size after 3 cycles of chemotherapy was taken as the gold standard to assess response based on RECIST. Total 22 primary masses, 32 lymph nodes and 18 liver metastases were evaluated. Baseline ADC was compared between responders and non-responders. To assess response to chemotherapy percentage ADC change at early time point was compared between responders and non-responders.
Results: Mean percentage increase in ADC at early time point for primary mass, lymph nodes and liver metastases was significantly higher in responders (24.8%, 29.6%, 15.9%) than non-responders (11.5%, 6.9%, 0.8%) respectively (p= 0.02, 0.0001, 0.04). There was no significant difference between baseline ADC of responders and non-responders in primary mass (p= 0.46). Area under curve (AUC) for percentage change in ADC for differentiating responders at early time point was 0.79 for primary mass, 0.89 for lymph nodes 0.79 for liver metastases respectively.
Conclusion: Increase in ADC can be used for early assessment of response to chemotherapy in Ca GB. However baseline ADC cannot predict response to chemotherapy.

B-0173 11:34

CT-based tumour heterogeneity analysis in pancreatic carcinoma allows prediction of progression

J.P. Steinacker[1], N. Stanescu-Siegmund[1], T. Ettrich[1], M. Baumhauer[2], T.F.E. Barth[1], M. Kornmann[1], A. Beer[1], M. Beer[1], S.A. Schmidt[1]; [1]*Ulm/DE*, [2]*Dossenheim/DE*

Purpose: Imaging in pancreatic cancer is a challenge regarding therapy response evaluation. Tumour size, attenuation, and perfusion are widely used as measurable parameters, but are often limited by blurry tumour borders and missing qualitative parameters. We tested this new CT-based approach of tumour heterogeneity feature analysis for monitoring therapy response.
Methods and Materials: 13 patients with pancreatic adenocarcinoma undergoing portalvenous abdominal computed tomography according to standard as baseline imaging with clinical follow-up and imaging (timespan median 64 days) under systematic therapy (FOLFIRINOX/Gemcitabin) were retrospectively analysed. Progression was defined as new lesions (6 patients) and local tumour spread (3 patients). Tumour heterogeneity analysis was performed using mintLesion®. Image features included tumour volume, entropy, kurtosis, mean positivity of pixels (MPP), skewness, uniformity of distribution of positive pixels (UPP), and uniformity of pixels. Statistical analysis were performed with spearman's rank correlation and Mann-Whitney-U-test.
Results: During follow-up tumour volume did not significantly change between our groups with overall progression (local and systemic) and progression free patients (p=0,661). MPP values were significantly higher in patients without progression compared to patients with progression (p=0.030). There was a significant negative correlation between changes in kurtosis and the time till local tumour spread (p=0.008) or systemic progression (p=0.017).
Conclusion: Results suggest that analysis of tumour heterogeneity may provide valuable information from routine acquired images regarding therapy response evaluation; this may help adjusting therapy regimes and is easily integrated in clinical workflows. Furthermore, this procedure may predict therapy response and, hence may regarded as a marker for progression-free survival.

B-0174 11:42

Sarcopenia is an independant prognostic factor for poor overall survival among patients with pancreatic adenocarcinoma

A. Lambert, J. Salleron, C. Gavoille, A. Viard, A. Ayav, T. Conroy, V. Laurent; *Vandoeuvre-lès-Nancy/FR (a.lambert@nancy.unicancer.fr)*

Purpose: Our purpose was to evaluate sarcopenia as an independent prognostic factor for overall survival in patients with pancreatic adenocarcinoma to predict early relapses or progressive disease and to help decision-making for treatments.
Methods and Materials: From 2009 to 2015, all the patients with pancreatic adenocarcinoma were retrieved (N=114). A retrospective review of the total psoas area (TPA) was performed for each scan (N=713). The TPA was measured on a single cross-sectional image through the third lumbar vertebrae normalised for stature. The percentage decrease in the value of the TPA during the follow-up was also analysed.
Results: In univariate analysis, a TPA level under 420 during the follow-up whatever the time of the measure HR=3.419 ([2.168;5.394]; 95% CI; p<0.0001) and a TPA decrease of more than 20% from baseline HR=7.169 ([4.526;11.353]; 95% CI; p<0.0001) were independent prognostic factors of death. The multivariate analysis, confirmed the results with HR=5.799 ([3.418; 9.839]; 95% CI; p<0.0001) in the non-surgical group and HR=8.089 ([2.157; 30.339]; 95% CI; p=0.0019) in the surgical group for TPA decrease of more than 20% from baseline during the follow-up.
Conclusion: Our analysis shows that regardless of the time of the measurement, a TPA value under 420 and a TPA decrease of more than 20% during the follow-up are strong and independent death risk prognostic factors in patients with pancreatic adenocarcinoma. We now provide a tool to evaluate patients at diagnosis or during iterative consults of treatment or surveillance.

10:30 - 12:00 **Room M 5**

Neuro

SS 211b

White matter diseases

Moderators:
E. Avdagic; Sarajevo/BA
C. Lukas; Bochum/DE

K-02 10:30

Keynote lecture

M.P. Wattjes; *Amsterdam/NL (m.wattjes@vumc.nl)*

B-0175 10:39

Microbleed location is related to white matter lesion morphology

L.G.M. Cremers, J.G.J. Verbruggen, M. de Groot, W.J. Nlessen, M.A. Ikram, M.W. Vernooij; *Rotterdam/NL (l.g.m.cremers@erasmusmc.nl)*

Purpose: The location of microbleeds is thought to reflect the underlying pathology, with lobar microbleeds suggestive of cerebral amyloid angiopathy and deep microbleeds more related to hypertensive or atherosclerotic microangiopathy. Such dichotomy is also presumed to be present for white matter lesions (WML), but has not been studied in relation to WML morphology. We hypothesize that WML differs morphologically, depending on location of concomitant microbleeds and underlying pathology.
Methods and Materials: This study is embedded within the Rotterdam study. Participants underwent multi-sequence MRI scanning to assess microbleed presence and location, and presence and morphology of WML. We calculated the surface-to-volume ratio of the WML. A high surface-to-volume ratio indicates punctate WML, while a low ratio indicates larger, more confluent lesions. We assessed differences in WML morphology between presence of lobar versus deep microbleeds using linear regression models.
Results: We found 601 (13.0%) participants with solely lobar microbleeds and 145 (3.2%) participants with solely deep microbleeds. WML found in participants with solely lobar microbleeds had a higher surface-to-volume ratio compared to WML in persons with deep microbleeds, after adjusting for age and sex (B= 0.04, 95%CI=0.01; 0.06, p<0.01). The association attenuated after correcting for intracranial volume, total white matter volume and WML volume, but remained borderline significant (B=0.01, 95%CI= -0.00; 0.03, p=0.08).
Conclusion: WML in people with solely lobar microbleeds have a more punctate morphology compared to larger, confluent WML in people with solely deep microbleeds. These findings warrant further investigation of lesion morphology in relation to the location of cerebral microbleeds.
Author Disclosures:
W.J. Nlessen: Founder; Quantib BV.

B-0176 10:47

MR features and cerebrospinal fluid and plasma oxidative stress biomakers in different clinical phenotypes of neuroinflammatory acute attacks

D. Stojanov, S. Ljubisavljević, I. Stojanovic, S. Vojinovic; *Nis/RS (drstojanov@gmail.com)*

Purpose: To correlate MRI features with plasma and CSF lipid peroxidation product-malondialdehyde (MDA), catalase (CAT), and superoxide dismutase (SOD) activity in patients with clinically isolated syndrome (CIS) and relapsing remitting multiple sclerosis (RRMS).
Methods and Materials: Cross-sectional study included 50 CIS patients, 57 RRMS patients, and 20 control patients with nonspecific neurological symptoms. We calculated the number of T2W hyperintense lesions and load of T1W Gd-enhancing lesions as volume. Patients were divided into those with mild and severe MRI changes. Concentration of MDA was determined by modified TBA method. SOD and CAD were measured by spectrophotometry.
Results: MDA values were higher in plasma and CSF of all study patients with a higher number of total T2W lesions (p<0.05). The CSF/plasma MDA ratio was higher in RRMS patients. CAT activity was higher in CIS and RRMS patients with lower number of T2W lesions (p<0.05). SOD activity was higher in CIS and RRMS patients with lower number of T2W lesions, but these differences were significant only for plasma SOD activity changes (p<0.05). The positive correlations were observed in MDA levels in plasma and CSF, and Gd-enhancing lesion volume, for CIS and RRMS patients, and a negative correlation in SOD activity in plasma ad Gd-enhancing lesions volume, only for CIS patients (p<0.01).
Conclusion: Beyond MDA plasma, CSF values, SOD activity in plasma of CIS patients, and their MRI features, no correlation was observed between MRI and other biomarkers. It may be the consequence of a relatively small number of MRI scans.

B-0177 10:55

Decreased white matter integrity (WMI) in SLE patients: a DTI study

J.S.B. Nystedt, M. Nilsson, A. Jönsen, P.M. Sundgren; *Lund/SE (jessika.nystedt@med.lu.se)*

Purpose: To investigate WMI in SLE patients without neuropsychiatric complaints and relation to the concomitant depression and fatigue commonly described in lupus patients.
Methods and Materials: 26 female SLE patients (age: 23-52 years, mean: 36 years) and 20 aged-matched, healthy controls (age: 19-52 years, mean: 36 years) underwent cognitive testing (CNS-VS) and self-assessment questionnaires screening for depression and fatigue. All patients underwent 3T MRI and DTI. Software used for analyses of DTI data was developed in-house in Math-lab. The diffusion tensor was fitted using linear least squares minimisation. FA and MD were measured in the corpus callosum (CC) and the cingulum bundle, both associated to the default mode network. The cinguli were segmented primary focusing on the rostral and hippocampal parts. CC was segmented with main interest in the forceps minor which has been related to depression and fatigue. For statistical evaluation of WMI Kruskal-Wallis test was used. For correlation analysis, Spearman's Rho was used.
Results: Decreased FA values was demonstrated in rostral cinguli (p=0.044) and in left rostral cingulum in SLE patients (p= 0.03). Decreased MD was demonstrated in the left hippocampal cingulum (p=0.036) and decreased FA (p=0.002) and MD (p=0.042) was observed in the forceps minor of the lupus group and was associated with fatigue (rho=-0.015) and depression (rho=-0.026).
Conclusion: WMI in areas crucial for attention, mood and cognitive functions such as verbal memory, and consolidation of memories, might be altered in lupus patients without neuropsychiatric complaints. The disintegrity of the left hippocampal cinguli could contribute to the cognitive decline common in lupus patients.

B-0178 11:03

Phase sensitive inversion recovery improved identification of intracortical lesions in multiple sclerosis comparison with FLAIR and T2WTSE MR imaging

H. Naghibi, K. Firouznia, M. Shakiba, A. Azimi, V. Shahabian, H. Soroush, P. Sabet Rasekh; *Tehran/IR*

Purpose: Accurate detection and classification of purely intracortical lesions in multiple sclerosis (MS) are important in understanding their role in disease progression and impact on the clinical manifestations of the disease. Conventional MRI can not show cortical lesions, but some new MRI sequences have been proposed to be dedicatein this relation.Here, we want to evaluate efficacy of phase-sensitive inversion recovery (PSIR) for detection of cortical lesions of MS patients.
Methods and Materials: Fifty MS patients underwent MRI scanning on a 1.5 Tesla scanner. PSIR, T2W-TSE and fluid-attenuated inversion recovery (FLAIR) images were acquired and inspected by 2 experts, aNeuroradiologist and a MS *Fellowship*. The lesions were classified as purely intracortical, mixed gray-white matter, and juxtacortical. The difference in the number of lesions detected in each category was compared between PSIR and FLAIR and T2W-TSE.
Results: Cortical brain lesion load and the number of lesions were significantly higher on PSIR compared to both FLAIR and T2-TSE (P<0.001). Also the contrast between GM-WM was excellent in PSIR. PSIR consistently allowed a clearer classification and delineation of MS plaque.
Conclusion: PSIR is a promising technique to detect cortical lesions and could be beneficial in monitoring of cortical damage and disease progression in MS patients.

B-0180 11:11

The role of multivoxel proton MRS in differential diagnosis of multiple sclerosis disease courses

A. Bogdan, J. Khomenko, G. Kataeva, L. Prakhova, A. Ilves; *St. Petersburg/RU (andrey.a.bogdan@gmail.com)*

Purpose: Evaluation of brain metabolic changes in relapsing-remitting and secondary-progressive multiple sclerosis (RRMS and SPMS) with proton magnetic resonant spectroscopy (H-MRS).
Methods and Materials: Concentration ratios of main MRS-detectable metabolites of 47 patients with multiple sclerosis (MS) including 27 RRMS and 20 SPMS, and 21 normal subjects where compared in 9 regions of interest (ROI) of supraventricular normal appearing white matter (NAWM) and medial cortex. H-MRS was performed on Achieva 3T (2D PRESS, TE/TR=144/2000 ms). Localization: multivoxel MRS study (8*9 voxels (10*10*15 mm), whole volume 80*90*15 mm) was divided into 6 ROIs (anterior, medium and posterior ROIs bilaterally) in NAWM and 3 ROIs of gray matter (GM) in medial cortex. NAA/Cr, NAA/Cho, Cho/Cr ratios (NAA - N-acethylaspartate, Cr - creatine, Cho - choline) where analyzed.
Results: NAA/Cr ratio was significantly lower in RRMS-patients in NAWM (posterior frontal lobe bilaterally) and medial frontal lobe cortex compared to healthy subjects. In SPMS-patients NAA/Cr was significantly lower in all observed regions compared with RRMS-patients. NAA/Cho ratio was lower in NAWM of posterior frontal lobe bilaterally in RRMS-patients and, in case of SPMS in all observed regions, compared with normal controls. Ratio of Cho/Cr did not show any difference between the investigated groups.
Conclusion: In MS, metabolic changes precede the structural ones. The markers of neuronal and axonal dysfunction (decrease of NAA/Cr in the NAWM and GM) are registered in the early stages and aggravate during disease courses. Differences in metabolic ratios levels can be useful in differential diagnosis of MS disease courses.

B-0181 11:19

Diagnostic value of contrast-enhanced T2 FLAIR in multiple sclerosis disease: a preliminary experience in 49 patients

M. Perri[1], R. Balzano[1], R. Izzo[2], G. Guglielmi[1], T. Popolizio[1]; [1]*San Giovanni Rotondo/IT*, [2]*Naples/IT (marco-perri@tiscali.it)*

Purpose: The aim of this study is to assess the diagnostic value of CE-FLAIR for the detection of new active plaque in clinically suspected relapsing phase of the Multiple Sclerosis (MS) disease.
Methods and Materials: The institutional review board approved this prospective study in which all subjects provided written informed consent. A total of 49 patients with clinically definite MS disease underwent brain MRI. All examinations were performed using 1.5 T MR scanner, with standard protocol for brain including pre and post contrast SPGR T1-Weighted Image (CE-T1WI) and in adjunct Susceptibility Weighted Imaging (SWI) and CE-FLAIR. Two neuroradiologists, blinded to the clinical disease activity, evaluated by consensus all images to assess presence or absence of enhancement in MS lesions. Chi- square and T student tests were used for testing variables.
Results: Fourteen out of 49 patients had no active plaques in post contrastographic sequences being in remitting phase; SWI confirmed only the presence of iron storage as disease biomarker in white matter. A total number of 83 enhanced lesions was detected in 35 patients. CE-T1WI detected 51 lesions (61.4% of total) in 22 patients; all these lesions showed an enhancement in the post-contrast FLAIR sequence while CE-FLAIR images showed 32 (38.5%) new enhanced lesions in 13 patients, therefore classified as in a new relapsing phase.
Conclusion: Our results demostrate that CE-FLAIR sequence has a very high sensitivity in the detection of enhanced MS lesions compared to conventional CE-T1WI sequence.

B-0182 11:27

Subpial cortical demyelination (SCD) in multiple sclerosis: a MRI study in patients of recent onset

S. Iafrate, L. Panebianco, S. Quarchioni, L. Patriarca, M. Varrassi, A. Splendiani, C. Masciocchi; *L'Aquila/IT (sonia.iafrate87@gmail.com)*

Purpose: A growing body of evidence shows that subpial cortical demyelination (SCD) is associated with demyelinated cortex in patients affected by multiple sclerosis (MS). SCD is also found in biopsy cases with early MS and in experimental model. Recently, it has been shown that local meningeal inflammatory cells infiltrations contributes to the pathogenesis of SCD. In this study, we aimed to investigate the subpial cortical demyelination (SCD), in patients affected by recent-onset multiple sclerosis (MS).
Methods and Materials: We enrolled 146 recent-onset (< 6 months) MS patients, fulfilling Mc Donald's criteria, in a prospective study. All patients underwent 3T MRI exams; SCD was evaluated performing post-contrast axial Flair images on 3T MRI scan.
Results: Post-contrast axial Flair images showed the presence of enhanced meningeal rim referable to SCD in acute phase in 32% of our population. A large percentage (78%) of patients with SCD showed female gender. In 17% of our cases, SCD precedes the appearance of classic white matter plaques.
Conclusion: The evaluation of SCD may suggest a possible pathogenic role of meningeal inflammation in recent-onset MS patients. Targeting the cells and molecules mediating these inflammatory responses within the meninges may offer future promising therapies for MS.

B-0183 11:35

Perfusion and brain volume changes connected to cognitive dysfunction in multiple sclerosis patients

I. Krotenkova; *Moscow/RU (irina.krotenkova@mail.ru)*

Purpose: To investigate perfusion changes in NAWM and thalamus in relapsing-remitting MS (RRMS), secondary progressive MS (SPMS), to access volume changes and to investigate the correlation between these measures and neurological disability and cognitive status.
Methods and Materials: 20 RRMS and 20 SPMS patients underwent conventional MRI, 3D T1 MPRAGE for VBM, CT-perfusion and neurological examination, including EDSS and MSFC with PASAT for cognitive function.

Different perfusion characters were detected in thalamus and NAWM. 20 healthy controls underwent MRI.
Results: Compared to RRMS, SPMS patients experienced decrease of perfusion measures in frontal NAWM and thalamus. RRMS showed a negative correlation between amount of correct answers in PASAT and TTD, MTT in frontal NAWM (r= -0,38, p=0,01 and r= -0,36, p=0,018, respectively). SPMS showed a negative correlation between amount of correct answers in PASAT and PMB in parietal NAWM, that reflects changes in blood-to-brain barrier permeability (r=-0,46, p=0,032) and cortical left temporal lobe volume(r=0,677, p=0,011). RRMS, SPMS patients experienced significantly higher thalamus atrophy (p<0.05) compared to healthy controls, but there was no significant difference between both types of MS. There were no correlations between blood flow and thalamus volume in any of groups.
Conclusion: This study shows reduced cerebral blood perfusion in SPMS compared to RRMS patients in thalamus and normal appearing white matter, that means a presence of pathologic process in intact brain matter either in demyelination lesions. Cognitive functions are connected to pathology of normal appearing white matter and cortical GM atrophy.
Author Disclosures:
I. Krotenkova: Author; V. Bryukhov, M. Zakharova, M. Krotenkova, L. Askarova. Speaker; I. Krotenkova.

B-0184 11:43

MRI characteristics of early cerebral lesions in asymptomatic boys with X-linked adrenoleukodystrophy
P.A. Caruso; *Boston, MA/US (pcaruso@partners.org)*

Purpose: X-linked adrenoleukodystrophy (ALD) a rapidly progressive form of inflammatory demyelination. Identification of cerebral lesions prior to onset of symptoms is paramount in selecting patients who will benefit from rescue therapies. We set out to analyse cerebral lesions in a unique cohort of asymptomatic boys with CCALD.
Methods and Materials: We reviewed 193 brain MRIs from 44 neurologically asymptomatic (neurologic functional scale=0) boys with biochemical or genetically confirmed ALD followed at Massachusetts General Hospital between 2001 and 2015. Two neuroradiologists blinded to clinical information recorded the number of patients with lesions, the Loes score, the pattern of white matter involvement, and the presence and pattern of enhancement.
Results: Of the 44 boys, 59% (26) showed small subtle brain lesions (median age 6.7 years; range 3.6-15.5 years). The median Loes score found was 3.0 points (range 0.5-11). The most frequent lesion pattern was parieto-occipital white matter and splenium of corpus callosum (58%) followed by frontal white-matter and genu of corpus callosum, and frontopontine/corticospinal tracts. Among all patients with lesions, 85% (22/26) had contrast enhancement, either at baseline (50%) or on follow-up MRI (50%). Ten patients showed normal baseline MRI and subsequently converted to CCALD (median age 6.4 years).
Conclusion: MRI can detect brain lesions and development of disease in the absence of neurological symptoms. As newborn screening is implemented, familiarity with the characteristics of early lesions will help improve disease detection and guide monitoring and treatment in ALD.

14:00 - 15:30 **Room B**

Abdominal Viscera

SS 301a

Liver: advances in CT and MRI

Moderators:
O.V. Kucheruk; Moscow/RU
L. Marti-Bonmati; Valencia/ES

B-0185 14:00

Transient severe motion artifact related to gadoxetic acid enhanced liver MRI: incidence and risk evaluation at a European institution
L. Well, V.H. Rausch, G. Adam, F.O. Henes, P. Bannas; *Hamburg/DE (l.well@uke.de)*

Purpose: Varying incidences (5-18%) of contrast-related transient severe motion (TSM) imaging artifacts during gadoxetic disodium-enhanced arterial phase liver MRI have been reported. Since previous reports originated from the United States and Japan, we aimed to determine the incidence of TSM at a European institution and to correlate it with potential risk factors and previously published results.
Methods and Materials: Two age and sex matched groups were retrospectively selected (gadoxetate disodium n=89; gadobenate dimeglumine n=89) from dynamic contrast-enhanced MRI examinations. Respiratory motion related artifacts in non-enhanced and dynamic phases were assessed independently by two readers blinded to contrast agents on a 4 point scale. Scores of ≥ 3 were considered as severe motion artifacts. Severe motion artifacts in arterial phases were considered as TSM if scores in all other phases were < 3. Potential risk factors for TSM were evaluated via logistic regression analysis.
Results: For gadoxetate disodium, the mean score for respiratory motion artifacts was significantly higher in the arterial phase (2.2±0.9) compared to all other phases (1.6±0.7) (p<0.05). Incidence of TSM was significantly higher with gadoxetate disodium (n=19; 21.1%) than with gadobenate dimeglumine (n=1; 1.1%) (p<0.001). The incidence of TSM at our institution is in the upper range of previously published reports. Logistic regression analysis did not show any significant correlation between TSM and risk factors (all p>0.05).
Conclusion: No associated risk factors for TSM could be identified. However, we revealed a high incidence of TSM at a European institution, undermining the importance of a diagnosis-limiting phenomenon.

B-0186 14:08

Liver function is significantly correlated with liver to portal vein contrast ratio during the hepatobiliary phase with Gd-EOB-DTPA-enhanced MR at 3 Tesla
W. Zhang, C. Hu; *Suzhou/CN (jszwgys@163.com)*

Purpose: To quantitatively evaluate the correlation of the liver-to-portal vein contrast ratio (LPC) and liver function on gadolinium ethoxybenzyl diethylenetriamine pentaacetic acid (Gd-EOB-DTPA)-enhanced MR imaging.
Methods and Materials: A total of 102 patients who underwent Gd-EOB-DTPA-enhanced 3Tesla MR imaging (normal liver, n=20; Child-Pugh class A, n=55; B, n=21; and C, n=6) were included in this restrospective study. LPC was defined as the enhancement ratio of hepatic parenchyma and potal vein at hepatobiliary phase(HBP) 20min, and it was compared between normal and cirrhosis livers. The correlation between LPC and hepatic function parameters at HBP after injection was quantitatively analysed as well.
Results: The degree of LPC differed between normal and cirrhosis livers (P<0.001) significantly. LPC constantly and significantly decreased as the severity of cirrhosis increased at HBP imaging (P<0.001). Total bilirubin (P<0.001), albumin (P<0.001), platelet count (P<0.001), and model for end stage liver disease score (P<0.001) were independent predictors of LPC at HBP imaging.
Conclusion: The index of hepatic LPC on Gd-EOB-DTPA HBP imaging can predict the severity of cirrhosis and is correlated with clinical hepatic function parameters.

B-0187 14:16

Magnetic resonance elastography for prediction of radiation-induced liver disease after stereotactic body radiation therapy
S. Ichikawa, U. Motosugi, M. Oguri, H. Onishi; *Chuo-shi, Yamanashi/JP (si99006@yahoo.co.jp)*

Purpose: To evaluate the usefulness of magnetic resonance elastography (MRE) for prediction of radiation-induced liver disease (RILD) after stereotactic body radiation therapy (SBRT) in patients with hepatocellular carcinoma (HCC).
Methods and Materials: Seventeen patients who underwent SBRT (dose: 28-60Gy in 4-10 fractions) for HCC (size: 14-68mm) had pretreatment liver stiffness measured by MRE. Diagnosis of RILD was determined by the following criteria: (i) anicteric elevation of alkaline phosphatase to a level at least twice the upper limit of the normal level, or (ii) elevation of transaminases, to at least five times the upper limit of the normal, or five times the pretreatment level within 16 weeks after SBRT. The following variables were analysed as potential predictors of RILD: age; sex; body weight; etiology of hepatitis; liver stiffness measured by MRE; tumour size blood test results; tumour markers; Child-Pugh score; Karnofsky performance status; indocyanine green retention rate at 15min; and parameters of SBRT (fraction size, total dose, V20 (percentage of normal liver volume that received >20Gy), and VS15 (volume spared from ≥15Gy)).
Results: Pretreatment liver stiffness measured by MRE in patients with RILD (n=4; median 8.3kPa) was significantly higher than that in patients without RILD (n=13; median 5.0kPa) (P=0.0090). Other variables showed no significant differences between the two groups. No patient died of RILD.
Conclusion: Pretreatment liver stiffness measured by MRE can be a predictor of RILD after SBRT in patients with HCC.

B-0188 14:24

Self-gated 4D-MRI of the liver: comprehensive real-time imaging of hepatic enhancement
J. Weiss, A.E. Othman, P. Martirosian, M. Kolb, C. Ruff, J. Taron, K. Nikolaou, M. Notohamiprodjo; *Tübingen/DE (jakob.weiss@uni-tuebingen.de)*

Purpose: To evaluate a free-breathing self-gated volumetric interpolated breath-hold examination (VIBE) with compressed sensing (CS) for continuous dynamic contrast-enhanced (DCE) MR imaging of the liver.
Methods and Materials: 25 patients underwent gadobutrol contrast-enhanced MRI of the liver on a 1.5T scanner. A free-breathing prototype VIBE-sequence

with CS and automated respiration gating ($VIBE_{CS}$) was continuously acquired for 128 seconds starting with the administration of the contrast agent. From the acquired raw data, 16 consecutive series with a temporal resolution of 8 seconds and spatial resolution of 1.2x1.2x3 mm were reconstructed. The unenhanced, arterial, portal-venous and venous phase series with the subjectively most satisfying image quality were selected and compared to a clinical routine VIBE-sequence ($VIBE_{std}$). Image quality was assessed qualitatively (overall, sharpness, lesion conspicuity, motion/other artefacts; two readers independently; 5-point-Likert scale; 5=excellent) and quantitatively (coefficient-of-variation (CV); mean liver SI).
Results: Overall image quality, lesion conspicuity and motion artefacts showed no significant differences between the sequences (p≥0.07). Image sharpness was significantly higher in the portal-venous (4.9±0.2) and venous phase (4.9±0.3) images of $VIBE_{CS}$ as compared to $VIBE_{std}$ (4.2±0.6; p=0.01). However, $VIBE_{CS}$ showed a significant appearance of bow-like reconstruction artefacts (3.8±0.5), which were not present in $VIBE_{std}$ (5.0±0.0; p≤0.001). Mean liver SI was significantly higher in $VIBE_{std}$ (200.1±85.1) than in $VIBE_{CS}$ (170.3±68.3; p=0.002) whereas CV calculations revealed no significant differences among the sequences (p=0.1).
Conclusion: $VIBE_{CS}$ is applicable for continuous self-gated DCE-MRI of the liver with similar overall image quality and lesion conspicuity and improved image sharpness as compared to a $VIBE_{std}$.

B-0189 14:32

Evaluation of transient dyspnea during gadoxetic acid-enhanced liver MRI using free-breathing T1WI

J. Yoon[1], M. Yu[1], B. Hur[2], G. Robert[3], Y. Son[1], B. Kiefer[3], K. Block[4], H. Chandarana[4], J. Lee[1]; [1]*Seoul/KR*, [2]*Goyang/KR*, [3]*Erlangen/DE*, [4]*New York, NY/US (jmlshy2000@gmail.com)*

Purpose: To observe transient dyspnea pattern after gadoxetic acid administration and prove clinical feasibility of free-breathing gadoxetic acid-enhanced liver magnetic resonance imaging (MRI) using golden-angle radial sparse parallel imaging (GRASP) with respiratory gating.
Methods and Materials: In this IRB-approved prospective study, 60 patients have been enrolled and informed consent was obtained from all patients. Dynamic T1-weighted image (T1WI) was obtained using GRASP in free-breathing manner. Development of transient motion after gadoxetic acid administration was monitored using respiratory motion recording. In addition, subjective symptom, oxygen saturation and heart rate were monitored. Early arterial, late arterial and portal venous phases with different temporal resolution (13sec vs. 6sec) and respiratory gating were reconstructed for evaluating image quality and motion artifact.
Results: In 40.0% (23/59), transient motion (mean duration: 21.5±13.0 seconds) was observed and it developed in 15 seconds after gadoxetic acid administration in 73.9% (17/23). There were no significant difference of subjective symptom and vital signs between groups with and without transient motion (P=0.25~0.99). Motion artifact reduced after respiratory gating, and there was no significant difference of motion artifact on early and late arterial phases between the two groups (P=0.42) whereas significantly higher motion artifact was observed on non-gated 13sec-T1WI in patients with transient motion (P=0.001). Gated 6-sec-T1WI provided significantly lower image quality than gated 13-sec-T1WI.
Conclusion: Free-breathing T1WI using GRASP and incoherent undersampling technique provided timely and acceptable arterial phase consistently in patients with transient motion which is potentially influential on arterial phase.
Author Disclosures:
J. Yoon: Research/Grant Support; Bayer Healthcare. Speaker; GE Healthcare, Bayer Healthcare, Philips Healthcare. **G. Robert:** Employee; Siemens Healthineers. **Y. Son:** Employee; Siemens Healthineers Korea. **B. Kiefer:** Employee; Siemens Healthineers. **H. Chandarana:** Advisory Board; Siemens Healthineers. Grant Recipient; RSNA. **J. Lee:** Research/Grant Support; Philips Healthcare, Bayer Healthcare, GE Healthcare, Guerbet. Speaker; Philips Healthcare, Bayer Healthcare.

B-0190 14:40

Rapid continuous multiarterial MRI of hepatic arterial dominant phase during free-breathing

A. Othman, J. Weiss, K. Nikolaou, M. Notohamiprodjo; *Tübingen/DE (ahmed.othman@uni-tuebingen.de)*

Purpose: To evaluate the feasibility of multiarterial MRI of hepatic arterial dominant phase (HAD) using a free-breathing self-gated spoiled gradient-echo sequence with compressed sensing (CS).
Methods and Materials: 40 patients who underwent contrast-enhanced liver MRI with gadobutrol were included. Each 20 patients were examined in 1.5 and 3T (Magnetom Aera and Skyra, Siemens Healthineers), respectively. Multiarterial imaging was performed for 64s beginning with contrast injection using a rapid free-breathing prototype volume-interpolated-breath-hold examination (VIBE) sequence with CS and automated respiration gating (iVIBE, 1,2x1,2x3mm^3). 8 consecutive arterial subphases were reconstructed (8s/phase). Two readers selected and assessed the best HAD phase on a five-point Likert scale (5=excellent) regarding image quality, respiratory artefact compensation, enhancement of abdominal aorta and hepatic artery, lesion detectability and diagnostic confidence. Signal intensity (SI) and SNR were measured in the liver and in the abdominal aorta.
Results: HAD phase varied among patients (3rd - 7th phase). Image quality and respiratory artefact compensation were good (median=4, 3-5) without significant differences among field strengths (p≥.089). Lesion detectability, contrast enhancement of aorta and diagnostic confidence were excellent (median 5, 3-5) without significant differences among field strengths (p≥.165). Signal intensity and liver SNR were significantly higher in 3T (p≤.015). SNR in abdominal aorta was high in both field strengths without significant differences (p.=637).
Conclusion: Acquisition of continuous multiarterial MRI of hepatic arterial dominant phase during free-breathing using iVIBE is feasible and yields good image quality and excellent arterial enhancement with good compensation of respiratory artefacts resulting in excellent diagnostic confidence in both 1.5T and 3T.

B-0191 14:48

Gadoxetic acid-enhanced MR imaging of transient hepatic enhancement difference: another cause of hypointense observation on hepatobiliary phase

C. Torrisi, D. Picone, M. Midiri, G. Brancatelli; *Palermo/IT (chiaratorrisi84@gmail.com)*

Purpose: To determine the frequency, natural history and factors associated with the presence of transient hepatic enhancement difference (THED) showing hypointensity in the hepatobiliary phase (HBP) of gadoxetic acid-enhanced MR imaging.
Methods and Materials: Gadoxetic acid-enhanced MR imaging of 125 patients (91 males; mean age: 68 years; range 26-84 years) with THED were retrospectively reviewed. Three readers qualitatively and quantitatively evaluated MR imaging features of THED and evolution at follow up. Fisher's exact test and Mann-Whitney-Wilcoxon test were used for statistical analysis.
Results: THED were wedge-shaped (n=106 (85%)), hypervascular on HAP (125 of 125; 100%) and isointense on both HBP (105 of 125; 84%) and fat-suppressed T2-weighted imaging (n = 100 (80%)). Hypointense THED on hepatobiliary phase were more commonly wedge-shaped (P < .05), hyperintense on T2-weighted imaging (P < .05), and were associated with previous locoregional treatment (P < .05). Of 12 patients with hypointense THED on HBP who had follow-up MR, nine showed reduction in size.
Conclusion: Hypointensity on HBP is not uncommonly observed in THED, and might be explained with chronic portal hypoperfusion and or biliary obstruction resulting from previous locoregional treatment of adjacent tumour and leading to hepatocellular dysfunction, fibrotic changes and parenchymal atrophy.

B-0192 14:56

Intravoxel incoherent motion diffusion-weighted imaging of hepatic warm ischemia-reperfusion injury in a rabbit model

Q. Ji, Z. Chu, W. Shen; *Tianjin/CN (jiqianq@aliyun.com)*

Purpose: To investigate the diagnostic efficacy of intravoxel incoherent motion (IVIM) MRI in the grade of hepatic warm ischemia-reperfusion injury (WIRI) in rabbit models.
Methods and Materials: Fifty rabbits were randomly divided into sham-operation group (n=10) and four test groups (n=10 for each group) according to different hepatic warm ischemia time. IVIM was performed on a 3T MR scanner with 11 b values of 0 to 800 s/mm^2. Rabbits were sacrificed for biochemical and histomorphological analysis. Interobserver variability, the parametric, non parametric methods and receiver operating characteristic (ROC) curves were used to determine diagnostic efficacies.
Results: Apparent diffusion coefficient (ADC), true diffusion (Dslow), pseudodiffusion (Dfast) and perfusion fraction (PF) showed moderate to excellent interobserver reproducibility. Significant differences were found between different grades of hepatic WIRI by ADC, Dslow, Dfast, and PF (P <0.001). IVIM parameters corresponded well with biochemical parameters (P <0.01). ROC analysis showed that the differences in ADC, Dslow, Dfast, and PF among different grades of hepatic WIRI were significant (P <0.05), and the area under the ROC curve (AUC) of PF was the largest.
Conclusion: The grades of hepatic WIRI could be effectively evaluated by using IVIM in a rabbit model, with PF being the most accurate parameter.

B-0193 15:04

Liver function evaluation at magnetic resonance imaging: comparison between liver enhancement and MELD

M. Di Martino, V. Ceci, S. De Vizio, A. Capalbo, K. Koryukova, C. Catalano; *Rome/IT (micdimartino@hotmail.it)*

Purpose: To evaluate the enhancement of the liver parenchyma in patients with different grade of liver cirrhosis.
Methods and Materials: Seventy-five patients scheduled for liver transplantation were divided according to the MELD (< 15 and ≥ 15) and Child-Pugh (A, B, C) classifications for liver cirrhosis. Fourty-one patients reported also hepatocellular carcinoma with 63 lesions (1-4 per patients). All subjects underwent MRI at 1.5T (Avanto, Siemens). MR acquisitions comprised unenhanced breath-hold T2W images and volumetric 3D gadoxetic acid enhanced (0.1 mmol/kg bodyweight) T1W GRE images acquired at 25s, 60s, 180s (dynamic phases) and 20 minutes (hepatobiliary phase). Quantitative analysis comprised: enhancement ratio (ER) of liver parenchyma, signal-to-noise ratio of liver parenchyma (SNR) and contrast-to-noise ratio (CNR) between signal intensity of lesions and liver parenchyma. Comparisons among different classes were performed with ANOVA or Kruskall-Wallis test and Mann-Whitney U and Student's t test. P values of < 0.05 were considered statistically significant.
Results: Patients with MELD score lower than 15 reported a significant higher ER and CNR (0.47 vs 0.35 and -11.6 vs -0.09). The same result was observed between Child-Pugh groups A - B and C (0.46 - 0.52 and 0.31). Regarding CNR a significant difference was found between class B and C (-11.8 vs. -0.929; p=0.03). No significant differences were reported on SNR.
Conclusion: Liver enhancement during the hepatobiliary phase should be useful to distinguish different grade of liver function.

B-0194 15:12

Prediction of liver stiffness measurement using liver surface analysis on CT scan

M. Seong, T. Kang, M.-R. Kwon, J. Kim, S. Yang, J. Lee; *Seoul/KR (seong.minjung@gmail.com)*

Purpose: To develop a prediction method using liver surface analysis based on the computed tomography (CT) for liver stiffness measurement in patients with liver cirrhosis.
Methods and Materials: This retrospective study was approved by the institutional review board, and the requirement for informed consent was waived. 47 patients with liver cirrhosis who had received transient elastography for liver stiffness measurement and liver CT were retrospectively analyzed. We assessed the inflection/length of liver surface (left lateral segment) using auto-segmentation method based on the CT images to evaluate the degree of surface serration. The correlations between inflection/length of liver surface and the degree of fibrosis stage F1 from F4 on the METAVIR scale were assessed using simple regression analysis.
Results: Median liver stiffness values measured using transient elastography was 8.9 kPa (range, 7.2-52.3 kPa). The degrees of liver stiffness according to the fibrosis stage in the patients included were 2.4-7.1 in F1, 7.2-8.0 kPa in F2, 8.1-10.9 kPa in F3, and 11.0-52.3 kPa in F4, respectively. The inflection/length of liver surface using auto-segmentation method showed a stepwise increase with increasing degree of fibrosis stage ($\rho = 0.43$; $p = 0.018$).
Conclusion: Liver surface analysis using CT auto-segmentation method could stratify the degree of liver fibrosis in patients with liver cirrhosis.

B-0195 15:20

Baseline values of DCE-CT of liver in patients with colorectal cancer

A. Bevilacqua[1], S. Malavasi[1], M. Ronot[2], J.-L. Daire[2], B.E. Van Beers[2], V. Vilgrain[2]; [1]*Bologna/IT*, [2]*Clichy/FR (s.malavasi@unibo.it)*

Purpose: Assessment of baseline values in CT perfusion (CTp) studies is as much difficult as it plays a crucial role for an accurate computation of perfusion parameters. Besides that, the unenhanced stage of CTp provides repeated measures of baseline. This study aims at computing and analysing the voxel-based baseline values of normal liver in a set of patients with colorectal cancer.
Methods and Materials: 40 patients with colorectal cancer, free from any hepatic diseases, underwent axial CTp examinations of liver at colorectal cancer diagnosis. A large region of interest (ROI) was drawn on one central section of the liver, avoiding large vessels. Baseline portion (BP) of each TCC of the ROI was determined through the use of an adaptive 3D filtering and the relative baseline value (HU) was computed as the mean of the TCC concentration values over BP. Mean, median, and standard deviation values were computed for each patient as well as for the entire cohort.
Results: For each patient, mean and median baseline values coincide, thus suggesting quite symmetric distributions. The average and standard deviation (std) of baseline mean values of all patients are 61.7HU (range 32-79HU), and 10.1, with 73% of values within one std interval (51-71HU). Moreover, baseline colorimetric maps showed a high spatial correlation.
Conclusion: Baseline values of normal liver of patients with colorectal cancer are compliant with values of normal liver in healthy subjects reported in the literature. The spatial coherence hints at a local similarity of tissue features.

14:00 - 15:30 **Room C**

GI Tract

SS 301b

Imaging of the colon and pelvic floor

Moderators:
A. Laghi; Latina/IT
N.N.

B-0196 14:00

Costs of a colorectal cancer screening with CT colonography in Italy

P. Mantellini, G. Lippi, L. Sali, G. Grazzini, B. Mallardi, M. Falchini, M. Mascalchi, L. Ventura, M. Zappa; *Florence/IT (lapo.sali@unifi.it)*

Purpose: Unit costs of screening CT colonography (CTC) can be useful for cost-effectiveness analyses and for health care decision-making. We evaluated the unit costs of CTC as a primary screening test for colorectal cancer in the setting of a randomised trial in Italy.
Methods and Materials: Data were collected within the randomised SAVE trial. Subjects were invited to screening CTC by mail and requested to have a pre-examination consultation. CTCs were performed with 64- and 128-slice CT scanners after reduced or full bowel preparation. Activity-based costing was used to determine unit costs per-process, per-participant to screening CTC and per-subject with advanced neoplasia.
Results: Among 5242 subjects invited to undergo screening CTC, 1312 had pre-examination consultation and 1286 ultimately underwent CTC. Among 129 subjects with a positive CTC, 126 underwent assessment colonoscopy and 67 were ultimately diagnosed with advanced neoplasia (i.e. cancer or advanced adenoma). Cost per-participant of the entire screening CTC pathway was € 196.80. Average cost per-participant for the screening invitation process was € 17.04, while it was € 9.45 for the pre-examination consultation process. Average costs per-participant of the CTC execution and reading process was € 146.08 and of the diagnostic assessment colonoscopy process was € 24.23. Average cost per-subject with advanced neoplasia was € 3777.30.
Conclusion: Our data suggest that the more relevant cost of screening CTC, amenable of intervention, is related to CTC execution and reading process.

B-0197 14:08

Retrospective analysis of patient position errors and impact of MSCT dose in virtual colonscopy: single centre experience

C. Tudisca, S. Salerno, L. Scopelliti, M. Marrale, C. Terranova, G. Lo Re, G. La Tona, A. Lo Casto, R. Lagalla; *Palermo/IT (chiaratudisca@gmail.com)*

Purpose: Virtual-colonoscopy (VC) is a well known and valid technique for evaluation of colon wall and detection of new lesions. The main drawback for its execution is patient exposition to ionizing radiations. Indeed, guidelines recommend standardized low dose acquisition procedures aimed to minimize radiation exposition. We retrospectively examined the impact in term of radiation exposure of patient position and scan length mislead.
Methods and Materials: A two-year retrospective analysis of multi-slice-computed-tomography (MSCT) acquisition data of 106 patients that underwent a VC at our institution. Exams were performed in a MSCT 128 slice with low-dose protocol. The parameters that characterise the examinations and could induce an increase of absorbed dose were: patient position with respect to the gantry isocenter and scan length that could exceed the area of interest.
Results: Mean value of patient position resulted below isocenter for 48±25mm and 29±27mm in prone and supine positions, respectively. On the basis of previous literature experience the dose increase in our patient population, due to the incorrect positioning, was estimated to be about 30% (~1.5mSv) and 20% (1mSv) for prone and supine positions, respectively.Moreover, we found that the scan exceeded the correct position below the anal orifice for an average length of 36±25mm e 48±28mm in prone and supine positions, respectively, exposing sensitive anatomic organs.
Conclusion: Errors in acquisition parameters, eluding the optimized protocols, should be avoided given the increase in the dose.Nowadays acquisition technique is one crucial focus on daily practice, giving the major spread of ionizing radiations in routine exams.

B-0198 14:16

Accuracy of CT colonography in staging colon cancer: a metanalaysis

M.J. Lahaye[1], E. Nerad[2], D.M.J. Lambregts[1], M. Maas[1], G.L. Beets[1], R.G.H. Beets-Tan[1]; [1]*Amsterdam/NL*, [2]*Eindhoven/NL (nerad19@hotmail.com)*

Purpose: Computed tomography colonography (CTC) is an established tool in the screening for colon cancer. Furthermore CTC can be used in the staging of colon cancer, which is imperative with the possibility of neo-adjuvant treatment in the nearby future (FOXTROT trial). Therefore the aim of this study is to determine the accuracy of CTC in the detection of important prognostic factors being; tumour invasion beyond the bowel wall and nodal involvement of colorectal carcinomas.
Methods and Materials: A literature search was performed in Ovid, Embase and Pubmed to identify studies reporting on the accuracy of CTC for local staging of colon cancer with histology as reference standard. Data were extracted by two observers in consensus. A hierarchical summary ROC (HSROC) model was used to construct a summary ROC curve and to calculate summary estimates of sensitivity, specificity and diagnostic odds ratios (DOR).
Results: Fourteen studies fulfilled the inclusion criteria for detection of tumour invasion beyond the bowel wall (combined total of 1257 lesions). The pooled sensitivity, specificity and DOR were 90% (95% CI: 88-92%); 87% (95% CI: 83-90%) and 19,6 (95% CI: 10,2-41,5) respectively. For nodal involvement nine studies were included (combined total of 525 patients) the estimates were 84% (95% CI: 80-88%); 66% (95% CI: 59-72%); 5,8 (95% CI: 2,5-9,4) respectively.
Conclusion: CTC is an accurate tool in the staging of colon cancer with a good sensitivity for the detection of T3/T4 tumours and an improved specificity than standard CT. However, the accuracy in detecting nodal involvement is mediocre.

B-0199 14:24

Colorectal cancer vs chronic diverticular disease: differential diagnosis at CT colonography

M. Chincarini, M. Signorini, N. Faccioli, R. Pozzi-Mucelli; *Verona/IT (marco.chincarini@gmail.com)*

Purpose: To retrospectively identify the most significant morphologic findings at CT colonography (CTC) for differentiating between sigmoid cancer and chronic diverticular disease.
Methods and Materials: Two experienced radiologists reviewed the CTC examinations of 54 Patients, 33 with proven chronic diverticular disease and 21 with proven sigmoid cancer, and identified a subgroup of 26 Patients with a mass lesion (15 Patients with chronic diverticular disease and 11 with carcinoma). The readers looked at specific morphological criteria established from a literature review for CT findings of chronic diverticular disease and colon cancer. Sensitivity, specificity, positive predictive value (PPV), negative predictive value (NPV) and interval of confidence were calculated.
Results: The most suggestive morphologic findings for carcinoma are: absence of diverticula in the affected segment (NPV 82.6%, PPV 93.5%); straightened growth pattern (NPV 83.3%, PPV 83.3%); presence of shoulder phenomenon (NPV 93.1%, PPV 76%); completely distorted mucosal folds pattern (NPV 96.2, PPV 71.4). In the “mass lesion subgroup”, the distortion of mucosal folds (NPV 87.5%, PPV 55.6%) and the straightened growth pattern (NPV 75%, PPV 70%) have significantly lower diagnostic performance. In this latter group, the two strongest morphological features suggestive of carcinoma are the absence of diverticula in the affected segment (NPV 93.3%, PPV 90.9%) and the presence of shoulder phenomenon (NPV 91.7%, PPV 71.4%).
Conclusion: The most useful morphological sign to differentiate chronic diverticulitis from colorectal cancer is the presence of diverticula in the affected segment.

B-0200 14:32

CT colonography: effect of electronic cleansing of tagged fecal residuals on the size of submerged colorectal polyps in screening patients

C. Bräuer[1], H. Ringl[1], P. Lefere[2], S. Gryspeerdt[2], P. Apfaltrer[1], M. Scharitzer[1], D. Berzaczy[1], A. Graser[3], T. Mang[1]; [1]*Vienna/AT*, [2]*Roeselare/BE*, [3]*Munich/DE (christian_braeuer@msn.com)*

Purpose: To assess whether there is a difference in the size of colorectal polyps before and after electronic cleansing (EC) of tagged residuals in screening CT colonography (CTC) studies.
Methods and Materials: A database of 894 colonoscopy-validated CTC patient-datasets of a low prevalence cohort was retrospectively reviewed to identify patients with polyps ≥6mm that were entirely submerged in tagged residuals in at least 1 of 2 scanning positions. 2D measurements of the largest diameter of each identified polyp were performed independently by ten radiologists before and after EC in colon, bone, and soft tissue windows in a fully randomised order. Differences of size and of polyp count before and after EC were calculated for size-categories ≥6mm, ≥10mm. Statistical testing involved 95% CI, Intraclass Correlation and mixed model ANOVA.
Results: 37 patients with 48 submerged polyps (34 adenomas, 14 non-adenomas) ≥6mm were identified by reference-standard. Mean polyp size before EC was 9.8mm in colon, 9.9mm in bone and 8.2mm in soft tissue windows. After EC the mean polyp size decreased significantly to 9.4mm in colon, 9.1mm in bone, and 7.1mm in soft tissue windows. Compared to the unsubtracted colon window, EC, performed in bone and soft tissue windows, leads to a shift of 10 (20.8%) and 25 (52.1%) polyps ≥6mm and 1 (6.7%), and 5 (33.3%) polyps ≥10mm into the next smaller size category.
Conclusion: EC significantly reduces the size of polyps submerged in tagged residuals. Polyp measurements should be performed in unsubtracted image data in a colon window setting.

B-0201 14:40

Diagnostic performance and influence on computer-assisted-diagnosis (CAD) of ultra-low dose CT colonography (ULD-CTC) with model-based iterative reconstruction (MBIR)

G. De Paoli Barbato, M. Bassi, E. Raimondi, A. Spiller, R. Rizzati, M. Tilli, M. Giganti, G. Benea; *Ferrara/IT (dplgcm@unife.it)*

Purpose: To compare perfomance of standard-dose (SD) and ultra low-dose (ULD) in CT-Colonography (CTC), using hybrid-iterative reconstruction (HIR) and model-based iterative reconstruction (MBIR), and to asses the effect of different reconstruction algorithms on computed-aided diagnosis (CAD).
Methods and Materials: Fifty patients (31 males, 19 females, mean age 69,7) underwent CTC with SD (120kV, 50mAs 4,6±1,3mSv) and ULD (120kV, 10mAs, 0,95±0,2mSv); images were reconstructed with HIR and MBIR; CAD system was applied complementary to all reconstructions. Two independent radiologists review obtained images separately randomized to avoid recall-bias, and recorded colonic findings (polyps/cancer), extracolonic findings and CAD detections. Polyps were classified by size (<5mm, =5-10mm, ≥10mm), shape (flat, sessile, peduncolated) and location (rectum, sigmoid, descending, transverse, ascending, caecum). Extracolonic findings ≥E4 (C-RADS) were recorded. CAD results were reported and significant findings were selected.
Results: Nine polyps were found in 8 patients, six <5mm, two between 5-10mm and one ≥10mm; 8 were peduncolated and 1 flat, 2 were in caecum, 3 ascending, 2 transverse, 1 descending, 1 sigmoid tract; colonic-findings records were super-imposable for both radiologist between SD and ULD reconstructions; 2 extracolonic findings ≥E4 were recorded in all reconstructions. MBIR-CAD results compared to HIR-CAD showed a mean 13,56% increment at SD and 32,92% at ULD, with no change in terms of significant results. Colonic findings were confirmed by optical-colonscopy (OC).
Conclusion: ULD-MBIR CTC showed promising results in terms of diagnostic performance and inter-reader reproducibility for intra-colonic findings. CAD detection was influenced by MBIR, with no decrease in diagnostic value.

B-0202 14:48

Protocol optimisation of MR colonography for polyp detection using pig colonic phantom: influence of magnetic field strength, colonic distension technique, and MRI sequence

E.-S. Cho, J. Kim, J. Choi, Y. Choi; *Seoul/KR (jjondol@yuhs.ac)*

Purpose: To compare the diagnostic performance and image quality of MR Colonography (MRC) using pig colon phantoms and to evaluate the influence of magnetic field strength (1.5-T or 3.0-T), colonic distension technique (bright- or dark-lumen), and MRI sequences.
Methods and Materials: Six pig colon segments (60-92 cm) with 56 artificial colon polyps (0.4-1.6 cm) were placed in plastic container containing soybean oil. The colon was distended using room air for dark-lumen MRC and with tap water or a gadolinium-chelate based enema fluid for bright-lumen MRC. Each colon phantom was scanned on both 1.5-T and 3.0-T scanners using the following sequences: 2D fast-imaging with steady-state precession, T2-weighted 2D single-shot fast-spin-echo (SSFSE), and/or T1-weighted 3D gradient-echo (GRE) sequences. Two radiologists evaluated the presence of polyps and analysed the image quality.
Results: For polyp detection sensitivity and image quality, MRC obtained at 1.5-T was better than that obtained at 3.0-T, and a bright-lumen technique was superior to a dark-lumen technique. Bright-lumen MRC at 1.5-T was most sensitive for polyp detection ($p < 0.001$) and gave the highest image quality ($p < 0.05$) regardless of polyp size and shape (flat or sessile). SSFSE and 3D GRE sequences at bright-lumen MRC at 1.5-T had highest sensitivity for polyp detection (83.9% and 83.0%, respectively) and highest image quality.
Conclusion: The most effective sequences of MRC for polyp detection were SSFSE- or 3D GRE-based bright-lumen MRC obtained with a 1.5-T scanner. These sequences had the highest polyp detection rate and the best image quality.

B-0203 14:56

Apparent diffusion coefficient as a potential marker of tumour aggressiveness in colon cancer

E. Nerad[1], A. Delli Pizzi[2], D.M.L. Lambregts[3], M. Maas[3], F. Bakers[4], G.L. Beets[3], R.G.H. Beets-Tan[3], M.J. Lahaye[3]; [1]*Eindhoven/NL*, [2]*Chieti/IT*, [3]*Amsterdam/NL*, [4]*Maastricht/NL (nerad19@hotmail.com)*

Purpose: To investigate the role of magnetic resonance imaging (MRI) as a potential tumour marker in predicting the aggressiveness of colon cancer tumours with the apparent diffusion coefficient (ADC), and its potential in discriminating between low and high-risk colon cancer patients.
Methods and Materials: Thirty patients (21M, 9F) were included retrospectively. All patients received a 1.5T MRI of the colon including T2 and DWI sequences. ADC maps were automatically constructed for all diffusion weighted magnetic images with b factors of 0 and 1000 s/mm(2). ADC measurements of each colon tumour were performed by two readers in concensus using regions of interest with IntelliSpace Discovery research platform (Philips Healthcare, The Netherlands). High-risk colon cancer patients were defined if one or more of the following parameters were present with histology as the reference standard: direct invasion of tumour into surrounding structures/organs (T4), nodal involvement (N+) and/or distant metastasis (M+). The student t-test was used to assess the differences between the ADC means of low and high-risk colon cancer tumours.
Results: The mean ADC of the high risk patients (n=16) was 1129.7 and for low-risk patients (n=14) 1231.8 with a significant difference between the mean ADC intensity of high versus low risk tumours (p=0.002). The optimal cut off value was 1178.8 with an area under the curve (AUC) of 0.83 and a sensitivity and specificity of 81% and 86% respectively.
Conclusion: ADC has potential to discriminate between low and high-risk colon cancer patients with lower ADC values significantly associated with high-risk colon tumours.

B-0204 15:04

CT differentiation of poorly-differentiated colorectal neuroendocrine tumours from well-differentiated neuroendocrine tumours and colorectal adenocarcinoma

J. Kang, S. Kim, J. Han; *Seoul/KR (kangjihee1@gmail.com)*

Purpose: To find differential CT features of colorectal poorly-differentiated neuroendocrine tumours (PD-NETs) from well-differentiated NETs (WD-NETs) and adenocarcinomas (ADCs).
Methods and Materials: CT features of 25 pathologically-proven colorectal WD-NETs, 36 PD-NETs and 36 ADCs were retrospectively reviewed. The following CT items were analysed: size, longitudinal location, morphology, homogeneity, the presence of intact overlying mucosa, necrosis, calcification, homogeneity, degree of enhancement on each CT phase, the presence of enlarged lymph node (LN), and metastasis. Significant CT variables were determined using the chi-square test, Fisher's exact test, and Student t-test. Receiver operating characteristic analysis was used to determine the optimal cut-off value of tumour and LN size.
Results: Large size, rectum location, ulceroinfiltrative morphology, absence of intact overlying mucosa, heterogeneous CT attenuation with necrosis, presence of ≥3 enlarged LNs, and metastasis were found to be significant variables to differentiate PD-NETs from WD-NETs (P<0.05). The optimal cut-off value for tumour size in differentiating PD-NETs from WD-NETs was 1.5cm (AUC=0.958, sensitivity=100%, specificity= 84%, P<0.0001). High attenuation on arterial phase, persistent high enhancement pattern, presence of ≥6 enlarged LNs, large LN size, and wash-in/wash-out enhancement pattern of liver metastasis were significant variables to differentiate PD-NETs from ADCs (P<0.05).
Conclusion: Compared to WD-NETs, colorectal PD-NETs usually appear as large, ulceroinfiltrative, heterogeneous rectal mass without intact overlying mucosa and accompany with enlarged LNs and metastasis. High attenuation on arterial phase, presence of enlarged LNs with larger size and greater number, and wash-in/wash-out enhancement pattern of liver metastasis can be useful CT discriminators of colorectal PD-NETs from ADCs.

B-0205 15:12

Value of MR defecography parameters used in diagnosis of obstructed defecation

K. Schawkat[1], H. Heinrich[1], H. Parker[1], B. Barth[1], R.P. Mathew[1], D. Weishaupt[1], M. Fox[2], C.S. Reiner[1]; [1]*Zurich/CH*, [2]*Basel/CH (k_schawkat@hotmail.com)*

Purpose: To assess the value of MR-defecography (MRD) parameters used in diagnosis of obstructed defecation.
Methods and Materials: Twenty-two consecutive patients (16 women, 6 men; mean age 51±19.4) with obstructed defecation and twenty healthy volunteers (11 women, 9 men; mean age 33.4±11.5) underwent MRD in a closed-configuration 3.0T MRI-system in supine position. MRD included midsagittal T2-weighted images at rest and during defecation after filling the rectum with 250ml water-based gel. Two independent and blinded radiologists measured pelvic floor descent in reference to the pubococcygeal line (PCL) and HMO-lines during defecation, anorectal angle (ARA), qualitatively assessed grade of evacuation (GE), paradoxical contraction (PC), and missing sphincter relaxation (MSR).
Results: Interreader agreement for PCL-, HMO-, and ARA-measurements was good to excellent (Intraclass-correlation-coefficient [ICC], 0.60-0.99), for GE excellent (κ-value, 0.76-0.80), and for PC and MSR fair to moderate (κ-value, 0.24-0.47). Posterior compartment descent, H-, M-line and ARA were significantly greater in patients compared to volunteers (p<0.05). 30-50% of volunteers had mild anterior and middle compartment descent and hiatal enlargement. 50% of volunteers had moderate rectal descent. Impaired evacuation was seen in 9/20 (45%) volunteers and 9/22 (41%) patients. Also PC and MSR were equally found in volunteers (40%, 40%) and patients (41%, 32%).
Conclusion: Quantitative, but not qualitative MRD-parameters show both excellent interreader agreement and ability to differentiate patients with obstructed defecation from healthy volunteers. However, pelvic floor descent values considered abnormal according to PCL and HMO-system are found in a substantial number of healthy volunteers and therefore need to be redefined.

B-0206 15:20

Dynamic MRI of the pelvic floor in different body positions: success rate of MR defecography in supine vs left lateral body position

K. Schawkat[1], B. Pfister[1], H. Parker[1], H. Heinrich[1], B. Barth[1], D. Weishaupt[1], M. Fox[2], C.S. Reiner[1]; [1]*Zurich/CH*, [2]*Basle/CH (k_schawkat@hotmail.com)*

Purpose: To assess the success rate of MR-defecography (MRD) performed in supine versus lateral body position and assess differences in pelvic floor measurements.
Methods and Materials: 22 consecutive patients (16 women, 6 men; mean age 51±19.4) with obstructed defecation underwent MRD in a closed-configuration 3.0T MRI-system in supine and lateral position. MRD included midsagittal T2-weighted images at rest and during defecation after filling the rectum with 250ml water-based gel. Two independent radiologists measured pelvic floor descent in reference to the pubococcygeal line (PCL) and assessed grade of evacuation (GE) in both body positions. Image quality (IQ) was rated on a 5-point-scale (5=excellent, 1=poor).
Results: Grades of middle and posterior compartment descent were similar in supine and lateral position (p>0.05). Anterior compartment descent was significantly higher in lateral position, but still normal to small in the majority of patients (4.6±23.1 cm vs. 8.9±25.2 cm, p<0.042). When attempting to defecate in supine position 6/22 (27%) patients showed no evacuation, while in lateral position only 3/22 (14%) were not able to evacuate. Image quality was equal at rest (4.4±0.5 and 4.7±0.6, p>0.05) and slightly better in supine compared to the lateral position during defecation (4.5±0.4 vs. 3.9±0.9, p<0.017).
Conclusion: In lateral position more patients were able to evacuate with similar grades of pelvic floor descent compared to supine position. Image quality was slightly degraded during defecation in lateral position. MRD in lateral position is a valuable alternative for patients unable to defecate in supine position.

14:00 - 15:30 **Room X**

Vascular

SS 315

Carotid / cerebrovascular imaging

Moderators:
M. Köcher; Olomouc/CZ
R.N. Planken; Amsterdam/NL

K-06 14:00

Keynote lecture
C. Loewe; *Vienna/AT*

B-0207 14:09

Correlation of cerebrovascular reactivity and MRI pattern of carotid atherosclerotic plaque
A. Maksimova, E. Bobrikova, I. Bukhovets, M. Plotnikov, W. Ussov; *Tomsk/RU (asmaximova@yandex.ru)*

Purpose: Comparison of patients with carotid atherosclerosis, the structure of atherosclerotic plaques imaged using MRI with cerebral vascular reactivity quantified by echo.
Methods and Materials: Everyone of 21 persons with carotid artery stenosis >70%, quantified with high-resolution MRI of arterial wall. To assess the cerebrovascular reactivity transcranial ultrasound of middle cerebral artery was carried out with quantification of blood flow parameters at rest and during the stress tests: first with breath holding test and then with hyperventilation one, with calculation of reactivity index (RI). The patterns of auto-regulative reaction to the stress test were assigned to the following conventional types: positive reaction (RI=1.1-1.4); negative reaction (RI=0.9-1.1); paradoxical reaction (RI<0.9). From visual evaluation of MRI of carotid stenoses four types of plaques were assembled: mixed plaque with severe fibrosis and lipid core, plaque with lipid component, with intraplaque haemorrhage and calcified plaque.
Results: It was found that at breath holding hypercapnic test there is a statistically significant association between MRI plaque structure and type of the reaction, whereas at the test with hyperventilation no significant differences were found. At breath hold test in 56% of patients with MR images of plaque hypointense on T1-weighted scans and hyperintense on T2-weighted ones unidirectional positive response was observed; pathologic unidirectional negative response or multidirectional response were observed in patients with MR evidence of haemorrhagic plaques hyperintense on T1-weighted scans and hypointense on T2-weighted ones.
Conclusion: Atherosclerotic lesions of the internal carotid artery with intra-plaque haemorrhage are accompanied with critical deterioration of cerebrovascular reactivity.

B-0209 14:17

Spontaneous intracranial artery dissection: HR-MRI and MRA diagnosis
M. Dreval, M.V. Krotenkova, L.A. Kalashnikova, L.A. Dobrynina; *Moscow/RU (shusheek@yandex.ru)*

Purpose: To compare the diagnostic capabilities of MRA and HR-MRI in spontaneous intracranial dissection detection.
Methods and Materials: The study included 61 patients (27 males, 31 females) with spontaneous artery dissection manifested by ischaemic stroke or isolated head or neck pain. In every time point MRI was performed on 1.5 T scanner. Data of 3D TOF MRA of the cervical and intracranial arteries and 3D spc T1 fat suppression sequence of the neck and head were obtained. Intramural haematoma (IMH), and muscle signal intensity was measured and contrast index was calculated.
Results: After statistical analysis of the data with the use of non-parametric statistical methods (Mann-Whitney U test) it was revealed that value of the contrast index of IMH in 3D spc T1 fat suppression sequence was higher than that in 3D TOF MRA ($p<0.05$). The contrast index of IMH in intracranial and cervical artery dissection did not differ significantly in 3D spc T1 fat suppression sequence. The subjective visual analysis showed the same results.
Conclusion: 3D spc T1 fat suppression sequence of the neck and head has the advantage of identifying both intracranial and cervical artery dissection before 3D TOF MRA and allows reducing the study protocol up to one sequence.

B-0210 14:25

The risk of MR-detected carotid plaque haemorrhage on recurrent or first-time stroke or any cerebrovascular events: a meta-analysis of individual patient data
A.T.R. Schindler[1], R. Schinner[1], N. Altaf[2], M.E. Kooi[3], A.R. Moody[4], H. Poppert[1], M.F. Reiser[1], D.P. Auer[2], T. Saam[1]; [1]*Munich/DE*, [2]*Nottingham/UK*, [3]*Maastricht/NL*, [4]*Toronto, ON/CA (Andreas.Schindler@med.uni-muenchen.de)*

Purpose: To obtain precise estimates on the cerebrovascular risk of MR-detected carotid-plaque-haemorrhage (PH) during follow-up in symptomatic and asymptomatic individuals in a meta-analysis based on individual patient data.
Methods and Materials: Individual patient data of published cohorts on the association of PH with ischaemic symptoms was collected, including clinical course from diagnosis of PH until first treatment or last available follow-up. Risk of ischaemic stroke alone and of ischaemic events (stroke, TIA, amaurosis fugax) after 3, 12, and 24 months was estimated by survival-analysis. Baseline predictors of outcome were investigated by an adjusted COX/Frailty model.
Results: Datasets of 722 individuals from seven studies were obtained (symptomatic=77.6%, prevalence of PH at baseline=46.8%). During 1.205 person-years of follow-up 70 strokes (annualised event rate; AER=5.81%), and a total of 131 ischaemic events were observed (AER=10.9%). Presence of PH increased the risk of stroke in symptomatic, asymptomatic, and all patients by 7.1-, 3.5-, and 6.1-fold, and for ischaemic symptoms by 4.8-, 5.8-, and 5.3-fold, respectively. Cumulative risk for ischaemic stroke after 3, 12, and 24 months was 6.3, 13.7 and 24.4% in PH^+ vs. 0.5, 0.9, and 2.5% in PH^- patients. In the adjusted model presence of PH (HR 9.1, 4.6-18.1; $p<0.0001$), and diabetes (1.9, 1.1-3.2; $p=0.0192$) significantly increased the risk of recurrent ischaemic stroke.
Conclusion: This IPD meta-analysis overcomes limits of previous meta-analyses and provides more precise risk estimates on the association of PH with ischaemic symptoms and -more importantly- for ischaemic stroke alone which can be used for planning of intervention trials.

B-0211 14:33

A population-based investigation of cerebral vascular stenosis
S. Yan, M. Li, F. Zhai, Y. Zhu, S. Zhang, Z. Jin; *Beijing/CN (ysh19a@163.com)*

Purpose: To investigate the population-based prevalence of cerebral vascular stenosis and the relationship between it and other vascular diseases.
Methods and Materials: This research comprised 1183 participants (aged 55.8±9.57 years, 38.1% male) from an ongoing community-based cohort study. All the participants underwent brain MRI and carotid ultrasound. MRI images were collected at 3T MRI scanner and the sequences mainly included 3D T1 MPRAGE, T2-FLAIR, SWI and TOF-MRA. Used kappa test to estimate the inter-observer agreement and logistic regression adjusted for vascular risk factors to evaluate associations between cerebral vascular stenosis and other imaging biomarkers.
Results: Based on the MRA images, we observed cerebral vascular stenosis in 13.9% persons of all the participants, included 8.9% persons with mild stenosis and 5% with severe stenosis and occlusion. The value of inter-observer agreement was 0.755. There was a significant association between higher prevalence of cerebral vascular stenosis and the presence of carotid plaque, odds ratio (OR) = 2.040 (95% confidence interval [CI]: 1.471-2.830), $p < 0.001$. Also the prevalence of cerebral vascular stenosis was significantly associated with the deep white matter hyperintensities (OR=1.497, 95%CI: 1.071-2.093, p=0.018) and lacunes (OR=2.563, 95%CI: 1.442-4.554, p=0.001).
Conclusion: This high prevalence of cerebral vascular stenosis might remind us of the prevention of cerebral ischaemic diseases in the future. The outcomes of logistic regression might help us reveal the relationship between intracranial and extracranial stenosis, also showed evidences of the relationship between cerebral vascular atherosclerosis diseases and cerebral small vessel diseases.

B-0212 14:41

Variants of the circle of Willis and association with internal carotid artery stenosis
A. Varga[1], G. Di Leo[2], P.V. Banga[1], C. Csobay-Novak[1], M. Kolossvary[1], K. Hüttl[1]; [1]*Budapest/HU*, [2]*Milan/IT (vargand26@yahoo.com)*

Purpose: To provide an overview of anatomical variants of the circle of Willis (CoW) in patients with internal carotid artery (ICA) stenosis, in relation to clinical data.
Methods and Materials: After Institutional Review Board approval, two independent readers retrospectively studied 544 patients (331 males, mean age 69±8 years) that underwent carotid endarterectomy without shunting and had an adequate carotid and cranial CT angiography. The presence and the diameter of the individual segments and the anterior and two posterior parts of the CoW were evaluated as well as four reclassified groups based on the

number of hypoplastic and absent segments. Intraobserver and intraobserver agreement were estimated.
Results: Variants of CoW were found in 97% of patients. Aplasia of the posterior communicating artery (41%) was the most common finding; compromised posterior collaterals were observed in 78% of patients; circles with ≥2 hypoplasic or ≥1 absent segments in 86%. Compromised CoW was more frequent in patients with symptoms and was also correlated to ICA stenosis (p=0.012). Intraobserver and intraobserver agreement was excellent for almost all segments of the CoW.
Conclusion: A high prevalence of CoW variants and compromised CoW, in particular compromised posterior collaterals, was observed in a large cohort of patients undergoing carotid endarterectomy. The CoW variations reported here may contribute to our understanding of cerebral collateralisation in steno-occlusive carotid disease.

B-0213 14:49

Coexistence of cardiovascular risk factors and the volume of carotid bodies determined by computed tomography angiography of the carotid arteries

P. Jazwiec, P. Gac, M. Poreba, G. Mazur, R. Poreba; *Wroclaw/PL (pawelgac@interia.pl)*

Purpose: The study aimed at evaluation of the relationship between comanifestation of cardiovascular risk factors (CVRF) and the volume of carotid bodies (CB) determined by computed tomography angiography (CTA) of the carotid arteries.
Methods and Materials: The study was conducted on 52 persons (mean age of 68.32±12.31 years). Anamnesis, physical examination and laboratory tests allowed to characterise every patient in respect to CVRFs, i.e. smoking of cigarettes, arterial hypertension, hypercholesterolaemia, hypertriglyceridaemia, type 2 diabetes mellitus and overweight/obesity. Among the participants, subgroups were distinguished with 1-2 CVRF (group A, n=23), with 3-4 CVRF (group B, n=21) or with 5-6 CVRF (group C, n=8). In all patients, the volume of carotid bodies was evaluated at the basis of scans obtained by CTA of the carotid bodies.
Results: The volume of carotid bodies proved to be significantly higher in groups B and C than in group A (A: 23.66±12.02 mm^3, B: 42.17±14.85 mm^3, C: 45.77±24.71 mm^3, $p_{A-B, A-C}<0.05$). Positive correlation could be noted between the number of CVRF and the volume of carotid bodies (r=0.56, p<0.05). Regression analysis allowed to demonstrate that in the study group manifestation of arterial hypertension, followed by type 2 diabetes mellitus and smoking of cigarettes, were linked to the highest probability of the increased volume of carotid bodies.
Conclusion: In the study group, a positive relationship was found between the number of cardiovascular risk factors and the volume of carotid bodies. Arterial hypertension involved the CVRF linked to the highest probability of the increased volume of carotid bodies.

B-0214 14:57

Carotid resistive index as a marker of cardiovascular risk in adults without symptomatic cardiovascular disease

K.D. Hurtado Ortiz, F. Lubinus Badillo, V.M. Herrera; *Floridablanca/CO (kevinkorporation@hotmail.com)*

Purpose: Equations and markers of atherosclerosis such as the intima-media thickness (IMT) allows risk stratification in cardiovascular disease. The resistive index, an easily measured haemodynamic marker, might contribute this task; however, little is known about its relationship to cardiovascular risk factors (CVRFs) or IMT.
Methods and Materials: We conducted a cross-sectional study in adults (>40) from Bucaramanga, Colombia. Non-current smokers and individuals without symptomatic cardiovascular disease (i.e. myocardial infarction, stroke or peripheral artery disease) were eligible. CVRFs were determined by interview, anthropometry, ambulatory blood pressure (BP) monitoring, and quantification of fasting blood glucose and lipid fractions. IMT and RI were measured by ultrasonography (Toshiba Aplio 500 PLT-805AT) at the common carotid (CCA), and CCA and internal carotid (ICA) arteries, respectively.
Results: We evaluated 429 participants (mean age: 57.3 years; 22% male). IMT was larger at the posterior compared to the anterior CCA walls (0.69 vs. 0.64; p<0.05) and RI was larger in the CCA than the CCI (0.73 vs. 0.64, p<0.05). RI was associated with IMT (β [age and sex-adjusted] = 0.006 per 0.1 mm, p<0.05) without hypertension or atheromatous plaque-by-interaction. RI was larger in men than in women, and positively correlated to age, waist-to-hip ratio, BP, and glucose; however, in multivariate analyses only BP was a statistically significant predictor (0.022 per 10 mmHg [systolic] and -0.019 per 5 mmHg [diastolic]).
Conclusion: Our results, first from a Latin American population, confirms RI as a marker of cardiovascular risk, mainly explained by BP, and haemodynamic correlate of subclinical structural abnormalities.

B-0215 15:05

Effects on radiation dose, image quality and accuracy for the detection of carotid stenosis of 90-kVp low-tube-voltage carotid and intracerebral CT-angiography combined with ADMIRE

D. Leithner, J.L. Wichmann, L. Lenga, S.S. Martin, S. Mahmoudi, M. Beeres, M.H. Albrecht, T.J. Vogl, J.-E. Scholtz; *Frankfurt a. Main/DE*

Purpose: To evaluate radiation exposure, image quality, artefact and detection of carotid stenosis of low-tube-voltage 90-kVp acquisition combined with advanced modelled iterative reconstruction algorithm (ADMIRE) for carotid and intracerebral CT-angiography (CCTA).
Methods and Materials: We evaluated 43 patients (33 male; mean age: 61.7) retrospectively who underwent dual-energy CCTA on a third-generation 192-slice dual-source CT. 90-kVp and linearly-blended 120-kVp images were compared. Attenuation and noise of CCA at shoulder height, CCA at bifurcation, ICA at carotid syphon, MCA and BA were measured to calculate contrast-to-noise ratio (CNR). Subjective image quality was rated by three independent reviewers using 5-point grading scales regarding artefact and suitability. Detection and grading of carotid stenosis was performed. Interobserver agreement was calculated using intraclass correlation coefficient (ICC). Radiation dose was expressed as dose-length product (DLP).
Results: Attenuation and noise of all arteries were higher in 90-kVp compared to standard 120-kVp (all p<0.001), resulting in significantly increased CNR in 90-kVp (ICA, 38.2±13.5 vs 22.4±8.0 HU; p<0.001). Artefact and suitability were excellent in both series without significant differences.Highest artefact level, still with excellent suitability was rated at shoulder height without significant difference (90-kVp, 4.9±0.4; 120-kVp, 4.8±0.5). Detection of carotid stenosis was excellent in both series with no significant difference (stenoses in 32 of 129 segments; ICC, 0.94).DLP was reduced by 40.3% using 90-kVp acquisition (110.6±32.1 vs 185.4±47.5 mGy·cm, *P*<0.001).
Conclusion: 90-kVp CCTA combined with ADMIRE results in increased CNR, excellent suitability with low artefacts and significant reduction of radiation dose. Detection and quantification of carotid stenosis maintains excellent.

B-0216 15:13

Wavelet-based angiographic reconstruction of CT perfusion data: diagnostic value in cerebral venous sinus thrombosis

W.G. Kunz, F. Schuler, M.P. Fabritius, L. Havla, M.F. Reiser, W.H. Sommer, K.M. Thierfelder; *Munich/DE (wolfgang.kunz@med.lmu.de)*

Purpose: To test the diagnostic value of wavelet-based angiographic reconstruction of CT perfusion data (waveletCTA) to detect cerebral venous sinus thrombosis (CVST) in patients who underwent whole-brain CT perfusion (WB-CTP).
Methods and Materials: Datasets were selected from a cohort of 2863 consecutive patients who underwent multiparametric CT including arterial CTA (artCTA) and WB-CTP. The angiographic waveletCTA signal is generated by voxel-based wavelet-transform of time attenuation curves (TAC) from WB-CTP data. Two blinded readers analysed waveletCTA for presence of CVST. Venous CT/MR angiography (venCTA/venMRA) served as reference standard. Diagnostic confidence for CVST detection and quality of depiction for 13 different venous sections were evaluated on 5-point Likert scales. Thrombus length and the flowing blood-to-thrombus (FBtT) ratio of mean CT attenuation and waveletCTA signal were quantified.
Results: Sixteen patients were included: 10 with venCTA-/venMRA-confirmed CVST, and 6 with artCTA-suspected but follow-up-excluded CVST. waveletCTA reconstruction was successful in all patients. Among patients with confirmed CVST, waveletCTA correctly demonstrated presence, location and extent of the thrombosis in 10/10 cases. Among the patients with artCTA-suspected but follow-up-excluded CVST, waveletCTA correctly ruled out CVST in 5/6 patients. Additional reading of waveletCTA significantly increased diagnostic confidence compared to artCTA (4.4 vs 3.6, p=0.044). waveletCTA provided higher FBtT ratios (146.2 vs 2.6, p<0.001) and better depiction of all venous sections (4.2 vs 2.6, p<0.001) compared to artCTA.
Conclusion: waveletCTA was technically feasible in CVST patients and reliably identified CVST. waveletCTA might serve as an additional reconstruction to rule out or incidentally detect CVST in patients who underwent WB-CTP.

14:00 - 15:30 **Room Z**

Interventional Radiology

SS 309

Radioprotection in interventional radiology (IR)

Moderators:
V. Bérczi; Budapest/HU
N. Karunanithy; London/UK

B-0219 14:00

Personalised dose feedback to medical staff involved in fluoroscopy-guided interventions: a new era in radiation dose monitoring

A.M. Sailer[1], L.W.M. Vergoossen[2], L.E. Paulis[2], W.H. van Zwam[2], M. Das[2], J.E. Wildberger[2], C.R.L.P. Jeukens[2]; [1]*Stanford, CA/US*, [2]*Maastricht/NL (laura.vergoossen@mumc.nl)*

Purpose: Ionizing radiation is a major concern for the medical community as well as society. We hypothesize that providing weekly personal dose feedback will increase awareness and ultimately will lead to optimized behaviour. Therefore, we designed and implemented a personalized feedback of procedural and personal doses for medical staff involved in fluoroscopy-guided interventions.
Methods and Materials: Staff (physicians and technicians, n=27) involved in fluoroscopy-guided interventions were equipped with electronic personal dose meters (PDMs). Procedural patient dose data including the dose area product (DAP) and effective doses from PDMs were prospectively monitored for each procedure over an 8 months period (n=1082). A personalized feedback form was designed displaying the DAP individually and personal dose per procedure, as well as the relative and cumulative doses. This study consisted of two phases: (1) month 1-5: staff did not receive feedback (n=701); (2) month 6-8: staff received weekly individual dose feedback (n=381).
Results: For the first technician, the average relative dose was significantly lower in the feedback phase compared to the pre-feedback phase (mean relative dose±SD: 0.60±1.42 µSv/Gy·cm² (phase 1) versus 0.32±0.95 µSv/Gy·cm² (phase 2), p=0.002). The average relative first physician dose showed a non-significant trend towards a lower relative dose during the feedback phase (mean relative dose ±SD: 1.19±1.81 µSv/Gy·cm² (phase 1) versus 0.95±1.32 µSv/Gy·cm² (phase 2), p=0.099).
Conclusion: Personalized dose feedback to staff involved in fluoroscopy-guided interventions proofed feasible and valuable to improve individual awareness and overall radiation safety.

B-0218 14:08

Evaluation of radiation exposure in central venous catheter (CVC) placement in paediatric patients using two fluoroscopy protocols on a flat-panel system

R. Gerasia[1], S. Degiorgio[2], C. Tafaro[1], G.S. Gallo[1], A. Cucchiara[1], K. Cortis[2], L. Maruzzelli[1], R. Miraglia[1]; [1]*Palermo/IT*, [2]*Msida/MT (ctafaro@ismett.edu)*

Purpose: Evaluation of radiation exposure in paediatric patients undergoing image-guided CVC placement procedures using two different fluoroscopy protocols (FP).
Methods and Materials: We reviewed 110 consecutive CVCs placed in 62 paediatric patients in our centre between 7/2010 and 9/2016. Mean age was 14±12 months (median 12, range 1-48); mean weight was 8.3±3.3kg (median 8,8, range 3.5-13.5). 62 CVCs were placed using 50% of the nominal dose (FP50) whereas 58 CVCs were placed using 35% of the nominal dose (FP35) with technical parameters adjusted for paediatric protocol. DAP and fluoroscopy time (FT) were recorded for each procedure. DAP was normalised (nDAP) per unit fluoroscopy time and means for both groups were compared. Every FP35 procedure was completed successfully without changing protocol. No complications were recorded during these procedures. In addition, between October 2015 and September 2016 (20 procedures), radiation dose to operators was measured using electronic personal dosimeters, and effective dose (E) calculated.
Results: For FP50 protocol, mean nDAP was 0.30±0.17cGy*cm^2/s (median 0.25, range 0.09-0.75). For FP35 protocol, mean nDAP was 0.18±0.11cGy*cm^2/s (median 0.15, range 0-0.41). The difference between mean nDAP was statistically significant (p=0.004). E for radiologist was 0.04±0.07µSv (median 0, range 0-0.24), for anesthesia nurse 0.01±0.01µSv (median 0, range 0-0.03) and for radiographer 0±0.01µSv (median 0, range 0-0.03).
Conclusion: The use of low-dose paediatric adjusted protocols for CVC placement results in a statistically significant radiation exposure reduction by 39.5% and a very low effective dose to operators performing it.

B-0217 14:16

Procedural DAP can be used for relative dose estimation for staff dose in fluoroscopy-guided interventions

L.W.M. Vergoossen[1], A.M. Sailer[2], L.E. Paulis[1], J.E. Wildberger[1], C.R.L.P. Jeukens[1]; [1]*Maastricht/NL*, [2]*Stanford, CA/US (laura.vergoossen@mumc.nl)*

Purpose: Monitoring of effective staff doses only does not allow for judgment whether individual and procedural radiation safety can be optimized. Therefore, the relative dose was introduced, which relates the personal staff dose to a reference, measured by personal dose meters (PDMs). Our aim was to investigate the correlation between dose-area-product (DAP) and reference PDM dose and furthermore whether relative staff dose can be estimated by using the DAP.
Methods and Materials: Staff members (n=27) were equipped with PDMs and a reference PDM was mounted at a fixed position on the C-arm of the fluoroscopy system, thereby measuring scattered radiation. Clinical procedures (n=1082), grouped by procedure type were monitored prospectively. The median relative staff dose ($Dose_{Staff}/Dose_{Reference}\cdot100\%$) was calculated. The correlation between DAP and reference PDM dose was analyzed by comprehensive measurements with an Alderson anthropomorphic phantom for different scenarios of patient anatomy, operator height, acquisition techniques and C-arm angulations. Phantom measurements were compared to clinical data.
Results: DAP correlated strongly with reference PDM dose in clinical procedures (R^2=0.94, R^2=0.91, R^2=0.93 for cerebral, thoracic and abdominal procedures, respectively). Phantom measurements indicated that this correlation was mainly depending on the spectrum, i.e. kVp (mean grouped by kVp R^2=0.97, all data-points R^2=0.93; slopes: 4.07, 4.76, 5.75 µSv/Gy·cm^2 for kVp <70, 70-75, 75-80, respectively) and additional filtration, which is influenced by patient anatomy and acquisition technique.
Conclusion: We conclude that procedural DAP can be used as a reliable substitute to calculate a relative staff dose measure, increasing its applicability in daily practice.

B-0220 14:24

Radiation dose estimation for lumbar spine pain relieving interventional procedures: comparison of CT fluoroscopy and conventional CT techniques

N. Rasouly; *Kabul/AF (nrasouly@gmail.com)*

Purpose: The purpose of this study is to compare the radiation dose in lumbar spine pain relieving interventional procedures (steroid and local anesthetic injection in the facet joint, perineural and epidural spaces) under conventional computed tomography (CT) and computed tomography fluoroscopy (CTF) guidance.
Methods and Materials: From Jan 2008 to March 2014, we retrospectively obtained the data from 80 CT-guided and 56 CT fluoroscopy-guided interventional procedures performed in 74 patients with injections of steroid and local anesthetics in the facet joints, epidural space and neural foramina to estimate the radiation dose in the radiology department of Jean Minjoz university hospital, Besancon France. The data consisted of starting time, ending time, DLP measurements, patient's age and sex, site of procedure and number of procedures.
Results: 74 patients with total number of 136 procedures were included in the study, 30 (42%) male and 44 (58%) female with mean age of the 56.6 years (age range, 23-93 years). The mean DLP differed significantly between the two procedures showing marked dose reduction using CT fluoroscopy compare to conventional CT scan.
Conclusion: CT fluoroscopy significantly decreases the overall procedure time with marked reduction in radiation dose compared with conventional CT scan technique.
Author Disclosures:
N. Rasouly: Author; Prof Bruno KASTLER. Speaker; Dr Najibullah RASOULY.

B-0221 14:32

Comparison of shoulder strain relief between radiation protection aprons

A.M. Koenig[1], D. Sasse[1], R. Etzel[2], A.H. Mahnken[1]; [1]*Marburg/DE*, [2]*Giessen/DE*

Purpose: In interventional radiology radiation protection for staff has become increasingly important during the last recent years. In this study, we compared different commercially available staff's radiation protection concepts regarding their shoulder strain relief.
Methods and Materials: The tested radiation protection systems were a one-piece coat apron, a two-piece apron (vest and skirt), and the zero-gravity system (Biotronik, Germany). Shoulder strain was measured by a pressure sensor (FSR 406, Interlink Electronics, USA), which changes the electrical resistance depending on the applied pressure. This electrical resistance was measured using a portable multimeter (VC850 with bluetooth-adapter VC810,

Voltcraft, Switzerland). By generating a calibration graph, we were able to calculate the physical force of the shoulder pressure. Each apron was measured on two subjects, with focus on the right and on the left shoulders.
Results: The physical force of the shoulder pressure obtained from the one-piece coat apron, the two-piece apron, and the zero-gravity system was measured to be 29.2±2.1 N, 19.2±4.0 N, and 6.2±0.5 N, respectively. Inter-comparison between both shoulder sites showed different pressure values: the one-piece apron showed a shoulder weight of 27.4±1.5 N and 30.8±0.7 N for the right and left shoulder, respectively. While the two-piece apron was measured to be 16.9±2.1 N (right) and 21.8±4.0 N (left).
Conclusion: Compared to a one-piece coat apron, both the two-piece apron and the zero-gravity system showed substantial shoulder strain relief. Besides, we detected a significant higher pressure on the left shoulder when wearing the one-piece or two-piece aprons.

B-0222 14:40

Characteristics of a new C-arm imaging system used during uterine artery embolisation for uterine fibroids treatment: reduced radiation exposure and improved image quality

R. Schernthaner[1], R.R. Haroun[2], S. Nguyen[2], R. Duran[2], K. Hong[3], J.-F.H. Geschwind[2], M. Lin[4]; [1]*Vienna/AT*, [2]*New Haven, CT/US*, [3]*Baltimore, MD/US*, [4]*Cambridge, MA/US*
(ruediger.schernthaner@meduniwien.ac.at)

Purpose: To compare radiation exposure and image quality between a new C-arm system and the preceding generation system during uterine artery embolisation (UAE).
Methods and Materials: In this retrospective, IRB approved two-arm trial, 54 patients with symptomatic uterine fibroids were treated with UAE on two different C-arm systems. The new system includes optimised acquisition parameters and real-time image processing algorithms. Air Kerma (AK), dose area product (DAP) and acquisition time for digital fluoroscopy (DF) and digital subtraction angiography (DSA) were recorded. Body mass index was noted as well. DF image quality was assessed objectively by image noise measurements. DSA image quality was rated by two blinded and independent readers on a four-rank scale. Unpaired t tests and Wilcoxon rank-sum tests were used to assess statistical differences between the systems.
Results: There was no significant difference between the patients treated on the new (n=36) and the old system (n=18) regarding age (p=0.10), BMI (p=0.18), DF time (p=0.35) and DSA time (p=0.17). The new system significantly reduced the cumulative AK and DAP by 64% and 72%, respectively (median 0.58 Gy and 145.9 Gy*cm^2 vs. 1.62 Gy and 526.8 Gy*cm^2, p<0.01 for both). Specifically, DAP for DF and DSA decreased by 59% (75.3 vs. 181.9 Gy*cm^2, p<0.01) and 78% (67.6 vs. 312.2 Gy*cm^2, p<0.01), respectively. The new system achieved a significant decrease in DF image noise (p<0.01) and a significantly better DSA image quality (p<0.01).
Conclusion: The new imaging system significantly reduced radiation exposure and significantly improved image quality during UAE procedures.
Author Disclosures:
R. Schernthaner: Grant Recipient; Max Kade Foundation, Inc., NY, USA. **J.H. Geschwind:** CEO; PreScience Labs, LLC. Consultant; Nordion, Biocompatibles/BTG, Bayer Healthcare. Founder; Prescience Labs, LLC. Research/Grant Support; NIH, Philips Medical, DOB, Biocompatibles/BTG, Bayer Healthcare, Nordion, Context Vision, SIR, RSNA, Guerbet. **M. Lin:** Employee; Philips Research North America. Research/Grant Support; NIH.

B-0223 14:48

Evaluation of reduction in time and radiation exposure using a robotic tracking system for CT-guided percutaneous bone procedures - our experience

S. Quarchioni, F. Bruno, F. Smaldone, F. Arrigoni, S. Mariani, L. Zugaro, A. Barile, C. Masciocchi; *L'Aquila/IT (di.gao@hotmail.it)*

Purpose: To evaluate the advantages of using a robotic tracking system for CT-guided percutaneous bone procedures in terms of technical success, procedure's time, perfect centering of the lesion and radiation exposure to the interventional radiology (IR) and patients.
Methods and Materials: In the period between June 2015 and February 2016 we performed 28 CT-guided percutaneous procedures of bone's lesion in 28 patients (16 biopsy, 6 crioablations, 6 RFA). 14 procedures (7 biopsy, 3 crioablations, 4 RFA) were performed with "free hand" standard technique, meanwhile 14 procedures (7 biopsy, 3 crioablations, 4 RFA) were performed using a robotic tracking system. For all procedures the final positioning of the needle was confirmed with Fluoro-CT. We used for the CT scans the following parameters: 50mAs, 120Kv, Slice Thickness 3mm.
Results: Fluoro-CT scans confirmed the correct position of the needle using the robotic tracking system with a single entry in 12 patients (92%). Technical success for both procedures was 100%. The mean execution time was 16 minutes for the procedures assisted with the robotic system and 25 minutes for the standard procedures. The mean radiation dose for the patients after the first CT-scans used for the visualisation of the lesion, was 3.5±1mSv in the standard procedures, and 0.92±0.78mSv in the procedures with the robotic system. The radion dose for the IR was 0.
Conclusion: The robot tracking system is an innovative medical device that allows to reduce the procedure's time, the number of CT-scans and consequently the radiation's dose for the patients and IR.

B-0224 14:56

Evaluation of a novel needle positioning system for CT-guided interventions: preliminary results

W.J. Heerink[1], M. Arnolli[2], R. Vliegenthart[1], J.-P. Pennings[1], G. Sieders[1], I.A.M.J. Broeders[2], M. Oudkerk[1], K.P. de Jong[1]; [1]*Groningen/NL*, [2]*Enschede/NL (w.j.heerink@umcg.nl)*

Purpose: To determine the accuracy of a novel table-mounted needle placement system (NPS) and compare it to regular free-hand CT-guided needle placement.
Methods and Materials: A novel table-mounted needle placement system (DEMCON, Enschede, the Netherlands) for CT-guided interventions is introduced and tested in a gelatin phantom, with chamois leather skin, containing 12 targets (six in-plane and six out-of-plane) at a depth of 12cm. Two experts approached 6 of the targets with regular free-hand CT-guidance and 6 using the NPS, for a total of 24 approaches.
The distance between the tip of the needle and the center of the target was measured as placement error. The needle was not repositioned if it was within 5mm of the target or after 5 needle manipulations. The mean (range) of the placement error, the number of needle manipulations and the number of CT scans acquired were determined for the NPS and free-hand group and were compared using independent samples t-tests.
Results: The mean placement error was 2.3mm (0.8-4.8mm) and 6.6mm (2.7-13.2mm; p=0.001), the mean number of needle manipulations was 1 (1-1) and 4.6 (3-5; p<0.001), and the number of CT scans was 3.2 (2-4) and 5.9 (3-8; p<0.001), for the NPS and free-hand group, respectively.
Conclusion: The use of the NPS increases the accuracy of needle placement and reduces the number of repositioning attempts and CT scans. It has the potential to reduce complications and patient radiation in CT-guided biopsy and ablative procedures.
Author Disclosures:
M. Arnolli: Employee; DEMCON Advanced Mechatronics B.V.

B-0225 15:04

Increased freedom in AEC parameter selection can reduce dose and increase efficiency in interventional cardiology x-ray systems

M. Dehairs, N. Marshall; *Leuven/BE (michiel.dehairs@uzleuven.be)*

Purpose: This work compares 3 exposure parameter (3P) AEC control to a more flexible 5-parameter (5P) method to investigate the possible benefits of increasing AEC parameter freedom.
Methods and Materials: A phantom composed of 15 composite PMMA/aluminium plates, was imaged on a Siemens Artis Q interventional cardiology system. Standard 3P acquisition parameter settings (tube potential, tube current, pulse length) vs 5P settings (extra copper filtration, focus size) and entrance air kerma rate (EAKR) were measured vs phantom thickness. Signal difference to noise ratio (SDNR) was measured using an iron insert, centred in the phantom. SDNR was then multiplied by MTF based correction factors for focal spot and motion blurring, giving a spatial frequency dependent parameter: SDNR(f). These MTF correction factors were evaluated at a spatial frequency of 1.4mm^{-1} and object motion of 25mm/s, which are typical for cardiac imaging. A generalised figure of merit (FOM) SDNR(f)²/EAKR was calculated for the 3P and 5P data.
Results: AEC control using 5P versus 3P technique showed clear improvements, when considered over all thicknesses (~78mm to ~390mm water equivalent): EAKR was reduced by 24% and 34% for fluoroscopy and acquisition modes respectively, while the FOM increased by 27% and 87% respectively. Averaging over smaller thicknesses (~78mm to ~209mm) gave even higher increases in FOM of 50% and 139% for fluoroscopy and acquisition, respectively, suggesting further benefit for paediatric procedures.
Conclusion: Increasing the number of controlling AEC parameters from three to five enables increased image quality at reduced entrance air kerma for interventional cardiology systems.
Author Disclosures:
M. Dehairs: Research/Grant Support; Siemens Healthcare.

B-0226 15:12

Occupational radiation doses to operators performing fluoroscopically guided diagnostic and therapeutic hepatobiliary interventional procedures: a single-centre study

R. Gerasia[1], S. Degiorgio[2], C. Tafaro[1], G.S. Gallo[1], A. Cucchiara[1], K. Cortis[2], L. Maruzzelli[1], R. Miraglia[1]; [1]*Palermo/IT*, [2]*Malta/MT (rgerasia@ismett.edu)*

Purpose: Evaluation of effective radiation doses (E) of radiologist, nurses and radiographers performing hepatobiliary FG procedures.
Methods and Materials: Over a 10-month period (October 2015-August 2016), 459 FG hepatobiliary procedures were performed in a single center in 240 adult patients. Electronic personal dosimeters were used to measure radiation doses to radiologist, anaesthesia nurse and radiographer. Patients' radiation dose was measured using Dose Area Product (DAP) and Fluoroscopy Time (FT).
Results: Chemoembolisation of HCC: mean E for the radiologist was 0,66 µSv (SD 1.09, range 0-9.96), for the anaesthesia nurse 0.18 µSv (SD 0.49, range 0-4.65), for the radiographer 0.05 µSv (SD 0.10, range 0-0.99); range for patients' DAP was 4.68-421.98 Gy*cm^2, for FT range 115-4035 sec. Percutaneous biliary procedures: mean E for the radiologist was 2.86 µSv (SD 3.26, range 0-54.54), for the anaesthesia nurse 0.261 µSv (SD 0.59, range 0-4.05), for the radiographer 0.43 µSv (SD 3.04, range 0-38.01); range for patients' DAP was 0,29-218.49 Gy*cm^2, for FT 35-4192 sec. TIPS: mean E for the radiologist was 1.37 µSv (SD 2.50, range 0.15-12.18), for the anaesthesia nurse 0.20 µSv (SD 0.62, range 0-3.99), for the radiographer 0.57 µSv (SD 1.02, range 0-4.83); range for patients' DAP was 7,22-644,44 Gy*cm^2, for FT range 213-2604 sec.
Conclusion: Mean E of operators varies with complexity of procedure performed, position of operator in angiosuite and use of adjunct leaded shield when possible.

B-0227 15:20

Radiation dose reduction during bronchial artery embolisation with a new imaging technology

C. Spink, M. Avanesov, T. Schmidt, M. Grass, G. Schoen, A. Koops, G. Adam, H. Ittrich, P. Bannas; *Hamburg/DE (c.spink@uke.de)*

Purpose: To compare the patient radiation doses during bronchial artery embolisation (BAE) before and after an imaging processing technology upgrade.
Methods and Materials: In a retrospective single-center-study, cumulative air kerma (AK), cumulative dose area product (DAP), total fluoroscopy time and contrast agent were gathered from a BMI- and age-matched population of 60 patients during BAE. 32 procedures were performed before and 28 after the technology upgrade from Philips Allura Xper to Philips AlluraClarity. Mean values were compared using two-tailed t-tests. Independent readers assessed DSA image quality using a four-rank likert scale and the Wilcoxcon test.
Results: Using the new imaging technology a significant reduction in mean DAP (187.7 vs 77.3 Gycm^2, p<0.001) and a significant reduction in mean AK (1.5 vs 0.6 Gy, p<0.001) could be achieved. The number of exposure frames (251 vs 231 frames, p=0.60), fluoroscopy time (35.3 vs 33.5 min, p=0.68) and amount of contrast agent (139.5 vs 155.1 ml, p=0.29) did not differ significantly between the two groups. Image quality after the technology upgrade was not rated significantly inferior (2.81 vs 2.94, p=0.62).
Conclusion: The new imaging technology significantly reduces patient radiation dose up to 58% maintaining an adequate image quality. Fluoroscopy time, the number of exposure frames and the amount of contrast agent did not significantly increase.

14:00 - 15:30 **Room O**

Chest

SS 304

Interstitial lung disease (ILD) and COPD: quantification and function

Moderators:
J. Broncano; Cordoba/ES
P.A. Grenier; Paris/FR

B-0228 14:00

Is CT visual score able to demonstrate significant differences in distribution and progression of IPF abnormalities on the basis of smoking habit and treatment?

C. Romei, E. Perrone, A. De Liperi, L. Tavanti, D. Nieri, L. Carrozzi, R. Morganti, A. Palla, F. Falaschi; *Pisa/IT (chiara.romei@gmail.com)*

Purpose: To evaluate the role of smoking habit in patients with idiopathic pulmonary fibrosis (IPF) regard to the distribution of the main CT abnormalities (honeycombing and reticulation) and their progression during the follow-up. To assess the mortality of these patients in relation to smoking habit and treatment.
Methods and Materials: 56 patients with multidisciplinary diagnosis of IPF were distributed into three groups on the basis of smoking habit (18 non-smokers, 14 ex-smokers less than 20 pack-year (PY) and 24 ex-smokers more than 20 pack-year). We also classified the population in two groups; treated with Pirfenidone and untreated. The distribution of different abnormalities were visually scored by a radiologist at baseline and during the follow-up. The correlation with mortality rate were assessed.
Results: In the 3 groups no significant differences in the distribution of reticulation and honeycombing were found. A significant increase of honeycombing and reticulation in ex-smokers was demonstrated. The percentage of reticulation and honeycombing increases faster in untreated patients; the progression was quantified in 1,6 versus 2,3 points/year for honeycombing and 0,5 vs 3 points/year for reticulation. No significant difference in mortality rate was observed.
Conclusion: In our study CT visual score was not able to demonstrate any significant difference of IPF abnormalities distribution on the basis of smoking habit. Conversely a greater progression of abnormalities was showed in heavy smokers and untreated patients.

B-0229 14:08

Volumetric texture analysis in the characterisation of interstitial lung diseases in lung transplant patients

F. Gentili, V. Nardone, D. Spina, D. Bennett, A. Fausto, P. Tini, P. Rottoli, L. Volterrani, M.A. Mazzei; *Siena/IT (francescogentili@gmail.com)*

Purpose: Diagnosing usual interstitial pneumonia (UIP) with chest CT is fundamental because of the new treatment options that could modify the prognosis of this disease; however, it still represents a challenge for radiologists. The aim of this work was to investigate the possibility of volume texture analysis (TA) in differentiating UIP from non-UIP fibrosis, comparing TA parameters with histological specimens.
Methods and Materials: We selected the pre-transplant chest CT examinations of 47 patients (35 males); eighteen of them (38.3%) suffered from UIP. The lung was segmented into three regions of interest (ROI), the apex (A-ROI), the middle (MD-ROI) and the lower lobe region (B-ROI), using the lung autosegmentation of the FocalPro software, Elekta ©. All the ROIs were analysed with LifeX Software © and TA parameters were extracted, including the grey level co-occurrence matrix feature (GLCM), neighbourhood grey-level dependence matrix (NGLDM), grey-level run length matrix (GLRLM), grey-level zone length matrix (GLZLM), sphericity and indices from the grey-level histogram. Univariate and multivariate analyses, with ROC curve calculation, between all these parameters and the pathological evidence of UIP/non-UIP fibrosis were performed.
Results: Only B-ROI TA parameters resulted significantly correlated with the diagnosis in univariate analysis (histogram kurtosis, p:0.016; GLCM-contrast, p:0.016; GLCM-dissimilarity, p:0.011; NGLDM-contrast, p:0.034; GLZLM-zp, p:0.042). The logistic regression analysis produced significant results for TA parameters B-ROI histogram skewness (p:0.011), GLCM-dissimilarity (p:0.005), LGRE (p:0.020) and A-ROI GLRLM-LRE (p:0.020), with an R^2 of 0,645 and an AUC of 0.897.
Conclusion: Volumetric TA seems to improve the differential diagnosis of pulmonary fibrosis.

B-0230 14:16

Utility of 3D computer-aided diagnosis system for pulmonary functional loss and treatment response assessments in connective tissue disease patients

Y. Ohno[1], A. Yaguchi[2], T. Okazaki[2], K. Aoyagi[3], S. Kaminaga[3], Y. Kishida[1], S. Seki[1], T. Yoshikawa[1], K. Sugimura[1]; [1]*Kobe/JP*, [2]*Kawasaki/JP*, [3]*Otawara/JP (yosirad@kobe-u.ac.jp)*

Purpose: To evaluate the capability of a 3D computer-aided diagnosis (CAD) system of thin-section CT for quantitative pulmonary functional loss and treatment response assessment in connective tissue disease (CTD) patients.
Methods and Materials: 37 consecutive CTD patients underwent thin-section CT and pulmonary function test as follow-up examinations. In this study, total 135 follow-up examinations were divided as following three groups at each time point: stable (n=103), acute exacerbation (n=16), and after treatment (n=16) phases. In this study, all CT data were analysed by our proprietary software, and percentages of following six volume extents to total lung volume were automatically calculated in each CTD patient: normal lung, GGO and reticulation, nodular, honeycombing, consolidation, and emphysema. To determine the capability of pulmonary functional loss assessments, step-wise regression analyses were performed. To evaluate the capability for treatment response assessment, each volume and pulmonary functional changes were compared among three groups by Tukey's HSD test.
Results: In the step-wise regression test, VC change was significantly affected by the following two factor changes: the first-step factor was GGO and reticulation, and the second-step factor was honey comb (r=0.39, p<0.05). On comparison of each volume change, stable and after treatment phase groups had significant differences with acute exacerbation phase group (normal lung, GGO and reticulation, honeycomb and consolidation: p<0.0001). In addition, consolidation volume change had significant difference between stable and after treatment phase groups (p=0.0002).
Conclusion: 3D CAD system for thin-section CT has a potential for pulmonary functional loss and treatment response assessments in CTD patients.
Author Disclosures:
Y. Ohno: Research/Grant Support; Toshiba Medical Systems Corporation. **A. Yaguchi:** Employee; Toshiba Corporation. **T. Okazaki:** Employee; Toshiba Corporation. **K. Aoyagi:** Employee; Toshiba Medical Systems Corporation. **S. Kaminaga:** Employee; Toshiba Medical Systems Corporation. **S. Seki:** Research/Grant Support; Toshiba Medical Systems Corporation. **T. Yoshikawa:** Research/Grant Support; Toshiba Medical Systems Corporation. **K. Sugimura:** Research/Grant Support; Guerbet.

B-0231 14:24

Interstitial lung disease in systemic sclerosis: comparison between quantitative CT and visual-scoring system before and after therapy

G. Cicchetti[1], M. Occhipinti[2], M. Rucco[1], S. Bosello[1], A. Larici[1], L. Bonomo[1]; [1]*Rome/IT*, [2]*Florence/IT (cicchetti.giuseppe88@gmail.com)*

Purpose: To compare quantitative computed tomography (qCT) analysis with semiquantitative visual analysis for the evaluation of interstitial lung disease (ILD) in systemic sclerosis (SS). To evaluate the role of radiological scores during treatment follow-up.
Methods and Materials: 15 patients with ILD in SS were evaluated both clinically and radiologically with high-resolution computed tomography (HRCT) scans before and during treatment with immunosuppressive therapy. Semiquantitative evaluation was performed by 2 chest radiologists independently using Goh's visual-scoring system. Qualitative analysis was made using texture-analysis software CALIPER (Imbio, Minnesota), which can assess extent of 5 different patterns: normal, ground-glass, reticular, honeycombing, and hyperlucent. Results were compared with respiratory function tests (RFT).
Results: 30 HRCT scans were evaluated. For the semiquantitative analysis overall interobserver agreement between radiologists was good, whereas agreement between Goh's scoring system and CALIPER was fair for ground-glass and poor for reticular. The extent of ground-glass and reticular patterns were inversely correlated with RFT both with Goh's score and CALIPER, while the latter showed greater correlation at the analysis of Pearson's coefficient (P<0.001 for FVC and P=0.001 for DLCO). In particular, patients with FVC<79% and DLCO<50% showed significantly greater extent of each pattern of disease for both scores (P<0.05). ROC curve analysis did not identify any cutoff of radiological involvement extent to predict functional deterioration.
Conclusion: Both scores showed significant correlation between the extent of ILD and RFT. Despite the fair agreement with Goh's score, CALIPER showed good performance in assessing disease extent and a greater correlation with RFT than Goh's score.

B-0232 14:32

Three dimensional structures of alveoli and alveolar ducts on magnified 3D print model based on micro CT of the lung specimen

H. Natori[1], H. Takabatake[1], M. Mori[1], H. Homma[1], M. Oda[2], K. Mori[2], H. Koba[1], H. Takahashi[1]; [1]*Sapporo/JP*, [2]*Nagoya/JP (hnatori@sapmed.ac.jp)*

Purpose: Virtual microscopic images of the peripheral lung specimen by micro CT disclosed structures of the alveolar duct and alveolus. However, fine 3D structures of the alveoli and alveolar ducts have not been reported. Author reported those structures in fine visible form at a glance by magnified 3D print model.
Methods and Materials: Inflated fixed lung specimen was prepared by Heitzman's method. Size of 5 mm cubic sample was used. FOV of micro CT was 5 or 10 mm in diameter. Data were processed by the original application named as micro-NewVES and NewVES system for 3D vision and virtual endoscopy, created by co-author KM. Magnified 3D model was printed from micro CT data. Non-destructive analyses of internal structures were performed with virtual image of the magnified print model by high resolution CT for clinical use.
Results: Virtual micro endoscopic observation disclosed the orifice of the respiratory bronchiole, and then the alveolar duct was appeared. Magnified model and its virtual images disclosed structures of the alveolar ducts. The alveolar duct was constructed circular arrangement of 6 alveoli as one unit. Several units were successively connected one after another. At the dead end of the alveolar duct, there is one alveolus in the center that surrounded by 6 alveoli were found.
Conclusion: Magnified 3D model and virtual endoscopy of the model give us easy to understand complicated structures of peripheral lung at a glance. This method is useful to establish basics for image analysis of COPD and many diseases with alveolar involvement.

B-0233 14:40

Quantitative CT analysis in COPD: do coexisting fibrotic changes influence pulmonary function in patients with advanced emphysema?

F.W. Feldhaus[1], D. Theilig[1], R.-H. Huebner[1], J. Kuhnigk[2], F. Doellinger[1]; [1]*Berlin/DE*, [2]*Bremen/DE (felix.feldhaus@charite.de)*

Purpose: Aim of this retrospective study was to find out if there is significant correlation of fibrotic changes with pulmonary function tests (FEV1) in patients with severe pulmonary emphysema (GOLD 3-4).
Methods and Materials: 86 patients with pulmonary emphysema underwent CT followed by pulmonary function tests. All CT-scans were performed with identical scanning parameters. Quantitative analysis of CT-data was performed with MeVisPULMO 3D v3.42 (Fraunhofer MEVIS, Bremen, Germany) to detect low (LAV) and high (HAV) attenuation volumes, defined by a threshold (LAV: <-950HU; HAV: >-700HU). HAV was considered the measurable correlate of fibrotic changes of lung tissue. HAV-extent was classified in three groups (<7%, 7-10%, >10% of lung volume). Peripheral lung volumes within a subpleural space of 2cm width were considered as the lungs "peel". In multivariate regression-analysis results were correlated with FEV1 and LAV.
Results: There was no significant correlation of HAV and FEV1 compared with LAV. Even when more than 10% of all lung voxels accounted for HAV, LAV showed a significant higher negative correlation with FEV1 (r= -.309, R^2=.096, p=.003) than HAV (no correlation, p=.786). The highest decrease of FEV1 was registered in expiration-CT and core volumes (r= -.377, p<.001 vs. HAV with p=.376). Neither in in-/expiration series nor in core-/peel-volumes HAV showed a significant correlation with FEV1.
Conclusion: Only emphysematous changes have a significant influence on FEV1 whilst coexisting fibrotic changes do not. In contrast to CPFE (chronic pulmonary fibrosis and emphysema) emphysema-score seems to show best correlation with lung function in COPD.

B-0234 14:48

CT abnormalities in never-smoking HIV patients

R. Scaglioni, G. Besutti, G. Ligabue, A. Santoro, S. Zona, A. Malagoli, G. Guaraldi, P. Torricelli; *Modena/IT (riccardo.scaglioni@hotmail.it)*

Purpose: To assess the prevalence and risk factors for CT signs of chronic lung disease in a large cohort of never-smoking HIV-infected patients.
Methods and Materials: 329 never-smoking HIV-infected patients (49.6±8.9 years, 73.9% men) underwent ECG-gated chest CT scan for the evaluation of coronary artery calcium score (CACs) and CT slices at the level of L4-L5 for the assessment of subcutaneous and visceral adipose tissue (SAT-VAT). CT signs of chronic lung disease (emphysema, respiratory bronchiolitis (RB), bronchiectasis, bronchial wall thickening, fibrosis and non-calcified nodules) were collected. Lung emphysema was graded with a semi-quantitative visual score (0-4 for each lobe). Epicardial adipose tissue (EAT) was calculated in a subset of 153 patients. Univariable and multivariable logistic regression analyses were performed to identify factors independently associated with the presence of emphysema.

Results: Emphysema was found in 52 patients (15.6%, 13 patients with score>4), RB in 39 (11.7%), bronchiectasis in 52 (15.8%) and nodules in 33 (10%). Univariable analysis showed significant associations between the presence of emphysema and: male sex (p=0.09), age (p<0.01), BMI (p=0.05), Framingham risk score (p<0.01), CACs (p<0.01), VAT (p<0.01), and EAT (p<0.01). No significant association was found with HIV-related factors and inflammatory markers. In a multivariable model, significant predictors of emphysema were: age (OR=1.098; p=0.01), and EAT (OR=1.015; p=0.03).
Conclusion: CT signs of chronic lung diseases are common in never-smoking HIV patients. Emphysema was associated with epicardial and visceral adiposity, but not with HIV-related variables, underlying a common pathogenetic mechanism linking lung CT abnormalities and ectopic fat accumulation.

B-0235 14:56

Xenon-enhanced ADCT: utility for functional and morphological assessments of smokers as compared with ventilation SPECT/CT

S. Seki[1], Y. Ohno[1], Y. Kishida[1], T. Yoshikawa[1], Y. Fujisawa[2], N. Sugihara[2], E. Suehiro[1], T. Sekitani[1], K. Sugimura[1]; [1]*Kobe/JP*, [2]*Otawara/JP*
(yosirad@kobe-u.ac.jp)

Purpose: To prospectively and directly compare the utility of xenon-contrast enhanced area-detector CT (Xe-ADCT) for pulmonary functional and disease severity assessments in smokers, when compared with ventilation SPECT/CT.
Methods and Materials: 46 consecutive smokers underwent prospective unenhanced and xenon-enhanced ADCTs, krypton ventilation SPECT/CT and pulmonary function tests. Xe-ADCT was generated from unenhanced and xenon-enhanced ADCT. Then, all smokers were divided into 4 groups as follows: 'Non-COPD', 'Mild COPD', 'Moderate COPD' and 'Severe or Very Severe COPD' groups. For each method, regional ventilation was assessed by 10-point scoring system on a per-lobe basis. Then, ventilated lung volume (VLV) on each method, functional lung volume (FLV) and wall area percent (WA%) in each subject were calculated according to past literatures. To evaluate the capability of each index for pulmonary functional loss assessment, all indexes were correlated with $\%FEV_1$ by step-wise regression analyses. To compare each index among all groups, Tukey's HSD test were performed.
Results: In the step-wise regression test, $\%FEV_1$ (r=0.62, p<0.001) was significantly affected by the following three factors: the first-step factor, VLV on Xe-ADCT; the second-step factor, WA%; the third-step factor, FLV. All indexes of 'Non-COPD' and 'Mild COPD' groups had significant difference with those of 'Severe or Very Severe COPD' groups (p<0.05), and all indexes except VLV on SPECT/CT had significant difference between 'Moderate COPD' and 'Severe or Very Severe COPD' groups.
Conclusion: Xenon-enhanced ADCT had equal to or better capabilities for pulmonary functional and disease severity assessments in smokers as compared with ventilation SPECT/CT.
Author Disclosures:
S. Seki: Research/Grant Support; Toshiba Medical Systems Corporation. **Y. Ohno:** Research/Grant Support; Toshiba Medical Systems Corporation. **T. Yoshikawa:** Research/Grant Support; Toshiba Medical Systems Corporation. **Y. Fujisawa:** Employee; Toshiba Medical Systems Corporation. **N. Sugihara:** Employee; Toshiba Medical Systems Corporation. **K. Sugimura:** Research/Grant Support; Guerbet.

B-0236 15:04

Quantitative CT analysis of pulmonary vessels using virtual gradationally peeled off lung in COPD patients: interrelation with emphysema, air trapping and pulmonary function

E. Lee, S. Lee, J. Seo, N. Kim, J. Bae, S. Lee, S. Oh, J. Lee, Y.-M. Oh;
Seoul/KR (eslee0214@gmail.com)

Purpose: To analyse quantitatively pulmonary vessel using virtual peeled off lung in COPD patients and interrelation with emphysema index (EI), air trapping index (ATI) and PFT.
Methods and Materials: 100 COPD patients (M:F=93:7; 65.2±0.8years) have non-contrast 3D inspiration/expiration CTs, PFT and DLco were enrolled. AView Lung software was used to analyse pulmonary vessel. Closed plane having an even distance (6mm~24mm, 3mm interval) from the fissure and surface regarding whole lung were automatically generated. Number of vessels per square centimeter, mean diameter of vessels, and percent of vessel area per surface were semi-automatically measured on all generated planes. EI (percentage of area HU≤-950), ATI (percentage of area subtracted HU≤60HU between inspiration CT and registered expiration CT), and mean of bronchiolar wall area percentage (WA%) were also measured. Correlations between parameters of vessels and EI, ATI, WA%, PFT, DLco were evaluated.
Results: All level of number of vessels per square centimeter and percent of vessel area per surface showed significant negative correlation with EI (r=-0.606~-0.811), ATI (r=-0.310~-0.423), RV (r=-0.331~-0.463) and positive correlation with WA% (r=0.264~0.340), and PFT parameters (r=0.243~0.552). They also showed significant positive correlation with DLco (r=0.241~0.443) except vessel area per surface on 6mm plane. Mean diameter of vessels showed significant negative correlation with EI, and ATI on 9~18mm level plane (r=-0.216~-0.370). All detailed results are showed in Table 1.
Conclusion: CT measured parameters of pulmonary vessels are related with CT measured emphysema, air trapping, airway wall thickness and clinical pulmonary functions.

B-0237 15:12

Cardiac remodelling in COPD: An effect of reduced preload or increased afterload?

J. Weir-McCall, A. Struthers, B. Lipworth, J. Houston; *Dundee/UK*
(jweirmccall@doctors.net.uk)

Purpose: The classic cardiac complication of those with chronic obstructive pulmonary disease (COPD) is that of cor pulmonale. However this has typically been described in those with end stage disease or based on echo measures which is known to be poor for right ventricular (RV) assessment and even worse in a COPD cohort. Thus the aim of the current study was to use cardiac MRI to assess cardiac remodelling in COPD.
Methods and Materials: 21 healthy volunteers (HV) free from cardiovascular disease and 60 patients with COPD were recruited. Those with COPD were screened with echocardiography, and those with silent left ventricular (LV) systolic dysfunction excluded. All patients underwent spirometry and cardiac MRI for mass and volume assessment on the same visit.
Results: With increasing severity of COPD both left and right ventricular end diastolic volumes (EDV) fell (LVEDV: 60±10ml in HV vs. 44±18ml in severe COPD, p=0.011; RVEDV 60±13 in HV vs. 42±16 in severe COPD, p=0.017) and as did stroke volumes (SV) (LVSV: 36±5ml in HV vs. 25±10ml in severe COPD, p=0.001; RVSV 37±6 in HV vs. 24±11 in severe COPD, p=0.001). Left ventricular mass (LVM) also fell with increasing severity of COPD (LVM: 41±7g in HV vs. 33±14g in severe COPD, p=0.024), while RV mass remained unchanged (p=0.24).
Conclusion: Increasing severity of COPD results in reduced cardiac volumes and mass, suggesting the predominant cause of cardiac remodelling in COPD is due to reduced preload rather than the classical cor pulmonale model of increased afterload.

B-0238 15:20

Pulmonary hypertension secondary to diffuse lung diseases: correlations between radiological findings and haemodynamic assessment

A. Poerio, A. Bruno, F. Ciccarese, V. Cosi, F. Ragusa, A. Conficoni, F. Niro, D. Attinà, M. Zompatori; *Bologna/IT (a.poerio@alice.it)*

Purpose: To evaluate the different correlations between radiological findings and haemodynamic parameters in a cohort of patients with pulmonary hypertension (PH) secondary to diffuse lung diseases (DLD) of different types and varying severity.
Methods and Materials: We retrospectively evaluated CT-pulmonary angiography (CTPA) and right heart catheterization (RHC) of 48 patients with PH secondary to DLD. Radiological assessment included: pattern of DLD (fibrosis, emphysema, CPFE); extension of disease (expressed as visual score: VS); radiological signs of PH. RHC values considered were: mean pressure of the main pulmonary artery (mPAP), pulmonary vascular resistance (PVR), pulmonary capillary wedge pressure (PCWP) and cardiac index (CI). We divided patients into 2 main groups based on VS (</≥40%) and into 3 sub-groups based on DLD pattern. Correlations between radiological and haemodynamic parameters among various groups were evaluated.
Results: In the group of patients with VS <40% we found a significant direct correlation between mPAP, RVP and the radiological signs of PH such as pulmonary trunk diameter (p: 0.04 and 0.02, respectively) and pulmonary trunk diameter to ascending aorta diameter ratio (p: 0.006), while in the group with VS ≥40% the significance was lost and even observed a trend to an inverse relation, especially in the CPFE sub-group, in which we found also a lower CI, predictive of worst prognosis.
Conclusion: Our results confirm the high potential of the CT pulmonary angiography in the assessment of PH secondary to DLD and highlight the usefulness of the visual score, expressed as percentage of total lung volume, to improve the sensitivity of imaging in the PH screening.

14:00 - 15:30 **Room N**

Genitourinary

SS 307

Kidney and urinary tract II

Moderators:
P.K. Prassopoulos; Alexandroupolis/GR
K.K. Pyra; Lublin/PL

B-0239 14:00

Comparison between contrast-enhanced CT (CECT) and contrast-enhanced ultrasound (CEUS) in patients with clinical suspicion of complicated acute pyelonephritis (c-APN)

C. Montalto, E. Raimondi, Z. Ferrante, M. Tilli, M. Giganti, G. Benea; *Ferrara/IT (edoardo.raimondi@unife.it)*

Purpose: To assess the value of contrast-enhanced ultrasonography (CEUS) in clinical suspicion of complicated acute pyelonephritis (c-APN), in terms of nature and extent of disease, compared with contrast-enhanced computed tomography (CECT) findings (reference standard).
Methods and Materials: From January 2016 to September 2016, 39 patients (33 women, 6 men; mean age 26 years, range 18-67) with clinical suspicion of complicated-APN, underwent both CEUS and CECT 72 hours after admission, performed in a blinded manner by two different operators. Prior informed consent, CEUS was performed evaluating both kidneys, after injection of 5 ml of US-contrast agent. CECT study (multislice 64-row scanner) was performed after injection of 100ml of iodinated contrast agent. All renal parenchymal changes were independently reported for both studies.
Results: At CECT 34/39 patients (87%) showed renal parenchymal changes suggestive for focal c-APN, confirmed in 33/34 (97%) at CEUS; the remaining case was false negative at CEUS (US anatomic limitation). 24/34 patients (70.5%) had unilateral and 4 /34 (11.7%) had bilateral focal APN. CECT showed 6/34 cases of renal abscesses, all confirmed at CEUS. In 5/39 cases there was no evidence of renal disease at CEUS or CT.
Conclusion: CEUS showed to be almost as equally accurate as CECT in patients with clinical suspicion of c-APN, allowing detection of renal parenchymal changes as focal APN and/or renal abscesses. Considering CECT-associated radiation and potential nephrotoxicity of iodine contrast media, in c-APN patients (frequently young women) CEUS should be considered as first-step imaging technique to depict the extension and entity of renal infection.

B-0240 14:08

Detection and characterisation of urolithiasis using photon-counting-CT in a clinical setting

R.P. Marcus[1], J.G. Fletcher[2], T.J. Vrtiska[2], M.L. Wells[2], A.F. Halaweish[3], F.T. Enders[2], S. Leng[2], C.H. McCollough[2]; [1]*Tübingen/DE*, [2]*Rochester, MN/US*, [3]*Malvern, PA/US (roy.marcus@med.uni-tuebingen.de)*

Purpose: To compare the performance of an experimental photon-counting-detector CT (PCCT) with clinical dual-energy-CT (DECT) in detecting and characterising urolithiasis.
Methods and Materials: Non-contrast-enhanced DECT stone detection/characterisation exams were performed in thirty patients using a 2nd-generation dual-source-CT-system (SOMATOM Flash, Siemens) using 80/140Sn kVp or 100/140Sn kVp, depending on patient size. Subsequently, a similar exam was performed using the PCCT at 140 kV with energy thresholds at 25 and 75 keV, and CTDIvol matched between exams. 1 and 5 mm images were reconstructed using a D30 kernel. Two radiologists examined in a blinded fashion DECT mixed and low kV images, and PCCT low energy threshold (25-140 keV) and bin1 (25-75 keV) images. Confidence in stone presence was graded in consensus (1=definitely present, 2=probably present, 3=questionably present, 4=not seen). Stone characterisation was performed using commercial software (Syngo DE, Siemens) based on low- and high-kV-images for DECT and bin1 and bin2 images (25-75 and 75-140 keV) for PCCT.
Results: 160 stones (5.4±9.3 mm) were detected in total, with 91 stones ≤ 3mm. No difference in confidence for stone presence between DECT and PCCT was detected for 1mm images (p= 0.38-0.81). Stones were more likely to be definitely present with 1mm images compared to 5 mm images (p<.0001). Automatic stone characterisation was more successful in PCCT than DECT (112 vs. 87 stones), especially for small stones (45 vs.25). Agreement in stone composition between scanners (κ=.65) was substantial.
Conclusion: Detection confidence for stones was identical in both modalities. PCCT demonstrated improved stone characterisation results.
Author Disclosures:
R.P. Marcus: Research/Grant Support; Siemens AG. **J.G. Fletcher:** Grant Recipient; Siemens AG. **A.F. Halaweish:** Employee; Siemens Healthcare. **C.H. McCollough:** Research/Grant Support; Siemens AG.

B-0241 14:16

New radiologic classification of renal angiomyolipomas

B. Park, S. Song; *Seoul/KR (1436park@gmail.com)*

Purpose: To introduce a new radiologic classification of renal angiomyolipoma (AML).
Methods and Materials: Between 1995 and 2014, CT or MR images in 98 patients with histologically proven 98 AMLs were reviewed independently by a radiologist and a resident. The lesions were classified as (a) 53 fat-rich AML (≤ -10HU), (b) 22 fat-poor AML (> -10HU) with tumour-to-spleen ratio (TSR) <0.71 or signal intensity index (SII)>16.5%, and (c) 23 fat-invisible AML (>-10HU) with TSR≥0.71 and SII≤ 16.5%. Inter-reader agreement was assessed with a weighted kappa value. Fat-poor and fat-invisible AMLs were compared in terms of attenuation value, TSR, and SII using unpaired t-test.
Results: The weighted kappa value was 0.956 (95% confidence interval, 92.0 - 99.1%). When a region of interest (ROI) was placed within the most hypodense area on unenhanced CT or within the most signal-dropped area on chemical shift image, the mean attenuation values, TSRs, and SIIs of fat-poor versus fat-invisible AMLs were 19.5±8.1 HU versus 38.1±9.9 HU, 0.59±0.19 versus 0.96±0.01, and 43.7±16.9% versus -5.4±21.1%, respectively (p<0.0001). When a ROI was placed within the other area on CT or chemical shift images, 90.1% (48/53) of fat-rich AMLs were misclassified as fat-poor or fat-invisible AML and 50% (11/22) of fat-poor AMLs as fat-invisible AML.
Conclusion: The new radiologic classification of renal AML is feasible for clinical practice. ROI location is important in differentiating the types of AMLs.

B-0242 14:24

Two-point Dixon in the detection and evaluation of renal angiomyolipoma: does the fat-water fraction measurement have a contributing effect?

H. Demirtas, B. Değirmenci, A.O. Çelik, M. Kara, A.R. Aktaş, H.A. Ekşili, H. Orhan; *Isparta/TR (demhakan@yahoo.com)*

Purpose: The aim of this study was to compare the effectivity of 3D two-point Dixon sequence and in- and opposed-phase sequence in the detection of renal AML and in the detection of size and localisation of these lesions and also to evaluate interobserver differences.
Methods and Materials: The retrospective study included 35 patients who underwent renal mass MRI protocol that included Dixon sequences [in-phase (IP), opposed-phase (OP), water-only (WO), and fat-only (FO)]. The differences between sequences relating to tumour size and localisation were evaluated. The four sequences were compared in terms of lesion detection rate and interobserver differences were also evaluated.
Results: The lesion detection rates in the OP and FO sequences were 80% and 86% for Reader 1 and 91% and 96% for Reader 2, respectively. The rates in the WO and IP sequences were 66% and 74% for Reader 1 and 48% and 52% for Reader 2. The number of detected lesions smaller than 5mm was slightly higher in FO sequence. The evaluations indicated that small-size tumours were significantly more difficult to identify as compared to large-size tumours for both readers (Reader 1, p=0.039; Reader 2, p=0.047). The detectability of peripherally located lesions with regards to their localisation was significantly higher in the WO and IP sequences (Reader 1, p=0.014; Reader 2, p=0.004).
Conclusion: The OP and particularly the FO sequences are highly effective in the diagnosis of AML and centrally located lesions.The FO sequence can be useful in the detection of lesions smaller than 5mm in size.

B-0243 14:32

Characterisation of adrenal lesions with histogram analysis using unenhanced MRI

V. Romeo, R. Cuocolo, S. Dell'Aversana, M. Coppola, P. Mainenti, M. Imbriaco, S. Maurea, A. Brunetti; *Naples/IT (valeria.romeo@unina.it)*

Purpose: To investigate the role of quantitative histogram analysis applied to T1-weighted in-phase (IP), opposed-phase (OP) and T2-weighted sequences (T2w) in discriminating among lipid-rich adenomas (LRA), lipid-poor adenomas (LPA), and non-adenomas (NA).
Methods and Materials: Forty-five patients with unilateral adrenal lesions (18 LRA, 7 LPA, 20 NA) at MRI examination have been retrospectively enrolled. Each detected adrenal lesion was manually segmented with Itksnap through placement of a spherical ROI on IP, OP and T2w images. The ROIs were successively imported on a dedicated software (MITK) to calculate first-order histogram-derived statistics. Data were compared among LRA, LPA and NA lesions and differences were evaluated using Mann-Whitney tests. A p value ≤ 0.05 was considered statistically significant.
Results: Among the extrapolated parameters, entropy on T2w (e-T2w), standard deviation on T2w (sd-T2w), uniformity on T2w (u-T2w) and kurtosis on OP (k-OP) were significantly different between LRA and NA (p<0.05) and between LPA and NA (p < 0.05), while were not statistically different between LRA and LPA (p>0.05).

Conclusion: Several of the extrapolated parameters (mainly extracted from the T2w sequence) may play a role in the discrimination between adenomas (both LRA and LPA) and non-adenomas; however, the additional role of these parameters in characterizing adrenal lesions on standard unenhanced MRI protocol have to be investigated in a larger patient population to confirm our preliminary results.

B-0244 14:40

Quantitative ultrasound evaluation of cystic and solid tumours of the kidney: a fancy toy or an useful tool?

C. Bruno, A. Bucci, C. Dallaserra, R. Pozzi-Mucelli; *Verona/IT (costanza_bruno@libero.it)*

Purpose: To assess if ARFI can be a reliable technique in distinguish ccRCCS from other solid and fluid-containing small renal masses.
Methods and Materials: 50 small (less than 4 cm) renal masses (40 solid - 24/40 ccRCCs, 5/40 papillary RCCs, 4/40 chromophobe RCCs, 4 oncocytomas and 3 angiomyolipomas - and 10 cystic - 4 simple cysts, 1 MEST, 1 cystic nephroma, 1 mucinous tubular tumour, 1 tubulocystic tumour and 1 an Xp translocation RCC) were prospectively evaluated using US and ARFI. Each lesion was assigned an ARFI value obtained from the average of 12 measurements. Complex cysts were evaluated in the solid portion. All the solid masses underwent resection; among the 10 cystic lesions 4 were Bosniak 2, so were evaluated with follow-up, the other 6 underwent resection too.The difference existing between the two groups was evaluated by means of Student's t test. A cut off value was determined to distinguish between ccRCCs and other lesions and sensibility, specificity, PPV, NPV and accuracy were determined.
Results: ccRCCs are characterised by an higher ARFI value and - when compared with all the other lesions - the difference existing between the two groups was statistically significant (p<0.001). Considering a cut off value of 1.95 m/sec sensibility, specificity, PPV, NPV and accuracy were respectively 91%, 69.2%, 72.4%, 90% and 79.6%.
Conclusion: ccRCC is characterised by an higher ARFI value which can be used to distinguish it from other solid and fluid containing masses.

B-0245 14:48

Perfusion CT in the evaluation of renal cell carcinoma

S.S. Chauhan, R. Dixit, V. Chowdhury, N. Khurana; *New Delhi/IN (drshaan54@gmail.com)*

Purpose: The purpose of this study is to determine perfusion characteristics of renal cell carcinoma (RCC) using perfusion CT technique and compare them with histopathological findings.
Methods and Materials: 21 patients (18 clear cell, 2 papillary and 1 chromophobe subtype) of RCC underwent perfusion CT on a 128 slice MDCT scanner (Siemens Somatom Definition AS CT Scanner). A non-contrast scan of the upper abdomen was done to localize the region of interest (ROI) followed by dynamic CT acquisition of ROI. Perfusion parameters including blood flow (BF), blood volume (BV), permeability (PMB), mean transit time (MTT) and time to peak (TTP) were obtained from the tumour cross section (CS) and maximally enhancing area (MEA) of RCC and the contralateral renal cortex.
Results: Mean BF, BV and PMB were significantly reduced in both the tumour CS and MEA of RCC in comparison to contralateral renal cortex (p=0.00l). MTT was significantly increased both in tumour CS and MEA of RCC in comparison to contralateral renal cortex [(p=0.002) and (p=0.001) respectively]. TTP (sec) was significantly increased only in MEA of RCC in comparison to contralateral renal cortex (p=0.042). Mean BF and BV in the MEA were highest in clear cell RCC (88.83+/-49.74 ml/100ml/min and 19.64+/-10.10 ml/100ml) followed by papillary (49.74+/-7.94 ml/100ml/min and 10.48+/-2.26 ml/100ml) and lowest in chromophobe subtype (27.41 ml/100ml/min and 5.68 ml/100ml).
Conclusion: CT perfusion parameters show significant difference between the RCC and normal renal cortex and between various subtypes of RCC, thus can be used for preoperative subtype differentiation.

B-0246 14:56

Elastography point quantification and chronic renal diseases

E. Danse, C. Lenfant, M. Jadoul, F. Houssiau, S. Aydin, J. Cosyns, N. Demoulin, P. Trefois, N. Michoux; *Brussels/BE (etienne.danse@uclouvain.be)*

Purpose: Evaluation of the correlation between the renal cortex stiffness in chronic kidney disease (CKD) evaluated with elastography point quantification (ElastPQ) and the FIAT score of renal fibrosis in CKD.
Methods and Materials: 16 consecutive adults patients with CKD and 16 healthy volunteers underwent ElastPQ elastography. The elastographic measurements of the renal cortex were expressed with kPa values. 10 patients with CKD had a clinically indicated biopsy for which interstitial fibrosis was evaluated by the FIAT score. Correlation was evaluated between elasticity values and echographic (US), biological and histopathologic data for the patients comparison; US and biological results were used for the comparison of data between patients and volunteers.
Results: Renal cortical stiffness did not correlate with biological or US parameters. A significant correlation was observed between cortical stiffness and the FIAT score (r=0.7, p=0.0282). No significant difference were found between the renal cortical stiffness of the control group and the diseased group.
Conclusion: Renal cortical stiffness in CKD by ElastPQ was correlated with the FIAT score. A significant difference was observed between the grade 1 and 2 of the FIAT score with a thershold of 5.66kPa. This result offers pesrpectives in evaluation and detection of CKD with the possibility to reduce the number of biopsies.

B-0247 15:04

Evaluation of diffusion kurtosis imaging for detecting and grading the renal clear-cell carcinoma

Q. Feng; *Weifang/CN (fengqiang1975@163.com)*

Purpose: To investigate the detection of clear-cell renal cell carcinoma (CCRCC) by diffusion kurtosis imaging (DKI) and evaluate the association between DKI-derived parameters and pathologic factors.
Methods and Materials: In this study, 20 low-grade and 15 high-grade were performed. DKI with b values (0,500, 1000s/mm^2) and DWI data wtih b values (0,800s/mm^2) were acquired. In patients with histologically proven CCRCC, a representative region was determined on coronal T2WI. DKI parameters (D_{app} and K_{app}) and ADC values of the ROIs in tumour and contralateral areas were calculated. The receiver operating characteristic (ROC) were calculated for DKI parameters and ADC values. A subgroup analysis was performed to determine the aggressiveness of CCRCC using D_{app} and K_{app}.
Results: In the 35 patients, D_{app} was significantly lower in tumour compared with control regions (2.85±0.22 vs 2.93±0.27, P<0.05), and K_{app} was significantly higher (0.58±0.08 vs 0.51±0.06, P<0.05). D_{app} was significantly higher than standard ADC both in tumour regions and in controls (2.85±0.22 vs 2.72±0.24 and 2.93±0.27 vs 2.79±0.31, P<0.05). ROC revealed a significant difference between DKI and ADC for detection of CCRCC. Sensitivities ranged from 79% to 91% for DKI parameters; specificities ranged from 81% to 92%. Kurtosis was positively correlated with tumour histologic grade (r=0.83), diffusivity was negatively (r=-0.81), the significant difference were found for discrimination between high- and low-grade (P<0.05).
Conclusion: For detection and grading of CCRCC, DKI was better than standard ADC.
Author Disclosures:
Q. Feng: Author; zhijun ma, wei fang.

B-0248 15:12

Four-dimension dynamic imaging by 640-slice multidetector CT for the diagnosis of urine flow related diseases

J. Guan, Y. Guo, H. Wang; *Guangzhou/CN (usefulkey0077@hotmail.com)*

Purpose: To explore the value of diagnosis on urine flow related diseases by applying of 640-slice MDCT four-dimension dynamic imaging.
Methods and Materials: Sixteen patients were clinically diagnosed with urine flow related diseases, and detail diagnostic information could not be provided by other routine imaging exam. Four-dimension dynamic CT imaging was performed for diagnosis by the 640-slice MDCT with a 160-mm detector, which was approved by the hospital ethics committee. According to the location of lesion, degree of hydronephrosis, status of bladder and so on, all cases received low dose CT scan with personalised scan protocols. Multi-planner reformation was performed for getting 4-dimension dynamic imaging.
Results: Four cases of slight urine reflux were confirmed. Four cases of stenosis of lower ureter were found (2 of moderate stenosis, and 2 of severe stenosis). The locations of ectopic ureter were accurately defined in five cases. The precise locations and sizes of fistula of fistulas were shown in three cases (1 of vesico-vaginal fistula, and 2 of vesico-rectal fistula). Compared with traditional cystography, 4-dimension dynamic CT imaging was a non-invasive examination.
Conclusion: Four-dimension dynamic imaging by the 640-slice MDCT is a new choice of imaging exam for urine flow related disease, and can directly and clearly show direction and route of urine flow, and provide detail and rich information for diagnosis.
Author Disclosures:
J. Guan: Author; Huanjun Wang, Yan Guo.

B-0249 15:20

3T multiparametric MRI in differentiating muscular-invasive and non muscular-invasive bladder cancer

M. Grompone; *Rome/IT (mdgrompone@libero.it)*

Purpose: The differentiation of muscular-invasive bladder cancer and non muscular-invasive bladder cancer is crucial for an effective treatment. Purpose of the study is to demonstrate the rule of 3T multiparametric MRI in differentiation and staging of muscular-invasive and non muscular-invasive bladder cancer.
Methods and Materials: 61 patients with suspected or confirmed bladder lesion underwent 3T multiparametric MRI exam. MRI protocol included T2W morphological sequences, dynamic sequences (PWI),b-500, b-800 and b-1000 diffusion sequences (DWI) and diffusion tensor imaging (DTI) with post-processing bladder wall reconstruction. MRI data were read in both qualitative (T2W, PWI, DWI and DTI) and quantitative (PWI, DWI and DTI) way. Endoscopic cystoscopy was performed for histological diagnosis of the lesion.
Results: The accuracy of mpMRI exam was 90%, 93%, 86% and 90% in T2W, PWI, DWI and DTI sequences respectively with the best performance combining and interpreting T2W, DWI and PWI sequences together. DTI helped to correctly categorize uncertain lesions and in cases of DWI and ADC interpretative doubt about bladder invasion.
Conclusion: 3T Multiparametric MRI can be considerd a valid tool in bladder cancer diagnostic pathway replacing diagnostic cystoscopy, that means just a therapeutical rule for interventional procedures.
Author Disclosures:
M. Grompone: Author; Maurizio Del Monte, Elena Lucia Indino, Vincenzo Salvo, Carlo Catalano, Valeria Panebianco.

14:00 - 15:30 **Room L 8**

Head and Neck

SS 308

Head and neck cancer: value of multiparametric and advanced imaging techniques

Moderators:
P. De Graaf; Amsterdam/NL
N.I. Traykova; Plovdiv/BG

B-0250 14:00

RECIST 1.1, WHO and 3D CT-scan methods predict vocal cord remobilisation after induction chemotherapy in patients with T3 laryngeal squamous-cell carcinoma

G.C.T.E. Garcia[1], P. Gorphe[1], S. Ammari[1], C. Even[1], Y. Tao[1], C. Balleyguier[1], A. Varoquaux[2], F. Bidault[1]; [1]*Villejuif/FR*, [2]*Marseilles/FR (gabrielgarcia1988@gmail.com)*

Purpose: After induction chemotherapy (ICT) for head and neck squamous cell carcinomas (SCC) CT scan is used to assess tumour response (TR) but lacks rationalized measurement methods. In T3 laryngeal SCC, vocal cord remobilisation (VCR) is a major TR criterion. We compare the performances of RECIST 1.1, WHO and volumetric methods with CT-scan to predict remobilisation.
Methods and Materials: Contrast-enhanced cervical CT-scans were acquired before and during ICT from 43 patients treated for T3 laryngeal SCC with vocal cord fixation. Tumour size was assessed according to RECIST 1.1 (1D), WHO (2D) and volumetric (3D) methods. Tumour shrinkage after ICT was evaluated as predictor of VCR. Areas under the curve (AUC) of receiver operating characteristic curves were compared and sensitivity and specificity of optimal cutoffs were determined.
Results: AUCs were 0.763 (95%CI [0.615; 0.911]) for 1D, 0.779 (95%CI [0.63; 0.971]) for 2D and 0.763 (95%CI [0.623; 0.904]) for 3D evaluations with no significant difference (1D vs 2D p = 0.78; 2D vs 3D p = 0.66; 1D vs 3D p = 1). Optimal cutoffs were -29% (Se = 70.8%; Sp =68.4%), -47% (Se = 91.7%; Sp = 63.2%) and -64% (Se = 75%; Sp = 63.2%) for 1D, 2D and 3D evaluation, respectively.
Conclusion: RECIST 1.1, WHO or volumetric measurements with CT-scan equally predict, VCR after ICT in patient with T3 laryngeal SCC. Cutoff values were very close to these methods' usual thresholds, we could thus use them to assess TR when vocal cord fixation is absent.

B-0251 14:08

Correlation between locally advanced HPV positive oropharyngeal squamous cell carcinoma and quantitative MRI parameters

M. Leali, E. Tononcelli, E. Lleshaj, A. Grammatica, M. Ravanelli, D. Farina, R. Maroldi; *Brescia/IT (michela.leali@icloud.com)*

Purpose: to evaluate the association between quantitative MR parameters and HPV status in advanced oropharyngeal squamous cell carcinoma (OPSCC).
Methods and Materials: 24 patients with locally advanced OPSCC underwent pre-treatment MR. Histogram analysis was performed on TSE-T2, DWI and post-gadolinuim 3D-VIBE sequences before and after application of a Laplacian of Gaussian spatial scale filter (ssf) at the primary tumour site. Search of HPV DNA on biopsies was performed to evaluate HPV status. Mann-Whitney test was used to assess differences in quantitative MR parameters between HPV+ and HPV- groups.
Results: 10 patients were HPV-positive (41,7%). Mean ADC was significantly lower in HPV+ compared to HPV- patients (0.83 vs 1.04 x $10^{-3}mm^2/s$ respectively, p=0.015). Skewness measured on 3D-VIBE with 1mm-ssf was significantly higher in HPV+ compared to HPV- patients (p=0.03).
Conclusion: quantitative MR parameters, especially mean ADC, may reflect microstructural differences between HPV+ and HPV- OPSCC.

B-0252 14:16

DWI can distinguish between morphologically differentiated and undifferentiated thyroid carcinoma

S. Schob; *Leipzig/DE (stefan.schob@medizin.uni-leipzig.de)*

Purpose: Thyroid carcinomas represent the most frequent endocrine malignancies. Recent studies were able to distinguish malignant from benign nodules of the thyroid gland with diffusion weighted imaging (DWI). Although this differentiation is undoubtebly helpful, presurgical discrimination in between well differentiated and undifferentiated carcinomas would be crucial in order to define the optimal treatment algorithm. Therefore the aim of this study was to investigate if DWI is able to differentiate between differentiated and undifferentiated subtypes of thyroid carcinomas.
Methods and Materials: 14 patients with different types of thyroid carcinomas who received preoperative DWI using a RESOLVE sequence were included in our study. In all lesions ADCmin, ADCmean and ADCmax and D were estimated on basis of region of interest (ROI) measurements after coregistration with T1 weighted, postcontrast images. All tumours were resected and analysed histopathologically. Ki-67 index, p53 synthesis, cellularity, total and average nucleic areas were estimated using ImageJ version 1.48
Results: ANOVA revealed a statistically significant difference of ADCmean values between differentiated and undifferentiated thyroid carcinomas (p=0.022). Spearman-Rho calculation identified significant correlations between ADCmax and cell count (r=0.541, p=0.046) as well as between ADCmax and total nuclei area (r=0.605, p=0.022).
Conclusion: DWI can distinguish between differentiated and undifferentiated thyroid carcinomas.

B-0253 14:24

Prognostic significance of pre-treatment FDG PET-CT parameters in laryngeal and hypopharyngeal squamous cell carcinoma

S. Vaidyanathan[1], R. Prestwich[1], F. Slevin[1], G. McDermott[1], E. Ermis[2], P. Gopalan[1], A.F. Scarsbrook[1]; [1]*Leeds/UK*, [2]*Kahramanmaraş/TR (srivaidyanathan@gmail.com)*

Purpose: To evaluate the prognostic value of adaptive-threshold based metabolic tumour volume (MTV), maximum (SUV_{max}) and mean (SUV_{mean}) standardised uptake value and total lesional glycolysis (TLG) measured prior to radiotherapy on FDG PET-CT in patients with laryngeal and hypopharyngeal cancer.
Methods and Materials: 43 patients with locally advanced laryngeal or hypopharyngeal squamous cell carcinoma who underwent ^{18}F-FDG PET-CT before curative-intent (chemo)radiotherapy in a single centre (2009-2014) were retrospectively analysed. Imaging parameters including SUV_{max}, SUV_{mean}, MTV and TLG were calculated for both tumour and nodal disease using an adaptive thresholding method (Homburg algorithm). Univariate and multivariate analyses were used to identify clinico-pathological and imaging variables associated with progression-free survival (PFS) and overall survival (OS). Univariate analyses included the following variables: age, sex, T and N classifications, overall TNM stage, tumour size, nodal size, SUV_{max}, MTV, and TLG.
Results: The median SUV_{max}, MTV, and TLG were 11.1 (range, 0-53.9), 3.5 ml (2.0-42.9 ml), and 72.5 g (0-744.9 g) respectively. Univariate analyses showed that there were significant correlations between T stage (p = 0.013), primary tumour MTV (p = 0.031) and nodal TLG ([= 0.001) and overall survival. Multivariate analyses revealed that T stage, tumour MTV and nodal TLG were independent variables for PFS.

Conclusion: Pre-treatment values of MTV and TLG are independent prognostic factors in patients with laryngeal and hypopharyngeal tumours and may help predict subsequent patient outcome.

B-0254 14:32

Utility of T2-weighted magnetic resonance imaging, MR spectroscopy and diffusion-weighted imaging of thyroid to differentiate malignant from benign nodules

P. Yadav; *Pune/IN (yadavpratiksha@hotmail.com)*

Purpose: To evaluate the diagnostic performance of T2WI mean signal intensity combined with diffusion-weighted imaging and MR spectroscopy to differentiate thyroid carcinomas from benign thyroid nodules.
Methods and Materials: Study included 32 patients (12years to 67years) who had 41 solid thyroid nodules detected on high resolution ultrasonography. T2WI,T1WI & STIR sequences were acquired followed by DWI and MR spectroscopy. T2W mean signal intensity and ADC values of each thyroid nodule were calculated.MRS was done to observe the choline value. Histopathology was done in all the cases after MRI.
Results: Papillary carcinoma detected in 14 lesions,metastasis in 5 and lymphoma detected in one lesion ,5 detected thyroiditis and 7 lesions detected adenoma and 9 lesions confirmed colloid nodule on histopathology.T2W SI was lower in the thyroid carcinoma ranging 205-298 mean was 247.4 as compare to benign thyroid nodules ranging from 275-512, mean 391.72. Mean ADC values was 1.32+-38 x10^{-3} mm^2/s in malignant nodules and was 2.58+-53 x10^{-3} mm^2/s in benign nodules. ADC value was significantly lower in malignant nodules as compare to benign (p<0.001). MRS showed high choline value in the malignant nodules though choline was not raised in the benign nodules.Sensitivity to detect malignant lesion by DWI was 80% (95% CI 58.4-91.93),specificity 85.7%,(95%CI 65.36-95.02),PPV 84.2% and NPV 81.82%. Sensitivity by MRS was 75%(95%CI 53.13-88.8) and specificity 90.48%,(95% CI 71.09-97.35), PPV 88.24% and NPV 79.17%.
Conclusion: MRI thyroid is an efficient non-invasive imaging modality to differentiate thyroid carcinoma from benign nodules on the basis of MRI T2W SI, ADC values and MR spectroscopy.

B-0255 14:40

Is quantitative ultrasound elastography valuable in the assessment of cervical lymphadenopathy?

V. Selvadasan, A. Prakash, V. Chowdhury, A. Gulati, S. Jain, A. Garg; *New Delhi/IN (dr.vinayagamani@gmail.com)*

Purpose: Cervical lymphadenopathy frequently poses a diagnostic challenge as neither clinical nor imaging assessment can reliably differentiate between benign and malignant lymphadenopathy. Non-invasive differentiation between the two may help to reduce the number of FNAC or biopsy. The purpose of this study was to evaluate whether the new ARFI technique (Virtual Touch Quantification), in conjunction with greyscale sonography and colour Doppler, can help in the characterisation and differentiation of benign from malignant cervical lymphadenopathy.
Methods and Materials: Fifty adult patients with cervical lymphadenopathy were included in the study and sonoelastography of the enlarged nodes was done. ARFI (SWV) measurements in benign and malignant enlarged lymph nodes were compared using the Student *t* test and ROC curve was used to arrive at the Youden index , sensitivity, specificity, PPV, NPV and diagnostic accuracy.
Results: Sonographic patterns indicative of malignancy includes heterogenous echopattern, short axis/long axis ratio >0.5, absent echogenic fatty hilum and mixed vascular pattern. The sensitivity, specificity, PPV, NPV and accuracy in differentiation between the benign and malignant lymph nodes using ARFI elastography was 79.17%, 100% , 100%, 83.9% and 89.9% respectively. ROC curve analysis of SWVs for differentiation between the malignant and benign lymph nodes gave a cut-off value of 2.8m/s with an area under curve (AUC) of 0.892.
Conclusion: ARFI imaging technique provides quantitative information about the tissue stiffness of cervical lymph nodes which also complement sonography non-invasively and objectively in characterisation and differentiation of benign from malignant lymph nodes.

B-0256 14:48

Can qualitative and semi-quantitative ultrasound elastography contribute to the diagnosis of salivary gland tumours?

C.Z. Karaman, Y. Durum, A. Eryılmaz, F. Taşkın, E.H. Navaei; *Aydın/TR (yasemindurum@gmail.com)*

Purpose: The aim of this study was to investigate the contribution of qualitative and semi-quantitative strain sonoelastography in differential diagnosis of salivary gland tumours.
Methods and Materials: Fifty-seven patients (29 men and 28 women) with salivary gland mass, aged between 16 and 85 years (mean age 56,12±15) were enrolled in this prospective study. All masses were examined by qualitative and semi-quantitative strain elastography techniques. The most representative images were recorded to be evaluated according to a 4-scale scoring system. Score 1-2 were accepted to be benign and 3-4 malignant. The strain index of the mass in respect to surrounding parenchyma was measured.
Results: Fifty-three (%92.9) masses were located in the parotid gland, the rest in the submandibular gland (7.02%). Forty-seven (82.4%) masses were benign, and pleomorphic adenomas lesions were in the majority (44.6%). There were 10 malignant lesions (17.5%). Sensitivity, specificity, PPV and NPV were calculated for both qualitative scoring and strain index ratio. For qualitative assessment these values were 90%, 44,6%, 25,7%, 95,4%, respectively. Using the ROC analysis, sensitivity and specificity at the cutoff value of 2.44 for strain ratio were 70% and 100%, respectively (P=0.002). All the lesions with strain indices were malignant.
Conclusion: High sensitivity and negative predictive values for qualitative method may be better to recognise benign rather than malignant. High specificity of strain ratio at proper cutoff values may be helpful for verification of malignant tumours. Qualitative and semi-quantitative sonoelastography may be helpful in deciding the nature of salivary gland masses.

B-0257 14:56

Combination of diffusion weighted imaging and dynamic contrast-enhanced MRI improves differentiation of benign and malignant orbital masses

E.Y.L. Dai, A.T. Ahuja; *Hong Kong/HK (dai.eunice@gmail.com)*

Purpose: Diffusion weighted imaging (DWI) and dynamic contrast-enhanced MR imaging (DCE-MRI) allow assessment of lesion cellularity and vascularity respectively. We evaluated the combined use of DWI and time-signal intensity curve (TIC) analyses to differentiate benign from malignant orbital masses.
Methods and Materials: We retrospectively studied 54 patients with orbital masses who underwent MR imaging using DWI and DCE-MRI at either 1.5 or 3 Tesla. We calculated apparent diffusion coefficient (ADC) values and performed qualitative assessment of TIC curve patterns generated by DCE-MRI.
Results: 47 (87.0%) patients had benign orbital masses (4 benign tumours, 19 cavernous hemangiomas, 15 inflammatory lesions, 9 vascular malformations); while 7 (13.0%) patients had malignant orbital masses. All malignant masses were histologically proven while benignity was established by histology or clinical follow-up. Mean ADC values were significantly different for benign and malignant subgroups (ANOVA p=0.007). Benign masses had significantly higher ADC values compared with malignant masses (1.49±0.50 vs 0.97±0.45, p=0.01). Type of TIC curve was also significantly different amongst subgroups (p=0.04). 71.4% of benign masses had type 1 TIC pattern while none of the malignant lesions had type 1 pattern (p=0.01). Cavernous hemangiomas were predominantly associated with type I TIC pattern, and the predictive value of a type 1 TIC pattern for cavernous hemangioma was associated with high sensitivity (89.5%) and modest specificity (60.0%). In comparison, vascular malformations had heterogeneous TIC patterns.
Conclusion: Benign and malignant orbital masses have significantly different diffusion and perfusion characteristics and combination of ADC values and TIC pattern analysis improves their differentiation.

B-0258 15:04

Usefulness of microvascular ultrasonography in differentiation between pleomorphic adenoma and Warthin tumour of salivary glands

S. Chae, I. Ryoo, S. Suh, A. Park, M. Ku, H. Seol; *Seoul/KR (csyloo@naver.com)*

Purpose: Pleomorphic adenoma (PA) and Warthin tumour (WT) are the most common salivary gland tumours. It is important to differentiate between them because at least partial parotidectomy is necessary for PA, whereas enucleation is sufficient to WT. This study aimed to evaluate the usefulness of vascular pattern analysis using microvascular ultrasonography in differentiation of PA and WT of salivary glands.
Methods and Materials: Sixty-three patients with pathologically proven PA (n=39) and WT (n=24) were included. For all tumours, gray-scale, power-Doppler and microvascular ultrasonography (Superb-Microvascular Imaging) were performed. Differences between vascular patterns (internal vascularity and vascular distribution) on power-Doppler and microvascular ultrasonography and other sonographic features (size, shape, echogenicity, border, cystic change and heterogeneity) on gray-scale ultrasonography for PA and WT were evaluated. Comparison of diagnostic performance of gray-scale with power-Doppler ultrasonography and gray-scale with microvascular ultrasonography was performed. The level of inter-observer agreement of two reviewers in diagnosing tumours was evaluated.
Results: No sonographic features on gray-scale ultrasonography showed significant difference between two tumours. Internal vascularity and vascular distributions on power-Doppler (p=0.002 and 0.008, respectively) and microvascular ultrasonography (all p<0.0001) were significantly different. Diagnostic accuracy of gray-scale with microvascular ultrasonography (79.4%) is higher than that of gray-scale with power-Doppler ultrasonography (73.0%).

This difference was significant according to McNemar test (p=0.004). Inter-observer agreement was excellent in diagnosing tumours on both gray-scale with power-Doppler ultrasonography(κ=0.83) and gray-scale with microvascular ultrasonography(κ=0.94).
Conclusion: Vascular pattern analysis using microvascular ultrasonography with other sonographic features is helpful in differentiation between PA and WT in salivary glands.

B-0259 15:12

Thyroid nodules: utility of ultrasound combined to cytopuncture results in diagnosing malignant nodules that must be biopsied
G. Berrada, N. El Benna, O. Amriss, N. Moussali; *Casablanca/MA (berradaghita1988@gmail.com)*

Purpose: To highlight the high utility and accuracy of the ultrasound-guided cytopuncture of the suspect thyroid nodules detected by ultrasonography in assessing malignancy risk and selecting patients for surgery.
Methods and Materials: 19 patients were eligible to participate in a prospective study from March to June, 2016. The mean age of our patients was 51 years old (range, 29-65). It was about 17 women and 2 men. B-scan Ultrasonography, color Doppler imaging and pulsed method was performed using a linear high frequency probe (5-18MHz) (HITACHI). The cytopuncture was performed using 22-gauge fine needle.
Results: Using the risk stratification system for thyroid nodules TIRADS (Thyroid Imagind Reporting And Data System),we found 7 TIRADS "category 3" nodules (36,85%), 7 TIRADS "category 4a" nodules (36,85%) and 5 TIRADS "category 4b" nodules (26,3%). The cytologic results revealed 1 patient with benign cytology (5,27%), 6 with suspect nuclear atypia (31,58%), 5 with cytologic atypia that needs a checking (26,32%), 7 with hypocellular material and hematic cytology (36,85%).
Conclusion: The ultrasonography is the first line examination to select suspect thyroid nodules but the fine-needle cytopuncture of these nodules is the most efficient examination to assess malignancy risk to select the nodules that must be confirmed by tissue examination. Hence the utility of the duo ultrasonography / Ultrasound-guided cytopuncture.

B-0260 15:20

MRI-based treatment response assessment for head and neck tumours chemoradiotherapy
N. Plakhotina, D. Kuplevatskaya, A. Smirnova, M. Anishkin, A. Mikhailov; *St. Petersburg/RU (mikhail.a.cherkashin@gmail.com)*

Purpose: To create and implement MRI-based treatment response assessment algorithm in head and neck tumours after chemoradiotherapy (CRT).
Methods and Materials: Study involved 37 patients (age 41-76 years). 1.5T scanner was used. Sagittal T2, T1 WI, axial T1 WI with FS with large-field scanning were used, axial T2 STIR WI and sagittal or coronal T2 STIR WI were added depending on tumour localisation. Axial DWI and ADC maps were calculated. Post-contrast T1 WI sequences with FS were performed in 3 planes. Slice thickness 1-3 mm. MR examinations were performed before CRT and each 3 months after. For local failure confirmation, PET/CT was performed in 7 cases.
Results: In 37.8% (14 patients) early postradiation changes were detected. DWI helped to distinguish between tumour fragments with high cellularity and oedema and to trace increasing of ADC as sign of tumour regression. If area of pathological changes did not extend beyond area of radiation exposure, such changes were regarded postradiation alterations. Increasing postradiation necrosis was observed on average up to 8 months, with later swelling decreasing. Signs of clinically significant postradiation necrosis were not detected in our studies. In 16 patients tumour regression signs were detected. In 4 patients tumour progression was detected. All cases were confirmed by PET/CT.
Conclusion: Reactions of head and neck tumours after CRT characterised by heterogeneity. Most MR characteristics of tumour progression and postradiation changes are similar. Standard MRI is not enough to differentiate them, it is necessary to perform DWI and compare with PET/CT.

B-0261 15:28

Accuracy of diffusion-weighted imaging and dynamic contrast-enhanced MRI for differentiating benign from malignant non-cystic lesions in floor of the mouth
Y. Yuan, X. Tao; *Shanghai/CN (yuany83@163.com)*

Purpose: The aim was to evaluate the potential use of diffusion-weighted imaging (DWI) and dynamic contrast-enhanced MRI (DCE-MRI) in differentiating benign from malignant lesions in floor of the mouth (FOM).
Methods and Materials: A retrospective review was conducted of patients with pathologically confirmed non-cystic FOM lesions between January 2010 and December 2014. The apparent diffusion coefficient (ADC) and time-signal intensity curve (TIC) pattern were assessed. Receiver operating characteristic (ROC) and logistic regression analyses were performed to evaluate their differential value and association with malignancy.
Results: Significant differences were detected between benign and malignant lesions in ADC value and TIC pattern (p=0.015 and p<0.001). The areas under the curve (AUCs) for ADC and TIC pattern were 0.754 and 0.704, respectively. The joint association of ADC and TIC with malignancy was most prominent in lesions with both ADC≤1.23×10^{-3} mm^2/s and plateau/wash-out TIC pattern. The AUC of combined use of ADC value and TIC pattern was 0.820 (best sensitivity: 98.3%; best specificity: 88.9%).
Conclusion: Our results suggested that DWI and DCE-MRI contribute to differential diagnosis of non-cystic MOF lesions, especially when used in combination. Additional larger studies are warranted to confirm our findings.

14:00 - 15:30 **Room E1**

Computer Applications

SS 305

Machine learning in image interpretation

Moderators:
T. Bäuerle; Erlangen/DE
E. Svedström; Turku/FI

K-04 14:00

Keynote lecture
N.N.

B-0262 14:09

Evaluation of CAD-RADS in coronary CTA: man vs machine
B. Szilveszter, M. Kolossváry, J. Karády, Z. Bagyura, M. Károlyi, A. Panajotu, Á. Jermendy, B. Merkely, P. Maurovich-Horvat; *Budapest/HU (szilveszter.balint@gmail.com)*

Purpose: The Coronary Artery Disease - Reporting and Data System (CAD-RADS) has been recently introduced to facilitate interdisciplinary communication of coronary CT angiography (CTA) results. The accuracy of readers to determine CAD-RADS has not been tested. Our aim was to assess readers' performance ("Man") using an automated structured reporting software ("Machine").
Methods and Materials: We prospectively analysed the reports of 149 patients who underwent coronary CTA. The scans were read by four expert readers with 2-6 years' experience using a structured reporting platform blinded to the automated CAD-RADS results. The readers recorded the CAD-RADS stenosis categories (0,1,2,3,4A,4B,5) and modifiers (V,N,S,G). The reporting platform ,,machine" automatically determined the CAD-RADS classification, which was validated previously and applied as the reference standard. We compared reader's and the machine's performance using Cohen's kappa.
Results: The agreement in stenosis categories was 93.3%, kappa:0.80. Whereas the agreement in modifiers was only 85.9%, kappa:0.73. Stenosis categories: 0: 18.1% vs 16.8%, 1: 31.5% vs 24.2%, 2: 19.5% vs 24.8%, 3: 9.4% vs 12.1%, 4A: 6.0% vs 8.7%, 4B: 0.0% vs 0.7% and 5: 5.4% vs 5.4%, reader vs machine, respectively. Modifiers: N: 10.1% vs. 7.4%, V: 9.4% vs 17.5%, N: 10.7% vs 12.1%, G: 2.7% vs 3.4%, S:4.7% vs 8.7%, readers vs machine, respectively.
Conclusion: Despite the fact that automated CAD-RADS classification uses data filled in by the readers it performs better than the clinical readers by preventing human errors and inattention. Structured reporting platforms with automated score calculations might improve data quality and support clinical decision making.
Author Disclosures:
M. Kolossváry: Shareholder; Shareholder of Bioscreen Ltd.. **Z. Bagyura:** Shareholder; Shareholder of Bioscreen Ltd.. **P. Maurovich-Horvat:** Shareholder; Shareholder of Bioscreen Ltd..

B-0263 14:17

A new computer-aided decision (CAD) system based on artificial neural networks for detecting breast lesions on MRI
M. Telegrafo, V. Bevilacqua, S. De Ceglie, A. Stabile Ianora, G. Angelelli, M. Moschetta; *Bari/IT (mikitele@hotmail.it)*

Purpose: To evaluate the role of a computer-aided decision (CAD) system based on medical imaging for detecting regions of interest (ROI) including breast lesions on breast MRI, having contrast-enhanced MR and hystological findings as the reference standard.
Methods and Materials: 20 patients underwent MR examination on a 1.5T device with a diagnostic protocol including morphological (T2-TSE, STIR) and dynamic (THRIVE) sequences. The overall number of the obtained slices from MR examinations was 3735. An innovative preliminary step for segmenting

ROIs was used. Significant features were extracted from ROIs in order to obtain artificial neural networks (ANNs) architecture-based on error back propagation training algorithm. CAD sensitivity, specificity, positive predictive value (PPV), negative predictive value (NPV) and diagnostic accuracy for detecting ROIs including breast lesions on breast MRI were calculated.
Results: 192/3735 slices were considered as positive basing on the proposed CAD system while the remaining 3543/3735 were considered as negative. By comparing the obtained results with the reference standard, 102 false positive and 4 false negative slices were found. Sensitivity, specificity, PPV, NPV and diagnostic accuracy for the proposed CAD system were respectively of 96%, 97%, 47%, 100% and 97%.
Conclusion: The high negative predictive value and diagnostic accuracy of the proposed CAD System allows to select ROIs on breast MRI excluding areas which do not require further assessment.

B-0264 14:25

Why big image analytics is essential for imaging biobanks: an osteoporosis radiomics study

K.S. Mader[1], T.J. Re[2], J. Cyriac[2], B. Stieltjes[2]; [1]*Zurich/CH*, [2]*Basle/CH (kevinmader@4quant.com)*

Purpose: Imaging biobanks are becoming increasingly popular and active efforts from a number of different institutions in Germany, the UK, and US are making significant progress in collecting, storing, and organising large sets of image data. These large cohorts of data contain very diverse data from different sources, with different resolutions, and quality which makes large-scale analysis challenging. In this study, we aim to develop large-scale tools for processing and extracting meaningful bone information and statistics from a heterogenous set of CT data collected for other purposes.
Methods and Materials: The training and validation data are created by a trained radiologist that manually contoured all of the bone regions in 179 images from 60 different patients. These segmentations were augmented by adding noise and deformations and were then used to train a multi-layered convolutional neural network (CNN) until both the training and validation had above 95%.
Results: Our tools link the PACS directly to a computing cluster and allow the analysis to be run on any CT dataset immediately and scales linearly to 133,000 patients per hour. The results were very robust against noise, contrast, different body regions, energy, and dose settings. Compared to state of the art threshold and morphology approaches, it had 1000 fewer misclassified pixels at TPR of 99%.
Conclusion: The study presents the basis for conducting large scale studies to extract meaningful quantitative information from imaging biobanks. To analyse 80M images, these algorithms could be run in 10 days on a cluster (60 nodes).
Author Disclosures:
K.S. Mader: Board Member; 4Quant Ltd.. Founder; 4Quant Ltd.. Shareholder; 4Quant Ltd.. **B. Stieltjes:** Shareholder; HQ Imaging.

B-0265 14:33

Fully-automated mean bone density calculation on 1,000,000 CT scans: groundwork for opportunistic osteoporosis screening

T.J. Re, A.W. Sauder, E.M. Merkle, B. Stieltjes; *Basle/CH (tomjre@gmail.com)*

Purpose: Osteoporosis is estimated to causes more than 8.9 million fractures annually worldwide. Risk assessment of osteoporotic fracture currently relies on dual-energy x-ray absorptionmetry measurement of bone mineral density. We evaluate the possibility of utilizing CT data already present in our PACS for opportunistic screening of osteoporotic fracture risk.
Methods and Materials: We developed a software package, named “PACS Crawler”, for identifying, downloading, and post-processing CT images from the PACS. It was used to automatically identify all CT series performed between the years of 2010 to 2015 and currently stored in the PACS. It then randomly choose 1,000,000 samples and all samples were automatically post-processed to calculate a mean bone density and standard deviation from density range and shape-based bone segmentation.
Results: A total of approximately two million (1,903,715) CT series were identified in the PACS in the selected six-year period from which 1,000,000 samples were randomly selected. Fitted trend lines were calculated as f(x)= 245.5x-0.278 with R2=0.16 for females and f(x)= 219.0x-0.208 with R2=0.30 for males. Thus, as expected, bone density decrease over age was found to be more pronounced in women.
Conclusion: Automated bone density extraction from CT data using the developed pipeline is feasible and delivers plausible results. Future studies will be performed to evaluate the value of these measurement considering fracture risk prediction.

B-0266 14:41

Automatic vertebrae localisation in arbitrary field-of-view spine CT using decision forests

A. Jiménez-Pastor, E. Tomás-González, Á. Alberich-Bayarri, D. García-Juan, F. García-Castro, L. Martí-Bonmatí; *Valencia/ES*

Purpose: Diagnosis of spine abnormalities, vertebrae deterioration and bone characterisation from CT scans is a frequent task of radiologists. Our goal was to propose an algorithm based on supervised classification forests to automatically locate, identify and characterise vertebrae in spine CT scans.
Methods and Materials: The artificial intelligence (AI) technique used in this project was decision forests, based on supervised learning. For each voxel, hundreds of intensity-based features and their location were used as inputs and their corresponding label as output. These labels were: C1-C7, T1-T12, L1-L5, S1, B (vertebrae and background). The first step consisted on dataset preparation for training the forest algorithm. To build the input data, a total of 200 spine CT scans with arbitrary field of views were used, including healthy and pathological studies. The scans were manually labelled by selecting vertebrae centroids. To determine which label corresponded to each voxel, first of all we calculated the probability of each voxel to be part of each vertebra. Once the probabilities map was obtained, the label matrix was calculated. Finally, we trained our decision forest and then we tested it using new spine scans.
Results: The decision forest created to automatically determine vertebrae locations from new CT datasets was tested against 20 new cases with a mean performance of 95% correct classification of the voxels of a vertebra.
Conclusion: Automatic localisation and identification of vertebral bodies can be addressed with excellent results by all methods to improve diagnosis workflow and characterise bone structure.

B-0267 14:49

Quantitative CT metrics outperform pulmonary function testing for diagnosis of bronchiolitis obliterans syndrome after lung transplantation

E.J.M. Barbosa Jr.[1], H. Shou[1], S. Simpson[1], N. Tustison[2], J. Gee[1], J. Lee[1]; [1]*Philadelphia, PA/US*, [2]*Charlottesville, VA/US (eduardo.mortani@gmail.com)*

Purpose: Chronic lung allograft dysfunction after lung transplantation (LTx) manifests as a sustained decline in FEV1, indicative of bronchiolitis obliterans syndrome (BOS). Our hypothesis is that quantitative CT (QCT) metrics may be superior to PFTs and semi-quantitative image scores (SQS) to diagnose BOS.
Methods and Materials: Paired inspiratory-expiratory CT scans and PFTs of 178 LTx patients were analysed retrospectively, and separated into BOS (79) and non-BOS (99) cohorts. SQS were assessed by 2 radiologists and graded from 0-3 for features including mosaic attenuation and bronchiectasis. PFTs included FEV1 and FVC. QCT included lung volumes and air trapping volumes, by lobe. Multivariate regression modelling was performed using logistic and principal component analysis.
Results: Multivariate logistic regression using QCT metrics outperformed models using SQS or PFTs (area under the ROC curve of 0.95, 0.64, 0.80; respectively), to distinguish BOS from non-BOS LTx patients. Principal component regression of normalised variables determined that the first 3 components captured 79% of the variability of data, and the first two components heavily weighted a linear combination of QCT metrics in lieu of PFTs or SQS to predict BOS status.
Conclusion: While no single QCT metric was sufficient to determine BOS status, the constellation of QCT metrics dominate both multivariate logistic and principal component regression and are superior to PFTs and SQS to predict BOS status. This suggests that latent information on paired volumetric CT may be useful for early diagnosis of BOS in LTx patients, via computation of QCT metrics and multivariate modelling.

B-0268 14:57

Semi-automatic software for time-efficient CT-based quantification of abdominal adipose tissue

A. Schaudinn, N. Linder, A. Hudak, R. Stange, N. Garnov, G. Stocker, U. Hacker, T. Kahn, H. Busse; *Leipzig/DE (Alexander.Schaudinn@medizin.uni-leipzig.de)*

Purpose: Quantification of visceral and subcutaneous adipose tissue (VAT, SAT) based on CT-images is gaining importance in risk assessment in patients with metabolic disease or cancer, or prior to abdominal surgery. The aim of this study was to present a custom-made tool (*MatLab*-tool) for semi-automatic AT quantification.
Methods and Materials: Twenty normal to overweight patients (14 male, 6 female, mean BMI: 29.4 kg/m²) underwent IRB-approved abdominal CT (Somatom Sensation 64, Siemens, slice thickness 5 mm). Total volumes of VAT (V_{VAT}) and abdominal SAT (V_{SAT}) (diaphragm to pelvic floor) were determined with MatLab-tool using supervised automatic segmentation (under MatLab, MathWorks). Default AT-range was set between -190 and -30 HU. Analyses were repeated with a common commercial tool (SliceOmatic,

TomoVision). Agreement was determined by coefficients of determination (R^2) and standard deviations (SD) of the volume differences (Bland-Altman).
Results: Mean volumes were V_{VAT}=5.6L and V_{SAT}=8.6L. Processing involved an average of 83 slices and took a mean time of 15min (MatLab-tool) and 41min (SliceOmatic) per patient. Coefficient R^2 was 0.99 in both compartments while bias and SD (SD%) were 108ml and 73ml (1.2%) for V_{VAT} and -221ml and 165ml (1.9%) for V_{SAT}.
Conclusion: The presented tool provides a reliable and time-efficient option for CT quantification of adipose tissue, with an average time-saving of 26 minutes for each patient compared to commercial tools.

B-0269 15:05

Using 3D image features for the prediction of survival in patients after liver transplantation

D. Pinto dos Santos, M. Wand, S. Brodehl, C. Li, R. Klöckner, T.C. Hadler, M. Sprinzl, E. Schömer, P. Mildenberger; *Mainz/DE (pintodos@uni-mainz.de)*

Purpose: To explore whether automated extraction of 3D imaging features from CT scans and machine learning allow for the prediction of survival in patients with liver cirrhosis undergoing liver transplantation.
Methods and Materials: A total of 313 patients undergoing liver transplantation for final stage liver cirrhosis between 1989 and 2015 were included in this study. Clinical data, such as transplantation date, patient characteristics and survival were retrieved from the patient's records. Relevant imaging studies (i.e. CT scans of the abdomen) were retrieved from the PACS. An algorithm was developed that applied a linear max-margin classifier (SVM) to a bag-of-visual-words descriptor based on histograms of oriented 3D gradients. A pipeline was then designed where CT image data was processed through this algorithm. Results were validated on a separate randomised test dataset. Both, training and validation set were randomly sampled such that an equal number of positive and negative cases were present. Visual features identified by the algorithm could then be visualized on the respective CT data to allow for anatomical correlation.
Results: The training process took a few hours of computation time and was run on a standard workstation using the training dataset. Thereafter, the classification process based on the trained model could be performed within a few seconds per scan using the testing dataset. With this setup we achieved a prediction-accuracy of around 80% on the validation dataset.
Conclusion: Low-level 3D image feature statistics in CT scans can potentially help identifying patients that have a longer survival after liver transplantation.
Author Disclosures:
M. Wand: Grant Recipient; from the special focus area "computer-based methods in life-sciences" of the Johannes Gutenberg-University Mainz. **C. Li:** Research/Grant Support; partially funded by the Intel Vision Computing Institute.

B-0270 15:13

Machine learning in whole-body oncology: fully automatic, multi-organ segmentation in whole body-MRI, using classification forests and convolutional neural networks

I. Lavdas, B. Glocker, D. Rueckert, H. Mair, A. Sandhu, E. Aboagye, A.G. Rockall; *London/UK (a.rockall@imperial.ac.uk)*

Purpose: As part of a programme to develop automatic tumour detection methodology for whole-body MRI, we initially developed and compared two algorithms for automatic, multi-organ segmentation in healthy volunteers.
Methods and Materials: Algorithm A was based on 'classification forests' and algorithm B on 'convolutional neural networks'. Healthy volunteers were scanned with multi-parametric whole-body MRI at 1.5T. MRI data were used as input data to the algorithms, while training was based on manual annotations by clinical experts. 5-fold cross-validation experiments were run on 34 subjects. We report the Dice overlap coefficient between the manual and automatic segmentations. Performance between the two algorithms was compared with a Mann Whitney U test.
Results: Both methods facilitated simultaneous multi-organ segmentation. The algorithms were efficiently trained using a relatively small number of data, an important consideration in the clinical setting. The mean Dice coefficient (±SD) for algorithms A/B, was: right and left lung: 0.92±0.02/0.94±0.01, liver: 0.90±0.02/0.91±0.04, gallbladder: 0.38±0.25/0.25±0.22, right kidney: 0.79±0.06/0.85±0.05, left kidney: 0.73±0.13/0.74±0.17, spleen: 0.67±0.15/0.72±0.11, pancreas: 0.55±0.11/0.54±0.13, bladder: 0.74±0.18/0.70±0.22, spine: 0.83±0.03/0.86±0.05, pelvic bones: 0.74±0.05/0.78±0.05. Algorithm B returned significantly higher Dice coefficient than algorithm A ($P<0.05$) for both lungs, the liver and the spinal/pelvic bones.
Conclusion: We report two robust algorithms for automatic multi-organ segmentation in whole-body MRI with good agreement to manual segmentations performed by clinical experts. Algorithm B outperforms algorithm A in terms of Dice coefficient for a number of structures, but with the penalty of training complexity/time. The methods are currently being optimised for automatic tumour lesion detection.

B-0271 15:21

Fully automated segmentation of rectal carcinomas using supervised learning techniques with expert-reader input

S. Trebeschi[1], J.J.M. van Griethuysen[1], H.J.W.L. Aerts[2], D.M.J. Lambregts[1], M.J. Lahaye[1], F.C.H. Bakers[3], N.H.G.M. Peters[4], M. Verheij[1], R.G.H. Beets-Tan[1]; [1]*Amsterdam/NL*, [2]*Boston, MA/US*, [3]*Maastricht/NL*, [4]*Heerlen/NL (j.v.griethuysen@nki.nl)*

Purpose: To perform fully automated segmentation of locally advanced rectal carcinomas (LARCs) via a supervised learning technique (SLT) trained and validated using delineations performed by expert-readers.
Methods and Materials: We selected the MRI scans (1.5T, T2-weighted and b1000 DWI) of 140 LARC-patients. Manual whole tumour volume delineation, performed by an expert radiologist (on b1000 DWI, was used as the standard reference). From each image, 500 pixels within the tumour and 500 pixels outside the tumour were randomly sampled. For each pixel, we extracted the surrounding patch of 25x25 in all MRI sequences. By fitting the resulting three patches as color channels, we could build a multiparametric representation of the image. The architecture consisted of three convolutional layers. A fully connected layer of 256 neurons was placed between the convolutional layers and the output layer. From each patient, 1000 patches were extracted. Both classes were balanced due to randomised sampling procedure. Patients were randomly and equally divided between training and testing.
Results: The algorithm was trained until it reached a stable condition. The trained algorithm was then applied on the test set, reaching an AUC of 0.94 based on the probability of being tumour for each pixel.
Conclusion: Automatic segmentation using an SLT is able to reproduce manual expert segmentations with an AUC of >0.90, suggesting that it can be a time-efficient solution to help delineation in daily practice.

14:00 - 15:30 **Room E2**

Neuro

SS 311a

Stroke: CT and MRI

Moderators:
S. Jefic; Banja Luka/BA
U. Lamot; Ljubljana/SI

B-0272 14:00

Detection of single-phase CTA-occult vessel occlusions by CT perfusion post-processing predicts favorable response to IV thrombolysis in acute ischaemic stroke

W.G. Kunz, M.P. Fabritius, C. Höhne, L. Havla, M.F. Reiser, W.H. Sommer, K.M. Thierfelder; *Munich/DE (kolja.thierfelder@med.lmu.de)*

Purpose: To study the predictive value of single-phase CTA (spCTA)-occult occlusions detected using CT perfusion-based wavelet-transformed angiography (waveletCTA) on morphologic and clinical response to IV thrombolysis (IVT) in acute ischaemic stroke.
Methods and Materials: Patients were selected from a cohort of 1351 consecutive subjects who underwent multiparametric CT including whole-brain CT perfusion. Inclusion criteria were: (1) significant cerebral blood flow (CBF) deficit, (2) absence of spCTA occlusion, and (3) follow-up confirmed infarction. waveletCTA defines angiographic signal by voxel-based fitting of time attenuation curves to generic contrast bolus curves. waveletCTA was analysed by two blinded readers. Morphologic outcome was defined as final infarction volume divided by CBF deficit volume, of which smaller values were considered favorable. Favorable clinical outcome was defined as decrease in modified Rankin scale (mRS) score of ≥1 from admission to discharge (ΔmRS) and a decrease of National Institutes of Health Stroke Scale (NIHSS) score of ≥3 from admission to 24 hours (ΔNIHSS). Linear and logistic regression analyses were performed to identify independent associations.
Results: Among all included patients (N=106) with negative spCTA, 50 patients (47%) showed an occlusion on waveletCTA. In patients treated with IVT (N=50), regression analyses showed that the presence of a waveletCTA-detected occlusion was an independent predictor of a favorable morphologic outcome (beta=-0.524, p=0.015) and favorable clinical outcome (ΔmRS: OR=9.018, p=0.047; ΔNIHSS: OR=5.810, p=0.024), while it failed to predict outcome in patients who did not receive IVT (N=56; all p>0.05).
Conclusion: Detection of spCTA-occult vessel occlusions using waveletCTA independently predicts favorable response to IVT.

B-0273 14:08

Crossed cerebellar diaschisis in acute ischaemic stroke: impact on morphologic outcome, functional outcome and stroke-related complications

W.G. Kunz, W.H. Sommer, M.P. Fabritius, F. Schuler, M.F. Reiser, K.M. Thierfelder; *Munich/DE (wolfgang.kunz@med.lmu.de)*

Purpose: Crossed cerebellar diaschisis (CCD) is the phenomenon of hypoperfusion of the contralateral cerebellar hemisphere caused by dysfunction of related supratentorial regions. We analysed the clinical relevance of CCD in acute ischaemic stroke as assessed by whole-brain CT perfusion (WB-CTP).
Methods and Materials: Subjects with follow-up confirmed stroke caused by a vessel occlusion of the anterior circulation were selected from a cohort of 1644 consecutive patients who underwent multiparametric CT including WB-CTP. Two blinded and experienced readers evaluated the posterior fossa in terms of CCD presence (CCD+) or absence (CCD-). Final infarction volumes (FIV), modified Rankin scale (mRS) scores at discharge and at 90 days as well as the occurrence of stroke-related complications served as outcome indicators. Linear and logistic regression analyses were performed to determine the association of CCD occurrence with these indicators.
Results: In total, 156 patients matched the inclusion criteria, encompassing 102 patients (65.4%) categorised as CCD- and 54 (34.6%) as CCD+. In linear and logistic regression analyses, no significant association between CCD and FIV (β=-0.440, p=0.972), discharge mRS≤2 (OR=1.897, p=0.320), or 90-day mRS≤2 (OR=0.531, p=0.492) were detected. CCD+ patients had larger supratentorial cerebral blood flow deficits compared to CCD-patients (median: 164ml vs 115 ml; p=0.001). In logistic regression analyses of complications, the occurrence of CCD was associated with parenchymal haematoma formation (OR=4.793, p=0.035).
Conclusion: CCD is a frequent WB-CTP imaging finding in acute anterior circulation stroke. CCD was associated with parenchymal haematoma formation but did not prove to significantly influence either morphologic or functional outcome.

B-0274 14:16

Quantitative assessment of hyperacute cerebral infarction with intravoxel incoherent motion MR imaging: initial experience in a canine stroke model

S. Lu, Q. Gao, X. Xu, X. Liu, H. Shi, S. Liu; *Nanjing/CN (lushan1118@163.com)*

Purpose: To evaluate the feasibility of intravoxel incoherent motion (IVIM) for the measurement of diffusion and perfusion parameters in hyperacute stroke.
Methods and Materials: An embolic ischaemic model was established with an autologous thrombus in 20 beagles. IVIM imaging was performed on a 3.0 T platform at 4.5 h and 6 h after embolisation. Ten b values from 0 to 900s/mm^2 were fitted with a biexponential model to extract perfusion fraction f, diffusion coefficient D, and pseudo-diffusion coefficient D*. Additionally, the apparent diffusion coefficient (ADC) was calculated using the mono-exponential model with the maximum b value. Statistical analysis was performed using the pairwise Student's t-test and Pearson's correlation test.
Results: A significant decrease in f and D was observed in the ischaemic area compared to that in the contralateral side at 4.5h (p=0.001 and p=0.000) and 6h (both p=0.000) after embolisation. No significant difference was observed in D* between the two sides at either time point. f in the stroke area at 6h was significantly lower than that at 4.5h (p = 0.016). A significantly positive correlation was detected between ADC and D in both stroke and contralateral sides at 4.5h and 6h (both p=0.000). Significant correlation between ADC and f was observed in the contralateral side at 4.5h and 6h (p=0.019 and 0.026).
Conclusion: IVIM imaging could simultaneously evaluate the diffusion and microvascular perfusion characteristics in hyperacute stroke.

B-0275 14:24

Automated assessment of early ischaemic damage on CT scans: as good as an expert?

C. Goncalves[1], S. Bowman[1], S. Liyanage[1], R. OrathPrabakaran[1], S. Shah[1], S. Gerry[2], P. Harman[1], P. Guyler[1]; [1]*Southend-on-Sea/UK*, [2]*Oxford/UK*

Purpose: The ASPECTS (Alberta stroke program early CT score) is an established 10-point quantitative topographic score to assess early ischaemic changes on unenhanced CT. Recently, a software (e-ASPECTS, Brainomix Ltd.) has become available for automated scoring of ASPECTS regions and ischaemic damage.
Methods and Materials: 2640 (132 patients x 20 regions) ASPECTS regions were scored by 3 neuroradiologists (NRAD). The ground truth was determined by a corelab with access to follow-up scans (24h CT +_ DWI, CT Perfusion). Sensitivity, specificity and accuracy (SSA) for region-based and score-based analysis, ROC curves, Bland-Altman plots and Matthews correlation coefficients (MCC) relative to the ground truth were calculated and comparisons were made between NRADs and different pre-specified e-ASPECTS operating points. The non-inferiority margin was set to 10% for both sensitivity and specificity on region-based analysis.
Results: Mean time from symptoms onset to baseline CT was 146+/-124 min and median NIHSS was 11 (6-17 interquartile range (IQR)). Median ASPECTS for ground truth on follow-up imaging was 8 (6.5-9 IQR). In the region-based analysis, two e-ASPECTS operating points (SSA of 44%, 93%, 87% and 44%, 91%, 85%) were statistically non-inferior to all three NRADs (all p values <0.003). Both MCCs for e-ASPECTS were higher (0.36 and 0.34) than those of all NRADs (0.32. 0.31 and 0.3).
Conclusion: e-ASPECTS was non-inferior to three neuroradiologists in scoring ASPECTS on unenhanced CTs of acute stroke patients.

B-0276 14:32

MRI stroke protocol: one-stop shop in setting of acute infarct with multiple comorbids

F. Mubarak; *Karachi/PK (fatima.mubarak@aku.edu)*

Purpose: Purpose of our study is to predict progression of infarct size as depicted by venous congestion on susceptibilty weighted imaging (SWI).
Methods and Materials: We retrospectively enrolled all diagnosed cases of stroke from January, 2013 to December, 2015.We included only thirty patients since we had stringent incluion and exclusion criterias. Inculsion criteria were: 1. acute infarct on diffusion weighted imaging (DWI) in MCA, ACA or ICA territory. 2. stroke protocol performed including DWI and SWI on first day and repeat DWI with in three days.Exclusion criteria were: 1. tissue plasmineogen activator (TPA) given.2. Haemorrhagic infarction on initial presentation. 3. Watershd infarcts.Patients were imaged on 1.5T Siemens and 3T Toshiba machines.Venous congestion was defined as numerous and larger veins with greater hypointensity comapred with contralateral hemisphere.We used (ASPECTS) scoring system to estimate infarct size.Degree of venous congestion was graded as none, moderate and extensive on the basis of ASPECTS scoring.SPSS 21 version was used for analysis.The venous congestion grading was used to predict infarct growth.
Results: There was interval increase in ASPECT score on DWI in 15 patients with moderate degree of vascular congestion on SWI. The extent of venous congestion was significantly correlated with infarct growth (P<0.001). In 2 patients there was development of haemorrhage with stable size of infarct. In 13 patients there was no vascular congestion and no increase in size of infarct.
Conclusion: Venous congestion seen in infarcted territory is related to poor prognosis and this can be reliably used as a surrogate marker of oxygen extraction in penumbra.

B-0277 14:40

Intraluminal thrombus detection in patients with acute ischaemic stroke using three-dimensional black blood contrast-enhanced MRI: comparison on SWI

W. Jang, H.-S. Kwak, G.-H. Chung; *Jeonju/KR (weon0315@gmail.com)*

Purpose: To evaluate the accuracy of three dimensional black blood contrast-enhanced MR imaging in the detection of intra-arterial thrombus in patients with acute ischemic stroke
Methods and Materials: 47 patients with acute ischemic stroke involving anterior circulation underwent MR imaging within 6 hours of clinical onset. MR examination included SWI, DWI, PWI, TOF MR angiography, and three dimensional black blood contrast-enhanced T1-weighted imaging. Cerebral angiography for thrombectomy was used as the reference standard to establish the diagnosis of occlusion of intracranial artery. Two neuroradiologists interpreted three data sets as blinded study: 1, DWI + 3D BB contrast-enhanced MR imaging; 2, DWI + SWI; 3, DWI + 3D BB contrast-enhanced MR imaging + SWI. The diagnostic accuracy of both methods was evaluated using ROC analysis.
Results: For both observers, the Az values of the data 1 and 3 set included 3D BB contrast-enhanced MR imaging was significantly higher than that of the data 2 set included only SWI(observer 1; 0.978 vs. 0.915; p = .002, observer 2; 0.977 vs. 0.904; p = .000). The sensitivity of the data 1 set included 3D BB contrast-enhanced MR imaging was significantly higher than that of the data 2 set included SWI (observer 1; 95.7 vs. 83.0, p = .004 observer 2; 95.7 vs. 80.9; p = .009). The k-value of all data set was excellent (0.861).
Conclusion: Detection of intra-arterial thrombus using 3D BB contrast-enhanced MR imaging provides accurate detection of thrombus in patients with acute ischemic stroke.

B-0278 14:48

Site and rate of arterial occlusive disease in acute ischaemic stroke: a CT-angiography study of 50'807 cervico-cerebral arterial segments

D.C. Rotzinger, P.J. Mosimann, R.A. Meuli, P. Maeder, P. Michel; *Lausanne/CH (david.rotzinger@chuv.ch)*

Purpose: CT angiography (CTA) can rapidly and accurately depict arterial abnormalities in acute ischaemic stroke (AIS) patients. Our purpose was to determine the pattern of significant stenoses and occlusions at Admission based on CTA in a representative AIS population.
Methods and Materials: Data from consecutive AIS patients admitted to a single centre (CHUV) between 2003 and 2012 were prospectively collected in the Acute Stroke Registry and Analysis of Lausanne (*ASTRAL*) database. All patients with a good quality CTA within 24 hours from symptom onset were selected. All intracranial and cervical arterial stenoses ≥50% or occlusions were registered and classified according to 31 pre-specified segments per patient.
Results: Among 2'209 patients (42.6% females, median age 71 years), 1'177 (53.3%) had significant arterial CTA anomalies. Among the 50'807 examined arterial segments, 2'259 were abnormal: 1'851 (82%) were within the ischaemic territory, whereas 408 (18%) were considered asymptomatic. The arteries most frequently affected by symptomatic anomalies were the proximal MCA (20.1% of all segments), followed by the cervical ICA (16.7%) and the distal MCA (12.1%). In AIS patients imaged by CTA within 6 hours of onset, 40.7% had occlusions potentially amenable to endovascular therapy.
Conclusion: This study shows that CTA obtained within 6h of symptom onset can depict large, proximal segmental arterial occlusive disease amenable to endovascular therapy in more than 40% of AIS patients. The annual case load of CTAs performed in AIS patients may therefore serve to estimate how many acute endovascular treatments can be expected per stroke center or region.

B-0279 14:56

The application of Alberta Stroke Program Early CT Score (ASPECTS) to acute ischaemic stroke initial CT brain imaging and haemorrhagic transformation rates

M. Hanley, T. Tarmey, L. Morrison, C. Judge, M. Costello, K. Donlon, P.A. McCarthy, R. Ó'Caoimh; *Galway/IE (marionhanley98@gmail.com)*

Purpose: Predicting Haemorrhagic transformation (HT) in patients with acute ischaemic stroke often proves difficult, and the implications of this extends to clinical decisions such as the timing of reinstating anticoagulation therapy.
Methods and Materials: Data was collected from a single centre, University Hospital Galway (UHG). Patients were identified using a database of stroke patients presenting to UHG over a two year period. The initial CT brain images were reviewed, ASPECTS applied and high risk HT features were identified. Repeat CT brain images prior to initiating anticoagulation were then reviewed for HT.
Results: 150 patients were identified as having ischaemic stroke and atrial fibrillation. The average age was 77 years (33-100), 106 (70.9%) were male. 95 (61.3%) infarcts were not identified on initial CT brain imaging. 30 (20%) were small infarctions, 20 (66.7%) were medium, and 5 (3.33%) were large posterior infarctions. ASPECTS was applied to 68 (45.3%) initial CT brain images; average ASPECTS was 8.5 with 4.5% (15) having an ASPECTS of less than or equal to 7. Of these, 30% (5) were associated with haemorrhagic transformation, accounting for 4.8% HT overall. 105 (70%) initial CT images showed one or more high risk radiological features for HT.
Conclusion: ASPECTS and other high risk radiological features are important predictors of haemorrhagic transformation in the acute ischaemic stroke setting and greater weight should be emphasised on these features when making clinical decisions, such as, the timing of introducing or reinstating anticoagulation.

B-0280 15:04

Intracranial arterial calcification in black Africans with acute ischaemic stroke

R.B. Olatunji, A.J. Adekanmi, A.O. Ogunseyinde; *Ibadan/NG (richard_olat@yahoo.com)*

Purpose: Intracranial arterial calcification (IAC), a recognised marker of atherosclerosis on cranial computed tomography (CT), is an independent risk factor for ischaemic stroke. This study aimed to determine the prevalence, distribution, severity and associations of IAC in adults with acute ischaemic stroke at the University College Hospital, Ibadan, Nigeria.
Methods and Materials: Cranial CT images of 130 consecutive adults who presented with acute ischaemic stroke were acquired on a 64-slice multi-detector Toshiba Aquilion scanner and evaluated for IAC in bone window on Vitrea software using a semi-quantitative scoring method for extent, thickness and length of calcifications in the large intracranial arteries. Association of IAC with clinical and laboratory data was determined by statistical analysis at $p<0.05$.
Results: There were 71 male (54.6%) and 59 female (45.4%) patients with mean age of 63.0±13.2 years. IAC was found in 121 patients (93.1%), predominantly in the carotid siphon (86.1%) followed by the intracranial vertebral arteries (9.3%), middle cerebral arteries (2.4%), basilar artery (1.2%) and the anterior cerebral arteries (1%). Severity of the burden of IAC ranged from mild (17.4%), moderate (52.1%) to severe (30.6%). IAC was associated with age (p=0.003), diastolic blood pressure (p=0.03) diabetes mellitus (p=0.02) and elevated serum low-density lipoprotein (p=0.04) but not with sex (p=0.35).
Conclusion: The burden of intracranial arterial calcifications is high among black African patients with acute ischaemic stroke and preferentially involves proximal inflow arteries. Therefore, the role of large vessel atherosclerosis in ischaemic stroke in black Africans should be explored in future multicentre, multimodality studies.

B-0281 15:12

Haemodynamic disturbances in CT perfusion (CTP) for infarct core volume prediction during acute Ischaemic stroke (AIS) in large vessel multiple occlusion

E. Puglielli, R. Lattanzi, G. Esposito, V. Di Egidio; *Teramo/IT (edopug@hotmail.com)*

Purpose: To evaluate the impact of haemodynamic disturbances due to multiple intra- and/or extracranial vessel occlusions upon automated CT perfusion analysis tool during AIS.
Methods and Materials: We review our database retrospectively (876 pts) for all cases of endovascular treatment of AIS (from April 2009 to September 2016), with anterior circulation occlusion, baseline CTP and full recanalisation (mTICI III) (114pts). The infarct core was accurately measured using automated normalised, threshold and voxel-wise analysis in real time with CTP and time to peak enhancement TTP, mean transit time MTT, and cerebral blood volume CBV.
Results: CT angiography can well define the occlusion site, depict arterial state, grade collateral blood flow, and characterise atherosclerotic status. Comparison between multiple 68.4% (78/114) and non-multiple 31.5% (36/114) occlusion groups revealed similar baseline ischaemic core (21±19 vs 18±24cm^3; p=0.8), MTT>6s (175±105 vs 156±115cm^3; p=0.6), MTT>10s (92±84 vs 95±91cm^3; p=0.9) and final infarct volumes (44±46 vs 36±41cm^3; p=0.5). The mean difference between estimated core and final infarct volume was similar between patients with and those without multiple occlusion (23±43 vs 16±13 cm^3; p=0.5).
Conclusion: Automated CTP imaging is not significantly influenced by presence of intra- or extracranial carotid steno-occlusive disease in large vessel AIS and thus may be useful to select patients who will benefit from endovascular reperfusion therapy.

B-0282 15:20

Correlation between iodine extravasation after mechanical revascularisation in acute ischaemic cerebrovascular stroke and haemorrhage development

M. Bonatti[1], F. Lombardo[1], A. Comai[1], G.A. Zamboni[2], G. Bonatti[1]; [1]*Bolzano/IT*, [2]*Verona/IT (matteobonatti@hotmail.com)*

Purpose: To correlate iodine extravasation presence, distribution and concentration after mechanical revascularisation in acute ischemic cerebrovascular stoke with subsequent haemorrhage development.
Methods and Materials: We included in our IRB-approved retrospective study 9 consecutive patients who developed intracranial haemorrhage after mechanical revascularisation for ischemic stroke (group A) and 21 controls who didn't develop it (group B). All patients underwent post-procedural dual-energy CT of the brain. Iodine presence, distribution pattern (deep white matter (DWM), cortical or both) and maximum concentration (mgI/ml) were evaluated by means of a commercially available software.
Results: Iodine extravasation was present in 9/9 patients in group A and in 13/21 patients in group B (p>0.05). In group A, 4/9 patients presented DWM iodine distribution, 1/9 patients cortical distribution and 4/9 patients both. In group B, 4/13 patients presented DWM iodine distribution, 0/13 patients cortical distribution and 9/13 patients both. None of the distribution patterns was significantly associated with haemorrhage development. Mean maximum iodine concentration was 7.5±3.7 mgI/ml in group A (range 1.4 - 27.7 mgI/ml) and 1.3±0.3 mgI/ml in group B (range 0 - 4.2 mgI/ml) (p=0.0145). According to ROC analysis, a cut-off value of 1.3 mgI/ml had 100% sensitivity and 57% specificity for detecting patients who will develop haemorrhage.
Conclusion: Post-procedural intracerebral iodine extravasation with maximum concentration equal or greater than 1.3 mgI/ml can identify patients at higher risk of post-procedural haemorrhage development with excellent sensitivity and good specificity.

14:00 - 15:30 **Room F2**

Emergency Imaging

SS 317

Non-traumatic emergencies

Moderators:
A. van Randen; Amsterdam/NL
S. Wirth; Munich/DE

B-0283 14:00

MDCT assessment of esophageal perforations in the emergency setting

C. Liguori, A. Pinto, G. Ponticiello, C. Stavolo, S. Nicotra, L. Romano;
Naples/IT (carlo.liguori@gmail.com)

Purpose: To investigate how accurately MDCT can diagnose the level of upper GI tract perforation especially assessing site and entity of esophageal leakages.
Methods and Materials: MDCT studies in 55 patients with surgically confirmed esophageal perforation were retrospectively evaluated. MDCT scans were obtained with 64-detector CT; submillimetre axial images and multiplanar reconstruction (MPR) images were generated for all patients. Intravenous contrast enhancement was performed in all patients and in 35 oral contrast was also administered. Two experienced radiologists reviewed the images for direct findings (free air, ruptured esophageal wall, oral contrast leak) and indirect findings (inflammatory changes, fluid collection, focal thickening of the GI tract wall) and attempted to identify the perforation site in each patient.
Results: Free air was seen in more than 95% of the patients with perforation at sites; rupture of the esophageal wall was directly visualised in 32%; oral contrast leakage was appreciated in 90%. Indirect signs: wall thickening and periesophageal inflammatory changes were present in 95% of cases, fluid collections in 87%. The perforation site was correctly diagnosed in 90% of the patients when the radiologists referred to both direct and indirect findings.
Conclusion: MDCT is a robust technique for esophageal perforation identification. Intravenous contrast and oral contrast administration are key factor for a confident diagnosis.

B-0284 14:08

Application of model-based iterative reconstruction algorithm in CT pulmonary angiography in emergency setting: dose reduction and image quality

L. Riva, D. Ippolito, C.R.G.L. Talei Franzesi, A. De Vito, C. Cangiotti, S. Sironi;
Monza/IT (luca.riva89@gmail.com)

Purpose: To compare radiation dose and image quality of low-dose CT pulmonary angiography with new model-based iterative reconstruction protocol (IMR), with a standard CTPA, in patients with suspect of pulmonary embolism (PE).
Methods and Materials: A total of 87 patients investigated for PE were enrolled in our study.The study group was evaluated using a new 256-MDCT (iCT elite,Philips) with low-kV (100 kV; automated tube-current modulation), low volume of CM and IMR algorithm to reconstruct raw data. Control group underwent standard CTPA study on 16-MDCT scanner, with the same volume of CM (120 kV; 150-250 mAs; FBP reconstruction). Two radiologists performed quantitative evaluation measuring vessels contrast enhancement and calculating SNR and CNR. A 4-point scale was used to perform the qualitative evaluation. Radiation dose exposure data was recorded as DLP, CTDIvol and ED.
Results: The intra-vessel density was higher in study group than in control group, while background noise was significantly lower ($p<0.05$) in study group than the control one. The SNR and CNR of the low-kV MBIR-CTPA were better than standard FBP-CTPA ($p<0.05$). DLP, CDTIvol and ED in study group were significantly lower than those in control group ($p<0,05$), with a 34% reduction in CTDIvol and 25% reduction in ED for study group, having SNR and CNR higher than those of standard FBP-CTPA. Moreover, the overall image quality rating score was higher for MBIR-CTPA than FBP-CTPA both for the two readers ($p<0.05$; C.Alpha=0.91).
Conclusion: Low-kV setting combined with MBIR can improve the diagnostic image quality of CTPA in pulmonary embolism, compared to a standard CTPA reconstructed with FBP, allowing to reduce the radiation dose to patients.

B-0285 14:16

Use of whole-body CT to detect patterns of CPR-related injuries after sudden cardiac arrest

A. Perez-Girbes[1], G.M. Dunham[2], F. Bolster[3], K. Sheehan[2], K.F. Linnau[2];
[1]*Valencia/ES*, [2]*Seattle, WA/US*, [3]*Dublin/IE (perez_alegir@gva.es)*

Purpose: Patients with Sudden Cardiac Arrest (SCA) commonly undergo cardiopulmonary resuscitation (CPR) in order to maintain, and ultimately restore return of spontaneous circulation (ROSC). CPR related injuries are common and may be detectable with whole-body computed tomography (WBCT). We have recently implemented a dedicated SCA- WBCT protocol to evaluate SCA patients with ROSC post-CPR. The aim of this study is to evaluate the number and pattern of CPR-related injuries in ROSC patients with SCA-WBCT.
Methods and Materials: Single-centre retrospective review of 39 patients (13 female; 26 male, mean age 51.8 yrs) with non-traumatic, out-of-hospital SCA and ROSC and evaluation with dedicated SCA-WBCT over a 10 month period (January to September 2016). SCA-WBCT-protocol includes non-enhanced head CT, ECG-gated CTA chest, and portal-venous CT abdomen and pelvis. Medical records were reviewed for demographic, CPR-related, and patient outcome data. Two radiologists reviewed all SCA-WBCTS by consensus.
Results: In-hospital mortality was 46%. Chest injuries were most common on WBCT: 84.6% (33) subjects had rib fractures (mean of 8.5 fractures/subject); 30.8% (12) sternal fractures; 12.8% (5) mediastinal haematoma; 10.3% (4) pneumothorax; 7.7% (3) pneumomediastinum and 2.6% haemothorax (1). Three subjects (7.7%) had abdominal injuries on WBCT, including one hepatic laceration with active haemorrhage."
Conclusion: CPR-related injuries on WBCT after ROSC are common, with serial rib fractures detected most commonly. An unexpectedly high rate of abdominal injuries was detected on SCA-WBCT. Radiologists need to be attuned to the spectrum of CPR-related injuries in WBCT, including abdominal injuries.

B-0286 14:24

Role of high-frequency ultrasound in ocular emergencies

S.S. Sachar; *Bareiily/IN (drsacharsaurabh@gmail.com)*

Purpose: To examine the effectiveness and accuracy of HFUSG for evaluation of acute ocular pathologies in emergency. 5% cases presenting to casualties are ocular emergencies and their evaluation can be limited by lack of specialised equipment, training, and ophthalmologic backup. Investigations such as CT, MRI, etc. are time-consuming, costly and may be unavailable. However, with the advent of HFUSG, many acute ocular pathologies, e.g. orbital trauma, rupture, retinal detachment (RD) central retinal artery or vein occlusion can be safely and non-invasively diagnosed at the bedside.
Methods and Materials: Prospective study was carried out in the casualty of teaching institutes named above during 06 months in which 44 patients were assessed who had acute ocular related complaints. A 10MHz linear array transducer with Doppler was used.
Results: Out of 44, 28 (64 %) were found to have serious acute ocular pathologies other than soft tissue swelling, including globe rupture, RD, vitreous haemorrhage, etc.
Conclusion: Acute ocular pathologies resulting from conditions such as trauma can be accurately and quickly diagnosed at the bedside itself by HFUSG resulting in immediate and correct therapeutic Intervention and lower costs for patients and must form an integral part of diagnostic protocol.

B-0287 14:32

Low-dose abdominal CT using pure iterative reconstruction in patients presenting to the emergency department with acute abdominal symptoms

F. Molony, M. Tomey, D. Ryan, K. James, T. Grey, N. Moore, M. Murphy, O. O'Connor, M. Maher; *Cork/IE (karl.m.james@gmail.com)*

Purpose: To evaluate the diagnostic ability of low-dose abdominopelvic CT using pure MBIR to accurately diagnose non-trauma patients presenting acutely with abdominal symptoms.
Methods and Materials: 57 patients were scanned using a split dose technique whereby 80-90% of the standard CT effective dose (ED) was used to generate a control study (CD) and was immediately followed by a low-dose CT (LD) using the remaining 10-20% of the standard ED CT dose. Dose measurements from both scans were obtained. Blinded reads by 2 experienced radiologists performed objective and subjective measures of image quality from both datasets and the ability to identify pathology and reach a diagnosis was compared between the two study types.
Results: The ED was significantly lower in the LD group by an average factor of 3 ($p<0.0001$). The LD CT study had significantly increased subjective image noise and poorer contrast and diagnostic resolution ($p<0.0001$). 28 of the 57 studies had an identifiable pathology and the low dose study was able to correctly identify this pathology in all but one of the abnormal studies. There

were 5 cases where there was discrepancy in the detail of the pathology (e.g. acute appendicitis vs. perforated appendicitis). The positive predictive value and negative predictive value of the LD compared with the CD studies were 96.4% (95% CI: 81.7%-99.9%) and 96.6% (95% CI 82.2%-99.9%) respectively.
Conclusion: Although more difficult to interpret, LD CT with MBIR provides diagnostic images in patients presenting with acute abdominal pain while imparting a significantly lower patient dose.

B-0288 14:40

Dengue fever: markers on ultrasound predicting prolonged hospital stay and complications

P. Khokhani, K. Dhamecha, H. Shah; *Anand/IN (khokhani1988@gmail.com)*

Purpose: Dengue fever during epidemics assumes very high hospital admissions. However these patients receive supporting management, our purpose of study was to elaborate the USG findings in general and grave findings in particular, concerned with prolonged hospital stay and complications.
Methods and Materials: The study was performed during peak epidemic between months of June to September 2016. Inclusive criteria are serologically and biochemically positive indoor patients. Informed consent of the patients and referring physician was taken. The ethical committee approval was obtained. The patients were subjected to USG of abdomen and chest with routine protocol. Machine used was Mind-Ray DC7, probes 3-5MHZ and 8-12MHZ.
Results: The findings of dengue positive patients were classified as general and in particular (which we focussed upon in study). Study comprised of 100 inward patients referred for USG. General findings comprised of: hepatomegaly (90%), splenomegaly (60%), gallbladder wall oedema (95%), clear ascites (90%). In particular findings to be focussed upon are: septated perinephric fluid (20%) and particulate ascites and periportal oedema (25%). In particular findings were associated with a platelet count of <20,000/mm3 and prolongation of hospital stay (>7 days) as compared to their counterparts having general findings. Here, the chi-square test of relevance showed $p<0.05$.
Conclusion: We conclude from this study, during dengue epidemic the findings on USG of septated perinephric fluid and particulate ascite with periportal oedema represents significant platelet loss, patient debility and prolongation of hospital stay.

B-0289 14:48

CT findings in impending rupture of atherosclerotic abdominal aortic aneurysms: a case control study

M. Giannotta, M. Piolanti, E. Pisano, L. Rignanese, F. Magnoni, A. Pilato, M. Zompatori, M. Imbriani; *Bologna/IT (marica.giannotta@studio.unibo.it)*

Purpose: Patients with impending rupture of atherosclerotic Abdominal Aortic Aneurysm (AAA) usually present with abdominal or back pain, that may mimic several abdominal emergencies. Prompt recognition of impending rupture is mandatory, since rupture is a life-threatening emergency. The purpose of this study is to value whether CT may correctly identify the presence of an impending rupture.
Methods and Materials: We retrospectively assessed CT findings in two groups of patients: 22 patients with impending rupture (symptomatic AAA without retroperitoneal haemorrhage at CT) and 27 patients with asymptomatic AAA (electively studied with CT). The groups were matched for size, age and sex. Presence of blebs, hyper-attenuating crescents, linear thrombus dissections, draped aorta sign, peri-aortic stranding and vertebral scalloping were blindly assessed by 2 experienced radiologists. The study was approved by the Institutional Review Board.
Results: No sign showed acceptable sensitivity for the diagnosis of impending rupture. Several signs showed high specificity with a satisfactory positive predictive value (PPV): draping aorta sign (specificity 96%, PPV 66%), hyper-attenuating crescents of the aortic wall (specificity 96%, PPV 80%), linear dissections of the thrombus (specificity 96%, PPV 80%) and peri-aortic stranding (specificity 100%, PPV 100%).
Conclusion: Various signs have been associated with AAA impending rupture in literature, although their reliability have never been assessed. Our results point out that no sign is sufficiently sensitive or has acceptable negative predictive value. Contrarily, there are some findings which have good specificity and PPV, that have to be taken in account when assessing AAAs.

B-0290 14:56

MDCT signs accuracy in detection of acute perforated appendicitis

M. Porta, C. Liguori, S. Daniele, T. Cinque, C. D'errico, L. Romano; *Naples/IT (m.elenaporta@gmail.com)*

Purpose: Presence of perforated appendicitis significantly increases morbidity, mortality and the risk of complications after surgical period. The aim of this study is to evaluate MDCT accuracy in detecting perforated appendicitis signs in the preoperative setting.
Methods and Materials: From January 2013 to August 2016, retrospective study included 73 patients (mean age 37.5y; 16y-68y) admitted to the emergency department with clinical suspicious of acute appendicitis. Intravenous contrast media was administered. Two Radiologists with 10- and 15-year experience in emergency imaging classified the six most frequent signs of perforated appendicitis as follow: 1) enlarged lumen calibre >6 mm (aspecific sign); 2) enhancing defect foci of the wall; 3) abscess presence; 4) phlegmon presence; 5) extraluminal air (also divided into 2-groups based on an anterior-posterior abdomen-Visceral Diameter -aVD- in axial plane); 6) extraluminal appendicolith. Perforated appendicitis imaging findings were compared with final pathology/clinical proven as standard of reference.
Results: 11 patients were excluded because of artefacts and/or no-appendicitis diagnosis. 62 (85%) had pathologically/clinical proven perforated appendicitis. Six individual CT signs sensitivity and specificity were respectively determined for each patient: 1(100%, 100%); 2(95%, 97%); 3(29%, 98%); 4(45%, 95%); 5(60%, 90%); 6(40%, 99%). Extraluminal air sign sensibility was also divided for aVD less(20%) or more(65%) than 15cm.
Conclusion: MDCT is a high sensitive/specific technique in setting of acute perforated appendicitis; enhancing defect foci of the wall and abscess presence showed the statistically most significant association with perforated appendicitis. Extraluminal air sign showed lower sensitivity in subjects with <15cm aVD.

B-0291 15:04

Interobserver variability in detection of acute abdominal bleeding with CT

J. Rabczak, M. Powerski, M. Pech, S. Penzlin, S. Neumann, R. Damm, B. Friebe, P. Schindler, S. Titz; *Magdeburg/DE (joanna.rabczak@med.ovgu.de)*

Purpose: Acute intra-abdominal bleeding is a common emergency indication to CT-angiography in daily routine as well as during off-hours. It is a sensitive and fast first-line modality not only to diagnose an active bleeding but also to plan the subsequent therapy. The main purpose was to evaluate accuracy of a radiologist in detection of active bleeding in abdomen with angiography as reference standard according to different level of experience of a proband.
Methods and Materials: Eight radiologists were assigned to three groups: with no practical clinical knowledge, in the fourth and fifth year of residency and a group of specialists with experience in interventions. Any of them reviewed independently CTA of 50 patient's abdomen. For each patient, a potential bleeding status was scored as positive, possible, uncertain, dubious or negative. The results of each group were analysed by the receiver operating characteristic curve analysis with consecutive assessment of interobserver agreement.
Results: The sensitivity for the youngest group was 77.3%, for the middle-experienced 80.6 % and for the group of interventionists 83.8%, the specificity subsequently 62%, 82.7% and 91%. The rate of ROC AUC was analogically 0.786, 0.842 and 0.905. Kappa analysis showed good agreement between the two more experienced groups, fair agreement between the novices and interventionists and poor agreement between the novices and the intermediate group.
Conclusion: The study shows some disparities between radiologist's interpretation that vary from personal experience and abilities which may significantly influence the outcomes of patients care.

B-0292 15:12

To die or die hard? Plain radiography for acute non-traumatic abdominal pain presenting to the emergency department

M.E. Abd El Bagi, B. Almutairi, S. Alsolamy, S. Alrashidi, I. Alrashidi, N. Ashraf, M. Reutener, A. Mohammed, N. Alrasheed; *Riyadh/SA (drm_bagi@hotmail.com)*

Purpose: To evaluate the utilisation of plain abdominal radio-graphs (PAR's) for imaging of acute non-traumatic abdominal pain (ANTAP) presenting to the emergency department(ED) in the era of low dose CT.
Methods and Materials: This is a retrospective study conducted at the ED of an 800 bed tertiary care hospital during the period from 01.06.2014 to 30.06.2014. The records of all adults who underwent PAR's due to ANTAP were reviewed. Trauma, gynecologic and paediatric cases were excluded.
Results: 756 patients were referred for PAR's due to ANTAP. 379(49.6%) of those were males, and 385(50.4%) were females. Age range was 15 to 92 years. Mean age was 46 years. Commonest presentation was unclassified abdominal pain in 679 (89.8%). PAR's were the only requested procedure for the vast majority of cases 594(78.57%). In 103(13.6%) conventional dose contrasted CT was added and in 33(4.3%) low dose CT was added. Abdominal ultrasound (US) was added in 52(6.8%). MRI was added for only one patient. When both PAR's and CT were used, there was a poor diagnostic congruence of 50% in cases of nonspecific pain, 43% in cases with non-significant findings and only 35.7% in abnormal cases.

Conclusion: Although of lower sensitivity, PAR's are still commonly used as a one stop shop for ANTAP presenting to the ED despite CT availability. When both CT and PAR's were used, there was a poor congruence of findings due to higher CT sensitivity but at a higher radiation dose. However, the new ultra-low- dose CT may soon replace PAR's.

B-0293 15:20

Suspicion of acute appendicitis in adults: the value of ultrasound

G. Benedetto, A. Llavata Solaz, M. Ferrer Puchol; *Alzira/ES*

Purpose: To evaluate the accuracy of ultrasonography for the diagnosis of acute apendicitis (AA) in adult patients, to calculate the negative apendicectomy rate (NAR) in operated patients and to identify statistically significant signs and symptoms of acute appendicitis.
Methods and Materials: In this prospective study, every ultrasound requested in a one-year period from the emergency department for adult patients (age 15 years and older) with pain in the right iliac fossa (RIF) was registered upon completion. Clinical symptoms, signs and ultrasound findings were recorded and a presumptive diagnosis was formulated in the report (normal, non-visible appendix and no indirect signs, non-conclusive, probable appendicitis, appendicitis). Optimal sample size was calculated and statistical analysis of the data was performed by means of the software Stata14 (descriptive analysis, t-test, Chi-square, Roc curve and diagnostic tests) and compared with the final post-surgical pathological findings.
Results: We studied 139 patients (45% men, 55% women), mean age: 33 (15-84). Statistically significant clinical signs and symptoms were RIF pain, fever, leukocytosis and left shift. Significant US findings were visible appendix, non-compressibility, echogenic fat, appendicolith and free fluid. NAR: 0%. Mean appendiceal diameter without AA: 5mm (5.53-6.58 with 95% CI), with AA: 9mm (7.84-9.15 with 95% CI). AUC of the ROC curve (with a 50% prevalence in our population for the categories of certain and probable AA with 95% CI): 0.935. Sensibility: 94.3%, specificity: 92.8%, PPV: 93%, NPV: 94%.
Conclusion: The ultrasonography yields excellent results and makes the correct diagnosis in case of suspected AA in adults.

14:00 - 15:30 **Room D**

Musculoskeletal

SS 310

Tumours and inflammation

Moderators:
R. Campbell; Liverpool/UK
N.N.

K-05 14:00

Keynote lecture

A. Oktay; *Izmir/TR*

B-0294 14:09

Spondyloarthropathy (SpA): is sacroiliac (SI) joint imaging sufficient?

S. Gupta, J.P. Singh; *Gurgaon/IN (drsaurabhjmu@gmail.com)*

Purpose: To assess the utility of including sagittal STIR sequence of dorsolumbar spine and coronal STIR/PD fat saturated sequence through both hips, to routine SI joint MR imaging protocol, in patients clinically suspected to have SpA.
Methods and Materials: Observational study was conducted between February 2013 and October 2016 on clinically suspected SpA patients referred to our department for imaging. The images obtained using this new SI joint protocol were evaluated for findings suggesting SpA diagnosis as per the Assessment of SpondyloArthritis international Society criteria. Other differentials in symptomatic patients without radiologic SpA were also evaluated.
Results: Of the 308 patients (225M; 83F), 192 had features confirming the diagnosis of SpA and 116 had no radiological manifestations of SpA (29 were normal and 87 had other findings to suggest clinical symptoms e.g. degenerative spondyloarthropathy, Pott's spine, skeletal metastases, early AVN of hip, cysticercus, iliofemoral impingement etc.). 18/192 patients had normal SI joints but other findings to suggest diagnosis of SpA, e.g. romanus lesions, costovertebritis/costotransversitis, pubic symphysitis, inflammatory hip arthropathy, enthesitis, iliofemoral/trochanteric bursitis. 27/49 patients with chronic sacroilitis had disease activity in spine/hip.
Conclusion: Inclusion of sections through dorsolumbar spine and both hips to routine SI joint protocol, helped identify: (a) early disease in 18 patients, who had normal SI joints and may have otherwise been missed with routine SI joint imaging protocol, (b) additional findings in SpA related sacroiliitis, (c) disease activity in chronic sacroilitis and (d) other causes of low back pain, and thus helped in further patient management.

B-0295 14:17

Presence of bone marrow edema on MRI of the sacroiliac joints is predictive of subsequent (5 years) radiographic progression in early onset non-radiographic axial spondyloarthritis

A. Feydy, M. Dougados, A. Sepriano, R. Landewe, C. Dermattei, A. Molto, M. de Hooge, V. Navarro, M. Reijnierse; *Paris/FR (antoine.feydy@aphp.fr)*

Purpose: The aim of this study was to evaluate the rate of radiographic progression and its predisposing factors after a 5 years follow-up period in patients with recent onset axial SpA.
Methods and Materials: Patients: Recent onset (<3 years) axial SpA enrolled in the Cohort DESIR. Outcome measure: Radiographic SIJ status according to the mNY criteria after 5 years follow-up. Reading of the SIJ-X-Rays: 3 trained readers unaware of the chronology of baseline, 2-year and 5-year films and of the clinical and other imaging data.
Results: Of the 708 patients enrolled in the cohort 482 (68.1%) completed the 5 years follow-up. Complete x-ray data was available in 379 patients. 326/ 379 patients were mNY negative at baseline and 23 (7.1%) of these were found positive at year 5. Conversely, 53/379 patients were mNY positive at baseline and 5 (5.7%) were found negative at year 5 (net progression of 1.4%). BME on MRI-SIJ was found in 15 (71.4%) of the patients who switched from mNY-negative at baseline to mNY-positive at year 5 and only in 51 (16.8%) patients who remained mNY-negative throughout the 5 years follow-up period. In the multivariable analysis, presence of BME on MRI was the strongest predictor of radiographic progression (OR=4.85 [95% CI: 2.95-7.97]).
Conclusion: These data suggest that 5-year radiographic progression in SIJ of patients with early onset SpA is modest and demonstrate that a positive MRI of the SIJ (presence of BME) is the strongest predictor of radiographic progression in the SIJ of these patients.

B-0296 14:25

Whole spine MRI findings in SAPHO syndrome

W. Xu, C. Li, X. Shao, X. Zhao, W. Zhang; *Beijing/CN (xuwr0122@163.com)*

Purpose: To systematically document the whole spine MRI findings in a large cohort of synovitis-acne-pustulosis-hyperostosis-osteitis (SAPHO) syndrome.
Methods and Materials: 38 SAPHO patients (26 female, 46.3±9.3 years) were perspectively enrolled. MRI examinations of the whole spine were performed with standardised protocols. All the images were evaluated in a blinded manner, and discrepancies were reached in consensus after discussion.
Results: A total of 310 vertebrae were involved in 35 SAPHO patients. All the 35 patients had a multiple-vertebra involvement pattern (median: 7, range: 2-24), with a predilection on lumbosacral spine. 80.3%(249/310) affected vertebrae were continuously involved, while 19.7%(61/310) were separately involved. For the 310 affected vertebrae, a total of 567 lesions were observed. 35.8%(203/567) of the lesions were confined to vertebral corners, while 64.2% (364/567) also implicated adjacent endplate. Abnormal signal intensity (SI) of a mixture of bone marrow edema (BME) and fat deposition was found in 49.2%(279/567) lesions, while abnormal SI of solely BME or fat deposition was observed in 13.9%(79/567) and 36.9%(209/567) lesions, respectively. Cortical bone erosion was found in 50.6% (287/567) lesions. Vertebral collapse and bony bridge were observed in 0.6%(2/310) and 6.8%(21/310) affected vertebrae. Adjacent disk space was narrowed in 37.4%(116/310) affected vertebrae, but only 6.8%(21/310) were accompanied by hyperintensity on T2-weighted images. 1.3%(4/310) apophyseal joints were observed with hyperintensity on T2-weighted images. Thickening of anterior longitudinal ligaments was observed in 7.1%(22/310) affected vertebrae.
Conclusion: Imaging features of spinal disorders in SAPHO syndrome may facilitate better understanding of this rare disease and avoid misdiagnoses.

B-0297 14:33

Initial experience with dual-phase hybrid ^{18}F-Fluoride PET/MRI in patients with ankylosing spondylitis

L.M. Sawicki[1], S. Lütje[2], X. Baraliakos[3], J. Kirchner[1], V. Ruhlmann[2], H.H. Quick[2], L. Umutlu[2], G. Antoch[1], C. Buchbender[1]; [1]*Düsseldorf/DE*, [2]*Essen/DE*, [3]*Herne/DE (Linomorris.sawicki@med.uni-duesseldorf.de)*

Purpose: Increased ^{18}F-F uptake during blood-pool phase PET represents regional hyperaemia, while indicating osteoblastic activity during mineralisation phase PET. This study aimed to assess the feasibility of dual-phase ^{18}F-F PET/MRI of the sacroiliac joints (SIJ) in ankylosing spondylitis (AS) and find an association between regional hyperaemia and osteoblastic activity in different AS lesions.
Methods and Materials: Thirteen patients underwent dual-phase ^{18}F-F PET/MRI. Blood-pool phase PET was acquired 6 and mineralisation phase PET 40 min after ^{18}F-F injection. We analysed PET image quality (DIQ) and co-registration of blood-pool and mineralisation phase ^{18}F-F PET/MRI. SIJ quadrants (SQ) were assessed for presence of bone marrow oedema (BME), erosion, fatty deposits (FD), sclerosis, or ankylosis on MRI and focal ^{18}F-F uptake on PET.

Results: DIQ of both ^{18}F-F PET datasets was high, albeit DIQ of mineralisation phase PET was better than that of blood-pool phase PET (p<0.001). Image co-registration was equally good. BME alone was associated with focal ^{18}F-F uptake in 90.9% SQ on mineralisation phase and 63.6% SQ on blood-pool phase. FD, erosion, sclerosis, ankylosis were not associated with focal ^{18}F-F uptake on blood-pool or mineralisation phase. SQ with BME had a significantly higher (p<0.001) percentage of focal ^{18}F-F uptake on blood-pool phase (47.7% SQ) and mineralisation phase (86.4 % SQ) than SQ showing AS lesions without BME (6.7% and 11.7% SQ, respectively).
Conclusion: Dual-phase ^{18}F-F PET/MRI of SIJ is feasible with high image quality. Inflammatory AS lesions presenting with BME rather than structural changes are associated with regional hyperaemia and osteoblastic activity.

B-0298 14:41

Monitoring of tocilizumab treatment in patients with rheumatoid arthritis using selected imaging techniques

M. Dura[1], P. Zuchowski[1], S. Jeka[1], M. Waszczak-Jeka[2], E. Sokolska[1], T. Barczynska[1], M. Wegierska[1]; [1]*Bydgoszcz/PL*, [2]*Warsaw/PL (martadura83@gmail.com)*

Purpose: The aim of the study was to assess the usefulness of imaging techniques vs. disease activity score (DAS28) for therapy monitoring in patients with rheumatoid arthritis (RA).
Methods and Materials: The study included 24 RA patients (mean (SD) age 53 (12) years; disease duration 9.8 (8.5) years; 88% anti-CCP positive, 96% rheumatoid factor positive). At baseline, 17 patients had high disease activity (DAS28 > 5.1), and 7 patients had moderate disease activity (3.2 < DAS28 ≤ 5.1). All patients received tocilizumab for a year. Hand x-ray and MRI scans, power Doppler ultrasound (PDUS) of the metacarpophalangeal joints (MCP) as well as DAS28 measurement were performed at enrolment and completion of the study. At month 6 of the study, PDUS was performed and DAS28 was calculated. PDUS (semiquantitative scoring (0-3)) scans were performed by one rheumatologist. X-ray and MRI scans were interpreted by one radiologist.
Results: At month 6, remission (DAS28 ≤ 2.6) was observed in 15 (63%) patients, and the absence of synovitis was confirmed by PDUS in 16 (67%) patients. At month 12, remission (DAS28 ≤ 2.6) was observed in 24 (100%) patients; the absence of synovitis was confirmed in 19 (79%) patients by PDUS and in 17 (71%) patients by MRI. All patients showed no radiographic progression.
Conclusion: PDUS and MRI allow for detection of subclinical lesions, which are not identified by DAS28. The use of imaging techniques may prevent premature treatment modification in patients with remission as evidenced by DAS28.

B-0299 14:49

Ultrasound superb microvascular imaging in the evaluation of synovial vascularity: a preliminary study

S. Gitto[1], D. Orlandi[2], A. Corazza[1], E. Silvestri[2], M.A. Cimmino[2], L.M. Sconfienza[1]; [1]*Milan/IT*, [2]*Genoa/IT (sal.gitto@gmail.com)*

Purpose: Superb microvascular imaging (SMI) is an advanced flow-detection ultrasound (US)-based modality able to detect very low-flow vessels with high detail and definition. Our aim was to evaluate the use of SMI in patients with early rheumatoid arthritis (RA) and RA under treatment with rituximab also comparing the diagnostic performance of SMI with that of power Doppler (PDI) and B-mode US.
Methods and Materials: 30 patients (18 women, mean age 45±11 years) affected by RA with remission-to-moderate disease activity were examined. Ulnar recess, metacarpophalangeal I-to-V and proximal interphalangeal II-to-V joints of both hands were evaluated using a high-end US system equipped with a 7-18MHz broadband linear-array transducer, PDI and SMI module. From each US examination, short video clips showing B-mode US, PDI and SMI of synovial vascularity were registered and exported for image analysis. Two radiologists reviewed video clips registered for all patients evaluating synovial vascularity intensity with a semi-quantitative scoring system.
Results: SMI demonstrated the presence of synovial vessel signals in a significantly higher number of patients than PDI (P=0.02). Inter-observer agreement for B-mode US, PDI and SMI semiquantitative scoring was moderate (k=0.59), almost perfect (k=0.87) and almost perfect (k=0.82), respectively.
Conclusion: SMI detects more vessels than B-mode US and PDI in assessing synovial abnormalities in RA patients. This may allow for early diagnosis of synovial inflammation as well as monitoring its dynamic changes under therapy.

B-0300 14:57

MRI grading of cartilaginous tumours: comparison of texture analysis with visual MRI analysis

B. Fritz, D.A. Müller, R. Sutter, M.C. Wurnig, M. Wagner, C.W. Pfirrmann, M.A. Fischer; *Zurich/CH (benjamin.fritz@balgrist.ch)*

Purpose: To assess diagnostic accuracy and inter-reader agreement of MRI texture analysis (TA) for grading of cartilaginous neoplasms of bone in comparison to visual MRI analysis.
Methods and Materials: MRI of 101 cartilaginous neoplasms (grade 0-4) were retrospectively included. T1w-, T2w-, STIR- and contrast-enhanced T1w fs-images were analysed qualitatively and quantitatively by four independent musculoskeletal radiologists. Qualitative visual MR-features (N=14) included tumour morphology as well as cortical bone, bone marrow and soft tissue abnormalities, whereas quantitative TA-parameters (N=19) included grey-level histogram, co-occurrence and run-length-matrix features. Inter-reader reliability, univariate, multivariate and ROC analysis were performed for MR- and TA-parameters separately and for combined models to determine independent predictors and diagnostic accuracy for grading of cartilaginous lesions.
Results: Mean inter-reader agreement of visual MR- and TA-features were 0.49 (range: 0.08-0.82) and 0.81 (range: 0.34-0.99) respectively. Diagnostic accuracies for differentiation of benign vs. malignant as well as for benign vs. low-grade cartilaginous lesions were 92.6% and 95.1% using a combined model of visual MR- and TA-predictors, 89.5% and 78.7% using visual MR-predictors, and 87.2% and 86.9% using TA-predictors exclusively. For differentiation of low-grade vs. high-grade chondrosarcoma no significant independent TA-predictors existed, whereas a model containing visual MR-predictors exclusively had a diagnostic accuracy of 87.4%.
Conclusion: TA showed substantial higher inter-reader reliability compared to visual MRI analysis. A model combining visual MR- and TA-features showed a higher diagnostic accuracy for differentiation of benign vs. malignant as well as for benign vs. low-grade cartilaginous lesions compared to models using exclusively visual MR- or TA-predictors.

B-0301 15:05

Use of shear wave elastography to differentiate benign and malignant fatty soft tissues tumours

N. Regnard, S. Charlon, A. Buisson, A. Feydy, J. Drape, R. Campagna; *Paris/FR (nregnard@yahoo.fr)*

Purpose: It is not easy to discriminate, thanks to imaging, benign lipomas and atypic lipomatous tumours (ALT). The objective was to discriminate benign and malignant fatty soft tissues tumours with shear wave elastography.
Methods and Materials: All patients were included consecutively and prospectively in our institution. The multidisciplinary staff decided a biopsy under ultrasonography guidance. All patients had ultrasonography with shear wave elastography mode (Toshiba Aplio 500). We selected fatty lesions. We assessed the size of the tumour, the elasticity (value and ratio under subcutaneous fat), and the histology of the tumour. We compared the group with benign soft tissue tumours (lipomas) and malignant tumours (Atypic lipomatous tumours).
Results: 33 tumours were included (24 lipomas and 9 ALT). The mean age was 51.8 (+/- 15) in the benign group and 61.3 (+/- 15.1) in the malignant group (p=0.13) . The greater sizes were 82.2 mm (+/- 51) in the benign group vs 164 mm (+/- 89.2) in the malignant group (p= 0.03). The average volumes were 336.3 cc in the benign group vs 1463.3 cc in the malignant group (p=0.08). The average ratio between elasticity of the tumour and subcutaneous fat was 0.95 in malignant lesions vs 0.57 in benign lesion (p=0.05). The sensitivity and the specificity of this ratio to discriminate benign and malignant lesions were 77.8% and 75% with Area Under the Curve of 0.750 (p=0.01) with a threshold superior to 0.68.
Conclusion: We can discriminate benign and malignant fatty soft tissue tumours with shear wave elastography.

B-0302 15:13

PETMR evaluation of the relationship between metabolic activity on PET and cell-density on DWI for bone metastases

C. Giraudo, M. Weber, M. Hartenbach, P.A.T. Baltzer, M. Mayerhoefer; *Vienna/AT (chiara.giraudo@meduniwien.ac.at)*

Purpose: To assess the diagnostic performance of PETMR and DWI for bone metastases and evaluate whether, metabolic activity, on PET, and cell-density, on diffusion-weighted MRI, correlate in bone metastases.
Methods and Materials: Patients with histological proven cancer undergoing a PETMR (fully integrated system) for staging or restaging, with whole-body-DWI implementing the protocol, were evaluated. PETMR was rated positive when at least one hypointense lesion on T1w with high, non-inflammatory, uptake on PET (i.e., FDG, PSMA, Dotanoc) was shown.DWI was separately evaluated.PETMR and PETMR-DWI agreement (k) with the reference standard

(i.e., histology and/or follow-up/previous examination) was assessed.The relationship between bone metastases' metabolic activity (SUVmax, SUVmean) and cell-density (ADCmin, ADCmean) was investigated (Spearman correlation coefficient).
Results: One-hundred-three patients were evaluated (70 males; mean age±SD 58.29±16.76 years; 47 staging and 56 restaging). Sixty-four patients had lymphoma, 23 prostate cancer, six melanoma, two breast-, three gastrointestinal cancer, soft tissue sarcoma, bladder, ovarian, thyroid and neuroendocrine tumour one patient each. Thirty-four patients were correctly rated as positive at PETMR and 33 at PETMR-DWI. PETMR and PETMR-DWI showed a high agreement with the reference standard (k=.915 and k=.852, respectively). SUVmax, SUVmean, ADCmin and ADCmean, mean±SD values, were 12.62±10.50, 5.82±5.58, 629±238.37 and 895.52±278. No correlation emerged between SUVmax and ADCmin (r=.013; p=.941) and between SUVmean and ADCmean (r=-0.001; p=.996) neither, separately, at staging (r=.289, p=.296; r=.475, p=.074) or restaging (r=-.023, p=.925; r=-.293, p=.211).
Conclusion: PETMR and DWI demonstrated a high diagnostic performance for bone metastases.SUV and ADC seem to be independent imaging biomarkers for bone metastases, but further studies focused on cancer type and PET tracer, are necessary to fully assess this evidence.
Author Disclosures:
C. Giraudo: Research/Grant Support; Austrian Science Fund (FWF), project KLIF 382.

B-0303 15:21

Patient dose evaluation for whole-body skeletal CT using 100Sn filter for spectral shaping at 100kV in multiple myeloma
M. Meyer, N. Vogler, H. Haubenreisser, M.M. Ong, S.O. Schönberg, T. Henzler; *Mannheim/DE*

Purpose: To prospectively compare radiation dose parameters and image quality of an unenhanced whole-body CT protocol performed with 100kVp tube voltage in combination with a dedicated tin-filter (Sn-filter) for spectral shaping and a standard whole-body CT protocol performed with 120kVp tube voltage.
Methods and Materials: Twenty-five prospectively enrolled patients (18 men; median age 68 years) with proven multiple myeloma underwent a whole-body unenhanced 100kVp Sn-filter CT protocol. All scans were performed on a 3rd generation dual-source CT, using the following scan parameters: 100kVp tin filter, ref. mAs 280, 192 mm × 0.6 mm detector collimation, pitch 1.2. Each patient had undergone a previous CT whole-body standard protocol with 120 kVp within one year. Subjective and objective image quality was assessed in various anatomic regions and radiation dose was compared. Comparisons between the groups were analyzed with two-way ANOVA or Wilcoxon-Rank-Sum Test depending on the distribution of the data.
Results: All studies were rated as diagnostic. There was no significant difference between both protocols for subjective image quality (p>0.05). Objective image quality revealed significant higher attenuation values for the standard protocol, when compared to the 100 tin protocol for bone tissue, lung tissue and liver tissue (all p<0.05). Radiation dose was significantly less for the 100kVp tin protocol when compared to the standard protocol (mean dose-length-product 161±30 mGy*cm vs 1233±211 mGy*cm; p<0.0001).
Conclusion: 100 kVp spectral shaping whole-body CT by means of a tube-based tin-filter allows 88% dose reduction when compared to a standard 120 kVp.

14:00 - 15:30 **Room G**

Physics in Medical Imaging

SS 313
Innovations in radiology

Moderators:
H. Bosmans; Leuven/BE
I. Sechopoulos; Nijmegen/NL

B-0304 14:00

Evaluation of a new x-ray imaging system based on Talbot-Lau interferometry: initial images of the knee joints of healthy volunteers
Y. Hara[1], J. Tanaka[1], M. Niitsu[1], Y. Hoshino[2]; [1]*Saitama/JP*, [2]*Hachioji/JP (jtanaka@saitama-med.ac.jp)*

Purpose: To evaluate the characteristics of images of the knee obtained in a hospital from normal volunteers using an x-ray interferometry system that does not require either a synchrotron or a microfocus x-ray tube, and instead uses a practical x-ray tube (Talbot-Lau interferometry).
Methods and Materials: The cartilage in the four knee joints of healthy volunteers was imaged using our test system via the differential phase image technique, and its visibility was evaluated. Adequate positioning of the knee joint was examined so that the x-ray beam could pass through the joint space properly, using a specially designed fixing device with a weight of 2-4kg. The average exposure time was 7 seconds and the maximum skin radiation dose was 8mGy. This trial was performed based on results using cadaveric knee joints and with the approval of the university ethics committee.
Results: In all case, the joint cartilage and part of the menisci were well depicted.
Conclusion: This new x-ray imaging system based on Talbot-Lau interferometry can be used to image the cartilage and menisci to some extent, but more quickly and inexpensively than with MRI. The thickness of the joint cartilage and menisci can be measured in these images. The potential of this technology for diagnostic applications should be explored further. We have already started to examine other joints, such as the hands and elbows, using this system, to advance the clinical application of this new device.
Author Disclosures:
Y. Hara: Author; Junji Tanaka.

B-0305 14:08

Chest imaging with x-ray dark-field radiography: first human body experience
A.A. Fingerle[1], K. Willer[2], L. Gromann[2], F. de Marco[2], T. Koehler[3], K. Rindt[3], K. Hellbach[1], F. Pfeiffer[2], P.B. Noël[1]; [1]*Munich/DE*, [2]*Garching/DE*, [3]*Hamburg/DE (alexander.fingerle@tum.de)*

Purpose: To evaluate the performance of an experimental x-ray dark-field radiography system for chest imaging in humans and to compare with conventional diagnostic imaging.
Methods and Materials: The study was institutional review board (IRB) approved. A single human body (52years, female, height: 173cm, weight: 84kg, chest circumference: 97cm) was imaged within 24 hours postmortem on the experimental x-ray dark-field system. In addition, the body was imaged on a clinical CT system to obtain a reference scan. The grating-based dark-field radiography setup was equipped with a set of three gratings to enable grating-based dark-field contrast x-ray imaging. The prototype operates at an acceleration voltage of up to 70kVp and with a field-of-view large enough for clinical chest x-ray (>35x35cm^2).
Results: It was feasible to extract x-ray dark-field signal of the whole human thorax, clearly demonstrating that human x-ray dark-field chest radiography is feasible. Lung tissue produced strong scattering, reflected in a pronounced x-ray dark-field signal. The ribcage and the backbone are less prominent than the lung but are also distinguishable. Finally, the soft tissue is not present in the dark-field radiography. The regions of the lungs affected by oedema, as verified by CT, showed less dark-field signal compared to healthy lung tissue.
Conclusion: Our results reveal the current status of translating dark-field imaging from a micro-scale (small-animal) to a macro-scale (patient). The performance of the experimental x-ray dark-field radiography setup offers, for the first time, obtaining multi-contrast chest x-ray images (attenuation and dark-field signal) from a human body.
Author Disclosures:
T. Koehler: Employee; Philips Healthcare. **K. Rindt:** Employee; Philips Healthcare.

B-0306 14:16

Impact of aspiration on dark-field signal intensities in chest radiographs of living pigs

K. Hellbach[1], A. Bähr[2], P.B. Noël[1], S. Reu[1], A. Yaroshenko[3], T. Köhler[3], J. Mohr[4], M.F. Reiser[1], F. Pfeiffer[5]; [1]*Munich/DE*, [2]*Oberschleißheim/DE*, [3]*Hamburg/DE*, [4]*Eggenstein-Leopoldshafen/DE*, [5]*Garching/DE*
(katharina.hellbach@med.uni-muenchen.de)

Purpose: The purpose of this study was to assess the effect of aspiration on dark-field signal intensities in chest radiographs of living pigs.
Methods and Materials: Experiments were performed using 2.5 months old, wild-type German landrace pigs (n=5). Before image acquisition all animals were anesthetized, intubated, and mechanically ventilated. Pigs were imaged with an experimental grating-based large animal scanner to acquire x-ray transmission and dark-field radiographs in posterior-anterior (p.a.) and lateral direction under respiratory arrest. This was done prior to aspiration and 45 minutes after intrabronchial administration of 0.05M hydrochloric acid (HCl). Subsequently, pigs were sacrificed and their lungs were obtained for detailed histopathological analysis. ROIs were placed into the lungs to quantify signal intensities in dark-field and transmission images.
Results: When comparing the scans of the living pigs´ lungs prior to aspiration with the lung images after aspiration had been induced, a visible loss of dark-field signal intensity in the affected parts of the lungs was found.
Conclusion: We were able to show - for the first time - the impact of aspiration on the dark-field images of living large animals. Understanding the properties of this new imaging technique in the depiction of lung pathologies is an absolutely essential step towards transferring this experimental imaging method to a clinical setting.

B-0307 14:24

A fully functional prototype for establishing electrochemotherapy in interstitial usage with drug application and a Q factor optimisation model

A. Ritter, J. Pfeffer, P. Isfort, M. Baumann, P. Bruners; *Aachen/DE*
(aritter@ukaachen.de)

Purpose: Irreversible electroporation (IRE) and electrochemotherapy (ECT) are two innovative electroporation-based minimally-invasive therapies for the treatment of cancer. Combining non-thermal properties of IRE with local application of chemotherapy, ECT is an established treatment modality for superficial malignancies of the skin. In ECT the induced nanopores facilitate the intracellular uptake of the chemotherapeutic agent. The application of ECT in solid organs has not yet been described, so we developed a prototype applicator for ECT in solid organs.
Methods and Materials: Computer simulations were used to design a needle-shaped applicator for percutaneous image-guided ECT in solid organs. To rate the criteria, a Q factor model with weighting coefficients has been developed to optimize the geometric and electric parameters dispassionately. In clinical application, the physician can adapt the 3D field distribution, i.e. the desired ablation zone to the patient individual situation.
Results: With the results of an electric field simulation processes we built up a fully functional needle-shaped prototype with a shaft diameter of 3.2 mm. The cylindrical applicator contains four expandable hollow electrodes in a semicircular configuration used both for interstitial injection of the chemotherapeutic agent as well as the creation of the electric field. First ex-vivo as well as in-vivo tests demonstrate promising results with excellent conformity of simulated and resulting ablation volumes.
Conclusion: Using the ECT prototype system promising results legitimate the next steps, i.e. broad animal studies, including the best strategy of chemotherapy application (intravenous, intra-arterial, interstitial). One of the main efficient advantages is one stich for five electrodes.

B-0308 14:32

Multispectral magnetic particle imaging for real-time 3D MPI-guided treatment of a vessel stenosis

J. Salamon, M. Hofmann, C. Jung, M.G. Kaul, R. Reimer, A. vom Scheidt, G. Adam, T. Knopp, H. Ittrich; *Hamburg/DE (j.salamon@uke.de)*

Purpose: The aim was to establish a real-time multispectral (multicoloured) visualization of multiple MPI tracers and MRI/MPI-roadmapping for MPI-guided interventions on a vessel stenosis model. Since MPI visualizes the spatial distribution of superparamagnetic iron oxide particles (SPIOs) one challenge is the lack of anatomical background information. A multispectral blood pool agent or MRI/MPI road-mapping might overcome this problem.
Methods and Materials: A standard guide wire and balloon-catheter were labelled with a magnetic lacquer. A vessel phantom with a stenosis was either filled with saline or SPIOs (MM4). In vitro stenosis treatment was performed inflating the balloon either with MM4 or with saline. MPI data were acquired at a rate of 46 frames/s. For analysis of the magnetic lacquer marks electron microscopy and micro-computed tomography were performed.
Results: Real time multicolored visualization of the different tracers' distinct magnetic fingerprints at a rate of 6 frames/s as well as MRI/MPI-roadmapping using bimodal fiducial markers was feasible allowing MPI-guidance for PTA. The magnetic lacquer consisted of 10-20 nm thick iron plates with a size of 0.5 to 90µm (10.6 mg Fe/ml). Micro-CT showed a maximum lacquer thickness on the instruments of 80-100 µm allowing for coaxial use. Successful angioplasty was verified by MPI and MRI.
Conclusion: Multicoloured MPI allows for 3D real-time guidance of endovascular instruments and PTA. A combination of MPI/MRI for an anatomical road map in addition to multispectral interventions with a blood pool agent might emerge as a promising tool for radiation free interventions.

B-0309 14:40

Impact of temporal resolution on quantitative renal perfusion MRI: assessment using a single contrast injection and a continuous golden angle radial sampling technique

J. Budjan[1], P. Riffel[1], R. Grimm[2], K. Block[3], F.G. Zoellner[1], S.O. Schönberg[1], U.I. Attenberger[1], D. Hausmann[1]; [1]*Mannheim/DE*, [2]*Erlangen/DE*, [3]*New York, NY/US*

Purpose: Dynamic contrast-enhanced (DCE) MRI is an established method for the quantitative assessment of renal perfusion. However, temporal resolution of DCE sequences varies in literature; there is no definite consensus on the minimal temporal resolution required for reliable quantitative perfusion assessment. Purpose of this study was the in-vivo evaluation of different temporal resolutions for quantitative renal DCE using a single contrast injection.
Methods and Materials: 22 patients (7 female; 58.7±21.2 years) underwent a prototypical fat-suppressed, contrast-enhanced, golden-angle radial stack-of-stars T1-weighted 3D spoiled gradient-echo examination (GRASP) for 3min during free breathing. Using this single acquisition, 4 datasets were retrospectively reconstructed for each patient with a temporal resolution of 9.7s, 5.9s, 3.6s and 1.3s, respectively. Renal plasma flow (rPF) was calculated for the entire renal volume using a voxel-by-voxel deconvolution approach on all datasets and manual kidney segmentation. rPF values were compared between the individual patients' datasets using paired t-testing and Blant-Altmann analyses.
Results: Using the datasets with the highest temporal resolution (1.3s), mean rPF was 216±93ml/100ml/min. The analysis of the lower temporal resolution datasets yielded similar values; no statistically significant differences between the groups were found (p>0.09 for all pairs).
Conclusion: DCE MRI for quantitative renal perfusion assessment performed with temporal resolutions between 1.3s and 9.7s results in comparable rPF values. An increase in temporal resolution does not seem to result in relevant changes of rPF parameters.
Author Disclosures:
R. Grimm: Employee; Siemens.

B-0310 14:48

Novel high quantum efficiency photodiode for x-ray imaging

M.A. Juntunen, J. Heinonen, V. Vähänissi, P. Repo, A. Vaskuri, H. Savin; *Espoo/FI (mikko.juntunen@aalto.fi)*

Purpose: Performance of x-ray imaging using photodiodes with scintillators, for example computed tomography, is limited by radiation dose. Improving photodiode sensitivity helps reduce dose at given image quality or improve image quality at given dose. A novel high quantum efficiency photodiode applicaple to scintillator based imaging is introduced.
Methods and Materials: Present-day photodiodes notably suffer from optical losses, and generated charge carriers are often lost via recombination. Here we demonstrate a device characterized by very high external quantum efficiency. Instead of a conventional p-n junction, we use negatively charged alumina to form an inversion layer that generates a collecting junction. We enhance the collection efficiency further by nanostructuring the photodiode surface, forming black silicon, which dramatically reduces reflectance and allows for high response also at high incident angles. This enhances collection of diffuse light emitted by scintillators giving additional response improvement in comparison with planar photodiodes.
Results: External quantum efficiency of the sample diodes exceeds 96% over the wavelength range between 250 and 950 nm. Extremely low reflectance was measured up to 70 degrees incident angle. Signal from scintillator under x-ray beam was >20% higher than with similar size commercial planar photodiode.
Conclusion: Black Silicon photodiodes were shown to achieve very high optical quantum efficiency and to collect scintillator light signal far better than conventional planar diodes, giving possibility to improve performance of scintillator based x-ray imaging, like CT and SPECT, or to reduce radiation dose.

Author Disclosures:
M.A. Juntunen: Research/Grant Support; Tekes – the Finnish Funding Agency for Innovation. **J. Heinonen:** Research/Grant Support; Tekes – the Finnish Funding Agency for Innovation. **V. Vähänissi:** Research/Grant Support; Tekes – the Finnish Funding Agency for Innovation. **P. Repo:** Research/Grant Support; European Metrology Research Program, Research Excellence Grant.

B-0312 14:56

Bone mineral density measurements on digital radiography systems: an experimental comparison between IBEX MAP technology and a DEXA system

A. Ratcliffe[1], B. Lopez[2], J. Cowling[1], P. Scott[1], D. Rawlings[3]; [1]*Sedgefield/UK*, [2]*Durham/UK*, [3]*Newcastle upon Tyne/UK (j.cowling@ibexinnovations.co.uk)*

Purpose: DEXA measurements are performed to assess bone health in patients with low impact fractures. IBEX's Multi-Absorption Plate (MAP) allows generation of BMD information on standard DR systems without compromising diagnostic image quality. This study compares bone composition measurements from DEXA and IBEX systems to assess IBEX BMD measurement as a potential replacement for DEXA.
Methods and Materials: A Hologic "Discovery" DEXA machine was compared with an IBEX MAP-equipped DR system (x-ray tungsten target source, Rayence 1417 FPD, 115cm source to detector distance). Phantoms were constructed of tissue- and bone-equivalent materials giving a "ground truth" against which to compare the two measurements. Phantoms ranged in total thickness from 3cm to 6cm with 50% to 100% tissue-equivalent material giving a BMD range from approximately 0 to 1 g/cm^2.
Results: Bone thickness was compared to BMD values obtained from each system. A set of DEXA data produced a simple calibration to align the output of the IBEX system to the DEXA results, allowing BMD values to be compared directly. Plotting BMD against bone simulant thickness we find agreement between linear models associated with BMD outputs from both machines. A standardised distance between model gradients of 0.9389 suggests no evidence that IBEX's methodology does not give an unbiased estimator for DEXA BMD. The residual standard error of the IBEX system is calculated to be 0.0434g/cm^2.
Conclusion: IBEX technology enables BMD to be measured on a DR system, and therefore presents a potentially viable alternative to further patient referral and use of DEXA.
Author Disclosures:
A. Ratcliffe: Employee; IBEX Innovations. **B. Lopez:** Research/Grant Support; IBEX Innovations funded PhD. **J. Cowling:** Employee; IBEX Innovations. **P. Scott:** Employee; IBEX Innovations. **D. Rawlings:** Consultant; IBEX Innovations.

B-0311 15:04

Gridless scatter removal on standard digital radiography systems using the IBEX material identification technology

P.D. Scott[1], B. Lopez[1], A. Ratcliffe[1], J. Cowling[1], I. Argyridis[2], K. Robson[2]; [1]*Sedgefield/UK*, [2]*Newcastle Upon Tyne/UK (p.scott@ibexinnovations.co.uk)*

Purpose: A process has been developed for accurate scatter prediction and removal using materials information generated by IBEX materials identification technology. This enables scatter to be removed without the dose impact of an anti-scatter grid (ASG) and also provides quantitative materials information required for diagnostic techniques such as bone mineral density (BMD). Currently, ASGs are used to remove scattered x-rays when imaging larger body parts. ASGs improve feature contrast at the cost of increased radiation dose or increased Poisson noise. This study compares IBEX's scatter removal method (SRM) to a standard ASG, for a range of phantoms and cadavers and shows the potential for gridless x-ray imaging and BMD measurements on a standard DR detector.
Methods and Materials: The technology has been applied to a standard FPD (Rayence 1417) and GE VMX+ mobile x-ray source with an accompanying simulator developed in GEANT4. The model provides information relating to sample specific scattering characteristics which is used to identify materials and remove scatter present within the x-ray image. The technology has been demonstrated on both x-ray phantoms and cadaveric donors.
Results: Early data demonstrates removal of scatter to a level equivalent to that of an ASG. This results in a factor six CNR improvement when compared to an uncorrected image as well as providing quantitative materials information.
Conclusion: A gridless scatter removal method using the IBEX materials identification technology has demonstrated improvements in CNR and a reduction in patient dose. This offers clear benefits to both patients and clinicians in medical diagnostics.

B-0313 15:12

Novel segmentation method using absorption- and phase-contrast x-ray images

A. Yoneyama[1], R. Baba[1], K. Hyodo[2]; [1]*Kokubunji/JP*, [2]*Tsukuba/JP (akio.yoneyama.bu@hitachi.com)*

Purpose: To finely identify inner structures of biomedical samples and precisely distinguish between normal and tumour tissues, a novel segmentation method based on absorption- and phase-contrast x-ray images was tested using three-dimensional images of a phantom and a rat tail obtained under ideal conditions.
Methods and Materials: Three-dimensional absorption- and phase-contrast images were obtained using a Talbot interferometric imaging system with 17.8-keV monochromated synchrotron radiation. A phantom composed of small spheres made of five kinds organic material (glass, polyurethane, polypro pine, acryl, and nylon) and a formalin-fixed rat tail were used as demonstrative samples. The obtained images were segmented using the proposed method, which uses a ratio of absorption and phase-shift CT values at the same pixel in each image.
Results: The segmented image of the phantom clearly depicts each sphere made of different materials, which cannot be distinguished using the absorption- and phase-contrast imaging method only. Artefacts caused by heavy material was also identified clearly and removed easily. The segmented image of the rat tail also shows hair, muscle, and bone clearly.
Conclusion: These results show that the proposed segmentation method effectively identifies organic materials and biomedical regions, and therefore, is expected to provide a new way to finely segment biomedical samples, especially to precisely distinguish between normal and tumour tissues.

B-0314 15:20

Application of a single-energy electron-density reconstruction in radiation therapy planning

A. Ritter, B. Schmidt, R. Raupach; *Forchheim/DE (andre.ritter@siemens.com)*

Purpose: In radiation therapy, a tube-voltage-dependent conversion from CT value (HU) to electron density is needed for dose calculation on CT images. It is common practice to use a fixed tube voltage. A new single-energy electron-density reconstruction, can remove the need for a tube-voltage-dependent conversion. We discuss properties of this reconstruction and their implications for the application in radiation therapy planning.
Methods and Materials: The reconstruction is based on a material decomposition, which takes place partly in image and projection domain, to compute the effective thicknesses of water and bone in the projection domain. Both effective thicknesses are used to synthesize line integrals of electron density, from which images of electron density are reconstructed. The reconstruction is tested with the Gammex 467 Tissue Characterisation Phantom using different arrangements of the tissue substitutes and different tube voltages. Additionally, this method is compared to a conventional conversion from CT value to electron density.
Results: The accuracy of the electron density reconstruction increases with higher tube voltage and tends to be at least as high as for tube-voltage-dependent conversion from standard images. Additionally, effects of beam hardening, such as streaks between high-density bone-like tissues or systematic changes of image values due to different substitute arrangements, are decreased.
Conclusion: The improved stability of electron density estimation might be advantageous for the accuracy of dose calculation in radiation therapy. Systematic changes of image values due to changes in tube voltage are reduced, which opens the opportunity to introduce the benefits of tube-voltage-adaption to radiation therapy.
Author Disclosures:
A. Ritter: Employee; Siemens Healthcare GmbH. **B. Schmidt:** Employee; Siemens Healthcare GmbH. **R. Raupach:** Employee; Siemens Healthcare GmbH.

14:00 - 15:30 **Room K**

Radiographers

SS 314
MR imaging

Moderators:
L. Natale; Rome/IT
K. Taylor; Cambridge/UK

B-0315 14:00

Short-term effects during examinations in an actively shielded 7T MR

B. Hansson[1], P. Höglund[1], O. Johan[1], K. Markenroth-Bloch[1], M. Nilsson[1], J. Frankel[2], J. Wilén[2], T. Owman[1], J. Arborelius[1]; [1]*Lund/SE*, [2]*Umeå/SE (boel.hansson@med.lu.se)*

Purpose: To evaluate frequency and quality of short-term effects reported by research persons after research examinations performed in an actively shielded 7T MR.
Methods and Materials: 124 research persons undergoing 154 7T MR examinations (77% brain) answered a web-based questionnaire on occurrence (n) and strength (VAS, visual-analogue-scale) of inconsistent movement, dizziness, nausea, headache, metallic taste, twitches and light flashes, and regarding temperature, noise, communication system, information status, motion sickness and willingness to repeat a scan. Scanner output on predicted peripheral nerve stimulation (PNS) values was recorded in 85 research persons.
Results: Short-term effects reported were dizziness (84% of examinations), inconsistent movement (70%), nausea (53%), headache (53%) and metallic taste (43%). Mixed model analyses showed in all positions (in, inside, out, outside) significantly higher VAS values for inconsistent movement ($p<0.001$) and dizziness ($p<0.002$) when scanned head first compared to feet first, but no significant differences were found for nausea, headache and metallic taste. Twitches, an expression of PNS, was reported in 67% of examinations, occurred primarily in torso, hand and arm, and tended to increase with higher predicted PNS values. 23% of the research persons experienced light flashes. Scanner noise levels were well tolerated. The communication system was well perceived. Willingness to undergo a future 7T MR was high both as research person and patient (90%, 96%).
Conclusion: Actively shielded 7T MR examinations are well tolerated, although short-term effects such as inconsistent movement, dizziness and twitches are more commonly reported compared to literature on passively shielded 7T MRs.

B-0316 14:08

Assessment of incidental findings detected on research MRI scans of healthy volunteers

A. Ljimani, H.-J. Wittsack, J. Aissa, G. Antoch, R. Lanzman; *Düsseldorf/DE (alexandra.ljimani@med.uni-duesseldorf.de)*

Purpose: To assess the frequency and clinical significance of incidental findings in healthy volunteers undergoing research MRI scans.
Methods and Materials: Research MRI scans of 324 healthy subjects (178 male, 146 female, mean age 31.5±11.6 years) performed in our department over a two year period were considered for this analysis. Research scans of the brain (n=92), spinal cord (n=149), kidneys (n=20), liver (n=3), hands (n=22), hips (n=34) and knees (n=4) were systematically reviewed by board certified radiologists for incidental findings. Incidental findings and subsequent recommendations were analysed.
Results: Incidental findings were reported in 19 of 324 (5.9%) subjects in scans of the spinal cord (n=15), brain (n=3) and knee (n=1). Most frequently prolapsed vertebral discs (n=7), enlarged ovarian cysts (n=3) and inguinal lympadenopathies (n=3) were reported. Furthermore, dilated bile ducts (n=1), a meniscus tear in the knee (n=1), microangiopathic changes in the brain (n=1), a state following hip necrosis (n=1), a retroperitoneal mass/metastasis (n=1) and a lesion in the clivus that was suspicious for a chondroma (n=1) were reported. Further medical examination or treatment based on the incidental findings was required in 8 of 19 (42%) subjects.
Conclusion: Incidental findings may occur in up to 6% of healthy volunteers undergoing research MRI scans and might often (42%) require further examinations. Therefore, MRI research scans should be systematically evaluated for incidental findings.

B-0317 14:16

Artefact evaluation in MRI of new materials for hip prostheses: a phantom study

D. Sousa[1], P. Martins[1], C. Ferreira[2], S. Francesco[1], M. Castelo-Branco[2], R. Silva[1]; [1]*Aveiro/PT*, [2]*Coimbra/PT (pmartins@ua.pt)*

Purpose: MRI is a well-established imaging method for diagnostic purposes. Nevertheless, it is prone to several artefacts like those coming from magnetic susceptibility ones, which can compromise image quality. Development and use of new materials is a promising alternative concerning the reduction of this type of artefacts. Silicon nitride ceramics coated with nanocrystalline diamond (SND) developed by CICECO-Aveiro University show excellent characteristics of wear resistance and biocompatibility. Our aim is to evaluate the magnetic susceptibility artefacts caused by this prosthesis and compare it with others available on the market.
Methods and Materials: Cobalt-chromium (CC), oxinium (Ox), zirconia-toughened alumina (ZTA), silicon nitride (SN) and SND femoral head prosthesis placed in a custom-made plastic phantom were used to compare image artefacts. T1-weighted images were acquired with spin-echo and gradient-echo sequences at 3 and 1.5Tesla. Quantitative analysis of the images and 3D reconstruction of the artefact was performed with MeVisLab2.7.1 using region-growing method to calculate artefact volume.
Results: All prosthesis showed higher artefact volumes at 3Tesla when compared with 1.5Tesla, as expected. At 3Tesla, artefact volume was 445.14cm^3, 60.39cm^3, 3.67cm^3, 2.45cm^3, 2.52cm^3 for CC, OX, ZTA, SN and SND, respectively, with a similar pattern at 1.5Tesla. Ceramic materials (ZTA,SN and SND) present considerably smaller artefacts than metallic ones (CC and OX) both at 1.5 and 3Tesla. SND produce comparable artefacts (even lower) than ZTA prosthesis, the gold standard in clinical practice.
Conclusion: Our preliminary results pointed to an excellent performance (reduced artefact volume) of diamond-coated ceramic prosthesis, even in high-field imaging. However, a more comprehensive evaluation should be carried out.

B-0318 14:24

Investigation of radiographer and radiologist ability to manage MR image quality issues for abdomen and pelvis examinations in Saudi Arabian and Irish centres

S. Al Dahery, A. McGee, L. Rainford; *Dublin/IE (shrooq_talal@hotmail.com)*

Purpose: The study aimed to identify the current knowledge and confidence of MR radiographers and radiologists from Saudi Arabia and Ireland with regard to image quality management for MR abdomen and pelvis examinations. Findings would inform any future training requirements needed to ensure high-quality imaging standards.
Methods and Materials: A qualitative approach was applied. Public, private, military and academic hospitals in the western region of Saudi Arabia (SA) were invited to participate, as were Irish centres. Institutional review board ethical approval was attained. Semi-structured interviews were designed to investigate both the radiographer's and radiologist's professional role in the two countries, how they dealt with image quality issues and perceived personal development in MR and what they viewed as required regarding image quality training to support their work. Chief radiographers, radiographers, and radiologists working in MR were included. Coded interviews were recorded and then transcribed.
Results: Nvivo 10 files (n=87): Saudi Arabia (n=10 centres); Ireland (n=12 centres) were created. Coding resulted in 2071 references grouped into nodes, later becoming three themes: healthcare professional: factors affecting image quality, image quality, and departmental policy. An interrelationship across and between data was identified. A variety of experience and participant knowledge of image quality was noted, as where the challenges of achieving optimal quality levels. Differences between countries were identified as was the impact of experience and education level.
Conclusion: Image quality training and subsequent assessment of professional skills are required to support radiographers and radiologist in the routine management of MR image quality.

B-0319 14:32

Magnetic resonance imaging of anterior cruciate ligament tears: evaluation of standard orthogonal and tailored paracoronal imaging

L.M. Deguara, P. Demicoli, F. Zarb; *Msida/MT (ldeg0010@um.edu.mt)*

Purpose: To evaluate the diagnostic efficiency of using the standard magnetic resonance planes with an additional paracoronal plane in the diagnosis of anterior cruciate ligament (ACL) tears.
Methods and Materials: Ten MR examinations of the knee using proton density fat saturated sequences were prospectively compiled. The visibility of anatomical structures was used for the evaluation of image quality. Repeat MR examinations facilitated intra and inter rater reliability. Two radiologists performed absolute visual grading analysis (VGA). Data was analysed using

visual grading characteristic curves (VGC) and the area under the curve (AUC) determined which plane offers the best image quality for each anatomical structure. The one sample t-test was performed to establish significant differences in image quality.
Results: Overall image quality scores were higher for coronal (VGC_{AUC} 0.76) and sagittal (VGC_{AUC} 0.51) over the paracoronal plane, whilst the paracoronal showed better image quality over the axial plane (VGC_{AUC} 0.48). The coronal plane was significantly better in the visualization of 3 anatomical structures: anteromedial bundle of the ACL (p-value 0.04), posterolateral bundle of the ACL (p-value 0.04) and lateral insertion of the collateral ligament (p-value 0.02). The paracoronal plane was significantly better than the axial plane in the visualization of the distal insertion of the ACL (p-value 0.02). None of the structures showed significant image quality differences (p&gt0.05) on the sagittal plane.
Conclusion: The addition of the paracoronal plane might be of added benefit when used in conjunction with the orthogonal planes for further investigations concerning the distal insertion of the ACL.

B-0320 14:40

Assumed factor analysis of MRI safety processes by MRI personnel: a FMEA approach

A. De Bock, A. Stadler, W. Schima; *Vienna/AT (anke.de.bock@live.be)*

Purpose: Due to the broadening, the field of MRI applications using high-field scanners and the growing number of examinations, hazardous events in MR units do occur. The role of MR safety officers in the MR environment and the perceived level of safety among MRI personnel was assessed.
Methods and Materials: A questionnaire was designed with q-set.at, and sent out to MR institutions. Reply from MRI personnel (n=175) was analysed regarding subjective feeling of safety in MR institutions, objective occurrence of adverse events in the MRI suite, and the role of MR safety officers. The statistic tests used were contingency coefficient and the Mann-Whitney-U-test (significance level 0.05, test power with a probability ≥ 0,8).
Results: MRI personnel feels safe (scale 0-20) with a value of 16.6. There is a higher level of safety feeling in an MRI department with an MRI safety officer present (p=0.002). However, there is no association between the presence of an MRI safety officer and the amount of serious events regarding MR safety (C=0,014; p=0,894). There is no association between the number of educated radiographers and the safety feeling if working in the MRI department (C=0,239; p=0,101).
Conclusion: The presence of MRI safety officers causes a higher level of subjective safety feeling of the MRI personnel, which, however, does not correlate with a lower number of hazardous events. The results of this survey show the importance of an MRI safety education to ensure safety for patients and personnel.

B-0321 14:48

Brain imaging: comparison of T1 FLAIR BLADE with conventional T1 SE

E. Lavdas[1], E. Giankou[2], A. Tsikrika[3], E. Kapsalaki[3], G. Batsikas[3], S. Kostopoulos[1], D. Glotsos[1], K. Ninos[1], D. Kavouras[1], P. Mavroidis[4]; [1]*Athens/GR*, [2]*Paros/GR*, [3]*Larissa/GR*, [4]*Chapel Hill, NC/US (eleonoragiankou@gmail.com)*

Purpose: The objective of this study is to compare the quality of T1W-FLAIR BLADE images and the quality of T1W-SE images in the MR imaging of the brain.The goal is to highlight which sequence can better eliminate artifacts and visualise lesions and surrounding tissues.
Methods and Materials: Brain examinations with T1W-FLAIR BLADE images and T1W-SE were performed on 55 patients using 1.5T SIEMENS (AVANTO) scanner.These techniques were evaluated by two radiologists for a) qualitative analysis i.e. presence of artifacts, CSF nulling, and b) quantitative analysis of signal-to-noise ratios (SNR), contrast-to-noise ratios (CNR) and relative contrast (ReCon).The evaluation was performed by the Kruskal-Wallis non-parametric system.
Results: In the quantitative analysis, T1W-SE appeared to have higher values in the majority of cases regarding the SNR measurements, whilst T1W-FLAIR BLADE had higher values on CNR and ReCon measurements. In the qualitative analysis BLADE sequences had a higher scoring than the conventional sequences in all the cases.The overall image quality was better on T1W-FLAIR BLADE.Motion and flow-related artifacts, as well as susceptibility errors were lower in T1W-FLAIR BLADE.T1 FLAIR BLADE offered a better imaging for metastases, AVMs, ischaemic strokes, multiple sclerosis and vessels.
Conclusion: T1W-FLAIR BLADE sequence is superior to T1W-SE in overall image quality, reduction of motion and flow-pulsation artifacts, susceptibility errors and in nulling CSF. T1W-FLAIR BLADE is preferred by the clinicians and may be an alternative approach to brain MRI imaging. We suggest the use of T1 FLAIR BLADE in AVM's, metastases, ischaemic strokes and multiple sclerosis.

B-0322 14:56

Patients' MRI acoustic noise exposure in different protocol exams

V.M.F. Silva, I.M. Ramos, J.A. Moreira, M. Marques; *Porto/PT (vitorsoft@gmail.com)*

Purpose: Time-varying gradient fields are the main source of acoustic noise associated with an MRI procedure. Lorenz forces are produced during each procedure, deforming and vibrating the three main gradient coils. Various types of acoustic noise are produced in each protocol exam. Problems associated from this hazard for patients include annoyance, anxiety, verbal communication difficulties, psychological distress, temporary hearing loss, headaches and, in extreme cases, the potential for permanent hearing impairment. Acoustic noise may pose a particular and substantial problem to specific patient groups. There is legislation to rule acoustic noise levels that are divided in two types of exposure: equivalent continuous sound level (Lex, 8h) and peak sound pressure level (Lc peak).
Methods and Materials: Different exam protocols used in brain, spine and abdominal MRI were tested in a 1.5T scanner, with a sound level meter. It was used ISO 9612:2009 for determination of acoustic noise exposure.
Results: Lex, 8h ranged from 58.6 dB(A) in T2 FLAIR sequence used in brain and 80.3 dB(A) used in time of flight (TOF) 2D sequence used in MRI angiography.While Lc peak ranged from 98.63 dB(C) in T2 FLAIR sequence and 118.84 dB(C) used in abdominal echo planar imaging (EPI) diffusion sequence.
Conclusion: Lex, 8h is higher in TOF 2D sequences used in brain MRI and EPI sequences used in abdominal MRI, while Lc peak is higher in EPI sequences used in all diffusion and perfusion MRI protocols. Manipulating some MRI parameters, maintaining image quality, it is possible to lower exposure noise levels.

B-0323 15:04

Application of the tractography method in the study of magnetic resonance imaging in paediatric patients in selected clinical situations

A. Przepióra; *Poznań/PL (agnieszkaprzepiora@gmail.com)*

Purpose: Correlation of the impact of technical conditions on quality of the images obtained using diffusion tensor imaging (DTI) in the study of magnetic resonance imaging (MRI) of paediatric patients' heads.
Methods and Materials: From January to November 2015, in the department of paediatric radiology of the K. Jonscher Clinical Hospital No. 5 in Poznań, MRI of brain has been performed with the use of DTI and visual representations of nerve fibres have been made using the tractography technique. 25 patients have been examined. The patients were from 3 days to 17 years old. The study has been performed with the 3T scanner. The dependency between age, clinical condition of a child, size of the imaged area and resulting image quality has been analysed.
Results: The objective of the study was to analyse the technical conditions of the study taking into account patient's individual features. It has been shown that in most of studies (84%) tractography was possible to perform from the data collected during diffusion imaging. For the operator of the study an important factor is age of an examined patient and size of the imaged area. Examination of the youngest patients needed a significant modification of existing technical settings.
Conclusion: For the operator who performs the examination, information on the individual characteristics of the patient is important for the selection of appropriate technical conditions for the sequence. Proper technical settings are in correlation with the obtained image quality of the tractography.

B-0324 15:12

Patients knowledge about ultrasound, computed tomography and magnetic resonance

P. Ferreira, R.P.P. Almeida, A.F. Abrantes, L.P.V. Ribeiro, N. Pinto, K.B. Azevedo, J.P. Pinheiro; *Faro/PT (lpribeiro@ualg.pt)*

Purpose: To study the level of patients knowledge about ultrasound (US), computed tomography (CT) and magnetic resonance imaging (MRI) and to assess patients understanding of the main general aspects of these examinations.
Methods and Materials: A self-applied questionnaire developed by Chesson, Mckenzie and Mathers (2001) in UK was validated for the Portuguese population with permission of the authors and assigned to 143 outpatients who perfomed US (55), CT (48) and MRI (40) examinations. The questionnaires used 15 main questions, an answer scale with 3 options (True, False or Don't Know) and were interpreted and statistically analysed through descriptive statistics, Phi and Cramer's V tests.
Results: Only 22,4% of the patients indicated they sought information about the type of investigation they had been referred for and 63,6% had performed US, CT or MRI examinations before. Considering the three mentioned techniques, patients answered more accurately to questions related to situations experienced during the examination (darkness of the examination

room, presence of the radiographer in the examination room and viewing images on a monitor) than items related to specific issues (use of ionizing radiation, use of contrast media, preparations and respiratory instructions).
Conclusion: Patients were not well informed regarding these examinations, especially relating to specific issues. Since this could have implications in the information-giving strategies, it becomes necessary to raise awareness and educate patients, allowing the social development of information on this topic as well as radiographer intervention in the exam procedure.

B-0325 15:20

MRI safety procedures during the dismantling of one scanner

T. De Bondt, F. Vanhevel, M. Geldof, F. Deferme, P.M. Parizel; *Antwerp/BE (timo.debondt@gmail.com)*

Purpose: To describe issues regarding MRI safety during the unusual situation of the dismantling of an MRI scanner, and to identify potential associated risks.
Methods and Materials: Our hospital received the Joint Commission International (JCI) accreditation in 2015. To achieve this, MRI safety procedures were put in place, following the American College of Radiology (ACR) guidance document. Two capital aspects of these measures are the screening procedure and the site-access restriction through the zoning system. Zone 1 is accessible for the general public, Zone 2 is the reception and screening area, Zone 3 is only accessible for patients under supervision of MR personnel and Zone 4 is the scanner room. Our MRI facility had 4 MRI systems, 3 of which are still operational and 1 was dismantled by Hegele Logistics.
Results: The normal access door for unscreened patients needed to be removed because of the scanner size. This door was removed for 2 days; after working hours, wooden plates were put in place to prevent free access. Additionally, during transportation of the scanner, all physical barriers between Zone 1 and Zone 3 were not in place. Therefore, radiographers were instructed to increase alertness when unscreened patients moved throughout the MRI-site Zone 3. No incidents occurred during the dismantling.
Conclusion: During the unusual situation of a scanner dismantling, several established safety precautions can temporarily be rendered useless. These events need special attention in terms of improvised safety measures, and need to be discussed and communicated in advance.
Author Disclosures:
T. De Bondt: Consultant; GE Healthcare.

14:00 - 15:30 **Room M 2**

Cardiac

SS 303

Cardiac function: what's hot?

Moderators:
M. Gardarsdottir; Reykjavik/IS
B. Graca; Coimbra/PT

B-0326 14:00

Rapid functional cardiac imaging between gadolinium injection and late enhancement: evaluation of a highly accelerated sequence with sparse data sampling and iterative reconstruction

J. Budjan, H. Haubenreisser, S. Sudarski, C. Doesch, T. Henzler, M. Borggrefe, S.O. Schönberg, U.I. Attenberger, T. Papavassiliu; *Mannheim/DE*

Purpose: To create and evaluate a time-efficient, patient-friendly cardiac magnetic resonance imaging (CMRI) protocol that uses the idle time between gadolinium injection and late enhancement acquisition for volumetric assessments.
Methods and Materials: 20 consecutive patients (14 male, 56±19 years) underwent a CMRI examination including a fully-sampled multi-breath-hold sequence as gold standard (Ref) as well as an highly accelerated real-time CINE TrueFISP sequence based on sparse data-sampling with iterative reconstruction (SSIR) acquired in single-breath-hold (SSIR-BH) and under free breathing (SSIR-nonBH). SSIR sequences were acquired 4 minutes after gadolinium injection (0.2mmol/kg body weight Gd-DOTA). Right (RV) and left ventricular (LV) volumetric parameters as well as regional wall movement (RWM) were evaluated and compared between Ref and SSIR.
Results: Despite reduced contrast between myocardium and intra-ventricular blood, volumetric as well as regional wall movement assessment revealed high agreement between both SSIR sequences and Ref. For the volumetric LV assessment, excellent correlation and narrow limits of agreements were found for both SSIR-BH and SSIR-nonBH when compared to Ref (mean LV ejection fraction [EF] Ref: 52.8%, SSIR-BH 52.3%, SSIR-nonBH 52.5%). For the RV analysis, both SSIR sequences showed an excellent correlation and high agreement with Ref (mean RV EF Ref: 52.7%, SSIR-BH 52.0%, SSIR-nonBH 52.2%). In the RWM analysis, 314/320 segments (98%) received identical ratings in all three sequences.
Conclusion: Even when acquired in the idle time between gadolinium injection and LGE acquisition, the highly accelerated SSIR sequence delivers accurate volumetric and regional wall movement information. It thus seems ideal for very time-efficient CMRI protocols.
Author Disclosures:
H. Haubenreisser: Speaker; Bayer and Siemens. **S. Sudarski:** Speaker; Siemens. **T. Henzler:** Speaker; Siemens.

B-0327 14:08

Cross-modality accuracy of dual-step prospective ECG-triggered dual-source CT compared with echocardiography and cardiac MR in the follow-up of heart-transplanted patients

D. Curione, C. Rutigliano, D. Di Molfetta, C. Grippo, B. Merlino, L. Natale, R. Marano, L. Bonomo; *Rome/IT*

Purpose: To evaluate the role of dual-step prospective ECG-triggered dual-source CT (pECGdualstep-DSCT) in the follow-up of heart-transplanted-patients (HTPs) for the assessment of both left ventricular function (LVF), in comparison with Echocardiography (Echo) and Cardiac Magnetic Resonance (CMR), and the coronary arteries.
Methods and Materials: Prospective blinded evaluation of 11 HTPs: 1. left ventricular ejection fraction (EF), end-diastolic (EDV), end-systolic (ESV), stroke volume (SV), cardiac output (CO), and mass on pECGdualstep-DSCT (2 independent readers), Echo (single operator) and CMR (single reader) performed on the same day (heart-rate (HR) recorded during all exams); 2. coronary arteries on pECGdualstep-DSCT. pECGdualstep-DSCT technique: sequential scan (10-90% R-R interval) applying variable tube current (full during systole (35-45%) and reduced (20%) during the remaining acquisition).
Results: 1. EF was slightly lower on pECGdualstep-DSCT (55.7%±5.0) than Echo and CMR, but without a statistically significant difference. pECGdualstep-DSCT showed statistically significant higher EDV (153.7±24.2mL), ESV (67.8±11.5mL), SV (85.9±17.6mL), CO (6.4±1.2L/min), and mass (120.6±28.7g/m2) ($p<0.01$) compared with Echo and CMR, but with a high correlation coefficient (rho), mainly with CMR ($p<0.05$ up to <0.001) and particularly for CO (rho=0.959). HR was statistically significant lower on pECGdualstep-DSCT (75.6±7.8bpm, $p<0.001$). Inter-reader agreement on pECGdualstep-DSCT was excellent for all parameters (concordance correlation coefficient≥0.97, $p<0.001$). 2. No significant coronary artery disease was detected. Mean effective radiation dose was 6.4±1.9mSv.
Conclusion: pECGdualstep-DSCT allows reliable and reproducible LVF assessment in HTPs, with good correlation with Echo and CMR, and with simultaneous coronary artery evalutation in one single fast acquisition with a limited radiation dose.

B-0328 14:16

The effect of contrast administration on the treshold-based cardiac magnetic resonance (CMR) evaluation

F. Suhai, I. Csécs, C. Czimbalmos, A. Tóth, Z. Dohy, B. Horváth, B. Szilveszter, B. Merkely, H. Vágó; *Budapest/HU (suhaiimi987@gmail.com)*

Purpose: The aim of our study was to investigate the effect of the contrast administration on left and right ventricular (LV,RV) parameters evaluated by a threshold-based quantification software (MassK).
Methods and Materials: We prospectively evaluated CMR data of 19 patients without any functional, structural abnormalities or delayed contrast enhancement (mean age:38±4 years) and 14 patients with previous myocardial infarction (mean age:57±15 years). The CMR scans were performed on a 1.5T Philips Achieva, assessements were performed using Medis, QMASS 7.6 software. We performed precontrast short axis cine images (SACI) before iv. Gadovist administration (0.15 mmol/kg) and postcontrast SACI which were taken 2 minutes after the contrast administration. We assessed the LV, RV volumes and masses using the conventional and the MassK method.
Results: With the MassK algorithm the LV, RV volumes were significantly higher and LV, RV masses were lower on the postcontrast compared to the precontrast evaluation in both groups.
The median LV end-diastolic volume index (LVEDVi) was in the control group:71 ml/m^2 [67-87] vs. 67ml/m^2[60-81], LV mass:141g[62-88] vs. 149g[112-180] ($p<0.002$). Median LVEDVi in the infarction group:74.5 ml/m^2[61-95] vs. 64.5 ml/m^2[62-88] LV mass:152g[130-184] vs. 164g[135-189] ($p<0.002$).
With the conventional method there were no differences in LV, RV volumes and masses in control group. In the infarction group the postcontrast LVEDVi was lower compared to the precontrast (median LVEDVi:92.4 ml/m^2[77.7-114] vs. 93.4 ml/m^2[79.6-113.6] ($p=0.0023$).
Conclusion: These preliminary results show that contrast administration has a significant effect on the threshold-based quantification method which have to take into account during the post-processing evaluation.

B-0329 14:24

Assessment of left ventricular deformation in patients with ebstein's anomaly by cardiac magnetic resonance tissue tracking

X. Liu, Z.-G. Yang, Y.-K. Guo, R. Li, K.-Y. Diao; *Chengdu/CN (liuxihsd@163.com)*

Purpose: The aim of this study was to clarify the feasibility of myocardial strain using cardiovascular magnetic resonance (CMR) for the evaluation of left ventricular (LV) deformation in patients with Ebstein's anomaly (EA).
Methods and Materials: We recruited 32 EA patients and 30 controls for CMR examination and measured LV function, dimension and tissue tracking parameters (the global and regional radial, circumferential and longitudinal peak strain), together with the right ventricle (RV) dimension. LV strain parameters were compared among the controls, patients with preserved LV ejection fraction (LVEF; ≥55%), and patients with reduced LVEF (<55%).
Results: The global strain parameters all decreased significantly in the EA group compared with the control group (all $P < 0.05$). Furthermore, the global radial and circumferential peak strain (PS) were obviously even lower in the reduced LVEF group than the strain measured in preserved LVEF groups (28.64% vs. 37.39%, $p< 0.05$; and -8.20% vs. -17.89%; $p< 0.05$). The regional strain abnormalities in EA patients were mainly involved in basal and middle segments. The results also demonstrated a significant correlation between the ratio of the RV end-diastolic dimension to the LV end-diastolic dimension (RVEDD/LVEDD index) with the global circumferential PS ($r = 0.508$) and the longitudinal PS ($r =0.474$), as well as a good correlation between radial PS and LVEF ($r = 0.465$).
Conclusion: LV strain serves an earlier and more comprehensive measurement of LV dysfunction than LVEF in EA, which could potentially be included as a supplementary diagnostic procedure in the evaluation of EA.

B-0330 14:32

Non-invasive evaluation of left ventricular function using CT and MRI: a meta-analysis

M. Kaniewska[1], G.M. Schütz[1], S. Willun[1], P. Schlattmann[2], M. Dewey[1]; [1]*Berlin/DE*, [2]*Jena/DE (malwina.kaniewska@ksb.ch)*

Purpose: To compare the diagnostic accuracy of CT in the assessment of global and regional left ventricular function with MRI established as the gold standard examination.
Methods and Materials: We have systematically reviewed databases of MEDLINE, EMBASE, and ISI Web of Science. Evaluation included: ejection fraction, end-diastolic volume, end-systolic volume, stroke volume, and left ventricular mass. Differences between modalities were analysed using limits of agreement. Publication bias was measured by Egger's regression test. Heterogeneity was evaluated using Cochran's Q test and Higgins I2 statistic. In the presence of heterogeneity the DerSimonian-Laird method was used for estimation of heterogeneity variance.
Results: 53 studies including 1814 patients were identified. The mean difference between CT and MRI was -0.56% (-11.6 to 10.5%) for EF, 2.62 ml (-34.1 to 39.3 ml) for EDV and 1.61 ml (-22.4 to 25.7 ml) for ESV, 3.21 ml (-21.8 to 28.3 ml) for SV and 0.13 g (-28.2 to 28.4 g) for LVM. CT detected wall motion abnormalities on a per-segment basis with 90% sensitivity and 97% specificity.
Conclusion: CT is accurate for assessing global LV function parameters but the limits of agreement in comparison to MRI are moderately wide. However, in CT examination wall motion deficits are detected with high accuracy.
Author Disclosures:
P. Schlattmann: Research/Grant Support; FP7 Program of the European Commission for the randomized multicenter DISCHARGE trial (603266-2, HEALTH-2012.2.4.-2, the Joint Program of the German Research Foundation (DFG), the German Federal Ministry of Education and Research (BMBF) for meta-analyses (01KG1013, 01KG1110, 01KG1110). **M. Dewey:** Author; Editor of Coronary CT Angiography and Cardiac CT, both published by Springer, Offers hands-on workshops on cardiovascular imaging (www.ct-kurs.de). Consultant; Associate editor of Radiology and European Radiology, Consultant to Guerbet and one of the principal investigators of multi-center studies (CORE-64 and CORE-320) on coronary CT angiography sponsored by Toshiba Medical Systems.. Research/Grant Support; From the Heisenberg Program of the DFG for a professorship (DE 1361/14-1), the FP7 Program of the European Commission for the randomized multicenter DISCHARGE trial (603266-2, HEALTH-2012.2.4.-2), the European Regional Development Fund (20072013 2/05, 20072013 2/48), the German Heart Foundation/German Foundation of Heart Research (F/23/08, F/27/10), the Joint Program of the German Research Foundation (DFG), German Federal Ministry of Education and Research (BMBF) for meta-analyses (01KG1013, 01KG1110), GE Healthcare, Bracco, Guerbet, and Toshiba Medical Systems, Institutional master research agreements exist with Siemens Medical Solutions, Philips Medical Systems, and Toshiba Medical Systems.. Speaker; Lecture fees from Toshiba Medical Systems, Guerbet, Cardiac MR Academy Berlin, and Bayer (Schering-Berlex).

B-0331 14:40

Left ventricular absolute wall thickening: a unifying theory of heart failure?

J.C.L. Rodrigues[1], B. Rooms[1], K. Hyde[1], S. Rohan[1], M.C.K. Hamilton[1], A.K. Nightingale[1], J.F.R. Paton[1], N.E. Manghat[1], D.H. MacIver[2]; [1]*Bristol/UK*, [2]*Taunton/UK (jonrodrigues@doctors.org.uk)*

Purpose: No single well-established hypothesis for the mechanisms of heart failure exists. Left ventricular ejection fraction (LVEF) is widely used to dichotomise heart failure into reduced and preserved LVEF cohorts. We hypothesised that a common myocardial mechanism occurs in heart failure regardless of cause. We quantify the relationship of absolute wall thickening (AWT) with LVEF across a range of global cardiac pathology with varying degrees of end-diastolic wall thickness (EDWT) using cardiac magnetic resonance (CMR).
Methods and Materials: 183 subjects underwent 1.5T CMR: 53 idiopathic dilated cardiomyopathy (DCM), 36 amyloid cardiomyopathy, 55 hypertensives (HTN) and 39 normal controls. LV volumes and LVEF were calculated. EDWT and end-systolic wall thickness (ESWT) were measured in basal and mid-myocardial segments from long-axis cines. AWT (ESWT-EDWT) and relative AWT (rAWT=AWT/LV end-diastolic internal diameter) were calculated. Longitudinal and circumferential strain were measured.
Results: There was a range of LVEF: normal (controls 64±7% and HTN 66±8%), moderately reduced (amyloid 49±16%) and severely reduced (DCM 30±11%). There were significant differences in EDWT between subgroups (controls: 8±1mm, DCM: 8±1mm, HTN: 11±3mm and amyloid: 14±3mm, $P<0.0001$). Reduced longitudinal ($R=-0.457$, $P<0.0001$) and circumferential strain ($R=-0.710$, $P<0.0001$) were associated with reduced AWT. AWT was strongly related to LVEF ($R=0.812$, $P<0.0001$). Changes in rAWT accounted for >75% LVEF variability across the entire cohort ($R^2=0.766$).
Conclusion: LVEF is determined by changes in rAWT across a range of global LV disease of varying EDWT. Our findings offer a unifying mechanism to explain heart failure with preserved and reduced LVEF.

B-0332 14:48

Value of post contrast Cine-SSFP images for visual assessment of global left ventricular function at 3T

A. Preuß[1], S. Wyschkon[1], M. Elgeti[2], B. Hamm[1], T. Elgeti[1]; [1]*Berlin/DE*, [2]*Los Angeles, CA/US*

Purpose: At higher field strengths, B0-inhomogeneitis and the resulting dark-band artefacts can degrade delineation of myocardial contours on steady-state free precession (SSFP) magnetic resonance (MR) images and thus impair visual assessment of myocardial functional abnormalities. We therefore tested if gadobutrol (Gd)-enhanced post-contrast Cine- SSFP images allow visual assessment of global cardiac function on cardiac long-axis views.
Methods and Materials: Pre- and post-contrast (single standard dose of gadobutrol) Cine-SSFP loops in the four-chamber view of 20 patients who underwent contrast-enhanced cardiac MR imaging at 3T (Magnetom Trio, Siemens) were evaluated. Contrast-to-noise ratios (CNR) were calculated. Standard deviation (SD) of left ventricular (LV) signal intensity was measured to quantify signal heterogeneity of LV blood pool. Presence of artefacts (dark band, flow) in both ventricles and delineation of the endocardial LV border were rated by two observers in consensus using a four-point Likert scale (lower=better). Results are given as mean±SD. Measurements were compared using Student´s t-test and qualitative results were assessed using the non-parametric Wilcoxon signed-rank test.
Results: Pre- and post-contrast CNR was 33±17 and 40±18 ($p=0.052$), SD of LV blood pool was 43±32 and 31±15($p=0.062$). Presence of artefacts was rated 3±0.9 in pre- and 1.9±0.9 in postcontrast images ($p=0.001$). Endocardial delineation was rated 2.7±0.9 (precontrast) and 1.7±0.6 (postcontrast) ($p=0.002$).
Conclusion: If Gd-based contrast medium is used (e.g., for delayed Gd-enhancement imaging), post-contrast Cine-SSFP images show comparable CNR by significantly reduced dark band and flow artefacts thus improving the visual assessment of global cardiac function.
Author Disclosures:
B. Hamm: Research/Grant Support; 1. Abbott 2.Actelion Pharmaceuticals, 3. Bayer Schering Pharma 4. Bayer Vital 5. BRACCO Group, 6. Bristol-Myers Squibb 7. Charite, research organisation GmbH 8. Deutsche Krebshilfe 9. Dt. Stiftung Herzf, 10.Essex Pharma 11.EU Programmes, 12.Fibrex Medical Inc. 13.Focused Ultrasound Surgery Foundation, 14.Fraunhofer Gesellschaft 15. Guerbet 16.INC, Research, 17.InSightec Ud. 18.IPSEN Pharma, 19.Kendlel MorphoSys AG 20. Lilly GmbH 21. Lundbeck GmbH, 22. MeVis, Medical Solutions AG 23. Nexus Oncology 24. Novartis 25. Parexel CRO Service, 26. Perceptive 27. Pfizer GmbH, 28.Philipps, 29.sanofis-aventis S.A 30. Siemens 31.Spectranetics GmbH, 32.Terumo Medical Corporation 33.TNS Healthcare, 34. Toshiba, 35.UCB Pharma 36.Wyeth Pharma 37.Zukunftsfond Berlin(TSB), 38.Amgen 39.AO Foundation, 40.BARD 41.,

Braun (Sponsoring eines Workshops) 42. Boehring Ingelheimer, 43. Brainsgate 44. PPD(CRO), 45.CELLACT Pharma 46.Celgene 47.CeloNova BioSciences, 48.Covance 49.DC Deviees, Ine., 50.Ganymed 51.Gilead Scienees 52. Glaxo Smith Kline 53.ICON (CRO), 54.Jansen 55. LUX Bioseienees, 56. MedPass 57. Merek 58. Mologen, 59. Nuvisan 60. Pluristem 61. Quintiles 62. Roehe,, 63. Sehumaeher GmbH, 64. Seattle Geneties 65. Symphogen 66. TauRx Therapeuties, 67. Accovion 68. AIO:69.ASR Advanced sleep research 70. Astellas 71. Theradex, 72. Galena 73. Chiltern 74.PRAint 75.Inspiremd, 76. Medronic 77. Respicardia 78. Silena Therapeutics, 79. Spectrum Pharmaceuticals, 80. St. Jude Medical 81.TEVA 82. Theorem.

B-0333 14:56

Left ventricular diastolic function estimation from magnetic resonance real-time cine imaging

C. Reiter[1], G. Reiter[1], A. Schmidt[1], A. Greiser[2], M. Fuchsjäger[1], U. Reiter[1]; [1]*Graz/AT*, [2]*Erlangen/DE (Clemens.Reiter@medunigraz.at)*

Purpose: To evaluate if cardiac magnetic resonance (CMR) cine real-time imaging-derived volumetric parameters of the left heart allow grading of left ventricular diastolic dysfunction similar to routinely used early-to-late diastolic transmitral (E/A) and systolic-to-early diastolic pulmonary venous (S/D) flow ratios.
Methods and Materials: Eleven patients with coronary heart disease without aortic and mitral insufficiencies (age = 66±9 years; male/female = 8/3) underwent 3T CMR 4D flow and cine real-time imaging covering the left heart in 4-chamber orientation. E/A and S/D ratios were derived from 4D flow data. Left ventricular and atrial volumes were semi-automatically segmented in cine images to determine the ratios of early-to-late diastolic left ventricular peak filling rates (volumetric E/A) and of systolic atrial peak filling to early-diastolic peak emptying rate (volumetric S/D). Relations between flow and volumetric ratios were analysed by correlation and regression analysis; means were compared with paired t test.
Results: Whereas mean values of E/A and volumetric E/A did not differ (0.87±0.34 vs. 0.76±0.20; p=0.11), mean values of S/D and volumetric S/D differed (0.98±0.42 vs. 1.55±0.40; p<0.0001). Flow and volumetric ratios correlated strongly (E/A, r=0.87; S/D, r=0.92). Standard deviations from the regression lines of flow against volumetric ratios were small (0.10 in case of E/A and 0.17 in case of S/D).
Conclusion: A close relationship between flow and volumetric-derived E/A ratio and S/D ratio was found. Cine real-time imaging of the left heart might present a fast alternative in the assessment of diastolic dysfunction.
Author Disclosures:
G. Reiter: Employee; Siemens Health Care Diagnostics GmbH. **A. Greiser:** Employee; Siemens Healthcare GmbH.

B-0334 15:04

Subclinical changes in cardiac functional parameters as determined by MRI in patients with sleep apnea and snoring: findings from UK Biobank

A. Curta[1], H. Hetterich[1], R. Schinner[1], W. Sommer[1], N. Aung[2], M.M. Sanghvi[2], S. Neubauer[3], S.K. Piechnik[3], S.E. Petersen[2]; [1]*Munich/DE*, [2]*London/UK*, [3]*Oxford/UK (adrian.curta@med.uni-muenchen.de)*

Purpose: Obstructive sleep apnoea (OSA) is a common disorder that shows an increased risk for left ventricular (LV), more rarely right ventricular (RV) dysfunction. We explored subclinical alterations in cardiac MRI in patients participating in the UK biobank study.
Methods and Materials: We analysed data from 5000 subjects. Patients with known heart disease were excluded. The rest was divided into three groups: a) individuals with OSA, b) individuals with snoring and c) individuals with no OSA or snoring (n=35, 2049 and 2666 respectively). We researched demographic parameters, cardiovascular risk factors, LV and RV functional parameters.
Results: Our analysis showed significantly increased LV mass (109±25g vs 94±25g vs 85±23g, p<0.001), LV end diastolic volume (167±29ml vs 148±35ml vs 139±32ml, p<0.001), LV end systolic volume (67±18ml vs 61±21ml vs 57±19ml, p<0.001), LV stroke volume (100±19ml vs 87±20ml vs 82±18ml, p<0.001), RV end diastolic volume (179±34ml vs 157±38ml vs 147±36ml, p<0.001), RV end systolic volume (80±20ml vs 70±23ml vs 65±22ml, p<0.001) and RV stroke volume (100±20ml vs 88±20ml vs 82±18ml, p<0.001) in patients with OSA and snoring compared to the control group. There was no significant difference in LV or RV ejection fraction.
Conclusion: Our results indicate that not only sleep apnoea but also snoring, although at a smaller degree, could be associated with dilation of both ventricles and LV hypertrophy. A differentiation between alterations caused by OSA and by associated cardiovascular risk factors such as hypertension and obesity still remains a challenge.
Author Disclosures:
S.E. Petersen: Consultant; Circle Cardiovascular Imaging Inc., Calgary Canada.

B-0335 15:12

Cardiac MRI correlates of patient functional improvement after advanced pharmacotherapy for pulmonary arterial hypertension (PAH)

S. Terpenning, L. Melendres, M. Boivin, C. Bunn, L. Ketai;
Albuquerque, NM/US (STerpenning@salud.unm.edu)

Purpose: To identify cardiac MRI correlates of improved patient functional capability in response to advanced pharmacotherapy for pulmonary arterial hypertension (PAH).
Methods and Materials: Retrospective analysis identified 28 patients with PAH who underwent cardiac MRI and 6-minute walk testing before initiating or intensifying vasodilator treatment. Ten of these patients underwent repeat cardiac MRI and six-minute walk testing > 4 months after change in therapy. Two cardiothoracic radiologists independently analysed the pre and post-treatment MRIs masked from walk results. Cardiac outputs (CO) were calculated from right (RV) and left (LV) ventricular volumes. Relationship between walk distance and cardiac parameters was analysed with linear regression.
Results: Mean change in six-minute walk distance was 18m±57m, p>.05, with a range of -106m to +100m. Measurements from one reader showed significant positive correlation between change in RVCO and change in walk distance (R=.79, R2=.62, p<.01), while correlation between other reader's RVCO measurements and walk distance did not achieve significance. (R=.62, R2=.38, p = 0.6). Both readers measurements demonstrated significant correlation between change in LVCO and change in walk distance, (R=.75, R^2=.56, p=.01) and (R=.65, R^2=.42, p<.05). For both readers change in LVEDV showed the strongest correlation with change in walk distance (R=.89, R^2=.80, p=.001) and (R=.82, R^2=.68, p<.01). Neither reader's measurements of change in RVEDV correlated significantly with changes in walk distance.
Conclusion: Changes in patient functional capability after advanced pharmacotherapy for PAH correlate with changes in CO and may be more strongly associated with changes in LV rather than RV morphology.

B-0336 15:20

Evaluation of myocardial strain by cardiac MRI: correlation with myocardial iron overload and echocardiography speckle tracking

C. Tudisca[1], A. Meloni[2], F. Pizzino[3], C. Gerardi[4], M. Midiri[1], A. Pepe[2]; [1]*Palermo/IT*, [2]*Pisa/IT*, [3]*Messina/IT*, [4]*Sciacca/IT (chiaratudisca@gmail.com)*

Purpose: Magnetic resonance (MR) tagging analyzed by dedicated tracking algorithms allows precise measurements of myocardial motion and characterization of regional myocardial function.Our aim was to quantitatively assess regional myocardial contractility in thalassemia major (TM) patients and correlate it with myocardial iron overload, global biventricular function and strain values in speckle tracking ehocardiography (STE).
Methods and Materials: One-hundred and one TM patients (59 F; 3.3±9.0 yrs) enrolled in the MIOT network underwent MR (1.5T). Among these, 25 patients underwent STE on the same day. Three short-axis tagged MR-images were analyzed offline using harmonic-phase methods, and circumferential shortening (Ecc) was evaluated for all the 16 myocardial segments.The same short-axes were acquired by a T2* GRE-multiecho technique to assess myocardial iron overload.Bi-ventricular function parameters were quantitatively evaluated by cine-images. In the patients that underwent STE was evaluated the strain in the 3 directions.
Results: Global-Ecc and T2* values were -12.2±2.6 and 27.2±13.2, respectively, not significantly correlated. Global-Ecc value was not associated to left ventricle (LV) volumes and ejection fraction (with a P> 0.5 in all the comparisons), while was significantly correlated with LV mass and cardiac output (p<0.05).Mean-Ecc was significantly different among 4 cardiac regions (anterior, septal, inferior and lateral; p<00001). In the 25 patients who underwent STE we found a significant correlation between the mean Ecc value and the mean global longitudinal deformation (GLD) value, (R= 0.593, p=0.002).
Conclusion: In TM patients mean global Ecc is significantly correlated with LVmass and cardiac output, and with the GLD evaluated with the STE.

14:00 - 15:30 **Room M 3**

Oncologic Imaging

SS 316

Female genitourinary cancers

Moderators:
S. Guerrini; Siena/IT
S. Kharuzhyk; Minsk/BY

B-0337 14:00

Differential diagnosis of ovarian tumours: value of multiparametric MRI
A.E. Solopova, A.D. Makatsaria, S.K. Ternovoy; *Moscow/RU (dr.solopova@mail.ru)*

Purpose: The objective was to evaluate the value of magnetic resonance imaging with quantitative DCE and DWI analysis for differential diagnosis of complex ovarian tumours (OT).
Methods and Materials: MRI was performed in 141 patients (173 OT) using the following protocol: Sg T2, Ax T2, Co T1, DCE using dynamic T1-FS, and DW MRI (b-values 0, 1000 v/vv2). Following quantitative parameters were evaluated: amplitude of contrast agent accumulation (ACAA), period of rise of signal intensity (HRSI), the maximum curvature (MC), apparent diffusion coefficient (ADC). All MRI results were compared with histological verification.
Results: The tumour grade distribution: benign tumours (BTs)—49%, borderline (BrTs)—12%, malignant (MTs)—39%. ACAA was significantly higher in MT—165% (118.5-211.1%) than in BTs—68.2% (40.5-96.2%) (P<0.001) and BrTs—82.7% (59.1-141.5%), (P=0.05); HRSI was significantly higher in BTs—35.1 s (31.0-41.2 s) than the BrTs—27.6 s (23.1-29.4 s), (P=0.05), and BTs—23.6 s (21.9-30.2 s) (P = 0.01). MC was 1.75 (1.0-2.4), 2.8 (2.04-3.7) and 6.04 (4.25-9.26) for BTs, BrTs and MTs, respectively, and was significantly higher in MTs (P<0.01). Mean ADC values of MT's solid component were significantly lower than in BTs (1.013 ± 0.12 and 1.41 ± 0.3, respectively (P<0.05)). The diagnostic efficiency of multiparametric MRI was as follows: the accuracy of 93.4%, sensitivity of 92.9% and specificity of 95.1%.
Conclusion: Quantitative multiparametric MRI should be obligatorily included into preoperative assessment of indeterminate adnexal masses, allowing clear distinction the degree of OT malignancy, to optimise the treatment strategy.

B-0338 14:08

Delayed detection of recurrence on postoperative PET-CT in patients with advanced ovarian cancer: a study of initially missed lesions on MDCT
H. Bae, D.C. Jung, S.Y. Park, Y.T. Oh; *Seoul/KR (hbae07@yuhs.ac)*

Purpose: To describe patterns of erroneous postoperative multi-detector row CT (MDCT) interpretation of recurred peritoneal lesions in patients with advanced ovarian cancer (AOC).
Methods and Materials: Between 2011 and 2016, we reviewed postoperative follow-up PET-CT images of 223 patients with suspected recurrence based on images, who had a history of initially diagnosed AOC (International Federation of Gynaecology and Obstetrics (FIGO) stage IIIC-IV) and underwent primary cytoreduction. Under the awareness of the recurred location, we re-evaluated MDCT images taken right before the recurrence was detected on PET-CT and categorised the cases as either absence of lesion or presence of lesion (missed case). We performed region-based comparisons of the missed cases according to predefined peritoneal locations. In the same period, preoperatively neglected lesions in AOC patients were analysed for comparison.
Results: Re-evaluation of follow-up MDCT revealed that 42.6 % (95/223) of recurrent lesions were missed. According to region-based comparisons of the missed cases, the most commonly missed site was pelvic cavity (18.9%, 18/95) followed by porta hepatis (14.7%, 14/95) and para-aortic/aortocaval lymphadenopathy (12.6%, 12/95). Compared to postoperative images, the most commonly neglected site in preoperative staging evaluation was porta hepatis followed by small bowel mesentery and pelvic cavity.
Conclusion: The most commonly missed location on post-op CT imaging was pelvic cavity followed by upper abdominal lymphadenopathy while porta hepatis was equally overlooked on both pre- and postoperative evaluations. Compared to preoperative evaluations, missed rate of mesenteric implants was lower in relapsed cases. Familiarity with these imaging features may aid in detection of recurrence.

B-0339 14:16

Diagnostic efficiency of DW MRI in detection of peritoneal carcinomatosis
I.Y. Sychenkova, N.A. Rubtsova; *Moscow/RU (sichiu@rambler.ru)*

Purpose: To determine the diagnostic efficiency of DW MRI in detection of abdominal and pelvic peritoneal dissemination in oncological patients.
Methods and Materials: The study included 32 patients of both sexes with cancer of various localizations. In case of suspicion for the peritoneal implants presence patients underwent MRI, which was performed in two stages: the first one was carried out with the use of a protocol that included Sg T2, Ax T2, Cor T2 FatSat, Obl-Ax T2, Obl-Cor T2 and Co T1; the 2nd - with addition of DWI.
Results: When carrying out MRI under the standard protocol full compliance of MRI data with histopathological examination was determined in 18 (56,2%) cases, which were considered as true positive (TP) results, false positive (FP) results were obtained in 2(6,3%) cases. True negative (TN) results were determined in 4(12,5%) patients, false negative (FN) - in 8(25,0%) patients. The indicators of MRI diagnostic efficiency when using the standard protocol were the following: accuracy 69%, sensitivity 69%, and specificity 67%. During the assessment of diagnostic value of DW MRI, 25(78,1%) cases demonstrated TP results, 1(3,1%) - FP results, TN results were obtained in 4(12,5%) cases, and FN results were shown in 2(6,3%) cases. The informativity measures when using the DWI method increased to: 91% for accuracy, 93% for sensitivity and 80% for specificity.
Conclusion: The use of DWI significantly increases the diagnostic efficiency measures of MRI in detection of abdominal and pelvic peritoneal dissemination for cancer of various localizations.

B-0340 14:24

Dedicated diffusion-weighted MR imaging for staging peritoneal metastases: a preoperative selection tool for cytoreduction surgery (CRS) candidates
I. van't Sant-Jansen, S. Chandrasegaram – Shanmuganathan, D.M.J. Lambregts, W. van Driel, N.F.M. Kok, R.G.H. Beets-Tan, G.L. Beets, A.G.J. Aalbers, M.J. Lahaye; *Amsterdam/NL (MJ.Lahaye@gmail.com)*

Purpose: The peritoneal cancer index (PCI) quantifies the extent of peritoneal metastases found at surgery. To prevent unnecessary surgical staging procedures in patients whose peritoneal tumourburden is too extensive to benefit from CRS/HIPEC, patient selection based on preoperative imaging would be ideal. Computed tomography is inaccurate in predicting the PCI. Therefore, we compare the PCI estimated preoperatively by DW-MRI with the PCI found at surgery to assess whether DW-MRI can be used to select CRS/HIPEC candidates.
Methods and Materials: In this ongoing study eighteen consecutive patients (April-September 2016, M/F=3/15) with histologically proven peritoneal carcinomatosis from either colorectal (n=13) or ovarian (n=5) origin were included. Patients were scheduled for exploratory laparoscopy and/or CRS/HIPEC and underwent preoperative dedicated DW-MRI (scan time=30min). Two independent readers prospectively determined the PCI on DW-MRI. Patients were categorised as low-risk (PCI 0-21) versus high-risk (PCI 22-39); in our center considered operable versus non-operable. Reference standard was PCI found at surgery. Quadratic weighted kappa was used to evaluate the interobserver agreement.
Results: At surgery the mean PCI was 11.3 (range 0-26). For reader 1 the mean PCI was 11.5 (0-29) and for reader 2 9.8 (0-29). Both readers categorized 17 out of 18 patients correctly (accuracy 94%) when compared to surgical findings. Both readers understaged the same patient.
The interobserver agreement was perfect (k=1.0).
Conclusion: These data suggest that DW-MRI is an accurate selection tool to noninvasively select patients who could potentially benefit from CRS/HIPEC. No overstaging occurred with DW-MRI, meaning no patients would have been denied potential curative surgery if DW-MRI would have been used as a selection tool.

B-0341 14:32

The usefulness of preoperative radiological assessment of peritoneal cancer index (PCI) as predictive factor for optimal debulking and survival: a preliminary study
G. Avesani[1], M. Arshad[2], J. Liang[2], A. Thornton[2], H. Lu[2], A.G. Rockall[2]; [1]*Bolzano/IT*, [2]*London/UK (giacomo.avesani@gmail.com)*

Purpose: To evaluate if the radiological assessment of PCI on preoperative CT of patients with ovarian cancer can be predictive of complete surgical debulking and whether the radiological PCI (rPCI) is correlated with Overall Survival (OS) and Progression Free Survival (PFS).
Methods and Materials: We considered all patients with a diagnosis of ovarian cancer, a preoperative CT, up-front cytoreductive surgery at a single institution between 2004 and 2009 and a complete clinical follow-up after surgery, to December 2015 (51 patients). We recorded the surgical outcome and the OS and PFS after surgery. An expert radiologist retrospectively evaluated the CT examinations and assigned rPCI following Sugarbaker's diagram. We correlated rPCI score with the results of surgery using ROC curve analysis and with OS and PFS using Kaplan-Meier curve.
Results: 32 (62.7%) patients had complete cytoreduction and 31 (60.8%) died due to the cancer; the median value of OS was 42 months (2-113) and of PFS was 15 months (7-56). The median value of rPCI was 11 (0-31). ROC curve analysis identified a PCI of 18 as significant threshold useful to predict complete surgical cytoreduction (p=0,05). Patients with a rPCI >16 has a

shorter OS (p=0.02; Hazard Ratio=2.13). Similarly, patients with a rPCI >7 has a shorter PFS (p=0.03; HR=1.9).
Conclusion: rPCI on preoperative CT could help in predicting surgical outcome and seems to correlate positively with both OS and PFS. This may be helpful in better evaluating prognosis in patients with high FIGO stage who may have very different peritoneal extension.

B-0342 14:40

Diagnosis of peritoneal metastases: comparison of DWIBS MR imaging with FDG 18PET CT

R. Balaji; *Chennai/IN (ravikanthbalaji@gmail.com)*

Purpose: Assess diagnostic performance and accuracy of diffusion weighted imaging with background signal suppression (DWIBS) compared with ^{18}Fluorodeoxyglucose positron emission tomography (FDG-PET) in detection of peritoneal metastases.
Methods and Materials: The study included 64 patients with ovarian and colonic malignancies and lymphomas with peritoneal deposits. DWIBS imaging was performed on a 1.5T scanner (Achieva, Philips Medical Systems, Netherlands) within mean period of two days after ^{18}FDG-PET/CT study. b-value of 800 s/mm^2 was used. ^{18}FDG-PET/CT was performed on Philips, Gemini PET/CT system after intravenous injection of FDG. Axial images and coronal MIP images of MR and PET CT images were obtained and blinded review of PET/CT and DWIBS images was performed separately to avoid bias and all lesions detected were recorded. DW MR images were also assigned colour scale based on diffusion restriction and ADC values to display PET like images. The findings detected on DWIBS and PET/CT images were compared on a per-lesion basis using PET/CT as gold-standard.
Results: FDG-PET/CT revealed 380 malignant lesions in 64 patients. DWIBS showed 368 lesions with a detection rate of 96% compared with ^{18}F FDG-PET/CT which was the gold standard. The study exhibited relatively good concordance between detection rates of DWIBS and FDG-PET/CT irrespective of primary pathology.
Conclusion: DWIBS allows for fast and robust imaging with low technical and operational efforts and is cost effective. Patients are comfortable as there is no injection of contrast and no exposure to radiation. DWIBS is as accurate as FDG PET/CT in assessment of peritoneal metastases.

B-0343 14:48

Added value of diffusion-weighted magnetic resonance imaging in the staging of cervical carcinoma

S.M. Mansour, S. Fakhry; *Cairo/EG (shery4@yahoo.com)*

Purpose: Assess the diagnostic accuracy of diffusion-weighted imaging (DWI) versus dynamic contrast-enhanced MRI (DCE-MRI) and T2 fast spinecho-weighted images (T2WI) in the preoperative staging of cervical carcinoma.
Methods and Materials: MRI pelvis using T2WI, DCE sequence and DWI were done for 50 cases with cancer cervix after initial biopsy confirmation for pre-management staging. In dynamic imaging we used T1 THRIVE (High Resolution Isotropic Volume Examination) technique that enables images acquisition at one pre-contrast, and six sequential post-contrast phases at 40, 80, 120, 160, 200 and 240sec. On DWI, scanning acquired by b values: 0, 500, 1000 and 1500.Analysis considered signal intensity (SI) at b1000 and the mean ADC values for the solid components of the masses. Surgical staging was the standard reference.
Results: The staging accuracy in all cases were 66.6% for T2WIs, 83.3% for DCE-MRI and 91% for DW-MRI.Upon assessment of parametrial infiltration, T2 detected 36%(n=18), DCE-MRI detected 35.4% (n=17) and DWI detected 32% (n=16). Assessment of locally advanced and advanced stages was comparable among T2WIs, DWI and DCE-MRI.While on assessing metastatic lymph nodes T2WIs was positive for lymphadenopathy in 15 cases (30%), DWI in 14 cases (28%) and DCE-MRI in 7 cases (14.6%).The overall accuracy of T2WIs, DW-MRI and DCE-MRI in staging cervical carcinomas was 74%, 88% and 83.3% respectively.
Conclusion: DWIs supported by conventional MRI data can improve detection of small tumours, increase overall accuracy, increase reader's confidence in evaluation of parametrial infiltration and help in proper detection of locally advanced and advanced stages of cancer cervix.

B-0344 14:56

Histological type of cervical cancer: can it be evaluated with mpMRI

E. Tarachkova, M. Shorikov, V. Panov, I. Tyurin, B. Dolgushin; *Moscow/RU (tarachkovaelenavlad@gmail.com)*

Purpose: To show if combined MRI data can improve differential diagnostics of the histological type of cervical cancer (CC).
Methods and Materials: 91 patients with histologically verified diagnosis of CC (cervical squamous cell carcinoma, CSCC: 74; cervical adenocarcinoma, CAC: 17); for some grade of the tumour had been determined: SCCC: G1-6, G2-23, G3-24; CAC: G1-5, G2-5, G3-4) MRI (1.5 & 3T): T2WI TSE native/fat saturated (fs); DWIfs+ADC-maps; T1WIfs VIBE before and 4 min after i.v. injection of MRCA (1.0 M; 0.1 ml/kg); 35 series DCE T1WIfs TWIST after MRCA injection, time resolution=5s. Signal intensity (SI) and standard deviation (SD) in CC and the gluteus maximus muscle (15-30 pixels) were measured (SD, SI/SD for heterogeneity; SI(CC), SI(CC)/SI(muscle) for intensity).
Results: DCE: both types showed active SI increase at first 10-20 s after the occurrence of MRCA in pelvic arteries with following change of signal (inflection point), after relative SI (rSI) for DCE was calculated as rSI(t)= 100%* (SI(t)-SI (inflection))/SI (inflection); CAC was more heterogeneous at 110 s ($p < 0.03$) and had higher rSI ($p < 0.003$-0.04). Additionally areas under DCE curves were significantly different: CAC>CSCC, $p < 0.005$, CSCC curve had an additional inflection point before plateau at about 60-70th second while CAC continually accumulated MRCA, rSI (60s) had maximum accuracy (Sen/Sp=0.75/0.76) or Sen/Sp=0.27/0.95 T2WIfs: CAC was brighter, less heterogeneous ($p<0.05$). A regression model showed that T2WIfs and DCE combined data significantly differentiate CSCC and CAC: $p<0.0015$, Sen/Sp=0.80/0.85 or 0.67/0.95. SD of SI of the tumours on postcontrast T1WI-VIBE for CAC of G1 and G3 grades were significantly different from each other and from all other types of CC: SD(CAC(G1)) > SD (SCCCs,CAC(G2)) > SD (AC(G3)), $p<0.02$. Sp/Sen (CAC(CAC(G1)) = 0.75/0.95;Sp/Sen (CAC(G3)) = 1.00/0.83.
Conclusion: T1WI after MRCA injection, T2WI with fat saturation can be used to estimate histological type of CC.

B-0345 15:04

Invasive stromal cancer cervix post-therapy: MRI pulse sequences comparative diagnostic merits

S.A. Hussein, M.K.A. Asran, M.H. El Naggar, R.M. Kamal, T.A. Raafat; *Cairo/EG (samar.ahmad@nci.cu.edu.eg)*

Purpose: The aim of the study was to assess the diagnostic merits of each of the applicable MRI pulse sequences in the evaluation of tumour residual, recurrence or post treatment complications of cervical cancer aiming to assess the possibility of use of Diffusion weighted imaging instead of Contrast enhanced studies especially in patients with deteriorated renal functions.
Methods and Materials: Our study included 48 patients with histopathologically proven cancer cervix and a control group of 20 patients. All patients underwent post treatment Contrast Enhanced and Diffusion weighted MRI examinations to assess, confirm or exclude the presence of residual/recurrence mass lesions or post therapy complications.The reported MRI findings of both studies were correlated with histopathology results and/or with follow -up imaging.
Results: The sensitivity and specificity of DWI were 96.8 % and 100% respectively as compared to sensitivity and specificity of 87.5 % & 87.5% respectively calculated for contrast enhanced MRI studies. The mean ADC value of malignant post-treatment tumour (1+/- 0.18 x 10-3 mm2/sec) was significantly different than those of benign post -treatment changes (1.56 +/- 0.03 x 10-3 mm2/sec) and from values calculated for the control group (1.57 +/- 0.2 x 10-3 mm2/sec) (P value< 0.0001). The initial mean ADC value of complete responders were also significantly less than that of partial responders and those with recurrent disease (P value< 0.0001).
Conclusion: Quantitative DW imaging provides a better assessment tool than Contrast enhanced MRI in the characterisation of post-treatment changes.

B-0346 15:12

DW-MRI: an early predictive assay for treatment outcome in locally advanced cervical cancer

A.M. Telesca, M. Miccò, B. Gui, M. Giuliani, E. Rodolfino, F. Cambi, P.P. Grimaldi, A.L. Valentini, L. Bonomo; *Rome/IT (annamariatelesca@gmail.com)*

Purpose: The purpose of this study was to investigate the clinical value of DW-MRI as early predictor of treatment response in patients with locally advanced cervical cancer (LACC) receiving preoperative chemoradiotherapy (CRT) through the measurement of ADCm. Correlation with histopathological findings.
Methods and Materials: This prospective study was approved by our Ethical Committee. 88 patients receiving CRT for LACC (FIGO staging IB2 or more advanced) were enrolled and underwent 1.5 T pelvic MRI including DWI before CRT (baseline) and after 4 weeks (early). ADCm (b-values: 0-800 s/mm^2), determined at baseline and early MRI, were compared with histopathologic findings after radical hysterectomy (good responders (R) vs. poor-R). For ADCm values, differences between good-R and poor-R were assessed by T-test. Its discriminatory capability for detection of good-R was compared with receiver operating characteristics (ROC) analysis.
Results: Early ADCm values were significantly higher for good-R than for poor-R (1.12×10^{-3} mm^2/sec vs 1.04×10^{-3} mm^2/sec; p=0.02), but no significant differences were observed for ADCm at baseline MRI (p= 0.40) between the two groups. The area under the ROC curve for prediction in treatment response was higher for early ADCm comparing to baseline ADCm (0.63 vs 0.52). A cut-off value of 1.10×10^{-3} mm^2/sec was determined for early ADCm

with a sensibility, specificity, VPP, VPN and accuracy of 74%, 67%, 50%, 85% and 90%.
Conclusion: Early evaluation of ADCm might provide useful information for predicting outcome and selecting high-risk patients for more aggressive therapy.

B-0347 15:20

Factors affecting inferior vena cava retrieval: 5-year experience from a district hospital

H. Lee, W. Wong, C. Chan; *Hong Kong/HK*

Purpose: This study aims to evaluate factors related to IVC filter (IVCF) retrieval rate and factors that affect success rate in retrieval attempts.
Methods and Materials: All patients with IVCF insertion in a district hospital from 10/2011 to 8/2016 were retrospectively included. Data regarding patient demographics, comorbidities, indications for and type of IVCF, IVCF tilting, and time to retrieval were obtained.
Results: 75 patients with 76 IVCF placement were included. IVCF retrieval rate was 30% (23 out of 76). IVCF retrieval success rate was 82% (23 out of 28 attempts). In patients with DVT and contraindicated for anticoagulation due to operation, the rate of IVCF retrieval was significantly higher than that of patients with IVCF placed for other indications (63% vs 17%, p<.05). Patients with malignancy had a significantly lower rate of IVCF retrieval compared to patients without malignancy (17% vs 39%, p<.05). IVCF angulation >15 degree was observed more in patients with failed retrieval attempt (3/5), compared to patients with successful retrieval (0/23). This difference was statistically significant (p<.05). There were no significant differences between successful and failed attempts in terms of age, sex, history of malignancy, placement route, type of filter, and time to filter retrieval.
Conclusion: IVCF retrieval is more likely in patients with IVCF placed for DVT and contraindication for anticoagulation due to operation, and in patients with no known malignancy. Unsuccessful IVCF retrieval attempts are more likely to occur in IVCF which are angulated.

14:00 - 15:30 **Room M 5**

Neuro

SS 311b

Functional MRI

Moderators:
T. Auer; Egham/UK
C. Calli; Izmir/TR

B-0348 14:00

Independent component and seed-based analyses in localisation and lateralisation of Broca's and Wernicke's areas with resting state fMRI

L. Makovskaya[1], R. Vlasova[2], E. Mershina[1], E. Pechenkova[1]; [1]*Moscow/RU*, [2]*Los Angeles, CA/US (lmak@fbm.msu.ru)*

Purpose: To compare SCA and ICA methods in mapping Broca's and Wernicke's areas with resting-state fMRI (rsfMRI) data in healthy volunteers.
Methods and Materials: Each of 52 volunteers (25 left-handed) performed two task-based and one rsfMRI session in the Siemens Avanto 1.5T scanner. Each of the Broca's and Wernicke's areas was localised by three methods: using one of the speech tasks (SPM12 software); ICA analysis of rsfMRI data and the language network mask (GIFT v4.0); and SCA analysis of the rsfMRI data with a seed region in the other speech area revealed by the independent speech task (Conn v.14). Location and laterality index (LI) of the speech areas identified with the two rsfMRI methods were cross-validated with the task-based data.
Results: The average overlap of the speech areas localized by task-based and rsfMRI (either SCA or ICA) has not exceeded 25%. However, correlation between LI across SCA and task-based analyses was moderate for Broca's area (r=0.67, p<0.001) and high in Wernicke's area (r=0.71, p<0.001). The ICA showed no LI correlation with the task-based data: r=0.26 (p=0.06) for Broca's area and r=0.08 (p=0.57) for Wernicke's.
Conclusion: Unlike task-based and SCA-based results, the speech areas localized by ICA analysis of rsfMRI were bilateral in all volunteers. Therefore, speech areas are better lateralized by SCA method of rsfMRI rather than ICA. It is still to be empirically tested whether the flexible adjustment of the statistical thresholds on the individual basis may improve the consistency of task-based and rsfMRI data.

B-0349 14:08

Functional connectivity analysis in differential diagnostics of chronic disorders of consciousness

E.I. Kremneva, E. Zmeykina, L. Legostaeva, A. Poidasheva, A. Chervyakov, D. Sergeev, J. Ryabinkina, N. Suponeva, M. Piradov; *Moscow/RU (moomin10j@mail.ru)*

Purpose: To perform functional connectivity analysis based on resting-state fMRI data for differential diagnostics between vegetative (VS) and minimal consciousness states (MCS).
Methods and Materials: In 14 patients with chronic disorders of consciousness (DOC) (CRS-rVS=4, CRS-rMCS-=5, CRS-rMCS+=5, mean age 26+-2.0) rsfMRI (3T Siemens Verio) was performed followed by data preprocessing in SPM8 and connectome construction in CONN. As regions of interest (ROI) we accepted full standard brain atlas. We obtained connectome with functional connections showing correlation of BOLD signal in ROIs. Also, we analysed correlation coefficients in default mode network's (DMN) nodes. Statistical results were thresholded using a combination of a connection-level threshold (FDR-corrected p values on individual ROI-to-ROI connections) and seed-level thresholds (F test on multivariate connectivity strength for each seed ROI).
Results: MCS- group showed appearance of three connections with a positive correlation, and MCS + group showed significant increase of the amount of connections. Improving of the level of awareness is associated with increase of the correlation coefficient between medial prefrontal cortex (MPFC) only and other areas outside the DMN. Values of correlation coefficients between MPFC and left lateral parietal cortex were: -0.01 (VS), 0.05 (MCS-), 0.05 (MCS+); between MPFC and posterior cingulate cortex: -0.01 (VS), 0.1 (MCS-), 0.1 (MCS+); between MPFC and right lateral parietal cortex: -0.12 (VS), 0.1 (MCS-), 0.14 (MCS+).
Conclusion: The connectoms' number of connections in ROI multiplies with the level of consciousness increase. MPFC may be of most important value for further investigations because of its relations with other DMN zones.
Author Disclosures:
E.I. Kremneva: Research/Grant Support; The study is supported by Russian Science Foundation grant No 16-15-00274.

B-0350 14:16

Altered interactions of cortical cores in patients with type 2 diabetes mellitus: a resting state functional MRI study

D. Liu; *Chongqing/CN (liudaihong121@163.com)*

Purpose: To investigate the change patterns of cortical cores and their interactions in type 2 diabetes mellitus (T2DM) patients using combined degree centrality (DC) and Granger Causality Analysis approaches.
Methods and Materials: Forty-seven T2DM patients and 47 healthy controls (HCs) matched for age, sex, education and BMI were enrolled in the blood biometric measurement, neuropsychological tests and resting-state brain MRI scanning. DPARSF v4.1 software was applied to preprocess the MRI data. REST v1.8 software was applied to analyse the difference of DC pattern between the two groups and verify the candidate cortical cores influenced by T2DM. Granger Causality effect among these cores was also calculated with REST v1.8 software. Proportion was examined with χ^2 test. Independent samples *t* test and Mann-Whitney U test were applied to normally distributed continuous data and to non-normally distributed data, respectively. P<0.05 was considered as statistically significant.
Results: In T2DM patients, significantly higher DC values were observed in left anterior cingulate gyrus (ACG), and significantly lower DC values in bilateral superior/middle occipital gyrus (S/MOG) and right precentral gyrus. There was negative causal effect from left ACG to left S/MOG that negatively correlated with fasting insulin (r=-0.360, P=0.013) and C-peptide (r=-0.363, P=0.012) in T2DM patients. No effective connectivity was found among the cores in HCs.
Conclusion: The altered interactions of cortical cores may provide insights into the neurological mechanisms underlying the T2DM-associated cognitive impairment. Patients may benefit from anti-diabetic therapy to prevent brain function decrement.
Author Disclosures:
D. Liu: Author; Shanshan Duan, Chaoyang Zhou, Xuntao Yin, Ping Wei, Jiuquan Zhang, Jian Wang. Research/Grant Support; the National Natural Science Foundation of China (81471647), the Innovation Fund for Younger Investigators of Southwest Hospital of the Third Military Medical University (SWH2013QN09).

B-0351 14:24

Physiological artefacts correction at pre-surgical task-related functional MRI

M. Kiss, J. Martos, V. Gál; *Budapest/HU (kissmate20@gmail.com)*

Purpose: Pre-surgical functional MRI (fMRI) is rapidly becoming a standard method to detect the eloquent brain areas. Breathing and pulsation cause significant artefacts, which are decreasing the localisation sensitivity and specificity. We would like to demonstrate the effectivity of physiological artefact removal - based on physiological parameter recordings - on the sensitivity and selectivity of the fMRI mapping.
Methods and Materials: Siemens Magnetom Verio 3T MRI system was used to collect data. The physiological parameters (breathing, pulse and ECG) were recorded with the built-in devices. 20 patients - with brain tumour - data were evaluated with SPM12. RETROICOR/RVHR was applied to detect the relevant physiological artefacts. We compared the statistical maps before and after the physiological correction.
Results: The physiological correction improved the specificity: we found false-positive activation around the main brain vessels. The main relative activation value of the eloquent areas did not change significantly after the correction, albeit the standard deviations were lower. The correction improved the statistical maps in 11 patients. We detected minimal changes in 5 patients as a result of low pulse and slow breathing.
Conclusion: The physiological correction increased the specificity of statistical maps, so we are able to detect the eloquent regions more reliably, which allows more reliable pre-surgical planning.

B-0352 14:32

Repeated application of realtime-fMRI neurofeedback in tobacco dependent patients after smoking cessation

M. Paolini, D. Keeser, S. Gschwendtner, A. Reckenfelderbäumer, H. Jeanty, B. Rauchmann, B. Ertl-Wagner, T. Rüther, S. Karch; *Munich/DE (Marco.Paolini@med.uni-muenchen.de)*

Purpose: To evaluate the effect of repeated application of real-time(rt)-fmri neurofeedback in patients with tobacco dependency with respect to smoking cessation success.
Methods and Materials: Tobacco-dependent patients (n=43) were randomized into two groups receiving either real feedback (n=26) of an addiction associated brain region (ACC, insula, DLPFC) or sham feedback. The aim was to reduce neural activity in the region of interest during nicotine cue exposure in 3 sessions within a period of 4 weeks after professionally assisted smoking cessation. Preprocessing and statistical analysis of functional images were conducted in BrainVoyagerQX taking patients' smoking status after 6 months into account (persistent tobacco abstinence/ significant reduction or complete relapse). Clinical data were assessed by established questionnaires (QSU, BDI, BIS, FTND).
Results: The fixed effect analysis of all patients with known smoking status after 6 months (real feedback, group) revealed brain activity reduction in addiction associated brain region in both abstinent/ less smoking patients (n=17) and completely relapsed patients (n=7) during neurofeedback sessions (3rd versus 1st run, $p<0.05$, Bonferroni corrected). However, in contrast to relapsed patients, abstinent/ less smoking patients had reduced brain activity in the ACC and the nucleus caudatus in several runs and enhanced brain activity in thalamic and parietal regions, especially in the 2rd and 3rd run of each session (between-group-comparison, $p<0.05$, Bonferroni corrected).
Conclusion: Neurofeedback based on rt-fmri may reveal and induce specific anti-addiction changes of brain state in tobacco dependent patients after smoking cessation and probably be used as a diagnostic and therapeutic tool.

B-0353 14:40

Assessment of executive functions in bipolar disorder: a voxel-based meta-analysis of fMRI studies

F. Tian, Z. Jia; *Chengdu/CN (1534748929@qq.com)*

Purpose: To identify executive function deficits assessed in functional magnetic resonance imaging (fMRI) studies of bipolar disorder (BD) through a voxel-based meta-analysis.
Methods and Materials: Web-based publication databases were searched to perform this meta-analysis of whole brain fMRI studies up to July 2016. A new improved voxel-based meta-analytic method, signed differential mapping (SDM), was developed to examine regions of activated or deactivated grey matter regions in the BD patients vs. healthy controls during a variety of executive functioning tasks.
Results: Eighteen datasets comprising 461 people with BD and 423 healthy controls met the inclusion criteria. Compared with age-matched healthy control participants, participants with BD showed reliable patterns of hyperactivation in bilateral gyrus rectus, extending to bilateral anterior cingulate cortex (ACC) and right middle temporal gyrus; hypoactivation in left cerebellum crus I, left precentral gyrus, right precuneus, right dorsolateral prefrontal gyrus (DLPFC). A sensitivity analysis as well as analyses of subgroups further confirmed these findings. Meta-regression analyses showed that studies that included individuals with older age of onset were significantly more likely to report hyperactivation area in the right ACC.
Conclusion: These findings suggest that BD pts show greater activation mainly in the prefronto-temporal gyrus during executive function tasks which could represent a major neural functional correlate of their illness as defined in DSM-V.

B-0354 14:48

Stroke-related brain plasticity of the human mirror-neuron system during audio-motor transformation: fMRI and DTI study

O. Omelchenko; *Kiev/UA (ol.omelchenko@gmail.com)*

Purpose: Audio-motor transformation (AMT) is a good model for perception to action information flow. Human mirror-neuron system (MNS) consisted of ventral premotor and inferior parietal cortices and was shown to participate in AMT. We propose brain activation, structural and functional connectivity analysis for the focal-stroke-related plasticity changes in AMT.
Methods and Materials: Three groups (G1, G2, G3) of right-handed subjects were studied. G1: 5 healthy subjects (3F, 45-63 y.o.), G2: 3 primary sensorimotor stroke patients (1F, 41-76 y.o.), G3: 2 left supramarginal gyrus stroke patients (1F, 44-58 y.o.). We used 1.5T SIGNA (GE, USA) for DTI and fMRI. Finger tapping was used for activation. EPI was used for BOLD imaging (TR/TE=3000/71ms, voxel 4x4x5mm) and DTI (b=1000, TR/TE=8000/100ms, voxel 0.9x0.9x4mm, encoded directions =25). Data processing was done using FSL (Oxford, GB) and BrainWavePA (GE, USA).
Results: Decrease of FA (G3=0.08, G1=0.4) and fiber density was shown for G3 at ischaemic focus location. Altered AMT-related brain activation was found in G3, in comparison to G1, G2. G1, G2 AMT activation pattern: primary sensorimotor cortex, supplementary motor area, bilateral temporal cortex, suparamarginal, inferior frontal cortices (MNS). G3 showed altered AMT-related activation: lesion nearby left supramarginal gyrus slight activation, bilateral temporal cortices. Thus, one of the mirror-neuron nodes' impairment led to the decrease of MNS AMT functioning, resulting in decreased auditory stimulus response and voice command execution.
Conclusion: fMRI and DTI could reveal stroke-related brain plasticity. Left supramarginal gyrus plays important role in MNS functioning during AMT.

B-0356 14:56

Mapping of brain regions associated with deception by functional magnetic resonance

M. Perez, H. Ferreira, N. Pereira; *Lisbon/PT (mafaldaperez13@gmail.com)*

Purpose: Functional magnetic resonance imaging (fMRI) had been used for lie perception. Our study prompts to reproduce these studies and also to test a novel paradigm, which consists of displaying images of the stolen object amongst images of various other objects.
Methods and Materials: Nine healthy subjects, aged 21 to 36, were studied after given their consent and being screened for their aptitude to understand the paradigms. The subjects were asked to commit a mock crime: stealing only one of two objects, a watch or a ring, and hiding it in a specific locker. Two fMRI experiments were done: a slideshow with ten images of various objects including the watch and the ring; and a mixed-design questions paradigm where subjects were instructed either to confirm or deny (lie about) the theft. The data was collected in a 1.5 Tesla MRI scanner with a button box to record the subjects' responses in the second experiment. The fMRI data analysis was done using FEAT and response times were evaluated.
Results: In the first and second experiments it was possible to correctly identify the stolen object in 67% and 87.5% of subjects, respectively. The parietal area showed overall higher brain activity in both experiments, and response times denounced 87.5% of subjects in the second experiment.
Conclusion: The questions paradigm together with time reaction analyses seems to play an important role to perception of brain activity areas associated with the action of lying.

B-0357 15:04

Functional and structural changes in brain's default mode network in early stages Parkinson's disease patients according to voxel-based morphometry and resting-state fMRI comparison

E. Seliverstova, Y. Seliverstov, M. Krotenkova, R. Konovalov, S. Illarioshkin, I. Krotenkova; *Moscow/RU*

Purpose: To assess pattern of functional and structural changes in neurodegeneration comparing to physical examination and healthy controls by resting-state fMRI (RsfMRI) and voxel-based MRI (VBM) is very prospective nowadays study, especially changes within default mode network (DMN).
Methods and Materials: We have exanimated, compared 3 independent right-handed groups - 41 patients with PD in early steps in pharmacological treatment and newly diagnosed, 20 healthy volunteers were investigated

summary and underwent 1.5 T RsfMRI, T1-MPR MRI scanning for fMRI, VBM data acquisition.
Results: We had some results (p<0,005): in group of newly diagnosed PD patients we observed significant greater volume of right precuneus (part of DMN) comparing to patients in pharmacological treatment and healthy volunteers, in group of patients in treatment we marked volume loss in right precuneus comparing to newly diagnosed PD patients and healthy volunteers. Comparing fMRI data and volume changes in precuneus in group of newly diagnosed PD patients we observed direct correlation (than higher volume of precuneus that greater areas of spontaneous neuronal activity in precuneus), in group of patients in treatment we observed inversed correlation (than smaller precuneus volume that significant greater areas of spontaneous neuronal activity in precuneus).
Conclusion: Our findings may indicate about compensatory hypertrophia of precuneus as compensatory mechanisms of neuroplasticity phenomena in early stages of PD, at that time volume loss of precuneus in PD patients in treatment may reflect increasing atrophy in neurodegenerative process. Correlation between fMRI and VBM-analysis data may be demonstration of multivariants of compensatory mechanisms in neurodegeneration.

B-0358 15:12

Mirror imaging

A. Sharma[1], J. Lay[1], I.Q. Grunwald[2], A.L. Kühn[3], P. Harman[1], S. Bowman[1], S. Kelavkar[1], R. Aspinall[2], C. Law[4]; [1]*Southend-on-Sea/UK*, [2]*Chelmsford/UK*, [3]*Worcester, MA/US*, [4]*Palo Alto, CA/US*

Purpose: Mirror therapy is an effective rehabilitation therapy after stroke. A mirror is placed between the patient's arms or legs so that the image of the non-affected limb gives the illusion of normal movement in the affected limb. Despite the overwhelming evidence of adult brain's capacity to reorganize after stroke, it remains unclear whether and to what extent specific peri-lesional or full brain adaptation is responsible for motor-function recovery.
Methods and Materials: In a randomised study, starting with either conventional or Mirrorbox Therapy, we used a repetitive task specific approach (forearm, wrist and hand) 3x15 minutes/day) for 3 weeks at which time patients switched therapy group. Resting-state-fMRI was performed at baseline, crossover (3 weeks) and 6 weeks.
Results: Resting-state fMRI showed changes in inter-hemispheric synchronization of neuronal signalling and reorganization of the motor execution network after stroke rehabilitation. This was more pronounced after Mirror therapy compared to conventional rehabilitation. There was specific activation of the temporal gyrus, precuneus and the posterior cingulate cortex (PCC).
Conclusion: It appears that alterations in functional brain networks are interrelated to the structural plasticity of the underlying neuronal architecture. Activation of the temporal gyrus, precuneus and the PCC might be related to improved self-awareness and spatial attention.

Thursday, March 2

10:30 - 12:00 **Room B**

Abdominal Viscera

SS 601a

Focal liver lesions: characterisation and therapeutic response

Moderators:
A. Filippone; Chieti/IT
P. Rodríguez; Madrid/ES

B-0366 10:30

The role of quantitative analysis on T2WI and DWI in differentiating haemangiomas from malignant liver tumours

K. Ozturk, E. Soylu Ozturk, C. Bilgin, G. Savci; *Bursa/TR*
(keremov54@hotmail.com)

Purpose: To determine if haemangiomas and malignant liver tumours could be differentiated on the basis of T2-weighted imaging (T2WI) and diffusion-weighted imaging (DWI) by using quantitative measures.
Methods and Materials: 384 patients with liver tumours (250 haemangioma, 134 malignant tumours) underwent 3-T MRI examination with breath hold turbo spin echo T2WI (TR = 3,000 ms; TE = 80 ms) and respiratory-triggered DWI (b = 0, 500, 1000). The both T2WI and DWI images were evaluated with independent and blinded technique. The measurement of lesion to liver signal intensity ratios (SI) for T2WI and b1000/ b0 true diffusion signal intensity ratios for DWIs were assessed quantitatively. Histopathologic evaluation, contrast-enhanced MR images and long period follow-up images were used as the gold-standard.
Results: The mean SI ratio of the haemangiomas and malignant tumours on T2WI found to be 2.9 ± 0.5 and 1.5 ± 0.3 (P < .001) and on DWI 0.22 ± 0.10 and 0.36 ± 0.09 (P < .001) respectively. A cut-off value of 3.1 on T2WI images gave a performance (100% sensitivity, 92% specificity) which is better than DWI with cut-off value of 0.25 (92% sensitivity, 95% specificity). Combination of two sequences didn't provide additive diagnostic performance (90% sensitivity, 88% specificity) (P < 0.05).
Conclusion: Our results indicate that quantitative analysis of both sequences offers high diagnostic performance separately in distinguishing haemangiomas from malignant liver tumours (T2WI is better than DWI) which may have impact on adaption of non-contrast MR techniques.
Author Disclosures:
K. Ozturk: Author; Kerem Ozturk. Founder; Kerem Ozturk. Owner; Kerem Ozturk. Patent Holder; Kerem Ozturk. Speaker; Kerem Ozturk. **E. Soylu Ozturk:** Board Member; Esra Soylu Ozturk. CEO; Esra Soylu Ozturk. Employee; Esra Soylu Ozturk. Investigator; Esra Soylu Ozturk. Shareholder; Esra Soylu Ozturk. **C. Bilgin:** Consultant; Cem Bilgin. Employee; Cem Bilgin. Shareholder; Cem Bilgin. **G. Savci:** Advisory Board; Gursel Savci. Author; Gursel Savci. Equipment Support Recipient; Gursel Savci. Grant Recipient; Gursel Savci. Research/Grant Support; Gursel Savci.

B-0359 10:38

Usefulness of a multi-arterial phase protocol for MRI characterisation of hypervascular liver lesions using Gadoxetic Acid

L. Grazioli[1], R. Ambrosini[1], R. Faletti[2], B. Frittoli[1], G. Battisti[3]; [1]*Brescia/IT*, [2]*Turin/IT*, [3]*Spoleto/IT (lgrazioli@yahoo.com)*

Purpose: To assess the usefulness of a multi-arterial phase MRI technique (Controlled Aliasing In Parallel Imaging Results in Higher Acceleration - CAIPIRINHA) for assessment of enhancement characteristics of hypervascular liver lesions using Gadoxetic Acid, in comparison to a single arterial phase protocol.
Methods and Materials: 148 consecutive patients have been examined: 70 with a single phase protocol and 78 using the CAIPIRINHA multi-arterial technique. MRI exams were carried out using a 1.5T scanner with a phased array coil and automated contrast injection of Gadoxetic Acid (Primovist - Bayer, 0.025 mmol/kg @1ml/sec). We analysed SI from Aorta, Portal vein, Liver parenchyma and Lesions on both protocols and classified lesions identified on triple arterial phase CAIPIRINHA protocol as follows: A=maximum lesion-to-liver contrast ratios (LLCR) at 1st phase, B=maximum LLCR at 2nd phase and C=maximum LLCR at 3rd phase of the examination.
Results: The single-phase protocol detected 33 hypervascular lesions, the CAIPIRINHA protocol showed 50 hypervascular lesions. The comparison between the two protocols showed that Aortic enhancement resulted significantly higher with the single-phase technique if compared to the 1st arterial phase of the CAIPIRINHA protocol (p<0.0001). All the other measured values resulted in between the observed ones in the first two arterial phases of the CAIPIRINHA protocol, and significantly lower to the values measured in the latest arterial phase (p=0.0003).
Conclusion: The possibility to obtain and assess three arterial phases allows to detect more hypervascular lesions and to better assess lesions enhancement respect to a single phase protocol.

B-0360 10:46

A breakthrough in non-contrast MR characterisation of hepatic focal lesions

W.R.A. Abdel Hamid, R. Salah Eldein, Y. Abbas; *Cairo/EG*
(w.gforever@yahoo.com)

Purpose: Our work aimed at evaluating the role of intravoxel incoherent motion (IVIM) as a non-contrast imaging biomarker in the characterisation of hepatic focal lesions (HFLs) as an attempt to reduce health care cost and introduce an alternative for patients with contraindications for IV contrast.
Methods and Materials: This retrospective study includes 130 patients with a total of 200 HFLs. They were assessed using a 3T MR scanner adding IVIM to the established MR protocol. Post-processing analysis was performed to measure IVIM parameters of D, D*, fp & ADC. fp was compared to percent of arterial enhancement of hepatic focal lesions using Pearson correlation test. MedCalc Software was used to assess sensitivity, specificity, PPV and NPV.
Results: Moderate correlation between fp & % of arterial enhancement of hepatic focal lesions (r= 0.686). fp showed high sensitivity (86.27%), low specificity (60.71%), PPV (80%) and NPV (70.83%) to % of enhancement. D showed high sensitivity (83.02%), low specificity (65.38%), PPV (83.02%) and NPV (65.38%). ADC showed lower sensitivity (72.9%) and PPV (77.78%), yet comparable specificity (65.52%), and NPV (63.38%) when compared to D.
Conclusion: fp and D values are promising non-contrast MR tools in the characterisation of hepatic focal lesions that can readily replace IV contrast.

B-0361 10:54

Role of 3-Tesla diffusion-weighted magneic resonance imaging in differentiation between benign and malignant hepatic lesions

M.T.A.A. Ali, D.M. Nabil, M.F. Osman, M.D. Homos; *Cairo/EG*
(mtalatali@hotmail.com)

Purpose: To evaluate the ability of DWIs to distinguish between benign and malignant focal hepatic lesions (FHLs) using 3T MR.
Methods and Materials: A total of 73 FHLs in 48 patients were evaluated. There were 28 benign lesions including 13 hemangiomas (17.8%), 8 hepatic cysts (10.9%), 4 regenerating hepatic nodules (5.4%), 2 adenomas (2.7%) and 1 focal fatty infiltration (1.3 %). The others 45 lesions were malignant including 28 hepatocellular carcinoma (38.3%), 15 metastases (20.5%) and 2 cholangiocarcinoma (2.7%). The study used two b values (0 and 800 sec/mm2) and the ADC values were calculated.
Results: The mean ADC value for simple liver cysts was 2.58 ± 0.35 x 10^{-3} mm^2/sec, for solid benign lesions was 1.63 ± 0.41 x 10^{-3} mm^2/sec and for malignant lesions was 1.21 ± 0.38 x 10^{-3} mm^2/sec with statistical difference (p<0.0001). We found that the best cut off was 1.49 x 10^{-3} mm^2/sec ADC value with accuracy of 83.6% in differentiation between the all benign and malignant FHLs. While with exclusion of the cystic hepatic lesions, the best cut off was reduced to be 1.35 x 10^{-3} mm^2/sec ADC value, with accuracy of 78.5%.
Conclusion: DWI can be used to differentiate between the benign and malignant FHLs.

B-0362 11:02

Visibility of hepatic focal lesion: comparison between kupffer phase images of sonazoid-enhanced ultrasound and hepatobiliary phase images of gadoxetic acid-enhanced MRI

W. Yang, H. Park, Y. Kim, M. Yu, S. Jung, H. Jeon; *Seoul/KR*
(20130094@kuh.ac.kr)

Purpose: To assess the agreement between Kupffer phase images of Sonazoid-enhanced ultrasound and hepatobiliary phase images of gadoxetic acid-enhanced MRI in the visibility assessment of hepatic focal lesions.
Methods and Materials: One hundred and fifty eight hepatic focal lesions in 158 patients who underwent both Sonazoid-enhanced ultrasound and gadoxetic acid-enhanced liver MRI were included in this retrospective study. Visibility of hepatic focal lesions on Kupffer phase images of Sonazoid-enhanced ultrasound was graded as 0 (invisible; isoechoic), 1 (vaguely visible; vaguely hypoechoic), and 2 (clearly visible; clear hypoechoic), while that on hepatobiliary phase images of gadoxetic acid-enhanced MRI was graded as 0 (invisible; high/iso SI), 1 (vaguely visible; weak low SI), and 2 (clearly visible; strong low SI). Pairwise comparison of lesion visibility between the two modalities was performed and inter-modality agreement was assessed.
Results: On Kupffer phase imaging, 38 (24.1%) lesions were invisible, 14 (8.9%) were vaguely visible, and 106 (67.1%) were clearly visible. On hepatobiliary phase of MR, 5 (3.2%) lesions showed high SI, 4 (2.5%) lesions showed iso SI, 45 (28.5%) lesions showed weak low SI, and 104 (65.8%) showed strong low SI. Regarding the visibility, 77.8% (123/158) of the lesions showed agreement between the two modalities. Among the 35lesions showing the discrepancy, 32 (91.4%) visible lesions on MR images were invisible on US

images, while only three(8.6%) visible lesions on US images were invisible on MR images. Overall inter-modality agreement regarding the lesion visibility was fair (weighted *k*=0.213).
Conclusion: Visibility of hepatic focal lesion showed discrepancy in approximately22% between the Kupffer phase images of Sonazoid-enhanced ultrasound and hepatobiliary phase images of gadoxetic acid-enhanced MRI.

B-0363 11:10

Radiological-pathological correlation of hepatocellular adenoma and focal nodular hyperplasia with atypical clinical or radiological features on Gd-BOPTA enhanced MRI

B. Gest, R.L. Miclea, M.G.J. Thomeer, F.E.J.A. Willemssen, R.S. Dwarkasing; *Rotterdam/NL (b.gest@erasmusmc.nl)*

Purpose: The typical radiological features of HCA and FNH on MRI allow for confident diagnosis. However, little data is available when these tumours have an atypical presentation. The aim of this retrospective study was to investigate HCA and FNH with atypical findings on gadobenate dimeglumine (Gd-BOPTA) enhanced MRI (GB-MRI).
Methods and Materials: Between 2008 and 2016, 451 patients underwent GB-MRI of the liver. Patients with histopathological (PA) proven lesions (n=110) were included. Indication for PA was reviewed in the patient dossier. Exclusion criteria were patients with unequivocal HCA or FNH, preexistent liver disease, history of malignancy. Lesions with atypical findings were reviewed by 2 radiologists blinded to the PA result. Interobserver agreement was measured using kappa statistics.
Results: 31 patients (all women, mean age 42.3±10 yrs) with 33 lesions were included. Indications for biopsy were: possible malignancy (n=14, 42.4%), unable to differentiate between HCA and FNH (n=11, 33.3%), interval lesion growth (n=3, 9.1%), HCA >5 cm, (n=3, 9.1%) and miscellaneous (n=2, 6.0%). Interobserver agreement between the 2 readers was good (kappa=0.77, 95% CI=0.58-0.96).
Pathological diagnosis revealed inflammatory HCA (n=15, 45.4%), FNH (n=7, 21.2%), HCA not otherwise specified (n=4, 12.1%), steatotic HCA (n=3, 9.1%), chronic autoimmune hepatitis (n=1, 3.0%), β-catenin mutated HCA with foci of HCC (n=1, 3.0%), HCC (n=1, 3.0%), and cholangiocarcinoma (n=1, 3.0%). All malignant lesions (n=3, 9.1%) were initially characterized as “possible malignancy” on GB-MRI.
Conclusion: Inflammatory HCA represents the majority (45%) of HCA and FNH cases with an atypical presentation. Almost one in ten cases is malignant.

B-0364 11:18

Intra-patient comparative MRI study of MultiHance and Primovist to differentiate HCA from FNH

I.J.S.M. Vanhooymissen, M.G. Thomeer, B. Gest, S. van Koeverden, L.M.M. Braun, R.S. Dwarkasing, R.A. De Man, J. IJzermans; *Rotterdam/NL (ingevanhooymissen@hotmail.com)*

Purpose: At present, imaging guidelines do not recommend which hepatobiliary contrast agents should be used preferably to differentiate hepatocellular adenoma (HCA) from focal nodular hyperplasia (FNH). We analysed the intra-patient differences of the hepatobiliary phase using gadobenate dimeglumine (Gd-BOPTA, MultiHance) and gadoxetate disodium (Gd-EOB-DTPA, Primovist)-enhanced magnetic resonance imaging (MRI) to characterise a benign liver lesion in non-cirrhotic patients.
Methods and Materials: We reviewed the hepatobiliary phase of 43 patients with 112 lesions (69 HCA; 43 FNH). All patients underwent Gd-BOPTA and Gd-EOB-DTPA-enhanced MRI. Signal intensities, inter-observer correlation and degree of certainty for scoring lesions in the hepatobiliary phase were assessed by two observers. Sensitivity and specificity to diagnose HCA and FNH were calculated for both contrast agents.
Results: Almost perfect agreement was found between the two observers for scoring signal intensities with both contrast agents. In 25 out of 112 lesions (22%) there was a difference in signal intensity in the hepatobiliary phase between both contrast agents. For distinguishing HCA from FNH with Gd-BOPTA sensitivity was 55% (38/69) and specificity was 93% (40/43). With Gd-EOB-DTPA sensitivity was 83% (57/69) and specificity was 98% (42/43). We found no significant difference between the two contrast agents in the degree of certainty for scoring a lesion by the observers.
Conclusion: These results indicate that there is a difference in the usefulness of both contrast agents to differentiate HCA from FNH in the hepatobiliary phase. According to our findings, Gd-BOPTA-enhanced MRI would misclassify a significant proportion of HCAs as FNH.

B-0365 11:26

Role of CT perfusion in differentiating haemangiomas from liver metastasis in patient with known primary tumour: initial experience

J. Singh[1], S. Sharma[2], K. Kaur[3], S. Singh[2], N. Aggarwal[2], S. Sood[2]; [1]*New Delhi/IN*, [2]*Shimla/IN*, [3]*Chandigarh/IN (drjagjeetsingh86@gmail.com)*

Purpose: The purpose of the study was to determine whether CT perfusion shows any difference in perfusion parameters in haemangiomas and metastatic hepatic lesions in patients with known primary malignancy.
Methods and Materials: This study was approved by the institutional review board. All the patients provided informed consent. CT perfusion was performed on 64 MDCT in 72 patients with 54 cases of metastasis, 18 cases of haemangiomas. Data was analysed to calculate BF, BV, PS, MTT, HAF and IRFTO. CT perfusion parameters at the periphery of lesions and background liver parenchyma were compared.
Results: Significant changes were observed in the perfusion parameters at the periphery of haemangiomas and metastatic lesions. Of all the perfusion parameters BF, HAF and IRFTO showed most significant changes. BF cut-off value of more than 400ml/100g/min at the periphery of the lesions showed sensitivity of 88.9%, specificity of 83.3%, PPV of 57.1% and NPV of 96.7% in differentiating haemangiomas from hepatic metastasis. HAF cut-off value of more than 60% showed sensitivity of 77.8%, specificity of 86.1%, PPV of 58.3% and NPV of 93.9% in differentiating haemangiomas from hepatic malignancy. IRFTO cut-off value of more than 3 seconds showed sensitivity of 77.8%, specificity of 86.1%, PPV of 58.3% and NPV of 93.9% in differentiating haemangiomas from hepatic malignancy .
Conclusion: Perfusion CT is a helpful tool in differentiating haemangiomas from hepatic metastasis by determining changes in perfusion parameters at the periphery of the lesions.

B-0367 11:34

Detection and viability of colorectal liver metastases after neoadjuvant chemotherapy: a multiparametric PET/CT-MR study

V. Dunet[1], N. Halkic[1], A. Anaye[2], J.O. Prior[1], C. Sempoux[1], A. Denys[1], S. Schmidt[1]; [1]*Lausanne/CH*, [2]*Vevey/CH (sabine.schmidt@chuv.ch)*

Purpose: To compare the value of combined gadoxetic-acid-enhanced (Gd-EOB-DTPA) and diffusion-weighted (DW) MRI, with intravenously (IV) contrast-enhanced 18-F-FDG-PET/CT for the detection and viability assessment of colorectal liver metastases (CLMs) after neoadjuvant chemotherapy (NAC).
Methods and Materials: Following NAC forty-five patients with CLMs were prospectively enrolled and underwent combined Gd-EOB-DTPA-enhanced and DW-MRI and contrast-enhanced 18-F-FDG-PET/CT. Forty patients subsequently underwent surgery including peroperative ultrasound (US), which served as reference standard. The number of metastases detected by each technique was compared. In 69 resected metastases, SUVmean, SUVmax, maximum target-to-background ratio (TBR), TBRmean, total lesion glycolysis (TLG), metabolic tumour volume (MTV), ADCmean and ADCmin were correlated to corresponding tumour viability (TV) assessed on histological specimens.
Results: Peroperative US revealed 153 CLMs of whom 122 were resected. Detection rate of MRI and contrast-enhanced 18-F-FDG-PET/CT were similar (p>0.31) while detection rate of 18-F-FDG-PET was lower (p=0.0005). SUVmax and ADCmin were negatively correlated (r=-0.34, p=0.005) on preoperative imaging after NAC. However, TV was significantly correlated with TBRmax (r=0.33, p=0.006) and TBRmean (r=0.37, p=0.002), unlike with ADCmin (r=-0.02, p=0.9) or ADCmean (r=0.01, p=0.9).
Conclusion: While both combined Gd-EOB-DTPA-enhanced and DW-MRI and contrast-enhanced 18-F-FDG-PET/CT allow confident detection of CLMs, only 18-F-FDG-PET metrics are able to predict TV after NAC.
Author Disclosures:
S. Schmidt: Research/Grant Support; Bayher Healthcare, Switzerland.

B-0368 11:42

Prediction and response assessment after chemotherapy of colorectal liver metastases: can ADC values evaluated at 3T MRI represent a reliable biomarker?

F. Pacciardi, F. Donati, P. Boraschi, R. Cervelli, M. Castagna, L. Urbani, R. Gigoni, D. Caramella; *Pisa/IT (federica.pacciardi@libero.it)*

Purpose: To determine the usefulness of ADC values at 3T MRI as a biomarker for prediction and response assessment after neoadjuvant chemotherapy (nCT) in colorectal liver metastases.
Methods and Materials: Eighteen patients with colorectal liver metastases underwent MR imaging at 3T device (GE DISCOVERY MR750; GE Healthcare) before and after nCT. Diffusion-weighted-MRI (DW-MRI) was performed using a spin-echo echo-planar sequence with multiple b-values (150,500,1000,1500 sec/mm²), obtaining an ADC map. Fitted ADC values were calculated by two observers in conference for each liver lesion (more than 1cm of diameter) in both examinations drawing two ROIs: the former

around the entire tumour (eADC) and the latter in the peripheral area of the lesion (pADC). Pre- and post-nCT e- and pADC values and the difference between the eADC values (ΔeADC) and the pADC values (ΔpADC) before and after nCT were histopathologically related to tumour regression grading (TRG) of surgically resected liver metastases. Statistical analysis was performed on a per-lesion basis.
Results: In our 18 patients e- and pADC values were calculated in 43 and 35 colorectal liver metastases before and after nCT, respectively. The e- and pADC values obtained in the post-nCT and the ΔeADC and ΔpADC were statistically related to TRG classification ($p<0.0052$, $p<0.0001$, $p<0.222$ and $p<0.0203$, respectively). On the contrary, the e- and pADC values obtained in the pre-nCT MRI were not related to the pathologic staging.
Conclusion: ADC values at 3T MRI can be helpful as a biomarker for response assessment after nCT in colorectal liver metastases.

B-0369 11:50

Posttherapeutic changes of the liver parenchyma on hepatobiliary MR imagigng after radioembolisation
R. Seidel, M. Mehrmann, P. Fries, G. Schneider, A. Buecker, A. Massmann; *Homburg/DE (melina.mehrmann@uks.eu)*

Purpose: To investigate changes in the uptake of liver specific contrast media after radioembolization (RE) in correlation to liver function.
Methods and Materials: In 31 patients with various tumours undergoing RE the signal intensity of the liver in correlation to the spleen (liver- spleen ratio, LSR) was determined in the hepatobiliary phase 60 to 90 minutes after administration of Gd-BOPTA. Imaging was performed on a 1.5 T scanner before and 3 to 4 months after RE. Image analysis was processed on a separate workstation based on a fat suppressed T1 w GRE Sequence (TR/TE 108/4.76ms, flip angle 70°, matrix 256x256) by two readers in consensus. 5 regions of interest (ROI) were placed in the treated liver volume and 3 ROI in the splenic parenchyma avoiding vessels and tumour. LSR and laboratory findings (i.e. gamma glutamyl transpeptidase (GGT), international normalized ratio (INR) and Bilirubin) were statistically analyzed.
Results: LSR before RE with a mean of 1.39 (SD 0.33; CI1.27 to 1.50) and LSR post RE with a mean of 1.18 (SD 0.27; CI 1.08 to 1.28) differed significantly ($p=0.0003$). Difference mean was -0.21 (CI -0.11 to -0.31). A significant increase of GGT was observed with a mean 279.3 U/l (SD 264.4, CI 180.6 to 378.1) before and 349.3 U/l (SD 324.2; CI 223.6 to 475.0) after RE ($p=0.0074$). No correlation for laboratory values and LSR was found.
Conclusion: Liver specific imaging reflects parenchymal changes after RE. This might be useful to determine tissue at risk for further interventional procedures.
Author Disclosures:
G. Schneider: Consultant; Bracco, Italy. **A. Buecker:** Consultant; Aachen Resonance, Germany. Equipment Support Recipient; Siemens, Healthcare, Germany.

10:30 - 12:00 **Room C**

GI Tract

SS 601b
New insights into inflammatory bowel disease

Moderators:
S. Kinner; Essen/DE
Z. Tarján; Budapest/HU

B-0370 10:30

Increasing efficiency of MRE for detecting Crohn's disease activity through proper sequence selection
J. Rimola[1], A. Cofiño[2], I. Alfaro[1], S. Rodríguez[1], I. Ordás[1], J. Panes[1]; [1]*Barcelona/ES*, [2]*Gijón/ES (jrimola@clinic.cat)*

Purpose: The aim of this study is to compare different Magnetic Resonance Enterogrphy (MRE) sequence strategies for grading activity in patients with Crohn's disease (CD).
Methods and Materials: MRE and ileocolonoscopies performed within 1 month were compared. Intestinal segments were assessed using, T2, Diffusion Weighted Imaging (DWI) or combination of both, and categorically classified as inactive, active or severe. The findings were matched with those obtained using contrast-enhanced gadolinium sequences using MaRIA score. Simplified Endoscopy Score for CD (SES-CD) was considered the gold standard.
Results: 224 segments were included. Sensitivities of T2, DWI or combination of both for detecting activity were 0.81, 0.83, 0.76; and specificities were 0.97, 0.69, 0.96 respectively. For severity, sensitivities were 0.93, 0.7, 0.93; and specificities 0.88, 0.90, 0.83, respectively. For detecting active inflammation, T2 sequence had a similar sensitivity but superior specificity and accuracy to DWI. T2 had higher sensitivity than DWI for identifying severe disease. Compared with T2 sequence, the MaRIA had higher specificity and accuracy for identifying severe inflammation.
Conclusion: Our results support the use of a T2 sequence as a first screening step, and proceed with a full MRE examination only when abnormal findings are identified in the initial T2 sequence.

B-0371 10:38

Magnetic resonance enterography in the evaluation of anti-TNF alpha therapy response
I. Martini, C. Briani, F. Landolfi, G.M. Barelli, E. Iannicelli; *Rome/IT (isabella.martini88@gmail.com)*

Purpose: Identify possible correlations between magnetic resonance enterography (MRE) parameters and endoscopic data, in patients with Crohn's disease, with the aim to evaluate anti-TNF alpha therapy response.
Methods and Materials: 40 patients with Crohn's disease underwent MRE and ileo-colonoscopy before and after 1 year of anti-TNF alpha therapy. Different MRE parameters were analysed: pathological segment extension, bowel wall thickening, pattern and degree of contrast enhancement, presence of hyperaemia of mesenteric vessels (comb sign). CDEIS was used to evaluate endoscopic activity.
Results: After 1 year of treatment, 50% of patients had ileo-colonoscopy suggestive for active disease and an MRE stable and unchanged. Meanwhile, 50% of patients had ileo-colonoscopy suggestive of non-active disease. In the last group of patients we found statistically significant correlations between pathological segment extension ($p=0.001$), bowel wall thickening ($p=0.001$), comb sign ($p=0.011$) and endoscopic data. In particular, 80% of patients had regression of disease extension and bowel wall thickening and 60% of patients had also disappearance of comb sign.
Conclusion: In patients with non-active Crohn's disease, bowel wall thickening, comb sign and pathological tract extension are the MRE findings that statistically significantly correlate with endoscopic data. Finally, evaluation of these parameters before and after 1 year of anti-TNF alpha treatment can be useful to assess therapy response.

B-0372 10:46

Detectability of inflammatory bowel disease in Diffusion-weighted MR imaging (DWI): which imaging plane and b-values should be preferred?
C. van Rijswijck[1], T. Lauenstein[2], S. Kinner[1]; [1]*Essen/DE*, [2]*Düsseldorf/DE (Christine.Lipponer@uk-essen.de)*

Purpose: MR imaging (MRI) plays an important role in the diagnostic work up of patients with inflammatory bowel disease (IBD). Diffusion-weighted imaging (DWI) has gained more importance in body MRI including IBD, but has been performed differently in different institutions. The aim of this study was to evaluate which imaging planes and b-values are most helpful for DWI to differentiate inflammatory lesions.
Methods and Materials: 50 consecutive patients with known/suspected IBD and a standard MR of the bowel including DWI in axial and coronal planes with b-values of 50, 500 and 1000 were included. Standard bowel MR sequences served as reference for inflammatory lesions. 2 radiologists reviewed axial and coronal DWI images and scored on a 3-point Likert scale the detectability of lesions (1: not detectable, 2: weakly detectable, 3: clear detectable). Best b-value for detectability was evaluated in consensus. A Wilcoxon rank sum test was used for statistical analysis.
Results: According to the standard MRI sequences suspected bowel lesions in DWI were detected in 46/50 patients. In coronal DWI radiologists were able to detect 32/29 lesions clearly and 14/17 lesions weakly. In axial DWI readers rated 32/33 lesions respectively as clearly detectable, and rated 14/13 as weakly detectable. There was no significant interobserver difference (Kappa-value=0.79). A b-value 1000sec/mm^2 was noted to be best in lesion-detection.
Conclusion: DWI offers a high detectability of abnormal bowel parts in patients with IBD. Axial DWI was rated higher than coronal DWI. High b-values turned out to present the pathology most clearly in both orientations.

B-0373 10:54

Bowel distention degree does influence DWI ADC values throughout the whole bowel length: results from two consecutive studies in healthy subjects
I. Apine, S. Atteka, J. Pokrotnieks, M. Leja, G. Krumina; *Riga/LV (dr.ilze.apine@gmail.com)*

Purpose: To compare ADC values in different bowel distention degrees in MR Enterography (MRE) examinations to assess reliability of DWI ADC in diagnosis of inflammatory bowel disease (IBD) in subjects with various bowel distention degrees.
Methods and Materials: ADC values of bowel walls with high SI in DWI images at b=600 grading bowel filling level as “distended”, “partially distended” and “collapsed” were measured in two consecutive studies (for small and large bowels separately) including 406 small bowel segments from 42 patients and

269 large bowel segments from 26 patients with no evidence of IBD were included. Bowel distention was maintained with 1-1.5 l of 2.5% mannitol solution orally and MRE were performed by 1.5T MR systems using DWI of b=0, 100 and 600. ADC differences between bowel filling grades were assessed with t-test and Wilcoxon signed-rank test.
Results: There were statistically significant differences ($p<0.05$) among ADC values of different bowel distention degrees being 1.84×10^{-3} mm^2/s and 2.73×10^{-3} mm^2/s for collapsed and distended state of jejunum, 2.46×10^{-3} mm^2/s and 2.89×10^{-3} mm^2/s for collapsed and distended state of ileum. In large bowel the mean ADC values were 1.45×10^{-3} mm^2/s, 1.79×10^{-3} mm^2/s and 2.49×10^{-3} mm^2/s for collapsed, partially distended and distended bowel walls, respectively.
Conclusion: Bowel distention degree has influence on ADC and ADC values of collapsed and inflamed bowel walls can overlap which has to be considered in diagnosis of IBD.

B-0374 11:02

Semi-automatic assessment of the small bowel and colon in Crohn's disease patients using MRI (the VIGOR++ project)
C.A.J. Puylaert[1], P.J. Schüffler[2], R.E. Naziroglu[3], J.A.W. Tielbeek[1], Z. Li[3], L.J. van Vliet[3], J. Stoker[1], S.A. Taylor[4], F.M. Vos[3]; [1]*Amsterdam/NL*, [2]*New York, NY/US*, [3]*Delft/NL*, [4]*London/UK (c.a.puylaert@amc.uva.nl)*

Purpose: MRI scores show promise for evaluation of Crohn's disease (CD) activity, although reported reproducibility is variable. Potentially, reproducibility could be improved using software assisted semi-automated measurements. The aim of this study was to develop and validate a predictive MRI activity score for ileocolonic CD activity based on software assisted semi-automatic measurement of MRI features.
Methods and Materials: 104 patients (59 female, median age 32) patients with known CD were prospectively recruited from two centres to undergo consecutive MRI and ileocolonoscopy. An MRI-based disease activity score (the "VIGOR" score) was developed based on both subjective radiologist observations and semi-automatic measurements of bowel wall thickness, excess volume and contrast enhancement (initial slope of increase; ISI) using a retrospective cohort of 27 patients with known CD and endoscopic reference standard (CDEIS). A second score was developed based only on the subjective radiologist observations. For validation, both scores were applied to the prospective dataset, along with two existing MRI activity scores (MaRIA and the London score) by two observer groups. Interobserver agreement was evaluated using the intraclass correlation coefficient (ICC).
Results: The VIGOR score (20.5*ISI+0.2*excess volume+2*mural T2) and the subjective model had comparable correlation to CDEIS as the MaRIA and London score (Ob1/2, r=0.55/0.60, 0.40/0.53, 0.38/0.47 and 0.37/0.49, respectively). The VIGOR score however had a significantly higher ICC compared to the other activity scores (0.82 vs 0.45-0.58, $p<0.001$).
Conclusion: The new VIGOR score achieves comparable accuracy to conventional MRI activity scores, but with significantly improved reproducibility.
Author Disclosures:
J. Stoker: Consultant; Consultant for Robarts. **S.A. Taylor:** Consultant; Consultant for Robarts. **F.M. Vos:** Grant Recipient; The VIGOR++ project was funded through a research grant from the European Union's Seventh Framework Programme (project number 270379)..

B-0375 11:10

Comparative study with magnetic resonance of bowel and perianal disease between adult and paediatric patients affected by Crohn's disease
D. Bencardino, F. Maccioni, V. Buonocore, F. Mazzamurro, C. Catalano; *Rome/IT*

Purpose: Perianal disease is considered a disabling complication and a negative prognostic factor in patients with Crohn's disease (CD), particularly in children. Comparative studies are necessary to mark any distinguishing features between paediatric and adult population.
Methods and Materials: 350 consecutive 1.5 Tesla MRI examinations performed on adult (>20 yo) and paediatric (<20 yo) patients affected by CD were retrospectively reviewed. Main inclusion criteria: CD confirmed with endoscopy and biopsy; no previous intestinal resections or surgical treatments for perianal fistulas. MR-enterography and high-resolution pelvic MRI were considered as gold standard. Nine intestinal localisations were considered, from jejunum to rectum. Disease activity grading was obtained considering the following activity parameters: wall thickening, overall length of CD lesions, wall Gd-enhancement, T2w wall signal and local active lymph nodes, according to published papers. Perianal fistulas were staged using Parks and St James's Hospital classification.
Results: 219 patients were selected (54% adult). The prevalence of perianal disease in paediatric and adult population was 35.6% and 17.8% (OR 2.5, $p=0.0031$ with Fisher exact test). Children have a higher risk of rectum involvement ($p=0.0042$), as well as of perianal disease in the presence of rectal involvement, than adults ($p=0.0007$). Paediatric patients with severe colorectal CD have a significantly increased risk of perianal disease ($p=0.0274$). No significant differences emerged regarding fistulas staging.
Conclusion: Paediatric patients with CD have a higher incidence of colorectal involvement and higher risk of perianal fistulas than adult patients. Evaluation of the perianal region should be always performed during MRI-enterography, particularly in children.

B-0376 11:18

Time is money: ultrashort protocol of MRI fistulogram for perianal fistulae
A. Balani[1], S. Shaikh[2], A. Kumar[1], S. Alwala[1], S. Marda[1], C. Chatur[2]; [1]*Secunderabad/IN*, [2]*Hyderabad/IN (drankitbalani@gmail.com)*

Purpose: To formulate state of art ultra-short protocol for imaging perianal fistulae and to evaluate its accuracy by correlating imaging findings with intraoperative findings.
Methods and Materials: 45 patients with suspicion of perianal fistula were included. Ultra-short protocol was done utilizing phased-array coil on GE 1.5T machine which included only two sequences, i.e. 3D-T2 fat suppressed FSE (4 min 55 sec) and T2 axial (4 min 24 sec). Observations were tabulated under headings of age, gender, patterns of abnormalities [types of fistulas,branching tracts,inflammatory collections] and surgical findings. Accuracy was assessed by correlating with surgical findings.
Results: The most common age group was 31-50 years with 82.2% males. Intersphincteric fistula was the most common type (25 cases, 55.5%), followed by transsphincteric type (17 cases, 37.7%). 1 patient(2.2%) had extrasphincteric fistula and 2 (4.4%) had no perianal fistula. In 23 (51.1%) patients, MRI showed additional findings like branching tracts (22.2%) or inflammatory collection (8.8%) or both (20%). Of the 45 patients, MRI correctly identified the fistulous tract in 44. In one patient, only one amongst the two fistulas was identified. Of 21 patients having secondary tracts intraoperatively, MRI correctly identified them in 19. All inflammatory collections were correctly identified. Thus the sensitivity was 93%, specificity was 100% and the accuracy was 93.3%. This is comparable to the previously reported sensitivity of 91% by Buchanan etal, 97% by Beckingham et al.
Conclusion: Ultra-short MRI protocol (9 min 19 sec) is highly accurate in mapping perianal fistulae with results comparable to studies done utilizing detailed protocols. The protocol significantly reduces scan time, improving patient co-operation and patient throughput and obviates the need of contrast administration.

B-0377 11:26

Virtual monoenergetic dual-energy CT enterography: optimisation of KeV settings and the added value for small bowel diseases
S. Lee, S. Kim, S. An, H.-J. Kang, J. Kang, J. Han; *Seoul/KR (twin393@hanmail.net)*

Purpose: To find the optimal keV setting for obtaining maximum contrast-to-noise (CNR) on dual-energy CT enterography (DE-CTE) and to investigate the added value of virtual monoenergetic image for the diagnosis of small bowel (SB) diseases.
Methods and Materials: Forty-five consecutive patients who underwent DE-CTE were prospectively enrolled. Images were reconstructed with iterative reconstruction algorithm (iDose[4]) and virtual monoenergetic settings at 40 keV, 55 keV, and 70 keV. For quantitative analysis, CNR for normal and abnormal bowel wall were measured and compared. Thereafter, two successive review sessions for the diagnosis of SB diseases were independently performed by three radiologists with different expertise using a 5-point confidence scale. At the first session, reviewers interpreted DE-CTE images reconstructed with iDose[4]. At the second session, monoenergetic images were additionally provided to the reviewers. To assess improvement in radiologists' performance, the multi-reader multi-case receiver operating characteristic method was used.
Results: CNR for both normal (16.1, 7.6, 3.0, 2.5; $P<0.001$) and abnormal (9.1, 6.5, 5.0, 3.5; $P=0.005$) bowel wall was significantly greatest on 40 keV images, followed by 55 keV, 70 keV, and iDose. When 40 keV images were added on iDose[4] images, mean area-under-the-curve (AUC) of three radiologists was significantly improved from 0.926 to 0.954 for the diagnosis of Crohn's disease ($P=0.028$). For SB tumours, AUC was improved from 0.708 to 0.954, but statistical significance was not achieved ($P=0.423$).
Conclusion: Lowest (40 keV) monoenergetic images provide best CNR on DE-CTE. Regardless of radiologists' expertise, diagnostic performance for the diagnosis of Crohn's disease can be significantly improved with the addition of 40 keV monoenergetic images.
Author Disclosures:
S. Lee: Founder; the Basic Science Research Program through the National Research Foundation of Korea [NRF] funded by the Ministry of Science, ICT & Future Planning (2016R1A2B4007762. **S. Kim:** Research/Grant Support; the Basic Science Research Program through the National Research Foundation of Korea [NRF] funded by the Ministry of Science, ICT & Future Planning (2016R1A2B4007762).

B-0378 11:34

The value of CT enterography in predicting the need of surgery in Crohn's disease: what advises can radiologists give to gastroenterologists in advance?

M. Jiang, X. Li, Z. Li; *Guangzhou/CN (1063345769@qq.com)*

Purpose: When to perform a surgery and how to choose the right lesions needed for surgery are critical for CD patients, in order to reduce surgical complications and avoid "short bowel syndrome". Thus, the purpose of this study was to assess the efficacy of CTE in predicting the need of surgery for CD patients.
Methods and Materials: 156 consecutive CD patients were evaluated and stratified as surgery group (n=83) and non-surgery group (n=73) according to clinical outcome in observation time. Compared between the two groups, the CTE findings with statistical significance were listed as risk factors. According to the number of CTE risk factors, the patients were divided as low-risk group, median-risk group and high-risk group. Survival analysis was used to predict the need for surgery.
Results: The CTE findings with significant differences between surgery and non-surgery group included number of lesion, fibrofatty proliferation of the mesentery, mesenteric lymph nodes, bowel thickness, enhanced density, proximal bowel dilation, perienteric stranding , ulceration, comb sign, abscess and fistulas (all P<0.05). All these risk factors were analysed using a cumulative risk-score shown as surgery-free survival curve. An enterography-based cumulative risk-score (low-risk, 1-4 CTE risk factors; median-risk, 5-8 CTE risk factors; high-risk,>8 CTE risk factors) derived from multivariate analysis was able to differentiate at different risk for surgery (P=0.001).
Conclusion: CTE helps pick out high-risk CD patients to closely monitor and can accurately predict the need for surgery for CD patients.

B-0379 11:42

Correlation study of quantitative parameters derived from a dual-layer spectral CT with endoscopic and clinical indicators for evaluation of Crohn's disease

Y. Tang, Y. Jiang, F. Yan, Q. Han; *Shanghai/CN (yanjiangcs@hotmail.com)*

Purpose: To investigate the correlation of quantitative parameters derived from a dual-layer spectral CT with endoscopic and clinical indicators for evaluation of Crohn's disease.
Methods and Materials: 24 patients with diagnosed Crohn's disease underwent dynamic abdomen CT using a dual-layer spectral CT (IQon spectral CT, Philips Healthcare) and gastrointestinal endoscopy with an interval not more than 2 days. Bowel wall thickness, CT attenuation and iodine concentration (IC) in the areas with the greatest thickening of different phases were recorded. Difference of CT attenuation and IC between arterial and venous phases was calculated. Clinical disease activity index (CADI) and Crohn's disease endoscopic index of severity (CEDIS) were evaluated for analysis. The correlation between spectral CT parameters with CADI and CEDIS was analysed by Pearson coefficients.
Results: Only bowel wall thickness presented significant correlation with CADI (r=0.492, p=0.017), no other CT quantitative parameters presented correlation with CADI. No CT quantitative parameters presented significant correlation with CEDIS. A significant correlation presented between CADI and CEDIS (r=0.567, p=0.005).
Conclusion: Bowel wall thickness is an important indicator for evaluation of Crohn's disease, which exhibits significant correlation with CADI.

B-0380 11:50

CT enterography: farewell to colonoscopy? - diagnostic accuracy of qualitative predictors of inflammatory bowel disease and its activity (prospective study from a tertiary centre)

S.T. Laroia, A. Rastogi, K. Yadav, M. Haroon, A.S. Bhadoria, G. Kumar, S.K. Sarin; *New Delhi/IN (thaparshalini@gmail.com)*

Purpose: To study the CT Enterography (CTE) findings in inflammatory bowel disease (IBD) for accuracy of qualitative imaging features of primary disease and its activity in comparison to histopathology of the affected segment
Methods and Materials: A prospective study on patients who underwent CTE followed by enteroscopy/colonoscopy and histopathology within one week was conducted during 2010-16 at a tertiary hospital. Parameters such as mural thickening, stratification, pericolonic congestion, lymph nodes and extra-intestinal manifestations were assessed for diagnostic accuracy and qualitative predictors of IBD and its activity
Results: Out of 203 patients, 106 (67 males, age 41.9±14.6, range 12-73 years) were found to have IBD (Ulcerative colitis 47%, Crohn's disease 42.5%, indeterminate disease 10.4% patients) on histopathology. Most common site of involvement was sigmoid colon (65.1%) followed by rectum (60.4%). Increased mucosal enhancement (53%Vs27%) and mural thickening (71.1%Vs30%) were found to be predictors of IBD with odds of 3.13 (95%CI, 1.03-4.91) and 3.16 (95%CI, 1.07-5.72), respectively. Pericolonic vascular congestion (58.5%Vs19.7%) showed borderline significance with OR of 2.74 (CI 0.91-5.23). Other indices were not significant. Toxic megacolon was seen in 5%Vs0.9%7.5%Vs3.1% patients underwent surgery for emergency and elective management. CTE revealed a sensitivity and positive predictive value (PPV) of 83.3% and 86.2% respectively in diagnosis of IBD. Sensitivity and PPV for determination of disease activity was 83.7% and 88.5% respectively
Conclusion: Our study revealed that CTE and its qualitative indices are accurate in diagnosis of IBD and its activity and have the potential to replace invasive scopic studies and histopathology

10:30 - 12:00 **Room Z**

Interventional Radiology

SS 609

Urogenital interventions

Moderators:
J.M. Pulido; Las Palmas/ES
A. Rebonato; Perugia/IT

B-0381 10:30

Percutaneous varicocele embolisation: a retrospective cohort study of recurrence, pain and fertility on follow-up in a single centre 7-year study

H. Shiwani[1], S. Shaikh[2]; [1]*Leeds/UK*, [2]*Bradford/UK (hshiwani@gmail.com)*

Purpose: A varicocele is a collection of dilated and tortuous veins due to dilation of the spermatic vein caused by impaired drainage of blood. Varicoceles impair spermatogenesis, are painful and appear unsightly. Radiologic embolisation of the spermatic vein is an alternative to surgical varicocele ligation which is linked to hydrocele formation and testicular atrophy. In this study, we aimed to determine the outcomes in patients following percutaneous varicocele embolisation.
Methods and Materials: A retrospective single-group cohort study included patients who underwent percutaneous varicocele embolisation in a 7-year period between 1st January 2009 to 1st January 2016 in a single centre at the Bradford Royal Infirmary, Bradford, UK. All patients were followed up and questioned on pain (on a scale of 1 to 10), unsightly appearance (Not at all, A little, Moderately, Extremely) and the outcome of successful pregnancy.
Results: A total of 26 patients underwent percutaneous varicocele embolisation. Follow-up information was obtained for 21 of the 26 patients. There was 1 recurrence (This patient underwent re-embolisation 6 years later) and no reported side-effects. Median length of follow-up was 2.1 years (IQR= 3.1 years). There was a median decrease of 4 in the pain score (out of 10) after the procedure compared to before the procedure. All recorded an improvement in appearance. For those that attempted pregnancy after the procedure, 8 (50%) had a successful pregnancy and 8 (50%) did not.
Conclusion: Varicocele embolisation is an effective treatment for improving pain and the unsightly appearance of a varicocele with minimal complications.

B-0382 10:38

Salvage cryoablation after curative treatment in locally recurrent prostate cancers

M. Barat, L. Colleter, P. Mongiat Arthus, F. Desgrandchamps, E. de Kerviler; *Paris/FR (maxime.barat89@gmail.com)*

Purpose: 20 to 30% of patients have a local recurrence after a curative treatment in prostate cancer. We report our series of salvage cryoablation in locally recurrent prostate cancers.
Methods and Materials: 28 patients underwent cryoablation for intra-prostatic (n=21) or extra-prostatic (n=7) locally recurrent prostate cancers.
Results: Mean follow-up was 428 days. Among the 21 intra-prostatic recurrent patients, Procedure was successful in 13 patients with a PSA blood level drop of -3.72ng/L. Two patients had an insufficient treatment. Six patients had a biological recurrence (average time: 15 months) among them 3 had bones metastasis that required hormone deprivation therapy. Among the 7 patients with extra-prostatic recurrence, (4 seminal vesicle, 3 lymph nodes), 4 procedures were successful with a PSA blood level drop of 1.33ng/ml, and the remaining 3 had an early biological recurrence (3 seminal vesicles) that required hormonotherapy.
Conclusion: Salvage cryoablation of locally recurrent prostate cancer after a curative treatment is a safe and efficient technique allowing delay initiation of hormone deprivation therapy.

B-0383 10:46

Leiomyoma-based selection of patients for uterine artery embolisation: which leiomyomas are best suited for embolisation?

N.N.N. Naguib, N.-E.A. Nour-Eldin, T. Gruber-Rouh, M. Al-Subhi, T.J. Vogl; *Frankfurt a. Main/DE (nagynnn@yahoo.com)*

Purpose: To study which leiomyomas are best suited for uterine artery embolization (UAE) based on pre-embolization MRI for proper selection of patients.
Methods and Materials: The study was retrospectively performed on 38 females (mean: 45.5+/-4.43) with 108 leiomyomas. The following leiomyoma characteristics were studied: leiomyoma enhancement (ratio leiomyoma: piriform muscle enhancement), leiomyoma location (pedunculated submucous, submucous, interstitial, subserous and pedunculated subserous), leiomyoma position (fundal, anterior, posterior and cervical) and size (maximal diameter <3 cm, 3 to <6 cm, 6 to <9 cm, 9 to <12 cm and 12 cm or more). Individual parameters were tested for significance against leiomyoma volume change at 3-month follow-up.
Results: No significant difference between patients was found regarding the size, enhancement or location of leiomyomas. The mean initial leiomyoma volume was 66.38 ml+/-131.61 (range: 1.23-987.34). The maximal diameter was 4.27 cm+/-2.42 (range: 1.4-14.4). At follow-up, the mean volume was 43.69 ml+/-110.45 (range: 0.03-875.05). The mean percentage volume change at follow-up was 55.58% [reduction]+/-26.1 (range: 40.05% [increase]-99% [reduction]). No significant correlation was seen between the leiomyoma position and volume change at follow-up (p=0.79). Degree of enhancement, location and size showed statistically significant correlation with percentage volume change at follow-up (p=0.043, p<0.001 and p<0.001, respectively).
Conclusion: Leiomyoma location, maximal diameter and degree of enhancement correlate significantly with the volume changes of leiomyoma at follow-up and can be used for proper patient selection.

B-0384 10:54

To evaluate the effectiveness and the safety of magnetic resonance-guided focused ultrasound (MRgFUS) in the treatment of submucosal uterine fibroids

S. Iafrate, I. Capretti, M. Di Luzio, F. Arrigoni, S. Mascaretti, G. Mascaretti, C. Masciocchi; *L'Aquila/IT (sonia.iafrate87@gmail.com)*

Purpose: To evaluate the effectiveness and the safety of magnetic resonance-guided focused ultrasound (MRgFUS) in the treatment of submucosal uterine fibroids.
Methods and Materials: From December 2013 to December 2015, we submitted to MRgFUS treatment 17 patients (age range 23-52 years) affected by submucosal uterine leiomyomas, studied with MRI and classified with the FIGO staging system. Twenty-one submucosal fibroids of type 0, 1 and 2 were treated, measuring between 1 and 3.5 cm (7 of type 0, 5 of type 1, 9 of type 2). After treatment, an evaluation of the non-perfused-volume (NPV), representing the treated area, was performed on the c.e. T1-weighed sequences (MRI). Symptoms severity score questionnaire (UFS-QOL) was used to assess the severity of clinical features.
Results: Each patient was treated in one session alone. After MRgFUS treatment, a mean NPV extension of 93% was observed without major complications or side effects. At control studies up to 2-years, 7 out of 17 patients showed progressive reduction of the volume with regularisation of the uterine wall. Ten out of 17 patients showed significant reduction of fibroid volume (about 80%). All the patients experienced a reduction of UFS-QOL symptoms severity score, when compared with the pre-treatment score.
Conclusion: MRgFUS is a valid mininvasive and radical approach in the treatment of submucosal fibroids.

B-0385 11:02

Pre-abortion uterine arterial embolisation in high haemorrhage risk pregnancies

P. Venetucci[1], F. Venetucci[2], S. Pizzetta[1], R. Basile[1], F. Pane[1], A. Brunetti[1]; [1]*Naples/IT*, [2]*Rocchetta Sant'Antonio/IT (pierovenetucci@gmail.com)*

Purpose: Interventional radiology has a well-defined role in the management of many gynaecological conditions (postpartum haemorrhage, fibromas, placentation abnormalities). Through our experience, we wanted to analyse the pre-abortion interventional radiology role in high haemorrhage risk pregnancies such as caesarean scar pregnancy (CSP) and vesicular mola.
Methods and Materials: In the past two years, we performed 12 pre-abortion precautionary embolisation procedures: 10 patients with CSP and 2 with vesicular mola. All the patients came for a planned therapeutic procedure, except one (CSP) who arrived unstable, with an uterus laceration. Embolisation was achieved through a right common femoral artery access with a 5F catheter. Left uterine artery was embolised before the right one using temporary embolisation material.
Results: Significant bleeding reduction has been obtained; less than 500 ml blood loss in 11 patients, and between 500 and 1000 ml in only 1 patients. In CSP group menstrual function has been preserved in 6 patients while one is still in the 6-month follow-up term; hysterectomy has been performed on 3 patients, 1 due to procedure complications. Interventional radiology techniques proved to be, in our experience, an important and successful step in the therapeutic planning of high haemorrhage risk pregnancies that cannot be carried to full term. Between the two patients with vesicular mola, 1 is still in the 6-month follow-up for menstrual function recovery and 1 underwent hysterectomy.
Conclusion: Interventional radiology techniques proved to be an important and successful step in the therapeutic planning of high haemorrhage risk pregnancies that cannot be carried to full term.

B-0386 11:10

Uterine fibroids treated with MRI-guided high-intensity focused ultrasound (MRgFUS): clinical outcomes in comparison to current therapeutic strategies

A. Napoli, R. Scipione, M. Anzidei, F. Andrani, S. Dababou, C. Catalano; *Rome/IT (alessandro.napoli@uniroma1.it)*

Purpose: To prospectively evaluate clinical outcomes in patients affected by uterine fibroids and treated using MRI-guided focused ultrasound (MRgFUS), uterine artery embolisation (UAE) or surgery.
Methods and Materials: 570 women affected by symptomatic uterine fibroids referred our department for MRgFUS treatment. Pre-treatment evaluation assessed fibroids MR characteristics and MRgFUS eligibility. 166 of 182 eligible patients (group A) were treated with MRgFUS, while 388 resulted ineligible. Of these, 33 patients underwent UAE (group B), 140 myomectomy (group C) and 58 hysterectomy (group D). Clinical efficacy for each treatment was determined by symptoms severity score (SSS) reduction from baseline to 3- and 12-month follow-up. Further data concerning number and type of complications, days of hospitalisation and days of convalescence were also compared.
Results: MRgFUS group showed a mean SSS decrease of 24.6% at 3 months and 55.8% at 12 months. SSS drop for UAE was 51.2% and 57.4%, respectively, for myomectomy 71.5% and 66.0%, for hysterectomy 96.6% and 94.5%. MRgFUS group had the least number of adverse events (1.8%), while UAE group experienced the major rate (26.4%). MRgFUS patients were treated in outpatient setting, while mean days for hospitalisation and convalescence for other groups were, respectively, 3.1±2 and 12.4±9 days for group B, 4.5±2 and 17.2±12 for group C, 4±1 and 26.3±14 for group D.
Conclusion: MRgFUS clinical efficacy for uterine fibroids treatment is comparable to UAE and slightly lower than myomectomy. However, MRgFUScan be performed in an outpatient setting and complication rate is significantly inferior to other treatments.

B-0387 11:18

Role of embolisation with N-butyl cyanoacrylate in recurrent post-surgical varicoceles

M.M. Zaitoun, E.R. Elsayed, S.B. Elsayed; *Zagazig/EG (zaitoun2015@gmail.com)*

Purpose: To evaluate the role of n-butyl cyanoacrylate (NBCA) embolisation in recurrent post-surgical varicoceles and to detect the most common cause of recurrence after surgery.
Methods and Materials: During 2 years, 36 consecutive patients with recurrent post-surgical varicoceles were embolised with n-butyl Cyanoacrylate (NBCA) emulsified in lipidol using a 4-F hydrophilic catheter. Mean age was 23 years. Follow-up with Doppler US was performed after 1 month then every 3 months for 1 year.
Results: The technical success was 100%. Neither major complications nor non-targeted embolisation were detected. Only 6 patients had pain following the embolisation and were treated medically for 10 days. In the follow-up by the Doppler US, all the patients showed complete resolution of the varicocele. Duplication of the gonadal veins was the main observation in this study as a cause of recurrent varicocele after surgery.
Conclusion: Embolisation with n-butyl cyanoacrylate (NBCA) is ideal for post-surgical recurrence of varicoceles with 100% technical success and no major complications as well as it is an inexpensive and safe technique. Duplication of the gonadal vein is the most common cause of varicocele recurrence after surgery.

B-0388 11:26

Renal angiomyolipoma: effects of selective arterial embolisation on glomerular filtration rate

A.M.K. Abdel Aal, R. Oser, S. Saddekni, S. Moawad, A. Abouarab, K. Mahmoud, A. Almehmi; *Birmingham, AL/US (akamel@uabmc.edu)*

Purpose: Selective arterial embolisation (SAE) is a surgery-sparing treatment for renal angiomyolipoma (AML). However, limited data are available on the effects of SAE on glomerular filtration rate (GFR). The outcomes of contrast exposure on GFR during SAE procedure remain unknown. The aim of this study is to evaluate the change in serum creatinine and GFR in patients with AML who underwent SAE.
Methods and Materials: Retrospective review of AML cases that were treated with SAE procedure at our center from 2004 to 2015. Data on demographics, tumour side and size, and other laboratory values were collected. Serum creatinine and calculated GFR were assessed immediately prior and 3 months after SAE procedure.
Results: This study included 42 patients. The indications for SAE included back pain, haematuria and retroperitoneal haemorrhage. Baseline characteristics were: median age 42 (32-64) years; 81% females; 66% whites. Hypertension and tuberous sclerosis were present in 33% and 42.9% of patients, respectively. Tumour size was median 5.9 (4.7-8.5) cm. Acute kidney injury (AKI) was encountered in 2 patients (4.7%) following the SAE procedure. However, both cases had a full renal recovery. Although the mean serum creatinine increased from 0.98 to 1.15 mg/dl (p=0.001), no statistically significant difference was noted in GFR (70 vs 60 ml/min;p=0.125).
Conclusion: SAE is a safe, surgery-sparing treatment for renal AML. Despite contrast exposure and partial parenchymal loss, renal function did not change after SAE procedure. AKI is a rare complication after SAE that occurred in only 4.7% of the patients with complete renal recovery.
Author Disclosures:
A.M.K. Abdel Aal: Consultant; St jude medical, Boston Scientific, WL Gore, Baxter Healthcare, Bard Peripheral Vascular Inc.. Grant Recipient; BTG, Covidien, Bard, Boston Scientific, Sirtex. Research/Grant Support; Celonova, Boston Scientific. **S. Saddekni:** Consultant; St Jude medical.

B-0389 11:34

Comparison of radiofrequency and cryoablation for renal masses exceeding 3cm

J. Gregory, C. Delavaud, J. Dbjay, A. Khairoune, O. Helenon, J.-M. Correas; *Paris/FR (jgregory111@gmail.com)*

Purpose: To compare the efficacy and complications of cryoablation and radiofrequency in the treatment of renal masses larger than 3cm.
Methods and Materials: The study was approved by our institution's local Ethics. Patients were included in two groups: group 1 with all patients referred for cryoablation treatment of renal tumours exceeding 3cm from September 2013 to March 2015. Group 2 with all patients referred for radiofrequency treatment of renal tumours exceeding 3cm from December 2010 to August 2013, when radiofrequency was the treatment of choice. Clinical and laboratory data were collected from medical records. All patient underwent constant CT and MRI during a one-year follow-up.
Results: Forty-three patients were included in each group. The mean tumour diameter was significantly higher in the cryoablation group (4.0 ± 0.8 cm) than in the RF ablation group (3.5 ± 0.6 cm) ($p < 0.01$). Tumours treated by cryoablation were of higher complexity according to the RENAL score than those treated by RFA ($p < 0.01$). Local recurrence-free survival rates at 12 months for cryoablation and RFA were 72.1% (95% CI, 60-87) and 76.7% (95% CI, 65-91) respectively ($p = 0.65$). According to the Clavien-Dindo classification, 29 (67%) of the cryoablation and 35 (81%) of the RF ablation procedure lead to no complication at all. ($p = 0.18$).
Conclusion: The efficacy and safety of radiofrequency and cryotherapy for renal tumours larger than 3 cm are not different in our study.

B-0390 11:42

Trans-rectal- ultrasound (TRUS) guided biopsy with MRI-TRUS fusion: feasibility study using a multipurpose magnetic tracking system

G. Bizzarri[1], A. Bianchini[1], D. Valle[1], L. Di Vito[1], L. Velari[1], L. Lodigiani[1], A. Dell'Era[1], V. Anelli[2]; [1]*Albano Laziale/IT*, [2]*Rome/IT (bizzarrigiancarlo@libero.it)*

Purpose: Purpose. TRUS guided biopsy with MRI fusion is a promising technique as it combines the accuracy of prostate multiparametric MRI (mpMRI) with TRUS guided biopsy that is well recognized to be friendly, well-tolerated and inexpensive. We report a feasibility study using a multipurpose Virtual Navigation (VN) system based on magnetic tracking technology for TRUS guided biopsy with MRI-TRUS fusion.
Methods and Materials: Methods and Materials. A MyLabTwice ultrasound scanner equipped with VN software and hardware was used (ESAOTE, Italy). The procedure was performed on 20 patients (mean age 75) with EC123 (3-9 MHz) endfire transrectal probe with single use guiding system and reusable tracking brackets for magnetic sensor (CIVCO Medical Solutions,Kalona,Iowa,USA).For each patient prostate mpMRI performed within one month was loaded on the VN system. After periprostatic local anesthesia, US-MRI coregistration was performed on the sagittal plane and NV modality activated. Fusion accuracy was evaluated using internal markers (seminal vesicles and retention cysts). Targeted and systematic biopsies were performed using a 18G trucut needle.
Results: Results. TRUS and mpMRI fusion was a rapid procedure (mean time 4 minutes). The use of the magnetic tracking system did not required any change in the standard TRUS biopsy technique. The error of TRUS-mpMRI fusion, checked using internal markers, never exceeded 5 mm.. The learning curve required 5 procedures.
Conclusion: Conclusion. Our experience demonstrates that TRUS guided prostate biopsy with mpMRI-TRUS fusion is easy, reliable and accurate despite the use of a multipurpose VN system available in a large number of radiological departments.

B-0391 11:50

Renal sympathicolysis by transaortic periarterial ethanol injection in pigs with the use of an experimental injections catheter: a feasibility study

P. Freyhardt[1], J. Schütze[2], R. Donners[2], J. Schnorr[2], N. Stolzenburg[2], J.-L. Rinnenthal[2], R.W. Günther[2], F. Streitparth[2]; [1]*Krefeld/DE*, [2]*Berlin/DE (patrick.freyhardt@helios-kliniken.de)*

Purpose: Evaluation of feasibility, safety and efficacy of renal sympathetic denervation after transaortic periarterial ethanol injection with an experimental injection catheter in pigs.
Methods and Materials: Percutaneous unilateral periarterial transaortic injection of 10 ml of an ethanol-bupivacaine-accupaque-mixture (7:2:1) was performed in 11 normotensive pigs. Catheter advancement and injections were performed under fluoroscopic guidance in all animals. CT scans of the kidneys and perirenal structures and blood pressure measurements were performed immediately pre- and post-intervention and 4 weeks after treatment. After euthanasia the norepinephrine (NE) concentration of both kidneys was determined. A histopathologic analysis of the renal arteries and the surrounding tissue was performed to assess induced nerve fibre degeneration.
Results: All procedures were technically successful with good periarterial injectant distribution. In two animals, a slight distribution to the contralateral side was observed. One animal died immediately after the intervention due to cardiac arrest. NE concentration of the renal parenchyma was significantly lower on the treated side in eight of ten pigs with a decrease of up to 68% and an average decrease of 37%. Histopathological analysis revealed mild to severe circumferential nerve degeneration correspondingly.
Conclusion: Renal sympathetic denervation by transaortic periarterial ethanol injection was feasible, effective and safe in a pig model. This approach may be an alternative to catheter-based RFA or other methods of renal denervation.

10:30 - 12:00 **Room O**

Chest

SS 604

Pulmonary nodules and screening

Moderators:
M.-P. Revel; Paris/FR
M. Simic; Zagreb/HR

B-0392 10:30

Subsolid and part-solid nodules in lung cancer screening: comparison between visual and computer-aided detection

M. Silva[1], G. Capretti[1], N. Sverzellati[1], C. Jacobs[2], F. Ciompi[2], B. van Ginneken[2], C.M. Schaefer-Prokop[2], A. Marchianò[3], U. Pastorino[3]; [1]*Parma/IT*, [2]*Nijmegen/NL*, [3]*Milan/IT (mario.silva@unipr.it)*

Purpose: To compare visual detection and computer aided diagnosis (CAD) for detection of non-solid nodules (NSN) and part-solid nodules (PSN), in a lung cancer screening trial.
Methods and Materials: Baseline low-dose computed tomography (LDCT) of 2303 subjects were assessed by 2 independent operators: a) visual detection (VD); b) CAD software (CIRRUS Lung Screening). CAD was run also on first and second incidence round. Rate of agreement was calculated by weighted k test. Sensitivity and negative predictive value (NPV) were calculated according to cumulative number of subjects with detected nodules (VD and CAD). LDCT features were compared between CAD-only and VD-only detected nodules.
Results: Nodules were detected in 215/2303 subjects (dominant nodule: 171/215 NSN and 44/215 PSN), notably 149 were CAD-only detected (113 NSN and 36 PSN), 27 were VD-only detected (25 NSN and 2 PSN), and 39 were CAD and VD detected (33 NSN and 6 PSN). The agreement was fair

(weighted k=0.276). Sensitivity and NPV for CAD 87.4% and 98.7%, and for VD 30.7% and 93.3%. Automatic and manual caliper were similar for the assessment of maximum diameter (p=0.111). CAD-only and VD-only detected nodules showed similar nodule diameter (p=0.727) and proportion of PSN (p=0.073). Volume of CAD-only detected nodules was significantly smaller (p=0.019). Among the 27 VD-only detected nodules, 11 NSN were subsequently detected by CAD at the incidence rounds.
Conclusion: Detection of NSN and PSN showed only fair agreement between VD and CAD. Combined assessment of LDCT by both VD and CAD is needed to achieve optimal sensitivity.

B-0393 10:38

'Non-nodule' appearance of early lung cancer in CT screening: retrospective evaluation of 281 lung cancers detected

M. Minotti, S. Calloni, C. Rampinelli, M. Bellomi; *Milan/IT*
(marta.minotti@alice.it)

Purpose: Pulmonary nodule is the typical presentation of lung cancer. However, there is a spectrum of focal lesions that cannot be defined as pulmonary nodule, but really represent early manifestation of lung cancer. Therefore, we aimed to evaluate the features of early stage lung cancers which are depicted on low-dose CT as 'non-nodule' lesion.
Methods and Materials: Two experienced radiologists in lung CT screening retrospectively reviewed the radiological features of 281 lung cancers detected during 10 years of screening trial (5203 heavy smokers, >50-year-old). The readers in consensus assessed if lung cancer appearance at time of diagnosis was consistent ('nodule') or not ('non-nodule') with the Fleischner Society definition of 'pulmonary nodule'. 'Non-nodule' lung cancers were further classified as: 1) bulla-like, 2) scar-like, 3) endobronchial, 4) other. In case of disagreement, a third radiologist (>15-year experience) resolved the discrepancies.
Results: Twenty-four lung cancers (24/281, 8.5%) were defined as 'non-nodule' lesions: 7 (2.9%) were bulla-like, 9 (3.7%) scar-like, 4 (1.6%) endobronchial and 4 (1.6%) other. The mean diameter at time of diagnosis was 16.2 mm (range: 7.5-65 mm). Nineteen were adenocarcinomas, two SCC, two NSCLS non-otherwise-specified, and one SCLC. Nineteen were diagnosed in stage I, four in stage III and one in stage IV.
Conclusion: A non-negligible proportion (8.5%) of screening-detected lung cancers has a 'non-nodule' appearance. Bulla-like and scar-like lesions are predominant and should be carefully evaluated. The awareness of these atypical lung cancer presentations can avoid missed diagnosis and should be considered in management of screening-detected focal lesions.

B-0394 10:46

The implications of internal vessel and bronchial changes within pure ground-glass opacity lung adenocarcinoma on CT

Z. Shaohong, Y. Nie, X. Jin, Y. Yang; *Beijing/CN*
(cjr.zhaoshaohong@vip.163.com)

Purpose: To investigate the implications of vessel and bronchial changes within lesion on CT by comparing with histopathologic subtypes of lung adenocarcinoma with pure ground-glass nodule (pGGN).
Methods and Materials: One hundred and ninety patients (201 lesions) of lung adenocarcinomas with pGGN who underwent curative resection were included. All patients were categorized into two groups according to the abnormalities of vessel and bronchus: abnormal group and normal group. Histopathologic subtypes were classified into preinvasive lesions (atypical adenomatous hyperplasia [AAH] and adenocarcinoma in situ [AIS]), minimally invasive adenocarcinoma (MIA) and invasive pulmonary adenocarcinoma (IPA). Pearson Chi square test was used to analyze the relationships between vessel and bronchial abnormalities and histopathologic subtypes. Mann-Whitney rank test and t-test were used to identify the correlation of vessel and bronchial abnormalities with the density and diameter of pGGN.
Results: There were 4 with vessel abnormalities and 1 with bronchial abnormalities in 35 preinvasive lesions, 26 and 18 in 53 MIAs, 80 and 55 in 113 IPAs, respectively. There were statistically significant differences of vessel and bronchial abnormalities among histopathologic subtypes (P=0.000, 0.000). There were significant differences in vessel and bronchial abnormalities with pGGN diameter (P=0.000, 0.000), but not with density (P=0.303, 0.966). There were no significant difference between vessel convergence and vessel dilation or distortion among these three subtypes (P=0.115).
Conclusion: Vessel and bronchial abnormalities within the pGGN may indicate the invasiveness of lung adenocarcinoma and were correlated with the lesion diameter.

B-0395 10:54

Quantitative analysis for determining the optimal computed tomography threshold value to detect invasive foci in subsolid nodules

D. Lee, C. Park, T. Kim; *Seoul/KR (edahyunle@gmail.com)*

Purpose: To establish the optimal CT threshold value for detecting the solid components of subsolid nodules, using invasive foci as reference.
Methods and Materials: Thin-section non-enhanced chest CT scans were retrospectively reviewed for 25 patients (M:F=7:18; age, 55.9±12.7 years) with pathologically confirmed MIA. The solid portion was assumed as the surrogate marker of invasive foci of MIA. It was defined as the area with higher attenuation than the threshold and measured using the maximum diameter on multiplanar reconstruction images with various HU thresholds ranging from −600 to −100 HU in 50-HU intervals. A linear mixed model for considering repeated measures from various thresholds was used to evaluate bias in each threshold, using the pathological size of invasive foci as the reference.
Results: The size of the 25 MIA was 9.2±1.33 mm, with mean attenuation of −539.1±96 HU. The size of the pathologically invasive foci was 3.56±1.33 mm. The maximum size (mm) of the solid portion was 0.31±0.87 on −100 HU, 0.55±1.06 on −150 HU, 0.93±1.31 on −200 HU, 1.39±1.6 on −250 HU, 2.00±1.67 on −300 HU, 2.76±2.22 on −350 HU, 3.58±2.39 on −400 HU, 4.52±2.39 on −450 HU, 5.44±2.47 on −500 HU, 6.67±2.34 on −550 HU, and 7.75±2.56 on −600 HU. At the threshold of −400 HU, the bias was lowest (−0.0176) between the solid portion and invasive foci, showing an insignificant difference (p=0.963).
Conclusion: For quantitative analysis, −400 HU might be the optimal threshold to define the solid portion of subsolid nodules as a surrogate marker of invasive foci.

B-0396 11:02

Small pulmonary nodules on negative mode lung window images

M.U. Nasir, G. Masood, A. Iqbal, I.K. Niazi; *Lahore/PK*
(dromernasir@gmail.com)

Purpose: To compare normal and negative mode axial images of lung windows of multi detector computed tomographic CT data for detection of small intrapulmonary nodules.
Methods and Materials: Prospective analysis of 500 oncology patients who underwent standard dose thoracic multi detector CT was done. Axial thin slice CT images were reviewed on standard workstations. Two consultant radiologists and registrars were involved in data collection and analysis.Parameters observed included mean, minimum and maximum reading time per examination and per radiologist. The nodules detected and confirmed by two consensus of two observers served as the reference standard. Descriptive statistics were calculated with P value of 0.05 indicating a significant difference. The McNemar's test and confidence intervals for differences between methods were used to compare the sensitivities.
Results: Negative mode images of lung windows were superior to the normal images. There was significant difference in detection rate and reporting time of nodules smaller than 10 mm in diameter for both set of observers. Sensitivity of negative mode images ranged from 89 % to 98% while the sensitivity of normal axial images of lung windows was 70 to 84 %.
Conclusion: Negative mode images of lung windows are the superior to normal axial lung widows for the detection of small intrapulmonary nodules.

B-0397 11:10

Comparison of lung nodule detection performance on 3D CAD system among filtered back projection and iterative reconstruction methods at different radiation-dose levels

Y. Ohno[1], K. Aoyagi[2], Q. Chen[3], S. Kaminaga[2], Y. Fujisawa[2], N. Sugihara[2], Y. Kishida[1], S. Seki[1], T. Yoshikawa[1]; [1]*Kobe/JP*, [2]*Otawara/JP*, [3]*Beijing/CN*
(yosirad@kobe-u.ac.jp)

Purpose: To compare the nodule detection capability on a 3D computer-aided detection (CAD) system among filtered-back projection (FBP) and iterative reconstruction (IR) methods at standard-, reduced- and ultra-low-dose CTs (SDCT, RDCT and ULDCT).
Methods and Materials: Forty patients prospectively underwent chest CT examinations with SDCT (250mA), RDCT (50mA) and ULDCT (10mA) protocols, and CT data were reconstructed into 1-mm-thick images with and without commercially available IR method (i.e. AIDR 3D). Therefore, the following CT data set in each patient was reconstructed: SDCT with and without AIDR 3D, RDCT with and without AIDR 3D, and ULDCT with and without AIDR 3D. Then, nodule detections were automatically performed by our proprietary CAD software. To determine the utility of IR method for improving nodule detection capability, sensitivity and false positive rate (/case) of the CAD system were also compared among all protocols by means of McNemar's test or signed rank test.
Results: Although there were no significant difference of false-positive rate among all protocols, sensitivities of RDCT and ULDCT with AIDR 3D (RDCT:

72.3%, ULDCT: 66.3%) were significantly higher than that without AIDR 3D (RDCT: 56.4%, p<0.0001; ULDCT: 35.6%, p<0.0001). Sensitivity of SDCT with and without AIDR 3D (with AIDR 3D: 73.3%, without AIDR 3D: 76.2%) were significantly higher than that of RDCT without AIDR 3D (p<0.0001) and ULDCT with and without AIDR 3D (p<0.0001).
Conclusion: Iterative reconstruction method is useful for improving nodule detection performance on a 3D CAD system at reduced- and ultra-low-dose CTs as compared with filtered-back projection method.
Author Disclosures:
Y. Ohno: Research/Grant Support; Toshiba Medical Systems Corporation, Smoking Research Foundation. **K. Aoyagi:** Employee; Toshiba Medical Systems Corporation. **Q. Chen:** Employee; Toshiba Medical Systems (China) Co., Ltd. **S. Kaminaga:** Employee; Toshiba Medical Systems Corporation. **Y. Fujisawa:** Employee; Toshiba Medical Systems Corporation. **N. Sugihara:** Employee; Toshiba Medical Systems Corporation. **S. Seki:** Research/Grant Support; Toshiba Medical Systems Corporation, Smoking Research Foundation. **T. Yoshikawa:** Research/Grant Support; Toshiba Medical Systems Corporation, Smoking Research Foundation.

B-0398 11:18

Effect of detectability of pulmonary nodules with lowering dose based on nodule size, type and body mass index with different iterative reconstruction algorithms

V. Vardhanabhuti[1], C.-L. Pang[2], S. Tenant[2], J. Taylor[2], C.J. Hyde[3], C.A. Roobottom[2]; [1]*Hong Kong/HK*, [2]*Plymouth/UK*, [3]*Exeter/UK*

Purpose: To determine the diagnostic accuracy of lung nodule detection in thoracic CT using 2 reduced-dose protocols comparing 3 available CT reconstruction algorithms (filtered back projection-FBP, adaptive statistical reconstruction-ASIR and model-based iterative reconstruction-MBIR) in a western population.
Methods and Materials: A prospective single-center IRB-approved study recruited 98 patients with written consent. Standard-dose (STD) thoracic CT followed by 2 reduced-dose protocols using automatic tube current modulation (RD1) and fixed tube current (RD2) were performed and reconstructed with FBP, ASIR and MBIR with subsequent diagnostic accuracy analysis for nodule detection.
Results: 108 solid nodules, 47 subsolid nodules and 89 purely calcified nodules were analysed. RD1 was superior to RD2 for assessment of solid nodules ≤4mm, and subsolid nodules ≤5mm. Deterioration of RD2 is correlated to patient's body mass index and least affected by MBIR. For solid nodules ≤4mm, MBIR area under curve (AUC) for RD1 was 0.935/0.913 and AUC for RD2 was 0.739/0.739, for rater 1/rater2 respectively. For subsolid nodules ≤5mm, MBIR AUC for RD1 was 0.971/0.986 and AUC for RD2 was 0.914/0.914, for rater 1/rater2 respectively. For calcified nodules excellent detection accuracy was maintained regardless of reconstruction algorithms with AUC >0.97 for both readers across all dose and reconstruction algorithms.
Conclusion: Diagnostic performance of lung nodule is affected by nodule size, protocol, reconstruction algorithm and patient's body habitus. The protocol in this study showed that RD1 was superior to RD2 for assessment of solid nodules ≤4mm, and subsolid nodules ≤5mm and deterioration of RD2 is related to patient's body mass index.

B-0399 11:26

Influence of reconstruction methods to measurement accuracy for computer-aided volumetry (CADv) at standard-, reduced-, low-dose and ultra-low-dose CT in QIBA phantom study

T. Sekitani[1], E. Suehiro[1], N. Negi[1], K. Fujii[2], Y. Fujisawa[2], N. Sugihara[2], K. Aoyagi[2], T. Yoshikawa[1], Y. Ohno[1]; [1]*Kobe/JP*, [2]*Otawara/JP (atieinks-toshi@nifty.com)*

Purpose: To directly compare the capability of three reconstruction methods using forward projected model-based iterative reconstruction (FIRST), adaptive iterative dose reduction using 3D processing (AIDR 3D) and filtered back projection (FBP) for radiation dose reduction and accuracy of computer-aided volumetry (CADv) measurements on chest CT examination in the QIBA recommended phantom study.
Methods and Materials: An thoracic phantom with 30 simulated nodules of three density types (100, -630, and -800 HU) and five different diameters was scanned with an area-detector CT at tube currents of 270, 80, 40, 20, and 10 mA. Each scanned data was reconstructed with three methods. CT value and image noise were measured, and compared among three reconstruction methods at each tube current by Tukey's HSD test. For comparison of the capability for CADv at each tube current, Tukey's HSD test was used to compare the percentage of absolute measurement errors for three reconstruction methods.
Results: Image noises of FIRST and AIDR 3D for each nodule type were significantly lower than that of FBP at each tube current (p<0.05). In addition, image noises of FIRST were significantly lower than that of AIDR 3D at all tube currents except 270mA (p<0.05). Mean absolute measurement errors of AIDR 3D and FIRST for each nodule type were significantly lower than those of the FBP method at 20mA and 10mA (p<0.05).
Conclusion: FIRST and AIDR 3D methods are more effective than the FBP method for radiation dose reduction, while yielding better measurement accuracy of CADv for chest CT examination.
Author Disclosures:
K. Fujii: Employee; Toshiba Medical Systems Corporation. **Y. Fujisawa:** Employee; Toshiba Medical Systems Corporation. **N. Sugihara:** Employee; Toshiba Medical Systems Corporation. **K. Aoyagi:** Employee; Toshiba Medical Systems Corporation. **T. Yoshikawa:** Research/Grant Support; Toshiba Medical Systems Corporation. **Y. Ohno:** Research/Grant Support; Toshiba Medical Systems Corporation, Koninklijke Philips NV, Bayer AG , DAIICHI SANKYO Group, Eisai Co. Ltd, Fuji Pharma Co. Ltd, FUJIFILM RI Pharma Co. Ltd, Guerbet SA.

B-0400 11:34

Effect of image reconstruction with ADMIRE in low-dose and ultra-low-dose CT volumetry of solid pulmonary nodules: a phantom study

M. Eberhard, D. Stocker, T. Nguyen-Kim, M. Wurnig, T. Frauenfelder, S. Baumüller; *Zurich/CH (matthias.eberhard@usz.ch)*

Purpose: To investigate the influence of ultra-low-dose CT and iterative reconstruction with ADMIRE on volumetry of solid lung nodules.
Methods and Materials: CT scans were obtained with third-generation dual-source CT at standard dose, 1/8, 1/20 and 1/70 of standard dose using an anthropomorphic chest phantom containing solid microspheres (4-10mm). An extension ring was used for different phantom sizes (M, L). Image reconstruction was performed with FBP, ADMIRE3 and 5. Three oberservers independently measured nodule volumes semi-automatically. Relative percentage error (RPE) was computed to evaluate measurement accuracy. To assess influence of various parameters on RPE univariate ANOVA with post hoc Bonferroni-Test was applied. P<.05 was considered significant.
Results: Intra-class correlation coefficient for RPE between observers was 0.862 (95%CI: 0.838-0.883). Phantom size, nodule diameter, CT dose protocol and reconstruction algorithm significantly contributed to RPE (all p<.001). Underestimation of mean nodule volume among all dose protocols was -5.3±6.0% with ADMIRE3,-7.0±5.6% with ADMIRE5, and-2.7±8.5% with FBP (all p<.001). Overall scanning with 1/70 dose protocol showed higher underestimation of mean volume (-7.3±10.3%) compared with standard dose (-4.1±4.0%), 1/8 (-4.6±4.3%) and 1/20 (-4.1±7.3%) dose (all p<.001). There were no significant differences between other dose values. Overall volume underestimation was highest in 6mm nodules (-10.3±5.4%), compared to 4 (-1.3±10.3%), 8 (-3.2±2.8%) and 10mm (-4.7±1.9%) nodules. Phantom size L (-5.8±7.9%) showed significant lower overall mean RPE compared to size M (-4.2±6.0%; p<.001).
Conclusion: Our study indicates that image reconstruction with ADMIRE3 and 5 and scanning with 1/70 dose leads to little but significant underestimation of solid nodule volume.

B-0401 11:42

Comparison of the effect of model-based iterative reconstruction (MBIR) and filtered back projection (FBP) algorithms on software measurements in pulmonary ground-glass nodules

J.G. Cohen[1], H. Kim[2], S. Park[2], B. Van Ginneken[3], C. Lee[2], J. Goo[2], C. Park[2]; [1]*Grenoble/FR*, [2]*Seoul/KR*, [3]*Nijmegen/NL (jcohen@chu-grenoble.fr)*

Purpose: To evaluate the differences between filtered-back-projection (FBP) and model-based iterative reconstruction (MBIR) algorithms on semi-automatic measurements in subsolid nodules (SSNs).
Methods and Materials: Unenhanced CT-scans of 73 SSNs obtained using the same protocol and reconstructed with both FBP and MBIR algorithms were evaluated by two radiologists. Diameter, mean-attenuation, mass, and volume of whole nodules and its solid components were measured. Intra-, inter-observer variability and differences between FBP and MBIR were then evaluated using Bland-Altman method and Wilcoxon tests.
Results: Longest diameter, volume and mass of nodules and those of its solid component were significantly higher using MBIR (p<0.05) with mean differences of 1.1% (limits of agreement, -6.4 to 8.5%), 3.2% (-20.5 to 27%), 3.2% (-20.9 to 27.3%), 6.3% (-51.9 to 64.6%), 2.9% (-16.9 to 22.7%), and 6,6% (-50.1 to 63.3%), respectively. The limits of agreement between FBP and MBIR were within the range of intra- and inter-observer variability for both algorithms with respect to the diameter, volume and mass of nodules and its solid components. There were no significant differences in intra- or inter-observer variability between FBP and MBIR (p>0.05).
Conclusion: Semi-automatic measurements of SSNs significantly differed between FBP and MBIR, however, the differences were within the range of measurement variability.

B-0402 11:50

Deep learning applied to automated chest x-ray screening

B. Fos Guarinos[1], A. Alberich-Bayarri[2], A. Ten-Esteve[2], I. Bosch-Roig[2], L. Martí-Bonmatí[2]; [1]*Sueca/ES*, [2]*Valencia/ES (befogua@etsii.upv.es)*

Purpose: One of the most performed examinations by radiologists is chest radiography, providing information of important anatomical structures of the body. Reporting chest x-rays is a demanding task and very important medical-legally, sometimes neglected. The aim is setting up a screening tool for giving priority to the abnormal radiographs and facilitate the reporting task. New techniques based on artificial intelligence have emerged (field of computer vision). We propose to use deep learning (convolutional neural networks, CNN) in a computer-aided diagnostic (CAD) system to help radiologists to perform automated screening of chest radiographs.
Methods and Materials: A database of chest x-ray images (7470) from the Indiana University was used for the study. A subset of cases was selected consisting of 2242 A-P, divided into different groups (abnormal, cardiomegaly, nodule, opacity, atelectasis, pleural effusion, each one versus normal). The AlexNet CNN (pretrained with ImageNet) was implemented to extract features from the different groups needed to train binary support vector machine classifiers. An NVIDIA Tesla K40 GPU was used to optimize the computing performance.
Results: A software tool was successfully implemented obtaining an area under curve (AUC) of 0.86 for abnormal, 0.91 for cardiomegaly, 0.92 for pleural effusion, 0.70 for nodule, 0.90 for atelectasis group and 0.86 for opacity.
Conclusion: Using a pretrained CNN as an automatic feature extractor for training an SVM classifier is a good approach to get relevant results in chest x-ray screening tasks.

10:30 - 12:00 **Room N**

Genitourinary

SS 607

Male urogenital system I

Moderators:
A. Lebovici; Cluj-Napoca/RO
E. Sala; New York, NY/US

B-0403 10:30

Sarcopenia assessed using preoperative CT-scans as a predictor of postoperative complications following radical cystectomy

B.J.U. Hensen[1], M. Kramer[2], M. Jansen[1], M. Hennig[2], M. Hupe[2], H. Tezval[1], M. Kuczyk[1], A. Merseburger[2], F. Wacker[1]; [1]*Hannover/DE*, [2]*Lübeck/DE (hensen.bennet@mh-hannover.de)*

Purpose: Urothelial carcinoma is usually treated with radical cystectomy (RC). However, patients face a relevant risk of postoperative complications on variable factors. Recent reports described that sarcopenia, which is defined by a loss of sceletal muscle body composition may enhance risk stratification.
Methods and Materials: Our retrospective study includes 200 patients (154 men, 46 women, mean age: 68 years) which were treated with RC (2005-2014). Median follow-up time was 26 months. Computed tomography (CT) scans were performed within 60 days prior to surgery. Skeletal muscle index (SMI) were measured with MeVisLab 2.7 by manually segmentation of preoperative CTs. The fat mass index (FMI) was calculated based on the same CT slides. Cut off points were developed for men and women separately. Additionally, complications were assessed using the Clavien-Dindo-Classification.
Results: SMI (cm^2/m^2), FMI (kg/m^2) and BMI (kg/m^2) for men were calculated with median scores of 50.6, 9.7 and 26.8, respectively. The corresponding calculated means for women were 38.6, 9.2 and 24.8. The SMI for mid-term complications (<Grade IIIa) were statistically significant (p = 0.017).
Conclusion: The presence of sarcopenia may improve risk stratification in patients undergoing radical cystectomy. BMI and FMI may not be used in risk stratification models. Further research is needed to validate the current findings. Noninvasive and semiautomatic calculation of SMI in preoperative CT scans may improve risk stratification in patients undergoing radical cystectomy and thus could reduce mortality.

B-0404 10:38

Stiffness of benign and malignant prostate tissue measured by shear-wave elastography

O. Rouviere[1], C. Melodelima[2], A. Hoang-Dinh[1], F. Bratan[1], G. Pagnoux[1], T. Sanzalone[1], S. Crouzet[1], M. Colombel[1], F. Mège-Lechevallier[1], R. Souchon[1]; [1]*Lyon/FR*, [2]*Grenoble/FR (olivier.rouviere@netcourrier.com)*

Purpose: To measure benign and malignant prostate tissue stiffness using shear-wave elastography (SWE).
Methods and Materials: Thirty consecutive patients underwent transrectal SWE in axial and sagittal planes before prostatectomy. After reviewing prostatectomy specimens, two radiologists measured stiffness in regions corresponding to cancers, lateral and median benign peripheral zone (PZ) and benign transition zone (TZ).
Results: Cancers were stiffer than benign PZ and TZ. All tissue classes were stiffer on sagittal than on axial imaging, in TZ than in PZ, and in median PZ than in lateral PZ. At multivariate analysis, the nature of tissue (benign or malignant; P<0.00001), the imaging plane (axial or sagittal; P<0.00001) and the location within the prostate (TZ, median PZ or lateral PZ; P=0.0065) significantly and independently influenced tissue stiffness. On axial images, the thresholds maximizing the Youden index in TZ, lateral PZ and median PZ were respectively 61.5 kPa, 32.8 kPa and 48.9 kPa. On sagittal images, the thresholds were 76.4 kPa, 49.5 kPa and 72.4 kPa, respectively.
Conclusion: SWE can distinguish prostate malignant and benign tissues. Tissue stiffness is influenced by the imaging plane and the location within the gland.

B-0405 10:46

Chronic prostatitis: retrospective cohort-study of persistence of signs on T2-weighted MR-images

U.G. Mueller-Lisse[1], M.K. Scherr[2], U.L. Mueller-Lisse[1], A. Meister[1], M.F. Reiser[1], M. Kuhn[1]; [1]*Munich/DE*, [2]*Murnau am Staffelsee/DE (ullrich.mueller-lisse@med.uni-muenchen.de)*

Purpose: Chronic prostatitis may elevate prostate-specific-antigen-levels (PSA) in patients with negative prostate-biopsy (NBX) and show at T2-weighted MR-imaging (T2WI) with diffusely-low (DLSI), focally-non-nodular-low (FLSI), nodular-low (NLSI), or unremarkable signal-intensity (UNSI). Persistence of T2WI-signs of chronic prostatitis was analysed in a retrospective cohort from a prospective data-base.
Methods and Materials: With ethics-committee-approval, 19 patients with prior prostate-MR-examinations 3.7+/-2.7 years ago (average+/-standard-deviation) showing signs of chronic prostatitis, age, 63.7+/-7.4 years, PSA, 9.4+/-2.6 ng/ml, median 2 NBX (range, 1-5), median 12 samples/NBX (2-20), without previous prostate-therapy except for antibiotics, were identified in a prospective database of 210 prostate-MR-examinations. All current and 4/19 prior MR-examinations were at 3.0T with multi-channel-surface-coils; 15/19 prior MR-examinations were at 1.5T with phased-array/endorectal-coil-systems. Presence and temporal/spatial persistence of DLSI, FLSI, NLSI, and UNSI on T2WI were compared in peripheral-zone-(PZ)-regions and central-zone-(CZ)-regions, applying the PI-RADSv2-39-region-prostate-scheme. McNemar's-chi-square-test was significant for p<0.05 in two-by-two-tables (first-second T2WIs, changed-unchanged); Cohen's kappa was substantial >0.60.
Results: DLSI persisted in 194/225 (86%) and newly developed in 41/113 regions (36%, chi-square, 1.125, 0.25<p<0.50, agreement, 79%, kappa 0.51), FLSI in 34/51 (67%), new in 15/287 (5%, 0.0313, p>0.5, 91%, 0.62), NLSI in 0/1, new in 3/337 (1%, 0.25, p>0.5, 98.8%, 0), and UNSI in 34/61 (56%), new in 17/277 (6%, 2.0511, 0.1<p<0.25, 87%, 0.53). Four CZ-regions were non-evaluable.
Conclusion: DLSI appears to be the most frequent, most persistent, and most often newly-developing sign of chronic prostatitis at T2WI. Both FLSI and UNSI appear to decrease insignificantly over time, while NLSI appears to be an infrequent finding.

B-0406 10:54

Interobserver agreement in the volumetric assessment of peri-prostatic fat, a marker of prostate tumour aggressiveness

D. Nörenberg[1], C. Kelly-Morland[2], V. Goh[2], G. Cook[2], D. Cahill[2]; [1]*Munich/DE*, [2]*London/UK (dominik.noerenberg@med.uni-muenchen.de)*

Purpose: Previous studies have shown peri-prostatic fat volume is associated with prostate cancer Gleason score and outcome. This study aimed to assess the inter-reader reliability of measurements of peri-prostatic fat volume.
Methods and Materials: The pelvic MRI scans of 100 men (mean age 60 (41-75)) with prostate cancer who subsequently underwent a robotically assisted radical prostatectomy were reviewed. The following measurements were performed by two independent radiologists with 6 and 3 years of pelvic MRI experience; the peri-prostatic fat volume (PPFV), ischio-anal fossa fat volume (IAFV), anterior prostatic fat depth (APFD), subcutaneous fat depth (SCFD)

and prostate volume (PV).Intra-class correlation coefficients (ICCintra) and Bland-Altman analysis were performed.
Results: ICC results showed substantial agreement for PPFV 0.61 (0.42-0.74) and IAFV 0.72 (0.62-0.8) excellent for SCFD 0.87 (0.79-0.91) and PV 0.94 (0.88-0.96) and moderate for APFD 0.48 (0.32-0.62).
Conclusion: Excellent or substantial agreement was found for all parameters with the exception of the anterior prostatic fat depth indicating assessment of peri-prostatic fat is reproducible.

B-0407 11:02

Effectiveness of intramuscular hyoscine butylbromine compared with intravenous administration in improving image quality in pelvic MRI

M.B. Taylor, A. Kilburn, L. McDaid, C. Shepherd, D. Ryder, S. Bonington, B. Carrington; *Manchester/UK (ben.taylor@christie.nhs.uk)*

Purpose: To determine whether intramuscular (IM) hyoscine butylbromide (HBB) is as effective as intravenous (IV) HBB in reducing movement artefact during pelvic MRI.
Methods and Materials: Institutional ethical approval and patient consent were obtained. 321 patients attending for pelvic MRI on 400 occasions were recruited to this prospective study. At each attendance the patient was randomised to receive 20 mg HBB either IM or IV. T2-weighted image series were anonymised and assessed for image quality (IQ) and lesion visualisation using a 4 point scale by 3 radiologists blinded to the route of injection. The primary aim was demonstration of similar proportions of median IQ scores for the 3 observers of 3 or 4 (slight or no artefact) for both sagittal and transverse series between the IM and IV groups. A one tail non inferiority test with an inferiority margin (IM-IV) of -10% was used.
Results: There were 385 attendances included in the analysis (15 examinations not completed to protocol). Non-inferiority of IM was demonstrated with 169/194 (87.1%) having both IQ scores of 3 or 4 in the IM arm compared to 165/191 (86.4%) in the IV arm (point estimate for the difference (IM - IV) of 0.7% with 95% CI (-6.0%, 7.5%) (p=0.001). Interobserver agreement for image scoring was fair to moderate (k=0.383-0.537).
Conclusion: IM HBB is as effective as IV injection in reducing movement artefact in pelvic MRI. IM HBB may be preferred as an antiperistaltic in pelvic MRI due to patient preference and ease of administration.

B-0408 11:10

Effect of hyoscine butylbromide on prostate multiparametric MRI anatomical and functional image quality

I. Caglic[1], N. L. Hansen[2], A. J. Patterson[1], T. Barrett[1]; [1]*Cambridge/UK*, [2]*Aachen/DE (iztokcaglic@gmail.com)*

Purpose: To evaluate the effect of the spasmolytic agent hyoscine butylbromide (HBB) on the quality of anatomical and functional prostate multiparametric (mp) MRI.
Methods and Materials: 87 patients received 20mg intravenous hyoscine butylbromide (HBB group), 86 patients did not (non-HBB group) in this retrospective study. 3T-MRI was performed using a 32-channel body coil. Quality of T2WI, diffusion-weighted imaging (DWI) and ADC maps, was evaluated using a 5-point Likert scale. DWI was further assessed for distortion and artefact, and T2WI for motion or blurring. Dynamic contrast-enhanced (DCE) sequences were assessed by recording the number of corrupt data-points on the contrast curve.
Results: HBB group T2W image quality was significantly higher than the non-HBB group (3.63±1.11 versus 2.84±0.899); p<0.001. The HBB group showed significantly less T2W motion and blur than the non-HBB group (23.0% and 51.7% versus 53.5% and 83.7%, respectively; p<0.001). However, there was no significant improvement in DWI/ADC image quality, distortion or artefact. There was a trend towards fewer corrupted DCE data points in the HBB group (2.47±2.44 versus 3.68±2.64), but this did not reach significance (p=0.052). Substantial inter-reader agreements were achieved for T2W Image Quality (k=0.670), DWI distortion (0.741) and ADC Image Quality (0.630). Agreements for T2W Motion (k=0.514), DWI image quality (0.441) and DWI artefact (0.427) were moderate, agreement for T2W Blur was fair (0,341).
Conclusion: Administration of HBB significantly improves the image quality of T2-weighted images. These results provide evidence for the use of HBB in routine patient preparation prior to prostate mpMRI.

B-0409 11:18

Screening of prostate cancer by means of fast MR protocol: feasibility study

G. Foti, E. Demozzi, F. Cavicchioli, A. Molinari, S. Cavalleri, G. Carbognin; *Negrar/IT (gfoti81@yahoo.it)*

Purpose: To compare diagnostic accuracy of different magnetic resonance (MR) protocols in diagnosing prostate tumour.
Methods and Materials: Multiparametric MR (mpMR) of 185 consecutive patients (mean age 62.3 years) with elevated serum level of prostate-specific antigen (PSA) studied with 1.5 Tesla scanner were retrospectively reviewed by two experienced radiologists. Four reading sessions separated by 1 month gap were performed, starting by reading only axial T2+DWI (PR-1), and progressively including coronal and sagittal T2 (PR-2), pre-contrast T1 (PR-3) and dynamic contrast-enhanced sequences (PR-4), respectively. Sensitivity (se), specificity (sp) and accuracy (acc) values in diagnosing prostate cancer were assessed using radical prostatectomy as reference standard and compared by using Mc-Nemar test, A value of p<0.05 was considered statistically significant. Inter-observer variability was calculated by using k-statistics.
Results: At pathology, prostate cancer was diagnosed in 115/185 patients (mean size index lesion 12 mm). Best accuracy was achieved by reading PR-4 for reader 1 and 2 (se 85.2% and 83.4%, sp 87.1% and 84.2%, acc 85.9% and 83.7%, respectively). For both readers, accuracy did not drop significantly by reading PR-3 (se 83.4% and 83.4%, sp 85.7% and 83.4%, acc 84.3% and 83.2%, respectively), PR-2 (se 83.4% and 82.6%, sp 82.8% and 81.4%, acc 83.2% and 82.1%, respectively) and PR-1 (se 82.6% and 80.9%, sp 81.4% and 77.1%, acc 82.2% and 79.4%, respectively). Inter-observer variability was excellent (k=0.92).
Conclusion: Fast PR-1 MR protocol did not give significant drop in overall accuracy if compared to mp-MR protocol (p<0.05).

B-0410 11:26

Multiparametric magnetic resonance imaging of the canine prostate gland as an animal model prior to MRgFUS

K. Lorenc, K. Skierbiszewska, T. Jasinski, K. Siewruk, Z. Gajewski; *Warsaw/PL (kamil_lorenc@sggw.pl)*

Purpose: Multiparametric magnetic resonance imaging (mp-MRI) is an evolving technique used in the diagnostic protocol for prostate cancer (PCa) detection, localisation, risk stratification and staging of clinically significant prostate cancers in humans. It has also opened up opportunities for focal treatment of PCa. PCa in dogs and humans share similar features: extracapsular extension, pulmonary and bone metastases, as well as are diagnosed at later age. Wherefore, dogs are used as a pre-clinical, animal model for PCa diagnosis and therapy management. The aim of the study was to create and apply an mp-MRI protocol for PCa imaging in dogs based on the PI-RADS™ v2 human protocol and its implementation on a 3.0T MR scanner before future ablation procedures (MRgFUS).
Methods and Materials: 10 male dogs, age 4-14, with confirmed prostatic gland pathologies with ultrasound examination were enrolled into the study. Anaesthetised dogs were positioned (prone, feet first) on the MRI table. Protocols were validated with MR imaging on clinical scanner discovery MR750w 3.0T, coils GEM anterior array and GEM large flex depending on canine size.
Results: Final protocol consisted of: T1WI axial FSE, T2WI sagittal FRFSE, T2WI axial FRFSE, T2WI coronal FRFSE, DWI focus axial: b-value 0, 50, 200, 800 s/mm^2.
Conclusion: MRI examination including mp-MRI in canine model is challenging due to a small field of view and thin slices, which increases scan time, distortion, and noise level. Canine model is particularly useful for the study of diagnostic and therapeutic methods used in PCa in humans.

B-0411 11:34

Comparison of the Likert score and a quantitative model in characterising prostate focal lesions on pre-biopsy multiparametric MRI

A. Hoang-Dinh[1], R. Souchon[1], C. Melodelima[2], F. Bratan[1], F. Mège-Lechevallier[1], A. Ruffion[3], S. Crouzet[1], M. Colombel[1], O. Rouviere[1]; [1]*Lyon/FR*, [2]*Grenoble/FR*, [3]*Pierre Bénite/FR (olivier.rouviere@netcourrier.com)*

Purpose: To assess in patients referred for pre-biopsy multiparametric MRI (mpMRI) a quantitative model trained at characterising Gleason ≥7 cancers.
Methods and Materials: We trained a model combining the 10th percentile of ADC and the time-to-peak for distinguishing Gleason ≥7 cancers in 106 retrospectively-selected patients treated by prostatectomy who had pre-operative 3T mpMRI (T2-weighted, diffusion-weighted and Dynamic Contrast-enhanced imaging) on a General Electric (n=72) or a Philips (n=34) scanner.Then, we prospectively selected 131 consecutive patients referred for prostate biopsy who had pre-biopsy mpMRI on the same GE (n=108) or Philips (n=23) scanners. The uroradiologist performing the biopsy prospectively assigned a 5-level Likert score of suspicion to each targeted lesion (cognitive guidance). The model was then used to estimate the probability the lesion was a Gleason ≥7 cancer.
Results: Using targeted biopsy as reference, the model outperformed the Likert score at per-patient (AUC=0.94 [95% confidence interval (CI): 0.90-0.98] versus AUC=0.81 [(CI): 0.75-0.88]; p=0.0002), per-lobe (AUC=0.90 [CI: 0.84-0.95] versus AUC=0.84 [CI: 0.78-0.89]; p=0.015) and per-lesion (AUC=0.88 [CI: 0.83-0.93] versus AUC=0.80 [CI: 0.74-0.86]; p=0.01) analysis. The model significantly outperformed the Likert score at the three levels of analysis for PZ lesions and for radiologists with <1 year of experience, and at per-patient analysis for radiologists with >1 year of experience. It was outperformed by the Likert score in the 15 patients with suspicious lesions of the transition zone.

Conclusion: The quantitative model outperformed the Likert score in PZ lesions. This approach may help less experienced readers characterising focal lesions seen on mpMRI.

B-0412 11:42

T2 correlated PSA density

K. Ozturk, Y. Kordan, G. Savci; *Bursa/TR (keremov54@hotmail.com)*

Purpose: To evaluate the value of new tool such as T2-correlated PSA (prostate specific antigen) density (T2-correlated PSAD) in detecting prostate cancer (PCa) on 3-Tesla magnetic resonance (MR) system.
Methods and Materials: Eighty-five patients with a negative DRE and PSA level between 4-20 ng/ml suspected for PCa underwent TRUS-guided cognitive biopsies with the result of multiparametric-MRI including T2-Weighted (T2-WI), diffusion weighted, and spectroscopy imaging. Total volume and mean signal intensity of the prostate gland were determined in axial T2-WI. PSAD was obtained by dividing serum PSA level to the prostate volume. Mean T2 signal intensity of the prostate gland was adjusted with signal intensity of internal obturator muscle. T2-Weighted PSAD was calculated by multiplying PSAD with the mean T2 signal intensity of the prostate gland. Accuracy of PSAD and T2-correlated PSAD were analyzed using the receiver operating characteristic curve while relationship between two method was assessed using the un-paired t-test.
Results: PCa was detected in 12 patients (14%) with TRUS biopsies. The positive predictive value of PSAD with cut-off level of 0.12 ng/mL/cm and T2-correlated PSAD with cut-off level of 0,023 ng/ml/cm for detection of PCa were found to be 28% and 39%, respectively. The performance of T2-correlated PSAD was better than that of PSAD alone (P<0.01).
Conclusion: In patients who have negative DRE and PSA levels between 4-20 ng/ml, the application of T2-correlated PSAD would have prevent 63% of patients from an unnecessary biopsy, without missing any PCa. T2-correlated PSAD is better indicator of detecting PCa compare to PSAD.
Author Disclosures:
K. Ozturk: Author; Kerem Ozturk. Founder; Kerem Ozturk. Investigator; Kerem Ozturk. Owner; Kerem Ozturk. Patent Holder; Kerem Ozturk. Speaker; Kerem Ozturk. **Y. Kordan:** Board Member; Yakup Kordan. Consultant; Yakup Kordan. Equipment Support Recipient; Yakup Kordan. **G. Savci:** Advisory Board; Gursel Savci. Author; Gursel Savci. Consultant; Gursel Savci. Equipment Support Recipient; Gursel Savci. Grant Recipient; Gursel Savci. Research/Grant Support; Gursel Savci.

B-0413 11:50

Efficacy of PSA density for predicting prostate cancer utilising volumes from mpMRI and TRUS

A. Ushinsky, S. Fardin, M. Nguyentat, C. Green, E. Uchio, C. Lall, T.B. Nguyen, R. Houshyar; *Orange, CA/US (tbnguyen@uci.edu)*

Purpose: To compare the efficacy of prostate-specific antigen (PSA) density based on prostate volume from mpMRI versus transrectal ultrasound (TRUS).
Methods and Materials: We retrospectively reviewed 137 patients who underwent prostate mpMRI and subsequent MRI/TRUS fusion biopsy. For each patient, MRI prostate volume was estimated using measurement technique per PI-RADS version 2, and US prostate volumes were obtained during fusion biopsy. Two PSA densities were then calculated by dividing serum PSA concentration by prostate volume using each modality. MRI-based and US-based PSA densities were compared using paired and independent T test. The classification function was evaluated with ROC analysis, and then areas under the curves (AUCs) were compared.
Results: Based on histopathology, 53 patients had clinically significant prostate cancer (Gleason score ≥ 7) and 84 patients had non-clinically significant cancer. PSA density was significantly higher in patients identified with clinically significant cancer versus non-clinically significant cancer when calculated with both MRI (0.22 vs 0.12, p=0.001) and US (0.19 vs 0.12, p=0.001). MRI-based versus US-based PSA density was not statistically different in patients with clinically significant cancer (p= 0.057) nor in those with non-clinically significant cancer (p= 0.439). Also, the AUCs were not statistically different (0.681 vs. 0.671, P= 0.87) between the two methods of PSA density in diagnosing clinically significant cancer.
Conclusion: These results suggest that US and MRI-based PSA density calculations are not significantly different and the two modalities' estimates of prostate volume are consistent. Therefore, PSA density calculations may likely be performed with either US or MRI.

Oncologic Imaging

SS 616
Imaging rectal cancer

Moderators:
R. García Figueiras; Santiago de Compostela/ES
N.N.

K-11 10:30

Keynote lecture

V.J. Goh; *London/UK*

B-0414 10:39

Radiomics of primary staging diffusion-weighted MRI to predict neoadjuvant treatment response in rectal cancer

J.J.M. van Griethuysen[1], S. Trebeschi[1], D.M.J. Lambregts[1], M.J. Lahaye[1], F.C.H. Bakers[2], R.F.A. Vliegen[3], E. Voest[1], R.G.H. Beets-Tan[1], H.J.W.L. Aerts[4]; [1]*Amsterdam/NL*, [2]*Maastricht/NL*, [3]*Heerlen/NL*, [4]*Boston, MA/US (j.v.griethuysen@nki.nl)*

Purpose: Assessing robust radiomics signature of rectal carcinoma most likely to respond to neoadjuvant chemoradiation (nCRT).
Methods and Materials: We assessed primary staging (pre-treatment) diffusion-weighted MRI scans (b-values 0-1000/1100) of 140 patients with locally advanced rectal carcinoma, treated with nCRT. Tumours were semi-automatically segmented on b1000-DWI by a region-growing algorithm and then manually adapted by 4 readers (2 expert; 2 non-expert), adding to a total of 5 segmentations. Radiomics features were extracted from these segmentations. Feature stability was assessed using the intraclass correlation coefficient (ICC) across different readers/segmentations. Predictive performance to distinguish between complete tumour regression and residual tumour was assessed by ROC-curve analysis with False Detection Rate (FDR) 10%.
Results: 112 features were identified, of which 1010 were stable across readers (ICC ≥0.75, mean 0.82, range 0.76-0.88). For the manually-adjusted delineations 129/1129 features per reader showed significant performance after FDR-correction, however, none of these remained significant after FDR-correction for the semi-automated segmentation. A final subset of 60 features remained stable and performant across all readers. These 60 features resulted in a mean AUC of 0.67 (range 0.65-0.69) to predict a complete response and a mean ICC of 0.83 (range 0.73-0.88).
Conclusion: Robust radiomics features exist that can aid in predicting a complete tumour response to nCRT. Features extracted from semi-automated segmentation show inferior performance compared to features extracted from manually adjusted segmentations, emphasising the need for adequate tumour segmentation. Interestingly, delineations by inexperienced and experienced readers showed comparable results, suggesting that highly expert input is not required.

B-0415 10:47

T2-weighted MR image registration of rectal tumours and mesorectum during radiotherapy

A. Bani Yassien[1], G. Ghobadi[2], M. Staring[2], B. van Triest[1], D.M. Lambregts[1], A. Betgen[1], C.A.M. Marijnen[2], U.A. van der Heide[1]; [1]*Amsterdam/NL*, [2]*Leiden/NL (a.baniyassien@nki.nl)*

Purpose: To monitor tumour changes in rectal cancer patients undergoing sequential MRI during radiotherapy, deformable image registration (DIR) is required. However, applying DIR may result in unrealistic tissues expansion or folding, particularly in the case of tumour shrinkage. We developed and evaluated two registration approaches of T2-weighted (T2W) MRI for spatial mapping of tumour and mesorectum.
Methods and Materials: Thirteen patients received weekly repeated T2W-MRI (3T) for five weeks (n=62 scans). Both approaches were implemented in Elastix, using a B-splines transformation and mutual information as a similarity metric. For registration of non-tumour structures in the mesorectum manually selected landmarks and/or rectum contours were utilized to refine the registration when needed. For tumour mapping, the transit point from tumour to normal rectum wall was used for tumour alignment assuming tumour volume preservation.
Results: Registration of non-tumour structures resulted in average dice similarity coefficient (DSC) of 90±6% and mean surface distance (MSD) of 1.53±0.48 mm between mesorectum segmentations. Refinement using landmarks was required for one patient improving MSD and DSC, from 18.0 to 1.27 mm and 62% to 96% respectively. Refinement using rectum contours was required for another patient improving MSD form 3.0 to 2.7 mm. Tumour mapping resulted in satisfactory alignment when evaluated visually. For an

average-sized tumour (~30cc) with 44% volume shrinkage MSD was 1.5 mm between rectum delineations.
Conclusion: We obtained accurate registrations between T2W-MRIs over time within the mesorectum. This can be used for monitoring tumour response and toxicity of normal tissue in radiotherapy of rectal tumours.

B-0416 10:55

Pathological complete responders after chemoradiotherapy in rectal cancer, what can be learned from imaging for the selection?
M. Maas[1], M. van der Sande[1], B. Hupkens[2], M. Martens[3], D. Lambregts[1], S. Breukink[2], F. Bakers[2], G. Beets[1], R.G.H. Beets-Tan[1]; [1]*Amsterdam/NL*, [2]*Maastricht/NL*, [3]*Sittard/NL (moniquemaas@live.nl)*

Purpose: Many complete responders(CRs) after CRT for rectal cancer are missed, leading to overtreatment of CRs.Aim is to assess what can be learned from operated pathological CRs who were missed on post-CRT MRI+DWI+endoscopy.
Methods and Materials: Patients with a pCR after CRT and surgery were retrospectively selected.The MRI+DWI+endoscopy were re-evaluated by expert readers (MRI: radiologist and endoscopy: surgeon) who scored likelihood for CR by following updated (according to current knowledge) selection criteria for a CR.Patients were categorised into groups:(1) residual tumour at reassessment and (2) (near) CR.Several other imaging parameters about the primary tumour, volume and morphology/aspect were assessed.At endoscopy aspect of the scar (normal/ulcer/polyploid) was noted.
Results: 32 patients were included with a pCR after surgery.Main reason for missing CR were heterogeneous T2W-MRI signal, residual focal/massive diffusion-restriction, massive fibrosis ycN+ disease and residual mucosal lesions at endoscopy.In distal rectal tumours CRs are more easily missed.20/32 (63%) were deemed to have residual tumour (non-CR group), the remaining 12 (37%) had (near) CR (CR group).In the non-CR group heterogeneous signal on T2W-MRI was present more often than in the CR group (75% vs 25%,p=0.01), just as massive/spicular fibrosis (90% vs 58%,p=0.07) and residual diffusion restriction (58% vs 27%,p=0.11). Nodes were scored false positive in 7/32 patients, mostly due to irregular morphology.
Conclusion: Reasons for missing a CR after CRT are heterogeneous T2W-MRI signal, massive/spicular fibrosis, residual focal/massive diffusion-restriction, ycN+ disease, residual mucosal lesions at endoscopy and distal tumour. Knowledge about these features can help improve selection of patients for a watch-and-wait strategy.

B-0417 11:03

Nodal staging in complete responders (ypT0) after CRT for rectal cancer, how can we better select the ypN0 patients for organ preservation?
M. Maas[1], M. van der Sande[1], B. Hupkens[2], M. Martens[3], D. Lambregts[1], F. Bakers[2], S. Breukink[2], G. Beets[1], R.G.H. Beets-Tan[1]; [1]*Amsterdam/NL*, [2]*Maastricht/NL*, [3]*Sittard/NL (moniquemaas@live.nl)*

Purpose: To evaluate nodal staging accuracy and identify factors that might improve nodal staging in patients with ypT0 after CRT.
Methods and Materials: 42 patients with ypT0 after surgery were identified. Nodes were re-evaluated by one expert reader, who scored a confidence level for likelihood of residual N+ disease and described the morphology of the nodes after CRT. Diagnostic performance was assessed by ROC curves and area under the curve (AUC). Differences between pN+ and pN0 patients and between incorrectly staged patients and correctly staged patients were assessed.
Results: Nine patients had ypT0N+ disease, the remaining 33 had ypT0N0. AUC for nodal staging was 0.91 (0.81-1.00). Sensitivity was 100%; specificity was 75%, PPV was 53%, NPV was 100%. 8 patients were overstaged, of which 7 had irregular nodal morphology. Of the 9 patients with ypN+ disease 6 had irregular nodes. All patients with normalised nodes (n=10) were ypN0.
Conclusion: Nodal staging in the subset of patients with a complete response (ypT0) after CRT is more accurate than nodal staging in the general post-CRT population. No residual ypN+ disease was missed but overstaging was found in almost 50%, mostly due to the irreliable feature of irregular morphology. Irregular morphology was encountered in almost all patients with ypN0, but also in 67% of patients with ypN+ disease. Normalisation of nodes was associated with ypN0 in 100%.

B-0418 11:11

Evaluation of rectal cancer response to therapy: role of MR-tumour regression grade to predict pathological complete response
S. Picchia[1], M. Rengo[2], D. Bellini[2], D. Caruso[2], T. Biondi[2], A. Laghi[2]; [1]*Latina/IT*, [2]*Rome/IT (lisiva@alice.it)*

Purpose: To evaluate the accuracy of magnetic resonance tumour regression grade (MR-TRG) for the identification of complete responders after chemoradiotherapy in a population of patients with locally advanced rectal cancer.
Methods and Materials: 65 patients, diagnosed with locally advanced rectal cancer were prospectively enrolled in the study. All patients underwent MRI on a 3-Tesla before, during and after chemoradiotherapy (CRT). All patients underwent total mesorectal excision (TME). MR-TRG was evaluated on TSE T2-weighted axial images as the fibrosis/tumour ratio. Results were grouped into favourable (>75% fibrosis) and unfavourable (<74%) classes. Measurements were performed on the entire tumour volume using a dedicated software. MR-TRG was compared to pathologic TRG. Disease-free survival (DFS) and overall survival (OS) were compared between MR-TRG classes. Sensitivity and specificity for the detection of CR were evaluated with ROC analysis.
Results: A complete pathological response was observed only in patients with favourable MR-TRG. A good correlation with pathologic TRG was observed (r2=0.874). Good sensitivity (96%) and specificity (78%) were observed on ROC analysis (AUC =0.947). A significant difference was observed between MR-TRG classes in terms of DSF (p=0.028) and OS (p=0.012).
Conclusion: MR-TRG is an accurate predictor of complete response after CRT and correlates with patients survival. When an unfavourable MR-TRG is observed the persistence of disease should be suspected. This method, applied also during therapy, may reduce the time to surgery.

B-0419 11:19

Rectal cancer: comparison of MR-TRG, volume ratio and signal intensity decrease for the identification of complete responders after radiochemotherapy
S. Picchia[1], M. Rengo[2], D. Caruso[1], D. Bellini[1], M. Zerunian[1], A. Laghi[1]; [1]*Latina/IT*, [2]*Rome/IT (lisiva@alice.it)*

Purpose: To compare three methods to identify complete responders after CRT in a population of patients with locally advanced rectal cancer.
Methods and Materials: 65 patients, diagnosed with locally advanced rectal cancer were prospectively enrolled in the study. All patients underwent MRI on a 3-Tesla before, during and after chemoradiotherapy (CRT). All patients underwent total mesorectal excision (TME). MR-TRG, volume reduction ratio (VR) and signal intensity percentage decrease (SI) were compared. Measurements were performed on the entire tumour volume using a dedicated software. MR-TRG, VR and SI were compared with histology. DFS, OS and ROC analysis were evaluated and compared among the three groups. Patients were stratified according to the histology result in complete responders (CR) and partial or non-responders (PNR).
Results: MR-TRG and VR were significantly different in CR and PNR patients (P=0,0005) while no significant differences were observed for SI (p=0.14). Significantly higher sensitivity and specificity were observed for MR-TRG compared to VR and SI (p=0.001). MR-TRG was also more accurate to predict the OS and DFS (p=0.002).
Conclusion: MR-TRG is more accurate than VR and SI for the identification of CR and correlates with patients' survival.

B-0420 11:27

The value of diffusion kurtosis imaging to assess pathological complete response to neoadjuvant chemoradiation therapy in rectal cancer
F.-X. Hu, T. Tong, W.-J. Peng; *Shanghai/CN (fxhu14@fudan.edu.cn)*

Purpose: The aim of this study was to compare diffusion kurtosis imaging (DKI) with conventional diffusion-weighted imaging (DWI) for assessing the pathological complete response (pCR) to neoadjuvant chemoradiation therapy (CRT) in locally advanced rectal cancer (LARC).
Methods and Materials: Fifty-six consecutive patients diagnosed with LARC were prospectively enrolled and underwent MRI before and after CRT on 3T MRI. The DWI and DKI parameters were compared between patients with pCR and non-pCR, using the nonparametric Mann-Whitney U test. Receiver operating characteristic (ROC) curve analyses were performed to characterize each parameter in terms of its value for predicting the CRT outcome.
Results: The MK_{pre} and MK_{post} values were significantly lower for the pCR patients (mean±SD, 0.72±0.09 and 0.56±0.06, respectively) than for the non-pCR patients (0.89±0.11 and 0.68±0.08, respectively) ($p<0.001$). The ADC_{post} and the ratio of apparent diffusion coefficient (ADC_{ratio}) values were significantly higher for the pCR patients (mean±SD, 1.31±0.13 and 0.64±0.34, respectively) than for the non-pCR patients (1.12±0.16 and 0.33±0.27, respectively) ($p<0.001$ and $p=0.001$, respectively). In addition, the MD_{post} and MD_{ratio} (2.45±0.33 vs 1.95±0.30, $p<0.001$; 0.80±0.43 vs 0.35±0.32, $p<0.001$, respectively) were also increased. The area under the receiver operating characteristic curve (AUROC) for the assessment of pCR were greater using MK_{post} (0.908, cut-off value=0.6196) compared with other parameters.
Conclusion: Both DKI and conventional DWI exhibited potential for predicting treatment response to neoadjuvant chemoradiation therapy in rectal cancer. The DKI parameters, especially MK_{post}, showed higher specificity than did conventional DWI for assessment of pCR and non-pCR in patients with LARC.

B-0421 11:35

DW MRI by 3T in the response assessment of locally advanced rectal cancer after chemioradiotherapy: apparent diffusion coefficient value as an imaging biomarker

R. Cervelli, P. Boraschi, F. Donati, F. Pacciardi, A. Cacciato Insilla, D. Campani, D. Caramella; *Pisa/IT (rosa.cervelli@virgilio.it)*

Purpose: To investigate the usefulness of the apparent diffusion coefficient (ADC) value by 3T-device in response assessment of locally advanced rectal cancer after neoadjuvant chemoradiotherapy (n-CRT).
Methods and Materials: Twenty-one patients affected by locally advanced rectal cancer underwent 3.0T MRI (GE DISCOVERY MR750; GE Healthcare) before and after n-CRT. After the conventional preliminary acquisition of high-resolution T2-weighted sequences, diffusion-weighted MR images (DW-MRI) were acquired using a spin-echo echo-planar sequence with multiple b-values (150, 500, 1000, 1500 sec/mm2) and an ADC map was obtained. Fitted ADC values were calculated for each rectal lesion before and after nCRT, by drawing a hand-made ROI around the tumour outline. All patients underwent surgery and the pathologic staging (classified according to TNM and to tumour regression grading, TRG) represented the reference standard. Pre-treatment ADC value (p-ADC), ADC value obtained after n-CRT (n-ADC) and the difference between p-ADC and n-ADC (ΔADC) were correlated with both the TNM and the TRG staging systems, in each patient.
Results: The ADC value obtained in the post-nCRT examination was statistically related both to TRG and TNM stages by histopathology (p=0.0019; p=0.0497, respectively). On the contrary, the ΔADC and the p-ADC values were not related to the pathologic staging.
Conclusion: DW-MRI, using ADC map and value, can be useful to assess the efficacy of neoadjuvant chemoradiation therapy in locally advanced rectal tumours; in fact post-nCRT ADC value improves the MR capability in the evaluation of nCRT response assessment.

B-0422 11:43

Role of MRI and added value of diffusion-weighted and gadolinium-enhanced MRI for the diagnosis of local recurrence from rectal cancer

V. Molinelli, N. Tarallo, F. Piacentino, E. Macchi, M. Angeretti, E. Bracchi, C. Fugazzola; *Varese/IT (va.la@hotmail.it)*

Purpose: To evaluate whether the addiction of gadolinium-enhanced and diffusion weighted (DWI) MRI improves standard pelvic MRI performance for diagnosis of local recurrence (LR) from rectal cancer; to asses which one is better in formulating this diagnosis and interobserver agreement among readers with different experienc.
Methods and Materials: 43 patients with suspected LR from rectal cancer underwent pelvic MRI with T2 weighted (T2) sequences, gadolinium fat-suppressed T1 weighted (T1mdc) and DWI MR sequences. Three readers (expert:G, intermediate:E, resident:V) scored the likehood of LR on T2, T2+DWI and T2+T1mdc.
Results: 18 Patients had LR; on T2 images the expert reader achieved AUC 0.916, se 88,9%, sp 96%; for intermediate reader were 0.890, 88.8% and 92%, respectively; for resident 0.852, 88.8% and 88%. DWI significantly improved AUCs value for expert radiologist up to 0.999 (p=0,0492), while T1mdc significantly improved AUC for resident up to 0.950 (p=0,0432). For intermediate reader, both T2+DWI AUC and T2+T1mdc AUC were better than T2 AUC (0.976 and 0.980 respectively), but with no statistical difference. No statistically significant difference was achieved from comparison between T2+DWI AUCs and T2+T1mdc AUCs in none of three readers.
Conclusion: Both DWI and gadolinium-enhanced MRI increase diagnostic performances for LR diagnosis compared to T2, in particular, DWI may be helpful in patients with contraindications to i.v. administration of gadolinium.

B-0423 11:51

Diffusion-weighted MRI and ADC value: their role in detection of metastatic lymph nodes in patients with primary rectal cancer

A. Ferrari[1], F. Schirru[1], G.F. Satta[1], A. Restivo[1], F. Scintu[1], L. Zorcolo[1], M. Cerci[1], J. Suri[2], L. Saba[1]; [1]*Cagliari/IT*, [2]*Pocatello, CA/US (ferrant.1986@gmail.com)*

Purpose: The aim of our study is to demonstrate the diagnostic value of DWI and ADC value in detection of metastatic lymph nodes in patients with primary rectal cancer.
Methods and Materials: In this retrospective study, 9 patients with rectal cancer were studied with MRI morphological T2W and DWI sequences. Surgical treatment and lymphadenectomy was performed successively on all patients. Total 68 lymph nodes were included in the study. Lymph nodes were classified as suspected and no-suspected considering dimension (diameter greater than 4 mm), morphology and T2 signal inhomogeneity. ADC values were then compared with the histopathological data.
Results: Of the 68 considered nodes (36 metastatic and non-metastatic 32), we excluded 11 lymph nodes with clear necrotic characteristics that showed extremely high ADC values (mean value of 1,57 ± 0:47 × 10-3 mm2/s). The mean ADC of the metastatic LNs (0.75 ± 0.29 × 10−3 mm2/s) was lower than that of the non-metastatic LNs (1.08 ± 0.26 × 10−3 mm2/s); the area under the ROC curve was 0,715 (95% confidence interval, 0,58-0,83 P < 0,002). Choosing an ADC value of 0,95 × 10−3 mm2/s as the cut-off, we got a sensitivity of 76% and a specificity of 68%.
Conclusion: Although T2W nodes characteristic is still the gold standard in defining the N Stage of a tumour, ADC value could be useful in differentiating between benign and metastatic pelvic lymph nodes in patients with rectal carcinoma, especially in doubtful nodes.

10:30 - 12:00 **Room L 8**

Molecular Imaging

SS 606

Experimental and preclinical molecular imaging

Moderators:
B. Bennani-Baiti; Vienna/AT
F.M.A. Kiessling; Aachen/DE

B-0424 10:30

Non-invasive monitoring of therapeutic response in sorafenib-treated orthotopic hepatocellular carcinoma mouse models using photoacoustic and fluorescence imaging

S. Lee, J. Kim, J. Lee, J. Han; *Seoul/KR (seunghyun.lee.22@gmail.com)*

Purpose: To investigate the changes in oxygen saturation (sO_2) and radiant efficiency (R_E) in sorafenib-treated hepatocellular carcinoma (HCC) mouse models using photoacoustic (PI) and fluorescence imaging (FI).
Methods and Materials: BALB/c nude mice, implanted with human HepG2-RFP cells in left lobe of the liver, were randomized to the sorafenib-treated group (n = 21), or the control group (n = 20). Sorafenib (30 mg/kg) was administered orally to the treated group during 1-week. The changes in tumour volume, sO_2 of HCC and liver parenchyma, and R_E were measured at baseline and after 1-week. Pathologic changes including necrotic fraction and microvessel density were compared using unpaired t-test and correlation analysis.
Results: In the sorafenib-treated group, tumour volume and R_E showed lower values than those in the control group at 1-week (94.77 ± 42.24 vs. 159.10 ± 77.32 mm^3 and 4.89 ± 2.57 vs. 7.02 ± 3.89 x 10^{11} [p/sec/cm^2/sr]/ [μW/cm^2], P = .003 and P = .044). The sO_2 of HCC and liver parenchyma were also lower in the treated group than in the control group at 1-week (42.89 ± 8.16% vs. 49.40 ± 8.52% and 54.16 ± 7.91% vs. 59.14 ± 5.29%, P = .017 and P = .023). The sO_2 change in HCC showed a significant correlation with higher necrotic fraction (r = .427, P = .005) and lower microvessel density (r = -.421, P = .006) in the treated group.
Conclusion: The changes in sO_2 and R_E by sorafenib can be useful markers for non-invasive monitoring of therapeutic response in orthotopic HCC mouse models.

B-0425 10:38

Hyperpolarised MRS using 13-C-pyruvate reveals alterations in the metabolic phenotype of DEN-induced HCC in a rat model not revealed by 18F-FDG-PET

G. Kaissis, E. Bliemsrieder, D. Keim, L.S. Gebrekidan, G. Topping, F. Schilling, M. Schwaiger, E.J. Rummeny, R. Braren; *Munich/DE (g.kaissis@tum.de)*

Purpose: The propensity of tumour cells for aerobic glycolysis as opposed to mitochondrial oxidative phosphorylation, termed the "Warburg-Effect", is a potential target for oncologic pharmacotherapy in HCC. Magnetic Resonance Spectroscopy (MRS) with hyperpolarized substances such as C-13-Pyruvate allows non-invasive evaluation of tumour metabolism to identify candidate tumours.
Methods and Materials: HCC was induced in Wistar rats with oral Diethyl Nitrosamine. 20 HCCs were imaged using high-resolution T2w imaging and Free Induction Decay-Chemical Shift Imaging (FID-CSI) after i.v. injection of Hyperpolarised 13-C-Pyruvate. 6 healthy control animals were also imaged. A subset of 5 tumours was also examined with 18F-FDG-PET. Tumours and livers were excised and histologically examined. Tumour-ROI and liver spectra were generated and label exchange between C13-pyruvate, lactate and alanine was evaluated.
Results: Ratios of 13-C-pyruvate to lactate and 13-C-pyruvate to alanine label exchange (lac/ala-ratio) were significantly higher in HCC than in normal liver tissue (1.69±0.44 in HCC vs 1.05±0.12 in normal liver, p=0.002). There was marked intertumoural heterogeneity in lac/ala-ratio (σ^2=0.19) compared to normal liver (σ^2=0.016). Tumours with similar standardised uptake values in PET demonstrated markedly different lac/ala ratios.

Conclusion: C-13-Pyruvate-MRS allows in vivo visualisation of HCC metabolics and offers an imaging correlate to the "Warburg-phenotype" by directly demonstrating increased lactate production from pyruvate in HCC compared to normal liver. This technique could offer additional information about tumour biology compared to PET, since tumours with similar SUVs were found to demonstrate distinctly heterogeneous lactate/alanine production.

B-0427 10:46

Time-lapse MRI: single-cell tracking in experimental autoimmune encephalomyelitis

M. Masthoff, S. Gran, X. Zhang, L. Wachsmuth, L. Sorokin, J. Roth, M. Eisenblätter, M. Wildgruber, C. Faber; *Münster/DE (max.masthoff@ukmuenster.de)*

Purpose: Time-lapse MRI was recently introduced for MRI cell tracking studies. Here, via repetitive acquisition of the region of interest not only a static, single impression but also dynamic observation of cell migration can be obtained. Our purpose was to optimise the temporal resolution of time-lapse MRI and evaluate this technique in a specific disease model.
Methods and Materials: After inducing experimental autoimmune encephalomyelitis (EAE) in C57BL/6J mice via myelin oligodendrocyte glycoprotein injection, iron nanoparticles (Resovist®, 1.3ml per kg/BW) were injected i.v. 24h prior to MRI scan. MRI of the brain was performed on a 9.4T small animal MRI at different EAE disease levels (symptomatic n=8, presymptomatic n=2, healthy control n=3) using a T2* multi-gradient echo sequence with following scan parameters: TR 649ms, TE: 8.0ms, FA: 60°, averages 4, slice thickness 300µm, scan time 8min 12s (single time frame), respectively, 2h 44min with 20 repetitions. After MRI mice were sacrificed and brains prepared for histology.
Results: Time-lapse MRI sequence was improved to a temporal resolution of 8 minutes per time frame covering the entire brain. The technique allowed for tracking of patrolling leukocytes labelled with iron nanoparticles. The number of detected events changed significantly in EAE mice compared to healthy control mice.
Conclusion: By optimising time-lapse MRI towards an improved temporal resolution this technique is now applicable for single-cell tracking in animal models. Application in EAE disease shows the feasibility of detection of alternated immune cell dynamics.

B-0428 10:54

High resolution magnetic resonance imaging of HPF-labelled mouse natural Killer cell

L. Zheng[1], Z. Zhang[2], A. Larson[2]; [1]*Shanghai/CN*, [2]*Chicago, IL/US*

Purpose: To develop and optimise clinically translational protocol using US FDA approved drugs ferumoxytol, heparin and protamine to form HPF nanocomplexes and label specific mouse NK cell line (LNK) and determine in vitro and in vivo quantitative MRI properties.
Methods and Materials: LNK cells were labelled with self-assembled HPF nanocomplexes and optimise by varying the amount of HPF-nanocomplex. Labelling was confirmed the iron uptake with TEM, Prussian blue staining and ICP-MS. Cell viability and function were evaluated with Trypan blue staining and flow cytometry. Using a 7 Tesla MRI scanner, the labelled LNK MRI properties including signal intensity, R2* value and SNR were assessed with T2*W sequence. Finally, in Panc02 C57BL/6 mice model, changes of T2* signal, R2* value and SNR of labelled cells injection area were analysed by serial MRI detection after delivery of these labelled cells via percutaneous and intra-tumoural injection procedures, respectively.
Results: The HPF nancomplexes were internalised and encapsulated in labelled LNK cell as electron-dense nanoparticles. No significant difference between labelled LNK and control(unlabelled) LNK cells($p<0.05$, n=6) . No influence of HPF on both dead cell and early apoptosis were observed with exception of 200 µg/ml HPF-labelled LNK cells ($p<0.05$, compared with control).There is statistical significance between labelled and unlabelled LNK cells for both SNR and R2* in vivo and in vitro, respectively (all $p<0.05$).
Conclusion: LNK can be labelled with clinical applicable HPF-nanocomplex for MRI imaging in vitro and in vivo and has the potential to translate for longitudinal monitoring during NK cell immunotherapy.

B-0429 11:02

Directing neuronal differentiation of stem cells with a small interfering RNA-complexed MRI-visible cationic polymersome to counteract inhibitory microenvironment in stroke

L. Lu, J. Shen, X. Duan, F. Zhang, W. Young, M. Chen; *Guangzhou/CN (luliejingsysu@163.com)*

Purpose: Poor neural differentiation limits therapeutic prospects of exogenous neural stem cells (NSCs) to stroke,myelin associated inhibitory factors played critical inhibitory roles in axonal regeneration and neuronal differentiation of NSCs. A MRI-visible cationic polymersome system was used to delive siRNA targeting NgR gene, a common receptor of myelin associated inhibitory factors to direct neuronal differentiation of NSCs.
Methods and Materials: Superparamagnetic iron oxide nanoparticles loaded polyethyleneimine polylactic acid polymeric vesicle was synthesized and used to deliver NgR-siRNA into NSCs.Then, we assess the capability of this MRI-visible cationic polymersome to deliver siRNA targeting NgR into NSCs and the consequent effectiveness of directing neuronal differentiation of NSCs. The therapeutic benefits, long-term biological behaviour and safety of such epigenetic modification of NSCs are further tracked by the structural and functional changes of the host brain.
Results: This multifunctional nanocarrier enables efficient and safe blockage of NgR gene and can efficiently direct neuronal differentiation of NSCs both in vitro and in vivo. Meanwhile, this nanosystem can non-invasively monitor the migration and retention of NSCs in real time, without affect their therapeutic benefits.
Conclusion: These results demonstrate that the cationic polymersome-based multifunctional nanocarrier can provide robust epigenetically control over stem cell differentiation via RNA interference to counteract inhibitory microenvironment in stroke. This nanosystem will offer an opportunity for delivery of proneurogenic genes and simultaneous real-time monitoring of dynamics of stem cells, which will facilitate develop new stem cell therapy paradigm for stroke.

B-0430 11:10

Alanine loaded HMSNs: a potential contrast agent for MRS imaging

J. Wang, Z. Yao; *Shanghai/CN (jingwang_hs@foxmail.com)*

Purpose: To explore distinctive exogenous MRS contrast agents (CAs) to reliably distinguish brain glioma from other diseases.
Methods and Materials: Herein, β-alanine loaded hollow mesoporous silica nanospheres (AMSNs) have been synthesised and used as exogenous CAs for contrast-enhanced MRS based on the following two major merits: (1) β-alanine (ALA) is a kind of safe nutrition that is absent in the central nervous system. In the characteristic MRS spectrum, the peak of ALA at 2.562ppm should not be interfered by other metabolites in brain; (2) Hollow mesoporous silica nanospheres (HMSNs) can serve as nanocarriers to encapsulate large amounts of ALA with remarkable bio-safety and flexible facile modification.
Results: Our investigations have demonstrated that AMSNs with high biosafety could serve as specific MRS CAs for brain glioma's detection both ex-situ and in-situ, which helps to greatly enhance the diagnostic accuracy in comparison with the conventional MRS.
Conclusion: In summary, the constructed AMSNs with a characteristic MRS spectrum have been synthesised and used as remarkably efficient MRS CAs for brain glioma diagnosis. Our investigations show that the outstanding contrast-enhanced MRS using the biocompatible AMSNs can substantially promote the diagnostic efficiency and improve the diagnostic confidence of glioma. To our best knowledge, this is the first time to study on the exogenous specific MRS CAs. Similarly, specific MRS CAs may find a universal application in the accurate diagnosis of other diseases, which is hopeful to further accelerate the progress and break the shackle of current MRS technology.

B-0431 11:18

Histological correlation of dGEMRIC and T2 mapping in an ovine femoroacetabular impingement model: preliminary results

F. Schmaranzer[1], L. Arendt[2], N. Wolfer[2], C. Zurmühle[1], T. Lerch[1], K. Nuss[2], P. Kircher[2], B. von Rechenberg[2], M. Tannast[1]; [1]*Berne/CH*, [2]*Zurich/CH (schmaflo@gmail.com)*

Purpose: DGEMRIC and T2 mapping are increasingly used to judge prearthritic cartilage quality in femoroacetabular impingement (FAI) but the correlation between histology and both techniques is not well established. We asked whether dGEMRIC and T2 indices correlate with histological cartilage degeneration in a validated, experimental ovine FAI model.
Methods and Materials: This experimental, controlled, prospective study on 5 sheep (10 hips) was conducted after IRB approval. Five sheep underwent surgical induction of FAI by varus intertrochanteric osteotomy unilaterally, which rotates the naturally aspherical ovine femoral head into the acetabulum, inducing typical focal chondrolabral damage as seen in humans. Correction of the deformity was performed after 70 days. No surgery was performed in the 5 contralateral hips. Sheeps were sacrificed after further 70 days. One hour before sacrifice sheep received i.v gadolinium-DTPA and roamed free. Hips were dissected to fit into the coil. dGEMRIC and T2 maps were obtained at 3T using inversion recovery techniques. Histologic samples were stained with toluidine blue and cartilage degeneration was graded with the Mankin score. DGEMRIC and T2 indices of acetabular and femoral cartilage were radially measured at the 12 clock-face positions and correlated to Mankin scores (linear regression analysis; $p< 0.05$).
Results: Overall and regional (up to $R= -0.742$; $p<0.007$) inverse correlation was found between dGEMRIC indices and Mankin scores. No overall correlation was found between T2 indices and Mankin scores.

Conclusion: dGEMRIC correlates well with histological cartilage degradation, while we could not find such a correlation between T2 indices and Mankin scores.
Author Disclosures:
M. Tannast: Research/Grant Support; SNF-support.

B-0433 11:26

Whole-body imaging of mice using a long circulating blood pool tracer to perform multi-patch MPI
C.S.L. Jung[1], J. Salamon[1], P. Szwargulski[1], M.G. Kaul[1], G. Adam[1], K.M. Krishnan[2], A. Khandahr[2], T. Knopp[1], H. Ittrich[1]; [1]*Hamburg/DE*, [2]*Seattle, WA/US*

Purpose: The purpose was to perform multi-patch MPI using LS-008 as long circulating blood tracer to achieve mice whole body imaging in a high-spatial resolution.
Methods and Materials: MPI Scans of FVB mice (n=4) were carried out using a 3D imaging sequence (2.5T/m gradient strength, 14mT drive-field strength). Ten minutes after the iv injection of 60µl of LS-008 six different drive-field patches (two cranial, two median and two caudal) each taking 1.5min were performed. As MPI delivers no anatomic information, MRI scans at 7T ClinScan (Bruker) were performed using a T2-weighted 2D turbo spin echo sequence. Fiducial markers were used to enable MRI/MPI image fusion. Image reconstruction was performed offline using a custom reconstruction framework developed in the programming language Julia using the join formulation.
Results: The combined MRI/MPI measurements were carried out successfully. The reconstruction of the drive-field patches generated no artefacts at the margins resulting in a whole mice body MP imaging. Compared to previous experiments using a lower gradient strength of 1T/m the multi-patch method with a gradient strength of 2.5T/m resulted in a higher spatial resolution. Therefore we were able not only to visualise the inferior vena cava, the heart and the liver but also the cerebral vessels, the thoracic aorta and the kidneys.
Conclusion: In vivo whole-body imaging of mice using multi-patch MPI is feasible. The long circulating blood tracer enabled us to visualize whole mice without motion artefacts that would occur using short half-life contrast agents.

B-0434 11:34

Insulin-dependent triglyceride-rich lipoprotein uptake into brown adipose tissue visualised by 7T MRI and intravital microscopy
C.S.L. Jung, M. Heine, N. Mangels, M.G. Kaul, G. Adam, H. Ittrich, J. Heeren; *Hamburg/DE*

Purpose: The aim was to determine the activity of brown adipose tissue (BAT) and its dependence on signalling pathway mediated by insulin using superparamagnetic iron oxide nanoparticles (SPIO) or quantum dots (QD) embedded into triglyceride-rich lipoproteins (TRL).
Methods and Materials: BAT activity of C57BL/6J wild-type was stimulated by treatment with the β3 receptor agonist CL316, 243. Inhibition of insulin secretion was induced using the potassium channel agonist diazoxide. MRI at 7T ClinScan (Bruker) was performed before and 20min after iv injection of TRL-SPIOs using a T2*w Multiecho-GRE sequence (TR/TE_{first} 400/2ms, ETL 12, ES 1ms, FA 25°). ΔR2* in BAT was estimated. In addition intravital microscopy (IVM) analysis was performed for real time imaging of TRL-QD uptake. In order to quantify TRL clearance, the fate of radioactively labelled TRLs was analysed.
Results: For control mice no signal difference in BAT before and after the injection of TRL-SPIO was detectable, while a significant signal drop and increase of ΔR2* ($82.9s^{-1}$; $p<0.001$) was estimated for CL treated, BAT activated mice. Inhibition of insulin signalling resulted in a significant lower uptake of TRL-SPIO into BAT ($\Delta R2^* = 21.1s^{-1}$; $p<0.001$). IVM analysis and quantitative metabolic studies using radioactive lipid tracers confirmed MRI results. In both set-ups inhibition of insulin secretion using diazoxide diminished TRL uptake into BAT.
Conclusion: β3-receptor activation via CL with following acute insulin release lead to BAT activation, which can be visualized *in vivo* by MRI using TRL-SPIO and estimating ΔR2*. Accordingly, the inhibition of insulin signalling blocks TRL uptake into BAT.

10:30 - 12:00 **Room E1**

Breast

SS 602a

Breast density and background parenchymal enhancement

Moderators:
W. Alomaim; Dublin/IE
R.A. Kubik-Huch; Baden/CH

B-0444 10:30

Single nucleotide polymorphisms in relation to mammographic density in women with breast cancer
H. Sartor, J. Brandt, O. Melander, S. Zackrisson; *Malmö/SE (hannasartor@med.lu.se)*

Purpose: Certain single nucleotide polymorphisms (SNPs) are associated with mammographic density and breast cancer. Our purpose was to investigate whether certain SNPs known from literature (i.e., candidate SNPs) were associated with mammographic density in women with breast cancer in a large Swedish cohort - the Malmö Diet and Cancer Study (MDCS).
Methods and Materials: From 1991-2007 a total of 826 women with breast cancer have been identified in the MDCS and radiological parameters for those women have been registered. Genotyping was performed on 762 nonrelated women with breast cancer. 15 SNPs in relation to mammographic density (fat involuted and moderately dense vs dense) were analysed with logistic regression yielding odds ratios (OR) with 95% confidence intervals (CI) adjusted for age at diagnosis, body mass index, and hormone replacement therapy (at baseline).
Results: For SNP rs6557161, the minor homozygote allele showed a significant relation to high mammographic density as compared to the major homozygote (OR_{adj} 1.91 (1.12-3.26)). For SNP rs7289126, the minor homozygote (OR_{adj} 0.60 (0.37-0.97)) and the heterozygote allele (OR_{adj} 0.65 (0.45-0.94)) showed a significant relation to low mammographic density. For 13 of the selected SNPs no relation to mammographic density was observed.
Conclusion: We have found that two SNPs were associated with mammographic density in a large Swedish cohort, the MDCS, and further analyses on breast cancer survival will be performed. Increased knowledge regarding a potential shared genetic basis for mammographic parameters such as density could potentially help in the development of breast cancer risk scores including SNPs.
Author Disclosures:
S. Zackrisson: Speaker; SZ has received speaker' s fees and travel support by Siemens Healthcare AG and Astra Zeneca.

B-0435 10:38

Determining factors of radiation dose in digital breast tomosynthesis (DBT) and full-field digital mammography (FFDM) utilising automated breast density and volumetric measurements
L.H.Y. Sinn, C.S.Y. Lo, E.Y.W. Chan, M.W.M. Law, W. Wong, T.P.W. Lam, W.W.M. Lam; *Hong Kong/HK (lorriesinn@gmail.com)*

Purpose: To determine the factors affecting the radiation dose of stand-alone DBT versus FFDM.
Methods and Materials: IRB-approved study on women attending their surveillance mammography from February 2015 to March 2016 were performed. All women had both FFDM and DBT performed at same time under same degree of compression.The breast density and volumetric measurements were generated Quantra software (version 2.2, Hologic Inc, USA). The correlation between average glandular dose (AGD) per view with age, compressed thickness, and volumetric data of both FFDM and stand-alone DBT were performed with regression analysis.
Results: Retrospective analysis performed on 4283 study sets with mean AGD per view of FFDM and DBT equals 1.58mGy and 1.53mGy respectively.On regression analysis, there is positive correlation of AGD with compressed thickness, volume of fat, fibroglandular tissue and total breast volume for both FFDM and DBT, and negative correlation with age. All these parameters show stronger correlation in FFDM compared to DBT with better goodness of fit (R^2) values, as well as larger regression coefficients. Among all, compressed breast thickness and volume of fibroglandular volume demonstrated largest regression coefficient measuring 0.039 and 0.0057 respectively, R^2 = 57% and 32% respectively in FFDM, while for DBT the regression coefficient measured 0.021 and 0.0029 respectively.

Conclusion: The increase in compressed thickness and volume of fibroglandular tissue resulted in more significant increment in radiation dose in FFDM than in DBT, indicating that there was relatively less radiation dose in patients having stand-alone DBT compared to FFDM in population with predominantly dense breasts.

B-0436 10:46

Comparison of automated volumetric breast density measurements by two different applications

A. Shimauchi[1], Y. Machida[1], M. Yakabe[2], K. Nii[2], H. Namba[3], A. Saita[1], E. Fukuma[4]; [1]*Chuo-ku/JP*, [2]*Minato-ku/JP*, [3]*Miyazaki/JP*, [4]*Kamogawa/JP (akikoshima@gmail.com)*

Purpose: To compare automated volumetric breast density measured by two different applications.
Methods and Materials: Mammograms of 110 women using a spectral photon-counting scanner (MicroDose mammography SI; Philips), from Jan 2015 to Feb 2016, were used. Breast volume (BV) (cm^3), glandular volume (GV) (cm^3), and volumetric breast density (VBD) (%) of two views of each breast were obtained from spectral energy data at the time of acquisition, using Breast Density Measurement (Philips). Three parameters were also obtained by Volpara (version 1.5.1; Volpara Solutions) using the raw data. Correlation coefficients (R) between MLO and CC views of the same breast for each system, and between two systems for each view were calculated. Weighted κ analyses were performed for density scores between the two systems, and between visual assessment and each system.
Results: Both systems showed very strong correlations between CC and MLO, for BV, GV and VBD (R=0.970, 0.977, 0.990 by Philips, R=0.963, 0.898, 0.864 by Volpara). BV and GV of two systems showed very strong correlations (R=0.993-0.997, 0.865-0.880), whereas VBD showed strong correlation (R=0.775-0.794). Density scores between Philips and Volpara, visual assessment and Philips, and visual assessment and Volpara showed moderate agreement (κ=0.510, 0.523, and 0.419).
Conclusion: Volumetric measurements of BV, GV, and VBD by both systems showed good precision. Philips system showed slightly better performances in correlation of VBD between CC and MLO, and agreement of density scores with visual assessment, which may be because direct measurements of spectral energy data are undertaken instead of processing of raw digital data.

B-0437 10:54

Reproducibility of automated mammographic density measures between two digital mammography device vendors

M. Abdolell, K.M. Tsuruda, P. Brown, J.S. Caines, C.B. Lightfoot, S.E. Iles; *Halifax, NS/CA (sian.iles@nshealth.ca)*

Purpose: This study examined the reproducibility of automated mammographic density measures for mammograms acquired from two digital mammography device vendors during a one year period. Continuous measures of mammographic density included percent breast density, dense breast area, and total breast area; categorical measures of mammographic density included a 3-category scale and the 4th edition BI-RADS density scale.
Methods and Materials: Pairs of "for presentation" digital mammography images were obtained from two mammography units for 128 women who had a screening mammogram on one vendor unit followed by a diagnostic mammogram on a different vendor unit. All exposures occurred within a single department by the same group of mammography-certified technologists and under the direction of a single medical director, technical manager, and quality assurance officer. A fully-automated density software was used to generate mammographic density measures from all available standard screening view images from the two vendors. Intra-class correlation coefficients (ICC), Pearson's correlation coefficient (PCC), weighted kappas, and scatter plots were used to evaluate mammographic density measures between vendors.
Results: ICCs of 0.94, 0.90, and 0.98 and PCCs of 0.94, 0.92, and 0.99 were observed for percent density, dense breast area, and total breast area measurements respectively. Weighted kappas for a 3-category scale and the 4th edition BI-RADS scales were 0.85, 0.83 respectively.
Conclusion: Overall agreement of mammographic density measures automatically generated from pairs of "for presentation" digital mammography images was almost perfect between the two vendors.
Author Disclosures:
M. Abdolell: CEO; Densitas Inc. Founder; Densitas Inc. **K.M. Tsuruda:** Employee; Densitas, Inc.

B-0438 11:02

Reliability of automated breast density measurements vs visual assessment in mammography

C.S.Y. Lo, L.H.Y. Sinn, K.W.M. Wong, T.P.W. Lam, W.W.M. Lam; *Hong Kong/HK (chrissy.lo@gmail.com)*

Purpose: To compare the reliability of automated breast density (ABD) measurements and visual assessment in terms of reproducibility.
Methods and Materials: 159 women (excluding those with previous breast operation) attending surveillance mammography at least once with digital breast tomosynthesis (DBT) from October 2014-June 2016 recruited with IRB approval. Breast density assigned using BIRADS 5th edition (Fatty: a, scattered fibroglandular tissue: b, heterogeneously dense: c, markedly dense: d). Simply dense (category c+d) and non-dense breast (category a+b) grouping done and analysed. Quantra software [version2.2; Hologic Inc, USA] utilised for ABD. For visual assessment, two blinded radiologists (Readers 1&2) assigned breast density to same group of patients for visits 1 and 2. Kappa statistics used to assess agreement between different comparison groups.
Results: [Same visit] Agreement of Quantra ABD of both breasts (assuming symmetrical) compared: Kappa coefficient 0.8 (CI 0.6-0.9). As only one measurement was given to each patient in visual assessment, agreement of Readers 1 and 2 assigned breast density assignment compared for same visit, but kappa coefficient was only 0.27 (CI 0.13-0.41). [Same patient, different visits] Agreement of Quantra assigned breast density category at two visits compared: Kappa co-efficient 0.82 (CI 0.73-0.91). For visual assessment reproducibility, the agreement of the Reader 1 in the first visit was compared with Reader 2 in the second visit, but kappa coefficient was only 0.16 for visual assessment (CI 0-0.3).
Conclusion: Automated breast density is more reliable in terms of reproducibility of breast density assessment than visual assessment, which has high inter-observer variability.

B-0439 11:10

Accuracy of fully automated volumetric FGT measurement with MRI of the breast: correlation with anthropomorphic breast phantoms

G.J. Wengert, K. Pinker, T.H. Helbich, W.-D. Vogl, S. Spijker, H. Bickel, S. Polanec, P.A.T. Baltzer; *Vienna/AT (georg.wengert@meduniwien.ac.at)*

Purpose: To investigate the accuracy of fully automated measurements of the amount of fibroglandular tissue (FGT) with magnetic resonance imaging (MRI) using different MRI sequences based on anthropomorphic breast phantoms as the ground truth.
Methods and Materials: In this study, ten anthropomorphic breast phantoms that consisted of different known fractions of adipose and fibroglandular tissue, which closely resembled normal breast parenchyma, were developed. Anthropomorphic breast phantoms were imaged with a 1.5 Tesla unit (Siemens, AvantoFit) using an 18-channel breast coil. The sequence protocol consisted of an isotropic Dixon sequence (Di), an anisotropic Dixon sequence (Da), and T1 3D FLASH sequences with and without fat saturation (T1). Fully automated, quantitative, volumetric measurement of FGT for all anthropomorphic phantoms and sequences was performed and correlated with the amount of fatty and glandular components in the phantoms as the ground truth.
Results: Fully automated quantitative measurements of FGT with MRI were performed successfully in all phantoms 6.71-59.72% (mean 32.82%) and for all sequences; Di, Da, and T1 ranged from 6.98-58.05% (mean 32.89%), 7.43-61.05% (mean 34.76%), and 6.44-54.69% (mean 34.67%), respectively. All sequences yielded good correlation with actual FGT content. However the best correlation of FGT measurement results and anthropomorphic breast phantoms was identified for Dixon sequences; Di (R2=0.998), Da (R2=0.997), and T1 (R2=0.910).
Conclusion: Fully automated quantitative measurements of FGT with MRI provide accurate information on the actual amount of FGT. Dixon type sequences showed the highest correlation and reproducibility of automated, quantitative FGT measurements on anthropomorphic breast phantoms, compared to conventional sequences.

B-0440 11:18

Breast MRI background parenchymal enhancement: a potential bridge to molecular cancer subtype?

G. Dilorenzo, M. Telegrafo, V. Ranieri, A. Cirilli, C. Giardina, A.A. Stabile Ianora, G. Angelelli, M. Moschetta; *Bari/IT (giuseppedlr@live.it)*

Purpose: To evaluate the distribution of MRI BPE among different breast cancer subtypes searching for any correlation with immunohistochemical and receptorial panel (Estrogen Receptor -ER, Progesterone Receptor - PR, Human Epidermal Growth Factor Receptor 2 - HER2).
Methods and Materials: 41 consecutive patients affected by breast cancer underwent breast DCE-MRI. Two radiologists evaluated all subtracted MR enhanced images for classifying normal BPE. ER, PR and HER2 expression was assessed by immunohistochemical analysis. ER and PR status was evaluated using Allred score (positive values: score ≥3). The intensity of the c-erbB-2 staining was scored as 0, 1+, 2+, or 3+ (positive values: ≥ 3+; negative: 0 and 1+; 2+ value assessed with silver in-situ hybridisation). Patients were subdivided into four categories based on cancer subtypes: ER/PR+HER2+, ER/PR+HER2-, ER/PR-HER2+, ER/PR-HER2- (triple negative). Distribution of BPE into the four categories was assessed and any significant difference was

calculated with the comparison of proportions, with p≥0.05 considered as significant.
Results: 6/41 (14.5) patients were ER/PR+Her2+, 24/41 (58.5%) were ER/PR+HER2-, 2/41 (5%) were ER/PR-HER2+, 8/41 (19.5%) were ER/PR-HER2-. No significant correlation between BPE pattern and receptor expression among breast tumours was found (p>0.05). Mild/moderate BPE were the most prevalent patterns in ER/PR+HER2+, ER/PR+HER2-, ER/PR-HER2+ groups; in the ER/PR-HER2- (triple negative) group, moderate/marked BPE prevailed.
Conclusion: BPE shows no significant correlation with breast tumour receptorial panel, except for triple negative breast tumours, in which an atypical trend for moderate/marked BPE prevalence could be supposed. Further studies need to be performed to confirm this preliminary data.

B-0441 11:26

Association of breast density and region of interest size with apparent diffusion coefficient value of normal fibroglandular tissue at MRI

N. Radovic, G. Ivanac, M. Crnogorac, E. Divjak, T. Cicvara-Pecina, J. Petrovic, B. Brkljacic; *Zagreb/HR (niko.radovic@gmail.com)*

Purpose: To determine association of breast density and region of interest (ROI) size with apparent diffusion coefficient (ADC) value of normal fibroglandular tissue on diffusion-weighted imaging (DWI) at MR.
Methods and Materials: The retrospective study included 28 women who underwent clinical MR exams. Breast density was evaluated at MRI and divided into low and high density category, the former including breasts interpreted as being fatty or having scattered fibroglandular tissue, and the latter including heterogeneously dense and dense breasts. DWI was performed at 1.5T using b = 0, b = 400 and b = 800. ADC of normal fibroglandular tissue was calculated by manually drawing two sets of multiple circular ROI´s of sizes equalling 15 mm^2 and 30 mm^2. Areas of fibroglandular tissue not large enough to encompass the larger ROI were excluded from measurements to avoid partial volume averaging. Intrasubject mean ADC values for the two ROI sizes were compared by Pearson's correlation coefficient. Association between mean ADC and breast density level was assessed using Student's t-test.
Results: Mean ADC of fibroglandular tissue was 1.79 ±0.18 $x10^{-3}$ mm^2/s and 1.8±0.2 $x10^{-3}$ mm^2/s on smaller and larger ROI respectively. Intrasubject ADC measurements for the two ROI sizes were highly correlated (r=0.954, p<0.001). ADC was not associated with breast density level (p>0.5).
Conclusion: ADC reflects microstructural characteristics of fibroglandular tissue unrelated to breast density or ROI size. Contrast between lesions and fibroglandular tissue on DWI will not be affected by breast density.

B-0442 11:34

Effect of parenchymal pattern in women with dense breasts, variation with age and impact on screening outcomes: observations from a UK screening programme

L. Ward[1], S. Heller[2], S. Hudson[1], L. Wilkinson[1]; [1]*London/UK*, [2]*New York, NY/US (lauraward@doctors.org.uk)*

Purpose: To analyse mammographic parenchymal pattern (PP) in women with densest breasts; to determine how tissue pattern varies with age and impacts recall and cancer detection.
Methods and Materials: Breast density data (Volpara™, 5th ed.) was obtained in a subset of women screened in a regional programme (April 2013-March 2015). Cases with densest breasts (Volpara Grade d [VGd]) were selected for PP categorization. All assessed VGd cases and 100 randomly selected VGd cases from non-assessed women were reviewed. Ten readers classified PP on a 1-5 scale (1-very smooth to 5-very nodular). Mean PP classification was compared between age groups and for assessed vs non-assesed women. Reader agreement was analysed using intraclass correlation. Likelihood of biopsy, cancer diagnosis and cancer characteristics were analysed by age and PP.
Results: 4,331/40,760(10.6%) screened women were VGd. Proportions of PP categories were similar at all ages for controls (p = 0.145) and for 280 assessed women (p=0.657). Inter-rater reliability for scoring PP in controls was good (ICC = 0.6302). 155 women underwent biopsy of which 34 had cancer. PP (1-5) ratios did not vary significantly with age in these groups (p = 0.580). There was significant correlation between cancer and nodular PP (p = 0.043). Cancer characteristics did not differ by age or PP.
Conclusion: Ratio of smooth to nodular pattern in women with the densest breasts did not vary with age. PP did not affect likelihood of recall to assessment or biopsy. There was a significant association between nodular PP and cancer diagnosis.

B-0443 11:42

Positive predictive values by breast density in the Norwegian Breast Cancer Screening Programme

N. Moshina, M. Roman, S. Sebuodegard, S. Hofvind; *Oslo/NO (nataliia.moshina@kreftregisteret.no)*

Purpose: To investigate the trends of PPV-1 (the percentage of screening detected breast cancers among the recall examinations due to abnormal mammographic findings) and PPV-2 (the percentage of screening detected breast cancers among the recall examinations that include an invasive diagnostic procedure) by categories of subjectively assessed mammographic density (MD).
Methods and Materials: We used information from 6363 recall examinations obtained from 5666 women screened with full field digital mammography in the Norwegian Breast Cancer Screening Programme, 2003-2010. The radiologists who performed the recall examination classified the mammograms into three categories based on MD: MD-1 (<30% of fibroglandular tissue), MD-2 (30-70%), and MD-3 (>70%). We used chi-square trend statistics to estimate trends of PPVs across MD categories. Logistic regression was used to estimate the odds ratio (OR) of screening detected breast cancer associated with MD among recalled women, adjusting for age.
Results: PPV-1 and PPV-2 decreased by increasing MD category (p<0.05 for the trend). MD-2 and MD-3 were associated with lower odds of breast cancer among recalled women compared with MD-1. Adjusted OR was 0.79 (95% CI: 0.68-0.92) and 0.75 (95% CI: 0.58-0.97) for MD-2 and MD-3, respectively.
Conclusion: High MD was associated with a higher amount of false positive results, and thus decreased radiologists' performance, compared with low MD in the national screening programme in Norway.
Author Disclosures:
N. Moshina: Research/Grant Support; ExtraStiftelsen via the Norwegian Breast Cancer Society.

B-0445 11:50

Reliability of 5th edition vs 4th edition BI-RADS mammographic density scales

M. Abdolell[1], K.M. Tsuruda[1], P. Brown[1], J.S. Caines[1], G. Schaller[2], C.B. Lightfoot[1], S.A. Raza[2], S.E. Iles[1]; [1]*Halifax, NS/CA*, [2]*Sydney, NS/CA (pbpete@gmail.com)*

Purpose: This study examined the variability in inter-rater reliability between radiologists assessments of mammographic density using the 4th and 5th edition of the BI-RADS density classification scales.
Methods and Materials: Six radiologists assessed mammographic density for 375 cases using the 4th and 5th editions of the BI-RADS density scale. A consensus assessment was calculated based on the majority assessment. Chance-corrected inter-rater agreement was evaluated using the weighted kappa statistic for all pairs of radiologists and between each radiologist and the consensus measure.
Results: Inter-rater agreement between all pairs of radiologists was moderate to almost perfect for the 4th edition scale (mean Kappa=0.76, range=0.53-0.90), and substantial to almost perfect for the 5th edition scale (mean Kappa=0.79, range=0.71-0.83). Inter-rater agreement between each radiologist and the consensus measure was substantial to almost perfect for the 4th edition scale (mean Kappa=0.85, range=0.69-0.92) and almost perfect for the 5th edition scale (mean Kappa=0.86, range=0.81-0.91).
Conclusion: In the absence of strict percent density cut-points in the BI-RADS 5th edition density scale, inter-rater agreement is significantly better than for the BI-RADS 4th edition density scale. The range of inter-rater variability between pairs of raters and between raters versus the consensus measure was considerably less for the 5th edition BI-RADS density scale compared to the 4th edition scale. Visual assessment of density using the BI-RADS 5th edition density scale may be more reliable than using the BI-RADS 4th edition density scale.
Author Disclosures:
M. Abdolell: CEO; Densitas Inc. Founder; Densitas Inc. **K.M. Tsuruda:** Employee; Densitas Inc..

10:30 - 12:00 **Room E2**

Neuro

SS 611

Stroke: endovascular treatment

Moderators:
S. Rohde; Dortmund/DE
M.A. van Buchem; Leiden/NL

K-08 10:30

Keynote lecture
A. Krainik; *Grenoble/FR*

B-0446 10:39

Iatrogenic complications during mechanical thrombectomy for acute ischaemic stroke: potential mechanisms, rescue strategies, and clinical outcomes in a multicentre study
C. Parra-Fariñas, A. Tomasello Weitz, P. Cardona Portela, M. de Miquel, M. Gomis Cortina, C. Castaño Duque, J. Blasco, X. Urra, M. Ribó Jacobí; *Barcelona/ES (carmenparrafarinas@gmail.com)*

Purpose: Mechanical thrombectomy has emerged as valuable armamentarium for acute ischaemic stroke. Complications due to arterial rupture and dissection have not been formally described. This study aimed to report our intra-procedural vessel damage and discuss its technical details and clinical significance.
Methods and Materials: We studied patients prospectively included in SONIIA registry (2011-2015), a mandatory, externally audited registry that monitors the quality of reperfusion therapies in Catalonia during practice. Successful recanalisation (TICI grade ≥2b), procedural time, symptomatic intracranial haemorrhage (SICH), dramatic neurological improvement (≥10 points decrease in the NIHSS score at 24 hours), independent functional outcome (mRS ≤2) at three months, and iatrogenic arterial injury were recorded.
Results: Among the 1640 patients included, iatrogenic complications occurred in 3.6% (2.0% dissection, 1.6% perforation, 40% middle cerebral artery occlusion, 52.1% left side, 21.7% posterior circulation). Median NIHSS score was 17 (12-21) on arrival and 9 (3-18) at 24 hours. Complications were not related to general anaesthesia: 26.7% vs. 73.3% (RR, 1.7; 95% CI, 1.0-3.0; p=0.061). Complications were associated with less successful recanalisation: 36.7% vs. 79.3% (RR, 6.0; 95% CI, 3.6-10.1; p=0.000) and longer procedural time: 108.1±55.2 min vs. 87.4±73.32 min (p=0.031). SICH: 18.3% (81.8% perforation vs. 18.2% dissection, p=0.002) vs. 2.5% (p=0.000). Good early response: 15.1% vs. 71.0% (p=0.000). Functional independence: 18.4% vs. 48.9% (p=0.000). Mortality: 60.0% vs. 17.4% (p=0.000).
Conclusion: Intra-procedural vessel damage was rare, but when it occurred was associated with high unfavourable outcome. However, 18.4% had functional independence, suggesting that in some complicated patients good neurological recovery is achievable.

B-0447 10:47

Should mechanical thrombectomy be considered in patients with M2 occlusion?
I.Q. Grunwald[1], M. Sneade[2], B. Bock[1], V. Janardhan[3], L. Ammar[4], A. Kühn[5], S. Shah[6], C. Goncalves[6], S. Sit[4]; [1]*Chelmsford/UK*, [2]*Oxford/UK*, [3]*Dallas, TX/US*, [4]*Alameda, CA/US*, [5]*Worcester, MA/US*, [6]*Southend-on-Sea/UK*

Purpose: The preponderance of evidence suggests that vessel location is an important predictors of outcomes in acute ischemic stroke. However, few studies have examined the natural history of a cohort of patients with persistent M2 vessel occlusion who would have been eligible for, but remained untreated with mechanical thrombectomy.
Methods and Materials: The SOS and FIRST trials were prospective, multicenter studies evaluating the natural history of a stroke cohort eligible for mechanical thrombectomy but did not receive the treatment. Enrolled patients presented with symptoms of acute ischaemic stroke due to large vessel occlusion and were refractory or ineligible for rtPA treatment. Functional independence was defined as a mRS score 0-2 at 90 days. Incidence of death, intracranial hemorrhage, serious adverse events, and mortality were assessed for association with vessel location.
Results: 238 patients (median age: 71) met study criteria. Occlusions of the M2 alone were reported in 8.9%. At 90 days only 75% of Middle Cerebral Artery M2 patients did not achieve functional independence as defined by a mRS score of 0-2. Mortality rate was 10%.
Conclusion: Persistent occlusion of the M2 MCA is associated with a low rate of functional independence and a high mortality, posing the question if this patient group should be considered for mechanical thrombectomy.

Author Disclosures:
V. Janardhan: Consultant; Penumbra. **L. Ammar:** Employee; Penumbra Inc.. **S. Sit:** Employee; Penumbra Inc..

B-0448 10:55

Manual aspiration thrombectomy using penumbra catheter in patients with acute migrated MCA occlusion
S. Baik; *Jeonju/KR (mdshbaik@gmail.com)*

Purpose: Our study aimed to retrospectively assess the efficacy and safety of a manual aspiration thrombectomy (MAT) using Penumbra in patients with acute migrated middle cerebral artery (MCA) occlusion.
Methods and Materials: We conducted a retrospective review of patients who underwent MAT using Penumbra 4 or 5 MAX reperfusion catheters for treatment of acute MCA occlusion between January 2012 and December 2015. Migrated thrombus was defined as distal migration above> 1cm on initial cerebral angiography compared with preprocedural angiographic findings. We evaluated immediate angiographic results and clinical outcomes through reviewing of patient's electrical medical records. We compared with clinical outcomes between migrated MCA occlusion and non-migrated MCA occlusions.
Results: During this period, 98 patients underwent MAT using Penumbra catheters for treatment of acute MCA occlusions. Of these patients, 19 (19.4%) had a migrated MCA thrombus on initial cerebral angiography compared with preprocedural angiographic findings. The overall rate of successful recanalisation (TICI grade ≥ 2b) was 90.8%. The rate of successful recanalisation on migrated thrombus group was 94.7% (18/19). Overall favourable clinical outcomes (mRS score at 3 months ≤ 2) were seen in 64 patients (65.3%). Although it is not significant, favourable clinical outcomes in migrated thrombus group was higher compared with non-migrated thrombus groups (78.9% vs. 60.8%, p = .231).
Conclusion: MAT appears to be safe and is capable of achieving high rate of successful recanalisation and favourable clinical outcomes in patients with acute MCA occlusion. A migrated thrombus group was more favorable clinical outcomes.

B-0449 11:03

Single-centre experience using the 3MAX reperfusion catheter in the treatment of acute ischaemic stroke with distal arterial occlusion
K. Premat, B. Bartolini, E. Shotar, F. Barronet-Chauvet, V. Degos, N. Sourour, F. Clarençon; *Paris/FR*

Purpose: Recently published data reported promising results with tromboaspiration devices such as the Penumbra System (Penumbra, Alameda, California) combined with the Penumbra MAX series reperfusion catheters by using the ADAPT technique. The aim of this study was to report our initial experience with the 3MAX (3.8F) reperfusion catheter for the recanalisation of occluded distal intracranial arteries.
Methods and Materials: From August 2015 to December 2016, 28 consecutive patients (15 women [54%] and 13 men [46%]; mean age=69±18.7y, [range: 22-94]) for 34 distal occlusions underwent mechanical thrombectomy (MT) using the 3MAX catheter. The occluded vessels were: M2 (n=24; 70.6%), M3 (n=2; 5.9%), P1 (n=2, 5.9%), P2 (n=2, 5.9%), P3 (n=2, 5.9%), A3 (n=1, 2.9%) and superior cerebellar artery (SCA) (n=1, 2.9%). The primary endpoint was the Thrombolysis In Cerebral Infarction (TICI) score after thromboaspiration attempts alone using the 3MAX.
Results: In 1/34 (2.9%) cases, the 3MAX could not be navigated into the target artery. Successful recanalisation (TICI 2b/3) after aspiration with the 3MAX alone was achieved in 59% of the cases. Overall recanalisation rate was 76%. Six (17.6%) procedure-related complications occurred, including four (11.8%) 3MAX-related complications (two clot migration in the same territory; 2 clot migration in another territory). Overall mortality rate was 15.8%. No procedure-related mortality was recorded. mRS 0-2 was observed in 47.3% of the cases at last follow-up (average delay: 108±70 d).
Conclusion: The 3MAX reperfusion catheter is a safe device and provides interesting results for recanalisation of distal occlusions.
Author Disclosures:
N. Sourour: Consultant; Medtronic. **F. Clarençon:** Consultant; Medtronic, Codman Neurovascular.

B-0450 11:11

Comparison of dual-layer spectral CT with MRI in differentiation between haemorrhage and extravasation of iodinated contrast medium after endovascular treatment of ischaemic stroke

I. Riederer, A. Sauter, M. Renz, J. Dangelmaier, J.S. Kirschke, A.A. Fingerle, E.J. Rummeny, P.B. Noel, D. Münzel; *Munich/DE (isabelle.riederer@tum.de)*

Purpose: To evaluate the advantages of dual-layer spectral omputed tomography (CT) for distinguishing between intracerebral haemorrhage and iodine extravasation due to disruption of the blood brain barrier in ischaemic stroke patients after mechanical thrombectomy.
Methods and Materials: Twenty patients who had received mechanical thrombectomy, were examined with a dual-layer spectral CT (IQon spectral CT, Philips Healthcare, USA) 11 +/- 3h after revascularisation. Virtual non-contrast (VNC) images and iodine overlay maps (IOM) were calculated and evaluated using a dedicated software (IntelliSpace Portal, Philips Healthcare, USA). Region of interests (ROIs) analyses were performed within the hyperdense areas in the conventional CT, IOM and VNC images. As a standard of reference data from Magnetic Resonance Imaging (MRI), acquired during the follow-up procedure, are utilised. Sensitivity, specificity and positive predictive value (PPV) for the presence of haemorrhage in dual-layer spectral CT are calculated.
Results: A total of twenty hyperdense areas in twelve patients were seen in dual-layer spectral CT. In comparison to follow-up MRI as a gold standard, it was possible to correctly classify haemorrhage (n=8), extravasation of iodine (n=8), or both (n=4) in spectral CT images. The ROI analysis showed HU of 64 +/- 2 (“conventional CT”) and 51 +/-2 (VNC) for haemorrhage and 61 +/- 3 (“conventional CT”) and 22 +/-2 (VNC) for iodine, respectively.
Conclusion: Dual-layer spectral CT improves the capability to distinguish between intracerebral haemorrhage and extravasation of iodinated contrast medium due to disrupted blood brain barrier in patients with acute stroke after intra-arterial thrombectomy.

B-0451 11:19

Catheter thrombo-aspiration in acute ischaemic middle cerebral artery stroke: first results

M. Voormolen, T. van der Zijden, O. d'Archambeau, L. Yperzeele, T. Menovsky, P.M. Parizel; *Antwerp/BE (maurits.voormolen@uza.be)*

Purpose: To assess the efficacy and safety of thrombo-aspiration (TA) using Penumbra catheters in patients with acute middle cerebral artery (MCA) occlusion.
Methods and Materials: We evaluated immediate angiographic results and prospective clinical outcomes after treatment of 33 consecutive patients undergoing endovascular treatment of MCA occlusions, treated with Penumbra aspiration catheters and pump system, between January 2015 and July 2016, involving 12 men and 21 women, with a median age of 69 years (range 25-88). Seventeen patients had left MCA arterial occlusion (52%). Inclusion criteria were defined as: patients with neurological symptoms (NIHSS≥6), treatment within 6 hours after symptom onset, brain CT scan showing infarct <50% MCA territory and catheter angiography showing thrombo-embolic MCA occlusion.
Results: Recanalisation by TA was achieved in 24 patients (73%), with successful recanalisation (TICI 2b/3) in 22 patients. Seven patients were additionally treated with stent retrievers (21%). In 9 patients TA was unsuccessful, because of access difficulties in tortuous arteries (n=4) or shortness of catheters (n=2), or impossibility to aspirate thrombus (n= 3). Except one carotid artery dissection and a thrombo-embolus in another vascular territory, no procedure related complications occurred. At admission, median NIHSS was 16 (range 6-29), with decrease to 10 at discharge (range 1-29). Median mRS at 3 months was 1 (range 0-6). Favorable clinical outcome at 3 months (mRS≤2) was seen in 21 patients (64%).
Conclusion: In our experience, catheter thrombo-aspiration is a safe procedure, with high rates of successful recanalisation and favorable clinical outcomes in patients with acute ischemic MCA stroke.

B-0452 11:27

Primary aspiration technique in acute stroke treatment with ACE 64 in 121 patients

M. Alexandrou, M. Politi, L. Meyer, C. Roth, P. Papanagiotou; *Bremen/DE (mariapoliti@hotmail.com)*

Purpose: To evaluate the safety and affectivity of primary aspiration technique in endovascular stroke treatment.
Methods and Materials: Between July 2014 and December 2015 107 acute ischaemic stroke patients with large vessel occlusion and mean NIHSS 14 were treated with primary aspiration technique. The ACE 64 aspiration catheter (Penumbra inc.) was used in all patients. Procedural and clinical data were selected for analysis.
Results: The primary aspiration technique was successful in achieving thrombolysis in cerebral infarction (TICI) 2b or 3 revascularization in 65% of cases. In 60% of these cases procedure time was <40min. The additional use of stent retrievers in 37 cases improved the TICI 2b/3 revascularisation rate to 89%. The functional outcome (modified Rankin Scale (mRS) 0-2) at discharge was 49.5 %, mRS 6 in 14%.
Conclusion: Primary aspiration technique is an alternative strategy for mechanical thrombectomy as it allows high recanalisation rates with small procedure times.

B-0453 11:35

Endovascular treatment of basilar artery occlusion: RELOBA study group experience

A. Giorgianni[1], F. Biraschi[2], D. Mardighian[3], G. Pero[4], M. Crispino[5], M. Pavia[3], S. Strocchi[1], L. Valvassori[4]; [1]*Varese/IT*, [2]*Rome/IT*, [3]*Brescia/IT*, [4]*Milan/IT*, [5]*Cremona/IT (f.biraschi@gmail.com)*

Purpose: Acute basilar artery (BA) occlusion is considered among the most severe medical conditions, with very high morbidity and mortality. The aim of this study is to present 5 years experience of 12 centers of the Lumbardy area of Italy, in BA occlusion endovascular treatment (EVT) and to evaluate prognostic factors that may improve clinical outcomes and recanalisation rate.
Methods and Materials: The RELOBA registry is a retrospective multicenter collection of basilar artery occlusion undergone to EVT in the period 2010-2015. 102 patients (mean age 65 years) with proven basilar artery occlusion treated with EVT were included. Clinical, procedure and neuroradiological data were collected. Recanalisation (TICI score 2b-3) was assessed by local interventional neuroradiologist. Good (moderate) outcome was defined as a mRS score of 0 to 2 (0-3) assessed at 3 months.
Results: 39% patients had good and 46% had moderate mRS clinical outcome at 3 months. Mortality was 30%. TICI 2b-3 recanalisation was achieved by 62%. Univariate analysis showed that age, NIHSS at onset, total time to recanalisation, recanalisation TICI grade were all statistically significant ($p<0.05$) in predicting clinical outcome. Multivariate logistic regression showed total time, age, NIHSS at onset as significant independent predictors of good outcome.
Conclusion: Mechanical thrombectomy is feasible and effective in patients with acute basilar artery occlusion. A better understanding of the factors that influence the prognosis could dramatically improve patient outcome. These initial results must be confirmed by further prospective studies within a randomised-controlled settings.

B-0454 11:43

Low admission blood glucose favours good neurologic outcome and smaller final infarct size in stroke thrombectomy

T. Huber[1], M. Kaesmacher[1], J.F. Kleine[2], C. Zimmer[1], J. Kaesmacher[1]; [1]*Munich/DE*, [2]*Berlin/DE (thomas.huber@med.uni-muenchen.de)*

Purpose: High levels of peripheral blood glucose on admission (AG) are associated with a deteriorated outcome in stroke. Different pathophysiologies have been suggested, including inhibitory effects on the efficacy of IV rtPA, blood-brain barrier breakdown and reduced salvage of the penumbra. The association of AG in the context of stroke thrombectomy has not been evaluated in detail up to date.
Methods and Materials: 325 consecutive patients with acute MCA occlusion undergoing mechanical thrombectomy (MT) between 2008 and 2016 were included in this retrospective study. AG was classified on an ordinal scale ranging from normoglycaemia to severe hyperglycaemia. Final infarct volume (FIV) was segmented on postinterventional, diffusion-weighted MR images. Short-term neurologic outcome was assessed using dichotomised NIHSS variables (good outcome: discharge-NIHSS <5; substantial improvement: compound criterion of either NIHSS at discharge ≤1 or NIHSS-improvement ≥8).
Results: Higher levels of AG were associated with older age, higher admission-NIHSS, larger FIV and more severe neurologic disability (all $p<0.05$). These associations were present in all subgroups, irrespective of recanalisation results, time to recanalisation and administration of IV rtPA bridging. Higher AG was found to be an independent risk factor for lower rates of good neurologic outcome and substantial neurologic improvement (aOR 0.744, 95%-CI: 0.568-0.975 and aOR 0.745, 95%-CI 0.600-0.925, respectively).
Conclusion: Higher levels of AG are significantly associated with a poor neurologic outcome in patients undergoing MCA-thrombectomy. These findings challenge the hypothesis that an association between acute hyperglycaemia and patients' outcome may be mediated through altering the efficacy of thrombolysis and thereby favours others pathophysiologic explanations.
Author Disclosures:
T. Huber: Consultant; Brainlab AG until 09/2016 (Feldkirchen, Germany) - not related to the present study. **C. Zimmer:** Advisory Board; Philips, Bayer Schering, Clinical Neuroradiology - not related to the present study. Research/Grant Support; Biogen Idec, Quintiles, MSD Sharp & Dome,

Boehringer Ingelheim, Inventive Health Clinical UK Ltd., Advance Cor, Brainsgate, Pfizer, Bayer-Schering, Novartis, Roche, Servier, Penumbra,, WCT GmbH, Syngis, SSS Internartional Clinical Research, PPD Germany GmbH, Worldwide Clinical Trials Ltd., Phenox, Covidien, Actelion, Medivation, Medtronic, Harrison Clinical Research, Concentric,, Pharmtrace, Reverse Medical Corp., Premier Research Germany Ltd., Surpass Medical Ltd. and GlaxoSmithKline - not related to the present study.. Speaker; Philips, Bayer Schering - not related to the present study.

B-0455 11:51

Impact of thrombectomy maneuver count on recanalisation and clinical outcome in patients with ischaemic stroke

F. Seker, J. Pfaff, M. Wolf, S. Nagel, S. Schönenberger, C. Herweh, M.A. Möhlenbruch, M. Bendszus, M. Pham; *Heidelberg/DE*

Purpose: The effectiveness of thrombus retraction in patients with acute stroke using stent retrievers is variable. Here, we studied the impact of thrombectomy maneuver count on recanalisation and clinical outcome.
Methods and Materials: We retrospectively analysed data of 99 consecutive patients with acute occlusion of the terminal internal carotid artery or M1 segment of the middle cerebral artery treated with thrombectomy. Successful recanalisation was defined as TICI score of 2b or 3. Good clinical outcome was defined as mRS score of ≤2 at 90 days after stroke onset.
Results: Median thrombectomy maneuver count was 3 (range 1-10). Multivariate logistic regression analyses identified increasing maneuver count as an independent predictor of both unsuccessful recanalisation (adjusted OR 0.39, 95% confidence interval 0.22 to 0.59, P<0.001) and unfavorable clinical outcome (adjusted OR 0.56, 95% confidence interval 0.34 to 0.88, P=0.018). In cases where the thrombectomy procedure was finished within two maneuvers, a good outcome was significantly more likely compared to cases where three or four maneuvers or even more than four maneuvers were required (P<0.001). Besides, maneuver count was not associated with the occurrence of intraprocedural complications (unadjusted OR 1.01, 95% CI 0.99-1.03, P=0.436).
Conclusion: The number of thrombectomy maneuvers is strongly associated with the probability of successful recanalisation and good clinical outcome. A good outcome appears to be unlikely, if recanalisation is not achieved within four maneuvers.
Author Disclosures:
J. Pfaff: Other; JP has received travel expenses from Siemens and Stryker. **S. Nagel:** Other; SN received consulting honoraria, speakers honoraria and travel support from Boehringer-Ingelheim, Bayer, Pfizer and Brainomix Ltd.. **C. Herweh:** Other; CH has received travel expenses from Covidien. **M.A. Möhlenbruch:** Other; MAM has received consulting honoraria, speaker honoraria and travel support outside this work from Acandis, Codman, Covidien, MicroVention, Phenox and Stryker. **M. Bendszus:** Other; MB has received consulting honoraria and speaker honoraria from Codman, Guerbet, Novartis, Roche, Bayer, Teva and Vascular Dynamics. **M. Pham:** Other; MP has received speaker honoraria and travel reimbursement from Penumbra and Covidien.

10:30 - 12:00 **Room F2**

Breast

SS 602b

Contrast-enhanced spectral mammography and other new techniques

Moderators:
E.M. Fallenberg; Berlin/DE
K. Pinker-Domenig; Vienna/AT

B-0456 10:30

One step beyond contrast-enhanced spectral mammography: malignancy potential score as a new diagnostic tool in mammography

E. Nikolentzou, C. Tzimas, E. Gioutlaki, E. Feida, A.N. Chalazonitis; *Athens/GR (christostzimas@yahoo.com)*

Purpose: To propose a new score estimated quickly by the sum of BIRADS score and Contrast Enhanced Spectral Mammography strength enhancement, termed as “Malignancy Potential Score” (MPS).
Methods and Materials: From September 2014 to September 2015, 216 females underwent diagnostic mammograms, followed by CESM. 10 of these females had bilateral findings; so, 226 lesions were examined in total. We collected data from women only with BIRADS 3-5 findings. CESM findings were evaluated based on the intensity of lesion enhancement compared with background breast enhancement (-1 to 2). The score of BIRADS was added to the score of CESM. This new score served as the final diagnostic score. Histopathology reports were compared with imaging assessment. Receiver-operating characteristic (ROC) curves were used to determine the sensitivity and specificity and also to extrapolate the optimum cut-off value for MPS.
Results: 98 of 226 lesions were malignant and 128 of 226 lesions were benign. The sensitivity, specificity and accuracy rates were 91.83, 80.47 and 85.40%, respectively, when a best MPS cut-off point of 4, to distinguish benign from malignant, was used. The diagnostic accuracy and specificity of MPS were superior to that of digital mammography or CESM alone.
Conclusion: Combining the well-documented experience of digital mammography with the power of type of enhancement of CESM into one score improves diagnostic accuracy and specificity compared with digital mammography or CESM alone.MPS seems to be an efficient tool in clinical management in every-day practice serving as an additional problem-solving method in breast imaging.

B-0457 10:38

Contrast-enhanced spectral mammography for the evaluation of breast calcifications: diagnostic performance and impact on surgical planning

M.B.I. Lobbes[1], I. Houben[1], S. Vanwetswinkel[1], V. Kalia[2], P. Nelemans[1], E. Heuts[1], M. Smidt[1], J.E. Wildberger[1]; [1]*Maastricht/NL*, [2]*Reykjavik/IS (marclobbes@planet.nl)*

Purpose: To evaluate the diagnostic accuracy of contrast-enhanced spectral mammography (CESM) in breast (micro)calcifications and its impact on surgical decision making.
Methods and Materials: All screening recalled patients with suspicious microcalcifications that underwent CESM in the period October 2012 till September 2015 were included. First, radiologists provided a BI-RADS classification for the low-energy (mammographic) images only. In a session simulating a tumour board meeting, two breast surgeons (in consensus) decided on the preferred surgical treatment (breast conservative (BCT) versus mastectomy, blinded for final histopathology) for all (pre)malignant cases. After eight weeks, the evaluation was repeated for the entire CESM exam (i.e. including the recombined image with contrast information). Sensitivity, specificity, PPV and NPV were calculated using BI-RADS>4 being malignant as cut-off value. In addition, differences in surgical decision making were analysed and compared using the McNemar test.
Results: In total, 147 women were included in this study (mean age 61 years). Pathology showed 82 benign and 32 malignant lesions, with 33 ductal carcinoma in situ cases. Diagnostic performances of CESM (with differences compared to low-energy images in brackets) were: sensitivity 94% (+3%), specificity 38% (-3%), PPV 56% (0%), NPV 88% (+4%). Based on low-energy images, surgeons suggested BCT in 89% of the cases. Based on the CESM exam, their decision making did not change statistically significant (86% BCT).
Conclusion: CESM is not of added value in breast (micro)calcifications, as it neither improve their evaluation, nor helpful in guiding surgical decision making.

B-0458 10:46

The added value of contrast-enhancing mammography in assessment of breast asymmetry

R.W. Abdel Rahman; *Cairo/EG (rashakao@yahoo.com)*

Purpose: To evaluate the clinical performance of CEDM on asymmetries detected on mammogram.
Methods and Materials: This study is a retrospective analysis that included 125 females, 33 (26.4%) were presented for screening and 92 (73.6%) were presented for diagnostic mammogram in the period from March, 2015 to March, 2016 .Their age ranged from 25-81 years (mean 48.87). None of them were treated with hormonal replacement therapy. Enhanced spectral mammography (CESM) was performed using Senographe Essential; (Seno DS; GE, Buc, France) that is adapted to obtain low- and high-energy images for each mammography view. Reference stander was histopathology after core or surgical biopsy, as well as follow-up (6months) for non-enhanced asymmetry classified as normal variants.
Results: The study included 125 females. 9/125 (7.2%) had asymmetry, 92/125 (73.6%) had focal asymmetry, 23/125 (18.4%) had global asymmetry and 1/125 had developing asymmetry (0.8%). There is a significant correlation between focal and global asymmetries showing mass or non-mass enhancement and malignancy (p value ≤0.001), while asymmetry showing non-mass enhancement has significant correlation with benign pathology (p value ≤0.001). There is significant correlation between non-enhancing asymmetrical findings and benign pathology provided no associated suspicious mammographic finding (p value ≤0.001).
Conclusion: Contrast enhanced mammography provided clinical impact on breast asymmetrical density by figuring out underlying lesions and high lightening the management of asymmetry whether to be followed-up or to biopsied .
Author Disclosures:
R.W. Abdel Rahman: Author; Dr.Mohamed Gomaa, Dr. Mona Fouad, Dr .Sherief Mokhtar.

B-0459 10:54

3T multiparametric MR: contrast-enhanced (DCE) MR with DWI and single-voxel spectroscopy could predict the assessment of prognostic indicators in breast cancer?

L. Camera, C. Cavedon, I. Baglio, G. Meliadò, G. Barbazeni, S. Montemezzi; *Verona/IT (camera.lfmad@gmail.com)*

Purpose: To test whether 3T multiparametric magnetic resonance could predict the assessment of prognostic indicators in breast cancer.
Methods and Materials: 318 patients were prospectively studied with a 3T MR. We considered lesion volume, dynamic curve, apparent diffusion coefficient (ADC) provided by DWI and total choline (tCho) peak obtained from spectroscopy (single-voxel technique, volume 10x10x10mm^3). tCho signal-to-noise ratio (SNR) was used as an index of tCho concentration. The pathologic examination of surgical specimens was the standard reference. For each lesion we considered: histological type, nuclear grade, the expression of oestrogen receptor [ER], progesterone receptors [PgR], HER2 and Ki-67, categorised as subtypes luminal A, luminal B, HER2 enriched, triple negative as reported by Perou et al. [Nature(2000); 406:747-752]. Correlations were investigated by logistic regression analysis.
Results: 320 invasive malignant lesions with volume >1cm^3 were included. DCE-MRI and DWI were successfully performed in all patients; regarding spectroscopy, the spectrum quality was considered acceptable in 281/320 lesions with 83 cases that showed tChoSNR≥2. The distribution in the prognostic categories was: 112/320 luminal A; 136/320 luminal B, 39/320 HER2 enriched, 33/320 triple negative lesions. We found that high volumes were correlated with triple-negative group (P=0.002); similar results were obtained with type of curve (type 3 was correlated with triple-negative lesions, P=0.008). No statistically significant correlation was found between ADC values and the different categories. tCho was significantly correlated with the aggressiveness of cancer (P=0.003). Tumours with high volume, curve III and tCho≥2 were more likely triple-negative cancers.
Conclusion: Multiparametric breast MR could predict the assessment of breast cancer prognostic indicators.

B-0460 11:02

Role of magnetic resonance spectroscopy using choline peak as a malignancy marker in diagnosis of breast lesions classified BIRADS III and IV

M.M.K.M. Barakat, N. Chalabi; *Cairo/EG (nivine.chalabi@gmail.com)*

Purpose: To assess the diagnostic value of MR spectroscopy using choline peak as a malignancy marker in diagnosis of breast lesions categorised by mammography and/or ultrasound as (BIRADS III,IV) and correlation with histopathological findings or follow-up.
Methods and Materials: 35 female patients underwent breast MRI with single-voxel MRS performed, on a 1.5 T Philips machine. All patients included had lesions classified as BIRADS III and IV by Mamography+/- US.Single-voxel MR spectroscopic data were collected. MR spectroscopic findings were defined as positive if the signal-to-noise ratio of the choline resonance peak was 2 or greater and as negative in all other cases. MR spectroscopic results were then compared with histologic findings or at least 1 year follow-up , and statistical analysis was performed.
Results: 18 out of 35 patients had BIRADS III Lesions and 17 were BIRADS IV. 25 lesions were benign (71.4%) (7 of them were BIRADS IV lesions and 18 were BIRADS III lesions), and 10 were malignant (28.6%) (all of them BIRADS IV lesions). A choline peak was present in 13 lesions (37.1%) of 35 and in 3 of 18 benign lesions. Calculated MR spectroscopy sensitivity was 100% and specificity 88%. Positive predictive value was 76.9%, false positive rate was 12.0%, correct classification was 91.4%, misclassification was 8.6%.
Conclusion: Breast single MR scan increase the specificity of the conventional dynamic MRI in evaluating breast lesions classified as (BIRADS III and BIRADS IV) and hence reduced the number of unnecessary biopsies.

B-0461 11:10

Adjunct screening with 3-D functional infrared imaging in women with dense breasts: interim-analysis of a prospective study

R. Hellgren[1], A. Sundbom[1], P. Dickman[1], K. Czene[1], P. Hall[1], D. Izhaky[2]; [1]*Stockholm/SE*, [2]*Air Port City/IL (karmakamera99@gmail.com)*

Purpose: 3D functional infrared imaging (3DIRI) has shown high accuracy in assessment for the likelihood of breast cancer based on multiparametric evaluation of metabolic imaging biomarkers1. In this prospective study, we conducted a trial of adjunct screening with 3DIRI in women with dense breasts to evaluate the incremental cancer detection rate.
Methods and Materials: Women with breast density greater than 7.5% on their most recent mammogram were recruited at the time of their subsequent routine screening mammography to undergo additional 3DIRI. The 3DIRI findings were classified into healthy or possibly suspicion of cancer. Women with a negative mammography, but positive 3DIRI result, were referred to contrast-enhanced MRI. Diagnosis of breast cancer was verified after biopsy or surgery and histopathologic examination.
Results: 1728 women (median age 56 years) underwent digital mammography and 3DIRI screening procedures. Mammography detected 7 cancers in 7 women. Two of these 7 women had a positive 3DIRI score and 5 had a normal score. Of 1692 women with negative mammography, 225 women had a positive 3DIRI result and were referred to contrast-enhanced MRI, of which 219 completed the MRI. An additional 6 cancers were identified in 5 women, increasing cancer detection rate from 0.4% to 0.7%, demonstrating incremental cancer detection rate of 86%
Conclusion: The use of 3DIRI to select women for an MRI can result in the detection of additional cancers in women with mammographically dense breasts. Additional studies are necessary to evaluate the role of 3DIRI as adjunct to mammography for women with dense breast.
Author Disclosures:
D. Izhaky: Employee; Real Imaging Ltd..

B-0462 11:18

Detection of breast masses in dense breast tissue with a contrast-enhanced cone-beam breast CT

S. Wienbeck, V. Stahnke, E. von Fintel, J. Lotz, U. Fischer; *Göttingen/DE*

Purpose: To evaluate the conspicuity of breast lesions in dense breasts with a contrast-enhanced cone-beam breast-CT (CE-CBBCT) in comparison to noncontrast CBBCT and mammography in the diagnostic setting.
Methods and Materials: In this prospective, institutional review board approved clinical trial, women with ACR density types c and d and a BI-RADS 4 or 5 assessment in mammography and/ or ultrasound of the breast, underwent noncontrast and CE-CBBCT (Koning Corp.). Two radiologist independently scored lesion conspicuity for the different imaging modalities. Patient age, breast density type, lesions size and histopathological results were recorded. Mean lesion voxel intensity was measured in Hounsfield units (HU) of each mass and the surrounding tissue with three measurements within the same coronal slices before and after administration of contrast media.
Results: In this ongoing study non-contrast and CE-CBBCT has be done in 30 women with 49 lesions (12 benign, 18 semimalignant, 29 malignant). All malignant lesions were seen at CE-CBBCT, with a better visibility in comparison to noncontrast CBBCT or mammography. Benign lesions enhanced in median 38.9±3.5 HU. Semimalignant lesions enhanced in median 42.8±2.5 HU and malignant lesions enhanced in median 66.2±3.2 HU after contrast administration.
Conclusion: The first results with CBBCT show that the lesion detection is improved at CE-CBBCT for women with ACR types c and d in comparison to mammography and noncontrast CBBCT. Semimalignant and malignant lesions show a higher density after contrast administration in comparison to benign lesions. Quantifying lesion enhancement may aid in the detection and diagnosis of breast cancer.

B-0463 11:26

Quantitative optoacoustic imaging detects increased haemoglobin in malignant lesions

O. Abeyakoon, S. Morscher, M. Wallis, P. Moyle, S. Bohndiek, F.J. Gilbert; *Cambridge/UK (oshi.creativity@googlemail.com)*

Purpose: Optoacoustic imaging is an emerging technology, which has the potential to differentiate between benign and malignant breast tissue by exploiting the differential absorption characteristics of endogenous chromophores. Our study aims to detect quantitative changes in haemoglobin concentration/oxygenation to facilitate the differentiation of benign and malignant breast lesions
Methods and Materials: Optoacoustic images from 12 solid malignant lesions (9 no specific type NST, 2 ductal carcinoma in-situ DCIS and 1 invasive lobular carcinoma ILC) and 8 benign lesions (5 fibroadenomas, 1 post-op scar, 1 fibrocystic change, 1 sclerosing-adenosis) were analysed using Matlab. Images taken from the total haemoglobin-weighted (800nm) and deoxyhaemoglobin-weighted (700nm) images were analysed.
A region of interest was drawn around the outline of breast lesion based on anatomical information from ultrasound. All results are presented as mean and standard deviation.
Results: The lesion size ranged from 0.5-3cm. The depth range was 0.3-2.5cm. Lesion signal intensity in the total haemoglobin-weighted image increased from 11.54±1.037 in benign lesions to 15.09±1.221 in malignant lesions (p=0.0398). The result was statistically significant. An increase was also observed in the deoxyhaemoglobin-weighted image, with a rise from 13.94±0.9145 in benign lesions to 15.34±1.258 in malignant lesions. However, the increase was not statistically significant.
Conclusion: Preliminary results from the quantitative analysis of optoacoustic images are encouraging. Development of algorithms for depth correction (fluence correction) and multispectral unmixing algorithms have the potential to further refine the clinical value of quantitative optoacoustic imaging.

B-0464 11:34

Systematic review: translation of optoacoustic imaging into the breast clinic

O. Abeyakoon, S. Morcher, S. Bohndiek, F.J. Gilbert; *Cambridge/UK (oshi.creativity@googlemail.com)*

Purpose: Optoacoustic imaging is an emerging technology that measures endogenous-chromophores relevant in breast cancer. These include total haemoglobin, oxy- and deoxy-haemoglobin, water and collagen. Our systematic review (PRISMA Guidelines) evaluates the current status of clinical translation.
Methods and Materials: Four data-bases (PubMed, Scopus, Biosis, Web of Science) and one search-engine (google-scholar) were searched using the terms “optoacoustic” “photoacoustic” “photo-acoustic” “opto-acoustic” AND “breast” “mamm*”. Eligibility criteria included studies performed in humans and use of histopathology as the gold standard for diagnosing malignancy. Data extracted included prototype design, scan protocol, demographics of women scanned, cancer detection rate and correlation with other modalities where available and reasons for failure.
Results: Nine eligible publications were found with 7 prototype machines (6 with 2D probes, 1 3D probe). One prototype used a single wavelength, 4 prototypes used two wavelengths and two prototypes used four wavelengths. The resolution ranged from 0.25-4mm with depths of 2.6-6cm. In the four studies published between 2007-2014 45/73 (61.7%) invasive cancers were detected. As the technology evolved in the 5 studies published from 2014-2016 68/79 (86%) invasive breast cancers and 7/7 (100%) cases of DCIS were seen. The most common reasons for non visualisation were position of the lesion within the breast, technical and operator errors/limitations. 5 mammographically occult cancers were seen. 9/11 cancers had good co-localisation with MRI.
Conclusion: Optoacoustic imaging is a promising technique that could enhance breast cancer diagnosis. The molecular information provided has the potential to be a prognostic biomarker of outcome.

B-0465 11:42

Study of the nipple-areola complex with MRI and microcoils

M.E. Munoz, M.S. Munoz, L. Mignini, A.M. Pendino; *Rosario/AR (memf@fibertel.com.ar)*

Purpose: To evaluate Magnetic Resonance Imaging with microcoils in the study of the nipple-areolar complex.
Methods and Materials: MR with commercially available microcoils were acquired from 52 patients. The type of secretion, dilated duct (>3 mm) and 4 types of enhancements, defined as unifocal, multifocal in scattered nodes, non-mass enhancement of clustered rings (volume reconstructions showed them as sponges), and mixed pattern (nodes, rings and cyst), were registered. Three-dimensional reconstruction, with the high resolution provided by microcoils, was shared with the surgeon and pathologist.
Results: The duct diameter showed dilated in 66.7% of the cases, which was related to mass enhancement or mixed pattern (p &lt 0.0001). Of the 17 cases with non-dilated duct diameter, 13 showed hematic secretion. Among 34 cases with dilated duct, 28 had serohematic secretion (p &lt 0.0001). Unifocal enhancement was found in 38.8% of the cases, mixed enhancement in 24.5%, rings in 22.4%, and nodes in 12.2%. Of the 16 cases with non-dilated duct diameter, 10 presented enhancement as rings (sponges). 36 patients were referred to surgery; the pathologists found 13 instances of cancer and 10 papillomas. The remaining 13 cases did not present cancer. 9 of 10 papillomas presented dilated conducts and mass enhancement. 11 of the 19 cases with hematic secretion showed no dilated ducts and ring enhancement (sponges) representing micropapillary and cribriform carcinoma
Conclusion: The method is simple and effective, and claims to be used as a first line treatment of thelorrhagia and in the examination of the nipple-areolar complex.

B-0466 11:50

Performance of deep artifical neural networks in the diagnosis of breast cancer in mammography

A.S. Becker, M. Marcon, S. Ghafoor, M.C. Wurnig, T. Frauenfelder, A. Boss; *Zurich/CH*

Purpose: To evaluate the diagnostic performance of a deep artificial neural network (ANN) for the detection of breast cancer in an independent, dual-centre mammography dataset.
Methods and Materials: Mammographies from 2012 at our institution were reviewed (n=3271). Patients diagnosed with cancer or borderline lesions were identified (n=143). I) A matched control cohort was selected from the remaining patients. The ANN was trained with this dataset. From a publicly available dataset, patients with cancer and a matched control cohort were selected (n=35x2). The performance of the trained ANN was tested with this external dataset by receiving operator characteristic (ROC) analysis. II) Cases from Jan-Sept were used for training, from Oct-Dec for testing. Three radiologists (3, 5 and 10 years of experience) evaluated both test datasets. The area under the ROC curves (AUC) between readers and the ANN were compared. A Bonferroni-corrected p value of <0.016 was considered statistically significant.
Results: Mean age of patients with a lesion was 59.6 years (range: 35-88y), and in controls 59.1y (35-83y). Diagnoses were invasive ductal carcinoma in 90, ductal in situ carcinoma in 13, invasive lobular carcinoma in 13, mucinous carcinoma in 3 and borderline lesion in 12 patients. I) AUC of the trained ANN was 0.81 and comparable on the test cases 0.79 (p=0.63). One of the radiologists showed comparable performance (0.83, p=0.17), while two were significantly better (0.91 and 0.94, p<0.016). II) The ANN (0.82) performed comparable to the radiologists (0.77-0.87, p>0.016).
Conclusion: Cancer detection in mammographies with ANN shows similar diagnostic performance when compared to radiologists.

10:30 - 12:00 **Room D**

Musculoskeletal

SS 610

Bone health and osteoporosis

Moderators:
J.L. Bloem; Leiden/NL
T. Zahel; Munich/DE

B-0467 10:30

Dose reduction in MDCT-based bone mineral density and microstructure assessment: effects of low-dose simulation and sparse sampling

B.J. Schwaiger[1], K. Mei[1], F.K. Kopp[1], R. Bippus[2], A.S. Gersing[1], E.J. Rummeny[1], J.S. Kirschke[1], P.B. Noël[1], T. Baum[1]; [1]*Munich/DE*, [2]*Hamburg/DE*

Purpose: To evaluate whether in-vivo quantitative bone mineral density (BMD) and microstructure assessment after simulated dose reduction and sparse sampling combined with statistical iterative reconstruction (SIR) is still feasible for differentiating subjects with and without vertebral fractures.
Methods and Materials: In 12 subjects with osteoporotic vertebral fractures and 12 controls pairwise-matched for age and sex undergoing routine thoracic/abdominal MDCT examinations, lower radiation doses were simulated by virtual lower tube current (10, 25 and 50% of the original current) and sparse sampling (10, 25 and 50% of the original raw data). All images were reconstructed with SIR. BMD and trabecular bone microstructure parameters (including bone fraction and trabecular thickness) were extracted from the reconstructed images in T10 to L5.
Results: Effective dose of the original scan was 10 mSv, and 5, 3, 1 mSv for the 50, 25, 10% sparse sampled/low-dose simulated data, respectively. All BMD measurements calculated from different virtual lower tube currents and different sparse samplings were significantly lower in subjects with fractures compared to controls (range: 89-110 vs. 125-187 mg/ml; $P<0.003$ for all). Analogously, bone fraction (0.31-0.47 vs. 0.50-0.52, $P<0.004$ for all), and trabecular thickness were consistently lower in subjects with fractures (1.1-1.3 vs. 1.7-2.4 mm; $P<0.011$ for all).
Conclusion: After simulated dose reduction and sparse sampling, BMD and microstructure parameters obtained from MDCT examinations and processed with statistical iterative reconstruction were still significantly different in subjects with and without vertebral fractures, suggesting osteoporosis diagnosis to be feasible in low-dose protocols.
Author Disclosures:
R. Bippus: Employee; Philips GmbH Innovative Technologies.

B-0468 10:38

Establishing a method to measure bone density using spectral CT

M. Ramyar[1], C. Leary[2], R. Aamir[1], N. de Ruiter[1], A.P.H. Butler[1], T.B.F. Woodfield[1], N.G. Anderson[1]; [1]*Christchurch/NZ*, [2]*Portland, OR/US (mohsenramyar@gmail.com)*

Purpose: Combining bone structure and density measurement in 3D is required for site-specific bone quality assessment. Spectral molecular imaging can measure bone density in relation to bone structure by quantifying calcium hydroxyapatite (CaHA) in 3D space. This study aimed to optimise spectral CT methodology to measure bone density in excised human bone samples.
Methods and Materials: MARS CT with CdTe Medipix3RX detector was used with brass filter in four energy binds between 26 and 118 keV for following experiments. Two energy protocols were tested using a Perspex phantom containing four concentrations of CaHA (50, 200, 800 and 1200 mg/cm^3) to assess the linear relationship between attenuation and density and to detect anomalies in measured mass attenuation curve. Using the chosen protocol, linear response and mass attenuation curves were compared with theoretical values for CaHA and $CaCl_2$ phantoms. Two parts of the same human femoral

head were prepared in two conditions (in air and in PBS) then scanned to assess the effect of intra-osseous air on trabecular bone density measurement.
Results: The protocol with energy bins [30-45, 45-60, 60-78 and 78-118 keV] displayed linear response and anticipated mass attenuation behaviour for both CaHA and $CaCl_2$. Due to partial volume effect at bone-air interface, trabecular CaHA density measured 172 ± 46 mg/cm^3 (air present) versus 319 ± 20 mg/cm^3 (prepared in PBS).
Conclusion: We established a bone density protocol for quantifying bone density with spectral CT. In future, this method could be combined with bone structure measurement to study site-specific bone quality.
Author Disclosures:
A.P.H. Butler: Board Member; MarsBioImaging Ltd. **N.G. Anderson:** Shareholder; Mars BioImaging Ltd.

B-0469 10:46

L1 vertebra CT density measurements are too variable with different scanning protocols to be used as a simple screening test for osteoporosis

E.-L. Gerety, M.A. Hopper, P.W.P. Bearcroft; *Cambridge/UK (emma@dormand.com)*

Purpose: Osteoporosis is an increasing problem in the aging population, with insufficiency fractures causing significant morbidity and mortality. CT density of the L1 vertebral body has previously been found to correlate with bone mineral density. There has been recent interest in screening for osteoporosis in patients undergoing CT by measuring their L1 density. We aimed to determine the feasibility of a simple L1 density threshold to identify patients with osteoporosis. We investigated some of the parameters causing variability in L1 density measurements.
Methods and Materials: Retrospective study of 200 randomly selected patients from a previous audit of CT reporting of vertebral fractures. The L1 density was measured on 864 CT scans with a variety of scanners, kVp and iv contrast protocols.
Results: L1 densities for the same patient with multiple scans within 6 months varied by a mean of 27.5 HU (95%CI 23.8-31.1 HU). Iv contrast resulted in a mean increase of 24.5 HU (95%CI 21.6-27.4 HU). Changing the scan kVp from 100 kVp to 130 kVp lead to a mean decrease of 24.1 HU (95%CI 13.45 - 34.8 HU). Increasing age decreased the L1 density by approximately 1.7 HU per year.
Conclusion: There is too much variation in L1 CT density due to patient and scanning parameters to define a single threshold to identify those at risk of osteoporosis. Previous studies have been performed on more defined subsets of patients. Patient age and scanning protocol have significant effects on the measured CT density of the L1 vertebral body.

B-0470 10:54

CT-based bone strength prediction using finite element analysis: how much dose is needed?

T. Baum[1], D. Anitha[2], K. Mei[1], F.K. Kopp[1], P. Foehr[1], P.B. Noel[1], J.S. Kirschke[1], K. Subburaj[2]; [1]*Munich/DE*, [2]*Singapore/SG (thbaum@gmx.de)*

Purpose: Multi-Detector Computed Tomography (MDCT) image-based finite-element (FE) analysis has shown significant improvement in prediction of vertebral bone strength beyond bone mineral density (BMD). However, high radiation exposure limits its use in clinical routine. This study aimed to evaluate the effect of dose reduction, by means of tube exposure reduction, on bone strength prediction from FE analysis.
Methods and Materials: Fresh thoracic midvertebral specimens (n = 11) were imaged in a water bath to simulate the soft tissue environment using MDCT with different x-ray tube exposures (80, 150, 220 and 500 mAs). Differences in image quality and geometry of each specimen were measured. FE analysis was performed on all specimens to predict fracture load. Paired t-tests were used to compare the results obtained, using the highest MDCT dose (500 mAs) as reference.
Results: Dose reduction had no significant impact on FE-predicted fracture loads, with significant correlations obtained with reference to 500 mAs, for 80 mAs (R^2 = 0.997, p < 0.001), 150 mAs (R^2 = 0.998, p < 0.001) and 220 mAs (R^2 = 0.987, p < 0.001). There were no significant differences in volume quantification between the different doses examined.
Conclusion: MDCT radiation dose could be reduced substantially with no impact on strength estimates obtained from FE analysis. This finding may enable early diagnosis and advanced monitoring of osteoporosis and associated fracture risk.

B-0471 11:02

Femoral neck strength prediction in osteoporosis patients: trabecular bone analysis using tomosynthesis images

M. Fujii, T. Aoki, S. Yamaguchi, Y. Hayashida, K. Nakano, Y. Okada, K. Saito, Y. Tanaka, Y. Korogi; *Kitakyushu/JP*

Purpose: Although bone mineral density (BMD) by dual x-ray absorptiometry (DXA) has been used for the diagnosis of osteoporosis, bone marrow quality also has important implications in bone strength prediction. The purpose of this study is to determine the value of trabecular bone analysis using tomosynthesis (TS) images to BMD in femoral neck strength prediction of osteoporosis patients.
Methods and Materials: Forty-seven consecutive osteoporosis patients were included in this study. They underwent DXA, TS, and CT covering the hip joints within a week. We extracted the trabecular patterns of TS images, and obtained the total strut length (TSL), the bone volume per tissue volume (BV/TV) and the textural features (HOM: homogeneity, ENT: entropy, COR: correlation, CON: contrast, VAR: variance) as the indices of TS images. Failure load of the femoral neck, determined by the CT-based finite-element method (FEM), was used as the gold standard for bone strength. Stepwise multiple regression analysis for evaluating the availability of the TS image indices was performed.
Results: Amongst the combinations of the BMD and each index of TS images, the combination of BMD with the TSL and the VAR showed the highest correlation to the failure load by CT-FEM. The correlation between the failure load and the BMD with the TSL and the VAR (r^2=0.72) was significantly higher than that between the failure load and the BMD alone (r^2=0.67; p=0.0397).
Conclusion: TS-based trabecular bone analysis in combination with BMD measurements can potentially be used in predicting bone strength in osteoporosis patients.

B-0472 11:10

Validation of bone volume percentage and pore size measurements extracted from MR and MDCT against synthetic bone phantom

A. Ten-Esteve[1], R. García-Marcos[1], F. García-Castro[1], L. Martí-Bonmatí[1], M. Pérez[2], A. Alberich-Bayarri[1]; [1]*Valencia/ES*, [2]*Zaragoza/ES (ten_ama@gva.es)*

Purpose: The characterisation of the bone microarchitecture from MR or CT is significantly relevant to predict the risk of bone fracture. Our purpose was to evaluate the accuracy of the bone analysis methodology and compare it to the reference standard under different imaging modalities.
Methods and Materials: The reference is based on synthetic bones, consisting of 10 samples, 5 with 15% and 5 with 30% of material density that were acquired from SAWBONES® (Washington, USA) with known mass, density and pore size and were scanned using MDCT and MR. The voxel size in MDCT was of 0.234x0.236x0.67mm. The MR sequence was a T2-GRE with a voxel of 0.146x0.146x0.5mm. The image processing steps were different in MDCT and MR, according to a methodology developed in our group. Bone volume to total volume (BV/TV) was measured to define the bone percentage in the volume. Trabecular separation (Tb.Sp) was quantified by taking into account consecutive voxels corresponding to marrow cavities.
Results: Mean relative errors of 9% and 27% were obtained for MDCT and MR measurements of BV/TV, with a tendency to overestimate the parameter in 15% density samples but underestimate in 30% density samples with similar errors. Mean relative errors for Tb.Sp were of 4% and 34% for MDCT and MR, respectively.
Conclusion: MR and MDCT measurements of trabecular bone volume percentage and pore size were calibrated against the known ground truth from synthetic bones. These results add insight into the validation of bone microarchitecture imaging biomarkers.

B-0473 11:18

Characterisation of sharp force trauma and thermal injuries on human bone samples: a forensic MicroCT study

G. Pelletti[1], G. Cecchetto[1], D. Miotto[1], G. Viel[1], P. Fais[2], M. Montisci[1], S.D. Ferrara[1], C. Giraudo[3]; [1]*Padua/IT*, [2]*Bologna/IT*, [3]*Vienna/AT (chiara.giraudo@meduniwien.ac.at)*

Purpose: Identification of sharp force and thermal injuries is a main challenge in forensic medicine.Thus, aim of this study was to investigate the role of MicroCT for the detection of experimentally produced saw marks and the characterization of bone structural parameters after fire exposure.
Methods and Materials: Saw-marks were experimentally produced on eight human bone samples using either a 24-teeth-per-inch (TPI) with alternating-set or a 18-TPI with wavy-set rip-cut-saw (ie.,four samples each). Each sample was then examined by MicroCT before and after exposure to open-flame fire for two and ten minutes. For all investigated conditions, saw-marks' detectability and structural cortical (bone volume (BV_c), bone surface (BS_c), bone surface/bone volume (BS/BV_c)) and trabecular bone parameters (BV_t,

BS_t, BS/BV_t, structural model index, anisotropy degree, trabecular thickness, -spacing, -number, -pattern factor) were collected and compared using a one-way-repeated measures ANOVA with Greenhouse-Geisser correction and Bonferroni post-hoc tests.
Results: All saw-marks (n=8) were recognizable at each investigated condition (i.e., fresh, after two and ten minutes of fire exposure). BV_t and BS_t significantly decreased comparing two (BV_t mean±SD=5.16±2.96 mm^3; BS_t=133.40±69.13 mm^2) and ten (BV_t=3.48±2.23 mm^3;BS_t=97.15±56.72 mm^2) minutes exposure ($p<0.05$, each). BV_c decreased whereas BS/BV_c increased at all tested condition (BV_c values: 139.95±67.18 mm^3,131.66±71.64 mm^3,119.89±68.91 mm^3; BS/BV_c values: 5.30±1.06%, 5.48±1.29%, 5.94±1.17%, respectively fresh, at two and at ten minutes fire exposure; $p<0.05$,each). All other cortical and trabecular parameters did not show any significant difference ($p>0.05$).
Conclusion: MicroCT demonstrated to be an accurate forensic tool to investigate bone saw marks, even after thermal injuries, providing information about heat-induced bone modifications. Future studies including prolonged fire exposure are necessary to further assess these evidences.
Author Disclosures:
C. Giraudo: Research/Grant Support; Austrian Science Fund (FWF), project KLIF 382.

B-0474 11:26

The effect of vertebral osteoarthrosis (VO) and vertebral fractures (VF) on trabecular bone score (TBS): preliminary results
A. Poloni[1], C. Monaco[1], S. Rapisarda[1], G. Di Leo[2], C. Messina[1], L.M. Sconfienza[1]; [1]*Milan/IT*, [2]*San Donato Milanese/IT (alessandropoloni.md@gmail.com)*

Purpose: TBS is a textural score that provides an indirect index of trabecular microarchitecture from lumbar spine (LS) dual energy x-ray absorptiometry (DXA). We evaluated the effect of VO and VF on bone mineral density (BMD) and TBS.
Methods and Materials: We retrospectively identified all patients that performed an LS DXA in January-March 2015 together with an LS x-ray/MRI (maximum interval with DXA=6 months). Among them, we included patients with VO or VF diagnosed on LS x-ray/MRI with a maximum of two vertebrae involved. We calculated the BMD/TBS difference between vertebrae affected by VO/VF and the adjacent vertebrae with the greater values of BMD/TBS; between vertebrae affected by VO/VF and the average L1-L4 BMD/TBS (average value included the vertebrae with VO/VF).
Results: Out of 258, we included 20 patients (19 females, age=72±10y) with VO (n=13) or VF (n=7). Mean BMD (g/cm2): vertebrae with VO/VF = 1.004±0.167; adjacent-vertebrae = 0.935±0.154; L1-L4 = 0.946±0.127. Mean TBS: vertebrae with VO/VF = 1.300±0.122; adjacent-vertebrae = 1.252±0.122; L1-L4 = 1.261±0.091. Considering VO+VF together, all differences were significant ($p<0.05$), except for BMD difference between vertebrae with VO/VF and adjacent-vertebrae ($p=0.082$). Considering only VO vertebrae, all differences between vertebrae were significant ($p<0.05$). Considering only VF vertebrae, no differences were found with adjacent-vertebrae/L1-L4 for BMD and TBS ($p>0.119$). Correlations between BMD and TBS for vertebrae with VO/VF were all significant ($p<0.05$): R=0.5247 (VO+VF), R=0.6194 (only VO), R=0.9224 (only VF).
Conclusion: Compared to adjacent vertebrae and L1-L4, VO significantly impacts both on BMD and TBS, while no differences were found for VF. BMD and TBS are positively correlated, especially for VF.

B-0475 11:34

Lumbar bone marrow perfusion in osteoporosis rabbit with dynamic contrast enhancement MRI: correlation with BMD and MVD
H. Yang, Y. Li, F. Lv, O. Yu; *Chongqing/CN (frankyang119@126.com)*

Purpose: To use dynamic contrast enhancement (DCE-MRI) to assess lumbar spine bone marrow blood perfusion in osteoporosis rabbit and correlate perfusion with bone mineral density (BMD) and microvessel density (MVD).
Methods and Materials: 22 New Zealand white rabbits were randomly divided into 2 groups, including experimental group (n=12) and control group (n=10). Bilateral ovariectomies (OVX) were applied in experimental group. DCE-MRI, DEXA and immunohistochemistry exam were respectively performed both groups in 3, 5, 7 moths after OVX. Vertebral maximum percentage of enhancement (Emax), enhancement slope (ES), BMD and MVD were measured from them.
Results: BMD of lumber spine in OVX group in postoperative 7m was obviously decreased compared to control group ($P<0.05$). In postoperative 3 and 5m lumber spine bone marrow Emax and ES had no difference both groups($P>0.05$), however the significant difference were found in postoperative 7m ($P<0.05$), Emax and ES were significantly decreased in OVX group. MVD of vertebral marrow was 67.58±11.6 in control group and 39.32±9.54 in OVX group, which were significant difference between them ($P<0.05$).Vertebral marrow Emax and ES were significant positive correlation with BMD and MVD in 7m OVX group (r=0.714, 0.820, 0.866 and 0.771,$P<0.05$).
Conclusion: Lumbar bone marrow perfusion is significantly decreased in osteoporosis rabbit, similarly vertebral MVD obviously reduce too. DCE-MRI can provide more information about osteoporosis blood perfusion. Emax and ES are significant correlation with BMD and MVD. This result may suggest a vascular component in the pathogenesis of OP and is helpful to diagnosis and treatment of OP.

B-0476 11:42

Prediction of fracture non-union healing using clinical scores, contrast-enhanced ultrasound (CEUS) and dynamic contrast-enhanced MRI (DCE-MRI)
M.-A. Weber, T. Bruckner, G. Schmidmaier, H.-U. Kauczor, C. Fischer; *Heidelberg/DE (marcandre.weber@med.uni-heidelberg.de)*

Purpose: To assess whether dynamic contrast-enhanced magnetic resonance imaging (DCE-MRI) and contrast-enhanced ultrasound (CEUS) can predict fracture non-union consolidation after revision surgery.
Methods and Materials: Perfusion within non-unions of extremities was prospectively quantified in 205 patients (mean, 51.5 years; 76 female) before revision surgery and at 6, 12, 26, 52 and more weeks follow-up. 3-Tesla DCE-MRI derived signal-intensity-curves obtained from a region-of-interest analysis were normalized to adjacent muscle tissue and non-unions were classified as vascularised or not depending on the contrast uptake within the non-union. Potential infection was measured by positive microbiologic culture of the resected non-union tissue. In addition, CEUS was performed in 43 patients (mean, 46.8 years; 14 female). The ability to predict successful outcome with osseous consolidation at CT of DCE-MRI and CEUS parameters, body mass index (BMI), and the non-union scoring system (NUSS) was estimated by receiver-operating-characteristic analysis.
Results: 103/169 (61%) non-unions eventually healed and demonstrated higher perfusion than in failed consolidation at 6 ($p=0.023$), 12 ($p=0.025$) and 26 ($p=0.009$) weeks follow-up (sensitivity/specificity of DCE-MRI at 26 weeks for prediction of consolidation: 75%/87%, false classification rate: 19%). 50% of all non-unions consolidated within 14 months after revision surgery. Both a low BMI ($p=0.041$) and NUSS ($p<0.0001$) were associated with eventual consolidation. CEUS detected preoperatively increased perfusion kinetics in infected non-unions (n=16/43, rise time ($p=0.024$), time to peak ($p=0.011$), sensitivity/specificity: 93%/65%).
Conclusion: DCE-MRI at 26 weeks after revision surgery of non-unions predicts successful outcome. Preoperative vascularity in CEUS, NUSS and BMI are important prognostic factors concerning consolidation.

B-0477 11:50

Quantitative MR T_2* relaxometry in osteoporosis of ovariectomised rabbits
H. Yang, Y. Li, F. Lv, Y. Ouyang; *Chongqing/CN (frankyang119@126.com)*

Purpose: To establish a primary osteoporosis rabbit model by ovariectomy (OVX) and measure lumbar spine T_2* and R_2* MR relaxation parameters in osteoporosis rabbit and compare them with bone mineral density (BMD) and histomorphology.
Methods and Materials: 22 New Zealand white rabbits were randomly divided into 2 groups, including experimental group (n=12) and control group (n=10). Bilateral ovariectomies were applized in experimental group. MRI, DEXA and pathohistology exam were respectively performed both groups in 3, 5, 7 moths after OVX. T_2*, R_2* and BMD of lumber spine were obtained.
Results: BMD of lumber spine in OVX group in postoperative 7m was obviously decreased compared to control group ($P<0.05$). In postoperative 3m lumber spine T_2* and R_2* value had no difference both groups; but the significant difference were found in postoperative 5m ($P<0.05$) and 7m ($P<0.001$), T_2* was significantly increased and R_2* was obviously decreased. Histomorphological characteristics showed the trabecular bone were thinner, interrupted and trabecular spaces enlarged and trabecular number lessened in OVX group. Lumber spine T_2* value was significant inverse correlation with BMD in OVX group ($r=-0.599$, $P< 0.001$), and R_2* was positive association with BMD ($r=0.746$, $P< 0.001$).
Conclusion: T_2* and R_2* MR relaxation time can sensitively detect trabecular bone micro-architecture changes in osteoporosis rabbit and are significant correlation with BMD. Combination with T_2*, R_2* and BMD can better reflect bone strength and bong quality variation in early OP.

10:30 - 12:00 **Room G**

Physics in Medical Imaging

SS 613

Radiation dose estimation, measurement and reduction

Moderators:
X. Lopez Rendon; Leuven/BE
I.A. Tsalafoutas; Athens/GR

K-10 10:30

Keynote lecture
A. Trianni; *Udine/IT*

B-0478 10:39

Dose evaluation in dental, interventional and radiotherapy CBCT: the EFOMP-IAEA-ESTRO guidelines
H. de las Heras[1], R.M. Sánchez Casanueva[2], K. Mair[3], A. Baumgartner[4], F. Schöfer[1]; [1]*Zorneding/DE*, [2]*Madrid/ES*, [3]*Kempten/DE*, [4]*Munich/DE*
(hugo@quart.de)

Purpose: Investigate the applicability of the dose action levels provided in the recent EFOMP-IAEA-ESTRO guidelines for quality control of CBCT devices, and introduce one measure for patient dose estimation.
Methods and Materials: Empty scans of the most common protocols were performed in a linac, C-arm and dental scanner. The incident air kerma ($K_{a,i}$) at the flat panel was measured using a solid-state probe. The dose in the field of view D_{FOV} and the average $K_{a,i}$ at the skin of a hypothetical patient head $K_{a,i}$(skin) were subsequently calculated. A kerma-area product (KAP) meter was attached to the exit of the tube and the scan was repeated with the same exposure parameters.
Results: The KAP meter attenuates the beam intensity by 8 % (125 KVp) up to 13 % (80 KVp). The corresponding D_{FOV}, KAP and $K_{a,i}$(skin) were respectively for the dental scanner 23.1±1.4 mGy, 0.86±0.05 Gycm^2 and 3.3 ±0.2 mGy; for the interventional C-arm (high-dose protocol) 42±2 mGy, 19.8±1.2 Gycm^2 and 23.4±1.3 mGy; and for the linac (full-trajectory head protocol) 8.8±0.5 mGy, 2.74±0.16 Gycm^2 and 5.0±0.3 mGy.
Conclusion: The action level for the D_{FOV} (50 mGy) seems appropriate for common CBCT protocols (excluding high resolution). The three suggested quantities can be used for constancy tests accompanied by image quality evaluations. The $K_{a,i}$(skin), as opposed to the other quantities, represents actual patient exposure and it is sensitive to changes in the field of view and the scanning geometry. Therefore, it can be useful for both quality control and patient dose estimations.
Author Disclosures:
H. de las Heras: Consultant; QUART GmbH. **A. Baumgartner:** CEO; Baumgartner & Rath. **F. Schöfer:** CEO; QUART GmbH.

B-0479 10:47

Patient dose in CT: what is the impact of the generation of the CT scanner? Results of a decade of patient dose collection in France
P. Roch, D. Celier, S. Dreuil, C. Etard; *Fontenay-aux-Roses/FR*
(serge.dreuil@irsn.fr)

Purpose: To assess evolution of patient dose in CT since implementation of diagnostic reference levels (DRLs) in France in 2004.
Methods and Materials: Volume Computed Tomography Dose Index ($CTDI_{vol}$) and Dose Length Product (DLP) per sequence are annually collected from all CT departments by the French national institute for radiation protection (IRSN) in order to update national DRLs, defined as the 75th percentile of the distributions ($CTDI_{vol,75}$ and DLP_{75}). Evolution of $CTDI_{vol,75}$ and PDL_{75} from 2006 to 2015 was analyzed for chest, head and abdomen/pelvis CTs, based on 500 to 12700 patient dose data per examination per year. The influence of the age of the CT scanner on DLP_{75} was studied on 2013 to 2015 data.
Results: The $CTDI_{vol,75}$ for chest, head and abdomen/pelvis CTs decreased by 36%, 38% and 24% respectively, whereas the reductions in DLP_{75} were evaluated to 28%, 27% and 20%. The DLP_{75} increased significantly with the age of the CT scanner. For abdomen/pelvis CT, an increase by 35% was noticed between CT scanners commissioned in 2015 and 5 year old ones, all brands taken together.
Conclusion: Recent CT scanners enable effective patient dose reduction, mainly due to iterative reconstruction algorithms and detectors' improvement. Based on these results, French DRLs per sequence in CT (published in 2011) should be consequently reduced by 34% in average. Nevertheless, in order to optimize the global exposure of the patient, clinical DRLs taking into account all the sequences of an examination, remain necessary.

B-0480 10:55

Dental scan MDCT: comparison of dose levels and image quality assessment between three centres in two European countries
S. Puggina[1], S. Galo[2], M. Calderone[3], L. Best[4], K. Katsari[5], R. Illing[5]; [1]*Monselice/IT*, [2]*Évora/PT*, [3]*Padova/IT*, [4]*London/UK*, [5]*Amsterdam/NL*
(stefano.puggina@affidea.it)

Purpose: To analyse the relationship between radiation exposure and diagnostic image quality of dental multidetector Computed Tomography (MDCT) protocols, to determine best practice and compare to published dose figures from cone beam CT (CBCT).
Methods and Materials: Data was collected for 90 anonymised, unenhanced dental MDCT examinations from three centres in two European countries. Protocols from three MDCT scanner models were compared; Discovery 750 HD 128 with ASiR, LightSpeed VCT 64 with ASiR (GEHC, Mil. USA) and Somatom Sensation 64 with Care Dose option (Siemens Healthineers, Erlangen, Germany). GEHC DoseWatch recorded and analysed protocol parameters, gender, age, CTDIvol, DLP and Effective Dose. Images were evaluated by three radiologists using a 5-level scale for subjective quality. For visualisation of pathology, a 3-level scale was used. VGA, VGC and inter-rater reliability analysis were used in correlation with statistical analysis of the dose values. Dose values were compared to those published for dental CBCT.
Results: None of the centres were deemed to produce significantly inferior image quality on blinded assessment, but one of the three centres did give significantly less dose. Published Effective Dose figures for CBCT varies between 11µSV and 1073µSV.
Conclusion: It is possible to significantly reduce dose while maintaining image quality for dental MDCT. Work is underway to reproduce the lowest dose CT protocol on the other systems across the network. Although historical dose figures for CBCT may be lower than MDCT, without assessment of comparative imaging, conclusions as to the best method of examination cannot be drawn.

B-0481 11:03

Effective and equivalent organ doses conversion factors in coronary angiography and percutaneous coronary interventions with a radial access
M. Brambilla, B. Cannillo, R. Mathoeud, A. Bongo, A. Carriero; *Novara/IT*
(marco.brambilla@maggioreosp.novara.it)

Purpose: To derive Effective dose (ED), organ dose (H_T) and conversion factors with the Dose Area Product (DAP) in Coronary angiography (CA) and percutaneous coronary intervention (PCI) with a radial access.
Methods and Materials: The patient population included 34 patients referred for CA and 31 for PCI. ED, HT and risks were derived from in-the-field DAP measurements using Monte Carlo methods embedded in the PCXMC software.
Results: Median DAP of 23.2 and 56.8 Gy cm2 and ED of 6.9 and 20.0 mSv were found for CA and PCI, respectively. Conversion factors between DAP and effective dose were 0.30±0.04 mSv Gy-1 cm-2 for CA and 0.33±0.05 mSv Gy-1 cm-2 for PCI. The correlation between E and DAP was excellent for both CA (r= 0.99) and PCI (r=0.96). The correlation between HT and DAP for different organs/tissues ranged from r=0.87 to r=1 and from r=0.71 to r=0.98 for CA and PCI, respectively.
Conclusion: A single factor, the total DAP, can be used to reliably estimate ED and H_T without the need of a detailed analysis for each patient. While this circumstance favorably solves the issues of reliability in the estimation of ED and H_T using conversion factors, the issues of accuracy of such estimates still remains challenging. The disparities in ED/DAP and H_T/DAP conversion factors (a factor of 3) predominantly arose from differences in the phantoms used. This is of concern also considering that specific methods for organ dose estimation are being embedded in software for radiation dose data collection and reporting.

B-0482 11:11

Radiation exposure during CT-guided interventional procedures for adults
N. Guberina, S. Suntharalingam, K. Nassenstein, J. Theysohn, A. Ringelstein, M. Forsting, A. Wetter; *Essen/DE*

Purpose: The purpose of this study was to examine radiation dose levels of CT-guided interventional procedures at a large multicenter institute.
Methods and Materials: In a retrospective study design altogether 1219 CT-guided interventional procedures of different organ regions ((A) abdomen (n= 516), (B) chest (n= 528), (C) spine (n= 134) and (D) extremities (n= 41)) at different CT-scanner generations ((I) SOMATOM Definition AS+, (II) Somatom Definition Volume Zoom, (III) Emotion 6) were included in the time period from 2013-2016. Important CT-parameters, as well as standard dose descriptors like $CTDI_{vol}$ and DLP were examined. Additionally, effective and organ doses

were calculated using Monte Carlo simulation, following recommendations by ICRP103.
Results: The mean effective dose [$CTDI_{vol}$; DLP] for each of the four procedures is summarised as follows: (A) (I) 9.3 mSv [10.8 mGy; 655 mGy*cm; SSDE12.2 mGy]; (II) 13.9 mSv [13.3 mGy; 813 mGy*cm; SSDE13.2 mGy]; (B) (I) 7.3 mSv [7.8 mGy; 440 mGy*cm; SSDE8.8 mGy]; (III) 11.4 mSv [9.5 mGy; 684 mGy*cm; SSDE11.9 mGy]; (C) (I) 6.3 mSv [13.3 mGy; 460 mGy*cm]; (II) 7.4 mSv [14.4 mGy; 620 mGy*cm]; (D) (I) 4.3 mSv [9.1 mGy; 257 mGy*cm]; (II) 10.8 mSv [14.7 mGy; 777 mGy*cm].
Conclusion: This is the first data acquisition of radiation exposure during various CT-guided interventional procedures at a large interventional and diagnostic radiological centre in Germany. The assessment of radiation exposure is crucial for the determination of diagnostic reference levels. Employment of newer CT-scanner generations is recommended for CT-guided interventions in order to reduce radiation exposure.

B-0483 11:19

Monte-Carlo evaluation of mean glandular dose in spot compression mammography

A. Sarno[1], D.R. Dance[2], R.E. van Engen[3], K.C. Young[2], P. Russo[1], F. Di Lillo[1], G. Mettivier[1], K. Bliznakova[4], I. Sechopoulos[3]; [1]*Naples/IT*, [2]*Guildford/UK*, [3]*Nijmegen/NL*, [4]*Varna/BG (ioannis.sechopoulos@radboudumc.nl)*

Purpose: To characterise the dependence of mean glandular dose (MGD) on image acquisition and breast model parameters and evaluate alternative dose-related metrics in spot compression mammography.
Methods and Materials: Using a previously validated Geant4-based Monte Carlo simulation, three different previously-proposed dose related metrics for spot compression mammography were characterised: the standard normalised glandular dose to the entire breast (DgN), the normalised MGD to only the directly irradiated portion of the breast (DgN_v), and the DgN weighted by the ratio of irradiated breast mid-height area to the entire breast area (DgN_m). The variation of each with field-of-view size, spot area thickness, x-ray energy, spot area and position, breast shape and size, and system geometry using a standard breast model was studied. Comparison of the simple model results to estimates with patient-based heterogeneous breast models was also performed.
Results: As expected, DgN is lower than DgN_v for all partial breast irradiation areas, especially so for clinically used spot compression areas. DgN_m underestimates DgN by up to 14%. In spot compression, unlike in full field mammography, DgN varies considerably with breast area. Neither the difference in breast thickness between the spot compressed area and the uncompressed area, nor the position and size of the compressed area introduce a variation in DgN.
Conclusion: The results provide insight in how DgN and two alternative dose metrics behave with various image acquisition and model parameters. This will be used as part of the development of a new breast dosimetry model undertaken by the AAPM and EFOMP.
Author Disclosures:
I. Sechopoulos: Research/Grant Support; Siemens, Toshiba. Speaker; Siemens.

B-0484 11:27

SSDE calculations in thoracoabdominal CT: comparison of different approaches

C. Aberle[1], M. Obmann[1], B. Stieltjes[1], S. Schindera[2]; [1]*Basle/CH*, [2]*Aarau/CH (christoph.aberle@usb.ch)*

Purpose: To evaluate SSDE (Size Specific Dose Estimate) calculations for thoracoabdominal CT compared to the recommended method described in the AAPM Report 220.
Methods and Materials: SSDE values of 115 adult thoracoabdominal exams (52 male, 63 female, BMI-range 15.8 to 42.9 kg/m^2) from three CT scanners (Siemens Somatom Definition AS+, Flash and Edge) were evaluated using three methods. First, the study's reference was calculated according to the AAPM Report 220. A dedicated reconstruction with non-overlapping slices and a 500 mm field of view was used. Slice by slice, the water-equivalent diameter (WED) was calculated excluding the patient table, the $CTDI_{vol}$ was extracted and the SSDE was determined. The average over all slices was used as the reference SSDE. Secondly, the WED of only one slice at the center of the scan region was calculated and the SSDE was obtained using the mean $CTDI_{vol}$. Thirdly, the SSDE value was extracted from a dose-monitoring software (Radimetrics, Bayer HealthCare).
Results: The ratios of the SSDEs from the central slice method to the reference SSDEs averaged 0.96 with a standard deviation of 0.04. The ratios of the SSDEs from the dose-monitoring software to the reference SSDEs averaged 0.95 with a standard deviation of 0.04.
Conclusion: The SSDE values from the dose-monitoring software and from the central slice method are in good agreement with the reference SSDEs. They both have a root mean square deviation of less than 10% relative to the reference, which is a quality criterion proposed in the AAPM Report 220.
Author Disclosures:
C. Aberle: Research/Grant Support; The Radiology and Nuclear Medicine department receives support from Bayer. **S. Schindera:** Research/Grant Support; Siemens AG, Ulrich GmbH & Co KG. Speaker; Bayer AG Speakers Bureau.

B-0485 11:35

Accuracy of size specific dose estimate (SSDE) calculation from water-equivalent diameter of the center slice in computed tomography

J. Boos, P. Kröpil, O.T. Bethge, J. Aissa, G. Antoch, C. Thomas; *Düsseldorf/DE (Johannes.Boos@med.uni-duesseldorf.de)*

Purpose: To quantify the impact of patient size on accuracy of SSDE calculation from central slice with water-equivalent diameter (Dw).
Methods and Materials: 1812 CT scan series (1583 adult: 1195 abdominal, 388 chest, 61.5±15.7years, BMI 26.0±5.6kg/m²; 229 paediatric: 26 abdominal, 203 chest, 9.3±5.0years, BMI 17.6±4.3kg/m²) were included in this retrospective study. Dw was automatically calculated for all slices of each CT using a self-developed Matlab tool (The Mathworks, Natick, MA). SSDE were calculated: 1. based on Dw from the centre slice and overall CTDIvol; and 2. based on Dw and CTDIvol from all slices of the volume, which was regarded as the reference standard. Impact of patient weight, height and BMI on SSDE accuracy was assessed.
Results: The mean absolute relative difference between overall SSDE and the centre slice approach was 3.9±3.4% (range 0-30.5%) for adult abdominal, 5.0±3.2% (0-17.2%) for adult chest, 3.1±2.6% (0-9.2%) for paediatric abdominal and 2.0±1.7% (0-15.5%) for paediatric chest CT. Accuracy of the centre slice SSDE approach correlated with patient size (BMI: r=0.15 in paediatric chest to r=0.43 in adult abdominal CT; body weight r=0.26 in paediatric chest to r=0.49 in paediatric abdominal CT) with a tendency for dose overestimation in small and underestimation in large patients.
Conclusion: SSDE calculation using the centre slice approach leads to a mean relative absolute error of 2-5% compared to SSDE calculation with all slices of the scan volume. Accuracy of the centre slice approach is related to patient size with SSDE underestimation in large and overestimation in small patients.

B-0486 11:43

Initial estimation of an optimal dose protocol for evaluation of the lumbar spine of human cadaveric specimens in the upright position with a novel 3D x-ray system

R.M. Benz[1], D. Harder[1], J. Voigt[2], A. Fieselmann[2], F. Amsler[1], R. Menz[1], A.L. Falkowski[1], B. Stieltjes[1], A. Hirschmann[1]; [1]*Basle/CH*, [2]*Erlangen/DE (robyn.benz@usb.ch)*

Purpose: To estimate the optimal dose protocol and assess image quality and radiation dose of the lumbar spine of cadaveric specimens with a different BMI in the upright position using a prototype 3-D x-ray system and compare it to conventional CT.
Methods and Materials: The lumbar spine of five formalin-fixed cadaveric human specimens (BMI 22-35) was assessed in the upright position using 3D tomography (Multitom Rax/Siemens Healthineers/Erlangen/Germany). Specimens were scanned at a detector surface dose (DSD) of 0.696µGy with varying kV-levels (70/81/90/100/109/121kV). With the optimal kV DSD was varied (0.278/0.435/0.548/0.87/1.09µGy). Conventional CT (Somatom Definition Flash/Siemens Healthineers/Erlangen/Germany) was performed. Images were rated qualitatively (visibility of cortex/end plates/facet-joints/trabeculae/neuroforamina/posterior alignment/spinal canal/nerve roots). Noise and radiation dose were assessed quantitatively. Descriptive statistics were used ($p<0.05$).
Results: For specimens with a BMI<32 81kV and for BMI≥32 121kV and 0.87uGy yielded the best image quality. In specimens with a BMI<32, depiction of all structures was good and comparable to CT except for nerve roots. For specimens with a BMI≥32, image quality was limited. Noise did not differ significantly (1.3 vs 0.8). Dose measurements were higher in 3D tomography (mean DLP; 984±412 vs 387±102 mGycm).
Conclusion: An optimal dose protocol for 3D-tomography in the upright position of the lumbar spine in cadaveric specimens was estimated. Image quality is comparable to CT in specimens with BMI<32 and limited for soft tissue structures and specimens with BMI≥32. Patient dose is higher in 3D tomography than CT.
Author Disclosures:
J. Voigt: Employee; Siemens. **A. Fieselmann:** Employee; Siemens.
A. Hirschmann: Research/Grant Support; Siemens.

B-0487 11:51

How contrast data management complements dose data management: preliminary results

L. Pyfferoen[1], K. Van De Moortele[1], F. Zanca[2], M.-S. Walgraeve[1], C. Lafay[2], J.W. Casselman[1]; [1]*Bruges/BE*, [2]*Buc/FR (lotte.pyfferoen@azsintjan.be)*

Purpose: Increasingly medicine is being defined and evaluated based on patient outcome. The aim of this study was to assess how implementation of a contrast data management software can help in achieving best practices and better patient outcome.
Methods and Materials: In June 2015, an existing dose tracking system (DoseWatch, GE Healthcare) was upgraded with a contrast tracking module. Contrast administration data of CT-protocols using intravenous Iodine administration were collected from a GE-Revolution CT-scanner for a 7-months period. The injected volume per patient was analysed and compared to hospital specific used volume (fixed volume, adapted to patient habitus, kidney function and age) for thorax, abdomen, thorax-abdomen and neck CTs. Image quality was quantified by measuring Hounsfield Units (HU) of selected organs. The operator's impact on the administered volume was also assessed.
Results: Non-standard procedures for the investigated CT-protocols were identified. For CT-thorax-abdomen exams the contrast volume was infrequently adapted to patient habitus, resulting in large variations in image quality (e.g. liver, 351% variation in HU). The contrast volume was adapted to patient age only in 62% of patients above 80 years. Operator dependence was also observed, with less trained operators using fixed contrast volumes more often.
Conclusion: The implementation of contrast data management as a complementary tool to dose management, allows identifying unwanted variations in the administered contrast volume and therefore image quality for the same CT-protocol. As a consequence, contrast protocols optimisation and standardisation have been put in place along with increased awareness and management of the patient risk.
Author Disclosures:
F. Zanca: Employee; GE Healthcare. **C. Lafay:** Employee; GE Healthcare.

10:30 - 12:00 **Room K**

Radiographers

SS 614

Dose optimisation

Moderators:
M. Mechl; Brno/CZ
L.A. Rainford; Dublin/IE

B-0489 10:30

Radiation dose to obese patients in projection radiography: where we are

S.J.M. Alqahtani[1], K.M. Knapp[1], R. Welbourn[2], J.R. Meakin[1], R. Palfrey[1], K. Thomson[2], S.J. Rimes[2]; [1]*Exeter/UK*, [2]*Taunton/UK (sa512@exeter.ac.uk)*

Purpose: The increasing prevalence of obesity in the UK has brought new challenges in imaging this group of patients. This study aimed to investigate the dose delivered to obese patients and its relation to patient's size.
Methods and Materials: Data from 1964 patients from a bariatric clinic were reviewed with relevant approval. Patients' dose data were collected for all projection radiography and gastrointestinal fluoroscopy procedures. Multiple exams in one day including only one dose area product (DAP) reading and exams with missing DAP and exposure factors were excluded. Correlations were calculated and data analysed to yield the third quartile for each examination using STATA 14.
Results: A total of 630 patients matched the inclusion criteria. The national diagnostic reference level (NDRL) was used as a comparison. The 3rd quartile of DAP is used here. The lumbar spine (30.3 Gy.cm^2, 34 patients), abdomen (17.6 Gy.cm^2, 50 patients), pelvis (5.69 Gy.cm^2, 27 patients), cervical spine (0.9 Gy.cm^2, 16 patients) and chest (0.32 Gy.cm^2, 183 patients) all exceeded the NDRL. Weak to moderate correlations were found between DAP in abdominal x-ray and BMI (r= 0.42), height (r= 0.38) and weight (r= 0.52) with p <0.005, DAP in chest x-ray and BMI (r= 0.20), weight (r= 0.25) with p <0.005 and height (r= 0.15) with p <0.05.
Conclusion: Obese patients receive a significantly greater doses compared to the NDRL. Due to the weak to moderate correlations between DAP and patient's size, further research is needed to explore the variation of the doses delivered to obese patients.

B-0490 10:38

Do post-processing algorithms influence radiographic exposure factors?

M. Hardy[1], B. Snaith[2], A. Martin[3], C. Quinn[2]; [1]*Bradford/UK*, [2]*Wakefield/UK*, [3]*Bolton/UK (M.L.Hardy1@bradford.ac.uk)*

Purpose: The move from film-screen to digital imaging technologies was rapid in dissemination and implementation. Radiographers previously used image appearance to subjectively determine under/over exposure and adequacy of exposure factors adopted. With digital systems, image appearance is determined by computer algorithms and is not overtly visibly responsive to the exposure factors adopted. A number of studies have considered the limited impact of exposure factors on digital image appearance. This study examines whether radiographers have embraced digital measures of receptor dose adequacy or whether subjective assessment of image appearance persists.
Methods and Materials: 200 neonatal mobile chest images were randomly selected from 2 geographically distinct hospital Trusts in the North of England (100 at each site). Each site used different computed radiography image capture systems and mobile equipment. The routine exposure factors listed were identical across sites. Trends in exposure factors were determined from recorded patient and examination data. Study was registered as a service evaluation/audit in each Trust.
Results: A significant difference in proportion of Exposure Index measures that fell within, above and below locally determined thresholds was noted between sites (Chi2 = 48.996; P<0.001). Controlling for other factors, radiographer exposure factor selection appeared to be influenced by image appearance.
Conclusion: Image capture technologies have altered dramatically over last 20 years but radiographer technology interaction and its influence on decision making have been slower to evolve. A consequence of this may be the production of image of sub-optimal quality which is partially masked by the post-processing algorithms adopted.
Author Disclosures:
M. Hardy: Grant Recipient; ISRRT Award, HEE Award, CCIP HEIF Award. Other; President UKRC, Associate Editor JMIRS Journal, Editorial Board Member Radiography Journal.

B-0491 10:46

Factors influencing the effective dose and dose reduction for abdominal radiography

J. Jang, Y. Cho, J.-H. Park; *Seoul/KR (jsjang@amc.seoul.kr)*

Purpose: To identify the independent factors associated with increased radiation dose and to evaluate the effect of a patient's position on the effective dose for abdominal digital radiography.
Methods and Materials: We retrospectively evaluated the effective dose for abdominal digital radiography in 222 patients in both the supine and standing positions. The patients were divided into two groups with a cutoff value of 0.311 mSv which is the upper third quartile of the dose distribution. Using logistic regression analysis, the independent factors associated with the increased effective dose were identified. The effect of a patient's position on the effective dose was also evaluated using the paired t-test.
Results: Multivariate logistic regression analysis revealed that a high BMI (odds ratio [OR], 25.201; 95% confidence interval [CI], 8.576-74.051; P<0.001) and ascites (OR, 25.132; 95% CI, 5.381-117.376; P<0.001) were significantly associated with an increased effective dose. The effective dose was significantly decreased (22.6%) with a patient in the supine position compared with that in the standing position (P<0.001). Among them, patients with a high BMI or ascites and who were placed in the supine position received a lower 22.5% or 15.3% effective dose, respectively, compared to those in the standing position.
Conclusion: High BMI and ascites were the independent factors associated with an increased effective dose in abdominal digital radiography. The significant dose reduction in patients with these factors may be achieved by the patient being placed in the supine position during abdominal digital radiography.

B-0492 10:54

The anode heel effect: a dose reducing approach in digital thoracic spine radiography?

F. Glynn; *Dublin/IE (mae.94@hotmail.com)*

Purpose: Use of the anode heel effect to optimise image quality has been widely reported but has little, if any importance in digital radiography. No studies investigating dose optimisation by utilising the anode heel effect in thoracic spine radiography could be identified. This study set out to measure the dose to critical organs when the anode-cathode alignment and kVp and mAs exposure factors were varied for thoracic spine projections.
Methods and Materials: A Rando phantom and thermoluminescent dosimeters (TLD 100H) were used to measure the absorbed radiation dose at various sites corresponding to critical organs (thyroid, superior lung, breast,

stomach, and transverse colon). Each antero-posterior (AP) projection was recorded in two phantom orientations, first with the phantom head placed towards the cathode-end of the x-ray tube, and then in the reverse direction, while exposed at a range of 70-90kVp in intervals of 5kVp.
Results: The differences in dose to all organs between the two anode-cathode alignments were statistically significant (p-values <0.05). The greatest dose savings occurred above 80kVp. At 80kVp and 20mAs, with the anode-end of the x-ray tube towards the phantom head, the breast, superior lung and thyroid received an average dose of 35%, 33% and 163% lower, respectively in the AP projection, than those obtained in the reverse orientation. The pattern of dose distribution at the two tube orientations applies to each exposure factor combination investigated.
Conclusion: Patients should be positioned with the head placed towards the tube's anode for thoracic spine radiographs to achieve significant dose reductions.

B-0493 11:02

An evaluation of the size-specific dose estimates (SSDE) in fast kVp switching dual-energy imaging

K. Yagami[1], T. Miyoshi[1], S. Shigeyama[1], H. Okada[1], S. Suzuki[2]; [1]*Gifu/JP*, [2]*Toyoake/JP (yagami@gifu-u.ac.jp)*

Purpose: The aim of this study was to evaluate the SSDE in fast kVp switching (gemstone spectral imaging [GSI]) dual-energy CT (DECT) imaging by comparing with the measured absorbed dose.
Methods and Materials: The 64 detector row CT system was used for dose measurement. A human equivalent phantom with thermo-luminescent dosimeters inside and on the surface was used to measure the SSDE and the absorbed dose. The tube current was 360mA and the tube voltage was GSI. The scanning conditions were the same as those used in clinical practice, and the scanning range was set from the thyroid gland to the symphysis pubis. The conversion factor and the SSDE were calculated based on AAPM report 204.
Results: The indicated CTDIvol. was 10.34mGy. The conversion factor in each slice of the human equivalent phantom was minimum at 1.35 and maximum at 1.80. The SSDE was lowest at 14mGy and highest at 19mGy. The measured absorbed dose was lowest at 14mGy and highest at 25mGy. The differences between the measured absorbed dose and the SSDE were within 10% in the thoracic and pelvic regions, while the measured absorbed dose was approximately 35% higher than SSDE in the abdominal region. The SSDE was lower than the measured absorbed dose in thoracic, abdominal, and pelvic regions.
Conclusion: This phantom study suggested that the SSDE may be lower than the measured absorbed dose in GSI imaging.

B-0494 11:10

An investigation into knowledge of radiation dose as an influential factor in collimation practice

J. Doyle, K. Matthews; *Dublin/IE (jenniferannedoyle@gmail.com)*

Purpose: To investigate influences on current collimation practices in Irish radiography departments, and establish whether knowledge of actual radiation dose differences could be used to compel improved collimation practice.
Methods and Materials: The study was conducted as an online image-based survey in which four radiographs were rated on a Likert scale of acceptability for six clinical situations. Stratified sampling was applied to the population of Irish radiographers and 57 responses were obtained. Non-parametric analysis of variance (Wilcoxon signed-ranks test) was performed to establish whether acceptability of the images changed significantly depending on the situation. Images were presented first without information, and secondly alongside associated organ doses. Variance between mean Likert scores with and without dose information was analysed using Wilcoxon signed-ranks test. Dose information was measured in an x-ray laboratory using TLD100Hs. Participants also rated influences on their practice when collimating the primary beam and post-processing images.
Results: Radiographer tolerance of poor collimation varied significantly based on clinical situation ($p<0.003$), with poor collimation least acceptable in co-operative patients and most acceptable in difficult patients. When presented alongside organ doses poor collimation was considered less acceptable, with significant differences when breast and thyroid doses were presented ($p<0.05$), but no significant difference with colon or peripheral lung dose.
Conclusion: A variety of factors influence radiographers' collimation practice. Radiographers have different acceptability levels depending on the clinical situation. Radiographers could be encouraged to collimate more accurately by education on organ doses associated with poor collimation and radiation sensitivity weighting factors of radiosensitive organs.

B-0495 11:18

Impact of the anode heel effect on image quality and effective dose for AP pelvis: a pilot study

C. Buissink[1], M. Bowdler[2], A. Mohammed[2], S. Al-Murshedy[2], T.K. Urdahl[3], S.C. Soares[4], Y.R. Rey[5], J. Jorge[5], L. Peters[1]; [1]*Groningen/NL*, [2]*Manchester/UK*, [3]*Oslo/NO*, [4]*Lisbon/PT*, [5]*Lausanne/CH*

Purpose: This study proposes a method together with pilot data to determine whether the anode heel effect has an impact on image quality and effective dose (E) for AP pelvis.
Methods and Materials: An adult CIRS ATOM dosimetry phantom with high sensitivity TLDs and an adult anthropomorphic pelvis phantom were positioned with feet towards anode and feet towards cathode. For each anthropomorphic phantom orientation exposures were made using 75, 80 and 85kVp and 18, 22 and 27mAs at 110cm SID. Twelve images were taken of the anthropomorphic phantom in each orientation and then assessed for physical and visual quality by signal-to-noise ratio (SNR) and two-alternative-forced-choice (2AFC). Six exposures were then made of the ATOM phantom in each orientation using 75, 80 and 85kVp and 18, 22 and 27mAs at 110cm SID; E was calculated from organ dose data.
Results: For 2AFC data, no significant difference ($p=0.811$) was found in image quality between orientations; SNR achieved significance between the two orientations ($p<0.05$). E showed no significant difference ($p=0.207$) between the two orientations.
Conclusion: No significant difference in visual image quality, or E was observed. Whilst significance was achieved for SNR this is not likely to have any clinical impact as image interpretation is a visual task. The method proved fit for purpose however the findings should be treated with caution. Further work is proposed, to increase the number of images to be evaluated and doses to be compared for the two orientations along with a lesión detection performance study.

B-0497 11:26

Steps to an optimisation process

J. Santos[1], C. Almeida[2], G. Paulo[1]; [1]*Coimbra/PT*, [2]*Lisabon/PT (joanasantos@estescoimbra.pt)*

Purpose: Analyse the exposure parameters and dose levels of three most common procedures per image modality in order to audit and implement optimisation measures.
Methods and Materials: Exposure parameters and dose values of plain radiography (in terms of dose area product- DAP), computed tomography (CT) (in terms of CTDI and DLP) and interventional neuroradiology (in terms of DAP) procedures were directly collected on the equipment's with daily quality control. During this prospective study, patient data as examination identification (ID), gender, weight and height was also collected before the examination.
Results: Standard patients were selected from the 300 patients analysed data and diagnostic reference levels were calculated for chest, abdomen and pelvis radiographs (11, 280 and 372 mGy.cm); head, abdomen and abdomen-pelvic CT in terms of CTDI and DLP (1000, 300, 500 mGy.cm); diagnostic cerebral angiography, cerebral aneurism embolisation and stroke emergency treatment (320, 242, 280 mGy.cm).
Conclusion: Considering the obtained results, optimisation measures were implemented and data is being collected in order to analyse and compare the impact on dose levels. The examination ID will be also used to compare image quality pre- and post-optimisation.

B-0498 11:34

Universal dose electronic ID (UdoseeID): a step into the future without barriers

L.P.V. Ribeiro, A. Abrantes, L. Guerra, R.P. Almeida, F. Ramos, S. Rodrigues, J. Guerreiro, A. Ribeiro; *Faro/PT (luispedroribeiro@hotmail.com)*

Purpose: The European Directive 2013/59/Euratom was unanimously adopted by the Council of the European Union and it was expected to have a relevant and positive impact on European radiology. It put on paper the need for justification of medical exposure introduces requirements concerning patient information and strengthens those for recording and reporting doses from radiological procedures.The main objective of this project was to create, apply and develop a universal application on site for registration and monitoring of radiation doses to which patients are exposed in radiological exams in all of health facilities that use ionizing radiations for clinical purposes.
Methods and Materials: We have developed a multi-profiled site, based on user authentication permissions, where the radiographers (including nuclear medicine radiotherapy professionals) can registry the dose exposure and in cases when in which its institutions are not registered on the site patients provide credentials that allows to do it. The patient with the dose electronic ID has the ability to consult and provide information from clinical exposures through a simple internet login.

Results: According to the directive, the professionals involved in medical exposure are fundamental to ensure adequate protection of patients undergoing medical radiodiagnostic and radiotherapeutic procedures. With the provided tool and the patient collaboration the universal dose electronic ID, could be the answer for acomplishing the European Directive 2013/59/Euratom.
Conclusion: This tool is universal and gives the possibility to the patient to have long-life registry of all doses that is subjected in medical imaging and radiotherapy procedures.

B-0488 11:42

Evidence of dose optimisation with a single UK radiology department
A. England[1], L. Harding[2], R. Penney[2], R. Wilde[3], F. Dunn[3], A. Manning-Stanley[1], P. Evans[2]; [1]*Manchester/UK*, [2]*Warrington/UK*, [3]*Liverpool/UK (A.England@salford.ac.uk)*

Purpose: Optimisation is a fundamental requirement of radiographic practice. The degree in which this is routinely undertaken is likely to vary and is difficult to quantify. The aim of this study was to assess levels of dose optimisation within common radiographic projections.
Methods and Materials: Within a large state hospital DICOM information was extracted from three digital radiography rooms over a two-month period. Radiographic examinations assessed included chest, abdomen, shoulder and knee. Data extraction was by bespoke software and included demographics and all available procedure/dose-related parameters. Study data were then compared with default protocols to identify evidence of optimisation. Patients under the age of 16 were excluded and all projections were subject to visual scrutiny.
Results: Data from a total of 1250 examinations were collected. With paediatric patients removed data analysis was undertaken on 1245 (99.6%) examinations (724 women; mean (SD) age 57 (18) years). Examinations were equally split between the four anatomical areas. In terms of kVp, for chest radiography, parameters were adjusted from the default in six (2.4%) cases. For abdominal radiography parameters were adjusted in a greater number of cases (29/247; 11.7%). For shoulder and knee radiography kVp settings were adjusted in 3.2% of cases. For mAs (non-AEC examinations) 6 out of 581 (1.0%) projections (knee/shoulder) had adjustments from the baseline protocol.
Conclusion: Based on this initial assessment of DICOM header data exposure factors appear to be infrequently adjusted and this raises questions regarding levels of dose optimisation within clinical practice.

B-0496 11:50

Radiation dose from pelvic radiography: a comparison of three digital radiography (DR) systems
A. England[1], P. Evans[2], F. Dunn[3], A. Manning-Stanley[1], L. Harding[2], E.M. Taylor[2]; [1]*Manchester/UK*, [2]*Warrington/UK*, [3]*Liverpool/UK (A.England@salford.ac.uk)*

Purpose: To compare the radiation dose and image quality between the three digital radiography (DR) systems when undertaking examinations of the pelvis.
Methods and Materials: Using a Carestream Directview, Siemens Ysio and a Samsung XGEO, a series of antero-posterior (AP) pelvic images were obtained using a phantom. Images were obtained using 75 kVp, outer AEC chambers and the source to image distance (SID) was varied from 115 to 140cm, 5cm intervals. The phantom was also imaged across two orientations, outer AEC chambers nearest the head and then the feet. Field size, centring point, grid usage and focal spot were fixed throughout the study. For each examination tube potential, mAs and source to skin distance were recorded. Entrance surface dose including scatter (ESD) and effective dose (ED) were calculated using the PCXMC software. The resultant images were independently assessed for image quality by two blinded observers using a previously established scoring system.
Results: The lowest ED (0.105 mSv) was achieved at 125 cm, outer AEC nearest the feet and when using Siemens DR. The highest dose (0.161 mSv) was at 105 cm, outer AEC chambers nearest the head and when using Samsung DR. When compared with a reference image (current parameters) the image obtained with the lowest ED was graded as having the same image quality.
Conclusion: Based on the equipment and acquisition factors investigated there are differences in ED between systems. Such differences should be factored into dose optimisation strategies or attempts should be made to normalise doses between systems.

10:30 - 12:00 **Room M 1**

Cardiac

SS 603
Myocardial infarction

Moderators:
M. Hrabak Paar; Zagreb/HR
A. Tóth; Budapest/HU

K-07 10:30

Keynote lecture
M. Gutberlet; *Leipzig/DE*

B-0499 10:39

An experimental study on use of 7T MRI for evaluation of myocardial infarction in SD rats
Y. Zhang[1], L. Yang[1], F. Gao[2]; [1]*Guizhou/CN*, [2]*Sichuan/CN (102651873@qq.com)*

Purpose: This study aims to build the myocardial infarction model in SD rats transfected with pcDNA 3.1(+)/VEGF$_{121}$ plasmid and study the effect of the transfection using 7T MRI.
Methods and Materials: Twenty-four male SD rats were randomly divided into 2 groups, plasmid transfection group (with improved coronary perfusion delivery) and myocardial infarction model group. Cardiac cine magnetic resonance imaging (Cine-MRI), T2-mapping and late gadolinium enhancement (LGE) cardiac imaging were performed at 24h, 48h, 72h and 7d after myocardial infarction, respectively. The signal intensity, area at risk (AAR), myocardium infarction core (MIC) and salvageable myocardial zone (SMZ) were compared. The hearts were harvested for anatomic characterisation, which was correlated to pathological examination (TTC staining, HE staining, Masson staining and immunohistochemical staining).
Results: The Cine-MRI results showed that plasmid transfection group had higher end-diastolic volume (EDV) with a reduction in MIC and SMZ, as compared with the myocardial infarction model group. MIC, SMZ and AAR of the plasmid transfection declined over time. At 7d, the two groups did not differ significantly in AAR and T2 value. According to Western Blotting, VEGF was up-regulated, while CaSR and caspase-3 were downregulated in the plasmid transfection group, as compared with the model group.
Conclusion: 7T CMR provide a non-invasive quantification of the treatment efficacy. The myocardial protection of the plasmid transfection group may be related to the inhibition of myocardial apoptosis, vascular endothelial cell (VEC) proliferation and collagen proliferation. The CaSR signaling pathway may contribute to reversing the apoptosis.
Author Disclosures:
Y. Zhang: Author; Yan Zhang. **L. Yang:** Author; Li Yang. **F. Gao:** Shareholder; Fabao Gao.

B-0500 10:47

Prospect CMR study: prognostic stratification in patients with stelevation myocardial infaction over transthoracic echocardiography by CMR
G. Pontone[1], D. Andreini[1], G. Ferro[2], A. Guaricci[3], M. Guglielmo[1], S. Mushtaq[1], A. Baggiano[1], P. Carità[2], M. Pepi[1]; [1]*Milan/IT*, [2]*Palermo/IT*, [3]*Bari/IT (gianluca.pontone@ccfm.it)*

Purpose: We sought to evaluate additional value of a multiparametric cardiac magnetic resonance (CMR)score in comparison with traditional TIMI (Thromolysis in Myocardial Infarction) score and transthoracic echocardiography (TTE) score in prognostic stratification of ST-elevation myocardial infarction (STEMI) reperfused by primary percutaneous coronary intervention (PCI).
Methods and Materials: 209 STEMI patients reperfused by primary PCI underwent TTE and CMR 3 days after the index event. We measured: TIMI score, left ventricle ejection fraction (EFTTE), left ventricle end-systolic volume (LVESVTTE) and number of myocardial segment with wall motion abnormalities (WMITTE) measured by TTE, left ventricle ejection fraction (EFCMR), left ventricle end-systolic volume (LVESVCMR) and number of myocardial segment with wall motion abnormalities (WMICMR) measured by CMR, myocardial salvage index (MSI) and presence of microvascular obstruction(MVO). The primary clinical endpoint of study was the occurrence of major adverse cardiac events (MACE) defined as combined endpoint of hospitalisation, acute coronary syndrome, implantable defibrillator and cardiac death.
Results: Patients experiencing MACE showed higher TIMI score, LVESVTTE, WMITTE,LVESVCMR,WMICMR,prevalence of MVO and lower EFTTE, EFCMR and MSI.Two different models based on a binary score were created: a) Model 1 based on clinical parameters andTTE: TIMI <3=0 or >3=1; LVESVTTE<25ml/m2=0 or >25ml/m2=1; EFTTE>50%=0 or <50%=1;

WMITTE<7=0 or >7=1; b)Model 2 based on CMR:LVESVCMR<55ml/m2=0 or >50ml/m2=1; EFCMR>50%=0 or <50%=1; WMICMR<7=0 or >7=1;MSI>0.47:0 or <0.47:1; MVO: absence=0 or presence=1. Clustering the study population for both model with a score threshold of 2,model 2 provide a better prognostic stratification as compared to model 1 with a significant incremental prognostic value on the top of traditional outcome model.
Conclusion: A multiparamteric approach with CMR including markers of myocardial damage provide incremental prognostic information.

B-0501 10:55

T1 and T2 Mapping cardiovascular magnetic resonance to differentiate acute from chronic myocardial infarction

E. Tahir, M. Sinn, K. Muellerleile, S. Bohnen, M. Avanesov, J. Starekova, C. Stehning, G. Adam, G. Lund; *Hamburg/DE (e.tahir@uke.de)*

Purpose: Novel T1 and T2 mapping CMR techniques could provide incremental information to differentiate acute from chronic myocardial infarction (MI). We compared these techniques to standard T2-weighted CMR.
Methods and Materials: 67 patients with first-time AMI were enrolled. CMR were obtained at 8 ±5 days after infarction (baseline) and 6 ±1.4 months. All acquisitions were performed on end-diastolic LV short-axes. T2 relaxation times were quantified using a free-breathing, navigator-gated multiecho sequence. T1 relaxation times were measured using the modified Look-Locker inversion recovery sequence. Parametric maps were generated using a plug-in for OsiriX software (Pixmeo, Switzerland). Two experienced observers independently placed ROIs in the infarcted areas using LGE as a reference standard. A T2w-ratio was also generated: T2w-ratio = Mean SIinfarct/Mean SIremote.
Results: Native T1 had an almost perfect discriminative performance between acute and the chronic MI (AUC of 0.984), which was significantly superior to the T2w-ratio with an AUC of 0.906 (P<0.05) and to T2 with an AUC of 0.903 (P<0.05). ECV had a poor discriminative performance with an AUC of 0.655, which was significantly inferior to the other techniques (P<0.001). The cut-off of ≥1138 ms for native T1 provided a sensitivity and specificity of 96% and 100%, respectively. The other cut-offs were as follows: ≥3.3 for T2w-ratio, ≥69ms for T2 and ≥39% for ECV.
Conclusion: Native T1 is the best discriminator between acute and chronic MI and should preferably be used as an objective truly quantitative parameter to differentiate between the acute and chronic stage of MI.
Author Disclosures:
G. Lund: Grant Recipient; Deutsche Forschungsgemeinschaft.

B-0502 11:03

Feature tracking assessment using cardiovascular MRI for the prediction of adverse left ventricular remodelling after STEMI

J. Lee, S. Kim, J. Kim, M.-R. Kwon, M. Seong, S. Yang, Y. Choe; *Seoul/KR (sig.jhl@gmail.com)*

Purpose: To investigate the feasibility of feature-tracking assessment using cardiac MRI (CMR) for the prediction of adverse LV remodelling after ST-elevation myocardial infarction (STEMI).
Methods and Materials: We retrospectively searched our institution's database between July 2010 and September 2015 for patients with a history of STEMI, who underwent reperfusion therapy, post-reperfusion CMR, and follow-up CMR. A total of 83 patients were included in the analysis. CMR included cine imaging and late gadolinium enhancement imaging. Feature-tracking assessment for myocardial strain was performed using steady-state free-precession cine imaging. Volumetric analysis and evaluation for presence of intramural haemorrhage, microvascular obstruction, and oedema were also performed.
Results: Patients were divided into two groups, ac0cording to the presence of adverse LV remodelling; STEMI without adverse remodelling (n=64) and STEMI with adverse remodelling (n=19). Significant differences in global longitudinal strain (GLS) using 2D analysis (-13.3±3.5 vs - 10.9±3.6, p = 0.01), GLS using 3D analysis (-13.4±2.8 vs -11.4±2.4, p < 0.01), and global circumferential strain using 3D analysis (-14.2±3.1 vs - 12.6±2.9, p = 0.048) were observed. Univariate logistic regression models using GLS showed significance with an AUC of 0.687 and 0.702, in 2D and 3D analyses, respectively.
Conclusion: Global longitudinal strain in both 2D and 3D analyses were significantly different between groups with and without adverse LV remodeling. CMR strain analysis, early after reperfusion for STEMI, may aid in the prediction of adverse LV remodelling.

B-0503 11:11

Depiction of adverse remodelling after ST segment elevation myocardial infarction by T1 mapping and ECV on 3 Tesla MRI

Ö. Ates[1], K. Ercan[1], A. Ertem[1], F. Eyüpkoca[1], F. Arslan[2], C. Şabanoğlu[1], T. Çimen[1], Z. Güven[1], E. Kızıltunç[1]; [1]*Ankara/TR*, [2]*Utrecht/NL (omfarat@hotmail.com)*

Purpose: To demonstrate adverse remodelling in the remote myocardium of post myocardial infarction patients as well as comparison of native-T1 values and ECV values between post-MI patients and normal controls.We also evaluate the prognostic value of T1-relaxation and ECV scores post-MI patients.
Methods and Materials: Patients with history of ST elevated MI(first-MI) and healthy controls were included the study.Patients with diseases that may affect myocardial remodelling other than current MI, and patients having suboptimal imaging quality were excluded.Follow-up were scheduled at two weeks and sixth month post-MI;prognostic indicators including EF, end-diastolic volume, MI volume and extent, transmurality and microvascular obstruction were assessed using cardiac magnetic resonance imaging.Remote myocardium were used to perform T1 mapping and ECV calculation.Native-T1 values and ECV scores were compared between patients with MI and adverse remodelling, patients with MI without adverse remodelling and control group.Association of prognostic indicators, T1 values and ECV scores were also evaluated.
Results: 31 patients (11 adverse remodelling, 7 MVO) and 22 healthy control were included to study.There was no difference in native-T1 value between MI and control group, but ECV scores were significantly higher in MI group (ECV scores in MI group vs.control group p<0.001). In MI group, MI ratio and MI extent, transmurality, MVO, native-T1 values and ECV scores of remote myocardium had significant correlation with adverse remodelling. Moreover, ECV scores alone had significant correlation with MI extent, 2. weeks LVEDV, 6. months LVEDV and MI area ratio.
Conclusion: ECV and Native-T1 may be used to demonstrate adverse remodelling in post-MI remote myocardium and ECV scores may also be correlated with poor prognostic factors.

B-0504 11:19

Towards quantitative cardiac CT imaging: texture analysis of myocardial infarction

R.M.M. Hinzpeter, M.W. Wagner, M.C. Wurnig, R. Manka, H. Alkadhi; *Zurich/CH (Ricarda.Hinzpeter@usz.ch)*

Purpose: To investigate the ability of texture analysis (TA) for CT imaging to distinguish through quantitative image information between healthy subjects and patients with acute myocardial infarction (MI).
Methods and Materials: Twenty patients (8 females; mean age 42±15.2 years) with no cardiac abnormalities (hereafter termed controls) and twenty patients (5 females; mean age 56±10.3 years) with proven acute MI underwent cardiac CT. Short axis reformations of the left ventricle (LV) were reconstructed at slice thicknesses of 1mm, 2mm, and 5mm. Two independent, blinded readers segmented the LV myocardium in controls and patients. TA was performed yielding first-level features (based on the histogram), second-level features based on the grey-level co-occurrence matrix (GLCM), and third-level features based on the grey-level run-length matrix (GLRLM).
Results: Inter- and intrareader agreement was good to excellent for all first and second-level features (ICC:0.661-0.988), and was variable for the third-level features (ICC:-0.115-0.991). Multivariate logistic regression analysis showed the single best feature from each level to be an independent predictor of acute MI (kurtosis, OR 0.86, P=0.019; correlation, OR 0.97, P=0.22; short run high grey-level emphasis, OR 1856, P=0.79). The AUC showed best results when combining the features kurtosis and short run high grey-level emphasis (AUC:0.985) and when using the 5mm short axis reformations.
Conclusion: TA can be used in cardiac CT for distinguishing healthy from acutely infarcted myocardium with most reproducible and accurate results at a short axis slice thickness of 5mm.

B-0505 11:27

Reproducibility and agreement of early synthetic PSIR imaging as compared to the conventional LGE approach for myocardial infarct areas

R. van Dijk, D. Kuijpers, T. Kaandorp, P. van Dijkman, R. Vliegenthart, P. van der Harst, M. Oudkerk; *Groningen/NL (r.van.dijk02@umcg.nl)*

Purpose: Synthetically reconstructed enhancement images in adenosine magnetic resonance perfusion imaging show potential for the assessment of myocardial viability. We compared Early Synthetic Phase-Sensitive-Inversion-Recovery (PSIR) images from post-contrast T1-mapping to the conventional PSIR late Gadolinium enhancement (LGE) approach and assessed reproducibility and agreement of quantification of myocardial infarct areas.
Methods and Materials: Presence of LGE was assessed in 214 consecutive patients suspected of myocardial ischemia. The volume of myocardial infarct

areas was quantified on a per-segment basis in both synthetic (2-3 min post-Gadolinium) and conventional (9 min post-Gadolinium) PSIR images by two independent observers twice using semi-automatic LGE volume quantification software (MASS analytical software, Medis, Leiden). Pearson correlation and Bland-Altman analysis were performed to assess inter- and intra-observer correlation (R^2) and agreement (mean difference) of LGE quantification between synthetic and conventional PSIR images.
Results: There were 37 infarct-related LGE areas [RV1] in 21 patients with a median volume of LGE of 1.9 [0.4;7.3] mL in the synthetic images and 2.1 [0.4;7.2] mL in the conventional images (p-value: 0.386). Correlation and agreement between synthetic and conventional images were excellent with R^2 = 0.995 and mean difference of -0,028±0,289). Inter-observer R^2 was 0.998 for both synthetic (mean difference, -0,056±0,079) and conventional (mean difference, -0,057±0,087) images. Intra-observer R^2 between synthetic and conventional images were 0.995 (mean difference -0,028±0,156), and 0.994 (mean difference -0,029±0,157) for observer 1 and observer 2, respectively.
Conclusion: Synthetic images calculated from T1 mapping early post-contrast show high reproducibility and agreement for myocardial LGE areas compared with conventional LGE images.

B-0506 11:35

Assessment of cardiac dynamics in a mouse model of myocardial infarction by optoacoustic imaging
F. Lohöfer[1], H.-C. Lin[2], X. Déan-Ben[2], M. Kimm[1], H. Haas[1], D. Razansky[2], M. Wildgruber[3]; [1]*Munich/DE*, [2]*Neuherberg/DE*, [3]*Münster/DE*
(fabian.lohoefer@tum.de)

Purpose: The aim of this study is the evaluation of contrast-enhanced three-dimensional optoacoustic (OA) imaging without cardiac gating in a mouse model of myocardial infarction.
Methods and Materials: Contrast-enhanced three-dimensional optoacoustic (OA) imaging at high volumetric frame rate was used. Real-time volumetric cardiac perfusion parameters were measured using indocyanine green (ICG) as optical contrast agent. A murine myocardial infarction model optimised for acquisition of artefact-free optoacoustic imaging was used. Functional parameters, including pulmonary transit time and non-linearity of the heartbeat, were compared between infarcted and healthy mice. MRI was used as a reference for assessment of cardiac function.
Results: Optoacoustic imaging was able to extract key cardiac parameters, such as pulmonary transit time and heart rate, on a beat-by-beat basis. Infarcted hearts (N=9) could be differentiated from healthy controls (N=3) with a significantly higher pulmonary transit time (2.35s (2.07s-2.4s) versus 1.25s (1.20s-1.32s), p=0.0195). Non-linear heartbeat dynamics was stronger in the healthy hearts, as evinced by the second and third harmonic components in the heartbeat spectra. MRI revealed that the pulmonary transit time increases with the size of infarction and increases with reduced ejection fraction.
Conclusion: Optoacoustic imaging can depict cardiac anatomy, function and molecular signatures, both with high spatial and temporal resolution. Beat-by-beat volumetric optoacoustic characterization of cardiac dynamics can provide new insights into the pathophysiological mechanisms of myocardial ischaemia.

B-0507 11:43

VINTAGE study: diagnostic Value of QT evaluation In aNterior STsegment elevAtion myocardial infarction for predictionof myocardial salvaGE index, as compared to CMR
A. Guaricci[1], G. Pontone[2], P. Carità[3], D. Andreini[2], M. Guglielmo[2], S. Mushtaq[2], A. Baggiano[1], M. Verdecchia[4], M. Pepi[2]; [1]*Bari/IT*, [2]*Milan/IT*, [3]*Palermo/IT*, [4]*Chieti/IT*

Purpose: Myocardial salvage index (MSI) measured by cardiac magnetic resonance (CMR) allows to evaluate the myocardial damage in ST elevation myocardial infarction (STEMI). QT interval corrected for heart rate at ECG (QTc) prolongs in all patients with early transmural ischaemia. We sought to evaluate the correlation between QTC time change after STEMI and MSI as detected by CMR in STEMI patients underwent primary percutenous intervention (PCI).
Methods and Materials: Fifty anterior STEMI patients reperfused by primary PCI underwent quantitative ECG repolarization analysis and CMR. The difference (ΔQTc) between QTc of ischaemic myocardium (maximum QTc in anterior leads) versus remote myocardium (minimum QTc in inferior leads) over the first week, left ventricle end-diastolic (LVESVCMR) and end-systolic volume (LVESVCMR), numbers of myocardial segments with wall motion abnormalities (WMA index), ventricle ejection fraction (EFCMR) and myocardial salvage index (MSI) were measured.The endpoint was defined as MSI>0.6.
Results: The QTc in anterior leads was longer than QTc in inferior leads (p<0.0001) over the first week.There was a significant correlation between ΔQTc at 6th day and percentage of LGE (r:0,49, p 0.0007) and MSI (r:0.48; p:0.0012). At univariate analysis peak myocardial enzymes, LVEDVCMR, LVESVCMR, AWM index and ΔQTC at 6th day were independent predictor of high MSI (>0.6),while at multivariate analysis only WMA index (p:0.05) and ΔQTC at 6th day (p:0.02) still remained as predictors of endpoint.The receiver operative curve of ΔQTC at 6th day showed a AUC of 0.78 to predict a MSI>0.6.
Conclusion: ΔQTC is inversely correlated with MSI and it could represent an easy tool to evaluate the myocardial damage after PCI in STEMI patient

B-0508 11:51

Effect of inversion time on the precision of myocardial late gadolinium enhancement quantification evaluated with synthetic inversion recovery MR imaging
A. Varga-Szemes[1], R.J. van der Geest[2], B. Spottiswoode[3], C.N. De Cecco[1], G. Muscogiuri[1], J.L. Wichmann[1], R. Vliegenthart[4], P. Suranyi[1], U.J. Schoepf[1]; [1]*Charleston, SC/US*, [2]*Leiden/NL*, [3]*Chicago, IL/US*, [4]*Groningen/NL*
(vargaasz@musc.edu)

Purpose: To simulate the influence of inversion time (TI) on the precision of myocardial late gadolinium enhancement (LGE) quantification using synthetic inversion-recovery (IR) imaging in patients with myocardial infarction (MI).
Methods and Materials: Fifty-three patients with suspected prior MI underwent 1.5T cardiac magnetic resonance imaging (MAGNETOM Avanto, Siemens, Germany) with conventional magnitude IR (MagIR) and phase-sensitive IR (PSIR) LGE imaging and post-contrast myocardial T1-mapping. T1-based synthetic MagIR and PSIR images were calculated with a TI ranging at 5ms intervals from -100 to +150ms relative to the optimal TI (TI_0). LGE was quantified using a 5 standard deviation threshold (5SD) and full-width at half-maximum (FWHM). Differences in LGE size at various TIs were compared using one-way analysis of variance.
Results: The $MagIR_{sy}$ technique provided precise assessment of LGE area at TIs ≥TI_0, while precision was decreased below TI_0. The LGE area showed significant differences at <25ms than TI_0 using 5SD (P<0.001), and <-65ms using the FWHM approach (P<0.001). LGE measurements did not show significant difference over the analyzed TI-range in the $PSIR_{sy}$ images using either of the quantification methods. The conventional and synthetic IR techniques yielded similar areas of infarct using the 5SD (4.38 and 5.68cm^2, P=NS) and FWHM (3.21 and 4.09cm^2, P=NS) thresholds.
Conclusion: T1-map-based $PSIR_{sy}$ images provide precise quantification of MI independent of TI at the investigated time-point post-contrast. $MagIR_{sy}$-based MI quantification is precise at TI_0 and at longer TIs while showing decreased precision at TI values below TI_0.
Author Disclosures:
A. Varga-Szemes: Consultant; Guerbet. **B. Spottiswoode:** Employee; Siemens. **C.N. De Cecco:** Consultant; Guerbet. **U.J. Schoepf:** Consultant; Bayer, Bracco, GE Healthcare, Guerbet, Medrad, and Siemens Healthcare. Research/Grant Support; Bayer, Bracco, GE Healthcare, Guerbet, Medrad, and Siemens Healthcare.

10:30 - 12:00 **Room M 2**

Paediatric

SS 612
Paediatric abdominal imaging

Moderators:
K. Iliadis; Brighton/UK
M. Raissaki; Iraklion/GR

K-09 10:30

Keynote lecture
M. Haliloglu; *Ankara/TR*

B-0509 10:39

Advanced virtual monoenergetic reconstruction of dual-energy abdominal CT angiography of children: comparison with conventional monoenergetic reconstruction
H. Choi, Y. Choi, J.-E. Cheon, W. Kim, I.-O. Kim; *Seoul/KR*

Purpose: To determine the most effective advanced virtual monoenergetic imaging (VMI) energy level for maximising the abdominal arterial image quality in dual-energy contrast-enhanced liver CT of children, and to assess the improvement compared with conventional monoenergetic reconstruction, and linearly-blended images.
Methods and Materials: From January 2014 to October 2015, 19 consecutive liver CT scans (7boys and 12girls; mean age 6.7years) acquired in dual-energy CT scanner were retrospectively reconstructed at 7VMI energy levels from 40 to 100keV in 10-keV increments using both conventional (Mono) and advanced (Mono+) monoenergetic reconstruction techniques. Mean attenuation, image noise, signal-to-noise ratio (SNR), and contrast-to-noise ratio (CNR) in the common hepatic artery (CHA), superior mesenteric artery (SMA), splenic artery (SA), and left renal artery (LRA) were analysed. VMI series with the best SNR

or CNR were selected from each monoenergetic reconstruction technique, and were compared with linearly-blended images (M_0.5; 50% of 80kV, 50% of 140kV).
Results: The noise was lowest at 80keV (Mono+), and 70keV (Mono). The maximal SNRs in all arteries were observed at 50keV (Mono+), and 70keV (Mono), and maximal CNRs were observed at 40keV (Mono+), and 60keV (Mono). The SNRs, and CNRs of Mono+ was higher than those of Mono in all investigated arteries at all energy level except for the SNRs at 70keV in CHA, and LRA. The optimal VMI energy level was 50keV for Mono+ and 60keV for Mono. The SNR, and CNR of Mono+ 50keV was higher than 60keV Mono and linearly-blended (M_0.5) images.
Conclusion: The Mono+ reconstruction of dual-energy CT angiography of the abdomen at 50keV (optimal energy level) maximises image quality compared with Mono or linearly-blended(M_0.5) images.

B-0510 10:47

Advanced virtual monochromatic reconstruction of dual-energy abdominal CT in children: optimisation of kiloelectron volt settings to improve image contrast
T. Kim, Y. Choi, J.-E. Cheon, W. Kim, I.-O. Kim; *Seoul/KR (kjambong@gmail.com)*

Purpose: To compare quantitative image quality parameters in paediatric abdominal dual-energy CT using advanced (Mono+), conventional (Mono) monochromatic reconstructed images at different kiloelectron volt (keV) levels and standard linearly blended M_0.5 images (50% 80kV, 50% 140kV).
Methods and Materials: Thirty-seven consecutive abdominal dual-energy CT scans (27 boys and 10 girls; mean age 9.65 ± 5.33 years) were retrospectively included. Mono+ and Mono images were reconstructed at seven energy levels from 40 to 100keV at 10keV intervals and as standard linearly blended M_0.5 images. The contrast-to-noise ratio (CNR) and signal-to-noise ratio (SNR) of the liver, pancreas and aorta were objectively measured and compared.
Results: The maximal CNR values for all investigated organs were observed at 40keV and 60-70keV in Mono+ and Mono reconstructions, respectively. Mono+ images showed a significantly higher CNR at 40, 50 and 60keV compared to M_0.5 images for all measured organs except liver at 60keV. Mono images showed no significant superiority in CNR for all energy levels compared to M_0.5 images. The CNR of Mono+ at 40keV increased by 134% and 133% on average among all measured organs compared to the best CNR of Mono and M_0.5 images respectively. SNRs of Mono+ and Mono images showed no improvement compared to linearly blended images.
Conclusion: Mono+ showed superior CNRs at low keV levels of abdominal dual-energy CT compared to Mono and linearly blended images. The CNR in Mono+ peaked at 40keV and showed significant improvement compared to the best CNR of Mono and M_0.5 images.

B-0511 10:55

Plicae palmatae on MRI in paediatric population
M. Kitami; *Sendai/JP (rad.med3@gmail.com)*

Purpose: The ridges of plicae palmatae (RPP) are ridge of uterine cervical folds, previously considered as the remnant of fusion of Mullerian duct. Earlier studies have shown RPP could be seen on MRI in adult population, but there has been no reports regarding paediatric population. Besides, clinical significance could be different in neonate. RPP is usually important because RPP mimic uterine septum, potentially leading to unnecessary invasive procedure. In neonate, RPP could have tumourous appearance on sonography, but there is no report on MRI. Thus, the purpose of this study is to examine the depiction rate of RPP on MRI, and its appearance in paediatric population.
Methods and Materials: We retrospectively examined consecutive 117 pelvic MRI studies with patients aged from 0 to 15 years. Depiction rate in each age group (every one-year-old) was analysed, and the appearance was recorded whether tumourous or not.
Results: Depiction rate (from 0 to 15 years-old, every one-year-old) was following; 3/6 (50%); 3/8 (37.5%); 5/6 (82.5%); 0/5 (0%); 0/2 (0%); 2/6 (33%); 0/3 (0%); 3/7 (43%); 1/3 (33%); 2/6 (33%); 2/9 (22%); 4/7 (57%); 8/13 (62%); 9/12 (75%); 11/14 (79%); and 1/2 (50%). There was no case with tumourous appearance on MRI in every age group.
Conclusion: Depiction rate of RPP varied according to age groups on MRI, although RPP are relatively common feature also in paediatric population. There was no case showing tumour-mimicking appearance on MRI.

B-0512 11:03

MRI and transient elastography for the assessment of hepatic steatosis and elasticity in non-alcoholic fatty liver disease of children
J. Shin, H. Shin, H. Yoon, M.-J. Kim, M.-J. Lee, H. Koh; *Seoul/KR (drshinjs@yuhs.ac)*

Purpose: To evaluate MRI and transient elastography (TE) for assessing hepatic steatosis and elasticity in children with non-alcoholic fatty liver disease (NAFLD).
Methods and Materials: We retrospectively reviewed the records of children with clinically NAFLD who underwent hepatic MR elastography (MRE) and TE from January 2015 to August 2016. Hepatic fat fraction on MRI and hepatic steatosis by the Controlled Attenuation Parameter (CAP, dB/m) on TE was measured. Liver elasticity was also estimated on both MRE and TE. The patients were divided into normal and obese groups using the cut-off of 95 percentile body mass index (BMI). The results were analysed using Pearson's correlation.
Results: Total 76 children (M:F=53:23) were included with the mean age of 13.3±3.0 years. The mean BMI was 26.4±4.5kg/m^2 with 49 patients in the obese group. Hepatic elasticity on MRE (2.6±0.8 kPa) showed positive correlation with that on TE (6.4±2.5 kPa) (ρ=0.608, p<0.001). Hepatic fat fraction on MRI (21.7±12.1%) was significantly correlated with CAP (311.9±45.7 dB/m) (ρ=0.508, p<0.001). Both groups showed positive correlation between MRE and TE (ρ=0.646, p<0.001 in normal; ρ=0.575, p<0.001 in obese), as well as liver fat quantification on MRI and CAP (ρ=0.655, p<0.001 in normal; ρ=0.361, p=0.013 in obese).
Conclusion: In children with NAFLD, hepatic elasticity can be estimated non-invasively by MRE as well as TE. Hepatic fat quantification using CAP was also correlated with MR fat fraction. However, the obese group shows less correlation between CAP and MR fat fraction than the normal group.

B-0513 11:11

The significance of radiographic and ultrasonographic findings in the management of necrotising enterocolitis - results from a survey
M. Ahle[1], E. Rubesova[2], H. Ringertz[2]; [1]*Linköping/SE*, [2]*Stanford, CA/US (margaretaahle@gmail.com)*

Purpose: To investigate the perceived significance of various radiographic and ultrasonographic findings in necrotising enterocolitis (NEC) as reported by involved specialists.
Methods and Materials: 70 neonatologists, 58 paediatric surgeons and 74 radiologists from various countries answered a web-based questionnaire on their use of imaging in NEC. The results were descriptively analysed, using proportions with 95% confidence interval to evaluate differences between subgroups.
Results: In abdominal radiography (AR), pneumoperitoneum (PP) was stated to be of great importance by 97%, pneumatosis intestinalis by 96%, portal venous gas (PVG) by 89%, and "fixed loop" on sequential radiographs by 69%. On ultrasound, the most frequently evaluated signs were focal fluid collections, PVG, echoic fluid, and thickening of the intestinal wall, all used by over 90% of those stating that ultrasound is used for NEC in their hospital (58% of all). Among indications for surgery, PP on AR was considered possible by 99% and definite by 88%. PP on US was regarded a definite indication by 50%, significantly less than for AR. PVG in AR was considered a possible indication for surgery by 65% and PVG on US by 50%. Turbid or localised fluid on US was more often regarded an indication for surgery where US was used for NEC than where it was not.
Conclusion: There is greater consensus on possible signs of NEC, as well as the significance of these findings, on AR than on US. The perceptions are partly influenced by the respondents' experience of US in NEC.

B-0514 11:19

Analysis of clinical and ultrasound determinants of adnexal torsion in children and adolescents
R. Jourjon, B. Morel, S. Irtan, E. Audureau, H. Ducou le Pointe, E. Blondiaux; *Paris/FR (eleonore.blondiaux@aphp.fr)*

Purpose: To assess the performance of transabdominal ultrasonography (US) for diagnosis of adnexal torsion (AT) in children and adolescents and evaluate its clinical and US determinants.
Methods and Materials: We retrospectively (2004 to 2014) studied data for children referred for acute or sub-acute pelvic pain who underwent US and included children 3 months to 18 years old who underwent surgical exploration and/or clinical and radiological follow-up for at least 3 months. The evaluation of US diagnostic performance was based on the proposed diagnosis after US: AT or no AT (NAT) with or without mass. Clinical and US predictors of AT were identified by regression analysis.
Results: Among 65 girls included (mean age 11.75±4.49 years), 33 (50.8%) had AT. The sensitivity, specificity, positive predictive value, negative predictive value and accuracy of US for AT were 90.9%, 68.7%, 75%, 88% and

80%, respectively. Overall, 20/33 (60.6%) AT patients had a mass, including 33% with mature teratomas. Patients with AT versus NAT more frequently showed vomiting (64% vs 28%, p=0.008), ovarian edematous stroma with a peripheral distribution of follicles (45.5% vs 9.4%, p=0.002) and a mass of pluritissular aspect (40% vs 0%, p<0.0001). The quantitative US predictors of AT were total area ratio (ovary and mass) / area of the contralateral ovary ≥4.9 (p=0.0002) and surface area ≥18.5 cm2 (p=0.0003).
Conclusion: US has high sensitivity but low specificity for the diagnosis of AT in children. The predictive criteria are vomiting, presence of a pluritissular mass, ≥4.9 area ratio or surface area ≥18.5 cm2.

B-0515 11:27

Value of sonographic pseudogestation sac sign in diagnosing Meckel diverticulum in children presenting with bleeding per rectum: a decade's experience

V.N. Zefov, S.M. El-Maadawy, N.A. Abdelrahman, D. Abdul Rahman, A.R. Mustafawi; *Dubai/AE (samarmaadawy@gmail.com)*

Purpose: Meckel diverticulum is the most common congenital anomaly of the gastrointestinal tract. Gastrointestinal bleeding is the most frequent complication of Meckel diverticulum in the paediatric population. The purpose of our prospective study is to assess the value of using the ultrasound pseudogestation sac sign in diagnosing Meckel diverticulum in children presenting with bleeding per rectum.
Methods and Materials: 59 children were included in our study. All cases were referred with a clinical suspicion of Meckel diverticulum due to bleeding per rectum. Data were collected from 2005 to 2016. All children were examined by a paediatric radiologist using a high resolution linear or curvilinear probe with colour Doppler imaging. The results were correlated with nuclear studies, operative and histopathology findings.
Results: The ratio of boys to girls in our study population was 4:1. The age ranged from 1 month to 12 years with a median of 2 years. 42 cases were operated and 17 cases were treated conservatively and followed by ultrasound. The pseudogestation sac sign was identified in 32 cases. 2 cases were operated despite negative nuclear studies and proved later to be Meckel by histopathology. Using the ultrasound pseudogestation sac sign, the sensitivity, specificity, positive and negative predictive values for Meckel diverticulum were 87.1%, 82.1%, 84.4%and 85.2% respectively.
Conclusion: We believe that the sonographic pseudogestation sac sign is a reliable diagnostic tool for diagnosing Meckel diverticulum in children presenting with bleeding per rectum. The sonographic diagnosis of Meckel diverticulum complies with the international efforts of "Image Gently".

B-0516 11:35

Anorectal malformations: diagnostic value and reliability of MRI distal pressure colostogram in comparison with the fluoroscopic examination

D. Maslava, Z. Holubová, M. Kynčl, L. Poš, R. Škába; *Prague/CZ (darya.maslava@fnmotol.cz)*

Purpose: Application of gadolinium into the colostomy during MRI study (MRI-DPCG) of patients with anorectal malformations (ARM) facilitates demonstration of the presence and precise localization of fistula. This anatomical information and identification of other malformations by MRI guides the surgical approach. The aim of our study was to compare the diagnostic accuracy of fluoroscopic distal pressure colostogram (DPC) and MRI-DPCG in the pre-operative work-up of patients with ARM.
Methods and Materials: A retrospective study of patients with ARM admitted to the surgical department between the years 2011-2015 was conducted. DPC and MRI-DPCG were analysed and the results of these examinations were compared with intra-operative findings. The presence and location of the rectal fistula and length of the common channel in cloacal malformations in girls were evaluated.
Results: 16 colostomized patients with ARM were included in our cohort (13 boys, 3 girls). Median age at the time of MRI was 12.5 weeks. MRI revealed rectovesical fistula in 2 patients, rectourethral prostatic fistula in 2, rectourethral bulbar fistula in 5, without fistula in 4. There were 3 cloacal malformations - 2 low type cloacas and 1 high cloaca. There was full agreement between MRI-DPCG and intra-operative findings. DPC was identical in 15 patients in comparison with the intra-operative findings and didn't show bulbar fistula in 1 patient.
Conclusion: As shown in our study, MRI-DPCG provides accurate evaluation of ARM and should be considered a serious alternative to fluoroscopic imaging during preoperative work-up.

B-0517 11:43

Utility of dynamic sequence in defeco-MRI for the evaluation of patients with ano-rectal malformation

C. Tudisca, S. Salerno, C. Geraci, G. La Tona, A. Lo Casto, M. Midiri; *Palermo/IT (chiaratudisca@gmail.com)*

Purpose: Patients operated for correction of anorectal malformation (MAR) could have variables post-surgery complications, such as constipation and/or incontinence. Aim of the study was to evaluate morphologically and functionally the organs and muscle-sphincter pelvic structures involved in defecation in patients treated for MAR with post-surgery complications, by using MR-defecography technique.
Methods and Materials: 10 adolescents (17.2 ± 2.4 years), operated in childhood for MAR with defecatory difficulties were analysed by MR-defecography static and dynamic sequences. The static MRI exam assessment included evaluation of: -position the neo rectum, -perineal muscles, -expansion of the superior rectus, -abnormalities of the spinal cord and sacrum. In dynamic sequences were evaluated: -erniation of muscle and/or peritoneal fat, -position of the perineum plane, -rectal emptying.
Results: In 6 (60%) cases there was an asymmetry of the levator ani, in particular 3 patients had an hypotrophy of the right levator ani and contralateral compensatory hypertrophy. In dynamic sequences in maximum evacuative phase 8 (80%) patients presented an incomplete emptying of the rectum and minimum variation of the anorectal angle between the static phase and the phase of incomplete emptying, as from obstructed defecation syndrome. In 7 (70%) cases it was detected abnormality of the coccyx tract.
Conclusion: MR-defecography can be an important diagnostic tool in the evaluation of the postoperative regional anatomy and of perianal functionality with dynamic sequences that allow you to identify the causes of defecatory obstruction and/or incontinence.

B-0518 11:51

Modified-Seldinger technique for paediatric percutaneous nephrostomy

K. Rangarajan, D. Kandasamy, M. Jana, L. Singh, V. Ramalingam; *New Delhi/IN (krithikarangarajan86@gmail.com)*

Purpose: To describe a new technique for paediatric Percutaneous Nephrostomy (PCN). Compare the technique with the conventional Seldinger technique in terms of success rate, number of attempts and procedure time.
Methods and Materials: PCN was performed in 18 children under 4 years of age with hydronephrosis in whom renal function was expected to improve after percutaneous drainage. 8 children underwent PCN with the new technique using 14 G puncture needle. Ten children underwent PCN with Seldinger technique. Procedure time, number of attempts and success of procedure were noted for each patient.
Results: In the conventional technique it was seen that though the puncture needle entered the pelvicalyceal system, the dilators and catheter tended to push the renal parenchyma, rather than piercing it, leading to deployment of the catheter within the parenchyma or in the perinephric space. This problem was encountered in 3 patients out of 10, of which in 2 patients the procedure was abandoned as the system got decompressed. In 1 patient the catheter was deployed in the second attempt. Procedure time was 10 to 15 minutes. Fluoroscopy was used in 5 patients to confirm position of guide-wire. Using the new technique, catheter could be deployed in the first attempt in all 8 patients, without using fluoroscopy. Procedure time was under 8 minutes from local anesthesia to sutures.
Conclusion: This technique is useful for paediatric PCN to overcome the elasticity of tissues and aids successful deployment of catheter. It reduces procedure time, improves success rate and eliminates radiation exposure.

10:30 - 12:00 **Room M 3**

Computer Applications

SS 605

Image quantification, texture analysis and imaging biomarkers

Moderators:
M.E. Mayerhöfer; Vienna/AT
N.N.

B-0519 10:30

Texture-based analysis of dual-energy CT and monochromatic imaging for quantification of steatosis hepatitis: correlation with pathology

B. Hoppel[1], K. Goatman[2], P. Rogalla[3]; [1]*Vernon Hills, IL/US*, [2]*Edinburgh/UK*, [3]*Toronto, ON/CA (bhoppel@tmriusa.com)*

Purpose: To analyse texture-based parameters with dual-energy and monochromatic CT imaging in patients with suspected fatty liver disease and compare to simultaneously acquired histo-pathology.
Methods and Materials: Following REB approval, patients (n=44) with clinically indicated non-focal liver biopsy for assessment of fatty liver disease underwent biopsy within the CT area. After biopsy needle placement, a dual-energy non-contrast CT volume (16 cm, 320 slices) was acquired over the liver with the needle in-situ, which is apparent in the CT image. Single energy (80KVP/135KVP) and monochromatic images in 5 KEV increments were reconstructed from the dual-energy data. Both local and volumetric liver segmentation was performed. Data analysis used over 2000 statistical and filter methods including Grey level co-occurrence matrices (GLCM), Run Level Emphasis (RLE), Law's texture filters and first order statistical measures and were correlated to pathology.
Results: DECT images of 80kVp and 60KEV showed the highest correlations with fat and fibrosis quantification from biopsy. Overall in non-contrast images, fat had a strong correlation but fibrosis had a weak correlation. The Pearson correlation (Fat/Fibrosis) for GLCM; Autocorrelation (-0.701/-0.398), ClusterProminence (-0.692/-0.407), ClusterShade (-0.737/ -0.409), ClusterTendency (-0.744/-0.398) RLE parameters also correlated well with fat; High Gray Level Run Emphasis (-0.745/ -0.404), Short Run High Gray Level Emphasis (-0.735/-0.422), Long Run High Gray Level Emphasis (-0.673/-0.402), Mean_Long Run High Gray Level Emphasis (-0.710/ -0.415), Mean_High Gray Level Run Emphasis (-0.800 /-0.33). Law's filters were less correlated but show promise; Iso-edge-wave-Mean (0.457/0.256), Iso-edge-wave-standard Deviation (0.4212/0.228), Iso-spot-Mean (0.440/0.228), Iso-spot-wave-mean (0.460/ 0.223).
Conclusion: Histopathological measures of fat correlated well with several of DECT texture analysis parameters, which may allow for non-invasive stratification of hepatic steatosis in patients with diffuse disease. In the future, a combination of these parameters may improve prediction.
Author Disclosures:
B. Hoppel: Employee; Toshiba Employee. **K. Goatman:** Employee; TMVS employee. **P. Rogalla:** Research/Grant Support; Research support from Toshiba Medical.

B-0520 10:38

Early diagnosis of bronchiolitis obliterans syndrome after lung transplantation using functional respiratory imaging

E.J.M. Barbosa Jr.[1], F. Ferreira[2], W. Vos[2], C.V. Holsbeke[2], L. Nuyttens[3], W. De Backer[4], J. De Backer[4], J.C. Lee[1]; [1]*Philadelphia, PA/US*, [2]*Kontich/BE*, [3]*North Brunswick, NJ/US*, [4]*Antwerp/BE (eduardo.mortani@gmail.com)*

Purpose: Chronic lung allograft dysfunction after lung transplantation (LTx) manifests as a sustained decline in FEV1, heralding the onset of bronchiolitis obliterans syndrome (BOS). Identifying regional disease in the lungs could lead to earlier diagnosis of BOS and potentially improved outcomes. Functional Respiratory Imaging (FRI) using quantitative CT image processing may predict the onset of BOS.
Methods and Materials: Paired inspiratory-expiratory CT scans of 41 LTx patients were analyzed retrospectively. The BOS cohort experienced a reduction in FEV1>10% compared to baseline (BOS 0-p). FRI yielded regional parameters: lung volumes (iVlobe), airway volumes (iVaw) and airway resistance (iRaw). Differences between the two groups were analyzed via multivariate regression modelling to determine the FRI parameters most predictive of FEV1 decline.
Results: A significant increase in transplanted iVlobe at FRC was demonstrated in the BOS cohort, with no statistically significant difference in FEV1 between the two groups. In the BOS cohort, distal iVaw at FRC, transplanted iVlobe at FRC and TLC were identified as predictors of FEV1 decline, while in the non-BOS cohort FEV1 decline is driven by central iVaw at FRC and TLC of the non-transplanted lung.
Conclusion: FRI could differentiate early BOS from non-BOS in LTx patients, whereas FEV1 could not. FEV1 decline in the BOS cohort appears to be particularly associated with changes in the transplanted lung, while in the non-BOS cohort, metrics from the non-transplanted lung are more associated with FEV1 changes. These results illustrate the potential of FRI as a diagnostic tool for early diagnosis of BOS.

B-0521 10:46

Role of 320-row CT with semi-automatic 3D analysis software for evaluating the response to systemic theraphy of multicentric HCC according to the mRECIST criteria

M. Moschetta, M. Telegrafo, G. Dilorenzo, G. Di Giovanni, I. Cornacchia, A. Stabile Ianora, G. Angelelli; *Bari/IT (marco.moschetta@gmail.com)*

Purpose: To evaluate the role of 320-row CT with 3D analysis software in the follow-up of multicentric hepatocellular carcinoma (HCC) treated with systemic therapy according to the mRECIST criteria.
Methods and Materials: In the period between December 2013 and June 2016 38 patients with multicentric HCC undergoing systemic therapy were assessed twice a year by MDCT before and after injection of contrast medium with three-phasic technique. Two blinded radiologists evaluated multi-planar images (MPR) classifying the response to therapy in PR (partial response), PD (progressive disease), SD (stable disease) and CR (complete response) by using the mRECIST criteria. 30 days later, the same two blinded radiologists evaluated the same target lesions applying the 3D semi-automatic analysis software. The differences between the two evaluating systems were assessed using the analysis of variance (ANOVA test). The inter-observer agreement for both the evaluating systems was calculated using Cohen's kappa statistics.
Results: In 10/38 cases (26%) PR was found; in 6/38 (16%) PD; in 22/38 (58%) SD. The analysis of variance did not detect statistically significant differences between the two systems of measurement ($p>0.05$). The inter-observer agreement (k) was 0.62 for the measurements in MPR and 0.86 for the measurements performed by using the 3D analysis software, with a significantly higher value for the proposed semi-automatic software ($p<0.05$).
Conclusion: The semi-automatic 3D analysis software represents a reliable method for evaluating the HCC response to therapy according to the mRECIST criteria and could be proposed in the clinical practice.

B-0522 10:54

Fully automated method for lung emphysema quantification from multidetector CT images

I. Mayorga-Ruiz, D. García-Juan, A. Alberich-Bayarri, F. García-Castro, P. Calvillo, L. Martí-Bonmatí; *Valencia/ES*

Purpose: Lung emphysema is considered one of the main changes in chronic obstructive pulmonary disease (COPD) disease. Our aim was to develop an automated algorithm for segmentation of lungs, vessels, airways and emphysema areas.
Methods and Materials: New methodology for automated lung emphysema quantification was developed and tested in 28 standard-of-care thorax MDCT scans. Lungs, main airways and blood vessels were segmented using thresholding, clustering and region growing techniques, applying as initial seed a previously computed trachea centroid. The emphysema detection was performed using either fixed or adaptative thresholding (algorithm patented by QUIBIM, Valencia, Spain). A value of -950 HU was applied in the first algorithm while the second implemented the computation of a slice-wise air adaptive threshold. Lung parenchyma HU levels were also analysed to provide meaningful information about parenchyma status. Finally, the percentage of emphysema and the total lung parenchyma volume were calculated.
Results: The complete automated algorithm execution took 25 minutes on average. Emphysema ratio, blood vessels, lung parenchyma and emphysema volumes were computed from the 28 CT studies with an initial execution efficiency of 86%. The algorithm could not analyse the rest due to lung hyperinflation. Adaptative thresholding outperformed fixed threshold emphysema segmentation due to image-specific air threshold.
Conclusion: Automated lung emphysema quantification can be used for the diagnosis and follow-up of COPD, helping radiologist to integrate a quantitative evaluation when reporting these patients. Adaptive thresholding is capable to provide a better characterization of lung emphysema due to the image-specific thresholding.

B-0523 11:02

Cerebral white matter, grey matter and cerebrospinal fluid segmentation in CT using VCAST: a volumetric cluster annotation and segmentation tool

S. van de Leemput, F.J.A. Meijer, M. Prokop, R. Manniesing; *Nijmegen/NL (silvandeleemput@gmail.com)*

Purpose: Segmentation of cerebral white matter (WM), grey matter (GM) and cerebrospinal fluid (CSF) in head CT is important for subsequent quantitative analysis and automated detection of cerebral pathology. We introduce VCAST, a new volumetric annotation tool aimed at delineating soft tissue in non-contrast CT (NCCT) and CT perfusion (CTP).
Methods and Materials: VCAST supports traditional 2D visualizations and annotations, and provides functionalities to facilitate 3D segmentations based on pre-calculated grids of volumetric clusters where the clusters are spatially coherently grouped based on HUs. Clicking a cluster in a 2D-plane allows for inclusion of the 3D-cluster in the output segmentation. Ten patients with suspicion of ischaemic stroke were included in this retrospective study, five NCCTs and five whole-brain CTPs (320-row detector scanner). Temporal average CTA was reconstructed from CTP and in one slice in arbitrary direction, WM, GM and CSF were annotated two times by one observer using VCAST. In NCCT, a subvolume of approximately 22 mm^3 was randomly selected in which CSF was annotated by one observer, using VCAST either with 2D (slice-based) or 2D and 3D (cluster-based) annotation support. Dice coefficients and annotation times were reported.
Results: Dice coefficients were 0.86±0.04, 0.91±0.02, 0.87±0.02 for CSF, GM and WM respectively. CSF annotation times reduced from 16±9 to 8±5 minutes with 3D cluster support (p=0.02). CSF Dice similarity was 0.81±0.03.
Conclusion: VCAST is a volumetric annotation tool which reduces the time to obtain 3D segmentations in head CT while maintaining good overlap with a slice-based approach.
Author Disclosures:
S. van de Leemput: Research/Grant Support; Toshiba Japan.
R. Manniesing: Grant Recipient; Toshiba Japan.

B-0524 11:10

Validation of a semi-automated technique to accurately measure abdominal fat distribution using CT and MRI for clinical risk stratification

M. Waduud, A. Sharaf, I. Roy, R. Lopez-Gonzalez, A. Hart, D. McGill, G. Roditi, J. Biddlestone; *Glasgow/UK (m.a.waduud@doctors.org.uk)*

Purpose: Positive correlations exist between measurements of total abdominal fat (TAF), intra-abdominal fat (IAF), extra-abdominal fat (EAF) and abdominal waist circumference (AWC) [collectively; abdominal fat distribution (AFD)] on Computer Tomography (CT) and Magnetic Resonance (MR) imaging when performed in immediate succession. This study investigated the comparability of retrospective measurements of AFD on CT and MR imaging performed solely on clinical merit without predefined research criteria and undertaken at different times.
Methods and Materials: All patients were identified retrospectively from a local database of patients planned to undergo flap-based breast reconstruction as the Canniesburn Plastic Surgery Unit. Patients with both preoperative CT and MR imaging were identified from the Patient Archiving Computer System. Image analysis was performed using the Image-J software package. Linear regression analysis was performed between values obtained from both modalities for the individual parameters of AFD. Intra-observer and inter-observer differences were assessed using Bland-Altman plots.
Results: The AFD was quantified at the level of the umbilicus on paired CT and MRI scans from 15 patients. In total 30 scans were analysed. The mean time between the imaging modalities was 68 days (77.8 days SD, range 1 to 255). Pearson's correlation demonstrated strong relationships between imaging modalities for TAF (R=0.846, p<0.001***), IAF (R=0.858, p<0.001***), EAF (R=0.844, p<0.001***), and AWC (R=0.617, p<0.05*). Interchangeable mathematical models were subsequently developed.
Conclusion: A strong interchangeable relationship exists between calculations of AFD on retrospective CT and MR imaging performed out with strict research criteria. Results are comparable to previously published prospective studies.

B-0525 11:18

3D CT texture analysis of neuroendocrine pancreatic neoplasms

M. D'Onofrio, V. Ciaravino, N. Cardobi, R. De Robertis, R. Pozzi-Mucelli; *Verona/IT (valentinaciaravino@gmail.com)*

Purpose: To evaluate the added value of CT texture analysis in the study of neuroendocrine pancreatic neoplasms.
Methods and Materials: 24 patients with PNETS were included in this study. All tumours were pathologically diagnosed after resection or with biopsy. Histological grade of these neoplasms was available in all cases. There were 7 G1, 7 G2, and 10 G3 neoplasms with presence of metastases in 21/24 (87%) cases. 3D CT texture analysis of primary tumour was performed comparing results with tumour grading. CT texture analysis results (Mean Value, Variance, Skewness, Kurtosis) were compared by using Wilcoxon correlation test.
Results: Included PNETS were located in the head of the pancreas in 7/24 (29%) cases; in the body-tail in 17/24 (71%) cases. G1 neoplasms show mean dimension of 41 mm (range: 9 - 112 mm). G2 neoplasms show mean dimension of 42 mm (range: 21 - 73 mm). G3 neoplasms show mean dimension of 50 mm (range:16 - 111 mm). CT texture analysis was finalised in all cases. There was no statistical significant difference regarding all the parameters of CT texture analysis among G1, G2, and G3 neoplasms. Higher value of kurtosis was found in G3 (Kurtosis median= 2,1499000) in respect to G1 (Kurtosis median = 0,1128400) and G2 (Kurtosis median = 1,3848000) neoplasms. Grouping together G1 and G2 neoplasms, statistical significant difference (p< 0,05) was found regarding the only kurtosis CT texture analysis parameter.
Conclusion: This preliminary results show that CT texture analysis parameters can be complementary data for PNETS grade prediction.

B-0526 11:26

Quantitative CT metrics from the transplanted lung may predict FEV1 after lung transplantation

E.J.M. Barbosa Jr.[1], H. Shou[1], S. Simpson[1], N. Tustison[2], J. Gee[1], J. Lee[1]; [1]*Philadelphia, PA/US*, [2]*Charlottesville, VA/US (eduardo.mortani@gmail.com)*

Purpose: Chronic lung allograft dysfunction after lung transplantation (LTx) manifests as a sustained decline in FEV1, indicative of bronchiolitis obliterans syndrome (BOS). Our hypotheses are that quantitative CT (QCT) metrics may predict FEV1 better than semi-quantitative scores (SQS), and that the transplanted lung behaves differently from the native lung in unilateral LTx.
Methods and Materials: Paired inspiratory-expiratory CT scans and PFTs of 178 LTx patients were analyzed retrospectively, and separated into unilateral left (43), unilateral right (40) and bilateral (95) LTx. SQS were graded from 0-3 (absent, mild, moderate, severe) for features including mosaic attenuation, tree in bud nodules and bronchiectasis. QCT included lung volumes and air trapping volumes, by lobe, in inspiration and expiration. Multivariate Pearson correlation analysis was performed to measure the strength of association between QCT metrics and FEV1.
Results: QCT metrics demonstrated stronger correlation (r) with FEV1 than SQS. In bilateral LTx, whole lung volume difference (WLVD) (r=0.69), left lung volume difference (LLVD) (r=0.69) and right lung volume difference (RLVD) (r=0.65) were better than the sum of SQS (r=-0.54). Interestingly, in left LTx we obtained r=0.81, r=0.86, r=0.25 and r=-0.39, respectively. In right LTx we obtained r=0.69, r=0.49, r=0.68 and r=-0.31, respectively.
Conclusion: QCT metrics demonstrate much stronger correlations with FEV1 and therefore are better predictors of pulmonary function than SQS. SQS performs moderately well in bilateral LTx, but poorly on unilateral LTx. In unilateral LTx, QCT metrics from the transplanted lung are better predictors of FEV1 than QCT metrics from the non-transplanted lung.

B-0527 11:34

A new integrated biomarker for IVIM/diffusion MRI: clinical feasibility study

D. Le Bihan; *Gif-Sur-Yvette/FR (denis.lebihan@gmail.com)*

Purpose: IVIM/diffusion MRI results are often expressed as model parameters (ADC, Kurtosis) which are cumbersome to estimate, resulting in variable results across centers. A new integrated diffusion biomarker (Signature Index, S) which directly provides a diagnosis statement without requiring any model computation is introduced, as well as its extension to obtain angiograms and tissue shear stiffness without using contrast agents or mechanical vibrations.
Methods and Materials: The feasibility of this approach was evaluated in 30 patients (breast, head and neck, liver tumours and fibrosis). "Key b values" which provide highest sensitivity to changes in IVIM, Gaussian and non-Gaussian diffusion were first identified for the organs under evaluation. The S Index was calculated on a voxel-by-voxel basis from the "distance" between lesions MRI signals acquired at those key b values and those of typical tissues (eg, malignant/benign) to produce color-encoded diagnostic maps, which were also used for texture analysis (such as stratified conspicuity). The S Index was also tailored to identify specific tissue features, such as vessels, to generate angiograms, or converted into tissue shear stiffness to generate quantitative elastograms.
Results: The performance of the S index to identify malignant and benign lesions was excellent (AUC=0.89) with specificity and sensitivity close to 90%. The correlation between shear stiffness obtained from IVIM virtual MRE and standard MRE in liver patients was very high (R^2=0.89, p=1.02 10^{-7}), allowing accurate fibrosis staging (F0-4).
Conclusion: This integrated S index provides tissue features recognition with high accuracy without the need to estimate diffusion model parameters.
Author Disclosures:
D. Le Bihan: Patent Holder; Le Bihan D.

B-0528 11:42

Automatic visual-like classification of lung tumour heterogeneity in DCE-CT sequences

S. Baiocco[1], D. Barone[2], A. Bevilacqua[1], G. Gavelli[1]; [1]*Bologna/IT*, [2]*Meldola/IT (s.baiocco@unibo.it)*

Purpose: Tumour heterogeneity is an important prognostic factor, as high intra-tumour heterogeneity showed to be associated with higher tumour grades. However, its assessment is still mostly accomplished subjectively through visual procedure. This work presents an automatic approach to classify the heterogeneity levels in lung tumour as performed through visual analysis.
Methods and Materials: 40 datasets referring to 13 patients (age range 36-81 years) with NSCLC, who underwent axial DCE-CT, were considered. Two 25-year experienced Readers chose the most representative slices in the DCE-CT sequences, outlined each lesion and its most significant regions. Then, each slice was assigned a class, according to a proper taxonomy for heterogeneity levels previously defined: homogeneous, macro-inhomogeneous (i.e., different homogeneities together), and micro-inhomogeneous. A statistical voxel-based index was devised to quantify the heterogeneity, then represented in colorimetric maps. The values were grouped into regions subsequently compared with those drawn by radiologists.
Results: Results for the three classes were computed in terms of specificity (SP) and sensitivity (SE). Our approach proved to be extremely specific, mostly for homogeneous (SE=77%, SP=93%) and macro-inhomogeneous (SE=75%, SP=90%) tissues. On the other hand, the most indefinite micro-inhomogeneous tissue also shows a high specificity (SE=86%, SP=87%).
Conclusion: The approach developed allows an automatic classification of heterogeneities, with a reduction of both intra- and inter-observer variability. This represents a novel approach acting as a second radiologist in the heterogeneity assessment, which could yield a great benefit for patient stratification and constitutes a valid tool to assist radiologists in daily clinical activities.

B-0529 11:50

Design and implementation of a parallel filter for real-time fluoroscopy imaging

A. Brusan, F.A. Durmaz, I.B. Erguder, A. Yaman, C. Ozturk; *Istanbul/TR (altay_bn@yahoo.com)*

Purpose: Design and implementation of a parallel filter for real-time fluoroscopy imaging.
Methods and Materials: A digital filter was designed to exploit a 3D spatio-temporal averaging kernel over a queue of images captured by a digital fluoroscopy camera. The filter was implemented on both CUDA and OpenCV platforms to use their parallelization foundations. As a benchmark, a step phantom was used to figure out image noise characteristics and its dependency on contrast level. The filtering operation was performed with different spatio-temporal kernel sizes, image bit-depths, camera gain and exposure parameters to model the performance of the filter with regards to both Signal to Noise Ratio (SNR) and execution speed. Subsequently, this model is used to find optimum tune parameters of the filter.
Results: The speed was correlated with image bit-depth and spatio-temporal kernel size. Increasing bit-depth or kernel size consequently reduced the speed proportionally. However, in contrast to non-parallel algorithms, the parallel implementation brought up to twelve times speed-up. The SNR level was dependent on the contrast. At high-contrast regions the filtered image quality was (SNR: 18.37%, STD: 6.48) in contrast to (SNR: 13.97%, STD: 12.37) of non-filtered images and at the low-contrast regions the quality factors were (SNR: 13.64%, STD 11.53) in compare to respective (SNR: 12.04%, STD: 16.53) of non-filtered images.
Conclusion: CUDA and OpenCV based parallelization has been applied in machine learning and Image processing for a while. This study put these platforms under the limelight for utilizing them in real-time fluoroscopy image processing.

14:00 - 15:30 **Room B**

Abdominal Viscera

SS 701a

Benign and malignant pancreatic diseases: advances in imaging

Moderators:
N. Alberti; Bordeaux/FR
D. Weishaupt; Zurich/CH

B-0530 14:00

Pancreatic lipid deposition is determined by environmental rather than genetic factors: a classical twin study

A. Panajotu, M. Kolossváry, S. Papp, Á.L. Jermendy, D.L. Tárnoki, J. Karády, F.I. Suhai, B. Merkely, P. Maurovich-Horvat; *Budapest/HU (panajotualexisz@gmail.com)*

Purpose: Intrapancreatic fat can be assessed by non-contrast-enhanced computed tomography (CT) and is associated with beta-cell dysfunction. The role of genetic and environmental factors in pancreatic lipid accumulation is unclear. Therefore, we sought to evaluate the contribution of genetics and environmental factors on pancreatic lipid content within a cohort of adult twins.
Methods and Materials: We investigated 77 twin pairs (47 monozygotic [MZ] and 30 dizygotic [DZ] same gender pairs) with a 256-slice CT-scanner. Using non-enhanced CT images we measured the average value of pancreatic attenuation (Hounsfield units [HU]) in three regions of interest. Blood samples were collected before the CT scan. Intra-pair correlations were calculated and structural equation model was used for evaluating additive genetic (A), dominant genetic (D) and unique environmental (E) components.
Results: Main clinical and laboratory findings of the twins were: age 56.1±9.4 years, BMI 27.7±5.3kg/m^2, fasting glucose 97.5±25.7mg/dL, HbA1c 5.5±1.0% (mean±SD). Average pancreatic attenuation was 47.2±11.3 HU in MZ and 47.6±11.8 HU in DZ twins. The intra-pair correlation between HU values were stronger in MZ as compared to DZ twins (rMZ=0.498, p<0.001; rDZ=0.080, p=0.674). Using the structural equation model, a predominant environmental influence (E: 59%) and a moderate additive genetic dependence (A: 41%) was found. Dominant genetic influence was not identified (D: 0%).
Conclusion: We found a moderate genetic and a much stronger environmental dependence of pancreatic lipid accumulation in our twin cohort indicating that environmental factors and lifestyle characteristics are predominantly involved in the development of fat accumulation in the pancreas.

B-0531 14:08

Differences in pancreatic proton-density fat fraction by MRI in subjects with prediabetes, diabetes, and controls from the general population

S.D. Heber[1], H. Hetterich[2], R. Lorbeer[2], C. Bayerl[2], J. Machann[1], S. Auweter[2], C. Schlett[3], A. Peters[4], F. Bamberg[1]; [1]*Tübingen/DE*, [2]*Munich/DE*, [3]*Heidelberg/DE*, [4]*Neuherberg/DE (sophia.heber@uni-tuebingen.de)*

Purpose: To determine differences in pancreatic adipose tissue between subjects with prediabetes, diabetes, and normal controls as measured by magnetic resonance imaging (MRI) and its association with other adipose tissue compartments.
Methods and Materials: Subjects without history of cardiovascular disease with established diabetes or prediabetes as well as normal controls were included from a population-based cohort study and underwent whole-body 3T MRI. The imaging protocol included a 3D multi-echo Dixon sequence for derivation of proton-density fat fraction of the pancreas ($PDFF_{panc}$) and liver ($PDFF_{hepatic}$) as well as a two-point Dixon to determine subcutaneous and visceral adipose tissue (SAT and VAT, respectively). Univariate and multivariate analyses were employed to determine associations.
Results: A total of 385 subjects were included (median age: 57 years, 58.2% males) and the prevalence of diabetes and prediabetes was moderate (13.8% and 24.7%, respectively). The median $PDFF_{panc}$ was 5.2% [IQR 3.3; 9.4], and significantly higher in subjects with prediabetes and diabetes as compared to controls (6.2% [3.5; 12] vs. 8.6% [4.3; 17.5] vs. 4.9% [3.1; 7.4], respectively; p_{Trend}<0.001). After adjusting for age, gender and BMI, the association was attenuated. In addition, while in univariate analysis BMI, $PDFF_{hepatic}$, SAT and VAT were associated with $PDFF_{panc}$ (all p<0.05), only VAT predicted $PDFF_{panc}$ independently (Beta: 0.02; p<0.001).
Conclusion: While there is a significant difference in $PDFF_{panc}$ between subjects with prediabetes, diabetes and controls, this association is largely confounded by the amount of VAT. Thus, VAT may play a prominent role in the pathophysiology of the development of hyperglycaemic states.

B-0532 14:16

Optimising quality and diagnostic performance of the MDCT by using low tube voltage in patients with suspected pancreatic adenocarcinoma

E. Kondratyev, V.J. Aznaurow, I.A. Blokhin, P. Davydenko, G.G. Karmazanovsky; *Moscow/RU (evgenykondratiev@gmail.com)*

Purpose: Attenuation characteristics of the pancreatic adenocarcinoma(PA) and contrast material uptake vary depending on histologic grade, pancreatic parenchyma condition and scanning parameters. The purpose of this study was to evaluate the impact of low-tube voltage multiphase contrast-enhanced MDCT on tumour conspicuity and overall diagnostic performance.
Methods and Materials: 42 consecutive patients with clinically suspected PA and indications for MDCT were enrolled in the study and randomized into two groups based on the tube voltage (group 1 - 120 kV and group 2 - 100 kV). We compared mean tumour and parenchyma attenuation, noise, effective dose as well as qualitative score between groups. Relative tumour enhancement ratio (RTE) was calculated for each contrast enhancement (CE) phase.
Results: The mean BMI was 25.5±3.56kg/m^2 and 26.3±3.14kg/m^2, respectively (p=0.552). 34 PA and 8 chronic pancreatitis were identified by CT. Parenchyma attenuation was significantly higher during arterial and venous phase in 100kV group - 106±17 HU and 95±18 HU vs 91±14 and 89±9 HU in 120kV group, respectively (p<0,0001). Arterial RTE in 100kV group was -0.73±0.13 (-0,88±0,05 in 120kV group, p<0.001), venous RTE was -0.33±0.23 (-0,45±0,25 in 120kV group, p>0.05), delayed RTE was 0.59±0.27 (0,21±0,53 in 120kV group, p>0.05). Qualitative analysis showed better lesion conspicuity in 100kV group, especially on arterial and delayed phases. Diagnostic accuracy of the MDCT was higher in 100kV group (sensitivity 97,3 vs 91,3%, specificity 84,1 vs 80%).
Conclusion: Low-tube-voltage scanning protocol may be used for improving diagnostic quality and performance of the multiphase contrast-enhanced MDCT during pancreatic adenocarcinoma diagnostic workflow.

B-0533 14:24

Timing-specific contrast media protocol enhances image quality at reduced contrast volume and radiation dose during computed tomography of the pancreas

C. Saade, J. Chokr, L. Naffa, W. Faraj, A. Shamseddine, D. Mukherji, S. El Sageyh, R. Assi, A. Haydar; *Beirut/LB (charbel.saade@aub.edu.lb)*

Purpose: To investigate the opacification of the pancreatic vasculature and parenchyma during CT utilizing a patient-specific contrast formula.
Methods and Materials: This hybrid prospective and retrospective study was institutional review board approved. In 220 consecutive patients, pancreatic CT was performed with one of two protocols: protocol A, 100mL of contrast material injected via timed bolus triggering technique; or protocol B, employing a patient-specific contrast media protocol specifically timed at the gastroduodenal artery. Measured attenuation of pancreatic parenchymal, arterial and venous vasculature. Effective dose was calculated. Data were compared with the independent two-sample t-test. Receiver operating characteristic (ROC), visual grading characteristic (VGC) and Cohens' kappa analyses were performed.
Results: Pancreatic measurements in each of the segments during the arterial and venous phase were significantly higher in Protocol B (mean±standard deviation, art: 96.59HU±27.37; venous: 91.28HU±20.88) compared to A (art:77.86HU±21.14; venous: 73.99HU± 14.75) (p<0.0001). Arterial opacification was significantly higher in protocol B compared to A (p<0.036). In the venous circulation, the inferior vena cava, superior mesenteric, portal and splenic veins demonstrated reduction in vascular opacification protocol B compared to A(p<0.001). The contrast media volume in protocol B (57.60±12.25 mL) was significantly lower than in protocol A (100±1 mL) (p<0.001). Effective dose was significantly reduced in protocol B (2.75±0.63mSv) compared to A (4.015±0.89mSv) (p<0.001). ROC and VGC analysis demonstrated significantly higher area under the curve for protocol B (p<0.0001)(p<0.034) respectively, with inter-reader agreement increasing from good to excellent in pancreatic lesion detection.
Conclusion: Timing-specific contrast media protocol enhances image quality at reduced contrast volume and radiation dose during CT of the pancreas.
Author Disclosures:
C. Saade: Grant Recipient; GE Healthcare.

B-0534 14:32

CT features of non-hypervascular endocrine tumours of the pancreas: a comparison with pancreatic adenocarcinoma

G. Zamboni, M. Chincarini, M.C. Ambrosetti, F. Lombardo, R. Negrelli, E. Boninsegna, R. Pozzi-Mucelli; *Verona/IT (marco.chincarini@gmail.com)*

Purpose: To review the CT features of non-hypervascular endocrine tumours of the pancreas (nonH-NETs) and compare them with those of pancreatic adenocarcinomas.
Methods and Materials: We reviewed the multiphasic MDCTs performed on 38 nonH-NETs. These were compared with 38 pancreatic adenocarcinomas matched by size. All patients underwent multiphasic MDCT after administration of a weight-based amount of high-concentration contrast agent. One reader evaluated tumour size, margins, homogeneity, enhancement pattern (subjectively increasing enhancement from arterial to venous phase vs other patterns) and presence of vascular invasion. All diagnoses were confirmed at pathology. Data were analysed with Fisher's test.
Results: Mean tumour diameter was 46 mm for nonH-NETs and 45.5 mm for adenocarcinomas (p=ns). 41/57 nonH-NETs had well-defined margins, in contrast to 15/57 adenocarcinomas (p<0,0001). Calcifications were seen in 5/57 nonH-NETs and none of the adenocarcinomas (specificity 100%). No difference in tumour homogeneity was observed between the two groups (p=ns). 33/57 nonH-NETs were hypodense in the arterial phase and 22/57 were isodense, 54/57 adenocarcinomas were hypodense and 3/57 isodense (p<0,0001). 15/57 nonH-NETs and 11/57 adenocarcinomas showed increasing enhancement from the arterial to the venous phase (p=ns). The MPD upstream to the tumour had significantly larger calibre in adenocarcinomas (5.8 vs 2.2 mm; p<0,0001). No difference was observed for arterial or venous invasion between the two groups (p=ns).
Conclusion: Non-hypervascular endocrine tumours have well-defined margins, cause less MPD dilatation, and are more commonly isodense than adenocarcinoma. The presence of tumoural calcifications is specific for nonH-NETs.

B-0535 14:40

Insulinoma detection with cross-sectional imaging: comparison of biphasic-enhanced CT, volume perfusion CT and 3T multiparametric MR

L. Zhu, H.-D. Xue, Z.-Y. Sun, P. Li, Z.-Y. Jin; *Beijing/CN (zhuliang_pumc@163.com)*

Purpose: To evaluate the diagnostic performance of biphasic contrast-enhanced CT (CECT), volume perfusion CT(VPCT) and multiparametric MR (mp-MR) at 3T, in patients with clinically suspected insulinomas.
Methods and Materials: Sixty-four patients with clinically suspected insulinomas were prospectively enrolled. All patients underwent biphasic CECT, VPCT and 3T mp-MR with identical protocols. Two radiologists independently determined the presence/absence of tumour using a 5-scale confidence level. Conspicuity of the lesion and clarity of tumour-to-pancreatic duct distance were graded. CECT, VPCT and mp-MR were evaluated in random order, with time interval of at least 7 days. Receiver operating characteristic (ROC) analysis was performed to compare the radiologists' diagnostic confidence.
Results: Forty-seven patients were tumour positive, with a total of 51 tumours. The Az values for tumour detection were as follows: 0.715 (CECT), 0.903 (VPCT) and 0.955 (mp-MR) for reader 1, and 0.738 (CECT), 0.895 (VPCT) and 0.956 (mp-MR) for reader 2. VPCT and mp-MR were significantly more accurate than CECT for insulinoma detection (p=0.02 and 0.01 for reader 1, and p=0.03 and 0.01 for reader 2). Lesion conspicuity was better on mp-MR and VPCT compared to CECT (both p<0.01). Tumour-to-pancreatic duct distance was better appreciated on MR, compared to CECT and VPCT (both p<0.01). The weighted k values indicate good to excellent agreement between observers for determining tumour presence/absence (k=0.64 for CECT, 0.80 for VPCT and 0.84 for mpMR).
Conclusion: VPCT and mp-MR were significantly more accurate than CECT for insulinoma detection, and mp-MR demonstrate better tumour conspicuity and clearer tumour-to-duct distance.

B-0536 14:48

Correlation between appearance of the retroportal fat plane at preoperative CT and pathology findings in resected adenocarcinoma of the pancreatic head

F. Lombardo[1], G.A. Zamboni[2], M.C. Ambrosetti[2], M. Chincarini[2], M. Bonatti[1], G. Malleo[2], G. Marchegiani[2], R. Pozzi-Mucelli[2]; [1]*Bolzano/IT*, [2]*Verona/IT (fabio.lombardo@me.com)*

Purpose: To correlate the CT and pathology findings in resected adenocarcinomas of the pancreatic head (PDAC).
Methods and Materials: We included 48 patients with resected PDAC of the pancreatic head (24M, 24F, mean age 65 years). All patients underwent multiphasic preoperative MDCT less than 30 days before surgery. All cases

were re-evaluated at pathology for the state of the retroportal lamina, lymphatic and perineural invasion. CT images were reviewed in consensus by two radiologists for assessment of the fat plane between the pancreatic head and the mesenteric vessels: this was graded in two categories (clear, effaced/infiltrated). Fisher's test was used to assess the correlation between CT and pathology findings.
Results: A clear fat plane between the pancreatic head and the mesenteric vessels was significantly associated with a negative retroportal lamina at pathology (p=0.0037). No different results were observed between effaced and clearly infiltrated fat. No association was observed between the appearance of the fat planes at CT and the presence of lymphatic or perineural invasion (p=ns).
Conclusion: A clear fat plane between the pancreatic head and the mesenteric vessels is significantly associated with negative retroportal lamina at pathology. CT is not accurate in predicting lymphatic or perineural invasion.

B-0537 14:56

Body composition parameters, pancreatic volume and texture as radiological predictors of pancreatic fistula after Whipple procedure

I. Shrainer, V. Voropaev, E.A. Mershina, Z.A. Kovalenko, V.K. Lyadov, V.E. Sinitsyn; *Moscow/RU (shrainer@gmail.com)*

Purpose: Patients after Whipple procedure (pancreatoduodenectomy) experience postoperative complications in up to 50-60% of cases. Many surgical and radiological reports describe pancreatic fistula (PF) as the most frequent complication (10-24%). Aim was to find out the radiological predictors of PF in patients after Whipple procedure.
Methods and Materials: We retrospectively analysed 32 patients who underwent Whipple procedure and had a preoperative CT scan as staging in our centre. CT images were processed to obtain measures of pancreatic texture (density in nonenhanced scan), whole pancreatic volume, volume of pancreatic remnant and body composition parameters including whole body fat-free mass index (FFMI), whole body fat mass index (FMI), L3 skeletal muscle index (SMI).
Results: PF occurred in 15 patients who were included in the first group, the other 17 patients did not have PF and were included to the second group. There were significant differences ($p \leq 0.05$) between the two groups in the whole pancreatic volume (32.1+/-3.4cm^3 vs 21.4+/-3.0cm^3), texture of the pancreas (38.5+/-3.6HU vs 21.7+/-3.0HU) and volume of pancreatic remnant (18.4+/-2.1cm^3 vs 12.1+/-1.4cm^3). The significant difference of SMI (44.3 ± 8.3cm^2/m^2 vs 40.5 ± 8.8cm^2/m^2), FFMI (15.4 ± 2.4kg/m^2 vs 14.3 ± 2.5kg/m^2), FMI (8.8±2.5kg/m^2 vs 9.5±2.5kg/m^2) was not determined.
Conclusion: Pancreatic texture, preoperative whole pancreatic volume and volume of pancreatic remnant are independent predictors of pancreatic fistula. Body composition parameters (FFMI, FMI, SMI) do not affect the development of pancreatic fistula.

B-0538 15:04

Evaluation of perfusion in pancreas graft using 640-slice computed tomography

M.S. Khubutia, S.K. Ternovoy, R.S. Muslimov, Y.A. Anisimov, A.V. Pinchuk, N.S. Serova; *Moscow/RU (transfer498@yahoo.com)*

Purpose: To define feasibility of the 640-slice dynamic volume computed tomography in diagnostics of vascular complications and assessment of pancreas graft's (PG) perfusion.
Methods and Materials: 23 patients after pancreas transplantation were investigated using Toshiba 640-slice computer tomography. The contrast was injected through the central venous 16G-catheter. Data acquisitions were done without breath holding. Arterial blood flow parameters (AF, ml/min/100ml) were measured at the level of graft head, body, tail areas, and the time of maximum PG's tissue peak (TTP, sec.) contrasting was determined. The obtained results were analysed and compared with those of others authors dealing with perfusion of native pancreas.
Results: 12 cases showed adequate PG's blood flow at both arteries with normal organ function. The TTP-19[17;21], AF-117[97;123], 113[98;125], 104[89;126]. 9 cases revealed blood flow absence in a PG's superior mesenteric artery (PG blood flow was going separately through splenic artery's system). There were neither clinical nor laboratory signs PG dysfunction. AF-137[117;160], 126[120;132], 125[105;137], TTP-18[17;19] and statistically didn't differ from first patients group and a native pancreas perfusion. Also there were in 2 patients expressed depression of PG's blood supply in both arteries which resulted in depressed perfusion: AF - 44[20;66], 52[18;85], 57[21;92], TTP - 11[9;13]. Clinical and laboratory signs of PG's dysfunction were also found in this patients.
Conclusion: 640-slice dynamic volume perfused computed tomography allows to visualise whole-PG's vascular structure and anatomy. It also helps objectively estimate the adequacy of PG's blood supply and clinical importance of vascular complications.

B-0539 15:12

Diagnostic role of new generation multidetector-CT scanner in detection and characterisation of incidental pancreatic cystic lesions: comparison with MRCP

D. Ippolito, A. Nasatti, C. Talei Franzesi, A. De Vito, E. Orsini, S. Lombardi, S. Sironi; *Monza/IT (davide.atena@tiscalinet.it)*

Purpose: To compare the diagnostic accuracy of MDCT to MRI with MRCP sequences, in detecting pancreatic cystic lesion and those features useful for their characterization.
Methods and Materials: We evaluated 50 patients with no history of pancreatitis, neoplasm and prior surgical procedures in pancreas, who underwent both MDCT and MRI with MRCP (time interval lower 90 days),for pancreatic cysts characterization. The reviewer recorded number of lesions detected in each patients and the main morphologic features of defined target lesion: location (head,uncinate process,neck,body,tail), number, size, communication with main pancreatic duct (MPD), maximum MPD diameter, presence of septa, mural enhancing nodules. Data were analysed to compare diagnostic performance of MDCT and MRI.
Results: A greatest number of pancreatic cysts was identified on MRI than CT examinations (227 vs 128); however ICC value of 0.76 suggested a good agreement.Very good agreement (ICC 0.98) was found regarding the diameter of target lesions(21.4 mm on CT vs 21.8 mm on MRI),location of target lesion (κ=0.90), and detection of MPD dilatation (κ=1.00) and septa (κ=0.86). Fair agreement about the evaluation of MPD communication (κ=0.33) and calcifications (κ=0.22) was found.
Conclusion: MDCT can be consider almost equivalent to MRI with MRCP in the evaluation of pancreatic cystic lesion, offering detailed morphologic features helpful for their characterisation and those correlated with a high risk of malignancy.

B-0540 15:20

MDCT vs endoscopic USG in evaluation of pancreatic masses

S. Gupta; *Delhi/IN (surabhig27@gmail.com)*

Purpose: Compare the diagnostic accuracy of 256 multislice CT and endoscopic ultrasound (EUS) in characterization and assessment of resectability of pancreatic masses. - Comparison of 256 slice MDCT and EUS findings with histopathological/operative findings.
Methods and Materials: Total of 36 patients with pancreatic masses were included. Clinical and laboratory findings were recorded followed by dual phase examination using pancreatic protocol. EUS was performed using transducer of 5-13 MHz. FNAC was done wherever feasible. Parameters regarding tumour size, location, imaging morphology and vessel involvement were recorded. Findings were compared with histopathological /operative diagnosis/clinical follow up.
Results: Out of 36 patients, MDCT and EUS established diagnosis consistent with tissue diagnosis in 30 (83%) and 22 (61%) patients respectively. However, best results were obtained with combined use of MDCT and EUS ie 34 (95%) patients. The number of patients categorized as inconclusive by MDCT were lower compared to EUS (2/36 cases on MDCT vs 10/36 cases on EUS) -MDCT showed specificity and PPV of 100% in assessment of resectability of pancreatic adenocarcinoma compared to EUS which had specificity and PPV of 75% and 92.3% respectively. The sensitivity and NPV was 100% for both modalities.
Conclusion: MDCT is first line imaging modality in detection, characterization of pancreatic masses and assessment of resectability in malignant solid neoplasms. The specificity and PPV of MDCT was higher than EUS in determining resectability of pancreatic adenocarcinoma. -EUS is beneficial in detection of masses <2 cm in size causing only mild pancreatic contour deformity on CT, and for guiding FNAC.
Author Disclosures:
S. Gupta: Author; Dr S.K. Puri.

14:00 - 15:30 **Room C**

GI Tract

SS 701b

Bowel imaging: inflammation, obstruction and beyond

Moderators:
E. Biscaldi; Genoa/IT
D.J.M. Tolan; Leeds/UK

B-0541 14:00

Reduced scan range abdominopelvic CT in patients with suspected acute appendicitis: impact on diagnostic accuracy and effective radiation dose

D. Zinsser, M. Maurer, P.-L. Do, J. Weiß, M. Notohamiprodjo, K. Nikolaou, F. Bamberg, A. Othman; *Tübingen/DE*

Purpose: To compare a reduced-range CT in patients with suspected acute appendicitis to a standard abdominal CT regarding diagnostic performance and effective radiation dose.
Methods and Materials: We retrospectively included 90 patients (43 female, mean age 56.7±17 years) with suspected acute appendicitis who underwent an abdominopelvic CT. From those, we reconstructed images with a reduced scan range from L1 to the top of the pubic symphysis. Two radiologists assessed full-range and reduced-range datasets for coverage of the appendix, presence/absence of appendicitis and presence of differential diagnoses. Effective radiation doses as well as organ doses were calculated using a commercially available dose management platform.
Results: The appendix was covered by the reduced-range CT in all cases. In 66 patients CT confirmed the presence of appendicitis. In 17 patients, other relevant differential diagnoses were identified by CT. No relevant findings were detected in 7 patients. Both readers identified all patients with appendicitis on both full- and reduced-range CT. For reduced-range CT, total effective dose was 40 % lower than for full-range CT (4.99±1.76 vs. 8.34±2.95 mSv; p≤0.001). Notably, a remarkable reduction of organ doses in the female breast by 96 % (0.18±0.1 vs. 4.12±3.79 mSv; p=0.003) and in the testicles in males by 66 % (6.61±7.61 vs. 19.7±10.32 mSv; p≤0.001) was observed for reduced-range CT compared to full-range CT.
Conclusion: In patients with suspected acute appendicitis, reduced-range abdominopelvic CT results in a comparable diagnostic performance with a remarkable reduction of total effective radiation dose and organ doses as compared to full-range CT.

B-0542 14:08

Impact of low-dose abdominal CT on diagnostic accuracy and image quality in patients with suspected appendicitis

C. Storz[1], M. Kolb[1], J. Weiß[1], J. Kim[2], F. Bamberg[1], A. Othman[1]; [1]*Tübingen/DE*, [2]*Seoul/KR (corinna.storz@med.uni-tuebingen.de)*

Purpose: To determine the impact of radiation dose reduction on diagnostic image quality and accuracy of abdominal CT for detection of acute appendicitis.
Methods and Materials: Consecutive patients with suspected appendicitis who underwent contrast-enhanced abdominal CT (120kV, CARE dose reference 160-200mAs) following inconclusive ultrasound were retrospectively analyzed. Realistic reduced-dose simulation was used to generate low-dose datasets with 75%, 50% and 25% of the original-dose level. Two independent readers determined objective (signal-to-noise ratio [SNR]), subjective image quality (5-point Likert scale) and presence of appendicitis and complications, including abcess formation or perforation.
Results: Among 50 patients (mean age: 47±17 years, 68% female), 200 data sets were generated and 48% had surgically confirmed appendicitis. SNR and subjective image quality of all low-dose CTs was significantly lower compared to original datasets (all p<0.005). Appendicitis was correctly identified in all original and low-dose datasets (sensitivity: 100%, NPV: 100%). The presence of complications was correctly detected in original, 75% and 50% datasets, whereas on 25% datasets the diagnostic accuracy was significantly lower (sensitivity: 75%). Similarly, diagnostic confidence was high for original and low-dose datasets down to 50% but significantly decreased for 25% datasets (p<.001). Inter-observer-agreements was high for original, 75% and 50% datasets but moderate for 25% datasets (κ=1 and κ=0.66, respectively).
Conclusion: Abdominal CT acquisitions with 50% reduced radiation exposition provide high diagnostic image quality and accuracy for the detection of appendicitis, while further reduction of exposition is associated with decreased diagnostic performance.

B-0543 14:16

The impact of CT findings in resolving appendicitis

K. Ozturk, E. Soylu Ozturk, G. Savci; *Bursa/TR (keremov54@hotmail.com)*

Purpose: To establish the outcome of patients with radiological diagnosis of acute appendicitis and to predict the significance of resolving appendicitis.
Methods and Materials: 114 patients having positive CT criteria for acute appendicitis in an emergency setting were evaluated. 26 patients with mild clinical presentation were treated conservatively. CT findings such as appendix wall thickening and enhancement, maximum appendix diameter, presence of an appendicolith, local lymphadenopathy, infiltration around peri-appendiceal fat, fluid collections and focal cecal thickening obtained from images. An univariate analysis was conducted to identify statistically significance of CT findings. Logistic regression analysis was performed in order to find the factors related to the discrimination of resolving appendicitis.
Results: Mean diameter of appendix was over 6 mm in all patients. However, mean diameter of the appendix was significantly lower in patients with resolving appendicitis compared to the non-resolving appendix, 10.9 ± 2.2 mm vs 13.4 ± 2.3 mm, respectively, (P < 0.05). In addition, the degree of infiltration of peri-appendiceal fat was milder in patients with resolving appendicitis (P < 0.05). Patients with appendix diameter over 12 mm (odds ratio [OR] 5.6) and presence of infiltration around appendiceal fat (OR 5.5) seem to have more severe and non-resolving course. The other parameters did not reached to a statistically significant level.
Conclusion: Our results indicate that CT findings using regression model can accurately predict the resolving appendicitis. It seems that it is logical to correlate the radiological findings with clinical findings to prevent unnecessary surgery.
Author Disclosures:
K. Ozturk: Author; Kerem Ozturk. Founder; Kerem Ozturk. Owner; Kerem Ozturk. Patent Holder; Kerem Ozturk. Speaker; Kerem Ozturk. **E. Soylu Ozturk:** Board Member; Esra Soylu Ozturk. CEO; Esra Soylu Ozturk. Employee; Esra Soylu Ozturk. Investigator; Esra Soylu Ozturk. Shareholder; Esra Soylu Ozturk. **G. Savci:** Advisory Board; Gursel Savci. Author; Gursel Savci. Consultant; Gursel Savci. Equipment Support Recipient; Gursel Savci. Grant Recipient; Gursel Savci. Research/Grant Support; Gursel Savci.

B-0544 14:24

MDCT experience of male anterior peritoneal reflection: investigate and measurement in patients with appendicitis

J. Xu; *Shanghai/CN (drxujun@yahoo.com)*

Purpose: To investigate the MDCT experience of anterior peritoneal reflection in male patients with appendicitis and see if pelvic fluid can influence the measured distance from the anal verge to the anterior peritoneal reflection.
Methods and Materials: 80 valid MDCT studies of 121 male appendicitis patients between July 2014 and June 2015 were retrospectively analysed with a Reformat application (GE Advanced Workstation version 4.5). The visualisation of anterior peritoneal reflection, the exist of pelvic fluid of each patient were investigated and the measured distances from anterior peritoneal reflection to the anal verge were recorded.
Results: In male appendicitis patients, anterior peritoneal reflection is a V-shaped line with high density along superior bladder margins and seminal vesicle and then inserting onto rectum. The mean distance from the anal verge to the anterior peritoneal reflection was 9.6±1.3 cm. Pelvic fluids were found in 29 patients, and the mean distance of patients with and without pelvic fluid were 9.2±1.3cm and 10.1±1.2cm, respectively, with statistically significant differences (P=0.0027<0.05, F=0.627).
Conclusion: Pelvic fluid may influence the distance from the anal verge to the anterior peritoneal reflection, thus, using perioperative CT or MRI to determine the location of rectal cancer with respect to the peritoneal reflection may unreliable.

B-0545 14:32

CT findings of terminal ileum wall thickening in differential diagnosis of right lower quadrant pain

M.M. Baris, O. Hatem, O. Topalak, O. Sagol, M. Secil; *Izmir/TR (mustafa.secil@deu.edu.tr)*

Purpose: The aim of this study was to investigate the direct and accompanying CT findings in terminal ileum wall (TIW) thickening in patients with right lower quadrant (RLQ) pain.
Methods and Materials: A retrospective evaluation of PACS was performed for patients presenting with RLQ pain and TIW thickening. The investigated CT parameters included the length, thickness and symmetricity of thickened segment, the presence of mural enhancement, target sign, mesenteric fat stranding, fluid or abscess in the abdominal cavity. The presence, number and the greatest diameter of lymph nodes (LN) were recorded. The final diagnoses were obtained from hospital records. Histopathological findings obtained by

operation or colonoscopy and/or long term follow-up findings were considered as the reference standards.
Results: The investigation detected 84 patients (51 male, 33 female) that met the inclusion criteria. Clinical/pathological diagnoses of these patients were acute appendicitis in 25 (29.8%), non-specific ileitis (NSI) in 32 (38.1%) and Crohn's disease (CD) in 27 (32.1%). The measurement of TIW thickening, the number and diameter of LN were shown to have statistically significant difference between appendicitis, CD and NSI (p= 0.026, p=0.003, p=0.021). There was also statistically significant difference between three groups for mural enhancement, target sign, mesenteric fat stranding, and presence of abscess.
Conclusion: The parameters of TIW thickness measurement, the number and diameter of involved LN may be used as practical parameters in differential diagnosis of terminal ileum findings in patients presenting with RLQ pain.

B-0546 14:40

Systematic evaluation of the effect of low-dose CT on diagnostic performance in patients with suspected acute diverticulitis
S. Walter[1], M. Maurer[1], J. Weiss[1], F. Bamberg[1], J. Kim[2], K. Nikolaou[1], A. Othman[1]; [1]*Tübingen/DE*, [2]*Seoul/KR (sven.walter@uni-tuebingen.de)*

Purpose: To examine the effects of radiation dose reduction on image quality and diagnostic accuracy in low-dose computed tomography in patients with acute diverticulitis and its complications.
Methods and Materials: Consecutive patients presenting with symptoms of acute diverticulitis who underwent routine abdominal CT with rectal and intravenous contrast injection (120 kVp, CareDosexxx, CTDI) were included. Low-Dose-CT datasets (25%, 50% and 75% of the original dose) were generated using a realistic low-dose simulation technique based on sinogram synthesis and quantum noise modeling. Image analysis included assessment of objective (Signal-to-noise-ratio, SNR) and subjective image quality (5-point Likert scale) and the presence of acute diverticulitis and associated complications (abscess, fistula formation or perforation) by two independent readers.
Results: Among 31 subjects of whom none was older than 40 years (mean age: 32.1 years, 12.9% female), the prevalence of the clinical diagnosis of acute diverticulitis was high (64.5%). Subjective image quality and SNR for all datasets were highest for 100% and lowest for 25% exams (both p<0.001). Similarly, diagnostic confidence was highest for 100%, 75%, and 50%, while 25% had significantly lower certainty (p<0.001). The diagnostic accuracy was excellent for all low-dose and original datasets (sensitivity: 100%, NPV: 100%) whereas associated complications (prevalence: 45%) could be detected in 25% datasets with decreased sensitivity (77.8%, NPV: 91.3%; sensitivity: 100% and NPV: 100% for all >25% low-dose exams).
Conclusion: Low-Dose CT acquisition with 50% of the standard radiation exposure permits high diagnostic confidence and accuracy for the diagnosis of acute diverticulitis and its complications.

B-0547 14:48

To use CT for management decision in small intestinal obstruction: surgery or conservative treatment?
J.-D. Chen, C.-M. Tiu, Y.-H. Chou; *Taipei/TW (jdchenjdchen2013@gmail.com)*

Purpose: To verify whether CT can differentiate the patients with small bowel obstruction (SBO) who need surgery from those who need not.
Methods and Materials: We retrospectively reviewed consecutive cases with SBO in one-year period. The patients who needed surgery for SBO constituted the study group, and those who recovered from conservative treatment, the control group. CT were evaluated for the followings: largest bowel diameter (BD) proximal to and smallest BD distal to transition zones, maximal proximal-to-distal BD ratio, proximal bowel content, small bowel faeces sign, bowel wall thickening, shape and enhancing patterns of transition zones, presence of closed loop, mesenteric fat stranding, mesenteric vascular engorgement, interloop/mesenteric fluid and ascites. All CT features were compared between two groups with Student t test or Chi-square test accordingly for statistical analysis.
Results: 128 cases with SBO were included in this study, including 84 males and 44 females with mean age 72 years. 64 cases received surgery for SBO and 64 recovered after conservative treatment. The maximal proximal-to-distal BD ratio was significantly larger in study group (mean 8.36 ± 3.05 vs 7.03 ± 2.81, *p*=0.01). The following CT features were more significantly present in study group: mesenteric fat stranding (71.9% vs 29.7%, *p*<0.001), closed loop pattern (21.9% vs 6.3%, *p*=0.02), and interloop/mesenteric fluid (70.3% vs 35.9%, *p*<0.001).
Conclusion: CT helps to facilitate management decision in SBO. When presence of larger maximal proximal-to-distal BD ratio, mesenteric fat stranding, closed loop pattern, and associated interloop/mesenteric fluid on CT, surgery should be appropriate for these patients with SBO.

B-0548 14:56

Can the characteristics of bowel wall and signs on CT differentiate the aetiology of bowel obstruction?
E. Güler, N. Elmas, M. Harman, S. Türk, T. Köse; *Izmir/TR (gulerezgi@yahoo.com)*

Purpose: To evaluate performance of bowel wall characteristics and findings on CT images in determining the aetiology of bowel obstruction accompanied with bowel wall thickening.
Methods and Materials: CT scans of 63 patients with bowel obstruction accompanied with thickened bowel wall, who were admitted to our institution between January 2015 and September 2016 were retrospectively reviewed. Bowel wall thickness, length of involvement, bowel wall attenuation in arterial and portal venous phase contrast-enhanced images were measured. Patient age, presence of small-bowel faeces sign, ascites, lymphadenopathy, liver metastasis, comb sign, mesenteric oedema, omental thickening, thrombosis of mesenteric vessels were noted. Causes of bowel obstruction were divided into 4 main groups: malignancy (n=14), adhesions (n=12), ischaemia (n=11), inflammatory bowel disease (IBD) (n=9). Comparisons between groups were evaluated using Mann-Whitney U or post-hoc tests. Pearson's chi-square test was applied to assess associations between variables and aetiology.
Results: Comparisons of adhesion-IBD, malignancy-adhesion, malignancy-IBD, malignancy-ischaemia groups were statistically significant for bowel wall thickening. Length of involved bowel wall thickening was significant in comparison of IBH-ischaemia. Differences of age were significant in comparisons of IBH-adhesion, IBH-malignancy groups. Presence of faeces sign, comb sign, thrombosis of vessels were significantly associated with comparisons of groups. There was a statistically significant difference between ischaemia and other groups in terms of bowel wall enhancement calculated using a ratio between two phases of contrast-enhanced images (p<0.05).
Conclusion: Differences of bowel wall thickening can be helpful in differentiating malignancy from other causes of bowel obstruction. A ratio of bowel wall attenuation can be useful in distinguishing ischaemia.

B-0549 15:04

Mesenteric panniculitis: is malignancy associated with higher grade of CT changes?
T. Grubesic, Z. Matana Kastelan, D. Miletic; *Rijeka/HR (tianagrubesic@yahoo.com)*

Purpose: Mesenteric panniculitis (MP) is a disorder of mesenteric adipose tissue, a subgroup of sclerosing mesenteritis, presented by inflammation and fat necrosis. Both aetiology and association with various disorders remain unclear. Our objective was to assess if there exits a difference in severity of MP in "neoplastic" and "non-neoplastic" patients.
Methods and Materials: In period between June 1, 2015 and October 1, 2016, 54 patients, 32 male and 22 female, mean age 69.13±3.33, who underwent abdominal CT were diagnosed with MP. Based on their clinical data, patients were classified as "neoplastic" (n=35 or 64.81%) or "non-neoplastic" (n=19 or 35.19%). Two radiologists independently reviewed CT examinations evaluating 5 parameters: inhomogenous higher attenuation of mesenteric fat tissue, presence of lymph nodes, hypoattenuated fatty halo around vessels, mass effect on neighbouring structures and presence of pseudocapsule. Each sign was assigned with four possible grades: absent (0), discrete (1), moderate (2) or marked (3), with overall grade of MP as minimal (≤5), moderate (6-9) or marked (10-15).
Results: In "neoplastic" group, MP was classified as minimal in 3 patients (8.57%), moderate in 22 patients (62.86%) and marked in 10 patients (28.57%), with mean score of 8.09. MP in "non-neoplastic" group was graded as minimal in 3 patients (15.79%), moderate in 10 patients (52.63%) and marked in 6 patients (31.58%). Mean score was 7.89.
Conclusion: CT grade of MP does not significantly differ in neoplastic patients in comparison to non-neoplastic in our series, so its predictive value in course of the disease is not relevant.

B-0550 15:12

Evaluation of dynamic ultrasound scanning in the diagnosis of equivocal abdominal hernias with surgical comparison
P.R. Jayaram, J. Barrett; *Bury St Edmunds/UK (premruben@yahoo.com)*

Purpose: Ultrasound has become the modality of choice for diagnosing equivocal hernias in many centres worldwide. However, there is no quantification of its effectiveness when compared to surgery. This study aims to compare dynamic abdominal sonography for hernias (DASH) with surgical findings and establish its accuracy in equivocal cases.
Methods and Materials: A retrospective review of all patients who underwent an abdominal ultrasound scan between June 2011 and June 2015 was performed. The word 'hernia' in the referral information was the sole inclusion criterion. Patients who were under 18 years of age, found to have an unrelated hernia or had a known hernia were excluded. No distinction was made

between the types of abdominal hernias. These patients were followed up for at least 6 months and operation notes, if any, were also analysed.
Results: 348 scans were included this study (F=198, M=150, F:M ratio=1.32:1). The mean age was 53.4 years (range 18-97 years). 101 scans were positive for hernias (29.0%), 189 were negative (54.3%), and 58 had other findings (e.g. seroma, lipoma, etc.; 16.7%). 54 patients were taken to surgery (15.5%), including 5 who were found to be negative on ultrasound. Of these patients, 45 were true positives, 4 true negatives, 4 false negatives, and 1 false positive, giving a sensitivity of 91.8%, specificity of 80.0% and positive predictive value of 97.8%.
Conclusion: This study provides evidence that DASH has high sensitivity, specificity and positive predictive value, and confirms the effectiveness of DASH when investigating for equivocal abdominal hernias.

B-0551 15:20

Noise insertion in abdominal computed tomography for suspected body packing: where is the limit of extensive dose reduction?
J. Aissa, L. Sawicki, P. Heusch, E. Appel, P. Kröpil, C. Thomas, G. Antoch, J. Boos; *Düsseldorf/DE (joel.aissa@med.uni-duesseldorf.de)*

Purpose: To evaluate abdominal CT at different dose levels in patients suspected of body packing in regards to image quality and capability to detect foreign body packets.
Methods and Materials: We retrospectively included 27 subjects (20 male, 7 female; 378±11years) who underwent abdominal CT (80kV, automated tube current modulation, eff. dose 2.1±1.3mSv) in clinical routine. Images were reconstructed with simulated radiation dose levels of 50%, 10%, 5% and 1% of the initial dose using a validated noise-insertion software. The initial reconstruction at 100% dose served as the reference standard. Three independent readers blinded to the dose level and findings reviewed all images in a random order and assessed: 1. the presence and composition of foreign bodies, 2. the overall image quality using a 5-point scale, and 3. the presence of incidental findings.
Results: Image quality was comparable between 100% and 50% dose simulated images (p>0.05). Further dose reduction produced significantly worse image quality compared to the 100% images (p<0.0001). The threshold for correct identification of all incidental findings was 10% of the original dose (eff. dose 0.21±0.13mSv). The threshold for correct identification of all 8 body packets by all three readers was 5% (eff. dose 0.1mSv) (p<0.008). A dose reduction to only 1% led to 3 false positive cases suspected of solid cocaine packets.
Conclusion: An effective dose of 0.1 mSv seems sufficient to detect body packets in abdominal CT. However, overall image quality is reduced and a dose of 0.21mSv is necessary to reliably detect incidental findings.

14:00 - 15:30 **Room Z**

Interventional Radiology

SS 709

Non-vascular interventions

Moderators:
B. Kastler; Paris/FR
L. Ponhold; St. Pölten/AT

B-0552 14:00

Prospective randomised MIRA trial: microwave vs radiofrequency ablation of hepatocellular carcinoma - first results
T.J. Vogl, L.-M. Klohmann, T. Gruber-Rouh, R. Hammerstingl, N.-E. Nour Eldin; *Frankfurt a. Main/DE (t.vogl@em.uni-frankfurt.de)*

Purpose: To prospectively determine and compare therapy response and safety of microwave (MWA) and radiofrequency ablation (RFA) of hepatocellular carcinoma (HCC) in a randomised trial.
Methods and Materials: In this prospective study 36 patients (31 men, 5 women; mean: 65 years; range 42-82) with 36 HCC lesions (mean: 2.4cm; range 0.9-5cm; MWA 2.5cm, RFA 2.2cm) underwent CT-guided thermal ablation. Location of HCC and changes in size, volume, necrotic area, diffusion and ADC value were evaluated using MRI. First MRI was performed before ablation. Follow-up MRI was performed 24h after ablation and then in 3-month intervals for 12 months.
Results: Mean volume 24h after ablation was 47.3cm^3 (62cm^3 for MWA, 32.7cm^3 for RFA). Complete ablation was observed in 83.3% (30/36), 66.7% (12/18) in MWA and 100% (18/18) in RFA. Local recurrence rate within one year for both groups was 16.7% (6/36). Local recurrences were only documented in the MWA-group. New malignant formations in another location than the ablated lesion were documented in 19.4% (7/36) and only in the RFA-group. 16.7% (6/36) of patients underwent thermal ablation before participating in this trial, 19.4% (7/36) received again thermal ablation in other segments of the liver while being part of this trial. The mortality rate for this trial was 0% with no major complications.
Conclusion: First data of the MIRA trial show no significant differences in mortality or complication rates between RFA and MWA. MWA generates greater ablation volumes and 1-year follow-up of the MWA-group shows a higher rate of local recurrences vs RFA.

B-0553 14:08

MWA of liver tumours with thermosphere technology: prospective analysis of ablation zone predictability in vivo with different liver conditions and operative approaches
P. Marra, M. Colombo, F. Ratti, F. Cipriani, C. Sallemi, M. Venturini, L. Aldrighetti, A. Del Maschio, F. De Cobelli; *Milan/IT (marra.paolo@hsr.it)*

Purpose: The high power/frequency MW-system with Thermosphere-technology allows ablation of liver tumours in short time. Ablation-zone (AZ) volume prediction relies on ex vivo animal studies on normal livers, with concerns about reproducibility and safety in humans. We aimed to investigate if MW effects produced in vivo on human livers reflect the ex vivo model and vary with liver conditions (normal/cirrhotic/chemotherapy-treated) and approaches (percutaneous/intraoperative).
Methods and Materials: From October-2014, 54 patients prospectively underwent MWA for the treatment of 74 liver nodules (HCC=30;mets=44), percutaneously (P=28), during laparotomy (LT=28) or laparoscopy (LP=18) in normal (N=19), cirrhotic (C=30) and chemotherapy-treated (ChT=25) livers, with a 2450MHz/100W MW-generator (EmprintTM-Medtronic). Contrast-enhanced-CT was performed 1 month after the procedure to verify complete-ablation (CA) and to quantify AZ volume and sphericity.
Results: AZ volumes were linearly correlated with ablation times (R=0.67; p<0.01) with no differences between in vivo results and the ex vivo model at regression analysis. The time/volume linear correlation was confirmed for each subgroup with no differences related to operative approach or liver condition. We observed a higher time/volume linear correlation in cirrhotic (R=0.81; p<0.01) versus non-cirrhotic (R=0.73; p<0.01) and chemotherapy-treated (R=0.59; p<0.01) livers. Mean AZ roundness-index was 0.77±0.07. MWA efficacy in terms of CA at 1 month was slightly better in intraoperative procedures (LT=100%vs LP=100%vs P=93%; p=ns). No complications occurred.
Conclusion: The extent of AZ reflected animal models in all liver conditions and operative approaches. Our results confirm that Thermosphere technology produces highly predictable AZ and is effective and safe for the treatment of liver tumours.

B-0554 14:16

Percutaneous microwave ablation of exophytic tumours in hepatocellular carcinoma patients: safe or not?
X. Jing, J. Ding, Y. Zhou, Y. Wang; *Tianjin/CN (dr.jingxiang@aliyun.com)*

Purpose: To compare the long-term therapeutic outcomes and safety of microwave ablation (MWA) of exophytic tumours with those of non-exophytic subcapsular tumours in hepatocellular carcinoma (HCC) patients.
Methods and Materials: From July 2010 to July 2014, 856 consecutive patients with HCC underwent ultrasound-guided MWA ablation. Among them, 132 patients were enrolled in this retrospective study. Those patients were divided into exophytic group (n=71) and non-exophytic group (n=61) according to the location of their tumour(s). The local tumour progression (LTP), progress free survival (PFS) and overall survival (OS) were analyzed using Kaplan-Meier and Log-rank tests.
Results: The follow up periods ranged from 6 to 62 months, with a median of 31 months in exophytic group, and ranged from 5 to 61 months, with a median of 27 months in non-exophytic group. Local progression rate was 11.3% (8/71) in exophytic group and 11.5% (7/61) in non-exophytic group (P=0.733). The 1-, 2-, 3-, 4- and 5 year PFS rate were 84.5%,53.7%,31.2%,25.6% and 21.3% in exophytic group and 82.0%,53.5%,38.6%,30.4% and 24.3% in non-exophytic group, respectively(P=0.489). The 1-, 2-, 3-, 4- and 5 year OS rate were 100.0%,87.4%,75.7%,65.5% and 52.9% in exophytic group and 95.0%,83.0%,73.8%,69.2% and 61.5% in non-exophytic group, respectively (P=0.980).There were no procedure-related mortality and major complications in both exophytic and non-exophytic group.
Conclusion: MWA is a safe and effective treatment for exophytic tumours in HCC patients. Treated by MWA, the patients with exophytic tumours can get the similar local response and long-term outcome with those with non-exophytic subcapsular tumours.

B-0555 14:24

Comparison of multi-modality and mono-modality fusion imaging using ultrasound in the intraoperative immediate evaluation of the therapeutic response of liver thermal ablation

E. Xu, Y. Long, K. Li, Z. Su, S. Lv, Q. Zeng, R. Zheng; *Guangzhou/CN (xuerjiao@126.com)*

Purpose: Purpose of the study is to investigate the value of multi-modality fusion imaging combined computed tomography or magnetic resonance imaging with ultrasound (CT/MRI-US fusion imaging) and mono-modality fusion imaging using ultrasound (US-US fusion imaging) in the intraoperative immediate evaluation of therapeutic response of liver thermal ablation.
Methods and Materials: From Aug. 2015 to Dec. 2015, 157 liver cancers in 115 patients which were undergone US-guided thermal ablation were enrolled. Both US-US fusion imaging and CT/MRI-US fusion imaging were performed to immediately evaluate the therapeutic response intraoperatively. The CT/MRI results after one month were taken as references. The applicable rates, success rates of registration and complete ablation rates were compared between two types of fusion imaging by Chi-square test.
Results: The applicable rate of US-US fusion imaging was only 61.8%(95/157) because of the ill-defined lesions in US. It was lower than that of CT/MRI-US fusion imaging (99.7%(155/157)) (P<0.05). However, the success rate of registration in US-US fusion imaging (91.7%(89/95)) was superior to that of CT/MRI-US fusion imaging (81.3%(126/155)) (P<0.05). The complete ablation rates (98.7%(81/82) vs 99.2%(118/119)) were no statistical difference between two types of fusion imaging (P>0.05).
Conclusion: Both US-US fusion imaging and CT/MRI-US fusion imaging are useful means to evaluate the therapeutic response of liver thermal ablation. US-US fusion imaging could be the priority in the assessment. When the lesions are ill-defined in US, CT/MRI-US fusion imaging could be selected preferentially instead.
Author Disclosures:
E. Xu: Research/Grant Support; National Natural Science Foundation of China (No.81401434), Science and Technology Planning Project of Guangdong Province, China (No. 2014A020212136). **R. Zheng:** Research/Grant Support; National Natural Science Foundation of China (No. 81430038).

B-0556 14:32

Cone-beam CT for percutaneous drainage of abdominal and pelvic collections: technical considerations, success rates, complications and dose compared to CT-fluoroscopic guidance

J. Das, D. Lohan, I. Davidson, D. Sheppard, R. McLoughlin, G. O'Sullivan; *Galway/IE (jjeeban@hotmail.com)*

Purpose: Cone-beam Computed Tomography (CBCT) utilises a flat panel detector and C-arm system in the Interventional Radiology suite allowing 3D reconstruction of the imaged volume of tissue. This study compares performace of CBCT with conventional CT guidance in draining abdominopelvic collections.
Methods and Materials: 111 CT drainages of abdomino-pelvic collections were performed in 108 patients between December 2010 and July 2016. 55 patients underwent drainage with CBCT (Dyna CT™, Siemens, Erlangen, Germany), 53 patients had conventional CT fluoroscopic drainage (Siemens Sensation™ 64-slice, Forchheim, Germany) Patient demographics, collection size and depth, technical success, microbiology, incidence of complications and dose were recorded.
Results: Successful collection drainage was achieved in 51/57 (89.5%) in the CBCT group and 49/54 (90%) of the CT fluoroscopy group (p=0.4). The average abdominopelvic collection size was 10.6cm vs 8.8cm in the CBCT and CT-fluroscopy guided groups respectively (p=0.6). The average depth of collection was 7.5cm in CBCT vs 7.9cm in CT fluoroscopy (p=0.07) A 12 F (or smaller) drain was placed in 41 patients in the CBCT group vs 43 in the conventional CT guided cohort. The mean duration of procedure in the CBCT group was 36 minutes, in the conventional CT group the mean time was 48 minutes (p=0.35) The average dose was lower in CBCT group vs CT-fluoroscopy (11mSv vs 17.4mSv, p=0.05). No immediate complications were recorded in either group.
Conclusion: CBCT is comparable to CT-Fluoroscopic guidance for abdominopelvic collection draininge in terms of success with the advantage of reduced dose and shortened procedure time.

B-0557 14:40

Microwave ablation of pulmonary neoplasms with enabled constant spatial energy control to achieve a predictable spherical ablation zone: retrospective evaluation

T.J. Vogl, H. Ackermann, N.-E. Nour Eldin, N.N.N. Naguib, L. Basten; *Frankfurt a. Main/DE (t.vogl@em.uni-frankfurt.de)*

Purpose: To evaluate performance of microwave ablation (MWA) with enabled constant spatial energy control (Thermosphere™) for treatment of lung malignancies in formation of a spherical ablation zone.
Methods and Materials: In this retrospective study 45 patients (23 men, 22 women; mean 58.6 years; range 27-75) were treated in 45 sessions between 05/2014 and 11/2015, after giving written informed consent, using MWA with Thermosphere™. To provide three-dimensional evaluation for each ablation zone section in each transverse and longitudinal CT slice two perpendicular diameters were measured and their ratios computed. Calculating average of all ratios per single ablation zone resulted in a final sphericity value for each ablation zone. This final value is stated as deviation from 1.0, corresponding to an ideal sphere. Same parameters were retrospectively evaluated of 45 sessions using conventional low-frequency (LF) MWA. Results of both groups were compared using Wilcoxon-Mann-Whitney test.
Results: Thermosphere interventions succeeded in 97.8%, LF-MWA in 100%. Overall complication rate was 22.2% with Thermosphere and 31.1% with LF-MWA, minor 17.8% and 20.0%, major 4.4% and 11.1% (p=0.474). Mean duration was 7.98 min (median:8.0 min) for Thermosphere and 9.59 min (median:10.0 min) for LF-MWA with a significant difference (p=0.005). Deviation from ideal sphericity was median 0.194 (range: 0.078-0.500, 25th-percentile: 0.158, 75th-percentile: 0.291) for Thermosphere interventions and 0.384 (range: 0.218-0.610, 25th-percentile: 0.312, 75th-percentile: 0.450) for LF-MWA with a significant difference (p<0.0001).
Conclusion: MWA of lung malignancies using Thermosphere™ achieves a distinctly more spherical ablation zone to facilitate complete ablation in significantly shorter duration heading towards fewer complications.

B-0558 14:48

Respiratory phase tracking with visual patient feedback facilitating consistent level of breath-hold during image-guided interventions: an exploratory study

W.J. Heerink, M.D. Dorrius, H.J. Groen, R. Vliegenthart, M. Oudkerk; *Groningen/NL (w.j.heerink@umcg.nl)*

Purpose: To validate a novel respiratory phase feedback system that facilitates consistent level of breath-hold during image-guided interventions.
Methods and Materials: A commercially available depth camera (KinectV1, Microsoft) is used to determine the mean distance to thorax and abdomen in real-time. The camera is mounted to the CT table and aimed into the gantry. After breathing instruction and breath-hold, the system is set to this specific depth-of-breath. Subsequently, visual feedback for patient and radiologist can be provided on a screen with a ball moving up and down with respiration and a stationary circle corresponding to target level of breath-hold. For eight healthy volunteers, a conversion factor from mean thoracic depth to depth-of-breath (mL) was determined in supine and prone position using spirometry. After breathing instruction and initial breath-hold, the volunteers were asked to return to the same level of breath-hold 10 times, with and without visual feedback, in both positions. Without feedback, the volunteers did receive regular breathing instructions. Mean error from initial breath-hold and standard deviation were determined for both positions, with and without feedback and compared using independent samples t tests.
Results: Without feedback, the volunteers returned to within 169±153 mL and 234±194 mL of initial breath-hold in supine and prone position, respectively. With feedback, this was reduced for all volunteers, with a mean of 42±36 mL (p<0.001) and 30±25 mL (p<0.001), respectively.
Conclusion: The system provides accurate feedback enabling healthy volunteers to return to a consistent level of breath-hold, thereby elimination potential targeting errors in image-guided interventions caused by respiratory movement.

B-0559 14:56

Performance of a robotic assistance device in computed tomography-guided percutaneous diagnostic and therapeutic procedures

A. Smakic, N. Rathmann, M. Kostrzewa, S.O. Schönberg, C. Weiß, S. Diehl; *Mannheim/DE (arman.smakic@medma.uni-heidelberg.de)*

Purpose: To evaluate a novel commercially available robotic assistance device for computed tomography-guided diagnostic and therapeutic interventions compared to standard manually performed CT-scan-guided interventions in terms of precision, exposure to radiation and intervention time.
Methods and Materials: 55 patients were treated using robotic assistance (group A) and compared to a control group of 101 patients treated with a standard CT-scan-guided, manually performed, approach (group B). Evaluated

parameters were precision, radiation exposure and time of intervention. Evaluations were performed with regard to complexity and type of anesthesia (general vs local anesthesia).
Results: Precision parameters were in general significantly better in the robotic assistance group (p<0.01) with a mean deviation of 1.2mm(±1.6 mm) compared to 2.6mm(±1.1 mm) in the comparison group. Regarding the sub-groups differences in deviation in both groups were smaller in procedures performed under general anesthesia compared to local anesthesia (Group A: 0.5mm (±0.9mm) vs 2.1mm (±1,9mm) group B: 1.9mm (±1.3 mm) vs 3.4mm (±1.1 mm) (both p<0.001). Mean number of needle replacements that there were necessary to reach the target was 0.3 (±0,4) in the robotic assistance group compared 1.8 (±0.7) in the comparison group (p<0.001).
Conclusion: Compared to manual placement the use of a robotic assistance device in out of plane CT-guided interventions under general anesthesia allows probe placement with high precision, reduces intervention time with no increase of exposure to radiation to the patient and zero radiation for the physician. These characteristics render it a useful tool, especially in complex interventions like irreversible electroporation or microwave ablation.

B-0560 15:04

Ablation zone geometry in microwave ablation of the liver - comparison of two systems using a semi-automatic segmentation software
V.D. Vo Chieu[1], F. Wacker[1], C. Rieder[2], C. Schumann[2], H. Ballhausen[2], K.I. Ringe[1]; [1]*Hannover/DE*, [2]*Bremen/DE (vochieu.vandai@mh-hannover.de)*

Purpose: To evaluate ablation zone geometry in CT-guided microwave ablation (MWA) of the liver using two different ablation systems by means of a semi-automatic segmentation software.
Methods and Materials: 27 patients referred for CT-guided MWA with a total of 40 lesions (HCC n=17, CCC n=3, metastases n=20) were analysed. Two different systems were used: System 1 (2.45 GHz) or system 2 (915 MHz) with each 20 ablated lesions. Semi-automatic ablation zone segmentation and ellipticity index calculation was performed using SAFIR (Software Assistant for Interventional Radiology). For validation of semi-automatic software calculations, results were compared with those of manual analysis (Pearson's correlation, Mann-Whitney U test).
Results: Manually measured mean maximum ablation zone diameters were 32mm (system 1) and 27mm (system 2). Correlations between manual and semi-automatic measurements were very good for maximum axial and transversal diameter (both r=0.83, p<0.0001) and moderate for minimum transversal diameter (r=0.46, p=0.003). Ablation zones created with system 1 had a significantly lower ellipticity index compared to system 2 (1.17 vs 1.86, p<0.0001) in non-automatic analysis, whereby an ellipticity index of 1 indicated a perfect spherical ablation zone, correlating well with software measurements (r=0.79, p<0.0001).
Conclusion: The 2.45 GHz microwave ablation system generated a significantly more spherical ablation zone compared to the 915 MHz system. Semi-automatic assessment of ablation zone geometry using SAFIR seems feasible and significantly correlates with manual measurements, while at the same time providing further information. Software evaluation of ablation zones can prove beneficial while and before performing complex ablation procedures.

B-0561 15:12

Hybrid dynaCT-guided hookwire localisation of pulmonary lesions prior to surgical resection in the same hybrid operating theatre
C. Chu, E. Dai, C. Ng, R. Lau, R. Wong, S. Yu; *Shatin/HK*

Purpose: Hybrid DynaCT-guided hookwire localisation of pulmonary lesions immediately prior to surgical resection by radiologist in same hybrid operating theatre is a new one-stop technique, which our centre is the world's first in performing such procedure. We aim to compare safety and efficacy of this new technique with conventional MSCT-guided hookwire procedure.
Methods and Materials: Retrospective case-control study performed in a university-based hospital from Feb 2014 to Jan 2016. 18 patients with lung lesion who underwent Hybrid DynaCT-guided hookwire localisation utilizing Siemens Artis Zeego system compared against 10 age- and sex-matched controls who underwent conventional MSCT guided hookwire localisation. All cases performed under local anaesthesia.
Results: Mean lesion size was significantly smaller in DynaCT group compared with MSCT (5.96±1.92min vs 8.42±3.30mm, p=0.02). All interventions met primary endpoint of satisfactory hookwire positioning. There was no hookwire dislodgement in both groups. DynaCT associated with significantly shorter transfer times (38.28±16.95min vs 98.7±35.24min, p<0.001) and a trend towards lower pneumothorax rate (22% vs 50%, p=0.13). Effective dose of DynaCT was not significantly different from MSCT (16.41±14.99mSv vs 8.26±3.88mSv, p=0.11). DynaCT had longer procedure time (55.39±19.01min vs 23.30±9.99min, p<0.001) than MSCT. Lesion size inversely correlated with procedural time (r=-0.50, p=0.01). This may suggest that smaller target lesion size may contribute towards longer procedure time in DynaCT group.
Conclusion: Hybrid DynaCT-guided hookwire localisation of pulmonary lesions immediately prior to surgical resection in same hybrid operative theatre is a pioneer one-stop technique; which is associated with shorter interdepartmental transfer time and lower post-procedure pneumothorax rate when compared with conventional MSCT procedure.

B-0562 15:20

Clinical significance of postinterventional contrast medium injection after CT-guided drainage
H. Goessmann, M. Haimerl, W. Uller, L. Bayer, V. Teusch, F. Poschenrieder, L.-M. Dendl, A. Schreyer; *Regensburg/DE (holger.goessmann@ukr.de)*

Purpose: The aim of this study was to evaluate the added clinical value of an additional postinterventional control-scan after CT-guided drainage placement with contrast medium (CM) via the newly placed drain.
Methods and Materials: All CT-guided drainages of fluid collections between January 2014 and September 2016 in a maximal care hospital were included in this study. The patients were divided into 2 subgroups, patients that underwent surgery before developing the fluid collection and patients that did not. Drainages that were additionally flushed with CM were evaluated to which extend the additional scan was helpful for either detecting the source of the fluid collection (e.g. anastomosis insufficiency) or additional cofactors (e.g. intestinal fistulas in pancreatitis) and whether or not these information led to an immediate change of therapy.
Results: A total of 499 drainages in 352 patients (123 female, mean age 60 years, range 11-87 years) were detected, 197 thereof were postinterventionally flushed with CM. 51 (26%) of those showed a clinically significant additional finding. An immediate change of therapy was found in 19 cases (9%). The group that underwent surgery (120 CM-drainages; 32 (27%) additional findings; 13 (11%) immediate change of therapy) showed no statistically significant difference to the group that did not (77 CM-drainages; 19 (25%) additional findings; 5 (6%) immediate change of therapy).
Conclusion: An additional scan with CM injection via the newly placed drain revealed clinically significant additional information in almost 26% in this study. In 9% of the cases this information led to an immediate change of therapy.

14:00 - 15:30 **Room O**

Chest

SS 704

Pulmonary vessels and perfusion

Moderators:
T.N.H. Matin; Oxford/UK
E. Mershina; Moscow/RU

B-0563 14:00

Are patients' age, height, weight and heart rate relevant in pulmonary CTA?
J. Sagasta Urrutia, S. Santos Ochoa de Eribe, L. Alonso Irigaray, E. De las Heras Diez, R. Cobos Campos, J. Etxano; *Vitoria-Gasteiz/ES (jone.sagastaurrutia@osakidetza.net)*

Purpose: To analyze the influence of patients´ characteristics in pulmonary CT angiography (CTA).
Methods and Materials: From June 2016 to October 2016, 127 patients with intermediate-high suspicion of pulmonary embolism according to Well´s criteria were prospectively recruited. All of them underwent a CTA with same technical paramethers, contrast injection dose and rate (300mg/ml, 70 ml, 4ml/s). Patients´ age, weight, height and heart rate before the acquisition of the CTA were obtained. Mean value (UH) at the main pulmonary artery was calculated drawing a region of interest. All the examinations were classified in two groups according to the enhancement of the pulmonary artery: good (>250UH) and poor (<250UH). Multivariate analysis was performed to evaluate the influence of each variable in the enhancement of the pulmonary artery. Differences between studies with poor and good enhancement were analyzed using Mann Whitney´s U test. A p<0.05 was considered significant.
Results: Out of 127 studies, 12 (9.4%) were classified as poor and 115 (90.6%) as good. Multivariate analysis showed significant association between UH and age (p=0.01), weight (p=0.01), height (p=0.025) and heart rate (p=0.037). Differences in weight (median=86kg p25-75=74-90kg vs median=70kg p25-75=60-82kg p=0.021), age (median=61years p25-75=44-76years vs median=75years p25-75=64-83years p=0.046), height (median=170cm p25-75=161-181cm vs median=162cm p25-75=156-170cm p=0.01) and heart rate (median=85beats/min p25-75=74-98beats/min vs median=76beats/min p25-75=68-90beats/min p=0.062) were found between poor and good studies.

Conclusion: The knowledge of patients' age, height, weight and heart rate are relevant in pulmonary CTA. Patients with poor enhancement in pulmonary CTA studies are younger, have higher weight, height and heart rate than patients with good enhancement studies.

B-0564 14:08

CT pulmonary angiography during pregnancy: radiation dose of commonly used protocols and the effect of z-axis optimisation

B.M.F. Hendriks[1], R.S. Schnerr[1], G. Milanese[2], C.R.L.P. Jeukens[1], S. Niesen[1], J.E. Wildberger[1], M. Das[1]; [1]*Maastricht/NL*, [2]*Parma/IT*
(babs.hendriks@mumc.nl)

Purpose: Evaluating radiation dose and the simulated effect of an optimised z-axis for pregnant women undergoing commonly used CTPA scan-protocols.
Methods and Materials: 120 CTPA datasets, acquired using 4 scan protocols (n=30 per protocol), were mapped to Cristy phantoms; simulating 120 non-pregnant women (NP) and 120 women in the first (FT), second (ST) and third trimester (TT) of pregnancy, including fetal dose in second and third trimester. Scan protocols: single-source 64-slice helical scan at 120kV (protocol A), high pitch dual-source acquisition at 100kV (protocol B), dual-energy acquisition at 80/140kV (protocol C) and automated-kV-selection high pitch scan at $100kV_{ref}$ (protocol D). Effective radiation dose (in mSv) for woman and fetus was calculated for all scan protocols and repeated after z-axis optimisation: lung apex - top of lower diaphragm.
Results: Mean effective dose per protocol: A; NP 7.6±1.5mSv, FT 10.2±3.0mSv, ST 10.5±3.1mSv, TT 10.6±3.1mSv. B: respectively 4.5±0.8mSv, 5.2±1.2mSv, 5.4±1.3mSv and 5.5±1.3mSv. C: 7.7±0.8mSv, 9.1±1.0mSv, 9.4±1.2mSv and 9.7±1.1mSv. D: 2.0±0.6mSv, 2.6±1.1mSv, 2.7±1.1mSv and 2.7±1.1mSv. Mean effective dose increase during pregnancy (NP to TT) was highest for protocol A; 3mSv or 39%. Fetal dose was highest in third trimester: 1.53±0.6mSv, 0.54±0.2mSv, 0.96±0.4mSv and 0.2±0.1mSv for the respective protocols. Z-axis optimisation showed largest benefit in 3rd trimester, reducing fetal dose by 84% for protocol A, 78% for B, 78% for C, 80% for D.
Conclusion: Careful scan protocol selection and subsequent z-axis optimisation for CTPA during pregnancy can result in significant radiation dose reduction for expecting mother and the fetus in particular.
Author Disclosures:
B.M.F. Hendriks: Research/Grant Support; Bayer, Philips. **J.E. Wildberger:** Research/Grant Support; Siemens, Philips, Bayer, AGFA. Speaker; Siemens, Bayer. **M. Das:** Research/Grant Support; Bayer, Siemens, Philips, Cook.

B-0565 14:16

Influence of 90-kVp low-tube-voltage pulmonary CT-angiography on radiation dose, image quality and diagnostic accuracy for the detection of pulmonary embolism using ADMIRE

L. Lenga, M. Beeres, D. Leithner, J.L. Wichmann, S. Martin, M. Albrecht, T.J. Vogl, J.-E. Scholtz; *Frankfurt a. Main/DE (l.lenga@gmx.de)*

Purpose: To compare low-tube-voltage 90-kVp acquisition using advanced modelled iterative reconstruction algorithm (ADMIRE) and standard linearly blended dual-energy images for pulmonary CT angiography (CTPA) regarding radiation exposure, image quality, diagnostic accuracy and suitability for depiction of pulmonary embolism (PE).
Methods and Materials: 40 patients suspected of PE were included (21 male, 19 female; mean age: 56 years) . Intraindividual comparison of 90-kVp and linear blended M_0.6 images was performed. Signal attenuation and image noise of the pulmonary trunk were measured, signal-to-noise (SNR) and contrast-to-noise ratios (CNR) were calculated. Presence of and suitability for central and segmental PE and overall visualisation of pulmonary arteries were evaluated by three radiologists. Interobserver agreement was calculated using intraclass correlation coefficient (ICC). Radiation exposure was measured as dose-length-product (DLP).
Results: Attenuation and noise of the pulmonary trunk were significantly increased in 90-kVp images compared to linear blended images. CNR in 90-kVp images was significantly increased (15.4±6.3 vs. 11.3±4.6, P<0.001). Interobserver agreement (mean ICC 0.83) and detection of PE were excellent in both image series with no significant difference. Overall suitability for the evaluation of PE was rated excellent for both image series with slightly but significantly lower ratings for 90-kVp. The calculated average DLP was reduced by 37.2% with 90-kVp acquisition compared to dual-energy CTPA (77.5±44 vs. 123.4±51.1 mGy•cm, P<0.001).
Conclusion: 90-kVp CTPA using ADMIRE provides increased CNR with excellent diagnostic accuracy for the evaluation of PE. Radiation exposure is significantly reduced while maintaining excellent suitability for the assessment of central and segmental pulmonary arteries.

B-0566 14:24

ECG-gated pulmonary CT angiography for the prediction of right ventricular dysfunction in patients suspected of acute pulmonary embolism

N.A. Nikitin, S.M. Minin, M.E. Amelin; *Novosibirsk/RU (n_nikitin@outlook.com)*

Purpose: Right ventricular dysfunction (RVD) is an important prognostic factor of 30-day mortality in patients with acute pulmonary embolism (PE). The purpose of this study was to investigate and compare prognostic role of ECG-gated computed tomography (CT) signs, including 3-dimensional ventricular volume measurements and the left ventricular (LV) and right ventricle (RV) functions for predicting RVD in patients with acute PE.
Methods and Materials: We evaluated 10 patients with acute PE for the following CT signs of RVD obtained on retrospectively ECG-gated pulmonary CT angiography: abnormal position of the interventricular septum, inferior vena cava contrast reflux, RV diameter to LV diameter ratio on axial sections (RV/LV_{axial}), and 4-chamber views ($RV/LV_{4\text{-}ch}$), 3-dimensional RV volume to LV volume ratio (RV/LV_{volume}), RV and LV end-diastolic volumes (EDV), end-systolic volumes (ESV) and ejection fractions (EF). The results were compared with echocardiographic data. Echocardiographic examination for cardiac function analysis was performed on the same day.
Results: The RV/LV_{axial}, $RV/LV_{4\text{-}ch}$, RV/LV_{volume}, EDV_{RV} were significantly increase in patients with acute pulmonary embolism. There were strong correlations between RV/LV_{volume} ratio and EDV_{RV} r=0,872, also between echocardiography-derived pulmonary arterial systolic pressure and RV/LV_{volume}, r=0,914.
Conclusion: ECG-gated pulmonary CT angiography can accurately quantify RV and LV function. The RV function is impaired in patients with acute PE.

B-0567 14:32

Value of low-dose ECG cardiac gating for the assessment of right ventricular dysfunction in patients with suspected pulmonary embolism

J.C. Schaefer, H. Haubenreisser, M. Meyer, S.O. Schönberg, T. Henzler; *Mannheim/DE (JulCaSch@t-online.de)*

Purpose: Right ventricular dysfunction (RVD) is the main predictor of short-term mortality in patients with acute pulmonary embolism. However, the role of ECG-gating for the assessment of RVD using computed tomography pulmonary angiography (CTPA) is still unclear. The aim of this prospective study was to investigate the differences between systolic and diastolic measurements using a novel low-dose ECG-gated CTPA protocol.
Methods and Materials: Sixty patients (32 female, age 64.6+/-17.5 years) underwent a high pitch CTPA examination with 80cc of iodinated contrast material. 5s after the end of the CTPA a retrospectively ECG-gated cardiac CT examination with a 80% reduced tube current was started. Ejection fraction of both ventricles (RVEF, LVEF), endsystolic (RV/LV 4ch sys) and enddiastolic 4-chamber view ratio (RV/LV 4ch diast), endsystolic (RV/LV EDV) and enddiastolic volume ratio (RV/LV ESV) were assessed. In the CTPA, RV/LV ratio was measured in the axial plane and 4-chamber view. Correlation between RV/LV ratios and RVEF and statistical difference between corresponding systolic and diastolic RV/LV ratios were calculated.
Results: Systolic RV/LV ratios showed higher values than the corresponding diastolic RV/LV ratios (RV/LV 4ch sys = 1.30+/-0.40, RV/LV 4ch diast = 1.01+/-0,21, RV/LV ESV = 2.18+/-1.23, RV/LV EDV = 1.33+/-0.40) with a significant difference between endsystolic and enddiastolic 4ch ratios (p=<.0001) and volume ratios (p=<.0001). RV/LV EDV had the strongest correlation of all RV/LV ratios with RVEF (r = -0.543).
Conclusion: RV/LV EDV correlates best with RVEF. Further studies have to evaluate the proposed CTPA protocol regarding its additional value for risk stratification.
Author Disclosures:
H. Haubenreisser: Speaker; Siemens, Bracco, Bayer. **M. Meyer:** Speaker; Siemens, Bracco. **S.O. Schönberg:** Speaker; Siemens. **T. Henzler:** Speaker; Siemens.

B-0568 14:40

Small left atrium: a sign of pulmonary embolism

A.E. Mahfouz, F. Al-Khafaji, H. Sherif; *Doha/QA (falkhafaji@hamad.qa)*

Purpose: To assess the small size of the left atrium as a diagnostic sign and a follow-up parameter for pulmonary embolism patients.
Methods and Materials: Contrast-enhanced CT examinations of the chest of 50 patients with clinical and CT evidence of pulmonary embolism and 50 control patients were retrospectively evaluated. The initial and follow-up CT of the pulmonary embolism patients have been evaluated. In all cases; the ratio between the pulmonary artery diameter and the anteroposterior dimension of the left atrium (PA/LA ratio) has been calculated. Statistical analysis has been done by the student's t-tests.
Results: The PA/LA ratio has been 0.97±0.26 for pulmonary embolism patients and 0.73±0.12 for control (p ≤0.0001). At the cut-off value of ≥ 0.81;

the PA/LA ratio has sensitivity, specificity, positive predictive value, negative predictive value and accuracy of 68%, 72%, 70.8%, 69.2% and 70% respectively for the diagnosis of pulmonary embolism. On follow up, 31 of the pulmonary embolism patients showed improvement while 19 showed CT evidence of either recurrence or persistence of the emboli. In the first group, the PA/LA ratio has changed from 0.95 ± 0.24 to 0.78 ± 0.22 (p ≤0.0001). In the second group, the PA/LA ratio showed no statistically significant change.
Conclusion: The PA/LA ratio on contrast-enhanced CT has been significantly higher in patient with pulmonary embolism compared to control. The ratio has significantly decreased on CT follow up of patients with improvement of their pulmonary embolism and remained unchanged in patients with no improvement.

B-0569 14:48

Diagnostic value of CT measurements as a predictor of pulmonary hypertension in TAVI patients

M. Eberhard, J. Pavicevic, M. Mastalerz, T. Frauenfelder, F. Tanner, T. Nguyen-Kim; *Zurich/CH (matthias.eberhard@usz.ch)*

Purpose: To assess the diagnostic value of computed tomography (CT) measurements for detection of pulmonary hypertension (PH) in a cohort of patients undergoing transcatheter aortic valve implantation (TAVI) with known severe left heart disease.
Methods and Materials: 257 consecutive patients (median age 83.0±6.1 ys,134 f) with symptomatic severe aortic valve stenosis undergoing TAVI at the University Hospital Zurich(Switzerland) from 03/2008 to 12/2014 were retrospectively analysed. Patients underwent right heart catheterisation (RHC) and CT within 3 consecutive days. Previously described CT measurements for assessment of PH were examined. Measurements were compared between PH and no PH patients using Mann-Whitney-U- and Chi-Square-test. P-value <0.05 was considered statistically significant.
Results: 161 patients had PH (83.0±6.4y, 90f). Diameters of pulmonary artery trunk (PA) (p<0.001), right (p=0.037) and left pulmonary artery (p=0.044), anterior pericardial recess (PR) (p=0.003) as well as ratios of PA/ascending aorta (AA) (p<0.001) and PA/descending aorta (DA) (p=0.003) were significantly higher in PH patients. Pleural fluid (p<0.001) and positive segmental artery-bronchus ratio (ABR) in patients with PA diameter ≥29mm (p=0.021) were significantly more common in patients with PH. Sensitivity, specificity, NPV and PPV for presence of pleural fluid (42.0%, 90,5%, 47.7%, 88.3%), positive ABR score (28.9%, 84.0%, 43.4%, 73.7%), PA diameter ≥31mm (38.9%, 77.9%, 42.8%, 75.0%) and PR ≥10mm (37.3%, 81.7%, 43.4%, 77.6%) were computed. ROC analysis for PA, PR, PA/AA ratio and PA/DA ratio showed AUC of 0.63; 0.61; 0.62 and 0.62, respectively.
Conclusion: In our study CT showed limited diagnostic value for detection of PH in TAVI patients.

B-0570 14:56

Non-invasive estimation of mean pulmonary arterial pressure in suspected pulmonary hypertension based on automated 3D volumetry of pulmonary CT angiography

C. Melzig[1], S. Wörz[1], B. Egenlauf[1], S. Partovi[2], K. Rohr[1], E. Grünig[1], H.-U. Kauczor[1], C.P. Heussel[1], F. Rengier[1]; [1]*Heidelberg/DE*, [2]*Cleveland, OH/US (claudius1.melzig@med.uni-heidelberg.de)*

Purpose: To non-invasively estimate mean pulmonary arterial pressure (mPAP) in patients being evaluated for pulmonary hypertension (PH) by using automated 3D volumetry of central pulmonary arteries based on CT pulmonary angiography (CTPA).
Methods and Materials: 73 consecutive patients (mean age 66.3 years, 50 female) undergoing CTPA, right heart catheterisation (RHC) and echocardiographic pulmonary arterial systolic pressure measurement (PASP) for suspected PH in our institution were retrospectively reviewed. Patients with chronic thromboembolic PH were excluded. Patients were randomised to a derivation (n=36, mean age 66.4 years) and a validation cohort (n=37, mean age 66.1 years). Automated segmentation of CTPA data was performed using in-house developed software. Volumes of the main as well as right and left pulmonary artery were calculated and corrected for vessel length and body surface area (MPA-volume and RLPA-volume). A linear regression model was established in the derivation cohort to estimate mPAP and diagnostic accuracy compared to gold standard RHC assessed in the validation cohort.
Results: Mean mPAP was 29.2 mmHg in the derivation cohort and 28.9 mmHg in the validation cohort. Regression analysis yielded the following formula: estimated mPAP = -2.353 + (11.04 x MPA-volume) + (13.82 x RLPA-volume) + (0.489 x PASP) (r=0.92). When applied to the validation cohort sensitivity and specificity for prediction of PH (mPAP >= 25 mmHg) were 86% and 100%, respectively.
Conclusion: Non-invasive estimation of mPAP using automated 3D volumetry of central pulmonary arteries based on CTPA can predict the presence of PH as confirmed by RHC with high sensitivity and specificity.

B-0571 15:04

Low-kilovoltage chest CT angiography at the recirculation phase: a new option to optimise the image quality?

A. Hutt, S. Gicquel, J.-B. Faivre, M. Remy-Jardin, J. Remy; *Lille/FR (martine.remy@chru-lille.fr)*

Purpose: To reduce beam-hardening artifacts on single-energy chest CT angiograms (CTA).
Methods and Materials: The study population comprised 100 patients who underwent a chest CTA with a fixed scan delay (60s), using 90-110mL of a 35% contrast agent and a low kVp (80, 90, 100 or 110 kVp depending on the b.w.) (Group 1). The image quality was compared to that of standard chest CT examinations (Group 2; n=25) obtained with a similar injection protocol at the exception of the use of a bolus tracking technique and a kilovoltage set at 100 or 120 kVp.
Results: Homogeneous enhancement of systemic veins was significantly more frequent in Group 1 than in Group 2 (superior vena cava [95% vs 8%]; inominate vein ipsilateral [89% vs 28%] and controlateral [92% vs 4%] to the side of injection; p<0.0001). The severity scores of artifacts significantly differed between the two groups with no artifacts at the level of 2R (95%), 2L (96%), 4R (98%), 4L (100%), 7 (100%) nodal stations in Group 1 (Group 2: 2R [16%]; 2L [76%], 4R [16%], 4L [52%],7 [76%]) (p<0.0001). In Group 1, the mean level of attenuation was 219±44.38 HU in the pulmonary trunk with arteries analysable down to the subsegmental level in 80% of cases; an 209.7±44.73 HU in the descending aorta.
Conclusion: CT scanning at a recirculation phase and low kVp allows suppression of most beam-hardening artifacts while providing a diagnostic level of vascular enhancement in all vascular compartments.
Author Disclosures:
M. Remy-Jardin: Research/Grant Support; Siemens Healthcare. **J. Remy:** Consultant; Siemens Healthcare.

B-0572 15:12

Intra-individual comparison of direct subtraction vs dual-energy for imaging of pulmonary perfusion: a feasibility study

D.J.M. Grob[1], E.J. Smit[2], M. Prokop[1], L.J. Oostveen[1], M.M. Snoeren[1], C.M. Schaefer-Prokop[2], I. Sechopoulos[1], M. Brink[1]; [1]*Nijmegen/NL*, [2]*Amersfoort/NL (Dagmar.Grob@radboudumc.nl)*

Purpose: Iodine mapping as surrogate of lung perfusion can be achieved using dual-energy acquisition (DE) or direct subtraction (s-CT), requiring image registration. Purpose of the study was to compare image quality and detection of perfusion inhomogeneities (PI) in patients suspected for acute pulmonary embolism (PE).
Methods and Materials: Prospectively included 55 consecutively patients with suspected PE underwent CTPA in addition to an unenhanced scan (100kV), allowing for intra-individual comparison of both techniques. Five blinded radiologists independently evaluated the image quality of both types of iodine maps overlaid on CTA using visual grading analysis on a 5-point scale (1=excellent, 5=non-diagnostic) and assessed the presence and underlying causes of PI. McNemar tests were used to compare proportions.
Results: Median DLPs were 172mGy-cm for DE and 162mGy-cm for subtraction. The mean proportion of iodine maps rated as showing excellent or good overall image quality was 36% (range: 5-69%) for DE and 67% (31-80%) for subtraction (p< 0.05 for 4 radiologists), mainly because of fewer artefacts. Mean proportion of PI positive scans was 46% (31-98%) for DE and 51% (29-98%) for subtraction, mostly related to airways pathology. Of 6 patients with PE, readers detected on average 90% of PE-related PIs with DE compared to 70% with subtraction.
Conclusion: Pulmonary iodine mapping of the lung in CTA is feasible with subtraction at the same radiation dose as DE, but with superior image quality. In the small group of patients with PE, DE detected more PE-associated perfusion inhomogeneities.
Author Disclosures:
D.J.M. Grob: Research/Grant Support; Toshiba Medical Systems. **E.J. Smit:** Research/Grant Support; Toshiba Medical Systems. Speaker; Toshiba. **M. Prokop:** Research/Grant Support; Toshiba Medical Systems. Speaker; Bracco, Bayer, Toshiba. Other; Thirona, Veolity. **L.J. Oostveen:** Research/Grant Support; Toshiba Medical Systems. **I. Sechopoulos:** Speaker; Siemens. Other; Research agreement: Siemens, Research agreement: Siemens. **M. Brink:** Research/Grant Support; Toshiba Medical Systems.

B-0573 15:20

Ventilation/perfusion ratio map by dual-energy CT after xenon inhalation and intravenous contrast media

N. Honda[1], H. Osada[1], W. Watanabe[1], K. Aoki[1], K. Izumi[1], M. Nakayama[1], T. Itoh[2], K. Otani[2]; [1]*Kawagoe/JP*, [2]*Tokyo/JP (honda.nyasie@gmail.com)*

Purpose: Ventilation/perfusion (V/Q) ratio represents efficiency of pulmonary blood oxygenation. The purpose of the study was to report a method to create V/Q ratio map from dual-energy CT.
Methods and Materials: Twenty-six patients of lung caner treated with lobectomy were included. The study was approved by IRB and informed consent was obtained. The first CT of the chest after a vital-capacity inhalation of xenon-oxygen mixture in 35/65% ratio, and the second CT at individualised pulmonary artery phase were acquired consecutively both in dual-energy mode. Ventilation and perfusion CT was generated through material decomposition applied to each CT data. V/Q ratio map was created by pixel-by-pixel division between the ventilation and perfusion CT images. Mean V/Q ratio, SD, mode, median and fractal dimension (FD) was calculated. Paired *t*-test was applied.
Results: Mean age, SD, range and male/female ratio were 67, 1.9, 51 to 86 years and 12:16. Mean, SD, mode, median and FD of the V/Q ratios were 0.877, 0.392, 0.797, 0.703, and 2.511 before and were 0.912, 0.346, 0.842, 0.768, and 2.522 after the lobectomy, respectively. The difference was non-significant in all. All of the patients maintained activities of daily living after the lobectomy.
Conclusion: V/Q map was generated from CT using xenon CT and perfusion CT. No changes in the mean, SD, median, mode and FD of V/Q ratios after the lobectomy may indicate that enough compensation to restore V/Q ratio was present as all of the patient regained activities of daily living after the operation.

14:00 - 15:30 **Room N**

Genitourinary

SS 707

Male urogenital system - prostate cancer: diagnosis and PIRADS scoring

Moderators:
B.K. Barth; Zurich/CH
P. Puech; Lille/FR

B-0574 14:00

Prostate volume assessed by TRUS and its correlation with post-void residue

A. Mereu, E. Scapin, L. Saba; *Monserrato/IT*

Purpose: To analyse whether there is a correlation between prostate volume measured by transrectal ultrasonography (TRUS), post-void residual urine volume and post-void/pre-void urine volume ratio.
Methods and Materials: 493 TRUSs (age range 28-88 years) were retrospectively analysed. Prostate volume, post-void residual urine volume and post-void/pre-void urine volume ratio were assessed. Included patients were categorised into three groups: subjects who did not have transurethral resection of the prostate (TURP) (473 cases, 96%), subjects who had TURP (20 cases, 4%) and all the subjects. Statistical analysis was performed using the two-tailed unpaired Student's t test and the Pearson's r.
Results: Weak correlations between prostate volume and post-void residual urine volume (r value: 0.133 in non-TURP, -0.093 in TURP, 0.132 in all) and between prostate volume and post-void/pre-void urine volume ratio (r value: 0.243 in non-TURP, -0.272 in TURP, 0.239 in all) were found using the Pearson's r. No statistically significant difference was observed between prostate volume, post-void residual urine volume, post-void/pre-void urine volume ratio of non-TURP and TURP patients, determined using the two-tailed unpaired Student's t test (p value=0.146 of prostate volume, p value=0.084 of post-void residual urine volume, p value=0.055 of post-void/pre-void urine volume ratio).
Conclusion: Our study results showed that prostate volume does not have a statistically significant correlation neither with post-void residual urine volume nor with post-void/pre-void urine volume ratio. Furthermore, these measurements do not differ significantly statistically between non-TURP and TURP patients. Therefore, evaluation of all these parameters should be considered.

B-0575 14:08

Role of multiparametric MRI in the follow-up of patients with a clinical suspicion of prostate cancer

G. Cappello, S. Mazzetti, V. Giannini, L. Vassallo, F. Russo, D. Regge; *Candiolo/IT (giovanni.cappello@ircc.it)*

Purpose: To investigate patients in follow-up (FU) with a clinical suspicion of prostate cancer (PCa) after a negative mp-MR of the prostate or previous negative prostate biopsy.
Methods and Materials: The dataset comprised 368 subjects with suspicion of PCa who underwent diagnostic mp-MRI. Of these, 97 patients (26%) showed at least one suspicious lesion at mp-MRI, while 271 (73.6%) had a negative mp-MR and were monitored with clinical FU. Among the 97 subjects with a positive mp-MR, 21 had a negative biopsy and they also underwent clinical FU. The final dataset was composed of 292 patients.
Results: Among the 292 patients, 13/292 (4.4%) had a PSA doubling time (PSA-DT) less than 3 years: 5/13 (38.4%) had a positive mp-MR and, therefore, they underwent prostate biopsy resulting in 3/5 (60%) patients with pathologically confirmed PCa. 8/292 (2.7%) patients repeated mp-MR after a positive digital rectal examination: all of them resulted negative at the repeated mp-MR. Overall, 3/292 (1.02%) patients had a positive biopsy during FU, resulting in a negative predictive value (NPV) of 99%.
Conclusion: The results suggest that mp-MR of the prostate has high NPV in predicting PCa reducing the number of useless biopsy and the risk to overdiagnose and overtreat low-risk cases, with limitation in patient's quality of life.

B-0576 14:16

Sub-differentiating equivocal PI-RADS 3 lesions in multiparametric MRI of the prostate

N.L. Hansen[1], B. Koo[2], A. Warren[2], C. Kastner[2], T. Barrett[2]; [1]*Cologne/DE*, [2]*Cambridge/UK (nienke.hansen@uk-koeln.de)*

Purpose: To evaluate if equivocal PI-RADS 3 lesions on multiparametric magnetic resonance imaging (mpMRI) of the prostate can be further differentiated using pre-defined T2- and diffusion-weighted imaging criteria in order to aid in the biopsy decision process.
Methods and Materials: 143 patients with an index PI-RADS 3 lesion on mpMRI underwent transperineal MR/US fusion biopsy from 2013 to 2016. Two radiologists with 2 years and 7 years of experience performed a blinded retrospective second-read of each lesion and gave a recommendation whether or not to biopsy. Inter-reader agreement, Gleason score (GS), positive (PPV) predictive values (+-95% confidence intervals) were calculated and compared by exact Fisher test.
Results: 43% (61/143) patients had any cancer and 21% (30/143) GS 7-10 cancer in the biopsy. Using shape, border, homogeneity, and diffusion restriction as objective imaging criteria had a significant effect on PPV. When asked to make a subjective biopsy recommendation, agreement between the two readers was observed in 62% of cases (89/143). PPV for finding any cancer decreased from 0.43 (±0.08) for all PI-RADS 3 to 0.21 (±0.10) with "defer biopsy" and increased to 0.61 (±0.11) with "biopsy recommended"; p=0.0001. PPV for GS 7-10 cancer decreased from 0.21 (±0.07) for all PI-RADS 3 to 0.08 (±0.07) with "defer biopsy" and increased to 0.32 (±0.10) with "biopsy recommended"; p=0.0003.
Conclusion: Identification of certain imaging criteria, as well as a subjective biopsy recommendation can help to increase the PPV of PI-RADS 3 prostate lesions and aid the decision to biopsy, even without using contrast enhancement.
Author Disclosures:
N.L. Hansen: Research/Grant Support; RWTH Aachen University Rotation Program. **A. Warren:** Research/Grant Support; National Institute for Health Research Cambridge Biomedical Research Centre UK. **C. Kastner:** Speaker; Siemens Healthcare, MedCom GmbH. **T. Barrett:** Research/Grant Support; Cancer Research UK, National Institute of Health Research Cambridge Biomedical Research Centre, Engineering and Physical Sciences Research Council Imaging Centre in Cambridge and Manchester and the Cambridge Experimental Cancer Medicine Centre.

B-0577 14:24

Clinically significant prostate cancer: evaluation of PI-RADS v2 score 3 lesions on prebiopsy MRI

J. Kim, C. Kim, M.-R. Kwon, R. Kim, J. Yim; *Seoul/KR (ssakpo.kim@samsung.com)*

Purpose: To evaluate the value of score 3 lesions on Prostate Imaging Reporting and Data System (PI-RADS) v2 at prebiopsy magnetic resonance imaging (MRI) in predicting clinically significant cancer (CSC).
Methods and Materials: 103 consecutive patients underwent prebiopsy 3-T multiparametric MRI, followed by radical prostatectomy. Two independent readers performed PI-RADS v2 scoring. Based on the histopathological

findings, the CSC was defined when a tumour had Gleason score 7 or greater, tumour volume ≥ 0.5 cm^3, or extraprostatic extension. Statistical analysis was performed using receiver operating characteristics (ROC) curve analysis and κ statistics.
Results: Of 103 patients, 81 (78.6%) had 107 lesions of CSCs on surgical specimen. In patient-based analysis, the CSCs of each PI-RADS assessment category in both readers were 60.0% (9/15) and 56.3% (9/16) for score 1-2, 68.4% (13/19) and 70.6% (12/17) for score 3, 75.8% (25/33) and 77.5% (31/40) for score 4, and 94.4% (34/36) and 96.7% (29/30) for score 5. The PI-RADS score 3 lesions rated from both readers were 68 and 66 on MRI, respectively and of these, 22 (32.3%) and 21 (31.8%) lesions had CSCs. For predicting CSCs, the area under the ROC curve for both readers was 0.71 and 0.72. The inter-reader agreement for PI-RADS scoring was good (κ = 0.65).
Conclusion: PI-RADS v2 score 3 lesions on prebiopsy MRI might harbor substantial CSCs in patients with prostate cancer. Thus, a targeted biopsy needs a lesion with PI-RADS v2 score 3 or greater.

B-0578 14:32

Multiparametric MRI of the prostate: prospective evaluation of PIRADSv2 in detection of prostate cancer using ISUP grading system for validation

S. Bednarova[1], S. Mehralivand[2], J.H. Shih[3], F.V. Mertan[4], S. Gaur[4], R. Girometti[1], M.J. Merino[4], B.J. Wood[4], P.A. Pinto[4], P.L. Choyke[4], B. Turkbeyi[4]; [1]*Udine/IT*, [2]*Mainz/DE*, [3]*Rockville, MD/US*, [4]*Bethesda, MD/US (sandra.bednarova@gmail.com)*

Purpose: To prospectively assess prostate cancer detection rate (CDR) of PIRADSv2 using the new ISUP grading system.
Methods and Materials: 339 consecutive treatment naïve patients (mean age=64years, mean PSA=8.3 ng/mL) prospectively underwent mpMRI scored with PI-RADSv2, 12 core systematic and TRUS/MRI guided biopsy (Fbx) between May 2015-May 2016. The highest Gleason score for each PCa lesion was assigned an ISUP score, ISUP≥2 represented clinically significant (CS) PCa. CDRs for all and CS PCa were determined for each PIRADS score for the entire prostate, peripheral and transition zone. CDRs of each PIRADS score was compared.
Results: Overall, 737 lesions detected at mpMRI underwent Fbx. 346 lesions were positive for PCa, 237/346 lesions were CS PCa, resulting in CDR of 47% and 32% for all and CS PCa, respectively. CDRs for PIRADS scores 1, 2, 3, 4 and 5 for all PCa were 25%, 20.2%, 24.8%, 39.1% and 86.9%, respectively, while for CS PCa CDRs were 0%, 9.6%, 12%, 22.1% and 72.4%, respectively. For all and CS PCa, differences in CDRs between PIRADS4 and 5 scores, as well as between PIRADS3 and 4 scores were statistically significant ($p<0.05$). Overall PIRADS score 4 had unexpectedly high false positive results; whereas corresponding T2W PIRADS score 4 had higher CDR compared to overall PIRADS score 4 (39% vs 51%, p<0.001).
Conclusion: CDR increases with higher PIRADS scores for all and CS PCa lesions. PIRADS4 score had a high false positive rate, but the additional use of T2W scores can improve the CDR of PIRADS4 lesions.

B-0579 14:40

Updating prostate image reporting and data system version 2 (PI-RADS v2) for the detection of clinically significant prostate cancer in patients with elevated PSA level

C.-C. Wang, J.-S. Huang; *Kaohsiung City/TW (chunchiehwang1221@gmail.com)*

Purpose: To determine the predictive value of prostate image reporting and data system (PI-RADS v2) for the assessment of clinically significant prostate cancer by multiparametric MRI (mp-MRI) patients with elevated PSA level.
Methods and Materials: A retrospective and prospective study was performed in 221 patients with elevated prostate-specific antigen (PSA) level by 1.5T or 3T mp-MRI. MRI studies containing T2 weighted, diffusion weighted, and dynamic contrast enhancement images. Two experienced abdominal radiologists reviewed images and reported all the studies according to recent PI-RADS v2 scoring system. All suspected lesions were recorded due to multifocal prostate cancer, and then we focused on index lesions (defined by PI-RADS v2) in each patient. Patients who had PI-RADS 3, 4, 5 received either targeted core biopsies and systemic core biopsies. Clinically significant prostate cancer was defined by PI-RADS v2 (Gleason score (GS) ≥ 3+4 or tumour volume ≥ 0.5 ml). ROC curve for clinically significant prostate cancer using PI-RADS v2 category was analyzed.
Results: 205 patients diagnosed as prostate cancer, 183 patients tumour volume ≥0.5 ml (any Gleason score) , 22 tumours <0.5 ml (18 with GS =3+3, 4 with GS≥3+4). Area under ROC curve for clinically significant prostate cancer using PI-RADS was 0.981. For the threshold of PI-RADS scores of 3 or greater, sensitivity was 91.89%, positive predictive value (PPV) was 90.91%. Interobserver agreement for PI-RADS scoring system was good (k=0.80).
Conclusion: PI-RADS v2 can be a simple and valuable diagnostic tool for the detection of clinically significant prostate cancer before biopsy.

B-0580 14:48

Quantitative analysis of dynamic contrast-enhanced MRI for prostate cancer detection: is there an added value compared to PI-RADS v.2 classification?

G. Cristel, A. Esposito, S. Antunes, G. Brembilla, L. Brunetti, A. Briganti, F. Montorsi, A. Del Maschio, F. De Cobelli; *Milan/IT (cristel.giulia@hsr.it)*

Purpose: To assess whether there is a significant difference in pharmacokinetic dynamic contrast-enhanced MRI (DCE-MRI) parameters between benign and malignant prostatic lesions, in order to improve multiparametric MRI (mpMRI) diagnostic performance.
Methods and Materials: Among a total of 339 patients who underwent prostatic mpMRI (1.5T) from February to September 2016, we selected all the lesions, with available corresponding histological specimen (n=61) obtained through target biopsies. The imaging protocol consisted of multiplanar T2W, diffusion-weighted imaging and DCE-MRI. For each lesion the following pharmacokinetic parameters were assessed: transfer constant (Ktrans), rate constant (Kep), extravascular extracellular volume fraction (Ve), fractional plasma volume (Vp) and area under the curve (AUC). The association between the analysed parameters and the histological result was then evaluated basing on Gleason score ≥7 (GS).
Results: Malignant lesions showed higher Ktrans, Kep and AUC compared to the benign ones, all p<0.01. Moreover a significant difference among the Gleason score groups was observed, with more aggressive tumours showing higher values, all p<0.01. ROC curve analysis was used to identify a Ktrans cut-off value of $180x10^{-3}$/min (AUC 0.81) which in turn predicted the presence of GS≥7 with sensitivity, specificity, NPV, PPV and accuracy respectively of: 95%, 65%, 96%, 59% and 75%. The corresponding values basing on PI-RADSv.2 were as follows: 100%, 38%, 100%, 46%, 59%. The application of Ktrans cut-off on PI-RADS≥3 cases shifted 13 false positives to true negatives with the loss of 1 true positive.
Conclusion: DCE-MRI pharmacokinetic analysis may improve PI-RADSv.2 capability of prostate lesions' characterisation.

B-0581 14:56

Monocentric experience in the detection of prostate cancer comparing PI-RADS Version 1 and Version 2: the role of dynamic contrast enhancement (DCE)

G. Michelini, L. Panebianco, A. Mancini, A. Pace, C. Gianneramo, C. Marsecano, I. Capretti, R. Manetta, C. Masciocchi; *L'Aquila/IT (giuliamichelini.gm@gmail.com)*

Purpose: To compare two system of PIRADS score, Version 1 (PiradsV1) and 2 (PiradsV2), and analyse the effectiveness of DCE to detect prostate lesions.
Methods and Materials: Two dedicated MRI-prostate radiologists (A and B) retrospectively and independently evaluated 90 multiparametric 3T MRI (mpMRI) (mr750w GE, with pelvic phased-array 32 channel coil + endorectal coil) performed between February 2015 and February 2016, with both PiradsV1 and PiradsV2. From PiradsV1 the score (1-5) of only DCE was considered, from PiradsV2 the score (1-5) of ESUR 2015 guidelines. Patients Median age:62,6 years. Exclusion Criteria: contraindications to mpMRI, previous prostatectomy, radiotherapy or ormonotherapy. Contrast media: Gadobutrol (1mmol/ml/Kg). For each patient the histological report was obtained, and a histological score was assigned to it (PI): normal=1; prostatitis=2; Atypical Small Acinar Proliferation (ASAP)=3; prostatic intraepithelial neoplasia (PIN)=4; Prostate cancer (CaP) (GS≥6)=5. The PI was subtracted from the two Pirads Scores (PiradsV1-PI and PiradsV2-PI) to obtain an absolute value that is truer the more it nears to 0 (maximum correlation between PR and PI). The statistical analysis was performed with Student t test.
Results: All values are expression of an average. Concordance between PiradsV1 and PiradsV2 from A and B: A-PiradsV1=2,37, B-PiradsV1=2,71 (p=0,5); A-PiradsV2=2,96, B-PiradsV2=2,92 (p=0,16). Statistically significant differences between PiradsV1-PI e PiradsV2-PI: A-PiradsV1-PI=1,66, A-PiradsV2-PI=0,58 (p<0.05); B-PiradsV1-PI=1,75, B-PiradsV2-PI=0,66 (p<0.05).
Conclusion: The study confirms the usefulness of PIRADS systems for structured and concordant report. Introduction of PiradsV2, which subtracts importance to DCE, in our experience has resulted in higher correlation with histological report.

B-0582 15:04

Multiparametric MRI of prostate cancer for the prediction of lymph node metastasis

G. Brembilla, A. Esposito, G. Cristel, F. Giganti, L. Brunetti, P. Dell'Oglio, A. Briganti, F. Montorsi, F. De Cobelli; *Milan/IT (brembilla.giorgio@hsr.it)*

Purpose: To investigate the role of pre-operative mp-MRI of prostate cancer (PCa) in predicting lymph node involvement (LNI).
Methods and Materials: 87 PCa patients treated with radical prostatectomy (RP) and extended pelvic lymph node dissection at a single tertiary care referral center were included in our study. All patients underwent pre-operative

MRI. For each patient PSA dosage, pre-operative biopsy Gleason score and MRI-related parameters (PI-RADS score, tumour ADC, tumour volume, MRI stage) were assessed. Logistic regression analyses and ROC curves were performed in order to identify the predictors of LNI.
Results: Overall, 18 (20,7%) had LNI at final pathology. At univariate analysis all the MR parameters were predictors of LNI (all p <0.05). At multivariate analysis tumour ADC, tumour volume and extracapsular extension (ECE) were significantly associated with LNI (all p <0.05). Sensitivity, specificity, PPV and NPV in predicting LNI were respectively 89%, 87%, 65% and 97% for an ADC value <0.7 x 10^{-3} mm^2/s (AUC = 0.89) and for a tumour volume > 0.9 cc (AUC = 0.93); 89%, 78%, 53% and 96% for ECE (AUC = 0.83). The presence of seminal vesicle invasion (SVI) was 98% specific with 91% PPV.
Conclusion: Pre-operative MpMRI of PCa is a promising tool in the prediction of LNI. High tumour volume (> 0.9 cc), low ADC (< 0.7 x 10-3 mm2/s), presence of ECE and SVI at MRI correlate with LNI at post-operative pathologic examination.

B-0583 15:12

Evaluation of clinical outcome for prostate cancer after radical prostatectomy using PI-RADS v2

R. Kim, C. Kim, J. Yim, J. Park; *Seoul/KR (ran1001.kim@samsung.com)*

Purpose: To determine whether the Prostate Imaging and Reporting and Data System (PI-RADS) v2 helps predict the clinical outcome for prostate cancer (PCa) after radical prostatectomy (RP).
Methods and Materials: From February 2005 to January 2007, 166 consecutive patients with localized PCa underwent multiparametric MRI (mpMRI) at 3T before RP. The PI-RADS v2 score was performed per patient. Biochemical recurrence-free survival (RFS) and progression-free survival (PFS), cancer-specific survival (CSS) and overall survival (OS) were assessed using Kaplan-Meier curves. Preoperative clinical and imaging parameters were evaluated using Cox proportion hazards regression analysis.
Results: During a median follow-up of 9.1 years, 16 patients (9.6%) died. The biochemical recurrence and disease progression were identified in 67 patients (40.4%) and 55 patients (33.1%). No clinical and imaging parameters were significantly associated with CSS and OS. On univariate analysis, prostate-specific antigen, Gleason score, number of positive cores, PI-RADS score and tumour apparent diffusion coefficient were significantly associated with RFS and PFS. On multivariate analysis, Gleason score, number of positive core and PI-RADS score were independent predictors of RFS [hazard ratio (HR)= 1.45, p= 0.006; HR= 1.20, p=0.026; HR= 1.43, p= 0.041] and PFS (HR= 1.46, p= 0.017; HR= 1.32, p= 0.001; HR= 1.62, p= 0.016]. The PI-RADS score < 3 was significantly associated with better RFS (p= 0.002) and PFS (p= 0.013). The inter-reader agreement of PI-RADS score was fair (κ= 0.353).
Conclusion: PI-RADS v2 score on mpMRI may be a useful marker for predicting RFS and PFS after RP in patients with PCa.

B-0584 15:20

Usefulness of PI-RADSv1 vs PI-RADSv2 in multiparametric MR imaging of prostate cancer recurrence after radical radiotherapy

J. Rembak-Szynkiewicz[1], A. Hebda[1], K. Kansy[1], A. Badzinski[2], B. Bobek-Billewicz[1]; [1]*Gliwice/PL*, [2]*Sosnowiec/PL (remszyn@wp.pl)*

Purpose: PI-RADS is used for prostate cancer detection. PI-RADSv1 was applied until 2014; currently PI-RADSv2 is used. Prostate assessment after radiotherapy is difficult due to intensified fibrotic and inflammatory changes, atrophy, and necrosis. To analyse the usefulness of PI-RADSv1vs PI-RADSv2 to assess focal prostate cancer recurrence after radiotherapy.
Methods and Materials: We analysed 118 patients (mean age: 71 yrs) treated with radical radiotherapy due to prostate cancer with microscopically confirmed local recurrence. Mp MR examination was done using a 3T scanner. T1-w, T2-w, DWI and DCE images were obtained.
Results: For PI-RADSv1 T2-w, DWI and DCE were assessed using a 5-point score. For PI-RADSv2 T2-w and DWI were assessed using a 5-point score, DCE +/- images were applied to assess local recurrences. Mean “index lesion” size was 17mm. In PI-RADSv1 and v2 focal recurrent size correlated with a point score (p <0.0001). PI-RADSv2 (≥4) result: “cancer is likely to be present” in 91/118 (77.1%) recurrences. PI-RADSv1 (≥9) result: “cancer is likely to be present” in 89/118 (75%) recurrences. For T2-w images 30.5% lesions had PI-RADS in both versions highly suggestive of malignancy. Diffusion restriction was confirmed in 79.7% of local recurrences. DWI ≥4for PI-RADSv1:91/118 (77.1%), for PI-RADSv2: 86/118 (72.9%). Positive DCE result in PI-RADSv2 was observed in 82.7% recurrences, but DCE influenced the final PI-RADS result in only 6%, resulting in a change from 3 (intermediate) to 4 (cancer likely to be present).
Conclusion: Usefulness of PI-RADSv1 is similar to PI-RADSv2 in the assessment of focal recurrence of prostate cancer.

14:00 - 15:30 **Room L 8**

Head and Neck

SS 708

Temporal bone imaging: hearing loss and vestibular symptoms

Moderators:
P. Gołofit; Koszalin/PL
B. Verbist; Leiden/NL

B-0585 14:00

Abnormal regional activity and functional connectivity in resting-state brain networks associated with aetiology confirmed unilateral pulsatile tinnitus in the early stage of disease

H. Lv, P. Zhao, Z. Liu, R. Li, L. Zhang, P. Wang, F. Yan, L. Liu, Z. Wang; *Beijing/CN (chrislvhan@126.com)*

Purpose: The abnormal neural activities revealed by the resting-state functional magnetic resonance image (rs-fMRI) are defined by the regional activity and functional connectivity (FC) of the networks in the brain. This study was designed to demonstrate the network alterations in the patients with pulsatile tinnitus (PT).
Methods and Materials: In this study, we recruited 45 patients with unilateral PT in the early stage of disease (less than 48 months of disease duration) and 45 normal controls. We used the regional homogeneity (ReHo) and seed-based FC analytic methods to reveal the resting-state brain activities associated with pulsatile tinnitus.
Results: Compared with healthy controls, PT patients showed regional abnormalities mainly in the left middle occipital gyrus (MOG), posterior cingulate gyrus (PCC), precuneus and right anterior insula (AI). When set as seeds, we demonstrated widespread modification of interaction between the auditory and non-auditory networks. The auditory network was positively connected with cognitive control network (CCN), which was associated with tinnitus related distress. Both altered regional activities and changed FC with other brain areas were found in the visual network. The modification of interaction of higher order networks were mainly found in DMN, CCN and limbic networks. Functional connectivity between left MOG and left parahippocampal gyrus could also be an index to reflect the disease duration.
Conclusion: This study helped us to have a better understanding of the characters of neural network modification in patients with pulsatile tinnitus.

B-0586 14:08

Evaluation of cochlear implants with Dyna CT previous and after surgery: what the radiologist needs to know/what the otologist wants to know

P. Largo Flores, E. Barcena Ruiz, X. Santos Sala, C. Sierra, M. Calderon Sanchez; *Madrid/ES (plargoflores@gmail.com)*

Purpose: To evaluate the anatomy of the temporal bone with a flat panel CT. To measure diameter A, B and insertion depth angle (IDA) and evaluate the interclass correlation (ICC) between two observers. To analyse the intracochlear electrodes position and possible dislocations after surgery.
Methods and Materials: Prospective study with 24 patients and different deaf causes. Two different observers evaluated the temporal bones before and after the cochlear implant with a flat panel CT. Flat diameter A (largest distance measured from the centre of the round window to the lateral wall) and diameter B (largest perpendicular cochlear measurement of “A”) were measured before the intervention to evaluate the interobserver correlation. After surgery, electrodes position, the IDA and possible dislocations were evaluated with a new CT.
Results: Preliminary results show that the mean distance A was 9.74 +/- 0.38 mm (observer 1) and 9.65 +/- 0.45 (observer 2) and ICC of 0.7. The mean distance B was 6.70 +/- 0.43 mm (observer 1) and 6.63 +/- 0.37 mm (observer 2) (95% IC) and ICC of 0.74. The mean IDA was 509.79 +/- 87.68 degrees (observer 1) and 509.38 +/- 87.57 degrees for (observer 2) with an ICC >0.95. Electrodes of the cochlear implants had no signs of dislocations.
Conclusion: Flat panel CT showed advantages on demonstrating the critical landmarks of the cochlea previous to cochlear implants and the evaluation of the position of intracochlear electrodes after surgery. A good ICC was demonstrated between both observers in the measurement of the diameter A, B and the IDA.

B-0587 14:16

MR imaging strategies in cochlear implants with novel self-aligning magnets, 1.5T vs 3T, high-bandwidth vs WARP artefact reduction: a phantom study

A. Pomschar, M.F. Reiser, B. Ertl-Wagner; *Munich/DE (Andreas.Pomschar@med.uni-muenchen.de)*

Purpose: Susceptibility artefacts caused by magnets in cochlear implants pose a significant problem for cranial MR imaging. Novel CIs are MR-compatible up to 3T without explanation of their magnet. Artefacts caused consist of a large central loss of signal and extensive surrounding distortion. Little information on reducing these artefacts is available. We aimed to optimise the cranial imaging protocol in patients with cochlear implants.
Methods and Materials: We examined a 3T compatible CI with self-aligning magnet (Synchrony, MED-EL) in a plastic phantom at 1.5 and 3T (Aera and Skyra, SIEMENS), comparing different bandwidth (low, middle, high) and WARP metal artefact reduction with VAT (view angle tilting). Penetration depth of the signal loss was measured. Distortion and visual image quality were rated on a 5-point Likert scale.
Results: For reducing penetration depth 1.5T was superior to 3T by 21.4%±7.7; WARP showed a general reduction of 12%±6.5; at 1.5T T1 generated smaller artefacts than T2 (-8.3%±3.3) but slightly larger artefacts at 3T (2.9%±3.5); low vs medium vs high bandwidth reduced the artefact from 7.5cm to 7 to 6.8. Distortion was greatly reduced using WARP by 1.8±0.5 points and by increased BW (low vs medium vs high) 4±1.1 vs 2.9±1.1 vs 2.5±1.2. Using WARP reduced sharpness at low BW but only slightly at medium and high BW.
Conclusion: From this preliminary phantom results we conclude that scanning at 1.5T with intermediate bandwidth and using WARP should yield the best results for whole brain imaging. However, specific areas of interest can be scanned at 3T as long as they have a certain distance from the implant.
Author Disclosures:
A. Pomschar: Equipment Support Recipient; CI was provided by Med-El.

B-0588 14:24

Longstanding sensorineural hearing loss: impact of aetiology of hearing loss on the size of the cochlear nerve

N.N.N. Naguib, N.-E.A. Nour-Eldin, T. Gruber-Rouh, B. Kaltenbach, T.J. Vogl; *Frankfurt a. Main/DE (nagynnn@yahoo.com)*

Purpose: To test whether the size of the cochlear nerve measured in the internal auditory canal using multiplanar reconstruction (MPR) of the high-resolution MRI sequence correlates with the aetiology of hearing loss in patients with longstanding sensorineural hearing loss (SNHL).
Methods and Materials: The retrospective study was performed on 64 patients with longstanding SNHL due to different diseases of the inner ear. High-resolution MRI was performed using a T2-weighted SPACE sequence with 0.6 mm slice thickness. The cross-sectional surface area of the cochlear nerve was measured by drawing a region of interest around the circumference of the nerve. The correlation between the cochlear nerve size measured in MPR and the aetiology of hearing loss was tested using the Kruskal-Wallis test.
Results: The aetiology of SNHL was genetic disorder in 14 patients, sudden hearing loss in 10 patients, infection in adulthood in 8 patients, chronic otitis media in 4 patients, perinatal infection in 3 patients, toxic in 2 patients, due to congenital anomaly in 2 patients and idiopathic in 21 patients. The median size of the cochlear nerve in the different aetiologies was $1.2mm^2$, $1.1mm^2$, $1.25mm^2$, $1.2mm^2$, $1.3mm^2$, $1.25mm^2$, $1.17mm^2$ and $1.1mm^2$, respectively. Statistical analysis showed no statistically significant correlation between the aetiology of hearing loss and the size of the cochlear nerve ($p = 0.923$).
Conclusion: The size of the cochlear nerve in patients with longstanding SNHL does not correlate with the aetiology of hearing loss.

B-0589 14:32

The new classification system for inner ear malformations: the INCAV system

Z.H. Adıbelli, L. Isayeva, A.M. Koc, T. Catlı, H. Adıbelli, L. Olgun; *Izmir/TR (m_leyla_87@hotmail.com)*

Purpose: This study was conducted to explore a more specific, definitive classification system which was based on radiological criteria for inner ear malformations.
Methods and Materials: We found 43 patients who had inner ears malformations, magnetic resonance (MR) and computed tomography (CT) imaging together with the retrospectively evaluation of the medical records between August 2010 and February 2015. We separated the inner ear structures into 5 anatomical subgroups; internal acoustic canal (I), cochlear nerve (N), cochlea (C), vestibular aqueduct (A) and vestibule (V). Based on their malformations, these anatomical structures have been assigned grades and have been classified by using increasing numbers which were dependent to increasing order of severity of the malformation. We defined typical incomplete partition type II (IP-II) by using INCAV system as $I_0N_0C_1A_0V_2$; Mondini as $I_0N_0C_1A_1V_2$; IP-I as $I_0N_0C_4A_0V_4$; IP-III as $I_1N_0C_2A_0V_0$; Michel aplasia as $I_3N_3C_6A_0V_6$.
Results: Among these 43 patients, there were 80 inner ear malformations and 6 normal inner ears ($I_0N_0C_0A_0V_0$). All of the ears were defined successfully by the INCAV system, even 26.25% of the patients, who could not be categorised with existing classification schemes, could be defined successfully by using the INCAV system.
Conclusion: The proposed INCAV system standardises reporting of inner ear malformations; gives adequate information about the structures of inner ear; defines the ears which could not be classified before; helps in the selection of the ear as the cochlear implant candidate. Also the INCAV system is easy-to-use for radiologists, is useful to the referring otolaryngologists.

B-0590 14:40

Diagnostic accuracy of the perilymphatic signal drop on a 3D FIESTA C sequence at 3 Teslas to differentiate vestibular schwannomas from meningiomas of the internal auditory canal

A. Venkatasamy, A. Karol, A. Charpiot, C. Debry, F. Proust, N. Meyer, F. Veillon; *Strasbourg/FR (aina.v@hotmail.fr)*

Purpose: The perilymphatic signal changes on a 3D FIESTA C sequence may be a reliable diagnostic tool to differentiate obstructive vestibular schwannoma (VS) from IAC (internal auditory canal) meningioma (M), through a compartmental analysis of the signal intensity of inner ear fluids.
Methods and Materials: 203 patients with all criteria for a typical VS or IAC M, on a T1-weighted contrast-enhanced sequence, were retrospectively enrolled. 64 healthy subjects (G1), 190 typical VS and 13 typical IAC M (G5) were included. The VS were separated in non-obstructive VS (G2), CSF-border VS (G3) and obstructive VS (G4). All subjects underwent a gradient-echo 3D FIESTA C on a 3T MRI. Two radiologist analysed the signal intensity of the perilymph (vestibular cistern and cochlea) and endolymph (saccule and utricle).
Results: Obstructive VS (G4) presented with a marked perilymphatic signal drop in the vestibular cistern (RCiCSF=0,62) and cochlea. IAC M(G5) presented with a significant but more moderate drop (RCiCSF=0,81). For RCiCSF above 0.70, the tumour was more likely a meningioma, with a high Se=92%, Sp=83% and PNV=0.99. The perilymphatic signal drop was correlated to the degree of IAC's obstruction and no endolymphatic signal changes were observed.
Conclusion: The more pronounced drop of the perilymphatic signal on a 3D-FIESTA-C sequence in obstructive VS provides an additional tool to differentiate obstructive VS from IAC M, which may be useful to overcome the insufficiency of the morphological analysis itself. A cut-off value RCiCSF=0.70 enables the reader to differentiate between these two tumours with a high Se and Sp.

B-0591 14:48

Effect of the duration of hearing loss on the size of the cochlear nerve in patients with longstanding sensorineural hearing loss

N.N.N. Naguib, N.-E.A. Nour-Eldin, T. Gruber-Rouh, M. Al-Subhi, T.J. Vogl; *Frankfurt a. Main/DE (nagynnn@yahoo.com)*

Purpose: To test whether the size of the cochlear nerve measured in the internal auditory canal correlates with the duration of hearing loss in patients with longstanding sensorineural hearing loss (SNHL).
Methods and Materials: The retrospective study was performed on 98 patients who were divided into two groups. In group 1 (n = 68, test group), patients presented with bilateral longstanding SNHL and in group 2 (n = 30, control group) normal hearing patients referred for MRI of the inner ear for other diseases. High-resolution MRI was performed using a T2-weighted SPACE sequence with 0.6 mm slice thickness. The cross-sectional surface area of the cochlear nerve was measured by drawing a region of interest around the circumference of the nerve in the multiplanar reconstructed images.
Results: For group 1, the mean cross-sectional surface area of the cochlear nerve was $1.2mm^2$ (standard deviation: 0.35, range: 0.31-2.2). For group 2, the mean cross-sectional surface area of the cochlear nerve was $1.5mm^2$ (standard deviation:0.34, range: 1-2.5). Patients with SNHL (Group 1) had a statistically significant ($p=0.001$) smaller size of the cochlear nerve than normal hearing patients (group 2). A statistically significant ($p=0.0019$) weak negative correlation (rho= - 0.2) between the cochlear nerve size and the duration of hearing loss in patients with longstanding SNHL was noted.
Conclusion: Patients with longstanding SNHL have a significantly smaller size of the cochlear nerve compared to those with normal hearing. The cochlear nerve size correlates negatively with the duration of SNHL.

B-0592 14:56

Diagnostic performance of reformatted isotropic thin-section helical CT images in the detection of superior semicircular canal dehiscence

G. Sparacia[1], F. Agnello[1], A. Anastasi[1], A. Iaia[2], K. Traylor[2], M. Midiri[1];
[1]*Palermo/IT*, [2]*Newark, DE/US (fra.agnello@libero.it)*

Purpose: To assess the diagnostic performance of highly collimated isotropic CT reformatted images in detection of superior semicircular canal (SSC) dehiscence.
Methods and Materials: Forty-two patients, with sound- and/or pressure-induced vestibular symptoms, and forty-two control subject, underwent CT with highly collimated beam (0.5-mm). Reformatted images of the vestibular labyrinth structures were obtained from volumetric CT data in standard axial, and coronal planes (group A images). Additionally, reformatted images in a plane oriented to be parallel (plane of Pöschl) and perpendicular (plane of Stenver) to the SSC were obtained (group B images). Group A and group B images were evaluated separately by two neuroradiologists in consensus to establish whether a dehiscence of the SSC was present at the arcuate eminence.
Results: Diagnostic performance of group A images measured by the AUC was 0.929 (sensitivity 85.7%, specificity 100%, TP 36, TN 42, FP 0, FN 6) with an overall accuracy of 92.9%. Diagnostic performance of group B images measured by the AUC was 0.988 (sensitivity 97.6%, specificity 100%, TP 41, TN 42, FP 0, FN 1) with an overall accuracy of 98.8. Although differences between two AUCs were not statistically significant, group B images alone showed an improved diagnostic performance over the group A images alone.
Conclusion: Thin-section isotropic voxel CT with reformatted images oriented in the plane parallel (plane of Pöschl) and perpendicular (plane of Stenver) to SSC improves diagnostic accuracy in assessing for SSC dehiscence in comparison to CT images with reconstructions limited to traditional axial and coronal planes.

B-0593 15:04

MRI findings in infants with auditory neuropathy spectrum disorder due to thiamine deficiency

P.A. Caruso; *Boston, MA/US (pcaruso@partners.org)*

Purpose: A group of 11 Israeli children who developed encephalopathy due to nutritional thiamine deficiency has previously been reported. These children later developed moderate to severe hearing loss with features of auditory neuropathy spectrum disorder. Our purpose is to describe the MRI findings in this unique cohort.
Methods and Materials: The clinical records were reviewed for demographics, age at presentation, duration of nutritional thiamine deficiency, findings confirmatory of ANSD, outcome of the hearing loss following treatment with thiamine supplementation, and for neurologic sequelae. The MRIs were reviewed for abnormal findings along the auditory pathway from the external auditory canal to the cerebral cortex. All MRIs included T1- and T2-weighted images. Post-gadolinium T1-weighted images were available in six patients and DWI in five patients. Four children underwent additional MR imaging following thiamine supplementation.
Results: The study group included 7 infants: five female and two male aged 3-10 months. Along the auditory pathway, abnormal signal on the T2-weighted images was seen in the cochlear nuclei in six patients, in the trapezoid body in four patients, in the lateral lemnisci in four patients, in the inferior colliculi in five patients. Abnormal diminished diffusion was seen in the tectum, brainstem, posterior thalami, and the basal ganglia.
Conclusion: Our report describes for the first time the MR findings along the auditory pathway in infants with auditory neuropathy spectrum disorder due to nutritional thiamine deficiency.

B-0594 15:12

Detection and measurement accuracy of cholesteatomas: a comparison between non-EPI RESOLVE DWI and 3T MRI vs EPI DWI PROPELLER on 1.5T MRI

P.G. Chan, M. Thong, W. Maclaurin, S. Kerr, H. Kavnoudias, V. Cousins;
Melbourne/AU (pchan713@gmail.com)

Purpose: PROPELLER non-EPI DWI is highly sensitive and specific for the diagnosis of cholesteatoma, with a 98% clinical and radiological concordance rate. The aim of this study is to determine if 3T RESOLVE EPI DWI is equivalent in cholesteatoma detectability and accuracy compared to 1.5T PROPELLER non-EPI DWI.
Methods and Materials: All consecutive patients aged 18 or above who had undergone MRI for investigation for cholesteatoma, and received both PROPELLER and RESOLVE DWI imaging, were reviewed from June 2014 and September 2016. The images were independently reviewed by two head and neck consultant radiologists. Detection of cholesteatoma was the primary endpoint for each sequence. Lesions were measured along maximal dimensions and compared for concordance as the secondary endpoint.
Results: There were 28 patients who underwent 32 examinations. 14 lesions (PROPELLER) and 4 lesions (RESOLVE) were identified by both radiologists in total. Radiologist A detected 11 lesions and Radiologist B detected 13 lesions on PROPELLER; three lesions were identified on RESOLVE by each radiologist. All lesions (100%) that were detected by RESOLVE were detectible by PROPELLER. Concordance rates between the sequences were 27.27% (Radiologist A) and 23.08% (Radiologist B). The interobserver concordance rate for PROPELLER was 71.43% and 50% for RESOLVE. Six measurements were obtained in only four lesions. The mean percentage size concordance between the sequences was 78.8% (range 45.45% - 110.20%).
Conclusion: 3T RESOLVE EPI DWI has been shown to be inferior in both cholesteatoma detection and lesion size equivalence when compared to 1.5T PROPELLER non-EPI DWI.

B-0595 15:20

Comparison between a flat-panel angiography system and a 64-slices multisection computed tomography scanner in the cross-sectional imaging of the temporal bone

G. Conte, E. Scola, C. Sina, S. Calloni, R. Brambilla, L. Lombardi, F. Triulzi;
Milan/IT (giorgioconte.unimed@gmail.com)

Purpose: To compare the image quality and radiation dose between a flat-panel angiography (FPA) system and a 64-slices multisection computed tomography (MSCT) scanner in the cross-sectional imaging of the temporal bone.
Methods and Materials: We retrospectively collected 29 FPA and 29 MSCT of normal whole-head temporal bones. Image quality was assessed by two neuroradiologists who rated the visualisation of 30 anatomic structures with a three-point ordinal scale. Radiation dose was assessed using an anthropomorphic Rando Alderson Phantom in which thermoluminescent dosimeters were inserted in sites corresponding to organs and tissues.
Results: FPA showed better image quality than MSCT in depicting anterior and posterior crura of the stape, footplate of the stape, stapedius muscle, anterior ligament of the malleus ($p<0.05$). On the contrary CT showed better image quality than FPA in assessing tympanic membrane, bone marrow of the malleus and incus, tendon of tensor tympani, interscala septum and modiulus of the cochlea ($p<0.05$). No statistical difference, in terms of image quality, was found for the remaining anatomic structures. FPA had a significantly higher overall image quality rate than FPA ($p = 0.035$). A reduction of the effective dose of about 40% was proved for FPA compared to MSCT, with a reduction of 76% of dose for the lenses of the eye and 40% for the thyroid.
Conclusion: FPA is a convincing technique for cross-sectional imaging of the temporal bone. It provides better image quality in depicting the normal anatomy at lower radiation exposure compared to 64-slices MSCT.

14:00 - 15:30 **Room E1**

Breast

SS 702a

Digital breast tomosynthesis

Moderators:
G. Gennaro; Padua/IT
N. Radovic; Zagreb/HR

B-0596 14:00

Digital breast tomosynthesis: rate of recalls and screen-detected breast cancer in a population-based screening program by previous screening acquisition

S. Hofvind[1], T. Hovda[2], Å.S. Holen[1], J.L. Albertsen[3], H. Bjørndal[2], S.H.B. Brandal[1], L. Romundstad[2], E. Vigeland[3], P. Skaane[1]; [1]*Oslo/NO*, [2]*Drammen/NO*, [3]*Tønsberg/NO (solveig.hofvind@kreftregisteret.no)*

Purpose: To compare the recall rate and rate of screen-detected breast cancer using synthetic images and digital breast tomosynthesis (DBT) by previous screening acquisition in the Norwegian Breast Cancer Screening Program (NBCSP).
Methods and Materials: The study population included women screened with DBT at the NBCSPs screening unit in Oslo, 2014 and 2015, who also attended screening two years earlier, 2012 and 2013 respectively (n=23 154). The women were stratified by screening technique used at their previous screening examination, DBT (n=9947) or DM (n= 13 207). Data on women with a previous DBT were retrieved from the Oslo Tomosynthesis Screening Trial, 2012. Z-test was used to test for statistical significance ($p<0.05$) between the groups.
Results: Women with a previous DM had a higher recall rate compared to women with a previous DBT (2.4% and 1.9% ($p=0.02$), respectively). The rate of screen-detected breast cancer did not differ statistically significantly for

women with a previous DBT (8.6/1000 screened) compared to a previous DM (10.1/1000 screened) (p=0.27).
Conclusion: The results imply that fewer women are recalled when screened with DBT for two consecutive screening rounds. However, it does not affect the rate of screen-detected breast cancer.

B-0597 14:08

Interpretation time for digital breast tomosynthesis vs digital mammography in a population-based screening program

H.S. Aase[1], C.W. Frøland[1], Å.S. Holen[2], T.K. Neraas[1], K. Obst-Gleditsch[1], C.K. Sandvik[1], K.T. Søvik[1], I.M.O. Ulvik[1], S. Hofvind[2]; [1]*Bergen/NO*, [2]*Oslo/NO (solveig.hofvind@kreftregisteret.no)*

Purpose: To compare interpretation time for initial and consensus reading using digital breast tomosynthesis (DBT) versus digital mammography (DM) in the Norwegian Breast Cancer Screening Program.
Methods and Materials: As part of a randomized controlled trial performed in Bergen, interpretation time was registered at initial reading and consensus for DM (n=3694 and 242, respectively) and DBT (n=3765 and 227, respectively), January-June 2016. Mean time was calculated, while t-test with a 95% confidence interval (CI) was used to test for statistical significance between the two means.
Results: Mean initial interpretation time was 38 seconds (95% CI: 37-39) for DM and 01:12 minutes (95% CI: 01:11-01:13) for DBT, p<0.01. Mean interpretation time at consensus was 02:03 minutes (95% CI: 01:54-02.13) for DM and 03:24 (95% CI: 03:07-03:41) for DBT, p<0.01. For DM, mean time for initial reading decreased from 51 seconds in January to 27 seconds in June (p<0.01), while it decreased from 01:56 minutes to 58 seconds (p<0.01) for DBT. For consensus, the time decreased from 03:05 to 01:42 minutes (p<0.01) for DM and from 05:44 to 03.34 (p<0.01) for DBT during the study period.
Conclusion: The mean interpretation time at initial reading at DBT was double that of DM and a longer interpretation time should be expected when reading DBT images, also at consensus. The decreasing interpretation time might be related to the start-up of the randomized trial, indicating that the readers became more familiar with the protocol and reading DBT after six months.

B-0598 14:16

Syntetic 2D + tomosynthesis for population breast cancer screening: first year of a pilot study

F. Caumo[1], G. Romanucci[1], S. Brunelli[1], P. Bricolo[1], L. Cugola[1], C. Fedato[2], M. Zorzi[3], S. Montemezzi[1]; [1]*Verona/IT*, [2]*Dorsoduro (VE)/IT*, [3]*Padova/IT (francescacaumo@gmail.com)*

Purpose: To assess advantages and limitations of Synthetic 2D + tomosynthesis (C-view + 3D) for population breast cancer screening.
Methods and Materials: From 1st April 2015 to 1st April 2016, 16755 women (aged 50-69 years) underwent screening C-view + 3D examinations at our institute and satellite centres. Participants were asymptomatic women at standard risk (population) for breast cancer. All examinations was interpreted on double-reading whereby recall was decided based on recall by either radiologist. Outcome measures were: incremental of storage, reading time, number of detected cancer, the number of detected cancer per 1000 screens, recall rate and pTN category. We also compared data with conventional 2D-mammography screening performed on previous screening round (14510 women screened from 1st April 2014 to 31th March 2015).
Results: Among C-view + 3D screening participants, 157 breast cancer were detected (vs 80 detected at 2D screening). Recall rates were 4,9% (vs 5,5% in 2D screening), cancer detection rate were 10,1% (vs 6,5% in 2D screening), T2+ were 16% (vs 26,4%), conservative treatment 88,5% (vs 79% in 2D screening). The incremental of storage increased from 532.862 MB to 5076.176 MB. The mean number of studies interpreted in hour was 38,5 +/- 0.55 (standard deviation) for C-view + 3D and 60 +/- 0.55 (standard deviation) for 2D alone.
Conclusion: Despite a consequential increase of reading time, C-view + 3D significantly increased cancer detection rates and conservative treatment and lowered T2+ cancer in breast screening population.

B-0599 14:24

The accuracy of digital breast tomosynthesis (DBT) and spot compression views for the diagnosis of different soft tissue breast lesions in a screening programme

J.J. James[1], E.J. Cornford[1], Y. Chen[2], A.E. Turnbull[3]; [1]*Nottingham/UK*, [2]*Loughborough/UK*, [3]*Derby/UK (jonathan.james@nuh.nhs.uk)*

Purpose: To compare the accuracy of DBT and spot compression views in the diagnosis of masses, asymmetric densities (AD) and parenchymal deformities (PD) in women recalled for further investigation following screening mammography.
Methods and Materials: The women recruited received both spot compression views and two-view DBT. The radiologists working up the case first prospectively recorded their suspicion of malignancy on a five-point scale when reading standard two-view digital mammograms (DM) together with spot compression views. They then prospectively recorded scores for DM read in conjunction with two-view DBT. Pathology data were obtained.
Results: 334 lesions were assessed. The breast lesions were masses (51%), AD (15.5%) and PD (33.5%). There were 107 malignant and 227 benign/normal cases. The overall performance of DBT (as determined by ROC analysis) was equivalent to spot compression views for the assessment of each type of breast lesion (AUC was 0.94996 and 0.91055, respectively, for masses; 0.98913 and 0.95897 for AD; 0.86943 and 0.8679 for PD - all non-significant). DBT demonstrated significantly higher absolute sensitivity for malignancy manifesting as an AD (p=0.039). There was no significant difference in specificity or negative and positive predictive values for each technique.
Conclusion: DBT can be used to assess all types of soft tissue breast lesions with overall accuracy at least equivalent to spot compression views. For a malignant lesion presenting as an AD, a significant improvement in sensitivity was demonstrated when DBT was used to characterise the lesion.
Author Disclosures:
E.J. Cornford: Research/Grant Support; GE Health Care. **A.E. Turnbull:** Research/Grant Support; GE Health Care.

B-0600 14:32

Added value of one-view digital breast tomosynthesis combined with digital mammography according to readers concordance: changing in BIRADS rate and follow-up management

F. Galati, F. Marzocca, E. Bassetti, M. Luciani, F. Pediconi, C. Catalano; *Rome/IT (flaminia.marzocca@gmail.com)*

Purpose: To evaluate the added value of Digital Breast Tomosynthesis (DBT) when combined with Digital Mammography (DM): changing in BIRADS assessment and follow-up management.
Methods and Materials: From February 2014 to April 2015, 214 patients underwent one-view DBT and two-view DM. Two readers, with 15 and 10 years experience in breast imaging, independently reviewed all exams in two steps: DM and DM+DBT, according to BIRADS classification. Patients with BIRADS 0, 3, 4 and 5 were recalled for work-up. Inter-reader concordance of BIRADS rate and work-up rate were evaluated using Cohen's Kappa.
Results: K value for BIRADS classification was 0.58 for DM and 0.8 for DM+DBT. DM+DBT increased BIRADS 1 and 2 (Reader 1: DM 29.44%, DM+DBT 60.28% - Reader 2: DM 21.96%, DM+DBT 63.55%; p<0.01) and BIRADS 4 and 5 (Reader 1: DM 18.22%, DM+DBT 31.78% - Reader 2: DM 16.83%, DM+DBT 28.51%; p<0.01). While reduced BIRADS 0 and 3 compared to DM alone (Reader 1: DM 52.34%, DM+DBT 7.94% - Reader 2: DM 61.21%, DM+DBT 7.94%; p<0.01). K value for work-up rate was poor for DM and substantial (0.7) for DM+DBT. DM+DBT reduced work-up rate for both Reader 1 (DM 85.98% vs DM+DBT 52.8%, p<0.01) and Reader 2 (DM 97.2 % vs DM+DBT 55.14%, p<0.01).
Conclusion: The combination of DM and DBT increased the concordance between the readers for BIRADS classification and work-up rate. DBT+DM also increased the number of BIRADS 1-2 and BIRADS 4-5, while reduced the number of BIRADS 0 and 3 (uncertain cases) for both readers.

B-0601 14:40

One-view digital breast tomosynthesis as a standalone modality for breast cancer detection: do we need more?

A. Rodríguez-Ruiz, A. Gubern-Mérida, M. Imhof-Tas, S. Lardenoije, N. Karssemeijer, R. Mann, I. Sechopoulos; *Nijmegen/NL (alejandrorzrz@gmail.com)*

Purpose: To compare the performance of three different implementations of digital breast tomosynthesis (DBT) as a replacement or an adjunct to digital mammography (DM) for breast cancer detection.
Methods and Materials: Two radiologists retrospectively reviewed 181 unilateral DBT and DM cases (79 malignant, 49 benign, and 53 normal). All non-malignant cases had >1 year of negative imaging follow-up. A sequential study with three steps per case was used, displaying different protocols. Step 1: only medio-lateral oblique (MLO) DBT. Step 2: MLO-DBT plus cranio-caudal (CC) DM. Step 3: CC and MLO from both modalities. Lesions were annotated and scored following BI-RADS (for diagnostic performance analysis) and level of suspiciousness (for jackknife alternative free-response receiver operating characteristic (JAFROC) analysis). Inter-reader variability was assessed using Cohen's kappa.
Results: Inter-reader agreement was moderate for all steps (k>0.46). Averaged across readers, sensitivity increased significantly from step 1 to step 2 (71% vs 77%; p<0.01) but step 3 had no added value (78%). Specificity decreased in step 2 (75% vs 72%; p=0.04), but was similar between steps 1 and 3 (step 3: 76%). The JAFROC figure of merit was comparable between steps 1 and 2 (p=0.66), but significantly greater for step 3 (p<0.05). Sub-analysis by lesion type and breast density showed that additional views improved performance only for detection of microcalcifications and in dense breasts.

Conclusion: One-view DBT has similar diagnostic performance whether or not the CC-DM is added, but the performance increases slightly when scoring the full breast exam. Studies with additional readers are ongoing.
Author Disclosures:
A. Rodríguez-Ruiz: Research/Grant Support; Siemens Healthcare S.L.U.

B-0602 14:48

Galactography in tomosynthesis technic - renaissance of a method?
R. Schulz-Wendtland[1], P. Fasching[1], C. Löhberg[1], M. Lux[1], M.W. Beckmann[1], M. Uder[1], M. Müller-Schimpfle[2]; [1]*Erlangen/DE*, [2]*Frankfurt a. Main/DE*
(ruediger.schulz-wendtland@uk-erlangen.de)

Purpose: The conventional galactography was used as the only imaging method in case of pathological nipple discharge for decades. Aim of our study was the comparison of the ductal oriented sonography with the contrast-enhanced galactography in tomosynthesis technique and of this generated reconstructed synthetic 2D-full-field digital mammographies.
Methods and Materials: From 01.10.2014 bis 31.03.2016 we investigated a total of 100 patients with a ductal oriented sonography as well as a contrast-enhanced galactography in tomosynthesis technique and of this generated reconstructed synthetic 2D-full-field digital mammographies. The mean age of the patients was 54.2 yrs (minimum 21 yrs, maximum 83 yrs). The evaluation of the three methods was made and correlated with the final histology.
Results: About all three investigators the results were: ductal oriented sonography with a sensitivity of 79.7%, a specificity of 58.3%, a ppV of 77.3% and a npV of 61.8%; for synthetic 2D-full-field digital mammography resp. 80.0%, 60.0%, 78.8% and 61.8% and the 3D-digital tomosynthesis resp. 90.9%, 73.9%, 92.1% and 73.9%. The accuracy, separated for the three methods: the ductal oriented sonography 0.72, synthetic 2D-full-field digital mammography 0.73 and the 3D-digital tomosynthesis 0.87.
Conclusion: First application of tomosynthesis in the galactography with significant better results in comparison to the ductal oriented sonography. This might become a renaissance of this method and an expansion of the spectrum of tomosynthesis in the complementary breast diagnostic. The generated reconstructed synthetic 2D-full-field digital mammographies are comparable with these of the ductal oriented sonography in high resolution.

B-0603 14:56

To compare total radiation dose of FFDM alone and FFDM+DBT when additional views were considered
C.S. Lo, L.H.Y. Sinn, K.W.M. Wong, T.P.W. Lam, W.W.M. Lam; *Hong Kong/HK*
(chrissy.lo@gmail.com)

Purpose: To compare total radiation dose of FFDM alone and FFDM+DBT when additional views were considered.
Methods and Materials: Retrospective analysis of women attending annual surveillance mammography to assess number of additional views before (FFDM only: 1/10/2012-31/03/2013) and after implementation of combined FFDM+DBT (01/04/2015-31/03/2016) utilising same mammography unit. Average glandular dose (AGD) estimates obtained from DICOM images. Total radiation for each examination and additional views compared with Fisher exact test for periods A and B. Statistical significance considered when $p<0.05$.
Results: 2181 and 2701 women were included in period A (FFDM) and Period B (FFDM+DBT) respectively. Additional views dropped from 242 (11.1%) to 50 (1.9%). Mean AGD per view of FFDM in Period A and B shows no significant difference (1.51mGy to 1.53mGy). Mean AGD measures 3.09mGy in period B when combined with DBT. Significant increase in mean AGD per view (1.11mGy to 2.56mGy, $p<0.01$) and total radiation dose from additional views (1.86mGy to 4.23mGy, $p<0.01$) in period B. Average total radiation dose per patient including additional views increased from 5.27mGy to 11.4mGy, $p<0.01$.
Conclusion: Significant reduction in recall rate for additional views after implementation of combined FFDM and DBT. Radiation dose per additional view was considerably higher in period B, possibly attributed by decreased compression force and increased compression thickness. No significant difference in radiation dose when initial FFDM dose compared with stand-alone DBT, implying potential significant reduction in radiation dose when synthesised mammography used in lieu of FFDM in clinical practice.

B-0604 15:04

Comparison of detectability and characterisation of micro calcifications with digital mammography (DM), synthesised 2D mammography (SM) and digital breast tomosynthesis (DBT)
L.H.Y. Sinn, W. Wong, T.P.W. Lam, S.H.Y. Lam, V.W.H. Lau, J.J.K. Ip, G. Ho, H. Leung, W.W.M. Lam; *Pokfulam/HK (lorriesinn@gmail.com)*

Purpose: Comparison of the ability of detection and characterisation of benign and malignant microcalcifications in DM, SM and DBT.
Methods and Materials: Women attending surveliiance mammography since October 2014 were recruited with informed consent. Combined DM and DBT performed at same time for all cases with reconstruction of SM from DBT data. 9 radiologists reviewed the images without access to prior examinations / clinical history. Characterisation of the lesions and calcifications are documented.
Results: Interim analysis of 1067 study sets showed there were 475 sets demonstrated presence of benign microcalcifications in all three modalities. 61.9% sets showed increase in benign microcalcifications on SM, while only 13.1% showed increase benign microcalcifications when interpreting SM with DBT. When comparing BIRADS assignment of benign microcalcifications with DM, 14 and 19 cases were changed from BIRADS 0 to 1/2 in SM and DBT respectively. None of the cases were being upgraded from category 1/2 to 4/5 or downgraded vice versa in both SM and DBT groups. 15,15 and 16 cases with suspicious microcalcifications (BIRADS 4/5) were found in the DM, SM and DBT groups with respective sensitivity of 33%, 33% and 37.5%.
Conclusion: Increase benign microcalcifications were found when interpreting SM compared to DM, but most “overcalled” could be eliminated when interpreting together with DBT. None of the cases were upgraded from normal/benign findings in DM to BIRADS 4 or 5 or downgraded vice versa in both SM and DBT. Diagnostic performance of suspicious microcalcifications of DM and SM group was comparable.

B-0605 15:12

Is digital breast tomosynthesis (DBT) favourable for the evaluation of breast microcalcifications and for pre-procedural study of stereotactic biopsy?
G. Choi[1], O. Woo[1], H. Shin[1], K. Cho[1], B. Seo[2]; [1]*Seoul/KR*, [2]*Ansan/KR*
(cgyjulie@gmail.com)

Purpose: To investigate the diagnostic power of digital breast tomosynthesis (DBT) in evaluation of breast microcalcifications and usefulness as a pre-procedural study for stereotactic biopsy in comparison with full-field digital mammogram (FFDM) and FFDM plus magnification images (FFDM+MAG).
Methods and Materials: An IRB approved retrospective observer performance study on DBT, FFDM, and FFDM+MAG was done. Image quality was rated in 5-point scoring system for lesion clarity (1, very indistinct; 2, indistinct; 3, fair; 4, clear; 5, very clear) and compared by Wilcoxon test. Diagnostic power was compared by diagnostic values and AUC with 95% confidence interval. Additionally, procedural report of biopsy was analysed for patient positioning and adequacy of instruments.
Results: DBT showed higher lesion clarity (median 5, interquartile range 4-5) than FFDM (3, 2-4, p-value<0.0001), and no statistically significant difference to FFDM+MAG (4, 4-5, p-value=0.3345). Diagnostic sensitivity and specificity of DBT were 86.4% and 92.5%; FFDM 70.4% and 66.7%; FFDM+MAG 93.8% and 89.6%. The AUCs of DBT (0.88) and FFDM+MAG (0.89) were larger than FFDM (0.59, p-values<0.0001) but there was no statistically significant difference between DBT and FFDM+MAG (p-value=0.878). In 2 cases with DBT, petit needle could be appropriately prepared; and other 3 without DBT, patient repositioning was needed.
Conclusion: DBT showed better image quality and diagnostic values than FFDM and equivalent to FFDM+MAG in evaluation of breast microcalcifications. Evaluation with DBT as a pre-procedural study for breast stereotactic biopsy can lead to more accurate localisation and successful biopsy and also waive the need for additional magnification images.

B-0606 15:20

To what extent is the detectability of breast microcalcifications and spiculated lesions dependent on display luminance level?
C. Ferranti, A. Primolevo, F. Cartia, C. Cavatorta, M. Lualdi, E. Pignoli, M. Plebani, P. Verderio, G. Scaperrotta; *Milan/IT*
(claudio.ferranti@istitutotumori.mi.it)

Purpose: Evaluation of the influence of the calibrated luminance level of medical displays in the detectability of microcalcifications and spiculated lesions in Digital Breast Tomosynthesis (DBT) images.
Methods and Materials: Four models of medical displays with calibrated maximum and minimum luminance respectively ranging from 500 to 1000cd/m^2 and from 0.5 to 1.0cd/m^2 were investigated. Forty-eight studies were selected by a senior radiologist: 16 with microcalcifications, 16 with spiculated lesions and 16 without lesions. All images were anonymised and blindly evaluated by

one senior and two junior radiologists. For each study, lesion presence/absence and localisation statements, interpretative difficulty level and overall quality were reported. Cohen Kappa statistic was computed between monitors and within/between radiologists to estimate the reproducibility in correctly identifying lesions; for multi-reader-multi-case (MRMC) analysis, weighted Jackknife Alternative Free-response Receiver Operating Characteristic (wJAFROC) statistical tools were applied.
Results: Intra-radiologist reproducibility ranged from 0.75 to 1.00. Inter-reader as well as reader-truth agreement values were >0.80 and higher with the two 1000cd/m^2 luminance displays than with the lower luminance displays for each radiologist. Performances in the detectability of breast lesions were significantly greater with the 1000cd/m^2 luminance displays when compared to the display with lowest luminance value (p<0.001).
Conclusion: Our findings highlight the role of display luminance level on the accuracy in detecting breast lesions.

14:00 - 15:30 **Room E2**

Neuro

SS 711

Brain tumours: lesion characterisation and treatment evaluation

Moderators:
M.A. Lucic; Sremska Kamenica/RS
S. Thust; London/UK

B-0607 14:00

Tumour vascular pattern on MRI: a new and promising potential biomarker of glioblastoma survival
A. Gimeno[1], G. Blasco[1], P. Daunis-i-Estadella[1], C. Biarnés[1], J. Sanchez-Gonzalez[2], A. Alberich-Bayarri[3], M. Puigdemont[1], S. Pedraza[1], J. Puig[1]; [1]*Girona/ES*, [2]*Madrid/ES*, [3]*Valencia/ES (fredigimeno1989@gmail.com)*

Purpose: Vascularity correlates with shortened survival. We aimed to determine whether the tumoural vascular pattern on MRI (TVP-MRI) of newly diagnosed glioblastomas is useful in predicting survival, and to correlate TVP-MRI with dynamic susceptibility contrast (DSC) perfusion and diffusion parameters for contrast-enhancing lesion (CEL) and surrounding non-CEL.
Methods and Materials: Ninety-seven patients (59 men; mean age, 61 years) with histologically proven glioblastoma underwent 1.5T-MRI including anatomical sequences, first-pass DSC images and post-contrast T1-weighted SE images after gadobutrol (Gadovist; Bayer Schering Pharma, Berlin, Germany) at 0.1 mmol/kg) with a 1 mm isometric voxel. Volumes of interest for CEL, non-CEL, and contralateral tissue were obtained for relative cerebral blood volume (rCBV), relative cerebral blood flow (rCBF), delay time (DT), mean temporal maximal intensity projection (tMIP), and apparent diffusion coefficient (ADC) using Olea Sphere V.3.0 software (Olea Medical, La Ciotat, France). Tumours over 5 vessels were classified as hypervascular (hyper-TVP-MRI) on post-contrast 1 mm-T1SE images. Prognostic factors were evaluated by Kaplan-Meier survival and Cox proportional hazards analysis.
Results: Fifty-five (56.7%) glioblastomas were hyper-TVP-MRI. Patients with hyper-TVP-MRI, mean age, volume-CEL, ADC-CEL, DT-CEL, rCBV-CEL, rCBV-nonCEL and tMIP-CEL were higher and DT-nonCEL lower. Mean survival for hypo- and hyper-TVP-MRI glioblastomas treated with surgery and with radiotherapy plus chemotherapy was 12.9±7.7 and 8.3±6.9 months, respectively. TVP-MRI was the best survival predictor for glioblastoma at 1 year (AUC 0.84, 88.5% sensitivity, 77.9% specificity, 82.3% positive predictive value, 87.8% negative predictive value).
Conclusion: TVP-MRI might be a new and promising potential biomarker for predicting survival in newly diagnosed glioblastoma.

B-0608 14:08

Medulloblastoma in adults: identifying imaging biomarkers of genetic status in a prospective multi-centre study
V.C. Keil[1], M. Warmutz-Metz[2], C. Reh[1], J. Enkirch[1], H.H. Schild[1], T. Pietsch[1], E. Hattingen[1], P. Hau[3]; [1]*Bonn/DE*, [2]*Würzburg/DE*, [3]*Regensburg/DE (vera.keil@ukb.uni-bonn.de)*

Purpose: Medulloblastomas are rare in adults. Histopathological and molecular profiles are known to influence the course of disease. This study is a first radiogenomic approach to identify MR imaging biomarkers of molecular subtypes in adults with medulloblastomas, which may facilitate pre-operative tumour assessment and elucidate differences between adult and paediatric tumours. This is a subanalysis of the multi-center NOA-07 study.
Methods and Materials: Between 2008 and 2014, 18 neuro-oncological centers recruited 28 patients above 21 years with confirmed and molecularly sub-grouped medulloblastomas and full pre-operative MRI datasets (T1w, T2w, FLAIR and contrast-enhanced T1w sequences). Morphological characteristics (predefined as: enhancement pattern, T1 and T2 signal, hemorrhage) and further tumour and edema volumes, location, Chang criteria and hydrocephalus were evaluated by 3 experienced neuroradiologists. These MR findings were matched to histological and molecular subtypes (Fischer and ANOVA testing). Results were compared to findings from the only radiogenomic medulloblastoma study in children (S Perreault et al., AJNR 2014).
Results: Relation to the 4th ventricle and lower rhombic limb, edema volume, CNS metastases, non-enhancing tumour volume (Chang larger 2) and hydrocephalus differed significantly between molecular subtypes (P=0.01 to 0.04 respectively). None of these criteria matched with corresponding findings in paediatric medulloblastomas. Perifocal edema was larger in the desmoplastic subtype (P=0.01). Except for hemorrhage, none of the predefined MR-morphological characteristics could differentiate between the molecular or histopathological subtypes.
Conclusion: There are indicators that prognostically different molecular subtypes of adult medulloblastoma can be preoperatively identified based on MRI imaging. These seem distinct from findings in children.

B-0609 14:16

Apparent diffusion coefficient and permeability parameters from dynamic contrast-enhanced perfusion MR imaging: preliminary correlation study with glioma genetic profiles
J. Zhao, J.-P. Chu, Y.-L. Wang, X.-B. Li, J.-Y. Wang, Y.-K. Song; *Guangzhou/CN (zhaojing_sysu@126.com)*

Purpose: Preliminary evaluation of the efficacy of diffusion and DCE-MR imaging in predicting major genetic alterations in glioma.
Methods and Materials: 30 gliomas (male: 19, female: 11; mean age: 37.3 y) were retrospectively included and they all underwent DWI and DCE-MRI. ADC and permeability parameters (K^{trans}, Ve, Kep and iAUC) maps were generated. 5~10 ROIs were placed on tumour parenchyma. The max, min, mean value of ADC and the median, mean value of permeability parameters were recorded. Four major glioma genetic alterations (IDH-1; n=27), (MGMT; n=26), (ATRX; n=27) and Ki-67 (n=29) were included and their associations with ADC and permeability parameters were analysed.
Results: The max and mean value of ADC and mean value of Ve and iAUC in IDH-1 mutated group were significantly higher than those of the IDH-1 negative group (P<0.040) and the max value of ADC showed the highest diagnostic value; The mean value of ADC and Ve demonstrated the highest sensitivity (96.8%) and specificity (94.8%), respectively. Compared with ATRX-negative group, the max and mean value of ADC also significantly higher (P<0.001) and it demonstrated the highest diagnostic value. Further, in the analysis of MGMT-positive group, the mean/median value of K^{trans}, Kep, ADC and the max/mean value of ADC were significantly higher; in addition, we found that only Kep and ADC values were negatively correlated with Ki-67 (P<0.022).
Conclusion: Tumours with mutated IDH-1, ATRX and MGMT prone to have a higher permeability and ADC value. Thus, DWI and DCE-MRI, especially DWI, might be helpful in predicting genetic alterations.

B-0610 14:24

Hybrid methionine PET/MRI and MR spectroscopy in the diagnostic workup of primary brain tumour
C. Deuschl, S. Göricke, T. Pöppel, H. Quick, M. Forsting, L. Umutlu, M. Schlamann; *Essen/DE (cornelius.deuschl@uk-essen.de)*

Purpose: The objective of this study was to assess the diagnostic value of integrated 11C-methionine positron emission tomography/magnetic resonance imaging (methionine PET/MRI) and MRI with magnetic resonance spectroscopy (MRS) for suspected primary brain tumour.
Methods and Materials: Thirty-four consecutive patients with suspected primary brain tumour were prospectively enrolled for an integrated 11C-methionine PET-MRI with MRS. 5 Spectra were non diagnostic (25.6%); therefore, 29 spectroscopic data sets were available for definitive evaluation (85.3%). Reference standard was the histopathological report in 21 patients, whereas in the remaining 8 patients follow-up imaging was used. Two radiologists evaluated the integrated PET/MRI data sets and the MRI datasets with MRS regarding the most likely diagnosis and diagnostic confidence on a 5-point Likert-scale.
Results: In 29 patients 30 lesions were detected and classified by the reference standard. Twenty-seven lesions were primary brain tumour: 15 low-grade glioma (LGG), 12 high-grade glioma (HGG). Three lesions were classified as non-oncologic lesions. MRI with MRS correctly identified 27 of the 30 lesions (90%), whereas integrated PET/MRI was correct in 26 of the 30 lesions (Fig 1). Diagnostic confidence was better for MRI with MRS vs. integrated PET/MRI (4.3±0.8 vs. 4.1±1.1), but did not reach significance (p < 0.17).
Conclusion: This is the first study comparing the clinical impact of integrated PET/MRI and MRI with MRS. MRI with MRS was more sensitive and reached a higher diagnostic confidence than integrated PET/MRI, even though it was not significant.

B-0611 14:32

Micro-fractionated brain cancer high-dose radiosurgery observed using 3D x-ray phase contrast CT

G.E. Barbone[1], P. Romanelli[2], G. Battaglia[3], A. Mittone[4], M.F. Reiser[5], S. Auweter[5], T. Gaaß[5], A. Bravin[4], P. Coan[5]; [1]*Garching/DE*, [2]*Milan/IT*, [3]*Pozzilli/IT*, [4]*Grenoble/FR*, [5]*Munich/DE*
(Giacomo.Barbone@physik.uni-muenchen.de)

Purpose: Current limitations in brain imaging, especially the lack of tissue discrimination at the cellular level, lead to the inability to detect microscopic spread of cancerous tissue and to verify the survival of cancer cells following surgical resection, chemo- or radio-therapy. We used high sensitivity of x-rays Phase Contrast micro-computed tomography (PCI-CT) to non-invasively study the effects of a novel spatially fractionated single-stage high-dose radiotherapy technique, Microbeam Radiation Therapy (MRT), administered in-vivo to both healthy and cancerous rat brains.
Methods and Materials: 9 Fisher rats implanted with 9L gliosarcoma were treated with MRT (75 microns-thick micro-beams reaching up to 600Gy peak doses) and then imaged by PCI-CT (with 32 keV x-rays and an imaging CCD camera with voxel size of 8^3 micron³).
Results: PCI-CT allows recognition and differentiation of brain anatomical details down to cellular level, and identification of single cancerous cells, microscopic cancerous cell-clusters far from the main lesion, tissue necrosis, neuronal degeneration, tumour oedema, high-density calcifications as well as micrometric MRT-transections. Furthermore, the technique permits the segmentation of full brain vessel networks down to blood micro-capillaries.
Conclusion: The ability of PCI-CT to replicate the accuracy of histology and to provide far more anatomical detail than MRI opens a fascinating novel avenue for brain imaging. This technique appears to be well suited for post-mortem studies of brain cancer dissemination and radiotherapy effects. In the future, PCI-CT may provide image-guidance during radiotherapy, e.g. by directing focused x-ray irradiation in the ablation of inlets of cancerous cells.

B-0612 14:40

Assessment of intracranial meningioma-associated calcifications using susceptibility-weighted magnetic resonance imaging

L.C. Adams, S.M. Böker, Y.Y. Bender, E. Fallenberg, M. Wagner, R. Buchert, B. Hamm, M. Makowski; *Berlin/DE (lisa.adams@charite.de)*

Purpose: To determine the diagnostic performance of susceptibility-weighted magnetic resonance imaging (SW-MRI) for the detection of intracranial meningioma-associated calcifications compared to standard MR sequences, using computed tomography (CT) as a standard of reference.
Methods and Materials: MRI scans of 354 patients, who received a clinical brain MR with SW-MRI sequences between January 2014 and July 2016, were retrospectively evaluated and 316 patients were included. 50 patients had positive findings for intracranial meningioma-associated calcifications on CT scans. Calcification diameter was used to assess correlation between imaging modalities. Sensitivity and specificity as well as intra- and interobserver reliability were calculated for SW-MRI and standard MRI sequences.
Results: SW-MRI reached a sensitivity of 94% (95% CI: 83-99%) and a specificity of 95% (95% CI: 92-98%) for the detection of meningioma-associated calcifications, while standard MR yielded a sensitivity of 64% (95% CI: 49-77%) and a specificity of 94% (95% CI: 90-96%). Diameter measurements between SW-MRI and CT showed a close correlation (R^2= 0.993, p<0.001) with a slight overestimation of size, which, however, did not reach significance level (SW-MRI: 8.2 mm ± 7.2; CT: 6.8 mm ± 6.4, p>0.05). Interobserver-agreement for size measurements of calcifications was high on SW-MRI (κ = 0.85, p < 0.0001) and fair on standard MRI (κ = 0.29, p < 0.001).
Conclusion: The combination of SW magnitude and phase images enables an accurate detection of intracranial meningioma-associated calcifications, using CT as standard of reference, and offers a higher sensitivity and specificity than standard MRI sequences.
Author Disclosures:
B. Hamm: Grant Recipient; Grant money from more than 100 companies or nonprofit organizations to the Department of Radiology. **M. Makowski:** Grant Recipient; Financial support from the Deutsche Forschungsgemeinschaft.

B-0613 14:48

The role of diffusion-weighted imaging for radiological identification of molecular subgroups of medulloblastoma in children

L. Filograna, A. Mastronuzzi, E. Miele, C. Carducci, A. Cacchione, A. Napolitano, A. Carai, E. Ferretti, G.S. Colafati; *Rome/IT (chi.carducci@gmail.com)*

Purpose: Recent studies on genomic characterisation of medulloblastoma (MB) prompted the development of new classification combining histopathological and molecular approach.The identified subgroups have shown potential for improved risk stratification. The aim is to verify if DWI and ADC maps are able to predict new subgroups of MB.
Methods and Materials: Twenty-six patients with diagnosis of MB, with pretreatment MR imaging, histologic, genomic characterisation after surgery, were retrospectively selected. ADC maps were coregistered with T1w post-contrast and FLAIR images. ROIs were double-blindly selected (ADC): restricted, intermediate, not restricted areas and (post-contrast) absent, inhomogeneous, homogeneous areas. Standard t test was performed to evaluate differences among paired MB subgroups.
Results: No statistical significance was detected. A trend in differences was found for both restricted ADC values between WNT and group 3 (0.61+/- 0.36 vs 1.29+/- 0.10) and ADC values in areas of homogeneous contrast enhancement (0.44 +/- 0.26 vs 1.13 +/- 0.15). Mean values along with standard deviations: for areas of restricted ADC (WNT: 0.67+/- 0.03; SHH: 0.72 +/- 0.06; group 3: 0.81+/- 0.14; group 4: 0.74 +/- 0.11).
Conclusion: The study shows no statistically significant correlation between ADC values and T1 post-contrast between and within different MB subgroups. However, a trend was identified in restricted ADC value and ADC in areas of homogeneous contrast enhancement between WNT and group 3. The study demonstrates that it is not possible to predict the type of medulloblastoma based on ADC/contrast enhancement characteristics. A larger cohort of patients is needed to clarify their real potential to discriminate molecular MB subgroup before surgery as suggested by observed trend.

B-0614 14:56

Residual tumour identification with intra-operative CEUS during glioblastoma resection

F. Prada[1], M. Del Bene[1], A. Martegani[2], L. Aiani[2], L.M. Sconfienza[3], G. Mauri[3], L. Solbiati[4], B. Pollo[1], F. DiMeco[1]; [1]*Milan/IT*, [2]*Como/IT*, [3]*San Donato/IT*, [4]*Rozzano/IT (io@lucasconfienza.it)*

Purpose: Our purpose was to assess contrast-enhanced ultrasound (CEUS) capability to identify residual tumour mass during glioblastoma (GBM) surgery, in order to increase the extent of resection.
Methods and Materials: We prospectively evaluated 10 patients who underwent surgery for GBM removal with navigated ultrasound guidance. Navigated B-mode and CEUS were performed prior to resection, during resection and after complete tumour resection. Areas suspected for residual tumours on B-mode and CEUS were localised within the surgical field with navigated ultrasound and sent separately for histopathological analysis to confirm tumour presence.
Results: In all cases tumour remnants were visualised as hyperechoic areas on B-mode, highlighted as CEUS positive areas and confirmed as tumoural areas on hystopathological analysis. In 1 case only CEUS partially failed to demonstrate residual tumour because the residual hyperehoic area was devascularised prior to ultrasound contrast agent injection. In all cases CEUS enhanced B-mode findings.
Conclusion: As already shown in other neoplastic lesions in other organs CEUS is extremely specific in the identification of residual tumour. CEUS distinction between tumour and artefacts/normal brain on B-mode is based on its capability to show the vascularisation degree and not the echogenicity of the tissues. Therefore, CEUS can play a decisive role in the process of maximising GBM surgical resection.

B-0615 15:04

Texture analysis on diffusion-tensor imaging: discriminating glioblastomas from single brain metastasis

K. Skogen[1], A. Schulz[1], E. Helseth[1], J.B. Dormagen[1], B. Ganeshan[2], A. Server[1]; [1]*Oslo/NO*, [2]*London/UK (kaskog@ous-hf.no)*

Purpose: Texture analysis has been used to stage, differentiate and predict prognosis in many oncologic tumours. It has been used on CT, MRI and PET. The purpose of this study was to determine the diagnostic accuracy of discriminating glioblastoma (GBM) from single brain metastasis (MET) by assessing the heterogeneity of both the solid tumour and the peritumoural oedema with MRI texture analysis (MRTA).
Methods and Materials: Preoperative MRI examinations done on a 3T scanner of 44 patients were included, 23 GBM and 21 MET. MRTA was performed on the DTI in a representative ROI. The MRTA was assessed using a commercially available research software program (TexRAD) which applies a

filtration histogram technique for characterising tumour and peritumoural heterogeneity. The filtration step selectively filters and extracts texture features at different anatomical scales varying from 2mm (fine) to 6mm (coarse). Heterogeneity quantification was obtained by the statistical parameter entropy. A threshold value to differentiate GBM from MET with sensitivity and specificity was calculated by receiver operating characteristics (ROC) analysis.
Results: Quantifying the heterogeneity of the solid part of the tumour showed no significant difference between GBM and MET. However the heterogeneity of the GBMs peritumoural oedema was significantly higher than the oedema surrounding MET, differentiating them with a sensitivity of 90% and specificity of 80%.
Conclusion: Assessing the peritumoural heterogeneity can increase the radiological diagnostic accuracy when discriminating GBM and MET. This will facilitate the medical staging and optimise the planning for surgical resection of the tumour and postoperative management.
Author Disclosures:
K. Skogen: Shareholder; Yes. Speaker; Yes. **B. Ganeshan:** Shareholder; Yes.

B-0616 15:12

Progressive disease in glioblastoma: benefits and limitations of semi-automated volumetry

T. Huber, G. Alber, S. Bette, J. Kaesmacher, J. Gempt, B. Meyer, C. Zimmer, B. Wiestler, J.S. Kirschke; *Munich/DE (thomas.huber@med.uni-muenchen.de)*

Purpose: Definite detection of glioblastoma (GB) progression in follow-up MRIs is essential, both for clinical trials and everyday clinical routine. 3D-volumetry provides quantification of tumour extent, and might therefore facilitate unbiased disease assessment. Aim of the present study was to evaluate the utility of absolute changes in volume (delta) or regional, segmentation-based subtractions for detecting disease progression in longitudinal MRI follow-ups.
Methods and Materials: 165 high-resolution, 3-Tesla MRIs of 30 GB patients (23m, mean age 60y) were retrospectively included. Contrast enhancement (CV) and tumour-associated signal alterations in FLAIR images (FV) were semi-automatically segmented. Delta volumes (dCV, dFV) as well as regional subtractions (sCV, sFV) were assessed. For every follow-up, disease progression was classified according to the histopathologic results of resected specimen, decisions of the local multidisciplinary CNS tumour board and a consensus rating of the radiologic report.
Results: A generalized logistic mixed model for disease progression (yes/no) and the input variables dCV, dFV, sCV and sFV showed that only dCV was significantly associated with prediction of disease progression (P = .005). Delta volumes had a better accuracy than regional, segmentation-based subtractions (79 % versus 72 %) and a higher area under the curve in ROC analysis (.83 vs .75).
Conclusion: Absolute volume changes of the contrast enhancing tumour part were the most accurate volumetric determinant to detect progressive disease in GB follow-ups and outweighed FLAIR changes as well as regional image subtractions. This volumetric parameter might be valuable in upcoming objective response criteria for glioblastoma
Author Disclosures:
T. Huber: Consultant; Brainlab AG until 09/2016 (Feldkirchen, Germany) - not related to the present study. **S. Bette:** Consultant; Brainlab AG (Feldkirchen, Germany) - not related to the present study. **J. Gempt:** Consultant; Brainlab AG (Feldkirchen, Germany) - not related to the present study. **B. Meyer:** Consultant; Brainlab AG (Feldkirchen, Germany) - not related to the present study. **C. Zimmer:** Advisory Board; Philips, Bayer Schering, Clinical Neuroradiology - not related to the present study. Research/Grant Support; Biogen Idec, Quintiles, MSD Sharp & Dome, Boehringer Ingelheim, Inventive Health Clinical UK Ltd., Advance Cor, Brainsgate, Pfizer, Bayer-Schering, Novartis, Roche, Servier, Penumbra,, WCT GmbH, Syngis, SSS Internartional Clinical Research, PPD Germany GmbH, Worldwide Clinical Trials Ltd., Phenox, Covidien, Actelion, Medivation, Medtronic, Harrison Clinical Research, Concentric,, Pharmtrace, Reverse Medical Corp., Premier Research Germany Ltd., Surpass Medical Ltd. and GlaxoSmithKline - not related to the present study.. Speaker; Philips, Bayer Schering - not related to the present study.

B-0617 15:20

Quantitative analysis of brain tumours perfusion with contrast-enhanced ultrasound

F. Prada[1], C. Richetta[1], M. Del Bene[1], L.M. Sconfienza[2], G. Mauri[2], L. Solbiati[3], F. DiMeco[1]; [1]*Milan/IT*, [2]*San Donato/IT*, [3]*Rozzano/IT (io@lucasconfienza.it)*

Purpose: Neuroimaging plays an essential role in brain tumours resection which is a major prognostic factor in order to increase the survival rate. Contrast enhanced ultrasound (CEUS) using intravascular contrast media enhances image quality and allows visualization of tumour's perfusion. Perfusion quantification is one of the newest application of CEUS and it may give a clue about tumour's biological features and vascularisation. Even though this technique is already well established in other fields, it has never been applied to Neurosurgery before. The aim of the study is to evaluate quantitatively different histological types of brain tumours in order to detect specific perfusion patterns which may correlate with molecular parameters and with antiangiogenetic treatment response.
Methods and Materials: We evaluated 102 DICOM clips recorded during brain tumour excision with the perfusion quantification software Vuebox©.
Results: Only 27 video clips were amenable for quantitative analysis. However we found that some parameters, particularly PE, mTTI and FT, seem to be related with tumour's grade and histology.
Conclusion: The use of Vuebox© underlined some conditions which may increase data variability or make the images inadequate for the quantitative evaluation. This allowed us to define a precise protocol for video clip acquisition which should make data loss less likely. Thanks to quantitative analysis we detected some differences in perfusion patterns between tumours with different histology.

14:00 - 15:30 **Room F1**

Oncologic Imaging

SS 716

Imaging nervous system and musculoskeletal tumours

Moderators:
F.A. Gallagher; Cambridge/UK
B.M. Schaarschmidt; Düsseldorf/DE

B-0618 14:00

Radiomics reveals prognostic information from baseline MRI in patients with glioblastoma

M. Ingrisch[1], M.J. Schneider[1], D. Nörenberg[1], G. Negrao de Figueiredo[1], K. Maier-Hein[2], B. Suchorska[1], M.F. Reiser[1], J.C. Tonn[1], B. Ertl-Wagner[1]; [1]*Munich/DE*, [2]*Heidelberg/DE (dominik.noerenberg@med.lmu.de)*

Purpose: Radiomics has recently gained much attention as a tool that promises to extract the maximal amount of information from standard-of-care images. The present study investigates whether a radiomics analysis can predict overall survival from T1-weighted contrast-enhanced baseline MR images in a uniformly treated cohort of glioblastoma patients.
Methods and Materials: This retrospective study was approved by the institutional review board and informed consent was waived. MR images from 66 patients with newly diagnosed GBM from a previous prospective study were analyzed. Tumour segmentation was performed manually on contrast-enhanced 3D T1-weighted images. Using these segmentations, n=100 quantitative image features characterizing tumour shape, signal intensity and texture were calculated by automated high-throughput analysis and prognostic models based on random survival forests were trained on the data. For each patient, mortality was predicted using leave-one-out cross validation and average prediction error was recorded. Association of predicted mortalities with overall survival was assessed using Kaplan-Meier analysis and univariate proportional hazard models.
Results: The final prognostic model predicted a median mortality of 32.3% (range 7.1% - 61%) with a prediction error of 34.5%. Kaplan-Mayer analysis clearly distinguished two patient groups with high and low predicted mortalities (p=8.0e-4). Low predicted mortality was found to be a favorable prognostic factor for overall survival in a univariate Cox proportional hazard model (p=1.7e-04).
Conclusion: Baseline MR imaging in GBM patients contains strong prognostic information, which become accessible by radiomics analysis using random survival forests.
Author Disclosures:
J.C. Tonn: Research/Grant Support; received honoraria and travel grants from BrainLab and Siemens.

B-0619 14:08

Cerebrovascular events in glioblastome multiforme patients

T. Auer, M. Renovanz, F. Marini, M.A. Brockmann, Y. Tanyildizi; *Mainz/DE (y.tanyildizi@gmx.net)*

Purpose: Bevacizumab (BVZ) is a monoclonal antibody directed against vascular endothelial growth factor (VEGF) and has been suspected to increase the incident of ischemic stroke (IS) and intracranial hemorrhage (ICH) in GBM patients.
Methods and Materials: In this study 364 MRI of 82 GBM patients were eligible for analyses. All patients were treated with basic treatment. Out of the 82 patients, 40 were treated with BVZ in addition to basic treatment. (BVZ-group) The cohorts matched in age and gender. Vascular risk factors were analyzed retrospectively. The KPS was captured at the beginning and end of

the observation, and before and after the event. Chi-square test was used to evaluate the level of significance.
Results: In seven (8 % / 7/82) out of 82 patients a vascular pathology was detected with MRI. 4 (4.8 % / 4/82) of them revealed an IS, while ICH was detected in 3 (3.6 % / 3/82). 4 of them had been treated with BVZ- with a total of 3 IS (7.5% 3/40), and 1 ICH (2.5% / 1/40). Three of them were part of the control-group, with a total of 1 IS (2.3% / 1/42) and 2 ICH (4.7% / 2/42).
Conclusion: The incidence of vascular events did not differ significantly between patients receiving BVZ and the control group. Thus, BVZ treatment does not seem to be associated with an elevated risk for vascular events in GBM patients.

B-0620 14:16

1H magnetic resonance spectroscopy of supratentorial WHO grade II gliomas

A. Hebda, B. Bobek-Billewicz, G. Stasik-Pres, P. Wawrzyniak; *Gliwice/PL (ahebda@io.gliwice.pl)*

Purpose: Comparison of supratentorial WHO grade II gliomas spectroscopic image.
Methods and Materials: Group of 45 patients with supratentorial WHO grade II gliomas: 26/45 (58%) Astrocytoma fibrillare, 10/45 (22%) Astrocytoma fibrillare partim gemistocyticum, 9/45 (20%) Oligodendroglioma. All patient had their 1HMRS study in Cancer Center Gliwice before surgery. Studies were performed on 1.5 T or 3T scanners. Single voxel PRESS method was used with long (135 ms), and also in 43 patients short (30 ms) echo time (TE). Reference spectra were obtained from healthy tissue of contralateral hemisphere (ref). Spectra were analyzed with LCModel. Following metabolite ratios were calculated for TE135ms: Cho/Cr, NAA/Cr, Cho/NAA, Gly/Cr in lesion and reference and Cho lesion/ Cho ref, NAA lesion/NAA ref and Gly lesion/Gly ref. In TE30ms: mI/Cr, Glx/Cr in lesion and reference and mI lesion/mI ref, Glx lesion/Glx ref. Metabolite integrals between lesion and healthy tissues were compared with statistical methods using STATISTICA 10 software.
Results: Maximal and minimal values in groups: Astrocytoma fibrillare: Cho/Cr 1.17-3.96, NAA/Cr 0.31-2.19, Cho/NAA 0.69-6.21, Gly/Cr 0.04-0.72, mI/Cr 0.19-1.36, Glx/Cr 0.03-5.13, mIlesion/ mIref 0.55-3.09, Glxlesion/Glxref 0.01-2.00, Cholesion /Choref 0,27-3,60, NAAlesion/NAAref 0,06-0,69. Astrocytoma fibrillare partim gemistocyticum: Cho/Cr 1.09-6.40, NAA/Cr 0.50-1.33, Cho/NAA 1.40-5.07, Gly/Cr 0.21-0.98, mI/Cr 0.37-0.92, Glx/Cr 0.29-4.16, mIlesion/mIref 0.70-1.95, Glxlesion/Glxref 0.27-2.00, Cholesion/Choref 0.87-2.80, NAAlesion/NAAref 0.01-0.40.
Oligodendroglioma: Cho/Cr 1.01-7.23, NAA/Cr 0.50-1.54, Cho/NAA 0.68-4.07, Gly/Cr 0.50-1.11, mI/Cr 0.35-0.74, Glx/Cr 0.81-3.35, mIlesion/mIref 0.88-2.34, Glxlesion/Glxref 0.29-1.10, Cholesion /Choref 0.93-5.08, NAAlesion /NAAref 0.30-0.68.
Conclusion: No significant differences in 1HMRS were found between groups: Astrocytoma fibrillare, Astrocytoma fibrillare partim gemistocyticum and Oligodendroglioma.

B-0621 14:24

Multiparametric MRI assessment of glioblastoma for predicting patient survival

A. Gimeno[1], G. Blasco[1], P. Daunis-i-Estadella[1], C. Biarnés[1], J. Sanchez-Gonzalez[2], A. Alberich-Bayarri[3], M. Puigdemont[1], S. Pedraza[1], J. Puig[1]; [1]*Girona/ES*, [2]*Madrid/ES*, [3]*Valencia/ES (fredigimeno1989@gmail.com)*

Purpose: MRI biomarkers role in prognosis of newly diagnosed glioblastoma remains unclear. We retrospectively determined the usefulness of dynamic susceptibility contrast (DSC), permeability maps, diffusion parameters, extensive battery of qualitative findings for contrast-enhancing lesion (CEL) and surrounding non-CEL in predicting survival.
Methods and Materials: Before treatment, 72 consecutive patients (45 men; mean age, 64 years) with histologically proven glioblastoma underwent 1.5T MRI (anatomical, first-pass DSC, DWI and post-contrast T1-weighted sequences). Perfusion maps were computed with the Bayesian approach. Volumes of interest for cerebral blood (CB) volume ratio, CB flow ratio, mean transit time (MTT), time-to-peak, delay time (DT), permeability constant (k_2), and apparent diffusion coefficient (ADC) in CEL, non-CEL, and contralateral tissue using Olea Sphere V.3.0 software (Olea Medical, La Ciotat, France) we determined. We evaluated 26 VASARI descriptors. Patients were classified by survival:<1year and >1year. Surgery, radiotherapy and chemotherapy was considered complete treatment.
Results: Forty-nine patients (68%) survived<1year. Thirty-nine (54.16%) underwent complete treatment. Survival groups differed in age (62.21±12.53 vs 50.63±15.1years;P<0.001), ADC-CEL (0.98±0.97 vs 0.78±0.05mm^2/s;P=0.032), delay-CEL (-0.41±0.82 vs 0.07±0.54sec; P=0.043), DT-nonCEL (-0.26±0.58 vs 0.18±0.47sec;P=0.01) and treatment (P<0.001), for <1 and >1year survival, respectively. In univariate analysis, complete treatment best predicted survival at 1 year (AUC=0.774, 60.6% sensitivity, 94.3% specificity, 95.6% positive predictive value, 54.1% negative predictive value). However, DT-CEL and age yielded the best combined prediction of survival (AUC=0.859, 86.7% sensitivity, 73.3% specificity, 86.7% positive predictive value, 73.3% negative predictive value).
Conclusion: Beyond well-known survival factors, our data suggests perfusion parameter DT might help predict survival in newly diagnosed glioblastoma.

B-0622 14:32

Evaluation of deep brain large metastasis after hypofractioning stereotactic radiotherapy

A.V. Smirnova, O. Lukina, N. Plakhotina, P. Ivanov, A. Kuzmin, I. Zubatkina; *St. Petersburg/RU (smirnova_alina@bk.ru)*

Purpose: To asses by MRI the dynamic changes of deep brain large metastases after hypofractionation stereotactic radiation therapy.
Methods and Materials: In retrospective analysis, 146 patients (mean age 55 y.o.) with 215 brain metastases, treated by hypofractioning radiotherapy were included (dose 8-10 Gy, mean metastasis volume 1.5 cm^3). 1.5 and 3.0T scanners were used with T13D sequences 1mm before and after contrast enhancing, T2 WI tra 2mm, flair tra 1-3mm, T2 WI cor 2mm, DWI. In 21 patients SWI was added. Tumour volume control was performed by GammaPlan 10.1 station. Patients were assessed before treatment, after 1 month, then, every 3 months.
Results: We have detected 6 radiologic patterns: tumour dimensions changes (68%), structural necrosis (28%), metastasis contrasting decreasing (64%), contour changes (83%), perifocal swelling area reduction (97%), intratumour haemorrhage (14%). The most variable were dimensions and volume changes: volume reduction or stabilisation, volume increasing by necrosis or disease progression, volume increasing on 1st control, then decreasing on 2nd control (necrosis), then increasing by haemorrhage.
Conclusion: Brain metastases reaction after radiotherapy characterised by heterogeneity. Imaging results (volume and contour changes, haemorrhage) are non-specific and may be signs of local disease progression or postradiation reactions. To clarify these findings, well-designed prospective multi-centre clinical trials are needed in future.

B-0623 14:40

Image-based response evaluation of intracranial lesions after cyberknife robotic radiosurgery: a radiological review

S. Kadri, N. Ahmed, K. Saeed, T. Mahmood; *Karachi/PK (shaziaum_wk@yahoo.com)*

Purpose: To study the radiological response of Cyber Knife Robotic Radiosurgery for treating intracranial tumours by tailored MRI sequences in providing maximum details.
Methods and Materials: 653 patients from Dec. 2012 to 2015 were selected with tumour less than 6 cm size, post-operative residual/recurrent tumour and surgically unresectable tumour. Follow-up MRI with 3D T1 contrast done every three monthly with added sequences according to need.
Results: Out of 653 patients, 35% of benign tumours showed reduction in size and 63% remain stable and 2% were resolved radiologically with clinical improvement in 80% whereas 47% of malignant tumours were reduced, 31% remain stable and 22% showed progression but 70% of patients showed clinical improvement. Considering meningiomas, 33% reduced, 65% stable and 2% resolved. In AVM, 82% reduced,13% remained stable and 5% were resolved. In gliomas, 64% low-grade gliomas and 58% high-grade gliomas were reduced with clinical improvement of 86% and 73%, respectively. Acoustic neuromas were 20% reduced and 80% stable. Metastasis were 83% reduced with 85% clinical improvement. Pituitary adenomas, 52% were reduced and 76% clinically improved and craniopharyngioma 53% were reduced and 88% were clinically improved.
Conclusion: Cyberknife is highly effective in controlling benign tumours and a good palliative modality for recurrent malignant and metastatic brain tumours. T1 3D contrast is the sequence of choice for most of the intra-cranial lesions after treatment follow-up, while in some cases, we utilized BTFE for cranial nerve definition. Longer follow-up is mandatory.

B-0624 14:48

Brain gliomas recurrence imaging after chemoradiation therapy

A.V. Smirnova[1], O. Lukina[1], N. Plakhotina[1], I. Lobanov[2], A. Kuzmin[1], A. Tkachev[3]; [1]*St. Petersburg/RU*, [2]*Nizhny Novgorod/RU*, [3]*Volgograd/RU (smirnova_alina@bk.ru)*

Purpose: To assess gliomas reaction after different types of radiation therapy.
Methods and Materials: In prospective trial 101 patients with brain gliomas were included. Patients were stratified into 2 groups: group A with grade I-II (n=58), group B with grade III-IV (n=43). 1.5 and 3.0T scanners were used with T13D sequences before and after contrast enhancing, T2 WI tra 2mm, flair tra 1-3mm, T2 WI cor 2mm, DWI. Tumour volume control was performed by GammaPlan 10.1 station. First assessment was before treatment, then after 1 month, next - every 3 months. For disease progression evaluation, stereotactic brain biopsy, PET-CT and CT-perfusion were used.

Results: We have detected 4 postradiation patterns: tumour dimension changes (reduction in 23% in group A and 9% in group B, stabilisation in 46 and 18%, respectively, increasing and then decreasing due to necrosis or haemorrhage - 15 and 7%, respectively, disease progression - 16 and 66%, respectively), contrasting decreasing (17% in group A and 8% in group B), contour changes (54 and 82%, respectively), intratumour haemorrhage (5% in group A and 12% in group B).
Conclusion: Postradiation reaction in patients after gliomas radiotherapy characterised by heterogeneity. Grade III-IV is the serious prognostic risk factor for disease recurrence. MRI-based only disease assessment potentially may be nonspecific and the complex diagnostic tools (included PET-CT and brain biopsy) should be used.

B-0625 14:56

MRI evaluation of sacral chordoma treated with carbon ion hadron therapy

D. Stoppa, S. Camisa, L. Preda, G. Viselner, G. Fontana, M. Fiore, P. Fossati, E. Ciurlia, R. Orecchia; *Pavia/IT (dvdstoppa@gmail.com)*

Purpose: To compare Response Evaluation Criteria in Solid Tumours (RECIST 1.1) to volume modifications, in order to evaluate the response in patients with sacral chordoma, not suitable for surgery, treated with carbon ions radiotherapy (CIRT) alone. Secondarily, to detect if baseline ADC values could predict response to treatment.
Methods and Materials: 39 patients were retrospectively studied, considering baseline (03/2013 - 04/2016) and follow-up multiparametric MR exams (mean follow-up 18 months, range 3-37), for a total of 195 examinations. The exams were performed with a 3T MR scanner (Siemens Magnetom Verio). For each exam, lesion maximum diameter and volume were obtained from T2w axial images. Lesion segmentations were consequently aligned to the ADC maps calculated from DWI sequences. The baseline ADC values within the lesion volume were analyzed.
Results: Considering maximum diameter changes between baseline MRIs and the last available follow-ups, according to RECIST 1.1, patients were classified: Partial Response (PR) 0%, Stable Disease (SD) 89.7% and Progressive Disease (PD) 10.3%. Considering lesion volume changes, applying the same response criteria, PR were 53.8%, SD 35.9% and PD 10.3%. The assessment of baseline examinations ADC maps, using Wilcoxon test, demonstrated significantly higher median ADC values of PD vs both PR and SD (p=0.0306 and p=0.0143 respectively).
Conclusion: Our study demonstrates that lesion volume measurement may be more accurate than maximum diameter to better stratify the response of sacral chordoma treated with CIRT. Preliminary results suggest that baseline ADC values could be predictive of response to CIRT, particularly to detect potential non responders.

B-0626 15:04

Does elevated glucose metabolism correlate with higher cell density in neurofibroma?

D. Berzaczy, T. Traub-Weidinger, M. Mayerhoefer; *Vienna/AT (dominik.berzaczy@meduniwien.ac.at)*

Purpose: To investigate wether elevated glucose metabolism in neurofibroma determined by [18F]-FDG-PET is correlated with cell density in MRI as expressed through the apparent diffusion coefficient.
Methods and Materials: Maximum and mean standardised uptake values (SUVmax, SUVmean) on [18F]-FDG-PET/CT and [18F]-FDG-PET/MR were compared, and correlated with minimum and mean apparent diffusion coefficients (ADCmin, ADCmean).
Results: 12 (6 male/6 female, mean age was 16,2 ± 5,2 years) patients were prospectively included and analysed on a per-lesion (n=39) basis. The SUVmean of examined neurofibroma loci showed a moderate negative correlation of the ADC mean (r:-.441) and ADCmin (r:-.477), which both proved to be statistically significant (p=.005 and p=.002); the SUVmax of respective lesions however, showed a weaker negative correlation for ADCmean (r: -.311) and ADCmin (r: -.300) and did not reach statistical significance (p=.054 and p=.057).
Conclusion: Our data suggest that the ADCmean and min could possibly supersede the SUVmean as a potential determinant of malignant transformation in neurofibromatosis 1.

B-0627 15:12

3D texture analysis distinguishes low-grade chondrosarcoma from enchondroma

C.S. Lisson[1], C.G. Lisson[1], R. Mayer-Steinacker[1], T.F.E. Barth[1], A. von Baer[1], M. Schultheiss[1], M. Baumhauer[2], M. Beer[1], S.A. Schmidt[1]; [1]*Ulm/DE*, [2]*Heidelberg/DE (catharinavonend@gmail.com)*

Purpose: Differentiation of low-grade chondrosarcoma from enchondroma is both a radiologic and histologic challenge. Benign lesions do not require surgery, whereas curative surgical resection is mandatory in treatment for chondrosarcoma. Texture analysis is a promising tool in oncologic imaging. This study evaluates the performance and accuracy of MRI-based 3D texture analysis for the discrimination of G1-chondrosarcoma from enchondroma.
Methods and Materials: 22 patients were retrospectively evaluated: 11 patients with chondrosarcoma confirmed by histopathological diagnosis; 11 patients with enchondroma confirmed by histopathology or with a follow-up greater 5 years without changes in radiological features. Texture analysis was performed using the commercially available software mint Lesion by Mint Medical, a spinoff from the German Cancer Research Center (DKFZ). It allows 2D-and volumetric measurements and multiparametric texture analysis. Mann-Whitney U test and ROC-analysis were performed to identify the most discriminative texture features (kurtosis, entropy, skewness, MPP, uniformity), and by Youden's index optimal cut-off-values were selected.
Results: Significant differences were found in 6 out of 20 texture parameters ($p<0.05$). The area-under-the-ROC-curve for this 6 parameters to discriminate chondrosarcoma from enchondroma were 0.876 and 0.826 for kurtosis and skewness in ceT1-fs, respectively; in non-contrast T1 the values were 0.851, 0.793 and 0.822 for entropy, MPP and uniformity, respectively; in STIR it was 0.802 for MPP. Highest discriminatory power had kurtosis in ceT1-fs with an optimal cut-off ≥3.15 (82% sensitivity, 91% specificity, accuracy 86%).
Conclusion: MRI-based 3D texture analysis has the potential to distinguish low-grade chondrosarcoma from enchondroma by kurtosis in ceT1-fs having the highest power of discrimination.
Author Disclosures:
M. Baumhauer: CEO; Mint Medical GmbH.

B-0628 15:20

Ewing's sarcoma: comparative diagnostic merits of different MRI pulse sequences

M.M. Saleh, T.A. Raafat, Y.M. Said, M.K.A. Asran, N.M. Abdel Wahab; *Cairo/EG (Mahmoud.m.ali@interns.kasralainy.edu.eg)*

Purpose: The aim of the study is to investigate the role of MRI using conventional and DWI sequences in initial evaluation and follow-up of pathologically proven cases of Ewing's sarcoma family of tumours.
Methods and Materials: Our study included 35 patients with pathologically proven Ewing's sarcoma family of tumours. We recorded the conventional and diffusion-weighted MR features of the examined lesions at initial presentation and after neo-adjuvant treatment including tumour location, size, signal characteristics, enhancement and breaking down. The diffusion images with ADC of the minimum and mean values were obtained.
Results: This study included (35) patients, their ages ranges from 2 to 41 years (mean age 17.2 years). Intermediate signal intensity on T1WI was noted in 77.1% of Ewing's sarcoma cases while high signal intensity on T2WI was noted in 62.9%. Our cases showed homogeneous contrast pattern and avid intensity contrast uptake in 45.7% and 74.3% respectively. Intra-tumoural breaking down was noted in 25.7% of the patients at initial assessment as compared to 65.7 % in patient post neo-adjuvant therapy with statistically significant P=0.005. The initial mean ADC of the Ewing's sarcoma family of tumours ($0.68x10^{-3}$ mm²/sec) was significantly different from that after neo-adjuvant treatment ($1.60x10^{-3}$ mm²/sec) with mean difference (-0.9125) and P<0.001.
Conclusion: MR imaging is the method of choice in the initial evaluation and follow-up of Ewing's sarcoma family of tumours. Diffusion-weighted MR imaging has the potential of being an additional non-invasive tool offering means for a more detailed analysis of these lesions and assessment of their therapeutic response.

14:00 - 15:30 **Room F2**

Breast

SS 702b

Breast MRI

Moderators:
C.S. Balleyguier; Villejuif/FR
V. Dominelli; Milan/IT

B-0629 14:00

A survey by the European Society of Breast Imaging on the utilisation of breast MRI: technical notes

P.A.T. Baltzer[1], P. Clauser[1], R. Mann[2], A. Athanasiou[3], K. Pinker[1], T.H. Helbich[1], F. Sardanelli[4], G. Forrai[5], H. Prosch[1]; [1]*Vienna/AT*, [2]*Nijmegen/NL*, [3]*Athens/GR*, [4]*Milan/IT*, [5]*Budapest/HU (patbaltzer@gmail.com)*

Purpose: While breast MRI is recognised as a powerful diagnostic tool in breast cancer diagnosis, standardisation in acquisition and interpretation still remain a matter of debate. The European Society of Breast Imaging (EUSOBI) launched a survey to gather data on MRI acquisition and interpretation in clinical practice.
Methods and Materials: A survey reviewed by the board and committees of the EUSOBI was distributed to the members online using a dedicated platform (SurveyMonkey). Data were extracted and summarised. Statistical analysis was performed using SPSS.
Results: 27.4% of the EUSOBI members answered the survey. The majority were radiologists (90.5%) based in a university hospital (51.9%). The majority of responders used exclusively 1.5T (57.3%) magnets. 22.6% used exclusively 3T and 19.5% both. Other field strengths were seldom used (0.6%). The majority of participants employed a dedicated breast coil with at least 7 channels, and an automatic injector for contrast medium (78.4% and 82.3%, respectively). 3D gradient echo (GE) imaging for dynamic contrast-enhanced sequences was used by 73.2%, 2D GE by 21.1% and both alternatively by 5.7%. Fat saturation (FS) was favoured over non-fat saturated (NFS) sequences for both T1 and T2 weightings (77% used FS-T1w alone and 71.4% used FS-T2w alone or along with non-FS sequences). 40% of the responders did not acquire DWI regularly.
Conclusion: Dedicated equipment (coils, injector), 1.5T and 3D dynamic GE sequences were used by majority of the survey participants. Of note, the majority prefers FS protocols and only a large minority uses new techniques such as DWI.

B-0630 14:08

A survey by the European Society of Breast Imaging on the utilisation of breast MRI: clinical indications

P. Clauser[1], H. Prosch[1], R. Mann[2], A. Athanasiou[3], K. Pinker[1], T.H. Helbich[1], F. Sardanelli[4], G. Forrai[5], P.A.T. Baltzer[1]; [1]*Vienna/AT*, [2]*Nijmegen/NL*, [3]*Athens/GR*, [4]*Milan/IT*, [5]*Budapest/HU (clauser.p@hotmail.it)*

Purpose: Breast MRI as a highly sensitive breast imaging modality is applied to a variety of clinical indications. Although consensus recommendations have been published, institutional and national variations in the use of breast MRI are a matter of debate. The European Society of Breast Imaging (EUSOBI) launched a survey to gather data on MRI application in clinical practice.
Methods and Materials: A survey reviewed by the executive board and the committees of the EUSOBI was distributed to the members online using a dedicated software platform (SurveyMonkey). Data were extracted and summarised. Statistical analysis was performed using SPSS.
Results: 27.4% of the EUSOBI-members answered the survey. The majority were radiologists (90.5%) based in university hospitals (51.9%). The majority of responders used MRI in the preoperative setting (85.7%). Differences in subgroups that receive MRI were found: in southern countries MRI was commonly performed in all cancer patients, while in northern countries it was performed according to recommendations (P<0.003). Other common indications were: carcinoma of unknown primary (89.6%), neoadjuvant chemotherapy (NAC) (84.2%), high-risk screening and nipple discharge (83.9%). MRI was performed as problem-solving by 83.0% of the responders. Evaluation of nipple discharge was more common in southern countries (P<0.001). In eastern countries, HR screening and evaluation of response during NAC were less frequent (P<0.036). MR-guided interventions were performed by only a minority of participants (35.4%).
Conclusion: Recommendations were generally followed. MRI was frequently used for preoperative staging and problem-solving but substantial international variations were noted. The availability of MRI-guided interventions could seemingly be improved.

B-0631 14:16

Kinetic breast MRI parameters of normal parenchyma in healthy individuals and invasive ductal carcinoma patients

M. Nadrljanski, Z. Jokovic, Z. Milosevic; *Belgrade/RS (dr.m.nadrljanski@gmail.com)*

Purpose: Dynamic contrast-enhanced MRI (DCE-MRI) kinetic parameters: wash-in (WI), washout (WO), and positive enhancement integral value (PEI) - the semiquantitative kinetic parameters were obtained from normal breast parenchyma of healthy individuals and patients with invasive ductal carcinoma (IDC).
Methods and Materials: Initial DCE-MRI exams of 30 patients with confirmed IDC (n1=30) were compared to those of the paired 30 healthy individuals (n2=30). The exams were realized on 1.5T MRI system with the full diagnostic protocol (T2W-STIR, T2W-TSE, T1W-TSE, 3D T1W C+ five series) with the generated parametric maps for the semiquantitative kinetic parameters: WI, WO and PEI. The region of interest was defined in the normal breast parenchyma for both groups.
Results: The average WI and WO values for the normal parenchyma in patients with IDC were significantly different compared to those of the healthy individuals (WI: 39.43 +/- 7.89 vs 29.42 +/- 2.71, p less than 0.01 and WO: 35.10 +/- 7.58 vs 25.23 +/- 3.35, p less than 0.01). The same applies to the PEI values, where the value for the normal parenchyma in IDC patients was 101.7+/-18.72, compared to 72.02+/-9.85 in healthy individuals (p less than 0.01) - considered statistically significant.
Conclusion: DCE-MRI kinetic parameters (WI, WO and PEI) in normal breast parenchyma, may be considered associated with IDC, therefore should the results of the large studies confirm the data, these parameters may serve as the potential cancer risk markers, together with morpho-dynamic and functional imaging parameters.

B-0632 14:24

Occult nipple-areola complex (NAC) involvement in breast cancer patients: can we predict it with preoperative MRI before nipple sparing (NSM) or skin sparing (SSM) mastectomy?

C. Berzovini, F. Esposito, M. Durando, G. Mariscotti, M. Brunetti, L. Bergamasco, P. Fonio, G. Gandini; *Turin/IT (claudioberzovini@yahoo.it)*

Purpose: To identify clinically occult NAC involvement using preoperative MRI, to properly select patients with newly diagnosed breast cancer eligible for NSM; to compare MRI findings with histopathological features and intraoperative evaluation of retroareolar tissue.
Methods and Materials: Retrospective monocentric analysis of 180 patients, who underwent preoperative breast MRI between January 2010 and June 2016 before NSM/SSM. Tumour features at MRI [mass-non mass lesion, diameter, lesion-NAC distance (LND)] and pathology (diameter, histopathological type, receptor status) were recorded, as well as type of surgery (NSM/SSM) and presence (NAC+) or absence (NAC-) of tumour at intraoperative evaluation of retroareolar tissue. Mann-Whitney test, multivariate and ROC curve analysis were applied.
Results: Over the study period, 109 patients were NAC- and 71 NAC+ (61 NSM and 119 SSM performed). Among the examined imaging and histological features, only MRI LND was associated with NAC+, being LND statistically different between NAC+ and NAC- patients (p<0.001). MRI LND proved to be a good discriminant between the two groups (area under the ROC-curve 0.8): the best cutoff was determined at 12mm, with sensibility 73%, specificity 82%, odds ratio=13 (vs 86%, 48% and 5, respectively, for 20mm distance cutoff). The analysis of this subgroup showed no further features statistically associated with NAC+.
Conclusion: MRI is able to identify most NAC+ patients. LND≤12mm is associated with increased risk of NAC+; this cutoff has higher specificity than 20mm LND cutoff (p<0.0001), allowing a larger proportion of patients to be selected for NSM, even though intraoperative retroareolar tissue examination remains mandatory.

B-0633 14:32

MRI to predict nipple-areola complex (NAC) involvement: an automatic method to compute the 3D distance between the NAC and tumour

V. Giannini, S. Mazzetti, V. Doronzio, E. Tabone, F. Arabia, S. Pedalino, D. Regge, L. Martincich; *Candiolo/IT (valentina.giannini@ircc.it)*

Purpose: To describe and test an innovative and automatic method able to compute the 3D tumour-NAC distance and to assess its role in predicting NAC involvement.
Methods and Materials: 99 patients scheduled to NAC sparing mastectomy underwent MR examination at 1.5T. The method developed consists of different steps. First, the NAC and the lesion were automatically segmented on the T2w sagittal and the maximum intensity projection over time images, respectively. Then, the 3D distance was computed between the base of the NAC and the nearest margin of the lesion. 3D distance was compared with

manual 2D measurements. NAC involvement was defined by the presence of invasive ductal/lobular carcinoma and/or ductal carcinoma in situ/ductal intraepithelial neoplasia.
Results: The tumour-NAC distance was computed on a dataset of 95/99 patients (25 having NAC involvement), since 3 patients were discarded because their lesions were not segmented and one was removed because the NAC was not detected by the system. Area under the ROC curve was equal to 0.830 (95%CI: 0.749-0.911), 0.676 (95%CI: 0.557-0.796), 0.664 (95%CI: 0.542-0.786), 0.664 (95%CI: 0.542-0.783) for the automatic, manual axial, manual sagittal, minimum manual distances, respectively. The best performances were obtained by the automatic distance (cutoff=21mm) with sensitivity, specificity, positive predictive value and negative predictive value of 72%, 80%, 56% and 89%, respectively.
Conclusion: The proposed automatic method outperformed the manual 2D measurements in assessing the NAC involvement and it could provide reliable information for surgical planning and intraoperative management of candidate patients to the NAC sparing mastectomy.

B-0634 14:40

MRI evaluation of post-mastectomy irradiated breast implants: prevalence and analysis of complications

M. Telegrafo, L. Rella, A. Cirilli, V. Ranieri, A. Stabile Ianora, G. Angelelli, M. Moschetta; *Bari/IT (mikitele@hotmail.it)*

Purpose: To evaluate the effect of post-mastectomy radiation therapy (RT) on breast implants as detected by magnetic resonance imaging (MRI) searching for short-term complications.
Methods and Materials: 140 patients (total of 144 implants) were evaluated by MRI; 80 (group 1) had undergone RT, whereas the remaining 60 patients (group 2) underwent mastectomy with implant reconstruction without RT. Two radiologists evaluated MRI images searching for implant rupture signs, sub-capsular seromas, capsular contracture, soft-tissue oedema, peri-implant fluid collections. Implant ruptures were classified as severe complications; seromas and capsular contractures as moderate complications; oedema and fluid collections as mild complications. The prevalence of MRI findings in two groups was calculated and compared by unpaired t-test. Cohen's kappa statistics was used to assess interobserver agreement.
Results: 69/144 (48%) implants presented pathological findings at MRI with complication rates of 47.5 and 48.4 for groups 1 and 2, respectively. Two (5%) severe complications, 10 (26%) moderate complications, and 26 (69%) mild complications occurred in group 1 and surgical treatment was performed in 10 cases. Two (6%) severe, seven (23%) moderate and 22 (71%) mild complications occurred in group 2 and surgical treatment was performed in eight cases. No significant difference between the two groups was found ($p>0.1$). Almost perfect agreement between the two radiologists was found ($k=0.86$).
Conclusion: RT does not seem to cause a significant effect on breast implants in terms of complication rate in patients undergoing implant-based breast reconstruction. One-stage immediate implant-based breast reconstruction performed at the same time as mastectomy could be proposed.

B-0635 14:48

Multi-parametric MRI in differentiation of benign and malignant breast lesions: imaging interpretation and radiology-pathology correlation

Y.G.S.E. Shokry, R.M.K.E. Kamal, M.R.L. Louis, S.A.M.S. Salem; *Cairo/EG (youstina_youanna@yahoo.com)*

Purpose: The additive role of functional MRI (diffusion-weighted MRI and MR-spectroscopy) to dynamic contrast-enhanced MRI in characterization of breast lesions.
Methods and Materials: 35 female patients with 47 breast lesions were examined using 1.5 T MRI. Morphology and dynamic curves of the lesions were assessed. Analysis of DWI was done at b values 0, 500 and 850 s/mm² followed by quantitative analysis of ADC values. SV-MRS was done using (PRESS) technique for Choline peak measurement. Agreement between the results of each MRI modality and histopathological results was done.
Results: 47 breast lesions (pathologically proven 32/47 malignant and 15/47 benign) were analysed. The sensitivity and specificity were 87.5% and 93.3% respectively using morphology, 96.9% and 73.3% using dynamic curve pattern, 96.9% and 66.7% using DWI and 74.2% and 71.4% using MRS. The suggested ADC cut-off value was 1.063×10^{-3}mm²/s. The suggested cut-off value of Choline was 0.36 mmol/l. Combining dynamic curve with morphology increased the sensitivity and specificity to become 100% and 93.3%. Sensitivity and specificity were also increased after combining DWI with morphology to become 100% and 93.3%. Combining MRS with morphology increased the sensitivity to 90.3%, but the specificity was slightly reduced to 92.9%.
Conclusion: Post-processing and addition of DWI to dynamic contrast-enhanced MRI have improved the diagnostic performance of MRI. Addition of MRS has increased the sensitivity but slightly decreased the specificity of MRI. DWI and MRS are not recommended as standalone diagnostic modalities for breast lesions but should be interpreted in combination with morphological features and dynamic curves.

B-0636 14:56

Breast cancer radiomics in the semantic feature space: association with therapeutically relevant subtypes

P. Clauser[1], P. Kapetas[1], R. Woitek[1], M. Bernathova[1], F. Leone[2], K. Pinker[1], T.H. Helbich[1], P.A.T. Baltzer[1]; [1]*Vienna/AT*, [2]*Monza/IT (clauser.p@hotmail.it)*

Purpose: To identify semantic lesion features on breast MRI associated with therapeutically relevant breast cancer subtypes.
Methods and Materials: Prospectively collected consecutive patients with a diagnosis of invasive breast cancer undergoing multiparametric (high temporal resolution DCE, T2w, DWI) breast MRI at 3T were included in this IRB-approved observational study. Two experienced breast radiologists evaluated semantic lesion features: T2w signal intensity; size; number and type of lesions (mass, non-mass, both); presence of blooming sign; perifocal oedema; feeding vessels; most suspicious curve type (I-III). Oestrogen receptor (ER) status, HER-2neu status and MIB-1/Ki67 were assessed according to international recommendations. A multivariate, 10-fold cross-validated data mining approach was run on the semantic feature space to predict dichotomised ER, HER-2neu and MIB-1/Ki67 status.
Results: 77 patients (mean age: 56 years, range 29-85) with 77 index lesions (55 mass and 22 mass with non-mass) were included. Signal intensity on T2w TSE sequences was high in 90.9% of the lesions with a high MIB-1/Ki67 ($P=0.001$). 97.4% of lesions not presenting with perifocal oedema were ER positive ($P<0.001$). Absence of non-mass components was highly specific (92.7%) for HER-2neu negativity ($P=0.005$). The remaining semantic features did not provide incremental information to further distinguish these subtypes.
Conclusion: Semantic lesion features such as intensity on T2w sequences, perifocal oedema and lesion type were found useful for characterising therapeutically relevant subtypes of invasive breast cancer by MRI.

B-0637 15:04

The spatial relationship of malignant and benign breast lesions to the fat-gland interface in three-dimensional magnetic resonance imaging

S. Shin[1], W. Kim[2], W. Moon[1]; [1]*Seoul/KR*, [2]*Daegu/KR (dominica84@naver.com)*

Purpose: To investigate the location of malignant and benign breast lesions based on the spatial relationship of the fat-gland interface using MR imaging in women under 50 years old.
Methods and Materials: A total of 881 women (≤50 years) with 792 malignant and 165 benign lesions were included. The location of 957 lesions based on the spatial relationship of the fat-gland interface was reviewed using MR imaging with five categories (within gland; near interface, gland side; interface; near interface, fat side; and within fat). The shortest distance between lesion center and fat-gland interface was measured for quantitative analyses. We calculated percentages of breast lesions and breast volumes within 2mm and 1cm from the fat-gland interface.
Results: Most breast lesions were located in or near the interface in qualitative (89.7%) and quantitative (90.0%, 1cm within the interface) analyses. Malignant lesions were located in or near the interface in significantly higher proportions in qualitative (94.3% vs 67.3%, $P<.0001$) and quantitative (49.7% vs 34.5%, $P=.0004$, 2mm within the interface) analyses than benign lesions. The calculated percentages of breast volumes within 2mm and 1cm from the interface were 12.3% and 55.7%, respectively.
Conclusion: Most breast lesions were located in or near the fat-gland interface, with a higher proportion in malignant lesions being found in this region than benign lesions in women under 50 years old. This phenomenon may reflect a biological importance of the fat-gland interface in breast cancer development and progression.

B-0638 15:12

MRI for the assessment of malignancy in mammographic microcalcifications

B. Bennani-Baiti[1], M. Dietzel[2], P.A.T. Baltzer[1]; [1]*Vienna/AT*, [2]*Erlangen/DE (barbara.bennani-baiti@meduniwien.ac.at)*

Purpose: Assess the performance of breast MRI to diagnose breast cancer in BI-RADS 4 microcalcifications detected by mammography.
Methods and Materials: This retrospective, IRB-approved study included 248 consecutive contrast-enhanced breast MRI (1.5T, protocol in accordance with EUSOBI recommendations) performed to further diagnose BI-RADS 4 microcalcifications detected at mammography during a 3-year period. Standard of reference had to be established by histopathology. Routine consensus reading results by two radiologists were dichotomised as positive or negative

and compared with the reference standard (benign vs malignant) to calculate diagnostic parameters.
Results: There were 107 malignant and 141 benign microcalcifications. Malignancy rates were 18.3% (23/126 BI-RADS 4a), 41.7% (25/60 BI-RADS 4b) and 95% (59/62 BI-RADS 4c). There were 103 true-positive, 116 true-negative, 25 false-positive, and 4 false-negative (one invasive cancer, three DCIS; 2 BI-RADS 4c, 1 BI-RADS 4b on mammography) breast MRI findings, effecting a sensitivity, specificity, PPV, and NPV of 96.3% (95%-CI 90.7-99.0%), 82.3% (95%-CI 75.0-88.2%), 80.5% (95%-CI 72.5-87.0%) and 96.7% (95%-CI 91.7-99.1%), respectively.
Conclusion: MRI is an accurate tool to further diagnose BI-RADS 4 microcalcifications. MRI may be particularly helpful to exclude invasive cancer before surgery and may allow to obviate unnecessary biopsies in microcalcifications not highly suspicious for malignancy.

B-0639 15:20

Correlation of the radiological findings with the Baker score of capsular contracture: does it have added value?
G. Bar On, H. Maresky, V. Kent, G. Landau, I. Wiser, P. Gottlieb, S. Tal;
Zrefin/IL (galiam2004@gmail.com)

Purpose: The purpose of our research was to determine and whether there is a correlation between the clinical and the radiological findings of capsular contracture and if the MRI has added value.
Methods and Materials: Our retrospective study included 29 patients (with an age range of 39 - 55.75, average 48) who had undergone cosmetic breast augmentation or breast reconstruction surgery with silicone implants, 58 breast with clinical features of capsular contracture. The reports were performed by two breast imaging specialists and correlated with the Baker score. These assessments were made by two plastic surgeons using palpation.
Results: The clinical examination proved the following distribution of the Baker score: Baker grade I - II 39 (69.6%), Baker grade III - IV 17 (30.4%). Our findings include a change in the shape of the implant 14 (25.0%), a thickening of the fibrous capsule 0.19 (0.15-0.22) cm, enhancement of the capsule and the presence of implants rupture 30 (53.6%). The thickening of capsule was not associated with Baker grade (p=0.613). 21.4% (3/14) of patients with no enhancement, 29% (7/24) of mild to moderate enhancement, 16.7% (2/12) with severe enhancement had Baker of III-IV (p=0.741). There are no difference between enhancement and thickening of the capsule mean (SE) thickness: no enhancement 0.25 (0.017), mild to moderate enhancement 0.26 (0.022), with severe enhancement 0.26 (0.026), p=0.941.
Conclusion: There is no association between the Baker score and radiological findings. This emphasises the need of MRI imaging. It is an important objective measurement which can add value for physical examinations.

14:00 - 15:30 **Room D**

Musculoskeletal

SS 710

Cartilage and osteoarthritis

Moderators:
J. Oudeman; Amsterdam/NL
K. Verstraete; Ghent/BE

K-13 14:00

Keynote lecture
G. Guglielmi; *Andria/IT*

B-0640 14:09

Meniscus T2 relaxation time and knee joint degeneration
R. Kijowski, B. Beduhn, F. Liu; *Madison, WI/US (rkijowski@uwhealth.org)*

Purpose: To investigate changes in meniscus T2 relaxation time at various stages of knee joint degeneration.
Methods and Materials: T2 mapping was performed on the knees of 121 patients with meniscus tears who underwent subsequent knee arthroscopy. T2 of the torn and untorn portions of the meniscus with a tear and the T2 of the contralateral untorn meniscus were measured. The severity of radiographic osteoarthritis was assessed using the Kellgren-Lawrence (KL) grading scale. The severity of cartilage loss within the knee joint at arthroscopy was numerically scored. Kruskal-Wallis tests were used to compare meniscus T2 between KL0, KL1, and KL2 subjects, while Spearman correlation coefficients were used to correlate T2 of the meniscus and severity of cartilage loss in the same compartment of the knee joint.
Results: There was a significant difference (p<0.001) in meniscus T2 between KL0, KL1, and KL2 subjects in both the torn and untorn portions of the meniscus with a tear and within the untorn contralateral meniscus with KL2 subjects having highest T2 and KL0 subjects having lowest T2. There was a significant direct moderate correlation (rho=0.535, p<0.001) between meniscus T2 and severity of adjacent cartilage loss.
Conclusion: Meniscus T2 was progressively higher in individuals with worsening radiographic knee joint degeneration indicating that joint degeneration leads to changes in the composition and microstructure of both torn and untorn meniscus. The direct correlation between meniscus T2 and the severity of adjacent cartilage loss indicates the important inter-relationship between changes in meniscus and cartilage during joint degeneration.

B-0641 14:17

Assessment of meniscal and cartilage damage of the knee with ultrahigh field imaging at 7Tesla: a comparison to 3Tesla imaging with arthroscopic correlation
B. Friebe, M. Richter, S. Penzlin, C. Staerke, F. Godenschweger, J. Ricke, S. Kropf, F. Fischbach, O. Speck; *Magdeburg/DE (bjoern.friebe@med.ovgu.de)*

Purpose: To determine the diagnostic accuracy of ultrahigh-field MRI at 7Tesla (7T-MRI) in meniscal tears and cartilage damage compared to clinical routine MRI at 3Tesla (3T-MRI).
Methods and Materials: 41 patients with suspected meniscal damage or mild osteoarthritis (Kellgren-Lawrence 0-2) received 7T-MRI as well as clinical routine 3T-MRI consecutively. The imaging protocol in both field strengths consisted of a PD-weighted fat saturated and a T1-weighted turbo spin echo (TSE) sequence with a higher resolution at 7T-MRI. Images were read blinded regarding field strength and patient characteristics by three readers with different experience in musculoskeletal MRI (3 years, 6 years and 10 years) according to a modified whole-organ magnetic resonance imaging score of the knee in osteoarthritis (WORMS). Arthroscopic reports as a gold standard were available for twelve patients.
Results: A multifactorial mixed model analysis was performed. The mean cumulated diagnostic score in 7T-MRI was significantly closer to the gold standard compared to 3T-MRI in patients where gold standard was available (p<0.001). In all 41 patients 7T-MRI detected significantly more severe damages in cartilage (p<0.001) and in meniscus (p<0.001). No difference in interreader variability between 3T and 7T was observed. Imaging acquisition time was similar.
Conclusion: Morphologic imaging of cartilage and meniscal damage of the knee in ultrahigh-field MRI at 7T with T1- and PD-weighted TSE-sequences has a significantly higher diagnostic accuracy than compared to 3T-MRI and can be performed with equal acquisition times exploiting higher resolution of 7T-MRI. 7T-MRI detected significantly more severe damages in cartilage as well as in meniscus.

B-0642 14:25

Weight loss regimens in obese and overweight individuals impact cartilage degeneration: 96-month data from the Osteoarthritis Initiative
G.C. Feuerriegel[1], A.S. Gersing[1], B.J. Schwaiger[1], J. Zarnowski[1], P.M. Jungmann[1], C.E. McCulloch[2], M.C. Nevitt[2], E.J. Rummeny[1], T.M. Link[2];
[1]*Munich/DE*, [2]*San Francisco, CA/US (g.feuerriegel@gmail.com)*

Purpose: To investigate MR-based cartilage biochemical degeneration and morphologic joint abnormalities over 96 months in overweight and obese subjects with stable weight and weight-loss and to assess how these changes are affected by different weight loss regimens.
Methods and Materials: Subjects with a BMI>25kg/m^2 from the Osteoarthritis Initiative (n=760; age 62.6±9.0y; 465 females) with risk factors for or radiographic mild to moderate osteoarthritis were included. Subjects losing weight (>5% of baseline BMI; N=380) were frequency matched to controls with stable weight (N=380) and categorised into groups regarding the weight-loss method (diet and exercise, diet only, exercise only). 3T MRI of the right knee was performed at baseline, 48-and 96-months. T2 changes of cartilage composition, including laminar and texture analysis as well as morphological knee abnormalities, assessed with Whole-Organ-Magnetic-Resonance-Imaging-Scores (WORMS) were analysed using mixed random effects models to calculate associations between weight-loss degree and regimen.
Results: Progression of cartilage WORMS was significantly lower in the weight-loss group compared to controls (P<0.001) over 96 months. Subjects with weight-loss showed significantly less T2-value increase in the bone layer of all compartments (P<0.03, for each). Rates of increase in cartilage T2 averaged over all compartments were lowest in the diet and diet and exercise groups compared to the stable weight group (P=0.042 and P=0.003, respectively). Weight-loss through exercise alone was not beneficial.
Conclusion: Results suggest that cartilage degeneration is slowed through weight-loss in obese and overweight subjects over 96-months. This protective effect was strongest in subjects losing weight through combined exercise and diet programs.

B-0643 14:33

Risk factors for biochemical cartilage alterations in young asymptomatic individuals

A.F. Tschischka, B. Bittersohl, N. Heinzler, J. Boos, A. Joel, F. Fichter, G. Antoch, C. Schleich; *Düsseldorf/DE (Alexander.Tschischka@med.uni-duesseldorf.de)*

Purpose: To assess the glycosaminoglycan (GAG) content of lumbar intervertebral discs (IVD) in healthy volunteers with facet tropism (FT) and sagittal facet joint (FJ) orientation using glycosaminoglycan chemical exchange saturation transfer imaging (gagCEST).
Methods and Materials: Seventy-five lumbar IVDs of twenty-five young, healthy volunteers without any history of lumbar spine pathologies (13 female; 12 male; mean age: 28.0 ± 4.4 years; range: 21 - 35 years) were examined with a 3T MRI scanner. Orientation of FT and FJ were assessed for L3/4, L4/5 and L5/S1 using standard T2 weighted images. Biochemical gagCEST imaging was used to determine the GAG content of each nucleus pulposus (NP) and annulus fibrosus (AF).
Results: Significantly higher gagCEST values of NP were found in volunteers without FT and normal FJ orientation compared to volunteers with FT and sagittal FJ orientation > 45° ($p < 0.0001$). GagCEST values were significantly higher in volunteers without FT compared to volunteers with moderate or severe FT (moderate FT: $p < 0.0001$; severe FT: $p = 0.0033$). Volunteers with normal FJ orientation showed significantly higher gagCEST values compared to those with sagittal FJ orientation > 45° ($p < 0.001$). We found a significant, negative correlation between gagCEST values and higher angels in sagittal FJ orientation ($rho=-0.459$; $p < 0.0001$).
Conclusion: GagCEST analysis indicated lower GAG values of NP in young volunteers with FT and sagittal orientated FJ, indicating that FT and sagittal orientation of the FJ represent risk factors for the development of early biochemical alterations of lumbar IVDs.

B-0644 14:41

Simultaneously measured T2 and dGEMRIC indices do not correlate in an experimental, ovine FAI model

F. Schmaranzer[1], L. Arendt[2], N. Wolfer[2], T. Lerch[1], S. Steppacher[1], K. Nuss[2], P. Kircher[2], B. von Rechenberg[2], M. Tannast[1]; [1]*Berne/CH*, [2]*Zurich/CH (schmaflo@gmail.com)*

Purpose: dGEMRIC and T2 mapping estimate glycosaminglycan respectively water content and collagen fiber network organisation. These techniques are increasingly used in prearthritic conditions such as femoroacetabular impingement (FAI). However their correlation is yet to be established. Hence we aimed to correlate T2 and dGEMRIC indices in a validated, experimental ovine FAI model.
Methods and Materials: This experimental, controlled, prospective study on 5 sheep (10 hips) was conducted after IRB approval. Five sheep underwent unilateral surgical induction of FAI by varus intertrochanteric osteotomy, which rotates the naturally aspherical ovine femoral head into the acetabulum, inducing typical focal chondrolabral damage as seen in humans. Correction of the deformity was performed after 70 days. No surgery was performed in the 5 contralateral hip. Sheep were sacrificed after further 70 days. One hour before sacrifice sheep received i.v gadolinium-DTPA and roamed free. Hip were dissected to fit into the coil. dGEMRIC and T2 maps (inversion recovery technique) were obtained at 3T. dGEMRIC and T2 times were fitted and merged with radial PD-w morphologic slices using a specifically developed software (GT1*map, Gyro Tools) to enable simultaneous dGEMRIC and T2 measurements in the same region of interest. Peripheral and central regions of interest measured at the 12 acetabular and femoral clock-face positions were correlated using linear regression analysis ($p<0.05$).
Results: No correlation between acetabular/femoral dGMERIC and T2 indices could be found.
Conclusion: No correlation between dGEMRIC and T2 indices was observed which suggests that both techniques show complementary effects in cartilage.
Author Disclosures:
M. Tannast: Research/Grant Support; SNF-support.

B-0645 14:49

Can the offset correction in experimentally induced ovine, cam FAI stop the process of biochemical and histologic cartilage degeneration: a pilot study

F. Schmaranzer[1], L. Arendt[2], N. Wolfer[2], C. Zurmühle[1], S. Steppacher[1], K. Nuss[2], P. Kircher[2], B. von Rechenberg[2], M. Tannast[1]; [1]*Berne/CH*, [2]*Zurich/CH (schmaflo@gmail.com)*

Purpose: The potential of hip preservation surgery for correction of femoroacetabular impingement (FAI) to prevent osteoarthritis progression is unclear. We asked whether offset creation in an ovine, cam FAI model can stop cartilage degeneration assessed with dGEMRIC and histologic Mankin scores.
Methods and Materials: This experimental, prospective study on 5 sheep (10 hips) was conducted after IRB approval. Five sheep underwent surgical FAI induction by varus intertrochanteric osteotomy unilaterally, which rotates the naturally aspherical ovine femoral head into the acetabulum, inducing typical focal chondrolabral damage as seen in humans. Offset was corrected after 70 days `FAI`. No surgery was performed in the 5 contralateral hips `No FAI`. Sheep were sacrificed after further 70 days. One hour before sacrifice sheep received i.v. gadolinium-DTPA and roamed free. Hips were dissected to fit into the coil. dGEMRIC maps (inversion recovery) were obtained at 3 T. Acetabular and femoral cartilage dGMERIC indices were measured radially at the 12 clock-face positions. Cartilage samples were stained with toluidine blue and degeneration was graded with the Mankin score. Unpaired T-tests were used for comparison ($p<0.05$).
Results: Acetabular and femoral dGEMRIC indices decrease after FAI induction and correction (411 ± 151ms vs 371 ± 110ms; $p<0.04$ respectively 391 ± 141ms vs 351 ± 91ms; $p<0.017$) while only femoral Mankin scores [0-15 points] increased (4 ± 3 vs 7 ± 3; $p<0.001$).
Conclusion: Despite a uniform dGEMRIC decrease no general histologic osteoarthritis progression was observed which underlines the potential of joint preservation hip surgery to stop the degenerative process.
Author Disclosures:
M. Tannast: Research/Grant Support; SNF-support.

B-0646 14:57

Follow up after matrix based autologous chondrocyte transplantation of the hip vs microfracture: a comparative 3T-MRI-study

J. Haubold, J.M. Theysohn, C. Geis, K. Körsmeier, S. Landgraeber, O. Kraff, A. Lazik-Palm; *Essen/DE (johannes.haubold@uk-essen.de)*

Purpose: To evaluate the regeneration of acetabular cartilage repair tissue after matrix based autologous chrondrocyte transplantation (ACT) vs. microfracture (MF) using proton density weighted (PDw) high resolution 3T-MRI.
Methods and Materials: The hips of patients with acetabular focal cartilage defects resulting from CAM-impingement were examined 6 and 12 months after ACT (n = 20) and MF (n = 16) using 3T high-resolution PDw sequences. The cartilage repair tissue was evaluated using an adapted MOCART score rating the integrity, surface and signal-intensity of the repair tissue as well as surrounding pathologies to a maximum of 85 points. MOCART scores were compared between the groups using Student's t-test and one-way Anova with Bonferroni correction.
Results: Six and 12 months after MF the characteristics of the repair tissue were nearly stable with a mean MOCART score of 51 and 49 points respectively. After ACT the MOCART score increased from a mean of 58 points after 6 months to a mean of 66 points after 12 months mainly because of a proceeding defect filling (35% of the points increase). The absolute scores after 12 months ($p < 0.01$; one-way Anova with Bonferroni correction) as well as the individual differences between the 6- and 12-month follow up ($p < 0.001$; Student's t-test) were significantly higher after ACT compared to MF.
Conclusion: With PDw 3T MRI significant better cartilage regeneration could be shown in the follow up after ACT vs. MF. After ACT MOCART scores were significantly higher compared to MF in a one-year follow-up.

B-0647 15:05

Cartilage repair tissue composition assessed with 3T MRI correlates with trabecular bone remodeling in patients with spongiosa augmented matrix-associated chondrocyte implantation

A.S. Gersing, G. Feuerriegel, C. Holwein, A. Suchowierski, D.C. Karampinos, T. Baum, B.J. Schwaiger, E.J. Rummeny, P.M. Jungmann; *Munich/DE (alexandra.gersing@tum.de)*

Purpose: To investigate whether maturation of cartilage repair tissue is associated with maturation of the subchondral bone in patients after spongiosa augmented matrix-associated autologous chondrocyte implantation (MACI).
Methods and Materials: Both knees of patients (n=25, 25.5±7.8y; 10 female) were examined 2 years after unilateral spongiosa augmented MACI at one femoral condyle or patella using 3T MRI. Cartilage composition was assessed in all knee compartments using MRI T2 relaxation time mapping. Three dimensional phase-cycled balanced steady state free-precision (bSSFP) sequences were used in order to quantify the subchondral trabecular bone structure. Cartilage T2 values in the compartment treated with MACI (patella, medial or lateral femur condyle) that were higher than those of the corresponding compartment of the contralateral knee were considered as elevated. Values were compared using t-tests.
Results: Cartilage T2 values were significantly higher in compartments undergoing cartilage repair compared to the corresponding compartment of the contralateral knee (mean±standard error, 41.1±1.2ms vs. 38.8±1.6ms, P=0.035). Apparent trabecular thickness and bone fraction were also significantly higher in the compartment undergoing cartilage repair compared to the contralateral side (each comparison, P<0.001). Apparent trabecular thickness in the compartment undergoing cartilage repair was significantly

higher in patients with elevated cartilage T2 in the cartilage repair compartment (n=17; 0.37±0.05mm) compared to those without elevated cartilage T2 (n=8; 0.27±0.05mm; *P*=0.042).
Conclusion: After spongiosa augmented MACI, patients with elevated cartilage T2 values of the cartilage repair tissue showed thickened subchondral trabecular bone structure. The observed findings suggest a synergetic maturation of cartilage and subchondral bone after osteochondral transplantation.

B-0648 15:13

Standing CT imaging to enable earlier and more accurate detection, diagnosis, and longitudinal monitoring of knee osteoarthritis features
N. Segal[1], A. Guermazi[2]; [1]*Kansas City, KS/US*, [2]*Boston, MA/US (segal-research@kumc.edu)*

Purpose: Radiographs are insensitive, requiring years to detect signs of knee osteoarthritis (OA). The optimal knee flexion angle and x-ray beam tilt to visualize the joint surface is person-specific and difficult to reproduce, further complicating radiographic detection of OA features before joint damage is advanced. This line of research was initiated to accelerate detection of knee OA through improving sensitivity and reliability of knee OA imaging.
Methods and Materials: Advances in cone beam CT have enabled lower limb imaging while standing (SCT). SCT has the same Relative Radiation Level as x-ray, while enabling weight-bearing 3D imaging that places physiological stress on the cartilage and menisci. Knees of older adults were imaged with fixed-flexion radiographs, MRI and pulsed SCT (isotropic resolution of 0.37 mm; FOV of 20x35cm; SCT footprint 121x147 cm) were read for OA features. Diagnostic performance as well as test-retest reliability statistics were compared between modalities.
Results: In comparison with fixed-flexion radiography, SCT demonstrated (1) higher sensitivity (93%, 100%) and accuracy (95%, 99%) for detection of osteophytes and subchondral cysts respectively, (2) high reliability for joint space width (JSW) measurements (ICC=0.94-0.97), and (3) significantly better correlation with central medial tibia cartilage morphology by MRI (SCT, r_s=0.84; radiographs, r_s=-0.66); and better differentiation between cartilage and subchondral bone compared with MRI.
Conclusion: SCT imaging offers greater diagnostic performance for tibiofemoral and patellofemoral OA features than radiographs, without increasing radiation dose. SCT is unique in offering 3D weight-bearing imaging of the bilateral legs and holds potential for wide-spread implementation.
Author Disclosures:
N. Segal: Equipment Support Recipient; CurveBeam, LLC provided the CT scanner for the research.. Patent Holder; Dr. Segal is named on patent 2015/116573 for the alignment frame used.. Research/Grant Support; NIH/NIA grant AG-18832. **A. Guermazi:** Shareholder; Boston Imaging Core Labs.

B-0649 15:21

MRI scoring of osteoarthritis of the ankle
S.M. Aboelmagd, S.B.L. Low, J.G. Cahir, A.P. Toms; *Norwich/UK (sharief.aboelmagd@nnuh.nhs.uk)*

Purpose: To develop a semi-quantitative MR-based scoring system for osteoarthritis of the ankle, and to determine its inter and intra-observer reproducibility. To examine association between MR features and radiographic osteoarthritis severity.
Methods and Materials: A retrospective sample of 50 patients who underwent MRI and plain radiographs were included. Features included were bone marrow lesions, bone marrow oedema, cysts, osteophytes and cartilage integrity. Anatomical zones were based on existing published systems. MR examinations were graded using the proposed system by two consultant radiologists and two residents. Radiographs were graded using a published Kellgren-Lawrence ankle score. Inter and intra-observer reproducibility were examined using a weighted kappa statistic (kw), and association between MR and radiographic severity using Spearman's Rho.
Results: Inter-reader reproducibility was "almost perfect" for all features for total joint scores (kw 0.88-0.97) except osteophyte scoring between the residents that was "substantial" (kappa 0.64). Zonal-based assessment demonstrated "substantial agreement" between the residents (kw 0.63-0.75), and "substantial" or "almost perfect" agreement for the consultants (kw 0.73-0.92). Intra-reader reproducibility was "substantial" or "almost perfect" for total joint scores (kw 0.79-0.97) and "moderate" to "almost perfect" for the zonal approach (kw 0.51-0.89). Confidence intervals were narrow for total joint scores although variable for the zonal approach. There was strong positive correlation between all features and radiographic severity (rho 0.75-0.85) except cysts which demonstrated positive although weaker correlation (rho 0.35).
Conclusion: This new grading system demonstrated "substantial" to "almost perfect" inter and intra-observer reproducibility. This tool may be useful in clinical OA and epidemiological studies.

14:00 - 15:30 **Room G**

Physics in Medical Imaging

SS 713

Performance optimisation in medical imaging

Moderators:
S. Savolainen; Helsinki/FI
S. Wildner; Vienna/AT

B-0650 14:00

Initial evaluation of image performance of a novel 3D x-ray system: phantom-based comparison of 3D tomography with conventional computed tomography
R.M. Benz[1], M. Garcia[1], F. Amsler[1], J. Voigt[2], A. Fieselmann[2], A.L. Falkowski[1], B. Stieltjes[1], A. Hirschmann[1]; [1]*Basle/CH*, [2]*Erlangen/DE (robyn.benz@usb.ch)*

Purpose: Phantom-based performance assessment of a prototype 3D x-ray system and comparison with conventional computed tomography (CT).
Methods and Materials: A 3D-image quality phantom (Cone Beam Phantom/ QRM/ Moehrendorf/ Germany) was scanned with a prototype of a novel 3D x-ray system (Multitom Rax/ Siemens Healthineers/ Erlangen/ Germany) using three dedicated trajectories of 163° (table), 188° (upright) and 200° (side) scanning angles and 160 projections. Images were obtained with 60/70/81/90/100/121kV and 0.348/0.696/1.740/3.480µGy/p as well as conventional CT (Somatom Definition Flash/ Siemens Healthineers/ Erlangen/ Germany) with a clinical protocol. Spatial resolution was assessed as well as soft tissue contrast resolution. Signal-to-noise ratio (SNR) and contrast-to-noise ratio (CNR) were calculated. Additionally, radiation dose was measured for the x-ray system as well as the CT. Descriptive and ANOVA analyses (P<0.05) were performed.
Results: Using 3D x-ray a maximum of 16lp/cm were visible and best soft tissue contrast resolution was 2mm at 30HU compared to CT with 10 lp/cm and 4mm at 20HU, respectively. Mean SNR and CNR were significantly lower in the upright trajectory (mean SNR: upright, 7.7±2.9/side, 9.7±3.8/table, 9.1±4.1/CT, 9.1±1.6 [P<0.05]). Radiation dose was significantly higher using 3D tomography than CT (P<0.05).
Conclusion: The 3D x-ray system renders an equal or higher spatial resolution and comparable soft tissue contrast to conventional CT for medium and high dose protocols in the side and upright trajectory, but with increased radiation doses.
Author Disclosures:
J. Voigt: Employee; Siemens. **A. Fieselmann:** Employee; Siemens.
A. Hirschmann: Grant Recipient; Siemens.

B-0651 14:08

A human cadaver study to evaluate automatic image quality assessment in chest CT
C. Franck[1], A. De Crop[2], B. De Roo[1], P. Smeets[1], E. Achten[1], T. Van Hoof[1], K. Bacher[1]; [1]*Ghent/BE*, [2]*Roeselare/BE (caro.franck@ugent.be)*

Purpose: The evaluation of clinical image quality (IQ) is important to optimise CT protocols and to keep patient doses as low as reasonably achievable. Considering the significant amount of effort needed for human observer studies, automatic IQ tools are a promising alternative. The purpose of this study was to evaluate automatic IQ assessment in chest CT using Thiel embalmed cadavers.
Methods and Materials: Chest CT's of Thiel cadavers were acquired at different exposures. Clinical IQ was determined by performing a visual grading analysis. Physical-technical IQ (noise, contrast-to-noise and contrast-detail) was assessed in a Catphan phantom. Soft and sharp reconstructions were made with filtered back projection and two strengths of iterative reconstruction. A filtering algorithm (IQs) was used for automatic IQ evaluation. Normalisation of IQs allowed comparison of soft and sharp reconstruction kernels.
Results: Correlation coefficients between IQs and physical-technical parameters varied from 0.882 to 0.990. The correlations between IQs and clinical IQ were 0.824 (soft reconstructions) and 0.930 (sharp reconstructions).
Conclusion: IQs can be used in clinical practice for the evaluation of chest CT scans. It allows to monitor the IQ of a clinical chest protocol over time, without human intervention. Different reconstruction kernels can be compared after normalisation of the IQs.

B-0652 14:16

Clinical use of digital scatter correction in bedside chest radiography to improve image quality and reduce patient dose

C. Cases[1], D. Mentrup[2], A. Ruíz[1], R. Pallerol[1], A. Gimenez[1], I. Gich[1], M. Ribas[1], A. Capdevila[1]; [1]*Barcelona/ES*, [2]*Hamburg/DE (ccasadevall@santpau.cat)*

Purpose: Accumulation of bedside chest radiographs can lead to significant patient dose in an intensive care unit (ICU). Anti-scatter grids improve image quality (IQ) at the expense of increasing patient dose and workflow complexity. Recently, digital scatter correction (DSC) which simulates grid-like image contrast has been introduced as an alternative. We evaluated the influence of DSC on IQ and dose.
Methods and Materials: 50 ICU patients received clinically indicated bedside chest radiographs on two consecutive days. First-day images were acquired using the institution's standard protocol (80kVp, 2mAs, no grid). On the second day, dose was reduced up to 40% depending on the exposure index. The visibility of six anatomical features plus a general score was evaluated by two senior radiologists using a 10-point scale (1=insufficient, 10=excellent) with and without DSC (SkyFlow, Philips Healthcare). ANOVA tests were used to evaluate the influence of DSC on IQ.
Results: Scores with DSC were significantly higher (ANOVA test, $p<0.001$) than those without DSC with a mean difference greater than 1 point for each feature. Pairwise comparison showed that dose reduction resulted in lower image scores on 4 (out of 6) features and on general judgement ($p<0.05$). However, dose-reduced images with DSC obtained significantly higher scores (mean 7.5) than standard-dose images (mean 5.7) without DSC ($p<0.001$) for all anatomical features and for the general judgement.
Conclusion: Even with a dose reduction of up to 40%, usage of DSC results in significantly higher image scores for bedside chest radiographs compared with images acquired without grid.
Author Disclosures:
C. Cases: Founder; Philips. **D. Mentrup:** Employee; Philips. **A. Ruíz:** Founder; Philips. **R. Pallerol:** Founder; Philips. **A. Gimenez:** Founder; Philips. **I. Gich:** Founder; Philips. **M. Ribas:** Founder; Philips. **A. Capdevila:** Founder; Philips.

B-0653 14:24

Towards automated clinical image quality assessment in CT: 3D model observer applied to simulated images of a virtual lung phantom

I. Hernandez-Giron[1], W.J.H. Veldkamp[1], G.J. Streekstra[2]; [1]*Leiden/NL*, [2]*Amsterdam/NL (irene.debroglie@gmail.com)*

Purpose: To develop a method for clinical image quality assessment in CT. As a proof of concept the detectability of nodules embedded in an anthropomorphic lung phantom was investigated with a 3D model observer analyzing simulated CT images.
Methods and Materials: A virtual phantom representing the distribution and sizes of lung vessels was generated using a custom algorithm in MATLAB. For nodules, 10 spheres, (3-5-8mm diameter), were digitally inserted in different locations, mimicking attenuations (-800,-630,-500,-250HU). Two levels of Gaussian white noise were added to the phantom images, which were then blurred with the PSF of a CT standard lung kernel. As proof of concept, a 3D model observer with Gabor channels was used to calculate the detectability of the nodules (d') based on test-statistics measured in samples with/without nodule, extracted from the images.
Results: For equivalent locations in the phantom d' increased with object attenuation, diameter and decreasing noise. For 3mm diameter objects (-800,-630,-500,-250HU) the average (d'±σ) were (3.8±0.3, 7.3±0.6, 9.9±0.4, 15.0±0.7) and (5.3±0.3, 10.2±0.4, 14.0±0.3, 21.2±1.0), for high and low noise simulated images, respectively. Regarding d'vsobject size, for (-800HU and 3-5-8mm), d' was (3.8±0.3, 7.9±1.0, 16.5±2.6) and (5.3±0.3, 11.1±1.9, 23.1±2.5) for each noise level.
Conclusion: A 3D model observer was successfully used to analyze the detectability of nodules in matematically generated lung structures with CT-like colored noise simulated images. The 3D model observer is a promising tool to assess clinical image quality in CT. As a next step, the 3D model performance will be compared to human observers.
Author Disclosures:
I. Hernandez-Giron: Author; Wouter J. H. Veldkamp, Geert Streekstra. Research/Grant Support; STW (CLUES project). **W.J.H. Veldkamp:** Research/Grant Support; STW (CLUES project).

B-0654 14:32

Performance evaluation of a dual-layer spectral CT: initial results

P.B. Noel, S. Ehn, T. Sellerer, A. Fingerle, J. Dangelmaier, R. Braren, F. Pfeiffer, E.J. Rummeny, D. Muenzel; *Munich/DE (peter.noel@tum.de)*

Purpose: We present a performance evaluation of a recently introduced spectral computed tomography system equipped with a dual-layer detector.
Methods and Materials: A semi-anthropomorphic abdomen phantom for CT performance evaluation was imaged on a dual-layer spectral CT (IQon Spectral CT, Philips Healthcare, USA) with three different radiation dose levels. The phantom was equipped with a specific spectral insert. The insert included the following material: water, adipose tissue, muscle, liver, bone, and a variation of iodine concentrations. Additionally, the phantom was enlarged with four different extension rings to simulate obese patients. With these acquisitions we have evaluated the contrast-to-noise (CNR) ratio over the range of available virtual monoenergetic images (MonoE) and the quantitative accuracy of MonoE Hounsfield Units (HU), effective Z-maps and iodine concentrations.
Results: For all evaluated tasks the results are within the calculated theoretical range of the spectral inserts. Especially for lower contrasts at low energies, the CNR could be boosted by a factor up to 200% with respect to the conventional image. The quantitive accuracy of MonoE images, effective Z-maps and iodine concentrations are well below 10% and the quantitive difference between normal to obese patients is on average around 6%.
Conclusion: Dual-layer spectral CT offers excellent quantitative CT capabilities over the whole field of view without any compromise in radiation dose or image quality.

B-0655 14:40

Objective comparison of high- and low-contrast detectability for three clinical protocols on eight CT scanners

D. Racine[1], A. Viry[1], F. Becce[1], S. Schmidt[1], A. Ba[1], A. Schegerer[2], F.R. Verdun[1]; [1]*Lausanne/CH*, [2]*Oberschleißheim/DE (damien.racine@chuv.ch)*

Purpose: To objectively compare computed tomography (CT) scanner performances for three clinically relevant protocols using a task-based image quality assessment method in order to assess the potential for radiation dose reduction thanks to technological developments.
Methods and Materials: Eight CT scanners from 4 manufacturers released between 2003 and 2014 were compared using ideal model observers: Prewhitening (PW) model for high-contrast detectability (HCD) and channelised Hotelling (CHO) model with Laguerre-Gauss channels for low-contrast detectability (LCD). HCD was assessed using a custom-made phantom to estimate task transfer function, and noise power spectrum. LCD was assessed using an abdominal phantom providing equivalent diameters of 24, 29.6, and 34.6 cm. Three protocols were reviewed: a head (trauma) and an abdominal (urinary stones) protocol were applied to assess HCD; and another abdominal (focal liver lesion) protocol was applied for LCD. The last protocol was tested with fixed and modulated tube currents.
Results: Compared to older generations, newer CT systems did not yield major improvements for HCD; one recent system had even lower performances than its predecessor. The use of the CHO model revealed that excellent image quality for LCD could be obtained with newer scanners at a significantly lower dose level.
Conclusion: This study shows that model observers can objectively benchmark CT scanners using a task-based image quality method, thus helping to estimate the potential for further dose reductions offered by the latest technology. Such an approach may be useful for adequately comparing clinically relevant image quality between various scanners.

B-0656 14:48

Properties of primary MDCT x-ray source spectra: influence on total energy deposition and spatial absorption distribution

A. Steuwe, H.-U. Kauczor, W. Stiller; *Heidelberg/DE (andrea.steuwe@med.uni-heidelberg.de)*

Purpose: X-ray spectra of different MDCT sources differ by shape and mean photon energy (E_{mean}) due to different anode geometries, materials and filtration. Nonetheless, a variety of spectra and monoenergetic x-rays are applied in Monte-Carlo simulations of CT, despite possible differences in total energy deposition and spatial absorption distribution. This study aims at assessing resulting differences and implications.
Methods and Materials: The effect of different 120kV$_p$-x-ray spectra ([a] Toshiba CXB-750D MegaCool (E_{mean}=57.7keV, reference spectrum measured in-house), "Siemens Healthcare Online tool for the simulation of x-ray Spectra"-spectra without [b] and with [c] 3.3mm aluminum-filtration matching E_{mean} of the reference spectrum) and monoenergetic x-rays ([d] 57.7keV, [e] 120.0keV) on total energy deposition and spatial distribution in a water phantom (Ø=32cm, d=16cm) was determined with Monte-Carlo simulations (Geant4). Simulations were performed using stationary x-ray sources with/without bowtie filter.

Results: Compared to reference spectrum [a], differences in total energy deposition are: +63.5% [e], -1.5% [d], -5.0% [b] and +0.5% [c]. Approximate maximum differences in spatial absorption distribution are larger: 400% for [e] and 20% for [d], with underestimation in the phantom periphery and overestimation at its center. Differences of [b] are 20%, whereas added aluminum-filtration decreases differences to 5% [c]. Ignoring bowtie filtration causes up to 250% difference in energy distribution, especially in the phantom periphery.
Conclusion: Total energy deposition and spatial distribution are comparable for different spectra, if tube potential and E_{mean} match. Monoenergetic sources are not suited for x-ray source modeling. Simulations of correct spatial absorption distributions require modeling of bowtie filtration.
Author Disclosures:
H.-U. Kauczor: Research/Grant Support; Siemens, Bayer. Speaker; Böhringer Ingelheim, Bracco, GSK, Novartis, Siemens, Almirall.

B-0657 14:56

Reducing mean contrast volumes in small patients and harmonising chest-abdomen CT-image quality using personalised contrast volumes
M.-S. Walgraeve[1], L. Pyfferoen[1], K. Van De Moortele[1], C. Lafay[2], F. Zanca[2], J.W. Casselman[1]; [1]*Bruges/BE*, [2]*Buc/FR (marie-sofie.walgraeve@azsintjan.be)*

Purpose: To achieve consistent contrast enhancement across different patients, patient-tailored contrast protocols should be considered. The aim of this study was to evaluate the effect of fixed contrast volumes compared to patient-tailored contrast volumes on contrast-enhanced chest-abdomen CT-images.
Methods and Materials: Data of 77 patients who underwent two contrast-enhanced chest-abdomen CT-examinations over a one-year period were collected. First exam was performed with a fixed contrast volume (95 ml), follow-up exam with a patient-tailored contrast protocol (based on patient body surface area and heart rate). Contrast volumes were compared and contrast enhancement of liver, spleen, portal vein and aorta was assessed by 2 radiologists. Wilcoxon-rank-sum test and Kruskal-Wallis test were used to assess significant differences.
Results: Reduced contrast volumes were administered in 51 (66%) patients and mean contrast volumes were significantly (p=0.002) lower (-17%) in female patients using a patient-tailored contrast protocol compared to a fixed contrast volume. There was a significant reduction in variance of enhancement of spleen and portal vein in all patients across different BMI categories (fixed protocol, p=0.001 and 0.0007, respectively; patient-tailored, p=0.18 and 0.12) and there was a significant reduction in variance of liver enhancement across different BMI categories in female patients (fixed protocol, p=0.02; patient-tailored, p=0.15).
Conclusion: A patient-tailored contrast protocol can reduce mean contrast volumes in small patients, especially females. It also improves CT-image quality by harmonising contrast enhancement of spleen, portal vein and liver across different BMI categories. This avoids administration of inappropriate high contrast volumes in small patients and inadequately low contrast enhancement in large patients.
Author Disclosures:
C. Lafay: Employee; GE Healthcare. **F. Zanca:** Employee; GE Healthcare.

B-0658 15:04

Optimisation of abdominal CT protocols using a mathematical model observer: a multicentre study
D. Racine, N. Ryckx, A. Viry, F. Becce, F.R. Verdun, S. Schmidt; *Lausanne/CH (damien.racine@chuv.ch)*

Purpose: To highlight the spread of patient exposure and image quality performances for comparable clinical questions.
Methods and Materials: An abdominal phantom containing spheres of 5 and 8 mm at 10 and 20HU was scanned on 58 CT machines of 50 different institutions using locally clinical settings of the native phase for the detection of focal liver lesions (FLL). Objective image quality was assessed with a Channelised Hotelling Observer (CHO) with ten dense differences of Gaussian channels. The area under the ROC curve (AUC) was used the figure of merit (FOM). Because of various reconstructed slice thickness, the product of the CTDIvol and slice thickness, dose-slice thickness product (DSP) was used as radiation dose metric.
Results: No significant differences in AUC were noted between FBP and iterative reconstructions, but the DSP varied from 2.6 to 61mGy.mm and the reconstructed slice thickness varied from 2 to 5mm. For the 5mm-20HU target, 49% of the CTs gathered around an AUC range of 0.86-0.98 for a DSP range of 5-20mGy.mm. Nevertheless, 10% of the CTs were outliers because of relatively high dose levels and limited AUC scores.
Conclusion: The use of a CHO model showed that the majority of institutions performed reasonably well when searching FLL. However, the limited spread in objective image quality was associated with a large spread in the chosen dose indicator. In the future, an expected level of low-contrast detectability should be used as FOM to ensure that the optimisation process does not impair the diagnostic goal.

B-0659 15:12

Effect of acquisition geometry on image quality of a digital tomosynthesis system for general radiography
A. Maldera, M. Sutto, P. Colombo, A. Torresin; *Milan/IT (angela.maldera@gmail.com)*

Purpose: In tomosynthesis system, the optimization process is strongly related to the acquisition geometry: sweep angle(θ) and number of projections(p). We investigated the relationships between acquisition geometry and image quality (IQ) metrics as artefact spread function(ASF), blurring ripple, in-plane/in-depth resolution and signal difference to noise ratio(SDNR).
Methods and Materials: All exposures were performed on a Fujifilm FDR AcSelerate with 55kVp, 1.25mAs/projection and reconstructed with FBP, 1mm pitch. θ(20°-60°) and p(20-60) were changed with the sampling angle. Agatha phantom was used to evaluate ASF, ripple and in-depth resolution(z-PSF). Copper steps of different thickness were imaged to assess SDNR and MTF (edge method). All IQ metrics were evaluated on the reconstructed images.
Results: Sweep angle is the only parameter affecting ASF and z-PSF: they both improve with larger scan angles. FWHM of ASF ranges from 16.7mm for θ =20° to 10.6mm for θ =60°. FWHM of z-PSF ranges from 5.0mm for θ =20° to 1.5mm for θ =60°. Blurring ripple is affected by sampling angle: ripple is reduced or eliminated when the sampling angle is narrower.In plane MTF was found to be anisotropic: MTF50%=1.99±0.04 (1.21±0.12)lp/mm for the edge parallel or orthogonal to the tube-travel direction, respectively; regardless the acquisition geometry.SDNR depends only on total exposure, i.e. number of projections, no matter the sweep angle.
Conclusion: This study showed that for Fujifilm FDR AcSelerate wider sweep angles improve in-depth resolution and narrower sampling angle reduces off-focus blurring. The choice of the optimal configuration needs to take into account also SDNR and the total dose.

B-0660 15:20

Impact of detector type, dose and image processing on the quality of digital neonatal chest x-ray images
M.-H. Smet, L. Breysem, E. Mussen, H. Bosmans, N.W. Marshall, L. Cockmartin; *Leuven/BE (Marleen.Smet@uzleuven.be)*

Purpose: To study the impact of different detector types, dose levels and processing algorithms on image quality (IQ) of digital chest x-ray imaging using a neonatal chest phantom.
Methods and Materials: An absolute visual grading analysis (VGA) study was performed on 400 x-ray images of the Gammex^{R} neonatal chest phantom mimicking hyaline membrane disease, pneumothorax and additional vascular lines. Three Agfa HealthCare detectors (CR powder phosphor (PIP), CR needle crystal based phosphor (NIP) and CsI DR detector (DXD)), and a Carestream CsI DR detector (CRX) were included. For each detector, 10 images at 5 dose levels were acquired with 2 processing algorithms for each vendor. Three experienced paediatric radiologists scored the reproduction of important normal anatomical structures following European quality criteria, with additional questions on the visibility of vascular lines, noise and disease simulation. Visual grading characteristic (VGC) analysis compared the different detectors while ordinal regression was used to test the effect of dose and processing on VGA score.
Results: No significant differences were found between the NIP, DXD and CRX detectors (p>0.05) whereas the PIP detector had significantly lower VGA score (p< 0.0001). Processing did not influence the VGA scores (p=0.819) whereas increasing dose level resulted in significantly higher VGA scores (p<0.0001). VGA identified a ~2.3μGy detector air kerma as optimal working point for NIP, DXD and CRX.
Conclusion: VGA score could identify differences between detectors and dose levels but was not sensitive for image processing. VGA shows the dose values above which perception of quality does not improve.

14:00 - 15:30 **Room K**

Radiographers

SS 714

Breast imaging

Moderators:
C. Falzon; Sta. Lucija/MT
S. Zackrisson; Malmö/SE

B-0661 14:00

A multicentre international study to develop and validate a reproducible assessment tool for evaluating the image quality of screening mammograms

K. Taylor[1], D. Parashar[2], A. Poulos[3], R. Gullien[4], R. Aarre[5], M. Wallis[1]; [1]*Cambridge/UK*, [2]*Warwick/UK*, [3]*Sidney/AU*, [4]*Oslo/NO*, [5]*Hvidovre/DK (kathryn.taylor@addenbrookes.nhs.uk)*

Purpose: Optimum mammography positioning technique is necessary to maximise cancer detection. Current criteria for mammography evaluation lack reliability and validity with a need to develop a more objective system. We aimed to establish current international practice in assessing image quality (IQ), of screening mammograms then develop and validate a reproducible assessment tool.
Methods and Materials: A questionnaire sent to centres in countries undertaking population screening identified practice, participants for an expert panel (EP) of radiologists/radiographers and a testing panel (TP) of radiographers. The EP developed category criteria and descriptors using a modified Delphi process to agree definitions. The EP scored 12 screening mammograms to test agreement then a main set of 178 cases. Weighted scores were derived for each descriptor enabling calculation of numerical parameters for each new category. The TP then scored the main set. Statistical analysis included ANOVA, t-tests and Kendalls coefficient.
Results: 11 centres in 8 countries responded forming an EP of 7 members and TP of 44 members. The EP showed moderate agreement when the scoring the mini test set W=0.50 p<0.001 and the main set W=0.55 p<0.001, 'posterior nipple line' being the most difficult descriptor. The weighted total scores differentiated the 4 new categories Perfect, Good, Adequate and Inadequate (p<0.001).
Conclusion: We have developed an assessment tool by Delphi consensus and weighted consensus criteria. We have successfully tabulated a range of numerical scores for each new category providing the first validated and reproducible mammography IQ scoring system.

B-0662 14:08

The impact of image blurring on lesion detection performance in full field digital mammography FFDM

A.K. Abdullah[1], J. Thompson[1], C. Mercer[1], R. Aspin[1], J. Kelly[2], P. Hogg[1]; [1]*Salford/UK*, [2]*Chester/UK (P.Hogg@salford.ac.uk)*

Purpose: Image blurring is a known phenomenon in FFDM, but no research has quantified its impact on lesion detection performance. This study investigates the detection of malignant masses and microcalcifications using FFDM with varying magnitudes of simulated blurring.
Methods and Materials: Seven observers (15±5 years' reporting experience) evaluated two image sets for three conditions; each set consisted of 124 cases (62 normal; 62 abnormal). Abnormal cases contained malignant masses and microcalcifications; these were confirmed as malignant by biopsy. Images were evaluated for 3 conditions - without blurring (0mm), and two magnitudes of simulated blurring (0.7mm and 1.5mm), introduced by mathematical simulation. A free-response observer study was conducted to compare lesion detection performance in blurred and non-blurred images. Equally weighted jackknife alternative free-response receiver operating characteristic (wJAFROC) analysis was used for statistical analysis. Test alpha was set at 0.05 to control probability of Type I error.
Results: A statistically significant difference was evident for the detection of masses (F(2,21)=6.01, P=0.0084) and microcalcifications (F(2,20)=6.12, P=0.0082). Statistical differences were found between multiple pairs (0.0mm v 0.7mm) and (0.0mm v 1.5mm) for both masses and microcalcifications. No difference was detected between 0.7mm and 1.5mm for masses or microcalcifications. The observer averaged wJAFROC figures of merit are 0.905(0.859, 0.952) [0mm], 0.869(0.814,0.924) [0.7mm] and 0.862(0.810,0.915) [1.5mm] for masses, and, 0.894(0.856,0.931) [0mm], 0.813 (0.757,0.870) [0.7mm] and 0.802(0.714,0.890) [1.5mm] for microcalcifications.
Conclusion: Simulated image blurring has a statistically significant impact on lesion detection performance (increasing false-negative and false-positive); this has implications for clinical practice.

B-0663 14:16

Radiation doses received by women attending BreastScreen NSW in 2014

M.E. Suleiman, P.C. Brennan, P. Kench, M.F. McEntee; *Lidcombe/AU (msul1801@uni.sydney.edu.au)*

Purpose: To review radiation doses received by women attending BreastScreen NSW Australia in a period of two months in 2014. To compare doses with doses from international digital mammography screening programmes.
Methods and Materials: Anonymised mammograms (52,405 mammograms for 12,034 women) across 61 mammography units taken over a period of two months, had their metadata and QA data examined. Exposure information was extracted from DICOM headers and medical physics QA reports were collected for all mammography units. Women between 20-110mm breast thickness, with no breast implants were included. Mammograms with incomplete exposure or QA information were excluded. Mean glandular dose (MGD) was calculated using methods described by Dance et al., using an in-house developed Microsoft Excel workbook.
Results: Mean breast thickness was 58mm. Median MGD for all images, CC view and MLO view were 1.39, 1.43mGy respectively. DRLs (75th percentile) suggested for a breast thickness range of 60±5mm for the whole population and for three different detector technologies were for all data, 2.06mGy; CR, 2.22mGy; DR, 2.04mGy; Photon counting, 0.79mGy.
Conclusion: Mean MGD was lower than the latest UK dose audit (1.79mGy) and higher than some international published mean MGDs. Breast thickness and detector technologies have a big impact on dose, hence DRLs have been reported separately for different breast thickness ranges and each detector technology.

B-0664 14:24

Students, teaching-staff and clinical radiographers' perspectives about difficulties and challenges in mammography education and training

C.S. Reis[1], J. Pires Jorge[2], B. Strøm[3], N. Richli Meystre[2], A. Henner[4], T. Kukkes[5], E. Metsala[6]; [1]*Perth/AU*, [2]*Lausanne/CH*, [3]*Bergen/NO*, [4]*Oulu/FI*, [5]*Tartu/EE*, [6]*Helsinki/FI (Jose.JORGE@hesav.ch)*

Purpose: To identify the main challenges and difficulties in mammography education around Europe according to three perspectives - students, teaching-staff and radiographers.
Methods and Materials: Questionnaires were developed and applied in five European countries to collect data regarding individual profile, academic background, challenges, difficulties and education needs. Before sending by email, the questionnaires were translated into national languages and tested.
Results: Students, teaching-staff and radiographers fulfilled 254 questionnaires. 76(out of 97) students from 5 European countries identified 5 topics that could promote difficulties in mammography education/training: teaching-related (45 answers), breast positioning-related (16 answers), image evaluation (10 answers), lack of resources (7 answers) and human interaction (6 answers). The transition from theory to practice and breast positioning in media-lateral oblique were highlighted as very demanding by students and radiographers. The need to providing an explanation to the patients about the role of the students inside mammography room was identified by radiographers as difficult. The challenges identified by this group were supervising students practice (22.6%) and perform exams and teach at the same time (22.6%). The majority of the students (60.8%) and radiographers (80%) reported the need of update their knowledge and skills in breast imaging areas.
Conclusion: The difficulties and challenges identified were similar for all participants. The transition from theory to practice due to the reduced time allocated to mammography education in undergraduates studies was pointed out as one of the main reasons. Regarding these findings, it could be possible to identify pedagogical strategies and develop recommendations to harmonise education and training around Europe.

B-0665 14:32

Assessing risk of pain in mammography

S. Pacifici; *Rome/IT (s_pacifici@virgilio.it)*

Purpose: According to literature, a wide percentage of women reports pain or discomfort during the procedure that may undermine compliance with periodic or follow-up mammography. Firstly, the study focuses on identifying the factors that determine the risk of pain with special attention to the woman-related factors, the procedure itself and the staff. Secondly, it sets out to define recommendations to reduce the pain experienced during mammography.
Methods and Materials: 300 women 40-70 years old were interviewed immediately before and after undergoing mammography. Pre-test interview was used to evaluate the expected pain and the risk factors. Subsequently, after an appropriate counselling and the given option over the control the pressure, mammography was performed. In post-test interview the women were questioned about the pain they experienced, the difference between their

experience and their expectations, and the most stressful part of the entire procedure.
Results: A number of women-related factors, staff-related and procedural factors were found significant in assessing the risk of pain, besides anxiety related to anticipatory representations of possible positive diagnosis. Anticipation of pain and discomfort were the dominant factor explaining a pain experience. Despite the most of assessed women expected that mammography would be painful, most of those who anticipated pain has reported that the severity experienced during current test was much lower than the anticipated severity.
Conclusion: Study results emphasise the need for a careful assessment of the emotional state of the woman and an appropriate pre-mammography counselling to address those factors which may interfere with future test compliance.

B-0666 14:40

Ergonomic analysis in mammography: strategies to improve radiographers' activity and postures

N. Cernean[1], F. Serranheira[1], P. Gonçalves[1], C.S. Reis[2]; [1]*Lisbon/PT*, [2]*Perth/AU (nicolaicernean@gmail.com)*

Purpose: To investigate the ergonomic characteristics of mammography equipment and identify strategies to improve radiographers' postures to reduce the risk of work-related musculoskeletal disorders (WRMSDs).
Methods and Materials: The study was conducted in two phases. During the first phase, the standard breast positions used in mammography exams were simulated (craniocaudal - CC and mediolateral-oblique - MLO). In the second phase interventions were performed (radiographer and/or patient stead; elevation of the patient using a step). The postures were analysed in both contexts for several anthropomorphic combinations through photo/video. Angles were measured using the kinovea0.8.15 software and classified according to European-Standards (EN1005-4:2005+A1:2008).
Results: For a radiographers taller than patient (180cmm/153cm) were identified postures that could lead to WRMSDs, mainly during the MLO positioning. The measured angles in this context were 139º for arm flection, -24º head/neck, 120º arm abduction and 72º for trunk/back, being classified as non-acceptable according to European-Standards- After the introduction of corrective actions (radiographer seated), the measured angles were 60º for arm flection, 99º arm abduction, 0º head/neck and 14º for trunk/back. The classification of angles was acceptable after corrective measures.
Conclusion: The radiographers can develop WRMSDs while they are positioning the breast to acquired CC and MLO views. The introduction of corrective measures improved the positioning procedure and demands, considering several anthropomorphic characteristics of patients and workers. These improvements have potencial to reduce the risk of WRMSDs for radiographers.

B-0667 14:48

The effect of mean glandular dose variations on effective risk from full-field digital mammography in screening

R.M.K. M.Ali, A. England, A.K. Tootall, C.E. Mercer, P. Hogg; *Manchester/UK (P.Hogg@salford.ac.uk)*

Purpose: Investigate the effect of Mean Glandular Dose (MGD) variations of 16 Full Field Digital Mammography (FFDM) machines on the risk of radiation-induced cancer from screening mammography.
Methods and Materials: Organ doses from FFDM screening exposures (craniocaudal and mediolateral oblique) were measured using a simulated approach involving average breast thickness and adult ATOM phantoms with 16 FFDM machines. Doses were measured using TLDs accommodated inside the ATOM phantom; examined breast MGD was calculated. Total effective risk during a client's lifetime was calculated for 150 screening scenarios of different screening commencement ages and frequencies. For each scenario, a set of conversion factors was graphically obtained to convert MGD values into total effective risk.
Results: The examined breast received the highest radiation dose. For the 16 FFDM machines, MGD contributes approximately 98% of total effective risk. Although total effective risk decreases as screening commencement age increases, MGD contribution remains approximately constant because the radio-sensitivity of all body tissues, including breast tissue, reduce with age. The high breast tissue dose makes variations due to other tissues very small. Three sets of conversion factors were obtained for three screening frequencies (annual, biennial, triennial). Three relationship graphs between screening commencement age and total effective as percentages of MGD were established.
Conclusion: The use of graphical representation of total risk could be an easy way to illustrate the total effective risk during a client's lifetime. Screening frequency, commencement age, and MGD are good predictors for total effective risk generating more understandable data by clients than MGD.

B-0668 14:56

Radiographers' practice in mammography departments: challenges in training and clinical performance

E. Metsälä[1], N. Richli[2], J. Jorge[2], A. Henner[3], T. Kukkes[4], C. Reis[5]; [1]*Helsinki/FI*, [2]*Lausanne/CH*, [3]*Oulu/FI*, [4]*Tartu/EE*, [5]*Lisbon/PT (eija.metsala@metropolia.fi)*

Purpose: The aim of this study was to identify European radiographers' most common challenges of clinical performance and mammography training.
Methods and Materials: An extensive search was performed to identify studies focused on clinical practice and on training in mammography published in the English language between January 2010 and December 2015. Several electronic databases were used in search engines EBSCO Host, Pro Quest, MEDLINE and the Open Access Theses and Dissertations database (OATD). The data were analysed by using deductive thematisation analysis.
Results: A total of 27 full text articles were reviewed in the first stage, 11 were excluded due to the content and 16 were used to perform the integrative review. Most common challenges of clinical performance in mammography among European radiographers involved technical performance, quality of practices and patient-centred care. The main challenges of training were related to the need of more education in mammography, the structure and organisation of education and radiographer-related challenges.
Conclusion: Introduction of harmonised guidelines across Europe may serve as an evidence-based tool to be implemented in mammography education. However, the variability in human and material resources across Europe as well as the different cultures contexts should be considered in the introduction of improvements in this field of radiographers practice.

B-0669 15:04

Importance of training the radiographer in communication technique with female patient with breast cancer

H. Mohammed; *Doha/QA (hessa-salem@hotmail.com)*

Purpose: This paper seeks to explore the benefits of radiographer training regarding communication with woman breast cancer patients. The study targets women patients undergoing breast imaging procedures. It aims to show that it is beneficial for patients to be aware of how the radiographer is relaying the patient's health condition.
Methods and Materials: The procedure involved administering multiple-choice questionnaires. The multiple questions helped to determine if patients are comfortable with being taken through the imaging process due to communication between the radiographer and the patient. Another survey was conducted to gage whether patient's knowledge of their imaging procedure experience helped radiologists avoid mistakes in diagnosis or improved the accuracy of the diagnosis. This was done by administering the questionnaire to radiologists. The aim was to discover if radiographer interaction with patients who understood the breast imaging procedure eased the diagnosis process.
Results: Two-third of patients respondents expressed interest in understanding breast imaging procedures. Half of the radiologists who responded acknowledged that patients who understand breast imaging procedures make the diagnosis process a smoother process, as those patients comprehend the importance of the procedure.
Conclusion: Radiographer communication training can ease communications with all patients who are undergoing cancer treatment. Such an arrangement improves the quality and speed of cancer diagnosis procedures.

B-0670 15:12

Radiographer's role in the conscious participation in breast screening: the importance of interpersonal aspects and communication

M. Simoncini[1], M. Biondi[1], M. Virgilio[2], L. Giuliani[2], C. Ottonello[1]; [1]*Pomezia/IT*, [2]*Rome/IT (marta.simo@hotmail.it)*

Purpose: To evaluate the role of mammographic screening dedicated radiographer in: 1) improving patient awareness; 2) promoting patient's active participation; 3) better managing the patient's emotional component.
Methods and Materials: In the last three years we have organised an information campaign based on: 1) explanatory leaflets on the screening programme; 2) research and development of more effective communication channels (verbal and non-verbal) in order to better interact with patient with more empathy. That was possible through few precise details and by paying more attention to the emotional state of women, in close collaboration with radiologist, in order to create a safe and welcoming environment and improving a better response at screening examination call.
Results: With an information programme consisting in awareness screening flyers and by searching an effective and more empathic communication channel (verbal and non-verbal) we observed a progressive increase of mammographic call response up to 37,71% from 2012 to 2015.

Conclusion: Radiographer-patient communication channel is an important element in clinical practice, as seen as the first contact with a breast unit. The whole examination procedure is therefore optimised not only because of improving imaging quality but also because of improving full and conscious patient compliance.

B-0671 15:20

Mathematical modelling of radiation-induced caner from screening mammography

R.M.K. M.Ali, A. England, A.K. Tootall, C.E. Mercer, P. Hogg; *Manchester/UK (P.Hogg@salford.ac.uk)*

Purpose: Establish a mathematical model to predict radiation risk from Full Field Digital Mammography (FFDM) screening.
Methods and Materials: Radiation risk from screening mammography was quantified using effective risk. For effective risk calculations, organ doses and examined breast mean glandular dose (MGD) were used. Screening mammography was simulated by exposing a breast phantom (cranio-caudal and medio-lateral oblique) for each breast using 16 FFDM machines. An ATOM phantom loaded with thermo-luminescent dosimeters was positioned in contact with the breast phantom to simulate the client's body. Effective risk data were analysed to establish a regression model to predict the effective risk of any screening programme. Graphs were generated to extrapolate the effective risk of all screening programmes.
Results: Screening commencement age and number of screening visits are the most important factors which influence total effective risk (correlation coefficients >0.5). The regression model shows that 87% of total effective risk variability can be predicted by commencement/end ages and number of screens. Since tissue radio-sensitivity reduces with age, the secession age does not result in noteworthy effect on total effective risk.
Conclusion: Regression modelling can be used to predict total effective risk for breast screening clients but it cannot be used for exact assessment of total effective risk (standard error of estimate=91.13case/10^6, 31.21%). Graphical representation of risk could be a better and easy way to represent risk in a manner which might be helpful to clients and clinicians, unlike MGD which is not readily understandable within certain populations.

14:00 - 15:30 **Room M 1**

Cardiac

SS 703a

Atherosclerosis and plaque imaging

Moderators:
T.C. Walter; Berlin/DE
F. Wolf; Vienna/AT

B-0672 14:00

High-risk plaque and calcification at coronary CT to predict future events after second generation drug eluting stent implantation

N. Tomizawa, K. Yamamoto, S. Inoh, T. Nojo, S. Nakamura; *Matsudo/JP (tomizawa-tky@umin.ac.jp)*

Purpose: To investigate whether high-risk plaque (HRP) and calcium detected by coronary CT could predict future events after second generation drug eluting stent (DES) implantation.
Methods and Materials: We included 317 patients from December 2012 to April 2015 who received second generation DES implantation (everolimus-eluting, zotalorimus-eluting or biolimus-eluting stent) because coronary artery disease was suspected by coronary CT and confirmed by coronary angiogram or functional tests. Patients were divided into three groups for further analysis: high-risk group (HRG) as possessing HRP (low-attenuation and positive remodelling or napkin-ring sign) with Agatston score ≥400, low-risk group (LRG) as Agatston score <400 without HRP and the remaining patients as intermediate-risk group (IRG). The primary endpoint was a composite of all-cause mortality, myocardial infarction, fatal arrhythmia or repeated revascularisation.
Results: During the median follow-up period of 26.3 months, primary endpoint was observed in 74 patients (23%). Primary endpoint occurred more frequently in the HRG (42%, p=0.0001), and the IRG (26%, p=0.02) than the LRG (12%). Cox regression model adjusting for baseline characteristics showed that HRG and IRG were significant predictors of the primary endpoint (hazard ratio, 2.7 and 1.9, 95% confidence interval 1.3−5.7 and 1.0−3.8, p=0.001 and 0.04, respectively).
Conclusion: The presence of coronary HRP and calcium detected by CT would be an independent risk factor for future cardiovascular events after second generation DES implantation.

B-0673 14:08

Different anticoagulation regimes affect stenosis and plaque composition in patients with atrial fibrillation

C. Beyer, F. Plank, G. Friedrich, M. Wildauer, W. Dichtl, G. Feuchtner; *Innsbruck/AT (christoph.beyer@student.i-med.ac.at)*

Purpose: Vitamin K Antagonists (VKA) are associated with an increase of vascular calcification which may lead to a higher cardiovascular event risk. However, the mechanism has not yet been fully understood. If new anticoagulants(NOACs) have similar vascular effects is unclear. Therefore, we analysed patients with atrial fibrillation(AF) and different anticoagulation regimes regarding coronary stenosis and plaque morphology by CTA.
Methods and Materials: Three patient cohorts matched for age, gender and cardiovascular risk factors (total N=132, mean60.8years) in patients with AF and VKA, without anticoagulation and a control group without arrhythmia underwent coronary CTA.To compare results of VKA to NOACs, an additional matched patient cohort (N=45) has been analysed. Images were evaluated for plaque types (non-calcified,mixed,calcified) and stenosis (<50%;50-70%,>70%). Segment involvement score (SIS) and non-calcified SIS were calculated. High risk plaque features (HRP; napkin ring sign, low attenuation plaque, spotty calcifications, positive remodelling) were quantified.
Results: Patients under AF using VKA had equal degrees of stenosis, overall plaque burden and calcification, however, increased rates of non-calcified plaques (ncSIS 0.9vs.0.3vs.0.3,p<0.001). Especially HRP features were increased (37%vs.14%vs.16%,p<0.001). Also, low attenuation plaques had significantly lower CT-attenuation levels (40.2vs.46.0vs.49.9HU,p<0.05). Patients under AF and NOACs showed inverse results: equal non-calcified plaques and HRP, however, increased overall plaque burden (SIS 3.2vs.1.4vs.1.4,p<0.05) and calcium score (240vs.58vs.146HU,p<0.05).
Conclusion: Patients in AF using VKA had increased vulnerable and lipid-rich plaques, whereas patients under NOACS had a higher rate of calcification and overall plaque burden. Therefore, NOACs may not attenuate overall CV risk while conventional VKA may be associated with higher rates.

B-0674 14:16

Calcified coronary artery disease: advanced calcium subtraction improves luminal visualisation and diagnostic confidence in dual-energy coronary CT angiography

D. De Santis, M.H. Albrecht, M. Eid, C.N. De Cecco, A. Varga Szemes, T.M. Duguay, U.J. Schoepf; *Charleston, SC/US (domenico.desantis@hotmail.it)*

Purpose: To evaluate a prototype algorithm for calcium subtraction and its impact on luminal visualisation in patients with calcified coronary artery disease (CAD) using dual-energy coronary computed tomography angiography (DE-CCTA).
Methods and Materials: Twenty-nine patients (62% male; mean age, 62 ± 9 years) who had undergone DE-CCTA were retrospectively included in this IRB-approved study. Linearly-blended M_0.6 (60% low-kV spectrum) and calcium subtracted (CS) images were reconstructed. Two independent readers assessed luminal visualisation of the coronary arteries in a segment-based analysis, as well as subjective image quality and diagnostic confidence using 5-point Likert scales. Contrast-to noise ratios (CNR) for both datasets were calculated. Wilcoxon testing and Cohen's κ were used for statistical comparisons.
Results: CS images showed higher lumen visualisation (P=0.008), with excellent inter-reader agreement (mean score, 3.3; κ=0.82), compared to standard M_0.6 series (mean score, 2.9; κ=0.77). The CS algorithm granted a higher diagnostic confidence in comparison with linearly-blended reconstructions (mean scores, 4.0 and 3.1, respectively; P<0.001). No significant differences between CS and M_0.6 datasets were found in terms of image quality (subjectively - mean scores, 4.1 and 4.2, respectively; P = 0.442, and objectively - mean CNR, 37.0 and 38.2, respectively; P = 0.733).
Conclusion: A prototype algorithm for CS substantially improves coronary lumen visualisation and diagnostic confidence in patients with calcified CAD without deteriorating image quality.
Author Disclosures:
C.N. De Cecco: Consultant; Guerbet. Research/Grant Support; Siemens.
A. Varga Szemes: Consultant; Guerbet. **U.J. Schoepf:** Consultant; Guerbet. Research/Grant Support; Astellas, Bayer, Bracco, GE, Medrad, Siemens.

B-0675 14:24

Assessing genetic and environmental influences on epicardial and abdominal fat quantities: a classical twin study

A.L. Jermendy[1], M. Kolossvary[1], Z.D. Drobni[1], A.D. Tarnoki[1], D.L. Tarnoki[1], J. Karady[1], S. Voros[2], B. Merkely[1], P. Maurovich-Horvat[1]; [1]*Budapest/HU*, [2]*Richmond, VA/US (adam.jermendy@gmail.com)*

Purpose: Increased quantity of epicardial and abdominal adipose tissue compartments are linked to elevated cardiometabolic risk. The role of genetic and environmental factors in the lipid accumulation of different fat compartments is unclear. This study aims to assess the genetic and environmental effects on epicardial and abdominal adipose tissue quantities within a cohort of adult twin pairs.
Methods and Materials: We investigated 180 twin subjects (mean age: 55.8±9.6) of whom 57 were monozygotic (MZ) pairs and 33 were dizygotic (DZ) same-gender pairs. Epicardial adipose tissue (EAT) volume as well as subcutaneous and visceral adipose tissue (SAT and VAT) compartments at the upper abdominal level were quantified by a 256-slice CT-scanner. Values of MZ and DZ twin pairs were separately analysed and compared. Intra-pair correlations and multi-trait structural equation model were used to assess genetic and environmental influences.
Results: In co-twin analysis, MZ twins had higher degree correlations (r values) than DZ twins for EAT (rMZ = 0.81, rDZ = 0.32) and also for SAT and VAT quantities (rMZ = 0.80, rDZ = 0.68 and rMZ = 0.79, rDZ = 0.48, respectively). In multi-trait model fitting analysis the overall contribution of genetic factors to EAT, SAT and VAT quantities was 80%, 78% and 70% whereas that of environmental factors was 20%, 22% and 30%, respectively.
Conclusion: In our twin cohort, genetic effects strongly predominated over environmental influences in the phenotypic appearance of EAT, SAT and VAT quantities.

B-0676 14:32

PARISK (Plaque At RISK) study: the association between intraplaque haemorrhage and thrombin generation in symptomatic carotid atherosclerotic plaques

G.A.J.C. Crombag[1], H. Spronk[1], A. van der Lugt[2], J. Hendrikse[3], P.J. Nederkoorn[4], J.W. Wildberger[1], H. ten Cate[1], R.J. van Oostenbrugge[1], M.E. Kooi[1]; [1]*Maastricht/NL*, [2]*Rotterdam/NL*, [3]*Utrecht/NL*, [4]*Amsterdam/NL (g.crombag@maastrichtuniversity.nl)*

Purpose: Carotid atherosclerosis is an important cause of stroke. Intraplaque hemorrhage (IPH) on MRI increases the ischaemic stroke risk. Little is known, however, about mechanisms leading to IPH development. Thrombin is an essential enzyme in haemostasis. Recent animal studies have shown that direct thrombin inhibitors attenuate atherosclerosis. We hypothesize that thrombin generation affects IPH and plaque development and may be a suitable blood biomarker for IPH on MRI. To investigate whether thrombin generation parameters are associated with MRI plaque parameters in stroke patients.
Methods and Materials: Patients were included in the Plaque-AT-RISK study and underwent multi-sequence carotid 3.0T MRI and blood sampling. Presence and volume of IPH, lipid-rich necrotic core and fibrous cap status were assessed on MRI using dedicated software by trained observers. The thrombin generation was assessed in platelet-poor plasma, resulting in the following parameters: lag time, peak height, endogenous thrombin potential and velocity index. Binary logistic regression was used to investigate the association between MRI and thrombin generation parameters.
Results: Valid MR plaque imaging results were available in 224/244 patients; in 161 patients blood samples also were available. IPH was present in 65/161 patients. There were no significant associations between the various MRI parameters and the different thrombin generation parameters.
Conclusion: Plaque MRI parameters show no strong association with thrombin generation in stroke patients. Systemic thrombin generation does not seem to affect IPH. The identification of IPH on MRI remains the method of choice to identify this important hallmark of plaque vulnerability.

B-0677 14:40

Epicardial adipose tissue and pericoronary fat tissue thickness in patients with essential hypertension environmentally exposed to cigarette smoke

P. Gac, P. Jazwiec, M. Poreba, G. Mazur, R. Poreba; *Wroclaw/PL (pawelgac@interia.pl)*

Purpose: The determination of the influence of the environmental exposure to cigarette smoke on epicardial adipose tissue and pericoronary fat tissue thickness in patients with hypertension.
Methods and Materials: The research has covered 96 people with hypertension: 48 non-smokers, declaring the environmental exposure to cigarette smoke (group A, mean age: 65.83±10.86 years) and 48 non-smokers declaring the lack of environmental exposure to cigarette smoke (group B, mean age: 64.67±10.24 years). In all patients 128-slice multidetector computed tomography of coronary vessels (coroCT) was carried out. Scans acquired in coroCT were evaluated with regard to epicardial adipose tissue thickness (EATT) and pericoronary fat tissue thickness (PFTT). EATT was measured on the right ventricular anterior free wall. PFTT was determined in 3 localisations: at the region of the right coronary artery ($PFTT_{RCA}$), left anterior descending ($PFTT_{LAD}$) and left circumflex ($PFTT_{LCX}$).
Results: In group A the average values of EATT, $PFTT_{RCA}$, $PFTT_{LAD}$, $PFTT_{LCX}$ were significantly higher than in group B (EATT [mm] - 6.18±1.94 vs 5.43±1.57; $PFTT_{RCA}$ [mm] - 14.98±3.67 vs 13.48±3.18; $PFTT_{LAD}$ [mm] - 6.15±1.96 vs 5.12±2.01; $PFTT_{LCX}$ [mm] - 12.57±3.91 vs 11.06±2.84; $p<0.05$). In regression analysis it was documented that passive smoking constitutes a risk factor for higher values of EATT, $PFTT_{RCA}$, $PFTT_{LAD}$ and $PFTT_{LCX}$.
Conclusion: In patients with hypertension the environmental exposure to cigarette smoke is connected with the thickening of epicardial adipose tissue and pericoronary fat tissue.

B-0678 14:48

Iterative model reconstruction improves semiautomated plaque quantification in coronary CT angiography

I. Kocsmar, M. Karolyi, B. Szilveszter, M. Kolossvary, J. Karady, A. Jermendy, A. Bartykowszki, B. Merkely, P. Maurovich-Horvat; *Budapest/HU (ildi.kocsmar@gmail.com)*

Purpose: The performance of automated plaque quantification in coronary CT angiography (CTA) dependents on image quality. It has been demonstrated that hybrid iterative reconstruction (HIR) technique improves CTA image quality compared to standard filtered back projection (FBP) allowing more accurate plaque quantification. Our aim was to evaluate the effect of iterative model reconstruction (IMR) on automated coronary plaque assessment, as compared to HIR and FBP.
Methods and Materials: We studied 20 consecutive patients (80.0% male, mean age 66.7±8.9 years) with coronary artery disease using 256-slice multidetector-row coronary CTA. All CTA datasets were reconstructed with FBP, HIR and IMR. Total plaque volume of the three main coronaries were quantified using automated plaque quantification software. Lumen and outer vessel wall contours were manually corrected, if necessary. Fixed window settings were used for CTA reading.
Results: Overall volume was larger without manual correction, as compared to manually adjusted measurements using FBP (924±367 vs 823±333 mm^3, $p=0.013$). Using HIR, we also found significant difference between the non-adjusted and manually adjusted plaque volumes (852±331 vs 784±325 mm^3, $p=0.043$). However, no difference was found between the non-adjusted and manually corrected measurements for overall plaque volume using IMR (801±328 vs 709±297 mm^3, $p=0.078$).
Conclusion: IMR-based fully automated plaque quantification leads to similar values as the manually corrected measurements. Therefore, IMR might result in a more efficient and less observer-dependent coronary CTA plaque quantification as compared to FBP and HIR.

B-0679 14:56

Contrast-enhanced MRI of inflammatory component of coronary atherosclerosis in patients with acute coronary syndrome

W.Y. Ussov, N.V. Belokopytova, T.A. Shelkovnikova, E.A. Aleksandrova, E.Y. Pushnikova, V.D. Aptekar; *Tomsk/RU (wolfussov@yandex.ru)*

Purpose: We evaluated the patterns of contrast enhancement (CE) of arterial walls of coronary arteries in CE-MRI of the heart in patients with myocardial infarction due to stenosis or in non-stenotic coronary atherosclerosis.
Methods and Materials: Of 23 patients with myocardial infarction in 11 no coronary stenosis over 40% of lumen was revealed whereas in 12 the coronary stenosis was > 50%. In everyone the CE-MRI of the heart included imaging with contrast as 0,1 mM/Kg of BW and acquisition of slices depicting the descending and circumflex branches of the left coronary artery. Volume of myocardial damage (V_{md}, cm^3) and index of enhancement (IE), were calculated.
Results: V_{md} in patients with and without coronary stenosis did not differ significantly and was 14,5 ± 2,6 cm^3 and 13,8 ± 3,5 cm^3 ($p > 0,1$). Highly intense uptake of paramagnetic was seen in patients with coronary stenosis in infarction-related CA for as long as 19 — 31 mm (in average 24 ± 4 mm), IE = 1,57 ± 0,09 for the infarction itself and IE = 1,87 ± 0,12 for the region of stenosis. In patients with "pure" coronary arteries the IE for infarction region = 1,68 ± 0,14, and the infarction-related coronary artery IE = 2,67 ± 0,21 (1,58 — 5,89), superior to values in group of persons with myocardial infarction and critical stenosis.
Conclusion: CE-MRI of coronary arteries provides imaging of coronary inflammatory response in patients with myocardial infarction both due to and without coronary critical stenosis.

B-0680 15:04

Relationship between complications during pregnancy and coronary atherosclerosis later in life in African-American women assessed by coronary computed tomography

J.L. Wichmann[1], J.H. Nunez[1], R. Vliegenthart[2], K. Otani[3], S.E. Litwin[1], P.B. Morris[1], T.J. Vogl[4], N.K. Wenger[5], U.J. Schoepf[1]; [1]*Charleston, SC/US*, [2]*Groningen/NL*, [3]*Tokyo/JP*, [4]*Frankfurt a. Main/DE*, [5]*Atlanta, GA/US (docwichmann@gmail.com)*

Purpose: To compare the prevalence and degree of coronary atherosclerosis detected by coronary computed tomography angiography (CCTA) in African-American women with and without a history of complications during prior pregnancy.
Methods and Materials: We retrospectively evaluated patient characteristics and CCTA findings in groups of African-American women with a history of pregnancy complications including preterm delivery (n=154), preeclampsia (n=137), or gestational diabetes (n=148), and a matched control group of African-American women who gave birth without such complications (n=445). Univariate and multivariate analyses were performed to assess predictors of coronary atherosclerosis.
Results: Average age at delivery and CCTA, number of pregnancies, smoking history, body mass index, and prevalence of hypertension or hyperlipidaemia were similar between groups (all P>0.2). All groups with a history of pregnancy complications showed higher rates of any (=20% luminal narrowing) and obstructive (>=50% luminal narrowing) coronary atherosclerosis (preterm delivery: 29.2% and 9.1%; preeclampsia: 29.2% and 7.3%; gestational diabetes: 47.3% and 15.5%) compared to control women (23.8% and 5.4%). After accounting for confounding factors at multivariate analysis, gestational diabetes remained a strong predictor of any (OR 3.26; 95% confidence interval 2.03-5.22; P<0.001) and obstructive coronary atherosclerosis (OR 3.00; 95% confidence interval 1.55-5.80; P<0.001) on CCTA.
Conclusion: A history of pregnancy complications was associated with a higher prevalence of coronary atherosclerosis on CCTA in African-American women, but only a history of gestational diabetes represented an independent predictor of any and obstructive coronary atherosclerosis in our study.
Author Disclosures:
J.L. Wichmann: Speaker; Siemens Healthcare, GE Healthcare. **K. Otani:** Employee; Siemens Japan K.K.. **U.J. Schoepf:** Research/Grant Support; Bayer, Bracco, GE Healthcare, Medrad, Siemens Healthcare.

B-0681 15:12

Sensitivity and specificity of epicardial adipose tissue thickness measured with 128-slice computed tomography as a marker predicting significant lesions in coronary arteries

P. Gac, P. Jazwiec, O. Kornafel-Flak, R. Poreba; *Wroclaw/PL (pawelgac@interia.pl)*

Purpose: To determine the sensitivity and specificity of epicardial adipose tissue thickness measured by 128-slice computed tomography as a marker predicting significant lesions in coronary arteries in patients with the suspicion of coronary artery disease (CAD).
Methods and Materials: The study group included 99 patients with the suspicion of CAD who were sent for 128-slice multidetector computed tomography of coronary vessels (coroCT). Mean age in the study group was 60.53±12.65 years. Scans obtained in coroCT were evaluated in order to find significant lesions in coronary arteries and to estimate epicardial adipose tissue thickness (EATT). Significant lesion of coronary artery was defined as stenosis exceeding 50%. EATT was measured on the right ventricular anterior free wall.
Results: The presence of the significant stenosis in coronary arteries in the study group was confirmed in 15.15% of patients. Mean value of EATT was 5.42±1.82mm. On the base of ROC curve EATT value was estimated, as an optimal cut-off point of the prediction of the significant stenosis in coronary arteries in the study group, giving the result of 6.7mm. The area under the curve for EATT was 89.7%. Sensitivity, specificity and accuracy of the EATT ≥6.7mm as a predictor of the significant stenosis in coronary artery were, respectively, 0.893, 0.867 and 0.889.
Conclusion: In a study group of patients with suspicion of CAD the determination of epicardial adipose tissue thickness in computed tomography angiography of the coronary arteries may constitute a good predictive marker of the significant lesions in coronary arteries.

B-0682 15:20

Downstream investigation of non-cardiac incidental findings in patients undergoing CT coronary angiography: findings from the multi-center randomised controlled SCOT-HEART trial

M.C. Williams[1], A. Hunter[1], J. Dreisbach[2], J.R. Weir-McCall[3], M. Macmillan[1], S. Mirsadraee[1], E.J.R. van Beek[1], D.E. Newby[1], G. Roditi[2]; [1]*Edinburgh/UK*, [2]*Glasgow/UK*, [3]*Dundee/UK*

Purpose: The prospective multi-centre randomized controlled Scottish COmputed Tomography of the HEART (SCOT-HEART) trial showed CT coronary angiography (CTCA) improved diagnostic certainty, changed management and reduced myocardial infarction. Here we assessed non-cardiac findings (NCF), and the impact of changes in lung nodule guidelines.
Methods and Materials: Trial radiologists reported NCF and assessed whether they were responsible for symptoms (yes, probable, unlikely, no). Significant NCF were those requiring further investigation, follow-up or treatment. Lung nodule follow-up recommendations were provided using 2005 Fleischner Guidelines. We assessed potential changes to management using the 2015 British Thoracic Society (BTS) Guidelines.
Results: NCF were reported in 677 (38%) of 1778 patients who underwent CTCA, with 173 (9.7%) defined as significant. NCF were the cause of symptoms in 22 (1.2%), and probably the cause in 33 (1.9%). Five patients (0.3%) had pulmonary emboli, 135 patients (7.6%) required further imaging for NCF and 41 (2.5%) required additional clinic consultations. Lung nodules or masses were identified on 200 scans (11%) and 81 had follow-up CT (4.6%). Malignancy was subsequently diagnosed in 7 patients (0.4%), all of whom had either lung nodule >10mm or mediastinal lymphadenopathy. Application of the BTS guidelines would mean 22 patients (27%) did not require follow-up, none of whom have developed evidence of lung malignancy.
Conclusion: Although common in outpatients undergoing CTCA, most NCF are not clinically important and only a small number are the cause of chest pain. Application of new lung nodule guidelines will reduce follow-up imaging, without the risk of missing malignancy.
Author Disclosures:
E.J.R. van Beek: Speaker; Toshiba Medical Systems. **D.E. Newby:** Speaker; Toshiba Medical Systems. **G. Roditi:** Speaker; Toshiba Medical Systems,Bracco, Bayer-Schering, GE Healthcare and Guerbet.

14:00 - 15:30 **Room M 2**

Cardiac

SS 703b

Acute chest pain and non-ischaemic cardiomyopathies

Moderators:
S. Feger; Berlin/DE
S. Harden; Southampton/UK

K-12 14:00

Keynote lecture

V.E. Sinitsyn; *Moscow/RU*

B-0683 14:09

Triple rule out in patients with acute chest pain: economic aspects

M. Fusaro, G. Tessarin, M. Milana, M. Tessarin, L. La Torre, G. Morana; *Treviso/IT (tessarin.giovanni@gmail.com)*

Purpose: To asses economic impact of triple rule out with second generation dual source CT in the management of patients with atypical acute chest pain.
Methods and Materials: Blinded prospective observational cohort study to conduct a cost-effectiveness analysis of TRO CT versus standard care in patients with atypical acute chest, with negative ECG and troponin test, arriving to ED from March 7, 2016 to July 7, 2016. Endpoints were costs (euro) and length of hospitalization (hours) per patient. The descriptive analysis of the data was performed with SPSSv13 and with WinPEPI v11.5. Z test (p<0.05) was used to compare all means (euro and length of hospitalization).
Results: 70 patients (53.9yo ±10.3), 44 (62.9%) males, were enrolled: 44 (62.9%) were free of CAD, 23 (32.9%) had <50% CAD and 3 (4.3%) had a >50% CAD. No pulmonary embolism or aortic dissection were observed. The mean length of hospitalization per patient was significantly lower for the TRO protocol (8.41 hours vs. 63.21 hours, p<0,05). Invasive coronary angiography (ICA) was performed in 5 patients, suggested by CT only in 2 cases. The mean costs per patient were significantly lower for the TRO protocol than the standard of care (376.64 € vs 976.28 €, p<0,05).
Conclusion: In patients with atypical acute chest pain, properly stratified, triple rule out with second generation dual source CT is more cost-effective compared to the standard of care of our institution.

B-0684 14:17

Acute chest pain CT in comparison with standard treatment: a cost-effectiveness study

J.L. Wichmann[1], K. Otani[2], C.M. Carr[1], C. Tesche[1], S.E. Litwin[1], R.R. Bayer[1], C.N. De Cecco[1], T.J. Vogl[3], U.J. Schoepf[1]; [1]*Charleston, SC/US*, [2]*Tokyo/JP*, [3]*Frankfurt a. Main/DE (docwichmann@gmail.com)*

Purpose: To evaluate the cost-effectiveness of coronary CT angiography (CCTA) in comparison with traditional management protocols in patients presenting to the emergency department (ED) with chest pain.
Methods and Materials: We performed a retrospective single-centre analysis in 2,156 patients who presented to the ED with acute chest pain. Patient cohorts matched by patient characteristics and pretest likelihood for coronary artery disease (CAD) had undergone CCTA as the primary imaging test (n=1,139) or traditional standard of care (n=1,017). Cost-relevant factors of ED visits, utilisation of downstream tests and total patient care cost were compared.
Results: No significant differences between cohorts were observed for age, gender, race, BMI, or CAD risk factors (all P>0.08). In addition, no significant differences in the diagnosis of CAD were observed (all P>0.11). Time to discharge (4.5 vs 7 hours), hospital admission rate (12.6% vs 54.2%), length of hospital stay (48 vs 72 hours) and readmission rate within 30 days (3.5% vs 14.6%) were significantly lower in CCTA patients (all P>0.001). Reduced rates of additional downstream testing (e.g. nuclear stress test) and invasive coronary angiography (4.9% vs 22.7%; P<0.001), and ultimately lower total cost per patient (11,783$ vs 18,996$, P<0.001) were observed in the CCTA cohort.
Conclusion: In this large single-center study, the use of CCTA as the initial imaging test in patients presenting to the ED with acute chest pain was associated with shorter ED and hospital stays, lower readmission rates and ultimately reduced total cost, mostly due to reduced utilisation of additional downstream tests.
Author Disclosures:
J.L. Wichmann: Speaker; Siemens Healthcare, GE Healthcare. **K. Otani:** Employee; Siemens Japan K.K.. **C.N. De Cecco:** Research/Grant Support; Siemens Healthcare. **U.J. Schoepf:** Research/Grant Support; Bayer, Bracco, GE Healthcare, Medrad, Siemens Healthcare.

B-0685 14:25

Coronary CT angiography-derived plaque quantification in patients with acute coronary syndrome

C. Tesche, D. Caruso, C.N. De Cecco, T.M. Duguay, D.C. Shuler, J.D. Rames, M.H. Albrecht, A. Varga-Szemes, U.J. Schoepf; *Charleston, SC/US (tesche.christian@gmail.com)*

Purpose: To assess the discriminatory value of quantitative atherosclerotic plaque markers derived from coronary CT angiography (cCTA) in patients with acute coronary syndrome (ACS) compared to patients with stable coronary artery disease (CAD).
Methods and Materials: 40 patients (56.9±9.3years, 55% male) admitted for ACS were retrospectively analysed and compared to Framingham risk score matched controls with stable CAD. All patients underwent cCTA followed by invasive catheter angiography (ICA). ACS-related culprit lesions were identified using ICA. Total plaque volume (TPV), calcified and non-calcified plaque volumes (CPV, NCPV), plaque burden (PB), remodeling index (RI), lesion length (LL), presence of napkin-ring sign, segment involvement score (SIS), and segment stenosis score (SSS) were derived from cCTA and compared between both groups on a per-lesion and per-patient level.
Results: Patients with ACS showed significantly more obstructive CAD, and higher values for SSS, SIS, NCPV, LL, and RI compared to the stable CAD group (all p<0.05). Culprit lesions had significantly higher values for PB, TPV, NCPV, RI, LL, and prevalence of napkin-ring sign in comparison to non-culprit lesions (all p<0.05). A ROC analysis showed that clinical risk scores and plaque markers demonstrated incremental discriminatory power in identifying ACS on a per-patient (AUC 0.92, p<0.0001) and per-lesion (AUC 0.88, p<0.0001) level.
Conclusion: cCTA-derived culprit plaque markers show discriminatory value on a per-patient and per-lesion level. A combination of markers added to the Framingham risk score yields the greatest discriminatory ability and may aid in the identification of patients at risk for ACS over clinical risk scores alone.
Author Disclosures:
C.N. De Cecco: Consultant; Guerbet. Research/Grant Support; Siemens. **A. Varga-Szemes:** Consultant; Guerbet. **U.J. Schoepf:** Consultant; Guerbet. Research/Grant Support; Astellas, Bayer, Bracco, GE, Medrad, and Siemens.

B-0686 14:33

Global and regional left ventricular myocardial deformation in cardiac amyloid light-chain amyloidosis: assessment with cardiovascular magnetic resonance tissue tracking

R. Li, Z.-G. Yang, Y.-K. Guo; *Chengdu/CN (ddtwg_nsmc@163.com)*

Purpose: To clarify the feasibility of cardiovascular magnetic resonance (CMR) derived tissue tracking strain analysis for assessing the difference of LV myocardial deformation between normal subjects and light-chain amyloid (AL) cardiac amyloidosis (AL-CA) patients.
Methods and Materials: Thirty-two AL-CA patients, including 19 with preserved systolic function and 13 progressed to systolic dysfunction (LVEF<50%), and 26 healthy controls underwent CMR examination. LV global and regional radial, circumferential and longitudinal myocardial peak systolic strain values (PSS) and rates (PSSR), as well as peak diastolic strain rates (PDSR) were compared among three patients groups. Receiver operating characteristic analysis (ROC) was performed to determine if myocardial deformation parameters could help discriminating LV dysfunction between normal subjects and AL-CA patients with preserved LVEF.
Results: AL-CA patients, regardless of LVEF, had significantly reduced PSS and PDSR (radial, circumferential and longitudinal) compared with normal subjects (all P<0.05). Patients with AL-CA and impaired LVEF showed lower radial, circumferential and longitudinal PSS and circumferential PDSR in basal, mid and apical levels, reduced radial PSSR and PDSR in mid and apical level, and decreased longitudinal PSSR in basal and mid slices compared with AL-CA patients with preserved LVEF (all P<0.05). The ROC curve analysis revealed that global and regional circumferential and longitudinal PSS, and radial PDSR may be used as indicators for differentiating LV dysfunction between AL-CA patients with preserved LVEF and normal subjects.
Conclusion: The differences in LV myocardial deformation between normal subjects and AL-CA patients can be monitored using tissue tracking CMR.

B-0687 14:41

Myocardial contractile disfunction is correlated with maximum wall thickness and myocardial lipid accumulation in Fabry's disease: a CMR study with tissue tracking technique

N. Galea, R. Ammendola, M. Francone, A. Fiorelli, F. Ciolina, A. Frustaci, C. Catalano, I. Carbone; *Rome/IT (rosamaria.ammendola@gmail.com)*

Purpose: Our purpose was to investigate the relationships between degree of left ventricular (LV) hypertrophy, function impairment and lipid accumulation in patients with Fabry Disease Cardiomyopathy (FDC) using cardiac magnetic resonance (CMR) tissue tracking technique (TTT).
Methods and Materials: 22 FDC biopsy-proven consecutive patients (9 males, age 53.4 years) underwent to CMR exam on 1.5 Tesla unit acquiring STIR-T2w, cineMR, late enhancement and Modified Look Locker inversion recovery (MOLLI) sequence before and 15 minutes after injection of 0.2mmol/Kg Gd-DOTA for extracellular volume fraction (ECV) measurement. LV volumes, maximal wall thicknesses (MWT), native T1 (nT1) and ECV were analysed. Global longitudinal strain (GLS), circumferential strain (GCS) and radial strain (GRS) were measured on cineMR images by a dedicated software (Cvi42, Circle Cardiovascular Imaging). Patients were categorised into 4 groups (pre-hypertrophic, mild, moderate and severe hypertrophy) according to MWT (<11mm,11-15mm,16-18,>18mm). Correlations between tracking parameters, glicosphingolipids accumulation (measured by nT1) and myocardial fibrosis (LGE and ECV) among four groups were investigated.
Results: nT1 was lower in patients with severe (908ms), mild (910ms) and moderate (920ms) hypertrophy than with no-hypertrophy (959ms). 14 patients showed typical LV inferolateral scar and 4 patients had areas of myocardial oedema. Mean LV ejection fraction was preserved in all groups. Significant correlations were found between all TTT features and hypertrophy degree (p<0.01 for all) and between GCS and nT1 (p<0.05). No associations were noted between tracking parameters and ECV.
Conclusion: In FDC, contractile disfunction assessed by CMR-TTT is correlated to hypertrophic degree and lipid accumulation.

B-0688 14:49

Myocardial strain analysis using feature-tracking CMR approach for the differential diagnosis of amyloidosis vs HCM: a novel approach besides conventional imaging sequences?

G. De Rubeis, F. Cilia, N. Galea, I. Carbone, M. Francone, C. Catalano; *Rome/IT (derubeis.gianluca@gmail.com)*

Purpose: To evaluate the potential role of global radial and circumferential peak myocardial strain, calculated with CMR feature-tracking technique, in the differential diagnosis between amyloidosis and HCM.
Methods and Materials: We evaluated the global radial (GRS) and circumferential myocardial (GCS) strain peak, through CMR feature-tracking technique, in 12 patients with known cardiac amyloidosis and 32 patients with

histologically proven or clinical referral for HCM. All patients presented, in at least one segment, a myocardial thickening >13 mm.
Results: Patients' median age was 55±16 years, and 64% were male; per group analysis shows significant younger age in HCM group compared with amyloidosis ones (50±16 vs 66±10 years; p<0.05). GRS was lower in amyloidosis group than HCM group (25.0±10.6% vs 34.0±7.4%; p<0.01), while GCS was higher (-13.6±4.2 vs -16.4±2.9%; p<0.05). However, with a multiple regression analysis weighted for age, the r partial coefficients were 0.31 (p = 0.07) for GRS and 0.38 (p=0.02) for GCS. Using ROC curves, the optimal cutoffs for radial and circumferential strain were, respectively, ≤24.09% and >-15.18%. The sensitivity, specificity and AUC were 58.3, 93.75 and 0.779 for GRS and 66.7, 71.87 and 0.702 for GCS. Comparing the two ROC curves no statistically significant differences were highlighted (differences between areas=0.0768; p=0.17).
Conclusion: GRS and GCS can help in the differential diagnosis between cardiac amyloidosis and HCM likely reflecting diffuse intracellular accumulation of amyloid material with subsequent disease-dependent global contraction impairment. This might help in differentiating between two forms mostly in patients with negative or non-specific LGE findings.

B-0689 14:57

Denoising effect on T2* values in magnetic resonance imaging with application in iron load of patients with thalassaemia major

M. Dodangeh, S. Gholami Bardeji, Z. Gholami Bardeji, S. Sefidbakht, R. Jalli; *Shiraz/IR (dodangeh@sums.ac.ir)*

Purpose: To investigate the effect of noise and denoising on the measurement of magnetic resonance imaging (MRI) T2* values at interventricular septum of the heart in thalassaemia major patients. A second objective is to estimate the T2* value based on the improvement of Signal to Noise Ratio (SNR).
Methods and Materials: Different levels of Rician and Gaussian noises were added to the cardiac T2* MR images of 5 thalassaemia major patients. The state-of-art denoising methods were applied to the obtained noisy images. T2* values of the interventricular septum and SNR were measured in both series of images by Segment and Matlab software, respectively.
Results: With respect to the Gaussian noisy and denoised images in different noise levels, although SNR improved, there were no significant differences between T2* values in original, noisy and denoised images. On the other hand, after denoising images with Rician noise a relation between improvement of SNR and T2* value is noticed. A predictor model is constructed based on the level of Rician noise for each method.
Conclusion: In the case of existence Gaussian noise, the results confirm that denoising is not effective on the measurement of T2* value. In the case of image distortion by Rician noise, a predictor model is proposed to estimate the original T2* value. The predictor model is used to estimate the T2* value of new patients. The predicted T2* values were in a good agreement with the corresponding original T2* values.

B-0690 15:05

The cardiac MRI sphericity index in the dilated cardiomyopathy: new diagnostic and it prognostic marker

A. Zidi, I. Ben Amara, R. Aouini, A. Ben Halima; *Tunis/TN (drzidiasma@yahoo.fr)*

Purpose: Study the diagnostic and prognostic value of left ventricular sphericity in dilated cardiomyopathy.
Methods and Materials: Retrospective study of 132 patients, 44 diagnosed with dilated cardiomyopathy (DCM+) and 88 control patients with normal ventricular function and volumes (DCM-). All patients underwent a cardiac MRI with standerdized clinical protocol : cine-acquisition in short axis, 4-chamber and long axis views and late enhancement data sets acquired 10 minutes after intra-venous administration of extracellular gadolinium contrast agent. The sphericity index (SI) = left ventricular short axis end-diastolic length / long axis end-diastolic length x 100. Statistical investigation of correlations between SI and Left ventricular ejection fraction (LVEF) and occurrence of cardiac events
Results: In our study, SI was inversely correlated with LVEF (P<0,001), and positively correlated with end-systolic LV volume (p=0,03). For patients with LVEF >50%, SI was ≤ 63,5% (sensitivity = 90,9% and specificity = 92%). In DCM+ group, the mean SI was 72,7% ± 7 and the mean LVEF was 30%. Occurrence of a cardiac event was noted in 45% of patients and it was correlated to a high SI (p<0,001).
Conclusion: Few studies have investigated the IS which proves to be according to our study a good diagnostic marker reflecting cardiac dysfunction and prognostic predictor ECM occurred.

B-0691 15:13

Stratification of arrhythmic risk in HCM patients on the basis of oedema and myocardial scar on late gadolinium enhancement-cardiac magnetic resonance (LGE-CMR): a 11-year follow-up study

S. Bertugno, L. Nocetti, F. Fiocchi, A. Barbieri, Y. Bartolacelli, P. Torricelli, G. Ligabue; *Modena/IT (serena.bertugno@libero.it)*

Purpose: To investigate the role of LGE-CMR to predict the risk of Ventricular Tachyarrhythmia (VT) in HCM patients throughout a LGE% cut-off determination associated with the presence of oedema.
Methods and Materials: LGE-CMR was performed in 150 consecutive HCM patients (mean age: 57±17 years; 73% males) using a 1.5T scanner to determine cardiac functional parameters. LGE images were obtained 15 minutes after injection of 0.2 mmol/kg of Gadolinium. LGE was quantified using 6SD method. Indexed end-diastolic left ventricular mass (IEDLVM) was determined and LGE extension was defined as percentage of IEDLVM. We assessed myocardial fibrosis and oedema according to the 17 AHA (American Heart Association) segment-model. Occurrence of VT during a follow-up of 11 years were recorded. Multivariate analysis was performed to determine independent CMR parameters with a statistically significant correlation with VT. ROC analysis was performed to determine the optimal cut-off value for the parameter already individuated.
Results: The mean IEDLVM was 89±27 g/m^2. On LGE-CMR 116 (77%) patients showed myocardial scar (mean LGE%:6.4±7.8) and 61 (41%) oedema. During the follow-up 33 (22%) VT were recorded. Multivariate analysis revealed that both LGE% and oedema were independently associated with VT (P<0.001 both). According to the ROC curve, patients with a LGE>6%, have a high risk to present VT (sensitivity:82%; specificity:77%; AUC:0.882). If we considered oedema associated with a LGE>4% both the sensitivity and the specificity increased (respectively 85% and 85%; AUC:0.858).
Conclusion: Extension of fibrosis and oedema detected with LGE-CMR predict the occurrence of VT in HCM patients.

B-0692 15:21

Age- and gender-specific differences and magnetic resonance characteristics of hypertrophic cardiomyopathy

Z. Dohy, C. Czimbalmos, I. Csécs, A. Tóth, F. Suhai, B. Horváth, E. Dinya, B. Merkely, H. Vágó; *Budapest/HU*

Purpose: The aim of our study was to investigate age- and gender-specific differences and the prognostic value of cardiac magnetic resonance imaging (CMR) in patients with HCM.
Methods and Materials: CMR examination was performed on 152 adults (89 male; 47.6±13.7 years) and 24 children (17 male; 11.8±3.0 years) with HCM. Using cine short-axis images we evaluated left ventricular ejection fraction (EF), end-diastolic (EDVi) and end-systolic volume indices (ESVi), stroke volume index (SVi), mass index (LVMi) and maximal end-diastolic wall thickness (MEDWT). The amount of fibrosis was quantified on delayed contrast enhancement images. During the clinical follow-up adverse cardiac events (ACE) were recorded.
Results: Male patients had higher ESVi (34.8±9.8 vs 29.4±7.9 ml/m2), EDVi (92.8±17.2 vs 80.9±13.2 ml/m2), SVi (59.2±10.6 vs 51.5±9.4 ml/m2) and LVMi (98.9±33.0 vs 79.3±23.0 g/m2) (p<0.001). LVMi was higher in female children than in adult women (107.7±27.2 vs 79.3±19.8 g/m2) (p<0.01). The amount of fibrosis correlated positively with LVMi and MEDWT (p<0.001), negatively with EF (p<0.05). In 16 male patients with apical HCM morphology LVMi (83.5±13.7 vs 102.2±35.0 g/m2, p<0.05) and MEDWT (17.4±2.8 vs 23.5±5.4 mm, p<0.001) were lower. Obstructive form was found in 20 male patients, who had higher EDVi (99.6±18.1 vs 90.8±16.5 ml/m2) and MEDWT (25.1±6.2 vs 21.6±5.1 mm) (p<0.05). During clinical follow-up (1216±449 days) the incidence of ACE was higher in HOCM patients (p<0.05). Age, LVMi and EDVi combined had an effect on the incidence of ACE.
Conclusion: HCM seems to be influenced by gender-specific differences and CMR may have an essential role in complex risk stratification.

Friday, March 3

10:30 - 12:00 **Room A**

Oncologic Imaging

SS 1016a

Imaging in prostate cancer

Moderators:
P.A.T. Baltzer; Vienna/AT
M. Spahn; Berne/CH

B-0693 10:30

Effect of PIRADSv2 instead of PIRADSv1 in the analysis of multiparametric prostate MRI at 310 prostatic lesions proven by MR-guided biopsy at 3T vs 1.5T

A. Malich, I. Papageorgiou, R. Chelaru, A. Kott; *Nordhausen/DE (ismini.e.papageorgiou@gmail.com)*

Purpose: To verify diagnostic potential of PIRADS-V2 at the exact localisation of prostate lesions being histologically proven by MR-guided biopsy; to verify the influence of field strength on PIRADS-analysis and histopathological outcome.
Methods and Materials: 2080 patients underwent mp-prostate-MRI at our hospital (2009-2016) (T2w, DWI/ADC b-values: 0, 100, 400, 800, 1000; dynamic analysis >5min, single series: 13sec). 310 lesions were, after inconclusive sonographically-guided biopsy, scored as suspicious justifying an endorectally performed MR-guided biopsy (18G gun, 2 samples/lesion; access planning using DYNACAD-software and InVIVO at 3T Philips Ingenia and 1.5T Philips Achieva, respectively).
Results: Histopathological outcome was (1.5T/3T): PCA: 32/97(33%) vs 101/213(47%); ASAP: 9/97(9%) vs 20/213(10%); prostatitis: 26/97(27%) vs 33/213(15%); BPH: 14/97(14%) vs 31/213(15%); other findings: 16/93(16%) vs 28/213(14%). Gleason6: 10/32(32%) vs35/101(35%); Gleason7: 17/32(55%) vs 49/101(49%); Gleason8: 4/32(13%) vs 7/101(7%); Gleason9: 1/32(3%) vs 8/101(8%); Gleason10: 0 vs 2/101(2%). Using PIRADS-V1 17(5.5%) lesions were scored as PIRADS3 (3xPCA; remaining benign); 156 (50.3%) as PIRADS4 (42 PCA; 16 ASAP; all other benign) and 137 (44.2%) lesions as PIRADS5 (88 PCA, 13 ASAP; all other benign). When applying PIRADS-V2 9 lesions (2.9%) were downgraded as PIRADS2 (1/9 ASAP, all other benign), 23 lesions (7.4%) as PIRADS3 (1/23 PCA, 4/23 ASAP, all other benign), 162 lesions (52.3%) as PIRADS4 (70/162 PCA; 18/162 ASAP; other benign). 93 lesions (30.0%) revealed PIRADS5 (60/93 PCA; 4/93 ASAP). Consequently, sensitivity remained stable, specificity raised by V2, confirmed by ROC-analysis to be significant. No side effects or complications occurred. Mean scan time was 30min/intervention.
Conclusion: Application of PIRADSv2 reduces significantly the number of unnecessary MR-guided biopsies on the one hand and strengthens the indication for biopsy especially by upgrading suspicious lesions from PIRADS 4 to 5 with a high PPV.

B-0694 10:38

The role of PI-RADSv2 in determining who needs active surveillance or definitive treatment according to PRIAS

B. Park, J. Park; *Seoul/KR (1436park@gmail.com)*

Purpose: To evaluate the role of Prostate Imaging Reporting and Data System version 2 (PI-RADSv2) in triaging patients with prostate cancer according to Prostate Cancer Research International: Active Surveillance (PRIAS).
Methods and Materials: This HIPPA-compliant study was approved by IRB. Between January 2012 and December 2014, 456 patients with biopsy proven cancer underwent MRI and then radical prostatectomy. Two radiologists independently reviewed MR images using PI-RADSv2. According to PRIAS, cancer suitable for AS was defined as insignificant lesion with clinical stage <T3, prostate specific antigen (PSA) ≤10ng/mL, PSA density <0.2ng/mL^2, Gleason score (GS) ≤6, and the number of positive cores ≤2. According to PI-RADSv2, an insignificant cancer was defined when an index lesion scored <4. Standard reference was prostatectomy, in which insignificant cancer was defined as a small (<0.5cm^3) organ-confined lesion with GS ≤6. Sensitivity and specificity for insignificant cancer were obtained with PRIAS, PI-RADSv2, and both. Comparison of diagnostic performances was multiplied by two according to Bonferroni method.
Results: Of 456 patients, 82 (18.0%) were histologically diagnosed as insignificant cancer. The sensitivity and specificity with PRIAS were 82.9% (68/82) and 70.9% (265/374), respectively. PI-RADSv2 by two readers decreased the sensitivity to 61% (50/82)-80.5% (66/82), but increased the specificity to 77.8% (291/374)-90.8% (340/374). Combination of PRIAS and PI-RDASv2 increased significantly the specificity to 89.6% (335/374)-92.8% (347/374) (P<0.001).
Conclusion: PRIAS can identify a greater number of insignificant cancers than PI-RADSv2. However, PI-RADSv2 helps detect many significant cancers which are misdiagnosed as insignificant cancer with PRIAS.

B-0695 10:46

Clinical outcome following a low-suspicious multiparametric MRI or benign MRI-targeted biopsies for prostate cancer detection: a 3-year follow-up study

L. Boesen, N. Nørgaard, V. Loegager, H.S. Thomsen; *Herlev/DK (lars.boesen@dadlnet.dk)*

Purpose: To asses the clinical impact and time-varying risk of being diagnosed with significant prostate cancer (sPCa) following either a low-suspicious multiparametric (mp)-MRI or benign mp-MRI targeted biopsies (mp-MRI-bx) in men with prior negative transrectal ultrasound guided biopsies (TRUS-bx).
Methods and Materials: 289 patients were included and underwent mp-MRI followed by re-TRUS-bx and mp-MRI-bx of suspicious lesions at baseline. Of these, 194 patients had either a low suspicious mp-MRI or benign mp-MRI-bx and were selected for this analysis. Men diagnosed with PCa by re-TRUS-bx were classified as mp-MRI false-negative. Men without cancer were followed for at least three years to assess how many had a diagnosis of PCa within follow-up. The negative predictive values (NPV) of mp-MRI and mp-MRI-bx for ruling out any PCa, significant grade (Gleason score≥7) PCa and clinical sPCa were calculated.
Results: PCa was detected in 38/194 (20%) patients during the entire follow-up period. The overall NVP of mp-MRI and mp-MRI-bx to rule out any PCa and significant grade PCa (GS≥7) was 80% (156/194) and 95% (185/194), respectively. In addition, the NPV of clinical sPCa was 88% (170/194) caused by 15 patients with Gleason score 6 cancer having a PSA-density >0.15 ng/ml/cc. No patients with low suspicious mp-MRI features had significant grade PCa detected.
Conclusion: A low suspicious mp-MRI in patients with previous negative TRUS-bx has a high NVP for ruling out sPCa in a longer term. Thus, immediate repeated biopsies have only diminutive clinical impact and could be avoided even in men with persistent elevated PSA-levels.

B-0696 10:54

Accuracy of multiparametric MRI with PI-RADS V2 assessment in detecting infiltrations of the neurovascular bundles prior to prostatectomy

M. Sauer, J. Weinrich, G. Salomon, G. Adam, D. Beyersdorff; *Hamburg/DE (m.sauer@uke.de)*

Purpose: To evaluate multiparametric MRI (mpMRI)-based assessments of neurovascular bundle (NVB)-infiltration and to determine the value of PI-RADS V2 scores for the prediction of NVB infiltration before prostatectomy.
Methods and Materials: Our institutional review board approved the study. 198 patients underwent standardised mpMRI at 3T prior to surgery, including high resolution T2w-TSE-imaging in 3 planes, T1-w-TSE, DWI with ADC map, PD-TSE and Gd-DCE with post-processing of images. Assessment for NVB-infiltration was made for each side of each prostate (n=396). Maximum PI-RADS-V2 scores were determined for the posterolateral areas adjacent to the NVB (n=396). MRI-findings were correlated to pathologic analysis as reference standard, where NVB-infiltration was defined as tumour invasion into the NVB or extraprostatic expansion in the posterolateral area adjacent to the NVB.
Results: Overall T-staging accuracy, sensitivity, specificity, positive predictive value (PPV) and negative predictive value (NPV) of mpMRI were 78.3%, 64.4%, 89.2 %, 82.4% and 76.2%, respectively. In 396 cases infiltration of the NVB was predicted with 89.4%, 75.2%, 94.0%, 80.2% and 92.1% overall accuracy, sensitivity, specificity, PPV and NPV, respectively. By correlating 365 maximum PIRADS-V2 scores to the pathology of adjacent NVBs, infiltration was demonstrated in 13 NVBs despite low likelihood of cancer presence (PI-RADS 1 or 2 scores), amounting to 14% false negative predictions.
Conclusion: mpMRI-based assessment of NVB-infiltration should be acknowledged when nerve sparing surgery is considered. However, areas without tumour suspicion (PI-RADS 1 or 2) might demonstrate NVB-infiltration in pathology causing false negative predictions.

B-0697 11:02

Validation of prostate imaging reporting and data system version 2 using a MR-ultrasound fusion biopsy in prostate cancer diagnosis

Y. Nam, S. Kim, Y. Yeo; *Daegu/KR (nyk3435@gmail.com)*

Purpose: The purpose of our study was to prospectively assess PI-RADS version 2 to use a MR-ultrasound fusion biopsy for the diagnosis of clinically significant prostate cancer (csPCa).
Methods and Materials: This study included 295 consecutive patients with 478 lesions who underwent multiparametric MR imaging and subsequent MR-ultrasound fusion biopsy between December 2014 and September 2016. Lesions were assessed using an overall score of PI-RADS version 2. One radiologist assessed the presence or absence of csPCa in the whole gland,

and subgroups of peripheral zone and transition zone using cut-off values ≥4 and 3. Histologic examination of MR-ultrasound fusion biopsy specimens was used as the reference standard. Sensitivity, specificity, PPV and NPV, and accuracy were calculated to assess the ability of PI-RADS version 2 for the diagnosis of csPCa.
Results: The overall scores of the PI-RADS version 2 showed an accuracy of 82.2% (393 of 478) for the whole gland, with a cut-off value ≥4 granting sensitivity of 90.0% (90/100), specificity of 80.1% (303/378), PPV of 83.3% (90/108), and NPV of 81.8% (303/370). For the peripheral zone, the overall scores showed an accuracy of 84.7% (301/355), and an accuracy of 74.7% (92/123) in the transition zone. In applying an arbitrary overall score ≥3, overall score showed an accuracy of 68.6% (328/478), a sensitivity of 94.6% (124/131), specificity of 58.7% (204/347), PPV of 51.6% (124/240), and NPV of 85.7% (204/238).
Conclusion: PI-RADS version 2 has moderate overall performance for the diagnosis of csPCa.

B-0698 11:10

Manual adjustment in mpMRI-directed prostate biopsy significantly improves the detection rate of prostate cancer: experience in 180 patients
S. Alessi, L. Nicosia, P. Pricolo, B. Jereczek-Fossa, V. Cubadda, G. Renne, O. De Cobelli, M. Bellomi, G. Petralia; *Milan/IT (Sarah.Alessi@ieo.it)*

Purpose: To compare the results of software-guided sampling with those obtained after manual adjustment in multiparametric prostate magnetic resonance imaging directed prostate biopsy (mpMRI-PB), and evaluate the percentage of core involvement at mpMRI-PB and lesion diameter at surgery.
Methods and Materials: 180 patients with suspicious prostate cancer (PCa) and a lesion visible on multiparametric prostate magnetic resonance underwent mpMRI-PB between November 2014 and September 2016. After calibration of the biopsy device the first sample was obtained using the coordinates provided by the device software to guide the needle along a trajectory to the target lesion. The trajectory of subsequent samples was manually adjusted to improve localisation to the target lesion.
Results: Biopsy was positive for PCa in 0/14 PIRADS 2, 13/58 PI-RADS 3, 47/78 PI-RADS 4 and 26/30 PI-RADS 5 lesions. Of the 86 lesions with positive biopsy, just 47 were obtained with the first sample, whereas biopsy with manual adjustment was positive in all 86 lesions. The additional 39 positive biopsies correspond to an increase in detection rate of 83% (p<0,0001; McNemar's Test). To date, 32 of the patients have undergone radical prostatectomy; the core involvement averaged 59% (range 10-90%) and lesion diameter in the surgical specimen 10,2 mm (range 5-16mm).
Conclusion: Manual adjustment of needle trajectory significantly improves the detection rate of PCa with mpMRI-PB. The percentage of core involvement in mpMRI-PB is high relative to literature values for conventional biopsy, suggesting that the criteria for clinical decision-making in these patients should be re-examined.

B-0699 11:18

Early dynamic imaging increases the detection rate of local recurrence in prostate cancer patients with biochemical relapse referred for ^{68}Ga-PSMA-11 PET/CT
C. Uprimny, A. Kroiss, C. Decristoforo, B. Warwitz, L. Scarpa, E. von Guggenberg, J. Bektic, W. Horninger, I. Virgolini; *Innsbruck/AT (Christian.UPRIMNY@tirol-kliniken.at)*

Purpose: ^{68}Ga-PSMA-11 PET/CT has proved to establish a very accurate imaging modality in prostate cancer (PC) patients with biochemical relapse after primary therapy. Despite a high overall detection rate visualisation of local recurrence remains challenging due to high physiological tracer accumulation in the urinary bladder on whole-body ^{68}Ga-PSMA-11 PET usually performed 60 min post injection (p.i.). The purpose of this study was to evaluate whether early dynamic PET-imaging allows differentiation of PC lesions from urinary bladder activity and thereby probably increasing detection rate of local recurrence.
Methods and Materials: 64 PC patients with biochemical relapse (median PSA: 1.7ng/ml) referred for ^{68}Ga-PSMA-11 PET/CT were retrospectively analysed. In addition to whole-body imaging 60 min p.i. early dynamic acquisition of the pelvis in the first 8 min p.i. was performed.
Results: On whole-body PET 13 patients exhibited pathological lesions in the prostatic fossa consistent with local recurrence, which were also positive on early dynamic imaging. However, in 6 additional patients pathological lesions suspicious for local recurrence could only be detected on early dynamic PET. Combination of early dynamic PET and whole-body PET increased the detection rate of local recurrence compared to imaging 60 min p.i. alone (29.4% versus 20.3%).
Conclusion: Early dynamic imaging of the pelvis enhances detection rate of local recurrence in PC patients with biochemical relapse and should be integrated in the routine acquisition protocol of ^{68}Ga-PSMA-11 PET/CT.

B-0700 11:26

Detection rate of PET/CT in patients with biochemical relapse of prostate cancer using [68Ga]PSMA I&T and comparison with published data of [68Ga]PSMA HBED-CC
C. Berliner[1], M. Tienken[1], Y. Kobayashi[1], U. Kirchner[1], S. Klutmann[1], L.H. Budäus[1], H.-J. Wester[2], J. Mester[1], P. Bannas[1]; [1]*Hamburg/DE*, [2]*Munich/DE (caberliner@gmail.com)*

Purpose: To determine the detection rate of PET/CT in biochemical relapse of prostate cancer using [^{68}Ga]PSMA I&T and to compare it with published detection rates of [^{68}Ga]PSMA HBED-CC.
Methods and Materials: We performed a retrospective analysis in 83 consecutive patients with biochemical relapse after prostatectomy. All patients underwent whole-body [^{68}Ga]PSMA I&T PET/CT. PET/CT images were evaluated for presence of local recurrence, lymph node metastases, and distant metastases. Proportions of positive PET/CT results were calculated for six subgroups with increasing prostate specific antigen (PSA) levels (<0.5 ng/ml, 0.5 to <1.0 ng/ml, 1.0 to <2.0 ng/ml, 2.0 to <5.0 ng/ml, 5.0 to <10.0, >10.0 ng/ml). Detection rates of [^{68}Ga]PSMA I&T were statistically compared with published detection rates of [^{68}Ga]PSMA HBED-CC using exact Fisher's test.
Results: Median PSA was 0.81 (range: 0.01-128) ng/ml. In 58/83 patients (70%) at least one [^{68}Ga]PSMA I&T positive lesion was detected. Local recurrent cancer was present in 18 patients (22%), lymph node metastases in 29 patients (35%), and distant metastases in 15 patients (18%). The tumour detection rate was positively correlated with PSA levels, resulting in detection rates of 52% (<0.5 ng/ml), 55% (0.5 to <1.0 ng/ml), 70% (1.0 to <2.0 ng/ml), 93% (2.0 to <5.0 ng/ml), 100% (5.0 to <10.0 ng/ml), and 100% (>10.0 ng/ml). There was no significant difference between the detection rate of [^{68}Ga]PSMA I&T and published detection rates of [^{68}Ga]PSMA HBED-CC (all p>0.05).
Conclusion: In our retrospective study, [^{68}Ga]PSMA I&T PET/CT has high detection rates of recurrent prostate cancer that are comparable to [^{68}Ga]PSMA HBED-CC.
Author Disclosures:
H. Wester: Shareholder; Scintomics.

B-0701 11:34

Assessing early treatment induced changes on diffusion signal of prostate cancer: comparison of two radiotherapy schemes
N. Papanikolaou[1], G. Manikis[2], I. Santiago[1], A. Gaivao[1], C. Greco[1], Z. Fuks[1], C. Matos[1]; [1]*Lisbon/PT*, [2]*Iraklion/GR (npapan@npapan.com)*

Purpose: To assess radiation therapy induced early changes in patients with prostate cancer, and compare the effects on diffusion biomarkers of two different treatment schemes.
Methods and Materials: Twelve patients with locally confined prostate cancer underwent either single dose radiotherapy (SDRT; 24Gy, n=7) or hypo-fractionated radiotherapy (HYPO; 9Gy per fraction repeated daily for 5 days, n=5). Multiple diffusion sequences were acquired beginning at 15 minutes after treatment completion up to 40min, to detect early diffusion signal changes. A bi-exponential diffusion model was applied to quantify true Diffusion coefficient (D), pseudo-diffusion coefficient (D*) and micro-perfusion fraction (f), in visible lesions. The diffusion sequence utilised comprised of 7 b values (0, 50, 100, 200, 500, 1000 and 1500 s/mm^2).
Results: A major decrease in f values along with an increase in D, as early as 15min after the end of the treatment, was noted forming a plateau configuration in both D and f , till 40min after treatment. In patients with HYPO treatment there was a major reduction of D that returned to the baseline value at 40min and a moderate reduction of f that resulted in a minor increase of the f value at 40min after the end of treatment. No clear changes were observed on D* in both types of treatment.
Conclusion: Our preliminary results indicate that diffusion related biomarkers can detect early treatment induced changes. They may therefore have the potential to be used for assessing treatment effects of different radiotherapy schemes.

B-0702 11:42

IVIM of prostate cancers: assessing grade and response to treatment
R. Balaji; *Chennai/IN (ravikanthbalaji@gmail.com)*

Purpose: Investigate use of intravoxel incoherent motion (IVIM) diffusion-weighted imaging of prostatic cancers, correlation with Gleason score and assess response to treatment.
Methods and Materials: 35 patients with histologically proven prostate cancer underwent IVIM diffusion imaging on 1.5 Tesla MR scanner using 11 b values 0, 10, 20, 30, 50, 80, 100, 200, 400, 800 and 1000 s/mm^2. Biexponential fits were applied to diffusion decay curves to calculate molecular diffusion coefficient (D), perfusion-related Diffusion coefficient (D*), and perfusion fraction (f). Grading of tumours was based on correlation of ADC, D and f

values with Gleason score. Post treatment imaging was performed after 3 months to assess changes in ADC, D and f values.
Results: D values were significantly reduced within tumour foci compared to normal parenchyma. High grade tumours had lower D values 0.70 +/- 0.23 x 10^{-3} mm^2/s compared to low grade tumours which had higher D values 0.92 c 0. 27 10^{-3} mm^2/s. f values were increased in tumours at b-values below 800 s/mm^2 - 7+/- 2.6 %. When higher b-values were used f values in tumours was indistinguishable from normal prostatic glandular tissue.D values increased after treatment with radiotherapy - 1.22 +/- 0.23 x 10^{-3} mm^2/s with decrease in f values 3.4 +/- 2.4 %.
Conclusion: True diffusion (D)obtained by IVIM technique is a much superior biomarker of malignancy, grade of tumour and response to treatment. f values are also an important indicator of malignancy at b values below 800 s/mm^2 in the prostate gland.

B-0703 11:50

Multiparametric MRI of prostate cancer bone disease: correlation with bone biopsy histological and molecular features
R. Perez Lopez, D. Nava Rodrigues, J. Mateo, M. Rata, Z. Zafeiriou, D.J. Collins, D.-M. Koh, J.S. de Bono, N. Tunariu; *London/UK (Raquel.PerezLopez@icr.ac.uk)*

Purpose: To assess multiparametric MRI (MP-MRI) of metastatic and non-metastatic bone in patients with prostate cancer and correlate with histological features from bone metastases biopsies.
Methods and Materials: Patients with metastatic castration resistant prostate cancer (mCRPC), MP-MRI, bone metastases biopsies and biopsy tract visible on a subsequent CT between May 2012 and March 2016 were included. A cohort of 10 consecutive CRPC patients with MP-MRI and no bone metastases was also analysed. Associations of MRI parameters (apparent diffusion coefficient [ADC], normalised DWI [nDWI] signal and fat fraction [FF]) with bone marrow biopsy histological characteristics were evaluated using Mann Whitney test; Spearman's correlations were assessed. Univariate and multivariate analyses were performed using logistic regression models.
Results: Forty-three bone marrow biopsies from 33 patients (median age 72, range 48-84 years) were included. In the non-metastatic bone cohort, 10 patients were included (median age 69, range 53-75 years). The median ADC in bone metastases and non-metastatic bone was $993x10^{-6}mm^2/s$ (IQR 872.5-$1093.5x10^{-6}mm^2/s$) vs $601.8x10^{-6}mm^2/s$ (IQR 545-$667x10^{-6}mm^2/s$), the median nDWI signal was 4 AU (IQR 2.6-6.7 AU) vs 1.6 AU (IQR 1.4-2.7AU) and the median FF was 16% (IQR 9-45%) vs non 63% (IQR 60-76%); p<0.001 in all cases. There was a significant inverse correlation of ADC and FF and positive correlation of nDWI signal with tumour cellularity; p<0.001.
Conclusion: MP-MRI parameters correlate with histological characteristics of bone marrow biopsies in mCRPC. These data further supports clinical qualification of DWI as a prognostic and response biomarker in mCRPC.

10:30 - 12:00 **Room C**

Abdominal Viscera

SS 1001

New techniques in abdominal imaging

Moderators:
D. Prezzi; London/UK
C. Stoupis; Männedorf/CH

B-0704 10:30

Evaluation of different methods to optimise contrast media amount in abdominal CT of obese patients
F. Rivosecchi, D. Caruso, M. Rengo, D. Bellini, M. Zerunian, A. Laghi; *Latina/IT (flaminiarivosecchi@gmail.com)*

Purpose: To prospectively compare two different approaches for calculating the lean body weight (LBW) and the amount of intravenous contrast media (CM) for MDCT of the abdomen in obese patients.
Methods and Materials: Nineteen patients (9 men, 10 women) with a BMI greater than 35 kg/m2 were included in this prospective study and underwent MDCT of the abdomen. The amount of CM injected was computed according to the patient's LBW which was estimated using either the Boer formula (Group A) or the James formula (Group B). The following variables were compared and analysed between the two groups: patient's characteristics, CM volume and iodine dose. CNR of liver, kidney, portal vein, aorta and pancreas was also calculated.
Results: Patients in Group A has a superior BMI than Group B (38.56±6.31 vs. 37.23±5.54 kg/m2) while an inferior LBW was observed for Group A vs Group B (59.15±12.23 vs 59.79±12.68 kg). Group A provided greater CNR (liver 3.64±1.12; kidney 13.53±7.2; portal vein 10.22±6.34; aorta 11.93±3.45; pancreas 2.51±0.98) during the portal venous phase compared to CNR of Group B (liver 3.38±2.11; kidney 9.87±6.55; portal vein 7.70±3.43; aorta 8.07±2.69; pancreas 2.35±1.12). A significant difference was observed for CNR of kidney, portal vein and aorta (p<0.05) although a lower amount of CM was administered in Group A compared to Group B (115.45±13.3 ml vs 116.64±12.56, p>0.05).
Conclusion: The optimisation of contrast media volume using Boer formula significantly improves parenchymal enhancement in obese patients although a lower amount of contrast media was administered.

B-0705 10:38

Clinical robustness of accelerated and optimised abdominal DWI
J. Taron, P. Martirosian, J. Weiß, A. Stemmer, A. Othman, K. Nikolaou, M. Notohamiprodjo; *Tübingen/DE (taronjana@yahoo.com)*

Purpose: To assess the robustness of accelerated and optimised diffusion-weighted imaging (DWI) in routine abdominal MRI using the simultaneous-multislice (SMS) technique for scan time reduction and a 3D Diagonal diffusion mode to improve image quality.
Methods and Materials: A total of 152 patients (88 male, 64 female; mean age 62 years) were included in this study. All received the institutional standard abdominal MRI protocol including an optimized diffusion-weighted sequence (DWI_{OPT}: TR/TE 3100/56ms; b-values 50, 400 and 800s/mm²; diffusion mode 3D Diagonal; SMS factor 2; scan time 1:44min). A subgroup of 41 patients (mean age 62 years) additionally received standard DWI (DWI_{STD}: TR/TE 5100/60ms; b-values 50, 400 and 800s/mm²; diffusion mode 4-scan-Trace; scan time 2:35min) as reference. Image quality criteria, lesion conspicuity (rated on a 5-point Likert-scale; 5=excellent) and ADC-values (measured in a region-of-interest-analysis) in DWI_{STD} and DWI_{OPT} were compared interindividually using dedicated statistics. P-values <.05 were considered significant.
Results: Interindividually DWI_{OPT} proved superior to DWI_{STD} in comparison of overall image quality (DWI_{OPT}: 4.6 ±0.7; $DWI_{STD:}$ 4.2 ±0.8; p=.025); lesion conspicuity was comparable (p=.461); ADC-values showed no statistically significant difference (right hepatic lobe p=.107; kidney p=.098). The patients receiving DWI_{OPT} only showed very high overall image quality and lesion conspicuity (4.7±0.6 and 4.7±0.6, respectively).
Conclusion: Integrating the SMS technique- and a 3D-Diagonal diffusion mode abdominal DWI can be accelerated and optimised with superior image quality and similar ADC-values compared to standard DWI. This approach proved stable in a larger patient cohort, so that we can recommend it for clinical routine application.
Author Disclosures:
J. Taron: Equipment Support Recipient; Nonfinancial support from Siemens Health Care. **A. Stemmer:** Employee; Employee of Siemens Health Care. **M. Notohamiprodjo:** Equipment Support Recipient; Nonfinancial support from Siemens Health Care.

B-0706 10:46

Diagnostic value and radiation dose reduction of model-based iterative reconstruction compared with hybrid iterative reconstruction in routinely upper abdominal CT study
A. De Vito, D. Ippolito, C.R.G.L. Talei Franzesi, L. Riva, S. Drago, S. Sironi; *Monza/IT (a.devito@campus.unimib.it)*

Purpose: To evaluate dose reduction and image quality of upper abdominal CT images reconstructed with model-based iterative reconstruction (IMR) compared with hybrid iterative reconstruction (iDose4).
Methods and Materials: We prospectively enrolled 72 patients who underwent to upper abdominal CT scan;36 patients were examined using a low-kV setting (100kV) while the other 36 patients were investigated using standard kV setting (120kV), on the same 256-row CT. In the first group (Study Group) images were reconstructed using IMR algorithm while in the second group (Control Group) we used iDose4 technique. CTDIvol, DLP and Estimate Doses (ED) were evaluated. Region of interests were drawn in three different points in the liver and spleen; signal-to-noise ratio (SNR) and contrast-to-noise ratio (CNR) were calculated. A four-point scale was used to subjectively evaluate the imageS in both groups.
Results: Mean CTDI Volume was 9,2 ± 1,2 mGy and 17,7 ± 2,5 mGy for low-kV IMR CT scans and standard dose iDose4 CT scans, respectively. Compared to iDose4-CT, low kV IMR CT showed significant lower DLP (570,5 ± 8,3 mGy x cm) and ED (6,3 ± 1,8 mSv). Low kV IMR images yielded higher attenuation values (HU) and higher SNR and CNR in the liver and spleen, compared with standard dose iDose4 images.The subjective image quality of both groups was comparable.
Conclusion: Low-kV MBIR technique allows significant reduction of radiation doses exposure maintaining high image quality (i.e. attenuation values, SNR and CNR in the liver and in the spleen) at routine abdominal CT, compared with standard-dose HIR technique.

B-0707 10:54

Contrast dose variability depending on morphometric values: a retrospective analysis on patients undergoing multi-phase abdominal CT

M. Zanardo[1], F.M. Doniselli[2], A. Esseridou[2], S. Tritella[2], G. Di Leo[2], F. Sardanelli[2]; [1]*Milan/IT*, [2]*San Donato Milanese/IT* *(moreno.zanardo90@gmail.com)*

Purpose: The dose of contrast material for multi-phase abdominal CT is usually based on patient body weight (BW). Inter-patient morphometric variables, such as muscular and adipose tissues or blood pool extent, are implicated in variations of parenchymal contrast enhancement (CE). We assessed their impact on liver CE.
Methods and Materials: We retrospectively evaluated 200 abdominal CT exams in 106 males and 94 females, intravenously injected with Iopamidol (370mg/ml). Body mass index (BMI), lean body weight (LBW) and body surface area (BSA) were estimated using validated formulas. Liver CE, defined as the absolute difference in HU between portal and basal phases, was measured. Data were reported as mean±standard deviation; bivariate correlation and multivariate regression analyses were performed.
Results: Patient age was 66±13 years, with a BW of 72±15kg and a LBW of 53±11kg. The contrast dose was 1.2±0.2 ml/kg of BW or 1.7±0.2 ml/kg of LBW; the liver CE resulted 43±9 HU. A negative correlation was found between BW and dose (r=-0.686, p<0.001). Liver CE weighted on iodine grams positively correlated with the BW (r=0.704, p<0.001), LBW (r=0.665, p<0.001) and BSA (r=0.712, p<0.001). At multivariate regression analysis, the contrast dose per kg of BW was the only independent predictor of contrast enhancement variability, with a standardised correlation coefficient of 0.268 (p=0.002).
Conclusion: We found a high variability of administered dose due to radiologist's adjustment based on patient morphometry and comorbidities. To reduce liver CE variability, further studies are needed to find out a more patient-centered way to calculate contrast dose.
Author Disclosures:
G. Di Leo: Other; Congress Sponsorship from Bracco Imaging SpA.
F. Sardanelli: Advisory Board; Bracco Imaging SpA.

B-0708 11:02

Material suppressed iodine using dual-energy spectral CT: feasibility and influencing factors

H. Zhao; *Zhengzhou/CN (kindergirl@sina.cn)*

Purpose: To investigate the feasibility of material suppressed iodine (MSI) images derived from spectral CT to replace true noncontrast-enhanced (TNC) images and assess the effect of contrast agent dose and body mass index (BMI) on MSI images.
Methods and Materials: Sixty patients who underwent spectral CT were divided into two scan protocols based on BMI (n = 30 each; protocol A, 80 kVp/300 mgI/kg, 18-23.9kg/m^2; protocol B, 100 kVp/400 mgI/kg, 24-29kg/m^2). TNC images (A1 and B1) were obtained while MSI images with adaptive statistical iterative reconstruction (ASIR) were reconstructed during the arterial phase (A2 and B2) and venous phase (A3 and B3). Image noise, CT value and contrast-to-noise-ratio (CNR) of liver, aorta and portal vein were compared between MSI images and TNC images and between protocols A and B.
Results: Intra-group: image noise in A3> A2>A1 and B3>B2, in B1 was similar to those of B2 and B3. The CT values of liver in A1 were similar to A3 but higher than A2, in B1>B3>B2. The CT values of vessels in MSI images were similar to TNC images except B2> B1 in aorta and A3>A1 in portal vein.The CNR values of liver and vessels were similar except A1>A2 and A1>A3 in aorta and portal vein. Inter-group: compared with protocol B, protocol A showed higher image noise but lower CT values of vessels.
Conclusion: The image quality of MSI images might be able to replace TNC images; the increase of contrast material dose and BMI might improve the image quality of MSI images.
Author Disclosures:
H. Zhao: Author; Peijie Lv, Jianbo Gao, Liying Zhang.

B-0709 11:10

Feasibility of material suppressed iodine using dual-energy spectral CT with optimised adaptive statistical iterative reconstruction (ASIR) in abdominal CT

H. Zhao; *Zhengzhou/CN (kindergirl@sina.cn)*

Purpose: To assess the image quality of material suppressed iodine (MSI) images derived from spectral CT imaging with different percentages of ASIR.
Methods and Materials: Forty-six patients underwent conventional non-contrast-enhanced (TNC) and arterial-phase (AP) and venous phase (VP) with CT spectral imaging mode. MSI images generated from spectral CT were reconstructed with different percentages of ASIR (0%, 30%,50%, 70%) during the arterial phase (B1, C1, D1, E1) and venous phase (B2, C2, D2, E2). TNC images (A) were reconstructed with 0% ASIR and compared with MSI images in image noise, CT value and contrast-to-noise ratio (CNR) of liver, aorta and portal vein. Volume CT dose index (CTDIvol) was recorded.
Results: Image noise in E1<D1<C1<B1<A, C2<D2<B2<E2<A (all *P* values <0.05). The CT values of the liver in B1<C1<D1<E1<A (all *P* values <0.05), C2<B2<D2<E2<A (all *P* values> 0.05). The CT values of the aorta and portal vein of MSI images were similar to those of TNC images, and the CT value of MSI with 70% ASIR was close to the TNC images. There were significant differences in CNR of liver: E1>B1>C1> D1>A, C2>E2>D2>B2>A. There was no significant difference between MSI images and TNC images in CNR of aorta and portal vein (all P values >0.05).The CTDIvol could be reduced by 9.92mGy (34%) without TNE scan.
Conclusion: MSI images with 70% ASIR might replace TNC images and could reduce 34% radiation dose.
Author Disclosures:
H. Zhao: Author; Peijie Lv, Jianbo Gao, Liying Zhang.

B-0710 11:18

Fast abdominal imaging with high parallel-imaging factors: comparative study of a 60-channel receiver coil with the standard coil setup

A. Othman, J. Weiss, J. Taron, K. Nikolaou, M. Notohamiprodjo; *Tübingen/DE (ahmed.othman@uni-tuebingen.de)*

Purpose: To assess a novel 60-channel receiver coil setup regarding signal-to-noise ratio (SNR) and image quality in fast abdominal imaging as compared to a standard 30-channel coil setup.
Methods and Materials: All imaging data were acquired on a 3T MR scanner (Magnetom Skyra, Siemens Healthineers). 3D-T1-GRE imaging with different PAT factors (CAIPIRINHA: none,2,3,2x2,3x2,2x3,3x3) was performed in a water-phantom and in 5 volunteers using a novel 60-channel (30-channel anterior+posterior) receiver coil setup and standard 30-channel (18-channel-body and 12-channel-spine coil)-setup. SNR was measured on phantom images. Image quality assessed by two radiologists (5-point Likert scale; 5=excellent quality). In a further step, standard contrast-enhanced abdominal 3D-T1-GRE imaging with PAT 2 and accelerated imaging with PAT 2x2 and 3x2 was performed in 17 patients who were assigned into two groups (60-channel, n=8; 30-channel, n=9). Image quality was compared between the two patient groups.
Results: In comparison to the 30-channel coil, SNR gain for the 60-channel setup was observed for all acquisitions except for PAT=none. Relative SNR gain for the 60-channel coil ranged between 2.21% for PAT=2 and 22.69% for PAT=3x2. Comparison of image quality in healthy participants revealed significantly higher ratings of the 60-channel setup for all acquisitions (p≤.046), except for PAT=none (p≥.180). In patients, similar results were observed with comparable image quality at lower PAT factors (PAT=2; p≥.069) and significantly superior image quality of the 60-channel setup for higher PAT factors (2x2 and 3x2; p≤.036).
Conclusion: The 60-channel coil setup improves image quality and, therefore, enables fast abdominal imaging at high PAT factors with diagnostic image quality.

B-0711 11:26

Assessment of bolus tracking for the acquisition of a single dual-energy iodine map as a quantitative imaging biomarker replacing abdominal CT perfusion

S. Skornitzke, F. Fritz, P. Mayer, M. Koell, T. Hackert, H.-U. Kauczor, W. Stiller; *Heidelberg/DE (Stephan.Skornitzke@med.uni-heidelberg.de)*

Purpose: To quantitatively evaluate dual-energy (DE) computed tomography (CT) iodine concentration maps acquired using bolus tracking with different trigger delays as a dose-reduced replacement of CT-perfusion maps for diagnosis and treatment response assessment of abdominal tumours, such as pancreatic carcinoma.
Methods and Materials: For 22 patients with pancreatic carcinoma, DECT perfusion sequences were dynamically acquired using dual-source DECT at tube potentials of 80kV$_p$ and 140kV$_p$ with tin filtration. After deformable motion-correction, perfusion maps were calculated from 80kV$_p$ image series and DECT iodine maps were calculated for each of the 34 DECT acquisitions per patient. Measurements of perfusion and iodine concentration were performed in regions of interest in healthy pancreatic tissue and carcinoma. For each patient, 34 iodine maps at different acquisition delays were evaluated with regard to correlation to perfusion and inter-group differences between healthy tissue and carcinoma, simulating acquisitions triggered by bolus tracking by using the timing of bolus tracking of prior three-phase contrast-enhanced CT as a reference (threshold 120HU in abdominal aorta).
Results: Average perfusion measured in healthy pancreatic tissue and carcinoma was 87.6±28.4ml/100ml/min and 38.6±22.2ml/100ml/min, respectively. Correlation between iodine concentrations and perfusion was statistically significant for bolus tracking with trigger delay greater than 0s (r_{max}=0.89). Differences in iodine concentrations between healthy pancreatic tissue and carcinoma were statistically significant for DECT acquisitions corresponding to trigger delay of 15-21s.

Conclusion: DECT iodine maps acquired using bolus tracking with appropriate trigger delay could serve as a quantitative imaging biomarker in the abdomen, providing a dose-efficient replacement of CT-perfusion.
Author Disclosures:
H.-U. Kauczor: Research/Grant Support; Siemens, Bayer. Speaker; Böhringer Ingelheim, Bracco, GSK, Novartis, Siemens, Almirall.

B-0712 11:34

Image quality comparison of low-dose contrast-enhanced abdominal CT with different protocols: reduced tube voltage or reduced tube current?
S. Ying[1], F. Chen[1], J. Yao[1], G. Yang[1], G. Lei[1], Y. Jiang[2]; [1]*Hangzhou/CN*, [2]*Shanghai/CN (ysh0609@126.com)*

Purpose: To determine a better optimised scan protocol between reduced tube voltage and reduced tube current for low-dose-enhanced abdominal CT.
Methods and Materials: 41 patients who were randomly assigned into 2 groups underwent enhanced abdominal CT. The scan protocols were 100kV/150mAs with ATCM for group 1, and 120kV/100mAs with ATCM for group 2. Images were reconstructed with filtered back projection (FBP), hybrid iterative reconstruction (HIR) and iterative model reconstruction (IMR) algorithms, respectively. Images acquired in portal vein phase were used for analysis. CT attenuation, image noise and CNR of liver parenchyma were measured. Subjective image quality assessments were performed according to the features of structure delineation, noise, artefacts, image distortion, and diagnostic confidence.
Results: No difference was found in mean $CTDI_{vol}$ between two groups. Image noise was higher in group 1 than group 2 in FBP and HIR images; however, no difference of image noise was observed in IMR images. No difference was found in CNR between groups. FBP images in both groups failed to reach acceptable subjective image quality, although images in group 2 exhibited better scores than group 1. HIR images in both groups reached acceptable image quality with no difference between each other. IMR images in both groups reached excellent image quality with better score in group 1 than group 2.
Conclusion: Both reduced tube voltage and tube current protocols can be used in low-dose abdominal CT with HIR and IMR. Reduced tube voltage protocol tends to exhibit better image quality when using IMR.

B-0713 11:42

Spleen stiffness: an index marker of oesophageal varices in patients with liver cirrhosis
N. Balpande[1], D. Aditi[1], K. Meera[1], K. Sudhakar[1], K. Ajairamcharan[1], M. Ipsit[2]; [1]*Chennai/IN,* [2]*Kozhikode/IN (drnikb@gmail.com)*

Purpose: To correlate spleen stiffness (SS) measured by ARFI (acoustic radiation force impulse) with upper GI endoscopy for the presence of esophageal varices (EV) in patients of cirrhosis.
Methods and Materials: Our study included 78 patients of cirrhosis (66 males, 12 females). We performed 5 measurements in each and a median value was obtained. Patients were examined by endoscopy and grade of EV was noted.
Results: A cut-off value of 3.04 m/s for spleen stiffness by ARFI showed sensitivity of 78.2%, specificity of 78.3%, PPV of 89.5% and NPV of 60% for differentiating those with and without EV. SS in patients with grade 3 EV was significantly higher than those with grade 1 EV. Spleen size in patients with EV was significantly higher than those without EV. Within the group of patients with EV, those with higher grades of EV had higher values of spleen size.
Conclusion: 1) SS is significantly higher in patients of cirrhosis than in normal individuals. 2) In patients of liver cirrhosis, SS by ARFI can be used to predict the presence of EV; and endoscopy being an invasive procedure can be avoided in rest of the patients who do not have EV. 3) SS in patients with grade 3 EV was significantly higher than those with grade 1 EV. Thus it could predict the severity of EV.

B-0714 11:50

Focal splenic lesion: to remove or not to remove?
S. Jang[1], J. Kim[1], B. Hur[2], I. Joo[1], S. Ahn[1], M. Kim[2], J. Han[1]; [1]*Seoul/KR*, [2]*Gyeonggi-do/KR (junemiru@gmail.com)*

Purpose: To assess the important CT findings and clinical features for differentiating malignant from benign focal splenic lesions.
Methods and Materials: From 2003 to 2015, among 673 patients with splenectomy in two institutes, we included 114 patients with focal splenic lesion who underwent preoperative CT scans (malignant=66, benign=48). Two radiologists retrospectively accessed CT findings including size of spleen, multiplicity, nature (mainly cyst vs mainly solid), margin (well- vs ill-defined), presence of wall, calcification, and enhancement pattern. They also graded the possibility of malignancy. Clinical features including presence of underlying malignancy, fever, and leukocytosis were assessed. Multivariate logistic regression analysis was performed to identify significant predictors for malignant lesion. We used receiver operating curve analysis for diagnostic performance.
Results: Statistically common features for malignant lesions included enhanced, mainly solid nature, ill-defined margin, absence of splenomegaly, absence of wall and calcification, and presence of underlying malignancy ($p<0.05$). In multivariate analysis, mainly cystic nature (OR, 7.428, P=0.005) and presence of underlying malignancy (OR, 15.017, P=0.001) were significant predictors for malignant lesion. Diagnostic performance for differentiating malignant lesions were 0.856 and 0.893 for each reviewers with substantial interobserver agreement (κ=0.6336). Malignant lesion (3.9+3.2cm) was smaller than benign lesion (5.9+3.3cm). Using the 4.25cm as a cut-off value, sensitivity and specificity were 66.7% and 72.7%.
Conclusion: CT and clinical features were useful for prediction of malignant splenic lesion. Mainly solid nature and presence of underlying malignancy can be helpful when differentiating malignant splenic lesion.

10:30 - 12:00 **Room Z**

Vascular

SS 1015
Pulmonary circulation

Moderators:
G. Balázs; Budapest/HU
S. Haneder; Cologne/DE

K-16 10:30

Keynote lecture
K. Malagari; *Athens/GR*

B-0715 10:39

4D-flow MRI in patients with Fontan circulation for evaluation of pulmonary artery blood distribution
A. Curta, A. Lehner, U. Walter, R. Dalla-Pozza, M. Fischer, N. Haas, H. Kramer; *Munich/DE (harald.kramer@med.lmu.de)*

Purpose: To implement 4D-phase-contrast-flow MRI (4D-flow MRI) in the workup of patients with congenital heart disease and Fontan (FO) circulation and to evaluate the feasibility to assess caval blood flow distribution towards the pulmonary arteries (PA).
Methods and Materials: 4D-flow MRI scans were acquired in 10 FO patients (12.8±4.2 years) with extracardiac tunnel. 4D-flow MRI was performed with a velocity encoding (VENC) of 100cm/s, spatial resolution of 2.2x1.8x1.8mm and 10 time-frames/heart beat (HB). Flow pattern and distribution to the PAs were visualised using colour-coded path lines. All acquired data were processed offline using vendor prototype software.
Results: Blood from the Glenn and Fontan tunnel drained predominantly to the right PA (53% vs 47%). Left PA blood supply tended to be lower but with higher flow velocity compared to the RPA (12.68 ml/HB vs 15.68 ml/HB; 62.2 cm/s vs 49.7 cm/s), consistent with anatomically smaller or distorted LPAs. Path lines revealed Fontan blood predominantly draining to the RPA within our patient cohort on the contrary to recently published data. However, within our group, Glenn and Fontan tunnels were rather placed orthogonal to each other than with a distinct offset to one or the other side as reported by others.
Conclusion: 4D-flow MRI in Fontan patients was feasible with promising results. This work can serve as pilot data for further studies with larger patient numbers to correlate different surgical methods to the resulting PA blood flow distribution and its possible impact on late complications of the Fontan operation-like protein-losing enteropathy.

B-0716 10:47

Optimising image quality in CT pulmonary angiography using low contrast media volume and automated tube voltage selection
B.M.F. Hendriks, N.G. Eijsvoogel, B. Horehledova, M. Kok, B. Martens, L.F. Carati, J.E. Wildberger, M. Das; *Maastricht/NL (babs.hendriks@mumc.nl)*

Purpose: Evaluating image quality of ultra-low contrast media (CM) volume and ultra-low radiation dose computed tomographic pulmonary angiography (CTPA) using automated tube voltage selection (ATVS).
Methods and Materials: 140 consecutive patients receiving CTPA at 70, 80 and 90kV as selected by ATVS on a 3rd generation MDCT (SOMATOM Definition Force, Siemens Healthcare) were analysed. Scan protocol: 105 $mAs_{qual.ref}$, 100 kV_{ref}, pitch 1.2, 1 mm slice, 0.7 mm increment, iterative reconstruction strength 3 (ADMIRE). CM (Iopromide 300 mgI/ml, Bayer) was adapted to body weight and kV-setting via iodine delivery rate based on an 8 s injection time. Objective image quality (IQ) was assessed in the pulmonary trunk (PT; attenuation measurements [HU]), contrast-to-noise and signal-to-noise ratio (CNR/SNR). Variables are reported as mean±SD. Subjective IQ was assessed at central, lobar, segmental and subsegmental level.
Results: Mean body weight was: 70±14 kg for 70 kV (n=42), 71±13 kg for 80 kV (n=67)and 92±14 kg for 90 kV (n=31), p-value between 70/80 kV and 90

kV<0.01. Mean effective radiation dose for 70 kV: 1.2±0.2 mSv, 80 kV: 1.7±0.4 mSv and 90 kV: 2.1±0.6 mSv. Mean CM bolus was 24±3 ml, 28±3 ml and 38±3 ml, respectively. Mean PT attenuation was similar for 70, 80 and 90 kV: 397±99 HU, 396±97 HU and 378±101 HU. CNR/SNR: 14±6/14±4, 16±6/14±4 and 14.±7/13±4 for 70, 80 and 90 kV (p>0.6). Eight scans (4 at 70 kV, 3 at 80 kV and 1 at 90 kV) were rated non-diagnostic on subsegmental level; all other segments were graded as diagnostic/excellent IQ.
Conclusion: CTPA can be individually optimised using ATVS in combination with CM application adapted to body weight and kV, resulting in very low radiation and CM doses for patients.
Author Disclosures:
B.M.F. Hendriks: Research/Grant Support; Bayer, Philips. **N.G. Eijsvoogel:** Research/Grant Support; Bayer. **B. Horehledova:** Research/Grant Support; Siemens. **J.E. Wildberger:** Research/Grant Support; Siemens, Philips, Bayer, AGFA. Speaker; Siemens, Bayer. **M. Das:** Research/Grant Support; Bayer, Siemens, Philips, Cook.

B-0717 10:55

Virtual monoenergetic imaging and iodine perfusion maps improve diagnostic accuracy of dual-energy CT pulmonary angiography with suboptimal contrast attenuation

D. Leithner, J.L. Wichmann, T.J. Vogl, J. Trommer, S.S. Martin, S. Jan-Erik, B. Bodelle, M.H. Albrecht; *Frankfurt a. Main/DE (doris.leithner@googlemail.com)*

Purpose: To evaluate the impact of virtual monoenergetic imaging (VMI+) and perfusion maps (DECT-PM) on diagnostic accuracy and reader confidence in dual-energy CT pulmonary angiography (DE-CTPA) examinations with suboptimal contrast attenuation, compared to standard linearly-blended series.
Methods and Materials: DE-CTPA examinations with suboptimal contrast attenuation of 68 patients with suspected pulmonary embolism (PE) were included in this IRB-approved retrospective study. VMI+ series at 40keV, DECT-PM and linearly blended images (M_0.6 - 60% 90 kV spectrum) were reconstructed. Contrast-to-noise (CNR) and signal-to-noise ratios (SNR) within the pulmonary trunk were calculated. Four independent radiologists assessed the presence of PE and their diagnostic confidence using three DE-CTPA reconstruction protocols: protocol 1: M_0.6 images; protocol 2: M_0.6 series and DECT-PM; protocol 3: M_0.6, DECT-PM, and VMI+ series. Receiver operating characteristic (ROC) analysis was performed.
Results: 14 patients showed central and 29 segmental PE. Higher CNR and SNR values were measured in VMI+ series at 40keV in comparison to M_0.6 images (P<0.001). Diagnostic accuracy for segmental PE detection was as follows: protocol 1: 69.1%; protocol 2: 86.8%; protocol 3: 92.6%. Protocol 3 resulted in a significantly greater area under the curve (AUC) for diagnosing segmental PE (0.991, P≤0.033), compared to protocol 1 and 2 (0.897 and 0.951, respectively), and provided the highest diagnostic confidence (P<0.001).
Conclusion: A reconstruction protocol including 40keV VMI+ series and DECT-PM improves reader confidence and diagnostic accuracy for segmental PE detection compared to standard M_0.6 images in DE-CTPA with suboptimal contrast attenuation.

B-0718 11:03

Validation and error quantification of pulmonary artery 4D-flow MRI in a digital broadband 3T-MR setup

C. Berlin, T.H. Oechtering, M. Sieren, D. Droemann, J. Barkhausen, A. Frydrychowicz; *Lübeck/DE (thekla.oechtering@uksh.de)*

Purpose: 4D-flow MRI offers a yet unmet potential diagnosing pulmonary hypertension. Until now, there has been no comprehensive validation of the sequence at a system with digital broadband technique, which promises an increased signal-to-noise ratio. Therefore, our aim was to validate 4D-flow MRI in the pulmonary arteries (PA).
Methods and Materials: The PA of 23 healthy volunteers (14f, 38±18y) were examined at 3T (Philips Ingenia) with a 4D-flow MRI sequence. Using GTFlow (GyroTools, CH), planes transecting the main, right, and left PA (MPA, RPA, LPA, respectively) were analysed. The MPA stroke volume (SV) was measured in 4D data and compared to 1) a static phantom acquisition, 2) 2D phase contrast (2DPC) acquisitions, 3) right ventricular SV (RVSV) derived from a bSSFP-sequence, and 4) a conservation of mass analysis (COM). Statistical analyses included Bland-Altman analysis and Student's t test.
Results: Using 4D flow-MRI, the MPA SV was 93.0±26.1 vs. 90.5±25.3ml/s with phantom correction, respectively, compared to 2DPC with 87.3±19.1 and 87.4±19.0ml (uncorrected p<0.05, corrected p=0.241). The average difference between 4D flow-MRI and 2DPC was 5.7±10.6ml and improved to 3.1±12.3ml after phantom correction. Compared to RVSV (92.9±15.6ml), the average difference was 5.5±17.2ml and improved to -0.1±20ml (p=n.s.) after phantom correction. The average difference to the COM analysis was 2.2±15.6ml which worsened through correction to 7.7±15.9ml (p=n.s.; p<0.05).
Conclusion: Quantitative 4D-flow MRI in the pulmonary artery is comparable to alternative MR approaches. The improvement of the already good data after phantom correction and the standard deviation may be explained by imperfectly corrected phase offsets.

B-0719 11:11

Comparison of unenhanced and contrast-enhanced MRI in the detection of pulmonary AV-malformations in patients with hereditary haemorrhagic telangiectasia

P. Jagoda, J. Stroeder, A. Massmann, A. Buecker, G. Schneider; *Homburg/DE*

Purpose: The aim of our study was to compare Gd-enhanced MR angiography with unenhanced MR imaging techniques for the detection of pulmonary AV-Malformations (PAVMs) in patients with hereditary hemorrhagic telangiectasia (HHT).
Methods and Materials: 122 patients with HHT underwent 188 MR examinations between 2011 and 2015. During each examination a non contrast enhanced SPACE (3D TSE-sequence/TR 4.733 ms/TE 101 ms/FLIP 150°) and a contrast enhanced 3D GRE MRI sequence (TR 2,87ms/TE 1,07 ms/FLIP 25°, 0.1 mmol/kg BW MultiHance) were acquired. Both examinations were read by two experienced radiologists and the number of detected AV-Malformations was reported in mutual agreement for each examination. The contrast enhanced images were always read first and after an interval of 6 weeks, the SPACE was read. In those patients that underwent interventional treatment, catheter angiography and in all other patients CE-MRA served as the gold standard. A paired t-test was utilised for statistical evaluation.
Results: 4 Examination were excluded due to respiratory artifacts in both sequences. 60 AV-malformations requiring therapy were reported in 35 patients. Using contrast enhanced images, an overall significantly higher number of AV-malformations was detected (166 vs. 96, p<0.001) but none of the AV-malformations requiring therapy were missed using the unenhanced SPACE sequence.
Conclusion: The detection of clinical relevant pulmonary AV-malformations can be safely performed in patients with contraindications for i.v. contrast medium (e.g. pregnancy) by using a SPACE sequence.

B-0720 11:19

C-arm computed tomography (CACT) in patients with chronic thromboembolic pulmonary hypertension and a positive V/Q SPECT/CT: evaluation of additive diagnostic information

J. Hinrichs, T. Werncke, M.M. Hoeper, K.M. Olsson, T. Brunkhorst, F.K. Wacker, J.M. Sohns, B.C. Meyer, C. von Falck; *Hannover/DE*

Purpose: To evaluate the potential additional diagnostic information of C-arm computed tomography (CACT) in patients suffering from chronic thromboembolic pulmonary hypertension (CTEPH) with a positive ventilation/perfusion (V/Q) SPECT/CT.
Methods and Materials: Seventeen patients (11 men, 6 women, 73±11 years) with CTEPH who had undergone SPECT/CT, followed by CACT and right heart catheterisation (RHC) were included. Two independent readers reviewed SPECT/CT and another two readers the CACT images. CTEPH-indicating findings and their location (segmental or sub-segmental) were identified (V/Q mismatch in SPECT/CT and vascular pathologies in CACT). Inter-observer agreement was calculated and consensus reading was done for calculation of inter-modality agreement (Cohen´s Kappa).
Results: Overall, 306 pulmonary artery segments were assessed in SPECT/CT and CACT. SPECT/CT identified 128/306 (41%) arterial segments without and 178/306 (59%) with CTEPH-indicating V/Q mismatch. CACT detected 57/306 (19%) segments without abnormal findings and 249/306 (81%) with CTEPH-indicating findings. Inter-observer agreement was good for both modalities (SPECT/CT κ=0.73; CACT κ=0.77, respectively). Inter-modality agreement after consensus reading was fair (κ=0.28). Discrepant findings were mostly attributed to a higher frequency of sub-segmental pulmonary arterial pathologies on CACT (79 sub-segmental CTEPH-indicating findings) rated as normal on SPECT/CT.
Conclusion: In patients with CTEPH, contrast-enhanced CACT detects additional findings as compared to V/Q SPECT/CT. CACT indicates abnormalities even in segments without V/Q abnormalities.
Author Disclosures:
M.M. Hoeper: Research/Grant Support; Fees from Actelion, personal fees from Bayer, personal fees from GSK, personal fees from Pfizer, outside the submitted work. **F.K. Wacker:** Research/Grant Support; Grants from Siemens Healthcare, grants from DFG, Rebirth-Cluster of Excellence, grants from BMBF, German Centre for Lung Research (DZL), grants from Promedicus Ltd., outside the submitted work. **B.C. Meyer:** Research/Grant Support; Grants from Siemens Healthcare, during the conduct of the study, outside the submitted work; grants from Promedicus Ltd., outside the submitted work.

B-0721 11:27

Model-based iterative reconstruction on low-dose CT pulmonary angiography: diagnostic image quality and radiation dose saving compared with hybrid iterative reconstruction CTPA

A. De Vito, D. Ippolito, C.R.G.L. Talei Franzesi, L. Riva, E.B. Orsini, S. Sironi; *Monza/IT (a.devito@campus.unimib.it)*

Purpose: To evaluate dose reduction and image quality of low-dose CT pulmonary angiography (CTPA) reconstructed with model-based iterative reconstruction (IMR) and compared with hybrid iterative reconstruction (iDose4).
Methods and Materials: 69 patients were prospectively enrolled and investigated for pulmonary embolism; a study group of 39 patients underwent low-kV setting (100kV;automated mAs) CTPA study, while a control group of 30 patients underwent standard CTPA protocol (120 kV;automated mAs); all patients were examined on 256 MDCT scanner (iCT elite;Philips). In the first group (Study Group) images were reconstructed using IMR technique while in the second group (Control Group) we used iDose4 technique. CTDIvol, DLP and Estimate Doses (ED) were evaluated in both groups. Region of interests were drawn in the three main pulmonary vessels; signal-to-noise ratio (SNR) and contrast-to-noise ratio (CNR) were calculated. A four-point scale was used to subjectively evaluate the image quality of iDose4-CTPA and low kV IMR-CTPA.
Results: Compared to iDose4-CTPA, low kV IMR-CTPA presented lower CTDIvol (9,68 ± 3,54 vs 16,7 ± 5,34 mGy) and DLP (352,48 ± 3,59 vs 673,5 ± 36,9 mGy x cm). ED were 4,93 ± 1,8 vs 9,64 ± 3,05 mSv. Moreover IMR-CTPA showed higer values of attenuation in the three main pulmonary vessels and a significantly higher SNR (p<0,0001) and CNR (p<0,0001). The subjective image quality of low kV IMR-CTPA was also higher compared with iDose4-CTPA.
Conclusion: Low kV IMR-CTPA allows a significant dose reduction and improves attenuation values, SNR and CNR in the pulmonary vessels, as compared with standard kV iDose4-CTPA.

B-0722 11:35

Analysing pulmonary artery haemodynamics with 4D-flow MRI: comparison to 2D phase contrast MRI in patients with pulmonary hypertension and healthy volunteers

M. Sieren, C. Berlin, T. Oechtering, P. Hunold, D. Droemann, J. Barkhausen, A. Frydrychowicz; *Lübeck/DE (malte.sieren@uksh.de)*

Purpose: 2D and 4D phase-contrast MRI (2DPC, 4D flow MRI) are increasingly being used to non-invasively diagnose pulmonary hypertension (PH). It was the goal of this study to compare 2DPC and 4D flow MRI in the pulmonary vessels with respect to previously established diagnostic parameters to distinguish healthy volunteers from patients diagnosed with PH.
Methods and Materials: 11 patients with PH (4f, 63±15y), 15 age-matched healthy volunteers (9f, 56±11y), and 20 young healthy volunteers (13f, 23±2y) were scanned at 3T (Philips Ingenia). A retrospective ECG-gated 4D flow MRI sequence with respiratory gating was applied. Data were reconstructed to spatial resolution=2mm^3 and temporal resolution=20 frames. A standard clinical 2DPC-MRI sequence with 40 frames was acquired during breath holds in the main pulmonary artery (MPA). GTFlow (GyroTools, CH) was used to extract various flow-, velocity- and vessel area-derived parameters.
Results: There was good agreement between 2DPC and 4D flow MRI across all participants with a tendency of 4D flow MRI to overestimate values. Only differences in flow volume and time to maximum flow revealed statistical significance, the average Bland-Altman differences were acceptably small. Both 2DPC and 4D flow MRI revealed concordant results to differentiate patients from healthy individuals, especially with strain (4D: Vol 34.8±13.3% vs. Pat 24.5±8.8%; 2D: Vol 41.2±12.4% vs. Pat 21.2±7.3%; for all p<0.05).
Conclusion: This study confirms that haemodynamic parameters used for the diagnosis in pulmonary hypertension can be gathered using 4D flow MRI within reasonable clinical limits of agreement. Despite its unfavourable spatial and lesser temporal resolution, the identification of diseased study participants was possible.

B-0723 11:43

Feasibility of a low dose and low contrast media protocol for CT pulmonary angiography

S. Suntharalingam, C. Mikat, Y. Erfanian, K. Nassenstein; *Essen/DE*

Purpose: To evaluate the image quality and radiation dose of a low dose and low contrast media protocol for CT pulmonary angiography (CTPA).
Methods and Materials: Sixty patients with suspected pulmonary embolism were examined with two different protocols (n = 30 each, group A, 100 kVp, ref. mAs 150, 60 ml of contrast medium; group B, 80 kVp, ref. mAs 115, 25 ml of contrast medium. Image quality and radiation dose were evaluated and compared.
Results: Signal intensities in main pulmonal artery (351.4 vs. 291.8; p=0.08), left pulmonal artery (339.2 vs. 311.6; p=0.42), right pulmonal artery (340.8 vs. 309.9; p=0.37), lobar artery (368.9 vs. 343.0; p=0.49), segmental artery (347.6 vs. 323.4; p=0.50) and subsegmental artery (334.4 vs. 330.4; p=0.91) were slightly, but not statistically significantly higher in group A. SNR and CNR values were comparable between both groups (all p>0.05). Subjective image analysis revealed no significant differences between the two groups. All exams were rated as good to excellent or adequate. Compared with group A, radiation dose of group B was reduced by 71.8 % (2.4 vs. 0.7 mSv; p<0.001).
Conclusion: A low dose protocol at 80 kV can obtain sufficient image quality for CT pulmonary angiography with 25 ml of contrast media and reduce radiation dose by 71.8 % compared to a standard protocol.

B-0724 11:51

Vascular rings: contrast-enhanced MR angiography in comprehensive evaluation of broncho-vascular anatomy in children.

E. Karavaeva[1], J. Finn[2]; [1]*Moscow/RU*, [2]*Los Angeles, CA/US (lenakara-23@mail.ru)*

Purpose: To evaluate feasibility and sufficiency of high resolution, contrast-enhanced MR Angiography (CEMRA) in detailed assessment of 3D vascular and proximal airway anatomy in children with suspected vascular rings.
Methods and Materials: 42 paediatric patients (25 male, 17 female; 6.14 +/- 4.07 years, range 1m to 13 y) with clinical suspicion of vascular rings underwent multiphase, high spatial resolution CEMRA at 3.0T (31 patients) or 1.5T (15 patients) with gadolinium-based contrast medium. Using standardised scoring system 2 independent radiologists scored the studies for image quality, artifacts, visibility of upper airways. Additionally, all studies were evaluated for presence of pathology, including vascular rings and trachea-bronchial compression, by the same two radiologists and a third independent radiologist. Correlation with chest x-ray was available in all patients and with chest CT in 12 patients.
Results: All scans were scored as highly diagnostic with good or excellent image quality. Visualisation of the trachea and bronchi was assessed as confident, the interobserver agreement was considered as 'good' and 'excellent' (Cohen's kappa ranged from 0.607 to 0.846 depending on scored segment). A total of 10 vascular rings with tracheobronchial compression were detected with excellent interobserver agreement (Fleiss' kappa = 1). The mean difference between MR and CT measurements of trachea diameter at 3 different levels was 0.45 +/- 0.3 mm.
Conclusion: High resolution CE MRA is feasible for confident assessment of both vascular and relevant 3D trachea-bronchial anatomy in children with suspected vascular rings, and may make supplemental CT imaging unnecessary in appropriate patient groups.

10:30 - 12:00 **Room O**

Chest

SS 1004

Chest CT dose reduction and image quality

Moderators:
L.F. Alva López; Tlalpan/MX
C. Heilmaier; Zurich/CH

B-0725 10:30

Lung image quality of a prototype ultra-high resolution CT scanner: comparison to current clinical standard

P. Rogalla[1], A. Sirajuddin[2], S. Kandel[1], J. Kavanagh[1], M. Prokop[3], A. Blum[4], J. Schuzer[1], B. Hoppel[1], M. Chen[2]; [1]*Toronto, ON/CA*, [2]*Bethesda, MD/US*, [3]*Nijmegen/NL*, [4]*Nancy/FR (Patrik.Rogalla@uhn.ca)*

Purpose: To compare the lung image quality of a prototype ultra-high resolution CT (UHR-CT) scanner with a current state-of-the-art CT scanner.
Methods and Materials: 20 patients (mean BMI 25.1 ± 3.1, age 55.5) underwent a chest CT on a prototype whole body (0.25mm x 128 detector matrix) scanner (Toshiba) for cancer staging. Images were compared to prior scans acquired on a standard CT (Vision, 0.5 x 80 detector matrix). Images were iteratively reconstructed on the clinical scanner at 0.5 mm and 512 image matrix (series I), and on the prototype scanner at 0.25 mm, 512 (series II) and 1024 image matrix (series III). Five blinded reviewers (1-24 years of expertise) forced-ranked the images in order of their individual preference. Image noise was measured in the aorta, muscle, air; radiation dose was recorded.
Results: Mean ranking for series I, II, II was 2.78, 2.15, and 1.07 (p<0.0001), with the exception of two patients ranked by three readers, the 0.25 mm slices at 1024 matrix always ranked best, followed but the 0.25 mm slices at 512 matrix (p=0.0013). Mean SD of image noise in air/muscle/aorta for series I, II, and III was 19.7/39.4/34.5, 25.2/57.9/50.0, and 33.5/77.7/69.0, respectively

(p<0.0001). Radiation dose was 18% higher on the prototype scanner (mean DLP: 386.8, SD 98.3) than on the clinical scanner (mean DLP: 325.4, SD 109.1).
Conclusion: Radiologists preferred the UHR-CT over the current clinical standard. Thinner slices at higher matrix improved subjective image quality of the lung at the cost of higher radiation dose.
Author Disclosures:
P. Rogalla: Research/Grant Support; Institutional Research Grant, Toshiba Medical Systems. **A. Sirajuddin:** Research/Grant Support; Institutional Research Grant, Toshiba Medical Systems. **M. Prokop:** Research/Grant Support; Institutional Research Grant, Toshiba Medical Systems. **J. Schuzer:** Employee; Toshiba Medical Systems. **B. Hoppel:** Employee; Toshiba Medical Systems. **M. Chen:** Research/Grant Support; Institutional Research Grant, Toshiba Medical Systems.

B-0726 10:38

Prototype ultrahigh-resolution CT for chest imaging: initial human experience
S.M. Shanbhag[1], J.L. Schuzer[2], C. Steveson[3], S. Rollison[1], M.S. Stagliano[1], K.C. Bronson[1], M.Y. Chen[1]; [1]*Bethesda, MD/US*, [2]*Vernon Hills, IL/US*, [3]*Otawara/JP (Shanbhagsm@nhlbi.nih.gov)*

Purpose: To evaluate a prototype, ultrahigh-resolution computed tomography CT scanner which offers imaging at a significantly higher matrix (1024x1024) and spatial resolution (140 microns) for chest imaging.
Methods and Materials: 100 consecutive patients (age 49.9±16.8 years, BMI 24.7±3.8 kg/m^2) were prospectively enrolled for this IRB-approved study. Each patient underwent a helical CT on a prototype, ultrahigh-resolution CT with 128-detector rows and 0.25mm detector width. CT images were reconstructed at a standard resolution matrix of 512x512 and at high-resolution 1024x1024 matrix. Each set of reconstructions was graded for image quality by 2 expert readers blinded to clinical data and reconstruction on a Likert scale (1=excellent, 5=non-diagnostic) for noise, artefacts, contrast, small detail, lesion conspicuity, image sharpness and diagnostic confidence. Image noise was quantified.
Results: All CT acquisitions were diagnostic image quality. Image noise was higher on the 1024 compared to 512 matrix reconstruction (20.2±4.0 vs. 17.2±3.8, respectively, p<0.001) and had a worse rating (1.98±0.63 vs. 1.75± .61, respectively, p<0.001). However, 1024 matrix performed significantly better than 512 matrix with regard to artefacts (1.37±0.43 vs. 1.50±0.48, respectively, p<0.001), contrast (1.50±0.56 vs. 1.62±0.57, respectively, p<0.001), small detail (1.06±0.19 vs. 2.02±0.22, respectively, p<0.001), lesion conspicuity (1.08±0.23 vs. 2.02±0.24, respectively, p<0.001), image sharpness (1.09±0.24 vs. 2.02±0.28, respectively, p<0.001), and diagnostic confidence (1.09±0.25 vs. 1.18±0.34, respectively, p<0.001).
Conclusion: Ultrahigh-resolution CT with higher 1024x1024 image matrix improves image quality compared to conventional 512x512 image matrix reconstruction, despite a small increase in image noise. This technological advancement in resolution may enhance the detection of disease.
Author Disclosures:
J.L. Schuzer: Employee; Toshiba Medical Research Institute. **C. Steveson:** Employee; Toshiba Medical. **M.Y. Chen:** Research/Grant Support; Research agreement with Toshiba Medical.

B-0727 10:46

Overscanning in chest CT: comparison of incidence among five Swiss hospitals and its impact on radiation dose
F.R. Schwartz[1], B. Stieltjes[1], Z. Szucs-Farkas[2], A. Euler[1]; [1]*Basle/CH*, [2]*Biel/CH (fides.schwartz@usb.ch)*

Purpose: To compare the incidence of overscanning in chest CT among five Swiss hospitals and its impact on radiation dose.
Methods and Materials: Scout images of 250 chest CT scans from five hospitals (A-E), which participate in a regional dose registry, were reviewed using a radiation dose tracking software (RTS) (Radimetrics, Bayer Healthcare). The RTS offers the possibility to virtually alter the cranial and caudal scan limits on each scout image and to estimate the changes in radiation dose, based on Monte Carlo simulations. Incidence of cranial and caudal overscanning was assessed by comparing the actual scan limits of each scan to optimized scan limits determined by a third-year radiology resident. In the optimised scan limits, 2 cm of safety margin were added to the cranial and caudal anatomic borders to account for patient's respiration and operator dependency. Changes in effective dose were calculated by the RTS. Descriptive statistics and Wilcoxon matched pairs test were applied.
Results: Cranial overscanning was observed in 24%, 28%, 30%, 0%, 14% of scans; caudal overscanning in 66%, 32%, 6%, 10%, 6%; both cranial and caudal overscanning in 20%, 10%, 2%, 0%, 0% for hospital A, B, C, D and E, respectively. Simultaneous caudal and cranial overscanning increased the effective dose on average by 0.36 mSv, 0.37 mSv, 0.02 mSv, 0 mSv, 0 mSv for A, B, C, D, E, respectively.
Conclusion: Substantial differences in the incidence of overscanning in chest CT exist among different hospitals resulting in excessive effective dose to the patient.
Author Disclosures:
A. Euler: Research/Grant Support; GE Healthcare.

B-0728 10:54

Radiation dose reduction using orthogonal tomogram associated with topogram-based automatic tube voltage and current modulation for lung CT scanning
X. Liu, L. Zhang; *Shenyang/CN (xiaofeicmu@sina.com)*

Purpose: A new feature for advanced CT is to use tomogram a priori knowledge to modulate tube voltage or current in the real acquisition. This study is to evaluate tomogram's effectiveness on radiation dose and image quality for a set of lung scanning follow-up patients.
Methods and Materials: 38 patients were enrolled in our study. Scanning protocol was identical for both baseline and follow-up examinations. However, in baseline, only anteroposterior (AP) tomogram was applied, while in the follow-up, both AP and lateral (LAT) tomograms were performed. Topogram-based longitudinal-angular automatic current control and automated tube potential selection were "on" during all the scans. Radiation dose, subjective and objective image quality evaluations were compared. Meanwhile, the dose reduction ratio was further analysed in different BMI groups using ANOVA.
Results: In 34.2% (13) of the patients, tube voltage was automatically adjusted to lower kV when using orthogonal tomogram. Radiation dose was lower in follow-up group with an average of 16.9% reduction (5.38±1.37 vs 4.47±1.56mSv, p<0.05). Image noise, signal-to-noise ratio and objective image quality showed no differences between baseline and follow-up. Dose reduction in different BMI groups was not equivalent which intends to be more benefit for overweighted populations.
Conclusion: Using orthogonal tomogram can affect not only tube current modulation but also the selection of tube voltage. Total radiation dosage can even be saved without any compromise on image quality. Furthermore, this advantage was found to be of much more benefit for oversized patients.

B-0729 11:02

Impact on image quality and radiation dose of a novel spectral filtration 150 kV tin-filtered chest CT protocol in patients after lung transplantation
A. Wresenegger[1], C. Schestak[1], H. Prosch[1], H. Ringl[1], G. Apfaltrer[2], P. Apfaltrer[1]; [1]*Vienna/AT*, [2]*Graz/AT (Alexander.wressnegger@meduniwien.ac.at)*

Purpose: The purpose of this study was to investigate the radiation dose and image quality of non-enhanced chest CT using spectral filtration with a novel 150kVSn filter in patients after lung transplantation.
Methods and Materials: This retrospective study included 35 patients (51.4% male, mean age 49.5±15.5 years) who had undergone routine unenhanced chest CT follow-up after lung transplantation on both, a second-generation dual-source CT system (DSCT) using standard chest CT protocol and on a third-generation DSCT using a novel spectral filtration chest protocol (150kVSn). Signal-to-noise (SNR) was measured in 6 standardised regions in lung and soft tissue window to assess objective image quality. Subjective image quality was graded on a 5-point Likert scale for the assessment of ground glass opacities, bronchiectasis, traction, consolidation, architectural deformation, volume loss and hilus retraction after lung transplantation. Radiation metrics were compared using Student's t test.
Results: All studies were considered of diagnostic quality. Mean DLP and effective dose were 77.7±33.8mGy*cm and 1.4±0.6mSv at Sn150 kVp chest protocol vs 196.4±57.5mGy*cm and 3.5±1.0 mSv at conventional chest CT protocol (p<0.001) equivalent to a 60% reduction in radiation using the novel Sn150 kVp. There was no significant difference in image noise (54.1±2.7HU vs 45.0±2.3HU; p=0.097) and SNR (4.1±3.5 vs 5.1±3.5; p=0.054) between 150kVSn-CT and standard protocol. The median score in subjective analysis was equal for both protocols [25th-75th percentile]: 1[1-2] vs 1[1-2], (p>0.05).
Conclusion: Using a non-contrast 150kVSn chest CT protocol allows for substantial radiation dose reduction without compromising diagnostic image quality in the follow-up of patients after lung transplantation.

B-0730 11:10

Sub-millisievert (mSv) third-generation dual-source chest CT with advanced modeled iterative reconstruction: image quality and lesion conspicuity
F. Sodagari, H. Savas, R. Agrawal, T.H. Grant, V. Yaghmai; *Chicago, IL/US (Rishi.Agrawal@nm.org)*

Purpose: To determine the lowest CT radiation dose parameters for detection of various lung pathologies in a phantom model.
Methods and Materials: An anthropomorphic adult-sized chest phantom containing six pathologies (ground glass opacity, bronchial polyp, solid nodule, ground glass nodule, bronchiectasis, tree-in-bud) was scanned with a third-

generation dual-source scanner. Scans were performed with 70, 80, 100 and 120 kV and fixed mAs ranging from 7 to 75 mAs and were reconstructed using advanced modeled iterative reconstruction algorithm. Two blinded chest radiologists reviewed the images independently and scored overall image quality and lesion conspicuity using a five-point scale. A score of 3 was considered acceptable for both image quality and lesion conspicuity. Radiation dose and noise were recorded for each acquisition and CNR was calculated.
Results: The lowest radiation dose parameters with acceptable conspicuity score for bronchial polyp, solid nodule, ground glass nodule, ground glass opacity, and bronchiectasis were 70 kVp/7 mAs (0.05 mSv). The conspicuity for tree-in-bud pathology was acceptable at 70 kVp/40 mAs (0.28 mSv). The lesion conspicuity scores between the two radiologists were comparable (P>0.05) for all lung pathologies studied. The lowest radiation dose parameters for acceptable image quality were 70 kVp/10mAs (0.07 mSv). Subjective image quality was directly proportional to the CNR (r=0.736; P=0.015) and inversely proportional to the image noise (r= -0.925; P=0.0001) for each acquisition.
Conclusion: Robust reduction in radiation dose for chest CT examinations, at levels similar to a chest radiograph, is possible at low kV settings with advanced modeled iterative reconstruction.
Author Disclosures:
F. Sodagari: Grant Recipient; Educational Grant, Siemens.

B-0731 11:18

Influence of reconstruction methods for lung densitometry among model-based and hybrid type IR and FBP methods on ADCT from standard to low-dose levels at QIBA phantom study

E. Suehiro[1], T. Sekitani[1], W. Tani[1], N. Negi[1], Y. Fujisawa[2], N. Sugihara[2], K. Fujii[2], T. Yoshikawa[1], Y. Ohno[1]; [1]*Kobe/JP*, [2]*Otawara/JP*
(yosirad@kobe-u.ac.jp)

Purpose: To directly compare the influence of reconstruction method on area-detector CT (ADCT) from standard- to low-dose levels to COPD density measurement accuracy in QIBA phantom study.
Methods and Materials: QIBA recommended phantom for CT densitometry standardisation was scanned on a ADCT system at three tube current as 400mA, 100mA, and 10mA levels. In this study, three reconstruction methods such as FIRST (i.e. model-based iterative reconstruction <IR>), AIDR 3D (i.e. hybrid-type IR) and FBP methods were applied. To determine the influence of reconstruction methods, correlations between measured and actual densities at different simulated phantoms within QIBA recommended phantom were statistically evaluated by Pearson's correlation analyses. To evaluate the influence of reconstruction method on ADCT to CT densitometry assessment for COPD, CT values within lung phantom between measured and actual values were compared among all methods by Tukey's HSD test. Finally, the limits of agreement of each scan was assessed by Bland-Altman's analysis.
Results: There were significant and excellent correlations between measured and actual CT values on each scan method at all tube current setting (r=0.999, p<0.0001). On comparison of CT density assessment, there were no significant difference among all reconstruction methods at three different tube current sets (p>0.05). The limits of agreement of each reconstruction method between measured and actual CT density at different tube current settings were ranged as follows: FIRST, -0.7−1.1HU; AIDR 3D, -2.5−-1.4HU; FBP, -3.5−-1.4HU.
Conclusion: Reconstruction methods on ADCT at different tube current settings have little influence to accuracy of CT densitometry in QIBA phantom study.
Author Disclosures:
Y. Fujisawa: Employee; Toshiba Medical Systems Corporation. **N. Sugihara:** Employee; Toshiba Medical Systems Corporation. **K. Fujii:** Employee; Toshiba Medical Systems Corporation. **T. Yoshikawa:** Research/Grant Support; Toshiba Medical Systems Corporation. **Y. Ohno:** Research/Grant Support; Toshiba Medical Systems Corporation.

B-0732 11:26

Influence of scan methods to lung density measurement accuracy using ADCT from standard- to low-dose CT levels at QIBA phantom study

N. Negi[1], T. Sekitani[1], E. Suehiro[1], W. Tani[1], Y. Fujisawa[2], N. Sugihara[2], K. Fujii[2], T. Yoshikawa[1], Y. Ohno[1]; [1]*Kobe/JP*, [2]*Otawara/JP*
(yosirad@kobe-u.ac.jp)

Purpose: To determine the influence of scan method difference on area-detector CT (ADCT) from standard- to low-dose CT levels for COPD density measurement accuracy in Quantitative Imaging Biomarker Alliance (QIBA) recommended phantom study.
Methods and Materials: QIBA recommended phantom for densitometry standardisation in COPD was scanned by means of helical scans as 64-detector row CT (HS 64) and 80-detector row CT (HS 80) and non-helical scan (i.e. wide-volume scan: WV) at tube currents as 400 mA (standard-dose), 100 mA (reduced-dose) and 50 mA (low-dose) levels. To determine the influence of scan method to COPD densitometry assessment, correlations between measured and actual densities were statistically evaluated by Pearson's correlation analyses. To evaluate the influence of scan methods on ADCT at different tube current set to CT densitometry assessment for COPD, CT values within lung phantom were compared among all methods by Tukey's HSD test. Finally, the limits of agreement of each scan was also assessed.
Results: There were significant and excellent correlations between measured and actual CT values on all data set (r=0.999, p<0.0001). On comparison of CT density assessment, there were no significant difference among all scan methods at different tube currents (p>0.05). The limits of agreement of each scan method between measured and actual CT density at different tube current settings were ranged as follows: HS 64, -6.9−-5.0HU; HS 80, -4.6−-2.5HU; and WV, -3.5−-1.4HU.
Conclusion: Scan methods at ADCT with different tube current settings have little influence to accuracy of CT densitometry in QIBA phantom study.
Author Disclosures:
Y. Fujisawa: Employee; Toshiba Medical Systems Corporation. **N. Sugihara:** Employee; Toshiba Medical Systems Corporation. **K. Fujii:** Employee; Toshiba Medical Systems Corporation. **T. Yoshikawa:** Research/Grant Support; Toshiba Medical Systems Corporation. **Y. Ohno:** Research/Grant Support; Toshiba Medical Systems Corporation.

B-0733 11:34

Effects of the ASiR-V algorithm on objective and subjective image quality in chest MDCT

D.C. Rotzinger, D. Racine, K. Alfudhili, N. Keller, F.R. Verdun, C. Beigelman-Aubry, F. Becce; *Lausanne/CH (david.rotzinger@chuv.ch)*

Purpose: To investigate the effects of implementing ASiR-V on subjective and objective image quality (IQ) using appropriate physical metrics, in routine oncologic chest MDCT. Secondly, to determine the optimal ASiR-V level for the analysis of lung parenchyma at regular dose level.
Methods and Materials: Twenty patients underwent oncologic thoraco-abdominal MDCT performed on a 64-MDCT scanner at regular dose level (CTDIvol=12mGy) with images reconstructed using FBP. The same patients subsequently underwent (mean time interval=10months) follow-up imaging on a 256-MDCT scanner with 20% dose reduction (CTDIvol=9.6mGy) with images reconstructed using six ASiR-V levels (0%-100%, 20% increments). Subjective IQ was assessed by two independent and blinded radiologists. Objective IQ was evaluated on patient MDCT images by measuring standard deviation (SD), SNR and CNR, and on phantom images by computing detectability indices (d') with the Non-prewhitening with eye filter model observer.
Results: Regarding subjective IQ comparison between both CT systems, ratings from the two observers diverged. However, in subjectively determining the optimal ASiR-V level, both observers preferred 80% due to perceived lack of subtle details at 100%, with substantial interrater agreement (weighted kappa=0.69). Concerning objective assessment, ASiR-V significantly impacted IQ. Increasing ASiR-V level up to 100% significantly decreased SD, while concomitantly increasing SNR and CNR (p<0.001) on clinical images. On phantom images, d' indices gradually increased to peak at ASiR-V 100% (p<0.001).
Conclusion: ASiR-V at a level of 80% in oncologic chest MDCT enhances objective IQ for the analysis of lung parenchyma, while concomitantly enabling a dose reduction of 20% as compared with FBP.

B-0734 11:42

Comparison of the diagnostic performance of ASIR-V ultra-low-dose and standard low-dose CT protocols for basic chest CT findings

M. Ludwig[1], J. Cohen[1], E. Reymond[1], B. Ycart[2], G. Ferretti[1]; [1]*La Tronche/FR*, [2]*Saint-Martin-d'Hères/FR*

Purpose: To evaluate diagnostic performances of ultra low-dose CT (ULDCT, DLP<10mGy.cm) vs Low dose CT (LDCT) for basic chest CT findings.
Methods and Materials: 3 radiologists of different experience reviewed 50 patients on ULDCT (Noise index:80, ASIR-V: 70%) and LDCT (Noise index:40, ASIR-V: 40%) consecutive acquisitions obtained on a GE-Healthcare Revolution CT scanner. For each patient and CT protocol, 37 items taken from the Fleischner glossary were rated on a 4 degrees certainty scale. Ratings were then compared with a proportion test. Interreader agreements were computed using Fleiss Kappa for each item; then mean of the differences between protocols was calculated using Student paired t-test.
Results: Mean patients' age and BMI were 61+/-29 years old and 24,4+/-9,3, respectively. Mean DLP was 8,7+/-0,9 mGy.cm and 98,3+/- 34,3 mGy.cm for LD and ULDCT acquisitions respectively. There were no significative differences for the ratings between CT protocols (p>0.05), except for traction bronchiectasis (p=0,001), crazy paving (p=0,047) and tree-in-bud disposition (p=0,012). Observers' confidence significantly decreased on ULDCT (181 vs 27 doubts, p=1.1*10^-26), especially for ground glass opacities and nodules, and emphysema. Mean of the differences of Fleiss kappa was significantly higher and positive within LDCT compared to ULDCT (0.12 ; p=3.9x10^-05).
Conclusion: An ASIR-V ultra-low-dose CT protocol significantly reduces radiation exposure with a conserved diagnostic performance for most chest CT-findings, at the cost of a decreased certainty and decreased interreader agreement.

B-0735 11:50

Optimal low-dose chest CT parameters for monitoring interstitial lung disease: a systematic simulation study

S. Ley[1], L. Fidler[2], H. Schenk[1], M. Durand[3], T. Marras[2], N. Paul[2], S. Shapera[2], S. Mittoo[2]; [1]*Munich/DE*, [2]*Toronto, ON/CA*, [3]*Pietermaritzburg/ZA (ley@gmx.de)*

Purpose: HRCT is preferred imaging technique to evaluate interstitial lung disease (ILD). We set out to establish an optimal low-dose CT (LDCT) protocol for monitoring ILD to identify the lowest radiation dose with optimal diagnostic accuracy and image quality.
Methods and Materials: 25 Patients underwent HRCT (120kV, 50-300mA, 1mm thickness) during routine evaluation. Image reconstructions with varying combinations of tube current (50mA, 20mA, 10mA) and image slice thickness/increment (1/1mm, 3/2.4mm, 5/4mm) were simulated from raw data. Two radiologists independently reviewed all images and reported on image quality, ILD-specific features (ground-glass opacity, reticulation, honeycombing, disease extent), ILD pattern.
Results: 204 CTs were reviewed by each radiologist. There were no significant differences in sensitivity and specificity across LDCT imaging series. Diagnostic accuracy was best in 20mA series with a mean across group of 91%, compared with 50mA (84%, p=0.014) and 10mA series' (82%, p=0.018). Image quality was reduced in grouped 10mA (p=0.0003) and 1mm (p<0.0001) thickness series compared with other series. At 10mA series, a higher percentage of ground-glass opacity (p=0.003), reticulation (p=0.015), total extent of ILD (p=0.003) was reported. No difference in extent of honeycombing was found (p=0.227). Following successive evaluation of diagnostic accuracy and image quality between series, the 20mA/3mm, 20mA/5mm, 50mA/3mm, 50mA/5mm were found to be equivalent. Of these, the series with the lowest estimated radiation dose was 20mA/5mm.
Conclusion: Evaluating ILD patterns using a LDCT protocol of 20mA and 5mm slice thickness reduces patient radiation exposure without significantly compromising diagnostic accuracy and image quality in comparison to HRCT.

10:30 - 12:00 **Room N**

Genitourinary

SS 1007

Male urogenital system II

Moderators:
A. Graser; Munich/DE
N.N.

B-0736 10:30

Diffusivity and diffusion anisotropy for diagnosis of prostate cancer: a systematic investigation of quantification strategies

S.H. Polanec, G. Wengert, H. Bickel, C. Spick, T.H. Helbich, M. Susani, K. Pinker, P.A.T. Baltzer; *Vienna/AT (stephan.polanec@meduniwien.ac.at)*

Purpose: To assess the impact of region-of-interest (ROI) statistics on diagnostic performance and reproducibility in the assessment of diffusivity and diffusion anisotropy for diagnosis of prostate cancer at 3T-MRI.
Methods and Materials: In this IRB-approved, retrospective study, 65 prostate lesions (35 malignant, 30 benign) verified by MRI-guided biopsy in 65 men (mean age 62.8y) were investigated. Two radiologists independently and repeatedly measured minimum, mean, and maximum Apparent Diffusion Coefficient (ADC) and Fractional Anisotropy (FA) on DTI-images (TR, TE, b-values: 1000mm2/; 6 diffusion directions) by placing a 2-dimensional region of interest around the lesions targeted by subsequent biopsy. Diagnostic performance and reproducibility statistics were calculated for all lesions and stratified by lesion location.
Results: Minimum ADC showed the best diagnostic performance (AUC 0.759). Dependent of the zonal location of a lesion in the transitional zone of the prostate, minimum and mean ADC values showed equal AUC (0.854, P>0.05). In the peripheral zone minimum ADC showed the best diagnostic performance (0.806). In the fibromuscular stroma minimum FA achieved the highest AUC (0.714). Minimum ADC showed highest intra- and interreader reproducibility.
Conclusion: Mean and minimum ADC values showed the best diagnostic performance and minimum ADC the highest reproducibility of all investigated parameters in diagnosis of prostate cancer. Diffusion anisotropy may be of particular value in the fibromuscular stroma.

B-0737 10:38

Diffusion-weighted imaging of the prostate: should we use quantitative metrics to better characterise focal lesions originating in the peripheral zone?

T. Pierre, L. Colleter, F. Beuvon, P. Legmann, F. Cornud; *Paris/FR (p_thibaut@hotmail.fr)*

Purpose: To compare the interreader agreement of the qualitative DW-MRI score ≥3 (PI-RADSv2), with that of quantitative DW-MRI parameters to characterise peripheral zone (PZ) focal lesions.
Methods and Materials: Two experienced radiologists in prostate MRI independently reviewed the T2W- and DW-MR images (computed b-value: 1500s/mm^2) to evaluate 92 DWI-score ≥ 3PZ focal lesions. Quantitative parameters were the mean ADC value, two different ADC ratios with two ROI's as reference areas: PZ mirror area (ADCrmirror) or the rest of the whole prostate surface (ADCrWP), and the mean whole-lesion ADC value with the 10th, 25th and 50th percentiles. Finally, very high b-values (b-3000 and b-6000s/mm^2) were computed and Signal Intensity Ratios (lesion/rest of the prostate surface) were calculated for b-values ≥1500s/mm². Surgical histology and MRI-TRUS fusion-biopsy findings were the reference standard for tumours and benign foci, respectively. Interreader agreement was assessed by the kappa and intraclass correlation coefficients (ICC). Univariate and multivariate regressions were used to determine which factor was the most predictive of cancer.
Results: Fifty abnormalities were malignant (50/92,54%). Interreader concordance for qualitative assessment was moderate (k=0.49 [95%CI:0.30-0.64]), but excellent for quantitative assessment (ICC≥0.80 [95%CI:0.70-0.88]) for all variables. At univariate analysis, all quantitative parameters were significant to predict cancer for both readers. At multivariate analysis, the only independent variable was the ADCrWP for both readers (reader1, OR=12.24 [95%CI:2.7-55.6], p=0.0012; reader 2, OR=12.86 [95%CI: 4.64-35.64], p<0.0001). Sensitivities and specificities were 76-72% and 93-83%, at a cut-off value of 0.62-0.60, respectively.
Conclusion: Quantitative DW-MRI improves the qualitative interreader concordance and the accuracy for the characterisation of focal PZ lesions.

B-0738 10:46

Diagnostic test accuracy meta-analysis of diffusion and T2 weighted-imaging for prostate cancer detection: which b-value is most accurate?

T. Syer, K.C. Godley, T. Smith, P. Malcolm; *Norwich/UK (kcgodley@googlemail.com)*

Purpose: To investigate the role of Diffusion-weighted imaging (DWI) and T_2-weighted imaging (T2WI) in combination for the detection of prostate cancer, specifically assessing the role of high *b*-values (&gt1,000), with a systematic review and meta-analysis of the published data.
Methods and Materials: The electronic databases MEDLINE, EMBASE and OpenSIGLE were searched between inception and 8th March 2016. Eligible studies were those that reported the sensitivity and specificity of both DWI and T2WI for the diagnosis of prostate cancer by visual assessment using a histopathological reference standard. The QUADAS-2 critical appraisal tool was used to assess the quality of included studies. A meta-analysis with pooling of sensitivity, specificity, was undertaken, as well as constructing a summary receiver operating characteristics (sROC) curve and determining the Area Under the Curve (AUC). Predetermined subgroup analysis was also performed.
Results: Twenty-six studies were included in the final analysis, evaluating 1,987 patients. The pooled sensitivity and specificity respectively was 0.68 (95% CI 0.67-0.69) and 0.84 (95% CI 0.84-0.85) and the sROC AUC was 0.83 (95% CI 0.796-0.861). Sub-group analysis showed significantly higher sensitivity using a *b*-value over 1000 (0.77 (95% CI 0.75-0.78)), compared to 1,000 and less (0.64 (95% CI 0.62-0.65)).
Conclusion: The diagnostic accuracy of DWI and T2WI for prostate cancer detection is good. The use of high *b*-values significantly improved the sensitivity while maintaining specificity. Therefore, *b*-values over 1000 should be considered for all DWI protocols for prostate cancer assessment.

B-0739 10:54

Prediction of extracapsular extension in prostate cancer using qualitative and quantitative multiparametric MRI

J. Kim, C. Kim, M.-R. Kwon, R. Kim, J. Yim, W. Kim; *Seoul/KR (ssakpo.kim@samsung.com)*

Purpose: To investigate the predictive value of multiparametric MR imaging (mpMRI) for extracapsular extension (ECE) in prostate cancer (PCa).
Methods and Materials: Enrolled 292 patients who received radical prostatectomy underwent preoperative mpMRI at 3T. For predicting ECE, the likelihood of ECE was assessed qualitatively on T2-weighted imaging (T2WI) and combined T2WI and diffusion-weighted imaging (DWI) or dynamic contrast-enhanced imaging (DCEI). Quantitative MRI parameters were

measured in PCa based on histopathological findings. Two predictive models of ECE including imaging and clinical parameters were developed using multivariate analysis: model 1 excluding combined T2WI and DWI and DCEI and model 2 excluding combined T2WI and DWI, and combined T2WI and DCEI. Diagnostic performance of imaging parameters and models was evaluated using the area under the receiver operating characteristics curve (Az).
Results: For predicting ECE, the specificity, accuracy and Az of combined T2WI and DWI or DCEI were statistically better than those of T2WI (P< 0.001), and all quantitative MRI parameters showed statistical difference between the patients with and without ECE (P< 0.001). On multivariate analysis, significant independent predictors in model 1 were combined T2WI and DWI, combined T2WI and DCEI and K^{trans} (P< 0.05). In model 2, significant predictors were combined T2WI and DWI and DCEI, K^{trans}, K_{ep} and Ve (P< 0.05). The Az values of model 1 and 2 were 0.944 and 0.957, respectively.
Conclusion: mpMRI may be useful to improve diagnostic accuracy of predictive models for ECE in PCa.

B-0740 11:02

Comparison between different DWI protocols using high b values with or without perfusion fraction in differentiating prostate cancer
E.L. Indino, M.D. Grompone, M. Del monte, D. Fierro, C. Catalano, V. Panebianco; *Rome/IT (elenaindino87@gmail.com)*

Purpose: To investigate the ability of a DWI/ADC protocol which exclude perfusion component in distinguishing prostate carcinoma(PCa) to normal prostatic gland and benign prostate hyperplasia (BPH),using histopathologic analysis as reference standard for tumour identification.
Methods and Materials: 120 patients with suspected PCa underwent mp-MRI of the prostate performed at 3.0T(GE MR750). 73 patients were histologically-proven PCa. Two different protocols of DWI/ADC were used: 1) b-values 0, 500, 1000, 3000 s/mm^2, and 2) b=200,500,1000,3000s/mm^2. Two radiologists blinded delineated probable tumour based on T2-weighted, DWI and ADC maps. DWI signal for ADC and ADC-P analyses were taken in pathologic (ROI1), contralateral (ROI2) and central gland(BPH) regions (ROI3).All analyses were performed using SPSS (version 22) and Spearman's rank correlation test was performed to determine the relationship between ADC, ADC-P with Gleason score(GS) and PIRADS.
Results: Differences between ADC and ADC-P values were detected for all the GS in all pathological ROIs. The percentage differences between the two measured parameters [(ADC-ADC-P)/ADC-P] corresponds to the perfusion component of the DWI signal. By using the Youden test, we found 5.71 and 4.6 mm^2/s as best ADC and ADC-P values, respectively. The ADC-P parameters showed the same PPV but higher values for PPN, sensitivity, specificity and accuracy of the diagnostic test with respect to ADC.
Conclusion: Our data showed that ADC-P maps which derived from protocol 2, which exclude b value lower than 200s/mm^2 (in order to exclude the perfusive contribution) can help in the differential diagnosis from significant tumour to indolent disease.

B-0741 11:10

High yield of DWI-based MR-guided targeted prostate biopsy with predominantly intermediate to high risk cancer
S. Heijmink, P. de Koekkoek-Doll, J. de Jong, H. van der Poel, R.G.H. Beets-Tan; *Amsterdam/NL (swheijmink@live.com)*

Purpose: The purpose of the study was to analyse the learning curve and the accuracy of DWI-based MR-guided prostate biopsy as well as determine the accuracy in detecting intermediate and high grade prostate cancer.
Methods and Materials: 66 patients with elevated PSA levels and previously negative TRUS-guided biopsy or low grade prostate cancer underwent a 3T mpMRI of the prostate, which included T2w, DWI and DCE imaging. This was followed by MR-guided in bore biopsy of lesions scored as suspicious of intermediate/high grade disease on DWI. Two radiologists without prior prostate MR-biopsy experience performed all procedures. Biopsy Gleason score was the standard of reference. In patients who subsequently underwent prostatectomy, results were also compared with prostate specimen histopathology.
Results: A total of 34/71 (48%) biopsies in 30/66 (45%) patients were positive for prostate cancer. The biopsy yield in the second half of patients was significantly higher than the first half of patients (36% vs 69%, p<0.05). In 65% (22/34) of biopsies, the detected cancer was Gleason 7 or higher. In 78% (14/18) patients who underwent prostatectomy, MR-guided biopsy correctly predicted the final prostatectomy Gleason score on prostatectomy as intermediate or high grade.
Conclusion: A learning curve was observed for DWI-based MR-guided biopsy, suggesting that at least 30 procedures have to be performed to provide a sufficient level of experience. A majority of cancers detected were intermediate/high grade. The biopsy Gleason score correlated well with the final score on prostatectomy, thereby reducing undergrading and optimizing patient risk stratification.

B-0742 11:18

Comparison of image quality and signal-to-noise ratio between four different diffusion-weighted sequences for MRI of the prostate
D. Stocker, A. Manoliu, A. Becker, B.K. Barth, D. Nanz, M. Klarhöfer, O.F. Donati; *Zurich/CH (daniel.stocker@usz.ch)*

Purpose: To compare image quality and signal-to-noise-ratio (SNR) of four different magnetic resonance (MR) diffusion-weighted imaging (DWI) sequences in the prostate.
Methods and Materials: Axial T2-weighted turbo-spin echo images (TSE-T2w) and axial DWI echo planar imaging (EPI) sequences, including single-shot spin-echo (ss-EPI), readout-segmented multi-shot (rss-EPI), selective-excitation reduced field of view (sTX-EPI) and prototype single-shot sequence applying slice-selective shim-settings (prot-EPI) sequences were acquired at 3T in ten healthy volunteers (mean age 25.9 ± 3.8; BMI 23.2 ± 3.0). Two radiologists, blinded to the type of DWI, independently rated DWI-sequences on a 5-point Likert scale regarding subjective image quality features (resolution, demarcation of prostate capsule, zonal anatomy). Interreader agreement was assessed using the intra-class correlation coefficient (ICC). Quantitative image analysis was performed, evaluating the SNR in the transitional and peripheral zone. Significant differences were calculated using the Wilcoxon rank sum test with Benjamini-Hochberg correction for qualitative parameters and analysis of variance (ANOVA) for quantitative parameters.
Results: Interreader agreement was good to excellent (ICC 0.712 - 0.792) for all qualitative features. Subjective IQ regarding "resolution" was significantly better for ss-EPI as compared to rss-EPI (p=0.031) and sTX-EPI (p=0.046) as well as for prot-EPI as compared to rss-EPI (p=0.031) and sTX-EPI (p=0.047). There was no significant difference regarding capsule demarcation and zonal anatomy. SNR was significantly higher in prot-EPI than sTX-EPI (p=0.015).
Conclusion: ss-EPI and prot-EPI showed a tendency towards superior image quality and SNR compared with rs-EPI and sTX-EPI.
Author Disclosures:
M. Klarhöfer: Employee; Siemens Healthcare.

B-0743 11:26

Correlation between ADC and Gleason score in the evaluation of peripheral zone prostate cancer
G. Michelini, L. Panebianco, A. Mancini, A. Pace, C. Gianneramo, C. Marsecano, I. Capretti, R. Manetta, C. Masciocchi; *L'Aquila/IT (giuliamichelini.gm@gmail.com)*

Purpose: To evaluate the correlation between Apparent Diffusion Coefficient (ADC) obtained with b3000 DWI from 3T Multiparametric Magnetic Resonance of Prostate (mpMRI), and Gleason Score (GS) in patients with peripheral prostate cancer (CaP).
Methods and Materials: Between February and December 2015 we retrospectively evaluated 127 patients, aged 45-75 years, who underwent mpMRI 3T (mr750w GE, with both pelvic phased-array 32 channel coil and endorectal coil) for suspicious CaP. Exclusion criteria: patients previously subjected to radiotherapy or ormonotherapy, patients with general contraindications to mpMRI, patients with central zone lesions. 75 were found to be positive for peripheral zone CaP after Fusion biopsy (MRI-Transrectal Ultrasound Image Fusion Biopsy). ADC map was obtained from Diffusion Weighted Imaging (DWI) at b0 and b3000 mm^2/sec. Minimum (ADC_{min}) and mean (ADC_{mean}) ADC value of the suspected region were calculated, drawing a region of interest with a minimum area of 5 mm, excluding margins. The values were compared with GS.
Results: An inverse correlation between ADC and GS resulted. Malignant lesions had ADC_{min} e ADC_{med} values included between 500-1000 x10^{-6} mm^2/sec. 46 patients (61,3%) had ADC between 800-1000 x10^{-6}mm^2/sec; 44 of them (95,6%) had an histological GS between 5 and 7(3+4) and 2 (4,4%) had GS≥7(4+3). 29 patients (38,6%) had ADC between 500-800 x10^{-6}mm^2/sec; 28 of them (96,5%) had GS≥7(4+3) and 1 (3,5%) had GS<7(4+3).
Conclusion: Our experience with mpMRI confirmed an inverse correlation between ADC values and GS stages. Therefore, ADC value proves useful for noninvasive characterisation of prostate cancer aggressiveness and could improve therapeutic planning.

B-0744 11:34

Prostate MRI: relationship between apparent diffusion coefficent (ADC) and pathological Gleason score (pGS) in prostate cancer
S. Cavanna, A. De Libero, C. Arese, C. Saviolo, C. Lario, M. Petracchini, S. Cirillo; *Turin/IT (cavannaste@gmail.com)*

Purpose: The aim of our study was to investigate the correlation of DWI (ADC and ADCratio) with the pathological Gleason score (pGS) and subsequently its ability in predicting the aggressiveness of prostate cancer.
Methods and Materials: 41 patients with prostate cancer underwent multiparametric MRI scan with 1.5T and subsequently subjected to radical surgery. ADC and ADCratio (rADC) were calculated using a contralateral and

symmetrical area of healthy prostate ($rADC_{mirror}$) and bladder ($rADC_{bladder}$) as a reference. Patients were divided by three grouping methods: according to pGS, clinical risk or primary Gleason pattern. The degree of association between ADC or rADC and pGS was analyzed using ANOVA test and ROC curves.
Results: 3 patients presented a pGS of 6, 22 of 7 (3+4), 8 of 7 (4+3), 8 of 8. 25 patients had a primary Gleason pattern 3 and 16 a primary pattern 4. ADC and rADC showed a statistically significant association with the degree of tumour aggressiveness, being significantly lower in patients with higher tumour grade. $rADC_{mirror}$ presented the better diagnostic performance in discriminating between primary pattern 3 and 4, with an AUC of 0.835 ($p<0.001$). For this variable has been identified a cutoff value of $0.645x10^{-3}mm^2/s$ able to discriminate between the two different primary pattern with a sensitivity and specificity of 87% and 80% respectively.
Conclusion: ADC and rADC are significantly associated with Gleason score. The $rADC_{mirror}$ shows greater degree of association and the better diagnostic performance in identifying cancers with primary Gleason pattern 4.

B-0745 11:42

Diagnostic value of high-field MRI for Peyronie's disease
H. Wang, J. Guan, Y. Guo; *Guangzhou/CN (usefulkey0077@hotmail.com)*

Purpose: To analyse the MRI findings of Peyronie's disease and further to investigate the diagnostic value of using 3.0 Tesla MR.
Methods and Materials: 14 patients with clinically diagnosed Peyronie's disease underwent 3.0T MR examination using a loop coil (11cm) were included. MR Imaging protocol including routine sequences (T1WI, T2WI and enhanced T1WI) and susceptibility weighted imaging (SWI) was performed. Each patient received 2-4 times of penile ultrasound examinations previously (total 43 times of ultrasound), which were compared with MRI results.
Results: Totally 25 penile plaques of 14 patients were detected by MRI. 3 cases with 7 inflammatory plaques, 4 cases with 8 fibrotic plaques, and 7 cases with 10 calcified plaques were detected. All of 10 calcified plaques presented hypo-intense signal on SWI, which also can be stably detected by ultrasound. 7 cases with 10 calcified plaques were sensitively detected in all 20 times of ultrasound (20/20). Patients with inflammatory or fibrotic plaques could not be sensitively or accurately detected by ultrasound. Only 6 fibrotic plaques in 4 cases were found in 3 times of ultrasound (3/14). None of inflammatory plaques was detected by ultrasound (0/9). The combination of routine sequences and SWI was necessary for detection of calcified plaques, and the diagnostic rates of ultrasound for inflammatory (0/7) and fibrotic (6/8) plaques were significantly lower than MRI ($P<0.05$).
Conclusion: High-field MRI can provide high diagnostic sensitivity and accuracy for Peyronie's disease since plaques in all different stages can be detected by using multi-parametric MRI.

B-0746 11:50

"One-stop" evaluation of obstructive azoospermia: combined application of loop and body coil MR imaging
H. Wang, J. Guan, J. Lin, Y. Guo; *Guangzhou/CN (usefulkey0077@hotmail.com)*

Purpose: To evaluate the diagnostic value of combined loop and body coil MR imaging applied in "one stop" examination for obstructive azoospermia.
Methods and Materials: 78 infertile men with azoospermia undergoing 3.0 Tesla MR examination were prospectively recruited. Loop and body coil were alternatively used in pelvis scan. Epigastrium (mainly kidneys) will be included based on medical requirements during MRI scanning. Seminal tract as well as renal anatomy will be evaluated in "one stop". Subject including criteria: semen analysis, seminal plasma biochemistry and sex hormone tests within 2 weeks before MR examination, additional percutaneous testis biopsy within 2 months after MR scan also should be performed. MR findings were compared with final confirmed diagnostic results.
Results: Totally 42 patients were included, all lesions can be obviously observed on MR images. Lesions limited in scrotal were found in 23 patients (findings according to loop coil). Lesions in 11 cases were detected localised in pelvis (findings according to body coil). And multifocal lesions or syndrome were detected in 8 cases (findings according to combined coil). Lesions detection sensitivity according to loop coil, body coil and the two combination were 54.8% (23/42),26.2% (11/42),19.0% (8/42) respectively.
Conclusion: Abnormal findings in seminal tract can be clearly and completely shown on "one-stop" MRI examination method using the combination of loop and body coil at one time of MR scanning.

10:30 - 12:00 **Studio 2017**

Oncologic Imaging

SS 1016b

Hybrid imaging in oncology

Moderators:
G. Cook; London/UK
B.D. Klumpp; Tübingen/DE

K-17 10:30

Keynote lecture
G. Cook; *London/UK*

B-0747 10:39

Is it possible to predict tumour burden of peritoneal carcinomatosis from ovarian cancer with PET/MRI?
M. Alemany, B. Jonsdottir, A. Bergman, H. Ahlström, K. Stålberg; *Uppsala/SE (montserrat.alemany.ripoll@akademiska.se)*

Purpose: Successful surgery of peritoneal carcinomatosis (PC) is correlated with tumour burden, often evaluated by peritoneal cancer index (PCI). Sensitivity of different imaging techniques in diagnosing PC varies broadly. Our main aim was to validate preoperative assessment of PCI with PET/MRI using surgical PCI as gold standard. A second aim was to evaluate if PET/MRI was superior to MRI alone for this assessment.
Methods and Materials: PET-MRI was performed in 24 patients with PC from ovarian cancer 0 to 29 days (mean: 9, median: 6) before cytoreductive surgery. A radiologist blinded to surgical-PCI calculated PET-MRI and MRI-PCI score for each patient, based on size and location of peritoneal implants (PCI range: 0-39). A PCI below 20 was considered low/moderate tumour burden whereas PCI over 20 indicated high tumour burden. MRI evaluation of PCI was based on DWI. Preoperative assessment of PCI imaging was compared with surgical PCI.
Results: Surgical PCI was <20 in 10/24 (41%) patients and > 20 in 12/24 (58%). PET/MRI classified correctly 9/10 (90%) patients as low/moderate tumour burden and correctly 12/14 (86%) as high tumour burden, accuracy 21/24 (87%). MRI alone classified correctly 10/10 (100%) patients as low/moderate and 11/14 (78%) as high tumour burden, accuracy 21/24 (87%). Correlation index between surgical PCI and imaging PCI was 0.77 for PET-MRI and 0.69 for MRI.
Conclusion: Our study showed a good correlation between imaging PCI (both for PET/MRI and MRI) and surgical PCI as gold standard. No significant difference was found between PET/MRI and MRI.

B-0748 10:47

Comparison of integrated ^{18}F-FDG PET/MRI and MRI alone for pre-therapeutic tumour staging of patients with primary cervical cancer
J. Grueneisen[1], M. Al-bayati[1], L.M. Sawicki[2], J. Kirchner[2], V. Ruhlmann[1], M. Forsting[1], A. Wetter[1], L. Umutlu[1]; [1]*Essen/DE*, [2]*Düsseldorf/DE (johannes.grueneisen@uk-essen.de)*

Purpose: To evaluate and compare the diagnostic performance of ^{18}F-FDG PET/MRI and MRI alone for dedicated primary tumour staging of cervical cancer patients.
Methods and Materials: A total of 47 consecutive patients with histopathologically confirmed cancers of the uterine cervix underwent a whole-body^{18}F-FDG PET/MR scan prior to the start of therapy. Two experienced physicians analysed the MR datasets, followed by an evaluation of ^{18}F-FDG PET/MR data. They were instructed to determine the local tumour spread of primary tumours as well as to identify the presence of nodal or distant metastases.
Results: ^{18}F-FDG PET/MRI allowed for a correct determination of the T-stage in 40 (85%) cases, while MRI alone enabled a correct evaluation of the tumour stage in 41 (87%) cases. In 22 of the 47 patients lymph node metastases were present. For the identification of nodal positive patients, ^{18}F-FDG PET/MR revealed higher values for sensitivity (86% vs. 73%), specificity (92% vs. 84%) and diagnostic accuracy (89% vs. 78%) in comparison to MRI alone. Additionally, ^{18}F-FDG PET/MR showed better results for the detection of distant metastases then MRI alone (sensitivity: 85% vs. 69%, specificity: 94% vs. 88%, diagnostic accuracy: 91% vs. 83%)
Conclusion: The results of the present study demonstrate the usefulness of ^{18}F-FDG PET data as a valuable additive to MRI alone for more accurate assessment of nodal or distant metastatic spread in patients with primary cervical cancer. For the determination of the local tumour spread ^{18}F-FDG PET data do not provide an additional benefit to MRI alone.

B-0749 10:55

Evaluation of a fast ^{68}Ga-DOTATOC PET/MRI protocol for whole-body staging of neuroendocrine tumours: a comparison with ^{68}Ga-DOTATOC PET/CT

L.M. Sawicki[1], C. Deuschl[2], K. Beiderwellen[2], T.D. Poeppel[2], P. Heusch[1], D. Fuehrer[2], M. Forsting[2], G. Antoch[1], L. Umutlu[2]; [1]*Düsseldorf/DE*, [2]*Essen/DE (Linomorris.sawicki@med.uni-duesseldorf.de)*

Purpose: To compare the diagnostic performance of a fast ^{68}Ga-DOTATOC PET/MRI protocol with ^{68}Ga-DOTATOC PET/CT in whole-body staging of patients with neuroendocrine tumours (NET).
Methods and Materials: The local ethics committee approved this study. Thirty consecutive patients with histopathologically confirmed NET underwent ^{68}Ga-DOTATOC PET/CT and ^{68}Ga-DOTATOC PET/MRI in a single injection protocol. For PET/MRI a fast (30min) whole-body protocol was applied. PET/CT and PET/MRI were retrospectively evaluated regarding lesion count, localisation, nature (NET/non-NET/indeterminate), and conspicuity (4-point scale). The reference standard was based on histopathology and follow-up imaging. Sensitivity, specificity, positive predictive value (PPV), negative predictive value (NPV), and diagnostic accuracy of PET/CT and PET/MRI were compared using McNemar's chi^2 test. Wilcoxon tests assessed differences in SUVmax and lesion conspicuity. Correlation analysis of SUVmax was performed using Pearson's correlation coefficient (r).
Results: According to the reference standard, 197 NET lesions were present in 25 patients. On a per-patient basis, PET/MRI and PET/CT each correctly identified 96.0% of these patients. In a lesion-based analysis, the sensitivity, specificity, PPV, NPV, and diagnostic accuracy of PET/MRI was 90.0%, 100%, 100%, 80%, and 92.9%, respectively. Corresponding values for PET/CT were 86.6%, 98.2%, 99.2%, 74.0%, and 89.8%. Differences in the diagnostic performances were not statistically significant (p=0.38). SUVmax was strongly correlated (r=0.86; p<0.001) and did not differ significantly (p=0.35). Overall and NET lesion conspicuity was significantly higher on PET/MRI than on PET/CT (p<0.01, each).
Conclusion: ^{68}Ga-DOTATOC PET/MRI provides an equivalent diagnostic performance for whole-body staging of NET patients as compared with PET/CT.

B-0750 11:03

Comparing the diagnostic performance of integrated 18F-FDG PET/MRI and MRI for the identification of local recurrences of soft tissue sarcomas

Y. Erfanian[1], J. Grueneisen[1], J. Kirschner[2], L. Podleska[1], T. Poepel[1], K. Herrmann[1], L. Umutlu[1]; [1]*Essen/DE*, [2]*Düsseldorf/DE (y.erfanian@gmail.com)*

Purpose: Comparing the diagnostic performance of integrated 18F-FDG PET/MRI and MRI for the identification of local recurrences of soft tissue sarcomas.
Methods and Materials: A total of 41 patients with a clinically suspected tumour relapse of STS underwent an 18F-FDG- PET/MRI examination for assessment of local recurrence. Two experienced physicians interpreted the MRI data and subsequently the PET/MRI datasets in two separate reading sessions and were instructed to identify potential local tumour recurrences. Additionally, the diagnostic confidence in each reading for the identification of malignant lesions was determined. A McNemar test was applied to test for differences of both ratings and a Wilcoxon signed-rank test was used to identify differences of the confidence levels. Histopathological verification as well as follow-up imaging was applied as the standard of reference.
Results: A tumour relapse was present in 27/41 patients. Calculated sensitivity, specificity, positive predictive value, negative predictive value and diagnostic accuracy for the detection of local tumour recurrence was 81%, 85%, 91%, 70%, 82% for MRI and 96%, 75%, 89%, 91%, 90% for PET/MRI (p > 0.05). Furthermore, PET/MRI showed significantly higher confidence levels (p<0.05) for the determination of malignant lesions.
Conclusion: Our results demonstrate 18F-FDG PET/MRI to be an excellent imaging method in the evaluation of recurrent STS after surgical excision, as it displays superior detection accuracy as compared to routine MRI follow-up examinations.

B-0751 11:11

Diagnostic value of bi-disciplinary PET/MRI reading for the assessment of malignancies

F. Celebi, B. Unalan, N.C. Balcı; *Istanbul/TR (elbuken.filiz@gmail.com)*

Purpose: To evaluate nuclear medicine and radiology joined PETMRI reading compared to separate evaluation of PET and MRI datasets.
Methods and Materials: PETMRI datasets of 53 patients with known primary malignancies were retrospectively evaluated. FDG PET and T1 weighted Turboflash fused images were read by a nuclear medicine physician, contrast enhanced Whole Body MRI without FDG PET fusion was read by a radiologist. All datasets were reevaluated in a joint session with the combination of contrast enhanced whole body MRI and FDG PET Turboflash MRI. Contrast enhanced Whole body MRI protocol consisted of dynamic contrast enhanced MRI of the upper abdomen with the use of 3D VIBE, contrast enhanced MRI of the whole body with the use of coronal 3D Dixon VIBE sequence.
Results: The mean numbers of malignancies on FDG PET T1 W Turboflash MRI and Whole Body Contrast Enhanced MRI were 11.8 ± 17.6 and 13.2 ± 18.5, respectively. There was significant difference for the total number of malignancies (p=0.031). The joint reading of FDG PET T1 W Turboflash MRI and Whole Body Contrast Enhanced MRI revealed mean number of 15.9 ± 22.4 malignancies. There was significant difference between joint reading and separate reading of contrast enhanced whole body MRI (p=0.005) or FDG PET T1 W Turboflash MRI (p=0.002).
Conclusion: Combined reading of PET and MRI datasets by a Radiologist and Nuclear Medicine physician depicts more malignancies than separate reading of datasets.

B-0752 11:19

Assessment of PET/MR, including DWI, for diagnosing skeletal muscle metastases

C. Giraudo, M. Weber, G. Karanikas, P.A.T. Baltzer, H. Markus, M. Mayerhoefer; *Vienna/AT (chiara.giraudo@meduniwien.ac.at)*

Purpose: To evaluate the diagnostic performance of PETMR, with and without DWI, for skeletal muscle metastases (SMM) in oncologic patients.
Methods and Materials: Patients with histological proven cancer who underwent a PETMR (fully integrated system), including whole-body-DWI, for staging or restaging from January 2014 until December 2015 were included in this retrospective study. PETMR was considered positive if a muscle lesion was visible on MR images (i.e., T1w and/or T2w) and showed a pathologic, not inflammatory, uptake (i.e., FDG, PSMA, Dotanoc); DWI was then separately assessed. Muscles of the following areas were investigated: neck, thorax, abdomen, pelvis, upper and lower extremities. Sensitivity and specificity were calculated using histology and/or follow-up/previous examination as reference standard. The relationship between SMM's metabolic activity (SUVmax, SUVmean) and cell-density (ADCmin, ADCmean) was examined (Pearson correlation).
Results: One-hundred-three patients met the inclusion criteria (70 males; mean age±SD 58.29±16.76 years; 47 staging and 56 restaging). Histology revealed lymphoma (n=64), prostate cancer (n=23), melanoma (n=6), breast cancer (n=2), soft tissue sarcoma, esophageal-, pancreatic-, bladder-, gastric-, ovarian-, thyroid- and neuroendocrine tumour (n=1,each). Overall six SMM were diagnosed in five patients (4.85%) at PETMR (83.3% [95%CI 35.88-99.58%] sensitivity, 100% [95%CI 96.27-100%] specificity). Seven SMM were diagnosed in six patients (5.8%) at PETMR-DWI (100% sensitivity [95%CI 54.07-100%], 100% specificity [95%CI 96.31-100%]). Pelvic muscles were mostly affected (i.e., four out of seven lesions). A negative non-significant relationship emerged between SUVmax and ADCmin (r=-.64; p=0.16) and between SUVmean and ADCmean (r=-.39; p=0.43).
Conclusion: Even if SMM rarely occur in oncologic patients, according to our preliminary results, DWI demonstrated to improve PETMR diagnostic performance, at staging and restaging.
Author Disclosures:
C. Giraudo: Research/Grant Support; Austrian Science Fund (FWF), project KLIF 382.

B-0753 11:27

Simultaneous C11 choline PET and multiparametric MRI in high-risk prostate cancer patients: interim report

L.-J. Wang, J.-R. Tseng, S.-P. Pang; *Taiwan/TW (lijenwang0918@gmail.com)*

Purpose: To evaluate the agreements of diagnosing lymph node and bone metastasis between C11 choline PET (chPET) and multiparametric prostate MRI (mpMRI) in high-risk prostate cancer (hrPCA) patients.
Methods and Materials: From January, 2014 to January, 2015, all consecutive hrPCA patients were prospectively enrolled for undergoing simultaneous chPET and mpMRI. Their ages, prostate surface antigen (PSA) titers before examination and Gleason scores (GS) of prostate cancer biopsies were recorded. Agreements of diagnoses of lymph node and bone metastases between chPET C11 and mpMRI were analysed.
Results: Twenty-six patients underwent PET/MRI and 4 patients were excluded by fitting exclusion criteria. The 22 patients had a mean age of 68.8 years, a mean PSA titer of 49.1 ng/mL and GS of biopsy specimens of 6-10. MRI and choline PET had concordant results of regional lymph node metastasis in 20 patients (90.9%) and discordant results in 2 patients (PET and MRI detect 1 more positive result, respectively). For non-regional lymph node metastasis, mp-MRI and chPET had concordant results in 21 patients (95.4%); chPET detected non-regional lymph node metastasis in one more patient than mpMRI. For bone metastasis, mpMRI and ch-PET had concordant results in 19 patients (86.4%); mpMRI detected bone metastasis in 3 more patients than ch-PET.

Conclusion: ch-PET and mp-MRI have good agreements of lymph node and bone metastasis in hr-PCA patients. Ch-PET is less sensitive in detecting bone metastasis but more sensitive in showing non-regional lymph node metastasis than mpMRI.

B-0754 11:35

Comparison of PET-CT MR (3.0T) with 68Ga-PSMA for evaluation of prostate cancer patients with biochemical recurrence

M. Garcia, O. Alonso, E. Henry; *Montevideo/UY (margarita.garciafontes@cudim.org)*

Purpose: The aim of this study was to compare the detection rate of PET-MR versus 68Ga-PSMA PET-CT in prostate cancer recurrence.
Methods and Materials: A sample of patients with PSA relapse were included. We used a trimodality PET-CT-MR (3.0 T) setup including a 64-slice PET-CT, with a dose of approximately 280MBq of 68Ga-PSMA. An abbreviated MRI protocol was used with panoramic and high-resolution thin slices with T2 sequence at prostate loggia and diffusion (DWI) and ADC maps. Two blinded and independent readers asessed all images.
Results: 37 patients were enrolled of whom 25 (68%) had undergone radical prostatectomy and 12 treated with radiotherapy. The median PSA level was 3.5ng-mL. Both techniques were positive in 20 patients (54%) and negative in 7 patients (19%). Eight patients were only positive with 68Ga-PSMA alone (22%) and 2 with MR only (5%). In 11 patients (30%), PET-CT showed metastatic lesions outside the pelvis. Local relapse was detected in 16 (43%) and 12 (32%) patients, pelvic bone metastases in 6 (16%) and 2 patients (5%), and pelvic lymph nodes in 11 (30%) and 3 (8%) patients, for PET-CT and MR, respectively. A statistically significant difference was found for lymph node relapses (P-0.013). MR was useful in indeterminate cases by means of PET-CT alone.
Conclusion: 68Ga-PSMA PET-CT detects better pelvic lymph nodes and extrapelvic metastasis and PET-CT-MR adds clinically relevant information for patient management.

B-0755 11:43

Evaluation of 18F-FDG PET and MR datasets in integrated PET/MRI: a comparison of different MR sequences for whole-body restaging of breast cancer patients

J. Grueneisen[1], A. Wetter[1], L.M. Sawicki[2], S. Kinner[1], V. Ruhlmann[1], M. Forsting[1], L. Umutlu[1]; [1]*Essen/DE*, [2]*Düsseldorf/DE (johannes.grueneisen@uk-essen.de)*

Purpose: To investigate the diagnostic value of different MR sequences and 18F-FDG PET data for whole-body restaging of breast cancer patients utilizing PET/MRI.
Methods and Materials: 36 patients with a suspected tumour recurrence of breast cancer were prospectively enrolled for a whole-body PET/MR examination. The MR protocol comprised: Diffusion-weighted imaging, a T2w HASTE and a post-contrast T1w VIBE sequence. Two readers were instructed to identify the total number of tumour lesions in subsequent MR and PET/MR readings, utilizing different MR sequence constellations for each PET/MR reading session. Additionally, the diagnostic confidence for each detected lesion (3-point ordinal scale) was qualitatively rated.
Results: Tumour recurrence was present in 25/36 (69%) patients. All three PET/MRI readings showed a significantly higher accuracy as well as higher confidence levels for the detection of recurrent breast cancer lesions when compared to MRI alone ($p<0.05$). Furthermore, all three PET/MR sequence constellations showed comparable diagnostic accuracy for the identification of recurrent tumour lesions ($p>0.05$), yet increasing diagnostic confidence levels after the application of contrast-agent. However, highest confidence levels were obtained, when all three MR sequences were used for image interpretation.
Conclusion: Integrated PET/MRI provides superior restaging of breast cancer patients than MRI alone. Facing the need for efficient whole-body PET/MR imaging, our results show the feasibility of fast and morphologically adequate PET/MR protocols. However, considering an equivalent accuracy for the detection of breast cancer recurrences in the three PET/MR readings, the application of contrast-agent and the inclusion of DWI in the study protocol seems to be debatable.

B-0756 11:51

The diagnostic value of hybrid PET/MRI in the assessment of gastrointestinal tumours

F. Celebi, B. Unalan, N.C. Balci; *Istanbul/TR (elbuken.filiz@gmail.com)*

Purpose: To evaluate the diagnostic performance of positron emission tomography (PET)/magnetic resonance (MR) imaging in the assessment of gastrointestinal tumours and metastases.
Methods and Materials: 44 patients with histopathologically proven primary gastrointestinal tumour underwent FDG PET/MR imaging for initial staging and therapy monitoring. PET/MR imaging was performed with the acquisition of axial serial contrast-enhanced 3D FS VIBE images in the upper abdomen, whole-body coronal FS VIBE Dixon and axial 3D FS VIBE for the brain.Total number of lesions determined on CE (contrast enhanced) PET/MR imaging were compared to NCE (non-contrast enhanced) PET data.
Results: Total number of lesions determined with CE PET/MR protocol were 106 HCC, 37 cholangiocellular carcinoma, 194 liver, 2 brain, 112 bone, 175 lymph node and 62 lung metastases. 7 patients were evaluated as peritoneal metastasis. With the use of FDG PET data alone 50 HCC, 24 cholangiocellular carcinoma, 130 liver, 1 brain, 49 bone, 175 lymph node and 20 lung metastases were determined. 3 patients were evaluated as peritoneal metastasis. CE FDG PET/MR was compared to NCE FDG PET data for the detection of lesions and statistically significant difference analysed between them ($p<0.03$)
Conclusion: CE FDG PET/MR protocol is more effective than NCE FDG PET protocol for lesion and metastasis detection in gastrointestinal tumours.

10:30 - 12:00 **Room L 8**

Head and Neck

SS 1008

Skull base and face

Moderators:
S. Connor; London/UK
M. Ravanelli; Brescia/IT

K-15 10:30

Keynote lecture

N.N.

B-0757 10:39

US-sialography in diagnostics ductal system of major salivary gland

Y. Vasil'eva; *Moscow/RU (Drugya@yandex.ru)*

Purpose: Efficiency evaluation of salivary ultrasonography with ductal system contrast (US-sialography) using universal liquid substance.
Methods and Materials: Echographic examination was performed on a total number of 73 patients (age 18 to 79) with confirmed chronic major salivary gland disorders as well as allergic reaction to iodine. Considering inability to perform an MSCT-sialography, all patients were examined using US-sialography with up to 4ml of normal saline solution in ductal system. Normal saline solution was used as a universal liquid substance for echographic imaging of the entire ductal system. For the purpose of keeping the solution inside the ductal system for its continuous tight filling, after contrast infusion the catheter was blocked by a plug without being removed from the opening of the duct. Examination was carried out using the iU-22 ultrasound system (Philips, Netherlands) and the dedicated compact pen-transducer with 7 to 15 MHz operating frequency range. Primary diagnostics and dynamic case observation (in 45% of cases) were performed.
Results: In 100% of cases US-sialography allowed not only to evaluate gland parenchyma, but also to visualise up to distal duct segments, give its full anatomic characteristics, define its pathological changes. All results had clinical confirmation.
Conclusion: US-sialography can be a method of choice in diagnostics of salivary gland ductal system disorders for patients with contraindications to MSCT-sialography and to avoid radiation exposure.

B-0758 10:47

Key anatomical features of Vidian canal on skull base CT

M.E. Adin[1], C.A. Özmen[1], N. Aygün[2]; [1]*Diyarbakir/TR*, [2]*Baltimore, MD/US (emin.adin@gmail.com)*

Purpose: To investigate the key anatomical features of Vidian canal that have critical role in planning and performing endoscopic skull base surgeries.
Methods and Materials: We reviewed high-resolution skull base CT images of 640 consecutive subjects. Multiple anatomical features of Vidian canal were analysed in all three planes along with oblique reconstructions. Rostral-caudal course of the Vidian canal, length of the Vidian canal, dehiscence of the Vidian canal, and position of the Vidian canal with respect to petrous ICA were examined. Classification of the amount of pneumatisation around Vidian canal was done in four different degrees.
Results: The average length of the Vidian canal was 15.4 ± 2.0 mm in females and 16.6 ± 1.7 mm in males and difference between both genders was statistically significant ($P<0.001$). The most common rostral-caudal course of Vidian canal was medial to lateral and was followed by straight course, tortuous course, and lateral to medial course, respectively. The frequency of pneumatisation pattern was found as type 0, III, II and I, respectively. Of 342 evaluated instances, Vidian canal was located below the level of petrous ICA in

303 (89%) instances, at same level with petrous ICA in 25 (7%) instances, and above the level of petrous ICA in 14 (4.1%) instances.
Conclusion: Various anatomical features of the Vidian canal were defined. Unlike what was reported in most previous studies, we showed that inferior-medial drilling of the Vidian canal may not be always safe, as it could be located superior to the level of petrous ICA.

B-0759 10:55

Dynamic contrast-enhanced MRI of the TMJs in patients with juvenile idiopathic arthritis

P.A. Caruso; *Boston, MA/US (pcaruso@partners.org)*

Purpose: Our purpose is to determine the dynamic enhancement curves of inflamed TMJ synovia in juvenile idiopathic arthritis that may provide a basis for the assessment of response to therapeutic interventions such as intraarticular steroid injections.
Methods and Materials: MRI parameters include a pre-contrast coronal T1 sequence followed by 10 consecutive post-contrast T1-weighted sequences each with a scan time of 1 minute for a total duration of 10 minutes. A region of interest (ROI) was placed in the synovium of the left and right TMJ with a reference ROI placed in the longus capitus muscle belly. Dynamic enhancement characteristics of the inflamed TMJs were determined and compared to clinical exam findings of synovitis.
Results: The synovia in the JIA patients demonstrated an initial peak enhancement at 5 minutes after contrast administration followed by a second peak at 10 minutes and showed twice the intensity of enhancement compared to normal controls. The synovia of control subjects demonstrated peak enhancement at approximately 3-4 minutes after contrast administration and slowly decreased in enhancement thereafter. The synovia of asymptomatic TMJs in JIA patients showed a peak at 5 minutes but above that of control subjects without JIA.
Conclusion: This study demonstrates proof of concept and the utility of dynamic post-contrast-enhanced images of the TMJs in patients with synovitis. This method demonstrates peak enhancement of inflamed synovia and maximal difference between inflamed and non-inflamed synovia at 5 minutes postinjection, and may be utilised to evaluate treatment-related response in patients with JIA.

B-0760 11:03

CT findings in patients with zygomatic complex fractures and trismus

P.A. Caruso; *Boston, MA/US (pcaruso@partners.org)*

Purpose: A subset of patients with zygomatic complex fractures (ZCFs) develop trismus and limitation of jaw opening. We hypothesise that in the group with trismus the ZCF results in closer approximation of the zygoma to the coronoid process of the mandible.
Methods and Materials: The clinical and CT imaging findings of 30 patients, 22 male and 8 female (median age, 37 years; age range, 14-85 years), with zygomatic complex fractures, were retrospectively reviewed. Patients with mandibular fractures or h/o prior facial surgery were excluded. The CTs were reviewed for fractures in the maxillae, zygomae, sphenoid, and temporal bones, for retroposition of the fractured zygomatic body, and for the distance between the coronoid process of the mandible and the fractured zygomatic body, zygomatic arch, and the posterolateral wall of the maxilla. The results of the trismus and nontrismus groups were then compared by standard T test and a p value was calculated.
Results: 16 of the 30 patients reported trismus following ZCF. There were statistically significant differences between the trismus and nontrismus groups in the relative retroposition of the fractured zygomatic body compared to the unfractured side. In the group with trismus, the zygomatic body and the zygomatic arch more closely approximated the coronoid process compared to the non-trismus group and this difference reached statistical significance.
Conclusion: Our study confirms that in patients with ZCF fractures and trismus, the fractured zygoma more closely approaches the coronoid process compared to those patients with ZCF without trismsus.

B-0761 11:11

Cephalometric evaluation of soft tissue changes in the upper and lower lips and chin after gap arthroplasty for the correction of temporomandibular joint bony ankylosis

A.M.K.E. Ibrahim; *Cairo/EG (abeermk7@gmail.com)*

Purpose: Correction of postankylotic deformity is a major intention for patients with temporomandibular joint ankylosis (TMJ) ankylosis after release of ankylosis. The aim of present study is to evaluate the changes of soft tissue of the lips and chin area after gap arthroplasty.
Methods and Materials: Twenty-four patients suffering from TMJ ankylosis were subjected to gap arthroplasty. They were selected from Outpatient Clinic of Faculty of Oral and Dental Medicine, Cairo University. Lateral cephalometric view was performed preoperatively and 3 months postoperatively. Special reference points As, PrSs, Bs, PrIs, and Pogs were selected on the soft tissue cephalometric tracing of upper and lower lips and chin were measured in relation to vertical and horizontal axes. These points were assessed to evaluate their changes postoperatively.
Results: The entire group of patients (24 patients) showed statistically significant downward movement of soft tissue of the upper and lower lips, whereas the chin moved downward and backward 3 months postoperatively. In unilateral cases (12 patients), the upper lip did not moved downward as in bilateral cases (12 patients) postoperatively.
Conclusion: The present study revealed downward movement of the soft tissue of upper lip, lower lip, and chin 3 months postoperatively. The soft tissue of the chin also showed backward movement. These changes must be taken into consideration with surgical planning in postankylotic orthognathic surgery.

B-0762 11:19

The capabilities of ultrasound in the diagnosis of foreign bodies in the maxillofacial region

Y. Shumina; *Moscow/RU (yana.shu92@gmail.com)*

Purpose: To assess the capability of ultrasonography of soft tissue in the identification of foreign bodies in the maxillofacial region.
Methods and Materials: 18 patients aged 18 to 45 with suspicion regarding the existence of foreign bodies in maxillofacial region were surveyed . The study was carried out on ultrasonic scanner IU-22 (Philips, Netherlands) using intraoperative linear sensor with a frequency of 7-15MHz in B-mode and Color Doppler.
Results: The study revealed the following foreign bodies in the soft tissues of the maxillofacial region of 18 examined patients: intubation tube in the tear ducts (n=1), drainage tube in the parotid duct (n=2), mustache shrimp into the floor of the oral cavity (n=1), a fragment of plastic in the main excretory duct of the parotid gland (n=1), husk of sunflower seed in the area of the sublingual salivary gland duct (n=1), ear of cereal plants (rye) (n=1), glass splinters in the cheek area (n=2), helminth disease (dirofilariasis) of the upper eyelid (n=1) and parotid-masticatory area (n=1). There have also been identified fillers after contour plastics (n=7), silicone in the lip area (n=3), polyacrylamide gel in nasolabial fold (n=2), hyaluronic acid in nasolabial fold (n=2). 14 patients have been operated, 4 patients are subjected to dynamic ultrasound monitoring.
Conclusion: Thus, ultrasound allows to visualise the foreign bodies in the maxillofacial region, to determine their precise location, the depth of occurrence, the relation to surrounding structures and to predict the possible nature of it.

B-0763 11:27

Lateral cephalometric analysis for treatment planning in orthodontics based on MRI compared with radiographs: a feasibility study in children and adolescents

A. Heil, E. Lazo Gonzalez, T. Hilgenfeld, P. Kickingereder, A. Sommer, M. Bendszus, S. Heiland, C.J. Lux, S. Zingler; *Heidelberg/DE (alexander.heil@med.uni-heidelberg.de)*

Purpose: To evaluate whether magnetic resonance imaging (MRI) can serve as a non-ionizing alternative modality to lateral cephalometric radiographs (LCR, “gold standard”) in cephalometric analysis.
Methods and Materials: This prospective study was approved by the local research ethics committee, informed patient consent was obtained. The applied MRI technique was optimized for detection of cephalometric landmarks and geometric accuracy. Prior to orthodontic treatment, 20 patients (mean age ± SD, 13.95 years ± 5.34; 8 females) received MRI and LCR. MRI datasets were postprocessed into lateral cephalograms. Based on 19 landmarks 24 widely used cephalometric measurements (14 angles, 10 distances) were taken twice by two observers for both modalities. Statistical analysis was performed by using intraclass correlation coefficient (ICC), Bland-Altman analysis and two one-sided tests (TOST) with an equivalence margin of ± 2 °/mm.
Results: Geometric accuracy of the MRI technique was confirmed. Mean intraobserver ICC were 0.977/0.975 for MRI and 0.975/0.961 for LCR. Average interobserver ICC were 0.980 for MRI and 0.929 for LCR. Bland-Altman analysis showed high of levels agreement between the two modalities, bias range (mean ± SD) was -0.66 to 0.61 mm (0.06 ± 0.44) for distances and -1.33 to 1.14 ° (0.06 ± 0.71) for angles. Except for the interincisal angle (P = .17) all measurements were statistically equivalent (P < .05).
Conclusion: MRI datasets can be transformed into lateral cephalograms allowing reliable measurements as applied in orthodontic routine with high levels of agreement to the corresponding measurements on LCR. Thus, MRI-based orthodontic treatment planning appears feasible.
Author Disclosures:
A. Heil: Grant Recipient; Dietmar Hopp Foundation. **S. Heiland:** Grant Recipient; Dietmar Hopp Foundation. **C.J. Lux:** Grant Recipient; Dietmar Hopp Foundation. **S. Zingler:** Grant Recipient; Dietmar Hopp Foundation.

B-0764 11:35

Assessment of SRCMT of nasal and paranasal sinus by ADC value

K. Xue, J. Cheng; *Zhengzhou/CN (xuekang08yx@163.com)*

Purpose: The apparent diffusion coefficient (ADC) value is a non-invasive imaging parameter that can be used to effectively assess small round cell malignant tumours (SRCMT) of nasal and paranasal sinus.
Methods and Materials: 143 patients with SRCMT and non-SRCMT of nasal and paranasal sinus were consecutively enrolled.All patients underwent DWI, and quantitative analysis of ADC values were performed.Difference in ADC values between SRCMT and non-SRCMT was evaluated. ROC were used to determine the cut-off points to differentiate SRCMT from non-SRCMT, and the areas under the ROC were calculated.
Results: All lesions were solitary. There were 98 SRCMT, of which 20 lesions were rhabdomyosarcoma (RMS), 19 lesions were non-Hodgkin's lymphoma (NHL),14 lesions were malignant melanoma (MM), 14 lesions were neuroendocrine carcinoma (NEC), 12 lesions were Ewing's sarcoma/primitive neuroectodermal tumour (Ewing/PNET), 11 lesions were extramedullary plasmacytoma (EMP), and 8 lesions were olfactory neuroblastoma (ON). There were 45 non-SRCMT, of which 28 lesions were squamous cell carcinoma (SCC) and 17 lesions were adenoid cystic carcinoma (ACC). The mean ADC value of SRCMT ($0.66\pm0.12\times10^{-3}$mm²/s) was significantly different (P<0.01) from non-SRCMT ($1.02\pm0.16\times10^{-3}$mm²/s). All of 7 kinds of SRCMT were divided into 3 groups according to ADC values: NHL/MM/NEC/EMP, RMS/Ewing/PNET and ON, there was statistically significant difference among all 3 Groups (F=39.743, P<0.01). The area under the ROC was 0.975.An ADC value of 0.82×10^{-3}mm²/s was used as the threshold with a sensitivity of 97.8%, specificity of 89.8%, and accuracy of 92.3%.
Conclusion: The ADC value is a non-invasive imaging parameter that can be used to effectively assess SRCMT of nasal and paranasal sinus.

B-0765 11:43

Imaging features of myoepithelial carcinoma in the nasopharynx and paranasal sinus

C. Zhang, J.-L. Cheng; *Zhengzhou/CN (13733891344@163.com)*

Purpose: To analyze the imaging features of myoepithelial carcinoma(MEC)in the nasopharynx and paranasal sinus.
Methods and Materials: 11 patients with MEC in the nasopharynx and paranasal sinus confirmed by pathology were analyzed retrospectively. 4 underwent CT, MR, DWI and DCE-MRI.3 underwent MR, DWI and DCE-MRI.4 underwent CT.
Results: 11 cases were one bilateral, irregular shape and unclear boundary.The diameter of tumours was larger than 2.3 cm. The aggressive nature was demonstrated by bone destruction and invasion of adjacent structures. Among 8 patients under going CT, tumour centres were located in nasopharynx in 4 cases,3 in maxillary sinus,1 in nasal cavity and ethmoid sinus.8 cases were soft tissue density.5 lesions demonstrated destruction of the adjacent bone structure.2 cases had cervical lymph node metastasis.1 lesion showed slight enhancement. Among 8 patients under going MRI, tumour centres were located in nasopharynx in 5 cases,1 in maxillary sinus and 1 in ethmoid sinus.On T_1WI,4 showed equal signal and 3 showed low signal.On T_2WI,7 showed sligthly high or high signal. After contrast agent injection, 6 patients showed obvious heterogeneous enhancement,1 showed obvious homogeneous enhancement and 1 with circular enhancement of cervical lymph node. The mean ADC value was$(0.87\pm0.04)\times10^{-3}$mm^2/s.
Conclusion: CT and MRI appearances can show tumours' features.MEC in the nasopharynx and paranasal sinus easily has osteolytic destruction on CT and owns certain characteristic features on MR and ADC value. These features are helpful to the clinical diagnosis and treatment plan formulation.

B-0766 11:51

Inflammatory pseudotumour (IPT) of the skull base. MR and CT findings

A. Lo Casto, P. Purpura, F. Di Naro, C. Lunetta, G. La Tona, S. Salerno; *Palermo/IT (pierpaolopurpura@gmail.com)*

Purpose: Inflammatory pseudotumour is a benign condition mimicking malignant tumours, due to its infiltrative behaviour. MR and CT findings in 4 patients affected by skull base IPT are described.
Methods and Materials: Clinical records and imaging findings of 4 patients (2 men, 2 women, age range 42-75 years), complaining multiple cranial nerve neuropathies, including tinnitus, dysphagia, hoarseness, dysphonia, and haemitongue palsy, were reviewed. Patients were studied by MR and CT of the head and neck with different clinical suspicion, as nasopharynx tumour, paraganglioma, otitis. The diagnosis of IPT was made basing on of clinical data, response to systemic corticosteroids and MR findings.
Results: On 4/4 patients the IPT was located in the carotid space, in two involving the hypoglossal canal. On 3/4 patients an otomastoiditis was present, two of them had diabetes, while the third had a nasopharynx carcinoma treated some years before by radiotherapy with osteonecrosis and recurrent bilateral petrous bone osteomyelitis. Masticatory space was involved in 2/4 patients, hemipharynx in 1/4 patients; 1/4 patients had a jugular vein and sigmoid sinus thrombosis. 2/4 patients had a hypoglossal nerve palsy. Typical MR findings were areas of moderately diffuse enhancement after i.v. Gadolinium, that showed only slight hyperintensity and/or hypointensity on T2 images. At MR follow up at 1-3 months findings were significantly decreased and symptoms dramatically improved.
Conclusion: Radiologists and other specialists should be aware of IPT among disease involving the skull base, in order to differentiate this condition especially from tumours and avoiding more and unnecessary invasive treatment.

10:30 - 12:00 **Room E1**

Breast

SS 1002

Multimodality breast imaging

Moderators:
M.B.I. Lobbes; Maastricht/NL
M. Sklair-Levy; Tel Aviv/IL

B-0767 10:30

Preoperative digital breast tomosynthesis added to conventional imaging: can we reduce the re-excision rate in patients with breast carcinoma?

A. Milan, G. Mariscotti, M. Durando, P. Campanino, E. Caramia, P. Fonio, G. Gandini; *Turin/IT (alessiamilan.ptc@gmail.com)*

Purpose: To compare the re-excision rate for positive or close margins in patients undergone to breast cancer surgical treatment, previously staged with 2D digital mammography (DM) and breast ultrasound (US) versus digital breast tomosynthesis (DBT) added to DM and US.
Methods and Materials: We conducted a retrospective observer study, including 925 patients with newly diagnosed breast cancer who consecutively underwent breast surgery (662 conservative surgeries, 263 non-conservative surgeries) between January 2010 and December 2015. Patients were divided into two groups: 1) 537 patients staged with DM+US; 2) 388 patients staged with DBT+DM+US. A statistical analysis was performed, assuming definitive histology as a gold standard, to compare the re-excision rates between the two groups (Chi-square test with Yates correction). Statistical significance was set at p<0.05.
Results: On a total of 73/925 (7.9%) patients with positive margins at definitive histology, in group 1 the re-excision rate (53/537, 10%) was significantly higher (p<0.01) than in group 2 (20/388, 5%). The re-excision planning was less extensive for patients in group 2 (1/20 mastectomies) compared to group 1 (20/53 mastectomies). The two groups did not significantly differ for breast cancer characteristics, age and risk factors.
Conclusion: In this series, the adjunction of DBT to preoperative DM and US significantly reduced the re-excision rate of breast cancer surgical treatment. Although this result is biased (not randomised), it may be interesting for next studies including patients staged with breast MRI.

B-0768 10:38

Preoperative staging in women with known breast cancers: comparison between digital breast tomosynthesis and magnetic resonance imaging

F. Galati, F. Marzocca, E. Miglio, M. Luciani, F. Pediconi, C. Catalano; *Rome/IT (francesca.galati3@gmail.com)*

Purpose: To evaluate the accuracy in tumour extent and size assessment of Digital Breast Tomosynthesis (DBT) and Magnetic Resonance Imaging (MRI) in women with known breast cancers.
Methods and Materials: From May 2014 to April 2016, 59 patients (mean age 54.9) with known breast cancer were enrolled. All patients underwent DCEMR exam using Gd-BOPTA and GE DISCOVERY 750 3T, with bilateral breast coil and dedicated protocol, and DBT projections with Siemens Mammomat Inspiration system. A radiologist with 15 years of experience in breast imaging, evaluated blindly each imaging set. Sensitivity, PPV and accuracy of MRI and DBT were calculated, using histology as the gold standard. McNemar test was used to compare MR and DBT sensitivity. Lesions' tumour size and correlation coefficient were also evaluated comparing MRI vs Histological Examination, DBT vs Histological Examination and MRI vs DBT. Measurements were considered concordant if they were within ±3 mm.
Results: On histological examination 71 lesions were detected. MRI had a sensitivity of 100%, PPV 93%, and accuracy 97%; DBT sensitivity was 81%, PPV 89%, and accuracy 77%. McNemar p-value was 0.0003. The correlation coefficient of MRI vs Histological Examination was 0.98, DBT vs Histological Examination was 0.92 and MRI vs DBT was 0.93.

Conclusion: MRI provided higher diagnostic performance than DBT in disease extent evaluation, especially in dense breasts. However, DBT showed good accuracy and sensitivity, proving to be a valid tool in pre-operative staging.

B-0769 10:46

Impact of an image fusion technique, a coordinated US and MRI system, on tissue sampling for conventional B-mode-occult, MRI-detected breast lesions a prospective multicenter study

S. Nakano[1], T. Uematsu[2], M. Futamura[3], T. Mizoo[4], S. Akashi-Tanaka[5], I. Isomoto[6], H. Satake[7], S. Yamamoto[8], M. Gosho[9]; [1]*Nagakute/JP*, [2]*Sunto-gun/JP*, [3]*Gifu/JP*, [4]*Okayama/JP*, [5]*Shimagawa-ku/JP*, [6]*Nagasaki/JP*, [7]*Nagoya/JP*, [8]*Ube/JP*, [9]*Tsukuba/JP*

Purpose: An image fusion technique has recently been developed that uses either real-time virtual sonography (RVS) or volume navigation (Vnav), and can overlay an US image with the MRI image of the same site in real time. The aim of this prospective multicenter study was to evaluate the utility of RVS/Vnav for conventional B-mode (cB-mode)-occult, MRI-detected breast lesions.
Methods and Materials: In 4 Japanese centres, 32 patients who had cB-mode-occult, MRI-detected lesions on prone MRI were enrolled in this study from 2014 to 2016. Written informed consent was acquired, and then an additional supine MRI using a body surface coil was performed. Targeted US using RVS/Vnav applied supine MRI data was performed after a repeat targeted US using cB-mode alone. Pathological findings were confirmed by a RVS/Vnav-guided vacuum-assisted biopsy or excision for targeted US-detected lesions.
Results: Of the 32 lesions, 1 (3%) was detected with repeat targeted US using cB-mode alone, whereas 30 (94%) were detected with targeted US using RVS/Vnav (p<0.0001). The mean lesion size on MRI was 14 mm. Lesion types based on enhancement patterns were 2 focus, 6 mass, and 22 non-mass. The mean RVS/Vnav examination time required to detect the target lesion was 6.4 min. The success rate of tissue sampling was 75% (24/32). Of the 24 lesions, 3 (13%) were DCIS and 2 (8%) were invasive ductal carcinoma.
Conclusion: Our results suggest that RVS/Vnav-guided biopsy is a time-efficient approach that increases the tissue sampling success rate for cB-mode-occult, MRI-detected lesions.

B-0770 10:54

Digital breast tomosynthesis plus mammography, magnetic resonance imaging plus mammography and mammography alone: a comparison of diagnostic performance in symptomatic women

W. Tang, W. Peng; *Shanghai/CN (12111230002@fudan.edu.cn)*

Purpose: To compare the diagnostic value of digital mammography (DM), digital breast tomosynthesis (DBT) plus (DM) and magnetic resonance imaging (MRI) plus DM in symptomatic women.
Methods and Materials: 197 patients with 238 histologically proven lesions underwent DM, DBT and MRI. All images were interpreted independently by two experienced radiologists. A receiver-operating characteristic (ROC) curve was used to evaluate the diagnostic performance of each method. The accuracy, sensitivity, specificity, positive predictive value (PPV) were compared using McNemar's test and Fisher's exact test. A Kappa test was used to assess the interobserver agreement.
Results: The diagnostic performance was lower in DM alone (Radiologist1 [R_1], 0.849; Radiologist2 [R_2], 0.850) than DBT (R_1, 0.907, P=0.0204; R_2, 0.900, P=0.0239) and MRI plus DM (R_1, 0.939, P=0.0006; R_2, 0.935, P=0.0009). However, the difference between DBT and MRI plus DM was not significant (R_1, P=0.1262; R_2, P=0.0843). The accuracy (R_1, 85.3%; R_2, 83.6%) and sensitivity (R_1, 92.1%; R_2, 90.8%) of DBT plus DM were lower than those of MRI plus DM (accuracy: R_1, 90.3%; R_2, 90.7%; sensitivity: R_1, 94.7%, R_2, 95.4%) but without statistical difference (accuracy: R_1, P=0.644; R_2, P=0.360; sensitivity: R_1, P=0.502; R_2, P=0.359).The interobserver agreement of each method was excellent (k=0.894, 0.919 and 0.882 for DM, DBT and MRI plus DM, respectively).
Conclusion: The diagnostic performance of DBT and MRI plus DM is superior to that of DM alone in symptomatic women; the accuracy and sensitivity of MRI plus DM is slightly better than that of DBT plus DM, but not statistically significant.

B-0771 11:02

Breast MRI for detecting and characterising papillary lesions: comparison with conventional digital ductography and histological findings

M. Moschetta, M. Telegrafo, C. De Leo, T. Introna, L. Coi, V. Ranieri, A. Cirilli, A. Stabile Ianora, G. Angelelli; *Bari/IT (marco.moschetta@gmail.com)*

Purpose: To evaluate the role of breast contrast-enhanced MR imaging (CE-MR) for detecting and characterising papillary lesions and to compare the obtained results with conventional digital ductography, having the histological findings as the reference standard.
Methods and Materials: 49 consecutive patients with spontaneous, unilateral, single-pore nipple discharge underwent conventional digital ductography and CE-MRI (1.5 Tesla device) with morphological (T2-TSE, STIR) and dynamic sequences (THRIVE). Sensitivity, specificity and diagnostic accuracy values for both ductography and CE-MRI were calculated having post-surgical histological examination (n=43) and 12 month MR follow-up (n=6) as the reference standard. The obtained performance values were compared by using Mc Nemar test searching for any statistical significant difference between the two imaging tools.
Results: CE-MRI detected papillary lesions in 41/49 (84%) patients (mass like enhancement, n=30 - papillomas; ductal enhancement, n=7 - papillomatosis; linear enhancement, n=4 - papillary carcinomas) with sensitivity, specificity and accuracy values of 95%, 100% and 96%, respectively. Conventional digital ductography detected papillary lesions in 33/49 (67%) patients (single filling defects, n=26 - papillomas; multiple filling defects, n=4 - papillomatosis; filling stops with ductal distortions, n=3; papillary carcinomas) with sensitivity, specificity and accuracy values of 77%, 100% and 80%, respectively. A significant difference between the two imaging tools was found in terms of sensitivity and diagnostic accuracy (p<0.05).
Conclusion: Breast CE-MRI represents an accurate and non-invasive tool for diagnosing and classifying papillary lesions with higher sensitivity and accuracy values as compared with conventional ductography.

B-0772 11:10

Does the immunohistochemical pattern of breast cancer influence the detection by mammography, US or tomosynthesis?

P. Bartolomé, A. Quílez, F. Martinez Regueira, A. Fernandez Montero, A. Elizalde, L. Pina; *Pamplona/ES (aquilez@unav.es)*

Purpose: To assess the influence of the immunohistochemical patterns in the sensitivity of mammography, tomosynthesis and US.
Methods and Materials: This retrospective, single-centre, lesion-based study was approved by the IRB. 247 invasive cancers, histologically confirmed, were reviewed from October 2011 to September 2016. One expert breast radiologist, blindly reviewed all the mammographic (MX), ultrasound (US) and tomosynthesis (DBT) examinations. All the cases were classified according to the BI-RADS categories, considering positive categories 3-5. The cancers were divided into 3 immunohistochemical patterns: Luminal A, Luminal B and non-Luminal (pure Her2 and triple negative). A McNemar test (IBM SPSS 21.0) was used to compare the sensitivity of the combination of different techniques in the three immunohistochemical patterns.
Results: The sensitivities of MX, MXUS and MXDBT for Luminal A were: 46%, 84% and 78%; for Luminal B: 60%, 90% and 74%; for non-Luminal: 65%, 93% and 73%. For both Luminal A and B, whatever the additional technique (US, DBT), the sensitivity was higher than MX alone (p<0.001). The comparison between MXUS and MXDBT was similar in Luminal A (84% vs 78%; p=0.18) but not for Luminal B (90% vs 74%; p<0.001). In the non-luminal group, the combination MXUS was superior to MXDBT (93% vs 73%; p<0.001) and MXDBT was similar to MX (73% vs 65%; p=0.25).
Conclusion: Additional US significantly increased the sensitivity of mammography in all immunohistochemical patterns, while tomosynthesis only in Luminal A and B. The combination mammography-US was better than mammography-DBT for Luminal B and non-Luminal cancers.

B-0773 11:18

Radiological and epidemiological features of breast cancer in women previously exposed to chest and mantle radiation therapy: single center experience

F. Cartia, A. Primolevo, C. Ferranti, G. Scaperrotta; *Milan/IT (francesco.cartia@gmail.com)*

Purpose: Aim of this study was to evaluate the epidemiological and radiological features of breast cancer in women previously exposed to chest radiation therapy.
Methods and Materials: From the paediatric registry we retrospectively analysed imaging of breast cancer in patients who had been exposed to radiation therapy at a young age.
Results: we identified 22 patients with 24 breast cancer who performed imaging studies in our Institute. The commonest reason for irradiation was Hodgkin's Lymphoma.Mean latency period between exposure and breast cancer presentation was 21.7 years.Mean dose given during radiation therapy was 33 Gy Nineteen of 24 tumours were invasive, 5 were ductal carcinoma insitu. The upper-outer quadrant was the commonest tumour location (15/24 cases).Detection rate for DM and US was 74% and 77% was respectively. In 23 mammograms available, 12 presented as a nodular mass and 5 showed microcalcifications only, 6 were occult to digital mammogram (DM).In 22 ultrasound (US) available 17 showed a hypoechoic mass.The predominant MR features in 8 cases available included: 5/8 mass-like lesions.Mass-like lesion presented irregular margins, homogenous contrast enhancement and hyperintensity on T2weighted images.Enhancement pattern "denditric" and "patchy" have been identified in non mass-like lesion.

Conclusion: women treated with supra-diaphragmatic radiation therapy in young age have a higher risk to develop breast cancer at an earlier age.Longterm active surveillance strategies including annual MR are mandatory, starting at least 8-10 years after primary radiation treatment, because BCs in this cohort is expected to develop more frequently before 50 years.

B-0774 11:26

MRI features, FDG PET/CT and clinical characteristics of triple negative breast cancer: comparison with non-triple negative breast cancer

T. Kang, K. Kim, Y. Kim, J. Seo, C. Hwang, Y. Cho, M. Lee; *Daejeon/KR (taesun524@naver.com)*

Purpose: To compare magnetic resonance (MRI) findings and standardised uptake values (SUV) in positron emission tomography-computed tomography (PET-CT) of triple-negative breast cancer (TNBC) with those of breast cancers that are either endocrine-receptor positive or HER-2 positive or triple positive (non-TNBC).
Methods and Materials: 120 breast cancer cases were examined in 116 women (mean age 54.17 years; range 30-87 years). Among them, 23 cases of surgically-confirmed TNBC and 97 cases of non-TNBC were identified. The cases were evaluated using MR (n=93) and PET-CT (n=91). MR findings were discussed in the aspect of the tumour shape, margin, internal enhancement, T2 signal intensity, and kinetic curve. Peak SUVs (p-SUV) of the cancer lesions were measured using PET-CT. Histologic grade was classified according to the degree of differentiation. These findings were compared between TNBC and non-TNBC.
Results: In MR, large size, circumscribed mass were significantly associated with TNBC ($p<0.05$). 12 of 15 masses (80%) had rim enhancement pattern in TNBC ($p<0.05$). In PET-CT, the p-SUV of TNBC (7.575±3.942) was significantly higher than that of non-TNBC (3.715±3.172) ($p<0.05$). In histopathology, TNBC (78.3%) had a higher proportion of poorly differentiated type than non-TNBC (46.4%).
Conclusion: TNBC has a tendency to have large round mass, a rim enhancement pattern in MR, a higher p-SUV in PET-CT and higher pathologic grade.

B-0775 11:34

Correlation of diffusion-weighted imaging with apparent diffusion coefficient value, the standardised uptake values of PET/CT with prognostic factors for breast cancer

T. Kang, K. Kim, Y. Kim, J. Seo, Y. Cho, C. Hwang, M. Lee; *Daejeon/KR (taesun524@naver.com)*

Purpose: This study was carried out to retrospectively correlate the apparent diffusion coefficient (ADC) value, peak standardised uptake value (pSUV) and pSUV/ADC with pathological and clinical prognostic factors in breast ductal calcinoma.
Methods and Materials: Sixty-two breast cancers of 58 women (range 30-87 years) who underwent MRI including DWI, FDG PET/CT and immunohistological staining of the surgical specimens were enrolled. The relationships of ADC value, pSUV and pSUV/ADC with clinicopathological prognostic factors (age, tumour size, histologic grade of tumour, hormone receptors, HER-2 expression status, nodal metastasis) were evaluated by using statistical methods.
Results: The histologic type of breast cancer included DCIS (n=10), IDC (n=52, grade 1= 10, grade 2=14, grade 3=28). As tumour size increased, pSUV and pSUV/ADC become higher ($p<0.05$). There was significant association between the ADC value and HER-2-negative expression. The pSUV/ADC was significantly associated with tumour size and histologic grade ($p<0.05$). As the histologic grade become higher, the pSUV/ADC increased. The nodal metastasis was significantly associated with ADC value, pSUV and pSUV/ADC. The characterisation accuracy of pSUV/ADC (76.4%) was higher than pSUV (73.7%) and ADC values (43.3%) alone for diagnosis of breast cancer.
Conclusion: pSUV and pSUV/ADC were correlated with nodal metastasis, tumour size and histologic grade. The ADC value was associated with nodal metastasis and HER-2-negative expression. The pSUV/ADC had a high accuracy for grading of breast cancer. Therefore, pSUV and ADC value are useful indexes for predicting the prognosis of breast cancers.

B-0776 11:42

The role of fusion between breast MRI and 18F-FDG PET in staging of breast cancer

A. Quilez[1], P. Bartolomé[1], P. Martinez Miravete[2], A. Elizalde[1], M. Garcia Velloso[1], M. Ribelles[1], A. Fernandez Montero[1]; [1]*Pamplona/ES*, [2]*Zaragoza/ES (aquilez@unav.es)*

Purpose: To evaluate the diagnostic accuracy of magnetic resonance imaging (MRI) fused with prone 18F-fluoro-deoxyglucose (FDG) positron emission tomography (PET) in primary tumour staging of patients with breast cancer.
Methods and Materials: This retrospective study included 45 women with 49 pathologically proven invasive breast carcinoma. MRI and prone PET/CT scans with time-of-flight and point-spread-function reconstruction were performed with the same dedicated breast coil. The studies were assessed by a radiologist and a nuclear medicine physician and the evaluation of fused images was made by consensus. The final diagnosis was based on pathology (90 lesions) or follow-up ≥24 months (17 lesions).
Results: The study included 72 malignant and 35 benign lesions with a median size of 1.8 cm (range 0.3-8.4 cm), being 31 focal, 9 multifocal and 9 multicentric cases. In lesion-by-lesion analysis, sensitivity, specificity, positive and negative predictive values were 97%, 80%, 91% and 93% for MRI, 96%, 71%, 87%, and 89% for prone PET, and 97%. 94%, 97% and 94% for MRI fused with PET. Areas under the curve (AUC) were 0.953, 0.850, and 0.983, respectively ($p<0.01$).
Conclusion: MRI fused with FDG-PET is more accurate than FDG-PET in primary tumour staging of breast cancer patients and increases the specificity of MRI.

B-0777 11:50

Sonographic and MRI evaluation of complex cystic lesions of the breast: imaging findings in malignancy

P. Gupta, M.B. Popli, N. Sharma, D. Arse; *New Delhi/IN (dr.pranavg@gmail.com)*

Purpose: The aim of this study was to evaluate complex cystic lesions (CCL) of breast by ultrasonography (USG) and advanced MRI techniques in order to differentiate benign lesions from malignant.
Methods and Materials: 160 patients presenting with palpable or mammographically detected breast lesions were evaluated using USG and 44 patients with 50 sonographically detected CCL were included in the study. Morphological characteristics were assessed on USG according to BI-RADS and lesions were subclassified into four types. Dynamic contrast enhanced MRI along with diffusion weighted imaging and MR spectroscopy were then used to further establish benign and malignant findings. All findings were correlated with histopathology which was taken as gold standard and appropriate statistical tools were applied.
Results: Of the 50 CCL, 32 proved to be benign while 18 were malignant on histopathology. The USG descriptors of irregular shape (88.8%), not circumscribed margins (66.7%) and anti parallel orientation (72.2%) showed high positive predictive value (PPV) for malignancy which was statistically significant ($p<0.001$). Among the four types of CCL, PPV for malignancy was highest for type IV lesions (70%). MRI features of heterogeneous enhancement (72.2%), Type III kinetic curve (72.2%), reduced apparent diffusion coefficient (100%) and tall Choline peak (94.4%) were strong predictors of malignancy. The kappa score of 0.780 between ultrasound and MRI shows good agreement between the two modalities.
Conclusion: Combination of USG and advanced MRI techniques provides a high level of diagnostic confidence in characterisation of CCL of the breast thus allowing early diagnosis of breast malignancies.

10:30 - 12:00 **Room E2**

Neuro

SS 1011a

Brain tumours: imaging techniques

Moderators:
M. Herman; Olomouc/CZ
C.M. Perez Fernandez; Berlin/DE

B-0778 10:30

Incidences of tumour progression and treatment-induced pseudoprogression in high-grade gliomas, a systematic review and meta-analysis.

A.W. Abbasi, H.E. Westerlaan, G.A. Holtman, K.M.A. Aden, P.J. van Laar, A. van der Hoorn; *Groningen/NL (a.van.der.hoorn@umcg.nl)*

Purpose: High-grade gliomas are the most common primary brain tumours. Treatment-induced pseudoprogression describes the false appearance of radiation-induced progression on MRI. Differentiation should be made between true tumour progression to correctly plan treatment. However, there is wide variation of reported pseudoprogression. We thus aimed to establish the incidence of treatment-induced pseudoprogression and tumour progression in high-grade glioma patients with a systematic review and meta-analysis.
Methods and Materials: We searched PubMed, Embase, and Web of Science on the incidence of treatment induced pseudoprogression and tumour progression in adult high-grade glioma patients from 2005. Histology or imaging follow-up was used as reference standard. Extracted data included number of patients with progression on T1 post-contrast and/or T2/FLAIR,

treatment-induced pseudoprogression and tumour progression. Study quality was assessed with the NIH Tool. Heterogeneity was tested with the chi-square and I^2. Pooling of the results was done with random models using metaprop in STATA.
Results: We identified 73 studies. MRI progression occurred in 2603 patients. Of these, 36%, (95%CI 33-40%) demonstrated treatment-induced pseudoprogression, 60% (95%CI 56-64%) tumour progression and unknown outcome was present in the remaining 4% (range 1-37%).
Conclusion: We demonstrated a higher than previously thought incidence of treatment induced progression. This highlighted the full extent of the limitation of conventional MRI as currently used in the RANO criteria for treatment evaluation in high-grade gliomas. The need for more accurate treatment response evaluation using advanced imaging to aid in greater diagnostic accuracy and more accurate therapeutic approach is underscored.

B-0779 10:38

MR perfusion perilesional oedema difference between glioblastoma and metastasis

F. Aparici, A. Perez Girbes, M. Mazon, J. Carrreres, J. Garcia; *Valencia/ES (aperezgirbes@gmail.com)*

Purpose: To analyse MR perfusion of the closest peritumoural oedema tumour to normal white matter in patients with glioblastoma or unique brain metastasis.
Methods and Materials: The study was conducted on patients diagnosed with brain tumours between January 2010 and December 2015, 15 GBM and 15 metastases, with histopathologic confirmation. We analysed for each area of oedema the CBV, CBF, MTT, Ktrans, ve and Kep. All perfusion biomarkers were normalised against the white matter contra-lateral unaffected by the lesion.
Results: The results show a greater heterogeneity in peritumoural oedema area in GBM patients relative to oedema concerning patients with metastases. A gradual retreat is observed in perfusion parameters of the oedema, much more pronounced in cases of GBM.
Conclusion: This work supports the hypothesis of GBM tumour infiltration in the perilesional oedema, distal to the area of enhancement.

B-0780 10:46

Diffusion tensor imaging metrics as a tool for the grading of cerebral gliomas with histopathological correlation

H.A.M.M. Abdel Daiem, A.M. Elnekiedy, M. Elsheikh, Y. Eladawy, R. Darweesh; *Alexandria/EG (hanan.morsi@yahoo.com)*

Purpose: To evaluate the role of quantitative diffusion tensor imaging measurements including, fractional anisotropy (FA) and mean diffusivity (MD) values in the grading of cerebral glioma.
Methods and Materials: 11 patients with gliomas of low histological grades (WHO grade I and II) and 15 patients with high histological grades gliomas (WHO grade III and IV) were examined by MRI 1.5T. Mean FA, FA tumour/normal tissue ratio in the solid tumour components and corresponding mean MD, MD tumour/normal tissue ratio were measured and compared statistically among different tumour grades.
Results: There was statistically significant difference in mean FA values and FA ratios between low grade gliomas (LGGs) and high grade gliomas (HGGs). LGGs showed low FA values and ratios (mean 0.19$\pm$0.06 and 0.40$\pm$0.07, respectively) compared to that of HGGs (mean 0.35$\pm$0.06 and 0.56$\pm$0.08, respectively) p<0.001. Mean MD values and ratios were significantly higher in LGGs (mean 1.49$\pm$0.47 and 1.95$\pm$0.64, respectively) than that of HGGs (mean 1.10$\pm$0.23 and 1.43$\pm$ 0.36, respectively) p<0.010 and 0.013 respectively.
Conclusion: MR diffusion tensor imaging metrics could increase the diagnostic accuracy in the preoperative grading of cerebral glioma.

B-0781 10:54

Diffusion-weighted imaging for predicting and monitoring primary central nervous system lymphoma treatment response

J.B. Wen, W.X.Z. Xu, D.Y. Geng; *Shanghai/CN (wen123jianbo@163.com)*

Purpose: This study assessed the minimum ADC correlated with treatment response in patients with primary central nervous system lymphoma undergoing methotrexate-based chemotherapy.
Methods and Materials: Thirty-five patients with primary central nervous system lymphoma underwent conventional MR imaging and DWI before chemotherapy and after 1 and 5 cycles of chemotherapy.Pretreatment minimum ADC, minimum ADC after 1 cycle, minimum ADC after 5 cycles, and change in minimum ADC were compared among the different response groups.The Pearson correlation test was calculated between these ADC parameters and tumour response.
Results: The pretreatment minimum ADC of the progressive disease group was lower than that of the complete response and partial response groups, but there was no significant difference among them. A comparison among groups showed that Minimum ADC after 1 cycle, minimum ADC after 5 cycles, minimum ADC change, and the percentage of minimum ADC change were all significantly different among the 3 groups. A significant positive correlation was observed between the percentage of minimum ADC after 1 cycle of chemotherapy and the size reduction percentage after 5 cycles of chemotherapy. The minimum ADC change and the percentage of minimum ADC change performed better in the differentiation of the final treatment response, specifically in complete response and partial response from progressive disease.
Conclusion: The minimum ADC after 1 cycle and minimum ADC changes were better correlated with the treatment response than the pretreatment minimum ADC. Minimum ADC after early therapy may potentially to be used to predict and monitor the response of primary central nervous system lymphoma to chemotherapy.

B-0782 11:02

True progression vs pseudoprogression in glioma: a comparative study of arterial spin labelling and dynamic susceptibility contrast imaging

Q. Xu[1], K. Xu[1], J. Wu[2], J. Qu[2]; [1]*Xuzhou/CN*, [2]*Shanghai/CN (xuqianxz@126.com)*

Purpose: The purpose of this study was to differentiate true progression from pseudoprogression of gliomas treated with concurrent chemoradiotherapy (CCRT) with temozolomide (TMZ) using 3D pseudo-continuous arterial spin labelling (3D-ASL) technique and dynamic susceptibility contrast perfusion magnetic resonance imaging (DSC-MRI).
Methods and Materials: Twenty-six consecutive patients who showed new or enlarged, contrast-enhancing lesions within the radiation field after CCRT were assessed by use of 3D-ASL and DSC-MRI. These patients were classified into groups of tumour recurrence (n=16) or pseudoprogression (n=10) based on pathologic analysis or clinical-radiologic follow-up. The extent of susceptibility artefacts in the enhanced lesions was scored from 1 to 3 (1 = no susceptibility artefacts and 3 = extensive susceptibility artefacts (maximum diameter>2 cm)). A quantitative analysis was performed with cerebral blood flow values (ASL-CBF), relative cerebral blood flow values (ASL-rCBF, DSC-rCBF) and relative cerebral blood volume values (DSC-rCBV) in the region of interest (ROI) with maximum signal enhancement.
Results: ASL had a lower susceptibility-artefact score than DSC-MRI (p=0.01). There was a statistically significant difference between tumour recurrence group and pseudoprogression group for all parameters. There was good correlation between DSC-rCBF and ASL-rCBF values, as well as DSC-rCBV and ASL-rCBF values with correlation coefficients of 0.8 and 0.727.
Conclusion: 3D-ASL is an alternative to DSC-MRI for the evaluation of perfusion in differentiating true progression from pseudoprogression of gliomas treated with CCRT. The method has fewer susceptibility artefacts than DSC-MRI and can be used in patients with renal failure because no contrast injection is needed.

B-0783 11:10

Necrosis in tumour bed-radiation necrosis vs tumour necrosis: is there any role of dynamic contrast-enhanced perfusion MRI? First step - clinical feasibility study

F. Mubarak; *Karachi/PK (fatima.mubarak@aku.edu)*

Purpose: To assess adequacy of cerebral blood volume (CBV) and permeability index in differentiating radiation necrosis and tumour growth.
Methods and Materials: In this study we analysed rCBV and permeability index from the enhancing areas to the contralateral white matter in10 post-treatment malignant brain lesions.The lesions were compatible with features of MR-morphological tumour progression. The diagnosis (real progression vs radiation necrosis) was determined by histopathology or by clinical/MRI-follow-up.
Results: Significant differences between tumour progression (N=5) and radiation necrosis (N=4) and mixed (N=1). An increased rCBV and permeability index is highly predictive of tumour progression.
Conclusion: Initial results of CBV and permeability map in differentiating tumour necrosis and tumour growth was highly promising.

B-0784 11:18

Prediction of survival in patients affected by Glioblastoma multiforme evaluated with perfusion MRI: a histogram analysis

A. Di Napoli, L. Pasquini, A. Romano, A. Boellis, A. Bozzao; *Rome/IT*

Purpose: Currently the most predictive prognostic marker for longer survival in patients with newly diagnosed glioblastoma is the MGMT promoter methylation status. The aim of this study was to verify which parameters rCBV data (kurtosis, skewness, average, maximum value, median) obtained by histogram analysis of perfusion acquisitions could predict the survival at 1 year in patients with GBM after surgical procedure.
Methods and Materials: Thirty-four patients with newly diagnosed histologically verified GBM were retrospectively evaluated. All patients received postoperative focal radiotherapy plus concomitant daily temozolomide, followed by adjuvant TMZ therapy. Each subject underwent the same MR

examination with standard sequences and dynamic susceptibility-weighted contrast-enhanced perfusion. The CBVratio was then automatically calculated by the software. Histograms were generated from multiple ROIs covering the tumour and the histogram pattern was statistically evaluated for kurtosis, skewness, mean, median and maximum value of rCBV. Survival curves of histogram parameters were performed and compared to methylation status of GBM.
Results: Only kurtosis showed a significant difference comparing subjects survived more and less than a year. A significant correlation was evident between OS and rCBV kurtosis. According to ROC analysis, the rCBV kurtosis value of 1,26 represented an optimized cutoff useful to distinguish subjects survived more and less than a year. Survival curves showed a better survival condition with rCBV kurtosis more than 1,26. No similar results were appreciable in survival curves of methylated and unmethylated subjects.
Conclusion: The histogram analysis could represent a valid method to predict survival in patients affected by GBM.

B-0785 11:26

Contrast-enhanced MRI vs contrast-enhanced ultrasound: a comparison in glioblastoma surgery using intra-operative fusion imaging
F. Prada[1], V. Vitale[2], M. Del Bene[1], C. Boffano[1], L.M. Sconfienza[1], G. Mauri[3], L. Solbiati[3], G. Sakas[4], F. DiMeco[1]; [1]*Milan/IT*, [2]*Lecco/IT*, [3]*Rozzano/IT*, [4]*Darmstadt/DE (io@lucasconfienza.it)*

Purpose: To compare intraoperative contrast enhanced ultrasound (CEUS) images to the correspondent co-planar T1 weighted contrast-enhanced magnetic resonance images (gdMRI) using fusion imaging between CEUS and pre-op MRI in glioblastoma (GBM).
Methods and Materials: Ten patients with GBM diagnosis were retrospectively enrolled. All patients underwent tumour excision guided by navigated intra-operative US (ioUS) based on fusion imaging between ioUS and pre-operative MRI. Navigated CEUS scans were performed after intravenous administration of ultrasound contrast agents (CA), before tumour resection. Using fusion imaging we compared CEUS contrast enhancement (location, morphology, margins, dimensions, and pattern) to that of gdMRI.
Results: Registration between pre-operative gdMRI and ioUS demonstrated an error less the 2mm. In all cases CEUS highlighted the lesion. Contrast enhancement of gdMRI and CEUS was superimposable in all cases for location, margins, dimensions, and morphology while the pattern was the same in 9/10 cases; in one case the pattern was different.
Conclusion: CEUS contrast enhancement location, margins, morphology, and dimensions are superimposable to that provided by pre-operative gdMRI in all cases; while the pattern is the same in most of the cases. Taking into account that the goal of GBM resection is to remove all the gdMRI enhanced area, the information obtained with CEUS are of paramount importance in surgical management of GBM.

B-0786 11:34

Could new reconstruction CT techniques challenge MRI for the detection of brain metastasis in the context of initial lung cancer staging?
D. Millon, D.L. Byl, S.E. Cambier, A.G. Van Maanen, A. Vlassenbroek, E.E. Coche; *Brussels/BE (domitille.millon@uclouvain.be)*

Purpose: To evaluate the diagnostic performance of brain CT images reconstructed with a model-based iterative algorithm and acquired at conventional and reduced dose in the staging work-up of lung cancer.
Methods and Materials: 115 patients with histologically proven lung cancer were prospectively included between July 2014 and September 2015. Patients underwent 2 brain CT acquisitions, during the same initial staging session. Acquisitions were performed on a 256-slice MDCT (Philips Healthcare, Cleveland OH) at standard (CTDIvol: 41.4mGy) and half dose (CTDIvol: 20.7mGy). Both images datasets were reconstructed with Filtered Back Projection (FBP) and model-based iterative reconstruction algorithm (IMR, Philips HealthCare, OH). Brain MRI was performed within 7 days and was considered as the gold standard. 2 blinded independent readers analysed the images. Diagnostic performance and inter-observer agreement were calculated.
Results: 93 patients underwent all examinations. MRI showed 56 metastasis on 17 patients. At the standard dose, 8 patients presented metastasis on both FBP and IMR CT images with 15 and 17 lesions, respectively. At half-dose, 6 (FBP) and 7 patients (IMR), presented 13 and 15 lesions, respectively. Specificity, negative and positive predictive values were excellent for all CT techniques.The test couldn't highlight any significant difference between the standard dose IMR and the half dose FBP techniques (p=0.12>0.05).
Conclusion: Even using new CT reconstructions techniques, MRI is still the best imaging tool to detect brain metastases at the initial staging of lung cancer. No significant difference could be demonstrated between the 2 CT techniques.

B-0787 11:42

Exact differentiation of tumoural borders in patients with glioma by MRS and diffusion magnetic resonance imaging
G. Amjad, D. Firouznia, D. Zeinalizadeh, H. Ghanaati, A. Jalali, M. Shakiba, P. Sabetrasekh, N. Ghavami; *Tehran/IR (Ghazal_1986_amjad@yahoo.com)*

Purpose: Most of patients with glioma are planned for surgical intervention in whom, exact localisation of tumour borders is so critical as this could optimize the surgery to remove as much as tissues involved by tumour and preserve intact tissues. Here, we want to assess the exact differentiation of tissues involved by glial tumoural cells vs non-involved areas by MRS and perfusion MRI.
Methods and Materials: Ten patients with glioma diagnosis based on conventional MRI features were enrolled [mean age: 35.3±13.2, range: 20-62, 6 males]. All patients underwent 3T MRI in which tumour mapping based on MRS was featured and according to this mapping, different tumoural and peritumoural locations [including tumoural core, infiltrative oedema, reactive oedema and normal tissue] were determined. Quantitative diffusion and MRS measurements on these locations were performed. Then, using a biopsy navigation system, biopsies were taken from different mentioned locations and histopathological assessment results were considered as gold standard. MRI quantitative measurements of different locations were compared together.
Results: Among 48 pathologic samples,36 (75%) contained tumoural cells [including 9 tumoural core, 26 infiltrative tissues and 1 necrosis]. Based on primary mapping, 7 (19.4%) of these positive samples were missed [five were diagnosed as reactive oedema and 2 as normal tissue] [kappa: 0.67, P value<0.001]. Mean of ADC was statistically higher in tumoural samples (P=0.002). Median of NAA and NAA/Chol was different between positive and negative samples (P value<0.001). Mean ADC and median Chol/NAA were statistically different in missed reactive oedema samples than normal and correctly diagnosed reactive oedema samples together (P values <0.05).
Conclusion: Detailed diffusion and MRS quantitative measurements could be new measurements for more exact delineating peritumoural borders of gliomas.

B-0788 11:50

Radiographic response of tectal gliomas following proton radiotherapy
P.A. Caruso; *Boston, MA/US (pcaruso@partners.org)*

Purpose: Proton radiotherapy is an effective modality for the treatment of paediatric brainstem tumours. Many tumours including tectal gliomas may respond to proton radiotherapy initially by increasing in size that may be misinterpreted as tumour progression. The purpose of our study is to assess the quantitative response of tectal gliomas by performing serial MRI measurements of tumour volume over time to identify a predictable trend in tumour response to proton radiotherapy.
Methods and Materials: Following IRB approval, a retrospective clinical database search was performed for patients with tectal gliomas. Patients aged 0 through 25 years with tectal gliomas who underwent proton radiotherapy were included. Patients with tumours previously treated with radiotherapy or surgical resection were excluded. Cubic volume measurements were obtained from FLAIR MRI scans at all available timepoints.
Results: Five subjects met inclusion criteria with median age 14.4 years (average, 16.2 years; range, 12.6-20.8 years). Median imaging follow-up was 2.6 years (average, 3.0 years; range, 1.4-5.4 years) with a median of 8 post-treatment timepoints (average, 7.6; range, 4-10). Each of the five tumours followed a pattern of post-radiotherapy enlargement followed by reduction in size. The peak tumour volume occurred at a median of 6.9 months (average, 6.2 months; range, 3.5-8.2 months) from initiation of radiotherapy.
Conclusion: Following proton radiotherapy, tectal gliomas demonstrate a predictable trend of enlargement and subsequent reduction in tumour size. This trend may be helpful in distinguishing radiographic response from tumour progression.

10:30 - 12:00 **Room F1**

Molecular Imaging

SS 1006

Clinical molecular imaging

Moderators:
J. Grimm; New York, NY/US
I. Mendichovszky; Cambridge/UK

K-14 10:30

Keynote lecture
M.R. Makowski; *Berlin/DE*

B-0789 10:39

Ultra-fast ^{18}F-FDG PET/MRI compared to ^{18}F-FDG PET/CT and CT in whole-body staging of females with recurrent pelvic malignancies

J. Kirchner[1], L.M. Sawicki[1], S. Suntharalingam[2], J. Grüneisen[2], V. Ruhlmann[2], C. Deuschl[2], K. Herrmann[2], G. Antoch[1], L. Umutlu[2]; [1]*Düsseldorf/DE*, [2]*Essen/DE (Julian.Kirchner@med.uni-duesseldorf.de)*

Purpose: To evaluate the diagnostic feasibility of an ultra-fast ^{18}F-FDG PET/MRI protocol, including T2-w and contrast-enhanced T1-w imaging as well as metabolic assessment (PET) in comparison to 18F-FDG PET/CT and CT for whole-body staging of female patients with suspected recurrence of pelvic malignancies
Methods and Materials: 43 female patients with suspected tumour recurrence were included in this study. All patients underwent a PET/CT and a subsequent PET/MRI examination. Two readers were asked to evaluate ultra-fast PET/MRI, PET/CT as well as CT datasets of PET/CT separately for suspect lesions regarding lesion count, lesion localization and lesion characterization. Statistical analyses were performed both, on a per-patient and a per-lesion basis.
Results: Tumour relapse was present in 38 of 43 patients. Based on CT readings 25/38 tumour relapses were correctly identified. PET/CT enabled correct identification of 37/38 patients, PET/MRI correctly identified 36/38 patients with recurrent cancer. On a lesion-based analysis PET/MRI enabled the correct detection of more lesions, comprising a lesion-based sensitivity, specificity, positive predictive value, negative predictive value and diagnostic accuracy of 50%, 58%, 76%, 31%, and 53% for CT, 97%, 83%, 93%, 94%, and 92% for PET/CT and 98%, 83%, 94%, 94%, and 94% for PET/MRI, respectively. Mean scan duration of ultra-fast PET/MRI, PET/CT and whole-body CT amounted to 18.5 ± 1 minutes, 18.2 ± 1 minutes and 3.5 minutes, respectively.
Conclusion: Ultra-fast PET/MRI provides equivalent diagnostic performance and examination time when compared to PET/CT and superior diagnostic performance to CT in restaging female patients suspected to have recurrent pelvic cancer.

B-0790 10:47

Characterisation of complicated and recurrent urological infections using molecular imaging of the chemokine receptor CXCR4 in combination with diffusion-weighted MRI

K. Hueper[1], F. Gueler[1], J.H. Bräsen[1], H.-J. Wester[2], T.L. Ross[1], H. Haller[1], F. Wacker[1], F. Bengel[1], T. Derlin[1]; [1]*Hannover/DE*, [2]*Garchingen/DE (hueper.katja@mh-hannover.de)*

Purpose: To obtain mechanistic insights into complicated recurrent urological infections in patients after kidney transplantation using molecular imaging of chemokine receptor CXCR4-expression by means of positron emission tomography (PET) in combination with diffusion-weighted magnetic resonance imaging (MRI).
Methods and Materials: Twelve patients with suspected acute kidney transplant infection were examined using PET with the specific CXCR4-ligand, gallium-68- (Ga-68-)pentixafor as well as diffusion-weighted MRI (10 b-values). The spatial distribution and intensity of up-regulation of CXCR4-expression on PET and diffusion restriction as determined by apparent diffusion coefficients (ADCs) on MRI were analyzed, and compared to serum and urine analyses, microbiologic evaluation and immunohistochemistry of kidney biopsy specimens.
Results: Patterns consistent with acute transplant infection were detected in 7/12 patients on PET and MRI. In focal lesions, ADC was reduced compared to unaffected parenchyma (1.110±0.125 vs. 1.577±0.028*10^{-3} mm^2/s, p<0.001). Areas of ADC-reduction corresponded to up-regulated CXCR4-expression compared to parenchyma (SUVmean 5.37±2.37 vs. 3.63±1.92, p<0.01). In the other patients, imaging detected no signs of renal involvement, consistent with lower urinary tract infection. Leukocyturia was present in all patients with evidence for renal inflammation. Immunohistochemistry of biopsies of acute transplant infection showed CXCR4-expression in infiltrating leukocytes.
Conclusion: Combined PET/MR imaging with Ga-68-pentixafor detects acute renal infections and provides insights into the pathophysiology of the disease. Up-regulated CXCR4-expression in infiltrating leukocytes corresponded to areas of increased cell density on MRI. Combined PET/MRI may have the potential to confirm the presence, extent and localization of acute renal infection providing relevant information for the therapeutic management of patients.

B-0791 10:55

PET/MR radiogenomics of invasive ductal breast cancer: an exploratory study

O.A. Catalano[1], U. Mahmood[1], A. Soricelli[2], M. Salvatore[2], C. Catana[1], B.R. Rosen[1]; [1]*Boston, MA/US*, [2]*Naples/IT (onofriocatalano@yahoo.it)*

Purpose: To explore the potentialities of CE-FDG PET/MR to provide insights into genetics and grade of differentiation of ductal invasive breast cancer.
Methods and Materials: 21 non-operated invasive ductal breast cancer patients, with known degree of expression of oestrogen receptor (ER), progesterone receptor (PR), human epidermal growth factor 2 (HER2), antigen Ki-67 (Ki67), and histology grading, underwent CE-FDG PET/MR. SUV_{max}, $Ktrans_{mean}$, Kep_{mean}, Ve_{mean}, iAUC, and ADC_{mean} were compared with the expression of ER, PR, HER2, KI67 and with grading, using Student's t-test.
Results: Of the explored biomarkers only Kep_{mean}, ADC_{mean}, and SUV_{max} were capable of discriminating expression of ER, PR, HER2, Ki67, and grading. Higher Kep_{mean} and SUV_{max} differentiated ER- and PR- from ER and/or PR+ cancers (Kep_{mean} 9234±1320min^{-1}versus 6492±2359min^{-1}, p=0.011; SUV_{max} 14.19±7.17 versus 6.18±4.34, p=0.005). ADC_{mean}, Kep_{mean}, and SUV_{max} were higher in HER2- rather than in HER2+ tumours (ADC 1303±121 x10^{-6}mm^2/s versus 1022±280 x10^{-6}mm^2/s, p=0.009; Kep_{mean} 8599±2122min^{-1} versus 6322±2241min^{-1}, p=0.028, and SUV_{max} 11.79±7.65 versus 6.17±4.02, p=0.046, respectively). Only ADC_{mean} discriminated Ki67≤14% versus Ki67>14% cancers (964±242x10^{-6} mm^2/s versus 1252±214x10^{-6} mm^2/s, p=0.011). Both Kep_{mean} and SUV_{max} demonstrated lower values in G2 rather than in G3 cancers (Kep_{mean} 6638±2392 min^{-1} versus 8944±1765 min^{-1}, p=0.036; SUV_{max} 6.83±4.73 versus 12.89±8.08, p=0.042).
Conclusion: ADC_{mean}, Kep_{mean}, and SUV_{max} correlated with expression of ER, PR, HER2, and Ki67 in ductal breast cancer and also with grading. CE-FDG PET/MR has the potentiality to non-invasively provide insight into genetics and grading of invasive ductal breast cancer. This might aid better patient management optimizing personalized therapy.

B-0792 11:03

PET imaging of chemokine receptor CXCR4 in patients with primary breast carcinoma

T. Vag, A. Rossmann, S. Metz, J. Ettl, M. Niemeyer, H. Wester, M. Schwaiger; *Munich/DE (tibor.vag@tum.de)*

Purpose: CXCR4 is a chemokine receptor that was reported to be overexpressed in invasive breast cancer and seems to play a major role in signalling pathways of metastases. The aim of this study was to assess the feasibility of CXCR4-directed imaging in patients with breast cancer using the novel CXCR4-targeted PET probe 68Ga-pentixafor.
Methods and Materials: 12 patients suffering from primary breast cancer underwent PET imaging (either PET/MR or PET/CT) using 68Ga-pentixafor. The lesions included 10 invasive ductal carcinomas (IDC) and two invasive lobar cancers (ILC). Five patients were known to have lymph node or distant metastases detected by previously performed imaging modalities. Maximum standardised uptake values (SUVmax) and tumour-to-background ratios (T/B ratio) were determined in the breast cancer lesions.
Results: 8 of 12 primary breast cancers were visually detectable with a mean SUVmax of 2.75 (range 1.7 to 4.5) and a mean T/B ratio of 2.2. The visually undetectable lesions included the two cases of ILC, and two cases of IDC (G2). Highest SUVmax T/B rations of 4.37/3.9 and 4.5/3.5, respectively, were demonstrated in an IDC (G3) with evidence of bone and lymph node metastases and in an IDC (G2) without any metastases. A statistical significant correlation between SUVmax, T/B ratios and occurrence of metastases was not observed.
Conclusion: CXCR4-directed PET imaging of breast cancer is feasible. Based on our first observations in this small patient cohort, tracer accumulation was significantly higher in IDC compared to ILC.
Author Disclosures:
H. Wester: CEO; H.J. Wester is CEO of Scintomics, provider of Pentixafor.

B-0793 11:11

Does bone scan add any value to whole body FDG-PET/CT in staging and restaging breast carcinoma?

M.M. Abouzied, H. Al-Refai, M. AlQahtani, A. Elsaadany, A. Almuhideb, A. Fathala, Z. Khan, A. Alsugair, A. Abu-zaid; *Riyadh/SA (mohei.abouzied@gmail.com)*

Purpose: To evaluate the efficacy of fluorine-18 fluorodeoxyglucose positron emission tomography/computed tomography (^{18}F-FDG PET/CT) compared to ^{99m}Tc-methylene diphosphonate (^{99m}Tc-MDP) bone scan in detecting bone metastases in patients with breast cancer.
Methods and Materials: Total of 526 patients with breast cancer were retrospectively identified in our database who had underwent ^{18}F-FDG PET/CT, from January 2006 to May 2016. Of whom, 133 patients met our inclusion criteria — namely, biopsy-proven breast cancer, and ^{18}F-FDG PET/CT and bone scan within 30 days. Comparison was made on a lesion-by-lesion analysis. MRI, multi-detector CT, and the clinical course of the patients were used as reference standard.
Results: ^{18}F-FDG PET/CT identified 506 bone lesions in 47 patients, in addition to distant metastases in solid organs (brain, lymph nodes, lung, liver and adrenals). Bone scan missed 4 patients with confirmed bone metastases and was false positive in 3 patients. ^{18}F-FDG PET/CT showed neither false-positive nor false-negative results. The overall sensitivity, specificity, and accuracy was 100, 100 and 100% for ^{18}F-FDG PET/CT and 91.5, 96.5 and 94.7%, for bone scan, respectively.
Conclusion: ^{18}F-FDG PET/CT is superior to ^{99m}Tc-MDP bone scan in detecting bone metastases from breast cancer, not adding benefit for bone scan.

B-0794 11:19

Correlation of apparent diffusion coefficient value on diffusion-weighted imaging and SUV values on PSMA PETCT in patients with biopsy-proven prostate cancer

S. Shivalingappa, K. Kallur, I. Desai, M.A. Kumar, G.R. Prashanth, S. Neelakantan, S. Sampangi, A. Kesari, P.S. Sridhar; *Bangalore/IN (dr.shivaswami@gmail.com)*

Purpose: Correlation of apparent diffusion coefficient value on diffusion-weighted imaging and SUV values on PSMA PETCT in patients with biopsy-proven prostate cancer.
Methods and Materials: This is a prospective study conducted in our hospital, department of molecular imaging over last 6 months. 22 patients with biopsy-proven prostate cancer were included. All these patients underwent PSMA PETCT imaging as a staging investigation and were subjected to prostatic pelvic MRI (3T SKYRA 48 channels). PSMA PETCT images were analysed on GE work station (AW 4.6). Mean and maximum SUV values were obtained. MRI images were analysed on MMWP work station and ROIs were drawn for the ADC values at the regions of elevated SUV values. ADC values were compared with SUV values using one-way Pearson bivariate relationships were determined between SUV and ADC. T2W MR images were also correlated with ADC values and PET-MRI fusion with T2 W axial images was performed to assess the extent of the lesion.
Results: There was a significant negative correlation between SUV max with mean ADC (r =-525, p=0.01). There was a significant negative correlation of max SUV with min ADC (r= -0.602, p=0.005). There was a significant negative correlation between min SUV with mean ADC (-0.61, p=0.004) . The ADC values were significantly low and mean SUV values were high with Gleason's score above 8.
Conclusion: Quantitative ADC values in correlation with PSMA PETCT help in localisation, assessing the extent of the disease and also determining the aggressiveness of the disease.

B-0795 11:27

Diagnostic accuracy of integrated 68-Ga-PET/MRI in suspected recurrent prostate cancer

S. Lütje[1], J. Cohnen[1], J. Grüneisen[1], L.M. Sawicki[2], T. Pöppel[1], L. Umutlu[1], A. Wetter[1]; [1]*Essen/DE*, [2]*Düsseldorf/DE (axel.wetter@uk-essen.de)*

Purpose: To evaluate diagnostic accuracy of ^{68}Ga-PSMA- PET/MRI in suspected recurrent prostate cancer.
Methods and Materials: 25 patients with suspected recurrent PCa underwent ^{68}Ga-PSMA PET/CT followed by integrated PET/MRI. Data from both investigations were analysed separately and compared regarding tumour detection rate, image quality and radiotracer uptake in tumour lesions and muscle tissue. Image analysis was prospectively performed by different groups of nuclear medicine physicians and radiologists with respect to the detection of lymph node metastases, bone metastases and local recurrence of the tumour. Image quality was evaluated visually based on a three-point ordinal scale.
Results: ^{68}Ga-PSMA-PET/MRI provided diagnostic image quality in all examined patients. Overall detectability of PET-positive lesions was higher with PET/MRI compared to PET/CT (43 vs 36), identifying 14 vs 9 PET-positive local recurrences, 23 vs 20 PET-positive lymph nodes, 2 vs 3 PET-positive soft-tissue lesions, and 4 vs 4 PET-positive bone lesions, respectively. Mean PET image quality obtained with ^{68}Ga-PSMA-PET/MRI and -PET/CT was 2.8±0.4 and 2.7±0.5, respectively (p=0.1604).
Conclusion: ^{68}Ga-PSMA-PET/MRI is superior to ^{68}Ga-PSMA-PET/CT in the detection of PSMA-expressing prostate bed recurrences and lymph node lesions and as reliable as ^{68}Ga-HBED-CC-PSMA-PET/CT in the detection of bone lesions.

B-0796 11:35

Detection efficacy of hybrid ^{68}Ga-PSMA ligand PET/CT in prostate cancer patients with biochemical recurrence after primary radiation therapy defined by Phoenix criteria

I. Einspieler, I. Rauscher, C. Düwel, M. Krönke, C. Rischpler, G. Habl, M. Schwaiger, T. Maurer, M. Eiber; *Munich/DE (ingo.einspieler@tum.de)*

Purpose: The aim of this study was to evaluate the detection rate of ^{68}Ga-PSMA PET/CT in patients with biochemical recurrent prostate cancer defined by Phoenix criteria after external beam radiotherapy or brachytherapy as primary treatment.
Methods and Materials: 118 patients were included for this retrospective analysis. Of these, 45 were receiving androgen deprivation therapy (ADT) within at least 6 months prior to the PET/CT. The detection rates were stratified by PSA. The influence of primary Gleason score (GS) and ADT was assessed. Correlations between standardised uptake values (SUV) and GS or ADT in patients with positive findings were analysed.
Results: 90.7% (107/118) patients showed pathological findings indicative for tumour recurrence in ^{68}Ga-PSMA PET/CT. The detection rates were 81.8% (36/44), 95.3% (41/43) and 96.8% (30/31) for PSA of 2 to <5, 5 to <10 and ≥10 ng/mL, respectively. The detection rate was significantly higher in patients with ADT (97.7%) vs without ADT (86.3%, p=0.0381), but independent from primary GS ≥8 (92.0%) vs ≤7 (90.2%, p=0.6346). SUVmax and SUVmean were significantly higher in patients with ADT (p=0.0025 and 0.0044, respectively) and a clear trend to higher values was observed for patients with GS ≥8 (p=0.0502 and 0.0514, respectively).
Conclusion: ^{68}Ga-PSMA PET/CT demonstrates high detection rates in patients with biochemical recurrence of prostate cancer after primary radiation therapy. The detection rate positively correlated to increasing PSA as well as concomitant ADT. ^{68}Ga-PSMA PET/CT enables discrimination of local vs systemic disease and thus might have a crucial impact on further clinical management.

B-0797 11:43

Improved detection of transosseous meningiomas using 68Ga-DOTATATE PET-CT compared to MRI

W.G. Kunz, L. Jungblut, P.M. Kazmierczak, A. Rominger, N.L. Albert, M.F. Reiser, C.C. Cyran; *Munich/DE (wolfgang.kunz@med.lmu.de)*

Purpose: To analyse the diagnostic performance of 68Ga-DOTATATE PET-CT and contrast-enhanced MRI for detection of transosseous extension of intracranial meningiomas and to find associations with imaging parameters.
Methods and Materials: In this retrospective study, subjects were selected from a cohort of 325 consecutive patients who underwent 68Ga-DOTATATE PET-CT of the head for evaluation of confirmed or suspected meningioma. Inclusion criteria were (1) MR imaging within 1 month of either pre- or postoperative matching PET-CT imaging, and (2) as standard of reference pathology-confirmed meningioma diagnosis with inclusion or exclusion of transosseous extension. Imaging was independently analyzed by two readers with respect to osseous involvement, absolute tracer uptake measured as SUVmax, volume of meningioma and surrounding edema. Chi-square, Mann-Whitney U or exact McNemar's tests as well as receiver operating characteristics (ROC) analyses were performed to compare variables and diagnostic test performance.
Results: Eighty-two patients fulfilled the inclusion criteria. Patients with transosseous meningiomas (n=67) showed significantly larger lesions (median 10ml vs 3ml, p=0.002) and significantly higher SUVmax (median 14 vs 8, p=0.032) compared to extraosseous meningiomas. 68Ga-DOTATATE PET-CT in comparison to MRI performed at a considerably higher sensitivity (98.5% vs 55.2%) while maintaining high specificity (86.7% vs 100.0%); statistically significant differences between the tests were observed (p<0.001). In ROC analysis, PET-CT assessment performed best (AUC: 0.933), followed by MRI assessment (0.866), meningioma volume (0.765) and SUVmax (0.680) while surrounding oedema added no valuable information (0.483).
Conclusion: 68Ga-DOTATATE PET-CT enables improved detection of the transosseous extension of intracranial meningiomas compared to MRI.

B-0798 11:51

Development of the helmet-neck PET prototype for high sensitivity brain imaging

H. Tashima[1], E. Yoshida[1], Y. Iwao[1], H. Wakizaka[1], Y. Takado[1], C. Seki[1], T. Suhara[1], T. Yamashita[2], T. Yamaya[1]; [1]*Chiba/JP*, [2]*Tokyo/JP*
(tashima.hideaki@qst.go.jp)

Purpose: There is an emerging demand for dedicated brain PET for the study and diagnosis of neurological disorders such as dementia. We have proposed a helmet PET geometry with add-on detector for high sensitivity, high resolution and low cost brain PET. Our first prototype had an add-on detector at the chin position (helmet-chin PET). However, the gantry design gave oppressive feeling to the patient and the movement of the chin detector was inconvenient for the patient set-up. On the other hand, our previous simulation showed that add-on detectors covering the neck has equivalent effect. In this study, therefore, we developed a helmet-neck PET, which has additional detectors at the neck.
Methods and Materials: We developed the helmet PET prototype using 54 four-layer depth-of-interaction detectors with 16×16×4 array of 2.8×2.8×7.5 mm^3 GSO crystals. In the prototype, 47 detectors were arrangement in a hemisphere, and seven detectors were placed as the add-on detector. We compared the helmet-chin PET and the helmet-neck PET regarding the effects of the add-on detectors for increasing the sensitivity.
Results: The sensitivity measured with a hemispherical phantom for the brain region was increased by 12% in the helmet-chin PET and by 19% in the helmet-neck PET compared with the geometry without add-on detectors. This is because the arrangement of the detector at chin required larger margin for designing gantry, in which detector position became farther than the case of neck.
Conclusion: The helmet-neck PET has promising performance for high sensitivity brain imaging and improved convenience for patient studies.
Author Disclosures:
H. Tashima: Grant Recipient; Research Grant from ATOX Co. Ltd.. Patent Holder; U.S. and Japanese Patent for the helmet PET. **E. Yoshida:** Grant Recipient; Research Grant from ATOX Co. Ltd. **Y. Iwao:** Grant Recipient; Research Grant from ATOX Co. Ltd.. **T. Yamaya:** Grant Recipient; Research Grant from ATOX Co. Ltd.. Patent Holder; U.S. and Japanese Patent for the helmet PET.

10:30 - 12:00 **Room F2**

Emergency Imaging

SS 1017

CT virtopsy and other "hot" topics

Moderators:
F.H. Berger; Toronto, ON/CA
F. Macri; Nîmes/FR

K-18 10:30

Keynote lecture

F.H. Berger; *Toronto, ON/CA*

B-0799 10:39

Errors in out of hours radiology reports due to telephone interruptions

G.P. Tarr, R. Mitchell; *Auckland/NZ (greg.tarr@otago.ac.nz)*

Purpose: Errors in out of hours radiology reports may contribute to adverse outcomes in emergency patients. Radiology trainees are often required to report in non-ideal environments with high acuity patients and frequent interruptions. While a number of studies have examined rates of reporting error, there is a paucity of data on factors contributing to error. The aim of this study was to assess whether phone call interruptions while reporting raised the risk of errors.
Methods and Materials: Institutional ethical approval was obtained with waiver for informed consent. Patients undergoing out of hours CT at our institution between May 2015 and March 2016 were included. Time stamps for the on-call radiology phone were obtained. Reporting errors were identified by the presence of a standard proforma inserted into each report when the responsible consultant judged that a clinically significant discrepancy had occurred between the preliminary and final reports. Statistical analysis was performed with Stata 13.0.
Results: A total of 4738 CTs with 260 errors (5.5%, 95% CI: 4.8 to 6.1%) were included. There were 14458 phone calls, with a median of 2 phone calls (IQR 1 to 6) received per during the creation of each report. There was no association between phone call interruptions and error rate. Errors were more frequent in junior registrar reports and in reports created later in shifts.
Conclusion: Phone call interruptions were not associated with increased risk for discrepancies in preliminary reports. Inexperience and fatigue may be more important risk factors.

B-0800 10:47

Calculation of body weight by means of CT using dose modulation

D. Gascho, L. Ganzoni, M.J. Thali, T.D. Ruder; *Zurich/CH*
(dominic.gascho@irm.uzh.ch)

Purpose: Documentation of the visual appearance is required in any forensic report, including body weight of the decedent. Due to a failure of our in-house, floor-embedded weighting scale, we developed a method for body weight estimation based on post-mortem computed tomography (PMCT) using automated dose modulation. The aim of this study was to evaluate the correlation between effective milliampere second (mAs^{eff}) values, based on automatic exposure control, and body weight for the purpose of determining body weight just by the means of PMCT.
Methods and Materials: The study population comprised 349 (114 female, 234 male) decedents. In a retrospective evaluation the PMCT mAs^{eff} values of the automatically provided patient protocol were correlated with the actual body weight measurements (as performed by a calibrated weighting scale). Correlations were calculated for men/women both separately and together as well as with regard to the post-mortem interval (PMI).
Results: There was an excellent correlation between mAs^{eff} values and body weight for both men and women with a PMI of less than 4 days. Correlation significantly decreased in decomposed cadavers (PMI larger or equal 4 days). Based on the data a formula to calculate individual body weight based on mAs^{eff} values was developed.
Conclusion: This study offers a reliable mean to rapidly determine the body weight of non-decomposed human cadavers. The method shows potential for further application areas in clinical radiology, e.g. in paediatric radiology for weight-based application of contrast media for CT in the emergency room.

B-0801 10:55

The role of ultrasound screening in combat surgical trauma

E. Konjukhova, I. Aseeva, V. Trojan; *Moscow/RU*
(executive-committee@yandex.ru)

Purpose: Analyse complex ultrasound analysis of battle-scarred persons with the object to the early effective medical care at several kinds of surgical trauma during early examination phase and in temporal treatment.
Methods and Materials: It was examined totally 107 (100%) patients with combat trauma in different anatomical areas.
Results: The transabdominal analysis with intraoperative evidence elicited free water at 35 (33%) of patients, the spleen rupture at 2 (2%), the liver rupture at 1 (1%) patient, the kidneys subcapsular rupture at 2 (2%). During the low limbs veins US analysis, the thrombosis was elicited: the thrombus with floating apex in popliteal vein -1 (1%). The several localisation soft tissue haematomas were detected at 86 (80%) patients. The hydrothorax was elicited at 80 (75%) patients: the signs of pneumonia were suspected at 23 (21%) of patients, the lung atelectasis were suspected at 7 (6%) patients, all with later confirmation during the roentgenologic examination. In the same way, the fractures of one or more than one ribs with the later confirmation during the x-ray examination were diagnosed. The foreign bodies (debris) in soft tissue of buttock area and low limbs were found at 25 (23%) patients with confirmation during the CT examination.
Conclusion: It can concluded on the basis of our analysis that as a result of the timely performed US analysis at the screening phase, the definite and quick patient evacuation by designation with the object to the quality medical care under the armed conflicts and war conditions is possible to performing.

B-0802 11:03

MR perfusion to identify candidates more suitable to endovascular recanalisation therapy than iv-tPA in MCA occlusion

T. Mori, Y. Tanno, S. Kasakura, K. Yoshioka, N. Nakai; *Kamakura/JP*
(moritkama@icloud.com)

Purpose: To investigate if MR perfusion (MRp) can identify candidates suitable to endovascular therapy (EnT) rather than iv-tPA alone.
Methods and Materials: We included patients 1) admitted between 2005 and 2015 within 3.5 hours, 2) with MCA occlusion, 3) with DWI-ASPECTS of 6 or more, 4) with CBF-grade of 2 or 3 and 5) treated with iv-tPA alone. We defined proximal M1 occlusion as MCA-grade1, distal M1 occlusion as MCA-grade2, and M2 occlusion as MCA-grade3 and no occlusion on MRA as MCA-grade4. At the bilateral MCA territories, we compared time intensity curves (TIC) of MRp in the affected side (a) with contralateral side (c), defined TICa divided as TICc as CBF% and CBF% of less than 0.2 as CBF-grade1, CBF% of 0.2 or more and less than 0.7 as CBF-grade2 and CBF% of 0.7 or more as CBF-grade3. We evaluated relations among MCA-grade, CBF-grade and favorable clinical outcome (fCO) of mRS 0-2 at 3 months.

Results: Thirty-four patients were analyzed. Nine patients in MCA-grade1, 9 in MCA-grade2, 15 in MCA-grade3 and 1 in MCA-grade4. Twenty-three patients in CBF-grade2 and 11 in CBF-grade3. Only 2 patients (22%) obtained fCO in MCA-grade1. In MCA-grade2, 4 (57%) of 7 patients in CB-grade2 obtained fCO and 2 (100%) of 2 in CBF-grade3 obtained fCO. In MCA-grade3,6 (67%) of 9 in CBF-grade2 obtained fCO and 5 (83%) of 6 in CBF-grade3 obtained fCO. One patient in MCA-grade4 obtained fCO.
Conclusion: Patients with MCA-grade1, MCA-grade2 and CBF-grade2, or MCA-grade3 and CBF-grade 2 were candidates for EnT.

B-0803 11:11

Current imaging practice for potentially thrombolysable ischaemic strokes in NHS Lothian with the introduction of a thrombectomy service

D.A.J. Smith, G.J. McNeill; *Edinburgh/UK (derekxii@gmail.com)*

Purpose: Evaluation of current imaging practice for potentially thrombolysable ischaemic strokes and impact of a new CT angiography (CTA) policy identifying patients who may benefit from endovascular thrombectomy.
Methods and Materials: Retrospective review over 10 consecutive weeks from October 2015, and a further 10 weeks following new CTA/thrombectomy criteria in June 2016. Analysis of cases from the major emergency department in NHS Lothian, with primary outcomes including number of thrombolysis requests, imaging findings and CTAs performed anticipating thrombectomy. Secondary outcomes were inclusion of onset-time and NIH stroke scale (NIHSS) score in CT requests, radiologists' reporting time and proportion of cases progressing to thrombolysis/thrombectomy.
Results: 87 potential thrombolysis requests were analysed in the initial group. 74 did not demonstrate contraindication to thrombolysis (haemorrhage or tumour), 13 (18%) underwent thrombolysis. Five CTAs were performed, with significant arterial occlusion on three. One patient progressed to thrombectomy. 52 (60%) requests included a time-of-onset, only one with NIHSS score. Radiologists issued 59 (67%) of reports in under 1 hour.
Following the thrombectomy policy, 110 requests were analysed. Nine demonstrated imaging contraindications, with 22 (20%) receiving thrombolysis. Three CTAs were performed, but no treatable occlusions were identified. Two other patients were considered for thrombectomy, but CTA was not performed. No requests recorded NIHSS score, 83 (75%) included onset-time. 78 (71%) reports were issued in under 1 hour.
Conclusion: Increased awareness of thrombectomy criteria among referring teams and radiologists, with inclusion of onset-time and NIHSS in initial imaging requests, could aid triage and identification of thrombectomy candidates.

B-0804 11:19

Discrepancies between preliminary resident and finalised consultant reviewed CT brain reports

A.H. Rajaram; *Bangalore/IN (akashrajaram@gmail.com)*

Purpose: To determine the rate of discrepancy between preliminary resident and finalised consultant CT brain reports.
Methods and Materials: One radiologist retrospectively reviewed all the preliminary and final CT brain reports of patients presenting with acute neurological symptoms from March 2015 to February 2016. Of the 1543 scans, 1283 had a preliminary resident report followed by a consultant report and were evaluated for minor or major discrepancy. Major discrepancy was considered when the primary diagnosis was changed between the preliminary and final report. Minor discrepancy was considered when any other amendment was made between the preliminary and final report that did not affect the overall diagnosis.
Results: No discrepancy was seen in the final report of 161/1283 (12.54%) patients. 42 (3.27%) had a major discrepancy, out of which 19 (45.23%) were false negative and 11 (26.19%) were false positive for acute infarct. Others were false negative for contusion (n=4), subdural haemorrhage (n=3), space occupying lesion (n=3) and diffuse cerebral oedema (n=2). Major discrepancies were found in 2nd (n=20) and 3rd (n=22) year resident reports. There was no correlation between resident level of training and rate of discrepancy. Third year residents had an overall higher error rate. Second year residents had significantly more false positive misinterpretations ($p<0.05$). Common sites for misinterpretation were basi-frontal lobes and posterior fossa. Discrepancy rate was highest between 5:00 p.m. and 9:00 p.m.
Conclusion: There is a low discrepancy rate between preliminary resident and final reports. However, the resident reports may be further improved in certain areas.

B-0805 11:27

Validity of head CT examinations in the emergency department

L. Skrule, A. Tarasova, D. Sosars, A. Lice, M. Radzina; *Riga/LV (ligitaskrule@gmail.com)*

Purpose: To evaluate validity of head computed tomography (CT) examinations, their impact on patient radiation exposure risk and triage management.
Methods and Materials: This cross-sectional retrospective study enrolled patients with head CT scan at the emergency department, data were assessed within one calendar month from clinical university hospital. Computed tomography scan indications and results were analysed according to the diagnostic hypothesis in admission documents, CT request forms in combination with patient clinical symptoms and history.
Results: A total of 647 consecutive CT procedures were performed in the emergency department. There were 343 (53.01%) male and 304 (46.98%) female, mean age 54 years (range 18-94). Pathology was proved in 226 (34.93%) patients (symptomatic 101/226 patients), with high correlation between referral and final diagnosis only in symptomatic patients with trauma and cerebrovascular disorders ($p=0.0001$). In asymptomatic group 46/144 (31.9%) patients had pathological CT findings (11 cerebrovascular, 3 tumours, 32 trauma, 26 other entities, e.g. arteriovenous malformation and intracranial aneurysm) with no statistically significant OR differences among patients with or without symptoms. Mean radiation exposure for all scanned patients were DLP 1186 mGy*cm (IQ range 572-1275) with estimated effective dose 2.60 mSv.
Conclusion: Considering high rate of emergency head CT scans with normal findings in symptomatic patients and unnecessary radiation exposure, the minor rate of asymptomatic patients with pathology, we need additional clinical criteria for validation of this examination, omitting patients with trauma and cerebrovascular disorders.

B-0806 11:35

Syncope, vertigo and seizure: what is the utility of imaging in the emergency department?

K. Ozturk, C. Bilgin, E. Ozturk, M. Parlak; *Bursa/TR (keremov54@hotmail.com)*

Purpose: Our purpose was to evaluate abnormal findings on cranial CT or MR in patients admitted to the emergency department with either one or in combination of symptoms such as vertigo, syncope or seizure.
Methods and Materials: The database were retrospectively reviewed for all patients underwent cranial CT or MRI, having the symptoms of syncope, seizure or vertigo. Patients were included only if they were from the emergency department and excluded if were under 18 years of age, had known recent intracranial pathology, having a history of trauma. Primary outcome was assumed as abnormal head CT or MRI including intracranial haemorrhage, infarction, acute or subacute stroke and newly diagnosed brain mass. Concurrent clinical symptoms and age were evaluated with logistic regression analysis, important parameters to indicate pathology in either CT or MR scan with either symptoms were investigated.
Results: Total of 24210 head CT and 4502 cranial MRI were searched, 2537 CT and 655 MRI were found to be eligible for this study. 1230 (38%) syncope, 1413 (44%) vertigo and 549 (18%) seizure were identified. Of those in head CT scan, only 60 (2.3%) patients have had clinically significant pathology requiring admission to the hospital. However, in 43 (6.5%) of MRI studies significant abnormalities has been noted.
Conclusion: Our study indicates that most patients presenting with vertigo, syncope or seizure may not take advantage of head CT and MRI. Abnormal findings related to the syncope were observed in only 37 patient, vertigo in 42 patients and seizure in 24 patients.
Author Disclosures:
K. Ozturk: Author; Kerem Ozturk. Founder; Kerem Ozturk. Investigator; Kerem Ozturk. Owner; Kerem Ozturk. Patent Holder; Kerem Ozturk. Speaker; Kerem Ozturk. **C. Bilgin:** Employee; Cem Bilgin. Equipment Support Recipient; Cem Bilgin. **E. Ozturk:** Author; Esra Soylu Ozturk. CEO; Esra Soylu Ozturk. Employee; Esra Soylu Ozturk. Investigator; Esra Soylu Ozturk. Research/Grant Support; Esra Soylu Ozturk. Shareholder; Esra Soylu Ozturk. **M. Parlak:** Advisory Board; Mufit Parlak. Board Member; Mufit Parlak. Grant Recipient; Mufit Parlak. Research/Grant Support; Mufit Parlak.

B-0807 11:43

The role of radiology in body identification and in determination of the cause of death in shipwrecked refugee casualties

G. Lo Re[1], A. Argo[1], S. Zerbo[1], S. Salerno[1], D. Mazzarelli[2], M. Midiri[1], C. Cattaneo[2], R. Lagalla[1]; [1]*Palermo/IT*, [2]*Milan/IT (giuseppe.lore12@gmail.com)*

Purpose: In April 2015 an overcrowded boat with an estimated 700 migrants drowned off the Libyan coasts. Italian navy recovered the boat and thanks to a "Memorandum of Understanding" between the Ministry of Interiors, the Ministry of Education and the Commissioner's-Office-for-Missing-Persons, post mortem

activities aimed at the identification of the victims was signed. Cadavers were recovered and kept inside body bags in refrigerated trucks. Forensic pathologists and anthropologists from several Italian Universities, were recruited along with the Police Forces for this activity. Radiologists were asked to cooperated in this activity in order to facilitate identification and give a proper burial to these migrants.
Methods and Materials: In July 2016, 149 body bags were scanned before conventional autopsy through a mobile 8-channel-CT placed at the NATO's Melilli base in Sicily, next to the tents where forensic studies were being performed. Images were studied according to the guidelines provided by the Internal Ministry through a workstation with MPR, MIP and 3D-VR reconstructions.
Results: Study of number, type, congruency, calluses, fractures and anthropometric measurements of bones, teeth, growth-plate cartilages and internal/external genitals helped in sex and age assessment. Foreign objects were encountered in many cases: some of them were potentially dangerous for the coroners, while others were useful for body identification.
Conclusion: Our data clearly demonstrate the pivotal role of radiology in mass disasters and when anthropological identification is required. We also demonstrate that radiological assessment in mass disasters is feasible, but full cooperation between different medical and legal professional figures is advisable.

B-0808 11:51

Thoraco-abdominal injuries of manual and device-assisted resuscitation on postmortem CT
A.R. Bayat, D.G.H. Bosboom, W.M. Prokop, M. Brouwer, W.M. Klein;
Nijmegen/NL (alireza.bayat@radboudumc.nl)

Purpose: Resuscitation has been associated with different kind of injuries, such as fractures of sternum and ribs. Device-assisted resuscitation seems to use more power than manual CPR. We compared fractures and haemorrhages of cadavers who died after either manual or device-assisted resuscitation.
Methods and Materials: We retrospectively included cadavers who had undergone total body postmortem CT (PMCT) if aged >18 years and natural cause of death, and divided into 3 groups: no CPR versus manual CPR versus device-assisted CPR (AutoPulse). The resuscitation injuries scored at PMCT were: rib fracture anterior or posterior, sternal and spine fractures, pneumothorax, pleural haemorrhages (HU>25), pleural fluids in mm (HU<25), haemoperitoneum (HU>25), retroperitoneal haemorrhages (HU>25), lacerations of the abdominal organs (surrounding fluid (HU>25) and induration of the epigastric fat. Univariate analyses with χ^2 and Mann-Whitney U tests were performed.
Results: 93 Cadavers with PMCT were included: 26 after device-assisted CPR, 23 manual CPR and 44 no CPR. The cadavers without CPR showed no injuries. Significantly more rib fractures (20 vs 6, p<0.001) and especially posterior were identified in the device-assisted CPR cadavers than in the manual CPR cadavers (12 vs 9, p=0.016). Other injuries including haematothorax, fractured vertebra and liver laceration were not different between the CPR groups.
Conclusion: Both manual and device-assisted CPR result in several serious injuries. Posterior rib fractures are significantly found more after device-assisted CPR. Prospective study is needed to investigate the effective and traumatic results of manual versus device-assisted CPR.

10:30 - 12:00 **Room D**

Musculoskeletal

SS 1010

Shoulder and wrist

Moderators:
P. Omoumi; Lausanne/CH
C.W.A. Pfirrmann; Zurich/CH

B-0809 10:30

Subtendinous extensor carpi ulnaris (ECU) bone marrow edema as a predictor of peripheral triangular fibrocartilage tears and ECU tendon pathology
M.T. Nevalainen[1], A.C. Zoga[2], W.B. Morrison[2], J.B. Roedl[2]; [1]*Oulu/FI*, [2]*Philadelphia, PA/US (mikaneva@paju.oulu.fi)*

Purpose: To determine the association between peripheral triangular fibrocartilage (TFC) tears and extensor carpi ulnaris (ECU) pathology and to evaluate subtendinous ECU bone marrow edema (BME) at the styloid process of the ulna as a diagnostic marker for TFC and ECU pathology on MRI.
Methods and Materials: The presence of TFC tears, ECU pathology (tenosynovitis, tendinosis, tears and subluxation) and subtendinous ECU BME were determined on MRI and correlated with arthroscopy. These findings were assessed in a study group of 64 patients with peripheral TFC tears and in two age- and sex-matched control groups: 64 patients with central TFC tears, and 64 patients without TFC tears (all proven with arthroscopy).
Results: Among the 64 patients without TFC tears on arthroscopy, 1.2% (8/60) had ECU pathology (all with mild ECU tendinosis, no ECU tenosynovitis, no ECU subluxation) and 0% (0/60) had subtendinous ECU BME. In the 64 patients with central TFC tears on arthroscopy, 9 (1.4%) had ECU pathology and 0% (0/60) had subtendinous ECU BME. Among the 64 patients with peripheral TFC tears, 46/60 (78%) had ECU pathology and 34/60 (70%) had subtendinous ECU BME. All 34 patients with subtendinous ECU BME (100% specificity) had both a peripheral TFC tear and ECU pathology (combined injury). 45/46 of patients with a combined injury had subtendinous BME yielding a 98% sensitivity.
Conclusion: Peripheral TFC tears are highly associated with ECU pathology. Subtendinous ECU BME on MRI indicates a combined peripheral TFC and ECU injury with 100% specificity and 98% sensitivity.

B-0810 10:38

The posterior radioscaphoid angle is related to the severity of degenerative cartilage damage of the wrist in patients with scaphoid nonunion
C.M. Phan, A. Miquel, C. Pradel, C. Quach, Y. Menu, M.D. Crema; *Paris/FR (catherine.phan@aphp.fr)*

Purpose: To determine whether the posterior radioscaphoid angle evaluated on CT-arthrography, reflecting posterior displacement of the distal pole in cases of scaphoid nonunion, is related to the cartilage damage severity of the wrist.
Methods and Materials: CT-arthrography images from 35 patients with scaphoid nonunion (cases) and from 35 patients without fractures or ligament injury (controls) were retrospectively reviewed by one experienced musculoskeletal radiologist. Cartilage morphology of the wrist including both radiocarpal and midcarpal joints was graded from 0 to 6 using a modified WORMS system. Scaphoid nonunion advanced collapse (SNAC) was graded from 0 to 3. Five carpal angles were assessed: radio-scaphoid (RS), posterior radioscaphoid (PRS), radio-lunate (RL), scapho-lunate (SL), and capito-lunate (CL). Independent sample T test was performed to test if carpal angles were able to discriminate cases from controls, as well as the different SNAC grades. Pearson correlation analysis was used to assess the correlations between carpal angles and the sum of WORMS scores (severity of the global cartilage damage).
Results: All carpal angles were able to discriminate between cases and controls (p<0.001). Only the PRS angle was able to discriminate between radiocarpal (SNAC 1 and 2) and midcarpal (SNAC 3) involvement (116.1±12.8 vs. 127.9±13.6; p=0.015). The PRS angle (0.70) better correlated with the severity of global cartilage damage than did the SL (0.64) and RS (0.46) angles (p <0.0001).
Conclusion: The PRS angle was able to discriminate between radiocarpal and midcarpal involvement (SNAC) and demonstrated better correlation with global cartilage damage severity in patients with scaphoid nonunion.

B-0811 10:46

Diffusion tensor imaging in carpal tunnel syndrome (CTS): is there any correlation with ultrasound?
M.M.H. Abd Ellah, C. Kremser, W. Jaschke, E. Gizewski, A.S. Klauser;
Innsbruck/AT (dr_m_hamdy2006@hotmail.com)

Purpose: To study the correlation between quantitative analysis of diffusion tensor imaging (DTI) of median nerve (MN) and CTS severity determined by delta cross-sectional area measurement (Δ-CSA).
Methods and Materials: Thirty-seven CTS patients (25 females and 12 males) [mean age 58.11± Std] were examined using a 3T MR scanner (Skyra, Erlangen, Germany). The examination protocol included diffusion tensor imaging (DTI) in addition to routine sequences (coronal T1 VIBE, axial T1 and T2 TIRM) for anatomical correlation. All patients underwent ultrasound examination using 5-18 MHz (HI Vision Preirus, Hitachi Aloka Medical, Ltd, Tokyo) for diagnosis of CTS. Δ-CSA measurement represented the difference in CSA between MN at distal forearm and carpal tunnel. Patients were divided into three groups based on Δ-CSA (mild, moderate and severe). Mean apparent diffusion coefficient (ADC) and fractional anisotropy (FA) were correlated to Δ-CSA.
Results: Patients were classified as follows (mild = 8, moderate = 9 and severe = 25). Mean ADC and FA values were $1.482x10^{-3}$ and $0.541x10^{-3,}$ respectively. A significant mild to moderate correlation was shown between FA and Δ-CSA (r=0.311, *P*=0.044), however, no correlation between ADC and Δ-CSA. Mean FA values were 602.4, 560.2 and 523 for mild, moderate and severe groups, respectively, with a significant difference between severe and mild groups (*P*=0.027).

Conclusion: Quantitative analysis of diffusion using ADC and FA proved feasible with a mild to moderate correlation between FA and severity grade of CTS determined by Δ-CSA, with a significant difference between severe and mild groups.

B-0812 10:54

Comparison of T2 BLADE PD and isotropic three-dimensional fast spin echo cube (3D T2 SPACE) sequences with conventional protocols in wrist lesions using 3T MRI

H. Soroush, H. Naghibi, M. Shakiba, F. Faeghi, H. Hashemi; *Tehran/IR (SOROUSH_HEDAYAT@YAHOO.COM)*

Purpose: Magnetic Resonance Imaging (MRI) of wrist is a useful diagnostic method for different wrist structures, however the efficacy could be optimized. In this study we compared new protocols of 3D T2SPACE, PD BLADE and T2 BLADE with the conventional protocols, including T2 FSE, PD FSE and T1 FSE for wrist imaging.
Methods and Materials: Twenty patients (12 men) with history of wrist trauma or suspected wrist lesions were enrolled. All protocols were carried out on all patients; then quality of each protocols was assessed by two musculoskeletal radiologists and one hand surgeon.In addition, signal to noise ratio (SNR) and contrast to noise ratio (CNR) in specific regions of interests (ROIs) [including TFCC,cartilage and bone] were measured. At the end, all of qualitative and quantitative assessments were compared between protocols.
Results: SNR of cartilage, TFCC on 3D T2SPACE and T1 FSE was better than other sequences (P<0.001). SNR of bone on PD BLADE was significantly higher than that of conventional protocols (P<0.001). PD BLADE images showed significantly higher bone-cartilage CNR and bone-TFCC CNR (P<0.001 to P<0.001). CNR of cartilage-TFCC on T1 FSE was better than other sequences, but no statistically significant difference was seen. Qualitative assessment showed better wrist imaging in SPACE and BLADE protocols in comparison to conventional sequences (P<0.001).
Conclusion: PD BLADE, 3D T2SPACE and T2 BLADE MRI protocols were superior compared to conventional sequences in wrist imaging. High-SNR and CNR in SPACE and BLADE MR sequences could be a promising method to diagnose wrist lesion.

B-0813 11:02

Injuries of the finger in rock climber

F. Schellhammer[1], T. Schwarz[2], A. Boberg[3], K.-A. Riel[4], A. Vantorre[3]; [1]*Cologne/DE*, [2]*Gelnhausen/DE*, [3]*Frankfurt a. Main/DE*, [4]*Groß-Gerau/DE (fschellhammer@severinskloesterchen.de)*

Purpose: Indoor rock climbing is gaining increasing popularity. Thus the incidence of climbing related injuries is rising. About 40% of these are to the fingers. Out of the entirety of injuries of the upper extremity, we demonstrate lesions of the finger which were evident in a network for rock climbing medicine.
Methods and Materials: Between 05/2012 and 06/2016, a total of 227 finger injuries were seen. Following clinical examination, MR-imaging was performed. In case of a lesion to the flexor-tendon-pulley-system, a 4-step grading system was used.
Results: MR-imaging disclosed characteristic dilatation and thickening of the interdigital joint capsule in almost all cases. Stress fractures were evident in 19 cases (adult fracture: 1, physeal fracture: 18). Capsular lesions were seen in 6 cases (capsular rupture: 4, plantar plate rupture: 2). Lesions of the flexor tendon were found in 39 cases. 1 lumbrical shift syndrome and 1 calcified stenosis of the A2-annular pulley were disclosed. Lesions of the flexor-tendon-pulley-system were seen in 162 cases (GI: n=22, GII: n=103, GIII: n=46, GIV: n=1).
Conclusion: Knowledge of the anatomy and the biomechanics is important to differentiate physiologic chances from true injuries. MR-imaging is important for classification of GII lesions of the flexor-tendon-pulley-system, which are the most common and of high sport physiologic importance. Furthermore, MR-imaging allows distinguishing complex lesions, which may require surgical repair.

B-0814 11:10

Impact of delimitation on the healing of rotator cuff injury after a tension band arthroscopic repair

C. Dekimpe, O. Andreani, C. Ranc, N. Amoretti, P. Boileau; *Nice/FR (dekimpe.chloe@gmail.com)*

Purpose: Arthroscopic repair of transfixing rotator cuff lesions using the « tension band » technique gives good results. The impact of tendon delamination is less known than the degree of tendon retraction on the anatomical result. The aim of our study was to assess the impact of delamination on tendon healing after arthroscopic cuff repair made with the « tension band » technique.
Methods and Materials: 117 patients with a transfixing lesion of the rotator cuff operated thanks to the « tension band » technique, over a 5-year period, were clinically and anatomically evaluated. The delaminated or not status of the rotator cuff injury and the stage of retraction was set intraoperatively. All patients had a 6 months minimum follow-up. Tendon healing was evaluated by ultrasound and functional outcome using the adjusted Constant score.
Results: 80 patients had a non-delaminated rotator cuff injury and 37 a delaminated one. The healing rate was 78% and 57% respectively (p = 0.0287). Patients were comparable preoperatively in terms of age, sex, BMI, Subjective Shoulder Value, strength and adjusted Constant score. There were no significant differences in the subgroup analysis for the stage 1(77% versus 75%), and stage 2 (75% versus 60%) retracted lésions. There was a significant difference for the stage 3 retracted lesions (83% versus 45%; p <0.05).
Conclusion: Delamination appears as a key factor in the healing of arthroscopic repair of rotator cuff lesions. Ultrasound was a useful tool to assess the anatomical result of the surgery.

B-0815 11:18

Combined quantitative MR imaging assessment of the rotator cuff integrity at 3.0T by multi-echo Dixon-based fat quantification and diffusion tensor imaging

Q.M. Hamie, L. Issler, E. Ulbrich, D. Nanz, N.A. Farshad-Amacker, R. Guggenberger; *Zurich/CH (mustafa.hamie@usz.ch)*

Purpose: To establish quantitatively normative values of fractional fat content (FF%) and diffusion tensor imaging (DTI) parameters (fractional anisotropy [FA] and apparent diffusion coefficient [ADC]) of normal rotator cuff (RC)-muscles.
Methods and Materials: 40 patients underwent standard direct MR arthrography of the shoulder including 3D multi-echo Dixon and 3D echo-planar DTI sequences (15 gradient encoding directions, b-value 600 s/mm^2) at equal spatial resolution. RC-muscles and tendons were qualitatively assessed. Goutallier gradings >1 and tendon tears were excluded from further analysis. FF%, FA and ADC were evaluated quantitatively by region-of-interest (ROI) measurements at Y-position of the scapula by two independent radiologists. Intraclass correlation coefficients (ICC) were calculated. Pearson correlation, Student's t-test, Chi-Square test and one-way ANOVA testing were performed to correlate measurements with age and gender and to compare different RC muscles and two Goutallier groups (0 and 1).
Results: Interreader agreements for quantitative measurements were perfect (ICC: 0.90-0.99). Goutallier 0 muscles showed significant positive correlations of FF% and FA with age (R=0.269, p<0.01 and 0.206, p<0.05) as well as FF% with FA (R=0.351, p<0.001). Significant differences were seen among different RC muscles in Goutallier group 0 for FF% and ADC (p=0.011 and p=0.001) but not in Goutallier group 1 (p>0.05). ADC is significantly different between Goutallier groups for all RC muscles (p<0.05).
Conclusion: Quantitative MR assessment of RC-muscle integrity delivers high interreader agreement. In normal RC muscles FF% and FA increase significantly with age. ADC allows best to differentiate between Goutallier group 0 and 1 in all RC-muscles.

B-0816 11:26

Preoperative MR imaging characteristics of full-thickness rotator cuff tendon tears do not correlate with changes in clinical outcome scores following repair

P.C. Thurlow, R. Kijowski; *Madison, WI/US (pthurlow@uwhealth.org)*

Purpose: The purpose of this study was to evaluate whether preoperative MR imaging features of full-thickness rotator cuff tears correlated with changes in subjective and functional outcomes following surgical repair.
Methods and Materials: This retrospective study included 208 patients who underwent conventional shoulder MRI examination within 12 months of full-thickness rotator cuff tendon tear repair and performed preoperative and 12 month postoperative clinical outcome scoring. Clinical outcome scoring systems utilised were SF-12, QuickDASH, and SANE. A musculoskeletal radiologist evaluated all MRI for tear size, tendon retraction, tendinosis, atrophy, fatty infiltration, glenohumeral cartilage loss, biceps tendinosis or tear, and labral tear. Pearson correlation coefficients, Student's t-test, and one-way ANOVA was used to analyse for statistically significant correlation between clinical outcome score changes and MR imaging features.
Results: Overall, there were statistically significant postoperative improvements in SANE scores, QuickDASH scores, and bodily pain, physical functioning, and physical health composite scale scores from the SF-12 (p<0.01). Female patients demonstrated greater improvement in QuickDASH scores than did male patients (p<0.05). Average size of the tears measured 2.6 cm in anteroposterior dimension with an average of 2.3 cm of retraction. There was no statistically significant correlation between any of the measured MR imaging characteristics and postoperative changes in SF-12, QuickDASH, or SANE clinical outcome scores.
Conclusion: MR imaging features of full-thickness rotator cuff tendon tears do not correlate with changes in clinical outcome scores following repair of full thickness rotator cuff tears.

B-0817 11:34

Associating MRI findings of adhesive capsulitis with the clinical orthopedic exam

C.K. Ho, E.S. Gould, M. Huang, M. Badalamente, J. Yang, D. Yin;
Stony Brook, NY/US (corey.ho@stonybrookmedicine.edu)

Purpose: The purpose of our study is to investigate the association of MRI findings of adhesive capsulitis (AC) with the clinical examination.
Methods and Materials: Following IRB approval, 256 subjects with untreated, unilateral idiopathic AC for 3 to 12 months were enrolled in a clinical trial for treatment and all received shoulder MRI. Clinical evaluation included calculation of American Shoulder and Elbow Surgeons Shoulder function and pain scores, and multi-directional shoulder range of motion (ROM). Two radiologists blindly reviewed the studies for AC MR Characteristics. The most prevalent findings were graded using a 4-point Likert scale (normal, mild, moderate, and severe), including coracohumeral ligament thickening, capsular thickening at axillary pouch, edema within axillary pouch, and synovitis along superior border of subscapularis tendon, and overall assessment of AC severity.One-way Analysis-of-Variance models were used with significance level set at 0.05.
Results: Multi-directional ROM and clinical exam scores were grouped, thus, our p-values are reported as a range. All MRI findings showed some significant correlation. Edema within axillary pouch was associated with clinical exam scores (p 0.004-0.035), active ROM (p <0.001-0.021), and passive ROM (p <0.001-0.007). Overall assessment of AC severity was associated with the clinical exam scores (p <0.001-0.005), active ROM (p <0.001-0.041), and passive ROM (p <0.001-0.028). These two findings demonstrated most significant association.
Conclusion: The strong association between MRI characteristics and clinical exam scores in patients with clinically confirmed AC suggests MRI can serve as a tool for grading severity and therefore guide clinical treatment.

B-0818 11:42

Glenoid surface measuraments by means of 3D MRI: comparison between healthy volunteers and first time dislocators

G. Foti, E. Demozzi, P. Avanzi, G. Carbognin; *Negrar/IT (gfoti81@yahoo.it)*

Purpose: To identify any differences in glenoid area measuraments in healthy volunteers, in comparison to post-traumatic and non-traumatic anterior shoulder dislocators.
Methods and Materials: IRB approval was obtained for this prospective study and written informed consent was obtained from patients enrolled. A total of 124 patients (84 males, 40 females; range 14-62 years) studied with MRI including an isotropic 3D sequence were evaluated. By using the best-fit circle method, glenoid surface area was measured in the following patients subgroups: GR1=35 healthy volunteers; GR2=54 post-traumatic dislocators; GR3=35 non-traumatic dislocators. Two measurements were performed by two experienced radiologists, independently, on a dedicated workstation with at least 1 month gap. Differences between subgroups were calculated by using Student t test and Pearson correlation. A value of p<0.05 was considered statistically significant. Intra and Inter-reader variation was determined with the interclass correlation coefficient.
Results: As regards glenoid surface area, differences were not significant between GR1 (mean 484, range 355-562 square millimiters) and GR2 (mean 491, range 364-586 square millimiters); conversely a significant difference (p=0.025) was determined between GR1 and GR3 (mean and range values of 441 and 323-537 square millimiters, respectively) and between GR2 and GR3 (p=0.02). The difference was not significant when comparing GR2 to GR3 (mean 6.2%, range 1-27%). There was excellent intra- and inter-reader correlation (R=0.94 and R=0.98 respectively).
Conclusion: Glenoid area of patients undergoing non-traumatic shoulder dislocation is significantly smaller if compared to a control-group of healthy volunteers and to patients undergoing post-traumatic shoulder dislocation.

B-0819 11:50

Added value of combined acromiohumeral distance and critical shoulder angle measurements on conventional radiographs for the prediction of rotator cuff pathology

Q.M. Hamie, V. Grunder, T. Finkenstädt, M. Marcon, N.A. Farshad-Amacker, R. Guggenberger; *Zurich/CH (mustafa.hamie@usz.ch)*

Purpose: To investigate the role of acromiohumeral distance (AHD) and critical shoulder angle (CSA) measurements from conventional radiographs (CR) in isolation and combined as predictors of transmural rotator cuff tendon tears (RCT) and critical fatty degeneration (CFD).
Methods and Materials: In this retrospective study in 127 AHD and CSA were measured on CR. MR Arthrograms served as reference standard and were screened for RCT and CFD (Goutallier stages ≥2). Statistical analysis for inter-reader agreement, Spearman's rank correlation, linear stepwise regression and diagnostic performance at different cut-off values for AHD and CSA both isolated and combined were performed.
Results: In 90 subjects (17 females, mean age 36.1±14.1) no RCT were found on MR imaging and served as control group. In 37 patients (13 females, mean age 58.7±13.2) at least one RCT was found. Inter-reader agreements rated between κ=0.42-0.82 for categorical and 0.91-0.96 for continuous variables. No significant correlation of AHD and CSA with either age or gender was seen (p=0.28 and p=0.74, respectively). Case group had significantly smaller mean AHD (8.7±3.2 vs 10.8±2.2 mm; p<0.001) and larger mean CSA (36.5±4.5° vs 33.1± 4.0°; p<0.001). Combination of AHD-CSA-measurements increased specificity and positive predictive value (PPV) for prediction of RCT and CFD.
Conclusion: RCT and CFD correlate with smaller AHD and larger CSA. Combination of AHD and CSA measurements leads to increased specificity and PPV for detection of RCT or CFD. Goutallier stage of the infraspinate muscle is associated with small AHD and large CSA.

10:30 - 12:00 **Room K**

Radiographers

SS 1014

Professional issues in radiography

Moderators:
M. Hailemichael; Lund/SE
J. Reponen; Raahe/FI

B-0820 10:30

An investigation of mobile phone use in the radiology department and the success of an awareness campaign at reducing the associated nosocomial infection risks

C. Crofton, S. Foley; *Dublin/IE (crofton.ciara@gmail.com)*

Purpose: To determine whether a mobile phone infection control awareness campaign will improve radiographers' phone and hand hygiene practices.
Methods and Materials: 36 radiographers in two tertiary hospitals (convenience sampling) volunteered to have their mobile phones swabbed and tested using an adenosine triphosphate (ATP) meter to numerically quantify surface cleanliness. A survey determined their current practices and awareness levels. Subsequently, a poster campaign took place for one month in one hospital. The ATP testing and survey were repeated in both sites and compared. Changes were measured using simple descriptive analysis and Wilcoxon signed rank testing (survey data) and Mann Whitney U testing (ATP results).
Results: 100% (n=36) of radiographers used their phone at work. However, the majority were uninformed of the associated infection risks with only 6% being informed. 33% had been performing adequate phone disinfection and 0% performed adequate hand hygiene following phone use. Following the campaign, there was a significant improvement (p=0.028) in the frequency of phone disinfection. Utilisation of the optimal phone disinfection method increased (33% vs 7% in control). The ATP meter readings showed numerical reductions (p>0.05) and there were negligible changes in hand hygiene practices. Radiographers considered the ATP testing just as effective as the campaign at improving their awareness.
Conclusion: Radiographers are unaware of mobile phone infection risks. Although significant improvements in phone cleanliness and hygiene habits were not achieved, the improvements in phone hygiene practices indicate that an awareness campaign could play an important role as an educational tool to improve awareness.

B-0821 10:38

The radiologist and the radiographer: how do they compare in image quality judgement?

R.G.L. Decoster, R. Toomey, M.-L. Bulter; *Dublin/IE (decoster.robin@gmail.com)*

Purpose: In radiology departments, radiographers are concerned with the production of the radiograph, and radiologists report the findings. Disagreement on the clinical acceptability of radiographs may lead to unnecessary retakes or insufficient image quality to report on, with a needless exposure of patients in both cases. This study compares the agreement on image quality and clinical acceptability between these professions.
Methods and Materials: Five radiographers and five radiologists evaluated the image quality of 22 chest radiographs using, respectively, a secondary and a primary class monitor to mimic reality. Participants rated the reproduction of five anatomical structures on a scale from 1 to 5. These data were assessed using a VGC approach. They also judged the clinical acceptability of the radiograph using the RadLex categories and expressed their confidence concerning their decision. The responses for the two groups were compared using Nagelkerke Pseudo R-Square.

Results: No significant (p>0.05) difference was found in the area under the curve between the groups for none of the structures. The judgement of clinical acceptability by radiographers is significantly different (Pseudo-R^2 0.076, p<0.01) from the radiologists. Radiographers rejected 21% more radiographs then the radiologists and were less confident in 29% of their decisions, especially in cases with limited quality.
Conclusion: These findings indicate that radiographers and radiologists agree on the evaluation of anatomical structures. On the contrary, they do not agree on the clinical acceptability, indicating that the decision of accepting or rejecting a radiograph is based on other information then purely the visualisation of anatomy.

B-0822 10:46

Patient perceptions of radiation therapist communication skills
S. Teixeira, L.P.V. Ribeiro, A.F. Abrantes, M. Ramos, F. Serra, O. Lesyuk, S. Rodrigues; *Faro/PT (lpribeiro@ualg.pt)*

Purpose: The improvement of results in healthcare through the transmission of information to the patient within a relation of empathy and trust is already a verified hypothesis. Healthcare professionals should base themselves on interpersonal competences throughout their daily work routine, to promote quality in radiotherapy, patient safety and technical excellence. The aim of this study was the exploration of patient's perceptions regarding the performance of the radiation therapist in terms of interpersonal communication skills.
Methods and Materials: The instrument used was the questionnaire "Communication Assessment Tool" (Makoul et al. 2007) adapted to the professional reality of the radiation therapists. A total of 118 valid questionnaires (including 15 questions with a 5 point Likert scale) from patients aged between 22 to 87 years old from a private radiotherapy center. The patients have performed at least 5 radiotherapy sessions to be included in this study.
Results: The internal consistency of the questionnaire was excelent (Cronbach's alpha = 0.97). Highest ratings were for radiation therapist behavior items, such as "paying attention to the patients" (4.45), "respect for the patients" (4.43) and "using comprehensive language and terms" (4.42). Lowest ratings were "explained the treatment plan" (4.00), "encouraged to make questions" (4.07) and other items related with being involved in decision-making process.
Conclusion: Patients demonstrated high levels of confidence in their therapist and feel well treated during the sessions. Despite the overall positive results, "Radiation Therapist - Patient" relationships can be strengthened and patient outcomes improved through improved communication.

B-0823 10:54

Evidence-based practice in radiology: the radiographer perspective
C. Costa[1], A.F. Abrantes[1], L.P.V. Ribeiro[1], K.B. Azevedo[1], R.P.P. Almeida[1], O. Lesyuk[1], C.A. Silva[2]; [1]*Faro/PT*, [2]*Évora/PT (kbazevedo@ualg.pt)*

Purpose: Analyse the application of the Evidence-Based Practice (EBP) in Radiology by the radiographers' in their daily practice in CT departments.
Methods and Materials: A self-applied questionnaire to assess EBP was addressed to 97 radiographers working in 5 public hospitals. A total of 65 valid questionnaires (including 3 main sections with a total of 103 items, and a 7 point Likert scale format) were interpreted and statistically analysed through descriptive statistics. T-student and ANOVA tests were used for groups' comparison.
Results: 80% of radiographers applied the principles of EBP in their daily practice. However, the major limiting factors highlighted by the radiographers for the application of EBP were: "Knowledge to transfer the results of literature/scientific articles in their daily practice" (18,5%), "Existence of legislation/regulation about practices" (18,5%), "Knowledge of EBP concepts" (15,4%) and "Professional motivation" (15,4%). Regarding the training and updating of knowledge, the item "Specific training to be able to apply an EBP model in professional activity" had the highest mean score (5,25) and the item "Regular attendance in courses about EBP and research topics" had the lowest (3,49).
Conclusion: Despite the general application of EBP by radiographers, thanks to regular consultation of CT guidelines and decision-making processes based on literature review and scientific articles, this group of professionals would benefit from further training. Such approach would be well received and help the radiographers to enhance their knowledge and technical skills, which would ultimately result in an increase of the deparment's quality.

B-0824 11:02

Radiographers knowledge about infection control measures during radiological examinations
M. Ramalho, L.P.V. Ribeiro, A.F. Abrantes, O. Lesyuk, S. Rodrigues, A.M. Ribeiro, J.P. Pinheiro, R.P.P. Almeida; *Faro/PT (jppinheiro@ualg.pt)*

Purpose: To Assess the appropriate use of infection control principles/measures by radiographers during radiological examinations and to establish whether infection control guidelines are necessary.
Methods and Materials: A self-applied questionnaire about infection prevention and control measures was applied to 48 radiographers within 3 different public hospitals. Besides, using an observational grid, 20 of them were observed during the performance of radiological examinations to check if the infection prevention measures were applied. Efficiency of alcohol based solution and hand-scrubbing technique were evaluated with ultraviolet light after procedure.
Results: 58,3% of radiographers had training in hospital infection control measures and 62,5% of them indicated the use of individual equipment protection, such as gloves and aprons when necessary. During the observation, only 1 radiographer disinfected their hands before placing gloves and 8 of them never did it after removing gloves. During the evaluation of hand scrubbing technique using ultraviolet light, it was observed that only 20% of radiographers presented a total area of disinfected hand.
Conclusion: Radiographers were aware of infection control guidelines but several of them failed to apply these procedures during the radiological examinations. Therefore, radiographers must be given periodic training in infection control procedures, written protocols and legislation must be outlined to monitor the use of infection control procedures during work and there should be a periodic monitoring of practice of infection control procedures by radiographers.

B-0825 11:10

Humour: what do they think? On opinions of students and professional radiographers
E. Cordier[1], S. Lantheaume[2], L. Motak[3]; [1]*Grenoble/FR*, [2]*Guilherand-Granges/FR*, [3]*Aix-en-Provence/FR (cordieretienne@gmail.com)*

Purpose: To gather opinions of radiographers regarding the use of humour among students and professionals, and to apprehend possible positive and/or negative impacts of its use on the care relationship.
Methods and Materials: *Sample.* Six hundred forty-one senior radiographers and 411 first, second or third year undergraduate radiographers, for a total sample of 1052 subjects from all over France. *Material.* Within a quantitative phase, both professionals radiographers and radiographers-in-training were assessed on several Likert-type scales involving concepts such as the functions of humour, and a second, qualitative phase based on open survey questions further focused on investigating the most salient concepts, notably within the senior radiographer sample.
Results: Although radiographer apprentices saw the major benefits of humour in their relationships with patients (i.e. building a trust relationship, distraction technique), the senior radiographers put forward benefits especially regarding their colleagues or their own person (pleasant working environment, coping strategy during stressful events). Positive aspects of humour do prevail over the negative ones in both radiographer groups, but professionals emphasize the contextualized aspects of humour and warn that it may infringe on patients and their dignity.
Conclusion: Considering humour as a personal and a professional value among the samples studied opens new perspectives on use of humour and its training within both institutional and educational contexts, preventing any possible harmful use.

B-0826 11:18

Consultant radiographers: a study to assess activity and impact
B. Snaith, A. McGuinness, A. Coates, L. Field, R. Clarke, S. Yunis; *Wakefield/UK (bev.snaith@midyorks.nhs.uk)*

Purpose: Consultant radiographers' roles are currently unique to the UK and evidence of their impact is limited, particularly at an organisational level. This study reviews the activity of consultant practitioners across their 4 key functions (clinical practice, leadership, research and education), evidencing the impact this has on patients, staff and the organisation.
Methods and Materials: The study was a prospective exploratory study using activity diaries and comprised interval sampling by 6 consultant radiographers employed within a busy multisite English NHS Trust. All radiographers work a standard 37.5 hour week across a range of specialities/modalities. Data were collected using a coded list and recorded in fifteen-minute intervals over the period of one week to establish the relative hours of activity.
Results: The mean number of hours worked within the study week was 45.8 (range 41.3-50.8). All individuals evidenced activities in the 4 key functions; however, the proportions varied. Clinical work predominated and comprised

43.9% of the worked hours (mean=20.1). Support for other staff was a key component of all roles, undertaking one-on-one teaching or assessment, case discussion or problem solving. The individuals evidenced strategic working at an organisational and national level. Multi-tasking was common, with interruptions of work a feature of the accessibility of the role.
Conclusion: This localised study provides a snapshot of the breadth and complexity of the activities performed by consultant radiographers. The individuals appear to be routinely performing functions which have an impact on patients, colleagues, the organisation and profession.
Author Disclosures:
B. Snaith: Advisory Board; Radiography journal.

B-0827 11:26

Assessment of image quality criteria from digital radiography
A. Mendes, A.M. Ribeiro, L.P.V. Ribeiro, A.F. Abrantes, R.P.P. Almeida, K.B. Azevedo, S. Rodrigues; *Faro/PT (lpribeiro@ualg.pt)*

Purpose: To assess the image quality criteria from examinations in digital radiography based on quality control charts and to demonstrate the importance of implementing an image quality control system.
Methods and Materials: A retrospective study was conducted in a public radiology department using a random sample of 1200 radiographs grouped in 60 smaller samples, each one with 20 radiographs. Using a checklist based on the "*American College of Radiology Practice Guidelines for the Performance* of abdominal, chest and extremities radiographs", the conformities and non-conformities found were recorded and used to establish three types of quality control chars: (1) the proportion of conformities and non-conformities (p chart); (2) the total number of non-conformity exams (np chart) and (3) the total number of non-conformities in each sample (c chart), in order to suggest corrective actions for improvement.
Results: Considering all exams, 473 were classified as non-conform (39.42%) and 727 were classified as conform (60.58%). Considering the non-conform exams group, the quality criteria "incomplete or incorrect image post-processing" presented the highest number of non-conformities (58,92%), followed by "incorrect patient positioning" (35,32%) and "artefacts" (5,77%). Chest radiograph showed the highest number of non-conformities (174).
Conclusion: The existence of suitable quality control of the image is essential to achieve high quality standards. Strategies for improving radiographers performance must be implemented to ensure that digital radiography examinations are performed in compliance with all the quality criteria established.

B-0828 11:34

Computer-assisted diagnostics and the importance of optimised integration into the clinical setting
T. Butcher[1], C. Goncalves[1], S. Shah[1], S.P. Kelavkar[1], M. Johnson[1], P. Harman[1], P. Guyler[1], A. Kuhn[2], I. Grunwald[1]; [1]*Southend-on-Sea/UK*, [2]*Worcester, MA/US*

Purpose: The CE-marked e-ASPECTS software (Brainomix, Oxford) assists clinicians in detecting areas of acute ischaemic stroke on CT using the validated ASPECTS score. Instant access to the processed results is crucial in stroke and depends on optimised software integration into the clinical pathway. We evaluated the main 3 integration strategies available.
Methods and Materials: Feasibility, time and user friendliness (questionnaire) of the following integration options were evaluated. 1) Images for processing sent from CT to cloud-based server, results returned to PACS. 2) Images sent from PACS to local sever, processed images returned to PACS. 3) Images automatically sent from CT to hospital-based server (accessible via ipad user interface), results returned to PACS.
Results: All 3 integration solutions were feasible. Local server compared to cloud-based processing significantly decreased time ($p<0.05$), the remote Internet transfer adding 2 minutes. Transferring images from PACS for post-processing incurred varying time delay, depending on PACS data load and system (max 6 min). Option 2 required most user interaction, associated with potential user errors. The fastest solution (Option 3) allowed near instant access to post-processed images (<1min) via a hospital-based server, utilising a dedicated iPad interface. This was also judged as the user-friendliest option in the acute setting. In the non-acute setting Option 2 was also judged to be important to accommodate requirements of different users (e.g. researchers, neurologists).
Conclusion: The value of computer-assisted diagnostics can be increased by optimised integration into the clinical pathway, thus increasing user friendliness, speed and potentially outcome.
Author Disclosures:
I. Grunwald: Founder; Brainomix Limited. Shareholder; Brainomix Limited.

B-0829 11:42

The implementation of a radiology hospital inpatient turnaround team (HITT) to reduce radiology waiting times
C. Roche, G. Naughton, T. Fallon, T. Glavey, S. Ruddy, S. McNulty; *Galway/IE (stevemac182@hotmail.com)*

Purpose: To estabish a radiology "Hospital Inpatient Turnaround Team" (HITT). To reduce inpatient radiology waiting times through better integration and organisation of staff and resources.
Methods and Materials: A series of radiology multidisciplinary team meetings culminated with the establishment of a radiology HITT, with representation from all relevant disciplines. Regular HITT meetings resulted in many changes being implemented in order to improve departmental efficiency. The HITT developed a clear inpatient workflow process and introduced brief daily meetings between the scheduling radiographer, clerical officer and porter. Necessary resources such as IT support were also addressed. A "turnaround time" KPI was introduced to measure the time from an x-ray order being placed to the time that order was completed on the RIS. Updates on this KPI were posted weekly around the department. A competition to name the inpatient radiography area was held to improve morale and highlight departmental focus on the area. The PACS manager carried out a retrospective audit to measure how these changes had influenced the KPI.
Results: The audit demonstrated reduction in mean inpatient waiting times of 26.2%. Median inpatient waiting times also decreased from 3 hours, 34 minutes to 2 hours, 38minutes; a reduction of 30.7%.
Conclusion: Significant improvements in efficiency are possible through closer integration of the many disciplines that make up a radiology department. The creation of a multidisciplinary team to implement a clear workflow process, with input from all disciplines, can lead to decreases in median inpatient radiology waiting times of over 30%.

B-0830 11:50

Infection control for x-ray cassettes in a radiology department
A. Brás, K.B. Azevedo, A.F. Abrantes, L.P.V. Ribeiro, S. Rodrigues, A.M. Ribeiro, R.P.P. Almeida; *Faro/PT (kbazevedo@ualg.pt)*

Purpose: To verify if the presence of pathogens in contact areas of x-ray cassettes (Image Plates) can cause nosocomial infections and to establish whether infection control guidelines are necessary.
Methods and Materials: The methodology used consisted, initially, in observing hygiene practices performed by radiographers in the cleaning of x-ray cassettes, through an observation grid. After, the second fase involved the swabbing of contact areas to check the general levels of bacterial contamination and also to verify the presence or absence of payhogen agents.
Results: The results demonstrated that there were large levels of growth of samples taken from contact areas and developed in the Microbiology Department. The existence of colonies varies according to the method for obtaining samples from contact areas. Streptococcus, Staphylococcus epidermidis, Staphylococcus aureus, Enterococcus and Proteus were all identified.
Conclusion: In order for cross contamination to be kept to a minimum an effective infection control policy needs to be employed and this should be to carry out regular cleaning of contact areas of x-ray cassettes (Image Plates). Therefore, radiographers must be given periodic training in infection control procedures, written protocols and legislation must be outlined to monitor the use of infection control procedures during work and there shoud be a periodic monitoring of practice of infection control procedures by radiographers.

10:30 - 12:00 **Room M 1**

Cardiac

SS 1003

Myocardial ischaemia and perfusion imaging I

Moderators:
P.T. Klimeczek; Krakow/PL
M. Pirnat; Maribor/SI

B-0831 10:30

Diagnostic performance of stress Echo, SPECT, PET, stress CMR, CTCA, CTP and FFRCT for the assessment of CAD vs invasive FFR: a meta-analysis

G. Pontone[1], A. Guaricci[2], M. Verdecchia[3], D. Andreini[1], M. Guglielmo[1], A. Baggiano[1], P. Carità[4], G. Ferro[4], M. Pepi[1]; [1]*Milan/IT*, [2]*Bari/IT*, [3]*Chieti/IT*, [4]*Palermo/IT (gianluca.pontone@ccfm.it)*

Purpose: Stress echocardiography (Echo),stress single photon emission computed tomography (SPECT), positron emission tomography (PET),stress cardiac magnetic resonance (CMR), cardiac computed tomography (CTCA), stress computed tomography(CTP) and computed tomography fractional flow reserve (FFRCT) have been proposed as gatekeeper to invasive coronary angiography (ICA).We sought to determine the diagnostic accuracy of all these non-invasive tests as compared to invasive FFR(FFRi) for the detection of haemodynamically significant coronary artery disease(CAD).
Methods and Materials: We searched for studies evaluating Echo, SPECT, PET, CMR, CTCA, CTP and FFRCT for non-invasive diagnosis of functionally significant CAD compared with FFRi. Inclusion criteria were English language, clinical indication of index test for suspected CAD, raw data of pervessel and/or perpatient model available or derivable and FFRi as reference standard.Pooled diagnostic accuracy (Ac) vs FFRi were assessed and compared.
Results: We analysed data (14256 vessels and 6285 patients) from 97 out of 638 relevant abstracts of fulltext articles. At vessel level the mean prevalence of CAD was 29.63% and the diagnostic accuracy of Echo, SPECT, PET, CMR, CTCA alone,CTP, FFRCT, CTCA+PET, CTCA+CTP and CTCA+FFRCT were 82% (7885), 75% (7377), 87% (8588), 89% (8890), 76% (7577), 86% (8488), 79% (7782), 93% (9195), 88% (8690), 80% (7289), respectively. At patient level the mean prevalence of CAD was 45.1% and the diagnostic accuracy of Echo, SPECT, PET, CMR, CTCA alone, CTP, FFRCT, CTCA+PET, CTCA+CTP were 77 (7481), 77 (7580), 87% (8489), 87%(8589), 69% (6771), 86% (8290), 79% (7682), 91% (8795), 88% (8492), respectively. CTCA+PET showed the highest accuracy at vesselbased analysis (p<0.001) while CTCA+PET showed similar accuracy vs CTCA+CTP and CMR but higher accuracy as compared to other non-invasive tests(p<0.001).
Conclusion: In patients with intermediate prevalence of CAD, CTCA+PET, CTCA+CTP or CMR are all more accurate to detect haemodinamically significant CAD. Echo, SPECT and CTCA are less suited to this aim.

B-0832 10:38

Diagnostic accuracy of rapid on-site fractional flow reserve CT

P. Maurovich-Horvat[1], M. Kolossvary[1], J. Karady[1], P.A. Ball[2], S. Kelly[2], D. Fitzsimons[2], C. Celeng[1], B. Merkely[1], P.M. Donnelly[2]; [1]*Budapest/HU*, [2]*Belfast/UK (maurovich.horvat@gmail.com)*

Purpose: Fractional flow reserve derived from coronary CT angiography (FFR-CT) is a novel tool for the diagnosis of ischemic coronary lesions. Our aim was to evaluate the diagnostic performance of a novel on-site FFR-CT. Furthermore, we sought to determine if the diagnostic performance is altered by the adjustments to the lumen segmentation performed by two different readers.
Methods and Materials: We have enrolled consecutive patients who underwent coronary CTA and invasive coronary angiography (ICA) in two centres. ICA examinations with FFR measurements were performed within 60 days after the coronary CTA. An FFR value ≤ 0.8 was considered haemodynamically significant. All coronary CTA scans were evaluated by two readers, who manually adjusted the semi-automated coronary lumen segmentations.
Results: In total 44 patients (mean age 63.0±8.0 years, 24.4% female) were enrolled in our two-centre prospective study. Overall, we analysed 60 coronary atherosclerotic lesions. Average quantitative coronary CT cross-sectional area stenosis was 60.3±19.7%. The average FFR-CT was 0.77±0.15 and 33 (54.1%) lesions were considered to be haemodynamically significant (FFR-CT≤0.8). Sensitivity of FFR-CT was 90.5%, specificity 71.8%, positive predictive value 63.3%, negative predictive value 93.3% and accuracy of 78.3%. Area under the receiver operating curve of the two expert readers did not show any significant difference (0.89 versus 0.88; p=0.63).
Conclusion: Rapid on-site FFR-CT simulation is feasible and it has excellent diagnostic performance. Importantly, the diagnostic performance did not differ between the readers who corrected the automated lumen contour segmentations.

B-0833 10:46

Non-invasive assessment of coronary stenoses by CT myocardial perfusion imaging during pharmacologic coronary vasodilatation

R. Boughrarou, B. Mansouri; *Algiers/DZ (rafikalinda@hotmail.com)*

Purpose: Computed tomography angiography (CTA) has be shown to be accurate in detecting anatomic coronary arterial obstruction, but is limited for the detection of myocardial ischaemia. The primary aim of this study was to assess the accuracy of 320-row computed tomography perfusion imaging (CTP) to detect atherosclerosis causing myocardial ischaemia.
Methods and Materials: One hundred patients underwent a comprehensive cardiac computed tomography (CT) protocol that included 320- CTA, followed by dipyridamole stress CTP. CTA was evaluated for stenosis. CTP images were analysed for the presence of subendocardial perfusion deficits, using the transmural perfusion ratio (TPR) and 17 segments model.
Results: The protocol was successfully completed for 100 patients, with an average radiation dose of 14mSv. CTA alone was a limited predictor of myocardial ischaemia. CTP was a better predictor of myocardial ischaemia, with a sensitivity, specificity, PPV and NPV of 94%, 71%, 69%, 95%, respectively; using quantitative angiography and SPECT, as gold standard.
Conclusion: Computed tomography perfusion imaging with rest and dipyridamole stress 320- row CT is accurate in detecting atherosclerosis causing myocardial ischaemia.

B-0834 10:54

Prognostic value of coronary CT angiography-derived fractional flow reserve of non-culprit lesions in patients with acute coronary syndrome

T.M. Duguay, C. Tesche, C.N. De Cecco, H. Lin, M.H. Albrecht, A. Varga-Szemes, D. De Santis, U. Ebersberger, U.J. Schoepf; *Charleston, SC/US (duguay@musc.edu)*

Purpose: To investigate the prognostic value of coronary CT angiography (CCTA)-derived fractional flow reserve (CT-FFR) assessment of non-culprit lesions in patients with acute coronary syndrome (ACS).
Methods and Materials: 48 patients (55.8±9.6 years, 60% male) admitted for ACS who underwent dual-source CCTA followed by invasive coronary angiography (ICA) were retrospectively analyzed. ACS-related culprit lesions on CCTA were identified using ICA. Non-culprit lesions with ≥30% luminal stenosis on CCTA that were considered non-critical on ICA were evaluated using CT-FFR for the presence of lesion-specific ischemia. Follow-up was performed to monitor the occurrence of major adverse cardiac events (MACE) related to the non-culprit lesions. The prognostic value of CT-FFR to predict MACE was assessed.
Results: CT-FFR evaluation showed 23 of 81 non-culprit lesions had lesion-specific ischemia. MACE occurred in 14 patients (29%) (2 cardiac deaths, 12 additional ACS cases related to a non-culprit lesion; median follow-up interval: 19.5 months). The following markers carried predictive value with a univariable Cox regression analysis (hazard ratio [HR]): Dyslipidemia (HR 2.35, *p*=0.048), diabetes mellitus (HR 2.98, *p*=0.036), and CT-FFR ≤0.80 (HR 3.77, *p*=0.007). In a risk-adjusted model controlled for diabetes mellitus and dyslipidemia, CT-FFR ≤0.80 (HR 1.78, *p*=0.047) remained a predictor for MACE. A combined model receiver operating characteristics analysis including clinical characteristics and CT-FFR (AUC 0.77) showed incremental discriminatory power compared to clinical characteristics alone (AUC 0.65, *p*=0.034).
Conclusion: CT-FFR accurately depicts the haemodynamic significance of non-culprit lesions in patients with ACS and portends prognostic value in identifying patients at risk for future MACE.
Author Disclosures:
C.N. De Cecco: Consultant; Guerbet. Research/Grant Support; Siemens.
A. Varga-Szemes: Consultant; Guerbet. **U.J. Schoepf:** Consultant; Guerbet. Research/Grant Support; Astellas, Bayer, Bracco, GE, Medrad, and Siemens.

B-0835 11:02

Improved on-site FFR-CT accuracy by coronary tree standardisation

H. Nickisch[1], M. Freiman[2], S. Prevrhal[1], M. Vembar[3], P. Donnely[4], P. Maurovich-Horvat[5], L. Goshen[2], H. Schmitt[1]; [1]*Hamburg/DE*, [2]*Haifa/IL*, [3]*Cleveland, OH/US*, [4]*Belfast/UK*, [5]*Budapest/HU (hannes.nickisch@philips.com)*

Purpose: Fractional flow reserve (FFR) simulation based on standard coronary CT angiography (CCTA) may be an alternative to invasive FFR measurements. This study evaluated the robustness of our toolchain to generate patient-specific coronary tree models and simulate FFR against variations in manual input, with the goal to allow full on-site processing.
Methods and Materials: We collected CCTA datasets from 44 subjects from two different sites, along with invasive reference FFR measurements

conducted on 60 coronary lesions. Readers at both sites used our software to manually adjust the automatic extraction of coronary centerlines and lumen. From these, complete coronary trees were generated and then standardised following specific rules and geometric constraints to reduce operator and image quality dependency. FFR was simulated from both complete and standardised coronary trees using a non-linear, machine learning-accelerated lumped model trained earlier on computational fluid dynamics simulations. We finally used invasive FFR measurements as the reference standard with a cut-off value of 0.8 to determine changes in predictive performance and diagnostic accuracy resulting from coronary tree standardisation.
Results: Standardising the trees improved the diagnostic accuracy and area under the ROC curve for the two readers from 73±1.3% to 78±1.6% and 0.83±0.01 to 0.89±0.014 (reader 1), and 70±1.4% to 77±1.6% and 0.81±0.015 to 0.88±0.009 (reader 2), respectively. Furthermore, the variance between the two readers is reduced.
Conclusion: Coronary tree standardisation prior to patient-specific non-invasive FFR simulation can reduce operator dependency thereby improving CCTA-based lesion specific ischaemia assessment.
Author Disclosures:
H. Nickisch: Employee; Philips. **M. Freiman:** Employee; Philips. **S. Prevrhal:** Employee; Philips. **M. Vembar:** Employee; Philips. **L. Goshen:** Employee; Philips. **H. Schmitt:** Employee; Philips.

B-0836 11:10

Non-invasive on-site estimation of fractional flow reserve: initial experience using coronary CTA-derived patient-specific lumped parameter models

R.W. van Hamersvelt[1], M. Voskuil[1], P. Maurovich-Horvat[2], P.A. de Jong[1], M.J. Willemink[1], T. Leiner[1]; [1]*Utrecht/NL*, [2]*Budapest/HU*
(R.w.vanhamersvelt-3@umcutrecht.nl)

Purpose: To report initial experiences with a novel coronary computed tomography angiography (cCTA)-derived algorithm for on-site non-invasive estimation of fractional flow reserve (FFR) based on patient-specific lumped parametric models.
Methods and Materials: Fourteen patients who underwent a cCTA (256-slice CT scanner) and an invasive catheter-based FFR measurements of 17 coronary segments were retrospectively selected. Haemodynamically significant stenoses were defined as FFR≤0.8. FFRct measurements were performed on the 17 segments and compared to the invasive FFR measurements in a blinded fashion. For FFRct, a prototype based on patient-specific lumped parameter models was used. In each coronary artery, the observer semi-automatically defined the centre line, subsequently lumen segmentation was automatically performed and manually corrected. The location for FFRct simulation was selected to match that of the pressure wire used for invasive FFR. Time was measured for each FFRct simulation.
Results: Total simulation time after the completion of segmentation was ≤10 seconds. True haemodynamically significant stenoses (invasive FFR≤0.8) were present in 5 patients (36%) and 6 (35%) segments. FFRct identified 5 (100%) patients and 5 segments (83%) with significant stenosis correctly. On a per-segment basis, our initial results showed a performance (%true), sensitivity, specificity, positive predictive value and negative predictive value of 71%, 83%, 63%, 55% and 88%, respectively. On a per-patient basis this was 79%, 100%, 67%, 63% and 100%, respectively.
Conclusion: These preliminary results suggest that this rapid, on-site FFRct prototype, based on lumped parameter models, has the potential identify haemodynamically significant stenosis.
Author Disclosures:
M.J. Willemink: Speaker; Speakers Bureau, Koninklijke Philips NV. **T. Leiner:** Research/Grant Support; Bayer A, Bracco Group.G Research Grant. Speaker; Speakers Bureau, Koninklijke Philips NV.

B-0837 11:18

Stress-rest CMR for the assessment of myocardial perfusion reserve index modification after coronary sinus stent implantantion

A. Palmisano, A. Esposito, A. Botta, F. Giannini, A. Colombo, F. De Cobelli, A. Del Maschio; *Milan/IT (palmisano.anna@hsr.it)*

Purpose: The management of patients with angina refractory to revascularisation procedures and medical therapy is challenge. The implantation of a coronary sinus stent named "Reducer" seems to improve patient' symptoms but the physiopathological mechanism underlying this effect is not clear. Aim of the study was to evaluate the modification in myocardial perfusion reserve occurring after Reducer implantation using a stress-rest CMR study.
Methods and Materials: 9 patients eligible for implantation of the "Reducer" underwent clinical evaluation (CCS Angina Class and 6minutesWT) and a stress-rest CMR study with dipyridamole before the implantation and after 3 months. Segmental and global myocardial perfusion reserve index (MPRI) was measured using stress-rest CMR. Simultaneously, MRI morpho-function parameters of LV were analysed.
Results: All patients reported an improvement of ≥ 2 CCS ($p < 0.0001$) and a 60% increase in the average distance during the 6minutesWT ($p=0,004$). The global value of MPRI has increased on average by 35% ($p=0.047$). The analysis per cardiac segments showed, patient by patient, an increase of MPRI in the ischemic territories on average by 72% ($p=0.03$) while the necrotic areas, post-infarction, present in 2/9 patients, did not show significant changes ($p=0.623$).
Conclusion: The preliminary data of this study suggest, for the first time, that this device is really able to determine a positive redistribution of myocardial blood flow, providing a new insight about its pathophysiological mechanism of action, with consequent improvement of angina symptoms, quality of life and exercise tolerance.

B-0838 11:26

Inversion of T1 reactivity in patients with caffeine intake prior to adenosine myocardial perfusion imaging

D. Kuijpers, R. van Dijk, N. Prakken, R. Vliegenthart, P. van Dijkman, P. van der Harst, M. Oudkerk; *Groningen/NL (r.van.dijk02@umcg.nl)*

Purpose: Caffeine intake before adenosine stress myocardial perfusion imaging may cause false negative findings. We hypothesised that the antagonistic effect of caffeine can be measured by T1 relaxation times in rest and adenosine cardiac magnetic resonance imaging (CMR), as T1 mapping techniques are sensitive to changes in myocardial blood volume.
Methods and Materials: CMR was performed in 105 consecutive patients at 1.5T using a Modified Look-Locker Inversion Recovery sequence with stress and rest T1 mapping. The change in T1 (T1 reactivity) was calculated by subtracting $T1_{stress}$ from $T1_{rest}$. Self-reported caffeine intake was <4 hours (<4H) prior to CMR in fifteen patients and >8 hours (>8H) in ten patients. These groups were compared to a control group of fifty patients with normal CMR, twelve patients with myocardial infarction, and eighteen patients with myocardial ischaemia.
Results: T1 reactivity in the <4H group showed an inverted response of -7.8% and (T1rest 975 ± 42 ms, T1stress 898 ± 51 ms, $p<0.0005$) and was significantly lower as compared to both the >8H (T1 reactivity +1.8%, T1rest979 ms, T1stress 997 ms), and the control group (T1 reactivity +4.3%, T1rest 977 ± 40 ms, T1stress 1018 ± 40 ms), $p<0.0005$. Ischaemic and infarcted myocardium showed minimal T1 reactivity (0.2 and 0.3 %, respectively).
Conclusion: Caffeine intake prior to adenosine MR perfusion causes an inversion of the effects of adenosine as measured by T1 mapping. T1 reactivity can be used the assess the adequacy of adenosine during vasodilator MR perfusion.

B-0839 11:34

Dynamic CT analysis of myocardial perfusion parameters comparing different temporal sampling rates using a third generation dual-source CT

M. van Assen[1], G. Pelgrim[1], E. Slager[1], S. van Tuijl[2], U.J. Schoepf[3], R. Vliegenthart[1], M. Oudkerk[1]; [1]*Groningen/NL*, [2]*Eindhoven/NL*, [3]*Charleston, SC/US (m.van.assen@umcg.nl)*

Purpose: To evaluate the influence of different temporal sampling rates, in dynamic CT myocardial perfusion imaging (CTMPI) on myocardial blood flow (MBF) using a 3th generation dual-source CT (DSCT), in an ex-vivo porcine heart model.
Methods and Materials: Three porcine hearts were perfused with an isolated heart model in Langendorff mode (Physioheart®, LifeTec Group, Eindhoven, The Netherlands). Haemodynamic monitoring was performed during the experiment. Third generation DSCT was used to perform dynamic CTMPI in three different modes: electrocardiographic (ECG)-triggered shuttle-mode (70kVp,350mAs/rot,z-range10.2cm) and non-shuttle-mode with continuous

stationary tube rotation (70KVp, 230mAs/rot, z-range 5.8cm, merged A and B-tube) and in non-ECG-triggered continuous-rotation-mode (70kVp, 230mAs/rot, z-range 5.8cm). Multiple fractional flow reverse (FFR) values were simulated in the circumflex artery by artificially creating a stenosis. The ECG-triggered scan were analysed with Volume Perfusion CT (VPCT) Myocardium software. The non-ECG triggered scans were analysed with MASS research version combined with an in-house Matlab script. MBF(mL/g/min) was calculated for non-ischaemic segments only.True MBF was calculated using input flow in non-stenosis situation and weight of the hearts.
Results: Heart rate, model blood flow and blood pressure were stable during the experiments. Significant differences were found between shuttle, non-shuttle and continuous-mode with median MBF 0.87 (IQR:0.72-1.00), 1.20 (IQR:1.07-1.30) and 1.65 (IQR:1.40-1.88), respectively. The median MBF values increased 44% by increasing the temporal sampling rate from shuttle to non-shuttle mode and by 98% increasing the sampling rate from shuttle to continuous mode.
Conclusion: Dynamic CTMPI using increased temporal sampling rates, results in higher and more accurate MBF values compared to the currently used shuttle technique.
Author Disclosures:
S. van Tuijl: Employee; LifeTec Group. **U.J. Schoepf:** Consultant; Bayer, Bracco, GE, Siemens, Astellas, Guerbet, Medrad.

B-0840 11:42

Coronary CT angiography with computational fractional flow reserve for therapeutic decision making
T.M. Duguay, C. Tesche, C.N. De Cecco, J.W. Nance, M.H. Albrecht, D. De Santis, M.C. Langenbach, A. Varga-Szemes, U.J. Schoepf;
Charleston, SC/US (duguay@musc.edu)

Purpose: To investigate the performance of coronary CT angiography (cCTA) with computational fractional flow reserve (cFFR) compared to invasive coronary angiography (ICA) with fractional flow reserve (FFR) for therapeutic decision making in patients suspected of having coronary artery disease (CAD).
Methods and Materials: 74 patients (62.2±10.6 years, 62% male) who underwent a clinically indicated dual-source cCTA and ICA with FFR measurement for the assessment of CAD within 3 months were retrospectively analyzed. cCTA datasets were visually evaluated for the presence of significant CAD (≥50% stenosis). cFFR calculation for the functional assessment of CAD significance was performed. The therapeutic strategy and appropriate revascularization procedure were defined using cCTA and cFFR. The diagnostic accuracy for detecting obstructive CAD and selection of therapeutic strategy was calculated and compared using ICA as the reference standard.
Results: 36 patients (49%) had obstructive CAD based on ICA. The diagnostic accuracy for cCTA to identify obstructive CAD and to select the appropriate therapeutic strategy was 86% and 85%, respectively. cCTA with cFFR yielded significantly superior diagnostic accuracy over cCTA alone for the detection of obstructive CAD and the selection of the correct therapeutic decision with 99% and 99%, respectively.
Conclusion: cCTA alone shows modest performance while cCTA with cFFR showed excellent diagnostic accuracy in identifying patients with and without need of revascularization and in selecting the appropriate revascularization strategy in patients with suspected CAD. cCTA with cFFR has the potential to reduce unnecessary ICA procedures showing non-obstructive CAD and to inform therapeutic decision making for revascularization.
Author Disclosures:
C.N. De Cecco: Consultant; Guerbet. Research/Grant Support; Siemens.
A. Varga-Szemes: Consultant; Guerbet. **U.J. Schoepf:** Consultant; Guerbet. Research/Grant Support; Astellas, Bayer, Bracco, GE, Medrad, and Siemens.

B-0841 11:50

Splenic switch-off: a reliablesign of understress by Adenosin?
A.S. Sträter, J. Nadjiri, M. Rasper, T. Stadlbauer, H.-H. Eckstein, E.J. Rummeny, A. Huber; *Munich/DE (Alexandra.Straeter@gmail.com)*

Purpose: While myocardium shows a faster and greater enhancement under adenosin-stress it was recently described spleen enhancement under adenosin stress decreases compared to rest. It was proposed patients that without this signal are understressed. MR scans (stress and rest) were performed to investigate 1. number of patients with no splenicswitch-off and 2. number of patients with decreased myocardial Perfusion reserve index (MPRI) but no relevant coronary artery disease.
Methods and Materials: MR Perfusion scans were performed in 37 patients with suspision of coronary artery disease. SR-gradientecho-sequence in a 3 tesla MR scanner was used. All scans were followed by a selective coronar-angiographie done for clinical indications. Peak Enhancement (PE) is the difference of maximum signalintensity and baseline signalintensity. Upslope is the gradient from the footpoint to the maximum of the signal-intensity-curve. The quotient of stress-valueand rest-value is the MPRI.
Results: For PE myocardium had a mean of 48± 13, spleen of 56 ± 23 at rest. Under adneosin-stress mean was 60 ±17 for myocardium, 48± 28 for spleen. In the selective coronaryangiographie 57 % (21 of 37 patients) had one relevant coronary artery stenosis. PE showed splenic switch-off in 59 % (22 of 37 patients) by analysing PE. 60 % without splenic switch-off showed normal MPRIUpslope while 40 % (6 of 15) decreased MPRIUpslope (<1,5). In patients with no splenic switch-off and decreased MPRIUpslope 50 % showed a relevant coronary artery Stenosis in invasive coronary angiographie.
Conclusion: Splenic switch-off showed a low specificity for detection of understress in adenosin-stress perfusion-scans.

10:30 - 12:00 **Room M 3**

Computer Applications

SS 1005

Radioprotection and dose management

Moderators:
A. Alberich-Bayarri; Valencia/ES
R. Kikinis; Boston, MA/US

B-0842 10:30

Implementation of size specific dose estimates (SSDE) into an automated institutional CT dose monitoring system: feasibility and initial results
N. Heinzler, C. Thomas, O. Bethge, P. Kröpil, G. Antoch, J. Boos;
Düsseldorf/DE

Purpose: To implement SSDE calculation based on water-equivalent diameters (Dw) of all slices of the CT scan volume into automated CT dose monitoring and to compare SSDE values with scanner indicated CTDIvol in chest and abdominal CT.
Methods and Materials: 1476 consecutive clinical abdominal and chest CT examinations (517 chest/905 abdominal, age 62±15yrs; 850male/626female, BMI 25.5±5.0kg/m²) were analysed. An in-house developed Matlab image segmentation device (The Mathworks, Natick, MA) was used to automatically calculate Dw of every slice of the scan volume. SSDE were automatically calculated using the mean Dw of the scan volume and transferred into the institutional CT dose monitoring software. Two radiologists independently evaluated the accuracy of the image segmentation algorithm in 100 consecutive CTs (one random slice per exam) on a 5-point scale (1=false segmentation, 5=perfect segmentation). SSDE values were compared to CTDIvol.
Results: The accuracy of the image segmentation algorithm was excellent (median rating 5, inter quartile range 4-5) and false segmentation was not identified. Automated calculation and transfer of SSDE into the CT dose monitoring system was successful in 1476/1476 (100%) exams. SSDE were higher compared with CTDIvol in chest CT (5.8±3.6mGy vs. 5.4±3.2mGy) and in abdominal CT (10.7±6.1mGy vs. 8.8±5.6mGy)(p<0.001, respectively).
Conclusion: Automated correction of CT dose data to patient size using SSDE based on mean water-equivalent diameter of the scan volume is feasible. Implementation into automated CT dose monitoring allows for large scale analysis and initial results demonstrate that mean SSDE is higher than the uncorrected CTDIvol in abdominal and chest CT.

B-0843 10:38

How to reduce the overdose in conventional x-rays using a centralised electronic system in paediatric patients
E. Fraile[1], C. Benito[1], P. Fraga[2], J. Azpeitia[3], J. Albillos[1], E. Dominguez[4], J. Galobardes[5]; [1]*S. Sebastian de los Reyes/ES*, [2]*Coslada/ES*, [3]*Madrid/ES*, [4]*Arganda del Rey/ES*, [5]*Parla/ES (eduardo.fraile@salud.madrid.org)*

Purpose: To analyse the causes of alerts of overdose in conventional x-ray departments using and electronic centralise system and how we can reduce it using continuing education programmes.
Methods and Materials: We compare the number of alerts examination in conventional x-ray using a centralise electronic platform in six general hospitals in patient under 21, before and after implementation of educational programme for radiographers. The electronic system of record dose per examination allows us to know the causes of overdose and implementation solutions to fix it.
Results: We analysed 21778 examines from six hospitals during one month, of which 4024 were patients under 21. The number of alerts were 3796 (17.4%) and 191 (4.74%) were in patients under 21. The main causes were problems related with collimation and radiographer technique applied. After six month and the implementation of educational programme to the technician, the dose of radiation decrease between a 20% and 8% depended on age and type of examination.
Conclusion: Dose control systems and programmes of continuing education allow us reduce the overdose in paediatrics patients in conventional x-ray.

B-0844 10:46

Optimising cardiac CTA procedures: a practical multi-step approach using a dose management software

T. De Bondt[1], R. Salgado[1], M. Faure[1], P. Van Herck[1], F. Zanca[2], B. Shivalkar[1], P. Parizel[1]; [1]*Antwerp/BE*, [2]*Buc/FR (timo.debondt@gmail.com)*

Purpose: Defining an optimization strategy for cardiac CTA procedures and assessing its impact on radiation dose and image quality (IQ), using a dose management solution.
Methods and Materials: Data from 362 ECG-gated cardiac CTA procedures performed on a GE VCT 64-slice scanner were collected during a 5-month period, using DoseWatch (GE Healthcare). As data showed that dose exceeded the national dose reference level (DRL), multi-disciplinary meetings were held between radiologists, cardiologists, imaging technicians and a medical physicist to define a prudent 4-step plan aiming to optimize cardiac CTA doses. Interventions consisted of: 1/ protocol standardization, 2/ mAs range reduction for zero calcium-score patients, 3/ mAs range reduction for all patients with normal weight, 4/ scan length reduction. IQ was evaluated by a radiologist and a cardiologist, using the IQ-voting system in DoseWatch.
Results: Before the interventions, average DLP and CTDI were 741 mGy.cm and 42.12 mGy respectively - both above the DRLs of 490 mGy.cm and 35 mGy. Each step of the plan gradually reduced patient dose, with a final result of 556 mGy.cm and 33.73 mGy. Step 4 was less effective, because imaging technicians were reluctant to reduce the scan margin at the cost of missing relevant anatomy. IQ ratings indicate no diagnostic value loss.
Conclusion: Using a multi-step approach, we were able to reduce dose by approximately 25%. Open discussions across specializations and education of imaging technicians are of capital importance to safeguard quality of healthcare. Dose management software tools facilitate responsible optimization processes, with regard for IQ.
Author Disclosures:
T. De Bondt: Consultant; GE Healthcare. **F. Zanca:** Employee; GE Healthcare.

B-0845 10:54

Potential dose reduction in abdominal computed tomography using a model-based iterative reconstruction algorithm

B. Kataria[1], J. Nilsson Althén[1], Ö. Smedby[2], A. Persson[1], H. Sökjer[1], M. Sandborg[1]; [1]*Linköping/SE*, [2]*Stockholm/SE (bharti.kataria@liu.se)*

Purpose: The main advantage of Model-based Iterative Reconstruction (MBIR), as an alternative to filtered back projection (FBP), is noise reduction which may facilitate reduction in patient dose. The aim is to compare visual image quality in an abdominal CT examination between FBP and a commercial MBIR (ADMIRE) and to estimate potential dose reduction while image quality is maintained.
Methods and Materials: Fifty patients referred for an abdominal CT examination were recruited. A Siemens dual-source Somatom Force was used to obtain three data sets per patient with 30%, 70% and 100% tube loads. Four image criteria from the European Guidelines for Image Criteria for CT, together with overall noise and image quality were assessed in a pairwise fashion by five radiologists. Visual Grading Regression (VGR) was used to estimate potential dose reduction, controlling for fixed and random effects, when comparing FBP with MBIR. Weighted kappa (κ_w) was used to calculate inter-observer and intra-observer agreements. The limit of significance was set at p=0.05.
Results: A significant strong effect of log mAs and ADMIRE was seen, with potential dose reduction of 22-47% for strength 3 and 34-74% for strength 5 compared with FBP ($p< 0.001$) for almost all image criteria. Inter-observer reliability showed an agreement of 71-76% (κ_w 0.201 to 0.286) and intra-observer reliability (κ_w 0.525 to 0.783) with an agreement of 82-96%.
Conclusion: MBIR (ADMIRE) showed improved image quality compared with FBP. A positive correlation between ADMIRE strength and increasing potential dose reduction was found for some, but not all, image criteria.

B-0846 11:02

Determination of iterative reconstruction dose reduction potentials in CTA with a novel image quality assessment method based on forced-choice comparisons

S. Ellmann[1], F. Kammerer[1], M. Brand[1], T. Allmendinger[2], M.S. May[1], M. Uder[1], M. Lell[3], M. Kramer[1]; [1]*Erlangen/DE*, [2]*Forchheim/DE, Erlangen/DE*, [3]*Nürnberg/DE (stephan.ellmann@uk-erlangen.de)*

Purpose: Iterative reconstructions (IR) permit CT dose-reduction potential. Diagnostic quality of dose-reduced images is mostly assessed using Likert-scales, but their ordinal character prohibits calculations of e.g. standard deviations or confidence intervals. This study presents a novel image quality assessment method devoid of statistical restrictions accompanying Likert Scales and exemplarily determined dose-reduction potentials of Circle-of-Willis CTA.
Methods and Materials: Dose-reduced CTA images of 10 patients undergoing head CTA were reconstructed using Sinogram-affirmed iterative reconstruction (SAFIRE) and compared with full-dose FBP in pairwise manner by five observers with 3,000 ratings in total. Images differed in the degree of dose reduction, IR-strength (3 vs 5) and the size of the vessels of interest.
Regression curves were calculated from the observers' preferences for dose-reduced IR over FBP images. Regression curve progression facilitated conclusions on the level where dose-level IR-images were equal to full-dose-FBP images in terms of vessel definition.
Results: Dose reduction potential in head CTA was significantly dependent on the size of the vessel of interest and on the strength of the IR algorithm. Large vessels reconstructed with SAFIRE 5 offered a dose reduction potential of 84% (95% CI 82.9-85.8%), whereas small vessels reconstructed with SAFIRE 3 permitted dose reductions of 40% (35.2-45.8%).
Conclusion: This study presents a novel method to determine CT dose reduction potentials, which in contrast to other established methods permits exact calculations and versatile statistical analyses. For an exemplary investigation of Circle-of-Willis CTA, considerable radiation dose reductions were achievable, which were nonetheless dependent on vessel situation and clinical question.
Author Disclosures:
T. Allmendinger: Employee; Siemens Healthineers. **M.S. May:** Speaker; Siemens. **M. Uder:** Speaker; Bracco, Medtronic, Siemens, and Bayer Schering. **M. Lell:** Grant Recipient; Bayer and Siemens. Speaker; Bayer and Siemens.

B-0847 11:10

Image quality of ultra-low-dose CT examinations in overweighed patients using iterative model-based reconstruction

N. Große Hokamp, K. Slebocki, K. Mamadov, J. Salem, J. Herden, D. Maintz, D.-H. Chang; *Cologne/DE (nils.grosse-hokamp@uk-koeln.de)*

Purpose: Iterative model-based reconstruction methods (IMR) enable improvement of image quality. Purpose of this study was to assess image quality and diagnostic confidence in overweighed patients in ultra-low-dose CT examinations (ULD-CT).
Methods and Materials: Image quality and radiation dose (dose-length product) were retrospectively reviewed for overweighed patients (BMI ≥ 25 kg/m^2) who underwent ULD-CT for the evaluation of acute flank pain and suspected urolithiasis. All scans were performed at 100 kVp and a fixed tube current (50mAs). Images were reconstructed using filtered back projection (FBP), iterative reconstruction (iDose) and IMR. Image quality was objectively evaluated as contrast-to-noise-ratio (CNR) and subjectively by 2 readers for diagnostic confidence, delineation of ureters, noise and sharpness on a 4-point Likert Scale, respectively. Statistic significance was assessed using ANOVA and Friedman-Multiple-Comparison-Testing with Bonferoni and Dunn post-hoc.
Results: 20 patients with a BMI of 31.6 ± 7.4 kg/m^2 were enrolled in this study. Urolithiasis was detected in 17 patients (85%). Mean DLP was 106.8 ± 34,3 mGy*cm.In relative terms, use of IMR yielded a 370% and 122% improvement in CNR relative to FBP and iDose ($p\leq0.001$). Subjective image quality with IMR always received higher ratings as compared to FBP and iDose for all criteria and from both readers. In particular, diagnostic confidence was significantly higher using IMR (3.2/4, 2.4/4 vs. 1.6/4 $p\leq0.05$).
Conclusion: ULD-CT protocol using IMR in overweighed patients was feasible in all examinations. IMR should be preferred to FBP and iDose as both image quality and diagnostic confidence are improved.

B-0848 11:18

Improved image quality of low-dose CT combining with iterative model reconstruction algorithm for response assessment in patients after treatment of malignant tumour

X. Xin[1], J. Shen[1], S. Yang[1], S. Liu[1], M. Wang[1], A. Hu[1], Y. Jiang[2], Z. Sheng[1], Q. Han[2]; [1]*Nanjing/CN*, [2]*Shanghai/CN (yanjiangcs@hotmail.com)*

Purpose: To evaluate the image quality of low-dose CT combining with iterative model reconstruction (IMR) algorithm for response assessment in patients after treatment of malignant tumour.
Methods and Materials: 47 patients (mean age 57.8±10.9, 30 men, BMI 22.09±2.35kg/m^2) after treatment of malignant tumour underwent chest and abdomen CT twice for response assessment with an interval of 6 months according to clinical routine. The first CT scans were performed with routine dose (RD) protocol at 120kV and images were reconstructed with filtered back projection (FBP) algorithm; while the second scans were performed with low-dose (LD) protocol at 100kV and images were reconstructed with FBP and IMR respectively. All scans were performed using automatic tube current modulation technique with image quality index of 18. Objective image quality including CT attenuation, image noise, and CNR, subjective image quality including artefacts,visualization of small structures and diagnostic confidence, as well as lesion detection were assessed and compared.
Results: Effective radiation dose of LD-CT scans was reduced 51.5% compared to RD-CT scans (30.5±7.4mSv vs. 14.8±2.7mSv). Higher CT

attenuation were found in both LD-IMR and LD-FBP images compared to RD-FBP images. Better subjective image quality and CNR as well as lower objective noise were found in LD-IMR images (all, p<0.05). Two small lesions (diameter <= 1cm) were missed on LD-FBP images, which can be observed in LD-IMR images.
Conclusion: IMR can help 50% radiation dose reduction without compromising image quality in patients after treatment of malignant tumours to repeated chest and abdomen CT for response assessment.

B-0849 11:26

Reduction of iodinated contrast dose and increase quality of practice on CTPA with a programme for data recording and dose personalisation P3T and the use of an 18G for venous access

M. Perez-Pena, E. Diaz, J. Vazquez, I. Gutiérrez, S. Shehadeh, C. Quispe, C. Huerta, H. Bernardo, R. Diaz; *Mieres/ES (mar_perez@yahoo.com)*

Purpose: We present our experience in the performance of CT of pulmonary arteries (CTPA) using a programme for iodinated contrast data recording and dose personalisation P3T, and a venous access of 18G on antecubital location.
Methods and Materials: 125 patients underwent CTPA (January-June 2016), 64 women-61 men, using a programme for iodinated contrast data recording and dose personalisation that calculates amount of contrast based on various factors, among which weight is the most determinant. We used a venous access of 18G needle placed on the elbow flexure. We analysed our data using SPSS V.11 and compared with our old protocol, in which we used a fixed amount of 90 ml.
Results: Our results showed a significant difference on the amount of contrast used, mean value 79,5ml per patient in comparison to 90ml of our old protocol (p< 0,001), with a decrease in contrast injected per patient of -10,44ml (95% confidence interval (-12.05, -8.83). There is also significant difference between men and women related to weight (p<0,001). Mean flux was 5,9ml/sec, and by using a venous catheter of 18G placed in the elbow flexure we suffered one extravasation. This programme provides a data recording of the injection protocol and sends a report to the PACS.
Conclusion: The use of P3T on CTPA decreases the dose required antecubital location of needle and 18 gauge decreases extravasations P3T provides a data recording of the injection protocol and sends a report to the PACS, thus increasing the quality of practice.

B-0850 11:34

Comparison of radiation dosage and image quality: digital breast tomosynthesis (DBT) vs full-field digital mammography (FFDM)

Y. Choi[1], O. Woo[1], H. Shin[1], G. Choi[1], K. Cho[1], B. Seo[2]; [1]*Seoul/KR*, [2]*Ansan/KR (yoom880103@gmail.com)*

Purpose: With increasing concern of individual radiation exposure doses, studies analyzing radiation dosage in breast imaging modalities are required. Aim of this study is to compare radiation dosage and image quality between DBT and FFDM.
Methods and Materials: 221 patients (mean age 51.7 years) who studied both DBT and FFDM were retrospectively reviewed. Radiation dosage data were obtained by radiation dosage scoring and monitoring program: Radimetrics (Bayer HealthCare, Whippany, NJ). Entrance dose and mean glandular doses in each breast were obtained in both imaging modalities. To compare the image quality of DBT with two-dimensional synthesized mammogram (2DSM) and FFDM, 5-point scoring system for lesion clarity was assessed and compared. The parameters of radiation dosages (entrance dose, mean glandular dose), and image quality (lesion clarity scoring) were compared between two modalities by using paired t-test and Wilcoxon rank sum test.
Results: For entrance dose, DBT had lower mean dosage (12.7mGy) compared with FFDM (28.3mGy, p-value <0.0001). Mean glandular doses for both breasts were lower in DBT (Left 3.34, Right 3.42) compared with FFDM (Left 3.98, Right 4.02, p-value 0.03, 0.008). The lesion clarity score was higher in DBT with 2DSM (mean score 4.59) compared with FFDM (3.32, p-value <0.0001).
Conclusion: DBT showed lower radiation entrance dose and also lower mean glandular doses to both breasts compared with FFDM. Also, DBT with 2DSM had better image quality than FFDM, suggesting that DBT may have a potential to be performed as an alternative to FFDM.

B-0851 11:42

Effect of QuantaStream denoising on image quality and diagnostic accuracy of low-dose CT in patients with suspected appendicitis

M.M. Kolb[1], C. Storz[1], J. Kim[2], D. Ketelsen[1], F. Bamberg[1], K. Nikolaou[1], A.E. Othman[1]; [1]*Tübingen/DE*, [2]*Seoul/KR (m_m_kolb@web.de)*

Purpose: To determine the effect of a novel denoising technique on image quality and diagnostic accuracy on low-dose CT in patients with suspected appendicitis.
Methods and Materials: 50 consecutive patients with suspected appendicitis who underwent contrast-enhanced abdominal CT (120kV, CARE dose reference 160-200mAs) were retrospectively included. Low-dose CT datasets were generated using realistic reduced dose simulation at 25% of the original exposition. Low-dose datasets were then denoised using a novel QuantaStream technique. All original, low-dose (ND25) and denoised (D25) datasets (n=150) were evaluated regarding objective (signal-to-noise ratio, SNR), subjective image quality (5-point Likert scale by overall quality, image noise, and diagnostic confidence) and appendicitical signs (including perforation or abscess formation) by two independent readers.
Results: SNR of ND25 were significantly lowest (p<.001) with no significant difference between original and D25 (p>0.14). Similarly, subjective image quality was rated highest for original and D25 and lowest for ND25 (all p<.05). Appendicitis was correctly identified in all datasets (n=24, sensitivity: 1.00, NPV: 1.00). Diagnostic confidence was highest for original, followed by D25 and was lowest for ND25 (p=.001). Presence of complications was correctly identified on original and D25 datasets (sensitivity: 1.00, NPV: 1.00) whereas 3 and 1 features were not identified on ND25 (respectively sensitivity: .75/.92, NPV: .25/75). Inter-reader agreements were perfect for original and D25 (κ=1.0) and fair for ND25 (κ=0.66).
Conclusion: QuantaStream Denoising of lower dose abdominal CTs (25% of original exposition) maintains high diagnostics image quality and diagnostic accuracy in patients with suspected acute appendicitis and associated complications.

B-0852 11:50

The analysis of 2-year cumulative effective radiation dose and cumulative organ dose on regular follow-up CT scans in patients with breast cancer

J. Lee, H. Yong, O. Woo, E.-Y. Kang, G. Choi, Y. Choi; *Seoul/KR (ljw2000e@naver.com)*

Purpose: The aim of this study is to evaluate 2-year cumulative effective radiation dose and cumulative organ dose on regular follow-up CT scans in patients with breast cancer and to establish personalised low-dose CT protocol.
Methods and Materials: A retrospective study was performed on the patients with breast cancer who were diagnosed and managed consistently on the basis of routine breast cancer follow-up protocol between January 2012 and June 2016. Based on ICRP 103, the cumulative effective radiation doses of each patient for 2-year follow-up were analysed using the commercial radiation management software (Radimetrics, Bayer healthcare). The personalized effective doses on each organ were analysed in detail by the software-providing Monte Carlo simulation.
Results: A total of 3822 CT scans on 490 patients was evaluated (age 52.32 ± 10.69). The mean scan number on each patient was 7.8 ± 4.54. Each patient was exposed 95.54 ± 63.24 mSv of radiation for 2 years. The cumulative CT radiation dose was significantly higher in patient with lymph node metastasis (p=0.00). The HER-2 positive patients were more exposed to radiation compared to estrogen or progesterone receptor positive patient (p=0.00). There was no difference in the cumulative effective radiation dose with different age groups.
Conclusion: To acknowledge how much radiation exposed to a patient is a starting point of management of radiation exposure for patients with long-term CT follow-up. Precise and personalized protocol as well as iterative reconstruction may reduce hazard from unnecessary radiation exposure.

10:30 - 12:00 **Room M 5**

Neuro

SS 1011b

Vascular disorders

Moderators:
P. Due-Tønnessen; Oslo/NO
I.Q. Grunwald; Southend-on-Sea/UK

B-0853 10:30

A new brick in the wall? Use of vessel wall magnetic resonance imaging in the evaluation of intracranial vasculopathies

M. Reis Lima, M. Longo, R. Menegatti, J. dos Santos Muller, F. Aesse, B. Bressan Valentini, L. Vedolin; *Porto Alegre/BR (marjanalima@hotmail.com)*

Purpose: Vessel wall magnetic resonance imaging (VWMRI) is a tool in development that presents as an alternative for differentiation of cerebral vasculopathies. This study aims to evaluate applicability in differentiating intracranial atherosclerosis (IA), central nervous system vasculitis (CNSV) and reversible cerebral vasoconstriction syndrome (RCVS).
Methods and Materials: This is a retrospective cohort study. We reviewed imaging findings in patients who went through VWMRI for suspected intracranial vasculopathy. Among findings, we considered specially thickening and enhancement, which were correlated with gold-standard diagnosis (clinical and biochemical parameters).
Results: 18 patients were evaluated, with 37 altered vessels - 11 RCVS, 14 CNSV and 12 IA. 11 patients with CNSV presented wall thickening, while only 1 RCVS patient had it (p=0,008). There was no difference in thickening between CNSV and IA (p=0,586). All patients with CNSV and IA presented enhancement, while none RCVS had it. Between groups there were significant differences in enhancement: CNSV presented higher enhancement degree compared with IA (p=0,08). Regarding the pattern, CNSV showed diffuse pattern while IA showed heterogeneous pattern (p=0,002). In some cases, we noticed wall enhancement in V4 segment of vertebral arteries without other changes.
Conclusion: Our evaluation's preliminary results show satisfactory performance in differential diagnosis of intracranial vascular pathologies.

B-0854 10:38

Diagnostic performance of different perfusion algorithms for the detection of cerebral vasospasm

S. Afat[1], C. Brockmann[1], O. Nikoubashman[1], M. Müller[1], M. Brockmann[2], K. Nikolaou[3], M. Wiesmann[1], A. Othman[3]; [1]*Aachen/DE*, [2]*Mainz/DE*, [3]*Tübingen/DE (safat@ukaachen.de)*

Purpose: In this study, we aimed to assess the diagnostic performance of different perfusion algorithms for the detection of cerebral vasospasm as compared to angiography.
Methods and Materials: 39 datasets from 25 patients (57.5±10.8y) with suspected cerebral vasospasm were included. Volume Perfusion CT (VPCT) and angiography were performed within 6 hours. Perfusion maps were generated using a maximum slope (MS) and a deconvolution-based approach (DC). Two blinded neuroradiologists evaluated presence and severity of vasospasm on MS and DC perfusion maps on a 3-point Likert scale (0=no vasospasm, 1=vasospasm affecting <50%, 2=vasospasm affecting >50% of vascular territory). A third neuroradiologist assessed the angiography using the same 3-point Likert scale. Perfusion maps were evaluated regarding diagnostic accuracy for vasospasm with angiography as reference. Correlation analysis on perfusion maps and on angiography was performed. The agreement between MS and DC and the inter-reader agreement was assessed.
Results: DC perfusion maps yielded significantly higher diagnostic accuracy than MS perfusion maps (DC: AUC=.821; MS: AUC=.755; p=.014) with remarkably higher sensitivity for DC compared to MS (DC: sensitivity=.724; MS: sensitivity=.590). Findings on DC maps showed significantly higher correlation with angiography compared to MS (DC: R=.664; MS: R=565; p=.007). Findings in MS and DC showed substantial agreement (Kappa=.732). Regarding inter-reader analysis, (almost) perfect inter-reader agreement was observed for both MS and DC maps (Kappa≥.980).
Conclusion: Results of this study indicate that DC yields significantly higher diagnostic accuracy for the detection of cerebral vasospasm and higher correlation with angiographic findings compared to MS.

B-0855 10:46

Monitoring cerebral perfusion change after revascularisation by using arterial spin labeling in patients with Moyamoya disease

S. Lee, T. Yun, R.-E. Yoo, K. Kang, S. Choi, J.-H. Kim, H.-S. Kang, C.-H. Sohn, M. Han; *Seoul/KR (seunghyun.lee.22@gmail.com)*

Purpose: To evaluate whether arterial spin labeling (ASL) MRI can help identify the change in cerebral blood flow (CBF), collateral blood flow, and anastomosis site patency after revascularisation in patients with moyamoya disease (MMD).
Methods and Materials: This retrospective study was conducted in 140 patients with MMD who underwent middle cerebral artery (MCA)-superficial temporal artery anastomosis. Pre- and early/late postoperative ASL and digital subtraction angiography images were analysed. The absolute CBF (CBF_{MCA}) and normalised CBF values adjusted with respect to non-anastomosis side ($nCBF_{MCA}$) and cerebellum ($nCBF_{CbII}$) were calculated in MCA territory. A collateral grading in MCA territory according to ASPECTS methodology and an anastomosis site patency were also assessed. The change in CBF was compared by using one-way analysis of variance with a Bonferroni correction for multiple comparisons, and inter-modality agreement was determined by kappa statistics.
Results: Significant increases in CBF_{MCA}, $nCBF_{MCA}$, and $nCBF_{CbII}$ were found after revascularisation (for pre- and early/late postoperative values, CBF_{MCA}; 35.2 [ml/100g/min]) ± 7.8, 56.3 ± 16.8, 51.5 ± 12.0, $nCBF_{MCA}$; 0.74 ± 0.12, 1.17 ± 0.23, 1.12 ± 0.16, and $nCBF_{CbII}$; 0.73 ± 0.14, 1.11 ± 0.25, 1.01 ± 0.18, respectively, P values < .001 for all). The agreements for collateral grading and anastomosis patency were moderate to good, with weighted kappa values of 0.77 (0.74-0.79) and 0.49 (0.32-0.66), respectively.
Conclusion: ASL MRI can identify the perfusional change after revascularisation, and it has the potential to serve as a non-invasive imaging tool to monitor the perfusional change after revascularisation in patients with MMD.

B-0856 10:54

Evaluation of AICA and vestibulocochlear nerve relationship in patients with vertigo

A. Öztek, I. Çakar, K. Karaali, U. Şenol; *Antalya/TR (alpoztek@gmail.com)*

Purpose: To establish the course of AICA, type of contact with the vestibulocochlear nerve (CN-VIII) and vascular contact at the root entry zone (REZ) in patients with vertigo.
Methods and Materials: CISS images of 125 consecutive patients who had temporal MRI were retrospectively evaluated by the radiologists independently. The course of AICA was: cisternal, abutting the internal acoustic meatus, looping into the proximal or distal half of IAC. Its relation to the CN-VIII was: touching, looping around, indenting or not touching it. Contact by any vessel in REZ was also noted. The control group consisted of asymptomatic sides of patients with unilateral symptoms and patients with symptoms not related to the CN-VIII. Types of AICA course, types of contact with the CN-VIII and presence of vascular contact at REZ were compared in symptomatic patients and the control group.
Results: Fifty-eight patients had vertigo and 67 patients were in the control group. Vascular contact near the origin of the nerve was significantly more common in the vertigo group (p<0.001). AICA loops into the proximal or distal halves of the IAC were more common in the vertigo group (p=0.041). There was no relationship between the type of contact and the presence of vertigo (p=0.264). There was good agreement between the two radiologists regarding vascular contact at REZ (K=0.650); but poor agreement in evaluation of the type of contact of AICA (K=0.422).
Conclusion: AICA loops into the IAC and vascular contact at REZ are more common in patients with vertigo.

B-0857 11:02

Impact of the global outflow angle on recanalisation after endovascular treatment of MCA bifurcation aneurysms

Y. de la Torre; *Poitiers/FR (yannick.delatorre@outlook.fr)*

Purpose: Intracranial aneurysm recanalization after endovascular treatment remains a major problem. The main goal of this study was to find new predictive factors of recanalization after EVT, by calculating 3D angle values between the arteries of the MCA bifurcation, and in particular the Global Outflow Angle.
Methods and Materials: Ninety-six aneurysms of MCA bifurcation, ruptured or not, treated only by endovascular approach, were included. Clinical factors, aneurysm anatomic parameters, postoperative occlusion class, percentage of packing volume and morphological parameters were studied. Angles were measured in 3D reconstructions of initial DSA, using three-dimensional coordinates of key points. The Global Outflow Angle was the sum of the two lateral angles of MCA bifurcations.

Results: Recanalization occurred in 25 cases (26%), retreatment performed in 11 cases (11%). Only one patient (1%) had a rebleeding. Univariate analysis established as predictive factors of recanalization: high blood pressure, the aneurysm size, neck size, postoperative occlusion class, the percentage of packing volume, the two Outflow Angles, and the Global Outflow Angle. Multivariate analysis established two independent risk factors of recanalization: the Global Outflow Angle (OR=1.05; 95% CI, 1.02-1.08; p<0.002) and the aneurysm width (OR=0.67; 95% CI, 0.46-0.96; p=0.031). A Global Outflow Angle threshold <192° was found to be a risk factor of recanalization (OR=13.75; 95% CI, 4.46-42.44).
Conclusion: This study emphasizes that a new parameter, the Global Outflow Angle, could be predictive of recanalization for MCA bifurcation aneurysms treated by EVT. This should be kept in mind during the periprocedural management of this subgroup of patients.

B-0858 11:10

Role of endovascular intervention in intracranial arterial pseudoaneurysms

N. Khandelwal, C.K. Ahuja, V. Gupta, A. Kumar, P. Singh, K.K. Mukherjee; *Chandigarh/IN (ajay2509@gmail.com)*

Purpose: Latrogenic traumatic intracranial aneurysms are rare occurrences, but their clinical impact is significant due to the high risk of intracranial haemorrhage and eventual demise. We describe a short series of 11 such cases and discuss the diagnosis and management of these.
Methods and Materials: Last 8 years database of the Interventional neuroradiology section was analysed. All cases of intracranial pseudoaneurysms were extracted and the records were analysed pertaining to the following parameters: primary disease, intervention done, secondary complaints, imaging, treatment offered, if any and follow-up.
Results: 11 cases of iatrogenic intracranial pseudoaneurysms were extracted from the last 8 years DSA database. Of these, 7 were secondary to transsphenoidal surgery for pituitary macroadenomas, 2 were the result of transcranial surgery for meningiomas and the remaining 2 secondary to surgical clipping of ruptured aneurysms. Eight patients were managed by endovascular means (endosaccular coiling and parent artery occlusion/trapping using sandwich technique). Of these, 1 patient had undergone stent graft placement but eventually required a parent artery occlusion due to significant endoleak. Three patients succumbed due to massive bleed prior to any attempt of treatment. All the patients treated had a successful outcome, the follow-up duration being 3 months to 18 months.
Conclusion: Endovascular management with embolisation currently forms the mainstay of treatment of intracranial pseudoaneurysms with reasonably good success rates. Quick diagnosis and prompt treatment is the key to prevent fatality.

B-0859 11:18

Endovascular therapy vs thrombolysis in patients with anterior circulation stroke in everyday clinical practice

M. Politi, M. Alexandrou, B. Gemes, C. Roth, P. Papanagiotou; *Bremen/DE (mariapoliti@hotmail.com)*

Purpose: In patients with large vessel occlusions, endovascular treatment has been shown to be superior to intravenous thrombolysis in recent trials. The aim of this study was to analyse the impact of endovascular treatment on clinical and radiological outcome in everyday clinical practice.
Methods and Materials: We compared the rates of good outcome (modified Rankin scale ≤ 2 at discharge) and in-hospital mortality in patients with distal intracranial carotid artery, M1 and M2 occlusions during two time periods. From January 2008 to October 2012, a total of 509 patients were treated with intravenous thrombolysis and from November 2012 to December 2014, a total of 270 patients received endovascular treatment (with or without intravenous thrombolysis).
Results: Significantly, more patients in the endovascular treatment group than in the intravenous thrombolysis group had a good outcome (37% vs. 27%, $p < 0.01$). An excellent clinical outcome (mRS 0-1) was seen in 20% of the patients in the endovascular treatment group vs 13% of the patients in the intravenous thrombolysis group. There was no difference concerning in-hospital mortality in the two groups.
Conclusion: In everyday clinical practice and compared with intravenous thrombolysis, endovascular treatment significantly improved clinical outcome.

B-0860 11:26

Hypoplasia of the anterior cerebral artery A1 segment is a risk factor for post-treatment recanalisation of anterior communicating artery aneurysms

V. Onofrj, M. Cortes, D. Tampieri; *Montreal, QC/CA (valeriaonofrj@gmail.com)*

Purpose: The purpose of this study is to assess an association between the presence of anatomical variants of the anterior cerebral artery (ACA) in patients receiving treatment for an anterior communicating artery (ACoA) aneurysm and post-treatment recurrence.
Methods and Materials: 194 patients received treatment with coiling for an ACoA aneurysm between 2001 and 2016. Presence of anatomical variants of the ACAs and ACoAs were retrospectively assessed and the geometry of the aneurysm was evaluated by assessing if the aneurysm main axis direction was parallel to that of the parent vessel. 113 of the treated patients received regular follow-up with MRA and/or angiography up to 6 years after treatment. Aneurysm neck and sac recanalisation were measured at each follow-up. We analysed the association between recanalisation of the aneurysm, the presence of anatomic variant of the anterior cerebral artery and the aneurysm configuration.
Results: In 48% of patients hypoplasia of the A1 segment contralateral to the side of the aneurysm was identified. 58% of the aneurysms were oriented parallel to the parent vessel. Aneurysm size and shape were similar between groups ($p>0.05$). Overall recurrence was significantly more frequent in patients with A1 hypoplasia ($P<0.01$) and in patients with both A1 aplasia and which aneurysms main axis was oriented parallel to the axis of the parent artery ($p=0.03$). Cox regression showed A1 hypoplasia was a significant predictor of time to recurrence (hazards ratio=2.48, 95% CI, $p<0.01$).
Conclusion: A1 hypoplasia is a predictor of post-treatment recanalisation of ACoA aneurysms.

B-0861 11:34

Role of CT and MR angiography in follow-up of intracranial aneurysms

N. Khandelwal, C.K. Ahuja, V. Gupta, A. Kumar, S.K. Gupta; *Chandigarh/IN (ajay2509@gmail.com)*

Purpose: Intrarterial digital subtraction angiography (IADSA) is currently the gold standard for the follow-up of treated intracranial aneurysms. The study evaluated the performance of CTA and MRA in the follow-up evaluation of clipped and coiled aneurysms.
Methods and Materials: After institute IRB approval, a total of 42 patients (47 intracranial aneurysms) were enrolled in the study which comprised clipping arm (Group I; 24 patients; 29 aneurysms) and coiling arm (Group II; 18 patients; 18 aneurysms). CTA, DSA and MRA were performed within 1 week of each other. The following parameters were assessed: the quality of the images, the presence of clip/coils and motion artefacts, presence/absence of the aneurysm remnant, completeness of the occlusion of the aneurysm, duration of examination and cost of the study.
Results: Reasonably good aneurysm detectability was obtained in 70.2% patients (combined groups I and II) by CTA; 96.7% in group I and 27.8% in group II. CTA underestimated residual aneurysm size (2.214±1.4392 mm) compared to 3D-DSA (2.7727±1.67874) which; however, was not significant. 100% aneurysm detectability was achieved in all patients on MRA in Group II; however, it was less than 60% in Group I (done in only 10 patients). Mean size was nearly similar (2.875±1.6520 mm) with 3D-DSA (2.946±1.7012). Procedure duration, cost and adverse effects of both CTA and MRA were significantly less as compared to DSA.
Conclusion: CTA is a reasonably efficacious alternative to DSA in detection of clipped aneurysm remnants while MRA performs well for the detection of coiled aneurysm remnants.

B-0862 11:42

Sinovenous outflow restriction outweighs cortical venous drainage as a parameter associated with haemorrhage in dural arteriovenous fistulas in the transverse-sigmoid sinus

Y.-S. Hu, C.-J. Lin, H.-M. Wu, W.-Y. Guo, C.-B. Luo, C.-C. Wu, W.-Y. Chung, K.-D. Liu, H.-C. Yang; *Taipei/TW (sam6526@hotmail.com)*

Purpose: The haemorrhage rates in dural arteriovenous fistulas (DAVFs) with cortical venous drainage (CVD) vary widely and sinovenous outflow restriction (SOR) contributes to haemorrhage. We hypothesize that SOR plays a more important role in DAVF haemorrhage than does CVD.
Methods and Materials: Retrospectively (1995-2016) recruited 163 cases of DAVFs in the transverse-sigmoid (T-S) sinus were divided into haemorrhage and non-haemorrhage groups based on initial presentation. Their angiograms and magnetic resonance imaging were evaluated, with evaluators grading the sinovenous outflow patency as the combined sinovenous conduit score (CCS), ranging from 0 (total occlusion) to 8 (fully patent). The median CCS was compared between the haemorrhage and non-haemorrhage groups. We

established 2 logistic regression models based on the CVD and CCS, respectively, to compare their performances in predicting DAVF haemorrhage.
Results: Sinovenous outflow was significantly more restrictive (lower median CCS) in the haemorrhage group than in the non-haemorrhage group (1 versus 6.5; $p < 0.001$). A CCS ≤ 2 best discriminated between the groups with a sensitivity of 90.0% and a specificity of 88.1%. By contrast, CVD predicted the presence of haemorrhage with a sensitivity of 80.0% and a specificity of 73.4%. The CCS model had a better predictive performance than did the CVD model ($p = 0.018$).
Conclusion: The grading system semiquantifies SOR and SOR may represent a stronger imaging parameter associated with haemorrhage in DAVFs of T-S sinus than does CVD, which may offer potential guidance in therapeutic decision making.
Author Disclosures:
C. Lin: Research/Grant Support; the Ministry of Science and Technology, ROC (MOST 104-2314-B-010-037).

B-0863 11:50

Ruptured MCA aneurysms with a concomitant intraparenchymal haematoma: single centre treatment strategy evaluation in 81 patients

I.A.J. Zijlstra; *Amsterdam/NL (ij.a.zijlstra@amc.uva.nl)*

Purpose: The prognosis of patients with ruptured middle cerebral artery (MCA) aneurysms and an associated intraparenchymal haematoma (IPH) is bad, even after aggressive surgical therapy. The role of the haematoma volume in determining treatment strategy has not been extensively studied and little data are available on coiling with or without clot removal in these patients.
Methods and Materials: We retrospectively studied the clinical data and the imaging of consecutive patients with a ruptured MCA aneurysm and an IPH admitted between January 2006 and December 2015. The influence of IPH +/- intrasylvian haematoma volume (ISH) on the followed treatment strategies (coiling or clipping with or without clot removal and/ or decompression) and on clinical outcome was evaluated.
Results: Outcome data were available in 76 patients. Overall favorable outcome (mRs 0-3) rates after 3-6 months and mortality rates were 54%/ 18% after coiling and 43%/ 38% after clipping (p=0.46/ 0.10). Brain stem compression (BSC) before treatment was significantly associated with worse clinical outcome (p<0.01), IPH + ISH volume not. In patients with brain stem compression that needed decompression favorable clinical outcome rates and mortality rates were 11%/44% after coiling and 23%/ 54% after clipping.
Conclusion: Brain stem compression is a more important factor than IPH (+ISH volume) in determining the treatment strategy of patients with a ruptured MCA aneurysm and an associated IPH. In patients with BSC, clipping with decompression might be the preferred treatment strategy. In patients without BSC the treatment strategy can be based on aneurysm configuration and local expertise.

Saturday, March 4

10:30 - 12:00 **Room C**

Abdominal Viscera

SS 1401

Pancreas and bile ducts: imaging assessment

Moderators:
M. Bonatti; Bolzano/IT
B.I. Choi; Seoul/KR

B-0864 10:30

Definition of age dependent reference values for diameter of the common bile duct and pancreatic duct on MRCP from a population based cohort study

M.-L. Kromrey, F. Kasprowicz, J. Mayerle, M.M. Lerch, J.-P. Kühn, G. Beyer; *Greifswald/DE (marie-luise.kromrey@uni-greifswald.de)*

Purpose: To define new reference values for diameters of pancreaticobiliary ducts on magnetic resonance cholangiopancreatography (MRCP) in general population and to identify factors influencing duct size.
Methods and Materials: Study subjects were recruited from the population based Study of Health in Pomerania (SHIP) and had whole body MRI + MRCP (1,5T). Diameters of pancreatic duct (PD) and common bile duct (CBD) were measured on MRCP before and after administration of secretin by an investigator blinded to other subject data.
Results: 1,385 subjects were initially scanned, 865 measured PDs and 938 CBDs were included for further analysis (median age 53y, 48.5% female). Subjects were excluded for missing data or evidence of pancreaticobiliary disease. The diameters increased with age (PD median (range) 1.-3. Quartile: 20-29y 1,33mm (1.20 - 1.57), >70y 2.49 (1.85 - 3.01); CBD median (range) 1.-3. Quartile: 20-29y 4.53 (3.87 - 5.17), >70y 6.50 (5.10 - 8.23)) and the historic upper limit of normal of 3mm for PD and 7mm for CBD were exceeded by 11% and 18.2% respectively. Subjects that underwent cholecystectomy presented with significantly increased diameter of CBD, but not PD (CBDw/oCCE: 5.30mm±1.893 SD vs. CBDw/CCE: 8.18mm±2.841 SD, p<0.01; PDw/oCCE: 1.84mm±.778 SD vs. PDw/CCE: 2.06mm±.868 SD, p>0.01).
Conclusion: Up to 18% of healthy volunteers would have undergone diagnostic workup for enlarged CBD or PD above the current reference standard. The width of the pancreaticobiliary ducts increases in an age dependent manner in asymptomatic volunteers. An increase of the CBD after cholecystectomy can be observed, the PD remains unaffected.

B-0865 10:38

CT texture analysis of downstaged ductal adenocarcinoma after chemoteraphy in predicting treatment response

M. D'Onofrio, V. Ciaravino, N. Cardobi, R. De Robertis, R. Pozzi-Mucelli; *Verona/IT (valentinaciaravino@gmail.com)*

Purpose: To evaluate the added value of CT texture analysis in the estimation of tissue changes in resected ductal adenocarcinoma after chemotherapy.
Methods and Materials: Patients with ductal adenocarcinoma downstaged after neoadjuvant treatment and therefore resected were included in this study. All the tumours were unresectable or borderline resectable at first evaluation. A pre-treatment and post-treatment CT study were obtained. The pancreatic phase of pre- and post-treatment CT study were used to evaluate the texture analysis. Tumour volume reduction was obtained in all cases based on which successfully tumour resection was performed in all cases. CT texture analysis results (Mean Value, Variance, Skewness, Kurtosis, Entropia) were compared by using Wilcoxon correlation test.
Results: 17 patients reached the resectable stage after neoadjuvant treatment. CT texture analysis was finalized in all cases. The comparison between Mean Value, Variance, Skewness and Entropia pre-treatment (MV median = 1082.70; V median = 876.31; S median = -0.23; E = 0,5520) in respect to post-treatment results (MV median = 1081.10; V median = 28.14; S median = - 0.09; E = 0,5520) shows no statistical significant difference (p > 0.05). The comparison between Kurtosis pre-treatment (K median=0.34) and Kurtosis post-treatment (K median -0.51) shows statistical significant difference (p < 0.05). Pathological correlation were performed.
Conclusion: This preliminary results on CT texture analysis of downstaged ductal adenocarcinoma show that this evaluation may represent an added value in the judgment of changes in tumour tissue, especially in those cases of ductal adenocarcinoma with no evident downsizing after chemotherapy.

B-0867 10:46

Patient-adapted respiratory training improves image quality of respiratory-triggered 3D MRCP in painful pancreaticobiliary disorders

L. Zhu, Z.-Y. Sun, D. Liu, P. Li, H.-D. Xue, Z.-Y. Jin; *Beijing/CN (zhuliang_pumc@163.com)*

Purpose: To compare the image quality of respiratory-triggered magnetic resonance cholangiopancreatography (RT-MRCP) with and without a patient-adapted respiratory training before the examination, in clinical patients with painful pancreaticobiliary disorders.
Methods and Materials: Hospitalised patients with painful pancreaticobiliary disorders who were scheduled for MRCP study were prospectively enrolled (n=31). The maximal numerical rating scale (NRS) of abdominal pain during the course of disease and the immediate NRS before the MRCP examination were recorded. Patient-adapted respiratory training was conducted before the examination. A sex- and age-matched group of patients with painful pancreaticobiliary diseases who underwent MRCP during the same time period served as control (n=62), who received ordinary instructions only. Acquisition time was recorded. General image quality, visualization of 12 segments of the pancreaticobiliary tree and diagnostic confidence based on 3D MRCP images were rated on a five-point scale and compared between the two groups.
Results: Maximal and immediate NRS of pain was comparable between the two groups. Image quality and diagnostic confidence were significantly improved (p<0.01 and p=0.02) in patients receiving respiratory training. Visualisation of left intrahepatic duct (p=0.02 for the trunk and p<0.01 for medial and lateral branches) and pancreatic duct (p<0.01 for head, body and tail segments) was also significantly better. The other segments showed no significant difference. The acquisition time was shorter (176±54s vs 253±67s, p<0.01) in the group with patient-adapted respiratory training.
Conclusion: Patient-adapted respiratory training is feasible in clinical practice and improves the image quality of RT-MRCP in patients with painful pancreaticobiliary disorders.

B-0868 10:54

Bile duct obstruction: diagnosis using contrast-enhanced ultrasound (CEUS)

F.J.P. Fontán, A.R. Reboredo, S. García Dubra, C. Rodríguez López, F. Vidal Filgueira; *Corunna/ES (carmenrlopez86@gmail.com)*

Purpose: The aim of this study was to investigate the value of contrast-enhanced ultrasound (CEUS) for evaluating biliary obstruction and in differentiating between benign and malignant causes.
Methods and Materials: Between November 2006 and September 2016, 124 patients with bile duct dilatation without visible cause in baseline ultrasound underwent CEUS study. All ultrasound studies were performed by the same radiologist .The enhancement and posterior washout were analysed in real time all along the study duration (5'). Final diagnosis provided by CEUS was compared with histologic diagnosis (47.58%) or with radiologic follow-up with TC, RM or ERCP.
Results: Final diagnoses included 89 malignant lesions (cholangiocarcinoma n=41, pancreatic carcinoma n=19, metastases n=16, hepatocarcinoma n=4, gallbladder carcinoma n=4, ampullary carcinoma n=2, lymphoma n=2 and neuroendocrine pancreatic tumour n=1); and 34 patients with benign condition, (lithiasis or sludge n=24, pancreatitis n=2, abscess n=1, xanthogranulomatous cholecystitis n=1, pancreatic serous cystoadenoma n=1, biliar elastance loss=4 and indeterminate n=2). CEUS correctly identified 74 of 89 malignant lesions (sensibility 83,14%) and 26 of 35 benign lesions (specificity 74.28%). The positive predictive value was 89.15% while the negative predictive value was 63.41%.
Conclusion: CEUS is useful to differentiate between benign and malignant causes of biliary obstruction, improves the detection of bile duct invasion in hepatic neoplasms and permits better evaluation of intra- and extraductal extension of hilar hepatobiliary tumours.

B-0869 11:02

Impact of MR elastography in patients with biliary obstruction

D. Kim, Y. Jeong, M.-S. Park, M. Kim; *Seoul/KR (kdk7118@yuhs.ac)*

Purpose: To investigate the impact of liver stiffness measured by MR elastography in patients with cholestasis due to biliary obstruction.
Methods and Materials: Sixty-nine patients who underwent pancreaticobiliary MR with MRE without history of diffuse liver disease were retrospectively included. Quantitative MR parameters including liver stiffness (LS), ADC, R2*, and fat fraction (FF) were measured. Laboratory results including aspartate transaminase (AST), alanine transaminase (ALT), total bilirubin (TB) were obtained. Patients were divided into two groups: patients with normal bilirubin level (group 1) and patients with cholestasis (group 2). Quantitative parameters were compared by independent t-test between two groups. Correlation between parameters was analyzed by Pearson correlation. Diagnostic performance and clinical impact of MR parameters was analyzed by ROC.

Results: Forty-nine patients classified into group 1 and twenty patients belonged to group 2. LS was higher in group 2 (3.8 ± 0.7 kPa) than group 1 (2.8 ± 0.5, p < 0.001), whereas other MR parameters were not different between two groups. There were positive correlation between LS and TB (r=0.611, P < 0.001), as well as the level of AST (r=0.350, P=0.004) and ALT (r=0.258, P=0.035). Furthermore, there was negative correlation between the degree of biliary decompression 1 week after bile drainage and LS (r= -0.71, P=0.003). When cut-off value was set at 4.0 kPa using ROC curve, the sensitivity and specificity for predicting biliary decompression was 84.6% and 100%, respectively.
Conclusion: LS measured by MRE increased as increasing cholestasis and can be a predictive factor for biliary decompression after biliary drainage.

B-0870 11:10

Validation of feasibility of MRI for measurement of depth of tumour invasion in distal bile duct cancer

J. Lee, N. Han, J. Kim, M. Kim, B. Park, D. Sung, K. Sim, S. Cho; *Seoul/KR (serendipish@gmail.com)*

Purpose: The aim of this study was to develop and validate a method for measuring depth of tumour invasion (DoI) on MRI and to investigate the diagnostic performance of measured DoI for the stratification of T classification in patients with distal bile duct cancer.
Methods and Materials: In this retrospective, institutional review board-approved study, 54 patients (30 men, 24 women; age range, 43-81 years) with distal bile duct cancer with available preoperative MRI were registered. A study coordinator and a pathologist developed 'provisional method' for measuring DoI based on published studies. Thereafter, 'improved method' was developed after compensating the defect. Two reviewers independently measured DoI on MRI using 'improved method' and correlations with histopathologic reference standard were evaluated by intraclass correlation (ICC). To evaluate the diagnostic performance of MRI for T classification using DoI, the study population was radiologically and histopathologically assigned into three groups according to the DoI.
Results: ICC between reviewers' measured DoI using 'improved method' and histopathologic DoI was very good or good (ICC coefficient, 0.885 and 0.784) and its' values were significantly higher than that using 'provisional method' (ICC coefficient, 0.501; p-value = 0.00000 and 0.00075). The overall accuracy of the use of MRI for stratifying bile duct tumours using DoI was 68.5 % to 85.2 %.
Conclusion: With the suggested method for measuring DoI on MRI in our study, we can reliably measure DoI on MRI T2-weighted image and MRI is a feasible tool for the preoperative T classification based on DoI.

B-0871 11:18

CT differentiation of benign and malignant gallbladder wall thickening

H. Yang[1], J. Lee[1], S. Lee[1], J. Park[2]; [1]*Seoul/KR*, [2]*Busan/KR (gedanken.yang@gmail.com)*

Purpose: To retrospectively analyse the CT imaging features to characterise gallbladder wall thickening as benign or malignant.
Methods and Materials: CT scans obtained including the portal venous phase in 108 patients with pathologically proven benign (n = 68), uncertain of malignant potential (n = 3), or malignant (n = 41) gallbladder wall thickening were retrospectively reviewed. Two blinded readers independently analysed concentricity, evenness, mucosal smoothness and layered pattern of the gallbladder wall thickening. Presence of multiple tiny enhancing dots in the thickened gallbladder wall, so-called "strawberry dot sign", was also investigated.
Results: Concentric and even wall thickening, smooth contour of the mucosa and double layering enhancement were significant predictors for benign gallbladder wall thickening (p&lt: 0.01 for each finding). Strawberry dot sign was significantly more frequent in benign wall thickening (p&lt: 0.01), particularly in adenomyomatosis (p>0.05). Sensitivities of strawberry dot sign in diagnosing adenomyomatosis were 92% in the reader 1 and 100% in the reader 2. On the contrary, strawberry dot sign was not observed in 70% (reader 1) and 68% (reader 2) of the cases with malignant diseases or uncertain of malignant potential entities.
Conclusion: Analysing the contour and layering of gallbladder wall thickening, and presence of strawberry dot sign on CT is helpful in differentiating benign entities from malignancy.

B-0872 11:26

Bile leakages after hepatic surgery and orthotopic liver transplantation: value of Gd-EOB-DTPA-enhanced MR cholangiography

F. Pacciardi, R. Cervelli, P. Boraschi, F. Donati, S. Salemi, R. Gigoni, M. Della Pina, F. Falaschi, D. Caramella; *Pisa/IT (federica.pacciardi@libero.it)*

Purpose: To assess the diagnostic value of Gd-EOB-DTPA-enhanced MR cholangiography in the detection of bile leakages after hepatic surgery and orthotopic liver transplantation.
Methods and Materials: Thirty-two patients with previous hepatic resection (n=20) or orthotopic liver transplantation (n=12) underwent MR imaging at 1.5T/3T device due to strong suspicion of bile leak, based on a combination of clinical, laboratory and previous imaging findings. After the acquisition of axial T1w/T2w images and conventional MR cholangiography (thin-slab 3D FRFSE and thick-slab SSFSE T2w sequences), 3D fat-suppressed coronal and axial LAVA sequences were performed before, 20 minutes and between 25 and 120 minutes after intravenous administration of 10ml Gd-EOB-DTPA (Primovist®, Bayer HealthCare). Two radiologists in conference evaluated all the images for the presence or absence of bile leak, and its location when present. Imaging results were correlated with direct cholangiography, percutaneous drainage of fluid collection and/or imaging follow-up.
Results: A well-defined collection containing contrast material was detected in 14 out of our 32 patients (one false negative case on MRI). Gd-EOB-DTPA-enhanced MR cholangiography yielded an overall sensitivity of 93%, specificity of 100%, PPV of 100%, NPV of 94% and accuracy of 97% for the diagnosis of an active bile leak. However, the sensitivity of 20 minutes delayed MR images was 47%.
Conclusion: Gd-EOB-DTPA-enhanced MR cholangiography utilizing delayed phase images is a highly reliable technique for the detection of active bile leakages after hepatic surgery and orthotopic liver transplantation. The images obtained 25-120 minutes after hepato-biliary contrast agent injection significantly increased the detection of leaks.

B-0873 11:34

Diagnostic value of Gd-EOB-DTPA-enhanced MR cholangiography in non-invasive detection of postoperative bile leakage

M. Kul, G.A. Erden, E. Düsünceli Atman; *Ankara/TR (melahatkul@yahoo.com)*

Purpose: To assess the value of dynamic T1-weighted (T1w) gadolinium ethoxybenzyl diethylentriamine penta-acetic acid (Gd-EOB-DTPA)-enhanced MR Cholangiography (MRC) for the diagnosis of active bile leaks.
Methods and Materials: A total of 28 patients with suspected biliary leakage who underwent routine T2w-MRC and T1w-GD-EOB-DTPA-enhanced MRC at our institution from February 2013 to June 2016 were included in this study. The image sets were retrospectively analysed in consensus by 3 radiologists. T1-weighted -Gd-EOB-DTPA-enhanced MRC findings were correlated with clinical data, follow-up examinations and findings of invasive-/surgical procedures. Patients with positive bile leak findings in Gd-EOB-DTPA-enhanced MRC were divided in hepatobiliary phase (HBP) (20-30 min) and delayed phase (DP) group (60-390 min) according to elapsed time until detection of bile leak after Gd-EOB-DTPA injection. These groups were compared in terms of laboratory test results (total bilirubin, liver function tests) and presence of bile duct dilatation in T2w-MRC images.
Results: The accuracy, sensitivity and specificity of dynamic Gd-EOB-DTPA-enhanced T1w-MRC in detection of biliary leaks were 92.9%, 90.5%, and 100%; respectively (P<0.001). Nineteen of 28 patients had bile leak findings in MRC, with 7 patients (36.8%) in HBP group and 12 patients (63.2%) in DP group. There was no statistically significant difference in terms of laboratory test results and presence of bile duct dilatation between HBP and DP group (P>0.05).
Conclusion: Dynamic T1-weighted Gd-EOB-DTPA-enhanced MRC is a useful non-invasive diagnostic tool to detect bile leak and prolonged delayed phase imaging may be required if extravasation of Gd-EOB-DTPA is not visible in HBP.

B-0874 11:48

An investigation into the use and outcomes of percutaneous transhepatic cholangiogram (PTC)

M. Renton, A. Ganeshan; *Birmingham/UK (mary.renton@nhs.net)*

Purpose: Percutaneous transhepatic cholangiogram (PTC) provides imaging of the biliary system. PTC is indicated for investigation and treatment of biliary obstruction. We investigate the use of PTC and factors that potentially predict outcomes.
Methods and Materials: We conducted a one-year retrospective case-note review of PTC procedures at Birmingham Heartlands hospital from September 2014. The following was recorded:-Patient: diagnosis and bloods-Procedure: intervention, antibiotics and technical success-Outcomes: bloods (day 1, 7 and month 1) and complications.

Results: 162 PTCs were performed in n=108 (59 male, mean 70.4 years). Malignant disease accounted for 76% of diagnoses, with 91% palliative cases. Baseline bloods included: bilirubin 194.73umol/L, albumin 23.09g/L and INR 1.25 with 16.3% >1.4. Procedures included 115 drains, 28 biopsies and 54 stents. Reduction in bilirubin occurred at day 1 (13.48 ±7.6), 7 (64.63 ±101.2) and persisted at month 1 (132.03 ±139.9). Sepsis occurred in 19% and fatal haemorrhagic pancreatitis developed in one patient. Hospital stay was 9.83days (±11.9) with 9% failed discharges. 7- and 30-day mortality were 12 (11%) and 28 (26%), respectively. Baseline bilirubin, haemoglobin and INR predicted mortality (p=0.015, 0.014, 0.018). Baseline albumin predicted delta bilirubin post-PTC (at all follow-up intervals p=0.02, 0.046 and 0.041) and hospital stay (p=0.002). Benign disease is a negative predictor for sepsis, p=0.006.
Conclusion: PTC is primarily used for palliative management of malignancy. It has a high technical success rate with substantial risk. Bilirubin, haemoglobin and INR should be considered in risk profiling to optimise patient selection.

10:30 - 12:00 **Room X**

Vascular

SS 1415

Assessing venous and lymphatic diseases

Moderators:
M.A. Aschauer; Graz/AT
C. Floridi; Varese/IT

B-0875 10:30

Feasibility of high-resolution MR lymphangiography in planning lymphaticovenous anastomosis treatment: a single-centre experience
F. Gentili, F.G. Mazzei, P. Gennaro, D. Notaro, A. Fausto, M.A. Mazzei, L. Volterrani; *Siena/IT (francescogentili@gmail.com)*

Purpose: To demonstrate the feasibility of MR lymphangiography (MRL) for imaging lymphatic vessels in patients with lymphoedema, its accuracy in distinguishing lymphatic vessels from veins, and its utility for planning lymphaticovenous anastomosis (LVA) treatment.
Methods and Materials: We prospectively enrolled 16 consecutive patients (13 female, range 18-70). All the patients underwent MRL, using a 1.5 T MR unit (Signa Twin Speed Hdxt; GE), after the intracutaneous injection of gadobenate dimeglumine (Gd-BOPTA) with a little dose of lidocaine into the interdigital webs of the dorsal foot or hand. Lymphatic vessels and veins identified for the LVA at MRL were histologically confirmed after surgery. Enhancement of lymphatic vessels and veins at different times after injection of contrast medium and their diameters were measured.
Results: Pathological lymphatic vessels were clearly recognised because of their tortuous and beaded appearance, whereas, the adjacent veins were straight with focal bulging only at the level of venous valve; the enhancement kinetic of the two different structures were different ($p<0.05$); the mean diameter of affected lymphatic vessels was similar to the adjacent veins ($p>0.05$). Thirty-four out of 38 specimens of presumed lymphatic vessels at MRI, collected during surgery, resulted positive at the immunoistochemical marker d2-40, with a significant association (Chi square=40.421, DF=1, $p<0.05$, contingency coefficient 0.644).
Conclusion: MRL is easy and safe to use and combines extensive informations on the anatomy and functionality of lymphatic vessels and veins in a single process; therefore, it could be useful in planning LVA treatment in patients with lymphoedema.

B-0876 10:38

Vector flow imaging evaluation of stenotic and functioning haemodialytic accesses
M. Raciti[1], I. Fiorina[1], A. Goddi[2], F. Calliada[1]; [1]*Pavia/IT*, [2]*Varese/IT (mariavittoria.raciti@libero.it)*

Purpose: The aim of this retrospective study is to evaluate the different features of the flow in arteriovenous fistulas (AVFs) between well functioning and stenotic accesses through vector flow imaging and in comparison with conventional Doppler.
Methods and Materials: Ultrasound VFI describes the flow through the use of many coloured vectors, representing velocity, magnitude and direction in every point of the vessel. 2 experienced radiologists examined vascular accesses of 6 patients (2 females, 4 males; age ranging from 32 to 83 years, median age 57.5 years), comparing vector flow imaging and Doppler through Resona 7 ultrasound scanner (Mindray, Shenzen, China).
Results: Doppler examination showed the presence of significant stenosis in 2 cases and good AVFs patency in 4 patients but did not provide any information regarding the flow layers' direction. VFI evidenced the presence of high-velocity vectors (mean 45-50 cm/s) directed against the vascular walls in correspondence of the stenosis, despite lower velocity orthogonal arrows (mean 20-25 cm/s) in well-functioning accesses.
Conclusion: The development of significant stenosis in arteriovenous fistulas could be correlated with wall shear stress, determined by the presence of orthogonal components of the flow against the vessel wall. VFI can help to show and identify high-velocity vectors facing the vascular surface. Further studies are in progress to demonstrate this relationship.
Author Disclosures:
A. Goddi: Consultant; Esaote, Mindray, SuperSonic. **F. Calliada:** Consultant; Mindray, Hitachi, Toshiba.

B-0877 10:46

Acute or subacute DVT - role of real time elastography for determining the age of thrombi
A. Aslan[1], E. Ayaz[1], H. Barutca[1], C. Kocaaslan[1], M. Aslan[1], I. Inan[2], S. Sahin[1], A. Yıkılmaz[1]; [1]*Istanbul/TR*, [2]*Adıyaman/TR (ercan_ayaz@yahoo.com)*

Purpose: Exact age of deep venous thrombosis (DVT) is of high importance for an appropriate treatment. The elasticity imaging could be a good way to estimate the age of DVT. In this study, real time elastography (RTE) which measures the hardness of tissue is used to detect and characterise changes in stiffness of thrombus in vessels semiquantitatively.
Methods and Materials: Patients who were diagnosed with CDUS and serum D-dimer level as acute DVT were enrolled into study and scheduled for follow-up imaging by CDUS after 15-30 days from initial diagnosis. RTE was performed together with CDUS and stiffness of thrombi classified into 3 as soft, intermediate, hard.
Results: 44 patients of acute DVT were enrolled in the study and 27 of them came back for control imaging. RTE could not be performed in 3 patients with acute DVT and 6 patients with subacute DVT. The elasticity patterns of 41 acute DVT were; 10 (24.4%) hard, 20 (48.8%) intermediate, 11 (26.8%) soft. The elasticity patterns of 21 subacute DVT were; 8 (38.1%) hard, 7 (33.3%) intermediate, 6 (28.6%) soft. But there was no statistically significant difference between elasticity patterns of acute and subacute DVT ($p = 0.463$)
Conclusion: In contrast to most of the previous studies which were strongly suggest that RTE can determine the age of DVT, we did not find any statistical significant difference between acute and subacute DVT in terms of tissue stiffness that is obtained by RTE.

B-0878 10:54

Venous thromboembolism in radiation oncology: retrospective trial
M. Cherkashin, N. Berezina, A. Serov, N. Vorobyov; *St. Petersburg/RU (mikhail.a.cherkashin@gmail.com)*

Purpose: To generate clinical evidence for VTE risk assessment in patients with radiation therapy.
Methods and Materials: In retrospective analysis, 3280 medical record were included (1612: RT and 1668: chemotherapy). Inclusion criteria: RT in outpatient setting, chemotherapy in outpatient setting. Exclusion criteria: combined radiochemotherapy, hospitalisation, central venous catheter, palliative treatment. We have selected 360 patients, stratified into 3 groups: group I (n=120) 3D-conformal RT for brain tumours or brain metastasis; group II (n=120) RT for body tumours (abdominal, retroabdominal, pelvic, chest, breast); group III (n=120) was control - brain and body tumours on chemotherapy. Mean fraction numbers - 25 (11 - 32), mean total dose - 52 Gy.
Results: Deep vein thrombosis (DVT) was detected in 7 cases (5.8%) in group I, in group II - 2 cases and in control - 1 case. VTE patients has a different tumours (right parietal area astrocytoma, brain trunk tumour, skull basis cancer, rectal cancer, breast cancer). 3 patients were available for long-term outcomes assessment (12 months after RT). During 1-year period we haven't detected thrombosis recurrence. Posthrombotic disease was developed without severe venous insufficiency. Difference between VTE incidence for group I and group III characterised by statistical significance ($p<0.05$). Risk difference for these groups was 5% ($p<0.05$)
Conclusion: External beam radiation therapy potentially may be an independent risk factor for VTE development in outpatient setting. These patients need to be strongly assessed for VTE prophylaxis

B-0879 11:02

Anatomy of the collateral venous drainage in late pregnancy in different positions
S.A. Mirjalili, G.P. Tarr, G. Williams, P. Stone; *Auckland/NZ (greg.tarr@otago.ac.nz)*

Purpose: Sleeping position has been associated with stillbirth, with increased risk in supine position. The gravid uterus can cause hypotension by compression of the inferior vena (IVC), but the path of venous drainage is not known in this setting. The aim of this study is to investigate collateral systemic venous drainage in late pregnancy in different positions.

Methods and Materials: After obtaining ethics approval and written consent, 5 healthy pregnant women 35-38 weeks gestation underwent MR in supine and left decubitus position (Siemens Skyra 3T) with T2 TRUFI and phase contrast flow. Measurements were obtained of cardiac output, calibre of inferior vena cava, azygous vein and abdominal aorta). Paired t-tests were used to compare intra-individual measurements.
Results: Cardiac output was unchanged in both positions. The IVC was completely collapsed at its origin in supine position in all cases. Compared to the decubitus position, supine positioning was associated with decreased cross sectional area of the IVC at the level of the liver (3.5 cm^2 [95% CI 2.7 to 4.3 cm^2] vs 5.5 cm^2 [95% CI 3.8 to 7.1 cm^2], p = 0.049) and increased cross sectional area of the azygous vein (0.36 [95% CI 0.03 to 0.68 cm^2] vs 0.77 cm^2 [0.48 to 1.06 cm^2], p = 0.008).
Conclusion: Healthy pregnant women without symptomatic supine hypotension maintain cardiac output when lying flat with increased distention of collateral venous drainage via the azygous venous system. These findings may help elucidate the contribution of systemic venous drainage to risk of stillbirth.

B-0880 11:10

Role of MRI in detecting lower limb incompetent perforator veins
B.K. Soni[1], H. Sahni[2], A. N[1]; [1]*Bangalore/IN*, [2]*Jorhat/IN*
(taureandoc@gmail.com)

Purpose: To differential incompetent perforators from competent perforator on the basis of size on MRI.
Methods and Materials: The prospective study was carried out in 30 patients during a period of six months at a tertiary care hospital in India after approval from institutional ethical committee. There were a total of 81 perforators studied and evaluated by both colour Doppler and True FISP, fat saturated axial sequence of MRI. The number and location of the perforators detected on Colour Doppler and MRI were documented and correlated.
Results: The study results shows that any perforator more than or equal to 2.8mm has got a positive predictive value of more than 95% for being incompetent and any perforator more than or equal to 3.4mm has got a 100% positive predictive value for being incompetent. The mean diameter of incompetent perforator was 3.57 and that of competent perforator was 2.27mm.
Conclusion: Addition of MRI to the colour Doppler in assessment of incompetent perforators in assessment of varicose veins is of tremendous importance especially in those patients planned for Foam Sclerotherapy. It is non-operator dependent and entire set of images is available for review and comparison.

B-0881 11:18

Recent diagnostic opportunities in ultrasound diagnostics of lower extremities deep veins thrombosis
A. Demidova, A. Zubarev, N. Krivosheeva, I. Rychkova; *Moscow/RU*
(333555.78@mail.ru)

Purpose: The aim of our study was to analyse physical basis and assess opportunities and advantages of new ultrasound technologies quantitative assessment of acoustic structures (Acoustic Structure Quantification, ASQ), ultrasound elastography (USE), mapping of microvascular bedflow with high spatial and temporal resolution (Superb Microvascular Imaging, SMI) in evaluation of patients with venous thrombosis of lower extremities.
Methods and Materials: The study involved 72 patients (41 men - 56,9% and 31 women - 43,1%) aged 42-85 with venous thrombosis of lower extremities (144 lower extremities). All patients had undergone standard ultrasound investigation including B-mode, colour duplex or power Doppler imaging modes. In addition to standard modes we used new ultrasound technologies announced by Toshiba Medical Systems in ultrasound system Aplio™ 500.
Results: We assessed condition of main veins of lower extremities, including revealing of thrombotic changes and estimation of the spreading level and composition of thrombotic masses. During dynamic follow-up signs of the initial stages of recanalisation were revealed and comparison of thrombolysis process intensity with further follow-up studies was performed. A significant advantage of new technologies in comparison with a standard ultrasound examination was established.
Conclusion: ASQ, USE and SMI of Toshiba Medical Systems can be effectively used for examining patients with venous thrombosis in the system of inferior vena cava. Taking into consideration the fact that these technologies are highly informative, not time consuming and simple in everyday use they can be recommended to be included into standard ultrasound investigation for precise assessment of revealed abnormalities.

B-0882 11:26

MR-venography in the diagnosis of post-thrombotic iliac vein obstruction and extravascular compression
V. Shebryakov, Y. Stoyko, M. Yashkin, G. Karmazanovskiy, D. Lutarevich;
Moscow/RU (VSHEBRYAKOV@MAIL.RU)

Purpose: Evaluate the information value of magnetic resonance imaging (MRI) in the diagnosis of post-thrombotic iliac vein obstruction and extravascular compression.
Methods and Materials: The study included 28 patients with CVD (clinical class C3-C6 according to the CEAP classification), including 7 men and 21 women. The average age was 43.6±11.6 years. Studies were performed from December, 2014 to June, 2016 on Optima MR360 MRI using a special protocol non contrast MR-venography in the sequences: 1. BH FIESTA (TRA, COR, SAG) using samples of Valsalva; 2. INHANCE 3D (SAG or COR) on the free breathing, with subsequent MIP and 3D reconstruction. Scan time no more than 15 min.
Results: Thirteen patients have been diagnosed with stenosis of the left common iliac vein due to compression of the right common iliac artery, with the lumen of the left common iliac vein was 4.1±1.6 mm, and the length of stenosis was 16.8±5.5 mm. One patient underwent stenting of left common iliac vein (self-expanding stent Wall-stent Uni Endoprotesis) with the syndrome Mey-Turner, the velocity of blood flow on Doppler ultrasound before the operation had the following characteristics: 55-63 cm/sec before stenosis and 84-110 cm/sec after. After stenting, the linear velocity of blood flow in the OPV was 40-45 cm/sec.
Conclusion: Non-contrast MR-venography is the most optimal screening method in the diagnosis of the causes of extra - and intravenous pathology of the IVC and its basin. 3D-reconstruction of the IVC and iliac veins can be used for planning reconstructive, corrective and reconstructive operations.

B-0883 11:34

Arterialisation of venous thrombosis as an indicator of tumoural vascular spread
G.G. Leal, J. Crosta, M. Centurion, M. Diaz Fusi, D. Sanchez, F. Abramzon;
Buenos Aires/AR (grettelealh@gmail.com)

Purpose: To describe the sonographic findings of venous thrombosis with arterial vascularisation within the tumour thrombus associated disease. Demonstrate the presence of arterial flow with color Doppler and spectral in the thrombotic material. Report enhancement with contrast ev of these thrombosis in the tomographic study. Emphasise the importance of these signs to suspect the presence of a tumour and vascular spread it.
Methods and Materials: Descriptive study. Case series. Ultrasonographic and tomographic images of three patients of our institution without prior cancer diagnosis, in which deep vein thrombosis by Doppler ultrasound was diagnosed in different anatomical territories are presented. Also presented with color Doppler and spectral, arterialisation of thrombosis, detected as arterial flows within the venous lumen occupied. It was detected in a nearby tumour posteriorly, checking vascular spread. Tumour pathologies were detected hepatocellular carcinoma, uterine sarcoma and pancreatic adenocarcinoma.
Results: Images are shown with the following findings: the presence of venous thrombosis level, arterial flows into the venous thrombus, the existence of tumoural pathology associated to thrombosis, enhancement with contrast ev. Thrombus in tomographic study. In US Doppler of the three patients it was observed thrombotic material endoluminal level in the scanned veins, with blood flow within the thrombus. Arterialisation demonstrated by spectral analysis. Also completed checking tomographic study thrombus enhancement with contrast ev.
Conclusion: The arterialisation venous thrombus in patients with no known history of tumour pathology should be suspected a hidden tumour and must be emphasised in the search for a primary for a final diagnosis.

B-0884 11:42

Time of flight MR venography - an important tool for evaluation of lower limb venous abnormalities
M.M. Kulkarin; *Mumbai/IN (makarand_kul@yahoo.com)*

Purpose: Time of flight (TOF) MR venography (MRV) is an effective, non-contrast technique which gives a road map of deep venous system to vascular surgeons. Doppler is an operator dependant modality leading to discrepancy in Interpretation. Contrast CT and contrast MRV lead to contamination of superficial veins and arteries leading to difficulty in visualisation of deep venous system.
Methods and Materials: We studied 175 patients of venous insufficiency on TOF MRV and Doppler. MRV was performed on 1.5 and 3 Tesla MRI with patient in supine position using surface body array coil. The saturation band was placed at the kidney level to block the arterial signals. Doppler was performed independently.

Results: We found discrepancy between the Doppler and TOF MRV in 44 patients (25%). Doppler was normal in 16 patients (9.4%) while MRV showed evidences of chronic deep vein thrombosis, mainly in pelvic veins. MRV gave important information about other causes of venous insufficiency like pelvic vein compression by adjacent artery (89%) or by tumour (1.6%). MRV also helped in therapeutic planning (venoplasty) in the patients with deep vein thrombosis in pelvic veins.
Conclusion: TOF MRV is an important adjuvant to Doppler in evaluation of patients with lower limb venous insufficiency with main advantage in the diagnosis of the pelvic vein abnormalities. It gives an anatomical depiction for the vascular surgeon while doing interventions. Due to static images, it is difficult to diagnose varicose veins and incompetent perforators which is limitation of this modality.

B-0885 11:50

May-Thurner syndrome: no pain, no gain
P. Armelin; *Campinas/BR (plinioarmelin@hotmail.com)*

Purpose: To spread knowledge of this disease and demonstrate the technical aspects of angiotomography for the accurate diagnosis, its treatment and possible complications.
Methods and Materials: We selected 20 cases with suspicion of May-Thurner syndrome. Patients underwent angiotomography with podalic contrast injection technique.The podalic venous puncture is more painful than the antecubital vein. However, the contrast injection flow is lower. The collateral circulation is better demonstrated, as well the identification of complications.
Results: The May-Thurner syndrome is a rare disease caused by compression of the left common iliac vein by the right common iliac artery, providing a number of symptoms depending on the degree of compression. Among them: asymmetrical swelling of the left lower limb, pain, unilateral varicose veins, ulcers and deep vein thrombosis. The syndrome is diagnosed in 2-5% of patients with chronic venous diseases. Most patients are women between the 2nd and 4th decades of life. This technique showed to be superior to the conventional techniques, such as Doppler ultrassound, conventional angiotomography, conventional angioresonance and venography. The endovascular treatment is safe, effective and reduces symptoms in most patients. It is associated with high rates of vascular patency and is the best option compared to conventional techniques and clinical treatment.
Conclusion: The angiotomography with podalic contrast injection technique was more effective in screening and diagnosis of May-Thurner syndrome, enabling the treatment planning and assessment of associated complications.

10:30 - 12:00 **Room Z**

Interventional Radiology

SS 1409

Portal interventions

Moderators:
R. Golfieri; Bologna/IT
M. Krokidis; Cambridge/UK

B-0886 10:30

Psoas muscle density predicts survival of cirrhotic patients undergoing transjugular intrahepatic portosystemic shunt
M. Shoreibah, S. Kim, S. Moawad, A. Abouarab, K. Mahmoud, B. Jackson, M.O. Massoud, S. Saddekni, A.M.K. Abdel Aal; *Birmingham, AL/US (snkim@uabmc.edu)*

Purpose: Sarcopenia is a common complication in cirrhotic patients and is also an independent predictor of survival in patients undergoing liver transplantation. The purpose of our study is to determine if the psoas muscle density (PD) can be used as a predictor of survival in cirrhotic patients who had transjugular intrahepatic portosystemic shunt (TIPS) placement.
Methods and Materials: We retrospectively reviewed the medical records of 216 patients who had TIPS placed between June 2005 and June 2015. We compared PD using the non-enhanced pre-TIPS CT scans. The primary endpoint was to determine if PD correlates with patient survival after TIPS. The secondary endpoint was to determine a threshold sensitivity of pre-TIPS PD for assessing mortality.
Results: The study included 134 (62%) males, 148 Caucasians (68.5%) with an average age of 56 years (SD=9.6). The main causes of cirrhosis were nonalcoholic steatohepatitis (30.6%), hepatitis C (23.2%), & alcoholic cirrhosis (20.8%). No significant difference between the pre-TIPS PD in the different etiologic groups (p=0.95). TIPS was performed for intractable ascites & variceal bleeding in 50.9% and 49.1% of the patients respectively. Mean MELD score was 13 and 16 before and after TIPS respectively. A higher pre-TIPS PD was associated with lower risk of mortality [HR= 0.52, 95%CI (0.32, 0.85), p=0.0088]. Threshold sensitivity of pre-TIPS psoas muscle density for assessing mortality was 43.63 HU (p=0.0049).
Conclusion: PD is a predictor of survival after TIPS placement in cirrhotic patients. A PD of more than 43.63 HU is associated with lower risk of mortality.
Author Disclosures:
S. Saddekni: Consultant; St Jude Medical. **A.M.K. Abdel Aal:** Consultant; St Jude Medical, Boston Scientific, WL Gore, Baxter Healthcare, Bard Peripheral Vascular Inc.. Grant Recipient; BTG, Covidien, Bard, Boston Scientific, Sirtex. Research/Grant Support; Celonova, Boston Scientific.

B-0887 10:38

5 years of portal vein embolisation prior to major hepatectomy
J.H. Luz, P. Luz, H. Gouveia, H. Martin, I. Faria, R. Souza, H. de Souza; *Rio de Janeiro/BR (jhugoluz@gmail.com)*

Purpose: To assess the efficacy, safety and lessons learned from portal vein embolisation prior to major hepatectomy, performed along 5 years in a single reference cancer centre, applying cyanoacrylate and lipiodol mixture as the embolic material.
Methods and Materials: From August 2011 through August 2016 forty-one patients (mean age: 55.9 years [5-80 year]) underwent trans-hepatic portal vein embolisation for colorectal liver metastases (n=29), hepatocellular carcinoma (n=2), cholangiocarcinoma (n=5), occult primary liver metastases (n=1), Wilms tumour liver metastases (n=1), Gist liver metastases (n=1) and hepatoblastoma (n=2). Assessment of future liver remnant was achieved by computed tomography volumetric measurements before and 4 weeks after portal vein embolisation. Adverse events were recorded for all patients.
Results: Technical success was 98% (one patient was submitted to a second portal embolisation procedure because of a patent segment VI branch). Three serious complications occurred: 1 patient died within 30 days of portal vein embolisation due to progressive liver insufficiency, 1 patient had unintentional cyanoacrylate migration to liver segment III and 1 patient developed a large biloma which was drained percutaneously. Resection was performed in 29/41 patients. After the waiting period (follow-up computed tomography was performed 21-46 days [median, 31 days]), the future liver remnant volume and future liver remnant to total liver volume ratio increased significantly (from a median value of 491g to 654g - Wilcoxon signed rank test p<0.001).
Conclusion: Although portal vein embolisation with cyanoacrylate-lipiodol mixture effectively produces future liver remnant augmentation, proficiency in the embolic agent usage must accompany this type of technique.

B-0888 10:46

Transjugular intrahahepatic stent-shunt (TIPSS) placement using C-arm cone-beam CT (CBCT) real-time 3-D-guidance-initial clinical experience
G. Böning[1], W. Lüdemann[1], J. Chapiro[2], M. Jonczyk[1], G. Wieners[1], D. Schnapauff[1], B. Gebauer[1], R.W. Günther[1], F. Streitparth[1]; [1]*Berlin/DE*, [2]*New Haven, CT/US (georg.boening@charite.de)*

Purpose: One of the technically most challenging procedures in interventional radiology is the placement of a transjugular intrahahepatic stent shunt (TIPSS). Aim of this study was to evaluate the feasibility of Cone-Beam CT (CBCT)-based real-time 3-D-guidance in TIPSS placement and relative dose of CBCT.
Methods and Materials: Real-time, 3-D-guidance based on a C-arm acquired CBCT (Allura Xper FD20 and XperCT, Philips Healthcare, Andover, USA) was used in 13 patients. Indications for TIPSS placement were therapy-refractory ascites in 12 cases and acute bleeding in 1 patient. Technical success of TIPSS-placement, puncture-time to assess portal-venous system, number of punctures needed and applied radiation dose of the intervention as well as relative dose of CBCT were documented.
Results: TIPSS could be successfully implanted in 12 of 13 patients (92 %). CBCT-based guidance for portal vein puncture was possible in all patients. Due to difficult anatomical situation in one patient the TIPSS could not be implanted neither after using additional US-guidance. Mean puncture time was 12±14 minutes, with 3±3 punctures needed in the 12 patients with technical success. During intervention total applied dose (dose area product, DAP) was 479±222Gy/cm². Relative dose of CBCT was 5±3%.
Conclusion: The use of CBCT-based real-time 3-D-guidance for portal vein puncture in TIPSS-placement was feasible and the relative dose of CBCT is low compared to total dose of intervention. This guidance technique has the potential to facilitate the TIPSS implantation, which has to be proven in further studies.

B-0890 10:54

Worsening of sarcopenia after transjugular intrahepatic portosystemic shunt
A.M.K. Abdel Aal, S. Kim, S. Moawad, B. Jackson, A. Abouarab, K. Mahmoud, N. Ghaleb, M.O. Massoud; *Birmingham, AL/US (akamel@uabmc.edu)*

Purpose: Sarcopenia is a common complication in cirrhotic patients and adversely affects the morbidity and mortality in these patients. The purpose of our study is to determine the change in psoas muscle density (PD) after

transjugular intrahepatic portosystemic shunt (TIPS) placement and its correlation with model of end-stage liver disease (MELD) score.
Methods and Materials: We retrospectively reviewed the medical records of 84 patients who had TIPS placed between June 2005 and June 2015. We compared the PD on the pre and post-TIPS non-enhanced CT scans.
Results: The study included 60 males (71.4%), 62 Caucasians (73.8%) with an average age of 53.9 years (SD=7.9). TIPS was performed for intractable ascites (50.9%) and for variceal bleeding (49.1%). There was a decrease in the PD (47.98 to 46.34HU) after TIPS placement but was not statistically significant (p=0.14). The change in PD did not vary significantly based on the MELD score. There was a significant increase in the MELD score after TIPS (12 to 15, p<0.0001) and decrease in serum albumin (2.8 to 2.61g/dL,p=0.04). There was no significant correlation between the change in PD and MELD score (r=0.03, p=0.81) or serum albumin (r=-0.09, p=0.40). There was a statistically significant negative correlation between PD and BUN (r=-0.301, p=0.0053), Cr (r=-0.221, p=0.0446), and bilirubin (r=-0.290,p=0.0082) after TIPS.
Conclusion: PD worsens after TIPS placement in cirrhotic patients. The change in PD does not correlate with MELD score or serum albumin. Further prospective studies with larger patient population are required to assess the validity of these results.
Author Disclosures:
A.M.K. Abdel Aal: Consultant; St Jude Medical, Boston Scientific, WL Gore, Baxter Healthcare, Bard Peripheral Vascular Inc.. Grant Recipient; BTG, Covidien, Bard, Boston Scientific, Sirtex. Research/Grant Support; Celonova, Boston Scientific.

B-0891 11:02

Transjugular intrahepatic portosystemic shunt prior to abdominal surgery: outcomes in cirrhotic patients

M. Shoreibah, S. Kim, M. Naseemuddin, A. Abouarab, K. Mahmoud, S. Moawad, A.M.K. Abdel Aal; *Birmingham, AL/US (snkim@uabmc.edu)*

Purpose: Abdominal surgery in patients with liver disease has been associated with an increased risk of perioperative mortality related to increased porto-systemic gradient (PSG). The purpose of our study is to evaluate pre-operative Transjugular intrahepatic portosystemic shunt (TIPS) placement in patients with cirrhosis and its effect on perioperative mortality.
Methods and Materials: A retrospective study of 16 patients with cirrhosis who had TIPS placement prior to abdominal surgery between 2010 and 2015. We used the Mayo Clinic post-operative (PO) mortality risk calculator to determine the expected 30-day mortality and compared it to the observed mortality in our cohort.
Results: Sixteen patients with cirrhosis (75% males, mean age of 50.3+10 years) were included. Fifteen patients had decompensated cirrhosis (ascites: 93%, variceal bleeding: 26.7% and hepatic encephalopathy: 60.0%) while 1 patient had ascites due allograft dysfunction after orthotopic liver transplant. The mean PSG was reduced from 14.8±5.0 mmHg pre-TIPS to 5.3±2.7 mmHg. The MELD score increased from 13.6±4.4 to 15.7±4.5. Median time to surgery was 39 days. Median hospital stay was 4 days. The mean expected PO 30-day mortality risk was 27.3±21.6%. Observed 30-day PO mortality rate was found to be 0%. Data was available on 12/16 patients at one year and the observed mortality was 8%. One patient, with a PO 30-day mortality risk of 43.6%, died (78 days from the procedure) and 5 patients received liver transplant.
Conclusion: Our retrospective review indicates that pre-operative TIPS placement in patients with decompensated cirrhosis, especially ascites, can help reduce the PO mortality.
Author Disclosures:
A.M.K. Abdel Aal: Consultant; St Jude Medical, Boston Scientific, WL Gore, Baxter Healthcare, Bard Peripheral Vascular Inc.. Grant Recipient; BTG, Covidien, Bard, Boston Scientific, Sirtex. Research/Grant Support; Celonova, Boston Scientific.

B-0892 11:10

Correlation between port-systemic pressure gradient and changes in platelet count following transjugular intrahepatic portosystemic shunt

A.M.K. Abdel Aal, S. Kim, M. Shoreibah, M. Babi, B. Jackson, M. Massoud, S. Moawad, A. Abouarab, A.S. Moustafa, S. Saddekni; *Birmingham, AL/US (snkim@uabmc.edu)*

Purpose: Platelet count is an important laboratory metric that reflects the change in portal pressure after transjugular intrahepatic portosystemic shunt (TIPS) placement. The purpose of this study is to demonstrate if there is a correlation between the changes in platelet count after TIPS with the change in portosystemic pressure gradient (PSG).
Methods and Materials: We retrospectively reviewed the medical records of 306 patients who had TIPS placed between January 2004 and December 2015. We stratified the patients into 4 groups according to the pre-TIPS platelet count: group1 (0-20), group2 (20-50), group3 (50-100), group4 (100-150). We calculated the percent change in platelet count before and after TIPS as well as the percent change in PSG for each group.
Results: The study included 193 (63%) males and 113 (37%) females, 208 Caucasians (68%), with a mean age of 56.6 years. There was an overall increase in the platelet count after TIPS (mean=17%, SD=62%). Patients in groups 1,2,3 and 4 showing a mean of 243%, 59%, 25% and 0.26% increase in platelet counts respectively which was significant between the groups. There was a negative correlation between the change in the platelet count and the change in PSG which decreased after TIPS (mean=67%, SD=17%) and was not significantly different between the groups.
Conclusion: Pre-TIPS platelet count is an important indicator of the improvement in platelet count after TIPS. The change in the platelet count correlates with the change in PSG, and can be used as an indicator for improvement of PSG after TIPS.
Author Disclosures:
A.M.K. Abdel Aal: Consultant; St jude medical, Boston Scientific, WL Gore, Baxter Healthcare, Bard Peripheral Vascular Inc.. Grant Recipient; BTG, Covidien, Bard, Boston Scientific, Sirtex. Research/Grant Support; Celonova, Boston Scientific. **S. Saddekni:** Consultant; St Jude Medical.

B-0893 11:18

Use of C-arm cone-beam CT for intraprocedural image fusion and 3D guidance in portal vein embolisation

W. Lüdemann[1], G. Böning[1], J. Chapiro[2], M. Jonczyk[1], R.W. Günther[1], B. Gebauer[1], B. Hamm[1], F. Streitparth[1]; [1]*Berlin/DE*, [2]*New Haven, CT/US (willie-magnus.luedemann@charite.de)*

Purpose: Portal vein embolisation (PVE) is applied to patients with extended oncologic liver disease and is meant to induce hyperplasia of non-embolised liver segments to make surgery feasible. Sonographic guidance is the gold standard for percutaneous portal vein access. This study evaluated the feasibility and safety of C-arm cone-beam computed tomography (CBCT) for needle guidance.
Methods and Materials: 10 patients with an indication for PVE and limited sonographic visualisability of the intrahepatic portal vein or unsuccessful previous PVE procedure were enrolled. Puncture was performed under 3D needle guidance in a volumetric data set. CT or MR baseline scans were either registered to a native CBCT or a contrast enhanced CBCT was generated. Technical feasibility, technical success, dose parameters as well as puncture time, defined as time between CBCT acquisition and successful portal vein access were evaluated.
Results: All interventions were technically successful. The mean number of puncture attempts was 4±3. The mean applied dose (dose area product, DAP) of the interventions was 346±251 Gy/cm². The relative share of CBCT-related radiation exposure in relation to the entire intervention was 5.9±3.4%. The puncture time was 20.1±17.8 minutes.
Conclusion: CBCT-guided PVE is feasible and safe and the relative dose of CBCT is low compared to total dose of intervention. This technique may be a promising approach especially for difficult anatomic situations that limit the use of sonography for needle guidance.

B-0894 11:26

Portal vein malignant thrombus recanalisation by endoportal RFA with metal stent placement (VesOpen procedure): rationale, technique and application

M. Mizandari[1], T. Azrumelashvili[1], N. Habib[2]; [1]*Tbilisi/GE*, [2]*London/UK (mgmizandari@gmail.com)*

Purpose: The novel technique of PV thrombus recanalisation is presented.
Methods and Materials: 18 patients underwent percutaneous endoportal RF treatment attempt. PV tributary is accessed under US guidance; manipulation by 5 Fr diameter guiding catheter is used to conduct the guidewire across the blocked segment and portography is performed. 15 Watts power was applied for 2 minutes using bipolar endoluminal RF device (Habib™ EndoHPB, EMcision Ltd., London, UK), placed in PV blocked segment according the guidewire. The number of RF application sessions depends on tumour thrombus extent as shown on portography. After RF application self-expanding 14 mm diameter vascular stent is positioned and PV patency restoration is documented by final portography. Procedure is completed by procedure track RF ablation and/or coil embolisation.
Results: The procedure was completed in 13 (72.2%) cases; in 3 (16.7%) cases we could not conduct the wire across the thrombus; in 2 (1.1%) cases we failed to conduct the RF device and procedure was completed by stenting. Portal vein obstructed segment showed the restored blood flow in all completed cases as documented by postprocedure portography, follow-up Doppler and CT studies; this resulted in liver function improvement in 8 (61.5%) of procedure technical success cases. Recanalised PV patency varied from 3 weeks to 22 months; in 4 cases patients underwent successful TACE procedure after PV recanalisation.
Conclusion: PV thrombus percutaneous recanalisation by endoportal RFA with subsequent stenting is an effective technique and should be suggested as a possible treatment option for HCC patients, complicated with PVT.

B-0895 11:34

Spontaneous portosystemic shunts embolisation in cirrhotic patients with recurrent hepatic encephalopathy: more than ten years of experience

C. Parra-Fariñas, M. Perez Lafuente, I. Díez Miranda, C. González-Junyent, Q. Ordi-Camprubí, M. Salcedo Allende, S. Dyer Hartnett, J. Prat Matifoll, A. Segarra Medrano; *Barcelona/ES (carmenparrafarinas@gmail.com)*

Purpose: Spontaneous portosystemic shunts (SPSS) provide an explanation for hepatic encephalopathy (HE) persistence in cirrhotic patients. Medical treatment alone may have limited success and frequently needs subsequent hospitalisation. This study aimed to assess the efficacy and safety of SPSS endovascular management.
Methods and Materials: From February 2002 to October 2016, a prospective study of 36 consecutive cirrhotic therapy-refractory HE patients who underwent SPSS embolisation was performed. Baseline characteristics, diagnostic workup, therapeutic method, and clinical and radiological outcomes were recorded.
Results: Mean age was 61.8±14.6, 52.8% male. Chronic liver damage was caused by alcoholic abuse (34.7%), HCV (23.1%), cryptogenic (23.1%), non-alcoholic steatohepatitis (11.5%), primary biliary cirrhosis (3.8%), and autoimmune hepatitis (3.8%). Prior to embolisation, seven patients had liver transplants. Doppler-colour ultrasound, CT-angiography and/or portography provided proof of the shunt. SPSS included spleno-renal (67.6%), meso-caval/renal (20.6%), gastro-azygos/renal (8.8%), and recanalised para-umbilical veins (3.0%). Approaches were common femoral vein (61.5%), internal jugular vein (26.9%), transhepatic (7.7%), and transplenic (3.9%). Used materials were coils (72.0%), occlusion devices (24.0%), or combination (4.0%). Secondary procedures were performed in four patients after identification of revascularised SPSS. All patients improved autonomy and decreased severity of the worst HE episode. Follow-up range was 3-31 months. One patient had transient low cardiac output due to acute shunt-closure. There were no other procedure-related complications, portal hypertensive gastropathy or varices development.
Conclusion: SPSS embolisation served as an effective and safe complementary or curative treatment for cirrhotic patients with recurrent HE, even after liver transplantation, improving quality of life by reduction of hospitalisations.

B-0896 11:42

Safety of catheter embolisation of pulmonary AVMs in Osler patients: evaluation of peri-interventional complications on pre- and post-interventional MRI

G. Schneider, P. Raczeck, L. Fenzel, A. Bücker, A. Massmann; *Homburg/DE (dr.guenther.schneider@uks.eu)*

Purpose: Recommended treatment of PAVMs in HHT patients (hereditary haemorrhagic telangiectasia/Osler disease) is catheter embolisation. To evaluate safety of this procedure we evaluated patients undergoing PAVM treatment pre- and post-intervention by MRI for detection of clinical insignificant cerebral infarctions.
Methods and Materials: 94 HHT patients (male/female = 40/54; mean age 45.7+/-16.7 (range 5-86)) with pre-diagnosed PAVMs underwent embolisation therapy. The number of PAVMs treated per patient ranged from 1 to 8 PAVMs. Depending on the size of the feeding vessel and the anatomical situation either coils or vascular plugs were used for embolisation. During the procedure, each patient received iv injection of 2500 IE heparin. MRI was performed immediately before and 4 hours and 3 months post-embolisation therapy applying a T2w sequence and DWI.
Results: DWI post-interventional therapy only showed small, diffuse clinical silent emboli in one patient who underwent re-embolization of a vessel previously treated with tungsten coils that corroded over time. The patient already before treatment had several episodes of brain emboli and re-embolisation had to be performed in the already placed coils for anatomic reasons. Post-re-embolisation the patient did not experience any further brain emboli. All other patients, either initial- or re-embolisation did not show any pre-interventional ischaemic brain lesion.
Conclusion: This prospective study in 94 patients undergoing interventional treatment of PAVMs shows that catheter embolisation, using the described technique, is a safe method for treatment and does not even result in clinical inconspicuous cerebral ischaemia.

10:30 - 12:00 **Room N**

Genitourinary

SS 1407

Male urogenital system - prostate cancer: diagnosis and intervention

Moderators:
M. de Rooij; Nijmegen/NL
J.C. Vilanova; Girona/ES

K-19 10:30

Keynote lecture

A.R. Padhani; *London/UK*

B-0897 10:39

Automated computer-based analysis of all multiparametric MRI data (T2w, DWI and dynamic data) in prostate cancer diagnostics: a useful tool to detect clinically relevant PCA?

A. Thon[1], I. Papgeorgiou[1], A. Malich[1], U. Teichgräber[2]; [1]*Nordhausen/DE*, [2]*Jena/DE (annika_thon@web.de)*

Purpose: Quantitative assessment of multiparametric MRI by means of computer-aided diagnosis (CAD) is the current challenge in prostatic cancer (PCa) diagnostics. An innovative CAD-software (Watson Elementary™) was proposed to achieve high sensitivity, specificity as well as to predict Gleason grade. The aim wa to assess Watson Elementary™ accuracy in our hospital´s database of MRI-guided prostate biopsies.
Methods and Materials: We retrospectively evaluated 104 MR-guided biopsied histologically verified lesions (47 PCa, 57 benign) from 79, 64.61±6.64 y.o. patients using 3T T2w, ADC (b-values 0; 100; 400; 1000) and dynamic contrast enhancement series. Watson Elementary™ computes a scalar MRI-based Gleason grade predictor termed “malignancy attention index” (MAI). The MAI-outcome of predefined ROIs was compared with the histologic outcome of the corresponding biopsy cores at the exact position of the biopsy (needle imaging during biopsy).
Results: CAD detected 36/104 lesions, thus revealing a sensitivity of 34.62% for mixed dignity lesions and 46.80% for PCa with false negative rate 0.53/pt. Specificity for PCa turned out to be 75.43% with positive predictive value 61.11%, negative predictive value 63.23% and false discovery rate 38.89%. CAD detected PCa and benign lesions with equal probability (P 0.06, χ^2 test) and the computed ‘malignancy attention index’ (MAI) revealed no significant correlation with Gleason grade (P 0.60, Pearson correlation). Receiver operating characteristic (ROC) analysis suggests a poor predictive value for MAI with AUC < 0.65.
Conclusion: Watson Elementary™ did not qualify for PCa diagnostics and Gleason grade prediction, image-guided biopsy remains the golden standard. Controversies with previously published outcomes of the same CAD-Software will be discussed.

B-0898 10:47

Target performance of MRI-ultrasound fusion guided prostate biopsy in a cohort of patients with suspected prostate cancer

M. Zadory[1], J.-L. Fehr[1], C. Moeckel[1], S. Hailemariam[2], J. Froehlich[1], M.A. Patak[1]; [1]*Zurich/CH*, [2]*Aarau/CH (matthias.zadory@akroswiss.ch)*

Purpose: To determine the target performance of the ARTEMIS MRI-ultrasound fusion guided prostate biopsy (ART-PBx) procedure to detect clinical significant prostate cancer.
Methods and Materials: In a single-centre study we retrospectively reviewed 245 patients with suspected prostate cancer who underwent in total 293 prostate biopsies. Subjects had all undergone a standardized multi-parametric MRI (indication: PSA rise / abnormal digital rectal exam) resulting in a cancer suspicious lesions. Lesions with high PIRADS classification (3, 4 or 5) underwent a standardized ART-PBx procedure by fusing the previously acquired MR images to biopsy ultrasound using the ARTEMIS-System. Subsequently, histopathological results were correlated with MRI findings indicating the target performance of the ART-PBx procedure. Furthermore, the target performance was subanalysed for the single lesions based on their initial PIRADS classification (excluding unclassified lesions).
Results: The final study population consisted of 194 patients with a mean age of 67 ± 1 years, and with an average PSA of 8.05 ± 0.82 ng/ml. 129 out of 243 cancer-suspicious lesions were positively biopsied for clinical significant prostate cancer yielding an overall ART-PBx target performance of 53.1%. On a patient level, 56.3% of 194 patients were positive. Sub-analysis of the PIRADS criteria delivered an escalating target performance increasing with the PIRADS scoring (PIRADS 3: 14,7%, PIRADS 4: 39.8%, PIRADS 5: 71.4% of all lesions, respectively).

Conclusion: The target performance of ART-PBx to detect clinical significant prostate cancer is robust increasing with higher PIRADS scoring advocating the use of MRI to select patient and lesion candidates for biopsies.

B-0899 10:55

Improvement of biopsy accuracy (target in target) with WATSON elementary CAD system in the detection rate of prostate cancer (csPCa): histopathological correlation

R. Campa, V. Salvo; *Rome/IT*

Purpose: To validate the role of a new algorithm based on a per voxel correlation with malignancy Watson elementary CAD system in the detection rate of clinically significant prostate cancer (PCa).
Methods and Materials: 3T multiparametric MRI (mpMRI), including T2-weighted, diffusion-weighted, and dynamic contrast-enhanced MRI and targeted biopsy of 31 consecutive patients have been performed. The target biopsy area according to PIRADS (V.2) has been considered. Two radiologists retrospectively re-evaluated the exams using PI-RADS v2 and WATSON elementary ® CAD system. The MRI data were compared with histopathological whole-mount step-section slides.
Results: Overall performance for detection rate biopsy was 85% for clinically significant cancer (csPCa) for both PIRADS and Watson systems; in addition, the CAD increases the percentage of tumour per core (25%), targeting the precise zone into the lesion to be biopsied (target in target).
Conclusion: The diagnostic performance of WATSON elementary in the detection rate of PCa is similar to PI-RADS v2. Furthermore, the Watson CAD is useful in identifying the most involved area by cancer within the focus bordered with MRI. So Watson can help in directing the prostatic targeted biopsy to improve the detection rate of biopsy in terms of percentage of tumour per core.

B-0900 11:03

Correlation between PIRADS score and fusion MR-TRUS biopsies (FMR-TB) in the detection of prostate cancer: a monocentric experience

L. Panebianco, G. Michelini, A. Mancini, A. Pace, C. Gianneramo, C. Marsecano, I. Capretti, R. Manetta, C. Masciocchi; *L'Aquila/IT (panebianco.luca@gmail.com)*

Purpose: To compare FMR-TB outcomes with PIRADS score assessed with pre-biopsy MRI.
Methods and Materials: In a period between 2/2015 and 10/2015, FMR-TB outcomes of 46 patients were retrospectively analysed in comparison with PIRADS2 v2 score assigned with pre-biopsy MRI. 2 patients were excluded from the study for previous radical prostatectomy, 1 for radiotherapic treatment. Exams were performed with a 3T scanner using both endorectal and surface 32-channel body coil.
Results: For correlation purposes we considered bioptic findings of prostatic intraepithelial neoplasia (PIN) as negatives, since these alterations are clearly beyond current MRI detection possibilities. 3 patients were scored with PIRADS 1, and their biopsy outcomes were all negative (normal prostatic tissue). 18 patients were scored with PIRADS 2; of these, 4 were assessed as adenomatous hyperplasia, 11 as chronic inflammation, 2 as high-grade (PIN), 1 as adenocarcinoma Gleason 6 (3+3). 4 patients were scored with PIRADS 3; at the biopsy, one was assessed as high-grade PIN and 3 as adenocarcinoma Gleason 6 (3+3). 11 patients were scored with PIRADS 4; of these, 3 were adenomatous hyperplasia, 6 adenocarcinoma Gleason 6 (3+3), 2 adenocarcinoma Gleason 7 (3+4). 7 patients were scored with PIRADS 5; of these, 1 was regular prostatic tissue, 1 adenocarcinoma Gleason 5 (3+2), 1 adenocarcinoma Gleason 6 (3+3), 3 adenocarcinoma Gleason 7 (4+3), 1 adenocarcinoma Gleason 9 (4+5).
Conclusion: MRI evaluation using PIRADS score correlates well with localisation and histologic nature of prostatic pathology.

B-0901 11:11

Sensitivity and negative predictive value of multiparametric MRI utilising PI-RADSvs2: a validation study using MRI/transrectal ultrasound (TRUS) fusion biopsy

M. Nguyentat, A. Ushinsky, C. Green, C. Lall, T.B. Nguyen, R. Houshyar; *Orange, CA/US (TanBNguyen@gmail.com)*

Purpose: Use a combination biopsy method (12-core plus MRI/TRUS fusion biopsies) to evaluate the accuracy of multiparametric MRI (mpMRI), utilising Prostate Imaging - Reporting and Data System version 2 (PI-RADSv2), for detecting clinically significant prostate cancer (csPCa) in the overall gland, the peripheral zone (PZ) and transitional zone (PZ).
Methods and Materials: An IRB approved retrospective analysis of patients who underwent prostate mpMRI and subsequent MRI/TRUS fusion biopsy was performed. We identified 137 men with a total of 231 mpMRI prostate lesions. Subjects were retrospectively graded utilising PI-RADSv2 criteria by a radiologist blinded to biopsy results. Spearman's correlation, chi-squared analysis, and logistic regression were performed. A multiparametric predictive model for csPCa was developed.
Results: There was positive correlation between PI-RADSv2 score and Gleason score ($p < 0.001$). For csPCa in the PZ, mpMRI had a 100% sensitivity, 100% negative predictive value (NPV), 9.0% specificity, and 35.9% positive predictive value (PPV), compared to 100%, 100%, 41.1%, and 27.1%, respectively, for TZ lesions. When predicting csPCa, employing PI-RADSv2 score in a multiparametric model with predictive factors for csPCa (BMI, PSA density, DRE result) increased the AUC from 0.797 to 0.886 (95% CI 0.030 - 0.039, $p < 0.01$).
Conclusion: PI-RADSv2 in conjunction with 12-core and MRI/TRUS fusion biopsies is accurate in detecting csPca with excellent sensitivity and NPV for both PZ and TZ lesions. However, compared to PZ lesions, the specificity and AUC for TZ lesions is greater. PI-RADSv2 contributes to a highly accurate predictive model when included in a multivariate analysis.

B-0902 11:19

The role of semi-quantitative dynamic contrast-enhanced MR imaging in characterisation of prostate cancer

Y. Yeo, S. Kim, Y. Nam; *Taegu/KR (omiri86@naver.com)*

Purpose: To retrospectively assess diagnostic value of semi-quantitative DCE-MR imaging in characterisation of prostate cancer.
Methods and Materials: 102 consecutive patients underwent DCE imaging. Regions of interest were drawn on 288 foci, including 133 cancers (Gleason grade 6 [30], Gleason grade 7 [72] and Gleason grade 8 or higher [31]), 55 benign hyperplasia and 100 healthy-tissues, by using histopathologic correlation. Semi-quantitative parameters derived from time-intensity curves (C_{peak}, TTP, Wash-in and Wash-out), and the curves types were evaluated as following type 0, 1, 2, or 3. The *k* was calculated to evaluate inter-radiologist agreement for the curve types of different tissue types and Gleason grades. Comparisons between these groups were performed by using one-way analysis of variance.
Results: The agreements between curve types were excellent (all $k \geq 0.85$). The values of C_{peak} and Wash-in in overall cancer foci and Gleason grade 8 or higher were significantly higher than those of healthy-tissue foci and Gleason grade 6, respectively (C_{peak}: 130.3±15.43 and 138.3±27.23 vs 115.3±13.24 and 122.3±23.43; P=0.032 and P=0.014, Wash-in: 18.8±9.55 and 26.5±8.62 vs 9.2±4.73 and 12.7±7.93; P=0.025 and P=0.010). The values of Wash-out in overall cancer foci and Gleason grade 8 or higher were significantly lower than those of healthy-tissue foci and Gleason grade 6, respectively (-0.52±1.59 and -0.75 ± 1.48 vs 0.37±1.72 and -0.44 ± 1.68; P=0.026 and P=0.020).
Conclusion: Semi-quantitative DCE-MR imaging poorly perform for differentiation of cancer from benign hyperplasia and healthy-tissue. Only Gleason grade 6 potentially enabled differentiation of Gleason grade 8 or higher in cancer grading.

B-0903 11:27

Searching for prostate cancer by fully automated magnetic resonance imaging classification: deep learning vs non-deep learning

L. Wang; *Wuhan/CN (1311935212@qq.com)*

Purpose: To develop deep learning with deep convolutional neural network (DCNN) versus non-deep learning methods to distinguish PCa from prostate benign conditions (BCs) including prostatitis and prostate benign hyperplasia (BPH).
Methods and Materials: We obtain 2,602 MR images of the prostate. We use deep learning with deep convolutional neural network (DCNN) versus non-deep learning methods to distinguish PCa from prostate benign conditions (BCs) including prostatitis and prostate benign hyperplasia (BPH). We validate the difference in fully automated PCa differentiation from prostate BCs between two methods was statistically significant (p-value<=0.05).
Results: Deep learning demonstrates fully automated PCa differentiation aggressiveness with accuracy of 63.6% for Gleason score (GS)<=6, 60.0% for GS 7 and 89.5% for GS>=8.
Conclusion: Our results suggest that deep learning with DCCN can be used to assist, or even partly replace radiologist to search for PCa by fully automated MR imaging classification.

B-0904 11:35

Detection of MRI index lesion with transrectal ultrasound-MRI fusion-guided prostate biopsies: is it correspondent with histopathology?

M. Del Monte, V. Salvo, M. Grompone, E. Indino, V. Panebianco, C. Catalano; *Rome/IT (delmonte_maurizio85@libero.it)*

Purpose: To assess the histopathological correspondence of "MRI index lesion" between magnetic resonance imaging (MRI)/ transrectal ultrasonography (TRUS) fusion and radical prostatectomy.
Methods and Materials: We enrolled 101 consecutive patients treated with radical prostatectomy for a clinically localised prostate cancer detected on magnetic resonance imaging (MRI)/transrectal ultrasonography (TRUS) fusion.

For each patient 3 to 5 biopsy specimen was performed for each “MRI index lesion". A correlation analysis between magnetic resonance imaging (MRI)/transrectal ultrasonography (TRUS) fusion and pathological findings of radical prostatectomy was performed.
Results: We found with regard to the “MRI index lesion” a detection rate of 100% for the dimensions (from 7 mm to 30 mm); the correspondence between biopsy and prostatectomy results was 83% in terms of Gleason score. In the 36% of patients the “MRI index lesion” corresponds to the more aggressive lesion.
Conclusion: MRI-transrectal ultrasound fusion biopsy shows a good correlation between “MRI index lesion” and definitive histopathological diagnosis.

B-0905 11:43

Detection of potentially malignant lesions of the prostate gland with targeted biopsy using a computer-assisted diagnostic tool based on multiparametric MRI

E. Alberioli, C. Cicero, B. De Concilio, A. Casarin, S. Canestrini, G. Zeccolini, A. Celia, L. Genesio, A. Guarise; *Bassano del Grappa/IT (enricoalberioli@gmail.com)*

Purpose: To estimate the capability of a computer-assisted diagnostic system (Watson Elementary®), based on the analysis of MR images, in identifying and localising potentially malignant lesions within the prostate gland.
Methods and Materials: 33 patients with suspected prostate gland malignancy were studied with multiparametric MRI, applying the European Society of Urogenital Radiology criteria; these sequences were used by an automated analysis tool to localise suspected lesions by the fusion of various series. The PI-RADS values of the studied lesions were 3 in 2 cases, 4 in 15 cases and 5 in 16 cases. Targeted biopsies were performed in all patients.
Results: Of 33 patients who underwent to targeted biopsy, in 20/33 (60,6%) patients the suspected lesion was confirmed to be malignant (prostate cancer) and in 13/33 (39,4%) the biopsied lesion resulted to be benign prostatic hyperplasia. PI-RADS was 5 in 13/16 cases of malignancy and in 3/16 cases of benign lesions. In 1/14 patients the suspected lesion at mpMRI was considered as a negative area by the automated diagnostic system while resulted to be prostate cancer at biopsy. The obtained sensitivity was of 95%, while no true negative cases resulted from this study.
Conclusion: The automated analysis system, thanks to the fusion of multiparametric MR images, has to be considered as an efficient additional tool available to the radiologist to improve the ability to identify, localise and biopsy potential malignant lesions of the prostate gland.

B-0906 11:51

Peripheral prostatic cancer detection in a biopsy-naive patient population: a biparametric MR study

G. Rusconi, A. Stanzione, S. Cocozza, N. Longo, A. Brunetti, M. Imbriaco; *Naples/IT (rusconi.giovanni@gmail.com)*

Purpose: Recent evidences suggested that Biparametric Magnetic Resonance Imaging (BP-MRI) is a feasible tool for detection of prostatic cancer (PCa). However, no direct evidences with respect to the zonal prostatic anatomy are available. Therefore, we aimed to analyse the diagnostic accuracy of a BP-MRI protocol to identify PCa of the peripheral zone, which is the most frequent localisation, in a biopsy-naïve patient population.
Methods and Materials: From an initial group of 84 patients (mean age: 66±9 years old) with suspicion of PCa, based on abnormal prostate-specific antigen (PSA) levels and/or digital rectal examination, 29 cases of PCa of the peripheral zone were identified. All included patients underwent a MR scan, including a T2-weighted imaging and diffusion-weighted imaging (with the correspondent apparent diffusion coefficient maps). All subjects subsequently underwent a prostate biopsy. Two radiologists reviewed prostate MR scan to establish a radiological diagnosis.
Results: The mean PSA level of these patients was 9.9±11.1 ng/ml, with a Gleason score ranging from 2+4 to 5+4. The evaluation of the sequences included in the BP-MRI protocol showed an accurate performance in terms of diagnostic accuracy (92.2%), correctly identifying 24/29 subjects with peripheral PCa (82.8% of sensitivity), with only one false negative (97.9% of specificity).
Conclusion: Our results confirm that BP-MRI prostate protocol is feasible for the detection of a PCa of the peripheral zone, showing both a high sensitivity and specificity and suggesting its possible inclusion in clinical routine diagnostic protocols for PCa imaging.

Oncologic Imaging

SS 1416
Imaging of liver and pancreas

Moderators:
M. Chouhan; London/UK
A. Luciani; Creteil/FR

B-0907 10:30

CT-based tumour response criteria compared after combined treatment for liver metastases of colorectal cancer

A. Varotto[1], L. Di Grazia[2], C. Aliberti[1], F. Bergamo[1], M. Nardin[1], F. Pomerri[1]; [1]*Padua/IT*, [2]*Chioggia/IT (ale.varotto86@gmail.com)*

Purpose: The aim of this analysis is to compare different tumour response criteria (TRC) after chemotherapy combined with bevacizumab in liver metastases from colorectal cancer (mCRC) to ascertain the best early prognostic indicator of response.
Methods and Materials: 103 target liver metastases from 65 mCRC patients treated with chemoterapy plus bevacizumab were examined at the Istituto Oncologico Veneto IOV-IRCSS (March 2008-January 2013). All patients had baseline CT and at least one follow-up scan. Tumour response was retrospectively analyzed by two radiologists using RECIST1.1, modified Choi, and Chun morphologic criteria. Tumour response, classified as good (complete or partial response) or poor (stable or progressive disease), was compared with progression-free survival (PFS) at first follow-up (t1) and time of best response. Interobserver agreement and concordance between TRC were measured.
Results: At t1, 32.31% showed a good response according to RECIST1.1 (median PFS 11.1), 84.62% according to Choi (median PFS 10.8). These percentages rose to 49.23% (median PFS 12.1) and 87.69% (median PFS 10.8), respectively, at the time of best response. According to Chun, 67.69% showed a good response at the time of best response (median PFS 10.8). The Choi criteria detected a higher proportion of good responders at t1, showing a better correlation with PFS; all methods correlated with PFS at the time of best response.
Conclusion: The Choi criteria proved more consistent in the early detection of response in mCRC treated with chemotherapy plus bevacizumab, underscoring the importance of using these criteria in the early assessment of response to combined treatment.

B-0909 10:38

Towards volumetric thresholds in RECIST 1.1: therapeutic response assessment in hepatic metastases

K.S. Winter, F.O. Hofmann, K.M. Thierfelder, N. Hesse, A.B. Baumann, V. Heinemann, M.F. Reiser, W.H. Sommer, M. D'Anastasi; *Munich/DE (stella.winter@med.uni-muenchen.de)*

Purpose: To empirically determine thresholds for volumetric assessment of liver metastases in line with standardised unidimensional thresholds (RECIST 1.1).
Methods and Materials: This study included patients with metastatic colorectal cancer from a multicentre clinical phase III trial who had undergone CT at baseline and follow-up. The longest axial lesion diameters were determined according to RECIST 1.1. Lesion volumes were calculated using semi-automatic segmentation. The sum of diameters and volumes of 1, up to 2 and up to 5 metastases were compared to all previous examinations. Volumetric thresholds corresponding to RECIST 1.1 thresholds (-30% and +20%) were each predicted using a regression model. Sensitivity analysis was performed to assess the concordance of the proposed thresholds with the weight-maximising thresholds and the results from regression. Classification concordance for measurements of up to 2 metastases was analysed.
Results: For measurements of up to 2 metastases, 348 patients with a total of 629 metastases were included, resulting in 4773 value pairs. Regression analysis yielded volumetric thresholds of -65.3% and +64.6%, corresponding to a diameter change of -30% and +20%. When comparing measurements of unidimensional RECIST assessment with volumetric measurements, there was concordance of significant progress (>+20% diameter / >+65% volume) in 98.0% and of non-significant progress (<+20% / <+65%) in 87.2% of the cases. Concordance of significant response (<-30% / <-65%) was found in 87.8% and of non-significant response (>-30% / >-65%) in 94.4% of the cases.
Conclusion: The evaluation of patients with hepatic metastases yields volumetric thresholds corresponding to RECIST 1.1 of +65% and -65%.
Author Disclosures:
V. Heinemann: Research/Grant Support; by Merck KGaA Darmstadt, Germany.

B-0910 10:46

Tumour response criteria after first line combined therapy (Bevacizumab + Chemotherapy) in unresectable liver metastases of colorectal cancer: RECIST 1.1 vs Choi in short-term follow-up

E. Raimondi, M. Bassi, G. De Paoli Barbato, S. Gamanji, M. Tilli, R. Rizzati, M. Giganti, G. Benea; *Ferrara/IT (edoardo.raimondi@unife.it)*

Purpose: Evaluate the predictive value of RECIST 1.1 and Choi criteria for early response to first line combined therapy.
Methods and Materials: Forty-one patients with colorectal-liver metastases (CLM) were retrospectively observed after first-line therapy, imaged with MD-CT at baseline and after therapy at 2 and 5 months (T1/T2). Tumour responses following RECIST 1.1 and Choi criteria were paired with time-to-progression (TTP) and overall-survival (OS).
Results: Median-TTP was 281 days (95% CI:175.555-386.445) for RECIST, 361 days (95% CI:324.131-397.869) for Choi; median-OS was 644 days (95% CI:457.624-708.376). At T1-RECIST showed no complete response (CR), while 14pts (34.1%) showed partial response (PR). Stable disease (SD) was found in 16pts (39%), whereas 11pts (26.8%) showed PD. At T1-Choi, no patient qualified for CR, 37pts (90.2%) showed PR, 3pts (7.3%) SD, and 1pt (2.4%) PD. At T2-RECIST, 6pts (14.6%) showed PR, 24pts (58.8%) SD and 11pts (26.8%) PD. At T2-Choi, 23pts (56.1%) showed PR, 10pts (24.4%) SD, and 8pts (19.5%), rated PR at T1-Choi, were rated PD. Based on TTP data, we categorised pts as Responders (CR+PR+SD) and Non-Responders (PD); we compared mTTP among these subgroups showing shorter mTTP for NR vs R (T1 99 vs 375 days, p<0.0001; T2 172 vs 357 days p<0.0001) according to RECIST, while significant-shorter mTTP for NR vs R (172 vs 357 days p<0.0001) only at T2 according to Choi criteria.
Conclusion: The best predictive marker of therapeutic response in this setting of cancer treatment seems to be the absence of progression, no matter which response evaluation criteria applied.

B-0911 10:54

TACE therapy assessment of HCC using iodine concentration in comparison with volume perfusion CT and RECIST/mRECIST

W. Thaiss[1], U. Haberland[2], S. Kaufmann[1], C. Kloth[1], H. Preibsch[1], D. Ketelsen[1], K. Nikolaou[1], M. Horger[1], A.W. Sauter[3]; [1]*Tübingen/DE*, [2]*Forchheim/DE*, [3]*Basle/CH (alexander.sauter.imaging@googlemail.com)*

Purpose: Assessment of pre- and posttreatment iodine concentration (IC) using 80 kVp CT as response assessment marker of transarterial chemoembolization (TACE) in hepatocellular carcinoma (HCC) lesions and comparison with volume perfusion CT (VPCT) and response evaluation criteria in solid tumours (RECIST, mRECIST).
Methods and Materials: 33 HCC lesions in 25 patients who underwent VPCT before and after TACE were included. Iodine maps 7 sec after aortic peak enhancement (APE) were processed and lesion iodine concentrations were calculated. VPCT and angiography were read in consensus to classify responding and non-responding lesions.
Results: In responding HCC lesions, IC was 118.1 ± 47.0 mg/100 mL (before TACE) and 17.0 ± 25.2 mg/100 mL (after TACE), BF 90.1 ± 28.7 mL/100 mL/min (before TACE) and 32.1 ± 19.0 mL/100 mL/min (after TACE). In non-responding lesions, IC was 100.9 ± 43.6 mg/100 mL (before TACE) and 118.8 ± 50.6 mg/100 mL (after TACE), BF 76.8 ± 35.6 mL/100 mL/min (before TACE) and 73.5 ± 36.1 mL/100 mL/min (after TACE). Absolute differences (before and after TACE) in IC revealed a sensitivity of 95.8% and specificity of 88.9%, absolute differences in BF reached a sensitivity of 66.7% and specificity of 88.9%. IC only derived from posttreatment measurements was on a par with pre- and post-TACE parameter differences.
Conclusion: IC 7 sec after APE is a useful perfusion marker for TACE response monitoring in HCC. This information can be used for further radiation dose savings in VPCT and optimization of dual energy CT acquisition.
Author Disclosures:
U. Haberland: Employee; Siemens AG, Healthineers. **K. Nikolaou:** Speaker; Siemens AG, Bracco Group, Bayer.

B-0912 11:02

Discrimination malignant from bland portal vein thrombosis: could DWI MRI help?

A.K. Fayed, M. Rezk, H. Samy, R. Hachem, A.H.K. Abdelmaksoud, B.E. Mahmoud Hussein, M.F. Osman; *Cairo/EG (ahmedkarm@outlook.com)*

Purpose: to determine the role of DW imaging in differentiating between the benign and malignant portal vein thrombosis in patient with HCC.
Methods and Materials: 74 patients with pathological or radiological proof of HCC and visible portal vein thrombosis were examined using 3 T MR Unit Philips scanner via abdominal surface coil. Axial T1 ,T2 and SPAIR sequences as well as DWI were performed before the dynamic study using single-shot spin echo echoplanar sequence with scan time 3-4 min. ADC values were calculated via ROIs of the hepatic tumour and the portal vein thrombus. The mean and standard deviation of the ADC as well as the ratio of the ADC of the thrombus to the ADC of the tumour were calculated and compared in each group by using the t-test. P value of 0.05 was chosen as the threshold for statistical significance.
Results: No statistically significant difference was between the ADC of HCC in the neoplastic and bland cohorts (P = 0.843). No statistically significant differences between the ADC values of the thrombi in the neoplastic and bland cohorts (P = 0.584). ADC ratio was significantly different between the neoplastic and bland cohorts (P= 0.001). The cutoff of value = 1.2 mm 2 /sec for the ADC ratio helped distinguish between neoplastic and bland portal vein thrombi with 98% sensitivity and 70% specificity.
Conclusion: ADC ratio may have a role in differentiation between the malignant and bland portal vein thrombosis.

B-0913 11:10

Dynamic contrast-enhanced CT-protocol for detection of colorectal liver metastases

L. Van Camp[1], P. Deak[2], M. Haspeslagh[1], K. Coenegrachts[1]; [1]*Bruges/BE*, [2]*Milwaukee, WI/US (laurent.vancamp@gmail.com)*

Purpose: To compare a dynamic contrast-enhanced (DCE) CT-protocol with venous CT-protocol for detecting colorectal liver metastases (CRLMs).
Methods and Materials: A DCE-CT protocol (Johnson-Wilson model) and venous CT scan were performed using Revolution CT (GEHC, Milwaukee, USA). Twenty patients (naïve to anti-tumour treatment) were examined. DCE-CT of the liver was performed using 50 ml of contrast agent (Xenetix® 350, Guerbet, France), followed by a saline flush of 40 ml injected at 4 ml/s. 5 s after start of IV injection, DCE-CT was performed. The first 23 DCE-CT scans were performed every 2 s, followed by 9 DCE-CT scans every 10 s. A second contrast agent injection of 40 ml was performed and venous CT was acquired at the end of injection. Perfusion maps were calculated. The number of detected CRLMs using perfusion maps (e.g. permeability surface area product (PS), blood volume (BV), hepatic arterial blood flow (hep.art.BF)) was compared with venous CT.
Results: 86 CRLMs were detected only on perfusion maps with hep.art.BF and BV parameter. Untreated CRLMs showed an elevated hep.art.BF and decreased BV parameter. Venous CT missed 5 CRLMs (2 missed (diameter 10 mm and 14 mm) in a patient having 4 CRLMs; 1 missed (diameter 15mm) in a patient having 1 CRLM; 2 missed (diameter 10 mm and 12 mm) in a patient having 2 CRLMs). Paired sample t-test results in t = 1.751 with significance of 0.096.
Conclusion: DCE-CT protocol appears to increase detection of CRLMs especially for lesions less than 15mm when compared with venous CT.

B-0914 11:18

Tumour subregion analysis of colorectal liver metastases using DCE-MRI: comparison with histological subregions and impact on PK analysis

J.M. Franklin[1], B. Irving[1], B.W. Papiez[1], J. Kallehauge[1], E.M. Anderson[1], L. Wang[1], R. Goldin[2], M. Brady[1], F.V. Gleeson[1]; [1]*Oxford/UK*, [2]*London/UK (jamiemfranklin@hotmail.com)*

Purpose: To use a novel segmentation methodology based on dynamic contrast-enhanced MRI (DCE-MRI) to define tumour subregions, to compare these with histology, and to use these to compare extracted pharmacokinetic (PK) parameters between tumour subregions.
Methods and Materials: This ethically approved prospective study recruited eight patients with CRC and ≥1 hepatic metastasis scheduled for hepatic resection from December 2013. Patients underwent DCE-MRI pre-metastasectomy. Histological sections of resection specimens were spatially matched to DCE-MRI acquisitions and used to define histological subregions of viable and non-viable tumour. A semi-automated voxel-wise image segmentation algorithm based on the DCE-MRI contrast-uptake curves was used to define imaging subregions of viable and non-viable tumour. Overlap of histologically-defined and imaging subregions was compared using the Dice similarity coefficient (DSC). DCE-MRI PK parameters were compared for the whole tumour and histological and imaging subregions (Student T-test).
Results: Direct histological comparison with imaging was possible in six patients. Mean DSC for viable tumour subregions defined by imaging and histology was 0.783 (range 0.635-0.930). There were significant differences between K^{trans} for viable and non-viable subregions ($p<0.05$) and between whole lesions and viable subregions ($p<0.05$). For k_{ep} ,a trend towards significant differences between viable and non-viable subregions ($p=0.05$) and a significant difference between whole lesions and viable subregions ($p<0.05$) were observed.
Conclusion: We demonstrate good concordance of viable tumour segmentation based on pre-operative DCE-MRI, with a post-operative histological gold-standard. This can be used to extract tumour-specific values from quantitative image analysis, and could improve treatment response assessment in clinical practice.
Author Disclosures:
M. Brady: Board Member; MIrada Medical.

B-0915 11:26

Perfusion CT changes in liver metastases from pancreatic neuroendocrine tumours during everolimus treatment

M. D'Onofrio, V. Ciaravino, S. Crosara, R. De Robertis, R. Pozzi-Mucelli; *Verona/IT (valentinaciaravino@gmail.com)*

Purpose: To evaluate modifications of perfusional parameters assessed by perfusion CT (P-CT) in liver metastases (LM) from pancreatic neuroendocrine tumours (PanNETs) during everolimus treatment, aiming to identify responding patients at an early stage of treatment.
Methods and Materials: All patients with LM from G1-2 PanNETs undergoing everolimus treatment between January 2013 and January 2015 were prospectively evaluated with PCT at baseline (T0), after 2 (T1) and 4 (T2) months of therapy. Treatment response was evaluated using RECIST 1.1 criteria. Size, perfusion (PF), blood volume (BV), peak enhancement intensity (PEI) and time to peak (TTP) of each lesion were calculated; morphological and perfusional modifications were compared between responder and non-responder lesions.
Results: Thirty-three LM from 9 patients with G1-2 PanNETs were prospectively evaluated: 23/33 (69.7%) were responders, 10/33 (30.3%) were non-responders. Among perfusional parameters, only PEI significantly differed between the two groups at baseline (p=0.043). BV increase was the most significant perfusional modification to identify responding lesions, even at an early stage of treatment (T1), with high positive predictive value (89.47%). A trend towards PEI decrease in responding lesions was observed; combining PEI decrease with BV increase did not improve response prediction. PF and TTP modifications were not significantly different between responders group and non-responders.
Conclusion: P-CT seems to be useful for response prediction to everolimus in LM from PanNETs. Baseline PEI values are significantly higher in responding compared to non-responding lesions. Significant BV increase was found in responding lesions, with high predictive value of response even in an early phase.

B-0916 11:38

Improved PET/CT-discrimination of hepatocellular cancer after carbohydrate-restricted diet and delayed imaging?

C. Cronberg, P. Björkman, L.-L. Johansson, S. Valind, P. Wollmer, S. Zackrisson; *Malmö/SE (carin.cronberg@med.lu.se)*

Purpose: Hepatocellular cancer (HCC) is often diagnosed too late. Using diet restrictions and delayed ^{18}F-FDG PET/CT imaging we investigated the potential effect on enhanced tumour detection in relation to the background parenchyma.
Methods and Materials: 18 patients with chronic hepatitis B or C and a lesion suspicious of HCC were included. ^{18}F-FDG PET/CT with a full dose CT-scan including intravenous and oral contrast media was performed 1 hour after FDG-injection. At 3 hours a PET scan was performed with low dose CT. After 48 hours on carbohydrate-restricted diet patients were examined by another two low dose PET/CT:s at 1 and 3 hours. Lesion SUV_{max}, liver SUV_{mean}, ratio lesion/liver reported as median and interquartile range in relation to change over time and diet were assessed using Wilcoxon signed-rank test.
Results: Lesion SUV_{max} decreased significantly over time, median -0,6 (IQR -0,7 to -0,3), ($p<0,05$) as did SUV_{mean} of the liver, median -0,3 (IQR -0,4 to -0,2). However, the ratio lesion/liver did not change significantly, median -0.1 (IQR -0,2 to 0,1). After carbohydrate-restricted diet SUV_{mean} of the liver was significantly higher than after normal diet after 1 hour (median 0,1; IQR 0-0,5 but not after 3. Lesion SUV_{max} or the ratio lesion/liver was not enhanced by carbohydrate depletion.
Conclusion: In this limited study sample the visibility of HCC was not enhanced by carbohydrate depletion or delayed imaging. SUV decreased slightly more over time in the parenchyma indicating that even later imaging in a larger study, may demonstrate such an effect more clearly.
Author Disclosures:
S. Zackrisson: Author; Sophia Zackrisson has received speaker's fees and travel support by Siemens Healthcare AG and Astra Zeneca..

B-0917 11:42

Mixed hepato-cholangiocellular carcinoma: LI-RADS analysis and radiologic-pathologic correlation

C. Khouri Chalouhi, F. Alessandrino, L. Di Tommaso, M. Roncalli, L. Balzarini; *Rozzano/IT (claudiakhouri@msn.com)*

Purpose: To correlate biphenotypic hepatic tumour imaging features analysed with LI-RADS categories to their relative histopathological composition of intrahepatic cholangiocarcinoma, hepatocellular carcinoma and stem cells.
Methods and Materials: We reviewed a total of 20 patients (6 females, mean age±SD: 69 ± 7.22 years; range: 78-47 years) with histologically confirmed biphenotypic hepatic tumour who underwent 9 contrast-enhanced CT and 11 contrast-enhanced MRI before liver resection. Imaging findings were classified into three categories, according to LI-RADS classification, as follows: hepatocellular carcinoma, probably hepatocellular carcinoma, and intrahepatic cholangiocarcinoma. Chi-square ($\chi 2$) or Fisher exact test was performed to assess the statistical association between LI-RADS categories and prevalent pathologic morphology or prevalent stem cell morphology.
Results: In total, 6 cases were labeled as hepatocellular carcinoma (5MR, 1 CT), 10 cases as intrahepatic cholangiocarcinoma (4 MR, 6 CT) and 4 cases (2 MR, 2 CT) as probably hepatocellular carcinoma according to LI-RADS classification. No significant association between imaging diagnosis and prevalent pathologic morphology and prevalent stem cells morphology was observed. Concerning association between single imaging features and prevalent pathologic morphology, only capsular retraction was significantly associated with prevalent intrahepatic cholangiocarcinoma pathologic morphology (p=0.03).
Conclusion: Our study showed that differentiation of biphenotypic hepatic tumours on the basis of LI-RADS categories is not feasible, when their relative histopathological composition is taken into account. Association between single imaging features and prevalent pathologic morphology was observed only for capsular retraction, significantly more frequent in cases with prevalent intrahepatic cholangiocarcinoma pathologic morphology.

10:30 - 12:00 **Room E1**

Breast

SS 1402a

Imaging the axilla

Moderators:
K. Kinkel; Chêne-Bougeries/CH
P.A.C. Teixeira; São Paulo/BR

B-0918 10:30

Benefits and risks of preoperative axillary staging in a low-risk screening population

M. Wallis[1], F. Kilburn-Toppin[1], K. Taylor[1], S. Taylor-Phillips[2]; [1]*Cambridge/UK*, [2]*Coventry/UK (matthew.wallis@addenbrookes.nhs.uk)*

Purpose: Preoperative staging of the axilla with ultrasound and needle biopsy is said to preferentially identify women with higher risk disease allowing node positive women to go direct to axillary node dissection (ALND) or neoadjuvant chemotherapy (NAC). ACOSOG-Z0011 questions the need for ALND in women with low risk axillary disease suggesting that some women with positive needle biopsy are being over treated.We sought to identify the risks and benefits for a population who should be at low risk.
Methods and Materials: All surgically treated invasive cancers detected between 01/04/2008 and 31/03/2016 were extracted from the records of one UK breast screening service. Axillary staging was compared with final pathology and treatment.
Results: 193 of 899 (21.7%) surgically treated invasive cancers were node positive. 101 (11.4%) had an axillary biopsy, 63 were positive (32.6% of the node positive cases). Of these 26 (41.3%) had NAC and 37 (58.7%) proceeded directly to ANLD, of which 18 (48%) had 3 or more nodes positive. 69.8% of women with a positive needle biopsy were heavily node positive or promoted to NAC compared to 23 (17.7%) of the 130 women with a positive sentinel lymph node biopsy. Balanced against this 19 (30%) were potentially over treated with ALND (mean node count 14.6).
Conclusion: This series confirms preoperative axillary staging picks up advanced disease but significant numbers of women are being potentially over treated. A much larger data set is required to predict who benefits from preoperative axillary staging. We are seeking funding to analyse UK data set.

B-0919 10:38

Dynamic contrast-enhanced magnetic resonance imaging and diffusion-weighted imaging for the prediction of axillary lymph node metastasis in early breast cancer

E.H. Jeong, E.J. Choi, E.H. Park, J.S. Song; *Jeonju-si/KR (ceh914@hanmail.net)*

Purpose: To evaluate dynamic contrast-enhanced breast magnetic resonance imaging (DCE-MRI) and diffusion weighted imaging (DWI) features for axillary lymph node (ALN) metastasis in the early breast cancer.
Methods and Materials: From January 2011 to April 2015, we retrospectively reviewed 580 early breast cancer patients. Among them, 240 patients who underwent 3.0-T DCE-MRI, including DWI with b value 0 and 1,000 s/mm^2, were enrolled. We compared MRI features (background parenchymal enhancement, internal enhancement, adjacent vessel sign, whole-breast vascularity, initial enhancement pattern, kinetic curve types, quantitative kinetic parameters, tumour-apparent diffusion coefficient (ADC), pretumoural maximum-ADC, and peritumour-tumour ADC ratio) and clinico-pathologic

variables (age, stage, histologic grade, nuclear grade, existence of lymphovascular invasion and extensive intraductal carcinoma component, and immunohistochemical profiles) between patients with ALN metastasis and no LN metastasis.
Results: On breast MRI, moderate or prominent ipsilateral whole-breast vascularity (moderate, odds ratio [OR], 3.45; 95% confidence intervals [CI], 1.28-9.51 vs. prominent, OR, 15.59; 95% CI, 2.52-96.46), signal enhancement ratio (SER) (OR, 1.68; 95% CI, 1.09-2.59), and peritumour-tumour ADC ratio (OR, 6.77; 95% CI, 2.41-18.99) were independently associated with ALN metastasis. Among clinico-pathologic variables, HER-2 positivity was independently associated with ALN metastasis (OR, 23.71; 95% CI, 10.50-53.54). The area under the receiver operating characteristic curves (AUC) of combining the selected MRI features and clinic-pathologic variables was higher than that of clinico-pathologic variables. (P < 0.05).
Conclusion: On breast MRI, moderate or prominent increased whole breast vascularity, SER, and peritumour-tumour ADC ratio could be useful for predicting ALN metastasis in patients with early breast cancer.

B-0920 10:46

The diagnostic performance of gadofosveset-enhanced axillary MRI for nodal (re-)staging in breast cancer patients: final results of a validation study

T. van Nijnatten[1], R.-J. Schipper[1], M. Smidt[1], P. Nelemans[1], B. de Vries[2], L. van Roozendaal[1], J. Wildberger[1], M.B.I. Lobbes[1], R.G.H. Beets-Tan[3]; [1]*Maastricht/NL*, [2]*Heerlen/NL*, [3]*Amsterdam/NL* *(t.vannijnatten@maastrichtuniversity.nl)*

Purpose: To evaluate the diagnostic performance of gadofosveset-enhanced axillary MRI for nodal (re-)staging in newly diagnosed breast cancer patients.
Methods and Materials: Ninety patients underwent dedicated axillary MRI, consisting of standard T2W-MRI and gadofosveset-enhanced T1W-MRI (GDF-MRI). Two radiologists independently scored each lymph node on a confidence scale, first on T2W-MRI, subsequently adjusting the score based on the GDF-MRI if necessary. Diagnostic performance parameters were calculated based on node-by-node and patient-by-patient validation with histopathology of axillary surgery as gold standard. To investigate the presence of a learning curve for reading GDF-MRI, diagnostic performance of the first 30 patients was compared to patients 31-60 and to the last 30 patients.
Results: Overall, node-by-node validation on T2W and GDF-MRI, showed a diagnostic performance with an AUC of 0.760 and 0.819 (p=0.022) for reader 1 and AUC of 0.771 and 0.771 (p=0.997) for reader 2. For patient-by-patient validation, AUC of standard and GDF-MRI were 0.749 and 0.770 (p=0.731) and 0.785 and 0.721 (p=0.156), for reader 1 and 2 respectively. The AUC for reader 1 of the first 30 patients was 0.671, improving to 0.727 (p=0.745) after 60 patients and further improving to 0.906 (p=0.089) for the remaining 30 cases. Sensitivity, specificity, PPV and NPV were 28.6%,82.6%,33.3% and 79.2% and improved to 50.0%,87.5%,50.0%, and 87.5% for reader 1. The AUC of reader 2 improved from 0.742 to 0.774 (p=0.598).
Conclusion: The current study demonstrated that GDF-MRI has potential as non-invasive method for nodal (re-)staging in breast cancer. A learning curve exists for reading GDF-MRI.
Author Disclosures:
T. van Nijnatten: Research/Grant Support; Kankeronderzoekfonds Limburg, Carla Boetes Fund.

B-0921 10:54

Are MR morphological and dimensional lymph node features predictive of axillary metastasis in breast cancer?

F. De Narda, A. Linda, R. Girometti, C. Zuiani; *Udine/IT (denardaf@gmail.com)*

Purpose: To investigate whether standard MR Mammography (MRM) performed for pre-operative staging of breast cancer may predict axillary metastasis evaluating morphological and dimensional lymph node (LN) features.
Methods and Materials: We retrospectively evaluated 306 consecutively patients with newly diagnosed invasive primary breast cancer who underwent preoperative MRM and pathological N-staging after surgery between September 2012 and June 2014. A state-of-the-art MRM protocol was performed, with no additional dedicated axillary sequences. According to histopathological results, patients were assessed to LN metastasis (LNM) or no-LNM group. Images were evaluated by two radiologists in consensus who recorded the presence of irregular margins, cortical inhomogeneity, loss of fatty hilum, perifocal edema, short axis diameter exceeding 1 cm, long axis to short axis ratio smaller than 1,5 cm and asymmetry. Imaging findings were compared among LNM and no-LNM patients using chi-square test. Multivariate logistic regression analysis was performed to determine whether MR findings predict LNM.
Results: Among 306 patients, 118 (38,6%) presented LNM. With the exception of the margins irregularity, all the features considered demonstrated a significant difference (p<0.05) between LNM and no-LNM groups. In particular, cortical inhomogeneity, loss of fatty hilum, perifocal edema, short axis diameter and asymmetry showed a p<0,001 while long axis to short axis ratio demonstrated a p=0,035. Our multivariate analysis showed that only short axis was independently associated with LNM (p<0,001) with an OR of 21,81 (CI 4,96-95,90).
Conclusion: Short axis diameter of axillary LN greater than 1 cm is predictive of LNM in breast cancer patients on standard MRM.

B-0923 11:02

Differentiating between benign and malignant axillary lymph nodes in breast cancer patients using sono-elastography and diffusion-weighted MRI

Y.M. Abdo, M. Abdel Latif, M. Shady; *Mansoura/EG* *(yaramohamedabdo@gmail.com)*

Purpose: To evaluate feasibility of sonoelastography and DWI in differentiating benign from malignant axillary lymph nodes.
Methods and Materials: From July 2014 to July 2015, 30 patients with enlarged axillary LNs were enrolled in this prospective study. First, B mode US was done to assess 4 morphological criteria; T diameter, L/T ratio, cortical thickness and hilum state. Then, sonoelastography was done to determine Elasticity score and Strain ratio. After that, DWI was done for visual assessment and estimation of ADC values. LNs were divided into benign (12 LNs) and malignant (18 LNs) groups based on pathological results. In the two groups, ES and visual DWI were compared using chi-squared test, SR and ADC values were compared using t test. ROC curve analysis was constructed to obtain best cut-off values.
Results: Elasticity Score >2 and restricted diffusion were significantly associated with malignancy (P <0.0001),(P= 0.0002) respectively. The Mean SR of malignant nodes (8.26) was significantly higher than that of benign nodes (2.08) (P <0.0001). The Mean ADC value of malignant nodes (0.7) was significantly lower than that of benign nodes (1.4) (P <0.0001). Comparing results of the three imaging modalities showed that DWI had higher sensitivity and accuracy (100%, 96.4%, respectively) than sonoelastography (88.89%, 93.33%, respectively) with both modalities having the same specificity (91.67%). while both DWI and sonoelastography had higher sensitivity, specificity, accuracy than B-mode ultrasound (77.78%, 66.7%, 73.3% respectively).
Conclusion: Sonoelastography and DWI improve the characterization of enlarged axillary lymph nodes than B-mode Ultrasound. Therefore, reducing the unnecessary invasive biopsies.

B-0924 11:10

Role of IVIM MRI: predicting axillary lymph node metastases in breast malignancies

R. Balaji; *Chennai/IN (ravikanthbalaji@gmail.com)*

Purpose: To evaluate potential for using IVIM MRI to predict axillary lymph node metastases in patients with invasive breast cancer.
Methods and Materials: 36 patients with invasive breast malignancies underwent DCE MRI using 8 channel dedicated breast coil on a 1.5 Tesla scanner (Achieva, The Best, Netherlands). IVIM images were acquired in an axial plane with 11 b values - 0, 20, 30, 50, 80, 100, 200, 400, 80, 1000 and 1200 s/mm^2. Nodes more than or equal to 1 cm were included in the study. 110 nodes were found suitable and evaluated for IVIM parameters - f fraction that represents vascular volume fraction, D the true diffusion coefficient and and D* that represents pseudo diffusion coefficient. This was correlated with histopathology results.
Results: Nodal metastases were observed in 71 nodes. The mean size of the metastatic nodes was larger than that of benign nodes- 1.3 cm versus 0,85 cm. ADC and D values of metastatic nodes were lower while f values were higher. Malignant nodes ADC 0.93 x 10^{-3} mm^2/s D value 0..82,x 10^{-3} mm^2/s, f values 12 % D* 13.95. Benign nodes ADC 1.9 x 10^{-3} mm^2/s D value 1.73, x 10^{-3} mm^2/s, f values 5 % D* 33.6.
Conclusion: Bio imaging markers derived from IVIM studies may provide a more reliable method of distinguishing benign from malignant axillary nodes in patients with invasive breast malignancies.

B-0925 11:18

Axillary assesment in breast cancer: imaging features to improve detection of metastasis

L. Metaxa, R. Aggarwal, A. Khan, L. Jones, T. Suaris; *London/UK* *(lindamet25@gmail.com)*

Purpose: Determine the sensitivity/specificity for detecting axillary lymph node (LN) metastases on preoperative US according to cortical thickness. Explore why some metastatic LN appeared 'normal' on US: false negatives (FN).
Methods and Materials: We performed a retrospective analysis on 627 patients, with primary breast cancer, between 1/1/2012-31/12/2015, undergoing surgical breast and axillary procedure at our institution. We recorded morphology and size of LN. LN with cortical thickness above 2.3mm were considered abnormal and underwent pre-surgical sampling.

Results: 607 patients with valid data were included in further analysis. The metastatic IDC cases were 17.0% of all cases, with PPV 53.4% in the pre-surgery imaging. However, 46.6% of those were FN. In 81.5% of all cases, the LN reported as normal with a FN rate of 9.7%(49/495). In 18.5% of all cases the LN reported as abnormal, with PPV 49.1%. but, in the pre-surgical sampling, 37.5% reported as abnormal (FN for biopsy 11.6%). Our sensitivity was 83.5% and specificity 63.4%. Regarding morphology of LNs, 3.1% cases had round shape with PPV 100%. 96.9% LN were ovoid with PPV14,3%.
Conclusion: 48 patients had FN assessment of the axilla with cortical thickness cut off at 2.3 mm (9.7% of all cases, 46.6% of the metastatic IDC). Is there a better modality, that can detect the metastasis to the LN? Our sensitivity/specificity are within national standards. Can we improve with more structured scanning technique for the axilla. Focus for the future is on morphology and number of abnormal nodes, as these factors guide management of axillary disease.

B-0926 11:26

Predicting axillary lymph node metastasis in breast cancer with multimodality imaging

J. Cho, J. Moon, S. Koh, H. Hwang, S. Park; *Anyang si/KR (cobblack@hallym.or.kr)*

Purpose: The purpose of this retrospective study is to compare the diagnostic performances of mammography, ultrasound (US), magnetic resonance imaging (MRI) and positron emission tomography/computed tomography (PET/CT) and their various combinations to evaluate preoperative axillary lymph node metastasis (ALNM).
Methods and Materials: From January 2011 to December 2014, we included 322 patients with breast cancer completed four preoperative imaging examinations (mammography, US, MRI and PET/CT) up to 3 weeks before surgery. All patients underwent breast conserving surgery or mastectomy and either ipsilateral sentinel lymph node biopsy (SLNB) or axillary lymph node dissection (ALND). The pathology from either ANLM or SLNB was used as the reference standard. The diagnostic performance, sensitivity, specificity, positive predictive value (PPV) and negative predictive value (NPV) of each modality and their various combinations (i.e., combinations of two, three, or all four modalities) were evaluated.
Results: Out of all possible combinations, mammography and US (MG+US) showed the best diagnostic performance. Regarding each single modality, mammography showed the highest specificity, however, its sensitivity was much lower than the other types of imaging. Furthermore, US revealed the highest diagnostic performance compared with the other three imaging modalities. The combination of all four imaging combination showed the highest sensitivity.
Conclusion: Routine basic studies using MG+US are enough for patients with breast cancer prior to ALNM. The addition of other modalities (e.g., MRI or PET/CT) is not necessary to evaluate ALNM; in fact it might decrease the specificity and PPV.

B-0927 11:34

Whole-body MRI DWIBS vs FDG-PET/CT in assessment of breast cancer patients

M.M.A. Rezk, M. Maher, Y. Labib, N. Abdelshafi, E. Elfayoumy, M. Gomaa, N. Abdelrazek, H. Fathy, M. Kotb; *Cairo/EG (medical1430@yahoo.com)*

Purpose: To assess the diagnostic performance of WB-DWIBS versus FDG-PET/CT in assessment of breast cancer patients.
Methods and Materials: 50 patients with pathologically proven breast cancer underwent both F-18-FDG-PET/CT and WB-MRI/DWIBS. The sequences acquired are whole-body DWI, coronal T1 and coronal STIR. FDG-PET/CT was performed on an integrated PET/CT system. Whole-body F18 FDG-PET/CT was performed using standard technique. Both F-18-FDG-PET/CT and WB-MRI/DWIBS were independently interpreted using visual qualitative and quantitative analysis in the term of SUVmax and ADC values respectively. Using pathological data and/or combined clinical/radiological follow-up as a reference standard, sensitivity, specificity, PPV, NPV and overall accuracy were estimated for both techniques.
Results: F-18-FDG-PET/CT demonstrated slightly higher specificity indices than MR-DWIBS while the MR-DWIBS displays higher sensitivity indices than FDG-PET/CT in particular in loco-regional assessment. In addition, high sensitivity indices of DWIBS were depicted in assessment of nodal and bone marrow lesions with fair specificity indices. A high degree of agreement also existed between DWIBS and PET/CT with little better accuracy of FDG-PET/CT more appreciated in the pulmonary lesions assessment.
Conclusion: WB-MRI/DWIBS is a promising tool in evaluation of loco-regional breast cancer and assessment of metastasis with no radiation exposure.

B-0928 11:42

The research of radiological methods reliability

G. Letautaite; *Vilnius/LT (g.letautaite@gmail.com)*

Purpose: To assess the sensitivity of mamography, ultrasonography (US) and magnetic resonance (MR) imaging in detection of multifocal/multicentric breast cancer.
Methods and Materials: The study was carried out using data of 2015-2016 from National Cancer Institute (Lithuania) and 2016 from private clinics Affidea (Lithuania). All the results were anonymous. Results of bilateral mammography, US and contrast-enchanced MRI were analysed from 456 consecutive findings with known or suspected invasive breast cancer of which 52 were found multifocal/multicentric BC. All the results were correlated with histopathologic findings. Statistical analysis was performed by using SPSS software version 23, for statistical reliability to check the use of $\chi 2$ test and t-test for independent samples. Selected statistical significance level of $p<0,05$.
Results: The final research group included 52 patients and it was 11,4% from all MRI examinations. The average age ±SD 50,7±10,54 years. Multifocal/multicentric BC were seen in 71% of the ultrasound examination, 56% of mammography examination and 100% of MRI. Sensitivity of US is 71%, 55,85% of mammography examination and 100% of MRI. Histological analyses of multifocal/multicentric BC: 23,53% invasive lobular carcinoma, 70,59% invasive ductal carcinoma, 5,88% invasive lobular and ductal carcinoma. Spread to lymph nodes was detected in 47,06%.
Conclusion: MRI is the most sensitive techniqe to detect multifocal/multicentric BC, US showed higher sensitivity than mammography according to results of 2015-2016. Standard test methods should be used in conjunction with MRI for assessing multifocal/multicentric BC because it would be more sensitive than any other individual test.

10:30 - 12:00 **Room E2**

Neuro

SS 1411

The ageing brain: cognition and dementia

Moderators:
L. Hermoye; Brussels/BE
A. Negaard; Lørenskog/NO

B-0929 10:30

Patterns of aging in functional connectivity: the Rotterdam study

H.I. Zonneveld, R.H.R. Pruim, D. Bos, H.V. Vrooman, W.J. Niessen, M.A. Ikram, M.W. Vernooij; *Rotterdam/NL (h.zonneveld@erasmusmc.nl)*

Purpose: Non-invasive markers for preclinical dementia are much needed. Structural brain changes are promising, but occur rather late in the disease process. Functional connectivity changes may yield earlier markers of dementia. Yet, little is known on how functional connectivity changes as individuals age. Therefore, we investigated the association of age with functional connectivity, using resting state fMRI, in middle-aged and elderly persons.
Methods and Materials: 2,398 stroke-free and non-demented persons from the population-based Rotterdam study (mean age 65.7 years, 54.4% women) underwent brain MRI on a 1.5 Tesla scanner. We studied age-related changes in resting state functional connectivity (RSFC) for ten well-known resting state networks derived from our data, using FMRIB software library. We used non-parametric permutation testing on linear regression models to study how RSFC differed within and between these networks with aging, and whether these RSFC changes were independent of macrostructural MRI markers (e.g., global grey matter volume, white matter lesions) and cardiovascular risk factors.
Results: With increasing age, higher and lower connectivity was observed within and between the ten resting state networks. Associations became weaker after adjustments for macrostructural MRI markers and cardiovascular risk factors.
Conclusion: In a community-dwelling population, resting state functional connectivity changes with age. The observed higher connectivity with increasing age in some networks may suggest a compensation mechanism of the brain in response to decreased connectivity in other networks. Further research needs to explore the (spatial) role of structural MRI markers as a mediator in the association between age and functional connectivity.
Author Disclosures:
W.J. Niessen: Founder; Quantib BV. Shareholder; Quantib BV.

B-0930 10:38

The neural substrate of cognition: the Rotterdam study

H.I. Zonneveld, G.V. Roshchupkin, H.H.H. Adams, W.J. Niessen, M.A. Ikram, M.W. Vernooij; *Rotterdam/NL (h.zonneveld@erasmusmc.nl)*

Purpose: Variations in cognition are thought to be reflected in the structure of the brain. Yet, global measurements of brain structure (e.g. brain volume) do not account for all variability in brain morphology. Hypothesis-free approaches that study brain structure at the highest resolution, i.e. the voxel, in relation to cognitive ability are typically lacking or underpowered. We investigated the neural substrate of cognition in the large population-based Rotterdam study including middle-aged and elderly subjects.
Methods and Materials: 4,480 stroke-free and non-demented persons (mean age 66.3 (±10.3) years; 55.8% women) underwent brain MRI including high-resolution 3D T1-weighting imaging. Cognition was assessed using an extensive cognitive test battery and grouped into four independent domains (fine motor speed, executive functioning, memory and information processing speed). Voxel-based morphometry (with permutation testing) was performed to investigate the association between local grey matter density and cognitive function.
Results: Memory was associated with higher grey matter density in the thalamus and both hippocampi. Lower grey matter density in Broca's area was related to worse executive functioning. Executive functioning was associated with higher and lower grey matter density in different parts of both putamina. Fine motor speed was related to higher grey matter density in both caudate nuclei, right putamen and with lower density in the cingulate gyrus.
Conclusion: Associations of grey matter density with cognition are localised to specific parts of the brain. Both positive and negative associations were observed within the same structure. Detailed brain maps of cognition may provide insight into the pathways of cognitive decline.
Author Disclosures:
W.J. Niessen: Founder; Quantib B.V.. Shareholder; Quantib B.V..

B-0931 10:46

Hippocampal subregions provide information beyond gross hippocampal volume for cognitive function and risk of dementia

T.E. Evans[1], H.H.H. Adams[1], S. Licher[1], F.J. Wolters[1], A. van der Lugt[1], M. Ikram[1], M. O'Sullivan[2], M.W. Vernooij[1], M. Ikram[1]; [1]*Rotterdam/NL*, [2]*London/UK (t.evans@erasmusmc.nl)*

Purpose: Hippocampal volume is related to various cognitive functions as well as risk of dementia. The hippocampus is a complex and highly organised structure, consisting of various subregions. Research on hippocampal subregions has focused on memory and subtasks. It remains unclear how hippocampal subregions relate to other cognitive domains and risk of dementia.
Methods and Materials: From the population-based Rotterdam ,study 5,035 non-demented and stroke-free persons underwent MRI (1.5T) followed by automatic segmentation of the hippocampus and its subregions using the FreeSurfer software (version 6.0). A cognitive test battery was used to assess a range of cognitive functions. Subsequently, persons were followed up for the incident dementia. Association of the hippocampal subregion volumes with cognition and incident dementia was tested using linear and Cox regression models, respectively. All analyses were adjusted for age, sex, education, and gross volume of the hippocampus.
Results: Mean age was 64.33 years (SD 10.58) with 56% women. The volume of the hippocampal fimbria, fissure, pre-subiculum and subiculum showed the most significant associations with all cognitive domains, except memory. During follow-up (mean 5.5 years), 76 persons became demented. Subiculum volume was associated with risk of dementia (hazard ratio per decrease in 1 SD volume: 6.70, 95% CI: 3.39, 13.24; P: 4.33 $^{x10-08}$, adjusted for gross volume and CV risk factors).
Conclusion: Hippocampal subregions provide additional information beyond its gross volume for various aspects of cognitive functioning, but surprisingly not for memory. Furthermore, our results suggest that the subiculum is a marker for predicting dementia.

B-0932 10:54

Acupoint-specific effect of acupuncture in Alzheimer's disease: a functional MRI study

Y. Shan[1], Y. Bian[2], Z. Wang[1], Z. Zhao[1], M. Zhang[1], J. Lu[1], K. Li[1]; [1]*Beijing/CN*, [2]*Hefei/CN (shanyiedu@hotmail.com)*

Purpose: Acupuncture has been a major therapeutic method in Chinese medicine for treating Alzheimer's disease (AD) with validation and safety. In this study, we use functional magnetic resonance imaging (fMRI) to investigate the acupoint-specific effect of acupuncture in treating for AD.
Methods and Materials: 35 subjects were recruited including 21 patients with AD (followed DSM-IV and NINCDS-ADRDA criteria) and 14 age-matched healthy controls. AD patients were randomly divided into real and sham acupoint groups. MRI data acquisition was performed on a 3-Tesla scanner (Verio; Siemens, Germany). We adopted a 16-minute single-block experimental design to obtain functional images: After acquiring baseline data for 3 minutes, acupuncture stimulation was administered while fMRI went on scanning for the next 3 minutes. Finally, needles were withdrawn and the scan continued acquiring data for another 10 minutes. Data analysis was performed using AFNI software. Intra-group comparisons were performed through paired t-test between two statistical maps.
Results: In AD patients, acupuncture at real acupoints activated brain areas primarily in the left uvula, right superior temporal gyrus and right uncus. However, acupuncture at sham acupoints only activated areas in the left insula. Brain regions that were activated more by real acupoint were mostly located in the left medial frontal gyrus, while brain areas in the right lentiform nucleus/putamen and right insula showed less activation. In healthy controls, acupuncture at real acupoints activated extensive regions in bilateral cortical structures.
Conclusion: Acupoint-specific effect of acupuncture demonstrated with fMRI may help to facilitate its clinical use in AD treatment.

B-0933 11:02

Application of multi-echo T2 relaxation technique in Alzheimer's dementia and Mild Cognitive Impairment

E. Kavroulakis, G. Kalaitzakis, P. Simos, I. Zaganas, T.G. Maris, E. Papadaki; *Iraklion/GR (fpapada@otenet.gr)*

Purpose: Multi-echo T2 relaxation technique provides quantitative measurements of the long-T2 component (80-100ms), attributed to intra/extracellular brain water and short -T2 component (20-35ms) originating from myelin water. Myelin water fraction (MWF) correlates with histological measures of myelin in animal and human brains. The aim of this study is to investigate: (1) regional changes in long/short-T_2 and MWF values in the normal appearing white matter (NAWM) of Alzheimer's Disease (AD) and Mild Cognitive Impairment (MCI) patients, (2) associations between MWF/ T2 values and neuropsychiatric test scores and 3) indirect impact of age on neuropsychiatric function, through changes in T2 /MWF values.
Methods and Materials: Multiple Echo Spin Echo (MESE) sequence with 32 echoes and detailed neuropsychological assessment was performed in 25 AD, 43 MCI and 35 healthy controls (HC). MWF/ T2 values were measured in 20 NAWM areas.
Results: AD patients showed significantly increased long-T2, increased short -T2 and reduced MWF values in temporal, parietal and periventricular NAWM, compared to HC and MCI patients. MWF/ T2 values in several NAWM regions correlated with neuropsychiatric test scores in MCI patients, who have, also, age-related increases on Dementia Rating Scale (DRS) scores and decline in episodic memory capacity, through Short-T2 and MWF values.
Conclusion: There are changes in short-T2, MWF and long-T2 values in NAWM areas of AD and MCI patients, probably due to demyelination, coupled with axonal loss and gliosis. Enhanced age-related demyelination exists in prodromal dementia states (MCI) and is associated with the severity of episodic memory deficiency and DRS scores.

B-0934 11:10

Characterising brain iron deposition in patients with subcortical vascular mild cognitive impairment using QSM: a potential biomarker

Y. Sun, Y. Zhou, Y. Wang, X. Han, W. Ding, Y. Zhang, Q. Xu, J. Xu; *Shanghai/CN (cjs1119@hotmail.com)*

Purpose: The presence and pattern of iron accumulation in subcortical vascular mild cognitive impairment (svMCI) or their effects on cognition has rarely been investigated. The aim of this study was to examine the brain iron deposition in svMCI patients using quantitative susceptibility mapping (QSM) and its correlation with the severity of cognitive impairment.
Methods and Materials: Twenty svMCI patients and 19 controls were recruited and underwent QSM using a 3.0T MRI system. Susceptibility maps were reconstructed from a vivo data. Then, regions of interest were drawn manually on the map of each subject. The inter-group differences of susceptibility value were explored in deep gray matter nuclei including bilateral subthalamic nucleus, head of caudate nucleus, globus pallidus, putamen, hippocampus, substantia nigra, and red nucleus. The correlations between regional iron deposition and the composite z-score, memory z-score, language z-score, attention/executive z-score and visuospatial z-score were assessed partial using correlation analysis, with age and gender as covariates.
Results: Susceptibility values were found to be elevated within bilateral hippocampus and right putamen in svMCI group compared with controls. The susceptibility value in right hippocampus was negatively correlated with memory z-score and positively correlated with language z-score, the susceptibility value in right putamen was negatively correlated with attention/executive z-score in svMCI group. However, composite z-score were not related to susceptibility values.

Conclusion: Our result suggests that brain iron deposition which relation to cognition indicates the clinical relevance of the biomarker. It provides further evidence for the pathophysiological mechanism underlying the cognitive deficit in svMCI patients.

B-0935 11:18

Diffusion tensor imaging for evaluating changes in the microstructural integrity of white matter in patients with mild cognitive impairment

A.A. Ojeda, P. Acevedo, M.B. Nallino, N. Lori; *Rosario/AR (ojedaheleg@hotmail.com)*

Purpose: Neuroscientists have focused increasing attention on white matter connections in the brain and on the effects of ageing and cognitive impairment. Novel methods of neuroimaging like diffusion tensor imaging (DTI)have enabled biological tissue to be investigated in vivo. White matter (WM) fractional anisotropy (FA) is thought to be related to WM integrity and decline in FA is often used as an index of decreasing WM health. The goal of this paper is to detect white matter abnormalities not shown with conventional acquisition sequences in patients with mild cognitive impairment compared to cognitively normal subjects.
Methods and Materials: We prospectively recruited 18 people with mild cognitive disorders without or with mild unspecific WM abnormalities and 8 healthy control subjects age-controlled. They were scanned on a 3T MRI with 3D FLAIR, T1 weighted 3D sequences, T2* and DTI 6 directions. DTI preprocessing and voxelwise statistical analysis diffusion data were performed using FSL tools, to calculate voxel wise differences between MCI and controls.
Results: Compared to controls, MCI subjects revealed low FA predominantly in posterior body of the corpus callosum, left cingulate gyrus (anterior portion), and right anterior corona radiata all with p<0.05; and anterior cingulum with p<0.07. The mean FA values were calculated for the most significant voxel in these regions, and for each of the 2 groups.
Conclusion: The results suggest that patients with MCI show microstructural abnormalities of specific WM fibers compared to controls, which may give an insight of early landscape pathology in cognitive disorders.

B-0936 11:26

A normal swallow tail sign on MRI has high negative predictive value in Lewy body dementia

S. Shams[1], D. Fällmar[2], S. Schwarz[3], L.-O. Wahlund[1], D. van Westen[4], O. Hansson[4], E.-M.B. Larsson[2], S. Haller[2]; [1]*Stockholm/SE*, [2]*Uppsala/SE*, [3]*Nottingham/UK*, [4]*Lund/SE (sara.shams@ki.se)*

Purpose: MRI has a blind spot for the diagnosis of Lewy body dementia (LBD), in the absence of simple MRI signs. The swallow tail sign has been proposed as an accurate sign for Parkinson Disease (PD). Due to similar disease pathophysiology between PD and LBD, we hypothesised that this sign would be likewise applicable in LBD.
Methods and Materials: This retrospective cross-sectional multicenter study received institutional review board approval. We included 97 patients (mean age 65±10, 46%female), consisting of: controls (n=21), LBD (n=19), frontotemporal lobe dementia (n=20), Alzheimer's disease (n=20) and mild cognitive impairment (n=17). All patients underwent brain MRI, with susceptibility weighted imaging at 1.5T (n= 46) / 3.0T (n= 51). The swallow tail sign was assessed independently by two experienced raters, and consensus reading was done with a third, in case of discordance.
Results: Inter-rater agreement was moderate (kappa 0.4) between raters (1.5 & 3.0T). An abnormal swallow tail sign was most common in LBD 63% (95%CI: 41-85%, p<0.001) and had a predictive value only in LBD with an odds ratio of 9 (95% CI: 3-28, p<0.001), on 1.5T and 3T. On 1.5 and 3.0T / 1.5T / 3.0T values in LBD were respectively, sensitivity 63% / 60% / 64%; negative predictive value 89% / 93% / 86%; accuracy 76% / 71% / 80%.
Conclusion: Assessment of the swallow tail sign is clinically applicable during the work-up of dementia on 1.5 and 3.0T scanners, with higher accuracy at 3.0T. Due to the high sensitivity and negative predictive value, a normal swallow tail suggests exclusion of a LBD diagnosis.

B-0937 11:34

Follow-up research in patients with amnestic mild cognitive impairment using 3D arterial spin labelling

Y. Liu, H. Yuan, X. Zeng, Z. Wang; *Beijing/CN (lyyulia@163.com)*

Purpose: To follow up the changes of cerebral blood flow (CBF) values in patients with amnestic mild cognitive impairment (aMCI) using 3D pseudo-continuous arterial spin labeling (pcASL).
Methods and Materials: Patients with aMCI (n=10, mean age 74.80±3.26 years) were recruited. All patients were follow-up, the average scanning interval was (10.36±2.14) months. MMSE and MoCA scores were measured twice. All MRI examinations were performed on a GE750 3.0T scanner. 3D pcASL and 3D-SPGR sequences were employed. All patients were scanned twice. Voxel-based analysis was used to analyze CBF data (SPM8). CBF values (First time) were compared with CBF values (Second time) in patients with aMCI.
Results: 1. The first test: mean MMSE scores were (26.80±1.48), mean MoCA scores were (22.70±2.45). Follow up: mean MMSE scores were (26.50±0.85), mean MoCA scores were (22.60±2.32). There were no significant differences of MMSE scores and MoCA scores between the first test and the second test in patients with aMCI(*P*>0.05).
2.Compared to patients with aMCI (First time), we found significant decreases of CBF values in left middle temporal gyrus and left inferior temporal gyrus in patients with aMCI (Second time) (P<0.001, T=4.50, uncorrected for multiple comparisons, cluster size>50).
Conclusion: There were more areas involved in aMCI patients with the progress of the disease. Although there were no scores changes, CBF values might serve as a more sensitive tool to detect and characterize subtle changes in patients with aMCI.

B-0938 11:42

Dynamical analysis techniques for connective graph networks

A. Meyer-Baese; *Tallahassee, FL/US (ameyerbaese@fsu.edu)*

Purpose: Neurodegenerative disease evolution is poorly understood and treatment strategies are consequently only limited efficient. Fusing modern dynamic graph network theory and modelling strategies at different timescales yields a novel transformational paradigm in neurodegenerative diseases research regarding disease evolution at the patient level, treatment response evaluation and revealing some central mechanism in a network that drives alterations in many diseases.
Methods and Materials: The structure of many functional connective networks is determined by a sparse graph structure; however, containing many hubs. While static graph network theory helps modelling and understanding a "snapshot" in the disease evolution described by the graph structure, the longitudinal time behaviour is poorly understood since a modelling paradigm of the dynamic transient graph behaviour was missing. We propose to model and analyse functional connectivity networks in neurodegenerative diseases as two timescale sparse dynamic graph networks with hubs (clusters) representing the fast sub-system and the interconnections between hubs the slow sub-system.
Results: This novel modelling paradigm will help determining the so-called controlling regions in functional connectivity networks which are the "key drivers" when it comes to control the dynamics of the network. We will present a simple method to detect those drivers and will show how they impact the disease evolution.
Conclusion: We have established a new method to detect the key nodes that control the aberrant dynamics of the functional connectivity network and have tremendous applications on the understanding of disease evolution and the subsequent development of therapeutic solutions.

B-0939 11:50

Specificity of white matter hyperintensitiy location related to cognition

L. Lampe[1], S. Kharabian-Masouleh[1], J. Kynast[1], C.J. Steele[2], V. Witte[1], M.L. Schroeter[1], A. Villringer[1], P.-L. Bazin[1]; [1]*Leipzig/DE*, [2]*Montreal, QC/CA (lampe@cbs.mpg.de)*

Purpose: White matter hyperintensities (WMH), a correlate of cerebrovascular disease, are related to dementia. We assessed how the WMH location in the white matter affects different cognitive functions.
Methods and Materials: WMH were assessed with T1-weighted MPRAGE and FLAIR (1 mm isovoxel respectively) in 700 healthy, elderly participants (60-82 years) via LesionTOADS, a revalidated segmentation algorithm originally designed for multiple sclerosis lesions. Cognitive factors were extracted with an exploratory factor analysis (16 cognitive variables from a cognitive testing battery, including CERAD and SIDAM). Binary WMH masks were registered into standardized space, multiplied by z-scored values of cognitive factor, and added to return WMH probability masks.
Results: Factor 1 (executive function), Factor 2 (memory/learning), and Factor 3 (motor speed performance) were significantly related to total WMH volume. All three cognitive factors showed circumscribed clusters in different locations throughout the white matter. Factor 1 was primarily clustered in the frontal white matter adjacent to the frontal horns; Factor 2 showed the highest cluster size in the parietal white matter; Factor 3 was related to WMH clustering in the upper deep white matter, including the corticospinal tract. All clusters were symmetrical.
Conclusion: WMH have differing impacts on cognitive functions depending on their location in the white matter. Frontal WMH are mostly related to executive function, WMH in the parietal white matter are more related to worse performance in memory/learning, and WMH in the upper deep white matter is mostly related to a decrease in motor speed performance.

10:30 - 12:00 **Room F2**

Breast

SS 1402b

Breast cancer risk estimation

Moderators:
D. Baditescu; Bucharest/RO
A. Van Hoyweghen; Edegem/BE

B-0940 10:30

New insights in the risk of breast cancer recurrences in BRCA1, BRCA2 and CHEK2 patients

H. Ghunaim[1], C. Anthierens[2], A. Laenen[2], J. Soens[2], P. Neven[2], K. Punie[2], A. Smeets[2], H. Wildiers[2], C. Van Ongeval[2]; [1]*Medina/SA*, [2]*Leuven/BE (dr.had.g@hotmail.com)*

Purpose: To adjust follow-up strategies, prevalence of breast cancer recurrence (BCR) and contralateral BCR (CBCR) in BRCA1, BRCA2 and CHEK2 patients compared to a control group with sporadic breast cancer (CG) was investigated.
Methods and Materials: In a retrospective analysis (2000-2014), 278 gene mutation carriers (GMC) were diagnosed with breast cancer (98 BRCA1, 133 BRCA2, 45 CHEK2) as first cancer event. Risk of BCR was compared to CG (4,638), analyzing time interval between breast cancer and first BCR/CBCR and between first and second BCR. Cox regression was used, correcting for age, grade, ER and lymph node status.
Results: Average age at diagnosis is 44.0y in GMC, 59.0y in CG. Grade 3 tumours were most frequently seen in BRCA1 (70.41%), compared to BRCA2 (45.31%), CHEK2 (42.22%) and CG (38.57%). The risk of first recurrence is significantly higher in the 3 GMC groups compared to CG: hazard ratio (HR) of 4.6 (2.245; 9.654) in CHEK2, 3.1 (1.731; 5.642) in BRCA2 and 3.6 (1.839; 7.138) in BRCA1, with the highest risk of first BCR after 3 years for CHEK2 (11.59%), compared to 5% (BRCA groups) and 1.74% (CG). In 16% BRCA1 and 15% BRCA2 a second recurrence was found. The risk of CBCR is also significantly higher in the 3 GM groups compared to CG: CHEK2 (HR 9.7), BRCA2 (5.8), BRCA1 (8).
Conclusion: BCR risk is significantly higher in BRCA1/2 and CHEK2 compared to CG, with CHEK2 showing most frequently a second BC and a CBCR: adjustment of radiological/clinical follow-up strategies is necessary.

B-0941 10:38

Enhanced breast cancer screening for increased risk women with a family history: is it worthwhile?

L. Davies[1], G. Stevens[2], D. Bailey[3], M. Lewis[3], A. Murray[2], K. Gower Thomas[2]; [1]*Swansea/UK*, [2]*Cardiff/UK*, [3]*Pontypridd/UK (kgt77@hotmail.co.uk)*

Purpose: Women referred on the basis of possible familial higher risk for developing breast cancer are offered early annual breast cancer screening. The effectiveness of such enhanced screening programmes has been questioned and we present our results following the implementation of such a service in Wales.
Methods and Materials: Prospectively collected data were available for all women referred for enhanced screening by genetic services since its inception in 2001. This aggregate data included numbers of referral, screen episodes and cancers detected.
Results: Genetic service referred 4,807 women for enhanced screening. There were 4,601 prevalent and 17,669 incident screen episodes. Uptake of prevalent screen was 95.7%, with 9.9% of those women recalled and 20 cancers identified (0.43% of women screened). Incident screens had a 5.6% recall rate and detected a further 64 cancers (0.36% of screen episodes). The screen detected and interval cancer rates were 3.8 and 1.5 per 1000 screens, respectively. For this enhanced programme the sensitivity, specificity and positive predictive values were 71.2%, 93.8% and 5.8%, respectively. The screening programme detected 71.2% of the cancers in this group.
Conclusion: The enhanced screening service for women at additional familial risk had a 60% lower cancer detection rate per screen compared with the routine programme and thus may be resulting in harm from unnecessary investigations and emotional distress. However, on a pragmatic level over 70% of cancers in this group are detected at enhanced screening. Alternative, less resource intensive screening programmes should be explored for women at increased familial risk.

B-0942 10:46

Rim sign and histogram analysis of apparent diffusion coefficient value on diffusion-weighted MRI in triple-negative breast cancer: comparison with ER-positive subtype

Y. Choi, S. Kim, B. Kang, K. Lee; *Seoul/KR (charismakkang@hanmail.net)*

Purpose: To compare the clinicopathologic and diffusion-weighted MRI features between triple-negative and ER-positive breast cancer and to investigate their correlation with recurrence.
Methods and Materials: 221 breast cancer patients with pre-operative MRI taken from August 2009 to March 2015 were retrospectively included. All patients had pathologically confirmed diagnosis of invasive ductal carcinoma and were grouped into ER-positive (149) and triple-negative (72) subtypes. DWI rim sign and various ADC parameters (mean, mode, 25, 50, 75 percentile, skewness, and kurtosis) between ER-positive and triple-negative subtypes were compared. The same comparison was made between recurred (11) and non-recurred (211) patients. Univariate and multivariate regression analysis were used for statistical comparison.
Results: 221 breast cancer patients with pre-operative MRI taken from August 2009 to March 2015 were retrospectively included. All patients had pathologically confirmed diagnosis of invasive ductal carcinoma and were grouped into ER-positive (149) and triple-negative (72) subtypes. DWI rim sign and various ADC parameters (mean, mode, 25, 50, 75 percentile, skewness and kurtosis) between ER-positive and triple-negative subtypes were compared. The same comparison was made between recurred (11) and non-recurred (211) patients. Univariate and multivariate regression analysis were used for statistical comparison.
Conclusion: Poor histologic grade, higher Ki-67 and higher ADC kurtosis value were correlated with triple-negative subtype. More DWI rim signs and higher ADC values were found in recurrent patients. Rim signs and histogram analysis of ADC values are helpful parameters in predicting prognosis of breast cancer.

B-0943 10:54

Significance of parametric diffusion tensor imaging correlation with immunochemistry of pathology

T.-H. Chang, H.-H. Hsu; *Taipei/TW (m10708@mail.ndmctsgh.edu.tw)*

Purpose: IHC stains of breast cancer pathology, including ER, PR, and HER2, are important to breast cancer treatment. Our goal is to observe the relationships between the parameters of diffusion tensor imaging (DTI) and IHC stains.
Methods and Materials: During 2014-2015, 34 breast cancers were included for breast DTI examination randomly. Breast DTI were performed by 1.5T whole body MRI scanner (GE HDx) with 8-channel breast coils with the following protocols, TE: minimal, TR: 6275, FOV: 21, slice: 5.0mm, b value: 0/600, 6 directions, matrix: 96x96. DTI parameters were selected and calculated on the AW server (GE®). The region of interests of tumours were judged by a senior radiologist, who is an expert on breast MRI for 9 years. Statics were calculated by MedCalc® 16.4.3 version (2016).
Results: Of these 34 breast cancers cases, 8 cases were DCIS, and 26 cases were invasive carcinoma. Parametric DTI (λ_1, λ_2, λ_3, λ_1-λ_3, FA, anisotropic index, ADC) reveals no significant relationship with IHC stains (ER/PR/Her2). However, anisotrpic index and λ_1-λ_3 revealed significant results on the Box-and-whisker graphs. In the scatter diagrams, “ER” revealed significance on the anisotropic index. The correlation coefficient (r) was calculated as -0.4294 (p=0.0286). Additionally, most of invasive carcinomas revealed peritumoural anisotropy on the FA maps (22/26), and more than half of DCIS cases showed no peritumoural anisotropy (5/8).
Conclusion: Anisotropic index of DTI revealed significance over the “ER stain”. It can be meaningful in the treatment of breast cancer. The phenomenon of peritumoural anisotropy might predict invasive cancer.

B-0944 11:02

Utility of 18F-FDG PET/CT and MRI imaging findings for predicting the clinicopathologic subtypes of triple negative breast cancer

K. Kubota, T. Fujioka, A. Toriihara, Y. Saida, U. Tateishi; *Tokyo/JP (kbtmrad@tmd.ac.jp)*

Purpose: Breast cancer is known to be a heterogeneous group of distinct disease entities, and the treatment approach is sophisticated based on each intrinsic subtypes. Genetically, triple-negative breast cancer (TNBC) is classified into 7 subtypes, and pathological classification corresponding to these subtypes has been known. We assessed the utility of 18F-FDG PET/CT and MRI imaging findings for predicting the clinicopathological subtypes of TNBC.
Methods and Materials: We retrospectively analysed the cases of 46 patients with TNBC of over 10mm in diameter who underwent 18F-FDG-PET/CT and/or MRI before therapy. The maximum standardised uptake value (SUVmax) was evaluated on FDG-PET/CT. Tumour shape, margins, size, and kinetic patterns

and intratumoural necrosis were evaluated on dynamic contrast-enhanced MRI. The imaging findings of each subtype were retrospectively evaluated with pathological diagnoses.
Results: There were 34 invasive ductal carcinoma of no special type (IDC-NST), 6 apocrine carcinomas, 2 spindle cell carcinomas, 2 medullary carcinomas, and 2 adenoid-cystic carcinomas. Both PET/CT and MRI were performed in 40 cases. Higher SUVmax values were significantly associated with IDC-NST and spindle cell carcinoma (p=0.02). Intratumoural necrosis was only seen in IDC-NST or spindle cell carcinoma. Multivariate analysis showed that the SUVmax was the only independent predictor of IDC-NST or spindle cell carcinoma (p=0.03).
Conclusion: There is a possibility that the sub-classification of TNBCs can be performed based on imaging findings.

B-0945 11:10

Does MRI background enhancement correlate with breast cancer risk? A systematic review and meta-analysis

B. Bennani-Baiti, P.A.T. Baltzer; *Vienna/AT*
(barbara.bennani-baiti@meduniwien.ac.at)

Purpose: Assess the possible correlation between MRI Background Parenchymal Enhancement and breast cancer risk.
Methods and Materials: Two investigators independently performed a systematic review using predefined search terms. Studies that applied contrast enhanced MRI for assessment of lesions rated BI-RADS 3-6 in patients that had not previously undergone chemo- or hormonal therapy were eligible. Standard of reference had to be established by histopathology or clinical follow-up. Study design, technical parameters, and level of BPE with regard to outcome, were extracted from the original publications, and possible bias was determined using the QUADAS 2 applet. Statistical analysis included data pooling, forest plot construction, and heterogeneity testing.
Results: Six eligible studies comprising 1933 lesions (959 benign and 974 malignant) were identified. Dichotomized assessment (minimal/mild vs. moderate/marked BPE) revealed a pooled OR of 1.06 for lesions associated with moderate/marked BPE and significant heterogeneity (I^2=88%,P<0.001). Subgroup analysis displayed a pooled OR of 0.46 (I^2=0%,P<0.5) in non-high risk cohorts, a pooled OR of 0.94 (I^2=0%,P<0.6) for mixed cohorts (30-50% high risk) and a pooled OR of 4.77 (I^2=0%,P<0.5) for high-risk cohorts.
Conclusion: Our analysis based on a limited number of studies shows that the discrepant findings in the literature on BPE in regard to breast cancer risk could be explained by the different patient cohorts that were investigated. High levels of BPE in high risk patients seem to be associated with an increased risk of malignancy while high levels of BPE in non-high risk patients are not. Further studies are needed to confirm this finding.

B-0946 11:18

Correlation between background parenchymal enhancement (BPE) and whole breast vascularisation of the breast at contrast-enhanced MRI

C.G. Monaco[1], N. Berger[2], G. Lo Bue[1], L.A. Carbonaro[3], F. Sardanelli[3];
[1]*Milan/IT*, [2]*Zurich/CH*, [3]*San Donato Milanese/IT*
(cristianmonaco87@gmail.com)

Purpose: A positive correlation between BPE and breast cancer risk was suggested by literature. Our aim was to investigate the association among the breast vascularization with BPE, fibro-glandular tissue(FGT) and breast size at MRI.
Methods and Materials: 46 women with intermediate risk for breast cancer (dense breasts or lifetime risk 15-20%), who underwent dynamic contrast-enhanced MRI from Sep/2013 to Nov/2015, were evaluated. Vascularization was scored 0 to 3, based on the number of vessels per breast ≥3cm-long and with a diameter ≥2mm-large; BPE and FGT were evaluated with BI-RADS classifications; breast size(nipple-pectoral distance) was measured. Statistical analysis was performed on per-breast basis. χ^2-test for categorical variables or Student's t test and ANOVA evaluation for continuous variables were used.
Results: 92 breasts were evaluated. Vascularization showed a score 0 in 42 breasts (46%), 1 in 20 breasts (22%), 2 in 28 breasts (30%) and 3 in 2 breasts(2%). Low breast vascularization(score 0) showed 17% (7/42) of BPE 3 and 4 while high breast vascularization (score 2-3) showed 63% (19/30) of BPE 3 and 4 (P < .001). Breast vascularization showed a negative correlation with FGT and a positive correlation with breast size (P<0.001); FGT showed a negative correlation with breast size (P<0.001). BPE and FGT did not showed a statistically significant correlation (P=0.552)
Conclusion: High values of BPE were significantly rarer in presence of low whole breast vascularization at MRI. When high BPE was evaluated as a risk factor, a potential difference in breast cancer risk between women with high or low breast vascularization at MRI might be considered.

B-0947 11:26

Quantitative assessment of residual fibroglandular breast parenchyma after mastectomy on MRI

R. Woitek, G. Pfeiler, A. Farr, P. Kapetas, J. Furtner, M. Bernathova, P.A.T. Baltzer, T.H. Helbich; *Vienna/AT (ramona.woitek@meduniwien.ac.at)*

Purpose: Skin-sparing and nipple-sparing mastectomies (SSM/NSM) are performed to remove the breast's fibroglandular tissue, thereby reducing the risk of new breast cancer or cancer relapse. The postoperative presence of residual fibroglandular parenchyma (RFGP) is associated with remaining cancer risk. This study evaluated the role of MRI for the quantitative assessment of RFGP and skin envelope thickness after NSM and SSM.
Methods and Materials: The postoperative MRI scans (in accordance with EUSOMA recommendations, including T2-TSE and T1 GRE sequences) of 58 patients (85 breasts) who had undergone mastectomies with immediate reconstructions, between 2003 and 2013, were retrospectively evaluated. Skin envelope thickness was measured and volumetry of hypointensities that were suggestive of RFGP was performed using standard software (ImageJ). Hypointensities >1cm³ were considered positive for RFGP.
Results: Of 58 patients, nine had NSM and 49 SSM. RFGP was found in 16 patients (27.6%; volume range = 1.1 - 14.5cm³). Retromamillary RFGP ($RFGP_{rm}$) was found only after NSM (mean volume = 2.8 ± 1.7cm³). RFGP in other locations ($RFGP_{other}$) was found in 24.2% (mean volume = 4.2 ± 3.6 cm³). The volumes of both $RFGP_{other}$ and $RFGP_{rm}$ were significantly higher after NSM than SSM (p = .023; p <.001). Skin envelope thickness correlated significantly with $RFGP_{other}$ in left-sided breasts (p = .018).
Conclusion: In almost 25% of patients, MRI showed $RFGP_{other}$ after SSM and NSM, apart from $RFGP_{rm}$ after NSM. Preoperative MRI is recommended to improve preoperative planning to avoid RFGP and the associated cancer risk.

B-0948 11:34

Correlation of quantitative multiparametric ultrasound with immunohistochemical expression of breast tumours

P. Kapetas, R. Woitek, P. Clauser, K. Pinker, M. Bernathova, T.H. Helbich, P.A.T. Baltzer; *Vienna/AT (panagiotis.kapetas@meduniwien.ac.at)*

Purpose: To evaluate the correlation of quantitative ultrasound (US) parameters with immunohistochemical expression of breast cancer.
Methods and Materials: 64 patients, each with one malignant, biopsy-proven breast lesion were included in this prospective, IRB-approved study. Each lesion was examined with B-mode US, elastography (acoustic radiation force impulse (ARFI)), Doppler US and contrast-enhanced US (CEUS). Quantitative indices were recorded for each modality as follows: shear wave velocity (SWV) for ARFI, pulsatility (PI) and resistive index (RI) for Doppler US, and peak enhancement (PE), wash-in area under the curve (WiAUC), rise time (RT), mean transit time (local) (mTTl), time to peak (TTP), wash-in rate (WiR), wash-in perfusion index (WiPI), wash-out AUC (WoAUC), fall time (FT) and wash-out rate (WoR) for CEUS. For each lesion, histologic study determined tumour grade, oestrogen (ER) and progesterone receptor (PR), human epidermal growth factor receptor 2 (HER2), Ki67 proliferation index and tumour protein p53. Paired and unpaired nonparametric statistics were applied for comparisons as appropriate. Spearman's correlation coefficient was used to evaluate the correlation of sonographic quantitative indices with immunohistochemical parameters.
Results: There was a significant yet weak negative correlation between ER positivity and PE (r_s=-0.258,p<0.05), WiAUC (r_s=-0.329,p<0.01), WiWoAUC (r_s=-0.309,p<0.05) and WoAUC (r_s=-0.294,p<0.05) as well as PR and PE (r_s=-0.248,p=0.05), WiWoAUC (r_s=-0.279,p<0.05) and WoR (r_s=-0.294,p<0.05). A significant but weak correlation was shown between tumour grade and RI (r_s=0.314,p<0.05).
Conclusion: Several quantitative US indices show significant (yet weak) correlation to immunohistochemical parameters of breast tumours. The clinical relevance of this finding has yet to be explored.

B-0949 11:42

3D quantitative ultrasound analysis of breast carcinoma can non-invasively detect important pathological prognostic factors

A.S.S. Meel-van den Abeelen, G. Weijers, J.C.M. van Zelst, J.M. Thijssen, R.M. Mann, C.L. de Korte; *Nijmegen/NL*
(aisha.vandenabeelen@radboudumc.nl)

Purpose: In breast cancer, tumour grade and biological markers (oestrogen receptor (ER), progesterone receptor (PR), and human epidermal growth factor receptor 2 (HER2)) are predictive factors for medical treatment response and important for patient prognosis. 3D quantitative breast ultrasound (3DQBUS) may be used to guide histological biopsy. We investigated the correlation of 3DQBUS features with tumour grade and receptor status and assessed its predictive value.
Methods and Materials: 3D US examinations of 81 breast tumours were included. Per tumour, 3 regions of interest were defined: LES (ellipsoid

covering the hypoechoic part of the LESion), PER (PERitumoural border: 0.5mm around LES, capturing the halo), and POS (POSterior-tumoural region, capturing the posterior acoustic effect). Mean and variance of the echo level within the regions was calculated, and for LES and POS, the attenuation coefficient was calculated. Logistic regression was used to test the associations of 3DQBUS with receptor status and tumour grade. Additionally ROC-analysis was performed.
Results: Of 81 IDCs, 58 were ER- or PR-positive and 23 were ER- and PR negative, of which 16 were also HER2 negative. 37 were low-grade and 32 were high-grade tumours (unknown in 12). 3DQBUS provided good discrimination between tumours that were ER or PR positive versus ER/PR- (AUC=0.86) and triple negative tumours (AUC=0.89) and also allowed separation of low- and high-grade tumours (AUC=0.84).
Conclusion: 3DQBUS allows non-invasive separation of breast cancers with a different prognosis. This may be used to target the most aggressive part of a tumour during biopsy.

B-0950 11:50

Upgraded malignancy from high-risk and borderline lesions: correlated with immunohistochemical and clinical findings
J.-H. Choi[1], B. Kang[2], S. Kim[2]; [1]*Gyeonggi-do/KR*, [2]*Seoul/KR*
(mchjjh2@naver.com)

Purpose: We investigated the immuohistochemical characteristics of upgraded malignancy from high-risk and borderline lesions and correlated with clinical and imaging findings.
Methods and Materials: We reviewed the image-guided biopsy record retrospectively. We included all women with high-risk and borderline lesions and followed them for later breast cancers. We evaluated the clinical and imaging findings and we correlated the clinical and imaging factors with upgrade to malignancy. After surgery, the pathologic results were reviewed. When the lesion was updated to malignancy, the immuohistochemical characteristics were analysed.
Results: From January 2011 to July 2015, 340 high risk or borderline lesions confirmed by image-guided biopsy were included. Of the total 340, 81.2% (n=276) was not upgraded, 13.5% (n=46) was upgraded to carcinoma in situ, and 5.3% (n=18) was upgraded to invasive cancer. The upgrade rates were higher in patients with older age, larger lesion size, and with ADH than with other pathologic type (p<0.05). In the surgical proven malignancy (n=64), there was no lymph node metastasis (0%). ER positive (93.9%), PR positive (87.5%), HER2 negative (90.6%), Ki-67 negative (82.8%), EGFR negative (84.4%) were more frequent. Luminal A (76.6%) was most frequent, and then there were luminal B (17.2%), HER2 positive (1.6%), basal type of triple negative (1.6%), and non-basal type of triple negative (0.6%).
Conclusion: This immunohistochemical approach may form a useful addition to the clinical and imaging evaluation of high-risk and borderline lesion of the breast.

10:30 - 12:00 **Room D**

Musculoskeletal

SS 1410

Spine

Moderators:
I. Boric; Zabok/HR
N. Farshad-Amacker; Zurich/CH

B-0951 10:30

3D-x-ray-tomographies of lumbar spine performed with twin robotic x-ray: quantitative results of lumbar neural foramens in supine and upright position
A.L. Falkowski, R.M. Benz, S. Schön, L. Rizzo, E. Sommer, A. Hirschmann;
Basle/CH

Purpose: Tomographic examinations of lumbar spine are generally performed in supine non-weight-bearing position. This position is unphysiologic and might underestimate pathologies due to lack of body-weight. Evaluation of changes of lumbar neural foramina in supine non-weight-bearing and upright weight-bearing position using 3D-x-ray-tomography.
Methods and Materials: Lumbar spines of 48 patients (14 male; 34 female) with a mean age of 67.8±13.0 years were examined in upright weight-bearing position using a twin robotic x-ray unit (Multitom Rax, Siemens Healthineers). Supine non-weight-bearing scan was either performed using x-ray unit or CT. All patients were prospectively enrolled after IRB-approval. Images were reformatted according to intervertebral disc and axis of the spine at each lumbar level. Sizes of neural foramina (area and cranio-caudal diameter) were measured by two readers independently on sagittal reformats. Wilcoxon signed rank test (P<0.05) was used and interreader reliability was defined by intraclass correlation coefficient.
Results: Area of neural foramina significantly decreased at nearly all levels for both readers from supine (reader 1; L5: 1.20±0.36cm^2) to upright (1.15±0.41cm^2; P=.005) position, except for L4. Cranio-caudal diameter of neural foramina decreased in all levels L1-3 and at left L5-level for both readers. Interreader reliability for area was fair to excellent (0.504-0.894) and showed a wide range of variability for cranio-caudal distance (0.322-0.744).
Conclusion: Upright weight-bearing position decreases size of neural foramina causing potential risk factors for neural nerve compression that might be not evident on routine supine examinations. Thus, more specific diagnoses in unclear cases might be made using 3D-tomography.

B-0952 10:38

Can listhesis on upright radiographs predict the Schizas grade of lumbar spinal canal stenosis assessed on MRI?
T. Finkenstaedt[1], N. Bolog[2], J. Burgstaller[1], F. Del Grande[3], F. Del Grande[3], N. Ulrich[1], J. Steurer[1], G. Andreisek[1], S. Winklhofer[1]; [1]*Zurich/CH*, [2]*Bucharest/RO*, [3]*Lugano/CH (tim.finkenstaedt@usz.ch)*

Purpose: To assess the correlation between the grade of degenerative listhesis on upright radiographs with the grade of central spinal stenosis on supine magnetic resonance imaging (MRI) in patients with lumbar spinal stenosis (LSS).
Methods and Materials: Conventional radiographs and MR images of 141 consecutive patients (77 female, mean age 73) were retrospectively evaluated in this IRB-approved study. The grade of listhesis (in millimeter [mm]) was assessed on upright radiographs and on supine MRI of the lumbar vertebral segment 4/5. In addition, the grade of central spinal stenosis of the same segment was evaluated according to the classification of Schizas and correlated to the listhesis severity in radiographs. Kappa and ICC statistics were performed.
Results: Listhesis was detected in significantly more patients in radiographs (n = 53; 38 %) compared to MRI (n = 27; 19 %), p < 0.001. Pairwise comparison demonstrated a significant larger extension of listhesis in radiographs (mean 8.6 ± 2.8 mm) compared to MRI (mean 5.6 ± 1.9 mm), p < 0.001, each. A significant positive correlation was found regarding the grade of listhesis measured in radiographs and the grade of stenosis in MRI (Pearson correlation 0.48, p < 0.001). The interreader agreement was excellent for the presence of listhesis (Kappa = 0.938) and for the grading of listhesis (ICC = 0.913).
Conclusion: The grade of listhesis on radiographs is highly correlated with the grade of central LSS on MRI.

B-0953 10:46

Intravoxel incoherent motion (IVIM) analysis of vertebral bone marrow changes after radiation exposure from diagnostic imaging and interventional procedures
M. Yoon[1], S.-J. Hong[1], C. Kang[1], K.-S. Ahn[1], B. Kim[2]; [1]*Seoul/KR*, [2]*Gyeonggi-do/KR (mina11360@gmail.com)*

Purpose: To assess changes in vertebral bone marrow diffusion and perfusion using intravoxel incoherent motion diffusion-weighted magnetic resonance imaging (IVIM-DW MRI) after exposure to ionizing radiation from diagnostic imaging and interventional procedures in hepatocellular carcinoma (HCC) patients.
Methods and Materials: A total of 21 IVIM-DW MRI sets in 20 HCC patients, consisting of baseline and follow-up liver MRI with an interval less than 100 days were reviewed, after varying levels of radiation exposure from transarterial chemoembolisation (TACE), dynamic computed tomography (CT) of the liver, and plain radiography of the abdomen. IVIM parameters (apparent diffusion coefficient (ADC), true diffusion coefficient (D), pseudodiffusion coefficient (D*), and perfusion fraction (PF)) of the lower thoracic and lumbar vertebral bone marrow were analysed for significant differences between baseline and follow-up MRI using Wilcoxon signed-rank test, and for correlations with cumulative effective dose, as well as time interval between the last radiation exposure and follow-up MRI using Spearman's correlation.
Results: Compared to baseline MRI, ADC, D* and PF values decreased on follow-up MRI with statistical significance (p<0.05). Cumulative effective dose was moderately correlated with decrease in D* (r=0.434). In addition, longer intervals between the last exposure and follow-up MRI were moderately and negatively correlated with changes in D and ADC (r=-0.352 and -0.333, respectively).
Conclusion: Vertebral bone marrow diffusion and perfusion parameters were significantly changed after exposure to medical radiation.

B-0954 10:54

Evaluation of sclerosis in modic changes of the spine using susceptibilityweighted magnetic resonance imaging

S.M. Böker, Y.Y. Bender, L. Adams, M. Wagner, E.M. Fallenberg, B. Hamm, M. Makowski; *Berlin/DE (Sarah-maria.boeker@charite.de)*

Purpose: Evaluation of the diagnostic performance of susceptibility-weighted magnetic resonance imaging (SWMR) to differentiate between sclerotic and non-sclerotic Modic changes (MC) of the spine compared to computed tomography (CT) and radiographs.
Methods and Materials: SWMR and standard T1/T2 MR of the cervical (n=21) and/or lumbar spine (n=34) were performed in 54 patients. 21 subjects served as control. CT was performed in 18 patients; in all other patients radiographs were available. 67 Modic changes were identified on T1/T2 MR. On SWMR changes were classified as sclerotic and non-sclerotic based on signal intensity measurements. Sensitivity and specificity of SWMR and T1/T2 MR for differentiating between sclerotic and non-sclerotic Modic changes were determined. CT and radiographs were used as reference standard.
Results: Signal measurements between sclerotic and non-sclerotic Modic changes differed significantly ($p<0.01$) on SWMR. In contrast on T1- and T2-weighted MR no significant difference ($p>0.05$) was measured. Using a specific cut-off value on SWMR, a reliable differentiation between sclerotic and nonsclerotic Modic changes could be achieved, with a sensitivity of 98% and specificity of 95%. T1-/T2-weighted MR yielded a significantly lower sensitivity to detect sclerosis (20 %).
Conclusion: Using CT and radiographs as reference standard, SWMR allows a reliable detection of sclerosis in Modic changes with a higher accuracy compared to standard spine MR sequences.
Author Disclosures:
B. Hamm: Research/Grant Support; DFG, BMBF and more. Shareholder; more than 50 biotechnical companies. **M. Makowski:** Grant Recipient; Deutsche Forschungsgemeinschaft.

B-0955 11:02

Facet joint effusion on supine MRI in patients with lumbar spinal stenosis: correlation with listhesis on upright radiographs

N.V. Bolog[1], T. Finkenstaedt[1], G. Andreisek[1], J. Burgstaller[1], J. Steurer[1], F. Del Grande[2], A.F. Mannion[1], S. Winklhofer[1]; [1]*Zurich/CH*, [2]*Lugano/CH (nbolog@phoenixswissmed.com)*

Purpose: To asses the correlation between facet joints effusion in MRI and grade of listhesis on upright conventional radiographs in patients with clinically suspected lumbar spinal stenosis (LSS)
Methods and Materials: MR images and upright conventional radiographs of 50 consecutive patients (31 female, 19 male, mean age 73 years) with LSS were retrospectively evaluated in this institutional review board-approved study. The grade of listhesis was assessed on upright radiographs and was measured in millimetres (mm). The facet joint effusion (in mm) was evaluated in the corresponding segment of the listhesis in axial T2-weighted images. Intraclass correlation coefficient statistics were performed to investigate into the inter-reader agreement. Pearson analysis was conducted to assess the correlation between facet joint fluid in MRI and grade of listhesis in upright radiographs.
Results: The mean listhesis in radiographs was 6.6 +/- 3mm. The mean facet joint effusion was 1.4 +/- 1.4 mm (range 0-5mm). A significant positive correlation was found regarding the amount of fluid in the facet joints in MRI and the grade of listhesis measured on radiographs (p less than 0.005). ICC values demonstrated an excellent inter-reader agreement for listhesis (ICC=0.91) and substantial agreement (0.55) for inter-reader agreement regarding joint fluid.
Conclusion: Lumbar fact joint effusion on supine MRI correlates with listhesis on the upright radiographs in patients with clinically lumbar spinal stenosis. Thus, the thickness of the fluid within the facet joints may be an indicator for the extent of listhesis on upright position.
Author Disclosures:
N.V. Bolog: Research/Grant Support; This study was supported by the Helmut Horten Foundation, OPO-Foundations, Symphasis Foundation, Baugarten Foundation and Pfizer-Foundation for geriatrics and research in geriatrics. Other; On behalf of the LSOS working group.

B-0956 11:10

Feasibility of ADC value in lumbar disc degeneration at 1.5T

C. Kim; *Sungnam-si/KR (hello.hello.chohee@gmail.com)*

Purpose: Grading of disc degeneration based on T2-weighted image has some ambiguity. To evaluate feasibility of ADC value in lumbar disc degeneration is introduced based on the both Pfirrmann and modified Pfirrmann grading systems.
Methods and Materials: Lumbar spine T2-weighted and diffusion-weighted with b-value 0 and 500 1.5T MR imaging scans in our single institution from March 2014 to December 2014 were retrospectively reviewed. A total of 210 lumbar discs of 70 patients were analyzed. Severity of lumbar disc degeneration was graded by two independent observers using Pfirrmann's and modified Pfirrmann's scales, and the weighted value of kappa is calculated to measure the degree of disagreement between two readers. ADC values were recorded by the third observer for each disc within the center of disc in midsagittal plane. ADC values of disc were tested by correlation with visual grading systems, age, and gender.
Results: Intervertebral disc degeneration was negatively correlated with ADC values at lumbar levels except between grade 4 and 5 in Pfirrmann's scale and except above grade 5 in modified Pfirrmann's scale. Inter-observer agreements were good (κ_P=0.74, κ_{mP}=0.76) in both grading systems. And intra-observer agreements were very good in both grading systems (κ_P=0.92, κ_{mP}=0.84). Multiple linear regression analysis revealed ADC value had statistically correlation with grading systems, not age and gender.
Conclusion: Using ADC values to evaluate degenerative lumbar disc can be alternative approach supplementing visual grading system and while directly quantifying subtle changes.

B-0957 11:18

Role of fractional anisotropy (FA) in diffusion tensor imaging (DTI) for assessing degenerative lumbar disc disease: a preliminary study in 75 patients

M. Perri[1], R. Balzano[1], R. Izzo[2], G. Guglielmi[1], T. Popolizio[1]; [1]*San Giovanni Rotondo/IT*, [2]*Naples/IT (ro.balzano@gmail.com)*

Purpose: To evaluate the imaging features of the lumbar disc degenerative disease using FA in DTI imaging and comparing them with those obtained by standard MR protocol.
Methods and Materials: Medical Ethical Committee approval and informed consent were obtained. We selected 75 patients (mean age 42,3) composed by 20 healthy volunteers and 55 patients with already documented pathology whose 16 with extrusion, 19 with protrusion and 20 with bulging disc. All patients underwent MRI 1,5 T scanner examinations . Axial DTI images were performed using b value =600 s/mm^2 and diffusion directions = 30. FA values and corresponding images were extraced from the axial DTI images. Disc levels were also studied using standard MR protocol. Two expert radiologists evaluated MRI exams according to the recommended Nomenclature of the combined task forces of the ASSR, ASNR, and NASS. Chi-Square Test was performed for statistical analysis.
Results: All 20 healthy volunteers showed no significant alterations of the annulus fibers as on MR standard protocol as on FA ($p>.01$). Twelve out of 20 patients with documented bulging disc, showed on FA annulus fissures and were classified as intraannular herniation ($p<.01$). In 10 out of 19 patients, classified as protrusions showed on FA no annulus fissures ($p<.01$). All 16 patients with extrusions showed annulus fissures on both standard sequences and FA ($p>.01$).
Conclusion: The FA could demonstrate the integrity or rupture of the annulus fibers and could be added to the standard MRI protocol for obtaining more information on the disc structure.

B-0958 11:26

Lumbar plexus neuropathy in diabetic patients: an MRI evaluation study

F.I. Rozalli, N. Mohd. Ramli, K. Rahmat, F. Fadzli, N. Sulaiman, N. Shahrizaila, F.N. Zulkilpully; *Kuala Lumpur/MY (izzrozalli@aol.com)*

Purpose: There is a high prevalence of peripheral neuropathy among diabetics in Malaysia. This is usually assessed clinically and via nerve conduction study. Our goal is to assess the feasibility of utilising Diffusion Tensor Imaging (DTI) to assess severity of peripheral neuropathy and to predict concurrent muscle atrophy.
Methods and Materials: 30 diabetic patients and 10 age-matched healthy controls were prospectively recruited. The neuropathy was classified using the Toronto Clinical Scoring System (TCSS). MRI 3-Tesla with DTI was performed on the dominant leg to evaluate sciatic and peroneal nerves. Fractional anisotropy (FA) values were obtained for each nerve. Axial in-out-phase of the calf was used to determine the presence of muscle atrophy and is classified into severity by using Goutallier classification on the lateral gastrocnemius muscle.
Results: Spearman correlation test on neuropathy severity level with sciatic nerve and peroneal nerve was done and proved that the neuropathy severity (TCSS) had strong negative correlation with sciatic FA (r^2=-0.61, $p<0.05$) and poor negative correlation with peroneal FA (r^2=-0.39, $p<0.05$). This concludes that the worse the neuropathy severity, the worse the FA values for both nerves. There is no association between medial gastrocnemius atrophy severity with neuropathy severity level ($p<0.05$). There is no significant association between the mean FA values for both nerves with HbA1c control, age and duration of diabetes.

Conclusion: DTI is a good predictive tool to assess peripheral neuropathy severity among diabetic patient as it correlates well with TCSS severity. However, muscle atrophy is not directly related to neuropathy severity.
Author Disclosures:
F.I. Rozalli: Research/Grant Support; BK045-2015.

B-0959 11:34

Stir and diffusion MR neurography of the lumbar and sacral plexus: findings in asymptomatic individuals
M.L. Zanatta, M.R. Abreu, W. Ezequiel Neto; *Porto Alegre/BR (matheuszanatta@gmail.com)*

Purpose: Evaluate and compare image quality of lumbar and sacral plexus anatomy with DW (diffusion weighted) and STIR (short tau inversion recovery) magnetic resonance (MR) neurography sequences.
Methods and Materials: MR neurography of the spine and hip were performed in 30 asymptomatic individuals (20-60 y) utilising DW and STIR sequences on a 1,5 tesla siemens MAGNETOM espree. Nerve and ganglia morphology analysis and measurements were performed by two musculoskeletal radiologists employing MPR (multiplanar reconstruction) and MIP (maximum intensity projection) on an advanced workstation.
Results: The visualisation of nerve roots and ganglia was possible in all patients through DW sequences with and without MIP reconstructions, meanwhile were only demonstrated in 80% of STIR sequence images without MIP and in 90% with MIP. The neural structures on DW images were easier to read than STIR sequences, whereas the surrounding vessels appeared on the same intensity as some nerve roots. DW also had a higher concordance ratio between the observers in comparison with STIR (Pearson 0.8).
Conclusion: Lower lumbar and sacral nerve roots and its ganglia were successfully assessed using DW neurography, specially after using the MIP technique, and surpassed STIR imaging on evaluation of the nerves anatomy and surrounding structures.

B-0960 11:42

Dual-layer spectral CT: reduction of metallic artefacts from posterior spinal fusions
J. Dangelmaier, B.J. Schwaiger, M. Renz, A. Sauter, I. Riederer, D. Münzel, A. Fingerle, E.J. Rummeny, P.B. Noël; *Munich/DE (julia.dangelmaier@gmx.de)*

Purpose: To evaluate the clinical potential of virtual monoenergetic images (monoE) generated with a dual-layer spectral Computed Tomography (CT) system and determine the optimal settings for reduction of metal artifacts from posterior spinal fusions of diverse extent and different spine levels.
Methods and Materials: Twenty patients with posterior spinal fusion who underwent a spectral CT scan (IQon Spectral CT, Philips Healthcare, USA) for various clinical indications were included into this study. Two independent readers evaluated axial 0.9 mm slides with a window center of 50 HU and width of 380 HU. Image quality of the conventional scan was compared with monoE images at 40, 60, 80, 100, 120, 140, 160, 180 and 200 keV. A four point Likert-scale was used to document subjective impression of diagnostic image quality and the Hounsfield unit of the area with the most pronounced streak artefact was documented for every keV-setting. Additionally, the optimal monoE (OPTkeV) setting for all patients was determined.
Results: Quantitative and qualitative analysis showed statistically significant artefact reduction for higher monoE levels and especially for the OPTkeV compared to conventional images. Optimal keV-settings ranged from 120 to 140 keV. Our results reveal high inter-reader agreement for quantitative and qualitative evaluations.
Conclusion: Virtual monoenergetic images of higher energy levels (120-140 keV) provide significant reduction of metallic artefacts from posterior spinal fusions compared to conventional scans. Compared to previous results, with dual-layer spectral CT our findings can be applied to the whole field-of-view and to all patients without any compromises.

B-0961 11:50

Value of dedicated iterative metal artefact reduction algorithms in CT following spinal instrumentation
J. Aissa, C. Thomas, L. Sawicki, J. Caspers, P. Kröpil, G. Antoch, J. Boos; *Düsseldorf/DE (patric.kroepil@med.uni-duesseldorf.de)*

Purpose: To investigate the value of CT iterative metal artifact reduction (MAR) algorithms in patients after spinal instrumentation.
Methods and Materials: Twenty-four patients (13 male, 11 female; age 60.1±16.6) with post-surgical spinal CT between March 2015 and July 2016 were retrospectively included. CT Images were reconstructed with weighted filtered back projection (WFBP) and with two iterative MAR algorithms (MAR-Algo1, adjusted to spinal instrumentations and MAR-Algo2, adjusted to large metallic implants). A medium smooth kernel (B30f) and a sharp kernel (B70f) were used for image reconstruction. Frequencies of density changes were measured to assess quantitative artefact strength. Two independent readers rated visibility of anatomic structures including the central canal, the spinal cord, neural foramina and vertebral bone (0 = structure not identifiable to 5 = structure visible with high diagnostic confidence).
Results: Both algorithms quantitatively reduced artefacts compared with WFBP (MAR-Algo1: 59527.2±70182.6; MAR-Algo2: 89593.3±41590.5, WFBP: 123273.4±104734.9, $p < 0.001$). Subjectively, both algorithms improved visualization of bone (median MAR-Algo1: 3; inter quartile range (IQR): 3-4; MAR-Algo2: 4; IQR: 4-5) and soft tissue structures (median MARAlgo1: 3; IQR: 1.5-3; MAR-Algo2: 4; IQR: 3.5-4) compared with WFBP (bone structures: median 2; IQR: 1-3; soft tissue: median 2; IQR: 0.5-2) ($p<0.001$). Compared with MAR-Algo1, quantitative artefact reduction and visualization of soft tissue and bone structures was improved with MAR-Algo2 ($p<0.001$).
Conclusion: Both iterative MAR algorithms improved image quality and reduced artefacts compared with WFBP, however, the algorithm with dedicated settings for large metallic implants was superior to the algorithm specifically adjusted to spinal implants.

10:30 - 12:00 **Room G**

Physics in Medical Imaging

SS 1413
Advances in medical imaging methodology

Moderators:
M. Costagli; Pisa/IT
J.N. Vassileva; Vienna/AT

B-0962 10:30

Fat quantification in MRI and MRS - an in vitro validation
N.P. Linder, T. Rakete, A. Schaudinn, T. Kahn, H. Busse; *Leipzig/DE (linder@uniklinik-leipzig.de)*

Purpose: MR is a well established technique for quantification of adipose tissue (fat). Current techniques involve MR imaging, mainly based on the Dixon technique and MR spectroscopy. There is little evidence on the exactness of this fat quantification, which is addressed in this project.
Methods and Materials: Two separate sets of fat emulsions (E1 and E2) were generated by two independent pharmaceutical laboratories. Concentrations ranged from zero (water only) to 100% in steps of 10%. Using a standard 1.5 T MR scanner (Archieva, Philipps, Best, NL) MR sequences performed were 2 (slice thickness 10 mm, FOV 530 x 530 mm, TE1 3.45 ms, delta TE 1.44 ms) and 11-point Dixon (10 mm, 384 x 288 mm, 0.93 ms, 0.77 ms), stimulated echo acquisition mode (STEAM) proton spectroscopy (VOI 20 x 20 x 20 mm, TE 10 ms, TR 4000 ms) and point resolved spectroscopy (PRESS) (30 x 30 x 30 mm, 29 ms, 3500 ms). Results were blotted and compared by a linear regression true the origin by the resulting coefficient of determination (R2) and Bland Altman Blots.
Results: Overall Performance of the MR techniques was moderate to good with best results shown in the 11-point Dixon technique: R^2 values for 2p Dixon, 11p Dixon, STEAM and PRESS were 0.7479, 0,9831, 0.340 and 0.9823 for E1 and 0.8065, 0.9853, 0.342 and 0.9267 for E2, respectively.
Conclusion: Both 11 point Dixon and PRESS techniques are a reliable choice for fat quantification over a wide range of fat concentration.

B-0963 10:38

Estimation and correction of susceptibility-related distortions in MRI
I. Seimenis[1], E.P. Pappas[2], A. Moutsatsos[2], E. Georgiou[2], P. Karaiskos[2]; [1]*Alexandroupoli/GR*, [2]*Athens/GR (iseimen@med.duth.gr)*

Purpose: To propose and implement a methodological approach for the differentiation, evaluation and correction of susceptibility-related distortions in MR images.
Methods and Materials: A custom-made, head-sized, CT- and MR-compatible phantom, encompassing 947 control points (CPs) and two inserts, was constructed. CT provided the reference locations for inserts and CPs. Following 1.5T imaging, distortions were estimated with either the read gradient reversal or phase difference mapping technique. Distortions related to Bo inhomogeneity were estimated with phantom and inserts filled with copper sulphate solution, whilst susceptibility effects were evaluated with air or gadolinium (Gd) solution (5-10 mmol/ml herein) within the inserts. Correction schemes were based on the average-image and phase unwrapping techniques.
Results: Read gradient reversal effortlessly highlights areas of increased distortion, although CPs analysis is required to quantitatively assess distortion. The phase difference method proves excellent at high-signal regions but lack of phase information at low-signal areas, often encountered in patient images, results in unwrapping errors. For the protocol employed and volume scanned, Bo inhomogeneity distortion reaches 1 mm. The presence of air or Gd within

the inserts results in approximately 0.5 mm disposition which is read gradient direction dependent.
Conclusion: The presented methodology employing a prototype phantom effectively untangles complex distortion phenomena present in patient images. Under specific conditions applied, Bo inhomogeneity constitutes the predominant source of sequence-dependent distortion compared with susceptibility effects. A correction approach employing the average-image method is the simplest and most efficient method to improve geometric accuracy in demanding applications.
Author Disclosures:
E.P. Pappas: Research/Grant Support; This work was financially supported by the Greek State Scholarships Foundation through the program 'Research Projects for Excellence IKY/SIEMENS'.

B-0964 10:46

X-ray dark-field imaging to monitor the development of acute lung injury in mice

K. Hellbach[1], F. Meinel[1], T. Conlon[2], A. Yaroshenko[3], S. Auweter[1], M.F. Reiser[1], O. Eickelberg[2], F. Pfeiffer[3], A.Ö. Yildirim[2]; [1]*Munich/DE*, [2]*Oberschleißheim/DE*, [3]*Garching/DE*
(katharina.hellbach@med.uni-muenchen.de)

Purpose: The aim of this study was to evaluate the assessment of acute lung injury (ALI) in a murine model of pulmonary emphysema with grating-based x-ray dark-field imaging in vivo.
Methods and Materials: ALI was induced in female, 8-10 week old C57Bl/6N mice by orotracheal instillation of porcine pancreatic elastase (80 U/kg BW) (n=11). Control mice (n=10) received orotracheal instillation of PBS. Mice were imaged immediately before and 1 day after the application of elastase or PBS to assess acute changes in pulmonary structure due to ALI. Subsequently, 6 mice from each group were sacrificed and their lungs were lavaged and explanted for histological analysis. 7, 14 and 21 days later the remaining mice were imaged to assess the development of acute lung injury as well as emphysema progression. All images were acquired with a prototype grating-based small-animal scanner. At day 21, lungs were lavaged and obtained for histopathological analysis.
Results: Lavage confirmed that mice had developed ALI one day after administration of elastase. Additionally, lungs showed signs of early pulmonary emphysema, which continuously worsened until the end of the experiment. ALI was visible as a striking decrease in signal intensity of the pulmonary parenchyma on dark-field images at day 1. Quantitative analysis confirmed that dark-field signal intensity at day 1 was significantly lower than signal intensities measured at the remaining timepoints. There was no significant alteration in median transmission signal intensity.
Conclusion: The development of ALI in vivo can be monitored with dark-field radiography.

B-0965 10:54

X-ray dark-field radiography for the depiction of pneumothoraces in living pigs

K. Hellbach[1], A. Bähr[2], J. Herzen[3], P.B. Noël[1], A. Yaroshenko[4], T. Köhler[4], J. Mohr[5], M.F. Reiser[1], F. Pfeiffer[3]; [1]*Munich/DE*, [2]*Oberschleißheim/DE*, [3]*Garching/DE*, [4]*Hamburg/DE*, [5]*Eggenstein-Leopoldshafen/DE*
(katharina.hellbach@med.uni-muenchen.de)

Purpose: The aim of this study was to investigate whether pneumothorax diagnosis in a large animal model can be facilitated using x-ray dark-field radiography.
Methods and Materials: Experiments were performed using 2.5 months old, wild-type German landrace pigs (n=8). The animals were anesthetized, intubated, and mechanically ventilated during the experiments. All pigs were imaged with an experimental grating-based large animal scanner to acquire x-ray transmission and dark-field radiographs before and after induction of a unilateral pneumothorax. All scans were performed in abdominal position and posterior-anterior (p.a.) direction under respiratory arrest. Image contrast-to-noise ratios (CNR) between lung tissue and the air filled pleural cavity were quantified for both, transmission and dark-field radiograms.
Results: Lateral pneumothoraces were clearly visible as areas with no dark-field signal next to the adjacent lung parenchyma, which generated a strong dark-field signal. CNR between the air filled pleural cavity and the adjacent lung tissue was significantly higher in dark-field (3.65 ± 0.9) than in transmission images (1.14 ± 1.1; $p < 0.01$). Due to abdominal positioning of the pigs some of the animals developed a dorsal pneumothorax, which was also visible in dark-field images.
Conclusion: This study shows increased contrast between lung parenchyma and air in the pleural space in x-ray dark-field radiography as compared to conventional chest x-ray in a large animal model in p.a. images. This makes this technique a promising tool for facilitated diagnosis of pneumothoraces.

B-0966 11:02

Channel data recycling in CEUS imaging

G. McLaughlin, D. Napolitano, R. Steins, J. Baun; *Mountain View, CA/US (glen@zonare.com)*

Purpose: Investigate CEUS performance enhancement possibilities through the use of Channel Data Recycling (CDR), and Synthetic Steered Continuous Transmit/Receive Focusing (SSCTRF), to extracting and compound multiple minimally correlated images from a single CEUS transmit/receive sequence for the purpose of improving contrast resolution, improving SNR, minimising microbubble destruction, and enhancing temporal resolution. For example, 9 minimally correlated CEUS images can be generated from a 4-pulse sequence set, along with 3 B-mode reference images for compounding.
Methods and Materials: CEUS loops were collected from a ZONARE ZS3 system using two different transducers (C9-3&L14-5w). These loops were then processed with traditional methods, where single cubic-fundamental and single B-mode images were extracted. They were also processed to extract up to 6 cubic-fundamental images and 3 harmonic images along with 3 B-mode images. The 6 cubic-fundamental images consisted of 2 images that were constructed by weighting and adding combinations of the pulse sequence, and 4 images that were than constructed through SSCTRF techniques to generate 2 steered left and 2 steered right images. The same technique was used to generate the 3 harmonic and 3 B-mode images.
Results: The CEUS loops generated from the CDR data sets utilising SSCTRF showed improved contrast resolution, improved SNR, and improved border delineation while maintaining tissue perfusion kinetics along with no additional bubble destruction. This resulted in enhanced visualisation and higher diagnostic confidence.
Conclusion: CDR with SSCTRF is a viable technology to improve SNR and contrast resolution in CEUS imaging while maintaining temporal resolution with no additional bubble destruction.
Author Disclosures:
G. McLaughlin: Employee; Mindray/ZONARE. **D. Napolitano:** Employee; Mindray/ZONARE. **R. Steins:** Employee; Mindray/ZONARE. **J. Baun:** Employee; Mindray/ZONARE.

B-0967 11:10

Conventional ultrasound speed of 1540 m/s is inappropriate for examinations of obese patients at second trimester of pregnancy

B. Chauveau[1], C. Auclair[1], A. Legrand[1], H. Laurichesse[1], R. Mangione[2], L. Gerbaud[1], F. Venditelli[1], L. Boyer[1], D. Lémery[1]; [1]*Clermont-Ferrand/FR*, [2]*Bordeaux/FR (benoitchauveauaconf@gmail.com)*

Purpose: Obesity impairs the quality of ultrasound images. All ultrasound scanners are calibrated for an ultrasound propagation speed of 1540 m/s, although the speed in fatty tissue is only 1450 m/s. Our objectives were to compare the quality of mid-trimester foetal scans set at different ultrasound propagation velocities and to see whether patient characteristics affected this choice.
Methods and Materials: This cross-sectional study collected image triplets of four recommended scanning planes from 32 obese pregnant women at their mid-trimester foetal scan. Each of them was obtained at three different speeds (1540 m/s, 1480 m/s, and 1420 m/s). A panel of 114 experts assessed the quality of 100 triplets (online, with the speed settings masked), grading them from A to C. The grades were converted to a score (10, 5, 0). The analysis used Kappa coefficients, ANOVA, Chi^2, Student's t, and non-parametric Mann-Whitney tests, with the Bonferroni correction.
Results: The experts had a mean of 18.1 (±10.2) years of experience. The grade distribution (A, B, C) differed significantly between the three propagation velocities tested ($P<0.0001$), with 1480 m/s ranked highest (5.6±1.0), followed by 1420 m/s (4.9±1.1); the conventional speed of 1540 m/s (4.5±1.0; $P<0.0001$) was rated worst. Regardless of the scanning plane, the thicker the abdominal wall, the lower the preferred speed ($P<0.0001$).
Conclusion: Image construction set for ultrasound propagation velocities lower than 1540 m/s significantly improves image quality for mid-trimester fetal scans of obese patients.

B-0968 11:18

A platform to investigate photon counting detectors for dedicated spectral breast CT imaging

M. Tornai, D. Coccarelli, J. Greenberg, M. Gehm; *Durham, NC/US (martin.tornai@duke.edu)*

Purpose: Photon counting detectors promise low dose, spectroscopic, in vivo x-ray CT imaging. A prototype platform is investigated which could be incorporated for theranostic purposes into our existing fully-3D dedicated breast SPECT-CT imaging system.
Methods and Materials: Six 128-element x-ray detector modules having 800micron CdZnTe pixels with 64 energy-channels (MultiX ME100) form a 60cm linear array. This array is irradiated by a 1.2mm focal-spot tungsten

anode tube (Aerosino SAXG1701). With 3mm slat collimation through 5cm lead bricks, this system creates a fan beam geometry on a 145cm SID. Material phantoms imaged for 720 projections on the rotation stage at the center-of-rotation include: low/high scatter rods/tubes (1.1-4.7mm diameters), 6 materials (2cm diameter delrin, acrylic, breast glandular- and fat-equivalent plastics, polyethylene, and oil cylinders), and a cadaveric human breast supported in a 12cm diameter breast cup. Various source filtration conditions including heavy-K-edge Ce-filtration yielding a quasi-monochromatic x-ray beam and detector-energy windowing are investigated. Data is reconstructed using fan-beam filtered back-projection, and compared with an ordered subsets iterative method.
Results: Measured energy spectra from 70-120kVp without/with filtration were representative of those in the literature. For both low/high scatter phantoms, rods greater than 1.5mm were easily visualised. For the cylinders, measured attenuation coefficients were within 6% of true narrow-beam values, and were easily separable in histograms of reconstructions. Reconstructions of breast slices yield glandular, adipose tissues along with skin boundaries.
Conclusion: With optimisation, linear arrays of photon counting detectors could be used to distinguish tissue composition in low-dose dedicated breast CT.

B-0969 11:26

High-pitch emergency CT of the abdomen in obese patients in third generation dual-source CT: a radiation dose pilot study
R. Forbrig[1], F. Schwarz[2], M. Ingrisch[1], R. Stahl[1], M.F. Reiser[1], C. Trumm[1]; [1]*Munich/DE*, [2]*Augsburg/DE (robert.forbrig@med.uni-muenchen.de)*

Purpose: In the field of radiation dose reduction in 3rd generation dual-source computed tomography (DSCT) several modern techniques have been introduced recently. However, only little practical data exist in obese patients. We therefore investigated radiation dose in selected patients with a high body mass index (BMI) referred to our university hospital emergency unit undergoing high-pitch CT of the abdomen on a 3rd generation DSCT scanner.
Methods and Materials: 18 patients (11 female, mean age 52 years) with a BMI ≥ 30 kg/m^2 were examined between October 2014 and June 2016 on a 3rd generation DSCT scanner (SOMATOM Force, Siemens Healthcare, Forchheim, Germany). The standard CT protocol comprised the following parameters: Rotation time 0.25 s, pitch 1.55, slice collimation 192 x 0.6 mm, slice width 0.75 mm, increment 0.3 mm, kernel Br36, flow rate 2.5 mL/s, start delay 95 s and scan direction cranio-caudal. Radiation dose optimization was performed with automated tube current and voltage modulation. Radiation dose indices (volumetric CT dose index [$CTDI_{vol}$] and dose-length product [DLP]) were recorded.
Results: Mean BMI was 40.1 kg/m^2 (range, 30.0 - 50.3 kg/m^2). Mean tube current time product was 256 mAs (range, 95 - 410 mAs). Tube voltage ranged between 90 and 130 kV (mean 110 kV). Mean $CTDI_{vol}$ was 13.4 mGy (range, 6.4 - 23.6 mGy) and mean DLP was 659.2 mGy*cm (range, 264.1 - 1338.3 mGy*cm).
Conclusion: In 3rd generation DSCT high-pitch CT of the abdomen provides tolerable radiation dose in obese patients.

B-0970 11:34

Automatic tube voltage selection on a 320-slice CT-scan: a strategy to reduce the iodine load in routine contrast-enhanced CT? - a retrospective and a phantom study
P. Leyendecker[1], A. Labani[1], V. Noblet[2], M. Riou[1], A. Lallement[2], K. Haioun[3], M. Ohana[1], C. Roy[1]; [1]*Strasbourg/FR*, [2]*Illkirch/FR*, [3]*Puteaux/FR (pierre.leyendecker@chru-strasbourg.fr)*

Purpose: Retrospective study and phantom assessment of automatic tube voltage selection (ATVS) in iodine load reduction. To develop individualised low-volume contrast media (CM) protocols adapted to tube voltage in patients undergoing routine portal venous phase contrast-enhanced computed tomographic (CT) scan.
Methods and Materials: 70 patients underwent a 320-slice CT scan, without ATVS (group 1), and with ATVS (group 2). A quantitative analysis was performed in thoracic and abdominal aorta. A modified CM protocol based on these results was designed with the aim to obtain a homogeneous vascular attenuation across tube voltages. Secondly, an ex-vivo experiment in a phantom was performed to confirm the results of the clinical study by determining iodine attenuation curves for each selected tube voltages.
Results: Linear regression was used to test in objective image quality between the automatically selected tube voltages. Thus, in group 2, a CM dose saving of 20% could be achieve at 100 kV (p=0.002) with a constant contrast in the ascendant thoracic aorta compared with 120 kV. Phantom experiments revealed tube voltage-dependent iodine attenuation curves. Mean iodine attenuation in terms of CM concentration follows these equations respectively at 120 kV, y=70x-200 (R^2=0.97) and at 100 kV, y=92x-226 (R^2=0.95). A CM dose saving of 23.9% could be obtained at 100 kV (p=0.001) compared to 120 kV protocol.
Conclusion: The use of an individualised low-volume CM protocol adapted to the tube voltage enables significant iodine load reduction compared with a standard weight-based CM protocol for routine enhanced CT-scan using ATVS.

B-0971 11:42

Feasibility of very low volume of low iodine concentration contrast media and 80-kVp protocol at CT angiography of renal arteries
Y. Choi, J. Kim, J. Choi, E.-S. Cho; *Seoul/KR (mirr0412@gmail.com)*

Purpose: To investigate the feasibility of 80-kVp protocol using low volume of low iodine concentration contrast media (LC-CM) for CT angiography (CTA) of the renal arteries by comparison with a 120-kVp protocol using low volume of high-concentration contrast media (HC-CM). In addition, we tried to further reduce the volume of LC-CM in 80-kVp setting.
Methods and Materials: 36 volunteers underwent CTA of the renal arteries using one of three protocols: Group A, 120-kVp and 48mL of HC-CM (350mgI/mL-CM); group B, 80-kVp and 48mL of LC-CM (270mgI/mL-CM); group C, 80-kVp and 32mL of LC-CM. The attenuation and contrast-to-noise ratio (CNR) of the renal arteries, image qualities, and radiation dose were compared among three groups.
Results: Among three groups, mean attenuations, CNR and image quality in group B (303.3 ± 73.6 HU and 29.4 ± 13.7, respectively) were significantly higher than those in group A (226.2 ± 70.4 HU, 13.8 ± 7.7) or group C (266.4 ± 84.8 HU and 23.2 ± 16.5). There was no significant difference in the mean attenuations, CNR and image quality between groups A and C. Radiation dose of groups B or C was significantly lower than group A by 22.0%.
Conclusion: The use of 80-kVp with LC-CM (group B) could improve arterial enhancement and CNR and provide superior image quality with a smaller amount of iodine administration and a lower radiation dose, compared with 120-kVp with HC-CM (group A). Furthermore, it enables to reduce the volume of LC-CM by 28.9% while maintaining arterial attenuation and CNR.

B-0972 11:50

CT protocolmanagement: from the perspective of a large-scale cancer institution
X. Liu, D. Cody, W. Stefan, J. Rong; *Houston, TX/US (xliu@mdanderson.org)*

Purpose: To develop a data-base core CT protocol management system and maintain CT protocol parameters effectively in a large-scale cancer institution.
Methods and Materials: The number of 21 CT scanners of different models and approximately 300 protocols on each scanner combine to produce over a half-million of parameters to manage in our routine operation. A data-base core software program was developed and running on a Dell PowerEdge R720 server to retrieve protocol files, scanned protocols, and dose Notification Value log from each scanner daily. It allows for editing/viewing permissions to be controlled and keeps track of protocol changes with time stamps.
Results: Managing and implementing the protocol changes becomes more challenging than assembling the protocol itself. The web-based protocol management interface allows for the flexibility of editing and reviewing process. It provides a powerful tool to compare/monitor protocol changes between scanners of different model/vendor, or when several regional imaging facilities are expected to produce exams with the same quality. Protocol changes are notified daily to minimise the potential mistakes in scan parameters. NV notifications are triggered within an hour of the event so investigation and action can be taken timely. As one measure of the success, the number of CT Image Quality reports generated that were protocol parameter specific has reduced substantially in recent 5-years compared with prior to the implementation of this new program.
Conclusion: The data-base core CT protocol management approach has resulted in more reliable imaging outcomes and facilitated a vast improvement in our overall CT operation.

10:30 - 12:00 **Room K**

Radiographers

SS 1414

Radiography education

Moderators:
D. Akata; Ankara/TR
P. Cosson; Teeside/UK

K-20 10:30

Keynote lecture
K. Knapp; *Exeter/UK*

B B-0973 10:39

Do radiographers find evidence-based practice (EBP) a suitable tool for developing guidelines or protocols in imaging departments?
L. Hammerstrøm; *Oslo/NO (linda.hammerstrom@hioa.no)*

Purpose: To investigate if radiographers find EBP suitable for developing guidelines or protocols in imaging departments in Norway.
Methods and Materials: The study has a qualitative inductive design with phenomenological approach. Data collection took place in individual, semi-structured interviews. Inclusion criteria: Radiographers with experience in developing guidelines or protocols in imaging departments. Managers in eight imaging departments received information about the study and inclusion criteria by email, to help in recruitment by suggesting participants. Fourteen suggested participants received information about the study by email. Seven radiographers in five different imaging departments who met the inclusion criteria choose to participate in the study. The author transcribed and analysed all interviews.
Results: The study reveals shortcomings and certain misunderstandings regarding EBP. It suggests that brief encounters with patients and complex high-tech equipment stands out as factors that can complicate the use of EBP in imaging diagnostics. Few respondents have had training or courses in EBP. Radiographers who have, believes that the method is suitable for developing guidelines and protocols. Radiographers that has little knowledge regarding EBP has the perception that the method is unnecessary and complicated. There seems to be a clear connection between the extent of knowledge radiographers have about the method, and to what extent they find EBP suitable for developing guidelines and protocols.
Conclusion: The findings in this study suggests that further focus on EBP, education-courses and time to search for research articles is needed in order to fully utilize EBP in developing guidelines and protocols.

B-0974 10:47

Radiographer and elderly people in x-ray examinations: is there a need for radiographers' further education?
A. Henner[1], L. Karhumaa[1], E. Riippi[2], H. Kiuttu[3]; [1]*Oulu/FI*, [2]*Pori/FI*, [3]*Rovaniemi/FI (anja.henner@oamk.fi)*

Purpose: Population in developed countries is ageing strongly. Increased life expectancy results increase in chronic illnesses. Number of elderly people using health services is increasing and more than half of all elderly patients are daily patients in many hospitals. The purpose of this study was to find out radiographer's opinions towards elderly people who are coming to radiological examinations and to find out further education needs of radiographers.
Methods and Materials: Radiographers working in magnetic resonance imaging, computer tomography, mammography, ultrasound and x-ray imaging were included in this survey. A link to questionnaire was sent by Webropol to radiographers (N=152) and data was analysed with Webropol data analysis and survey tools programme. The open questions were analysed using textual analysing methods.
Results: Radiographers want more information about physiological and physical changes following ageing. Radiographers felt that they know how to work with elderly patients and how to change procedures to fit better to patient's needs, but agree that some procedures are harder with elderly. Most difficult modalities are magnetic resonance and x-ray imaging. There is enough knowledge about elderly, but radiographers are still open for information and further education. Radiographers felt that the knowledge about elderly and co-operation with them was learnt more through practice than in academic lectures during the basic education.
Conclusion: Radiographers are aware of the needs of elderly patients but there is still need for further education to deepen knowledge, e.g. in physiological senescence.

B-0975 10:55

Effect of training and experience on quality of radio stereometric analysis (RSA) examinations
O. Muharemovic[1], A. Troelsen[1], M.G. Thomsen[1], H.R. Siebner[1], K.K. Gosvig[2]; [1]*Hvidovre/DK*, [2]*Herlev/DK (omarradiograf@hotmail.com)*

Purpose: Producing x-ray images for the purpose of Radio Stereometric Analysis (RSA) is a demanding radiography technic resulting in high percentage of exposure repetition. The aim of this study is to investigate if RSA focused training and experience in performing RSA examinations, have effect on development of radiographers' skills and improvement on quality of RSA x-ray images.
Methods and Materials: Four radiographers are selected for the study group. Assessment of radiographers' performance is divided in two phases in this project identified as cyclus1 and cyclus2. Each cycle includes 20 examinations on phantom followed by 10 patient examinations. The quality of all x-ray images performed during the two cycles will be measured by number of beads visible (NB) and the centre position of prosthesis (CP) compared to centre of calibration field (CCF). The number of re-exposures used to obtain a usable image during patient examinations will be recorded
Results: After a workshop training on phantom and gaining experience on the patient examinations radiographers projecting images where CP is in average 36,1mm closer to the CCF ($p<0,001$), NB visible increase significantly with 3,1 ($p<0,001$) and radiographers use between 2, 1 and 2, 9 exposures less to obtain a usable images during patient examinations in cyclus2 ($p<0,001$).
Conclusion: Experience and training implemented in this project have significant effect on development of radiographers' skills and improvement on quality of RSA x-ray images. This improvement will results in decreasing of radiation dose delivering to the RSA patients.

B-0976 11:03

The impact of innovative technological change on employee motivation: a case study of radiographers working in the public healthcare in Malta
D. Chetcuti; *Msida/MT (chetcutidaniella@gmail.com)*

Purpose: Explores how innovative technological change has an impact on the level of motivation in radiographers and develop useful strategies to overcome innovation resistance and increase user acceptance of technology.
Methods and Materials: The impact of innovative technological change on employee motivation was identified using a cross-sectional, non-experimental research design. 70 radiographers participated in an online questionnaire survey, which enquired about employees' motivation factors, use of technology, sources of occupational stress and resistance to change.
Results: This study reveals which factors motivate radiographers and the causes for employee dissatisfaction. It also demonstrates that innovative technology improves quality of their work and enables a more efficient service. Although radiographers are prepared for the challenges brought about by innovative change, they are uncertain and under-confident on the introduction of an innovative technology in their work. This research establishes which employees are more likely to resist an innovation, and identifies the factors contributing to resistance to change.
Conclusion: Based on the findings of the study, it was concluded that there is a significant association between innovative technological change and employee motivation in radiography. The author has put forward a number of conclusions and recommendations which offer effective means of improving innovative change in radiography, with the aim of increasing employee motivation and user acceptance of technology, while reducing dissatisfaction and resistance to change.

B-0977 11:11

Small group facilitation: reflections of inexperienced tutors
L. Robinson[1], C. Mercer[1], J. Coward[1], S. Labouchere[2], P. Tavakol[3], C. Palmqvist[3], J. Lowe[4]; [1]*Salford/UK*, [2]*Lausanne/CH*, [3]*Huddinge/SE*, [4]*Dublin/IE (l.robinson@salford.ac.uk)*

Purpose: The 3-week OPTIMAX summer school involves approximately 50 international students working in facilitated groups. As well as being pedagogically valuable for students, OPTIMAX provides tutor learners (TLs) with an opportunity to develop facilitation skills. We aimed to provide TLs with a structured learning framework involving peer observation. We report our method and findings
Methods and Materials: Following a preparatory tutorial on observation and facilitation, TLs observed their allocated facilitator using a template developed for the project until data had been saturated (typically 3 hours). Post-observation, TLs and the facilitator being observed, reflected together on observations to clarify and verify interpretation. TLs then wrote up these reflections. TLs attended a consensus meeting to develop a thematic framework related to themes grounded in the reflective observations. This framework was then circulated along with all the reflective reports for detailed analysis and framework refinement.

Results: 6 TLs observed 7 facilitators in a variety of permutations: paired, singly, and over the length of Optimax. This allowed us to consider intra- and inter-observer differences, group dynamics, and changes in facilitator behaviour over time. **Key themes:** (i) tutor emotion/ personality heavily influenced group dynamic and development; (ii) experience in facilitating learning was more important than topic knowledge; (iii) effective facilitation engaged students in demonstrating their understanding rather than just stating it; (iv) group configuration is important.
Conclusion: Facilitators strongly influence group development so should be adequately prepared for their role. Experienced tutors and TLs found peer-observation informative for professional development.

B-0978 11:19

Can motion capture technologies enhance radiography skills development?

M. Hardy, H. Ugail, K. Fenemore, A. Al-Dahoud, Z. Sayed; *Bradford/UK (M.L.Hardy1@bradford.ac.uk)*

Purpose: Radiographic practice encompasses knowledge of imaging technologies, radiation safety, anatomy and patient care in order to produce images of diagnostic quality. While computer programmes can enhance simulated learning of the image acquisition process, the practice of positioning patients and reviewing anatomical appearances on resultant images has required clinical placement experience and supervised exposure of patients to x-radiation. This proof of concept study explores whether motion capture technologies might be developed to simulate real life clinical radiographic practice.
Methods and Materials: Using an XSENS MVN motion capture suit and configured hardware, we developed a purposeful coding programme to link body position of suit wearer to CT and radiographic image data of a chest phantom to simulate varying degrees of sagittal rotation.
Results: The motion capture technology permitted students to practice chest radiography within the university simulation suite and allowed real time evaluation of the relationship between patient position and chest image appearances without exposure to x-rays. The technology also enabled students to discuss image acceptability and repeat imaging thresholds as well as develop confidence in 'touching' patients during positioning and appreciate patient experience in a meaningful way.
Conclusion: Motion capture technologies are well established within the film and media industry and could be developed to create a simulated radiography education environment that reflects actual practice. This is the first study to explore this concept and consider the potential of motion capture technologies to enhance the development of radiography practical skills and reduce the risks associated with 'learning on patients'.
Author Disclosures:
M. Hardy: Grant Recipient; CCIP HEIF Award; Health Education England Award. Other; President of UKRC.

B-0979 11:27

An evaluation of the educational requirements to practise radiography in the European Union

J.G. Couto[1], C. Hughes[2], S. McFadden[2], P. McClure[2], P. Bezzina[1]; [1]*Msida/MT*, [2]*Newtownabbey/UK (jose.g.couto@um.edu.mt)*

Purpose: The aim of this research was to compare the requirements to practise radiography across the EU. As a health-care profession that uses ionising radiation, this profession has a great impact on the health and safety of the population. Due to the free movement of professionals across borders (Directive 2005/36/EC), it is important to explore the education and competencies required of staff across the EU to ensure this health and safety is maintained.
Methods and Materials: A descriptive, non-experimental, qualitative methodology was used. Competent authorities were identified through the Regulated Profession Database (RPD) of the European Commission and the requirements to practise the profession were requested. Inductive analysis of the data was performed using thematic analysis.
Results: Twenty-seven out of the 28 EU member states have the profession regulated and although most countries require some level of education they vary considerably in level, subjects covered and branches/specialisms. Fourteen different English titles were identified in the RPD under the generic name of “Radiographer/Radiotherapist”, indicating different branches and levels of autonomy.
Conclusion: There is no uniformity in the title and requirements to practise radiography in the EU, leading to a lack of uniformity in education. This limits free movement of professionals since the level and subjects covered by the professional are verified prior to registration in the host country. It is, therefore, important to identify and close the educational gaps between countries to ensure that feasibility of professional movement and patient safety are not compromised.

B-0980 11:35

Subsequent publication of orally presented original studies within five years presented at the European Congress of Radiology 2010

M. Dollinger[1], F. Zeman[2], L.P. Beyer[2], C. Stroszczynski[2], T. Bley[1], P. Wiggermann[2]; [1]*Würzburg/DE*, [2]*Regensburg/DE (marco.dollinger01@gmail.com)*

Purpose: To determine the rate at which original studies that were presented orally at the European Congress of Radiology (ECR) 2010 were published in Medline-indexed journals and to identify factors predictive of publication.
Methods and Materials: The Scientific Program of ECR 2010 was reviewed by one reader. A total of 869 abstracts were included in the study. A Medline search of articles published between March 2010 through February 2015 was conducted to identify articles written by the first, second, and/or last authors of all abstracts published in the Scientific Program of ECR 2010. The year of publication, journal, country origin of the abstract, subspecialty, and nature of the research (i.e., human, animal, or technical) were recorded.
Results: 450 abstracts were expanded into manuscripts that were subsequently published in Medline-indexed journals (overall publication rate, 52%). Subspecialty molecular imaging and cardiac radiology studies had the highest publication rates (75% and 62%, respectively), whereas computer applications studies had the lowest (28%). The publication rate also differed substantially according to the nature of research. The articles were published in a total of 125 journals, most of them in radiology journals (317/450, 70%), and chiefly in European Radiology (50 cases, 11% of published studies). Of all published manuscripts 87% (393/450) were published within a 3 year time Frame.
Conclusion: More than half of original studies presented orally at the ECR 2010 were subsequently published in Medline-indexed journals. More articles were published in the journal European Radiology than in any other identified journal.

B-0981 11:43

A tool to supervise the radiographer clinical placement

L.P.V. Ribeiro, A.F. Abrantes, L. Guerra, R.P.P. Almeida, K. Azevedo, J. Guerreiro, J.P. Pinheiro, A.M. Ribeiro; *Faro/PT (luispedroribeiro@hotmail.com)*

Purpose: Radiographer trainee supervisors have a permanent need to communicate and exchange information between the hospital and the university. The aim of this work was to develop a tool to help the monitoring and assess the trainees in different clinical placement locations.
Methods and Materials: Recurring to Google sites, we have developed a multi-profiled site, based on user authentication permissions, where the supervisor can consult information regarding the place of internship and trainees, and fill out trainee's individual assessments. The evaluation form with the criteria is provided for all supervisors. The supervisors from the university as administrators can consult and compile all of the information available in a daily basis.
Results: The trial version is functional and answering the initial needs requested by the hospital supervisors. Trainees monitoring and assessment is simplified, reducing the number of dislocations between hospitals and the university.
Conclusion: This tool provides clearly written up-to-date learning outcomes/objectives (the learning outcomes are reviewed and assessed) appropriate to the practice placement environment.

B-0982 11:51

E-learning tool in students ultrasound education: increase stable perception of organic structures

B. Kraus, H.T. Zipko, M. Schratter, W. Wadsak, M. Kundi; *Vienna/AT (barbara.kraus@fh-campuswien.ac.at)*

Purpose: Ultrasound examiners are medical doctors from different areas like radiologists, internists, gynaecologists and also radiographers, physiotherapists and biomedical scientists. Optimal training procedures for all groups involved in medical imaging is of real importance. Medical ultrasound examinations are a powerful alternative to more expensive and/or invasive imaging modalities. Worldwide, different training procedures are in place, but little is known about the cognitive processes that lead to the transformation of the visual information provided by the ultrasound image into an anatomical and pathological assessment.
Methods and Materials: A prospective quasi-experimental study design was applied to compare the visualization performance of radiographer students in Ultrasound imaging, evaluating two groups, one with traditional method, the other with augmented e-Learning method. Overall 97 of 6th Semester Bachelor degree radiographer students at University of Applied Sciences FH Campus Wien participated in this descriptive-statistical evaluation, 41 assigned to the traditional group and 56 to the augmented e-Learning group.

Results: The e-Learning group had a faster increase of correct visualizations. But the difference declined during follow-up. Greatest problems in correct assignment of anatomical structures were detected for middle upper epigastric region (pancreas-region, vessels), retroperitoneal-region as well as for the correct orientation during three-dimensional dynamic measurements.
Conclusion: E-Learning tools may have advantages in early stages of ultrasound examiner education. Training of three-dimensional dynamic measured procedures should be forced due to the difficulty to maintain stable perception of organic structures.

10:30 - 12:00 **Room M 1**

Cardiac

SS 1403a

Myocardial ischaemia and perfusion imaging II

Moderators:
R. Maksimović; Belgrade/RS
E. Pershina; Moscow/RU

B-0983 10:30

Adenosine and adenosine triphosphate (ATP) have a similar stress effect in patients undergoing stress/rest perfusion cardiac magnetic resonance examinations

P. Bartolomé Leal, A. Quilez Larragan, A. García Baizán, M. Millor Muruzábal, J. Pueyo Villoslada, G. Bastarrika Alemañ; *Pamplona/ES (pbartolome@unav.es)*

Purpose: Adenosine is generally employed in stress perfusion cardiac magnetic resonance (CMR) examinations. Little is known about usefulness of adenosine triphosphate (ATP), a cheaper adenosine analogue. This study was conducted to evaluate the stress effect of ATP compared with adenosine in routine perfusion CMR examinations.
Methods and Materials: Thirty patients (15 in each group) prospectively underwent a clinically indicated CMR examination with a conventional stress/rest perfusion protocol following intravenous contrast injection of a total dose of 0.2 mmol/kg of gadobutrol. Individuals were randomly assigned to ATP (160 mckg/kg/min) or adenosine (140, 180 or 210 mckg/kg/min, as necessary). The vasodilator effect of both drugs was analyzed by comparing differences in heart rate, symptoms during the stress, and myocardial and splenic perfusion values, including time to peak, signal intensity, area under the curve of each sector, tissue perfusion values, splenic and myocardial signal intensity ratios and the splenic-to-myocardial signal intensity ratio.
Results: No statistically significant differences were found in heart rate variation (26.1±19.1 bpm vs 21.7±17.3 bpm, p=0.68) and myocardial perfusion reserve index between the two stress agents (1.81±0.61 and 2.29±0.89 for ATP and adenosine, respectively, p=0.11). Spleen to myocardium ratio was also similar (ATP=0.90±0.39 vs adenosine=0.71±0.24, p=0.202). During pharmacologically induced stress, patients receiving ATP referred less pronounced clinical symptoms compared with those receiving adenosine.
Conclusion: ATP and adenosine have similar stress effect based on patients vital signs, myocardial blood flow reserve and splenic switch-off and can be safely employed in patients undergoing stress/rest CMR perfusion examinations.

B-0984 10:38

Role of T1 mapping on the evaluation of cardiac perfusion during adenosine stress CMR in CAD patients

E. Cannizzaro, P. Palumbo, L. Panebianco, F. Bruno, L. Patriarca, V. Vellucci, R. Masi, E. Di Cesare, C. Masciocchi; *L'Aquila/IT (estercannizzaro@hotmail.it)*

Purpose: The aim of this study was to evaluate the capability of T1 mapping at rest and during adenosine stress in identifying cardiac involvement in coronary artery disease (CAD) patients.
Methods and Materials: We retrospectively analysed 44 CAD patients who underwent stress CMR (3.0-T). CMR protocol included MOLLI, first-pass perfusion imaging during adenosine stress, cineMR sequences, STIR T2w and LGE after administration of a bolus of 0.2mmol/kg gadoterate dimeglumine (Gd-DOTA). MOLLI images were acquired before and during adenosine injection and were analysed with a dedicated software (Cvi42, Circle). Results are expressed on mean±SD and compared with Student's t test, Pearson correlation and Wilcoxon test.
Results: A total of 44 patients with CAD was analyzed. 20 patients showed infartuated or ischaemic myocardium, with high value of T1 mapping at rest (1306.62±68.36ms) and no significant response during adenosine infusion (p vale:0,305). 24 patients showed normal myocardial perfusion and no LGE. 16 of these had high value of T1 mapping at rest (1243±184ms) and no significant modification during stress (p value:0,21). The remaining 8 had lower T1 mapping value at rest (1138±112ms) with significant modification during adenosine infusion (p value: 0.0167; r: 0.844).
Conclusion: T1 mapping during adenosine infusion can help to identify an early myocardial involvement also in CAD patients without other MRI signs of cardiac disease. Therefore, T1 mapping alterations are earlier than other MRI sign.

B-0985 10:46

Value of transluminal attenuation gradient of stress CCTA for diagnosis of haemodynamically significant coronary artery stenosis - comparison with stress perfusion CMR

J. Lee, H. Yong, H.-Y. Kim, E.-Y. Kang; *Seoul/KR (ljw2000e@naver.com)*

Purpose: This study aimed to evaluate the value of the transluminal attenuation gradient (TAG) of stress coronary computed tomography angiography (CCTA) using a wide detector in patients with coronary artery disease comparing to stress perfusion cardiac magnetic resonance (CMR).
Methods and Materials: From May 2012 to January 2015, 21 patients with moderate coronary stenosis on invasive coronary angiography were prospectively included. All patients underwent adenosine stress single-shot CCTA with a rest CCTA scan using a wide area detector CT. Coronary artery stenosis was evaluated on both stress and rest CCTA images, and TAG was manually obtained for all vessels. Stress perfusion CMR using a 3.0T scanner was used as a reference standard. A TAG cut off value of 15.1 HU/10 mm was considered significant. The diagnostic accuracies of TAG and CMR were estimated and compared.
Results: TAG of stress CCTA in all coronary arteries had a sensitivity, specificity, PPV, and NPV of 90.5%, 90.0%, 86.4%, and 93.1%, respectively. Corresponding values for TAG of rest CCTA in all coronary arteries were 42.9%, 83.3%, 64.3%, and 67.6%, respectively, whereas those for TAG of coronary arteries with moderate stenosis on stress CCTA were 93.3%, 100%, 100%, and 92.3%, respectively. Mean effective radiation doses for stress and rest CCTA were 10.6 ± 2.6 mSv and 2.3 ± 1.3 mSv, respectively.
Conclusion: TAG of CCTA provides high diagnostic accuracy for detecting haemodynamically significant coronary artery stenosis. TAG of stress CCTA was more diagnostically accurate than rest CCTA, especially in coronary arteries with moderate stenosis.

B-0986 10:54

A multiple regression analysis of determinants of myocardial perfusion as measured by CT

T. Rienmüller[1], V.N. Makarenko[2], O.L. Bockeria[2], I.E. Rychina[2], V. Bereznitsky[2], C. Baumgartner[1], L.A. Bockeria[2], P. Ourednicek[3], R. Rienmüller[1]; [1]*Graz/AT*, [2]*Moscow/RU*, [3]*Brno/CZ (theresa.rienmueller@tugraz.at)*

Purpose: To assess the relationship between global myocardial perfusion (MP) values and of some of its (possible) determinants using multiple regression analysis.
Methods and Materials: 34 patients (25 male) with known/suspected coronary heart disease underwent dynamic CT perfusion measurements with ECG-gating, i.v. contrast agent and 80/100/120kV (weight dependent). All patients signed informed consent (study NCT02361996). Functional determinants as heart rate (HR), systolic/diastolic blood pressure (SBP/DBP), left ventricular muscle mass (LVMM), and stroke volume (SV) were registered together with potential risk factors for decreased perfusion (calcium score, stenotic lesions, high body mass index (BMI)). Descriptive statistics are provided as mean±standard deviation/percentages, respectively. Mean MP values were compared for different risk factors (Wilcoxon rank-sum test and Kruskal-Wallis test (more than two groups)). A multivariate model was computed using a stepwise regression algorithm (all statistics at 0.05 level of significance).
Results: Age: 62.4±11.1 years, BMI: 27.9±4.3 kg/m^2, HR: 66.2±11.8 bpm, SBP: 134.7±20 mmHg, DBP: 81.7±8.7mmHg, LVMM: 170.3±42.2g, SV: 92.3±22.6ml, stenoses: no: 21%, <50%: 11%, >50%: 26%, >85%: 42%, overweight: 35%, MP: 78±17ml/100g/min. Overweight led to a (not significant) decrease of 4ml/100g/min, stenotic lesions >50% to a (not significant) decrease of 9ml/100g/min, stepwise regression provided a statistically significant model including age, BMI, sex, HR, SBP, SV, LVMM, calcium score, severity of stenosis (p<5e-04, average relative error: 0.04).
Conclusion: Our results confirm the close relationship between functional determinants and MP and demonstrate the effectiveness of the studied risk factors in reducing MP implying the need to consider the MP-values and its determinants in clinical settings simultaneously.
Author Disclosures:
P. Ourednicek: Employee; Philips Healthcare.

B-0987 11:02

Fractal analysis of the transition region in perfusion imaging to characterise the pathophysiology of perfusion defects - application in chronic myocardial ischaemia

F. Michallek, M. Dewey; *Berlin/DE (florian.michallek@charite.de)*

Purpose: The introduced concept of fractal analysis (FA) will allow characterisation of the pathophysiology in abnormally perfused tissue by addressing the transition region in perfusion imaging. This study establishes a method to differentiate the pathophysiological composition in chronic myocardial ischaemia regarding its macrovascular (coronary artery disease, CAD) and microvascular (coronary microvascular dysfunction, CMD) components and to evaluate severity of ischaemia.
Methods and Materials: The ischaemic transition region was studied with FA using specifically developed software ("FraktalWandler"). Fractal dimensions (FD) were calculated in dynamic, contrast-enhanced magnetic resonance imaging data acquired from 26 patients. FD values during first-pass ($FD_{first\text{-}pass}$) and recirculation ($FD_{recirculation}$) were evaluated to conclude on the predominating pathophysiology or severity of ischaemia, respectively. Percent diameter stenosis on coronary angiography (ICA) was used as reference standard. Receiver operating characteristics (ROC), univariate and bivariate analysis were performed.
Results: 108 ischaemic myocardial segments were studied. ROC analysis demonstrated $FD_{first\text{-}pass}$=2.358 as optimal operating point for pathophysiological classification. Mean±standard deviation of $FD_{first\text{-}pass}$ or $FD_{recirculation}$, respectively, was 2.449±0.035 or 2.215±0.085 in classified CAD lesions, and 2.280±0.039 or 2.127±0.044 in classified CMD lesions. A linear correlation was found between $FD_{recirculation}$ and percent diameter stenosis in ICA in classified CAD (r=0.472, p=0.001) but, as expected, not in classified CMD lesions (r=0.082, p=0.6).
Conclusion: This novel pathophysiology-driven, modality-independent concept was successfully applied in chronic myocardial ischaemia to delineate CAD and CMD and evaluate severity of ischaemia, which have been clinical challenges. The approach can be extended to study a variety of perfusion abnormalities.
Author Disclosures:
F. Michallek: Patent Holder; The authors have filed a patent application for the presented invention (PCT/EP2016/071551). **M. Dewey:** Patent Holder; The authors have filed a patent application for the presented invention (PCT/EP2016/071551).

B-0988 11:10

Iodine quantification using dual energy CT in first generation dual layer CT and third generation dual source CT

G. Pelgrim[1], R.W. Van Hamersvelt[2], M.J. Willemink[2], M. Oudkerk[1], T. Leiner[2], R. Vliegenthart[1]; [1]*Groningen/NL*, [2]*Utrecht/NL (g.j.pelgrim@umcg.nl)*

Purpose: To investigate the accuracy of quantification of iodine concentration using dual energy CT (DECT) on two high-end CT systems: third generation dual source CT (DSCT) and first generation dual layer CT (DLCT).
Methods and Materials: Five tubes with increasing iodine concentrations (0, 5, 10, 15 and 20 mg/mL) were inserted in an anthropomorphic phantom. Small, medium and large patient sizes were simulated using two fat-equivalent rings. Tube voltage combinations of 150Sn with 70, 80, 90 or 100 kVp, and 140/80kVp were used to acquire DSCT data. DLCT data were acquired at 120 and 140kVp. Images were reconstructed using four iterative reconstruction levels (ADMIRE 0,1,3,5 for DSCT and Spectral 0,2,4,6 for DLCT); all scans were repeated 3 times. Vendor-specific iodine quantification software was used to calculate iodine concentrations based on the DECT scan data. Median normalized differences between CT-measured and known iodine concentrations, and absolute differences were compared for the different imaging protocols.
Results: Iodine concentration quantification was not influenced by iterative reconstruction level. For DSCT, median measurement error was lowest for the 150Sn/70kVp combination, -0.5%(interquartile range [IQR]: -2.0-2.0%) and highest for the 140/80kVp combination, 4.5% (IQR:1.3-6.5%). For DLCT, median measurement error was -3.3% (IQR:-4.9 - -1.5%) for 140kVp, and -4.6% (IQR:-6.0 - -3.6%) for 120 kVp. Increase in simulated patient size resulted in higher variation of iodine measurements.
Conclusion: Quantification of iodine concentration was accurate for both high-end CT systems with different spectral imaging approaches. Images acquired with larger energy separation resulted in the most accurate iodine concentration calculation for both systems.

B-0989 11:18

Pixel-wise quantification of myocardial blood flow from dynamic contrast-enhanced magnetic resonance imaging: the impact of deconvolution method

C. Kräuter, U. Reiter, C. Reiter, A. Schmidt, M. Fuchsjäger, R. Stollberger, G. Reiter; *Graz/AT (corina.kraeuter@gmx.at)*

Purpose: To study the impact of different commonly employed deconvolution methods on pixel-wise quantification of myocardial blood flow (MBF) from dynamic contrast-enhanced magnetic resonance imaging (DCE-MRI).
Methods and Materials: Eight patients with coronary heart disease underwent 3T pre-contrast T1 mapping and cardiac DCE-MRI at rest using a saturation recovery fast low angle shot sequence. Gadolinium-based contrast agent was administered as bolus at a dose of 0.05 mmol/kg. After coil sensitivity and motion correction of DCE series as well as T1-mapping-based conversion of signal intensity to contrast agent concentration, MBF was calculated pixel-wise by deconvolution using three different methods: Fermi modelling, Tikhonov regularisation with B-splines and autoregressive moving average (ARMA) modelling. The relationships between different pixel-wise evaluated MBFs and between resulting global MBFs were analysed by correlation analysis; mean global MBFs were compared with paired t-test.
Results: Mean global MBFs determined by deconvolution using Fermi modelling (0.72±0.13 ml/min/g), Tikhonov regularisation (0.67±0.10 ml/min/g) and ARMA modelling (0.84±0.16 ml/min/g) differed ($p<0.02$ for all comparisons). The MBFs correlated strongly, both pixel-wise (r=0.95, 0.86, and 0.83 for Fermi modelling vs Tikhonov regularisation, Fermi modelling vs ARMA modelling, and Tikhonov regularisation vs ARMA modelling, respectively) and globally (r=0.93, 0.86, and 0.85 for Fermi modelling vs Tikhonov regularisation, Fermi modelling vs ARMA modelling, and Tikhonov regularisation vs ARMA modelling, respectively).
Conclusion: There is a close relationship between pixel-wise myocardial blood flows determined by different commonly employed deconvolution methods, especially between Fermi modelling and Tikhonov regularisation with B-splines. Absolute values of myocardial blood flow, however, differ.
Author Disclosures:
G. Reiter: Employee; Siemens Healthcare Diagnostics GmbH.

B-0990 11:26

Quantitative assessment of salvaged myocardial zone and intramyocardial haemorrhage by 7T MRI

Y. Zhang[1], L. Yang[2], F. Gao[3]; [1]*Guizhou/CN*, [2]*Beijing/CN*, [3]*Sichuan/CN (102651873@qq.com)*

Purpose: To determine the myocardial area at risk (AAR), infarction-core size (IS) and the salvaged myocardial zone (SMZ), and to evaluate the imaging and histological characteristics of intramyocardial haemorrhage (IMH) after myocardial infarction using non-contrast T2-mapping on 7T MRI.
Methods and Materials: Twenty Sprague-Dawley (SD) rats were randomly divided into the sham and model groups (n=10 for either group). In the model group, myocardial infarction models were established by left anterior descending branch ligation. All animals were imaged on a 7.0 Tesla system with cine spiral imaging, T2-mapping LGE after 24 h. Then, the rats were sacrificed for measurement of the IS and AAR using TTC and HE staining. T2-mapping revealed the AAR in the model group was significantly higher than sham group.
Results: No remarkable T2 value was noted in the entire heart of the sham group. LGE and TTC staining demonstrated similar IS. T2-mapping and HE staining revealed similar AAR as well. T2 mapping characterized the IMH as a phenomenon resulting from the area of hypointensity in the hyperintensity involving infarct-core zone and corresponding T2 value (28.6±1.52) ms with IMH vs. (35.8±2.61) ms without IMH: n=3 with 18 slices, P=0.032). Non-contrast T2-mapping was a reliable approach to quantitatively evaluate the SMZ and IMH.
Conclusion: This present study was designed to establish a stable and reliable platform using a non-invasive technique to assess the SMZ and IMH in a rat model despite a high heart rate.

B-0991 11:34

Identification of the best CMR technique for quantitative assessment of myocardial salvage using a systematic comparison

J. Kihlberg[1], V. Gupta[1], H. Haraldsson[2], A. Sigfridsson[3], S.I. Sarvari[4], T. Ebbers[1], J. Engvall[1]; [1]*Linköping/SE*, [2]*San Francisco, CA/US*, [3]*Stockholm/SE*, [4]*Oslo/NO (johan.kihlberg@regionostergotland.se)*

Purpose: Several cardiac magnetic resonance (CMR) techniques exist for the quantitative assessment of myocardial salvage that is vital in planning coronary revascularisation. The purpose of the current study is to identify the best technique for this assessment by systematic comparison with late gadolinium enhancement (LGE).

Methods and Materials: Data from 81 patients (mean age: 66 ± 6 years; 58 men) with suspect coronary artery disease were analysed. Analysis were performed using three commonly used CMR techniques, cine steady state free precession (SSFP) imaging for feature tracking (FT), tagging (current gold standard), and Displacement Encoded Stimulated Echoes (DENSE). The data were analysed using Tomtec software, Harmonic Phase Imaging (HARP), and an in-house algorithm, respectively. SSFP was included in standard CMR protocols while tagging and DENSE required separate acquisitions. The comparison was performed using circumferential strain in the myocardial segments with transmurality ≥ 50% LGE.
Results: 23 patients were identified with transmurality ≥ 50% LGE (49 segments). The area-under curve (AUC) value from the receiver-operating curve (ROC) for detecting transmurality ≥50% LGE was 0.87 for DENSE, 0.74 for FT and 0.66 for HARP. The Pearson Correlation between global circumferential strain and left ventricle end systolic volume was 0.76 (DENSE) and 0.73 (FT) at a significance level of 0.01, and 0.27 (HARP) at a significance level of 0.05.
Conclusion: DENSE outperformed FT and tagging in detecting regional dysfunction caused by coronary artery disease.

B-0992 11:42

How to assess haemodynamic aspect of not-evaluable plaques by cardiac CT? Use of CCO and role of stress CMR

P. Palumbo, E. Cannizzaro, L. Panebianco, F. Bruno, L. Patriarca, V. Vellucci, R. Masi, E. Di Cesare, C. Masciocchi; *L'Aquila/IT*
(palumbopierpaolo89@gmail.com)

Purpose: Stress myocardial perfusion imaging by cardiac magnetic resonance (CMR) and corrected coronary opacification (CCO) can help to assess calcified plaques not correctly evaluable by standardised method of cardiac-CT analysis.
Methods and Materials: We retrospectively analysed 26 patients who had undergone cardiac-CT and stress CMR, with match of calcified plaques not certainly evaluable at cardiac-CT. Evidence of stress myocardial perfusion imaging by CMR was compared with attenuation values in coronary lumen (CCO). The CCO difference across the calcified plaque was measured proximally and distally to the calcified plaque, in an axial plane, and normalised to the descending aorta at same slice.
Results: A total of 30 calcified plaques were assessed. Eight calcified plaques were not haemodynamically significant, and showed a low CCO difference (0.062). Ten calcified plaques determined reversible perfusion alteration under stress, with a significant correlation with an intermediate CCO difference (0.20; r: 0.7530; p value: 0.0012). Twelve calcified plaques determined irreversible perfusion alterations under stress with a significant correlation with a high CCO difference (0.364; r: 0.8152; p value: 0.0002).
Conclusion: Stress myocardial perfusion imaging by CMR and CCO analysis by cardiac-CT, offers interesting similar information about haemodynamic significance of calcified plaques not evaluable due to "blooming effect". Correlation of these two methods permits an effective management of patients with not-evaluable calcified plaques.

B-0993 11:50

Myocardial texture analysis for the detection of ischaemic heart disease on routine non-contrast cardiac MRI sequences

P. Talarczyk, J. Weir-McCall, S. Waugh, P. Guntur Ramkumar, G. Houston; *Dundee/UK*

Purpose: Texture analysis allows quantification of tissue heterogeneity and has been proven to provide powerful diagnostic and prognostic data in oncological imaging. However to date this technique has not been applied to the assessment of the myocardium. The hypothesis of the current study was that those with ischaemic heart disease (IHD+) have a more heterogenous myocardial texture than those without (IHD-).
Methods and Materials: Cardiac MRI was performed in 52 study participants on a 3T scanner, with routine bSSFP and late gadolinium enhancement sequences. 23 IHD+ patients with myocardial scarring confirmed on late gadolinium enhancement images were compared with 29 IHD- volunteers with no cardiovascular disease and absence of myocardial scarring. Image analysis was performed on a pre-contrast bSSFP short axis mid-ventricular slice at end systole. Texture features were measured using MazDa software, with co-occurrence matrix and run-length matrix.
Results: IHD+ had significantly increased measures of myocardial heterogeneity compared to the IHD- group. On a forward condition entry binary logistic regression model Grey Level Variance (IHD+ 3.2±1.3 vs IHD- 4.3±2.1, p=0.035), Grey Level Non-uniformity (IHD+ 4.8±1.2 vs IHD- 3.8±0.8, p=0.001) and Mean signal intensity (IHD+ 164±34 vs IHD- 206±54, p=0.002) were the strongest predictors for the presence of IHD showing 73% accuracy (ROC 0.84). When all 29 measures of texture were applied in the same model, there was 100% accuracy (ROC 1.0).
Conclusion: Myocardial heterogeneity on routine non-contrast sequences can predict the presence of myocardial fibrosis in those with ischaemic heart disease potentially obviating the need for contrast sequences.

10:30 - 12:00 **Room M 2**

Paediatric

SS 1412
Foetal and paediatric brain imaging

Moderators:
H.-J. Mentzel; Jena/DE
S. Stafrace; Doha/QA

B-0994 10:30

Evaluating a new objective indicator of idiopathic intracranial hypertension (IIH) on routine paediatric brain CT scan

T. Bartsikhovsky, S. Tal, S. Nagieva, M. Vaiman, P. Gottlieb, I. Bekerman; *Tzrifin/IL (hatul.ratz@gmail.com)*

Purpose: The aim of this study was to establish optic nerve sheath diameter (ONSD) to eyeball transverse diameter (ETD) index value as sign of elevated ICP on brain CT scan in paediatric patients and correlate this data with papilloedema on ophthalmologic examination.
Methods and Materials: We retrospectively reviewed brain CT studies and medical files of paediatric patients for a period 2014-2015 years, selecting patients who had normal CT scans. Total study population included 153 patients (75 male, 78 female, mean age 11.1±5.2). Patients who were admitted to the emergency department with complaints of headache and/or one of the signs of elevated ICP and underwent ophthalmological evaluation were selected and stratified into two groups: with no signs of papilloedema and with papilloedema. The control group included subjects who underwent brain CT studies for various reasons not related to elevated ICP and are unlikely to have papilloedema. All measurements were held manually on axial images of routine brain CT scans obtained by the 256-slice CT scanner.
Results: ONSD/ETD index had significantly higher values ($p<0.001$) in patients with papilloedema (median 0.24, IQR=0.22-0.25) compared to patients with no signs of papilloedema (median 0.18, IQR=0.16-0.19) and control group (median 0.17, IQR=0.15-0.18). The ONSD/ETD index of 0.21 is 82% sensitive and 93% specific for papilloedema and therefore increased ICP in paediatric patients with with headache.
Conclusion: A strong correlation between papilloedema on ophthalmologic examination and elevated values of the ONSD/ETD index was established making it a simple and reliable sign of elevated ICP in paediatric patients.

B-0995 10:38

Mechanical thrombectomy for acute ischaemic stroke: what about children, should we include them?

C. Parra-Fariñas, I. Delgado Álvarez, Á. Sánchez-Montanez, M. Ribó Jacobí, A. Tomasello Weitz, P. Coscojuela Santaliestra, A. Macaya Ruiz, C. Hernández Giraldo, É. Vazquez Mendez; *Barcelona/ES*
(carmenparrafarinas@gmail.com)

Purpose: Acute ischaemic stroke in children is difficult to diagnose and manage due to atypical presentation and imaging challenge. Recent trials have demonstrated mechanical thrombectomy success in adults, but there is a lack of evidence-based data concerning children. This study aimed to analyse the safeness and effectiveness of endovascular approach in paediatric intracranial recanalisation.
Methods and Materials: From October 2012 to October 2016, a prospective study of four patients younger than the age of 18 who underwent mechanical thrombectomy was performed. Baseline characteristics, successful recanalisation (TICI grade ≥2b), procedural time, dramatic neurological improvement (≥10 points decrease in NIHSS score at 24 hours), and independent functional outcome (mRS ≤2) at three months were recorded.
Results: Mean age at treatment was 14±1.2, all female. Patients presented with hemiparesis (n=2) and aphasia (n=1). Median NIHSS score was 13 (7-19) on arrival and 4 (1-5) at 24 hours. Two patients needed general anaesthesia. Occlusion site was middle cerebral artery (n=3) and basilar artery (n=1). All four patients achieved successful recanalisation. Procedural time was 62.3±23.9 min. We combined stent-retriever technology plus distal aspiration in three patients (median number of passes: 2) and direct aspiration first pass technique in one (duration of aspiration: 30 s). All procedures resulted in good early response and functional independence at three months. No complications were reported.
Conclusion: The current four patients treated with modern devices reported that children presenting with acute large-vessel embolic occlusion should be considered for mechanical thrombectomy to allow safe, effective, and prompt recanalisation to improved outcomes.

B-0996 10:46

Feasibility of T1-weighted dynamic contrast-enhanced MR imaging in paediatric neuroradiology in a 1.5T MRI

B.-B. Rochetams, J.-P. Cottier, L. Morales, C. Sembely-Taveau, J. Buraschi, H. Daurel, D. Sirinelli, B. Morel; *Tours/FR*

Purpose: The aim of this study is to evaluate the feasibility of T1-weighted dynamic contrast enhanced (DCE) MR imaging in paediatric patients at 1.5T with a low peripheral intravenous gadoteric acid injection rate of 1 ml/s.
Methods and Materials: Children with neurological symptoms underwent prospectively conventional MRI and T1-weighted DCE MR imaging. An MR perfusion analysis method (syngo MR Tissue 4D, Siemens Healthcare GmbH, Erlangen, Germany) was used to obtain time-concentration curves (persistent pattern, type-I; plateau pattern, type-II; washout pattern, type-III) and to calculate pharmacokinetic parameters. Two radiologists manually defined ROIs in the greatest enhancement part of the tissular lesion and in the surrounding or contralateral tissue. Tissular lesion/surrounding or contralateral tissue pharmacokinetic parameter ratios were calculated. Tumours were categorised by grade (I-IV) by using the WHO Grade. Mann-Whitney testing was performed.
Results: 9 boys and 9 girls (mean age 10.5 years) were included. Lesions consisted of 10 brain tumours, 3 inflammatory diseases, 3 arteriovenous malformations and 2 strokes. We obtained analysable concentration time curves for all patients (6 type-I, 9 type-II, 3 type-III). Ktrans between tumoural tissue and surrounding or contralateral tissue was significantly different (p=0.034). Tissular lesion/surrounding or contralateral tissue Ktrans ratios were significantly different between Grade I tumours and Grade IV tumours (p = 0.027).
Conclusion: The results establish the feasibility of paediatric T1-weighted DCE MR imaging at 1.5T with an intravenous injection rate of 1 ml/s. The proposed procedure allows obtaining quantitative concentration time curves which could be of great value for differentiating brain tumour grades.

B-0997 10:54

Gadolinium deposition in paediatric brain: findings after multiple exposures to gadobenate dimeglumine

G. Schneider, P. Raczeck, A. Bücker; *Homburg/DE (dr.guenther.schneider@uks.eu)*

Purpose: The possibility of gadolinium (Gd) deposition in the paediatric brain following Gd-based contrast agents (GBCA) is a potentially serious issue. We determined if T1-signal changes potentially indicative of Gd-deposition occur in paediatric brain structures after multiple exposures to gadobenate dimeglumine (MultiHance; Bracco).
Methods and Materials: 34 patients (Group 1; 17M/17F; mean age: 7.18 years; range: 9 months-17 years; mainly oncologic patients) that received between 5 and 15 injections (mean: 7.8 injections; each at 0.05 mmol/kg bw) of gadobenate over a mean of 2.24 years (range: 9 months-7 years) were compared with 24 control patients (Group 2; 16M/8F; mean age: 8.78 years; range: 7 months-17 years) never exposed to any GBCA. Five blinded readers independently determined the SI at regions-of-interest placed in the dentate nucleus (DN), globus pallidus (GP), pons, and thalamus on unenhanced T1-w images. Unpaired t tests were used to compare SI values.
Results: Mean SI in the DN, GP, pons and thalamus of patients exposed to gadobenate ranged 366.4-389.2, 360.5-392.9, 370.5-374.9, and 356.9-371.0, respectively. Corresponding values in control subjects were not significantly different (p>0.05), ranging from 368.3-374.3, 377.0-383.4, 364.4-385.4, 363.2-376.8, respectively. Similarly, no significant differences were noted by any reader for comparisons of mean DN-to-pons and GP-to-thalamus SI ratios.
Conclusion: SI increases in the DN, GP, pons and thalamus that are potentially indicative of Gd-deposition are not seen in paediatric patients after multiple exposures to gadobenate dimeglumine, even in patients with 15 injections over a time interval of 6 years.
Author Disclosures:
G. Schneider: Investigator; Siemens, Bracco, Guerbet. Research/Grant Support; Siemens, Bracco. Speaker; Siemens, Bracco, Guerbet. **A. Bücker:** Investigator; Siemens, Bracco, Guerbet. Research/Grant Support; Siemens, Bracco.

B-0998 11:02

Arterial spin labelling performance in rhombencephalitis diagnosis in children: a study over the last year at Necker Hospital in Paris

I. Cosmina Dana; *Paris/FR (ianc.cosmina.dana@gmail.com)*

Purpose: The aim of our study was to highlight the arterial spin labelling performance in imaging features of rhombencephalitis of the brain and spinal cord.
Methods and Materials: Retrospective and observational study reviewing records of patients hospitalized in neurology department at Necker Hospital between November 2015 and September 2016. MRI was performed with a 1.5-T and a 3-T units in 76 patients with suspected rhombencephalitis within maximum 4 hours after the onset of symptoms. The sequences consisted of spin-echo T1-weighted images, T2-weighted images , enhanced T1-weighted images with the intravenous injection , DWI and ASL.
Results: Between the 76 children suspected with rhombencephalitis, 28 were diagnosed with the infection . Clinical check-up showed respiratory and gastroenterological signs, supratentorial and cranial nerves damage brainstem dysfunction , signs of myelitis .MRI showed FLAIR and T2 hyperintensities in the brainstem in 36% of the children, in the cerebellum in 25.5%, at the supratentorial level in 28% , in the bone marrow in 36% . 36% had hyperintensities in combined territories. ASL was positive in 66% of the cases and was the only positive sign in 33% of the entire confirmed group.
Conclusion: Arterial spin labelling a non-invasive technique that provides absolute cerebral blood flow information within a brief period. It has been increasingly used in our department especially in diagnosis of SNC infections .Our results demonstrate the accuracy of ASL in imagining diagnosis of rhombencephalitis and its performance compared to techniques that relay only to T1, T2, DWI and contrast enhanced imaging.

B-0999 11:10

Robustness of kurtosis acquisition via multi-slice EPI: a test-retest study in children

A. Napolitano[1], C. Carducci[1], L. Filograna[1], V. Cannata[1], T. Beck[2], G. Colafati[1]; [1]*Rome/IT*, [2]*Erlangen/DE (gstefania.colafati@opbg.net)*

Purpose: Diffusion kurtosis imaging is an emerging technique based on non-Gaussian diffusion of water in biologic systems. The method provides complementary information to the traditional diffusion. Unfortunately, diffusion kurtosis suffers from long acquisition times. However, a recent technique, named simultaneous multi-slice (SMS) acquisition, allows simultaneous acquisition of multiple slices and thus reducing the acquisition time. The purpose of this work is then to investigate the robustness of diffusion kurtosis in children when using SMS.
Methods and Materials: Ten 6-10-year-old children were recruited. Two DTI acquisitions at the beginning and the end of scanning were acquired. The DTI protocol was acquired using a prototyping sequence from Siemens (acceleration factor =2). Diffusion images were preprocessed in matlab to account for eddy current and movement artefact. The actual kurtosis processing was performed on DKE toolbox. FA, kFA, kmean maps were calculated. ROIs were placed in anterior (AWM) and posterior (PWM) white matter, right (RSC) and left (LSC) semiovale centre. The absolute difference (AD) between the first and last scan scaled by the mean was used to evaluate the variability of the measure.
Results: The AD FA was AWM: 4.0+/-2.0%; PWM: 7.0+/-3.0%; RSC: 6.7+/-3.1%; RSC: 7.8+/-5.9%. The AD kFA was AWM: 6.0+/-4.0%; PWM: 12.8+/-9.0%; RSC: 9.5+/-5.4%; RSC: 9.7+/-6.9%. The AD kmean was AWM: 3.3+/-1.8%; PWM: 3.0+/-1.6%; RSC: 3.9+/-3.6%; RSC: 2.9+/-1.4%.
Conclusion: The AD estimates for FA, kFA and kmean are around 7% of the mean values of each measurements and the AD kurtosis estimates are also comparable to the more stable measurement of FA.

B-1000 11:18

Role of proton MR spectroscopy of the brain in neonatal hyperbilirubinemia

R.H. Hashem, I. El Hawary, W. Shaarawy, M. Elsayed.; *Cairo/EG (rania.hachem@yahoo.com)*

Purpose: The purpose of this study was to analyse proton ((1)H) MR spectroscopic data of infants with severe hyperbilirubinemia ,and wether it can be used to differentiate bilirubin encephalopathy from just severe hyperbilirubinemia in neonates, to compare the MRS findings with that of conventional MRI.
Methods and Materials: 10 patients aged 3 days to 2 weeks, with severe hyperbilirubinemia (indirect NH more than 20 mg/d) divided into 2 equal groups based on wether or not having clinical encephalopathy . All the patients underwent MR imaging and proton MR spectroscopy with a single-voxel point-resolved spectroscopic sequence. The voxel of interest was centered in the basal ganglia. metabolite ratios relative to creatine were evaluated. The ratios were compared to normal ratios for age in former studies. We compare their clinical , laboratory and radiological data.
Results: 3 out of the 10 patients had abnormal MR signal in the globi pallidi and the subthalamic nuclei. All the 5 Patients with clinical encephalopathy were having an abnormal MRS findings.3 out of the 5 with no clinical encephalopathy were having an abnormal MRS findings .2 out of the group with no clinical encephalopathy were free on MRI and MRS basis. The most frequently encountered MRS abnormality was a decrease in the Ch /Cr ,decrease in the NAA/Cr, then increase Glx /Cr ratio.
Conclusion: Neonatal hyperbilirubinemia with encephalopathy has a characteristic detectable (1)H-MR spectroscopic changes. Proton MRS could be used for early detection of bilirubin encephalopathy in neonates.

B-1001 11:26

SMI of the neonatal brain: assessment of feasibility and morphological features

K. Göral, A. Hojreh, G. Kasprian, K. Klebermass-Schrehof, K. Vergesslich-Rothschild, M. Weber, J.M. Patsch; *Vienna/AT (janina.patsch@meduniwien.ac.at)*

Purpose: Superb microvascular imaging (SMI) is a novel ultrasound application capable of depicting micro-vasculature throughout the body. To the best of our knowledge, there are no systematic reports on feasibility and morphologic features of brain SMI in healthy neonates.
Methods and Materials: Following study approval by institutional review and written informed consent, we performed transcranial ultrasound in healthy term-born neonates (n=19; Toshiba Applio 4000). Routine examinations (including Doppler) were performed and documented according to national standards. SMI ultrasound was performed according to a structured examination protocol, using two linear 18mHz and 14mHz transducers: superficial and deep scans were acquired in the coronal and parasagittal plane, using the left and right superior frontal gyrus as anatomical landmarks. All SMI views were imaged by monochrome and colour SMI and documented as video sequences. Videos were batch-read by a board-certified radiologist.
Results: On superficial coronal scans, cortical micro-vessels were identifiable in 89.5-100%(depending on region and scan mode). Medullary micro-vessels were visible in 94.7-100%. SMI performance was better on coronal views than on sagittal views (cortical in sagittal: 29.4-73.7%; medullary in sagittal: 82.4-89.5%). Color SMI improved overall SMI performance in only one of eight superficial assessment regions. On deep scans, cortical and medullary micro-vessels were visible in all cases. Periventricular micro-vessels were seen in 88.2% of cases. Thalamic micro-vessels were identifiable in 70.6% of cases.
Conclusion: SMI ultrasound of the neonatal brain is feasible and captures cortical, medullary, periventricular, and thalamic micro-vessels without the use of contrast.

B-1002 11:34

Malformations of cortical development associated with corpus callosum dysgenesis (CCD): diagnostic value of foetal MRI in prenatal counseling

A. Antonelli, S. Bernardo, E. Marchionni, V. Vinci, M. Saldari, A. Pizzuti, C. Catalano, L. Manganaro; *Rome/IT (amanda.antonelli@hotmail.it)*

Purpose: To define the diagnostic role of foetal MRI in the assessment of cortical dysplasias and other malformations of the developing cerebral cortex, in foetuses with different forms of Agenesis of the Corpus Callosum (ACC).
Methods and Materials: 104 MR images of foetal CNS with a US suspicion of ACC were retrospectively reviewed. Foetal MRI was performed at 1.5 T Magnetom Avanto (Siemens, Erlangen, Germany) without mother-foetal sedation. Polymicrogyria, lissencephaly, schizencephaly, subependymal heterotopias and migration disorders were evaluated. Cortical findings were compared to three types of ACC (complete agenesis, partial agenesis and hypoplasia). Genetic tests were collected. Post-natal MRI or foetopsy for diagnostic confirmation were collected.
Results: On 104 foetuses, fetal MRI was able to detect cortical malformations in 32 cases even in early gestational ages (<24GW). The mean Gestational Weeks (GW) at MR diagnosis was 26 (range: 22-36GW). MR imaging found 13/32 polymicrogyria, 7/32 lissencephaly, 5/32 schizencephaly, 4/32 subependymal heterotopias and 3/32 neuronal migration disorders. 22/32 had complete ACC, 4/32 had partial ACC and 6/32 had CC hypoplasia. Statistically significant correlations ($p<0.005$) between complete ACC, focal polymicrogyria and cortical dysmorphism affecting frontal lobes were found.
Conclusion: Fetal CNS MRI can detect cortical development malformations in complex ACC, providing further information for the clinician to assess the severity of perinatal outcome. MRI is a useful tool in improving obstetrical genetic prenatal counselling to predict pregnancy and foetal prognosis.

B-1003 11:42

Real-time virtual sonography: a new integrated approach for the evaluation of foetal CNS pathologies?

S. Bernardo, A. Antonelli, M. Saldari, V. Vinci, C. Catalano, L. Manganaro; *Rome/IT (silviabernardo@live.it)*

Purpose: The aim of this prospective study is to evaluate the feasibility and ability of foetal MRI-US real-time fusion imaging (RVS: real-time virtual sonography) in the assessment of the main cerebral pathologies, on foetuses with a US suspicion of CNS anomalies.
Methods and Materials: Fusion imaging (Hitachi HI Vision Ascendus) was offered to 35 patients who had undergone foetal MRI for a US suspicion of cerebral anomaly. Acquired MRI were loaded into the fusion system using a CD support and images were displayed together in real time with US images. Both sets of acquisition were then manually synchronised and images were recorded: this allowed the possibility to retrospectively re-evaluate examinations.
Results: RVS was technically possible in all cases. Data registration, matching and fusion imaging were performed in 25 minutes at the beginning and in less than 15-20 minutes after practice. The ability of RVS imaging to assess the main foetal CNS anatomy and anomalies was evaluated and compared with standard US and MRI. The principal application of RVS was the study of midline, cerebral gyration and vascular malformations because it also allowed adding a real-time Doppler signal on MRI images. Fusion imaging helped the diagnosis in 25%. In 25/35 cases of encephalic pathology, fusion imaging improved the diagnosis; in 10/35 MRI was superior to US even using RVS.
Conclusion: Both techniques are complementary but still independent and the retrospective synthesis of these exams allows optimal analysis of foetal cerebral anomalies. However, RVS is currently limited to the research area.

B-1004 11:50

Can foetal MRI predict the need for neonatal emergency procedures in cases of head and neck congenital masses?

M. Saldari, A. Antonelli, V. Vinci, C. Catalano, L. Manganaro; *Rome/IT (matteo.saldari@gmail.com)*

Purpose: To evaluate the role of foetal MRI in predicting the need and helping the planning of neonatal emergency procedures in cases of congenital head and neck masses.
Methods and Materials: In this prospective study we enrolled 24 consecutive pregnant women with ultrasound detection of foetal head and neck masses possibly requiring a post-partum surgical procedure or anaesthetic management and referred to our department of radiology for a foetal MRI. Foetal MRI protocol included T1 and T2-weighted, TrueFISP and DWI sequences on a 1.5 T unit. A Radiologist with more than 10 years of experience in foetal MRI, reviewed the images in order to detect the presence of findings suggestive for the necessity of a neonatal surgical or anaesthetic intervention.
Results: Foetal MRI confirmed the US suspicion of: cystic hygroma (n=8), lymphangioma (n=9) and cervical teratoma (n=7). All prenatal diagnoses were confirmed surgical or pathological findings. In 7 cases Foetal MRI highlighted the need for emergency neonatal surgery, whereas in 10 cases excluded it, suggesting a medical management until respiratory and cardiovascular status were stabilized. In 7 cases Foetal MRI suggested the necessity of an emergency EXIT procedure.
Conclusion: Foetal MRI provides useful information for a proper neonatal intervention to prevent a fatal outcome in cases of head and neck congenital masses.

10:30 - 12:00 **Room M 3**

Cardiac

SS 1403b

Transcatheter aortic valve implantation (TAVI), valves and stents

Moderators:
E. Blondiaux; Paris/FR
O. Duvernoy; Uppsala/SE

B-1005 10:30

Correlation of manual and semi-automated evaluation of aortic root in TAVI candidates

B. Horehledova[1], C. Mihl[1], C. Schwemmer[2], B.M.F. Hendriks[1], N. Eisvoogel[1], B.L.J.H. Kietselaer[1], J.E. Wildberger[1], M. Das[1]; [1]*Maastricht/NL*, [2]*Forchheim/DE (barbora.horehledova@mumc.nl)*

Purpose: Preprocedural TAVI planning requires highly sophisticated and time-consuming manual measurements performed by experienced readers. Semi-automatic software may assist with partial automation of assessment of multiple parameters. The aim was to evaluate differences between manual and semi-automated measurements, also in the light of the time needed for this assessment.
Methods and Materials: 120 pre-TAVI candidates referred for retrospectively ECG-gated CTA (Somatom Force/Flash, Siemens Healthcare GmbH, Forchheim, Germany) were evaluated. Fully manual and semi-automated measurements of aortic root dimensions were assessed in the 20%phase of the R-R interval. Semi-automated assessment was performed with a prototype version of dedicated software (Valve Pilot, syngo.CT Cardiac Planning, Syngo.via™VB20A, Siemens). Inter-software agreement was calculated using the Intraclass correlation coefficient (ICC) in a 2-way mixed effects model. Reading time was compared using paired samples t-test.
Results: Mean values (manual;semi-automated assessment) are stated in mm: aortic annulus (AA) short axis (21.9±2.2;22.2±2.3), AA long axis (27.7±2.7;27.7±3.0), AA area (469.1±85.8;486.3±92.1), AA perimeter (79.1±6.8;79.5±7.5), AA effective diameter derived from cross-sectional area

(24.3±2.3;24.8±2.3), AA effective diameter derived from perimeter (25.2±2.2;25.3±2.4), long axis at left coronary ostium (35.7±4.4;34.1±4.0), long axis at right coronary ostium (33.0±4.6;33.0±4.0), widest portion of coronary sinuses (36.6±4.3;35.1±4.1), long axis at sinotubular junction (31.0±4.6;31.8±4.0). Excellent inter-software agreement was found (ICC=0.84±0.1; range:0.64-0.95). Time needed for aortic root evaluation using semi-automated assessment (3min 24sec±1min 7sec) was significantly lower (p<0.001) compared to a fully manual approach (6min 31sec±1min 1sec).
Conclusion: Use of semi-automatic software in pre-TAVI evaluation results in comparable results in respect of measurements, while necessary reading time is significantly lower.
Author Disclosures:
B. Horehledova: Research/Grant Support; Institutional Research Grant Siemens. **C. Mihl:** Speaker; Bayer. **C. Schwemmer:** Employee; Siemens Healthcare GmbH. **B.M.F. Hendriks:** Research/Grant Support; Institutional Research Grant Bayer. **N. Eisvoogel:** Research/Grant Support; Institutional Research Grant Bayer. **J.E. Wildberger:** Research/Grant Support; Institutional Research Grants Siemens, Philips, Bayer, AGFA. Speaker; Siemens, Bayer. **M. Das:** Research/Grant Support; Institutional Research Grants Bayer, Siemens, Philips, Cook.

B-1006 10:38

Calcifications of the aortic arch: angio-CT quantification and correlation with cerebrovascular events in patients undergoing TAVI
M. Muca, M.G. Belgrano, J. De Groodt, A. De Luca, M.A. Cova; *Triest/IT (matilda02@hotmail.it)*

Purpose: To assess accuracy of Angio-CT in quantification of calcium amount on aortic arch and valve and to establish how this impact the occurrence of Cerebrovascular events (CVEs) in patients that undergo trans-catheter aortic valve implantation (TAVI), during six months of follow up.
Methods and Materials: We retrospectively measured on Angio-CT examination the calcium amount on aortic arch and valve of 98 patients who underwent TAVI with trans-femoral o trans-aortic approach, using dedicated software. The quantification was made with three different attenuation threshold (AT: 500-1500 HU, 700-1500 HU, 800-1500 HU).
Results: 6 of 98 (6,12%) patients had a CVE, 3 patients had TIA and 3 ischemic ictus. In all 98 patients the average of calcium amount in the aortic valve was 0,72 cm³ with AT 500-1500 HU, 0,17 cm³ with AT 700-1500 HU, 0,09 cm³ with AT 800-1500 HU; in the aortic arch was 5,7 cm³ with AT 500-1500 HU, 1,02 cm³ with AT 700-1500 HU, 0,45 cm³ 800-1500 HU. In patients who have had CVEs we measured a calcium amount in the aortic valve of 3,06 cm³ with AT 500-1500 HU, 0,57 cm³ with AT 700-1500 HU, 0,13 cm³ with AT 800-1500 HU; in the aortic arch an amount of 16,77 cm³, 1,8 cm³ and 0,78 cm³ respectively with the three different attenuation threshold.
Conclusion: We observed a significant correlation (P<0.001) between Angio-CT's evidence of high calcium burden in aortic arch and occurrence of CVEs. We identified the AT with lower limit higher than 700 HU more accurate.

B-1007 10:46

Diagnostic accuracy of third generation Dual Source CT with FLASH protocol for the detection of significant coronary artery stenosis in patients candidates for TAVI procedure
P. Toia[1], E. Maffei[2], C. Mantini[3], S. Seitun[4], A. Clemente[5], C. Lario[6], L. La Grutta[1], M. Midiri[1], F. Cademartiri[2]; [1]*Palermo/IT*, [2]*Montreal, QC/CA*, [3]*Chieti/IT*, [4]*Genoa/IT*, [5]*Massa/IT*, [6]*Turin/IT (toiapatrizia@gmail.com)*

Purpose: To evaluate the performance in the assessment of coronary arteries of high-pitch spiral acquisition, using 3rd generation dual-source CT equipment, in a selected patients' population candidate for TAVI and undergoing thoraco-abdominal CT angiography screening.
Methods and Materials: High-pitch thoraco-abdominal CT angiography was performed in 120 consecutive patients (mean age 80.2±11.5yrs); using a dual-source system (2x192 0.6mm sections, 0.25s rotation time, 66 ms temporal resolution). Tube settings were automatically modulated both for kV and mAs (CARE-kV and CARE-Dose). Data acquisition was prospectively electrocardiographically-triggered at 60% of the RR interval using a pitch of 3.2, corresponding to a table feed of 737 mm/s. Diagnostic accuracy was assessed using conventional coronary angiography as the reference standard. Image quality was evaluated using a three-point scale (1=excellent; 2=moderate; 3=poor).
Results: Image quality was of diagnostic value in 55% of the segments. In 30% of the patients diagnostic image quality was observed for all segments. Diagnostic accuracy was: sensitivity 95%, specificity 83%, PPV 78%, NPV 99%. Average heart rate was significantly (p<.001) higher in patients with at least one non-diagnostic coronary segment compared to those without. All patients with an average heart rate <65 bpm had diagnostic image quality in all coronary segments. Radiation dose was always <3mSv and contrast material volume was always below 70ml.
Conclusion: High-pitch thoraco-abdominal CT angiography for non-coronary purposes enables simultaneous diagnostic evaluation of the coronary arteries at a low contrast material dose and low radiation dose in patients candidate for TAVI.

B-1008 10:54

Reduction of metal artifacts after transcatheter aortic valve implantation in cardiac CT: value of iterative metal artifact reduction
K. Higashigaito, M. Mannil, H. Alkadhi; *Zurich/CH (Kai.Higashigaito@usz.ch)*

Purpose: To assess metal artifact reduction (MAR) capabilities of iterative metal artifact reduction (iMAR) in patients after transcatheter aortic valve implantation (TAVI) in cardiac CT.
Methods and Materials: First, MAR capabilities of three different prototype iMAR settings were evaluated in a phantom study by placing four different TAVI devices in a commercially available human chest phantom. Second, the best iMAR setting was then selected and tested in patients after TAVI which were scanned on a third generation dual source CT. Images were reconstructed with and without iMAR. Two blinded readers independently assessed qualitative image quality in three locations (center, anterior and lateral of TAVI device) by using a 5-point Likert scale (5=excellent, no artifacts, 1=non diagnostic, severe artifacts). Quantitative image quality was assessed on the same regions by measuring image noise. Intraclass correlation coefficients (ICCs) and Cohen's κ were calculated to evaluate interreader agreements. Wilcoxon signed-rank test and the student's T-test were used to compare qualitative and quantitative image quality.
Results: Agreements between both readers were good to perfect (all, κ ≥ 0.683) for qualitative and high (ICC ≥ 0.98) for quantitative image quality. As compared to images reconstructed without iMAR, images reconstructed with iMAR achieved significant higher qualitative (average image score: 4.1 vs. 3.2) and quantitative (average image noise: 37±9 HU vs. 52±17 HU) image quality in all three locations and all TAVI systems (all p>0.05).
Conclusion: iMAR significantly improves qualitative and quantitative image quality by reducing metal artifacts produced by TAVI devices.

B-1009 11:02

Comparison of aortic root dimensions by multimodal measurement before transcatheter aortic valve implantation
R. Qi; *Hangzhou/CN (tsirea@163.com)*

Purpose: We sought to compare 3 methods(TTE, TEE, and MSCT)of measurements of aortic root in patients of severe aortic stenosis, and to evaluate their potential clinical impact on TAVI strategy.
Methods and Materials: Aortic root dimensions were measured using 3 methods within 1 month in 138 consecutive patients referred for TAVI. The difference among the measurements of aortic annulus diameter was compared. The accuracy of the multimodal measurement before TAVI was evaluated with postoperative follow-up.
Results: Mean aortic annulus diameter was 24.9 ± 2.03mm using TTE and 25.3 ± 1.92mm using TEE (p = 0.21) and correlation between TTE and TEE was excellent (r = 0.86). The mean of long-and short-axis diameters (24.7 ± 2.01mm) using MSCT did not differ from the TTE and TEE measurements (p = 0.05, p = 0.08). Correlations between the diameter derived from the circumference (25.8 ± 2.23mm) and the diameter derived from the cross-sectional area (25.4 ± 2.19mm) were good in comparison with the measurements using TTE (r = 0.77, r = 0.79) or TEE (r = 0.81, r = 0.85). Implantation, performed in 118 patients (85.5%) based on MSCT measurements, was successful in all but 3 patients with worse than moderate paravalvular leakage and 1 patient with valve-in-valve implantation because of prosthetic valve restenosis.
Conclusion: In patients referred for TAVI, measurements of the aortic root using TTE, TEE, and MSCT were close but not interchangeable. In the absence of a gold standard, a strategy based on comprehensive consideration would provide good clinical results.

B-1010 11:10

Pressure recovery determination by cine MRI is feasible and leads to significant re-classification of aortic stenosis severity
F. Sagmeister[1], S. Herrmann[2], M. Weininger[3], T. Bley[2], H. Köstler[2], D. Hahn[2], F. Weidemann[4], M. Beer[1]; [1]*Ulm/DE*, [2]*Würzburg/DE*, [3]*Mutlangen/DE*, [4]*Unna/DE (florian.sagmeister@gmail.com)*

Purpose: Pressure recovery (PR) is an essential haemodynamic process to maintain the energy of forward flow distal the aortic valve. We tested the feasibility of cine-MRI for estimation of PR in AS and its potential clinical impact.
Methods and Materials: Twenty-five patients with severe aortic stenosis (AS) according to echocardiography were re-evaluated by cine MRI measurements (mean age 68±10 years). The echocardiographic AS-severity parameters were corrected for pressure recovery by MRI-measurements of ascending aorta in three chamber view. Pressure recovery, indexed pressure recovery and energy

loss index were calculated. The values were compared between different measurement positions of aorta and measurements at the beginning and end of systole.
Results: Measurements of sinotubular junction in three chamber view (3CV) at the beginning of systole resulted in a PR of 18±7.3 mmHg, indexed PR (iPR) of 25±9.2% and energy loss index of 0.56±0.24 cm^2/m^2. Severe AS using indexed effective orifice area was found in 22/25 (88%) of patients. After PR-correction and using energy loss index as parameter severe AS was only found in 16/25 (64%) of patients. This corresponds to a downward classification of AS-severity in 6/25 (24%) of patients There were only small variations of PR and iPR depending on measurement position in ascending aorta and depending of time point of measurements.
Conclusion: The estimation of PR is feasible by CINE-MRI. The estimation of PR by MRI resulted in a downward classification from severe to moderate AS-severity in up to 24% of patients.
Author Disclosures:
H. Köstler: Grant Recipient; HK receives research support from Siemens Healthcare (Erlangen, Germany).

B-1011 11:18

Impact of pulmonary valve replacement (PVR) and right ventricular (RV) remodelling on global and regional left ventricular (LV) mechanics in repaired tetralogy of Fallot (rTOF)

L. D'Errico, R. Wald, K. Hanneman, C. Silversides, M. Farkouh, B.J. Wintersperger; *Toronto, ON/CA (luigia.derrico@uhn.ca)*

Purpose: To evaluate the impact of PVR and consecutive RV remodelling on global/regional LV function assessed by cine MRI in patients with rTOF.
Methods and Materials: 44 patients (28m/16f;32.7±11.7y) with rTOF underwent cardiac MRI pre/post-PVR with standard short and long axes cine SSFP (6-8mm/2mm; TR less than 50ms) as well as cardiopulmonary exercise testing. RV/LV end-diastolic volume (EDV) and ejection fraction (EF) were assessed according to standard approaches. LV global longitudinal strain (GLS) and global circumferential strain (GCS) were performed using deformable registration algorithms (DRA). Analysis included assessment of global RV and LV remodelling post-PVR and changes in LV strain. ANOVA was performed to assess for possible predictors of LV functional recovery after PVR.
Results: In addition to LV EF (n=20; 45%) peak LV strain assessment identified additional patients with abnormal LV (n=10; 23%). Pre-PVR LV GLS significantly correlated to indexed RV EDV(P=0.029) while LV EF (P=0.18) and LV GCS (P=0.35) did not. Patients with impaired LV EF pre-PVR demonstrated no significant post-PVR improvement of global function (48.5±5.8% vs 46.9±7.2%;P=NS) or GLS (-13.0±2.2 vs -12.2±2.7%; P=NS) while GCS demonstrated significant improvement (-15.0±2.3 vs -13.0±3.1%;P=0.008). Post-PVR improvement of peak vO_2 correlated significantly to the improvement in RV EF (P=0.0008) while changes in any of the global or regional LV parameters did not correlate with peak vO_2 changes.
Conclusion: Cine MR-based LV strain analysis provides additional insight into LV dysfunction in patients with rTOF scheduled for PVR. Post-PVR changes of the LV do not correlate to improved exercise testing.

B-1012 11:26

Mitral valve prolapse: diagnostic value of MRI

S. Pradella, G. Grazzini, M. Brandani, L. Calistri, V. Miele, S. Colagrande; *Florence/IT (pradella3@yahoo.it)*

Purpose: Mitral valve prolapse (MVP) is a common valvulopathy affecting 2-3% of population. MVP has been associated with an increased risk of arrhythmic complications including atrial/ventricular arrhythmias and sudden cardiac death. Echocardiography is the first-line imaging modality for MVP. Cardiac magnetic resonance (CMR) represents an ideal, non-invasive diagnostic tool as an alternative or complementary modality to echocardiography providing systolic function, ventricular volume, regurgitant fraction and presence of fibrosis.
Methods and Materials: In 2015-16, consecutive patients with MVP underwent a comprehensive CMR examination at 1.5T with multiplanar cine imaging, phase-contrast flow acquisitions (at mitral annulus, proximal aorta and pulmonary valve), T1 mapping pre- and post-gadolinium administration. Expert readers independently and blindly analysed CMR and echocardiographic data. Inter-rater comparison was made by concordance correlation coefficient (CCC) with 95% confidence intervals.
Results: 32 patients mean age 56.8 ± 6.3, male 18 (56%). LGE was present in 13 (40%). CMR regurgitant fraction reproducibility was excellent (CCC 0.95, 0.86-0.98). Severity grading by CMR had good inter-observer agreement (CCC 0.85, 0.62-0.95). T1 mapping was significant in confirming LGE and more sensitive in identifying alterations.
Conclusion: CMR performs very well in MVP, with excellent reproducibility. A further unique strength of the exam is its ability to characterize myocardial tissue changes (LGE), which has further expanded with the implementation of T1 mapping techniques (relevant information regarding the amount and distribution of replacement fibrosis; over conventional LGE to identify diffuse interstitial fibrosis). The information derived from CMR may be the optimal key towards personalised therapy in MVP.

B-1013 11:34

Assessment of anatomic substrates for electrical instability in mitral valve prolapse (MVP) patients: a cardiac magnetic resonance (CMR) study

D. Palumbo[1], M. Cava[2], A. Esposito[1], S. Ravelli[1], G. La Canna[1], A. Del Maschio[1], F. De Cobelli[1]; [1]*Milan/IT*, [2]*Alessandria/IT (palumbo.diego@hsr.it)*

Purpose: MVP is a common condition due to improper leaflets atrial prolapse; often asymptomatic, it may be complicated by insidious conditions, as ventricular arrhythmias. Our aim was to investigate the CMR role in the evaluation of potential anatomic substrates for arrhythmogenic risk in MVP.
Methods and Materials: We enrolled 33 patients (47.4±17.8yrs, 21F, 12M); CMR protocol included evaluation of ventricular (LV and RV) function, myocardial oedema (T2-STIR) and late gadolinium enhancement (LGE). In order to assess MVP we measured prolapsed distance of posterior valve leaflet (maximum leaflet excursion beyond the mitral annular plane during systole, MVPE).
Results: All patients showed systolic mitral valve leaflets excursion towards left atrium >2mm, with mean MVPE of 8.5±5mm. Mean mitral indexed annular diameter (MADi) was 23.7±5.1mm; MADi and MVPE were directly related (p=0.008, r=0.473). 22 patients showed a bulging of LV inferior wall near mitral valve annulus during systole and higher values of MVPE (10.6±4.6 vs 4.2±2mm p<0.001) and MADi (25.5±4.3 vs 19.5±4.4mm p=0.004). 20 patients showed LGE, in 6 cases involving the posterior papillary muscle (PP), in 7 cases the infero-lateral LVwall, in 7 cases both. Patients with LGE in PP demonstrated systolic bulging in 92.3% of cases (p=0.044) and had greater MVPE (11.9±4.5 vs 6.2±3.8mm p<0.001). In 20 cases patients complained about arrhythmic events (2 VF, 11 NSVT, 6 LBBB, 1 AVblock); these events were significantly associated with presence of ventricular LGE (p=0.010).
Conclusion: In patients with MVP, CMR may characterise structural alterations of myocardium, probably representing a potential arrhythmogenic risk substrate.

B-1014 11:42

Coronary stent image subtraction using monochromatic CCTA derived from a dual-layer spectral CT

W. Yang, L. Qin, F. Yan, Y. Jiang, Q. Han; *Shanghai/CN (yanjiangcs@hotmail.com)*

Purpose: To investigate the coronary stent image subtraction using spectral tools derived from a dual-layer spectral CT as well as to compare the image quality among subtracted images and routine images.
Methods and Materials: 15 patients with 21 stents underwent CCTA using a dual-layer spectral CT (IQon Spectral CT, Philips Healthcare). Conventional, monochromatic and virtual non-contrast (VNC) images were reconstructed from the raw data of one scan in the same cardiac phase. Stent subtraction images were acquired by subtracting stent on VNC images from monochromatic (100keV) and conventional images ($Mono_{sub}$ and $Conv_{sub}$). Mean in-stent lumen diameter and reader confidence were assessed and compared among both subtraction images, monochromatic images and conventional images. One-way ANOVA and Friedman M test were used for statistical analysis.
Results: Significant difference were found in in-stent lumen diameter for all comparison combinations among different image sets ($Mono_{sub}$ > $Conv_{sub}$> Monochromatic > Conventional, all p<0.05). Higher reader confidence were found in $Mono_{sub}$, $Conv_{sub}$, monochromatic images compared to conventional images. No difference was found in reader confidence among two subtracted images sets and monochromatic images.
Conclusion: Subtracted images derived from monochromatic images exhibited largest in-stent diameter and better reader confidence, which indicated that stent subtraction using dual-layer spectral CT helps to improve in stent luminal visualisation and reader confidence.

B-1015 11:50

Image quality study of monochromatic coronary stent imaging with a dual-layer spectral CT: initial experience of optimal mono-energy exploration

W. Yang, F. Yan, L. Qin, Y. Jiang, Q. Han; *Shanghai/CN (yanjiangcs@hotmail.com)*

Purpose: To investigate the image quality of coronary stent imaging using a dual-layer spectral CT. Additionally, to explore the optimal monochromatic energy for coronary stent imaging.
Methods and Materials: 15 patients with 21 stents underwent CCTA using a dual-layer spectral CT (IQon Spectral CT, Philips Healthcare). Conventional series and monochromatic series (40-200keV, with an interval of 10keV) were reconstructed from the raw data of one scan. CT attenuation in both coronary artery near stents and aorta root for all series were measured. Difference between coronary luminal and aortic attenuation was calculated as an indicator for blooming artefacts. In-stent lumen diameter and subjective image quality were recorded.
Results: An increase in monochromatic energy was associated a decrease in luminal attenuation and blooming artefacts indicator. In-stent lumen diameter in 90keV and 100keV series was larger compared to other series, while series below 80keV as well as conventional series exhibited significant reduced lumen diameter due to severe blooming artefacts. Subjective image quality scores were higher in 90keV, 100keV and 110keV compared to other series.
Conclusion: Monochromatic CCTA using a dual-layer spectral CT improved image quality of stent imaging compared to conventional CCTA. 90keV and 100keV may be the optimal monochromatic energy for coronary stent imaging.

14:00 - 15:30 **Room M 1**

Cardiac

SS 1503

Coronary angiography

Moderators:
C.K. Atasoy; Ankara/TR
N. Galea; Rome/IT

B-1017 14:00

The ratio of coronary artery diameters predicts left main diameter and coronary dominance

M. Kolossváry, B. Szilveszter, K. Júlia, Á. Jermendy, M. Károlyi, A. Bartykowszki, A. Panajotu, B. Merkely, P. Maurovich-Horvat; *Budapest/HU (marton.kolossvary@cirg.hu)*

Purpose: Coronary artery stenosis is defined as the percent of maximal diameter stenosis compared to an adjacent normal segment. In cases of diffuse left main(LM) stenosis, such reference does not exist. Our goal was to assess how the LM diameter could be predicted from the left anterior descending(LAD) and the left circumflex(LCX) aretries' diameters. Furthermore, we sought to assess the diagnostic accuracy of the ratio of the LM and the right coronary artery(RCA) diameters for determining coronary dominance.
Methods and Materials: We included 952 consecutive patients (age:59.8±11.7; women:43.3%) who underwent 256-slice coronary CT angiography. We measured coronary artery ostium diameters on curved multiplanar reconstruction views on dedicated cardiac workstations.
Results: Coronary artery diameters were as following: LM:4.7±0.7mm; LAD:3.8±0.6mm; LCX:3.5±0.7mm; RCA:3.9±0.8mm. There was a significant difference between the diameters of the LM, LCX, RCA between left and right dominant coronary systems ($p<0.001$ for all), while there was no significant difference between LAD diameters ($p=0.24$). The ratio of the LM diameter as compared to the average of LAD and LCX was: 0.61±0.1, with no significant differece between right and left coronary systems ($p=0.88$). The ratio of the LM and RCA could predict coronary dominance with high diagnostic accuracy (AUC=0.95).
Conclusion: The average of the LAD and LCX ostium diameters can be used to estimate LM diameters (LM=1.64* (LAD+LCX) /2) both in right and left coronary systems. The ratio of the LM and RCA defines coronary dominance. These simple ratios might support clinical decision making especially in patients with severe coronary artery disease or unusual coronary anatomy.

B-1018 14:08

Diagnostic accuracy of coronary CT angiography performed in 100 consecutive patients with coronary stents using a novel whole organ high-definition CT scanner

D. Andreini, G. Pontone, S. Mushtaq, A. Annoni, A. Formenti, M. Mancini, C. Fiorentini, A. Bartorelli, M. Pepi; *Milan/IT (daniele.andreini@ccfm.it)*

Purpose: To evaluate image quality, interpretability, diagnostic accuracy and radiation exposure of coronary CT angiography (CCTA) using a new generation CT scanner in consecutive patients with coronary stents, including those with high heart rate (HR) and atrial fibrillation (AF).
Methods and Materials: We enrolled 100 consecutive patients (85 males, mean age 65±10 years) with previous coronary stent implantation scheduled for clinically indicated non-emergent invasive coronary angiography (ICA). A novel whole organ high-definition CT scanner was used. Image quality score, using a 4-point Likert scale on a per-stent level, coronary interpretability and diagnostic accuracy vs ICA were evaluated and the effective dose (ED) was recorded.
Results: Mean HR during the scan was 67±13 bpm. Twenty-six patients had >65 bpm HR during scanning and 13 patients had AF. Overall, image quality was high (Likert=3.2±0.9). Stent interpretability was 95.8% (184/192 stents). Among 192 stented segments, CCTA correctly identified 32 out of 33 with >50% in-stent restenosis (ISR) at ICA (sensitivity 97%). In the stented-based analysis, specificity, positive and negative predictive values and diagnostic accuracy for ISR detection were 97%, 86%, 99% and 97%, respectively. Overall, mean ED was 2.4±1.2 mSv.
Conclusion: A new whole organ high-definition CT scanner was able to evaluate coronary stents with high image quality, stent interpretability, diagnostic accuracy and low radiation exposure, also in the presence of unfavourable HR and heart rhythm.

B-1019 14:16

Standardized description of coronary artery disease by means of CAD-RADS: a better method?

G. Tabacco, G. Finetto, M. Poletti, M. Vettori, R. Malagò, R. Pozzi-Mucelli; *Verona/IT (giuliatabacco23@gmail.com)*

Purpose: CA-CTMS is a procedure of considerable usefulness in the study of cardiovascular diseases, particularly those resulting from coronary artery disease. To maximize the clinical impact of coronary CTA, CAD-RADS, a standardized reporting system for coronary CTA results was recently introduced. We analysed the data collected at our institute, classifying coronary artery lesions according to this system.
Methods and Materials: 1565 patients (953 M, 612 F, average age 63 years) underwent CA-CTMS, from April 2008 to April 2016, with a 64-slice CT scanner (Brilliance 64, Philips, Best, The Netherlands). We reconstructed and analysed each exam using a Philips workstation, classifying the detected lesions and plaques according to the CAD-RADS system.
Results: 470/1565 (30.5%) patients resulted free of plaques or stenosis (CAD-RADS 0). 156/1565 (10%) patients were classified as CAD-RADS 1, 579/1565 (37%) as CAD-RADS 2, 234/1565 (15%) as CAD-RADS 3, 78/1565 (5%) as CAD-RADS 4, 8/1565 (0,5%) as CAD-RADS 5, 40/1565 (2%) as CAD-RADS N, 313/1565 (20%) patients had CAD-RADS S as modifier, 6/1565 (0,4%) CAD-RADS G and 175/1565 (11%) CAD-RADS V.
Conclusion: The CAD-RADS classification allowed us to group our patients into a uniform, updated and evidence-based way, according to their risk profile. Through it we can provide to the patients a better follow-up and therapeutic approach.

B-1020 14:24

Diagnosticefficacy of coronary artery three-dimensional steady-state free precessionmagnetic resonance angiography in comparison with invasive coronaryangiography for detection of coronary artery disease

A. Mohammadzadeh[1], F. Faeghi[1], N. Sahraee[1], H. Pouraliakbar[1], R. Kiani[1], M. Mohammadzadeh[1], P. Entezari[1], A. Borhani[1], V. Mohammadzadeh[1], S. Kadivar[2]; [1]*Tehran/IR*, [2]*Rasht/IR (mralimohammadzadeh@yahoo.com)*

Purpose: To assess the diagnostic value of three-dimensional steady-state free precession magnetic resonance angiography (3D-SSFP MRA) for detecting coronary artery disease (CAD).
Methods and Materials: Patients, suspected of CAD based on clinical evaluation, underwent invasive coronary angiography (CAG) and cardiac MRA (CMRA). Collected data in favour of any CAD findings in CMRA were compared to ICA results as the standard diagnostic method in CAD detection. Analysis was performed on per-patient, per-vessel and per-segment basis.
Results: A total of 30 patients (mean age: 43±10 years, 19 male) enrolled in the analysis. On per-patient analysis, sensitivity, specificity, positive predictive value (PPV), negative predictive value (NPV) and area under receiver operator characteristic (ROC) curve of CMRA for detection of coronary artery stenosis were as follows, respectively: 100% (CI95%: 75%-100%), 50% (CI95%: 18%-

81%), 73.33% (CI95%: 46%-90%), 100% (CI95%: 47%-100%) and 0.827. On per-vessel analysis, CMRA had a sensitivity of 89.29% (CI95%: 71%-97%), specificity of 80.56% (CI95%: 63%-91%), PPV of 78.13% (CI95%: 60%-90%), NPV of 90.63% (CI95%: 74%-98%) and area under ROC curve of 0.845. On per-segment analysis sensitivity, specificity, PPV and NPV of CMRA for segmental stenosis detection were as follows, respectively: 77.78% (CI95%: 60-89%), 87% (CI95%: 81%-92%), 62% (CI95%: 46%-76%), 93.89% (CI95%: 88%-97%). Area under ROC curve was 0.835 on per-segment analysis.
Conclusion: 3D SSFP CMRA provides a promising non-invasive diagnostic tool in the assessment of coronary artery disease.

B-1021 14:32

Monochromatic imaging improving accuracy of coronary stenosis with heavy calcification compared with conventional imaging and invasive coronary angiography

Y. Yi, R.-Z. Wu, S. Yan, X.-M. Zhao, S.-H. Yu, M. Wang, Y. Wang, Z.-Y. Jin, Y.-N. Wang; *Beijing/CN (xy_yiyan@sina.com)*

Purpose: To investigate the performance of monochromatic imaging in assessing the stenosis with heavy calcification by coronary CT angiography (CCTA), compared with conventional 120 kVp image and invasive coronary angiography (ICA) as reference.
Methods and Materials: Seventeen patients (9 men and 8 women; 63.7±13.1 years) underwent CCTA and ICA. CCTA images were acquired on a dual-layer spectral detector CT. The conventional and monochromatic image were acquired within one scan. Monochromatic images from 50 to 150 keV with 10 keV increment were reconstructed. The degree of each coronary stenosis was quantitatively measured at all keV levels. The best keV is defined at which the stenosis degree is close to the result of ICA. The degree of stenosis on the best keV and conventional 120 kVp images was recorded.
Results: Forty-three stenosis were included in analysis. The keV images were selected at 80 and 90 keV in 35% and 53% cases. When using the best keV image, the mean and standard deviation for the difference of stenosis grade between monochromatic image and ICA is 0.35% ± 1.60%. While using the conventional images, the mean and standard deviation for the difference of stenosis grade between conventional image and ICA is 7.9% ± 5.4%. The difference of conventional image is significantly larger than that of the best keV images using ICA as the reference ($p < 0.001$).
Conclusion: The monochromatic images (e.g. 80 and 90keV) improve the accuracy of the stenosis evaluation in heavily calcified coronary artery, compared with the conventional images in CCTA.

B-1022 14:40

Cardiac allograft vasculopathy assessment with coronary computed tomography in heart transplanted patients

M. Károlyi, M. Kolossváry, A. Bartykowszki, I. Kocsmar, B. Szilveszter, Á. Jermendy, J. Karády, B. Merkely, P. Maurovich-Horvat; *Budapest/HU (karolyimisi@gmail.com)*

Purpose: Cardiac allograft vasculopathy (CAV) affects >50% of the heart transplanted (HTX) patients within 10-years of transplantation and has poor prognosis. Coronary CT angiography (CTA) has been proposed for the routine annual assessment of CAV. We sought to assess the feasibility of quantitative assessment and follow-up of CAV with coronary CTA in HTX patients.
Methods and Materials: 20 patients (12 males, age 54 [IQR:47;58] years) underwent 256-slice coronary CTA one year after HTX and an additional coronary CTA as part of the routine yearly follow up. We quantified the total vessel wall volume in all coronaries up to 2 mm luminal diameter using a semi-automated software. Fixed threshold settings were used to assess various vessel wall components: calcified lesions (>350HU), non-calcified lesions (75-350HU) and low-attenuation non-calcified lesions (<75HU).
Results: The average time between the baseline and follow-up scans was 368 [IQR:359;394] days. Total lumen volume did not change between baseline and follow-up studies (p=0.39). The total vessel wall volume showed significant progression during the follow-up period (464 [IQR:318;600] vs. 486 [IQR:359;600] mm^3, p=0.01). The volume of non-calcified and low-attenuation noncalcified components showed progression (401 [IQR:249;502] vs. 416 [IQR: 265;498] mm^3, p=0.05 and 11 [IQR: 7;17] vs. 16 [IQR: 9;34] mm^3, p=0.01, respectively), while the calcified volume did not change between baseline and followup CTAs (63 [IQR: 12;103]) vs. 49 [IQR: 16;88] mm^3, p=0.53).
Conclusion: Quantitative CAV assessment is feasible with coronary CTA in HTX patients. CAV progression within the first years after HTX is mainly attributable to noncalcified lesions.

B-1023 14:48

Predictors of clinical significance of moderate coronary stenosis in multiple lesions of culprit arteries in 256 multi-detector coronary CT angiography one-beat acquisitio

J.-L. Sablayrolles, P. Guyon, L. Macron, J. Feignoux, I. Timofeeva; *Saint-Denis/FR (dr.irina.timofeeva@gmail.com)*

Purpose: To identify morphological coronary CT angiography (CCTA) predictors for the clinical significance of moderate coronary artery stenosis using the fractional flow reserve (FFR) studying by quantitative coronary angiography (QCA).
Methods and Materials: A total of 61 arteries (43 consecutive patients) underwent CCTA and QCA associated with a lesion-specific FFR measurement were retrospectively analyzed. CCTA was performed on a 256-MDCT one-beat acquisition, three-phase injection protocol by using smart shot dual injector. Stenosis from 50-69% considered as moderate. FFR ≤0,80 was considered as functionally significant. The degree and length of stenosis was evaluated on CCTA and QCA.
Results: The mean age was 67,9±10,1, BMI 27,3±4,4 kg/m^2 and 75% were males. No difference between coronary stenosis degree and length measured by CCTA and QCA (p=0,10 and p=0,94 respectively) were observed.
29% patients (18 arteries) have clinically significant moderate stenosis with FFR ≤0,8; 23% (n=14) have moderate but not clinically significant stenosis and 48% (n=29) were presented by 30-49% stenosis.
All of stenosis <50% by CCTA were functionally non significant with FFR>0,8 (p<0,05, 100% negative predictive value (NPV)).
As CT-predictors for the clinical significance of moderate coronary stenosis (FFR≤0,8) were revealed: stenosis length ≥16 mm (sensitivity (ss) 78%, specificity (sp) 79%, PPV 82%, NPV 73%, p=0,004) and multiple stenosis in calcified arteries with the stenosis's length ≥16 mm (sp 86%, PPV 85%, p=0,012).
Conclusion: Moderate coronary artery stenosis evaluated by CCTA are clinically significant (FFR≤0,8) if their length is more than 16 mm in calcified arteries, particularly in culprit arteries with multiple stenosis.

B-1024 14:56

CT angiography for the diagnosis and subcategorisation of unroofed coronary sinus syndrome

A. Zhi[1], Z. Pei[1], D. Ruping[1], M. Weiguo[2], L. Bin[1], J. Shiliang[1]; [1]*Beijing/CN*, [2]*New Haven, CT/US (Zhiah@163.com)*

Purpose: To evaluate the role of CT angiographic (CTA) in diagnosis and classification of unroofed coronary sinus syndrome (URCSS).
Methods and Materials: We retrospectively analyzed 46 URCSS patients diagnosed by CTA from 2005-2015. Based on defect location and size, URCSS were divided into 4 types: complete defect as type I, partial defect of proximal coronary sinus (CS)as type II, partial defect of distal CS as type III, partial defect in which a communication occurs between CS and left atrial as type IV. In accordance with or without persistent left superior vena cava (LSVC), all types were divided into two subtypes as a and b.
Results: Based on CTA findings, URCSS type I was observed in 23 cases (Ia 7, Ib 16), type II in 10 cases (IIa 3, IIb 7), type III in 12 (IIIa 3, IIIb 9), and type IV in 1 case classified as IVb subtype. In type I patients, CS diameter was larger than other types (P <0.05). The CS diameter between type I, II and III, IV were significantly different (p <0.05). In these 46 cases, 21 were detected by echocardiography correctly as URCSS (46%). 22 patients were treated successfully by surgery and confirmed diagnosis of URCSS, types I, II and IIIa differs significantly from patients with types IIIb and IV ($p < 0.05$).
Conclusion: CT imaging can provide excellent anatomical structure and precise diagnosis of URCSS. URCSS classification in this paper is simple and easy to practice and very important for clinical diagnosis and treatment.

B-1025 15:04

Accuracy of CT for selecting revascularisation method based on mortality predictions: combined with the SYNTAX II score

S. Lee, B. Choi, Y. Suh, K. Han; *Seoul/KR (sieun@yuhs.ac)*

Purpose: To investigate the diagnostic performance of coronary CT angiography for selecting revasclarisation method based on mortality predictions according to combination of the 2011 American College of Cardiology Foundation (ACCF) and American Heart Association (AHA) guidelines for CABG surgery and SYNTAX score II, which enables individulised approach with clinical charcteristics.
Methods and Materials: From January to May 2011, a total of 160 patients who underwent both coronary CT angiography and invasive coronary angiography within 30 interval days were included. We reviewed coronary CT angiography and invasive coronary angiography for selecting CABG cadidates and calculated SYNTAX score. Diagnostic performances of coronary CT angiography, coronary CT angiography plus CT-SYNTAX score I and plus CT-SYNTAX score II were analyzed by using invasive angiography counterparts

as references. We suggested a method to dichomotise the results of the SYNTAX score II and investigated the added value of SYNTAX score II over I.
Results: The overall sensitivity, specificity, positive predictive value (PPV), and negative predictive value of coronary CT angiography for selecting CABG surgery candidates were 89.3%, 84.6%, 75.8%, and 93.6%, respectively. Combined coronary CT angiography with a CT-SYNTAX score I had higher specificity and PPV (94.3% and 65.2%, respectively) than did coronary CT angiography alone (67.1% and 30.3%, respectively; P<.0001). CT-SYNTAX score II showed high accuracy (94.4%) using ICA-SYNTAX II as reference.
Conclusion: Coronary CT angiography combining with a CT-based SYNTAX score II can be reliable method for selecting CABG surgery candidates.

B-1026 15:12

Prognostic implications of coronary CT angiography-derived quantitative markers for the prediction of major adverse cardiac events

C. Tesche, F. Plank, C.N. De Cecco, T.M. Duguay, M.H. Albrecht, A. Varga-Szemes, J. Yang, I.L. Jacks, U.J. Schoepf; *Charleston, SC/US (tesche.christian@gmail.com)*

Purpose: To evaluate quantitative markers derived from coronary CT angiography (CCTA) as predictors of major adverse cardiac events (MACE).
Methods and Materials: Datasets from two centers were retrospectively analyzed. 46 patients (65.5±8.1 years, 62% male) with suspected coronary artery disease (CAD) who underwent dual-source CCTA and experienced a MACE within 12 months were included and compared to a Framingham risk score matched cohort (*n*=46) without MACE. CCTA-derived quantitative markers were compared between both groups: total plaque volume (TPV), calcified and non-calcified plaque volumes (CPV and NCPV), plaque burden (PB), remodelling index (RI), lesion length (LL), presence of Napkin-ring sign, segment involvement score (SIS), and segment stenosis score (SSS).
Results: Patients suffering MACE had significantly more obstructive CAD with higher PB, SSS, and SIS (all $p<0.05$) compared to controls. MACE lesions showed more TPV, NCPV, LL, PB, and Napkin-ring sign (all $p<0.05$). On multivariate analysis, odds ratios (OR) for MACE on a per-patient level were 1.07 for PB ($p=0.0002$) and 1.13 for SSS ($p=0.049$). On a per-lesion basis OR for LL was 1.05 ($p=0.042$), 1.03 for PB ($p=0.018$), 1.28 for RI ($p=0.026$), and 1.68 for the Napkin-ring sign ($p=0.031$). A receiver operating characteristics analysis showed a combination of markers (Framingham risk score, Napkin-ring sign, LL, RI) showed the highest predictive value for MACE (AUC 0.92, $p=0.013$).
Conclusion: CCTA-derived markers portend predictive value for MACE on a per-patient (PB, SSS) and per-lesion level (LL, PB, RI, Napkin-ring sign). A combination of markers with the Framingham risk score has the highest predictive power.
Author Disclosures:
C.N. De Cecco: Consultant; Guerbet. Research/Grant Support; Siemens.
A. Varga-Szemes: Consultant; Guerbet. **U.J. Schoepf:** Consultant; Guerbet. Research/Grant Support; Astellas, Bayer, Bracco, GE, Medrad, and Siemens.

14:00 - 15:30 **Room M 2**

Paediatric

SS 1512

Paediatric musculoskeletal and oncological imaging

Moderators:
R.A.J. Nievelstein; Utrecht/NL
L.-S. Ording Müller; Oslo/NO

B-1027 14:00

Wrist angle measurements: are they applicable to the paediatric population in the trauma setting?

E.A. Joyce, T. Farrell, J. McMorrow, A. Snow; *Dublin/IE (joyceea@tcd.ie)*

Purpose: The purpose of this study is to assess the reliability of standard adult carpal angle measurements, specifically the scapholunate and capitolunate angles, in the assessment of the paediatric wrist in the trauma setting.
Methods and Materials: The study cohort comprised of male and female children who underwent a wrist radiograph for the evaluation of suspected wrist or forearm injuries post trauma. In order to ensure an accurate technique of carpal angle measurement, only individuals with a sufficiently ossified carpus and an adequately positioned lateral wrist radiograph were included. In addition, we determined wrist angle measurements on a gender matched adult population in order to assess if the two groups were comparable. Adults between the ages of 18-40 who underwent wrist radiographs for evaluation of suspected injury post trauma were included and similar exclusion criteria were applied.
Results: Carpal angle measurements were performed on the lateral wrist radiographs of 256 individuals between the ages of 5 and 17 years (mean 11.2 years , SD± 2.5 years). The mean scapholunate angle was 48°(SD± 7). The mean capitolunate angle was 10°(SD± 6). The mean scapholunate and capitolunate angles of the adult cohort were 49°(SD± 8°) and 11°(SD± 6°) respectively. No statistically significant difference was observed between the scapholunate or capitolunate angle measurements in the two groups (p=0.57 and p=0.92 respectively).
Conclusion: The data suggests that standard adult assessment techniques and values for scapholunate and capitolunate angle radiographic measurements are applicable to the paediatric population provided the carpus is sufficiently ossified.

B-1028 14:08

Pertinence of the micro-dose biplanar radiographs in children's pangonometry

C. Tillaux, H. Lerisson, E. Amzallag-Bellenger, A. Cebulski-Delebarre, L. Deruyter, E. Nectoux, F. Avni, B. Herbaux, N. Boutry; *Lille/FR (c.tillaux@outlook.com)*

Purpose: To evaluate the dose and reliability of micro-dose biplanar radiographs (BPR) in children's pangonometry.
Methods and Materials: From September 2015 to February 2016, children aged 6-18 years followed up for lower limb malalignment were prospectively included. Body mass index (BMI) was calculated for each patient. Morphotype was selected according to hip width: M1 (< 25cm), M2 (25 to 35cm), M3 (> 35cm). For each patient, standing full-length lower limb BPR were acquired using randomly either a standard low-dose protocol or a micro-dose protocol. Pangonometry was performed independently by two observers. Reliability of measured parameters was compared for each protocol and morphotype subgroups, using the intraclass correlation coefficient (ICC). For each patient, dose area product (DAP) and skin dose using two thermoluminescent dosimeters were registered.
Results: We studied 260 consecutive children (100 girls and 160 boys).The mean age was 12 years (SD: 3 yo); 74 children in M1 (mean BMI: 15.7 kg/m²), 149 in M2 (BMI: 19.8 kg/m²) and 40 in M3 (BMI: 30,2 kg/m²). In micro-dose protocol, reliability was excellent for lower limb lengths (ICC = 0.99), good for alignment (ICC = 0.85), comparable to low dose (ICC = 0.99 and 0.89). No correlation was found between BMI and measurements reliability in both protocols. DAP and skin dose was significantly lower ($p < 0.001$) in micro-dose protocol for all morphotypes (0.21 mGy vs 1.13 mGy).
Conclusion: Micro-dose BPR can be reliably used in pangonometry and allows a significant dose reduction in paediatric lower limb examinations.

B-1029 14:16

Conventional radiography in juvenile idiopathic arthritis: joined recommendations from the French societies for rheumatology, radiology, paediatric radiology

P. Marteau[1], C. Adamsbaum[2], L. Rossi-Semerano[2], M. De Bandt[3], I. Lemelle[4], C. Deslandre[2], T. Tran[5], A. Lohse[6], E. Solau-Gervais[7], C. Sordet[8], P. Pillet[9], B. Bader-Meunier[2], J. Wipff[2], C. Gaujoux-Viala[5], S. Breton[2], V. Devauchelle-Pensec[1]; [1]*Brest/FR*, [2]*Paris/FR*, [3]*Fort-de-France/FR*, [4]*Nancy/FR*, [5]*Nîmes/FR*, [6]*Belfort/FR*, [7]*Poitiers/FR*, [8]*Strasbourg/FR*, [9]*Bordeaux/FR (pa.marteau@hotmail.fr)*

Purpose: To provide guidelines concerning conventional radiography (CR), in every subtype of juvenile idiopathic arthritis (JIA) (let alone systemic JIA)
Methods and Materials: A multidisciplinary task force of 15 French rheumatologists, paediatricians, radiologists and two patients representatives was convened. Following the GRADE method for recommendations, they expressed a series of research questions. Systemic JIA was ruled out. An exhaustive literature review was performed. Articles in English describing structural damage (joint space narrowing, erosions, growth abnormalities) were considered. Several assessments were proposed, based on literature data and expert opinion when evidence-based medicine was lacking. This first draft was sent to a group of 14 independent French-speaking reviewers. It was then reconsidered by the authors, and accordingly modified. A final version was submitted for evaluation to each author and reviewer, for evaluation by a Delphi process.
Results: 72 articles were included in the literature review. Often, radiographic course was a secondary outcome. Four general statements and 28 recommendations were produced. Agreement between experts was high, ranking from 8.05 to 9.70. Grades of recommendations were mostly C and D, due to lack of power of the studies. We recommend systematic CR of hands, wrists and feet at diagnosis and follow-up when the structural threat is high. In oligoarticular JIA, CR should be performed in specific situations guided by clinical apprecation. CR is not the best imagery for axial skeletton.
Conclusion: This is the first work providing practical guidelines concerning CR in JIA - when to, and when not to, perform them.

B-1030 14:24

Femoral torsion assessment with MRI in children and adolescents: should we use the bony or cartilaginous contours?

A.B. Rosskopf, C.A. Agten, L.E. Ramseier, C.W.A. Pfirrmann, F.M. Buck; *Zurich/CH (andrea.rosskopf@balgrist.ch)*

Purpose: To assess whether the use of cartilaginous contours at the femoral condyles instead of bony contours significantly changes femoral torsion measurements in children and adolescents.
Methods and Materials: Femoral torsion was measured in 32 girls (mean age 10.1 years ±2.3 standard deviation) and 42 boys (10.9 years ±2.5) by two independent readers (R1,R2). The femoral condyle angle was measured twice using once the cartilaginous and once the bony contours of the distal femur. Cartilage thickness at femoral condyles was assessed. Intraclass-correlation-coefficient (ICC) and Pearson`s correlation were used for statistical Analysis.
Results: Mean difference between cartilaginous and bony femoral torsion in girls was -1.1°±1.75 (range, -5.4° to 3.1°) for R1 and -1.64°±1.67 (-6.3° to 2.1°) for R2, in boys -1.5°±1.87(-8.4° to 1.1°) for R1 and -2.28°±1.48 (-4.3° to 9.7°) for R2. Weak-to-moderate correlations between difference of cartilaginous-versus-bony measurements and cartilage thickness (r=-0.15 to -0.55,P<0.001-0.46) or age (r=-0.33 to 0.46,P<0.001-0.006) were found for both genders. Intermethod-ICC for cartilaginous versus bony femoral torsion measurements was 0.99/0.99 for R1/R2 in girls, and 0.99/0.98 in boys.
Conclusion: There is no benefit in the use of cartilaginous condyle contours instead of bony contours for femoral torsion assessment in children and adolescents, since measurement results are interchangeable.

B-1031 14:32

Human long bone development in intrauterine growth restriction: in vivo analysis of the distal femoral epimetaphysis on prenatal MR imaging

U. Nemec, S. Nemec, P. Brugger, D. Prayer; *Vienna/AT (ursula.nemec@meduniwien.ac.at)*

Purpose: To investigate human long bone development in fetuses with intrauterine growth restriction (IUGR) by analyzing distal femoral epimetaphyseal structures and bone morphometrics on prenatal MR imaging.
Methods and Materials: This retrospective study included 14 fetuses (mean gestational age, 26 weeks 2 days; range, 21 weeks 3 days to 33 weeks) with IUGR caused by placental insufficiency, without other brain or body abnormalities, as well as a total of 192 age-matched normal fetuses. On 1.5-T echo-planar MR images, diaphyseal and epiphyseal morphometric measurements were assessed, and, using a grading system, the cartilaginous epiphyseal and metaphyseal shape, secondary ossification, and the perichondrium were qualitatively analyzed. Student's t-testing was used to compare the morphometric measurements of IUGR fetuses with normal fetuses, and descriptive statistics were used to compare the qualitative bone characteristics.
Results: The morphometric measurements of the IUGR fetuses did not exceed the minimum normative measurements at any gestational age (diaphyseal length: p <0.0001 - 0.0053; epiphyseal length: p <0.0001 - 0.0022; epiphyseal width: p <0.0001 - 0.0032). Overall, the same grading for cartilaginous epiphyseal shape as observed in IUGR fetuses was found in 28.6% - 100% of normal fetuses, for the metaphyseal shape in 7.1% - 94.4%, for secondary ossification in 16.7% - 100%, and for the perichondrium in 12.5%- 91.7%.
Conclusion: On prenatal MR imaging, fetuses with placental-based IUGR exhibit long bone shortening, whereas their qualitative bone characteristics appear within normal limits. Consequently, the presence of qualitative bone abnormalities should include the differential diagnosis of various fetal skeletal disorders.

B-1032 14:40

Role of MRI to assess skeletal age in paediatric celiac disease

S. Bernardo, E. Tomei, M. Martino, A. Laghi; *Rome/IT (silviabernardo@live.it)*

Purpose: Coeliac children are often subject to weight loss and lower somatic growth rate, compared to healthy children of the same age. The purpose of this study was to asses the feasibility of magnetic resonance imaging (MRI) of the hand and the wrist to assess skeletal age and growth delay.
Methods and Materials: We enrolled in our study 39 coeliac children (13 males and 26 females) affected by histological proven coeliac disease, with a chronological age ranged between 5 years and 1 month and 16 years and 4 months (mean age of 10years, +/- 3 years and 8 months standard deviation). A single MRI sequence (T13D SE, acquisition time: 1 minute 31 seconds) of the hand and wrist in coronal plane was performed of each patient to estimate the skeletal age. Patients' data were compared with a population of normal subjects.
Results: The preliminary results showed a delay in skeletal age in children affected by coeliac disease in 85,7% of the simple study, with a delay of maturity of 0.83 years (+/- 2,2 years of SD). Only 3 children showed advance MRI skeletal age when compared to normal subjects.
Conclusion: MRI of hand/wrist to assess skeletal age may be considered as a reliable indicator of somatic growth. MRI, without radiation exposure, can be an used as a diagnostic tool in skeletal delay. It could play an important role in the follow up of coeliac children, after glutenfree diet.

B-1033 14:48

MRI T2* mapping for bone marrow iron overload assessment in patients with beta-thalassemia

E. Nazarova, G. Tereshchenko, A. Gvozdev, D. Ibragimova; *Moscow/RU (evelina.nazarova@fccho-moscow.ru)*

Purpose: To estimate iron distribution in the bone marrow of vertebrae according to the grade of liver siderosis.
Methods and Materials: MRI T2* mapping followed by liver biopsy was performed in 43 children with beta-thalassemia (mean age - 9 years). According to the grade of liver siderosis, patients were divided into 4 groups: group 1 - without iron overload (N=8); group 2 - mild iron overload (N=8); group 3 - moderate iron overload (N=10); group 4 - severe iron overload (N=17). Quantitative estimation was conducted by Phillips Achieva 3T with T2* - mapping using Multi echo GRE pulse sequence (TR=350 ms, TE=0.9 ms, ΔTE=0.9 ms, Breath Hold).
Results: From the perspective of regression analysis, we found correlations between the values of T2* signal intensity from liver and bone marrow. 1 group - LIC (Liver iron concentration) > 2.5 ms (0.1 - 2 mg/g dry weight), VIC (Vertebrae iron concentration) > 2.5 ms, r= 0.82 (R^2=0.67); 2 group - LIC of 1.5 - 2.5 ms (2-7 mg/g dw), VIC of 1.3-2.9 ms, r=0.47 (R^2=0.22); 3 group - LIC of 1.0 -1.5 ms (7-15 mg/g dw), VIC of 1.0-2.8 ms, r=0.67 (R^2=0.45); 4 group - LIC of 0.6-1.0 ms (>15 mg/g dw), VIC of 0.6-1.0 ms, r= 0.91 (R^2=0.83).
Conclusion: VIC is an indication of severe liver iron overload in children with beta-thalassemia.

B-1034 14:56

Diffusion-weighted MRI and FDG-PET in children with mediastinal lymphoma: does the apparent diffusion coefficient (ADC) discriminate between benign and malignant masses?

M.A. Stoffels, J. Herrmann, M. Groth, C. Berliner, S. Klutmann, G. Adam, M. Regier; *Hamburg/DE (m.stoffels@uke.de)*

Purpose: To intraindividually evaluate the role of diffusion weighted MRI (DWI) with ADC measurement as a marker of malignancy in children with mediastinal lymphoma in comparison to standardized uptake values (SUV) calculated by positron emission tomography computed tomography (PET-CT).
Methods and Materials: DWI-MRI and PET-CT were performed in 16 consecutive patients with histologically proven Hodgkin's and Non-Hodgkin's lymphoma before initiation of chemotherapy, comprising a total amount of 104 malignant nodes. DWI was performed at 3T with the following imaging parameters: TR/TE 2000/66ms; FOV 425mm; slice thickness 4mm; b-values 0, 25, 50, 75, 150, 500 and 900. By placing a region of interest (ROI) encovering the entire tumour manifestation, the minimum (ADC_{min}), mean (ADC_{mean}) and maximum (ADC_{max}) ADC as well as the mean and maximum SUV (SUV_{mean} and SUV_{max}) were determined by two independent radiologists. The results of DWI and PET-CT were statistically compared on a per-node base applying Pearson's correlation coefficient.
Results: The comparison of the ADC_{min} and SUV_{max} indicated a statistically significant inverse correlation (r=0.91; p=0.02). In contrast, no correlation was found between ADC_{mean} and SUV_{mean} (r=0.37; p=0.51). Higher tracer uptake at PET-CT and lower ADC were determined in Hodgkin's lymphoma compared to Non-Hodgkin's lymphoma.
Conclusion: The minimum ADC values demonstrate a higher tumour metabolism, as confirmed by SUV measurements, and allows the discrimination of benign and malignant mediastinal masses. In paediatric patients, DWI with ADC measurement should be considered as a powerful, radiation-free complementary tool in the diagnostic workup of mediastinal lymphoma.

B-1035 15:04

Vessel wall changes after radiochemotherapy in former paediatric medulloblastoma patients: a high-resolution MRI

Y. Tanyildizi, S. Keweloh, M.-A. Neu, A. Russo, A. Wingerter, A. Tropine, J. Faber, M.A. Brockmann; *Mainz/DE*

Purpose: High-resolution MRI (HR-MRI), including vessel wall imaging (VWI), is an emerging tool for evaluating intracranial vessel disease. Going along with the improved survival of medulloblastoma (MB) patients, an increasing number of long-term MB survivors experiences cerebrovascular late sequelae of the applied radiochemotherapy (RCT), including early occurrence of atherosclerotic lesions. This study evaluates radiation-induced intracranial vascular changes, imaged through HR-MRI.
Methods and Materials: In this prospective study, 22 former MB patients were enrolled (range 10-53 years, mean age 25.8 years). The internal carotid artery (ICA) and the basilar artery (BA) were analysed. Following MR sequences

were performed: precontrast 3D TOF-MRA, precontrast 2D T1- and 2D T2-VWI sequences and postcontrast 2D T1-VWI sequences. Vessel wall thickening, postcontrast enhancement (CE) and luminal narrowing were analysed in every image.
Results: In 7 (31%) and 5 (22%) out of 22 patients vessel wall alterations in the right and left ICA, respectively, were found. Alterations in the BA vessel wall were found in 13 (59%) patients. In total, 59% of the patients presented vessel wall changes. TOF-MRA did not reveal any alteration of the ICA or BA, respectively.
Conclusion: Cerebrovascular changes after RCT gain importance, as treatment and overall survival for MB patients is improving. In this study, vessel wall alterations were imaged with high-resolution MRI. In more than 50% vessel wall alterations were identified. Further studies are needed to image the progression of sequelae after RCT and to determine the time for preventive treatment, regarding vessel stenosis.

B-1036 15:12

MR imaging of post-treatment local bone marrow alterations in paediatric soft tissue sarcomas of the extremities
G. Pasquotti[1], G. Bisogno[1], G. Cecchetto[1], R. Stramare[1], M. Weber[2], T. Toffolutti[1], C. Giraudo[2]; [1]*Padua/IT*, [2]*Vienna/AT*
(giulio.pasquotti@sanita.padova.it)

Purpose: To retrospectively assess, by MRI, post-treatment local bone marrow abnormalities (BMA) occurring in paediatric patients affected by soft tissue sarcomas of the extremities (eSTS).
Methods and Materials: Paediatric patients with histologically proven eSTS, a follow-up of at least two years from diagnosis, and both pre- and post-treatment MRI scans of the affected limb were included.Two radiologists independently reviewed for BMA all available restaging examinations.Size, pattern, contrast-enhancement and site of involvement, as long as the risk (10 points-scale) for each BMA to be a metastasis (BMM), were assessed;intraclass correlation coefficient (ICC) and 95% confidence interval were calculated.
Results: Twenty-nine patients (age-range 1mo-20 yrs) met the inclusion criteria.Histology showed 12 alveolar and 4 embrional rhabdomyosarcomas, 3 fibromyxoid and Ewing sarcoma, 2 synovial sarcomas;angiosarcoma, extraskeletal osteosarcoma, epitelioid, fibrosarcoma and liposarcoma, in one patient each.Two patients were treated only with surgical excision, 2 only with chemotherapy, 6 only with radiotherapy and 19 with radio and chemotherapy.Seventeen BMA were diagnosed in nine patients.Most of the BMA were nodular or patchy (*n=5*) and smaller than 3 cm (*n=11*);all, except one, showed contrast-enhancement.The mean rate for BMM's risk was 2.12, with a high ICC (0.890;95%CI 0.721-0.959).Only one BMA (later on, histologically proven metastases in a patient with known wide-spread disease) showed a significant risk of 7. At the latest available follow-up, all other BMA solved.
Conclusion: To optimally assist the clinicians and avoid the risk of overrating,radiologists should carefully interpret BMAs occurring at local restaging in children treated for eSTS, which rarely represent malignant dissemination.
Author Disclosures:
C. Giraudo: Research/Grant Support; Austrian Science Fund (FWF; Project KLIF 382).

14:00 - 15:30 **Room M 3**

Neuro

SS 1511

Brain infection and trauma

Moderators:
M. Garbajs; Ljubljana/SI
R.F. Oot; Hollis, NH/US

B-1037 14:00

Clinical impact of delayed enhancement in brain MRI for patients with AIDS
A.A. Drozdov, V.M. Cheremisin, I.G. Kamishanskaya, A.A. Yakovlev, V.B. Musatov, I.P. Fedunyak, O.I. Fedunyak, M.N. Artem'eva;
St. Petersburg/RU (a_a_drozdov@mail.ru)

Purpose: To compare early and delayed enhancement in routine brain MRI for patients with AIDS; to identify optimal postcontrast delay.
Methods and Materials: 42 patients with profound AIDS with mean CD4+ 42±14/ml prospectively underwent brain MRI after intravenous Gd-DTPA group contrast injection (0.2mmol/kg body weight). MR scanning (1.5T) was performed immediately and in 20 minutes after the contrast administration. Two experienced radiologists independently compared early and delayed postcontrast images and rated by 0 (no new findings identified) or 1 (when new findings were identified). Those studies where new findings were identified were discussed with 2 experienced infectiologists, who rated them by 0 (for findings not implying change of treatment) or 1 (for findings implying change of treatment).
Results: Areas of pathological contrast enhancement were identified in 20 (47,6%) of the 42 cases. New findings at images after late enhancement were identified in 8 (40%) of the 20 cases with no areas of pathologic enhancement at early images in 3 cases. Among 8 cases 4 were associated with toxoplasmosis, 2 with tuberculomas and for 2 cases etiology of contrast enhancement was not identified. In 4 cases (9.5%) out of 42 changing in treatment was indicated. Two patients with toxoplasmosis and 2 patients with intracranial tuberculomas underwent imaging at multiple time points to identify the optimal postcontrast delay. Optimal postcontrast delay was between 10-15 minutes for toxoplasmosis and between 15-20 min for tuberculomas.
Conclusion: Optimal imaging protocol with delayed enhancement scanning is crucial for appropriate treatment in patents with profound AIDS.

B-1038 14:08

Conventional brain MRI data as an indicator to perform a HIV test
A.A. Drozdov, V.M. Cheremisin, I.G. Kamishanskaya, A.A. Yakovlev, I.P. Fedunyak, V.B. Musatov, O.I. Fedunyak, M.N. Artemjeva;
St. Petersburg/RU (a_a_drozdov@mail.ru)

Purpose: Evaluate the ability of conventional brain MRI to serve as an indicator to perform HIV-testing by working out MR-scoring system.
Methods and Materials: In our retrospective study we enrolled 21 patients (mean age 38,99±3,13) with AIDS (CD4+<200) and without signs of opportunistic or mass lesions based on conventional brain MRI. Control group included 12 healthy volunteers with negative HIV test (age 37,49±4,24). Brain MR images were reviewed with series of different structures measurements and with reporting features, that are usually low yield. Data for two groups of patients have been compared with One-way ANOVA or Chi-square methods ($p<0.05$) to identify features and measurements that were statistically significant and score 0-2 was given to significant findings with 0 being more common for non-HIV infected and 1-2 for finding associated with HIV infection.
Results: Six findings had statistical significance: ratio of maximal transverse length of the skull to distance between external margins of bodies of the lateral ventricles (score 0-2), number of focal white matter hyperintensities (0-2), effusion in the mastoid air cells (0-1), edema of mucosal lining of the paranasal sinuses (0-1), distention of perivascular spaces in the basal ganglia (0-1), distention of perivascular spaces in the centrum semiovale (0-1). The average score for HIV-infected patients was 4.1 while in the control group the average score was 1.75. Using 3 as a cut of criteria it had a 85% sensitivity, 67% specificity.
Conclusion: Conventional brain MRI is an effective diagnostic tool that might serve as a strong indication for HIV-testing.

B-1039 14:16

Role of diffusion-weighted imaging and magnetic resonance imaging in differentiation of intracranial abscess and neoplasms with necrosis
A.A. Jain, N. Bahri, H. Parekh, S. Chudasama; *Jamnagar/IN*
(a.jain56@yahoo.com)

Purpose: The aim of our study was to determine the utility of dffusion-weighted imaging (DWI) with calculated apparent diffusion coefficient (ADC) and MR spectroscopy (MRS), to distinguish brain abscess from necrotic tumour in patients presenting with an intracranial mass.
Methods and Materials: We studied patients referred for an MRI of the brain for evaluation of an intracranial mass. All patients underwent an MRI study on a 1. 5T Siemens Magnetom essenza. DWI was obtained with single-shot echo planner imaging spin echo sequences. Multi-voxel MR spectroscopy was performed. Imaging findings were compared with the histopathological diagnosis.
Results: We enrolled a total of 30 patients. 16 (53%) patients had glioblastoma multiforme (GBM), 12 (40%) patients of cerebral abscess, 2 (6%) patients of lymphoma. The ADC of abscesses was significantly lower than that of necrotic tumours, consistent with restricted diffusion in abscesses vs free diffusion in tumours. On spectroscopic evaluation, the lipid lactate peak with an absent choline peak was observed in 100% of abscesses. While necrotic neoplasms demonstrated an absent lipid lactate peak in most of the cases, an elevated choline peak and decreased NAA.
Conclusion: DWI and MRS can be used to differentiate between intracranial abscess and necrotic neoplasms. Abscesses demonstrate a much lower ADC value than GBM or metastasis, whereas specific MRS findings with selective peak and spectral pattern are seen with abscess vs necrotic neoplasms.

B-1040 14:24

Can new interferon-free therapy lead to white matter tracts recovery in HCV-infected patients?

J. Bladowska, K. Fleischer-Stepniewska, B. Knysz, A. Zimny, M. Inglot, W. Rymer, M. Waliszewska-Prosol, M. Ejma, M. Sasiadek; *Wroclaw/PL (asia.bladowska@gmail.com)*

Purpose: The aim of the study was to evaluate the selected white matter tracts using diffusion tensor imaging (DTI) in HCV-positive patients before and after 24 weeks after completion of interferon-free therapy.
Methods and Materials: Ten HCV-positive patients (mean age 50.1) treated with ombitasvir/paritaprevir/r and dasabuvir ± ribavirin and 17 control subjects were enrolled in the study. DTI examinations were performed with 1.5T MR scanner. Fractional anisotropy (FA) and average diffusion coefficient (ADC) values were obtained with a small ROI method in middle cerebellar peduncles (MCP), inferior longitudinal fasciculi (ILF), inferior frontooccipital fasciculi (IFOF), genu (GCC) and splenium (SCC) of the corpus callosum, posterior limbs of the internal capsules (PLIC), superior longitudinal fasciculi (SLF) and posterior cingula (CG). Sustained viral response as well as liver fibrosis using elastography and APRI (AST to Platelet Ratio Index) were analysed.
Results: Significant increase of FA values ($p<0.05$) after therapy compared to values obtained before treatment was found in almost all white matter tracts apart from the right SLF and right CG. Significant decrease of ADC values ($p<0.05$) after treatment was observed in the right IFOF, SCC, left PLIC, left SLF, left CG. Compared to controls, HCV-positive patients showed significantly higher FA value in both MCP and the left CG after treatment. All patients achieved a sustained viral response. Liver fibrosis regression was also observed.
Conclusion: Efficient interferon-free therapy leads to white matter tracts recovery. This is the first report on impact of interferon-free therapy on microstructural cerebral changes in chronic hepatitis C patients.

B-1041 14:32

Diffusion kurtosis imaging in diffuse axonal injury: a novel diagnostic approach

N. Zakharova, G. Danilov, A. Potapov, I. Pronin, E. Alexandrova, A. Tonoyan, L. Fadeeva, A. Sichev, E. Pogosbekian; *Moscow/RU (nzakharova@nsi.ru)*

Purpose: Diffusion kurtosis imaging (DKI) is an advanced tool for non-Gaussian water diffusion detection. The aim of this study was to evaluate DKI in patients with diffuse axonal injury (DAI) compared to healthy controls.
Methods and Materials: DTI and DKI data for 12 patients with acute severe DAI and 8 healthy volunteers were compared. The main group consisted of 8 males and 4 females (29±11 y.o.). We assessed mean, axial, radial diffusivities (MD, AD, RD), mean, axial, radial kurtosis (MK, AK, RK), kurtosis anisotropy (KA) for white and grey matter, fractional and relative anisotropy (FA, RA), axonal water fraction (AWF), axial and radial extra-axonal diffusion (AxEAD, RadEAD) and tortuosity (TORT) parameters for white matter in bilateral regions of interest (ROI): centrum semiovale, internal capsules, thalami, putamen, corpus callosum and brain stem.
Results: We revealed a statistically significant KA reduction in the right (0.31 vs 0.45, p=0.003) and left (0.30 vs 0.43, p=0.0001) cerebral peduncles versus controls. AWF was reduced in several white matter ROIs (>.05). TORT showed similar tendency with the most pronounced changes in genu (3.02 vs 4.18, p=0.002) and splenium (2.42 vs 4.12, p=0.0002) of corpus callosum. AK in DAI tended to increase not only in white matter (centrum semiovale and cerebral peduncles), but also notably in right (0.65 vs 0.56, p=0.02) and left (0.67 vs 0.57, p=0.01) putamen.
Conclusion: Significant changes of DKI parameters reflected brain structure disintegration, demyelination and loss of axons in DAI.

B-1042 14:40

The effect of early MRI in the management of children with traumatic brain injury admitted to the PICU

P.A. Caruso; *Boston, MA/US (pcaruso@partners.org)*

Purpose: While CT is used most commonly for assessing head injury, MRI provides increased sensitivity for many traumatic lesions without radiation dose. We sought to determine the effect on management of early MRI in paediatric traumatic brain injury by analysing a consecutive series of 79 children requiring paediatric intensive care (PICU) admission who underwent MRI within days of injury.
Methods and Materials: The medical records were reviewed for each patient to determine the indications, MR imaging findings, and whether the study had influenced decisions to escalate, de-escalate, or redirect care. The images were reviewed by two neuroradiologists, a paediatric neurosurgeon, and a paediatric intensivist, using the NIH common data elements definitions dictionary.
Results: Different lesion patterns influenced management in different ways. Mass lesions including haemorrhages and evolving contusions, seen readily on T2 and FLAIR images, led to continued aggressive medical and/or surgical interventions. Findings of diffuse axonal injury with open cisterns led to de-escalation of sedation and monitoring. Early widespread diffusion abnormality or evidence of brainstem herniation or infarction was correlated with redirection of care.
Conclusion: Early MRI can play an important role in the targeted management of severe traumatic brain injury in children, allowing for prompt understanding of injury type and pathophysiology with acceptable reliability and reduced radiation. Cost-effectiveness analyses also will be needed to fully analyse this management approach.

B-1043 14:48

Sonographic texture analysis for neonatal white matter injury: focused on change according to follow-up cranial ultrasonography

A. Pak, S.-i. Suh, S. Chae, K. Cheol, I. Ryoo, H.-Y. Seol; *Seoul/KR (csyloo@naver.com)*

Purpose: In neonatal serial screening cranial ultrasound (cUS), diagnosis whether periventricular echogenicity (PVE) is progressed to periventricular leukomalacia (PVL) or not is difficult because of different ultrasound acquisition settings and interobserver variability. For early and objective diagnosis of PVL, we assess pattern of echotexture of PVE during follow-up cUS through quantitative texture analysis.
Methods and Materials: We included preterm neonates born between 25 and 34 weeks of gestation showed parietooccipital PVE on initial cUS within 1 week of birth (1st cUS), and underwent follow-up cUS on 2-3 weeks (2nd cUS) and 4-6 weeks (3rd cUS) of life respectively. Patients was diagnosed as PVL (n=10) or normal (n=10) from brain MRI or cUS after term-equivalent age. Texture analysis was performed with region of interest on PVE in coronal sections. Histogram, gradient, run-length matrix, co-occurrence matrix, autoregressive model and wavelet-derived parameters were analysed.
Results: Total 57 of 308 texture features showed statistically significant difference during follow-up cUS. The PVE texture features of 1st cUS showed no significant difference between two groups. The variance was significantly changed between 1st cUS and 2nd cUS in both two groups, which was decreased in normal (p=0.009) and increased in PVL (p=0.017) group. There was no significant difference of texture parameter change between PVL and PVE groups during 2nd cUS to 3rd cUS.
Conclusion: Assessment of change of PVE echotexture during serial cUS based on quantitative texture analysis may be important clue for early PVL diagnosis of preterm neonate within the first 2-3 weeks of life.

B-1044 14:56

The value of susceptibility-weighted imaging and T2-weighted gradient echo in imaging in assessment of mild traumatic brain injury

A. Brakus, M. Karan, J. Ostojic, S. Stojanovic, P. Vulekovic, S. Pena Karan, K. Petrovic; *Novi Sad/RS (alma.brakus@gmail.com)*

Purpose: Our aim was to analyse sensitivity of GRE-T2* sequences and SWI in detecting lesions in patients with symptoms of mild traumatic brain injury and normal CT findings.
Methods and Materials: We analysed clinical data and MRI findings in 34 patients suffering from mTBI and admitted at clinic for neurosurgery clinical centre of Vojvodina in two-year period. All patients had initial CT examination without signs of trauma. MRI examination including GRE-T2*w and SW sequence was performed in all patients in first 72 hours from trauma. Neuropsychological assessment was performed at 1 month and 6-9 months after injury.
Results: Evidence of axonal pathology reflected as signal change on T2w FLAIR was present in 44% (15p). On SWI: 61% (21p) had haemorrhagic lesions, 18 patients (53%) had lesion visible both on GRE T2* and SWI. One patient (3%) had lesions visible only on T2w (pure oedematous lesions), 30% (10p) had pure haemorrhagic lesions ; 31% (11p) had mixed lesions. We failed to establish connection between any clinical findings, such as GCS score, duration of amnesia or presence of vegetative disturbances and MRI detected signs of trauma.
Conclusion: Unusually high percentage of positive MRI findings can be explained with selection bias because analysed patients had more pronounced clinical presentation of mTBI that led to admission to hospital. SWI proves itself as the most sensitive sequence in detection of haemorrhagic lesions. MRI should be considered as diagnostic tool in patients with more severe clinical presentation.

B-1045 15:04

Limbic encephalitis, diagnostic pitfall in MR-imaging

A.-H. Schievelkamp, A. Jurcoane, B. Mädler, T. Rüber, L. Ernst, H. Schild, C. Elger, E. Hattingen; *Bonn/DE*
(Arndt-Hendrik.Schievelkamp@ukb.uni-bonn.de)

Purpose: Asymmetric high signal intensity (SI) of the amygdala on T2-weigthed (T2-w) images is typical for the limbic encephalitis (LE). These changes are often only discrete or can be absent. We investigated if these SI changes are measurable and if there is an increase of T2-relaxation time (T2).
Methods and Materials: 24 patients with clinical diagnosis of LE and 21 age-matched healthy controls were measured on a 3T-scanner. T2-Mapping was based on temporal-angulated, 2mm-coronar sequences with increasing TE (15,30,45,60,75,105,120ms). ROIs were manually drawn in the left and right amygdala. SI on respective T2-w (TE=105ms) and PD-w images (TE=15ms), as well as quantitative T2-values (qT2) were analysed. Laterally Index was used to analyse if there is an asymmetric involvement of the amygdala.
Results: There was no significant left-to-right difference of the amygdala in controls and in LE patients, neither for SI nor for qT2. qT2 was higher in LE patients (left 97±8ms (mean±SD) and right 98±9ms) compared to controls (left 90±5ms and right 89±6ms) with $p<0.01$. No significant differences were for found for SI in T2-w images between both groups. The SI in PD-w images was by trend lower in LE patients.
Conclusion: Patients with LE have elevated qT2-values in the amygdala. However, the expected SI increase in T2-w images was not found, and there were no left-to-right differences. The reason for this discrepancy might be explained by lower PD-values which can also reduce the T2-SI. This could explain the difficulty to recognize LE, despite the pathologic changes of the amygdala.

B-1046 15:12

Imaging features of neurocysticercosis, a radiologic-clinical correlation

M. Campos[1], S. Rivadeneira[2], D. Páez[3], R. Salinas[1]; [1]*Quito/EC*,
[2]*Buenos Aires/AR*, [3]*Murcia/ES (rr.sebastian@icloud.com)*

Purpose: To illustrate the most common radiological features of human neurocysticercosis, describing the recurrent locations and stages of the parasite in the CNS in order to help us launch the possible clinical manifestations.
Methods and Materials: Twenty two patients with NCC from the General Hospital Eugenio Espejo in Quito-Ecuador were initially referred to the Neurology department. The study focused on CNS imaging features. MR and CT imaging examinations were grouped based on the pathological stage (Escobar's classification: vesicular, colloidal, granular and nodular calcified), anatomical location and the clinical symptoms of each patient.
Results: Location: parenchymal cysticerci were commonly located in the cortical- juxtacortical junction (68%), basal ganglia (18%) and ventricular cysticerci were relatively rare with an incidence of 14% of our neurocysticercosis cases. Escobar's stages: the first group of 45% was found in the vesicular stage, most of them located in the cortico-subcortical interface, 59% had scolexes with an average size 13-17 mm. Secondly, 27% was in a colloidal stage and 9.5% were found in glanular stage and 18.5% was calcified nodular was better detected by CT.
Conclusion: Current strategies for diagnosis of NCC must include neuroimaging studies due to a wide variety of neurologic disorders can be associated with the disease. As in this study, the most common symptoms were headaches, followed by seizures and focal neurological deficits. We must learn the different radiological findings of the disease and take it into account the differential diagnosis of multiple intracranial lesions, particularly in patients from endemic areas.

B-1047 15:20

Brain MRI characteristics of anti-N-methyl-D-aspartate receptor encephalitis

T. Zhang; *Beijing/CN (zhangtian822@163.com)*

Purpose: To investigate the brain MRI characteristics of anti-N-methyl-D-aspartate (NMDA) Receptor Encephalitis and their associations with clinical disability at one-year follow-up.
Methods and Materials: We retrospectively enrolled 45 clinically defined anti-NMDA encephalitis patients. Brain MRI were acquired for all patients at onset phase including T1WI, T2WI and FLAIR. The brain MRI were categorised as normal and abnormal. We further classified the abnormal brain MRI as hippocampal lesion, non-hippocampal lesion, and lesions involving hippocampus and other brain areas. The modified Ranking Scale (mRS) at 1 year follow-up was assessed. The association between MRI characteristics at baseline and one-year follow-up mRS was evaluated.
Results: Twenty-six (26/45; 57.8%) NMDA patients had normal MRI at onset phase, while nineteen patients(19/45; 42.2%)presented abnormal MRI. Among brain MRI abnormalities, thirteen patients showed hippocampal lesions (13/19; 68%). Lesions were only located in hippocampus in 5 patients, and 8 patients showed lesions in brain areas besides hippocampus such as insula, thalamus,basal ganglia,and frontal, temporal, parietal lobes. Six patients (6/19, 31.6%) showed lesions in frontal lobe, thalamus, cerebellum and white matter lesions in corpus callosum. Abnormal MRI was observed more frequently in female patients (17/22) than male patients (9/23) ($p=0.025$). The patients with hippocampus lesions had higher mRS at one-year follow-up than patients without hippocampal lesions ($P=0.04$).
Conclusion: Hippocampal lesions were the most common lesions in NMDA encephalitis patients, but nearly one-third patients can have lesions in other brain areas without hippocampus involvement. The NMDA encephalitis patients with hippocampal lesions had worse prognosis than patients without hippocampus involvement.

Sunday, March 5

10:30 - 12:00 **Room C**

Abdominal Viscera

SS 1801
Technical innovations in liver imaging

Moderators:
C. Matos; Lisbon/PT
M. Ronot; Clichy/FR

K-21 10:30
Keynote lecture
H. Ringl; *Vienna/AT*

B-1048 10:39
Clinical feasibility of multiple arterial phases in free-breathing at gadoxetic acid-enhanced liver MRI
J.-Y. Park[1], J. Yoon[2], J. Lee[2], M. Yu[2], W. Chang[2], M.D. Nickel[3], Y. Son[2], B. Kiefer[3], J. Han[2]; [1]*Busan/KR*, [2]*Seoul/KR*, [3]*Erlangen/DE*
(kachulove@hanmail.net)

Purpose: To investigate clinical feasibility of free-breathing multi-arterial phase using Cartesian sampling and added value of motion resolved reconstruction in gadoxetic acid-enhanced liver magnetic resonance imaging (MRI).
Methods and Materials: This retrospective study was approved by IRB and the requirement of informed consent was waved. A total of 37 patients were included who underwent iterative three-dimensional gradient echo sequence for precontrast, early arterial, late arterial and portal venous phases of T1-weighted image (T1WI) in free-breathing manner. Timing, motion artifact, image quality were evaluation by four radiologists on a 4-point scale. In addition, respiratory motion-resolved reconstruction was performed for patients with below average score (score <3) of late arterial phase and reviewed in the same manner.
Results: Overall image quality of free-breathing T1WI was 3.30±0.59 on precontrast, 2.68±0.70, 2.93±0.65 and 3.30±0.49 on early arterial, late arterial and portal venous phases, respectively. Image quality of early and late arterial phase was significantly lower than precontrast and portal venous phase (P<0.0001~0.001). Eleven patients showed late arterial phase with below than average image quality (<3), but image quality of late arterial phase was significantly improved on motion-resolved reconstruction images using the same MRI data (P=0.007). In addition, none of the patients missed adequate arterial phase timing on multiarterial phase acquired in free-breathing manner.
Conclusion: Dynamic phase with acceptable image quality at gadoxetic acid-enhanced liver MRI can be achieved using Cartesian reconstruction in free-breathing manner.
Author Disclosures:
J. Yoon: Research/Grant Support; Bayer Healthcare. Speaker; GE Healthcare, Bayer Healthcare, Philips Healthcare. **J. Lee:** Research/Grant Support; Bayer Healthcare, GE Healthcare, Philips Healthcare, Guerbet. **M.D. Nickel:** Employee; Siemens Healthineers. **Y. Son:** Employee; Siemens Healthineers Korea. **B. Kiefer:** Employee; Siemens Healthineers.

B-1049 10:47
Virtual monochromatic image of detector-based spectral CT: improved image quality as compared with that obtained with conventional CT
H.-J. Kang, J. Lee, S. Lee, H. Yang, R. Kim, J. Nam, J. Han; *Seoul/KR*
(dr.kanghj@gmail.com)

Purpose: To compare image quality obtained in phantom with virtual monochromatic image of detector-based spectral CT (VMS) with that performed with conventional CT on various body size and dose right index (DRI) values.
Methods and Materials: Three different size of body phantoms with 8 FLLs were scanned with two conventional mode (80 and 120kVp) by detector-based spectral CT with iDose (level 4) reconstruction. The VMS is reconstructed from 120kVp iDose (level 4) image basis and displayed on vendor specific workstation. The noise and CNR in different body size, and subjective image quality and FLL conspicuity in small phantom were analysed with different DRI values (16, 19, 22 and 25).
Results: Image noise on VMS is always lower than that of 80kVp with higher CNR in low KeV ranges (from 40 to 69~73KeV) regardless of DRI values. Also comparing 120kVp, CNR of VMS is improved in low KeV ranges (from 40 to 75~81KeV) on each DRI values. On the qualitative analysis, diagnostic acceptability (p=0.015) and subjective noise (p<0.01) is significantly higher in VMS. Lesion conspicuity of low-contrast FLLs are significantly improved in VMS (all p<0.05) than 120kVp CT. Also, VMS present lesser stiff noise increment with higher CNR than those of 120 kVp as body size increases.
Conclusion: VMS of detector-based spectral CT, the up-to-date VMS technique, is presenting improved CNR, noise and subjective image quality, and it is especially valuable in large phantom and low-contrast FLLs.

B-1050 10:55
Respiratory motion artefacts during arterial phase imaging with gadoxetic acid: how can we minimise this drawback?
S. Polanec[1], H. Bickel[1], P.A.T. Baltzer[1], P. Thurner[1], F. Gittler[1], J. Hodge[1], M. Bashir[2], A. Ba-Ssalamah[1]; [1]*Vienna/AT*, [2]*Durham, NC/US*
(stephan.polanec@meduniwien.ac.at)

Purpose: To determine which of three gadoxetic-acid injection techniques, performed serially in the same patient, could produce liver MRI with fewer contrast-related arterial-phase motion artefacts.
Methods and Materials: This IRB-approved, retrospective study included a cohort of 78 consecutive patients. Each patient had serial gadoxetic acid-enhanced MRI of the liver performed with at least two of three injection techniques: M1-test bolus undiluted, power-injected; M2-test bolus, diluted 50% with saline, power-injected; M3-fixed delay, undiluted, manually injected. The injection dose was 0.025mmol/kg body weight in all three methods. Three readers independently rated the images for motion artifacts, timing, and lesion detectability based upon a four-point Likert scale.
Results: Respiratory artefacts related to gadoxetic-acid arterial phase images obtained by M3 were superior to M1 (p=0.0001). M2 was rated significantly better than M1 (p=0.012). The difference between M3 and M2 scores was not statistically significant (p=0.49). Arterial-phase timing was significantly better for M1 compared to M3 (p<0.0001). The AUC was 0.59-0.68. M2 significantly outperformed M3 in arterial phase timing (p<0.0001). There was no significant difference between M1 and M2 (p=0.35). With regard to lesion detectability, there was no significant difference in the ratings for all three-injection techniques (p>0.05).Inter-reader agreement was moderate to substantial (0.41-0.62).
Conclusion: There were significantly fewer contrast-related-motion-artefacts in the arterial phase when gadoxetic acid was administered undiluted manually (M3), or diluted power-injected (M2), compared to undiluted power injection (M1).The arterial phase timing was significantly better with test-bolus, power injection of contrast media, however the diagnostic performance for all three methods was not significantly different.

B-1051 11:03
Free-breathing undersampled radial VIBE as a salvage strategy for liver dynamics in patients unable to suspend respiration
B. Kaltenbach, A. Roman, T.J. Vogl, S. Zangos; *Frankfurt a. Main/DE*
(benjamin.kaltenbach@kgu.de)

Purpose: Respiratory motion artifacts are a frequent source for image degradation in abdominal MRI. The introduced free-breathing sequence can be used as a salvage strategy in patients with limited breath-holding capacity for dynamic liver imaging.
Methods and Materials: Twenty-seven consecutive patients with known liver metastases underwent dynamic liver MR imaging using a free-breathing undersampled radial sequence. Patients were eligible for the free-breathing protocol due to severe respiratory artifacts at the precontrast sequences. The introduced free-breathing sequence was compared to a standard dynamic breathhold VIBE. Overall image quality, liver edge sharpness, liver lesion conspicuity, hepatic vessel clarity, respiratory motion artifacts and streaking artifacts were independently, retrospectively and blindly scored by four experienced readers using a 5-point Likert scale. Contrast-enhancement ratio (CER) between native and arterial phases was measured to assess temporal resolution.
Results: Free-breathing VIBE received lower image quality scores than breathhold VIBE but presented with generally good image quality. Regarding patients with severe respiratory artifacts already at breathhold VIBE, free-breathing VIBE received significantly higher scores for overall image quality (4.1 vs 3.8, p=0.01) and hepatic lesion conspicuity (4.2 vs 3.8, p=0.02). There were generally more respiratory artifacts in breathhold VIBE (p<0.0001), whereas streaking was characteristic for the undersampled radial acquisition (p<0.0001). Temporal resolution assessed with CER showed higher values for free-breathing VIBE sequence (p=0.028).
Conclusion: The introduced free-breathing sequence is a promising alternative for liver dynamics in challenging patients. Accurate temporal resolution, low motion artifact susceptibility and good image quality qualify this sequence for daily routine.

B-1052 11:11

Accuracy of new real-time shear wave elastography for assessing liver fibrosis in chronic viral hepatitis patients

J. Han, S. Yeom, I. Choi, S. Lee, H. Chung, S. Cha, S. Suh, Y. Jung, H. Yim; *Ansan-si, Gyeonggi-do/KR*

Purpose: Recently, new real-time shear wave elastography (SWE, Aplio500®, Toshiba) has been released. In this study, the diagnostic performance of SWE and TE (transient elastography) in assessing liver fibrosis in chronic viral hepatitis was investigated. Differences in diagnostic performance of SWE were evaluated according to the obesity.
Methods and Materials: 53 chronic viral hepatitis patients who underwent liver biopsy were prospectively enrolled (23 with HBV, 30 with HCV). For each patient, liver stiffness was assessed by SWE and liver biopsy was performed in the same session (METAVIR score). TE was performed within two weeks of liver biopsy. AUROCs were performed and compared for each degree of liver fibrosis. Differences in AUROCs were investigated according to body mass index (BMI ≥25, and BMI≥ 30).
Results: Among 52 patients, 16 belonged to F0-F1 stage, 12 were F2, 16 were F3 and 9 were F4. TE was significantly more accurate for prediction of F ≥2 than SWE (AUC: SWE=0.630, TE = 0.810, P=0.02). However, there were no significant differences between SWE and TE in prediction of F≥3(AUC: SWE = 0.800, TE = 0.883, P = 0.20). In overweight patients(BMI ≥25), SWE showed good diagnostic performance (AUC:0.808 with cutoff value 18.9kPa with 69.23% sensitivity and 87.5% specificity) in prediction of F≥3. However, in obese patients (BMI ≥30), SWE showed poor diagnostic performance (AUC:0.667).
Conclusion: New SWE seems to be good method for assessing advanced liver fibrosis with similar predictive value to TE. SWE showed poor diagnostic performance for assessing advanced liver fibrosis in obese patients.

B-1053 11:19

Diffusion-weighted MRI in liver fibrosis staging: added value of normalised ADC using spleen and renal cortex as reference organs

T.F.T. Ali, M.A. El-Hariri; *Zagazig/EG (tamerfathi2008@yahoo.com)*

Purpose: To evaluate the potential value of the spleen and renal cortex as reference organs to improve the performance of DWI in the assessment of liver fibrosis.
Methods and Materials: 30 patients with chronic viral hepatitis and 14 volunteers were subjected to DWI. Liver ADC, normalised ADC (ratio between ADC of liver to spleen (S-ADC) and renal cortex (R-ADC) was calculated. Data was analysed to evaluate the performance of ADC, S-ADC and R-ADC.
Results: The mean S-ADC value was significantly lower in patients with different hepatic fibrosis stages in comparison to control group (P<0.001). Significant negative correlation was noted between S-ADC value and fibrosis stage (r=-0.75, p<0.001). It had significant difference between stage 0 compared to stage 2, 3, and 4 as well as between stage 4 in comparison to stage 1, 2 and 3. Significant negative correlation was noted between R-ADC value and fibrosis stage (r=-0.68, p<0.001). The mean R-ADC value was lower in patients with liver fibrosis compared to volunteers with significant difference between stage 0 and 3 and between stage 0 and 4 (P <0.001). It had significant difference between stage 0 compared to stage 3, and 4 as well as in stage 4 in comparison to stage 1 and 2. ROC curve showed higher performance using S-ADC in comparison to liver ADC and R-ADC while R-ADC had higher performance in comparison to liver ADC.
Conclusion: Normalised liver ADC increases the ADC performance of ADC in the evaluation of liver fibrosis which is highest in S-ADC.

B-1054 11:27

Evaluation of virtual monoenergetic images computed by new dual-layer CT in assessing hypervascularised liver lesions

N. Große Hokamp, A. Höink, T. Persigehl, D. Maintz, S. Haneder; *Cologne/DE (nils@grossehokamp.de)*

Purpose: Evaluation of both objective and subjective image quality of virtual monoenergetic (vME) images for assessment of arterially hypervascularized liver lesions in dual-layer CT (e.g. haemangiomas, metastases).
Methods and Materials: 50 liver lesions in 20 contrast enhanced CT examinations, acquired at dual-layer CT (IQon, Philips Healthcare) in arterial contrast phase, were identified and retrospectively analysed in vME (40-200 keV; 10 keV intervals) and in conventional images, respectively. Image noise was represented by standard deviation of liver parenchyma; signal- (SNR) and contrast-to-noise ratio (CNR) of lesions and liver parenchyma were calculated. To assess subjective image quality, vME-images (40-110 keV) were rated by two readers with regard to lesion delineation and overall image quality, compared to conventional images, on a 5-point-scale.
Results: SNR of liver parenchyma was significantly higher in 40- and 50-keV-vME-images as compared to conventional images (3.8, 2.8 vs 1.3; p≤0.001). SNR and CNR of lesions were significantly higher in 40/50/60-keV-vME-images, compared to conventional images (SNR: 17.8, 12.4, 8.8 vs 5.0; CNR: 14.2, 10.5, 7.7 vs 4.4; p≤0.001). Image noise was significantly lower in vME-images (50-200keV), while 40-keV-vME-images exhibited similar image noise as conventional images (12.1 vs 13.8). Subjective lesion delineation received best rating at 50-keV-vME-images, while overall image quality was rated inferior to equal at all vME-intervals, compared to conventional reconstructions.
Conclusion: Both objective image quality and subjective assessment of hypervascularised liver lesions are superior at vME images of 40-60 keV. However, improved CNR at low-keV-vME-images impairs overall image quality.Thus, vME-images of low-keV may be useful as screening reconstructions.

B-1055 11:35

Comparison between the conventional Couinaud method vs a semiautomatic software (Syngo.CT. liver analysis, Siemens) in the precise localisation of liver metastases

P. Bartolomé, A. Quilez, I. Gonzalez de la Huebra, A. García Baizán, I. Gonzalez, I. Vivas; *Pamplona/ES (pbartolome@unav.es)*

Purpose: To analyse the variability in the location of CT detected liver metastases using the conventional method of Couinaud (CM) or a semiautomatic software (SAS) for liver segmentation (Syngo.CT-*liver Analysis*©, Siemens Healthcare, Germany).
Methods and Materials: Two expert radiologists in abdominal imaging consecutively studied 25 oncologic patients with a total of 70 liver metastases detected on abdominal CT. Lesions were distributed by segments, following either the Couinaud method based on anatomical landmarks or the semiautomatic software *liver Analysis*©, which relies on the ramifications of portal branches. The global agreement between the two methods was calculated, as well as the Kappa agreement values for each segment.
Results: The kappa values for each segment were: I(1.0), II(0.79), III(0.9), IV(0.68), V(0.42), VI(0.65), VII(0.49), VIII(0.4). The global agreement between methods was of 62%. There agreement was only moderate for lesions localised on the segments V, VII and VIII. With CM it is difficult to differentiate the V-VI boundaries because the right hepatic vein is not well recognised in the inferior segments. Between segments VII-VIII at the dome the middle hepatic vein trajectory is not well depicted.
Conclusion: The Couinaud method alone, based on indirect anatomical landmarks is not reliable enough for the precise localisation of hepatic metastases, especially for the lesions located below the liver dome (segments V-VI, VII-VII) Software tools that are able to demarcate the liver segments using a more anatomical approach, based on the portal ramifications, are essential for an accurate localisation of liver metastases, especially in patients undergoing surgery.

B-1056 11:43

Volumetric iodine-uptake measurement for early assessment of therapy response after microwave ablation in rabbit model with intrahepatic VX2 tumour

L. Zhang, X. Liu, B. Feng; *Shenyang/CN (270973226@163.com)*

Purpose: To investigate the diagnostic value of volumetric iodine-uptake (VIU) in assessing early therapy response after microwave ablation in rabbit model with intrahepatic VX2 tumour.
Methods and Materials: Our institutional animal care committee approved all experiments. VX2 tumours were implanted into the livers of 14 rabbits. Dual-source CT (DSCT) was performed at baseline and 7 days after microwave ablation. 23 lesions were treated and evaluated for tumour response according to VIU, adapted Choi and standard AALSD measurement criteria. Disease control was defined as the sum of complete response (CR), partial response (PR) and stable disease (SD). Lesions were collected 8 days after microwave ablation for histological examination to verify the assessment result.
Results: According to Choi and VIU assessment, more lesions were considered as disease control (56% and 47%, respectively) than that with AASLD (13%) (p<0.05). 10/20 and 8/20 progression disease (PD) lesions assessment by AASLD were classified as PR by Choi and VIU, respectively. For disease control group, change in mean VIU ranges from 3.43 ± 1.504 mg/ccm to 1.88 ± 1.268 mg/ccm (decreased 51.47± 29.56%). For progressive disease group, change in mean VIU ranges from 2.33 ± 1.127 mg/ccm to 2.85 ± 1.140 mg/ccm (increased 36 .03±70.26%). VIU has moderate consistency with Choi (kappa = 0.574, p<0.05).
Conclusion: VIU measurement by DSCT can make an early assessment of therapy response after microwave ablation. VIU has the potential to reflect vital tumour burden, therefore, it is likely to be applied as an optimal tumour response biomarker for HCC treatment.

B-1057 11:51

Differentiation of malignant thrombus from bland thrombus of the portal vein in patients with cirrhosis: application of intravoxel incoherent motion diffusion-weighted MR imaging

J. Choi, E.-S. Cho, J. Kim, Y. Choi; *Seoul/KR (justice-cjm@yuhs.ac)*

Purpose: Our purpose of this study was to demonstrate the presence of blood flow within the malignant thrombus using intravoxel incoherent motion (IVIM) diffusion-weighted (DW) MR imaging and investigate the utility of IVIM in distinguishing bland thrombus from malignant tumour thrombus of the PV in patients with cirrhosis or hepatocellular carcinoma.
Methods and Materials: Forty three patients with PV thrombosis (malignant thrombus n=29 and bland thrombus n=14) examined with gadoxetic acid-enhanced MR imaging including IVIM were enrolled. IVIM DW imaging was acquired with free-breathing axial single-shot echo-planar two-dimensional imaging sequence and the following eight b values: 0,25,50,75,100,200, 500 and 800 sec/mm^2. Diffusion coefficient (D), pseudo-diffusion coefficient (D*), and perfusion fraction (f) were calculated with bi-exponential model using Matlab software and were compared between malignant and bland thrombi using unpaired t-test.
Results: D* of malignant thrombus (mean=67.51 x 10^{-3}mm^2/sec) was significantly higher than that of bland thrombus (9.31 x 10^{-3}mm^2/sec, $p < 0.001$). However, there was no significant difference in f between malignant (18.47 %) and bland thrombi (18.46 %). D of bland thrombus (1.35 x 10^{-3}mm^2/sec) was significantly higher than that of malignant thrombus (1.03 x 10^{-3}mm^2/sec, p=0.014). However, the mean D difference between the two thrombi was relatively small.
Conclusion: Increased pseudo-diffusion coefficient (D*) of malignant thrombus suggests higher intra-thrombus micro-perfusion, which might be due to blood flow by arterial neovascularisation within the malignant thrombus. Therefore, IVIM DW imaging appears to be a promising method for the discrimination between bland and malignant PV thrombi.

10:30 - 12:00 **Room X**

Vascular

SS 1815

Peripheral arteries / arteritis

Moderators:
B. Merlino; Rome/IT
B. Sekovski; Split/HR

B-1058 10:30

Voxel-wise bone and plaque subtracted datasets calculated from dynamic lower limb CT angiography - image quality compared to conventional datasets

N. Vogler, S. Sudarski, M. Meyer, H. Haubenreisser, S.O. Schönberg, T. Henzler; *Mannheim/DE (nils.vogler@medma.uni-heidelberg.de)*

Purpose: Static CT angiography of the lower limb (sCTA) and dynamic CT angiography of the calf (dCTA) are routinely used in patients with peripheral artery disease. However extensive calcification provides a diagnostic challenge and impairs image quality, especially in the calf. The aim of this study was to evaluate the diagnostic image quality of voxel-wise bone and plaque subtracted datasets calculated from dCTA in comparison to sCTA and the best-contrast phase from dCTA.
Methods and Materials: 15 patients were retrospectively included. The CT acquisition consisted of a sCTA (Dataset 1) and a 14-phase dCTA of the calf. The dCTA images were corrected for motion and noise and the best-contrast phase (Dataset 2) was selected. Subsequently the first non-contrast-enhanced phase was subtracted from the corresponding best-contrast phase generating a voxel-wise bone and plaque subtracted dataset (Dataset 3). Two independent readers evaluated all three Datasets on a per-segment basis for diagnostic confidence and overall image quality using a 5-point Likert scale.
Results: Dataset 3 showed significantly higher overall image quality then Dataset 1 and Dataset 2 ($p<0.0001$). Dataset 3 showed significantly higher diagnostic confidence then Dataset 1 and Dataset 2 ($p<0.0001$). Reader 1/2 reported good or excellent diagnostic confidence in 20.2/20.0%, 33.5/47.8% and 70.1/95.8% for Datasets 1, Datasets 2 and Datasets 3, respectively.
Conclusion: Voxel-wise bone and plaque-subtracted datasets calculated from motion and noise-corrected dCTA datasets are superior in terms of overall image quality and diagnostic confidence to sCTA and non-subtracted dCTA of the calf.
Author Disclosures:
M. Meyer: Speaker; Siemens AG, Bracco Group. **H. Haubenreisser:** Speaker; Siemens AG, Bayer AG. **S.O. Schönberg:** Research/Grant Support; Institutional research agreement, Siemens AG. **T. Henzler:** Research/Grant Support; Research support, Siemens AG. Speaker; Siemens AG.

B-1059 10:38

Clinical utility of quiescent interval single-shot (QISS) non-contrast MRA at 3 Tesla for the diagnosis of chronic lower limb arterial disease

Y. Ragab, K. Alhusseiny, A. Almarakby; *Cairo/EG (yragab61@hotmail.com)*

Purpose: To assess the diagnostic performance of ECG-gated non-contrast enhanced quiescent interval single-shot (QISS) magnetic resonance angiography at a magnetic field strength of 3 Tesla in patients with peripheral arterial occlusive disease (PAOD).
Methods and Materials: 19 patients with advanced PAOD Rutherford classification (stage 3 and higher) referred for peripheral magnetic resonance angiography (MRA) were included. Imaging was performed on a 3T whole body MR. Image quality and stenoses diameters were compared to contrast-enhanced MRA (CE-MRA) as standard of reference. Two blinded readers rated the image quality and the degree of stenosis for both ECG gated HR-QISS and CE-MRA in 26 predefined arterial vessel segments on 5-point Likert scales.
Results: Compared with CE-MRA, HR-QISS technique showed high sensitivity (93%), specificity (95%), positive (95.1%), and negative predictive value (96%) for the detection of significant (≥50%) stenosis. Interreader agreement for stenosis assessment of both HR-QISS and CE-MRA was excellent (κ-values of 0.94 and 0.95, respectively). As compared to CR-MRA, image quality of HR-QISS was significantly lower for the distal aorta, the femoral and iliac arteries (each with $p<0.01$), while no significant difference was found in the popliteal ($p=0.07$) and lower leg arteries ($p=0.9$).
Conclusion: Non-contrast QISS MRA has been shown to be technically comparable to CE MRA. QISS provides good early results for the detection of significant peripheral arterial stenotic disease. Accordingly, QISS MRA may prove valuable in patients with renal dysfunction by avoiding the use of gadolinium-based contrast agents in peripheral MRA.

B-1060 10:46

Popliteal artery aneurysm (PAA) surveillance: a 5-year retrospective cohort study

H. Shiwani, E. Taylor, J. Scott; *Leeds/UK (hshiwani@gmail.com)*

Purpose: Popliteal artery aneurysms (PAA) comprise up to 85% of all peripheral aneurysms. There are, however, no longitudinal studies tracking the progression of PAA size, which is the determinant of intervention. In this study, we aimed to track the progression of asymptomatic PAAs.
Methods and Materials: A retrospective single-group cohort study included patients who had a PAA of any size on arterial duplex ultrasound (USS) between the 1st of January 2011 and 1st of January 2016. Progression of PAA size and progression to event or intervention were the primary outcome measures.
Results: 3217 records were screened and a total of 22 patients (males = 15, females = 7) with PAA were identified (9 had bilateral PAAs) with a median age of 77 (IQR = 10.3). Eight had a previous open repair of an AAA or previous EVAR and five had an AAA under surveillance. The median size of PAA at diagnosis was 13.0mm (IQR = 5mm). Six limbs eventually proceeded to intervention. Median size at the time of intervention was 30mm (IQR = 13.5mm). The median time to event duration was 2.74 years. Seventeen patients with a growth rate of their PAA slower than 1mm a year were asymptomatic irrespective of initial size.
Conclusion: PAAs were frequently bilateral (40%) and were associated with AAA (59%). We recommend that all those with PAA should undergo screening for AAA and vice versa. We also recommend initial yearly surveillance for asymptomatic PAAs until there is a stable growth rate of <1mm per year.

B-1061 10:54

Image quality assessment of lower extremity quiescent-interval single-shot (QISS) MR angiography: comparison with CT angiography

A. Varga-Szemes[1], G. Muscogiuri[1], C.N. De Cecco[1], P. Suranyi[1], J.L. Wichmann[1], P.M. Cannao[1], S. Giri[2], U.J. Schoepf[1], T.M. Todoran[1]; [1]*Charleston, SC/US*, [2]*Chicago, IL/US (vargaasz@musc.edu)*

Purpose: To evaluate the qualitative image quality of non-contrast quiescent-interval single-shot (QISS) MRA in patients with peripheral artery disease (PAD).
Methods and Materials: Thirty patients (66±7 years, 16 male) with PAD referred for a clinically indicated lower extremity CTA underwent non-contrast lower extremity MRA on a 1.5T scanner using an investigational prototype QISS sequence (FOV 400x260mm^2, TR/TE 3.5/1.4ms, flip-angle 90°). Image evaluation was performed on a per-segment basis according to an 18-segment model. The overall image quality was subjectively rated by two observers according to a 3-point scale: (1) vascular segment not assessable due to severe image artifacts; (2) acceptable image quality with minor artifacts, marginal reader confidence; (3) excellent image quality, high reader confidence. Quality scores 2 and 3 were considered acceptable for diagnostic purposes.

Results: A total of 540 segments were evaluated. Overall subjective image quality was rated similarly with QISS-MRA (2.52 [2.46-2.57]) and CTA (2.49 [2.43-2.55], P=0.5062). Excellent inter-reader agreement was found in image quality ratings (κ>0.8). Forty-two segments (7.8%) in CTA were excluded from the analysis due to stent artifacts (11), heavy calcification (8), or suboptimal opacification (23), while 15 segments (2.8%) were non-diagnostic in MRA due to major image artifacts.
Conclusion: Image quality of QISS-MRA was comparable to that of contrast enhanced CTA. In certain circumstances, such as in heavily calcified segments or suboptimal opacification (i.e. the scanner outruns the contrast bolus), QISS-MRA provides superior vascular visualization compared to CTA. Such a non-contrast technique may have potential advantage in patients with contraindication to contrast media.
Author Disclosures:
A. Varga-Szemes: Consultant; Guerbet. **C.N. De Cecco:** Consultant; Guerbet. **S. Giri:** Employee; Siemens. **U.J. Schoepf:** Consultant; Bayer, Bracco, GE Healthcare, Guerbet, Medrad, and Siemens Healthcare. Research/Grant Support; Bayer, Bracco, GE Healthcare, Guerbet, Medrad, and Siemens Healthcare.

B-1062 11:02

Reference values of vessel diameters and stenosis prevalence of the lower limb arteries using MR angiography - a population-based approach
B. Mensel[1], A. Grotz[1], H. Völzke[1], W. Lieb[2], M. Dörr[1], J.-P. Kühn[1], R. Lorbeer[3]; [1]*Greifswald/DE*, [2]*Kiel/DE*, [3]*Munich/DE (menselb@uni-greifswald.de)*

Purpose: This study aims to determine reference values of vessel diameters and to assess the prevalence of stenosis of the lower limb arteries in a population-based sample.
Methods and Materials: Magnetic resonance angiography at 1.5 Tesla was performed in 756 male participants (median age=52 years, range=21-82 years) of the population-based Study of Health in Pomerania. Vessel diameters were measured in 9 predefined segments of the pelvic and leg arteries on both sides.
Results: Reference values of vascular diameters decreased from proximal to distal arteries: common iliac=1.18cm; internal iliac=0.75cm; external iliac=1.03cm; proximal femoral=1.02cm; distal femoral=0.77cm; popliteal=0.69cm; anterior tibial=0.42cm; posterior tibial=0.38cm; fibular=0.40cm. Body-surface area indexed reference values increased with age in all segments. A number of 53 subjects (7.0%) had at least one stenosis, mainly in the lower leg arteries anterior tibial (n=28, 3.7%), posterior tibial (n=18, 2.4%) and fibular (n=20, 2.6%). The risk of stenosis increased considerably with age (odds ratio=1.08; p<0.001).
Conclusion: We present reference values for different pelvic and leg artery segment diameters in men that decrease from proximal to distal and increase with age. Stenoses were most prevalent in lower leg arteries.
Author Disclosures:
B. Mensel: Research/Grant Support; SHIP is part of the Community Medicine Research Net of the University of Greifswald, Germany, which is funded by the Federal Ministry of Education and Research (01ZZ9603, 01ZZ0103, 01ZZ0403, 01ZZ0701,. **H. Völzke:** Research/Grant Support; SHIP is part of the Community Medicine Research Net of the University of Greifswald, Germany, which is funded by the Federal Ministry of Education and Research (01ZZ9603, 01ZZ0103, 01ZZ0403, 01ZZ0701,. **M. Dörr:** Research/Grant Support; SHIP is part of the Community Medicine Research Net of the University of Greifswald, Germany, which is funded by the Federal Ministry of Education and Research (01ZZ9603, 01ZZ0103, 01ZZ0403, 01ZZ0701,.

B-1063 11:10

CT angiography in peripheral artery disease - feasibility of low-contrast media volume protocol
B. Horehledova, C. Mihl, R. Brans, N.G. Eijsvoogel, B.M.F. Hendriks, J.E. Wildberger, M. Das; *Maastricht/NL (barbora.horehledova@mumc.nl)*

Purpose: This study evaluated image quality (IQ) of low-contrast media (CM) volume computed tomographic angiography (CTA) of the peripheral arteries in patients with peripheral artery disease (PAD).
Methods and Materials: 50 patients were scanned on 3rd generation DSCT scanner (Somatom FORCE, Siemens Healthcare, Germany) with the following scan characteristics: tube voltage 70kV, tube current 90mAs, collimation 0.6, pitch 0.6 from diaphragm to forefoot; images were reconstructed with a slice thickness 2/1.4mm and kernel Bf40. CM injection protocol consisted of 15ml test bolus and 30ml main bolus (Iopromide 300mgI/ml, Ultravist, Bayer), at an injection rate of 5ml/s (Iodine delivery rate:1.5gI/l, respectively), followed by a 40ml saline chaser at the same flow rate. Aorto-popliteal bolus transit times were used to calculate the overall acquisition time and delay. Objective (attenuation;contrast-to-noise (CNR)) and subjective IQ (4-point Likert score:1=non-diagnostic, 2=diagnostic, 3=good, 4=excellent) were assessed at the infrarenal aorta and five levels of peripheral arteries: common iliac artery (CIA), superficial femoral artery (SFA), popliteal artery (PA), anterior tibial artery (ATA), dorsalis pedis artery (DPA).
Results: Objective IQ mean attenuation values/CNR (HU±SD) at aorta: 383±89/21±9, and peripheral arteries were: left: CIA 410±100/23±13, SFA 414±93/24±13, PA 316±89/17±8, ATA 249±71/12±6, DPA 166±65/7±5 right: CIA 401±80/22±9,SFA 413±101/24±13, PA 329±88/18±10, ATA 272±76/14±7, DPA 199±89/9±5. Subjective IQ median Likert score value was: 4 at aorta, in peripheral arteries (left/right): CIA 4/4, SFA 4/4, PA 4/4, ATA 3/3, DPA 3/3.
Conclusion: CM volume can be reduced using 70kV protocols using the transit time approach, while maintaining sufficient IQ for evaluation of PAD.
Author Disclosures:
B. Horehledova: Research/Grant Support; Institutional Research Grant Siemens. **C. Mihl:** Speaker; Bayer. **N.G. Eijsvoogel:** Research/Grant Support; Institutional Research Grant Bayer. **B.M.F. Hendriks:** Research/Grant Support; Institutional Research Grant Bayer. **J.E. Wildberger:** Research/Grant Support; Institutional Research Grants Siemens, Philips, Bayer, AGFA. Speaker; Siemens, Bayer. **M. Das:** Research/Grant Support; Institutional Research Grants Bayer, Siemens, Philips, Cook.

B-1064 11:18

Multipath curved planar reformations of peripheral CT angiography: higher diagnostic accuracy and time-savings for vascular radiologists and radiology residents
M. Schreiner, H. Platzgummer, C. Loewe, S. Unterhumer, G. Mistelbauer, E. Groeller, M. Sramek, R.E. Schernthaner; *Vienna/AT (markus.schreiner@meduniwien.ac.at)*

Purpose: To compare diagnostic performance and time efficiency between multipath curved planar reformations (mpCPRs) and axial images of CT angiography for the assessment of peripheral arterial disease (PAD).
Methods and Materials: Forty patients (10 female, mean age: 72 years) were prospectively included and underwent peripheral CT angiography. A semi-automated toolbox was used to render mpCPRs. Twenty-one arterial segments were defined in each leg; for each segment, the presence of stenosis > 70% was assessed by two independent readers (one expert vascular radiologist, one resident), once on mpCPRs and once on axial images, with digital subtraction angiography as gold standard.
Results: Both readers reached lower sensitivity (Reader 1: 89% vs 93%, p = 0.03; Reader 2: 91% vs 94%, p = 0.08) but significantly higher specificity (Reader 1: 96% vs 95%, p = 0.01; Reader 2: 94% vs 89%, p < 0.01) with mpCPRs than with axial images. Whereas the expert vascular radiologist had similar overall accuracy in both evaluations (94% vs 94%, p = 0.96) the resident achieved even higher accuracy with mpCPRs (93% vs 91%, p = 0.02). Both readers read mpCPRs significantly faster than axial images (p < 0.01).
Conclusion: The assessment of PAD based exclusively on mpCPRs is time-saving, yields high diagnostic performance and should be considered an alternative to time-consuming axial image reading. In particular less experienced readers might benefit from the assessment of mpCPRs. However, further confirmation of these initial results is required.

B-1065 11:26

Lower limb angiography: utilising dynamic datasets to optimise contrast and radiation dose
H. Haubenreisser, M. Meyer, N. Vogler, S. Sudarski, S.O. Schönberg, T. Henzler; *Mannheim/DE (Holger.Haubenreisser@medma.uni-heidelberg.de)*

Purpose: To investigate the impact of the additional information from time-resolved CT angiography examinations with a 3rd generation DSCT on standard CTA protocols.
Methods and Materials: 80 patients with suspected lower limb arterial occlusive disease underwent a combined CTA protocol consisting of a high-pitch-CTA run-off study starting from the abdominal aorta as well as a time-resolved-CTA of the lower limbs over 80cm (10 sec delay, 72sec scan time (8x3sec, 8x6sec); 70kV; 40ml iomeprol400). Quantitative information was gathered in the 3 popliteal segments over the 16 scan phases. In addition, two radiologists and one vascular surgeon assessed the time-resolved examination regarding additional information leading to changes in patient management.
Results: Peak contrast enhancement of the P1 segment was found in Phase 6 (430HU 28s post contrast), in Phase 7 for P2 (388HU 31s post contrast) and in Phase 7 for P3 (366HU 31s post contrast). Diagnostic CNR values (>6) were found in Phases 4-9 (22-40s) in Segment P1, Phases 4-9 (22-40s) in Segment P2 and Phases 5-9 (25-40s) in Segment P3.
Conclusion: Using the gathered information in combination with scanner parameters for static CTA of the lower limbs, it is possible to optimise the protocols for optimal contrast. For example, if a scan time of 20s is chosen, a delay of 21s (31-20/2s) is suitable. Similarly, for a high pitch scan of 2s a delay of 30s should be used.
Author Disclosures:
H. Haubenreisser: Speaker; Siemens Healthcare, Bayer Healthcare. **M. Meyer:** Speaker; Siemens Healthcare. **T. Henzler:** Speaker; Siemens Healthcare.

B-1066 11:34

Low dose whole aorta angio CT in the evaluation of Takayasu vasculitis: a prospective study analysing anatomic classification and identification of disease activity criteria

A. Habouchi, A. Habba, C. Aimeur, M. Tabouche, D. Hakem, N. Slimani, A. Berrah, B. Mansouri; *Algiers/DZ (aminehabouchi@gmail.com)*

Purpose: Takayasu disease is an inflammatory periaortitis involving large and medium size vessels. By the absence of a standardised medical imaging protocol, we propose by this study, the evaluation of a reproducible and exhaustive angio-CT protocol in the statement and the follow-up of the disease.
Methods and Materials: We report the results of a prospective study, realised from January 2013 to December 2015, involving the evaluation by a triphasic angio-CT (non-contrast, arterial and late phase at 5mn), with ECG triggering, low dose protocol (80kv, automatic adaptation of mAs, post treatment with AIDR 3D), and ordinary protocol (120kv, 100mAs) on a 320 rows CT, patients responding to the 1990 ACR criteria of Takayasu disease. Quality of vascular enhancement, irradiation dose, classification of anatomic lesions and correlation of radiologic findings with biologic inflammatory status were recorded.
Results: We have explored 31 patients, 11 patients at active phase and 20 at late phase of the disease. Vascular enhancement quality was at mean 3.8/4, with a mean DLP measured at 1257.3mGy.cm for a low dose protocol and at 3003mGY.cm for a standard protocol. Patients' classification was different according if we integrated or not vascular wall thickening to the anatomic modifications. Late double ring enhancement, blurring and densification of perivascular environment, also densification of the anterior mediastinal fat presented a significant statistic correlation with the biological inflammatory status (p<0.001).
Conclusion: Aortic angio-CT is a reliable and relevant technique with an acceptable irradiation dose in the evaluation of Takayasu disease.

B-1067 11:42

Abdominal large vessel vasculitis: diagnostic value of T1 3D mVISTA-MRI

S. Maurus[1], N.N. Sommer[1], H. Kooijman[2], E. Coppenrath[1], J. Bock[1], T. Saam[1], K.M. Treitl[1]; [1]*Munich/DE*, [2]*Hamburg/DE (karlamaria.treitl@med.uni-muenchen.de)*

Purpose: To assess the value of a high-resolution T1-3D black-blood TSE sequence for the diagnosis of abdominal large vessel vasculitis (aLVV).
Methods and Materials: The mono centric study included 20 patients (51.9 yrs.) with aLVV diagnosed according to the diagnostic reference standard and 17 controls (44.1 yrs.), who underwent a 3.0T MRI scan using a navigated T1-3D modified Volumetric Isotropic TSE Acquisition (T1-mVISTA) sequence with peripheral pulse-unit triggering and a segmented T1 3D turbo-field-echo sequence (T1-3D eThrive). Two radiologists analysed the abdominal aorta and its main branches for concentric contrast enhancement and wall thickening (CCE/CWT), image quality, flow artefact intensity and diagnostic confidence (IQ/FAI/DCL). T1-mVISTA findings were compared to T1-eThrive using accuracy parameters and inter-reader agreement. The average aortic wall thickness was analyzed in post contrast T1-mVISTA and compared for both groups.
Results: The scan time of T1-mVISTA was 4:10min. at an average heart rate of 80bpm. IQ was rated good to excellent in 91.5% of 282 evaluated segments with no or minor FAI present in 85.4%. The inter-observer reproducibility and the DCL for CCE and CWT were high (0.92/0.93; P<0.001; 3.54±0.52/3.50±0.63). The distribution of segmental inflammation in T1-mVISTA significantly correlated with T1-eThrive (CCE/CWT: k=0.740/0.702; P<0.001), resulting in a sensitivity of 87.8%, a specificity of 83.3%, an accuracy of 85.2%, positive and negative predictive value of 79.6% and 90.2%. The supra- and infrarenal aortic wall thickness significantly differed between both groups (3.60±0.65/3.04±0.85mm vs 2.32±0.44/2.18±0.44mm; P<0.001).
Conclusion: Navigated T1-mVISTA allows the detection of aLVV with a high IQ.

B-1068 11:50

Fibromuscular dysplasia of renal arteries: comparison of computed tomography angiography with digital subtraction angiography

E. Charpentier[1], F. Thony[2], E. Mousseaux[1], P.-F. PLOUIN[1], L. Boyer[3], A. Azarine[1]; [1]*Paris/FR*, [2]*Grenoble/FR*, [3]*Clermont-Ferrand/FR (etienne.charpentier88@gmail.com)*

Purpose: To evaluate the accuracy of computed tomography angiography [CTA] with submillimeter section slice compared to digital subtraction angiography [DSA] to diagnose and evaluate stenosis severity in patients with renal artery fibromuscular dysplasia [FMD].
Methods and Materials: Datasets from prospective study ARCADIA including 500 patients with FMD from November 2009 to December 2014, were analysed. A total of 43 patients [6 male and 37 women; mean age: 49 +/- 18 years; age range: 19-89 years] who underwent both renal artery CTA and DSA within 3 months without angioplasty prior to the CTA were included. For each artery, the angiographic phenotype, the stenosis severity were reviewed by 2 blinded radiologists for CTA and one radiologist for DSA. Stenosis severity greater-than-or-equal 70% was evaluated in terms of Se, Spe, PPV, NPV by comparing CTA results to DSA.
Results: DFM was diagnosed in 41/43 patients and 49/103 RA (48%), 67% multifocal, 33% unifocal. Among 41 FMD patients, 10 (24%) had bilateral FMD with multifocal FMD in 8/10 (80%). Interobserver agreement for the diagnosis of FMD using CTA was 0.84 with an overall Se 91% and 98,5% Spe compared to DSA. For stenosis greater-than-or-equal 70% Se, Spe, PPV & NPV of CTA were respectively 73%, 93%,62%,96% for the experimented and 55% ,94%, 60% and 93% for the junior radiologist.
Conclusion: CTA is an accurate tool for the diagnosis of FMD per patient with good reproducibility. DSA technique with selective catheterisation still remains the gold standard.

10:30 - 12:00 **Room Z**

Interventional Radiology

SS 1809

Vascular interventions

Moderators:
R.F. Dondelinger; Liège/BE
P.M. Kitrou; Patras/GR

K-24 10:30

Keynote lecture

E. Brountzos; *Athens/GR*

B-1069 10:39

Preoperative splenic artery embolisation in patients who underwent splenectomy for hypersplenism

M. Zaitoun, S.B. Elsayed, A.A. Elsammak, T. Rushdy; *Zagazig/EG (zaitoun2015@gmail.com)*

Purpose: To identify the role of preoperative splenic artery embolisation in reduction of blood transfusion after splenectomy and compare the results with splenectomy without prior embolisation in patients with hypersplenism
Methods and Materials: During 2 years, 100 consecutive patients with hypersplenism were divided into 2 groups; group (1) 50 patients with hypersplenism underwent preoperative splenic artery embolisation with Polyvinyl alcohol (PVA) and group (2) 50 patients with hypersplenism underwent splenectomy without prior splenic artery embolisation. Mean age was 35.6 years, 57 (57%) were males.
Results: Mortality rate was zero in both groups. Significant difference was detected between the two groups concerning the postoperative blood transfusion as there was no need for blood transfusion in group (1) in 100 % of patients as the platelets count rose from mean 8500 u/µl before the embolisation of the splenic artery to 70000 u/µl after embolisation of the splenic artery with PVA while 45 (90%) of the patients in group (2) received blood transfusion post-splenectomy.
Conclusion: Preoperative embolisation of the splenic artery in patients who undergo splenectomy for hypersplenism significantly reduces blood transfusion in comparison to splenectomy without prior embolisation. Preoperative SAE is a safe procedure with neither morbidity nor mortality.

B-1070 10:47

Percutaneous endovascular aortic repair (PEVAR) in the radiological suite: a paradigm shift?

R. Thomas, T. Kowald, B. Schmuck, O. Eldergash, M. Book, V. Dikov, P. Dohmen, A. Chavan; *Oldenburg/DE (kowald.tobias@klinikum-oldenburg.de)*

Purpose: To evaluate the efficacy of percutaneous femoral access closure in endovascular aortic repair (PEVAR) in the radiological angiography suite.
Methods and Materials: All patients undergoing percutaneous endovascular aortic repair (PEVAR) using the Prostar XL device from January 2010 to May 2016 were retrospectively analysed for incidence of complications and their relationship to various access site characteristics which included artery size, degree of vessel calcification, skin to artery distance and sheath to artery ratio.
Results: Indications for PEVAR in altogether 92 patients (142 access sites) included thoracic and abdominal aortic aneurysms and dissections. Mean follow-up was 32.39 ± 21.66 months. Introducer system sizes ranged from 12F to 25F. The endograft implantation was successful in 91 patients. Primary haemostasis was achieved in 97.1% (138/142) of the access sites. Four access sites (2.8 %) had to be closed surgically due to inadequate haemostasis; in all four cases the introducer systems was ≥18F. Late complications including inguinal / scrotal haematoma (n=8), wound infection

(n=1), pseudoaneurysm (n=4) and late bleeding (n=4), occurred in 17 access sites (11.9%), of which 13 were managed conservatively. On account of the low complication rate, no correlation between the evaluated variables and observed complications could be established.
Conclusion: PEVAR is feasible and safe irrespective of sheath size and nature of aorto-iliac pathology. The technical success rate is high and the incidence of complications is low. Failed haemostasis occurs most often with sheath sizes ≥ 18 F. The majority of late complications can be treated conservatively.

B-1071 10:55

Endovascular aneurysmal repair in octogenarians: is it justified?
V.M. Vishwanath[1], J. Soares[1], A. Burahee[2], S. Latif[3], R. Pathak[3];
[1]*Manchester/UK*, [2]*Birmingham/UK*, [3]*Dudley/UK*
(doctorveenavishwanath@gmail.com)

Purpose: The use of endovascular aneurysmal repair (EVAR) is favoured in the ageing population.[1] Despite the results of the recent EVAR II Trial showing survival advantage with intervention, further studies are needed to show the questionable survival advantage in patients with limited life expectancy.[2] In this study, we report an institution's experience with octogenarians undergoing EVAR over an 8 year period. We analysed mortality rate, complications, rate of re-intervention, outcomes on perioperative renal function and overall reduction in aneurysmal size.
Methods and Materials: All patients who had undergone EVAR for infrarenal aneurysms between 2006-2014 were identified using an electronic patient database. Patients were stratified by the age of 80 years and above. Demographics, comorbidities, imaging and perioperative blood results were analysed.
Results: Of 129 octogenarians, mean age was 84 years. Mean preoperative aneurysmal sac size was 6.35cm. Of 129 patients, 30 day mortality rate was 1.6%. We established 1 year mortality in 103 patients which was 7.8%. We established 2 year mortality in 70 patients which was 12.9%. The incidence of perioperative acute kidney injury was 3.9%. Mean reduction measured in postoperative aneurysmal sac size was 0.84cm.
Conclusion: This study shows a high success rate for EVARs in octogenarians with 87.1% surviving greater than 2 years and 3.1% rate of re-intervention. There is minimal effect on perioperative renal function and a good reduction in aneurysmal sac size. Factors relating to a short perioperative survival period were a significant number of co-morbidities (>3) and emergency repair.

B-1072 11:03

Importance of angiosome-targeted vascular bed identification using DSA and MR techniques for endovascular treatment in patients with critical limb ischaemia
A. Chahal, S. Sharma, P. Jagia, A. Dhar; *New Delhi/IN*
(anuragchahal18@gmail.com)

Purpose: Angiosome targeted vessel bed localisation by DSA, CEMRA (3 station bolus chase) and T-MRA (dedicated BTK time resolved CEMRA) in patients with Critical limb ischaemia.
Methods and Materials: 41 patients with 43 affected limbs with chronic CLI (Rutherford category IV-VI) underwent MRA on 1.5 T and Intra-Arterial DSA with additional T-MRA in 31 patients with BTK disease. Images obtained by each of the modalities were analysed by 2-blinded radiologists. Quality of MRA and T-MRA in BTK station was compared and accuracy of all modalities in localising the affected angiosome was assessed taking affected clinical angiosome as the gold standard.
Results: MRA had excellent sensitivity, 87.1% (95% CI 84-90%) and specificity, 98.04% (95% CI, 98.4-99.2%) taking DSA as gold standard. MRA was non-diagnostic in BTK station in 30% (13/43) limbs. Primary factors deteriorating quality of MRA were venous overlay in 19(44.2%) and motion artifact in 10(23.2%) limbs. Overall, quality of T-MRA was excellent in 22(70.9%), adequate for diagnosis in 8(25.8%) and non-diagnostic in only 1 (3.2%) limb by avoiding venous overlay or motion artifact. TMRA (87.9%, 93.5%) was able to detect 15.5 % more cases of ATA disease and 10.6 % more cases of PTA disease as compared to MRA alone (72.2%, 82.9%). Peroneal disease has poor accuracy (72.7-76.9%) for all the modalities probably due to multiple collaterals for this territory.
Conclusion: Dedicated BTK time resolved MRA proved to be an essential addition to the routine 3 station bolus chase MRA for angiosomal localisation in patients with critical limb ischaemia.
Author Disclosures:
A. Chahal: Research/Grant Support; ICMR for MD thesis grant.

B-1073 11:11

Single-centre experience of endovascular treatment of visceral artery aneurysms (VAAs) and pseudoaneurysms with Viabahn stent graft in 30 patients
M. Colombo, M. Venturini, P. Marra, M. Alparone, F. De Cobelli,
A. Del Maschio; *Milan/IT (colombo.michele@hsr.it)*

Purpose: In endovascular treatment of VAAs, covered stenting, when feasible, can be preferred to trans-catheter embolisation and considered first therapeutic option. Our aim was to retrospectively assess technical aspects, complications, technical/clinical success, mid-term follow-up of covered stenting with stent graft in 30 patients.
Methods and Materials: From 2000 to 2015, 30 patients affected by VAAs were treated with peripheral self-expandable stents. Following data were recorded: aneurysms vs pseudoaneurysms number, involved artery, emergent vs elective procedure, trans-femoral vs trans-axillary approach, one vs more than one stent, proximal vs middle vs distal position, and stent placement modality: remodelling the affected artery vs occluding the affected artery. Follow-up was based on clinical monitoring and contrast-enhanced MDCT. Complications, technical success and clinical success after the procedure and at 6 months were evaluated.
Results: 15 VAAs and 15 pseudoaneurysms (10 splenic, 8 hepatic, 6 renal, 5 gastroduodenal, 1 superior mesenteric arteries) were treated with stents. The procedures were performed via trans-femoral in 27 cases, via trans-axillary in 3 cases. Stents (one in 23 cases, more than one in 7 cases) were placed in proximal (n=15), middle (n=10), distal (n=5) position and remodelling the affected artery in 22 cases, occluding the affected artery in 8 cases. No complications were recorded. At mid-term technical and clinical success were and 91%, respectively.
Conclusion: Covered stenting is a safe and effective treatment for VAAs and VAPAs. In our experience, VSG showed high rates of technical and clinical success, especially in elective procedures, with good clinical outcome in terms of aneurysm exclusion.

B-1074 11:19

Clinical outcome of transarterial embolisation for postgastrectomy arterial bleeding
J. Yoon, K. Han, M.D. Kim, J.Y. Won, D.Y. Lee, G.M. Kim, J.H. Kwon,
S.H. Noh, W.J. Hyung; *Seoul/KR (jkyoon87@yuhs.ac)*

Purpose: To retrospectively investigate the feasibility and safety of transcatheter arterial embolisation in the management of postgastrectomy arterial bleeding.
Methods and Materials: Between January 2004 and July 2015, 13,246 patients underwent total or subtotal gastrectomy at our institution. 24 patients (18 men; mean age, 66.8 years; range, 42-80 years) received transcatheter arterial embolisation for postoperative arterial bleeding identified on angiography.
Results: Postgastrectomy arterial bleeding occurred after subtotal gastrectomy in 14 patients (58%) and after total gastrectomy in 10 patients (42%), after a mean of 17 days (range, 1-57 days). It manifested as luminal bleeding in 10 patients and as abdominal bleeding in 14 patients. Technical success was achieved in all 24 patients (100%). The clinical success rate was 79% (19/24); there were three transcatheter arterial embolisation-related major complications resulting in 30-day mortality (12%), one recurrent bleeding, and one persistent bleeding. The most common bleeding focus was the gastroduodenal artery (46%, 11 patients), followed by the splenic artery (29%, 7 patients). By surgery type, the gastroduodenal artery was the most common site of bleeding in subtotal gastrectomy (64%, 9/14) and the splenic artery in total gastrectomy (50%, 5/10).
Conclusion: Transcatheter arterial embolisation demonstrated high technical and clinical success rates with an acceptable complication rate in the management of postgastrectomy arterial bleeding. However, transcatheter arterial embolisation may not be the best treatment option in patients who underwent subtotal gastrectomy and bled from the splenic artery owing to the high risk of infarctions of the remnant stomach and the spleen.

B-1075 11:27

Stent graft implantation in visceral arteries in acute life-threatening haemorrhage after upper abdominal surgery: a single center experience
B.M. Schaarschmidt, C. Buchbender, J. Boos, P. Kröpil, F. Kröpil,
R.S. Lanzmann, G. Fürst, G. Antoch, C. Thomas; *Düsseldorf/DE*,

Purpose: Haemorrhage due to hepatic or mesenteric artery arrosion following pancreatic fistula and bile leakage ("sentinel bleed") is a rare but severe complication after pancreatic surgery. Endovascular management of these cases is challenging as it is necessary to preserve the blood supply of the upper abdominal organs. The purpose of this study was to evaluate technical success, complications and short-term outcome after implantation of endovascular stent grafts in these patients.

Methods and Materials: Twenty-nine consecutive patients (22 male, 7 female, mean age: 66.4y) that underwent stent graft implantation (Gore Viabahn®) after pancreatic (n=26) or hepatic (n=3) surgery between 2009 and 2016 were retrospectively analyzed. Explorative data analysis for technical success, complications and short-term survival after 30 days was performed.
Results: Initial technical success (stent graft placement, complete sealing and patent outflow) was obtained in 24 patients (83%), with a surgical conversion rate of 17% (n=5). Peri-interventional complications were observed in 6 patients (21%), including severe reversible vasospasms (n=4), aneurysm rupture (n=1) and reversible stent graft occlusion (n=1). In eleven patients stent-related complications (38%) occurred within the follow-up interval (recurrence of bleeding, n=7; stent thrombosis, n=4); access-related complications due to transbrachial access were observed in three patients (10%). Short-term survival was 72%, while eight patients died due to mulitorgan failure (n=4), fatal abdominal haemorrhage (n=2), sepsis and a cardiac event (n=1, respectively).
Conclusion: Emergency endovascular stent-graft implantation in patients with life-threatening upper abdominal bleeding after major abdominal surgery is feasible but prone to a high complication rate.

B-1076 11:35

Imipenem/cilastatin sodium (IPM/CS) as a temporary embolic agent for non-tumoural acute abdominal haemorrhage: our promising experience
J. Valcarcel, J. Joudanin, D. León, E. Alba, E. Escalante, Q. Ordi, A. Sotomayor, P. Naval; *Barcelona/ES (j.valcarcel89@gmail.com)*

Purpose: To evaluate IPM/CS effectiveness as a temporary embolic agent for abdominal bleeding of non-tumoural origin, and its safety in minimizing the risk of distal ischaemia.
Methods and Materials: In a 4 month period we performed 28 embolisations for abdominal haemorrhage of non-tumoural origin. 8 upper and 1 lower-gastrointestinal bleeding were embolised with IPM/CS. This agent was used in cases that required proximal large vessel embolisation, which comprises a high risk of distal ischaemia.An IPM/CS-isosmolar contrast mixture was used (1:1 dilution). IPM/CS was used alone in 3 cases, while a “sandwich” technique was performed in another 3, and in conjunction with proximal coiling in the rest. A retrospective study was performed, analysing technical success (angiographic cessation of bleeding) and clinical success (blood haemoglobin, blood transfusion needs within 7 days, and reintervention within 14 days).
Results: The technical success rate was 100%, with an angiographic cessation of bleeding in all cases. Clinical success was satisfactory, with an improvement/non-worsening of haemorrhagic parameters in 8. None of the cases required reintervention within 14 days. In three patients a computed tomography was performed for other reasons, and no rebleeding or signs of ischaemia were evident in any of them. In the follow-up no clinical and laboratory signs suggestive of ischaemia were objectified.
Conclusion: This study’s promising results, though preliminary, suggest the effectiveness and safety of intravascular embolisation with IPM/CS for abdominal haemorrhage. The authors consider this agent of great potential use in cases that require proximal embolisation, with high risk of tissue ischaemia.

B-1077 11:43

Dual contrast agent-based spectral photon-counting computed tomography for detection of endoleaks following EVAR
J. Dangelmaier[1], D. Bar-Ness[2], D. Münzel[1], H. Daerr[3], F. Pfeiffer[4], R. Proksa[3], E.J. Rummeny[1], P. Douek[2], P.B. Noël[1]; [1]*Munich/DE*, [2]*Bron/FR*, [3]*Hamburg/DE*, [4]*Garching/DE (julia.dangelmaier@gmx.de)*

Purpose: After endovascular aortic repair (EVAR) discrimination of leaking contrast media and calcifications of similar attenuation within the aneurysm sac is challenging and often requires multiple CT acquisitions. Dual contrast agent based spectral photon-counting CT may provide reliable detection of endoleaks with a single CT acquisition.
Methods and Materials: To experimentally evaluate the potential of spectral photon-counting computed tomography (SPCCT), an aortic phantom was in-house designed and produced. A centrally located stent lined compartment was filled with water as well as iodine and gadolinium mimicking enhanced blood within the aortic lumen. Representing the endoleak, adjacent compartments contained either one of the contrast agents or calcium chlorine to mimic calcifications. After data acquisition with a modified clinical base, small field-of-view SPCCT prototype scanner with multi-energy bins, material decomposition was performed to generate iodine, gadolinium and calcium maps.
Results: In a conventional CT slice, Hounsfield Units of the different compartments were similar ranging from about 145 HU up 170 HU. Material specific maps clearly differentiate the distributions, within the compartments filled with iodine, gadolinium or calcium.
Conclusion: A single dual contrast agent based spectral photon-counting CT scan may replace conventional CT scans in native, arterial and delayed phase to detect endoleaks of different flow rates without interference from existing calcifications after endovascular aortic repair. It is a unique feature of our method to capture different contrast media dynamics in a single scan. Additionally, a significant reduction of radiation exposure is enabled.
Author Disclosures:
H. Daerr: Employee; Philips GmbH, Innovative Technologies, Research Laboratories, Hamburg, Germany. **R. Proksa:** Employee; Philips GmbH, Innovative Technologies, Research Laboratories, Hamburg, Germany.

B-1078 11:51

Neointimal coverage in polymer coated stents with and without antiproliferating agent
W. Hundt, M. Burbelko, D. Jones, M. Kalinowski; *Marburg/DE (hundt@med.uni-marburg.de)*

Purpose: Investigation of the development of restenosis and neointimal coverage in passive coated stents compared to active and passive coated stents.
Methods and Materials: The passive coated stent (Camouflage®-Stent) is in clinical use, however no data exist using this stent with an active antiproliferative component. Arteriosclerotic plaques with stenosis were induced in the common iliac arteries of 10 rabbits by induction of endothelium lesions. Four weeks later, percutaneous intervention was performed by implanting a passive coated stent (Camouflage®-Stent) in one common iliac artery and an active and passive coated stent (Sirolimus+ Camouflage®-Stent) in the other. After further four weeks, the animals were euthanized and the vessels were removed. Microscopic evaluation of neointimal proliferation was performed and analysed statistically.
Results: The passive coated stents showed more neointimal proliferation (86.6±4.0 µm per section) than the active and passive coated stents (74.1±2.6 µm per section; p = 0.008). In both groups, a significant restenosis rate was noted at the stent edges and in the middle of the stent. In the active and passive covered stents naked stent struts were found in 26.8% and extended overgrowth in 3.3%. In the passive covered stents missing stent coverage and an extended overgrowth was seen in 41.6% and 11.6%, respectively .
Conclusion: The active and passive coated stents showed lesser induction of in-stent restenosis because of lesser intimal proliferation than the passive coated stents.

10:30 - 12:00 **Room O**

Chest

SS 1804

Are we ready for routine application of MRI of the lung?

Moderators:
P. Ciet; Rotterdam/NL
X. Montet; Geneva/CH

K-23 10:30

Keynote lecture
H.-U. Kauczor; *Heidelberg/DE*

B-1079 10:39

Pulmonary nodules: diagnostic accuracy of MRI
O. Solyanik, K. Hellbach, M. Bonert, D. Bondesson, T. Gaaß, N. Thäns, M.F. Reiser, J. Dinkel; *Munich/DE (olga_solyanik@hotmail.com)*

Purpose: To evaluate the sensitivity of modern MR sequences for the detection of pulmonary nodules using a dedicated porcine chest phantom.
Methods and Materials: Four porcine lungs containing a total of 131 variable sized nodules made of agar were inflated inside a phantom. Two three-dimensional (3D) gradient-echo (GRE) and one steady-state free precession (SSFP) MR sequences were acquired with optimised short TE (0.01-0.6ms). Spiral computed tomography served as the standard of reference. Two blinded readers (with 2 (reader 1) and 4 (reader 2) years experience in chest radiology) analysed the MR images independently and recorded the size and location of the nodules.
Results: Pulmonary nodules were divided into four groups depending on the nodules' size: A: 1.0-1.9 mm (n=57); B: 2.0-2.9 mm (n=50); C: 3.0-3.9 mm (n=14); D: 4.0-4.9 mm (n=10). Interobserver agreement was excellent (k=0.9) for D nodules with a sensitivity of 0.95 for SSFP sequence and 0.75 for GRE sequences. The interobserver agreement decreased (k=0.46) with smaller nodules. Reader 1 showed a sensitivity of 0.60 (all nodules), 0.58 (A), 0.56 (B), 0.67 (C) for SSFP sequence and of - 0.54 (all nodules), 0.50 (A), 0.53 (B), 0.60 (C), 0.65 (D) for 3D-GRE sequences. Reader 2 showed a sensitivity of 0.77 (all nodules), 0.70 (A), 0.83 (B), 0.71 (C) for SSFP sequence and - 0.65 (all nodules), 0.58 (A), 0.68 (B), 0.71 (C), 0.80 (D) for 3D-GRE sequences.

Conclusion: MRI showed a high to good sensitivity for the detection of pulmonary nodules depending on the readers' experience and nodule size. The SSFP sequence showed higher sensitivity than 3D-GRE sequences reaching sensitivity of 0.95 in nodules bigger than 4mm.

B-1080 10:47

Lung cancer screening with MRI compared to low-dose CT: initial results after one year of screening

M. Meier-Schroers[1], R. Homsi[1], D. Dabir[1], D. Kütting[1], A. Feißt[1], J. Gieseke[2], H.H. Schild[1], D. Thomas[1]; [1]*Bonn/DE*, [2]*Hamburg/DE*

Purpose: To evaluate the suitability of non-enhanced MRI for lung cancer screening.
Methods and Materials: 224 participants of a lung cancer screening program were examined with low-dose CT and MRI, both without contrast media. Acquired MRI sequences were T2w MultiVane XD, steady-state free precession, T1w GRE, and DWI with a maximum examination time of 20 minutes. MRI was analyzed regarding focal lesions blinded to CT. Lesions with a minimum size of 6 mm were assessed, since these require further investigation according to LungRADS criteria to determine their dignity. In these cases, participants underwent follow up after three or six months, PET/CT, biopsy, or surgery. The other participants were scheduled for regular controls after twelve months.
Results: By CT/MRI, the following lesions were detected: 17/16 lesions 6-7 mm, 12/12 lesions 8-14 mm, and 4/4 lesions ≥ 15 mm. Seven lesions were histologically confirmed carcinomas, five of them underwent curative resection. The 6 mm lesion missed by MRI was fat containing and located in between hypoventilated lung parenchyma. There was size discrepancy in two 7 mm lesions, which were measured as 8 respectively 9 mm on MRI. When only MRI had been available, these lesions would have been controlled after three instead of six months. Sensitivity/specificity of MRI was 94%/100% for 6-7 mm, and 100%/100% for ≥ 8 mm. There were no false-positive results for MRI concerning lesions ≥ 6 mm.
Conclusion: Non-enhanced MRI has very high sensitivity/specificity for lesions ≥ 6 mm and is therefore suitable for lung cancer screening.

B-1081 10:55

MRI detection of pulmonary nodules: comparison between true FISP and contrast-enhanced VIBE

S.B. Barlas, O.L. Ulusoy, S. Server, A. Öz, B. Koyuncu Sökmen, N. İnan, N.C. Balcı; *Istanbul/TR (sezgibarlas@gmail.com)*

Purpose: To evaluate the diagnostic performance of true FISP and contrast-enhanced VIBE (CE VIBE) sequences for the detection of pulmonary nodules.
Methods and Materials: Ninety patients with 300 pulmonary nodules (211 nodules were <5 mm; 89 nodules were ≥5 mm) diagnosed by CT underwent lung MRI. MRI examination were performed on 1.5 T scanner. CT and MRI data were analysed independently by two radiologists. The detection rate of pulmonary nodules was calculated for whole MRI and for individual MRI sequence. In addition, subgroup analysis have been done as <5 mm, ≥5mm and sensitivities of each sequences were calculated.
Results: The overall sensitivity of MRI for the detection of pulmonary nodules was 35.33% and according to nodule size: 21.80% for nodules <5 mm; 67.41% for nodules ≥5 mm. MRI sequences yielded following sensitivities according to nodul size: 12.79% (true FISP), 21.80% (CE VIBE) for nodules <5 mm; 44.94% (true FISP), 67.41% (CE VIBE) for nodules ≥5 mm.
Conclusion: Contrast-enhanced VIBE sequence is more sensitive for lung nodule detection than true FISP sequence.

B-1082 11:03

Non-contrast MR imaging of the lung: differentiation of infective and malignant lesions

S.N. Nagel, D. Kim, T. Penzkofer, I.G. Steffen, B. Hamm, S. Wyschkon, S. Schwartz, T. Elgeti; *Berlin/DE (thomas.elgeti@charite.de)*

Purpose: To investigate non-contrast MR imaging of the lung at 3T for characterisation of solid pulmonary lesions in immunocompromised patients to differentiate infectious from malignant findings.
Methods and Materials: 17 immunocompromised patients (11 infections, 6 lymphomas) and 12 immunocompetent patients (4 pneumonias, 8 solid tumours) were imaged using fast breath hold T2-weighted turbo spin echo sequences and T1-weighted gradient echo sequences at 3T. Signal intensities (SI) were measured in the lesion (L), chest wall muscle (M) and subcutaneous fat (F). A scaled signal intensity ratio was calculated using the mean T2 SI: ssiT2 = (SI_L - SI_M) / (SI_F - SI_M) * 100. Furthermore, the lesion SI in T1-weighted images was normalised against muscle SI. Wilcoxon's signed rank test and ROC analysis were used as statistical methods.
Results: Infectious pulmonary lesions showed a higher ssiT2 (40.1 [14.6-56.0] vs 20.9 [2.4-30.1], $p < 0.05$). T1-ratio differed significantly between infectious and malignant findings with higher values in the latter (0.85 [0.68-0.94] vs 0.93 [0.87-1.09], $p < 0.05$). The optimal cutoff value to differentiate infectious from malignant lesions was 43 for ssiT2 (YI 0.61, sensitivity 0.71, specificity 0.91). Combining ssiT2 and T1-ratio using binary regression increased sensitivity (YI 0.72, sensitivity 0.77, specificity 0.95).
Conclusion: ssiT2 allows differentiation of acute infectious from malignant pulmonary lesions with high specificity. Adding T1-ratio further increases overall performance, especially regarding sensitivity.
Author Disclosures:
B. Hamm: Research/Grant Support; 1. Abbott, 2. Actelion Pharmaceuticals, 3. Bayer Schering Pharma, 4. Bayer Vital, 5. BRACCO Group, 6. Bristol-Myers Squibb, 7. Charite research organisation GmbH, 8. Deutsche Krebshilfe, 9. Dt. Stiftu, für Herzforschung, 10.Essex Pharma, 11.EU Programmes, 12.Fibrex Medical Inc., 13.Focused Ultrasound Surgery Foundation 14.Fraunhofer Gesellschaft, 15. Guerbet, 16.INC Research, 17.InSightec Ud.,, 18.IPSEN Pharma, 19.Kendlel MorphoSys AG, 20. Lilly GmbH, 21. Lundbeck GmbH, 22. MeVis Medical Solutions AG, 23. Nexus Oncology, 24. Novartis, 25. Parexel CRO Service, 26. Perceptive, 27. Pfizer GmbH,, 28. Philipps, 29.Sanofis-Aventis S.A, 30. Siemens, 31.Spectranetics GmbH, 32.Terumo Medical Corporation, 33.TNS Healthcare GMbH, 34. Toshiba, 35. UCB Pharma, 36.Wyeth Pharm, 37.Zukunftsfond Berlin tsb, 38.Amgen, 39.AO Foundation, 40.BARD, 41. BBraun (Sponsoring eines Workshops) 42. Boehring Ingelheimer, 43. Brainsgate, 44. PPD (CRO), 45.CELLACT Pharma, 46.Celgene, 47.CeloNova BioSciences, 48.Covance, 49. DC Deviees, Ine. USA 50. Ganymed, 51. Gilead Scienees, 52. Glaxo Smith Kline 53.ICON (CRO) 54.Jansen, 55. LUX Bioseienees, 56. MedPass, 57. Merek, 58. Mologen, 59. Nuvisan, 60. Pluristem,, 62. Roehe, 63. Sehumaeher GmbH (Sponsoring eines Workshops) 64. Seattle Geneties, 65. Symphogen, 66. TauRx Therapeuties Ud., 67. Accovion, 68.AIO: Arbeitsgemeinschaft Internistische Onkologie, 69.ASR, 70. Astellas, 71. Theradex, 72. Galena Biopharma, 73. Chiltern 74.PRAint, 75.Inspiremd, 76. Medronic, 77. Respicardia, 78. Silena Therapeutics 79. Spectrum Pharmaceuticals, 80. St. Jude.

B-1083 11:11

Assessment of contrast-enhancement in the lung parenchyma using 3D ultra-fast steady-state free precession MRI

G. Sommer, O. Pusterla, M. Wiese, F. Santini, D. Lardinois, J. Bremerich, G. Bauman, O. Bieri; *Basle/CH (gregor.sommer@usb.ch)*

Purpose: To investigate the signal intensity enhancement in the lung parenchyma in 3D ufSSFP MRI after administration of gadolinium-based contrast agents in healthy subjects and patients with lung cancer and chronic obstructive pulmonary disease (COPD).
Methods and Materials: Eight healthy subjects and three patients with lung cancer and/or COPD underwent ufSSFP and VIBE imaging at 1.5 T before and 3 min after i.v. injection of Gadobenate-Dimeglumine. Quality of images and contrast enhancement (CE) maps was compared for the two sequences. In the patients, CE-mapping was set against recent ^{99m}Tc-MAA-SPECT/CT.
Results: The acquisitions were successful and provided diagnostic image quality in all subjects. The signal enhancement seen with 3D ufSSFP after contrast agent injection was significantly higher in the lung parenchyma (101%±8%) than in other tissues (fat: 2%±4%, muscle: 26%±6%, liver: 33%±9%) and in the blood pool (83%±9%). The relative signal enhancement of the lung parenchyma seen after contrast agent injection was more than twice as high for ufSSFP than for VIBE (47%±13%) providing homogeneous CE-maps of the lung parenchyma in all healthy subjects. The CE-maps acquired in the three patients showed characteristic changes due to the underlying diseases. There was good visual agreement between ufSSFP-based CE-mapping and SPECT/CT.
Conclusion: 3D ufSSFP CE-mapping allows for a selective depiction of the contrast enhancement in the lung parenchyma. The method is feasible in healthy subjects and in lung cancer and COPD patients. It may be used as a simple, fast and radiation-free alternative to lung perfusion SPECT/CT for patients with pulmonary perfusion abnormalities.

B-1084 11:19

Self-gated non-contrast-enhanced functional lung (SENCEFUL) MRI for quantitative ventilation assessment in patients with cystic fibrosis

S. Veldhoen[1], A. Weng[1], A.S. Kunz[1], D. Stäb[2], C. Wirth[1], H.U. Hebestreit[1], U. Malzahn[1], H. Köstler[1], T.A. Bley[1]; [1]*Würzburg/DE*, [2]*Brisbande/AU (veldhoen_s@ukw.de)*

Purpose: To assess the clinical feasibility of SElf-gated Non-Contrast-Enhanced FUnctional Lung (SENCEFUL) MRI for quantitative ventilation imaging in patients with cystic fibrosis (CF).
Methods and Materials: Twenty patients with CF and 20 matched healthy volunteers underwent unenhanced functional 1.5-T lung MRI in free-breathing using the SENCEFUL approach. The lungs were manually segmented from ventilation-weighted images to obtain quantitative ventilation (QV) measurements, which were compared between groups. QV values of the patients were correlated with results of pulmonary function testing. Three radiologists rated the functional images for presence of ventilation deficits.

Results: QV of the lungs was lower for CF patients (0.09 vs. 0.11 ml/ml, p<0.01). QV ratios of upper to lower lung quadrants were lower in CF patients expressing less ventilation of upper parts (right, 0.84 vs. 1.16, p<0.001; left, 0.88 vs. 1.11, p=0.02). Accordingly, ventilation differences between the groups were larger in the upper quadrants (mean difference, 0.04 ml/ml,p<0.01). Mean breathing frequency was higher in CF patients with 20 respiratory cycles per minute vs. 16 in the controls (p<0.01). QV values of CF patients correlated with vital capacity (r=0.7, p=0.01), residual volume (marker for static hyperinflation, r =-0.8, p<0.01) and FEV1 (marker for airway obstruction, r=0.7,p=0.02). A pattern of widely distributed small ventilation deficits was found in 40% of the patients vs. 8% of the volunteers (p<0.001).
Conclusion: SENCEFUL-MRI is feasible for contrast-free quantitative ventilation assessment. CF patients show less ventilation of upper lung parts and lower overall QV values, which correlate with vital capacity and with markers for hyperinflation and airway obstruction.
Author Disclosures:
S. Veldhoen: Grant Recipient; Interdisciplinary Center of Clinical Science at the University of Würzburg (Z-3/45)., Universitätsbund Würzburg (14-14).
H. Köstler: Grant Recipient; Siemens Healthcare. **T.A. Bley:** Consultant; GSK, MSK. Equipment Support Recipient; Noras, Rapid. Grant Recipient; Deutsche Forschungsgemeinschaft. Speaker; Bayer, Bracco, Guerbet, GE, Siemens, and HeartFlow.

B-1085 11:27

SENCEFUL MRI for detection of lung perfusion deficits in CF patients
A.S. Kunz, A.M. Weng, C. Wirth, C. Kestler, F. Segerer, H. Hebestreit, H. Köstler, T.A. Bley, S. Veldhoen; *Würzburg/DE (kunz_a@ukw.de)*

Purpose: To identify lung perfusion deficits in CF-patients using SElf-gated non-contrast-enhanced functional lung (SENCEFUL)-MRI.
Methods and Materials: Unenhanced Fourier decomposition-based SENCEFUL-MRI at 1.5T was performed in free breathing on 38 participants, i.e. 19 patients with known Cystic Fibrosis (CF) and 19 healthy volunteers. Color-coded lung maps indicating semiquantitative lung perfusion and lung perfusion phase (i.e. temporal pulmonary distribution of blood flow) were reconstructed. Four readers blinded to all clinical aspects rated 1644 coronal lung maps (10 mm slice thickness). Lungs in each map were rated per quadrant using a 4-point Likert scale (1=healthy, 2=defect <25% quadrant area, 3=defect <50% quadrant area, 4=defect >50% quadrant area). Readers rated perfusion and phase maps separately followed by simultaneous assessment thereof. Phase data was plotted in histograms with subsequent Gaussian fit. Peak-to-offset ratio was determined as the maximum of the fitted curve divided by the mean outer 10%. Ratios were compared between groups and to the reader's scoring.
Results: In perfusion maps, readers attributed pathological/conspicuous scores to 25.3% of quadrants (controls) vs 56.5% (CF-patients;p<0.05). Phase maps were rated conspicuous in 20.9% vs 56.1% (p<0.05). Simultaneous assessment was scored with 15.1% vs 53.6% (p<0.05). ICC-analysis for Inter-Reader-Agreement regarding the 4-point scale showed excellent agreement (perfusion: 0.851, phase: 0.805, combined: 0.822). Objective assessment of peak-to-offset ratios showed a median of 63.8 in controls vs 15.3 in CF-patients (p<0.05).
Conclusion: SENCEFUL-MRI detects impairments of lung perfusion and phase distribution with good spatial resolution. Analysis revealed distinct differences between CF-patients and controls, plausibly attributed to Euler-Liljestrand-Mechanism/hypoxic vasoconstriction.
Author Disclosures:
H. Köstler: Grant Recipient; Siemens Healthcare. **T.A. Bley:** Consultant; GSK, MSK. Equipment Support Recipient; Noras, Rapid. Grant Recipient; Deutsche Forschungsgemeinschaft. Speaker; Bayer, Bracco, Guerbet, GE, Siemens, and HertFlow. **S. Veldhoen:** Grant Recipient; Interdisciplinary Center of Clinical Science at the University of Würzburg (Z-3/45)., Universitätsbund Würzburg (14-14).

B-1086 11:35

Non-contrast enhanced ventilation and perfusion magnetic resonance imaging in early cystic fibrosis lung disease
M.O. Wielpütz[1], S. Gehlen[1], P. Leutz[1], M.U. Puderbach[1], M. Eichinger[1], Y. Ohno[2], G. Bauman[3], H.-U. Kauczor[1], M.A. Mall[1]; [1]*Heidelberg/DE*, [2]*Kobe/JP*, [3]*Basle/CH (mark.wielpuetz@me.com)*

Purpose: Previous studies demonstrated that morpho-functional magnetic resonance imaging (MRI) detects structural and perfusion abnormalities in lungs of cystic fibrosis (CF) patients. With the present study we evaluate Fourier decomposition (FD-)MRI to detect ventilation and perfusion defects in infants and preschool children with CF without the need for exogenous contrast materials.
Methods and Materials: In total, 30 children with CF (age 1.8±2.0y range 0-6y at first exam) contributed 85 MRI studies. Balanced steady-state free-precession imaging was performed in free breathing in three coronary slices through the central lung for FD-MRI, in addition to a standardized T1- and T2-weighted protocol including contrast-enhanced perfusion imaging. For FD-MRI lungs were segmented manually, and percent of ventilation and perfusion defects calculated by custom software. The remaining MRI protocol was assessed using the MRI score as previously evaluated.
Results: Ventilation-weighted images could be generated from 81 (95%) and perfusion-weighted images from all 85 (100%) datasets. Ventilation correlated substantially with perfusion defects (r=0.67, p<0.001). Mean ventilation and perfusion defects tended to be higher in older patients with 20.8±9.7% and 26.8±3.3% at 6y compared to 10.9±6.9% and 21.6±4.4% in newborns, respectively. Ventilation defects moderately correlated with overall disease severity documented by the MRI score (r=0.56, p<0.001), but perfusion defects did not (r=0.21).
Conclusion: FD-MRI is feasible and detects ventilation and perfusion defects already in newborns, infants and preschool children with CF. These results support the development of FD-MRI for non-invasive functional lung imaging in this age group, and may render application of exogenous contrast materials unnecessary.
Author Disclosures:
M.O. Wielpütz: Advisory Board; Boehringer Ingelheim.

B-1087 11:43

MR imaging of airway mucus contrasts as a tool to diagnose allergic bronchopulmonary aspergillosis in cystic fibrosis
G. Dournes, J. Refait, A. Rispal, F. Laurent; *Bordeaux/FR (snek60@gmail.com)*

Purpose: Allergic broncho-pulmonary aspergillosis (ABPA) is a fungal complication of cystic fibrosis (CF) associated with acute and chronic respiratory function loss that requires specific antifungal therapy. We hypothesised that MR characterisation of mucus contrasts could diagnose ABPA in CF and be a tool for treatment response.
Methods and Materials: The study was approved by the local Ethic Committee and all patients gave written informed consent. 110 consecutive CF patients were screened between January 2014 and July 2015 were included. All patients underwent a non-contrast-enhanced MR protocol including routine T1-weighted and T2-weighted sequences. The presence of mucus of both high T1 and low T2 signal, that we call the IMIS (Inverted Mucoid Impaction Signal) sign was qualitatively and quantitatively assessed by 2 physicians blinded from any other data. The Gold Standard to diagnose ABPA was the Cystic Fibrosis Foundation Consensus Conference criteria. ABPA status was followed-up during 1 year.
Results: 108 CF patients were included, 18 with and 90 without ABPA. At lobar scale, inter and intra-reader reproducibility was excellent (kappa>0.90). IMIS had a 94% [73;99] sensitivity and 100% specificity [96;100] to diagnose ABPA. After 3-months of specific ABPA treatment, complete resolution of IMIS was observed in ABPA patients and was significantly correlated with a decrease in total IgE blood levels (rho=0.47;p=0.04).
Conclusion: IMIS sign appeared both highly specific and sensitive to diagnose ABPA in CF. Allergic fungal inflammation induces characteristic modifications of mucus properties which are quickly and easily assessable using a non-invasive, contrast-free and radiation-free chest MRI.

B-1088 11:51

MR pulmonary angiography: can it be used as an alternative to CT angiography in diagnosis of major pulmonary thrombosis
A.M. Osman, E.H. Abdeldayem, N.M. Osman; *Cairo/EG (DR_osman80@yahoo.com)*

Purpose: A comparative study between the non-contrast magnetic resonance pulmonary angiography and the computed tomography angiography in diagnosis of pulmonary embolism.
Methods and Materials: Fifty patients were included in our study. All patients admitted and/or referred to Chest Department with moderate to high clinical suspicious of pulmonary embolism. All patients underwent CT angiography and non contrast MR pulmonary angiography in the same day or within two consecutive days after written consents. The radiological examinations were interpreted by two different radiologists. The results were compared and statistically analyzed.
Results: The mean age of the selected patients was about 55 years old. Thirty one cases showed positive pulmonary embolism in both MR and CT. Four cases showed positive pulmonary embolism only in CT with two cases showed positive pulmonary embolism only in MR. The rest of cases showed negative results in both. The sensitivity of non contrast MR angiography was 88.5% with 86.6% specificity. The sensitivity and specificity also calculated per vessel and was 87.2% and 99.3% respectively.
Conclusion: The non-contrast MR pulmonary angiography has a reasonable sensitivity and specificity in diagnosis of pulmonary embolism especially in major branches. So, it can be used as an alternative to the CT angiography especially when the use of CT and gadolinium are contraindicated.

10:30 - 12:00 **Room N**

Genitourinary

SS 1807

Female urogenital system - uterus: imaging and intervention

Moderators:
M.-F. Bellin; Le Kremlin-Bicêtre/FR
M. Horta; Lisbon/PT

B-1089 10:30

Comprehensiveness of EHSRGE/ESGE classification of female genital tract anomalies: systematic review of cases by MRI

P. Yadav; *Pune/IN (yadavpratiksha@hotmail.com)*

Purpose: To find the comprehensiveness of the EHSRGE/ESGE classification in uterovaginal congenital anomalies on MR imaging. Comparison of the EHSRGE/ESGE classification with AFS classification in systematic review of cases.
Methods and Materials: Retrospective study included the 45 cases of congenital anomalies of female genital tract,detected on MRI pelvis.MRI performed on 1.5 Tesla Siemen's Avonto). Images were observed to evaluate the uterine contour,endometrium and vagina.Each case was classify according to AFS as well as EHSRGE /ESGE.
Results: Study included 45 cases of the uterovaginal anomalies.Observation of the uteus, cervix and vagina done on MR imaging.Uterus was the most frequently involved organ in 82% followed by cervix (20%) and vagina (17.7%). Single organ anomalies seen in 57.8% cases and multiple organ,complex anomalies in 42.2% cases. Ipsilateral renal agenesis seen in 8.8% cases and contralateral in 1 case.There was no separate class in the AFS for the bicornuate uterus with septum,in ESHRE/ESGE it is classified as U3c.One case of duplication vagina with agenesis of uterus and cervix can not be classified in any of the class in the AFS,in ESHRE/ESGE it is classified class VI.
Conclusion: Uterovaginal congenital anomalies can involve single or multiple organ. AFS classification has limitation in systematic categorization of uterovaginal anomalies EHSRGE system may provide an effective and comprehensive categorization of uterovaginal anomalies,with cervix and vaginal anomalies in the subclasses.ESHRGE system may overcome the limitation of the AFS in classification.It includes a separate class VI for few complex uterovaginal anomalies,subtle changes,duplication defects and ectopic mullerian tissue,which was not in the AFS classification.

B-1090 10:38

Evaluation of Mayer-Rokitansky-Küster-Hauser syndrome with magnetic resonance imaging: variable findings of uterine remnants, ovaries and related clinical settings

Y. Wang, J. Lu, L. Zhu, B. Jiang; *Beijing/CN (yuewang9203@sina.com)*

Purpose: To summarise the magnetic resonance imaging (MRI) features of Mayer-Rokitansky-Küster-Hauser (MRKH) syndrome.
Methods and Materials: Eighty-one females with MRKH syndrome consecutively attended our institution between July 2014 and Aug 2016 and all underwent MRI of the pelvic cavity. One case was excluded for poor image quality; images of the rest 80 cases were retrospectively reviewed by two experienced gynaecological radiologists in consensus. Characteristics including the volume of uterine remnants, endometrium, haematometra, ovarian location and endometriosis were assessed. Basic demographic and clinical information were acquired by reviewing electronic records. The Chi-square and U tests were used to test for differences.
Results: The unilateral uterine rudiments were significantly larger (68.4±19.0ml vs 6.5±3.2ml, P=0.000) than those in patients with bilateral uterine rudiments. And the incidence of endometrium (100% vs 21%, P=0.000), haematometra (64% vs 2%, P=0.000), ovarian endometriosis (43% vs 2%, P=0.000) were significantly higher in patients with unilateral rudimentary uterus as compared with those who showed bilateral uterine rudiments.Twenty-six patients (33%) showed abnormally located ovaries. Abdomen pain was more common (P=0.000) in patients with unilateral rudimentary uterus (64%) as compared with those who had no (12%) or bilateral uterine remnants (16%).
Conclusion: Unilateral rudimentary uteri were more voluble. The incidence of endometrium, haematometra and ovarian endometriosis were significantly increased in patients with unilateral uterine remnants. Pelvic pain was more common in patients with unilateral rudimentary uterus. Ectopic ovary was not rare. Knowledge of such disparities can facilitate the adjuvant diagnosis and subsequent optimal treatment option.

B-1091 10:46

3D and 2D ultrasound-based foetal weight estimation a single center experience

M.F. Farghaly Amin, L.A.M.S. Mohsen; *Minya/EG (dr.laila.adel77@gmail.com)*

Purpose: To evaluate two new 3D and two new 2D ultrasound formulae for foetal weight estimation against the modified Hadlock formula and compare their estimation to the actual foetal weight.
Methods and Materials: Fifty pregnant females were included. Inclusion criteria: singleton pregnancy, within five days of delivery and normal or IUGR pregnancy. 3D evaluation of the foetal thigh and arm was done to calculate mid-thigh and mid-arm volumes. The actual foetal weight was recorded at delivery and compared to the estimated weights.
Results: Modified Hadlock formula had higher accuracy, whereas fractional limb volume method had higher precision. Systematic errors for the modified Hadlock formula, Model 6 of fractional limb volume and the original mid-thigh soft tissue thickness methods were 2.3%, 4.8% and 11%, respectively, whereas the random errors were 7.7%, 6.2% and 13.8%, respectively. The percentage of cases estimated within 5%, 10% and 15% of actual foetal weight were 48%, 86%and 92%, respectively, for the modified Hadlock method, whereas for the fractional limb volume method, these were 40%, 78% and 98%, respectively.
Conclusion: Fractional limb volume method is a very promising method for foetal weight estimation. Its performance is not significantly different from the modified Hadlock method.

B-1092 10:54

Assessment of endothelial function in postpartum preeclamptic women using flow mediated dilation of brachial artery

P. Tripathy, M. Sahu, M. Singh, P. Mishra, J. Mohanty; *Cuttack/IN (dr.priyadarshini.tripathy@gmail.com)*

Purpose: Preeclampsia is associated with inflammation and dysfunction of the maternal vascular endothelium. However, it is unclear whether this problem persists postpartum, and whether it also predisposes patients to increased cardiovascular risk. Hence, we aimed to compare the vascular profile of postpartum preeclamptic women with that of normal postpartum women.
Methods and Materials: Forty-five women with previous preeclampsia and 40 age-matched normotensive controls were enrolled in this study, all within 6 months to 2 years postpartum status. The brachial artery was identified though colour Doppler in cubital fossa, and its baseline diameter was measured. It was occluded for 5 minutes with an inflated cuff, and a measurement was repeated 1 minute after initial occlusion. Flow mediated dilation (FMD) of the brachial artery was calculated as a diameter percentage change after baseline occlusion. We determined ambulatory blood pressure measurement (ABPM) and serum high sensitivity C-reactive protein (hs-CRP) levels. Parameters were compared across groups, adjusting for potential confounders.
Results: FMD was significantly reduced in women with preeclampsia compared to controls (3.47±6% versus 8.75±6%; $p < 0.05$). Serum hs-CRP levels were slightly higher in the preeclamptic group than controls, while ABPM showed higher mean arterial blood pressures in the preeclamptic group than controls (98±7 mmHg versus 91±4 mmHg, $p < 0.05$).
Conclusion: Endothelial dysfunction in women with previous preeclampsia is persistent for up to 2 years postpartum. As a result, brachial artery FMD might be a useful noninvasive tool to assess the risk of future vascular disease in postpartum preeclamptic women.

B-1093 11:02

MRI evaluation of invasive placentation in high-risk patients: accuracy and reproducibility in comparison with the reference standard

F. Monelli, F. Fiocchi, G. Besutti, A. Pecchi, E. Petrella, E. Bertucci, F. Fachinetti, P. Torricelli; *Modena/IT (mofilippo@hotmail.it)*

Purpose: The aim of this study was to assess accuracy and reproducibility of MRI in the diagnosis of invasive placentation (IP) in high risk patients, using histologic findings or clinical evaluation as the reference standard.
Methods and Materials: Sixteen patients with placenta previa and other risk factors for IP (mean age 36 yrs, 62.5% with previous uterine surgery) underwent 1.5 T MR examination including T2-weighted Turbo-Spin-Echo, Balanced Turbo-Field-Echo and THRIVE sequences acquired on the three uterine planes. Images were reviewed by two readers, who evaluated specific MRI signs of IP. The reference standard was histology in 7 patients who underwent hysterectomy, and clinical diagnosis in the remaining 9 patients. Sensitivity and specificity of MRI findings were calculated, reproducibility was estimated by using Cohen's K test.
Results: The prevalence of IP was 56.25%, placenta percreta was found in two patients (12.5%). MRI had sensitivity and specificity of 100% and 85.7%, respectively. MRI findings with higher sensitivity were placental heterogeneity (PH), uterine bulging, dark intraplacental bands (DIB), myometrial interruption (MI), and thinning of the uterine-placental interface; those with higher

specificity were uterine scarring from previous caesarean delivery (US), PH, MI and tenting of the bladder wall. MRI reproducibility was high (K=1); US, DIB, and MI were the most reproducible MRI findings.
Conclusion: MRI is an accurate and reproducible tool in the evaluation of IP. Placental heterogeneity and myometrial interruption are the most accurate MRI findings.

B-1094 11:10

Quantitative and qualitative analysis of DWI of gestational trophoblastic disease: can it predict progression of molar pregnancy to persistent disease?

F. Hosseini; *Shiraz/IR (f.hoseini88@gmail.com)*

Purpose: To describe diffusion-weighted imaging (DWI) appearance of gestational trophoblastic disease (GTD) and to determine and compare apparent diffusion coefficient (ADC) values of hydatidiform mole (HM), persistent trophoblastic neoplasia and non-molar early pregnancy bleeding.
Methods and Materials: During a period of 6 months, women with preliminary diagnosis of GTD based on ultrasound and ßhCG levels underwent 1.5T MRI (T2 high resolution and DWI; b values 50,400,800; sagittal and perpendicular to endometrium, and T1, T2 Turbo Spin Echo (TSE) axial images). Patients underwent 6-12 months follow-up for progression to persistent form of disease. ADC values and image characteristics were compared between HM and persistent neoplasia and also between GTD and non molar pregnancy using Mann Whitney U and Fissure`s exact tests respectively.
Results: among 23 patients, 19 (83%) were classified as molar and 5(17%) as non-molar base on pathology reports. After 6-12 months follow up 5 (26%) cases progressed to persistent disease and 14(74%) were benign HM. There was no significant difference between ADC values of HM and persistent neoplasia, ($1.93\pm0.33*10^{-3}$ mm²/sec) and ($2.03\pm0.28*10^{-3}$ mm²/sec) respectively (P=0.69). ADC of non molar pregnancy was ($0.96\pm0.46*10^{-3}$ mm²/sec) with significant difference with GTD ($1.96\pm0.32*10^{-3}$ mm²/sec) (p=0.001). Heterogeneous snowstorm appearance, focal intratumoural haemorrhage, myometrial contraction and prominent myometrial vascularity were more common in GTD compared to non-molar pregnancy ($p<0.05$).
Conclusion: Heterogeneous snowstorm appearance, focal intratumoural haemorrhage, myometrial contraction and prominent myometrial vascularity are imaging characteristics of GTD. We cannot use ADC values to predict progression to persistent disease.
Author Disclosures:
F. Hosseini: Author; Sepideh Sefidbakht, Bijan Bijan, Bahareh Hamedi, Tayyebeh Azizi. Speaker; Fatemeh Hosseini.

B-1095 11:18

The added value of DWI for appreciating the degree of placental invasion of the myometrum: do the results depend on observer's experience?

D. Costachescu, D. Malita; *Timişoara/RO (dan_costachescu@yahoo.com)*

Purpose: To evaluate the added value of DWI in the diagnosis of placental invasion of the myometrium as well as the depth of invasion both for senior radiologists as well as junior radiologists.
Methods and Materials: We included 21 pregnant women investigated by prenatal MRI (T1, T2 and DWI sequences without i.v. contrast); among them 12 had histopathologically proven placental invasion and 9 women without placental invasion used as control group.Two senior and two junior radiologists blindly and independently reviewed MR-examinations in two separate reporting sessions indicating the presence and degree of placental invasion (placenta increta, accreta or percreta). In the first session only T1 and T2 sequences were evaluated, while in the second session DWI sequence was also evaluated among T1 and T2.For each reader the sensibility, specificity, and receiver operating curve (ROC) were calculated for both of the two reporting sessions.
Results: Sensitivity and specificity for placental invasion without the DWI sequence was 86.9% and 74% for seniors and 72.8% and 61.8% for juniors, respectively. In the second reporting session which included DWI sequence the sensitivity and specificity where improved, both for the Seniors (92,3%/85,6%) and juniors alike (91,2%/83,2%). Seniors detected placental invasion and depth of infiltration with significantly higher diagnostic certitude than juniors ($p = 0.0010$ and $p = 0.0262$, respectively). The use of DWI significantly reduced the diagnostic discrepancies between seniors and juniors.
Conclusion: DWI can clearly define the border between the placenta and myometrium making it an excellent tool in the assessment of placental invasion of the myometrium.

B-1096 11:26

Contribution of diffusion-weighted MRI to conventional MRI in ovarian torsion: a prospective study for the detection of haemorrhagic infarction

O. Ozdemir, Y. Metin, N. Orhan Metin, M. Kadioğlu, E. Zengin, Ö. Şahin; *Rize/TR (droguzrad@hotmail.com)*

Purpose: The objective of this study was to assess the role of DWI in differentiation haemorrhagic ovary infarction from non-haemorrhagic one. To our knowledge, this is the first prospective study regarding preoperative DWI diagnosis of haemorrhagic infarction in ovary torsion.
Methods and Materials: For this prospectively designed study, of 117 female patients who presented with acute lower quadrant pain and underwent MRI for suspicion of ovary torsion, results of only 29 patients (mean age, 24.7; SD, ±5.7; age range, 18-37), with surgical and pathological confirmation of adnexial torsion, were included to the study. All patients underwent DWI after conventional MRI. Quantitative and qualitative analysis of both the torsed and contralateral normal ovary were performed. Results of conventional MRI and DWI were noted.
Results: At operation 15 patients were found to have haemorrhagic infarction while 14 had non-haemorrhagic infarction. Of the 29 patients, 16 torsed ovaries could be salvaged in a viable state. We found statistically significant correlation of the ADC values, between haemorrhagic and non-haemorrhagic ovary infarction. The ADC values were significantly lower in patients with haemorrhagic infarction than non-haemorrhagic ones ($p<0.001$). Using an ADC threshold of 1.27, the sensitivity of DWI for haemorrhagic infarction was 0.93 and specificity 0.85.
Conclusion: DWI may be used with a significant success for the preoperative diagnosis of haemorrhagic infarction. This may be useful for preemptive surgery in preserving ovarian viability.

B-1097 11:34

Endometriosis as an underestimated foe: can MRI help?

W.R.A. Abdel Hamid, Y. Abbas; *Cairo/EG (w.gforever@yahoo.com)*

Purpose: The current days have shown an increased concern about endometriosis attributed to its significant morbidity rates. Our study aims to assess the ability of MRI to detect solid endometriotic implants and verify active from quiescent lesions.
Methods and Materials: 30 female patients with clinically proven endometriosis were included in this study to verify their endometriotic load through a dedicated MR protocol covering the lower abdomen and pelvis (including T1W images with and without fat suppression, T2W images, DWI (diffusion-weighted Images), IVIM (intravoxel incoherent motion) and T1W post-contrast images with fat suppression) followed by laparoscopic correlation.
Results: In these 30 patients, 108 lesions were detected including 18 ovarian endometriomas, 37 lesions at uterosacral ligaments, 22 parametrial lesions, 3 mural bladder lesions (2 serosal and 1 full thickness mural involvement), 4 serosal bowel lining lesions, 13 anterior abdominal wall serosal lining lesions, 3 vesicovaginal pouch lesions and 8 uterine serosal lining lesions. MR results were correlated with laparoscopic results with a sensitivity of 95.29%, specificity of 75%, PPV 93.1% and NPV 81.8%.
Conclusion: Preliminary results have revealed a promising role of DWI and IVIM as an asset in the detection of solid endometriotic implants and furthermore differentiating between active and quiescent lesions with which we can reliably exclude contrast reducing both time and cost of the MR studies together with acting as a road map to point out lesions and highlight blind spots for laparoscopic planning.

B-1098 11:42

Rectal and vaginal opacification MRI in the diagnosis of deep pelvic endometriosis

C. Saracin, D. Malita, F. Birsasteanu, D. Costachescu; *Timişoara/RO (oana.cristina.voicu@gmail.com)*

Purpose: The paper's objective was to establish the sensitivity of MRI using vaginal and rectal opacification with ultrasound gel in the detection of deep pelvic endometriosis as well as to appreciate the need of an experienced radiologist for reporting this pathology.
Methods and Materials: Prospective, single-centre study. All patients with symptoms of endometriosis were included. Axial T2-weighted imaging was performed before and after gel opacification of the vaginum and rectum. Four blinded radiologists (2 experienced and 2 unexperienced) reported the images. MRI performance was evaluated without vaginal and rectal opacification (C-) and with opacification (C+) by calculating sensitivity, specificity and both positive and negative predictive values.
Results: Sensitivity and specificity for C- and C+ scans were calculated for all the 4 reviewers.Sensitivity and specificity increased after opacification for all the reviewers ($p<0.0001$). Although before opacification there was a significant difference between the experienced and unexperienced readers, after

opacification, there were no notable differences between readers.The interpretation time for all of the 4 reviewers was calculated for each scan. The mean reporting time without opacification dropped from 8.8 minutes to 6.9 minutes when the rectum and vaginum were opacified. Moreover, the mean reporting time between the experienced and unexperienced radiologists became almost equivalent.
Conclusion: Our study was intended to evaluate the use of ultrasound gel to opacify the rectum and vaginum in diagnosing deep pelvic endometriosis.The results show that this technique is generally accepted by patients, the sensitivity and specificity are extremely high and the differences in reporting between experienced and unexperienced radiologists are almost none.

B-1099 11:50

Uro colon CT in the diagnosis of pelvic deep infiltrating endometriosis
S. Zanardi, F. Coppola, D. Papadopoulos, D. Valerio, A. Di Vincenzo, L. Zannoni, R. Seracchioli, R. Golfieri; *Bologna/IT (sara.zanardi10@gmail.com)*

Purpose: To evaluate the diagnostic accuracy (DA) of the uro-colon-CT (U-CCT) with dose-reduction dedicated protocol in preoperative study of deep infiltrating endometriosis of the anterior and posterior compartments (aDIE and/or pDIE).
Methods and Materials: 73 patients with clinical suspicion of aDIE and/or pDIE were analysed retrospectively, undergone U-CCT between January 2012 and December 2014 before laparoscopic surgery, and imaging data were compared with the surgical and histological reports. We calculated sensitivity, specificity, PPV, NPV of U-CCT and evaluated the utility of this technique to select patients who need a more detailed presurgical planning.
Results: 74 surgical interventions were performed on 73 patients (one patient was exposed to surgery twice due to DIE relapse after two years). In 4/74 surgical interventions U-CCT with dose-reduction dedicated protocol was negative for DIE. The urologists were properly involved when DIE nodules concerning ureters and bladder (p=0,042); The colorectal surgeons were more often involved when DIE nodules concerning sigmoid colon, particularly in case of bowel stenosis >50% (p=0,031%). U-CCT attested better results in the evaluation of DIE nodules involving digestive tract (DA 81%; p=0,000) and bladder (DA 87,8%; p=0,000).
Conclusion: U-CCT with dose-reduction dedicated protocol proved to be a valid alternative to barium-enema x-ray and urography or in absence of MRI with targeted protocol, to elaborate a detailed presurgical planning in selected patients with DIE; in particular this method is very helpful to individuate DIE nodules involving digestive tract or bladder and to evaluate the correct involvement of the urologist and/or the colorectal surgeon.

10:30 - 12:00 **Studio 2017**

Oncologic Imaging

SS 1816

Improving imaging of metastatic disease: what's new?

Moderators:
R.G.H. Beets-Tan; Amsterdam/NL
K.N. De Paepe; Leuven/BE

B-1100 10:30

Radiogenomics: evaluation of CT imaging features of melanoma metastases compared with genomic expression
E. Khodak, M. Lotem, J. DiPoce, S. Goldberg, J. Sosna; *Jerusalem/IL (Jkhodak@gmail.com)*

Purpose: Imaging features and the distribution of metastases could serve as surrogates predictive of molecular genotype, contributing to the diagnosis, prognosis, and BRAF-dependent treatment response in melanoma. We aimed to identify imaging biomarkers for metastatic melanoma.
Methods and Materials: A database of 142 patients with metastatic melanoma, previously genotyped for BRAF mutation status, was retrospectively reviewed. Patients >18 years with imaging evidence of metastases prior to treatment (including radiation), with no other neoplastic disease, were included. CT and PET-CT were assessed for 182 imaging features, including distribution (10 organs) and characteristics (border, shape, calcifications, central necrosis, vascularity, size) of metastases with blinding to BRAF status. Associations between imaging characteristics and BRAF status were assessed (T-test of proportion, Bayesian analysis).
Results: 30 BRAF-positive (BRAF-POS) and 34 BRAF-negative (BRAF-WT) patients (total 64) met inclusion criteria. There were significant differences between groups in the distribution of 54 imaging features, which were merged into 16 clusters. There was a strong correlation for spread to the adrenals, soft tissue, and lymph nodes for the BRAF-POS genotype (adrenals 10% vs 0%; soft tissues 47% vs 15%, lymph nodes 70% vs 38%, for BRAF-POS and BRAF-WT, respectively, p<0.01), and spread to the liver for the BRAF-WT genotype (26% vs 10% for BRAF-WT and BRAF-POS, respectively, p<0.01).
Conclusion: The pattern of metastatic spread in melanoma varies with BRAF genotype. BRAF-positive patients tend to present adrenal, lymph node, and soft tissue metastases; BRAF-negative patients tend to present liver metastases. Future studies assessing prognostic implications of these findings are warranted.

B-1101 10:38

Reduced dose CT for staging in patients with melanoma: evaluation of radiation dose and diagnostic confidence in comparison to standard dose dual-energy CT
D. Zinsser, A. Othman, T. Eigentler, C. Garbe, K. Nikolaou, B.D. Klumpp; *Tübingen/DE*

Purpose: To compare reduced dose intermediate tube voltage CT to standard dose dual-energy CT (DECT) for staging in melanoma patients regarding radiation dose, image quality and diagnostic confidence.
Methods and Materials: We retrospectively included 118 melanoma patients (53 females, mean age 60.2±14.5) who underwent whole-body DECT with 100/150 kVp (Tube A/B). Two datasets were reconstructed: 100 kVp (reduced dose, Tube A) and mixed series (standard dose, 80 % Tube A/20 % Tube B). Image quality and diagnostic confidence using a 4-point Likert scale (1=poor, 4=excellent) and presence/absence of tumour were assessed. Target lesions according RECIST1.1 were recorded. SNR values of skeletal muscles of neck, thorax and abdomen were calculated.
Results: Based on fixed combination of both tubes, 100 kVp acquisition instead of mixed DE acquisition renders 27% dose reduction. Diagnostic confidence was rated equal for both datasets (3.29±0.66 vs. 3.30±0.66, p=0.317). For standard dose, we observed better subjective and objective image quality for thorax (3.78±0.44 vs. 3.65±0.5, p≤0.001, SNR 6.69±1.02 vs. 6.5±1.34, p=0.032) and better subjective image quality for abdomen (3.81±0.45 vs. 3.41±0.57, p≤0.001). There was nearly perfect accordance in size and number of metastases (102 target lesions, mean diameter 33.7±35.1 mm/33.3±34.8 mm, p=0.022, correlation r≥0.999, p≤0.001).
Conclusion: Reduced dose intermediate tube voltage CT provides a comparable diagnostic confidence regarding presence and extent of metastases at 27% dose reduction compared to standard dose DECT for staging of melanoma.

B-1102 10:46

Automated tube potential selection in cancer staging on a third-generation dual-source CT: comparison to second generation dual-source CT
M. Beeres, C. Park, C. Frellesen, J.L. Wichmann, J.E. Scholtz, M. Albrecht, A.M. Bucher, B. Bodelle, T.J. Vogl; *Frankfurt a. Main/DE (beeres@gmx.net)*

Purpose: Evaluation of latest generation automated attenuation-based tube potential selection (ATPS) impact on image quality and radiation dose in contrast-enhanced chest-abdomen-pelvis CT examinations for gynaecological cancer staging.
Methods and Materials: This IRB approved single-centre, retrospective study included a total of 100 patients with contrast-enhanced chest-abdomen-pelvis CT for gynaecological cancer staging. All patients were examined with ATPS for adaption of tube voltage to body habitus. 50 patients on a third-generation dual-source CT (DSCT), and another 50 patients on a second-generation DSCT. Predefined image quality setting remained stable between both groups at 120 kV and a current of 210 Reference mAs. Subjective image quality assessment was performed by two blinded readers independently. Attenuation and image noise were measured in several anatomic structures. Signal-to-noise ratio (SNR) was calculated. For the evaluation of radiation exposure, CT dose index ($CTDI_{vol}$) values were compared.
Results: Diagnostic image quality was obtained in all patients. The median $CTDI_{vol}$ (6.1 mGy, range 3.9-22 mGy) was 40% lower when using the algorithm compared with the previous ATCM protocol (median 10.2 mGy·cm, range 5.8-22.8 mGy). A reduction in potential to 90 kV occurred in 19 cases, a reduction to 100 kV in 23 patients and a reduction to 110 kV in 3 patients of our experimental cohort. These patients received significantly lower radiation exposure compared to the former protocol.
Conclusion: Latest generation automated ATPS on third-generation DSCT provides good diagnostic image quality in chest-abdomen-pelvis CT while average radiation dose is reduced by 40% compared to former ATPS protocol on second-generation DSCT.

B-1103 10:54

Radiation dose reduction with venous-arterial MDCT in breast cancer patients

A. Meldo, I. Burovik; *St. Petersburg/RU (anna.meldo@yandex.ru)*

Purpose: Traditionally in oncology biphasic CT (arterial and venous phases) is used. The new approach in MDCT - venous-arterial phase (VAP) in breast cancer patients is presented.
Methods and Materials: Venous-arterial MDCT is a technique, which composes characteristics of arterial and venous phases in one scanning - venous-arterial phase (VAP). To obtain VAP we divided contrast bolus is 2 parts (2:1). Next we programmed scanning protocol so that the end of the second bolus part corresponded to the 60th sec from the beginning of the first one. ROI of "bolus tracking" was set to the aorta. It started scanning according to the second part of the bolus. Thus, the first part of the bolus provides a venous phase image, the second one provides an arterial phase image. 50 patients with primary breast cancer were examined. We compared the density of the tumour, pulmonary artery, thoracic aorta in the native, arterial phases and VAP.
Results: CT density of the tumour in arterial and native phases was equal (36±9 HU and 33±8 HU, $p>0.05$). We find a statistically significant increase of breast tumour density in VAP (69±14 HU, $p<0.05$). Enhancement of pulmonary artery and aorta in VAP and in arterial phase was identical (PA: 270±58 HU and 272±47 HU, $p>0.05$; A: 234±46 HU and 249±40 HU, $p>0,05$). Method was patented in Russia (№ 2556619).
Conclusion: The venous-arterial MDCT is effective method for visualization of breast cancer and mediastinal vessels. Radiation dose is reduced in comparison with traditional biphasic scanning.

B-1104 11:02

Added value of the virtual non-calcium technique for the detection of bone metastases with computed tomography in breast cancer patients

L.J. Claeys, J. Alexiou, J. Moreau, S.-L. Chao, M. Lemort; *Brussels/BE (lionel.claeys@gmail.com)*

Purpose: To evaluate the added value of the virtual non calcium technique (VNC) on the diagnostic performance of conventional Computed Tomography (CT) for the detection of bone metastases (BM).
Methods and Materials: This single-center study approved by the institutional ethics committee was based on retrospective interpretation of prospectively acquired data. Fifty patients with known breast cancer who underwent dual-energy CT (DECT) and whole-spine MRI (the standard of reference) were included after signing informed consent. The presence of BM was assessed on MR images with a vertebra-based and patient-based analysis by one blinded independent reader. Sensitivity, specificity and matched pair analyses for reading CT images alone and when combining CT with VNC were determined based on the results of 2 readings sessions, separated by a 4 weeks interval, with 2 independent blinded readers. Cohen's kappa coefficient was used for interobserver agreement evaluation.
Results: Twenty-nine patients and 381 vertebrae showed BM at MRI. The impact of VNC images on the diagnostic performance of the readers was contradictory but no statistically significant difference was shown by the matched pair analyses but for the greater specificity of CT alone for the vertebra-based analysis for one of the readers. The interobserver agreement was excellent for both CT and CT with VNC images (kappa=0.85 and kappa=0.82 respectively) but was moderate for VNC-only images (kappa=0.51).
Conclusion: In our study, the VNC technique showed no added value to the detection of bone metastases in breast cancer patients.

B-1105 11:10

Diffusion whole-body MRI (DWB) in the management of metastatic breast cancer patients

F. Zugni, P. Pricolo, P.E. Summers, M. Iorfida, M.A. Colleoni, M. Bellomi, G. Petralia; *Milan/IT (fabio.zugni@unimi.it)*

Purpose: To compare the clinical impact of diffusion whole-body MRI (DWB) in the management of patients with metastatic breast cancer (BC), with computed tomography (CT) and CT with ^{18}F-FDG positron emission tomography (PET/CT).
Methods and Materials: A retrospective audit was performed of all DWB examinations performed on patients with BC between 2012 and 2015, who had undergone CT or PET/CT (control examination). All DWB were acquired on the same 1.5 T scanner (Avanto Siemens, Erlangen). Clinical records were consulted to assess whether the findings on DWB and on the control examination determined a therapeutic change.
Results: 472 DWB examinations were identified, of which 51 had a control examination (median time between examinations = 35 days). In 34/51 examinations, DWB and the control examination had comparable findings, leading to concordant disease assessments and therapeutic management. In 17/51 examinations, DWB and the control examination had discordant findings: one PET/CT showed disease undetected by DWB, with a subsequent therapeutic change, and 16 DWB showed metastatic disease undetected by the control examination, leading to a therapeutic change in 12 cases (12/51 cases, 23%). Notably, 7/12 of these were in a subgroup of 20 DWB performed in patients with invasive lobular BC.
Conclusion: DWB increased the detection of metastatic disease over CT and PET/CT, leading to therapeutic changes for nearly one fifth of all cases. This initial observation encourages us to implement DWB in the management of patients with BC, and draws interest in the dedicated use of DWB for invasive lobular BC patients.

B-1106 11:18

Oncological staging of 30 pregnant patients with diffusion whole-body MRI (DWB)

F. Zugni, P. Pricolo, S. Alessi, P.E. Summers, F.A. Peccatori, M. Bellomi, G. Petralia; *Milan/IT (fabio.zugni@unimi.it)*

Purpose: To evaluate the feasibility of diffusion whole-body MRI (DWB) for the systemic staging of tumours in pregnant women.
Methods and Materials: Between 2011 and 2015, 30 patients with a tumour diagnosed during pregnancy underwent DWB examination for staging on a 1.5 Tesla scanner (Avanto, Siemens, Erlangen) without administration of contrast agent, by means of both morphological and diffusion-weighted sequences. All images were prospectively reviewed by an expert oncological radiologist and by one in training. Data regarding tumour histology, pregnancy history and tumour treatment were collected. Suspicious findings were reassessed through either histopathology or further imaging studies.
Results: The patients (median age = 34 years, median gestational age = 22.5 weeks) had histories of breast carcinoma (22 cases), lymphoma (5 cases), and one case each of lung adenocarcinoma, colon adenocarcinoma and melanoma. All DWB examinations were completed successfully and were readable. DWB led to a diagnosis of metastatic disease in 13 patients, distributed as follows: 8 breast cancer patients (regional lymph-nodes confirmed at pathology, and in 2 cases bone metastases confirmed at follow-up DWB), 4 lymphoma (supra-diaphragmatic lymph-nodes confirmed by postpartum CT or PET/CT) and one lung adenocarcinoma (brain, skeleton, abdomen and chest metastases confirmed at a follow-up MRI). In one patient, the DWB finding was not confirmed (breast nodule benign at biopsy). In the remaining 16 patients DWB revealed no suspicious findings.
Conclusion: DWB was feasible for the staging of patients with tumour during pregnancy, thus providing a systemic staging without contrast agent administration and exposure to ionizing radiation.

B-1107 11:26

Whole-body MRI as the method of choice during oncologic follow-up at 3T: outcome after 400 examinations

A. Malich, D. Wiech, A. Kott; *Nordhausen/DE (ansgar.malich@shk-ndh.de)*

Purpose: Whole-body MRI might be a beneficial diagnostic option in the oncological follow-up, providing information beyond the detection of bone metastatic lesions. However, it has been criticised due costs, scanning times, number of incidental co-findings, triggering inevitable but frequently unnecessary additional imaging causing raise of follow-up-costs. In the current study we investigated the impact of 400 3T-based MR-examinations at 380 patients.
Methods and Materials: 400 whole-body-MRI scans: mDixon:T1w +/-contrast uptake; whole-body STIR:3mm slice thickness; 3T:Philips-Ingenia were analysed (exclusively oncologic patients) comparing diagnostic outcome to clinical data (follow up +1y), other diagnostics (ultrasound, x-ray, scintigraphy), incidental findings requiring additional investigation and its relevance.
Results: The average scanning time was 64min. In 135cases osseous metastases were described, in 64 cases scintigraphy was performed matching with MRI in 84%. Overall 126 patients underwent additional MRI within 1year after whole-body-MRI, just 39 cases (9.7%) in order to clarify findings of whole-body MRI. In 45 cases an additional tumour like finding was reported; in 50 cases other surgically or orthopaedically relevant findings were described. Other than bone metastases were found in 88 cases.
Conclusion: Total body MRI is a sensitive, precise and reliable tool in the oncological follow-up routine, sufficient to replace current standards-of-care such as basic ultrasound, bone scintigraphy or conventional imaging. Increased sensitivity in detection of metastatic and other tumour-like lesions sufficiently counteracts cost of incidental findings, which are within acceptable limits. The realistic limitations remain the scanning time and MR-availability.

B-1108 11:34

Assessment of informativity between static scintigraphy and full-body magnetic resonance imaging examinations in children with metastatic bone disease at Riga, Latvia

J. Baronenko, L. Štelce, I. Apine; *Riga/LV (jevgenijs.baronenko@gmail.com)*

Purpose: To evaluate retrospectively all the paediatric patients with primary malignant tumours examined at Children's Clinical University Hospital, Riga, Latvia, with both static bone scintigraphy and whole-body MRI (DWIBS) with proven cancer for assessment presence of bone metastases (MTS). To compare informativity of bone MTS identification in children with malignant tumours between full-body MRI DWIBS and the static scintigraphy.
Methods and Materials: A retrospective study was conducted based on data from clinical history and radiology reports from the hospital and radiology information systems from January 2013 till September 2016.
Results: The analysis of totally 61 patients under the age of 18 with histologically confirmed cancer was performed. Only patients who underwent both SC and MRI DWIBS examinations were studied. Bone metastases were found in 12 cases. Of them: 5 cases included multiple bone MTS in both SC and MRI DWIBS, 2 cases included multiple MTS in SC whereas MRI DWIBS did not show MTS, in 4 cases MTS were detected in MRI DWIBS whereas SC did not show MTS, in 1 case MRI DWIBS revealed multiple MTS whereas SC showed only 1 metastasis.
Conclusion: According to our study data, both investigation methods finding metastases in bones had the same results in less than half of the patients. When the results differed, MRI DWIBS was more accurate in diagnosing bone MTS. The sensitivity of both radiological investigation methods is most likely to depend on the histological type of cancer. A further cohort with increased number of participants is necessary.
Author Disclosures:
J. Baronenko: Author; Riga Stradins's University. **L. Štelce:** Author; Riga Stradins's University. **I. Apine:** Author; Riga Stradins's University.

B-1109 11:42

Diffusion-weighted MRI of solid bone tumours of the spine: the diagnostic value of the apparent diffusion coefficient

G. Pozzi, C. Messina, G. Cannella, J. Almolla, A. Zerbi, L.M. Sconfienza; *Milan/IT (carmelomessina.md@gmail.com)*

Purpose: To evaluate the utility of the mean apparent diffusion coefficient value (m-ADC) in differentiating between benign and malignant solid bone tumours of the spine.
Methods and Materials: We reviewed MRI images of 107 patients with biopsy-proven spinal tumours (ST) who underwent 1.5 T MRI with T1, T2 and DWI (b values: 0 and 1000 s/mm²) sequences between January 2010 and June 2015. Two radiologists independently measured m-ADC by placing region of interest in both pathologic and normal bone, and findings were compared to histology (reference standard). ST were classified into three groups: malignant primary tumours (MPT), bone metastases (BM) and benign primary tumours (BPT).
Results: M-ADC values of MPT (N=30), BM (N=63) and BPT (N=14) were: 0.99 (0.59-1.47) x 10^{-3} mm^2/sec, 1.05 (0.73-1.96) x 10^{-3} mm^2/sec and 1.34 (0.83-2.14) x 10^{-3} mm^2/sec, respectively. M-ADC showed significant difference between benign and all malignant lesions (p=0.008), between BM and BPT (p=0.04) and between MPT and BPT (p=0.02). No statistical difference was found between BM and MPT (p=0.09). Normal bone showed ADC values lower than those of bone lesions (m-ADC = 0,33 x 10^{-3} mm2/sec). ADC measurements had almost perfect interobserver correlation (average intraclass correlation coefficient = 0.97).
Conclusion: M-ADC values of BPT showed to be higher than malignant ST with almost perfect interobserver correlation. In association with conventional MRI sequences, ADC values can be a useful tool in differentiating between benign and malignant bone tumours of the spine.

B-1110 11:50

Added diagnostic value of complementary gadoxetic acid-enhanced MRI to ^{18}F-DOPA-PET/CT for liver staging in medullary thyroid carcinoma

P.M. Kazmierczak, A. Rominger, M. Brendel, W. Kunz, R. Stahl, J. Sargsyan-Bergmann, C. Spitzweg, M.F. Reiser, C.C. Cyran; *Munich/DE (Philipp.Kazmierczak@med.uni-muenchen.de)*

Purpose: To investigate the added diagnostic value of complementary gadoxetic acid-enhanced MRI to ^{18}F-DOPA-PET/CT for liver staging in medullary thyroid carcinoma (MTC).
Methods and Materials: 29 consecutive Patients (n=17 f, n=12 m, median age 58 years) with histologically confirmed MTC undergoing gadoxetic acid-enhanced liver MRI within one month of matching contrast-enhanced ^{18}F-DOPA-PET/CT between 2010 and 2015 were selected for retrospective analysis. ^{18}F-DOPA-PET/CT and multiparametric MRI data sets were read consecutively and liver lesions were categorized on a 5-point scale analogously to the LI-RADS criteria (1-definitely benign; 2-probably benign; 3-intermediate risk for metastasis; 4-probably metastasis; 5-definitely metastasis). It was noted if gadoxetic acid-enhanced MRI detected additional, ^{18}F-DOPA-PET/CT-occult metastases (category 5) or if gadoxetic acid-enhanced MRI allowed for a definite classification (categories 1 and 5) of lesions for which ^{18}F-DOPA-PET/CT remained inconclusive (categories 2-4).
Results: A total of n=141 liver lesions (^{18}F-DOPA-PET/CT n=107, MRI n=141; n=99 metastases, n=27 benign cysts, n=15 hemangiomas) were analyzed. N=34 additional lesions were detected by MRI, of which n=30 were additional metastases (median diameter 0.5 cm [0.4 - 1.9 cm]) occult on ^{18}F-DOPA-PET/CT. MRI allowed for a definite lesion classification (categories 1 and 5) in 89 % (125/141) (^{18}F-DOPA-PET/CT 69 %, n=74/107). MRI lead to a change in lesion categorization in n=17 cases (from category 2 to 1: n=10; from category 3 to 1: n=3; from category 4 to 5: n=4).
Conclusion: Gadoxetic acid-enhanced MRI allows for a more accurate liver staging in MTC patients compared to ^{18}F-DOPA-PET/CT alone, particularly for ^{18}F-DOPA-negative metastases and lesions <1 cm.
Author Disclosures:
C. Spitzweg: Advisory Board; Swedish Orphan Biovitrum AB, Bayer AG, Eisai Co, Ltd, AstraZeneca PLC. Speaker; Swedish Orphan Biovitrum AB, Bayer AG, Eisai Co, Ltd, AstraZeneca PLC. **C.C. Cyran:** Research/Grant Support; Bayer AG, Novartis AG. Speaker; Bayer AG.

10:30 - 12:00 **Room L 8**

Physics in Medical Imaging

SS 1813

Physics-based approaches to imaging, diffusion and motion

Moderators:
I. Seimenis; Alexandropolis/GR
N.N

B-1111 10:30

Motion vector field upsampling for precise respiratory motion compensation with cone-beam CT of the thorax region

S. Sauppe[1], C.M. Rank[1], M. Brehm[2], P. Paysan[2], D. Seghers[2], M. Kachelrieß[1]; [1]*Heidelberg/DE*, [2]*Baden-Dättwil/CH (Sebastian.Sauppe@dkfz.de)*

Purpose: To improve the accuracy of motion vector fields (MVFs) required for motion-compensated (MoCo) CT image reconstruction.
Methods and Materials: On-board CBCT images for radiation therapy suffer from patient respiratory motion artefacts. However, accurate information about patient motion is useful for precise radiation therapy. While respiratory gating improves the temporal resolution it leads to sparse view sampling artefacts. MoCo image reconstruction is able to significantly reduce motion artefacts while utilising 100% of the acquired data. In some cases, however, the MVF accuracy is still to be improved. We developed an approach to upsample MVFs (estimated by the our acMoCo algorithm) and thereby to double the temporal samples without increasing the reconstruction time. Our upsampling strategy interpolates the original MVFs by incorporating respiratory amplitude to drive the interpolation weights. For validation we use an artificially deformed clinical CT scan and patient data. We varied the upsampling factor (UF) from 2 up to higher values. The entropy and total variation (TV) are used as an image quality measure.
Results: For both phantom and patient data, in-phase motion blurring was considerably decreased when using MVF upsampling. This is visible in the reconstructed images and is reflected in an improved entropy (10.1%) and TV value (6.5%). It turns out that UF=2 produces the most significant improvement regarding image quality and is the optimal choice in terms computation time.
Conclusion: Upsampling the MVFs can improve the quality of the MoCo reconstruction substantially without increasing acquisition time, patient dose, streak, or noise artefacts.
Author Disclosures:
M. Brehm: Employee; Varian. **P. Paysan:** Employee; Varian. **D. Seghers:** Employee; Varian.

B-1112 10:38

Inflow effect correction in fast gradient-echo dynamic contrast-enhanced imaging in vitro and in vivo

F. Bidault[1], H. Wang[2], B. Asselain[1], K. Rachid[2], D. Rodríguez[2], X. Maître[2], N. Lassau[1]; [1]*Villejuif/FR*, [2]*Orsay/FR (francois.bidault@gustaveroussy.fr)*

Purpose: The inflow effect in the arteries (flow-related enhancement (FRE)) leads to a biased assessment on the Arterial Input Function (AIF) and further on the perfusion quantification. Here, the goal was to develop a correction method based on pre-saturation pulses in flow apparatus and applied to measure the AIF in the carotid of patients.

Methods and Materials: MR-compatible flow apparatus [CardioFlow 5000MR] generated a closed-circuit, mimicking-blood flow of glycerol-water to determine FRE versus velocity (0-50 cm/s). MRI was performed on 3T PET-MR [GE SIGNA] with head-neck coil using multi-phases Fast-SPGR and LAVA sequences with clinical practice-based parameters. Spatially-selective saturation bands (1-4 cm) were applied at imaging slab upstream to suppress FRE. To assess FRE with contrast agent (CA), MR injection system [Bayer MEDRAD] generated continuous flow (10 mL/s) of Gd-DOTA solution (0, 2.5mM) into an open-circuit. Same sequences were performed without and with pre-saturation (4cm). All acquisitions were repeated 5 times. The method was further applied to patients (n=4).
Results: FRE increased with velocity without pre-saturation. Saturation bands of 3 or 4cm allowed suppressing significantly FRE (6-fold FRE for SPGR and 17-fold for LAVA with v=20cm/s). In presence of CA, significant increase (one-way ANOVA, $p<0.01$) was observed in SI without pre-saturation compared to static reference, while pre-saturated SI was comparable to reference. The correction allowed obtaining more precise AIF in the carotid of patients with both sequences, compared to flat curves without pre-saturation.
Conclusion: The proposed method corrects efficiently FRE and provides a better precision on the AIF measurement.

B-1113 10:46

Reanimating patients using motion transfer: a cardiorespiratory motion ground truth based on clinical CT patient data

J. Mayer, S. Sauppe, C.M. Rank, M. Kachelrieß; *Heidelberg/DE (johannes.mayer@dkfz.de)*

Purpose: Respiratory and cardiac motion often leads to artefacts in CT, e.g. in cone-beam CT (CBCT) scans in radiation therapy or during interventional imaging. Our aim is to provide volumetric cardiac and respiratory motion ground truth (GT) patient data to optimize imaging protocols or to evaluate image reconstruction algorithms.
Methods and Materials: We developed a method that transfers motion extracted from a 4D CT scan of a source patient onto the anatomy of a motion-free destination patient. For the motion transfer (MT) the cardiac or respiratory motion vector fields (MVFs) of a source patient are determined. These are warped onto the destination anatomy with a deformable map describing the geometric relation between source and destination patient. The resulting MVFs serve as the motion information GT in the destination anatomy. Thereby 4D or 5D volumes without motion artefacts can be generated. We evaluated our recently developed motion compensation (acMoCo) algorithm, simulating a CT scan with gantry rotation speeds of 3° and 6°/s with the reanimated destination patient serving as the GT.
Results: MT was used to generate 4D cardiac CT and 4D respiratory MR data. By definition the transferred motion is correct in the destination anatomy. The evaluation of the acMoCo algorithm indicated an accuracy of about 1 mm in MVF estimation on average.
Conclusion: The MVF ground truth based on patient data provides an improved framework to quantify MoCo algorithms and to design optimised imaging protocols. It may thus help to bring these algorithms and scan modes into clinical routine.

B-1114 10:54

Diffusion coefficient and perfusion fraction parameters correlate with gestational age in normal human in vivo placenta: a preliminary study

A. Antonelli, M. Guerreri, A. Di Paolo, S. Bernardo, S. Capuani, C. Catalano, L. Manganaro; *Rome/IT (amanda.antonelli@hotmail.it)*

Purpose: To investigate the potential of diffusion parameters derived from a bi-exponential analysis as marker to evaluate the perfusion quality of normal in vivo placenta.
Methods and Materials: 18 normal pregnancies, fulfilling the study inclusion criteria, have been analysed at 1.5 T Magnetom Avanto (Siemens, Erlangen, Germany) without mother-foetal sedation. DW imaging was collected using seven b values: 0, 50, 100, 150, 400, 700, 1000 (s/mm²). Three regions of interest (ROIs) have been considered - central (C), peripheral (P) and umbilical (U) regions. A bi-exponential model was used to obtain perfusion fraction (f), pseudo-perfusion (D*) and apparent diffusion (D) coefficients. Pearson test was performed to investigate correlation between diffusion parameters and gestation weeks (GW), body mass index (BMI) and basal glycaemia (bG).
Results: The average values on all ROIs were $D=1.41\pm0.16\cdot10^{-3}$ (mm²/s), $D^*=1.81\pm1.28\cdot10^{-2}$ (mm²/s), $f=3.28\pm0.18\cdot10^{-1}$, in good agreement with the literature. In the C ROI, a positive correlation ($p<0.04$) was observed between f and GW. After 30 GW in the P ROI a positive correlation between f and GW ($p<0.05$) and a negative correlation between D and GW ($p<0.0001$) were found. No correlation was found between D, D*, f, BMI and bG.
Conclusion: The f increase reflects normal placenta perfusion physiology. On the other hand, the decrease of D highlights placental parenchyma maturation becoming more fibrotic during late gestational age. Bi-exponential model provides more and useful information about placental morphological changes compared to mono-exponential diffusion model.

B-1115 11:02

Detection rates of simulated microcalcifications in FFDM, Synthetic-2D and DBT using an antropromorphic phantom model

K. Krug[1], S. Peters[2], M. Hellmich[1], M. Püsken[1], O. Grinstein[1], L. Stahlhut[1], A. Storck[3], J. Kemper[1], D. Maintz[1]; [1]*Cologne/DE*, [2]*Wennigsen/DE*, [3]*Düsseldorf/DE (Barbara.krug@uk-koeln.de)*

Purpose: To compare the microcalcification detectability in an anthropomorphic phantom model in full-field digital mammography (FFDM), synthetically reconstructed two-dimensional images (Synthetic-2D) and digital breast tomosynthesis (DBT).
Methods and Materials: Simulated microcalcifications of different numbers, sizes and shapes were randomly scattered on 50 film phantoms each divided in 4 quadrants. FFDM and DBT x-rays were taken of each film with both x-ray mammography systems (SenoClaire, GE, Selenia Dimensions, Hologic) using an anthropomorphic scattering body and automatic exposure control. The exposure factors were similar to a clinical setting. Synthetic 2D-images were generated automatically on both systems. All FFDM, Sythetic-2D and DBT images were interpreted in randomised order and independently of each other by 6 radiologists using a structured questionnaire.
Results: The number categories of simulated microcalcifications were correctly evaluated in 55.3% of instances in FFDM, 50.9% in Synthetic-2D and 59.5% in DBT, summarised for 200 quadrants per reader for each device. FFDM was superior to Synthetic-2D (mean difference 4%, 95% CI 2-7%, $p<0.001$) and DBT was superior to both FFDM (4%, 2-7%, $p = 0.002$) and Synthetic-2D (9%, 6-11%, $p<0.001$). This trend was consistent in all subgroup analyses. The number of the smallest microcalcifications (100-399µm) was correctly evaluated in 25.2% of the FFDM, in 14.2% for Synthetic-2D and in 28.3% of the DBT images.
Conclusion: In the presented in-vitro environment standard FFDM was superior to Synthetic-2D in the detection of simulated microcalcifications. Further investigations are needed to assess the clinical impact of the in-vitro results.

B-1116 11:10

Model observer approach applied to an innovative method for LCD assessment in mammography: comparison with CDMAM evaluation including psychometric correction

R. Villa[1], N. Paruccini[1], N. Oberhofer[2], C. Spadavecchia[1], A. Baglivi[1], A. Crespi[1]; [1]*Monza/IT*, [2]*Bolzano/IT (raffaele.vill@gmail.com)*

Purpose: In mammography image quality assessment is usually carried out by automated low contrast detectability (LCD) evaluation of the CDMAM phantom (Artinis, The Netherlands) with psychometric correction for human observer. The current study proposes a different approach where human detection performance was evaluated with a Model Observer.
Methods and Materials: LCD, expressed in terms of mmAl and contrast, was estimated by means of a homemade phantom and a dedicated MATLAB software exploiting a statistical approach requiring only single images. The effect of human perception was considered through a NPWE model observer. The internal eye noise was introduced with a response degradation factor while the eye response function was evaluated for different distances between the observer and the screen. Method parameters were derived from 2D mammography images acquired on five equipment of different manufacturers with different exposure parameters and phantom thickness. Human detection of 95% was considered. A comparison with CDMAM results associated with the same acquisition parameters was carried out.
Results: The conversion curve produced by the model observer resulted to be independent from both the acquisition parameters and the equipment (percent error 4,5%). For each equipment the agreement with the psychometric corrected CDMAM analysis was very good, with a mean difference of 9% (1% to 19%).
Conclusion: The statistical approach with model observer correction resulted in accordance with the psychometric corrected automatic readout of CDMAM images, being less time-consuming compared to CDMAM analysis . Thus, the current method could be applied in image quality assurance protocols.

B-1117 11:18

Radiation dose comparison between photon counting and selenium mammography technology

R. Salvador Tarrason, K. Piccotti, X. Salvador Izquierdo, M. Vallespi, N. Riquel; *Barcelona/ES (rafasalvador@imaginebarcelona.com)*

Purpose: To compare the radiation dose received by patients during a screening mammography exam for breast cancer with a photon counting detector (PhC) and a selenium detector (Se).
Methods and Materials: This study includes patients who had mammography exam between June 2013 and December 2014, with the PhC (Philips MicroDose SI) and an exam with the Se (Fujifilm Amulet) within a two years period. Patients with missing paired organ radiation dose data were excluded

from this study. The exposure was compared between both examinations for each patient, by age group (<40, 40-49, 50-59 and >60), and breast density groups (A, B, C and D). Linear mixed models were used to compare radiation dose. Least square means (LSM) and 95% confidence intervals (CI) were estimated. The hypothesis of no differences in mean radiation exposure was evaluated using an F-test. All analyses were conducted using SAS version 9.3.
Results: 2286 women were included. The mean age 57 years. LSM estimates and CI for overall mean radiation dose for the Se and PhC showed a difference of 0.88mGy (0.84 - 0.92), p<0.0001 . Higher radiation was observed for Se in all the subgroups evaluated; 0.44 mGy (0.42 - 0.46). The dose differences by age subgroups were: 1.33; 1.06; 0.84; and 0.77 mGy. And for A to D breast density subgroups were: 0.75mGy, 0.64 mGy, 1.04 mGy and 1.68 mGy.
Conclusion: The use of PhC resulted in a significant radiation reduction. Most benefit was observed in younger patients and in patients with dense breast.

B-1118 11:26

Dose data in mammography: what a dose management software can tell us?

C. Heilmaier, E. Kummer, N. Zuber, D. Weishaupt; *Zurich/CH (christina.heilmaier@triemli.zuerich.ch)*

Purpose: Mammography is a frequently performed screening examination, thus, radiation protection is essential. The purpose of the present study was to establish local diagnostic reference levels (DRLs) for mammography with a dose management software, taking into account the differences in breast types.
Methods and Materials: Dose data of full-field digital mammographies (FFDM) conducted in a 6-month-period was analyzed with a dose management software (DoseWatch®, GE Healthcare). Analysis was carried out separately for cranio-caudal (CC)- and medio-lateral-oblique (MLO)-views, which were further subdivided concerning compressed breast thickness (CBT; <4 cm, ≥4-6 cm, ≥6 cm), glandular fraction (≤50 %, >50 %) and compression force applied (low, standard, high). Analysis focused on entrance surface air kerma (ESAK), average glandular dose (AGD), compression force, and CBT and included descriptive statistics, Mann-Whitney U tests and Spearman rank correlation coefficients.
Results: Analysis of n = 3,454 mammographic images revealed mean values ± standard deviation (ESAK/AGD/CBT/compression force) as follows: 7.07±3.19 mGy/1.55±0.48 mGy/4.87±0.96 cm/100.8±37.0 Newton (N), respectively. ESAK, AGD and CBT was considerably higher in MLO-compared to CC-views, in which higher compression force was seen (for all, P<0.001). Compared to smaller breast, CBT and ESAK/AGD correlated stronger in larger breasts with CBT ≥6 cm. In breasts with the same CBT, ESAK- and AGD-values were higher in the group with glandular fraction >50 %.
Conclusion: A dose management software in mammography allows obtaining local DRLs, which are specific for several breast types. As proven in the present study, CBT is the strongest indicator to predict radiation exposure to the breasts.

B-1119 11:34

Performance characterisation of digital breast tomosynthesis systems: the need for a standardisation

M. Chevalier, M. Castillo-García, A. Rodríguez-Ruiz, D. García-Pinto; *Madrid/ES (chevalier@med.ucm.es)*

Purpose: To evaluate possible dependencies on material, size, and position of test objects used in performance characterization and quality control (QC) of digital breast tomosynthesis (DBT) systems.
Methods and Materials: Four different DBT systems (A,B,C,D) underwent the same testing procedure, with testing objects of different size and material, placed at different locations. Modulation transfer function (MTF) of the projections was measured with a steel edge (1mm thick), positioned at different heights above the table. In-plane MTF of the reconstructed planes was estimated with an aluminium (Al) edge (0.1mm thick) and tungsten (W) wires of different diameters (25, 50, 100µm), at fixed height. Similar wires (but tilted) were used to calculate the in-depth PSF. Artefact spread function (ASF) was computed with 1 mm diameter W and Al beads, placed at different (x,y,z) locations.
Results: Projections' MTF on the tube-travel direction depends on height for systems that use a continuous tube motion (-42% averaged decrease in $MTF_{50\%}$ frequency from 0mm to 70mm). In-plane MTF in the anode-cathode direction improves with decreasing wire diameter (a factor 1.7 in average), but the 25µm wire often splits. In-plane MTF results from edge and wires are compatible. In-depth PSF does not differ with wire diameter. ASF values and their reproducibility change randomly across the bead (x,y) position, but are independent of height and material.
Conclusion: DBT performance parameters show a different dependency on material, size, and position of test objects to be taken into account when developing phantoms for QC of DBT systems.

B-1120 11:42

Adjustment of x-ray measuring instruments for a new x-ray beam quality for mammography

R. Klausz, F. Mattana, Y. Popova, A. Guerin, F. Jeunehomme Patoureaux; *Buc/FR (remy.klausz@ge.com)*

Purpose: Currently available semi-conductor based x-ray beam measuring instruments (air-kerma, kVp) may not be operating per specifications when used with a newly introduced mammography x-ray beam quality. The process and results of introducing new adjustments are described.
Methods and Materials: One year before the planned introduction of a mammographic equipment featuring a new beam quality (rhodium anode, 30 µm silver filter) three leaders in x-ray measuring instruments were contacted, and detailed characteristics of the new beam quality shared with them. When needed they designed new adjustments for measuring air-kerma, single-shot Half-Value-Layer (HVL), and High Voltage (HV) for their respective measuring instruments. Measurements with adjusted instruments were compared with reference measurements performed on prototype mammographic equipment, using mammography-dedicated ionisation chamber dosemeters, high accuracy aluminium sheets, and invasive voltage dividers.
Results: Depending on manufacturers the final adjustments were obtained 12 to 16 months after initial contacts. The current uncertainty specifications were extended to the new beam quality. Maximum measured deviations vs. references between 27 and 40 kV for the three instruments were respectively 1%, 0,7% and 2% for HV, 0,2%, 0,5% and 3% for air-kerma, and 4%, 0.6% and 4% for one-shot HVL.
Conclusion: It was possible to synchronize the availability of satisfactory x-ray measuring instruments with the first installations of the mammographic equipment featuring a new beam quality, allowing calibration at installation and acceptance testing. Adjustments and calibrations for the new beam quality are now available from three vendors for new measuring instruments or as an upgrade.
Author Disclosures:
R. Klausz: Employee; GE Healthcare. **F. Mattana:** Employee; GE Healthcare. **Y. Popova:** Employee; GE Healthcare. **A. Guerin:** Employee; GE Healthcare. **F. Jeunehomme Patoureaux:** Employee; GE Healthcare.

B-1121 11:50

Evaluation of the effectiveness of a new x-ray beam quality in digital mammography

M. Rouxel, R. Klausz, Y. Le Meur, H. Souchay, R. Shi, F. Jeunehomme Patoureaux; *Buc/FR (marionrouxel@ge.com)*

Purpose: Evaluate the performances of a new anode/filter combination in digital mammography in terms of image quality, patient dose and patient comfort.
Methods and Materials: A rhodium anode/30µm silver filter combination was evaluated in comparison with rhodium anode/25µm rhodium. Using a spectral model, the signal-difference-to-noise-ratio (SDNR) of 0.2mm thickness aluminium, average glandular dose (AGD) and exposure times, were compared for 28-36kVp and 35-75mm PMMA thickness in 10mm steps. A factor of merit (FOM) equal to $SDNR^2/AGD$ was computed. The kVp ranges providing optimal FOM values per thickness were determined. The FOM values and exposure times were also compared at constant SDNR.
Results: For both anode/filter combinations the FOMs were found optimal within 5% between 29 and 34 kVp over the whole PMMA thickness range. For 35mm the FOM for Rh/Ag is lower than for Rh/Rh by less than 2%. At 45mm PMMA, FOM and exposure time are similar. At 55, 65 and 75 mm PMMA the FOMs are, respectively, 3%, 5-8% and 8-11% higher for Rh/Ag depending on kVp. At 34 kVp, exposure times are reduced by 5%, 8% and 10% at 55, 65 and 75 mm PMMA with RhAg compared to Rh/Rh.
Conclusion: With a rhodium anode, replacing the rhodium filter with a silver filter allows improving the FOM with shorter exposure times. This reduces the risk of patient movement, improves her comfort, and may benefit to the patient throughput.
Author Disclosures:
M. Rouxel: Employee; GE Healthcare. **R. Klausz:** Employee; GE Healthcare. **Y. Le Meur:** Employee; GE Healthcare. **H. Souchay:** Employee; GE Healthcare. **R. Shi:** Employee; GE Healthcare. **F. Jeunehomme Patoureaux:** Employee; GE Healthcare.

10:30 - 12:00 **Room E1**

Breast

SS 1802a

Breast MRI: diffusion-weighted imaging

Moderators:
J. Camps Herrero; Valencia/ES
R.M. Mann; Nijmegen/NL

K-22 10:30

Keynote lecture
J. Camps Herrero; *Valencia/ES*

B-1122 10:39

The relationship between molecular subtypes of breast cancer and ADC values calculated with diffusion MRI
A. Tanyeri, F. Taşkin, M.B. Cildağ, V.S. Özturk, A. Ünsal, C.Z. Karaman; *Aydin/TR (dr.a.tanyeri@gmail.com)*

Purpose: To investigate the relationship between molecular subtypes of breast cancer and ADC values calculated with diffusion MRI.
Methods and Materials: 193 patients who had been preoperatively evaluated and diagnosed as breast cancer between January 2013 and January 2016 in our institution were retrospectively evaluated. ADC values of these lesions were calculated with diffusion MRI. These patients were classified according to the molecular subtypes of breast cancer. Difference between the average ADC values of each molecular subtype was compared. Independent sample T test was used for statistical analysis.
Results: Subtypes of breast cancer and average ADC values for each subtype in this study group were as following: luminal A (75 cases, 39%; ADC value: 0.96 ± 0.16), luminal B (68 cases, 35%; ADC value: 0.99 ± 0.15), triple negative (33 cases, 17%; ADC value: 1.02 ± 0.15) and Her-2 positive (17 cases, 9%; ADC value: 1.00 ± 0,12). Average ADC value for entire study population was 0.99+/-0.15 (range: 0.60-1.34). No statistically significant difference was found between the average ADC values of molecular subtypes of breast cancer.
Conclusion: Diffusion MR imaging contributes well to the diagnostic performance of breast MRI. Despite the slightly higher ADC values of triple-negative and HER2-positive groups, there was no significant relationship between molecular subtypes and ADC values in this study. On the contrary to morphologic MRI findings, ADC values may not contribute to distinguish the molecular subtypes of breast cancer. Further prospective and multicentre studies are needed to verify our findings.

B-1123 10:47

Correlating pericyte gene expression signatures with pharmacokinetic parameters of dynamic contrast enhanced MR and intravoxel incoherent motion imaging in invasive breast cancer
W. Tsai, K. Chang, K. Kao; *Taipei/TW (wctsai@kfsyscc.org)*

Purpose: To investigate whether quantitative dynamic contrast material-enhanced (DCE) parameters and intravoxel incoherent motion imaging (IVIM) are correlated with pericyte gene expression signature in invasive breast cancer.
Methods and Materials: With the IRB approval and signed informed consents from 119 breast cancer patients, we performed additional DCE breast MRI studies followed by diffusion-weighted images (DWI) at 11 b values values (from 0 to 1200 s/mm^2) on a 1.5T MR system before breast surgery. Gene expression profiling was conducted on fresh biopsy or frozen surgical breast cancer tissue. Expression of six genes (ACTA2, ANGPT1, CSPG4, LAMB1, PDGFRB and RGS5) associated with pericytes was measured and a combined expression score was determined by principal component analysis. Associations between quantitative parameters from DCE MRI (K^{trans}, K_{ep}, V_e, V_p), IVIM (D, f and D*), and the kinetic curve analysis, and pericyte gene signature scores were evaluated using Spearman's correlation analysis with a significance level of 0.05.
Results: Pericyte gene signature score showed significant negative correlation with DCE MRI parameters kep (r=-0.2544, p=0.0052), vp (r=-0.2429, p=0.0078) and max slope of signal increase(r=-0.2282, p=0.0133); and positive correlation with ve (r=0.3275, p=0.0003) and D(r=0.2675, p=0.0037).
Conclusion: Invasive breast cancer with higher pericyte gene score showed lower perfusion pharmacokinetic parameters (kep, vp), higher extra-vascular extracellular space (ve) and less restricted diffusion, which means fewer blood vessels and less leaky in tumour. These associations revealed that DCE-MR parameters could be considered in guiding anti-angiogenesis treatment of breast cancer.

B-1124 10:55

Correlation of diffusion-weighted apparent diffusion coefficient values with prognostic factors of invasive breast cancer
B. Ubeda, S. Vizcaya, J.L. Browne, F. Terrel; *Barcelona/ES (belube@dexeus.com)*

Purpose: To correlate the apparent diffusion coefficient (ADC) values of invasive breast cancer with pathological and molecular prognostic factors.
Methods and Materials: Magnetic Resonance (MR) and diffusion-weighted images (DWI) were retrospectively reviewed in 310 patients with pathologically proven invasive breast cancer (267 invasive ductal carcinoma (IDC), 34 lobular invasive carcinoma (ILC), 9 other types). DWI were acquired at b values of 0 and 600 s/mm^2. Mean ADC values were correlated with MR morphological type of lesion (mass vs non-mass), histological features and molecular subtypes. Histological evaluation included tumoUral type, tumour size and grade, expression of oestrogen and progesterone receptors (ER, PR), HER2 status and Ki67 index.
Results: Mean ADC values were 0.97 x 10^{-3} mm^2/s for IDC and 0.95 x 10^{-3} mm^2/s for ILC. No significant difference of ADC was found with tumour size or morphological type of lesion. Mean ADC value of grade I lesions was significantly higher than grade II and III lesions (0.998 ± 0.21 x 10^{-3} mm^2/s vs 0.96 ± 0.18 x 10^{-3} mm^2/s and 0.87 ± 0.86 x 10^{-3} mm^2/s). There was no significant correlation between ADC value and ER, PR and HER2 expression status. Mean ADC of Ki67 index positive cancers (0.934 ± 0.19 x 10^{-3} mm^2/s) was significantly lower than that of Ki67 index negative cancers (1.006 ± 0.21 10^{-3} mm^2/s).
Conclusion: Our study showed statistically significant association between ADC values and histological and molecular features of breast cancer related to increased cellular proliferation such as tumour grade and Ki67 index.

B-1125 11:03

Is DWI a stand-alone or complimentary parameter to DCE-MRI of the breast for cancer detection?
K. Pinker-Domenig[1], L. Moy[1], E. Sutton[1], M. Weber[2], M. Jochelson[1], S. Thakur[1], T.H. Helbich[2], E. Morris[1]; [1]*New York, NY/US*, [2]*Vienna/AT (pinkerdk@mskcc.org)*

Purpose: To assess whether DWI can serve as a stand-alone parameter for breast cancer detection and to compare it to DCE-MRI and multiparametric MRI (mpMRI).
Methods and Materials: In this IRB-approved retrospective study two experienced reader independently evaluated mpMRI of 110 breast tumours. DWI and DCE-MRIs were randomly assessed by independent review, i.e. readers assessed DWI without DCE-MRI and vice-versa. Additionally, mpMRI using the combined information of DWI and DCE-MRI were evaluated. Lesions were classified as normal/benign or suspicious and a BI-RADS classification was assigned. Histopathology was used as the standard of reference. Appropriate statistical tests were used to assess sensitivity, specificity and diagnostic accuracy for DWI, DCE-MRI and mpMRI.
Results: There were 42 benign and 68 malignant tumours. DCE-MRI was the most sensitive test for breast cancer detection (r1 100%, r2 97%). DWI as a stand-alone parameter was significantly less sensitive (r1 and r2=85%, p=0.001 and 0.003) but more specific (r1 and r2=86%, p=0.004 and 0.048) compared to DCE-MRI (r1=69%, r2=74%). MpMRI had a sensitivity of 96% for both readers,which was not significantly different from DCE-MRI (p=0.076 and 0.53) and a specificity almost as good as DWI (r1 81%, r2 86%, p=0.147 and 1) with the best diagnostic accuracy (r1 90%, r2 92%).
Conclusion: DWI cannot be used as a stand-alone parameter for breast cancer detection. DCE-MRI is the most sensitive test. MpMRI using DWI and DCE-MRI maintains a high sensitivity, increases specificity and maximises diagnostic accuracy for breast cancer.

B-1126 11:11

Synthetic biomarkers using IVIM and non-Gaussian diffusion MRI: diagnostic performance and comparison with BI-RADS categories in differentiation of malignant/benign breast tumours
M. Iima, M. Kataoka, S. Kanao, N. Onishi, M. Kawai, A. Ohashi, R. Sakaguchi, A.K. Ohno, K. Togashi; *Kyoto/JP (mamiiima@kuhp.kyoto-u.ac.jp)*

Purpose: To evaluate the diagnostic performance in differentiation of breast lesions using IVIM, non-Gaussian diffusion parameters and synthetic ADC, and compare the performance of DWI derived categories with BI-RADS categories.
Methods and Materials: 405 patients were prospectively enrolled and 210 lesions (malignant 158/ benign 52) were included. IVIM (fIVIM, D*) and non-Gaussian diffusion (ADCo, K) parameters using IVIM and Kurtosis model were estimated from DWI series with 16 b values up to 2,500 sec/mm^2. Synthetic ADC (sADC) obtained from different combinations of 2 key b values (200/1500, 400/1500, 400/2000, 600/2000 sec/mm^2) and standard ADC (0/800 sec/mm^2) were calculated. The IVIM/diffusion parameters in malignant and benign lesions were compared using Mann-Whitney test. Then, equivalent BI-RADS

categories were computed by mixing these IVIM/diffusion parameters, through two diagnostic approaches; combined parameter thresholds and Bayesian analysis. These categories derived from DWI datasets was compared with standard BI-RADs categories, by assigning category 2/3 as benign, while category 4/5 as malignant.
Results: All IVIM/diffusion parameters and sADCs were different between malignant and benign breast lesions (p< .01). AUC for sADC200_1500 was the highest (0.923). The sensitivity and specificity for diagnosis was 89.9% and 78.8% for sADC200-1500, 93.0% and 80.8% for the combined thresholds approach, 88.6% and 73.1% for Bayesian analysis, and 100% and 78.8% for BI-RADS.
Conclusion: Synthetic approaches combining various IVIM and non-Gaussian diffusion MRI parameters may provide BI-RADs equivalent category comparable to BI-RADS without the use of contrast agents. sADC showed a fairly high diagnostic performance for breast cancer.

B-1127 11:19

Is the necrosis/wall ADC ratio useful for the differentiation of benign and malignant breast lesions?

I. Durursubasi[1], A. Durur-Karakaya[2], A. Karaman[3], M. Seker[2], E. Demirci[3], F. Alper[3]; [1]*Ankara/TR*, [2]*Istanbul/TR*, [3]*Erzurum/TR (irmakdurur@yahoo.com)*

Purpose: To determine whether the necrosis/wall apparent diffusion coefficient (ADC) ratio was useful for the benign-malign differentiation of necrotic breast lesions.
Methods and Materials: Breast MRIs were performed using a 3T system. In this retrospective study, calculation of the necrosis/wall ADC ratio was based on ADC values measured from necrosis and from the wall of malignant and benign breast lesions by diffusion-weighted imaging (DWI). All the diagnoses were pathologically confirmed. Statistical analyses were performed with the independent samples t test and receiver operating characteristic (ROC) analysis.
Results: A total of 53 female patients were enrolled, 27 of whom had necrotic breast carcinoma and 26 of whom had breast abscess. ADC values were obtained from wall and necrosis. The mean necrosis/wall ADC ratio (±SD) of carcinoma was 1.49±0.26 and abscess was 0.61±0.11. The area under the curve (AUC) values for necrosis ADC, wall ADC and the necrosis/wall ADC ratio were 0.967, 0.027 and 0.991, respectively. A wall/necrosis ADC ratio cut-off value of 0.83 demonstrated a sensitivity of 100%, specificity of 93%, positive predictive value of 96%, negative predictive value of 92% and accuracy of 94% to determine the malign nature of a necrotic breast lesion.
Conclusion: Necrosis/wall ADC ratio seems to be a reliable and promising tool for discriminating breast carcinoma from abscess using DWI.

B-1128 11:27

Discrimination of malignant and benign breast masses using automatic segmentation and region of interest-based features extracted from MRI

X. Jiang, F. Xie, L.-Z. Liu, Y.-X. Peng, H.-M. Cai, L. Li; *Guangzhou/CN (jiangxh@sysucc.org.cn)*

Purpose: To investigate whether combining morphology, texture features and kinetic features with diffusion-weighted imaging (DWI) using quantitative analysis improves the accuracy of discriminating malignant from benign breast masses.
Methods and Materials: One hundred and four benign and 171 malignant lesions in 205 women were included. Thirteen texture and eleven morphology features were computed from each lesion using a semi-automated segmentation method. To increase prediction accuracy, a newly designed classification model, difference-weighted local hyperplane (DWLH), was used for statistical analysis of the combined effects of the features for predicting lesion type. The mean apparent diffusion coefficient (ADC) value for each lesion was calculated. Diagnostic performances of morphology and texture features, kinetic features and ADC alone and the combination of them were evaluated using receiver operating characteristics analysis.
Results: Malignant lesions had lower mean ADCs than benign lesions. By using ten-fold cross validation scheme, combined morphological and kinetic features achieved a diagnostic average accuracy of 0.87. Adding an ADC threshold of 1.37 × 10−3 mm2/s increased the overall averaged accuracy to 0.90. A multivariate model combining ADC values with six morphological and kinetic parameters best discriminated malignant from benign lesions.
Conclusion: Incorporating morphology and texture features, kinetic features and ADC into a multivariable diagnostic model improves the discriminatory power of breast lesions.

B-1129 11:35

Comparison between mono-exponential Gaussian diffusion and non-Gaussian kurtosis model for breast lesions evaluation

A. Christou[1], A. Ghiatas[2], D. Priovolos[2], K. Veliou[3], H. Bougias[3]; [1]*Doncaster/UK*, [2]*Athens/GR*, [3]*Ioannina/GR (alexandrachristou@gmail.com)*

Purpose: To compare Gaussian and non-Gaussian diffusion models in the characterisation and differentiation of breast lesions.
Methods and Materials: 49 patients with 53 breast lesions underwent magnetic resonance imaging (MRI). Diffusion-weighted imaging (DWI) was acquired on a 1.5T MRI utilising 5 b-values (0,400,800,1100,1300). The median ADC, Dapp (non-Gaussian apparent diffusion coefficient) and K (kurtosis) were calculated from the whole-lesion histogram analysis and compared by the Mann-Whitney U test (level of significance set at 0.05). Receiver operating characteristics (ROC) analysis was used to determine the most effective cut-off values for the differentiation between benign and malignant pathologies. Goodness-of-fit for each model was assessed using the Root Mean Square Error (RMSE).
Results: K values of benign lesions were significantly lower than those of malignant lesions. A cut-off value of 0.71 provided sensitivity 97.1% and specificity 93.7% with area under curve (AUC) 0.976. Dapp values of malignant lesions were lower than those of benign lesions at 1.57mm^2/sec sensitivity 91.2%, specificity 93.7%, AUC 0.949. Malignant ADC was significantly lower than benign ADC. A cutoff value of 1.09×10^{-3} mm^2/sec provided sensitivity 95.1% and specificity 91.7%, AUC 0.962. The kurtosis model provided the highest fitting performance. RMSE for the mono-exponential and kurtosis models was 3.8 and 0.8 for the malignant lesions (P<0.05) and 3.2 and 0.4 (P<0.05) for the benign lesions respectively.
Conclusion: Both diffusion models proved to have excellent accuracy rates with no significant difference. However, the kurtosis model measures also the deviation from the Gaussian diffusion model and thus characterise better heterogeneous masses.

B-1130 11:43

Your choice: not all sequences for diffusion-weighted imaging (DWI) of the breast yield the same results

F. Leone[1], R. Woitek[2], P. Clauser[2], P. Kapetas[2], K. Preidler[2], T.H. Helbich[2], P.A.T. Baltzer[2]; [1]*Monza/IT*, [2]*Vienna/AT (federica-leone@live.it)*

Purpose: While readout-segmented EPI sequences for DWI have been promoted as yielding superior results due to higher spatial resolution and less architectural distortion, the literature lacks a systematic comparison with standard EPI-DWI regarding image quality, reproducibility and diagnostic performance. This study aimed to address this field.
Methods and Materials: Consecutive patients undergoing multiparametric 3T (Siemens Skyra fit) breast MRI including readout-segmented (RESOLVE) and standard breast DWI (REVEAL) were prospectively collected for this IRB-approved observational study. Further inclusion criterion was histological verification of breast lesions visible on MRI. Two breast radiologists evaluated both sequences independently. Data collection included lesion conspicuity on an ordinal scale and mean as well as minimum ADC values from manually placed regions-of-interest. Statistical analysis included visual-grading characteristics, receiver-operating characteristics and inter-reader intraclass-correlation coefficient (ICC) calculation. P values <0.05 were considered statistically significant.
Results: 43 Patients with 43 index lesions (29 malignant, 14 benign) were included. ROC analysis revealed a significantly higher area under the ROC curve for REVEAL as compared to RESOLVE (P≤0.039, respectively). Measurement of minimum ADCs was not diagnostically superior to mean ADCs (P>0.05). Inter-reader ICCs did not differ between RESOLVE and REVEAL (0.985). Lesion conspicuity was equal for both sequences (P>0.05).
Conclusion: We found a superior diagnostic performance using standard EPI (REVEAL) compared to readout-segmented DWI (RESOLVE) for diagnosis of breast lesions. Reproducibility and lesion conspicuity did not differ between both sequences.

B-1131 11:51

Comparison of conventional imaging plus DWI and conventional imaging plus DCE-MRI in planning the surgical treatment of patients with breast cancer

L. Vassallo[1], E. Rachetta[1], G. Cappello[2], V. Doronzio[3], D. Regge[3], L. Martincich[3]; [1]*Savigliano/IT*, [2]*Avola/IT*, [3]*Candiolo/IT (lorenzo.vassallo1987@libero.it)*

Purpose: To compare conventional imaging plus DWI (Protocol 1) and conventional imaging plus DCE-MRI (Protocol 2) in planning surgical treatment of patients with breast cancer.
Methods and Materials: 66 consecutive patients with operable biopsy-proven breast cancer underwent pre-surgical MRI (1.5T magnet and 8-channel coil) consisting of DWI (axial EPI sequence; b-value 0 and 1500 s/mm2; thickness

4mm) and DCE-MRI (3DT1w sequence; thickness 2mm). Both protocols were independently reviewed. For DWI, areas of hyperintensity at large b-value were considered suspicious/suggestive for malignancy while DCE-MRI were reported according to ACR BI-RADS. Results were then prospectively used by multidisciplinary team in planning surgical treatment (mastectomy vs BCS, breast conservative surgery) and compared with pathology. McNemar and κ tests were used to assess diagnostic performance and inter-protocols agreement.
Results: 29 Patients underwent BCS while 37 mastectomy (2 for positive margins after BCS). Pathology identified 34 unifocal and 32 multiple cancers. Protocol 1 planned 34 BCS and 32 mastectomies while protocol 2 planned 31 BCS and 35 mastectomies. Inter-protocol agreement was excellent (k=0.9). Accuracy of protocol 1 and 2 were 92% (61/66) and 97% (64/66), respectively. Two multiple DCIS requiring mastectomy for positive margins after BCS were underestimated by both protocols. 2/3 cases in which protocol 1 incorrectly planned BCS were represented by multiple disease at pathology.
Conclusion: In planning surgical treatment, conventional imaging plus DWI shows more than acceptable accuracy (slightly lower than conventional imaging plus DCE-MRI) and could represent a reliable tool in pre-surgical setting. The study is still ongoing to confirm the results in a larger series.

10:30 - 12:00 **Room E2**

Neuro

SS 1811a
Spine and peripheral nerves

Moderators:
D. Maric; Banja Luka/BA
G. Pellicanò; Florence/IT

B-1132 10:30

Diffusion tensor imaging and fiber tracking biomarkers of intramedullary tumours of spinal cord for predictive resectabality scoring-observational comparitive study of 48 cases
R.S.V. Vadapalli, L. Chittem, V. Mudumba, A. Vadapalli, S. Bhattacharya; *Hyderabad/IN (rammohanvsv@yahoo.com)*

Purpose: The aim of this prospective study is to evaluate the role of Diffusion Tensor Imaging (DTI) in management of intramedullary spinal cord lesions (IMSCL) for predicting “safe resectibility” to assess subsequent outcomes.
Methods and Materials: DTI was performed in 65 patients with IMSCL along with conventional MRI. Tumour matrix fractional anisotropy (FA), tumour cord interface FA were assessed. Lesions were grouped into 3 groups as completely resectable, partially resectable, unresectable based on the presence of cleavage between the lesion and spinal cord. These results were compared and correlated with intraoperative findings, neurological outcome at the end of 1 year follow-up was assessed.
Results: There were 65 patients (38 male, 27 female; mean age of 37.5 years) in this study, 50 were neoplastic (19 ependymomas, 14 astrocytomas, 3 metastases, 4 hemangioblastoma, 5 cavernomas, 5 lipomas); 20 were non neoplastic (Tuberculoma (6), Neurocystecercosis (4) Tumefactive demyelination plaques (5) . DTI was used to classify the lesions as completely resectable (18), partially resectable (26) unresectable (6). The capability of DTI in predicting the presence of cleavage plane, resectability and prognostication were statistically significant. (P=<.001) Spearman’s Correlation coefficient between DTI prediction of cleavage plane and intra operative finding of plane was 0.84 (p value 0.0001) -significant. Correlation coefficient between DTI prediction of infiltration of tracts and neurological outcome (deteriorated or not) was 0.46 (p value 0.02) suggesting that DTI can be useful tool for prognosticating the IMSCL.
Conclusion: This study suggests that DTI is useful in predicting the safe resectability of IMSCL.

B-1133 10:38

Role of phase sensitive inversion recovery sequence compared to STIR and T2W_TSE in detection of cervical cord multiple sclerosis lesions
Z. Abidi; *Qaem Shahr/IR (abidi.z4805@yahoo.com)*

Purpose: Multiple sclerosis (MS) is a chronic inflammatory disease in brain and spinal cord. Spinal cord MS lesions usually are accompanied by brain lesions. But, about 20% of patients with spinal cord lesions have no plaques in their brain. T_2W_TSE, STIR (Short TI Inversion Recovery) sequences routinely are used in imaging study of MS patients to depict spinal cord MS lesions. We aimed to investigate the importance of PSIR(Phase Sensitive Inversion Recovery) sequence in detection of MS lesions in spinal cord.
Methods and Materials: Fifteen patients with MS underwent on a 1.5 Tesla Philips (Ingenia) MRI scanner using protocols included T2W_ TSE, STIR and PSIR sequences in sagittal plane with 3 mm thick slices.
Results: The contrast between MS lesions and surrounding tissues in spinal cord was significantly higher in PSIR compared to STIR and T2W images. Radiologist observed better delineation of lesions in PSIR compared to T2W_TSE and STIR sequences. The lesions in PSIR were shown more clearly. In addition to higher contrast, flow artifacts are less eminent in PSIR due to a short TE.
Conclusion: Spinal cord MRI would be beneficial for early diagnosis and recognising clinical subtypes of MS due to high spread of lesions in patients with definite MS. STIR is still considered as a gold standard sequence in detection of cervical cord lesions. but, the advantages of PSIR over STIR and T2-weighted images persuaded us to recommend PSIR as a complementary sequence to detect cervical cord MS lesions.
Author Disclosures:
Z. Abidi: Author; Fariborz Faeghi, Zahra Mardanshahi, Jamil Abdolmohammadi, Mohammad Sakhaei.

B-1134 10:46

Causes of spinal haemorrhage in a level one trauma centre
R. Riascos[1], E. Bonfante[1], J.A. Mora[2], C. Sitton[1], J. Choi[1]; [1]*Houston, TX/US*, [2]*Bogota/CO (juanchomora83@hotmail.com)*

Purpose: The goal of this study was to determine the etiology and characteristics of spinal haematomas; also the effectiveness of the initial images in the diagnosis.
Methods and Materials: Retrospective observational study with a time period of seven months (December 2014- July 2015) was determined, then all patients diagnosed with spine haemorrage.
Results: 61 patients diagnosed with spinal haemorrhage, 40 men and 21 women with a median age of 49-53 years were included. It was established as the main mechanism. Trauma 83%, postsurgical 6.5%, insufficiency fracture 3.2%, pathological fracture 3.2% and spontaneous bleeding 3.2%. Were found 53 epidural haematomas and eight subdural haematomas Twenty-two cases were located in the lumbar spine,18 in cervical spine, eight thoracic spine, six thoraco lumbar, three cervical- thoracic and one sacrum. The location within the spinal canal 54% anterior, 45% posterior and 3.2% lateral. The average longitudinal diameter bruising models was 66 mm, with an extension of three vertebral segment on average. Sixty-three percent spinal haematomas has compressive effect and 37% showed no signs of compression. Seventy-seven percent of patients presented vertebral fracture associated with an average of three fractured vertebrae.
Conclusion: It was established as the main etiological factor of spinal bleeding is trauma associated with vertebral fractures, the effective diagnosis is important because most of the haemorrhage has compressive effects on the spinal cord; also MRI proved to be the modality of choice for diagnosis and follow-up while CT show has a low sensitivity diagnosed.

B-1135 10:54

Effects of appropriateness of cauda equina imaging on clinical risks, workload and costs
S. Gargalas, S. Karia; *Oxford/UK (sergios@gargalas.org)*

Purpose: Cauda equina (CE) is a neurosurgical emergency that requires imaging within 24 hours from symptom onset for optimum intervention results. Despite its naturally infrequent occurrence, requests to exclude CE constitute a significant portion of our department's workload. We investigate the appropriateness of the requests for such imaging and its effect on the clinical outcomes, costs and workload within the National Health Service (NHS).
Methods and Materials: We identified patients who had lumbar spine MRI with strong clinical suspicion for CE between 2014 and 2015. The clinical history, progression and outcomes were compared. Costs for inappropriate imaging and effects on workload have been calculated.
Results: A total of 705 cases were identified, accounting for average of 1.2 emergent lumbar spine MRI per day. A total of 131 studies (18.6%) did not meet published criteria for neurosurgical intervention and furthermore did not have radiological evidence of cauda equina. Overall positive rate was 6.8%.
Conclusion: We found that inappropriate referrals to exclude CE constitute 3% of total MRI inpatient workload. Each inappropriate study burdens the NHS £146 in tariff costs; however, the economic implications of added workload burden and/or misdiagnosis, as well as delay in "less urgent examinations" is expected to be far greater. Strict imaging criteria is a clear target in attempt to reduce these inefficiencies.

B-1136 11:02

Quantitative MRI-based three-dimensional volumetry of dural sac and vertebral bodies improves diagnosis of dural ectasia in Marfan syndrome

F. Rengier[1], O. Naas[1], T. Norajitra[1], M. Messerli[2], K. Kallenbach[1], M. Karck[1], K. Maier-Hein[1], H.-U. Kauczor[1]; [1]*Heidelberg/DE*, [2]*Zurich/CH*
(fabian.rengier@web.de)

Purpose: Assess MRI-based three-dimensional volumetry of dural sac and vertebral bodies for diagnosis of dural ectasia in Marfan syndrome compared to dural sac diameter ratios as current clinical standard.
Methods and Materials: In 188 patients being evaluated for Marfan syndrome 2012-2015 a single slab 3D T2-weighted TSE sequence of the lumbosacral spine was acquired with a spatial resolution of 1x1x1mm³. A random sample of 20 patients (mean 32.0 years, 7 female) was included. In nine of these patients diagnosis of Marfan syndrome was confirmed according to the 2010 Revised Ghent Nosology, 11 patients served as controls. Dural sac and vertebral bodies L5 and S1 were segmented using the Medical Imaging Interaction Toolkit (MITK). For comparison with current clinical standard, anteroposterior diameters of vertebral bodies and dural sac were measured halfway between the superior and inferior endplates. Ratios between dural sac volume/diameter at the respective level and vertebral body volume/diameter were computed for L5 and S1.
Results: L5-/S1-dural sac volumes were 11.0/13.8ml in Marfan patients compared to 6.9/5.0ml in controls (both $p<0.05$). Sensitivity, specificity, positive predictive value and negative predictive value for diagnosis of Marfan syndrome were: for 3D volumetry using 7.7/6.4ml as cut-off 78%/91%/88%/83%, for criteria of Habermann et al. 78%/45%/54%/71%, and for criteria of Oosterhof et al. 67%/73%/67%/73%.
Conclusion: MRI-based 3D volumetry of dural sac and vertebral bodies for quantifying dural ectasia is feasible and particularly improved specificity for diagnosis of Marfan syndrome compared to published quantitative criteria based on dural sac diameter ratios as current clinical standard.

B-1137 11:10

Diagnostic value of 3D FIESTA sequence in imaging of lumbar radiculopathy

F. Abubacker Sulaiman; *Chennai/IN (fasulaiman@hotmail.com)*

Purpose: This study is being conducted for establishing a new protocol for lumbar radiculopathy and to document the superiority of 3D FIESTA over conventional MRI protocol.
Methods and Materials: The study was divided into two groups. The control group consisted of 15 healthy volunteers and the experimental group consisted of 58 patients.
Results: In all patients who were evaluated in our study with both FSE T2W and 3D FIESTA sequences statistically the visibility of the evaluated structures and lumbar radiculopathy was excellent for axial 2D T2w TSE and axial 3D FIESTA (MPR) (74.2, 100 percent), respectively. As the visualisation of the normal structures were comparatively excellent for 3D FIESTA with good spatial resolution and adequate T2/T1 ratio.
Conclusion: The detection of lumbar radiculopathy in terms of each affected dermatomes has always proved to be a diagnostic challenge both for the physician and the radiologist, the use of 3D FIESTA sequences has greatly enhanced detection rates.

B-1138 11:18

Diffusion tensor imaging of the arm nerves: tractography and quantitative analysis

V. Durante, R. Gasparotti; *Brescia/IT (vale.durante@hotmail.it)*

Purpose: Diffusion Tensor Imaging (DTI) is an emerging MRI method that reveals micro structural characteristics of biological tissue and offers quantitative parameters as FA (fractional anisotropy). This parameter, which resulting different in base of disease, represent an added value in the patient's diagnostic workup becouse increase the specificity of magnetic resonance exam. We calculated this value,in healthy subjects, at the level of the arm for median, ulnar and radial nerves, because there aren't reference literature parameters.
Methods and Materials: We study 10 healthy volunteers (5men,5 women; mean age 23 years) using single-shot-spin-echo planar imaging sequence (TR/TE, 10700/77ms; b-value, 0, 1000 s/mm^2). Two indipentent readers performed post-processing and fiber tractography. Fiber tracts of median, ulnar and radial nerves in the arm were calculated and the FA value was calculated.
Results: Fiber tractography generated significantly longer fibers for three arm nerves in all subjects. No statistically significant differences ($p=0,67$) were found between FA values calculated by two readers, Mean FA values were as follow: 0,53 for median nerve, 0,54 for ulnar nerve and 0,51 for radial nerve.
Conclusion: The study showed that it is possible to examine the nerves of the arm through optimised DTI sequences and perform on them a quantitative analisys. The FA values obtained in healthy subjects rapresent an important stage for a better characterisation of pathology in the patients with neuropathy, using magnetic resonance imaging.

B-1139 11:26

Ultrasound findings and anatomical correlations in periferal nerves damage neurosurgery

V. Dekan, A. Gaivoronsky, E. Zhurbin, A. Grishchenkov; *St. Petersburg/RU (dekanvs@mail.ru)*

Purpose: Research objective was to compare anatomic features of peripheral nerves of extremities and ultrasonographic findings in diagnostics of injuries of peripheral nerves and scheduling of neurosurgical treatment.
Methods and Materials: 25 patients with injuries of peripheral nerves, including gunshot wounds were examined by means of a sonography. All patients undergone surgical treatment. Sonography was performed with use of high resolution linear transducer. Main indicators which estimated at a sonography were:- identification of the site of injury of a nerve, definition of the true divergence of the ends at the complete break, definition of a depth of a nervous trunk and its ends, epicutaneous marking of localisation of a nervous trunk, place of its damage, ends of a nerve.
Results: In all cases the sonography allowed to locate damages of a trunk of a peripheral nerve, estimate a damage rate and its character, and also to define criteria, necessary for making decision on operative measure realization. Main types of pathology were: the complete transmural injury of a nerve with a divergence of the ends and formation of end neuromas (n=19), partial damage of a nervous trunk with preservation of an anatomic continuity (n=3), traction damage without violation of an anatomic integrity (n=3).
Conclusion: Ultrasound examination of injured peripheral nerves is high informative and accurate method of preoperative vizualisation and planning in various damages of peripheral nerves. This method is sufficient for final diagnostics and definition of indications to surgical treatment.

B-1140 11:34

Value of high resolution ultrasound in carpal tunnel syndrome diagnosis

S.P. Ivanoski[1], M. Bozinoska Smiceska[1], V. Vasilevska Nikodinovska[2]; [1]*Ohrid/MK*, [2]*Skopje/MK (v_vasilevska@yahoo.com)*

Purpose: To evaluate the diagnostic efficiency of high-resolution ultrasound in carpal tunnel syndrome (CTS) diagnosis in comparison to electromyography (EMG).
Methods and Materials: Prospectively, median nerves in 39 wrists of 22 patients with CTS diagnosed on EMG were evaluated sonographically. Majority of patients (77%) had bilateral CTS. 16 patients were women and 6 were men. 40 wrists of 20 asymptomatic volunteers consisted the control group. Ultrasound exam was performed by a radiologist with 5 years' experience in MSK ultrasound, within few days following the EMG. The radiologist was blinded with clinical and EMG data. Ultrasound criterion for carpal tunnel syndrome was a median nerve cross-sectional area ≥10 mm^2 at proximal carpal tunnel level. Sensitivity, specificity, positive and negative predictive value and accuracy of the method were evaluated.
Results: Ultrasound showed high sensitivity in diagnosis of carpal tunnel syndrome (87.18%), true positive finding was present in 34 of 39 patients diagnosed by EMG. Specificity was high (82.5%). There was positive predictive value of 82.93% negative predictive value of 86.84% and accuracy of 84.81% for ultrasound. Mean cross-sectional area in patients diagnosed with CTS was 13.7 mm^2, and 7.92 mm^2 in asymptomatic volunteers. Wrist/forearm ratio of median nerve was 2.11 in patients with proven CTS, compared to 1.45 in asymptomatic volunteers.
Conclusion: Ultrasound has high sensitivity, specificity and accuracy in diagnosis of carpal tunnel syndrome compared to EMG exam. Its availability, easiness of use, acceptance by patients and low cost make it quick and valuable method for evaluation of carpal tunnel syndrome.

B-1141 11:42

Diffusion tensor imaging in cervical and dorsolumbar spinal cord injury

M.K. Poonia, M.M. D'souza, A. Choudhary; *Delhi/IN (mahesh.poonia@gmail.com)*

Purpose: The study was performed to assess the role of diffusion tensor imaging (DTI) in assessment of spinal cord integrity after injury, beyond that delineated on conventional magnetic resonance imaging (MRI).
Methods and Materials: Conventional MRI and DTI of the cervical and dorsolumbar spine was performed using 3Tesla MR system (Magnetom Skyra, Siemens) on cases of spinal trauma (cervical n=20 and dorsolumbar n=10) and age- and sex-matched healthy controls (n=30). Fractional anisotropy (FA) and mean diffusivity (MD) of injured cord were compared with corresponding region of controls.

Results: Mean FA value at the level of trauma was lower in cases as compared to controls in cervical (0.43+/-0.08 vs 0.62+/-0.06 respectively, p <0.001) and dorsolumbar injury (0.29+/-0.07 vs 0.57+/-0.05 respectively, p <0.001). Additionally, mean MD value was higher in cases as compared to controls at the level of trauma (1.30+/-0.24 vs 1.07+/-0.12 respectively, p <0.001 for cervical and 1.39+/-0.16 vs 1.27+/-0.24 respectively, p <0.02 for dorsolumbar injury). 14 cases revealed significantly abnormal DTI indices, despite a normal conventional MR study. All patients with DTI abnormalities had sensorimotor deficit on clinical examination.
Conclusion: DTI appears to be a better diagnostic measure as compared to conventional MR imaging in depicting subtle changes in cord integrity after injury.

B-1142 11:50

Evaluation of neurovascular compression in trigeminal neuralgia using 3D-DRIVE MRI and correlation with surgical microvascular decompression

M.M.A.H. ElShafey, H.A.M.M. Abdel Daiem, A.H. Farhoud; *Alexandria/EG (mohamedeshafei@yahoo.com)*

Purpose: To present the role of 3D-CISS as a non-contrast enhancing high-resolution MR imaging sequence in the preoperative evaluation of neurovascular compression (NVC) in patients with trigeminal neuralgia (TN), and correlation with surgical microvascular decompression (MVD).
Methods and Materials: 30 patients with TN refractory to medical treatment performed 3D-CISS at 1.5 T MRI. Multiplanar reformation (MPR) was used for reconstruction of the source images in three dimensional planes. Assessment of trigeminal nerves was done on both sides for detection of the point of NVC (crushing point), it's site, length of affected segment and the offending vessel.
Results: Neurovascular compression was detected in all patients. The root entry zone (REZ) was the crushing point in all except one patient who showed NVC only at the cisternal segment of the trigeminal nerve. Five patients presented NVC at two points including REZ and the cisternal segment. Imaging findings were matching with the intraoperative findings in all patients. No significant postoperative complications encountered.
Conclusion: 3D-CISS MRI could be considered an essential diagnostic tool in the preoperative evaluation of TN patients.

10:30 - 12:00 **Room F2**

Breast

SS 1802b

Breast cancer screening

Moderators:
F. Kilburn-Toppin; Cambridge/UK
S. Zackrisson; Malmö/SE

B-1143 10:30

A randomised controlled trial to evaluate tomosynthesis vs digital mammography screening: preliminary results on baseline detection rate

V. Iotti[1], A. Nitrosi[1], C. Coriani[1], S. Caffarri[2], C. Campari[1], V. Ginocchi[2], R. Vacondio[1], P. Giorgi Rossi[1], P. Pattacini[1]; [1]*Reggio Emilia/IT*, [2]*Guastalla/IT (valentina.iotti@asmn.re.it)*

Purpose: We are conducting a randomised trial on the efficacy of breast cancer screening with digital breast tomosynthesis (DBT) compared with digital mammography (DM) in reducing advanced and interval cancer incidence (NCT02698202). We present interim baseline data on detection rate by cancer diameter and breast density.
Methods and Materials: Consenting women presenting for a new screening round at the population-based (45-70 age range) mammography screening, were randomised to DM (usual care) or DBT+DM two-view bi-lateral examinations, both with double independent reading. Breast density was classified according to the Peak Breast Density computed by the mammography system and stored in image header. We report relative detection rate (RDR) with 95% confidence intervals (95%CI).
Results: From March 2014 to March 2016, 9782 were randomised to DM arm and 9623 to DBT+DM arm; 45 (6 in-situ) and 79 (14 in-situ) cancers were detected in DM and DBT+DM arm, respectively; overall RDR was 1.8 (95%CI:1.2-2.6), in-situ RDR was 2.4 (95%CI:0.9-7.5, p for heterogeneity 0.52); there was no difference by breast density (RDR 1.6, 95%CI:1.0-2.8 and 1.9, 95%CI:1.0-3.9, in dense and fat breast, respectively, p for heterogeneity 0.74), despite the absolute detection rate was 2.8 folds higher in dense than fat breast. The RDR was 1.7 (95%CI 0.9-3.5), 2.6 (95%CI 1.2-5.8), and 0.7 (95%CI 0.2-2.7) for T1<1cm, T1c and T2, respectively (p for heterogeneity 0.18).
Conclusion: DBT identified 80% more cancers than DM in this randomised trial. The detection was increased similarly for in-situ and invasive, <1 cm and T1c cancers, in dense and fat breast.

B-1144 10:38

Digital breast tomosynthesis vs digital mammography - early performance measures in a population-based screening program

S. Hofvind[1], T. Hovda[2], Å.S. Holen[1], J.L. Albertsen[3], H. Bjørndal[2], S.H.B. Brandal[1], L. Romundstad[1], E. Vigeland[3], P. Skaane[1]; [1]*Oslo/NO*, [2]*Drammen/NO*, [3]*Tønsberg/NO (solveig.hofvind@kreftregisteret.no)*

Purpose: To compare recall rate and rate of screen-detected breast cancer after one year screening with synthetic images and digital breast tomosynthesis (DBT) versus digital mammography (DM) in the Norwegian Breast Cancer Screening Program (NBCSP).
Methods and Materials: A total of 18 172 women residing in Oslo were screened with DBT in 2014, while a control group of 30 883 women was screened with DM, in the NBCSP. We performed descriptive analyses, and z-test to test for statistical significance (p<0.05) between the two groups.
Results: The recall rate due to abnormal mammographic findings was 3.2% (576/18 172) and 3.3% (1007/30 883, p=0.58) for DBT and DM, respectively. The rate of screen-detected breast cancer was 9.3 per 1000 screened with DBT and 6.4 per 1000 (p<0.01) screened with DM. Both the rate of screen-detected Ductal Carcinoma in Situ and invasive breast cancer was statistically significantly higher for DBT compared with DM (p<0.01 and p=0.02, respectively).
Conclusion: The rate of screen-detected breast cancer was about 50% higher for women screened with DBT compared with women screened with DM.

B-1145 10:46

The risk of progression of atypia into invasive breast cancer among women attending the Norwegian Breast Cancer Screening Programme

M. Lilleborge, S. Sebuødegård, S. Hofvind; *Oslo/NO (marie.lilleborge@kreftregisteret.no)*

Purpose: To estimate the risk of progression from atypia into invasive cancer in the ipsilateral breast, among women attending the Norwegian Breast Cancer Screening Programme (NBCSP).
Methods and Materials: A total of 2,764,782 screening examinations were performed among 677,932 women aged 50-69 years in NBCSP, 1995-2015. Out of 83,891 recall examinations, 50,130 were concluded negative after additional imaging and ultrasound only, while 1,177 included biopsy with corresponding classification for both breasts. Ductal carcinoma in situ (DCIS) or invasive breast cancer was identified in 15,659 cases, and 19,279 cases were classified as benign. A total of 1,167 women, free from ipsilateral DCIS and breast cancer, were diagnosed with atypia (last digit in the SNOMED code: 1 or 5). We followed the women for invasive breast cancer until end of follow-up (31.12.2015, date of death, emigration or diagnosis of invasive breast cancer, whichever came first). Cox regression was used to study the risk of ipsilateral invasive breast cancer among the women classified with atypia, stratified by age.
Results: The risk of an invasive breast cancer in the ipsilateral breast after a screening detected atypia was 93% higher compared with a negative recall after additional imaging and ultrasound only [HR= 1.93; 95% CI: 1.38-2.69]. The risk increased by age at atypia (1-year-intervals) [HR= 1.04; 95% CI: 1.03-1.05].
Conclusion: The risk of developing invasive breast cancer in the ipsilateral breast was about twofold for women recalled and diagnosed with atypia compared with those recalled and ruled out negative with additional imaging and ultrasound only.

B-1146 10:54

Grade, size, invasive status and breast density of screen detected and interval cancers in breast screening in the UK

L.M. Warren[1], L. Wilkinson[2], M.G. Wallis[3], R. McAvinchey[1], R.M. Given-Wilson[2], M.D. Halling-Brown[1], M. Patel[1], D.R. Dance[1], K.C. Young[1]; [1]*Guildford/UK*, [2]*London/UK*, [3]*Cambridge/UK (lucy.warren@nhs.net)*

Purpose: To compare the characteristics of screen-detected and interval breast cancers.
Methods and Materials: Breast cancer cases were collected from three UK screening centres between April 2011 and Feb 2016. Size, grade and invasive status were reviewed for 3294 screen-detected cancers and 477 interval cancers. Here, an interval cancer was defined as an invasive or in situ cancer diagnosed between normal screens (round length = 3 years). Volumetric breast density (VBD) from Volpara v1.5.1 was available for 2436 of the screen-detected cancers and 220 prior screening images of the interval cancers. Significance was tested using chi-squared.
Results: Compared to screen-detected cancers, a greater proportion of interval cancers were invasive (p<0.0001). The interval invasive cancers were

of higher grade (p<0.0001) and had a larger median diameter (20.5mm v. 16.0mm, p=0.004). Intervals also had a larger proportion of lobular, and smaller proportion of ductal cancers than screen-detected cancers (p=0.009). Mean age did not differ significantly between women with screen-detected cancers and women at the screening episode prior to their interval cancer (60 v. 59 years, p=0.14). Breasts were denser in women with interval cancers compared with screen-detected cancers (mean VBD of 10.2% v. 8.1%, p=0.0007). The proportion of women with VBD<4.5%, VBD=4.5-7.5%, VBD=7.5-15.5% and VBD>15.5%, were 14%, 28%, 39% and 19% for interval cancers and 24%, 38%, 29% and 9% for screen-detected cancers respectively.
Conclusion: The characteristics of invasive interval cancers differ significantly from screen-detected cancers, in terms of invasive status, grade, size and volumetric breast density.

B-1147 11:02

Frequency and characteristics of additionally detected ipsilateral breast lesions following recall at screening mammography

J.L.R. Lameijer[1], M.M. Mourits[2], J. Nederend[1], A.C. Voogd[3], L.E.M. Duijm[2]; [1]*Eindhoven/NL*, [2]*Nijmegen/NL*, [3]*Maastricht/NL (joostlameijer@gmail.com)*

Purpose: To determine the frequency and outcome of additionally detected ipsilateral breast abnormalities following recall at screening mammography.
Methods and Materials: We included a consecutive series of 97799 screening mammograms performed between January 1, 2014 and July 1, 2015. All mammograms were double read by a team of 13 certified screening radiologists, each assessing more than 9000 screening mammograms yearly. Clinical data, breast imaging reports, biopsy results and breast surgery reports were collected of all recalled women.
Results: A total of 3061 women were recalled (recall rate, 3.1%). In 452 (14.8%) of these women, an additional lesion was detected in the breast for which she had been recalled. Biopsy was more frequently performed of recalled lesions than of additionally detected lesions (44.3% (1156/2609) vs 20.1% (91/452), p<0.005). Recalled lesions were more frequently malignant than additionally detected lesions (23.6% (615/2609) vs 12.8% (58/452), p<0.005). Of all 91 biopsy procedures performed of additionally detected lesions, 48 had been done to confirm or rule out breast cancer multifocality or multicentricity (62.3% (30/48) of these biopsies were malignant), 3 biopsies revealed breast cancer at a different location in the ipsilateral breast for which the woman had been referred, and the remaining 40 biopsies showed benign findings.
Conclusion: A substantial proportion of women are analysed for additional ipsilateral breast lesions following recall. These lesions are significantly less frequently biopsied than recalled lesions and have a significantly lower probability of malignancy, unless biopsy is performed to confirm or rule out breast cancer multifocality or multicentricity.

B-1148 11:10

Breast compression and radiation dose in mammographic screening

G.G. Waade, A. Sanderud, N. Moshina, S. Sæbuødegård, S. Hofvind; *Oslo/NO (Gunvor-Gipling.Wade@hioa.no)*

Purpose: Radiation protection and keeping the radiation dose as low as reasonably achievable is particularly important in mammographic screening as mainly healthy women are examined. Breast compression is used in mammography amongst other to reduce radiation dose. However, there is limited knowledge about the dose reduction by breast compression. We investigated radiation dose by compression force and compressed breast thickness for digital mammography in the Norwegian Breast Cancer Screening Programme.
Methods and Materials: Information regarding compression force, compressed breast thickness and radiation dose was available from 17,951 randomly selected screening examinations, performed at 14 breast centres, January-March 2014. We calculated mean compression force (Newton, N), compressed breast thickness (millimetre, mm) and radiation dose (milliGray, mGy) with 95% confidence interval (95% CI) for the left craniocaudal (CC) and mediolateral-oblique (MLO) mammograms. Further, radiation dose by quartiles of compression force and of compressed breast thickness were investigated. ANOVA and Tukey's HSD test were used to identify statistically significantly differences.
Results: Mean values were 116.3N (95% CI: 116.0-116.6) for compression force, 57.4mm (95% CI: 57.3-57.6) for compressed breast thickness, and 1.09mGy (95% CI: 1.09-1.10) for radiation dose. Mean radiation dose increased statistically significantly by quartiles of compression force (p<0.05), while it decreased statistically significantly by quartiles of compressed breast thickness (p<0.05).
Conclusion: Radiation dose increased by increasing compression force. Our findings raise concern about the current practice of using compression force to reduce breast thickness and subsequently the radiation dose.

B-1149 11:18

Breast compression variability in the Norwegian Breast Cancer Screening Programme

G.G. Waade[1], P. Hogg[2], N. Moshina[1], S. Sæbuødegård[1], S. Hofvind[1]; [1]*Oslo/NO*, [2]*Salford/UK (Gunvor-Gipling.Wade@hioa.no)*

Purpose: In mammography, breast compression is assumed to increase image quality and to reduce radiation dose. However, there are no evidence-based guidelines regarding the optimal compression force to use. We compared the compression force applied between screening centres in the Norwegian Breast Cancer Screening Programme.
Methods and Materials: Information regarding compression force was available from 17,951 randomly selected screening examinations performed at 14 of the 16 breast centres during January-March 2014. We calculated mean compression force (Newton, N) and 95% confidence interval (95% CI) for the left craniocaudal (CC) and mediolateral-oblique (MLO) mammograms, by breast centre. ANOVA and Tukey's HSD tests were used to identify any statistically significantly differences.
Results: Mean compression force for all the mammograms was 116.3N (95% CI: 116.0-116.6), 108.0N (95% CI: 107.6-108.4) for CC and 124.6N (95% CI: 124.2-125.0) for MLO. Comparing the breast centres, the lowest mean compression force was 90.5N (95% CI: 89.7-91.3) while the highest was 146.8N (95% CI: 145.0-148.5). Mean compression force differed statistically significantly for five breast centres when compared to all the others (p<0.05 for all).
Conclusion: We observed a substantial variations in mean compression force between the breast centres. This difference might influence image quality, radiation dose and patient experience. There is a need for establishing evidence-based recommendations for compression force in mammography.

B-1150 11:26

Breast arterial calcification on screening mammography can predict clinically significant coronary artery disease (CAD) in the BreastCheck screening cohort

E. Scanlon, B. Kelly; *Dublin/IE (emerscanlon1308@hotmail.com)*

Purpose: Breast arterial calcifications (BAC) are vascular calcifications observed at mammography. BAC has been associated with an increased risk of coronary artery disease (CAD). We investigated the association of BAC with findings on Computerised Tomography Coronary Angiography (CTCA) and thus CAD within the BreastCheck screening cohort.
Methods and Materials: Women aged between 50-64 who underwent CTCA between 2014-2015 were included. The BreastCheck mammography database was cross referenced to determine how many of these had both CTCA and digital mammography. BAC was scored as absent, mild, moderate or severe by specialist breast radiologists. CTCAs were scored according to the CAD-RADs system by specialist chest radiologists. Any findings significant in the CONFIRM trial were also recorded. History of chronic kidney disease, diabetes, hypertension, hypercholesterolaemia and smoking were recorded.
Results: 484 women had CTCA during that time period. 219 were within the 50-64 age category. Of these, 95 patients with no previous history of MI or CAD had both CTCA and mammography performed. Using standard multiple regression BAC was independently associated with a finding of CONFIRM significant CAD on CTCA (p=0.008) and with a CADRADs score of ≥3 (p=0.008). Furthermore using the Pearson method there was a significant positive correlation between the patients BAC score and their CADRAD score (p<0.001).
Conclusion: BAC diagnosed on 2 yearly screening mammography predicts CONFIRM significant CAD and CADRADs ≥3 disease. This information could be used to communicate cardiac risk to patients' primary care physician through the medium of the radiologic report to identify potentially undiagnosed CAD.

B-1152 11:34

Comparison of recall and breast cancer rates for spontaneous and organised screening mammograms performed in the same department

N. Voyvoda[1], L.A. Carbonaro[2], C.G. Monaco[3], F. Sardanelli[2]; [1]*Kocaeli/TR*, [2]*San Donato Milanese/IT*, [3]*Milan/IT (nuraykad@gmail.com)*

Purpose: Spontaneous screening mammography usually shows a recall rate of 8-12%, compared to 3-5% of organised screening programs. This study aims to evaluate and compare recall rates and breast cancer detection in a healthcare setting where spontaneous and organised screening is performed.
Methods and Materials: In 2013, 2818 organised screening mammograms (asymptomatic women 50-69 years old without breast cancer(BC) history) and 3430 spontaneous screening mammograms were performed in our department. Organised screening mammograms were read independently by two radiologists and patients were recalled when a suspect finding was detected by one of the two readers. Spontaneous mammograms were read by one radiologist. Throughout the year, both spontaneous and organised

screening mammograms were read by the same three radiologists(10-, 6-, and 2-year experience in screening and 11-, 8-, and 4-year experience in breast imaging) in rotation. Of 3430 spontaneous mammograms, all asymptomatic patients between 50 and 69 years old without symptoms and BC history were included to compare results with organised screening mammograms. Chi-square test was used; p value<0.05 was considered statistically significant.
Results: 907 spontaneous mammograms were included. Of these, 36(4.0%) were recalled. 135 organised screening mammograms(4.6%) were recalled (P=0.304). Six (6.6/1000) and 12 (4.3/1000) BCs were detected at spontaneous and organised screening mammograms, respectively (P=0.373). The positive predictive value of recalls was 16.7% for spontaneous and 8.9% for organised screening mammograms (P=0.177).
Conclusion: Recall rates of spontaneous mammograms performed in a single department where a screening organised program is performed can be maintained as low as the latter with comparable cancer detection rates.

B-1153 11:42

The value of routine screening mammography in women aged 35 to 39 years in a symptomatic breast unit
A. Buckley, N. Healy, S. O'Keeffe; *Dublin/IE (bucklear@tcd.ie)*

Purpose: To determine the breast cancer detection rate in women aged 35-39 attending a symptomatic breast clinic, on routine bilateral screening mammography, in women of population risk profile with a normal clinical examination.
Methods and Materials: A retrospective analysis of all mammograms performed on patients aged 35-39 at our institution from 2011 to 2015 was carried out. Patients with moderate or high familial risk of breast cancer, personal breast cancer history or chest radiation, males, GP and internal hospital referrals, and those with abnormal clinical examinations were excluded. Included women had “normal”, “benign” or undocumented examination findings. Results of imaging including ultrasound and histopathological results were extracted from the hospital’s electronic record systems.
Results: 4,087 patients aged 35-39 had bilateral mammograms from 2011 to 2015. 2,148 patients were excluded from analysis. Of 1,939 included women, 4 (0.21%) were diagnosed with breast cancer confirmed at histology based on mammographic findings: 2 invasive ductal carcinoma (8 and 2mm) and 2 DCIS (4.5mm high grade DCIS and 2 mm low grade DCIS). Other histological findings included 2 B3, 46 B2 and 3 B1 lesions. Overall, 115 biopsies were performed in this cohort; 55 (47.8%) were attributable to mammographic screening, producing a biopsy rate of 2.8% due to mammography alone.
Conclusion: 2.1 cases of cancer were detected per 1000 women screened. This figure would be below accepted international thresholds to undertake screening mammography and raises radiation protection issues. Additionally, a large number of benign biopsies were undertaken. Further studies could inform national guidance.

10:30 - 12:00 **Room D**

Musculoskeletal

SS 1810a
Musculoskeletal interventions

Moderators:
J.M. Cambronero Gómez; Girona/ES
N.N.

B-1154 10:30

Balloon sacroplasty (BSP), radiofrequency sacroplasty (RFS), vertebrosacroplasty (VSP) and cement sacroplasty (CSP) for the treatment of insufficiency fractures
R. Andresen[1], S. Radmer[2], J.R. Andresen[3], H.C. Schober[4]; [1]*Heide/DE*, [2]*Berlin/DE*, [3]*Vienna/AT*, [4]*Rostock/DE (randresen@wkk-hei.de)*

Purpose: To examine the feasibility and clinical outcome of the different treatment methods.
Methods and Materials: In 62 patients with a total of 93 sacral fractures, CT-guided cement augmentation was performed by means of BSP, RFS, VSP and CSP. Cement leakages were detected with a CT on the first postoperative day. Pain intensity was determined on a VAS before the intervention, on the second day, and 6, 12 and 18 months after the intervention.
Results: BSP, RFS, VSP and CSP were technically feasible in all patients. Leakage could be ruled out for the BSP - and the RFS group, in the VSP group there were 4 leakages in 17 fractures (24%) and in the CSP group 3 leakages in 19 fractures (16%). The mean pain score before the intervention was 8.6 in the BSP group, 8.8 in the RFS group, 8.6 in the VSP group and 8.7 in the CSP group. On the second postoperative day, a significant pain reduction was seen (p<0.001), with an average value of 2.5 for all groups. After 6 (12; 18) months, these values were stable at 2.2 (2.3; 2.0) for the BSP group, 2.3 (2.2; 2.0) for the RFS group, 2.4 (2.2; 2.0) for the VSP group and 2.4 (2.3; 2.2) for the CSP group.
Conclusion: BSP, RFS, VSP and CSP are interventional, minimally invasive procedures that achieve equally good pain reduction in the medium term. However, in the case of VSP and CSP, a higher rate of cement leakages is to be expected.

B-1155 10:38

Modic 1 signal evolution after intradiscal glucocorticoid injection (vs sham-procedure) for patients with chronic low back pain
A. Buisson, N.-E. Regnard, C. Nguyen, S. Poiraudeau, J.-L. Drape, A. Feydy; *Paris/FR*

Purpose: Assessment of the Modic signal evolution after intradiscal steroid injection versus sham-procedure for patients with chronic low back pain associated with active discopathy (Modic 1 MRI pattern).
Methods and Materials: Ninety chronic low back pain patients with active discopathy on MRI (Modic 1) and failure of first line treatments were included in a double-blinded, multicentric trial. Patients were randomized for an intradiscal injection of glucocorticoid or a sham-procedure. MRI before and twelve months after discography were assessed for evolution of the Modic type, extension and signal intensity, and the disc space narrowing, blinded to the procedure.
Results: At the 12 months evaluation, no significant difference were observed about the Modic signal changes between the 45 patients treated with an intradiscal glucocorticoid injection and the 45 patients with a single discography. The rate of persisting Modic 1 was similar in both groups (80% vs 73%, p = 0,62). The extent of endplate oedema did not change differently between the two groups, neither in volume (increase of 830 mm3 versus decrease of 99 mm3, p=0,60), nor in maximal height (-5% vs -1,7%, p=0,43), nor in maximal antero-posterior diameter (-6,1% vs -6,4%, p=0,95). The signal intensity changes after discography did not differ. The disc space narrowing at 12 months was similar in both groups (5% vs 3,9%, p=0,61).
Conclusion: Evolution of the vertebral body endplate oedema was similar after intradiscal injection of corticosteroids or after a sham-procedure. MRI should not be used as a predictive tool in the follow-up of patients with active discopathy.

B-1156 10:46

Predictive value of MR-arthrography of the shoulder for pain relief after glenohumeral corticosteroid injection
B. Fritz[1], F. Del Grande[2], R. Sutter[1], C.K. Peterson[1], C.W.A. Pfirrmann[1]; [1]*Zurich/CH*, [2]*Lugano/CH (benjamin.fritz@gmx.net)*

Purpose: To determine the predictive value of MR-arthrography of the shoulder for pain relief after glenohumeral corticosteroid injection.
Methods and Materials: This study enrolled prospectively 212 patients (mean age 51.4 years; range 15 - 90) who underwent fluoroscopy guided glenohumeral corticosteroid injection for pain relief. All patients had an MR-arthrography of the shoulder up to 3 months prior to the infiltration and returned questionnaires which assessed patients’ shoulder pain using the 11-point numeric rating scale (NRS), covering a 1 month follow-up period. MR-arthrograms were retrospectively assessed for abnormalities of the rotator cuff, long biceps tendon, glenohumeral bone and cartilage and labrum as well as for synovitis, bursitis and signs of adhesive capsulitis. MR-arthrography findings were compared to patients’ NRS-change using univariate and multivariate linear regression analysis.
Results: Pain level reduction of ≥2 points was considered to represent clinically relevant improvement, which was seen by 74.0% after 1 month post-injection. Univariate analysis of MRI-findings showed that a non-torn labrum and signs of adhesive capsulitis were associated with significantly higher NRS-reductions after 1 month in comparison to patients without these findings (3.7 vs. 2.6, p=0.003 and 4.0 vs. 3.0, p=0.007). Multivariate analysis proved both factors to be independent predictors of improved outcome after 1 month (beta=0.212, p=0.001 and beta=0.176, p=0.039).
Conclusion: Glenohumeral corticosteroid injections for pain relief have a high success rate with 74.0% of patients reporting clinically relevant improvement after 1 month, with a non-torn labrum and signs of adhesive capsulitis on MR-arthrography being independent predictors of an even better outcome.

B-1157 10:54

Clinical and radiological outcome of platelet-rich plasma (PRP) vs stromal vascular fraction (SVF) to treat Achilles tendinopathy: randomised controlled trial
C. Messina, C. Maccario, L. De Girolamo, A. Corazza, F.G. Usuelli, L.M. Sconfienza; *Milan/IT (carmelomessina.md@gmail.com)*

Purpose: Injections of PRP and adipose-derived mesenchymal stem cells contained in the SVF are considered effective treatments for non-insertional Achilles-tendinopathy (NIAT). We prospectively compared the clinical and

radiological outcome of the PRP and the SVF for the treatment of chronic NIAT.
Methods and Materials: Forty-four patients were randomly assigned to PRP group (n=23) and SVF group (n=21), treated unilaterally or bilaterally (total=28 tendons per group). Patients (age range 18-55y) were followed up at baseline and at 15/30/60/120/180 days from the injection via VAS, VISA-A, AOFAS and SF-36. Patients were also evaluated by US and MRI before and at 4 (US) and 6 months (MRI) after treatment. On MRI, mean preoperative (MPREA) and postoperative (MPOSTA) lesion area were assessed.
Results: Statistically significant differences in favor of the SVF group were just found at the earliest follow up: VAS scored significantly better at both 15 and 30 days in the SVF group in comparison to PRP ($p<0.05$), as well as AOFAS (15 days) and VISA-A (30 days) ($p<0.05$). At the following time points the scores were not significantly different between the two groups, even if SVF always showed better results than PRP. US/MRI evaluation did not reveal significant differences of thickness, echotexture, or signal intensity between the two groups before and after treatment. PRP: MPREA=8.93±2.10mm^2, MPOSTA=8.67±2.10mm^2 ($p>0.05$). SVF: MPREA=10.70±3.38mm^2, MPOSTA= 10.46±3.37mm^2 ($p>0.05$).
Conclusion: Both PRP and SVF showed to be effective for NIAT. Patients treated with SVF obtained faster results. US/MRI are not sensitive enough to detect NIAT changes after treatment.

B-1158 11:02

Validity of T2 mapping sequences at 3T for the assessment of knee cartilage repair after treatment with platelet rich plasma (PRP)
F. Bruno, S. Quarchioni, S. Mariani, F. Arrigoni, L. Patriarca, L. Zugaro, A. Barile, C. Masciocchi; *L'Aquila/IT (federico.bruno.1988@gmail.com)*

Purpose: To define the ability of T2 mapping sequences to evaluate the efficacy of PRP injections characterizing qualitatively and quantitatively the grade of knee cartilage repair in patients with patellofemoral and tibiofemoral chondropathy.
Methods and Materials: 40 patients (17 men, 23 women, mean age 35.8 years), with clinical suspicion of chondropathy were examined on a 3T MRI scanner. T1WI, T2WI, and PDWI sequences were used for morphological evaluation of cartilage lesions, using a modified WORMS score. T2 mapping sequences were correlated to the morphological findings and used for qualitative and quantitative analysis of cartilage by means of colour-scale representation and ROI measurements of T2 relaxation time values. Patients were randomly assigned to 2 groups: 20 patients (group A) were treated with intra-articular PRP injections (3 times, 3 weeks apart), 20 patients (group B, control) were submitted to conservative therapy. MRI follow-up was performed at 6 months.
Results: Patients of group A showed pre-treatment mean T2 values of 51.39msec, and post-treatment mean values of 44.19msec ($p<0,001$). In patients of group B pre-treatment and post-treatment mean T2 values were 51.86msec and 50.70msec respectively ($p=0,274$). Mean post-treatment T2 values between group A and group B were statistically significant ($p<0,001$). In the study group, the overall Worms score had a 25% improvement, in the control group the improvement was of 3%.
Conclusion: T2 mapping is a valuable approach for the evaluation of cartilage, allowing better monitoring of the disease and the treatment-related changes over time in addition to standard morphological MRI sequences.

B-1159 11:10

Ultrasound-guided percutaneous treatment of plantar fasciitis: 5-year follow-up of three different approaches
V. Buscarino[1], D. Orlandi[2], E. Silvestri[2], M. Moscatelli[1], M. Catapano[1], L.M. Sconfienza[1]; [1]*Milan/IT*, [2]*Genoa/IT (valentinabuscarino@gmail.com)*

Purpose: To compare the short- and long-term outcome of US-guided percutaneous treatment of plantar fasciitis based on dry needling and local injection of steroid compared to patients treated with simple steroid injection or dry needling.
Methods and Materials: Among 75 patients referred for US-guided treatment of plantar fasciitis, 25 (12 males; age 43.8±7.6y) were treated with dry needling and local injection of steroid together; 25 (12 males; age 46.2±12.3y) were treated with dry needling only; 25 (11 males; age 52.7±10.0y) were treated only with local injection of steroid. Pain was assessed using the visual analogue scale (VAS) at baseline and at 7, 14, 30, 90, 180, 360 days and at five years after the procedure; fascial thickness was measured with US scanning at baseline and at 180 and 360 days later.
Results: Patients treated with complete procedure had a faster and more permanent decrease of symptoms (VAS at 7 days=1.2±0.4; at 360 days=0.0± 0.1). Patients treated only with injection of steroid had a quick decrease of pain that was not permanent on a long-term basis (VAS at 7 days=1.2±0.6; at 360 days=5.2± 0.4). Patients treated only with needling had a permanent but very slow decrease of symptoms (VAS at 7 days=5.7±0.5; at 360 days VAS=0.1±0.2). Difference was statistically significant ($p>001$). At five-year follow-up, VAS was 0.9±1.9 for the complete procedure, 1.5±2.4 for steroids only, 1.1±1.9 for needling only.
Conclusion: Patients treated with the combined procedure had faster and better outcome than others. At five years, outcomes were not significantly different.

B-1160 11:18

Soft tissue sarcoma diagnosis by imaging-guided core-needle biopsy: yield and limitations
P. Naval, J. Narvaez, M. Huete, J. Hernandez-Gañan, J. Sardiñas, X. Sanjuan; *Barcelona/ES (jose_a_narvaez@hotmail.com)*

Purpose: To evaluate the diagnostic yield of core-needle biopsy (CNB) guided by ultrasound or CT for the diagnosis of soft tissue sarcomas (STS).
Methods and Materials: We retrospectively revised all the cases of STS visited in the multidisciplinary musculoskeletal tumour unit of tertiary hospital during 5 years (2011-2015). We found 120 cases of STS in which imaging-guide CNB was performed. There were 63 males and 57 females, with an average age of 58 years (range 22-90).
Results: Image-guided CNB correctly established the diagnosis of sarcoma in 105 patients, with a sensitivity of 87.5% and a specificity of 100%. False negatives of CNC (n=15) mainly corresponded to well-differentiated liposarcomas diagnosed as lipomas (n=4), small local recurrences misdiagnosed as fibrotic changes (n=3), low-grade fibromyxoid sarcoma (n=2) and synovial sarcoma (n=2). Excluding well-differentiated liposarcomas diagnosed as lipomas, sensitivity increased to 94.8%, with a specificity of 100%. Only 9 cases of high-grade STS were classified as low grade by image-guided CNB. Only one procedure was stopped due to pain (nerve damage). No other serious complications occurred.
Conclusion: Our results suggest that CNB can replace open biopsy in the diagnosis of STS. Nevertheless, in our experience, the differentiation between lipoma and well-differentiated liposarcoma and difficulty in discerning histopathologic degree of STS present lower yield, and were the two main limitations of CNB.

B-1161 11:26

Benign bone tumours other than osteoid osteoma percutaneous ablation
J. Martel[1], F. Ruiz-Santiago[2], Á. Bueno[1], L. Guzmán[2]; [1]*Alcorcon/ES*, [2]*Granada/ES (jmartel@fhalcorcon.es)*

Purpose: Bone tumours ablative thermal methods are being widely used, especially to the osteoid osteoma curative treatment. However, other benign tumours can also be treated by means of these techniques. We review the radiofrequency, microwave and cryoablation CT-guided methods usefulness to the treatment of benign tumour bone conditions different from osteoid osteoma
Methods and Materials: For the last fifteen years we have performed 35 percutaneous ablations for the treatment of different benign bone tumours other than osteoid osteoma. 13 (37%) patients were female and 22 (63%) male. Mean age: 23.5 years (range 13 to 58 years). Location: femur (9 cases), pelvic ring (7), tibia (6), foot (5), spine (4), humerus (2) and hand (2). Follow-up period: 24-36 months. Percutaneous radiofrequency thermal ablation was used in most (30) of the patients, microwave ablation in 3 and cryoablation in 2 patients. In 5 cases these techniques were combined with cementoplasty. Biopsy was performed in all cases in order to confirm the diagnosis, in 14 cases just before the ablation procedure. 9 tumours proved to be chondroblastoma, 8 osteoblastoma, 5 giant cell tumour, 3 enchondroma, 3 aneurysmal bone cyst, 2 mesenchymal tumours, 5 other.
Results: All procedures were technically successful. All of patients were pain-free by the seventh-tenth day except in three patients (one chondroblastoma and two osteoblastoma). Only two single complications were recorded.
Conclusion: CT-guided thermal ablation can be curative to other benign bone tumours other than osteoid osteoma, mainly osteoblastoma, chondroblastoma, giant cell tumour and aneurysmal bone cyst.

B-1162 11:34

Diagnostic findings (MRI and CT) in long term follow-up of osteoid osteomas treated with RFA and MRgFUS: a pictorial review with clinical correlation
F. Arrigoni, S. Mariani, L. Zugaro, A. Barile, C. Masciocchi; *L'Aquila/IT (arrigoni.francesco@gmail.com)*

Purpose: To review and describe the main diagnostic findings that feature the follow-up, up to 5 years, after treatment of OO with RFA or MRgFUS, and to investigate their evolution over the time and relationship with clinical data.
Methods and Materials: Retrospectively we evaluated MRI and CT performed after ablation procedure (6, 12, 24 and 60 months) of patients successfully treated with RFA or MRgFUS (23 and 20 respectively) looking for signs proving the good outcome or, eventually possibility of complications. The evaluation also took into account the site of lesions: intrarticular or extraarticular. For each patient, the study of the imaging was coupled with clinical data.

Results: The main outcome that proves the success of the procedure is clinical: the pain disappears mainly in one week and it is the most precocious sign of the success of the procedure. Imaging features of the disease do not modify before 6 months after treatment: only synovial reaction (in case of intrarticular lesions) disappears at the follow-up at 6 months, instead at this follow-up, the bone edema can be less evident but disappears completely 1 years after treatment. The "ring sign", if present, can last up two years. About the CT, only for the MRgFUS treatments, we observed in all cases within 2 years a complete "restitutio ad integrum" of the bone segment.
Conclusion: The imaging in the follow up of this type of treatment confirms the good outcome of the procedure, but the most precocious sign is the clinical improvement.

B-1163 11:42

The safety and short-term efficacy of MR-guided focused ultrasound surgery for bone metastases-induced pain palliation

H. Xiong, J. Zhang; *Shanghai/CN (xionghairui@gmail.com)*

Purpose: To evaluate the safety and short-term efficacy of MR-guided focused ultrasound surgery (MRgFUS) for pain palliation of bone metastasis patients.
Methods and Materials: 14 patients with painful bone metastases were recruited in a prospective, non-randomised, controlled study. The treating efficacy is characterised by the brief pain inventory quality of life (BPI-QOL) survey, numerical rating scale (NRS), and Karnosky performance status scale (KPS). On the basis of survey results, the adverse events that occurred pre- and post-treatment were analysed, and the short-term MRgFUS treatment efficacy for painful bone metastases was discussed.
Results: 14 metastatic bone lesions of these patients were treated with MRgFUS. The average treatment time and sonication number was (111.07±34.03) minutes and (17.43±6.86) times. One patient died from pneumonia during the follow-ups, one patient dropped out of the study due to chemotherapy. After the treatment, three patients reported lower extremities numbness which relieved spontaneously within 7 days; only one patient developed deep venous thrombosis in one week; two patients had soft tissue oedema around the lesions. According to the survey, the NRS decreases from 6.83±2.12 to 3.42±3.58 from pre-treatment to post-three months. The tendency of BPI-QOL and KPS rating are from 40.54±9.42 to 29.14±19.46, 76.67±12.31 to 60.0±26.97, respectively. Pain palliation efficiency reached 75%, compared with the NRS of pre-treatment was significantly different (P<0.05), with statistical significance.
Conclusion: MRgFUS is proved to be a novel, safe, and noninvasive approach for bone metastases-induced pain palliation, which is effective in short term.

B-1164 11:50

Effect of MRI-guided high intensity focused ultrasound on local control of bone metastases

A. Bazzocchi[1], A. Napoli[2], R. Scipione[2], C. Marrocchio[2], G. Guglielmi[3], C. Catalano[2], U. Albisinni[1]; [1]*Bologna/IT*, [2]*Rome/IT*, [3]*Foggia/IT (abazzo@inwind.it)*

Purpose: MRI-guided high-intensity focused-ultrasound (MRgHIFU or FUS) treatment was proved to be effective and safe for palliating pain of bone metastases. The aim of this work was to provide evidence about the effect of MRgFUS on local tumour control of bone metastases.
Methods and Materials: Patients with painful bone metastases were prospectively enrolled and underwent MRgFUS, with imaging (CT/MRI) before and 3, 6 and 12 months after treatment. The primary endpoint of the study was the number of lesions with partial or complete response at 3 months according to MD-Anderson criteria.
Results: Out of 105 patients, 18 were lost and missed the 3-month imaging check. Eighty-seven patients with 89 lesions were evaluated. The procedure was successful in terms of local tumour control at 3 months in 53/89 lesions (60%) - complete-31, partial-22. A stable disease was observed in 26 lesions and a progression in 10. The single element influencing the outcome was the size of the lesion (up to 16cm), with 7cm as reasonable cut-off for supporting successful ablation (p<0.01). Results were statistically independent of previous radiation therapy (59%), histology, and lesion type, though osteolytic (or mixed) pattern, with complete accessibility of the margins to the ultrasound beam were generally better candidates. BMI, age and sex did not play a role in the final outcome.
Conclusion: MRgFUS for painful bone metastases may achieve a local control. In the future, this opportunity should be further explored and addressed even to patients with a potential primary intent of tumour ablation.

Author Disclosures:
A. Bazzocchi: Grant Recipient; This work has been supported by the Programma di ricerca Regione-Università, Regione Emilia-Romagna, bando Giovani Ricercatori "Alessandro Liberati" 2013, Italy (public research call winner), The grant above refers to an official call of the Regional/National Healthcare System (public research call). Research/Grant Support; Grants to support congress participations, and sponsored study by InSightec Ltd. (not the reported study).

10:30 - 12:00 **Room G**

Musculoskeletal

SS 1810b
Hip and foot

Moderators:
C. Czerny; Vienna/AT
R. Sutter; Zurich/CH

B-1165 10:30

More than half of the patients with hip pain due to FAI present an abnormal femoral torsion

T.D. Lerch, I.A. Todorski, F. Schmaranzer, S.D. Steppacher, K.A. Siebenrock, S.F. Werlen, M. Tannast; *Berne/CH (inga.todorski@insel.ch)*

Purpose: Torsional deformities have been increasingly recognised as additional important factor in young patients with hip pain resulting from FAI or hip dysplasia. It is unknown how often torsional deformities are present in young patients with hip pain due to FAI. We questioned what is the prevalence of a pathological femoral torsion in hips with FAI or hip dysplasia?
Methods and Materials: An IRB-approved retrospective radiological study of 463 consecutive symptomatic FAI patients (539 hips) and MRI or CT scan to measure femoral torsion were performed. Out of 915 MRI we excluded 376 hips. The study groups were further classified into 10 groups (e.g. dysplastic (LCE<20°), valgus (CCD>139°), perthes hips(LCPD)). Femoral torsion was defined according to Tönnis et al. as angle between the axis of femoral neck and the posterior axis of the femoral condyles. Normal femoral torsion was defined 10-25°. Torsional deformities include decreased (<0°) and increased (>35°) femoral torsion.
Results: 51% of all 539 hips presented pathological values for femoral torsion. Torsion deformities (<0° or >35°) were measured in 17% of all hips with hip pain due to FAI.Analysis of Varianz (ANOVA) revealed significant differences (p<0,001) of torsion between normal (Mean: 17°) and dysplastic (Mean: 26°), valgus (Mean: 27°) and perthes hips (Mean: 32°).
Conclusion: More than half of the patients with FAI present an abnormal femoral torsion. In particular valgus, dysplastic and perthes hips have an abnormal high torsion. Femoral torsion should be measured in all patients with hip pain due to FAI or hip dysplasia.

B-1166 10:38

Pelvic inclination is not different in Pincer FAI due to acetabular retroversion compared to hip dysplasia

I.A. Todorski, T.D. Lerch, F. Schmaranzer, K.A. Siebenrock, S.D. Steppacher, M. Tannast; *Berne/CH (inga.todorski@insel.ch)*

Purpose: Pincer femoroacetabular impingement (FAI) can be due to overcoverage or acetabular retroversion. Pelvic inclination is a parameter for pelvic tilt and should be increased in hips with acetabular retroversion according to current literature. Pelvic incidence is a static parameter for sagittal balance and determines lumbar lordosis.Therefore we asked (1) Does pelvic inclination and (2) pelvic incidence differ in hips with pincer FAI compared to hip dysplasia?
Methods and Materials: A retrospective radiological controlled study including 151 consecutive patients (236 hips) with symptomatic FAI was performed. CT scan including the entire pelvis available for all hips allowed the calculation of pelvic inclination and pelvic incidence. These hips were allocated to 5 groups: overcoverage, acetabular retroversion, hip dysplasia, increased acetabular anteversion and valgus hips. Statistical analysis was performed using Analysis of Variance (ANOVA) with Bonferroni correction.
Results: (1) Pelvic inclination did not differ between 5 groups (p=0,311)(2) Pelvic incidence was significantly lower in hips with acetabular retroversion (42°) compared to dysplastic hips (55°), hips with increased acetabular anteversion (55°), valgus (54°) and overcoverage (54°) (p<0,001).
Conclusion: Pelvic inclination is not different in acetabular retroversion, but pelvic incidence was lower in patients with acetabular retroversion. This suggest that these patients should be present with decreased lumbar lordosis. Sagittal balance has to be considered during the clinical and radiological evaluation in patients with Pincer FAI.

B-1167 10:46

Is acetabular labrum size and tear pattern associated with femoral retrotorsion or increased femoral torsion in patients with FAI?

I.A. Todorski, T.D. Lerch, F. Schmaranzer, K.A. Siebenrock, S.D. Steppacher, M. Tannast; *Berne/CH (inga.todorski@insel.ch)*

Purpose: Acetabular labrum size and labral tears antero-superior are typical for femoroacetabular impingement (FAI). Femoral torsion (FT) is a novel cause for anterior FAI and influences labral size and tear pattern. Therefore, we asked (1) what is the anterior labral size and (2) which labral tear patterns are associated with femoral retrotorsion compared to hips with elevated FT.
Methods and Materials: Out of 620 consecutive MR arthrographies we excluded 491 hips with normal FT. An IRB-approved retrospective radiological study involving 129 hips with symptomatic FAI and abnormal FT was performed. Femoral retrotorsion was defined as FT <5° (58 hips), elevated FT was defined as >30° (71 hips). All patients underwent routine radiological evaluation using MR arthrography (3T) including distal femoral condyles for calculation of FT. Labral size and labral tear patterns were measured circumferentially on every clock position (15° intervals) on radial slices trough the femoral neck.
Results: (1) Anterior labral size was significantly decreased in hips with femoral retrotorsion (14mm2 vs 22mm2, p<0,001) compared to posterior in hips with elevated FT. Labral size was significantly smaller anterior compared to posterior hips with femoral retrotorsion (p<0,001). (2) Labral tear patterns were more frequently anterior (2 and 3 o'clock, p<0,001) in hips with elevated FT.
Conclusion: Anterior labrum was smaller in hips with femoral retrotorsion on the corresponding localisation of acetabular rim impingement. This has be considered during radiological diagnosis of FAI for hip-preserving surgery. Anterior labral tear patterns could be associated with anterior subluxation or instability in hips with elevated FT.

B-1168 10:54

MR hip arthrography: diagnostic perfomance of 3D-SSFP vs 2D TSE protocol

M. Kraus, U. Grosse, M. Notohamiprodjo, K. Nikolaou; *Tübingen/DE (mareen.kraus@med.uni-tuebingen.de)*

Purpose: To compare the diagnostic performance and image quality of an isotropic 3D-SSFP sequence to the current diagnostic standard 2D PD-TSE-protocol in hip MR arthrography (hMRA) with arthroscopy as a standard of reference.
Methods and Materials: Eighty-one patients (age 39.5 ± 11.1) with hip pain and suspected labral tears were included, who underwent hMRA at a 3T scanner. We acquired 2D PD-weighted TSE in 3 planes and a parasagittal 2D-SSFP sequence. Labral tears, cartilage pathology and bone marrow were assessed independently by two blinded experienced musculoskeletal radiologists using a 5-point Likert scale. In 39 patients, diagnostic accuracy could be determined using invasive arthroscopy as gold standard.
Results: Diagnostic confidence of labral and cartilaginour pathologies based on image quality was rated higher for 3D-SSFP (4.5 ± 0.8; 4.35 ± 0.7; p<0.0001). In the subset of patients with invasive arthroscopy, similar sensitivity (85.9%) but higher specificity (74.4% vs 42.9%), higher positive and negative predictive values were found for 3D-SSFP for evaluation of labral tears and cartilage alterations.
Conclusion: 3D-SSFP in hMRA offers an increased accuracy in detecting labral tears and cartilage alterations compared to 2D TSE-PD, whilst reducing the acquisition time. A major drawback of 3D-SSFP was the inferior diagnostic confidence for bone marrow evaluation; thus, 3D-SSFP should still be combined with conventional 2D-TSE-sequences.

B-1169 11:02

MRI hindfoot characteristics of genetic haemochromatosis: a case control study

A. Elstob, V. Ejindu, C.W. Heron, P.D.W. Kiely; *London/UK (alison.elstob@nhs.net)*

Purpose: From an early stage, many genetic haemochromatosis (GH) patients report arthropathy. There is an unexpectedly high prevalence of ankle involvement in GH, resembling primary osteoarthritis (OA). We evaluated distinguishing MRI features that might improve recognition of GH in undiagnosed cases.
Methods and Materials: Retrospective case-control study. Local ethical approval obtained. 30 MRI studies of GH patients with hindfoot arthropathy were identified from a specialist rheumatology database. 30 gender and age matched controls with primary hindfoot OA identified from PACS search. Anonymised MR images were independently scored by two specialist MSK radiologists using a semiquantative tool adapted from the MRI osteoarthritis knee score. The primary outcome score was bone marrow lesion (BML) and cyst size. Seven secondary outcomes were scored with scores generated for ankle joint and middle and posterior facets of the subtalar joint. Paired Student's T test and Chi squared test were used to compare outcome measures between GH and controls.
Results: BML/cyst size score at the ankle joint was significantly higher in GH cases compared with controls (p=0.001) but not at the subtalar joint (p=0.119, p=0.63). At the ankle joint, GH scores were significantly higher than paired controls for 5 of 7 secondary outcomes (p<0.05). At the middle facet subtalar joint, GH scores were significantly higher for 3 secondary outcomes (p<0.05).
Conclusion: In comparison to matched primary OA controls, GH patients have significantly higher MRI osteoarthritis scores at the ankle and middle facet subtalar joint. These MRI features may have potential diagnostic value for recognising GH.

B-1170 11:10

Talonavicular ligament: anatomy and stability

M. De Dea, C. Loizou, G. Allen, D. Wilson, N. Athanasou, P. Cooke, T. Cosker; *Oxford/UK (miriamdedea@yahoo.com)*

Purpose: To assess the anatomy of the talonavicular ligament (TNL) and its role in talonavicular joint stability.
Methods and Materials: 6 TNL were dissected from thawed cadaveric feet and sent for histological analysis. In further 6 feet the talonavicular joint was imaged with ultrasound (US) and two landmarks identified on each side of the joint in order to measure its movement caused by a stressing manoeuvre (great toe extension causing a rising of the arch of the foot as per windlass mechanism applied through the plantar aponeurosis). Measurements were taken at rest and with stress, with intact TNL and after its US guided division.
Results: The TNL is composed by bundles of collagen with parallel arrangement of fibres along its length. The talonavicular joint displacement assessed with US measured 0.18±0.08cm when the TNL was intact and 0.29±0.07 cm when divided (p<0.005).
Conclusion: The TNL has a structure suggesting a role in tensile force transmission. We have demonstrated by US that division of the TNL simulating a complete tear results in increased talonavicular joint displacement when the joint is stressed. A complete tear of the TNL may be implicated in later joint arthritis and symptomatology. It may be useful to include the TNL in the check list of ankle and foot: if injured early treatment might include immobilisation.
This abstract has been submitted in whole or in part to the British Orthopaedic Foot & Ankle Society Annual Meeting (2016).

B-1171 11:18

Ligament evaluation of the hind and midfoot: better depiction by using dixon method in ankle MRI

E. Park, S. Kim, E. Koh, E. Jung; *Jeonju/KR (kohesther@naver.com)*

Purpose: To determine if ankle magnetic resonance (MR) imaging using Dixon technique helps to depict hind and midfoot ligaments compared with those achieved without using Dixon technique.
Methods and Materials: From July to December 2015 ankle MRI using Dixon technique of 48 ankles was obtained from 25 asymptomatic healthy volunteers. Twenty-three ligaments from hind and midfoot were chosen for evaluation. Two experienced reviewers separately rated the depiction of 23 ligaments. Set 1 was MRI using Dixon technique which composed of all 7 sequences. Set 2 represented conventional MRI composed of subsets with 4 different sequences including 2 nonfat-suppressed and 2 fat-suppressed plane. Ligaments were divided in to two groups. Major ligament included ATFL, CFL, PTFL, Lisfranc ligament, deltoid ligament, spring ligament. Other ligaments were categorized as minor ligament. The depiction rate was calculated using generalized estimating equations.
Results: The depiction rate was significantly higher on set 1 compared with set 2; 91.3% versus 73.2 %, respectively. This was consistently observed for major ligament; 96.4% versus 76.1% (p<0.005). In set 2, the depiction rate was higher for subset with nonfat-suppressed axial and sagittal plane compared with those with axial and sagittal plane and coronal and saggital plane (82.7%, 77.6%, 70.7%, respectively).
Conclusion: For better depiction of hind and midfoot ligaments, all three axial, coronal and sagittal plane with non-fat suppressed sequences are required. The Ankle MRI using Dixon technique yielded better depiction rate of hind and midfoot ligaments by supplying both nonfat-suppressed and fat-suppressed sequences in single scan.

B-1172 11:26

High incidence of periprosthetic cystic lesions around CCI evolution ankle implant

S. Somodi; *Hvidovre/DK (sanja.somodi.03@regionh.dk)*

Purpose: The CCI evolution ankle prosthesis was abandoned due to failures and findings of bone loss at revision. The aim of this study was to a) determine our true revision rate, b) investigate prevalence, size and location of periprosthetic bone cysts through x-ray and CT c) relate these findings to patient-reported outcome measurements (PROMs) and alignment of implants.

Methods and Materials: 51 primary surgeries were performed - of these 36 patients were enrolled and underwent evaluation with metal artefact reduction CT-scans and conventional x-ray. They filled out 3 PROMs; SEFAS-da, SF-36, EQ-5D. Cyst volume larger than 0.1 ml was measured using VITREA volume tools and IMPAX built-in measuring tools. PROMs association to osteolytic volume and implant alignment was analysed by linear and logistic regression.
Results: 19 of the original 51 implants had secondary surgery; primarily because of large osteolytic lesions +/- non-traumatic fractures and non-union (9 true revisions), lesser osteolytic cyst cavities (5 allo-/auto-transplantations), exostosis (4 cases) and traumatic fractures (1 case). The 3- and 5-year rates were 14% and 18% for true-revisions and 17% and 29% for overall secondary surgeries. Cystic lesions were found in 81% of participants. Total cystic volume was not significantly related to PROM scores (P 0.16-0.5), but showed some association with implant alignment.
Conclusion: The implant investigated performs below standard, compared to public registries that report overall 5-year revision rates at 5-6.5% in comparable implants. Cysts were common, large and unrelated to PROMs. Malalignment of implants might be the cause of high failure rates.

B-1173 11:34

Follow-up study with sonoelastography after open surgery repair on Achilles tendon in professional athlets and balet dancers in comparance to non-sport related persons

V. Gazhonova, P. Pereyarchenko, V. Abelcev; *Moscow/RU (vx969@yandex.ru)*

Purpose: To compare strain ratio (SR) values in Achilles tendon after open surgery.
Methods and Materials: 39 patients (24 non-permanent sport persons, 15 active sportsmen and ballet dancers) with acute Achilles rupture after open surgical repair were included in the follow-up sonoelastography study. Rehabilitation was received in recommended amount according to time after surgery. Functional outcomes were assessed with AOFAS rating system. Sonoelastography Mean Strain Ratio values (SR1, SR2 values) of the regenerated Achilles tendon were measured in the longitudinal plane during the follow-up period (1 week, 3, 6, 12, 36-40 weeks after surgery). Student's t-test were used to consider statistical significance with $p<0.05$.
Results: There were significant differences with respect to the mean SR values and functional scores of the repaired Achilles tendon at 6, 12, and 24 weeks postoperatively between 2 groups. Tendon function was positively correlated with increase in SR values of the repaired Achilles tendon. Sport related patients showed more prominent and quick appearance of increase in stiffness of the regenerated tendon: SR 3 weeks 2.5+/-06, 4.1+/-1.4, p<0,001; SR6weeks 1.7+/-0.5, 3.6+/-1.7, p<0.005; SR12weeks 1.9+/-1.1, 3.8+/-1.3, p<0,007, correspondingly). Non-sport related patients showed prolongation in time for increase in tendon stiffness that result in longer rehabilitation time.
Conclusion: Sonoelastography is an effective method for monitoring regenerative processes of the Achilles tendon after operation, reflecting the elasticity of the collagen fibres which can be used for individual rehabilitation programs for sport related and non-sport related patients.

B-1174 11:42

Detecting fracture of ankle in MRI: improved sensitivity by Dixon technique including opposed phase imaging

E. Koh, E. Jung; *Jeonju/KR (kohesther@naver.com)*

Purpose: To evaluate if the opposed phase from Dixon image can increase sensitivity in the diagnosis of fracture of ankle compared with conventional MR imaging technique.
Methods and Materials: This study included 45 patients with 95 CT confirmed ankle fractures who performed MRI applying Dixon technique. The images were divided in to set 1; represented conventional MRI and set 2; opposed phase imaging. Two readers assessed 4 point confidence score to detect fracture. At first review session, readers were blinded to information and site of fractures. At second review, the information of site of the fracture was given. Sensitivity and positive predictive value (PPV) were calculated.
Results: In both session, the sensitivity of set 2 was significantly higher than those for the set 1 (session 1; 76.3 versus 62.6, respectively, session 2; 80.5% versus 65.3%). The PPV of set 2 was significantly lower compared with set 1 (85.8% versus 97.5%, respectively). While 8.9% showed lower movement of confidence score at set 2 compared with set 1, 33.6% of cases showed upper movement of confidence score. The devised possible causes of false lesions were small fractures, subcutaneous fat lobule, bone marrow edema, intraosseous vessel.
Conclusion: Opposed phase image from Dixon technique provides better sensitivity and better description of fractures compared with conventional MRI. However, cautions are required in opposed phase in diagnosis of fracture since it can be confused by adjacent BM edema or subcutaneous fat lobule.

B-1175 11:50

MRI study of plantar plate and associated lesions

B.C.S. Rabelo[1], R. Nobre Rodrigues[2], J. Mendes Torres[2], A. Abuhid Lopes[2], E. Salgado Ribeiro[2], M. Santana Firme[2], L. Gavio[2]; [1]*Itaúna/BR*, [2]*Belo Horizonte/BR (brenorabelomed@gmail.com)*

Purpose: Identify and provide data for comprehension of lesions that could be associated to metatarsophalangeal joint (MTPJ) instability and metatarsalgia based on analysis of MRI.
Methods and Materials: 52 forefoot MRI`s in 49 patients (mean age 59 years, ranging from 45-78) with plantar plate (PP) tear were retrospectively reviewed by two MSK radiologists using a 1.5T MRI. MRI was evaluated for MTP PP tear and for the presence of associated lesions.
Results: From 52 feet evaluated, 31 (59,6%) presented with PP tear only at the second MTF and 2 (3,8%) at the third MTF. 13 (25%) presented with combined lesions with 2 or more PP tears. 42 feet (81,6%) were classified as index minus. All feet had associated lesions with PP tear: hallux valgus (71,4%), Morton`s neuroma (63,3%), bursitis (55,1%), flexor tendonitis (46,9%), sesamoiditis (42,9%), arthrosis (30,6%), synovitis (24,5%). Most of the lesions (88.8%) were insertional, located at the base of the proximal phalanx.
Conclusion: The detection of associated lesions in patients with PP tear in MRI is crucial for adequate surgical planning, avoiding failure to correct lesions that may keep causing pain in the future and require further invasive interventions. The data from this study aims to help the evaluation of MRIs of feet with PP tear by providing predictability of the associated lesions in the feet, ultimately the high frequency of associated lesions shown is useful data and may contribute to differential diagnostic imaging of other causes of metatarsalgia.

10:30 - 12:00 **Room K**

Radiographers

SS 1814

Topics in general and paediatric imaging

Moderators:
B.T. Andersson; Lund/SE
D. Prayer; Vienna/AT

B-1178 10:30

Using programmable LED lighting to create a personalised ambience in the radiology environment

M.U. Knopp[1], M.M. Knopp[2], K. Binzel[3], C. Wright[3], M.V. Knopp[3]; [1]*Malibu, CA/US*, [2]*Atlanta, GA/US*, [3]*Columbus, OH/US (knopp@wcibmi.org)*

Purpose: Dedicated commercial solutions for ambient lighting have been available for years, however, broader utilisation has been limited due to their high costs. With programmable LED lighting now consumer products, we explored and assessed the feasibility and potential impact of deploying such systems in imaging environments.
Methods and Materials: We installed IP addressable LED lights using the ZigBee standard in different radiology rooms such as equipment, control, waiting and injection in order to assess a, the feasibility and b, how the different colours/hue are being perceived. In this feasibility study, we used staff and volunteers (n=13) in order to get base data to develop a clinical trial protocol. A visual perception assessment procedure was developed that used a questionnaire, pre-programmed light colour/hue settings and the ability of the subject to select the preferred setting that was found to be relaxing. The answers and setting such as RAL tone were tabulated.
Results: Technical implementation using consumer based LED lights was realized without any hardware/electric modifications. The installed IP programmable lights were readily controllable using smartphone/tablet based apps. The subject testing revealed substantial variabilities in light colour/hue perception, however clear trends were noted. In regard to which hue was perceived to enable a relaxed feeling, 62% indicated a blue tone, 23% a yellow and only 8% a red tone. Hue tones perceived to exacerbate anxiety were red 38%, yellow 38% and green 15%.
Conclusion: Programmable LED lighting can effectively and efficiently be implemented. Colour perception appears highly individualised suggesting a personalised approach is needed to create comforting atmospheres.

B-1179 10:38

Optimisation of fluoroscopic imaging of the Codman Hakim adjustable cerebrospinal fluid shunt valve

A. Bremnes, L. Kubosch, B. Ween; *Oslo/NO (alexander.bremnes@ahus.no)*

Purpose: To investigate the different fluoroscopic imaging techniques used to control the Codman Hakim adjustable valve (Codman/Johnson & Johnson, Raynham, Massachusetts) and to best practice in this image procedure. Cerebrospinal Fluid (CSF) Shunt valves, as the Codman Hakim valve, has become an important tool in hydrocephalus treatment. It has an adjustable valve and to control the adjustable valve settings fluoroscopic imaging is used.
Methods and Materials: Based on a survey on Codman Hakim imaging procedures used in hospitals in Norway, eight experimental images were acquired based on the imaging techniques seen in the hospitals. The images were measured for SNR values. Then evaluated and graded by 10 radiologists and 50 radiographers, subjectively and anonymously, using relative visual grading analysis.
Results: The image using the imaging technique with head support, grid, and the valve on the near side of the head when positioned towards the detector got 31% of the total score. The image using the imaging technique recommended by the manufacturer of the Codman Hakim adjustable valve got second highest total score with 22%. Image readers gave 64% of the total score to the imaging techniques with the valve on the near side of the head when positioned towards the detector.
Conclusion: The subjective and objective results show that images acquired using a head support, grid, and with the valve on the near side of the head when positioned towards the detector are most optimal. These is a potential to improve image optimisation in shunt radiography.

B-1180 10:46

The radiopaque anatomical side markers: have we forgot how to use them?

E. Saukko, J. Svegin, E. Svedström; *Turku/FI (ekaterina.saukko@tyks.fi)*

Purpose: The use of anatomical side markers within the primary beam of radiographs is considered as a best practice. CR and DR systems allow applying markers electronically during post-image processing and this has led to a decrease in use of radiopaque anatomical side markers. The aim of this study was to evaluate a clinical practice for use of anatomical side markers in radiography at our radiological department.
Methods and Materials: The use of anatomical side markers was evaluated from a total of 150 radiographic examinations of ankle, shoulder, cervical spine, lumbar spine and wrist. Data was collected consecutively from PACS during the period of five months in 2014 and each assessed examination consists of 1-3 images (n=330). An educational intervention was performed in 2015 and all radiographers were supplied with their own set of markers. After 12 months in 2016, a re-evaluation of anatomical side markers use was conducted by collecting the similar data to assess the impact of interventions.
Results: Results from 2014 demonstrate that anatomical side makers were used within primary beam on 28% of images, 74% of images had a marker added post-processing and 1.2% of images had an incorrect or absent anatomical side marker. In 2016 all assessed images were appropriately marked (100%) and 54% of them included anatomical side marker placed pre-exposure.
Conclusion: The use of radiopaque anatomical side markers was increased. Radiology departments should provide for radiographers an easy access to radiopaque anatomical side markers and carry out regular audits of practice.

B-1181 10:54

Radiation dose to newborns in a neonatal intensive care unit

L. Sousa, A.F. Abrantes, L.P.V. Ribeiro, J.P. Pinheiro, R.P.P. Almeida, S. Rodrigues, P. Sousa; *Faro/PT (jppinheiro@ualg.pt)*

Purpose: To assess the entrance surface doses (ESD) in newborns from chest radiographs performed in a neonatal intensive care unit of a public hospital.
Methods and Materials: A survey of technical parameters used in the mobile x-ray examinations was performed using a sample of 24 chest radiographs to determine the average parameters (kVp and mAs) according to the weight of the newborns (0-1000g; 1000-2000g; and >2000g). Using these parameters, ESD values were determined based on the mean and 75th percentile. Quality control of the mobile equipment was made with a semiconductor detector (Unfors Xi).
Results: The ESD values resulting for the 75th percentile was 27.3 µGy at 1 meter of Source-Image Distance (SID) and 16,17 µGy at 1.28 meters. Considering the weight intervals, ESD values for the 75th percentile were 18.4 µGy (0-1000g), 27.3 µGy (1000-2000g) and 34.76 µGy (>2000 g) at 1 meter of SID. The ESD values increased with the increase in the weight of newborn. The results of this study were also compared with three previous studies. The values of the ESD resulted from the mean of this study (23.1 µGy at 1 meter) only exceeded the results of a study which ESD was 20.0 µGy.
Conclusion: The results obtained did not exceed the limits required internationally. However, several actions should be pursued, including: remarking the ALARA (as low as reasonable achievable) concept, defining national guidelines for good newborn radiography and, retraining radiographers to be specialised for neonatal imaging and neonatal ionisation radiation hazards.

B-1182 11:02

Are radiographers prepared to meet children with special needs when seen for a radiographic examination?

B. Bjorkman; *Jönköping/SE (berit.bjorkman@ju.se)*

Purpose: Two previous national surveys showed, that none radiology and paediatric departments and a minority of anaesthesiology departments throughout Sweden use specific guidelines when interacting with children diagnosed with Autism Spectrum Disorders (ASD). Following, the purpose was to develop guidelines to use when caring for and preparing children with ASD for anaesthesia and callenging radiographic procedures.
Methods and Materials: A modified Delphi method was used, including 19 experts identified from the two aforementioned surveys. The questions considered in the Delphi process, proceeded from previous research and the results from the two national studies. The experts' responses regarding the importance of each item, were analysed and scrutinised between each round.
Results: The Delphi process resulted in guidelines consisting of 15 items and a checklist of 16 aspects. The items cover the areas: planning and involving parents/guardians, features in the environment, use of time, communication and the health care professionals. The checklist covers the child's pattern of communication, anxiety, sensory stimuli, special interests and likes/dislikes.
Conclusion: In order to obtain an optimum caring encounter with a child with ASD in the preoperative and radiology setting, a meticulous planning ahead to fulfil the needs of each specific child is important. Also the environment should be adjusted for the needs of the child and the health care professionals need to inherit knowledge about ASD in general and the specific needs of the individual child in particular. In order to accomplish this, guidelines need to be in place and be followed.

B-1183 11:10

Optimisation full-spine curvature radiography in paediatrics - impact of acquisition parameters

C.S. Reis[1], V. Harsaker[2], A. Bregman[3], R. Chêne[4], B. Cordeiro[5], T. Daniels[6], M. Johannessen[2], S. Vestli[2], M. Widmer[4], A. England[7], P. Hogg[7]; [1]*Perth/AU*, [2]*Oslo/NO*, [3]*Groningen/NL*, [4]*Lausanne/CH*, [5]*Lisbon/PT*, [6]*Bloemfontein/ZA*, [7]*Salford/UK (a.bregman@outlook.com)*

Purpose: To determine a set of acquisition parameters for infantile scoliosis in anteroposterior (AP) digita radiography using low effective dose (*E*) whilst retaining adequate image quality (IQ) for visual evaluation using 1 year-old anthropomorphic phantom.
Methods and Materials: 48 images of the phantom full spine were acquired in AP position varying beam energy (55-85kVp), source-to-image distance (SID) (160-200cm), beam intensity (6,3-0,8mAs) whilst applying the 10 kVp rule, air gap (with 20cm or without), added beam filtration (1mm Al+0,2mm Cu or without) to analyse the impact of E on IQ. IQ was evaluated by an objective approach using contrast-to-noise ratio (CNR) and a perceptual approach using 6 observers. Monte-Carlo modelling (PCXMC software) was used to estimate E. The Intraclass correlation coefficient (ICC) was used to calculate intra and inter-observer consistency.
Results: The results show that CNR was high at 65kVp, with SID of 180cm; but the lowest E was achieved using 160cm SID, 85kVp, 0.8mAs, no air gap and with a filtration of 1mm Al and 0.2mm Cu. The intra- and inter-observer ICC for visualising the anatomical structures was moderate to good varying between 0.596-0.890 and 0.631-0.988, respectively. Observers identified all relevant anatomical structures to draw the lines used for angle measurements in clinical practice.
Conclusion: The observers were able to perform the task related to diagnostic performance in the group of images produced with the lowest E. This study shows that it is possible to optimise radiography practice concerning infantile studies.

B-1184 11:18

Benefit-risk communication in paediatric imaging: an assessment of current practice among local referrers and practitioners

J.L. Portelli[1], J.P. McNulty[2], P. Bezzina[1], L. Rainford[2]; [1]*Msida/MT*, [2]*Dublin/IE (jonathan.portelli@um.edu.mt)*

Purpose: To investigate referrers' and practitioners' practice of providing benefit-risk information when imaging paediatric patients at a large general hospital in Malta.

Methods and Materials: A cross-sectional survey was conducted prospectively among 272 referrers and practitioners, namely: emergency medicine physicians (55), paediatricians (49), radiographers (146), and radiology practitioners (22). Apart from assessing whether participants had received any education or training in radiation protection, referrers and practitioners were asked about the type of information they generally provided to paediatric patients and their families; whether they would discuss benefits and/or risks associated with paediatric imaging examinations; and how confident they felt in their ability to communicate such information.
Results: A total of 168 participants (56 referrers and 112 practitioners) completed and returned the questionnaire, providing an overall response rate of 61.8%. Findings revealed that the practice of providing benefit-risk information varied, with a lower proportion of practitioners indicating that they would discuss associated benefits and risks of paediatric imaging examinations. Those who received education and training in radiation protection provided a significantly better ranking to their level of confidence and ability to communicate benefit-risk information, although only 36.7% of all participants actually indicated a high level of confidence in this regard.
Conclusion: The practice of discussing benefits and risks associated with paediatric imaging examinations is varied. Education and/or training activities are necessary to help improve referrers' and practitioners' confidence so as to encourage them to further engage in benefit-risk discussions with paediatric patients and their families.

B-1185 11:26

Wireless workflow in radiology: a pilot testing in portable x-ray
B.E. Koay, S. Li, S.K. Sanamandra; *Singapore/SG*
(koay.beng.ee@sgh.com.sg)

Purpose: The pilot test aims to simplify the work processes for the radiographers, reduce the reliance on paperwork and improve the turn-around-time (TAT) for the portable teams. This paper presents the findings from the pilot test
Methods and Materials: The LEAN thinking system was employed to evaluate the original workflows. Stakeholders identified valued, non-valued tasks and waste process from the workflow. Timing from the original workflow was benchmarked against the wireless workflow. For the wireless workflow, a Toughbook was issued to the portable team and RIS module was customized to facilitate readability and documentation on the Toughbook. Portable x-ray machine was configured to detect hospital Wi-Fi network. Both workflows were applied on the same portable team.
Results: Waste tasks contributed 25% to 30% to the total tasks. They posed potential errors in patient misidentification for ad-hoc additional procedures. With the removal of waste task and simplification of the process, lesser errors could occur. The process indirectly improved patient safety. Instructions were captured in RIS, allowing takeover shift to view outstanding issues from RIS worklist instead of paperwork. Equipped with an electronic signature pad, paperless workflow is achievable. By sending images wirelessly to PACS, the TAT for images to be available to physician improved by 27% to 40%. Overall, average time worked on a patient improved in the range of 12% to 21%.
Conclusion: Our pilot test showed improved results from the wireless workflow. This workflow could potentially extend to be paperless, saving 90 pieces of paper daily.

B-1186 11:34

Mobile radiography services in nursing homes: a systematic review of residents and societal outcomes
E. Kjelle[1], K.B. Lysdahl[2]; [1]*Kongsberg/NO*, [2]*Oslo/NO (elin.kjelle@hbv.no)*

Purpose: The purpose of this systematic review was to identify the outcomes of mobile radiography services for nursing home residents and society.
Methods and Materials: A systematic review based on searches in the Medline, Cochrane, PubMed, Embase and Svemed+ databases was performed. Titles and abstracts were screened according to a predefined set of inclusion criteria: empirical studies in the geriatric population, and reports of mobile radiography services in a clinical setting. All included publications were quality appraised using MMAT or CASP appraisal tools. Data were extracted using a summary table and results were narratively synthesised.
Results: 10 publications were included. Three overarching outcomes were identified: 1) reduction in hospitalisations and outpatient examinations or treatment, 2) reduction in transfers between hospitals and nursing homes and 3) increased access to x-ray examinations. These outcomes are interlinked with the more specific outcomes for residents and society reported in the literature. For residents there is a reduction in burdensome transfers, waiting time, an increase in adequate treatment and care. For society, released resources can be used more wisely, and overall costs are reduced substantially.
Conclusion: This review clearly indicates the benefits of mobile radiography services for nursing home residents, by reducing the burden of transfer, and providing more adequate Treatment and care. Mobile radiography services provide a better socio-economic solution compared to hospital or emergency room examinations. Further research is needed to evaluate the outcomes for residents and next of kin, and to estimate the cost-effectiveness.

10:30 - 12:00 **Room M 1**

Cardiac

SS 1803

Myocardial tissue characterisation and texture analysis I

Moderators:
U. Reiter; Graz/AT
R. Vliegenthart; Groningen/NL

B-1187 10:30

Quantification of fibrosis with cardiac MR-T1-mapping using histologic quantification as a gold-standard
P.-A. Barral, J.-J. Izaaryene, A. Jacquier; *Marseilles/FR*
(pierre-antoine.barral@ap-hm.fr)

Purpose: Fibrosis is characterised by fibroblast accumulation and excess deposition of extracellular matrix (ECM) proteins, which leads to distorted organ architecture and function. The contribution of fibrogenesis to impaired cardiac function is increasingly recognised. The goal of this study is to validate T1-mapping for myocardial fibrosis quantification against histological fibrosis quantification as a gold standard, and to assess the link between ECV quantification and blood biomarkers of fibrosis.
Methods and Materials: Thirty patients with aortic pathology needed aortic valve replacement were recruited from the department of cardiac surgery in our institution. Cardiac magnetic resonance (CMR) for ECV quantification and blood samples were performed. T1-mapping (MOLLI) using “look-locker” technique, were performed before and 15 minutes after injection of gadolinium to assess ECV. Standard blood samples and specific fibrosis bio-marker were sampled during the week before surgery. Muscular interventricular septum biopsy was fixed in the formol and stained with picrosirius red.
Results: We found a significant correlation between ECV quantification and histologic evaluation of fibrosis with red picrosirius (p=0.0026), with a 95% confidence interval of 0.2771 to 0.8524. Correlation between ECV and biomarkers was significant for timp 1 (p=0.0378) with 95% confidence interval of 0.026 to 0.69 and for mmp2 (p=0.0475) with 95% confidence interval of 0.0056 to 0.68, but no correlation with galectine, cic p, piinp and icp was found.
Conclusion: T1-mapping and ECV quantification can provide accurate evaluation of myocardial fibrosis. Two biomarkers have also a strong correlation with myocardial fibrosis.

B-1188 10:38

Left ventricular interstitial fibrosis drives left atrial enlargement and impairment in arterial hypertension: novel insights from T1 mapping
J.C.L. Rodrigues, T. Erdei, A. Ghosh Dastidar, A.E. Burchell, M.C.K. Hamilton, J.F.R. Paton, A.K. Nightingale, C. Bucciarelli-Ducci, N.E. Manghat; *Bristol/UK*
(jonrodrigues@doctors.org.uk)

Purpose: Hypertensive left atrial enlargement (LAE) predicts cardiovascular morbidity and mortality. Impaired left atrial (LA) function also confers poor prognosis. We hypothesised that the burden of left ventricular (LV) interstitial fibrosis would be associated with LAE and impaired LA function.
Methods and Materials: 86 hypertensives (49±15 years, 53% male, office SBP 168±30mmHg, office DBP 97±14mmHg) underwent 1.5T cardiovascular magnetic resonance. LV mass and volumes were measured. T1 mapping (with validated modified look-locker inversion-recovery sequence) enables non-invasively LV extracellular volume fraction (ECV) estimation. LA volumes were assessed using the biplane area-length method. The phasic volumetric method generated estimates of LA reservoir, conduit and pump function.
Results: Structurally, as indexed LV mass increased, so did LA size (R=0.345, P<0.001). Functionally, increasing indexed LV mass was associated with significant reductions in LA reservoir (R=-0.439, P<0.0001) and conduit (R=-0.345, P<0.0001) but not pump (R=-0.149, P=0.117) function. At the intra/extracellular myocardial level, increasing ECV was associated with increasing LA size (R=0.359, P<0.001). Furthermore, increasing indexed myocardial interstitial volume was associated with significant reductions in both LA reservoir (R=-0.437, P<0.0001) and conduit (R=-0.316, P=0.003) but not pump (R=-0.167, P=0.125) function. In multivariate regression (controlling for age, gender, BMI, SBP and DBP) ECV remained the only significant independent predictor of LAE (odds ratio[95% confidence interval]: 1.35 [1.09-1.68], P=0.006).

Conclusion: LV interstitial fibrosis is associated with LAE and impaired reservoir and conduit function. LA pump function is preserved which offers hope that future anti-fibrotic agents may be able to cause reverse remodelling of hypertensive LA structural and functional abnormalities.
Author Disclosures:
C. Bucciarelli-Ducci: Consultant; Circle Cardiovascular Imaging Inc, Calgary, Canada.

B-1189 10:46

Evaluation of myocardial fibrosis in patients affected by diabetes mellitus type II and its correlation to left ventricular functional impairment

N. Galea, F. Ciolina, R. Ammendola, E. Giannetta, M. Francone, I. Carbone, C. Catalano; *Rome/IT (nicola.galea@gmail.com)*

Purpose: In diabetic cardiomyopathy (DCM), the chronic metabolic injury determines progressive impairment of cardiomyocytes contractility and fibrotic tissue infiltration, leading to ventricular dysfunction and dilation. The purpose of our study is to non-invasively investigate the relationship between myocardial fibrosis, geometric/function features and clinical data.
Methods and Materials: Sixty-two diabetic patients with preserved ventricular function and no history of ischaemic disease and 20 matching controls underwent CMR. Imaging protocol included: modified look-locker sequence before and 20 minutes after 0.2 mmol/kg gadoterate meglumine injection; T2-mapping; ventricular function module; tagged-cine MR module; late gadolinium enhanced (LGE) imaging. Native myocardial T1 (nT1) and T2 values, extracellular volume fraction (ECV), ventricular torsion angle and myocardial strain values have been calculated and correlated to lab and clinical markers of disease. Pearson Correlation, Mann-Whitney test and unpaired T test were used for statistical analysis.
Results: Patient group had higher nT1 and ECV values compared to controls (1035±94 ms vs975±38 ms, 28.2±3.3%vs24.8±4.3%, respectively, p<0.05 for both), whereas no significant differences occurred in T2 measurements (46.1±2.3ms vs47.0±2.8ms, respectively, p=0.23). nT1 and ECV correlated with glycated haemoglobin (HbA1c, nT1:r2=0.98, ECV:r2=0.95, p<.001) and disease duration (nT1:r2=0.98; ECV:r2=0.55, p<.001) in diabetic patients. nT1 and ECV showed a positive correlation with torsion (nT1:r2=0.98; ECV:r2=0.89, p<.001) and a negative correlation with strain value in tagged-cine MR analysis (nT1:r2=-0.98; ECV:r2=0.92; p<.001). Ischaemic LGE areas were found in four patients as marker of silent infarction.
Conclusion: In diabetic patients with preserved ventricular function, HbA1c values and disease duration showed a correlation with myocardial nT1 and ECV increase, as reflection of diffuse fibrosis, and torsion modification.

B-1190 10:54

Myocardial tissue characterisation by CMR in subjects with prediabetes, diabetes and normal controls with preserved ejection fraction from the general population

C. Storz[1], H. Hetterich[2], R. Lorbeer[2], S. Auweter[2], W. Rathmann[3], C. Schlett[4], A. Peters[5], J. Schulz-Menger[6], F. Bamberg[1]; [1]*Tübingen/DE*, [2]*Munich/DE*, [3]*Düsseldorf/DE*, [4]*Heidelberg/DE*, [5]*Neuherberg/DE*, [6]*Berlin/DE*
(corinna.storz@med.uni-tuebingen.de)

Purpose: To characterise myocardial tissue in subjects with prediabetes, diabetes, and healthy controls using CMR in a sample from the general population.
Methods and Materials: Subjects without history of cardiovascular disease and preserved left ventricular ejection fraction (LVEF) but established diabetes, prediabetes, and normal controls from a population-based cohort underwent contrast-enhanced 3 Tesla CMR. Obtained parameters included left ventricular (LV) function and morphology, late-gadolinium enhancement (LGE) for assessment of focal fibrosis as well as T1-mapping and derivation of extra-cellular volume fraction (ECV) by modified Look-Locker inversion recovery for diffuse fibrosis. Myocardial fibrosis (MF) and cell volume (CV) were calculated.
Results: Among 343 subjects (mean age: 56.1±9.2 years, 57% males), 14% subjects were classified as diabetic, 23% as prediabetes, and 64% as controls. LVEF was preserved in all patients but LV remodeling index was significantly higher in participants with prediabetes and diabetes, independent of BMI, hypertension, age and sex (1.17, 95%-CI: 1.11 to 1.23 and 1.28, 95%-CI: 1.20 to 1.36, p<0,002 respectively). ECV was decreased in subjects with prediabetes and diabetes compared to healthy controls (23.1±2.4% and 22.8±3.0%, both p<0.007, respectively). In contrast, CV was significantly higher in subjects with prediabetes and in diabetics as compared to healthy controls (109.1±23.8 ml and 114.9±32.3 ml vs. 96.5±26.9 ml, both p<0.03, respectively).
Conclusion: Subjects with prediabetes and diabetes but preserved LVEF had higher LV remodeling indices and cell volume than controls, indicating a role for hypertrophy in the pathogenesis of diabetic cardiomyopathy, while diffuse fibrosis appears to be less relevant.

B-1191 11:02

T1 relaxation-times, epicardial fat volume and left ventricular contractility in obese individuals with normal systolic left ventricular function: a cardiac magnetic resonance study

R. Homsi, D. Kuetting, A. Sprinkart, S. Fischer, J. Luetkens, M. Meier-Schroers, D. Dabir, H. Schild, D. Thomas; *Bonn/DE*
(r.homsi@hotmail.com)

Purpose: To investigate left-ventricular (LV) strain, epicardial fat volumes (EFV) and T1-relaxation times (T1) in obese non-hypertensive and non-diabetic individuals with a preserved LV ejection fraction (LVEF).
Methods and Materials: 68 subjects (mean age 56±14years [y]; BMI 29kg/m2) were examined at 1.5 Tesla. 28 individuals were obese (>30kg/m²) and 40 were non-obese (<30kg/m²). T1-RTs, LV peak longitudinal and circumferential strain (LS; CS) as well as EFV and pericardial fat volumes (PFV) were evaluated.
Results: EFV was increased and LS and CS were both decreased in obese (EFV: 69±27ml/m²; LS: -20±3%; CS: -23±5%) compared to non-obese subjects (58±20ml/m²; LS: 23±3%; CS: -27±4%; p<0.05, each). Obese individuals showed increased T1-RTs (990±37ms vs. 972±30ms), however these differences did not reach statistical. There were no significant differences regarding age or gender.
Conclusion: Obesity is associated with an increased EFV, a reduced LV strain in spite of a preserved LVEF, as well as with a trend towards higher T1-RT - as a marker of myocardial fibrosis. Evaluation of these parameters may identify early cardiac changes associated with obesity.

B-1192 11:10

Role of late gadolinium enhancement, myocardium native T1 value and texture analysis in patients affected by dilated cardiomyopathy: clinical score and outcome correlation

A. Scavuzzo, E. Faietti, D. Farina, E. Gavazzi, C. Foletti, I. Zorza; *Brescia/IT*
(alessandro.scavuzzo@gmail.com)

Purpose: To correlate late gadolinium enhancement (LGE), myocardium T1 value, texture analysis and the outcome in patients affected by dilated cardiomyopathy (DMC).
Methods and Materials: Retrospective evaluation on 104 DMC affected patients who underwent cardiac MR (CMR) between January 2012 and May 2015. Exam protocol included morphologic sequences, cine MR, native T1 mapping and after gadolinium PSIR sequences. LGE was analysed drawing ROIs on short-axis PSIR, T1 delineating the cardiac septum on native short-axis ShMOLLI and texture analysis delineating the septum on short-axis cine MR using TexRad software. Outcome was set as major cardiac events (MACE) 6 months within the exam.
Results: 53/104 patients presented LGE and they showed a higher percentage of MACE compared to patients without LGE (37% vs 7%, respectively, p=0.001). The extension of LGE did not correlate with MACE, the ejection fraction or the end-diastolic volumes (t test, p=ns). T1 was measured on 34 patients, 21 with LGE (mean 1033msec) and 13 without LGE (mean 1008msec) (p=ns). Significant difference was shown between T1 of patients with MACE (11/34, mean 1045msec) and without MACE (23/34, mean 1011msec)(p=0.02). Texture analysis showed correlation between patients with and without MACE, with kurtosis at 1mm filter being the most significant value (t test, p=0.0019).
Conclusion: Both the presence of LGE and native T1 value of myocardium correlate with MACE. Correlation between T1 and LGE has not been proved. Texture analysis has demonstrated a potential on defining diffuse myocardium fibrosis (particularly with thin filters) and is easily applicable, but it is not still supported by enough literature data.

B-1193 11:18

Cardiovascular magnetic resonance in cardiomyopathies with viral genome incorporated in cardiac tissue

A. Michalek, M. Lanckoroński, A. Pawlak, M.I. Furmanek, R.J. Gil, A. Nasierowska, M. Przybylski, J. Walecki; *Warsaw/PL*

Purpose: The aim of this study was to identify characteristic pattern of cardiovascular magnetic resonance (CMR) findings in patients with acute myocarditis or chronic dilated cardiomyopathy who had viral genome detected in cardiac tissue.
Methods and Materials: Sixty three patients who presented for work - up of myocarditis or unclear cardiomyopathy underwent CMR and endomyocardial biopsy (EMB) with viruses identification by nested PCR.
Results: Viral genome was identified in 39 patients (62%). Parvovirus B19 was most prevalent virus (29 biopsies), we also detected HHV6 (6), Adenovirus (1), EBV (3), CMV (1). Left ventricular ejection fraction was impaired both in viral positive and viral negative hearts, 45,25 (+/- 18,8) % vs 41,2 (+/- 18,07) % respectively, p=0,2. There was no difference in presence of late gadolinium enhancement (LGE) in accordance of viral genome. Typical non-ischaemic

LGE was presented in 26 (66,7%) viral positive patients and in 12 (50%) viral negative patients, p=3,4. In both groups LGE was detected in all segment with the majority of mid - segments. LGE was detected in all walls, with prevalence of infero/lateral and antero/lateral walls (52,6%, 44,7% LGE positive cardiac scans) and least in anterior wall (21% LGE positive scans) but without any difference in accordance of viral genome. There were 6 cases in viral positive group and 3 cases in viral negative group with typical CMR oedema, p - 1,8.
Conclusion: There is no typical pattern of CMR LGE specific for cardiomyopathy with cardiac tissue positive for viral genome.

B-1194 11:26

Myocardial T1 mapping and extracellular volume fraction (ECV) comparing MOLLI and SMART1Map sequences in 3T-MRI

L. Panebianco, V. Vellucci, L. Patriarca, E. Cannizzaro, P. Palumbo, R. Masi, E. Di Cesare, C. Masciocchi; *L'Aquila/IT (panebianco.luca@gmail.com)*

Purpose: Assessing variability in T1 mapping and extracellular volume fraction values between MOLLI (Modified Look Locker Inversion Recovery) and SMART1Map (Saturation Method using Adaptive Recovery Time) sequences, using ARC (Autocalibrating Reconstruction for Cartesian imaging) and ASSET (Array Spatial Sensitivity Encoding Technique) parallel imaging algorithms.
Methods and Materials: 54 patients underwent contrast-enhanced cardiac magnetic resonance (CE-CMR) on a 3T MRI scanner, after collecting their haematocrit values. Data acquisition was achieved with a cardiac phased-array 32-channel coil, and T1 mapping sequences were performed: MOLLI ARC, MOLLI ASSET, SMART1Map ARC and SMART1Map ASSET, acquired in one slice in short axis plane at mid-ventricular height, with electrocardiographic gating and during expiratory apnoea, before and after intravenous administration of gadobenate dimeglumine 2mmol/kg. For each sequence ECV was obtained by measuring the signal intensity of the antero-septal wall myocardium and of blood pool placing circular ROIs in T1- maps and correlating it with the haematocrit.
Results: A statistically significant difference ($p < 0.05$) for both pre- and post-contrastographic T1 values was observed in SMART1Map sequences (SMART1Map Asset medium 1510.88; SD ± 92.32 and SMART1Map Arc average in 1560; SD ± 135.17) in comparison to the corresponding MOLLI sequences (MOLLI Asset media 1171.61; SD ±40.63 and MOLLI Arc average 1182.1; SD ±54.81); the results showed no significative difference relatively to ECV values. Continuous variables were represented as means and standard deviations, and comparisons between groups were obtained by Student's t test for independent samples.
Conclusion: MOLLI and SMART1Map resulted to provide significantly different values of T1.

B-1195 11:34

MRI atrial fibrosis after cryoablation in patients with atrial fibrillation: a prospective feasibility study and its relation to endovascular procedure

E. Caramia, R. Faletti, L.J. Pavan, D. Tore, M. Matta, M. Anselmino, P. Fonio, F. Gaita, G. Gandini; *Turin/IT (espiguinha@hotmail.it)*

Purpose: cryoablation (CA) is a well-established technique for atrial fibrillation (AF) treatment. Many studies used late gadolinium enhancement magnetic resonance imaging (LGE-MRI) to evaluate left atrial (LA) fibrosis, but there is a lack of data regarding post-procedural structural changes. Our aim was to define the role of LGE-MRI in the identification and quantification of LA ablation induced fibrosis.
Methods and Materials: eight consecutive patients (mean age 56,4) with AF underwent CA (procedure parameters: minimum temperature, freezing and heating time, procedure duration for each ostium). LGE-MRI was performed prior the procedure, at 24 hours and after 1 month. Atrial fibrosis was evaluated qualitatively and quantitatively. Statistical analysis was performed by univariate analysis using Kruskal-Wallis test for continuous variables and X^2 analysis for categoric variables.
Results: 30 out of 47 applications were effective, 9 repeated and 8 ineffective. A difference between procedure duration (p=0,014), minimum temperature (p=0,002) and heating time (p=0,001) was found between effective and ineffective procedures. Procedure duration was lower for right ostia. At 1-month, fibrosis was identified in 26/32 (81,3%) of pulmonary veins (PV) ostia. Circumferential fibrosis was observed in 12/32 (37,5%) PV ostia. Right inferior PV ostium has a lower amount of fibrosis both qualitatively (fibrosis foci p=0.0045; circumferential fibrosis p=0,046) and quantitatively (mean fibrosis 39% vs 14.9% p=0.0088).
Conclusion: fibrosis foci were detected in large amount of PV ostia, otherwise their circumferentially involvement is quite rare and related to treatment temperature and duration. Lowest amount of fibrosis was detected at right inferior PV according to complex anatomy.

B-1196 11:42

Acute myocardial tissue characterisation using magnetic resonance native T1 mapping at 3.0 T

A. Clemente[1], F. Avogliero[1], A. Di Giambattista[1], N. Martini[1], A. Barison[2], D. Della Latta[1], D. Chiappino[1]; [1]*Massa/IT*, [2]*Pisa/IT (andreadigia@gmail.com)*

Purpose: To investigate the ability of native T1 mapping at 3.0 T to identify inflammatory processes involved in acute myocardial diseases.
Methods and Materials: Native T1 maps in short-axis view were acquired from 91 subjects using a modified Look-Locker inversion recovery sequence at 3.0 T with heart rate independency. Patients were grouped based on CMR findings and consisted of subjects with acute myocardial infarction (IMA, n=12), acute myocarditis (AM, n=7) and controls (n=72). Six-segment analysis was performed with manually drawn regions-of-interest.
Results: Global myocardial T1 relaxation time was significantly increased in IMA (1248.8±38.8 ms, p<0.01) and AM (1237.9±70.7 ms, p<0.01) compared to controls (1163.1±34.9 ms, p<0.01). T1 values were higher in segments with LGE than in those with no LGE in IMA (with LGE 1309.9±70.0 ms versus no LGE 1187.9±18.0 ms, p<0.01). T1 values were higher in segments with LGE than in those with no LGE in AM (with LGE 1330.0±41.0 ms versus no LGE 1206.3±74.0 ms, p<0.05). T1 values were both higher in segments with no LGE compared to controls in IMA (1187.9±18.0 ms, p<0.05) and AM (1206.3±74.0 ms, p<0.01).
Conclusion: Native T1 mapping at 3.0 T was found to be significantly higher in acute myocardial processes involved in no LGE segments compared to healthy controls.

B-1197 11:50

Native T1 mapping comparison of mean and median assessment reveal reduced T1 in normal anterior and anterolateral segments compared to the rest of the myocardium

P. Triadyaksa, T.A. D'Antonoli, N.H.J. Prakken, M. Oudkerk, P.E. Sijens; *Groningen/NL (p.triadyaksa@umcg.nl)*

Purpose: In pixel-wise analysis of the myocardium, assessment of median segmental T2* values was previously found to produce more reproducible results than assessment of the means. To our knowledge, pixel-wise comparisons of reproducibility of median and mean signal intensities has not yet been reported for native T1 mapping. The purpose of this study was therefore to compare the reproducibility of normal native T1 mapping of the myocardium in using mean and median assessment.
Methods and Materials: Retrospective analysis of 1.5T MOLLI sequence MRI data acquired with motion correction was applied to map native T1 in the myocardium of 63 patients that turned out to have a normal heart ejection fraction and stroke volume. For the myocardium measured at three short-axis slices, pixel-wise T1 quantification (mapping) with mean and median assessment was done on 16 AHA segments. Fitting with assessment of R^2 was used to evaluate precision.
Results: Median myocardial native T1 values were significantly lower than the means (P<0.001). Median assessment produced significantly less segmental T1 variation between patients with higher fitting precision (P<0.001) in global and segmental analysis. Evaluated either way, the apical lateral segment, anterior segment at three slices, and anterolateral segment at mid-ventricular and basal slices had significantly lower native T1 values than the other ten segments (P<0.001).
Conclusion: Median assessment reduces measurement variability in global and segmental native T1 mapping of the myocardium. Variation of normal heart T1 values was apparent on segmental analysis, a novel finding with implications for pathological evaluation.

10:30 - 12:00 **Room M 4**

Computer Applications

SS 1805

Clinical decision support and structured reporting

Moderators:
M. Fatehi; Tehran/IR
N. Pyatigorskaya; Paris/FR

B-1198 10:30

Integrating clinical decision support for pulmonary embolism in the emergency department: a pilot study of feasibility and provider perspective

A. Goehler, J. Weinreb, H. Forman, C. Moore, A. Hsiao, J. Arango, L. D'Amato; *New Haven, CT/US (alexander.goehler@yale.edu)*

Purpose: In the context of a commercial EMR, we implemented a clinical decision support (CDS) intervention for CTA for pulmonary embolism (CTA-PE) in the emergency department (ED) and quantified its impact on ordering practices.
Methods and Materials: In a survey of 231 radiologists and clinicians in the ED, 78% identified CTA-PE as "overutilised". We developed an algorithm that combined established risk scores and local practice patterns to risk stratify PE workup. We integrated a mandated questionnaire for every CTA-PE study requested within the EMR. If answers were concordant with the clinical pathway, the study order was placed; if answers were discordant, alternative scenarios were recommended.
Results: Among the 853 studies conducted, 8.2% were positive for PE. The algorithm was highly accurate, with 10.4% and 10.0% positivity among studies that were recommended to proceed with CT or pursue D-dimer, respectively. In cases where cancellation was recommended, 2.6% of studies were positive, and one of these showed a clinically significant PE. Among the 879 studies requested, 479 (55%) were recommended to change their order: 6 (1.3%) studies were subsequently cancelled; 13 (2.7%) changed to a D-dimer, 460 (51%) proceeded with CTA despite the recommendation. Among providers who ordered ≥10 studies, concordance with the CDS recommendation ranged from 12 - 68% (mean 45%) with little (0.10) correlation between compliance and positivity rates.
Conclusion: While the CDS algorithm for PE was accurate, it had only a modest impact on ordering practices, in part due to substantial heterogeneity in physician adherence to the CDS intervention.

B-1199 10:38

Dematerialisation of informed consent in radiology: results from an Italian online survey

F. Coppola[1], L. Faggioni[2], C. Privitera[3], D. Regge[4]; [1]*Bologna/IT*, [2]*Pisa/IT*, [3]*Catania/IT*, [4]*Turin/IT (francesca_coppola@hotmail.com)*

Purpose: The aim of this study is to present the results of the Italian survey on dematerialisation of informed consent in radiology (DIC).
Methods and Materials: Two radiologists created an online survey using Survey Monkey. The survey consisted of 15 multiple-choice questions. Members of Italian Society of Medical Radiology (SIRM) were given 1 week to perform the survey.
Results: A total of 1791 radiologists, 18% of all SIRM members, participated. In Italy the radiological informed consent is used for CT and MRI (93.33%), interventional procedures (70.95%), ultrasound examinations with i.v. contrast media (42.40%), and for the exclusion of pregnancy in young women before x-ray examinations (70.22%). Seventy-two percent of radiologists evaluate the appropriateness of the diagnostic procedures before deciding to accept or reject the request. Ninety-five percent (n=1684) of responders have a positive opinion on DIC, while only 5% (n=93) have a negative one. The advantages are: storage and conservation of DIC is safer according to majority of responders (94.54%), its recovery is easier and faster (96.53%) in case of medico-legal disputes respectively and the reduction of paper used leads to reduced costs (90.67%). The disadvantages are: implementation of DIC is complex, in particular to obtain the preliminary approval for the utilization of advanced digital sign from each patients (51.76%) and to provide required dedicated area inside radiological unit (63.97%).
Conclusion: The majority of Italian radiologists are favourable on DIC. However, they have concerns that the implementation of DIC could be complex.
Author Disclosures:
F. Coppola: Other; I am EPOS reviewer.

B-1200 10:46

How to prescribe imaging tests and to make clinical decisions? - effectiveness of a virtual classroom for undergraduate students in radiology

A. Viteri Jusué[1], A. Tamargo Alonso[1], A. Bilbao González[2], D. Grande Icaran[2], T. Palomares Casado[2]; [1]*Vitoria-Gasteiz/ES*, [2]*Bilbao/ES (ainhoa.viterijusue@osakidetza.net)*

Purpose: To develop a virtual learning environment for teaching to medical students the following skills: prescribing imaging tests and making decisions based on their results. To assess its feasibility, effectiveness and students´ satisfaction.
Methods and Materials: An ad-hoc virtual classroom was implemented in the Moodle platform consisting on videolectures, practical exercises and e-learning resources. Sixth-grade students were recruited and gave informed consent prior to randomization into the experimental or the control group. Research Ethics Committee approved this project. Performance (ability to prescribe imaging tests and to take diagnostic-therapeutic decisions based on their results) was evaluated with objective structured clinical exams. Weighted scores from 0 to 100 were compared between experimental and control groups with the non-parametric Wilcoxon test (SAS System for Windows, version 9.2). Satisfaction was assessed with an eleven-items, five-level Likert scale.
Results: Twenty-six students were included (8M/18F, median age 23y) and randomized (13 experimental/13 control group). 76.9% students in the experimental group completed the practical assignments. Mean self-reported time devoted to the virtual course 7.17 hours. Satisfaction: median satisfaction was high or very high in 10 out of 11 items. Efficacy: students in the experimental group performed better at prescribing imaging tests (mean score 55.9% vs 37.1%, p=0.0042) and at making clinical decisions (mean score 40.0% vs 29.5%, p=0.0403).
Conclusion: The abilities to prescribe imaging tests and to make clinical decisions with their results can be taught effectively and satisfactorily to undergraduate medical students through a virtual learning environment. Its use will be generalized to the remaining students.

B-1201 10:54

Structured reporting: using the voice of the customer method to settle an ongoing debate about the future of radiology reporting

T. Heye, V. Gysin, D. Boll, E. Merkle; *Basle/CH (tobias.heye@usb.ch)*

Purpose: The presentation and clarity of a radiology report do not always meet the expectations of referring physicians. Meanwhile a debate about the future of radiological reporting is taking place. The purpose of this study is to assess the perception, preferences and expectations of recipients of radiology reports in terms of style and content.
Methods and Materials: A survey was conducted among general practitioner (GP) and hospital based physicians (HP) in north-western Switzerland. The questionnaire consisted of a demographic section, a part addressing current satisfaction and a section addressing expectations in content and structure. The participants were presented with four layouts of radiology reports (text, structured text, tables, images) and asked to rate each in comprehensibility and efficiency (range 1-10; 10 highest score).
Results: 434 participants (121GPs, 313HPs, 4 different hospitals) with 114 residents and 320 board-certified physicians completed the survey. Both GP and HP were equally satisfied with radiology reports with a mean of 7.2. Regarding layout preferences, structured text (mean 5.8-7.9;) and images (mean 6.6-8) rated highest in terms of readability, time savings and helpfulness in the communication with patients, when compared with tables (mean 4.5-5.4) and unstructured text (mean 3.3-4.6). Of all participants, 81% stated a report should allow for fast and efficient reading.
Conclusion: The voice of the customer approach offers valuable feedback and an indisputable argument in favor of structured reporting. Radiology has to facilitate easy communication while delivering comprehensive information. The form of this communication should be tailored to the referring physicians' preferences.
Author Disclosures:
T. Heye: Research/Grant Support; Siemens Healthcare. Speaker; Siemens Healthcare, GE.

B-1202 11:02

Guideline based query of conventional narrative "free text" radiological reports and structured reports: a solution for objective comparison

M.E. Maros[1], M. Frölich[2], C. Groden[1], W.H. Sommer[2], S.O. Schönberg[1], T. Henzler[1], H. Wenz[1]; [1]*Mannheim/DE*, [2]*Munich/DE (matt.maros@gmail.com)*

Purpose: Data on how well structured reports (SR) and conventional narrative reports (cFTR) comply with clinically relevant findings are scarce. A feasibility study of a text mining based scoring algorithm was performed to provide an objective intra-individual comparison of SR and cFTR by means of guideline-based key terms.
Methods and Materials: 25 suspected stroke patients with consecutive cMRI stroke protocol were re-assessed by two independent,blinded readers (experience:>2 [unxR]; >6yrs[exR]). SRs were generated using an online template-tool (www.smart-radiology.com) with additional free text (uxR:20/; exR:22/25). Corresponding pre-existing cFTR were retrieved from local database. A query-vector of key terms based on imaging recommendations for acute stroke and transient ischemic attack patients by the ASNR and the ACR was defined. Following automatic text retrieval, SR and cFTR were compared with guideline-query using term frequency-inverse document frequency based similarity index and Wilcoxon signed-rank test.
Results: All 18 (72%) cases with ischemia were identified by SR and cFTR (rho_{sp}=1, Cohen's Kappa=1). UnxR using SR had the highest median (0.82) and maximal (7.57) guideline similarity scores (GSS). SRs of exR had significantly (p_W=0.0020) higher GSS (median:0.72, range:0-5.4), than cFTR (median:0.57, range:0-5.7). Although SRs of unxU were not corrected by senior radiologist, they had similar GSS (p_W=0.50) like the reviewed cFTR,and were comparable to the SR of exR (Z=1.59,p=0.11).
Conclusion: An objective guideline-based comparison of SRs and cFTRs using term frequency is feasible and provides a scalable quality measure. In spite of additional free text, SR improved the adherence to guidelines of both senior- and junior radiologist when evaluating stroke suspected brain MRIs.
Author Disclosures:
M. Frölich: Employee; M. Frölich is an employee of Smart Reporting GmbH. **W.H. Sommer:** Founder; Wieland H. Sommer is a co-founder of Smart Reporting GmbH.

B-1203 11:10

Comparison of report characteristics of un- and experienced radiologists using an online-based structured reporting tool and conventional "free text" reports

M.E. Maros[1], M. Frölich[2], C. Groden[1], W.H. Sommer[2], S.O. Schönberg[1], T. Henzler[1], H. Wenz[1]; [1]*Mannheim/DE*, [2]*Munich/DE (matt.maros@gmail.com)*

Purpose: Online reporting tools (ORT) with predefined text blocks are gaining popularity to create structured reports (SR). However, their effects on report structure and reporting process are obscure. We compared SR of un-(uxR;>2yrs) and experienced radiologists (exR;>6yrs),and conventional narrative -"free text"- reports (cFTR) in the setting of MRI stroke diagnostics.
Methods and Materials: 25 patients with cMRI were randomly sampled from a population of suspected stroke cases (n=780). They were re-assessed blindly by uxR/exR using ORT (www.smart-radiology.com) and SR were created. Parameters of interest were: correctness, reporting time (RT), word count (Wc) of SR, and pre-existing cFTR. Factors like free text in SR (uxR|exR:20|22), extra MRI-sequence (13/25) and subjective case complexity (SCC; 5-point-Likert scale) were also considered. Inter-rater reliability, Spearman's rank correlation, Wilcoxon signed-rank test, and linear mixed models with outcomes RT, Wc including aforementioned factors were applied.
Results: There was perfect agreement (kappa=1) of ischemia (18/25) in all SR and cFTR. SCC was similar (r_{sp}=0.79,p<0.001) between users showing substantial association with RT (r_{uxR}=0.70;r_{exR}=0.67,p_{both}<0.01). ExR was significantly (p<0.01) faster (median=6.75min;range:2-12min) than uxR (8min;range:2-13.5min) using SR. SR of exR were significantly shorter (Wc) than SR of uxR (p<0.001) and cFTR (p<0.01) corrected by senior radiologists. SR of uxR had comparable Wc to supervised cFTR ($p_{findings}$=0.37;$p_{impresssion}$=0.70). SCC had the most decisive effect on Wc by both SR and cFTR when adjusted for aforementioned factors.
Conclusion: ORT enables a standardized, valid and time-effective SR creation, while improving RT and Wc of both senior- and junior radiologist when evaluating stroke suspected brain MRIs.
Author Disclosures:
M. Frölich: Employee; Smart Reporting GmbH. **W.H. Sommer:** Founder; Co-founder of Smart Reporting GmbH.

B-1204 11:18

Recall of unstructured radiology reports is significantly inferior to that of structured reports

B. Buckley, G.N. Allen, L. Daly, C.A. Ridge; *Dublin/IE (bryan.buckley@ucdconnect.ie)*

Purpose: To measure recall by clinicians immediately after reading a structured compared to an unstructured radiology report.
Methods and Materials: Institutional review board approval was obtained. A structured radiology report is a uniform report template that uses headings and subheadings followed by standardized statements to create uniformity and improve communication with referring physicians. A structured radiology report differs from the "freetext" radiology report, which lacks headings or a standardised format. Four hypothetical radiology reports were devised based on a review of common cross sectional imaging studies. Two structured and two unstructured reports followed immediately by a 7-response cloud-based multiple-choice questionnaire were used to survey physicians at multiple institutions whose demographics and training data were collected. The proportion of all correct answers, correct critical findings, sensitivity and specificity were recorded. A paired t-test was used to compare results.
Results: 148 physicians completed the survey. The frequency of incorrect diagnoses was 6.2% for structured reports compared to 18.2% for unstructured reports (p<0.001). Critical diagnoses were missed in 17.4 % of structured reports compared to 35% of unstructured reports (p <0.001). Average physician sensitivity and specificity was greater for structured reports (64.2% and 95.5%, respectively) compared to unstructured reports (59% and 83%, respectively) (p≤0.001).
Conclusion: Physician recall of unstructured radiology reports is significantly inferior to recall of structured reports immediately after reading a radiology report. Structured reports are a more accurate means of conveying the salient findings of a radiology study.

B-1205 11:26

Eye-tracking analysis of interpretation characteristics in detection of alimentary tract lesions on body CT

F. Ichinohe, A. Yamada, T. Nonaka, T. Aonuma, K. Oyama, K. Todoroki, M. Nakamura, Y. Fujinaga, M. Kadoya; *Matsumoto/JP (tattuqoltuae.42@gmail.com)*

Purpose: To clarify interpretation characteristics of radiologists in detecting alimentary tract lesions on body CT using eye-tracking technique.
Methods and Materials: 3 radiologists (1, 2, 12 years of experience) and 3 non-radiologists (2 residents and 1 medical student) were asked to detect lesions suspected as malignant tumours within 3 minutes without any clinical information on thoracic and abdominal CT obtained from 10 patients with histologically proven malignant tumours in the alimentary tract. Gaze path was recorded by eye-tracking technique during interpretation to calculate gaze time at each voxel (GTV) on CT. The lesion detection rate (LDR) and interpretation characteristics in eye movement were statistically analysed.
Results: GTV fitted to the Burr distribution (P<0.001); however, the observed GTV was relatively longer than estimated GTV from the Burr distribution above the 95th percentile. Therefore, the intentional gaze was defined where GTV was longer than 95th percentile GTV (GTV95%) estimated from the Burr distribution in this study. The mean value of LDR, GTV95%, and the percentage of gazed area in patient's body were 46.7%, 0.18 s, 25.0% in radiologists, 0%, 0.36 s, 16.1% in non-radiologists (P<0.001, P=0.002, P<0.001), respectively. The intentionally gazed lesions were significantly fewer than unintentionally gazed lesions in undetected lesions by radiologists (P=0.049).
Conclusion: Radiologists can detect more lesions than non-radiologists due to effective gazes and the diagnostic ability for intentionally gazed lesions. Undetected lesions were located more in unintentionally gazed area; therefore, making radiologists pay attention to the area utilizing gaze path information may improve their diagnostic performance.

B-1206 11:34

Radiological counseling, a new approach to radiologist-patient relationship

F. Rigiroli, D. Fazzini, A. Malasevschi, P. Arnaldi, B. Colombo, S. Papa, G. Cornalba; *Milan/IT (francesca.rigiroli@unimi.it)*

Purpose: The aim of the study is to analise the results of the Radiological Counseling (RC) service introduced in C.D.I. Diagnostic Imaging Department. By using this service the patients can meet the radiologist to get information about radiological exams and medical report, and to discuss diagnostic imaging issues.
Methods and Materials: The RC service started in September 2015 and the patients were informed about RC by a notice in the radiological report and in the institutional website. The service outcome has been investigated by a survey on the first 50 patients that used the RC: afterwards the meeting with

the radiologist, they answered to a questionary about their age and sex, the discussion satisfaction, as well as the preferred comunication modality in normal or pathologic findings.
Results: The survey shown complete satisfaction of the meeting with the radiologist, with a score of 4,5 of 5. The 60% of the cases are under 60 years-old. The majority of the patients answer that they prefer to receive the radiological report by a meeting with the radiologist: 50% if there are normal findings and 80% if pathological.
Conclusion: The RC is a useful service for the patient and can improve the relationship between the patient and the radiologist, who gains a new clinical role. We are satisfied about this results that will help us to improve this service to raise our patient's trust in our institution.

B-1207 11:42

Frequency & analysis of non-clinical errors made in radiology reports using the national integrated medical imaging system (NIMIS) voice recognition dictation software

R.E. Motyer, S. Liddy, W.C. Torreggiani, O. Buckley; *Dublin/IE (ronanmotyer@gmail.com)*

Purpose: Voice recognition (VR) dictation of radiology reports has become the mainstay of reporting in many institutions worldwide. Despite benefit, such software is not without limitations, and transcription errors have been widely report. We evaluated the frequency and nature of transcription error using VR software.
Methods and Materials: Retrospective audit of 378 finalised radiology reports. Errors were counted and categorised by significance, error type and sub-type. Data regarding imaging modality, report length and dictation time was collected.
Results: 67 (17.72%) reports contained ≥1 errors, with 7 (1.85%) containing 'significant' and 9 (2.38%) containing 'very significant' errors. A total of 90 errors were identified from the 378 reports analysed, with 74 (82.22%) classified as 'insignificant', 7 (7.78%) as 'significant' and 9 (10%) as 'very significant'. 68 (75.56%) errors were 'spelling and grammar', 20 (22.22%) 'missense' and 2 (2.22%) 'nonsense'. 'Punctuation' error was most common sub-type, accounting for 27 errors (30%). On average, complex imaging modalities had higher error rates, with computed tomography containing 0.57 errors per report compared to plain film with 0.08. Longer reports had a higher error rate, with reports >25 sentences containing an average of 1.23 errors per report compared to 0-5 sentences containing 0.09.
Conclusion: These findings highlight the limitations of VR dictation software. While most error was deemed insignificant, there were occurrences of error with potential to alter report interpretation and patient management. Longer reports and reports on more complex imaging had higher error rates and this should be taken into account by the reporting radiologist.

B-1208 11:50

Evaluation of a patient safety tool: the preferred reading of the radiology report - has it been useful?

P. Fraga, C. Benito, L. Garcia del Salto, J. De Miguel, A. Marco, E. Fraile; *Madrid/ES (patricia.fraga@salud.madrid.org)*

Purpose: To submit a software tool that allows us to warn about the preferred reading of those reports showing unexpected radiological findings, emergency and incidental findings that imply a change in clinical management of patients. To analyse its use and effectiveness in a radiological hospital service since its implementation.
Methods and Materials: A computer tool of radiological alert reports was implemented in 2012. We review its use, analysing its distribution by modality and requesting service. We analyse the most frequent causes that have produced these warnings and the implications for the management of patients. We also evaluated the problems found in its use.
Results: We review the alert filed in the 574,006 reports performed from January 2012 to September 2016 in our department. We send alerts in 0.13% of the reports, (CT 35,5% , MR 19,8%,US 15,1% and mammography 0,25%) , 94.2% of them were in out patients. The discovery of unsuspected tumour pathology is the main cause of that alert (45.2%). We found some problems, like the communication with primary care.
Conclusion: The radiological alert of preferred reading of a report is part of the radiology daily activity, both for, transmits unexpected or incidental findings and to enable rapid action on the patient. It is an important element for patient safety. It should be a useful, simple, and effective tool known by all physicians involved. 0.13% of our reports were subsidiaries of prioritising reading mainly CT and MR.

10:30 - 12:00 **Room M 5**

Neuro

SS 1811b

Technical developments in CT and MRI improving image quality and lesion analysis

Moderators:
M. Palm; Maastricht/NL
R. Riascos; Houston, TX/US

B-1209 10:30

Improvement of image quality in dual layer unenhanced head CT using virtual monoenergetic image reconstructions

V. Neuhaus, N. Abdullayev, N. Große Hokamp, C. Kabbasch, A. Mpotsaris, D. Maintz, J. Borggrefe; *Cologne/DE (victor-frederic.neuhaus@uk-koeln.de)*

Purpose: To determine optimal kiloelectron volt levels of virtual-monoenergetic-images (VMI) to yield optimal image-quality, in particular in regard to the assessment of grey-white matter differentiation (GWMD) and reduction of artefacts.
Methods and Materials: 40 patients that received unenhanced head-CT using a dual-layer-CT (DLCT, Philips, Amsterdam, Netherlands) were included. CTs were acquired at 120kV/320mAs and VMI were reconstructed in between 40-120keV. Attenuation and standard deviation of supra- and infratentorial grey and white matter were measured to calculate signal-to-noise-ratios (SNR) and contrast-to-noise-ratios (CNR). Artefacts were detected close to the calvarium (SAI) and in the posterior fossa (PFAI). Two radiologists rated image quality regarding GWMD and subcalvarial space.
Results: Continuously higher SNR and CNR of grey and white matter were observed at lower keV in VMI, which were superior to RCT (p<0,0001). Subcalvarial artefacts were significantly lower in VMI at higher keV (p<0,02). Artefacts measured in the posterior fossa were lower in VMI, however not statistical different. VMI were rated superior to conventional images in regard to all four quality criteria. Optimal assessment of GWMD was found at 65keV, optimal assessment of subcalvarial space was found at 120keV.
Conclusion: VMI reconstructed from unenhanced DLCT of the head improved image-quality compared to RCT. Even though CNR increases with decreasing keV and is greatest at 40 keV, subjective image analysis found 65 keV superior in the assessment of GWMD due to the artefacts caused by the calvarium at lower keV.

B-1210 10:38

Improved image quality of low-dose brain CT using knowledge-based iterative reconstruction technique: effect on the noise reduction and low-contrast detectability

Y. Lee, H. Seo; *Ansan/KR (younghen@korea.ac.kr)*

Purpose: To evaluate the image quality of low-dose brain CT obtained by knowledge-based iterative model reconstruction (IMR), we compared noise and low-contrast detectability of CT images between hybrid iterative reconstruction and IMR.
Methods and Materials: Based on the medical record review, we retrospectively identified the 40 patients (M:F=20:20, mean age 51.3±14.8 years) with unremarkable finding on non-contrast brain CT examination using our routine CT protocol during the recent two months. We then reconstructed the CT images using IMR routine level 1 (Philips Healthcare), in addition to our routine hybrid iterative reconstruction (iDose4, level 2, Philips Healthcare). At the same axial levels of supra- and infratentorial brain, the mean CT attenuation value, noise, signal to noise (SNR) and contrast to noise ratio (CNR) were calculated for basal ganglia, internal capsule, pons and adjacent cistern for a pairwise comparison between IMR and iDose4.
Results: With radiation at 100 peak kVp and 120mAs (effective dose: mean 0.46mSv), improvement of SNR was achieved in the CT images reconstructed with IMR compared to iDose 4 by the significantly decreased noise (mean 60.9% reduction) at both supra-and infratentorial brain levels (p<0.01), while their mean CT attenuation values were not significantly affected. Regarding to noise reduction and low-contrast detectability, the CT images reconstructed with IMR was significantly better than iDose4 (p<0.01).
Conclusion: IMR might be considered as a feasible technique to improve the image quality of brain CT examination at the lower radiation dose.

B-1211 10:46

Detection of vessel occlusion in acute stroke is facilitated by color-coded 4D-CTA

M. Meijs, S. Pegge, M. Prokop, B. van Ginneken, F.J.A. Meijer, R. Manniesing; *Nijmegen/NL (midas.meijs@radboudumc.nl)*

Purpose: To perform a pilot study to explore the effect of a new post-processing technique for 4D-CTA on speed and accuracy of the detection of intracranial vessel occlusions in acute stroke. This technique color-codes the contrast arrival time in the cerebral vasculature in 4D-CTA so that abnormally delayed vascular territories are easily detected.
Methods and Materials: We selected 10 patients without and 10 patients with a single vessel occlusion, confirmed by consensus reading, on CTA from our database of acute ischaemic stroke patients, so that occlusions of the ICA, MCA, ACA and PCA of varying subtlety were included. Whole-brain CT perfusion was performed on a 320 detector-row scanner. Color-coded 4D-CTA images were obtained by centering the color scale of vessel time-to-peak (TTP) on the modus of the TTP histogram. Temporal MIP of 4D-CTA with and without color-coding were evaluated in random order for the presence of vessel occlusion by two neuroradiologists. Time-to-detection and accuracy of detection of vessel occlusions were evaluated.
Results: One false-positive vessel occlusion was rated on color-mapping by both observers. Overall, the average time-to-detection decreased from 37.0s to 19.4s ($p<0.03$) and the average accuracy of vessel occlusion detection increased from 0.825 to 0.85 with color-mapping.
Conclusion: Color-mapping of cerebral vasculature in 4D-CTA improves the speed and may improve the accuracy of the detection of vessel occlusions in acute stroke patients.
Author Disclosures:
M. Meijs: Research/Grant Support; Toshiba Japan. **R. Manniesing:** Grant Recipient; Toshiba Japan.

B-1212 10:54

Robust segmentation of the cranial cavity in non-contrast CT and CT perfusion of the brain

A. Patel, F.J.A. Meijer, M. Prokop, B. van Ginneken, R. Manniesing; *Nijmegen/NL (Ajay.Patel@radboudumc.nl)*

Purpose: Cranial cavity segmentation in CT is the essential first step for subsequent image processing and automated detection of cerebral pathology. This becomes complicated in the presence of skull fractures, metallic foreign objects or due to connected soft tissues such as the orbit. A robust and accurate method is presented to segment the cranial cavity in CT images.
Methods and Materials: We propose a multi-atlas based method that uses atlas selection based on anterior skull variations, followed by a two-stage level set refinement. The method was developed using a set of 99 non-contrast CT and 18 CT perfusion (CTP) scans obtained for emergency indications on a 320-row detector CT scanner. It was evaluated on a different set of 200 non-contrast CT and 100 CTP scans obtained for the same indications. Quality of segmentations was visually assessed. The reference standard consisted of three randomly selected orthogonal slices per patient that were manually annotated by trained observers. The corresponding slices were extracted and compared to the reference standard. Dice similarity coefficient (DSC) and 95th percentile Hausdorff distance (95% HD) were reported.
Results: The segmentation results were evaluated as very good to excellent. The method achieved a mean DSC of 0.98±0.03 and mean 95% HD of 0.60±2.15 mm in comparison to the reference standard.
Conclusion: The proposed method is capable of accurate segmentation of the cranial cavity in non-contrast CT and CTP independent of gross pathology or foreign objects. The method provides a fundamental first step towards automated evaluation of cranial CT.
Author Disclosures:
A. Patel: Research/Grant Support; Toshiba Japan. **R. Manniesing:** Grant Recipient; Toshiba Japan.

B-1213 11:02

Parameters based on blood flow velocity obtained from 3D cine PC-MR on cerebral intracranial aneurysms: comparative study with computational fluid dynamics

K. Ishiguro[1], H. Isoda[1], Y. Takehara[1], M. Terada[2], T. Naito[3], C. Tanoi[2], T. Kosugi[4], Y. Ohnishi[5], A. Fukuyama[1]; [1]*Nagoya/JP*, [2]*Iwata/JP*, [3]*Kasugai/JP*, [4]*Hamamatsu/JP*, [5]*Tokyo/JP (ishiguro.kenta@d.mbox.nagoya-u.ac.jp)*

Purpose: Some studies regarding haemodynamic analysis of intracranial aneurysmal growth and rupture using computational fluid dynamics (CFD) have discussed parameters such as inflow concentration index (ICI), energy loss (EL) and pressure loss coefficient (Plc) based on blood flow velocity. The purpose of our study was to compare these parameters between magnetic resonance fluid dynamics (MRFD) and CFD quantitatively.
Methods and Materials: We performed 3D time-of-flight (TOF) MR angiography (MRA) and 3D cine phase contrast (PC) MR for 20 patients, each of who had an unruptured internal carotid artery aneurysm. We created patient-specific vascular geometries and obtained the patient-specific volume flow rate (VFR) of each vessel based on MR data sets using Flova. We performed CFD based on our acquired data. At peak systole we acquired spatially averaged inflow velocity into the aneurysm, ICI, EL and PLc with MRFD and CFD. We calculated the interclass correlation coefficient (ICC) of these parameters between MRFD and CFD. We also obtained scatter diagrams of these parameters and calculated their correlation coefficient between MRFD and CFD.
Results: ICC was >0.80 and correlation coefficient was >0.85 between MRFD and CFD for all parameters. Internal carotid arteries were large enough to be analysed with good accuracy. Therefore, MRFD showed accurate velocity and volume flow rate for each artery.
Conclusion: Average velocities, ICI, EL and PLc obtained by MRFD were similar to those obtained by CFD. MRFD may be a useful way to quantitatively analyse these parameters in the clinical setting.
Author Disclosures:
T. Kosugi: Employee; Renaissance of Technology Corporation.

B-1214 11:10

Comparison of spoiled gradient recalled acquisition and spin echo magnetic resonance images in detection of pituitary ACTH secreting adenoma

R. Kidzinski[1], E. Frankowska[1], M. Żabicka[1], M. Kania-Pudlo[1], A. Sciuk[2], K. Tomczykiewicz[1], G. Zielinski[1]; [1]*Warsaw/PL*, [2]*Houston, TX/US (rafalkidzinski@gmail.com)*

Purpose: The objective of the study was to compare the efficacy of spoiled gradient recalled acquisition (SPGR) and spin echo (SE) magnetic resonance images in detection of pituitary ACTH secreting adenoma. SPGR images have the potential to improve tumour detection because of better soft tissue contrast, thinner sections, higher image resolution and faster acquisition than SE images.
Methods and Materials: We compared SPGR and SE images in 7 patients (mean age 44 years) that underwent surgery with histological confirmation of the ACTH secreting adenoma. All patients had negative MR studies on 1.5T scanner. We obtained coronal pre- and postgadolinium SPGR and SE images using 3T scanner. SE scans were performed over 4:39 min with 16 cm field of view and contiguous slices 2.7 mm. SPGR scan parameters were analogically: 4:32 min, 16cm and 2.5mm. Three radiologists interpreted the images, pointing exact localisation and assessing visibility of tumours. Localisation of tumours proposed by radiologist was compared to findings at surgical resection.
Results: In retrospective assessment, tumours were not visible in 1 of 7 patients. Sensitivity of tumour detection was 44% for SPGR images and 39% for SE images.
Conclusion: 3T MR studies proved to be superior to 1.5T in Cushing syndrome. There was no significant difference between SPGR and SE images.

B-1215 11:18

Different consistency of pituitary adenomas evaluated with dynamic constrast MRI acquisition

A. Di Napoli, L. Pasquini, A. Boellis, A. Romano, A. Bozzao; *Rome/IT*

Purpose: Our hypothesis was that pituitary macroadenomas show different areas of consistency detectable by enhanced magnetic resonance imaging (MRI) with Dynamic study during gadolinium administration.
Methods and Materials: We retrospectively analysed 21 patients with pituitary macroadenomas between June 2013 and June 2015. The ethics committee of our Institution approved the study protocol and informed consent was obtained from all patients. All patients underwent trans-sphenoidal surgery and neurosurgeon described whether macroadenomas consistency was hard or soft considering a lower and an upper compartment. Similarly, two neuroradiologists manually drew regions of interest (ROIs) inside the solid-appearing portions of macroadenoma (upper and lower) and in the normal

white matter both on dynamic and post-contrast acquisitions. The ratio between these ROIs, defined as Signal Intensity Ratio (SIR), allowed obtaining signal intensity curves over time on dynamic acquisition and a single value on post-contrast MRI. SIR values best differentiating solid from soft macroadenoma components were calculated and correlated with pathologic patterns. A two-sample T-test and empiric receiver operating characteristic (ROC) curve of SIR was performed.
Results: According to ROC analysis, the SIR value of 1,92, obtained by dynamic acquisition, best distinguished soft and hard components. SIR values from post-contrast MRI didn't allow this differentiation. All the specimens from soft components were characterised by high cellularity, high representation of vascularisation and micro-haemorrhage and low percentage of collagen content. The reverse was evident in hard components.
Conclusion: We demonstrated that dynamic MRI acquisition could distinguish with good accuracy macroadenomas consistency.

B-1216 11:26

MRI tractography comparing diffusion tensor and kurtosis tensor imaging

J. Leote, R.G. Nunes, R. Loução, L. Cerqueira, H.A. Ferreira; *Lisbon/PT (jlleotte@gmail.com)*

Purpose: The topographical delineation of the corticospinal tract (CST) is of paramount importance for surgical procedures in primary brain tumours. We evaluated if diffusion kurtosis imaging tractography (DKI-tract) brings up additional resolution to the delineation of the CST obtained using conventional diffusion tensor imaging tractography (DTI-tract).
Methods and Materials: We recruited 6 patients with brain tumours and 8 healthy subjects to perform a 1.5T MRI with a 12-channel head coil. Scans comprised volumetric T1-weighted data and diffusion-weighted images (repetition/echo time of 5800/107 ms; 82x82 resolution; 3x3x3 mm^3 voxel size; b-values of 0, 1000, 2000 s/mm2, 64-32 directions). CST was estimated using DTI and DKI methods between cerebral peduncles and frontoparietal regions-of-interest (ROIs). We also selected a passing through ROI with 10% of the lesion volume. We extracted diffusion metrics of the tracts' courses and volumes at the strongest deviation point of the CST from the midline and compared the two methods in both groups and between hemispheres using an asymmetry index.
Results: It was possible to estimate the CST using both methods. However, the DKI-tract depicted significantly more volume than the DTI-tract in 83% of patients. The fractional anisotropy mean values were significantly lower in patients, with higher asymmetry index between hemispheres. Lower kurtosis metrics were denoted in pathological hemisphere despite no statistical difference.
Conclusion: DKI-tract showed a broader image of the CST than DTI. Since DKI image acquisition and analysis is also compatible with a high patient throughput, DKI-tract assessment seems to be safer than DTI for pre-surgical planning.

B-1217 11:34

Accuracy of SWI sequences compared to T2*-weighted gradiente echo sequences in the detection of cerebral cavernous malformation

G. Sparacia, A. Anastasi, C. Speciale, F. Bencivinni, A. Banco, M. Midiri; *Palermo/IT (andreaanastasi@hotmail.it)*

Purpose: To assess the accuracy of SWI sequences compared with GRE T2* sequences in assessing cerebral cavernous malformations (CCV).
Methods and Materials: We retrospectively evaluated 11 patients with familial form of CCV (4 men, 7 women; age: 32-77 years; mean age, 53,7 years). MR protocol included nonenhanced and contrast enhanced FSE T1w sequences, FSE T2w, FLAIR, GRE T2*w and SWI sequences. Images were reviewed by two expert neuroradiologist to assess location, number, size and conspicuity of the lesions on GRE and SWI sequences. Statistical differences of lesions seen on SWI and GRE images were assessed with the nonparametric Wilcoxon signed rank test.
Results: The number of cerebral cavernous malformations (CCV) was significantly higher (P <.001) on SWI images (n=152) than on T2*weighted GRE images (n=55). Lesion size was significant higher (P <.001) on SWI images (mean 0.42cm, SD ∓ 0.55) than on T2*weighted GRE sequences (mean 0.25cm, ∓ 0.51) and differences were statistically significant (P<.001). Lesion conspicuity was significant higher (P <.001) on SWI than T2*weighted GRE images. In one patient, who underwent two months followup for the onset of sudden neurologic symptoms, it was identified a cerebral haematoma in the site of a CCV demonstrated previously only on the SWI images.
Conclusion: SWI sequence allowed to identify malformations that didn't appear in GRE T2 * images. Thus, routine clinical neuroimaging protocols should contain SWI sequences for the evaluation of patients with or suspected cerebral cavernous malformations to assess the true prevalence of lesions in order to improve the diagnosis.

B-1218 11:42

Evaluation of the communication between arachnoid cysts and neighbouring cerebrospinal fluid spaces by T2W 3D-SPACE with variant flip-angle technique at 3T

O. Algin; *Ankara/TR (droktayalgin@gmail.com)*

Purpose: PC-MRI is a broadly used technique for determination of possible communication of arachnoid cysts (ACs). 3D-SPACE technique is a relatively new-method for 3D-isotropic scanning of entire cranium within a short time. In this research, we aimed to evaluate the usage of the 3D-SPACE technique in differentiation of communicating or non-communicating type's ACs.
Methods and Materials: We retrospectively examined 35 ACs in 34 patients. 3D-SPACE, PC-MRI and contrast-material enhanced cisternography (if present) images of the patients were analysed. Each cyst was described according to cyst size/location, third ventricle diameter, Evans ratio, and presence of hydrocephalus. Communication was defined as absent (score 0), suspected (score 1) or present (score 2) on each sequence. Results of PC-MRI and cisternography (if available) examinations were used as a gold standard techniques to categorize all cysts as communicating or non-communicating type. The results of 3D-SPACE were compared with gold standard techniques. The comparisons between groups were performed using Mann-Whitney and fisher's exact tests.
Results: There is a perfect agreement between 3D-SPACE and gold standard test findings (p<0.001). Correlation between 3D-SPACE and gold standard tests results is 97% for communication assessment of the cysts. For other analysed variables, there is a significant difference or correlation between the groups.
Conclusion: 3D-SPACE technique is an easy, useful and non-invasive alternative for the evaluation of morphology, topographical relationships, and communication status of ACs.

B-1219 11:50

Determination of intra-axial brain tumours cellularity through the analysis of T2 relaxation time of brain tumours before surgery using MATLAB software

J. Abdolmohammadi; *Baharan/IR (Abdolmohammadi.jamil@gmail.com)*

Purpose: Timely diagnosis of brain tumours could considerably affect the process of patient treatment. To do so, para-clinical methods, particularly MRI, cannot be ignored. MRI has so far answered significant questions regarding tumour characteristics, as well as helping neurosurgeons. In order to detect the tumour cellularity, neurosurgeons currently have to sample specimens by biopsy and then send them to the pathology unit. The aim of this study is to determine the tumour cellularity in the brain.
Methods and Materials: In this cross-sectional study, 32 patients (18 males and 14 females from 18-77 y/o) were admitted to the neurosurgery department of Shohada-E Tajrish Hospital in Tehran, Iran from April 2012 to February 2014. In addition to routine pulse sequences, T2W Multi echo pulse sequences were taken and the images were analysed using the MATLAB software to determine the brain tumour cellularity, compared with the biopsy.
Results: These findings illustrate the need for more T2 relaxation time decreases, the higher classes of tumours will stand out in the designed table. In this study, the results show T2 relaxation time with a 85% diagnostic weight, compared with the biopsy, to determine the brain tumour cellularity (p<0.05).
Conclusion: Our results indicate that the T2 relaxation time feature is the best method to distinguish and present the degree of intra-axial brain tumours cellularity (85% accuracy compared to biopsy). The use of more data is recommended in order to increase the percent accuracy of this techniques.

14:00 - 15:30 **Room A**

GI Tract

SS 1901a

Gastric cancer and upper GI tract diseases

Moderators:
I. Blazic; Belgrade/RS
S.A. Jackson; Plymouth/UK

K-26 14:00

Keynote lecture
S. Romano; *Naples/IT*

B-1220 14:09

Perfusion CT: a novel quantitative and qualitative imaging biomarker in gastric cancer
J. Kruk-Bachonko; *Lublin/PL (asiakruk1@wp.pl)*

Purpose: The aim of this research was to examine whether perfusion computed tomography (P-CT) exam can estimate gastric cancer neoangiogenesis in vivo. We attempted to explore whether and which P-CT parameters can be used in neoangiogenesis and neoadjuvant therapy effects evaluation. An additional aim was to recognise a positive prediction value of P-CT in responders and non-responders.
Methods and Materials: 51 patients with biopsy and/or clinically proved gastric cancer were involved in the P-CT exam. 26 of them were qualified for systemic treatment (16 patients received chemotherapy and 10 patients received radiochemotherapy). Perfusion-CT exam was conducted using 64-row GE tomograph, based on deconvolution model in first pass protocol perfusion. In P-CT exam, we estimated four parameters: blood flow (BF) - tumour vasculature and progression marker, blood volume (BV) - tumour vasculature and mitotic activity marker, mean transit time (MTT)- perfusion pressure parameter, permeability surface (PS) - vessels maturity and tightness marker.
Results: Patients with a positive treatment response showed decreased BF, BV, PS perfusion parameters with an increased MTT. Tumour dimension reduction after neoadjuvant therapy was significantly correlated with BF and PS. Neoadjuvant therapy was more effective for patients with higher output BF and PS values. We did not register a significant relationship between BV and MTT parameters and tumour dimension reduction.
Conclusion: P-CT exam allows non-invasive gastric cancer assessment in vivo. It enables neoadjuvant treatment monitoring and determines early treatment answer for chemotherapy and radiochemotherapy in gastric cancer. P-CT has positive predictive value in neoadjuvant therapy effects evaluation.
Author Disclosures:
J. Kruk-Bachonko: Author; Krupski Witold, Skoczylas Tomasz, Przemysław Mądro, Grzegorz Wallner. Speaker; Joanna Kruk-Bachonko.

B-1221 14:17

CT volumetry for primary gastric lesions in predicting pathologic response to neoadjuvant chemotherapy in locally advanced gastric cancer
I. Shrainer; *Moscow/RU (shrainer@gmail.com)*

Purpose: It is difficult to assess the response to neoadjuvant chemotherapy (NAC) in gastric cancer (GC) using standard CT-based RECIST criteria. CT volumetry might be a valuable alternative. We aimed to evaluate the accuracy of CT volumetry in terms of predicting response to NAC in locally advanced GC.
Methods and Materials: From February 2014 to April 2015 39 patients with stage II-III GC underwent 3 cycles of NAC followed by surgery. Contrast-enhanced CT was obtained after gastric distention with water before and after 3 cycles of chemotherapy. Pre- and post-chemotherapy volume of the tumour were measured using a dedicated 3D software and compared to histopathologic assessment of response.
Results: In 38 (97%) patients tumour size decreased. In 16 patients there was good tumour response (grade 1-2 according to Mandard score), other 23 patients had poor response (grade 3-4). In patients with good response, median tumour volume decrease was 54% (32-72%) vs 21% (0-48%) in patients with poor response, p<0.0001. Cutoff value was determined to be 37% by means of Youden's index, with sensitivity 92% and specificity 92%. Negative predictive value, positive predictive value, overall accuracy were 96%, 86%, 92%. respectively. Area under the ROC curve was 97%.
Conclusion: CT volumetry with a cutoff 37% of tumour volume reduction predicts good morphological response after 3 cycles of NAC in locally advanced GC with an overall accuracy of 92%. This finding needs further external validation and a larger cohort of patients to evaluate its predictive value after the first cycle of NAC.

Author Disclosures:
I. Shrainer: Author; Klimenko A.O., Lyadov V.K., Sinitsyn V.E., Mershina E.A., Ledin E.V, Ilina O.V., Milovanov V.V..

B-1222 14:25

Tumour volume at MDCT association with lymphatic invasion and N categories in resectable gastric adenocarcinoma: study in large surgical specimens
H. Li, X.-l. Chen; *Chengdu/CN (lihang111222@126.com)*

Purpose: To determine whether gross tumour volume (GTV) of resectable gastric adenocarcinoma at MDCT could predict presence of lymphatic invasion and N categories.
Methods and Materials: 350 consecutive patients with gastric adenocarcinoma who underwent gastrectomy in 1 week after contrast-enhanced MDCT were retrospectively identified. GTV was evaluated on MDCT images. Univariate and multivariate analyses were performed to determine whether GTV could predict presence of lymphatic invasion and regional lymph node metastasis (LNM). Mann-Whitney U test was performed to compare GTV among N categories. With pathologic confirmation, cutoffs of GTV were first investigated in 202 patients (group A) and then validated in an independent 148 patients (group B) for predicting presence of lymphatic invasion and N categories.
Results: Univariate analysis showed GTV could predict presence of lymphatic invasion and regional LNM (P<0.0001). Multivariate analyses indicated GTV as an independent risk factor of presence of lymphatic invasion (P=0.026,odds ratio=2.284) and regional LNM (P=0.000,odds ratio=7.991). The Mann-Whitney U test showed GTV could distinguish N0 from N1-N3 categories, N0-N1 from N2-N3, and N0-N2 from N3 (P<0.0001 for all). In group A, GTV could predict presence of lymphatic invasion (cutoff,16.6 cm^3; AUC, 0.780) and differentiate N0 from N1-N3 (cutoff, 12.3 cm^3; AUC, 0.870), N0-N1 from N2-N3 (cutoff, 16.6cm^3; AUC, 0.878) and N0-N2 from N3 (cutoff, 24.6cm^3; AUC,0.869). In group B, GTV could predict presence of lymphatic invasion (AUC,0.760), and differentiate N0 from N1-N3 categories (AUC, 0.853), N0-N1 from N2-N3 (AUC, 0.850), and N0-N2 from N3 (AUC,0.862).
Conclusion: GTV of resectable gastric adenocarcinoma at MDCT demonstrated capability in predicting presence of lymphatic invasion and N categories.

B-1223 14:33

Application of spectral CT in differential diagnosis of the gastric cancer and the high-risk gastric stromal tumours
X.-W. Wang; *Zhengzhou/CN (wxw0724@126.com)*

Purpose: To evaluate the application value of gemstone spectral imaging (GSI) in differential diagnosis of the gastric cancer and the high-risk gastric stromal tumours (GST).
Methods and Materials: Dual-phase enhanced CT scans by GSI mode were analysed retrospectively on 30 gastric cancer patients and 24 high-risk GST patients that confirmed by pathology.The spectral curve were obtained with GSI viewer software, and calculated the slopes for spectral curve in the 40~70,70~140 and 40~140keV energy ranges respectively. Iodine concentration (IC), water concentration (WC) and normalised iodine concentration (NIC) of tumours were also obtained. Data were analysed statistically by independent t test.
Results: During the vein phase,the IC (23.78±6.85) (100μg/m1) and NIC (0.54±0.15) of gastric cancer were higher than these of the high-risk GST (16.87±2.67) (100μg/m1) and (0.34±0.04) (P<0.05). The slope of the gastric cancer in the 40~70,70~140 and 40~140keV energy ranges (4.64±1.28, 0.68±0.21 and 1.87±0.53) were higher than these of the high-risk GST (3.35±0.52, 0.48±0.11 and 1.34±0.20) (P<0.05). And there was no significant difference in the WC between the two groups (P>0.05). During the artery phase, there were no significant differences in the IC, NIC, WC and the slope in every energy ranges between the two groups (P>0.05).
Conclusion: Spectral CT parameters are helpful in differential diagnosis of the gastric cancer and the high-risk GST.

B-1224 14:41

CT imaging features of internal hernia: post Roux-en-Y gastric Bypass - our experience in an Indian tertiary care setup
K. Sikund, G. Aggarwal, B. Aggarwal; *New Delhi/IN (ksikund@gmail.com)*

Purpose: To describe the CT findings in internal hernia seen after laparoscopic RYGB. To study the sensitivity of CT abdomen in diagnosing internal hernia.
Methods and Materials: Retrospectively data was collected of post bariatric laparoscopic RYGB patients (2009-2014) who presented with symptoms of abdominal pain, distention and vomiting in our institution. Records of 40 such patients were obtained in whom Internal hernia was diagnosed on diagnostic laparoscopy. Unfortunately CT records of only 21 patients were available. CT signs of internal hernia included: whirlpool sign- swirled appearance of

mesentery, mushroom shape of the hernia, clustered loops of small bowel, small bowel obstruction, small bowel other than duodenum posterior to superior mesenteric artery and right side location of distal jejunal anastomosis. Sensitivity of abdominal CT in diagnosing internal hernia was also calculated.
Results: CT findings of internal hernia were seen in 13/21 patients (sensitivity 61.9%) while remaining 8/21 patients had normal findings. CT findings - swirling of the mesentery was seen in 10/13 patients. Atypical bowel configuration with mushroom shape of the hernia was seen in 10/13 patients. Laparoscopy confirmed presence of internal hernia in 21 of these patients, with 5 showing peterson s defects, 10 mesenteric defects and 6 combined defects.
Conclusion: The sensitivity of abdominal CT in diagnosis of internal hernia in postoperative RYGB is 61.9% with mesenteric swirling snd mushrooming being the best CT indicator.

B-1225 14:49

MRI assessment of delayed gastric emptying and motility in Parkinson's disease: a feasibility study

J. Cho; *Seongnam/KR (jungheum.cho.md@gmail.com)*

Purpose: To examine the feasibility of evaluating delayed gastric emptying and motility in Parkinson's disease (PD) patients by magnetic resonance imaging (MRI), in comparison with healthy volunteers.
Methods and Materials: 38 PD patients without gastrointestinal illness (mean age, 67.3 years; 20 males; 18 females) and 5 healthy volunteers (mean age, 32.6 years; 3 males; 2 females) were recruited. Unified Parkinson's disease rating scale (UPDRS) and gastric symptom were assessed by self-reporting survey in each patient. After at least 6 hours of fasting, each participant underwent MRI of the stomach before and after a fluid meal (400 mL), which was followed up to 120 minutes. Gastric content volume and total gastric volume were measured by semi-automatic method using volume analysis software and gastric motility index (GMI) was calculated from measurements in cine MRI. Gastric emptying, accommodation, and GMI were compared between the two groups using repeated measures ANOVA and Mann-Whitney tests. Pearson's correlation analysis was also performed for UPDRS, gastric symptom score, gastric emptying, accommodation, and GMI.
Results: Gastric emptying tended to be delayed in PD patients at 10 minutes after meal (0.94 vs 0.90, P = .226) without statistical significance. Gastric accommodation (3.47 vs 5.89, P = .011) and GMI at 30 minutes (5.58 vs 12.09, P = .010) were decreased in patient group compared with control group. However, there was no significant correlation between UPDRS, gastric symptom scores, and MRI measurements.
Conclusion: MRI is feasible for assessment of delayed gastric emptying, decreased accommodation, and GMI in PD patients.

B-1226 14:57

Gastric remnant volume on radiology as a predictor of weight loss after laparoscopic sleeve gastrectomy for morbid obesity

A. Bertesso, I. Zotta, G. Barbiero, M. Zuliani, A.C. Frigo, L. Prevedello, M. Foletto, F. Pomerri; *Padua/IT (alberto.bertesso@gmail.com)*

Purpose: To correlate initial gastric remnant volume after laparoscopic sleeve gastrectomy (LSG) with volumetric changes and patient's weight loss (WL).
Methods and Materials: A retrospective review was conducted on 430 upper gastrointestinal contrast studies concerning 159 obese patients with body mass indexes (BMI) exceeding 40 kg/m^2 or 35 kg/m^2 and comorbidities who underwent LSG from 2007 to 2016 and were followed up for periods ranging from 3 months to 6 years. Radiological images of the gastric remnants were broken down into multiple components and volumes were calculated with appropriate software. Percent excess weight loss (%EWL) and reduction in BMI were also calculated in all patients at each follow-up. Relationships between variables were assessed with Spearman's rank correlation coefficient, Wilcoxon's signed-rank test and Student's t-test.
Results: The mean gastric remnant volume on the first postoperative day (t=0) was 130.7±53ml, and then increased at most of the follow-up intervals analysed (p<0.0001). The reduction in BMI was greatest at 1 year (57.3±40%), 2 years (79.2±70%), and 6 years (64.8±37%). The highest %EWL was identified at 6 months (44.8±20%), 2 years (52.7±26%), and 3 years (47.8±25%) and was positively correlated with a gastric remnant volume of 125ml or less at t=0 (p<0.05). No correlation emerged between gastric volumetric changes and %EWL.
Conclusion: A direct relationship was documented between an initial sleeve volume of ≤125ml and a satisfactory WL after LSG. The increase in gastric remnant volume on radiology after surgery did not affect the WL achieved over the long-term follow-up.

B-1227 15:05

Intestinal type ampullary adenocarcinoma vs duodenal adenocarcinoma: role of ampullary MDCT in preoperative differentiation

Z. Kovacevic, A. Ivanovic, D. Masulovic; *Belgrade/RS (zeljka.kovacevic.bg@gmail.com)*

Purpose: To evaluate the utility of ampullary MDCT in the non-invasive, preoperative differentiation of duodenal carcinoma and intestinal-type ampullary carcinoma.
Methods and Materials: In this retrospective study, 20 [8 females (age 38-77 years)] patients with resected ampullary adenocarcinoma and duodenal adenocarcinoma who underwent preoperative contrast-enhanced ampullary MDCT were included. Two radiologists, blinded to pathological diagnosis of adenocarcinoma subtype, evaluated the presence of five MDCT features in consensus. Correlation between MDCT findings with ampullary cancer subtypes was performed using $\chi 2$ and Fisher's exact test.
Results: When evaluated with ampullary MDCT, intestinal- type ampullary adenocarcinomas were significantly different in terms of lesion morphology (p:<0.0001), shape of the papilla (p:<0.0001), CBD infiltration (p:0.003) and dilation (p:0.0004) and duodenopancreatic groove infiltration (p:0.0009).Duodenal carcinomas were more often infiltrative in morphology (9/10 [90%]), showed retracted papilla (8/10 [80%]), CBD (3/10[30%]) and MPD infiltration (2/10 [20%]), dilated CBD (3/10 [100%] and MPD (2/10 [20%]), "fixed" duodenopancreatic groove appearance (5/10 [50%]). Intestinal-type ampullary carcinomas were significantly more frequently nodular in shape (10/10 [100%]), had a bulging papilla (9/10 [90%]), "free" duodenopancreatic groove appearance (10/10[100]).
Conclusion: A tailored ampullary MDCT protocol can be useful to differentiate intestinal adenocarcinoma from duodenal adenocarcinoma preoperatively.

B-1228 15:13

Radiological management after bariatric surgery

P. Venetucci[1], A.G. Tucci[1], A. Macca[1], F. Venetucci[2], M. Quarantelli[3], A. Brunetti[1]; [1]*Naples/IT*, [2]*Mercato San Severino/IT*, [3]*Portici/IT (pierovenetucci@gmail.com)*

Purpose: To illustrate an imaging protocol after bariatric surgery, based on upper gastrointestinal series and MDCT, in the presence or in the absence of complications.
Methods and Materials: 954 patients were evaluated with radiographic upper gastrointestinal series following the most common procedures for obesity: laparoscopic adjustable gastric banding (269), sleeve gastrectomy (525) and Roux en Y gastric bypass (160). In the presence or in suspect of early or late complications they performed also MDCT.
Results: 882 patients had normal post-operative findings after radiographic gastrointestinal series. 72 patients had signs suggestive of complications and they performed also MDCT scan. Major complications after gastric banding were 46 (26 band slippage and 20 small bowel obstructions); after sleeve gastrectomy were 16 (10 gastric leaks, 3 haemorrhages, 3 small bowel obstructions); 10 complications were found following Roux en Y bypass (3 internal hernias, 3 leaks, 3 anastomotic strictures, 1 volvulus). Upper gastrointestinal complications that required a new surgery occurred in 6% of patients (58/954).
Conclusion: Upper GI series and CT are essential tools for the evaluation of complications after bariatric surgery. All patients should perform upper gastrointestinal series as first step. In the presence of signs or in suspect of major complications, MDCT is necessary to identify and characterize the type of complication. This protocol can modify patient's outcome, directing to surgery patients who require reintervention.

B-1229 15:21

A MRI-guided high-intensity focused ultrasound-triggered wax-coated capsule for temporally and spatially supertargeted drug release

S. Matoori[1], M. Roveri[1], A. Romagna[1], O. Voznyuk Wuerthinger[1], P. Tiefenboeck[1], O. Kolokythas[2], J.M. Froehlich[2]; [1]*Zurich/CH*, [2]*Winterthur/CH*

Purpose: To prepare an orally-applied temperature-sensitive wax-coated capsule containing a gadolinium-based contrast agent (GBCA) to visualize drug release; and to test the release of its content upon applying a MRI-guided high-intensity focused ultrasound (HIFU) trigger.
Methods and Materials: A mixture of lanolin and cetyl alcohol was optimized to a suitable melting point. Cellulose capsules were coated using the Michelangelo method based on carving out the GBCA-containing capsule embedded in the wax mixture (n=10). The melting of the wax-coating was tested by applying a MRI-guided 200W HIFU beam (n=3). The release of the capsule content was verified with a T1-weighted MR-sequence visualizing the release of the encapsulated contrast agent (n=3).
Results: The capsules were coated with a 1:1-mixture of lanolin and cetyl alcohol (melting point 43°C, n=10). The coating resisted for 24h upon exposure to simulated gastrointestinal fluids (n=3). A 200 W MR-guided HIFU pulse was

able to selectively melt the coating and release the content of the capsule (n=3).
Conclusion: We provide a reproducible method to coat a capsule with a highly temperature sensitive waxy composition and a proof-of-concept of using MRI-guided HIFU to trigger the release of the capsule contents. This wax-coated capsule addresses a currently unmet clinical need in personalised medicine as it provides the opportunity for HIFU-MR-guided temporally and spatially supertargeted drug release. Therefore, this drug delivery system promises to enable targeted local therapy of gastrointestinal lesions.
Author Disclosures:
J.M. Froehlich: Consultant; JMF is a consultant for a contrast agent company.

14:00 - 15:30 **Room B**

Abdominal Viscera

SS 1901b

Pancreatic and biliary inflammation

Moderators:
M. Maher; Dublin/IE
B. Marincek; Kilchberg/CH

K-25 14:00

Keynote lecture
B. Marincek; *Kilchberg/CH*

B-1230 14:09

Focal autoimmune pancreatitis vs pancreatic adenocarcinoma in the pancreatic head: MRI-MRCP findings
R. Negrelli[1], E. Boninsegna[1], G.A. Zamboni[1], G. Avesani[2], S. Mehrabi[1], R. Manfredi[1], R. Pozzi-Mucelli[1]; [1]*Verona/IT*, [2]*Bolzano/IT*
(ricky.negrelli@gmail.com)

Purpose: Focal form of autoimmune pancreatitis (AIP) represents a challenging mimicker of pancreatic adenocarcinoma (PAD). The aim of our study is to retrospectively evaluate the MRI-MRCP findings of focal AIP and PAD, to find helpful patterns for the differential diagnosis.
Methods and Materials: 48 patients with a solid lesion of the pancreatic head underwent MRI-MRCP, 20 patients had focal AIP and 28 PAD. We excluded patients who underwent different imaging, lesions of the body-tail and diffuse AIP. Image analysis included: lesion volume, signal intensity abnormalities, enhancement pattern, common bile duct (CBD) caliber, main pancreatic duct (MPD) stenosis, presence of upstream MPD and side branches dilation.
Results: AIP lesions tend to be larger than PAD (p<0,001). Both AIP and PAD appeared hypointense on T1-WI and slightly hyperintense on T2-WI (p=NS). Although both lesions were hypovascular in the arterial-phase (p=NS), AIP presented progressive enhancement and contrast retention (p<0,001). The CBD resulted dilated in 9/20 (45%) cases of AIP and in 14/28 (50%) of PAD (p=NS). On MRCP, 60% of the AIP showed multiple stenoses of the MPD, opposed to none of the PAD (p<0,001). The caliber of the upstream MPD was larger in PAD (mean: 6,2mm) than in AIP (3,7mm; p<0,001); side branches dilation was found in 26/28 (93%) and in 12/20 (60%), respectively (p=0,02).
Conclusion: The most suggestive features of AIP are large mass-forming lesions, with contrast retention, delayed washout and multiple stenoses of the MPD, without a marked dilation of the upstream MPD at MRCP.

B-1231 14:17

Diagnostic performance of apparent diffusion coefficient in acute pancreatitis; correlation with revised Atlanta and Japanese severity score
R.M. El Kady, S.H. Bakr, H.I. Megally, W.A. Abbas, E. Abo Elhamd; *Assiut/EG (dr.eman_08@yahoo.com)*

Purpose: To investigate the role of apparent diffusion coefficient (ADC) in evaluating acute pancreatitis patients and rule out pancreatic necrosis.
Methods and Materials: Prospective study with 34 patients with acute pancreatitis and 20 control cases underwent magnetic resonance imaging using 1.5T machine include T1, T2 WI, SPIR, and DWI using b-values of (0,200,400,800). The ADC values of pancreatic head, body and tail were averaged and correlated with clinical scoring based on revised Atlanta classification and Japanese score.
Results: The mean ADC of normal pancreatic tissue, mild pancreatitis, moderate pancreatitis and necrotic tissue in severe pancreatitis was (1.54 ± 0.05), (1.18±1.16), (1.14± 0.06), (1.99±0.06) X 10-3 mm2/S respectively .The ADC significantly correlates with both revised Atlanta and Japanese classifications in differentiating normal cases from acute pancreatitis and in differentiating cases of moderate edematous pancreatitis from severe necrotising pancreatitis (p < 0.001 for each classification respectively). The ADC couldn't significantly differentiate between mild and moderate forms of acute pancreatitis. Using ROC curve analysis to differentiate normal cases from acute pancreatitis, the AUC was 0.85 and the best ADC cut-off value was 1.26 X 10-3 mm2/S with sensitivity 85.3% and specificity 95.8%. To differentiate mild to moderate acute pancreatitis from severe necrotising pancreatitis the AUC was 0.98 and the best ADC cut off value was 1.8 X 10-3 mm2/S with sensitivity 100 % and specificity 98%.
Conclusion: ADC measurement is helpful in evaluating acute pancreatitis patients. It provides a safe alternative to the use of contrast media in these patients.

B-1232 14:25

Characterisation of patients with abdominal pain and signs of acute pancreatitis on CT without threefold increase of normal serum lipase levels
M. Avanesov, A. Löser, J.M. Weinrich, G. Adam, J. Yamamura, M. Karul; *Hamburg/DE (m.avanesov@uke.de)*

Purpose: To evaluate the prevalence, severity and characteristics of patients with abdominal pain and signs of acute pancreatitis on contrast-enhanced CT(CECT) <3x increase of serum lipase (lip-) compared to patients with ≥3x increase of normal serum lipase levels (lip+).
Methods and Materials: 272 patients with abdominal pain, CT with signs of acute pancreatitis and serum lipase levels on admission were retrospectively evaluated. The severity of acute pancreatitis was assessed in 124 patients (61 lip-,63lip+) by 3 different CT severity scores for pancreatic (CTSI,mCTSI) and extrapancreatic changes (mCTSI,EPIC). A serum lipase of ≥180U/l was regarded as threefold increase.
Results: In 61 patients (22%, 53y, 48men) serum lipase levels were less than three-fold of the reference value (lip-) despite of signs of acute pancreatitis on CT, whereas 211 patients (56y,131men) belonged to the lip+ group. In lip- patients, CTSI and mCTSI scores revealed similar values (CTSI 4.3vs.4.8, p=0.2, mCTSI 5.3vs.6.1, p=0.1) compared with 63 lip+ patients, whereas EPIC score was significantly lower in lip- patients (2.6vs.3.4, p=0.01). In the lip- group, significantly more patients had an acute on chronic pancreatitis compared with the lip+ group (67% in lip- vs. 26% in lip+, p<0.001).
Conclusion: 22% of patients with abdominal pain and acute pancreatitis on CT belonged to the lip- group. In the lip-group acute on chronic pancreatitis was 3 times as common as in the lip+ group. Only the extrapancreatic changes assessed by EPIC score were significantly altered in both groups. In lip- patients a CECT is crucial for correct diagnosis of acute pancreatitis.

B-1233 14:33

Paraduodenal pancreatitis: MRI features and differential diagnosis with pancreatic adenocarcinoma
E. Boninsegna, R. Negrelli, G. Zamboni, G. Tedesco, R. Manfredi, R. Pozzi-Mucelli; *Verona/IT (boninsegnae@gmail.com)*

Purpose: Paraduodenal pancreatitis (PDP) is an uncommon type of chronic pancreatitis affecting the "groove", a region between the head of the pancreas and the duodenum. It has been recently defined and few studies have been conducted to define its imaging characteristics. It presents common features with pancreatic adenocarcinoma (PA) and differential diagnosis could be difficult. We evaluated its MRI aspects, to identify distinctive elements with PA.
Methods and Materials: 56 patients had been included; 28 were affected by PDP, 28 by PA; everyone had performed an MRI examination and a biopsy. For both groups we evaluated: size of the lesion, presence of cystic components, signal intensity on T1- and T2-weigthed images (WI), on DWI and after contrast medium administration, presence of dilatation of hepatic duct and main pancreatic duct.
Results: On T1-WI 18/28 (64,3%) PDP and 25/28 (89,3%) PA were hypointense to the healthy pancreas; on T2-WI 19/28 (67,9%) PDP were isointense and 18/28 (64,3%) PA were hyperintense (p>0,05). On DWI, 20/28 (71,4%) PDP were isointense and every PA was hyperintense (p<0,01). In the delayed phase 18/28 (64,3%) PDP were hyperintense and 14/28 (50%) PA were isointense (p<0,01). Cysts were present in 24/28 (85.7%) PDP; 15/28 (53,6%) PA presented the "double duct" sign; 11/15 (73.3%) PDP presented calcifications within the lesion. PDP mean volume was 59,9 cm^3, PA volume 10,7 cm^3 (p<0,01).
Conclusion: PDP features useful for the differential diagnosis with PA are: presence of cysts and calcifications, normal ADC values, high signal intensity on delayed phases and greater dimensions.

B-1234 14:41

Comparative evaluation of CT and MRI in non-invasive detection of infection in fluid collections of acute pancreatitis
N.A. Dikshit; *Chandigarh/IN (drnadz@gmail.com)*

Purpose: The study was undertaken to compare CT and newer MRI sequences namely DWI and MR Spectroscopy in non-invasive detection of infection in collections of acute pancreatitis.
Methods and Materials: Total of 30 patients diagnosed as acute pancreatitis with fluid collections and untreated suspected infection were included. They

underwent CECT and MRI followed by microbiological analysis (Gram stain and culture) of the guided diagnostic aspirate. Presence of gas bubbles in the collections on CT images were considered to be a criteria for diagnosing infection. Collections were analysed for diffusion restriction on b 400 and b 800 images and corresponding ADC maps. Objective assessment of the ADC values was also performed both from peripheral and central part of the collection. Multivoxel proton spectroscopy was applied to an area showing diffusion restriction and a control area within the collection.
Results: Culture detected infection in 13 collections, 11 showed qualitative and quantitative diffusion restriction with only 5 of them showing gas bubbles on CECT. Mean central and peripheral ADC values (b value=800) had a higher sensitivity (92.3%) and specificity (88.2%) for identifying infected collections. Mean I value of aminoacids showed 92.3% sensitivity and 58.8% specificity for identifying infected fluid collections.
Conclusion: DW-MRI can be used in non-invasive detection of infection in fluid collections of acute pancreatitis with higher sensitivity and accuracy than CT. MRS can substantiate the detection of pyogenic infection in collections by detection of amino acids at 0.9 ppm.This may obviate the need for unnecessary diagnostic and therapeutic aspirations.

B-1235 14:49

MRI for detailed assessment of pancreatic morphology and function in chronic pancreatitis

J. Frøkjær[1], A. Madzak[1], S. Olesen[1], I. Haldorsen[2], A. Drewes[1]; [1]*Aalborg/DK*, [2]*Bergen/NO (frokjaer@mail.tele.dk)*

Purpose: Chronic pancreatitis (CP) is characterised by abnormal pancreatic morphology and impaired endocrine and exocrine function. As little is known about the relationship between pancreatic morphology and function, and also the association to etiology and clinical manifestations of CP, the aim was to explore pancreatic morphology and function with advanced MRI.
Methods and Materials: Eighty-two CP patients and 22 healthy controls (HC) were included. Morphological imaging parameters included pancreatic main duct diameter, gland volume, Dixon fat signal fraction, and apparent diffusion coefficient (ADC) values. Functional imaging parameters included quantitative bowel fluid volume assessment of pancreatic secretion and changes in pancreatic ADC before and after secretin stimulation. Patients were classified according to the modified Cambridge and M-ANNHEIM classification system. Fecal elastase was collected as proxy for exocrine pancreatic function.
Results: All imaging parameters differentiated CP patients from HC. However, correlations between morphological and functional parameters in CP were weak. Patients with alcoholic and non-alcoholic etiology had comparable MRI findings. Fecal elastase was positively correlated to pancreatic gland volume (r= 0.68, P=0.0016) and negatively correlated to Cambridge classification (r =-0.35, P<0.001). Additionally, gland volume was negatively correlated to the CP duration (r=-0.39, P<0.001) and baseline ADC (r =-0.35, P=0.027). When stratified by clinical stage (M-ANNHEIM), pancreatic gland volume was significantly decreased in severe stages of CP (P=0.001).
Conclusion: Secretin-stimulated MRI provides detailed information about pancreatic morphology and function and represents a promising non-invasive imaging method for characterising pancreatic pathophysiology and may enable monitoring of disease progression in patients with CP.

B-1236 14:57

Comparison of radiological scoring systems, clinical scores, neutrophil-lymphocyte ratio and serum C-reactive protein level for severity and mortality in acute pancreatitis

N. Gezer, G. Bengi, A. Baran, P. Erkmen, Ö. Topalak, C. Altay, O. Dicle; *Izmir/TR (agahbaran1@gmail.com)*

Purpose: To compare radiological scoring systems, clinical scores, serum C-reactive protein (CRP) level and neutrophil-lymphocyte ratio (NLR) in predicting severity and mortality of acute pancreatitis (AP).
Methods and Materials: Demographic, clinical and radiographic data from 80 patients with AP were retrospectively evaluated. Harmless acute pancreatitis score (HAPS), systemic inflammatory response syndrome (SIRS), bedside index for severity in acute pancreatitis (BISAP), Ranson and Balthazar scores, modified computed tomography severity index (CTSI), extrapancreatic inflammation on computed tomography (EPIC) score and renal rim grade were recorded. Prognostic performance of scoring systems, NLR at admission and CRP level at 48 hours were compared for severity based on definition of revised Atlanta classification and mortality. Receiver operator characteristic curves and area under the ROC (AUROC) were calculated.
Results: Out of 80 patients, 19 (23.8%) had severe AP and 9 (11.3%) died. AUROC for BISAP score was 0.836 (95%CI: 0.735-0.937) having the highest value for severity. With a cut-off of BISAP ≥2, the sensitivity and specificity were 68.4% and 78.7%. AUROC for NLR was 0.915 (95%CI: 0.790-1) having the highest value for mortality. With a cut-off of NLR>11.91, the sensitivity and specificity were 76.5% and 94.1%. Among radiological scoring systems, EPIC score had the highest AUROC which was 0.773 (95%CI: 0.645-0.900) for severity and 0.851 (95%CI: 0.718-0.983) for mortality with a cut-off value ≥6.
Conclusion: BISAP score and NLR might be preferred as early determinants of severity and mortality in AP. EPIC score might be suggested among current radiological scoring systems.

B-1237 15:05

Detection of inflammation in primary sclerosing cholangitis using gadolinium-based contrast enhancement index (CEI)

S. Keller, J. Weinrich, C. Schramm, G. Adam, J. Yamamura; *Hamburg/DE (s.keller@uke.de)*

Purpose: To evaluate the feasibility of conventional magnetic resonance imaging (MRI) T2-weighted images (T2wI) and the T1wI relative contrast enhancement index (CEI) for detection of intrahepatic inflammation in patients with primary sclerosing cholangitis (PSC).
Methods and Materials: 3T MRI scans were retrospectively reviewed in 27 patients (42.9 ± 15.6 y) with known PSC and in healthy controls (n=19). Wedge-shaped areas with hyperintense signal in T2wI and PSC-typical MR imaging findings such as intrahepatic bile duct dilatation and irregularities were defined by two radiologists. The inter-observer agreement was calculated by using Cohen`s kappa coefficient. The patients' contrast enhancement index (CEI) was calculated both for wedge-shaped T2w hyperintense (CEI_{hyper}) and normal appearing (CEI_{normal}) areas and compared to one each other and also to the CEI of healthy controls ($CEI_{healthy}$). The CEI ratio (hyper/normal) in patients was correlated statistically to disease specific laboratory parameters.
Results: The inter-observer agreement for detection of hyperintense areas in T2wI was very good (κ = 0.92; 95% Confidence interval 0.78-1.0). In patients, the mean CEI_{normal} (53.53±6.5%) of normal appearing tissue in T2wI corresponded to the CEI of healthy controls (53.2±2.7%, p>0.97). The patients' CEI_{hyper} (81.7±10.68) was elevated compared to the CEI_{normal} (p=0.03) as well as to the controls (p=0.01). No correlation of the patients' functional laboratory parameters and the CEI ratio was observed.
Conclusion: The CEI is a useful additional tool for assessment of inflammatory alterations in PSC liver parenchyma.

B-1238 15:13

Image monitoring of hepatic oxygenation and Kupffer activity during preneoplastic changes induced with obstructive cholangitis and N nitrosodimethylamine in a mouse model

J. Kim, S. Lee, J. Lee, H. Eun, J. Han; *Seoul/KR (jhkim2008@gmail.com)*

Purpose: To investigate serial changes of the impaired phagocytic activity of Kupffer cells (KC) and liver oxygen saturation (sO_2) using Sonazoid-enhanced ultrasound imaging (SEUS) and photoacoustic imaging (PI) during preneoplastic changes induced with obstructive cholangitis and N-nitrosodimethylamine (NDMA) in a mouse model.
Methods and Materials: A mouse cholangitis model was created by ligation of the common bile duct (n=33, G1) and had taken NDMA for 8 weeks. The cholangitis group was compared to the control group (n=19, G2). Serial changes of echogenicity and sO_2 by SEUS and PI were measured at baseline, four, six, and eight weeks after NDMA administration. Serial pathologic changes including H&E staining and KC fraction using CD68 staining were compared using ANOVA and Unpaired t-test.
Results: Serial pathologic changes showed biliary epithelial hyperplasia, some foci of dysplasia. CBD ligation group showed serial decreased of parenchymal intensity (-29.8 dB vs. -30.5 dB, -35.0 dB vs. -30.4 dB, and -38.2 dB vs. -31 dB) on SEUS and liver oxygen saturation (45.2% vs. 51.9%, 43.0% vs. 49.0%, and 31.3% vs. 49.7%) of PI as compared with the control group at the 4th, 6th, and 8th weeks after administration, respectively (P<0.05). However, the KC fraction showed an increase in the ligation group than in the non-ligation group at 6th, and 8th weeks (P<0.05).
Conclusion: During preneoplastic changes induced with obstructive cholangitis and NDMA, SEUS and PI are a useful tool for monitoring of the serial change of impaired phagocytic activity of Kupffer cells and liver hypoxic state.

B-1239 15:21

Contrast-enhanced CT of abdomen in acute pancreatitis: can we predict the development of necrosis simply by CT number measurements?

N. Gezer, G. Bengi, A. Baran, Ö. Topalak, O. Dicle; *Izmir/TR (agahbaran1@gmail.com)*

Purpose: Pancreatic necrosis is an important prognostic factor in acute pancreatitis. It is associated with tissue ischaemia due to vasospasm of intrapancreatic arteries. However, ischaemic tissue may not always be observable early in the course by contrast-enhanced computed tomography (CT). Demonstration of enhancement on contrast-enhanced CT is a reliable sign of vascularisation and measurable as CT numbers expressed in Hounsfield Units (HU). Our aim was to evaluate if a routine contrast-enhanced CT of abdomen can detect tissue ischaemia and predict the development of necrosis by CT number measurements in acute pancreatitis.

Methods and Materials: 69 patients with acute pancreatitis (17 necrotic, 52 oedematous) whose contrast-enhanced CT images were obtained 48-72 hours after onset of symptoms were included in the study. The highest (relatively normal-HUp1) and lowest (presumably ishemic-HUp2) CT numbers of pancreatic tissue, CT numbers of spleen (HUs) and abdominal aorta (HUa) were measured. The follow-up CT examinations 3-4 weeks after were evaluataed to identify patients with necrotic or oedematous pancreatitis.
Results: In 6 (35%) of 17 necrotic pancreatitis, pancreatic necrosis was not diagnosed by initial CT but proved in the latter. Mean HUp1, HUp2, HUs and HUa of necrotic group were 70.5±11.3, 31.8±14.3, 94±24, 205.5±80.3. Mean HUp1, HUp2, HUs and HUa of oedematous group were 71±15.5, 47.7±17.6, 93.4±19.7 and 169.9±61.2. Statistical differences in HUp2, HUp1/HUp2, HUs/HUp2, HUa/HUp2 were shown between necrotic and oedematous pancreatitis.
Conclusion: CT number measurements on a standard contrast-enhanced CT of abdomen may help to distinguish between necrotising and oedematous pancreatitis.

14:00 - 15:30 **Room C**

Abdominal Viscera

SS 1901c

Liver fat, iron and fibrosis: assessment and quantification

Moderators:
O. Dahlqvist Leinhard; Linkoping/SE
B.E. Van Beers; Clichy/FR

B-1240 14:00

Liver fat storage in patients with NAFLD: differences between metabolic syndrome and genetic aetiology
M. Di Martino, A. Capalbo, K. Koryukova, S. De Vizio, C. Catalano; *Rome/IT (micdimartino@hotmail.it)*

Purpose: To compare the hepatic fat fraction (HFF) at Magnetic Resonance Spectroscopy (MRS) and proton density hepatic fat fraction (PD-HFF) in patients with genetic and metabolic syndrome determined NAFLD.
Methods and Materials: This prospective study comprised three groups: control group (50 patients), genetic NAFLD group (57 patients) and metabolic syndrome NAFLD group (55 patients). Magnetic Resonance (MR) examination was performed on a 3.0T scanner. MRS was acquired with a single voxel breath-hold PRESS sequence (TR 4000, TE 30-40) with an acquisition time of 24 s. PD-HFF was determined with a breath-hold low-flip angle, T1-weighted, 2D multiple-echo, spoiled gradient-echo (GRE) sequence (TR5.1/TE from 0.8 to 3.8, flip angle 5°, FOV 33-40 cm; section thickness, 10 mm; intersection gap, 0, matrix 128 × 128, acquisition time 2 × 17s) and with a 3D GRE T2* sequence (IDEAL-IQ GE; TR12.9 msec; TE 6 echos from 1.6 to 9.8 FOV, 35-40 cm; matrix, 224x 160; flip angle, 5°; section thickness, 10 mm. Differences between study groups were evaluated by ANOVA and Kruskall-Wallis test. Pearson's correlation coefficient was used for comparison among MR techniques.
Results: Patients with NAFDL reported a significantly greater HFF than healthy subjects, with a trend to a higher value in metabolic syndrome group (8.7% vs 24.7% and 31.4%; p < 0.0001). Good correlation was found between PD-HFF sequences and MRS (0.51 and 0.55 respectively).
Conclusion: Subjects with metabolic NAFLD have a higher hepatic fat than patients with genetic NAFLD. IDEAL-IQ sequence should replace MRSfor non-invasive diagnosis of liver steatosis.

B-1241 14:08

Simultaneous dual-energy CT based monochromatic imaging and US with normalised local variance analysis for quantification of hepatic steatosis: correlation with pathology
P. Rogalla, G. Guenette, A. Rattansingh, M. Roest, K. Mao, B. Hoppel; *Toronto, Ontario, ON/CA (Patrik.Rogalla@uhn.ca)*

Purpose: To analyse dual-energy monochromatic CT imaging in patients with suspected fatty liver disease and compare to simultaneously acquired normalised local variance (NLV) ultrasound imaging and histopathology.
Methods and Materials: 41 patients with clinically indicated liver biopsy for fatty liver disease were prospectively enrolled in this study. Biopsies were performed under US guidance (Aplio 500) within the CT suite (Toshiba Aquilion Vision). Prior to the liver biopsy, three measurements were performed using investigational US software that provides NLV of the target liver area in the right lobe. A single dual-energy CT volume (16 cm, 320 slices) was acquired with the needle in situ. Two cores were taken from the liver for clinical pathology evaluation. Monochromatic images were reconstructed in 5 keV intervals from 35 to 130 keV. Attenuation in 2 ROIs measured at the needle tip were curve fitted to generate DE-CT-I_0. NLV was measured in a 3 cm ROI (each with 12,000 samples) placed at the site of biopsy. All values were correlated to pathology.
Results: There were no biopsy related complications. The mean/SD for the pathology steatosis score, NLV, DE-CT-I_0 and HU for 80kVP and 135kVp images were 0.57/0.72, 1.16/0.13, 54.94/12.04, 45.8/11.0 and 52.84/11.24 respectively. The correlation/two tailed p-value of DE-CT-I_0 vs biopsy, NLV vs biopsy, and NLV vs DE-CT-I_0 were r^2= 0.76/p<0.01, r^2= 0.59/p<0.01 and r^2=0.61, p<0.01, respectively.
Conclusion: Both US and CT correlate well with each other and allow predicting the degree of hepatic steatosis, with monochromatic DE-CT performing slightly better than NLV analysis on US.
Author Disclosures:
P. Rogalla: Research/Grant Support; Institutional Research Grant, Toshiba Medical Systems. **G. Guenette:** Employee; Toshiba Medical Systems.
B. Hoppel: Employee; Toshiba Medical Systems.

B-1242 14:16

The performance of multi-echo chemical shift magnetic resonance imaging for the evaluation of liver steatosis: a meta-analysis
Y. Qu, J. Chen, B. Song; *Chengdu/CN (yali_qu_xray@163.com)*

Purpose: To evaluate the diagnostic performance of multi-echo chemical shift magnetic resonance imaging (CS-MRI) for the evaluation of liver steatosis (LS).
Methods and Materials: A systematic literature search was performed to identify relevant original studies. Quality analyses were conducted by Quality Assessment of Diagnostic Accuracy Studies (QUADAS-2). Diagnostic data were extracted for each steatosis stage (G0-G3). A bivariate mixed-effect binary regression model was used to produce pooled sensitivity, specificity and summary receiver operating (SROC) curves. The areas under SROC curve (AUC) were calculated as the indicator of the diagnostic accuracy.
Results: We included 10 studies with 11 subsets of data discriminating LS from normal (LS≧G1) and 5 studies differentiating moderate or severe LS from mild or no LS (LS≧G2). The sensitivity, specificity, diagnostic odds ratio and AUC for LS≧G1 were 0.92 (95% confidence interval (CI) 0.88-0. 95), 0.93 (95% CI 0.86-0.97), 160 (95% CI 79-327) and 0.97, and for LS≧G2 were 0.83 (95% CI 0.67-0.92), 0.86 (95% CI 0.79-0.91), 30 (95% CI 13-67) and 0.90.
Conclusion: Multi-echo CS-MRI revealed excellent diagnostic accuracy for the staging of LS≧G1 and LS≧G2. This technique shows notable potential in the evaluation of LS.

B-1243 14:24

Magnetic resonance spectroscopy for differentiation between non-alcoholic steatohepatitis and simple hepatic steatosis
K.-H. Yoon, T.-H. Ahn, R.-H. Kim, H. Jun, Y. Lee, M. Lee, E. Cho; *Iksan/KR (whitezombi88@naver.com)*

Purpose: To study the hepatic metabolite difference between patients with non-alcoholic steatohepatitis (NASH) and simple hepatic steatosis, and study the diagnostic accuracy of proton magnetic resonance spectroscopy (^{1}H-MRS) with long echo-time (TE).
Methods and Materials: The local institutional review board approved this study and waived written informed consent. ^{1}H-MRS measurements were performed on a localised voxel of the liver using a point-resolved spectroscopy sequence and hepatic metabolites of the alanine (Ala), lactate/triglyceride (Lac/TG), and TG were analyzed in patients with NASH (n=11), simple steatosis (n=15), and healthy controls (n=6). The group difference was tested with the ANOVA and Tukey's post-hoc tests, and diagnostic accuracy was tested by calculating the area under the receiver operating characteristics (ROC) curve. The values of metabolites were correlated with the histopathology and non-alcoholic fatty liver disease (NAFLD) activity scores.
Results: Patient with NASH showed significant elevated the Ala (p<0.001), Lac/TG (p<0.001), TG (p<0.05) concentration when compared with patients who had simple steatosis and healthy controls. The patients with NASH were significantly higher levels in Ala (mean ± standard deviation, 52.5±8.3 vs 2.0±0.9; p<0.001), Lac/TG (824.0±168.2 vs 394.1±89.8; p<0.05) than simple steatosis. The area under the ROC curve to distinguish NASH from simple steatosis was 1.00 (95% confidence interval; 0.1.0, 1.00) with Ala and 0.782 (95% confidence interval; 0.61, 0.96) with Lac/TG. The Ala and Lac/TG levels were well correlated with steatosis grade, lobular inflammation, and NAFLD activity scores.
Conclusion: ^{1}H-MRS with long TE would be useful for differentiation of patients with NASH and simple hepatic steatosis.

B-1244 14:32

Staging steatosis using quantitative ultrasound, validation with pathohistology

G. Weijers, I.D. Munsterman, A.S.S. MMeel-van den Abeelen, J.M. Thijssen, E.T.T.L. Tjwa, J.P.H. Drenth, C.L. de Korte; *Nijmegen/NL (Gert.Weijers@radboudumc.nl)*

Purpose: Quantitative ultrasound can be an attractive non-invasive alternative for liver biopsies to stage steatosis. We validated the Computer Aided Ultrasound (CAUS) method for staging human steatosis.
Methods and Materials: Analysis of a prospectively obtained dataset (biopsy and CAUS) of a cohort consisting of consecutive patients referred for liver biopsy with a variety of clinical indications. From this cohort retrospectively, patients (n=24) with positive histology scores for steatosis (Brunt score 1-3) were selected. As a reference, patients without steatosis and without fibrosis were selected (n=26). Five ultrasound image per patient were analysed using the CAUS protocol, which estimates average and depth dependent histogram and texture parameters. Mean and variance of 15 parameters as well as Pearson correlations to the Brunt score were obtained. Leave one out multiple linear regression analysis and receiver operating characteristics revealing the area under curve (AUC) were estimated.
Results: Highly significant correlations were found for 11 out of 15 US parameters. Best correlating parameters were: mean echo level (MU, R=0.801, p<0.01), residual attenuation coefficient (R=0.736, p<0.01) and depth dependent speckle signal to noise ratio (R=0.774, p<0.01). Regression analysis with these three parameters revealed an AUC of 0.944. Histology also revealed fibrosis in 75% of the patients, however only a weak correlation of the MU (R=0.414, p=0.019) with fibrosis score was observed.
Conclusion: The high AUC value indicates the potential of CAUS for screening a population for steatosis. Despite the presence of fibrosis, good predictive results for staging steatosis were obtained indicating the robustness of CAUS.

B-1245 14:40

Attenuation coefficient measurement (ACM) as a newest mode for ultrasound quantitative hepatic steatosis assessment

O. Dynnyk, N. Kobyliak, O. Fedusenko; *Kyiv/UA (Obdynnyk@Gmail.Com)*

Purpose: The presence of fat droplets in the hepatocytes (hepatic steatosis) under condition of chronic diffuse liver disease (CDLD) increases the attenuation of ultrasound (US). A group of Ukrainian scientists proposed an original algorithm for US attenuation coefficient measurement - ACM and accuracy navigation by B-mode.
Methods and Materials: From total of 3274 patients who underwent to comprehensive abdominal US (2015-2016) in our clinic, 949 have been diagnosed with fatty liver according to Hamaguchi criteria. All these patient we provide ACM (dB/cm) measurement by SoneusP7 device (Ultrasign, Ukraine), with a 1-6MHz convex transducer in the right lobes. For diagnostic accuracy assessment we used CT as standard and comparison with CAP by Fibroscan (Echosens, France) we included 142 patients for subanalysis.
Results: From total of 3274 patients who underwent to comprehensive abdominal US (2015-2016) in our clinic, 949 have been diagnosed with fatty liver according to Hamaguchi criteria. All these patient we provide ACM (dB/cm) measurement by SoneusP7 device (Ultrasign, Ukraine), with a 1-6MHz convex transducer in the right lobes. For diagnostic accuracy assessment we used CT as standard and comparison with CAP by Fibroscan (Echosens, France) we included 142 patients for subanalysis.
Conclusion: The ACM as novel real-time ultrasound approach can be used for non-invasive hepatic steatosis diagnosis, allows clinicians to follow-up disease progression and response to treatment.

B-1246 14:48

Accuracy of automated liver contouring, fat fraction and R2* measurement on T1-weighted q-Dixon magnetic resonance images

D. Stocker[1], K. Schawkat[1], M. Bashir[2], S. Kannengiesser[3], C.S. Reiner[1]; [1]*Zurich/CH*, [2]*Durham, NC/US*, [3]*Erlangen/DE (daniel.stocker@usz.ch)*

Purpose: To evaluate the accuracy of automated liver contouring and volumetry and its influence on automated fat signal fraction (FSF) and R2* measurements in the multi-echo T1-weighted q-Dixon magnetic resonance (MR) sequence compared with manual measurements in the liver.
Methods and Materials: Unenhanced multi-echo q-Dixon MR-images were retrospectively evaluated in 30 consecutive patients without prior liver surgery (21 females, 9 males; mean age 59±13.4 years; mean BMI 24.8±5.1) undergoing clinically indicated liver MRI on a 3T-scanner. Liver volume (LV), FSF_{vol} and $R2^*_{vol}$ measurements across the whole liver volume were automatically generated by the MR-scanner on q-Dixon images. Similar measurements were manually performed by one radiologist. Differences between automated and manual measurements were assessed with the related-samples Wilcoxon signed rank test and Bland-Altman plots.
Results: Automatic LV (1576.8 ± 434.8 ml) was significantly smaller than manual LV (1829.9 ± 758.5 ml) with a relative difference of -10±13.3% ($p < 0.01$). Mean automatic $R2^*_{vol}$ (80.7±65 s^{-1}) was slightly but significantly lower than manual $R2^*_{vol}$ (85.7±84.4 s^{-1}) with a relative difference of -2±7.5 % (range, -25.3% to 21.3%; $p < 0.01$). Mean automatically measured FSF_{vol} was 6.5±5.1% and was not significantly different to manual FSF_{vol} 6.8±4.6 % with a relative difference of -3.2±30.5% (range, -54.1% to 100.3%; p=0.185).
Conclusion: Automated liver contouring lead to slightly but significantly smaller liver volumes and lower R2* values compared to manual measurements. FSF_{vol} was not significantly influenced by differences in automated and manual liver contouring in this group of patients with normal to slightly elevated FSF.
Author Disclosures:
S. Kannengiesser: Employee; Siemens Healthcare.

B-1247 14:56

Liver iron measurement by R2* in comparison to R2 and biosusceptometry

J. Yamamura, S. Keller, B. Schönnagel, E. Tahir, P. Nielsen, R. Grosse, G. Adam, R. Fischer; *Hamburg/DE (j.yamamura@uke.de)*

Purpose: To develop a breathhold liver MRI-R2* sequence as an alternative method for SQUID biomagnetic liver susceptometry (BLS) reference method and compare the results with R2 rates from the literature.
Methods and Materials: 34 patients with transfusional siderosis (ß-thalassemia major n=24) underwent a gradient recalled ECG-gated multi-echo sequence. LIC by BLS is calculated from the SQUID. R2* is determined from a mono-exponential fit to the echo-time-dependent signal amplitudes averaged over a whole liver slice with constant signal level offset. A correlation between BLS and R2* was determined statistically.
Results: The expected non-linear relationship, $R2^* = 30 + (0.007\pm0.003)\cdot LIC \cdot (1 + LIC0.39\pm0.05)$ ($r2 = 0.97$), was found in the range between 100 and 8000 µg/g liver. The Spearman rank correlation coefficient RS = 0.98 ($p < 10\text{-}4$) was similar to the reported R2 calibration versus liver biopsy (St. Pierre et al., 2005). Mono-exponential fit convergence for R2*(TE) at LIC > 6000 µg/g was poor due to the available first echo-time of 1.3ms. A comparison with formerly measured R2 rates resulted in a conversion factor of 4.9 ± 0.3 for the approved MRI-R2 calibration by St. Pierre et al. (2005) using freeze-dried liver biopsies.
Conclusion: In patients, where liver susceptometry is spoiled by local magnetic contaminations (dental braces, etc.) or by severe obesity, alternative breathhold MRI-R2* method within known limitations can be used to determine the liver iron concentration.

B-1248 15:04

Non-invasive staging of liver fibrosis in patients with chronic viral hepatitis: performance of a shear wave measurement method

G. Ferraioli, L. Maiocchi, R. Lissandrin, A. De Silvestri, C. Tinelli, C. Filice; *Pavia/IT*

Purpose: This single center cross-sectional study aimed at prospectively assess the performance of a point shear wave measurement (SWM) method by using transient elastography (TE) as the reference standard.
Methods and Materials: Consecutive patients with chronic viral hepatitis were enrolled. Liver stiffness was assessed with the SWM method implemented in the HI VISION Ascendus ultrasound system (Hitachi Ltd, Japan) and with the TE method of the FibroScan device (Echosens, France). The liver stiffness measurements with the SWM method were performed before the measurements with TE. For staging liver fibrosis we used the TE cutoffs of a previous meta-analysis, i.e. 7.0, 9.5 and 12.0 kiloPascal, respectively, for significant fibrosis (F>=2), advanced fibrosis (F>=3), and cirrhosis (F=4). The diagnostic performance of the SWM method was assessed by calculating the area under the receiver operating characteristic (AUC) curve.
Results: 411 individuals [218 males, 193 females; mean age, 61.2 (13.2) years] were studied. 382 (92.9%) of them were affected by chronic hepatitis C. 179 (43.6%) individuals were in F0-F1 stage, 75 (18.2%) in F2 stage, 41 (10.0%) in F3 stage, and 116 (28.2%) in F4 stage. The optimal cutoff values of the SWM method for staging F>=2, F>=3, F=4, respectively, were 6.44, 7.82 and 8.40 kiloPascal. AUC calculations showed values of 0.92 (0.89-0.94) for F>=2 [sensitivity, 83.3% (77.4-88.2); specificity, 87.4% (81.4-92.0]; 0.92 (0.88-0.94) for F>=3 [sensitivity, 86.0% (78.8-91.5); specificity, 82.6% (77.2-87.2)]; 0.94 (0.91-0.96) for F=4 [sensitivity, 92.3% (84.8-96.9); specificity, 82.1% (77.1-86.5)].
Conclusion: These preliminary results show that the SWM method is a useful tool for non-invasively staging liver fibrosis in patients with chronic viral hepatitis.
Author Disclosures:
G. Ferraioli: Speaker; Philips Healthcare, Toshiba, Esaote, Hitachi Ltd..
C. Filice: Speaker; Esaote, Philips Healthcare, Toshiba, Hitachi Ltd..

B-1249 15:12

Diagnostic performance of 2D-shear wave elastography using comb-push techniques for liver fibrosis evaluation: a prospective study

S. Lee, J. Lee, J. Yoon, W. Chang, H.-J. Kang, H. Yang; *Seoul/KR (twin393@hanmail.net)*

Purpose: To evaluate the diagnostic performance of a new 2D-shear wave elastography (2D-SWE) using the comb-push technique in hepatic fibrosis detection using histopathology as the reference standard.
Methods and Materials: This prospective study was approved by the institutional review board, and informed consent was obtained from all patients. The liver stiffness (LS) measurements were obtained from 140 patients, using the 2D-SWE (GE LOGIQ E9), which uses comb-push excitation to produce shear waves and a time-aligned sequential tracking method to detect shear wave signals. Intraobserver reproducibility was evaluated in the 114 patients with histologic diagnosis, and interobserver reproducibility was evaluated in 20 patients without histologic diagnosis. LS values and histologic results were compared by using Spearman correlation and receiver operating characteristic (ROC) curve analysis.
Results: The technical success rate of 2D-SWE was 92.11% (105 of 114). Intraclass correlation of interobserver agreement was 0.873 and the value for intraobserver agreement was 0.951. LS values showed high correlation with estimation of fibrosis (r=0.712, p<0.001) and mild correlation with necroinflammation (r=0.340, P=0.0004), while steatosis did not show correlation with LS values (r=0.053, P=0.590). The area under the ROC curve (AUC) of LS values for stage F2 fibrosis or greater, stage F3 or greater, and stage F4 fibrosis was 0.874 (95% confidence interval [CI]: 0.794,0.930), 0.905 (95% CI : 0.832,0.954), and 0.894 (95% CI : 0.819,0.946), respectively.
Conclusion: 2D-SWE using the comb-push technique can be used as a reliable method for accessing hepatic fibrosis with excellent repeatability and reproducibility.
Author Disclosures:
S. Lee: Founder; National Research foundation of Korea. **J. Lee:** Founder; National Research foundation of Korea.

B-1250 15:20

Early changes of liver stiffness assessed using shear wave elastography after novel direct antiviral therapy in chronic hepatitis C virus induced liver fibrosis

S.R. Marticorena Garcia, J. Guo, H. Tzschätzsch, M. Dürr, F. Halleck, K. Jöhrens, B. Hamm, I. Sack, T. Fischer; *Berlin/DE (stephan.marticorena-garcia@charite.de)*

Purpose: Chronic hepatitis C virus (HCV) infection predisposes to liver fibrosis. The purpose of this study is to non-invasively monitor the liver elasticity using shear wave elastography (SWE) after direct antiviral therapy.
Methods and Materials: In this prospective study 8 patients with chronic HCV infection and liver fibrosis (age 52±14 years) were treated with direct-acting antivirals (Daclatasvir/Sofosbuvir), their liver stiffness was monitored over 6 months and compared to a healthy control group (ctr, n=7). In all patients liver biopsy and histopathological analysis were performed prior to the treatment. SWE was performed before (d0) and after antiviral treatment (3 and 6 months) at a high-end ultrasound device (Aplio500, Toshiba) with a 5 MHz broadband convex transducer. HCV load is assessed by real-time PCR over 6 months.
Results: Liver fibrosis was detected in 7 patients (stage 1-3). HCV load was below detectable levels after 19 days (range 8-29 days) of treatment initiation. SWE shows a decrease in liver shear wave velocities (SWV) after 6 months (SWV: d0, 2.12±0.61m/s; 3mo, 1.73±0.26m/s; 6mo, 1.54±0.23m/s; d0 vs. 3mo, ns; d0 vs. 6mo, *P*<0.05; one-way ANOVA). Significant differences in liver SWV between HCV patients and ctr were only seen before antiviral treatment (SWV, ctr: 1.48±0.23m/s; d0 vs. ctr, *P*=0.008; 3mo vs. ctr, *P*=0.052; 6mo vs. ctr, *P*=0.450; Mann-Whitney-test).
Conclusion: Direct antiviral therapy is associated with decrease of liver stiffness after 6 months and SWV could be used as biomarker for non-invasive monitoring of liver stiffness during therapy.
Author Disclosures:
M. Dürr: Research/Grant Support; research funds from Bristol–Myers Squibb and travel grants from Novartis and Roche. **B. Hamm:** Research/Grant Support; DFG, BMBF and more. Shareholder; >50 biotechnological companies. **T. Fischer:** Consultant; Toshiba, Siemens, Bracco.

14:00 - 15:30 **Room X**

Vascular

SS 1915

Aortic imaging

Moderators:
M.I. Furmanek; Warsaw/PL
N.N.

B-1259 14:00

Hypertension following aortic coarctation repair: is the 'selfish brain' to blame?

J.C.L. Rodrigues, M. Jaring, M.C.K. Hamilton, S.L. Curtis, J.F.R. Paton, E.C. Hart, N.E. Manghat; *Bristol/UK (jonrodrigues@doctors.org.uk)*

Purpose: 20-30% repaired aortic coarctation (CoA) patients develop hypertension, resulting in significant cardiovascular morbidity and mortality. We recently demonstrated that vertebral artery hypoplasia and incomplete posterior circle of Willis (VAH+ipCoW) is associated with increased cerebrovascular resistance and decreased cerebrovascular blood flow, which occur before increased sympathetic nerve activity in borderline hypertensives suggesting brainstem hypoperfusion may evoke hypertension to maintain cerebral blood flow: the 'selfish brain' hypothesis. We now assess whether similar mechanisms account for the pathogenesis of hypertension in repaired CoA.
Methods and Materials: CoW time-of-flight magnetic resonance angiography from 79 repaired CoA patients (33±12 years, 57% male, SBP135±23mmHg, DBP 76±11mmHg) was compared blindly with 33 normotensive controls (41±14 years, 48% male, SBP 124±10mmHg, DBP 76±8mmHg). VAH was defined as <2mm and ipCoW as hypoplasia of one or both posterior communicating arteries.
Results: VAH+ipCoW was significantly higher(P<0.05, Fisher's exact test) amongst CoA (26/79, 33%) than controls (3/33, 9%). Subgroup analysis by repair type (stent, balloon angioplasty, patch repair, subclavian flap or end-to-end anastomosis) revealed no significant difference in prevalence of VAH+ipCoW, suggesting it is not related to the cerebrovascular deformation. In multivariate logistic regression analysis controlling for age and gender, VAH+ipCoW was a significant independent predictor of hypertension (odds ratio 2.67 [95th confidence interval: 1.09-6.52], P=0.031).
Conclusion: VAH+ipCoW predicts hypertension in repaired CoA and is unrelated to repair type. CoA may be marker of a wider congenital vascular problem. Understanding the role of the 'selfish brain' in the pathogenesis of this condition will help guide future treatment strategies.

B-1251 14:08

Aortic wall thickness is associated with high serum concentrations of the thyroid-stimulating hormone: a cross-sectional population-based study

C. Klausenitz[1], T. Ittermann[1], R. Lorbeer[2], M. Dörr[1], A. Quadrat[1], T. Schneider[1], H. Völzke[1], B. Mensel[1]; [1]*Greifswald/DE*, [2]*Munich/DE*

Purpose: To investigate the influence of thyroid function by measuring the serum levels of thyroid-stimulation hormone (TSH) on promotive factors in the pathogeneses of artherosclerosis such as aortic wall thickness (AWT) and aortic diameter.
Methods and Materials: Data of 3,904 individuals from two independent population based trials of the Study of Health in Pomerania was analysed. Imaging of the aorta was performed on a 1.5-T MRI scanner. Measurements of AWT and aortic diameter were perfomed at the layer with concentration of the right pulmonary artery displaying the ascending and the descending aorta.
Results: There was a significant association between TSH, treated as a continuous variable, and the AWT of the descending aorta (p=0.015, ß=0.11, 95% confidence interval (CI) 0.02-0.21) but not with the AWT of the ascending aorta (p=0.081, ß=0.20, 95% CI -0.01-0.21). High serum levels of TSH (>3.29 mIU/L) were significantly associated with the AWT of the ascending aorta (p=0.018, ß=0.12, 95% CI 0.02-0.23) but not with the AWT of the descending aorta (p=0.212, ß=0.06, 95% CI -0.04-0.16). There were no statistical significant associations between serum TSH levels and aortic diameters.
Conclusion: The values of AWT increase with increasing levels of serum TSH. Therefore a hypothyreotic state might be considered as a precursor for aortic arteroscleroses. These findings are in line with previous investigations stating an increased atherosclerotic risk in the hypothyroid state.
Author Disclosures:

C. Klausenitz: Equipment Support Recipient; Siemens Healthcare, Erlangen, Germany. Founder; German Federal Ministry for Education and Research, Ministry for Education, Research and Cultural Affairs, Ministry for Social Affairs of the State Mecklenburg-West-Pomerania. Research/Grant Support; German Research Foundation, BMELV. **T. Ittermann:** Equipment Support Recipient; Siemens Healthcare, Erlangen, Germany. Founder; German Federal Ministry for Education and Research, Ministry for Education, Research and Cultural Affairs, Ministry for Social Affairs of the State Mecklenburg-West-Pomerania. Research/Grant Support; German Research Foundation, BMELV. **R. Lorbeer:** Equipment Support Recipient; Siemens Healthcare, Erlangen, Germany. Founder; German Federal Ministry for Education and Research, Ministry for Education, Research and Cultural Affairs, Ministry for Social Affairs of the State Mecklenburg-West-Pomerania. Research/Grant Support; German Research Foundation, BMELV. **M. Dörr:** Equipment Support Recipient; Siemens Healthcare, Erlangen, Germany. Founder; German Federal Ministry for Education and Research, Ministry for Education, Research and Cultural Affairs, Ministry for Social Affairs of the State Mecklenburg-West-Pomerania. Research/Grant Support; German Research Foundation, BMELV. **A. Quadrat:** Equipment Support Recipient; Siemens Healthcare, Erlangen, Germany. Founder; German Federal Ministry for Education and Research, Ministry for Education, Research and Cultural Affairs, Ministry for Social Affairs of the State Mecklenburg-West-Pomerania. Research/Grant Support; German Research Foundation, BMELV. **T. Schneider:** Equipment Support Recipient; Siemens Healthcare, Erlangen, Germany. Founder; German Federal Ministry for Education and Research, Ministry for Education, Research and Cultural Affairs, Ministry for Social Affairs of the State Mecklenburg-West-Pomerania. Research/Grant Support; German Research Foundation, BMELV. **H. Völzke:** Equipment Support Recipient; Siemens Healthcare, Erlangen, Germany. Founder; German Federal Ministry for Education and Research, Ministry for Education, Research and Cultural Affairs, Ministry for Social Affairs of the State Mecklenburg-West-Pomerania. Research/Grant Support; German Research Foundation, BMELV. **B. Mensel:** Equipment Support Recipient; Siemens Healthcare, Erlangen, Germany. Founder; German Federal Ministry for Education and Research, Ministry for Education, Research and Cultural Affairs, Ministry for Social Affairs of the State Mecklenburg-West-Pomerania. Research/Grant Support; German Research Foundation, BMELV.

B-1252 14:16

Dynamic 3D angiography in patients with aortic dissection as risk factor for chronic aortic expansion

M. Trojan[1], M. Müller-Eschner[1], D. Kotelis[1], S. Partovi[2], C. Karmonik[3], H. von Tengg-Koblingk[4], D. Böckler[1], H.-U. Kauczor[1], F. Rengier[1]; [1]*Heidelberg/DE*, [2]*Cleveland, OH/US*, [3]*Houston, TX/US*, [4]*Berne/CH (michael.trojan@med.uni-heidelberg.de)*

Purpose: Assess dynamic contrast-enhanced MR angiography in patients with chronic expanding or stable aortic dissection and evaluate its role as potential risk factor for chronic aortic expansion.
Methods and Materials: 20 patients with aortic dissection underwent dynamic contrast-enhanced 3D MR angiography of the aorta at 1.5T and follow-up CT (mean follow-up 6.1 years). 7 patients (mean 65.3 years) showed chronic aortic expansion, 13 patients (mean 64.3 years) had stable aortic diameters. MR angiographies were evaluated by placing regions of interest in the centre of the lumen of the non-dissected arch and of the false lumen of the descending aorta at the thoracoabdominal transition. From resulting time-intensity-curves the following parameters were calculated: full width at half maximum (FWHM), upward slope, downward slope, and time delay of peak intensity in the false lumen compared to the non-dissected aortic arch.
Results: The values were for the expansion/stable group: FWHM 0.19±0.02/0.41±0.17 (p=0.009), upward slope 10.97±3.11/7.64±2.68 (p=0.038), downward slope -6.55±0.87/-1.97±2.67 (p=0.013), time delay of peak intensity in the false lumen 1.32±0.25/1.42±0.24 (p=0.027).
Conclusion: Time-resolved 3D MR angiography showed significant differences of contrast dynamics between patients with chronic expanding and stable aortic dissection as an expression of accelerated inflow into and outflow from the false lumen. The technique may help to advance understanding of the complex pathophysiology of chronic expansion and has potential as a risk factor for aortic expansion.

B-1253 14:24

Morphological and functional CFD-based analysis for predicting abdominal aortic evolution

O. Meyrignac, C. Zadro, R. Moreno, L. Bal, B. Saint Lebes, A. Sewonu, A. Jacquier, P. Piquet, H. Rousseau; *Toulouse/FR (meyrignac.o@chu-toulouse.fr)*

Purpose: Abdominal aortic aneurysm (AAA) is a common pathology where the need for surgical intervention is mostly determined on maximal diameter. The purpose of this study was to identify volumetric and computational fluid dynamics (CFD) parameters to predict AAA evolution.
Methods and Materials: In our multicentre and prospective study, we included 82 patients with AAA between September 2012 and June 2014. Patients underwent two CT examinations separated by a one-year interval to assess aneurysms evolution. Fifty patients were eligible for CFD analysis. Based on a 10ml threshold of total volume progression we classified patients into slow and rapid progression groups. Initial aneurysm morphological parameters and CFD functional parameters were analysed including: maximal diameter and surface, thrombus and lumen volumes, maximal parietal pressure and wall shear stress (WSS).
Results: There was a significant difference between the two groups regarding aneurysm lumen volume (P=0.0051) and mean WSS variation (P=0.0240). Conversely, mean maximal diameters were identical (P=0.71). We found a significant correlation between lumen volume (R=0.47, P=0.0015), reduction of the mean WSS variation value (R=-0.42, P=0.0062) and total aneurysm volume evolution. We further used these parameters to compute a model to predict the progression of AAAs, displaying better area under ROC than the only measurement of maximal diameter (0.75 vs 0.52, P=0.0037). Depending on the threshold, our model yields either excellent sensitivity (95.00% [IC95% 75.1, 99.9]) or specificity (90.00% [IC95% 73.5, 97.9]).
Conclusion: Combined analysis of lumen volume and WSS provides better information than maximal diameter to assess rapid volumetric evolution risk.

B-1254 14:32

Aortic arch plaque characterisation by computed tomography angiography in acute ischaemic stroke: fast technique for high quality vessel analysis

C. Parra-Fariñas, J. Juega, M. Ribó Jacobí, A. Tomasello Weitz, P. Coscojuela Santaliestra, C. Vert Soler, E. Almazán Mesa, J. Pagola, Á. Rovira; *Barcelona/ES (carmenparrafarinas@gmail.com)*

Purpose: Aortic arch atheroma was suggested as critical ischaemic stroke determinant. Properly detection is of the utmost clinical importance. Computed tomography angiography (CTA) provides rapid plaque characterisation and high diagnostic accuracy. This study aimed to investigate CTA features to characterise aortic arch plaque in acute ischaemic stroke patients.
Methods and Materials: From March 2010 to August 2016, a prospective study of 199 consecutive patients who underwent CTA within 8 hours from symptoms onset was performed. Maximal plaque thickness was measured in ascending aortic arch, perpendicular to aortic wall, proximal and distal sections. Complex aortic plaques (CP) were defined as plaque ≥4 mm in thickness or those with irregular ulcerations. Ulcerated plaques (UP) were defined as having craters ≥2 mm in depth and width. Plaque instability gradation was assessed by its composition.
Results: Mean age was 69.0±13.5, 54.8% male. Proximal aortic arch was affected in 81.6% patients (mean plaque thickness: 1.5±1.8 mm) and distal in 89.7% (2.7±2.1 mm) (p=0.730). CP were detected in 34.2%: 2.5% proximal arch, 20.6% distal, 11.1% both proximal and distal. UP were detected in 8.5%: 0.5% proximal, 5.5% distal, 2.5% both. Proximal arch plaque composition was 57.9% fibrolipid, 3.7% calcic, 59.3% mixed. Distal arch plaque composition was 17.9% fibrolipid, 22,2% calcic, 60.3% mixed. Brachiocephalic artery was involved in 14.6%, left common carotid artery in 16.7%, left subclavian artery in 28.6%.
Conclusion: CTA allowed quick and accurate evaluation of aortic arch atheroma, being useful for measuring plaque thickness, discovering ulceration, and examining its components in acute ischaemic stroke.

B-1255 14:40

Automated tube voltage selection with adapted contrast media injection protocols in CT angiography of the thoraco-abdominal aorta

N. Eijsvoogel, B.M.F. Hendriks, M. Kok, C. Mihl, B. Horehledova, G.H. Schurink, B.M.E. Mees, J.E. Wildberger, M. Das; *Maastricht/NL (nienke.eijsvoogel@mumc.nl)*

Purpose: To optimise radiation dose and contrast media (CM) application for patients undergoing CTA of the aorta using automated tube voltage selection (ATVS).
Methods and Materials: 54 consecutive patients referred for thoraco-abdominal aortic CTA were included. kVp settings between 70-90 kVp were chosen automatically (CAREkV; Siemens Healthcare). Scans were acquired on a 3rd-generation DSCT (Somatom Definition Force, Siemens) with 2*192*0.6 mm collimation, pitch 0.6, gantry rotation time 0.5 s, quality reference tube current 150 mAs_{ref}, and image reconstruction at 1 mm slice thickness and increment 0.8mm (kernel Bv36/iterative reconstruction strength 3). CM (300 mgI/ml) injection was adapted to kVp setting (volume/flow rate): 40 ml/3.0 ml/s (70 kVp); 44 ml/3.3 ml/s (80 kVp); and 49 ml/3.7 ml/s (90 kVp), respectively. Patient characteristics (BMI) were collected. Objective and subjective image quality (SIQ) were determined by attenuation values (HU), contrast-to-noise ratio (CNR), signal-to-noise ratio (SNR) and 4-point Likert scale (1=non-diagnostic/2=sufficient IQ/3=good IQ/4=excellent IQ).
Results: Patient distribution was 39(70 kVp), 3(80 kVp) and 12(90 kVp). Overall attenuation was 362±71 HU, 312±46 HU and 311±48 HU for 70/80/90

kVp. Aortic attenuation was diagnostic (>200 HU), except for the lower aortic levels in eight cases (15%) in the 70 kVp/90 kVp group due to high BMI, contrast-pooling in large aneurysms and aortic stenosis. SIQ was diagnostic in all scans (59% excellent IQ). Mean CNR/SNR was 14±6/11±4 (70 kVp), 16±5/11±5 (80 kVp) and 18±8/14±4 (90 kVp). Overall effective radiation dose for different groups (70-90 kVp) was 1.8±0.3 mSv, 2.8±0.2 mSv and 3.7±0.5 mSv, respectively.
Conclusion: Optimising CTA protocols using ATVS shifts image acquisition to low kVp settings with significantly lower radiation and CM dose while maintaining diagnostic IQ.
Author Disclosures:
N. Eijsvoogel: Research/Grant Support; Bayer. **B.M.F. Hendriks:** Research/Grant Support; Bayer. **C. Mihl:** Speaker; Bayer. **B. Horehledova:** Research/Grant Support; Siemens. **J.E. Wildberger:** Research/Grant Support; Bayer, Siemens, Philips, AGFA. Speaker; Siemens, Bayer. **M. Das:** Research/Grant Support; Bayer, Siemens, Philips, Cook.

B-1256 14:48

Increased aortic wall shear stress and wall shear stress gradient in patients with an anatomically shaped sinus prosthesis using 4D flow-MRI
V. Schultz[1], T. Oechtering[1], M. Sieren[1], M. Scharfschwerdt[1], A. Hennemuth[2], M. Hüllebrand[2], H.-H. Sievers[1], J. Barkhausen[1], A. Frydrychowicz[1]; [1]*Lübeck/DE*, [2]*Bremen/DE (victoria.schultz@web.de)*

Purpose: Despite near physiological haemodynamics in the aortic bulb, patients with an anatomically shaped sinus prosthesis for valve-sparing aortic root replacement have altered flow characteristics distal to the prosthesis. Vessel wall parameters derived from blood flow such as the wall shear stress (WSS) may thus be altered. Hence, it was the aim of this study to analyse WSS using 4D flow-MRI.
Methods and Materials: 12 patients (1f, 55±15y) with sinus prosthesis and 12 age-matched volunteers (10f, 55±6 y) were examined on a 3T MR-scanner using a 4D flow-sequence. WSS was determined using GTFlow (GyroTools, CH) in 8 analysis planes with 8 segments, placed orthogonal to the aorta. The maximum WSS averaged over all segments per plane ($maxWSS_{avg}$), segmental temporal WSS minimum and maximum ($minWSS_{Seg}$,$maxWSS_{Seg}$) and the WSS gradient per plane ($gradWSS_{Seg}$=$maxWSS_{Seg}$-$minWSS_{Seg}$) were calculated.
Results: In patients, $maxWSS_{avg}$ showed a trend to be similar or lower close to the prosthesis and increased distal to the prosthesis with a maximum in the distal ascending aorta, differences not reaching statistical significance. Segmental $maxWSS_{Seg}$ was increased distal to the prosthesis with a maximum in the arch (1.22±0.45 vs 0.90±0.16N/m^2, p<0.05). Interestingly, the WSS gradient per segment ($gradWSS_{Seg}$) was increased throughout all planes, the maximum of 1.03.±0.43 vs 0.72±0.26N/m^2 (p<0.05) in the ascending aorta.
Conclusion: This study confirmed WSS alterations in patients after sinus prosthesis in comparison to age-matched healthy individuals. Of special interest was the WSS gradient with increased results throughout the entire aorta. Now larger patient cohorts are warranted to correlate findings with clinical outcome.

B-1258 14:56

70kV automated tube potential selection at third-generation high-pitch dual-source CTA of the whole aorta: comparison to a standard protocol
A.M. Bucher, A. Zierden, J.E. Scholtz, M.H. Albrecht, B. Kaltenbach, M. Kaup, B. Bodelle, T.J. Vogl, M. Beeres; *Frankfurt a. Main/DE*

Purpose: To compare the feasibility of low-voltage automated tube potential selection (ATPS) in an unselected patient population at high-pitch dual-source CT angiography (DS CTA) of the full aorta in third-generation dual-source CT against a standard DS CTA protocol.
Methods and Materials: Two groups of 65 consecutive patients each underwent clinically indicated DS CTA in high-pitch mode using ATPS on a second-generation (group 1) or third-generation (group 2) dual-source CT. Subjective image quality was scored by two independent readers, qualitative image quality parameters by an independent investigator. A reference of 70kV was set in group 2, a reference of 100kV in group 1, with the remaining image quality settings and contrast administration kept constant. Radiation exposure was compared according to CT-dose index and dose-length product.
Results: All images were of diagnostic quality. Patient characteristics were comparable (p>0.06 each). At constant overall image quality (p>0.08 overall) group 2 received substantially lower radiation doses compared to group 1 (p<0.001). Mean radiation dose in third-generation DS CTA was 3.1±1.8 mSv (group 2); in second-generation DS CTA 6.9±2.1 mSv (group 1). Overall dose reduction equalled 55%. Inter-reader agreement was very good (k=0.8, p=0.002). In group 1, ATPS indicated a level of 120kV for most cases; in group 2, 90kV was indicated in most cases.
Conclusion: Third generation high-pitch dual-source CTA using latest generation ATPS at low tube voltage selection is feasible in the clinical routine against a standard protocol and is associated with significantly lower radiation exposure.

B-1260 15:04

Diagnostic accuracy of free-breathing contrast-enhanced T1 sequences in comparison with breath-hold sequences, in the assessment of the aorta, having CT angiography as reference
C.R.G.L. Talei Franzesi, D. Ippolito, S. Drago, S. Lombardi, E.B. Orsini, S. Sironi; *Monza/IT (ctfdoc@hotmail.com)*

Purpose: To evaluate the diagnostic efficacy of contrast-enhanced T1 free-breathing gradient echo sequences in the evaluation of aortic disease, in comparison with standard MR-angiographic sequences and CT-angiography.
Methods and Materials: Forty-one patients, with known aortic disease established at CT-angiography evaluation, were prospectively enrolled. All patients were evaluated on a 1.5T magnet(Achieva,Philips),with a phased array multi-coil, after the intravenous injection of 0.1mL*Kg of gadobutrol, using standard MR angiography protocol with 3D-angiographic sequences and T1 breath-hold sequences (THRIVE). Multiplanar T1 free-breathing gradient-echo fat-suppressed (THRIVE-FB) sequences were additionally performed in all the examinations. Two radiologists independently compared the diagnostic quality of different MR-angiographic sequences with CT-angiography studies, in terms of visualization of aortic wall and lumen and main arterial branches. Vascular calipers measured at different aortic levels were compared between the MR-sequences and CT evaluations and statistically analyzed. Interobserver agreement was assessed using the Intraclass Correlation Coefficient(ICC).
Results: Free breathing sequences showed good diagnostic accuracy in the assessment of vascular calipers and walls, with no significant differences in comparison with standard breath-hold sequences and CT-studies.THRIVE-FB also demonstrated high sensitivity and specificity in the evaluation of vascular plaques, thrombus and adjacent structures.Not significant differences were obtained in terms of overall diagnostic quality between THRIVE-FB sequences, standard angiographic sequences and CT-angiography, with a good interobserver agreement (ICC of 0.84).
Conclusion: Free-breathing contrast-enhanced T1 gradient-echo fat-suppressed sequences, combined with high relaxivity contrast agent, demonstrated high diagnostic efficacy, permitting to correctly evaluate the aorta and its major branches, with no significant differences in comparison with standard breath-hold MR-sequences and CT-evaluations.

B-1261 15:12

The benefits of the evaluation of endoleaks with CT angiography using multiphase technique and high temporal resolution with iterative reconstruction
P. Armelin; *Campinas/BR (plinioarmelin@hotmail.com)*

Purpose: Assess the initial experiment, the viability and diagnostic performance of CT angiography with high temporal resolution protocol with 8 phases of low dose and iterative reconstruction (idose 4) after aortic aneurysm by endovascular technique compared to traditional phase angiotomographic study.
Methods and Materials: A retrospective study of 10 patients with aortic aneurysms treated with stent. The tests were performed in a CT scanner Phillips Brilliance 64-channel using injection pump Medtron AG, endovenous nonionic iodised contrast (60 ml), injected the speed of 5.0ml/s, followed by saline bolus of 100 ml; protocol 80 kV and 120 mA, 1,078 pitch composed of 8 layers of 3 seconds each with 27 cm scan range, after reconstruction processing using interactive idose 4.
Results: It conducted a comparative study evaluating the presence or absence of endoleaks and their classification, as well as compared to the total dose mSv of this protocol with the conventional three-phase study before used in our service. Following the principles ALARA total radiation dose is reduced by about 50% compared to conventional examination, despite the increase in noise level no loss in diagnostic quality of images. Furthermore, the contrast volume used is lower.
Conclusion: Angiotomography with high temporal resolution multiphase technique with iterative reconstruction proved to be more conspicuous in the detection and classification of endoleaks than conventional three-phase study.

14:00 - 15:30 **Room Z**

Interventional Radiology

SS 1909

Musculoskeletal interventions

Moderators:
X. Buy; Bordeaux/FR
G. Velonakis; Athens/GR

B-1262 14:00

Percutaneous discectomy in lumbar radiculalgia: an international multi-centric study about 77 patients (6 months follow-up)

G. Gallo[1], O. Andreani[2], F. Torre[2], N. Amoretti[2]; [1]*Menton/FR*, [2]*Nice/FR (giacomo.gallo83@gmail.com)*

Purpose: To show a new technique for the percutaneous treatment under CT guidance and local anaesthesia of lumbar radiculalgia due to an herniated disc in patients resistant to conservative treatment.
Methods and Materials: An international multi-centric study (four European centers) has been performed. Inclusion criteria were: lumbar radiculalgia with CT/MRI evidence of the hernia; pain lasting from more than one month; VAS (0-10) over 6. Both postero-lateral and trans-laminar accesses have been performed. VAS have been collected at 1 and 6 months of follow-up. Interventions have been performed under CT and fluoroscopic guidance with a percutaneous mechanised device that, once in the hernia, can turn around to soften and then aspirate the herniated material.
Results: The average VAS pre-intervention was 8 (6-10), one month after it decreased to 3 (0-8) (p <0.001). No significant differences were found between the different centres. Only three patients left the follow-up for surgery within the first month after the intervention. At 6-month follow-up, 91% of patients present a modification of the VAS not greater than 1 point.
Conclusion: The results show the high rate of effectiveness of this percutaneous therapy, which is performed under local anaesthesia, and that presents minimal risk compared to the surgical discectomy (such as failed back surgery syndrome or intracanalar fibrosis). It permits a faster return to normal life (usually within one week) with evident advantage in terms of quality of life. Furthermore, the failure of this intervention does not threaten the possibility of a surgical solution.

B-1263 14:08

CT-guided pulsed radio frequency treatment of the lumbar dorsal root ganglion (DRG) in patients with acute and sub-acute radicular low back pain

A. Napoli, R. Scipione, M. Anzidei, C. Marrocchio, H.-P. Erasmus, C. Catalano; *Rome/IT (alessandro.napoli@uniroma1.it)*

Purpose: To determine the clinical impact of pulsed radiofrequency for the treatment of patients with neuro-radicular low back pain.
Methods and Materials: Patients were eligible for this study if they presented acute or sub-acute neuro-radicular low back pain (EMG confirmed) refractory to usual treatments and if they could safely undergo pulsed radiofrequency procedure. Clinical evaluation was conducted with visual analogue scale (VAS) and Oswestry disability index (ODI) for quality of life assessment, both obtained at baseline and at 1-week, 1-month and 1-year follow-up.
Results: Over a 3-year period, 80 patients were treated with pulsed radiofrequency (Cosman). Median VAS scores decreased from 7.8 at baseline to 3.5 at 1 week after treatment, to 2.6 at 1 month and 1.3 at 1 year; median ODI scores decreased from 78.0 at baseline to 12.5 at 1 week, to 6.0 at 1 month and 5.5 at 1 year (p<0.001). Overall, 90.0% of patients reached a 0 VAS score within the first month after treatment, and 97.5% had a decrease of at least 20 points in ODI score in the same interval. There were 6 patients considered partial responders that required a second PRF session.
Conclusion: Pulsed radiofrequency has shown to be a promising and effective percutaneous treatment option for patients with acute or sub-acute neuro-radicular low back pain; the results of this study are superior to those reported from the literature for usual care strategies or injections and may avoid surgery for a substantial number of patients with sciatic disc compression.

B-1264 14:16

Vertebral augmentation with the Spine Jack device in non-acute (> 1 month) vertebral compression fracture

J. Chiras, E. Cormier, F. Clarençon; *Paris/FR (jacques.chiras@psl.aphp.fr)*

Purpose: The efficacy of Spinejack® device (Vexim SA) to reduce fresh vertebral fractures (≤1 month) is well established. Older painful fractures are usually treated by vertebroplasty. However, this technique may fail to reduce the kyphosis or may be potentially dangerous in Magerl's A3 fractures as it can be responsible of increased protrusion of bone fragment into the spinal canal. Vertebral augmentation with SpineJack®could be an alternative. The objective of the study is to evaluate the feasibility and efficacy of a vertebral augmentation with the SpineJack in vertebral compression Magerl's A3 fractures older than one month with major kyphosis.
Methods and Materials: Retrospective , monocentre, investigator initiated study. 19 patients (16 F, 3 M) with A3 vertebral fracture with important kyphosis (11 cases) (kyphosis angle: 20-37^0) and/or intra spinal bone fragments (17 cases) were treated with the Spinejack® expansion device between one month and one year after the fracture. The vertebral augmentation was performed under general anesthesia during a 2 days' hospital stay.
Results: Immediate kyphosis reduction >25% after procedure : 21/31.Bone fragment bulging : None.Clinical complications: None.Pain reduction: VAS pre op: 6.85 (3-9); VAS post op: 2.1 (0-7) MID TERM RESULTS: New fractures: 3/31 patients. 2 patients presented an adjacent fracture at 1 month post op; 1 patient presented a distant fracture at 6 months.
Conclusion: Vertebral augmentation with SpineJack® device is feasible in vertebral compression fractures older than 1 month. Significant kyphosis reduction is obtained in about 67% of the cases.

B-1265 14:24

Percutaneous screw fixation for complex pelvic fractures: a key role for the interventional radiologist

O. Andreani[1], A. Rudel[1], G. Gallo[2], F. Torre[1], N. Amoretti[1]; [1]*Nice/FR*, [2]*Menton/FR (andreani.olivier@gmail.com)*

Purpose: Therapeutic management of complex pelvic fractures is challenging. Although orthopaedic surgeons play a major role, interventional radiologists' role is crucial to treat some pelvic fractures. The goal of our study is to show the technical feasibility of acetabular roof and sacro-iliac lesion percutaneous screw fixation under CT-guidance.
Methods and Materials: We present a consecutive series of 20 patients treated for acetabular roof and/or sacro-iliac post-traumatic lesions. Therapeutic procedure were all made under general anaesthesia. Procedures were minimally invasive thanks to a percutaneous approach, under CT-guidance and fluoroscopy. Post-interventional CT-scan assessed the technical success or failure of the procedure.
Results: Procedures have been conducted in our 20 patients. Screw positioning was good in 19 cases. Approach was bilateral in 8 patients. The mean procedure time was less than 60 minutes. No major complications occurred during and after procedures.
Conclusion: Percutaneous screw fixation is a safe and effective procedure to manage acetabular roof and sacro-iliac fractures. CT-guidance allows a short learning curve.

B-1266 14:32

Hamstring tendinopathy: pre-procedural MRI correlation with clinical outcome in therapeutic image-guided injection

D.J. Bowden, C.A. Byrne, A. Alkhayat, E. Kavanagh, S.J. Eustace; *Dublin/IE (dermotbowden@gmail.com)*

Purpose: To assess the correlation between severity of hamstring tendinopathy on MRI with clinical outcome post-percutaneous hamstring injection of corticosteroid.
Methods and Materials: Patients undergoing image-guided hamstring injection were identified by chart review. Patients with pre-procedural MRI were selected for inclusion and imaging reviewed by two musculoskeletal radiologists. Severity of tendinopathy was graded: mild, moderate or severe. Discrepancies were resolved by consensus. At follow-up, outcome was assessed and the following data were recorded: resolution of pain: none, partial or complete; duration of resolution; timing of recurrences.
Results: 26 patients underwent injection with pre-procedural MRI during the study period. 23 were available for follow-up, 13 males, 10 females mean age 44.6 yrs (range 16-88). 12 mild, 9 moderate, 2 severe. 78% experienced improvement following injection, 26% partial, 52% complete. 7 experienced recurrence (39%) at mean of 6.1 months post-treatment. Mild group: equal proportions (33.33% - 4 patients each) reported no improvement, partial improvement and complete resolution. Recurrence rate 37.5% (3 of 8). Moderate group: 89% experienced benefit from treatment - complete resolution in 67%, partial in 22%. Recurrence rate was 25% (2 of 8) at mean of 2 months. Severe group: 2 patients had 100% resolution, but both patients experienced recurrence at mean of 10 months.
Conclusion: Image-guided hamstring injection is effective in the majority of patients; however, patients with moderately severe disease on pre-procedural MRI may be most likely to benefit from this treatment.

B-1267 14:40

Non-invasive MR-guided focused ultrasound (MRgFUS) therapy is associated with bone integrity restoration in patients with osteoid osteoma

R. Scipione, A. Napoli, M. Anzidei, C. Marrocchio, H.-P. Erasmus, C. Catalano; *Rome/IT (roberto.scipione@uniroma1.it)*

Purpose: To analyse MRgFUS outcomes for osteoid osteoma (OO) treatment, and the relationship of residual nidus vascularity with bone remodelling.
Methods and Materials: Patients with clinical and radiological diagnostic findings of OO, suitable for MRgFUS and anaesthesia, were recruited. The study was designed with an intention-to-treat protocol and bone behaviour was analysed before and after MRgFUS; patients underwent CT and dynamic contrast-enhanced (Gd-BOPTA, Bracco) MRI scans yearly, over a 3-year period. Nidus perfusion was measured using a semi-quantitative method; bone remodelling was determined with CT scans for complete or partial restoration. Multivariate analysis was conducted to understand the relationship between imaging and clinical outcomes (visual analogue scale, VAS) BMI, sex and age.
Results: Among 35 subjects recruited, 30 underwent MRgFUS; 28 had a complete clinical benefit with VAS=0 during follow-up; 2 patients required re-treatment with RFA at 1 month because of residual pain. At 36 months, absence of residual nidus perfusion was found in 76.7% of cases, with restitutio ad integrum in 30% of cases. Multivariate analysis demonstrated that restoration is associated with absence of perfusion and patient age: subjects younger than 18 years presented complete restoration, a 0% residual perfusion and a complete clinical response, while older patients more frequently showed variable results on restoration, irrespective of clinical outcome. These results are independent of BMI and sex.
Conclusion: MRgFUS is an effective treatment option for OO; results are dependent on subject age, and patient selection may be influenced by this factor in the future when seeking complete bone restoration.

B-1268 14:48

Middle- and long-time follow-up of percutaneous computed tomography and fluoroscopy-guided injection of bone cement in treatment of subchondral cysts

F. Torre[1], O. Andreani[1], A. Caudal[1], G. Gallo[2], A. Rudel[1], D. Palominos[1], B. Padovani[1], N. Amoretti[1], E. Benattar[2]; [1]*Nice/FR*, [2]*Menton/FR (fede.torre@libero.it)*

Purpose: To evaluate long-time follow-up of subchondral cysts treatment through percutaneous computed tomography and fluoroscopy-guided injection of bone cement.
Methods and Materials: A single-centre prospective study involving 23 patients (14 women, 9 men) with symptomatic subchondral cysts was developed. Average age was 61 years. Patients underwent percutaneous CT-guided injection of bone cement into the subchondral cysts. Surgical treatment was not indicated or refused by patients. All the lesions were localised in weight-bearing bones. A quantification of pain was evaluated using the visual analogue scale (VAS) before treatment, at one, six months and up to 8 years after treatment.
Results: Within 23 patients, 22 were satisfied after the procedure had been performed. The feasibility was 91%. We reported one case with para-articular asymptomatic cement leak at the knee and an unsatisfactory filling of the lesion. There were no other immediate or delayed complications observed. One patient had no relief of his pain after the treatment and underwent hip surgery. Our results show a significant decrease of the pain felt by patients between before procedure and one month after the procedure ($p<0.001$), six months after the procedure ($p<0.001$) and years after the procedure ($p<0.001$).
Conclusion: Percutaneous injection of bone cement under CT and fluoroscopy guidance seems to be a rapid, safe and efficient therapeutic option for symptomatic subchondral cysts. We suggest that significant decrease of patient's pain deal to consider this procedure as an alternative to classic surgery, when invasive interventions are contraindicated or refused by patients.

B-1269 14:56

Percutaneous image-guided screw fixation of bone lesions in cancer patients: double-centre analysis of outcomes including local evolution of the treated focus

R. Cazzato[1], X. Buy[2], J. Garnon[1], G. Koch[1], J. Caudrelier[1], G. Tsoumakidou[1], J. Palussiere[2], A. Gangi[1]; [1]*Strasbourg/FR*, [2]*Bordeaux/FR (gigicazzato@hotmail.it)*

Purpose: To review outcomes and local evolution of treated lesions following percutaneous image-guided screw fixation (PIGSF) of pathological/insufficiency fractures (PF/ InF) and impeding fractures (ImF) in cancer patients at two tertiary centres
Methods and Materials: 32 consecutive patients (mean age 67.5 years) with a range of tumours and prognoses underwent PIGSF for non/minimally displaced PF/InF and ImF. Screws were placed under CT/fluoroscopy or cone-beam CT guidance, with or without cementoplasty. Clinical outcomes were assessed using a simple 4-point scale (1 = worse; 2 = stable; 3 = improved; 4 = significantly improved). Local evolution was reviewed on most recent follow-up imaging. Technical success, complications, and overall survival were evaluated.
Results: 36 lesions were treated with 74 screws mainly in the pelvis/femoral neck (58.2 %); including 47.2 % PF, 13.9 % InF, and 38.9 % ImF. Cementoplasty was performed in 63.9 % cases. Technical success was 91.6 %. 87.1 % of lesions were improved at 1-month follow-up. Three major complications (early screw-impingement radiculopathy; accelerated coxarthrosis; late coxofemoral septic arthritis) and one minor complication were observed. Unfavourable local evolution at imaging occurred in 3/24 lesions (12.5 %) at mean 8.7-month follow-up, including poor consolidation (one case) and screw loosening (two cases, at least 1 symptomatic). There were no cases of secondary fractures.
Conclusion: PIGSF is feasible for a wide range of oncologic patients, offering good short-term efficacy, acceptable complication rates, and rapid recovery. Unfavorable local evolution at imaging may be relatively frequent, and requires close clinico-radiological surveillance.

B-1270 15:04

Trans-isthmic screw fixation with CT and fluoroscopy guidance: precision of the procedure

E. Cervantes, O. Andréani, N. Amoretti; *Nice/FR (elodie.cervantes@live.fr)*

Purpose: To evaluate the precision of the trans-isthmic screw fixation with CT and fluoroscopy guidance in the care of low-grade isthmic spondylolisthesis.
Methods and Materials: Fifty patients (28 women and 22 men mean age 50 years old [min 17-Max 80, SD 18.9]) presenting a low-grade isthmic spondylolisthesis, resistant to medical regimen, treated by percutaneous screw fixation. The procedure was performed under local anaesthetic with both CT and fluoroscopy guidance. The positioning of the screws was considered optimal on the control scanner, once all the surgical criteria were applied accordingly.
Results: Ninety-nine procedures were carried out in 50 patients. CT control by the end of the intervention confirms that 96 screws out of 99, or in 96.9% of the cases were correctly positioned. 99 screws had an optimal entry point, the trajectory and completion of 96 screws were optimal. The tree displacement failures (3%) were caused a suboptimal trajectory, not penetrating the isthmic defect through its centre thus breaking the medial cortex of the blade and having an intraosseous completion, but located in the lower third of the pedicle. No complication during or following the operation has been reported in case of good positioning.
Conclusion: These results confirm that the trans-isthmic screw fixation with CT and fluoroscopy guidance procedure performed under local anaesthesia is both precise and safe.

B-1271 15:12

MRI-guided high-intensity focused ultrasound: a new first-line technique in the treatment of osteoid osteoma?

A. Napoli[1], A. Bazzocchi[2], R. Scipione[1], M. Anzidei[1], S. Dababou[1], C. Catalano[1]; [1]*Rome/IT*, [2]*Bologna/IT (alessandro.napoli@uniroma1.it)*

Purpose: To demonstrate that non-invasive ablation of osteoid osteoma (OO) with MRI-guided focused ultrasound (MRgFUS) is a safe, effective and durable treatment option.
Methods and Materials: Patients with typical clinical and radiological diagnostic findings of OO, suitable for MRgFUS and anaesthesia, were enrolled in a dual-centre study. Safety (rate of complications) and clinical effectiveness (visual analogue scale [VAS] score reduction) were considered as primary outcomes, tumour control (nidus ablation) at imaging as secondary outcome. All patients underwent a 3-year follow-up.
Results: Among 50 subject screened, 45 were enrolled and underwent MRgFUS. No treatment-related complications were observed. A complete and durable response was achieved in 80% of cases. Median VAS score dropped from 8 (IQR: 7-9) to 0 at 1 week and all subsequent follow-ups (1 month, 6 month, 12 month, 24 month and 36 month). Scores evaluating interference of pain with sleep, physical and daily activities showed a similar trend. Among subjects with partial response (20%), 4 received a second treatment (3 with CT-guided radiofrequency ablation, 1 with MRgFUS), and 5 did not need any other treatment. All re-treated patients achieved a 0 VAS score. Overall, 87% of patients after MRgFUS treatment reached and maintained a stable 0 VAS score during follow-up. At 3-year MRI OO showed no vascularisation in 76% of patients.
Conclusion: MRgFUS is safe and effective in the treatment of OO. This technique provides relevant advantages in the treatment of such a small, benign, impairing disease affecting mostly young population: no ionising radiation, incisions, needles nor complications. MRgFUS is candidate as first-line treatment.

B-1272 15:20

US-guided injection of triamcinolone in Morton neuroma (MN) is safe and can avoid the need of surgical treatment: retrospective review of 307 procedures

A. Viteri Jusué[1], C. Morandeira Arrizabalaga[2], A. Bilbao González[2], R. Zabala Landa[2], I. Korta Gomez[2], J. Del Cura Rodríguez[2]; [1]*Vitoria-Gasteiz/ES*, [2]*Bilbao/ES (ainhoa.viterijusue@osakidetza.net)*

Purpose: To evaluate the feasibility, safety and effectiveness of ultrasound-guided intralesional triamcinolone injections for MN.
Methods and Materials: Retrospective review of all patients with MN treated at our department between Jan 2010 and Dec 2014. Institutional Review Board approval was obtained. Procedure: US-guided intralesional injection of 40 mg of triamcinolone acetate. Patients´ characteristics, treatment administration, complications, and therapeutic failure (measured as need of surgical rescue) were assessed. Statistical analysis: Chi-square and Fisher's exact test. Time to surgery: Kaplan-Meier. SAS System for Windows, version 9.2.
Results: We treated 143 patients (18.2% M /81.8% F, mean age 58.9y, SD 10.1) totaling 307 procedures in 174 neuromas. 86 pts (60.1%) underwent >1 procedures, and 17 pts (11.9%) underwent >3 administrations. Mild and reversible complications were seen after 10 procedures (3.2%): pain/haematoma/skin problems/other: 3/2/2/3. Complications only presented in patients with musculoskeletal comorbidity (p= 0.022). No statistically significant differences according to total dose of steroids or number of administrations were seen. Surgery-free survival at 5 years was 85.3%, with a trend towards higher surgical needs for female patients (17.1% vs 3.9%, p=0.084) and patients ≤ 60 years (17.5% vs 11.1%, p=0.28). No statistically significant differences were found for comorbidity, number of procedures or total steroid dose.
Conclusion: Ultrasound-guided intralesional injection of steroids in unselected patients with MN is safe and effective, and can be repeated to delay and/or avoid the need of surgical treatment. Thus, this remains the initial treatment in patients with MN in our institution.

14:00 - 15:30 **Room O**

Chest

SS 1904

Chest imaging and intervention

Moderators:
P. Dalal; London/UK
E.J. Stern; *Seattle, WA/US*

K-28 14:00

Keynote lecture

R. Schernthaner; *Vienna/AT*

B-1273 14:09

Diffusion-weighted imaging planning percutaneous lung biopsies

C.E. Zurstrassen, M. Guimaraes, A. Bitencourt, P. Barbosa, M.F. Arruda, C. Tyng, J. Italo, M. Amoedo, R. Chojniak; *Sao Paulo/BR (charles.zurstrassen@accamargo.org.br)*

Purpose: We prospectively evaluated the role of diffusion-weighted imaging (DW-MRI) in planning biopsies of suspicious lesions of lung cancer through the calculation of the mean values of apparent diffusion coefficient (ADC).
Methods and Materials: After the calculation of the mean values of ADC, were collected samples from both the area with the highest mean value of ADC, that we called hot area, as well as from the smallest mean value of ADC, that we called cold area. The results of biopsies from both areas were recorded and then compared with regard to histopathology and differentiation degree.
Results: Twelve patients were included, 6 men and 6 women, mean age 59.4 years (37-75 years). The mean lesion size was 75.4mm, varying from 33 to 110mm. The mean ADC value in the hot area was 1,129 x10-3mm^2/s (0.381 to 2.821 x10-3mm^2/s) and in the cold area was 1,706 x10-3mm^2/s (0.733 - 3,437x10-3mm^2/s), which was statistically significant (p and lt 0.001). There were correlation between histological diagnosis obtained in the two areas in most of the cases (n=9; 75.0%). However, in two cases (16.7%) the results were different, being insufficient for diagnosis in the cold area, and in 1 case (8.3%) the histological diagnosis from both areas were different.
Conclusion: The study by DW-MRI may be useful in the evaluation of suspected lung cancer lesions prior to the percutaneous biopsy. Misdiagnosis may occur in 25% of cases.

B-1274 14:17

Metabolic guidance in CT-guided lung biopsies: Does ^{18}F-FDG PET/CT increase the rate of successful biopsies and diagnostic yield?

A. Goldman[1], T. Jacob[1], M. Miligkos[2], T. Senbanjo[1], A. Witwit[1], S. Paramothayan[1], J. Vlahos[1], K. Stefanidis[1]; [1]*London/UK*, [2]*Larissa/GR (anouchka.goldman@gmail.com)*

Purpose: To evaluate the role of Fluorine-18 fluorodeoxyglucose (^{18}F-FDG) PET/CT as a metabolic guide in increasing the accuracy and diagnostic yield of CT-guided lung biopsy.
Methods and Materials: Retrospective analysis of consecutive patients with suspicious lung nodules, masses or extensive disease that underwent lung biopsy over a 2-year period. Patients were divided into two groups; those that had ^{18}F-FDG PET/CT metabolic information guiding needle position for biopsy and those who did not. Correlation was made with the histopathological result. Biopsy results were considered diagnostic if malignant cells were detected or malignancy could be excluded.
Results: A total of 219 patients were evaluated in our study. Of those, 15 patients were excluded. ^{18}F-FDG PET/CT findings were available for 82 cases prior to biopsy. 122 cases had CT-guided lung biopsies without metabolic information available. The overall rate of a diagnostic biopsy was 89% (n=204). The proportion of patients with a diagnostic biopsy result following an ^{18}F-FDG PET/CT was significantly higher than those who did not undergo an ^{18}F-FDG PET/CT scan (97.6% vs. 83.6%, p = 0.003). In patients with extensive disease (n=28), although 9/10 cases with ^{18}F-FDG PET/CT prior to biopsy yielded a diagnostic sample compared to 11/18 that did not have ^{18}F-FDG PET/CT, this did not reach statistical significance (90% vs 61%, p=0.24), likely due to the small number of patients.
Conclusion: Metabolic information provided by ^{18}F-FDG PET/CT can assist in guiding CT-guided lung biopsies, improve diagnostic accuracy and increase the probability of achieving a definite diagnosis.

B-1275 14:25

Lung lesion motion in the z-axis during CT-guided lung biopsy is greater in the lower lung and after intravenous sedation

G.N. Allen, C.D. Gillespie, L. Daly, C.G. Cronin, J.G. Murray, C.A. Ridge; *Dublin/IE (grainne.allen@ucdconnect.ie)*

Purpose: Operators hypothesize that lung lesion motion is least in the prone position, the lung apices and when sedation is not used. This study aims to test these hypotheses.
Methods and Materials: Institutional review board approval was obtained. Consecutive patients underwent CT-guided lung biopsy by experienced operators over a 3-year period. Lung lesions <4cm were included. Lung lesion motion in mm was determined by the table position of the lesion on axial images during CT-guided biopsy. z-axis motion was the difference between maximum and minimum table positions during the procedure. Lesion size, location, patient position, radiation and sedation use were recorded. A paired t-test and multivariate analysis were used to compare variables.
Results: 124 patients were included. Median z-axis lesion motion was 7 mm (0-43.5). Lower lung location and intravenous sedation increased z-axis motion ($p < 0.0001$ and $p = 0.0007$, respectively). Prone positioning did not decrease z-axis nodule motion. Median estimated radiation dose was 671 mGym/cm. z-axis motion was proportionate to total radiation dose ($r = 0.298$; $P = 0.001$)
Conclusion: Lung lesion motion in the z-axis is greatest in the lower lung and when intravenous sedation is administered. Prone positioning has no effect on nodule motion. Increased nodule motion is associated with increased radiation dose during CT-guided biopsy.

B-1276 14:33

CT-guided lung biopsy in the lateral decubitus position: effect on the incidence of pneumothorax and haemoptysis

O. Drumm, E. Joyce, T. Gleeson, E. McCarthy, J.F. Meaney, R. McDermott, P. Beddy; *Dublin/IE (odrumm@yahoo.co.uk)*

Purpose: To assess the effect of positioning the patient in the lateral decubitus position during CT-guided lung biopsy on the incidence of pneumothorax and haemoptysis.
Methods and Materials: This was a retrospective IRB approved study. Between March 2014 and January 2016, percutaneous CT-guided lung biopsy was performed in 277 patients. 145 biopsies were performed in the supine or prone position (group 1) and 132 were performed with the patient positioned in the lateral decubitus position with the tumour side down against the CT table (group 2). Standard biopsy was performed with an 18 or 20G co-axial technique. Patient demographics, lesion characteristics, biopsy technique and complications were assessed.
Results: There was no significant difference in the age, sex or incidence of emphysema between group 1 and 2. There was a significant difference ($p<0.01$) in the incidence of pneumothorax between groups 1 and 2, with 40 (27%) pneumothoraces in group 1 and 14 (10%) in group 2. Eight patients in

group 1 required a chest drain and five in group 2 (p=0.2). Eleven patients in group 1 had haemoptysis compared with seven in group 2 (p=0.2). Diagnostic samples were obtained in 95% of patients in group 1 and 98% in group 2.
Conclusion: CT-guided lung biopsy in the lateral decubitus position with tumour side down significantly reduces the rate of pneumothorax. The reduction in drain insertion and haemoptysis was not statistically significant.

B-1277 14:41

CT-guided percutaneous transthoracic core biopsy (PTCB) of deep thoracic lesions using pure virtual navigation guidance (PVNG) with magnetic-tracking system: preliminary experiences

G. Bizzarri, A. Bianchini, D. Valle, L. Di Vito, L. Velari, S. De Nuntis, A. Dell'Era; *Albano Laziale/IT (bizzarrigiancarlo@libero.it)*

Purpose: CT-guided PTCB is essential in the diagnosis of pulmonary and mediastinal tumour and cellular characterization. Usually it is performed under cognitive-CT-guidance. Reports continue to show major complications and death. Possible impact of PVNG for deep thoracic lesion not visible on US was explored.
Methods and Materials: MyLabTwice ultrasound scanner with Virtual Navigation (VN) software and hardware was used (ESAOTE,Italy). The procedure was performed with convex transducer CA541 (1-5 MHz) probe with single use guiding system and reusable tracking brackets for magnetic sensor (CIVCO, USA). Biopsy was performed using coaxial technique and 18G trucut needles. 15 patients with mediastinal or pulmonary lesions were enrolled. Preliminary CT scan was performed with reference tool fasten on patient skin. Images were coregistered with probe position and VN modality activated. After local anaesthesia coaxial needle was advanced using the probe-guiding system. CT scan was performed to rule out complications and, if the coaxial needle was in correct position, biopsy procedure was performed.
Results: 35 samples were obtained on 15 lesions (range 40-15mm.; mean 25) in 15 patients (age 45-85, mean 72). In all cases a single step procedure was possible without the necessity of needle repositioning. All biopsies were diagnostic (mets 3, lung carcinomas 12). No major complication were encountered. 4 pneumothorax and 3 parenchymal haemorrhages resolved spontaneously. Biopsies required 25-45min., mean 35.
Conclusion: PVNG is a promising technique for increasing the accuracy of needle positioning during thoracic biopsies potentially reducing major complications, time and radiations versus cognitive-CT-guidance. Technological improvements are mandatory.

B-1278 14:49

Risk factors for complications of CT-guided percutaneous transthoracic needle biopsy: utility of SIR classification of complications

A. Elshafee[1], A. Karch[1], K. Ringe[1], H.-o. Shin[1], H.-J. Raatschen[1], N. Soliman[2], F. Wacker[1], J. Vogel-Claussen[1]; [1]*Hannover/DE*, [2]*Mansoura/EG (elshafee.amany@mh-hannover.de)*

Purpose: To detect risk factors for complications of CT-guided transthoracic needle biopsy and to classify these complications using the Society of Interventional Radiology (SIR) classification.
Methods and Materials: 387 biopsies were evaluated. Studied risk factors were patient related (age, sex, position, chronic lung diseases), lesion related (size, location, lesion pleural distance and thoracic wall thickness at needle path), and procedure related risk factors (times of pleural puncture, number of tissue samples, fissures penetration, duration and images of the procedure, needle blood vessel angle, technical success, histopathology). Complications were classified into no or minor (SIR0-2) and major (SIR3-6). Data were analysed using logistic and ordinal regression.
Results: Complications were pneumothorax in 143 patients (37%) and pulmonary haemorrhage in 22 patients (6%). 341 patients (88%) were classified as SIR0-2, 46 patients (12%) were SIR3-4, no permanent injury (SIR5) or death (SIR6) occurred. Patient age, lesion size, lesion pleural distance, times of pleura punctures, fissure puncture, procedure duration and images were significant risk factors in univariable analysis. Lesion pleural distance remained the only significant factor in multiple logistic regression model (OR=1.7 per cm, p &lt 0.001). No statistical difference of complication rate between the radiologists performing the biopsies was observed.
Conclusion: Transthoracic CT-guided needle biopsy is a safe technique. Careful planning is necessary to traverse least amount of aerated lung.

B-1279 14:57

Patient selection prior to lung volume reduction: impact of FEV1 and emphysema score

F. Doellinger, R.-H. Huebner, D. Theilig; *Berlin/DE (felix.doellinger@charite.de)*

Purpose: Aim of this retrospective study was to evaluate the relevance of baseline forced expiratory volume in one second (FEV1) and baseline emphysema score to predict a clinical benefit after endoscopic lung volume reduction (ELVR) with endobronchial valves.
Methods and Materials: Sixty-two patients with severe chronic obstructive pulmonary disease (GOLD-stages III and IV) and pulmonary emphysema were treated with endobronchial valves in our institution. All patients underwent pulmonary function tests and computed tomography (CT) before and at least three months after the valve implantations. At both time points emphysema score was determined using quantitative CT analysis. Emphysema score was defined as the proportion of all lung voxels with a density below a threshold of -950 HU. Linear regression analysis including established influencing factors as well as baseline FEV1 and baseline emphysema score was performed to determine the impact of both parameters on a beneficial outcome, which was defined as an improvement of FEV1.
Results: In regression analysis, baseline FEV1 showed to have a statistically significant impact on clinical outcome after ELVR (coefficient of determination R^2 = .40). Baseline emphysema score did not show such statistical correlations.
Conclusion: In patients with severe COPD and pulmonary emphysema, a lower baseline FEV1 prior treatment seems to predict for a higher relative improvement of FEV1 after ELVR. Emphysema score prior to treatment did not show strong correlations with a beneficial clinical outcome.

B-1280 15:05

How to calculate an interlobar emphysema heterogeneity index in the context of lobar lung volume reduction therapy

D. Theilig[1], F. Doellinger[1], A. Poellinger[2], R.-H. Hubner[1]; [1]*Berlin/DE*, [2]*Berne/CH (dorothea.theilig@charite.de)*

Purpose: A standardised definition for interlobar emphysema heterogeneity in the context of endoscopic lung volume reduction (ELVR) is lacking. The aim of this study was to elucidate the most appropriate way to define a heterogeneity index (HI).
Methods and Materials: We retrospectively analysed 62 patients who had undergone ELVR with placement of one-way valves at our institution and were prospectively monitored using lung function tests and CT scans acquired in inspiration and expiration before and after ELVR. Quantitative analysis of the CT scans was performed and the HI of the targeted lobe was determined with six different methods, each from inspiratory and expiratory CT scans. The differently defined HIs were correlated with the increase in absolute forced expiratory volume in one second (FEV1) after ELVR and their predictive accuracy was assessed with receiver-operating characteristic (ROC) curve analysis assuming a minimum difference in FEV1 of 100ml to indicate a clinically important change. DeLong's test was used to test for significant differences between ROC curves.
Results: Most HIs showed a statistically significant, albeit weak, positive correlation with ELVR outcome assessed as FEV1 improvement. The HI defined as targeted lobe emphysema score minus emphysema score of the lung without the targeted lobe on inpiratory CT scans showed the best predictive accuracy in ROC analysis (AUC=0.68, p=0.019). However, the DeLong's test showed no statistically significant differences between the ROC curves.
Conclusion: This study reveals the most appropriate ways to calculate an emphysema heterogeneity index in the context of ELVR.
Author Disclosures:
D. Theilig: Grant Recipient; Dr. Theilig is participant in the Charité Junior Clinical Scientist Program funded by Charité - Universitätsmedizin Berlin and the Berlin Institute of Health. **R. Hubner:** Equipment Support Recipient; Dr. Hubner has received lecture fees from Pulmonx, the company of the one-way valves used in this study..

B-1281 15:13

Evaluation of three iterative metal artefact reduction algorithms in postsurgical chest computed tomography

J. Aissa, J. Boos, L. Sawicki, N. Heinzler, P. Kröpil, G. Antoch, C. Thomas, B.M. Schaarschmidt; *Düsseldorf/DE (Benedikt.Schaarschmidt@med.uni-duesseldorf.de)*

Purpose: To evaluate the impact of three iterative metal artefact reduction (MAR) algorithms on image quality in CT of patients with metallic devices.
Methods and Materials: Twenty-seven consecutive patients (68.1±11.1 years, 22 male/5 female) with thoracic implants who underwent postsurgical chest-CT were retrospectively included. Images were reconstructed using three different iterative MAR algorithms (iterative MAR-Algo1: cardiac algorithm, iterative MAR-Algo2 = pacemaker algorithm, iterative MAR-Algo3 = thoracic coils algorithm). Weighted filtered back projection (WFBP) reconstructions served as reference standard. Artefacts were subjectively classified into mild and severe. Subjective image quality was evaluated on a 5-point scale by two independent readers (1: severe artefacts, non-diagnostic; 5: no artefacts, excellent image quality). Objective image quality was assessed using region of interest measurements and measuring artefact strength (in Hounsfield Units, HU).
Results: Artifacts were significantly lower for the iterative MAR-Algo1 (58.9±36.HU), iterative MAR-Algo2 (52.7±43.9HU) and the iterative MAR-Algo3 (51.9±44.1HU) compared to WFBP (91.6±78.3HU, p<0.01 for all). Subjectively,

all MAR reconstructed images showed significantly lower mild artefacts (MAR-Algo1 and 2: 4.5±0.5, MAR-Algo3: 3.8±0.5) and severe artefacts (MAR-Algo1 and 2: 3.8±0.4, MAR-Algo3: 3.3±0.5) compared with WFBP (mild: 3.6±0.5; severe: 1.7±0.4)($p<0.01$, respectively). MAR-Algo2 and MAR-Algo3 decreased mild artefacts more effectively compared to MAR-Algo1 ($p<0.01$) while there was no difference for severe artefacts.
Conclusion: All three iterative MAR algorithms improved image quality and reduced artefacts compared to WFBP in postsurgical chest-CT after metallic device implementation. The iterative MAR-Algo2 and MAR-Algo3 were best for mild artefacts while iterative MAR-Algo1 was superior for severe artefacts.

B-1282 15:21

USG-guided thoracocentesis using pigtail catheter with or without pleurodesis in the palliation of recurrent/refractory malignant pleural effusions

A.K. Madayambath, S. Thulkar, A.S. Bhalla, S. Bhatnagar, S. Mishra, M. Jana; *New Delhi/IN (anoopmkcmc@gmail.com)*

Purpose: To evaluate the efficacy of ultrasound-guided pigtail thoracocentesis followed by pleurodesis in patients with symptomatic and refractory malignant pleural effusions.
Methods and Materials: We recruited 57 patients with malignant pleural effusions due to intrathoracic (n=17) and extrathoracic malignancies (n=40). Ultrasound-guided thoracocentesis was performed using 10F pigtail catheter. Those in whom the pigtail drain output dropped to <150ml/day and adequate re-expansion of the underlying lung occurred, pleurodesis was performed (n=33) by intrapleural instillation of Bleomycin (60 IU). Various factors precluded pleurodesis in the remaining patients (n=24). The post-pleuordesis follow-up ranged from 1 to 12 weeks. Pre- and postprocedural clinical scoring was done using NYHA dyspnoea and ECOG performance status scoring systems. Chest radiographs were performed at regular intervals to detect fluid re-accumulation.
Results: 17 patients followed till 12 weeks post-pleurodesis, showed improvement in their clinical and radiological status. Technical success rate of thoracocentesis was 100%, procedural success of pleurodesis was 91% and clinical success rate after Bleomycin in our study was 68%.
Conclusion: We concluded that pigtail thoracocentesis followed by pleurodesis is an effective and safe procedure for palliation of dyspnoea in malignant pleural effusions and hence, strongly recommend early consideration of pleurodesis with Bleomycin.
Author Disclosures:
A.K. Madayambath: Author; Dr Sanjay Thulkar Professor and Head Deaprtment of Radiodiagnosis BRA IRCH AIIMS.

14:00 - 15:30 **Room N**

Genitourinary

SS 1907

Female urogenital system: imaging and intervention

Moderators:
R. Forstner; Salzburg/AT
G. Tardaguila de la Fuente; Vigo/ES

K-29 14:00

Keynote lecture

R. Forstner; *Salzburg/AT*

B-1283 14:09

Dynamic MR of the pelvic floor: impact of the PCL on the grading of pelvic floor descent

S. Picchia, M. Rengo, D. Caruso, D. Bellini, D. De Santis, A. Laghi; *Latina/IT (lisiva@alice.it)*

Purpose: To evaluate the impact of three methods for drawing the pubococcygeal line (PCL) on the grading of pelvic floor descent.
Methods and Materials: Patients with suspected pelvic floor dysfunction were prospectively included. Exams were acquired on a 1.5 Tesla MR scanner. Rectum and vagina were filled with 200ml and 50ml of ultrasound gel. The acquisition protocol included TSE T2-weighted sequences on axial, sagittal and coronal planes for morphological evaluation. A steady-state sequence, in the midsagittal plane, was acquired during straining and defecation. The anterior aspect of all PCL was the pubic symphysis while posterior aspects were the tip of the coccyx (PCLtip), the sacrococcygeal joint (PCLsc) and the last coccygeal joint (PCLcc). The grade of pelvic floor descent was measured with the M line. Measurements of M line were compared as differences of absolute measures and differences of grading.
Results: A total of 29 consecutive female patients were included in the study (mean age 56.07 yy ± 10,52). M line measured using the PCLtip was significantly smaller than the one measured using both the PCLsc or PCLcc in all measurements. The grading of pelvic floor relaxation, using PCLtip, was underestimated in 13 patients (44%) at rest, in 19 patients (65%) during straining and in 16 patients (55%).
Conclusion: A significant difference was observed for the measurement of the M line according to the three PCL used. A significant underestimation of the pelvic floor descent was observed when the M line was measured using the PCLtip as reference.

B-1284 14:17

Intrauterine devices in MRI: not every IUD is safe and MR compatible

S. Bussmann; *Zurich/CH (bussimon88@gmail.com)*

Purpose: The lack of safety information on intrauterine devices (IUD) in MRI is a practical problem for radiologists. Thus, the aim of the study is the evaluation on safety and imaging compatibility in both 1.5T and 3.0T MRI of selected metallic IUD.
Methods and Materials: A variety of MR compatibility tests were performed in a 1.5T/3.0T MRI: assessment of displacement force, measurement of torque effects of the implant, evaluation of image artefacts (3.0T) and evaluation of heating effects (1.5/3.0T) were performed with the following IUD: Mona Lisa, Gold Luna, Nova T (gold/copper) and Chinese ring (steel).
Results: Most IUD (Mona Lisa, Gold Luna, Nova T) presented deflection angles of 0.33°, corresponding to a calculated magnetic force of 0.3mN. In contrast, in Chinese rings a distinct magnetic force (41.66° with an additional 58.1 g increase of mass) was induced corresponding to a calculated magnetic force of 5'706mN. Manual rotation of all IUD showed no signs of any torque effects at all. Heating measurements at 1.5T/3.0T showed a temperature increase of 1.4°C/3.4°C (Chinese ring), 3.2°C/3.8°C (Gold Luna), 3.3°C/4.8°C (Mona Lisa), 3.8°C/4.8°C (Nova T) and 2.2°C/3.6°C (negative control). The artefacts of the copper/gold IUD in the 3T MRI reach a diameter of 3.8mm ± 0.5mm while the Chinese ring achieves 20cm (gradient echo) and 14.9cm ± 0.2mm (spinecho), respectively.
Conclusion: Standard IUD consisting of copper/gold can be considered as safe, while the Chinese ring IUD disturbs images with big artefacts and is potentially harmful to patients during MRI due to significant magnetic forces.

B-1286 14:25

CT and MR imaging of clear-cell carcinoma of the ovary

Y. Shin, H. Joo; *Incheon/KR (joohaele_rd@hanmail.net)*

Purpose: We explored the clinical and imaging features in patients with pathologically proven clear-cell carcinoma (CCC) of the ovary.
Methods and Materials: Twenty patients with hitologically confirmed CCC of the ovary from 2005 to 2016 were enrolled. The staging of these patients is decided by surgical staging (FIGO staging). Retrospectively, two reviewers independently analysed by dividing into two groups. The one group is early stage and another group is advanced stage. And we found the common findings in each groups and also in all groups, regardless of stage. Imaging studies were evaluated for the following: (a) location, (b) maximal transverse diameter, (c) shape (d) margin (e) solid, solid and cystic regions, or cystic, (f) attenuation of the cystic portion, (g) enhancement pattern of the solid portions of the tumour, and (h) secondary manifestations.
Results: Contrary to previous study, our study revealed that the diagnosed stage of CCC of ovary is relatively advanced stage (III/IV). Common imaging findings of CCC was smooth margined cystic mass, unilocular cystic mass, relatively high attenuation in cystic portion (20-30HU). Predictable factor of early stage was mainly cystic tumour, a few and small, round or papillary luminal protruding mass. Predictable factor of advanced stage was mixed type tumour (higher proportion of solid portion than cystic portion), many and large, irregular luminal protruding mass.
Conclusion: The ovarian CCCs are rare tumours, and familiarity with clinical setting and imaging features will facilitate prompt and accurate diagnosis and treatment.

B-1287 14:33

Role of MRI in the staging of primary carcinoma cervix and its correlation with clinical FIGO/histopathological staging

N. Mohan, A. Prahladan, V. Jiji, K. Ramachandran; *Trivandrum/IN (drnehamohan@gmail.com)*

Purpose: To assess the role and accuracy of multiparametric MRI in staging primary carcinoma cervix and its agreement and correlation with clinical FIGO and histopathology. To assess the impact of MRI in revised FIGO staging and change in treatment plan. To study the role of ADC values in histological characterisation of carcinoma cervix.
Methods and Materials: MRI of 193 carcinoma cervix patients were studied. Non-parametric Spearman's rho (rank correlation) test and percentage agreement were calculated to assess the correlation between the MRI, clinical

stage and histopathology. For the surgically treated patients, histopathology was taken as gold standard and sensitivity, specificity, negative predictive value, positive predictive value, accuracy, over staging and under staging were calculated for MRI. Mean ADC values of different histopathological types were tested for significance using ANOVA and independent sample t test.
Results: MRI had a high tumour detection rate of 94.3%, over all staging accuracy of 78.26%, very strong correlation with histopathology (r = 0.886). Clinical FIGO and MRI based staging (r = 0.615) had agreement only in 51.81%. MRI changed the clinical stage in 48.19% patients and subsequent primary treatment plan in 26.6%. Mean ADC value was lower for squamous cell carcinoma (p 0.004).
Conclusion: MRI is highly accurate in evaluating carcinoma cervix and has high correlation with histopathology. Agreement between clinical and MRI based FIGO stage is low. ADC values are lower for squamous cell carcinoma. MRI has a considerable impact in altering treatment decisions and should be available to all patients with carcinoma cervix.

B-1288 14:41

Quantitative MRI analysis of cervical cancer treated with external beam chemoradiotherapy followed by MRI-assisted HDR intracavitary Brachytherapy

A. Jacques, K. Stavrou, V. Tse, S. Natas, O.A. Westerland, A. Winship, V. Mullassery, V.J. Goh; *London/UK (dianastavrou@gmail.com)*

Purpose: To evaluate quantitative morphological MRI parameters at baseline, pre & post brachytherapy in locally advanced cervical cancer and correlate with clinical outcome.
Methods and Materials: Quantitative assessment of T2 signal intensity(T2SI) was made in a subset of 33/100 patients(mean age 54.8 yrs) who were treated with External Beam Chemotherapy(EBRT) followed by brachytherapy(BT), at baseline, pre & 3 month post BT. Clinical data included age, histology, stage & follow up(median 30 months). Mean tumour T2SI & T2SI ratio(T2SIr) was calculated. Change & percentage change in T2SIr and estimated tumour size before & after BT were compared with outcome.
Results: 28/33(84.5%) had biopsy proven squamous cell carcinoma & 5/33(15.2%) adenocarcinoma. 30/33(90.9%) presented with FIGO stage 2b disease. 6/33(18%) relapsed. Median tumour size significantly reduced between treatments**;** 77.8% reduction post EBRT(p=0.00); 33.7% post BT(p=0.00) but did not differ signfiicanctly between relapse & non-relapse groups at all 3 time points. Persistent T2 hyperintensity was seen in 17/33 patients post BT & in 3/6 who subsequently relapsed. Median T2SIr measured 3.37 at baseline & decreased significantly to 2.7 pre BT(p=0.026) & 1.58 post BT(p=0.00), corresponding to visual lowering of signal intensity. Median T2SIr was significantly higher(1.9 vs 1.6; p=0.015) & corresponding T2SIr percentage change was lower in the relapse group(p=0.021) at 3 months.
Conclusion: Initial results suggest that simple quantitative morphological MR metrics are capable of showing significant differences post therapy for locally advanced cervical cancer, & suggest a potential biomarker for disease relapse in patients who may be suitable for early salvage surgery.

B-1289 14:49

The utility of apparent diffusion coefficient in differential diagnosis of neuroendocrine carcinoma of the uterine cervix

C. Zhang, J.-L. Cheng; *Zhengzhou/CN (13733891344@163.com)*

Purpose: To assess the value of diffusion weighted imaging(DWI) and apparent diffusion coefficient(ADC) in differential diagnosis of neuroendocrine carcinoma of the uterine cervix(NECUC).
Methods and Materials: A total of 12 NECUC,39 squamous carcinoma of the cervix(SCC)and 21 adenocarcinoma of the uterine cervix(AUC) confirmed by pathology were analyzed retrospectively. All the patients performed conventional and diffusion weighted MR scan. The ADC values were measured and compared between NECUC, SCC and AUC. Diagnostic performance of ADC was compared using receiver operating characteristic curves (ROC).
Results: The mean ADC value of NECUC, SCC and AUC was$(0.66\pm0.11)\times10^{-3}mm^2/s$, $(0.86\pm0.11)\times10^{-3}mm^2/s$ and$(1.04\pm0.17)\times10^{-3}mm^2/s$, with statistical differences among each group. The optimal cutoff values of ADC for differentiating NECUC and SCC was $0.681\times10^{-3}mm^2/s$ with sensitivity of 94.9%,specificity of 75.0% and accuracy of 90.2%. The optimal cutoff values of ADC for differentiating NECUC and AUC was $0.824\times10^{-3}mm^2/s$ with sensitivity of 95.2%,specificity of 91.7% and accuracy of 93.9%.
Conclusion: The differences of the mean ADC value are helpful in the differential diagnosis of NECUC, SCC and AUC.

B-1290 14:57

Assessing of depth of myometrial invasion and preoperative staging of endometrial cancer: the added value of diffusion-weighted imaging and dynamic contrast-enhanced MRI sequences

I. Alves[1], M. Ramalho[2], T.M. Cunha[2]; [1]*Funchal/PT*, [2]*Lisbon/PT (inesmpalves@gmail.com)*

Purpose: To compare T2-weighted image (T2WI) vs dynamic contrast-enhanced magnetic resonance imaging (DCE-MRI) vs diffusion-weighted imaging (DWI) for the evaluation of depth of myometrial invasion and preoperative overall staging of endometrial cancer.
Methods and Materials: This retrospective study included forty-four women with endometrial cancer who underwent 1.5 Tesla pelvic MRI as part of their initial preoperative staging. T2WI, DCE-MRI, and DWI sequences were obtained. Retrospectively, two radiologists performed a consensus interpretation of all images interpreted the depth of myometrial invasion, overall stage, and presence of pitfalls. Surgical histology was available for each case and was the gold standard for comparison. The accuracy, sensitivity, specificity, positive predictive value (PPV) and negative predictive value (NPV) for each method were assessed.
Results: Respective diagnostic accuracy, sensitivity, specificity, PPV and NPV in assessing the depth of myometrial invasion were: T2WI 61%, 58%, 64%, 55% and 67%; DCE-MRI 86%, 84%, 88%, 84% and 88%; DWI 95%, 95%, 96%, 95% and 96%. DWI correctly staged more patients (41/44) than DCE-MRI (34/44) and T2WI (22/44) ($P<0.05$). For overall cancer staging, κ values were 0.29 with T2WI, 0.59 with DCE-MRI, and 0.89 with DWI.
Conclusion: DWI considerably improved the diagnostic sensitivity and accuracy of MRI compared to DCE-MRI and T2WI in assessing both depth of myometrial invasion and overall staging in endometrial cancer.

B-1291 15:05

Collision tumour of ovary: pathological features and imaging diagnosis

H. Wang, J. Guan, M. Liu; *Guangzhou/CN (usefulkey0077@hotmail.com)*

Purpose: To explore imaging findings and pathological features of ovarian collision tumours, to further improve the imaging diagnosis.
Methods and Materials: 12 female patients with ovarian collision tumours were confirmed by surgical pathology. All imaging findings (9 CT, 2 CT and MRI, 1 non-enhanced MR) and pathological features were retrospectively analysed.
Results: All ovarian collision tumours in 12 cases consisted of two different types of tumours, originated from surface epithelial cells, germ cell, or sex cord-stromal cell. 7 masses localised in left ovary, and 5 were in right. Collision tumours in 9 consisted of surface epithelial tumour and germ cell tumour (6 with mucinous cystadenoma and teratoma, 1 with mixed cystadenoma and teratoma, 1 with serous cystadenoma and struma-ovarii, 1 with undifferentiated carcinoma and teratoma). Collision tumours in 3 consisted of surface epithelial tumour and sex cord-stromal tumour, mucinous cystadenoma and fibroma were detected in 2 and serous cystadenoma and fibroma were detected in 1. Imaging findings included: 1. All collision tumours presented large multiple cystic mass with complicated densities/signals in diameter from 9 to 28 cm. 2. Germ cell tumour or sex cord-stromal tumour were usually smaller (11/12), and lied inside (n=4) or on the wall (n=8) of surface epithelial tumour. The two types of tumours in collision tumour can be well differentiated. 3. Typical imaging features of different tumours in ovarian collision tumours can be detected on CT or MRI.
Conclusion: Pathological and imaging features of ovarian collision tumours are characteristic. Accurate preoperative diagnosis is possible.

B-1292 15:13

Factors influencing MRgFUS efficiency for uterine fibroids treatment

A. Hocquelet, T. Lerebour, N. Frulio, C. Salut, H. Trillaud; *Bordeaux/FR (nonobdx@gmail.com)*

Purpose: The aim of this study was to assess uterine fibroids stiffness and perfusion as independent factor associated with MRgFUS efficiency.
Methods and Materials: We present the preliminary results of the PERAGUS study (NCT02386137). Fibroids stiffness was assessed by ARFI and perfusion by contrast-enhanced US using Sonovue injection and VueBox software. MRgFUS efficiency was defined as the non-perfused volume/the total volume of treatment cells size.
Results: The first 20 patients were included corresponding to 20 fibroids with a median size of 145cc, with 14 grade 1, 4 grade 2 and 2 grade 3 of Funaki classification. The mean NPV was 40%. Funaki grade (P=0.01) and fibroid stiffness (P=0.046) were associated with MRgFUS efficiency. No CEUS perfusion parameter was associated with MRgFUS efficiency.
Conclusion: Fibroids stiffness assessed by ARFI is associated with MRgFUS efficiency like the well-documented Funaki grade.

14:00 - 15:30 **Studio 2017**

Oncologic Imaging

SS 1916

Haematological maligancies and lymphadenopathy revisited

Moderators:
C.A. Cuenod; Paris/FR
D. Simons; Heidelberg/DE

B-1293 14:00

Whole-body MRI with DWI in lesion detection, staging and response evaluation in FDG-avid lymphomas: comparison with 18F-FDG-PET/CT

M. Ciliberto, L. Calandriello, L. Leccisotti, A. Giordano, A. Larici, L. Bonomo; *Rome/IT (dott.mariociliberto@gmail.com)*

Purpose: To assess diagnostic capability of WBMRI with DWI in lesion detection, staging and response evaluation in FDG-avid lymphomas, namely Hodgkin lymphoma (HL) and diffuse large B-cell lymphoma (DLBCL), in comparison with PET/CT.
Methods and Materials: 16 patients with histologically proven HL and DLBCL underwent both 18F-FDG-PET/CT and WBMRI with morphological sequences and DWI (b values=0-50-1000) for initial staging and for treatment response evaluation. For each patient, 30 nodal and extra-nodal stations were evaluated. We assessed diagnostic accuracy of WBMRI in comparison with PET/CT for Ann Arbor staging. We also assessed sensitivity, specificity, PPV, NPV and accuracy of WBMRI in nodal and extra-nodal lesion detection, and concordance between the two imaging modalities in evaluating response to therapy. Gold standard was represented by PET/CT and concordance between the two modalities was assessed with Cohen's kappa.
Results: Sensitivity, specificity, PPV, PPN and accuracy for nodal and extra-nodal lesions were respectively 83.7, 96.3, 85.4, 95.8 and 93.8% for WBMRI with a very good agreement with PET/CT (k=0.81). Although these differences, there was a perfect agreement (16/16) between WBMRI and PET/CT in Ann Arbor staging. At the end of treatment WBMRI and PET-CT demonstrated excellent agreement in evaluating response to therapy (k=0.92) with only two discordant cases.
Conclusion: WBMRI with DWI, compared to PET/CT, showed a very good agreement and diagnostic accuracy in staging and therapy response assessment of FDG-avid lymphomas, and has the potential to be a "radiation-free" alternative modality in these patients.

B-1294 14:08

Whole-body MRI, FDG-PET/CT and bone marrow biopsy, for the assessment of marrow involvement in patients with newly diagnosed lymphoma

D. Albano, C. Patti, L. La Grutta, E. Grassedonio, A. Mulè, A. Costa, M. Midiri, R. Lagalla, M. Galia; *Palermo/IT (albanodomenico@me.com)*

Purpose: To compare whole-body MRI (WB-MRI) with diffusion-weighted imaging (DWI), FDG-PET/CT, and bone marrow biopsy (BMB), for the evaluation of bone marrow involvement (BMI) in patients with newly diagnosed lymphoma.
Methods and Materials: Two independent radiologists and one nuclear medicine specialist reviewed all WB-MRI and FDG-PET/CT scans prospectively performed on 104 patients with newly diagnosed lymphoma (53 males; 47 Hodgkin; mean age: 44, range 15-86) between 2013 and 2015. The delay between imaging scans and BMBs was up to 10 days. The diagnostic accuracy of WB-MRI (1.5 Tesla MR scanner, with T1w, T2w-STIR and DWI sequences) was evaluated using BMB and FDG-PET/CT as the reference standard. We applied Cohen's kappa coefficient to assess the inter-observer agreement in WB-MRI interpretation and to compare WB-MRI, FDG-PET/CT and BMB. The Student's t test was done to compare pelvic marrow ADC values of patients with positive and negative BMB. A p-value of <0.01 was considered significant.
Results: Inter-observer agreement was excellent (k=0.937). Agreement between WB-MRI and FDG-PET/CT was excellent, with a k=0.935. Agreement between WB-MRI and BMB was moderate (k=0.489), and fair between FDG-PET/CT and BMB (k=0.370). WB-MRI and FDG-PET/CT were falsely negative in four indolent non-Hodgkin lymphomas with BMI<30% of marrow cellularity. Conversely, WB-MRI and FDG-PET/CT detected all cases with a BMI>30% of marrow cellularity. Mean ADC values in patients with positive and negative BMB were not significantly different (p=0.049).
Conclusion: WB-MRI and FDG-PET/CT are valuable tools for the assessment of BMI.

B-1295 14:16

Whole-body diffusion-weighted MR and FDG-PET/CT in Hodgkin lymphoma: predictive role before treatment and early assessment after two courses of chemotherapy

D. Albano, C. Patti, D. Matranga, L. La Grutta, E. Grassedonio, C. Ortolano, M. Midiri, R. Lagalla, M. Galia; *Palermo/IT (albanodomenico@me.com)*

Purpose: To evaluate whether whole-body MR has a predictive role before treatment and may assess the response after two courses of chemotherapy in comparison to FDG-PET/CT.
Methods and Materials: We reviewed the whole-body MR and FDG-PET/CT scans performed on 41 patients (20 males, mean age: 32.6, 15-66; 21 females, mean age: 30.8, 16-56) with newly diagnosed Hodgkin Lymphoma, before and after two courses of chemotherapy (ABVD) between 2013 and 2016. We used the Multivariate GEE model to assess the statistical association between being-responder and baseline-SUV_{max}, pre- and post-treatment-ADC and size, percentage change of ADC and size during chemotherapy, site of disease, bulky and stage.
Results: After two ABVD, 10/41 patients (24%) were positive on interim-PET. Mean baseline-SUV_{max} was 11.18±5.58 (3.1-28.0) and baseline-ADC was 0.70±0.14 mm^2/s (0.39-0.98). Mean post-treatment-SUV_{max} of non-responder lesions was 5.68±3.13. Post-treatment-ADC was 1.83±0.34 mm^2/s (1.31-2.90) in responder lesions and 1.01±0.27 mm^2/s (0.49-1.48) in non-responder ones (p<0.001). There was a significant difference also based on post-treatment-size (p=0.009) and bulky (p=0.002). There was no significant difference based on baseline-SUV_{max} (p=0.713), baseline-ADC (p=0.253), percentage change of ADC (p=0.058), size changes (p=0.085), site of disease (p=0.209), stage (p=0.290), baseline-size (p=0.064).
Conclusion: Baseline-SUV_{max} and ADC do not have a predictive role. The occurrence of bulky is the most helpful imaging parameter to predict suboptimal response after two courses of chemotherapy. Post-treatment-ADC is useful for identifying non-responder lesions, whereas size changes are not helpful.

B-1296 14:24

Whole body MRI with DWI as surveillance imaging for lymphoma patients

A. Balbo Mussetto, C. Saviolo, S. Cavanna, M. Petracchini, C. Lario, A. Macera, C. Arese, T. Gallo, S. Cirillo; *Turin/IT (annalisa.balbomussetto@gmail.com)*

Purpose: The aim of our study was evaluating diagnostic performance of Wb-MRI-DWI in periodical surveillance after therapy and for recurrence identification in lymphoma patients compared with PET-CT.
Methods and Materials: 71 patients with previous lymphoma diagnosis (31 HL and 40 NHL) underwent to Wb-MRI-DWI for surveillance (mean 2,4 examination/patient for 42 mounts). When disease relapse was suspected, definitive diagnosis was obtained with FDG PET-CT or biopsy.
Results: During surveillance, Wb-MRI-DWI correctly identified all 13 patients with recurrence (4 HL, 7 DLCL, 3 FL, 1MCL, 1 ATCL). Only in 1 case both Wb-MRI-DWI and PET-CT suspected disease but biopsy was negative. Sensitivity and specificity, respectively, were 1.00 (I.C. 95% 0.77-1) and 0.98 (0.91-1) with NPV 1.00 (0.94-1) and PPV 0.93 (0.69-0.99).
Conclusion: Wb-MR-DWI thanks to its high sensitivity and NPV is a feasible examination for periodical surveillance in lymphoma patients.

B-1297 14:32

Comparing whole-body CT with x-ray skeletal survey for staging monoclonal plasma cell disease: results from an international, blinded reader study

S. Delorme[1], V. Koutoulidis[2], J. Mosebach[1], T. Hielscher[1], J. Hillengass[1], H.-P. Schlemmer[1], L.-A. Moulopoulos[2]; [1]*Heidelberg/DE*, [2]*Athens/GR (s.delorme@dkfz-heidelberg.de)*

Purpose: To compare the sensitivities of Whole-Body Low-Dose CT (WBLDCT) and conventional skeletal survey (CSS) for bone lesions due to monoclonal plasma cell disease.
Methods and Materials: CSS and WBLDCT from 8 international centres were read in consensus by 3 radiologists blinded for the presence of focal osteolyses or osteoporosis. Differences in sensitivity were tested with the exact McNemar test.
Results: 160/308 patients were previously untreated, and of these, 56 had smoldering multiple myeloma (SMM) according to CSS. 80/160 untreated patients were free of lesions with either modality, and 33 had lesions visible on both. In 38 patients, lesions were only visible with WBLDCT, and in 9 they were detected on plain films only (OR, 4.22 (p<0.0001)). WBLDCT was superior to CSS for the iliac bones, the thoracic and lumbar spine, and the ribs, but not for the proximal extremities. Osteoporosis was diagnosed with WBLDCT only in 29, with CSS only in 10, and with both techniques in 63 /157 patients (OR, 2.9 (p=0.003)). Out of the 56 patients with SMM, 12 (21.4 %) showed lytic bone lesions on WBLDCT (p=0.0005).

Conclusion: WBLDCT was significantly more sensitive for bone lesion detection than plain radiographs in the axial skeleton, ribs, and pelvis, but somewhat less sensitive for lytic lesions in the extremities, partly for technical reasons. On the whole, 20% of patients with SMM were upstaged to symptomatic myeloma based on WBLDCT findings. We suggest that imaging standards for multiple myeloma staging be reconsidered.
Author Disclosures:
S. Delorme: Advisory Board; Scientific advisory board: European Radiology. Springer, Heidelberg, Radiation Protection Commission, German Ministry of Environment. Author; Duale Reihe Sonographie. Textbook. Thieme, Stuttgart, Essentials Onkologie, textbook, Elsevier, Munich, Bildgebung in der Onkologie, textbook, Springer, Heidelberg. Board Member; Editorial board: Der Radiologe, European Radiology, Springer, Heidelberg. Research/Grant Support; International Myeloma Foundation, Deutsche Forschungsgemeinschaft, Dietmar Hopp Foundation. Speaker; Teacher at the ESTRO school.

B-1298 14:40

Prognostic relevance of focal lesions in whole-body MRI in multiple myeloma patients before and after allogeneic stem cell transplantation

J. Mosebach, S. Shah, N. Fard, H. Goldschmidt, S. Schönland, U. Hegenbart, H.-P. Schlemmer, S. Delorme, J. Hillengass; *Heidelberg/DE (j.mosebach@dkfz-heidelberg.de)*

Purpose: To investigate predictors of survival in patients with multiple myeloma before and after allogeneic stem cell transplantation (alloSCT) by assessing the tumour burden with whole-body-MRI.
Methods and Materials: Diagnostic WB-MRI was performed in 1.5 T scanners. Of initially 79 patients with stage II multiple myeloma or higher, according to the Salmon and Durie classification, 63 completed imaging before and after alloSCT. Lesions were characterised by corresponding focal signal changes in T1w-(hypointens) as well as in T2w- fat-saturated sequences (hyperintens) and size >5mm. Statistical analysis included univariable and multivariable Cox regression models. Distribution of survival times was estimated with the Kaplan-Meier method and Log rank test was used to determine prognostic impact of the presence of focal lesions on survival.
Results: Presence of focal infiltration was associated with a shorter progression free survival (PFS; 2nd MRI: HR 2.52, p=0.035 and 1st MRI: borderline statistical significance, HR 1.95 P=0.079) and overall survival (OS; 2nd MRI HR 3.8, p=0.032). Increasing number of focal lesions at baseline proved to be an additional adverse prognostic factor (PFS: HR 1.02, p=0.047; OS: HR 1.02, p=0.013). Kaplan-Meier estimates at 60 months of follow-up showed OS rates of 31% for patients with focal infiltration after therapy and 74% for patients without.
Conclusion: Multiple myeloma patients in this setting with any focal lesion have a higher risk of progression as well as shorter OS, and may benefit from continuous consolidating therapy. WB-MRI before and after alloSCT can be recommended to detect prognostic relevant lesions.
Author Disclosures:
J. Mosebach: Research/Grant Support; Deutsche Forschungsgemeinschaft SFB/TRR 79. **H. Goldschmidt:** Advisory Board; Janssen, Celgene, Novartis, Onyx, Amgen Takeda, BMS. Research/Grant Support; Celgene, Janssen, Chugai, Novartis, BMS, Millennium. Other; Honoraria: Celgene, Janssen, Novartis, Chugai, Onyx, Millennium. **U. Hegenbart:** Speaker; Janssen. **H.-P. Schlemmer:** Advisory Board; Siemens, Bracco, Curagita. Board Member; ICIS, ESOI, ABO-DKG. **S. Delorme:** Advisory Board; Scientific advisory board: European Radiology. Springer, Heidelberg, Radiation Protection Commission, German Ministry of Environment. Author; Duale Reihe Sonographie. Textbook. Thieme, Stuttgart, Essentials Onkologie, textbook, Elsevier, Munich, Bildgebung in der Onkologie, textbook, Springer, Heidelberg. Board Member; Editorial board: Der Radiologe, European Radiology, Springer, Heidelberg. Research/Grant Support; International Myeloma Foundation, Deutsche Forschungsgemeinschaft, Dietmar Hopp Foundation. Speaker; Teacher at the ESTRO school. **J. Hillengass:** Advisory Board; Amgen, Novartis, Janssen, BMS. Author; PRMA. Consultant; Amgen. Investigator; Novartis, Sanofi. Research/Grant Support; Novartis, Sanofi.

B-1299 14:48

Whole-body MR imaging vs conventional x-ray examination in patients with plasmacell neoplasia

A. Cassarà, A. Trisoglio, L. Sukhovei, G. Leale, S. Berardo, F. Buemi, L. De Paoli, A. Stecco, A. Carriero; *Novara/IT (alessandratrisoglio@outlook.it)*

Purpose: Multiple myeloma (MM) is the most common primary malignant neoplasm of the skeletal system. Radiological findings on conventional x-ray examinations of MM considered by International Myeloma Working Group criteria are multiple focal lytic lesions of the bone ≥5mm in size and >1 focal lesions on Magnetic Resonance Imaging (MRI) studies. In the next 10 years whole-body MRI (WB-MRI) has become an important additional tool. The aim of this study was to compare findings on conventional x-ray examinations with findings from wb-MRI to subsequently determine the influence of wb-MRI on therapy changes.
Methods and Materials: In 40 patients of Haematology Department with Plasmacell Neoplasia (including Smouldering Myeloma, Plasmocytoma and MM) with a mean age of 62.5+/-11.9 years, WB-MRI examinations were correlated with a recent conventional x-ray. The results were independently assessed by two radiologists. The disease was staged according to Salmon and Durie and Salmon and Durie PLUS.
Results: In all, 320 skeletal regions were compared; 38 regions were positive on conventional x-ray examination vs 95 regions on WB-MRI. An increased degree of infiltration was identified on wb-MRI with significant differences ($p < 0.05$) between the modalities in both lower extremities. Based on wb-MRI, tumour stage was upgraded in 13 of the 40 patients. In 11 out of these 13 patients, the WB-MRI results influenced for making the decision to initiate further therapy due to the degree of bone infiltration.
Conclusion: WB-MRI provides a more detailed assessment of the pattern of bone marrow infiltration and influences therapeutic strategies.

B-1300 14:56

Whole-body MRI in multiple myeloma: a retrospective study comparing ADC maps and dynamic contrast-enhanced imaging (DCE-MRI) in evaluation of post treatment response

P. Arcuri, S. Roccia, S. Molica, A. Anoia, D. Lagana', G. Fodero; *Catanzaro/IT (arppaolo@alice.it)*

Purpose: The aim of our study was to compare,in WB-MRI,the diagnostic capabilities of apparent diffusion coefficient (ADC) maps and dynamic contrast enhanced (DCE-MRI) in evaluation of post treatment response of Multiple Myeloma (MM).
Methods and Materials: The retrospective study includes forty-five patients affected by MM,all underwent radio/chemotherapy or autologous stem cell transplant.The protocol included coronal WB and sagittal (axial skeleton) TSE T1 ,STIR T2 and axial DWIBS (b: 0-1000 mm2/sec) sequences.Imaging post-contrast was performed immediately after injection during the first 2 min.Mean ADC values of focal suspected lesions and diffuse localisations were calculated. DCE-MRI images of the spine,were analysed with regions-of-interest (ROI) and Time-Intensity-Curves (TIC). Quantitative analysis was performed by means of K statistic.The qualitative interpretation of TICs based on the shape of the curve.Paraprotein evolution was considered the reference standard.
Results: DWI sensibility in detection disease remission was 88%, specificity 71%; in the relapse cases,(were considered positive the mean ADC values: 1.09±0.21x10-3 mm²/sec in focal lesions, 0.71±0.22x10-3 mm²/sec in diffuse involvement) sensitivity was 94%, specificity was 88%.DCE-MRI showed, in remission of disease,74% of sensitivity and 93% of specificity.In relapse of disease DCE-MRI showed 74% of sensitivity and 93% of specificity.In some patients (9%),progressive disease was detected earlier by WB-DW-MRI than by the routine biochemical follow-up.
Conclusion: DCE-MRI approach showed greater specificity in the evaluation of both remission and relapse of disease.WB-DWI-MR increase detection of relapse of disease in myeloma patients in comparison to DCE-MRI.A combined evaluation of DWI and DCE-MRI provides a comprehensive assessment of post treatment response in MM.

B-1301 15:04

Apparent diffusion coefficient (ADC) values in multiple myeloma patients: a potential noninvasive marker for bone marrow involvement characterisation at staging

P.A. Bonaffini[1], D. Ippolito[2], A. Nasatti[2], C. Talei Franzesi[2], S. Sironi[3]; [1]*Desio/IT*, [2]*Monza/IT*, [3]*Bergamo/IT (pa.bonaffini@gmail.com)*

Purpose: To assess the role of quantitative analysis of ADC maps in bone marrow involvement characterisation at staging for patients with multiple myeloma (MM).
Methods and Materials: Fifteen MM patients (focal 6, diffuse 6, combined 3), undergone a 1.5T Whole-Body MRI examination (Achieva, Philips) for staging purposes, were retrospectively analysed. Coronal (skull vertex-ankle) and sagittal (whole axial skeleton) short-tau inversion recovery (STIR) T2 and T1 TSE and axial DWIBS (*b:* 0-500-1000 mm^2/sec) sequences were acquired. According to visual-qualitative analysis, up to 3 target bone localisations per patient were chosen. Regions of interest (ROIs) were manually drawn on corresponding ADC maps, obtaining the mean ADC values for focal (ADC1) and diffuse (ADC3) localisations. ADC1 and ADC3 were compared each other and with ADC calculated in normal bone marrow (ADC2).
Results: A total of 22 neoplastic bone lesions (10 focal, 12 diffuse), with high signal intensity on DWIBS (compared to normal bone marrow), were retrospectively evaluated. The mean ADC values were $1.06\pm0.27\times10^{-3}$ mm²/sec, $0.75\pm0.19\times10^{-3}$ mm²/sec and $0.34\pm0.07\times10^{-3}$ mm²/sec in focal lesions (ADC1), diffuse involvement (ADC3) and normal bone marrow (ADC2) respectively. The ADC values were significantly lower (p=0.003) in cases of diffuse involvement than those of focal pattern. The values of MM bone localisations (ADC1-ADC3) were significantly higher (p=0.001) of those of normal bone marrow (ADC2).

Conclusion: Quantitative analysis of ADC maps in staging of MM patients provides data potentially useful for the non-invasive characterisation of normal bone marrow and its pathologic involvement, even in terms of the different patterns of disease.

B-1302 15:12

Comparison of normal and metastatic lymph nodes with multi-energy computed tomography

M. Femia[1], S. Rizzo[1], L. Preda[2], D. Radice[1], R. Vigorito[1], P. De Marco[1], D. Origgi[1], M. Bellomi[1]; [1]*Milan/IT*, [2]*Pavia/IT (marco.femia@unimi.it)*

Purpose: To evaluate whether multi-energy computed tomography (CT) could help in differentiating between normal and metastatic lymph nodes.
Methods and Materials: Mediastinal and abdominal lymph nodes (LN) with pathological evaluation, among patients who underwent multi-energy CT, were retrospectively evaluated. Regions of interest (ROI) were traced on the selected LN. Iodine/fat, Iodine/water, fat/iodine and water/iodine material decompositions were calculated and compared between normal and metastatic LN. Inter-observer variability between two readers was evaluated for the first 12 LN. P<0.05 was considered significant.
Results: 101 LN were selected: 53 were mediastinal LN (31 normal and 22 metastatic LN from lung cancer), and 48 were abdominal (28 normal and 20 metastatic LN from gynaecological malignancies). Iodine/fat material decomposition was significantly higher for normal LN (4.19±1.05 mg/cm^3; 95% P-tiles 2.80,5.47) than for pathologic LN (3.70±0.89 mg/cm^3; 95%P-tiles 2.31,4.93), p=0.003. At iodine/water material decomposition iodine content was higher in normal LN (29.7±10.3 µg/cm^3; 95% P-tiles 16.7,41.6) than in metastatic ones (25.0±8.6 µg/cm^3; 95% P-tiles 12.4,37.1), p=0.002. There was no significant difference between normal and metastatic LN at fat/iodine and water/iodine material decomposition. ROC curves were traced for the statistically significant parameters identifying an AUC of 0.6723 for iodine/fat decomposition density and an AUC of 0.6834 for iodine/water material decompositions. There was no significant inter-observer variability.
Conclusion: Multi-energy CT derived iodine/fat and iodine/water material decomposition differ significantly among normal and metastatic LN. Evaluation of iodine content by using multi-energy CT may help in differentiating normal from metastatic lymph nodes.

B-1303 15:20

Preoperative sentinel lymphnode (SLN) identification and mapping using SPION-MR in patients with prostatic cancer

T.S. Paulo, A. Winter, S.S. Amin, T. Kowald, P. Goos, S. Engels, H. Gerullis, F. Wawroschek, A. Chavan; *Oldenburg/DE*
(amin.sandeepsunder@klinikum-oldenburg.de)

Purpose: We assessed the role of intraprostatic super para magnetic iron oxid nanoparticle (SPION) injection for preoperative detection and mapping of sentinel lymphnodes (SLN) with MRI in patients with prostatic cancer (Pca) scheduled to undergo radical prosatectomie. To our knowledge, this has not been reported previously.
Methods and Materials: In a prospective study approved by the ethical committee, 50 patients with intermediate and high-risk PCa (PSA >10 ng/ml and/or Gleason score ≥7) received a transrectal intraprostatic SPION injection 1 day prior to radical prostatectomy. MRI (T1, T2 and T2*) was performed preoperatively one day before and after SPION injection. The number and localization of the visualized SLN was noted. Intraoperatively, the SLN were identified with the help of a magnetometer, their anatomical location noted before resection. Diagnostic rate was defined as number of patients with at least one detected lymph node / total number of patients.
Results: No adverse events attributable to SPION injection were observed. The diagnostic rate was 100% (50/50). SPION injection identified 890 SLNs (median 17.5; IQR 12-22.5). The anatomic distribution of the SLNs was: external iliac 19.21%, common iliac 16.63%, obturator fossa 15.84%, internal iliac 13.82%, presacral 12.13%, pararectal 12.02%, paraprostatic 3.71%, paravesical 2.25%, and other regions 4.38%.
Conclusion: SLN identification with MRI after intraprostatic SPION injection is feasible. SPION-MR reliably identifies SLNs draining the prostate in a high number of patients, especially outside the established extended node template. It has the potential to generate a reliable preoperative SLN- template to assist lymphadenectomy.

14:00 - 15:30 **Room L 8**

Head and Neck

SS 1908

Parathyroid and thyroid imaging: how to improve diagnosis?

Moderators:
J. Frühwald-Pallamar; Vienna/AT
N.N.

B-1304 14:00

Parathyroids: frequently overlooked or over-reported glands?

E. Scapin, A. Mereu, L. Saba; *Monserrato/IT*

Purpose: To analyse if a clinical request can drive sonographers to find parathyroids more frequently.
Methods and Materials: 14,968 neck or thyroid ultrasounds (11,835 females, 3,133 males, age range 0-97 years), performed by a team of several sonographers, were retrospectively assessed. Included cases were categorised into four groups: ultrasounds performed because of clinical requests concerning parathyroids, in which these were found or not and ultrasounds performed because of clinical requests not concerning parathyroids, in which these were found or not. We compared expected versus observed cases with a two-tailed Fisher's exact test.
Results: Parathyroids were observed in 484 cases (3.2%): ultrasounds were oriented by specific suspected pathologies in 219 cases (45.2%) and were not in 265 cases (54.8%). In 1 case only (0.4%) suspected pathological parathyroids were not visualised, thus giving a success rate of 99.6%. Parathyroids were observed in a mere 1.8% of ultrasounds performed when it has not been provided a clinical request concerning them. Out of 220 suspected parathyroid pathologies, only 44 ones were confirmed; whereas 50 cases were found incidentally, instead of 22 cases expected according to epidemiology. By comparing expected versus observed cases, with a two-tailed Fisher's exact test, we found a statistically significant difference (p value<0.001).
Conclusion: Effective exploration of parathyroids is difficult, and this somewhat challenging examination could stimulate the sonographer to find them only when requested and rarely if not. Our findings demonstrate that there could be a vast mismatch between expected and observed cases if parathyroid pathology is suspected or not.

B-1305 14:08

Diagnostic value of shear wave elastography for parathyroid lesions and comparison with cervical lymph nodes

A.V. Polat, M. Ozturk, B. Akyuz, C. Celenk, C. Polat; *Samsun/TR*
(dr.mesutozturk@gmail.com)

Purpose: The aim of this study was to prospectively assess the feasibility of the Virtual Touch tissue imaging quantification (VTIQ) method of Shear Wave Elastography (SWE) for the discrimination of parathyroid lesions and to compare the lesions' stiffness with that of cervical lymph nodes.
Methods and Materials: Institutional review board approval and written consent from all participating patients were obtained for this study. SWE using VTIQ was performed on 87 histologically proven parathyroid lesions and 31 cervical lymph nodes in 95 patients. Tissue stiffness was calculated as shear wave velocity (SWV) in meters per second (m/s) and two consecutive measurements were performed. Mean SWV of the lesions was compared and receiver operating characteristic curve analysis was used to evaluate diagnostic performance. Agreement between the measurements was assessed with intra-class correlation coefficient.
Results: Pathology results revealed 54 parathyroid adenomas and 33 parathyroid hyperplasia. Mean SWV of parathyroid adenomas (2.16 ± 0.33 m/s) significantly differed from parathyroid hyperplasia and lymph nodes (1.75 m/s ± 0.28 m/s and 1.86 ± 0.37 m/s respectively, p < 0.001). Selecting a cut-off value of 1.92 m/s for diagnosing adenoma led to 80% sensitivity and 70%specificity (AUC: 0.780 (95% CI: 0.697-0.864), p < 0.001). Agreement of the two SWV measurements was excellent as the intra-class correlation coefficient was 0.960 (95% CI: 0.943-0.973, p < 0.001).
Conclusion: The VTIQ method of SWE contributes to the discrimination of parathyroid adenoma from parathyroid hyperplasia and cervical lymph node.

B-1306 14:16

The 5-tiered categorisation system based on the 2015 ATA guidelines for classifying a small thyroid nodule on ultrasound: comparison with the modified 4-tiered categorisation system

J. Lee, K. Han, E.-K. Kim, H. Moon, J. Yoon, V.Y. Park, J. Kwak; *Seoul/KR (easywg@yuhs.ac)*

Purpose: To compare stratification of malignancy risk in small thyroid nodules with the 5-tiered categorisation system and the modified 4-tiered categorisation system based on the 2015 American Thyroid Association (ATA) management guidelines.
Methods and Materials: From January 2015 to December 2015, 737 thyroid nodules measured ≥1 cm and <2 cm in 723 patients were included in this study. Ultrasound (US) features of these lesions were evaluated retrospectively. Each nodule was assigned a category with the US patterns described by the 2015 ATA guidelines and the modified 4-tiered categorisation system. Univariate analysis was performed to assess malignancy risk in thyroid nodule and diagnostic performances were calculated for each category and compared.
Results: In total, 737 thyroid nodules were assessed. On univariate analysis, there was no significant difference of malignancy risk between low suspicion and very low suspicion of malignancy nodules (P=0.584). Therefore, we suggested a modified 4-tiered categorization system which combines very low suspicion nodules and low suspicion nodules into one category, the very low suspicion nodules. When comparing the diagnostic performances of the 2015 ATA guidelines and the modified 4-tiered categorisation system, specificity, PPV, and accuracy were higher with the modified 4-tiered categorisation system (P<0.001 for all), whereas sensitivity, and NPV were not significantly different (P=0.087, and P=0.370).
Conclusion: The modified 4-tiered categorisation system allows more efficient management with better diagnostic performance and avoiding unnecessary FNA than the 5-tiered categorisation systemof the 2015 ATA guidelines in small thyroid nodules.

B-1307 14:24

Efficacy of ultrasound elastography in diagnosing thyroid lesions and correlation with FNAC or biopsy

P. Dhayalan, D.S. Phansalkar, K. Chokka, H. Rao; *Pondicherry/IN (dsphansa@yahoo.com)*

Purpose: To determine shear wave velocity values of thyroid lesions using Virtual Touch Tissue Quantification (VTTQ) method by Acoustic Radiation Force Impulse (ARFI) technique of ultrasound elastography for differentiating malignant from benign lesions. To correlate shear wave velocity values with FNAC or biopsy results of thyroid lesions. To assess the sensitivity and specificity of ultrasound elastography shear wave velocity values in differentiating malignant and benign thyroid lesions.
Methods and Materials: Prospective diagnostic study of ultrasound elastography was done to determine shear wave velocity values of 88 thyroid lesions proved by 2D ultrasound imaging in 86 patients on Siemens Acuson S-2000. The findings were correlated in all patients with FNAC or biopsy results. Statistical methods were ROC curve and likelihood ratio analysis.
Results: Out of 88 lesions, 15 (17%) were malignant and 73 (83%) were benign on FNAC or biopsy. The optimal cut-off point for shear wave velocity values in differentiation was 2.87m/s. The mean shear wave velocity was 2.17±0.84m/s for benign and 6.17±2.72m/s for malignant lesions. The sensitivity was 86.7%, specificity 94.5%, positive predictive value 76.5%, negative predictive value 97.2%, accuracy 93.2%, positive likelihood ratio 15.76 and negative likelihood ratio 0.14 for shear wave velocity values in differentiating malignant from benign thyroid lesions.
Conclusion: Shear wave velocity estimation by ultrasound elastography has high potential to differentiate malignant from benign lesions and can reduce unnecessary invasive FNACs/biopsies.

B-1308 14:32

Acoustic radiation force impulse imaging in the differentiation of benign and malignant thyroid nodules

N.N. Pandey, G. Pradhan, A. Manchanda, A. Garg; *New Delhi/IN (nirajpandey2403@gmail.com)*

Purpose: To evaluate the role of ultrasound elastography using Acoustic Radiation Force Impulse (ARFI) imaging in characterising and differentiating malignant vs benign thyroid nodules.
Methods and Materials: A total of 40 thyroid nodules were evaluated with conventional sonography and ultrasound elastography using Acoustic Radiation Force Impulse (ARFI) imaging. The final diagnosis was obtained from histologic findings.
Results: A total of 14 malignant and 26 benign nodules were diagnosed on the basis of histologic examination. Majority of the malignant thyroid nodules demonstrated presence of intranodular vascular flow, hypoechoic echotexture, absent halo, irregular margins and microcalcifications. However, a considerable overlap was noted in the sonographic features of malignant and benign thyroid nodules. On ARFI imaging, the mean shear wave velocity (SWV) values (mean ± SD) of malignant and benign thyroid nodules were 3.131±0.921m/s and 1.691±0.513m/s, respectively. A significant difference was observed between the mean SWV values of malignant thyroid nodules and benign thyroid nodules (p<0.0001). Applying a cut-off value of 2.53m/s, the sensitivity, specificity, and the area under ROC curve for the differentiation were 85.71%, 96.15%, and 0.922 respectively.
Conclusion: ARFI imaging is a promising elastography technique that provides quantitative information about tissue stiffness. It provides additional information and complements sonography as an effective diagnostic tool in characterising and differentiating benign from malignant thyroid nodules.

B-1309 14:40

Distinguishing benign from malignant thyroid nodules: utility of superb microvascular imaging and ultrasound elastography

H. Ahn, J. Lee, M. Seo, S. Park, B.I. Choi, J. Yoo; *Seoul/KR (ach0224@gmail.com)*

Purpose: To prospectively investigate the utility of the combined use of superb microvascular imaging (SMI) and ultrasound strain elastography in distinguishing benign from malignant thyroid nodules.
Methods and Materials: We analysed 52 thyroid nodules (malignant=26, benign=26) and a reviewer scored the likelihood of malignancy for three data sets (i.e., B-mode ultrasonography alone, B-mode ultrasonography + SMI, and B-mode ultrasonography + strain elastography). The area under the receiver operating characteristic curve (Az) values, sensitivities, and specificities of each data set were compared.
Results: The mean lesion size was 1.27cm (range, 0.4-4.6 cm). Among the three data sets, the B-mode ultrasonography + SMI set showed the greatest Az value (average, 0.917; range, 0.807-0.975); however, it was similar to that of B-mode ultrasonography alone (average, 0.888; range, 0.770-0.959) and B-mode ultrasonography + strain elastography (average, 0.902; range, 0.788-0.967). The sensitivity and specificity based on the management decision of whether to perform fine-needle aspiration (FNA) of B-mode ultrasonography alone was 96.2% and 11.5%, respectively. B-mode ultrasonography + SMI and B-mode ultrasonography + strain elastography showed similar sensitivity (92.3%) to but significantly higher specificity (34.6%) than B-mode ultrasonography alone (P=0.032).
Conclusion: The combined use of SMI and ultrasound strain elastography showed similar diagnostic performance to conventional ultrasonography alone in distinguishing benign from malignant thyroid nodules. Moreover, the combined use could increase the specificity in decision making for FNA without any change in sensitivity.

B-1310 14:48

Diagnostic performance of computer-assisted diagnosis in evaluating thyroid masses on ultrasonography

M. Seong, E. Ko, B.-K. Han, J. Shin, S. Hahn, J. Bae, J. Lee, S. Yang, J. Kim; *Seoul/KR (seong.minjung@gmail.com)*

Purpose: To evaluate and compare the diagnostic performance of breast ultrasonography (US)-dedicated computer-assisted diagnosis (B-CAD) and thyroid US-dedicated CAD (T-CAD) in assessing thyroid masses on US.
Methods and Materials: We prospectively collected US images of 372 thyroid masses in 329 consecutive patients. All lesions were histologically confirmed or had long term follow up images. US findings were recorded according to Korean Thyroid Imaging Reporting and Data System (K-TIRADS) by radiologists who were expert in thyroid US. B-CAD and T-CAD were applied by another radiologist who was blind to the pathologic result. We evaluated the sensitivity, specificity, accuracy of B-CAD and T-CAD, and compared the performance of both CADs and radiologists. We also analysed the agreement of US descriptions among the B-CAD, T-CAD and radiologists.
Results: Overall sensitivity, specificity, accuracy of radiologists were 72.5%, 99.2%, and 89.3%. B-CAD showed 46.3%, 78.2%, and 67.4%, while T-CAD showed 53.3%, 92.9% and 79.4%. T-CAD showed good agreement with radiologists on the final diagnosis (kappa = 0.632), while B-CAD showed fair agreement with others. Among the US descriptors, radiologist and T-CAD showed moderate agreement in describing margin, echogenicity, and composition (kappa = 0.468, 0.505, and 0.446). B-CAD showed poor or fair agreement with others, except moderate agreement in describing composition with T-CAD (kappa = 0.407).
Conclusion: T-CAD showed good agreement with expert radiologists in final diagnosis, and showed better performance than B-CAD. Although T-CAD did not show comparable performance with expert radiologists, is suggested to provide a good assistance in diagnosing thyroid mass on US.
Author Disclosures:
E. Ko: Grant Recipient; Eun Young Ko. Research/Grant Support; Samsung Medison.

B-1311 14:56

Sonographic assessment for predictors of malignancy in Thy3a nodules

N.M. Hughes, A. Nae, J. Barry, L. Feeley, P. Sheahan; *Cork/IE (Nicolahughes@rcsi.ie)*

Purpose: Thy3a cytology poses difficult management decisions often leading to repeated ultrasound and FNA before undergoing diagnostic thyroid lobectomy. The purpose of this study was to assess sonographic features of these nodules for predictors of malignancy.
Methods and Materials: Preoperative ultrasounds of 67 patients with Thy3a cytology were retrospectively reviewed. The reviewing radiologist was blinded to histological diagnosis. Sonographic features evaluated included size, shape, echotexture, presence of a halo, margins, and micro- and macro-calcifications. All nodules were graded using the BTA classification system.
Results: There were 56 benign nodules and 11 malignant nodules. 4/11 malignant nodules were hypoechoic versus 12/56 benign thyroid nodules (p=0.44). 3/11 of the malignant nodules had a taller>wide shape versus 9/56 benign thyroid nodules (p=0.40). 8/56 benign thyroid nodules had irregular margins versus 3/11 malignant nodules (p=0.37). 4/11 malignant nodules had calcifications, 3 of which were microcalcifications compared with 17/56 of the benign nodules with any calcification, 13 of which were microcalcifications (p=0.73,p=0.72). 16/56 benign thyroid nodules and 3/11 malignant thyroid nodules had a halo (p>0.99). From the benign nodule group, 7/56 were correctly classified as benign(U2) and 26/56 were considered indeterminate(U3) but 23/56 were categorised as suspicious/malignant(U4/5). From the malignant nodule group, only 1/11 was classified as benign(U2), 4/11 were considered indeterminate(U3) and 6/11 were correctly categorised as suspicious/malignant(U4/U5).
Conclusion: 16.4% of Thy3a nodules were malignant. The histological and sonographic classification using the BTA guidelines did not correlate consistently in this subgroup. No statistically significant sonographic predictor of malignancy was identified when assessing Thy3a nodules.

B-1312 15:04

Role of ultrasound in predicting tumour invasiveness for follicular variant of papillary thyroid carcinomas

M.-r. Kwon, S. Hahn, J. Shin, J. Lee, S. Yang, J. Kim, M. Seong; *Seoul/KR (miri.kwon@samsung.com)*

Purpose: The purpose of this study was to assess the role of ultrasound (US) for predicting tumour invasiveness of follicular variant of papillary thyroid carcinomas (FVPTCs).
Methods and Materials: From Jan 2014 to May 2016, 151 patients surgically confirmed as FVPTCs were included. According to the pathologic analysis, we categorized FVPTCs into three groups (non-invasive follicular thyroid neoplasm with papillary-like nuclear features [NIFTP], invasive encapsulated FVPTC [iE-FVPTC], or infiltrative FVPTC [I-FVPTC]). The US pattern by the Korean Thyroid Imaging Reporting and Data System (K-TIRADS) and the American Thyroid Association (ATA) guidelines was assigned to each nodule. The correlation between the tumour invasiveness and the K-TIRADS category or ATA pattern was investigated using the Spearman's coefficient of rank correlation.
Results: Of total 152 FVPTCs, there were 48 NIFTPs (31.6%), 60 iE-FVPTCs (39.5%), and 44 I-FVPTCs (28.9%). Seventeen of the 152 FVPTCs (11.2%) were classified as “not specified” pattern by the ATA guidelines. All US characteristics of FVPTCs were significantly different according to tumour invasiveness (all P values ≤ 0.030). Tumour invasiveness significantly correlated positively with K-TIRADS (r = 0.591; P < 0.001) and ATA guidelines (r = 0.532; P < 0.001). According to both K-TIRADS and ATA guidelines, the most common subtype was NIFTP in low suspicion nodules (52.6% and 51.6%), iE-FVPTC in intermediate suspicion nodules (52.7% and 54.2%), and I-FVPTC in high suspicion nodules (82.5% and 69.4%), respectively.
Conclusion: US assessment with K-TIRADS and ATA guidelines is useful method for predicting tumour invasiveness for FVPTCs.

B-1313 15:12

Importance of thyroid microcalcifications in the absence of identifiable nodules

C. Whittle, E. Horvath, M. Garcia, C. Carrasco, J. Slater; *Santiago/CL (cwhittle@alemana.cl)*

Purpose: To analyse association of clinical and ultrasound (US) findings of thyroid microcalcifications in the absence of nodule with histological results. To determine the US and clinical findings associated with a higher risk of malignancy.
Methods and Materials: This was a IRB approved, retrospective study. All patients subject to US fine-needle aspiration biopsy (FNAB) for thyroid microcalcifications in the absence of sonographic nodules between 2008 and 2012 were identified. Demographic, clinical, US findings and pathological results were registered. Uni- and multivariable analysis was performed.
Results: 21 patients, mean age: 33.2 years (range 15 - 53 years). Mean age in patients with papillary carcinoma was 29.5 and 39 years in benign findings (p=0.0336). 18 patients were female (86%), no significant association among sex and cancer development was identified (p= 0.257). 11/21 patients had grouped microcalcifications and in 9 cases cancer was demonstrated. 10/21 patients had disperse microcalcifications and 4/10 had cancer. A non-statistically significant trend for association among cancer and grouped microcalcifications was found (p=0.063). 20/21 had findings suspicious for chronic thyroiditis. In all, Hashimoto’s thyroiditis was histologically confirmed. All patients with suspicious adenopathy in US (5/21) had FNAB positive for cancer. In multivariate analysis model for cancer, only age was significant OR=0.9 (p=0.05) with a discrimination capability of 79.3%. 13/21 patients had FNAB positive suspicious or diagnostic for cancer (62%). 11/13 had surgical thyroidectomy performed.
Conclusion: Our study suggests that the presence of thyroid microcalcifications without nodule is suspicious for papillary carcinoma. High suspicion should be considered in grouped microcalcifications in a background of Hashimoto’s thyroiditis.

B-1314 15:20

Utility of uptake rate in the thyroid bed measured by ^{123}I tracer study before ^{131}I radioactive iodine therapy for papillary thyroid carcinoma to predict treatment outcome

Y. Omiya, U. Motosugi, S. Ichikawa, T. Umeda, H. Onishi; *Yamanashi/JP*

Purpose: To predict the success of ^{131}I radioactive iodine therapy (RIT) for outpatients by measuring ^{123}I uptake rate in the thyroid bed in a pre-RIT tracer study.
Methods and Materials: Thirty-four patients (15 men and 19 women) with papillary thyroid carcinoma, who underwent total thyroidectomy and ^{131}I RIT, were included in the study. The mean age was 60.0 years (range, 37-80 years). Patients were enrolled from May 2011 to July 2016. No patients experienced distant metastases. An ^{123}I tracer study was performed before ^{131}I RIT, and the iodine uptake rate in the thyroid bed was measured. Initial RIT dose was 1,110 MBq ^{131}I. When RIT was completed with a single treatment, it was defined as “best indication.” We investigated whether “best indications” could be predicted using a pre-RIT ^{123}I tracer study. We analysed the following variables as potential “best indication” predictors: age, sex, tumour factor (lymph node metastasis, extrathyroidal extension, and differentiation), and the uptake rate in the thyroid bed after 4 and 24 hours.
Results: The uptake rate of ^{123}I tracer in the thyroid bed at 4 hours was significantly lower in the “best indication” group patients (n = 5; P = 0.0421), when compared to others (n = 29). No other significant differences were detected between the two groups. When 0.0033 was set as the cut-off value, negative predictive value was 100 % (5/5).
Conclusion: The uptake rate in the thyroid bed after 4 hours after in ^{123}I tracer study can predict “best indication” on ^{131}I RIT.

14:00 - 15:30 **Room E2**

Neuro

SS 1911a

Degenerative diseases of the brain

Moderators:
S. Shams; Stockholm/SE
N.N.

K-30 14:00

Keynote lecture

C. Calli; *Izmir/TR*

B-1315 14:09

Hypointensity of the primary motor cortex in SWAN images at 3T in patients with amyotrophic lateral sclerosis

G. Donatelli, A. Retico, E. Caldarazzo Ienco, P. Cecchi, M. Costagli, L. Biagi, G. Siciliano, M. Tosetti, M. Cosottini; *Pisa/IT (graziella_donatelli@hotmail.com)*

Purpose: Amyotrophic lateral sclerosis (ALS) is a neurodegenerative disease entailing both upper and lower motor neurons. Recent 7T-MR studies documented T2* hypointensity of deep layers of the primary motor cortex (M1) in ALS patients with severe upper motor neuron (UMN) impairment. Aim of this study was to investigate the ability of SWAN images in the assessment of M1 signal changes in ALS patients at 3T compared to 7T.
Methods and Materials: Nineteen ALS patients and 10 healthy subjects underwent a 3T-MR exam including a 3D multi-echo T2*-weighted sequence targeting M1. Signal intensity of M1 was assessed both visually by two observers and using a semiautomatic procedure. After drawing M1 profile, the algorithm produced a curve representing the average signal intensity along the

profile normalized with respect to that of the splenium of corpus callosum. M1 hypointensity was measured by the height of such curve. UMN impairment of patients was clinically assessed using the UMN-scale. Non-parametric statistics and ROC curve were used for analysis.
Results: At visual assessment, sensitivity was lower at 3T (0.42 and 0.58, respectively, for the two observers; inter-observer agreement=0.69) than that at 7T. At semi-quantitative analysis, M1 signal intensity was lower in patients than in controls ($p<0.0001$); sensitivity and specificity were 0.79 and 0.83 (AUC=0.88). In patients, M1 hypointensity correlated with the UMN impairment ($r=0.60$; $p<0.0001$).
Conclusion: Despite the unsatisfactory accuracy of qualitative assessment at 3T, semi-automated algorithms could increase the sensitivity in evaluating M1 signal changes in ALS patients with moderate-severe UMN impairment, reaching 7T performance.

B-1316 14:17

Retinal neurodegeneration is associated with structural MRI markers of cerebral neurodegeneration

U. Mutlu, M.A. Ikram, P. Bonnemaijer, L.G.M. Cremers, W.J. Niessen, C.C.W. Klaver, M.I. Ikram, M.W. Vernooij; *Rotterdam/NL (u.mutlu@erasmusmc.nl)*

Purpose: Retinal neurodegeneration, quantified using optical coherence tomography (OCT), is considered a potential biomarker for cerebral neurodegeneration, evaluated on magnetic resonance imaging (MRI). We investigated the association of retinal nerve fiber layer (RNFL) and ganglion cell layer (GCL) on OCT with structural markers of cerebral neurodegeneration on MRI.
Methods and Materials: We included 2585 participants (age&gt45 years) from the population-based Rotterdam Study (2007-2012) who had gradable quality OCT images and cerebral MRI scans. Thickness of RNFL and GCL were measured on OCT images. Structural markers of cerebral neurodegeneration were assessed on MRI. Associations between retinal layer thickness and structural MRI markers were examined using linear regression models, adjusting for age, sex, intracranial volume, and cardiovascular risk factors.
Results: We found that thinner GCL was associated with smaller grey matter volumes, adjusted mean difference per standard deviation decrease in GCL: -0.032; 95% confidence interval: -0.055; -0.010). Also thinner RNFL was associated with smaller white matter volume: -0.033 (-0.056; -0.010). Furthermore, both thinner RNFL and GCL were associated with poor white matter microstructure, adjusted mean difference in fractional anisotropy per SD decrease in RNFL and GCL: -0.061 (-0.097; -0.026) and -0.067 (-0.104; -0.029), respectively. Finally, we found that thinner RNFL was associated with less hippocampal volume, adjusted mean difference per SD decrease in RNFL: -0.081 (-0.113; -0.049).
Conclusion: Retinal neurodegeneration is associated with micro-and macrostructural MRI markers of cerebral neurodegeneration. These findings suggest that specific changes in retinal layers may be considered as novel markers for cerebral neurodegeneration.
Author Disclosures:
W.J. Niessen: Other; Wiro J. Niessen is Chief Scientific Officer of Quantib BV; Reports no disclosures for present work.

B-1317 14:25

Dorsolateral putaminal hypointensity on diffusion-weighted imaging in differentiating parkinsonism-predominant multiple system atrophy from Parkinson's disease

K. Zheng, L. Ma; *Beijing/CN (zhengkuihong1971@sina.com)*

Purpose: To evaluate the diagnostic value of dorsolateral putaminal hypointensity on diffusion-weighted imaging (DWI) for differentiating parkinsonism-predominant multiple system atrophy (MSA-p) from Parkinson's disease (PD).
Methods and Materials: Eleven patients with MSA-p, 18 patients with PD and 30 age-matched controls were included. All subjects were examined with 3.0 T MRI using conventional and DWI protocol. Putaminal atrophy, slit-like T2-hyperintense rim of the dorsolateral putamen, and hypointensity on DWI were evaluated. The pattern of dorsolateral putaminal hypointensity on DWI was measured using a visual grading scale.
Results: Putaminal atrophy, slit-like T2-hyperintense rim, and dorsolateral putaminal hypointensity on DWI (with a score ≥2) were recognised in MSA-p patients in 54.5% (6/11), 63.6% (7/11) , and 81.8% (9/11), respectively, but in none of PD or control group. The score of putaminal hypointensity on DWI was significantly higher in MSA-p than in those of other groups ($p < 0.001$), and a score of ≥ 2 well-differentiated MSA-p from PD. The specificity and sensitivity of the dorsolateral putaminal hypointensity on DWI for distinguishing MSA-p from PD were 100% and 81.8%, respectively.
Conclusion: Dorsolateral putaminal hypointensity on DWI, along with both putaminal atrophy and slit-like putaminal T2-hyperintense rim, is a reliable MR imaging biomarker in differentiating MSA-p from PD.

B-1318 14:33

The optimisation of magnetic resonance imaging pulse sequences in order to better detection of multiple sclerosis plaques

J. Abdolmohammadi; *Baharan/IR (Abdolmohammadi.jamil@gmail.com)*

Purpose: Magnetic resonance imaging (MRI) is the most sensitive technique to detect multiple sclerosis (MS) plaques. In some cases, the patients who were suspected to MS whereas MRI images are normal, but whether patients don't have MS plaques or MRI images are not enough optimised enough in order to show MS plaques? The aim of this study is evaluating the efficiency of different MRI sequences for better detection of MS plaques.
Methods and Materials: In this cross-sectional study which was performed at Shohada-E Tajrish in Tehran - Iran hospital between October, 2011 to April, 2012, included 20 patients who suspected to MS disease were selected and underwent routine brain Pulse sequences (Axial T2w, Axial T1w, Coronal T2w, Sagittal T1w, Axial FLAIR). Additional sequences such as: Sagittal FLAIR Fat Sat, Sagittal PDw-fat Sat, Sagittal PDw-water sat was also performed.
Results: The results in more than 19 lesions showed that, for the subcortical and infratentorial areas, PDWw sequence with fat suppression is the best choice, and in 33 plaques located in periventricular area, FLAIR Fat Sat was the most effective sequence than both PDw fat and water suppression pulse sequences.
Conclusion: Although large plaques may visible in all images, but important problem in patients with suspected MS is screening the tiny MS plaques. This study showed that for revealing the MS plaques located in the subcortical and infratentorial areas, PDw-fat sat is the most effective sequence, and for MS plaques in the periventricular area, FLAIR fat sat is the best choice.
Author Disclosures:
J. Abdolmohammadi: Author; Zahra Farshidfar.

B-1319 14:41

Longitudinal diffusion tensor imaging in early stage Parkinson's disease

T. Minett[1], L. Su[1], E. Mak[1], R.A. Lawson[2], A. Yarnall[2], G.W. Duncan[3], R.A. Barker[1], D. Burn[2], J.T. O'Brien[1]; [1]*Cambridge/UK*, [2]*Newcastle upon Tyne/UK*, [3]*Edinburgh/UK (tsm34@medschl.cam.ac.uk)*

Purpose: To verify whether white matter microstructural changes are predictors of cognitive decline in Parkinson's disease (PD), and if longitudinal white matter microstructural changes differ between patients with PD with normal cognition and those with mild cognitive impairment (MCI).
Methods and Materials: A total of 123 patients with early PD were enrolled (48 PD-MCI and 75 PD-normal cognition) along with 49 controls. Participants were part of the ICICLE-PD (Incidence of Cognitive Impairment in Cohorts with Longitudinal Evaluation) study and underwent clinical, cognitive and DTI investigations at baseline and 18 months later. Baseline and longitudinal fractional anisotropy (FA) and mean diffusivity (MD) changes were analysed voxelwise using Tract Based Spatial Statistics in generalised linear models. To verify if baseline FA and MD were independent predictors of cognitive decline, partial correlation (pr) analyses were performed. All analyses were controlled for age, sex, education, levodopa dose and visit intervals.
Results: At baseline, patients with PD had significantly higher widespread MD then controls regardless of their cognitive status. At follow-up, all groups showed a further significant FA decrease and MD increase. However, in patients with PD-MCI, MD deteriorated significantly faster in frontal brain areas when compared to those without MCI. Furthermore, baseline MD was a significant predictor of cognitive decline in patients with PD (pr 0.23; p 0.014).
Conclusion: MD represents an important correlate and predictor of cognitive decline in PD: DTI is potentially a useful tool in stratification of patients into clinical trials and to monitor the impact of treatment on cognition.

B-1320 14:49

Evolution of brain lesions in patients with antiphospholipid syndrome: a longitudinal MRI study

P. Svrckova, R. Jäger; *London/UK (psvrckova@doctors.net.uk)*

Purpose: Patients with antiphospholipid syndrome (APS) are prone to neurological complications, mainly ischaemic, frequently despite full anticoagulation. We conducted a longitudinal study with serial follow up to determine what types of brain lesions occur and in what proportion they progress.
Methods and Materials: All available MRI brain studies of 34 patients with APS under follow up at our regional haematology center were retrospectively reviewed. The brain lesions were categorised by type, chronicity and location. Comparison was made with previous imaging where available and note was made of any new lesions.
Results: The mean imaging follow up time was 3.5 (range 1.5-9.7) years. Of the 34 patients, 3 were excluded because of other significant pathology; 5 had had no interval scan. Of the 26 patients with follow up imaging, 14 had no new lesions and 12 had new lesions. 5 had a normal initial scan. The most frequently encountered lesions on initial scan were rounded/confluent white

matter lesions (WML; N=18), cortical infarct (N=9), basal ganglia/thalamic infarct (N=7), linear/wedge shaped WML (N=4) and venous thrombosis (N=3). The most frequently occurring new lesions on follow up imaging were rounded/confluent WML (N=12), cortical infarct (N=6), basal ganglia infarct (N=3), venous thrombosis (N=3) and linear/wedge shaped WML (N=1).
Conclusion: Despite maximum anticoagulation, a significant proportion of patients with APS develop new lesions, mainly WML, cortical and basal ganglia infarcts. Linear WML could potentially be venous infarcts. There is a need for optimisation of anticoagulation therapy to minimise the frequency of new lesions and associated disability.

B-1321 14:57

Associations among cognitive functions, plasma DNA, and white matter integrity in patients with early-onset Parkinson's disease

Y.-S. Chen, M.-H. Chen, C.-H. Lu, P.-C. Chen, H.-L. Chen, I.-H. Yang, N.-W. Tsai, W.-C. Lin; *Kaohsiung/TW (qqqqqq4545@cgmh.org.tw)*

Purpose: Early-onset Parkinson's disease (EOPD) patients are symptomatic at a relatively young age. Few studies have reported cognitive impairments in EOPD with diverse results. Furthermore, it is unclear what microstructural white matter (WM) changes are present in EOPD patients. We therefore conducted this study to investigate the microstructural WM changes experienced by EOPD patients and their association with cognitive function and plasma DNA levels.
Methods and Materials: We enrolled 24 EOPD patients and 32 sex- and age-matched healthy volunteers that underwent complete neuro-psychological testing (NPT) to evaluate their cognitive function and diffusion tensor imaging (DTI) scanning to determine their fiber integrity. The plasma DNA measurements included measurements of nuclear and mitochondrial DNA levels. Fractional anisotropy (FA) maps were compared using voxel-based statistics to determine differences between the two groups. The differences in DTI indices and NPT scores were correlated after adjusting for age, sex, and education.
Results: Our results demonstrate that EOPD patients have elevated nuclear DNA levels and wide spectrums of impairments in NPT, especially in the executive function and visuospatial function domains. Exploratory group-wise comparisons of the DTI indices revealed that EOPD patients exhibited lower DTI parameters in several brain locations. These poorer DTI parameters were associated with worse cognitive performances and elevated plasma nuclear DNA levels, especially in the anterior thalamic radiation region.
Conclusion: Our findings suggest that thalamus and its adjacent anterior thalamic radiation may be important in the pathogenesis of EOPD, as it appears to become involved in the disease process at an early stage.

B-1322 15:05

The morphometric parameters in MRI for differentiation progressive supranuclear Palsy from Parkinson's disease, multiple system atrophy and controls

E. Aydin[1], C. Eraslan[1], A. Acarer[1], E. Akyuz[2], Z. Colakoglu[1], C. Callı[1], O. Kitis[1]; [1]*İzmir/TR*, [2]*Aydın/TR (elcinaydin09@yahoo.com.tr)*

Purpose: The aim of this study was to evaluate the accuracy of magnetic resonance parkisonism index (MRPI) and cerebral peduncle angle compared with the other MRI measurements, in distinguishing progressive supranuclear palsy (PSP) from Parkinson's disease (PD), multiple system atrophy (MSA) and controls (C).
Methods and Materials: Nine PSP patients, 8 MSA patients, 6 PD patients, and 7 control subjects underwent MRI and, for each patient the pons area-midbrain area ratio (P/M) and MCP width-SCP width ratio (MCP/SCP) were used, and an index termed MR parkinsonism index was calculated [(P/M) _ (MCP/SCP)] and also the cerebral peduncle angle, that is, the angle between the two cerebral peduncles was measured. Differences in MR imaging measurements among groups were evaluated with Tukey HSD, Kruskal-Wallis test and Bonferroni correction.
Results: P/M and MCP/SCP were significantly larger in patients with PSP than in patients in MSA, PD and C groups. MRPI index value was significantly larger in patients with PSP (median, 17,75) than patients with PD (median, 7.42; P< .001), and control participants (median, 9.73; P <.001). The cerebral peduncle angle measurements were 64.28° (SD, 6.03°) in PSP patients, 54.79° (SD, 7.43°) in C group, 55.56° (SD, 1.15°) in patients with MSA, and 56.75° (SD, 2.07°) in patients with PD. MRPI and cerebral peduncle angle measurement showed higher accuracy to distinguish PSP from other groups (100% sensitivity and specificity).
Conclusion: MRPI and the cerebral peduncle angle are useful criterion for differentiating patients with PSP from PD, MSA patients and healthy persons.

B-1323 15:13

Combined R2* maps generated by IDEAL-IQ and cerebral blood flow by 3D-ASL as markers of cognitive deficit in Parkinson's disease

R.-H. Yan, X. Wei, J. Wang, Q. Wang; *Guangzhou/CN (yanrh@mail3.sysu.edu.cn)*

Purpose: To identify a PD-specific MRI pattern using combined iterative decomposition of water and fat with echo asymmetry and least-squares estimation quantitation (IDEAL-IQ) sequence and three-dimensional arterial spin labelling (ASL) to discriminate early cognitively impaired PD (PD-CI) from cognitively normal subjects and evaluate disease status.
Methods and Materials: Twenty-one PD-CI and 20 cognitively normal PD (PD-CN) patients,and 22 healthy controls underwent 3T MRI examination with R2* maps and cerebral blood flow (CBF) measurements. R2* and CBF in cerebral regions of interest (ROIs) were compared between three groups. Pearson's and Spearman's rank correlation analyses were performed to evaluate correlations between the above variables and clinical parameters. The stratified five-fold cross-validation was conducted to determine the efficacies of combined MRI parameters in evaluating cognitive status and diagnosing PD.
Results: Compared with controls, there was a susceptibility effect reflecting hyperintense on R2* maps in substantia nigra (SN) in both of PD-CI(p=0.001) and PC-CN (p=0.010),and declined perfusion in basal ganglia. The R2* in caudate nucleus (Cau) and putamen (Pu) were inversely correlated with cognitive deficit(Cau,r=-0.427,p=0.005;Pu,r=-0.321,p=0.041), whereas a positively correlation was observed between CBF and MMSE score in PD patients(Cau,r=0.449,p=0.003;Pu,r=0.344,p=0.028) . Stratified five-fold cross-validation identified Cau CBF and Pu R2* and the combination of them offered excellent accuracy (AUC 0.838) in distinguishing PD-CI from PD-CN.
Conclusion: This study characterises a multimodal approach using combined IDEAL-IQ and 3D-ASL for monitoring PD. These results demonstrate the changes in Cau CBF and Pu R2* values might serve as potential markers of early-stage cognitively impaired PD.

B-1324 15:21

White matter volume loss in amyotrophic lateral sclerosis: a metanalysis of voxel-based morphometry studies

G. Chen, B. Zhou, X. Huang, Q. Gong; *Chengdu/CN (cgx23ly2002@163.com)*

Purpose: To identify statistical consensus between published studies for white matter (WM) volume in amyotrophic lateral sclerosis (ALS).
Methods and Materials: A systematic search was conducted for the relevant studies with voxel-wise analysis of the WM volume in ALS. Effect-size signed differential mapping (ES-SDM) was applied to analyse the WM volume differences between ALS patients and healthy controls. Meta-regression was used to explore the effects of clinical characteristics on WM volume in patients with ALS.
Results: A total of 11 studies with 16 datasets including 283 patients and 255 healthy controls were identified. The pooled metanalysis revealed significant WM volume reductions in bilateral supplementary motor area (SMA), bilateral precentral gyri (PG), left middle cerebellar peduncle and right cerebellum in ALS patients relative to healthy controls. Fibre tracking indicated that the main WM tracts involved were the corticospinal tract, interhemispheric fibres running through the SMA, subcortical arcuate fibres and projection fibres to the striatum running through the PG, projection fibres from the cerebral cortex to pons and cerebellum running through the middle cerebellar peduncle. The ALSFRS-R was positively correlated with decreased WM volume in bilateral SMA. The duration of illness was negatively correlated with WM volume reduction in the right SMA and right PG.
Conclusion: This study provides a thorough profile of WM volume loss in ALS and further evidence that the involved brain regions include both motor and extramotor areas, supporting the view of ALS being a multisystem degenerative disorder.

14:00 - 15:30 **Room F2**

Breast

SS 1902a

Assessment of the effect of neoadjuvant therapy

Moderators:
F. Thibault; Paris/FR
R.M. Trimboli; Milan/IT

B-1325 14:00

Volume-based histogram analysis of breast cancer (BC) before neoadjuvant chemotherapy (NAC): could MRI features predict tumour response?

C. Losio, A. Della Corte, M. Panzeri, P. Panizza, A. Del Maschio, F. De Cobelli; *Milan/IT (claudiolosio@yahoo.it)*

Purpose: Response of locally advanced BC to NAC is difficult to predict. Identification of predictive factors with multiparametric breast MRI has been attempted by tracing peritumoural ROIs on axial images, with non-univocal results. Volume-based histogram analysis of MRI parameters, including first-order texture kinetics, is an emerging method for a more accurate assessment of tumour heterogeneity, intrinsic to more aggressive subtypes. Our work has explored the relationship between this analysis and subsequent response to NAC.
Methods and Materials: Sixty-nine patients with locally advanced, biopsy-proven BC, eligible for a taxane and anthracycline-based regimen, were retrospectively selected. Image data from baseline MRI (T2-TurboSpinEcho, DWI with b-values of 0.900 s/mm^2, T1-GradientEcho dynamic study) were post-processed (OLEA Sphere 2.4, Olea Medical), generating maps for apparent diffusion coefficient (ADC), T2 signal intensity and all perfusion semiquantitative parameters. Peri-lesional Volume of interest (VOI) was semiautomatically drawn on these maps, and a histogram analysis including first-order texture kinetics was performed for each parameter. Correlations between these values and response to NAC (evaluated on the surgical specimen) were finally assessed with univariate and multivariate analysis.
Results: Univariate analysis revealed a significant association between non-responders and higher AUCmax (p value=0.0338), AUCrange (p value=0.0311), TME75^{percentile} (p value=0.0452), and lower washout (10,20,25,30^{percentile} p value<0.05). A multivariate model was found for prediction of non-response, based on lower TMEmin (LogOR=-3.2202) and T260^{percentile}. No mean values yielded significant results.
Conclusion: Histogram-derived texture analysis of MR images can identify potential predictors of non-response to NAC, in women affected by locally advanced BC. A more heterogeneous angiogenesis, the presence of fibrosis or necrotic areas seem to be markers of chemoresistance.

B-1326 14:08

MR imaging after neoadjuvant therapy in subtypes of locally advanced breast cancer - correlation with predictive pathologic models of response

R.M. Lorente Ramos, J. Azpeitia Armán, T. Rivera García, M. Lara Alvarez, A. Martín Escobedo; *Madrid/ES (rlorenter@yahoo.es)*

Purpose: To review correlation of magnetic resonance (MR) imaging findings in patients with Neoadjuvancy, with different pathological systems of response evaluation, including Miller Payne and Residual Cancer Burden.To analyse correlation of the differente types of radiological response to neoadjuvant therapy in different tumour subtypes.
Methods and Materials: We retrospectively reviewed 53 patients with locally advanced breast cancer undergoing neoadjuvant therapy (NAC) previous to surgery between January 2009 and February 2015. Pre and posttreatment dynamic MR and diffusion-weighted sequences were performed. Parameters that were evaluated: on pathology tumour response was clasified according to Miller-Payne System based on changes in cellularity and grade and response in lymph nodes, and Residual Cancer Burden system.On MR: T2 signal, changes in tumour size, type and percentage of response, contrast enhancement kinetics, apparent diffusion coefficient (ADC), and response in lymph nodes.
Results: Tumour phenotypes were Luminal A (16.6%), Luminal B (43%), Triple Negative (16.6%), HER2+ (23%). After NAC, pathological complete response (pCR) was found in 30% of cases. On MR response was complete in 23%, and partial in 63%: fragmentation in 20% and concentric shrinkage in 43 %. Failures in MR-pathology correlation were found mostly in patients with fragmentation type response.
Conclusion: MR correlation with pathology is high in the evaluation of response both with Miller-Payne and RCB systems. Response may be overestimated by MR in patients with non-mass lesions and fragmentation response when residual tumour consists of small or scattered foci. MR stimation shows better correlation in patients with triple negative and Her2 subgroups.

B-1327 14:16

The relationship between tumour response to neo-adjuvant chemotherapy and response patterns seen on breast MRI

B. Goorts, K. Dreuning, J. Houwers, L. Kooreman, M. Moosdorff, T. van Nijnatten, E. Boerma, M. Smidt, M.B.I. Lobbes; *Maastricht/NL (marclobbes@planet.nl)*

Purpose: To investigate the relationship between breast MRI and histopathological tumour response patterns in patients treated with neoadjuvant chemotherapy (NAC).
Methods and Materials: Breast cancer patients treated with NAC and having baseline and half-way breast MRI exams in 2012-2015 were considered. Exclusion criteria were previous ipsilateral breast surgery, previous systemic treatment because and presence of distant metastasis at time of diagnosis. Tumours were classified into six shrinkage patterns: type 0 (complete radiologic response); type 1 (>5mm concentric shrinkage without surrounding lesions); type 2 (concentric shrinkage with crumbling and surrounding lesions); type 3 (crumbling: shrinkage into residual multinodular lesions); type 4 (stable disease, i.e. no increase or decrease of >5mm); type 5 (progressive disease). Percentage of patients with good pathologic tumour response (>50% tumour reduction, Pinder 1-2ii) for each MRI response pattern was calculated.
Results: Eighty primary breast tumours (76 patients) were included. Tumours with type 0, 1 or 3 pattern had significantly higher good pathologic response rates compared to type 2 or 4 (p<0.001). All crumbling tumours (type 3) showed good pathologic response. Tumours with type 0 or 1 pattern showed good pathologic response in 80% and 93%. Tumours with type 2 or type 4 pattern showed 47% and 40% good pathologic response. No tumour showed type 5 response.
Conclusion: Tumour response patterns on breast MRI are correlated to pathologic tumour response. Crumbling tumours on MRI have highest good pathologic response rates and tumours that don't show response halfway chemotherapy (type 4) show lowest response rates.

B-1328 14:24

Results of diffusion-weighted and dynamic contrast-enhanced MRI as biomarkers for evaluation of breast cancer response to neoadjuvant chemotherapy

O.S. Shliapkina, E.A. Mershina, Y.N. Nenakhova, V.E. Sinitsyn, V.K. Lyadov; *Moscow/RU (shlyapkinaolga571@gmail.com)*

Purpose: To analyse the changes of apparent diffusion coefficient (ADC) and contrast enhancement during neoadjuvant chemotherapy (NAC) for prediction of breast cancer response.
Methods and Materials: 23 patients (55±10 y.o.) with pathologically proven breast cancer T2-T4 stages (TNM) who underwent NAC followed by surgery were retrospectively enrolled. MRI was performed with 3T MR system before NAC, after 2rd and 4-6th NAC cycles including dynamic contrast-enhancement sequences and DWI. ADC value (mean of three tumour ROI), types of enhancement curves, percentage of wash-in and the largest tumour size were analysed. The patients had 2-5 grades of pathologic response based on the Miller-Payne system.
Results: The largest tumour diameter before treatment was 42±19mm. After NAC it significantly decreased to 24±13mm (p<0.01, t=4.259). Percentage enhancement in arterial phase (wash-in) significantly decreased from 226±88% to 132±60% after NAC (p<0.01, t=3.607). Enhancement curves changed from washout and plateau types to slow progressive enhancement in 74%.The tumour ADC increased from 1.035±0.391x10^{-3}mm^2/s before treatment to 1.392±0.388x10^{-3}mm^2/s after treatment (p<0.01, t=3.417). The tumour ADC increased from 1.035±0.391x10^{-3}mm^2/s before treatment to 1.392±0.388x10^{-3}mm^2/s after treatment (p<0.01, t=3.417). ADC for grade 2 (4 pts) before NAC was 1.118±0.171x10^{-3}mm^2/s, after NAC - 1.250±0.215x10^{-3}mm^2/s; for grade 3 (10 pts) - 1.104±0.484x10^{-3}mm^2/s and 1.518±0.570x10^{-3}mm^2/s; for grade 4 (3 pts) - 1.057±0.514x10^{-3}mm^2/s and 1.453±0.385x10^{-3}mm^2/s; for grade 5 (6 pts) - 0.967±0.281x10^{-3}mm^2/s and 1.409±0.404x10^{-3}mm^2/s.
Conclusion: CE MRI and DWI showed significant changes after NAC. Their results could be used as imaging biomarkers to predict and assess pathologic response of breast cancer tumours to chemotherapy. Bigger population of patients should be investigated.

B-1329 14:32

Texture and geometrical analysis in breast MRI: prediction of response to neo-adjuvant chemotherapy (NAC)

M. Panzeri[1], C. Losio[1], P. Panizza[1], F. Gallivanone[2], A. Del Maschio[1], F. De Cobelli[1]; [1]*Milan/IT*, [2]*Segrate/IT (panzeri.marta@gmail.com)*

Purpose: The role of baseline breast MRI in predicting response to NAC is debated, mainly due to the lack of standardised and accurate methods for imaging biomarkers extraction. Both texture and geometrical analysis of MR images are new promising tools to evaluate tumour heterogeneity, but few studies evaluated their usefulness in breast cancer (BC). Our purpose was to assess the role of accurate quantification of MRI advanced parameters before the beginning of NAC.
Methods and Materials: We included 38 women with biopsy-proven locally advanced BC addressed to NAC and subsequent surgery at our institution. All patients underwent a baseline breast MRI (T2-TSE; DWI: b-value=0,900 s/mm2; T1-3D-FFE dynamic study) 2 weeks before NAC. Geometrical and textural features were extracted from ADC maps, T2 and subtraction images and a logistic regression model was applied to assess the correlation to pathological complete response (pCR).
Results: MR intensity-based features "Entropy" and "Skewness" were found to be correlated with pCR (p-value<0.05). Limiting the sample to Triple Negative tumours, the analysis showed that the geomatrical features "Compactness" and "Spherical disproportion" were found correlated with pCR. At multivariate analysis an independent statistically significant association was found (p< 0.05) between pCR, "Sphericity","Surface to Volume ratio", "Entropy", "Skewness", "Standard Deviation" "Uniformity" (p< 0.05), and "Variance".
Conclusion: Our results show that the features "Entropy" and "Skewness" are significantly associated with pCR. These two parameters are indexes of the tumoural heterogeneity. Multivariate analysis confirmed this result and also suggested that the geometrical properties of tumour volume could be related to pCR.

B-1330 14:40

Background parenchymal enhancement: correlation with pathological response after NACHT and tumour biological subtypes

L. Ballesio, S. Gigli, C. Boldrini, C. Catalano; *Rome/IT (adrenalina_1@hotmail.it)*

Purpose: To analyse the possible role of background parenchymal enhancement (BPE) in predicting response after neoadjuvant chemotherapy (NACHT) and to evaluate its correlation with the different biological tumour subtypes.
Methods and Materials: We reviewed the MR exams of 63 patients and classified the BPE intensity before and after NACHT according to the BIRADS lexicon (1: absent, 2: mild, 3: moderate, 4: severe). The tumours were classified based on their biological profiles as Luminal A, luminal B, HER2 + and triple negative. The final pathological response after chemotherapy was assessed on the surgical specimen classified according to Miller and Payne system as complete (CR grade 5), partial (PR grade 3-4) and non-response (NR grade 1-2). Fisher test was used correlate BPE with the final pathologic response and with the different tumour biological profiles.
Results: BPE intensity (1/2/3/4) was, respectively, 28/12/18/5 before NACHT and 52/8/3/0 after NACHT. We observed an overall decreasing trend of BPE intensity after NACHT (p<0.005). Premenopausal patients achieved a greater BPE decrease than postmenopausal women (mean reduction, respectively :1.0 and 0.4 , p<0.005). Triple-negative cancer was more frequently associated with marked BPE before treatment (p<0.02). 16 patients achieved pCR. We observed a statistic association between complete response and marked BPE reduction (p<0.001).
Conclusion: BPE intensity decrease should be proposed as a predictive response factor to NACHT. Triple-negative cancer often presents marked BPE before treatment.

B-1331 14:48

Predictive factor affecting residual metastatic axillary lymph node disease in patient with negative axillary imaging after neoadjuvant chemotherapy for breast cancer

N. Jung, W. Kim; *Daegu/KR (nari14133@gmail.com)*

Purpose: To evaluate predictive factors affecting residual metastatic axillary lymph node (ALN) in patients with negative axillary imaging after neoadjuvant chemotherapy (NAC) for breast cancer.
Methods and Materials: Among 206 eligible patients with breast cancers who underwent NAC and curative surgery, 154 patients (mean age, 46.7 years) showed no suspicious ALN in negative axillary imaging including ultrasound, MRI and PET/CT after NAC. Data collected included age, clinical T, N stage, initial tumour size, histologic grade, hormonal receptor (HR), human epidermal growth factor receptor 2 (HER2), Ki-67, and percent tumour size change (≥ 30% decrease, < 30% decrease). Multivariate logistic regression analysis was performed between patients with and without residual metastatic ALN.
Results: Of the 154 patients who showed negative axillary imaging, 55 patients (35.7%, 95% confidence interval [CI]: 26.9% - 46.5%) had residual metastatic ALN disease on surgical histology. Among them, 43 patients had 1 - 3 residual metastatic ALNs (27.9%, 95% CI: 20.2% - 37.6%) and 12 had more than 4 residual metastatic ALNs (7.8%, 95%CI: 4.0% - 13.6%). Clinical N stage (*P* = .075), low to moderate tumour grade (odd ratio [OR] = 5.2, *P* = .009), positive HR status (OR = 6.6, *P* = .003), negative HER2 status (OR = 2.6, *P* = .048) were independently associated with residual metastatic ALN.
Conclusion: Low to moderate histologic grade and positive HR status are predictors for residual metastatic ALN in patients with negative axillary imaging after NAC for breast cancer.

B-1332 14:56

Impact of image fusion technique for the localisation of the achieved clinically complete response (cCR) lesions in breast conserving surgery after neoadjuvant chemotherapy

S. Nakano, K. Fujii, T. Ando, T. Ishiguchi; *Nagakute/JP (snakano1@aichi-med-u.ac.jp)*

Purpose: An accurate evaluation of the extent of residual disease after neoadjuvant chemotherapy (NAC) for breast cancer appears essential for successful clinical outcomes. However, there are some limitations in the localisation of the achieved clinically complete response (cCR) lesions in breast conserving surgery (BCS). Recently, we have developed an image fusion technique (real-time virtual sonography; RVS). RVS can overlay a real-time ultrasound (US) image with the previously acquired MRI/CT/US images of the same site in real time. The objective of our study was to determine the relative accuracy of RVS in detecting US/MRI occult lesions after NAC.
Methods and Materials: Five breast cancer patients who achieved a cCR after NAC with stage IIA-IIB were enrolled in this study. All patients underwent mammography, US, MRI/CT, and RVS before and after NAC. MRI was performed with a 1.5-T scanner in the supine position using a flexible body surface coil to achieve the same position as that used in US. Based on MRI/CT/US results of pre-NAC, we determined the surgical resection area by using RVS.
Results: The average age of patients was 49. The mean lesion size on MRI was 23mm. Applying pre-NAC MRI/CT/US images in RVS, we accurately localised the resection area on the body surface and performed BCS on all patients. Three of five were diagnosed pathological CR, and all surgical margins were negative.
Conclusion: RVS is a useful imaging technique for the localisation of the achieved cCR lesions in breast conserving surgery after NAC.

B-1333 15:04

Early evaluation of pathological response to neoadjuvant chemotherapy in breast cancer using quantitative 1H-MRS

M. Signorini, L. Camera, I. Baglio, G. Meliadò, C. Cavedon, S. Montemezzi; *Verona/IT (manuel.signorini@alice.it)*

Purpose: The aim of this study was to retrospectively assess the accuracy of changes in choline signal-to-noise ratio (SNR) after the beginning of neoadjuvant chemotherapeutic treatment (NACT), with the aim of predicting the pathological response.
Methods and Materials: The study included 28 Patients with histological diagnosis of breast cancer who underwent breast Magnetic Resonance (MR) between June 2012 and February 2016. For each Patient, tumour volume at the diagnosis, after two NACT cycles and at the end of the treatment (six cycles) was calculated. MR-spectroscopy was also performed at the beginning and after two NACT cycles. All Patients underwent mastectomy and histological evaluation of the specimen to establish the pathological rate of response. Sensitivity, specificity, positive (PPV) and negative predictive value (NPV) of choline SNR and volume changes as predictors of complete pathological response (cpr) were calculated; correlation between these parameters using Pearson correlation index was evaluated.
Results: SNR<2 after two NACT cycles to predict cpr showed sensitivity=83,3% (±29,8%, CI:95%), specificity=72,7% (±18,6%, CI:95%), PPV=45,5% (±29,4%%, CI:95%) and NPV=94,1% (±11,2%, CI:95%). There was no statistically significant difference between choline SNR and volume variation in distinguishing Patients achieving cpr from ones who did not. These two parameters showed a moderate correlation (ρ=0.5318), stronger in the subset of Patients with cpr (ρ=0,69) and weaker in that with a 10-50% residual cancer (ρ=0,43).
Conclusion: MRS showed moderate sensitivity, good specificity and high NPV in predicting early cpr after NACT. No statistically significant difference was observed between accuracies of MRS and volume variation.

B-1334 15:12

Comparative evaluation of MR spectroscopy choline signal-to-noise ratio (SNR) with ki-67 as a prognostic indicator

S.B. Grover, P. Jain, S. Suman, S. Jain, A. Mandal; *New Delhi/IN (shabnamgrover@yahoo.com)*

Purpose: Breast cancer is governed by several established histopathological prognostic parameters. Ki-67 is a nuclear protein, being used as a marker for cellular proliferation. Therefore, higher Ki-67 levels are associated with higher tumour grades. Prognostic factors help in individualistic management, decision on treatment protocols and in post treatment follow up. Imaging studies using choline detection as a marker of tumour aggressiveness are relatively newer techniques under evaluation for non-invasive prognosis prediction.
Methods and Materials: Forty-two female patients with newly diagnosed, biopsy proven breast cancer, larger than 2 cm, were included in the study approved by the Institute Review Board. Choline presence was recorded by MR proton spectroscopy using signal-to-noise (SNR), and was considered positive, when the peak was obtained at 3.2ppm with SNR>2.5. Ki-67 labelling index was obtained from biopsy specimens. The association between these two parameters, choline SNR and Ki-67, was estimated using the Spearmans rank correlation coefficient.
Results: Positive correlation was found between choline SNR and Ki-67 index with a correlation coefficient of 0.42 and p=0.005. Choline SNR was significantly higher for tumours with higher Ki-67 labelling index.
Conclusion: Significant correlation between choline SNR and histological prognostic factors indicates its potential role as a future non-invasive imaging biomarker in predicting tumour aggressiveness. Another promising application is the role of choline in predicting response to breast cancer treatment. Changes in choline levels within 24 hours after the first dose can serve as an early indicator for predicting clinical response to chemotherapy.

B-1335 15:20

Assessment of response to neo-adjuvant chemotherapy in breast carcinoma using shear wave elastography

V. Ramalingam, S. Hari, S.B. Paul, S. Thulkar, S. Vyas, A. Gogia, S.V.S. Deo, V. Seenu, S. Mathur, V. Sreenivas; *New Delhi/IN (drrvidyasagar@gmail.com)*

Purpose: Shear wave elastography (SWE) is a novel imaging technique for neo-adjuvant chemotherapy (NACT) response evaluation in breast cancer. Aim of this study is to evaluate NACT response in breast cancer using SWE.
Methods and Materials: Breast cancer patients scheduled for NACT were enrolled. B-mode ultrasound (US) and SWE were done prior to start of NACT (baseline), post-NACT after first and second cycles (between 7 and 14 days) and prior to surgery. SWE qualitative features -shape (Eshape), homogeneity (Ehomo), colour (Ecolour), and quantitative parameters of tissue stiffness - maximum (Emax), minimum (Emin), mean (Emean), ratio (Erat) were evaluated and baseline parameters and elasticity changes post-NACT were correlated with Miller-Payne scoring on histopathology post-surgery (gold standard).
Results: Twenty-eight patients with 29 masses were evaluated post-NACT. The mean baseline elasticity of responders (n=13) and non-responders (n=16) were not significantly different and showed poor correlation with Miller-Payne score (r=-0.086). The difference in mean elasticity (Δstiffness), however, was significantly higher in responders than in non-responders (49.50 Kpa vs 15.97 Kpa, P<.001) after the first cycle and showed the same trend on subsequent assessments. ROC analysis showed area under curve of 0.802 (p=0.001) for difference in the mean elasticity after first cycle. A Δ stiffness threshold for distinguishing between responders and nonresponders at 29.5 Kpa gives 83.3% sensitivity and 75% specificity. Of the qualitative parameters, Ecolour showed the best discrimination between responders and non-responders (p<0.05).
Conclusion: SWE is a promising technique to assess NACT response in breast carcinoma. Early prediction of NACT response using SWE would help tailor the management.

14:00 - 15:30 **Room D**

Musculoskeletal

SS 1910a

Performance optimisation in musculoskeletal imaging

Moderators:
D. Berritto; Acerra/IT
J. Hodler; Zurich/CH

B-1336 14:00

High prevalence of vitamin D insufficiency among radiologists: are we a profession at risk?

C.A. Agten, B. Fritz, S. Bensler, A.B. Rosskopf, L. Margaroli, C.W.A. Pfirrmann; *Zurich/CH (christoph.agten@gmail.com)*

Purpose: To assess prevalence of vitamin D insufficiency in radiologists. Our hypothesis was that radiologists have a higher prevalence of vitamin D insufficiency because of the generally dark working environment, compared to non-radiologists.
Methods and Materials: This study was approved by the local ethics committee. Informed consent was obtained from all participants. The study was conducted at the Swiss Congress of Radiology in May 2016. Attendees (radiologists and non-radiologists) were asked to give a venous blood sample to measure vitamin D(25-hydroxyvitamin) blood serum level. Vitamin D insufficiency was defined <50nmol/l. We collected information on age, gender, profession, vitamin D supplements, sunny vacation in the last two months, eating fish. We compared vitamin D between radiologists and non-radiologists.
Results: In total 301 blood samples, 137 radiologists (mean-age 38-years; 38.7% female) and 164 non-radiologists (mean-age 40-years; 65.9% female) were analysed. Mean vitamin D in radiologists was 49.7nmol/l, in non-radiologists 47.5nmol/l (p=0.374). Vitamin D insufficiency was more frequent in radiologists (58.4% (80/137) vs 53.7% (88/164)), however this was not statistically significant (p=0.479). 26 radiologists and 17 non-radiologists were under vitamin D supplementation with higher vitamin D than those without supplementation (70.4nmol/l vs 44.7nmol/l; p<0.0005). There was no difference in vitamin D between radiologists and non-radiologists without vitamin D supplementation (44.9nmol/l vs 44.6nmol/l; p=0.884). Subjects with a recent sunny vacation had higher vitamin D (55.0 vs 45.9nmol/l; p<0.0005). Eating fish had no relevant impact on vitamin D.
Conclusion: Vitamin D insufficiency is very common among radiologists (58.4%), but not significantly higher than in non-radiologists.

B-1337 14:08

Comparison study of growth plate fusion using MRI vs plain radiographs for age determination

A.A. Jain, N. Bahri, H. Parekh, S. Chudasama; *Jamnagar/IN (a.jain56@yahoo.com)*

Purpose: To compare the grade of fusion of the wrist distal growth plate between MRI and plain radiographs.
Methods and Materials: We conducted a study of twenty five cases, presented in span of 6 months. Patients were subjected MR imaging after taking informed written consent and ethical clearance of hospital committee was taken. Each participant had coronal T1-weighted MRI and plain radiograph of wrist. X-rays of wrist: 300m.A. Philips M.R.S. MRI- 1.5 TESLA 8 CHANNEL SIEMENS MAGNETOM ESSENZA (Germany).
Results: MRI of the wrist offers an alternative and superior non-invasive method of age determination in 13-18 year-old adolescents. The inter-rater reliability for grading was high (r=0.91 and 0.92); all correlations were highly significant (p<0.001). The average age increased with a higher grading of fusion, and the correlation between age and grade of fusion was highly significant (r=0.69, p<0.001).
Conclusion: Skeletal age is defined as the age at which healthy children of the same sex generally achieve the skeletal maturation stage for a determined chronological age. Thus, skeletal age should correspond to the chronological age in healthy children of the same sex in attaining a similar degree of skeletal development. The wrist was chosen as the distal radius and ulna epiphysial plates are the sites of maximal endochondral ossification and physeal fusion in the age group of interest. However, for the purposes of comparing the x-ray and MRI, the larger distal radial epiphysis was chosen. MRI has become very sensitive modality for detection of fusion of epiphysis.

B-1338 14:16

Computer-aided bone age assessment of the wrist and carpal bones in comparison to Greulich and Pyle atlas method

C. Booz, J.L. Wichmann, S. Martin, D. Leithner, A. Al Kamali, L. Lenga, M. Albrecht, T.J. Vogl, B. Bodelle; *Frankfurt a. Main/DE (boozchristian@gmail.com)*

Purpose: To investigate bone age assessment of the wrist and carpal bones in children using a computer-aided diagnosis (CAD) system and Greulich and Pyle (GP) atlas method.
Methods and Materials: Data from clinically indicated hand and wrist radiographs of 238 patients (137 male, 101 female) were included. Bone age of left radius and the carpal bones were analysed by two radiologists using GP atlas method. In comparison, the left distal radius of each patient was analysed by CAD system (BoneXpert). Correlations between bone age derived from CAD system and GP atlas method were performed by Pearson product-moment correlation coefficient and Bland-Altman analysis.
Results: Mean bone age of all distal radius determined by CAD was 9.6 years and of all left distal radius determined by two radiologists was 10.0 years. Mean bone age of all carpal bones estimated by two radiologists was 10.0 years. The statistic analysis demonstrated a higher correlation between bone age values of left distal radius determined by two radiologists and the CAD system (r=0.9697) than bone age values of left distal radius determined by CAD and the carpal bones determined by two radiologists (r=9.962).
Conclusion: The correlation between bone age values of left radius determined by radiologists and the CAD system was higher than bone age values of the left radius determined by CAD and the carpal bones. A method which determines the bone age without analysing the carpal bones should be more accurate than methods analysing the left hand including the carpals like the GP-method.

B-1339 14:24

Can initial radiographs prevent useless dual-energy CT for urate crystal detection in work-up of gouty arthritis?

T. Finkenstaedt, S. Kupfer, S. Winklhofer, S. Tok, A. Becker, H. Alkadhi; *Zurich/CH (tim.finkenstaedt@usz.ch)*

Purpose: Due to inherent methodological reasons, urate deposits can be detected with dual-energy CT (DECT) only in the presence of hyperdense soft tissue deposits when a certain attenuation threshold is exceeded. Thus, we examined whether initial radiographs are capable to rule in or out soft tissue deposits in the work-up of gouty acroarthritis.
Methods and Materials: This retrospective study included 143 patients (52 female, 57±12ys) with suspected gouty arthritis who underwent clinically indicated DECT of the hand/wrist (n=60) and feet/ankle (n=83). Two blinded readers independently evaluated DECT images for the presence/location of soft tissue and subsequently urate deposits. Additionally, both readers evaluated corresponding radiographs (standard projections) for the presence/location of soft tissue deposits 4 weeks later. Finally, both datasets (DECT/radiographs) were evaluated to examine whether the particular location/density of the deposits may influence the deposit detection likelihood on radiographs.
Results: Inter-reader agreement for detection of soft tissue/urate deposits with DECT was excellent (κ=0.91/0.92, respectively) as was its detection on radiographs (κ=0.95). DECT showed periarticular deposits in eighty-seven of the 143 patients (61%). Thirteen of these 87 patients (15%) only had detectable deposits on radiographs (p<0.05). In sixty-eight patients (92%) of the remaining 74 patients the low deposit density and in 6 patients (8%) the particular deposit location was regarded as the main reason for missed detection on radiographs.
Conclusion: Radiographs are not sufficiently capable to rule in or out soft tissue deposits and thus cannot aid a priori if a dual-energy CT is reasonable in the work-up of gouty acroarthritis.

B-1341 14:32

ETD score: a pre-surgical prognostic evaluation in acetabular labrum's pathology on magnetic resonance arthrography

S. Magnani[1], S. Sdao[2], M. Brioschi[1], E. Nocerino[1], C. Messina[1], S. Rapisarda[1], A. Aliprandi[1], F. Sardanelli[1]; [1]*Milan/IT*, [2]*San Donato Milanese/IT (dr.smagnani@gmail.com)*

Purpose: Nowadays surgeons have more treatment options in labrum's pathology and repair of the labrum allow better outcomes for patients in comparison to labrectomy. Arthro-MRI is the investigation of choice in the pre-surgical evaluation. Our aim is to investigate the prognostic value of a score called ETD, in the pre-surgical MRI evaluation of labrum pathologies.
Methods and Materials: 47 patients were selected who have made an arthro-MRI of the hip and subsequently they underwent arthroscopy with repair of the labrum or labrectomy. The pre-surgical arthro-MRI images were evaluated with 3D DESS sequence (Dual Echo Steady State) by a radiologist blinded to the arthoscopic results. We have identified 3 parameters generating the ETD score, an acronym of: E = extension of the lesion; T = thickness of the labrum, D = damage, indicating the type of structural damage. The resulting scores ranges from 3 points up to 10 with the higher values expressing an higher probability of labrectomy. The score differences between groups of patients were evaluated with the Mann-Whitney test.
Results: 35 of the 47 patients (74%), during arthroscopy underwent repair of the labrum, the remaining 12 patients (26%) were subjected to a labrectomy. The ETD score differences between the two groups of patients proved to be significant with a p<0.01.
Conclusion: Today the hip arthroscopy allows multiple therapeutic options in the treatment of labral damage. The arthro-MRI evaluation with the ETD score would allow a more complete prognostic evaluation during the pre-surgical phase.
Author Disclosures:
F. Sardanelli: Advisory Board; Bayer Healthcare. Research/Grant Support; Bracco Imaging, Bayer Healthcare, IMS-Giotto.

B-1342 14:40

Errors within the musculoskeletal system: anatomical based checklist derived from discrepancy meeting database

S.C. Chin[1], J.R. Weir-McCall[1], P.M. Yeap[2], R.D. White[3], M.J. Budak[1], G. Duncan[1], B. Oliver[1], I.A. Zealley[1]; [1]*Dundee/UK*, [2]*Leeds/UK*, [3]*Cardiff/UK (sookcheng@doctors.org.uk)*

Purpose: Discrepancy meetings are an integral part of continued professional development. Error types have been classified and but specific patterns of anatomical sites of error have not been previously evaluated in a systematic fashion. We set out to interrogate a large discrepancy meeting database with the aim of deriving a short "checklist" of specific anatomical review areas where errors occur commonly.
Methods and Materials: A discrepancy meeting database from a single centre was retrospectively reviewed from a period covering 5 years. Errors were classified by type, modality, body system and specific anatomical location. Frequency of anatomical location within the musculoskeletal system were then analysed to derive common anatomical locations of errors.
Results: There were 561 errors in 477 examinations, of which 125 (19.9%) occurred in the MSK system. Sixty eight errors occurred in the axial skeleton, 42 errors in the appendicular skeleton and 15 in the soft tissues. The most common sites for errors to occur were: spine (37), thoracic cage (12), pelvis (10), sacrum (7) and calvarium (7). Commonly missed pathologies were: missed metastases (35); overcalling of metastatic lesions in those with known primary non-bony malignancy (12); and missed fractures (7).
Conclusion: Over 50% of all perceptual errors occurred in just five anatomical sites suggesting an avenue for focused review at the end of reporting.

B-1343 14:48

Ampleness of pertinent patient history on MRI spine referral forms

A.H. Rajaram; *Bangalore/IN (akashrajaram@gmail.com)*

Purpose: To determine if clinician referrals for MRI spine provide adequate patient history and to establish if patient questionnaires can add valuable supplemental history.
Methods and Materials: 170 referrals for MRI spine were retrospectively identified from Jan 2015 to June 2015. Two radiologists independently reviewed patient history on referrals and rated the quality of the information as follows: 5 outstanding; 4 above average; 3 average; 2 below average; and 1 poor. Referrals were considered high quality for mean score ≥ 4.0 and low quality for mean score ≤ 2.0. Subsequently, they compared referral history with self-reported history from patient questionnaires and assigned a score on a 5-point scale: 5 referral clearly superior; 4 referral slightly more useful; 3 equal usefulness; 2 patient information slightly more useful; and 1 patient information clearly superior. Two cohorts were compared using unpaired t test, Fisher exact test, and chi-square test.
Results: The mean quality score ± SD was 2.86 ± 0.83 for all radiology referrals, with 2.84 ± 0.83 for clinician referrals versus 2.88 ± 0.83 for patient history (p=0.774). A total of 8.7% of all clinician referrals were of low quality and 17.0% were of high quality. In comparison of clinician referrals and patient questionnaires, patient history was superior to clinician referral history for 22.0%, equal for 64.0%, and inferior for 14.0%.
Conclusion: Clinicians provide low-quality patient history on 1 of every 12 MRI spine referrals. Patient questionnaires provide better or equivalent information than clinician referrals 86% of the time.

B-1344 14:56

Consultation in radiology: reducing unnecessary radiological examinations

S. Staparski Dobravec, Z. Kumše; *Ljubljana/SI*
(staparskidobravec@gmail.com)

Purpose: Clinical guidelines for managing back pain do not recommend x-ray imaging in 4-6 weeks from onset of pain. Strain on radiology departments with inappropriately indicated imaging of spine and pelvis, especially in patients from 25-45 years, has prompted introduction of non-mandatory consultations with radiologists.
Methods and Materials: Before x-ray imaging, radiologist interviews patients and estimates how data gained through imaging would affect further course of treatment. He excludes »red flags« and informs patients about effective dose of radiation they can expect to receive from imaging. A feedback to referral physicians is written report from radiologist. Our goal was to assess effectiveness and safety of new practice. A survey was sent to 497 patients, who had undergone consultation within past three years, as well as to 151 referring physicians. Response rate was 30% for patients, and 38% for physicians. We also analysed all referrals received within this period.
Results: Within three years, number of referrals to x-ray imaging of spine and/or pelvis has decreased by 39%. 52% of patients who had undergone the consultation, consequently decided not to have x-ray imaging and later showed no need for it. 95% of referral physicians who completed survey responded that practice is safe. 90% of patients assessed their consultation with radiologist as much as needed.
Conclusion: We believe that introduction of consultations with a radiologist is a simple and cost-effective measure that can reduce unnecessary exposure of the population to ionising radiation and bring relief to overburdened radiology departments.

B-1345 15:04

Structured reporting of dual-energy x-ray absorptiometry exams for osteoporosis evaluation: a time-saving approach to creating high-quality reports

F. Schoeppe, L. Sobez, J. Spiro, A. Curta, R. Bodensohn, M. Goepfert, F. Ceelen, E. Kampmann, W.H. Sommer; *Munich/DE*
(Franziska.Schoeppe@gmail.com)

Purpose: To compare reporting times and report quality of structured reports (SR) to conventional free text reports (FTR) of dual-energy x-ray absorptiomety exams (DXA).
Methods and Materials: FTR and SR of DXA were retrospectively generated by 2 radiology residents (RR) and 2 final year medical students (MS). Time was measured from the first view of the exam until the report was finished. A random sample of DXA reports was selected and sent to referring physicians for further evaluation of report quality.
Results: A total of 108 DXA reports (both FTR and SR) were generated and 48 randomly selected reports were evaluated by referring physicians. Reporting times were shorter for SR in both, RR and MS with median reporting times of 2.7min. (RR: 2.7, MS: 2.7) for SR and 6.1min. (RR: 5.0, MS: 7.5) for FTR. Information extraction was perceived to be significantly easier from SR vs FTR (P<0.001). SR were rated to answer the clinical question significantly better than FTR (P<0.007). Overall report quality of SR was rated significantly higher for SR compared to FTR (P<0.001) with 95.8% of SR vs 79.2% of FTR receiving of high or very high quality ratings. All participants (RR, MS and referring physicians) preferred SR over FTR for DXA.
Conclusion: Template-based SR of DXA might lead to shorter reporting times among residents as well as medical students. At the same time our results point to an increased report quality of SR compared to FTR.
Author Disclosures:
F. Schoeppe: Employee; background research on radiological diseases, creating and reviewing structured templates for Smart Reporting (a not-for-profit company for structured reporting templates). **W.H. Sommer:** Founder; Co-founder Smart Reporting GmbH.

B-1346 15:12

Structured reporting for x-ray examinations of the shoulder: is there an advantage over free text reports?

F. Schoeppe, W.H. Sommer, F. Schmidutz, D. Pförringer, M. Armbruster, K.J. Paprottka, J.L.V. Plum, F.G. Meinel, N.N. Sommer; *Munich/DE*
(Franziska.Schoeppe@med.uni-muenchen.de)

Purpose: To analyse structured reports (SR) and free text reports (FTR) of shoulder x-ray examinations evaluating the quality of reports and potential contributions to clinical decision-making.
Methods and Materials: We acquired 62 reports (FTR and SR) of patients with suspected degenerative changes who received an x-ray examination of the shoulder. For the SR a template was created based on the template ID 0000154 (Shoulder x-ray) from radreport.org and using an online software with clickable decision trees with concomitant generation of semantic SR. All reports were evaluated with regard to key features in terms of content, information extraction, clinical value and overall quality of the report.
Results: 62 reports were reviewed by two experienced orthopaedic and traumatology surgeons (5 and 7 years). SR achieved significantly higher mean ratings in all of the evaluated key features (p<0.05). The information on osteoarthritis were more complete in SR than in FTR (median rating: 10.0 vs 5.0; p<0.05). Information extraction was perceived to be easier in SR than in FTR (10.0 vs 2.5; p<0.05). SR were considered to answer the clinical question better than FTR (10.0 vs 5.0, p<0.05). The overall quality of SR vs FTR reports was significantly higher in structured reports (p<0.05); all of the SR received a high or very high overall quality rating (100%) compared to only 21% of FTR.
Conclusion: Structured reporting of x-ray examinations of the shoulder might provide reports of higher quality and better clinical decision support. It may thus lead to a higher satisfaction of referring surgeons.
Author Disclosures:
F. Schoeppe: Employee; background research on radiological diseases, creating and reviewing structured templates for Smart Reporting (a not-for-profit company for structured reporting templates). **W.H. Sommer:** Founder; Co-founder Smart Reporting GmbH. **M. Armbruster:** Founder; Co-founder Smart Reporting GmbH.

14:00 - 15:30 **Room G**

Musculoskeletal

SS 1910b

Knee

Moderators:
M. Shahabpour; Brussels/BE
E.J. Ulbrich; Zurich/CH

B-1347 14:00

Middle patellar tendon to posterior cruciate ligament (PCL): a new index for tibial tubercle position in patients with patellar instability (PI)

G. Pozzi[1], I. Merli[2], J. Almolla[1], R. Mesquita[3], L.M. Sconfienza[1]; [1]*Milan/IT*, [2]*San Donato Milanese/IT*, [3]*Lisbon/PT (ilaria.merli@gmail.com)*

Purpose: Tibial tubercle to trochlear groove (TT-GT) and tibial tubercle to PCL (TT-PCL) have been proposed as measures to establish PI risk. However, they need image post-processing for accurate calculation. We propose an alternate, easier method to calculate PI risk.
Methods and Materials: We reviewed knee MR images of 30 patients (13F,17M;45±17y) with history of PI. MR images of 60 patients with no history of PI (36F,24M;32±13y) served as controls. TT-PCL was calculated on two superimposed T2-weighted axial images separately by two operators. Then, the same operators separately selected the axial image where the PCL root was seen. There, the middle point of PT was calculated. A line parallel to the posterior tibial plateau was traced, two lines passing for the middle PT and medial edge of PCL were traced, and their distance calculated (PT-PCL). Differences of TT-PCL and PT-PCL between patients and controls, their correlation, and interobserver reproducibility were calculated.
Results: PT-PCL distance was 23.5±3.8mm in patients and 20.0±2.7mm in controls (P<0.001). TT-PCL distance was 22.9±3.9mm in patients and 20.5±2.7 mm in controls (P=0.002). Correlation between PT-PCL and TT-PCL was r=0.838, P<0.001. Interobserver reproducibility of PT-PCL and TT-PCL was very high (ICC=0.894, CI95%=0.839-0.930 and ICC=0.866, CI95%=0.796-0.912, respectively).
Conclusion: PT-PCL significantly correlates with TT-PCL with high interobserver reproducibility. Thus, PT-PCL may represent an alternate index to calculate PI risk, with the great advantage of being calculated on a single MR image, with no need of post-processing. A PT-PCL value >21.75mm may be used for increased PI risk.

B-1348 14:08

Suprapatellar fat-pad signal alteration on MRI is associated with degeneration of the patellofemoral joint over 48 months: data from the OAI

B.J. Schwaiger, J. Mbapte Wamba, A.S. Gersing, M.C. Nevitt, L. Facchetti, C.E. McCulloch, T.M. Link; *San Francisco, CA/US*

Purpose: To analyse associations of suprapatellar fat-pad (SPFP) hyperintense signal alterations and mass effect with progression of patellofemoral osteoarthritis (OA) and symptoms over 48 months.
Methods and Materials: Subjects from the Osteoarthritis Initiative (n=426; 51.8±3.8 years; 49.8% women) without radiographic OA underwent 3T-MRI of their right knees and clinical evaluation using the Knee Injury and Osteoarthritis Outcome Score at baseline and 48-months. Elevated SPFP signal compared to surrounding tissue was assessed on IW fat-saturated FSE images. Mass

effect was defined as convex posterior contour. Patellofemoral cartilage, bone marrow lesions (BML) and subchondral cysts were assessed with the Whole-Organ Magnetic Resonance Imaging Score (WORMS). Associations of SPFP imaging findings with morphologic and clinical progression were assessed using adjusted general linear models and logistic regressions.
Results: Baseline SPFP signal alterations were found in 51% of the subjects (n=217), of which 11% (n=23) additionally had a mass effect. Cartilage progression was significantly higher in subjects with signal alteration versus without (adjusted mean increases, 95% CI; patella: 0.29 [-0.07, 0.64] vs -0.04 [-0.40, 0.31]; p<0.001; trochlea: 0.47 [0.16, 0.77] vs 0.31 [0.01, 0.61]; p=0.007). BML progression was more likely in subjects with signal alteration (OR 1.75, 95% CI [1.09, 2.82]; p=0.021). Mass effect was not associated with joint degeneration and SPFP imaging findings were not associated with clinical worsening (p>0.18 for all).
Conclusion: Patellofemoral joint degeneration assessed with MRI over 48 months was significantly increased in subjects with SPFP signal alteration, suggesting the relevance of SPFP pathologies for the progression of patellofemoral OA.

B-1349 14:16

Contribution of SWI at 3T: detecting intraarticular haemosiderin accumulation in haemophilia patients

B. Akyüz, A.V. Polat, M. Ozturk, K. Aslan, L. Tomak, M.B. Selcuk; *Samsun/TR (behicakyuz@gmail.com)*

Purpose: To prospectively assess the feasibility of susceptibility-weighted imaging (SWI) at 3T to detect intraarticular haemosiderin accumulation in haemophilia patients.
Methods and Materials: We obtained Institutional Review Board approval and informed consent from all participating patients for this study. Forty-one joints in 24 haemophilia patients were imaged with conventional magnetic resonance imaging (MRI) and SWI sequences. Two experienced musculoskeletal radiologists (readers 1 and 2), and one radiologist with less experience in musculoskeletal imaging (reader 3), independently and separately rated images for haemosiderin accumulation: the final decision on accumulation was consensually determined by two experienced radiologists with both conventional MRI and SWI sequences. Diagnostic consistency of each MRI sequence with the reference, plus pairwise agreement between interpreters, was assessed with kappa statistics.
Results: Given conventional MRI sequences, diagnostic consistency of readers 1 and 2 was substantial with the reference (κ = 0.670 and κ = 0.658, respectively), diagnostic consistency of reader 3 with the reference was moderate (κ = 0.539). Interobserver agreement of readers 1 and 2 was almost perfect (κ = 0.869), whereas reader 3 (in conjunction with readers 1 and 2) was also substantial (κ = 0.655 and κ = 0.684, respectively). SWI interpretation by all readers demonstrated nearly perfect agreement with the reference (κ = 1, κ = 0.959, and κ = 0.959, respectively). Interobserver agreement was again almost perfect for all readers (κ = 1, κ = 0.959, and κ = 0.959, respectively).
Conclusion: SWI is an accurate and reliable method for determining intraarticular haemosiderin accumulation.

B-1350 14:24

MRI evaluation of knee osteochondritis dissecans treated with a cell-free biomimetic osteochondral scaffold vs microfracture technique: a multicenter randomised experience

L. Tonetti, M. Busacca, C. Tetta, A. Moio, S. Durante, G. Filardo, E. Kon, U. Albisinni, F. Perdisa; *Bologna/IT (lauratonetti.md@gmail.com)*

Purpose: To compare two arthroscopy approaches, biomimetic osteochondral scaffold implantation and microfractures, in treatment of knee osteochondritis dissecans (OCD) and to evaluate articular osteocartilaginous tissue's regeneration, using modified magnetic resonance observation of cartilage repair tissue (MOCART) score.
Methods and Materials: Thirty patients, affected by symptomatic knee OCD, were prospectively enrolled. Fifteen patients were treated with implantation of a three-dimensional multi-layered scaffold. The other fifteen patients underwent surgery treatment using Steadman microfracture technique. Two blinded radiologists, with more than 25 years of musculoskeletal imaging experience, prospectively evaluated MRI examinations, performed with a specific protocol at 1.5 or 3.0 Tesla, 6, 12 and 24 months after treatment, in 10 European centres. Modified MOCART score was assigned in MRI examinations.
Results: Modified MOCART score was compared among two groups of patients at 2-year follow-up. In group treated with biomimetic osteochondral scaffold implantation, 9 patients (60%) revealed improvement of modified MOCART score, in 2 patients (13.3%) MOCART score did not change and in the remaining 4 patients (26.7%) MOCART score decreased. In group which underwent surgery treatment with microfracture technique, 6 patients (40 %) showed MOCART score increased, in 3 patients (20 %) MOCART score did not change and in the remaining 6 patients (40 %) there was a decrease of MOCART score.
Conclusion: Biomimetic osteochondral scaffold was demonstrated to be a valid treatment option for knee OCD showing a good radiological outcome at 2-year follow-up. Modified MOCART score represented the best way to evaluate the osteocartilaginous tissue's regeneration after every arthroscopy approach.

B-1351 14:32

Patellar malalignment: a new method on knee MRI

H. Kurtul Yıldız, E.E. Ekin; *Istanbul/TR (eeeoner@gmail.com)*

Purpose: The medial patellofemoural ligament (MPFLL)/lateral patellar retinaculum (LPR) ratio were assessed in knees as a means to detect patellar malalignment. We also aimed to evaluate the prevalence of the various types of trochlear dysplasia in patients with patellar malalignment.
Methods and Materials: After approval of our institutional ethics committee, we conducted a retrospective study that included 450 consecutive patients to evaluate them for the presence of patellar malalignment. Parameters investigated were the trochlear type, sulcus angle, presence of a supratrochlear spur, MPFLL, LPR, patella alta, and patella baja by means of MRI. Overall, 133 patients were excluded because of the presence of major trauma, multiple ligament injuries, bipartite patella, and previous knee surgery. The Dejour classification was used to assess trochlear dysplasia. Two experienced radiologist evaluated the images. Their concordance was assessed using the kappa test.
Results: The frequencies of patellar malalignment and trochlear dysplasia were 34.7 and 63.7%, respectively. The frequency of trochlear dysplasia associated with patellar malalignment was 97.2%. An MPFLL/LPR ratio of 1.033-1.041 had high sensitivity and specificity for malalignment. The researchers' concordance was good (K=0.89, SE=0.034, Π<0.001).
Conclusion: Trochlear dysplasia is frequently associated with patellar malalignment. An increased MPFLL/LPR ratio is useful for detecting patellar malalignment on knee MRI, which is a novel quantitative method based on ligament length.

B-1352 14:40

T2-mapping correlates with histopathological degree of meniscal degeneration

S.M. Eijgenraam, F.A.T. Bovendeert, Y.M. Bastiaansen, D.E. Meuffels, J. Guenoun, S. Klein, M. Reijman, E.H.G. Oei; *Rotterdam/NL (s.eijgenraam@erasmusmc.nl)*

Purpose: To validate T2-mapping for meniscal tissue, by studying the correlation between T2 relaxation time and the degree of histopathological degeneration as the reference standard.
Methods and Materials: 10 patients undergoing surgery were included in this prospective observational study. From 5 patients, traumatically torn meniscal tissue was collected during arthroscopic partial meniscectomy. From the other 5 patients, degenerative menisci were obtained during total knee replacement surgery. All patients underwent a pre-operative MRI scan at 3 Tesla which included a 3D FSE T2-mapping pulse sequence with 5 echo times. Histopathological analysis was performed using the Pauli score, a validated semi quantitative grading system for human meniscal degeneration involving the following subdomains: surface integrity, cellularity, matrix and collagen organisation, and proteoglycan staining intensity. Mean T2 relaxation times were calculated in meniscal regions of interest corresponding with the areas scored histopathologically, using in-house developed post-processing software. The correlation between T2-mapping and histopathological degeneration was assessed using Spearman correlation tests.
Results: T2-mapping relaxation time was found to correlate well with the degree of histopathological degeneration in meniscal tissue (r_s = 0.64, P = 0.001). Meniscal tissue with mild to moderate degeneration was found to have statistically significantly higher T2 relaxation times compared to meniscal tissue without degeneration, 22.7 ± 3.0 ms and 18.2 ± 5.1 ms (P = 0.02) respectively.
Conclusion: T2-mapping relaxation time correlates well with histopathological degeneration in meniscal tissue and is a promising quantitative imaging biomarker to estimate meniscal degeneration.

B-1353 14:48

Microstructural evaluation of the anterior cruciate ligament (ACL) with MR-diffusion tensor imaging (DTI): correlations with knee stability

I. Voicu, L. Di Clemente, R. Navarra, P. Mattei, V. Panara, A. Cotroneo, M. Caulo; *Chieti/IT (p.voicu@rad.unich.it)*

Purpose: To assess if DTI metrics are correlated with microstructural anatomy of the anterior cruciate ligament (ACL) and with knee stability.
Methods and Materials: We examined both knees of 41 subjects: 23 healthy controls (11F, age 20-40) and 18 patients with previous ACL injury (9F, age 20-40). All subjects underwent clinical and KT1000 Knee Laxity Testing Compliance Index (CI) and an MR scan on a 1.5 T magnet. MR imaging protocol included conventional and axial DTI sequences. Quantitative analysis was performed by overlapping DTI sequences to T2 sequences. At least three ROI's on consecutive sections were manually drawn on the ACL. DTI metrics

were obtained using FMRIB Software Library (FSL). Differences of Fractional Anisotropy (FA) of ACLs between knees in healthy controls and patients were evaluated with a paired t-test. Correlations between FA and CI were evaluated with curve estimation analysis.
Results: FAs were significantly different in healthy and injured knees in the patient group (0.72±0.09, 0.60±0.09 respectively, p<0.001) but not in healthy control knees. Curve regression analysis indicated a statistically significant quadratic relationship between ACL FA and CI in controls (p=0.013) but no relationship in patients.
Conclusion: Injured knees presented a significant difference in ACL FA compared to healthy knees. This difference was not present when comparing contralateral knees in healthy subjects. The relationship between ACL FA and CI present in healthy subjects was not observed in injured knees. Further studies are required to determine if DTI FA could be used for early diagnostic, treatment evaluation and prognosis.

B-1354 14:56

MRI characteristics of torn and untorn menisci
R. Kijowski, A. Williams, H. Rosas, F. Liu; *Madison, WI/US (rkijowski@uwhealth.org)*

Purpose: To compare MRI characteristics of torn and untorn postoperative menisci.
Methods and Materials: The study group consisted of 140 patients with 148 partially resected menisci who were evaluated with repeat knee MRI examination and subsequent repeat knee arthroscopy. Two musculoskeletal radiologists retrospectively assessed the following MRI characteristics of the postoperative menisci: contour, T2 line through meniscus (no line, intermediate signal line, intermediate-to-high signal line, and high fluid signal line), number of images T2 line visualised, extent of T2 line though meniscus, and change in signal pattern through meniscus compared to baseline MRI. Positive predictive values (PPV) and negative predictive values (NPV) were calculated using arthroscopy as reference standard.
Results: All 36 menisci with no T2 line were untorn at surgery (100% NPV), while 46 of 79 menisci with intermediate T2 line, 16 of 18 menisci with intermediate-to-high T2 line, and 14 of 15 menisci with high T2 line were torn at surgery (58%, 89%, and 93% PPV respectively). Additional MRI characteristics associated with torn meniscus at surgery included irregular contour (86% PPV), T2 line on more than 5 images (82% PPV), T2 line extending through more than 75% of meniscus (66% PPV), and change in signal pattern (98% PPV).
Conclusion: Postoperative menisci with no T2 signal line are untorn at surgery. The most useful MRI characteristics to predict torn postoperative menisci at surgery are change in signal pattern compared to baseline MRI followed by high T2 line through meniscus, intermediate-to-high T2 line through meniscus, and irregular meniscus contour.

B-1356 15:04

T2 relaxation times in patients after ACL-repair with and without femoral notch sign
C. Behzadi, G.H. Welsch, A. Laqmani, F.O. Henes, G. Schoen, G. Adam, M. Regier; *Hamburg/DE (C.Behzadi@uke.de)*

Purpose: To quantitatively assess T2 relaxation times of articular cartilage of the anterolateral femoral condyle in patients after ACL-repair with and without a deep lateral femoral notch sign at initial MRI.
Methods and Materials: 58 patients underwent knee MRI at 3T 12 months after ACL-rupture and surgical treatment. In 27 of 58 re-evaluated patients a positive lateral femoral notch sign was present at posttraumatic MRI. For quantitative analysis, T2 relaxation time measurements (7 echo times ranging from 10-70 ms) were performed in sagittal orientation. By using the initial post-trauma MRI as an aid for orientation, a polygonal ROI encompassing the full cartilage layer was placed in the anterolateral femoral cartilage on the T2 map using a dedicated software tool (ImageJ). Statistical analysis included student t-test and 95%-confidence intervals.
Results: In patients with a positive lateral femoral notch sign, T2 relaxation times were significantly higher (14.1%) compared to those without a lateral femoral notch sign (p=0.003). In total, a mean relaxation time of 41.1ms (36.4-48.7ms) was determined for patients with a femoral notch sign, whereas a mean of 35.3ms (26.1-43.3ms) was calculated for patients with a negative femoral notch.
Conclusion: A trend towards elevated T2 relaxation times in the anterolateral femoral cartilage in patients with a positive femoral notch sign after ACL-rupture was noted compared to patients without a femoral notch sign. Therefore, a positive femoral notch sign in initial MRI seems to be associated with higher cartilage degradation and longitudinal studies are needed to further evaluate its clinical relevance.

B-1357 15:12

Diffusion tensor imaging of the anterior cruciate ligament graft at 3 Tesla: a feasibility and reliability study
P. Van Dyck[1], E. De Smet[1], M. Froeling[2], P. Pullens[1], M. Torfs[1], P. Verdonk[3], J. Sijbers[4], P.M. Parizel[1], B. Jeurissen[4]; [1]*Edegem/BE*, [2]*Utrecht/NL*, [3]*Antwerp/BE*, [4]*Wilrijk/BE (elinedesmet@hotmail.com)*

Purpose: A great need exists for objective biomarkers to characterize anterior cruciate ligament (ACL) graft healing. Our purpose was to demonstrate the feasibility and reliability of diffusion tensor imaging (DTI) to delineate the ACL graft and investigate its microstructural properties in vivo.
Methods and Materials: Axial DTI (b = 0, 400 and 800 s/mm^2 in 1, 10, and 10 directions repeated 16 times for a total of 336 diffusion weighted volumes; TR/TE: 1300/45 ms, voxel size: 1.5×1.5×6.0 mm^3, matrix: 128 × 128, slices: 10) of the knee was performed at 3T in twenty patients within 1 year after ACL reconstruction. Ttractography was performed by two independent observers to delineate the ACL graft. Fractional anisotropy (FA), mean diffusivity (MD), axial diffusivity (AD), and radial diffusivity (RD) were calculated within the graft. Interrater reliability was assessed using intraclass correlation coefficient (ICC) and scan-rescan reproducibility was evaluated based on the coefficient of variance (CV) across 20 repetition bootknife samples.
Results: In all subjects, the ACL graft was tracked successfully. Quantitative evaluation of diffusion properties of the graft yielded the following mean ± SD values: FA=0,224 ± 0,0424; MD=1,30± 0,125 x 10-3 mm^2/s; AD=1,60± 0,141 x 10-3 mm^2/s and RD=1,14± 0,125 x 10-3 mm^2/s. Interrater reliability was excellent (ICC= 0.907-0.981). Mean CVs for FA, MD, AD and RD were 5%, 4%, 4% and 4%, respectively.
Conclusion: This study demonstrates the feasibility and reliability of DTI for evaluating the ACL graft at 3T. These findings support the potential of DTI to serve as an objective biomarker to better characterize ACL graft healing.
Author Disclosures:
P. Van Dyck: Research/Grant Support; Senior Clinical Investigator of the Research Foundation Flanders Belgium. **B. Jeurissen:** Research/Grant Support; Postdoctoral fellow of the Research Foundation Flanders (FWO: 12M3116N).

14:00 - 15:30 **Room K**

Radiographers

SS 1914
Radiography practice

Moderators:
J.M. Saude; Porto/PT
D. Tscholakoff; Vienna/AT

B-1358 14:00

Elasticity characterisation of vastus lateralis muscle by ultrasound quasi-static elastography
R.A. Santos[1], M. Valamatos[2], P. Mil-Homens[2], P. Armada-da-Silva[2]; [1]*Coimbra/PT*, [2]*Lisbon/PT (rutemartinssantos@gmail.com)*

Purpose: To validate the use of QSE for muscle elasticity mapping as a possible clinical and quantitative tool and to compare quantitatively the QSE mapping obtained in the vastus lateralis muscles of young adults when submitted to a program of training.
Methods and Materials: Twenty-eight healthy males volunteers (mean age 20 ± 3.3 years), participated in this study, divided into two groups: control group and training group. From the training group, 11 performed a concentric training and 9 submitted an eccentric training, during 15 weeks, on a total of 45 training sessions. All the participants were submitted to an ultrasound evaluation of the vastus lateralis on transverse plan before and after the 12 weeks of training program.
Results: It was found high intra-evaluation reliability for colour mapping values by QSE ultrasound. In few cases, ICC was below the acceptable 0.70 levels. Vastus lateralis muscle was defined as a soft tissue, with higher percentage of green colour, followed by the blue colour when in rest. In generally, there were significant differences on red colour percentage between the first and second evaluations and between the rest and contraction, showing on these two evaluations a less percentage of red colour that is an increase on the tissue hardness after dynamic exercise.
Conclusion: QSE is a useful technique for monitoring of musculoskeletal changings principally on long programs of training, by evaluating the elasticity of muscle structures.

B-1359 14:08

Sonographer's ability to detect and grade pathological findings in shoulder radiograph

M.J. Pakanen, J. Haverinen, M. Heiskanen, E. Liukkonen, J. Niinimäki; *Oulu/FI (pakanemi@gmail.com)*

Purpose: The aim of this study was to evaluate and improve the knowledge and ability of sonographers, who perform shoulder ultrasonography examinations, to detect pathological findings in shoulder x-ray images and furthermore, to examine which pathological findings can be reliably detected by sonographers. The focus of this study was to examine the interpretation process primarily in the evaluation of degenerative changes.
Methods and Materials: Study material consisted of 50 anonymised shoulder x-ray examinations of patients who had shoulder ultrasonography within two months of the x-ray study. Three sonographers evaluated research material independently, a semi-structured evaluation, of GH-joint, osteophytes, tendon calcification, acromial shape, subacromial space, AC-osteoarthritis and other observations. Musculoskeletal radiologist evaluated images blinded to the interpretation of sonographers. The results were compared between radiologist and sonographers.
Results: Sonographers' detection rates compared to radiologist were; GH-joint 96,7%, GH-joint space 94%, GH-joint articular surfaces 81,3%, osteophytes 72,7%, tendon calcification 81,4%, acromial shape 69,3%, subacromial space 93,8%, AC-osteoarthritis 39,4% and other observations 76%.
Conclusion: Radiographers' ability to interpret and report x-rays have been studied widely and good results have been reported in the interpretation of trauma x-ray images. In our study, sonographers (Radiographer University of Applied Sciences) performed well in detecting degenerative radiographic findings of shoulder x-ray images. GH-joint, GH-joint space and articular surfaces, tendon calcification and subacromial space were most accurately evaluated when compared to radiologist's interpretation. The research material will be further utilised in education to improve the sonographers' skills to evaluate AC-osteoarthritis, acromial shape and osteophytes.

B-1360 14:16

Thickness and echo-intensity characterisation of quadriceps muscle by ultrasound

R.A. Santos, F. Alves, D. Matos, A. Fidalgo, A. André; *Coimbra/PT (rutemartinssantos@gmail.com)*

Purpose: To characterise the thickness and echo-intensity of the quadriceps femoris muscle and analyse its relationship with gender, practice of sports, number of training and practice time.
Methods and Materials: 61 young individuals were submitted to an ultrasound examination to assess the thickness and echogenicity of the quadriceps femoris muscle, through the acquisition of images in longitudinal sections. The ultrasound images were processed using the Image J software and the data were analysed through SPSS 20.0.
Results: The quadriceps femoris muscle has an average thickness between 1.12 and 1.34 cm, and an echo-intensity between 74.83 and 81.65 values. There are significant differences in the thickness of the left and right medial vastus muscle between males and females and significant differences in the thickness and echo-intensity of the quadriceps femoris muscle in relation to the practice of sport and practice time.
Conclusion: The thickness of quadriceps femoris muscle is greater in males than in females; however, the opposite is observed regarding the echo-intensity of it. The practice of sports, number of workouts and practice time influence the echo-intensity and thickness of the quadriceps femoris muscle.

B-1367 14:24

Bioethics education for radiographers in Europe

A. Santos; *Coimbra/PT (adelinosantos@estescoimbra.pt)*

Purpose: The knowledge that radiographers have on bioethics (and the legal framework of care) can have a direct impact on the type and quality of care that patients receive. This work has the goal of knowing what kind of bioethics unit contents are taught to future radiographers.
Methods and Materials: Semi-structured interviews with accountable pedagogical coordinators and meta-analysis on available official information about curricular unit contents in the major official schools were performed on 22 colleges, 15 countries. Data was examined to exclude significant bias; for qualitative variables, frequencies and percentages were calculated; averages and standard deviations for quantitative ones.
Results: The characterisation of radiographers high-level education showed that only a minority (36%) have bioethics and/or deontology training, with the duration equal or more than 1 semester. Regarding the characterisation of type and quality of the education, bioethical contents revealed that the most pertinent alluded topics are Professional Skills (83%) and Awareness (90%). However, reference authors highlight that ethical behavior should focus on tolerance, prudence and discrimination capacity. These features are bioethics discipline characteristics. Therefore, they cannot be scattered by well-meaning programmes that do not develop critical and reflective ethical thinking.
Conclusion: The educational environment should combat the incongruence of these results. If future professionals do not learn and integrate the importance of bioethics for clinical practice, patients may suffer needlessly and their self-determination rights are ignored. To avoid this situation priority to bioethics should be given, ensuring mandatory character in training plans of all these professionals.

B-1361 14:32

Sonographer's ergonomic pains, who cares

M. Abd El Bagi, F. Alkubaidan, A. Alkhalf, R. Albabtain, A. Wazira, N. Butt, A. Mohammed; *Riyadh/SA*

Purpose: Purpose work related injuries can affect staff well-being, decrease productivity and cause early career ending. The objective of this study is to determine whether our sonographers are suffering work related pains that require intervention and their awareness of ergonomics in comparison to a nationwide trend.
Methods and Materials: A questionnaire was conducted for the multinational practicing sonographers at an 800 bed tertiary care hospital. The general ultrasound sub-section was selected. The intervention, paediatric and women imaging sub-sections were excluded.
Results: 13 sonographers were involved.11 (85%) were females and 2 (15%) were males. Seven (54%) were Saudi's, five (38%) were Philipinos and one (8%) was Sudanese. Response rate was 100%. Only 3 (23%) were fully aware of ergonomics. 8 (62%) were suffering from various musculoskeletal pains compared to 89 (78%) nationwide of whom 58 (51%) suffered more severely and may consider leaving the profession. The vast majority of our staff 12 (92%) said they were over worked.
Conclusion: The issues of ergonomics are rarely addressed by management or staff. Our sonographers are mostly unaware of ergonomics. They are at risk of work related injuries and burn out syndrome but less than the nationwide pattern. An in-service education session was conducted by a physiotherapist. Subsequently regular staff exercise and stretching program was implemented at short breaks resulting in morale boosting. Impact on sick leave records was not studied.

B-1362 14:40

Our experience with gamma knife treatment planning

A. Fedorov, A. Lavrentyeva; *St. Petersburg/RU, (fedorov@ldc.ru)*

Purpose: To evaluate define (geometry tag error) in planning station in patient with metal frame before gamma knife radiosurgery.
Methods and Materials: 34 patients with gamma knife metal frame were assessed (20 by head TxRx, 4 by flex small, 10 by head matrix lower plus body). Aera 1.5T scanner was used with CIVCO planning accessories. 3 coil configurations were tested: 2 flex small combinations, head TxRx, head matrix lower plus body matrix 18. All patients were scanned with Leksell localiser and gamma plan station. T2 TSE and T1 VIBE with spatial resolution 1.0x1.0x1.0mm were used.
Results: The results of define due to using flex small coil and TxRx coil were 0.9±0.3. Satisfactory define (0.4±0.1) in planning station were reached with combination Head matrix lower plus Body Matrix 18, by channels increasing and scanning protocols optimisation. In these cases, B1 filter and reduced EC sensitivity were activated, and gradient system regime was changed from fast to low Sar.
Conclusion: CIVCO accessories and coils combination of head matrix lower plus body matrix 18 are useful for gamma knife treatment planning (in difference with standard protocols and coils).

B-1363 14:48

Radiation exposure assessment in educational setting: spine surgical programme with procedures simulated on cadavers

E.C. Antunes[1], M.S. Martins[2], M.M.C.P. Ribeiro[2], J.E.G. O'Neill[2], M.V. Casimiro[2]; [1]*Loures/PT*, [2]*Lisbon/PT (edgar.c.antunes@gmail.com)*

Purpose: Assess the amount of radiation dose in the spine surgical intervention in an educational setting, carried out in the dissection room using cadavers for training, and to evaluate if the exposure level is between the limits imposed by legislation to radiographers or medical students.
Methods and Materials: To evaluate the effective dose received by students, dosimetric evaluations were carried out in 6 students (five radiographers and one doctor) using thermoluminescent dosimeters (TLD-100) by (LiF:Mg,Li); bandwidth of 10μGy-10Gy, placed under the apron shield. In one student positioned in the place of the main surgeon, wrist and eye dosimeters were also used. The fluoroscopy time was obtained from the dose report print from the equipment (Ziehm Vision Vario 3D) used in pulsed emission mode. The data collection occurred during the all course time - 3 days.
Results: The effective dose measured under the apron for the whole body and in the eye gave the value of 0,00mSv for all students. The effective dose

results for the wrist were 0,69mSv Hp(0,07) and 0,74mSv Hp(10). The total time of exposition was between [11,51min-15,78Max]. The correlation between the cumulative dose and the exposition time was weak (R=0,29).
Conclusion: The radiation dose was lower than the limits imposed by legislation. We concluded that the training programs using fluoroscopy in cadavers revealed to be safe. It is safeguard the radiological protection for the students in lab area applying simulated techniques in cadaver, using the best practices that mimics the surgical theatre.

B-1364 14:56

Virtual autopsy: the role of CT and MRI
A. Silva, N. Pinto, A.F. Abrantes, L.P.V. Ribeiro, R.P.P. Almeida, K.B. Azevedo, J.P. Pinheiro; *Faro/PT (npinto@ualg.pt)*

Purpose: To demonstrate the role of CT and MRI examinations on the post-mortem analysis of a corpse.
Methods and Materials: In this case study, a person had to die in a violent manner by suicide or homicide (in these circumstances a conventional autopsy is mandatory according the nacional law) within the hospital area. For data collection purposes, the pathologist gave permission to be recorded during the course of conventional autopsy, and the radiology department agreed to perform the post-mortem imaging. The imaging was carried out with a 16 slices CT scanner and a 1.5 Tesla MRI.
Results: Both techniques viewed fluid in the thoracic cavity. Imaging did not detect the presence of sand in the larynx, pharynx, trachea and oesophagus, unlike conventional autopsy, but detected unspecific foreign bodies. In this parameter, the conventional autopsy was superior. However, this difficulty can be easily overcome since there are software programmes that enable the study of the tracheal lumen and the bronchial tree. In this case the imaging examinations were sufficient to determine the cause of death (drowning).
Conclusion: Literature reviews have shown good correlation between both techniques and this particular case study has shown that there was certainly a good congruence between the two modalities. The virtual method preserves the forensic evidence and, at the same time, represents an alternative to religious communities which do not accept the conventional autopsy. Virtual autopsy also creates another intervention field for radiographers, contributing to their professional development.

B-1365 15:04

Comparative study of plain radiography from three digital acquisition systems applied to works of Art
B. Barros, M.M.C.P. Ribeiro, D.A. Ramos, M.H.P. Martins, A. Candeias; *Lisbon/PT (beatrizcr-barros@hotmail.com)*

Purpose: In order to reinforce the cooperation between radiologic centres and the museums and enlarge the job-market of the Radiographers, this study aimed to give a contribution for a better understanding about the process used in the characterisation of radiography in painting and to optimise the exposition's parameters in 3 systems, comparing them.
Methods and Materials: With the help of an expert in Museology and Art History it was selected 5 paintings produced with different materials and techniques. The paintings underwent to three acquisition systems making a total of 21 images: 1-DR Siemens MultixSelect-DR; 2-CR Siemens Multix Pro combined with AGFA IP MD4.0 detector and scanner AGFA ADC Solo and 3-CR tube YXLON SMART 160E/0,4 belonging to José Figueiredo Lab from investigation and conservation of cultural heritage. All acquisition procedures were reproduced in all systems. Four observers classified the images: 2 experts in medical imaging and 2 in art. The dimensions of the check-list were: support conservation state; distinctness; contrast; contour; creative and technique process; components and materials.
Results: Globally the best images ranked by experts were obtained with the system 2 where was possible to see the fine contours, the brushstrokes or the matting of the canvas. However the system 3 gives some details inexistent in the others. The best acquisition parameters were the recommended by National Gallery's studies.
Conclusion: Radiography field and the knowledge of radiographers, through CR systems, may increase the image quality to expertise advice, validation and authentication of works of Art.

B-1366 15:12

An investigation into interface pressure (IP) and pressure ulcer (PU) risk of healthy volunteers whilst lying on medical imaging and radiotherapy tables
S.K. Angmorterh, A. England, J.-A. Webb, K. Szczepura, M. Stephens, P. Hogg; *Salford/UK (S.Angmorterh@edu.salford.ac.uk)*

Purpose: Determine whether IP risks exist on radiography/radiotherapy tables; determine the impact of a pressure relieving intervention on IP jeopardy areas.
Methods and Materials: Baseline study: An Xsensor pressure mapping system was used to measure IP of jeopardy areas in healthy volunteers (26 females, 23 males; aged 18-59 (mean=34.6±10.5)) on three radiography/radiotherapy tables. Volunteers also completed a pain/comfort questionnaire. Significant differences exist for mean IP for head, sacrum, and heels across the three tables ($p \leq 0.001$). Highest IP was recorded for the head (75.9±31.2mmHg) on the radiotherapy/planning table. This IP could induce tissue breakdown, predisposing to PU. Most pain occurred when lying on the radiotherapy table.
Results: Intervention study: A thin gel surface overlay, with low radiation attenuation, was assessed to reduce IP risk to the head. Pressure mapping was conducted on 20 healthy volunteers aged 25-53 years (mean=34.4±7.0). Significant difference in the mean IP with and without the intervention was identified (mean IP values of 62.4±6.1 and 83.9±8.1mmHg respectively, $p \leq 0.001$). There was a significant difference in the peak pressure index (PPI) of the head with and without the gel intervention (mean=159.8±26.8, and mean=205.1±28.2mmHg respectively, $p<0.05$).
Conclusion: IP and therefore PU risk exists for the head on radiotherapy/planning tables. A suitable intervention can reduce this risk. Further research is needed to assess interventions and also PU risk to high risk populations.

B-1368 15:20

Development of software for image quality assessment in cone-beam computed tomography
M.V.L. Oliveira[1], A.C. Santos[2], G. Paulo[2], P. Campos[1], J. Santos[2]; [1]*Salvador/BR*, [2]*Coimbra/PT (marcusradiology@gmail.com)*

Purpose: The purpose of this study was to develop free software, at low cost and with minimal time to evaluate the image quality in dental and maxillo-facial cone beam computed tomography (CBCT).
Methods and Materials: A polymethyl methacrylate (PMMA) phantom, CQP-IFBA, was scanned in three CBCT units with seven protocols. A macro-programme was developed, using ImageJ free software, to automatically evaluate the image quality parameters. The image quality evaluation was based on eight parameters: uniformity, signal to noise ratio (SNR), noise, contrast to noise ratio (CNR), spatial resolution (SR), artefact index, geometric accuracy and low contrast.
Results: The image uniformity was dependent on the applied protocols, as well as the noise. Regarding the CNR, the structures of high densities were more sensitive to the effect of scanning parameters. There were no significant differences between SNR and CNR in centered and peripheral objects. The geometric accuracy showed that all the distance measurements were lower than the real value. Low contrast resolution was influenced by scanning parameters and the 1mm rod was not depicted in three CBCT units. The smaller voxel sizes presented higher spatial resolution. There were no significant differences among protocols regarding artefact presence.
Conclusion: The package (phantom and macro) developed provided a fast, low cost and reproducible method for evaluation of image quality parameters in CBCT.

14:00 - 15:30 **Room M 1**

Cardiac

SS 1903

Myocardial tissue characterisation and texture analysis II

Moderators:
S. Bayraktaroglu; Izmir/TR
N.N.

B-1369 14:00

Fast, precise and accurate myocardium T1 mapping using a radial modified look locker NMR imaging sequence
B. Marty, B. Coppa, P.G. Carlier; *Paris/FR (b.marty@institut-myologie.org)*

Purpose: Quantitative NMR cardiac T1 mapping has become a popular modality to characterise myocardial tissue. The classical MOLLI sequence allows the acquisition of a single slice within a 17-heartbeat breath hold. Here, we developed a radial variant of the MOLLI (raMOLLI) allowing a decrease in acquisition time down to 5 heartbeats, while keeping high precision on T1.
Methods and Materials: After non-selective inversion, the raMOLLI sequence consisted in the acquisition of 5 shots of 80 radial spokes at end of diastole with a fast gradient echo readout. Fifty image were reconstructed using compressed sensing. The temporal signal evolution was fitted using Bloch equations to obtain a T1 map. The method was validated at 3T on phantoms, 4 healthy volunteers and a patient suffering from dilated cardiomyopathy. For comparison, conventional MOLLI was also acquired.
Results: In vitro, relative T1 differences were less than 3% between the raMOLLI and a gold standard sequence and the measures did not depend on the heart rate. On the four volunteers, the mean T1 estimated in the

myocardium were comparable between the two MOLLI variants. For the patient, the regions with decreased raMOLLI T1 values correlated with regions of late gadolinium enhancement.
Conclusion: The raMOLLI sequence offers several advantages compared to MOLLI. Acquisition time is substantially reduced and no effect of heart-rate on estimated T1 values were reported. Finally, the method allowed the reconstruction of a large number of images along the T1 recovery curve, providing a high robustness to the postprocessing.

B-1370 14:08

The value of feature/contour-based registration in quantification of myocardial extracellular volume fraction based on T1 mapping technique
L. Lin, X.-H. Zhou, M. Zheng, Q.-X. Xie; *Guangzhou/CN (xiangxiang_87@163.com)*

Purpose: Inconsistency of ventricular shape between pre- and post-contrast T1 maps or among T1 mapping images of different inversion time might cause artefacts, thus impact on the quantification of extracellular volume fraction (ECV). Feature/contour-based registration is a non-linear transformations using predefined myocardial contours to align multiple images before T1 map generation. We evaluated its influence on the accuracy of ECV quantification.
Methods and Materials: T1 mapping images of the mid-ventricular short axis slice (SAX) of 25 healthy volunteers were obtained using modified look-locker inversion recovery (MOLLI) on a 3.0T magnetic resonance imaging system (Magnetom Verio, Siemens). ECV was calculated using a software (cvi42 v5.3, circle cardiovascular imaging) by two methods: routine ECV by T1 maps automatically generated by the scanner, and registered ECV by T1 maps generated after feature/contour-based registration. Subjects were divided into deformation group (n=10) and control group (n=15) according to cardiac features. Paired comparison was done for ECVs within each group.
Results: There was statistical difference (P=0.025) between routine ECV (25.30±3.16%) and registered ECV (24.17±2.41%) of all the volunteers. In deformation group, routine ECV (26.76±3.47%) and registered ECV (24.03±2.10%) were statistically different (P=0.021). While in control group, there was no difference (P=0.707) between routine ECV (24.32±2.61%) and registered ECV (24.26±2.66%). 6 cases presented artefacts in routine ECV maps, which were eliminated or mitigated in registered ECV maps.
Conclusion: Feature/contour-based registration can improve the accuracy of ECV quantification in cases with ventricular shape deformation among source images.

B-1371 14:16

Diffusion weighted imaging in cardiac magnetic resonance for diagnosis of acute myocarditis: could it be the missing criteria?
L. Pavan, R. Faletti, F. Gentile, E. Caramia, M. Gatti, G. Schivazappa, A. Romano, P. Fonio, G. Gandini; *Turin/IT (lucajpavan@gmail.com)*

Purpose: In addition to Lake Louise criteria, T1- and T2-mapping are becoming very useful tools for diagnosis of acute myocarditis, although few MRI scanners provide them at the moment. The aim of our study was to assess diffusion weighted imaging (DWI) as a diagnostic criteria for acute myocarditis, since it is available on the majority of MRI scanners.
Methods and Materials: Fourteen patients were prospectively enrolled for this study: 7 patients affected by acute myocarditis with infarct-like presentation and positive to all Lake Louise criteria (mean age 32±17y) and 7 negative controls with no previous cardiac diseases (mean age 34±16y). All patients performed examination with a 1,5T MRI scanner with 32-channel phased-array coil. Image analysis was performed by two radiologists in consensus, T2-ratio and DWI-ratio (based on ADC values) between myocardial muscle and skeletal muscle of the same slice were calculated for each patient and compared between the two groups.
Results: Comparison of DWI-ratio between pathologic and control group showed a statistically significant difference (mean 0,58±0,08 vs 1,00±0,18; p<0,0001), as well as T2-ratio comparison (mean 2,28±0,42 vs 1,22±0,26; p<0,0001).
Conclusion: Our study suggests DWI could be introduced in cardiac magnetic resonance as a sequence for assessment of acute myocarditis and maybe considered as a major diagnostic criteria in addition to Lake Louise criteria, although larger studies are needed to assess it properly.

B-1372 14:24

Detection of cardiovascular disease with MRI myocardial texture changes on routine non-contrast sequences
P. Talarczyk, J. Weir-McCall, S. Waugh, P. Guntur Ramkumar, G. Houston; *Dundee/UK*

Purpose: Texture analysis allows quantification of tissue heterogeneity and has been proven to provide powerful diagnostic and prognostic data in oncological imaging. However to date this technique has not been applied to the assessment of the myocardium. The hypothesis of the current study was that those with diabetes and cardiovascular disease (CVD) would have more heterogenous myocardium than those without.
Methods and Materials: 143 enrolled subjects were divided into 4 groups: diabetics with (group 1, n=31) or without CVD (group 2, n=55), and non-diabetics with (group 3, n=28) or without CVD (group 4, n=29). Cardiac MRI was performed in a 3T scanner. Image analysis was performed on a pre-contrast bSSFP short axis mid-ventricular slice at end-systole. Texture features were measured using MazDa software, using the co-occurrence matrix (with fine and coarse filter) and run-length matrix.
Results: There were significant differences in coarse entropy (F-test =2.94, p=0.035), fine entropy (F-test =2.96, p=0.034), coarse sum of squares measure (F-test =3.48, p=0.018) and fine sum of squares measure (F-test =2.76, p=0.044) between the four groups. Post hoc analysis showed these differences to exist between group 3 and 4, with group 3 exhibiting significantly higher entropy (2.21±0.2 vs 2.33±0.2, p=0.041 for coarse, and 2.50±0.1 vs 2.58±0.1, p=0.025 for fine feature entropy).
Conclusion: Myocardial heterogeneity on routine non-contrast sequences is increased in those with cardiovascular disease compared with controls, suggesting this is a new and novel way of quantifying myocardial structure without the need for additional sequences.

B-1373 14:32

On the selection of region of interest in measurement of cardiac magnetic resonance imaging T2* in patients with thalassaemia major
S. GholamiBardeji, M. Dodangeh, Z. Gholami Bardeji, S. Sefidbakht, R. Jalli; *Shiraz/IR (s_gholami@sums.ac.ir)*

Purpose: To investigate the correlation between T2* values of different Regions of Interest (ROIs) in the heart with the means of estimating the cardiac iron content in the thalassaemia major patients. Another purpose is to design a model which predicts T2* value of inter-ventricular septum (Septum) based on T2* value of other ROIs.
Methods and Materials: 130 patients underwent ECG-gated cardiac Magnetic Resonance Imaging(MRI), and T2* values were measured in different ROIs. The statistical analysis carried out using Matlabr R2015b. Full-thickness ROIs are drawn manually in Septum, whole LV wall, the region of the best visual conspicuity (Sharp), and Left Ventricular (LV) free wall.
Results: In patients with the cardiac T2* ≤ 20, the statistical analysis confirms a significant correlation ($\alpha = 0.001$) between T2* values of Septum and the ROIs named above. Moreover, the statistical results become more concordant with decreasing T2* values. In addition for patients with a T2* > 20, a weak correlation is noticed between T2* values of different ROIs. Three predictor models are provided to estimate T2* value of Septum using T2*values of whole LV wall, Sharp regions, and LV free wall.
Conclusion: The T2* values of the LV free wall and the whole LV wall are reliable alternatives to estimate the T2* value of Septum. The predictor model based on T2* value of whole LV wall provides the best estimation.

B-1374 14:40

Myocardial fibrosis (MF) and its associated ventricular impairment in adults with repaired tetralogy of Fallot (rTOF): role of delayed enhancement cardiac magnetic resonance (DE-CMR)
G. Schivazappa, R. Faletti, F. Angelino, A. Romano, M. Gatti, E. Caramia, F. Misischi, P. Fonio, G. Gandini; *Turin/IT (giulia.schivazappa@gmail.com)*

Purpose: To define utility of DE-CMR in evaluating MF and its correlation with ventricular volume and function, essential prognostic factors in adults with rTOF.
Methods and Materials: Twenty-four patients (15 male, 9 female; mean age 34±12,9 years) with rTOF were subjected to CMR examination and compared with a control group (22 healthy patients: 11 male, 11 female; mean age 34±16,3 years). Protocol included inversion recovery turbo field-echo (IR-TFE) sequences to identify late enhancement (LE) after contrast medium intravenous administration (Gadobutrol). Qualitative analysis of IR-TFE images was performed using Kim et al. scheme. Indexed ejection fraction (EF) and volume (EDV) of both ventricles (right RV, left LV) were calculated using cine short-axis images from base to apex. Variables were compared with student-T test.
Results: LE was present (septum/ventricular junction) in 15/24 patients (group-A) and absent in 9/24 (group-B). Ventricular analysis showed statistically significant (SS) difference (p<0,01) comparing rTOF to control group for values of RV-EDV, RV-EF and LV-EF. Group-A demonstrated even more increased RV-EDV and decreased RV-EF compared to group-B (EDV/BSA (ml/m^2) group-A=143,87±49,17; B=91,55±13,23; EF (%) A=36,53±6,81; B=50,54±7,66), with SS values, and also showed a reduced LV-EF (group-A=39,82±5,77; B 45,65±7,18) with p=0,05.
Conclusion: DE-CMR in patients with rTOF proved to be an essential tool in early MF detection. Presence of LE is related to EF reduction in both ventricles and RV-EDV increase compared to healthy patients. Patients with rTOF and positive LE showed increased RV-EDV, decreased RV-EF and an apparent further LV-EF reduction compared to those without LE.

B-1375 14:48

Cardiac MRI with T1 and T2 mapping in patients with phenylketonuria (PKU)

T.C. Walter, G. Knobloch, N. Tiling, U. Plöckinger, D. Blaschke, T. Denecke, B. Hamm, M.R. Makowski; *Berlin/DE (thula.walter@charite.de)*

Purpose: Phenylketonuria (PKU) is one of the most common congenital defects of the amino-acid-metabolism. A vast body of research exists on neurological damage in PKU. However, there is very little data on potential cardiac effects of PKU in adult patients. Novel MR mapping techniques allow a more detailed evaluation of the myocardium, beyond mere morphological and functional assessment. The aim of this study was to evaluate changes in myocardial tissue composition in adult PKU.
Methods and Materials: 23 PKU patients (13 male) and 23 matched healthy controls were included in this study. Informed consent was obtained from all patients. The local ethics committee approved this study. All included patients underwent standard cardiac MRI (1.5 T, 32 channel coil, Siemens Avanto), which was amended by non-enhanced T1- and T2-mapping. T1- and T2-maps were segmented according to the AHA-17- Segment model. Cardiac function, mass and morphology were evaluated and compared between the two groups.
Results: Sex, age and BMI were similar in PKU patients and controls (p>0.05). Segmental non-enhanced T1 values showed a significant shortening of native T1 the mid-cavity posterior segment 10 (p=0.035). Late enhancement imaging and CINE-MRI showed no corresponding morphological alterations in this segment. T2 values, LV-morphology and function were similar for PKU patients and controls in all segments.
Conclusion: This study demonstrated that a significant shortening in T1-time can be measured in the posterior mid-cavity segment of PKU patients. The aetiology and clinical consequences of these signal alterations are currently unclear.

B-1376 14:56

Myocardial T1- mapping in daily cardiac magnetic resonance study in hypertrophic cardiomyopathy

O.Y. Dariy, S. Aleksandrova, M. Shlyappo, V. Makarenko, L. Bockeria; *Moscow/RU (dariiolyka@mail.ru)*

Purpose: The purpose of our study is to define the role of T1 mapping in hypertrophic cardiomyopathy diagnosis algorithm. To evaluate the end-diastolic wall thickness (EDWT) correlation with native and postcontrast myocardial T1-time, extracellular volume quantification (ECV), focal fibrosis degree and myocardial shortening.
Methods and Materials: We performed 21 cardiac magnetic resonance studies. In vivo T1 mapping was performed at a ventricular short-axis slice at three levels before and after the infusion of a contrast agent. T1 mapping with a modified Look-Locker Inversion Recovery (MOLLI) pulse sequence was used to calculate ECV. Assessment of T1 relaxation-time and ECV values was based on areas where focal fibrosis was excluded.
Results: There were the maximum hypertrophy at the anterior and posteriorseptal segments of the basal myocardium, the minimum one at the apical segments. Native myocardial MOLLI T1 was 1300±44ms (p<0.01) significantly higher than the multicenter study published in the normal myocardium, the post-contrast T1 (497±62ms p>0,05). The significant correlation of EDWT and T1 values was not received. The basal EDWT with native T1 showed the correlation (r=0,6) and with the focal fibrosis (r=0,6). The weak correlation of EDWT with the ECV (r=0,2). The midwall fractional shortening and native T1 had the weak correlation (r=0,5).
Conclusion: The advent of absolute T1 measurement techniques allows by definition of the ECV to quantify the entire range of fibrosis neither diffuse or focal. The values of T1 relaxation time and ECV does not depend on the degree of hypertrophy and are independent predictors of myocardial damage.

B-1377 15:04

Diagnostic significance of MRI in patients with myocarditis

M. Djurdjic, R. Maksimovic, B. Banko, I. Živković, I. Milinkovic, P. Seferovic; *Belgrad/RS (djurdjic_milica@yahoo.com)*

Purpose: The purpose of this study was to analyse significance of MRI parameters in assessment of patients with myocarditis and their relations to clinical data, ECG and laboratorory findings.
Methods and Materials: The study included 73 patients, predominantely males 55 (75.3%), average age 55.3 years. All patients underwent clinical examination, ECG, laboratory testing and MRI examination within 14 days of establishing suspected myocarditis. MRI parameters were: LVEDD, LVESD, LVEF, LVESV, LVEDV, presence of oedema and late gadolinium enchancement (LGE).
Results: The edema was present in 22 patients (30.1%), LGE in 42 (57.5%), both LGE and edema was seen in 11 (15.1%) of patients. Patients with oedema has significantly lower EF 42,7±21.7% in comparisson to those without oedema (53,7±16.7%), p<0.05, increased EDV (181,5±85,4 ml vs 161,0±55,9 ml, p<0.05, respectively) and increased ESV (126,9±96,1 ml vs 78,6±55,4 ml, p<0.01, respectively). Patients with LGE had decreased EDV (163,6±51,4 ml vs 171,6±87,4 ml, p<0.05, respectively) and decreased ESV (82,9±53,9 ml vs 105,3±94,3 ml, p<0.01, respectively) but LVEF was not significantly different among two groups, 52,4±17.5% vs 48,1±20.5%, respectively. There was a significant correlation between increased BNP and troponin and systolic parameters of LV function, ESV, r=0,45, p<0.05, r=-0,35, p<0.05, respectively. Troponin was also associated with presence of LGE, r=0,38, p<0.05.
Conclusion: Presence of myocardial oedema and LGE has been associated with systolic function of the left ventricle and therefore has great importance in final evaluation and furhter therapeutical decision making in these patients.

B-1378 15:12

Meta-analysis on pre-ablation late gadolinium enhancement predicting post-ablation recurrence of atrial fibrillation

K. Diao, Z. Yang, Q. Zhao, B. Hu, X. Liu; *Chengdu/CN (kaiyuediao@qq.com)*

Purpose: To explore whether the pre-ablation myocardial fibrosis could constitute an independent risk factor for recurrence of arrhythmia after catheter ablation, corresponding to the call from the newest clinical guidelines.
Methods and Materials: PubMed, Cochrane, web of Science, EMBASE were searched for studies demonstrating LGE's prognostic value in AF patients. Studies recording pre-ablation LGE analysis and recognizing AF recurrence as the primary end point were included. Pooling of the odds ratio was performed using a fixed- or random-effect model. Meta-regression and sub-group analysis were also performed to find a possible resource of heterogeneity.
Results: Data was included from 7 studies with a total of 1385 patients and proximately one year's follow-up. Included patients had a mean age of 63.6. Patients with higher level (>10%) of LGE had a much larger chance of AF recurrence than the lower level LGE ones (OR, 0.34; 95% confidence interval, 0.21-0.55; P<0.0001; I^2=71.6%). Meta-regression showed age could have an effect and considering which could greatly decrease the heterogeneity (revised I^2=26.43% vs I^2=71.6%, p=0.0023). Sub-group analysis showed little pre-ablation LGE (<5%) had prominently smaller OR than patients without moderate and severe level LGE (OR, 0.0602; 95% confidence interval, 0.0081-0.4453; P=0.0059; I^2=0.00%).
Conclusion: The severity level of pre-ablation LGE can predict the AF recurrence, and patients with milder myocardial fibrosis can get a better chance to recover to sinus rhythm without symptomatic recurrence through the catheter ablation.

B-1379 15:20

Pulmonary reperfusion injury following right ventricular outflow tract stenting

O.D. Garcia, J. Sandoval Jones, G. Aristizabal Villa; *Mexico City/MX (omarcillogarciag@yahoo.com.mx)*

Purpose: To determine if PRI (pulmonary reperfusion injury) was present (by chest x-ray) following right ventricular outflow tract (RVOT) stenting.
Methods and Materials: Prospective study including 12 consecutive children with ToF Tetralogy of Fallot (25% female) that underwent RVOT stenting between January and July, 2016. Clinical and procedural data were reviewed. A radiologist evaluated chest x-ray films before and after intervention to determine presence and severity of PRI, as well as its impact on days of ventilation and length of hospital stay.
Results: Mean age and weight were 32 months (range 1-139) and 10.8 kg (1.8-22) respectively. SaO2 increased from a mean of 71±9.8% to 97±6% post RVOT stenting (p<0.0001); PaO2 was 43±7.4 mmHg and 126±94 mmHg pre and post-stenting respectively (p<0.001). The radiological analysis results were as follows: of the 12 patients, diffuse lung opacifications were classified as severe in n=5(41%); moderate n=1(8%); mild n=3(25%); none n=3(25%) within 24 hs post-RVOT-stenting. Pulmonary infiltrates affected the right lung in 8(66.7) patients. Seventy-two hours post-RVOT-stent, 8(67%) patients had complete resolution of previous abnormal findings on chest x-ray. A positive correlation was found between diameter of the pre-stent RVOT and days of ventilation (r 0.851, p 0.032). Similarly, positive correlation was found between post-stent RVOT diameter (mm) and days of hospital stay (r 0.683 p 0.014).
Conclusion: Transient PRI is present after RVOT stenting. Degree of pre-stent RVOT stenosis is reflected by longer duration of ventilation and length of hospital stay.

14:00 - 15:30 **Room M 4**

Breast

SS 1902b

Image-guided breast interventions and radiologic-pathologic correlation

Moderators:
G. Forrai; Budapest/HU
J. Raposo; Lisbon/PT

K-27 14:00

Keynote lecture
G. Forrai; *Budapest/HU*

B-1380 14:09

Initial experience in percutaneous cryoablation for breast cancer
C. Pusceddu; *Cagliari/IT (clapusceddu@gmail.com)*

Purpose: To evaluate the safety and efficacy of breast cryoablation (CRA) as local therapy for patient with metastatic breast cancer.
Methods and Materials: thirty-nine breast lesions, mean size 2,1 (range 1 - 6,7 cm) in twenty-nine consecutive patients, mean age 51 (36-81) with core-needle biopsy-proven breast carcinoma and metastases were included in this study. Twenty-three patients had one lesion, 4 patients two lesions, 1 patient three lesions and 1 patient five lesions. Under local anaesthesia the tumour and surrounding breast tissue were ablated with percutaneous CT-guided CRA. Cryoablation consisted of 2 cycles each of 10 minutes of freezing followed by a 4-min active and 4-min passive thawing phase for each one. Twenty-four patients underwent one CRA session, four patients 2 CRA sessions and one patient underwent 3 CRA sessions.
Results: All CRA sessions were successfully completed and all breast tumours were ablated. Morbidity consisted in transient and mild ecchymotic changes and post-procedural oedema seen in ten cases. The therapeutic outcomes were evaluated by contrast-enhanced TC or MRI at 2-, 6-, 12-, and 18-month intervals. The absence of tumour enhancement TC or MR image was considered as indicating complete tumour necrosis. During the mean follow-up of 15 months (6- 28 months) 26 patients had shown complete response to the treatment. Only 3 patients out 29 (10%) showed relapse close to the treated lesion. These patients were treated with a second CRA procedure.
Conclusion: CRA of metastatic breast cancer is a safe and effective method which allows local control of the disease.

B-1381 14:17

Breast cancer cryotherapy in elderly patients
C. de Bazelaire[1], C. Jousset[1], R. Cazzato[2], X. Buy[2], S. Ferron[2], E. de Kerviler[1], J. Palussière[2]; [1]*Paris/FR*, [2]*Bordeaux/FR (cedric.de-bazelaire@aphp.fr)*

Purpose: Some elderly patients with breast cancer do not undergo operation despite a theoretical indication for this therapy because of contraindications or refusal. In such cases, cryotherapy could serve as an alternative therapy. The objective of this study was to evaluate the feasibility, tolerance, and effectiveness of cryotherapy for malignant breast lesions.
Methods and Materials: This was a retrospective two-center study. Between February 2012 and January 2016, tumour treatment via cryotherapy under CT and ultrasound guidance was proposed to 40 patients with malignant breast lesions less than 35mm in diameter. All procedures were performed under local anaesthesia. The patients received follow-up by their oncologist and underwent biannual MRI for an average of 18 months (range 3-48 months). The evolution of the disease was compared between the group of patients treated with primary surgery and the group treated with neoadjuvant hormone therapy and subsequent surgery.
Results: A total of 34 patients were disease-free at 24 months. After cryotherapy, two patients had skin necrosis or erythema. Two patients experienced local recurrence. Among this cohort of patients with the same cancer and comorbidities, the frequencies of complications and recurrence after 24 months were not different between patients who received cryotherapy and patients who received either primary surgery or neoadjuvant hormone therapy with subsequent surgery.
Conclusion: When surgery was not feasible, cryotherapy appeared to be an effective alternative to local treatment of breast lesions without major side effects.

B-1382 14:25

Dosimetric and clinical detail detectability performance of a new dedicated tomosynthesis-guided prone breast biopsy system
S. Grisotto, M. Borroni, E. Mazzarella, T. Giandini, C. Tenconi, A. Primolevo, F. Cartia, C. Ferranti, G. Scaperrotta; *Milan/IT (simone.grisotto@istitutotumori.mi.it)*

Purpose: To evaluate the main parameters affecting clinical practice of the first dedicated tomosynthesis-guided prone breast biopsy system Affirm™ Prone (Hologic, Danbury, USA) and to compare it with prone stereotactic system MultiCare Platinum™ (Hologic, Danbury, USA).
Methods and Materials: Average glandular dose (AGD) for breasts of different compressed thicknesses (21-90mm) was calculated according to Dance et al. (2011) exposing suitable polymethyl methacrylate slabs. AGD_{std}, i.e. the total AGD absorbed after a standard biopsy procedure which differs from one system to the other, was estimated. Detectability of different size lesions was semiquantitatively quantified by 9 operators of our institution evaluating images of 3 different thicknesses of a heterogeneous breast imaging phantom provided with 6 clusters of microcalcifications, 7 fibrils and 6 masses (CIRS 020 BR3D). Particularly, for every image, a detectability score (0, 0.5 or 1) relative to each lesion was independently assigned by all operators.
Results: AGD_{std} for MultiCare Platinum™ resulted 47%, 80% and 3% higher than for Affirm™ Prone, for small (21mm), medium (45mm) and large (75mm) breast sizes, respectively. For the first system, masses and fibrils detectability respectively decreased of about 50% and 85% with increasing phantom thickness. Affirm™ Prone detectability of all types of lesions remained almost constant at the different investigated thicknesses.
Conclusion: The new Affirm™ Prone system enables to perfom breast biopsy procedures with a limited amount of radiation dose, particularly with small and medium breast thicknesses. It also allows a much better visibility of clinical details, particularly fibrils and masses.

B-1383 14:33

Role of tomosynthesis-guided biopsy (3D VAB) in reducing uncertain biological potential lesions (B3) overtreatment, detected with tomosynthesis as architectural distortions
G. Romanucci[1], S. Brunelli[1], P. Bricolo[1], L. Cugola[1], A. Caneva[2], F. Caumo[1]; [1]*Verona/IT*, [2]*San Bonifacio/IT (giovi.romanucci@libero.it)*

Purpose: To evaluate the accuracy of tomosynthesis-guided biopsy in the characterisation of distortions detected with Synthetic 2D + tomosynthesis and in reducing lesions of uncertain malignant potential (B3) overtreatment.
Methods and Materials: Since April 1, 2015 we performed 102 3D VAB procedures on distortion (37%), 7.5% of which detected only with tomosynthesis, using a 9G needle with 20 mm aperture. All the 3D VAB procedures were performed with a double round the clock sampling, collecting 24 tissue samples instead of 12 samples (with an average weight of 3.4 g). The assessment of the post-biopsy residue was performed with tomosynthesis and a residue <10% was classified as complete removal of the lesions. All RS and PL (smaller than 15 mm) completely removed were classified as B2. Each histologic result has been subjected to multidisciplinary discussion for the therapeutic continuation and/or follow-up.
Results: B5 27 (25%), of which 9 detected only in 3D. B2 (55.9%): 42 RS, 2 PL, 13 benign lesions. RS and PL went to annual follow-up for 5 years. B3 (17.6%): 3 RS, 7 SR + ADH, 1 RS + LIN1, 1 RS FEA + ADH + 5 LIN. 66.7% were sent to therapeutic open surgical excision (50% were classified carcinomas at definitive histology), 33.3% were sent to follow-up.
Conclusion: 3D VAB procedures with 9G and 20 mm aperture needle allowed a more substantial and accurate biopsy thus avoiding overtreatment of low-risk malignant transformation lesions (RS and PL).

B-1384 14:41

Outcomes of vacuum-assisted biopsy for B3 breast lesions
N. Larkman, N. Sharma; *Leeds/UK (nisha.sharma2@nhs.net)*

Purpose: Management difficulties arise from the heterogeneous pathologies comprising B3 lesions. Vacuum assisted biopsy's (VAB) larger sampling compared to core biopsy means diagnostic surgery may be avoided. Our retrospective study looked at the grade of malignancies arising from B3 pathology.
Methods and Materials: A retrospective study from 2009 to 2014. Patients with B3 lesions on core biopsy from screening or symptomatic settings and a vacuum-assisted biopsy with pathology results were included. Upgrade rate at vacuum biopsy and surgery was reviewed.
Results: 735 B3 lesions on core biopsy. Of these 439 underwent VAB and 230 surgery. 95 had a VAB and surgery. Following VAB 89% (389) remained B3 or benign and 11% (50) were upgraded: 36 (72%) upgraded to B5a - 4 (8%) high grade in-situ disease, 12 (24%) upgraded to invasive B5b disease and 1 to B4. Of the VAB and surgery specimens; 6 (6%) downgraded from B5a to B3 following surgery. In these cases the DCIS was wholly removed by the VAB.

One B5b downgraded to B5a (invasive component excised in VAB), 7 (7%) upgraded from B3 to B5a, 1 (1%) was a B5a upgraded to a B5b - HGDCIS to ductal grade 1. One(1%) was a B3 upgraded to B5b - LCIS to ILC grade 2.
Conclusion: The reticence to use vacuum biopsy to manage B3 lesions is contributing to over diagnosis and treatment. If B3 lesions are upgraded the majority are low grade malignancies that will not have a negative impact on the women's life.

B-1385 14:49

Prospective follow-up of patients with B3 lesions over a 4-year period
N.D. Forester, N. Altaf; *Leeds/UK (nerysforester@mac.com)*

Purpose: Following introduction of large-bore vacuum-assisted biopsy (LVB) for diagnosis and management of B3 lesions in 2011, a prospective database of patients was developed. Following B3 lesion diagnosis on core biopsy, patients underwent LVB. If B5, patients had surgery; if B3 patients underwent 5 years annual surveillance mammography (ASM) or were discharged/returned to routine recall, depending on the presence of epithelial atypia. Patient outcomes were prospectively audited.
Methods and Materials: B3 lesion database analysed to ascertain number of ASMs performed, recall rate, symptomatic episodes and subsequent malignancy following B3 diagnosis.
Results: Between October 2011 and December 2015, 396 B3 lesions identified. 305 underwent second line LVB. 27 patients diagnosed with malignancy following LVB and 17 patients upgraded to malignancy following excision biopsy (unsuitable for LVB/pathology request). 352 patients had ASM/routine recall, together having 410 mammograms performed over 4 years. 9 patients were recalled from ASM (recall rate 2%). 20 underwent further breast investigations (19 presented symptomatically, 1 recalled from MRI high-risk surveillance). From additional investigations 3 cancers diagnosed (1 following high-risk surveillance MRI; 1 symptomatic presentation, 1 recall from ASM). There were also 4 further B3 lesions and 22 benign diagnoses.
Conclusion: LVB for B3 lesions is an excellent alternative to excision biopsy. However, ASM has a low recall rate and cancer detection rate, with only 1 of the 3 subsequent cancers detected by mammographic surveillance. This questions whether ASM is really necessary in this group of patients. Could they be safely returned to routine recall within the screening program?

B-1386 14:57

Non-surgical complete excision of small suspicious breast lesions using the breast lesion excision system BLES
N.M. Abdel Razek; *Cairo/EG (naglaabdelrazek@yahoo.com)*

Purpose: To assess the diagnostic efficiency of BLES in comparison to OB in diagnosis of small suspicious breast lesions.
Methods and Materials: The study included 435 patients with small suspicious non-palpable breast lesions. We included lesions categorised as BIRADS 4 & BIRADS 3 with positive family history for breast cancer.
Results: 435 suspicious lesions were successfully removed using the BLES,19.3 % (84/435) were diagnosed after histopathology as benign including fibrocystic disease, sclerosing adenosis, radial scars and papillomas without atypia. 38.2% (166/435) were diagnosed as high-risk lesions including, papillomas with atypia, ALH, ADH & 48.4% (142/435) were diagnosed as malignant including DCIS, LCIS,IDC&ILC. The maximum size removed was 12mm there was no underestimation encountered by the BLES. The margin was free in 40/142 (28.2%) and the margin was close in 45/142 (31.7%) and the margin was involved in 57/142 (40.1%) of the malignant cases.122/142 histopathologically proven malignant lesions were exposed to re-surgery and in 20/142, no surgery after BLES, only radiotherapy and sentinel node diagnosis. BLES outperforms the VAB in high-risk and malignant lesions. BLES is 100% as sensitive as the OB regarding the concordance and sensitivity with no underestimation. In 20/40 margin-free lesions, BLES excision was not followed by surgery, only sentinel node and radiotherapy.
Conclusion: BLES could be an efficient management for small carcinomas less than 8mm diameter if complete excision with free margin was achieved yet still it is the decision of the MDT and should be associated with sentinel node biopsy and focal radiotherapy.

B-1387 15:05

Gene expression profiling of breast cancer: associations among mammographic microcalcifications, ERBB2 and immunity
S. Shin, A. Chu, S. Song, W. Han, J. Kim, W. Moon; *Seoul/KR (shinsungui@gmail.com)*

Purpose: To investigate the associations between mammographic microcalcifications and breast cancer gene expression profiles using microarray analysis.
Methods and Materials: Gene expression analysis was performed using Affymetrix GeneChip® Human Gene 2.0 ST arrays in 168 breast cancer patients. Mammographic microcalcifications of these patients were reviewed by three radiologists and grouped into three groups: no microcalcifications (n=99); low-to-intermediate microcalcifications (n=37); and highly suspicious microcalcifications (n=32). To identify differentially expressed genes (DEGs) between these three groups, a one-way analysis of variance was performed with post hoc comparisons with Tukey's honest significant difference test, and a P value <0.05 was applied as the threshold for statistical significance. To explore the biological significance of DEGs, we used DAVID for gene ontology analysis and BioLattice for clustering analysis.
Results: Total 2551 genes showed differential expression among the three groups. Of these, 1838 DEGs were detected for the highly suspicious/no microcalcifications comparison, 484 DEGs for the highly suspicious/low-to-intermediate microcalcifications comparison, and 457 DEGs for the low-to-intermediate/no microcalcifications comparison. ERBB2 genes are up-regulated in highly suspicious microcalcifications group (P<0.001, fold change 2.474) . Both gene ontology and clustering analyses revealed that the immune, defense and inflammatory responses were decreased in the highly suspicious-microcalcifications group compared with the no-microcalcifications group (P<0.001).
Conclusion: Gene expression patterns are different according to the status of mammographic microcalcifications in breast cancer. Breast cancers with mammographic microcalcifications are associated with high levels of mRNA expression of ERBB2 and decreased immune system activity.
Author Disclosures:
S. Shin: Research/Grant Support; grant (#2015R1C1A1A01053362) from the Basic Science Research Program through the National Research Foundation of Korea (NRF) funded by the Ministry of Science, ICT & Future Planning.

B-1388 15:13

Triple-negative breast cancer: MR imaging findings associated with clinical-pathologic factors
K. Lee, S. Kim, B. Kang, I. Youn; *Seoul/KR*

Purpose: To compare the magnetic resonance imaging (MRI) findings and clinical-pathologic characteristics in patients with triple-negative cancer (TNC) with recurrence or advanced stage.
Methods and Materials: This study was approved by institutional review board. The informed consent for patients was waived. Two hundred eighty one patients with TNC between January 2009 and March 2016 who underwent preoperative MRI were included. Visual assessment of central T2 high signal intensity, rim-enhancement, DWI peripheral high signal intensity were performed by two radiologists. Measurement of ADC values of entire tumour, central and peripheral portion of the tumour was performed for 101 lesions. Clinical-pathologic data were collected including age, recurrence, stage, resection margin, histologic grade, tumour size, multiplicity, lymphovascular invasion (LVI), nodal involvement. Statistics for hazard ratio of recurrence performed using Cox proportional hazards model. Logistic regression analysis was performed to evaluate risk factors associated with advanced stage. The inter-observer reliability of ADC measurements was assessed using intra-class correlation coefficient.
Results: Of the 288 lesions, 36 (12.5%) lesions were recurred after a median follow-up of 18.0 months. Hazard ratio for recurrence was increased with LVI, tumour size, nodal involvement, advanced stage, rim-enhancement (p<0.05). Odds ratio for advanced stage was increased with LVI, tumour size, nodal involvement and recurrence (p<0.05). Intra-class correlation coefficient for ADC value of the whole tumour exceeded 0.80, indicating good agreement, but ADC values were not significantly associated with recurrence or advanced stage.
Conclusion: Rim-enhancement and several clinical-pathologic factors can be prognostic factors for recurrence and advanced stage in patients with TNC.

B-1389 15:21

Systematic review of breast lesions of uncertain malignant potential (B3 lesions) and their risk of malignancy
N.D. Forester, S. Lowes; *Newcastle/UK (nerysforester@mac.com)*

Purpose: Borderline breast lesions (B3 lesions) can coexist with malignancy. The magnitude of this risk varies between studies and lesion subtypes. This systematic review will determine an accurate estimate of the risk of invasive in-situ malignancy identified by surgical excision biopsy, following diagnosis of a B3 lesion at core biopsy, within each B3 lesion subtype, to guide risk stratification and improve management strategies.
Methods and Materials: Literature searches (MEDLINE, Embase, HMIC, Scopus and Web of Knowledge) identified relevant studies between 1980 and 2015. Literature appraisal, meta-analysis and subgroup analysis performed to determine malignancy risk for all subgroups of B3 lesions (Papilloma, Radial Scar, AIDP, Lobular Neoplasia and FEA).
Results: Searches returned 2289 citations, with 11 identified from other sources. Duplicates, unsuitable articles and abstracts/posters/reviews were excluded leaving 183 records. From these, 54 full-text articles did not meet inclusion criteria. Meta-analysis was performed from 129 studies. Rates of malignancy varied from 6% in a radial scar with no atypia, to 32% for a

papilloma with atypia. Differences in malignancy upgrade rates between atypical and non-atypical lesions were statistically significant (p<0.05). Study heterogeneity could not be explained by differences in core biopsy size or year of publication, however, a significant difference in upgrade rates to malignancy was observed between the US and non-US literature.
Conclusion: Studies have assessed the risk of malignancy following diagnosis of B3 lesions, but are often small and lack statistical power. This study is a comprehensive, inclusive assessment of the available literature, on which to base tailored management strategies.

14:00 - 15:30 **Room M 5**

Neuro

SS 1911b

Epilepsy and brain gadolinium deposition

Moderators:
N. Bargalló; Barcelona/ES
T. Rostovtseva; St. Petersburg/RU

B-1390 14:00

Integrated FDG-PET/MRI in patients with drug resistant epilepsy
C. Deuschl[1], T. Rüber[2], L. Ernst[2], J. Kirchner[3], V. Ruhlmann[1], T. Pöppel[1], M. Forsting[1], C. Elger[2], L. Umutlu[1]; [1]*Essen/DE*, [2]*Bonn/DE*, [3]*Düsseldorf/DE (cornelius.deuschl@uk-essen.de)*

Purpose: The aim of this study is to evaluate the diagnostic impact of simultaneous 18F-FDG PET/MRI for the detection of epileptogenic lesions in patients with drug resistant epilepsy.
Methods and Materials: Twelve patients with drug resistant epilepsy were enrolled in this ongoing prospective study (mean age: 40,1 years, range: 19-75 years, 6 female). All patients underwent a simultaneous 18F-FDG PET/MRI of the brain, comprising the following sequences: (1) non-enhanced MPRAGE, (2) 3D FLAIR, (3) STIR cor, (4) T2 ax, (5) SWI. Image analysis was performed by a neuroradiologist and a nuclear medicine specialist during consensus reading with subsequent reading of the (1)MRI, (2)PET and (3) fused PET/MR datasets regarding (a) lesion detection and (b) diagnostic confidence.
Results: All examinations were obtained successfully without any relevant (misregistration) artifacts. Based on morphologic MR readings, 8/12 patients were found to show suspicious lesions. Out of these 8 morphologically suspicious lesions, 5 lesions showed a corresponding lesion in FDG-PET (4 showed hypo- and one hypermetabolism). Based on the fused image analysis the diagnostic confidence was rated higher (mean 3,1) for PET/MRI when compared to sole morphologic reading (2.7). 4/12 patients did not show any pathologic findings in MRI and / or PET/MRI.
Conclusion: Our preliminary study results show an added diagnostic value of simultaneous 18-F-FDG PET/MRI in improving the diagnostic confidence for the detection of epileptogenic lesions, particularly for diagnosing temporal lobe epilepsy.

B-1391 14:08

Task specific alterations of the functional language connectome in patients with temporal lobe epilepsy
K.-H. Nenning, O. Fösleitner, C. Widmann, D. Prayer, C. Baumgartner, E. Pataraia, G. Langs, S.B. Bonelli, G. Kasprian; *Vienna/AT*

Purpose: Temporal lobe epilepsy (TLE) in the language dominant hemisphere may impair language function. In this study, we used functional MRI (fMRI) to 1. analyse the functional language connectome (LC) in healthy controls and 2. how it may be disrupted due to the underlying disease during two distinct language tasks in patients with left-sided TLE due to hippocampal sclerosis.
Methods and Materials: The functional LC was calculated on the basis of preoperatively acquired fMRI data (3 Tesla) during a verb-generation and a phrases task. A reference LC was established in 14 healthy controls and compared to the LC of 14 left TLE patients. The LC was calculated via task-regressed functional connectivity analysis (SPM12b, CONN toolbox), and differences in the connectome were quantified using Network Based Statistics (age and duration of disease were used as covariates).
Results: Analysis revealed widespread impairment of the LC in patients during verb-generation, involving frontal and temporal regions on the left hemisphere and regions in the contralateral cerebellum. The functional LC during the phrases task showed significantly decreased interhemispheric connectivity between the temporal lobes.
Conclusion: Analysis of the functional LC showed task-specific impairment of active language networks in left TLE, revealing that the left frontal language network within the ipsi- and to the contralateral hemisphere was impaired. This suggests a critical role for the left medial temporal lobe in language tasks.

B-1392 14:16

Correlation of language lateralisation with resting state hippocampal connectivity in temporal lobe epilepsy patients
A.M. Koc[1], A.Y. Oner[2], H. Ozer[2], M. Guryildirim[3], E.T. Tali[2]; [1]*Izmir/TR*, [2]*Ankara/TR*, [3]*Chicago, IL/US (alimuratcoach@yahoo.com)*

Purpose: Task-based fMRI allows easy calculation of language lateralisation index (LI) which is essential in preoperative evaluation of temporal lobe epilepsy (TLE) patients. Resting state (rs-) fMRI also can reveal brain connectivity networks. A method correlating resting state connectivity values with language lateralisation indices on single subject basis is introduced.
Methods and Materials: Task based and resting state fMRI data were gathered from a total of 45 subjects (15 subjects per Right-TLE, Left-TLE, healthy control groups) in 3T scanner. Brainvoyager QX, SPM and CONN softwares were used for preprocessing and functional data analysis. LI score of each subject was calculated and converted into normalised LI score (nLI). Intrahemispheric rs-connectivity analysis was performed between hippocampus and Broca regions on both sides. Correlation analysis was performed between these variables using SPSS software.
Results: Left intrahemispheric connectivity values showed moderate positive correlation with nLI values in Left-TLE patients (Rho=0,580; p:0,048) and whole subjects (Rho=0,560; p:0,001); strong positive correlation in Right-TLE patients (Rho=0,610; p:0,035) and control subjects (Rho=0,697; p:0,025). There were no positive or negative significant correlation between right intrahemispheric connectivity values and cLI scores in Left-TLE, Right-TLE patients, control and whole subjects (p:0,533; p:0,404; p:0,229; p:0,252 respectively).
Conclusion: Language LI estimation from rs-connectivity analysis in TLE patients could be a very useful tool eliminating the need for task based fMRI. This method seems to depict the correlation between hippocampal FC and nLI in epilepsy patients and healthy controls but further studies with increased sample sizes may demonstrate better outcomes covering all patients.

B-1393 14:24

Dynamic changes in internetwork functional connectivity of resting state networks in intractable mesial temporal lobe epilepsy
C. Zhang, K. Li, N. Chen, H. Yang; *Beijing/CN (chaozhang0328@hotmail.com)*

Purpose: To investigate the dynamic changes in functional connectivity (FC) between each resting-state networks (RSNs) in temporal lobe epilepsy (MTLE) patients before and after surgical treatment.
Methods and Materials: Resting-state fMRI data were acquired from 7 intractable unilateral MTLE patients and all this 7 patients received surgical treatment. The control group included 18 healthy volunteers. Subject-specific RSNs were estimated for three groups through group-information guided ICA. Nine meaningfull RSNs were identified via visual inspection. One-way ANOVA was used for analysing internetwork FC (iFC) differences among three groups. p<0.05 was considered statistically significant.
Results: Preoperative MTLE patients showed significantly increased iFC between pDMN (posterior default mode work) and AN (auditory network), CN (central network) and SMN (sensorimotor network) when compared with healthy volunteers, the significantly decreased iFC was found among AN, mVN (medial visual network) and SMN ($p < 0.05$). Posttreatment patients exhibited deceased iFC between DMN and SMN, CN and SMN, CN and parietal network, on the contrary, iFC between DMN and lVN (lateral visual network) increased when compared with preoperative patients ($p < 0.05$). However, there was no significantly change of iFC in posttreatment patients when compared with healthy volunteers.
Conclusion: Our study suggested that abnormal iFC in RSNs may reflect the characteristics of epileptic network. Furthermore, the dynamical changes of this functional organisation before and after surgical treatment may provide valuable information for further understanding of the pathophysiological mechanisms of intractable MTLE.

B-1394 14:32

Localisation of the epileptogenic neural network by the resting state fMRI in patients with temporal lobe epilepsy
O. Omelchenko, M. Makarchuk; *Kiev/UA (ol.omelchenko@gmail.com)*

Purpose: Temporal lobe epilepsy (TLE) exhibits recurrent seizures and has its epileptogenic zone. Hippocampus plays important role in seizure origin as it possesses large number of epileptogenic potassium ion channels. Localisation of epileptogenic zone and its delineation from eloquent cortex are crucial for successful surgery. We propose analysis of brain neural networks connectivity in the resting state (RS) and during movement execution in patients with TLE for the epileptogenic neural network localisation and motor cortex mapping.
Methods and Materials: Group of 8 patients (4M, 4F, age 19-49 y) was studied with the functional MRI. TLE was diagnosed by neurologist with the EEG. We used 1.5T SIGNA (GE) for routine MRI and fMRI. Finger tapping and RS acquisition was used for the fMRI. EPI was used for BOLD imaging

(TR/TE=3000/71 ms, voxel 4x4x5mm). FMRI data processing was carried out using FSL (Oxford, GB).
Results: FMRI data analysis revealed activation of the intact motor neural network of the brain: contralateral sensorimotor cortex, supplementary motor area and ipsilateral hemisphere of cerebellum. Deactivation of the left hippocampus was found. RS fMRI revealed increased functional connectivity of the anterior pole of the inferior temporal gyrus, posterior pole of the middle temporal gyrus, hippocampus and parahippocampal gyrus of the left hemisphere. This potentially depicts the epileptogenic neural network as it topographically coincides with the localisation of the EEG epileptiform activity.
Conclusion: RS fMRI could potentially depict epileptogenic neural network in TLE which includes regions of temporal lobe and hippocampus.

B-1395 14:40

Disrupted fronto-hippocampal language network in patients with temporal lobe epilepsy

K.-H. Nenning, O. Fösleitner, C. Widmann, D. Prayer, C. Baumgartner, E. Pataraia, G. Langs, S.B. Bonelli, G. Kasprian; *Vienna/AT*

Purpose: Temporal lobe epilepsy (TLE) in the language dominant hemisphere may impair language function. We used fMRI to study hippocampal and frontal language networks in patients with TLE and how it may be disrupted due to the underlying disease.
Methods and Materials: Functional connectivity (FC) analysis was based on preoperative fMRI data (3T, verb-generation task) of 27 patients with TLE (12 left) due to hippocampal sclerosis and 14 healthy controls. Data preprocessing was performed using Freesurfer and FSL, including the measurement of hippocampal volume (HV). For FC analysis the average time-series of 150 regions of interest (ROIs) were used (Freesurfer cortical parcellation), including 2 additional ROIs for the left and right hippocampus.
Results: Compared to right-TLE and controls, patients with left-TLE showed decreased FC within the language dominant network, and decreased FC from the left hippocampal ROI primary to frontal regions on both hemispheres. FC from Broca's region was reduced in left-TLE patients, within the left but also to the right hemisphere, which was not observed in right-TLE who showed a similar FC pattern as controls. Regression analysis revealed a relationship between HV and FC to frontal regions. These findings were corroborated by graph-based network analysis (efficiency, density), demonstrating impaired network structure in left-TLE.
Conclusion: FC analysis revealed that in left-TLE the left fronto-hippocampal language network was disrupted. Results indicated that the hippocampal integration in the frontal default mode network was disturbed, suggesting a critical role for the integration of the left hippocampus in the DMN during language tasks.

B-1396 14:48

Arterial spin labeling (ASL) in acute seizure

B. Law-Ye, M. Schertz, N. Pyatigorskaya, S. Belkacem, D. Dormont, D. Leclercq; *Paris/FR (brunolawye@hotmail.fr)*

Purpose: Seizure activity can mimic acute stroke. Arterial spin labeling (ASL) is a noninvasive method to measure cerebral blood flow. The objective of this study was to evaluate the characteristics of ASL imaging in acute seizure.
Methods and Materials: Among a cohort of patients presenting with a brutal neurological deficit in a national specialised stroke center, we retrospectively reviewed 24 cases of proven seizures who underwent magnetic resonance imaging (MRI) with ASL sequence at acute phase. We compared these data with electro-encephalographic findings.
Results: Hyperperfusion (high relative cerebral blood flow) was found in the cortical epileptogenic zone in all patients with a good correlation with clinical and electroencephalographic data. Additionally, 7 patients had a hyperperfused area in the homolateral pulvinar, and 5 patient had a hyperperfused area related to cerebellar diaschisis. Underlying causing lesions were found in 19 cases (ischemic sequelae n = 3, brain tumour n = 6, surgical scar n = 2, cortical dysplasia n = 2, haemorrhage n = 1, others n = 5). Associated diffusion abnormalities were found in 15 cases.
Conclusion: High cerebral blood flow in ASL can be observed in the cortical epileptogenic zone, in the homolateral pulvinar and in contralateral cerebellum (cerebellar diaschisis) of patients with acute seizure. The mechanism of hyperperfusion due to seizure activity may be related to transient loss of autoregulatory function in the surrounding vasculature. Arterial spin labeling is useful in the differential diagnosis of acute neurologic deficits. This sequence complements the traditional evaluation with electroencephalography (EEG).

B-1397 14:56

Does radiation therapy increase gadolinium accumulation in the brain: quantitative analysis of T1 shortening using R1 relaxometry in glioblastoma multiforme patients

W. Lim, S. Choi; *Seoul/KR (smtwh89@gmail.com)*

Purpose: To evaluate association between gadolinium accumulation in the brain and radiation therapy in glioblastoma multiforme (GBM).
Methods and Materials: From January 2010 to June 2015, 44 patients with supratentorial GBM were retrospectively identified, who completed standard treatment for GBM, and underwent pre- and post-radiation brain MR imaging including R1 map. All MR imagings were performed using gadobutrol (Gadovist, Bayer, Germany). Mean dose of used gadobutrol was 5.1 vials. Region of interests (ROIs) were drawn around primary tumours, which were located within 50-100% iso-dose lines of maximum radiation dose. ROIs were also drawn globus pallidus, thalamus, and cerebral white matters. Averages of R1 values (unit: sec^{-1}) before and after radiation therapy were compared using t-test or rank sum test as appropriate. R1 ratio (post-radiation R1 value / pre-radiation R1 value) was also calculated and compared according to radiation dose and radiation therapy type. Multiple regression analysis was examined to evaluate independent association factor for R1 increase.
Results: R1 value at peri-tumoural areas was significantly increased after radiation therapy (0.7901±0.0977 vs. 0.8146±0.1064; P=.0066). R1 ratio at high dose area was significantly higher than that of low dose area (1.0055±0.06539 vs. 0.9882±0.06419; P=.0003). R1 ratio of whom underwent hypofractionated radiation therapy was lower than that of whom underwent routine radiation therapy (1.0463±0.0633 vs. 0.9913±0.0740; P=.0758). Multiple regression analysis revealed only radiation type was significantly associated with R1 increase (P=.0212) around primary tumours.
Conclusion: Radiation therapy can enhance gadolinium accumulation in the brain, which can be explained by damaged blood-brain barrier.

B-1398 15:04

Evaluation of gadolinium brain deposits in melanoma patients: a retrospective study

J.L. Moreno Negrete, J.C. Soler, N. Borges Ribeiro Vaz, S. Podlipnik, L. Oleaga Zufiria; *Barcelona/ES (JLMORENO@clinic.ub.es)*

Purpose: The aim of the study is to retrospectively evaluate gadolinium brain deposits on MRI in the follow-up studies of patients with melanoma.
Methods and Materials: We performed a retrospective analysis of the contrast-MRI studies in 139 patients with localised melanoma. Mean age 52 years, all patients underwent more than 4 contrast-enhanced MRIs on the follow-up. Patients did not receive chemotherapy. A total of 1109 SE-T1W MRIs were evaluated, 92.24% of them were performed in three different 1,5T scanners and 6.67% in a 3.0T scanner. 87% of the patients underwent an average of 8 contrast-MRIs. Contrast agent used was gadobutrol at 0.1 mmol/kg dose. The variables recorded were creatinine, qualitative visualisation of the basal hyperintensity of the dens nucleus and globus pallidus on SE-T1W images, quantitative evaluation drawing ROIs on SE-T1W images of the dens and pallidum normalised with pons and thalamus respectively.
Results: Hyperintensity in the dens nucleus and globus pallidus was observed in 41% of the sample at the last MRI recorded. 12% of them at the 4th MRI and 54% between the 6th and 10th MRI. All cases visualised in a 1.5T scanner were positive on the 3.0T scanner. In contrast, some positive cases on the 3.0T scanner were not visualised in the immediate-next 1.5T study. All patients had normal renal function at first visit.
Conclusion: There is a significant association between dens nucleus and basal ganglia hyperintensity and the administration of cyclic-chelated gadolinium.

B-1399 15:12

Minimising the confounding effect of gadolinium contrast on subsequent ferumoxytol MRI in the brain

C.G. Varallyay, G. Toth, A. Horvath, L. Szidonya, E. Youngers, E.A. Neuwelt; *Portland, OR/US (varallyc@ohsu.edu)*

Purpose: Gadolinium enhanced MRI is the standard of care for various CNS pathologies. Ferumoxytol, used off label as an MRI contrast agent can visualize abnormal vascularity and can be used to create high resolution steady state CBV maps, which is not feasible with standard gadolinium. Clinically, it would be beneficial to extend gadolinium with subsequent ferumoxytol imaging, without confounding effects between the two contrast agents. The purpose of this study was to test if gadolinium administration alters the signal on T2*-weighted images, which are used for steady state CBV calculation with ferumoxytol.
Methods and Materials: Fifteen cases of 9 subjects with glioblastoma, enrolled in an ongoing imaging trial were analyzed. Two types of T2*-weighted acquisition techniques were tested: 3D gradient echo (the magnitude images of susceptibility-weighted imaging), and 2D gradient multiecho. Signal intensity

changes within the enhancing tumour were evaluated between pre and post standard gadolinium, as well as pre and post 7mg/kg ferumoxytol.
Results: Signal intensities post gadolinium (normalized to precontrast scan) increased substantially on the 3D T2*-weighted scans to 1.62±1.3 (Mean ± SD), while only minimally on the 2D T2*-weighted scans (to 1.1±0.08). Ferumoxytol caused signal drop on both sequences similarly, to 0.63±0.27 on the 3D and 0.64±0.14 on the 2D acquisitions.
Conclusion: Given the predominant T1 relaxation time shortening effect of gadolinium and T2* shortening effect of ferumoxytol early after injection, 2D T2*-weighted acquisition lacking substantial T1 effects is the best choice to image the intravascular space with ferumoxytol when added to standard of care gadolinium MRI.

B-1400 15:20

Gadolinium brain retention: detection and quantification of gadolinium based contrast agents in the cerebrospinal fluid in rats

G. Jost, J. Lohrke, T. Frenzel, H. Pietsch; *Berlin/DE (gregor.jost@bayer.com)*

Purpose: Increased signal (SI) intensity on unenhanced MRI in certain brain regions has been reported after repeated administrations of some gadolinium-based contrast agents (GBCAs). The pathway of GBCA entry into the brain and its distribution are unknown. One potential pathway, the infiltration of GBCAs from blood into the cerebrospinal fluid (CSF), was systematically evaluated in this rat study.
Methods and Materials: The infiltration and distribution of six marketed, multi-purpose GBCAs (three linear and three macrocyclic agents) in the CSF were investigated in healthy rats using repeated fluid-attenuated MRI after a single administration of 1.8 mmolGd/kg. Additionally, gadolinium in CSF and blood samples (obtained after 4.5 and 24 hours) was quantified by inductively coupled plasma mass spectrometry.
Results: Enhanced SI in the CSF spaces with similar kinetics was observed for all GBCAs. The SI time course suggests a GBCA entry from blood into the CSF via the choroid plexus and a further distribution with the CSF flow. No substantial differences in the gadolinium concentrations among the GBCAs were found in CSF and blood. After 4.5 hours, the concentration in the CSF (18.8-27.4 µM) was clearly higher than in blood (2.0-4.7 µM). After 24 hours CSF was almost completely cleared (0.08-0.28 µM) and the gadolinium concentration was lower than in blood (0.29-0.76 µM).
Conclusion: In contrast to the increased SI in some brain areas, no differences in infiltration and distribution into the CSF of healthy rats among the GBCAs were observed. After 24 hours an almost complete clearance from CSF was found.
Author Disclosures:
G. Jost: Employee; Bayer AG. **J. Lohrke:** Employee; Bayer AG. **T. Frenzel:** Employee; Bayer AG. **H. Pietsch:** Employee; Bayer AG.

Wednesday, March 1

12:30 - 13:30 **Room M 1**

Clinical Trials in Radiology 1

Moderators:
R. Baron; Chicago/US
M. Dewey; Berlin/DE

12:30

New insights into preoperative breast magnetic resonance imaging (MRI) from the multicentre individual patient analysis (MIPA) study

R.M. Trimboli[1], G. Di Leo[1], D. Sacchetto[2], M. Álvarez Benito[3], R.M. Mann[4], E. Wenkel[5], F. Cartia[6], M.B.I. Lobbes[7], K. Pinker-Domenig[8], J. Veltman[9], K. Siegmann-Luz[10], C. Zuiani[11], I.-M. Obdeijn[12], C. Balleyguier[13], U. Aksoy Ozcan[14], M. Docema[15], F. Pediconi[16], S. Weigel[17], J. Anderson[18], J. Camps Herrero[19], M. Calabrese[20], C. Losio[6], R. Ienzi[21], S. Harms[22], M. Van Goethem[23], G. Forrai[24], F. Gilbert[25], T.H. Helbich[8], H. Nehmat[26], F. Sardanelli[1]; [1]*San Donato Milanese/IT*, [2]*Turin/IT*, [3]*Cordoba/ES*, [4]*Nijmegen/NL*, [5]*Erlangen/DE*, [6]*Milan/IT*, [7]*Maastricht/NL*, [8]*Vienna/AT*, [9]*Almelo/NL*, [10]*Tübingen/DE*, [11]*Udine/IT*, [12]*Rotterdam/NL*, [13]*Villejuif/FR*, [14]*Istanbul/TR*, [15]*Sao Paolo/BR*, [16]*Rome/IT*, [17]*Münster/DE*, [18]*Perth/AU*, [19]*Alzira/ES*, [20]*Genoa/IT*, [21]*Palermo/IT*, [22]*Fayetteville, AR/US*, [23]*Antwerp/BE*, [24]*Budapest/HU*, [25]*Cambridge/UK*, [26]*Sydney/AU (trimboli.rm@gmail.com)*

Purpose: To show midterm results of the MIPA study.
Methods and Materials: Two concurrent groups of patients with newly diagnosed breast cancer, not candidate to neoadjuvant therapy, receiving or not receiving MRI, were prospectively enrolled in 28 centres. Data retrieval from clinical records. Statistics: McNemar, χ^2.
Results: Up to July 2016, 4944 patients were recruited, 2425 having data for analysis: 1201 (49.5%) without and 1224 (50.5%) with MRI. Of these 1224 MRIs, 210 (17%) were performed for screening (4%) or diagnostic purposes (13%). Of 1014 preoperative MRIs, 595 (59%) were ordered by radiologists alone (59%), 321 (32%) by surgeons alone; radiologist and surgeons were anyway involved in ordering MRI in 68% and 40% of the cases, respectively. Mastectomy rate planned at mammography/ultrasound was 185/1201 (15.4%) for non-MRI-group and 245/1224 (20.0%) for MRI-group (p<0.001). In MRI-group, 21 additional mastectomies (1.7%) were planned after MRI compared to those planned before MRI, while 25 patients planned with mastectomy shifted to conservative treatment (p=0.026). Of the 1004 patients planned for conservative treatment after MRI, MRI did not change surgery in 733 (73%), while prompted a wider surgery in 143 (12.5%), a less extensive surgery in 128 (12.7%). Mastectomy rate was 192/1201 patients (16%) in non-MRI-group and 257/1224 (21%) in MRI-group (p<0.001). Per-patient reoperation rate for close/positive margins were 135/1009 (13.4%) in non-MRI-group and 80/967 (8%) in MRI-group (p<0.001).
Limitations: Observational, non-randomised.
Conclusion: More than 1/6 (17%) of MRIs were performed for screening or diagnosis. Surgeons ordered MRI in 40% of cases but MRI prompted only 1.7% increase in mastectomy. MRI was frequently used as confirmation tool for an already planned mastectomy. MRI may allow a more tailored conservative surgery.

12:40
Discussant:
E.M. Fallenberg; *Berlin/DE*

12:45

The MICRA trial: Minimally Invasive Complete Response Assessment of the breast after neoadjuvant systemic therapy

M.E.M. van der Noordaa[1], F.H. van Duijnhoven[1], C.E. Loo[1], I. de Zwart[1], K. van den Vijver[1], G. Sonke[1], C.C. van der Pol[2], A. Francken[1], M.-J.T.F.D. Vrancken Peeters[1]; [1]*Amsterdam/NL*, [2]*Utrecht/NL (m.vd.noordaa@nki.nl)*

Purpose: We aim to omit surgery in breast cancer patients achieving pathologic complete response (pCR) after neoadjuvant systemic therapy (NST), thus preventing overtreatment and improving quality of life.
Methods and Materials: The MICRA-trial is a multicentre prospective cohort study. 440 breast cancer patients with a radiologic complete response on MRI after NST will be included. Prior to NST, a radioactive iodine seed is placed in the tumour. After NST, 8 ultrasound-guided biopsies are obtained from the region surrounding the iodine seed, while the patient is under general anesthesia. Immediately hereafter, breast surgery is performed. Pathology results of the biopsies and resected specimens are compared.
Results: Preliminary results: Until now, 39 patients have been included. The procedure was successful in 35/39 patients. Of these 35 patients, 46% had Her2+, 37% had TN tumours and 17% had HR+ tumours. Overall pCR (ypT0) was 63%. Our preliminary results show that out of 24 patients with pCR in biopsies, 4 patients had residual disease in the specimen (2 patients with near-pCR and 2 patients with ductal carcinoma in situ). All patients with residual disease in biopsies had residual disease in the specimen.
Limitations: Since biopsies are obtained in the operating room while the patient is under general anesthesia, identification of the iodine seed is more challenging for the radiologist.
Conclusion: With the MICRA-trial we aim to select a group of breast cancer patients in whom surgery of the breast after NST can be omitted, by predicting the presence of a pCR solely on biopsies.

12:55
Discussant:
F.J. Gilbert; *Cambridge/UK*

13:00

The MULTIPROS study - Multiparametric MRI with subsequent randomisation to MRI/US fusion guided biopsy vs TRUS biopsy in the diagnosis of prostate cancer

M.J. Szewczyk-Bieda, C. Wei, S. Vinnicombe, S. Lang, G. Nabi; *Dundee/UK (m.szewczyk-bieda@nhs.net)*

Purpose: To assess the reliability of pre-biopsy multiparametric MRI (MP MRI) in prediction of significant prostate cancer (PCa) and whether targeted US/MRI fusion-guided biopsies (FGB) allow accurate targeting of suspicious foci.
Methods and Materials: A prospective, multicentre study with subgroup randomisation. All patients with suspicion of localised PCa were considered. All enrolled participants underwent pre-biopsy MP MRI. In the positive MP MRI subgroup, (PIRADS v.2 score ≥3), patients were randomised to intervention (US/MRI FGB +TRUS) or TRUS biopsies alone. Patients diagnosed with PCa were offered standard stage-dependent treatment options. In the subgroup undergoing radical prostatectomy (RP) the specimen was sectioned using customised 3D printed molds, to allow slice-by-slice comparison with MP MRI.
Results: To date 107/600 participants have been recruited with 82 positive MP MRI, 39 randomised to US/MRI FGB (intervention group) and 43 to SC TRUS biopsy. In the intervention group, US/MRI FGB diagnosed 25 PCa and TRUS diagnosed 19 PCa; fusion biopsy targeted 22% more significant cancers than TRUS biopsy (p<0.05). A total of 46 MP MRI positive lesions were targeted in US/MRI FGB. Significantly more Gleason score ≥7 PCa were diagnosed in PIRADS 5 lesions (p=0.04). Preliminary data from 18 RP performed, suggest that performance of MP MRI was better for lesions larger than 10mm and situated in the peripheral zone.
Limitations: Health economics was not included in the study.
Conclusion: Preliminary results suggest that US/MRI FGB performs better than TRUS biopsy in patients with positive MP MRI.

13:10
Discussant:
P. Asbach; *Berlin/DE*

13:15

Study design and inclusion ROBINSCA trial: large-scaled population based (CT) screening trial for cardiovascular disease

C. van der Aalst[1], M. Vonder[2], J. Gratama[3], M.A. van Aerde[1], D. Kuijpers[4], H. de Koning[1], M. Oudkerk[2]; [1]*Rotterdam/NL*, [2]*Groningen/NL*, [3]*Apeldoorn/NL*, [4]*The Hague/NL (m.vonder@umcg.nl)*

Purpose: To give an overview of the study design and the first recruitment results of the ROBINSCA trial.
Methods and Materials: In three regions of the Netherlands, 400,000 people (age: 45-74 years) were invited to complete a questionnaire to assess eligibility. Eventually, 39,000 responders with elevated cardiovascular risk will be included and randomised (1:1:1) into either: 1) control group, 2) screening by SCORE method group, or 3) screening by coronary calcium CT scan group. Participants of group 2 and 3 will be stratified into risk categories and receive medical treatment according to their risk category. Risk categorisation for group 3 is based on the Agatston score, with low: 0-99, high: 100-399 and very high risk: ≥400.
Results: In the first phase, 135,862 persons were invited of which 33,918 (25%) responded of which 17,500 (51%) were eligible for randomisation, as expected. So far, 3140 participants (52% male, mean age 61.8 (SD 7.3)) were randomised to the CT screening group. Of these participants, 59.9% had a positive calcium score with a median Agatston score of 53.6 (range:1-7678). Percentage of participants per risk category was: low: 77.7%, high: 14.7%, very high: 7.5%.
Limitations: Only results of the first phase were included.
Conclusion: The inclusion of the first phase of the ROBINSCA trial shows optimal fulfilling of the parameters of the study design. Currently, participants at (very) high risk are treated with medication and in forthcoming years, results should show if population-based CT screening for CVD is more (cost) effective than screening by conventional risk factors or no screening.

13:25
Discussant:
M. Francone; *Rome/IT*

Thursday, March 2

12:30 - 13:30 **Room M 1**

Clinical Trials in Radiology 2

Moderators:
R. Baron; Chicago, IL/US
M. Dewey; Berlin/DE

12:30
Non-invasive treatment of osteoid osteoma with MRgFUS in paediatric patients only: a retrospective multicentre study
F. Arrigoni[1], A. Napoli[2], L. Zugaro[1], R. Scipione[2], A. Barile[1], C. Catalano[2], C. Masciocchi[1]; [1]*L'Aquila/IT*, [2]*Rome/IT (arrigoni.francesco@gmail.com)*

Purpose: To retrospectively evaluate in a multicentre study (two university hospitals), the effectiveness and safety of magnetic resonance-guided focused ultrasound (MRgFUS) as a definitive treatment for Osteoid Osteoma in paediatric patients. This pathology mostly affects patients in paediatric age: it is therefore crucial, to use the least invasive techniques.
Methods and Materials: Over a period of 4 years, we treated 27 patients (age <18 years, mean 11.7) affected by symptomatic non-spinal osteoid osteoma. Pretreatment pain, measured with visual analogue scale (VAS no pain: 0; the strongest imaginable pain 10) was 7.3 (CI: 4-10). Each lesion was treated in a single session. The outcome was evaluated with clinical and imaging follow-up over 5 years.
Results: After treatment, 25 patients reported no pain (93% of complete success, VAS:0), confirming the effectiveness of the procedure; 1 patient required another session for persistent pain (the VAS value dropped from 9 to 5) that finally completely resolved the symptoms; another patient reported VAS 1 during follow-up without requiring additional treatment. During follow-up, not disease relapse or complications occurred. The long-term imaging control showed a progressive "restitutio ad integrum" of the bone segments without signs of alteration of bone growth.
Limitations: No control group with alternative interventional radiology techniques.
Conclusion: MRgFUS is a safe and effective therapy. It may become the first line of treatment for paediatric patients with osteod osteoma.

12:40
Discussant:
L.-S. Ording Müller; *Oslo/NO*

12:45
Iodixanol versus iopromide in contemporary coronary CT angiography: lumen opacification and effect on heart rhythm in the randomised IsoCOR trial
M.M. Lubbers[1], A. Coenen[1], A. Niezen[1], M. Kock[2], T. Galema[1], M. Kofflard[2], T. Bruning[1], S. Kooij[2], F. Nous[1], H. van Valen[1], M. Dijkshoorn[1], R. Booij[1], R. Budde[1], K. Nieman[1]; [1]*Rotterdam/NL*, [2]*Dordrecht/NL (m.m.lubbers@erasmusmc.nl)*

Purpose: To demonstrate that using contemporary cardiac-CT protocols equal coronary lumen opacification can be achieved with iso-osmolar and low-osmolar contrast media, when injected at the same iodine delivery rate. In addition, we investigate the effect on heart rate.
Methods and Materials: Between November 2015 and August 2016, 306 patients who were clinically referred to cardiac CT and were at least 18years old and had a weight between 50-125 kg, were prospectively randomised to iso-osmolar iodixanol-270 (Visipaque) or low-osmolar iopromide-300 (Ultravist). Contrast media were injected to achieve a net iodine delivery rate of 1.5 gI/s (bodyweight 50-100 kg), or 1.75g I/s for larger patients (bodyweight 100-125 kg). All coronary segments were assessed for intraluminal opacification and image quality and compared using a student T-test. Heart rate, arrhythmia, patients discomfort and adverse events were also monitored.
Results: Measured coronary attenuation values were comparable between both contrast media (476 ± 160 HU vs 454 ± 158 HU, p=0.227). Adjusted for the lower iodine concentration, the mean iodixanol-270 bolus was larger compared to iopromide-300 (76.8 ± 11.6 ml vs. 69.7 ± 10.8 ml, p<0.001). The higher injection rate was associated with a higher injection pressure (111 ± 44 PSI vs 90 ± 36 PSI, p<0.001) while there were no differences in heart rate or rhythm between groups.
Limitations: While CT readers were blinded for randomisation, it was impossible to blind the CT technicians because of the different injection rates which resulted in similar iodine delivery rates.
Conclusion: If injected at comparable iodine delivery rates, the iso-osmolar contrast medium iodixanol-270 is not inferior to low-osmolar contrast medium iopromide-300 in terms of coronary opacification. Iodixanol-270 was associated with less heat discomfort, but did not affect heart rate differently compared to iopromide-300. The study was supported by an unrestricted grant from GE Healthcare.

Author Disclosures:
K. Nieman: Grant Recipient; Dutch Heart foundation. Research/Grant Support; Siemens, Bayer healthcare, Heartflow (all outside the submitted work).

12:55
Discussant:
G.A. Krombach; *Giessen/DE*

13:00
Comparison of Pretest Probability with Prevalence of Obstructive Coronary Artery Disease Using Invasive Coronary Angiography or Computed Tomography Angiography
S. Feger, M. Dewey, on behalf of the DISCHARGE consortium; *Berlin/DE (sarah.feger@charite.de)*

Purpose: To compare pretest probability of obstructive coronary artery disease (CAD) determined by using the pragmatic Diamond-Forrester (D+F) prediction models with prevalence of obstructive CAD by invasive coronary angiography (ICA) or computed tomography (CT).
Methods and Materials: Patients with suspected CAD and stable chest pain who were clinically referred for ICA or CT were prospectively included by clinical sites participating in the pilot study of the European multicentre DISCHARGE trial (www.dischargetrial.eu/EC-GA603266). Pretest probability of CAD was compared between the initial D+F model (1979) and the updated D+F model (2011).
Results: Overall, 1368 patients (611 female, 757 male) were included in 23 clinical sites from May, 2014 until July, 2016. Of these patients, 689 patients underwent CT (334 female, 355 male), while 679 underwent ICA (277 female, 402 male). The discriminative ability was higher for the updated D+F with an area under the receiver operating curve of 0.72 (AUC; 95% confidence interval 0.69-0.75), compared with an AUC of 0.64 for the initial D+F (0.62-0.68; P<0.001). The prevalence of obstructive CAD identified by using ICA and CT (32.0%, 443 of 1368 patients) was relevantly overestimated by both prediction models (pretest probabilities: initial D+F 57.8±25.3%, updated D+F 48.0±16.6%, P<0.001 respectively). However, overestimation of disease prevalence was less for the updated D+F compared with the initial version (P<0.001).
Limitations: Prevalence and pretest probabilities differ between both groups due to the non-randomised design.
Conclusion: Pragmatic pretest probability calculation relevantly overestimates the actual prevalence of obstructive CAD in patients with stable chest pain. To improve individually tailored decision-making according to chest pain guidelines for patients suspected having obstructive CAD, more accurate models to calculate pretest probability of CAD are needed. For the appropriate use of diagnostic tests further aspects should be considered, including cost-effectiveness and health related quality of life.

13:10
Discussant:
C. Loewe; *Vienna/AT*

13:15
Diagnostic value of novel MRI techniques for the primary staging and restaging of rectal cancer: multicentre study
D.M.J. Lambregts[1], M. Maas[1], R. Beckers[2], M. van Heeswijk[2], B. Hupkens[2], J. Houwers[3], N. Peters[4], R. Vliegen[4], P. Kint[5], J. Wijsman[5], B. Mearadji[1], P. Tanis[1], M. Osinga-de Jong[4], E. Belgers[4], R. Ooms[6], F. van Dielen[6], A. Daniels-Gooszen[7], H. Rutten[7], L. Oudenhoven[8], I. Faneyte[8], M. Lahaye[1], G. Beets[2], F. Bakers[3], R.G.H. Beets-Tan[2]; [1]*Amsterdam/NL*, [2]*Amsterdam/Maastricht/NL*, [3]*Maastricht/NL*, [4]*Heerlen/Sittard/NL*, [5]*Breda/NL*, [6]*Veldhoven/NL*, [7]*Eindhoven/NL*, [8]*Hengelo/Almelo/NL (doenja.lambregts@gmail.com)*

Purpose: To evaluate the performance of diffusion-weighted imaging (DWI) and lymph node contrast-enhanced MRI for rectal cancer (re-)staging.
Methods and Materials: Multicentre study of n=307 patients undergoing MRI including T2-weighted (='routine') plus additional DWI and (in n=125) lymph node (gadofosveset trisodium) contrast-enhanced (CE) sequences (='novel'). 145 patients were stratified for chemoradiotherapy (CRT) and underwent the same protocol again for restaging. Scans were evaluated by site radiologists (non-experts) and then re-assessed by a central expert radiologist. Main outcomes were defined as [1] discrimination between residual tumour (yT+) vs complete response (yT0) after CRT, and [2] discrimination between N0 vs N+ stage (both for primary staging and restaging after CRT). (Re-)staging results for experts and non-experts respectively were compared between 'routine' vs 'novel' MRI-methods using area under the receiver operating characteristics curve (AUCs)).
Results: AUC to predict tumour vs complete response for the non-expert was 0.81 on T2W MRI vs 0.79 on DWI (P=0.35); for the expert AUC was 0.80 on T2W-MRI vs 0.80 on DWI (P=0.61). AUC to predict N0 vs N+ stage for the

non-expert was 0.69 on T2W-MRI vs 0.74 on CE-MRI (P=0.70); for the expert AUC was 0.70 on T2W-MRI vs 0.81 on CE-MRI (P=0.05). AUC to predict yN0 vs yN+ stage after CRT for the non-expert was 0.82 on T2W-MRI vs 0.86 on CE-MRI (P=0.31); for the expert AUC was 0.80 on T2W-MRI vs 0.80 on CE-MRI (P=0.45).
Limitations: Not all patients received contrast agent.
Conclusion: Lymph node contrast may improve the performance of MRI for nodal staging; no significant effect was observed for addition of DWI on tumour restaging.

13:25
Discussant:
U. Attenberger; *Mannheim/DE*

C

Scientific and Educational Exhibits (C)

Abstracts and authors of EPOS™ presentations no longer appear in the Book of Abstracts. Full EPOS™ presentations are published at **epos.myESR.org** and can be cited by a Digital Object Identifier (DOI).

D

Satellite Symposia (D)

Wednesday, March 1

12:30 - 13:30 **Room Z**

organised by EUFUS & TRANS-FUSIMO

SY 1

Programme not available by date of publication

12:30 - 13:30 **Room N**

organised by SuperSonic Imagine

SY 2

Programme not available by date of publication

10:30 - 12:00 **Studio 2017**

jointly organised by Bayer HealthCare and Siemens Healthineers

SY 3a

Breast MRI: Current challenges and new trends

Moderator:
J. Barkhausen; Lübeck/DE

Preoperative breast MRI: first results from the MIPA study
F. Sardanelli; *San Donato Milanese/IT*

MIPA is an ongoing prospective observational multicenter study sponsored by Bayer, endorsed by EUSOBI and run by EIBIR/EuroAIM. Study was designed as an individual data analysis of two concurrent groups of women with a newly diagnosed first breast cancer, not candidate to neoadjuvant therapy, receiving or not receiving MRI before surgery. In 2012, after an web-based call, 96 centres applied and 34 (19 academic) were selected from 14 countries; 28 started the enrolment. Up to July 2016, 4,944 patients were enrolled, 2,425 with complete eCRF: 1,201 (49.5%) without and 1,224 (50.5%) with MRI. Gadobutrol (0.1 mmol/kg) was used in 70% patients; 84% had also DWI. A radiologist was involved in the MRI order in 68% of cases, a surgeon in 40%. Mastectomy rate planned after mammography/US was 185/1201 (15.4%) for non-MRI and 245/1224 (20.0%) for MRI-group (p<0.001). In MRI-group, 21 additional mastectomies (1.7%) were planned after MRI; bilateral surgery instead of bilateral was performed 13 (1.1%); of 1004 breasts conservatively treated after MRI, surgery was unchanged in 733 (73%), while a wider surgery or >1 excision wad done in 143 (12.5%) and a less extensive surgery was done in 128 (12.7%). Actual mastectomy rate was 192/1201 (16%) in non-MRI-group and 257/1224 (21%) in MRI-group (p<0.001; age/density-adjusted OR 1.4, 95% CI 1.3-1.6). Per-patient re-operation rate for close/positive margins was 135/1009 (13.4%) in non-MRI-group and 80/967 (8%) in MRI-group (p<0.001). These results show that already planned mastectomies prompt MRI, used as a confirmation tool, not vice versa and that MRI allows for tailoring conservative treatment.

First clinical experiences with a new 7ch breast imaging and biopsy coil
E. Wenkel; *Erlangen/DE*

A new coil for high-resolution imaging of the breast at 3T is presented. Whereas most breast coils have a high number of coil elements for diagnostic purposes but only a subset can be used during biopsy, the 7ch BI Breast Coil has a special design to facilitate imaging with the full number of elements in the biopsy scenario, thereby offering comparable image quality to the imaging scenario. Due to its open design, the coil is well suited for breast biopsy with lateral, medial and cranio-caudal access. Additional features like LED-lighting of the biopsy site simplify the workflow. During the presentation, first clinical cases and workflow experience with the new device are reported.

Gadolinium retention: impact on breast MRI?
J. Barkhausen; *Lübeck/DE*

Normal 0 false false false EN-GB X-NONE X-NONE /* Style Definitions */ table.MsoNormalTable {mso-style-name:"Normale Tabelle"; mso-tstyle-rowband-size:0; mso-tstyle-colband-size:0; mso-style-noshow:yes; mso-style-priority:99; mso-style-parent:""; mso-padding-alt:0cm 5.4pt 0cm 5.4pt; mso-para-margin-top:0cm; mso-para-margin-right:0cm; mso-para-margin-bottom:10.0pt; mso-para-margin-left:0cm; line-height:115%; mso-pagination:widow-orphan; font-size:11.0pt; font-family:"Calibri","sans-serif"; mso-ascii-font-family:Calibri; mso-ascii-theme-font:minor-latin; mso-hansi-font-family:Calibri; mso-hansi-theme-font:minor-latin; mso-fareast-language:EN-US;} More than 30 years ago, contrast-enhanced MRI emerged as a new technique in clinical breast imaging and over the last three decades numerous clinical studies have shown excellent results for the detection and characterization of breast lesions. Despite the most recent improvement of high-resolution and diffusion-weighted MRI, dynamic contrast-enhanced sequences are still considered as key component of any breast MRI examination. The applied gadolinium-based contrast agents (GBCAs) were considered as very safe compounds until the association between nephrogenic systemic fibrosis and GBCAs was suspected in 2006. Additionally, in late 2013 Kanda and colleagues described increased signal intensity in the dentate nucleus on unenhanced T1-weighted MR images as a consequence of repetitive previous GBCA administrations. Although no clinically relevant adverse events have yet been associated with the detection of gadolinium in the brain, the results of these studies must be taken seriously. With respect to breast MRI, these issues are especially important for repetitive breast cancer screening in high-risk patients, for example, with BRCA mutations. In this lecture, the results of the most recent clinical trials addressing these topics will be presented in a comprehensive manner and the impact of these studies on daily clinical routine will be discussed.
Learning Objectives:
1. To gain knowledge on the pharmacokinetics of different MR contrast agents.
2. To discuss the potential risks of gadolinium based contrast agents.
3. To learn about the most recent recommendations and guidelines.

12:15 - 13:45 **Studio 2017**

jointly organised by Bayer HealthCare and Siemens Healthineers

SY 3b

Multimodality lunch symposium: Dense breast and how to overcome the radiologist's "problem child"

Moderator:
L.J. Pina Instausti; Pamplona/ES

Dense breast and how to overcome the radiologist's "problem child"
L.J. Pina Insausti; *Pamplona/ES*

In BI-RADS 2003, the composition was based on the overall density resulting in ACR category 1 (<25% fibroglandular tissue), category 2 (25-50%), category 3 (50-75%) and category 4 (>75%). In BI-RADS 2013, the use of percentages is discouraged, because in individual cases it is more important to take into account the chance that a mass can be obscured by fibroglandular tissue than the percentage of breast density as an indicator for breast cancer risk. Four groups are used: a,b, c and d. The patterns c and d are considered as “dense”. Dense breasts reduce the sensitivity of mammography up to 50%. This is the main limitation of mammography. Fortunately, tomosynthesis can significantly increase the sensitivity of mammography, especially if wide angle is used (increment of detection rate up to +43%). Tomosynthesis is able to reduce the superimposition of tissue and the anatomic noise, allowing the detection of occult lesions. However, at least a small amount of fat surrounding the lesion is needed to be detected. Breast US is widely used as an adjunct to mammography and it improves the sensitivity in dense breasts. But US is a time-consuming, operator-dependent technique that detects too many benign lesions (false-positive results). This is why US cannot be used for population-based screening. MRI is not routinely used for the evaluation of dense breasts, although it can be very useful in some particular cases (preoperative planning, high-risk patients, etc.).
Learning Objectives:
1. To become familiar with the limitations of mammography in dense breasts.
2. To learn the role of Tomosynthesis to overcome the limitations of mammography in dense breasts.
3. To understand the role of breast US in dense breasts.

Volumetric breast density analysis in mammography and tomosynthesis: brief overview
H. Sartor; *Lund/SE*

High breast density is associated with an increased risk of breast cancer. However, qualitative measurements of breast density by radiologists may vary and be subjective. Automated VBDA, which is also associated with an increased risk of breast cancer, was developed to provide objective and reproducible measurements. To explore the possibilities and clinical use of VBDA, previous studies have described the agreement between different methods of measuring volumetric density (e.g. by software such as Volpara and Quantra) and radiologists' assessments in mammography (e.g. qualitative measurements such as BI-RADS and a visual analogue scale) with varying results. DBT is a promising technique and a potential screening modality and the possibility to measure breast density on DBT images is important. Our group has previously compared breast density that was measured by radiologists to measurements obtained from an automated VBDA tool from Siemens using the central projection image in DBT. The results suggested that VBDA could be used in DBT in addition to mammography. Taken together, the use of a robust VBDA is important and seems possible in both mammography and DBT, enabling it to be used in individualised screening programs and in breast cancer risk scores.
Learning Objectives:
1. To understand the clinical basics of volumetric breast density analysis (VBDA) based on previous studies.
2. To acknowledge the difference between radiologists' assessment of breast density and software measurements.
3. To discuss VBDA's potential use for mammography and digital breast tomosynthesis (DBT) in clinical practice.

Current role of MRI in imaging of dense breast tissue
C. Van Gils; *Utrecht/NL*

MRI is the most sensitive breast cancer imaging technique currently available and recommended for screening women with high breast cancer risk. Women with dense breasts have a moderately increased breast cancer risk. In addition, their dense tissue limits the detection of a tumour with mammography and, therefore, additional screening with MRI could provide a solution for these women as well. However, MRI is not included in screening recommendations for women with dense breasts. The effects of MRI, and also those of other supplemental imaging methods, on breast cancer outcomes remain as yet unclear due to a lack of comparative studies with interval breast cancer rates, stage at diagnosis or breast cancer mortality as the outcome. In this presentation I will outline the present evidence for MRI screening in women with dense breasts, and indicate which type of evidence is still needed to proove its additional value. DENSE, a large randomised controlled trial, that we are currently conducting, has been designed to deliver this proof. It investigates the value of additional MRI compared to usual screening practice, in women with extremely dense breasts and a negative digital mammography. Women are included solely on the basis of their breast density. A fully automatic and validated method is used to estimate mammographic density. The primary outcome is a difference in interval cancer rates between the two arms, the best proxy for a difference in breast cancer mortality.
Learning Objectives:
1. To understand the current evidence for MRI screening in women with dense breasts.
2. To learn what type of studies are needed to fully appreciate and weigh the benefits and harms of supplemental MRI screening in women with dense breasts.

The future of breast cancer screening: where can it help the dense breast?
M. Golatta; *Heidelberg/DE*

In most countries breast cancer screening is offered to women between (40)50 and 70(75). The organisation of the screening programs differ from country to country, but in general every two or three years mammography is offered to the participating women. In the past years, several breast imaging techniques have been developed which have the potential to improve breast cancer screening. Digital breast tomosynthesis is one method that has been developed. Multiple low-dose images are obtained and digitally edited and reconstructed as a 3D-image of a breast. The reconstructed 3D-image overcomes the weakness of standard mammography and enables reduction in false-positive findings as results of overlapping tissue. On the other hand, it also enables reduction in the false-negative findings in women with dense breast tissue. Studies have shown that combining ultrasound with mammography in screening settings can significantly improve the rate of found lesions. By adding US to the screening work flow the sensitivity can be improved especially in the dense breast. But US is very time consuming and the specificity goes down (more biopsies are necessary). To overcome these two weaknesses, an "automated breast volume scanner (ABVS)" and elastography can be used. Strain imaging ultrasound technology as Virtual Touch IQ(VTIQ) is a new method being used in breast ultrasound. Various studies have been able to show an increase of the diagnostic specificity without loss of sensitivity when combining the standard ultrasound BIRADS® classification with elastography. The improvement of the specificity will help to eliminate unnecessary breast biopsies in the future.
Learning Objectives:
1. To become familiar with new breast imaging techniques.
2. To understand that breast cancer screening could be improved by embedding new breast imaging techniques like tomosynthesis, US, elastography, ABVS.

14:00 - 15:30 **Studio 2017**

organised by Siemens Healthineers

SY 3c

Breast tomosynthesis symposium: Is digital breast tomosynthesis ready for mammo screening?

Moderator:
S.H. Heywang-Köbrunner; Munich/DE

Is digital breast tomosynthesis ready for mammo screening?
S.H. Heywang-Köbrunner; *Munich/DE*

For DBT, first systematic reviews of screening trials and of mostly retrospective data from the US confirm that DBT is clearly superior to mammography allowing significantly improved sensitivity. DBT leads to a slightly increased biopsy rate with comparable PPV compared to mammography screening with double reading. Unfortunately for a screening procedure, increased detection is not equivalent to mortality reduction, since increased detection could as well be caused by overdetection of "harmless" malignancy (overdiagnosis). So far no data on overdetection or mortality reduction exist for DBT. Even though important, they are generally difficult to obtain and require long-term follow-up. First indicators of effectiveness could include a significant reduction of interval cancers or an improved stage distribution of cancers detected during the follow-up round(s). Initial data on interval carcinomas are being published. However, first analyses show that evaluation of follow-up rounds remains essential. Thus, to date DBT remains the most promising new modality for screening. Further data allowing estimates of effectiveness and potential overdiagnoses are needed and are gradually expected. Logistic problems (longer reading time, fatigue, optimised hanging protocols, comparison with DM or DBT priors, etc.) should be investigated as well as the potential of stratified DBT vs mammography screening.
Learning Objectives:
1. To understand true benefits and risks of screening procedures.
2. To understand present data on diagnostic accuracy and the gap concerning data on screening effectiveness and potential overdiagnosis.
3. To understand logistic demands associated with future DBT screening.

Experiences from the Malmö breast tomosynthesis screening trial
K. Lang; *Malmö/SE*

The Malmö breast tomosynthesis screening trial is a prospective population-based single-arm study including randomly invited women 40-74 years old eligible for the screening programme in the city of Malmö, Sweden. Women underwent one-view BT and two-view DM. The images were read and scored separately in a blinded double-reading procedure. Interim results of 7,500 women showed a significant increase in cancer detection rate (6.3 to 8.9/1,000) and recall rate (2.6% to 3.8%). The additionally detected cancers were mainly invasive, with a tendency of downstaging (Lång 2015). Findings of stellate distortions simulating malignancy increased the false-positive rate with BT. The FP rate was reduced over time, suggesting a learning curve (Lång 2016). The BT images were acquired with reduced compression force which would be a great advantage for a new screening modality. Slabbing and reconstruction methods can be used to reduce the reading time and increase the image quality. The main challenge of implementing BT in screening is the reading time (x 2-4) (Bernardi 2012, Skaane 2013). CAD and AI could provide a solution. Hopefully, attempts to implement BT in screening could be a catalyst towards the development of individualised screening programmes.
Learning Objectives:
1. To describe the Malmö breast tomosynthesis screening trial.
2. To illustrate technical aspects of BT as a screening tool.
3. To recognise the challenges of implementing BT in screening.

Clinical performance of a synthetic mammogram (Insight 2D) and its role for screening procedures
M. Bernathova; *Vienna/AT*

Practical challenges in screening with digital breast tomosynthesis
C. Van Ongeval; *Leuven/BE*

Learning Objectives:
1. To evaluate the impact of the reading time on the use of digital breast tomosynthesis (DBT) in breast cancer screening.
2. To discuss the requirements of image transfer and data storage in breast cancer screening with DBT.
3. To evaluate additional tools in improving accuracy in reading of DBT in screening.

New tomo reconstruction algorithms: clinical experiences
D.F.P. Uhlenbrock; *Dortmund/DE*

Technical aspects of digital breast tomosynthesis
W. Lemish; *Melbourne/AU*

There are a number of digital breast tomosynthesis (DBT) systems in the market that have applied differing technologies to acquire the data necessary for tomosynthesis image reconstruction. The various techniques all have advantages and some potential limitations. These differences could potentially produce different clinical outcomes and the lack of uniformity may make the comparisons between clinical trials difficult. We will review the principles of DBT and discuss the likely advantages and possible limitations of different methods available.
Learning Objectives:
1. To review the physical principles of digital breast tomosynthesis.
2. To become familiar with the strengths and limitations of different technologies used in digital breast tomosynthesis.

16:00 - 17:00 **Studio 2017**

organised by Siemens Healthineers

SY 3d

Multimodality case discussion: Benign looking malignant lesions - malignant looking benign lesions

Moderator:
C. Van Ongeval; Leuven/BE

Breast MRI perspective
E. Wenkel; *Erlangen/DE*

Benign or malignant lesion: the radiologists dilemma. This interactive session will discuss the use of ultrasound, mammography, tomosynthesis and MRI in cases of challenging benign and malignant findings.
Learning Objectives:
1. To explain the relative strengths, advantages and limitations of each imaging technique in the detection and characterisation of breast lesions.
2. To understand the sequence of the use of different imaging technique in an up-to-date diagnostic work-up of breast lesions.

Mammography/tomosynthesis perspective
M. Bernathova; *Vienna/AT*

Benign or malignant lesion: the radiologists dilemma. This interactive session will discuss the use of ultrasound, mammography, tomosynthesis and MRI in cases of challenging benign and malignant findings.
Learning Objectives:
1. To explain the relative strengths, advantages and limitations of each imaging technique in the detection and characterisation of breast lesions.
2. To understand the sequence of the use of different imaging technique in an up-to-date diagnostic work-up of breast lesions.

Ultrasound perspective
M. Golatta; *Heidelberg/DE*

Benign or malignant lesion: the radiologists dilemma. This interactive session will discuss the use of ultrasound, mammography, tomosynthesis and MRI in cases of challenging benign and malignant findings.
Learning Objectives:
1. To explain the relative strengths, advantages and limitations of each imaging technique in the detection and characterisation of breast lesions.
2. To understand the sequence of the use of different imaging technique in an up-to-date diagnostic work-up of breast lesions.

12:30 - 13:30 **Room L 8**

organised by Mindray

SY 4

Programme not available by date of publication

Thursday, March 2

12:30 - 13:30 **Room X**

organised by Samsung

SY 5

Programme not available by date of publication

12:30 - 13:30 **Room O**

organised by Philips

SY 6

Photon counting technology for mammography and tomosynthesis*

Moderator:
C. Varian; Sutton/UK

Spectral photon counting technology for mammography and tomosynthesis*
J. Rehn; *Solna/SE*

Clinical study results on tomosynthesis* with photon counting and flat panel technologies
P. Panizza; *Milan/IT*

Comparison of spectral and non-spectral methods for automated volumetric breast density measurements
A. Shimauchi; *Sendai/JP*

Can photon counting tomosynthesis* improve lesion conspicuity and reduce average glandular dose compared to 2D mammography?
B. Wilczek; *Stockholm/SE*

**MicroDose 3D S90 spectral tomosynthesis is a work in progress*

12:30 - 13:30 **Room N**

organised by Siemens Healthineers

SY 7

Programme not available by date of publication

12:30 - 13:30 **Studio 2017**

organised by Siemens Healthineers

SY 8

Programme not available by date of publication

12:30 - 13:30 **Room L 8**

organised by Philips

SY 9

Programme not available by date of publication

12:30 - 13:30 **Room E1**

organised by Bracco

SY 10

Programme not available by date of publication

12:30 - 13:30 **Room E2**

organised by GE Healthcare

SY 11

Programme not available by date of publication

12:30 - 13:30 **Room F1**

organised by Bayer HealthCare

SY 12

Update and understanding on Gadolinium presence

Moderator:
V. Runge; Berne/CH

What do we know from the clinical research?
C.C. Quattrocchi; *Rome/IT*

Gd deposits in preclinical perspective
H. Pietsch; *Berlin/DE*

12:30 - 13:30 **Room F2**

organised by Toshiba Medical Systems

SY 13

Programme not available by date of publication

12:30 - 13:30 **Room G**

organised by GE Healthcare

SY 14

Programme not available by date of publication

12:30 - 13:30 **Room K**

organised by Hologic

SY 15

A paradigm shift in breast biopsy clinical practice: a European perspective

Moderator:
L. Fontaine; Marlborough, MA/US

Strategies for optimising the use of new breast biopsy technologies: a clinical perspective
S. Go; *Alkmaar/NL*

A new approach to breast biopsy in a national cancer institute: clinical impact on daily routine
G. Scaperrotta; *Milan/IT*

Tomosynthesis guided biopsy in the diagnostic and screening assessment: our choices and experience
A. Tejerina; *Madrid/ES*

12:30 - 13:30 **Room M 2**

organised by Bayer Healthcare Informatics

SY 16

A dose of reality: the need for active CT dose management

Moderator:
K. Strasdas; New York, NY/US

A dose of reality: the need for active CT dose management
R. Smith-Bindman; *San Francisco, CA/US*

Friday, March 3

12:30 - 13:30 **Room O**

organised by Philips

SY 17

Expanding the use of ultrasound

Moderator:
E. Danse; Brussels/BE

Utilising Shear Wave imaging and contrast in challenging cases
D.-A. Clevert; *Munich/DE*

Abdominal fusion/navigation in daily routine
A. McNeill; *Newcastle Upon Tyne/UK*

Prostate fusion: the benefit of prostate biopsy using MRI/ultrasound guided fusion!
M. Claudon, F. Lefèvre; *Vandoeuvre-les-Nancy/FR*

12:30 - 13:30 **Room N**

organised by Siemens Healthineers

SY 18

Twin robotic x-ray: a new player in your radiology department

Moderator:
A. Hebecker; Erlangen/DE

Multitom Rax in clinical practice: using fluoroscopy to improve standardisation in radiography
F. Jensen; *Malmö/SE*

3D tomography with Multitom Rax or CT: general overview of benefits and limitations
A. Falkowski; *Basle/CH*

Multitom Rax in trauma radiology: daily routine in an emergency department
I. Pössl; *Wels/AT*

12:30 - 13:30 **Studio 2017**

organised by Samsung

SY 19

Programme not available by date of publication

12:30 - 13:30 **Room L 8**

organised by Philips

SY 36

Programme not available by date of publication

12:30 - 13:30 **Room E1**

jointly organised by Bayer HealthCare and Siemens Healthineers

SY 20

Clear direction in CT: improved efficiency for better patient care

Moderator:
J.E. Wildberger; Maastricht/NL

Obtaining the optimal CT image the first time, every time: how to do it?
J.E. Wildberger; *Maastricht/NL*

12:30 - 13:30 **Room E2**

organised by Bracco

SY 21

Programme not available by date of publication

12:30 - 13:30 **Room F2**

organised by Toshiba Medical Systems

SY 22

Programme not available by date of publication

12:30 - 13:30 **Room G**

organised by Guerbet

SY 23

From brain hyperintensities to Gd deposition: what should we know?

Moderator:
M.M. Thurnher; Vienna/AT

Hyperintensities: state of the art and beyond
A. Radbruch; *Heidelberg/DE*

Gd deposition or retention?
E. Lancelot; *Villepinte/FR*

At risk population
D. Roberts; *Charleston, SC/US*

12:30 - 13:30 **Room K**

organised by GE Healthcare

SY 24

Programme not available by date of publication

12:30 - 13:30 **Room M 1**

organised by Bayer Russia

SY 25

Contrast enhancement in MRI - clinical practice: how and why?

Moderator:
I.E. Tyurin; Moscow/RU

Highlights on contrast applications in CNS
A.E. Tsoriev; *Ekaterinburg/RU*

ceMRI of prostate: why I do it
A. Mishchenko; *St. Petersburg/RU*

Avoiding pitfalls in the interpretation of enhanced MR liver imaging with Primovist®
G. Brancatelli; *Palermo/IT*

12:30 - 13:30 **Room M 3**

organised by HIMSS *(Healthcare Information and Management Systems Society)*

SY 26

Programme not available by date of publication

14:00 - 15:30 **Room O**

organised by GE Healthcare Russia

SY 27

Programme not available by date of publication

14:00 - 15:30 **Room N**

organised by Mint Medical

SY 28

Structured reporting in clinical oncology: approaches for an efficient and need-oriented implementation

Moderator:
D.-M. Koh; Sutton/UK

14:00 - 15:30 **Room M 3**

organised by HIMSS *(Healthcare Information and Management Systems Society)*

SY 29

Programme not available by date of publication

Saturday, March 4

12:30 - 13:30 **Room O**

organised by Philips

SY 30

Advancements in spectral detector based CT for routine and demanding clinical applications

Moderator:
P. Coulon; Orléans/FR

Introduction to spectral CT
P.B. Noel; *Munich/DE*

Spectral imaging experiences and expectations in oncology
D. Maintz; *Cologne/DE*

Spectral imaging in the cardiac department
P. Ball; *Belfast/UK*

12:30 - 13:30 **Room N**

organised by Siemens Healthineers

SY 31

Getting it right: radiation dose management

Moderator:
S. Ulzheimer; Forchheim/DE

Dose in breast tomosynthesis: where are we, where are we going, and what does it mean?
I. Sechopoulos; *Nijmegen/NL*

The introduction of digital tomosynthesis to breast imaging has brought about many questions regarding the dose involved in this new imaging modality. Questions on dose are especially important when the modality is or has the potential to be used for screening of asymptomatic patients. In addition, the uncertainty on how digital tomosynthesis will be incorporated into the clinic in the long term, i.e. as a replacement, adjunct, or some combination thereof of mammography, makes the dosimetric concerns more complicated. We will review the basic concepts of breast dosimetry, how they have changed for breast tomosynthesis, and the current levels used for dose from mammography and tomosynthesis. We will discuss the implications for patient breast dose that the different clinical implementations of tomosynthesis might result in.

CT dose reduction innovations and their impact on dose management
H. Alkadhi; *Zurich/CH*

The introduction of dual-source CT technology has revolutionised clinical CT imaging by enabling the radiologist to apply and combine a multitude of patient-tailored different dose reduction strategies. These include the technique for automated, attenuation-based tube potential selection, the tin filter technology for single-energy CT, high-pitch scanning and advanced iterative reconstruction algorithms. Combined application of these many options must be done carefully for fully exploiting the potential of the techniques for each individual patient. Optimal use of the techniques also allows for an individually tailored reduction of the amount of required contrast media for achieving a good image quality. This presentation will review the effect of these options on radiation dose, image quality and contrast media protocols and their impact on patient management and clinical decision making.
Learning Objectives:
1. To learn about the various individual and combined techniques for lowering and optimising the radiation dose of modern CT machines.

Radiation dose management made easy
F. Schellhammer; *Cologne/DE*

In modern radiology departments dose monitoring is gaining more and more interest. Based on regulations, legislation and recommendations from different associations, radiology departments commence to monitor the applied radiation. Team play provides the ability to gather all the information on the applied radiation dose and creates transparency in performance. By analysing dose values you gain knowledge and understanding what might cause dose outliers. As objectivity in dose monitoring and reporting is a must, team play helps to achieve this. In addition, team play supports to map customised scan protocols with the RADLEX Playbook coding that is created by the RSNA. We will experience how team play supports dose monitoring and how it is the base

12:30 - 13:30 **Studio 2017**

organised by Philips

SY 32

Programme not available by date of publication

12:30 - 13:30 **Room F2**

organised by Toshiba Medical Systems

SY 33

Programme not available by date of publication

12:30 - 13:30 **Room M 1**

organised by Olea Medical®

SY 34

Programme not available by date of publication

12:30 - 13:30 **Room M 5**

organised by Bracco

SY 35

Programme not available by date of publication

E

Authors' Index
(E)

Authors' Index

A

Authors' Index

Authors' Index

B

Authors' Index

Authors' Index

Authors' Index

Authors' Index

C

Authors' Index

Authors' Index

Authors' Index

D

Authors' Index

Authors' Index

Authors' Index

E

Authors' Index

F

Authors' Index

G

Authors' Index

Authors' Index

Authors' Index

H

Authors' Index

Authors' Index

Authors' Index

Authors' Index

K

Authors' Index

Authors' Index

Authors' Index

L

Authors' Index

Authors' Index

Authors' Index

M

Authors' Index

Authors' Index

Authors' Index

Authors' Index

N

Authors' Index

O

Authors' Index

P

Authors' Index

Authors' Index

Authors' Index

Q

R

Authors' Index

Authors' Index

Authors' Index

S

Authors' Index

Authors' Index

Authors' Index

Authors' Index

Authors' Index

T

Authors' Index

Authors' Index

Authors' Index

Authors' Index

Authors' Index

W

Authors' Index

Authors' Index

Authors' Index

F

List of Authors & Co-Authors (F)

List of Authors & Co-Authors

A

List of Authors & Co-Authors

B

List of Authors & Co-Authors

C

List of Authors & Co-Authors

List of Authors & Co-Authors

E

F

List of Authors & Co-Authors

G

List of Authors & Co-Authors

I

J

List of Authors & Co-Authors

K

List of Authors & Co-Authors

L

List of Authors & Co-Authors

M

List of Authors & Co-Authors

List of Authors & Co-Authors

N

O

P

List of Authors & Co-Authors

Q

R

List of Authors & Co-Authors

S

List of Authors & Co-Authors

List of Authors & Co-Authors

T

List of Authors & Co-Authors

U

V

W

List of Authors & Co-Authors

X

Y

Z

List of Moderators
(G)

List of Moderators

A

Ahuja B.: *RC 412*
Akata D.: *SS 1414*
Akhan O.: *BS 6*
Alberich-Bayarri A.: *SS 213, SS 1005*
Alberti N.: *SS 701a*
Alkadhi H.: *RC 503*
Alleman G.: *EM 4*
Alomaim W.: *SS 602a*
Alva López L.F.: *SS 1004*
Andersson B.T.: *SS 1814*
Andrade L.: *TF 1*
Antoniou K.M.: *ESR/ERS*
Aschauer M.A.: *SS 1415*
Atasoy C.K.: *SS 1503*
Auer T.: *SS 311b*
Avdagic E.: *SS 211b*
Aydingoz U.: *ESR/ESOR 2*

B

Bachmann Nielsen M.: *WG 4*
Baditescu D.: *SS 1402b*
Baert A.L.: *ER*
Balassy C.: *RC 1612*
Balázs G.: *SS 1015*
Balleyguier C.S.: *SS 702b*
Baltzer P.A.T.: *SS 1016a*
Bánsághi Z.: *SS 209*
Bargalló N.: *SS 1911b*
Barile A.: *RC 410*
Barkhausen J.: *SY 3a*
Baron R.: *CTiR 1, CTiR 2*
Barth B.K.: *SS 707*
Basilico R.: *E³ 926*
Bäuerle T.: *SS 305*
Bayraktaroglu S.: *SS 1903*
Beardmore C.: *RC 514*
Becker C.D.: *PI 3*
Beets-Tan R.G.H.: *SS 1816*
Bekiesinska-Figatowska M.: *BS 4*
Bellin M.-F.: *SS 1807*
Bennani-Baiti B.: *SS 606*
Bérczi V.: *SS 309*
Berritto D.: *SS 1910a*
Berger F.H.: *SS 1017*
Bilbao J.I.: *SS 215*
Biscaldi E.: *SS 701b*
Blazic I.: *SS 1901a*
Bloem J.L.: *SS 610*
Blondiaux E.: *SS 1403b*
Bogaert S.: *EM 4*
Bonatti M.: *SS 1401*
Bonomo L.: *EU 5*
Boric I.: *SS 1410*
Bosmans H.: *SS 313*
Brambilla M.: *EF 2*
Brink J.A.: *EM 2, EU 4, PI 1*
Brkljačić B.: *PI 2*
Broncano J.: *SS 304*
Buy X.: *SS 1909*

C

Calli C.: *SS 311b*
Cambronero Gómez J.M.: *SS 1810a*
Campbell R.: *SS 310*
Camps Herrero J.: *SS 1802a*
Cantisani V.: *WG 4*
Cassar-Pullicino V.N.: *E³ 24A, E³ 24B, E³ 24C, E³ 24D, E³ 24E, ESR/EANM*
Cevasco L.: *SS 201b*
Chodorowska A.: *RC 1204*
Choi B.I.: *SS 1401*
Chouhan M.: *SS 1416*
Ciet P.: *SS 1804*
Clément O.: *RC 406*
Connor S.: *SS 1008*
Cook G.: *SS 1016b*
Cosson P.: *SS 1414*
Costagli M.: *SS 1413*
Coulon P.: *SY 30*
Cuenod C.A.: *SS 1916*
Cyteval C.: *RC 510*
Czerny C.: *SS 1810b*

D

Dahlqvist Leinhard O.: *SS 1901c*
Dalal P.: *SS 1904*
Damilakis J.: *EF 1, EU 2, EU 4*
Danse E.: *SY 17*
De Graaf P.: *SS 308*
De Paepe K.N.: *SS 1816*
de Rooij M.: *SS 1407*
Derchi L.E.: *PS 1227*
deSouza N.M.: *ESR/EORTC*
Dewey M.: *CTiR 1, CTiR 2*
Dixon A.K.: *ER*
Dominelli V.: *SS 702b*
Domingo A.: *SS 202*
Dondelinger R.F.: *SS 1809*
Drzezga A.: *MC 528, MC 628, MC 728, MC 828*
Due-Tønnessen P.: *RC 811, RC 914, SS 1011b*
Duvernoy O.: *RC 903, SS 1403b*

E

Ebdon-Jackson S.: *EU 5*
Ehman R.L.: *EM 2*
Esen G.: *SS 202*
Esposito A.: *SS 203*

F

Fallenberg E.M.: *SS 602b*
Falzon C.: *SS 714*
Farshad-Amacker N.: *SS 1410*
Fatehi M.: *SS 1805*
Feger S.: *SS 703b*
Feragalli B.: *RC 1704*
Feuchtner G.: *SS 203*
Filippone A.: *SS 601a*
Fischer M.A.: *SS 210*
Floridi C.: *SS 1415*
Fohlen A.: *SS 216*
Fontaine L.: *SY 15*
Forrai G.: *SS 1902b*
Forstner R.: *SS 1907*
Franquet T.: *BS 2*
Freling N.J.M.: *SS 208*
Frija G.: *EU 1, EU 3*
Frühwald-Pallamar J.: *SS 1908*
Furmanek M.I.: *SS 1915*

G

Galea N.: *SS 1503*
Gallagher F.A.: *SS 716*
Gangi A.: *RC 109*
Garbajs M.: *SS 1511*
García Figueiras R.: *SS 616*
Gardarsdottir M.: *SS 303*
Gennaro G.: *SS 702a*
Gibbs V.: *PS 1227*
Golfieri R.: *SS 1409*
Gołofit P.: *SS 708*
Gourtsoyianni S.: *ESR/ESOR 1*
Gourtsoyiannis N.: *ESOR*
Graca B.: *SS 303*
Granata C.: *RC 1212*
Graser A.: *SS 1007*
Greffe J.-L.: *EM 4*
Grenier P.A.: *SS 304*
Grimm J.: *SS 1006*
Grunwald I.Q.: *SS 1011b*
Guerrero Gil J.L.: *EM 3*
Guerrini S.: *SS 316*

H

Hailemichael M.: *SS 1014*
Haneder S.: *SS 1015*
Harden S.: *SS 703b*
Hebecker A.: *SY 18*
Heilmaier C.: *SS 1004*
Herman M.: *SS 1011a*
Hermoye L.: *SS 1411*
Heywang-Köbrunner S.H.: *SY 3c*
Hjemly H.H.: *EM 4, RC 814*
Hodler J.: *SS 1910a*
Hogg P.H.: *RC 414*
Horta M.: *SS 1807*
Howarth N.: *E³ 25A, E³ 25B, E³ 25C, E³ 25D, E³ 25D*
Hrabak Paar M.: *SS 603*
Hricak H.: *E³ 126a, PI 3*
Huyskens J.: *RC 408*

I

Iliadis K.: *SS 612*
Ippolito D.: *SS 201a*

J

Jackson S.A.: *SS 1901a*
Jargiello T.: *RC 815*
Jefic S.: *SS 311a*

K

Karlovic-Vidakovic M.: *E³ 1726c*
Karunanithy N.: *SS 309*
Kastler B.: *SS 709*
Kelly B.E.: *Audit*
Kharuzhyk S.: *SS 316*
Kiessling F.M.A.: *SS 606*
Kikinis R.: *SS 1005*
Kilburn-Toppin F.: *RC 502, SS 1802b*
Kinkel K.: *SS 1402a*
Kinner S.: *SS 601b*
Kitrou P.M.: *SS 1809*
Klimeczek P.T.: *SS 1003*
Klumpp B.D.: *SS 1016b*
Köcher M.: *SS 315*
Koh D.-M.: *SY 28*
Krainik A.: *RC 911*
Krestin G.P.: *SS 207*
Krokidis M.: *SS 1409*
Kubik-Huch R.A.: *SS 602a*
Kucheruk O.V.: *SS 301a*

L

Laghi A.: *SS 301b*
Lamot U.: *SS 311a*
Leander P.: *PI 2*
Lebovici A.: *SS 607*
Lemmerling M.M.: *E³ 1726a*
Liu Y.: *ESR/EORTC*
Lobbes M.B.I.: *SS 1002*
Lopez Rendon X.: *SS 613*
Luciani A.: *SS 1416*
Lucic M.A.: *ESR/ESOR 3, SS 711*
Lukas C.: *SS 211b*
Lurie D.J.: *EF 2*

List of Moderators

M

Maas M.: *SS 217*
Macri F.: *SS 1017*
Magnano G.M.: *E³ 1526b*
Maher M.: *SS 1901b*
Maj E.: *RC 1311*
Maksimović R.: *SS 1403a*
Mann R.M.: *SS 1802a*
Maric D.: *SS 1811a*
Marincek B.: *SS 1901b*
Marti-Bonmati L.: *SS 301a*
Matin T.N.H.: *SS 704*
Matos C.: *SS 1801*
Mayerhöfer M.E.: *SS 605*
Mechl M.: *SS 614*
Mendichovszky I.: *SS 1006*
Mentzel H.-J.: *SS 1412*
Merlino B.: *SS 1815*
Mershina E.: *SS 704*
Mizzi A.: *RC 114*
Montet X.: *SS 1804*
Morozov S.: *PI 1*
Muscat K.: *SS 214*

N

Natale L.: *SS 314*
Negaard A.: *SS 1411*
Nievelstein R.A.J.: *SS 1512*
Nikolaou K.: *ESHI*
Njagulj V.: *RC 1210*

O

Occhipinti M.: *E³ 1526a*
Offiah A.C.: *RC 512*
Omoumi P.: *SS 1010*
Oner A.Y.: *SS 211a*
Oot R.F.: *SS 1511*
Ording Müller L.-S.: *SS 1512*
Oudeman J.: *SS 710*
Owens C.: *WG 1*
Oyen R.H.: *RC 1307*
Özbek S.S.: *BS 5*

P

Pagonidis K.: *RC 1603*
Palkó A.: *SS 214*
Palm M.: *SS 1811b*
Papadaki E.: *RC 814*
Papakonstantinou O.: *RC 1710*
Papanikolaou N.: *BS 3*
Parizel P.M.: *EM 1, EM 2, EM 3, ESOR*
Pediconi F.: *RC 1302*
Peer S.: *SS 210*
Pellicanò G.: *SS 1811a*
Pereira P.L.: *E³ 1326*
Perez Fernandez C.M.: *SS 1011a*
Pershina E.: *SS 1403a*
Pfirrmann C.W.A.: *E³ 1526c, SS 1010*
Pina Insausti L.J.: *SY 3b*
Pinker-Domenig K.: *SS 602b*
Pirnat M.: *SS 1003*
Planken R.N.: *SS 315*
Ponhold L.: *SS 709*
Prassopoulos P.K.: *SS 307*
Prayer D.: *SS 1814*
Prezzi D.: *SS 1001*
Puech P.A.B.: *RC 807, SS 707*
Pulido J.M.: *SS 609*
Puri S.K.: *RC 1301*
Pyatigorskaya N.: *SS 1805*
Pyra K.K.: *SS 307*

R

Radovic N.: *SS 702a*
Rainford L.A.: *SS 614*
Raissaki M.: *SS 612*
Raposo J.: *SS 1902b*
Ravanelli M.: *SS 1008*
Rebonato A.: *SS 609*
Reiser M.F.: *ER*
Reiter U.: *SS 1803*
Reponen J.: *SS 1014*
Revel M.-P.: *SS 604*
Riascos R.: *SS 1811b*
Riklund K.: *MC 528, MC 628, MC 728, MC 828*
Robinson S.: *RC 808*
Roding T.: *RC 914*
Rodríguez P.: *SS 601a*
Rohde S.: *SS 611*
Ronot M.: *SS 1801*
Rossi A.: *RC 912*
Rostovtseva T.: *SS 1911b*
Runge V.: *SY 12*

S

Sala E.: *SS 607*
Salvador R.: *SS 207*
Sappey-Marinier D.: *ESR/ESMRMB*
Saude J.M.: *SS 1914*
Savolainen S.: *SS 713*
Schaarschmidt B.M.: *SS 716*
Schaefer-Prokop C.M.: *ESR/ERS, SS 204*
Schmidt S.: *SS 201b*
Schönberg S.O.: *EIBIR 3*
Schueller G.: *RC 1617*
Sechopoulos I.: *SS 313*
Secinaro A.: *SS 212*
Seimenis I.: *SS 1813*
Sekovski B.: *SS 1815*
Shahabpour M.: *SS 1910b*
Shams S.: *SS 1911a*
Siemund R.: *RC 514*
Signore A.: *ESR/EANM*
Simeonov G.: *EU 1*
Simic M.: *SS 604*
Simons D.: *SS 1916*
Sklair-Levy M.: *SS 1002*
Smits M.: *ESR/ESMRMB*
Snoeckx A.: *SS 204*
Sosna J.: *SS 216*
Spahn M.: *SS 1016a*
Stadler A.: *SS 213*
Stafrace S.: *SS 1412*
Stern E.J.: *SS 1904*
Stiller W.: *EU 2*
Stoupis C.: *SS 1001*
Strasdas K.: *SY 16*
Sorantin E.: *SS 212*
Sutter R.: *SS 1810b*
Svare A.: *TF 1*
Svedström E.: *SS 305*
Syrgiamiotis V.: *RC 114*

T

Tack D.: *RC 904*
Taina M.: *SS 211a*
Takis F.: *SS 215*
Tali E.T.: *BS 1, RC 1211*
Tardaguila de la Fuente G.: *SS 1907*
Tarján Z.: *SS 601b*
Taylor K.: *SS 314*
Teixeira P.A.C.: *SS 1402a*
Tempels A.: *EM 4*
Thibault F.: *SS 1902a*
Thoeny H.C.: *E³ 126b*
Thurnher M.M.: *SY 23*
Thust S.C.: *SS 711*
Tolan D.J.M.: *SS 701b*
Torresin A.: *EF 1*
Tóth A.: *SS 603*
Traykova N.I.: *SS 308*
Trimboli R.M.: *SS 1902a*
Tsalafoutas I.A.: *SS 613*
Tscholakoff D.: *SS 1914*
Tsetis D.K.: *E³ 526b*
Tshering Vogel D.W.: *RC 108*
Tyurin I.E.: *SY 25*

U

Ulbrich E.J.: *SS 1910b*
Ulzheimer S.: *SY 31*

V

Vaidya S.: *SS 217*
Van Beers B.E.: *SS 1901c*
van Buchem M.A.: *SS 611*
van den Hauwe L.: *RC 414*
Van Hoyweghen A.: *SS 1402b*
Van Ongeval C.: *SY 3d*
van Randen A.: *SS 317*
Varian C.: *SY 6*
Vassileva J.N.: *SS 1413*
Velonakis G.: *SS 1909*
Verbist B.: *SS 708*
Verstraete K.: *SS 710*
Vilanova J.C.: *SS 1407*
Vilela P.: *RC 111*
Villeirs G.M.: *EM 1*
Vliegenthart R.: *SS 1803*

W

Walter T.C.: *SS 703a*
Weishaupt D.: *SS 701a*
Wildberger J.E.: *SY 20*
Wildner S.: *SS 713*
Wirth S.: *SS 317*
Wolf F.: *SS 703a*

Z

Zackrisson S.: *SS 714, SS 1802b*
Zahel T.: *SS 610*